F 1103 66 94

ACADÉMIE DE LA RÉPUBLIQUE SOCIALISTE DE ROUMANIE

REVUE ROUMAINE DE CHIMIE

TOME 32
N° 1
Janvier 1987

Rev. Roumaine Chim.

RRCHAX, 32, *1*, p. 1–110 (1987), Bucarest

EDITURA ACADEMIEI REPUBLICII SOCIALISTE ROMÂNIA

ACADÉMIE DE LA RÉPUBLIQUE SOCIALISTE DE ROUMANIE

COMITÉ DE RÉDACTION

Rédacteur en chef:

I. G. MURGULESCU, membre de l'Académie de la République Socialiste de Roumanie

Rédacteurs en chef adjoints:

A. T. BALABAN et V. EM. SAHINI, membres correspondants de l'Académie de la République Socialiste de Roumanie

Collège de rédaction:

EM. BRATU, ELENA CEAUŞESCU, ECATERINA CIORĂNESCU-NENITZESCU, CR. SIMIONESCU, membres de l'Académie de la République Socialiste de Roumanie ; P. SPACU, membre correspondant de l'Académie de la République Socialiste de Roumanie ; M. BANCIU, M. D. GHEORGHIU, I. HAIDUC, D. I. MARCHIDAN, G. NIAC et D. SĂNDULESCU

La Revue Roumaine de Chimie parait 10 fois par an. Toute commande de l'étranger sera adressée à ROMPRESFILATELIA — sectorul Export-Import Presă, P. O. Box 12—201, télex 10376 prsfi r 78 104 Bucarest, Calea Griviței nr. 64—66, Bucureşti, Roumanie

Les manuscrits, les livres et les revues proposés en échange, ainsi que toute correspondance seront envoyés à la rédaction:

REVUE ROUMAINE DE CHIMIE

125, Calea Victoriei, 79717 Bucarest, Roumanie, téléphone 50 76 80

EDITURA ACADEMIEI REPUBLICII SOCIALISTE ROMÂNIA
125, Calea Victoriei, 79717 Bucarest, Roumanie, téléphone 50 76 80

REVUE ROUMAINE DE CHIMIE

Tome 32, N° 1 **Janvier 1987**

ELENA CEAUȘESCU, R. BORDEIANU, P. GHIOCA, IRINA CERCHEZ, E. BUZDUGAN, RODICA STANCU, Dilute block copolymer systems. VI. Effect of polymeric diluents . . . . 3—20
F. SANDESCU and CR. I. SIMIONESCU, Interfacial phenomena on concentrated polymer solutions in the spinning process . . . . 21—28
C. I. CHIRIAC, A new synthesis of aromatic ureas from carbon dioxide and diamines using ethylene chlorophosphite in pyridine as reagent . . . . . 29—31
S. B. TAMBI, MADHU ANAND, NANDAN BHARGAVA and R. L. MITAL, Synthesis of some new fluorosubstituted tricyclic heterocycles. II. 3-Alkoxy-7-fluoro-10-{3-[4-(2-hydroxyethyl)-1-piperazinyl]-propyl}-2-methoxy phenothiazine derivatives . . . . 33—36
REKHA AGRAWAL, G. K. OBEROI, D. C. JAIN and R. L. MITAL, Studies in the synthesis of 10H-8-trifluoromethyl-1-azaphenothiazine *via* the smiles rearrangement . . . . 37—40
C. LUCA, N. BÎLBĂ, GH. MIHĂILĂ and I. AGHERGHINEI, Inclusion compounds of perhydrotriphenylene with aliphatic monocarboxylic acids 41—46
AIMEE ARIAS-CARBAJAL and ROBERTO CAO, Interaction product of N, N′-bis (Furfurylidene)ethylenediamine with cobalt(II) chloride 47—50
N. P. CID and L. O. GARCÍA VIOR, Oxidation of mordant blue 9 with bromate catalyzed by vanadium (V). Part I. Influence of variables (in Spanish) 51—62
NICULAE OLARU and ZENO SIMON, Electronic structure and reactivity indices for a series of purine derivatives, inhibitors of guanine phosphoribosyltransferase from *Escherichia Coli* . . . . 63—81
NICULAE OLARU and ZENO SIMON, Comparison between empirical and advanced molecular orbital calculations for some derivatives of nitrogen heterocycles . . . . 83—90
D. NEGOIU, S. NEAGOE, MARIA NEGOIU, ELENA BADAU and ELENA GHERMAN, Complex compounds of Pd(II) with thioethers. I. Investigation of some compounds of Pd(II) with thioethers of the bis(phenylthiomethyl) ether series . . . . 91—99
A. CĂLUȘARU and EUGENIA SAVIUC, Rate constants and activation energies of Fe(II) to Fe(III) oxidation reaction by hydroxylamine in normal and heavy water . . . . 101—108

BOOK REVIEWS . . . . 109—110

Rev. Roumaine Chim., 32, *1*, p. 1—110 (1987), Bucarest

Revue Roumaine de Chimie, **32**, *1*, 3–20 (1987)

DILUTE BLOCK COPOLYMER SYSTEMS. VI

EFFECT OF POLYMERIC DILUENTS[1]

ELENA CEAUȘESCU, R. BORDEIANU, P. GHIOCA, IRINA CERCHEZ,
E. BUZDUGAN and RODICA STANCU
Chemical Research Institute ICECHIM, 202 Spl. Independenței, 77208 Bucharest,
Romania

Received December 23, 1985

The effect of low-molecular weight polymeric diluents (polybutadienes, polypiperylenes and polybutenes) on mechanical and rheological properties of a butadiene-styrene triblock copolymer was investigated over a wide range of concentrations. Transitions in the variation of properties with diluent content, observed at low and high dilutions, were interpreted in terms of morphological changes and phase separation of the diluent. The concept of diluent-assisted transitions developed earlier for oil-diluted block copolymers was extended to systems containing polymeric diluents, the factor controlling the properties of dilute block copolymer systems being the diluent/polystyrene ratio. The use of failure envelopes in evaluating the suitability of polymeric diluents is also discussed.

The study of dilute block copolymer systems based on diene-styrene thermoplastic elastomers containing homopolymers incompatible with the glassy domains of the block copolymer is of considerable interest in view of the peculiarities exhibited by such systems. The effects of homopolybutadiene addition to diene-styrene block copolymers on mechanical properties,[2–4] morphology [4–7] and thermodynamics [8] have been explored. Special mention should be made of the works of Kawai and coworkers [9–12] who have established correlations between the molecular weight of the added homopolymer and its solubilization in the corresponding phase of the block copolymer. However, information on the mechanical properties of butadiene-styrene block copolymers diluted with polybutadienes of variable molecular weight and microstructure or with other homopolymers differing in chemical nature from the center block of the thermoplastic elastomer is still rather scarce.

A previous systematic investigation of oil-diluted butadiene-styrene block copolymers [13–17] has revealed that the mechanical and rheological properties of such systems do not obey simple additivity rules. The same applies for other physical characteristics (optical properties, chain orientation, etc.) as well. Morphological effects involving not only the glassy domains but also their surrounding interphase layers, as well as processes occurring in the matrix, seem to play an important part in determining the behaviour of oil-diluted block copolymers.

It was considered interesting to expand this investigation to butadiene-styrene triblock copolymers diluted with low-molecular weight polymers of various chemical structures. Three groups of diluents were chosen : polybutadienes, polypiperylenes and polybutenes *. Two high-molecular weight polybutadienes were also used as diluents : a polymer synthesized with a Ziegler-Natta catalyst, and an anionic polymer, actually a diblock copolymer containing a small polystyrene block at one end of the chain.

EXPERIMENTAL

The triblock copolymer used in this study was obtained by anionic polymerization with *n*-butyllithium in toluene using the sequential monomer addition process, and had the properties given in Table 1. The same polymer (coded L—1) was used in our previous studies on the properties of oil-diluted block copolymer systems,[13–17] which facilitates comparison between the effects of oil and polymeric diluents.

Table 1

Block copolymer properties

Property	Unit	Value
Styrene content	%	34.5
Total molecular weight ($\overline{M}_n$)	$g \cdot mole^{-1}$	123,200
Mol. wt. of polystyrene blocks	$g \cdot mole^{-1}$	21,200
Mol. wt. of polybutadiene block	$g \cdot mole^{-1}$	70,200
Tensile modulus at $\lambda = 4$	MPa	3.8
Hardness	°Sh A	69.5
Tensile strength	MPa	27.6
Extension ratio at break (λ_b)	—	8.43
Set at break (λ_s)	—	1.11
Initial Young's modulus	$daN \cdot cm^{-1}$	5.75
Melt viscosity at 170° ($\dot{\gamma} = 2.071\ s^{-1}$)	P	1,118,000

The properties of the polymeric diluents are given in Table 2. Commercial liquid polybutadienes of various molecular weights and microstructures were used as sold by the manufacturers. The high-molecular weight *cis*-1,4-polybutadiene (Z) is a commercial product of the Romanian rubber industry. The anionic polybutadiene (AN) is a developmental polymer synthesized at ICECHIM. The polypiperylenes were also obtained at ICECHIM by cationic polymerization of an unsaturated C_5 hydrocarbon fraction. The polybutenes were synthesized by cationic polymerization at the Research Institute for Petrochemistry and Oil Refineries (ICITPR—Ploieşti). With the exception of polymer MC-5, all the other low-molecular weight polymeric diluents were liquid at room temperature.

---

* Some of the properties of polypiperylene-containing systems are also discussed in another paper, [18] and are included here for the sake of unity.

Table 2

Properties of polymeric diluents

Chemical composition	Polybutadienes						Polypiperylenes			Polybutenes	
Designation	Lithene PM	Nisso B-1000	Plastikator 32	Polyöl 110	Z	AN*	MCL-3	MCL-4	MC-5	N-8	N-19
Origin	Revertex (U.K.)	Nippon Soda (Japan)	Buna-Schkopau (G.D.R.)	Hüls (F.R.G.)	Petrochem. Works Brazi	ICE-CHIM	ICE-CHIM	ICE-CHIM	ICE-CHIM	ICITPR Ploieşti	ICITPR Ploieşti
Molecular weight ($\overline{M}_n \times 10^{-3}$)	1.3	1.21	32	1.2	110	300	0.47	0.77	1.46	1.3	0.55
Microstructure											
cis-1.4	22	8	15	72	91	39	predominantly *trans*	*trans* + *cis*	predominantly *trans*	predominantly isobutylene units	
trans-1.4	33	5	40	27	6	53					
1.2	45	87	45	1	3	8					
Density (d_4^{20}, $g \cdot cm^{-3}$)	0.844	0.858	0.890	0.908	0.920	0.920	0.910	0.920	0.930	0.901	0.865

* Diblock copolymer containing a polystyrene block of $\overline{M}_n = 1500$

The diluents were blended with the triblock copolymer in toluene solution and films of approx. 0.8 mm thickness were obtained by spin casting using a method described in a previous paper.[19] The volume fraction of diluent in the network was calculated from blend composition, assuming ideal additivity of the specific volumes calculated from the densities given in Table 2, and with $v = 1.116$ for polybutadiene (rubber matrix of the triblock copolymer), neglecting the presence of the interphase layer.

Visual inspection of the blends showed that for all the liquid polybutadienes the cast films were clear over the entire range of concentrations. For polybutene-containing blends, as well as for the system diluted with polypiperylene MC-5, the films were cloudy even at low diluent concentrations (5—15 parts per 100 parts thermoplastic rubber — phr). Polypiperylene MCL-3 was slightly more compatible, the films becoming turbid beginning from 30 phr diluent in the block copolymer.

Tensile properties were determined at 25° on a Zwick Mod. 1454 tensile tester at a jaw separation speed of $0.5\ \mathrm{m \cdot min^{-1}}$, on dumbbell test pieces with an active length of 20 mm. Yield properties were determined at a jaw separation speed of $0.1\ \mathrm{m \cdot min^{-1}}$. Hardness was measured in the Shore A scale with a Zwick dead load hardness meter on film sheets piled up to a total thickness of 6 mm. Melt viscosity was measured at 170° and a shear rate of $2.071\ \mathrm{s^{-1}}$ on an Instron capillary rheometer fitted with a $4'' \times 0.06''$ capillary for which end effects are negligible.

RESULTS AND DISCUSSION

1. Large-Strain Tensile Modulus and Hardness

By diluting the elastic network of the triblock copolymer with polymeric diluents, the large-strain tensile modulus (f), i.e. the stress at an extension ratio $\lambda \equiv L/L_0 = 4$, shows, as in the case of systems diluted with mineral oils[13] a non-uniform decrease with increasing degree of dilution (expressed as volume fraction of rubber in the diluted matrix, Φ_R). Rather large differences in the shape of the respective $\log f - \log \Phi_R$ plots are found, depending mainly on the chemical nature of the diluent (Figure 1).

In the case of polybutadiene-diluted systems, a dependence of f on Φ_R similar to that found for oil-containing systems[13] is met : at low degrees of dilution modulus decreases slowly with Φ_R, after which a steeper descent follows. With the exception of the system diluted with the high-vinyl, low-molecular weight polybutadiene (Nisso), the length of the first zone is considerably shorter than for oil in the $\log f - \log \Phi_R$ diagram : for Plastikator, Lithene and Polyöl the onset of the transition lies around $\Phi_R = 0.78$, while for oil this transition was found to take place at $\Phi_R = 0.63$. High-molecular weight polybutadienes show a linear dependence of $\log f$ on $\log \Phi_R$. The smaller slope in the case of the anionic polybutadiene is probably due to the presence of a small block of polystyrene at the end of each chain. The polystyrene blocks of the diluent having a molecular weight similar to that of the polystyrene blocks of the triblock copolymer are largely compatible with the glassy domains of the thermoplastic elastomer. As a result, the diluent chains become anchored at one end with ensuing decrease in mobility.

In the polypiperylene series, although the slope of the first zone of tensile modulus variation with dilution is virtually equal to that found for oil-diluted systems, the slope of the second zone is dependent on the molecular weight of the diluent. Thus, while the lowest molecular weight polypiperylene (MCL—3) shows a slope similar to that of oil, the slope decreases with increasing molecular weight until, for polymer MC—5 which is solid at room temperature, the modulus shows only a slight increase with dilution, increasing again at high concentrations of diluent in the matrix.

In the case of systems diluted with polybutenes, an increase in modulus at low concentrations of diluent was observed. This apparent rigidization of the network might be linked with an antiplasticizing effect.

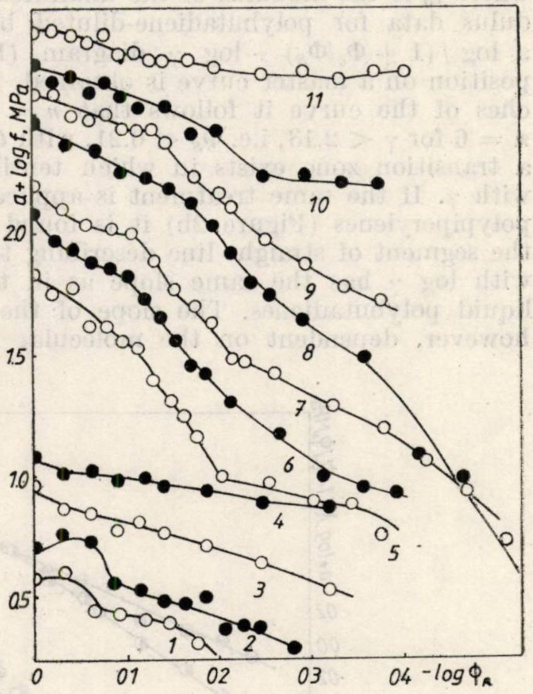

Fig. 1. — Dependence of large-strain tensile modulus on volume fraction of rubber in the diluted matrix (polymer designation as in Table 2). *1* — N-19, $a = 0$; N-8, $a = 0.125$; *3* — Z, $a = 0.375$; *4* — AN, $a = 0.5$; *5* — Plastikator, $a = 1.25$; *6* — Lithene, $a = 1.5$; *7* — Polyöl, $a = 1.625$; *8* — Nisso, $a = 1.875$; *9* — MCL-3, $a = 2$; *10* — MCL-4, $a = 2.125$; *11* — MC-5, $a = 2.25$.

The studies on oil-diluted block copolymers[13] have shown that the large strain tensile modulus can be described with reasonable accuracy by the following semiempirical equation:

$$f = (C_1' + C_2'/\lambda)\,(\lambda - 1/\lambda^2)\ \Phi_R^{1/3}\ (\Phi_{S,0}^{-1/2}\gamma)^n \qquad (1)$$

where, besides the symbols already explained, $\Phi_{S,0}$ is the volume fraction of polystyrene in the undiluted polymer, γ is the Guth-Smallwood function ($\gamma = 1 + 2.5\,\Phi_S + 14.1\Phi_S^2$ where Φ_S is the volume fraction of polystyrene in the diluted polymer), and C_1', C_2' are constants. For block copolymers diluted with paraffinic-naphthenic oils the exponent n is 4/3 for $\Phi_S > 0.20$ and 4 for $\Phi_S < 0.18$. It was later found, by more detailed investigations of the physical and mechanical properties of dilute block copolymer systems, that the onset of the transitions occurring in those properties correlates with the volume fraction of oil/ volume fraction of polystyrene ratio (Φ_o/Φ_S) rather than with Φ_R, supporting thus the assumption that the transitions are assisted by the diluent.[15] If this concept is extended to the variation of tensile modulus with dilution, Eq. (1) may be modified as follows:

$$f/f_0 = C(1 + \Phi_o/\Phi_S)\,(\gamma/\gamma_0)^n \qquad (2)$$

where f_0 is the modulus of the undiluted block copolymer. If tensile modulus data for polybutadiene-diluted block copolymers are plotted in a $\log f/(1 + \Phi_o/\Phi_S) - \log \gamma$ diagram (Figure 2a), a satisfactory superposition on a master curve is obtained. From the slopes of the two branches of the curve it follows that $n = 4.7$ for $\gamma > 2.4$ ($\Phi_S > 0.24$) and $n = 6$ for $\gamma < 2.13$, i.e. $\Phi_S < 0.21$, with $C = 1$. Between the two branches a transition zone exists in which tensile modulus varies more strongly with γ. If the same treatment is applied to the blends containing liquid polypiperylenes (Figure 2b) it is found that at low degrees of dilution the segment of straight line describing the variation of $\log f/(1 + \Phi_o/\Phi_S)$ with $\log \gamma$ has the same slope as in the case of systems diluted with liquid polybutadienes. The slope of the second branch of the curve is, however, dependent on the molecular weight of the diluent. The fact that for polypiperylene MCL-4 the second branch continues the first branch without any apparent change in slope is probably coincidental. Apart from their quantitative value, the plots given in Figure 2 demonstrate convincingly the existence of a transition in tensile modulus properties of block copolymers diluted with polymeric diluents.

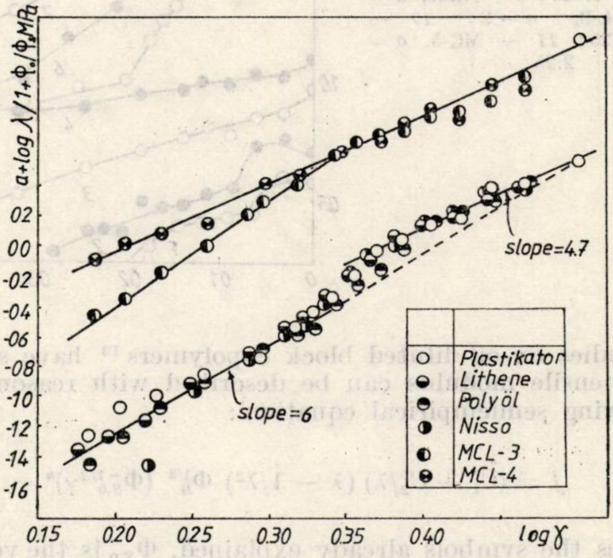

Fig. 2. — Variation of reduced tensile modulus with Guth-Smallwood function. *a* — Liquid polybutadienes ($a = 0$); *b* — Liquid polypiperylenes ($a = 0.6$).

The pattern of hardness variation with dilution follows in general that of large-strain tensile modulus.[14] It should be stressed that hardness testing involves small strain compression, in contrast to modulus testing which involves large strain tension. The similarity of the response of dilute block copolymer systems to the two kinds of strain becomes evident from the hardness data given in Figure 3. Moreover, the transitions found in the variation of hardness with the degree of dilution occur at roughly the same values of Φ_R as in the case of tensile modulus measurements. From a practical point of view it is interesting to note that, while low-molecular weight polybutadienes reduce rather strongly the hardness of dilute systems, the hardness of the triblock copolymer diluted with high molecular weight polybutadienes or the higher molecular weight polybutene remains virtually constant over a comparatively wide range of Φ_R (note also that the previously mentioned rigidization of the systems containing low amounts of polybutenes is absent). Not unexpected is the relative independence of hardness on the content of polypiperylene MC—5, a diluent solid at room temperature.

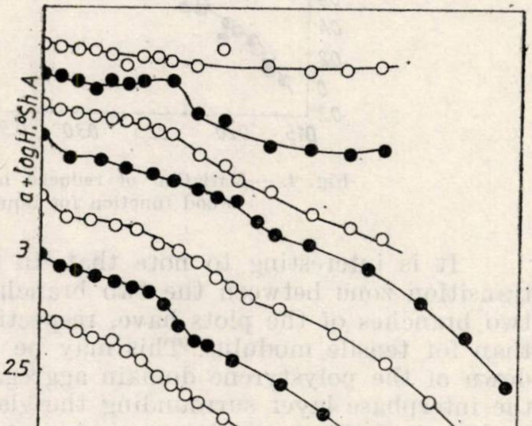

Fig. 3. — Dependence of hardness on volume fraction of rubber in the diluted matrix. *1* — N-19, $a = -0.125$; *2* — N-8, $a = 0$; *3* — Z, $a = 0.125$; *4* — AN, $a = 0.25$; *5* — Plastikator, $a = 0.875$; *6* — Lithene, $a = 1.125$; *7* — Polyöl, $a = 1.375$; *8* — Nisso, $a = 1.625$; *9* — MCL-3, $a = 1.75$; *10* — MCL-4, $a = 1.875$; *11* — MC-5, $a = 2$.

If the hardness data are reduced by using a model similar to Eq. 2, i.e. plotting $\log H/(1 + \Phi_o/\Phi_S)$ against $\log \gamma$, all the systems containing liquid polybutadienes fit reasonably well the master curve presented in Figure 4. As in the case of large strain tensile modulus two linear branches of different slope are evident, hence hardness variation can be adequately described by :

$$H/H_0 = C(1 + \Phi_o/\Phi_S)\,(\gamma/\gamma_0)^n \qquad (3)$$

where $n = 3.9$ and $C = 1$ for $\gamma > 2.4$ ($\Phi_S > 0.24$), and $n = 5.6$ and $C = 1.6$ for higher degrees of dilution. Obviously, the value of C, which is a lumped constant, will also depend on $\Phi_{S,0}$. The data presented in this study were obtained on blends based on only one block copolymer, hence they offer no information on the effect of initial polymer composition on hardness. The same applies for the modulus equation (Eq. 2) which, furthermore, lacks the dependence of f on λ.

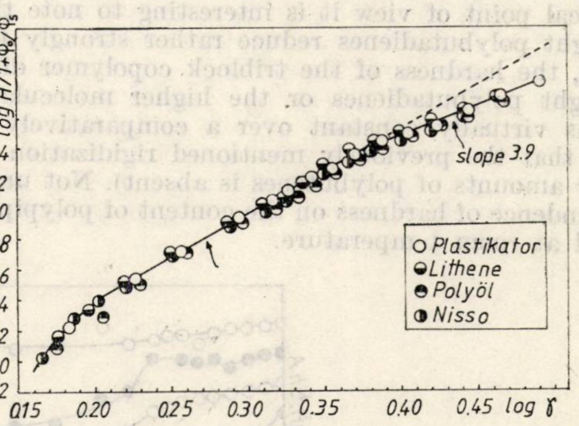

Fig. 4. — Variation of reduced hardness with Guth-Smallwood function for liquid polybutadienes.

It is interesting to note that, in contrast to tensile modulus, the transition zone between the two branches of the plot is absent and the two branches of the plots have, respectively, smaller slopes for hardness than for tensile modulus. This may be explained by the massive breakdown of the polystyrene domain aggregates in large-strain testing. Also, the interphase layer surrounding the glassy domains may play a significant part in this transition occurring at $\Phi_o/\Phi_S \approx 1$, as a collapse of that layer under stress at a critical degree of dilution is not improbable. For oil-diluted systems the transition mentioned above occurs at about the same value of Φ_o/Φ_S for both tensile modulus[13] and hardness.[14]

2. Ultimate Tensile Properties

The ultimate tensile properties (tensile strength, σ_b, elongation at break, λ_b, and set at break, λ_s) depend on the degree of dilution in a somewhat predictable manner and similar to that found for oil-diluted thermoplastic elastomers.[15] Thus, tensile strength (Figure 5) shows a general decrease with dilution but, as in the case of other properties of dilute systems, this dependence is not uniform. For virtually all the polymeric diluents investigated the decrease in tensile strength is slight at low degrees of dilution and, after a critical concentration of diluent has been reached, tensile strength decreases faster. A rather significant difference from oil-diluted systems[15] is the absence of the small increase n σ_b in the presence of small amounts of diluent. This is consistent with the explanation that the initial increase is brought about, in oil-diluted systems, by a reduction in matrix viscosity which, in its turn, leads to a more uniform stress distribution at the domain/matrix interface retarding thus the catastrophic failure of the glassy domains. Since even the lowest molecular weight polymeric diluent had a considerably higher viscosity than the mineral oils used in our previous study,[15] the plasticizing effect of the diluents was weaker and so was their ability of removing local stress concentrations on the interface.

While the length of the initial plateau seems difficult to correlate with the properties of the polymeric diluents, the slope of the second portion of the log σ_b — log Φ_R curves is to a large extent dependent on the chemical nature of the diluents: at high dilutions, the descendent slope of the curves for polybutadiene-diluted systems is the highest and apparently independent of microstructure and molecular weight. A different behavior is exhibited by the systems containing high-molecular weight polybutadienes: in contrast to all the other systems tensile strength decreases sharply over a narrow interval of degrees of dilution and then levels out at a comparatively low value. It must be recalled that the added polybutadienes had higher molecular weights than the middle block of the triblock copolymer, hence were incompatible with the matrix.[5-12] Due to the presence of the small polystyrene block, the anionic polybutadiene (AN) is "compatibilized" with the matrix,[25] which explains the different behavior of AN.

For the systems containing polypiperylenes, tensile strength shows a slower decrease with Φ_R in the high dilution range. Interestingly enough, the behavior in this respect of polymer MC-5 which is solid at room temperature is not significantly different from the other polypiperylenes. The systems containing polybutenes, although investigated over a more limited range of degrees of dilution, seem to exhibit the first (plateau) zone only.

If the concept of diluent-assisted transitions[15] is applied, then the Φ_o/Φ_S ratio rather than Φ_R should be the factor controlling the transitions of σ_b. Indeed, by plotting σ_b against $1 + \Phi_o/\Phi_S$ in a log-log diagram (Figure 6), it becomes clear that for all the four systems containing liquid polybutadienes the changes in slope occur at approximately the same values of Φ_o/Φ_S, which lends further support to the validity of extending that concept to polymer-diluted systems. However, the variation in the position of the transitions is an indication that the effects are complicated by structural characteristics of the polymeric diluents.

Elongation at break decreases in general as expected with Φ_R but again non-uniformly. The systems containing liquid polybutadienes show the strongest dependence of λ_b on diluent content in the network, similar to that found in oil-diluted triblock copolymers.[15] However, the maxima and minima found in the latter systems and assigned to morphological transitions are less marked. The effect of liquid polybutadienes on λ_b is dependent on both molecular weight and microstructure, as it becomes evident from a comparison of the respective curves given in Figure 7: while the slopes of the initial portions of the curves seem to be largely equal for all the polybutadienes, λ_b levels out sooner for Plastikator (the highest molecular weight member of the group); also, for roughly the same molecular weight the plateau is reached sooner for Polyöl than for Nisso which has the highest content of vinyl units in the chain.

The presence in the matrix of the slightly compatible or incompatible high-molecular weight polybutadienes, polypiperylenes or polybutenes leads to a much slighter increase in λ_b, due to the smaller disentanglement of polybutadiene blocks in the elastic network.

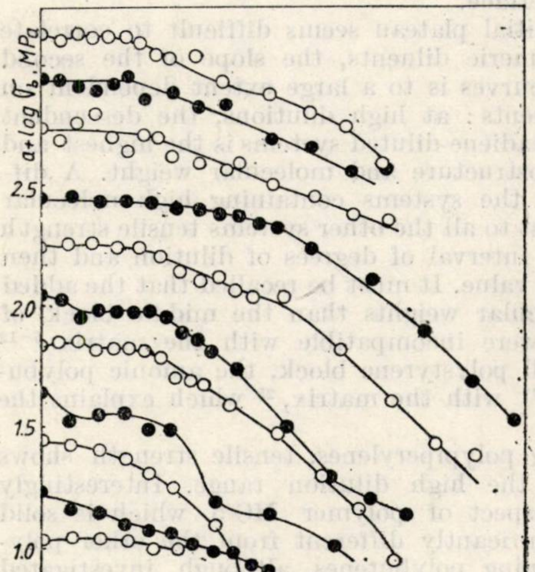

Fig. 5. — Dependence of tensile strength on volume fraction of rubber in the diluted matrix. *1* — N-19, $a = -0.4$; *2* — N-8, $a = -0.2$; 3 — Z, $a = 0$; *4* — AN, $a = 0.2$; *5* — Plastikator, $a = 0.4$; *6* — Lithene, $a =$ p.6; *7* — Polyöl, $a = 0.8$; *8* — Nisso, $a = 1$; *9* — MCL-3, $a = 1.3$; *10* — MCL-4, $a = 1.5$; *11* — MC-5, $a = 1.7$.

True tensile strength (σ_t), i.e. retractive force divided by cross-sectional area of sample at break, actually gives the combined effect of "engineering" tensile strength, σ_b, and elongation at break. Plots of σ_t as a function of the degree of dilution are given in Figure 8. In comparison with oil-diluted systems [15] the curves are less rich in characteristic features. Still, while polybutadiene-containing systems show a flat maximum similar to that found for oil-diluted systems, both polypiperilenes and polybutenes show only an initial plateau, followed by a descent with a slope which, in the case of polypiperylenes, is dependent on molecular weight.

By analogy between the known effects of temperature on the ultimate tensile properties of block copolymers [20] and the effects brought about by dilution, a failure envelope can be drawn[15] by plotting true tensile strength against elongation ratio $\varepsilon_b \equiv \Delta L/L_0$ for samples containing increasing amounts of diluents. Such failure envelopes are given in Figure 9 for liquid polybutadienes and polybutenes (a), high molecular weight polybutadienes (b) and polypiperylenes (c). The examination of these plots in which diluent concentration increases clockwise reveals striking differences between the various groups of diluents. The failure envelopes for systems containing liquid polybutadienes are largely similar to those for oil-diluted block copolymers.[15] With increasing dilution a maximum in σ_t and a further maximum in ε_b are reached. Both maxima ($\sigma_{t,\max}$ and $\varepsilon_{b,\max}$) are in the order : Nisso > Polyöl > Lithene > Plastikator, which probably reflects the order of compatibility between the respective polymers and the polybutadiene matrix of the triblock copolymer. Indeed, the higher the compatibility between diluent and matrix, the better the uniformization of stresses on the domain/ matrix interface (hence higher tensile strength due to failure retardation) and the stronger the disentanglement of the polybutadiene blocks of the thermoplastic rubber (hence higher elongation at break).

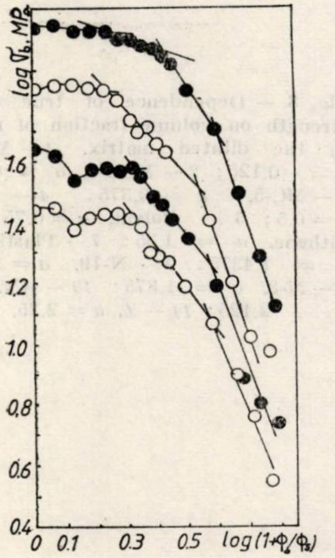

Fig. 6 — Dependence of tensile strength on diluent/ polystyrene ratio for systems containing liquid polybutadienes. 1 — Plastikator, $a = 0$; 2 — Lithene, $a = 0.2$; 3 — Polyöl, $a = 0.4$; 4 — Nisso, $a = 0.6$.

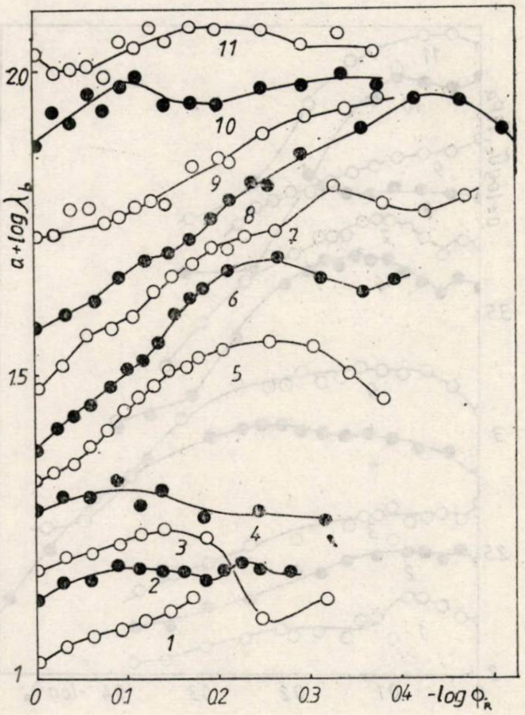

Fig. 7. — Dependence of elongation at break on volume fraction of rubber in the diluted matrix. 1 — N-19, $a = 0.1$; 2 — N-8, $a = 0.2$; 3 — Z, $a = 0.25$; 4 — AN, $a = 0.35$; 5 — Plastikator, $a = 0.4$; 6 — Lithene, $a = 0.45$, 7 — Polyöl, $a = 0.55$, 8 — Nisso, $a = 0.65$; 9 — MCL-3, $a = 0.8$; 10 — MCL-4, $a = 0.95$; 11 — MC-5, $a = 1.1$.

In contrast, for the two high-mol. wt. polybutadienes tested $\sigma_{t,\max}$ and $\varepsilon_{b,\max}$ are only insignificantly higher than the ultimate values for the undiluted polymer. The lower value of $\varepsilon_{b,\max}$ for the anionic diblock (AN) is probably due to the immobilizing effect of its polystyrene end block which anchors each chain of the diluent to a glassy domain of the triblock copolymer.

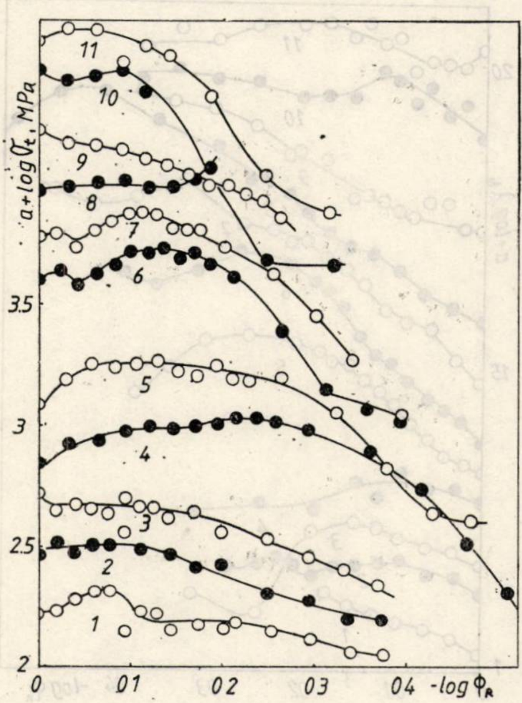

Fig. 8. — Dependence of true tensile strength on volume fraction of rubber in the diluted matrix. *1* — MCL-3, $a = -0.125$; *2* — MCL-4, $a = 0.125$; *3* — MC-5, $a = 0.375$; *4* — Nisso, $a = 0.5$; *5* — Polyöl, $a = 0.75$; *6* — Lithene, $a = 1.25$; *7* — Plastikator, $a = 1.4375$; *8* — N-19, $a = 1.625$; *9* — N-8, $a = 1.875$; *10* — AN, $a = 2.125$; *11* — Z, $a = 2.25$.

For both polybutenes and polypiperylenes the effects of incompatibility become obvious from the severely distorted shapes of the respective failure envelopes. As expected, in a given class of diluents incompatibility is increasingly severe the higher the molecular weight of the diluent. Thus, for polypiperylenes, both $\sigma_{t,\max}$ and $\varepsilon_{b,\max}$ decrease in the order: MCL-3 > MCL-4 > MC-5.

The usefulness of failure envelopes lies mainly in the fact that the user may evaluate at a glance the effects of a particular diluent on the properties of a given thermoplastic rubber and may easily choose the degree of dilution needed to achieve optimal ultimate tensile properties or compare the effects of different diluents. Thus, from a practical point of view, it may be concluded that polybutadienes of low molecular weight (not much higher than 10^3) are the best candidates as polymeric diluents for thermoplastic elastomers based on butadiene-styrene block copolymers.

The dependence of set at break (given here as $\lambda_s \equiv$ sample length after break and recovery/initial sample length) on Φ_R is given in Figure 10. No immediately obvious regularities can be detected in the shape of the curves and the data seem to be rather scattered. Parenthetically, this apparent scattering, common to virtually all elastomers, makes set at break data to be regarded as unreliable by most rubber technologists. However, at least for dilute block copolymer systems, λ_s data can provide some additional insight on the phenomena taking place at failure.

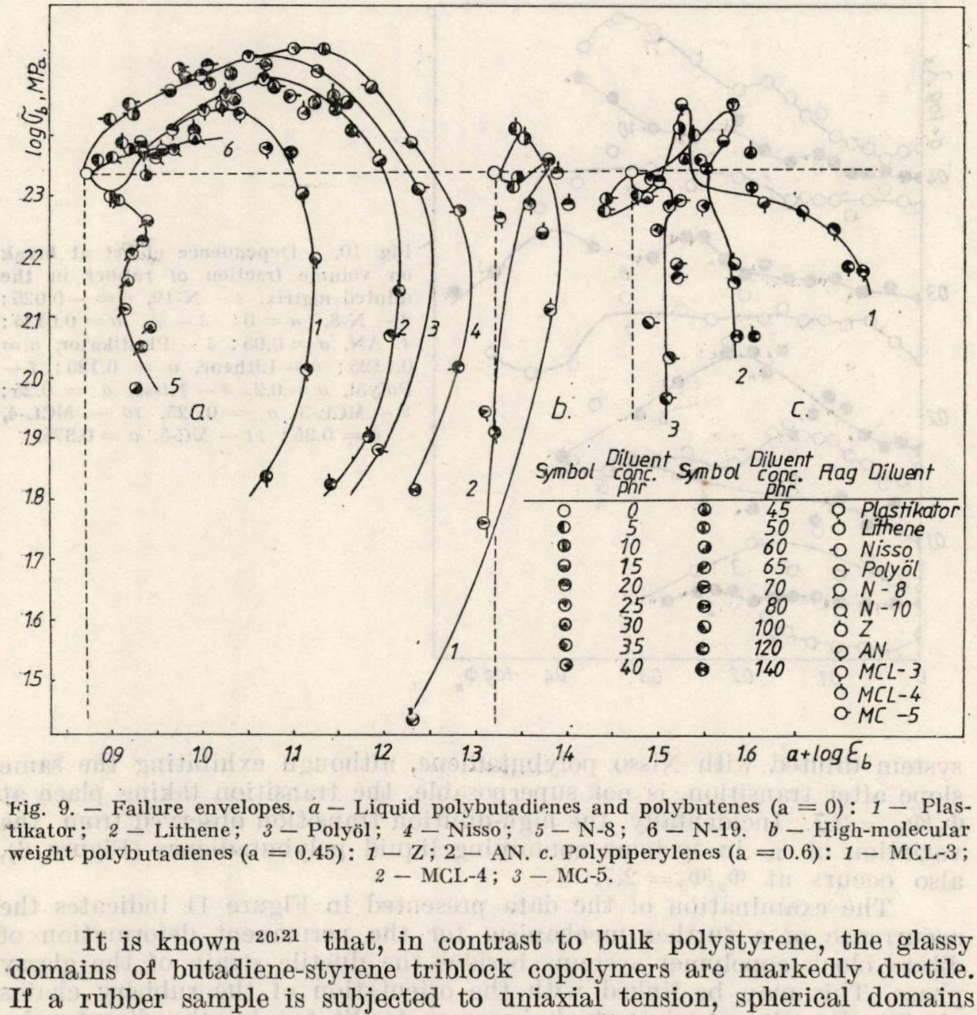

Fig. 9. — Failure envelopes. *a* — Liquid polybutadienes and polybutenes (a = 0) : *1* — Plastikator ; *2* — Lithene ; *3* — Polyöl ; *4* — Nisso ; *5* — N-8 ; 6 — N-19. *b* — High-molecular weight polybutadienes (a = 0.45) : *1* — Z ; 2 — AN. *c*. Polypiperylenes (a = 0.6) : *1* — MCL-3 ; *2* — MCL-4 ; *3* — MC-5.

It is known [20,21] that, in contrast to bulk polystyrene, the glassy domains of butadiene-styrene triblock copolymers are markedly ductile. If a rubber sample is subjected to uniaxial tension, spherical domains become ellipsoidal with the main axis parallel to the direction of the stress vector, while rodlike and lamellar domains undergo extensive fracture and deformation.[4] If the ductile deformation of the glassy phase, which is proportional to true tensile strength, is the main origin of set at break, then the λ_s/σ_t ratio should be constant irrespective of the degree of dilution. Indeed, if for systems containing liquid polybutadienes the λ_s/σ_t ratio rather than λ_s is plotted against the degree of dilution, it can be seen that for a considerable range of Φ_R the value of that ratio is constant. After a critical Φ_R is reached, λ_s/σ_t begins to increase with a constant slope for all the liquid polybutadienes. However, the transition point differs from diluent to diluent (Figure 11). A plot of λ_s/σ_t against $1+\Phi_o/\Phi_S$ brings a reasonable superposition of data for Plastikator, Lithene and Polyöl with a rather sharp transition at $\Phi_o/\Phi_S = 2.2$. The

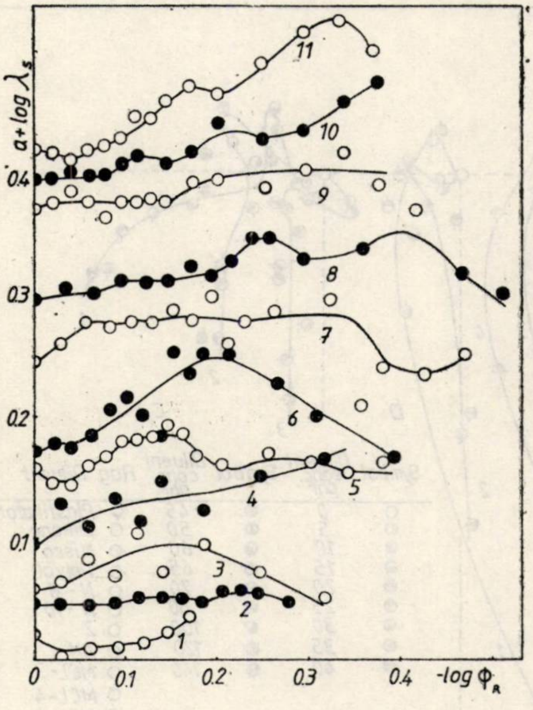

Fig. 10. — Dependence of set at break on volume fraction of rubber in the diluted matrix. *1* — N-19, $a = -0.025$; *2* — N-8, $a = 0$; *3* — Z, $a = 0.0125$; *4*. AN, $a = 0.05$; *5* — Plastikator, $a = 0.1125$; *6* — Lithene, $a = 0.125$; *7* — Polyöl, $a = 0.2$, *8* — Nisso, $a = 0.25$; *9* — MCL-3, $a = 0.325$, *10* — MCL-4, $a = 0.35$; *11* — MC-5, $a = 0.375$.

system diluted with Nisso polybutadiene, although exhibiting the same slope after transition, is not superposable, the transition taking place at $\Phi_o/\Phi_S = 2.7$. Incidentally, the high-dilution transition observed from the variation of σ_b in systems containing liquid polybutadienes (Figure 6), also occurs at $\Phi_o/\Phi_S = 2.7$.

The examination of the data presented in Figure 11 indicates the occurrence of a further mechanism for the permanent deformation of dilute block copolymer systems besides the ductile strain of the glassy phase. This may be linked with the orientation of the rubbery chains constituting the matrix, which becomes facilitated by the disentanglement of the polybutadiene blocks at high degrees of dilution. However, such an explanation would not be entirely consistent with the assistance by diluent (demonstrated by the superposability in the log λ_s/σ_t — log $(1+\Phi_o/\Phi_S)$ plot) which would necessarily involve the polystyrene domains and/ or their interphase layers. It must be stressed that at high diluent concentrations dilute block copolymer systems are thermodynamically unstable: the equilibrium concentration of paraffinic-naphthenic oil in the triblock copolymer used in the present study is of about 72 phr,[13] i.e. $\Phi_R = 0.47$ and $\Phi_o/\Phi_S = 2.6$. It may be assumed that at higher concentrations the diluent will tend to segregate forming a separate phase. This segregation will occur at lower concentrations for less compatible diluents. The most probable locus for beginning segregation is the interphase layer where, due to the presence of both butadiene and styrene units, the compatibility with the diluent is lower than in the matrix proper. Furthermore, the segregation is stress-induced and in the block copolymer the interphase layer which surrounds the rigid domains is the site of the highest local stresses. Hence, it seems probable that the transition at $\Phi_o/\Phi_S = 2.7$ is due to the phase separation of the diluent, beginning in the interphase layer.

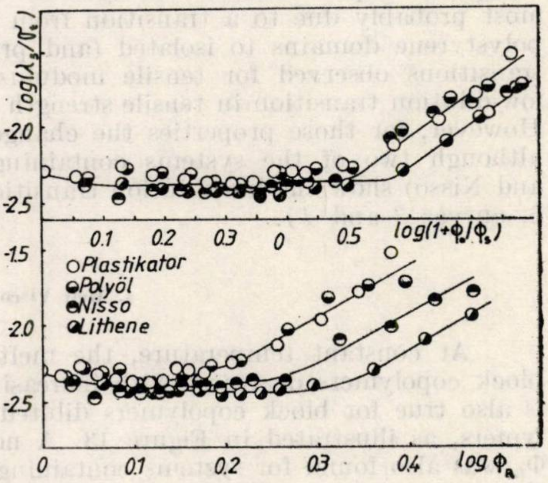

Fig. 11. — Variation of set at break/true tensile strength ratio. *a*, *b* — Liquid polybutadienes; *1* — Plastikator; *2* — Lithene; *3* — Polyöl; *4* — Nisso.

3. Small-Strain Properties

The films of triblock copolymer blends were cast from toluene, a good solvent for both polybutadiene and polystyrene blocks. This is conducive to the formation of frequent bridges between adjacent polystyrene domains.[21,23,24] When the volume fraction of the glassy phase is sufficiently large, an interpenetrating network of polystyrene and polybutadiene may result. At the first extension of the sample the small-strain behavior is governed by the continuous phase of polystyrene or the large aggregates of polystyrene domains, their breakdown giving rise to yielding and drawing (necking).[4,21] Hence, small-strain Young's modulus is useful in evaluating the coherence and long-range continuity of the glassy phase.[15]

In Figure 12 the small-strain Young's modulus data for the systems diluted with liquid polybutadienes are plotted against $1 + \Phi_o/\Phi_S$. It can be seen that a definite change in slope occurs at $\Phi_o/\Phi_S = 0.74$. A similar effect, with a transition occurring at the same Φ_o/Φ_S value, is found for polypiperylene-diluted systems.

In oil-diluted systems the pattern of variation is more complicated, maxima being found at $\Phi_o/\Phi_S = 0.58$ and 1.00, and two changes in slope at $\Phi_o/\Phi_S = 0.72$ and 1.57[15]. The causes of the difference in this respect between polymer- and oil-diluted systems are still obscure. The single change in slope found for the systems containing polymeric diluents is most probably due to a transition from increasingly loose aggregates of polystyrene domains to isolated (and probably spherical) domains. The transitions observed for tensile modulus and hardness, as well as the low-dilution transition in tensile strength were ascribed to the same effect. However, for those properties the change in slope occurs at $\Phi_o/\Phi_S \approx 1$, although two of the systems containing liquid polybutadienes (Polyöl and Nisso) show the low-dilution transition in σ_b at $\Phi_o/\Phi_S \approx 0.7$ (Figure 6, curves *3* and *4*).

4. Melt Viscosity

At constant temperature, the melt viscosity of butadiene-styrene block copolymers decreases with increasing degree of dilution.[16,26] This is also true for block copolymers diluted with low-molecular weight polymers, as illustrated in Figure 13. A non-uniform dependence of η on Φ_R was also found for systems containing mineral oils,[16] the maxima on the curves being ascribed to morphological transitions induced by dilution and assisted by the diluent[15,16] which confirm the composite character of block copolymers even in the melt, high above the glass transition temperature of polystyrene.[27] Such maxima are, with the possible exception of the system containing the lowest molecular weight polypiperylene, (MCL-3), comparatively less evident in the case of polymer-diluted systems and no immediately identifiable regularities in their positions can be found.

For oil-diluted butadiene-styrene block copolymers of various compositions and molecular architectures it was found[15] that the rheological features are rather well superposable in $\log \eta - \log(1 + \Phi_o/\Phi_S)$ plots. Such a plot is given in Figure 14 for the systems containing liquid polybutadienes or polypiperylenes. It can be seen that for all the systems the decrease in melt viscosity can be described with approximation by a single straight line whose slope, calculated by a restricted linear least squares fit, is about -2. Hence, the viscosity of polymer-diluted block copolymers in the melt is given by:

$$\eta/\eta_0 = (1 + \Phi_o/\Phi_S)^{-2} \tag{4}$$

where η is the melt viscosity of the diluted and η that of the undiluted block copolymer. Equation (4) also fits reasonably well the data for oil-diluted block copolymers presented in Ref. 15 for $\Phi_o/\Phi_S \leqslant 2$.

By the superposition of the viscosity curves, certain regularities in the deviation of experimental points from the least squares line become apparent, with rather diffuse maxima at $\Phi_o/\Phi_S \approx 0.5$, 1.3 and 2.2. The question if, in the case of polymer-diluted block copolymers, these maxima denote the presence of transitions occurring in the melt is, in our opinion still open and requires further investigations.

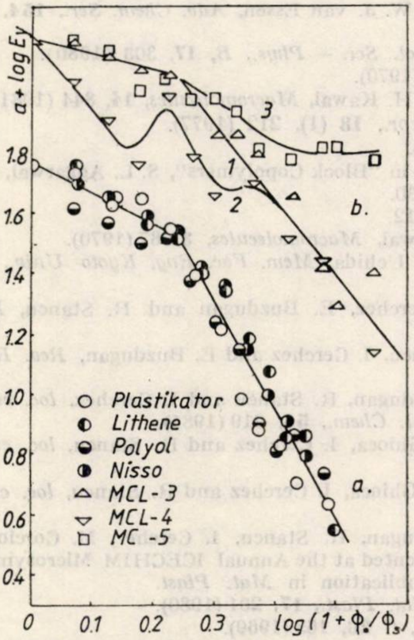

Fig. 12. — Dependence of initial Young's modulues on diluent/polystyrene ratio. *a* — Liquid polybutadienes ($a = 0$); *b* — Polypiperylenes ($a = 0.4$): *1* — MCL-3; *2* — MCL-4; *3* — MC-5.

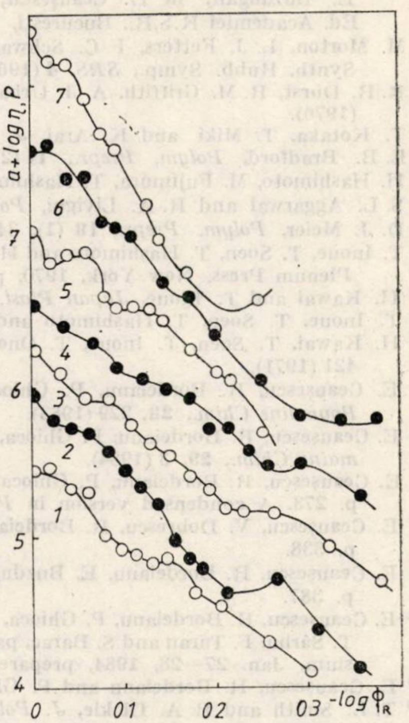

Fig. 13. — Dependence of melt viscosity at 170° (shear rate $2.071 s^{-1}$) on volume fraction of rubber in the diluted matrix. *1* — Plastikator, $a = 0.6$; *2* — Lithene, $a = -0.1$; *3* — Polyöl, $a = 0.2$; *4* — Nisso, $a = 0.5$; *5* — MCL-3, $a = 1$; *6* — MCL-4, $a = 1.5$; *7* — MC-5, $a = 2.3$.

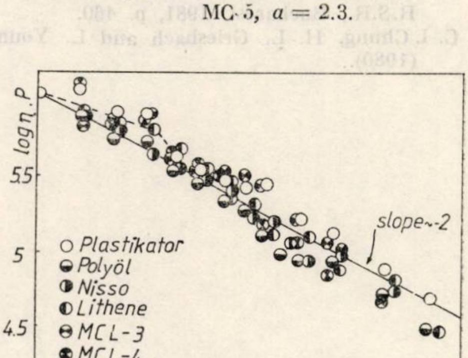

Fig. 14. — Dependence of melt viscosity of systems containing liquid polybutadienes and polypiperylenes on diluent/polystyrene ratio.

REFERENCES

[1] Part V of this series: E. Ceauşescu, R. Bordeianu, P. Ghioca, I. Cerchez, R. Stancu and E. Buzdugan, in E. Ceauşescu, "Cercetări în chimia şi tehnologia polimerilor", Ed. Academiei R.S.R., Bucureşti, 1983, p. 372.

[2] M. Morton, L. J. Fetters, F. C. Schwab, C. R. Strauss and R. F. Kammereck, Proc. 4-th Synth. Rubb. Symp., *SRS*, **4** (1969).

[3] R. R. Durst, R. M. Griffith, A. J. Urbanic and W. J. van Essen, *Adv. Chem. Ser.*, **154**, 239 (1976).

[4] T. Kotaka, T. Miki and K. Arai, *J. Macromol. Sci. — Phys.*, *B*, **17**, 303 (1980).

[5] E. B. Bradford, *Polym. Prepr.*, **11** (2), 392 (1970).

[6] H. Hashimoto, M. Fujimura, T. Hashimoto and H. Kawai, *Macromolecules*, **14**, 844 (1981).

[7] S. L. Aggarwal and R. A. Livigni, *Polym. Prepr.*, **18** (1), 212 (1977).

[8] D. J. Meier, *Polym. Prepr.*, **18** (1), 340 (1977).

[9] T. Inoue, T. Soen, T. Hashimoto and H. Kawai, in "Block Copolymers", S. L. Aggarwal, ed., Plenum Press, New York, 1970, pp. 19—30.

[10] H. Kawai and T. Inoue, *Japan Plast.*, **1970**, 12.

[11] T. Inoue, T. Soen, T. Hashimoto and H. Kawai, *Macromolecules*, **3**, 87 (1970).

[12] H. Kawai, T. Soen, T. Inoue, T. Ono and T. Uchida, *Mem. Fac. Eng. Kyoto Univ.*, **33**, 421 (1971).

[13] E. Ceauşescu, R. Bordeianu, P. Ghioca, I. Cerchez, E. Buzdugan and R. Stancu, *Rev. Roumaine Chim.*, **28**, 229 (1983).

[14] E. Ceauşescu, R. Bordeianu, P. Ghioca, R. Stancu, I. Cerchez and E. Buzdugan, *Rev. Roumaine Chim.*, **29**, 3 (1984).

[15] E. Ceauşescu, R. Bordeianu, P. Ghioca, E. Buzdugan, R. Stancu and I. Cerchez, *loc. cit.* [1], p. 273. A condensed version in *Pure Appl. Chem.*, **56**, 319 (1984).

[16] E. Ceauşescu, V. Dobrescu, R. Bordeianu, P. Ghioca, I. Cerchez and R. Stancu, *loc. cit.* [1], p. 338.

[17] E. Ceauşescu, R. Bordeianu, E. Buzdugan, P. Ghioca, I. Cerchez and R. Stancu, *loc. cit.* [1], p. 387.

[18] E. Ceauşescu, R. Bordeianu, P. Ghioca, E. Buzdugan, R. Stancu, I. Cerchez, M. Corciovei, T. Sârbu, F. Taran and S. Barac, paper presented at the Annual ICECHIM Microsymposium, Jan. 27—28, 1984, prepared for publication in *Mat. Plast.*

[19] E. Ceauşescu, R. Bordeianu and P. Ghioca, *Mat. Plast.*, **17**, 201 (1980).

[20] T. L. Smith and R. A. Dickie, *J. Polym. Sci.*, *C* **26**, 163 (1969).

[21] J. F. Beecher, L. Marker, R. S. Bradford and S. L. Aggarwal, *J. Polym. Sci.*, *C* **26**, 117 (1969).

[22] S. L. Aggarwal, *Polymer*, **17**, 938 (1976).

[23] P. S. Pillai, D. I. Livingston and J. D. Strong, *Rubb. Chem. Technol.*, **45**, 241 (1972).

[24] G. S. Fielding-Russell, *Rubber Chem. Technol.*, **45**, 252 (1972).

[25] E. Ceauşescu, V. Dobrescu, R. Bordeianu, P. Ghioca and I. Cerchez, *loc. cit.* [1], p. 345.

[26] E. Ceauşescu, S. Bittman, V. Dobrescu, R. Bordeianu, P. Ghioca, and I. Cerchez, in E. Ceauşescu, "Noi cercetări în domeniul compuşilor macromoleculari", Ed. Academiei R.S.R., Bucharest, 1981, p. 460.

[27] C. I. Chung, H. L. Griesbach and L. Young, *J. Polymer Sci., Polym. Phys. Ed.*, **18**, 1237 (1980).

Revue Roumaine de Chimie, **32**, *1*, 21–28 (1987)

INTERFACIAL PHENOMENA ON CONCENTRATED POLYMER SOLUTIONS IN THE SPINNING PROCESS*

F. SĂNDESCU [a] and CR. I. SIMIONESCU [b]

[a] Industrial Central for Chemical Fibres and Yarns, Săvineşti, Romania
[b] Institute of Macromolecular Chemistry "P. Poni", Iaşi, Romania

Received October 19, 1985

The present study deals with interfacial phenomena on ternary acrylic copolymer solutions, acrylonitrile/ vinyl acetate/ alpha-methyl styrene : 91/6/3 in ethylene carbonate (EC) aqueous solutions : 85/15 w. pr. as well as with phenomena taking place at the interface polymer solution/ coagulation bath(EC) aqueous solution in the spinning bath. The data were estimated with a tensiometer using the DE NOUY ring principle, both in the presence and in the absence of tensides of the type : $RCOOCH_2CH(OSO_3Na)COONa$, $RCOO(CH_2CH_2O)_nCH_2CH(SO_3Na)COONa$ and $RCOO(CH_2CH_2O)_n H$, R being an acrylic radical $C_{16} - C_{18}$ and $n = 6 - 10$. The surface tension σ decreases with the increase of polymer concentration, molecular weight, polar group content in the copolymer, as well as with temperature. The critical extrusion velocities increase with the decrease of the σ/η ratio, η being the spinning solution absolute viscosity. The entropy variations at the interface $\Delta S = d\sigma_{12}/dT$ are unimportant, whereas the enthalpy variations $\Delta H = \sigma_{12} + T \cdot \Delta S$ are significant. The latter can be minimized in the presence of surfactants.

The study of surface and interfacial tensions of melts and polymer solutions is a relatively new branch in the polymer science and the growing interest for such problems aims not only at theoretical aspects [1-3] but also at practical ones, related to polymer processing : extrusion of polymer solutions and melts in order to obtain fibres and films, [4-8] problems related to the polymer surface modification, [9-14] the coatings and adhesiveness techniques, [15-17] lubrication of fibres and wetting of textile surfaces in view of their processing. [18-21]

The present study focuses on the surface tensions of the acrylic copolymer solutions used for PAN fibres and on interfacial phenomena in the spinning process.

EXPERIMENTAL

There were used solutions of ternary copolymers acrylonitrile/ vinyl acetate/ alphamethylstyrene with the following composition : 91/ 6/ 3 weight percents, using as a solvent the aqueous solution 85 w. pr. of ethylene carbonate (EC).

---

* Paper communicated at the 30th Symposium of Macromolecules. The Hague, August 18—23, 1985 and at the Conference on Chemistry and Chemical Engineering, Bucharest, October 16—17, 1985.

The surface and interfacial tensions were determined with a tensiometer type TE-080-101 Q_1R_2, supplied by the firm MESSGERÄTE WERK DR. WOBSER-LAUDA, F.R.G., using the DE NOUY ring principle. The instrument measures electronically the force the liquid applies to the immersed measuring ring, by means of an inductive force transducer. The relative movement between the ring and the liquid is realized by a double walled tempering stage movement, the ring position being fixed. The sample beaker used for the measuring liquid is placed in the tempering stage. The force, which is proportional to the surface tension is converted to an analogous direct voltage and is measured digitally or recorded as a function of time.

The surface tension was calculated using the equation:

$$\sigma = \sigma_{\text{meas}} \cdot F(\text{dyn} \cdot \text{cm}^{-1}), \tag{1}$$

σ_{meas} being the measured surface tension, and F the Harkins — Jordan factor, depending on R^3/V, R being the ring radius (cm), and V the volume of the liquid lamella.

The Harkins-Jordan factors were determined by means of the modified stalagmometric method, using a 0.3575 cm capillary.

The modification applied to the stalagmometer consisted in that the viscous polymer solutions were pushed through the capillary tube under a constant nitrogen pressure of 2.5 bars, allowing the equal fluid drops to fall at a constant flow. The surface tension determined on the stalagmometer is calculated the usual way, as a function of the number of solution drops n, the solution density and the stalagmometer constant K:

$$\sigma_{st} = \frac{K}{n} \tag{2}$$

The Harkins — Jordan factors were determined by means of the relation:

$$F = \frac{\sigma_{st} \cdot 2 \cdot u}{K \max \cdot g} \tag{3}$$

where u is the ring circumference (cm), K max. is the force with which the liquid lamella is broken by the ring (g) and (g) represents the gravity acceleration (cm./s^2).

The interfacial tensions were measured at the interface of spinning solution/ ethylene carbonate aqueous solutions, both in the absence and in the presence of tensides type ethoxylated esthers of fatty acids: $RCOO(CH_2CH_2O)_nH$(EO), unethoxylated sulphonated esthers type $RCOOCH_2CH(SO_3Na)COONa$(S) and ethoxylated sulphonated esters type $RCOO(CH_2CH_2O)_nCH_2CH(SO_3Na)COONa$ (SO). In the above formulae R represents an alkylic saturated radical $C_{16}-C_{18}$ and $n = 6-10$.

RESULTS AND DISCUSSION

The modern theories consider the surface tension to be one of the main factors controlling the spinnability of copolymer solutions [4,5] in the extrusion process.

The filament formation process is controlled by the capillary break-up mechanism, as well as by the cohesive fracture mechanism. The break-up mechanism is controlled by the viscosity and the surface tension, but the cohesive fracture mechanism is controlled by the fluid jet deformation velocity and by the viscoelastic characteristics of the spinning dope. The material factor responsible for the break up of a fluid jet is the ratio of surface tension to viscosity (σ/η). The higher the ratio σ/η, the more probable is the break up of the fluid jet into drops. It is possible to calculate the critical velocity of filament formation as follows:

$$V_{cr} = \frac{2\sigma}{3\eta} \cdot \frac{l}{R_0} \tag{4}$$

l being the filament length and R_0 the filament diameter.

Some aspects related to the spinnability of the acrylic copolymer solutions were studied in previous papers.[22–24]

In the present paper, the data concerning the ratio σ/η and the critical velocities of filament formation at different temperatures are presented in the Table 1.

Table 1

The values of σ/η ratio and of the fibre forming critical velocities at different temperatures; $l = 1$ m; $R_0 = 80 \cdot 10^{-6}$ m

Temperature (°C)	50	70	80
σ/η (cm/s)	0.52	0.43	0.35
V_{cr} (m/min)	16.73	21.28	25.94

The responsible factors for the surface tension and polymer solution viscosities in the spinning process, for a defined solvent, are the temperature, the spinning dope, the molecular weight, and the polymer structure.

The viscosity evolutions with respect to each of these factors are well known from the literature.

Concerning the surface tension one can see that it decreases with the spinning dope (Fig. 1) and the temperature (Fig. 2).

In order to understand these evolutions it must be reminded that polymers belong to low surface energy compounds which by dissolution

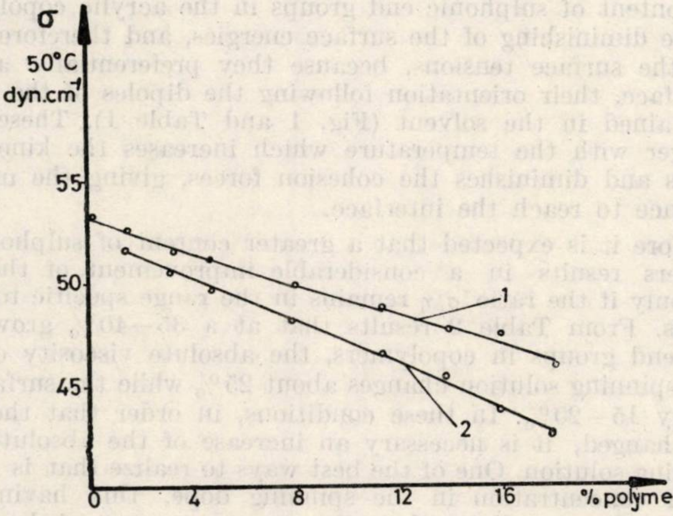

Fig. 1. — Evolution of the surface tension of acrylic copolymer solutions in ethylene carbonate 85 w. pr. aqueous solutions: *1* — $M_v = 50000$; Content of sulphonic end groups $-SO_3H=40$ μE/g; *2* — $M_v = 50000$; Content of sulphonic groups $-SO_3H = 55$ μE/g.

in a definite solvent diminish the surface tension of the latter. The greater the molecular weight of the polymer and the number of polar groups, the more this tendency emphasizes.

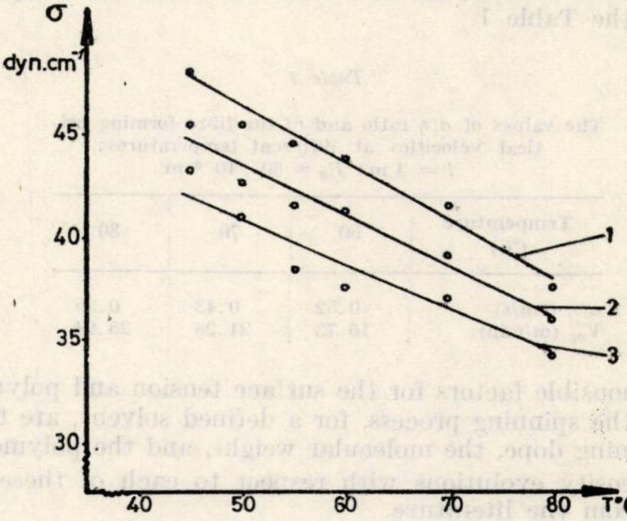

Fig. 2. — Evolution of the surface tension of 14 % acrylic copolymer solutions in ethylene carbonate 85 w. pr. aqueous solutions as a function of temperature and molecular weight: *1* — M_v = 42000; *2* — M_v = 48000; *3* — M_v = 52000.

The content of sulphonic end groups in the acrylic copolymers can influence the diminishing of the surface energies, and therefore the diminishing of the surface tensions, because they preferentially accumulate at the interface, their orientation following the dipoles of the water molecules contained in the solvent (Fig. 1 and Table 1). These processes grow stronger with the temperature which increases the kinetic energy of molecules and diminishes the cohesion forces, giving the molecules a greater chance to reach the interface.

Therefore it is expected that a greater content of sulphonic groups in copolymers results in a considerable improvement of the spinning conditions only if the ratio σ/η remains in the range specific to the spinning process. From Table 2 results that at a 35—40% growth of the content of end groups in copolymers, the absolute viscosity of the corresponding spinning solution changes about 25% while the surface tension changes only 15—20%. In these conditions, in order that the ratio σ/η remain unchanged, it is necessary an increase of the absolute viscosity of the spinning solution. One of the best ways to realize that is to increase the polymer concentration in the spinning dope, this having positive effects on the fiber quality and on the economic aspect of the equipment operation.

In the wet spinning, the interfacial tension copolymer solution/coagulation bath is one of the important factors which causes the capillary instability of the polymer jet submersed in the bath, having a decisive role on the extrusion velocity, as well as on the formed fiber structure.

Tables 3–5 present the experimental determinations at the interface polymer solutions/ ethylene carbonate aqueous solutions, with and without tensides of the type EO, S and SO.

Table 2

Surface tension and absolute viscosity variations in the case of the spinning solutions 16.5 w. pr. of acrylic copolymers AN/AV/α MS in the 85 w. pr. ethylene carbonate aqueous solution as a function of end groups HSO_3 in the acrylic copolymers

Content of $SO_3H(\mu E \cdot g^{-1})$	40	45	48	50	55
Surface tension ($dyn \cdot cm^{-1}$)	49	47	45	42	40
Absolute viscosity (*P*)	100	92	85	80	75

Table 3

Interfacial tensions σ_{12} spinning solution/EC aqueous solution at different EC and tenside EO concentrations. Temperature: 50°C

Tenside EO concentration g/L	EC concentration %			
	20	30	40	50
0	16.63	13.36	12.06	9.50
0.0005	1.53	1.48	1.20	1.18
0.0010	1.39	1.35	1.09	1.05
0.0050	1.25	1.22	0.96	0.92
0.0100	0.98	0.99	0.85	0.82
0.0500	0.85	0.88	0	0
0.1000	0.80	0	0	0
0.5000	0.63	0	0	0
1.0000	0	0	0	0

The addition of tensides in the coagulation bath causes a significant decrease of the interfacial tensions, even with very small concentrations. At concentrations above the critical micellar concentrations corresponding to the respective tensides, the interfacial tensions are equal to zero. Very good results can be obtained with the tenside EO.

It is known that the values of the interfacial tensions condition not only the change of enthalpy ΔH in the interfacial layer, but also the occasional change of the entropy ΔS. These can be estimated in thermodynamic terms:[1, 2, 15, 25]

$$\Delta H = \sigma_{12} + T \cdot \Delta S \tag{5}$$

Table 4

Interfacial tensions σ_{12} spinning solution/EC aqueous solution at different EC and tenside S concentrations. Temperature: 50°C

Tenside *S* concentration g/L	EC concentration %			
	20	30	40	50
0	16.63	13.36	12.06	9.50
0.0005	13.40	10.94	4.15	4.12
0.0010	13.25	10.79	3.82	3.90
0.0050	11.05	10.28	2.75	3.26
0.0100	10.98	9.89	2.40	2.55
0.0500	8.56	0	0	0
0.1000	5.05	0	0	0
0.5000	1.46	0	0	0
1.0000	0	0	0	0

Table 5

Interfacial tension σ_{12} spinning solution/EC aqueous solution at different ethylene carbonate and tenside SO concentrations. Temperature: 50°C

Tenside SO concentration g/L	EC concetration %			
	20	30	40	50
0	16.63	13.36	12.06	9.50
0.0005	8.09	3.92	2.88	2.35
0.0010	5.87	3.55	2.50	2.08
0.0050	4.37	3.02	1.98	1.62
0.0100	2.89	2.55	1.58	1.27
0.0500	1.90	0	0	0
0.1000	0	0	0	0
0.5000	0	0	0	0
1.0000	0	0	0	0

The entropy variation can be estimated from the data of the interfacial tension σ_{12} variation with temperature:

$$\Delta S = \mathrm{d}\sigma_{12}/\mathrm{d}T \tag{6}$$

using the experimental values from Figure 3.

The data are presented in Table 6.

The variations of the interfacial tension with the temperature, consequently the variation of entropy, are very small both in the presence and in the absence of tensides. This was to be expected since in the process of fibre forming there does not take place any chemical modification of the polymer which could affect the molecular structure.

The enthalpy variations are significantly greater with ethylene carbonate solutions having no tensides, but they diminish greatly in the presence of tensides. It is assumed that these tensides improve considerably the fibre forming conditions.

Using the data in Tables 3–5 there were accomplished spinning tests in the presence of tensides, in the conditions registered in Table 7.

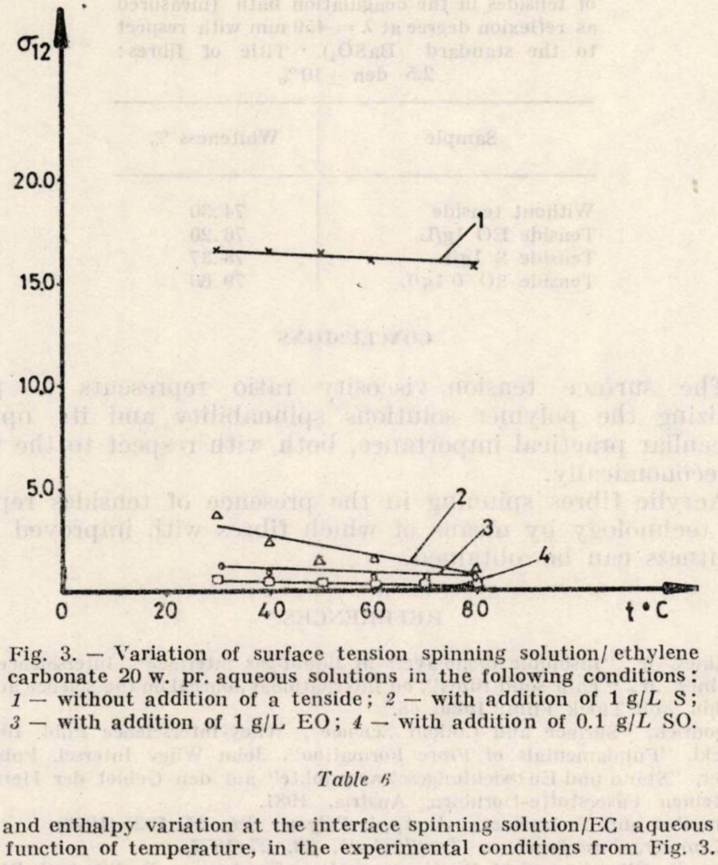

Fig. 3. — Variation of surface tension spinning solution/ ethylene carbonate 20 w. pr. aqueous solutions in the following conditions: *1* — without addition of a tenside; *2* — with addition of 1 g/*L* S; *3* — with addition of 1 g/L EO; *4* — with addition of 0.1 g/*L* SO.

Table 6

The entropy and enthalpy variation at the interface spinning solution/EC aqueous solution, as a function of temperature, in the experimental conditions from Fig. 3.

Thermodynamic parameters	Range of temperature °C					
	50–60		60–70		70–80	
No. cf. fig. 3.	ΔH erg/cm²	ΔS erg/cm²·°C	ΔH erg/cm²	ΔS erg/cm²·°C	ΔH erg/cm²	ΔS erg/cm²·°C
1	16.94	0.0125	16.91	0.0125	16.94	0.0125
2	5.3	0.060	5.4	0.060	5.5	0·060
3	1.34	0.00625	1.20	0.00625	1.17	0.00625
4	0.64	0.00625	0.61	0.00625	0.58	0.00625

The fibres obtained in the presence of tensides present a whiteness and a brightness more pronounced that the fibres spun the usual way, as well as a soft handle.

Remarkably advantageous results can be obtained in the presence of the tenside SO, the desired effect being better with a 10 times smaller quantity than the other 2 tested products.

Table 7

The whiteness of fibres spun in the presence of tensides in the coagulation bath (measured as reflexion degree at $\lambda = 459$ mm with respect to the standard $BaSO_4$). Title of fibres: 2.5 den ±10%

Sample	Whiteness %
Without tenside	74.30
Tenside EO 1g/L	76.20
Tenside S 1g/L	78.37
Tenside SO 0.1g/L	79.60

CONCLUSIONS

1. The surface tension/viscosity ratio represents a parameter characterizing the polymer solutions spinnability and its optimization is of a peculiar practical importance, both with respect to the fibre quality and economically.

2. Acrylic fibres spinning in the presence of tensides represents a potential technology by means of which fibres with improved whiteness and brightness can be obtained.

REFERENCES

[1] G. L. Gaines, Jr., "Insoluble monolayers at liquid-gas interface", Interscience Publ. 1970.
[2] G. L. Gaines, Jr., "Thin solid films", on International Journal on the Science and Tehnology of Thin and Thick Film, **1980**, 68.
[3] F. G. Goodrich, "Surface and Colloid Science", Wiley-Interscience Publ. 1969.
[4] A. Ziabicki, "Fundamentals of Fibre Formation", John Wiley Intersci. Publ. 1976.
[5] W. Berger, "Stand und Entwicklungeschwerpunkte" auf den Gebiet der Herstellung von ultrafeinen Faserstoffe-Dornbirn, Austria, 1981.
[6] H. P. Schreiber and Y. Marineau, *J. Appl. Polymer Sci.*, **24**, 1925 (1979).
[7] H. W. Kammer, *Faserforsch. u Textiltechnik*, **28**, 27 (1977).
[8] W. Berger, K. Olbricht and H. W. Kammer, *Faserforschung u Textiltechnik*, **21**, 7, 9 (1976).
[9] G. L. Gaines, Jr., *Macromolecules*, **12** (5), 1011 (1979).
[10] B. R. Vijayendron, *J. Appl. Polymer Sci.*, **23**, 733 (1979).
[11] P. Kassenbach and H. Huber, *Melliand Textilberichte*, **5**, 487 (1980).
[12] R. K. S. Chan, *Textile Res. J.*, 1059 December (1970).
[13] N. A. Pavlova, L. P. Zeicenko and A. A. Abramson, *J. prikl. himii*, **8**, 1970, (1982).
[14] J. A. Murashev, S. I. Koltsov and A. A. Abramson, *J. prikl. himii*, **7**, 495 (1982).
[15] H. W. Kammer, *Plaste u. Kautschuk*, **28** (10), 553 (1981).
[16] H. W. Kammer, *Acta Polymerica*, **34** (2), 112 (1983).
[17] A. J. Balchin, R. J. Clich and D. Wahren, *Advances in Colloid and Interface Science*, **14**, 251 (1981).
[18] F. Finoochiaro, G. Valk, E. Scholimayer and G. Heidemann, *Melliand Textilberichte*, **9**, 666 (1982).
[19] H. J. Jacobesch, *Textiltechnik*, **30**, 756 (1980).
[20] H. J. Jacobesch, I. Grosse, B. Thiel. B. Schmidt and J. Schiwertfeger, *Textiltechnik*, **32**, 176 (1982).
[21] G. V. Hornuff and R. Gärtner, *Melliand Textilberichte*, **8**, 935 (1970).
[22] F. Săndescu and D. Feldman, *Acta Polymerica*, **30**, 166 (1979).
[23] F. Săndescu, Doctoral Thesis, Polytechnic Institute, Iași 1981.
[24] F. Săndescu and C. I. Simionescu, *Rev. Roumaine Chim.*, **29**, 773 (1984).
[25] T. E. Lipatova, Sh. G. Vergarosskaia, A. E. Feinerman and L. S. Sheinino, *J. Polymer Sci* **21**, 2085 (1983).

Revue Roumaine de Chimie, **32**, *1*, 29–31 (1987)

A NEW SYNTHESIS OF AROMATIC UREAS FROM CARBON DIOXIDE AND DIAMINES USING ETHYLENE CHLOROPHOSPHITE IN PYRIDINE AS REAGENT

C. I. CHIRIAC

"P. Poni" Institute of Macromolecular Chemistry, Aleea Gr. Ghica-Vodă 41 A,
Iași, Romania

Received December 23, 1985

Various aromatic ureas are prepared in good yields by the reaction between aromatic amines and carbon dioxide in the presence of ethylene chlorophosphite as reagent in pyridine at 55–65°.

In a previous paper,[1] we have shown that ethylene chlorophosphite in pyridine is a good reagent for the synthesis of thioureas from aromatic amines and carbon disulfide at room temperature.

RESULTS AND DISCUSSION

In this paper we will describe the applicability of the above reaction in synthesis of aromatic ureas. This work will present detailed results of the reactions of ethylene chlorophosphite and aromatic primary amines with carbon dioxide in the presence of pyridine as a tertiary amine. Thus, when carbon dioxide was passed at 55–65° for 5–6 hours into a cylindrical flask containing ethylene chlorophosphite (2 moles + 30% excess) and aniline (4 moles) in dried pyridine, N, N′-diphenylurea was obtained in 82% yield (the yield was improved when we used a small excess of reagent). At room temperature, the yield is low (in the case of thioureas,[1] the yield is high even at room temperature, because the reactivity of carbon dioxide is lower in comparison with carbon disulfide). The pyridine was found to be the most suitable solvent for this reaction as well as an acceptor for hydrochloric acid.

The mechanism of this reaction is similar with the mechanism proposed by us in the case of aromatic thioureas prepared with the same reagent.[1] Thus by the addition of ethylene chlorophosphite to a solution of an aromatic amine (I) in pyridine at 0–20°, a reactive compound (II) results "in situ", which can react with carbon dioxide in the same conditions but at higher temperature (55—65°), affording (III) and (IV).

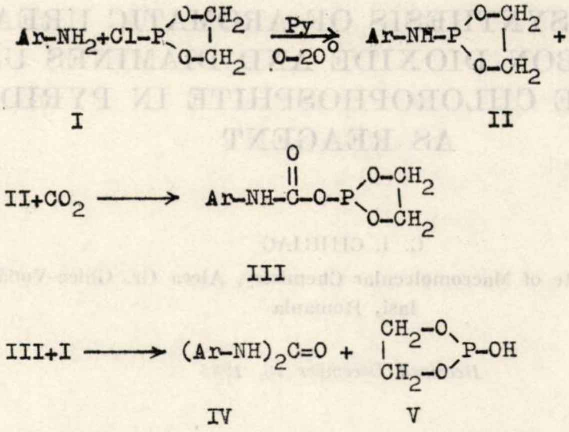
Ar-NH$_2$+Cl-P(O-CH$_2$)(O-CH$_2$)
Py
0-20°
Ar-NH-P(O-CH$_2$)(O-CH$_2$) + PyH$^+$Cl$^-$
I
II
II+CO$_2$
Ar-NH-C(=O)-O-P(O-CH$_2$)(O-CH$_2$)
III
III+I
(Ar-NH)$_2$C=O +
CH$_2$-O, CH$_2$-O, P-OH
IV
V

The by-products (V) and PyH^+Cl^- do not affect the reaction, similar to other cases.[1-3] We suppose, similar as in other cases,[1,4-6] that this reaction involves a four-centred transition state (VI).

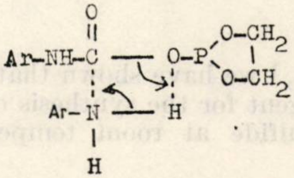

VI

In a typical procedure, to a solution of two moles (I) in dried pyridine cooled to 0°, one mole +30% excess ethylene chlorophosphite was added very slowly under stirring. Then, carbon dioxide was bubbled at a rate of about 350 mL/min. at 55—65° for 5—6 hours and the final product (IV) was separated by precipitation.

Table 1 shows the aromatic ureas obtained in this way. The yields ranged from 63 to 82%.

In conclusion, by this new synthesis we obtained aromatic ureas in high yield, the ethylene chlorophosphite being the first reagent with phosphorus and aliphatic structure used in this field.

EXPERIMENTAL

Diphenylurea

To a solution of 3.64 mL (0.04 moles) aniline and 10 mL dried pyridine in a cylindrical flask, 2.34 mL (0.02 moles + 30% excess) ethylene chlorophosphite[7] were added slowly under stirring and cooling with ice. The stirring is continued for one hour at room temperature, then dried carbon dioxide was bubbled at a rate of about 350 mL/min. at 55—65° for 5—6 hours. At the end of reaction, the obtained solution was poured into 80—100 mL water with ice when diphenylurea precipitated. The desired product was collected by filtration and washed with 50—70 mL 7% and three times with 20—40 mL water. After drying under vacuum at 100—120°C, 3.47 g diphenylurea were obtained with yield 82% calculated on aniline employed. After recrystallisation from ethanol, the final product has m.p. 237—239° (mixed m.p. with pure diphenylurea underpressed). Anal. Calculated for: $C_{13}H_{12}N_2O$; C, 73.58; H, 5.66; N, 13.20%. Found: C, 73.21; H, 5.54; N, 13.08%

In similar conditions, the other aromatic ureas (presented in table 1) were prepared.

Table 1

Aromatic ureas obtained from aromatic amines and carbon dioxide in the presence of ethylene chlorophosphite/ pyridine as reagent

$(Ar-NH)_2C=O$[a] Ar:	Yield[b] %	M.p.[c] °C	Reported m.p. °C
C_6H_5	82	237—239	328[8]
p-GH_3-C_6H_4	80	250—252	252—253
p-CH_3O-C_6H_4	77	237—233	232—234[9]
p-C_2H_5O-C_6H_4	81	224—226	224—226
m-CH_3-C_6H_4	72	216—218	217—219
m-Cl-C_6H_4	67	242—244	243[9]
m-Br-C_6H_4	63	262—264	262—263

[a] The products were identified by comparison of m.p. and IR spectra with those of authentic samples.

[b] Yields determined by isolation of the crude products.

[c] After recrystallisation

[d] From "Beilstein Handbuch der Organischen Chemie".

REFERENCES

C. I. Chiriac, *Rev. Roumaine Chim.*, **29**, 329 (1984).
N. Yamazaki, T. Iguchi and F. Higashi, *Tetrahedron*, **31**, 3031 (1975).
C. I. Chiriac, *Rev. Roumaine Chim.*, **26**, 1001 (1981).
H. G. Khorana, *J. Amer. Chem. Soc.*, **80**, 6204 (1958).
R. N. Ring and D. Davidson, *J. Org. Chem.*, **27**, 2428 (1962).
S. Goldschmidt and M. Wick, *Liebigs Ann. Chem.*, **575**, 297 (1952).
H. J. Lucas and F. W. Mitchell, *J. Amer. Chem. Soc.*, **72**, 5491 (1950).
N. Yamazaki and F. Higashi, *Tetrahedron Letters*, **1974**, 1191.
R. A. Franz and F. V. Morriss, *J Amer. Chem.*, **26**, 3311 (1961).

Revue Roumaine de Chimie, **32**, *1*, 33–36 (1987)

SYNTHESIS OF SOME NEW FLUOROSUBSTITUTED TRICYCLIC HETEROCYCLES. II[1]

3-ALKOXY-7-FLUORO-10-{3-[4-(2-HYDROXYETHYL)-1-PIPERAZINYL]-PROPYL}-2-METHOXY PHENOTHIAZINE DERIVATIVES

S. B. TAMBI, MADHU ANAND, NANDAN BHARGAVA and R. L. MITAL *
Chemical Laboratories, University of Rajasthan, Jaipur—302004, India

Received November 21, 1981
Revised July 25, 1986

3-Alkoxy-7-fluoro-10-{3-4-(2-hydroxyethyl)-1-piperazinyl]-propyl}-2-methoxy phenothiazines (IV) and (VII) have been synthesized by the condensation of 3-alkoxy-7-fluoro-2-methoxy phenothiazines (I) or (II) with 3-[4-(2-hydroxyethyl)-1-piperazinyl]-propyl chloride. Dioxalates of (IV) and (VII) have been oxidized with 30% H_2O_2 and the products were hydrolysed to afford sulphoxides of (IV) and (VII). 7-Fluoro-3-hydroxy-10-{3-[4-(2-hydroxyethyl)-1-piperazinyl]-propyl}-2-methoxy phenothiazine (IX) has also been reported, obtained by acid hydrolysis of (VII).

INTRODUCTION

In our previous publication[1] we reported some fluoro-substituted phenothiazines having N-methyl piperazinyl propyl side chain. Some of the possible metabolites of prochlorperazine[2,3] and trifluoperazine[4,5] have also been recently synthesized.

The investigations made on structure-antipsychotic activity correlation by Feinberg et al.[6] have shown that the increased potency of drugs was associated with piperazine side chain having N-hydroxyethyl group. Metabolic studies of fluphenazine[7] and perphenazine,[8] of this series, have been made by many workers.[9–11] Further, the well-known biological activity[12] of 10-[4′-(β-hydroxyethyl)-piperazinyl-1′]-alkyl or acyl phenothiazines induced us to synthesize some nuclear fluorinated phenothiazines having N-hydroxyethyl piperazinyl propyl side chain. In the present study we have synthesized 3-alkoxy-7-fluoro-10-{3-[4-(2-hydroxyethyl)-1-piperazinyl]-propyl}-2-methoxy phenothiazines (IV) and (VII) by direct condensation of 3-alkoxy-7-fluoro-2-methoxy phenothiazines[1] (I) or (II) with 3-[4-(2-hydroxyethyl)-1-piperazinyl]-propyl chloride[13] in the presence of sodamide under the atmosphere of nitrogen and alternatively by the reaction of piperazin ethanol with 3-alkoxy-10-(3-

chloropropyl)-7-fluoro-2-methoxy phenothiazines (III) or (VI), which were obtained by the reaction of (I) or (II) with 1-bromo-3-chloro-propane.

The stable dioxalates of (IV) and (VII), on oxidation with 30% H_2O_2 provided the corresponding sulphoxides, which on hydrolysis furnished 3-alkoxy-7-fluoro-10-{3-[4-(2-hydroxyethyl)-1-piperazinyl]-propyl}-2-methoxy phenothiazine-5-oxides (V) and (VIII). Acid hydrolysis of VII gave 7-fluoro-3-hydroxy-10-{3-[4-(2-hydroxyethyl)-1-piperazinyl]-propyl}-2-methoxy phenothiazine (IX).

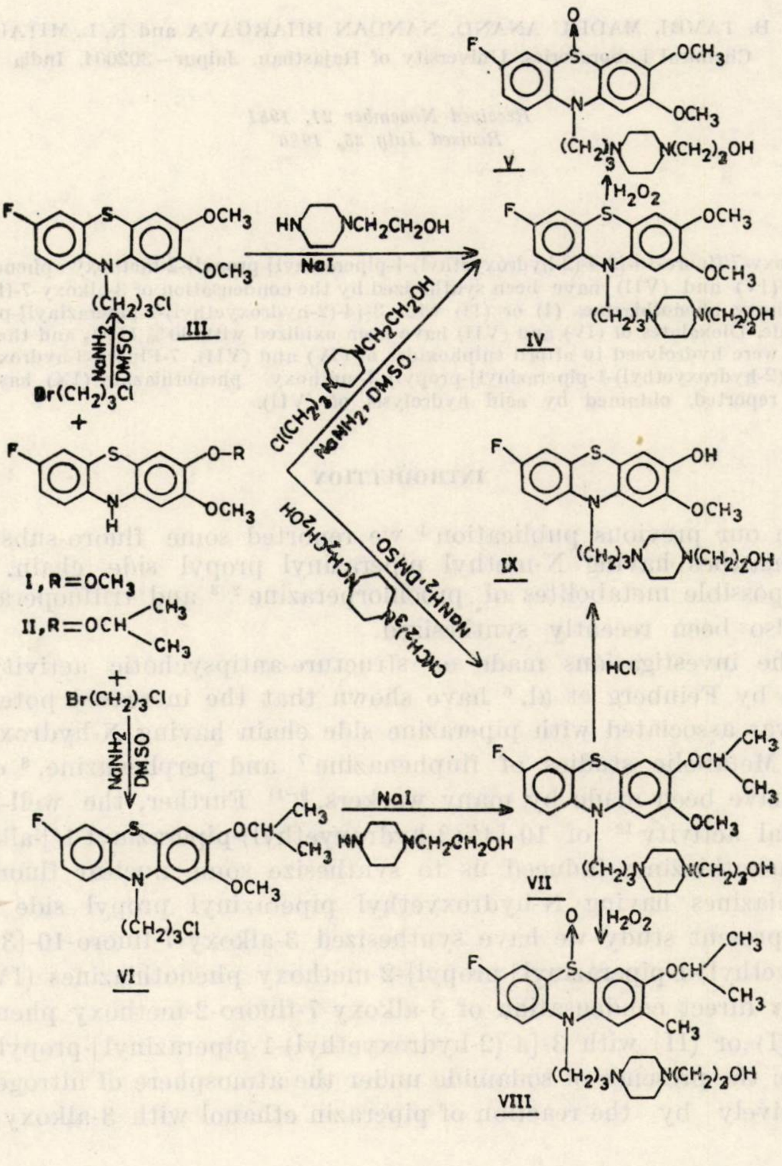
I, R=OCH3
II, R=OCH(CH3)2
III
IV
V
VI
VII
VIII
IX
Br(CH2)3Cl
NaNH2, DMSO
NaI
H2O2
HCl
Cl(CH2)3N NCH2CH2OH
NaNH2, DMSO
HOCH2CH2N NH
NaNH2, DMSO
HN NCH2CH2OH

EXPERIMENTAL*

10-(3-Chloropropyl)-7-fluoro-2,3-dimethoxy phenothiazine (III)

A mixture of 5.54 g (0.02 mole) of 7-fluoro-2,3-dimethoxy phenothiazine (I) in 50 mL of dried dimethylsulphoxide and 4.8 g (0.04 mole) of sodium hydride (20% dispersion in mineral oil) in 50 mL of dimethyl sulphoxide was stirred for 2 hours at room temperature and then refluxed for 20 hours after adding a solution of 5.50 g (0.035 mole) of 1-bromo-3-chloropropane in 60 mL of dimethyl sulphoxide. The mixture was filtered and cooled. On concentration a reddish-brown oil was obtained which was taken up in pet. ether. The ethereal solution was concentrated to afford a brown oil of title compound which could not be solidified. Yield 45%. It was used for the further reaction as such.
Anal. $C_{17}H_{17}FNO_2SCl$: Calcd. N : 3.96% ; Found N : 3.89%.

7-Fluoro-10-{3-[4-(2-hydroxyethyl)-1-piperazinyl]-propyl}-2,3-dimethoxy phenothiazine (IV

Method A :

To a suspension of 1.58 g (0.02 mole) of sodamide (50% dispersion in mineral oil) in 40 mL of dimethyl sulphoxide was added 4.43 g (0.016 mole) of (I) in 75 mL of sulphoxide. The reaction mixture was stirred for 2 hours at room temperature and then refluxed for 7—8 hours after adding a solution of 3-[4-(2-hydroxyethyl)-1-piperazinyl]-propyl chloride, 4.13 g (0.02 mole) in 30 mL of dimethyl sulphoxide. The product was poured into ice cold water containing ammonium chloride and then extracted with ether. The ethereal extract was treated with 10% HCl and the acid extracts were basified with 10% NaOH solution. The base so obtained was taken up in ether. The ethereal extract was dried, decolorized and concentrated to give a yellow oil which was converted into stable dioxalate (IV-a) of title compound. Melting point > 280°C. Yield 45%. IR 1260 $cm^{-1}\nu$ (C—F), 1400 cm^{-1} ($-OCH_3$) and 3450 cm^{-1} (—OH).
Anal $C_{27}H_{34}FN_3O_{11}S$: Calcd. C, 51.67% ; N, 6.69% ; Found C, 51.53% ; N, 6.64%.

Method B :

To a stirred suspension of sodium iodide 1.5 g (0.01 mole) and 3.17 g (0.009 mole) of (III) in 40 mL of ethyl methyl ketone was added 1.56 g (0.012 mole) of 2-hydroxyethyl piperazine and stirred at 80°C for 20 hours. The solution was concentrated on steam bath, cooled, poured into ice cold water and worked-up similarly as in the case of Method A to give (IV) as an oil. Yield 43%.

The melting points and IR spectra of the salts obtained by both methods are identical.

7-Fluoro-10-{3-[4-(2-hydroxyethyl)-1-piperazinyl]-propyl}-2,3-dimethoxy phenothiazin-5-oxide (V)

A solution of 4.38 g (0.007 mole) of (IV-a) in 60 mL of ethanol and 20 mL of water and 0.91 g (0.008 mole) of 30% H_2O_2 was heated under reflux for 8 hours. The solvent was evaporated on a steam bath and the resulting residue was washed with ethanol to give the corresponding sulphoxide, which was hydrolysed with sodium carbonate in water. The resulting suspension was stired for 30 min. at room temperature and at 40°C for an additional half an hour. The solution was evaporated, extracted with ether, dried and concentrated to afford pale yellow crystals of the title compound. Melting point 203°C.
Yield 60%. IR 1255 $cm^{-1}\nu$ (C—F) and 1035 cm^{-1} (sulphoxide).
Anal : $C_{23}H_{30}FN_3O_4S$: Calcd. C : 59.61%, N : 9.07% ; Found C : 59.67%, N : 9.06%.

---

* All the melting points are uncorrected.

All the reactions were done under the atmosphere of nitrogen and in the absence of direct light.

The samples were prepared as KBr pellets for recording IR spectra.

10-(3-Chloropropyl)-7-fluoro-3-isopropoxy-2-methoxy phenothiazine (VI)

The title compound was prepared similarly as (III) by taking 7-fluoro-3-isopropoxy-2-methoxy phenothiazine (II). The oil obtained was distilled under vacuum to afford a light brown oil of (VI) which could not be solidified.
Yield 62%.
Anal : $C_{19}H_{21}FNO_2SCl$: Calcd. N : 3.67% ; Found, N : 3.68%.

7-Fluoro-10-{3-[4-(2-hydroxyethyl)-1-piperazinyl]-propyl}-3-isopropoxy-2-methoxy phenothiazine (VII)

The title compound was prepared similarly as (IV), by taking 7-fluoro-3-isopropoxy-2-methoxy phenothiazine (II), in Method A and 10-(3-chloropropyl)-7-fluoro-3-isopropoxy-2-methoxy phenothiazine (VI) in Method B. The compound obtained as an oil was converted into its stable dioxalate (VII-a). Melting point > 300°C. Yield 46% (Method A) and 40% (in Method B). IR : 1255 cm^{-1} ν (C−F), two bands at 1380 cm^{-1} and 1360 cm^{-1} (gem dimethyl group and 3400 cm^{-1}(−OH)).
Anal : $C_{25}H_{38}FN_3O_{11}S$; Calcd. C : 53.12%, N : 6.41% ; Found C : 53.03%, N : 6.38%.

7-Fluoro-10-{3-[4-(2-hydroxyethyl)-1-piperazinyl]-propyl}-3-isopropoxy-2-methoxy phenothiazin-5-oxide (VIII)

The title compound was prepared similarly as (V) by taking (VII-a) to afford yellow crystals of (VIII). Melting point 197−98°C. Yield 55%. IR 1250 cm^{-1} ν (C−F) and 1065 cm^{-1} (sulphoxide).
Anal. $C_{21}H_{60}FN_3O_4S$; Calcd. N : 9.65% Found N : 9.69%.

7-Fluoro-3-hydroxy-10-{3-[4-(2-hydroxyethyl)-1-piperazinyl]-propyl}-2-methoxy phenothiazine (IX)

A solution of 4.75 g (0.01 mole) of (VII) in 75 mL of ethanol and 150 mL of conc. HCl was heated at 100−105°C for 1 hour. The mixture was cooled, filtered, poured into ice cold water and adjusted to pH 8 with 20% ammonium hydroxide solution. The resulting gum like substance was taken up in chloroform. Chloroform solution was dried, decolorized with Darco G-60, solvent was stripped off to provide reddish violet oil of (I), which was converted into its stable dioxalate (IX-a). Melting point 198°C, Yield 55%. IR 1250 cm^{-1} ν (C−F), 1170 cm^{-1} (−OCH_3) and 3500 cm^{-1} (−OH).
Anal. $C_{26}H_{32}FN_3O_{11}S$; Calcd. C : 50.89% ; N : 6.85% ; Found C : 50.97%, N : 6.81%.

ACKNOWLEDGEMENT. The authors are thankful to Prof. Y. K. Gupta, Head of the Chemistry Department, University of Rajasthan, Jaipur, for providing Laboratory facilities. One of the authors (S.B.T.) is indebted to the U.G.C., New Delhi, for awarding the Junior Research Fellowship. (M.A.) and (N.B.) are indebted to C.S.I.R., New Delhi for awarding Post-Doctoral Fellowship.

REFERENCES

[1] S. B. Tambi, R. K. Jain and R. L. Mital, *Rev. Roumaine Chim.*, **26**, 477 (1981).

[2] R. L. Mital, S. Mittal, V. Laxmi, M. Mittal and A. P. Shukla, *Indian J. Chem., Sec. B.*, **15B**, 577 (1977).

[3] R. L. Mital, V. Laxmi, M. Mittal and S. Mittal, *Acta. Cienc-Indica.*, **3**, 308 (1977).

[4] R. L. Mital, M. Mittal, A. P. Shukla, S. Mittal and V. Laxmi, *Indian J. Chem.*, **15B**, 1145 (1977).

[5] M. Mittal and R. L. Mital, *Z. Naturforsch.*, **33B**, 336 (1978).

[6] A. P. Teinberg and S. H. Snyder, *Proc. Nat. Acad. Sci. U.S.A.*, **72**, 1898 (1975).

[7] H. L. Yale and F. Sosinski, *J. Amer. Chem. Soc.*, **82**, 2039 (1960).

[8] M. Nakanishi, *Japan Patent*, **18**, 512 (1966); *Chem. Abstr.*, **66**, 37935 (1967).

[9] H. J. Gaertner, U. Breyer and G. Liomin, *Biochem. Pharmacol.*, **23**, 303 (1974).

[10] E. C. Schreiber and M. L. Grozier, *Therapie*, **28**, 441 (1973).

[11] L. B. Hansen, J. Elley, C. T. Rosted, N. E. Larsen, J. Naestoft and E. F. Hvidberg, *Br. J. clin. Pharmacol.*, **7**, 75 (1979).

[12] G. Sunagawa, M. Watatani, A. Mizukami and H. Takagi (*Sankyo Co. Ltd.*) *Japan Patent*, **14**, 585 (1963); *Chem. Abstr.*, **60**, 2960 (1964).

[13] L. J. Kitchen and C. B. Pollard, *J. Org. Chem.*, **8**, 338 (1943).

Revue Roumaine de Chimie, **32**, *1*, 37–40 (1987)

STUDIES IN THE SYNTHESIS OF 10H-8-TRIFLUOROMETHYL-1-AZAPHENOTHIAZINE *VIA* THE SMILES REARRANGEMENT

REKHA AGRAWAL, G. K. OBEROI, D. C. JAIN and R. L. MITAL *
Chemical Laboratories, University of Rajasthan, Jaipur-302004, India

Received August 14, 1981
Revised July 21, 1986

The condensation of zinc salt of 2-amino-4-trifluoro-methylbenzenethiol with 2-chloro-3-nitropyridine yielded an amine and a sulfide. The sulfide was acetylated with acetic anhydride. The acetylated sulfide undergoes Smiles rearrangement in acetone and KOH (2.22 mole) to give the title compound. The amine also gave the same compound when treated with dimethylsulfoxide and ethanolic potassium hydroxide. The acetylated sulfide rearranges to 10-acetyl derivative of the title compound when treated with one mole of potassium hydroxide in acetone.

INTRODUCTION

Azaphenothiazines have marked pharmaceutical properties as neuroleptics,[1] antitussives,[2] antihistaminics,[3] antihypertensives[4] etc. Little work has been reported on 1-azaphenothiazine and its derivatives.[5,6] In continuation of our works[7,9] on phenothiazines, we have synthesized 10H-8-trifluoromethyl-1-azaphenothiazine and its 10-acetyl derivative *via* Smiles rearrangement. The condensation of zinc salt of 2-amino-4-trifluoromethylbenzenethiol[10] (Ia) and 2-chloro-3-nitropyridine (Ib) in anhydrous sodium acetate and absolute ethanol yielded 2-amino-4-trifluoromethylphenyl 2′-(3′-nitro)pyridylsulfide (II), which on acetylation with acetic anhydride in pyridine gave 2-acetyl-amino-4-trifluoromethylphenyl 2′-(3′-nitro)-pyridylsulfide (III). The acetylated sulfide (III) rearranged in potassium hydroxide (2.22 mole) and acetone to give 10H-8-trifluoromethyl-1-azaphenothiazine. Compounds Ia and Ib were condensed in concentrated hydrochloric acid and ethanol to yield 2-mercapto-5-trifluoromethylphenyl 2′-(3′-nitro)-pyridylamine (IV), which on treatment with dimethylsulfoxide and ethanolic potassium hydroxide gave the title compound VI.

10-Acetyl-8-trifluromethyl-1-azaphenothiazine could be obtained when III was reacted with one mole of potassium hydroxide in acetone. Compound V on hydrolysis with concentrated hydrochloric acid and ethanol yielded VI. The overall reaction is shown in the following scheme.

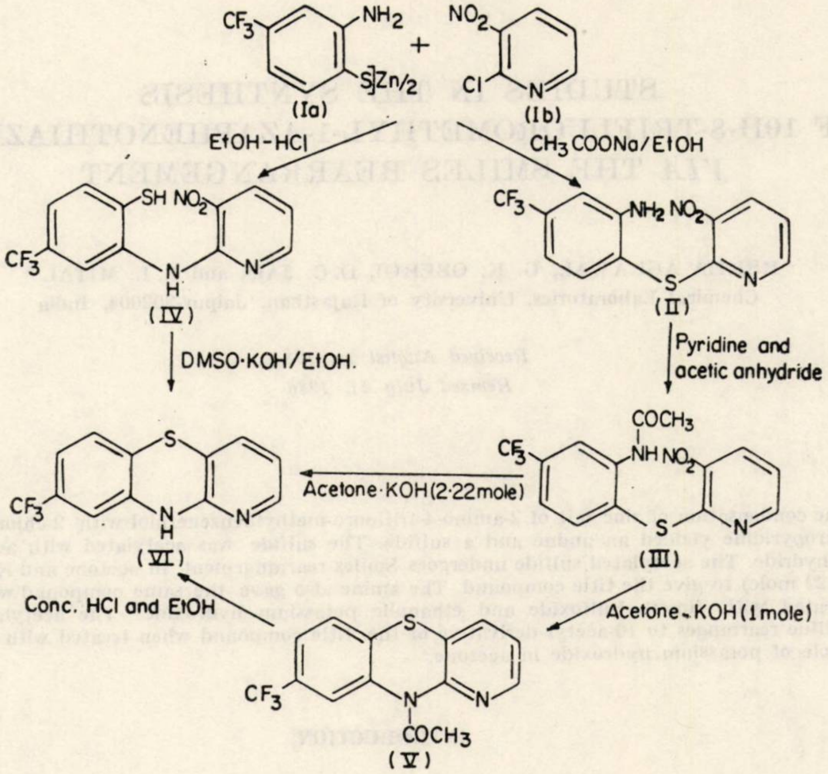

EXPERIMENTAL*

2-Amino-4-trifluoromethylphenyl 2′-(3′-nitro)pyridylsulfide (II)

A mixture of Ia (2.24 g, 5 mmole), Ib (1.58 g, 0.01 mole), anhydrous sodium acetate (2.0 g, 0.025 mole) and 15 mL of absolute ethanol was refluxed for 4 hours on a steam bath. The reaction mixture was cooled, filtered, washed with water and dried. Crystallization from ethanol gave yellow shining needles of II. Melting point 142—3°, yield 70%. *IR spectrum* (KBr, cm^{-1}) 3450m and 3350m ν (—NH_2), 2540w ν (—SH), 1330vs, 1570s (C—NO_2), 1130vs and 1160 vs ν (asymmetric CF_3), 1330 ν (symmetric CF_3). Found C, 45.65 ; H, 2.49 ; N, 13.28 ; Calcd. for $C_{12}H_8N_3SO_2F_3$, C, 45.71 ; H, 2.53 ; N, 13.33%.

2-Acetylamino-4-trifluoromethylphenyl 2′-(3′-nitro)-pyridylsulfide (III)

To II (1.6 g, 5.12 mmole) was added pyridine (0.4 mL, 0.005 mole) and acetic anhydride (4.8 mL, 0.047 mole) and the mixture was heated over a steam bath for 2 hours. The mixture was cooled to give yellow crystals of III. Melting point 122—3° (from isopropanol) ; yield 80%. *IR Spectrum* (KBr, cm^{-1}) 3320m ν(N—H), 1690s ν(C=O), 1330vs, 1580s (C—NO_2) 1130vs and 1170vs ν(asym. CF_3), 1330 ν(sym. CF_3). Found : C, 47.01 ; H, 2.75 ; N, 11.7 ; Calcd. for $C_{14}H_{10}N_3SO_3F_3$: C, 47.05 ; H, 2.80 ; N, 11.76%.

---

* All m. ps. are uncorrected. IR spectra have been scanned in KBr on a Perkin Elmer 577 Grating Spectrophotometer. NMR spectra were recorded on a Perkin Elmer R-12B spectrometer using tetramethyl silane as internal standard, approximately 5—10% solutions in DMSO-d_6. The resonance frequencies are denoted in ppm and coupling constants in hertzs.

2-Mercapto-5-trifluoromethylphenyl 2′-(3′-nitro)-pyridylamine (IV)

To a mixture of Ia and Ib (2.46 mmole each), 20 mL ethanol, 10 mL water and 1.5 mL concentrated HCl were added and the mixture was heated and evaporated over a steam bath to the half volume of constants. After cooling the separated solid was filtered, washed with hot water and dried.

Crystallization from acetone gave light orange crystals of IV. Melting point 186–7°; Yield 80%.

IR Spectrum (KBr, cm^{-1}). 3310m, ν (N–H), 1330 vs, 1580s ($C-NO_2$), 1130vs, 1165vs ν (asym. CF_3), 1330 ν (Sym. CF_3).

Found : C, 45.71 ; H, 2.53 ; N, 13.33 ; Calcd. for $C_{12}H_8N_3SO_2F_3$: C, 45.71 ; H, 2.53 ; N, 13.33%.

Smiles rearrangement of acetylated sulfide III

To a stirred, refluxing solution of III (1.35 g, 4 mmole) in 50 mL acetone 250 mg (8.88 mmole) of powdered KOH was added in small portions and the mixture was refluxed for 3 hours. After refluxing the acetone was distilled out and 50 mL water were added to the residue. The mixture was stirred, filtered and washed with water then dried.

Crystallization from benzene gave shining light yellow crystals of VI. Melting point 183–4°; Yield 45%.

IR Spectrum (KBr, cm^{-1}). 3310m ν (N–H), 1125vs, 1170vs (asym. CF_3), 1330vs (sym. CF_3).

The position of the substituents in compound VI is unequivocally demonstrated by ^1H-NMR spectrum. The main signals are as follows.

$\delta_{N-H}5.82$, δ_6 5.33, δ_7 5.30, δ_9 5.25, $J_{6\text{-}7}$ 7.3, $_{6\text{-}9}$ 0.7.

Found : C, 53.76 ; H, 2.59 ; N, 10.4 ; Calcd. for $C_{12}H_7N_2SF_3$: C, 53.73 ; H, 2.61 ; N, 10.44%.

10-Acetyl-8-trifluoromethyl-1-azaphenothiazine (V)

To a stirred mixture of 0.01 mole of KOH and 3.5 mL of ethanol, 120 mL of acetone were added under nitrogen. Then III (2.36 g, 6.6 mmole) was added to the mixture and acetone was distilled rapidly to a volume of 10 mL. Equal volume of water (10 mL) was added, filtered and dried. Crystallization from isopropanol gave yelow crystals of V melting point 105–6°; yield 55%.

IR Spectrum (KBr, cm^{-1}) 1720s ν (C=O), 1610s (C–N bending), 1140vs, 1165vs ν (asym. CF_3), 1330 ν (sym. CF_3).

In the ^1H-NMR spectrum of compound V the N-H signal disappeared. The other signals are as in compound VI.

Found : C, 54. 13 ; H, 2.87 ; N, 9.01 ; Calcd. for $C_{14}H_9N_2SOF_3$: C, 54.19 ; H, 2.90 ; N, 9.03%.

Hydrolysis of 10-acetyl-8-trifluoromethyl-1-azaphenothiazine (V)

A mixture of V (4 mole), 4.2 mL of ethanol and 0.7 mL concentraded HCl was refluxed for 2 hours and concentrated. The residue was treated with excess aqueous NH_3. The solid thus formed was filtered. The solid was dried by azeotropic distillation with benzene and the solvent was evaporated *in vacuo*. Crystallization from dry benzene yielded crystals of VI. Melting point 183–4°.

10H-8-Trifluoromethyl-1-azaphenothiazine from amine (IV)

To a stirred mixture of IV (0.630 g, 2.0 mmole) and 10 mL of DMSO a hot mixture of 15 mL DMSO, 170 mg KOH (3.0 mmole) and 10 mL ethanol was added and refluxed for 7 hours. After refluxing ethanol was distilled and 100 mL water was added to the residue. This mixture was three times extracted, washed with water then dried (Na_2SO_4). The solvent was removed *in vacuo*. Crystallization from benzene gave crystals of VI. Melting point 183–4°; Yield 40%.

ACKNOWLEDGEMENT. We thank the Council of Scientific and Industrial Research, New Delhi, for providing Junior Research Fellowships to two of us (R.A. and G.K.O.).

REFERENCES

[1] R. A. Loevstad, *Biochem. Pharmacols,* **25** (16), 1877 (1976).

[2] Olin Mathieson Chemical Corp (by W. L. Bryan, U. F. Nager and F. Y. Wiselogle); *Fr. M 2990,* Jan. 8, 1965; *Chem. Abstr.,* **62**, 16263 (1965).

[3] V. C. Saxena, S. K. Bapat and B. N. Dhawan, *Jap. J. Pharmacol.,* **19**(4), 477 (1969).

[4] Deutsche Gold- und Silber- Scheideanstalt Vorm. Roessler (by H. Beschka and W. Schuler), *Ger. 1,116,206,* Mar 26, 1964; *Chem. Abstr.,* **60**, 15887 (1964).

[5] Sandoz Ltd (by J. Renz, J. P. Bourguin, G. Gamboni, V. Theus and L. Ruesch), *Ger. 1,119,283* (Dec 14, 1961); *Chem. Abstr.,* **57**, 837 (1962).

[6] Deutsche Gold- und Silber- Scheideanstalt Vorm-Roessler. *Fr. M 1604,* (Jan. 7, 1963); *Chem. Abstr.,* **59**, 1652 (1963).

[7] H. L. Sharma, V. N. Sharma and R. L. Mital, *Tetrahedron Letters,* **1967**, 1657.

[8] R. L. Mital and S. K. Jain, *J. Chem. Soc. (C).,* **1969**, 2149.

[9] A. R. Goyal and R. L. Mital, *Gazz. chim. Ital.,* **109**, 205 (1979).

[10] A. Kirprianov and L. Yagupolskii, *Zhur. obshchei Khim.,* **22**, 2209 (1952).

Revue Roumaine de Chimie, 32, *1*, 41–46 (1987)

INCLUSION COMPOUNDS OF PERHYDROTRIPHENYLENE WITH ALIPHATIC MONOCARBOXYLIC ACIDS

C. LUCA, N. BÎLBĂ, GH. MIHĂILĂ and I. AGHERGHINEI*

Department of Chemical Technology, Polytechnic Institute, Splai Bahlui 71, Iaşi

* "Petru Poni" Institute of Macromolecular Chemistry, Aleea Gr. Ghica Vodă 41 A, Iaşi, Romania

Received January 25, 1986

Inclusion compounds of perhydrotriphenylene (PHTP) with aliphatic monocarboxylic acids, normally chained, have been synthesized and studied by IR spectroscopy, thermal differential analysis and X-ray diffraction. The PHTP — acids inclusion compounds exhibit a thermal stability higher than that of the individual compounds and belong to the hexagonal system. Acids are found to be associated as dimers in the channels of PHTP.

INTRODUCTION

The equatorial isomer *anti-trans-anti-trans-anti-trans* of PHTP forms very easily stable channel-like inclusion compounds, especially with linear molecules of hydrocarbons, esters, amines, halogenated compounds, *n*-alcohols, macromolecules etc. [1–5] Investigations concerning these compounds have been developed by Farina et al. [1,6,7] mainly on their structure.

In the present paper, using IR spectroscopy, differential thermal analysis and X-ray diffraction, the inclusion compounds of PHTP with normal chain, C_8—C_{18} aliphatic monocarboxylic acids, having even-number carbon atoms, synthesized by us, have been investigated.

EXPERIMENTAL

PHTP was synthetized as previously reported. [4]

The aliphatic monocarboxylic acids employed, namely, capronic, caprylic, caprinic, lauric, myristic, palmitic and stearic of high purity were supplied by Merck Co and used without further purification. Methylethylketone, employed as solvent, was of chromatographic grade, its boiling range was 79—80°C and its refractive index 1.380—1.381.

The inclusion compounds PHTP — monocarboxylic acids were prepared by their crystallization in solution. Thus, to a saturated solution of PHTP in methylethylketone at 60—65°C the pure monocarboxylic acid or its solution in methylethylketone was added and left for crystallization for about half an hour at room temperature. Under cooling, the inclusion compounds PHTP — monocarboxylic acid crystallizes as white colour acicular crystals. The obtained crystals are filtered under vacuum created by a water vacuum device, washed with methylethylketone and dried in air up to a constant weight. For example, to obtain the PHTP — capronic acid inclusion compound we started with 1 g PHTP dissolved in 30 mL methylethylketone and 0.5 mL capronic acid (an excess of 300% against PHTP) and to obtain the PHTP — stearic acid inclusion compound, we started with 1 g PHTP in 30 mL methylethylketone and 0.24 g stearic acid (an excess of 100 %) dissolved in 5 mL methylethylketone.

The IR spectra of the inclusion compounds have been performed in potassium bromide pellets, using a 577 Perkin-Elmer spectrophotometer.

Thermal analyses were carried out with a derivatograph MOM Budapest, under a heating rate of 10°/min. and sensitivity 1/3, using ignited α-alumina as reference material.

The structure of the synthetized products was determined on an X-ray diffraction apparatus TUR M — 61 Dresden, using the copper filtered radiation K_α ($\lambda = 1.54050$ Å).

RESULTS AND DISCUSSION

In the preparation of the PHTP-monocarboxylic acids inclusion compounds, methylethylketone was employed as solvent, because it dissolves both PHTP and monocarboxylic acids but does not form inclusion compounds with PHTP.

Utilization of certain excess of monocarboxylic acid led to the obtainment with high yield (about 90%) of a pure inclusion compound free of PHTP. This excess must be larger in the case of the acids with shorter chain, about 300% for capronic acid, because they are very soluble in methylethylketone. In the case of longer chain acids, the excess must be smaller, about 100% for stearic acid. The excess of monocarboxylic acid was removed by washing the crystals with methylethylketone. Characteristics of the synthesized compounds are presented in table 1.

Table 1

Characteristics of the inclusion compounds
PHTP — monocarboxylic acid, C_6—C_{18}

Inclusion compounds	Yield, %	Included acid, % by weight*	Weight ratio PHTP/acid	Molar ratio, PHTP/acid
PHTP-capronic acid	87.3	10.24	8.76	4.13
PHTP-caprylic acid	87.9	10.38	8.63	5.05
PHTP-caprinic acid	88.2	10.35	8.66	6.05
PHTP-lauric acid	88.9	10.41	8.61	7.00
PHTP-myristic acid	88.1	10.47	8.55	7.92
PHTP-palmitic acid	90.2	10.53	8.49	8.84
PHTP-stearic acid	90.6	16.51	8.51	9.82

*Determined by titration with 0.1 N NaOH solution.

By titration with 0.1 N solution of NaOH in hot ethanol, the content of monocarboxylic acid in the inclusion compound was determined. On the basis of the obtained results, the weight and molar ratio, PHTP to monocarboxylic acid, have been calculated. The weight ratio, PHTP to monocarboxylic acid, does not depend on chain length of included monocarboxylic acid; it is approximately constant and equal to 8.60. On the contrary, the molar ratios PHTP to monocarboxylic acid depend strongly on chain length of the included monocarboxylic acid, from 4.13 for capronic acid up to 9.82 for stearic acid, showing a linear dependency (figure 1).

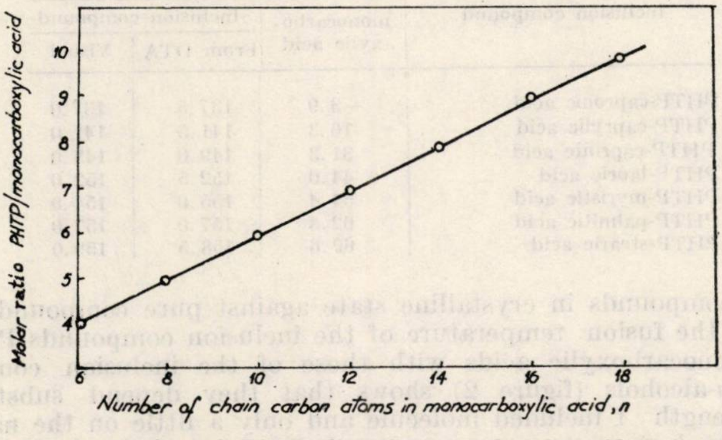

Fig. 1. — Molar ratio PHTP/ aliphatic monocarboxylic acids against the number of chain carbon atoms in included monocarboxylic acid molecule.

The IR spectra of the inclusion compound PHTP — monocarboxylic acids, $C_6 - C_{18}$, are similar to each other.

The region 700—1400 cm^{-1}, proper to PHTP, exhibits the following absorption bands: 834i, 896i, 918m, 938m, 960s, 978m, 1046m, 1068s, 1102s, 1127s, 1168m, 1205i, 1260s, 1284m, 1290s, 1322s, 1334s, 1346m, 1310s. These absorption bands are identical or very close to those attributed for PHTP by Farina and Audisio.[7] In this region, the inclusion compounds PHTP-monocarboxylic acids exhibit only one more absorption band at 720 cm^{-1}, proper to rocking vibration of the CH_2 groups in hydrocarbonate radical (γ_{CH_2r}).

In the region 1500—2000 cm^{-1}, except PHTP, in the IR spectra of the inclusion compounds PHTP-monocarboxylic acids there is an intense absorption band at 1700 cm^{-1}, proper to valence vibrations of the C=O bond (ν_{CO}), in the carboxylic group in the dimer form. The IR spectra show that all investigated monocarboxylic acids are found as dimers in the PHTP channels.

The thermal stability of the inclusion compounds PHTP — monocarboxylic acids, $C_6 - C_{18}$, was investigated by differential thermal analysis. In all cases, in the temperature range of 135—160°C, there is an endothermic peak that corresponds to fusion point of the inclusion compound and which moves continuously to higher temperatures as the chain length of monocarboxylic acid increases. The melting points of the inclusion compounds PHTP — monocarboxylic acids are higher than melting point of PHTP and of the monocarboxylic acid in pure state, table 2. This fact points out a higher thermodynamic stability of the

Table 2

Melting points of aliphatic monocarboxylic acids, C_6—C_{18}, and of the corresponding inclusion compounds with PHTP (M. p. of pure PHTP = 128 °C)

Inclusion compound	Melting point, °C		
	monocarboxylic acid	Inclusion compound	
		From DTA	Visual
PHTP-capronic acid	−3.9	137.5	137.0
PHTP-caprylic acid	16.3	141.5	141.0
PHTP-caprinic acid	31.3	149.0	148.0
PHTP-lauric acid	44.0	152.5	152.0
PHTP-myristic acid	54.4	155.0	154.0
PHTP-palmitic acid	62.8	157.0	157.0
PHTP-stearic acid	69.6	158.5	159.0

inclusion compounds in crystalline state against pure compounds. Comparison of the fusion temperature of the inclusion compounds PHTP — C_6—C_{18} monocarboxylic acids with those of the inclusion compounds PHTP — *n*-alcohols (figure 2) shows that they depend substantially on chain length of included molecule and only a little on the nature of the functional group.

For a certain chain length of the included molecule, thermal stability of the inclusion compounds PHTP — monocarboxylic acids is greater than that of the inclusion compounds PHTP — *n*-alcohols.

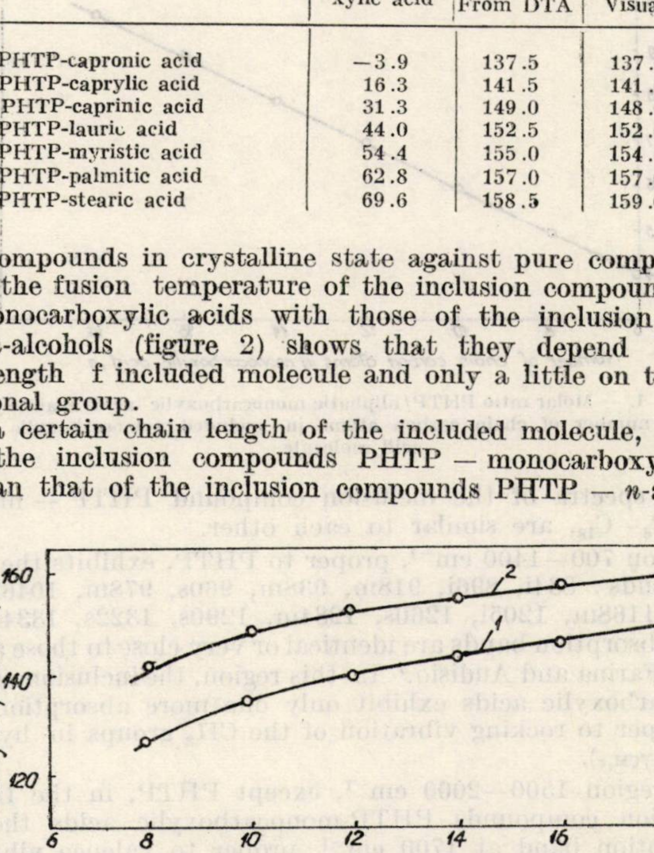

Fig. 2. — Melting point of the inclusion compounds of PHTP-against the number of chain carbon atoms in the guest molecule: 1-*n*-alcohol; 2 — aliphatic monocarboxylic acid with normal chain.

The X-ray spectra, proper to the inclusion compounds PHTP — monocarboxylic acids, are similar to one another, but different from that of PHTP in pure state. It is well known that PHTP crystallizes in the monoclinic system with an elementary cell having $a = 19.59 \pm 0.07$, $b = 15.39 \pm 0.06$, $c = 5.36 \pm 0.03$ A°, $\beta = 109.7 \pm 0.3$ and $V = 1522 \pm 0.0$ $A^{\circ 3}$. Using the analytical method of indexation, in the case of the inclusion compounds, a very good agreement was obtained between $\sin^2\theta_{calc.}$ and $\sin^2\theta_{obs.}$ for the hexagonal system.

The values of $\sin^2\theta_{calc.}$ were obtained from the equation proper to the hexagonal system:

$$\sin^2\theta = A(h^2 + hk + k^2) + Cl^2$$

where $A = \lambda^2/3a^2$ and $C = \lambda^2/4c^2$.

The constant A is specific to the lines having $l = 0$ and was computed taking into account the allowed whole values $(h^2 + hk + k^2)$ and the constant C was computed from the expressions cl^2 proper to diffraction lines for which their ratio is 1, 4, 9 etc.

The values $\sin^2\theta_{obs.}$, $\sin^2\theta_{calc.}$, interplanar distances $dhkl$, Miller's indices (hkl), relative intensity of reflexions for the range of θ of 2—23°, of the inclusion compounds PHTP — palmitic acid are summarized in table 3.

Table 3

X-Ray diffraction data of the inclusion compounds PHTP — palmitic acid, radiation CuK_{α_1} $(A = 0.00382;\ C = 0.0260)$

No. of line	$\theta_{obs.}$	$\sin^2\theta_{obs.}$	$\sin^2\theta_{calc.}$	*hkl*	d_{hkl}	I/I_0
1	3.56	0.00382	0.00382	100	12.405	100
2	6.13	0.01142	0.01146	110	7.2131	34
3	7.10	0.01530	0.01528	200	6.2317	9
4	9.40	0.02670	0.02674	210	4.7160	37
5	9.88	0.02948	0.02942	101	4.4890	5
6	10.69	0.03443	0.03438	300	4.1524	1.4
7	11.65	0.04075	0.04088	201	3.8144	1
8	12.37	0.04589	0.04584	220	3.5955	2
9	12.88	0.04966	0.04966	310	3.4554	4.4
10	14.32	0.06116	0.06112	400	3.1142	2.2
11	15.63	0.07257	0.07258	320	2.8589	1.1
12	16.45	0.08020	0.08020	410	2.7200	1.0
13	18.74	0.10324	0.10314	330	2.3975	4.5
14	19·10	0.10710	0.10696	420	2.3539	2
15	20.14	0.11854	0.11842	510	2.2370	1
16	21.36	0.13266	0.13256	421	2.1148	1.2
17	22.10	0.14150	0.14134	430	2.0473	1.3
18	22.70	0.14890	0.14898	520	1.9959	1.0

The data of table 3 point out that in the series of the studied inclusion compounds there is an increase in intensity of the (100), (110), (200), (210) and (310) and a decrease in intensity for the (101) lines as the carbon atom number in acid increases.

CONCLUSIONS

We summarize our results in the following statements:

1. PHTP forms inclusion compounds with C_6—C_{18} aliphatic monocarboxylic acids with the PHTP/acid weight ratio of about 8.6 and the molar ratio between 4.13 and 9.82.

2. The inclusion compounds PHTP – aliphatic monocarboxylic acids present a higher thermal stability than the individual compounds.

3. The aliphatic monocarboxylic acids are found to be associated as dimers in the channels of PHTP, $\nu_{CO} = 1700\ \mathrm{cm}^{-1}$.

4. The inclusion compounds PHTP – monocarboxylic acids are strictly isomorphous to one another and belong to the hexagonal system.

REFERENCES

[1] G. Allegra, M. Farina, A. Immirazi, A. Colombo, U. Rossi, R. Broggi and G. Natta, *J. Chem. Soc.* (B), **1967**, 1020.

[2] M. Farina, G. Allegra and G. Natta, *J. Amer. Chem. Soc.*, **86**, 516 (1964).

[3] C. Luca and V. Ababi, *Materiale plastice* (Bucharest), **13**, 89 (1976).

[4] C. Luca, A. Popa, N. Bîlbă and Gh. Mihăilă, *Rev. Roumaine Chim.*, **28**, 211 (1983).

[5] I. Agherghinei, C. Luca and Gh. Mihăilă, *J. Thermal Anal.*, **26**, 1, 1983.

[6] M. Farina, *Tetrahedron Letters*, **1963**, 2097.

[7] M. Farina and G. Audisio, *Tetrahedron*, **26**, 1827 (1970).

Revue Roumaine de Chimie, **32**, *1*, 47—50 (1987)

INTERACTION PRODUCT OF N,N'-BIS (FURFURYLIDENE)ETHYLENEDIAMINE WITH COBALT(II) CHLORIDE

AIMEE ARIAS-CARBAJAL* and ROBERTO CAO
Inorganic Chemistry Department, Faculty of Chemistry, University of Havana, Cuba

Received May 13, 1985

The complex [Co("furen")Cl_2] · EtOH obtained from N,N'-bis (furfurylidene)ethylenediamine ("furen") was investigated by thermogravimetric analysis, IR- and UV-spectra, electrical conductivity and magnetic susceptibility.

In the last years, Schiff bases derived from salycilaldehyde have been widely used for coordination compound syntheses. The methods of synthesis used were: a) "in situ" reaction of all components;[1,2] b) formation of the Schiff bases and their subsequent interaction with the corresponding salt;[3,4] c) the reaction between aldehyde and a complex of the selected amine.[5]

The reaction of the Schiff base N,N'-bis(furfurylidene)ethyleneamine ("Furen") has been investigated only with few divalent ions like Fe(II), Ni(II) and Cu(II);[4,6] for this reason in this work we investigated the product of its interaction with $CoCl_2$. With this purpose, the three above mentioned general methods were tried; it was found that only the interaction of the Schiff base with the metallic salt gave good results.

"Furen" was obtained by reaction of furfural with ethylenediamine (molar ratio 2:1) dissolved in benzene and further purification until a chloroformic solution of "furen" is obtained.

The "furen" solution was mixed with an ethanolic solution of anhydrous $CoCl_2$ (molar ratio 2.5:1) keeping the system in constant stirring and heating at 50°C during approximately 5 hrs. The dark green crystals obtained were washed with ethanol and ether, then dried over sodium hydroxide. Analysis: for [Co (furen) Cl_2]. EtOH(**1**) Calculated: Co: 15.03; Cl: 18.12 Found: Co: 14.76; Cl: 18.84%.

The resulting compound **1** decomposes in water and in methanol; it is insoluble in benzene, slightly soluble in ethanol, acetone, ethylic ether and chloroform, but it dissolves well in dimethylformamide (DMF).

---

* To whom correspondence should be addressed.

The thermogravimetric analysis of **1** recorded in air atmosphere shows a great stability of the compound up to 155°C. Two effects can be observed when temperature was varied from 155° up to 210°C : a very intensive exothermal effect which overlaps a slightly endothermal one.

These effects can be explained by the combination of various processes, among them, the loss of associated ethanol and the oxidation of "furen".

In Table 1 some of the most important IR frequencies are shown.

The stretching band of the C=N bond was shifted to lower frequencies in the obtained compound **1** in comparison with the free "furen". This fact can be due to the formation of Co-N bond. The small variations of the rest of the IR bands from the furanic ring can be attributed to the increasing mesomeric effects. The IR spectrum also shows bands in the region between 1040 and 1100 cm^{-1} which can be explained by the presence of ethanol. The large 3200 cm^{-1} band, characteristic for intermolecular hydrogen bond, along with the results of thermal analysis confirm the hypothesis of the strongly associated ethanol in the compound.

Table 1

Frequencies of most characteristic IR vibrations of "furen" and $[Co(furen)Cl_2]\cdot EtOH$ (**1**) (cm^{-1})

Vibration	Free furen [7]	$[Co(furen)Cl_2]\cdot$ $\cdot EtOH$
δ(=C−H) furan	780(s)	770(s)
ν(C−O−C) furan	(d) 1010(s)	1025(s)
Symmetric	1020(s)	
ν(C−O−C) furan	1265(s)	1260(m)
Antysymmetric	1265(s)	1260(m)
ν(C=N)Schiff	1640(s)	1630(s)
Base		

(s) = strong ; (m) = medium ; (d) = doublet

The electrical conductivity measurments of the $6 \cdot 10^{-4}$ $mol \cdot L^{-1}$ solutions of **1** in acetone and DMF gave the results shown in Table 2.

Table 2

Molar conductivities (λ) of the $6 \cdot 10^{-4}$ $mol \cdot L^{-1}$ $[Co(furen)Cl_2]\cdot EtOH$ (**1**) solutions at several times ($cm^2 \cdot ohm^{-1} \cdot mol^{-1}$)

Time (hours)	λ(acetone)	λ(DMF)
1	6.88	36.88
6	8.52	40.61
28	9.83	45.85
11	16.05	55.02

Compound **1** practically does not dissociate in acetone whereas in DMF dissociates a little more without reaching the condition of a 1 : 1 electrolyte.

The electronic absorption spectra in the visible region of the $6 \cdot 10^{-4}$ mol $\cdot$ L^{-1} solutions of **1** are shown in figure 1.

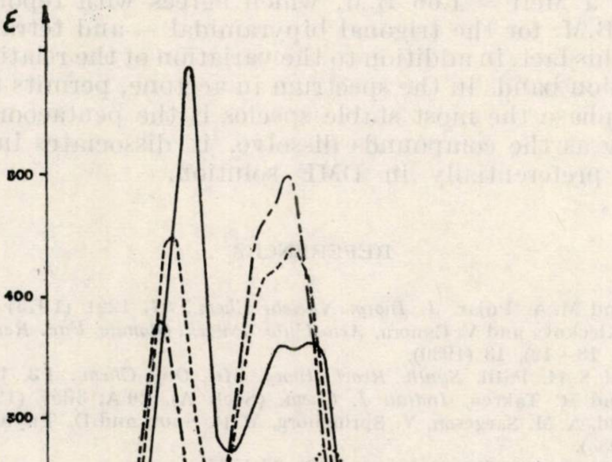

Fig. 1. — Electronic absorption spectra of [Co(furen)Cl$_2$] solutions in : .... DMF and in acetone : —— 1 hour ; ---- 6 hours ; - — - 28 hours.

The observed absorption in DMF with maxima at 14680 cm^{-1} ($\varepsilon \approx 280$) and 16160 cm^{-1} ($\varepsilon \approx 200$), did not change in time.

The obtained spectrum resembling that of the tetrahedric Co(II) compounds, corresponds to a band of a $^4A_2(F) \rightarrow {^4T_1}(P)$ transition, where the fine structure is caused by spin-orbit coupling.[7] However, in acetone solution the spectrum changes in time. In the fresh (1 hour) solution a double band at 15000–15400 cm^{-1} ($\varepsilon \approx 350$) and a symmetric one at 16800 cm^{-1} ($\varepsilon \approx 580$) can be observed. Both bands shift slightly towards larger wave-numbers as time passes, but also the relative intensities change. So, the molar absorption coefficient corresponding to 15000 cm^{-1} band increases while that of the 17000 cm^{-1} one diminishes.

This result could be explained by the existence of an equilibrium between polymeric pentacoordinated and tetrahedric species, since the pentacoordinated Co(II) compounds[8,9] exhibit a 15000 cm^{-1} band corresponding to a ${}^4A_2(F) \rightarrow {}^4E(F)$ transition along with a 17000 cm^{-1} band attributable to $a^4A_2(F) \rightarrow {}^4E(P)$ transition.

The magnetic measurements of the solid **1** performed by Faraday's method, gave a Meff = 4.66 B.M. which agrees with reported range[8, 9] of 4.4 to 4.7 B.M. for the trigonal bipyramidal — and tetrahedric Co(II) compounds. This fact, in addition to the variation of the relative intensities of the absorption bands in the spectrum in acetone, permits us to propose that in solid phase the most stable species is the pentacoordinated one, but as rapidly as the compounds dissolve, it dissociates into the tetrahedric form, preferentially in DMF solution.

REFERENCES

[1] N. S. Biradar and M. A. Pujar, *J. Inorg. Nuclear Chem.*, **37**, 1291 (1975).

[2] F. Brezina, M. Kleckova and V. Canora, *Acta Univ. Palacki Olomuc. Fac. Rerum. Nat.*, **61/65** (CHEMICA 18—19), 13 (1980).

[3] M. N. Patel and S. H. Patil, *Synth. React. Inorg. Met. Org. Chem.*, **13**, 133 (1983).

[4] P. R. Shukla and R. Takroo, *Indian J. Chem.* (Sect. A), **20** A, 3057 (1981).

[5] J. M. Harrowfield, A. M. Sargeson, V. Springborg, M. R. Snow and D. Taylor, *Inorg. Chem.*, **22**, 186 (1983).

[6] E. Z. Hoyer, *Anorg. u Allgem. Chem.*, **288**, 36(1956).

[7] R. M. Silverstein and G. C. Bassler "Spectrophotometric Identification of Organic Compounds", Wiley and Sons, New-York 3rd. edition, 1974.

[8] M. Ciampolini and J. Gelsomini, *Inorg. Chem.*, **6**, 1821 (1967).

[9] L. K. Thompson, B.S. Ramaswamy and E. A. Seymour, *Canad. J. Chem.* **55**, 878 (1977).

Revue Roumaine de Chimie, 32, *1*, 51–62 (1987)

OXIDACIÓN DE MORDANT BLUE 9 CON BROMATO CATALIZADA POR VANADIO (V). I

INFLUENCIA DE VARIABLES

N. P. CID y L. O. GARCÍA VIOR

Departamento de Química Inorgánica, Analítica y Química Física, Facultad
de Ciencias Exactas y Naturales — Universidad de Buenos Aires — Ciudad
Universitaria — 1428 Buenos Aires — República Argentina

Recibido: el 8 de Marzo de 1985
Revisto: el 19 de Julio de 1986

Se investiga la influencia de diversas variables en la oxidación de Mordant Blue 9 (MB9) por bromato con el fin de seleccionar las condiciones óptimas para la valoración del catalizador y para dar las bases de la cinética y mecanismo de la reacción. Se encontró que el **V** (V) forma un complejo 1 : 1 con MB9. Dicho complejo es un probable intermediario de la reacción. Las curvas de absorbancia vs. tiempo son lineales, luego de un periodo de inducción hasta que ca. 40 % del colorante ha sido oxidado. Las pendientes de estas curvas en la zona lineal, tgα, se utilizan como una medida de dicha velocidad.

The influence of different variables on the oxidation of MB9 by bromate is considered. This study allows to select the best conditions to determine the catalyst concentration and gives the basis of the mechanism and kinetics of the reaction. It has been found that vanadium forms a 1 : 1 complex with MB9 and this complex probably is an intermediary in the reaction. After the induction period, the absorbance *vs.* time curves are linear up when ca. 40% of the dye has been oxidated. The slopes of these curves, in the linear range, tgα, are used as measure of that rate.

INTRODUCCIÓN

Se han publicado diversos trabajos sobre las aplicaciones de los métodos cinéticos de análisis. Muchos de ellos se mencionan en las revisiones bienales del Analytical Chemistry. Resultan de particular interés en el análisis de trazas, debido a la elevada sensibilidad y reproducibilidad alcanzada para un gran número de elementos, en combinación con la aplicación de procedimientos relativamente sencillos y de bajo costo.[1–5] En condiciones adecuadas puede lograrse también, alta selectividad.[6–7]

Las reacciones homogéneas que se estudian para la valoración catalítica de iones pueden ser: aquéllas en que el catalizador no cambia su estado de oxidación[8–10] y en las que sí ocurre tal modificación, siendo éstas las más sensibles (del orden de ppb) y por lo tanto las más utilizadas. Es frecuente el empleo de reacciones entre halatos y especies inorgánicas u orgánicas, que al ser muchas de ellas de cinética lenta, permiten efectuar un análisis catalítico.[11–13]

En el presente trabajo se investiga la influencia de variables que intervienen en la reacción de oxidación de Mordant Blue 9 con bromato de potasio, catalizada por vanadio (V).

El Mordant Blue 9 (C.I. 14855)[14] posee la siguiente fórmula estructural:

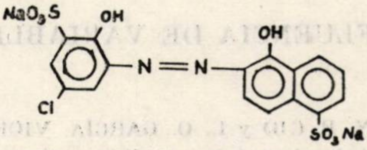

Este azo colorante fue descubierto por M. Kahn y R. Kothe en 1906.[14] Es ligeramente soluble en etanol, pero soluble en agua, originando soluciones violetas que cambian a rojo al acidificar. Cuando se oxida en medio ácido con bromato de potasio, produce inicialmente soluciones amarillas y finalmente incoloras.

PARTE EXPERIMENTAL

Aparatos

Se empleó un espectrofotómetro UV-visible Zeiss, modelo DMR-11 para la obtención de los espectros de absorción y seguir el curso de la reacción en el tiempo, y un Spectronic 20 para mediciones a longitudes de onda fija en la región visible. Las medidas de pH se efectuaron en un pH-metro Metrohm, modelo E 353 B con electrodo de vidrio Metrohm.

Reactivos

Mordant Blue 9: El colorante es 64,0% en Mordant Blue 9; 16,9% en NaCl y 19,1% en Na_2SO_4. La solución (0,03%) fue obtenida por disolución en agua.

Bromato de potasio 0,3M: El peso adecuado de bromato p.a, previamente secado a 120°C durante 1 hora, fue disuelto en agua.

Vanadio (V), 1000 mgV/L: Después de secar a 100°C por 1 hora, la cantidad requerida de NH_4VO_3 p.a, fue disuelta en agua.

Los reactivos auxiliares fueron en todos los casos de calidad p.a. y el agua usada para efectuar las diluciones fue bidestilada sobre cuarzo en un bidestilador Heraeus.

Procedimiento

Se añade el colorante, ácido acético, vanadio (V), bromato y la cantidad necesaria de agua bidestilada para completar el volumen a 10 ml. Se agita y se controla el tiempo con un cronómetro. La reacción se sigue espectrofotométricamente a temperatura controlada, midiendo la variación de la absorbancia con el tiempo a 510 nm, utilizando agua como blanco. Para la reacción no catalizada, el procedimiento es similar, sólo que se reemplaza el volumen usado de vanadio (V), por la misma cantidad de agua.

RESULTADOS Y DISCUSIÓN

1. Interacción vanadio-colorante

En la Fig. 1 se muestran los espectros de absorción del colorante y de los productos de oxidación en sus diferentes etapas para la reacción no catalizada. El reactivo presenta tres máximos: a 300 nm; 378 nm y 510 nm. Cuando la solución resultante es de color amarillo, desaparece el máximo a 510 nm, mientras que se observa una banda entre 400 nm y 450 nm (Fig. 1c), disminuyendo su intensidad en la medida que la oxidación continúa, hasta que llega a eliminarse totalmente (Fig. 1d).

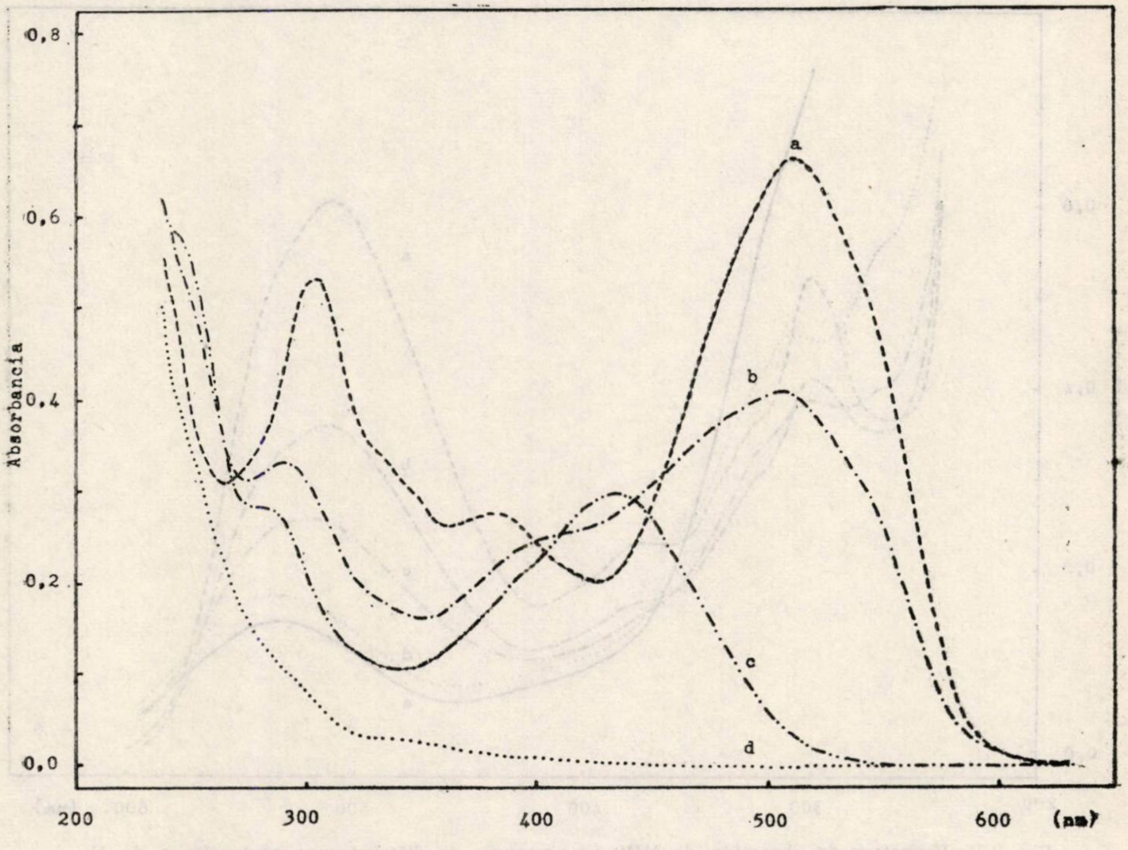

Fig. 1.–Espectros de absorción de MB9 y de sus productos de oxidación a diversos tiempos a: 0 min ; b : 45 min ; c : 150 min ; d : 290 min. $[MB9] = 3{,}8 \times 10^{-5}$; $[AcOH] = 3{,}4$ M ; $[BrO_3^-] = 0{,}015$ M.

El espectro de la Fig. 1a se ve modificado en presencia de trazas de vanadio (V) (Fig. 2). Al incrementarse la concentración de vanadio, el máximo a 510 nm sufre un desplazamiento batocrómico, decreciendo su intensidad. Por otra parte, la banda a 378 nm, si bien no varía su posición, queda eliminada para concentraciones de vanadio (V) de : 1 mgV/L o mayores. A partir de 1 mgV/L, la banda a 300 nm tiende a desaparecer, surgiendo un hombro a 270 nm y a 310 nm. Los espectros de la Fig. 2 indicarían una interacción metal-ligando. Aplicando el método de las variaciones contínuas, para el sistema colorante-vanadio (V) en medio de ácido acético a pH 2, la representación : $A_0 - A$ vs x_c (Fig. 3) conduce a una relación ligando : vanadio de 1 : 1. La constante condicional del complejo, K_1, es $2{,}1 \cdot 10^{-6}$ a 20°C y a fuerza iónica 0,01.

El vanadio (V), fundamentalmente como especie VO_2^+ a pH2[15], interaccionaría, en parte, a través de una unión coordinada con uno de los nitrógenos del grupo azo. Esta suposición se basa en la disminución de la banda a 378 nm, atribuible a una transición n → π^* (banda R) por su posición y baja intensidad,[16,17] donde estarían involucrados los electrones no enlazantes del nitrógeno. Los espectros de absorción del colorante en primera derivada, en la región de 378 nm, en diversas relaciones etanol : agua, producen un incremento en el desplazamiento batocrómico a medida que aumenta la concentración de etanol (Δλ : 2,3 nm para etanol 60 % (v/v)). Por otra parte, en medio ácido acético–agua ocurre un corrimiento hipsocrómico (Δλ : 2,1 nm para ácido acético 90 % (v/v)) mientras que en ácido clorhídrico–agua no se observa variación en la posición del máximo. Estas experiencias estarían de acuerdo con la asignación de la banda a 378 nm ya que al aumentar la polaridad del solvente, se produce desplazamiento hipsocrómico de la banda R.[17]

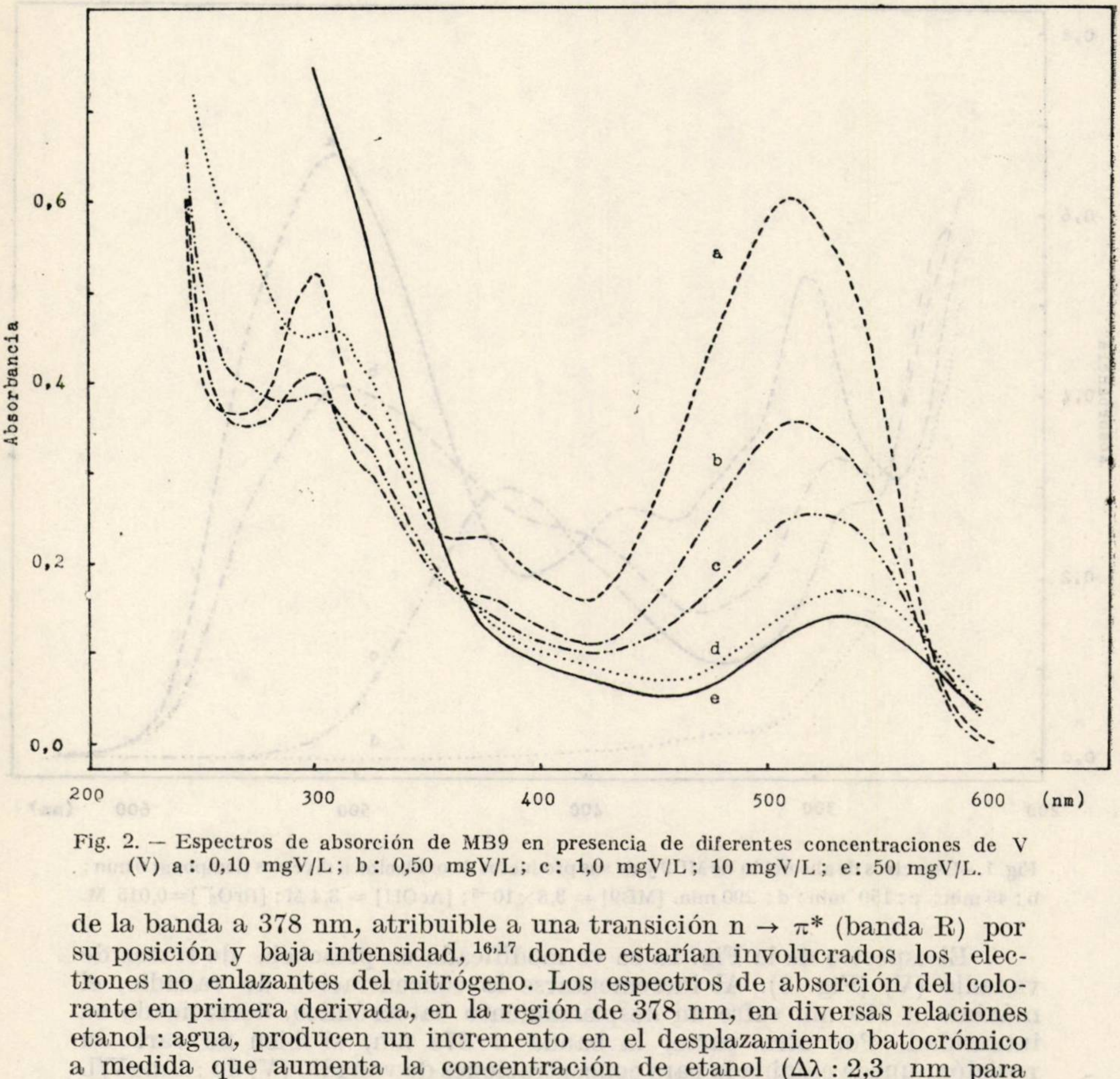

Fig. 2. – Espectros de absorción de MB9 en presencia de diferentes concentraciones de V (V) a : 0,10 mgV/L ; b : 0,50 mgV/L ; c : 1,0 mgV/L ; 10 mgV/L ; e : 50 mgV/L.

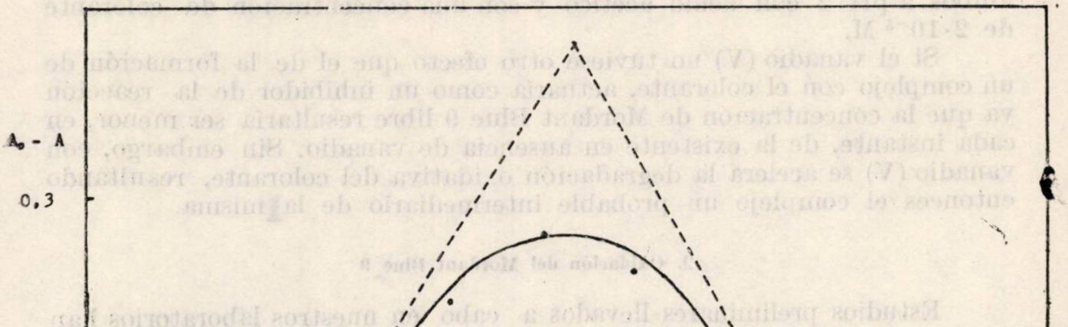

Fig. 3. — Método de las variaciones contínuas para el sistema MB9 — V (V). A_0 y A: absorbancia de MB9, en ausencia y en presencia de V(V), respectivamente; X_c: fracción molar de MB9.

A su vez, el vanadio (V) estaría unido a través de enlace iónico con uno de los oxígenos adyacentes al azo, pudiéndose entonces postular las siguientes estructuras:

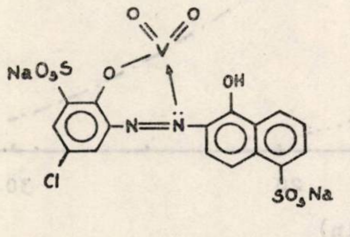

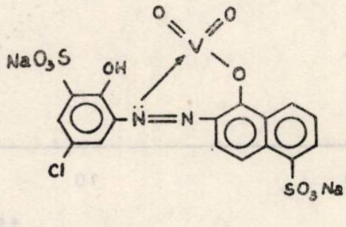

Esta suposición se apoya en el hecho que, en el Naranja de Metilo, sin hidroxilos adyacentos al azo, el espectro de absorción no sufre modificación apreciable respecto del obtenido en presencia de vanadio (0,5 mgV/L), ambos a pH 2 con ácido acético y con una concentración de colorante de $2 \cdot 10^{-5}$ M.

Si el vanadio (V) no tuviese otro efecto que el de la formación de un complejo con el colorante, actuaría como un inhibidor de la reacción ya que la concentración de Mordant Blue 9 libre resultaría ser menor, en cada instante, de la existente en ausencia de vanadio. Sin embargo, con vanadio (V) se acelera la degradación oxidativa del colorante, resultando entonces el complejo un probable intermediario de la misma.

2. Oxidación del Mordant Blue 9

Estudios preliminares llevados a cabo en nuestros laboratorios han demostrado que en la oxidación de dicho colorante con bromato en medio de ácido acético, la absorbancia de aquél disminuye linealmente con el tiempo, luego de un período de inducción, ejerciendo el vanadio (V) acción catalizadora.[18] La dependencia lineal observada (Fig. 4) indicaría, en primera instancia, una reacción de pseudo orden cero, ya que las concentraciones de bromato y de hidronio permanecen prácticamente constantes en el curso de la reacción por ser muy superiores a la de Mordant Blue 9.

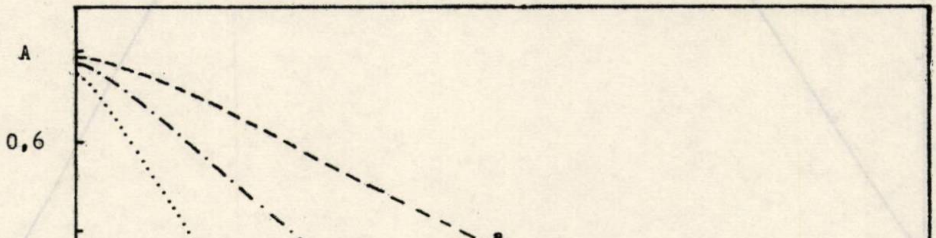

Fig. 4. — Variación de la absorbancia con el tiempo para varias concentraciones de V (V). [MB9] = $3,8 \times 10^{-5}$M; [BrO_3^-] = 0,015 M; [AcOH] = 3,4 M. a: sin V; b: 0,02 mgV/L; c: 0,05 mgV/L.

2.1. *Influencia de la concentración del catalizador*

Se estudió la influencia del vanadio en el ámbito de concentraciones de 0,01 a 0,30 mV/L, manteniéndose constantes las concentraciones de las otras especies. En la Fig. 5 se representa tg α vs concentración de vanadio (V), donde tg α son las pendientes de las curvas absorbancia vs tiempo para cada concentración de vanadio en la zona lineal de las mismas, siendo además una medida de la velocidad de reacción. Este tipo de representación es utilizado analíticamente para valorar ciertos catalizadores.[19,20] En nuestro caso se observa un aumento lineal hasta 0,1 mgV/L. Para concentraciones de vanadio por debajo de $5 \cdot 10^{-3}$ mg/L no llegan a obtenerse valores precisos de tgα ya que las velocidades de reacción catalizada y no catalizada son muy similares. Por encima de 0,3 mgV/L, la oxidación del colorante es prácticamente instantánea.

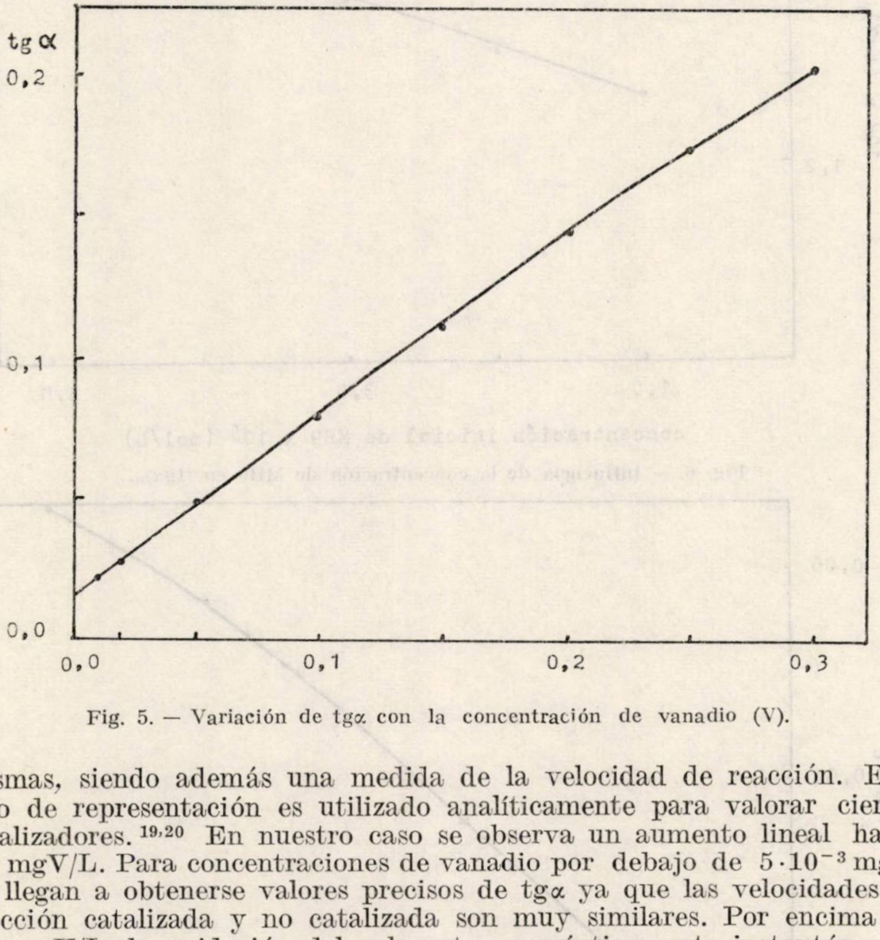

Fig. 5. — Variación de tgα con la concentración de vanadio (V).

2.2. *Influencia de la concentración de Mordant Blue 9*

A partir de las curvas absorbancia vs tiempo, tgα aumenta linealmente con la concentración de colorante en un ámbito de concentraciones de 10^{-5} a $5 \cdot 10^{-5}$M (Fig. 6). Si en la reacción catalizada se designa $(\text{tg}\alpha)_c$ a la diferencia entre las pendientes obtenidas en presencia del catalizador y en ausencia del mismo, cuando se representa $(\text{tg}\alpha)_c$ vs concentración de colorante (Fig. 7) se observa una ligera curvatura al incrementarse la concentración de Mordant Blue 9. Dado que la velocidad de la reacción

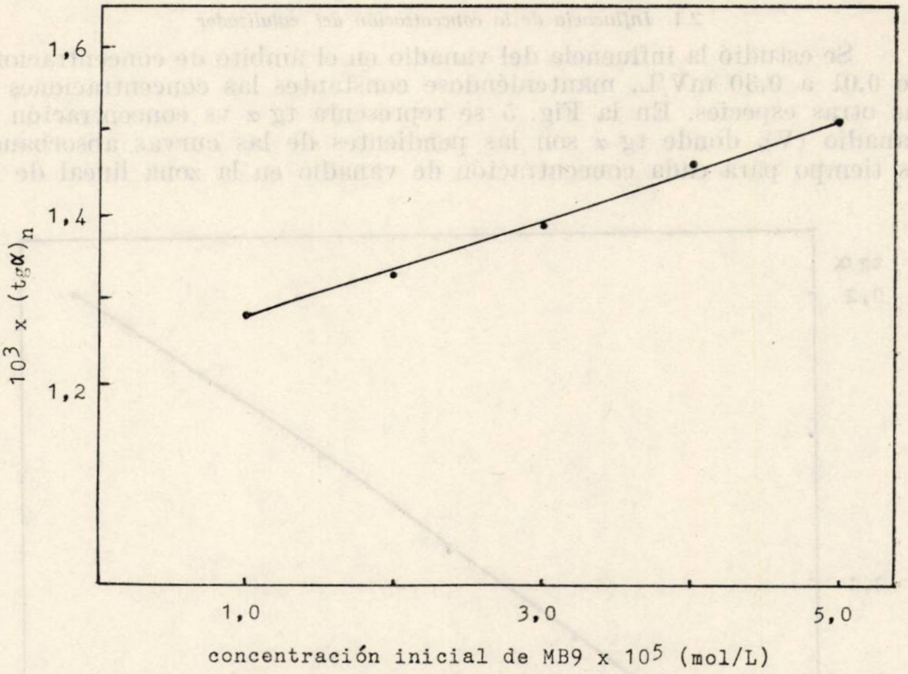

Fig. 6. — Influencia de la concentración de MB9 en $(tg\alpha)_n$.

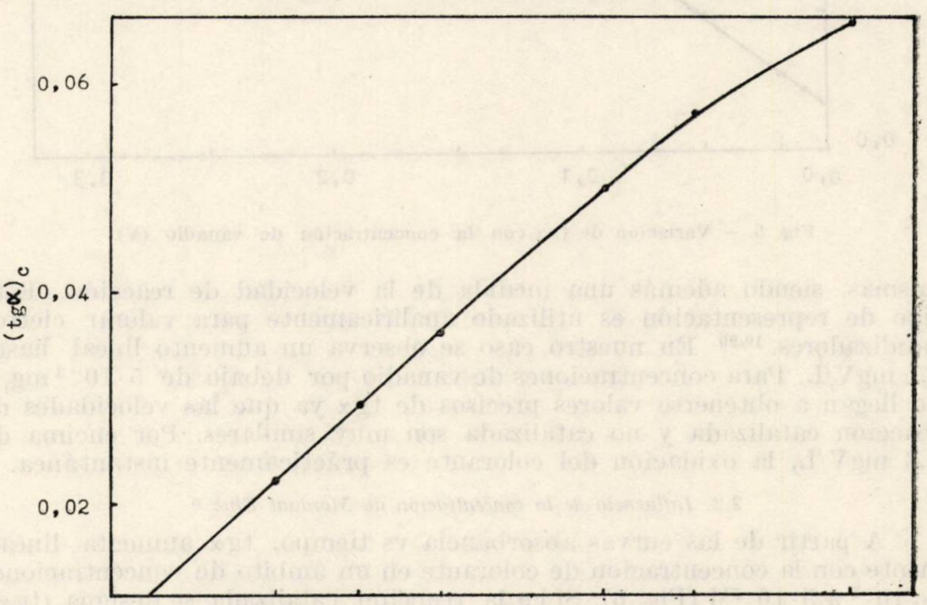

Fig. 7. — Influencia de la concentración de MB9 en $(tg\alpha)_c$.

total, v, es la suma de los términos de velocidad correspondientes a la reacción no catalizada, v_n, y catalizada, v_c,[21,22] $(\mathrm{tg}\,\alpha)_c$ es una medida de esta última.

2.3 *Influencia de la concentración del oxidante*

Las reacciones, catalizada y no catalizada, resultan muy lentas para concentraciones de bromato menores de 0,01 M, mientras que son excesivamente rápidas por encima de 0,12 M. A diferencia de lo observado con las variables anteriormente consideradas, un aumento en la concentración de bromato (de 0,015 M a 0,120 M), para la reacción no catalizada, produce un incremento no lineal en tg α. La curva resultante queda linealizada en una representación doble logarítmica (coeficiente de correlación, r, de 0,991) con una pendiente de 2,05. Esto indicaría un orden de 2 respecto de la concentración de bromato.

En la Fig. 8 y 9 se muestra la influencia de la concentración de bromato para ambas reacciones, encontrándose que el término v_c es independiente de dicha concentración.

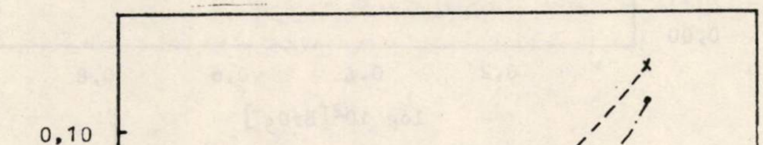

Fig. 8. — tgα versus concentración de bromato a: reacción global; b: reacción no catalizada; c: reacción catalizada.

Cabe aclararse que en la Fig. 9b la representación es lineal, no siendo así en la reacción catalizada (Fig. 9a). Esto puede justificarse en cierta medida considerando que:

$$(\mathrm{tg}\,\alpha)_n = \mathrm{K}\cdot[\mathrm{BrO_3^-}]^2 \quad \text{(reacción no catalizada)}$$

$$\mathrm{tg}\,\alpha = \mathrm{K}\cdot[\mathrm{BrO_3^-}]^2 + \mathrm{K}' \quad \text{(reacción global)}$$

donde K′ representa al término de la velocidad de la reacción catalizada.

Por otra parte, el bromato de potasio utilizado, aunque es de grado analítico, contiene bromuro como impureza mayoritaria (ca. 0,05 %).[25]

Fuller y col.[26] consideraron su efecto en la oxidación del Bordeaux con el mismo oxidante. En nuestro caso se estudió su influencia en la reacción no catalizada ([Mordant Blue 9]: $3{,}8 \cdot 10^{-5}$ M; $[BrO_3^-]$: $1{,}5 \cdot 10^{-2}$ M; [ác. acético]: 3,4M), agregando concentraciones conocidas de bromuro entre 0 y 5,0 $mgBr^-/L$, hallándose que $(tg\alpha)_n$ vs $[Br^-]$ agregado es lineal (r : 0,999, seis concentraciones de Br^-, pendiente $7{,}6 \cdot 10^{-3}$ y con ordenada al origen de $1{,}1 \cdot 10^{-2}$). El incremento en la velocidad de reacción en presencia de bromuro puede explicarse sobre la base de la reaccion:

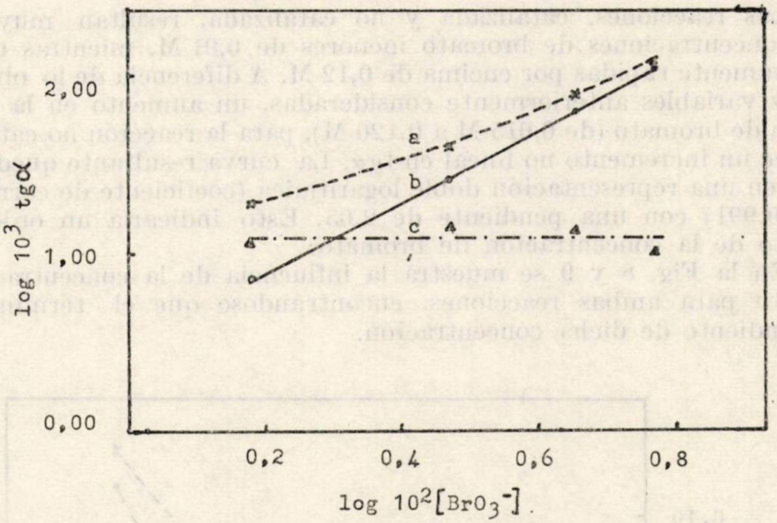

Fig. 9. — tgα versus log concentración de bromato. a: reacción global; b: reacción no catalizada; c: reacción catalizada.

$$BrO_3^- + 5Br^- + 6H^+ \rightleftarrows 3\,Br_2 + 3\,H_2O$$

El Br_2 formado actuaría junto con el ión BrO_3^- en la oxidación del colorante.

2.4 *Influencia de la concentración de iones hidrógeno*

Las condiciones de acidez más adecuadas para seguir la cinética de la reacción están acotadas dado que por debajo de pH 1 la velocidad de la reacción global es muy elevada y por encima de pH ca. 3 la reacción no catalizada es extremadamente lenta.

En la Fig. 10 se representa tgα vs $[H^+]$ para la reacción catalizada y no catalizada, ajustando la acidez con ácido perclórico.

Para el primer caso, log $(tg\alpha)_n$ vs pH conduce a una recta con pendiente 1,8 (orden con respecto de $[H^+]$ ca. 2) y coeficiente de correlación, r, de —0,9999 en el intervalo de pH ensayado: 1,20—2,35. En presencia de vanadio, log tgα vs pH, también da una recta, pero con pendiente 0,6 (orden respecto de $[H^+]$, ca. 1/2), con un valor de r : —0,9990 en un ámbito de pH : 1,20—2,55.

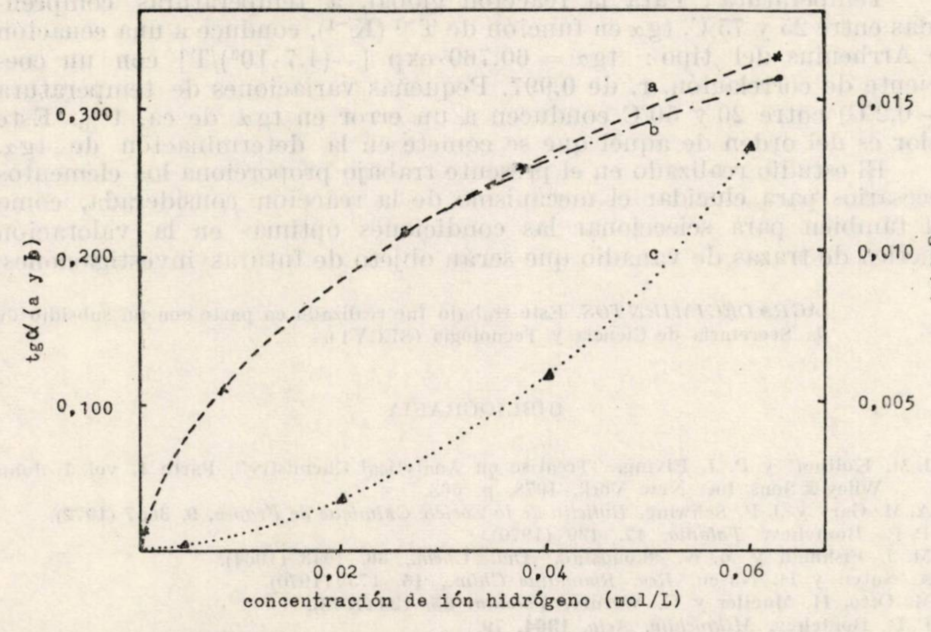

Fig. 10. — tgα en función de la concentración de ión hidrógeno a : reacción global ; b : reacción catalizada ; c : reacción no catalizada.

Es importante tener en cuenta qué especies intervienen en el ajuste del pH, ya que ciertos aniones pueden acelerar o inhibir las reacciones en cuestión. Así, con ácido clorhídrico se obtienen valores anormalmente elevados de $(tg\alpha)_n$ (Tabla 1), operando al mismo pH que con ácido perclórico. Ello se debe a que por su reacción con el oxidante se produce Br y Cl_2.[23] En medio de ácido acético, el incremento en la velocidad de reacción puede atribuirse a la formación de acetato de bromonio $(CH_3CO_2^- Br^+)$[24] que es más reactivo que el bromo que participa en la oxidación del Mordant Blue 9. De todos modos, en medio de ácido acético, $(tg\alpha)_c$ es aún significativa, no siendo así en ácido clorhídrico. Además, el poder regulador alcanzado con el primero es del 60 % superior al que se obtiene con ácidos fuertes al mismo pH.

Tabla 1

Influencia del ácido empleado en los valores de $(tg\,\alpha)_n$

ACIDO	$(tg\,\alpha)_n$	
	pH 1	pH 2
perclórico	0,03	$3,8 \cdot 10^{-4}$
acético	—	$1,4 \cdot 10^{-2}$
clorhídrico	0,30	—

2.5 *Influencia de otras variables*

Fuerza iónica : El estudio de la variación de la velocidad de reacción con la fuerza iónica, I, para el sistema Mordant Blue 9—bromato—vanadio (V)—ácido acético, se llevó a cabo modificando la fuerza iónica con perclorato de sodio. Se observó que para el ámbito de I estudiado (0,02—0,66), tgα, permanece prácticamente invariable.

Temperatura: Para la reacción global, a temperaturas comprendidas entre 25 y 75°C, tgα en función de T^{-1} (K^{-1}), conduce a una ecuación de Arrhenius del tipo: $tg\alpha = 60.760 \cdot \exp\,[-(4{,}7 \cdot 10^3)/T]$ con un coeficiente de correlación, r, de 0,997. Pequeñas variaciones de temperatura ($\pm$ 0,2°C) entre 20 y 50°C conducen a un error en tgα de ca. 1 %. Este valor es del orden de aquél que se comete en la determinación de tgα.

El estudio realizado en el presente trabajo proporciona los elementos necesarios para elucidar el mecanismo de la reacción considerada, como así también para seleccionar las condiciones óptimas en la valoración cinética de trazas de vanadio que serán objeto de futuras investigaciones.

AGRADECIMIENTOS. Este trabajo fue realizado en parte con un subsidio de la Secretaría de Ciencia y Tecnología (SECYT).

BIBLIOGRAFIA

[1] I. M. Kolthoff y P. J. Elving, "Treatise on Analytical Chemistry". Parte 1, vol. 1. John Wiley & Sons Inc. New York, 1978, p. 663.
[2] A. M. Gary y J. P. Schwing, *Bulletin de la Société Chimique de France*, **9**, 3657 (1972).
[3] P. R. Bontchev, *Talanta*, **17**, 499 (1970).
[4] M. J. Fishman y M. W. Skougstad, *Anal. Chem.*, **36**, 1643 (1964).
[5] A. Şuten y H. Naşcu, *Rev. Roumaine Chim.*, **15**, 1759 (1970).
[6] M. Otto, H. Mueller y G. Werner, *Talanta*, **25**, 123 (1978).
[7] P. R. Bontchev, *Mikrochim. Acta*, **1964**, 79.
[8] P. R. Bontchev y V. Michaylova, *J. Inorg. Nucl. Chem.*, **29**, 2945 (1967).
[9] H. Kroll, *J. Am. Chem. Soc.*, **74**, 2036 (1952).
[10] J. Kraljic, *Mikrochim. Acta*, **586** (1960).
[11] C. W. Fuller y J. M. Ottaway, *Analyst*, **95**, 34 (1970).
[12] G. López Cueto y J. A. Casado Riobó, *Talanta*, **26**, 127 (1979).
[13] H. Weizz y S. Pantel, *Anal. Chim. Acta*, **76**, 487 (1975).
[14] Color index, vol. 1, p. 1507; vol. 3, p. 3065; 2da ed. 1956. Suplemento 1963; p. S 137, Mass. (U.S.A).
[15] P. Souchay, "Ions minéraux condensés", Masson & Cie, 1968, p. 67.
[16] D. J. Pasto y C.R. Johnson; "Determinación de estructuras orgánicas", Ed. Reverté, 1977, p. 113.
[17] G. Serguéiev, N. Kazánskaia, B. Uzhinov, V. Papisova, V. Gurman, G. Melúsova, S. Zenin y V. Románov; ,,Métodos experimentales de la cinética química", Editorial Mir, Moscú, 1975, p. 12.
[18] N. P. Cid y L.O. García Vior, "Memoria del XIV Congreso Latinoamericano de Química", vol 1, San José, Costa Rica, 1—7 febrero 1981, p. 159.
[19] Ref. 1, p. 681.
[20] D. Costache, *Rev. Roumaine Chim.*, **16**, 849 (1971).
[21] Ref. 1, p. 679.
[22] G. Svehla, *Analyst*, **94**, 513 (1969).
[23] A. F. Clifford, "Inorganic Chemistry of Qualitative Analysis", Prentice-Hall, Inc., 1961, p. 389.
[24] A. L. Montes, "Bromatología", Editorial universitaria de Buenos Aires, Tomo II, 1969, p. 493.
[25] Laboratory Chemicals, Plastic ware and Lab. Safety Products, Malinckrodt, Inc., 1981—82, p. 235.
[26] C. W. Fuller y J. M. Ottaway, *Analyst*, **95**, 28 (1970).

Revue Roumaine de Chimie, **32**, *1*, 63–81 (1987)

ELECTRONIC STRUCTURE AND REACTIVITY INDICES FOR A SERIES OF PURINE DERIVATIVES, INHIBITORS OF GUANINE PHOSPHORIBOSYLTRANSFERASE FROM *ESCHERICHIA COLI*

NICULAE OLARU and ZENO SIMON*
Institute of Macromolecular Chemistry "P. Poni", Aleea Gr. Ghica-Vodă 41 A
Jassy-6600, Romania
* Institute of Medicine, Timişoara—1900, Romania

Received December 23, 1985

Reactivity indices and electronic structure for a series of 62 purinic derivatives, tested as inhibitors of guanine phosphoribosyltransferase (GPRT) from *Escherichia Coli*, are calculated using HMO and Del Re methods. Some quantitative structure activity relationships (QSAR) for a set of 13 compounds with similar steric structure are given. The correlational equations obtained show the importance of electronic control in the inhibition of GPRT.

The design of quantitative structure-activity relationships (QSAR) for molecules with relatively large, extended π-electron systems requires the knowledge of atomic charges and of other structural and reactivity indices, characterizing different atomic centres of the molecule. Such parameters are difficult to be obtained from experiment, but can be calculated by quantum chemistry.

In a previous note [1] we compared the net atomic charges calculated by different molecular orbital methods, and the good correlations of relative charge values, obtained by the simple HMO + Del Re methods and by other more advanced methods, allowed us to conclude that the results of simple methods are sufficiently accurate to be used in QSAR-studies.

Here we calculate electronic structure and reactivity indices for a series of 62 purinic derivatives tested as inhibitors of guanine phosphoribosyltransferase (GPRT) from *Escherichia Coli*. [2] These indices will be used in another note, [3] together with indices characterizing steric effects, to design QSAR's for this type of activity. Some QSAR's for a limited set of compounds with similar steric structure will be already given in this note.

ELECTRONIC STRUCTURE CALCULATIONS

The simple HMO + Del Re methods are used here, for above mentioned reasons and also in order to save the computer time required by more advanced methods for such a relatively large series of compounds.

The parameters used and details of calculations are described in our previous note. [1]

The molecular diagrams for the 62 molecules are depicted in Figure 1.

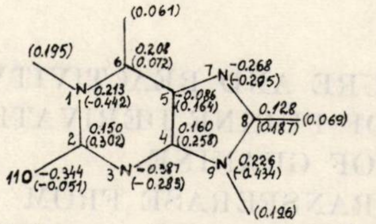
(0.061)
(0.195)
6
0.208
(0.072)
7
N
-0.268
(-0.295)
1
N
0.213
(-0.442)
5
-0.086
(0.164)
0.128
8
(0.187)
(0.069)
2
0.150
(0.302)
4
0.160
(0.258)
N
0.226
(-0.434)
9
11 O
-0.344
(-0.051)
3
N
-0.387
(-0.283)
(0.196)

1. 2-Hydroxypurine $\varepsilon_{LE} = \alpha - 0.549\beta$
$\varepsilon_{HO} = \alpha + 0.405\beta$

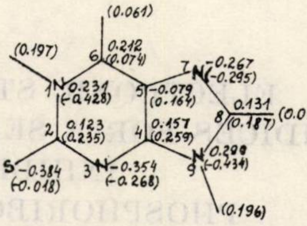
(0.061)
(0.197)
6
0.212
(0.074)
7
N
-0.267
(-0.295)
1
N
0.231
(-0.428)
5
-0.079
(0.164)
8
0.131
(0.187)
(0.069)
2
0.123
(0.235)
4
0.157
(0.259)
N
0.288
(-0.434)
9
11 S
-0.384
(-0.018)
3
N
-0.354
(-0.268)
(0.196)

2. 2-Mercaptopurine $\varepsilon_{LE} = \alpha - 0.545\beta$
$\varepsilon_{HO} = \alpha + 0.360\beta$

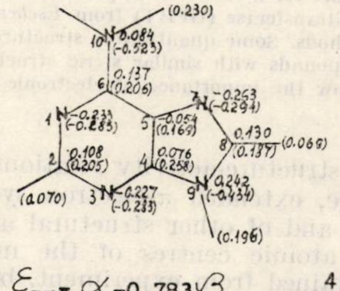
(0.230)
N
0.084
(-0.523)
0.137
6
(0.206)
7
N
-0.263
(-0.294)
1
N
-0.233
(-0.283)
5
-0.054
(0.169)
8
0.130
(0.187)
(0.069)
2
0.108
(0.205)
4
0.076
(0.258)
N
0.242
(-0.434)
9
(0.070)
3
N
-0.227
(-0.283)
(0.196)

3. Adenine $\varepsilon_{LE} = \alpha - 0.783\beta$
$\varepsilon_{HO} = \alpha + 0.640\beta$

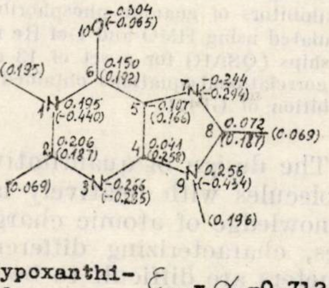
10 O
-0.304
(-0.065)
(0.195)
6
0.150
(0.192)
7
N
-0.244
(-0.294)
1
N
0.195
(-0.440)
5
-0.147
(0.166)
8
0.072
(0.187)
(0.069)
2
0.206
(0.187)
4
0.041
(0.258)
N
0.256
(-0.434)
9
(0.069)
3
N
-0.266
(-0.283)
(0.196)

4. Hypoxanthine $\varepsilon_{LE} = \alpha - 0.712\beta$
$\varepsilon_{HO} = \alpha + 0.415\beta$

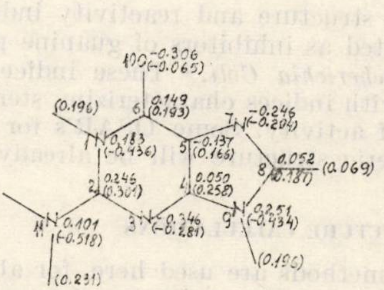
10 O
-0.306
(-0.065)
(0.196)
6
0.149
(0.193)
7
N
-0.246
(-0.294)
1
N
0.183
(-0.436)
5
-0.137
(0.166)
8
0.052
(0.187)
(0.069)
2
0.246
(0.301)
4
0.050
(0.258)
N
0.251
(-0.434)
9
3
N
-0.346
(-0.281)
11
N
0.101
(-0.518)
(0.231)
(0.196)

5 Guanine $\varepsilon_{LE} = \alpha - 0.811\beta$
$\varepsilon_{HO} = \alpha + 0.360\beta$

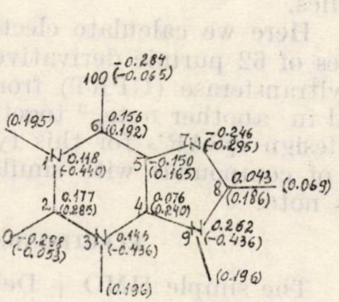
100
-0.284
(-0.065)
(0.195)
6
0.156
(0.192)
7
N
-0.246
(-0.295)
1
N
0.118
(-0.440)
5
-0.150
(0.165)
8
0.043
(0.186)
(0.069)
2
0.177
(0.285)
4
0.076
(0.240)
N
0.262
(-0.436)
9
11 O
-0.299
(-0.053)
3
N
0.145
(-0.436)
(0.196)
(0.196)

6. Xanthine $\varepsilon_{LE} = \alpha - 1.004\beta$
$\varepsilon_{HO} = \alpha + 0.489\beta$

Fig. 1. — Molecular diagrams and numbering of atoms for the 62 purinic derivatives.

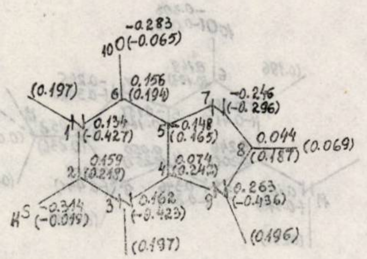
-0.283
10 O (-0.065)
(0.197)
6 0.156 (0.194)
7 N -0.246 (-0.296)
1 N 0.134 (-0.427)
5 -0.148 (0.165)
8 0.044 (0.187) (0.069)
2 0.159 (0.219)
4 0.074 (0.242)
9 N 0.263 (-0.436)
H S -0.314 (-0.019)
3 N 0.162 (-0.423)
(0.197)
(0.196)

7. 2-Mercapto-6-hydroxypurine $\mathcal{E}_{LE} = \alpha - 0.997\beta$ $\mathcal{E}_{HO} = \alpha + 0.479\beta$

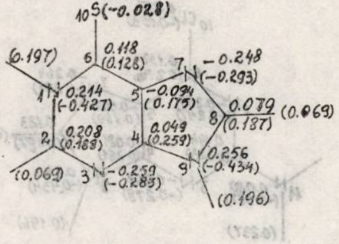
-0.324
10 S (-0.028)
(0.197)
6 0.118 (0.128)
7 N -0.248 (-0.293)
1 N 0.214 (-0.427)
5 -0.094 (0.175)
8 0.079 (0.187) (0.069)
2 0.208 (0.168)
4 0.049 (0.259)
9 N 0.256 (-0.434)
(0.069)
3 N -0.259 (-0.283)
(0.196)

8. 6-Mercaptopurine $\mathcal{E}_{LE} = \alpha - 0.708\beta$ $\mathcal{E}_{HO} = \alpha + 0.377\beta$

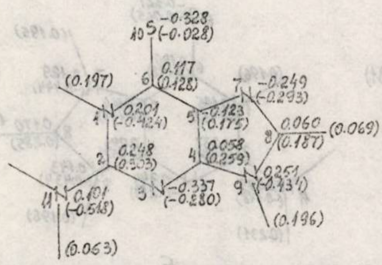
-0.328
10 S (-0.028)
(0.197)
6 0.117 (0.128)
7 N -0.249 (-0.293)
1 N 0.201 (-0.424)
5 -0.123 (0.175)
8 0.060 (0.187) (0.069)
2 0.248 (0.303)
4 0.058 (0.259)
9 N 0.251 (-0.431)
11 N 0.101 (-0.518)
3 N -0.337 (-0.280)
(0.196)
(0.063)

9. 2-Amino-6-mercaptopurine $\mathcal{E}_{LE} = \alpha - 0.806\beta$ $\mathcal{E}_{HO} = \alpha + 0.330\beta$

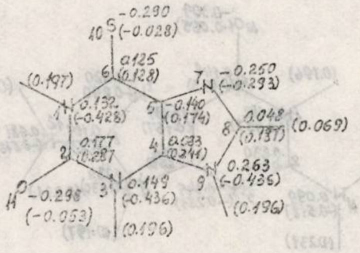
-0.290
10 S (-0.028)
0.125
6 (0.128)
(0.197)
7 N -0.250 (-0.293)
1 N 0.132 (-0.428)
5 -0.140 (0.174)
8 0.048 (0.187) (0.069)
2 0.177 (0.287)
4 0.083 (0.244)
9 N 0.263 (-0.436)
H O -0.298 (-0.053)
3 N 0.149 (-0.436)
(0.196)
(0.196)

10. 2-Hydroxy-6-mercaptopurine $\mathcal{E}_{LE} = \alpha - 0.980\beta$ $\mathcal{E}_{HO} = \alpha + 0.460\beta$

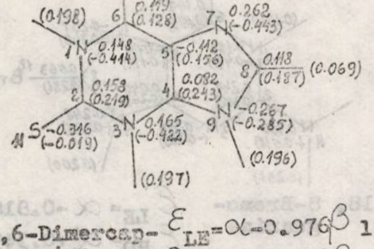
-0.287
10 S (-0.028)
(0.198)
6 0.149 (0.128)
7 N 0.262 (-0.443)
1 N 0.148 (-0.414)
5 -0.112 (0.156)
8 0.118 (0.187) (0.069)
2 0.158 (0.219)
4 0.082 (0.243)
9 N -0.267 (-0.285)
11 S -0.316 (-0.019)
3 N 0.165 (-0.422)
(0.196)
(0.197)

11. 2,6-Dimercaptopurine $\mathcal{E}_{LE} = \alpha - 0.976\beta$ $\mathcal{E}_{HO} = \alpha + 0.433\beta$

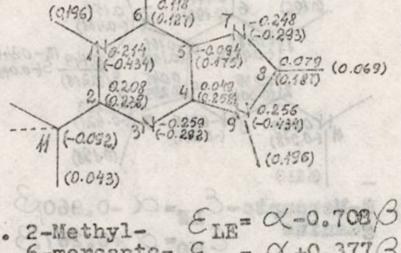
-0.324
10 S (-0.028)
(0.196)
6 0.118 (0.127)
7 N -0.248 (-0.293)
1 N 0.214 (-0.434)
5 -0.094 (0.175)
8 0.079 (0.187) (0.069)
2 0.208 (0.238)
4 0.049 (0.258)
9 0.256 (-0.434)
11 (-0.092)
3 N -0.259 (-0.282)
(0.196)
(0.043)

12. 2-Methyl-6-mercaptopurine $\mathcal{E}_{LE} = \alpha - 0.708\beta$ $\mathcal{E}_{HO} = \alpha + 0.377\beta$

Fig. 1b

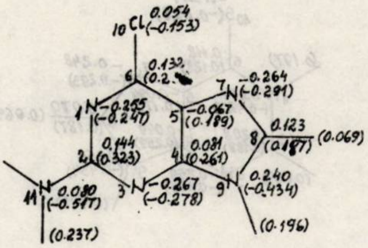
10 Cl 0.054 (-0.153)
6 0.132 (0.2
7 N -0.264 (-0.291)
1 N -0.255 (-0.247)
5 -0.067 (0.189)
8 0.123 (0.187) (0.069)
2 0.144 (0.323)
4 0.081 (0.261)
11 N 0.080 (-0.517)
3 N -0.267 (-0.278)
9 N 0.240 (-0.434)
(0.237)
(0.196)

13. 2-Amino-6-chloro-purine $\varepsilon_{LE} = \alpha - 0.798\beta$
$\varepsilon_{HO} = \alpha + 0.601\beta$

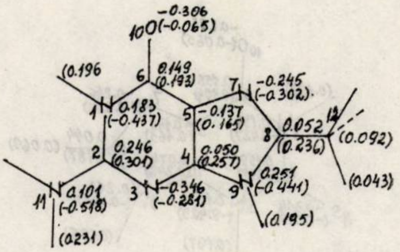
10 O -0.306 (-0.065)
(0.196
6 0.149 (0.193)
7 N -0.245 (-0.302).
1 N 0.183 (-0.437)
5 -0.137 (0.165)
8 0.052 (0.236)
12
(0.092)
2 0.246 (0.301)
4 0.050 (0.257)
9 N 0.251 (-0.441)
(0.043)
11 N 0.101 (-0.518)
3 N -0.346 (-0.281)
(0.195)
(0.231)

14. 8-Methyl-guanine $\varepsilon_{LE} = \alpha - 0.811\beta$
$\varepsilon_{HO} = \alpha + 0.360\beta$

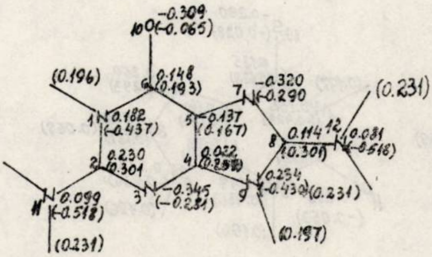
10 O -0.309 (-0.065)
(0.196)
6 0.148 (0.193)
7 N -0.320 (-0.290
(0.231)
1 N 0.182 (-0.437)
5 -0.137 (0.167)
8 0.114 (0.301)
12 N 0.081 (-0.516)
2 0.230 0.301
4 0.022 (0.25
9 N 0.254 (-0.430) (0.231)
11 N 0.099 (-0.518)
3 N -0.345 (-0.281)
(0.197)
(0.231)

15. 8-Amino-guanine $\varepsilon_{LE} = \alpha - 0.849\beta$
$\varepsilon_{HO} = \alpha + 0.280\beta$

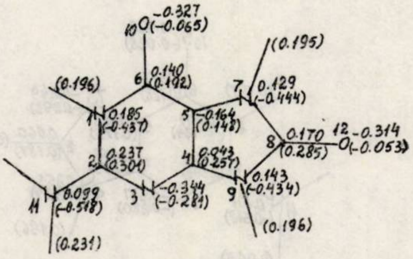
10 O -0.327 (-0.065)
(0.195)
(0.196)
6 0.140 (0.192)
7 N 0.129 (-0.444)
1 N 0.185 (-0.437)
5 -0.164 (0.148)
8 0.170 (0.285)
12 O -0.314 (-0.053)
2 0.237 (0.301)
4 0.043 (0.257)
9 N 0.143 (-0.434)
11 N 0.099 (-0.518)
3 N -0.344 (-0.281)
(0.196)
(0.231)

16. 8-Hydroxy-guanine $\varepsilon_{LE} = \alpha - 0.860\beta$
$\varepsilon_{HO} = \alpha + 0.278\beta$

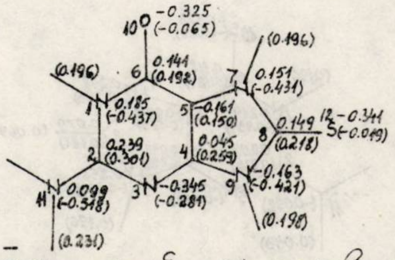
10 O -0.325 (-0.065)
(0.196)
(0.196)
6 0.144 (0.192)
7 N 0.151 (-0.431)
1 N 0.185 (-0.437)
5 -0.161 (0.150)
8 0.149 (0.218)
12 S -0.341 (-0.049)
2 0.239 (0.301)
4 0.045 (0.259)
9 N -0.163 (-0.421)
11 N 0.099 (-0.518)
3 N -0.345 (-0.281)
(0.198)
(0.231)

17. 8-Mercapto-guanine $\varepsilon_{LE} = \alpha - 0.860\beta$
$\varepsilon_{HO} = \alpha + 0.267\beta$

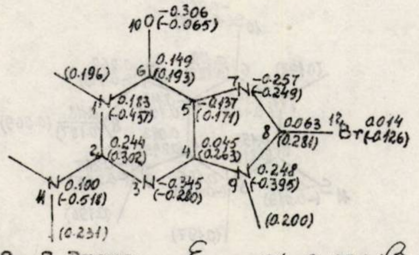
10 O -0.306 (-0.065)
(0.196)
6 0.149 (0.193)
7 N -0.257 (-0.249)
1 N 0.183 (-0.457)
5 -0.137 (0.171)
8 0.063 (0.281)
12 Br 0.014 (-0.126)
2 0.244 (0.302)
4 0.045 (0.263)
9 N 0.248 (-0.395)
11 N 0.100 (-0.518)
3 N -0.345 (-0.280)
(0.200)
(0.231)

18. 8-Bromo-guanine $\varepsilon_{LE} = \alpha - 0.818\beta$
$\varepsilon_{HO} = \alpha + 0.345\beta$

Fig. 1c

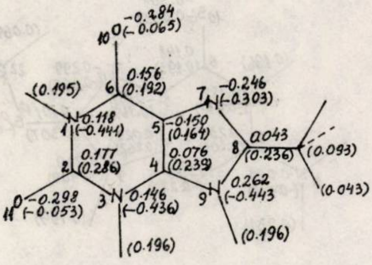
10 O −0.284 (−0.065)
(0.195)
6 0.156 (0.192)
7 N −0.246 (−0.303)
1 N 0.118 (−0.441)
5 −0.150 (0.164)
2 0.177 (0.286)
4 0.076 (0.239)
8 0.043 (0.236)
(0.093)
(0.043)
11 O −0.298 (−0.053)
3 N 0.146 (−0.436)
9 N 0.262 (−0.443)
(0.196)
(0.196)

19. 8-Methyl-xanthine $\varepsilon_{LE} = \alpha - 1.004\beta$
$\varepsilon_{HO} = \alpha + 0.489\beta$

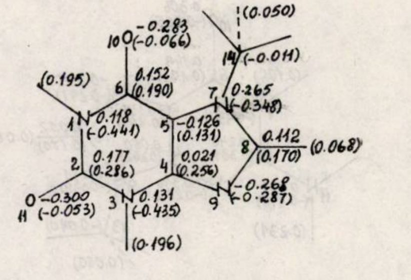
(0.050)
10 O −0.283 (−0.066)
14 (−0.011)
(0.195)
6 0.152 (0.190)
7 N 0.265 (−0.348)
1 N 0.118 (−0.441)
5 −0.126 (0.131)
8 0.112 (0.170)
(0.068)
2 0.177 (0.286)
4 0.021 (0.256)
O −0.300
11 (−0.053)
3 N 0.131 (−0.435)
9 N −0.268 (−0.287)
(0.196)

20. 7-Methyl-xanthine $\varepsilon_{LE} = \alpha - 0.848\beta$
$\varepsilon_{HO} = \alpha + 0.548\beta$

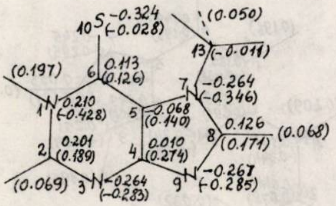
10 S −0.324 (−0.028)
(0.050)
13 (−0.011)
(0.197)
6 0.113 (0.126)
7 N −0.264 (−0.346)
1 N 0.210 (−0.428)
5 −0.068 (0.140)
8 0.126 (0.171)
(0.068)
2 0.201 (0.189)
4 0.010 (0.274)
(0.069)
3 N −0.264 (−0.283)
9 N −0.267 (−0.285)

21. 6-Mercapto-7-methyl-purine $\varepsilon_{LE} = \alpha - 0.725\beta$
$\varepsilon_{HO} = \alpha + 0.414\beta$

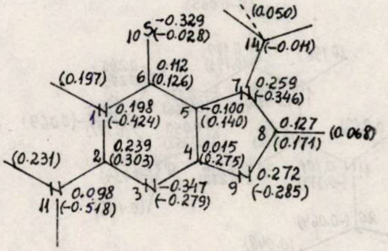
(0.050)
10 S −0.329 (−0.028)
14 (−0.011)
(0.197)
6 0.112 (0.126)
7 N 0.259 (−0.346)
1 N 0.198 (−0.424)
5 −0.100 (0.140)
8 0.127 (0.171)
(0.068)
(0.231)
2 0.239 (0.303)
4 0.015 (0.275)
9 N 0.272 (−0.285)
11 N 0.098 (−0.518)
3 N −0.347 (−0.279)

22. 2-Amino-6-mercapto-7-methyl-purine $\varepsilon_{LE} = \alpha - 0.773\beta$
$\varepsilon_{HO} = \alpha + 0.370\beta$

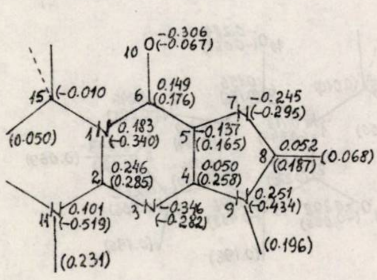
10 O −0.306 (−0.067)
15 (−0.010
6 0.149 (0.176)
7 N −0.245 (−0.295)
(0.050)
1 N 0.183 (−0.340)
5 −0.137 (0.165)
8 0.052 (0.187)
(0.068)
2 0.246 (0.285)
4 0.050 (0.258)
11 N 0.101 (−0.519)
3 N −0.346 (−0.282)
9 N 0.251 (−0.434)
(0.196)
(0.231)

23. 1-Methyl-guanine $\varepsilon_{LE} = \alpha - 0.811\beta$
$\varepsilon_{HO} = \alpha + 0.360\beta$

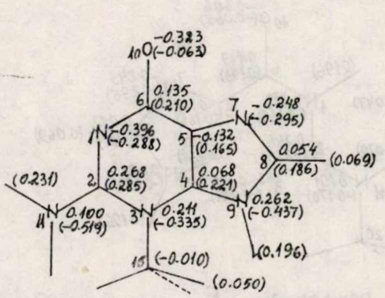
10 O −0.323 (−0.063)
6 0.135 (0.210)
7 N −0.248 (−0.295)
1 N −0.396 (−0.288)
5 −0.132 (0.165)
8 0.054 (0.186)
(0.069)
(0.231)
2 0.268 (0.285)
4 0.068 (0.221)
11 N 0.100 (−0.519)
3 N 0.211 (−0.335)
9 N 0.262 (−0.437)
(0.196)
15 (−0.010)
(0.050)

24. 3-Methyl-guanine $\varepsilon_{LE} = \alpha - 0.939\beta$
$\varepsilon_{HO} = \alpha + 0.495\beta$

Fig. 1d

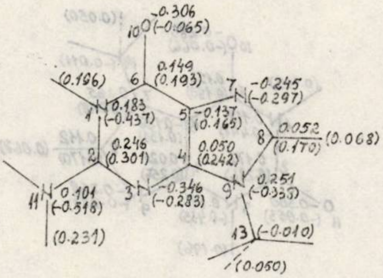
10
O
-0.306
(-0.065)
6
0.149
(0.193)
7
N
-0.245
(-0.297)
(0.196)
1
N
0.183
(-0.437)
5
-0.137
(0.165)
2
0.246
(0.301)
4
0.050
(0.242)
8
0.052
(0.170)
(0.068)
11
N
0.101
(-0.518)
3
N
-0.346
(-0.283)
9
N
0.251
(-0.333)
(0.231)
13
(-0.010)
(0.050)

25. 9-Methyl-guanine $\varepsilon_{LE} = \alpha - 0.811\beta$ $\varepsilon_{HO} = \alpha + 0.360\beta$

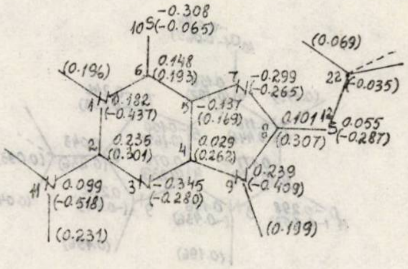
10
S
-0.308
(-0.065)
(0.196)
6
0.148
(0.193)
7
N
-0.299
(-0.265)
(0.069)
22
(-0.035)
1
N
0.182
(-0.437)
5
-0.137
(0.169)
8
0.101
(0.307)
12
S
0.055
(-0.287)
2
0.235
(0.301)
4
0.029
(0.262)
11
N
0.099
(-0.518)
3
N
-0.345
(-0.280)
9
N
0.239
(-0.409)
(0.231)
(0.199)

26. 8-Methyl-thioguanine $\varepsilon_{LE} = \alpha - 0.839\beta$ $\varepsilon_{HO} = \alpha + 0.303\beta$

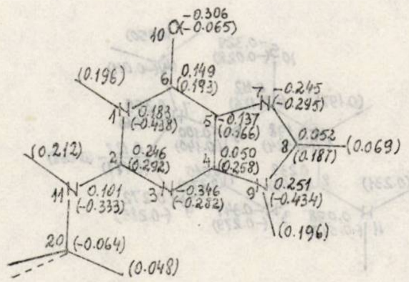
10
O
-0.306
(-0.065)
(0.196)
6
0.149
(0.193)
7
N
-0.245
(-0.295)
1
N
0.183
(-0.438)
5
-0.137
(0.166)
8
0.052
(0.187)
(0.069)
(0.212)
2
0.246
(0.292)
4
0.050
(0.258)
11
N
0.101
(-0.333)
3
N
-0.346
(-0.282)
9
N
0.251
(-0.434)
(0.196)
20
(-0.064)
(0.048)

27. 2-Methyl-amino-6-hydroxy-purine $\varepsilon_{LE} = \alpha - 0.811\beta$ $\varepsilon_{HO} = \alpha + 0.360\beta$

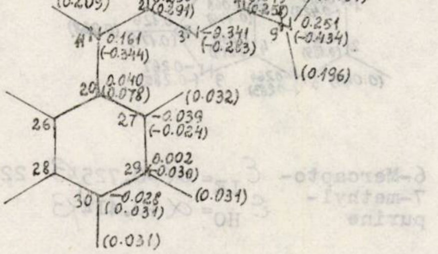
10
O
-0.306
(-0.065)
(0.196)
6
0.149
(0.193)
7
N
-0.245
(-0.295)
1
N
0.183
(-0.438)
5
-0.163
(0.166)
8
0.053
(0.187)
(0.069)
(0.209)
2
0.238
(0.291)
4
0.049
(0.250)
11
N
0.161
(-0.344)
3
N
-0.341
(-0.283)
9
N
0.251
(-0.434)
(0.196)
20
0.040
(0.078)
(0.032)
26
27
0.039
(-0.024)
28
29
0.002
(-0.030)
(0.031)
30
-0.028
(0.031)
(0.031)

28. 2-Anilino-6-hydroxy-purine $\varepsilon_{LE} = \alpha - 0.786\beta$ $\varepsilon_{HO} = \alpha + 0.353\beta$

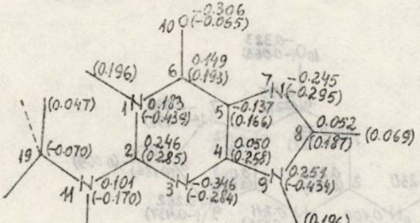
10
O
-0.306
(-0.065)
(0.196)
6
0.149
(0.193)
7
N
-0.245
(-0.295)
(0.047)
1
N
0.183
(-0.439)
5
-0.137
(0.166)
8
0.052
(0.187)
(0.069)
19
(-0.070)
2
0.246
(0.285)
4
0.050
(0.258)
11
N
0.101
(-0.170)
3
N
-0.346
(-0.284)
9
N
0.251
(-0.434)
(0.196)
20

29. 2-Dimethyl-amino-6-hy-droxypurine $\varepsilon_{LE} = \alpha - 0.811\beta$ $\varepsilon_{HO} = \alpha + 0.360\beta$

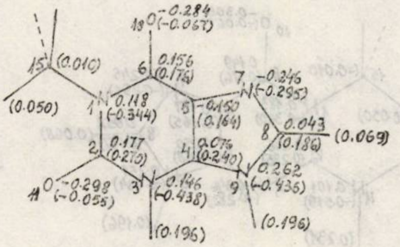
10
O
-0.284
(-0.067)
15
(0.010)
6
0.156
(0.176)
7
N
-0.246
(-0.295)
(0.050)
1
N
0.118
(-0.344)
5
-0.150
(0.164)
8
0.043
(0.186)
(0.069)
2
0.177
(0.270)
4
0.076
(0.240)
11
O
-0.298
(-0.055)
3
N
0.146
(-0.438)
9
N
0.262
(-0.436)
(0.196)
(0.196)

30. 1-Methyl-xanthine $\varepsilon_{LE} = \alpha - 1.004\beta$ $\varepsilon_{HO} = \alpha + 0.489\beta$

Fig. 1e

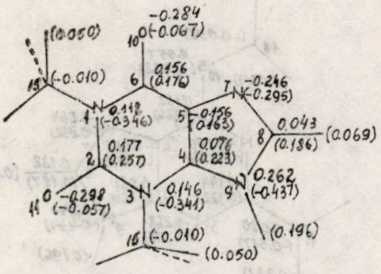
10 O -0.284 (-0.067)
(0.050)
15 (-0.010)
6 0.156 (0.176)
7 N -0.246 (-0.295)
1 N 0.118 (-0.346)
5 -0.156 (0.165)
8 0.043 (0.186) (0.069)
2 0.177 (0.257)
4 0.076 (0.223)
9 N 0.262 (-0.437)
11 O -0.298 (-0.057)
3 N 0.146 (-0.341)
(0.196)
16 (-0.010)
(0.050)

31. 1,3-Dimethyl-xanthine $\varepsilon_{LE}=\alpha-1.004\beta$ $\varepsilon_{HO}=\alpha+0.489\beta$

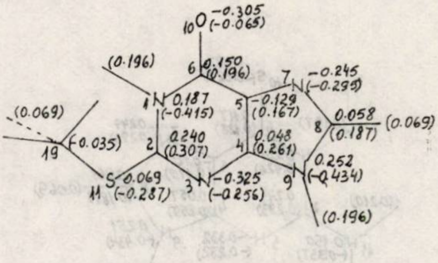
10 O -0.305 (-0.065)
(0.196)
6 0.150 (0.196)
7 N -0.245 (-0.295)
1 N 0.187 (-0.415)
5 -0.129 (0.167)
8 0.058 (0.187) (0.069)
(0.069)
19 (-0.035)
2 0.240 (0.307)
4 0.048 (0.261)
9 N 0.252 (-0.434)
11 S 0.069 (-0.287)
3 N -0.325 (-0.256)
(0.196)

32. 2-Methylthio-6-hydroypurine $\varepsilon_{LE}=\alpha-0.784\beta$ $\varepsilon_{HO}=\alpha+0.376\beta$

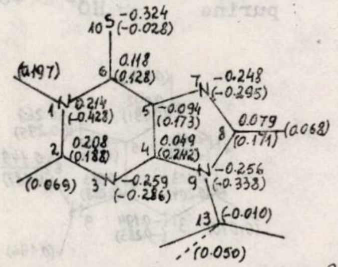
10 S -0.324 (-0.028)
(0.197)
6 0.118 (0.128)
7 N -0.248 (-0.295)
1 N 0.214 (-0.423)
5 -0.094 (0.173)
8 0.079 (0.171) (0.068)
2 0.208 (0.188)
4 0.049 (0.242)
9 N -0.256 (-0.338)
(0.069)
3 N -0.259 (-0.286)
13 (-0.010)
(0.050)

33. 6-Mercapto-9-methyl-purine $\varepsilon_{LE}=\alpha-0.708\beta$ $\varepsilon_{HO}=\alpha+0.377\beta$

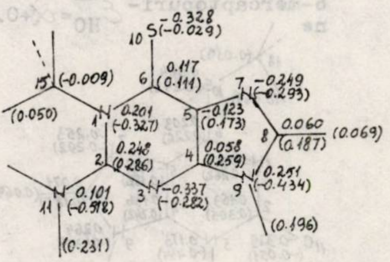
10 S -0.328 (-0.029)
15 (-0.009)
6 0.117 (0.111)
7 N -0.249 (-0.293)
(0.050)
1 N 0.201 (-0.327)
5 -0.123 (0.173)
8 0.060 (0.187) (0.069)
2 0.248 (0.286)
4 0.058 (0.259)
9 N 0.251 (-0.434)
11 N 0.101 (-0.518)
3 N -0.337 (-0.282)
(0.196)
(0.231)

34. 1-Methyl-2-amino-6-thiopurine $\varepsilon_{LE}=\alpha-0.806\beta$ $\varepsilon_{HO}=\alpha+0.330\beta$

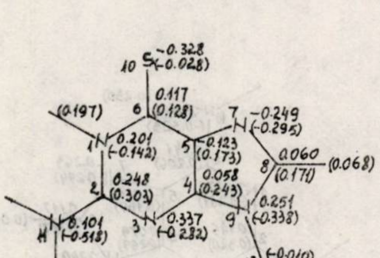
10 S -0.328 (-0.028)
(0.197)
6 0.117 (0.128)
7 H -0.249 (-0.295)
1 N 0.201 (-0.142)
5 -0.123 (0.173)
8 0.060 (0.171) (0.068)
2 0.248 (0.303)
4 0.058 (0.243)
9 N 0.251 (-0.338)
11 N 0.101 (-0.518)
3 N 0.337 (-0.282)
13 (-0.010)
(0.050)
(0.231)

35. 2-Amino-6-mercapto-9-methyl-purine $\varepsilon_{LE}=\alpha-0.806\beta$ $\varepsilon_{HO}=\alpha+0.330\beta$

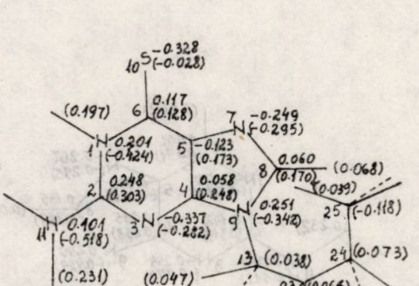
10 S -0.328 (-0.028)
(0.197)
6 0.117 (0.128)
7 N -0.249 (-0.295)
1 H 0.201 (-0.424)
5 -0.123 (0.173)
8 0.060 (0.170) (0.068)
2 0.248 (0.303)
4 0.058 (0.248)
(0.039)
25 (-0.118)
9 N 0.251 (-0.342)
11 N 0.101 (-0.518)
3 N -0.337 (-0.282)
13 (0.038)
24 (-0.073)
(0.047)
(0.231)
23 (0.066)
(0.039)
(0.038)

36. 2-Amino-6-mercapto-9-n-butyl-purine $\varepsilon_{LE}=\alpha-0.806\beta$ $\varepsilon_{HO}=\alpha+0.330\beta$

Fig. 1f

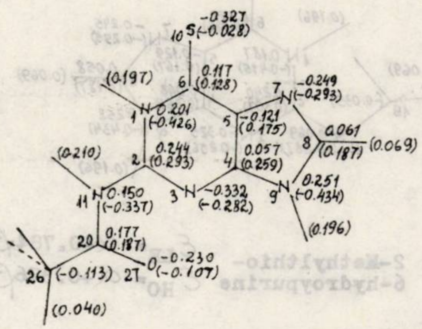
-0.327
10 S(-0.028)
(0.197)
6 0.117 (0.128)
7 N -0.249 (-0.293)
1 N 0.201 (-0.426)
5 -0.121 (0.175)
8 0.061 (0.187) (0.069)
(0.210)
2 0.244 (0.293)
4 0.057 (0.259)
11 N 0.150 (-0.337)
3 N -0.332 (-0.282)
9 N 0.251 (-0.434)
(0.196)
20 0.177 (0.187)
27 O -0.230 (-0.107)
26 (-0.113)
(0.040)

37. 2-Acetylamino-6-mercaptopurine $\varepsilon_{LE} = \alpha - 0.796\beta$
$\varepsilon_{HO} = \alpha + 0.331\beta$

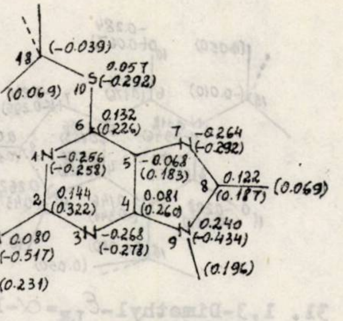
18 (-0.039)
0.057
(0.069) 10 S(-0.292)
6 0.132 (0.226)
7 N -0.264 (-0.292)
1 N -0.256 (-0.258)
5 -0.068 (0.183)
8 0.122 (0.187) (0.069)
2 0.144 (0.322)
4 0.081 (0.260)
11 N 0.080 (-0.517)
3 N -0.268 (-0.278)
9 N 0.240 (-0.434)
(0.231)
(0.196)

38. 2-Amino-6-methylthiopurine $\varepsilon_{LE} = \alpha - 0.799\beta$
$\varepsilon_{HO} = \alpha + 0.598\beta$

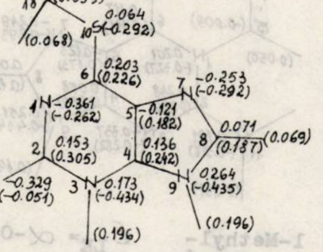
18 (0.039)
0.064
(0.068) 10 S(-0.292)
6 0.203 (0.226)
7 N -0.253 (-0.292)
1 N -0.361 (-0.262)
5 -0.121 (0.182)
8 0.071 (0.187) (0.069)
2 0.153 (0.305)
4 0.136 (0.242)
11 O -0.329 (-0.051)
3 N 0.173 (-0.434)
9 N 0.264 (-0.435)
(0.196)
(0.196)

39. 2-Hydroxy-6-methylthiopurine $\varepsilon_{LE} = \alpha - 0.732\beta$
$\varepsilon_{HO} = \alpha + 0.483\beta$

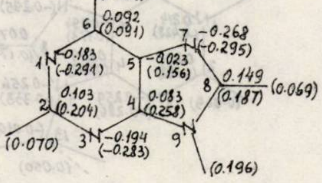
(0.062)
6 0.092 (0.091)
7 N -0.268 (-0.295)
1 N -0.183 (-0.291)
5 -0.023 (0.156)
8 0.149 (0.187) (0.069)
2 0.103 (0.204)
4 0.083 (0.258)
(0.070)
3 N -0.194 (-0.283)
9
(0.196)

40. Purine $\varepsilon_{LE} = \alpha - 0.757\beta$
$\varepsilon_{HO} = \alpha + 0.684\beta$

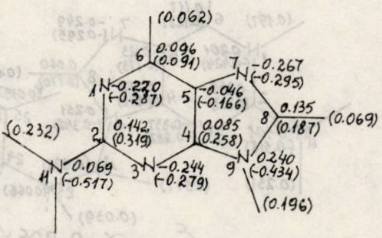
(0.062)
6 0.096 (0.091)
7 N -0.267 (-0.295)
1 N -0.270 (-0.287)
5 -0.046 (-0.166)
8 0.135 (0.187) (0.069)
(0.232)
2 0.142 (0.319)
4 0.085 (0.258)
11 N 0.069 (-0.517)
3 N -0.244 (-0.279)
9 N 0.240 (-0.434)
(0.196)

41. 2-Aminopurine $\varepsilon_{LE} = \alpha - 0.746\beta$
$\varepsilon_{HO} = \alpha + 0.636\beta$

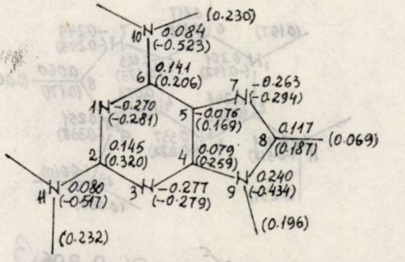
(0.230)
10 N 0.084 (-0.523)
6 0.141 (0.206)
7 N -0.263 (-0.294)
1 N -0.270 (-0.281)
5 -0.076 (0.169)
8 0.117 (0.187) (0.069)
2 0.145 (0.320)
4 0.079 (0.259)
11 N 0.080 (-0.517)
3 N -0.277 (-0.279)
9 N 0.240 (-0.434)
(0.196)
(0.232)

42. 2,6-Diaminopurine $\varepsilon_{LE} = \alpha - 0.819\beta$
$\varepsilon_{HO} = \alpha + 0.579\beta$

Fig. 1g

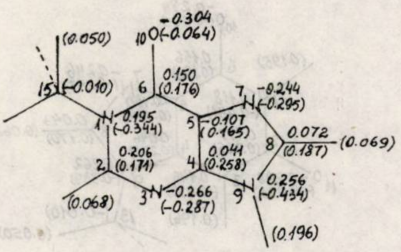
(0.050)
-0.304
10 O (-0.064)
15 (-0.010)
6
0.150 (0.176)
7 -0.244 (-0.295)
1 0.195 (-0.344)
5 -0.107 (0.165)
8 0.072 (0.187)
(0.069)
0.206 (0.171)
2
4 0.041 (0.258)
9 0.256 (-0.434)
(0.068)
3 -0.266 (-0.287)
(0.196)

43. 1-Methyl-hypoxanthine $\varepsilon_{LE}=\alpha-0.712\beta$ $\varepsilon_{HO}=\alpha+0.415\beta$

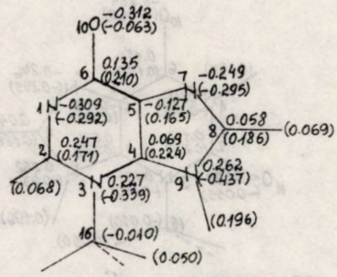
-0.312
10 O (-0.063)
6 0.135 (0.210)
7 -0.249 (-0.295)
1 -0.309 (-0.292)
5 -0.127 (0.165)
8 0.058 (0.186)
(0.069)
2 0.247 (0.171)
4 0.069 (0.224)
9 0.262 (-0.437)
(0.068)
3 0.227 (-0.339)
(0.196)
16 (-0.010)
(0.050)

44. 3-Methyl-hypoxanthine $\varepsilon_{LE}=\alpha-0.837\beta$ $\varepsilon_{HO}=\alpha+0.496\beta$

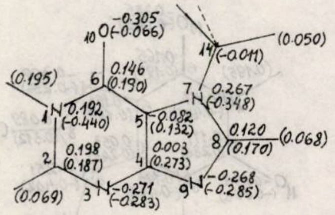
-0.305
10 O (-0.066)
14 (-0.011)
(0.050)
(0.195)
6 0.146 (0.190)
7 0.267 (-0.348)
1 0.192 (-0.440)
5 -0.082 (0.132)
8 0.120 (0.170)
(0.068)
2 0.198 (0.187)
4 0.003 (0.273)
9 -0.268 (-0.285)
(0.069)
3 -0.271 (-0.283)

45. 7-Methyl-hypoxanthine $\varepsilon_{LE}=\alpha-0.758\beta$ $\varepsilon_{HO}=\alpha+0.470\beta$

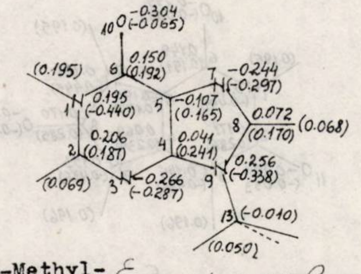
-0.304
10 O (-0.065)
(0.195)
6 0.150 (0.192)
7 -0.244 (-0.297)
1 0.195 (-0.440)
5 -0.107 (0.165)
8 0.072 (0.170)
(0.068)
2 0.206 (0.187)
4 0.041 (0.241)
9 0.256 (-0.338)
(0.069)
3 -0.266 (-0.287)
13 (-0.010)
(0.050)

46. 9-Methyl-hypoxanthine $\varepsilon_{LE}=\alpha-0.712\beta$ $\varepsilon_{HO}=\alpha+0.415\beta$

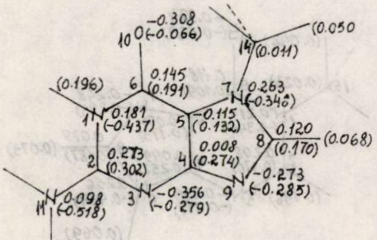
-0.308
10 O (-0.066)
14 (0.011)
(0.050)
(0.196)
6 0.145 (0.191)
7 0.263 (-0.346)
1 0.181 (-0.437)
5 -0.115 (0.132)
8 0.120 (0.170)
(0.068)
2 0.273 (0.302)
4 0.008 (0.274)
9 -0.273 (-0.285)
11 0.098 (-0.518)
3 -0.356 (-0.279)
(0.231)

47. 7-Methyl-guanine $\varepsilon_{LE}=\alpha-0.818\beta$ $\varepsilon_{HO}=\alpha+0.415\beta$

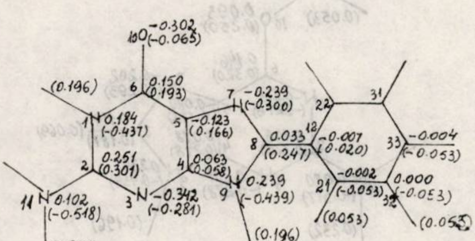
-0.302
10 O (-0.065)
(0.196)
6 0.150 (0.193)
7 -0.239 (-0.300)
1 0.184 (-0.437)
5 -0.123 (0.166)
8 0.033 (0.247)
12 -0.007 (0.020)
22
31
33 -0.004 (-0.053)
2 0.251 (0.301)
4 0.063 (0.058)
9 0.239 (-0.439)
21 -0.002 (-0.053)
32 0.000 (-0.053)
11 0.102 (-0.518)
3 -0.342 (-0.281)
(0.053)
(0.053)
(0.196)
(0.231)

48. 8-Phenyl-guanine $\varepsilon_{LE}=\alpha-0.633\beta$ $\varepsilon_{HO}=\alpha+0.310\beta$

Fig. 1h

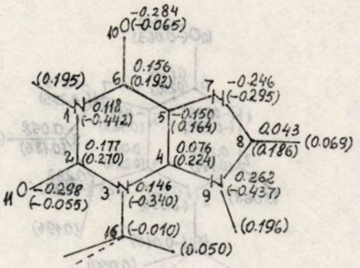
-0.284
10 O (-0.065)
(0.195)
6
0.156 (0.192)
7 N -0.246 (-0.295)
1 N 0.118 (-0.442)
5 -0.150 (0.164)
8 0.043 (0.186) (0.069)
2 0.177 (0.270)
4 0.076 (0.224)
9 N 0.262 (-0.437)
11 O -0.298 (-0.055)
3 N 0.146 (-0.340)
16 (-0.010)
(0.196)
(0.050)

49. 3-Methyl-xanthine $\mathcal{E}_{LE} = \alpha - 1.004\beta$ $\mathcal{E}_{HO} = \alpha + 0.489\beta$

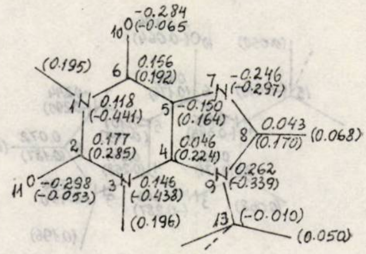
-0.284
10 O (-0.065
(0.195)
6
0.156 (0.192)
7 N -0.246 (-0.297)
1 N 0.118 (-0.441)
5 -0.150 (0.164)
8 0.043 (0.170) (0.068)
2 0.177 (0.285)
4 0.046 (0.224)
9 N 0.262 (-0.339)
11 O -0.298 (-0.053)
3 N 0.146 (-0.438)
(0.196)
13 (-0.010)
(0.050)

50. 9-Methyl-xanthine $\mathcal{E}_{LE} = \alpha - 1.004\beta$ $\mathcal{E}_{HO} = \alpha + 0.489\beta$

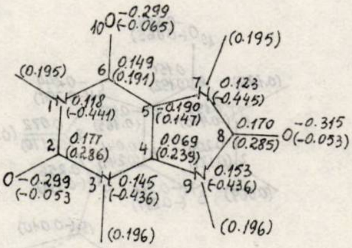
-0.299
10 O (-0.065)
(0.195)
(0.195)
6 0.149 (0.191)
7 N 0.123 (-0.445)
1 N 0.118 (-0.441)
5 -0.190 (0.147)
8 0.170 (0.285) O -0.315 (-0.053)
2 0.177 (0.286)
4 0.069 (0.239)
9 N 0.153 (-0.436)
11 O -0.299 (-0.053
3 N 0.145 (-0.436)
(0.196)
(0.196)

51. Uric acid $\mathcal{E}_{LE} = \alpha - 1.093\beta$ $\mathcal{E}_{HO} = \alpha + 0.359\beta$

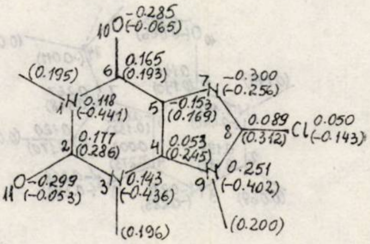
-0.285
10 O (-0.065)
(0.195)
6 0.165 (0.193)
7 N -0.300 (-0.256)
1 N 0.118 (-0.441)
5 -0.153 (0.169)
8 0.089 (0.312) Cl 0.050 (-0.143)
2 0.177 (0.286)
4 0.053 (0.245)
9 N 0.251 (-0.402)
11 O -0.299 (-0.053)
3 N 0.143 (-0.436)
(0.196)
(0.200)

52. 8-Chloro-xanthine $\mathcal{E}_{LE} = \alpha - 1.056\beta$ $\mathcal{E}_{HO} = \alpha + 0.417\beta$

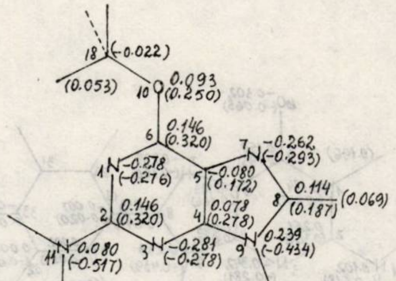
18 (-0.022)
(0.053)
10 O 0.093 (0.250)
6 0.146 (0.320)
7 N -0.262 (-0.293)
1 N -0.278 (-0.276)
5 -0.080 (0.172)
8 0.114 (0.187) (0.069)
2 0.146 (0.320)
4 0.078 (0.278)
9 N 0.239 (-0.434)
11 N 0.080 (-0.517)
3 N -0.281 (-0.278)
(0.232)
(0.196)

53. 2-Amino-6-methoxy-purine $\mathcal{E}_{LE} = \alpha - 0.830\beta$ $\mathcal{E}_{HO} = \alpha + 0.574\beta$

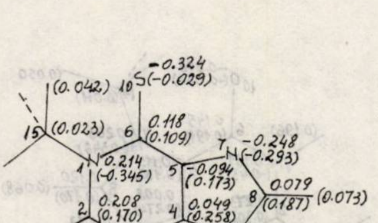
-0.324
10 S (-0.029)
(0.042)
15 (0.023)
6 0.118 (0.109)
7 N -0.248 (-0.293)
1 N 0.214 (-0.345)
5 -0.094 (0.173)
8 0.079 (0.187) (0.073)
2 0.208 (0.170)
4 0.049 (0.258)
9 N 0.256 (-0.434)
(0.196)
3 N -0.259 (-0.287)
(0.069)

54. 1-Methyl-6-thiopu-rine $\mathcal{E}_{LE} = \alpha - 0.708\beta$ $\mathcal{E}_{HO} = \alpha + 0.377\beta$

Fig. 1i

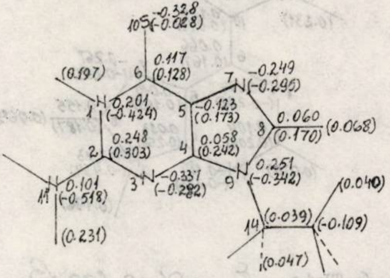
10 S -0.328 (-0.028)
6 0.117 (0.128)
(0.197)
1 N 0.201 (-0.424)
5 -0.123 (0.173)
7 N -0.249 (-0.295)
8 0.060 (0.170)
(0.068)
2 0.248 (0.303)
4 0.058 (0.242)
9 N 0.251 (-0.342)
3 N -0.337 (-0.282)
11 N 0.101 (-0.518)
(0.231)
14 (0.039)
(-0.109)
(0.040)
(0.047)

55. 2-Amino-
6-mercapto-
9-ethylpurine
$\varepsilon_{LE} = \alpha - 0.806\beta$
$\varepsilon_{HO} = \alpha + 0.330\beta$

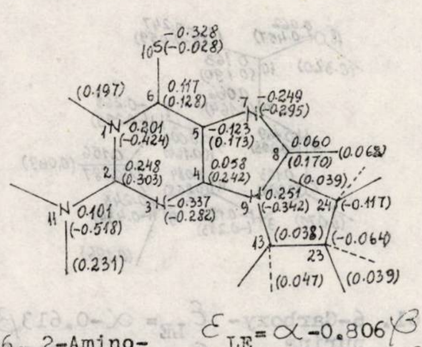
10 S -0.328 (-0.028)
6 0.117 (0.128)
(0.197)
1 N 0.201 (-0.424)
5 -0.123 (0.173)
7 N -0.249 (-0.295)
8 0.060 (0.170)
(0.068)
2 0.248 (0.303)
4 0.058 (0.242)
9 N 0.251 (-0.342)
3 N -0.337 (-0.282)
11 N 0.101 (-0.518)
(0.231)
(0.039)
24 (-0.117)
13 (0.038)
23 (-0.064)
(0.047)
(0.039)

56. 2-Amino-
6-mercapto-
9-n-propyl-
purine
$\varepsilon_{LE} = \alpha - 0.806\beta$
$\varepsilon_{HO} = \alpha + 0.330\beta$

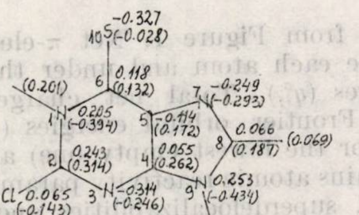
10 S -0.327 (-0.028)
6 0.118 (0.132)
(0.201)
1 N 0.205 (-0.394)
5 -0.114 (0.172)
7 N -0.249 (-0.293)
8 0.066 (0.187)
(0.069)
2 0.243 (0.314)
4 0.055 (0.262)
9 N 0.253 (-0.434)
11 Cl 0.065 (-0.143)
3 N -0.314 (-0.246)
(0.196)

57. 2-Chloro-
6-mercapto-
purine
$\varepsilon_{LE} = \alpha - 0.777\beta$
$\varepsilon_{HO} = \alpha + 0.345\beta$

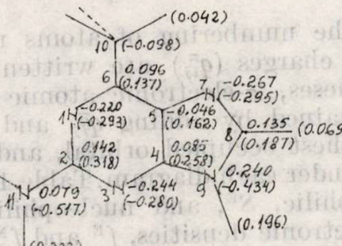
(0.042)
10 (-0.098)
6 0.096 (0.137)
7 N -0.267 (-0.295)
1 N -0.220 (-0.293)
5 -0.046 (0.162)
8 0.135 (0.187)
(0.069)
2 0.142 (0.318)
4 0.085 (0.258)
9 N 0.240 (-0.434)
11 N 0.079 (-0.517)
3 N -0.244 (-0.280)
(0.196)
(0.232)

58. 2-Amino-
6-methyl-
purine
$\varepsilon_{LE} = \alpha - 0.746\beta$
$\varepsilon_{HO} = \alpha + 0.636\beta$

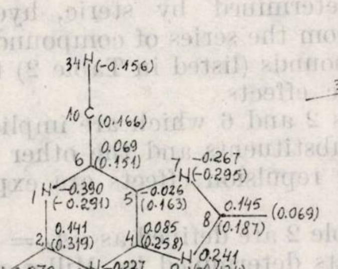
34 N (-0.156)
10 C (0.166)
6 0.069 (0.151)
7 N -0.267 (-0.295)
1 N -0.390 (-0.291)
5 -0.026 (0.163)
8 0.145 (0.187)
(0.069)
2 0.141 (0.319)
4 0.085 (0.258)
9 N 0.241 (-0.434)
11 N 0.079 (-0.517)
3 N -0.227 (-0.279)
(0.196)
(0.239)

59. 2-Amino-6-
cyanopurine
$\varepsilon_{LE} = \alpha - 0.521\beta$
$\varepsilon_{HO} = \alpha + 0.629\beta$

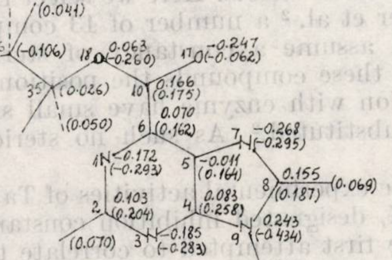
(0.041)
36 (-0.106)
18 O 0.063 (-0.260)
17 O -0.247 (-0.062)
35 (0.026)
(0.050)
10 0.166 (0.175)
6 0.070 (0.162)
7 N -0.268 (-0.295)
1 N -0.172 (-0.293)
5 -0.011 (0.164)
8 0.155 (0.187)
(0.069)
2 0.103 (0.204)
4 0.083 (0.258)
(0.070)
3 N -0.185 (-0.283)
9 N 0.243 (-0.434)
(0.196)

60. 6-Carbetho-
xypurine
$\varepsilon_{LE} = \alpha - 0.632\beta$
$\varepsilon_{HO} = \alpha + 0.717\beta$

Fig. 1j

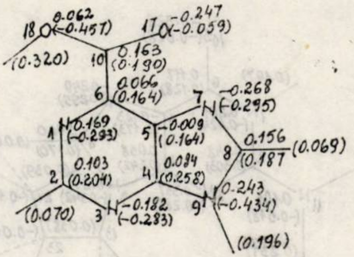
18
0.062
O(-0.457)
(0.320)
17
-0.247
O(-0.059)
10
0.163
(0.190)
6
0.066
(0.164)
7
-0.268
N(-0.295)
1
N
0.169
(-0.293)
5
-0.009
(0.164)
8
0.156
(0.187)
(0.069)
2
0.103
(0.204)
4
0.084
(0.258)
9
0.243
(-0.434)
(0.070)
3
N
-0.182
(-0.283)
(0.196)

61. 6-Carboxy-purine $\varepsilon_{LE} = \alpha - 0.613\beta$ $\varepsilon_{HO} = \alpha + 0.717\beta$

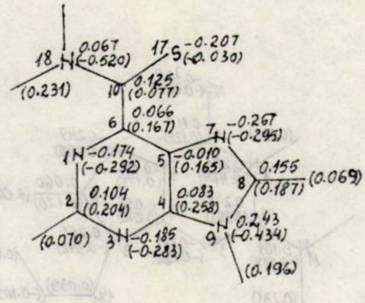
18
N
0.067
(-0.520)
(0.231)
17
S
-0.207
(-0.030)
10
0.125
(0.077)
6
0.066
(0.167)
7
N
-0.267
(-0.295)
1
N
-0.174
(-0.292)
5
-0.010
(0.165)
8
0.155
(0.187)
(0.069)
2
0.104
(0.204)
4
0.083
(0.258)
9
N
0.243
(-0.434)
(0.070)
3
N
-0.185
(-0.283)
(0.196)

62. 6-Thio-carbox-amido-purine $\varepsilon_{LE} = \alpha - 0.632\beta$ $\varepsilon_{HO} = \alpha + 0.717\beta$

Fig. 1k

The numbering of atoms results from Figure 1. Net π-electronic atomic charges (q_{ij}^{π}) are written beside each atom and under them, in parentheses, σ-electronic atomic charges (q_{ij}^{σ}). Total net charges (q_{ij}) are obtained by adding q_{ij}^{π} and q_{ij}^{σ}. Frontier orbital energies (ε_{HO}-for the highest occupied orbital, and ε_{LE}-for the lowest empty one) are also listed under each diagram. Table 1 contains atomic reactivity parameters :[4] electrophilic, S^{E}, and nucleophilic, S^{N}, superdelocalizabilities, and frontier electronic densities, f^{E} and f^{N}, for electrophilic and nucleophilic reaction, respectively.

STRUCTURE ACTIVITY RELATIONS WITH ELECTRONIC INDICES

Biologic activity is generally determined by steric, hydrophobic and electronic effects. Here we select from the series of compounds studied by Miller et al. [2] a number of 13 compounds (listed in Table 2) for which one can assume a constancy of steric effects.

In these compounds the positions 2 and 6 which are implied in the interaction with enzyme have small substituents and the other positions are unsubstituted.[2] As such no steric repulsion effects are expected to appear.

The experimental activities of Table 2 are defined as : $A_i = -\log K_i$, where K_i designated inhibition constants determined by Miller et al.[2]

We first attempted to correlate the activities A_i with net electronic charges q_{ij}. The best monoparametric correlation is obtained for the charge of the atomic position 2, q_{i2} :

$$\hat{A}_i = -5.437 + \underset{(4.297)}{10.844} q_{i2} \; ; \quad r = 0.792 \; ; \quad F = 18.462 \qquad (1)$$

In Eq. (1), $\hat{A}_i$ is the calculated activity, r and F are the linear correlation coefficient and the Fischer – test values, respectively, while the figur

Table 1

Reactivity atomic MO Indices for the 62 Purinic Derivatives Tested as Inhibitors of GPRT from *E. Coli*

Molecule	Atomic Index	Atom										
		1	2	3	4	5	6	7	8	9	10	11
0	1	2	3	4	5	6	7	8	9	10	11	12
1	S^E	1.172	0.330	1.884	0.559	1.120	1.065	1.224	1.056	1.111		1.112
	S^N	0.300	0.589	0.667	1.169	0.562	1.822	0.645	1.237	0.207		0.369
	f^E	0.116	0.005	0.512	0.005	0.257	0.336	0.195	0.259	0.087		0.230
	f^N	0.147	0.005	0.251	0.302	0.047	0.912	0.082	0.240	0.000		0.014
2	S^E	1.199	0.458	1.882	0.574	1.126	1.078	1.223	1.057	1.116		1.954
	S^N	0.330	0.721	0.671	1.185	0.570	1.839	0.646	1.240	0.214		0.446
	f^E	0.120	0.000	0.468	0.000	0.220	0.284	0.149	0.206	0.078		0.474
	f^N	0.156	0.010	0.234	0.314	0.042	0.913	0.080	0.224	0.001		0.026
3	S^E	0.974	0.755	1.019	0.760	0.889	0.721	1.108	0.910	1.010	1.132	
	S^N	0.660	1.032	0.704	0.879	0.623	1.056	0.616	1.189	0.242	0.087	
	f^E	0.012	0.236	0.179	0.148	0.250	0.263	0.334	0.408	0.045	0.125	
	f^N	0.003	0.351	0.265	0.000	0.089	0.426	0.162	0.600	0.065	0.041	
4	S^E	1.176	0.954	1.229	1.052	1.384	0.331	1.049	1.294	0.966	0.978	
	S^N	0.212	1.442	0.612	0.857	0.657	0.612	0.611	1.078	0.282	0.416	
	f^E	0.101	0.285	0.226	0.277	0.402	0.004	0.106	0.408	0.006	0.186	
	f^N	0.118	0.836	0.142	0.245	0.192	0.006	0.011	0.308	0.132	0.012	
5	S^E	1.155	0.824	1.583	1.057	1.605	0.335	1.075	1.467	0.985	1.021	1.131
	S^N	0.173	1.273	0.476	0.855	0.585	0.610	0.612	1.023	0.262	0.412	0.108
	f^E	0.062	0.207	0.319	0.229	0.426	0.005	0.098	0.410	0.011	0.171	0.064
	f^N	0.096	0.736	0.057	0.325	0.151	0.006	0.032	0.366	0.152	0.010	0.069
6	S^E	1.165	0.317	1.317	1.157	1.372	0.321	1.049	1.303	0.942	0.822	0.740
	S^N	0.065	0.623	0.105	0.944	0.520	0.625	0.613	0.975	0.260	0.441	0.376
	f^E	0.000	0.000	0.229	0.468	0.480	0.001	0.145	0.528	0.001	0.111	0.036
	f^N	0.004	0.008	0.048	0.641	0.049	0.016	0.205	0.736	0.260	0.022	0.011
7	S^E	1.182	0.476	1.333	1.156	1.376	0.321	1.049	1.306	0.943	0.823	1.214
	S^N	0.085	0.787	0.122	0.942	0.524	0.625	0.612	0.978	0.261	0.441	0.473
	f^E	0.002	0.001	0.244	0.439	0.467	0.001	0.137	0.508	0.001	0.099	0.101
	f^N	0.008	0.031	0.036	0.628	0.054	0.014	0.196	0.725	0.256	0.019	0.033
8	S^E	1.202	0.960	1.236	1.080	1.372	0.471	1.053	1.302	0.967	1.670	
	S^N	0.241	1.450	0.621	0.889	0.648	0.756	0.962	1.089	0.283	0.527	
	f^E	0.111	0.247	0.206	0.258	0.361	0.000	0.073	0.353	0.003	0.388	
	f^N	0.130	0.831	0.127	0.267	0.188	0.016	0.007	0.276	0.130	0.028	
9	S^E	1.179	0.828	1.592	1.084	1.594	0.424	1.079	1.477	0.986	1.757	1.131
	S^N	0.199	1.278	0.488	0.886	0.577	0.754	0.616	1.036	0.263	0.519	0.109
	f^E	0.070	0.183	0.290	0.217	0.387	0.000	0.072	0.365	0.004	0.353	0.054
	f^N	0.109	0.734	0.046	0.356	0.150	0.019	0.021	0.317	0.149	0.028	0.069
10	S^E	1.183	0.317	1.324	1.195	1.361	0.471	1.054	1.309	0.944	1.352	0.741
	S^N	0.086	0.623	0.112	0.985	0.510	0.780	0.618	0.983	0.262	0.577	0.376
	f^E	0.002	0.000	0.212	0.457	0.450	0.002	0.106	0.477	0.000	0.267	0.026
	f^N	0.020	0.005	0.069	0.834	0.094	0.152	0.050	0.377	0.224	0.168	0.007
11	S^E	1.201	0.476	1.340	1.194	1.365	0.471	1.054	1.312	0.945	1.353	1.215
	S^N	0.104	0.787	0.130	0.984	0.514	0.780	0.617	0.986	0.263	0.577	0.474
	f^E	0.000	0.000	0.226	0.437	0.445	0.001	0.104	0.468	0.000	0.245	0.074
	f^N	0.024	0.018	0.057	0.817	0.095	0.134	0.056	0.401	0.228	0.150	0.020

Table 1 (continued)

0	1	1	3	4	5	6	7	8	9	10	11	12
12	S^E	1.202	0.960	1.236	1.080	1.372	0.471	1.053	1.302	0.967	1.670	
	S^N	0.241	1.450	0.621	0.889	0.648	0.756	0.615	1.089	0.283	0.527	
	f^E	0.111	0.247	0.206	0.258	0.361	0.000	0.073	0.353	0.003	0.388	
	f^N	0.130	0.831	0.127	0.267	0.188	0.016	0.007	0.276	0.130	0.028	
13	S^E	1.015	0.696	1.115	0.760	0.942	0.745	1.119	0.951	1.016	0.971	1.130
	S^N	0.636	0.960	0.647	0.888	0.591	1.086	0.618	1.167	0.234	0.057	0.071
	f^E	0.010	0.236	0.204	0.156	0.283	0.216	0.293	0.410	0.039	0.047	0.105
	f^N	0.061	0.210	0.250	0.020	0.051	0.570	0.188	0.555	0.041	0.033	0.020
14	S^E	1.155	0.824	1.582	1.057	1.605	0.335	1.075	1.467	0.985	1.021	1.131
	S^N	0.173	1.273	0.476	0.855	0.585	0.610	0.612	1.023	0.262	0.412	0.108
	f^E	0.062	0.207	0.319	0.228	0.426	0.005	0.098	0.410	0.011	0.171	0.064
	f^N	0.096	0.736	0.057	0.325	0.151	0.006	0.032	0.366	0.152	0.010	0.069
15	S^E	1.186	1.014	1.686	1.371	1.844	0.345	1.479	1.459	0.989	1.117	1.171
	S^N	0.169	1.234	0.478	0.804	0.592	0.609	0.505	0.972	0.224	0.410	0.103
	f^E	0.052	0.211	0.255	0.270	0.390	0.007	0.183	0.328	0.001	0.154	0.058
	f^N	0.108	0.794	0.077	0.296	0.216	0.014	0.001	0.256	0.118	0.023	0.072
16	S^E	1.159	0.958	1.624	1.267	2.617	0.359	1.633	0.331	1.308	1.315	1.159
	S^N	0.176	1.243	0.477	0.827	0.655	0.597	0.092	0.612	0.101	0.399	0.104
	f^E	0.041	0.190	0.218	0.242	0.662	0.010	0.209	0.003	0.069	0.225	0.052
	f^N	0.130	0.842	0.078	0.319	0.381	0.037	0.039	0.000	0.034	0.061	0.076
17	S^E	1.159	0.959	1.623	1.265	2.616	0.360	1.653	0.481	1.327	1.316	1.159
	S^N	0.176	1.245	0.477	0.827	0.658	0.598	0.116	0.766	0.122	0.401	0.104
	f^E	0.037	0.178	0.197	0.231	0.626	0.010	0.212	0.001	0.075	0.212	0.048
	f^N	0.130	0.843	0.078	0.320	0.380	0.036	0.039	0.000	0.035	0.061	0.076
18	S^E	1.160	0.851	1.598	1.102	1.640	0.336	1.131	1.465	0.985	1.035	1.137
	S^N	0.172	1.266	0.476	0.846	0.586	0.610	0.593	1.016	0.256	0.411	0.108
	f^E	0.060	0.207	0.305	0.236	0.419	0.005	0.112	0.395	0.008	0.167	0.062
	f^N	0.098	0.747	0.060	0.321	0.162	0.007	0.024	0.348	0.146	0.012	0.070
19	S^E	1.164	0.317	1.317	1.157	1.372	0.321	1.049	1.303	0.942	0.822	0.740
	S^N	0.065	0.623	0.105	0.943	0.519	0.625	0.613	0.975	0.260	0.441	0.376
	f^E	0.000	0.000	0.229	0.469	0.480	0.001	0.145	0.528	0.001	0.111	0.036
	f^N	0.004	0.008	0.048	0.641	0.049	0.016	0.205	0.736	0.260	0.022	0.011
20	S^E	1.166	0.316	1.299	0.978	1.543	0.322	0.978	1.016	1.002	0.852	0.737
	S^N	0.067	0.622	0.086	0.765	0.690	0.626	0.296	1.151	0.565	0.471	0.372
	f^E	0.000	0.000	0.198	0.358	0.766	0.001	0.036	0.393	0.037	0.179	0.032
	f^N	0.011	0.000	0.019	0.192	0.381	0.094	0.240	0.779	0.127	0.157	0.000
21	S^E	1.193	0.882	1.253	0.932	1.533	0.467	0.991	1.006	1.030	1.712	
	S^N	0.232	1.372	0.638	0.741	0.809	0.752	0.307	1.179	0.593	0.569	
	f^E	0.113	0.217	0.213	0.211	0.502	0.001	0.028	0.212	0.003	0.500	
	f^N	0.127	0.519	0.057	0.205	0.395	0.098	0.157	0.273	0.004	0.166	
22	S^E	1.174	0.768	1.601	0.939	1.748	0.469	1.019	1.030	1.044	1.795	1.122
	S^N	0.194	1.219	0.498	0.741	0.732	0.749	0.295	1.182	0.581	0.558	0.100
	f^E	0.076	0.171	0.312	0.185	0.524	0.000	0.037	0.184	0.000	0.229	0.054
	f^N	0.087	0.260	0.010	0.224	0.348	0.133	0.189	0.489	0.037	0.206	0.025
23	S^E	1.155	0.824	1.583	1.057	1.605	0.335	1.075	1.467	0.985	1.021	1.131
	S^N	0.173	1.273	0.476	0.855	0.585	0.619	0.612	1.023	0.262	0.412	0.108
	f^E	0.062	0.207	0.319	0.228	0.426	0.005	0.098	0.410	0.011	0.171	0.064
	f^N	0.096	0.736	0.057	0.325	0.151	0.006	0.032	0.366	0.152	0.010	0.069

Table 1 (continued)

0	1	2	3	4	5	6	7	8	9	10	11	12
24	S^E	1.475	0.500	1.203	1.125	1.293	0.322	1.047	1.239	0.944	1.047	1.066
	S^N	0.478	1.225	0.193	0.920	0.544	0.596	0.609	1.002	0.260	0.431	0.099
	f^E	0.119	0.090	0.204	0.409	0.424	0.002	0.134	0.471	0.001	0.236	0.000
	f^N	0.213	0.638	0.016	0.157	0.037	0.032	0.157	0.522	0.124	0.048	0.054
25	S^E	1.155	0.824	1.582	1.057	1.605	0.335	1.075	1.467	0.985	1.021	1.131
	S^N	0.173	1.273	0.476	0.855	0.585	0.610	0.612	1.023	0.262	0.412	0.105
	f^E	0.062	0.207	0.319	0.228	0.426	0.005	0.098	0.410	0.011	0.171	0.064
	f^N	0.096	0.736	0.057	0.325	0.151	0.006	0.032	0.366	0.152	0.010	0.069
26	S^E	1.175	0.949	1.652	1.265	1.765	0.342	1.338	1.459	0.986	1.085	1.158
	S^N	0.170	1.245	0.478	0.817	0.590	0.609	0.532	0.990	0.234	0.410	0.106
	f^E	0.055	0.210	0.273	0.259	0.402	0.006	0.157	0.355	0.003	0.159	0.060
	f^N	0.105	0.782	0.072	0.305	0.199	0.011	0.005	0.286	0.127	0.019	0.072
27	S^E	1.155	0.824	1.582	1.057	1.605	0.335	1.075	1.467	0.985	1.021	1.131
	S^N	0.173	1.273	0.476	0.855	0.585	0.610	0.612	1.023	0.262	0.412	0.108
	f^E	0.062	0.207	0.319	0.228	0.426	0.005	0.098	0.410	0.011	0.171	0.064
	f^N	0.096	0.736	0.057	0.325	0.151	0.006	0.032	0.366	0.152	0.010	0.069
28	S^E	1.157	0.827	1.594	1.056	1.610	0.335	1.075	1.471	0.986	1.021	1.165
	S^N	0.175	1.276	0.488	0.854	0.591	0.611	0.612	1.027	0.263	0.412	0.143
	f^E	0.056	0.191	0.320	0.216	0.416	0.005	0.094	0.397	0.011	0.163	0.078
	f^N	0.094	0.706	0.069	0.279	0.148	0.005	0.023	0.319	0.134	0.010	0.037
29	S^E	1.155	0.824	1.582	1.057	1.605	0.355	1.075	1.467	0.985	1.021	1.131
	S^N	0.173	1.273	0.476	0.855	0.585	0.610	0.612	1.023	0.262	0.412	0.108
	f^E	0.062	0.207	0.319	0.228	0.426	0.005	0.098	0.410	0.011	0.171	0.064
	f^N	0.096	0.736	0.057	0.325	0.151	0.006	0.032	0.366	0.152	0.010	0.069
30	S^E	1.165	0.317	1.317	0.157	1.372	0.321	1.049	1.303	0.942	0.822	0.740
	S^N	0.065	0.623	0.105	0.944	0.520	0.625	0.613	0.975	0.260	0.441	0.376
	f^E	0.000	0.000	0.229	0.468	0.478	0.001	0.145	0.528	0.001	0.111	0.036
	f^N	0.004	0.008	0.048	0.641	0.049	0.016	0.205	0.736	0.260	0.022	0.011
31	S^E	1.164	0.317	1.317	1.157	1.372	0.321	1.049	1.303	0.942	0.822	0.740
	S^N	0.065	0.623	0.105	0.943	0.519	0.625	0.613	0.975	0.260	0.441	0.376
	f^E	0.000	0.000	0.229	0.468	0.480	0.001	0.145	0.528	0.001	0.111	0.036
	f^N	0.004	0.008	0.048	0.641	0.049	0.016	0.205	0.736	0.260	0.022	0.011
32	S^E	1.160	0.861	1.471	1.056	1.537	0.334	1.067	1.414	0.979	1.008	1.020
	S^N	0.183	1.322	0.508	0.856	0.603	0.611	0.612	1.037	0.267	0.413	0.077
	f^E	0.072	0.230	0.292	0.243	0.420	0.005	0.101	0.410	0.009	0.175	0.043
	f^N	0.103	0.773	0.077	0.302	0.163	0.006	0.024	0.346	0.146	0.011	0.049
33	S^E	1.202	0.960	1.236	1.080	1.372	0.471	1.053	1.302	0.967	1.670	
	S^N	0.241	1.450	0.621	1.889	0.648	0.756	0.615	1.089	0.283	0.527	
	f^E	0.111	0.247	0.206	0.258	0.361	0.000	0.073	0.353	0.003	0.388	
	f^N	0.130	0.831	0.127	0.267	0.188	0.016	0.016	0.276	0.130	0.028	
34	S^E	1.179	0.828	1.592	1.084	1.594	0.474	1.079	1.477	0.986	1.757	1.131
	S^N	0.199	1.278	0.488	0.886	0.577	0.754	0.616	1.036	0.263	0.619	0.109
	f^E	0.070	0.183	0.290	0.217	0.387	0.000	0.072	0.365	0.004	0.353	0.054
	f^N	0.109	0.734	0.046	0.356	0.150	0.019	0.021	0.317	0.149	0.028	0.069
35	S^E	1.179	0.828	1.592	1.084	1.594	0.474	1.078	1.477	0.986	1.757	1.131
	S^N	0.199	1.279	0.488	0.886	0.577	0.754	0.616	1.036	0.263	0.519	0.109
	f^E	0.070	0.183	0.290	0.217	0.388	0.000	0.072	0.365	0.008	0.353	0.054
	f^N	0.109	0.734	0.046	0.356	0.150	0.019	0.021	0.317	0.149	0.028	0.069

Table 1 (continued)

0	1	2	3	4	5	6	7	8	9	10	11	12
36	S^E	1.179	0.828	1.592	1.084	1.594	0.474	1.078	1.477	0.986	1.757	1.131
	S^N	0.199	1.278	0.488	0.886	0.577	0.754	0.616	1.036	0.263	0.519	0.109
	f^E	0.070	0.183	0.290	0.217	0.388	0.000	0.072	0.365	0.008	0.353	0.054
	f^N	0.109	0.734	0.046	0.356	0.150	0.019	0.021	0.317	0.149	0.028	0.069
37	S^E	1.181	0.834	1.574	1.083	1.582	0.474	1.077	1.468	0.985	1.752	1.091
	S^N	0.202	1.287	0.497	0.886	0.582	0.754	0.616	1.039	0.264	0.520	0.124
	f^E	0.071	0.185	0.287	0.218	0.386	0.000	0.072	0.363	0.007	0.353	0.051
	f^N	0.111	0.740	0.053	0.342	0.153	0.019	0.019	0.308	0.145	0.028	0.055
38	S^E	1.018	0.696	1.119	0.761	0.946	0.742	1.119	0.954	1.016	1.019	1.130
	S^N	0.633	0.960	0.645	0.887	0.590	1.083	0.618	1.165	0.234	0.060	0.071
	f^E	0.008	0.234	0.207	0.155	0.284	0.216	0.291	0.409	0.039	0.054	0.104
	f^N	0.060	0.212	0.249	0.019	0.051	0.567	0.189	0.558	0.041	0.035	0.020
39	S^E	1.563	0.322	1.223	1.010	1.188	0.529	1.072	1.175	0.945	0.985	0.990
	S^N	0.630	0.559	0.171	0.155	0.494	1.272	0.638	1.031	0.268	0.076	0.397
	f^E	0.372	0.002	0.164	0.378	0.371	0.000	0.102	0.404	0.000	0.000	0.207
	f^N	0.372	0.032	0.089	0.479	0.016	0.759	0.075	0.033	0.031	0.050	0.063
40	S^E	0.868	0.753	0.914	0.742	0.789	0.787	1.101	0.840	1.005		
	S^N	0.746	1.031	0.792	0.903	0.667	1.143	0.613	1.245	0.243		
	f^E	0.009	0.303	0.090	0.208	0.220	0.271	0.409	0.452	0.038		
	f^N	0.051	0.244	0.338	0.025	0.098	0.557	0.132	0.518	0.038		
41	S^E	0.955	0.695	1.040	0.749	0.872	0.789	1.114	0.903	1.013		1.131
	S^N	0.702	0.960	0.705	0.905	0.620	1.144	0.606	1.204	0.235		0.072
	f^E	0.047	0.264	0.153	0.177	0.262	0.213	0.311	0.414	0.034		0.125
	f^N	0.119	0.161	0.296	0.049	0.062	0.635	0.152	0.484	0.026		0.016
42	S^E	1.051	0.696	1.157	0.767	0.980	0.722	1.120	1.978	1.018	1.131	1.130
	S^N	0.610	0.960	0.624	0.880	0.580	1.056	0.619	1.151	0.234	0.086	0.071
	f^E	0.001	0.217	0.230	0.144	0.292	0.211	0.277	0.403	0.040	0.091	0.093
	f^N	0.039	0.235	0.226	0.009	0.048	0.526	0.204	0.592	0.050	0.049	0.022
43	S^E	1.176	0.954	1.224	1.052	1.384	0.331	1.049	1.294	0.966	0.978	
	S^N	0.212	1.442	0.612	0.857	0.657	0.612	0.611	1.078	0.282	0.416	
	f^E	0.101	0.285	0.226	0.277	0.402	0.004	0.106	0.408	0.006	0.186	
	f^N	0.118	0.835	0.142	0.245	0.192	0.006	0.011	0.308	0.132	0.012	
44	S^E	1.254	0.560	1.193	1.115	1.280	0.322	1.046	1.228	0.945	1.020	
	S^N	0.636	1.401	0.229	0.920	0.554	0.604	0.608	1.013	0.261	0.457	
	f^E	0.124	0.000	0.203	0.407	0.422	0.002	0.134	0.468	0.001	0.238	
	f^N	0.378	1.007	0.080	0.021	0.034	0.059	0.055	0.225	0.041	0.101	
45	S^E	1.165	0.874	1.245	0.899	1.556	0.331	0.992	0.978	1.031	1.004	
	S^N	0.201	1.361	0.628	0.704	0.829	0.612	0.308	1.149	0.593	0.442	
	f^E	0.104	0.264	0.250	0.229	0.612	0.003	0.045	0.233	0.003	0.256	
	f^N	0.117	0.150	0.111	0.173	0.470	0.043	0.151	0.210	0.001	0.081	
46	S^E	1.176	0.954	1.229	1.052	1.384	0.331	1.049	1.294	0.966	0.978	
	S^N	0.212	1.442	0.612	0.857	0.657	0.612	0.611	1.078	0.282	0.416	
	f^E	0.101	0.285	0.226	0.277	0.402	0.004	0.106	0.408	0.006	0.186	
	f^N	0.118	0.835	0.142	0.245	0.192	0.006	0.011	0.308	0.132	0.012	
47	S^E	1.149	0.763	1.590	0.908	1.770	0.334	1.019	1.002	1.045	1.045	1.122
	S^N	0.166	1.211	0.484	0.706	0.751	0.610	0.296	1.151	0.582	0.435	0.099
	f^E	0.067	0.204	0.363	0.196	0.616	0.005	0.054	0.196	0.000	0.232	0.068
	f^N	0.076	0.336	0.013	0.196	0.457	0.063	0.204	0.474	0.041	0.109	0.031

Table 1 (continued)

0	1	2	3	4	5	6	7	8	9	10	11	12
48	S^E	1.159	0.860	1.585	1.124	1.621	0.338	1.217	1.362	1.002	1.031	1.137
	S^N	0.176	1.309	0.478	0.922	0.601	0.613	0.754	0.917	0.279	0.422	0.114
	f^E	0.048	0.182	0.242	0.222	0.352	0.005	0.130	0.314	0.003	0.139	0.052
	f^N	0.031	0.275	0.003	0.221	0.004	0.001	0.216	0.293	0.131	0.003	0.030
49	S^E	1.164	0.317	1.317	1.157	1.372	0.321	1.049	1.303	0.942	0.822	0.740
	S^N	0.065	0.623	0.105	0.943	0.519	0.625	0.613	0.975	0.260	0.441	0.376
	f^E	0.000	0.000	0.229	0.468	0.480	0.001	0.145	0.528	0.001	0.111	0.036
	f^N	0.004	0.008	0.048	0.641	0.049	0.016	0.205	0.736	0.260	0.022	0.011
50	S^E	1.164	0.317	1.317	1.157	1.372	0.321	1.049	1.303	0.942	0.822	0.740
	S^N	0.065	0.623	0.105	0.943	0.519	0.625	0.613	0.975	0.260	0.441	0.376
	f^E	0.000	0.000	0.229	0.468	0.480	0.001	0.145	0.528	0.001	0.111	0.036
	f^N	0.004	0.008	0.048	0.641	0.049	0.016	0.205	0.736	0.260	0.022	0.011
51	S^E	1.167	0.318	1.368	1.387	2.220	0.334	1.554	0.330	1.321	1.002	0.754
	S^N	0.066	0.622	0.102	0.918	0.550	0.614	0.079	0.611	0.109	0.434	0.374
	f^E	0.001	0.001	0.156	0.412	0.718	0.005	0.258	0.003	0.141	0.161	0.027
	f^N	0.024	0.006	0.070	0.937	0.394	0.196	0.041	0.003	0.074	0.244	0.007
52	S^E	1.165	0.318	1.365	1.359	1.482	0.324	1.268	1.288	0.953	0.847	0.748
	S^N	0.065	0.622	0.101	0.905	0.519	0.624	0.533	0.947	0.253	0.440	0.375
	f^E	0.000	0.001	0.204	0.481	0.439	0.002	0.213	0.449	0.000	0.100	0.033
	f^N	0.008	0.008	0.054	0.748	0.111	0.045	0.090	0.593	0.242	0.059	0.011
53	S^E	1.063	0.696	1.171	0.769	0.993	0.712	1.121	0.988	1.018	1.025	1.130
	S^N	0.597	0.960	0.613	0.877	0.575	1.044	0.619	1.144	0.234	0.093	0.071
	f^E	0.000	0.215	0.238	0.143	0.296	0.211	0.276	0.404	0.040	0.084	0.091
	f^N	0.028	0.252	0.212	0.004	0.047	0.499	0.213	0.615	0.056	0.050	0.023
54	S^E	1.202	0.960	1.236	1.080	1.372	0.471	1.053	1.302	0.967	1.670	
	S^N	0.241	1.450	0.621	0.889	0.648	0.756	0.615	1.089	0.283	0.527	
	f^E	0.111	0.247	0.206	0.258	0.361	0.000	0.073	0.353	0.003	0.388	
	f^N	0.130	0.831	0.127	0.267	0.188	0.016	0.007	0.276	0.130	0.028	
55	S^E	1.179	0.828	1.592	1.084	1.594	0.474	1.078	1.477	0.986	1.757	1.131
	S^N	0.199	1.278	0.488	0.886	0.577	0.754	0.616	1.036	0.263	0.519	0.109
	f^E	0.070	0.183	0.290	0.217	0.388	0.000	0.072	0.365	0.008	0.353	0.054
	f^N	0.109	0.734	0.046	0.356	0.150	0.019	0.021	0.317	0.149	0.028	0.069
56	S^E	1.179	0.828	1.592	1.084	1.594	0.474	1.078	1.477	0.986	1.757	1.131
	S^N	0.199	1.278	0.488	0.886	0.577	0.754	0.616	1.036	0.263	0.519	0.109
	f^E	0.070	0.183	0.290	0.217	0.388	0.000	0.072	0.365	0.008	0.353	0.054
	f^N	0.109	0.734	0.046	0.356	0.150	0.019	0.021	0.317	0.149	0.028	0.069
57	S^E	1.185	0.870	1.467	1.083	1.518	0.473	1.070	1.417	0.979	1.728	0.974
	S^N	0.211	1.333	0.523	0.888	0.596	0.755	0.615	1.051	0.268	0.521	0.073
	f^E	0.083	0.205	0.263	0.231	0.380	0.000	0.073	0.362	0.006	0.365	0.033
	f^N	0.116	0.773	0.068	0.328	0.162	0.018	0.016	0.302	0.143	0.030	0.046
58	S^E	0.955	0.695	1.040	0.748	0.872	0.789	1.114	0.903	1.013		1.130
	S^N	0.702	0.960	0.705	0.905	0.620	1.144	0.616	1.204	0.235		0.072
	f^E	0.047	0.264	0.153	0.177	0.262	0.213	0.311	0.414	0.034		0.125
	f^N	0.119	0.161	0.296	0.049	0.062	0.635	0.152	0.484	0.026		0.016
59	S^E	0.975	0.688	1.024	0.745	0.862	0.741	1.102	0.887	1.010	0.462	1.130
	S^N	0.875	0.953	0.847	0.936	0.727	1.113	0.607	1.291	0.237	0.996	0.071
	f^E	0.035	0.245	0.155	0.163	0.252	0.204	0.292	0.392	0.033	0.001	0.114
	f^N	0.224	0.040	0.273	0.079	0.098	0.404	0.037	0.240	0.006	0.207	0.005

Table 1 (continued)

0	1	2	3	4	5	6	7	8	9	10	11	12
60	S^E	0.869	0.749	0.903	0.740	0.780	0.764	1.095	0.829	1.004	0.319	
	S^N	0.825	1.027	0.859	0.918	0.716	1.129	0.609	1.285	0.244	0.653	
	f^E	0.009	0.295	0.088	0.202	0.215	0.264	0.397	0.440	0.038	0.000	
	f^N	0.129	0.132	0.346	0.059	0.107	0.539	0.080	0.384	0.018	0.061	
61	S^E	0.861	0.748	0.893	0.738	0.772	0.766	1.094	0.822	1.003	0.283	
	S^N	0.846	1.027	0.878	0.923	0.729	1.133	0.608	1.297	0.244	0.743	
	f^E	0.144	0.116	0.346	0.065	0.110	0.525	0.072	0.363	0.016	0.089	
	f^N	0.416	0.391	0.003	0.496	0.081	0.056	0.040	0.305	0.157	0.024	
62	S^E	0.892	0.746	0.918	0.743	0.796	0.739	1.092	0.837	1.004	0.482	
	S^N	0.872	1.025	0.896	0.925	0.748	1.106	0.606	1.307	0.245	0.828	
	f^E	0.000	0.252	0.115	0.164	0.211	0.250	0.347	0.396	0.039	0.012	
	f^N	0.165	0.079	0.317	0.068	0.110	0.450	0.050	0.298	0.011	0.130	

Table 2

Experimental, A_i, and calculated with Eq. (5), $\hat{A}_5^i$, activities and the residuals, ΔA_i, for compounds $i = 1-13$

i	Name	A_i	$\hat{A}_5^i$	ΔA_i
1	2-Hydroxypurine	3.469	3.687	0.218
2	2-Mercaptopurine	3.081	3.015	−0.066
3	Adenine	3.000	2.545	−0.455
4	Hypoxanthine	3.745	3.892	0.147
5	Guanine	5.569	5.174	−0.395
6	Xanthine	4.319	4.122	−0.197
7	2-Mercapto-6-hydroxypurine	3.538	3.499	−0.039
8	6-Mercaptopurine	4.420	4.550	0.130
9	2-Amino-6-mercaptopurine	6.041	5.847	−0.194
10	2-Hydroxy-6-mercaptopurine	4.337	4.611	0.274
11	2,6-Dimercaptopurine	3.638	3.991	0.353
12	2-Methyl-6 mercaptopurine	4.959	4.930	−0.029
13	2-Amino-6-chloropurine	3.155	3.728	0.573

in parentheses, under the regression coefficient of q_{i2} represents the Student's t — test value for this parameter.

All these statistical tests are also repeated for the following regressional equations.

We next added a second electronic parameter to q_{i2} and the statistical tests for the resulted regressional equations were calculated. A significant increase in r and F was obtained in only three cases, excepting F for Eq. (4):

$$\hat{A}_i = \underset{}{25.654} + \underset{(4.379)}{8.933q_{i2}} + \underset{(2.953)}{46.419q_{i7}}\,; \quad r = 0.895\,; \quad F = 20.069 \tag{2}$$

$$\hat{A}_i = -1.400 + \underset{(6.141)}{10.887q_{i2}} - \underset{(-3.506)}{2.967q_{i10}}\,; \quad r = 0.912\,; \quad F = 24.859 \tag{3}$$

$$\hat{A}_i = -6.533 + \underset{(4.515)}{0.382q_{i2}} + \underset{(2.719)}{0.706S^E_{i10}}\,; \quad r = 0.886\,; \quad F = 18.295 \tag{4}$$

The best correlation for three electronic parameters obtained by us is the one using net charges of positions 1 and 2 (q_{i1}, q_{i2}) and the electrophilic superdelocalizability of position 10 (S^{E}_{i10}) :

$$\hat{A}_i = \underset{(4.870)}{0.682 + 8.167q_{i2}} + \underset{(2.740)}{2.997q_{i1}} + \underset{(3.739)}{0.759S^{\mathrm{E}}_{i10}}\,; \tag{5}$$

$$r = 0.940\,;\quad F = 22.636$$

One can consider that equation (5) is satisfactory from the statistical point of view. It indicates the importance of electronic control in the inhibition of this enzyme. Atoms 1 and 2 probably interact with nucleophilic zone of GPRT, while the oxygen or sulphur atom of position 10 interacts with an electrophilic zone, eventually with a Mg^{2+}-ion (the inhibition constants were determined in a solution containing $MgSO_4$).

CONCLUSIONS

The obtained correlational equations show the importance of the atoms 1, 2 and 10 in the electronic interactions between GPRT and inhibitors (or substrate). Also, the correlational results, especially those obtained with Eqs (3) and (5) suggest that electronic indices calculated with the simple Hückel + Del Re methods can be used with success for QSAR purposes. Details about the electronic structure parameters (as eigenvectors, etc.) for these and similar compounds can be obtained on request from one of us (dr. N. Olaru).

REFERENCES

[1] N. Olaru and Z. Simon, submitted to *Rev. Roumaine Chim.*

[2] R. L. Miller, G. A. Ramsey, T. A. Krenitsky and G. B. Elion, *Biochemistry*, **11**, 4723 (1972).

[3] N. Olaru, and Z. Simon in preparation.

[4] K. Fukui, T. Yonezawa and C. Nagata, *Bull. Chem. Soc. Japan*, **27**, 423 (1954); K. Fuku, T. Yonezawa and H. Shingu, *J. Chem. Phys.*, **20**, 722 (1952); K. Fukui, T. Yonezawa, C. Nagata and H. Shingu, *J. Chem. Phys.*, **22**, 1433 (1954).

Revue Roumaine de Chimie, **32**, *1*, 83–90 (1987)

COMPARISON BETWEEN EMPIRICAL AND ADVANCED MOLECULAR ORBITAL CALCULATIONS FOR SOME DERIVATIVES OF NITROGEN HETEROCYCLES

NICULAE OLARU and ZENO SIMON *
Institute of Macromolecular Chemistry "P. Poni", Aleea Gr. Ghica-Vodă 41 A
Jassy-6600, Romania
* Institute of Medicine, Timişoara-1900, Romania

Received December 23, 1985

Net atomic charges are calculated by the HMO + Del Re methods for adenine, guanine, purine, cytosine, uracil and thymine and compared with those calculated by more advanced molecular orbital methods (Pariser-Parr-Pople + Del Re, extended Hückel, iterative extended Hückel, CNDO/2, *ab initio* method by Clementi and by Mely). There are substantial differences between the charges calculated by different methods, but a rather good parallelism of the relative charges for different atomic positions. We conclude therefore that net atomic charges calculated by the simple HMO + Del Re methods can be used for quantitative structure-activity relations in large series of molecules.

INTRODUCTION

The calculation of intermolecular interaction energy using empirical potential functions, [1,2] requires the knowledge of several physico-chemical parameters such as dipole moments, polarizabilities, net atomic charges, ionization potentials. For relatively large molecules of the size interesting drug design, such parameters are rather difficult to be obtained using experimental methods, but they can be evaluated by quantum chemistry.

Several molecular orbital methods, from the simple HMO method to various *ab initio* methods, are available, but there are differences even between the most advanced methods as regards the absolute values of the mentioned parameters; however, a rather good parallelism between the relative values (for different atomic centres, as e.g.) exists. [3]

It is, therefore, of interest to study the intercorrelations between the results given by different molecular orbital methods. Thus, here we shall be concerned with the comparison of the net atomic charges obtained by HMO + Del Re, PPP + Del Re, EHT, IEHT, CNDO/2 and *ab initio* methods for adenine, guanine, purine, cytosine, uracil and thymine.

The abbreviations used here for atomic charges calculated by different methods are presented in Table 1.

This paper will present only the parametrization for the HMO and Del Re methods, which we use for molecular orbital calculations on large series of purinic derivatives and their analogues, for quantitative structure activity relationships (QSAR) purposes.[11,12]

Table 1

Abbreviations used for atomic charges

Charge abbreviation	Molecular orbital methods used for calculation.
QHD	Simple HMO for π-electrons and Del Re for σ-electrons [4]
QPD	PPP for π-electrons and Del Re for σ-electrons [5]
QEH	All-valence extended Hückel method [6] (EHT)
QIEH	All-valence iterative extended Hückel method [7] (IEHT)
QCD	All-valence SCF CNDO/2 method[8]
QABC	All-electrons *ab initio* method of Clementi [9]
QABM	All-electrons *ab initio* method of Mely and Pullman [10]

The molecular orbital and correlational calculations have been performed on the Felix C 32 computer of the "Petru Poni" Macromolecular Chemistry Institute of Jassy.

PARAMETRIZATION AND METHODS

The parameters used for Hückel + Del Re calculations are listed in Tables 2—4.

Table 2 lists the "coulombian", δ, and "resonance", η, parameters for the HMO method.[4,13] Table 3 lists the inductive $\gamma_{\mu(\nu)}$ parameters

Table 2

Parametres δ and η for the HMO method

Atom		δ	Bond		η
C	nitrile	0.1	$C=N$		1.0
C	aromatic	0.0	$C-F$		0.7
O	carbonyl	0.7	$C-N$	amino, pyrrole	0.8
O	hydroxyl	2.0	$C=O$	carbonyl	2.0
O	carboxyl	1.0	$C-O$	carboxyl	1.5
O	nitro	1.0	$C-O(-H)$		0.9
N	pyridine	0.4	$C-S(-H)$		0.7
N	amino	1.8	$C=S$		1.4
N	pyrrole	1.6	$C-Cl$		0.7
N	nitro	2.0	$C-Br$		0.3
S	sulfhydryl	2.0	$N-O$	nitro	0.7
S	thione	0.35	$C-C$		1.0
F		2.3	$C\equiv N$		1.4
Cl		2.1	$C-C(=O)O-H$		0.9
Br		1.6			

and Table 4 lists the δ_0 and $\varepsilon_{\mu(\nu)}$ parameters for the Del Re method.[14-17] The iterative method of Carbo[18] was used for our Del Re calculations.

Published results (see Table 5 for ref.) are used for net atomic charges calculated by the other molecular orbital methods.

Table 3

Parameters $\gamma_{(\mu\nu)}$ for the Del Re method

	H	C	N	O	Cl	Br	F	S
H	0.0	0.4	0.4	0.4	0.0	0.0	0.0	0.4
C	0.3	0.1	0.1	0.1	0.2	0.23	0.1	0.2
N	0.3	0.1	0.1	0.1	0.0	0.0	0.0	0.0
O	0.3	0.1	0.1	0.0	0.0	0.0	0.0	0.0
Cl	0.0	0.4	0.0	0.0	0.0	0.0	0.0	0.0
Br	0.0	0.5	0.0	0.0	0.0	0.0	0.0	0.0
F	0.0	0.1	0.0	0.0	0.0	0.0	0.0	0.0
S	0.3	0.4	0.0	0.0	0.0	0.0	0.0	0.0

Table 4

Parameters δ_0 and $\varepsilon_{\mu(\nu)}$ for the Del Re method

Atom		δ_0	Bond		$\varepsilon_{\mu(\nu)}$
H		0.00	C−C		1.00
C	aliphatic	0.07	C−H		1.00
C	olefine	0.12	C≡N		
N	pyrrole	0.30	C−N	pyrrole	0.70
N^+		0.31	C−N	amino	1.00
N	amino	0.24	$C-N^+R_3$		1.33
	pyridine	0.38	C−O		0.95
O	hydroxyl	0.40	C=O		0.70
O	carbonyl	0.28	$C-O^{-1/2}$		0.80
$O^{-1/2}$	nitro	0.33	C−Cl	aromatic carbon	0.60
S		0.18	C−Br		0.58
C		0.35	C−F		0.85
F		0.57	C−Cl	aliphatic carbon	0.65
Br		0.30	C=S		0.70
N	nitrile	0.50	N−H	amino	0.45
			C−S		0.45
			N−H	pyrrole	0.60
			O−H		0.45

Table 5

Total net atomic charges calculated by different methods

Charge	Atom 1	2	3	4	5	6	7	8	9	10	11	Ref.
						Adenine						
QHD	−0.518	0.313	−0.510	0.335	0.115	0.343	−0.558	0.317	−0.192	−0.439		this paper
QPD	−0.550	0.369	−0.516	0.287	0.098	0.352	−0.617	0.132	−0.066	−0.361		19
QEH	−0.949	0.636	−0.930	0.593	0.154	0.711	−1.049	0.618	−0.283	−0.648		20
QIEH	−0.277	−0.017	−0.266	0.070	0.014	0.077	−0.277	0.025	−0.044	−0.125		21
QCD	−0.264	0.207	−0.257	0.197	−0.039	0.266	−0.223	0.170	−0.123	−0.236		22
QABC	−0.309	0.018	−0.307	0.195	−0.024	0.234	−0.268	0.250	−0.456	−0.602		9
QABM	−0.511	0.178	−0.501	0.344	−0.003	0.405	−0.425	0.155	−0.670	−0.811		10
						Guanine						
QHD	−0.253	0.548	−0.626	0.308	0.029	0.342	−0.539	0.293	−0.183	−0.371	−0.417	this paper
QPD	−0.134	0.418	−0.667	0.227	0.098	0.408	−0.568	0.214	−0.048	−0.493	−0.370	19
QEH	−0.364	0.975	−1.019	0.624	0.117	1.089	−1.045	0.613	−0.277	−1.409	−0.647	20
QIEH	−0.055	0.138	−0.265	0.067	0.000	0.067	−0.283	0.016	−0.050	−0.494	−0.102	21
QCD	−0.210	0.400	−0.373	0.221	−0.095	0.355	−0.172	0.119	−0.103	−0.379	−0.245	22
QABC	−0.472	0.392	−0.361	0.193	−0.050	0.359	−0.239	0.000	−0.447	−0.368	−0.613	9
						Purine						
QHD	−0.474	0.308	−0.474	0.341	0.142	0.183	−0.563	0.335	−0.192			this paper
QPD	−0.482	0.355	−0.524	0.281	0.139	0.249	−0.606	0.261	−0.071			19
QIEH	−0.233	0.025	−0.207	0.105	0.037	0.015	−0.267	0.046	−0.026			21
QCD	−0.188	0.178	−0.209	0.174	0.021	0.101	−0.212	0.185	−0.150			23

Cytosine

QHD	−0.245	0.455	−0.663	0.401	−0.156	0.259	−0.431	−0.388		this paper
QPD	−0.133	0.509	−0.584	0.326	−0.164	0.113	−0.324	−0.512		19
QEH	−0.336	1.402	−1.024	0.776	−0.335	0.290	−0.661	−1.418		20
QIEH	−0.071	0.055	−0.296	0.062	−0.049	0.022	−0.134	−0.519		21
QCD	−0.175	0.422	−0.344	0.324	−0.163	0.190	−0.222	−0.419		22
QABC	−0.463	0.432	−0.335	0.240	−0.300	−0.018	−0.598	−0.407		9
QABM	−0.597	0.637	−0.461	0.363	−0.480	−0.013	−0.719	−0.520		10

Uracil

QHD	−0.283	0.461	−0.324	0.338	−0.187	0.191	−0.353	−0.350		24
QPD	−0.175	0.478	−0.182	0.370	−0.122	0.080	−0.451	−0.504		19
QEH	−0.291	1.389	−0.348	1.157	−0.288	0.343	−1.408	−1.395		20
QIEH	−0.021	0.168	−0.038	0.093	−0.012	0.056	−0.468	−0.451		21
QCD	−0.180	0.447	−0.240	0.374	−0.171	0.175	−0.358	−0.373		24

Thymine

QHD	−0.283	0.461	−0.324	0.335	−0.144	0.188	−0.353	−0.350	−0.104	this paper
QCD	−0.181	0.446	−0.239	0.366	−0.119	0.149	−0.356	−0.377	−0.010	22
QABC	−0.460	0.484	−0.463	0.335	−0.078	−0.057	−0.363	−0.406	−0.584	9
QABM	−0.708	0.771	−0.715	0.562	0.144	0.019	−0.498	−0.525	−0.820	10

For numbering of atoms – see Scheme 1; for the significance of the abbreviations of charges – see Table 1.

RESULTS

The numbering of atomic centres in adenine, guanine, purine, cytosine, uracil and thymine is indicated in the Scheme.

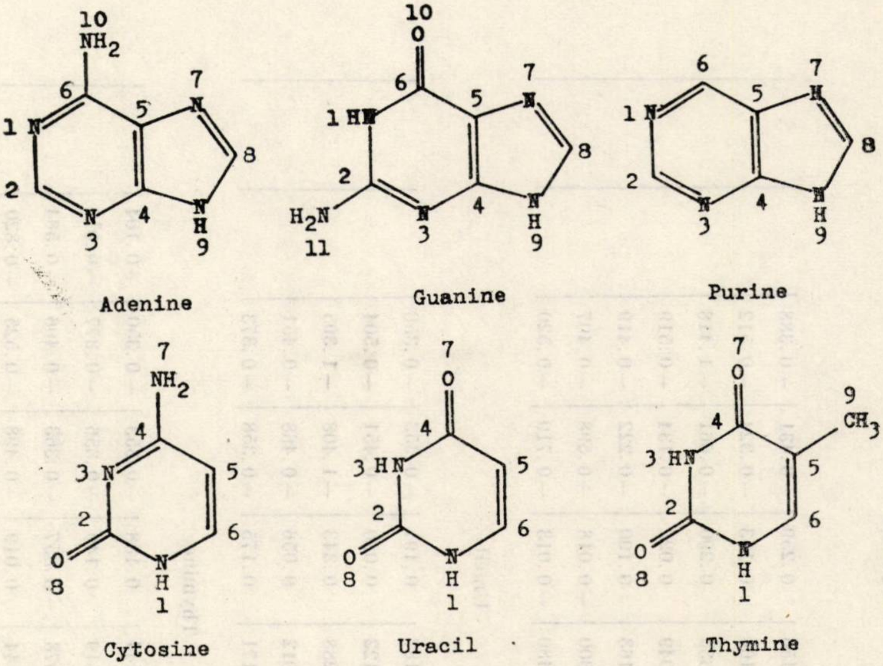

Adenine Guanine Purine

Cytosine Uracil Thymine

The atomic charges calculated by different methods are listed in Table 5. Results for hydrogen atoms are not considered here.

The intercorrelation coefficients between the sets of charges calculated by the above mentioned methods for the six bases are listed in Table 6.

DISCUSSIONS AND CONCLUSIONS

A comparison between net atomic charges calculated by different molecular orbital methods indicates rather large differences between their absolute values. One should certainly give more credit to the advanced methods, but even if we compare the results of the two *ab initio* methods (compare the lines QABC and QABM of Table 5), there are rather large differences between the pairs of net charges. Also, the parametrization of the HMO + Del Re methods, so designed as to obtain good results for dipole moments in model compounds, may yield rather realistic charge distributions. [4]

If the relative values of charges are compared, one observes a rather satisfactory parallelism for the atomic charges calculated by different

Table 6

Intercorrelation coefficients for sets of atomic charges calculated by different methods

	QHD	QPD	QEH	QIEH	QCD	QABC	QABM
Adenine							
QHD	1.000	0.987	0.996	0.935	0.972	0.864	0.901
QPD		1.000	0.993	0.954	0.953	0.776	0.833
QEH			1.000	0.945	0.973	0.833	0.876
QIEH				1.000	0.875	0.688	0.740
QCD					1.000	0.885	0.927
QABC						1.000	0.975
QABM							1.000
Guanine							
QHD	1.000	0.972	0.950	0.811	0.938	0.869	
QPD		1.000	0.970	0.883	0.918	0.975	
QEH			1.000	0.922	0.951	0.837	
QIEH				1.000	0.826	0.621	
QCD					1.000	0.907	
QABC						1.000	
Purine							
QHD	1.000	0.986		0.959	0.978		
QPD		1.000		0.967	0.945		
QIEH				1.000	0.884		
QCD					1.000		
Cytosine							
QHD	1.000	0.968	0.929	0.762	0.960	0.892	0.895
QPD		1.000	0.984	0.845	0.978	0.877	0.866
QEH			1.000	0.871	0.986	0.890	0.898
QIEH				1.000	0.837	0.604	0.599
QCD					1.000	0.914	0.925
QABC						1.000	0.995
QABM							1.000
Uracil							
QHD	1.000	0.951	0.930	0.737	0.990		
QPD		1.000	0.995	0.882	0.980		
QEH			1.000	0.914	0.968		
QIEH				1.000	0.804		
QCD					1.000		
Thymine							
QHD	1.000				0.986	0.893	0.906
QCD					1.000	0.847	0.852
QABC						1.000	0.997
QABM							1.000

methods. The set of charge calculated by the simple Hückel + Del Re methods correlates rather well with those calculated by more advanced methods; the sets of charges obtained by more advanced methods do not seem to give better intercorrelations. Most of resulted intercorrelation coefficients have values of about 0.9, excepting those obtained from the correlations with the set of charges calculated by the iterative extended Hückel method.

Net atomic charges and other molecular orbital results which characterize molecular structure and reactivity are required for structure-activity correlations in drug design. If one considers the correlational results for QSAR's, especially those for large series of molecules with a wider range of structural variations, the intercorrelation coefficients between sets of calculated charges are generally higher than those for QSAR's.

We conclude therefore that it is sound to use net atomic charges calculated by the simple HMO + Del Re methods for QSAR's with large series of molecules and it seems unlikely that such QSAR's would be sensibly improved by using results of more advanced methods.

REFERENCES

[1] D. F. Bradley, *J. Macromol. Sci. Chem.*, **4**, 739 (1970).

[2] A. M. Liquori, *Quart. Rev. Biophys.*, **2**, 65 (1969).

[3] A. Pullman, *Top. Current Chemistry*, **31**, 45 (1972).

[4] H. Berthod and A. Pullman, *J. Chim. phys.*, **62**, 942 (1965).

[5] H. Berthod, Cl. Giessner-Prettre and A. Pullman, *Theor. Chim. Acta*, **5**, 53 (1966).

[6] R. Hoffman, *J. Chem. Phys.*, **39**, 1397 (1963).

[7] A. Denis and M. Gilbert, *Theor. Chim. Acta*, **11**, 31 (1968).

[8] J. A. Pople and G. A. Segal, *J. Chem. Phys.*, **44**, 3289 (1966).

[9] E. Clementi, J. M. Andre, M. Cl. Andre, D. Klint and D. Hahn, *Acta Phys. Acad. Sci. Hung.*, **27**, 493 (1969).

[10] B. Mely and A. Pullman, *Theor. Chim. Acta*, **13**, 278 (1969).

[11] N. Olaru and Z. Simon, *Rev. Roumaine Biochim.*, **18**, 51 (1981).

[12] N. Olaru and Z. Simon, submitted to *Rev. Roumaine Chim.*

[13] W. P. Purcell and J. A. Singer, *J. Chem. and Eng. Data*, **12**, 235 (1967).

[14] G. Del Re, *J. Chem. Soc.*, **1958**, 4031.

[15] F. Peradejordi, A. N. Martin and A. Cammarata, *J. Pharm. Sci.*, **60**, 576 (1971).

[16] G. Del Re, B. Pullman and T. Yonezawa, *Biochim. Biophys. Acta*, **75**, 153 (1963).

[17] H. Berthod and A. Pullman, *C.R. Acad. Sci.*, **262**, 77 (1966).

[18] R. Carbo, *Theor. Chim. Acta*, **15**, 170 (1970).

[19] A. Pullman and B. Pullman, *Adv. Quantum Chem.*, **4**, 267 (1968).

[20] F. Jordan and B. Pullman, *Theor. Chim. Acta*, **9**, 242 (1968).

[21] A. Pullman, E. Kochanski, M. Gilbert and A. Denis, *Theor. Chim. Acta*, **10**, 231 (1968).

[22] C. Giessner-Prettre and A. Pullman, *Theor. Chim. Acta*, **9**, 279 (1968).

[23] B. Pullman, H. Berthod, F. Bergmann, Z. Neiman, H. Weiler-Feilchenfeld and E. D. Bergman, *Tetrahedron*, **26**, 1483 (1970)

[24] H. Berthod, Cl. Giessner-Prettre and A. Pullman, *Theor. Chim. Acta*, **8**, 212 (1967).

Revue Roumaine de Chimie, **32**, *1*, 91–99 (1987)

COMPLEX COMPOUNDS OF Pd(II) WITH THIOETHERS. I

I. INVESTIGATION OF SOME COMPOUNDS OF Pd(II) WITH THIOETHERS OF THE BIS(PHENYLTHIOMETHYL) ETHER SERIES

D. NEGOIU[a], S. NEAGOE[b], MARIA NEGOIU[a], ELENA BADAU[c] and ELENA GHERMAN[d]

[a] National Institute of Chemistry, Faculty of Chemical Technology, Department of Inorganic Chemistry, 1, Polizu Str., 78126-Bucharest, Romania

[b] Institute of Petroleum and Gas, 3, București—Ploiești Blvd. Ploiești, Romania

[c] Faculty of Pharmacy, 6, Traian Vuia Str., Bucharest, Romania

[d] Institute of Research and Technological Engineering for Petroleum and Refineries, Ploiești, Romania

Received December 20, 1985

Complex compounds of Pd(II) with ether-bisthioethers of the bis(phenylthiomethyl)-ether series were synthesized and investigated. The obtained compounds have the general formula [PdLCl$_2$], which was established on the basis of elemental chemical analysis, molecular mass determinations and thermal analysis. Electric conductivity measurements indicated that these compounds are nonelectrolytes, whereas infrared, ultraviolet/visible and nuclear magnetic resonance spectra are in agreement with their formulas.

INTRODUCTION

The pronounced donor character of sulfur allows for the formation of coordinative-type bonds. Thus, the thioether ligands form stable complex compounds with the salts of some heavy metals such as Hg, Cu, Au, Pd and Pt. The composition of the resulting compounds depends on the working conditions.

The donor properties of sulfur have drawn the attention of many researchers. Fehnel and Carmack [1] studied the UV spectra of some alkyl and aryl sulfides, Koch [2] noticed that the allyl and the benzyl sulfides absorb differently from the saturated dialkyl sulfides, and Phahov [3] — noticed that introduction of one or several CH$_2$ groups between the sulfur atom and the aromatic nucleus weakens very much or even eliminates completely the conjugation between the electrons of the thioetheric sulfur and the π electrons of the aromatic nucleus. Schmidt and Hoffmann [4] prepared and investigated some compounds of Pt and Pd with thioethers, showing, as expected, that the corresponding ligands are bidentate and form a stable, 6-membered ring with the central metal atom.

We give in this work the results of an investigation on the complex compounds of Pd(II) with ether-bisthioethers of the bis(phenylthiomethyl) ether (PTME) series [5]

$$Ar-S-CH_2-O-CH_2-S-Ar$$

where

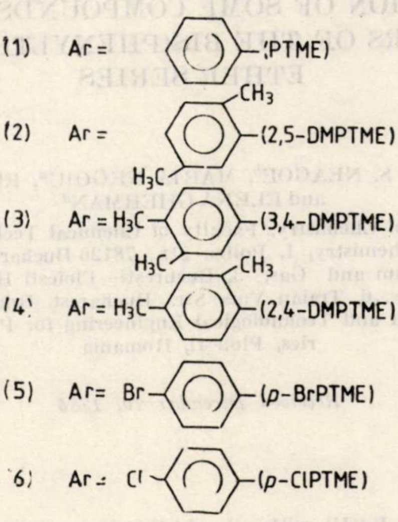

(1) Ar = (PTME)
(2) Ar = CH3 (2,5-DMPTME)
H3C
(3) Ar = H3C (3,4-DMPTME)
H3C CH3
(4) Ar = H3C (2,4-DMPTME)
(5) Ar= Br (p-BrPTME)
(6) Ar = Cl (p-ClPTME)

RESULTS AND DISCUSSION

The complex compounds of Pd(II) with ether-bisthioethers from the bis(phenylthiomethyl)ether group are microcrystalline powders, whose colour varies from yellow to red as a function of the nature of the ligand. They have higher melting points than the corresponding ligands and their solubility in common inorganic and organic solvents is low: however, they are easily soluble in dimethylsulfoxide (DMSO), dimethylformamide (DMF), dichloroethane (CH_2Cl_2) and somewhat less soluble in nitromethane.

The compounds were prepared by adding the solution of the thioether (dissolved in acetone) to the hydrochloric solution of palladium(II) chloride; the mixture was then either stirred for 0.5—3 hours or refluxed for 1—3 hours on a water bath.

The results of the elemental chemical analysis of the obtained compounds are presented in Table 1. These results allow to assign to the synthesised complexes the following general formula: $[PdLCl_2]$, where L are the ligands (1) to (6). This formula is confirmed by the molecular mass determinations as well as by the molar conductivity measurements, whose values are given in Table 2.

To determine the molecular masses we used the cryoscopic micromethod of Rast, [6] using camphor as solvent. The experimental values thus obtained agree with those calculated theoretically for the general formula given above.

The molar conductivities were measured in DMSO. [7] The values obtained experimentally confirm the fact that the investigated compounds are nonelectrolytes. Hence, the general formula proposed above for the compounds of Pd(II) with thioethers from the bis (phenylthiomethyl) ether group, *i.e.* [Pd*L*Cl_2], is correct.

Table 1

Results of the elemental chemical analysis of the bis-thioethers of the bis(phenylthiomethyl)ether series and of their complex compounds with Pd(II)

Compound/System	Analysed element $\frac{\text{theor.*}}{\text{exptl.}}$ (%)					Melting point (°C)
	Pd	C	H	S	Cl	
PTME	—	$\frac{66.00}{66.41}$	$\frac{6.21}{6.80}$	$\frac{22.07}{22.14}$	—	22
2,5-DMPTME	—	$\frac{67.92}{68.40}$	$\frac{6.91}{7.16}$	$\frac{20.13}{20.21}$	—	62
3,4-DMPTME	—	$\frac{67.92}{68.25}$	$\frac{6.91}{7.11}$	$\frac{20.13}{20.18}$	—	67
2,4-DMPTME	—	$\frac{67.92}{67.70}$	$\frac{6.91}{6.94}$	$\frac{20.13}{20.24}$	—	25
p-BrPTME	—	$\frac{40.01}{40.34}$	$\frac{2.87}{2.92}$	$\frac{15.26}{15.31}$	—	56
p-ClPTME	—	$\frac{50.75}{51.03}$	$\frac{3.65}{3.46}$	$\frac{19.35}{19.28}$	—	52
Pd(II)-(PTME)	$\frac{22.77}{22.65}$	$\frac{41.08}{41.59}$	$\frac{3.85}{4.00}$	$\frac{13.69}{14.00}$	$\frac{15.17}{15.25}$	170
Pd(II)-(2,5-DMPTME)	$\frac{21.46}{21.40}$	$\frac{43.57}{43.70}$	$\frac{4.43}{5.10}$	$\frac{12.90}{12.45}$	$\frac{14.30}{13.81}$	195
Pd(II)-(3,4-DMPTME)	$\frac{21.46}{21.72}$	$\frac{43.57}{44.10}$	$\frac{4.43}{4.22}$	$\frac{12.90}{12.75}$	$\frac{14.30}{14.83}$	205
Pd(II)-(2,4-DMPTME)	$\frac{21.46}{21.15}$	$\frac{43.57}{43.92}$	$\frac{4.43}{5.00}$	$\frac{12.90}{12.43}$	$\frac{14.30}{14.20}$	172
Pd(II)-(*p*-BrPTME)	$\frac{17.81}{18.00}$	$\frac{28.12}{28.76}$	$\frac{2.00}{2.44}$	$\frac{10.71}{10.92}$	$\frac{11.87}{12.16}$	176
Pd(II)-(*p*-ClPTME)	$\frac{20.92}{21.04}$	$\frac{33.05}{33.45}$	$\frac{2.36}{2.70}$	$\frac{12.59}{13.00}$	$\frac{27.88}{28.00}$	145

* For a proposed formula $PdLCl_2$ in the case of the Pd Compounds.

Table 2

Values of molecular masses and of molar conductivities for the complex compounds of Pd(II) with ether-bisthioethers

Compound	Molecular mass		Concentration ($\times 10^{-4}$ M)	Molar conductivity ($\Omega^{-1}cm^2mole^{-1}$)
	theor.	exptl.		
[Pd(PTME)Cl$_2$]	467.30	406.40	6.84	1.76
[Pd(2,5-DMPTME)Cl$_2$]	495.77	474.04	2.62	2.09
[Pd(3,4-DMPTME)Cl$_2$]	495.77	443.60	1.70	1.07
[Pd(2,4-DMPTME)Cl$_2$]	495.77	482.37	4.03	1.60
[Pd(*p*-BrPTME)Cl$_2$]	597.30	521.60	1.92	0.81
[Pd(*p*-ClPTME)Cl$_2$]	508.55	485.10	0.98	0.93

Thermal Analysis

We studied the thermal behaviour of the complex compounds of Pd(II) with ether-bisthioethers of the bis(phenylthiomethyl)ether series. The data acquired by analysing the DTA, DTG and TG curves of some of the compounds of Table 1 are given in Table 3.

Table 3

Results of the thermal analysis of the complex compounds of Pd(II) with ether-bisthioethers

Compound	Mol. mass	Residue		Temperature of some thermal effects		Final temp. of oxidn.	Thermal transformation of residue
		Form	theor. exptl.	Start of decompn.	First thermal effect		
[Pd(PTME)Cl$_2$]	467.30	Pd	22.77 23.04	150	170	540	850–870
[Pd(2,5-DMPTME)Cl$_2$]	495.77	Pd	21.46 22.34	120	195	670	850–870
[Pd(3,4-DMPTME)Cl$_2$]	495.77	Pd	21.46 23.13	120	205	600	850–860
[Pd(*p*-ClPTME)Cl$_2$]	508.55	Pd	20.94 21.23	130	145	500	860–870

The analysed complex compounds have a similar thermal behaviour. The experimental data given in Table 3 indicate that the decomposition of the compounds begins at 150°C for [Pd(PTME)Cl$_2$], at 120°C for [Pd(2,5-DMPTME)Cl$_2$] and [Pd(3,4-DMPTME)Cl$_2$], and at 130°C for [Pd(*p*-ClPTME)Cl$_2$]. These results suggest that the thermal stability of the investigated compound is influenced by the radicals bonded to the marginal benzenic rings.

The thermogravimetric curves present at least three ranges of decomposition of the compounds. The thermal effect of the transformation of the residue occurs between 800 and 875°C. This effect is typical to the reaction $PdO \rightarrow Pd + 1/2O_2$, mentioned in the literature. [8,9]

The data offered by the TG curves have allowed to estimate the value of the molar ligand/metal ratio at 1 : 1 (Tab. 1 and 3).

The endothermal effects on the DTA curves alternate with exothermal effects, which suggests that the decomposition and oxidation processes are simultaneous and, therefore, complex. We also can state that the palladium oxidation is only partial. A definite chemical composition was only observed for the corresponding residue.

IR Spectra

The frequencies of the bands observed in the IR spectra of the thioethers and of their complex compounds are compiled in Table 4 and discussed below according to spectral ranges.

In the 400—3100 cm^{-1} range, the bands which appear are due to ν_{CH}, $\nu_{sym.CH_3}$, $\nu_{asym.CH_3}$, $\nu_{asym.CH_2}$, $\nu_{sym.CH_2}$, $\nu_{C\overset{\cdots}{-}C}$, $\nu_{asym.C-O}$ and $\nu_{sym.C-O}$ valence vibration modes, as well as to ν_{CH} deformation mode. In what concerns the valence vibrations of the thioetheric groups, ν_{C-S}, an accurate estimate of the frequency of the corresponding bands is difficult, since these bands appear in the 600—700 cm^{-1} range, are weak and have shifting positions. [10]

We were able to assign the band due to the C—S bond by analysing comparatively the IR spectra of the thioethers and of their compounds with Pd(II). The assignment is based on the fact that this band has in the spectra of the complex compounds a much smaller intensity than in the spectra of the uncomplexed thioethers, and is frequently shifted.

Based on similar arguments, Schmidt and Hoffmann [4] have assigned the bands observed in the 690—750 cm^{-1} region to the vibrations of the C—S bonds in thioethers; these bands appear shifted to higher frequencies in the spectra of the compounds with Pt(II) and Pd(II).

From the data compiled in Table 4 it results that the bands corresponding to valence vibrations which appear in the spectra of the compounds with Pd(II), $\nu_{asym.CH_3}$, $\nu_{sym.CH_3}$, $\nu_{asym.CH_2}$ and $\nu_{sym.CH_2}$, have frequencies which differ from those measured in the spectra of the ligands. The obvious shifts and the change in the intensity of the bands corresponding to the valence asymmetrical and symmetrical vibrations ν_{CH_2}, due to the CH_2 groups neighbouring the thioetheric sulfur atom, —S—, lead to the conclusion that the vicinal thioetheric sulfur atoms are involved in the coordination with the central metal atom.

The bands characteristic of the $\nu_{C\overset{\cdots}{-}C}$ valence vibrations of the benzenic nuclei appear in the 1600—1400 cm^{-1} region. As compared to the spectra of the ligands, the bands occurring in the spectra of the corresponding complex compounds of Pd(II) either have the same frequency but a smaller intensity, or are shifted towards higher frequencies (within

Table 4

Characteristic frequencies of the bands observed in the IR spectra of the ether-bisthioethers of the bis(phenylthiomethyl)ether series and of their complex compounds with Pd(II) (in cm^{-1})

Compound	3100—3000 region	3000—2800 region				1600—1400 region	1100—1000 region	830—780 region	700—600 region
	ν_{CH}	$\nu_{sym.CH_3}$	$\nu_{as.CH_3}$	$\nu_{as.CH_2}$	$\nu_{sym.CH_2}$	$\nu_{C\cdots C}$	$\nu_{as.C-C}$	ν_{C-H}	ν_{C-S}
PTME	3020*s* 3040*w* 3085*m* 3090*w*	—	—	2926*m*	2860*m*	1480*s*	1055*s*	870*m*	700*s* 650*m*
2,5-DMPTME	3020*s* 3040*w* 3080*m* 3090*w*	2870*m*	2975*s*	2925*s*	2860*m*	1450*m* 1480*s* 1595*m*	1050*s*	810*s*	690*m* 650*s*
3,4-DMPTME	3025*w* 3045*sh* 3085*m*	2870*m*	2975*m*	2926*m*	2850*m*	1455*m* 1480*s* 1495*m*	1055*m*	810*s*	695*m* 650*m*
2,4-DMPTME	3020*s* 3030*m* 3080*m*	2872*m*	2970*m*	2925*m*	2855*m*	1445*m* 1485*s* 1590*m*	1055*m*	810*s*	695*m* 650*m*
***p*-BrPTME**	3020*s* 3040*sh* 3080*m*	—	—	2925*m*	2860*m*	1480*m*	1070*m*	810*s*	680*s* 650*m*
***p*-ClPTME**	3020*s* 3070*m*	—	—	2925*m*	2850*m*	1450*m* 1490*s*	1055*m*	815*s*	685*s* 660*m*
[Pd(PTME)Cl$_2$]	3025*w* 3075*w* 3090*sh*	—	—	2930*m*	2875*w*	1495*m*	1065*m*	870*w*	710*s* 665*m*
[Pd(2,5-DMPTME)Cl$_2$]	3015*w* 3030*sh* 3070*sh*	2870*w*	2990*w*	2930*m*	2845*sh*	1445*s* 1495*m* 1610*w*	1055*m*	820*s*	710*w* 675*m*
[Pd(3,4-DMPTME)Cl$_2$]	3020*sh* 3040*sh* 3085*sh*	2875*sh*	2990*w*	2926*sh*	2850*sh*	1445*s* 1490*w* 1495*s*	1070*s*	815*s*	680*m* 640*w*
[Pd2,4—DMPTME)Cl$_2$]	3015*w* 3030*sh* 3090*sh*	2870*w*	2980*w*	2925*w*	2870*w*	1450*w* 1475*w* 1605*m*	1055*s*	810*s*	705*w* 645*sh*
[Pd(*p*-BrPTME)Cl$_2$]	3020*sh* 3060*sh*	—	—	2910*sh*	2870*sh*	1470*s*	1075*m*	815*s*	680*m* 640*w*
[Pd(*p*-ClPTME)Cl$_2$]	3025*sh* 3060*sh*	—	—	2935*w*	2830*sh*	1445*m* 1480*s*	1065*m*	820*s*	695*sh* 675*s*

10 cm^{-1}). Such facts confirm that the p-π-type conjugation, which appears in the uncomplexed ligands, is perturbed as a result of complexation, since usually the donor sulfur atoms are situated in the vicinity of the benzenic nuclei of the ligand.

The bands corresponding to the asymmetric and symmetric valence vibrations, ν_{C-O-C}, appear in the 1300—1000 cm^{-1} region. Presence of the aliphatic ether characteristic bond in ligands is evidenced by a strong absorption at 1050—1070 cm^{-1} (Tab. 4). These bands appear as unmodified in the spectra of the corresponding complex compounds with Pd(II); this suggests that the etheric oxygen atom is not involved in the formation of the complex compounds.

UV/Visible Spectra

To elucidate the structure of the new complex compounds formed by Pd(II) with the mentioned thioethers, we also recorded the reflectance electronic spectra (for solid powders); the band assignment was made using the data given by Gray and Ballhausen.[11] By comparing the bands observed in the reflectance electronic spectra of the complex compounds of Pd(II) with thioethers with those of the $[PdCl_4]^{2-}$ and $[PdBr_4]^{2-}$ anions, we were able to make the following assignments:

— the band located at 415 nm (24,185 cm^{-1}) is assigned to the $e_g(\pi^*) \rightarrow b_{1g}(\sigma^*)$, $^1A_{1g} \rightarrow {}^1B_{1g}$ transition;

— the band located at 440 nm (22,773 cm^{-1}) is assigned to the $a_{1g}(\pi^*) \rightarrow b_{1g}(\sigma^*)$, $^1A_{1g} \rightarrow {}^1B_{1g}$ transition;

— the band located at 546 nm (18,386 cm^{-1}) is assigned to the $b_{2g}(\pi^*) \rightarrow b_{1g}(\sigma^*)$, $^1A_{1g} \rightarrow {}^1A_{2g}$ transition.

All these transitions are spin-allowed and parity-forbidden $d-d$ transitions. The relations such established lead to the conclusion that the complex compounds of Pd(II) with thioethers of the bis(phenylthiomethyl) ether series have a square-planar conformation with D_{4h} symmetry.

^{1}H-NMR Spectra

The ^{1}H-NMR spectra obtained in deuterated DMSO solutions contain signals which correspond to the organic group present in the compounds described. We give in Table 5 the values of the chemical shifts of the protons in 2,5-DMPTME and 3,4-DMPTME, as well as the coresponding values found in the spectra of the complexes with Pd(II).

The spectrum of bis(2,5-dimethylphenylthiomethyl)ether reveals that the protons of the methyl groups attached to the aromatic ring occur as a doublet ($\delta = 2.20$ and 2.26 ppm). After complexation, the two signals become superposed, which suggests that the electronic structure in the vicinity of the aromatic cycle has been modified. A slight influence is also observed at the methylene group bonded to the sulfur atom.

The aromatic protons show a slight de-screening, evidenced by the shape of the ^{1}H-NMR spectrum. The shift of the protons of the methylene group neighbouring the sulfur atom, as well of the marginal benzenic nuclei, directly bonded to the sulfur atoms, lead to the conclusion that the sulfur atoms in thioethers are involved in the coordination.

Table 5

Values of the proton chemical shifts of the complex compounds of Pd(II) with thioethers of the bis(phenylthiomethyl)ether series, as compared to the chemical shifts of the uncomplexed thioethers

Ligand			Complex combination		
Assignment	δ(ppm)	Multiplicity	Assignment	δ(ppm)	Multiplicity
2,5-DMPTME			Pd(2,5-DMPTME)Cl_2		
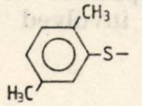	2.20	singlet	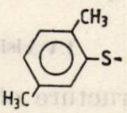	2.20	singlet
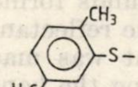	2.26	singlet			
$-O-CH_2-S-$	5.20	singlet	$-O-CH_2-S-$	5.14	singlet
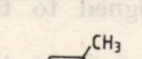	6.90	doublet			
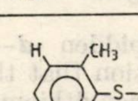	7.10	doublet	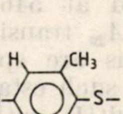	7.05— 7.26	doublet of doublets
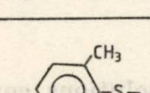	7.30	doublet			
3,4-DMPTME			Pd(3,4-DMPTME)Cl_2		
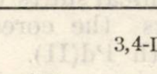	2.15	singlet	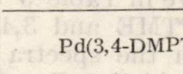	2.15	singlet
$-S-CH_2-O-$	5.13	singlet	$-S-CH_2-O$	5.13	singlet
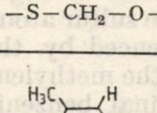	7.02— 7.23	multiplet	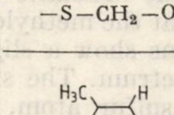	7.10— 7.30	multiplet

EXPERIMENTAL

Reagents : 0.02*M* solution of $PdCl_2$ in HCl ; 0.02*M* solution of thioethers in acetone.

Preparation of the complex compounds : Dichloro-bis(phenylthiomethyl)-ether-palladium (II), $[Pd(PTME)Cl_2]$, was prepared by adding 15 mL of the thioether solution in acetone to 10 mL of a 0,02*M* solution of $PdCl_2$. Then acetone was added until the opalescence disappeared and the mixture was stirred during 3 hours on a magnetic stirrer. Yellow crystals deposited, which were filtered, were washed and dried under vacuum.

Dichloro-bis(2,5-dimethylphenylthiomethyl)ether-palladium(II), $[Pd(2,5\text{-}DMPTME)Cl_2]$, and dichloro-bis(3,4-dimethylphenylthiomethyl)ether-palladium (II), $[Pd(3,4\text{-}DMPTME)Cl_2]$, were prepared by adding (under stirring) the acetone solution of the thioether to 10 mL of a 0.02*M* solution of $PdCl_2$, after which the mixture was heated during 5 minutes on a water bath. After 2 hours, red crystals deposited, which were filtered, washed and dried under vacuum.

Dichloro-bis(2,4-dimethylphenylthiomethyl)ether-palladium (II), $[Pd(2,4\text{-}DMPTME)Cl_2]$, was obtained by refluxing in a 100-mL flask, during 2 hours, 10 mL of a 0.02*M* solution of thioether in acetone with 10 mL of a 0.02*M* solution of $PdCl_2$. Red crystals deposited.

Dichloro-bis(*p*-bromophenylthiomethyl)ether-palladium (II) and dichloro-bis(*p*-chlorophenylthiomethyl)ether-palladium (II) were prepared by adding drop by drop and under stirring the solution of thioether in acetone to 10 mL of a 0.02*M* solution of $PdCl_2$. The yellow complex precipitated instantaneously and was separated on a G_4 sintered glass filter after one hour.

Instrumentation : The IR spectra of the thioethers and of their complex compounds were recorded with an UR 20 Carl Zeiss (Jena) Spectrometer, using samples prepared as KBr pellets. The UV/Vis reflectance spectra were recorded with a VSU-1 Carl Zeiss (Jena) Spectrometer, using MgO pellets.

CONCLUSIONS

This study established that the complex compounds of Pd(II) with ether-bisthioethers of the bis(phenylthiomethyl)-ether series have the formula $[PdLCl_2]$.

The elemental chemical analysis, molecular mass determinations and thermogravimetric analysis indicate that the palladium : ligand ratio is equal to 1 : 1. The electric conductivity measurements showed that the investigated complex compounds are nonelectrolytes. This suggests that a donor/acceptor-type bond may have been formed. Examination of the IR and ^{1}H-NMR spectra leads to the conclusion that the coordination is effected by means of the thioetheric sulfur atoms, so that the following structural formulas could be assigned to the complex compounds of Pd(II) with bis-thioethers.

REFERENCES

[1] E. A. Fehnel and M. Carmack, *J. Amer. Chem. Soc.*, **71**, 84, 231 (1949).

[2] H. P. Koch, *J. Chem. Soc.*, (1949) 387.

[3] V. A. Phahov, *Tr. Mosk. Khim.*, **61**, 146 (1969) ; *Chem. Abstr.*, **73**, 303/2C (1970).

[4] Von M. Schmidt and G. G. Hoffmann, *Z. Anorg. allg. Chem.*, **445**, 167 (1978).

[5] M. Iovu and E. Bădău, *Rev. Roumaine Chim.*, **26**, 1149 (1981).

[6] I. Tănăsescu and M. Ionescu, "Lucrări practice de chimie organică", Vol. 2, Ed. Tehnică, Bucharest, 1975, p. 143.

[7] W. J. Geary, *Coord. Chem. Rev.*, **7**, 81 (1971).

[8] D. N. Todor, "Thermal Analysis of Minerals", Abacus Press, Kent, 1976.

[9] C. D. Nenițescu, "Chimie generală", Ed. Tehnică, Bucharest, 1979.

[10] M. Avram and G. D. Mateescu, "Spectroscopia în infraroșu — aplicații în chimia organică", Ed. Tehnică, Bucharest, 1966.

[11] H. B. Gray and C. J. Ballhausen, *J. Amer. Chem. Soc.*, **85**, 260 (1963).

EXPERIMENTAL

Reagents : 0.02*M* solution of $PdCl_2$ in HCl; 0.02*M* solution of thioethers in acetone.

Preparation of the complex compounds : Dichloro-bis(phenylthiomethyl)-ether-palladium (II), [Pd(PTME)Cl_2], was prepared by adding 15 ml. of the thioether solution in acetone to 10 ml. of a 0.02*M* solution of $PdCl_2$. Then acetone was added until the opalescence disappeared and the mixture was stirred during 8 hours on a magnetic stirrer. Yellow crystals deposited, which were filtered, were washed and dried under vacuum.

Dichloro-bis(2,5-dimethylphenylthiomethyl)ether-palladium(II), [Pd(2,5-DMPTME)Cl_2], and dichloro-bis(3,4-dimethylphenylthiomethyl)ether-palladium (II), [Pd(3,4-DMPTME)Cl_2], were prepared by adding (under stirring) the acetone solution of the thioether to 10 ml. of a 0.02*M* solution of $PdCl_2$, after which the mixture was heated during 5 minutes on a water bath. After 2 hours, red crystals deposited, which were filtered, washed and dried under vacuum.

Dichloro-bis(2,4-dimethylphenylthiomethyl)ether-palladium (II), [Pd(2,4-DMPTME)Cl_2], was obtained by refluxing in a 100-ml. flask, during 2 hours, 10 ml. of a 0.02*M* solution of thioether in acetone with 10 ml. of a 0.02*M* solution of $PdCl_2$. Red crystals deposited.

Dichloro-bis(*p*-bromophenylthiomethyl)ether-palladium (II) and dichloro-bis(*p*-chlorophenylthiomethyl)ether-palladium (II) were prepared by adding drop by drop and under stirring the solution of thioether in acetone to 10 ml. of a 0.02*M* solution of $PdCl_2$. The yellow complex precipitated instantaneously and was separated on a G_4 sintered glass filter after one hour.

Instrumentation : The IR spectra of the thioethers and of their complex compounds were recorded with an UR 20 Carl Zeiss (Jena) Spectrometer, using samples prepared as KBr pellets. The UV/Vis reflectance spectra were recorded with a VSU-1 Carl Zeiss (Jena) Spectrometer, using MgO pellets.

CONCLUSIONS

This study established that the complex compounds of Pd(II) with ether-bisthioethers of the bis(phenylthiomethyl)-ether series have the formula [PdCl$_2$L].

The elemental chemical analysis, molecular mass determinations and thermogravimetric analysis indicate that the palladium : ligand ratio is equal to 1 : 1. The electric conductivity measurements showed that the investigated complex compounds are nonelectrolytes. This suggests that a donor acceptor $d\pi$-$p\pi$ bond may have been formed. Examination of the IR and ^{1}H-NMR spectra leads to the conclusion that the coordination is effected by means of the thioetheric sulfur atoms, so that the following structural formulas could be assigned to the complex compounds of Pd(II) with bis-thioethers.

REFERENCES

[1] E. A. Fehnel and M. Carmack, *J. Amer. Chem. Soc.*, **71**, 84, 231 (1949).
[2] H. P. Koch, *J. Chem. Soc.*, (1949), 387.
[3] V. A. Pikulin, *Ž. Neorg. Khim.*, **61**, 148 (1969); *Chem. Abstr.*, **74**, 92032 (1970).
[4] Von M. Schmidt and G. G. Hoffmann, *Z. Anorg. allg. Chem.*, **445**, 167 (1978).
[5] M. Davis and S. Kubota, *Rev. Roumaine Chim.*, **26**, 1349 (1981).
[6] I. Cănăsescu and M. Ionescu, "Lucrări practice de chimie organică", Vol. 2, Ed. Tehnică, Bucharest, 1973, p. 143.
[7] W. J. Geary, *Coord. Chem. Rev.*, **7**, 81 (1971).
[8] D. N. Todor, "Thermal Analysis of Minerals", Abacus Press, Kent, 1976.
[9] C. D. Nenițescu, "Chimie generală", Ed. Tehnică, Bucharest, 1972.
[10] M. Avram and G. D. Mateescu, "Spectroscopia în infraroșu – aplicații în chimia organică", Ed. Tehnică, Bucharest, 1966.
[11] H. B. Gray and C. J. Ballhausen, *J. Amer. Chem. Soc.*, **85**, 260 (1963).

Revue Roumaine de Chimie, 32, *1*, 101–108 (1987)

RATE CONSTANTS AND ACTIVATION ENERGIES OF Fe(II) TO Fe(III) OXIDATION REACTION BY HYDROXYLAMINE IN NORMAL AND HEAVY WATER

A. CĂLUŞARU* and EUGENIA SAVIUC**
* Institute of Chemical Research, Bucharest, Romania
**Department of Inorganic and Analytical Chemistry, Polytechnical Institute, Iaşi, Romania

Received March 17, 1986

During the polarographic reduction of Fe(III) to Fe(II) in the presence of hydroxylamine, a chemical reaction is superimposed on the electron transfer reaction (catalysed process), giving a kinetic character of the corresponding limiting currents. Using these polarographic currents it was posssible to determine the rate constants of the chemical reaction of Fe(II) oxidation by hydroxylamine in both normal water and deuterated systems. The kinetic isotope effect of the oxidation reaction in which participate isotopic molecules was calculated from the ratio of the corresponding rate constants: $k_H/k_D = (2.05 \times 10^2) / (1.51 \times 10^2) = 1.36$. At the same time, the isotope effects corresponding to the activation energies $E_H/E_D = 14.2/15.6 = 0.91$ and frequency factors $A_H/A_D = 1.355$ were calculated. It has been concluded that the origin of the isotope effect is the variation of the collision frequency of the isotopic molecules.

INTRODUCTION

Previous polarographic studies concerning the determination of the equilibrium constants and reaction rates in normal and heavy water showed that the isotopy gives information for a deeper understanding of the mechanism for the studied reaction.[1-3] The advantage of hydrogen substitution by deuterium is still higher when the magnetic properties of the atomic nucleus are considered, as in the case of the electron spin resonance.[4] The present work is a part of the systems where the redox couple represented by (low valence metal ion)/ (hydroxylamine) is a source of $^{\cdot}NH_2$ or $^{\cdot}NH_3^+$ radicals. This couple was studied also by the continuous flow ESR method.[5-7] Polarography[1-3, 8, 9] and pulse-polarography[10] were also used.

The unprotonated $^{\cdot}NH$ or $^{\cdot}NH_3^+$ radicals form depends on pH, but it has been found that even in acidic media, it is NH_2OH rather than NH_3^+OH which reacts with Ti(III).[10] However pulse radiolysis shows that by the reaction of e_{aq}^- with hydroxylamine ammoniumyl radical cation is observed, since the pK_a value is 6.7. Also in irradiated solid crystals of NH_4ClO_4 or ND_4ClO_4 the ESR spectra show always the radiolytic formation of the $^{\cdot}NH_3^+$ or $^{\cdot}ND_3^+$ radicals respectively.[11-13]

Extended works in normal water of the redox couple represented by (low valence metal ion) / (hydroxylamine) were carried out with Ti(III) ion. This system has been studied also polarographically in heavy water and deuterated components.[2]

It has been shown that Fe(II) can be oxidized to Fe(III) by hydroxylamine,[14, 15] forming $^{\bullet}NH_2$ or $^{\bullet}NH_3^+$ type radicals. The complexant triethanolamine media were used for this purpose. No data are available in the literature on the behaviour of this system in heavy water. This is why in the present work the oxidation reaction of Fe(II) to Fe(III) by hydroxylamine was studied in both normal and heavy water, in order to obtain data allowing the determination of the kinetic isotope effects and the explanation of the mechanism of this reaction.

EXPERIMENTAL

The polarograms were recorded in inert atmosphere with an LP 60 type polarograph. The anodic part of the polarographic cell was a saturated calomel electrode. The cathodic compartment was provided with a double wall space for keeping the work temperature by the flow of the hot water from a thermostat. The temperature was kept constant with a precision better than ±0.5°C.

The reagent grade deuterated hydroxylamine hydrochloride was furnished by VEB Berlin-Chemie Adlershof. The concentration of the both normal and deuterated hydroxylamine hydrochloride (about 10^{-1}M) was determined iodometrically.

The reagent grade triethanolamine was transformed into chlorhydrate salt and precipitated three times with ethyl alchool. The salt obtained was deuterated by solubilisation in heavy water and evaporation, therefore by the isotopic exchange method. This operation was repeated four times. In this way the hydrogen of the alcoholic groups was substituted with deuterium. A complete deuteration is not suitable, because in this case an additional mass effect is introduced, modifying the intrinsic effect, characteristic for the reaction center of the molecule.

The deuterated sodium hydroxide was obtained by the reaction between metallic sodium and heavy water.

The ferric sulphate was dried by heating and dissolved in normal or heavy water respectively.

EXPERIMENTAL RESULTS

In complex form with triethanolamine and in the presence of hydroxylamine, the ferric ion gives a kinetic polarographic current as it has been shown previously.[14,15] This current is higher in normal as compared with the same current in heavy water. The kinetic character of the current results in the oxidation by hydroxylamine of Fe(II) formed by cathodic reduction of Fe(III). Therefore this case represents a chemical reaction superimposed on an electron transfer reaction (catalysed process).

1. Effect of heavy water concentration on the kinetic current

The evidence of the isotope effect results in the decrease of the limiting current, when the concentration of the heavy water is increased. This behaviour is similar to the one found in acidic medium using titanium instead of ferric ions.[2]

Within the interval 0—7 mL in 10 mL solution, a linear relationship between the i_l/i_d ratio and deuterium content was found, as it is shown in Fig. 1 (i_l is the kinetic current and i_d the diffusion current of Fe(II) reduction to Fe(II)).

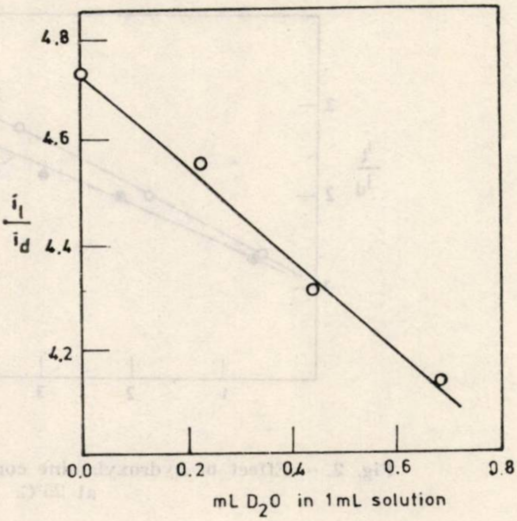

Fig. 1. — Ratio i_l/i_d as a function of deuterium content.

2. Effect of hydroxylamine concentration on the limiting currents in normal and heavy water

The oxidation of Fe(II) to Fe(III) by the both normal and deuterated forms of hydroxylamine is a bimolecular reaction, whose rate constant depends on both Fe(II) and hydroxylamine concentrations. This is why the variation of each component concentration produces a modification of the kinetic current, which is limited by the reaction rate constant. For the polarographic determination of the rate constant it is necessary to use an excess of one component in order to work in conditions of a pseudo-monomolecular reaction. For this case a quantitative treatment has been studied. [16]

The increase of the hydroxylamine concentration produces obviously an increase of the limiting currents. In Fig. 2 the values of the ratio i_l/i_d as a function of the hydroxylamine concentration for both normal and deuterated systems are shown. The current ratio increases with the increase of the hydroxylamine concentration, but for higher values the curves tend to a limiting value.

The general shape of the relationship variation is the same in both normal hydrogen and deuterated systems. However considerably lower values were found for i_l/i_d in deuterium containing media for the same hydroxylamine concentration. By using the values from Fig. 2 it is possible to determine the reaction rate constants of the oxidation reaction of Fe(II) to Fe(III) for both the studied systems.

3. Effect of temperature on the limiting currents

Since the kinetic currents are limited by the reaction rate, the variation of the temperature produces a much higher variation of the corresponding current values as compared with the diffusion currents.

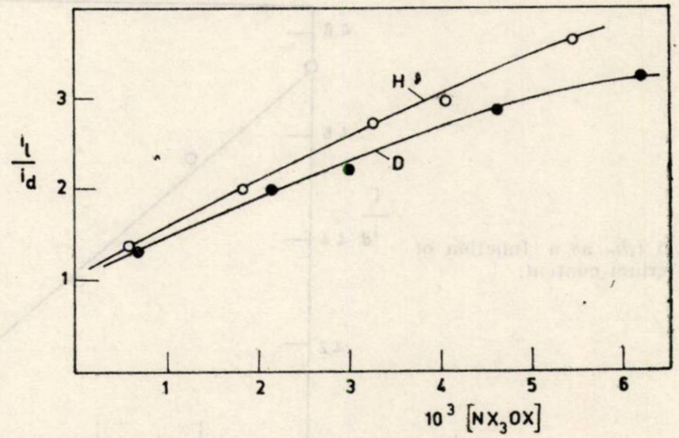

Fig. 2. — Effect of hydroxylamine concentration on the ratio i_l/i_d at 25°C.

The kinetic currents of the oxidation reaction of Fe(II) to Fe(III) increase considerably at higher temperatures both in the hydrogen and deuterium containing systems. This behaviour indicates high values for the activation energy of the reaction studied. In order to calculate the activation energy the logarithm of the rate constant as a function of the reciprocal value of the absolute temperature was plotted.

Using the Arrhenius equation:

$$\lg k = -0.43 \; E/RT + \text{const} \tag{1}$$

the following energies were calculated: (1) in hydrogen system $E_H = 14.2$ kcl mol^{-1} and (2) in deuterated medium $E_D = 15.5$ kcl mol^{-1}.

DISCUSSION

The present discussion concerns three aspects: (1) reaction mechanism, (2) rate constants and (3) isotope effects.

1. Reaction mechanism

As we have already shown the kinetic current is produced by the superimposition of the oxidation reaction of Fe(II) to Fe(III) by the hydroxylamine on the electron transfer reaction:

$$\text{Fe(III)} + e \rightarrow \text{Fe(II)} \tag{2}$$

For the chemical process several mechanisms can be proposed. If we consider the two forms of radicals generated during the reduction of hydroxylamine, then two reactions are possible (X is H or D):

(1) with formation of ammino-${}^{\bullet}NH_2$ radical:

$$Fe(II) + NX_2OX \rightarrow Fe(III) + {}^{\bullet}NX_2 + OX^- \quad (3$$

(2) with formation of ammoniumyl- ${}^{\bullet}NH_3^+$ radical:

$$Fe(II) + NX_2OX + X^+ \rightarrow Fe(III) + {}^{\bullet}NX_3^+ + OX^- \quad (4)$$

Since the Fe(III) complex with triethanolamine is formed in alkaline medium, reaction (3) appears to be the most probable, while reaction (4) applies in the case of Ti(III) oxidation[4] in acidic media.

The radical formed by hydroxylamine reduction can react *via* hydrogen atom abstraction from water:

$${}^{\bullet}NX_2 + X_2O \rightarrow NX_3 + {}^{\bullet}OX \quad (5)$$

and the ${}^{\bullet}OX$ radical oxidizes also the Fe(II) ion:

$$Fe(II) + {}^{\bullet}OX \rightarrow Fe(III) + OX^- \quad (6)$$

This mechanism was proved by continuous flow ESR studies using organic compounds substrates, such as alkenes and their derivatives.[4, 17–19]

The following reaction is however possible:

$$Fe(II) + {}^{\bullet}NX_2 + X_2O = Fe(III) + OX^- + NX_3 \quad (7)$$

proposed in older works.[14,15]

2. Rate constants

In a large excess of hydroxylamine the oxidation of Fe(II) to Fe(III) can be considered as a pseudo-monomolecular reaction. The overall oxidation reaction implies several stages, as it was shown in the previous section. For the determination of the rate constant the slowest reaction step must be considered. It is generally accepted[2, 14–16] that reaction (3) is the rate determining step and therefore the rate constant refers to this reaction.

In order to determine the rate constant the equation deduced by Koutecky for the pseudo-monomolecular conditions can be used.[20] This equation gives the relationship between the i_l/i_d ratio and a function, χ_1, defined by the relation:

$$\chi_1 = k_X[NX_3OX]t_1 \quad (8)$$

where X is H or D, k_X the rate constant of the Fe(II) to Fe(III) overall oxidation reaction, t_1 is the drop time and $[NX_3OX]$ the hydroxylamine concentration.

In this way the following rate constants were determined: (1) for hydrogen medium: $k_{H,\,25°C} = (2.05 \pm 0.25)\ 10^2$ L mol^{-1} s^{-1}; (2) for deuterated system: $k_{D,\,25°C} = (1.51 \pm 0.25)\ 10^2$ L mol^{-1} s^{-1}.

Using the average values for k_H and k_D determined experimentally (Fig. 2), the values of $\chi^{1/2}$ were calculated using the equation:

$$i_l/i_d = \Psi(\chi_1) \tag{9}$$

Plotting the i_l/i_d ratio as a function of $\chi_1^{1/2}$ for both normal and deuterium systems (Fig. 3) we can see that the asymptotic method can be applied in this case with a satisfactory precision.

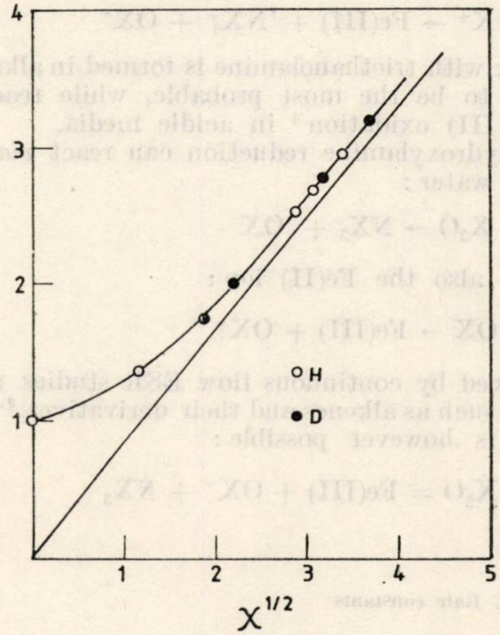

Fig. 3. — Variation of current ratio i_l/i_d as a function of $\chi_1^{1/2}$.

3. Isotope effects

From the literature data on the rate constant of Fe(II) to Fe(III) oxidation reaction in hydrogen containing media, only the corresponding values in normal water are available.[14, 15] If we compare these data with the value $k_{H, 25°C} = (2.05 \pm 0.25)\ 10^2$ L. mol^{-1} s^{-1} obtained in the present work we can see that this value is near to $k_{H, 25°C} = (1.98 \pm 0.08)\ 10^2$ L. mol^{-1} s^{-1} obtained by Koryta.[14] A different value was obtained in the case of the deuterium containing systems. This difference is produced by the isotope effect in the reactions, where different isotopic molecules participate, as can be seen in Fig. 2; here two different curves were obtained for hydrogen and deuterium by plotting the ratio i_l/i_d as a function of hydroxylamine concentration.

The kinetic isotope effect is defined by the ratio of the rate constants in the systems of different isotopes or isotopic molecules. In the present case the kinetic isotope effect is:

$$\frac{k_H}{k_D} = \frac{2.05 \times 10^2}{1.51 \times 10^2} = 1.36 \tag{10}$$

It should be of interest to know the origin of this isotope effect. In this respect the activation energies can be considered ; but as it results from the calculated data $E_H < E_D$ and therefore their ratio is less than unit :

$$\frac{E_H}{E_D} = \frac{14.2}{15.6} = 0.91 \tag{11}$$

The difference in activation energies cannot be the origin of the isotope effect of the oxidation reaction of Fe(II) to Fe(III).

Another source for the explanations of the influence of the isotopy results in considering the constant of the right part in equation (1), or in exponential form $k_X = A_X\, e^{-E_X/RT}$, the preexponential factor A_X. Since both reaction constant and activation energy in normal and deuterated systems are known, it is possible to calculate the isotope effect corresponding to the preexponential or frequency factor A_X :

$$\frac{A_H}{A_D} = \frac{k_H}{k_D} \times \frac{e^{-E_D/RT}}{e^{-E_H/RT}} = \frac{2.05 \times 10^2}{1.51 \times 10^2} \times \frac{e^{15.6/RT}}{e^{14.2/RT}} = 1.355 \tag{12}$$

The obtained value of 1.335 is practically the same as the ratio of the rate constants (10). Therefore the origin of the isotope effect of the oxidation reaction of Fe(II) by hydroxylamine consists in the difference of the collision frequency of the reactant particles in the normal and deuterated systems. The lower value of the rate constant of the reaction in which deuterated molecules are involved is due to the lower velocity of the hydroxylamine particles with four mass units in addition, as compared with the normal hydrogen containing molecules.

It has been possible in this way to know a peculiar aspect of the reaction mechanism by means of the isotopy as a tool for the study of the reaction involved in the present paper.

REFERENCES

[1] A. Călușaru, *Coll. Czech. Chem. Comm.*, **30**, 4061 (1965) ; A. Călușaru, I. Crișan and J. Kůta, *J. Electroanalyt. Chem.*, **46**, 51 (1973).

[2] A. Călușaru, *Isotopenpraxis*, **4**, 491 (1968).

[3] A. Călușaru, *Uspekhi Khim.* (Moscow), **58**, 221 (1979).

[4] B. C. Gilbert and P. R. Marriot, *J.C.S*, *Perkin II*, 987 (1977).

[5] C. Corvaja, H. Fischer and G. Giacometti, *Z. phys. Chem. (Frankfurt)*, **45**, 1 (1965) ; C. Corvaja, M. Brostolon, and G. Giacometti, *ibid.*, **66**, 279 (1969).

[6] J. Dewing, G. F. Longster, J. Myatt and P. F. Told, *Chem. Comm.*, **1965**, 391.

[7] D. J. Edge and R.O.C. Norman, *J. Chem. Soc.*, **B**, **1969**, 182.

[8] K. A. Blažek and J. Koryta, *Coll. Czech. Chem. Communs.*, **18**, 326 (1953).

[9] G. Farnia, D. Anselmi, and E. Vianello, *Ricerca sci.*, 1211 **1968** ; G. Farnia, R. Tomat and E. Vianello, *J.C.S. Perkin II*, **1975**, 763.

[10] R. Tomat and A. Rigo, *J. Electroanalyt. Chem.*, **35**, 21 (1972).

[11] J. S. Hyde and E. S. Freeman, *J. Phys. Chem.*, **65**, 1636 (1961).
[12] T. Cole, *J. Chem. Phys.*, **35**, 1169 (1961).
[13] J. P. Michaut and J. Roncin, *Nouveau journ. chim.*, **2**, 129 (1977).
[14] J. Koryta, *Coll. Czech. Chem. Comm.*, **19**, 666 (1954).
[15] O. Fischer, O. Dračka, and E. Fischerova, *Coll. Czech. Chem. Comm.*, **25**, 323 (1960).
[16] J. Heyrowsky and J. Kůta, "Principles of Polarography", Publishing House of the Czechoslovak Academy of Sciences, Prague, 1965.
[17] C. J. Albisetti, D. D. Coffman, F. W. Hoover, E. L. Jenner and W. E. Mochel, *JACS*, **81**, 1489 (1969).
[18] H. Claus, *Ber. Bunsengesellschaft Phys. Che.*, **78**, 702 (1974).
[19] M. Simic and E. Hayon, *JACS*, **93**, 5982 (1971).
[20] J. Koutecký, *Coll. Czech. Chem. Comm.*, **18**, 311 (1953).

Revue Roumaine de Chimie, **32**, *1*, 109–110 (1987)

BOOK REVIEWS

H. Engelhardt (Editor), "Practice of High Performance Liquid Chromatography. Applications, Equipment, and Quantitative Analysis", Springer Verlag, Berlin, 1986, 461 pp., hard cover, DM 198

The book contains 15 chapters written by 16 authors from the Federal Republic of Germany, three from USA, three from France, two from Holland, and one each from Sweden and Switzerland.

The qualities of the equipment influence markedly the analytical results; H. Colin, G. Guiochon and M. Martin review the HPLC equipment in the first and most substantial chapter of the book (65 pages), emphasizing recent trends such as the use of short (3–5 cm length) columns with fine (3–5 μm) particles, and data acquisition and processing for automated instruments requiring a short time for each analysis. The references are cited in an unusual way, by numbers starting from 1 in each section, but the discussion is detailed and objective, giving tabellar comparisons between pumps originating from various manufacturers, and reviewing all types of detectors.

J. Asshauer and H. Ullner review quantitative analysis in HPLC by starting from fundamentals and looking at the sources of errors. Intercomparisons show that the reproducibility between laboratories is half as good as within the same laboratory; standard errors of 2–3 % are normal, corresponding to reproducibilities R(95) of 5–9 %.

An important aspect, preparative HPLC, is discussed by A. Wehrli. Pumps and columns supplied by various manufacturers are described in table format. Strategies and trends (increase of pressure, repetitive operation over longer number of cycles) are reviewed.

Two brief chapters: 'Column Switching' by H. Hulpke and U. Werthmann, and 'Sample pretreatment and cleanup' by M. Uihlein describe on-line or off-line sample processing, respectively, for the analysis of complex mixtures, or for enriching trace components. Thus the bottleneck of long sample preparation times, especially for the determination of pharmaceuticals in biological materials, may be reduced.

J.C. Kraak and J. P. Crombeen review liquid-liquid chromatography, a method which has been neglected but which, thanks to high-pressure equipment and to the judicious selection of the liquid coating and the stationary porous support, can be used for delicate separations. An alternative technique, the use of ion pair HPLC, especially for bioactive molecules, has gained wide acceptance (chapter by B.A. Persson and B.L. Karger).

The following chapters review applications of HPLC in the separation of various types of compounds: inorganic (by H. J. Möckel) addictive, intoxicating or other compounds in forensic chemistry such as dyes or explosives allowing to trace the origin of illicit traders (by T. Daldrup, P. Michalke and S. Szathmary), lipids (by K. Aitzetmüller), nucleotide metabolites in physiological fluids (by A. P. Halfpenny and P. R. Brown), pharmaceutically important drugs, the most popular area, where HPLC has proved invaluable (a substantial chapter by G. Tittel and H. Wagner), psychotropic drugs in body fluids (by H.-J. Kuss), aminoacids and proteins (by H. Engelhardt who edits the book) and finally coal and oil products (by Th. Crispin and I. Halasz).

Although the history of HPLC is only 20 years old, this method is the most efficient one for separating non-volatile compounds. The importance of HPLC for pharmaceutical and toxicological analysis can hardly be overestimated; the most important physiologically active substances as well as the metabolites of proteins or polynucleotides can be separated by HPLC. For components lacking a chromophore such as lipids or non-aromatic aminoacids, the book indicates approaches for circumventing this drawback and for derivatization before or after separation, with a critical discussion of advantages and disadvantages of these methods.

The book will be a precious aid both for laboratories wishing to acquire new instrumentation (owing to the objective presentation of products supplied by various manufacturers) and to those wishing to keep abreast of new developments with the aid of authoritative up-to-date reviews by an international group of specialists.

Alexandru T. Balaban

Saraev V. V. and Schmidt F. C., "Electron Spin Resonance for Catalysts Based on Complex Combinations", (Russ.), Izd. Irkutskogo Univ., Irkutsk, 1985, 244 pages, 1.20 rbl.

The present work is a monograph concerning applications and recent development of electron spin resonance in the study of catalysis *via* complex combinations of transitional ions.

Catalysis is of crucial importance in chemical transformations, in living cells, as well as in its use for industrial processes, such as oxidation, hydrogenation, di- or oligomerization of olefins, etc.

The development of catalysis using complex combinations has stimulated the progress in modern physico-chemical methods, in order to obtain structural information at molecular level. In this field electron spin resonance has become a major tool, as intermediate paramagnetic species (including combinations of ions with incomplete *d* levels) may be investigated directly.

In turn, unusual valence states, or spherical configurations of intermediate combinations have facilitated theoretical advances in E.S.R. ; this progress is reviewed in the first part of the present work. Relationships between E.S.R. spectra and structural parameters of electronic configurations $3d^1 - 3d^9$ are discussed. A special stress is put on angular distortion, as the most important factor which has a marked influence on successive transformations from one geometry to another.

In the second part, there are presented E.S.R. experimental data concerning catalytic processes, *via* complex combinations. This very rich material has been divided according to the nature of transitional ions:

— titanium (Ti^{3+}, Zr^{3+}, Hf^{3+})
— vanadium (V^{4+}, V°, Nb^{4+}, Ta^{4+})
— chromium (Cr^{5+}, Cr^{4+}, Cr^{3+}, Cr^{1+}, Mo, W)
— manganese (Mn^{2+})
— iron (Fe^{3+}, Fe^{1+}, Fe^{1-})
— cobalt (Co^{4+}, Co^{2+}, Co°)
— nickel (Ni^{3+}, Ni^{1+}, Ni°)
— copper (Cu^{2+}, Au^{2+}, Ag^{2+}).

A critical inventory of these results allows pertinent conclusions on regularities noticed on structural features of complex compounds used as catalysts, on possibilities as well as limits inherent to E.S.R. method in solving homogeneous catalysis problems, and moreover, to show new research ways in the field of chemistry of complex compounds with transitional metals, having unusual oxidation states. Such abnormal valence states are the turning point in explaining sterical and structural properties, specific to complex compounds and finally their catalytic activity.

The main features revealed in E.S.R. spectra are correlated with the geometry of paramagnetic compounds the reciprocal position of ligands and the shape of wave function for the fundamental state of ions.

The last part is dedicated to the role of complex compounds containing Ti^{3+}, Co° and Ni^{1+} in hydrogenation and dimerization, stressing the nature of catalytic activity and the corresponding reaction mechanisms.

More than 500 references, up to date, are reviewed in a systematic way, increasing the monographic value of this work. Very useful are the numerous tables, containing data regarding E.S.R. spectra for systems with transitional ions.

This book, of a high scientific level, may be regarded as a must for research workers in the fields of organic catalysis and chemistry of complex compounds respectively.

Aurelia Meghea

NOTE POUR LES AUTEURS

La Revue Roumaine de Chimie publie des articles en anglais, français, russe, allemand ou espagnol. Les auteurs sont priés d'envoyer des articles et des comptes rendus inédits.

Les manuscrits seront dactylographiés à double interligne. La bibliographie, les tableaux et la légende des figures seront placés après le texte.

Si l'article fait partie d'une série numérotée, la partie précédente sera donnée comme première référence.

Chaque article sera précédé d'un résumé comprenant quinze lignes au maximum.

Les références bibliographiques dans le texte seront faites par des exposants sans parenthèses et paraîtront â la fin de l'ouvrage.

Les publications périodiques mentionnées dans la bibliographie seront présentées suivant les prescriptions internationales : le nom de l'auteur précédé de l'initiale du prénom, le titre du périodique abrégé conformément à « Chemical Abstract » et souligné par une ligne, le numéro du tome indiqué par des chiffres arabes et souligné par deux lignes, suivi de la première page de l'article : à la fin, l'année de la parution sera placée entre parenthèses. Le numéro de la revue ne sera pas indiqué si les pages du volume sont numérotées consécutivement.

Les textes des livres ou traités incluеront : le nom des auteurs, précédés de l'initiale du prénom, le titre du livre entre guillements et sans être souligné, le numéro du tome précédé par l'abréviation « vol. » (ou « Bd. »), le numéro de l'édition, les éditions (the publisher), la localité de la parution du livre, l'année de la parution et la page de la référence précédée(s) par l'abréviation « p » (ou « S »).

Les brevets seront indiqués comme suit : l'auteur ou la firme, le pays et le numéro du brevet, la date de la revue (*Chem. Abstr.*) Par.ex. : M. Jones (to Union Carbide Co.), Brit. Pat. 610 238, 2 Sept. 1959 ; cf. *Chem. Abstr.*, **54**, 12808 (1960).

Si la référence n'a pas été lue en original, on indiquera aussi la revue de références consultée.

Les diagrammes seront tracés à l'encre de Chine sur papier calque. Les tableaux et les figures (en nombre strictement nécessaire), ainsi que les courbes dans les figures seront numerotés par des chiffres arabes. Leur explication sera donnée dans la légende des figures. Prière de ne pas inscrire les mêmes données dans les tableaux et les figures. Chaque tableau aura un titre. On indiquera dans le texte la place approximative des tableaux et des figures. Les formules chimiques seront incluses dans le texte ; en outre, elles seront transcrites sur papier calque, à l'encre de Chine.

Les auteurs sont priés d'indiquer les caractéres italiques (en soulignant les lettres au crayon), ainsi que tout autre caractère spécial : les préfixes, *ortho*, *meta*, *para*, *cis*, *trans*, etc. seront soulignés pour indiquer leurs caractères italiques, et ne seront jamais écrits avec des majuscules.

Aucune correction à la main ne sera admise sur le manuscrit. Les correction seront frappées à la machine. Les lettres grecques ou d'autres symboles spéciaux seront insérés à la main à l'encre clairement.

Le manuscrit sera signé par l'auteur.

Le titre courant aura 50 lettres au maximum.

L'entière responsabilité du contenu des articles appartient aux auteurs.

Sur demande on peut obtenir une note plus complète.

PRINTED IN ROMANIA

NOTE POUR LES AUTEURS

La Revue Roumaine de Chimie publie des articles en anglais, français, russe, allemand ou espagnol. Les auteurs sont priés d'envoyer des articles et des comptes rendus inédits.

Les manuscrits seront dactylographiés à double interligne. La bibliographie, les tableaux et la légende des figures seront placés après le texte.

Si l'article fait partie d'une série numérotée, la partie précédente sera donnée comme première référence.

Chaque article sera précédé d'un résumé comprenant quinze lignes au maximum.

Les références bibliographiques dans le texte seront faites par des exposants sans parenthèses et paraîtront à la fin de l'ouvrage.

Les publications périodiques mentionnées dans la bibliographie seront présentées suivant les prescriptions internationales : le nom de l'auteur précédé de l'initiale du prénom, le titre du périodique, abrégé conformément à « Chemical Abstract » et souligné par une ligne, le numéro du tome indiqué par des chiffres arabes et souligné par deux lignes, suivi de la première page de l'article ; à la fin, l'année de la parution sera placée entre parenthèses. Le numéro de la revue ne sera pas indiqué si les pages du volume sont numérotées consécutivement.

Les textes des livres ou traités indiqueront : le nom des auteurs, précédés de l'initiale du prénom, le titre du livre entre guillemets et sans être souligné, le numéro du tome précédé par l'abréviation « vol. » (ou « Bd. »), le numéro de l'édition, les éditeurs (the publisher), la localité de la parution du livre, l'année de la parution et la page de la référence précédée(s) par l'abréviation « p » (ou « S »).

Les brevets seront indiqués comme suit : l'auteur ou la firme, le pays et le numéro du brevet, la date de la revue (*Chem. Abstr.*). Par ex. : M. Jones (to Union Carbide Co.), Brit. Pat. 610 238, 2 Sept. 1959 ; cf. *Chem. Abstr.*, 54, 12808 (1960).

Si la référence n'a pas été lue en original, on indiquera aussi la revue de références consultée.

Les diagrammes seront tracés à l'encre de Chine sur papier calque. Les tableaux et les figures (en nombre strictement nécessaire), ainsi que les courbes dans les figures seront numérotés par des chiffres arabes. Leur explication sera donnée dans la légende des figures. Prière de ne pas inscrire les mêmes données dans les tableaux et les figures. Chaque tableau aura un titre. On indiquera dans le texte la place approximative des tableaux et des figures. Les formules chimiques seront incluses dans le texte ; en outre, elles seront transcrites sur papier calque, à l'encre de Chine.

Les auteurs sont priés d'indiquer les caractères italiques (en soulignant les lettres au crayon), ainsi que tout autre caractère spécial : les préfixes, *orto*, *meta*, *para*, *cis*, *trans*, etc. seront soulignés pour indiquer leurs caractères italiques, et ne seront jamais écrits avec des majuscules.

Aucune correction à la main ne sera admise sur le manuscrit. Les correction seront frappées à la machine. Les lettres grecques ou d'autres symboles spéciaux seront insérés à la main à l'encre, clairement.

Le manuscrit sera signé par l'auteur.

Le titre courant aura 50 lettres au maximum.

L'entière responsabilité du contenu des articles appartient aux auteurs.

Sur demande on peut obtenir une note plus complète.

PRINTED IN ROMANIA

INDUSTRIAL CENTRAL FOR PLASTICS PROCESSING

BUCHAREST – ROMANIA

The Industrial Central for Plastics Processing coordinates the production, technical and development activity of 13 factories of plastics processing in Romania, among which the most important ones are those in Iași, Buzău, București, Orăștie and Focșani.

The enterprises, that have been set up and developed in the last two decades, have in their production activity the whole range of technologies and products from the domain of thermoplastics processing. Besides polymers processed by different, so-called classical technologies, namely: PVC, low and high density polyethylenes, polystyrene, ABS, high impact polystyrene a.s.o., during the last period the processing of engineering thermoplastics has been extended. Nowadays, a large variety of such materials – polyamides, polycarbonate, polyphenylene oxide etc. are used, simple, blended or reinforced. In addition, different types of polyurethanic foams are obtained – rigid, semiflexible and integral.

The main manufacturing share is given by the PVC and polyethylene products, among which the most important ones are: high density polyethylene sheets and unprinted sacks and bags.

AMONG THE PRODUCTS OFFERED:

— PVC granules for electrotechnical uses, shoes soles or other applications, manufactured on new types of high productivity equipments:

— PVC pipes and fittings obtained by extrusion;

— PVC carpets, plates and sheets of different colours, models and engravings obtained by calandering;

— containers and transportation boxes, bottles, barrels and cans obtained by injection or extrusion — blowing processes.

A very important field, especially for the national economy, is that of technical parts and devices meant to be used by the machine-building industry. These products are obtained from differently engineered plastic by injection moulding or from polyurethanes by different processes.

Plastics processing factories manufacture a large variety of products, mainly for internal consumption, but also for export.

The products that are exported are presented in catalogues and folders, accompanied by pictures and the necessary technical and commercial data.

We can offer, on your request, samples or the necessary quantities for tests, and also the technical assistance of our specialists, whenever demanded.

The products that are manufactured in our Central are marketed by:

DANUBIANA
FOREIGN TRADE COMPANY
BUCHAREST—ROMANIA
10, Republicii Blvd., P.O.B. 1—74
Telephone: 15 60 51, 15 60 52, Telex: 011184, 011697

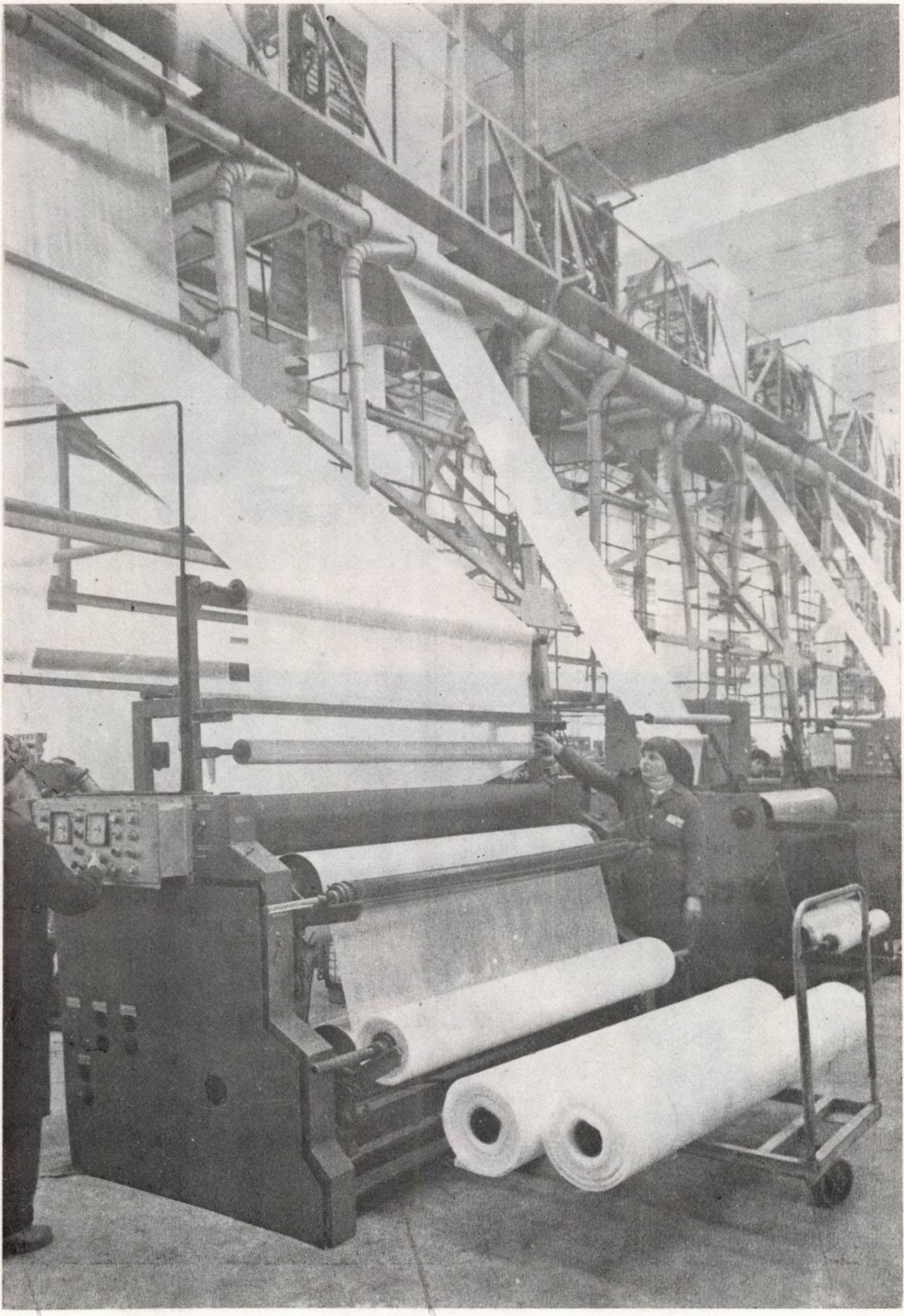

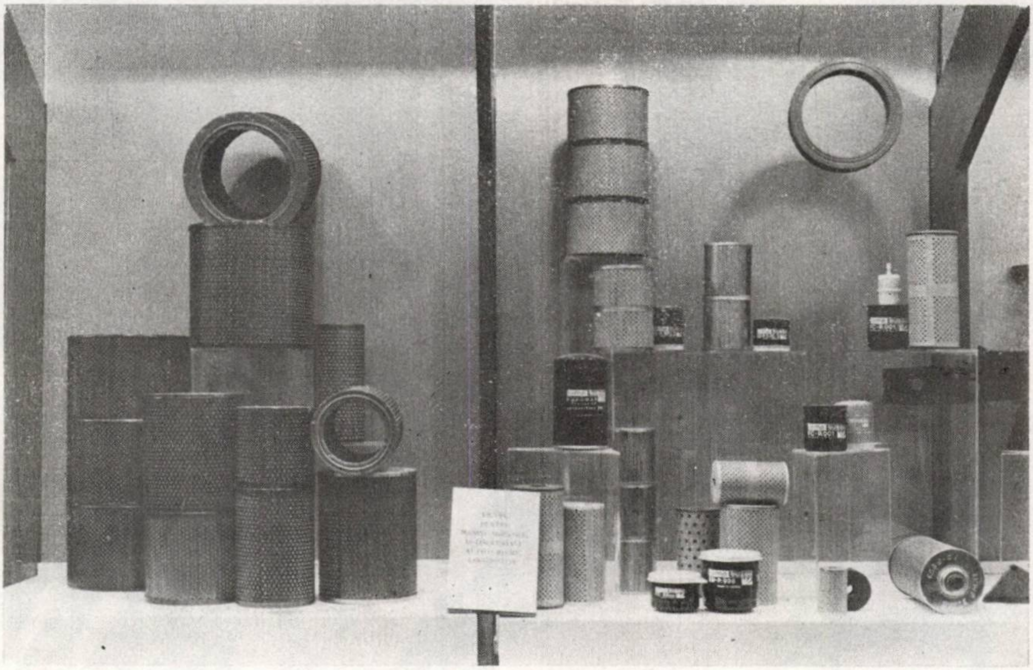

DE ANVELOPE

engineering
iprochim
ROMANIA

Si vous êtes intéressés à choisir une solution économique d'investissements dans l'industrie chimique, vous pouvez vous adresser en toute confiance à

IPROCHIM – ROMANIA

IPROCHIM — c'est une compagnie d'engineering, ayant un profil complexe. spécialisée en industrie chimique inorganique, industrie organique de base, industrie des engrais et industrie pétrochimique.

Pour toutes les usines chimiques et pétrochimiques existantes en Roumanie, IPROCHIM a élaboré indépendamment ou en collaboration avec des entreprises bien réputées, des études et toute la documentation de détail, donnant en même temps son avis pour la construction,le montage et la mise en fonction de toutes les installations de son profil.

Le potentiel technique dont IPROCHIM dispose, l'expérience accumulée pendant plus de 38 ans, l'étroite coopération avec les instituts de recherche, les centres universitaires et avec d'autres compagnies d'engineering du pays ainsi que la vaste coopération avec les autres compagnies étrangères, constituent la garantie de la qualité des services qu'IPROCHIM peut assurer, en assumant ses responsabilités pour :

- études de faisabilité, d'emplacement, de profil, d'optimisation et études technico-économiques ;
- cahiers de charges pour la réalisation des objectifs chimiques ;
- expertises techniques pour les installations en fonction visant leur modernisation ;
- documentation de licence et savoir-faire ;
- engineering de base (basic design) et projets d'exécution ;
- complexes pour les installations chimiques et pétrochimiques « à clef à main » ;
- organisation de la direction, du fonctionnement et de l'entretien des installations chimiques ;
- organisation des laboratoires de contrôle des procédés technologiques ;
- assistance technique à la construction, au montage et à la mise en marche des installations ;
- instruction du personnel d'opération et de contrôle dans les installations industrielles ;
- réalisation des maquettes de plan général et de montage des équipements, tuyauterie et contrôle ;
- calcul des installations et des équipements par des programmes propres.

Signe de notre capacité technique, sauf les plates-formes industrielles chimiques du pays, c'est l'élaboration des projets pour toute une série d'objectifs industriels importants réalisés à l'étranger, dont on mentionne les derniers :

- Installations de soude calcinée en Egypte et en Iran ;
- Installations d'engrais en Turquie, Syrie, Chine ;
- Installations d'acide sulfurique en Turquie, Egypte, Syrie ;
- Installations de Vitamine C en Corée Démocratique et au Mexique ;
- Installation d'aldéhyde phormique en URSS ;
- Installation de fibres de nitrile polyacrylique en Corée Démocratique ;
- Installation de bichromate de sodium en Turquie ;
- Installation d'aniline en URSS.

Les services sont offerts à l'exportation par l'intermédiaire des entreprises de commerce extérieur : ROMCONSULT, INDUSTRIALEXPORTIMPORT, UZINEXPORT et GEOMIN.

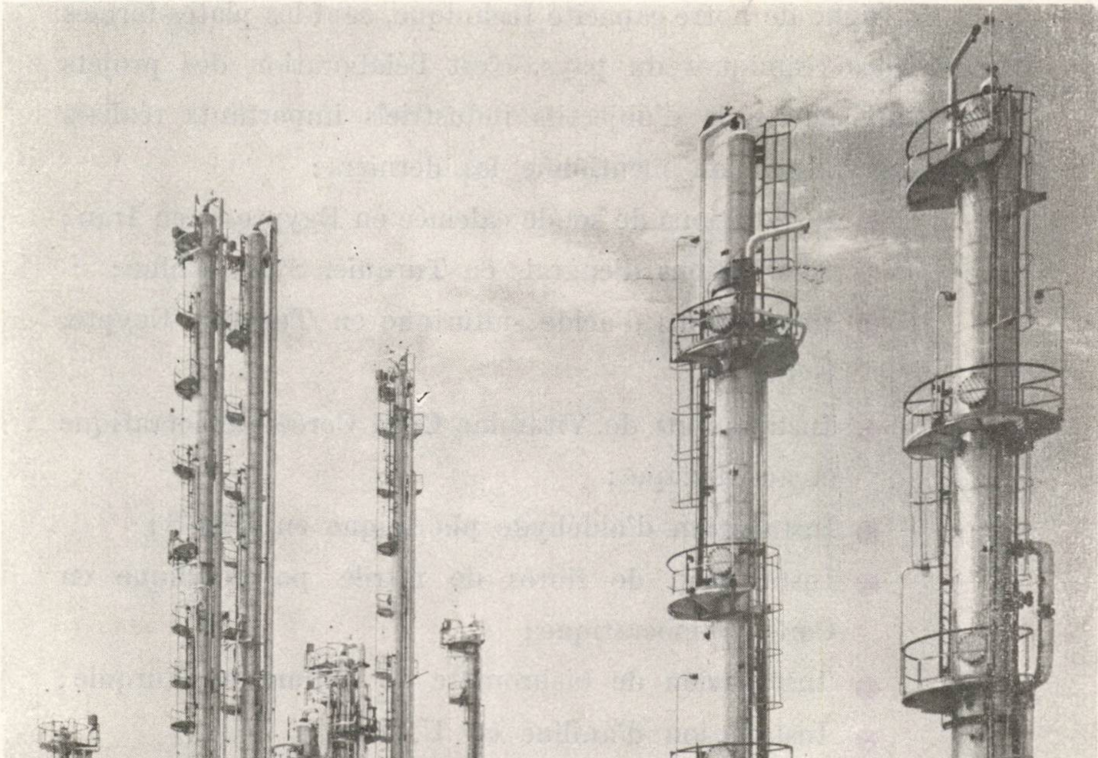

IPROCHIM
COMPAGNIE D'ENGINEERING POUR L'INDUSTRIE CHIMIQUE

Roumanie – Bucarest – 19–21 Rue Mihai Eminescu – Téléphone 49.64.48 ;
49.47.57, Telex 11907 Cab. TX. 735 IITPIC

TRAVAUX PARUS AUX ÉDITIONS DE L'ACADÉMIE DE LA RÉPUBLIQUE SOCIALISTE DE ROUMANIE

ELENA CEAUŞESCU, **Forschungen im Bereich der Chemie und Technologie der Polymere**, 1986, 444 p.

A. T. BALABAN et. al., **Labelled compounds and radio-pharmaceuticals applied in nuclear medicine**, coédition avec John Wiley and Sons 1986, 742 p.

I. G. MURGULESCU, O. M. RADOVICI, **Introducere în chimia fizică, vol. IV, Electrochimia**, 1986, 416 p.

D. PURDELA, **Nomenclatura chimiei anorganice**, 1986, 454 p.

V. DRĂGUŢAN, A. T. BALABAN, M. DIMONIE, **Olefin methathesis and ring-opening polymerization of cyclo-olefins**, coédition avec John Wiley and Sons, 1985, 544 p.

GH. MARCU, **Chimia compuşilor coordinativi**, 1984, 415 p.

E. CORDOŞ, C. MANOLIU, **Spectrometria de absorbţie şi fluorescenţă atomică**, 1984, 178 p.

C. BODEA (editeur), **Tratat de biochimie vegetală**, p. I, vol. 5, 1984, 438 p.

N. ASANDEI, A. GRIGORIU, **Chimia şi structura fibrelor**, 1983, 395 p.

N. IONESCU, M. CĂLDĂRARU, **Oxidarea catalitică a olefinelor inferioare**, 1983.

C. CAŞCAVAL, **Studiul polimerilor prin piroliză şi cromatografie de gaze**, 1983, 220 p.

C. I. SIMIONESCU, F. DANEŞ, **Originea vieţii**, 1983, 110 p.

C. BODEA (editeur), **Tratat de biochimie vegetală**, p. II, vol. IV, 1982, p. 408.

I. G. MURGULESCU, RODICA VÎLCU, **Introducere în chimia fizică, vol. III. Termodinamica chimică**, 1982, 624 p.

I. G. MURGULESCU, J. PĂUN, **Introducere în chimia fizică. Vol. I.3. Nucleul atomic, reacţii nucleare, particule elementare**, 1982, 606 p.

ELENA JERCAN, **Analiza cromatografică**, 1982, 286 p.

ELENA CEAUŞESCU, **Noi cercetări în domeniul compuşilor macromoleculari**, 1981, 536 p.

I. G. MURGULESCU, TATIANA ONCESCU, E. SEGAL, **Introducere în chimia fizică, Vol. II.2. Cinematică chimică şi cataliză**, 1981, 1024 p.

LYDIA-MARIA VAICUM, **Epurarea apelor uzate cu nămol activ. Bazele biochimice**, 1981, 218 p.

I. GĂLĂŢEANU, **Procese şi metode radiochimice în energetica nucleară**, 1981, 234 p.

O. IORDACHE, **Procese polistocastice aplicate la fenomenele de transfer**, 1981, 186 p.

CR. SIMIONESCU, VALERIA GORDUZA, **Polimeri biocompatibili şi biologic activi**, 1980, 479 p.

ELENA CEAUŞESCU, **Polimerizarea stereospecifică a izoprenului**, 1979, 307 p.

CONST. GH. MACAROVICI, **Analiza chimică cantitativă anorganică**, 1979, 457 p.

M. FLORESCU, **Metode ştiinţifice în dezvoltarea industriei chimice moderne**, 1979, 256 p.

I. G. MURGULESCU, E. SEGAL, **Introducere în chimia fizică. Vol. II. I. Teoria molecular-cinetică a materiei**, 1979, 1036 p.

S. STERNBERG, FL. DANEŞ, **Termodinamica chimică aplicată**, 1978, 400 p.

I. G. MURGULESCU, V. EM. SAHINI, **Introducere în chimia fizică. Vol. I.2. Structura şi proprietăţile moleculare**, 1978, 604 p.

I. ZUGRĂVESCU, MAGDA PETROVANU, **N-ylid chemistry**, coédition avec McGraw-Hill International Book Company, U.S.A., 1977, 396 p.

I. G. MURGULESCU, **Introducere în chimia fizică. Vol. I.1. Atomi, molecule, legătură chimică**, 1976, 560 p.

ELENA CEAUŞESCU, **Research work on synthesis and characterization of macromolecular compounds. Contributions**, 1974, 251 p.

CR. SIMIONESCU, VIORICA RUSAN, V. POPA, **Chimia algelor marine**, 1974, 212 p., 1 pl.

ISSN 0035—4090

I. P. INFORMAŢIA c. 2631

43 426

LEI 40

$ 80 (pour un abonnement annuel)

F1103 66

ACADÉMIE DE LA RÉPUBLIQUE SOCIALISTE DE ROUMANIE

REVUE ROUMAINE DE CHIMIE

TOME 32

N° 2

Février 1987

Rev. Roumaine Chim. RRCHAX, **32**, *2*, p. 111–226 (1987), Bucarest

EDITURA ACADEMIEI REPUBLICII SOCIALISTE ROMÂNIA

ACADÉMIE DE LA RÉPUBLIQUE SOCIALISTE DE ROUMANIE

COMITÉ DE RÉDACTION

Rédacteur en chef :

I. G. MURGULESCU, membre de l'Académie de la République Socialiste de Roumanie

Rédacteurs en chef adjoints :

A. T. BALABAN et V. EM. SAHINI, membres correspondants de l'Académie de la République Socialiste de Roumanie

Collège de rédaction :

EM. BRATU, ELENA CEAUȘESCU, ECATERINA CIORĂNESCU-NENITZESCU, CR. SIMIONESCU, membres de l'Académie de la République Socialiste de Roumanie ; P. SPACU, membre correspondant de l'Académie de la République Socialiste de Roumanie; M. BANCIU, M. D. GHEORGHIU, I. HAIDUC, D. I MARCHIDAN, G. NIAC et D. SĂNDULESCU.

La Revue Roumaine de Chimie paraît 10 fois par an. Toute commande de l'étranger sera adressée à ROMPRESFILATELIA — sectorul Export-Import Presă, P.O. Box 12—201, télex 10376, prsfir 78 104, 64—66, Calea Griviței, Bucarest, Roumanie

Les manuscrits, les livres et les revues proposés en échange, ainsi que toute correspondance seront envoyés à la rédaction

REVUE ROUMAINE DE CHIMIE

125, Calea Victoriei, 79717 Bucarest, Roumanie, téléphone 50 76 80

EDITURA ACADEMIEI REPUBLICII SOCIALISTE ROMÂNIA
125, Calea Victoriei, 79717 Bucarest, Roumanie, téléphone 50 76 80

REVUE ROUMAINE DE CHIMIE

Tome 32, N° 2 **Février 1987**

GH. SINGUREL, Study of the influence of the hydrogen bond on the electronic absorption bands of mandelic and 4-chloromandelic acids 113–120

S. STERNBERG, V. BRÂNZOI and LILIANA APĂTEANU, Effect of $CoSO_4$ additions on the $Pb/PbSO_4$ electrode 121–131

F. MATEI, GH. IONESCU, A. CECAL and A. DUCA, Study on Co^{2+} and Zn^{2+} behaviour in dialysis process 133–140

M. M. ABDEL BADEI and E. A. EL SAWI, Microdetermination of reducing sugars and ascorbic acid by indirect method using ferricyanide — thymolphthalin reagent 141–143

O. P. PANDEY, S. K. SENGUPTA and S. C. TRIPATHI, Synthesis, characterization, antifungal and antiviral activity of some transition metal complexes of cycloalkyl dithiocarbamates 145–150

F. CAPITÁN, P. ESPINOSA, F. MOLINA and L. F. CAPITÁN-VALLVEY, Study of the metallic complexes of Schiff bases derived from 2-thiophenecarboxyaldehyde, 2-pyridinecarboxyaldehyde and *ortho*-aminobenzenethiole (in Spanish) 151–154

ALEXANDRU T. BALABAN and EMIL STEPAN, Reactions of pyrylium salts with nucleophiles. XIX. Novel bispyridinium salts with potential biological activity 155–177

RODICA VLAD, F. BADEA and M. BANCIU, Kinetics of the acetolysis of 10,11-dihydro-10,5-propeno-5H-dibenzo[*a,d*]cyclohepten-11-yl bromide. Another example of double bond participation in ionisation 179–189

EMIL DUMITRIU, SPIRIDON OPREA and VASILE HULEA, Kinetic studies on the catalytic alkylation of toluene with methanol 191–197

N. DOCA and E. SEGAL, Dehydrogenation kinetics of low aliphatic alcohols on copper catalysts. III. Metallic copper with Fe and Ni as addition elements 199–202

N. P. CID and L. O. GARCÍA VIOR, Oxidation of mordant blue 9 with bromate catalyzed by vanadium(V). Part II. Kinetics and mechanism 203–213

B. C. JOSHI, YOGESH C. JOSHI, D. KISHORE and S. S. SHRIMALI, Proton catalysed rearrangement of N-alkyl arene sulphonanilides to *ortho*-alkylamino sulphones. Part III 215–221

C. I. CHIRIAC, Dimethyldichlorosilane as reagent for the synthesis of 1,3,4-oxadiazoles from diaroylhydrazines 223–226

Rev. Roumaine Chim. 32, *2*, 111–226 (1987), Bucarest

Revue Roumaine de Chimie, **32**, *2*, 113–120 (1987)

STUDY OF THE INFLUENCE OF THE HYDROGEN BOND ON THE ELECTRONIC ABSORPTION BANDS OF MANDELIC AND 4-CHLOROMANDELIC ACIDS

GH. SINGUREL
"Al.I. Cuza" University, Spectroscopy Laboratory, Iași, Calea 23 August 11, Romania

Received February 3, 1986

The results of the study of the hydrogen bond influence on the electronic absorption spectra of mandelic and 4-chloromandelic acids are presented. The study was performed both in ternary mixtures and neutral or proton acceptor or donor solvents.

INTRODUCTION

The IR spectral study of the mandelic acid and its derivatives in the valency oscillation region of the C=O and OH bands[1] showed the highly probable existence of an intermolecular hydrogen bond between hydroxyl group and the oxygen atom of the *cis*-carboxyl structure in respect of the C–O bond. The concentration and temperature dependence of the C=O band extinction of the solution of mandelic acid (**M**) and 4-chloromandelic acid (**4–Cl M**) in CCl_4^2 has shown that even at relatively low concentrations dimer formations, occurring by means of the carboxyl group, are present. At the same time the study in ternary mixtures emphasized the fact that on addition of a proton acceptor or a donor compound the breaking-up of the hydrogen intermolecular bond of the dimer and the formation of a new complex between the acid molecule and that of the added compound are possible.

The results of the study of the influence of the intermolecular interactions between the **M**-acid molecules and the **4–Cl M**-acid molecules respectively, as well as between the molecules of these acids and those of the proton acceptor and donor compounds on the electronic absorption spectrum are given.

EXPERIMENTAL

The electronic absorption spectra were recorded in *non-polar* and *polar solvents* (Tables 1 and 2), which are transparent within the spectral range 50000–30000 cm^{-1}, with a SPECORD UV–VIS C. Zeiss-Jena spectrometer. An absorbent layer (l) 1 mm and 10 mm thick was used.

The **M**-acid is very sparingly soluble in *non*-polar solvents, which renders the recording of the spectrum impossible, while for the **4–Cl M**-acid, which is more soluble, we could record the electronic absorption spectrum. Both the acids are very soluble in polar solvents, the concentration used being 10^{-3} mol/L.

The changes in the electronic absorption spectrum were also studied in ternary solutions made of the saturated solutions of the acid in *n*-hexane to which proton donor or acceptor compounds were added in known concentration.

The spectrum was also recorded by means of a differential method in order to establish some details of the interactions which occur in the ternary mixtures.

With the aim of recording the electronic absorption spectrum of the solid compounds, these were deposited in thin layers by evaporation on a quartz plate. The layers were then dissolved in ethanol and the spectrum of the solution was recorded to check up the alterations of the compound structure produced by evaporation.

RESULTS AND DISCUSSION

The mandelic acid. The electronic absorption spectrum recorded in *polar solvents* shows absorption ranges whose wavenumbers and extinction coefficients are given in Table 1. There is a high intensity absorption range ($\varepsilon \sim 10^4$L/mol × cm) corresponding to 50500 cm^{-1}. In the range of lower frequencies, at about 48600 cm^{-1}, a marked shoulder appears, and at 46000 cm^{-1} a very small one. Within the 40500—37000 cm^{-1} range, the **M**-acid displays an absorption band of low intensity ($\varepsilon \sim 200$ L/mol × × cm) with a marked vibrational structure, reminding of the benzene ^1L_b band. The spectrum recorded in solid state displays a very intense absorption for wavenumbers exceeding 50000 cm^{-1} and medium intensity absorption band at 45000 cm^{-1} which can be assigned to the M-acid associated molecules.

Table 1

The wavenumber (ν, cm^{-1}) and the molar absorption coefficient (ε, L/mol × cm) of the electronic absorption bands of the **M**-acid in various solvents

1. Methanol	υ	50800	48500	46000	40560	39640	38720	37800	37300
	a	132	92	47	sh	1.7	2.1	1.6	sh
2. Ethanol	ν	50640	48500	46000	40560	39640	38720	37800	37320
	a	129	103	54	sh	1.8	2.1	1.7	sh
3. Propanol	ν	50320	48500	46000	40560	39640	38720	37800	37320
	a	128	118	50	sh	1.8	2.2	1.7	sh
4. Ethylene glycol	ν	50450	48500	45800	—	39600	38680	37750	37320
	a	150	sh	54		2.1	2.2	1.7	sh
5. Diethyl ether	ν	49700	48720	46000	40500	39560	38640	37720	37320
	a	148	143	72	sh	3.0	3.2	2.5	sh
6. *Di-n*-buthyl ether	ν	49800	48640	45800	40500	39560	38680	37760	37320
	a	92	89	45	sh	1.6	2.1	1.5	sh

sh — shoulder, a = $\varepsilon \times 10^{-2}$

The 4-chloromandelic acid. In *non-polar solvents*, in saturated solutions ($C \sim 10^4$ mol/L), the spectrum displays an intense absorption at 50500 cm^{-1} and a second large absorption band with two maxima at 43560 cm^{-1} and 41000 cm^{-1}.

As it was also proved,[3-5] the experimental results allow the assignment of the absorption band with the maximum at 41000 cm^{-1} to the monomeric form of the acid and the band with the maximum at 43500 cm^{-1} to the molecules associated by hydrogen bond between the carboxyl groups. The shape of this absorption range is similar in all the *non*-polar solvents used, but the ratio between the extinctions of two maxima depends on the *non*-polar solvent employed. The form of this absorption range in *n*-pentane (a) and *n*-hexane (b) is given in Fig. 1 for various acid concentrations. Within the concentration range that we used no concentration

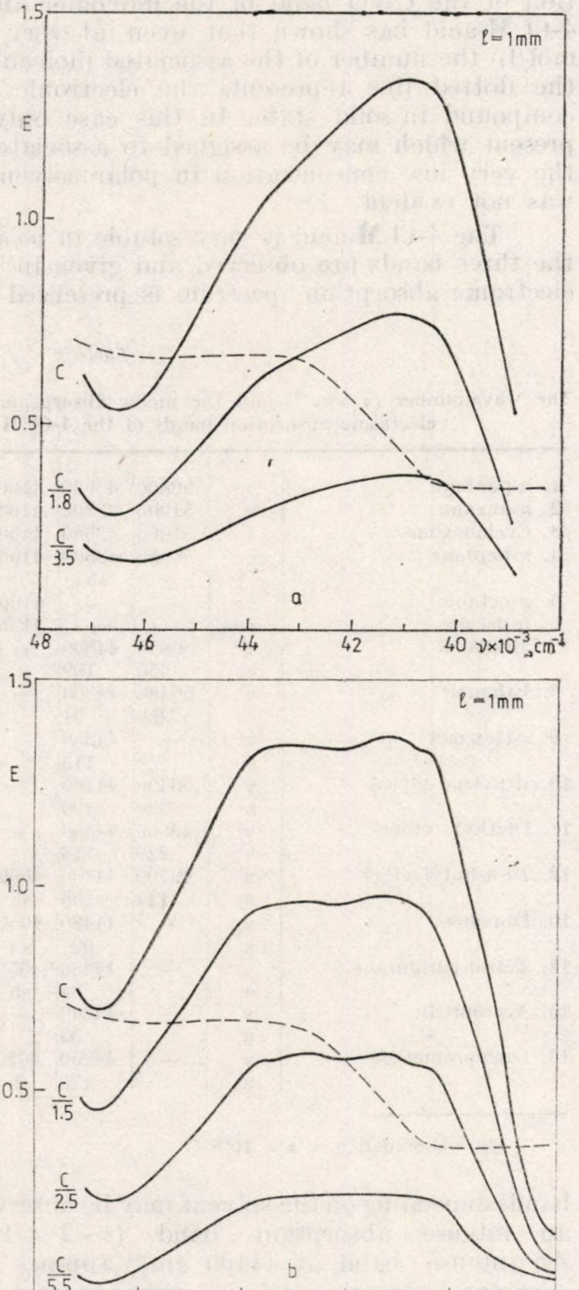

Fig. 1. — The electronic absorption band shape of the **4-Cl M**-acid monomer and dimer in *n*-pentane (a) and *n*-hexane (b), respectively. The dotted line represents the **4-Cl M**-acid absorption in solid state.

dependence was observed of the ratio between the extinctions of the two maxima. This shows that the intensity of the hydrogen bond of the formed dimer is high enough. The concentration dependence of the extinction of the C=O band of the monomer and the associated form of the **4-Cl M**-acid has shown that even at very low concentrations ($C \sim 10^{-5}$ mol/L) the number of the associated molecules is high enough. [2] In Fig.1 the dotted line represents the electronic absorption spectrum of this compound in solid state. In this case only the band of 43500 cm^{-1} is present which may be assigned to associated acid molecules. Because of the very low concentration in polar solvents the third absorption band was not evident.

The **4-Cl M**-acid is very soluble in *polar solvents* and in its spectrum the three bands are observed and given in Table 2. The structure of the electronic absorption spectrum is preserved but a shift of the absorption bands depending on the solvent may be observed. In the range of 50500 cm^{-1} an intense absorption band ($\varepsilon \sim 2 \times 10^4$ L/mol × cm) is noticed. An intense band at 44400 cm^{-1} appears in all polar proton donor or acceptor solvents, and in some cases a weak shoulder is evident at 40500 cm^{-1}. The band from 44400 cm^{-1}, hifted toward higher frequencies

Table 2

The wavenumber (ν, cm^{-1}) and the molar absorption coefficient (ε, L/mol × cm) of the electronic absorption bands of the **4-Cl M**-acid in various solvents

1. *n*-pentane	ν	50800	43640	41000					
2. *n*-hexane	ν	51000	43800	41000					
3. Cyclohexane	ν	51000	43680	41000					
4. *n*-heptane	ν	50000	43500	41000					
			sh						
5. *n*-octane	ν	—	—	41000					
6. *n*-decane	ν	—	—	41250					
7. Methanol	ν	50650	44600	—	38720	37560	36880	36320	35400
	a	350	109		3.7	3.4	2.5	2.2	sh
8. Ethanol	ν	50480	44500	—	38480	37480	36880	36250	35400
	a	256	91		2.9	2.7	2.0	1.7	sh
9. *s*-Hexanol	ν	—	44250	—	—	—	—	—	—
	a		113						
10. Ethylene glycol	ν	50400	44160	—	38720	37560	36800	36320	35240
	a	330	100		3.9	3.4	sh	2.2	sh
11. Diethyl ether	ν	49900	44400	—	38400	37350	36760	36250	35400
	a	220	118		2.6	2.9	sh	2.1	sh
12. *Di-n*-butyl ether	ν	49700	44400	40600	38480	37400	36850	36300	35560
	a	144	106	sh	2.9	3.0	sh	2.1	sh
13. Dioxane	ν	—	44480	40500	38480	37480	36850	36300	35560
	a		92	sh	2.4	2.6	sh	1.7	sh
14. Tetrahydrofurane	ν	—	44480	40500	—	—	—	—	—
	a		94	sh					
15. Acetonitrile	ν	—	44640	—	—	—	—	—	—
	a		92						
16. Dichlorometane	ν	—	44250	40500	38480	37480	36800	36300	35400
	a		170	sh	sh	3.5	sh	2.3	sh

sh = shoulder, a = $\varepsilon \times 10^{-2}$

as noticed in literature, [4] can be assigned to the complex occurred from **4-Cl M**-acid molecules and the proton acceptor or donor compound. In the range 38500—35500 cm^{-1} a weak absorption band appears ($\varepsilon \sim 300$ L/mol × cm) showing a vibrational structure similar to that observed in the **M**-acid.

*The interactions of the **4-Cl M**-acid molecules with proton acceptor or donor compounds.* The study of these interactions was performed in a ternary solution consisting of saturated acid solution ($C \sim 10^{-1}$ mol/L) to which well known quantities of proton acceptor or donor compounds were added. The concentration of the added compound varied between $0.5 \times \times 10^{-3}$ and 3×10^{-2} mol/L. An increase of the extinction of the 43500 cm^{-1} absorption band was found with increasing the concentration while the extinction of the band 41000 cm^{-1} decreases. The absorption range of these bands shown in Figs. 2, 3, 4 and 5(a) is recorded at various concentrations of tetrahydrofurane, dioxane, *di-n*-butylether and ethanol added to the saturated solution of the **4-Cl M**-acid in *n*-hexane, whose absorption is given by the first curve. The curves obtained at various concentrations of the added compounds intersect in the same spectral range and the extinction increases in a large absorption range between 42000—48000 cm^{-1}.

In Figs. 2, 3, 4 and 5(b) the same absorption range is shown recorded by differential method. Curve (1) represents the equilibrium line recorded when identical cells with saturated solutions of **4-Cl M**-acid in *n*-hexane were introduced in both the spectrometer beams. If one of the cells contains a ternary mixture consisting of the saturated solution in which one of the above mentioned compounds were added, then an unbalance of the beams appears determined by the interactions in the ternary mixture. Increasing the added compound concentration determines both the extinction increase in the range 42000—48000 cm^{-1} and its decrease in the range of 38000—42000 cm^{-1}. Within this range the absorption can be assigned to the complex generated by means of the hydrogen bond between a proton donor or acceptor molecule and the OH or C=O bond of the carboxyl group of the **4-Cl M**-acid. [2]

Using this method, the wavenumbers corresponding to the absorption band maximum of the monomeric form as well as some details of the shape of this band may be specified. One can notice in Figs 2, 3, 4 and 5 (b) that the monomer band shape with the proton acceptor compounds differs from that of the proton donor compounds and for the latter the intersection point is situated outside the equilibrium curve. The wavenumber of the intersection point of the curves recorded for various concentrations by the differential method coincides with the previous value.

The IR spectral study of the ternary mixture in the oscillation range of C=O of the **4-Cl M**-acid [2] has pointed out the competition between the process of dimer generation and the process of the complex generation, the latter prevailing, i.e. the complex bond energy exceeds the dimer bond energy. Accordingly, the wavenumbers of the maximum of the electronic absorption band of the formed complex will be higher than that of the dimer which may explain the shape of this absorption range as

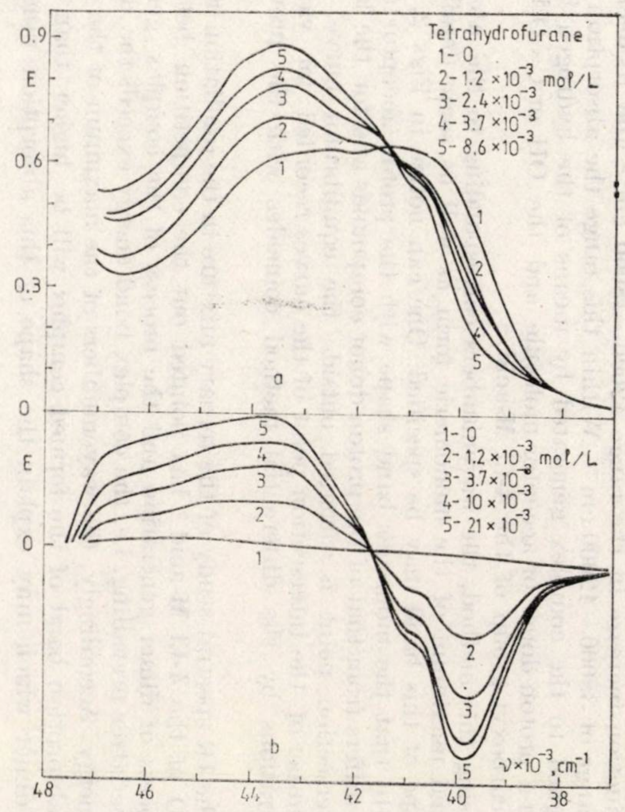

Fig. 2. — a) The electronic absorption band shape of the complex of the **4-Cl M**-acid and tetrahydrofurane at various concentrations in ternary mixture; b) the same band recorded by means of the differential method.

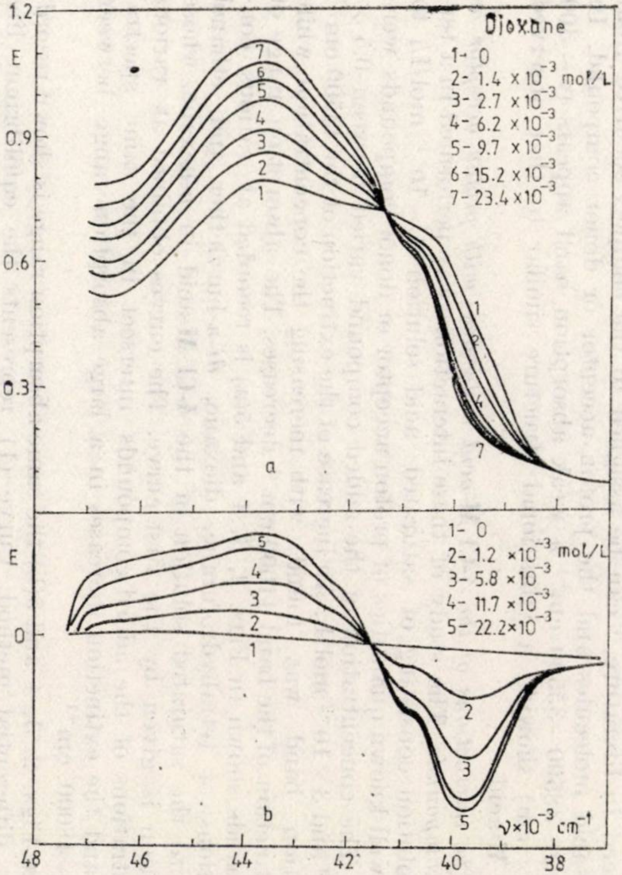

Fig. 3. — a) The electronic absorption band shape of the complex of the 4-Cl M-acid and dioxane at various concentrations in ternary mixture; b) the same band recorded by means of the differential method.

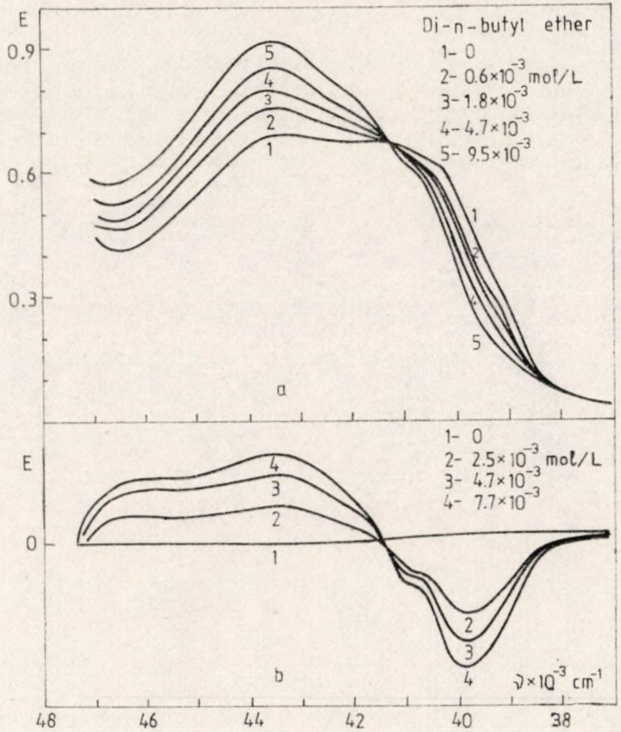

Fig. 4. — a) The electronic absorption band shape of the complex of the **4-Cl M**-acid and *di-n*-butyl ether at various concentrations in ternary mixture; b) the same band recorded by means of the differential method.

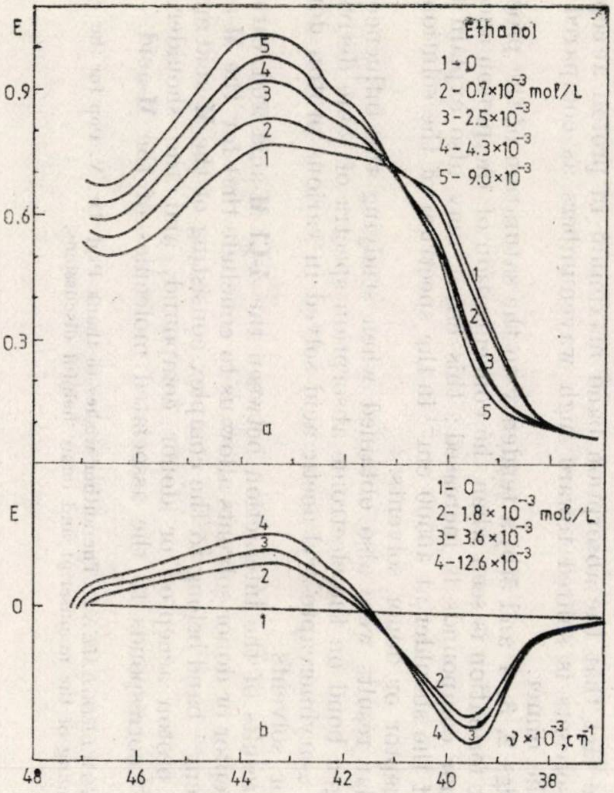

Fig. 5. — a) The electronic absorption band shape of the complex of the **4-Cl M**-acid and ethanol at various concentrations in ternary mixture; b) the same band recorded by means of the differential me thod.

well as the fact that the absorption band maximum in proton acceptor or donor solvents is shifted toward high wavenumbers as compared to those of the dimer.

In Figs 2, 3, 4 and 5(b) a tendency to the saturation of the process of complex formation is seen when the concentration of the proton acceptor or donor compounds is increased; this effect may also explain the presence of the shoulder at 40500 cm^{-1} in the spectrum of the solution in proton acceptor or donor solvents.

Similar results were also obtained when studying the influence of the hydrogen bond on the electronic absorption spectra of some derivatives of the α-arylmercapto-aryl acetic acid solved in various proton donor or acceptor solvents.

The results of the interaction between the **4-Cl M**-acid and various proton acceptor or donor solvents allow us to conclude that for the **M**-acid the 48500 cm^{-1} band belong to the complex consisting of the **M**-acid molecules and proton acceptor or donor compound, and the shoulder at 46000 cm^{-1} corresponds to the associated molecules of the **M**-acid.

ACKNOWLEDGEMENT. The author wishes to thank Prof. Dr. V. Pop for the critical reading of the manuscript and many helpful discussions.

REFERENCES

[1] N. Mori, Y. Asano, T. Irie and Y. Tsuzuki, *Bull. Chem. Soc. Japan*, **42**, 482 (1969).

[2] Gh. Singurel, *Rev. Roumaine Chim.*, **25**, 1469 (1979).

[3] W. F. Forbes and A. R. Knight, *Canad. J. Chem.*, **37**, 334 (1959).

[4] M. Ito, *J. Mol. Spectroscopy*, **4**, 125 (1960).

[5] M. Ito, *J. Mol. Spectroscopy*, **4**, 144 (1960).

Revue Roumaine de Chimie, **32**, *2*, 121 – 131 (1987)

EFFECT OF $CoSO_4$ ADDITIONS ON THE $Pb/PbSO_4$ ELECTRODE

S. STERNBERG*, V. BRÂNZOI* and LILIANA APĂTEANU**

* Polytechnic Institute of Bucharest, Dept. of Applied Physical Chemistry and Electrochemical Technology, Splaiul Independenţei 313, 76206 Bucharest, Romania

** Biochemical and Chemical Energetics Institute of Bucharest, Bucharest, Romania

Received November 4, 1985

The influence of $CoSO_4$ additions on the polarization behaviour of $Pb/PbSO_4$ electrode in H_2SO_4 ($d = 1.24$ g/cm^3) solution was studied by means of the potentiodynamic method. The lead microelectrode cycling was carried out within ($-1170 \div -870$) mV potential range. The $CoSO_4$ concentration in the electrolyte was changed from 3.5 ppm to 3 000 ppm. The following parameters were evaluated: the peak current intensity (I_p), the peak potential (E_p), the microelectrode behaviour during repeated cyclings characterized by the life time index η_{cycl}, the electricity amounts involved in the anodic (Q_a) and cathodic (Q_c) process, the Q_c/Q_a ratio, as well as the average anodic ($\bar{I}_a$) and cathodic ($\bar{I}_c$) currents. An optimum of η_{cycl} was found, at a $CoSO_4$ concentration of 125 ppm. In these conditions η_{cycl} is of about 2 times higher and Q_a and Q_c are of 4 to 9 times higher than in the H_2SO_4 solution, free of $CoSO_4$. This effect of the Co^{2+} ions addition in the electrolyte could be explained by the increase of the electrode active mass, determined by the cyclic process of deposition — dissolution of cobalt in the potential range under study.

INTRODUCTION

Previous papers [1-25] deal with the systematic study of the electrode processes occurring in the $Pb/PbSO_4$ (negative electrode) and $PbO_2/PbSO_4$ (positive electrode) systems, as well as of the influence of some additives (H_3PO_4, $CoSO_4$, Na_2SO_4, expanders etc.) in electrolyte on the functioning of the two electrodes from the lead acid batteries.

The present paper aims at elucidating the influence of $CoSO_4$ additions (in electrolyte) on the functioning of the negative electrode from the lead — acid batteries. On the basis of the experimental results, a mechanism of the Co^{2+} ion action on the electrode reactions in the $Pb/PbSO_4/H_2SO_4$ system was proposed, and the life time index (η_{cycl}) was evaluated, as a criterium of the negative microelectrode behaviour during the successive cyclings.

EXPERIMENTAL PART

Experiments were carried out by potentiodynamic method, using the microelectrode technique. The working electrode was a pure lead wire of 1.5 cm length and of 1.5 mm diameter. A platinum net was used as counterelectrode. All the potentials were measured vs. the

Hg/Hg_2SO_4/4 M H_2SO_4 reference electrode. The cell for the electrochemical polarizations, the scheme of the electric device, the working technique and the way of the microelectrode surface pretreatment were described in previous papers. [1–7] The potential of the working electrode was scanned within the (−1170 ÷ −870) mV range, with a scan rate of 150 mV/min, by means of a Model 173 Princeton Applied Potentiostat—Galvanostat — coupled with a low frequency pulses generator, type Orion EMG 1117/2. The potential-current characteristics were registered by means of an x—y recorder. The electricity amounts of the anodic (Q_a) and cathodic (Q_c) processes were simultaneously registered, by means of the Model 179 — Digital Coulometer of the potentiostat. The electrolytes were "pure" sulphuric acid solutions of 1.24 g/cm³ density and H_2SO_4 solutions ($d = 1.24$ g/cm³) containing $CoSO_4$ in concentration varying from 3.5 ppm up to 3000 ppm. A number of 40 cycles was realized for each determination, in order to obtain a porous microelectrode, with an active and reproducible surface.

RESULTS AND DISCUSSION

Figure 1 shows the potentiograms obtained on pure lead, in a sulphuric acid ($d = 1.24$ g/cm³) solution, at the potential scannig with a scan rate of 150 mV/min, from — 1170 mV up to —870 mV and back to — 1170 mV. The numbers on the figure represent the number of the cycle for which the potentiogram was registered. The overall electrode reaction, which occurs during a cycle, is the following:

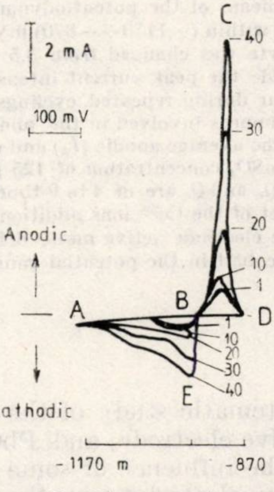

Fig. 1. — Potentiograms of pure lead microelectrode, obtained in a H_2SO_4 (d= =1.24 g/cm³) solution, as a function of the number of cycles; v=150 mV/min.

$$Pb + H_2SO_4 \rightleftarrows PbSO_4 + 2H^+ + 2e^- \quad (1)$$

At the increasing anodic potential scan, from −1170 mV up to — 870 mV, the lead dissolutions as Pb^{2+} ions occur, as well as the formation of an insoluble layer of $PbSO_4$ on the electrode surface, which passivates at the end. On the ascendent side (BC) of the curve the anodic process is controlled by the charge transfer, because the initial surface is free and clean. At the reverse potential scan, from −870 mV to −1170 mV, the electrode reduction of Pb^{2+} ions on the electrode surface occurs. This process (EA) is controlled by the diffusion of the Pb^{2+} ions through the $PbSO_4$ layer on the electrode surface. It is remarkable the asymmetry of the voltammograms : the anodic branch presents a sharp maximum (the peak C) which is much higher than the cathodic one (the peak E), that is $I_{p,c} \ll I_{p,a}$ because the solubility of $PbSO_4$ is very small, as well as the concentration of the Pb^{2+} ions.

The cobalt sulphate addition in electrolyte, independent of its concentration, does not sensibly change the shape of the curves, but changes the height of the anodic (C) and cathodic (E) peaks. Figure 2 shows the potentiograms obtained on pure lead (for the 40th cycle) in H_2SO_4 ($d = 1.24$ g/cm^3) solution containing $CoSO_4$ in concentrations which were changed from 3.5 ppm to 3 000 ppm, comparatively with the cyclovoltammogram obtained on pure lead in the H_2SO_4 ($d = 1.24$ g/cm^3) solution without addition of $CoSO_4$. Tables 1 and 2 show the values of the peak currents for the anodic and cathodic process, as a function of the $CoSO_4$ concentration and of the number of cycles.

Analysis of figure 2 and tables 1 and 2 shows that $CoSO_4$ addition leads to the increase of the anodic and cathodic peaks height, hence to the intensification of both anodic and cathodic processes. It is possible that Co^{2+} ions from the solution participate in a negligible extent in the anodic and cathodic currents, because their concentration is very low, but they probably activate the electrode surface by means of the change of its structure. Analysis of the normal electrode potentials, of the Pb/$PbSO_4$ and Co/Co^{2+} couples, vs. our Hg/Hg_2SO_4/H_2SO_4 reference electrode

Table 1

The peak current (I_p) variation as a function of the number of cycles and of the $CoSO_4$ concentration, for the anodic branch, at a potential scan rate of 150 mV/min

$I_{P(mA)}$	$CoSO_4$ concentration (mg/L)											
Number of cycles	0	3.5	7	12.5	25	50	125	250	500	1000	2000	3000
5	0.5	0.6	2.0	2.1	2.2	2.8	2.2	1.3	0.8	1.1	1.5	1.0
10	1.1	1.8	3.4	3.8	3.95	5.0	3.9	2.8	1.7	2.4	3.4	2.0
15	1.6	2.0	5.8	6.3	6.7	7.8	6.95	4.4	2.7	4.0	5.4	2.8
20	2.0	2.6	8.6	9.4	10.5	10.86	11.5	6.8	4.3	6.9	8.8	4.2
25	2.6	3.6	11.2	13.7	14.4	14.52	15.2	9.8	6.8	9.3	9.2	6.7
30	4.0	4.8	13.4	15.4	16.2	16.58	16.8	12.6	9.8	11.2	10.7	9.2
35	6.1	7.8	15.4	15.8	16.8	17.1	17.7	15.3	13.0	12.6	12.4	12.2
40	8.4	10.4	16.2	17.2	17.65	18.0	19.6	17.5	15.8	14.1	14.6	14.6

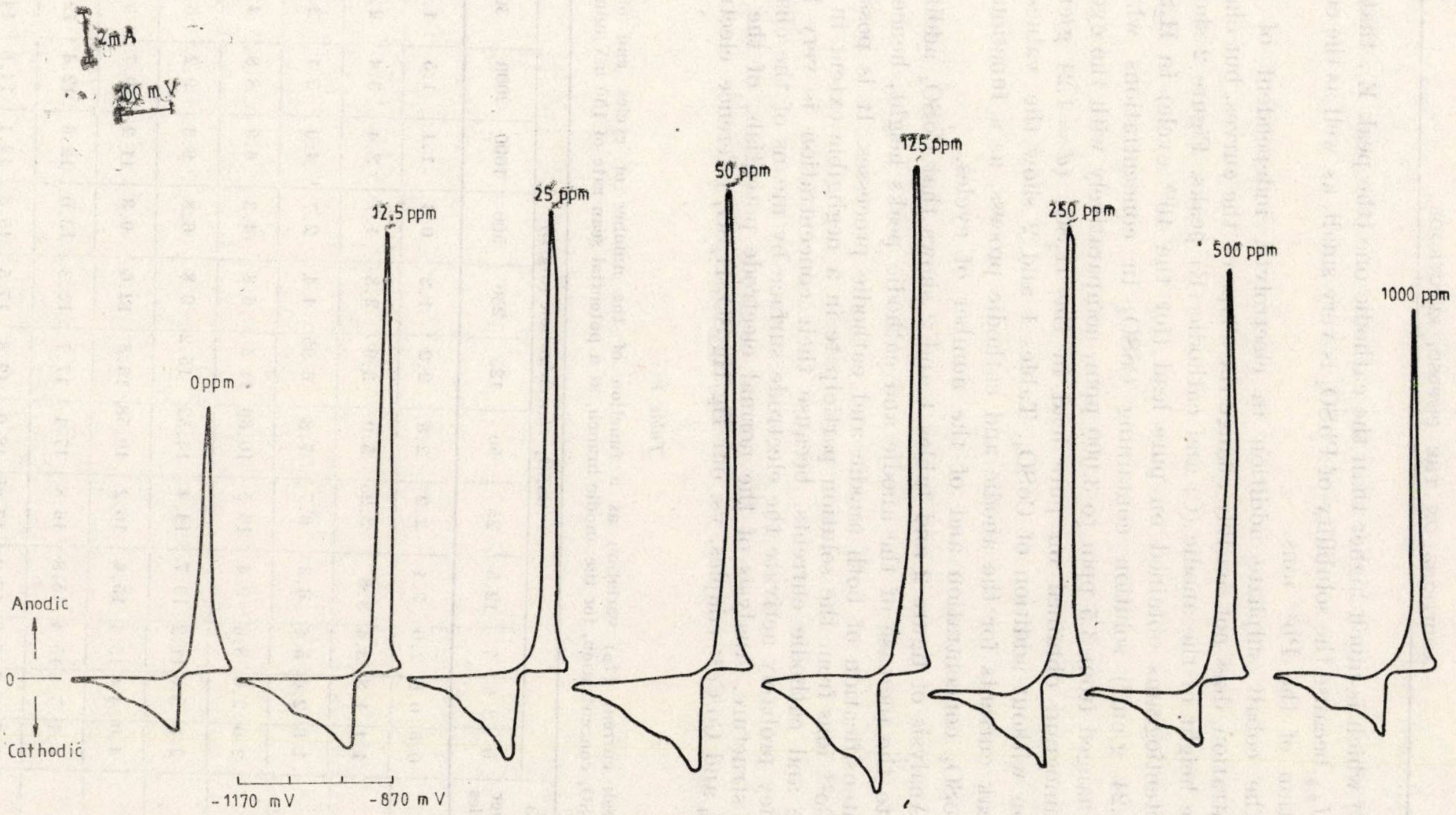

Fig. 2. — Potentiograms of pure lead microelectrode (for cycle 40) obtained in H_2SO_4 ($d=1.24$ g/cm^3) solutions containing $CoSO_4$ in concentration from O ppm to 1000 ppm ; $v=150$ mV/min.

Table 2

The peak current (I_p) variation as a function of the number of cycles and of the CoSO$_4$ concentration, for the cathodic branch, at a potential scan rate of 150 mV/min

$I_{P(mA)}$	The CoSO$_4$ concentration (mg/L)											
Number of cycles	0	3.5	7	12.5	25	50	125	250	500	1000	2000	3000
5	0.4	0.4	0.6	0.5	0.7	1.0	1.5	0.6	0.3	0.4	0.5	0.4
10	0.4	0.5	0.8	0.9	1.3	1.4	1.7	0.7	0.4	0.5	0.7	0.5
15	0.5	0.6	1.2	1.5	1.6	2.0	2.2	1.1	0.6	0.9	1.2	0.7
20	0.7	0.8	1.6	2.0	2.4	2.4	2.7	1.7	0.9	1.3	1.8	1.0
25	0.9	1.6	2.2	2.4	2.8	2.8	3.15	2.2	1.3	1.7	1.87	1.4
30	1.0	1.2	2.6	2.8	2.96	3.2	3.32	2.7	1.8	2.12	2.0	1.7
35	1.2	1.6	2.6	3.0	3.1	3.8	3.91	3.3	2.3	2.4	2.2	2.1
40	1.4	2.0	3.0	3.1	3.4	4.0	4.4	3.7	2.7	2.7	2.6	2.6

(see Table 3) shows that the two electrode potentials are very close, both being within the potential range under study.

Hence, simultaneously with the $Pb^{2+} \rightleftarrows Pb$ process, it is the the $Co^{2+} \rightleftarrows Co$ process which occurs, too, the difference being that PbSO$_4$ has a very small solubility and forms a passivating layer on the electrode surface, while CoSO$_4$ is completely soluble.

Table 3

Normal electrode potentials of the Pb/PbSO$_4$ and Co/Co^{2+} coup les [27]

Electrode	Normal electrode potential (in V), *vs*	
	Pt, $H_2/2H^+$	$Hg/Hg_2SO_4/H_2SO_4$*
Pb/PbSO$_4$	−0.355	−0.970
Co/Co^{2+}	−0.277	−0.892

* The normal electrode potential of the $Hg/Hg_2SO_4/H_2SO_4$ electrode vs. the Pt, $H_2/2H^+$ electrode is of +0.615 V.

It is possible that this cyclic process of cobalt deposition-dissolution increases the porosity of the PbSO$_4$ layer, that is the spongeous Pb amount which forms the microelectrode. This results in the increase of the anodic (Q_a) and cathodic (Q_c) electricity amounts (see tables 4 and 5). Concentrations of CoSO$_4$ higher than an optimum concentration of 125 ppm to a small decrease of Q_a and Q_c. However, Q_a and Q_c remain higher than in the H_2SO_4 solution without $CoSO_4$ addition. This behaviour could be explained by the fact that at high concentrations of Co^{2+} ions, their deposition occurs not only on the free sites of the spongeous lead, but also on $PbSO_4$, hindering its dissolution and leading to a small inhibition of both anodic and cathodic processes.

Table 4

The dependence of the electrochemical parameters of the $Pb/PbSO_4/H_2SO_4 + CoSO_4$ system on the $CoSO_4$ concentration (for cycle 40)

$CoSO_4$ concentration in H_2SO_4 (ppm)	Electrochemical parameter							
	$Q_a \cdot 10^2$ (C)	$Q_c \cdot 10^2$ (C)	$\bar{I}_a$ (mA)	$\bar{I}_c^{pr}$ (mA)	$\bar{I}_a^{rez}$ (mA)	$\bar{I}_c^{tot}$ (mA)	h (μ)	$\frac{h}{h_0}$
0	8.3	4.4	2.6	0.32	0.128	0.443	0.29	1.0
3.5	10.9	6.4	3.4	0.42	0.214	0.63	0.38	1.3
7.0	15.8	10.2	4.9	0.77	0.252	1.02	0.55	1.9
12.5	19.3	15.5	6.0	1.28	0.274	1.55	0.67	2.3
25	23.6	26.8	7.4	2.16	0.519	2.68	0.83	2.8
50	30.8	35.3	9.6	2.69	0.848	3.54	1.08	3.7
125	34.4	44.1	10.8	3.56	0.851	4.41	1.20	4.1
250	14.4	15.5	4.5	1.23	0.328	1.56	0.50	1.7
500	12.1	13.0	3.8	0.99	0.313	1.30	0.42	1.5
1000	12.0	12.9	3.7	0.98	0.310	1.29	0.42	1.4
2000	10.4	11.0	3.3	0.89	0.213	1.10	0.36	1.3
3000	10.3	10.7	3.2	0.87	0.200	1.07	0.36	1.2

$\bar{I}_a$ — the anodic average current; $\bar{I}_c^{pr}$ — the principal average current; $\bar{I}_c^{rez}$ — the rest cathodic average current; $\bar{I}_c^{tot}$ — the total cathodic average current; h — the thickness of the $PbSO_4$ layer formed on the microelectrode, at different $CoSO_4$ concentrations; h_0 — the thickness of the $CoSO_4$ layer formed on the microelectrode, in the H_2SO_4 solution free of $CoSO_4$.

Table 5

The dependence of the electrochemical parameters of the $Pb/PbSO_4/H_2SO_4 +$ $+ CoSO_4$ system on the $CoSO_4$ concentration (for cycle 20)

$CoSO_4$ concentration in H_2SO_4 (ppm)	Electrochemical parameter							
	$Q_a \cdot 10^2$ (c)	$Q_c \cdot 10^2$ (c)	I_a (mA)	I_c^{pr} (mA)	I_c^{rez} (mA)	I_c^{tot} (mA)	h (μ)	$\frac{h}{h_0}$
0	3.12	2.76	0.98	0.16	0.12	0.28	0.11	1.0
3.5	3.77	3.76	1.18	0.23	0.14	0.38	0.13	1.2
7	5.72	5.72	1.79	0.39	0.18	0.57	0.20	1.8
12.5	8.00	8.10	2.50	0.62	0.19	0.81	0.28	2.6
25	10.47	16.17	3.27	1.14	0.47	1.62	0.37	3.4
50	13.40	22.56	4.19	1.72	0.54	2.25	0.47	4.3
125	15.56	27.83	4.86	1.72	1.65	2.78	0.54	4.9
250	5.60	8.45	1.75	0.49	0.35	0.85	0.19	1.7
500	5.21	7.18	1.63	0.45	0.27	0.72	0.18	1.6
1000	5.14	7.02	1.61	0.42	0.28	0.70	0.18	1.6
2000	4.46	6.11	1.39	0.36	0.26	0.61	0.16	1.5
3000	3.88	5.03	1.21	0.25	0.25	0.50	0.14	1.3

In order to characterize the microelectrode behaviour during the successive cyclings, it was introduced the "life time index" parameter (η_{cycl}) defined by means of the relation:

$$\eta_{cycl} = \frac{Q_f - Q_c}{Q_o} = \frac{Q_f}{Q_o} - 1 \tag{2}$$

where Q_o represents the initial capacity of the microelectrode and Q_f the end capacity of this one, both in coulombs. From the experimental coulometric data, it is possible to evaluate the average currents for the anodic ($\bar{I}_a$) and cathodic ($\bar{I}_c$) processes. Tables 6 and 7 show the values of the life time index, η_{cycl}, as a function of the $CoSO_4$ concentration and of the number of cycles.

Table 6

The life time index (η_{cycl}) variation as a function of the number of cycles and of the $CoSO_4$ concentration, for the anodic branch, at a potential scan rate of 150 mV/min.

η_{cycl} Number of cycles	$CoSO_4$ concentration (mg/L)											
	0	3.5	7.0	12.5	25	50	125	250	500	1000	2000	3000
5	−0.40	−0.23	+0.04	0.22	0.26	0.25	0.25	0.18	0.22	0.21	0.18	0.15
10	+0.06	0.78	0.97	1.00	1.05	1.13	1.27	1.03	0.94	0.89	0.90	0.87
15	+0.50	1.12	1.82	2.14	2.10	2.34	2.78	2.05	1.37	1.30	1.30	1.27
20	+1.07	1.05	2.56	2.84	3.00	3.01	3.64	2.54	2.72	2.70	2.66	2.10
25	+1.77	2.99	3.32	3.45	3.62	3.74	4.52	3.28	4.06	4.25	4.11	3.26
30	+2.58	4.05	5.00	5.12	5.19	5.25	6.49	5.89	5.36	5.63	5.50	4.52
35	+3.50	5.61	7.10	7.15	7.23	7.40	8.10	7.43	6.59	6.33	6.21	5.79
40	+4.46	7.24	7.65	7.98	8.03	8.21	9.26	8.10	7.67	7.64	7.53	7.21

Table 7

The life time index (η_{cycl}) variation as a function of the number of cycles and of the $CoSO_4$ concentration, for the cathodic branch, at a potential scan rate of 150 mV/min

η_{cycl} Number of cycles	$CoSO_4$ concentration (mg/L)											
	0	3.5	7.0	12.5	25	50	125	250	500	1000	2000	3000
5	0.35	0.70	0.82	0.83	1.24	0.34	0.78	0.28	0.23	0.4	0.32	0.10
10	1.38	1.50	1.71	1.92	2.01	1.17	3.06	1.54	1.50	1.7	1.45	0.98
15	2.40	2.70	2.83	3.01	3.95	2.10	6.00	3.23	3.20	3.7	2.89	2.10
20	3.68	3.70	3.77	3.65	4.59	6.80	7.70	4.79	4.52	4.4	4.01	3.15
25	4.16	4.20	4.79	5.22	5.62	5.87	9.32	6.14	5.79	6.0	5.18	4.60
30	5.49	5.42	5.70	6.08	6.27	6.31	10.6	7.33	7.03	7.0	6.11	5.01
35	6.28	6.13	6.60	7.12	7.30	7.99	11.7	8.49	8.20	8.0	7.26	6.75
40	6.50	7.0	7.50	7.93	8.28	11.2	12.7	9.62	9.00	8.6	8.01	7.83

The total electricity amount Q is given by the relation:

$$Q = \int_{t_1}^{t_2} I \, dt = \bar{I} \cdot t \tag{3}$$

where $\bar{I}$ is the average current. Hence :

$$\bar{I}_a = \frac{Q_a}{t_a} \text{ and } \bar{I}_c = \frac{Q_c}{t_c} \tag{4}$$

The average currents can be calculated by the division of the anodic and cathodic electricity amounts by a corrected anodic and cathodic time respectively. Figure 2 shows the way of calculation of the average currents introduced by us. The Q_a and Q_c amounts are the experimental coulometric values. In order to calculate the $\bar{I}_a$ current, the back time t_a was neglected, because the back Q_a is practically null. For the cathodic process, at the reverse cathodic potential scan, a supplementary amount of electricity, Q_c^{rez}, is obtained, corresponding to the batched surface on figure 3. For this reason three average currents $\bar{I}_c^{\text{pr}}$, $\bar{I}_c^{\text{rez}}$ and $\bar{I}_c^{\text{tot}}$ were calculated for the cathodic process. $\bar{I}_c^{\text{tot}}$ is much smaller than $\bar{I}_a$, proving the irreversibility of the cathodic reaction, controlled by the diffusion. Interesting information concerning the Pb/PbSO$_4$ electrode behaviour can be obtained from the parameters η_{coul} and $\eta_{\bar{I}}$, too, given by the relations.

$$\eta_{\text{coul}} = \frac{Q_c}{Q_a} \tag{5}$$

$$\eta_{\bar{I}} = \frac{\bar{I}_c^{\text{tot}}}{\bar{I}_a} \tag{6}$$

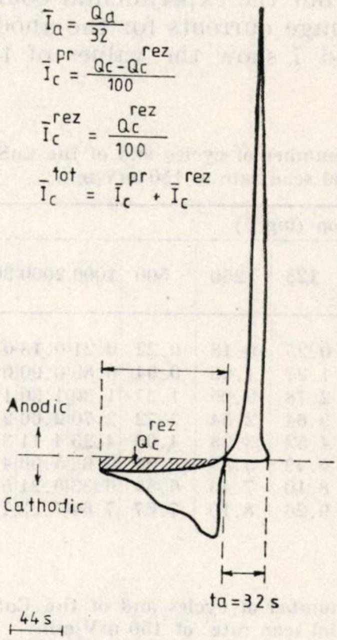

Fig. 3. — The illustration of the way of average currents calculation.

Figure 4 shows the dependence of the parameters $\eta_{\text{cycl},a}$ $\eta_{\text{cycl},c}$ η_{coul} and $\eta_{\bar{I}}$ on the CoSO$_4$ concentration in electrolyte.

Analysis of figure 4 shows that in solutions without CoSO$_4$, the parameter $\eta_{\text{coul}} < 1$, indicating that the PbSO$_4$ amount formed during the anodic potential scan, is not completely cathodically reduced. The cathodic process controlled by the diffusion occurs more slowly than the anodic process. For this reason $t_c \gg t_a$, and after the direct cathodic scan, there is a Q_c^{rez} as we showed. The CoSO$_4$ addition activates the PbSO$_4$ which probably forms a microcrystalline porous layer ; this one can be more easily reduced.

Out of the increase of the absolute values of Q_a and Q_c, there is an increase of the η_{coul} ratio which becomes close to unit. In the presence of CoSO$_4$, practically the whole PbSO$_4$ amount (anodically obtained) reduces during the cathodic process. The values higher than the unit, which obtain around the optimum concentrytion, could be explained by a supplementary reduction of hydrogen, within the cathodic potential range after the use of the $PbSO_4$ deposit. $\eta_{\bar{I}}$, which shows the relative reversibility of the cahodic process comparatively with the anodic one, increases with the $CoSO_4$ concentration, too, from 0.17 (in the solution without addition of $CoSO_4$) up to 0.41 (in the solutions containing 125 ppm $CoSO_4$). This decrease of the irreversibility of the cathodic process is due to the $PbSO_4$ layer activation, too. Figure 4 and tables 6 and 7 show that the life time index η_{cycl}, increases with the $CoSO_4$ concentration and with the number of cycles, too. All the curves presented in figure 4 have the same shape, with a maximum for the 125 ppm $CoSO_4$ concentration.

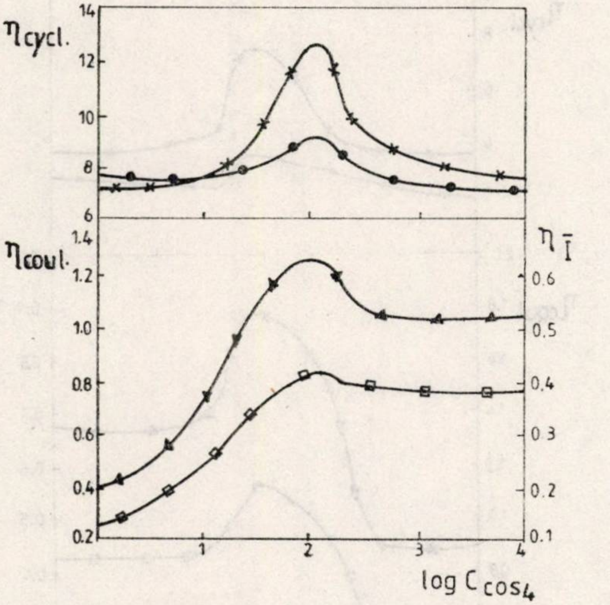

Fig. 4. — The dependence of $\eta_{cycl,a}$(·), $\eta_{cycl,c}$ (×), η_{coul} (Δ) and $\eta_{\bar{I}}$(□) parameters on the logarithm of the $CoSO_4$ concentration, for the 40th cycle.

From the coulometric data, registered for the anodic process, the thickness of the $PbSO_4$ layer formed on the microelectrode surface was calculated, using Faraday's law. Tables 4 and 5 show the values of the $PbSO_4$ layer thickness, on the microelectrode surface after 40 and 20 cycles, respectively, as a function of the $CoSO_4$ concentration. In this case, there is an optimum, too, for the 125 ppm $CoSO_4$ concentration, when the thickness of the $PbSO_4$ layer is of about 1.2 μ for the 40th cycle and of about 0.54 μ for the 20th cycle, respectively.

The electrochemical parameters presented in table 4 for the cycle 40, were calculated for the cycle 20, too; table 5 shows these values. As it was expected, the parameters values are smaller than those for the cycle 40, but the behaviour as a function of $CoSO_4$, concentration is the same, that is with maxima for the 125 ppm concentration; the same is the behaviour of $\eta_{cycl,a}$, $\eta_{cycl,c}\eta_{coul}$ and $\eta_{\bar{I}}$ parameters, too, for the 20th cycle (see Fig. 5).

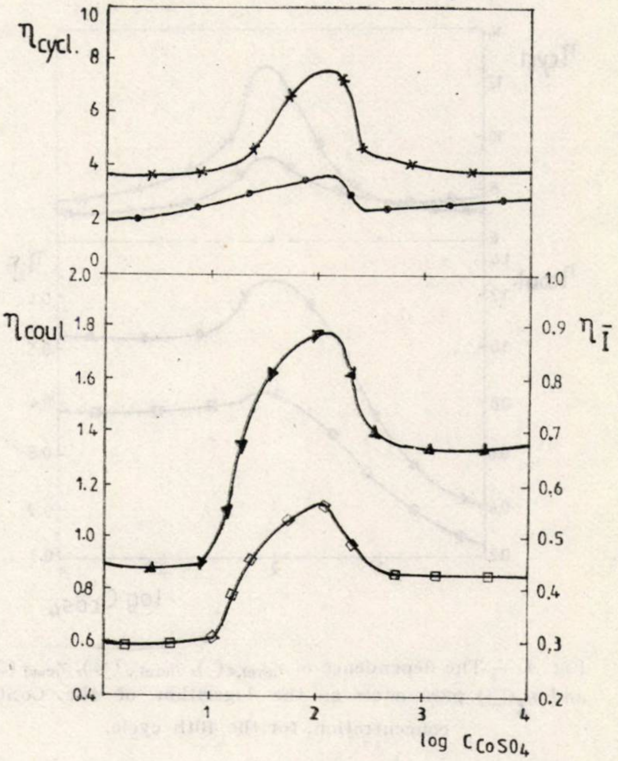

Fig. 5. — The dependence of $\eta_{cycl,a}(\cdot)$, $\eta_{cycl,c}$ $(\times)$, $\eta_{coul}(\Delta)$ and $\eta_{\bar{I}}(\square)$ parameters on the logarithm of the $CoSO_4$ concentration, for the 20th cycle.

That means that at the 20th cycle the behaviour of the lead microelectrode is the same as that at the 40th cycle. Hence, it is possible to obtain information concerning the influence of some additives on the functioning of $Pb/PbSO_4$ electrode from the lead — acid batteries, even after a smaller number of cycles; there is the possibility of a faster investigation of the way by which the different additives in the electrolyte influence the lead acid batteries performances. The conclusion is that the $CoSO_4$ addition leads to an activation of the $PbSO_4$ layer and to an increase of the $Pb/PbSO_4$ microelectrode capacity. Because the $Pb/PbSO_4$ microelectrode, cycled in the potential range under study, simulates the functioning of the negative electrode from the lead acid battery, we can conclude that the addition of small $CoSO_4$ amounts (up to 125 ppm) has a favourable influence on the performances of these batteries.

REFERENCES

[1] S. Sternberg, V. Brânzoi, L. Apăteanu and A. Mateescu, *Rev. Roumaine Chim.*, **28**, 583 (1983).
[2] S. Sternberg, A. Mateescu, V. Brânzoi and L. Apăteanu, *Rev. Roumaine Chim.* **29**, 727 (1984).
[3] S. Sternberg, V. Brânzoi and L. Apăteanu, *Rev. Roumaine Chim.*, **29**, 833 (1984).
[4] V. Brânzoi, S. Sternberg and L. Apăteanu, *Rev. Roumaine Chim.*, **30**, 199 (1985).
[5] S. Sternberg, V. Brânzoi, L. Apăteanu, C. Doboș and E. Comănescu *Rev. Chim* (București), **35**, 427 (1984).
[6] S. Sternberg, V. Brânzoi, L. Apăteanu and A. Mateescu "Proceedings of the 1st National Seminar of Applied Electrochemistry" Cluj-Napoca, 14—15 May 1982, p. 11.
[7] S. Sternberg, V. Brânzoi, L. Apăteanu and A. Mateescu, "Stocarea Energiei", 1982, p. 57, I.P.B.
[8] S. Sternberg, A. Mateescu, V. Brânzoi and L. Apăteanu, *Rev. Roumaine Chim.* (in press).
[9] S. Sternberg, A. Mateescu, V. Brânzoi and L. Apăteanu, *Rev. Roumaine Chim.* (in press).
[10] S. Sternberg, A. Mateescu, V. Brânzoi and L. Apăteanu, *Electrochim. Acta* (in press).
[11] S. Sternberg, A. Mateescu, V. Brânzoi and L. Apăteanu, *Rev. Roumaine Chim.* (in press).
[12] S. Sternberg, V. Brânzoi and L. Apăteanu, *Rev. Roumaine Chim.* (in press).
[13] K. R. Bullock and D.H.Mc Clelland, *J. Electrochem. Soc.* **123**, 327 (1976).
[14] K. R. Bullock, *J. Electrochem, Soc.*, **126**, 360 (1979).
[15] K. R. Bullock, *J. Electrochem Soc.* **124**, 1478 (1977).
[16] K. R. Bullock, *ibid.*, **126**, 662 (1980).
[17] B. K. Mahatto, *ibid.*, **126**, 365 (1979).
[18] B. K. Mahatto, *ibid.*, **8**, 127 (1980).
[19] B. K. Mahatto, *ibid.*, **7**, 128 (1981).
[20] V. Danel and V. Plichon, *Electrochim. Acta*, **28**, 781 (1983).
[21] V. Danel and V. Plichon, *ibid.*, **28**, 785 (1983).
[22] G. Archdale and J.A. Harrison, *J. Electroanalyt. Chem. and Interfacial Electrochem.*, **34**, 431 (1972).
[23] G. Archdale and J. A. Harrison, *ibid.*, **39**, 357 (1973).
[24] G. Archdale and J. A. Harrison, *ibid.*, **47**, 93 (1973).
[25] G. Archdale and J. A. Harrison, *ibid.* **43**, 321 (1973).
[26] A. Mateescu, Doctoral Thesis.
[27] D. Doboș "Elektrohimiceskie konstanty", MIR, Moskva, 1980.

Revue Roumaine de Chimie, **32**, *2*, 133–140 (1987)

STUDY ON Co^{2+} AND Zn^{2+} BEHAVIOUR IN DIALYSIS PROCESS

F. MATEI, GH. IONESCU, A. CECAL and A. DUCA
Analytical Chemistry and Physical Chemistry Departments, Polytechnic Institute,
Splai Bahlui 71, Iași 6600, Romania

Received December 9, 1985

Separation of $Co^{2+}-Zn^{2+}$ mixture by ion exchange membrane dialysis was studied. Separation is possible if the ions are complexed one by one only. The experimental data show that Zn^{2+} forms complexes with Cl^- ligand as $[Zn(Cl)_3|^-$ while in the presence of glycine $[Zn(Gly)_2|^0$ and $[Co(Gly)_3|^-$ complexes appear. In the former case, in a cell with anionic membranes, $[Zn(Cl)_3|^-$ is retained on the membranes and Co^{2+} remains in the solution, while in the latter, $[Co(Gly)_3|^-$ is retained on the membranes and $[Zn(Gly)_2|^0$ remains in the solution. With the Cl^- ligand the separation can be also performed with cationic membranes in the cell. In this case, Co^2 is retained on the membranes and $[Zn(Cl_3)|^-$ remains in the solution. The described procedure is advantageous for Co^{2+} and Zn^{2+} in dilute solutions to be separated from one another.

INTRODUCTION

The quantitative determination of the Co^{2+} and Zn^{2+} ions by electrochemical methods was discussed in a previous paper [1]. Owing to the similar properties of these ions the conclusion was drawn that the analysis of their mixture must be associated with a preliminary separation.

To separate these ions in a dilute solution the dialysis procedure was applied using ion exchange membranes.

The experiemental data obtained as well as the theoretical basis of these processes and the properties of ion exchange membranes led to the unanimously accepted conclusion that both cationic and anionic membranes have a good selectivity. The cationic and anionic exchange processes between the membranes and cations and anions, respectively, appear when membranes are immersed in the solution of the electrolyte mixture. [2]

Selectivity of an ionic membrane in ion exchange process as well as the permselectivity in its crossing by certain ions depend on the intrinsic properties and the properties of ions in the solution. Consequently, the selective character of a given ionic membrane might be improved by diversifying the size and electrical charge of the ions to be separated by the ion exchange membrane dialysis. In this connection the complexation of ions with adequate ligands is an important practical possibility leading to the modification of the initial ion size as well as to obtaining complexes either electrically neutral or of a contrary electrical charge toward the initial ion. [3]

The dialysis process with ionic membranes involving electrical charge shifts within the solution (in space) and must obey the "electroneutrality principle". That is to an ionic flux of a given species, moving from the solution to the ion exchange membrane, an ionic flux of another species from ion exchange membrane to the solution carrying the same amount of the electrical charge will correspond.

For instance, by immersion of an either cationic or anionic membrane in an electrolyte solution the electrical charge deficiency appearing in the solution by fixation of an either anion or cation on the membrane is exactly balanced by passing the cations and anions, respectively, from the membrane to the solution. Within the systems containing both cationic and anionic ions exchange membranes the strictly equivalent processes of charge exchange between the membrane and the solution, cation(1)-cation(2) and anion(1)-anion(2), respectively, proceed simultaneously.

In the present paper the study of the ion exchange membrane dialysis of the Co^{2+} and Zn^{2+} mixture both in the presence and the absence of complexing agents is reported and the possibility of separating these ions for their analysis made evident.

EXPERIMENTAL

A probable mechanism for a dialysis cell in which the solution compartment is bordered by two cationic membranes (C) is given in figure 1. The solution contains the electrolytes $(K_1^+A^-)$ and $(K_2^+A^-)$. The cations K_1^+ and K_2^+ may be retained on the membrane by a H^+ ionic exchange (the cationic membrane has the R^-H^+ cationic exchange group), while the anions A^- remain in the solution. By adding to the solution a new electrolyte (K^+L^-) whose anion is a ligand for the cation K_1^+ a complex of the form $[K_1(L)_2]$ is formed which remains in the solution compartment. Thus, the separation of K_1^+ and K_2^+ cations may be performed; the former remains in the solution as an anionic complex and the latter is fixed on the membrane. With membranes (C) of a high exchange capacity and low K_2^+ cation concentration the membrane regeneration in the (H^+) form will become necessary after several uses in the separation process. [3,13]

A similar mechanism may be supposed for the cell compartment with anionic membranes which perform the ionic exchange with the anions.

Besides the ion exchange membrane uses, in analytical purposes for the ions in the mixtures a spectacular application is the water desalting process developing in the cells with several chambers separated by alternately placed cationic and anionic membranes as the (H^+) and (OH^-) forms, respectively. In order to accelerate the ionic exchange phenomenon the dialysis cell is submitted to an electrical potential difference, this process being known under the denomination of electrodialysis. [4–6,14]

In order to separate the Co^{2+} and Zn^{2+} ions from their mixture by dialysis the ion exchange membranes supplied by SERVA, Entwicklungslabor, Heidelberg were used, namely Permaplex C-10 (H^+ form) and Permaplex A-20 (Cl^- form). The process was carried out in the dialysis cell with 3 compartments separated by two membranes (Fig. 2). In the central compartment the solution of the two ions and in the lateral ones the solvent were poured. Dialysis development *vs.* time was followed by the analysis of samples taken from the central compartment. The initial solution concentrations were of 10^{-4} M for each ion and the central compartment volume of 250 mL.

Concentration of Co^{2+} was measured both spectrophotometrically and radiochemically and that of Zn^{2+} by means of the atomic absorption method. [7–9]

The spectrophotometrical measurements were performed at 20°C on a VSU2-P, Carl Zeiss Jena (GDR) apparatus provided with a thermosetting device, by using the Nitrozo-R reagent, $\lambda = 525$ nm, pH $= 5.5$ in a cell of 0.5 cm in thickness. At 525 nm the reagent absorption is quite unsignificant in comparison with that of Co^{2+}-Nitrozo-R complex.

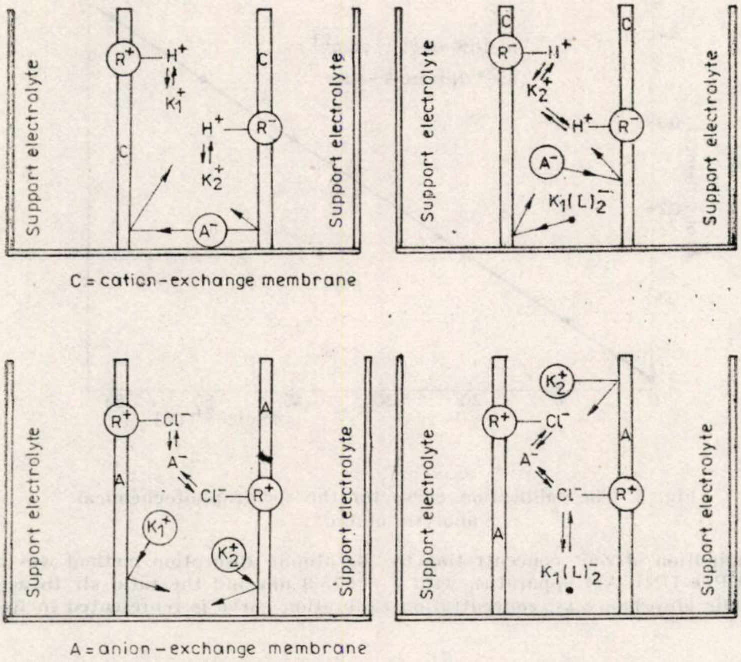
Support electrolyte
R^+
H^+
K_1^+
C
R^-
K_2^+
A^-
C = cation-exchange membrane
$K_1(L)_2^-$
Cl^-
A
A = anion-exchange membrane

Fig. 1. The possible mechanism scheme in a dialysis cell.

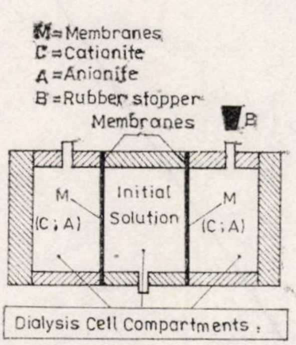
M = Membranes
C = Cationite
A = Anionite
B = Rubber stopper
Membranes
B
M (C ; A)
Initial Solution
M (C ; A)
Dialysis Cell Compartments

Fig. 2. The dialysis cell.

The absorbance-concentration calibration curve for the spectrophotometrical analysis is set out in figure 3. This function is seen to be a linear one and by statistical working of the data the following equation was derived:[10]

$$A = 0.015 + 6.727 \cdot c\,;\quad c - \text{mole/L} \tag{1}$$

In the radiochemical method $^{60}C_0^{2+}$ isotope supplied by IFIN-Bucharest was used. The initial solution was of the 10^{-4} M concentration showing a specific activity of 10^5 Bq/mL. A scintillation detector with $NaI(T_1)$ crystal connected to an NK-150 automatic energy selective scaler was used. The obtained results led to a linear calibration curve in the *R*(Puls/min.) — *c*(mole/L) (Fig. 4).

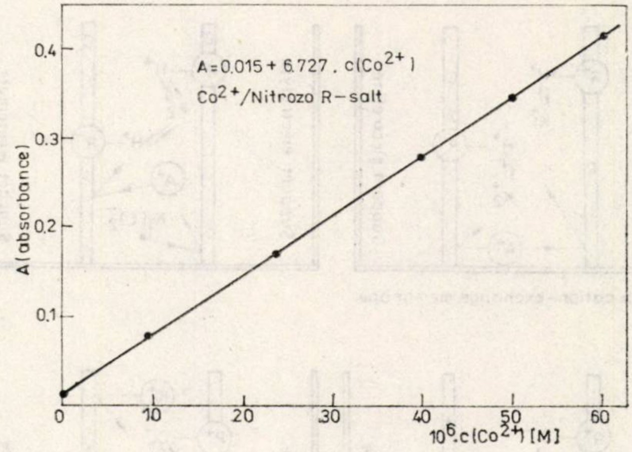

Fig. 3. The calibration curve for the spectrophotochemical analysis of Co^{2+}.

Determination of Zn^{2+} concentration by the atomic absorption method was performed on an SP-90 Pye UNICAM apparatus, with $\lambda = 213.9$ nm and the ratio air to acetylene of 1/5. The atomic absorbance *vs.* concentration calibration curve is represented in figure 5. In

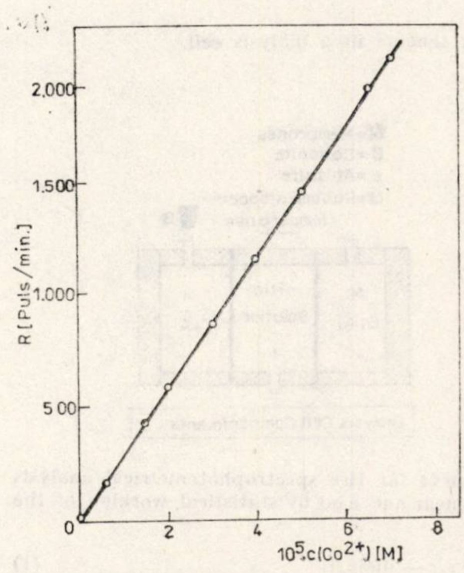

Fig. 4. The calibration curve for the radiochemical analysis of Co^{2+}.

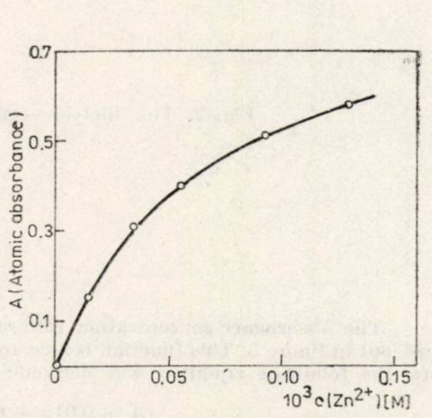

Fig. 5. The calibration curve for the atomic absorption analysis of Zn^{2+} in the *A*—*c* coordinates.

order to linearise this curve over a larger Zn^{2+} concentration range the A (atomic absorbance, vs. $\sqrt{c}$ was plotted, according to the equation,

$$A = 0.52 \cdot (10^2 \cdot \sqrt{c}) \tag{2}$$

and the dependence obtained set out in figure 6.

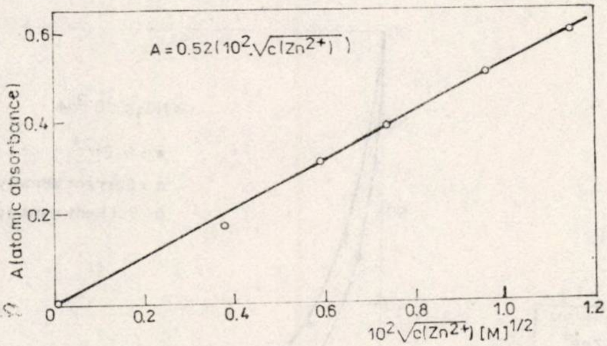

Fig. 6. The calibration curve for the atomic absorption analysis of Zn^{2+} in the $A-c$ coordinates.

RESULTS AND DISCUSSION

In order to prove that neither dialysis nor electrodialysis of the $Co^{2+}-Zn^{2+}$ mixture realises separation in the absence of adequate complexing agents two such experimental runs were performed by using the cells drawn in figure 2 and figure 7, respectively, with cationic Permaplex C-10 membranes. Moreover, two current densities were applied in electrodialysis to emphasize an eventual differentiation in the behaviours of the two ions during this process, i.e. 0.85 A/dm² and 1.15 A/dm². A previous paper[11] concerning the solvent influence over the ionic exchange rate between Permaplex C-10$-Co^{2+}$, Zn^{2+} ions concluded that the solvent must be H_2SO_4 acid solution of the 0.1...0.2 mole/L concentration.

Fig. 7. The electrodyalysis cell.

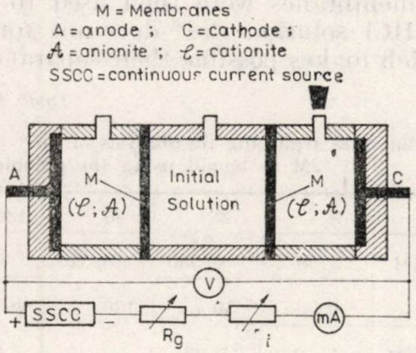
M = Membranes
A = anode ; C = cathode ;
𝒜 = anionite ; 𝒞 = cationite
SSCC = continuour current source
A
M
(𝒞; 𝒜)
Initial
Solution
M
(𝒞; 𝒜)
C
V
+
SSCC
−
Rg
mA
i

In electrodialysis the solvent influence is quite unsignificant in comparison with that of the electrical current having the role of assuring the electrical conductibility only in electrolyte. The two current densities may be obtained by means of a 10^{-3} mole/L KNO_3 solution (referred to as the support electrolyte). Variation of Co^{2+} and Zn^{2+} concentrations *vs.* time within the central compartments of the cells (Figs 8 and 9), points out that the two ions cannot be separated from one another.

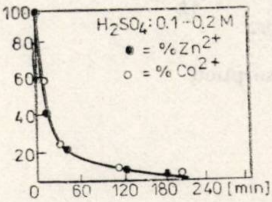

Fig. 8. Co^{2+} and Zn^{2+} dialysis curves in the absence of ligands.

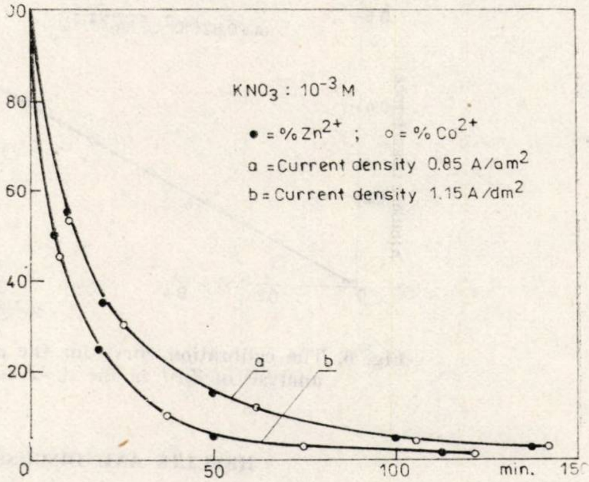

Fig. 9. Co^{2+} and Zn^{2+} electrodialysis curves in the absence of ligands.

Cl^- ion as complexing agent : As shown in a previous paper[11] Zn^{2+} gives in a 2 mole/L HCl solution a complex $[Zn(Cl)_3]$. On this way both the size and charge value and sign were modified. Two Permaplex A-20 anionic membranes were then used to make evident the fact that in 2 mole/L HCl solution Co^{2+} does not form a complex similar to that of Zn^{2+} which makes possible their separation. The data in table 1 show that

Table 1

Experimental data regarding the dialysis of Co^{2+} and Zn^{2+} mixture in the presence of HCl 2M as ligand using the anionic exchange membranes

t, min	0	50	80	130	190	310	410
$10^4 \cdot c(Co^{2+})$M	5.50	0.540	0.320	0.220	0.127	0.048	0.010
t, min	0	50	130	200	260	310	—
$10^4 \cdot c(Zn^{2+})$M	5.50	5.22	5.20	5.15	5.25	5.20	—

Zn^{2+} concentration in the central compartment decreases significantly while Co^{2+} concentration suffers much less modifications caused probably by the diffusion through membrane and not by the ion exchange process because Co^{2+} does not form anionic complexes with Cl^-. Consequently, an experiment like that might be efficient for separation of the two ions.

The same conclusions were drawn with an experiment in a cell containing two Permaplex C-10 cationic membranes. The experimental data are given in table 2.

Glycine as complexing agent : As mentioned in literature[12] the two ions complexing with glycine are different from one another both in size and charge, namely $[Co(Gly)_3]^-(K = 5.71 \cdot 10^{10})$ and $[Zn(Gly)_2]^-$(neutral, with $K = 9.10 \cdot 10^9$). In the case of the prevalence of these complexes over other complexes eventually formed between Co^{2+} and Zn^{2+} ions and glycine their mixture could be separated by using ion exchange membranes. This possibility was confirmed experimentally by using a cell with two Permaplex A-20 anionic membranes and a ligand concentration in the central compartment of 10^{-2} mole/L. The glycine excess is necessary to complexate Co^{2+} and Zn^{2+} as shown above. In table 3 the concentration variation of the two metallic ions *vs.* time is given for a solution of $5.2 \cdot 10^{-4}$ mole Co^{2+}/L, $5.0 \cdot 10^{-4}$ mole Zn^{2+}/L and 10^{-2} mole Gly/L concentration in the central compartment. These data support the hypothesis advanced on the nature of the complexes and on the possibility of the ions separation.

Table 2

Experimental data regarding the dialysis process of Co^{2+} and Zn^{2+} mixture in the presence of HCl 2M as ligand using the cationic exchange membranes

t, min	0	50	80	130	190	310	410
$10^4 \cdot c(Co^{2+})$M	5.50	0.540	0.320	0.200	0.127	0.048	0.010
t, min	0	50	130	200	260	310	—
$10^4 \cdot c(Zn^{2+})$M	5.50	5.220	5.200	5.150	5.250	5.200	—

Table 3

Experimental data regarding the dialysis process of Co^{2+} and Zn^{2+} mixture in the presence of glycine ligand using the anionic exchange membranes

t, min	0	50	80	130	190	310	410
$10^4 \cdot c(Co^{2+})$M	5.20	0.490	0.333	0.190	0.107	0.060	0.050
$10^4 \cdot c(Zn^{2+})$M	5.00	4.88	4.85	4.90	4.75	4.80	4.73

CONCLUSIONS

Starting from the behaviour of the ion exchange membranes during the ionic exchange process, as given in literature and applied practically, the following conclusions can be drawn:

1. Separation of Co^{2+} and Zn^{2+} ions by ion exchange membranes is not possible due to their similar behaviour in this process.

2. If one of them is complexed (either Zn^{2+} with Cl^{2-} or Co^{2+} with glycine) separation becomes possible by ion exchange membrane dialysis, hence a Co^{2+}, Zn^{2+} mixture can be analysed.

3. The experimental data and those in the literature agree on the complexing process of the two ions with the employed ligands.

REFERENCES

[1] A. Duca and F. Matei, *Rev. Chim. (București)*, **25**, 57 (1974).

[2] F. Helfferich, "Ion Exchange", McGraw-Hill, New York, 1962.

[3] S.T. Hwang and K. Kammermeyer, "Membranes in Separations", vol. VII, John Wiley, New York, 1975, chap. IX.

[4] T.E. Kressman, *Ind. Chemist.*, **30**, 99 (1954).

[5] A. G. Winger, G. W. Bodamer, R. Kunin, C. J. Prizer, and G. W. Harmon, *Ind. Eng. Chem.*, **47**, 50 (1955).

[6] K. S. Spiegler, "Ionoobmenaja Technollogja", Metallurgizdat, Moskva, 1959.

[7] M. Pinta., "Recherche et dosage des elements traces" Dunod Paris, 1962.

[8] J. Tölgyessy, V. Jenesak and T. Braun, "Radiochemical Methods of Analysis" IAEA. Wien, 1965.

[9] M. Pintea, "Spectroscopie d'absorbtion atomique" Masson et C-ie, Paris, 1971.

[10] K. Doerffel, "Statistik in der Analytischen Chemie", Carl Schorlemmer, Leipzig, 1966.-

[11] A. Duca and F. Matei, "Proceedings of the 3rd National Conference of Analytical Chemistry", Brașov, România, 1971.

[12] K. B. Jatzimirski and W. P. Wassiljew, "Instabilitätkonstanten von Komplexverbindungen", VEB. Deutscher Verlag der Wissenschaften, Berlin, 1963.

[13] R. E. Lacey, "Basis of Electromembrane Processes", in *Industrial Processing with Membranes*, Lacey R.E., Loeb S., Wiley-Interscience, New York, 1972.

Revue Roumaine de Chimie, **32**, *2*, 141–143 (1987)

MICRODETERMINATION OF REDUCING SUGARS AND ASCORBIC ACID BY INDIRECT METHOD USING FERRICYANIDE–THYMOLPHTHALIN REAGENT

M. M. ABDEL BADEI* and E. A. EL SAWI

Chemistry Department, Faculty of Science, Benha University, Benha, Qalubia and Chemistry Department, University College for Women, Ain Shams University Heliopolis, Cairo, Egypt

Received November 16, 1985

Microdetermination of D(−) arabinose, D(+) galactose, maltose, fructose, lactose and ascorbic acid have been developed. A measured excess of potassium ferricyanide is added to the sample solution to oxidize the compound under investigation and the surplus is measured spectrophotometrically by thymolphthalin at 592 nm. The method is simple, reproducible and accurate to ±0.1%.

INTRODUCTION

The literature concerning the determination of reducing sugars and ascorbic acid seems to be quite rich. However, reducing sugars, e.g. pentoses, have been determined by alkaline potassium permanganate;[1] colorimetrically;[2] spectrophotometrically[3,4] and iodometrically.[5] Ascorbic acid has been determined spectrophotometrically by molybdophosphate complex[6]; iron(III), 1,10 phenanthroline[7] or with ferricyanide.[8,10] Glucose[11,12] and ascorbic acid[13,14] have been determined titrimetrically by ferricyanide and ferrocyanide has been determined by thymolphthalin reagent.[15] Ferricyanidethymolphthalin has been recently used for microdetermination of some reducing agents.[16]

The present work deals with the microdetermination of D(−)arabinase, D(+)galactose, maltose, fructose, lactose and ascorbic acid. A measured potassium ferricyanide solution is added to the sample solution to oxidize the compound under investigation, the surplus is determined spectrophotometrically with thymolphthalin, which turns blue, by oxidative regeneration of thymolphthalein; the color produced obeys Beer's law.[15]

---

* To whom all correspondence should be addressed, Chem. Dept., Faculty of Science, Benha University, Benha, Qalubia. Egypt.

EXPERIMENTAL

REAGENTS

Thymolphthalin reagent. Prepared by mixing 0.4 g of thymolphthalein, 4 g of zinc dust, 4 g of sodium hydroxide and 20 mL of bidistilled water in a 50 mL round bottom flask, heating for 2 hours under reflux, cooling, filtering through a hardened filter paper and diluting to 100 mL with boiled bidistilled water. If kept in a dark bottle containing a few granules of zinc, the reagent remains colorless for at least one month. Before use 10 mL of it were diluted to 100 with oxygen free bidistilled water (9.29×10^{-4} M). *Potasssium ferricyanide.* A 4.72×10^{-4} M solution prepared from the analytical salt.

Stock solution of reducing sugars and ascorbic acid (10 μg/mL) were prepared.

PROCEDURE

Place a known volume of the test solution, containing an appropriate amount of sample (Note 1) into a 25 mL standard flask, raise the pH to 12—13 by adding one or two drops of 1 M sodium hydroxide, then add 3.5 mL of potassium ferricyanide, digest in a boiling water bath for 15 min. (Note 2) and cool to room temperature. Then add 4 mL of thymolphthalin reagent and dilute to the mark. The solution was left to stand for 15 min. From the recorded measurements with and without the test solution, the corresponding equivalent absorbances were predicted by difference.

NOTES

1. The sample contains 0.6—2.0 μg fructose, 1.0—2.4 μg galactose, 0.6—2.4 μg arabinose, 0.8—2.4 μg maltose, 0.8—2.0 μg lactose and 0.4.—1.6 μg ascorbic.
2. Ascorbic acid reacts rapidly and needs only 1 min. whereas galactose reacts slowly and needs digestion for 30 min

RESULTS AND DISCUSSION

The optimum conditions are developed adapting the above procedure. A very slow reaction takes place between reducing sugar with ferricyanide at temperatures below 50°C even in high pH. As temperature increases the rate of reaction increases and it was found that at 100°C, the reaction takes reasonable time to get quantitative reaction. About 10 min were necessary for all the sugars investigated except galactose, which requires 30 min.

The optimum alkalinity (pH 12—13) is found to be in the range 0.025—0.05 M hydroxide. Below this range of alkalinity and at 100°C the reaction proceeds with limited recovery and above it ferricyanide slightly decomposes during digestion, as confirmed by blank experiment.

Standard solution and ascorbic acid could be used as titrant for ferricyanide by Erdey and Svehla [13] at pH 5—6, whereas Sant [14] reversed the titration, by addition of zinc acetate as buffer and promoter. The results show uncomplete reaction on cold at pH range 5—12. The optimal conditions for determination of ascorbic acid are heating to 100°C for 1 min. at pH range 8—12.

A standard series of solutions containing varying amount of sugars investigated was tested according to the recommended procedure. The absorbance difference values (by substracting the absorbance values of sugar or ascorbic acid standards from that of the blank) are down against the concentration of compounds investigated. A straight line passing by the origin will be obtained. Table 1 indicates the range of validity of Beer's law.

Table 1
The range of validity of Beer's low

The compound	The concentration range
Arabinose	0.6–2.4 μg/ml
Fructose	0.6–2.0 μg/ml
Galactose	1.0–2.4 μg/ml
Maltose	0.8–2.4 μg/ml
Lactose	0.8–2.0 μg/ml
Ascorbic acid	0.4–1.6 μg/ml

THE PRECISION OF THE METHOD

The results for a series of ten determinations are shown in table 2- The results are satisfactory. The maximum error is 1.0%. Any other oxidant or reductant present will interfere if it is capable of reacting with the sample of ferricyanide or ferrocyanide, thymolphthalin or thymolphthalein.

Table 2

Sample	Taken μg	Found, μg	Standard deviation μg
Arabinose	0.8	0.8	0.1
Fructose	0.7	0.69	0.1
Galactose	1.0	0.99	0.2
Maltose	0.9	0.89	0.1
Lactose	1.2	1.19	0.2
Ascorbic Acid	0.7	0.7	0.1

REFERENCES

[1] W. L. Evans, C. A. Buchler, C. D. Looker, R. A. Crawford and C. W. Holl, *J. Am. Chem. Soc.*, **47**, 3085 (1925).

[2] S. Bose, S. Mukerji and A. N. Stivastava, *Shakara*, **3**, 7(1960).

[3] T. E. Timell, C. P. J. Glandmans and A. L. Currie, *Anal. Chem.*, **28**, 1916 (1956).

[4] I. H. Bath, *Analyst*, **83**, 451 (1958).

[5] M. I. Tomoda, *Yakugaku Zasshi*, **80**, 1696 (1960).

[6] A. De Vleeschanwet, W. Deschacht and H. Hendrickx, *Meded. Londb Hoogesch. Gent.*, **26(1)**, 149 (1961).

[7] O. Isao and U. Tadashi, *Bull. Chem. Soc. Japan*, **37**, 1314 (1964).

[8] N. Rukmini, V.S.N.P. Kavitha and V. K. Devendra, *Talanta*, **28**, 332 (1981).

[9] E. Vamos and E. S. Gabor, *Norburg*, **17**, 409 (1973).

[10] M. Muralikrishna, Y.V.S.K. Sesha Sagi and T.V. Raghu Ram, *J. Indian. Chem. Soc.*, **56**, 794, (1979).

[11] H. C. Hagedron and B. N. Jensen, *Biochem.*, **135**, 46 (1923).

[12] E. Paschke, *Mikrochim. Acta* (Wien), **1955**, 983.

[13] L. Erdey and G. Svehla, *Z. analyt. Chem.*, **150**, 407 (1956),

[14] B. R. Sant, *Chemist. Analyst*, **47**, 65 (1958).

[15] M. F. El-Shahat, A.B. El-Sayed, M.M. Abdel Badei and A.I. Amer, *J. of h: Chinese Chem. Soc.* (In Press.)

[6] M.M. Abdel Badei, A.B. El-Sayed and E.A. El-Sawi, (Submitted for publication).

Revue Roumaine de Chimie, 32, 2, 145—150 (1987)

SYNTHESIS, CHARACTERIZATION, ANTIFUNGAL AND ANTIVIRAL ACTIVITY OF SOME TRANSITION METAL COMPLEXES OF CYCLOALKYL DITHIOCARBAMATES

O.P. PANDEY, S.K. SENGUPTA* and S.C. TRIPATHI
Department of Chemistry, University of Gorakhpur, Gorakhpur — 273 009, India

Received November 28, 1985

Manganese(III), cobalt(III), nickel(II) and copper(II) complexes of two new cycloalkyldithiocarbamates viz., N-(cyclopentyl)-, N-(cycloheptyl)-dithiocarbamates have been prepared and characterized by elemental analyses, magnetic susceptibility, molecular weight and electrical conductance measurements and spectral (electronic and infrared) data. All these compounds have been tested against two species of fungi, *Aspergillus niger* and *Helminthosporium oryzae* and also against *cucumber mosaic* virus.

INTRODUCTION

Metal complexes of dithiocarbamates have been extensively studied for quite some time.[1–3] The keen interest in these complexes is due to their widespread applications in biological and biochemical field.[1] Various dithiocarbamates have been employed as inhibitors in research of enzymes due to their metal combining capacity and ability to interact with sulfhydryl containing compounds.[1,4] They were first used in experiments on the control of various dermatophytes and have been reported as fungicides, insecticides and acaricides.[5–10] Zinc and manganese salts of ethylene bisdithiocarbamic acid were found to be almost as effective as one of the best insecticides in the control of greenhouse whitefly.[11] Iron and zinc salts of dimethyldithiocarbamic acid and tetramethylthiuram disulphide are widely used as fungicides.[2] Since a change of a substituent at nitrogen of a dithiocarbamate ligand may markedly affect the structural, fungicidal and antiviral properties of the complexes, it is worthwhile investigating the synthetic, structural, fungicidal and antiviral properties of manganese(III), cobalt(III), nickel(II) and copper(II) complexes of two new dithiocarbamates containing cycloalkyl ring at the nitrogen, viz. N-(cyclopentyl)-and N-(cycloheptyl)-dithiocarbamates.

EXPERIMENTAL

All chemicals used were of analytical grade. The ligands sodium N-(cyclopentyl)- and sodium N-(cycloheptyl)-dithiocarbamates were prepared according to the method reported earlier.[12]

The metal complexes have been prepared by following a common procedure. Metal salt and sodium salt of the ligand (1 : 2 molar ratio) were heated in water on a water bath for 30—45 min. and the reaction mixture cooled. The coloured reaction products separated were filtered, washed thoroughly with water, recrystallised from acetone and dried over P_2O_5.

Details of elemental analyses and physical measurements have been described elsewhere.[13]

Fungicidal activity was evaluated against *Aspergillus niger* and *Helminthosporium oryzae* by the agar plate technique[14] at three concentrations, viz. 1000 ppm, 100 ppm, and 10 ppm, and the number of replications in each case was three. The average percentage inhibition after 96 hrs. of various compounds was calculated as:

$$\% \text{ inhibition} = \frac{(C - T) \times 100}{C}$$

where:

C = diameter of fungus colony in control plates after 96 hours,

T = diameter of fungus colony in tested plates after 96 hours.

The antiviral activity was evaluated by noting the reduction in number of local lesions produced by cucumber virus on *Chenopodium amaranticolor*, when mixed with the chemical. Standard extract of the virus was mixed in an equal quantity of chemical solution (1000 ppm). Inoculations were made by leaf rubbing method. One half of each leaf was inoculated with inoculum containing virus and chemical and the other half was inoculated with the standard virus extract. Infections on different samples were calculated on the basis of the local lesions produced by each treatment and percentage inhibition was calculated as:

$$\% \text{ inhibition} = \frac{\text{No. of local lesions by control} - \text{No. of lesions by treatment}}{\text{No. of lesions by control}} \times 100$$

RESULTS AND DISCUSSION

Elemental analyses (Table 1) reveal 1 : 2 metal to ligand stoichiometry for the nickel(II) and copper(II) complexes, and 1 : 3 for manga-

Table 1

Analytical data of the complexes

Compound	Colour	Found (Calcd.) %				
		C	H	N	S	M
$Mn(S_2CNRR')_3^a$ **1**	brown	40.2 (40.4)	5.6 (5.6	7.6 (7.8)	35.5 (35.9)	10.3 (10.3)
$Mn(B_2CNRR')_3^b$ **2**	brown	46.2 (46.5)	6.6 (6.8)	6.7 (6.8)	30.8 (31.0)	8.5 (8.8)
$Co(S_2CNRR')_3^a$ **3**	dark green	40.0 (40.0)	5.3 (5.6)	7.8 (7.8)	35.4 (35.6)	10.9 (10.9)
$Co(S_2CNRR')_3^b$ **4**	dark green	46.1 (46.2)	6.7 (6.7)	6.4 (6.7)	30.8 (30.8)	9.3 (9.4)
$Cu(B_2CNRR')_2^a$ **5**	brown	37.4 (37.5)	5.1 (5.2)	7.0 (7.3)	33.0 (33.3)	16.5 (16.5)
$Cu(S_2CNRR')_2^b$ **6**	brown	43.4 (43.7)	6.2 (6.4)	6.4 (6.4)	29.0 (29.1)	14.3 (14.4)
$Ni(S_2CNRR')_2^a$ **7**	green	38.0 (38.0)	5.3 (5.3)	7.2 (7.4)	33.6 (33.8)	15.5 (15.5)
$Ni(S_2CNRR')_2^b$ **8**	green	44.1 (44.2)	6.1 (6.4)	6.3 (6.4)	29.2 (29.4)	13.5 (13.5)

[a] where R = H and $R' = C_5H_9$, CPD

[b] where R = H and $r' = C_7H_{13}$, CHD

nese and cobalt complexes. The interesting feature lies in the preparation of manganese and cobalt complexes, where oxidation of Mn(II) and Co(II) to Mn(III) and Co(III) follows which can be assumed to occur through the action of aerial oxygen in the presence of an excess of the sulphur ligand. The complexes are soluble in common organic solvents particularly in acetone, benzene, chloroform, carbon tetrachloride, dimethylformamide and dimethylsulphoxide. Molecular weight determination in boiling benzene and conductance measurements in nitrobenzene indicate monomeric and non-electrolytic nature of all these complexes.

MAGNETIC MOMENTS AND ELECTRONIC SPECTRA

Manganese(III) complexes. Room temperature magnetic moment studies of manganese(III) complexes show their paramagnetic nature having μeff. value 4.80 B.M., corresponding to four unpaired electrons in the complexes.[15] Electronic spectra of the complexes resemble that of a d^4 octahedral complex.[16] These exhibit bands at 15000–19500–19800, and 24000–24500 cm^{-1}, which may be assigned to $^5B_{1g} \rightarrow {}^5A_{1g}$, $^5B_{1g} \rightarrow {}^5B_{2g}$ and $^5B_{1g} \rightarrow {}^5E_g$ transitions,[16] respectively.

Cobalt(III) complexes. Cobalt(III) complexes are diamagnetic. The electronic spectra of these complexes show two bands at ca. 15000–15500 and 21000–21500 cm^{-1}. The position of these bands indicates the octahedral geometry for cobalt(III) complexes.[16] Spin-paired Co(III) in an octahedral field gives rise[13] to two d-d bands corresponding to $^1A_{1g} \rightarrow T_{1g}$ and $^1A_{1g} \rightarrow {}^1T_{2g}$ transition with a separation of 7000–1000 cm^{-1} and two spin-forbiden transitions $^1A_{1g} \rightarrow {}^3T_{1g}$ and $^1A_{1g} \rightarrow {}^3T_{2g}$. In the present complexes the two bands observed may be assigned[17] to $^1A_{1g} \rightarrow {}^1T_{1g}$ and $^1A_{1g} \rightarrow {}^1T_{2g}$ transitions in an increasing order of energy. However, the spin forbidden transitions are not observed due to the strong charge transfer band in the near UV region.

Nickel(II) complexes. Nickel(II)complexes are diamagnetic. The electronic spectra of these complexes show two bands at *ca.* 15000–15500 and 18200–18500 cm^{-1} which can be assigned[16,18] to $^1A_{1g} \rightarrow {}^1B_{1g}$ and $^1A_{1g} \rightarrow {}^1A_{2g}$ transitions respectively. The fact that no band is observed below 10000 cm^{-1} indicates square planar stereochemistry for these complexes which may also be deduced from their diamagnetic nature.[18]

Copper(II) complexes. Magnetic moments of copper(II) complexes with N-(cyclopentyl)- and N-(cycloheptyl)-dithiocarbamato ligands are 1.78 and 1.81 B.M. respectively. The electronic spectra of both complexes show bands at *ca.* 17000, 19000, and 23000 cm^{-1}. The position of the bands indicates that these complexes have square planar stereochemistry. A large number of copper(II) complexes possessing a square planar structure is known,[16] but there still exists confusion regarding the ordering of orbitals in square planar copper(II) species. For instance, it has been shown that the highest orbital is $^2b_{1g}(d_{x^2-y^2})$ but beyond that there is little agreement. Hatfield and Piper[19] have made crystal field calculations and obtained the ordering $d_{x^2-y^2} > d_{z^2} > d_{xy} > d_{xz'}$, d_{yz}. On the other hand, Schuit et al. have placed the lowest d_{z^2} orbital on the basis of the Wofsberg-Helmholtz calculations.[20] In the present complexes, the bands appear to have their origin in $d-d$ transitions, which can be assigned[16] to $^2B_{1g} \rightarrow$ $\rightarrow {}^2A_{1g}$ and $^2B_{1g} \rightarrow {}^2E_g$ transitions in increasing order of energy. The appearance of a high energy band at *ca.* 23000 cm^{-1} is a subject of lively discussion in recent years. Some authors have attributed the presence of this band to polymeric structures of the copper complexes. However, in the present case it appears to be due to charge transfer phenomena.[21]

INFRARED SPECTRA

The dithiocarbamate ligand can be represented by the following resonating structures and hence can act both as monodentate and bidentate ligand upon complexation with the metal:

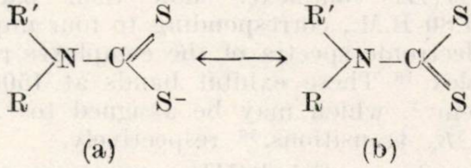

The extent to which the resonance form (c) contributes to the structure and its effect on physical and chemical properties of the complexes have been extensively studied.[23,24] The infrared spectra of free ligands and of complexes show that the $\nu(\mathrm{C}\overset{\cdots}{-}\mathrm{N})$ and $\nu(\mathrm{C}\overset{\cdots}{-}\mathrm{S})$ vibrational modes fall in the range 1465 – 1495 cm^{-1} and 970 – 1000 cm^{-1} respectively. Further observations reveal that there is shift in $\nu(\mathrm{C}\overset{\cdots}{-}\mathrm{N})$ frequency to higher value in the complexes in comparison with the ligand and also a strong band appears in the range mentioned above for $\nu(\mathrm{C}\overset{\cdots}{-}\mathrm{S})$ in all these complexes whereas doublet has been found in the same region for the ligands. Hence, the ligand behaves as bidentate ligand in these complexes and shows the maximum contribution of structure (c) on complexation. The far infrared spectra of the complexes show bands in the region 350 – 400 cm^{-1} which may be assigned[24] to $\nu(\mathrm{M-S})$.

ANTIFUNGAL ACTIVITY

The antifungal activity of two new dithiocarbamates viz., N-(cyclopentyl)- and N-(cycloheptyl)-dithiocarbamates and their complexes with Mn, Co, Cu and Ni was evaluated against *Aspergillus niger* and *Helminthosporium oryzae*.

The percentage inhibitions by various compounds are recorded in Table 2. Fungicidal action may be generalised as follows:

(i) All compounds have significant antifungal activity at 1000 ppm against both the fungi, the complexes being much more active than the corresponding ligands. Hence complexation increases the antifungal activity.

(ii) The antifungal activity has been found to decrease in the following order: Mn > Cu > Co > Ni.

(iii) All the compounds screened have been found to be more active against *H. oryzae* as compared to *A. niger*.

(iv) An increase in ring size results is an increase in activity.

Table 2

Antifungal activity of dithiocarbamate complexes

Compound No.	Average percentage inhibition after 96 hours					
	A. niger			*H. oryzae*		
	Conc. used (ppm)			Conc. used (ppm)		
	1000	100	10	1000	100	10
1	64.1	50.0	35.6	70.2	62.8	50.2
2	72.8	56.4	40.8	75.3	65.4	56.3
3	55.2	42.8	28.4	60.8	48.5	32.8
4	58.4	48.9	38.2	63.9	53.8	43.0
5	60.2	48.4	30.2	65.4	58.8	38.4
6	68.7	60.2	48.7	70.2	63.4	50.9
7	50.8	40.3	22.9	52.8	44.1	25.3
8	55.7	46.9	36.7	60.0	49.1	38.1
$(NaS_2CNRR')^a$	48.5	38.6	20.8	50.3	39.1	23.4
$(NaS_2CNRR')^b$	52.0	40.8	30.1	58.0	44.9	32.9

[a] where $R=H$ and $R' = C_5H_9$, CPD

[b] where $R=H$ and $r' = C_7H_{13}$, CHD

ANTIVIRAL ACTIVITY

The percentage inhibitions of *Cucumber mosaic virus* by various compounds are recorded in Table 3. All the compounds display very weak antiviral activity which decreases in the order: Cu>Mn>Ni≃Co. However, the complexes are found to be more active than their corresponding ligands.

Table 3

Antiviral activity of dithiocarbamate complexes*

Compound No.	*Cucumber mosaic virus Chenopodium amaranticolor* % inhibition
1	22.8
2	24.3
3	18.3
4	20.1
5	30.0
6	32.8
7	18.0
8	19.8
$(NaS_2CNRR')^a$	15.3
$(NaS_2CNRR')^b$	16.8

* Organism *Host plant* Concentration 1000 ppm

[a] where $R=H$ and $R'=C_5H_9$, CPD

[b] where $R=H$ and $r'=C_7H_{13}$, CHD

REFERENCES

[1] G. D. Thorn and R. A. Ludwig, "The Dithiocarbamates and Related Compounds", Elsevier Publishing Comp. New York, 1962.

[2] J. Willemse, J. A. Cras, J. J.Staggerda and G. P. Kiejers. *Structure and Bonding*, Berlin, **28**, 83 (1976).

[3] D. Coucouvanis, *Progr. Inorg. Chem.*, **11**, 233 (1970) ; **26**, 301 (1979).

[4] L. Cambi and A. Cagnasso., *Atti. Acad. Lincei.*, **14**, 301 (1979).

[5] H. Bode and F. Newman, *Z. analyt Chem.*, **169**, 410 (1959).

[6] H. Bode and F. Newman, *Z. analyt. Chem.*, **169, 410 (1959).**

[7] H. L. Klöpping, and G.J.M. Kerk Vander, *Rec. Trav. chim.*, **70**, 917, **949 (1951).**

[8] C. K. Jorgenson, *Inorg. Chim. Acta Rev.*, **2**, 65(1968).

[9] G.J.M. Vander Kerk, M.H. Raalte and A.K. Sijpesteijn, *Nature*, **176**, 308 (1955).

[10] F.P. Dwyer and D.P. Mellor, Chelating Agents and Metal Chelates, Academic Press, London, 1964.

[11] R.D. McMullen, *Nature*, **184**, 1335 (1959).

[12] S. Kumar and N.K. Kaushi, *J. Inorg. Nucl. Chem.*, **43**, 2679 (1981).

[13] S. K. Sengupta, S.K. Sahni, and R.N. Kapoor. *Indian J. Chem.*, **10**A, 703 (1980).

[14] J.G. Horsfall, *Bot. Rev.*, **11**, 357 (1945).

[15] B.N. Figgis, "Introduction to Ligand Fields", Wiley Eastern Ltd., New Delhi 1976.

[16] A.B.P. Lever, "Inorganic Electronic Spectroscopy", Elsevier, Amsterdam, 1968.

[17] A.B.P. Lever, *Coord. Chem. Rev.*, **3**, 119 (1968).

[18] H.B. Gray, "Transition Metal Chemistry", Marcel Dekker, New York, 1 1965.

[19] W.E. Hatfield and T.S. Piper, *Inorg. Chem.*, **3**, 841 (1964).

[20] D. Ros and G. C. A. Schuit, *Theor. Chim. Acta*, **4**, 1 (1966).

[21] I.N. Procter, B.J. Hathaway, and P.G. Hodgson, *J. Inorg. Nuclear Chem.*, **34**, 3698 (1972).

[22] J. Chatt, L.A. Duncanson and L.M. Venanzi, *Soumen Kemi*, B**29**, 75 (1956).

[23] G. Marcotrigiano, G.C. Pellacani, C. Preti and G. Tosi, *Bull. Chem. Soc. Japan*, **48**, 1018 (1975).

[24] S. K. Sengupta, S.K. Sahni and R.N. Kapoor, *Acta Chim. Acad. Sci. Hung.*, **104**, 89 (1980).

Revue Roumaine de Chimie, 32, 2, 151–154 (1987)

ESTUDIO DE COMPLEJOS METÁLICOS DE BASES DE SCHIFF DERIVADAS DEL 2-TIOFENCARBOXIALDEHIDO Y 2-PIRIDINCARBOXIALDEHIDO, Y *o*-AMINOBENCENOTIOL

F. CAPITÁN*, P. ESPINOSA, F. MOLINA y L.F. CAPITÁN-VALLVEY
Departamento de Química Analítica, Facultad de Ciencias, Universidad de Granada, 18071, Granada, España

Recibido: el 20 de diciembre de 1985

Se realiza un estudio de los compuestos aislados a partir de la reacción de la 2-(2-tienil) benzotiazolina y la 2-(2-piridil)benzotiazolina con diversas sales metálicas. Este estudio permite demostrar de manera clara que los complejos metálicos sintetizados son derivados de las bases de Schiff tautómeras respectivas, 2-(*o*-mercaptofeniliminometil)tiofeno y 2-(*o*-mercaptofeniliminometil)piridina.

A series of complexes isolated from the reaction of 2-(2-thyenilbenzothiazoline) and 2-(2-pyridyl)benzothiazoline with several metallic salts wás studied. The results obtained from this study support very well the fact that the resulting products are metal-complexes of the tautomeric Schiff bases, 2-(*o*-mercaptophenyliminomethyl)thiophene and 2-(*o*-mercaptophenyliminomethyl)pyridine.

INTRODUCCIÓN

La condensación de *o*-aminobencenotiol con un compuesto carbonílico no permite normalmente el aislamiento de una base de Schiff como cabría esperar, sino que se obtiene una tiazolina o una benzotiazolina. Esto se debe a algunas reacciones laterales que se dan en el transcurso de la condensación.

Se ha demostrado que en disolución existe un equilibrio tautomérico entre la tiazolina o benzotiazolina y la base de Schiff correspondiente, que se desplaza hacia la formación de esta última en medios muy básicos.[1,2–7] La reacción de una disolución de tiazolina o benzotiazolina con iones metálicos da lugar a la precipitación de los complejos metálicos de la base de Schiff tautómera. Algunos autores han postulado que el ión metálico retira a la forma base de Schiff de una mezcla de equilibrio. [3,4] Otros, sin embargo, postulan que en presencia de iones metálicos la estructura cíclica de la tiazolina o benzotiazolina se reordena para dar los quelatos metálicos de la base de Schiff de forma cuantitativa. [5,7]

A menudo, no obstante, los resultados aportados, basados fundamentalmente en estudios de IR y UV–VIS, no evidencian de forma clara cual es la naturaleza de los complejos obtenidos.

---

* Autor a quien debe enviarse la correspondencia

En publicaciones anteriores[8-10] hemos dado cuenta de los resultados obtenidos en el estudio de la actuación de la 2-(2-tienil)benzotiazolina* y la 2-(2-piridil)benzotiazolina* frente a iones metálicos. El objeto del presente trabajo es aportar nuevos datos que sirvan para dilucidar de una manera clara cual es la naturaleza del ligando presente en los complejos sólidos aislados.

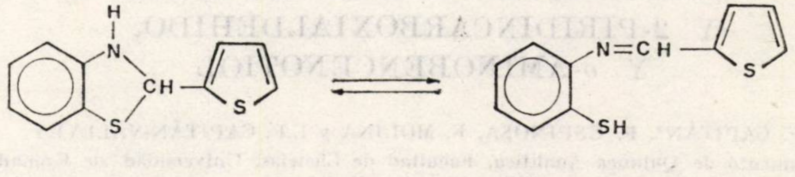

2-(2-tienil)benzotiazolina 2-(o-mercaptofeniliminometil)tiofeno

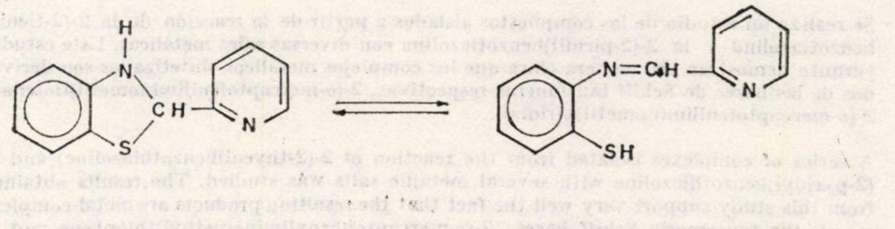

2-(2-piridil)benzotiazolina 2-(o-mercaptofeniliminometil)piridina

EXPERIMENTAL

SÍNTESIS DE LOS REACTIVOS

Los reactivos se han sintetizado por condensación en etanol de 2-tiofencarboxialdehido y 2-piridincarboxialdehido con *o*-aminobencenotiol según los procedimientos descritos en trabajos anteriores.[8,9] La 2-(2-tienil)benzotiazolina es un sólido cristalino de color amarillo pálido (p.f. 95 – 96°) y la 2-(2-piridil)benzotiazolina es un compuesto cristalino de color amarillo (p.f. 98.5 – 99°).

SÍNTESIS DE LOS COMPEJOS

El método mas adecuado para la preparación de los complejos consiste en calentar a reflujo durante aproximadamente media hora una mezcla etanólica de la benzotiazolina y de la sal metálica correspondiente (generalmente nitrato o acetato). El sólido formado se filtra, se lava con una mezcla hidroalcohólica 50 % v/v y se deja secar a vacio sobre $CaCl_2$ y H_2SO_4. Se obtenen así los complejos metálicos con una pureza alta y con elevados rendimientos.[8,9]

MEDIDAS FÍSICAS

Los espectros IR se registraron en un espectrofotómetro Beckman 4240 IR, en la región 4000 – 250 cm^{-1} en pastillas de KBr. Los espectros de absorción de los reactivos y de los complejos en DMSO se han registrado en un espectrofotómetro Bausch-Lomb mod. Spectronic 2000. Los espectros de ^1H–RMN en DMSO se han registrado en un espectrofotómetro Hitachi Perkin-Elmer mod. R – 20B usando TMS como referencia interna.

---

* Esta es la forma en que normalmente aparecen nombrados estos compuestos. También pueden encontrarse en la bibliografía nombrados como 2-tiazolin-2-iltiofeno, y 2-tiazolin-2-ilpiridina.

RESULTADOS Y DISCUSIÓN

El análisis de los espectros IR de los compuestos metálicos en estudio [8,9] sugiere que son quelatos metálicos de las bases de Schiff tautómeras de las benzotiazolinas. Este hecho se basa fundamentalmente en que en los espectros de los complejos se comprueba la desaparición de las bandas ν(N—H) y ν(C—S—C), presentes en los espectros de los reactivos en las regiones 3300—3200 cm^{-1} respectivamente y la aparición de una fuerte banda próxima a 1600 cm^{-1} atribuible a la vibración ν(C=N) coordinado. [11]

No obstante, resulta a veces muy difícil precisar la posición de la banda de tensión del C=N azometínico debido a la presencia en la misma zona de otras bandas intensas como las correspondientes a ν(C=C) aromáticos y ν(C=N) piridínico, así como las originadas por las vibraciones de tensión del grupo acetato en dos de los complejos aislados.

El análisis mediante espectrofotometría UV—VIS de estos compuestos pone de manifiesto lo siguiente: los espectros de los ligandos muestran dos bandas alrededor de 250 y 315 nm atribuibles a transiciones típicas de la forma cíclica benzotiazolina [1,3,12], mientras que en los espectros de los complejos estas bandas no experimentan apenas desplazamiento si bien todos ellos exhiben una nueva banda en la región visible (Tabla 1) atribuible a transiciones n—π^* o π—π^* implicando el doble enlace C=N azometínico.[12,13] Estos resultados apoyan a los anteriores respecto a que los complejos formados sean de las bases de Schiff pero sin que en ambos casos quede totalmente aclarada su naturaleza. Por ello hemos procedido a su estudio mediante ^1H—RMN.

Tabla 1

Datos espectroscópicos

Compuesto	^1H—RMN(δ ppm)				
	NH	—HC=D—	Aromáticos	λ(nm)	$\varepsilon(l \cdot mol^{-1} \cdot cm^{-1})$
$C_{11}H_9NS_2$	3.30	—	6.5—8.1	—	—
$Zn(C_{11}H_8NS_2)_2$		8.60	6.8—8.0	450	3.0×10^3
$Cd(C_{11}H_8NS_2)_2$	—	8.50	6.9—8.2	420	6.0×10^3
$Hg(C_{11}H_8NS_2)_2$	—	8.70	6.8—8.0	380	6.5×10^3
$Pb(C_{11}H_8NS_2)_2$	—	8.80	6.6—7.9	415	3.8×10^3
$Cd(C_{11}H_8NS_2)CH_3COO$	—	8.70	6.9—8.0	415	3.0×10^3
$C_{12}H_{10}N_2S$	3.40	—	6.2—8.4	—	—
$Zn(C_{12}H_9N_2S)_2$	—	9.40	6.9—8.8	520	5.0×10^3
$Cd(C_{12}H_9N_2S)_2$	—	9.15	6.9—8.7	500	6.4×10^3
$Hg(C_{12}H_9N_2S)_2$	—	9.30	6.7—8.8	505	5.4×10^3
$Pb(C_{12}H_9N_2S)CH_3COO$	—	9.40	6.8—8.8	485	1.6×10^3

Los espectros de ^1H—RMN de la 2-(2-tienil)benzotiazolina y de la 2-(2-piridil)benzotiazolina en DMSO constan de una señal a δ 3.30 ppm (aguda e intensa) y a 3.40 ppm (ancha, de intensidad media) respectivamente, que atribuimos al protón NH de la benzotiazolina, y multipls complejos en la región δ 6.40—8.70 ppm que atribuimos a los protones aromáticos (Tabla 1).

En los espectros ^1H-RMN de los complejos se observa fundamentalmente la desaparición de la señal debida al protón NH, y la presencia de un singlete agudo en la región 8.30—8.50 ppm en el caso de los derivados tiofénicos, y en la región 9.15—9.40 ppm en el caso de los piridínicos (Tabla 1), que hemos atribuido al protón azometínico, $-HC=N-$, de la forma imina presente en los complejos. La forma y posición de estas señales concuerda totalmente con la de compuestos similares conteniendo todos ellos la agrupación azometina.[12,14,15]. Así por ejemplo los espectros de ^1H-RMN en DMSO del 2-(*o*-hidroxifeniliminometil)tiofeno y de sus complejos (ML_2) de Zn y Cd exhiben la señal del protón azometínico a 8.80, 9.10 y 8.95 ppm respectivamente.[16]

En los acetato complejos de Cd y Pb estudiados se observa la señal de los protones del grupo metilo en forma de un singlete agudo a δ 1.80 y 1.60 ppm respectivamente.

De los resultados anteriores se desprende pues la gran utilidad que presenta la utilización de la ^1H-RMN en estos casos. Mientras que las bandas IR que podrían servir como criterio diagnóstico se presentan solapadas en la región 1630—1480 cm^{-1}, en los espectros de ^1H-RMN se presenta una situación inversa. La señal del protón azometínico aparece claramente diferenciada de las señales de los protones aromáticos, y en una región bastante alejada de la señal de los protones metilo de los acetato complejos estudiados.

BIBLIOGRAFÍA

[1] F.J. Goetz, *J. Heterocycl. Chem.*, **4**, 80 (1967) ; *Ibid.*, **5**, 501 (1968) ; *ibid.*, **5**, 509 (1968).

[2] L.F. Lindoy and S.E. Livingstone, *Inorg. Chim. Acta*, **1**, 365 (1967).

[3] E. Uhlemann and V. Pohl, *Z. Anorg. Allg. Chem.*, **397**, 162, (1973).

[4] L.F. Lindoy, *Coord. Chem. Rev.*, **4**, 41 (1969).

[5] H. Jadamus, Q. Fernando and H. Freiser, *J. Amer. Chem. Soc.*, **86**, 3056 (1964).

[6] E. I. Steifel, J.H. Waters, E. Billig and H.B. Gray, *J. Amer. Chem. Soc.*, **87**, 3016 (1965).

[7] E. Bayer and E. Breitmaier, *Chem. Ber.*, **101**, 1579 (1968) ; *ibid.*, **102**, 728 (1969).

[8] F. Capitán, F. Salinas et L.F. Capitán-Vallvey, *Bul. Soc. Chim. France*, **1—2**, 35 (1979) ; *ibid.*, **1—2**, 185 (1979).

[9] L.F. Capitán-Vallvey and P. Espinosa, *Polyhedron*, **2**, 1147 (1983).

[10] F. Capitán, L.F. Capitán-Vallvey, F. Molina y P. Espinosa, *Quim. Anal.*, **4**, 177 (1985).

[11] E. Uhlemann and V. Pohl, *Z. Chem.*, **9**, 385 (1969) ; M. Consiglio, F. Maggio, T. Pizzno and V. Romano, *Inorg. Nucl. Chem. Lett.*, **14**, 135 (1978).

[12] R.K. Sharma, R.V. Singh and J.P. Tandon, *J. Inorg. Nucl. Chem.*, **42**, 1267 (1980).

[13] N.S. Biradar, V.H. Mahabe and V.H. Kulkarni, *Inorg. Chim. Acta*, **7**, 267 (1973).

[14] K.A. Parry, P.J. Robinson, P.J. Sainsbury and M.J. Waller, *J. Chem. Soc.* (*B*), 700 (1970) ; A.F.M. Iqbal., *J. Org. Chem.*, **37**, 2791 (1972).

[15] A.S. Al-Tai, D.M. Hall and A.R. Mears, *J.C.S.*, *Perkin Trans*(*II*), 133 (1976) ; P.A.S. Smith and Chi Van Dang, *J. Org. Chem.*, **41**, 2013 (1976).

[16] F. Capitán, F. Molina, P. Espinosa and L.F. Capitán-Vallvey, *Acta Chimica Hungarica* (aceptado para publicación).

Revue Roumaine de Chimie, 32, 2, 155–177 (1987)

REACTIONS OF PYRYLIUM SALTS WITH NUCLEOPHILES. XIX[1]

NOVEL BISPYRIDINIUM SALTS WITH POTENTIAL BIOLOGICAL ACTIVITY

ALEXANDRU T. BALABAN[a] and EMIL STEPAN[b]

[a] Polytechnic Institute, Organic Chemistry Department, Splaiul Independenței 313, 76206 Bucharest, Romania

[b] Chemical Research Institute — ICECHIM, Splaiul Independenței 202, Bucharest, Romania

Received October 2, 1986

Biologically active bispyridinium salts are reviewed. New bispyridinium salts were prepared from pyrylium salts and the following classes of primary aromatic diamines : *m*- and *p*-phenylenediamine derivatives ; 2,7-naphthylenediamine ; 4,4′-diaminotriphenylmethane leading to a racemic dication by stepwise reaction with two different pyrylium salts ; various diaminodibenzyl derivatives ; diaminostilbene derivatives and 4,4′-diaminotolan ; and polyimino-polyethylenediamines. Steric and electronic factors influencing the reactivity are discussed, noting that in some cases the reaction stops at the monopyridinium cation stage.

1. KNOWN BIOLOGICALLY ACTIVE BISPYRIDINIUM SALTS

Literature data on known bispyridinium compounds with proven biological activity are numerous. The following survey will group references non-exhaustively into a few areas in order to present a systematic overview.

1.1. Reactivation of acetylcholinesterase blocked by organophosphorus compounds

Several organophosphorus compounds are able to block acetylcholinesterase by phosphorylating or phosphonylating it, leading to pronounced toxicity ; this is the basis for the neuroparalytic action of nerve gases and for the selective toxicity of pesticides. It was discovered in 1955 that two oximes : 4- or 2-hydroxy-iminomethyl-N-methylpyridinium (4-PAM and 2-PAM, respectively) are able to restore the activity of blocked acetylcholinesterase.[2] The latter is more active than the former. Poziomek and coworkers[3] tested 1,1′-(1,ω-polymethylene)bis-(4-hydroxyiminomethyl-pyridinium) salts **1** with $n = 2-5, 10$; these compounds are more active than 2-PAM, and the trimethylene dibromide **1** with $n = 3$ (TMB-4) proved to be the best, in association wih atropine. The decamethylene compound **1**, $n = 10$ is too toxic. Hobbiger et al.[4] investigated mono- and dioximes of bis-pyridinium salts **2**, with R,R′ = H or CH=NOH and n=1−5; the substituents were situated in positions 4,4′. Other authors[5] reported similar explorations, varying also the positions of the substituents. One oximic group is necessary and sufficient and the second group[6] is Alk, NR_2, NHAc, SR, SOR, Cl, I; the anion may be Cl^-, Br^-, I^-, or HF_2^-. Since 1,1′- (1,3-trimethylene) bispyridinium diiodide is inactive (**2**, R = R′ = H, n = 3, X = I),[7] the oximic group is essential.

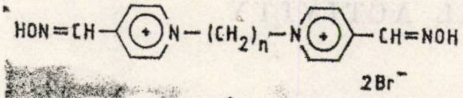

1

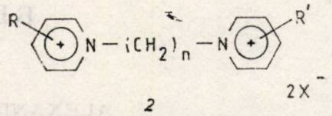

2

Studies with **1**, n = 1−6, 8, 10 using intact and blocked acetylcholinesterase revealed that the interaction with the active anionic centres of the enzyme is possible only when $n \geqslant 2$ with a flexible bridge between the two rings.[8] Two derivatives (R=H or Me) of the 1,1-[1,4-phenylenebis(methylene)]bispyridinium salt led to higher survival likelihood than 2-PAM in the presence of neuroparalytic agents, though their activity was lower.[9] Other derivatives of **3** were also found to be active.[10] 1,1′-[1,2-Phenylenebis(methylene)] bis (2-hydroxyiminomethyl-pyridinium) dibromide **4**, also known as OX-2, reactivates (in concentrations as low as 10^{-4} M) Sarin-blocked acetycholinesterase.[11] Loomis et al.[11] investigated N,N′-(*o*, *m*, or *p*-xylylene)bispyridinium salts related to **3** and **4**, and found that the *p*-xylylene derivatives are the most efficient, especially as alkali metal salts.[12]

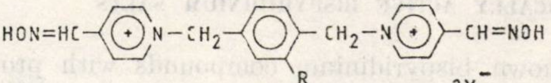

3

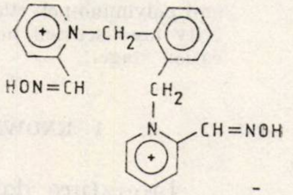

4

Lüttringhaus and Hagedorn[13] discovered the activity of ethers **5** with at least one 2- or 4-oximic group on one ring (one or two other substituents are placed on the other ring, preferably in *para*). The bis-4-oxime **5**, R = CH=NOH, R′=H is also known as Toxogonin; its monocation (one oximic group as CH=NONa) is active against toxic phosphoric esters.[12] Similar compounds proved to be effective,[14] and a mathematical model for the activity of **5** was proposed;[15] QSAR studies based on hydrophobicity and Verloop's steric parameter were reported.[16] Interestingly, esters similar to **5** with two 4,4′-groups CMe_3, CH=NOAlk, or $CO-C_6H_{11}$ (hexa-

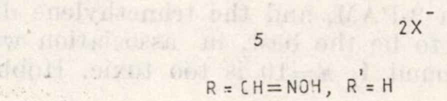

5

R = CH=NOH, R′ = H

hydrobenzoyl) were also active although they did not possess oximic groups.

The bridge between the two pyridinium rings may include the double bond of a 2-butene-1,4-diyl group, as in **6**;[9,18] the ability to restore blocked acetycholinesterase is 7–10 times higher than for **1**, $n=4$.[19] A tetroxime **7** is also active.[20]

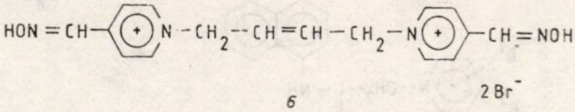

6

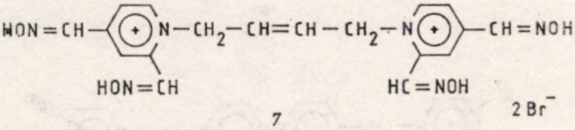

7

Other types of bridges include ketonic chains such as **8**, known as MBM-3,[21] which passes more easily the blood-brain barrier via retineal blood.[22] Other less active types of bridges include 2,5-thiophenediyl,[23] sulfide,[12] 1,2-dihydroxy-1,2-ethylene,[24] 2,5-dihydro-2,5-furanediyl,[25] and 2,5-tetrahydrofuranediyl;[26] the latter compound which is related with **1** $n=4$ and with **7**, blocks at high doses neuromuscular transmission like curare. Finally, a bispyridinium monoxime **9** is the only active compound whose oximic group is not attached directly to a pyridinium ring.[27]

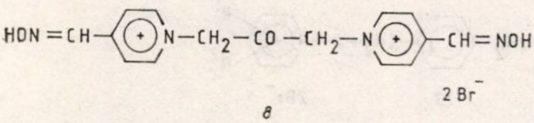

8

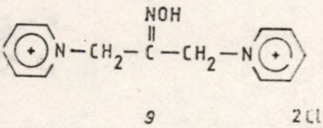

9

1.2. Parasympathetico-mimetic compounds, neuromuscular and ganglionar blocking agents

Studies of the bispyridinium systems **10** revealed that they inhibit acetylcholinesterase; they are less toxic than neostygmine and are antidotes for d-tubocurarine.[28] Other compounds with similar action are **11** (lower activity than physostigmine),[29] and **12**.[30] Cholinesterase inhibitors **12** and **13**,[31] and human pseudocholinesterase inhibitors **15**, **16**,[32] and **17**[33] were synthesized. In QSAR studies it was shown that **17**, R=H, $n=10$ is[33] the closest analogue of curare and the most potent compound with the distance between the two nitrogen heteroatoms close to 15 Å.[34] However, 1,1′-(1,6-hexanediyl)bispyridinium (**17**, $n=6$, R=H) is less active than analogous bisacridinium or bis(benzo[*c*]quinolinium) compounds.[35] Compounds **17**, R=NH_2 are synthetic analogues of acetylcholine and compete with it on receptors in electrical organs of *Electrophorus electricus*[36] or *Torpedo californica*; for $n=12$ and 14 the highest affinity is attained;[37] for $n=10$, comparative studies for the interaction with acetylcholinesterase were carried out.[38] Compounds **17**, R=$CONH_2$ or H, $n=2-6$, 9, 10 have a curare-like action[39] and are less toxic than tubocurarine or neurotoxins from *Cobra* venom; such systems **17**, $n=10$[40]

tested on cats, pigeons or chicken cause paralysis at the myoneural junction of skeletal muscles by inhibiting the depolarizing action of the acetyl-

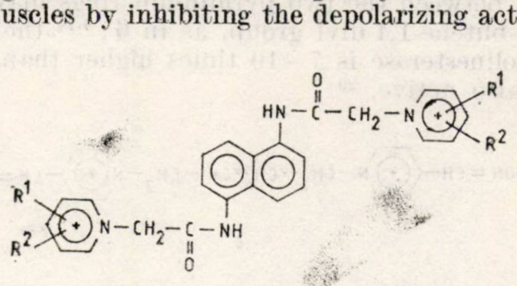

10

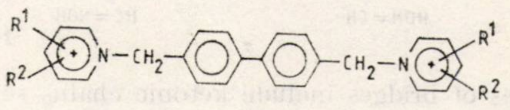

11

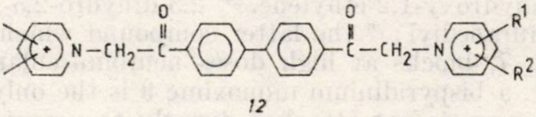

12

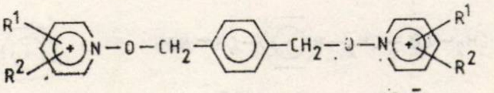

13 2Br⁻

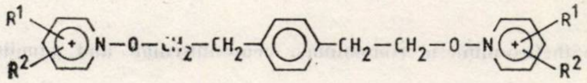

14 2Br⁻

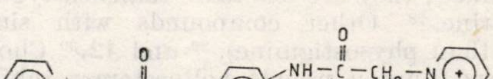

15 2Br⁻

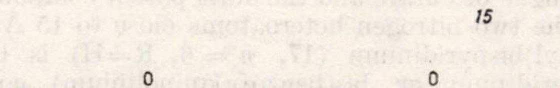

16 2Br⁻

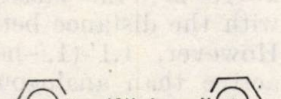

17 2Br

choline neurohormone. [41] A QSAR study based on π-electron densities in the pyridinium rings for 17, R=H, $n = 4$, 9 and 10 was correlated with tests on rats. [42]

2,2′-(1,ω-Polymethylene)bis(1-methylpyridinium) diiodides, **18**, $n = 3-8$, 11, 12 were synthesized by Bianchetti;[43] for lower n values, ganglionar blocking activity was observed, while for higher n values curare-like activity was manifested.[44]

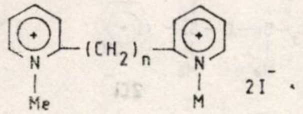
(CH2)n
N
Me
N
M
2I⁻

18

Substituted bispyridinium systems **19** related to **3** have a paralytic action on respiratory muscles,[45] comparable with pentamethonium salts. Esters such as **20** or **21** are ganglionar blocking agents.[31]

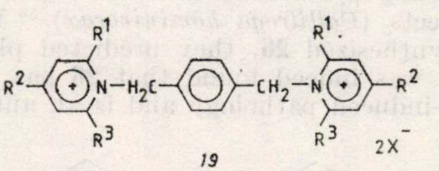
R1
R2
N–H2C
CH2–N
R1
R2
R3
R3
2X⁻

19

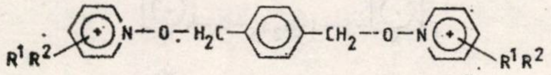
R1R2
N–O–H2C
CH2–O–N
R1R2
2Br⁻

20

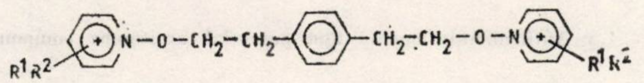
R1R2
N–O–CH2–CH2
CH2–CH2–O–N
R1R2
2Br⁻

21

1.3. Bispyridinium compounds with bactericidal and fungicidal action

A patent[46] claims that compounds **22**, R=SAlk, R′=H or a C_1-C_3 alkyl have a pronounced bactericidal and fungicidal activity; a similar activity was manifested by **22**, R=NMe_2, R′=H.[47] Other patents[48] provided evidence for activity against *Staphylococcus aureus*, *Escherichia coli* or *Candida albicans* of **22**, n=10 or 12, R′=H, R=NHAlk (C_7, C_8-alkyls) and of *m*- or *o*-isomers. The compound **22**, R′=H, R=C_8H_{17} is a skin disinfectant.[49]

Kharchenko and coworkers[50] reported that compounds **23**, some of which had been patented earlier by us,[51] have antimicrobial and antiviral activities comparable with that of rubomycine and bleomycine.

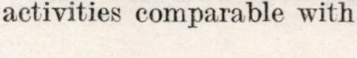
R
N–(CH2)n–N
R
R′
R′
2X⁻

22

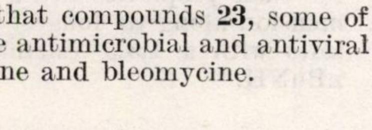
R1
R1
R2
N–(CH2)n–N
R2
R3
R3
2X⁻

23

Bispyridinium salts **24** are active against *Koch bacillus* and *Pseudomonas aeruginosa*; systems **25** are mouth disinfectants.[52]

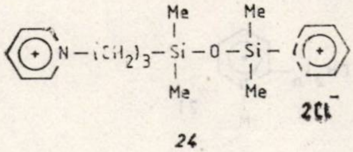

24

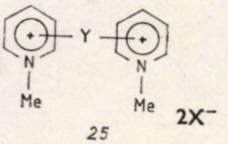

25

1.4. Chemosterilants and antisecretory compounds

1,1′-Methylenebispyridinium diiodide, **17**, R=H, n=1 is a chemosterilant for insects (*Callitroga hominivorax*).[53] When in 1966 Renault and Cartron[54] synthesized **26**, they predicted pharmacologic activity; later in 1980, it was indeed found that **26** has antisecretory activity; it inhibits stress-induced pathology and is an anti-ulcer agent.[55]

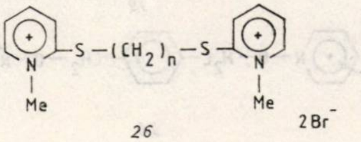

26

1.5. Antileukemic agents and potential antitumor compounds

Atwell and Cain discovered that bispyridinium compounds with planar geometry and a certain lipophilic/hydrophilic compromise possess antileukemic activity; whereas 2- and 4-acylaminopyridinium systems are inactive, their 3-acylamino congeners **27** (R=R′=R″=H) with a central terephthalic system,[56] or **28**[57] and **29**[58] with a central *p*-carboxycinnamic system, proved to be effective. Among various substituents which were tested for **27**, the most effective correspond to R′=R″=H, R=NH_2. A compound **30** lacking symmetry[59] is also active, but its synthesis is a long one. The symmetric compound **31** proved to have remarkable antileukemic properties.[60] Apparently, supplementary conditions for such properties are a certain molecular rigidity and a molecular dimension along its longest axis of about 40 Å.[61] Cytostatic bispyridinium salts with a 1,3,5-triazinic bridge were prepared with R = MeO or nBuNH.[62]

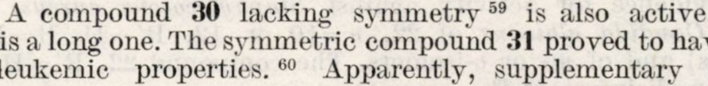

27

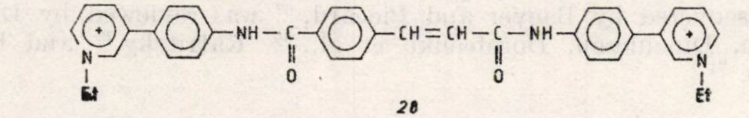

28

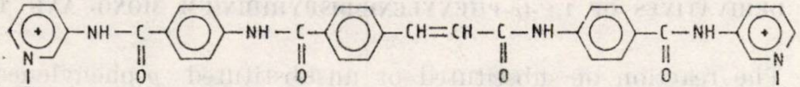

29

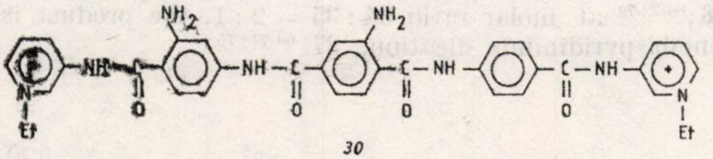

30

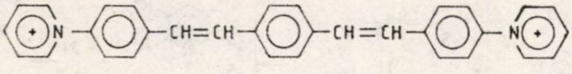

31

1.6. Bispyridinium herbicides and viologens

A vast literature exists on diquaternary bispyridinium salts since the discovery that **32** (diquat)[63] and **33** (paraquat)[64] possess selective phytotoxic properties enabling their wide-spread agricultural use. Biological tests, compounded with UV–VIS and ESR spectral studies and with electrochemical reduction data, led to a consistent explanation of their mode of action in plants involving formation of radical-cations. Methylviologen **33** (like related bispyridinium salts) has recently become an intense object of study because it sensitizes the conversion of solar energy into chemical energy, e.g. together with transition metal catalysts for hydrogen formation from water.

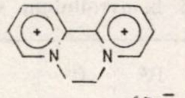

32

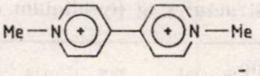

33

Both these vast areas are beyond the scope of the present literature survey because of the large number of references and of the rapid development of the field. A book on bispyridinium herbicides summarizes earlier literature data.[65]

The present paper reports the synthesis and spectra of several series of pyridinium salts obtained from pyrylium salts and diamines. The syntheses described in the above literature review were usually obtained by a different approach, namely Menshutkin quaternization of pyridines with alkyl halides or dihalides. Only a few earlier papers reported the formation of bispyridinium salts from pyrylium salts and diamines.[51,66] This reaction, discovered by Baeyer and Piccard,[67] was reviewed by Dimroth,[68] Balaban, Dinculescu, Dorofeenko et al.,[69] Katritzky[70] and by Polish authors.[71]

2. DERIVATIVES OF 1,1′-(*p*-PHENYLENE)BISPYRIDINIUM MONO- AND DICATIONS

The reaction of substituted or unsubstituted *p*-phenylenediamines (**35**) with 2,4,6-trisubstituted pyrylium salts (**34**) was described previously; at molar ratio 1 : 1, the result is a 1-(4-aminophenyl)-pyridinium monocation, **36**;[66,72,73] at molar ratio **34** : **35** = 2 : 1, the product is a 1,1′-(1,4-phenylene)bispyridinium dication, **37**.[66,73–75]

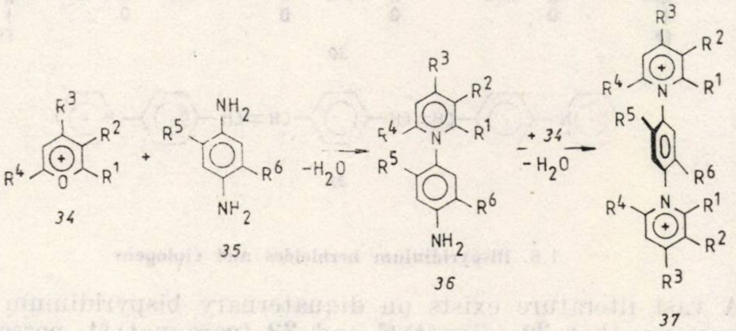

We report here that, along with the molar ratio, the nature and position of substituents on the pyrylium ring also influence the type of reaction product.

Thus, depending on all the above three parameters, one may isolate monocations, dications, or a mixture of both (Table 1).

Table 1

Structures of pyridinium (**36**) and bispyridinium salts (**37**)

Comp. 36, 37	R^1	R^2	R^3	R^4	R^5	R^6	Product
A	Me	Me	Me	Me	H	H	Mono, Bis
B	Me	Ph	Me	Me	H	H	Mono, Bis
C	Me	H	Me	Me	SO_3	H	Mono
D	Me	Ph	Me	Me	Cl	H	Mono
E	Me	H	Me	Me	Cl	Cl	Mono
F	Me	Ph	Me	Me	Cl	Cl	Mono
G	Me	Me	Ph	Me	H	H	Bis
H	Me	H	Me	iPr	H	H	Bis
I	Me	H	Me	Me	OMe	H	Bis
J	Ph	H	Ph	Ph	OMe	H	Bis
K	Me	H	Me	Me	Cl	H	Bis
L	Ph	H	Ph	Ph	Cl	H	Bis

2-Methoxy-1,4-diaminobenzene and 2,4,6-trimethyl- or 2,4,6-triphenylpyrylium perchlorates afford the bispyridinium dications **37 I, J**.

1,4-Diaminobenzene-2-sulfonic acid does not react with pyrylium salts, but its alkali metal salts react readily with pyrylium salts yielding an amphionic monopyridinium derivative **36C** in all conditions. Monocations **36E, F** are also the reaction products under any circumstance from 2,5-dichloro-1,4-diaminobenzene and pyrylium salts. However, one chlorine substituent on the 4-phenylenediamine ring may lead either to monocations (**36D**) or to dications (**37K, L**). 2,3,4,6-Tetrasubstituted pyrylium salts **34A, B** even in excess afford monocations **36** on refluxing with 4-phenylenediamines in lower alcohols (methanol, ethanol, isopropanol); however, in refluxing dimethylformamide at molar ratios **34** : **35**=2 : 1, only the bispyridinium salts **37A, B, G** were obtained.

Thus, one may obtain evidence for electronic factors controlling the course of the reaction (methoxy groups on the diamine facilitate the reaction, chloro substituents retard it) and for steric factors (dichloro substituents on the diamine stop the reaction to the monocation stage; an isopropyl group on pyrylium, **34H**, lowers its reactivity).

Table 2 presents ^{1}H-NMR data of pyridinium salts **36** and **37**. As reported in previous papers, [72,77]the ring current in the orthogonal systems **36** and **37** causes appreciable shielding of protons belonging to 2,6-methyls on the pyridinium rings. We have to take into account the ^{1}H-NMR data of N-(*o*-, *m*-, and *p*-methoxyphenyl)-2,4,6-trimethylpyridinium cations: [78] the chemical shift of the 2,6-methyl protons are 2.42, 2.48 and 2.50 ppm, respectively, in TFA. Therefore we can assign chemical shifts to 2,6-methyl protons in bispyridinium cations **37I** and **K**. In the latter dication, the assignment of 4-methyl protons and of 3-pyridinium protons is tentative and is based on the idea that the inductive effect of an N-(*m*-chlorophenyl) group deshields all protons relative to an N-(*o*-chlorophenyl) ring.

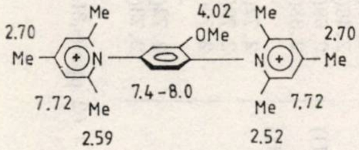

37I

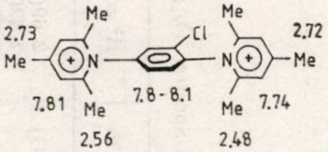

37K

3. DERIVATIVES OF 1,1'-(*m*-PHENYLENE)BISPYRIDINIUM DICATIONS

m-Phenylenediamine and its substituted derivatives **39** react readily with 2,4,6-trisubstituted pyrylium salts **38** forming bispyridinium cations **40**. [73,78,79]

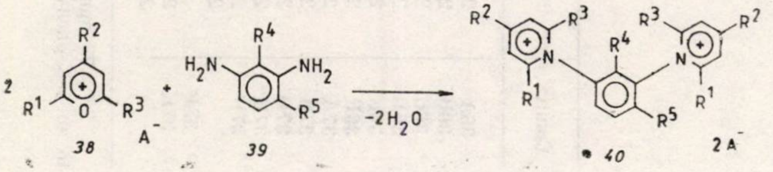

Table 2

^{1}H-NMR Spectra (δ, ppm) of pyridinium salts **36** and **37** in trifluoroacetic acid

Comp.	R^1 = 2-Me	R^2 = 3-Me	R^3 = 4-Me	R^4 = 6-Me	arom. H
36A	2.40(s, 3H)	2.53(s, 3H)	2.69(s, 3H)	2.44(s, 3H)	7.68(d, 2H) ; 7.75(s, 4H) ; 8.14(d, 2H)
36B	2.22(s, 3H)	—	2.42(s, 3H)	2.48(s, 3H)	7.62(m, 10H)
36C	2.48(s, 3H)	—	2.72(s, 3H)	2.48(s, 3H)	7.75(s, 2H) ; 8.16(m, 3H)
36D	2.28(s, 3H)	—	2.48(s, 3H)	2.57(s, 3H)	7.79(m, 9H)
36E	2.51(s, 3H)	—	2.76(s, 3H)	2.51(s, 3H)	7.84(s, 2H) ; 7.98(s, 1H) ; 8.27(s, 1H)
36F	2.23(s, 3H)	—	2.46(s, 3H)	2.54(s, 3H)	7.48(m, 5H) ; 7.93(s, 1H) ; 8.03(s, 1H) ; 8.27(s, 1H)
37A	2.52(s, 6H)	2.52(s, 6H)	2.69(s, 6H)	2.52(s, 6H)	7.72(s, 2H) ; 7.96(s, 4H)
37B	2.27(s, 6H)	—	2.38(s, 6H)	2.50(s, 6H)	8.02(s, 4H) ; 7.46(m, 12H)
37H	2.50(s, 6H)	2.60(s, 6H)	—	2.50(s, 6H)	8.07(s, 4H) ; 7.68(m, 12H)
37H[a]	2.50(s, 6H)	—	2.72(s, 6H)	1.40(d, 12H)	7.70(s, 2H) ; 8.02(s, 4H)
37I[b]	2.52(s, 3H) 2.58(s, 3H)[c]	—	2.70(s, 3H) 2.70(s, 3H)	2.52(s, 3H)[d] 2.58(s, 3H)[d]	7.72(s, 4H) ; 7.90(d, 1H) ; 7.47(m, 2H)
37J[c]	—	—	—	—	8.07(s, 3H) ; 8.10(s, 2H) ; 7.42(m, 33H)
37K	2.48(s, 3H)[d] 2.56(s, 3H)[e]	—	2.72(s, 3H) 2.73(s, 3H)	2.48(s, 3H)[d] 2.56(s, 3H)[d]	7.74(s, 2H) ; 7.81(s, 2H) ; 8.12(m, 3H)

---

[a] 2.73 ppm(septet, 2H, iPr) ; [b] 4.02 ppm(s,3H, MeO) ; [c] 3.68 ppm(s,3H,MeO) ; [d] A *m*-X-phenyl group deshields protons relative to an *o*-X-phenyl ring (X=Cl, OMe).

Table 3 presents the new systems **40A—H**, and Table 4 describes their ^{1}H-NMR spectra. Again, the R^1, R^3, R^4 and R^5 methyl groups are shielded by ring currents, unlike the R^2 methyl groups. The strongest shielding is manifest for the methyl R^4 in **40A** and **40B** owing to both pyridinium rings (in the latter case the phenyl substituents make additional contributions). The methyl R^5 is less shielded : only one pyridinium ring is responsible for most of the shielding in **40C, E** ; the additional shielding of R^5 in **40F** is due to the phenyl substituents on the pyridinium ring.

Table 3

Bispyridinium cations **40**

Comp.	R^1	R^2	R^3	R^4	R^5	A
40A	Me	Me	Me	Me	H	ClO$_4$
40B	Ph	Ph	Ph	Me	H	ClO$_4$
40C	Me	Me	Me	H	Me	BF$_4$
40D	Me	Me	Me	H	Me	ClO$_4$
40E	Me	Et	Me	H	Me	ClO$_4$
40F	Ph	Ph	Ph	H	Me	ClO$_4$
40G	Me	Me	Me	H	OMe	ClO$_4$
40H	Me	Me	iPr	H	OMe	ClO$_4$

2,3,4,6-Tetrasubstituted pyrylium salts **34** afford with 2-methyl-1,3-phenylenediamine (**39**, R^4 = Me, R^5 = H) only monocations, which were not investigated in detail.

4. DERIVATIVES OF 1,1′-(2,7-NAPHTHYLENE)BISPYRIDINIUM DICATIONS

A previous report[78] described the reaction of 1,8-diaminonaphthalene with pyrylium salts yielding a pyridinium monocation. Another paper [79] described the similar reaction of 1,2-diaminonaphthalene.

We report here that 2,7-diaminonaphthalene, having distant and sterically unencumbered amino groups, affords with 2,4,6-trisubstituted pyrylium salts the corresponding bispyridinium salts **41**.

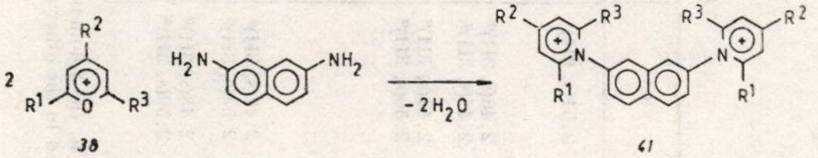

	R^1	R^2	R^3
41A	Me	Me	Me
41B	Ph	Ph	Ph

Table 4

^{1}H-NMR Spectra (δ, ppm) of bispyridinium salts **40** in trifluoroacetic acid

Comp.	R^1	R^2	R^3	R^4	R^5	arom. H
40A	2.51(s, 6H)	2.73(s, 6H)	2.51(s, 6H)	1.77(s, 3H)	—	7.78(s, 4H) ; 8.01(m, 3H)
40B	—	—	—	1.62(s, 3H)	—	7.68(m, 37H)
40C	2.46(s, 3H)^a 2.47(s, 3H)^a	2.63(s, 3H)^a 2.66(s, 3H)^a	2.46(s, 3H)^a 2.47(s, 3H)^a	—	2.18(s, 3H)	7.78(m, 7H)
40E	2.49(s, 3H)^a 2.50(s, 3H)^a	1.41(t, 3H)^a 2.97(q, 2H)^b 1.43(t, 3H)^a 3.00(q, 2H)^b	2.49(s, 3H)^a 2.50(s, 3H)^a	—	2.19(s, 3H)	7.90(m, 7H)
40F	—	—	—	—	1.87(s, 3H)	8.16(s, 2H) ; 8.21(s, 2H) 7.43(m, 3H)
40G	2.49(s, 3H)^a 2.52(s, 3H)^a	2.67(s, 6H)	2.49(s, 3H)^a 2.52(s, 3H)^a	—	4.04(s, 3H)	7.67(s, 4H)^a ; 7.84(m, 3H)^b
40H	2.48(s, 3H)^a 2.50(s, 3H)^a	2.70(s, 6H)	1.35(d, 6H)^a 2.97(sp, 1H)^c 1.45(d, 6H)^a 3.00(sp, 1H)^c		4.07(s, 3H)	7.60(m, 7H)

^{a}For **40 E**, the 2,6-methyls of the pyridinium ring closer to the methyl of the central phenylene group are shielded relatively to the α-methyls bonded to the other pyridinium ring ; the reverse is true for γ-methyls or methylene of **40E**. ^{b} Methyl of ethyl group. ^{c} Isopropyl methyls.

The ^{1}H-NMR spectrum of **41**, $R^1 = R^2 = R^3 =$ Me contains the following peaks (δ values, ppm): 2.52 (s, 12H, 2- and 6-Me); 2.72 (s, 6H,4-Me); 7.79(s, 4H, 3-H); 8.27 (m, 6H, naphthalene). Again, the shielding of 2- and 6-methyl hydrogens is apparent owing to the naphthalene ring current.

5. BISPYRIDINIUM SALTS WITH A BRIDGE BETWEEN TWO PHENYL RINGS

Earlier papers described bispyridinium salts with a central biphenyl moiety obtained from pyrylium salts and benzidine,[66] diphenyline,[80,81] and substituted benzidines.[80,81] One may consider such compounds as having a zero-atom bridge.

5.1. Bispyridinium salts with a monoatomic bridge between two benzene rings

Earlier papers reported some bispyridinium salts with a monoatomic bridge between two benzene rings, obtained from pyrylium salts and 4,4′-diaminodiphenylmethane,[66,82] 4,4′-diaminodiphenylsulfone,[66] 4,4′-diaminodiphenylether,[83] 4,4′-diaminodiphenylamine,[80,81] and 4,4′-diaminotriphenylmethane.[80,81] In all cases the compounds had symmetrical structure and were obtained from one mole of diamine and two moles of pyrylium salt.

A stepwise reaction of 4,4′-diaminotriphenylmethane with two different pyrylium salts was carried out, in order to obtain a racemic mixture of enantiomeric bispyridinium salts. 2,4,6-Triphenylpyrylium perchlorate and the diamine were mixed at 50° in dimethylformamide in equimolar amounts, yielding the monocation which was isolated and on further treatment with alkyl-substituted pyrylium salts afforded the bispyridinium cation **42**. The isopropyl group may serve for giving ^{1}H-NMR evidence

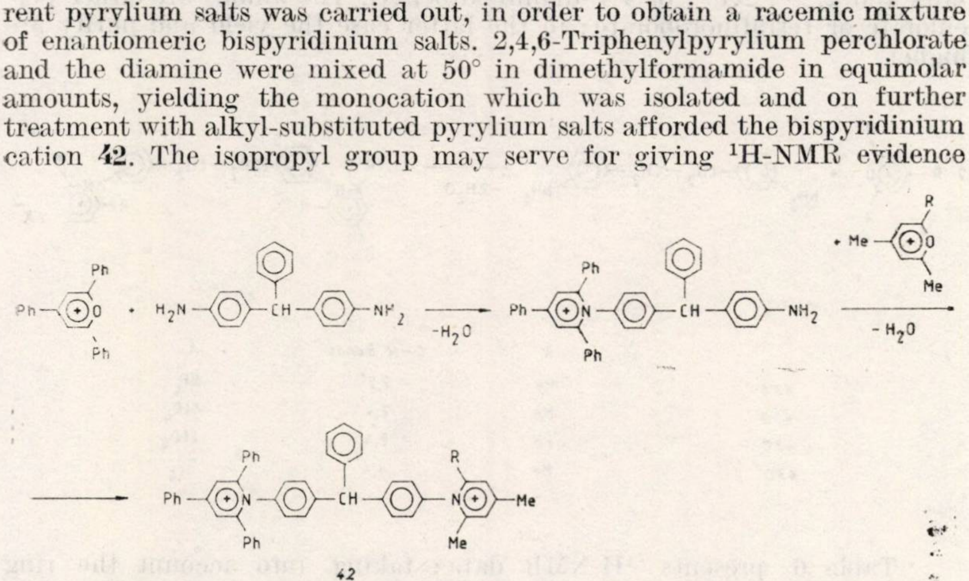

42

	R
42A	Me
42B	CHMe$_2$

for chirality by chemical shift non-equivalence of its two diastereotopic methyls. However, no splitting of the isopropyl peaks was observed in trifluoroacetic acid, and the low solubility of **42** precluded a more extensive ^{1}H-NMR study ; Table 5 presents ^{1}H-NMR data. As in previous. cases the 2- and 6-methyl protons are shielded by the phenyl ring current.

Table 5

^{1}H-NMR Spectra (δ, ppm) of bispyridinium salts **42** in trifluoroacetic acid

Comp.	R	2-Me	4-Me	6-Me	aliph. H	arom. H
42A	Me	2.45(s, 3H)	2.70(s, 3H)	2.45(s, 3H)	5.70(s, 1H)	7.51(m, 32H)
42B	$CHMe_2$	2.43(s, 3H)	2.73(s, 3H)	1.38(d, 6H)	5.72(sp, 1H)	7.72(m, 32H)

5.2. Bispyridinium derivatives with a saturated diatomic bridge between two benzene rings

Earlier papers reported a few bispyridinium compounds with a diatomic bridge between two phenyl rings obtained from pyrylium salts and 4,4′-diamino-diphenyldisulfide,[66,84] 4,4′-diaminoazobenzene,[66] 2,2′- and 4,4′-diaminodibenzyl.[80,81]

We report here new bispyridinium salts **43** obtained from pyrylium salts and 2,2′- ; 2,4′- ; or 4,4′-diaminodibenzyl. The anions are either perchlorate or tetrafluoroborate ; in the latter case the yield and purity are higher.

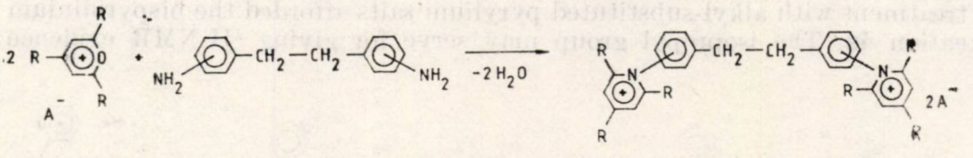

43

	R	C–N Bonds	A
43A	Me	2,2′	BF_4
43B	Me	2,4′	ClO_4
43C	Ph	2,4′	ClO_4
43D	Me	4,4′	BF_4

Table 6 presents ^{1}H-NMR data ; taking into account the ring current effects of phenyl and pyridinium rings, and the ^{1}H-NMR data of N-(*o*-, *m*-, and *p*-tolyl) pyridinium salts,[78] the assignments of chemical shifts are indicated on the formulas. A very strong shielding of one methylene group of the ethylene bridge, due to phenyl ring currents, is observed in the 2,4′-linked bispyridinium salt **43C**.

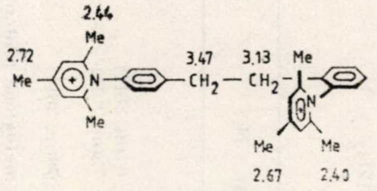

43B

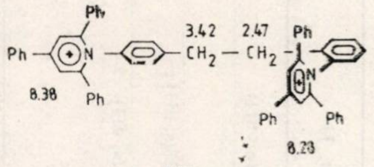

43C

5.3. **Bispyridinium derivatives with an unsaturated diatomic bridge between two benzene rings**

4,4′-Diaminostilbene-2,2′-disulfonic acid does not react with pyrylium cations but its sodium, potassium or ammonium salts react readily in water forming amphionic bispyridinium salts **44A**, **B**.

4,4′-Diaminotolan reacts sluggishly with 2,4,6-trimethylpyrylium perchlorate yielding the little soluble bispyridinium salt **44C** in modest yield. Table 7 presents ^{1}H-NMR data. A strong deshielding of the vinylene protons is observed in **44A**; owing to an even stronger deshielding in **44B**, the vinylene protons of **44B** are obscured by overlapping aromatic protons.

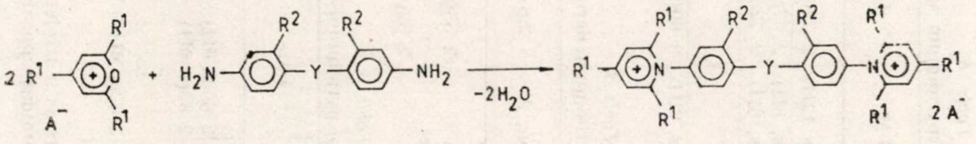

44

	R^1	R	Y	A
44A	Me	SO_3^-	HC=CH	None
44B	Ph	SO_3^-	HC=CH	None
44C	Me	H	C≡C	ClO_4

The presence of the ClO_4^- anion in **44C** is attested by analyses and by IR bands at 625 and 1100 cm^{-1}. The absence of such an inorganic anion in **44A** and **44B** is certified similarly by IR data; the amphionic structure of **44A** and **44B** is confirmed by the strong bands at 1215 and 1030 cm^{-1} characteristic for SO_3^- groups.

6. DERIVATIVES OF 1,1′-[x-IMINO-(x+1)ETHYLENE]BISPYRIDINIUM DICATIONS

According to the reaction conditions, the previously described reaction between aliphatic 1,ω-diamines and pyrylium salts may afford monopyridinium cations[78] or bispyridinium dications.[50, 51, 74, 78, 85–89] Some 1,1′-(1,ω-polymethylene)bispyridinium salts have antimicrobial and antiviral activity.[50]

Table 6

^{1}H-NMR Spectra (δ, ppm) of bispyridinium salts **43** in trifluoroacetic acid

Comp.	R	C–N bonds	Anion, A	2,6-Me	4-Me	CH_2	arom. H
43A	Me	2,2′	BF_4	2.37(s, 12H)	2.72(s, 6H)	2.63(s, 4H)	7.79(s, 4H); 7.42(m, 8H)
43B	Me	2,4′	ClO_4	2.40(s, 6H) 2.44(s, 6H)	2.67(s, 3H) 2.72(s, 3H)	3.13(t, 2H) 3.47(t, 2H)	7.48(m, 12H)
43C	Ph	2,4′	ClO_4	—	—	2.47(t, 2H) 3.42(t, 2H)	7.45(m, 38H); 8.28(s, 2H); 8.38(s, 2H)
43D	Me	4,4′	BF_4	2.44(s, 12H)	2.69(s, 6H)	3.26(s, 4H)	7.29(d, 4H); 7.67(s, 4H); 7.68(d, 4H)

Table 7

^{1}H-NMR Spectra (δ, ppm) of bispyridinium derivatives **44** in trifluoroacetic acid

Comp.	R^1	R^2	Y	Anion, A	2,6-Me_2	4-Me	HC=CH	arom. H
44A	Me	SO_3^-	HC=CH	None	2.53(s, 12H)	2.72(s, 6H)	7.61(d, 2H)	7.76(s, 4H); 8.46(m, 6H)
44B	Ph	SO_3^-	HC=CH	None	—	—	~8.00(d, 2H	8.65(s, 4H); ~8.00(m, 38H)
44C	Me	H	C≡C	ClO_4	2.52(s, 12H)	2.72(s, 6H)	—	7.73(m, 12H)

Table 8

^{1}H-NMR Spectra (δ, ppm) of bispyridinium salts **45** in trifluoroacetic acid

Comp.	R^1	R^2	Y	2,6-Me	4-Me	CH_2	CH_2	arom. CH
45A	Me	Me	H_2N^+	2.98(s, 12H)	2.60(s, 6H)	5.13(t, 4H)	4.02(t, 4H)	7.60(s, 4H)
45A[a]	Me	Me	NH	2.89(s, 12H)	2.55(s, 6H)	4.62(t, 4H)	3.22(t, 4H)	7.78(s, 4H)
45B	Ph	Ph	H_2N^+	—	—	5.03(t, 4H)	2.95(t, 4H)	8.08(s, 4H); 7.67(m, 30H)
45C	Me	Ph	H_2N^+	3.08(s, 6H)	—	5.03(t, 4H)	3.52(t, 4H)	8.05(s, 4H); 7.73(m, 20H)
45D[b]	Me	Me	$^+NH_2-CH_2-CH_2-H_2N^+$	2.99(s, 12H)	2.62(s, 6H)	5.12(t, 4H)	4.00(t, 4H)	7.60(s, 4H)
45E[c]	Ph	Ph	$^+NH_2-CH_2-CH_2-H_2N^+$	—	—	5.12(t, 4H)	3.40(t, 4H)	8.14(s, 4H); 7.78(m, 30H)

---

[a] Solvent: $(CD_3)_2SO + (CD_3)_2CO$; the NH proton appears as a triplet centered at 3.15 ppm; [b] The four central methylene protons appear as singlet at 4.10 ppm; [c] The four central methylene protons appear as singlet at 3.15 ppm.

Bispyridinium salts were obtained from N-aminoderivatives such as 1,4-diaminopiperazine,[90] or the dihydrazides of carbonic and oxalic acids.[91]

We report here that diethylenetriamine and triethylenetetramine react readily with pyrylium salts in water or lower alcohols at room temperature affording bispyridinium dications **45**.[92] The imino groups do not react under these conditions, although secondary amines are known to afford, with 2,4,6-trimethylpyrylium salts, 3,5-xylidine derivatives.[93] No bispyridinium salts could be isolated from reactions of tetraethylenepentamine under these conditions.

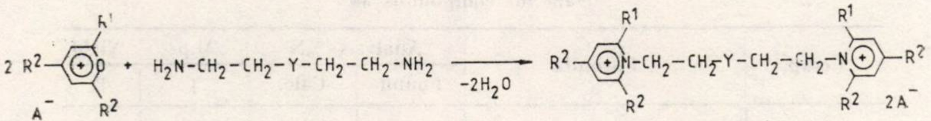

45

	R^1	R^2	Y	A
45A	Me	Me	NH	ClO_4
45B	Ph	Ph	NH	ClO_4
45C	Me	Ph	NH	ClO_4
45D	Me	Me	$HN-CH_2-CH_2-NH$	BF_4
45E	Me	Me	$HN-CH_2-CH_2-NH$	ClO_4
45F	Ph	Ph	$HN-CH_2-CH_2-NH$	ClO_4

^{1}H-NMR data were presented in Table 8. Unlike all compounds described in the present paper, in this case the 2,6-methyl protons resonate at lower field than 4-methyl protons, i.e. just as in alkyl-substituted pyrylium and pyridinium salts. For confirmation of NMR assignments, ^{1}H-NMR spectra of **45A** were recorded in solvents which protonate the —NH— group (trifluoroacetic acid) and in solvents which do not (a mixture of deuterated acetone and dimethylsulfoxide).

The assignment of the two types of methylene protons in **45A** is straightforward: the $\geqslant\overset{+}{N}-CH_2$ protons (α) are strongly deshielded relatively to the $NH-CH_2$ methylene protons (β) in non-protonating solvents. In protonating solvents the former protons are deshielded by an additional 0.5 ppm, and the latter protons by 0.8 ppm.

Interestingly, the shielding of methylene protons caused by the phenyl substituents in **45B**, **C**, **E** (manifested on the β-methylene groups only) is by 0.5 ppm for one 2-phenyl group (**45C**) and by 1 ppm for two 2,6-phenyl groups (**45B**). Even in **45E**, the central methylene protons are strongly shielded by comparison with **45D** which is devoid of phenyl groups; this fact indicates that despite electrostatic repulsions between the two pyridinium rings in the tetracation formed by **45E** in trifluoroacetic acid, this system adopts a folded conformation wherein the central methylene groups are shielded by the phenyl ring current.

7. EXPERIMENTAL PART

7.1. N-(4-Aminophenyl)-pyridinium monocations

A mixture of 2,4,6-tri- or 2,3,4,6-tetrasubstituted pyrylium perchlorate (10 mmol) and 10 mmol *p*-phenylenediamine or substituted derivative was refluxed in 20 mL ethanol for 4 hrs with stirring. The mixture was cooled, the crystalline precipitate was filtered off, treated with aqueous-ethanolic ammonia for removing unreacted pyrylium salt, filtered off again and washed with ethanol and ethyl ether. The products were recrystallized from aqueous acetic acid, colourless crystals (Table 9).

Table 9

Data for compounds **36**

Comp.	Formula	Analysis %N		M.p.	Yield
		Found	Calc.	°C	%
36A	$C_{15}H_{19}N_2(ClO_4)$	8.48	8.57	238–40	90
36B	$C_{20}H_{21}N_2(ClO_4)$	7.13	7.20	295–96	88
36D	$C_{20}H_{20}ClN_2(ClO_4)$	6.81	6.62	235–37	91
36E	$C_{14}H_{15}Cl_2N_2(ClO_4)$	7.89	7.34	245–46	90

1-(4-Aminophenyl-3-sulfonate)-2,4,6-trimethylpyridinium **(36C)** was prepared by dissolving in 20 mL water, 10 mmol $NaHCO_3$ and 10 mmol 1,4-diamino-2-benzenesulfonic acid at 70°; after complete solubilization, 10 mmol 2,4,6-trimethylpyrylium perchlorate was added and the mixture was refluxed with stirring for one hour. After usual work-up as above the product was recrystallized from water, colourless crystals with m.p. 317–320°, 87% yield. Found: N, 9.64%; $C_{14}H_{16}N_2O_3S$ requires N, 9.58%.

1(-4-Amino-2,5-dichlorophenyl)-2,4,6-trimethyl-3-phenylpyridinium perchlorate **(36F)**, was prepared from 10 mmol each of pyrylium salt and diamine in 20 mL dimethylformamide at 90° with stirring for two hrs. After cooling and dilution with water, the product was worked up as before. Pale yellow crystals, m.p. 123–125°, 88% yield. Found: N, 6.30%; $C_{20}H_{19}Cl_2N_2(ClO_4)$ requires N, 6.12%.

7.2. 1,1′-(1,4-Phenylene)bispyridinium dications (37)

Two synthetic variants were used:

a. For compounds **37H, I, K** the usual method as for monocations was used (refluxation with ethanol in a molar ratio **34** : **35** = 2 : 1).

b. The diamine (10 mmol) was dissolved in 50 mL dimethylformamide, and then 20 mmol of pyrylium salt were added. The mixture was heated at 100° with stirring for 6 hrs, then it was refluxed for 0.5 hrs. After cooling at 70°, 5 mL aqueous ammonia were added then the mixture was allowed to cool. The product was precipitated by adding water or ethyl ether. Recrystallization solvents are indicated in Table 10; products are colourless.

7.3. 1,1′-(1,3-Phenylene)bispyridinium dications (40)

Three synthetic variants were followed (Table 11).

a. Refluxing the pyrylium salt (20 mmol) and the diamine (10 mmol) in ethanol followed by the usual work-up.

b. As above in dimethylformamide; the product was precipitated with water and washed on the filter with ethanol.

c. 2,4-Diaminoanisole sulfate ($C_7H_{12}N_2O \cdot 1/2H_2SO_4$), 10 mmol, in 35 mL water was treated with 10 mmol $NaHCO_3$ with heating and stirring till dissolution was complete. Then 20 mmol pyrylium salt was added and the mixture was refluxed with stirring for three hours. The precipitate formed on cooling was filtered off and washed with aqueous ammonia and methanol, then recrystallized from water with decolorizing carbon.

Table 10

Data for compounds **37**

Comp.	Formula	Analysis %N		Recryst. from[a]	M.p. °C	Yield %
		Found	Calc.			
37A	$C_{24}H_{30}N_2(ClO_4)_2$	5.01	5.14	A	233–235	87
37B	$C_{34}H_{34}N_2(ClO_4)_2$	4.03	4.18	AW	350	82
37G	$C_{34}H_{34}N_2(ClO_4)_2$	4.25	4.18	A	350	79
37H	$C_{26}H_{34}N_2(ClO_4)_2$	4.92	4.88	AW	350	55
37I	$C_{23}H_{28}N_2O(ClO_4)_2$	5.14	5.12	AW	350	83
37J	$C_{53}H_{40}N_2O(ClO_4)_2$	2.83	3.05	A	340–342	89
37K	$C_{22}H_{25}ClN_2(ClO_4)_2$	5.22	5.08	AW	249–251	81
37L	$C_{52}H_{37}ClN_2(ClO_4)_2$	3.20	3.03	AAn	265–266	75

[a] Recryst. solvent : A = acetic acid, W = water, An = acetonitrile.

Table 11

Data for compounds **40**

Comp.	Formula	Analysis % N		Recryst. from[a]	M.p.	Yield
		Found	Calc.		C°	%
40A	$C_{23}H_{28}N_2(ClO_4)_2$	5.21	5.27	A	>350	83
40B	$C_{53}H_{40}N_2(ClO_4)_2$	3.20	3.10	AAn	161–163	89
40C	$C_{23}H_{28}N_2(BF_4)_2$	5.48	5.54	E	276–278	85
40D	$C_{23}H_{28}N_2(ClO_4)_2$	5.20	5.27	A	298–300	82
40E	$C_{25}H_{32}N_2(ClO_4)_2$	5.09	5.01	E	268–270	87
40F	$C_{53}H_{40}N_2(ClO_4)_2$	3.01	3.10	AAn	323–325	91
40G	$C_{23}H_{28}N_2O(ClO_4)_2$	5.34	5.12	W	296–299	84
40H	$C_{27}H_{36}N_2O(ClO_4)_2$	4.48	4.64	W	276–278	78

---

[a] Recrystallization solvent : A= acetic acid ; An = acetonitrile ; E = ethanol ; W= water.

7.4. 1,1′-(2,7-Naphthylene)bis(2,4,6-trimethylpyridinium) diperchlorate (41A)

A suspension of 20 mmol pyrylium salt and 10 mmol diamine was refluxed for 4 hrs with stirring in methanol. The product was filtered off after cooling, washed with aqueous ammonia and recrystallized from water with animal carbon. Colourless crystals with m.p. 302–304°, 83% yield. Found N, 4.99%; $C_{26}H_{28}N_2(ClO_4)_2$ requires N, 4.94%.

1,1′-(2,7-Naphthylene)bis(2,4,6,-triphenylpyridinium) diperchlorate, **(41B)**. The reaction was carried out according to procedure b, the product was precipitated with water and recrystallized from acetic acid. Colourless crystals with m.p. 313–315°, 78% yield. Found : N, 2.82%; $C_{56}H_{40}N_2(ClO_4)_2$ requires N, 2.98%.

7.5. Reaction of pyrylium salts with p,p′-diaminotriphenylmethane

2,4,6,-Trimethyl-1-[4-(2,4,6-triphenylpyridiniumyl-1)phenylmethylenedi-4,1-phenylene]-pyridinium diperchlorate **(42A)**.

A solution of 10 mmol 2,4,6-triphenylpyrylium perchlorate in 150 mL dimethylformamide (DMF) was added with a stirring to a solution of 10 mmol 4,4′-diamino-triphenylmethane in 40 mL DMF at 40–50° during one hour. Then the mixture was heated at 70° for one hour. The resulted solution was treated with 10 mmol 2,4,6-trimethylpyrylium perchlorate and heated for 4 hrs at 100° with stirring. After cooling, water and aqueous ammonia were added, and the precipitate was filtered off and washed with ethanol. Pale yellow crystals were obtained by recrystallization from acetic acid, m.p. 225–227°, yield 85%. Found: N, 4.05 ; $C_{38}H_{34}N_2(ClO_4)_2$ requires N, 3.90%.

2-Isopropyl-4,6-dimethyl-1-[4-(2,4,6,-triphenylpyridiniumyl-1)-phenylmethylenedi-4,1-phenylene]pyridinium diperchlorate (**42B**). The reaction was carried out similarly with the preceding procedure but using 2-isopropyl-4,6-dimethylpyrylium perchlorate [94] instead of trimethylpyrylium; yellowish crystals, m.p. 201–203°, 81% yield, Found: N, 3.98%; $C_{40}H_{38}N_3(ClO_4)_2$ requires N, 3.76%.

7.6. Derivatives of 1,1′-[1,2-ethanediyl-(2,1-phenylenebis)) pyridinium, 1,1′-(1,2-ethanediyl-(2,1-phenylene-4,1-phenylene)]bidspyridinium, and 1,1′-[1,2-ethanediyl-(4,1-phenylene)] bispyridinium, (43)

The synthesis was carried out with diamino-dibenzyl compounds in variant a for compounds **43A**, **43B** and **43D** with refluxing for 3 hrs, and in variant b for **43C**. Colourless crystals with data presented in Table 12.

Table 12

Data for compounds **43**

Comp.	Formula	Analysis %N		Recryst. from[a]	M.P. °C	Yield %
		Found	Calc.			
43A	$C_{30}H_{34}N_2(BF_4)_2$	4.82	4.70	E	229–231	92
43B	$C_{30}H_{34}N_2(ClO_4)_2$	4.62	4.51	W	271–272	92
43C	$C_{60}H_{46}N_2(ClO_4)_2$	2.73	2.82	AAn	204–206	89
43D	$C_{30}H_{46}N_2(BF_4)_2$	4.91	4.70	E	302–303	89

[a] Recrystallization solvent: E = Ethanol, W = Water, A = Acetic acid An = Acetonitrile.

7.7. Reaction of pyrylium salts with aromatic diamines having unsaturated bridges

1,1′-[1,2-Ethenediylbis(4,1-phenylene-3-sulfonate)]bispyridinium (**44A, B**). In a solution obtained from 20 mmol $NaHCO_3$, 10 mmol 4,4′-diaminostilbene-2,2′-disulfonic acid in 60 mL water, the pyrylium salt (20 mmol) was added, then the suspension was refluxed with stirring for 3 hrs. After cooling, 5 mL 20% aqueous ammonia were added and the mixture was heated at 70° for 15 minutes. The precipitate deposited on cooling was filtered off, washed with methanol, and recrystallized from aqueous acetic acid (**44A**) or acetonitrile (**44B**). Colourless crystals, as indicated in Table 13.

Table 13

Data for compounds **44**

Comp.	Formula	Analysis %N		Recryst. from[a]	M.P. °C	Yield %
		Found	Calc.			
44A	$C_{30}H_{30}N_2O_6S_2$	4.71	4.84	W	350	90
44B	$C_{60}H_{42}N_2O_6S_2$	2.90	2.95	W	113–115	87
44C	$C_{30}H_{30}N_2(ClO_4)_2$	4.66	4.54	An	190–192	60

[a] Solvents: W = Water; An = Acetontrile.

1,1′-(Ethinediyl-4,1-phenylene)bis(2,4,6,-trimethylpyrydinium) diperchlorate (**44C**) was prepared according to procedure a. Properties are presented in Table 13.

7.8. Derivatives of 1,1′-(iminodiethylene)bispyridinium and 1,1′-(diiminotriethylene) bispyridinium (45)

Two synthetic variants were used :

d. To a suspension of 20 mmol pyrylium perchlorate in 25 mL methanol, the diethylenetriamine or triethylenetetramine (10 mmol) in 10 mL methanol were added stepwise with stirring, then the mixture was stirred at room temperature for ten hrs, followed by refluxing for ten minutes. After cooling the precipitate was filtered off, washed with ammonia and methanol and recrystallized.

e. 2-Methyl-4,6-diphenylpyrylium sulfoacetate (20 mmol) was suspended in 30 mL methanol, and a solution of 10 mmol diethylenetriamine in 25 mL methanol was added with stirring. After 10 hrs' standing at room temperature the solution was refluxed for 0.5 **hrs**, then cooled and treated with 30 mmol 70 % perchloric acid. After filtration the precipitate was washed with ammonia and methanol, then recrystallized. Products are colourless. Data are presented in Table 14.

Table 14

Data for compounds **44**

Comp.	Formula	Analysis %N		Recryst. from[a]	M.p. °C	Yield %
		Found	Calc.			
45A	$C_{20}H_{31}N_3(ClO_4)_2$	8.17	8.20	W	254−256	90
45B	$C_{50}H_{43}N_3(ClO_4)_2$	5.15	4.75	E	180−182	84
45C	$C_{40}H_{39}N_3(ClO_4)_2$	5.24	5.12	AW	148−150	60
45D	$C_{22}H_{36}N_4(BF_4)_2$	10.42	10.57	M	170−171.5	78
45E	$C_{22}H_{36}N_4(ClO_4)_2$	9.95	10.09	W	174−176	81
45F	$C_{52}H_{48}N_4(ClO_4)_2$	5.63	6.04	AM	158−160	82

[a] Recrystallization solvents : A = acetic acid ; E=Ethanol ; M=Methanol ; W = Water.

ACKNOWLEDGEMENTS. Thanks are addressed to Drs. F. Chiraleu and M. D. Gheorghiu for ^{1}H-NMR spectra.

REFERENCES

[1] Preceding part, A. T. Balaban, G. Marton and I. Schiketanz, *Rev. Roum. Chim.*, **31**, 37 (1986).

[2] D. R. Davies and A. L. Green, *Discuss. Faraday Soc.*, **20**, 269 (1955) ; I. B. Wilson and S. Ginsburg, *Biochim. Biophys. Acta*, **18**, 168 (1955) ; I. B. Wilson and D. Nachmanson, *Arch. Biochem. Biophys.*, **64**, 456 (1956).

[3] E. J. Poziomek, B. E. Hackley Jr. and G. M. Steinberg, *J. Org. Chem.*, **23**, 714 (1958).

[4] F. Hobbiger and P. W. Sadler, *Brit. J. Pharmacol.*, **14**, 192 (1959) ; F. Hobbiger et al., *Nature*, **182**, 107, 1498 (1958).

[5] W. K. Berry, D. R. Davies and A. L. Green, *Biochem. J.*, **71**, 15P (1959) ; *Brit. J. Pharmacol.*, **14**, 186 (1959) ; D. R. Davies and A. L. Green, *Brit. J. Ind. Med.*, **16**, 128 (1959)

[6] K. Schoene and H. Oldiges, *Arch. Int. Pharmacodyn. Ther.*, **204**, 110, (1973).

[7] N. Golikov, V. I. Shchekoldina and I. G. Simonova, *Farmakol. Toksikol.*, **35**, 589 (1972)

[8] J. Patocka and J. Bielavsky, *Coll. Czech. Chem. Commun.*, **37**, 2110 (1972).

[9] B. E. Hackley, Jr., E. J. Poziomek and G. M. Steinberg, *U.S. Pat.*, 3,045,025, (1962) ; 3,093,539 (1963) ; 3,135,761 (1964).

[10] H. P. Benschop, L.P.A. De Long and L.A. Kepner, *Eur. Pat.* 23,378 (1979) ; L.P.A. De Long, H.P. Benschop, G.R. Van den Berg, G.Z. Wobung and D.C. De Korte, *Eur. J. Med. Chem.-Chim. Ther.*, **16**, 257 (1981).

[11] T. A. Loomis and L. Salafsky, *Toxicol. Appl. Pharmacol.*, **5**, 685 (1963) ; T. A. Loomis, M. J. Welsh Jr. and G. T. Miller, *ibid.*, **5**, 588 (1963).

[12] Farbenfabriken Bayer AG, *Ger Pat.*, 1, 200, 302 (1965).

[13] A. Lüttringhaus and I. Hagedorn, *Arzneimittel-Forsch.*, **14**, 1 (1964).

[14] D. Kuhnen-Clausen, *Toxicol. Appl. Pharmacol.*, **23**, 443 (1972); V. Deljac et al., *Acta Pharm. Jugosl.*, **29**, 107 (1979); **32**, 113 (1982); V. Simeon et al., *Arch. Toxicol.*, **41**, 301 (1979).

[15] V. P. Mager, *Pharmazie*, **36**, 450 (1981); **37**, 800 (1982).

[16] W. P. Hsiung and M. Chong, *Taiwan Yao Hsueh Tse Chih*, **35**, 32 (1983).

[17] I. Hagedorn, W. H. Guendel, I. Hoose and C. Henter, *Arzneimittel-Forsch.* **26**, 1273 (1976).

[18] B. E. Hackley Jr., E. J. Poziomek and G. M. Steinberg, *U.S. Pat.*, 3,054,799 (1962).

[19] J. Patocka, J. Bielavsky and F. Ornst, *FEBS Lett.*, **10**, 182 (1970).

[20] J. Bielavsky and F. Ornst, *Coll. Czech. Chem. Commun.*, **38**, 2788 (1973).

[21] Z. Binenfeld, B. Boskovic and M. Maksimovic, *Acta Pharm. Jugosl.* **17**, 35 (1967); Z. Binenfeld et al., *ibid.*, **31**, 5 (1981);M. Maksimovic, B. Boskovic and Z. Binenfeld, *Croat Chem. Acta*, **40**, 185 (1968).

[22] R. A. Andersen, J. A. B. Barstad and K. Laake, *Progr. Brain Res.*, **36**, 189 (1972).

[23] N. Engelhard and W. D. Erdmann, *Arzneimittel-Forchs.*, **14**, 870 (1964).

[24] K. Schoene and E. M. Strake, and *Biochem. Pharmacol.*, **20**, 1041 (1971).

[25] J. Pichler and J. Patocka, *Scr. Fac. Sci. Nat. Univ. Purkynianae Brun.*, **4**, 69 (1974); J. Pichler, *Czech. Pat.* 184, 005 (1980).

[26] L. Loits, M. V. Shimanskaya, V. Klusa and A. Kimenis, *Khim.—Farm. Zh.*, **11**, 70 (1977).

[27] V. Vittuci, *Gazz. Med. Mil.*, **128**, 72 (1978).

[28] R. A. Adamson, D. L. Boatman and J. P. Long, *Arch. Intern. Pharmacodyn.*, **141**, 22 (1963).

[29] G. L. Szendey, *Arzneimittel-Forsch.*, **22**, 1746 (1972).

[30] A. Z. Booth, J. P. Long and K. R. Long, *J. Pharm. Sci.*, **57**, 172 (1968); F. W. Benz and J. P. Long, *J. Pharmacol. Exp. Ther.*, **166**, 225 (1969); F. W. Benz and J.P.Long, *ibid.*, **168**, 315 (1969): F. W. Benz and J. P. Long, *J. Pharm. Pharmacol.*, **22** 20 (1970).

[31] K. B. Augustinsson and H. Hasselquist, *Acta Chem. Scand.*, **17**, 953 (1963).

[32] N. Moldoveanu, *Studii Cercetări Biochim. Acad. Rep. Populare Române*, **7**, 77 (1964).

[33] R. Hazard, J. Cheymol and E. Corteggiani, *Naunyn, Schmiedebergs Arch. Exptl. Pathol. Pharmacol.*, **220**, 62 (1953).

[34] H. Ozawa, M. Onda and S. Sato, *J. Farm. Soc. Japan*, **74**, 1267 (1954).

[35] Chen Wen-Sherng, G. H. Cocolas, C. J. Cavallito and Chai Kyung Ja, *J. Med. Chem.*, **20**, 1617 (1977); Chen Wen-Sherng, G. H. Cocolas and C. J. Cavallito, *J. Pharm. Sci.*, **68**, 1025 (1979).

[36] A. Maelicke, B. W. Fulpius, R. P. Klett, E. Reich and E. Dumaguing, *J. Biol. Chem.*, **252**, 4811 (1977).

[37] J. Bode, T. Moody, M. Schimerlich and M. Raftery, *Biochemistry*, **18**, 1855 (1979).

[38] T. Lee, V. Witzemann, M. Schimerlich and M. A. Raftery, *Arch. Biochem. Biophys.*, **183**, 57(1977); P. Taylor and S. Lappi, *Biochemistry*, **14**, 1989 (1975).

[39] R. Hazard, J. Cheymol, J. A. Gautier, E. Corteggiani and E. Leroi, *Arch. Intern. Pharmacodynam.*, **90**, 271 (1952).

[40] E. S. Lane, *Brit. Pat.* 717, 754 (1954); E. S. Lane, *J. Chem. Soc.*, 1172 (1953).

[41] A. F. Danilov, *Farmakol. Toksikol. (Moscow)*, **33**, 536 (1970).

[42] N. V. Khromov-Borissov, M. L. Indenbom and A. F. Danilov, *Dokl. Akad. Nauk. SSSR*, **183**, 134 (1968).

[43] G. Biancetti, *Farmaco (Pavia) Ed. Sci.*, **11**, 346 (1956); *ibid.*, **12**, 441 (1957).

[44] P. Mantegazza, *Farmaco (Pavia) Ed. Sci.*, **11**, 357 (1956).

[45] F. R. Domer and F. W. Schneler, *Arch. Intern. Pharmacodynam.*, **114**, 217 (1958).

[46] Dr. K. Thomae G.m.b.H., *Brit. Pat.* 914, 387 (1963).

[47] A. M. Badawi, M. M. El-Marzibani, B. Haroun and H. Soliman, *Curr.Sci.*, **52**, 1169 (1983).

[48] D. M. Bailey, *Ger. Pat.*, 2,708,331 (1977); D. M. Bailey, *U.S. Pat.*, 4,206,215 (1980).

[49] W. G. Gorman and K. E. Popp, *Eur. Pat.*, 24,031 (1981).

[50] N. A. Morozova, V. A. Sedavkina, L. K. Kulikova, M. K. Krasheninnikova and V. G. Kharchenko, *Khim. Farm. Zh.*, **17**, 1312 (1983).

[51] A. Dinculescu, A. T. Balaban and E. Stepan, *Roum. Pat.*, 73,504, (1978); see also E. Stepan and A. T. Balaban, *Rev. Roum. Chim.*, **28**, 707 (1983).

[52] P. N. Edwards, *Ger. Pat.*, 2,215,503 (1972).

[53] J. E. Oliver and M. M. Crystal, *J. Econ. Entomol.*, **65**, 303 (1972).

[54] J. Renault and J. C. Cartron, *Chim. Ther.*, 337 (1966).

[55] R. Crossley, *Brit. Pat.*, 2,038,327 (1980).

[56] G. J. Atwell, and B. F. Cain, *J. Med. Chem.*, **10**, 706 (1967).

[57] G. J. Atwell and B. F. Cain, *J. Med. Chem.*, **11**, 295 (1968).

[58] G. J. Atwell, B. F. Cain and R. N. Seelye, *J. Med. Chem*, **11**, 690 (1968).

[59] G. J. Atwell, B. F. Cain and R. N. Seelye, *J. Med. Chem.*, **11**, 300 (1968).

[60] W. A. Denny, G. J. Atwell, B. C. Baguley and B. F. Cain, *J. Med. Chem.*, **22**, 134 (1979).

[61] B. F. Cain, G. J. Atwell and R. N. Seelye, *J. Med. Chem.*, **12**, 199 (1969).

[62] Sandoz Ltd., *Belg. Pat.*, 636, 144 (1966).

[63] W. R. Boon, *Chem. Ind.*, 782 (1965); R. J. Fielden, R. F. Homer and R. L. Jones, *Brit. Pat.*, 785,732 (1957); R. C. Brian, R. F. Homer J. Stubbs and R. L. Jones, *Nature*, **181**, 446 (1958); J. Stubbs, *Proc. 4th Brit. Weed Control Conf. Brighton*, 251 (1958).

[64] R. C. Brian, G. W. Driver, R. F. Homer and R. L. Jones, *Ger. Pat.* 1,048,070 (1958); Imperial Chemical Industries Ltd., *Brit. Pat.* 813,531 (1959).

[65] L. A. Summers, "The Bispyridinium Herbicides", Academic Press, London, 1980.

[66] R. Neidlein and P. Witerzens, *Monatsh. Chem.*, **106**, 643 (1975).

[67] A. Baeyer and J. Piccard, *Liebigs Ann. Chem.*, **384**, 208 (1911); **407**, 332 (1915).

[68] K. Dimroth and K. H. Wolf, in "Newer Methods of Preparative Organic Chemistry", Ed. W. Foerst, vol. 3, p. 357, Academic Press, New York, 1964.

[69] A. T. Balaban, A. Dinculescu, G. N. Dorofeenko, G. W. Fischer, A. V. Koblik, V. V. Mezheritskii and W. Schroth, "Advances in Heterocyclic Chemistry, Supplement 2; Pyrylium Salts: Syntheses, Reactions and Physical Properties", Academic Press, New York, 1982.

[70] A. R. Katritzky, *Tetrahedron*, **36**, 679 (1980).

[71] W. Sliwa, G. Matusiak and A. Postawka, *Heterocycles*, **25**, 1513 (1985).

[72] C. Toma and A. T. Balaban, *Tetrahedron*, Suppl. **7**, 9 (1966).

[73] G. N. Dorofeenko, Yu. P. Andeichikov, E. A. Zvezdina, V. A. Bren, G. E. Trukhan, V. V. Derbevev and A. N. Popova, *Khim. Geterotsikl. Soedin.*, 1349 (1974).

[74] E. A. Zvezdina, M. P. Zhdanova, V. A. Bren and G. N. Dorofeenko, *Khim. Geterotsikl. Soedin.*, 944 (1978).

[75] R. M. Claramunt and J. Elguero, *Coll. Czech. Chem. Commun.*, **46**, 584 (1981).

[76] A. R. Katritzky, A. Krutosiková, C. A. Ramsden and J. Lewis, *Coll. Czech. Chem. Commun.*, **43**, 2046 (1978).

[77] A. Bota, A. T. Balaban and F. Chiraleu, *Rev. Roumaine Chim.*, **21**, 101 (1976).

[78] A. Dinculescu and A. T. Balaban, *Rev. Roumaine Chim.*, **25**, 1505 (1980); A. Dinculescu, H. N. Koutrakis and A. T. Balaban, *ibid.*, **24**, 439 (1979); A. T. Balaban, A. Dinculescu, H. N. Koutrakis and F. Chiraleu, *Tetrahedron Lett.*, 437 (1979).

[79] G. N. Dorofeenko, Yu. P. Andreichikov and G. E. Trukhan, *Khim. Geterotsikl. Soedin.*, 1344 (1974).

[80] E. Stepan and A. T. Balaban, *Roum. Pat.*, 79,547 (1982).

[81] E. Stepan and A. T. Balaban, *Rev. Roumaine Chim.*, **28**, 707 (1983).

[82] M. I. Knyazhanskii, Ya. R. Tymyanskii, N. V. Kholodova, G. E. Trukhan and Yu. P. Andreichikov, *Khim. Vys. Energ.*, **14**, 445 (1980).

[83] A. Dinculescu, M. Fahmy, F. Chiraleu and A. T. Balaban, *Rev. Roum. Chim.*, **28**, 699 (1983).

[84] K. Dimroth, Ch. Reichard and A. Schweig, *Liebigs Ann. Chem.*, **669**, 95 (1963).

[85] A. R. Katritzky, A. Chermprapai and R. C. Patel, *J. Chem. Soc. Chem. Commun.*, 238 (1979).

[86] A. R. Katritzky, U. Gruntz, A. A. Ikizler, D. H. Keny and B. P. Leddy, *J. Chem. Soc. Perkin Trans.* **1**, 436 (1979).

[87] N. F. Eweiss, A. R. Katritzky, Pai-Lin Nie and C. A. Ramsden, *Synthesis*, 634 (1977).

[88] A. R. Katritzky, U. Gruntz, N. Mongelli and M. Rezende, *J. Chem. Soc. Perkin Trans.* **1**, 1953 (1979).

[89] J. Grimshaw, S. Moore and J. Trocha-Grimshaw, *Acta Chem. Scand. Ser, B*, **B37**, 485 (1983).

[90] A. Dinculescu, V. Voroneanu, A. Ardeleanu and A. T. Balaban, *Roum. Pat.* 79,781 (1980).

[91] R. Neidlein and P. Witerzens, *Arch. Pharm.* (*Weinheim*), **309**, 649 (1976).

[92] E. Stepan and A. T. Balaban, *Roum. Pat.*, 81,908 (1983).

[93] O. Diels and K. Alder, *Ber. Dtsch. Chem. Ges.* **60**, 716 (1927).

[94] C. Uncuța and A. T. Balaban, *Rev. Roumaine Chim.* **21**, 251 (1976).

Revue Roumaine de Chimie, **32**, 2, 179–189 (1987)

KINETICS OF THE ACETOLYSIS OF 10,11-DIHYDRO-10,5-PROPENO-5H-DIBENZO [*a*, *d*] CYCLOHEPTEN-11-YL BROMIDE. ANOTHER EXAMPLE OF DOUBLE BOND PARTICIPATION IN IONISATION

RODICA VLAD, F. BADEA and M. BANCIU

Polytechnic Institute, Department of Organic Chemistry,
Splaiul Independenţei 313, 76206 Bucharest, Romania

Received October 5, 1986

The kinetics of the acetolysis at 50° and 110° of the title compound (6-Br) was studied. At 50° the main product (68 %) is the unrearranged acetate (*endo*-6-OAc) and the reaction follows a first-order kinetics in the first half-time. The integrated first-order rate constants decrease steeply in the second half-time and the production of bromide ion apparently ceases at 60–65 % conversion. The kinetics at 110° differs strikingly from that at 50°. The main reaction products (67–75 %) are the rearranged acetates 9-OAc and 10-OAc. The integrated first-order rate constants have a sharp decreasing trend from the very beginning of the reaction, and the extrapolated initial rates seem to be lower than the observed rates at 50°. A dependence upon sodium acetate concentration is also observed. The results are interpreted in terms of the collapse of the intermediate ion pair either into the solvolysis products or into an unreactive bromide (probably 9-Br).

INTRODUCTION

The participation of neighbouring groups in the ionisation step of the solvolyses of arenealkyl arenesulfonates is now an experimentally well documented fact.[1–5] Evidence is mainly based on kinetic measurements, coupled with product analyses. Thus, in previous works of our laboratory the solvolysis of 5,6-dihydrodibenzo[*a*,*e*]cyclooctene-5-yl bromide (**1**-Br) was studied.[6] Even at 0° in acetic acid, **1**-Br quantitatively rearranges into 5H-dibenzo[*a*,*d*]cycloheptene-5-yl-methyl bromide (**2**-Br). As compared with the saturated bromide, **3**-Br, the unsaturated bromide **1**-Br is about 10 times more reactive.

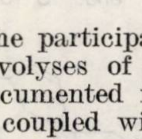

1–Br

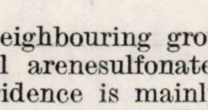

2–Br

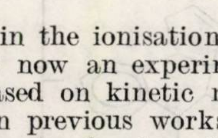

3–Br

Product analysis suggests the intermediate formation of a phenonium ion **4**. However, the high difference between the solvolysis rates of the unsaturated bromide **1**-Br and the saturated analogue **3**-Br indicated that the double bond must be in some manner involved into the ionisation step. A dibenzohomotropylium ion **5** was proposed [6–8] as reaction intermediate :

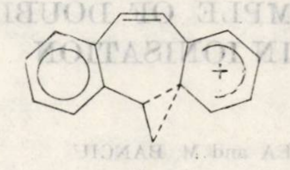

4

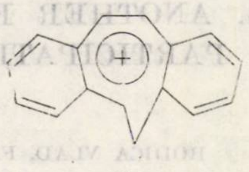

5

In an effort to compare the anchimeric assistance of a double bond with that of an aromatic ring, in this work we studied the acetolysis of *endo*-10,11-dihydro-10,5-propeno-5H-dibenzo[*a*,*d*]-cycloheptene-11-yl bromide (**6**-Br) related with bromide **1**-Br. The locations of the double bond and of the aromatic rings enable both π-route and phenonium route in the ionisation, without, however, allowing the formation of a more delocalized ion, such as **5** (in which both the initial double bond and the aromatic rings could be involved).

Scheme 1

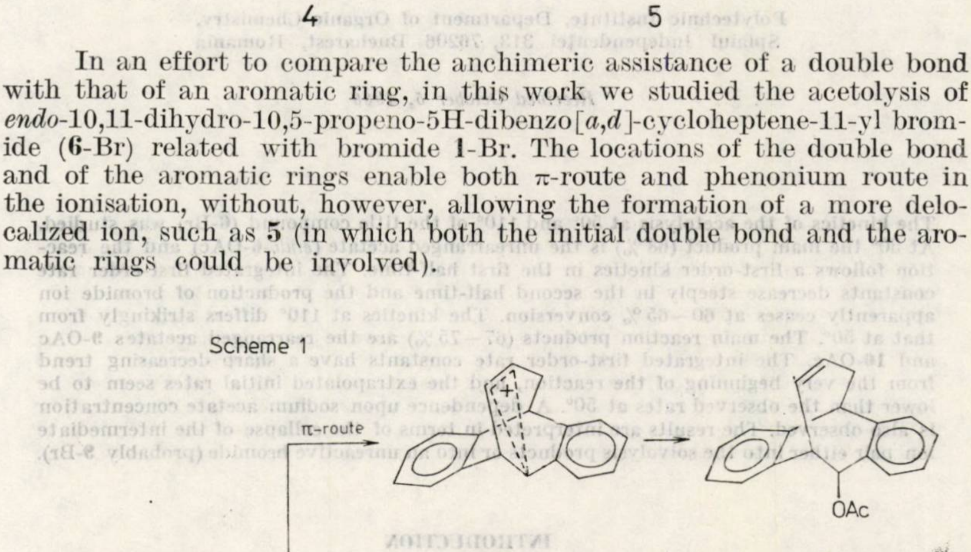

The present paper reports only the kinetic data obtained in the acetolysis of **6**-Br. A full account of the identification of the solvolysis products was published in a previous paper.[9]

RESULTS

1. *Products.*[9] The acetolysis of **6**-Br was performed in anhydrous acetic acid containing a small amount of acetic anhydride and sodium acetate as buffer.* At 56° the main reaction product (65–70%) is the *endo*-acetate **6**-OAc, with the structure and stereochemistry of the initial bromide **6**-Br. At 118° two rearranged acetates, **9**-OAc and **10**-OAc are formed, **9**-OAc representing 50–65% in the reaction mixture (see Scheme 1 and Table 1).

Table 1

Products formed in the acetolysis of bromide **6**-Br[a]

Temp. °C	Reaction time (hrs)	Products (% mol)[a]						
		Alcohols				Hydrocarbons		Other un-identified products
		endo-**6**-OH	*exo*-**6**-OH	**9**-OH	**10**-OH	**11**	**12**	
56	24.0	68.0	3.0	13.5	25.	1.6	6.5	4.9
118	6.6	4.2	—	65.0	10.0	5.0	13.5	2.3
118	24.0	2.3	1.2	52.0	15.0	14.2	8.5	6.8

[a] Determined by gas-chromatography after reduction with $LiAlH_4$. The ratio **6**-Br : NaOAc is 1 : 1.5 throughout.

It should be noted that the isomeric acetate **10**-OAc, as well as the diene **11** (see below) are favoured at 118° at a longer reaction time.

Bromide **6**-Br stored several months at room temperature is transformed quantitatively into bromide **9**-Br.

2. *Kinetics.* The progress of the solvolysis was followed by potentiometric titration of the bromide ion. At 50°, in the first half-time the acetolysis manifests a first-order kinetics, with the mean value of the first-order rate constant $k = (2.80 \pm 0.48) \cdot 10^{-4}\ s^{-1}$. However, in the second half-time, the integrated first-order rate constants fall steeply with increasing conversion and the formation of the bromide ion seems to stop at about 62% conversion (see Table 2).

The decreasing trend of the integrated rate constants is more evident in the acetolysis at 110° (Table 3).

The acetolysis at 110° presents two striking features. One of them is that the reaction rate is dependent upon the molar ratio **6**-Br : NaOAc, the extrapolated initial rate at the highest molar ratio used in this work being about 5 times larger than at the lowest concentration of the sodium acetate used as buffer. Another puzzling feature is that even at the highest natrium acetate concentration, the extrapolated rate constant is too small as compared with the rate constant determined at 50°. Moreover, at the molar ratio **6**-Br : NaOAc = 1 : 1.45 the extrapolated value seems to be even lower than the observed rate constant at 50°. It must be also noted that the apparent interruption of bromide ion formation occurs sooner at the lowest natrium acetate concentration.

---

* The batch-solvolyses were performed at 56° and 118° whereas the kinetic measurements at 50° and 110° C.

Table 2

Integrated first order rate constants of the acetolysis of **6**-Br at 50°C[a,b]

Time (s)	Conversion (%)	Integrated first-order rate constants $10^4k(s^{-1})$
0	0	—
120	3.79	2.98
240	6.82	2.95
660	19.72	3.30
1140	31.10	3.25
1560	35.65	2.85
3900	59.92	2.35
5100	62.19	1.95
8100	62.20	(1.22)[c]

[a] Initial concentration of **6**-Br=1.00×10^{-2}mol/L ; **6**-Br : NaOAc = 1 : 3 ; [b] Mean value of the rate constant : $(2.80 \pm 0.48) \cdot 10^{-4}$; [c] Not included in the mean value.

Table 3

The acetolysis of **6**-Br at 110° and at different molar ratios **6**-Br : NaOAc[a]

6-Br :NaOAc = 1 : 1.45			**6**-Br :NaOAc=1 : 4.4		
Time (s)	Conversion (%)	10^4k (s^{-1})	Time (s)	Conversion (%)	10^4k (s^{-1})
0	0	2^b	0	0	10^b
900	6.57	0.714	120	7.43	6.40
2100	7.46	0.352	600	8.95	1.55
3900	9.24	0.239	1860	11.23	0.64
7800	11.90	0.157	4800	18.05	0.415
15720	13.63	0.0907	16020	31.71	0.238
33300	13.63	—	26100	37.78	0.189

[a] Initial concentration of **6**-Br — 1.024 · $\cdot 10^{-2}$ mol/L ;

[b] Extrapolated value.

DISCUSSION

1. THE ACETOLYSIS OF 6-Ar AT 50°

The decreasing trend of the integrated first-order rate constants may indicate a reversible reaction. However, considering that the formed hydrogen bromide is buffered by an excess of sodium acetate, the interruption of the progress of the reaction at 62% conversion may more probably indicate two different pathways in the transformation of 6-Br : one producing bromide ion (and acetolysis products), the other leading to an unreactive organic bromide (Scheme 2):

Scheme 2

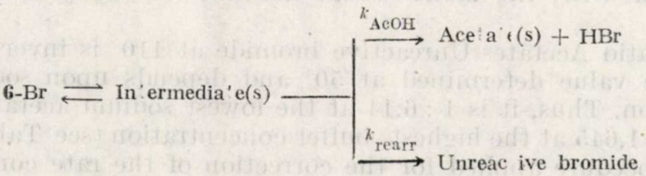

If all the reaction products are formed either from the same intermediate or from rapidly equilibrating intermediates, the ratio : Acetates/Unreactive Bromide$=k_{\text{AcOH}}/k_{\text{rearr}}$ must be constant throughout the acetolysis. Assuming that the transformation of bromide 6-Br is actually ended when the formation of bromide ion apparently ceases, the initial bromide being converted either into the acetolysis products or into the unreactive bromide, the ratio can be calculated from the highest observed conversion as $62.2/37.8 = 1.645$ (Table 2). Correcting the data of Table 2 for the actually transformed bromide, an overall rate constant $k_0=k_{\text{AcOH}} + k_{\text{rearr}}$ can be calculated (Table 4). The correct values are steadier with the progress of the reaction than the integrated rate cons-

Table 4

Corrected first-order rate constants for solvolysis and rearrangement of bromide 6—Br at 50°

Time (s)	Conversion in solvolysis products[a] (%)	Overall conversion[b] of initial bromide (%)	Corrected values 10^4 $(k_{\text{AcOH}} + k_{\text{rearr}})$ (s^{-1})
120	3.79	5.86	5.24
240	6.82	10.54	4.84
660	19.72	30.49	5.78
1140	31.10	48.08	6.08
1560	35.65	55.11	5.46
5100	62.19	100	mean : $k_0 = (5.48 \pm 0.48) \cdot 10^{-4}$

---

[a] See Table 2 ; [b] Considering the ratio : Solvolysis Products/ Unreactive bromide = 1.645 (see text).

tants, obtained directly from rate measurements. The error in the mean value is only $\pm 8.76\%$,whereas the error for the corresponding uncorrected value is larger ($\pm 17.15\%$). Thus, Scheme 2 seems to hold on.

The overall corrected rate constant (k_0) can be split into the individual rate constants : $k_{AcOH} = 3.33 \cdot 10^{-4} s^{-1}$ and $k_{rearr} = 2.15 \cdot 10^{-4} s^{-1}$. Both rate constants are lower than the isomerisation rate constant of **1**-Br into **2**-Br in acetic acid at 0°, but considerably larger than the solvolysis rate of **4**-Br in similar conditions. Indeed, the interpolation of the data published in the previous paper[6] for **4**-Br leads to a rate constant $k = 3 \cdot 10^{-6} s^{-1}$ (AcOH, 50°) bromide **6**-Br being thus more reactive than **4**-Br by a ratio of about two powers of ten. Only a benzylic ion may result from **4**-Br; if a similar intermediate would be produced in the acetolysis of **6**-Br, the latter would not differ sensibly in its reactivity from **4**-Br.

The ratio Acetates/Unreactive bromide at 110° is inverted with respect to the value determined at 50° and depends upon sodium acetate concentration. Thus, it is 1 : 6.14 at the lowest sodium acetate concentration and 1 : 1.645 at the highest buffer concentration (see Table 3). Moreover, the procedure applied for the correction of the rate constants at 50° cannot be used for correcting the data of the acetolysis at 110°. However, a better fit is observed if it is assumed that the ratio Acetates/Unreactive Bromide is not constant but decreases with increasing conversion.

2. THE MECHANISM OF THE ACETOLYSIS OF 6-Br AT 50°

The product data reported in Table 1 agree well with the simple mechanism depicted in Scheme 1. Thus, the main product, the *endo*-acetate **6**-OAc, as well as hydrocarbon **12** (dibenzobullvalene) are very likely formed from intermediate **7** :

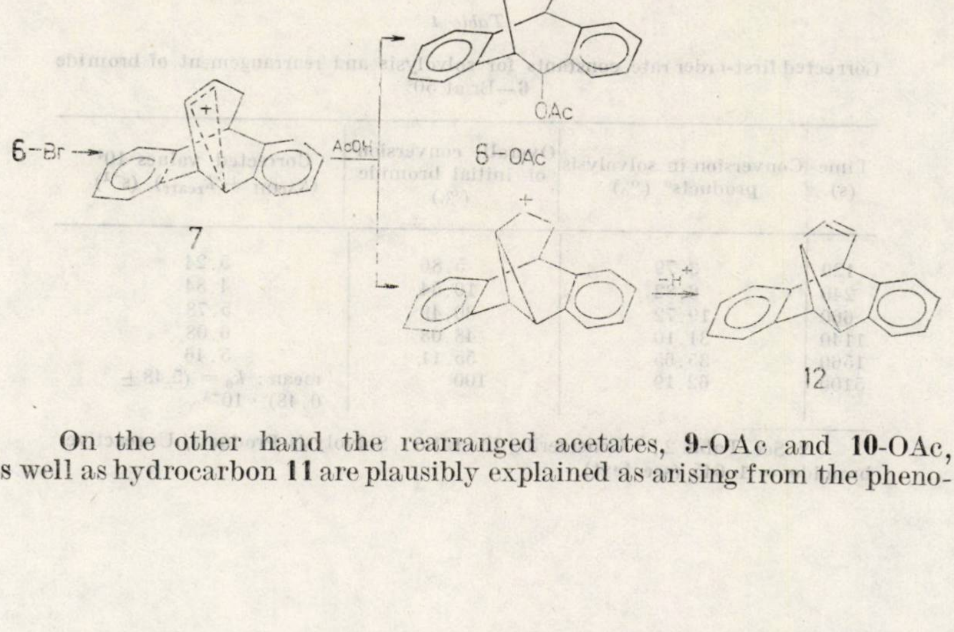

On the other hand the rearranged acetates, **9**-OAc and **10**-OAc, as well as hydrocarbon **11** are plausibly explained as arising from the phenonium ion **8**:

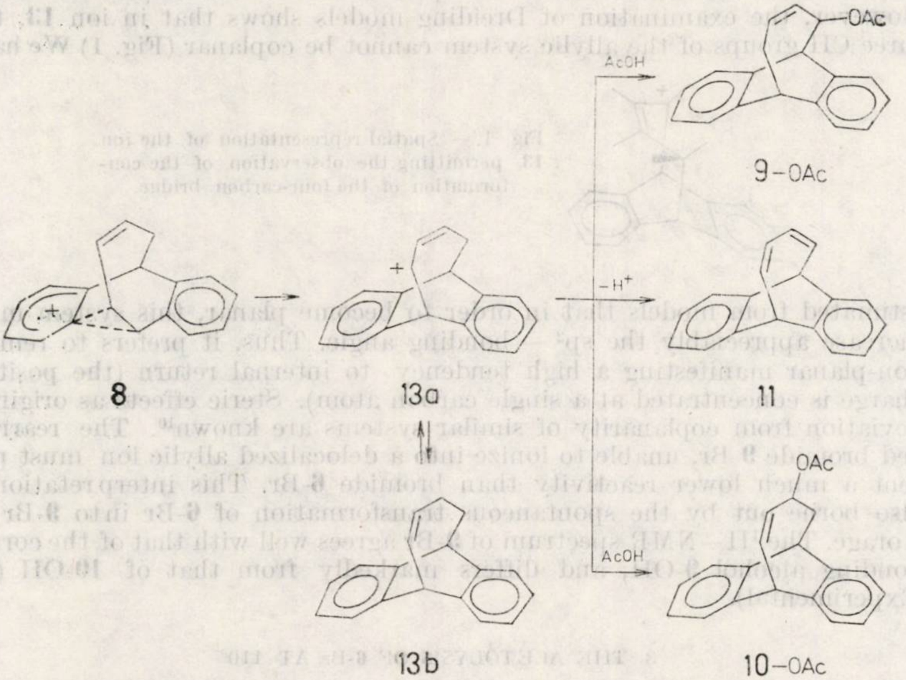
AcOH
9−OAc
−H⁺
8
13a
11
AcOH
13b
10−OAc

Even with these details, Scheme 1 does not explain the apparent interruption of bromide ion formation at about 60−65% conversion (see Table 2). As has been shown, a plausible interpretation of the kinetic data at 50° is offered by Scheme 2, in which we assume that **6**-Br forms in the initial step a mixture of rapidly equilibrating intermediates, which in their turn yield either the observed acetates or the unreactive bromide. It is reasonable to admit that the rapidly equilibrating intermediates are tight ion pairs R^-Br^+, the unreactive bromide resulting by return from such a pair (Scheme 3):

Scheme 3

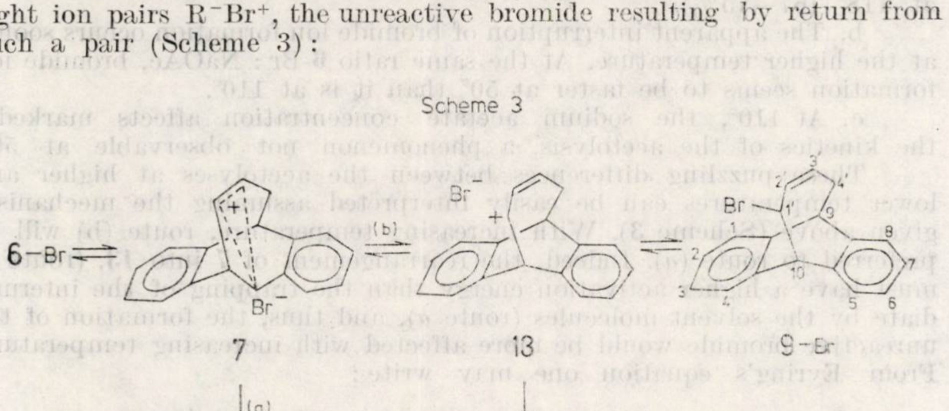
6−Br
Br
(b)
Br⁻
1
2
3
4
1'
2
3
4
9
10
8
7
5
6
Br
7
13
9−Br
(a)
6−OAc + 12
9−OAc + 10−OAc + 11

According to this scheme, the unreactive bromide could be **9**-Br (or **10**-Br) which seems to be unexpected, due to its allylic structure. However, the examination of Dreiding models shows that in ion **13**, the three CH groups of the allylic system cannot be coplanar (Fig. 1) We have

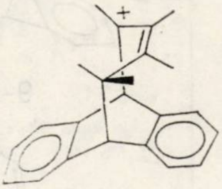

Fig. 1. — Spatial representation of the ion **13** permitting the observation of the conformation of the four-carbon bridge.

estimated from models that in order to become planar, this system must increase appreciably the sp^2 — bonding angle. Thus, it prefers to remain non-planar manifesting a high tendency to internal return (the positive charge is concentrated at a single carbon atom). Steric effects as origin of deviation from coplanarity of similar systems are known[10]. The rearranged bromide **9**-Br, unable to ionize into a delocalized allylic ion must present a much lower reactivity than bromide **6**-Br. This interpretation is also borne out by the spontaneous transformation of **6**-Br into **9**-Br on storage. The ^1H-NMR spectrum of **9**-Br agrees well with that of the corresponding alcohol **9**-OH, and differs markedly from that of **10**-OH (see Experimental).

3. THE ACETOLYSIS OF **6**-Br AT 110°

The data of Tables 1—3 clearly show that the phenomenon measured at this temperature is not the same with the phenomenon measured at 50°. The following observations sustain this statement :

a. At 56° the unrearraged acetate, **6**-OAc, is the main reaction product (68%), whereas at 118° it is formed only in small amounts (2.3%). The rearranged acetates, **9**-OAc and **10**-OAc are minor reaction products at 56° (16%), but overwhelm the other products in the reaction mixture at 118° (67—75%).

b. The apparent interruption of bromide ion formation occurs sooner at the higher temperature. At the same ratio **6**-Br : NaOAc, bromide ion formation seems to be faster at 50° than it is at 110°.

c. At 110°, the sodium acetate concentration affects markedly the kinetics of the acetolysis, a phenomenon not observable at 50°.

These puzzling differences between the acetolyses at higher and lower temperatures can be easily interpreted assuming the mechanism given above (Scheme 3). With increasing temperature, route (b) will be preferred to route (*a*). Indeed, the rearrangement of **7** into **13**, (route *b*) must have a higher activation energy than the trapping of the intermediate by the solvent molecules (route *a*), and thus, the formation of the unreactive bromide would be more affected with increasing temperature. From Eyring's equation one may write :

$$\ln\left(\frac{k_{\mathrm{rearr}}}{k_{\mathrm{AcOH}}}\right)_{T_2} - \ln\left(\frac{k_{\mathrm{rearr}}}{k_{\mathrm{AcOH}}}\right)_{T_1} - \ln\frac{T_2}{T_1} = \frac{\Delta G_1^{\ddagger} - \Delta G_2^{\ddagger}}{R}\left(\frac{1}{T_1} - \frac{1}{T_2}\right.$$

where $(k_{\text{rearr}}/k_{\text{AcOH}})T_2$ and $(k_{\text{rearr}}/k_{\text{AcOH}})T_1$ are the observed ratios at 110° and 50°, respectively and the difference $(\Delta G_1^{\ddagger} - \Delta G_2^{\ddagger})$ is the activation free energy difference between the formation of bromide **9**-Br and acetate **6**-OAc. Using this relation, a plausible value of about 10 kcal/mol can be appreciated for this free energy difference.

The formation of the rearranged acetates needs further comments. The dependence of the initial reaction rate upon sodium acetate concentration may either imply a bimolecular reaction between **9**-Br and acetate ion, or an ion pair collapse from an acetate ion pair. [11]

$$R^+ Br^- + AcO^- \rightleftharpoons R^+ AcO^- \longrightarrow R{-}OAc$$

The latter interpretation seems to be more probable. Indeed, a three-fold increase in sodium acetate concentration produces a five-fold increase in the initial rate constant (Table 3). On the other hand, secondary bromides in acetic acid follow the unimolecular pathway instead of the bimolecular reaction [12]. The formation of acetate ion pairs has been observed previously and is easily detected from product and kinetic data. [11]

The fact that the intermediate in the formation of **9**-OAc and **10**-OAc is not the delocalized allylic ion is suggested by Table 1. The ratio **9**-OAc/**10**-OAc at 110° is 6.5 : 1 at short reaction times (6.6 hrs) and 3.46 : 1 at longer reaction times (24 hrs). The latter acetate is thus formed from the former, and no ionisation mechanism from **9**-OAc is conceivable in the buffered acetic acid solution. Moreover, at similar reaction times, the larger amounts of **10**-OAc are formed at the higher temperature.

The formation of **10**-OAc from **9**-OAc does not need the involvement of an ionic species. Indeed, an allylic acetate is a 1,3-dioxahexa-1,5-diene which can suffer an allowed concerted process, corresponding to a Cope rearrangement [13] :

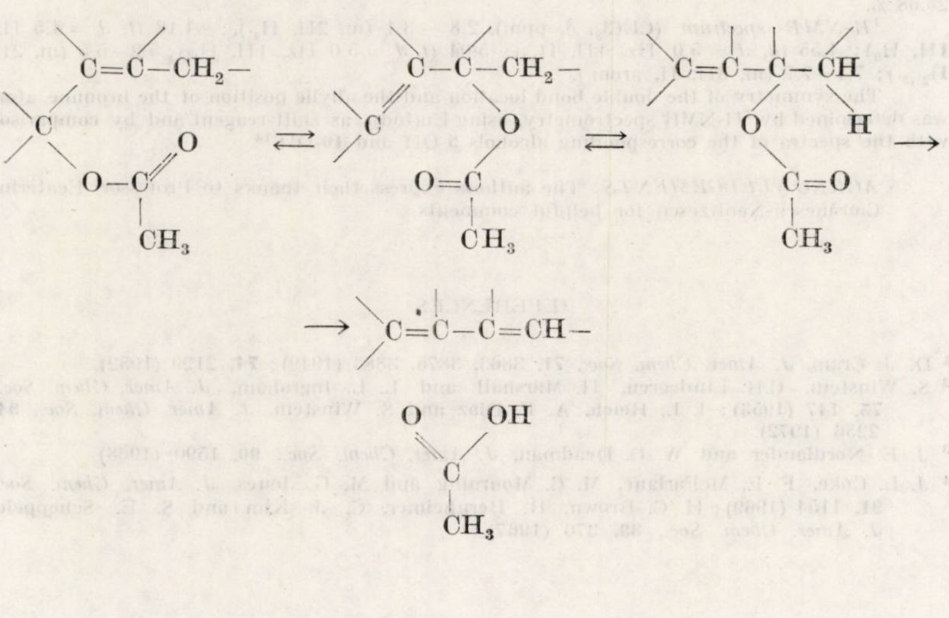

The formation of the rearranged acetate can be accompanied by a concerted elimination of acetic acid, leading to alkene **11**. As expected, a similar trend is observed under the reaction conditions in the formation of diene **11** as in the formation of acetate **10**-OAc.

The results reported herein are all in agreement with the collapse of ion pairs to unreactive reaction products.

EXPERIMENTAL

The acetic acid used in solvolyses was obtained by refluxing commercial acetic acid with acetic anhydride, followed by distillation on an efficient column (freezing point 16.4°C).

Sodium acetate solutions were obtained by dissolving anhydrous sodium acetate in acetic acid. The concentration of the solution was determined by titration of the solution with a 0.05 M solution of perchloric acid in acetic acid.

Bromide **6**-*Br*: The synthesis of this bromide was described previously.[9] Solutions of the bromide were obtained by weighing precisely the necessary amounts of **6**-Br.

Kinetic measurements. The ampoule technique was used. The liberated hydrogen bromide was indirectly titrated with a 0.05 M solution of $HClO_4$ (in acetic acid) after addition of an excess of a solution of NaOAc (in AcOH) in the presence of crystal-violet as indicator.

BROMIDE 9-Br FROM BROMIDE 6-Br

A sample of **6**-Br stored several months at room temperature was transformed quantitatively into bromide **9**-Br, which after recrystallization from cyclohexane indicated a melting point of 122—124°C.

Bromide **9**-Br was also obtained by bubbling (4 h) dried gaseous HBr (from tetraline and Br_2) in a cooled (-5°C) solution of bromide **6**-Br in anhydrous methylene chloride. The brown solution was left overnight, washed with water, Na_2CO_3 solution and again with water to neutral pH. After drying and evaporation of the solvent, the crude bromide **9**-Br was obtained in nearly quantitative yield. Purification of **9**-Br was achieved by chromatography on a short silica column (dried CH_2Cl_2 as solvent.)

1'-Bromo-9,10-(2'-buteno)-9,10-dihydroanthracene (**9**-Br), m.p. 122°—124°C;

Found: C, 69.44; H, 4.81; Br, 25.65; $C_{18}H_{17}Br$ requires: C, 69.47; H, 4.85; Br, 25.68 %.

^{1}*H-NMR spectrum* ($CDCl_3$, δ, ppm), 2.8 — 3.1 (m, 2H, $H_{4'}$),; 4.18 (*t*, $J = 4.5$ Hz, 1H, H_9); 4.55 (*d*, $J = 5.0$ Hz, 1H, H_{10}); 5.04 (*t*, $J = 5.0$ Hz, 1H, $H_{1'}$); 5.2—5.5 (m, 2H, $H_{2',3'}$); 7.1—7.7 (m, 8H, H, arom.).

The symmetry of the double bond location and the allylic position of the bromine atom was determined by ^{1}H-NMR spectrometry, using $Eu(fod)_3$ as shift-reagent and by comparison with the spectra of the corresponding alcohols **9**-OH and **10**-OH.[14]

ACKNOWLEDGEMENTS: The authors express their thanks to Professor Ecaterina Ciorănescu-Nenitzescu for helpful comments

REFERENCES

[1] D. J. Cram, *J. Amer. Chem. Soc.*, **71**, 3863, 3875, 3883 (1949); **74**, 2129 (1952).

[2] S. Winstein, C.R. Lindegren, H. Marshall and L. L. Ingraham, *J. Amer. Chem. Soc.*, **75**, 147 (1953); I. L. Reich, A. F. Diaz and S. Winstein, *J. Amer. Chem. Soc.*, **94**, 2256 (1972).

[3] J. E. Nordlander and W. C. Deadman, *J. Amer. Chem. Soc.*, **90**, 1590 (1968).

[4] J. L. Coke, F. E. McFarlane, M. C. Mourning and M. G. Jones, *J. Amer. Chem. Soc.*, **91**, 1154 (1969); H. C. Brown, R. Bernheimer, C. J. Kim and S. E. Scheppele, *J. Amer. Chem. Soc.*, **89**, 370 (1967).

[5] C. J. Lancelot and P.v.R. Schleyer, *J. Amer. Chem. Soc.*, **91**, 4291 (1969); C. J. Lancelot, J. J. Harper and P.v.R. Schleyer, *J. Amer. Chem. Soc.*, **91**, 4294 (1969); C. J. Lancelot, and P.v.R. Schleyer, *J. Amer. Chem. Soc.*, **91**, 4296 (1969); P.v.R. Schleyer and C.J. Lancelot, *J. Amer. Chem. Soc.*, **91**, 4297 (1969); D. J. Raber, J. M. Harris and P.v.R. Schleyer, *J. Amer. Chem. Soc.*, **93**, 4821, 4829 (1971).

[6] M. Voicu, F. Badea and A. Bucur, *Rev. Roumaine Chim.*, **17**, 1563 (1972).

[7] E. Ciorănescu, A. Bucur, F. Badea, M. Rentzea and C. D. Nenitzescu, *Tetrahedron Letters*, **1969**, 1867.

[8] G. Mateescu, C. D. Nenitzescu and G. Olah, *J. Amer. Chem. Soc.*, **90**, 6235 (1968).

[9] M. Banciu, R. Vlad, C. Drăghici and E. Ciorănescu, *Rev. Roumaine Chim.*, **22**, 1017 (1977).

[10] T. S. Sorensen, *Canad. J. Chem.*, **42**, 2768 (1964); see also: T. S. Sorensen, in "Carbonium Ions", vol. 2, G.A. Olah and P.v.R. Schleyer (Eds), Wiley, Interscience, New York, 1970, chapter 19.

[11] M. Voicu and F. Badea, *Rev. Roumaine Chim.*, **14**, 929 (1969).

[12] See for example: F. Badea, "Reaction Mechanisms in Organic Chemistry", Abacus Press, Tunbridge Wells, Kent, 1977, chapter 5.

[13] A. C. Cope and E. M. Hardy, *J. Amer. Chem. Soc.*, **62**, 441 (1940); E. Vogel, *Angew. Chem.*, **74**, 829 (1962); R. B. Woodward and R. Hoffmann, *J. Amer. Chem. Soc.*, **87**, 2511 (1965).

[14] R. Vlad, *Ph. Dr. Thesis*, Polytechnic Institute, Bucharest, 1984.

Revue Roumaine de Chimie, 32, 2, 191 – 197 (1987)

KINETIC STUDIES ON THE CATALYTIC ALKYLATION OF TOLUENE WITH METHANOL

EMIL DUMITRIU, SPIRIDON OPREA and VASILE HULEA
Department of Organic Chemical Technology, Polytechnic Institute of Jassy, Bahlui Stînga 71, Jassy 6600, Romania

Received March 4, 1986

A kinetic method allowing the quantitative estimation of the catalytic properties of zeolites in the alkylation reaction as well as of other catalytic processes or catalysts was developed. This method was applied to the study or the toluene alkylation with methanol in the presence of HY, HPrY and HNdY zeolites. It was stated that alkylation of xylene is a more rapid reaction than the toluene alkylation, but it depends on the type of catalyst. On the same kinetic basis was demonstrated that the toluene disproportionation has a minor role in the xylene formation. Other competitive reactions are also investigated.

It is generally admitted that the alkylation of aromatic hydrocarbons with alcohols implies more energetic conditions than the alkylation with other agents (olefines, alkyl halides etc.) due to the relatively low reactivity of alcohols. These conditions explain a series of secondary reactions which occur during the alkylation process. It is also recognized that the alkylation is an acid catalyzed process, the solid acids as zeolites having a very important role. [1–3]

From these reasons the alkylation of aromatic hydrocarbons, especially of toluene, was studied on various zeolites : faujazites, [2,4–6] ZSM-5[7] etc., but all these studies had as major aim only a qualitative investigation of the catalytic properties of zeolites, i.e. the catalytic activity and selectivity in relation to the nature of catalyst.

Therefore we intend here to develop a kinetic method which allows a quantitative estimation of the catalytic properties of zeolites in the alkylation reaction as well as for other catalytic processes or catalysts. This procedure, based on the determination of the reaction rates, was applied to the toluene alkylation with methanol, an intricate process due to the secondary reactions occurring at the same time with the proper alkylation reaction of toluene.

EXPERIMENTAL

Reagents. Methylic alcohol and toluene were purified by the common methods. [8]

Catalysts. All catalysts were prepared on the basis of NaY zeolite (LZ – Y 52 extrudate, VENTRON) having the following characteristics : 66.5% SiO_2, 20.8% Al_2O_3, 10.4% Na_2O, 0.23% Fe_2O_3 and 0.33% CaO (by weight); specific area was about 800 m^2/g and grain dimensions 1.5 × 2 mm. NaY was subjected to a partial ionic exchange with ammonium chloride, followed by washing with distilled water and drying for 3 hrs at 120°C to get NH_4NaY which on calcination at 500°C in dry air stream resulted in the H form. Various samples of deaminated zeolite were subjected to a subsequent ionic exchange referring to the residual Na^+ ions using aqueous solutions of $Pr(NO_3)_3$ or $Nd(NO_3)_3$. The percentage of exchanged ammonium was 58.0% and that of neodymium 20.12% and of praseodyum 10.62, 17.88, 23.06 and 25.39% respectively (in equivalents). It was proved, by X-ray diffraction, that zeolites did not lose their crystallinity during the exchange process.

Procedure. All experiments were carried out on an integral fixed bed flow reactor. The reactor was isothermally operated (with ±1.0°C accuracy) under atmospheric pressure. The feed rate of reagents was accurately maintained by a calibrated syringe pump and nitrogen free-moisture was used as diluent and as carrier gas. The reaction products were collected into a refrigerated trap at −32°C.

Analysis. The analysis of the liquid reaction products was performed by GC on a column of benton 34-dinonyl phthalate on Chromosorb W using a FID detector. The noncondensable products were analysed using a column of dimethylsulfolane-squalane on Cellite 22. The coke was determined either weighing or burning and measuring the CO_2 evolved.

KINETIC MODEL

This model was developed on the basis of the rate equations corresponding to the various reactions which take place during the alkylation process. Our previous studies [4,9] showed that the alkylation process consists of two groups of reactions: (i) – the catalytic transformations of aromatic hydrocarbons as alkylations, disproportionations, isomerizations etc., and (ii) – the catalytic conversion of methanol (dimethyl ether, paraffins, olefines and even the aromatic hydrocarbons formation).

Taking into account the most important reactions which imply important consumptions of reagents or products, a kinetic model can be elaborated allowing us to follow the competition among various reactions taking place during the catalytic process and also to state the catalytic properties of zeolites. Therefore, making the following notations: A_1 = toluene, A_2 = methanol, A_3 = xylenes, A_4 = benzene, A_5 = trimethylbenzenes, A_6 = dimethyl ether and A_7 = hydrocarbons resulting by the methanol conversion (i.e. paraffins and olefines), we can take into account the following reactions which describe the process:

— alkylation of toluene

$$A_1 + A_2 \xrightarrow{k_1} A_3 \tag{1}$$

— disproportionation of toluene

$$A_1 \xrightarrow{k_2} \frac{1}{2} A_3 + \frac{1}{2} A_4 \tag{2}$$

— alkylation of xylene

$$A_2 + A_3 \xrightarrow{k_3} A_5 \tag{3}$$

— formation of dimethyl ether

$$A_2 \xrightarrow{k_4} \frac{1}{2} A_6 \tag{4}$$

— methanol convesion

$$A_2 \xrightarrow{k_5} \nu A_7 \tag{5}$$

We must underline that this reaction scheme does not consider the true reaction mechanism so that dimethyl ether, which is a valuable alkylating agent, is here considered only as a reaction product, and the methanol conversion to hydrocarbons is shown as an overall process, irrespective of route. For the reversible reactions only the forward reactions have been considered.

Further we adopted the following notations which are useful for the model elaborations:

N_0 — the number of initial moles of toluene;

x_i — the fraction of initial mole number of reagent transformed in product, in the i-th reaction ($i = 1 ... 5$);

a — the initial mole ratio between toluene and methanol.

The mole number of each component at a given time will be:

$$N_{A_1} = N_0(1 - x_1 - x_2)$$

$$N_{A_2} = N_0(a - x_1 - ax_3 - ax_4 - ax_5)$$

$$N_{A_3} = N_0(x_1 + 1/2x_2 - ax_3)$$

$$N_{A_4} = 1/2 \cdot N_0 x_2$$

$$N_{A_5} = N_0 a x_3$$

$$N_{A_6} = 1/2 \cdot N_0 a x_4$$

$$N_{A_7} = N_0 a x_5$$

Now we can write the differential equations of the rate on the basis of Langmuir theory of adsorption and the theory of dynamic reaction process:

$$N_0 \frac{dx_1}{S_0 Ø \cdot dl} = k_1 \cdot \sigma_{A_1} \cdot \sigma_{A_2} \tag{6}$$

$$1/2N_0 \frac{dx_2}{S_0 Ø \cdot dl} = k_2 \cdot \sigma^2_{A_1} \tag{7}$$

$$N_0 \frac{dx_3}{S_0 Ø \cdot dl} = k_3 \cdot \sigma_{A_2} \cdot \sigma_{A_3} \tag{8}$$

$$1/2N_0 \frac{dx_4}{S_0 Ø \cdot dl} = k_4 \cdot \sigma^2_{A_2} \tag{9}$$

$$1/\nu N_0 \frac{dx_5}{S_0 Ø \cdot dl} = k_5 \cdot \sigma^2_{A_2}. \tag{10}$$

where : S_0 — the surface per unity of catalyst volume;
Ø — cross-section of reaction zone;
l — the length of reaction zone;
σ_{A_i} — the degree of coverage with component *i*.

If we want to analyse the competition between the *i* and *j* reactions, then we make the ratio of the corresponding rate equations and the following expression is obtained :

$$\frac{\mathrm{d}x_i}{\mathrm{d}x_j} = k_{ij} \frac{\alpha_0 + \sum\limits_{n=1}^{5} \alpha_n x_n}{\beta_0 + \sum\limits_{n=1}^{5} \beta_n x_n} \tag{11}$$

where $k_{ij} = k_i/k_j$ and α_0, β_0, α_n and β_n are constants having different values in relation to the considered reactions. If we note :

$$\gamma_{nj} = \frac{x_n}{x_j} \quad n = 1, \ldots 5; \tag{12}$$

equation (11) becomes :

$$\frac{\mathrm{d}x_i}{\mathrm{d}x_j} = k_{ij} \frac{\alpha_0 + \sum\limits_{n=1}^{5} \alpha_n \gamma_{nj} x_j}{\beta_0 + \sum\limits_{n=1}^{5} \beta_n \gamma_{nj} x_j} \tag{13}$$

It should be noted that x_i are experimentally determined values. This equation can be brought at a simpler from :

$$\frac{\mathrm{d}x_i}{\mathrm{d}x_j} = k_{ij} \frac{\alpha_0 + \alpha x_j}{\beta_0 + \beta x_j} \tag{14}$$

on the basis of the following notations :

$$\alpha = \alpha_j + \sum_{n=1}^{5} \alpha_n \gamma_{nj} = \text{const}$$

$$\beta = \beta_j + \sum_{n=1}^{5} \beta_n \gamma_{nj} = \text{const}$$

Equation (14) can be integrated and if the indices are particularized we can study the catalytic process especially in relation to the selectivity.

RESULTS AND DISCUSSION

We shall now consider the competition between the consecutive reactions of alkylation. In this case, equation (14) becomes :

$$\frac{\mathrm{d}x_3}{\mathrm{d}x_1} = k_{31} \frac{x_1 + \frac{x_2}{2} - ax_3}{1 - x_1 - x_2} \tag{15}$$

If we consider $a = 1$ and :

$$\gamma_{21} = \frac{x_2}{x_1}; \quad \gamma_{31} = \frac{x_3}{x_1} \tag{16}$$

by substituting relation (16) in equation (15) we obtain :

$$\frac{\mathrm{d}x_3}{\mathrm{d}x_1} = k_{31} \frac{(1 + 1/2\ \gamma_{21} - \gamma_{31})x_1}{1 - (1 + \gamma_{21})x_1} \tag{17}$$

This relation can be integrated :

$$x_3 = k_{31} \frac{1 + 1/2\,\gamma_{21} - \gamma_{31}}{1 + \gamma_{21}} \left\{ - \frac{1}{1 + \gamma_{21}} \ln[1 - (1 + \gamma_{21})x_1] - x_1 \right\} \tag{18}$$

and we obtain an equation which allows to estimate k_{31} constant (which is not a kinetic constant but a rate constant).

Therefore, by operating at various contact times different conversions are obtained, then the reaction products are analyzed (thus xi values are obtained) and the k_{31} values are calculated on the basis of integrated equation (18). The results are shown in Table 1.

Table 1

k_{31} values determined as a function of contact time ; $T = 425°\mathrm{C}$, $a = 1$, $N_2/F = 5/1$, HPrY-1

Contact time, s	x_n, mole ratio			k_{31}
	x_1	$x_2 \cdot 10^2$	x_3	
2.2	0.249	0.182	0.117	5.91
4.1	0.268	0.194	0.135	6.10
6.3	0.288	0.238	0.154	6.04
7.8	0.313	0.254	0.177	5.97

As it can be seen, equation (18) has an intricate form implying a laborious processing. When the mole fraction of toluene converted into benzene is very small, then we can neglect the ratio γ_{21}. Thus, equation (18) becomes :

$$x_3 = k_{31}(\gamma_{31} - 1)[x_1 - \ln(1 - x_1)] \tag{19}$$

The value calculated by equation (19), $k_{31} = 6.009$, is very close to that calculated by equation (18), i.e. $k_{31} = 6.007$.

Analysis of the data given in Table 1 shows that the alkylation reaction of xylene occurs at a higher rate than the toluene alkylation; this fact confirmes the literature data. [10]

It is known that the benzene ring is activated by the alkyl groups so that the reaction products consist in a mixture of mono- and polyalkylated products. This is possible due to the fact that the rate of alkylation is increased after the first substitution, so that the second substitution occurs more rapidly, though it is dependent on the steric hindrance. The confirmation of this supposition consists in the k_{31} values which are greater than the unity $(k_3/k_1) > 1$). It must be also mentioned the strong effect of temperature on the subsequent substitution, as it is shown in Figure 1.

As known, obviously, it should be desired that monoalkylation be the preponderent reaction, if only. Therefore we have investigated the catalytic properties of other zeolites according to this idea. In the same reaction conditions the following values of k_{31} for various catalysts are obtained (Table 2).

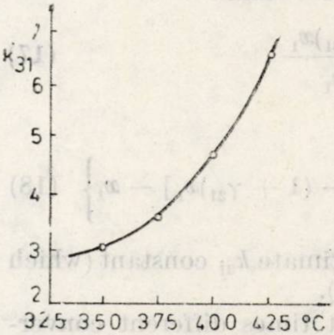

Fig. 1. — k_{31} *vs.* reaction temperature ; $N_2/F = 5/1$, HPrY-1.

We can remark some interesting aspects. HY catalyst shows an unsatisfactory selectivity in relation to the toluene alkylation. By the introduction of the rare earth cations (RE^{3+}) as result of the ionic exchange the selectivity for monoalkylation is increased to a certain extent. The best results are obtained using HNdY zeolite, but it can be also seen that by increasing Pr^{3+} content the selectivity is increased.

The developed model was also tested for other competitive reactions. For example, we show here the results obtained for monoalkylation — disproportionation competition. Therefore, we can write :

$$\frac{dx_2}{dx_1} = k'_{21} \frac{2(1 - x_1 - \gamma_{21}x_1)}{1 - (1 + \gamma_{31} + \gamma_{41} + \gamma_{51})x_1} \tag{20}$$

By integration of this equation we obtain :

$$x_2 = \frac{2k'_{21}}{1 + \gamma_{31} + \gamma_{41} + \gamma_{51}} \Big\{ (1 + \gamma_{21})x_1 + \tag{21}$$

$$+ \frac{\gamma_{21} - \gamma_{31} - \gamma_{41} - \gamma_{51}}{1 + \gamma_{31} + \gamma_{41} + \gamma_{51}} (\ln[1 - (1 + \gamma_{31} + \gamma_{41} + \gamma_{51})x_1] \Big\}$$

where $k_{21} = 2k'_{21}$

Table 2

Competitive alkylation as a function of catalyst nature: $T = 400°C$, $a = 1$, $N_2/F = 5/1$

Catalyst	Degree of Na^+ exchange, %		K_{31}
	NH_4^+	RE^{3+}	
HY	58.0	—	6.48
HNdY	58.0	20.12	4.75
HPrY-1	58.0	10.62	6.02
HPrY-2	58.0	17.88	5.73
HPrY-3	58.0	23.06	5.40
HPrY-4	58.0	25.39	5.21

We chose the experiments where the disproportionation of toluene is significantly, i.e. at 425°C. Solving equation (21) on the basis of x_1 and

x_2 values which are experimentaly determined we obtain the following results (Table 3).

As can be observed the model is also valuable for this case, the ratio k_{21} being approximately kept constant, irrespective of conversion. Taking into account the small values of k_{21} (e.g. $k_{21} = 6.67 \times 10^{-3}$), we can affirm that xylenes resulted as reaction products are formed more by toluene alkylation than by toluene disproportionation.

Table 3

k_{21} constant *vs.* conversion ; $T = 425°C$, $N_2/F = 5/1$, HPrY-1

x_n, mole fraction		$k_{21} \times 10^3$
x_1	$x_2 \cdot 10^2$	
0.249	0.182	6.77
0.268	0.194	6.22
0.288	0.218	6.81
0.313	0.254	6.49

Table 4

K' as a function of time factor (W/F) HPrY-1

W/F g.h. mole^{-1}	p %(g)	$k' \cdot 10^2$ mole$\cdot$g$^{-1}\cdot$h^{-1}
21	1.35	1.42
40	1.73	1.37
63	2.48	1.44
80	2.95	1.36

Finally, we tried to state the mathematical function which can be correlated with the catalyst deactivation. In such a case it is possible to estimate the formation of coke as a function of contact time by the expression :

$$p = \exp\left(k' \cdot \frac{W}{F}\right) \qquad (22)$$

where p is the formed coke.

On this basis the following equation is obtained :

$$p = e^{0.0139\ W/F}$$

To conclude, we can assert that the developed model is useful for the description of competitive reactions when a more complex catalytic process is studied. It was stated that the subsequent alkylation occurs at a higher rate than the monoalkylation of toluene and that the toluene disproportionation has not a significant contribution to the formation of xylenes. It was also stated that the contact time does not affect the relation between alkylation and other reactions. As it was expected the formation of coke is favoured by the contact time increasing.

REFERENCES

[1] P. B. Venuto, L. A. Hamilton and P. S. Landis, *J. Catal.*, **5**, 484 (1966).

[2] T. Yashima, H. Ahmad, K. Yamazaki, M. Katsuta and N. Hara, *J. Catal.*, **16**, 119 (1970).

[3] S. Zielinski and Z. Szabok, *React. Kinet. Catal. Lett.*, **16**, 119 (1981).

[4] Em. Dumitriu, Sp. Oprea and K. Yousef, *Rev. Chim.* (*București*), **35**, 906 (1984).

[5] M. Tuyen and C. Dimitrov, *React. Kinet. Catal. Lett.*, **22**, 215 (1983).

[6] B. Coughlan, W. M. Carrol and J. Nunan, *Chem. Ind.* (*London*), **14**, 480 (1979).

[7] N. Y. Chen, W. W. Kaeding and F. G. Dwyer, *J. Amer. Chem. Soc.*, **101**, 6783 (1979).

[8] A. I. Vogel, "Practical Organic Chemistry", Longmans Green and Co., London, 1956, pp. 169–173.

[9] Em. Dumitriu, Sp. Oprea and V. Hulea, *React. Kinet. Catal. Lett.*, (in press).

[10] J. B. Hendrickson, D. J. Cram and C. S. Hammond, "Chimie Organică", Ed. St. Enciclop., Bucharest, 1976, p. 704.

Revue Roumaine de Chimie, **32**, *2*, 199–202 (1987)

DEHYDROGENATION KINETICS OF LOW ALIPHATIC ALCOHOLS ON COPPER CATALYSTS. III

METALLIC COPPER WITH Fe AND Ni AS ADDITION ELEMENTS

N. DOCA* and E. SEGAL**

* Chemical Research Center, Blvd Mihai Viteazul 24, 1900 Timişoara, Romania
** Chair of Physical Chemistry and Electrochemical Technology, Faculty of Chemical Technology, Polytechnical Institute of Bucharest, Blvd Republicii 13, Bucharest, Romania

Received February 17, 1985

Metallic copper catalysts with 0.5, 1.0 and 1.5 at.% of Fe and Ni respectively, were prepared by hydrogen reduction of impregnated CuO, and were stabilised against reoxidation by adsorption of inert gases (N_2 and CO_2). Generally the apparent activation energy of dehydrogenation reaction, determined by the chromatographic pulse technique, decreases on these catalysts, comparatively with copper catalyst. The values of apparent activation energy increase as follows: EtOH<i-PrOH<n-PrOH<2-BuOH<n-BuOH.

The influence of small amounts of Fe and Ni on copper catalytic activity was studied in the same manner as described in our previous paper.[1] The laboratory equipment and working procedure were detailed in an earlier paper.[2]

CATALYST PREPARATION AND CHARACTERISATION

To a certain amount of CuO powder (prepared as in ref.[2]), the necessary volumes of $Fe(NO_3)_3$ and $Ni(NO_3)_2$, 0.1 N solutions were added, in order to obtain the desired composition, i.e. 0.5, 1.0 and 1.5 at% of Fe and Ni. After 2 h impregnation, the mixtures were dried for 5 h at 95–100° and calcined 5 h at 250°, then reduced with hydrogen and stabilised by nitrogen or carbon dioxide adsorption.

The variation of free enthalpy and equilibrium conversion *vs.* temperature for the metal oxide reduction was calculated using the well known equations and the data systematised in.[3]

The results presented in Tables 1 and 2 indicate a total reduction of NiO and a partial reduction of FeO. Thus the obtained catalysts were of the following types: metal and its oxide, deposited on metallic copper (for Fe); metal deposited on metallic copper (for Ni).

Table 1

Calculated variation of free enthalpy for metal oxide reduction with hydrogen

Oxide	ΔG_T^0, kJ /mol				
	T=473 K	573 K	673 K	773 K	873 K
CuO	−79.0	−77.3	−75.3	−72.9	−70.4
NiO	−22.4	−27.6	−32.3	−36.8	−41.2
FeO	7.5	7.1	8.2	10.6	13.8

Table 2

Calculated equilibrium constants (K) and conversions (α) for NiO and FeO reduction

Oxide		T=473	573	673	773	873
NiO	K	296	327	327	311	290
	$\alpha\times100$	100	100	100	100	100
FeO	K	0.148	0.225	0.230	0.192	0.149
	$\alpha\times100$	12.89	18.36	18.69	16.10	12.96

The experimental reduction conditions were : hydrogen flow — 0.5 cm³/s for 10 g catalyst ; heating rate up to 400° — 3°/min ; working temperature — 400° ; reduction time — 10 h for Ni + Cu and 9 h for Fe+Cu.

As stabilisation procedure, the treatment with stabilising gas which lasted for 60—120 min. at 200° was used, the temperature *vs.* time diagrames being presented in Figure 1.

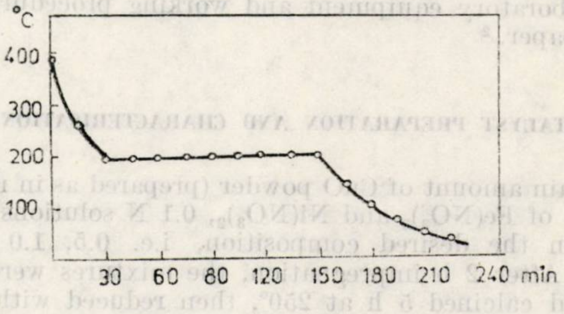

Fig. 1 — Temperature *vs.* time diagram of the stabilisation period.

The main characteristics of the catalysts are listed in Table 3.

The presence of easy reducible oxides increases strongly the reduction starting temperature,[1,2] which is rather independent of the amount of added metal (or metal oxides). The stability limits of the catalysts decreases for Ni-Cu systems, comparatively with the pure copper, while for Fe—Cu systems, these limits are relatively close.

Table 3

The main characteristics of the catalysts

Catalyst	Added element	Amount of added metal at. % *	Extrapol. red. beg. temp. °C	Stability, °C for**	
				CO_2	N_2
C_7	Ni	0.49	295	160	180
C_8	Ni	0.99	295	140	155
C_9	Ni	1.49	297	135	140
C_{10}	Fe	0.50	341	220	250
C_{11}	Fe	1.00	340	205	240
C_{12}	Fe	1.48	344	200	140

* in nitric solution with a Pye Unicam SP 1900 spectrophotometer, in air $-C_2H_2$ flame and wavelengths of 324.8, 232.0 and 248.33 nm for Cu, Ni and Fe respectively.

** comparatively with pure copper limits of 200° and 270° for CO_2 and N_2 respectively[2].

KINETICS OF ALCOHOLS DEHYDROGENATION

The apparent activation energy E_{ap} of ethylic, *n*-propylic, i-propylic, n-butylic and 2-butylic alcohols dehydrogenation on C_7—C_{12} catalysts was determined by the chromatographic pulse technique. The experimental conditions were: catalyst weight — 0.150 g; catalyst bed volume — 0.065 cm^3; volume of injected alcohol — 2 μL; catalyst bed temperatures — 200, 240 and 280°; eluent flow rates — 60, 90 and 120 cm^3 N_2/min.

The values of the apparent activation energy are presented in Table 4.

Table 4

Apparent activation energy (E_{ap}) kJ/mol

Reactant / Catalyst	EtOH	n-PrOH	i-PrOH	n-BuOH	2-BuOH
C_7	52.4	64.0	62.8	73.0	70.0
C_8	48.4	65.0	53.0	60.6	59.0
C_9	43.0	47.9	46.0	53.7	52.2
C_{10}	30.8	35.5	34.1	39.2	37.8
C_{11}	24.4	27.6	26.8	30.8	29.9
C_{12}	20.5	22.5	21.9	25.2	24.1

The presence of the added metal decreases E_{ap} as compared with the pure copper catalyst.[2] This effect is more significant in the case of Fe. The increase of added metal concentration determined a corresponding decrese of E_{ap}.

As in the previous work,[1] on the same catalyst, E_{ap} obtained for different reactants increases as follows: EtOH $<$ i-PrOH $<$ Nn-PrOH $<$ $<$ 2-BuOH $<$ n-BuOH.

CONCLUSIONS

1. A kinetic study concerning the dehydrogenation of ethylic, n-propylic, i-propylic, n-butylic and 2-butylic alcohols on copper catalyst with 0.5, 1.0 and 1.5 at.% Ni or Fe, was performed.

2. The presence on the surface of Ni/Cu and Fe, FeO/Cu junctions diminished the stabilising effect of inert gas adsorption on the freshly-reduced catalyst, but at the same time, these junctions determined a decrease of the apparent activation energy.

3. The particular values of E_{ap} depend both on the added metal concentration and reactant nature.

REFERENCES

[1] N. Doca, E. Segal, *Rev. Roumaine Chim.*, **31**, 567 (1986).
[2] N. Doca, E. Segal, *ibidem*, **30**, 949 (1985).
[3] M. H. Karapetiants, "Khimitscheskaia Termodinamika", Goskhimizdat, Moscow, 1953.

Revue Roumaine de Chimie, 32, 2, 203–213 (1987)

OXIDACIÓN DE MORDANT BLUE 9 CON BROMATO CATALIZADA POR VANADIO(V). II

CINETICA Y MECANISMO

N.P. CID y L.O. GARCÍA VIOR

Departamento de Química inorgánica Analitica y Química Física. Facultad de Ciencias Exactas y Naturales — Universidad de Buenos Aires — Ciudad Universitaria — 1428 Buenos Aires — República Argentina

Recibido el 8 de Marzo de 1985
Revisto el 19 de Julio de 1986

Se realiza un estudio cinético de oxidación de Mordant Blue 9 (MB9) por bromato de potasio catalizada por vanadio (V) y se propone un mecanismo para la reacción sin catalizar y catalizada. En ambos casos se plantean ecuaciones de velocidad, que, luego de ser integradas y con ciertas aproximaciones, permiten interpretar las curvas absorbancia vs. tiempo, obteniéndose buena concordancia con los resultados experimentales. La degradación del MB9 procede probablemente con la ruptura del grupo azo, dando en primer lugar, una sal de diazonio que se descompone para formar fenoles incoloros.

A kinetic study of the oxidation of MB9 by potassium bromate catalyzed by vanadium has been done and a mechanism for the reaction with and without the catalyst is suggested. The absorbance *vs.* time curves can be explained through rate equations, which agree with the experimental results. MB9 oxidation probably occurs in a first stage through the rupture of the azo group which leads to a diazonium salt that is finally transformed into colourless phenols.

INTRODUCCIÓN

Las reacciones de compuestos orgánicos e inorgánicos con halatos son frecuentemente lentas y susceptibles de ser catalizadas por iones inorgánicos.[1–3] Dada la complejidad de los sistemas, muchos de los trabajos publicados describen cualitativemente la cinética de las reacciones o bien se refieren estrictamente a aplicaciones analíticas. Sin embargo, el conocimiento de la cinética y mecanismo de las reacciones sin catalizar y catalizadas son muy útiles para optimizar las condiciones experimentales que conduzcan a los más bajos limites de detección con adecuada selectividad para el catalizador y predecir la influencia de ciertas especies que puedan actuar como activadores o inhibidores.

En la oxidación del azo colorante, Mordant Blue 9, con bromato de potasio, hemos encontrado, en base a los primeros resultados cinéticos obtenidos, que el vanadio (V) ejerce un notable efecto catalítico.[1,4]

En este trabajo se realiza un estudio cinético y se propone un mecanismo para dicha reacción. En una futura investigación se describirán las aplicaciones analíticas de la reacción catalizada.

PARTE EXPERIMENTAL

APARATOS Y REACTIVOS

Se utilizó un espectrofotómetro UV-visible Zeiss, modelo DMR 11 para seguir la cinéica de la reacción a temperatura controlada (25°C) por medio de un termostato marca Colora. Las medidas de RPE fueron realizadas con un espectrómetro Varian Associates, modelo V-4500 y los espectros IR se obtuvieron con un espectrofotómetro Perkin Elmer, modelo 710B. Los reactivos y el procedimiento utilizado fueron descriptos en la Parte I[1].

RESULTADOS Y DISCUSIÓN

1. REACCIÓN NO CATALIZADA

La reacción del bromato de potasio con Mordant Blue 9, (MB9), es lenta[1] y en las condiciones estudiadas exhibe propiedades autocatalíticas. Ello puede deberse a que el Br^- liberado en la reducción del BrO_3^- por el colorante reacciona con el BrO_3^- presente produciendo Br_2, que a su vez favorece la oxidación del azo compuesto, regenerándose Br^-. Estas suposiciones se basan en las siguientas experiencias: a) en los primeros instantes la velocidad se incrementa con el tiempo debido probablemente al aumento paulatino de la concentración de Br^- formado en el medio (Fig. 1); b) el agregado de Br^- incrementa la velocidad[1]; c) la presencia de pequeñas concentraciones de Hg(II) produce un efecto inhibidor sobre la reacción (Tabla 1) como consecuencia de la formación de complejos bromurados que reducirían la concentración de Br^- libre; d) la adición de cantidades crecientes de fenol (Tabla 1) produce una notable inhibición por su reacción con el bromo formado.

En virtud de lo dicho anteriormente, las posibles reacciones pueden ser:

$$BrO_3^- + C \xrightarrow{K_1} Br + P \quad \text{(muy lenta)} \tag{1.1}$$

$$BrO_3^- + 5Br^- + 6H^- \xrightarrow{K_2} 3Br_2 + 3H_2O \quad \text{(lenta)} \tag{1.2}$$

$$Br_2 + C \xrightarrow[H_2O]{K_3} 2Br^- + P + 2H^- \quad \text{(rápida)} \tag{1.3}$$

donde C representa al MB9 y P a su producto de oxidación.

La ecuación 1.1 corresponde a la zona I de la figura 1 (período de inducción) en la cual la velocidad aumenta con el tiempo debido a la aparición de Br^- en el medio.

Cuando finaliza el período de inducción, la concentración de Br^- alcanza un valor constante, pues el Br^- se regenera en un paso rápido (ecuación 1.3), es decir $[Br^-]_0 - [Br^-]_f = a$ (constante), donde $[Br^-]_0$ es la concentración de Br^- procedente del bromato de potasio, $[Br^-]$, es la concentración máxima de Br^- formado en la etapa inicial (ecuación 1.1) y „a" es la concentración de Br^- total.

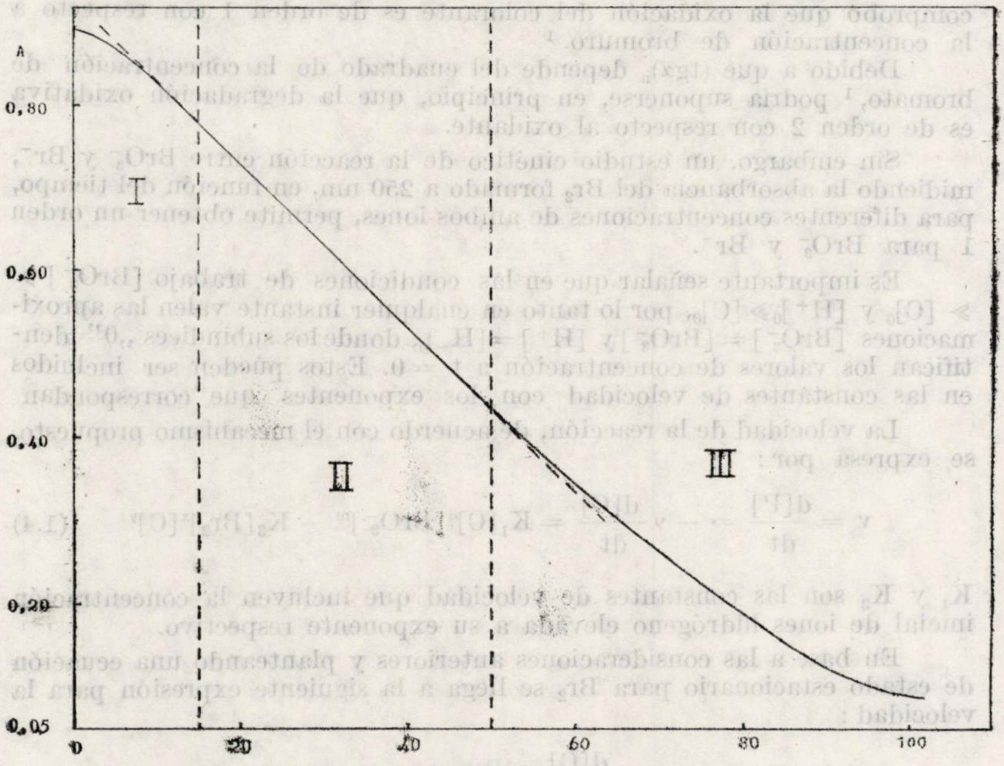

Fig. 1. — Variación de la absorbancia con el tiempo para la reacción no catalizada. $[MB9] = 5{,}0\ 10^{-5}M$; $[BrO_3] = 0{,}015M$; $[AcOH] = 3{,}4M$.

En el inicio de la zona II (figura 1) se ha alcanzado un estado estacionario, por lo tanto la velocidad de formación de Br_2 por la reacción entre el BrO_3^- y el Br^-, es igual a la velocidad de desaparición del Br_2 por la reacción con el colorante. La absorbancia disminuye linealmente con el tiempo y la velocidad de la reacción se mantiene constante.

En la zona III (figura 1) se observa une desviación de la linealidad y la velocidad de reacción disminuye con el tiempo.

Tabla 1

Influencia de mercurio (II) y fenol en los valores de $(tg\ \alpha)_n$

Concentración de interferencia (mg/L)	$(tg\ \alpha)_n$	
	Hg(II)	fenol
—	0,0148	0,0148
0,5	0,0110	—
1,0	0,054	0,0121
10,0	—	0,0059
100,0	—	0,0016

En base a la linealidad observada de la velocidad inicial $(\mathrm{tg}\,\alpha)_n$ extrapolada a $t \rightarrow 0$ en función de la concentración de colorante (10^{-5}M a 5.10^{-5}M), puede suponerse, en primera instancia, orden 1 con respecto al MB9.

Por agregado de concentraciones crecientes de Br^-, $[Br^-]_{ext.}$, se comprobó que la oxidación del colorante es de orden 1 con respecto a la concentración de bromuro.[1]

Debido a que $(\mathrm{tg}\alpha)_n$ depende del cuadrado de la concentración de bromato,[1] podría suponerse, en principio, que la degradación oxidativa es de orden 2 con respecto al oxidante.

Sin embargo, un estudio cinético de la reacción entre BrO_3^- y Br^-, midiendo la absorbancia del Br_2 formado a 250 nm, en función del tiempo, para diferentes concentraciones de ambos iones, permite obtener un orden 1 para BrO_3^- y Br^-.

Es importante señalar que en las condiciones de trabajo $[BrO_3^-] \gg [C]_0$ y $[H^+]_0 \gg [C]_0$, por lo tanto en cualquier instante valen las aproximaciones $[BrO_3^-] = [BrO_3^-]$ y $[H^+] = [H_+]_0$, donde los subindices ,,0'' identifican los valores de concentración a $t = 0$. Estos pueden ser incluidos en las constantes de velocidad con los exponentes que correspondan

La velocidad de la reacción, de acuerdo con el mecanismo propuesto, se expresa por:

$$v = \frac{d[P]}{dt} = -\nu\frac{d[C]}{dt} = K_1[C]^n[BrO_3^-]^m + K_3[Br_2]^x[C]^y \qquad (1.4)$$

K_1 y K_3 son las constantes de velocidad que incluyen la concentración inicial de iones hidrógeno elevada a su exponente respectivo.

En base a las consideraciones anteriores y planteando una ecuación de estado estacionario para Br_2 se llega a la siguiente expresión para la velocidad:

$$v = -\nu\frac{d[C]}{dt} = K_1'[C] + K_2'[Br^-] \qquad (1.5)$$

K_1' y K_2' son las constantes de velocidad que involucran los valores de concentración de bromato e ion hidrógeno iniciales elevadas a las potencias correspondientes.

En la zona I (figura 1) se cumple que:

$$v = K_1'[C] + K_2'\,[Br^-] + [Br^-]_0) \qquad (1.6)$$

En la región de interés analítico (zona 2) donde se mide $\mathrm{tg}\,\alpha)_n$:

$$v = K_1'[C] + K_2'a \qquad (1.7)$$

Por integración de esta ecuación entre 0 (inicio de la zona II) y t, para el tiempo, $[C]_0$ y $[C]$ para la concentración de colorante, se llega a que:

$$[C] = ([C]_0 + aK_2' \cdot K_1'^{-1})e^{-K_1't} - K_2'aK_1'^{-1} \qquad (1.8)$$

Por regresión no lineal[5] se obtiene $K'_2\,a = 1{,}102 \cdot 10^{-4}$ y $K'_1 = 3{,}8 \cdot 10^{-3}$ con coeficiente de correlación $r = 0{,}99996$, de modo que el exponencial puede desarrollarse en serie de Mc Laurin, considerando los dos primeros términos (función lineal en t) ya que $K'_1\,t$ es pequeño para valores de t dentro de la zona II.

Esta aproximación es válida para $t \leqslant 37$ minutos, experimentalmente entre 35 y 40 minutos ya se observa desviación de la linealidad.

Si se reemplaza $e^{-K'_1 t}$ por $1 - K'_1 t$ en 1.8, resulta:

$$[C] = [C]_0 - (K'_1[C]_0 + K'_2 a)t \tag{1.9}$$

La ecuación 1.9 justifica la linealidad observada en la zona II (figura 1), y

$$K'_1[C]_0 + K'_2 a = (\mathrm{tg}\,\alpha)_n / a_c \cdot b \tag{1.10}$$

donde b es la longitud del paso óptico y a_c es la absortividad molar del MB9.

Por representación gráfica de $(\mathrm{tg}\,\alpha)_n$ vs. $[C]_0$ se obtiene $K'_1 = 3{,}83 \cdot 10^{-3}$ que coincide, dentro del error experimental, con el obtenido por ajuste de la ecuación 1.8 a la curva de la figura 1.

A partir de la pendiente de la recta $(\mathrm{tg}\,\alpha)$ vs. $[Br^-]_{ext.}$ resulta $K'_2 = 0{,}039$, y de los parámetros de la ecuación 18 $a = 1{,}24 \cdot 10^{-5}$, con lo cual $[Br^-]_f = 4{,}84 \cdot 10^{-6}$.

En esta zona, la velocidad en función de las concentraciones de bromato, bromuro y colorante puede expresarse por:

$$v = -\nu \frac{d[C]}{dt} = K_1[BrO_3^-]_0[C] + K_2[BrO_3^-]_0 \cdot ([Br^-]_0 + [Br^-]_f) \tag{1.11}$$

Por lo tanto:

$$\frac{(\mathrm{tg}\,\alpha)_n}{a_c \cdot b} = [BrO_3^-]_0^2(K_1[C]_0 + K_2K + K_2[Br^-]_f/[BrO_3^-]_0) \tag{1.12}$$

En la ecuación 1.12 se ha reemplazado $[Br^-]$ por $K \cdot [BrO_3^-]_0$.

Se comprobó que la influencia del tercer término es pequeña para las concentraciones de bromato ensayadas, en consecuencia la ecuación 1.12 está de acuerdo con la suposición inicial de orden dos para bromato.[1]

En la región I, la concentración de bromuro es igual o proporcional a la fracción de colorante consumido por su reacción con el bromato, es decir $[C]_0 - [C]$.

Al reemplazar $[Br^-] = [C]_0 - [C]$ en 1.6 y resolviendo la ecuación diferencial, resulta:

$$\begin{aligned}[C] = \{[C]_0 &+ (K'_2[C]_0 + K'_2[Br^-]_0)/(K'_1 - K'_2) \cdot \\ &\cdot e^{-(K'_1 - K'_2)t} - (K'_2[C]_0 + K'_2[Br^-]_0)/(K'_1 - K'_2)\end{aligned} \tag{1.13}$$

Por regresión no lineal se obtiene: $-(K_1' - K_2') = 0{,}030$ y $K_2'[C]_0 + [Br^-]_0)/(K_1' - K_2') = 4{,}58 \cdot 10^{-5}$.

En la tabla 2 se comparan los valores estimados por la ecuación 1.13

Tabla 2

Comparación de absorbancias teóricas y experimentales en la región I

concentración MB9	tiempo (min)	absorbancia teórica	absorbancia experimental
$3{,}8 \cdot 10^{-5}$M	0	0,687	0,687
	1	0,683	0,680
	2	0,679	0,678
	3	0,674	0,675
	4	0,670	0,670
	5	0,665	0,665
	6	0,660	0,660
	7	0,655	0,652
	8	0,650	0,647
	9	0,644	0,640
	10	0,639	0,630
$5{,}0 \cdot 10^{-}M^{5}$	0	0,897	0,897
	2,5	0,884	0,887
	5	0,870	0,870
	7,5	0,855	0,850
	10	0,839	0,830
	12,5	0,821	0,805
	15	0,803	0,782

con los experimentales; las desviaciones típicas obtenidas para $[C]_0$: $3{,}8 \cdot 10^{-5}$ M y $5{,}0 \cdot 10^{-5}$ M son $1{,}6 \cdot 10^{-5}$ y $2{,}0 \cdot 10^{-4}$ respectivamente.

En la zona III, para t ca. 40 minutos, las absorbancias medidas son mayores que las predichas por la ecuación 1.8. Esto se explicaría en parte, porque puede presentarse una pequeña absorbancia residual debida a los productos que no fue tenida en cuenta en la deducción de la ecuación 1.8. Por otro lado, puede suponerse la existencia de un efecto de inhibición adicional por parte de los productos, o del proprio reactivo que consumirían Br_2 en reacciones laterales. Entonces, la velocidad de reacción desde $t = 0$ hasta $t \to \infty$ puede expresarse:

$$v = -\left.\frac{d[C]}{dt}\right|_{t_i} = K_1[BrO_3^-]_0^2[C] + K_2[BrO_3^-]_0[Br^-] - \sum_{i=1}^{n} K_i[Br_2]^{x_i}[P_i]^{y_i} \qquad (1.14)$$

siendo P productos que consumen el Br_2 formado en la etapa 1.2.

2. REACCIÓN CATALIZADA

En un trabajo previo se demostró que el vanadio(V) forma un complejo con el MB9[1]. Los espectros de resonancia paramagnética electrónica (RPE) del sistema V(V)−MB9 (figura 2) ponen en evidencia la formación de (V(VI) ya que esta especie es paramagnética y su resonancia es observada a temperatura ambiente con un ancho de línea relativamente angosto.[6-9] El V(IV) se forma por reducción del V(V) ($5.10^{-3}M$) con exceso de MB9 en ácido acético 5 M casi instantoneamente a 60°C o a las 48 horas a 25°C. En base a estas consideraciones, se propone que la reacción catalizada puede tener lugar de acuerdo con la siguiente secuencia de reacciones :

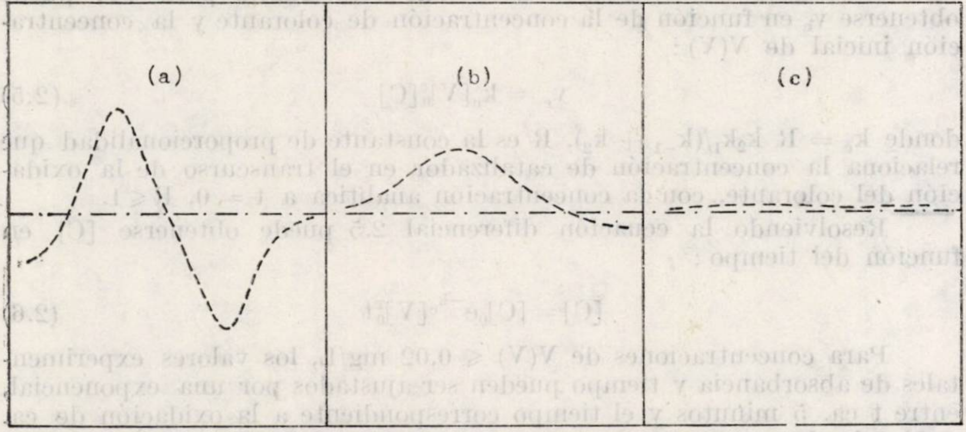

Fig. 2. — (a) — Espectro RPE de V(V)I a 25°C formado en el sistema V(V)-MB9. (b) —idem (a) en presencia de $KBrO_3$ $10^{-4}M$. (c) — idem (a) en presencia de $KBrO_3$ $3 \cdot 10^{-3}M$. Las condiciones experimentales fueron las mismas en los tres casos, excepto que la ganancia se incrementa de (a) a (c); $H_0 = 3 \cdot 500 \pm 500$ G.

$$\mathrm{V(V) + C \underset{k_{-1}}{\overset{k_1}{\rightleftharpoons}} V(V)C} \quad \text{(rápida)} \tag{2.1}$$

$$\mathrm{V(V)C \xrightarrow{k_2} V(IV) + P} \quad \text{(lenta)} \tag{2.2}$$

$$\mathrm{V(IV) + BrO_3^- \xrightarrow[H_2O/H^-]{k_3} V(V) + Br^-} \quad \text{(muy rápida)} \tag{2.3}$$

Esta secuencia se apoya, en parte, en el mecanismo propuesto por Bontchev para el estudio cinético de la oxidacion de aminas por halatos, cata lizada por V(V).[10]

Fuller y Ottaway[2] consideraron una interacción inicial BrO_3^- — — V(V) — colorante que da lugar al intermediario V(IV)

En cambió, en el caso del MB9, el V(IV) se forma como consecuencia de la descomposición del complejo estable V(V)C. La única función del bromato en la reacción catalizada consiste en la regeneración del catalizador con su estado de oxidación original (ecuación 2.3).

La velocidad de la reacción catalizada puede expresarse por :

$$v_c = \frac{d[P]}{dt} = -\nu \frac{d[C]}{dt} = k_2[VC] \tag{2.4}$$

donde VC representa el complejo formado entre el MB9 y el V(V), y V al catalizador con estado de oxidación V.

Como el V(V) se regenera en un paso rápido, puede considerarse que su concentración permanece constante en el transcurso de la reacción, e igual, o al menos proporcional a la concentración total a t=0 ($[V]_0^T$).[11]

Planteando una ecuación de estado estacionario para VC, puede obtenerse v_c en función de la concentración de colorante y la concentración inicial de V(V):

$$v_c = k_c[V]_0^T[C] \tag{2.5}$$

donde $k_c = R\ k_2k_1/(k_{-1} + k_2)$, R es la constante de proporcionalidad que relaciona la concentración de catalizador en el transcurso de la oxidación del colorante, con la concentración analítica a $t = 0$, $R \leqslant 1$.

Resolviendo la ecuación diferencial 2.5 puede obtenerse [C] en función del tiempo:

$$[C] = [C]_0 e^{-k_c[V]_0^T t} \tag{2.6}$$

Para concentraciones de V(V) $\leqslant$ 0,02 mg/L, los valores experimentales de absorbancia y tiempo pueden ser ajustados por una exponencial, entre t ca. 5 minutos y el tiempo correspondiente a la oxidación de ca. 40 % del colorante, para una concentración inicial de MB9 de $3{,}8 \cdot 10^{-5}$ M; $[BrO_3^-]_0 = 0{,}015$ M y $[AcOH] = 3{,}4$ M, obteniéndose $k_c = 3{,}96 \cdot 10^{-4}$.

En el intervalo de t mencionado, $k_c[V]_0^T t$ es pequeño, de modo tal que puede reemplazarse $\exp(-k[V]t) = 1 - k_c[V]_0^T t$ en la ecuación 2.6, con lo cual resulta:

$$[C] = [C]_0 - k_c[V]_0^T[C]_0\, t \tag{2.7}$$

siendo:

$$k_c[V]_0^T[C]_0 = (\mathrm{tg}\ \alpha)_c/a_c b \tag{2.8}$$

La aproximación realizada es válida para

$$t \leqslant 3{,}57 \cdot 10^{-6}/[V]_0^T \tag{2.9}$$

En la tabla 3 se compara el tiempo a partir del cual comienza a observarse desviación de la linealidad (t límite) experimentalmente, con el predicho por la ecuación 2.9.

Tabla 3

Relación de tiempos límites teóricos y experimentales con la concentración de vanadio

concentración total de V(V) (mg/L)	tiempo teórico (min)	tiempo experimental (min)
0,01	18	20
0,02	9	11

De acuerdo con 2.8 $(\mathrm{tg}\alpha)_c/a_c b$ deberá ser proporcional a la concentración analítica de V(V) y de colorante, que es lo que se verifica experimentalmente para concentraciones de catalizador inferiores a 0,1 mg/L y MB9 $\leqslant 3{,}0 \cdot 10^{-5}$M[1].

Para concentraciones de V(V) mayores que 0,1 mg/L la concentración de colorante libre en el sistema se ve disminuida por la formación del complejo VC. Planteando un balance de masa para el colorante y procediendo en forma similar que en la deduccion anterior se llega a que :

$$v_c = k_2[V]_0^T[C]^T/(k_S + [V]_0^T) = k_c[V]_0^T[C]^T \qquad (2.10)$$

donde $k_S = (k_{-1} + k_2)/k_1$ y k_c, la constante de velocidad para la reacción catalizada, que es en este caso, una función de la concentración analítica de catalizador. En estas condiciones :

$$(\mathrm{tg}\,\alpha)_c/a_c b = \{k_2[V]_0^T/(k_S + [V]_0^T)\}[C]_0^T \qquad (2.11)$$

Esto explica la curvatura observada en la representación de $(\mathrm{tg}\,\alpha)_c$ ó $(\mathrm{tg}\,\alpha)$ cuando $[V]_0^T > 0{,}1$ mg/L.

Por regresión no lineal[5] aplicada en 2.11 se obtiene $k_2 = 26{,}64$ y $k_S = 6{,}72 \cdot 10^{-4}$. En la tabla 4 se comparan los valores experimentales de $(\mathrm{tg}\,\alpha)_c/a_c b$ con los calculados a partir de 2.11 (desviación tipica[5] : $6{,}80 \cdot 10^{-8}$).

Tabla 4

Velocidades teóricas y experimentales para varias concentraciones de vanadio (V)

$[V]_0^T \times 10^7$	v_c teórica $\times 10^7$	v_c experimental $\times 10^7$
3,93	5,72	5,91
9,81	14,5	14,8
19,63	28,9	29,5
29,44	44,3	44,6
39,25	61,9	60,7
49,07	74,1	74,0
58,88	87,0	87,7

No se encontró una justificación aceptable para la curvatura de la representación gráfica $(\mathrm{tg}\,\alpha)_c$ vs. $[C]_0^{T1}$ para $[C]_0^T$ mayor que $3{,}0 \cdot 10$ M. Es posible que al aumentar la concentración analítica de colorante por encima del valor señalado, se manifieste algún efecto de inhibición debido a un retardo en la regeneración del catalizador (etapa 2.3), por formación de un complejo entre V(IV) y MB9. Se comprobó que el V(VI) Se comprobó que el V(IV) forma un complejo de estabilidad similar con el reactivo, lo que apoya en cierta medida la razón expuesta anteriormente. La formación de dicho complejo conduciría a una disminución de R (ecuación 2.8).

Si el catalizador es agregado al sistema con estado de oxidación IV, las curvas absorbancia vs. t, para distintas concentraciones de V(IV), son similares, resultando prácticamente iguales los valores de tg α. Esto surge como consecuencia de la oxidación instantánea del V(IV) por el BrO_1^- y está de acuerdo con el mecanismo propuesto, en especial en lo que respecta a la regeneración del V(V) en un paso rápido.

3. REACCIÓN GLOBAL

La velocidad de la reacción global (sistema con V(V) presente) puede expresarse como suma de las velocidades de las reacciones catalizada, v_c, y no catalizada, v_n.

$$v = k_1[BrO_3^-]_0^2[C]^T + k_2[BrO_3^-]_0([Br^-]_0 + [Br^-]) + \\ + k_2[V]_0^T[C]^T/(k_S + [V])_0^T \qquad (3.1)$$

Por integración y admitiendo la validez de las aproximaciones realizadas en el estudio de ambas reacciones, queda:

$$[C] = [C]_0^T - \{[BrO_3^-]_0^2(K_1[C]_0^T + K_2K + K_2[Br^-]_f/[BrO_3^-]_0) + \\ + k_2[V]_0^T[C]_0^T/(k_S + [V]_0^T)\}\, t \qquad (3.2)$$

siendo $(tg\,\alpha)a_cb$ los términos encerrados entre llaves. Como en presencia de V(V), ambas reacciones ocurren simultáneamente, en la expresión 3.2, la formación del complejo V(V)—MB9 afectaría también al primer término correspondiente a la reacción no catalizada. Sin embargo este efecto no modifica sensiblemente a v o $tg\,\alpha$ en el ambito de concentraciones ensayado para V(V).

4. PRODUCTOS DE REACCIÓN

Los espectros de los productos de oxidación del colorante entre 200 y 600 nm, usando como reactivo $KBrO_3$ o Br_2 son prácticamente idénticos.

Por otra parte, la oxidación del Naranja de metilo con $KBrO_3$ a pH = 2,1 (con AcOH), conduce a la formación de productos que dan espectros UV-visible similares a los que se obtienen por oxidación de aquél con Br^2_{12}. Estas experiencias constituyen una prueba adicional a lo expuesto para la reacción no catalizada de que el Br_2 formado como intermediario atacaría al azo compuesto, conduciendo a la formación de productos.

La diferencia entre el MB9 y el Naranja de Metilo en la oxidación con BrO_3^- es que en el primer caso aparece una banda con maximo en la zona de 430 nm, aproximadamente al cabo de dos horas. Dicha banda podría atribuirse a la formación, en primer lugar, de sales de diazonio, que, al estar sustituidas podrían ser las responsables del color amarillo observado. En esta etapa de la reacción si se agrega 1-naftilamina, se produce una coloración rojiza, probablemente debida a la copulación, siendo el espectro similar al obtenido a partir de la sal de diazonio del ácido sulfanílico con la amina mencionada (máximo de absorción en el visible: 520 y 512 nm, respectivamente).

Isac y col. [13] hallan que las sales de diazonio con sustituyentes atractores de electrones en posición para son térmicamente inestables y en su descomposición se forman fenoles. En nuestro caso, el espectro IR del producto incoloro finalmente obtenido indica la presencia de grupos fenólicos, sulfónicos además de las bandas propias de aromáticos. Dichos productos podrían ser:

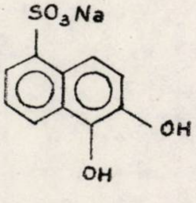

I

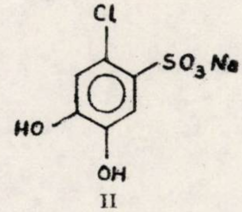

II

dependiendo de cómo se produzca la ruptura del grupo azo con la formación de la sal de diazonio correspondiente.

Por otra parte I y II sufrirían una posterior bromación. Mayores detalles sobre los productos intermedios y finales de la reacción serán objeto de una futura investigación.

AGRADECIMIENTOS. Se agradece al lic. J. Liwszyc por la confección de los programas de computación para regresión, como así también a CONICET, SECyT y Universidad de Buenos Aires por el aporte financiero.

BIBLIOGRAFÍA

[1] N. P. Cid y L. O. García Vior, XVI Congreso Latinoamericano de Química. Río de Janeiro, Brasil; 14 al 20 de octubre de 1984.
[2] C. W. Fuller y J. M. Ottaway, *Analyst*, **95**, 34 (1970).
[3] D. Costache y Gr. Popa, *Rev. Roumaine Chim.*, **15**, 1349 (1970).
[4] N. P. Cid y L. O. García Vior, XIV Congreso Latinoamericano de Química. San José, Costa Rica: 1 al 7 de frebrero de 1981.
[5] B. W. Clare, *Chemical Engineering*, **23**, 83 (1982).
[6] J. A. Mc. Millan. "Paramagnetismo electrónico", Monografía N° 14 O.E.A., Washington, 1975, pág. 70.
[7] G. F. Kokoszka, y G. Gordon, ,,Technique of Inorganic Chemistry", Editores H. B. Jonassen y A. Weissberger, Vol VII, IQterscience Publishers, New York, 1968, pág 238.
[8] A. J. Saraceno, D. T. Fanale y N. D. Coggeshall, *Anal. Chem.*, **33**, 500 (1961).
[9] T. Meisel y G.G. Guilbaut, *Anal. Chim. Acta.*, **50**, 143 (1970).
[10] P. R. Bontchev, *Talanta*, **17**, 499 (1970).
[11] G. Svehla, *Analyst*, **94**, 513 (1969).
[12] H. A. Laitinen y K. W. Boyer, *Anal. Chem.*, **44**, 920 (1972).
[13] D. Isac, M. Mracec, N. Proșteanu y Z. Simon, *Rev. Roumaine Chim.*, **25**, 29 (1980).

Revue Roumaine de Chimie, **32**, 2, 215–221 (1987)

PROTON CATALYSED REARRANGEMENT OF N-ALKYL ARENE SULPHONANILIDES TO *ORTHO*-ALKYLAMINO SULPHONES. PART III[1,2]

B.C. JOSHI*, YOGESH C. JOSHI, D. KISHORE and S.S. SHRIMALI
Department of Chemistry, University of Rajasthan, Jaipur-302004, India

Received September 9, 1985

Sulphonanilides (IA∼XIIA), obtained by condensing N-methyl and N-ethylaniline with sulphonyl chlorides of salicylic acid or its esters or 3-nitro derivatives of esters, were rearranged to the corresponding sulphones (IB–XIIB) in concentrated sulphuric acid. Structures of sulphonanilides (IA–XIIA) and sulphones (IB–XIIB) were established by elemental analysis, IR and ^{1}H–NMR spectral studies.

In earlier communications ,[1,2] it has been observed that sulphuric acid causes hydrolysis or rearrangement of N-alkyl arene sulphonanilides. According to Witt et al. [3,4] and later Halberkann, [5,7] electron donating groups in *para* position of the aniline ring increase the rate of the rearrangement while the electron withdrawing groups retard the rearrangement. Sometimes virtually no sulphone is formed and hydrolytic products are obtained. [7] However, electron withdrawing groups in the sulphonic acid moiety favours the rearrangement. Gennaro and Zanger [8] synthesized a number of sulphones by rearranging 1,2,3,4-tetrahydroquinoline sulphonamide with conc. sulphuric acid.

Since salicylic acid and its derivatives are medicinally important,[9,10] sulphonanilides and sulphones having this moiety have been synthesised by condensing their sulphonyl chlorides [11] with N-alkyl anilines followed with rearrangement of IA∼XIIA (the sulphonanilides) to the corresponding sulphones (IB∼XIIB). It has been observed that esters of salicylic acid gave better yield of sulphones as compared to salicylic acid.

Sulphonanilides and sulphones are obtained in 85–95% and 45–80% yields respectively. The introduction of nitrogroup in salicylic acid moiety however, increases the yield of both sulphonanilide and sulphones.

MECHANISM OF THE REARRANGEMENT

Various workers have tried to explain the mechanism of the rearrangement, [12–14] but it still remains to be fully elucidated. The intramolecular migration of sulphonylonium ion(z) (chart-II) to the *ortho*-position is confirmed by performing two experiments.

N-Methylaniline was acetylated followed by electrophilic substitution (Friedel-Crafts Reaction) of sulphonylonium ion (step-II, chart-II) at the *p*-position. The product on hydrolysis afforded *p*-N-methylamino-

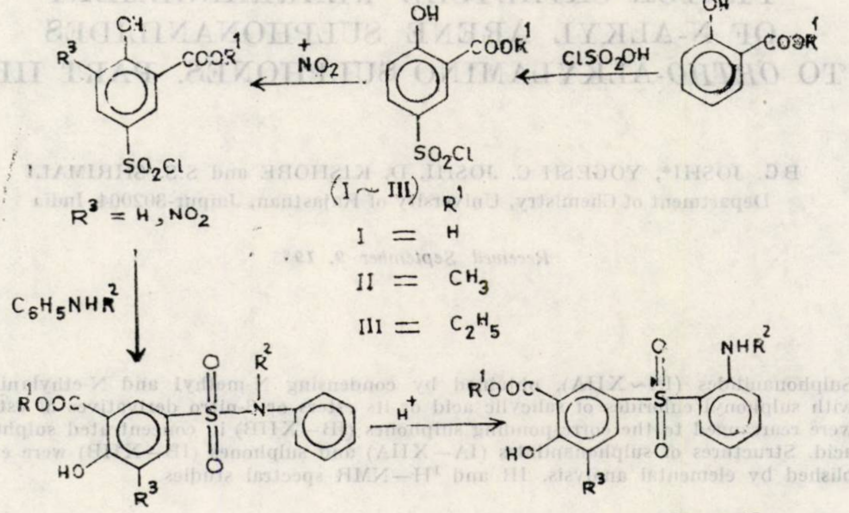

OH
COOR^1
ClSO$_2$OH
SO$_2$Cl
(I ~ III)
R^1
I = H
II = CH$_3$
III = C$_2$H$_5$
Cl
R^3
COOR^1
$\overset{+}{N}O_2$
R^3 = H, NO$_2$
C$_6$H$_5$NHR^2
ROOC
HO
R^3
R^2
H^+
NHR^2

IA ~ XIA

IB ~ XIIB

	R^1	R^2
IA , IB , VIIA , VIIB	H	CH$_3$
IIA , IIB , VIIIA , VIIIB	CH$_3$	CH$_3$
IIIA , IIIB , IXA , IXB	C$_2$H$_5$	CH$_3$
IVA , IVB , XA , XB	H	C$_2$H$_5$
VA , VB , XIA , XIB	CH$_3$	C$_2$H$_5$
VIA , VIB , XIIA , XIIB	C$_2$H$_5$	C$_2$H$_5$

(IA ~ VIA) , (IB ~ VIB) , R^3 = H

(VIIA ~ XIIA) , (VIIB ~ XII) , R^3 = NO$_2$

CHART – I

sulphone (B). An attempt to obtain (B) by the rearrangement of (A) with conc. sulphuric acid failed and gave (C). Thus the possibility of the formation of *p*-isomer is ruled out (cf. Chart II).

In another experiment two similar sulphonanilides (VIIIA with methyl substituent and XIIA with ethyl substituent) were rearranged with conc. sulphuric acid. The expected products (VIIIB and XIIB) could

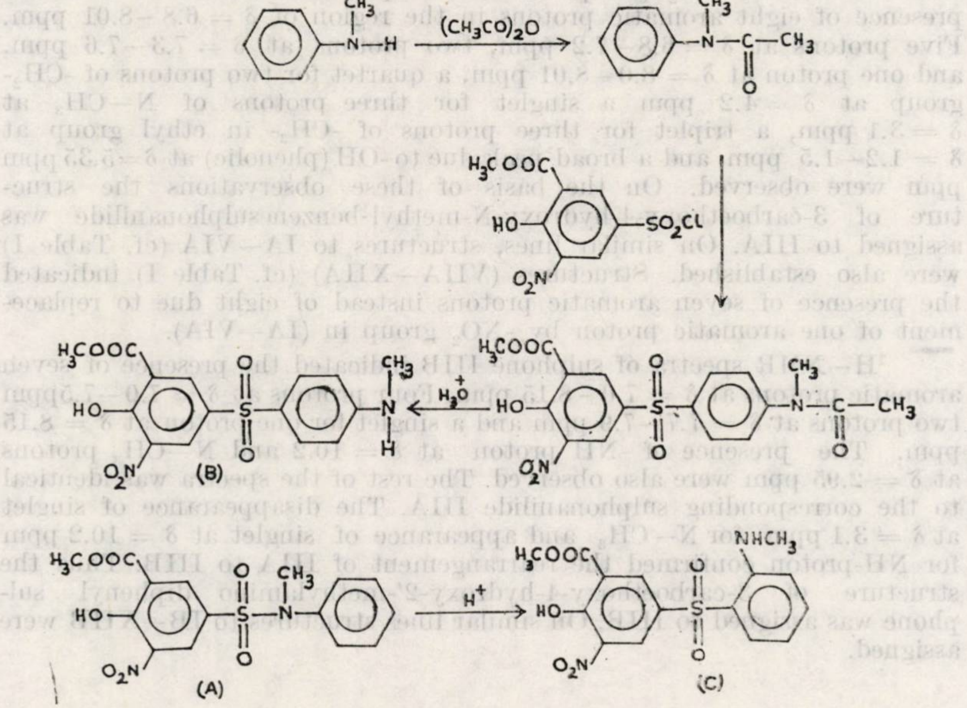

CHART-II

only be isolated through column chromatography. Non formation of cross products (XIB and IXB) indicates that the sulphonylonium ion (Z) had not been completely detached during migration.

STRUCTURAL ELUCIDATION

On the basis of elemental analysis and molecular weight determination (Rast method) the molecular formula to IIIA was assigned as $C_{16}H_{17}O_5NS$. IIIA and IIIB were found to have characteristic absorption bands at 3610 and 1200 cm^{-1} for phenolic and at 1730—1720 cm^{-1} for carboethoxy groups respectively. IIIA also showed absorption at 1180 cm^{-1} and 1330 cm^{-1} due to sulphonanilide group whereas IIIB indicated the band at 1150 and 1310 cm^{-1} due to $-SO_2-$ group. ^1H-NMR spectrum of IIIA indicated the presence of eight aromatic protons in the region of $\delta = 6.8-8.01$ ppm. Five protons at $\delta = 6.8-7.2$ ppm, two protons at $\delta = 7.3-7.6$ ppm, and one proton at $\delta = 8.0-8.01$ ppm, a quartet for two protons of $-CH_2-$ group at $\delta = 4.2$ ppm a singlet for three protons of $N-CH_3$ at $\delta = 3.1$ ppm, a triplet for three protons of $-CH_3-$ in ethyl group at $\delta = 1.2-1.5$ ppm and a broad peak due to -OH (phenolic) at $\delta = 5.35$ ppm ppm were observed. On the basis of these observations the structure of 3-carboethoxy-4-hydroxy-N-methyl-benzenesulphonanilide was assigned to IIIA. On similar lines, structures to IA—VIA (cf. Table I) were also established. Structures (VIIA—XIIA) (cf. Table I) indicated the presence of seven aromatic protons instead of eight due to replacement of one aromatic proton by $-NO_2$ group in (IA—VIA).

^1H-NMR spectra of sulphone IIIB indicated the presence of seven aromatic protons at $\delta = 7.0-8.15$ ppm. Four protons at $\delta = 7.0-7.5$ ppm two protons at $\delta = 7.7-7.9$ ppm and a singlet for one proton at $\delta = 8.15$ ppm. The presence of -NH proton at $\delta = 10.2$ and $N-CH_3$ protons at $\delta = 2.95$ ppm were also observed. The rest of the spectra was identical to the corresponding sulphonanilide IIIA. The disappearance of singlet at $\delta = 3.1$ ppm for $N-CH_3$ and appearance of singlet at $\delta = 10.2$ ppm for NH-proton confirmed the rearrangement of IIIA to IIIB. Thus the structure of 3-carboethoxy-4-hydroxy-2′-methylamino diphenyl sulphone was assigned to IIIB. On similar lines structures to IB—XIIB were assigned.

EXPERIMENTAL

All melting points are uncorrected. Purity of the compounds was ascertained by TLC using 0.25 mm thick plates coated with silica gel-G as stationary phase and benzene : ethanol : ammonia (7 : 2 : 1, upper layer) as mobile phase. The ^1H-NMR spectra were recorded in Perkin Elmer spectrophotometer using TMS as internal reference standard and $CDCl_3$ as solvent.

Synthesis of 3-carbomethoxy-4-hydroxy-N-methyl benzene sulphonanilide (IIA)

5.0 g (0.02M) of 3-carbomethoxy-4-hydroxy-benzene sulphonyl chloride (II) were treated with 2.6 g (0.024 mole) of N-methyl aniline in dioxane (30 mL) in the presence of anhydrous sodium acetate. The heat of the reaction was evident at room temp. The mixture was refluxed for four hrs and then poured into 50 mL conc. HCl and left overnight. On addition of water sulphonanilide (IIA) was precipitated. It was filtered, washed, dried and crystallised from alcohol-water (18 : 20). Yield 5.77 g (90%), m.p. 118°C. On similar lines sulphonanilide IA—XIIA was obtained by condensing corresponding sulphonyl chlorides and nitro sulphonyl chlorides with N-methyl aniline and N-ethyl aniline.

Synthesis of 3-carbomethoxy-4-hydroxy-2′-methylamino diphenyl sulphone (IIB)

3.21 g (0.01 mole) of IIA were added to conc. sulphuric acid (10 mL sp. gr. 1.84) in one lot. The mixture was heated on boiling water till the whole sulphonanilide was dissolved and turned to an intense red colour. Heating was continued for 10 min. and mixture was pou-

Table 1

^{1}H−NMR spectra (Chemical shifts are expressed in δ ppm)

Compound Number	Molecular formula	Aromatic protons	N−CH$_2$ and C−CH$_2$ protons	C−CH$_3$ protons	−COOCH$_3$ protons	N−CH$_3$ protons	OH protons
IA	$C_{14}H_{13}O_5NS$	6.8−8.01(m)−8H	—	—	—	3.1(s)−3H	5.35(b)−1H
IIA	$C_{15}H_{15}O_5NS$	6.8−8.01(m)−8H	—	—	4.05(s)−3H	3.1(s)−3H	5.35(b)−1H
IIIA	$C_{16}H_{17}O_5NS$	6.8−8.01(m)−8H	4.2(q)−2H	1.2−1.5(t)−3H	—	3.1(s)−3H	5.35(b)−1H
IVA	$C_{15}H_{15}O_5NS$	6.8−8.01(m)−8H	4.2(q)−2H	1.2−1.5(t)−3H	—	—	5.35(b)−1H
VA	$C_{16}H_{17}O_5NS$	6.8−8.01(m)−8H	4.2(q)−2H	1.2−1.5(t)-3H	4.05(s)−3H	—	5.35(b)−1H
VIA	$C_{17}H_{19}O_5NS$	6.8−8.01(m)−8H	4.15−4.8(m)−4H	1.2−1.8(m)-6H	—	—	5.35(b)−1H
VIIA	$C_{14}H_{12}O_7N_2S$	7.0−8.1(m)−7H	—	—	—	3.1(s)−3H	5.40(b)−1H
VIIIA	$C_{15}H_{14}O_7N_2S$	7.0−8.1(m)−7H	—	—	4.05(s)−3H	3.1(s)−3H	5.40(b)−1H
IXA	$C_{16}H_{16}O_7N_2S$	7.0−8.1(m)−7H	4.2(q)−2H	1.2−1.5(t)-3H	—	3.1(s)−3H	5.40(b)−1H
XA	$C_{15}H_{14}O_7N_2S$	7.0−8.1(m)−7H	4.2(q)−2H	1.2−1.5(t)-3H	—	—	5.40(b)−1H
XIA	$C_{16}H_{16}O_7N_2S$	7.0−8.1(m)−7H	4.2(q)−2H	1.2−1.5(t)-3H	4.05(s)−3H	—	5.40(b)−1H
XIIA	$C_{17}H_{18}O_7N_2S$	7.0−8.1(m)−7H	4.15−4.8(m)−4H	1.2−1.8(m)-6H	—	—	5.40(b)−1H

m = multiplet ; s = singlet, b = broad ; q = quartet, t = triplet.

Table 2

^1H-NMR spectra (chemical shifts in δ ppm)

Compd. No.	Molecular formula	Aromatic protons	N−CH$_2$ and C−CH$_2$ proton	C−CH$_3$ proton	COOCH$_3$ proton	NH−CH$_3$ proton	NH proton	OH proton
IB	$C_{14}H_{13}O_5NS$	7.0−8.15(m)−7H	−	−	−	2.95(s)−3H	10.2(b)−−1H	5.40(b)−1H
IIB	$C_{15}H_{15}O_5NS$	7.0−8.15(m)−7H	−	−	4.05(s)−3H	2.95(s)−3H	10.2(b)−1H	5.40(b)−1H
IIIB	$C_{16}H_{17}O_5NS$	7.0−8.15(m)−7H	4.2(q)−2H	1.2−1.5(t)−3H	−−	2.95(s)−3H	10.2(b)−1H	5.40(b)−1H
IVB	$C_{15}H_{15}O_5NS$	7.0−8.15(m)−7H	4.2(q)−2H	1.2−1.5(t)-3H	−	−	10.2(b)−1H	5.40(b)−1H
VB	$C_{16}H_{17}O_5NS$	7.0−8.15(m)−7H	4.2(q)−2H	1.2−1.5(t)-3H	4.50(s)−3H	−	10.2(b)−1H	5.40(b)−1H
VIB	$C_{17}H_{19}O_5NS$	7.0−8.15(m)−7H	4.15−4.8(m)−4H	1.2−1.8(m)-6H	−	−	10.2(b)−1H	5.40(b)−1H
VIIB	$C_{14}H_{12}O_7N_2S$	7.2−8.15(m)−6H	−	−	−	2.95(s)−3H	10.3(b)−1H	5.45(b)−1H
VIIIB	$C_{15}H_{14}O_7N_2S$	7.2−8.15(m)−6H	−	−	4.05(s)−3H	2.95(s)−3H	10.3(b)−1H	5.45(b)−1H
IXB	$C_{16}H_{16}O_7N_2S$	7.2−8.15(m)−	4.2(q)−2H	1.2−1.5(t)-3H	−	2.95(s)−3H	10.3(b)−1H	5.45(b)−1H
XB	$C_{15}H_{14}O_7N_2S$	7.2−8.15(m)−6H	4.2(q)−2H	1.2−1.5(t)-3H	−	−	10.3(b)−1H	5.45(b)−1H
XIB	$C_{16}H_{16}O_7N_2S$	7.2−8.15(m)−6H	4.2(q)−2H	1.2−1.5(t)-3H	4.05(s)−3H	−	10.3(b)−1H	5.45(b)−1H
XIIB	$C_{17}H_{18}O_7N_2S$	7.2−8.15(m)−6H	4.15−4.8(m)−4H	1.2−1.8(m)-6H	−	−	10.3(b)−1H	5.45(b)−1H

m = multiplet ; s = singlet, b = broad ; q = quartet, t = triplet.

red in crushed ice. The yellow coloured precipitated sulphone IIB was filtered, washed and crystallised from alcohol, yield, 1.60 g (50%), m.p. 155°C. On similar lines other sulphones (IB—XII) were synthesised.

ACKNOWLEDGEMENT. Authors are thankful to the Head of the Department of Chemistry, University of Rajasthan, Jaipur for providing necessary research facilities.

REFERENCES

[1] S. S. Shrimali, N. D. Sharma, S. Kumar, and B. C., Joshi, *Rev. Roumaine Chim.*, **23**, 613 (1978), part I.

[2] S. S. Shrimali, A. Iyer, R. K. Singhal, D. Kishore and B. C. Joshi, *Rev. Roumaine Chim.*, **24**, 597 (1979), part II.

[3] O. N. Witt and D. Uermenyi; *Ber. dtsch. Chem. Ges.*, **46**, 296 (1913); *Chem. Abstr.*, **7**, 1502 (1913).

[4] O. N. Witt, H. Truttwin, *Ber. dtsch. Chem. Ges.*, **47**, 2786 (1914); *Chem. Abstr.* **9**, 307(1915).

[5] J. Halberkann, *Ber. dtsch. Chem. Ges.*, **54**, 1833 (1921); *Chem. Abstr.*, **16**, 917 (1922).

[6] J. Halberkann, *Ber. dtsch. Chem. Ges.*, **54**, 1665 (1921); *Chem. Abstr.*, **15**, 3944 (1921).

[7] J. Halberkann, *Ber. dtsch. Chem. Ges.*, **55**, 3075 (1922); *Chem. Abstr.*, **17**, 734 (1923).

[8] A. R. Gennaro and M. Zanger, *J. Org. Chem.*, **36** 1321 (1971).

[9] T. R. Aalto, M. C. Firman and N. E. Rigler, *J. Am. Pharm. Assoc. Sci. Ed.*, **42**, 449 (1953).

[10] M. Gross and I. A. Greenberg, "The Salicylates. A critical Bibliographic Review", Hill House Press, New Haven, Conn. 1948.

[11] H. Gilmann and A. H. Blatt, "Organic Synthesis", Coll, Vol. I, Wiley, New York, 1951, p.8.

[12] C. K. Ingold, "Structure and Mechanism in Organic Chemistry", Cornell University Press, Ithaca, N.Y. 1953.

[13] H. W. Dieter, *Angew Chem.*, **86** 273, 1974.

[14] J. Sullivan and W. N. White, *Abstracts. 152nd. National Meeting of the American Chemical Society*, New York, N.Y. Sept. 1966, No. S. 83.

Revue Roumaine de Chimie, 32, 2, 223–226 (1987)

DIMETHYLDICHLOROSILANE AS REAGENT FOR THE SYNTHESIS OF 1,3,4-OXADIAZOLES FROM DIAROYLHYDRAZINES

C.I. CHIRIAC
"P. Poni" Institute of Macromolecular Chemistry, Aleea Gr. Ghica-Vodă 41 A, Iași, Romania

Received December 23, 1985

By the dehydration of diaroylhydrazines with dimethyldichlorosilane in dimethylformamide at 135–145° for 4–5 hours, substituted 1,3,4-oxadiazoles resulted in high yields.

Since R. Stollé, [1] prepared 2,5-diphenyl-1,3,4-oxadiazole from N,N′-dibenzoylhydrazine by dehydration at high temperature (250–300°), various dehydrating reagents have been used at lower temperatures as phosphorous oxychlorides, [2,3] thionyl chloride, [4] ethyl orthoformate, [5] etc.

RESULTS AND DISCUSSION

A previous communication from this laboratory [6] showed that phenyldichlorophosphite – dimethylformamide adduct is a useful reagent for the dehydration of diaroylhydrazines to 1,3,4-oxadiazoles.

In this work, we have investigated if dimethyldichlorosilane (a very reactive compound) is a suitable reagent for this dehydration. Thus by heating at 135–145° one mole dibenzoylhydrazine with two moles dimethyldichlorosilane in excess of dimethylformamide (DMF), 2,5-diphenyl-1,3,4-oxadiazole results in high yield (at smaller temperatures, the yield decreases). When we used only one mole of dimethyldichlorosilane the yield is smaller because this reagent having a low boilling point (70°) goes out from the hot solution (140°) and refluxes in the time of reaction. With trimethylchlorosilane which has a boilling point lower than dimethyldichlorosilane (57°), an excess of 3–3,5 moles reagent is necessary.

Dimethyldichlorosilane is a very reactive compound, which can react with DMF giving an adduct, similar with other reactive compounds.[7–9] But, by the reaction between one mole dimethyldichlorosilane and one mole DMF at room temperature, we could not obtain a solid adduct. Also infrared examination of a solution of dimethyldichlorosilane in DMF showed no new species to be present in comparison with DMF without reagent. These results are in agreement with those of Hall jr., [10] obtained in the case of reaction of benzoyl chloride with DMF. On the other hand, Rochow and coworkers,[11] demonstrated that chlorosilanes dissolved in DMF yield conducting solutions. In conclusion, the adduct between dimethyldichlorosilane and DMF must be present in small quantities (under 3%) unidentifiable by IR spectra but affording conducting solutions, the rest being only a solution of this reagent in DMF. This solution of dimethyldichlorosilane in DMF is the reagent for the dehydration of diaroylhydrazines to the corresponding oxadiazoles. Otherwise the dehydration reaction of dibenzoylhydrazine takes place only with dimethyldichlorosilane in great excess, without DMF as solvent, but the purity and the yield of the final product are lower. Using DMF, which is a very good solvent, this disadvantage is eliminated.

As a result of these investigations and similar with other cases,[6,9,12] we propose the following mechanism of reaction:

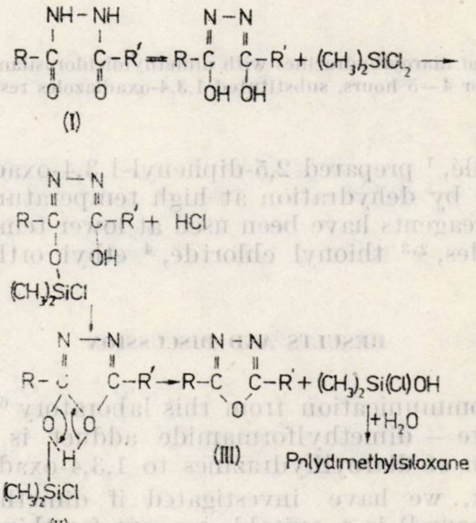

In this dehydration, polydimethylsiloxane results as by-product, by the precipitation with water at the end of reaction.[13] This by-product remains almost all stuck on the flask. The final product (III) is recrystallized from a suitable solvent.

In a typical procedure, two moles of dimethyldichlorosilane were added slowly to dried DMF under stirring. Then one mole (I) was added and heated for 4—5 hours at 135—145°. At the end of reaction, the obtained product is precipitated with water and ice. The yields of this method ranged from 73 to 94% (Table 1).

Thus, using dimethyldichlorosilane as a new reagent for the dehydration of diaroylhydrazines, we obtained substituted 1,3,4-oxadiazoles in high yields.

Table 1

Substituted 1,3,4-oxadiazoles obtained from diaroylhydrazines using dimethyldichlorosilane in DMF as reagent

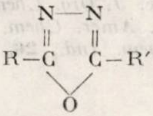

R	R′	Oxadiazoles [a]		
		Yield [b] %	Mp [c] °C	Reported m.p. °C
Phenyl	Phenyl	94	139—140	139—140[1]
Phenyl	4-Methoxyphenyl	90	144—146	146[2]
Phenyl	4-Chlorophenyl	81	161—163	162[2]
4-Methoxyphenyl	4-Methoxyphenyl	87	165—167	166—167[14]
4-Methylphenyl	4-Methylphenyl	93	173—175	175[14]
5-Bromophenyl	3-Bromophenyl	76	179—181	181—183[14]
Phenyl	4-Bromophenyl	73	165—167	167[2]

[a] The products were identified by comparison of m.p. and IR spectra with authentic samples.

[b] Yields calculated on diaroylhydrazines, before recrystallisation.

[c] After recrystallisation.

EXPERIMENTAL

2,5-Diphenyl-1,3,4-oxadiazole

To 15 mL dried DMF in a 50 mL three-necked flask 2.4 mL (0.02 moles) of dimethyldichlorosilane were added slowly under stirring and cooling. Then, 2.4 g (0.01 moles) dibenzoylhydrazine were added and the mixture was heated for 4—5 hours at 135—145°. At the end of reaction, the obtained solution was poured into a large volume of water with ice (50—70 mL) under vigorous stirring when the desired product precipitated. This solution was treated with 10% NaOH solution till pH = 9—10 and the product was collected by filtration, washed with 30—50 mL 7% HCl solution, three times with 30—40 mL water and dried under vacuum at 100—120°. 2,5-Diphenyl-1,3,4-oxadiazole, 2.1 g with m.p. 137—139° was obtained. Yield 94% (calculated on dibenzoylhydrazine employed). After recrystallisation from ethanol, m.p. 139—140° (mixed m.p. with pure product undepressed).
Anal. Found: C, 75.11; H, 4.18; N, 12.09. Calculated for $C_{14}H_{10}N_2O$; C, 75.60; H, 4.50; N, 12.60%.

Under similar conditions, the other oxadiazoles (presented in table 1) were prepared in good yields from the corressponding diaroylhydrazines.

REFERENCES

[1] R. Stollé, *Ber. dtsch. chem. Ges.*, **32**, 797 (1897).
[2] A. P. Grecov and L. N. Kulakova, *Zhur. obshcei. Khim.*, **29**, 3054 (1959); *Chem. Abstr.*, **54**, 13108 (1960).
[3] F. N. Hayes and B. S. Rogers, *J. Amer. Chem. Soc.*, **77**, 1850 (1955).
[4] Ciba Ltd., British. patent 816, 750 (July 15, 1959); *Chem. Abstr.*, **54**, 3457 (1960).
[5] G. Ainsworth, U.S. Pat. 2, 733, 245; *Chem. Abstr.*, **50**, 12. 115 (1956).
[6] C. I. Chiriac, *Rev. Roumaine Chim.*, **27**, 935 (1982).
[7] H. H. Bosshard, *Helv. Chim. Acta.*, **42**, 1658 (1959).

[8] F. Cramer and M. Winter, *Chem. Ber.*, **94**, 990 (1961).
[9] H. Bredereck, *Chem. Ber.*, **92**, 837 (1959).
[10] H. K. Hall, jr. *J. Amer. Chem. Soc.*, **78**, 2717 (1956).
[11] K. Gingold, E. G. Rochow and R. West, *J. Amer. Chem. Soc.*, **74**, 6306 (1952).
[12] E. A. Lawton and D. D. Mc Ritchie, *J. Org. Chem.*, **24**, 26 (1959).
[13] G. R. Lucas and R. W. Martin, *J. Amer. Chem. Soc.*, **74**, 5225 (1952).
[14] E. Baltazzi and A. J. Wysocki, *Chem. Ind.*, **26**, 1080 (1963).

M. I. Ch. — I. C. Ch.

IAMN

BUCUREȘTI

Ministry of Chemical Industry-
Chemical Research Institute
IAMN-Bucharest

PRODUCES:

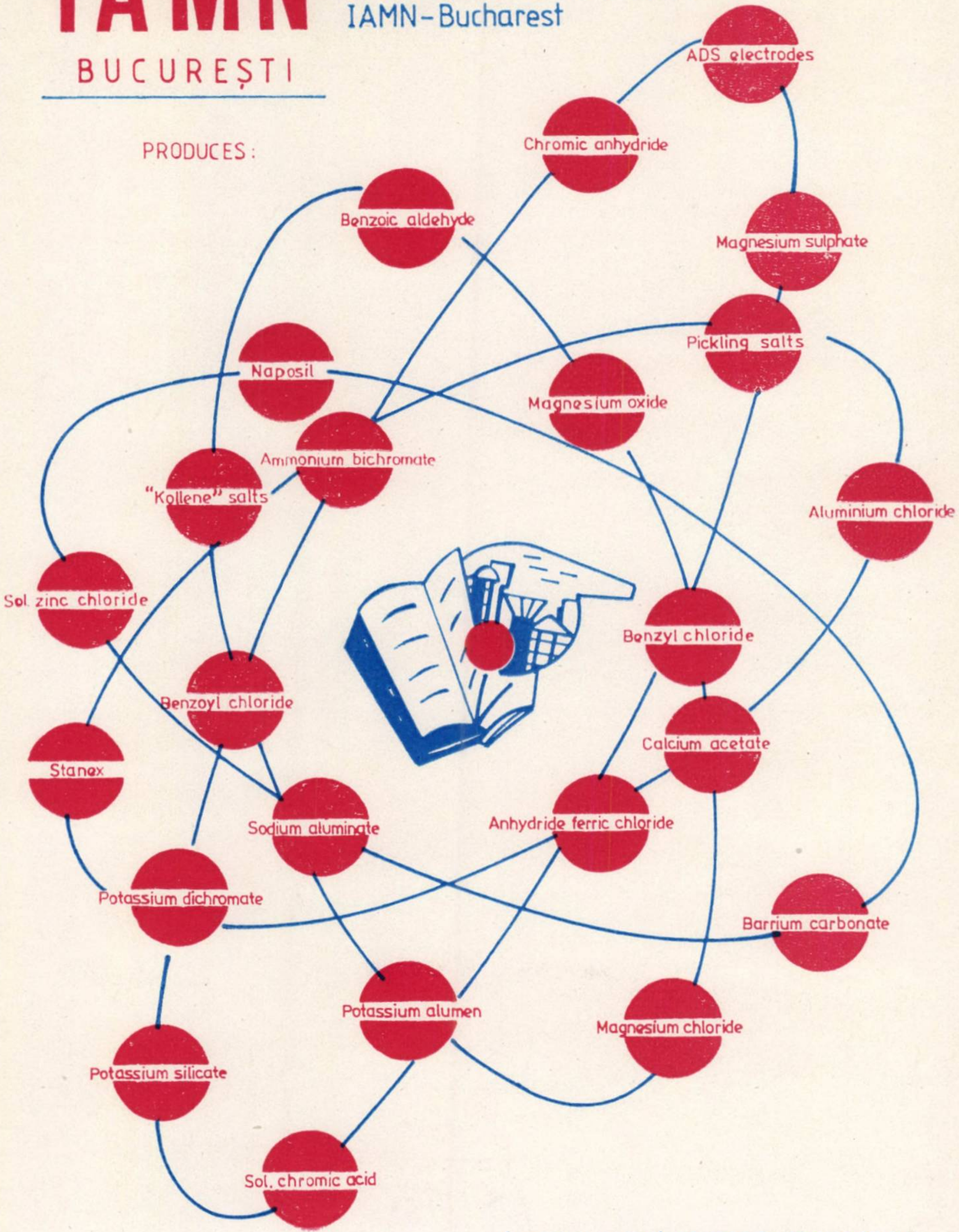

ADS electrodes
Chromic anhydride
Benzoic aldehyde
Magnesium sulphate
Pickling salts
Naposil
Magnesium oxide
Ammonium bichromate
"Kollene" salts
Aluminium chloride
Sol. zinc chloride
Benzyl chloride
Benzoyl chloride
Calcium acetate
Stanex
Sodium aluminate
Anhydride ferric chloride
Potassium dichromate
Barrium carbonate
Potassium alumen
Magnesium chloride
Potassium silicate
Sol. chromic acid

'TRANSILVANIA' RESEARCH DEPARTMENT
12 C Armata Roșie street
TURDA, ROMANIA

ORSZÁGOS MŰSZAKI INFORMÁCIÓS KÖNYVTÁR

NOTE POUR LES AUTEURS

La Revue Roumaine de Chimie publie des articles en anglais, français, russe, allemand ou espagnol. Les auteurs sont priés d'envoyer des articles et des comptes rendus inédits.

Les manuscrits seront dactylographiés à double interligne. La bibliographie, les tableaux et la légende des figures seront placés après le texte.

Si l'article fait partie d'une série numérotée, la partie précédente sera donnée comme première référence.

Chaque article sera précédé d'un résumé comprenant quinze lignes au maximum.

Les références bibliographiques dans le texte seront faites par des exposants sans parenthèses et paraîtront à la fin de l'ouvrage.

Les publications périodiques mentionnées dans la bibliographie seront présentées suivant les prescriptions internationales : le nom de l'auteur précédé de l'initiale du prénom, le titre du périodique abrégé conformément à « Chemical Abstracts » et souligné par une ligne, le numéro du tome indiqué par des chiffres arabes et souligné par deux lignes, suivi de la première page de l'article; à la fin, l'année de la parution sera placée entre parenthèses. Le numéro de la revue ne sera pas indiqué si les pages du volume sont numérotées consécutivement.

Les textes des livres ou traités inclueront : le nom des auteurs, l'initiale du prénom, le titre du livre entre guillemets et sans être souligné, le numéro du tome précédé par l'abréviation « vol. » (ou « Bd »), le numéro de l'édition, les éditions (the publisher), la localité de la parution du livre, l'année de la parution et la page de la référence précédée(s) par l'abreviation « p » (ou « S. »).

Les brevets seront indiqués comme suit : l'auteur ou la firme, le pays et le numéro du brevet, la date et la revue *(Chem. Abstr.)*. Par ex : M. Jones (to Union Carbide Co), Brit. Pat. 601 238, 2 Sept. 1959 ; cf. *Chem. Abstr.*, *54*, 12808 (1960).

Si la référence n'a pas été lue en original, on indiquera aussi la revue de référence consultée.

Les diagrammes seront tracés à l'encre de Chine sur papier calque. Les tableaux et les figures (en nombre strictement nécessaire) ainsi que les courbes dans les figures seront numérotés par des chiffres arabes. Leur explication sera donnée dans la légende des figures. Prière de ne pas inscrire les mêmes données dans les tableaux et les figures. Chaque tableau aura un titre. On indiquera dans le texte la place approximative des tableaux et des figures. Les formules chimiques seront incluses dans le texte ; en outre, elles seront transcrites sur papier calque à l'encre de Chine.

Les auteurs sont priés d'indiquer les caractères italiques (en soulignant les lettres au crayon), ainsi que tout autre caractère spécial ; les préfixes *ortho*, *meta*, *para*, *cis*, *trans*, etc. seront soulignés pour indiquer leurs caractères italiques et ne seront jamais écrits avec des majuscules.

Aucune correction à la main ne sera admise sur le manuscrit. Les corrections seront tapées à la machine. Les lettres grecques ou d'autres symboles spéciaux seront insérés à la main à l'encre clairement.

Le manuscrit sera signé par l'auteur.

Le titre-courant aura 50 lettres au maximum.

L'entière responsabilité du contenu des articles appartient aux auteurs.

Sur demande on peut obtenir une note plus complète.

PRINTED IN ROMANIA

TRAVAUX PARUS AUX ÉDITIONS DE L'ACADÉMIE DE LA RÉPUBLIQUE SOCIALISTE DE ROUMANIE

ELENA CEAUŞESCU, **Progrese în chimia şi tehnologia polimerilor**, 1986, 446 p.

ELENA CEAUŞESCU, **Forschungen im Bereich der Chemie und Technologie der Polymere**, 1986, 444 p.

A. T. BALABAN, I. GĂLĂŢEANU, G. GEORGESCU, L. SIMIONESCU, **Labelled compounds and radiopharmaceuticals applied in nuclear medicine**, coédition avec J. Wiley & Sons, 1986, 742 p.

RAUL MIHAIL, ION GROZEANU, **Estimarea secvenţială aplicată sistemelor chimice**, 1986, 406 p.

M. BREZEANU, L. PATRON, M. ANDRUH, **Combinaţii complexe polinucleare şi aplicaţiile lor**, 1986, 224 p.

V. Em, SAHINI, M. HILLEBRAND, **Chimia cuantică în exemple şi aplicaţii**, 1985, 380 p.

N. PERESCU, **Chimia extracţiei cu solvenţi şi aplicaţii**, 1985, 212 p.

V. DRĂGUŢAN, A. T. BALABAN, M. DIMONIE, **Olefin metathesis and ring-opening polymerization of cyclo-olefins**, coédition avec John Wiley & Sons, 1985, 544 p.

GH. MARCU, **Chimia compuşilor coordinativi**, 1984, 415 p.

E. CORDOŞ. C. MANOLIU, **Spectrometria de absorbţie şi fluorescenţă atomică**, 1984, 178 p.

C. BODEA, **Tratat de biochimie vegetală**, p. II, vol. 5, 1984, 438 p.

N. ASANDEI, A. GRIGORIU, **Chimia şi structura fibrelor**, 1983, 395 p.

N. IONESCU, M. CĂLDĂRARU, **Oxidarea catalitică a olefinelor inferioare**, 1983.

C. CAŞCAVAL, **Studiul polimerilor prin piroliză şi cromatografie de gaze**, 1983, 220 p.

C. I. SIMIONESCU, F. DANEŞ, **Originea vieţii**, 1983, 110 p.

C. BODEA, (editeur), **Tratat de biochimie vegetală**, II, Vol. IV, 1982, 408 p.

I. G. MURGULESCU, RODICA VÎLCU, **Introducere în chimia fizică, Vol. III. Termodinamica chimică**, 1982, 624 p.

I. G. MURGULESCU, J. PĂUN, **Introducere în chimia fizică, Vol. I.3. Nucleul atomic, reacţii nucleare, particule elementare**, 1982, 606 p.

ELENA JERCAN, **Analiza cromatografică**, 1982, 286 p.

ELENA CEAUŞESCU, **Noi cercetări în domeniul compuşilor macromoleculari**, 1981, 536 p.

I. G. MURGULESCU, TATIANA ONCESCU, E. SEGAL, **Introducere în chimia fizică. Vol.II, 2. Cinematică chimică şi cataliză**, 1981, 1024 p.

LIDIA-MARIA VAICUM, **Epurarea apelor uzate cu nămol activ. Bazele biochimice**, 1981, 218 p.

I. GĂLĂŢEANU, **Procese şi metode radiochimice în energia nucleară**, 1981, 234 p.

O. IORDACHE, **Procese polistocastice la fenomenele de transfer**, 1981, 186 p.

CR. SIMIONESCU, VALERIA GORDUZA, **Polimeri biocompatibili şi biologic activi**, 1980, 479 p.

ELENA CEAUŞESCU, **Polimerizarea stereospecifică a izoprenului**, 1979, 307 p.

CONST. GH. MACAROVICI, **Analiza chimică cantitativă anorganică**, 1979, 457 p.

M. FLORESCU, **Metode ştiinţifice în dezvoltarea industriei chimice moderne**, 1979, 256 p.

I. G. MURGULESCU, E. SEGAL, **Introducere în chimia fizică. Vol. II. 1. Teoria molecular cinetică a materiei**, 1979, 1036 p.

S. STERNBERG, FL. DANEŞ, **Termodinamica chimică aplicată**, 1978, 400 p.

I. G. MURGULESCU, V. EM. SAHINI, **Introducere în chimia fizică, Vol. I.2. Structura şi proprietăţile moleculelor**, 1978, 604 p.

I. ZUGRĂVESCU, MAGDA PETROVANU, **N-ylid chemistry**, coédition avec McGraw-Hill, International Book Company. U.S.A., 1977, 396 p.

I. G. MURGULESCU, **Introducere în chimia fizică. Vol. I.1. Atomi, molecule, legătură chimică**, 1976, 560 p.

ELENA CEAUŞESCU, **Research work on synthesis and characterization of macromolecular. compounds. Contributions**, 1974, 251 p.

CR. SIMIONESCU, VIORICA RUSAN, V. POPA, **Chimia algelor marine**, 1974, 212 p., 1 pl.

6 MAR 1987

ISSN 0035–4090

I. P. Informaţia c. 2698

43 426

Lei 40

$ 80 (pour un abonnement annuel)

1103

ACADÉMIE DE LA RÉPUBLIQUE SOCIALISTE DE ROUMANIE

REVUE ROUMAINE DE CHIMIE

TOME 32

N° 3

Mars 1987

Rev. Roumaine Chim.

RRCHAX, **32**, *3*, p. 227–340 (1987), Bucarest

EDITURA ACADEMIEI REPUBLICII SOCIALISTE ROMÂNIA

ACADÉMIE DE LA RÉPUBLIQUE SOCIALISTE DE ROUMANIE

COMITÉ DE RÉDACTION

Rédacteur en chef:

I. G. MURGULESCU, membre de l'Académie de la République Socialiste de Roumanie

Rédacteurs en chef adjoints:

A. T. BALABAN et V. EM. SAHINI, membres correspondants de l'Académie de la République Socialiste de Roumanie

Collège de rédaction:

EM. BRATU, ELENA CEAUȘESCU, ECATERINA CIORĂNESCU-NENITZESCU, CR. SIMIONESCU, membres de l'Académie de la République Socialiste de Roumanie ; P. SPACU, membre correspondant de l'Académie de la République Socialiste de Roumanie ; M. BANCIU, M. D. GHEORGHIU, I. HAIDUC, D. I. MARCHIDAN, I. MOLDOVAN, G. NIAC et D. SĂNDULESCU

La Revue Roumaine de Chimie paraît 10 fois par an. Toute commande de l'étranger sera adressée à « ROMPRESFILATELIA » — sectorul Export-Import, Presă, P.O. Box 12—201, télex 10376 prsfi r 78104, Calea Griviței nr. 64—66, București, Roumanie

Les manuscrits, les livres et les revue proposés en échange, ainsi que toute correspondance seront envoyés à la rédaction :

REVUE ROUMAINE DE CHIMIE
125, Calea Victoriei, 79717 Bucarest, Roumanie, téléphone 50 76 80

EDITURA ACADEMIEI REPUBLICII SOCIALISTE ROMÂNIA
125, Calea Victoriei, 79717 Bucarest, Roumanie, téléphone 50 78 60

REVUE ROUMAINE DE CHIMIE

Tome 32, N° 3 **Mars 1987**

MARCEL O. VLAD and E. SEGAL, The probability of reaction events in nonequilibrium chemical systems 229–234

F. MATEI, GH. IONESCU and AL. DUCA, Theoretical and experimental features of electrodialysis of $Cr_2O_7^{2-}$ ion on ion-exchange membranes . . . 235–242

E. A. GOMAA, A. H. EL-ASKLANY and M. N. H. MOUSSA, Dissociation of KCl in mixed hexamethylphosphortriamide—water solvents 243–247

P. SPACU, LUMINIȚA PATRON, SILVIA PLOȘTINARU, ADRIANA CONȚESCU, D. CRIȘAN and N. STĂNICĂ, Coordination compounds as raw materials for mixed oxides. IV. Mixed coordination compounds of lanthanides and Ni(II) with hydroxydiphenylacetic acid, as precursors of mixed Ln_2NiO_4 type oxides 249–253

I. GĂNESCU and CS. VÁRHELYI, Metal- and metal(III)-amine salts of the $H_2[Pt(SCN)_4]$ and $H_2[Pt(SCN)_6]$ acids 255–261

R. K. AGARWAL, M. B. L. SHARMA and A. K. SRIVASTAVA, Magneto, spectral and thermal studies of rare earth nitrate chelates of N, N, N′, N′-tetramethyl thiuram disulphide 263–269

ALEXANDRU T. BALABAN and CĂLIN DELEANU, Chemical graphs. Part 47. Valence isomers of [14]annulene 271–294

MISBAHUL AIN KHAN and RUBINA GHAFOOR, *IPSO*-Substitution of heterocyclic compounds. I. Nitration of 5-bromo-3,4-dimethyl-1-phenyl-1*H*, 6*H*-pyrano[2,3-*c*]pyrazol-6-one 295–296

M. I. ALI, A. M. ABD-ELFATTAH, H. A. HAMMOUDA and S. M. HUSSAIN, Reactions of homophthalic anhydride with some compounds containing two amino groups 297–303

F. GUTIERREZ-MARTÍN, A. RODRIGUEZ-PASTOR and F. MATA-PÉREZ, Phenylhydrazone formation from substituted benzaldehydes: substituent effect and structure-reactivity correlations 305–313

M. Z. A. BADR, M. M. ALY, S. A. MAHGOUB, A. M. FAHMY and F. F. ABDEL-LATIF, Photolysis of mono-, di- and tribenzylamine and the novel photocarbylamine reaction 315–320

B. C. JOSHI, YOGESH JOSHI, D. KISHORE and S. S. SHRIMALI, Proton catalysed rearrangement of N-alkyl-naphthalene-sulphonanilides to *ortho*-alkylamino-aryl-naphthalyl-sulphones. Part IV 321–324

MARIA BRUMĂ and ION SAVA, Poly-1,3,4-oxadiazolesterimides 325–328

CAROL CRISTESCU and CLAUDIU SUPURAN, *as*-Triazine derivatives with potential therapeutic action. XXII. A simplified method for the synthesis of 1,2,4-triazole nucleosides and 1,2,4-triazine-nucleosides 329–333

BOOK REVIEWS 335–340

Rev. Roumaine Chim. **32**, *3*, p. 227–340(1987), Bucarest

Revue Roumaine de Chimie, 32, *3*, 229–234 (1987)

THE PROBABILITY OF REACTION EVENTS IN NONEQUILIBRIUM CHEMICAL SYSTEMS

MARCEL O. VLAD * and E. SEGAL **
* CIMC, Bd. Chimiştilor 50, Bucharest, 78014, Romania
** Polytechnic Institute of Bucharest, Department of Physical Chemistry and Electrochemical Technology, Bd. Republicii 13, 70346, Romania

Received March 29, 1986

A stochastic model of a nonequilibrium system involving R linearly independent chemical reactions, can be formulated in the system own scale, by means of the numbers of reaction events. Assuming the validity of the van Kampen approximation, we prove that the probability distribution of the reaction events is normal.

The problem of determining the probability distribution of the numbers of reaction events has been formulated by Perrin.[1] In particular cases, analytical solutions of this problem were given by Šolc [2] and Vlad.[3,4]

The purpose of this note is to give a general solution to the problem of reaction events, within the framework of the van Kampen approximation.[5]

We consider a nonequilibrium chemical system involving R reactions:

$$\sum_{i=1}^{S} \nu_{ij}^{+} A_i \underset{k_j^-}{\overset{k_j^+}{\rightleftharpoons}} \sum_{i=1}^{S} \nu_{ij}^{-} A_i, \quad j = 1, \ldots, R, \; S > R, \tag{1}$$

where $\nu_{ij}^{\pm}$ are the stoichiometric coefficients and $k_j^{\pm}$ are the corresponding forward and backward rate constants. These reactions are linearly independent, that is, the rank of the stoichiometric matrix

$$\mathbf{F} = \|f_{ij}\|; \; f_{ij} = \nu_{ij}^{-} - \nu_{ij}^{+}; \; i = 1, \ldots, S; \; j = 1, \ldots, R; \; S > R, \tag{2}$$

is equal to R:

$$\mathit{rank}\ \mathbf{F} = R. \tag{3}$$

Denoting by N_i, $i = 1, \ldots, S$ the numbers of molecular species A_i, $i = 1, \ldots, S$, the state of the system (in the laboratory scale [2]) can be described by means of the composition vector:

$$\mathbf{N} = \|N_i\|, \; i = 1, \ldots S. \tag{4}$$

In the system own scale,[2] the state of the system is described by the numbers, E_i^+ and E_j^-, of the reaction events $\sum_i \nu_{ij}^+ A_i \to \sum_i \nu_{ij}^- A_i$ and $\sum_i \nu_{ii}^- A_i \to \sum_i \nu_{ij}^+ A_i$ occurring in the time interval t_0, t. The two descriptions are related through the obvious balance equations:

$$N_i(t) = N_i^0 + \sum_{j=1}^{R} f_{ij}(\mathrm{E}_j^+(t) - \mathrm{E}_j^-(t)), \quad i = 1, \ldots, S, \tag{5}$$

where

$$N_i^0 = N_i(t_0), \quad i = 1, \ldots, S. \tag{6}$$

The stochastic form of the mass action law [6] leads to the following expression for the transition rate from a state **N** to another state **N′**:

$$W(\mathbf{N} \to \mathbf{N}') = \sum_{j;\pm} \prod_{i=1}^{S} (\delta_{(N'_i)(N_i \pm f_{ij})}) W_j^{\pm}(\mathbf{N} \to \mathbf{N} \pm \mathbf{f}_j), \tag{7}$$

where

$$\begin{aligned} W_j^{\pm}(\mathbf{N} \to \mathbf{N} \pm \mathbf{f}_j) &= V k_j^{\pm} \prod_{i=1}^{S} \{N_i(N_i - 1) \ldots (N_i - \nu_{ij}^{\pm} + 1)/V^{\nu_{ij}^{\pm}}\} \cong \\ &\cong V k_j^{\pm} \prod_{i=1}^{S} \{N_i/V\}^{\nu_{ij}^{\pm}}, \quad j = 1, \ldots, R, \end{aligned} \tag{8}$$

$$\mathbf{f}_j = \|f_{ij}\|, \quad i = 1, \ldots, S; \; j = 1, \ldots, R, \tag{9}$$

V is the system volume and $\delta_{\alpha\beta}$ is the Kronecker symbol.

Introducing the conditional probability

$$P = P(\mathrm{E}^{\pm}, t|\mathbf{N}^0, t_0), \quad \sum_{\forall \mathrm{E}_j^{\pm} \geqslant 0} P(\mathrm{E}^{\pm}, t|\mathbf{N}^0, t_0) = 1, \tag{10}$$

with

$$\mathrm{E}^{\pm} = \|\mathrm{E}_j^{\pm}\|, \quad j = 1, \ldots, R. \tag{11}$$

Eqs. (7)—(9) lead to a phenomenological master equation:

$$\begin{aligned} \partial_t P = \sum_{j;\,\pm} [&W_j^{\pm}(\mathrm{E}_j^+ - \mathrm{E}_j^- \mp 1 \to \mathrm{E}_j^+ - \mathrm{E}_j^-) P(\mathrm{E}_j^{\pm} - 1) - \\ &- W_j^{\pm}(\mathrm{E}_j^+ - \mathrm{E}_j^- \to \mathrm{E}_j^+ - \mathrm{E}_j^- \pm 1) P], \end{aligned} \tag{12}$$

where

$$\begin{aligned} &W_j^{\pm}(\mathrm{E}_j^+ - \mathrm{E}_j^- \mp 1 \to \mathrm{E}_j^+ - \mathrm{E}_j^-) = \\ &= W_j^{\pm}(\mathbf{N}^0 \mp \mathbf{f}_j + \mathbf{F}(\mathrm{E}^+ - \mathrm{E}^-) \to \mathbf{N}^0 + \mathbf{F}(\mathrm{E}^+ - \mathrm{E}^-)), \text{ etc.} \end{aligned} \tag{13}$$

The initial condition corresponding to Eq. (12) is the following

$$\mathrm{P}(\mathrm{E}^{\pm}, t_0|\mathbf{N}^0, t_0) = \prod_{j;\,\pm} \delta_{(\mathrm{E}_j^{\pm})(0)}. \tag{14}$$

Applying to (12) the "van Kampen extensivity Ansatz",[5] i.e., assuming that the dependences $\mathrm{E}_j^{\pm} = \mathrm{E}_j^{\pm}(V)$ are given by

$$\mathrm{E}_j^{\pm} = V\langle \mathrm{e}_j^{\pm} \rangle + V^{\frac{1}{2}} \eta_j^{\pm} = V \mathrm{e}_j^{\pm}, \quad \mathrm{e}_j^{\pm} = \langle \mathrm{e}_j^{\pm} \rangle + V^{-\frac{1}{2}} \eta_j^{\pm}, \tag{15}$$

where $V\langle e_j^{\pm}\rangle$ and $V^{\frac{1}{2}}\eta_j^{\pm}$ are the deterninistic and the fluctuating contributions to $E_j^{\pm}$, with

$$\langle e_j^{\pm}\rangle,\ \ \eta_j^{\pm} \sim V^0, \tag{16}$$

and introducing the notations

$$\Psi(\boldsymbol{\eta}^{\pm},\ t)\,d\boldsymbol{\eta}^{+}d\boldsymbol{\eta}^{-} = V^{R}P(E^{\pm} = V\langle e^{\pm}\rangle + V^{\frac{1}{2}}\boldsymbol{\eta}^{\pm},\ t\,|\,\mathbf{N}^0 = V\mathbf{n}^0,\ t_0)\,d\boldsymbol{\eta}^{+}d\boldsymbol{\eta}^{-}, \tag{17}$$

$$r_j^{\pm} = k_j^{\pm}\prod_{i=1}^{S}\left[n_i^0 + \sum f_{il}(\langle e_l^{+}\rangle - \langle e_l^{-}\rangle)\right]^{\nu_{ij}^{\pm}}, \tag{18}$$

$$\mathbf{n}^0 = \|n_i^0\|,\ i = 1, \ldots, S;\ n_i^0 = N_i^0/V,\ i = 1, \ldots, S, \tag{19}$$

$$\Delta\eta_j^{\pm} = \eta_j^{\pm} - \langle\eta_j^{\pm}\rangle,\ j = 1, \ldots, R, \tag{20}$$

we get

$$d\langle e_j^{\pm}\rangle/dt = r_j^{\pm}, \tag{21}$$

$$d\langle\eta_j^{\pm}\rangle/dt = \sum_{l} b_{jl}^{\pm}\langle\eta_l^{\pm}\rangle, \tag{22}$$

$$\begin{aligned} d\langle\Delta\eta_j^{\alpha}\Delta\eta_k^{\beta}\rangle/dt = {} & \sum_{l} b_{jl}^{\alpha}\langle\Delta\eta_l^{\alpha}\Delta\eta_k^{\beta}\rangle + \\ & + \sum_{l} b_{kl}^{\beta}\langle\Delta\eta_l^{\beta}\Delta\eta_j^{\alpha}\rangle + \delta_{jk}\delta_{\alpha\beta}r_k^{\beta},\ \alpha, \beta = \pm, \end{aligned} \tag{23}$$

and

$$\frac{\partial}{\partial t}\Psi = -\sum_{j,l;\pm} b_{jl}^{\pm}\frac{\partial}{\partial\eta_j^{\pm}}(\eta_l^{\pm}\Psi) + \frac{1}{2}\sum_{j;\pm} r_j^{\pm}\frac{\partial^2\Psi}{\partial(\eta_j^{\pm})^2}, \tag{24}$$

where

$$b_{jl}^{\pm} = \frac{\partial r_j^{\pm}}{\partial(\langle e_l^{\pm}\rangle - \langle e_l^{\mp}\rangle)} = \pm\, r_j^{\pm}\sum_{i}\frac{\nu_{ij}^{\pm}f_{il}}{(n_i^0 + \sum_{k} f_{ik}(\langle e_k^{+}\rangle - \langle e_k^{-}\rangle))}. \tag{25}$$

The initial conditions corresponding to Eqs. (21)—(24) can be derived from (14) and (15), (17). We get

$$\langle e_j^{\pm}(t_0)\rangle\ = 0,\ \ \langle\eta_j^{\pm}(t_0)\rangle = 0,\ \langle\Delta\eta_j^{\alpha}(t_0)\Delta\eta_l^{\beta}(t_0)\rangle = 0, \qquad (26), (27), (28)$$

$$\Psi(\boldsymbol{\eta}^{\pm},\ t_0) = \prod_{j;\pm}\delta(\eta_j^{\pm}), \tag{29}$$

where $\delta(x)$ is the Dirac symbol. Eqs (21)—(24) and (26)—(29) determine the time evolution of $\langle e_j^{\pm}\rangle$, $\langle\eta_j^{\pm}\rangle$, $\langle\Delta\eta_j^{\alpha}\Delta\eta_j^{\beta}\rangle$ and Ψ.

Eqs. (22)—(24) are linear and can be integrated analytically, provided that the solutions

$$\langle e_j^{\pm}\rangle = \langle e_j^{\pm}(t)\rangle, \tag{30}$$

of the "deterministic equations" (21) with the initial conditions (26) are known. After some routine manipulations we come to :

$$\langle \eta_{jl}^{\pm}(t) \rangle = 0, \tag{31}$$

$$\langle \Delta \eta_j^{\alpha}(t) \Delta \eta_l^{\beta}(t) \rangle = \langle \eta_j^{\alpha}(t) \eta_l^{\beta}(t) \rangle = \delta_{\alpha\beta} \mathrm{M}_{jl}^{\alpha}(t), \tag{32}$$

$$\Psi(\boldsymbol{\eta}^{\pm}, t) = (2\pi)^{-\mathrm{R}} (\det \mathbf{M}(t))^{-1/2} \exp\left(-\frac{1}{2} \tilde{\mathbf{y}} \mathbf{M}^{-1} \mathbf{y} \right), \tag{33}$$

where

$$\tilde{\mathbf{y}} = (\tilde{\boldsymbol{\eta}}^{+}, \tilde{\boldsymbol{\eta}}^{-}), \tag{34}$$

$$\boldsymbol{\sigma}(\tau) = \| \sigma_{jl}(\tau) \|, \; j, \; l = 1, \ldots, \mathrm{R}, \tag{35}$$

$$\mathbf{M} = \begin{Vmatrix} \mathbf{M}^{+} & 0 \\ 0 & \mathbf{M}^{-} \end{Vmatrix}, \mathbf{M}^{\pm} = \| \mathrm{M}_{jl}^{\pm} \|, \tag{36), (37}$$

$\sigma_{jl}^{\pm}(\tau)$ are the solutions of the differential equations

$$\mathrm{d}\sigma_{jl}^{\pm}(\tau)/\mathrm{d}\tau = \sum_{k} b_{jk}^{\pm}(t_0 + \tau) \sigma_{kl}^{\pm}(\tau), \; \sigma_{kl}^{\pm}(0) = \delta_{kl}, \tag{38}$$

$$\mathrm{M}_{jl}^{\alpha}(t) = \sum_{\nu, \lambda, \mu} \sigma_{l\nu}^{\alpha}(t - t_0) \cdot \left(\int_0^{t-t_0} (\boldsymbol{\sigma}^{(\alpha)}(\tau))_{\nu\lambda}^{-1} r_{\lambda}^{\alpha}(t_0 + \tau) (\boldsymbol{\sigma}^{(\alpha)}(\tau))_{\mu\lambda}^{-1} \mathrm{d}\tau \right) \sigma_{l\mu}^{(\alpha)}(t - t_0), \tag{39}$$

and

$$r_j^{\pm}(t) = r_j^{\pm}(\langle \mathbf{e}^{\pm} \rangle = \langle \mathbf{e}^{\pm}(t) \rangle), \text{ with } t = t_0 + \tau, \tag{40}$$

$$b_{jk}^{\pm}(t) = b_{jk}^{\pm}(\langle \mathbf{e}^{\pm} \rangle = \langle \mathbf{e}^{\pm}(t) \rangle), \text{ with } t = t_0 + \tau. \tag{41}$$

In order to compare the above presented theory with other similar approaches[4, 7-9] we shall consider a chemical system at equilibrium. In this case the moments of random variables $N_1, \ldots, \; , \ldots, N_S$ are time invariant :

$$\langle N_i \rangle^{\mathrm{eq}} = \text{independent of } t, \tag{42}$$

$$\langle (N_i - \langle N_i \rangle^{\mathrm{eq}})(N_j - \langle N_j \rangle^{\mathrm{eq}}) \rangle = \text{independent of } t, \ldots, \tag{43}$$

wherefrom, taking into account (3), we get

$$\langle \mathrm{E}_j^{+} - \mathrm{E}_j^{-} \rangle^{\mathrm{eq}} = \text{independent of } t, \tag{44}$$

$$\langle (\Delta \mathrm{E}_j^{+} - \Delta \mathrm{E}_j^{-})(\Delta \mathrm{E}_l^{+} - \Delta \mathrm{E}_l^{-}) \rangle^{\mathrm{eq}} = \text{independent of } t, \; \Delta \mathrm{E}_u^{\pm} = \mathrm{E}_u^{\pm} - \langle \mathrm{E}_u^{\pm} \rangle^{\mathrm{eq}}. \tag{45}$$

For simplicity, we consider that the initial values N_i^0 are given by

$$N_i^0 = N_i^{\mathrm{eq}}, \; i = 1, \ldots, S. \tag{46}$$

Combining Eqs. (3), (5) and (46) it follows that in this case

$$\langle \mathrm{E}_j^{+}(t) \rangle^{\mathrm{eq}} = \langle \mathrm{E}_j^{-}(t) \rangle^{\mathrm{eq}}, \; \langle \mathrm{e}_j^{+} \rangle^{\mathrm{eq}} = \langle \mathrm{e}_j^{-} \rangle^{\mathrm{eq}}, \; j = 1, \ldots, R \tag{47), (48}$$

and thus, making use of (21) we have

$$r_j^+ = r_j^- = \bar{r}_j^{\mathrm{eq}} \Leftrightarrow k_j^+/k_j^- = \prod_{i=1}^{S} \langle n_i^{\mathrm{eq}} \rangle^{f_{ij}}, \; j = 1, \ldots, R, \tag{49}$$

$$b_{jl}^{\pm} = \pm \, \bar{r}_j^{\mathrm{eq}} \sum_{i=1}^{S} \frac{\nu_{ij}^{\pm} f_{il}}{\langle n_i \rangle^{\mathrm{eq}}}, \; j, \; l = 1, \ldots, R. \tag{50}$$

It is convenient to introduce the "coordinate transformation" :

$$\Xi_j = \mathrm{E}_j^+ - \mathrm{E}_j^-, \; j = 1, \ldots, R, \tag{51}$$

$$\mathrm{E}_j = \mathrm{E}_j^+ + \mathrm{E}_j^-, \; j = 1, \ldots, R. \tag{52}$$

Here Ξ_j are the reaction extents [10] attached to chemical reactions (1), and E_j are the total numbers of reaction events $\Sigma_i \nu_{ij}^+ A_i \to \Sigma_i \nu_{ij}^- A_i$, and $\Sigma_i \nu_{ij}^- A_i \to \Sigma_i \nu_{ij}^+ A_i$, $j = 1, \ldots, R$, occurring in the time interval t_0, t. Taking into account (15), Ξ_i and e_j can be scaled as

$$\Xi_j = V \langle \xi_j \rangle + V^{\frac{1}{2}} \chi_j, \; \xi_j = \langle \xi_j \rangle + V^{-\frac{1}{2}} \chi_j, \tag{53}$$

$$\mathrm{E}_j = V \langle \mathrm{e}_j \rangle + V^{\frac{1}{2}} \eta_j, \; \mathrm{e}_j = \langle \mathrm{e}_j \rangle + V^{-\frac{1}{2}} \eta_j, \tag{54}$$

where

$$\xi_j = \mathrm{e}_j^+ - \mathrm{e}_j^-, \; \chi_j = \eta_j^+ - \eta_j^-, \tag{55}$$

$$\mathrm{e}_j = \mathrm{e}_j^+ + \mathrm{e}_j^-, \; \eta_j = \eta_j^+ + \eta_j^-, \tag{56}$$

and

$$\langle \xi_j \rangle, \; \chi_j, \; \mathrm{e}_j, \; \eta_j \sim V^0. \tag{57}$$

Making use of Eqs. (55)–(56) and (31) we come to

$$\langle \chi_k \chi_v \rangle^{\mathrm{eq}} = \langle \eta_k^+ \eta_v^+ \rangle^{\mathrm{eq}} - \langle \eta_k^+ \eta_v^- \rangle^{\mathrm{eq}} - \langle \eta_k^- \eta_v^+ \rangle^{\mathrm{eq}} + \langle \eta_k^- \eta_v^- \rangle^{\mathrm{eq}}. \tag{58}$$

Combining (23), (25), (45), (48) and (58), yields the following equations for $\langle \chi_k \chi_v \rangle^{\mathrm{eq}}$:

$$2 \delta_{jl} \bar{r}_l^{\mathrm{eq}} = \bar{r}_j^{\mathrm{eq}} \Gamma_{jl} + \bar{r}_l^{\mathrm{eq}} \Gamma_{lj}, \tag{59}$$

with

$$\Gamma_{uv} = \Sigma_k \Omega_{uk} \langle \chi_k \chi_v \rangle^{\mathrm{eq}}, \tag{60}$$

and

$$\Omega_{uk} = \sum_{i=1}^{S} \frac{f_{iu} f_{ik}}{\langle n_i \rangle^{\mathrm{eq}}}. \tag{61}$$

If all $\langle n_i \rangle^{\mathrm{eq}}$ and $k_j^{\mp}$ are diferent from 0 we have

$$\bar{r}_j^{\mathrm{eq}} > 0, \tag{62}$$

$$rank \, \Omega = R, \; \Omega = \| \Omega_{uk} \|, \; u, \; k = 1, \ldots, R, \tag{63}$$

and the solution of Eqs. (59), (60) is given by [4]

$$\Gamma_{jl} = \delta_{jl}, \tag{64}$$

$$\langle \chi_k \chi_v \rangle^{\text{eq}} = (\Omega^{-1})_{kv}. \tag{65}$$

Eqs. (64) and (65) were previously derived within the framework of thermodynamic [7] or Kubo Matsuo Kitahara [8-9] approximations.

REFERENCES

[1] J. Perrin, "Les Atomes", Alcan, Paris, 1920, p. 201.

[2] M. Šolc, *Z. physik. Chem. Neue. Folge*, **92**, 1(1974).

[3] M. Vlad, *Rev. Roumaine Chim.*, **21**, 677 (1976).

[4] M. O. Vlad, *Phys. Lett.* **116A**, 453 (1986).

[5] N. G. van Kampen, *Canad. J. Phys.*, **39**, 551 (1961); *Adv. Chem. Phys.*, **34**, 245 (1976).

[6] G. Nicolis and I. Prigogine, "Self-Organization in Nonequilibrium System", Wiley, New York, 1977, Ch. 10.

[7] M. Vlad and M. Dragoş, *Rev. Roumaine Chim.*, **23**, 1233 (1978).

[8] M. O. Vlad, E. Segal and V. T. Popa, *Physica*, **127**A, 333 (1984).

[9] M. O. Vlad and V. T. Popa, *J. Phys. A : Math. Gen.*, **19**, 45 (1986).

[10] Th. De Donder, "L'Affinité", Gauthier Villars, Paris, 1936, Ch. 1.

Revue Roumaine de Chimie, **32**, *3*, 235–242 (1987)

THEORETICAL AND EXPERIMENTAL FEATURES OF ELECTRODIALYSIS OF $Cr_2O_7^{2-}$ ION ON ION-EXCHANGE MEMBRANES

F. MATEI, GH. IONESCU and AL. DUCA
Analytical Chemistry and Physical Chemistry Departments, Polytechnic
Institute of Jassy, Splai Bahlui stînga 71, Jassy 6600, Romania

Received February 15, 1986

A theoretical and experimental study on the separation of $Cr_2O_7^{2-}$ ion from aqueous solutions, by electrodialysis on an anion-exchange membrane in Cl^- form, Permaplex A–20, is reported. The significant physical amounts, useful in characterizing the process were correlated with time and current density. A good agreement between the equations derived theoretically and found experimentally was obtained. The conclusions of the study recommend the electrodialysis on ion-exchange membrane as an efficient process for separation, analysis and concentration of the investigated anion from diluted aqueous solutions.

1. INTRODUCTION

The electrodialysis became an extremely useful method for both the analytical separation of ionic species and the commercial purification of some waters contaminated with toxic ions.[1]

If in the dialysis process the neutral membranes are substituted for ion-exchange membranes (electromembranes [2]) the driving force of the ion separation significantly increases. This fact can be accounted for by the addition to the concentration gradient of an electric potential caused by the concentration difference of ion species passing through the membrane.

By means of dialysis using ion-exchange membranes the possibility also arises of ion passing from a compartment of low concentration into another of high concentration (the Donnan "pumping" phenomenon [3]).

The limitations of these advantages of dialysis in using ion-exhange membranes by the Donnan equilibrium principle and the low values of ionic flux obtained can be removed by applying an external potential in which case the dialysis becomes electrodialysis and was commercially applied by Meyer and Strauss.[2]

In the present paper a study on the separation of $Cr_2O_7^{2-}$ ion by using the electrodialysis process with ion-exchange membranes is reported.

2. EXPERIMENTAL

The $Cr_2O_7^{2-}$ ion is recognized as a strongly oxidizing reagent which can significantly affect the redox processes taking place on ion-exchange membranes and implicitly the exchange properties of the latter. To avoid the undesired effects the $Cr_2O_7^{2-}$ ion was converted into CrO_4^{2-} ion by the reaction,

$$Cr_2O_7^{2-} + 2HO^- \rightleftarrows 2CrO_4^{2-} + H_2O,$$

whose equilibrium at pH $\geqslant 7$ is completely shifted towards right.[5]

During the runs and in interpreting the results the concentration of CrO_4^{2-} ion was replaced by the proportional amount, the absorbance, A, of the solution. The constancy of absorbance, within 7 – 13 pH range supports the assumption of complete shifting towards the right of the equilibrium :

A	0.518	0.515	0.518
pH	7	9	13

2.1. Method of CrO_4^{2-} analysis

The determination of CrO_4^{2-} ion in the alkaline solutions used was accomplished spectrophotometrically. For determining the analytical wavelengths the absorption spectrum of an alkaline solution of CrO_4^{2-} was recorded, within the (330 – 500) nm spectral range (Fig. 1). The CrO_4^{2-} ion is noticed to exhibit the maximum absorbance at $\lambda = 370$ nm. The applicability of Lambert-Beer law was checked at this wavelength (Fig. 2).

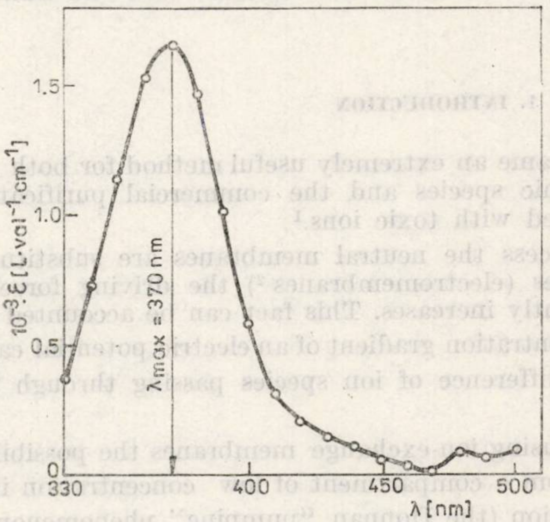

Fig. 1. — Absorption spectrum of CrO_4^{2-} in alkaline medium.

The equation of this linear function, obtained by working statistically the experimental data[6] is of the form :

$$A = a \cdot [10^4 \cdot c(CrO_4^{2-})] = 0.1695 \cdot [10^4 \cdot c(CrO_4^{2-})]$$

(c — Equiv/L ; $\lambda = 370$ nm ; pH = 8 ; $n = 10$ runs ; $P = 95\%$; $s_0 = 6.63.10^{-4}$ L/equiv. ; 20°C ; $\Delta a = 1.5.10^{-3}$).

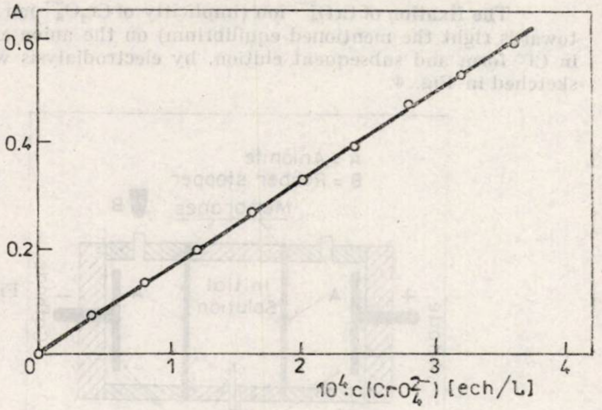

Fig. 2. — Plot of $A = A[c(CrO_4^{2-})]$ function, at pH = 8.

2.2. Experimental procedure of electrodialysis

The most common membrane stack is an alternate array of cation- and anion-exchange membranes between two electrodes as shown in Fig. 3. When a sufficiently high external electric potential is applied, the electric current carries cations of the feed stream into the transfer stream through the cation-exchange membrane facing the cathode. But anions are electrically transferred into the transfer stream on the opposite side through the anion-exchange membrane. On the other hand, cations in the transfer stream are rejected by the anion-exchange-membrane on the cathode side, and anions by the cation-exchange membrane on the opposite side. Thus, the feed stream is stripped of electrolyte solutes into the two transfer streams around the feed compartment, and the transferred ions remain in the transfer compartment. This electrically driven membrane process is generally called electrodialysis in the narrow sense.[7–8]

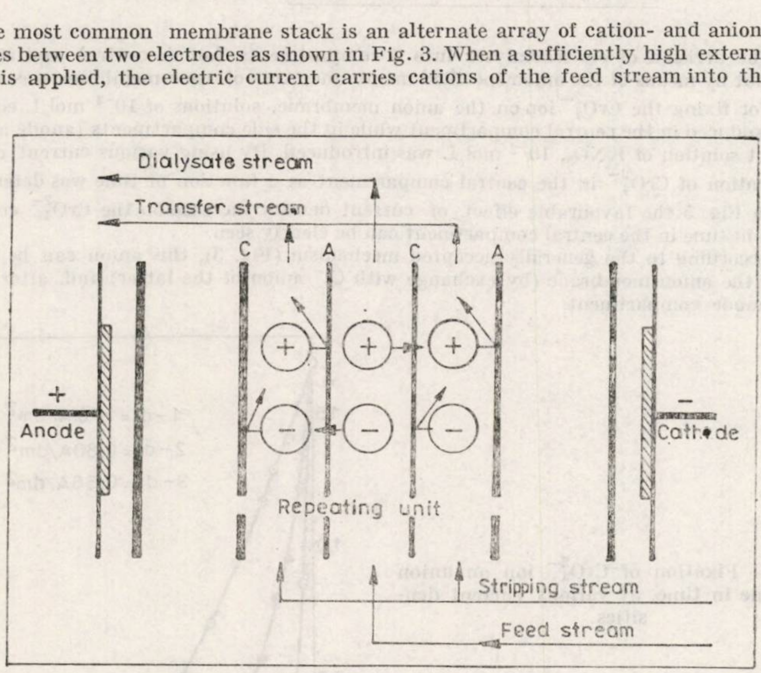

Fig. 3. — Electrodialysis diagram: C = cation-exchange membrane; A = anion-exchange membrane.

The fixation of CrO_4^{2-} ion (implicitly of $Cr_2O_4^{2-}$ ion by its conversion into CrO_4^{2-} by shifting towards right the mentioned equilibrium) on the anion-exchange membrane Permaplex A—20 in Cl^- form and subsequent elution, by electrodialysis were performed on the electrodialyser sketched in Fig. 4.

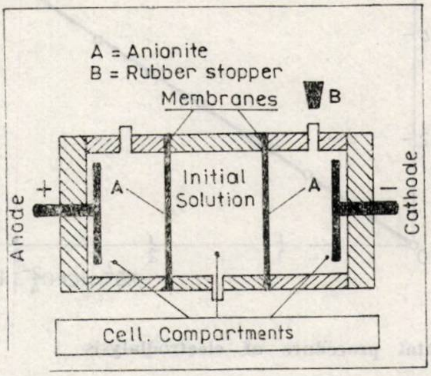

Fig. 4. — Electrodialyser.

The division of electrodialyser into 3 compartments (anode-central and cathode) was carried out by means of the anion specified membrane. Area of each membrane was of 21.5 cm^2.

For fixing the CrO_4^{2-} ion on the anion membrane, solutions of 10^{-3} mol/L concentration were introduced in the central compartment while in the side compartments (anode and cathode) a support solution of KNO_3, 10^{-2} mol/L was introduced. By using various current densities the concentration of CrO_4^{2-} in the central compartment as a function of time was determined.

In Fig. 5 the favourable effect of current density increase on the CrO_4^{2-} concentration decrease in time in the central compartment can be clearly seen.

According to the generally accepted mechanism (Fig. 3), this anion can be found only fixed on the anion membrane (by exchange with Cl^- anion of the latter) and, after saturation, in the anode compartment.

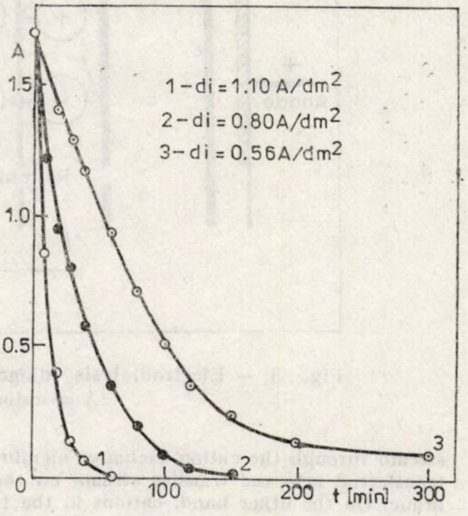

Fig. 5. — Fixation of CrO_4^{2-} ion on anion membrane in time, at various current densities.

This process of fixation before saturation was proved by the elution of CrO_4^{2-} ion; to this end a 10^{-1} mol/L NaCl solution was introduced in the central compartment and various current densities were applied. The increase of Cr_4^{2-} ion concentration in time in the anode compartment is depicted in Fig. 6 which also evidences the efficiency of increase of current density on the elution process.

In the fixation of CrO_4^{2-} on the anion membrane resulted in its removal from the solution in the central compartment the elution led to the recovery of this toxic but valuable ion. Depending on the ratio between the volumes of central and anode compartments the elution can result also not only in recovery of CrO_4^{2-} ion but also in its concentration.

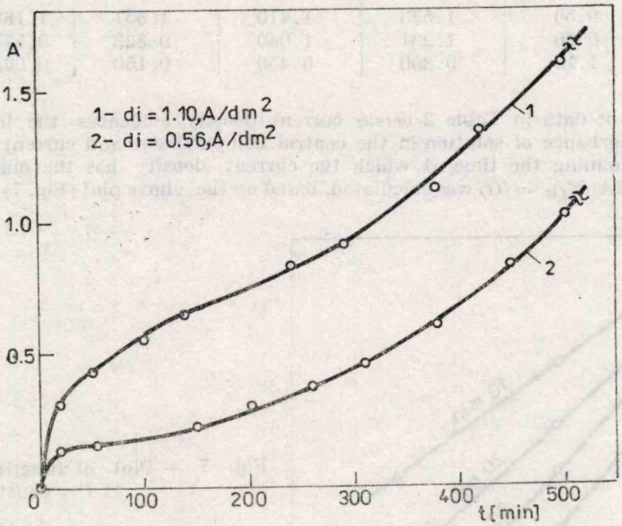

Fig. 6. — Variation in time of concentration of CrO_4^{2-} ion in the anode compartment as a consequence of elution process.

2.3. Discussion of experimental data on CrO_4^{2-} fixation

The experimental data listed in Table 1 were worked to find the influence of current density on the fixation of CrO_4^{2-} at constant time. The obtained data are listed in Table 1.

Table 1

Fixation of CrO_4^{2-} — ion on anion-membrane Permaplex A—20 (Cl^- form)[4]

t min.	d_i, A/dm²		
	0.56	0.80	1.10
	A	*A*	*A*
0	1.620	1.620	1.620
5	—	—	1.060
10	—	1.210	0.861
20	1.400	0.962	0.402
30	1.290	0.800	0.141
40	1.175	0.570	0.065
60	0.940	0.350	0.005
80	0.710	0.250	0.002
100	0.510	0.095	—
120	0.350	0.040	—
150	0.242	0.020	—
200	0.150	—	—
300	0.100	—	—

Table 2

Influence of current density: the function $A=A(d_i)$ at $t=\text{const.}$

d_i, A/dm^2	$t=10$ min.	$t=20$ min.	$t=30$ min.	$t=40$ min.
	A	A	A	A
0.56	1.533	1.410	1.331	1.184
0.80	1.231	1.040	0.823	0.575
1.10	0.800	0.450	0.150	0.065

The plot of data in Table 2 *versus* current density evidences the linear correlation between the absorbance of solution in the central compartment and current density (Fig. 7).

For determining the time at which the current density has the maximum influence the function $(-\mathrm{d}A/\mathrm{d}d_i)_t = f(t)$ was calculated, based on the above plot (Fig. 7) and then plotted in Fig. 8. In this way the linear influence of current density on the process of CrO_4^{2-} fixation on the anion membrane used at any process was evidenced.

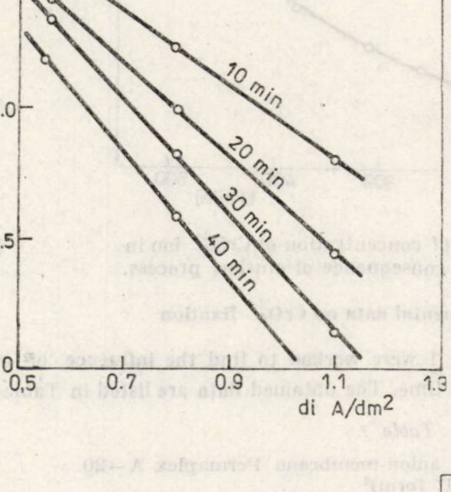

Fig. 7. — Plot of function $A = A(d_i)$, at $t = \text{const.}$

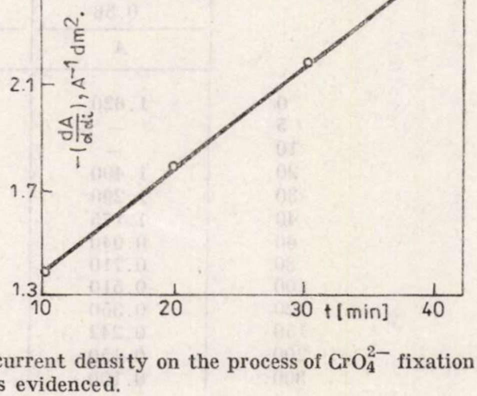

Fig. 8. — Plot of function $(-\mathrm{d}A/\mathrm{d}d_i)_t = f(t)$

The influence of current density in the rate of fixation process was also settled by calculating the process rate $(-\mathrm{d}A/\mathrm{d}t)d_i$, as a function of this variable. The corresponding plot in Fig. 9 also evidences a linear dependence.

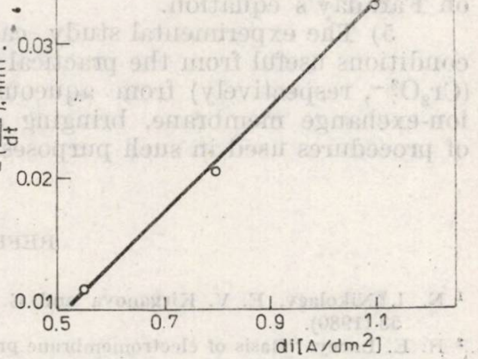

Fig. 9. — Plot of function $(-\mathrm{d}A/\mathrm{d}t)_{d_i} = f(d_i)$.

The linearity of the above functions can be theoretically proved starting from Faraday's equation:

$$m = k \cdot I \cdot t \text{ or, } \frac{m}{S} = k \cdot \frac{I}{S} \cdot t, \text{ whence,}$$

$$m = k \cdot S \cdot d_i \cdot t \quad \text{or} \quad m = k' \cdot d_i \cdot t$$

By dividing both members by the volume of solution in central compartment one obtains:

$$\frac{m}{V} = \frac{k'}{V} \cdot d_i \cdot t \Rightarrow c = k'' \cdot d_i \cdot t$$

By varying d_i and t, and differentiating the equation it results:

a) at $t = \text{const.}, (\mathrm{d}c/\mathrm{d}d_i)_t = k'' \cdot t$;

b) at $d = \text{const.}, (\mathrm{d}c/\mathrm{d}t_i)d_i = k'' \cdot d$.

The equation a) corresponds to Fig. 8 and the equation b) to Fig. 9. (The amounts in the above equations have the following meaning: m = mass of ion taking part into electrodialysis; k = proportionality constant; I = intensity of current in electrodialyser; t = process duration; S = surface of anion-exchange membrane; d_i = current density).

3. CONCLUSIONS

1) The separation from solution of $Cr_2O_4^{2-}$ can be accomplished by electrodialysis on anion membrane by converting it into CrO_4^{2-} ion in alkaline medium.

2) The fixation of CrO_4^{2-} on ion-exchange membrane Permaplex A—10 and the subsequent elution process can take place at current densities of about 1 A/dm^2 which assures durations useful from the practical point of view; under these conditions the electrolysis does not proceed with appreciable rate.

3) The useful amounts for caracterizing the efficiency of electrodialysis process, expressed as $(-\mathrm{d}A/\mathrm{d}t)_{d_i}$ and $(-\mathrm{d}A/\mathrm{d}d_i)_t$ derivatives are simple, linear functions of d_i and t variables.

4) These experimental relations can be theoretically proved based on Faraday's equation.

5) The experimental study carried out allowed the finding of those conditions useful from the practical point of view, of CrO_4^{2-} ion separation ($Cr_2O_7^{2-}$, respectively) from aqueous solutions by electrodialysis, on the ion-exchange membrane, bringing a contribution to the diversification of procedures used in such purposes.

REFERENCES

[1] N. I. Nikolaev, E. V. Kirganova and G. G. Ciuvileva, *Khimiceskaja promyshlenostj*, **4**, 53 (1980).

[2] R. E. Lacey, "Basis of electromembrane processes", in "Industrial processing with membranes", Lacey R.E. and Loeb S., Eds., Wiley-Interscience, New-York, 1972.

[3] F. G. Donnan, *Chem. Rev.*, **1**, 73 (1924).

[4] K. H. Meyer and W. Strauss, *Helv. Chim. Acta*, **23**, 795 (1940).

[5] L. Pauling, "Chimie generală", Ed. Ştiinţifică, Bucharest, 1972, p. 670.

[6] K. Doerffel, "Statistik in der analytischen Chemie", Leipzig, 1966.

[7] S. T. Hwang and K. Kammermeyer, "Membranes in separations", Wiley-Interscience Publication, John Wiley and Sons, New York, London, Sydney, Toronto, 1975, p. 193.

[8] N. F. Kizim *Izvest. VUZ, Khim. i khim. Tehnol.*, **22**, 1263 (1979).

Revue Roumaine de Chimie, **32**, 3, 243–247 (1987)

DISSOCIATION OF KCl IN MIXED HEXAMETHYLPHOSPHORTRIAMIDE – WATER SOLVENTS

E. A. GOMAA*, A. H. EL-ASKLANY and M. N. H. MOUSSA
Chemistry Department, Faculty of Science, Mansoura University, Mansoura, Egypt

Received February 15, 1986

From conductance measurements, the degree of dissociation, association constant and free energy of solvation of KCl in mixed hexamethylphosphortriamide (HMPT)-water solvents were estimated. The coulombic free energies of interaction of KCl in the mixed solvents were theoretically calculated. From their values also the non coulombic free energies of interaction were evaluated. Increasing the percentage of HMPT in the mixed solvents was accompanied by an increase in the association constant and free energies (coulombic, non coulombic and total) of solvation of KCl in HMPT–H_2O mixtures.

INTRODUCTION

When the solubility of an electrolyte and its association are reversible, the laws of the equilibrium are aplicable. Ostwald[1] assumed that the solution of the dissolved species has the ideal osmotic pressure. Besides being a direct and accurate technique[2] for determining ion association in solution, the conductance measurements can provide values of the mobility of ionic species. Since hexamethylphosphortriamide has a high dipole moment ($\mu = 5.39$),[3] it is expected to have a considerable effect on the dissociation and the thermodyamic quantities of KCl in mixed HMPT–H_2O systems.

EXPERIMENTAL

The conductance of KCl solutions was measured using Electronic Switchgear, model MC–1 conductivity bridge, which coupled with a circulating thermostat of the type Techne. HMPT from Merck-Co., Ovasol. The conductance of KCl in mixed HMPT–H_2O systems was measured at 25, 35, 45 and 55°C. The dielectric constants of the mixed solvents under consideration were measured using a Dekameter DK 300 (WTW) in Institut für Radiochemie der Technische Universität München.

RESULTS AND DISCUSSION

The conductance of KCl was measured at different temperatures in concentrations of 1, 2.5 and 10 mM using different volume percentages of HMPT (10, 30, 50 and 70). The experiments were carried out at those low concentrations of KCl to obtain limiting conductance value.[4] Plots conductance (Λ) *vs.* $\sqrt{C}$, when extrapolated to zero concentration gone the limiting Λ_0. The degree of dissociation (α) is related to $S(Z)$ by[5]:

---

* To whom correspondence should be sent.

$$\alpha = \Lambda S(Z)/\Lambda. \tag{1}$$

where

$$S(Z) = \{Z/2 + [1 + (Z/X2)^2]^{1/2}\}^2,\ Z = S\Lambda_0^{-3/2}(C\Lambda)^{1/2}$$

and $S = a\Lambda_0 + b$.

In the above equations $a = 0.82.10^6/(\varepsilon T)^{3/2}$ $b = 82.5/\eta(\varepsilon T)^{1/2}$ and C is the concentration of KCl. The estimated values are presented in Table 1. It shows evidence that increasing the percentage of HMPT is followed by a decrease in the dissociation value due to the association of HMPT dipoles with KCl dipoles in solution.

Table 1

Degree of dissociation (α) of KCl at different temperatures in mixed HMPT-H_2O solvent

Vol. % of HMPT	KCl conc. (mol/L)	α at			
		25°C	35°C	45°C	55°C
10	0.01	0.726	0.724	0.737	0.720
	2.5×10^{-3}	0.863	0.864	0.872	0.854
	1.0×10^{-3}	0.911	0.910	0.917	0.902
30	0.01	0.749	0.651	0.529	0.472
	2.5×10^{-3}	0.874	0.821	0.765	0.736
	1.0×10^{-3}	0.924	0.886	0.851	0.833
50	0.01	0.589	0.473	0.369	0.302
	2.5×10^{-3}	0.789	0.736	0.689	0.647
	1.0×10^{-3}	0.863	0.838	0.806	0.777
70	0.01	0.549	0.378	0.288	0.246
	2.5×10^{-3}	0.784	0.689	0.644	0.626
	1.0×10^{-3}	0.864	0.800	0.773	0.760

From α values the total dissociation constant K^T was evaluated using equation (2).

$$K^T = \frac{\alpha^2 C \gamma_\pm^2}{1 - \alpha} \tag{2}$$

The activity coefficient ($\gamma_\pm$) was calculated using the Debye-Hückel limiting law,[6] $\log \gamma_\pm = -A(\alpha C)^{1/2}$, where $A = 1.8246.10^6/(\varepsilon T)^{3/2}$. The values of K^T for KCl are listed in Table 2. These show a decrease in value by increasing HMPT percentages in the mixed solvent following the same trend of α values.

The total free energy of interaction of 0.01 M KCl in the mixed solvents used was obtained[7,8] by the application of equation (3).

$$\Delta G^T = -RT\ln K^T \tag{3}$$

Table 2

Total dissociation constant (K) KCl at different temperatures in mixed HMPT-H_2O solvents.

KCl conc. (mole/L)	Vol. % of HMPT	K^T at 25°C	K^T at 35°C	K^T at 45°C	K^T at 55°C
0.01	10	0.0192	0.0190	0.0210	0.019
	30	0.0223	0.0121	5.94×10^{-3}	4.220×10^{-3}
	50	8.440×10^{-3}	4.245×10^{-3}	2.158×10^{-3}	1.307×10^{-3}
	70	6.683×10^{-3}	2.297×10^{-3}	1.165×10^{-3}	8.026×10^{-3}
2.5×10^{-3}	10	0.0140	0.014	0.0150	0.0130
	30	0.0152	9.410×10^{-3}	6.230×10^{-3}	5.129×10^{-3}
	50	7.343×10^{-3}	5.130×10^{-3}	3.816×10^{-3}	2.965×10^{-3}
	70	7.114×10^{-3}	3.816×10^{-3}	2.913×10^{-3}	2.620×10^{-3}
1×10^{-3}	10	9.325×10^{-3}	9.20×10^{-3}	0.010	8.302×10^{-3}
	30	0.0113	6.890×10^{-3}	4.860×10^{-3}	4.155×10^{-3}
	50	5.436×10^{-3}	4.335×10^{-3}	3.349×10^{-3}	2.727×10^{-3}
	70	5.436×10^{-3}	3.200×10^{-3}	2.632×10^{-3}	2.406×10^{-3}

From ΔG^T values, the total free energy of transfer, ΔG^T (from water to mixed solvent) was determined by means of equation (4).

$$\Delta G_t^T = \Delta_w^s G^T = (G_s^T - G_w^T) \tag{4}$$

ΔG_s^T is the total free energy of interacton of KCl in HMPT$-H_2O$ solvent mixtures (s) and ΔG_w^T is the total free energy in water(w). It can be seen from the data in Table 3 that increase of the amounts of HMPT is followed by an increase in the total free energy of transfer of KCl solutions, due to the interaction with solvent dipoles.

The coulombic dissociation constants (K^c) were also calculated according to Fuoss's method[9] using equation (5):

$$K^c = \frac{4\pi N a^3}{3000} e^{\overline{\frac{e^2}{a\varepsilon kT}}} \tag{5}$$

N is Avogadro's number, ε the dielectric constant of the mixed solvent, a is the radius of the solvated KCl,[3] k the Boltzmann constant and T the absolute temperature.

From K^c values and on applying equations (3) and (4) the coulombic free energy of transfer (ΔG_t^c) was evaluated and tabulated in Table 3. The non coulombic free energy of transfer (ΔG_t^N) was calculated (Table 3) after Siekierski [10] and Abraham [11] by means of equation (6)

$$\Delta G_t^N = \Delta G_t^T - \Delta G_t^C \tag{6}$$

From the results shown in Tables 1, 2 and 3 it can be concluded that hexamethylphosphortriamide decreases both the dissociation of KCl and the total dissociation constant but increases ΔG^T, ΔG_t^T, ΔG_t^C and ΔG_t^N. This is due to the association of the high dipole moment organic solvent (HMPT) with potassium chloride electrolyte in mixed HMPT$-H_2O$

Table 3

Total free energy, total free energy of transfer, coulombic free energy of transfer and non coulombic free energy of transfer of 0.01 M KCl in HMPT – H_2O solvents at different temperatures (kcal/mole)

T	Vol. % of HMPT	ΔG^T	ΔG_t^T	ΔG_t^C	ΔG_t^T
25°C	0	2.216	0	0	0
	10	2.332	0.116	−0.023	0.139
	30	2.244	0.028	−0.082	0.110
	50	2.817	0.601	−0.183	0.784
	70	2.955	0.739	−0.361	1.10
35°C	0	2.267	0	0	0
	10	2.417	0.150	−0.024	0.174
	30	2.692	0.425	−0.084	0.509
	50	3.331	1.064	−0.188	1.252
	70	3.705	1.438	−0.375	1.811
45°C	0	2.305	0	0	0
	10	2.432	0.127	−0.024	0.151
	30	3.228	0.923	−0.086	1.009
	50	3.865	1.560	−0.194	1.754
	70	4.253	1.948	−0.385	2.333
55°C	0	2.306	0	0	0
	10	2.574	0.268	−0.025	0.293
	30	3.245	1.245	−0.09	1.335
	50	4.312	2.006	−0.201	2.207
	70	4.629	2.323	−0.397	2.721

solvents. On drawing the relation between ln K^T and $1/T$, straight lines are obtained with the slope of ΔH^0 values. The ΔH^0 values of 0.01 M KCl at 25°C in the mixed HMPT$-H_2O$ solvents are tabulated in Table 4 with the ΔH_t^0 (enthalpy of transfer) values. $T\Delta S^\circ$ and the entropy of transfer ($T\Delta S^0$) were calculated also from the free energies and enthalpies by using the well known equation $\Delta G = \Delta H - T\Delta S$. It is observed also from Table 4 that increasing the HMPT percentage in the mixed solvents was accompanied by increasing in the enthalpy and entropy of interaction between the KCl and the used mixed solvents.

Table 4

Enthalpies, entropies and their transfer values of 0.01 M KCl in mixed HMPT-H_2O solvents at 25°C (kcal/mole)

Vol. % of HMPT	ε	H^0	ΔH_t^0	$T\Delta S^0$	$T\Delta S_t^0$
0.0	78.5	−1.264	0	−3.48	0
10	76.5	0.396	1.66	−1.936	1.544
30	70.0	11.512	12.776	9.268	12.748
50	60.0	12.18	13.444	9.368	12.848
70	46.0	13.27	14.53	14.31	17.79

REFERENCES

[1] G. Kortüm, "Lehrbuch der Elektrochemie", Verlag Chemie, Weinheim, 1972.
[2] R. G. Bates, "Determination of pH, Theory and Practices", 2nd Ed., Wiley, 1977.
[3] J. I. Kim, *Z. phys. Chem.*, Neue Folge, **113**, 129 (1978).
[4] P. Dobye and E. Hückel, *Physik, Z.*, **24**, 57 (1923).
[5] J. Ananthaswamy, B. Sethuram and T. Navaneeth Rao, *Bull. Chem. Soc. Japan*, **52**, 3076, (1979).
[6] R. A. Robinson and R. H. Stokes, "Electrolyte Solutions", 2nd Ed., Butterworths, London, 1965, p. 230.
[7] A. J. Parker, *Chem. Rev.*, **69**, 1 (1969).
[8] O. Popovych, *Crit. Rev. Anal. Chem. Soc.*, **1**, 73 (1970).
[9] R. M. Fuoss, *J. Amer. Chem. Soc.*, **80**, 5059 (1958).
[10] S. Siekierski, *J. Radioanalyt. Chem.*, **31**, 335 (1976).
[11] M. H. Abraham and J. Liszi, *J. Inorg. Nuclear Chem.*, **53**, 143 (1981).

Revue Roumaine de Chimie, 32, *3*, 249–253 (1987)

COORDINATION COMPOUNDS AS RAW MATERIALS FOR MIXED OXIDES. IV.*

MIXED COORDINATION COMPOUNDS OF LANTHANIDES AND Ni(II) WITH HYDROXYDIPHENYLACETIC ACID, AS PRECURSORS OF MIXED Ln_2NiO_4 TYPE OXIDES

P. SPACU, LUMINIŢA PATRON, SILVIA PLOŞTINARU, ADRIANA CONŢESCU, D. CRIŞAN and N. STĂNICĂ

Center of Physical Chemistry, Bucharest, Romania

Received May 19, 1986

A new class of mixed coordination compounds of Ln(III) and Ni(II) with hydroxydiphenylacetic acid was synthesized. The complex compounds were characterized by elemental analysis, electronic and IR spectra, magnetic measurements. Thermogravimetric decomposition of these compounds gives mixed Ln_2NiO_4 type oxides (Ln = La—Ho). The pure oxide phases have been put in evidence by X-ray diffraction and characterized by physico-chemical methods.

The mixed oxides, whose applications are numerous nowadays, are generally obtained by classical methods of which the reaction of oxides in solid phase is most frequently employed. The decomposition of hydroxide coprecipitates or polynuclear complex compounds is seldom used in obtaining the mentioned oxides.

In earlier publications we reported the results regarding the preparation of mixed Ln(III) and Co(III) oxides of perowskite type, $LnCoO_3$ from polynuclear complex compounds as precursors, containing salicylic acid[1] and derivatives of acetic acid as ligands.[2]

This contribution, which aims at increasing the variety of mixed oxides of lanthanides with transition metals, presents the synthesis and characterization of polynuclear complex compounds of Ln(III) and Ni(II), as precursors of the mixed Ln_2NiO_4 type oxides.

It is worth emphasizing that the possibility of using complex compounds as precursors for oxidic phases in Ln—Ni—O system is not mentioned in the literature. The first data upon mixed complex compounds of 3d and 4f elements with oxalate and dithiooxalate were reported in 1985[3] and deal only with their synthesis and characterization.

---

* part III: Rev. Roumaine Chim., 31, 811(1986).

Because of the difference between the possibilities of coordination of Ln(III) and Ni(II) ions the selection of the ligand has aroused some problems. Complexation with various hydroxycarboxylic acids has been attempted; the best results were obtained with benzylic (hydroxydiphenylacetic)acid, (Bz).

Depending on the molar ratio of the two components Ln : Ni = 1 : 1 and Ln : Ni = 2 : 1, two series of complex compounds were obtained:

$$[LnNi(RCOO)_5] \cdot nH_2O \quad n = 6; \quad Ln(III) = La \ldots Er$$

and

$$[Ln_2Ni(RCOO)_8] \cdot nH_2O \quad n = 6-8; \quad Ln(III) = La \ldots Er$$

in both cases

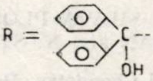

Thermal decomposition of the $[LnNi(RCOO)_5] \cdot nH_2O$ type complex compounds resulted in the formation of perowskite phase $LaNiO_3$[4] for Ln(III) = La.

The synthesized complexes are greenish-white powders, hardly soluble in water and in most common organic solvents. Their solubility in DMSO has allowed to determine the molar electric conductivity. The values obtained for both 1 : 1 and 2 : 1 compounds point to their non-electrolyte character (Table 1).

Table 1

Compound	$\lambda(\Omega^{-1}\ cm^2/mol)$
$[La_2Ni(C_{14}H_{11}O_3)_8] \cdot 8H_2O$	35.00
$[Sm_2Ni(C_{14}H_{11}O_3)_8] \cdot 8H_2O$	26.20
$[Ho_2Ni(C_{14}H_{11}O_3)_8] \cdot 6H_2O$	30.80
$[Er_2Ni(C_{14}H_{11}O_3)_8] \cdot 6H_2O$	35.21

Formation of polynuclear complex compounds was evidenced by X-ray diffraction and thermogravimetry. X-Ray diagrams and thermal decomposition curves of the mixed compounds synthesized are different in all respects from those recorded with the equimolar mixtures of simple compounds.

Information regarding the formation of complex compounds and the coordination of the ligand were obtained from the analysis of vibration spectra. IR spectra were recorded for mixed complex compounds and for the free ligand between 400 – 4000 cm^{-1}. Comparison of these spectra shows that the strong band at 892 cm^{-1}, corresponding to the distortion vibration of carboxylic hydroxyle, is present in the spectrum of the free acid but disappears on formation of complex compounds. Likewise, the absorption band at 1700 cm^{-1} in the spectrum of the acid corresponding to valence vibration of carbonyl group ($\nu C = O$) vanishes after complex compounds formation. This behaviour suggests the coordination of the metal ions by oxygen of the carboxylic group.

Replacement of hydrogen through the coordination of metallic ions is evidenced by existence in spectrum of the complex compounds of two vibration bands, $\nu_{\text{sym.}}$ and $\nu_{\text{asym.}}$, at 1370 – 1400 and 1600 cm^{-1}, respectively. Data regarding the structure of synthesized compounds were supplied by the study of electron reflectance UV and visible spectra. The UV spectrum of the mixed compounds is practically identical with that of the ligand, its bands being those characteristic of the ligand. Examination of the spectra in visible range (Fig. 1) suggests the assignment to Ni(II) ion of a tetrahedrally distorted octahedral configuration. Thus, the band at 25000 cm^{-1} (400 nm) is assigned to $^3A_{2g} \rightarrow {}^3T_{1g}(P)$ transition while that at 1400 cm^{-1} (700 nm) to $^3A_{2g} \rightarrow {}^3T_{1g}(F)$ transition; the splitting is due to spin-orbit coupling which causes mixing of $^3T_{1g}(F)$ and ^1E_g states. The band at about 9000 cm^{-1} (1100 nm) is assigned to $^3A_{2g} \rightarrow {}^3T_{2g}$ transition.

Because the spectrum of La(III) ion exhibits no bands in the visible range, in Fig. 1 is shown the electron spectra of the mixed complex containing Er(III) and Ni(II); it displays the bands characteristic of Er(III) in 450 – 600 nm range. These bands are due to the transition from the ground level to J excited levels of 4f configuration.

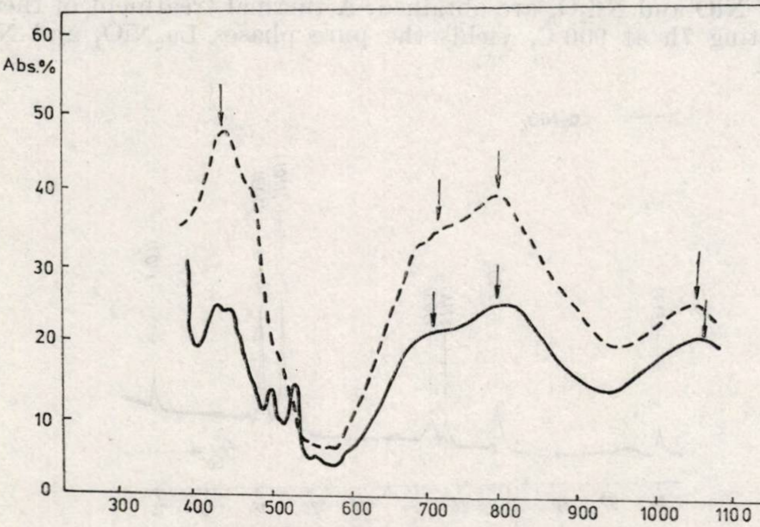

Fig. 1. – Electronic reflectance spectra of :
---- $Ni(Bz)_2 \cdot 2H_2O$
—— $[Er_2Ni(Bz)_8] \cdot 6H_2O$.

Measurements of magnetic susceptibility were carried out on mixed complexes containing Ln(III) = La, Nd, Gd and on simple compound of Ni(II). The values of magnetic moment for Ni(II) compound and of mixed complex containing La(III) are similar ($\mu_B = 3.28 - 3.30$ MB) which points to a high-spin O_h configuration (the La(III) ion is diamagnetic). The values of magnetic moment of Nd(III) and Gd(III) mixed compounds are higher due to the contribution of Ln(III) ion ($\mu_B = 5.51$ MB for Nd(III) and 10.55 MB for Gd(III) compounds).

Given the aim of this study — the preparation of mixed oxides by thermal decomposition of the complex compounds synthesized — we have performed a thermogravimetric study to establish the decomposition steps and the corresponding thermal effects. Thermolysis occurs in two steps : the former, between 24 and 160°C, corresponds to the elimination of water molecules and represents 5—6% weight loss ; the latter between 160 and 600°C, represents the decomposition of complex and the formation of oxide phase. The formation of oxide phase begins at 580°C. The thermogravimetric analysis carried out on complex compounds containing various lanthanides [La(III), Pr(III), Nd(III), Gd(III)] suggests that the temperature of oxide phase formation is not influenced by the nature of the lanthanide. The oxide phase represents in all cases 16.50—17.00%. The X-ray diagram of the oxide residue resulted from thermal decomposition points to a phase mixture. Calcination of the sample for 4h at 700°C yields La_2NiO_4 as main product, together with NiO, La_2O_3 and $La(OH)_3$. In the case of Nd(III), the compound Nd_2NiO_4, together with traces of NiO and Nd_2O_3 are obtained. A thermal treatment of these samples, lasting 7h at 900°C, yields the pure phases La_2NiO_4 and Nd_2NiO_4 (Fig. 2).

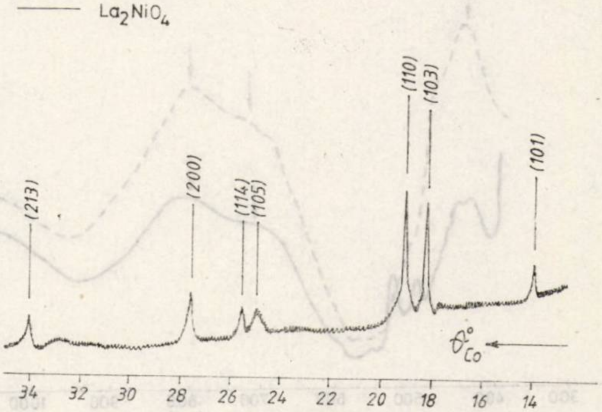

Fig. 2. — X-Ray diffraction pattern of La_2NiO_4.

The X-ray diagrams of Pr(III) and Gd(III) compounds obtained under similar conditions have evidenced only the mixture of component oxides.

Oxides of the Ln_2NiO_4 type assume a tetragonal or distorted K_2NiF_4 tetragonal structure.[5–7]

The oxide compounds obtained are black powders, slightly soluble in warm mineral acids. Their existence was evidenced through IR spectroscopy.

The IR spectra of double oxides differ from those of component oxides and therefore they may be used to identify them. Thus, the IR spectrum of the mixture of initial oxides ($NiO-Ln_2O_3$) exhibits characteristic maxima between 400 and 500 cm^{-1}. Mixed oxides of the Ln_2NiO_4 type exhibit — according to the literature — maxima between 600—660

cm^{-1}. In the IR spectrum of the mixed oxide La_2NiO_4 one band at 650 cm^{-1}, which was assigned to ν_{Ni-O} vibration, can be observed.

According to the literature the magnetic susceptibility of La_2NiO_4 obeys the Curie Weiss law at a higher temperature : the magnetic moment is $\mu_{eff} = 3.84$ MB and the Weiss constant is negative $\theta = -500$ K; this suggests a strong antiferromagnetic coupling in basal planes. Ganguly[5] has extended the measurements of magnetic susceptibility to the temperature of liquid He : $\mu_{eff} = 2.56$ MB and $\theta = -400$ K. The value of magnetic susceptibility determined in La_2NiO_4 sample at 298 K yielded $\mu_{eff} = 3.17$ MB. In Nd_2NiO_4 the susceptibility measured amounts to $\mu_{eff} = 5.19$ MB, lower than that calculated by summing up the moments of component oxides ($\mu_{eff} = 5.74-6.00$ MB), which suggests the existence of some antiferromagnetic interactions.

EXPERIMENTAL

Reagents were as follows: Ln_2O_3—99.9% (Mathey and Johnson); $Ni(NO_3)_2 \cdot H_2O$; benzylic acid (hydroxydiphenylacetic acid). For syntheses the lanthanide oxides were transformed in tonitrates. The mixed compounds were prepared in aqueous solution by treating the nitrate mixtures with a saturated benzylic acid solution. The precipitation of the complex compounds begins only after the addition of aqueous ammonia up to a pH = 7—8. After 24 hours, the precipitate is filtered, washed with water and acetone.

Elemental chemical analysis (C, H) was performed by microcombustion; Ni was determined by atomic absorption;

UV and visible spectra were recorded with a VSU—1 Zeiss Jena spectrophotometer, in the 249—980 nm range with MgO as standard;

IR spectra were recorded with a UR-10 Zeiss Jena spectrophotometer in KBr pellets;

Magnetic measurements, on solid samples were performed by the Faraday method, using Mohr salt as standard;

The differential thermal analyses were recorded with an MOM Budapest Paulik-Paulik-Erdey derivatograph.

REFERENCES

1. P. Spacu, S. Ploştinaru, L. Patron, A. Conţescu and E. Segal, *Rev. Roumaine Chim.*, **30**, 659 (1985).
2. P. Spacu, Ş. Ploştinaru, L. Patron, A. Conţescu and N. Stănică, *Rev. Roumaine Chim.*, **30**, 837 (1985).
3. C. Frasse, J. C. Trombe, A. Gleizes and J. Galy, *Compt. rend.*, **300**, 403 (1985).
4. P. Spacu, S. Ploştinaru, L. Patron, A. Conţescu, D. Crişan and N. Stănică, *Z. anorg. Chem.*, (in press).
5. P. Ganguly and C.N.R. Rao, *Mat. Res. Bull.*, **8**, 405 (1973).
6. J. B. Goodenough, *Mat. Res. Bull.*, **8**, 647 (1973).
7. M. Föex, *Compt. rend.*, **250**, 3027 (1960).

Revue Roumaine de Chimie, **32**, *3*, 255–261 (1987)

METAL- AND METAL(III)-AMINE SALTS OF THE $H_2[Pt(SCN)_4]$ AND $H_2[Pt(SCN)_6]$ ACIDS

I. GĂNESCU[a] and CS. VÁRHELYI[b]

[a] Faculty of Chemistry, University, 1100 - Craiova, str. Al. Ioan Cuza 13, Romania
[b] Faculty of Chemical Technology, University of Cluj-Napoca, 3400-Cluj-Napoca, str. Arany János 11, Romania

Received March 17, 1986

A number of 23 new cobalt(III)-amine salts of the $H_2[Pt(SCN)_4]$ and $H_2[Pt(SCN)_6]$ acids with monoacido-pentamine ($[Co(en)_2X(amine)]^{2+}$) and diacido-tetramine ($[Co(en)_2X_2]^+$, $[Co(DH)_2(amine)_2]^+$ type derivatives ("en"-ethylenediamine, DH_2 = dimethylglyoxime) were obtained and characterized. The derivatographic study of some transition metal salts (Cu, Ag, Hg, Pd) suggests that a linkage isomerisation process (Pt–SCN/Pt–NCS) may occur in the solid state, depending upon the nature of the external cation and temperature. The IR spectra of these salts compared with the analogous $M_3Cr(NCS)_6$ derivatives, show the presence of M′–NCS–M″ bridges in the solid state.

INTRODUCTION

The homogeneous thiocyanato-complexes of platinum : $[Pt(SCN)_4]^{2-}$ and $[Pt(SCN)_6]^{2-}$ are easily obtained by substitution reactions of $[PtCl_4]^{2-}$ and $[PtCl_6]^{2-}$ with KCNS or NH_4CNS.[1–3]. The free acids $H_2[Pt(SCN)_4]$ and $H_2[Pt(SCN)_6]$ can be also prepared from aqueous solutions of the lead and barium salts with an excess of diluted sulfuric acid[4,5] or by means of strong cation exchanger resins. The aqueous solutions of these dibasic acids evolve carbon dioxide from carbonates and hydrogen in the reaction with zinc metal. Some alkaline and transition metal salts of these acids have also been described. It is worth mentioning that the hydrochlorides of some heterocyclic amines and alkaloids (e.g. nicotine, codeine, sparteine, etc.) also form well defined crystalline salts with $H_2[Pt(SCN)_4]$ and $H_2[Pt(SCN)_6]$.[6] Spacu and Armeanu[7] reported some luteo- and purpureo-salts of this type, e.g. $[Co(NH_3)_6]_2[Pt(SCN)_6]_3$, $[Co(NH_3)_5Cl][Pt(SCN)]_6$.

It was observed that $[Pt(SCN)_6]^{2-}$ undergoes substitution reactions e.g. in reaction with NH_3 and pyridine, leading to a redox process: Pt(IV)→ → Pt(II) followed by the formation of *cis*-$[Pt(NH_3)_2(SCN)_2]$[8] and *cis*-$[Pt(Py)_2(SCN)_2]$[9] respectively.

RESULTS AND DISCUSSION

In the present paper a series of new cobalt(III) amine derivatives of the title complex acids are described. Besides the preparative work, the thermal behaviour of some transition metal salts (Cu, Ag, Hg, Tl) and of some cobalt(III)—amine derivatives and the IR spectra were studied.

We have observed, that cobalt(III) and chromium(III)-amines of different types : hexamines, monoacido-pentamines and diacido-teramines form well defined crystalline salts with $H_2[Pt(SCN)_4]$ and $H_2[Pt(SCN)_6]$. The solubility in water of the products is influenced by the charge of the cation and by the hydrophylic properties of the ligands. Generally, the solubility of thiocyanato platinites (II) – and platinates (IV) decreases in the order :

hexamines > monoacido pentamines > diacido-tetramines

A number of 23 new salts of the above mentioned class were obtained by double decomposition reactions. For these reactions some *cis*-$[Co(en)_2Cl(amine)]^{2+}$ type monoacido-pentamines and the following diacido-tetramines :$[Co(en)_2X_2]^+$, $[Co(pn)_2X_2]^+$ and $Co(DH)_2(amine)_2]^+$ were used.

As seen from tables 1 and 2, only neutral salts were obtained. Acidic salts of the types : Cation · $H[Pt(SCN)_4]$ and Cation.$H[Pt(SCN)_6]$ are not formed, either in the above mentioned conditions, or in acidic media (0.02 – 0.1 N H_2SO_4).

The new complexes are sparingly soluble in water, but are soluble in some organic polar solvents, e.g. acetone, dimethyl-formamide, dimethylsulphoxide, acetonitrile, etc. They decompose by heating with conc. HNO_3 and H_2SO_4.

The thermal behaviour of some cobalt(III)-amine derivatives of $H_2[Pt(SCN)_4]$ and $H_2[Pt(SCN)_6]$ was studied by derivatography. It was observed that the compounds are stable up to 180 – 230°C and decompose over this temperature, in some complex parallel and successive stages, with evolution of gaseous products, e.g. N_2, SO_2, NO, CO, CO_2, H_2O, amines, etc. in nonstoichiometrical ratios in a temperature range of 300 – 600°C (several exothermic peaks on the DTA curves). The residue at 800 – 850° is a stoichiometric mixture of Co_3O_4 + Pt. At 900 – 950°C another strong endothermic DTA peak appears corresponding to the Co_3O_4 – CoO transformation in all the studied cases. As compared to the thermal behaviour of the analogous tetranitro-platinites and hexanitroplatinates of the cobalt(III)-amines, the decomposition takes place much slower, without explosions.

The TG and DTA curves of Hg, Ag, Tl and Cu(I) salts of $H_2[Pt(SCN)_6]$ are presented in Fig. 1. These transition metal salts are anhydrous derivatives. The TG curves show no mass decrease up to 200 – 230°C. Over this temperature, up to 650 – 750°C the gradual decomposition of the platinum salts takes place. In air atmosphere 3 – 4 exothermic peaks appear on the DTA curves, corresponding to many oxidation processes. The end product of the pyrolysis of the mercury salt is metallic platinum ; a stoichiometric mixture : 2 Ag + Pt is formed in the case of the silver salt. The decomposition of $Tl_2[Pt(SCN)_6]$ leads to the formation of Tl_2O_3 + Pt

Table 1

New cobalt(III) amine salts of $H_2[Pt(SCN)_4]$ acid

No.	Formula	Shape and colour	Analysis		
			Calcd.		Found
1	*trans*-$[Co(pn)_2Cl_2]_2 \cdot A$	irregular green crystals	Co	11.93	11.84
			Pt	19.76	19.38
			N	17.00	16.88
2	*trans*-$[Co(en)_2Br_2]_2 \cdot A$	yellow-brown short prisms	Co	10.66	10.53
			Pt	17.66	17.38
			N	15.20	15.02
3	*trans*-$[Co(pn)_2(NCS)_2]_2 \cdot A$	red-brown irregular square prisms	Co	10.93	10.79
			Pt	18.10	17.99
			N	20.77	20.29
4	*cis*-$[Co(en)_2Cl(aniline)] \cdot A$	red-brown short prisms	Co	8.01	7.80
			Pt	26.56	26.19
			N	17.14	17.00
5	*cis*-$[Co(en)_2Cl(benzylamine)] \cdot A$	red-brown short prisms	Co	7.86	7.56
			Pt	26.06	25.90
			N	16.82	16.47
6	$[Co(DH)_2(NH_3)_2]_2 \cdot A$	yellow-brown dendrites	Co	10.93	10.62
			Pt	18.11	18.03
			N	20.78	20.59
7	$[Co(DH)_2(p\text{-phenetidine})_2]_2 \cdot A$	yellow-brown square prisms	Co	7.57	7.35
			Pt	12.53	12.35
			N	14.38	14.19
8	$[Co(DH)_2(m\text{-xylidine})_2]_2 \cdot A$	dark brown stars	Co	7.88	7.60
			Pt	13.06	12.89
			N	14.98	14.62
9	$[Co(DH)_2(m\text{-chloraniline})_2]_2 \cdot A$	yellow-brown rhombohedral plates	Co	7.73	7.48
			Pt	12.81	12.56
			N	14.70	14.59
10	$[Co(DH)_2(\alpha\text{-naphtylamine})_2]_2 \cdot A \cdot H_2O$	yellow-brown stars	Co	7.36	7.28
			Pt	12.20	11.95
			N	14.00	13.89
			H_2O	1.12	1.25
11	$[Co(DH)_2(aniline)_2]_2 \cdot A$	yellow-brown needles	Co	8.52	8.46
			Pt	14.13	13.98
			N	16.20	16.01

Table 2

New cobalt(III)-amine salts of the $H_2[Pt(CSN)_6]$ acid

No	Formula	Shape and colour	Analysis		
				Calcd.	Found
1	$[Co(pyridine)_4Cl_2]_2 \cdot B \cdot H_2O$	thick, brown tables	Co	8.00	7.82
			Pt	13.26	13.08
			N	13.31	13.10
			H_2O	2.44	2.08
2	*cis*-$[Co(en)_2Cl_2]_2 \cdot B$	short, brown prisms	Co	11.29	11.07
			Pt	18.70	18.39
			N	18.77	18.36
3	*cis*-$[Co(en)_2(NCS)_2]_2 \cdot B$	dark-yellow small prisms	Co	10.39	10.23
			Pt	17.21	16.95
			N	22.22	22.08
4	*trans*-$[Co(pn)_2Cl_2] \cdot B$	yellow-green needles	Co	10.71	10.24
			Pt	17.74	17.63
			N	17.81	17.59
5	*cis*-$[Co(en)_2Cl(benzylamine)] \cdot B$	red-brown irregular prisms	Co	6.81	6.48
			Pt	22.56	22.25
			N	17.80	17.66
6	*cis*-$[Co(en)_2Cl(aniline)] \cdot B$	red-brown tables	Co	6.92	6.77
			Pt	22.93	22.69
			N	18.09	17.86
7	*cis*-$[Co(en)_2Cl(p\text{-}toluidine)] \cdot B$	dark yellow microcrystals	Co	6.82	6.59
			Pt	22.59	22.30
			N	17.82	17.62
8	$[Co(DH)_2(NH_3)_2]_2 \cdot B \cdot H_2O$	yellow plates	Co	9.72	9.52
			Pt	16.10	15.97
			N	20.79	20.44
9	$[Co(DH)_2(m\text{-}xylidine)_2]_2 \cdot B$	yellow-brown needles	Co	7.31	7.18
			Pt	12.12	11.99
			N	15.64	15.29
10	$[Co(DH)_2\text{-}(m\text{-}toluidine)_2]_2 \cdot B$	red-brown square prisms	Co	7.58	7.29
			Pt	12.56	12.09
			N	16.21	16.02
11	$[Co(DH)_2(thiourea)_2]_2 \cdot B$	long, brown prisms	Co	8.24	8.62
			Pt	13.64	13.43
			N	21.53	21.19
12	$[Co(DH)_2(pyridine)_2]_2 \cdot B \cdot H_2O$	irregular cryst. aggregates	Co	8.07	7.92
			Pt	13.36	13.07
			N	17.25	17.20
			H_2O	1.23	1.03

"en" = ethylenediamine ; "pn" = 1,2-propylenediamine ;
"DH" = deprotonated dimethylglyoxime ; A = $[Pt(SCN)_4]^{2-}$; B = $[Pt(SCN)_6]^{2-}$

at 650°C. On the TG curve of $Cu_2[Pt(SCN)_6]$ $CuSO_4$ appears as intermediate product.

An interesting phenomenon can be observed on the DTA curves of the latter transition metal salts. Between 170 – 190°C appears a broad endothermal peak. This is, probably, due to a thiocyanato-isothiocyanato linkage isomerisation ($Pt-SCN \rightarrow Pt-NCS$), not influenced by the nature of the external cation. The same DTA peak temperature proves that no phase transition of the crystalline salts occurs.

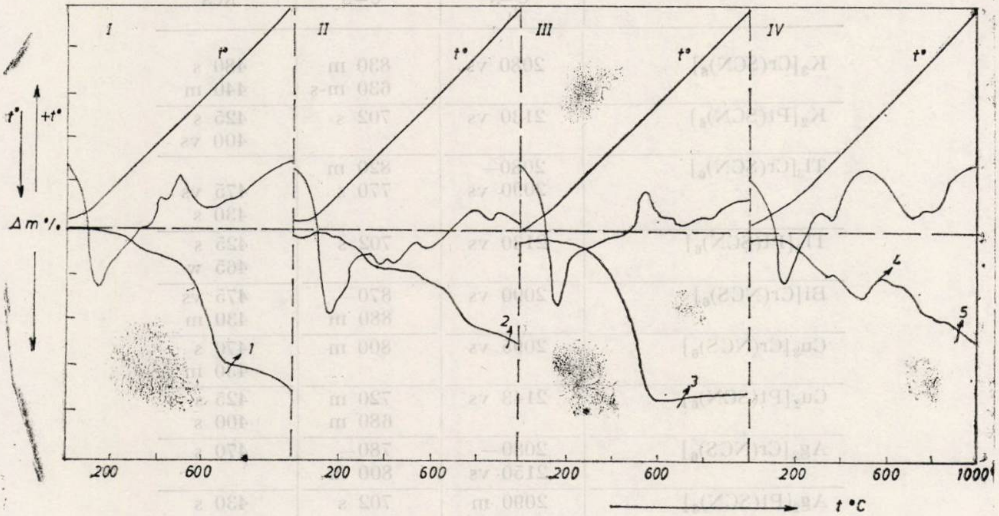

Fig. 1.—TG and DTA curves of some $M_2[Pt(SCN)_6]$ type salts : I. $Tl_2[Pt(SCN)_6]$, 1—$2Tl_2O_3+Pt$ II. $Ag_2[Pt(SCN)_6]$, 2—2 $Ag+Pt$; III. $Hg[Pt(SCN)_6]$, 3—2 Pt; IV. $Cu_2[Pt(SCN)_6]$, 4—2 $CuSO_4 + Pt$; 5—2 $CuO + Pt$.

The IR spectra of some $M_2[Pt(SCN)_6]$ salts were recorded in comparison with those of analogous $K_3[Cr(NCS)_6]$ derivatives.

Table 3

DTA peak temperature in the thermal decomposition of some $M_2[Pt(SCN)_6]$ type salts

Cation (M^{n+})	Endothermic peak	Exothermic peaks
Hg^{2+}	170–190°	400, 450, 550°
Cu^+	170–190°	350, 450, 600, 900°
Ag^+	170–190°	330, 550, 800, 900°
Tl^+	170–190°	300, 420, 470, 640, 700°

The characteristic NCS-frequencies of the studied complexes are presented in Table 4.

As shown, the $M_3[Cr(NCS)_6]$ complexes are isothiocyanato-derivatives with Cr-NCS bonding ($\nu_{C=N}$2060–2090 cm^{-1}). The $M_2[Pt(SCN)_6]$ salts are thiocyanato complexes with Pt-SCN bonding ($\nu C \equiv N$ over 2100

Table 4

Infrared spectral data of some $M_3[Cr(NCS)_6]$ and $M_2[Pt(SCN)_6]$ complexes

Compound	$\nu_{C \equiv N}$	ν_{C-S}	δ_{NCS}
$K_3[Cr(SCN)_6]$	2080 vs	830 m 630 m-s	480 s 440 m
$K_2[Pt(SCN)_6]$	2130 vs	702 s	425 s 400 vs
$Tl_3[Cr(SCN)_6]$	2080– 2090 vs	820 m 770 s	475 vs 430 s
$Tl_2[Pt(SCN)_6]$	2130 vs	702 s	425 s 465 w
$Bi[Cr(NCS)_6]$	2090 vs	870– 880 m	475 vs 430 m
$Cu_3[Cr(NCS)_6]$	2095 vs	800 m	470 s 430 m
$Cu_2[Pt(SCN)_6]$	2143 vs	720 m 680 m	425 s 400 s
$Ag_3[Cr(NCS)_6]$	2080– 2150 vs	780– 800 m	470 s
$Ag_2[Pt(SCN)_6]$	2090 m 2140 vs	702 s 630 m	430 s 460 w
$Pd_3[Cr(NCS)_6]_2$	2075 m 2130 s	800– 820 m	470 s
$Pd[Pt(SCN)_6]$	2115 s 2150 vs	700 m	430 s
$Hg_3[Cr(NCS)_6]_2$	2090 s 2120 vs	800 m	475 s 430 w
$Hg[Pt(SCN)_6]$	2125 vs 2186 vs	680 s	425– 430 s 460 w

vs = very strong, s = strong, m = medium, w = weak

cm^{-1}). In the case of the potassium and thallium salts only a single band appears in the mentioned wave number range. The Ag, Pd and Hg-salts of $H_2[Pt(SCN)_6]$ and $H_3[Cr(NCS)_6]$ exhibit an interesting feature, *i.e.* the splitting of the $\nu_{C \equiv N}$ vibration band. This means, the intermolecular $M-N^+ = C-S^- ..M^X$ bridging bonds appear in the crystalline state ($M = Cr, Pt$, $M^* = Hg, Pd, Ag$). A similar case was mentioned in the literature[10–12] in the IR spectrum of the mercury reineckate ($Hg[Cr(NCS)_4(NH_3)_2]_2$). One can assume that in the case of the $M_2[Pt(SCN)_6]$ complexes the formation of this bridging bond is due partially to a linkage isomerisation.

The $\nu_{C \equiv N}$ valence vibrations and the δ_{NCS} deformation vibration are not sensitive to the above mentioned behaviour.

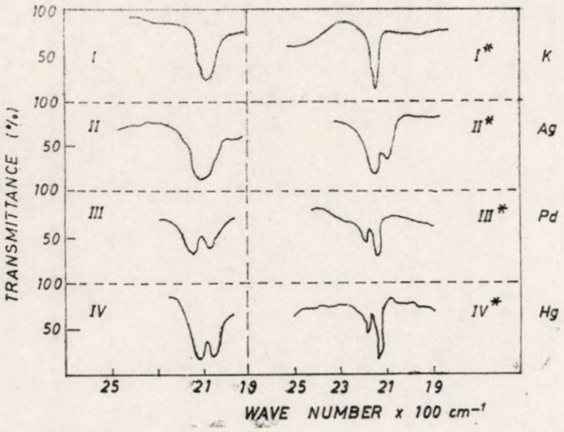

Fig. 2. — $\nu_{C\equiv N}$ stretching vibrations of some hexathiocyanatocomplexes: I. $K_3[Cr(NSC)_6]$; I^X — $Tl_2[Pt(SCN_6)]$; II. $Ag_3[Cr(NSC)_6]$; II^X — $Ag_2[Pt(SCN)_6]$; III. $Pd_3[Cr(NCS)_6]_2$; III^X — $Pd[Pt(SCN)_6]$; IV. $Hg_3[Cr(NSC)_6]_2$; IV^X — $Hg[Pt(SCN)_6]$.

EXPERIMENTAL

$K_2[Pt(SCN)_4]$ was obtained by the evaporation of a mixture of 1 mole $K_2[PtCl_4]$ and 4 moles of KCNS, in aqueous solution on a water bath. The crude product was recrystallized from alcohol.

$K_2[Pt(SCN)_6] \cdot 2H_2O$ was prepared by the evaporation of a mixture of 1 mole $K_2[PtCl_6]$ and 6 moles of KCNS solutions. The salt crystallizes in diamond brilliant thin, reddish-yellow plates. It is necessary to avoid the boiling of the mixture because of the formation of a resinous, insoluble material.

Tetrathiocyanato-platinites and hexathiocyanato-platinates of the cobalt(III)-amines

10 mmoles of the corresponding cobalt(III)-amine in 50—75 mL water or in dil. methano-(1 : 1) were treated with 3 mmoles $K_2[Pt(SCN)_4]$ or $K_2[Pt(SCN)_6]$ in 20—25 mL aqueous solution. After 30—60 min. the separated crystalline products were filtered off, washed with water and dried in air.

Analysis. The Co content was determined complexometrically after destruction of the samples with conc. H_2SO_4 and some crystals of KNO_3. Platinum was determined microgravimetrically as metallic platinum and nitrogen by means of the usual gasvolumetrical method.

Recovery od the platinum residues. The solutions of the platinum complexes and the solid residues were evaporated to dryness and calcinated at 800—900°C. The black porous mass was decomposed with. conc. H_2SO_4 and cryst. KNO_3 by boiling. After dilution with water the metallic platinum was filtered off from the violet solution of $CoSO_4$ formed.

The *IR spectra* were recorded in KBr pellets with a UR—20 Carl Zeiss Jena spectrophotometer.

The *thermal decomposition* of the complexes obtained was studied by means of a Derivatograph MOM Budapest up to 1000°C, with a heating rate of 20°/min. Sample weight : 100mg, atmosphere : static air. Reference material : α — Al_2O_3, Sample holder : platinum crucible.

REFERENCES

[1] G. B. Buckton, *Liebigs Ann. Chem.*, **92**, 286 (1854).

[2] G. B. Buckton. *J. prakt. Chem.*, **64**, 75 (1855).

[3] W. Peters, *Z. anorg. Chem.*, **77**, 18, 179 (1912).

[4] A. A. Grinberg, B. W. Ptizyn and W. N. Lavrentjev, *Zhur. fiz. Khim.*, **10**, 663 (1937).

[5] H. Grossmann, *Z. anorg. Chem.*, **37**, 437 (1903).

[6] J. Guareschi, *Giorn. Accad. Med. Torino*, **39**, 244 (1891).

[7] G. Spacu and V. Armeanu, *Bul. Soc. St. Cluj*, **7**, 614 (1933/34).

[8] A. A. Grinberg, *Z. anorg. Chem.*, **157**, 299 (1926).

[9] A. A. Grinberg. *Izvest. Akad. Nauk Sent. Platiny*, **6**, 122 (1928).

[10] M. Chamberlain and J. C. Bailar, *J. Amer. Chem. Soc.*, **81**, 6412 (1959).

[11] J. Chatt and L. A. Duncanson, *Nature*, **178**, 937 (1956).

[12] J. Fujita, K. Nakamoto and M. Kobayashi, *J. Amer. Chem. Soc.*, **78**, 3295 (1956).

Revue Roumaine de Chimie, 32, *3*, 263—269 (1987)

MAGNETO, SPECTRAL AND THERMAL STUDIES OF RARE EARTH NITRATE CHELATES OF N,N,N',N'-TETRAMETHYL THIURAM DISULPHIDE

R. K. AGARWAL[a], M. B. L. SHARMA[b]* and A. K. SRIVASTAVA[b]

[a] Department of Chemistry, Lajpat Rai Post-Graduate College, Sahibabad-201005, Ghaziabad, India

[b] Department of Chemistry, Meerut College, Meerut-250 001, India

Received December 20, 1985

A series of new complexes of rare earth nitrate of N,N,N',N'-tetramethyl thiuram disulphide (TMTDS) of the general composition $Ln(NO_3)_3 \cdot 2TMTDS$ were synthesized and characterized by elemental analyses, electrolytic conductivity, molecular weight, magnetic measurement, infrared and ^1H-NMR spectra. D.t.a. of the complexes were also investigated. In all the complexes TMTDS acts as a bidentate S—S chelating agent.

INTRODUCTION

Complexation of rare earth metals with various kinds of ligands has been the subject of interest for chemists in many diverse disciplines, both experimental and theoretical. Recently a large number of rare-earth compounds with oxygen and nitrogen donor ligands have been reported.[1-3] Comparatively very little is known about the complexes of sulphur donor ligands. The ligational behaviour of various sulphur donor ligands towards lanthanide ions viz. mercapto acid, [4,5] methyl 3-mercapto propionate, [6] furfuryl mercaptan, [7] 1-substituted tetrazaline 5-thiones,[8] thiosemicarbazide and thiosemicarbazone,[9] 2-thiopyridine N-oxide [10] and thiourea as well as substituted thioureas [11] is known. Trivedi[12] *et al.* have investigated the rare earth complexes of some multidentate sulphur containing ligands. Lanthanide complexes of N,N,N',N'-tetramethyl thiuram disulphide (TMTDS) have not been reported in the literature. It was therefore thought of interest to investigate the rare earth metal complexes of this ligand. The ligand of interest has four potential donor sites available for coordination to a metal ions but from steric considerations, it is expected to function either as a monodentate ligand coordinating through one of the thiocarbonyl sulphurs or as a bidentate ligand involving both the thiocarbonyl sulphurs.

---

* Author for correspondence.

EXPERIMENTAL

Materials

All the solvents and reagents were good quality products and were used as received. The ligand, an Aldrich Chemical Co. (U.S.A.) product was obtained and used as such.

Preparation of the complexes

A solution (25 mL) of lanthanide nitrate hexahydrate (1.0 mmole) in ethanol was mixed with 75 mL of an acetonic solution of the ligand (2.25 m mole) and refluxed for about 30 min. on water bath. The reaction mixture was concentrated on a water bath. After cooling the reaction mixture a precipitate was obtained, filtered, washed thoroughly with ethanol, acetone and finally with ether and dried over P_4O_{10} in a vacuum desiccator (yield $\sim 65\%$).

Physical measurements

Elemental analyses (C, H, N) were done at the C.D.R.I., Lucknow, while sulphur was estimated in the laboratory by Messenger's method. The metals were estimated as their oxides by direct combustion of complexes in platinum crucible as well as with standard EDTA method[13] using xylenol orange as indicator. The results from both the methods tallied within the experimental errors. Conductance measurements were carried out on a Toshniwal conductivity bridge type $CL^{01}/_{01}$ using a dip type cell in nitrobenzene. The molecular weight in freezing nitrobenzene was determined cryoscopically. The magnetic measurements were carried out at room temperature by Gouy's balance using anhydrous copper sulphate as a standard. The IR spectra of the complexes were recorded on a Perkin Elmer Infrared spectrophotometer model 521 in esI_2 in the range of 4000 – 200 cm^{-1}. Proton NMR spectra of the complexes and the ligand were recorded on a Varian T – 60 instrument using $CDCl_3$ as solvent. Differential thermal analyses were carried out on DTA-02 Universal (DDR) differential thermal analyser in air atmosphere and the heating rate was 10° min^{-1}.

RESULTS AND DISCUSSION

The interaction of rare earth nitrate with TMSDS results in the formation of complexes of the general composition, $Ln(NO_3)_3 \cdot 2TMTDS$ (Ln=La, Ce, Pr, Nd, Sm, Gd, Tb, Dy & Ho). The analytical data are given in Table 1. The compounds are non-hygroscopic, quite stable and can be stored for long periods: The compounds are fairly soluble in common organic solvents. The values of molar conductance of these complexes are low to account for any dissociation; these complexes may therefore be considered to be non-electrolytes. The molecular weight determinations are inconsistent with the same electrolytic nature of the complexes.

The magnetic moments of the rare earth complexes, recorded in Table 1, show little deviation from the Van Vleck values[14, 15] indicating thereby that 4*f* electrons do not participate in bond formation in these chelates. Thus, the magnetic moments of these complexes are within the range predicted and observed in the compounds of the lanthanide ions.[9,16]

Infrared spectra

Table 2 contains the partial IR bands of rare earth nitrato complexes of TMTDS and their assignments. These assignments were done by comparison with previously reported thiuram complexes.[17–20] The thiuram

Table 1

Analytical, magnetic and thermal data of TMTDS complexes of rare-earth nitrates

Compound	Found (Calcd.) %					Ω_m ohm^{-1} cm^2 mole^{-1}	Mol. Wt. Found (Calcd.)	$\mu_{eff.}$ B.M.	d.t.a. peak (°C)
	M	C	N	H	S				
$La(NO_3)_3 \cdot 2TMTDS$	17.32	17.96	12.42	3.06	32.10	5.89	798	Diamag.	310
	(17.26)	(17.88)	(12.17)	(2.98)	(31.80)		(805)		
$Ce(NO_3)_3 \cdot 2TMTDS$	17.51	17.97	12.29	3.09	31.62	4.76		2.62	—
	(17.38)	(17.86)	(12.15)	(2.97)	(31.75)		(806.12)		
$Pr(NO_3)_3 \cdot 2TMTDS$	17.41	17.98	12.39	3.12	31.96	4.98	803	3.62	315
	(17.47)	(17.84)	(12.14)	(2.97)	(31.72)		(807)		
$Nd(NO_3)_3 \cdot 2TMTDS$	17.67	17.97	12.28	3.09	31.84	4.99	804.62	3.61	320
	(17.80)	(17.77)	(12.09)	(2.96)	(31.59)		(810.24)		
$Sm(NO_3)_3 \cdot 2TMTDS$	18.72	17.86	12.19	3.08	31.68	5.06	811.92	1.56	330
	(18.41)	(17.63)	(12.00)	(2.93)	(31.35)		(816.35)		
$Gd(NO_3)_3 \cdot 2TMTDS$	19.32	17.59	12.21	3.06	31.42	5.08	819.30	7.84	340
	(19.10)	(17.49)	(11.90)	(2.91)	(31.09)		(823.25)		
$Tb(NO_3)_3 \cdot 2TMTDS$	19.42	17.69	11.61	2.86	30.91	6.06	820.16	9.21	350
	(19.27)	(17.45)	(11.87)	(2.90)	(31.03)		(825.00)		
$Dy(NO_3)_3 \cdot 2TMDS$	19.86	17.62	11.98	3.04	31.29	5.12	821.60	10.49	360
	(19.61)	(17.38)	(11.82)	(2.89)	(30.89)		(828.50)		
$Ho(NO_3)_3 \cdot 2TMTDS$	19.67	17.49	11.91	2.67	30.69	5.96	822.51	10.46	370
	(19.85)	(17.32)	(11.79)	(2.88)	(30.80)		(831.00)		

complexes possess four important bands in the region of 1500 – 800 cm^{-1}, a strong band at *ca.* 1500 cm^{-1} called "the thioureide band"; a band located at *ca.* 1280 – 1240 cm^{-1} due to the C – N vibration of the alkyl group; a band at 1000 – 970 cm^{-1} which corresponds to the C = S stretching mode, and a weak band at 860 – 820 cm^{-1} due to the C – S stretching mode.

Table 2

Pertinent IR spectral data (cm^{-1}) of tripositive rare-earth nitrate complexes of tetramethyl-thiuram-disulphide

Complex	$\nu(C\overset{\cdots}{-}N)$	$\nu(C_2-N)$	$\nu(C=S)$	$\nu(C-S)$	$\nu(M-S)$
TMTDS	1480(s)	1230(s)	960(s) 940(sh)	840(s)	—
La(NO$_3$)$_3$·2TMTDS	1538(s,br)	1245(m)	980(m)	890(w)	335(m)
Ce(No$_3$)$_3$·2TMTDS	1510(s)	1250(m)	970(m)	880(w)	340(m)
Pr(NO$_3$)$_3$·2TMTDS	1520(s)	1255(m)	975(m)	890(w)	340(m)
Nd(NO$_3$)$_3$·2TMTDS	1525(s)	1260(m)	975(m)	885(w)	315(m)
Sm(NO$_3$)$_3$·2TMTDS	1535(s)	1248(m)	975(m)	890(w)	315(m)
Gd(NO$_3$)$_3$·2TMTDS	1525(s)	1250(m)	982(m)	885(w)	325(m)
Tb(NO$_3$)$_3$·2TMTDS	1525(s,br)	1245(m)	980(m)	890(w)	330(m)
Dy(NO$_3$)$_3$·2TMTDS	1530(s)	1245(m)	982(m)	885(w)	335(m)
Ho(NO$_3$)$_3$·2TMTDS	1532(s)	1250(m)	978(m)	890(w)	330(m)

The frequency of the thioureide band is assigned to the $C\overset{\cdots}{-}N$ stretching mode since its value is intermediate between a C – N stretching frequency (1350 – 1250 cm^{-1}) and a C = N stretching frequency (1690 – 1640 cm^{-1}). The increase of the frequency of the thioureide band results from an increase in the double bond character of the C – N bond. This increase must be followed by a decrease in double bond character of the C = S bond as a result of the electron-donating properties of the ligand.

In far infrared region $\nu(M-S)$ vibrations further confirm the S-linkage to the metal ions in the complexes. In these complexes a $\nu(M-S)$ has been assigned in the region 340 – 310 cm^{-1}.[10]

The infrared frequencies of nitrato absorptions are presented in Table 3. In the present studies the non-electrolytic behaviour of TMTDS-nitrato complexes in nitrobenzene suggests that all the nitrate groups are covalently bound, this being confirmed by the absence of a band at 1350 cm^{-1} attributed to ionic nitrate.[21] Five bands attributed to the nitrate ions were observed for the corresponding complexes, indicating that these ions are coordinated to the tripositive lanthanides. The splittings observed for ν_4, ν_1 and ν_2 are attributed to solid effects. It is presumed that in complexes of the type described herein the nitrato group is bidentate if there is no evidence of the contrary. Such evidence (apart from X-ray evidence) might be (a) based on the occurrence of two types of nitrato groups IR spectra or (b) based on the apparent occurrence of an unreasonably high coordination number. The nitrato group IR absorptions of the complexes described herein show no indication of the existence of two types of coordination. Based on the previous observations[22,23] assuming that the nitrato groups are bidentate, the resulting probable coordination number is ten [3] in all the nitrato complexes. The coordination number is not unreasonably high having regard to the compact nature of the bidentate nitrato groups and the occurrence of the 12-coordinated cerous ion in $Ce(NO_3)_6^{3-}$.[24,25]

Table 3

IR frequencies (cm^{-1}) of the NO_3 ion

Compound	ν_4	ν_1	ν_2	ν_6	ν_3	ν(M—O) (Nitrato)
$La(NO_3)_3 \cdot 2TMTDS$	1510s	1315s	1035s 1025s	820s	735sh 730s	450w
$Ce(NO_3)_3 \cdot 2TMTDS$	1510s	1310s	1035s 1025sh	815s	740s	445w
$Pr(NO_3)_3 \cdot 2TMTDS$	1505s	1315s	1040s 1025s	815s	740s	440sh
$Nd(NO_3)_3 \cdot 2TMTDS$	1515s	1320s	1030s	820s	745s	450sh
$Sm(NO_3)_3 \cdot 2TMTDS$	1515sh 1500s 1480s	1315s	1030s 1020m 1020m	810s	735m	445m
$Gd(NO_3)_3 \cdot 2TMTDS$	1510sh 1500s 1485m	1310s	1035s 1025s	815s	740s	450m
$Tb(NO_3)_3 \cdot 2TMTDS$	1505s 1490m	1310s 1290sh	1040s 1025s	810s	735s	445w
$Dy(NO_3)_3 \cdot 2TMTDS$	1510s 1485sh	1320s 1290m	1035s 1025sh	820s	740s	450sh
$Ho(NO_3)_3 \cdot TMTDS$	1515s 1495sh	1305s 1285sh	1030s	815s	735s	450s

^{1}H-NMR spectra of some of the representative complexes have been recorded and data are tabulated in Table 4. ^{1}H-NMR spectra of the lingand show four peaks due to methyl protons with chemical shifts (δ) between 2.81—3.82 ppm. These four peaks are also present in ^{1}H-NMR spectra of these complexes. The change in intensity of the peaks of methyl protons and their upward shift may be due to the S—S chelation of the ligand.

Thermal studies

The thermal behaviours of TMTDS complexes of some metal ions have been studied to a limited extent.[26,27]

In the present studies, the differential thermal studies of tripositive lanthanide complexes of TMTDS have been discussed. There is no peak around 100°C clearly indicating that there is no water molecule either in coordination sphere or outside the sphere. These complexes decomposed endothermally in the 310—370°C temperature range (Table 1). At this stage all the ligand molecules are lost and finally at *ca.* 530°C, the end product is a mixture of M_2O_3 and M_2S_3. On the basis of decomposition temperature, the thermal stability of lanthanide-(III) complexes falls in the order :

$$Ho > Dy > Tb > Gd > Sm > Nd > Pr > La$$

Table 4

^{1}H-NMR spectral data of TMTDS and its complexes

Compound	Chemical shift (δ)	τ
TMTDS	2.81 3.25 3.49 3.58	7,19 6.75 6.51 6.42
$La(NO_3)_3 \cdot 2TMTDS$	2.92 3.24 3.48 3.82	7.08 6.76 6.54 6.18
$Pr(NO_3)_3 \cdot 2TMTDS$	2.88 3.25 3.64 3.69	7.12 6.75 6.36 6.31
$Sm(NO_3)_3 \cdot 2TMTDS$	2.91 3.24 3.65 3.79	7.06 6.76 6.41 6.20
$Gd(NO_3)_3 \cdot 2TMTDS$	2.91 3.26 3.65 3·81	7.09 6.71 6.54 6.21
$Dy(NO_3)_3 \cdot 2TMTDS$	2.89 3.26 3.51 3.90	7.10 6.76 6.55 6.21

REFERENCES

[1] T. Moeller, D. F. Martin, L. C. Thompson, R. Ferrus, G. R. Feistel and W. J. Randall, *Chem. Rev.*, **1**, 65 (1965).

[2] D. G. Karraker, *J. Chem. Educ.*, **47**, 424 (1970).

[3] J. H. Forsberg, *Coord. Chem. Revs.*, **10**, 195 (1973).

[4] L. S. Bear, G. R. Choppin and J. V. Quagliano, *J. Inorg. Nuclear Chem.*, **24**, 1601(1962).

[5] L. S. Bear, G. R. Choppin and J. V. Quagliano, *J. Inorg. Nuclear Chem.*, **25**, 593 (1963).

[6] R. S. Saxena and S. S. Sheelwant, *J. Inorg. Nuclear Chem.*, **35**, 1973 (1973).

[7] R. S. Saxena and S. K. Bhatia, *J. Inorg. Nuclear Chem.*, **37**, 309 (1975).

[8] Lakshmi and U. Agarwala, *J. Inorg. Nuclear Chem.*, **34**, 2255 (1972).

[9] M. C. Jain, R. K. Sharma, A. K. Srivastava and P. C. Jain, *J. Inorg. Nuclear Chem.*, **41**, 1305 (1979).

[10] D. X. West and C. A. Frank, *J. Inorg. Nuclear Chem.*, **41**, 49 (1979).

[11] M. B. Adi and A. S. R. Murty, *Current Sci.* (India), **47**, 539 (1978).

[12] C. P. Trivedi, O. P. Sunar and S. Tak, *Indian J. Chem.*, **10**, 1108 (1972).

[13] F. J. Welcher, "The analytical use of EDTA", Van Nostrand, New York, vol. 4, 1965.

[14] D. M. Yost, H. Russel and C. S. Garner, "The rare-earth elements and their compounds", Chp. 2, Wiley, New York, 1947.

[15] A. K. Garga, Thesis, Meerut University (India), 1975.

[16] N. M. Karayannis, C. M. Mikulski, L. L. Pytlewski and M. M. Labeş, *J. Less-Common Metals* **20**, 29 (1970).

[17] G. Contreras and H. Cortes, *Inorg. Nucl. Chem. Letters*, **6**, 225 (1970).

[18] G. Contreras and H. Cortes, *Inorg. Nucl. Chem. Letters*, **6**, 639 (1970).

[19] G. Contreras and H. Cortes, *J. Inorg. Nucl. Chem.*, **33**, 1337 (1971).

[20] C. F. Barrientos and J. G. Contreras, *A. Quim.*, **75**, 245 (1979).

[21] Soundararajan, *Proc. Chem. Symp.*, **1**, 203 (1970).

[22] D. R. Cousin and F. A. Hart, *J. Inorg. Nuclear Chem.*, **29**, 1745 (1967).

[23] D. R. Cousin and F. A. Hart, *J. Inorg. Nuclear Chem.*, **29**, 2965 (1967).

[24] M. D. Lind, B. Lee and J. L. Hoard, *J. Amer. Chem. Soc.*, **87**, 1611 (1965).

[25] A. Zalkin, J. D. Forrester and D. M. Templeton, *J. Chem. Phys.*, **39**, 2881 (1963).

[26] A. K. Srivastava, Veena Kapur and R. K. Agarwal, *Nat. Acad. Sci. Letters*, **4**, 361 (1981).

[27] A. K. Srivastava and R. K. Agarwal, *Thermochim. Acta*, **68**, 121 (1983).

Revue. Roumaine de Chimie, **32**, 3, 271–294 (1987)

CHEMICAL GRAPHS. PART 47.[1]

VALENCE ISOMERS OF [14]ANNULENE

ALEXANDRU T. BALABAN and CĂLIN DELEANU
Polytechnic Institute, Organic Chemistry Department, Splaiul Independenței 313, 76206 Bucharest, Roumania

Received October 10, 1986

All possible constitutional formulas for valence isomers of [14]annulene, represented by planar cubic graphs on 14 vertices, have been obtained by using a newly devised algorithm and a computer program. Isomorphism was eliminated by a subroutine based on the topological index *J′*, and another subroutine was used for listing cycles in each graph in order to obtain a unique notation for each of the 2140 constitutional valence isomers $(CH)_{14}$. The seven known valence isomers are indicated, mentioning briefly syntheses and interconversions.

INTRODUCTION

Previous papers have given a graph-theoretical definition for valence-isomers (as those hydrogen-depleted graphs which have the same partition of vertex degrees) and for constitutional valence-isomers of annulenes (as connected planar cubic multigraphs).[2,3] Graph-theoretical background information is available in papers [1-4] and books,[5,6] and will not be repeated here. By means of a constructive algorithm based on general graphs, all possible constitutional formulas for valence isomers of [*n*]annulenes where $n = 4-10$, [3,7] and 12, [8,9] were displayed. For avoiding trivial names and the cumbersome Baeyer-IUPAC notation of polycyclic systems, we adopted a notation formed by a string of integers $n-\beta-t-q-p-h-s$ indicating, in order, the numbers *n* of CH groups, β of double bonds and 3-, 4-, 5-, 6-circuits; the final number, *s*, is a serial integer number starting with 1, in case the previous numbers are the same for two or more graphs. Criteria for assigning non-arbitrarily serial numbers were listed previously.[10] In the present paper, we shall omit the number $n = 14$ from the notation, for simplification.

A different computer program enumerates connected and disconnected general cubic graphs.[11] We developed an algorithm for eliminating the chemically meaningles disconnected graphs, but so far no simple algorithm exists for enumerating non-planar or planar graphs. Chemically meaningful constitutional valence isomers of annulenes must be planar and connected. Comparison between the earlier ennumeration, *via* construction of structures, and numerical results *via* the latter program, gave full agreement for $n = 4, 6, 8, 10$, and 12.[11]

So far, no complete enumeration or construction of cubic multigraphs $(CH)_{14}$ exists. However, graph theoretical data exist for simple cubic graphs with $n = 14$ (no double bonds). This fact enabled us to simplify in the present paper the initial algorithm so as to allow the construction of cubic multigraphs with 14 vertices based on the cubic simple graphs and multigraphs with fewer vertices.

The problem of valence isomers of $[n]$annulenes is of fundamental importance for organic chemistry. The first valence isomer of an annulene, bitropyl $(CH)_{14}$, synthesized by Doering and Knox in 1957,[12] corresponds to a separable graph, i.e. to a graph which becomes disconnected by removing one edge. The first non-separable valence isomer of an annulene is Nenitzescu's hydrocarbon $(CH)_{10}$ prepared in 1960.[13] Later, the valence isomers of benzene were all explored and many of the possible valence isomers $(CH)_8$ and $(CH)_{10}$ were obtained. Some of these have extraordinary properties, e.g. semibullvalene and bullvalene which undergo degenerate rearrangements (automerizations, topomerizations). Several reviews of these valence isomers were published,[14,15] one in book form.[16] Interestingly, although the numbers of valence isomers $(CH)_{12}$, $(CH)_{14}$, etc. increase faster than exponentially with increasing n values, the known compounds are fewer and fewer for $n \geqslant 10$. Steric strain is smaller (on the average) for molecules with larger n values, therefore there exists a large unexplored field as a challenge for synthetic organic chemists.

ALGORITHMS AND COMPUTER PROGRAMS

The 133 structures of simple planar graphs on 14 vertices can be obtained from the comprehensive list published by Khvorostov;[17] all have $\beta = 0$.

Because we are interested only in generating valence isomers $(CH)_{14}$ with at least one double bond $(1 \leqslant \beta \leqslant 7)$, we shall use an algorithm which reduces the redundancy of generated graphs, leading to fewer isomorphic structures. This new algorithm no longer uses general graphs (which gave rise to non-planar graphs among the generated graphs), but only simple graphs and multigraphs $(CH)_{12}$.

There are two conversions of a $(CH)_{n-2}$ graph into a $(CH)_n$ multigraph with $\beta \geqslant 1$:

Conversion 1: two new vertices are created on any single line (edge) or on one line of a double bond, and these vertices are joined by a double bond, Fig. 1.

Conversion 2: a double bond together with its endpoints is replaced by a vertex linked to a cyclopropenyl residue, Fig. 2.

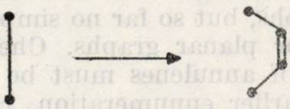

Fig. 1. — Conversion 1 applied to single bond.

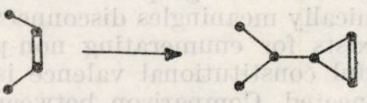

Fig. 2. — Conversion 2 applied to a double bond.

Conversion 1 was applied to all planar cubic graphs on 12 vertices, but conversion 2 was applied only to 12-vertex graphs having one double bond (disregarding double bonds in cyclopropenyl groups) because the graphs with cyclopropenyl groups which would result otherwise can be obtained by means of conversion 1; moreover, even for 12-vertex graphs having one double bond, it makes no sense in applying conversion 2 to a cyclopropenyl residue since the resulting vinylenecyclopropenyl derivative can also be obtained *via* conversion 1.

These two operations on the 357 connected planar graphs with 12 vertices were implemented by means of a computer program. The input data included information on the symmetry of each graph, in order to apply conversions 1 and 2 only once when more than one edge or double bond were equivalent by symmetry.

To eliminate all redundancies from the resulting 14-vertex multigraphs, were needed to screen these graphs for isomorphism. We conjectured that the highly discriminating topological index J',[18] related to the average distance sum connectivity J,[19] can serve for the purpose of finding and discarding isomorphic graphs. By definition:

$$J' = \sum_{\text{edge } ij} (s_i s_j)^{-\frac{1}{2}}$$

and the distance sum s_i is the sum of topological distances from vertex i to all other vertices in the graph, i.e. the sum over column i or row i in the distance matrix of the hydrogen-depleted cubic graph of order 14. For acyclic graphs $J' = J/q$, where q is the number of edges.[18-19]

Input data for each graph include the numbers of vertices and edges (14 and 21, respectively, in all cases), adjacencies, and the non-equivalent edges of the graph. A double bond is counted as two edges; the topological distance between two singly-connected vertices is 1, but between two doubly-connected vertices is considered to be 0.5. Thus the distance sums for the three isomeric methyl-1-pentenes (**1**—**3**) and the indices J' may be calculated as examples, as shown by Figure 3.

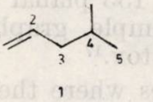

1

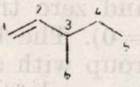

2

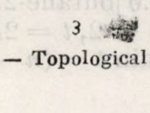

3

	1	2	3	4	5	6	s_i	J
1	0	0.5	1.5	2.5	3.5	3.5	11.5	
2	0.5	0	1	2	3	3	9.6	
3	1.5	1	0	1	2	2	7.5	0.5421
4	2.5	2	1	0	1	1	7.5	
5	3.5	3	2	1	0	2	11.5	
6	3.5	3	2	1	2	0	11.5	
1	0	0.5	1.5	2.5	3.5	2.5	10.5	
2	0.5	0	1	2	3	2	8.5	
3	1.5	1	0	1	2	1	6.5	0.5592
4	2.5	2	1	0	1	2	8.5	
5	3.5	3	2	1	0	3	12.5	
6	2.5	2	1	2	3	0	10.5	
1	0	0.5	0.5	2.5	3.5	1.5	9.5	
2	0.5	0	1	2	3	1	7.5	
3	1.5	1	0	1	2	2	7.5	0.5388
4	2.5	2	1	0	1	3	9.5	
5	3.5	3	2	1	0	4	13.5	
6	1.5	1	2	3	4	0	11.5	

Fig. 3. — Topological indices J' for the three isomeric 4-, 3-, and 2-methyl-1-pentenes, **1**—**3**.

A subroutine of the program takes care of checking J' and rejecting new graphs if they have a J' identical to one existing already within the file. It should be mentioned that topological indices J and J' do give degeneracy for certain classes of cyclic graphs with $n \geqslant 8$ and of acyclic graphs with $n \geqslant 12$ vertices,[20] but no such case was encountered for cubic multigraphs with $n \leqslant 12$ vertices. It is unknown if there is any case of accidental degeneracy for cubic multigraphs with $n = 14$ vertices; if there is, then the actual number of valence isomers of [14]annulene will be higher than that reported in the present paper.

A separate subroutine implements an earlier computer program and calculates all cycles with 2–6 vertices for each graph on the file;[21] the string of these cycle numbers serves for ordering the graphs. When all numbers in the string are the same for two or more graphs, a sixth (serial) number s discriminates among these graphs; otherwise this serial number is 1.

NUMBERS OF VALENCE ISOMERS

Tables 1–6 present the constitutional planar graphs of valence isomers $(CH)_{14}$ grouped according to increasing numbers β of double bonds, together with their notation (minus the initial number $n = 14$ throughout the series). The notation for separable graphs is enclosed in brackets; such graphs corresponds to legitimate valence isomers and have the advantage of an easy entry into the $(CH)_n$ valence-isomer field (only one C–C bond needs to be formed, in homo- or heterolytic reactions, unlike cycloadditions yielding non-separable graphs), but their reactions, interconversions and relationships to other valence isomers are poorer than for non-separable graphs. Drawings emphasize the graph-theoretical planarity. No consideration of stereoisomerism was taken into account, therefore the actual numbers of isomers are larger than those discussed below.

Numbers of constitutional valence isomers of [n]annulenes, grouped according to the numbers β of double bonds and t of three-membered circuits are presented in Table 7 for $n = 4$ to 14. The 133 planar graphs with $n = 14$ and $\beta = 0$ have been selected from the simple graphs with $n = 14$ (planar and non-planar) displayed by Khvorostov.[17]

We shall discuss in the following only the cases where there is a unique graph for a given pair of β and t values. Evidently, the [n]annulenes form such a group with $\beta = n/2$ double bonds and zero triangles (the bottom numbers 1 in the first column headed $t = 0$). The bottom numbers 1 in the column headed $t = 2$ form another group with a polyenic chain of k double bonds ($k = 0, 1, 2, \ldots$) and two cyclopropenyl end groups; for this group with $t=2$, we have $n = 6 + 2k$ and $\beta = k + 2$ double bonds, therefore $\beta = (n - 2)/2$. Another group has no double bonds ($\beta = 0$) and consists of a cycle grouping k bicyclo[1.1.0]butane-2,4-diyl units, where $k = 1, 2, \ldots$; in this case, $n = 4k$ and $t = 2k$, therefore $t = n/2$. A last group has a chain of k bicyclo[1.1.0]butane-2,4-diyl groups with two cyclopropenyl end groups; in this case, $\beta = 2$, $t = 2k + 2$, and $n = 4k + 6$; by eliminating $k = 0, 1, 2, \ldots$, we obtain $t = (n - 2)/2$.

Table 1

Connected planar cubic graphs of order 14 with $\beta = 0$, i.e. constitutional valence isomers $(CH)_{14}$ with no double bonds.

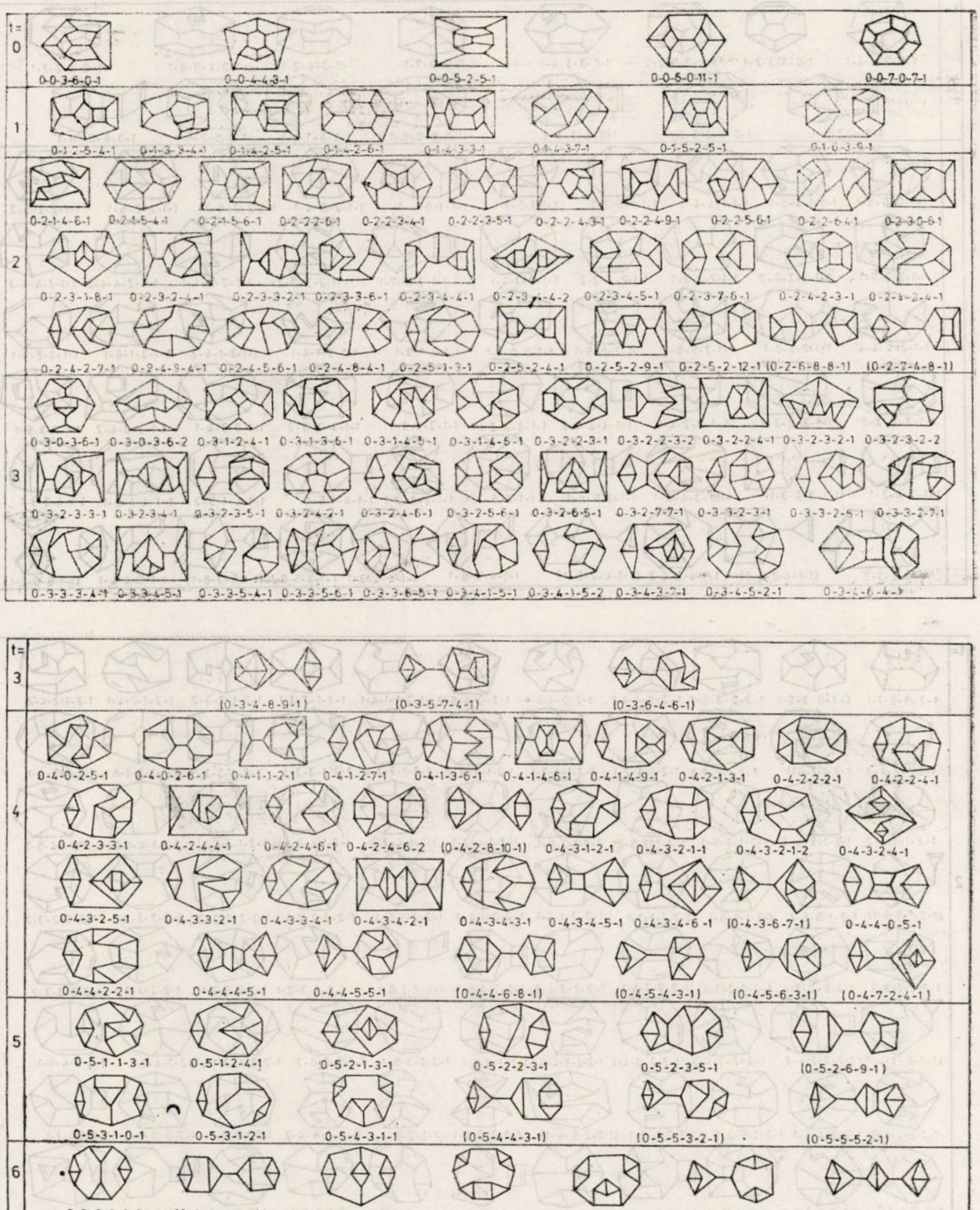
t=
0
0-0-3-6-0-1
0-0-4-4-3-1
0-0-5-2-5-1
0-0-6-0-11-1
0-0-7-0-7-1
1
0-1-2-5-4-1
0-1-3-3-4-1
0-1-4-2-5-1
0-1-4-2-6-1
0-1-4-3-3-1
0-1-4-3-7-1
0-1-5-2-5-1
0-1-6-3-9-1
2
0-2-1-4-6-1
0-2-1-5-4-1
0-2-1-5-6-1
0-2-2-2-6-1
0-2-2-3-4-1
0-2-2-3-5-1
0-2-2-4-3-1
0-2-2-4-9-1
0-2-2-5-6-1
0-2-2-6-4-1
0-2-3-0-6-1
0-2-3-1-8-1
0-2-3-2-4-1
0-2-3-3-2-1
0-2-3-3-6-1
0-2-3-4-4-1
0-2-3-4-4-2
0-2-3-4-5-1
0-2-3-7-6-1
0-2-4-2-3-1
0-2-4-2-4-1
0-2-4-2-7-1
0-2-4-3-4-1
0-2-4-5-6-1
0-2-4-8-4-1
0-2-5-1-3-1
0-2-5-2-4-1
0-2-5-2-9-1
0-2-5-2-12-1
(0-2-6-8-8-1)
(0-2-7-4-8-1)
3
0-3-0-3-6-1
0-3-0-3-6-2
0-3-1-2-4-1
0-3-1-3-6-1
0-3-1-4-5-1
0-3-1-4-5-1
0-3-2-2-3-1
0-3-2-2-3-2
0-3-2-2-4-1
0-3-2-3-2-1
0-3-2-3-2-2
0-3-2-3-3-1
0-3-2-3-4-1
0-3-2-3-5-1
0-3-2-4-2-1
0-3-2-4-6-1
0-3-2-5-6-1
0-3-2-6-5-1
0-3-2-7-7-1
0-3-3-2-3-1
0-3-3-2-5-1
0-3-3-2-7-1
0-3-3-3-4-1
0-3-3-4-5-1
0-3-3-5-4-1
0-3-3-5-6-1
0-3-3-6-5-1
0-3-4-1-5-1
0-3-4-1-5-2
0-3-4-3-7-1
0-3-4-5-2-1
0-3-4-6-4-1
t=
3
(0-3-4-8-9-1)
(0-3-5-7-4-1)
(0-3-6-4-6-1)
4
0-4-0-2-5-1
0-4-0-2-6-1
0-4-1-1-2-1
0-4-1-2-7-1
0-4-1-3-6-1
0-4-1-4-6-1
0-4-1-4-9-1
0-4-2-1-3-1
0-4-2-2-2-1
0-4-2-2-4-1
0-4-2-3-3-1
0-4-2-4-4-1
0-4-2-4-6-1
0-4-2-4-6-2
(0-4-2-8-10-1)
0-4-3-1-2-1
0-4-3-2-1-1
0-4-3-2-1-2
0-4-3-2-4-1
0-4-3-2-5-1
0-4-3-3-2-1
0-4-3-3-4-1
0-4-3-4-2-1
0-4-3-4-3-1
0-4-3-4-5-1
0-4-3-4-6-1
(0-4-3-6-7-1)
0-4-4-0-5-1
0-4-4-2-2-1
0-4-4-4-5-1
0-4-4-5-5-1
(0-4-4-6-8-1)
(0-4-5-4-3-1)
(0-4-5-6-3-1)
(0-4-7-2-4-1)
5
0-5-1-1-3-1
0-5-1-2-4-1
0-5-2-1-3-1
0-5-2-2-3-1
0-5-2-3-5-1
(0-5-2-6-9-1)
0-5-3-1-0-1
0-5-3-1-2-1
0-5-4-3-1-1
(0-5-4-4-3-1)
(0-5-5-3-2-1)
(0-5-5-5-2-1)
6
0-6-2-0-0-1
(0-6-2-4-8-1)
0-6-3-0-0-1
0-6-3-2-1-1
0-6-3-2-2-1
(0-6-5-2-0-1)
(0-6-7-4-0-1)

Table 2

Connected planar cubic multigraphs of order 14 with $\beta = 1$, i.e. constitutional valence isomers $(CH)_{14}$ with one double bond.

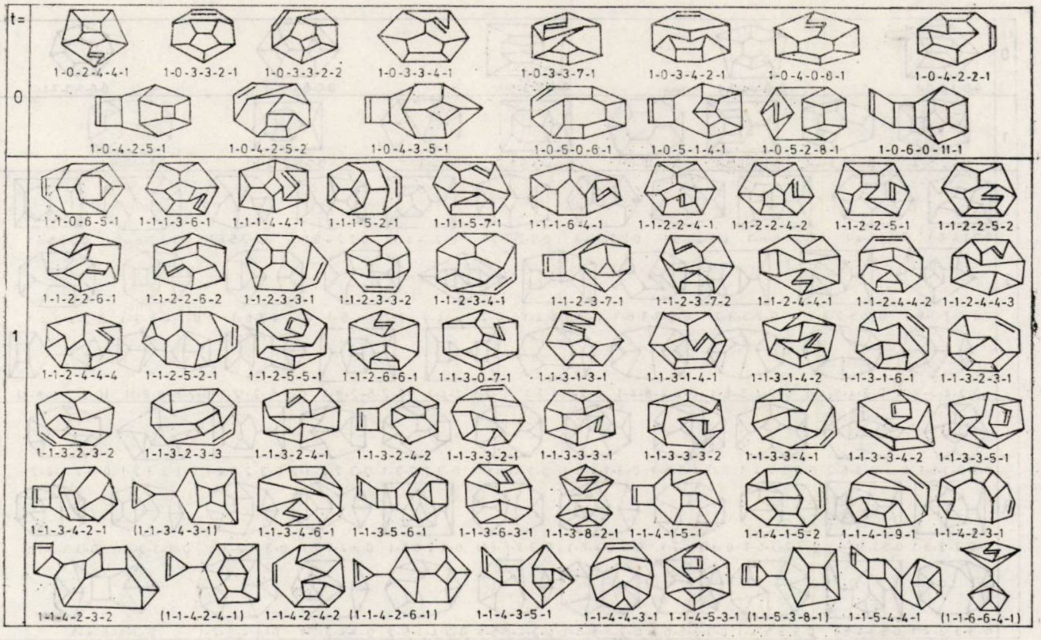
t=
0
1-0-2-4-4-1
1-0-3-3-2-1
1-0-3-3-2-2
1-0-3-3-4-1
1-0-3-3-7-1
1-0-3-4-2-1
1-0-4-0-8-1
1-0-4-2-2-1
1-0-4-2-5-1
1-0-4-2-5-2
1-0-4-3-5-1
1-0-5-0-6-1
1-0-5-1-4-1
1-0-5-2-8-1
1-0-6-0-11-1
1
1-1-0-6-5-1
1-1-1-3-6-1
1-1-1-4-4-1
1-1-1-5-2-1
1-1-1-5-7-1
1-1-1-6-4-1
1-1-2-2-4-1
1-1-2-2-4-2
1-1-2-2-5-1
1-1-2-2-5-2
1-1-2-2-6-1
1-1-2-2-6-2
1-1-2-3-3-1
1-1-2-3-3-2
1-1-2-3-4-1
1-1-2-3-7-1
1-1-2-3-7-2
1-1-2-4-4-1
1-1-2-4-4-2
1-1-2-4-4-3
1-1-2-4-4-4
1-1-2-5-2-1
1-1-2-5-5-1
1-1-2-6-6-1
1-1-3-0-7-1
1-1-3-1-3-1
1-1-3-1-4-1
1-1-3-1-4-2
1-1-3-1-6-1
1-1-3-2-3-1
1-1-3-2-3-2
1-1-3-2-3-3
1-1-3-2-4-1
1-1-3-2-4-2
1-1-3-3-2-1
1-1-3-3-3-1
1-1-3-3-3-2
1-1-3-3-4-1
1-1-3-3-4-2
1-1-3-3-5-1
1-1-3-4-2-1
(1-1-3-4-3-1)
1-1-3-4-6-1
1-1-3-5-6-1
1-1-3-6-3-1
1-1-3-8-2-1
1-1-4-1-5-1
1-1-4-1-5-2
1-1-4-1-9-1
1-1-4-2-3-1
1-1-4-2-3-2
(1-1-4-2-4-1)
1-1-4-2-4-2
(1-1-4-2-6-1)
1-1-4-3-5-1
1-1-4-4-3-1
1-1-4-5-3-1
(1-1-5-3-8-1)
1-1-5-4-4-1
(1-1-6-6-4-1)

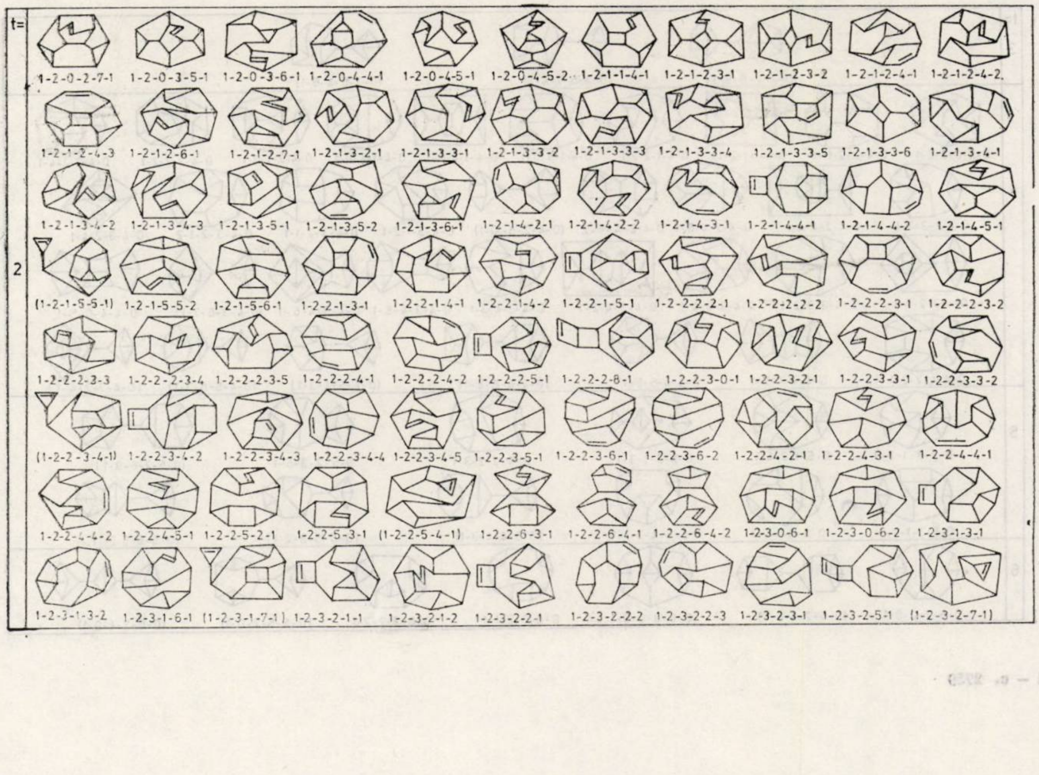
t=
2
1-2-0-2-7-1
1-2-0-3-5-1
1-2-0-3-6-1
1-2-0-4-4-1
1-2-0-4-5-1
1-2-0-4-5-2
1-2-1-1-4-1
1-2-1-2-3-1
1-2-1-2-3-2
1-2-1-2-4-1
1-2-1-2-4-2.
1-2-1-2-4-3
1-2-1-2-6-1
1-2-1-2-7-1
1-2-1-3-2-1
1-2-1-3-3-1
1-2-1-3-3-2
1-2-1-3-3-3
1-2-1-3-3-4
1-2-1-3-3-5
1-2-1-3-3-6
1-2-1-3-4-1
1-2-1-3-4-2
1-2-1-3-4-3
1-2-1-3-5-1
1-2-1-3-5-2
1-2-1-3-6-1
1-2-1-4-2-1
1-2-1-4-2-2
1-2-1-4-3-1
1-2-1-4-4-1
1-2-1-4-4-2
1-2-1-4-5-1
(1-2-1-5-5-1)
1-2-1-5-5-2
1-2-1-5-6-1
1-2-2-1-3-1
1-2-2-1-4-1
1-2-2-1-4-2
1-2-2-1-5-1
1-2-2-2-2-1
1-2-2-2-2-2
1-2-2-2-3-1
1-2-2-2-3-2
1-2-2-2-3-3
1-2-2-2-3-4
1-2-2-2-3-5
1-2-2-2-4-1
1-2-2-2-4-2
1-2-2-2-5-1
1-2-2-2-8-1
1-2-2-3-0-1
1-2-2-3-2-1
1-2-2-3-3-1
1-2-2-3-3-2
(1-2-2-3-4-1)
1-2-2-3-4-2
1-2-2-3-4-3
1-2-2-3-4-4
1-2-2-3-4-5
1-2-2-3-5-1
1-2-2-3-6-1
1-2-2-3-6-2
1-2-2-4-2-1
1-2-2-4-3-1
1-2-2-4-4-1
1-2-2-4-4-2
1-2-2-4-5-1
1-2-2-5-2-1
1-2-2-5-3-1
(1-2-2-5-4-1)
1-2-2-6-3-1
1-2-2-6-4-1
1-2-2-6-4-2
1-2-3-0-6-1
1-2-3-0-6-2
1-2-3-1-3-1
1-2-3-1-3-2
1-2-3-1-6-1
(1-2-3-1-7-1)
1-2-3-2-1-1
1-2-3-2-1-2
1-2-3-2-2-1
1-2-3-2-2-2
1-2-3-2-2-3
1-2-3-2-3-1
1-2-3-2-5-1
(1-2-3-2-7-1)

Table 2 (continued)

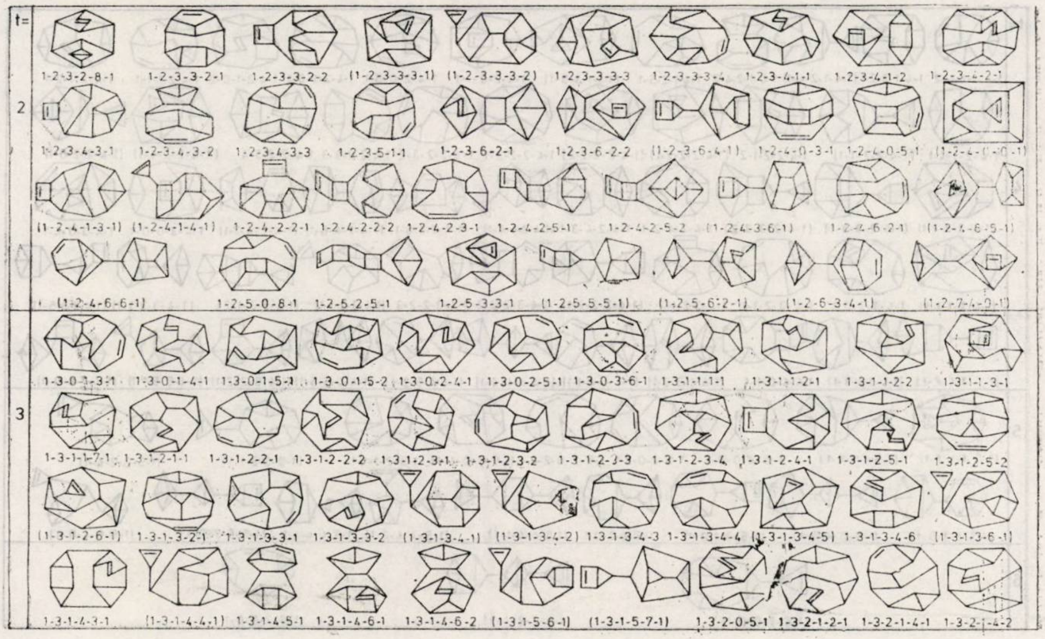
t=
2
1-2-3-2-8-1
1-2-3-3-2-1
1-2-3-3-2-2
(1-2-3-3-3-1)
(1-2-3-3-3-2)
1-2-3-3-3-3
1-2-3-3-3-4
1-2-3-4-1-1
1-2-3-4-1-2
1-2-3-4-2-1
1-2-3-4-3-1
1-2-3-4-3-2
1-2-3-4-3-3
1-2-3-5-1-1
1-2-3-6-2-1
1-2-3-6-2-2
(1-2-3-6-4-1)
1-2-4-0-3-1
1-2-4-0-5-1
(1-2-4-0-0-1)
(1-2-4-1-3-1)
(1-2-4-1-4-1)
1-2-4-2-2-1
1-2-4-2-2-2
1-2-4-2-3-1
1-2-4-2-5-1
1-2-4-2-5-2
(1-2-4-3-6-1)
1-2-4-6-2-1
(1-2-4-6-5-1)
(1-2-4-6-6-1)
1-2-5-0-8-1
1-2-5-2-5-1
1-2-5-3-3-1
(1-2-5-5-5-1)
(1-2-5-6-2-1)
(1-2-6-3-4-1)
(1-2-7-4-0-1)
3
1-3-0-1-3-1
1-3-0-1-4-1
1-3-0-1-5-1
1-3-0-1-5-2
1-3-0-2-4-1
1-3-0-2-5-1
1-3-0-3-6-1
1-3-1-1-1-1
1-3-1-1-2-1
1-3-1-1-2-2
1-3-1-1-3-1
1-3-1-1-7-1
1-3-1-2-1-1
1-3-1-2-2-1
1-3-1-2-2-2
1-3-1-2-3-1
1-3-1-2-3-2
1-3-1-2-3-3
1-3-1-2-3-4
1-3-1-2-4-1
1-3-1-2-5-1
1-3-1-2-5-2
(1-3-1-2-6-1)
1-3-1-3-2-1
1-3-1-3-3-1
1-3-1-3-3-2
(1-3-1-3-4-1)
(1-3-1-3-4-2)
1-3-1-3-4-3
1-3-1-3-4-4
(1-3-1-3-4-5)
1-3-1-3-4-6
(1-3-1-3-6-1)
1-3-1-4-3-1
(1-3-1-4-4-1)
1-3-1-4-5-1
1-3-1-4-6-1
1-3-1-4-6-2
(1-3-1-5-6-1)
(1-3-1-5-7-1)
1-3-2-0-5-1
1-3-2-1-2-1
1-3-2-1-4-1
1-3-2-1-4-2

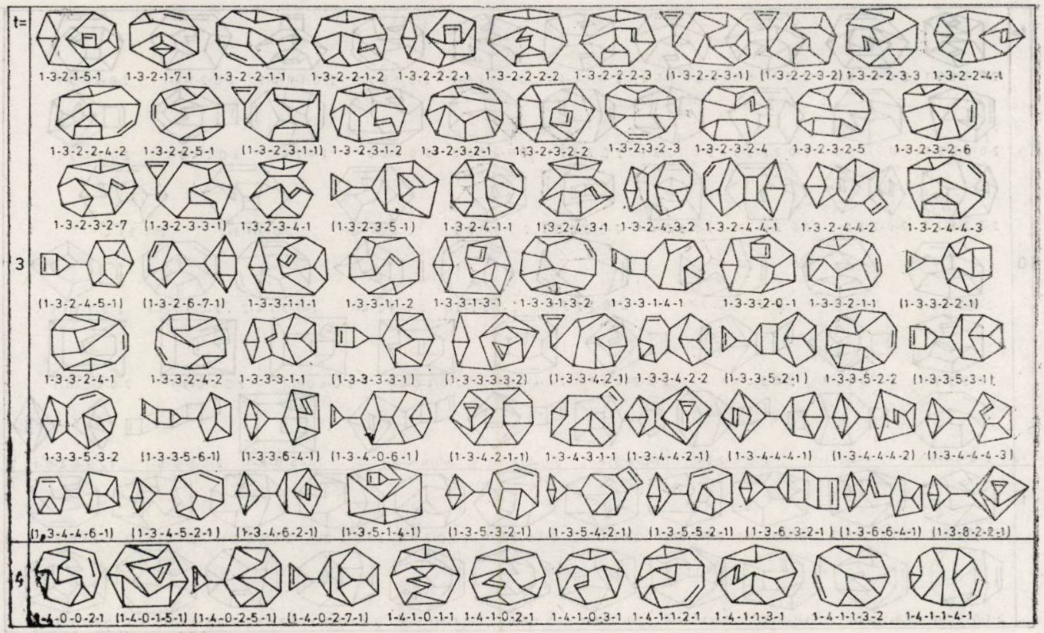
t=
3
1-3-2-1-5-1
1-3-2-1-7-1
1-3-2-2-1-1
1-3-2-2-1-2
1-3-2-2-2-1
1-3-2-2-2-2
1-3-2-2-2-3
(1-3-2-2-3-1)
(1-3-2-2-3-2)
1-3-2-2-3-3
1-3-2-2-4-1
1-3-2-2-4-2
1-3-2-2-5-1
(1-3-2-3-1-1)
1-3-2-3-1-2
1-3-2-3-2-1
1-3-2-3-2-2
1-3-2-3-2-3
1-3-2-3-2-4
1-3-2-3-2-5
1-3-2-3-2-6
1-3-2-3-2-7
(1-3-2-3-3-1)
1-3-2-3-4-1
(1-3-2-3-5-1)
1-3-2-4-1-1
1-3-2-4-3-1
1-3-2-4-3-2
1-3-2-4-4-1
1-3-2-4-4-2
1-3-2-4-4-3
(1-3-2-4-5-1)
(1-3-2-6-7-1)
1-3-3-1-1-1
1-3-3-1-1-2
1-3-3-1-3-1
1-3-3-1-3-2
1-3-3-1-4-1
1-3-3-2-0-1
1-3-3-2-1-1
(1-3-3-2-2-1)
1-3-3-2-4-1
1-3-3-2-4-2
1-3-3-3-1-1
(1-3-3-3-3-1)
(1-3-3-3-3-2)
(1-3-3-4-2-1)
1-3-3-4-2-2
(1-3-3-5-2-1)
1-3-3-5-2-2
(1-3-3-5-3-1)
1-3-3-5-3-2
(1-3-3-5-6-1)
(1-3-3-6-4-1)
(1-3-4-0-6-1)
(1-3-4-2-1-1)
1-3-4-3-1-1
(1-3-4-4-2-1)
(1-3-4-4-4-1)
(1-3-4-4-4-2)
(1-3-4-4-4-3)
(1-3-4-4-6-1)
(1-3-4-5-2-1)
(1-3-4-6-2-1)
(1-3-5-1-4-1)
(1-3-5-3-2-1)
(1-3-5-4-2-1)
(1-3-5-5-2-1)
(1-3-6-3-2-1)
(1-3-6-6-4-1)
(1-3-8-2-2-1)
4
1-4-0-0-2-1
(1-4-0-1-5-1)
(1-4-0-2-5-1)
(1-4-0-2-7-1)
1-4-1-0-1-1
1-4-1-0-2-1
1-4-1-0-3-1
1-4-1-1-2-1
1-4-1-1-3-1
1-4-1-1-3-2
1-4-1-1-4-1

Table 2 (continued)

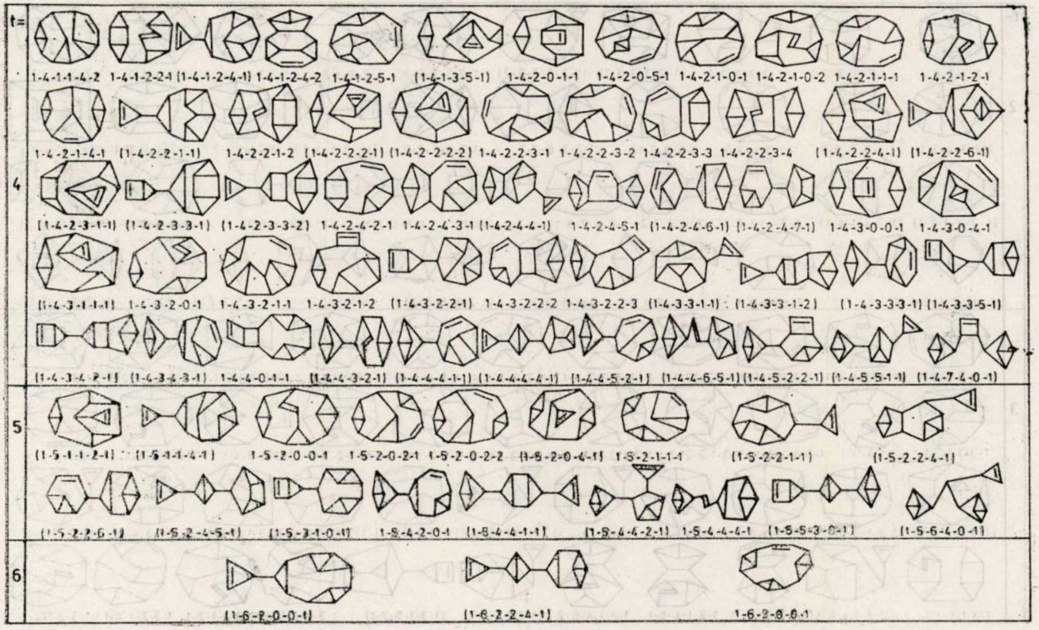
t=
1-4-1-1-4-2
1-4-1-2-2-1
(1-4-1-2-4-1)
1-4-1-2-4-2
1-4-1-2-5-1
(1-4-1-3-5-1)
1-4-2-0-1-1
1-4-2-0-5-1
1-4-2-1-0-1
1-4-2-1-0-2
1-4-2-1-1-1
1-4-2-1-2-1
1-4-2-1-4-1
(1-4-2-2-1-1)
1-4-2-2-1-2
(1-4-2-2-2-1)
(1-4-2-2-2-2)
1-4-2-2-3-1
1-4-2-2-3-2
1-4-2-2-3-3
1-4-2-2-3-4
(1-4-2-2-4-1)
(1-4-2-2-6-1)
4
(1-4-2-3-1-1)
(1-4-2-3-3-1)
(1-4-2-3-3-2)
1-4-2-4-2-1
1-4-2-4-3-1
(1-4-2-4-4-1)
1-4-2-4-5-1
(1-4-2-4-6-1)
(1-4-2-4-7-1)
1-4-3-0-0-1
1-4-3-0-4-1
(1-4-3-1-1-1)
1-4-3-2-0-1
1-4-3-2-1-1
1-4-3-2-1-2
(1-4-3-2-2-1)
1-4-3-2-2-2
1-4-3-2-2-3
(1-4-3-3-1-1)
(1-4-3-3-1-2)
(1-4-3-3-3-1)
(1-4-3-3-5-1)
(1-4-3-4-2-1)
(1-4-3-4-3-1)
1-4-4-0-1-1
(1-4-4-3-2-1)
(1-4-4-4-1-1)
(1-4-4-4-4-1)
(1-4-4-5-2-1)
(1-4-4-6-5-1)
(1-4-5-2-2-1)
(1-4-5-5-1-1)
(1-4-7-4-0-1)
5
(1-5-1-1-2-1)
(1-5-1-1-4-1)
1-5-2-0-0-1
1-5-2-0-2-1
1-5-2-0-2-2
(1-5-2-0-4-1)
1-5-2-1-1-1
(1-5-2-2-1-1)
(1-5-2-2-4-1)
(1-5-2-2-6-1)
(1-5-2-4-5-1)
(1-5-3-1-0-1)
1-5-4-2-0-1
(1-5-4-4-1-1)
(1-5-4-4-2-1)
1-5-4-4-4-1
(1-5-5-3-0-1)
(1-5-6-4-0-1)
6
(1-6-2-0-0-1)
(1-6-2-2-4-1)
1-6-3-8-6-1

Table 3

Connected planar cubic multigraphs of order 14 with $\beta = 2$, i.e. constitutional valence isomers $(CH)_{14}$ with two double bonds.

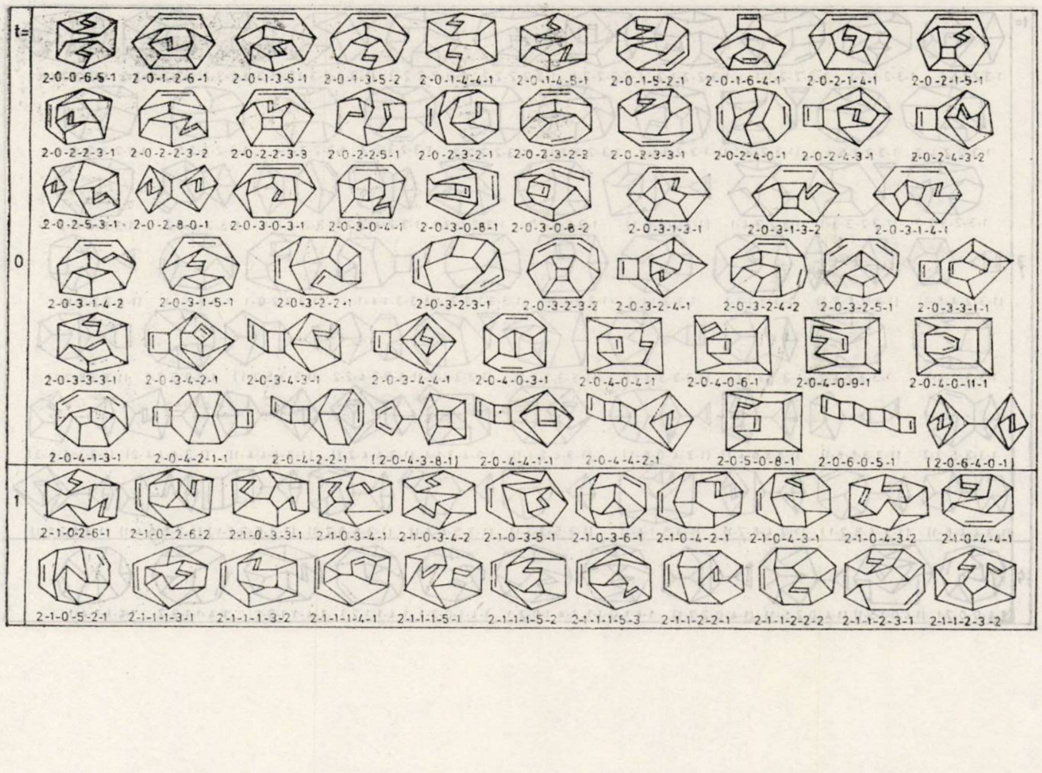
t=
2-0-0-6-5-1
2-0-1-2-6-1
2-0-1-3-5-1
2-0-1-3-5-2
2-0-1-4-4-1
2-0-1-4-5-1
2-0-1-5-2-1
2-0-1-6-4-1
2-0-2-1-4-1
2-0-2-1-5-1
2-0-2-2-3-1
2-0-2-2-3-2
2-0-2-2-3-3
2-0-2-2-5-1
2-0-2-3-2-1
2-0-2-3-2-2
2-0-2-3-3-1
2-0-2-4-0-1
2-0-2-4-3-1
2-0-2-4-3-2
2-0-2-5-3-1
2-0-2-8-0-1
2-0-3-0-3-1
2-0-3-0-4-1
2-0-3-0-8-1
2-0-3-0-8-2
2-0-3-1-3-1
2-0-3-1-3-2
2-0-3-1-4-1
0
2-0-3-1-4-2
2-0-3-1-5-1
2-0-3-2-2-1
2-0-3-2-3-1
2-0-3-2-3-2
2-0-3-2-4-1
2-0-3-2-4-2
2-0-3-2-5-1
2-0-3-3-1-1
2-0-3-3-3-1
2-0-3-4-2-1
2-0-3-4-3-1
2-0-3-4-4-1
2-0-4-0-3-1
2-0-4-0-4-1
2-0-4-0-6-1
2-0-4-0-9-1
2-0-4-0-11-1
2-0-4-1-3-1
2-0-4-2-1-1
2-0-4-2-2-1
(2-0-4-3-8-1)
2-0-4-4-1-1
2-0-4-4-2-1
2-0-5-0-8-1
2-0-6-0-5-1
(2-0-6-4-0-1)
1
2-1-0-2-6-1
2-1-0-2-6-2
2-1-0-3-3-1
2-1-0-3-4-1
2-1-0-3-4-2
2-1-0-3-5-1
2-1-0-3-6-1
2-1-0-4-2-1
2-1-0-4-3-1
2-1-0-4-3-2
2-1-0-4-4-1
2-1-0-5-2-1
2-1-1-1-3-1
2-1-1-1-3-2
2-1-1-1-4-1
2-1-1-1-5-1
2-1-1-1-5-2
2-1-1-1-5-3
2-1-1-2-2-1
2-1-1-2-2-2
2-1-1-2-3-1
2-1-1-2-3-2

Table 3 (continued)

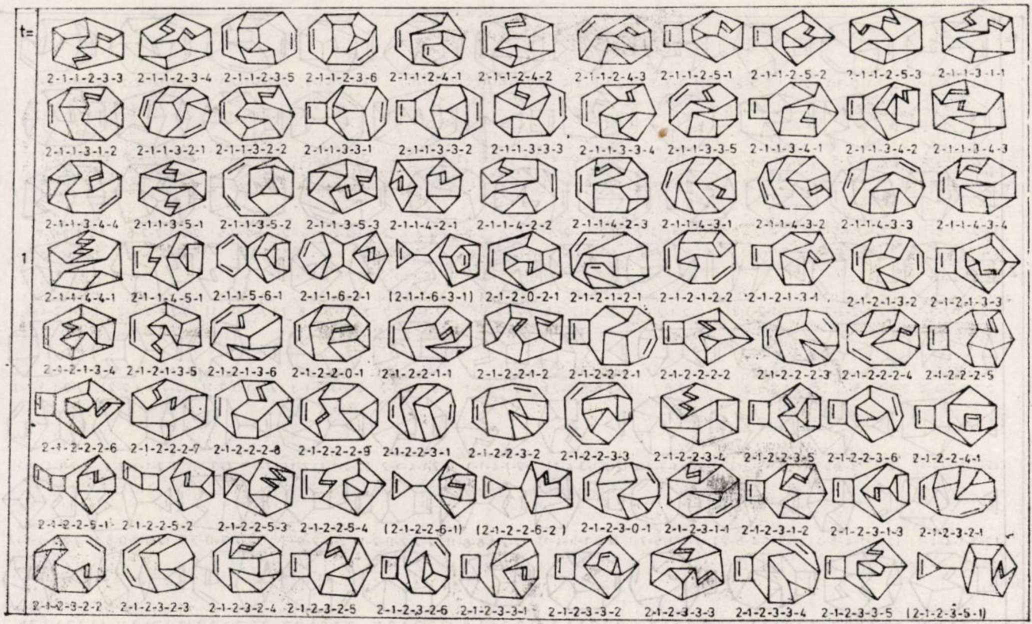
t=

1

2-1-1-2-3-3 2-1-1-2-3-4 2-1-1-2-3-5 2-1-1-2-3-6 2-1-1-2-4-1 2-1-1-2-4-2 2-1-1-2-4-3 2-1-1-2-5-1 2-1-1-2-5-2 2-1-1-2-5-3 2-1-1-3-1-1
2-1-1-3-1-2 2-1-1-3-2-1 2-1-1-3-2-2 2-1-1-3-3-1 2-1-1-3-3-2 2-1-1-3-3-3 2-1-1-3-3-4 2-1-1-3-3-5 2-1-1-3-4-1 2-1-1-3-4-2 2-1-1-3-4-3
2-1-1-3-4-4 2-1-1-3-5-1 2-1-1-3-5-2 2-1-1-3-5-3 2-1-1-4-2-1 2-1-1-4-2-2 2-1-1-4-2-3 2-1-1-4-3-1 2-1-1-4-3-2 2-1-1-4-3-3 2-1-1-4-3-4
2-1-1-4-4-1 2-1-1-4-5-1 2-1-1-5-6-1 2-1-1-6-2-1 (2-1-1-6-3-1) 2-1-2-0-2-1 2-1-2-1-2-1 2-1-2-1-2-2 2-1-2-1-3-1 2-1-2-1-3-2 2-1-2-1-3-3
2-1-2-1-3-4 2-1-2-1-3-5 2-1-2-1-3-6 2-1-2-2-0-1 2-1-2-2-1-1 2-1-2-2-1-2 2-1-2-2-2-1 2-1-2-2-2-2 2-1-2-2-2-3 2-1-2-2-2-4 2-1-2-2-2-5
2-1-2-2-2-6 2-1-2-2-2-7 2-1-2-2-2-8 2-1-2-2-2-9 2-1-2-2-3-1 2-1-2-2-3-2 2-1-2-2-3-3 2-1-2-2-3-4 2-1-2-2-3-5 2-1-2-2-3-6 2-1-2-2-4-1
2-1-2-2-5-1 2-1-2-2-5-2 2-1-2-2-5-3 2-1-2-2-5-4 (2-1-2-2-6-1) (2-1-2-2-6-2) 2-1-2-3-0-1 2-1-2-3-1-1 2-1-2-3-1-2 2-1-2-3-1-3 2-1-2-3-2-1
2-1-2-3-2-2 2-1-2-3-2-3 2-1-2-3-2-4 2-1-2-3-2-5 2-1-2-3-2-6 2-1-2-3-3-1 2-1-2-3-3-2 2-1-2-3-3-3 2-1-2-3-3-4 2-1-2-3-3-5 (2-1-2-3-5-1)

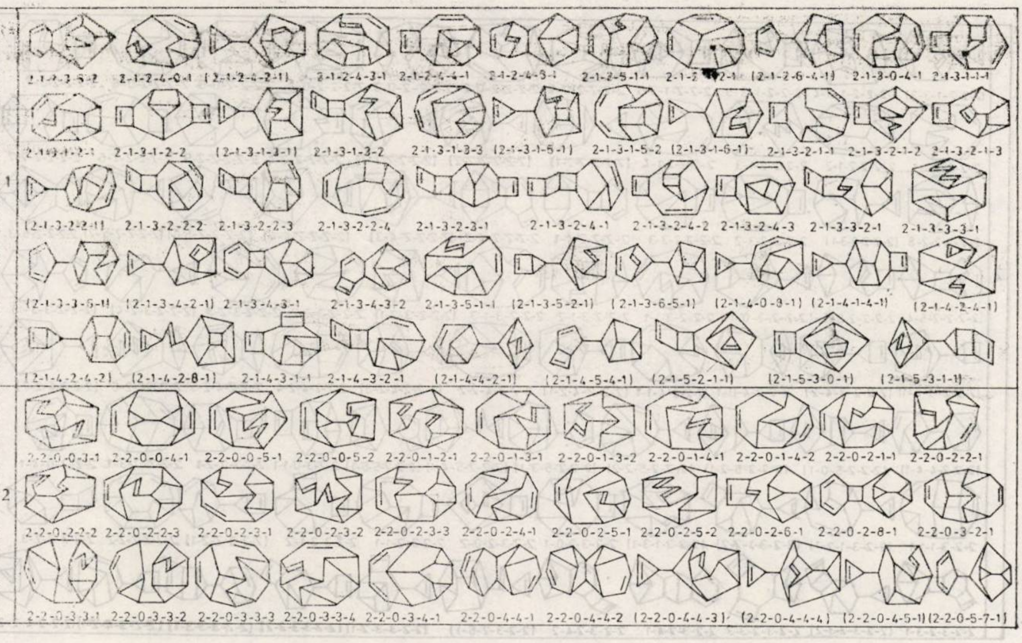
t=

1

2-1-2-3-6-2 2-1-2-4-0-1 (2-1-2-4-2-1) 2-1-2-4-3-1 2-1-2-4-4-1 2-1-2-4-5-1 2-1-2-5-1-1 2-1-2-[illegible]2-1 (2-1-2-6-4-1) 2-1-3-0-4-1 2-1-3-1-1-1
2-1-3-1-2-1 2-1-3-1-2-2 (2-1-3-1-3-1) 2-1-3-1-3-2 2-1-3-1-3-3 (2-1-3-1-5-1) 2-1-3-1-5-2 (2-1-3-1-6-1) 2-1-3-2-1-1 2-1-3-2-1-2 2-1-3-2-1-3
(2-1-3-2-2-1) 2-1-3-2-2-2 2-1-3-2-2-3 2-1-3-2-2-4 2-1-3-2-3-1 2-1-3-2-4-1 2-1-3-2-4-2 2-1-3-2-4-3 2-1-3-3-2-1 2-1-3-3-3-1
(2-1-3-3-6-1) (2-1-3-4-2-1) 2-1-3-4-3-1 2-1-3-4-3-2 2-1-3-5-1-1 (2-1-3-5-2-1) (2-1-3-6-5-1) (2-1-4-0-8-1) (2-1-4-1-4-1) (2-1-4-2-4-1)
(2-1-4-2-4-2) (2-1-4-2-8-1) 2-1-4-3-1-1 2-1-4-3-2-1 (2-1-4-4-2-1) (2-1-4-5-4-1) (2-1-5-2-1-1) (2-1-5-3-0-1) (2-1-5-3-1-1)

2

2-2-0-0-3-1 2-2-0-0-4-1 2-2-0-0-5-1 2-2-0-0-5-2 2-2-0-1-2-1 2-2-0-1-3-1 2-2-0-1-3-2 2-2-0-1-4-1 2-2-0-1-4-2 2-2-0-2-1-1 2-2-0-2-2-1
2-2-0-2-2-2 2-2-0-2-2-3 2-2-0-2-3-1 2-2-0-2-3-2 2-2-0-2-3-3 2-2-0-2-4-1 2-2-0-2-5-1 2-2-0-2-5-2 2-2-0-2-6-1 2-2-0-2-8-1 2-2-0-3-2-1
2-2-0-3-3-1 2-2-0-3-3-2 2-2-0-3-3-3 2-2-0-3-3-4 2-2-0-3-4-1 2-2-0-4-4-1 2-2-0-4-4-2 (2-2-0-4-4-3) (2-2-0-4-4-4) (2-2-0-4-5-1) (2-2-0-5-7-1)

Table 3 (continued)

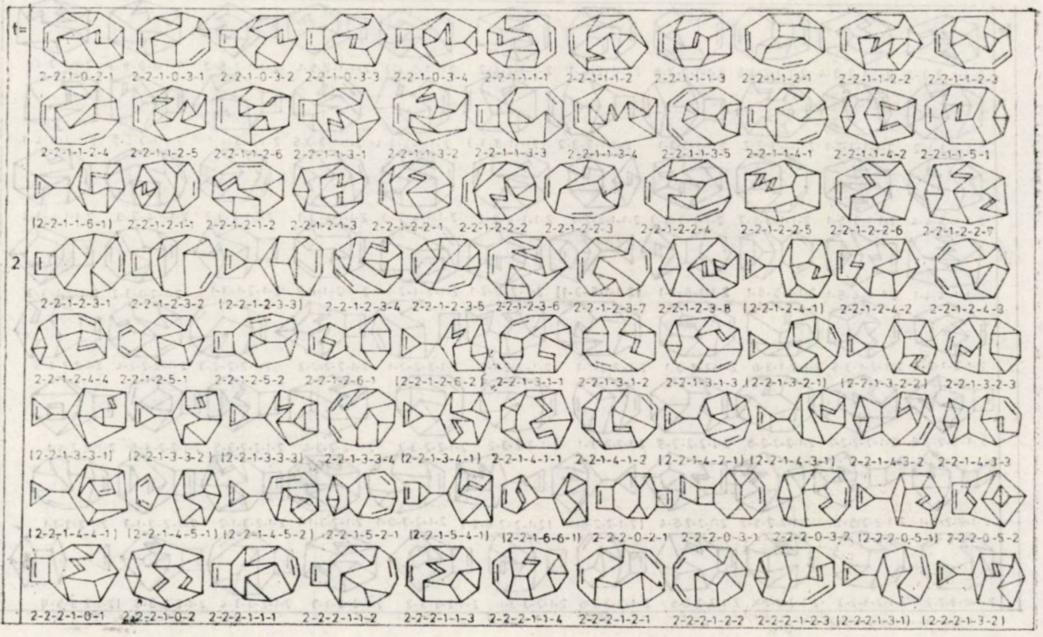
t=
2
2-2-1-0-2-1
2-2-1-0-3-1
2-2-1-0-3-2
2-2-1-0-3-3
2-2-1-0-3-4
2-2-1-1-1-1
2-2-1-1-1-2
2-2-1-1-1-3
2-2-1-1-2-1
2-2-1-1-2-2
2-2-1-1-2-3
2-2-1-1-2-4
2-2-1-1-2-5
2-2-1-1-2-6
2-2-1-1-3-1
2-2-1-1-3-2
2-2-1-1-3-3
2-2-1-1-3-4
2-2-1-1-3-5
2-2-1-1-4-1
2-2-1-1-4-2
2-2-1-1-5-1
(2-2-1-1-6-1)
2-2-1-2-1-1
2-2-1-2-1-2
2-2-1-2-1-3
2-2-1-2-2-1
2-2-1-2-2-2
2-2-1-2-2-3
2-2-1-2-2-4
2-2-1-2-2-5
2-2-1-2-2-6
2-2-1-2-2-7
2-2-1-2-3-1
2-2-1-2-3-2
(2-2-1-2-3-3)
2-2-1-2-3-4
2-2-1-2-3-5
2-2-1-2-3-6
2-2-1-2-3-7
2-2-1-2-3-8
(2-2-1-2-4-1)
2-2-1-2-4-2
2-2-1-2-4-3
2-2-1-2-4-4
2-2-1-2-5-1
2-2-1-2-5-2
2-2-1-2-6-1
(2-2-1-2-6-2)
2-2-1-3-1-1
2-2-1-3-1-2
2-2-1-3-1-3
(2-2-1-3-2-1)
(2-2-1-3-2-2)
2-2-1-3-2-3
(2-2-1-3-3-1)
(2-2-1-3-3-2)
(2-2-1-3-3-3)
2-2-1-3-3-4
(2-2-1-3-4-1)
2-2-1-4-1-1
2-2-1-4-1-2
(2-2-1-4-2-1)
(2-2-1-4-3-1)
2-2-1-4-3-2
2-2-1-4-3-3
(2-2-1-4-4-1)
(2-2-1-4-5-1)
(2-2-1-4-5-2)
2-2-1-5-2-1
(2-2-1-5-4-1)
(2-2-1-6-6-1)
2-2-2-0-2-1
2-2-2-0-3-1
2-2-2-0-3-2
(2-2-2-0-5-1)
2-2-2-0-5-2
2-2-2-1-0-1
2-2-2-1-0-2
2-2-2-1-1-1
2-2-2-1-1-2
2-2-2-1-1-3
2-2-2-1-1-4
2-2-2-1-2-1
2-2-2-1-2-2
2-2-2-1-2-3
(2-2-2-1-3-1)
(2-2-2-1-3-2)

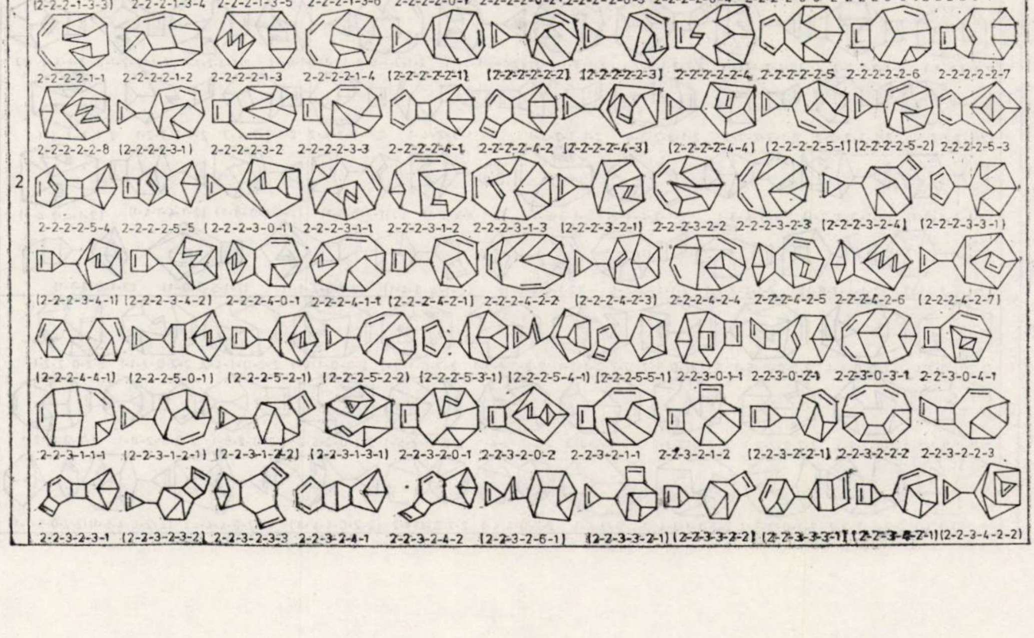
t=
2
(2-2-2-1-3-3)
2-2-2-1-3-4
2-2-2-1-3-5
2-2-2-1-3-6
2-2-2-2-0-1
2-2-2-2-0-2
2-2-2-2-0-3
2-2-2-2-0-4
2-2-2-2-0-5
2-2-2-2-0-6
2-2-2-2-0-7
2-2-2-2-1-1
2-2-2-2-1-2
2-2-2-2-1-3
2-2-2-2-1-4
(2-2-2-2-2-1)
(2-2-2-2-2-2)
(2-2-2-2-2-3)
2-2-2-2-2-4
2-2-2-2-2-5
2-2-2-2-2-6
2-2-2-2-2-7
2-2-2-2-2-8
(2-2-2-2-3-1)
2-2-2-2-3-2
2-2-2-2-3-3
2-2-2-2-4-1
2-2-2-2-4-2
(2-2-2-2-4-3)
(2-2-2-2-4-4)
(2-2-2-2-5-1)
(2-2-2-2-5-2)
2-2-2-2-5-3
2-2-2-2-5-4
2-2-2-2-5-5
(2-2-2-3-0-1)
2-2-2-3-1-1
2-2-2-3-1-2
2-2-2-3-1-3
(2-2-2-3-2-1)
2-2-2-3-2-2
2-2-2-3-2-3
(2-2-2-3-2-4)
(2-2-2-3-3-1)
(2-2-2-3-4-1)
(2-2-2-3-4-2)
2-2-2-4-0-1
2-2-2-4-1-1
(2-2-2-4-2-1)
2-2-2-4-2-2
(2-2-2-4-2-3)
2-2-2-4-2-4
2-2-2-4-2-5
2-2-2-4-2-6
(2-2-2-4-2-7)
(2-2-2-4-4-1)
(2-2-2-5-0-1)
(2-2-2-5-2-1)
(2-2-2-5-2-2)
(2-2-2-5-3-1)
(2-2-2-5-4-1)
(2-2-2-5-5-1)
2-2-3-0-1-1
2-2-3-0-2-1
2-2-3-0-3-1
2-2-3-0-4-1
2-2-3-1-1-1
(2-2-3-1-2-1)
(2-2-3-1-2-2)
(2-2-3-1-3-1)
2-2-3-2-0-1
2-2-3-2-0-2
2-2-3-2-1-1
2-2-3-2-1-2
(2-2-3-2-2-1)
2-2-3-2-2-2
2-2-3-2-2-3
2-2-3-2-3-1
(2-2-3-2-3-2)
2-2-3-2-3-3
2-2-3-2-4-1
2-2-3-2-4-2
(2-2-3-2-6-1)
(2-2-3-3-2-1)
(2-2-3-3-2-2)
(2-2-3-3-3-1)
(2-2-3-4-2-1)
(2-2-3-4-2-2)

Table 3 (continued)

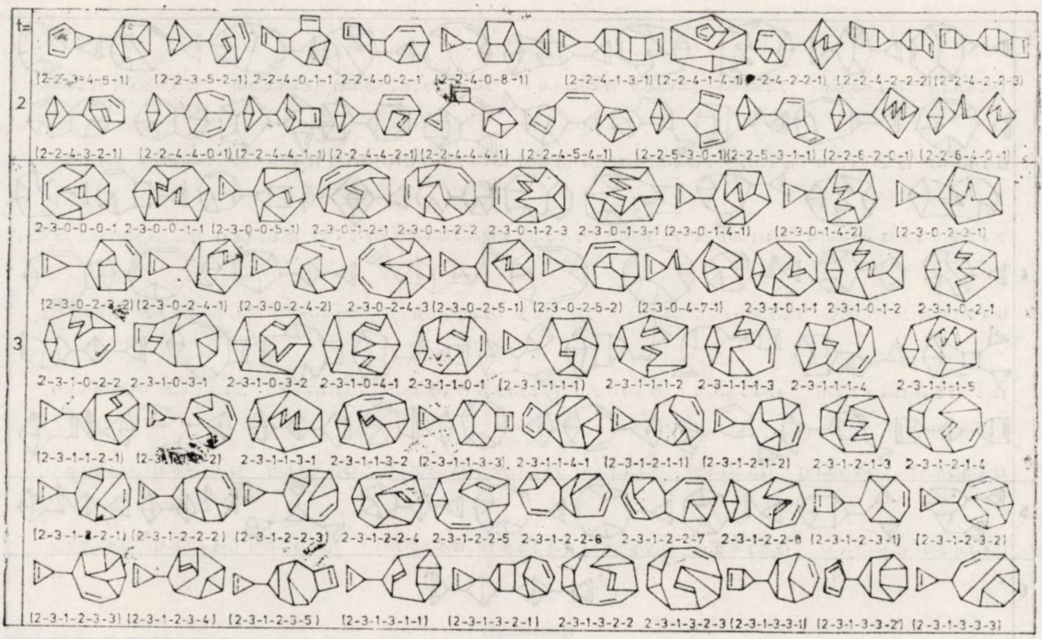
t=
2
(2-2-3-4-5-1)
(2-2-3-5-2-1)
2-2-4-0-1-1
2-2-4-0-2-1
(2-2-4-0-8-1)
(2-2-4-1-3-1)
(2-2-4-1-4-1)
[illegible]-2-4-2-2-1)
(2-2-4-2-2-2)
(2-2-4-2-2-3)
(2-2-4-3-2-1)
(2-2-4-4-0-1)
(2-2-4-4-1-1)
(2-2-4-4-2-1)
(2-2-4-4-4-1)
(2-2-4-5-4-1)
(2-2-5-3-0-1)
(2-2-5-3-1-1)
(2-2-6-2-0-1)
(2-2-6-4-0-1)
3
2-3-0-0-0-1
2-3-0-0-1-1
(2-3-0-0-5-1)
2-3-0-1-2-1
2-3-0-1-2-2
2-3-0-1-2-3
2-3-0-1-3-1
(2-3-0-1-4-1)
(2-3-0-1-4-2)
(2-3-0-2-3-1)
(2-3-0-2-3-2)
(2-3-0-2-4-1)
(2-3-0-2-4-2)
2-3-0-2-4-3
(2-3-0-2-5-1)
(2-3-0-2-5-2)
(2-3-0-4-7-1)
2-3-1-0-1-1
2-3-1-0-1-2
2-3-1-0-2-1
2-3-1-0-2-2
2-3-1-0-3-1
2-3-1-0-3-2
2-3-1-0-4-1
2-3-1-1-0-1
(2-3-1-1-1-1)
2-3-1-1-1-2
2-3-1-1-1-3
2-3-1-1-1-4
2-3-1-1-1-5
(2-3-1-1-2-1)
(2-3[illegible]2)
2-3-1-1-3-1
2-3-1-1-3-2
(2-3-1-1-3-3)
2-3-1-1-4-1
(2-3-1-2-1-1)
(2-3-1-2-1-2)
2-3-1-2-1-3
2-3-1-2-1-4
(2-3-1-2-2-1)
(2-3-1-2-2-2)
(2-3-1-2-2-3)
2-3-1-2-2-4
2-3-1-2-2-5
2-3-1-2-2-6
2-3-1-2-2-7
2-3-1-2-2-8
(2-3-1-2-3-1)
(2-3-1-2-3-2)
(2-3-1-2-3-3)
(2-3-1-2-3-4)
(2-3-1-2-3-5)
(2-3-1-3-1-1)
(2-3-1-3-2-1)
2-3-1-3-2-2
2-3-1-3-2-3
(2-3-1-3-3-1)
(2-3-1-3-3-2)
(2-3-1-3-3-3)

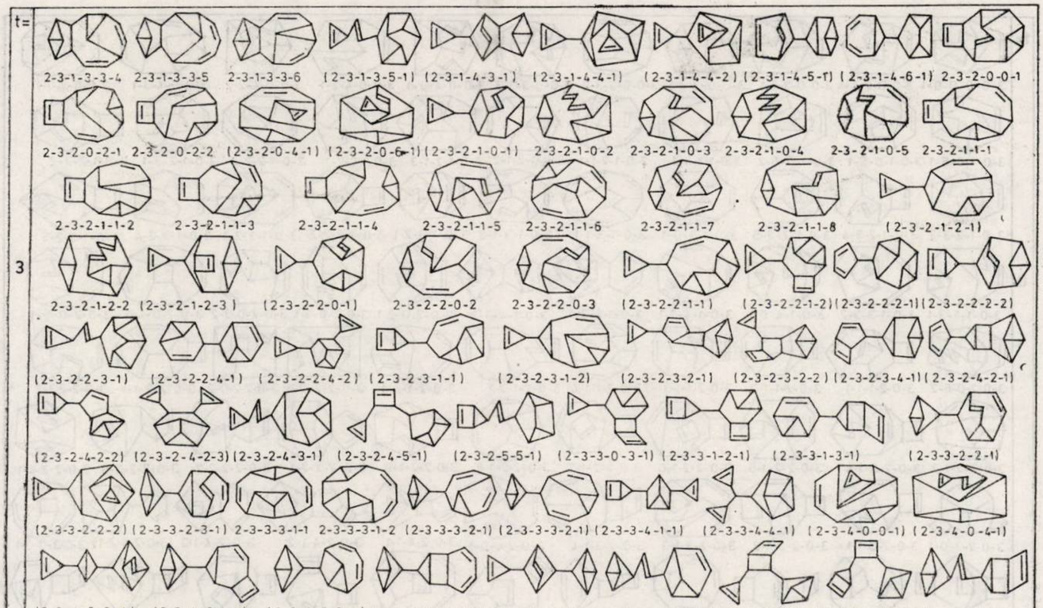
t=
3
2-3-1-3-3-4
2-3-1-3-3-5
2-3-1-3-3-6
(2-3-1-3-5-1)
(2-3-1-4-3-1)
(2-3-1-4-4-1)
(2-3-1-4-4-2)
(2-3-1-4-5-1)
(2-3-1-4-6-1)
2-3-2-0-0-1
2-3-2-0-2-1
2-3-2-0-2-2
(2-3-2-0-4-1)
(2-3-2-0-6-1)
(2-3-2-1-0-1)
2-3-2-1-0-2
2-3-2-1-0-3
2-3-2-1-0-4
2-3-2-1-0-5
2-3-2-1-1-1
2-3-2-1-1-2
2-3-2-1-1-3
2-3-2-1-1-4
2-3-2-1-1-5
2-3-2-1-1-6
2-3-2-1-1-7
2-3-2-1-1-8
(2-3-2-1-2-1)
2-3-2-1-2-2
(2-3-2-1-2-3)
(2-3-2-2-0-1)
2-3-2-2-0-2
2-3-2-2-0-3
(2-3-2-2-1-1)
(2-3-2-2-1-2)
(2-3-2-2-2-1)
(2-3-2-2-2-2)
(2-3-2-2-3-1)
(2-3-2-2-4-1)
(2-3-2-2-4-2)
(2-3-2-3-1-1)
(2-3-2-3-1-2)
(2-3-2-3-2-1)
(2-3-2-3-2-2)
(2-3-2-3-4-1)
(2-3-2-4-2-1)
(2-3-2-4-2-2)
(2-3-2-4-2-3)
(2-3-2-4-3-1)
(2-3-2-4-5-1)
(2-3-2-5-5-1)
(2-3-3-0-3-1)
(2-3-3-1-2-1)
(2-3-3-1-3-1)
(2-3-3-2-2-1)
(2-3-3-2-2-2)
(2-3-3-2-3-1)
2-3-3-3-1-1
2-3-3-3-1-2
(2-3-3-3-2-1)
(2-3-3-3-2-1)
(2-3-3-4-1-1)
(2-3-3-4-4-1)
(2-3-4-0-0-1)
(2-3-4-0-4-1)
(2-3-4-2-0-1)
(2-3-4-2-1-1)
(2-3-4-3-0-1)
(2-3-4-3-1-1)
(2-3-4-4-0-1)
(2-3-4-4-2-1)
(2-3-5-2-1-1)
(2-3-5-3-0-1)
(2-3-5-3-1-1)

Table 3 (continued)

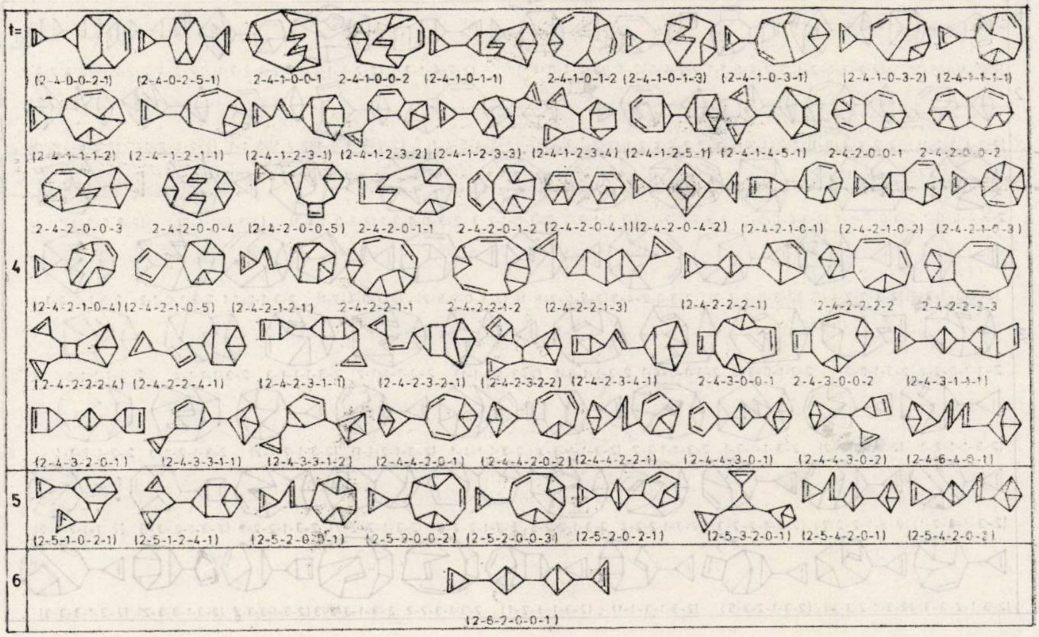
t=
4
5
6
(2-4-0-0-2-1)
(2-4-0-2-5-1)
2-4-1-0-0-1
2-4-1-0-0-2
(2-4-1-0-1-1)
2-4-1-0-1-2
(2-4-1-0-1-3)
(2-4-1-0-3-1)
(2-4-1-0-3-2)
(2-4-1-1-1-1)
(2-4-1-1-1-2)
(2-4-1-2-1-1)
(2-4-1-2-3-1)
(2-4-1-2-3-2)
(2-4-1-2-3-3)
(2-4-1-2-3-4)
(2-4-1-2-5-1)
(2-4-1-4-5-1)
2-4-2-0-0-1
2-4-2-0-0-2
2-4-2-0-0-3
2-4-2-0-0-4
(2-4-2-0-0-5)
2-4-2-0-1-1
2-4-2-0-1-2
(2-4-2-0-4-1)
(2-4-2-0-4-2)
(2-4-2-1-0-1)
(2-4-2-1-0-2)
(2-4-2-1-0-3)
(2-4-2-1-0-4)
(2-4-2-1-0-5)
(2-4-2-1-2-1)
2-4-2-2-1-1
2-4-2-2-1-2
(2-4-2-2-1-3)
(2-4-2-2-2-1)
2-4-2-2-2-2
2-4-2-2-2-3
(2-4-2-2-2-4)
(2-4-2-2-4-1)
(2-4-2-3-1-1)
(2-4-2-3-2-1)
(2-4-2-3-2-2)
(2-4-2-3-4-1)
2-4-3-0-0-1
2-4-3-0-0-2
(2-4-3-1-4-1)
(2-4-3-2-0-1)
(2-4-3-3-1-1)
(2-4-3-3-1-2)
(2-4-4-2-0-1)
(2-4-4-2-0-2)
(2-4-4-2-2-1)
(2-4-4-3-0-1)
(2-4-4-3-0-2)
(2-4-6-4-0-1)
(2-5-1-0-2-1)
(2-5-1-2-4-1)
(2-5-2-0-0-1)
(2-5-2-0-0-2)
(2-5-2-0-0-3)
(2-5-2-0-2-1)
(2-5-3-2-0-1)
(2-5-4-2-0-1)
(2-5-4-2-0-2)
(2-6-2-0-0-1)

Table 4

Connected planar cubic multigraphs of order 14 with $\beta = 3$, i.e. constitutional valence isomers $(CH)_{14}$ with three double bonds.

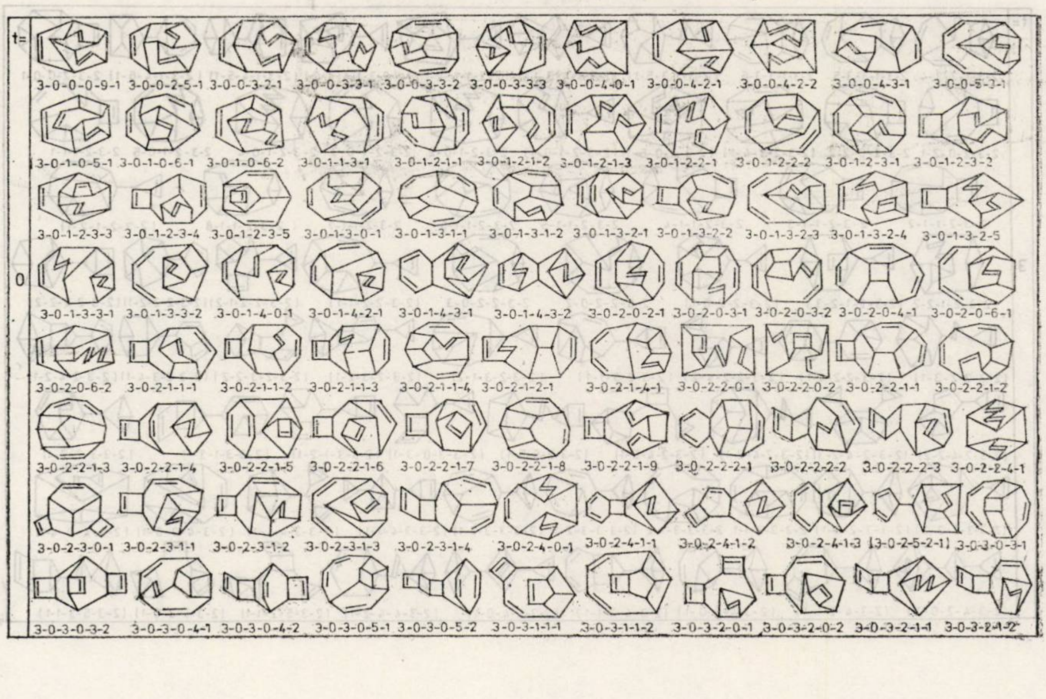
t=
0
3-0-0-0-9-1
3-0-0-2-5-1
3-0-0-3-2-1
3-0-0-3-3-1
3-0-0-3-3-2
3-0-0-3-3-3
3-0-0-4-0-1
3-0-0-4-2-1
3-0-0-4-2-2
3-0-0-4-3-1
3-0-0-5-3-1
3-0-1-0-5-1
3-0-1-0-6-1
3-0-1-0-6-2
3-0-1-1-3-1
3-0-1-2-1-1
3-0-1-2-1-2
3-0-1-2-1-3
3-0-1-2-2-1
3-0-1-2-2-2
3-0-1-2-3-1
3-0-1-2-3-2
3-0-1-2-3-3
3-0-1-2-3-4
3-0-1-2-3-5
3-0-1-3-0-1
3-0-1-3-1-1
3-0-1-3-1-2
3-0-1-3-2-1
3-0-1-3-2-2
3-0-1-3-2-3
3-0-1-3-2-4
3-0-1-3-2-5
3-0-1-3-3-1
3-0-1-3-3-2
3-0-1-4-0-1
3-0-1-4-2-1
3-0-1-4-3-1
3-0-1-4-3-2
3-0-2-0-2-1
3-0-2-0-3-1
3-0-2-0-3-2
3-0-2-0-4-1
3-0-2-0-6-1
3-0-2-0-6-2
3-0-2-1-1-1
3-0-2-1-1-2
3-0-2-1-1-3
3-0-2-1-1-4
3-0-2-1-2-1
3-0-2-1-4-1
3-0-2-2-0-1
3-0-2-2-0-2
3-0-2-2-1-1
3-0-2-2-1-2
3-0-2-2-1-3
3-0-2-2-1-4
3-0-2-2-1-5
3-0-2-2-1-6
3-0-2-2-1-7
3-0-2-2-1-8
3-0-2-2-1-9
3-0-2-2-2-1
3-0-2-2-2-2
3-0-2-2-2-3
3-0-2-2-4-1
3-0-2-3-0-1
3-0-2-3-1-1
3-0-2-3-1-2
3-0-2-3-1-3
3-0-2-3-1-4
3-0-2-4-0-1
3-0-2-4-1-1
3-0-2-4-1-2
3-0-2-4-1-3
(3-0-2-5-2-1)
3-0-3-0-3-1
3-0-3-0-3-2
3-0-3-0-4-1
3-0-3-0-4-2
3-0-3-0-5-1
3-0-3-0-5-2
3-0-3-1-1-1
3-0-3-1-1-2
3-0-3-2-0-1
3-0-3-2-0-2
3-0-3-2-1-1
3-0-3-2-1-2

Table 4 (continued)

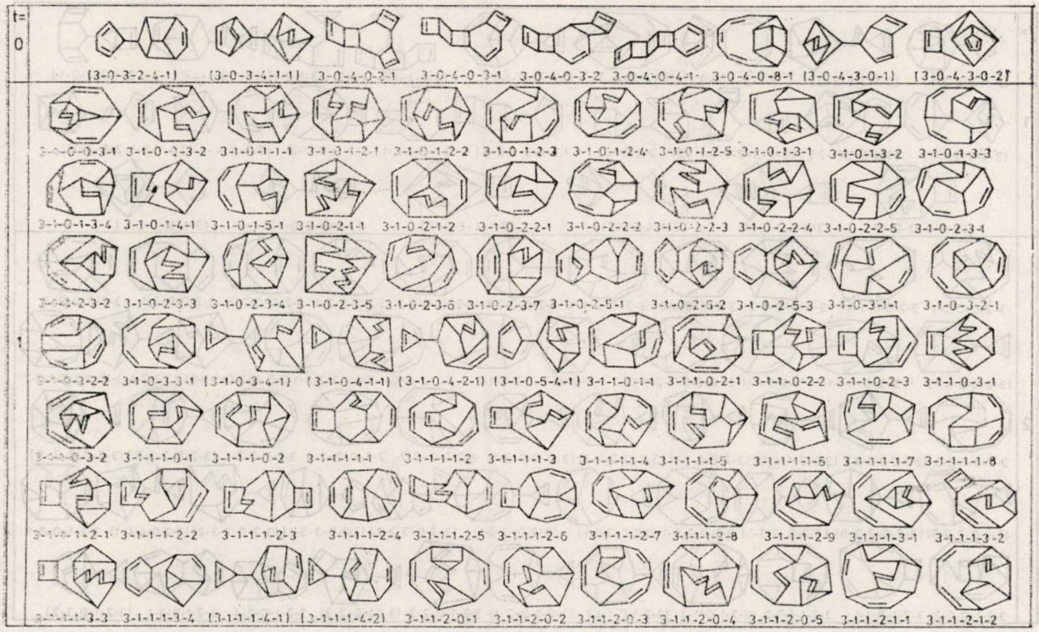
t=
0
(3-0-3-2-4-1)
(3-0-3-4-1-1)
3-0-4-0-2-1
3-0-4-0-3-1
3-0-4-0-3-2
3-0-4-0-4-1
3-0-4-0-8-1
(3-0-4-3-0-1)
(3-0-4-3-0-2)
3-1-0-0-3-1
3-1-0-0-3-2
3-1-0-1-1-1
3-1-0-1-2-1
3-1-0-1-2-2
3-1-0-1-2-3
3-1-0-1-2-4
3-1-0-1-2-5
3-1-0-1-3-1
3-1-0-1-3-2
3-1-0-1-3-3
3-1-0-1-3-4
3-1-0-1-4-1
3-1-0-1-5-1
3-1-0-2-1-1
3-1-0-2-1-2
3-1-0-2-2-1
3-1-0-2-2-2
3-1-0-2-2-3
3-1-0-2-2-4
3-1-0-2-2-5
3-1-0-2-3-1
3-1-0-2-3-2
3-1-0-2-3-3
3-1-0-2-3-4
3-1-0-2-3-5
3-1-0-2-3-6
3-1-0-2-3-7
3-1-0-2-5-1
3-1-0-2-5-2
3-1-0-2-5-3
3-1-0-3-1-1
3-1-0-3-2-1
1
3-1-0-3-2-2
3-1-0-3-3-1
(3-1-0-3-4-1)
(3-1-0-4-1-1)
(3-1-0-4-2-1)
(3-1-0-5-4-1)
3-1-1-0-1-1
3-1-1-0-2-1
3-1-1-0-2-2
3-1-1-0-2-3
3-1-1-0-3-1
3-1-1-0-3-2
3-1-1-1-0-1
3-1-1-1-0-2
3-1-1-1-1-1
3-1-1-1-1-2
3-1-1-1-1-3
3-1-1-1-1-4
3-1-1-1-1-5
3-1-1-1-1-6
3-1-1-1-1-7
3-1-1-1-1-8
3-1-1-1-2-1
3-1-1-1-2-2
3-1-1-1-2-3
3-1-1-1-2-4
3-1-1-1-2-5
3-1-1-1-2-6
3-1-1-1-2-7
3-1-1-1-2-8
3-1-1-1-2-9
3-1-1-1-3-1
3-1-1-1-3-2
3-1-1-1-3-3
3-1-1-1-3-4
(3-1-1-1-4-1)
(3-1-1-1-4-2)
3-1-1-2-0-1
3-1-1-2-0-2
3-1-1-2-0-3
3-1-1-2-0-4
3-1-1-2-0-5
3-1-1-2-1-1
3-1-1-2-1-2

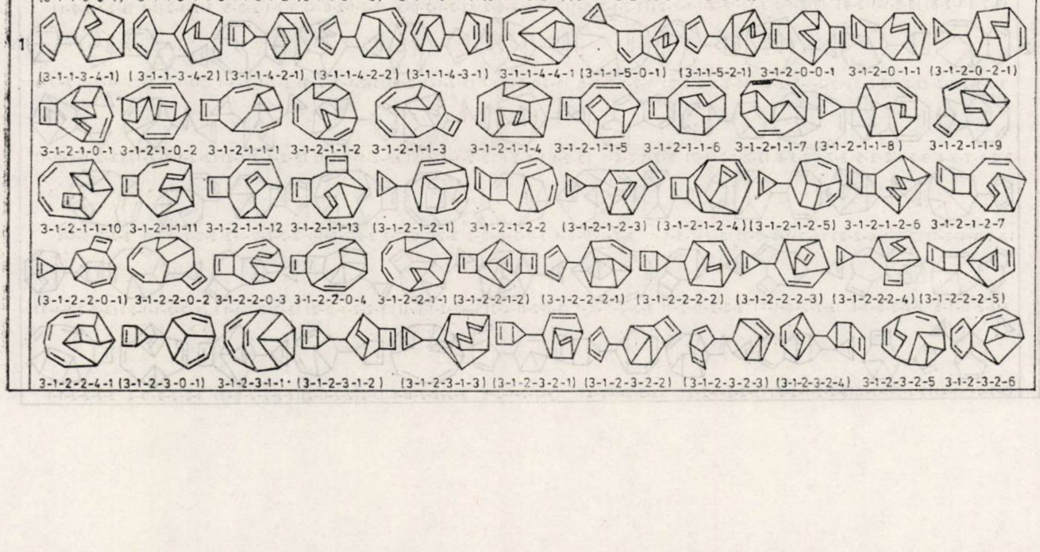
t=
1
3-1-1-2-1-3
3-1-1-2-1-4
(3-1-1-2-1-5)
3-1-1-2-1-6
3-1-1-2-2-1
3-1-1-2-2-2
(3-1-1-2-2-3)
3-1-1-2-2-4
(3-1-1-2-2-5)
(3-1-1-2-2-6)
3-1-1-2-2-7
3-1-1-2-2-8
3-1-1-2-2-9
3-1-1-2-2-10
3-1-1-2-2-11
3-1-1-2-2-12
3-1-1-2-3-1
3-1-1-2-3-2
3-1-1-2-3-3
3-1-1-2-3-4
3-1-1-2-3-5
3-1-1-2-3-6
(3-1-1-3-0-1)
3-1-1-3-1-1
3-1-1-3-1-2
(3-1-1-3-1-3)
3-1-1-3-1-4
(3-1-1-3-2-1)
(3-1-1-3-2-2)
3-1-1-3-2-3
(3-1-1-3-2-4)
(3-1-1-3-2-5)
3-1-1-3-2-6
(3-1-1-3-4-1)
(3-1-1-3-4-2)
(3-1-1-4-2-1)
(3-1-1-4-2-2)
(3-1-1-4-3-1)
3-1-1-4-4-1
(3-1-1-5-0-1)
(3-1-1-5-2-1)
3-1-2-0-0-1
3-1-2-0-1-1
(3-1-2-0-2-1)
3-1-2-1-0-1
3-1-2-1-0-2
3-1-2-1-1-1
3-1-2-1-1-2
3-1-2-1-1-3
3-1-2-1-1-4
3-1-2-1-1-5
3-1-2-1-1-6
3-1-2-1-1-7
(3-1-2-1-1-8)
3-1-2-1-1-9
3-1-2-1-1-10
3-1-2-1-1-11
3-1-2-1-1-12
3-1-2-1-1-13
(3-1-2-1-2-1)
3-1-2-1-2-2
(3-1-2-1-2-3)
(3-1-2-1-2-4)
(3-1-2-1-2-5)
3-1-2-1-2-6
3-1-2-1-2-7
(3-1-2-2-0-1)
3-1-2-2-0-2
3-1-2-2-0-3
3-1-2-2-0-4
3-1-2-2-1-1
(3-1-2-2-1-2)
(3-1-2-2-2-1)
(3-1-2-2-2-2)
(3-1-2-2-2-3)
(3-1-2-2-2-4)
(3-1-2-2-2-5)
3-1-2-2-4-1
(3-1-2-3-0-1)
3-1-2-3-1-1
(3-1-2-3-1-2)
(3-1-2-3-1-3)
(3-1-2-3-2-1)
(3-1-2-3-2-2)
(3-1-2-3-2-3)
(3-1-2-3-2-4)
3-1-2-3-2-5
3-1-2-3-2-6

Table 4 (continued)

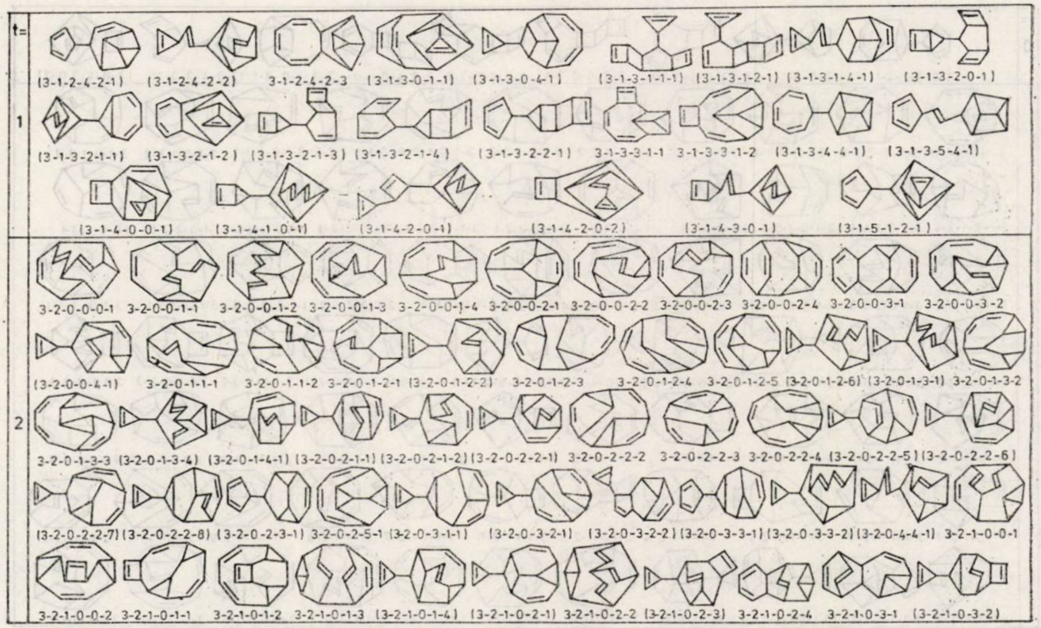
t=
1
(3-1-2-4-2-1)
(3-1-2-4-2-2)
3-1-2-4-2-3
(3-1-3-0-1-1)
(3-1-3-0-4-1)
(3-1-3-1-1-1)
(3-1-3-1-2-1)
(3-1-3-1-4-1)
(3-1-3-2-0-1)
(3-1-3-2-1-1)
(3-1-3-2-1-2)
(3-1-3-2-1-3)
(3-1-3-2-1-4)
(3-1-3-2-2-1)
3-1-3-3-1-1
3-1-3-3-1-2
(3-1-3-4-4-1)
(3-1-3-5-4-1)
(3-1-4-0-0-1)
(3-1-4-1-0-1)
(3-1-4-2-0-1)
(3-1-4-2-0-2)
(3-1-4-3-0-1)
(3-1-5-1-2-1)
2
3-2-0-0-0-1
3-2-0-0-1-1
3-2-0-0-1-2
3-2-0-0-1-3
3-2-0-0-1-4
3-2-0-0-2-1
3-2-0-0-2-2
3-2-0-0-2-3
3-2-0-0-2-4
3-2-0-0-3-1
3-2-0-0-3-2
(3-2-0-0-4-1)
3-2-0-1-1-1
3-2-0-1-1-2
3-2-0-1-2-1
(3-2-0-1-2-2)
3-2-0-1-2-3
3-2-0-1-2-4
3-2-0-1-2-5
(3-2-0-1-2-6)
(3-2-0-1-3-1)
3-2-0-1-3-2
3-2-0-1-3-3
(3-2-0-1-3-4)
(3-2-0-1-4-1)
(3-2-0-2-1-1)
(3-2-0-2-1-2)
(3-2-0-2-2-1)
3-2-0-2-2-2
3-2-0-2-2-3
3-2-0-2-2-4
(3-2-0-2-2-5)
(3-2-0-2-2-6)
(3-2-0-2-2-7)
(3-2-0-2-2-8)
(3-2-0-2-3-1)
3-2-0-2-5-1
(3-2-0-3-1-1)
(3-2-0-3-2-1)
(3-2-0-3-2-2)
(3-2-0-3-3-1)
(3-2-0-3-3-2)
(3-2-0-4-4-1)
3-2-1-0-0-1
3-2-1-0-0-2
3-2-1-0-1-1
3-2-1-0-1-2
3-2-1-0-1-3
(3-2-1-0-1-4)
(3-2-1-0-2-1)
3-2-1-0-2-2
(3-2-1-0-2-3)
3-2-1-0-2-4
3-2-1-0-3-1
(3-2-1-0-3-2)

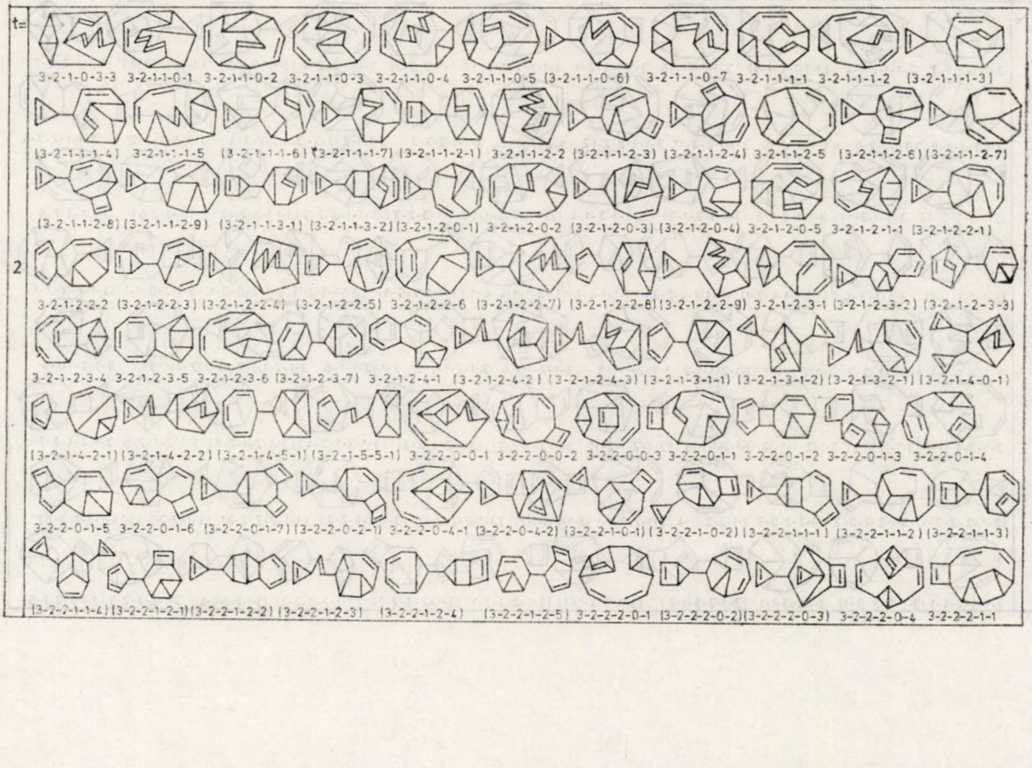
t=
2
3-2-1-0-3-3
3-2-1-1-0-1
3-2-1-1-0-2
3-2-1-1-0-3
3-2-1-1-0-4
3-2-1-1-0-5
(3-2-1-1-0-6)
3-2-1-1-0-7
3-2-1-1-1-1
3-2-1-1-1-2
(3-2-1-1-1-3)
(3-2-1-1-1-4)
3-2-1-1-1-5
(3-2-1-1-1-6)
(3-2-1-1-1-7)
(3-2-1-1-2-1)
3-2-1-1-2-2
(3-2-1-1-2-3)
(3-2-1-1-2-4)
3-2-1-1-2-5
(3-2-1-1-2-6)
(3-2-1-1-2-7)
(3-2-1-1-2-8)
(3-2-1-1-2-9)
(3-2-1-1-3-1)
(3-2-1-1-3-2)
(3-2-1-2-0-1)
3-2-1-2-0-2
(3-2-1-2-0-3)
(3-2-1-2-0-4)
3-2-1-2-0-5
3-2-1-2-1-1
(3-2-1-2-2-1)
3-2-1-2-2-2
(3-2-1-2-2-3)
(3-2-1-2-2-4)
(3-2-1-2-2-5)
3-2-1-2-2-6
(3-2-1-2-2-7)
(3-2-1-2-2-8)
(3-2-1-2-2-9)
3-2-1-2-3-1
(3-2-1-2-3-2)
(3-2-1-2-3-3)
3-2-1-2-3-4
3-2-1-2-3-5
3-2-1-2-3-6
(3-2-1-2-3-7)
3-2-1-2-4-1
(3-2-1-2-4-2)
(3-2-1-2-4-3)
(3-2-1-3-1-1)
(3-2-1-3-1-2)
(3-2-1-3-2-1)
(3-2-1-4-0-1)
(3-2-1-4-2-1)
(3-2-1-4-2-2)
(3-2-1-4-5-1)
(3-2-1-5-5-1)
3-2-2-0-0-1
3-2-2-0-0-2
3-2-2-0-0-3
3-2-2-0-1-1
3-2-2-0-1-2
3-2-2-0-1-3
3-2-2-0-1-4
3-2-2-0-1-5
3-2-2-0-1-6
(3-2-2-0-1-7)
(3-2-2-0-2-1)
3-2-2-0-4-1
(3-2-2-0-4-2)
(3-2-2-1-0-1)
(3-2-2-1-0-2)
(3-2-2-1-1-1)
(3-2-2-1-1-2)
(3-2-2-1-1-3)
(3-2-2-1-1-4)
(3-2-2-1-2-1)
(3-2-2-1-2-2)
(3-2-2-1-2-3)
(3-2-2-1-2-4)
(3-2-2-1-2-5)
3-2-2-2-0-1
(3-2-2-2-0-2)
(3-2-2-2-0-3)
3-2-2-2-0-4
3-2-2-2-1-1

Table 4 (continued)

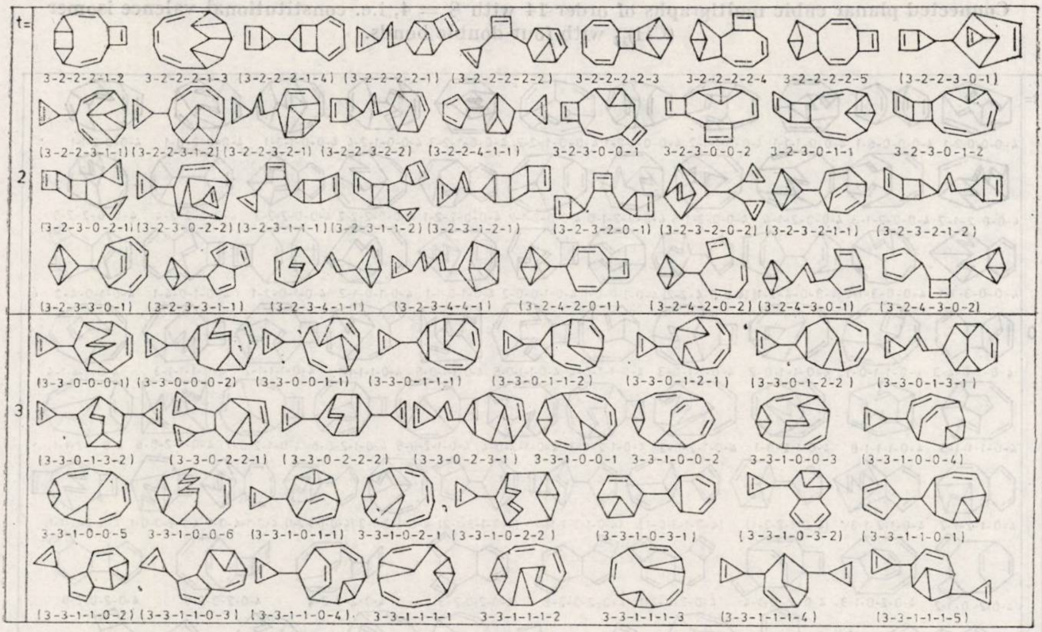
t=
2
3
3-2-2-2-1-2
3-2-2-2-1-3
(3-2-2-2-1-4)
(3-2-2-2-2-1)
(3-2-2-2-2-2)
3-2-2-2-2-3
3-2-2-2-2-4
3-2-2-2-2-5
(3-2-2-3-0-1)
(3-2-2-3-1-1)
(3-2-2-3-1-2)
(3-2-2-3-2-1)
(3-2-2-3-2-2)
(3-2-2-4-1-1)
3-2-3-0-0-1
3-2-3-0-0-2
3-2-3-0-1-1
3-2-3-0-1-2
(3-2-3-0-2-1)
(3-2-3-0-2-2)
(3-2-3-1-1-1)
(3-2-3-1-1-2)
(3-2-3-1-2-1)
(3-2-3-2-0-1)
(3-2-3-2-0-2)
(3-2-3-2-1-1)
(3-2-3-2-1-2)
(3-2-3-3-0-1)
(3-2-3-3-1-1)
(3-2-3-4-1-1)
(3-2-3-4-4-1)
(3-2-4-2-0-1)
(3-2-4-2-0-2)
(3-2-4-3-0-1)
(3-2-4-3-0-2)
(3-3-0-0-0-1)
(3-3-0-0-0-2)
(3-3-0-0-1-1)
(3-3-0-1-1-1)
(3-3-0-1-1-2)
(3-3-0-1-2-1)
(3-3-0-1-2-2)
(3-3-0-1-3-1)
(3-3-0-1-3-2)
(3-3-0-2-2-1)
(3-3-0-2-2-2)
(3-3-0-2-3-1)
3-3-1-0-0-1
3-3-1-0-0-2
3-3-1-0-0-3
(3-3-1-0-0-4)
3-3-1-0-0-5
3-3-1-0-0-6
(3-3-1-0-1-1)
3-3-1-0-2-1
(3-3-1-0-2-2)
(3-3-1-0-3-1)
(3-3-1-0-3-2)
(3-3-1-1-0-1)
(3-3-1-1-0-2)
(3-3-1-1-0-3)
(3-3-1-1-0-4)
3-3-1-1-1-1
3-3-1-1-1-2
3-3-1-1-1-3
(3-3-1-1-1-4)
(3-3-1-1-1-5)

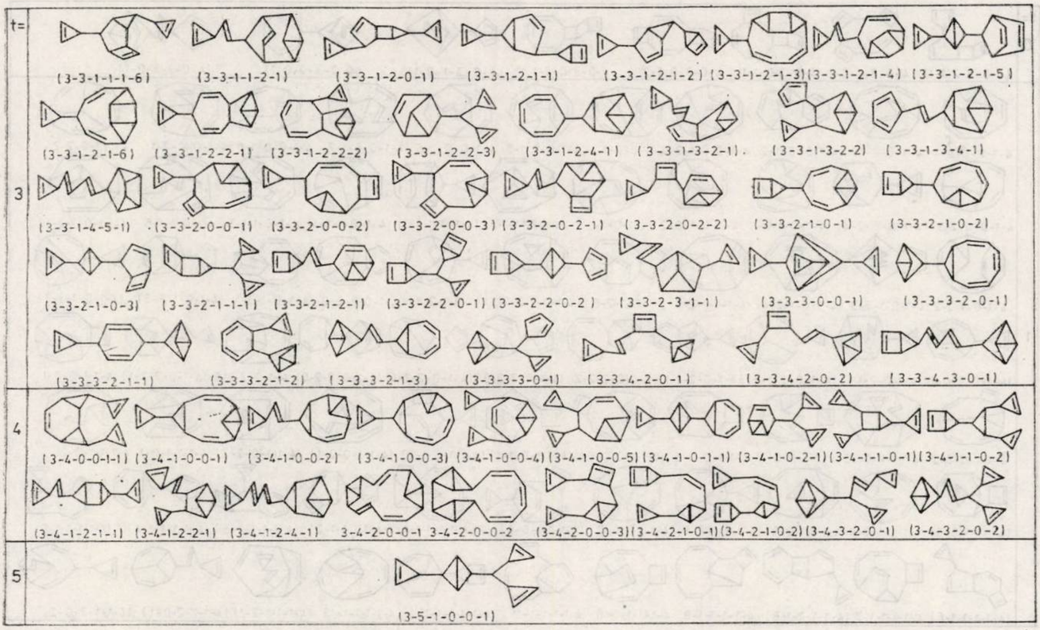
t=
3
4
5
(3-3-1-1-1-6)
(3-3-1-1-2-1)
(3-3-1-2-0-1)
(3-3-1-2-1-1)
(3-3-1-2-1-2)
(3-3-1-2-1-3)
(3-3-1-2-1-4)
(3-3-1-2-1-5)
(3-3-1-2-1-6)
(3-3-1-2-2-1)
(3-3-1-2-2-2)
(3-3-1-2-2-3)
(3-3-1-2-4-1)
(3-3-1-3-2-1)
(3-3-1-3-2-2)
(3-3-1-3-4-1)
(3-3-1-4-5-1)
(3-3-2-0-0-1)
(3-3-2-0-0-2)
(3-3-2-0-0-3)
(3-3-2-0-2-1)
(3-3-2-0-2-2)
(3-3-2-1-0-1)
(3-3-2-1-0-2)
(3-3-2-1-0-3)
(3-3-2-1-1-1)
(3-3-2-1-2-1)
(3-3-2-2-0-1)
(3-3-2-2-0-2)
(3-3-2-3-1-1)
(3-3-3-0-0-1)
(3-3-3-2-0-1)
(3-3-3-2-1-1)
(3-3-3-2-1-2)
(3-3-3-2-1-3)
(3-3-3-3-0-1)
(3-3-4-2-0-1)
(3-3-4-2-0-2)
(3-3-4-3-0-1)
(3-4-0-0-1-1)
(3-4-1-0-0-1)
(3-4-1-0-0-2)
(3-4-1-0-0-3)
(3-4-1-0-0-4)
(3-4-1-0-0-5)
(3-4-1-0-1-1)
(3-4-1-0-2-1)
(3-4-1-1-0-1)
(3-4-1-1-0-2)
(3-4-1-2-1-1)
(3-4-1-2-2-1)
(3-4-1-2-4-1)
3-4-2-0-0-1
3-4-2-0-0-2
(3-4-2-0-0-3)
(3-4-2-1-0-1)
(3-4-2-1-0-2)
(3-4-3-2-0-1)
(3-4-3-2-0-2)
(3-5-1-0-0-1)

Table 5

Connected planar cubic multigraphs of order 14 with β = 4, i.e. constitutional valence isomer $(CH)_{14}$ with four double bonds.

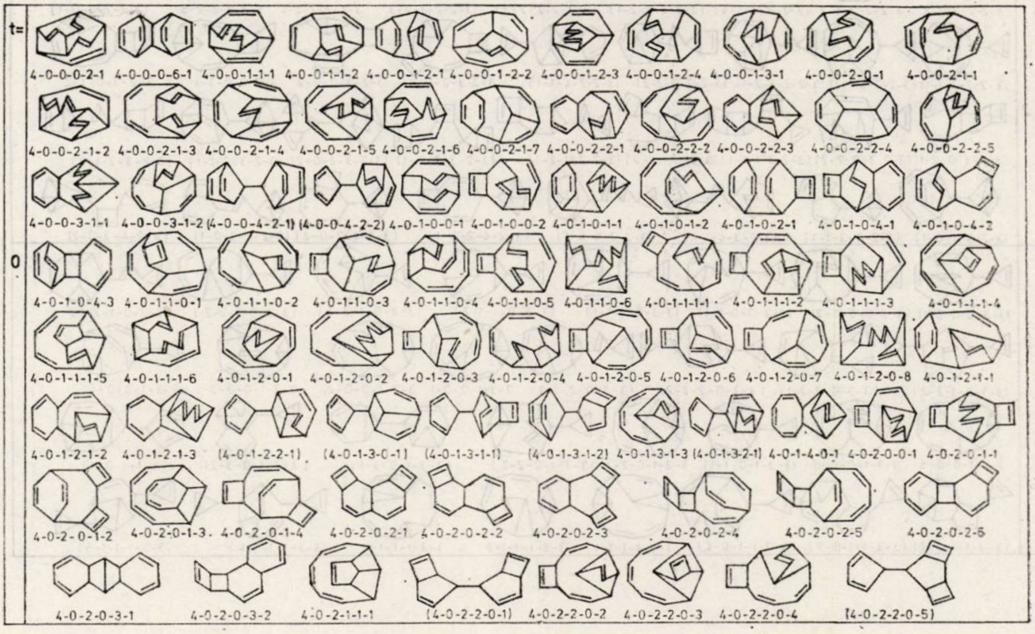
t=
0
4-0-0-0-2-1
4-0-0-0-6-1
4-0-0-1-1-1
4-0-0-1-1-2
4-0-0-1-2-1
4-0-0-1-2-2
4-0-0-1-2-3
4-0-0-1-2-4
4-0-0-1-3-1
4-0-0-2-0-1
4-0-0-2-1-1
4-0-0-2-1-2
4-0-0-2-1-3
4-0-0-2-1-4
4-0-0-2-1-5
4-0-0-2-1-6
4-0-0-2-1-7
4-0-0-2-2-1
4-0-0-2-2-2
4-0-0-2-2-3
4-0-0-2-2-4
4-0-0-2-2-5
4-0-0-3-1-1
4-0-0-3-1-2
(4-0-0-4-2-1)
(4-0-0-4-2-2)
4-0-1-0-0-1
4-0-1-0-0-2
4-0-1-0-1-1
4-0-1-0-1-2
4-0-1-0-2-1
4-0-1-0-4-1
4-0-1-0-4-2
4-0-1-0-4-3
4-0-1-1-0-1
4-0-1-1-0-2
4-0-1-1-0-3
4-0-1-1-0-4
4-0-1-1-0-5
4-0-1-1-0-6
4-0-1-1-1-1
4-0-1-1-1-2
4-0-1-1-1-3
4-0-1-1-1-4
4-0-1-1-1-5
4-0-1-1-1-6
4-0-1-2-0-1
4-0-1-2-0-2
4-0-1-2-0-3
4-0-1-2-0-4
4-0-1-2-0-5
4-0-1-2-0-6
4-0-1-2-0-7
4-0-1-2-0-8
4-0-1-2-1-1
4-0-1-2-1-2
4-0-1-2-1-3
(4-0-1-2-2-1)
(4-0-1-3-0-1)
(4-0-1-3-1-1)
(4-0-1-3-1-2)
4-0-1-3-1-3
(4-0-1-3-2-1)
4-0-1-4-0-1
4-0-2-0-0-1
4-0-2-0-1-1
4-0-2-0-1-2
4-0-2-0-1-3
4-0-2-0-1-4
4-0-2-0-2-1
4-0-2-0-2-2
4-0-2-0-2-3
4-0-2-0-2-4
4-0-2-0-2-5
4-0-2-0-2-6
4-0-2-0-3-1
4-0-2-0-3-2
4-0-2-1-1-1
(4-0-2-2-0-1)
4-0-2-2-0-2
4-0-2-2-0-3
4-0-2-2-0-4
(4-0-2-2-0-5)

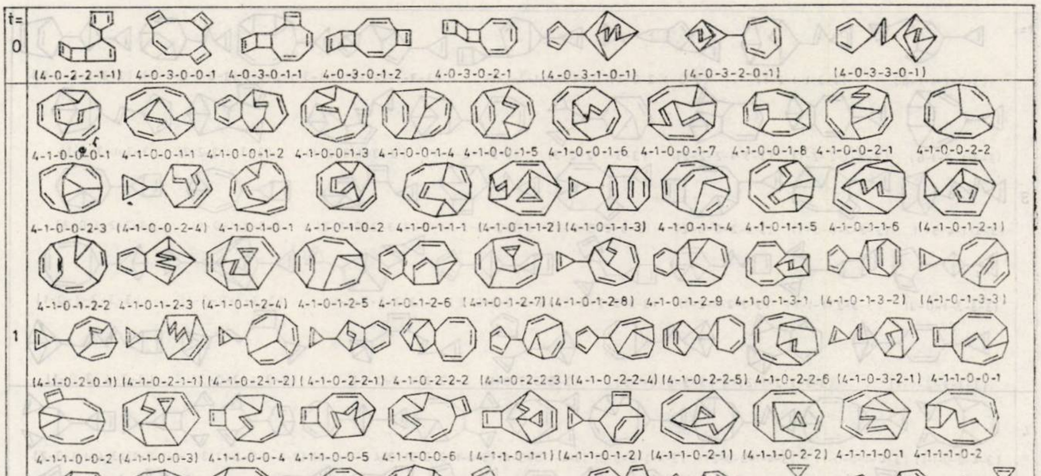
t=
0
(4-0-2-2-1-1)
4-0-3-0-0-1
4-0-3-0-1-1
4-0-3-0-1-2
4-0-3-0-2-1
(4-0-3-1-0-1)
(4-0-3-2-0-1)
(4-0-3-3-0-1)
1
4-1-0-0-0-1
4-1-0-0-1-1
4-1-0-0-1-2
4-1-0-0-1-3
4-1-0-0-1-4
4-1-0-0-1-5
4-1-0-0-1-6
4-1-0-0-1-7
4-1-0-0-1-8
4-1-0-0-2-1
4-1-0-0-2-2
4-1-0-0-2-3
(4-1-0-0-2-4)
4-1-0-1-0-1
4-1-0-1-0-2
4-1-0-1-1-1
(4-1-0-1-1-2)
(4-1-0-1-1-3)
4-1-0-1-1-4
4-1-0-1-1-5
4-1-0-1-1-6
(4-1-0-1-2-1)
4-1-0-1-2-2
4-1-0-1-2-3
(4-1-0-1-2-4)
4-1-0-1-2-5
4-1-0-1-2-6
(4-1-0-1-2-7)
(4-1-0-1-2-8)
4-1-0-1-2-9
4-1-0-1-3-1
(4-1-0-1-3-2)
(4-1-0-1-3-3)
(4-1-0-2-0-1)
(4-1-0-2-1-1)
(4-1-0-2-1-2)
(4-1-0-2-2-1)
4-1-0-2-2-2
(4-1-0-2-2-3)
(4-1-0-2-2-4)
(4-1-0-2-2-5)
4-1-0-2-2-6
(4-1-0-3-2-1)
4-1-1-0-0-1
4-1-1-0-0-2
(4-1-1-0-0-3)
4-1-1-0-0-4
4-1-1-0-0-5
4-1-1-0-0-6
(4-1-1-0-1-1)
(4-1-1-0-1-2)
(4-1-1-0-2-1)
(4-1-1-0-2-2)
4-1-1-1-0-1
4-1-1-1-0-2
(4-1-1-1-0-3)
4-1-1-1-0-4
(4-1-1-1-0-5)
(4-1-1-1-0-6)
4-1-1-1-0-7
(4-1-1-1-0-8)
4-1-1-1-1-1
(4-1-1-1-1-2)
(4-1-1-1-1-3)
(4-1-1-1-1-4)
(4-1-1-1-1-5)
(4-1-1-1-1-6)
4-1-1-1-1-7
(4-1-1-1-1-8)
4-1-1-1-1-9
4-1-1-1-1-10
4-1-1-1-1-11
(4-1-1-1-1-12)
4-1-1-1-1-13
(4-1-1-1-2-1)
(4-1-1-2-0-1)
(4-1-1-2-0-2)

Table 5 (continued)

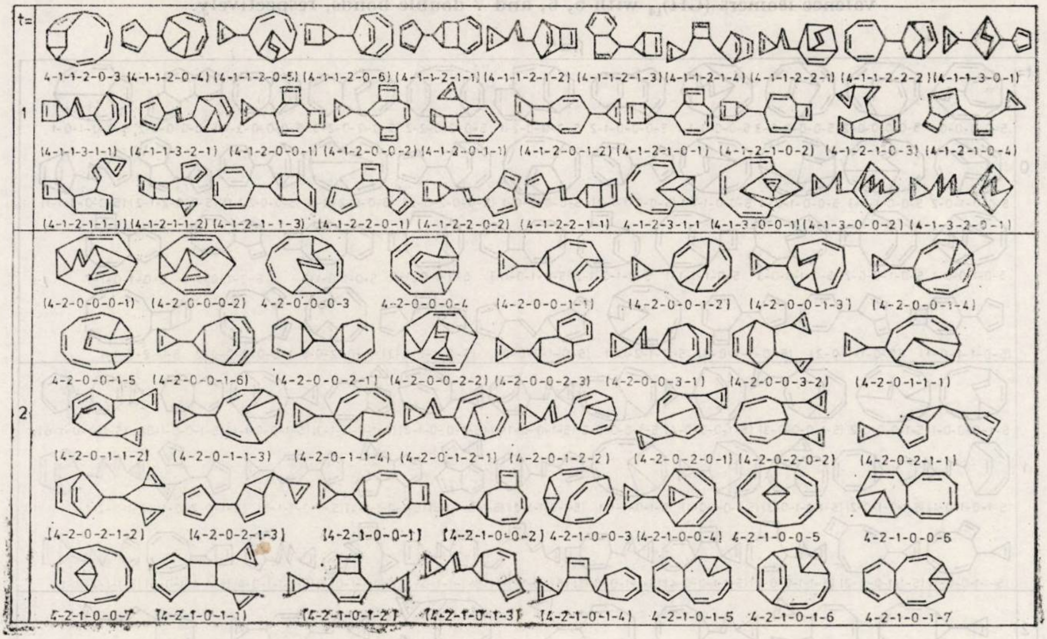
t=
1
4-1-1-2-0-3
(4-1-1-2-0-4)
(4-1-1-2-0-5)
(4-1-1-2-0-6)
(4-1-1-2-1-1)
(4-1-1-2-1-2)
(4-1-1-2-1-3)
(4-1-1-2-1-4)
(4-1-1-2-2-1)
(4-1-1-2-2-2)
(4-1-1-3-0-1)
(4-1-1-3-1-1)
(4-1-1-3-2-1)
(4-1-2-0-0-1)
(4-1-2-0-0-2)
(4-1-2-0-1-1)
(4-1-2-0-1-2)
(4-1-2-1-0-1)
(4-1-2-1-0-2)
(4-1-2-1-0-3)
(4-1-2-1-0-4)
(4-1-2-1-1-1)
(4-1-2-1-1-2)
(4-1-2-1-1-3)
(4-1-2-2-0-1)
(4-1-2-2-0-2)
(4-1-2-2-1-1)
4-1-2-3-1-1
(4-1-3-0-0-1)
(4-1-3-0-0-2)
(4-1-3-2-0-1)
2
(4-2-0-0-0-1)
(4-2-0-0-0-2)
4-2-0-0-0-3
4-2-0-0-0-4
(4-2-0-0-1-1)
(4-2-0-0-1-2)
(4-2-0-0-1-3)
(4-2-0-0-1-4)
4-2-0-0-1-5
(4-2-0-0-1-6)
(4-2-0-0-2-1)
(4-2-0-0-2-2)
(4-2-0-0-2-3)
(4-2-0-0-3-1)
(4-2-0-0-3-2)
(4-2-0-1-1-1)
(4-2-0-1-1-2)
(4-2-0-1-1-3)
(4-2-0-1-1-4)
(4-2-0-1-2-1)
(4-2-0-1-2-2)
(4-2-0-2-0-1)
(4-2-0-2-0-2)
(4-2-0-2-1-1)
(4-2-0-2-1-2)
(4-2-0-2-1-3)
(4-2-1-0-0-1)
(4-2-1-0-0-2)
4-2-1-0-0-3
(4-2-1-0-0-4)
4-2-1-0-0-5
4-2-1-0-0-6
4-2-1-0-0-7
(4-2-1-0-1-1)
(4-2-1-0-1-2)
(4-2-1-0-1-3)
(4-2-1-0-1-4)
4-2-1-0-1-5
4-2-1-0-1-6
4-2-1-0-1-7

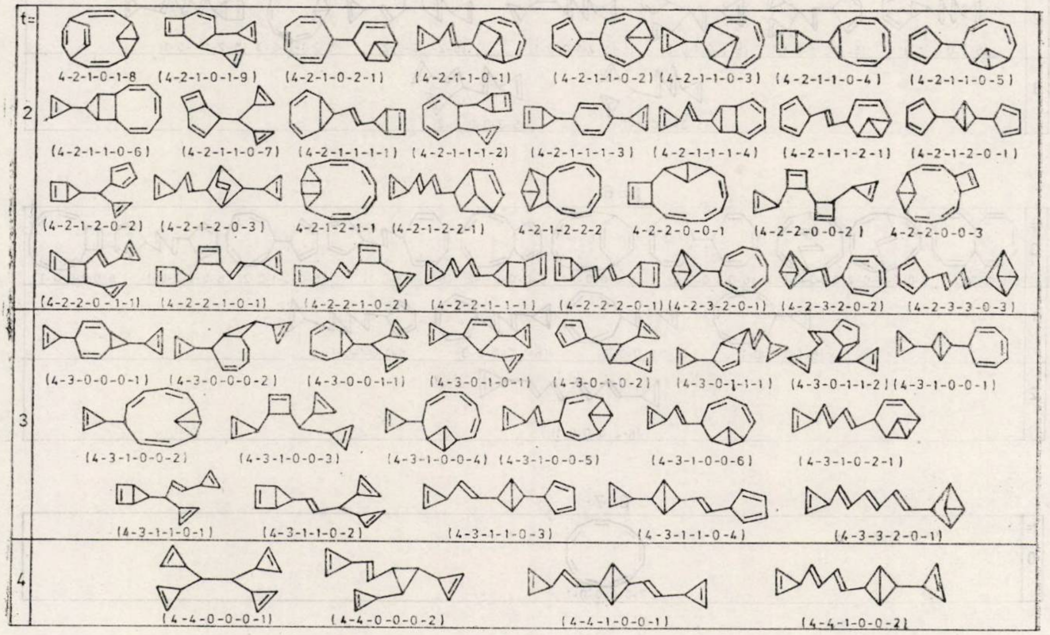
t=
2
4-2-1-0-1-8
(4-2-1-0-1-9)
(4-2-1-0-2-1)
(4-2-1-1-0-1)
(4-2-1-1-0-2)
(4-2-1-1-0-3)
(4-2-1-1-0-4)
(4-2-1-1-0-5)
(4-2-1-1-0-6)
(4-2-1-1-0-7)
(4-2-1-1-1-1)
(4-2-1-1-1-2)
(4-2-1-1-1-3)
(4-2-1-1-1-4)
(4-2-1-1-2-1)
(4-2-1-2-0-1)
(4-2-1-2-0-2)
(4-2-1-2-0-3)
4-2-1-2-1-1
(4-2-1-2-2-1)
4-2-1-2-2-2
4-2-2-0-0-1
(4-2-2-0-0-2)
4-2-2-0-0-3
(4-2-2-0-1-1)
(4-2-2-1-0-1)
(4-2-2-1-0-2)
(4-2-2-1-1-1)
(4-2-2-2-0-1)
(4-2-3-2-0-1)
(4-2-3-2-0-2)
(4-2-3-3-0-3)
3
(4-3-0-0-0-1)
(4-3-0-0-0-2)
(4-3-0-0-1-1)
(4-3-0-1-0-1)
(4-3-0-1-0-2)
(4-3-0-1-1-1)
(4-3-0-1-1-2)
(4-3-1-0-0-1)
(4-3-1-0-0-2)
(4-3-1-0-0-3)
(4-3-1-0-0-4)
(4-3-1-0-0-5)
(4-3-1-0-0-6)
(4-3-1-0-2-1)
(4-3-1-1-0-1)
(4-3-1-1-0-2)
(4-3-1-1-0-3)
(4-3-1-1-0-4)
(4-3-3-2-0-1)
4
(4-4-0-0-0-1)
(4-4-0-0-0-2)
(4-4-1-0-0-1)
(4-4-1-0-0-2)

Table 6

Connected planar cubic multigraphs of order 14 with $\beta = 5$, 6, and 7 i.e. constitutional valence valence isomers $(CH)_{14}$ with 5, 6, and 7 double bonds, respectively.

β=5

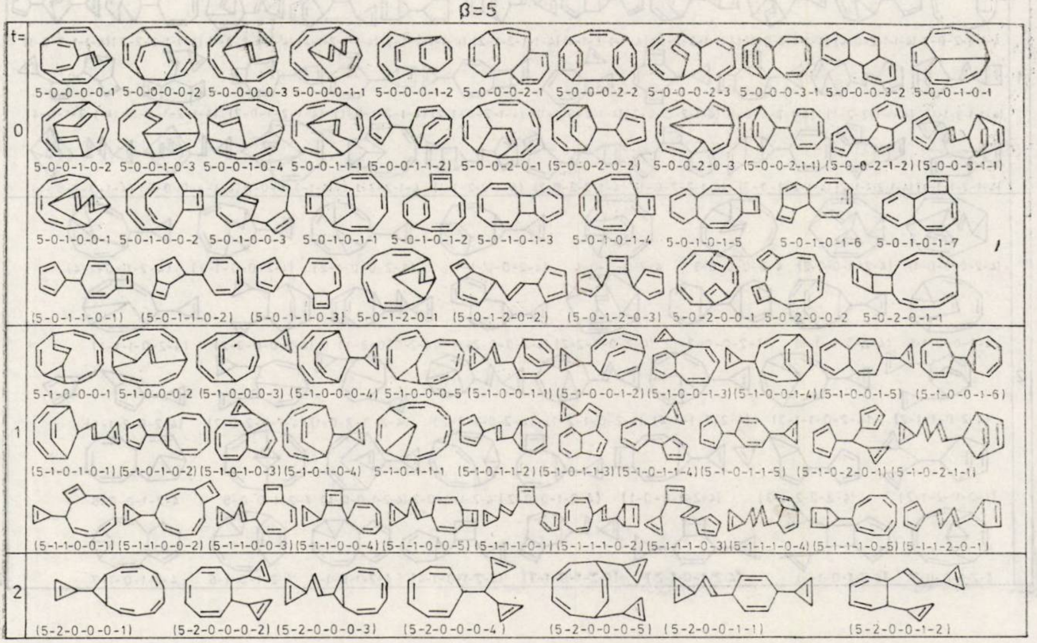
t=
0
5-0-0-0-0-1 5-0-0-0-0-2 5-0-0-0-0-3 5-0-0-0-1-1 5-0-0-0-1-2 5-0-0-0-2-1 5-0-0-0-2-2 5-0-0-0-2-3 5-0-0-0-3-1 5-0-0-0-3-2 5-0-0-1-0-1
5-0-0-1-0-2 5-0-0-1-0-3 5-0-0-1-0-4 5-0-0-1-1-1 (5-0-0-1-1-2) 5-0-0-2-0-1 (5-0-0-2-0-2) 5-0-0-2-0-3 (5-0-0-2-1-1) (5-0-0-2-1-2) (5-0-0-3-1-1)
5-0-1-0-0-1 5-0-1-0-0-2 5-0-1-0-0-3 5-0-1-0-1-1 5-0-1-0-1-2 5-0-1-0-1-3 5-0-1-0-1-4 5-0-1-0-1-5 5-0-1-0-1-6 5-0-1-0-1-7
(5-0-1-1-0-1) (5-0-1-1-0-2) (5-0-1-1-0-3) 5-0-1-2-0-1 (5-0-1-2-0-2) (5-0-1-2-0-3) 5-0-2-0-0-1 5-0-2-0-0-2 5-0-2-0-1-1
1
5-1-0-0-0-1 5-1-0-0-0-2 (5-1-0-0-0-3) (5-1-0-0-0-4) 5-1-0-0-0-5 (5-1-0-0-1-1) (5-1-0-0-1-2) (5-1-0-0-1-3) (5-1-0-0-1-4) (5-1-0-0-1-5) (5-1-0-0-1-6)
(5-1-0-1-0-1) (5-1-0-1-0-2) (5-1-0-1-0-3) (5-1-0-1-0-4) 5-1-0-1-1-1 (5-1-0-1-1-2) (5-1-0-1-1-3) (5-1-0-1-1-4) (5-1-0-1-1-5) (5-1-0-2-0-1) (5-1-0-2-1-1)
(5-1-1-0-0-1) (5-1-1-0-0-2) (5-1-1-0-0-3) (5-1-1-0-0-4) (5-1-1-0-0-5) (5-1-1-1-0-1) (5-1-1-1-0-2) (5-1-1-1-0-3) (5-1-1-1-0-4) (5-1-1-1-0-5) (5-1-1-2-0-1)
2
(5-2-0-0-0-1) (5-2-0-0-0-2) (5-2-0-0-0-3) (5-2-0-0-0-4) (5-2-0-0-0-5) (5-2-0-0-1-1) (5-2-0-0-1-2)

β=5

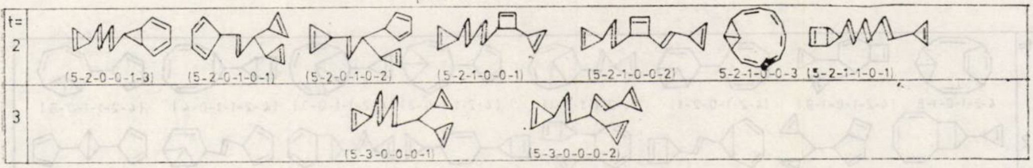
t=
2
(5-2-0-0-1-3) (5-2-0-1-0-1) (5-2-0-1-0-2) (5-2-1-0-0-1) (5-2-1-0-0-2) 5-2-1-0-0-3 (5-2-1-1-0-1)
3
(5-3-0-0-0-1) (5-3-0-0-0-2)

β=6

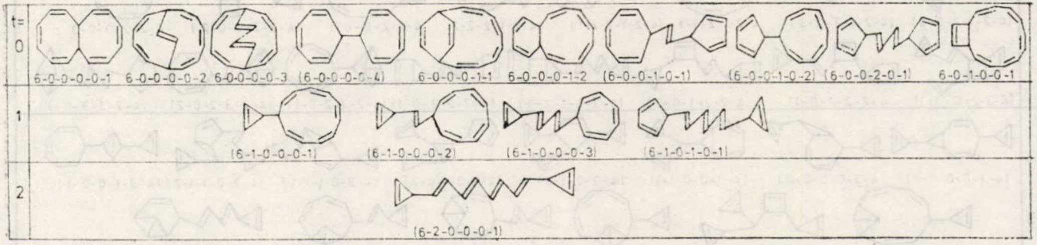
t=
0
6-0-0-0-0-1 6-0-0-0-0-2 6-0-0-0-0-3 (6-0-0-0-0-4) 6-0-0-0-1-1 6-0-0-0-1-2 (6-0-0-1-0-1) (6-0-0-1-0-2) (6-0-0-2-0-1) 6-0-1-0-0-1
1
(6-1-0-0-0-1) (6-1-0-0-0-2) (6-1-0-0-0-3) (6-1-0-1-0-1)
2
(6-2-0-0-0-1)

β=7

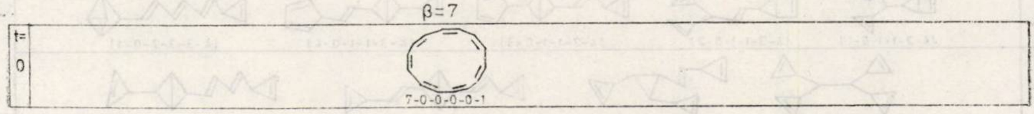

Table 7

Numbers of planar cubic multigraphs with $n = 4$ to 14 vertices, i.e. constitutional valence isomers $(CH)_n$ with β double bonds and t three-membered circuits

n	t β	0	1	2	3	4	5	6	Total
4	0	—	—	—	—	1	—	—	1
	1	—	—	—	—	—	—	—	0
	2	1	—	—	—	—	—	—	1
	total	1	0	0	0	1	0	0	**2**
6	0	—	—	1	—	—	—	—	1
	1	—	—	1	—	—	—	—	1
	2	1	—	1	—	—	—	—	2
	3	1	—	—	—	—	—	—	1
	total	2	0	3	0	0	0	0	**5**
8	0	1	—	1	—	1	—	—	3
	1	—	1	2	1	—	—	—	4
	2	2	1	2	—	—	—	—	5
	3	2	1	1	—	—	—	—	4
	4	1	—	—	—	—	—	—	1
	total	6	3	6	1	1	0	0	**17**
10	0	1	1	2	2	3	—	—	9
	1	1	3	7	4	1	—	—	16
	2	4	6	9	2	1	—	—	22
	3	6	5	4	1	—	—	—	16
	4	4	2	1	—	—	—	—	7
	5	1	—	—	—	—	—	—	1
	total	17	17	23	9	5	0	0	**71**
12	0	2	2	9	7	9	2	1	32
	1	4	13	26	19	11	2	—	75
	2	15	30	42	16	9	—	—	112
	3	21	30	26	7	2	—	—	86
	4	18	14	8	1	—	—	—	41
	5	6	3	1	—	—	—	—	10
	6	1	—	—	—	—	—	—	1
	total	67	92	112	50	31	4	1	**357**
14	0	5	8	31	35	35	12	7	133
	1	15	60	126	115	67	18	3	404
	2	56	161	229	134	57	9	1	647
	3	97	189	178	71	20	1	—	556
	4	91	108	72	19	4	—	—	294
	5	41	33	14	2	—	—	—	90
	6	10	4	1	—	—	—	—	15
	7	1	—	—	—	—	—	—	1
	total	316	563	651	376	183	40	11	**2140**

We conjecture that those groups lead to unique graphs in the $\beta - t$ triangular display, in other words that for these groups the numbers of triangles and double bonds are maximal for given numbers of double bonds and triangles, respectively.

It is interesting to note the numbers of graphs on any row marked Total are maximal for the row $t = 2$, in Table 7 (with the exception of $n = 4$ where no graph has exactly two triangles).

KNOWN VALENCE ISOMERS OF [14]ANNULENE

From the 2140 possible constitutional formulas (and about twice as much if stereoisomerism is taken into account), only seven constitutions have been obtained experimentally (two of these as substituted derivatives and not as the parent compounds). One structure is known to exist as two stereoisomers, namely [14] annulene. Table 8 presents all known valence isomers of [14] annulene **4**—**11** with the IUPAC and trivial names, in chronological order.

Bitropyl or *dihydroheptafulvalene* (**4**), (14—6—0—0—0—0—4), the first valence isomer of any annulene, is a separable graph $(CH)_{14}$ and is the most investigated compound among all those which will be reviewed here. Doering and Knox obtained it in 1957 *via* a smooth reduction of tropylium salts with zinc dust.[12] Other reductions leading to the same product involve electrochemical [22] or polarographic methods,[23] treatment with sodium amalgam,[24] manganese pentacarbonyl anions,[25] or photolysis.[26] The intermediate is a tropylium radical.[22,23] Alternative syntheses of **4** start from tropylidene and oxidize it to the same radical by (i) gamma irradiation (gamma source or Van der Graaf accelerator);[27] a ^{14}C-label becomes randomly distributed substantiating the intermediacy of a free radical;[27] (ii) 2,4,6-tri-t-butylphenoxyl radicals;[28] 9,10-dibromoanthracene;[29] (iii) sulfur monoxide;[30] (iv) Vilsmeyer reagent.[31] Oxidative methods have also been used starting from methyl tropenyl ether, *via* potassium tropenide.[32] Tropylium-chromium tricarbonyl perchlorate afforded with alkali cyanides a bis-(chromium tricarbonyl)bitropyl complex which on heating with diethylene-triamine was converted into **4**.[33]

Bitropyl **4** is a solid (m.p. 61°) with an electronic spectrum essentially identical with that of tropylidene.[12] The thermal reactions of **4** were extensively investigated.[34] Dissociation of the central bond needs[35] about 35 $\text{kcal} \cdot \text{mol}^{-1}$ (much less than in bibenzyl) and gives rise to tropylium radicals investigated mainly by ESR spectroscopy.[34-36] Thermolysis of molten **4** indicated:[36] $E_a = 34.4\ \text{kcal} \cdot \text{mol}^{-1}$; $\log A = 13.3$; $\Delta H^{\neq} = 32.8\ \text{kcal} \cdot \text{mol}^{-1}$; $\Delta S^{\neq} = -3.2\ \text{cal} \cdot \text{mol}^{-1} \cdot \text{grd}^{-1}$. Among thermolysis products occurring *via* tropylium radicals, bibenzyl was identified at 350°,[35] whereas benzene, toluene, xylene, bibenzyl and ethylbenzene were formed at 410°.[37] Isomeric hydrocarbons differing in the position of double bonds in the bitropyl skeleton were suggested to appear in the thermolysis of **4**.[36] Photolysis of **4** proceeds *via* double bond shifts (two consecutive suprafacial 1,7-H migrations).[26,38] Flash photolysis affords tropylium radicals [39] whereas UV-iradiation under oxygen in presence of methylene blue forms biphenyl and 7-phenyltropylidene along with different oxygenated com-

Table 8

Known valence isomers of [14]annulene in chronological order

Unsubstituted valence isomers of [14]annulene

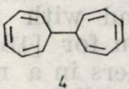 4	7,7′-bis-(1,3,5-cycloheptatrien-7-yl), Bitropyl, Dihydroheptafulvalene : (14 – 6 – 0 – 0 – 0 – 0 – 4)	1957 Doering and Knox [12]
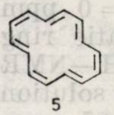 5 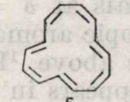 6	Cyclotetradeca -1,3,5,7,9,11,13 - heptaene, [14]Annulene : 14 – 7 – 0 – 0 – 0 – 0 – 1	1960 Sondheimer *et al.* [46,47]
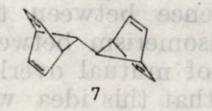 7	7,7′-bis-(Bicyclo[2.2.1]hepta-2,5-diene, 7,7′-bis-(2,5-Norbornadiene) : (14 – 4 – 0 – 0 – 4 – 2 – 1)	1965 Tanida *et al.* [53]
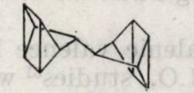 8	7,7′-bis-(Tetracyclo[2,2.1. ·$0^{2,6}$ ·$0^{3,5}$]heptane, bis-Quadricyclane : 14 – 0 – 4 – 2 – 8 – 10 – 1	1965 Tanida *et al.* [53]
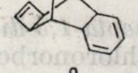 9	Tetracyclo[6.4.2.$0^{2,7}$ ·$0^{3,8}$]tetradeca-3,5,10,13-tetraene : 14 – 4 – 0 – 1 – 0 – 4 – 1	1981 Olgemöler and Beck[54] Hoffmann *el al.* [54]

Valence isomers of [14]annulene known only as derivatives

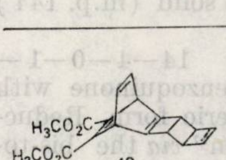 10	Bicyclo[6.6.0]tetradeca-2,4,6,9,11,13-hexaene : 14–6–0–0–0–0–1	1971 Sondheimer *et al.* [52]
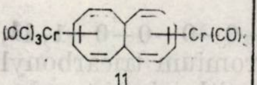 11	Pentacyclo[8.2.2.$0^{2,9}$ · $0^{3,8}$ · $0^{4,7}$]tetra-deca-5,11,13-triene : 14–3–0–3–0–5–2	1965 Schröder and Martin [55]

pounds.[40] Other reactions of **4** which may be mentioned are : oxidation to tropylium cations,[41] hydride abstraction,[42] hydrogenation,[42,43] ozonation,[27] reaction with dimethyl acetylene-dicarboxylate.[44,45]

[14]Annulene; *Cyclotetradeca*-1,3,5,7,11,13-*heptaene*, 14—7—0—0—0—0—1, **5** and **6**, were obtained by Jackman, Sondheimer *et al.* [46,47] starting from the acyclic tetradeca-4,10-diene-1,7,13-triyne *via* oxidative coupling of terminal acetylene carbons. The crystalline form was shown by X-ray crystallography [48] to have a non-planar centrosymmetric configuration with four "inner" hydrogens and with ring bond lengths in the range 1.35—1.47 Å (a wider range than for [18]annulene). In solution the compound exists as two stereoisomers in a ratio 11.5 : 1 at —10° ; the major component **5** gives rise at 40° to one ^{1}H—NMR peak at 5.58 ppm which misled initially, but which on cooling to —30° becomes flattened and at —60° is split into two signals at $\delta = 0$ ppm (4H) and 7.6 ppm (10H) ; these data indicate a diatropic aromatic ring current. On rapid dissolution of the crystals, only the above ^{1}H—NMR peaks may be seen. The minor stereoisomer **6** which appears in solution after about 30 minutes, gives rise at 40° to one peak at $\delta = 6.07$ ppm which decoalesces at much lower temperatures than the major isomer, hence is more mobile conformationally.[49] The difference between the two stereoisomers was first ascribed to conformational isomerism between two tri-*cis* conformations due to a different pattern of mutual overlap between the inner hydrogens, but later it was shown that this idea was incorrect : determination of the ^{1}H—NMR spectrum at very low temperatures showed that the minor component was a configurational stereoisomer **6**, with a tetra-*cis* configuration.

A 1,8-dimethyl-[14]annulene and its dihydro-octalenic valence isomer were prepared by Vogel *et. al.*[50] Semiempirical M.O. studies[51] were employed for studying equilibria of six stereoisomeric [14]annulenes. The reaction of [14]annulene with triaminotricarbonylchromium(0) led to the formation of a *trans*-dihydro-octalenic *bis*-chromium complex,[52] as indicated below for **11**.

7,7′-Bis-(2,5-norbornadiene) or *7,7′-bis-(bicyclo[2.2.1]hepta-1,5-diene)*, (14—4—0—0—4—2—1), **7**, results on treatment of 7-chloronorbornadiene with magnesium. Compound **7** is a solid (m.p. 63°) and presents characteristic IR and ^{1}H—NMR spectra.[53]

7,7′-Bis-(tetracyclo[2.2.1.0^{2,6}.0^{3,5}]heptane, bis-quadricyclane, (14—0—4—2—8—10—1), **8**, results on UV-iradiation of **7** as a solid (m.p. 144°) with characteristic IR and ^{1}H—NMR spectra.[53]

Tetracyclo[6.4.2.0^{2,7}.0^{9,12}]tetradeca-3,5,10,13-tetraene, 14—4—0—1—0—4—1, **9**, was obtained from the cycloadduct of *p*-benzoquinone with cyclooctatetraene (COT) in its bicyclic valence tautomeric form. Reduction of the quinonoid C=C double bond and "dehydration" *via* the bis-tosylhydrazone gave **9**. Formally this compound can be considered as an adduct of benzene and the bicyclic form of COT, and yields these two compounds on pyrolysis.[54]

Bicyclo[6.6.0]tetradeca-2,4,6,11,13-hexaene, 14—6—0—0—0—0—1, **11**, is known only as the *trans*-dihydro-octalenic *bis*-chromium tricarbonyl complex. It results in the reaction of [14] annulene (5) with triaminecarbonylchromium(0). Its structure was established by X-ray crystallography.

Interestingly, in solution this complex decomposes slowly at room temperature regenerating the monocyclic [14] annulene, rather than its bicyclic valence isomer.[52]

Pentacyclo[8.2.2.$0^{2,9}$.$0^{3,8}$.$0^{4,7}$]*tetradeca-5,11,13-triene*, 14–3–0–3–0–5–2, **10**, is known only as a substituted derivative with two carbomethoxy groups.[55]

CONCLUSION

By means of a new computer program implementing a novel algorithm, and on the basis of the conjectured non-degeneracy of topological index J' for cubic multigraphs of order 14, we have obtained the constitutional formulas of all possible $(CH)_{14}$ valence isomers (2140 cubic multigraphs of order 14); tables 1–6 presented these structures arranged according to their numbers β of double bonds and t of three-membered circuits, together with their notation found by means of yet another computer program which lists 4-, 5-, and 6-membered circuits.

The seven known valence isomers $(CH)_{14}$ were presented with their chemical data. Five of these, **4**–**9**, have been prepared as unsubstituted hydrocarbons and as derivatives; the remaining two, **10** and **11**, are known only as metallic complex and substituted derivative, respectively. For the monocyclic [14]annulene, two stereoisomeric forms, **5** and **6**, have been shown to exist. The stereochemistry of the other known $(CH)_{14}$ valence isomers has been little explored: no stereoisomers have been reported, although the possibility of stereoisomerism exists.

The above systematic listing of 2140 possible constitutional valence isomers $(CH)_{14}$ – and the above number will be approximately doubled if stereoisomerism is taken into account – constitute a challenge for future work by synthetic organic chemists.

REFERENCES

[1] Part 46, A. T. Balaban. *Rev. Roumaine Chim.* **31**, 795 (1986).

[2] A. T. Balaban, *Rev. Roumaine Chim.*, **11**, 1097 (1966).

[3] A. T. Balaban, *Rev. Roumaine Chim.*, **15**, 463 (1970).

[4] A. T. Balaban, *Math. Chem.*, **1**, 33 (1975).

[5] A. T. Balaban (Ed.), "Chemical Applications of Graph Theory", Academic Press, London, 1976.

[6] F. Harary, ,,Graph Theory", Addison-Wesley, Reading, Mass. 1969.

[7] A. T. Balaban and M. Banciu, *J. Chem. Educ.*, **61**, 766 (1984).

[8] A. T. Balaban, *Rev. Roumaine Chim.*, **17**, 865 (1972).

[9] M. Banciu, C. Popa and A. T. Balaban, *Chem. Scripta*, **24**, 28 (1984).

[10] A. T. Balaban, *Rev. Roumaine Chim.*, **19**, 1185 (1974).

[11] A. T. Balaban, R. Vancea, S. Holban and I. Motoc, *J. Chem. Inform. Comput. Sci.*, **26**, 72 (1986).

[12] W. von E. Doering and L. M. Knox, *J. Am. Chem. Soc.*, **79**, 352 (1957); W. von E. Doering and H. Krauch, unpublished results quoted in *Angew. Chem.*, **68**, 661 (1956).

[13] M. Avram, E. Şliam and C. D. Nenitzescu, *Liebigs Ann. Chem.*, **636**, 184 (1960).

[14] G. Maier, "Valenzisomerisierungen", Verlag Chemie, Weinheim, FRG, 1972.

[15] L. T. Scott and M. Jones Jr., *Chem. Rev.*, **72**, 181 (1972).

[16] A. T. Balaban, M. Banciu and V. Ciorba,"Annulenes, Benzo-, Hetero-, Homo-Derivatives and Their Valence Isomers", CRC Press, Boca Raton, 1987.

[17] P. V. Khvorostov, in "Mashinnyie metody obnaruzhenya zakonomernostei, analiza struktur i proektirovanya", Novosibirsk, Sbornik trudov, Edited by V. A. Skorobogatov, *Vychislitelnye systemy*, **92**, 80 (1982).

[18] A. T. Balaban, N. Ionescu-Pallas and T. -S. Balaban, *Math. Chem.*, **17**, 121 (1985).

[19] A. T. Balaban, *Chem. Phys. Lett.*, **80**, 399 (1982); *Pure Appl. Chem.*, **55**, 199 (1983); A. T. Balaban, and P. Filip, *Math. Chem.*, **16**, 163 (1983).

[20] A. T. Balaban and L. V. Quintas, *Math. Chem.*, **14**, 213 (1983).

[21] A. T. Balaban, P. Filip and T. -S. Balaban , *J. Comput. Chem.*, **6**, 316 (1985).

[22] R. Breslow and R. F. Drury, *J. Am. Chem. Soc.*, **96**, 4702 (1974); A. Stasko and P. H. Plesch, *Z. Phys. Chem.* (Leipzig), **256**, 418 (1975); A. M. Romanin, A. Venzo and A. Cecon, *J. Electroanal. Chem.*, *Interfacial Electrochem.*, **112**, 147 (1980); V. Vetani, T. Sato, T. Matsubayashi and T. Kashiwaya, *Denki Kagaku*, **34**, 124 (1966).

[23] S. I. Zhdanov and A. N. Frumkin, *Dokl. Akad. Nauk SSSR*, **122**, 412 (1958).

[24] M. E. Volpin and E. C. Teudoradze, *Izv. Akad. Kauk. SSSR, Ser. Khim.*, 1655 (1970).

[25] T. A. Whitesides and R. A. Budnik, *Chem. Commun.*, 1514 (1971).

[26] E. E. van Tamelen. R. H. Greeley and H. Schumacher, *J. Am. Chem. Soc.*, **93**, 6151 (1971).

[27] G. Juppe and A. P. Wolf, *J. Am. Chem. Soc.*, **83**, 337 (1961).

[28] C. M. Orlando Jr. and K. Weiss, *J. Org. Chem.*, **29**, 2493 (1964).

[29] H. Kondo, M. Mori and K. Kanematsu, *J. Org. Chem.*, **45**, 5273 (1980).

[30] R. M. Dodson and J. P. Nelson, *Chem Commun.*, 1159 (1969).

[31] T. Asao, S. Kuroda and K. Kato, *Chem. Lett.*, 41 (1978).

[32] H. J. Dauben Jr. and M. R. Rifi, *J. Am. Chem. Soc.*, **85**, 3041 (1963).

[33] J. D. Munro and P. L. Pauson, *J. Chem. Soc.*, 3484 (1961).

[34] G. Vinkow, M. L. Morell, W. V. Volland, H. J. Dauben Jr. and F. R. Hunter, *J. Am. Chem. Soc.*, **87**, 3527 (1965).

[35] A. G. Harrison, L. R. Honnen, H. J. Dauben Jr. and F. P. Lossing, *J. Am. Chem. Soc.*, **82**, 5593 (1960).

[36] W. V. Volland and G. Vinkow, *J. Am. Chem. Soc.*, **90**, 4537 (1968); G. Vinkov, H. J. Dauben Jr., E. R. Hunter and W. V. Volland, *ibid.*, **91**, 2823 (1969).

[37] M. Pomeranz and A. S. Ross, *J. Am. Chem. Soc.*, **97**, 5850 (1975).

[38] R. S. Givens , *Tetrahedron Lett.*, 663 (1969).

[39] B. A. Trush and J. J. Zwolenik, *Bull. Soc. Chim. Belges*, **71**, 642 (1962); *Proc. Chem. Soc.*, 339 (1962).

[40] H. Takaeshita and A. Mori, *Heterocycles*, **11**, 319 (1978).

[41] D. H. Geske, *J. Am. Chem. Soc.*, **81**, 4145 (1959); P. Beresford and A. Ledwith, *Chem. Commun.*, 15 (1970).

[42] P. Beresford, A. Ledwith and H. J. Woods, *J. Chem. Soc. B*, 257 (1970).

[43] R. B. Turner. W. R. Meador, W. von E. Doering, L. H. Knox, J. R. Mayer and D. W. Wiley *J. Am. Chem. Soc.*, **79**, 4127 (1957).

[44] J. Bordner and G. H. Wahl, Jr., *J. Org. Chem.*, **36**, 3630 (1971).

[45] G. H. Wahl, Jr. and K. Weiss, *J. Org. Chem.*, **35**, 3902 (1970).

[46] L. M. Jackman, F. Sondheimer, Y. Amiel, D. A. Ben-Efraim, Y. Gaoni, R. Wolovsky and A. A. Bothner-By, *J. Am. Chem. Soc.*, **84**, 1307 (1962).

[47] F. Sondheimer and Y. Gaoni, *J. Am. Chem. Soc.*, **82**, 5765 (1960). R. Gaoni, A. Melera, F. Sondheimer and R. Wolovsky, *Proc. Chem. Soc.*, 397 (1964).

[48] N. A. Bailey and R. Mason, *Proc. Roy. Soc. A*, **290**, 94 (1966); C. C. Chiang and J. C. Paul, *J. Am. Chem. Soc.*, **94**, 4741 (1972).

[49] Y. Gaoni and F. Sondheimer, *Proc. Chem. Soc.*, 299 (1964).

[50] E. Vogel, H. W. Engels, W. Huber, J. Lex and K. Müllen, *J. Am. Chem. Soc.*, **104**, 3729 (1982).

[51] D. Loos and J. Leska, *Coll. Czech. Chem. Commun.*, **47**, 1075 (1982).

[52] F. Sondheimer, K. Stökckel , T. A. Clark, W. Guss and R. A. Mason, *J. Am. Chem. Soc.*, **93**, 2571 (1971).

[53] H. Tanida, Y. Hata, Y. Matsui and I. Tanaka, *J. Org. Chem.*, **30**, 2259 (1965); H. Tanida. *Japan Pat.* 68—22862; *Chem. Abstr.*, **70**, 57297 (1969).

[54] R. W. Hoffmann, M. Lotze, M. Reiffen and K. Steinbach, *Liebigs Ann. Chem.*, 581 (1981); B. Olgemöler and W. Beck, *Chem. Ber.*, **114**, 867 (1981); W. Grimme and G. Reinhardt, *Angew. Chem. Int. Ed. Engl.*, **22**, 617 (1983).

[55] G. Schröder and W. Martin, *Angew. Chem. Int. Ed. Engl.*, **5**, 130 (1966).

Revue Roumaine de Chimie, 32, 3, 295–296 (1987)

IPSO-SUBSTITUTION OF HETEROCYCLIC COMPOUNDS.I.

NITRATION OF 5-BROMO-3,4-DIMETHYL-1-PHENYL-1*H*,6*H*-PYRANO[2,3-*c*]PYRAZOL-6-ONE

MISBAHUL AIN KHAN* and RUBINA GHAFOOR
Department of Chemistry, Islamia University, Bahawalpur, Pakistan

Received February 3, 1986

Nitration of the title compound gave 3,4-dimethyl-5-nitro-1-(*p*-nitrophenyl)-1*H*,6*H*-pyrano[2,3-*c*]pyrazol-6-one *via* an *ipso*-substitution.

Some derivatives of 1*H*,6*H*-pyrano[2,3-*c*]pyrazol-6-one have been shown to be good vasodilatators, hypotensive and hypoglycemic agents[1] and recently we reported the synthesis and reactions of various derivative of this system.[2] Here we would like to report the nitration of 5-bromo-3,4-dimethyl-1-phenyl-1*H*,6*H*-pyrano[2,3-*c*]-pyrazol-6-one (**1b**), which was earlier obtained from the bromination of **1a**.[2]

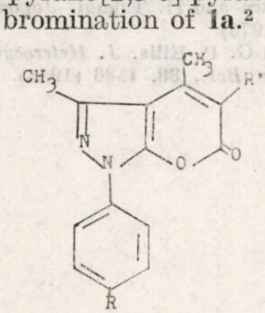

1a R=R'=H

1b R=H, R'=Br

1c R=R'=NO_2

1d, R=NO_2, R'=Br

During our investigations we found that the nitration of **1b** with "mixed acids" (sulfuric and nitric acid) leads to the formation of 3-4-dimethyl-5-nitro-1-(*p*-nitrophenyl)-1*H*,6*H*-pyrano[2,3-*c*]pyrazol-6-one (**1c**), identical with an authentic sample.[2] The expected "normal" reaction product, 5-bromo-3,4-dimethyl-1-(*p*-nitrophenyl)-1*H*,6*H*-pyrano[2,3-*c*]pyrazol-6-one (**1d**) was, however, not isolated in this reaction. This seems to be the first case of *ipso* substitution for this system. Replacement of a bromo substituent by a nitro group during nitration of a bromo methylpyrazole has earlier been reported by Huttel.[3] We are further investigating these *ipso* substitution reactions.

---

* Address for Correspondence : Prof. Dr. Misbahul Ain Khan, Chairman, Department of Chemistry, Islamia University, Bahawalpur, Pakistan

EXPERIMENTAL

Melting points were taken on a Gallenkamp melting point apparatus and are uncorrected. Infrared spectra were measured on a Beckmann and proton magnetic resonance spectra on a Hitachi L—24B, 60 MHz instrument (tetramethylsilane used as an internal reference).

Nitration of 1b

A mixture of 1 mL of concentrated sulfuric acid and 1 mL of concentrated nitric acid was added dropwise at 0° to a solution of 0.4 g of **1b**[2] in 1 mL of concentrated sulfuric acid. The reaction temperature was maintained at room temperature for half an hour after which the reaction mixture was poured over crushed ice, filtered, washed with ice-cold water and crystallized from ethyl acetate to give 0.3 g of 3,4-dimethyl-5-nitro-1-(*p*-nitrophenyl)-1*H*, 6*H*-pyrano[2,3-*c*]pyrazol-6-one (**1c**), m.p. 208—209°, mixed m.p., IR and ^{1}H—NMR spectra identical with an authentic sample.[2]

REFERENCES

[1] Y. Sato, Y. Shimoji, S. Kumakura and H. Takagi, *Japan Kokai*, **75**, 151, 896 (1975); *Chem. Abstr.*, **84**, 164771 (1976).

[2] M. A. Khan, A. G. Cosenza and G. P. Ellis, *J. Heterocyclic Chem.*, **19**, 1077 (1982).

[3] R. Huttel and F. Buchele, *Chem. Ber.*, **88**, 1586 (1955).

Revue Roumaine de Chimie, **32**, *3*, 297–303 (1987)

REACTIONS OF HOMOPHTHALIC ANHYDRIDE WITH SOME COMPOUNDS CONTAINING TWO AMINO GROUPS

M.I. ALI, A. M. ABD-ELFATTAH, H. A. HAMMOUDA and S. M. HUSSAIN

Chemistry Department, Faculty of Science, Cairo University, Giza, A. R. Egypt

Received March 24, 1986

Homophthalic anhydride was condensed with ethylenediamine, diphenylethylenediamine, anthranilamide, and orthanilamide to give I, VII, X and XIII, respectively. Compound I reacted with *p*-nitrosodimethylaniline to give VI and with arenediazonium salts to yield III which further reacted with Grignard reagents to give V.

In continuation of our previous studies,[1–3] the present communication reports on the behaviour of homophthalic anhydride toward some diamino compounds. Thus homophthalic anhydride reacted with ethylenediamine at 180°C to give a compound having very likely the structure I, *viz.*, 2,3-dihydroimidazo-[1,2-b]isoquinolin-5(1OH)one. The angular isomer 2,3-dihydroimidazo [2,1-a]isoquinolin-5(6H)-one (II) is excluded because it has been previously obtained from the reaction of 1-thio-1,3(2H, 5H)-isoquinolinedione with ethylenediamine [4] and is different from compound I. The IR spectrum of I showed an absorption at 1670 cm^{-1} (CO). The ^1H-NMR spectrum (TFA) of I showed peaks at δ4.64 ppm (m, 6H, $3CH_2$) and 7.92 (m, 4H, arom.).

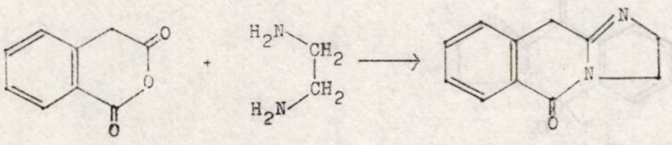

I

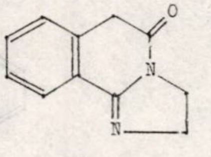

II

Compound I can be coupled with arenediazonium salts to give 2,3,5, 10-tetrahydroimidazo[1,2-b]isoquinoline-5,10-dione 10-arylhydrazones, III.

The IR spectum of IIIa showed CO absorption at 1675 cm^{-1}, almost with no shift from the CO absorption of the starting compound I. This is also in favour of the linear structure I. The UV spectrum of IIIa (CH_3OH) showed a maximum at 390 nm, which supports the hydrazone structure for compounds III.[5-7]

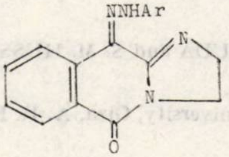

III

a, Ar = C_6H_5
b, Ar = $C_6H_4CH_3$-p
c, Ar = $C_6H_4OCH_3$-p
d, Ar = C_6H_4Cl-p
e, Ar = C_6H_4Br-p

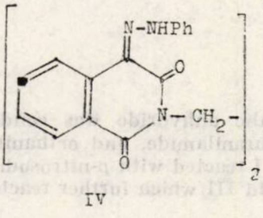

IV

In an attempt to prepare IIIa by condensing phthalonic anhydride phenylhydrazone[8] with ethylenediamine, the bis compound IV was obtained. The IR spectrum of IV showed two carbonyl absorption peaks at 1670 and 1625 cm^{-1}.

The addition of Grignard reagents to IIIa afforded compounds V which were separated as their dihydrochlorides.

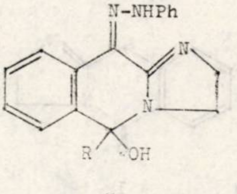

V

a, R = CH_3
b, R = C_2H_5
c, R = C_6H_5
d, R = $C_6H_4CH_3$-o

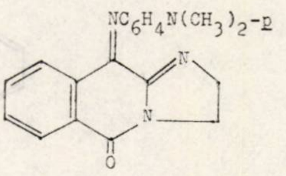

VI

Compound I could also react with *p*-nitrosodimethylaniline to give the deeply coloured azomethine, VI.

Homophthalic anhydride reacted with 1,2-diphenylethylenediamine in refluxing DMF to give 2,3-diphenyl-2,3-dihydroimidazo[1,2-b]isoquinolin-5(1H)-one(VII) or the angular isomer, VIII. The IR spectrum of the product showed NH absorption at 3270 cm^{-1} and a carbonyl band at 1655, thus favouring the linear structure VII.

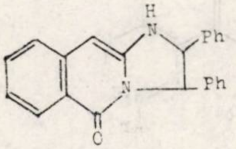

VII

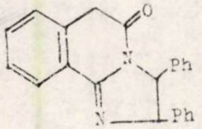

VIII

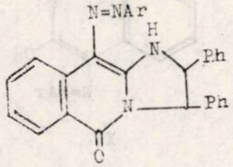

IX

a, $Ar = C_6H_5$

b, $Ar = C_6H_4Br$-p

Coupling of VII with diazonium salts gave the 10-arylazoderivatives, IX. The IR spectrum of IXa showed NH absorption at 3300cm^{-1} and CO absorption at 1660. The UV spectrum of IXa (EtOH) showed a maximum at 270 nm indicating an azo structure rather than a hydrazone form.[5-7]

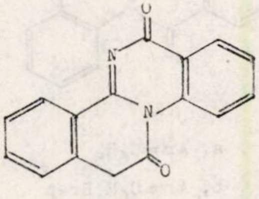

X

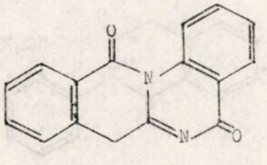

Xa

The reaction of homophthalic anhydride with orthanilamide at 180°C or in refluxing DMF led to the formation of a compound for which — due to the expected initial attack of the amino group of anthranilamide — one can assume structure X or Xa.

These formulations were also based on : a) molecular weight of this product which is 262 ; m/e, 262 (M), b) the presence of two CO absorption bands at 1680 and 1645 cm^{-1} and the absence of bands due to OH or NH in the IR spectrum. However, the presence of two different absorption bands in the CO region in the IR spectrum is in favour of structure X which has two different carbonyl groups.

Coupling of X with diazonium salts gave the arylazo derivatives XI. The IR spectrum of XIb showed only one carbonyl band at 1645 cm^{-1}

and a broad weak OH absorption at 3500–3300, indicating that XIb exists in the chelated structure XII.[9-10]

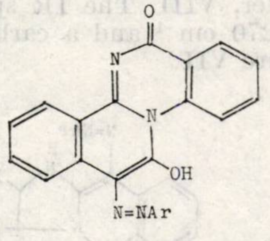

XI

a, Ar = C_6H_5

b, Ar = C_6H_4Br-p

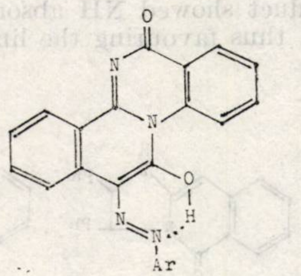

XII

Orthanilamide, on the other hand, reacted with homophthalic anhydride under the same conditions to give N-(*o*-aminosulphonylphenyl) homophthalimide, XIII indicating in the MS the characteristic peaks at m/e 316 (M^+) and 298 ($M^+ - H_2O$).

Boiling of XIII with acetic anhydride did not result in cyclisation. Thermal dehydration trials also were unsuccessful.

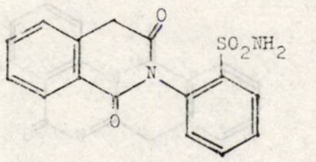

XIII

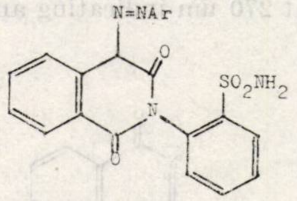

XIV

a, Ar = C_6H_5

b, Ar = C_6H_4Br-p

Coupling of XIII with diazonium salts gave the azo compounds XIV. The IR spectrum of XIVa showed carbonyl bands at 1660 and 1630 cm^{-1} and NH absorption at 3270 and 3200 cm^{-1}.

EXPERIMENTAL

Melting points are uncorrected. IR spectra were recorded using KBr discs on a Hitachi Grating IR Spectrophotometer Model EPI-G3. UV spectra were taken with a DK-Beckman recording spectrometer. ^1H–NMR spectra were taken with a Perkin-Elmer R12A instrument, expressed in δ ppm from TMS.

2,3-Dihydroimidazo [1,2-b]isoquinolin-5(1OH)-one (I)

A mixture of 4.1 g of homophthalic anhydride and 1.7 g of ethylenediamine was gently heated in an oil bath; the temperature was raised gradually and kept at 180°C for 10 minutes then cooled. The product was crystallized from ethanol to give 4 g (86 %) of I, m.p. 212°. Found: C, 70.95; H, 5.41; N, 14.04. Calcd. for $C_{11}H_{10}N_2O$: C. 71.21; H, 5.33; N, 15.17 %.

2,3,5,10-Tetrahydroimidazo[1,2-b]isoquinoline-5,10-dione 10-arylhydrazones (III). General procedure

A suspension of 1.86 g of I and 3 g of sodium acetate in 50 mL of ethanol was cooled in an ice bath, treated with an equimolar amount of the appropriate diazotized aniline, left for 1 hr and then poured into water. The precipitate formed was collected, dried and crystallized from AcOH (Table 1).

Table 1

Characterization data of compounds III and V

Compound*	m.p. °C	Yield %	Mol. Formula	Analyses % Calcd./Found C	H	N	X
IIIa	197	91	$C_{17}H_{14}N_4O$	70.33 70.09	4.86 5.11	19.30 19.52	
IIIb	172	94	$C_{18}H_{16}N_4O$	71.04 70.89	5.30 5.13	18.41 18.51	
IIIc	162	90	$C_{18}H_{16}N_4O_2$	67.49 67.32	5.03 5.26	17.49 17.58	
IIId	222	84	$C_{17}H_{13}ClN_4O$	62.87 62.61	4.03 4.19	17.25 17.41	10.92 10.67
IIIe	216	86	$C_{17}H_{13}BrN_4O$	55.30 55.48	3.55 3.72	15.17 15.01	21.64 21.33
Va	250	78	$C_{18}H_{20}Cl_2N_4O$	57.00 56.69	5.31 5.11	14.77 14.63	18.69 18.35
Vb	241	62	$C_{19}H_{22}Cl_2N_4O$	58.02 57.71	5.64 5.42	14.24 13.94	18.03 17.92
Vc	255	61	$C_{23}H_{22}Cl_2N_4O$	62.59 62.50	5.02 4.88	12.69 12.47	16.07 16.35
Vd	281	55	$C_{24}H_{24}Cl_2N_4O$	63.30 62.97	5.31 5.08	12.30 12.10	15.57 15.40

* Compounds IIIa—e and Vc were crystallized from acetic acid; Va from ethylene glycol; Vb, d from ethanol.

Reaction of phenylazohomophthalic anhydride with ethylenediamine. Formation of IV

Phenylazohomophthalic anhydride (2 g) was heated with an excess of ethylenediamine (ca. 0.7 g) as for the preparation of I. The product was crystallized from dioxane, m.p. 260°, yield 64 %. Found: C, 68.90; H, 4.41; N, 15.05. Calcd. for $C_{32}H_{24}N_6O_4$: C, 69.05; H, 4.35; N, 15.10 %.

5-Substituted 5-hydroxy-2,3,5,10-tetrahydroimidazo[1,2-b]-isoquinolin-10-one 10-phenylhydrazone dihydrochlorides (V.2HCl). General procedure

To a Grignard solution (prepared from 1.5 g of magnezium and the appropriate amount of alkyl or aryl halide in 100 mL of dry ether) 2 g of IIIa in 100 mL of dry ether were added. The mixture was refluxed on the steam bath for 2 hr, cooled and then decomposed with dil. HCl. The precipitate formed was filtered off, washed with water and crystallized (Table 1).

Condensation of I with p-nitrosodimethylaniline

A cold solution of 3.14 g of *p*-nitrosodimethylaniline hydrochloride in 100 mL of methanol was treated with a cold solution of 0.8 g of NaOH in 50 mL of methanol. The resulting mixture was added to a solution of 3.1 g of I in 50 mL of DMF. The reaction mixture was left overnight and then poured into cold water. The dark blue precipitate formed was collected, washed with water and then with ethanol and crystallized from benzene to give VI, m.p. 185°, yield 70 %. Found : C, 71.42 ; H, 5.52 ; N, 17.81. Calcd. for $C_{19}H_{18}N_4O$: C, 71.67 ; H, 5.71 ; N, 17.60 %.

2,3-Diphenyl-2,3-dihydroimidazo[1,2-b]isoquinolin-5(1H)-one (VII)

Homophthalic anhydride (2.4 g) and 1,2-diphenylethylenediamine (3.2 g) were refluxed in 30 mL of DMF for 1 hr and poured into cold water. The product was collected, washed with water, dried and crystallized from DMF-water (6 : 1), m.p. 277°, yield 68 %. Found : C, 81.92 ; H, 5.25 ; N, 8.22 ; Calcd. for $C_{23}H_{18}N_2O$: C, 81.63 ; H, 5.63 ; N, 8.28 %.

10-Arylazo-2,3-dihydro-2,3-diphenylimidazo[1,2-b]isoquinolin-5(1H)-ones (IXa, b)

The title compounds were prepared from VII and diazotized aniline or *p*-bromoaniline exactly as described for the preparation of III.

Compound IX, crystallized from acetic acid, m.p. 17 °, yield 79 %. Found : C, 78.91 ; H, 5.22 ; N, 12,69. $C_{29}H_{22}N_4O$ Calcd. : C, 78.71 ; H, 5.01 ; N, 12.66 %.

Compound IXb, crystallized from acetic acid, m.p. 275°, yield 86 %. Found : C, 67.08 ; H, 4.13 ; N, 10.91. Calcd. for $C_{29}H_{21}BrN_4O$: C, 66.80 ; H, 4.06 ; N, 10.75 %.

6,7-Dihydro-13H-isoquino[2,1-a]quinazoline-16,13-dione (X)

Method a). A mixture of homophthalic anhydride (1.62 g), anthranilamide (1.36 g) and DMF (20 mL) was refluxed for 2 hrs and left to cool. The separated crystals were collected and recrystallized from acetic acid to give X, m.p. 318°, yield 73 %.

Method b). A mixture of homophthalic anhydride (1.62 g) and anthranilamide (1.36 g) was heated and the temperature was raised gradually to 180° and kept for 45 minutes. The product was triturated with ethanol and the solid obtained was crystallized to give X, m.p. 318°. Found : C, 73.11 ; H, 3.70 ; N, 10.77. Calcd. for $C_{16}H_{10}N_2O_2$: C, 73.27 ; H, 3.84 ; N, 10.68 %.

7-Arylazo-6-hydroxy-13H-isoquino[2,1-a]quinazolin-13-ones (XI)

The title compounds were prepared from X and diazotized aniline or *p*-bromoaniline exactly as described for the preparation of III.

Compound XIa, crystallized from acetic acid, m.p. 284°, yield 90 %. Found : C, 72.39 H, 3.97 ; N, 15.34. Calcd. for $C_{22}H_{14}N_4O_2$: C, 72.12 ; H, 3.85 ; N, 15.29 %.

Compound XIb, recrystallized from dioxane, m. p.293°, yield 92 %.Found : C, 59.45 ; H, 2.98 ; N. 12.71 ; Br, 17.60. Calcd. for $C_{22}H_{13}BrN_4O_2$: C, 59.34 ; H, 2.94 ; N, 12.58 ; Br, 17.94 %.

N-(o-Aminosulphonylphenyl) homophthalimide (XIII)

A mixture of 1.62 g of homophthalic anhydride, 1.72 g of orthanilamide and 30 mL DMF was refluxed for 3 hr, cooled and poured into water. The product was filtered off, dried and crystallized from acetic acid, m.p. 280°, yield 72 %. Found : C, 5 .66 ; H, 3.68 ; N, 9.05 ; S, 10.1 . Calcd. $C_{15}H_{12}N_2O_4S$: C, 56.95 ; H, 3.82 ; N, 8.86 ; S, 10.14 %.

4-Arylazo-2-(o-aminosulphonylphenyl)-1,2,3,4-tetrahydroisoquinoline-1,3-diones (XIV)

The diazotized amine was added to an ice-cooled solution of XIII in pyridine. The mixture was refrigerated for 1 hr and poured into water. The product was filtered off, washed with water and crystallized from acetic acid.

Compound XIVa, m.p. 296°, yield 74 %. Found : C, 60.33 ; H, 4.10 ; N, 13.19 ; S, 7.67. Calcd. for $C_{21}H_{16}N_4O_4S$: C, 59.99 ; H, 3.84 ; N, 13.33 ; S, 7.63 %.

Compound XIVb, m.p. 305°, yield 76 %, Found : F, 50.66 ; ; H, .13 ; F. 11.17. Calcd. for $C_{21}H_{15}BrN_4O_4S$: C, 50.51 ; H, 3.03 ; N, 11.22 %.

REFERENCES

[1] M. I. Ali, A. A. El-Sayed and A. M. Abd-Elfattah, *J. Org. Chem.*, **37**, 3209 (1972).
[2] A. M. Abd-Elfattah, S. M. Hussain and M. I. Ali, *Tetrahedron*, **30**, 987 (1974).
[3] M. I. Ali, A. M. Abbd-Elfattah and S. M. Hussain, *Indian J. Chem.*, **14** B, 749 (1976).
[4] A. Mustafa, M. I. Ali and A. A. El-Sayed, *Liebigs Ann. Chem.*, **739**, 63 (1970).
[5] H. C. Yao and P. Resnick, *J. Amer. Chem. Soc.*, **84**, 3514 (1962).
[6] H. C. Yao, *J. Org. Chem.*, **29**, 2959 (1964).
[7] C. H. DePuy and P. P. R. Wells, *J. Amer. Chem. Soc.*, **82**, 2909 (1960).
[8] W. Dieckman, *Ber. dtsch. chem. Ges.*, **47**, 1428 (1914).
[9] D. Hadzi, *J. Chem. Soc.*, **1956**, 2143.
[10] K. Ueno, *J. Amer. Chem. Soc.*, **79**, 3066 (1957).

Revue Roumaine de Chimie, **32**, *3*, 305–313 (1987)

PHENYLHYDRAZONE FORMATION FROM SUBSTITUTED BENZALDEHYDES : SUBSTITUENT EFFECT AND STRUCTURE-REACTIVITY CORRELATIONS

F. GUTIERREZ-MARTÍN, A. RODRIGUEZ-PASTOR * and F. MATA-PÉREZ
Departamento de Química Física, Facultad de Ciencias, Universidad de Valladolid,
47011, Valladolid, Spain

Received September 9, 1985
Revised August 30, 1986

Kinetics of benzaldehyde phenylhydrazone formation from seven monosubstituted benzaldehydes has been investigated, in acidic medium, by a spectrophotometric method. Kinetic and thermodynamic parameters for both addition and hydrolysis reactions, and equilibrium were determined. Substituent effects have been analyzed by the Hammett equation, and elucidation of individual inductive, resonance and steric effects was carried out. Internal and external contributions at over-all ΔH and ΔS values have been obtained from the Hepler method, and both substituent and solvent effects were separately analysed. Finally, the relation of these parameters with the molecular grounds of the mechanism is discussed.

INTRODUCTION

It is clearly shown in a great number of works [1,2] that addition of nucleophiles (R_2NH, ROH, RSH, ROOH, . . .) to carbonyl group proceeds by a common mechanism ; in a first-step it gives rise to a simple carbon-nucleophile bond, in a second-step to the respective double bond when the nucleophile has two dissociable protons (as primary amines, hydroxylamine, semicarbazide and hydrazines, which undergo addition with formation of an aminoalcoholic intermediate and the suitable imine product) :

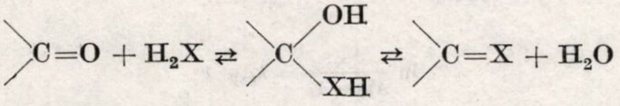

$$>C=O + H_2X \rightleftarrows >C(OH)(XH) \rightleftarrows >C=X + H_2O \qquad (1)$$

(X=N, O, S)

The above-mentioned investigations allowed the elucidation of a great number of questions about kinetic behaviour, catalysis and mechanism of both addition and hydrolysis reactions. However, the analysis of available material shows blanks when it is tried to correlate macroscopic kinetic and thermodynamic parameters on microscopic molecular grounds.

---

* Author to whom correspondence has to be addressed.

The main objective of this work is to study these problems in bezaldehyde phenylhydrazone formation and hydrolysis from seven monosubstituted benzaldehydes : $-H$, $p-N(CH_3)_2$, $m-OH$, $p-OH$, $o-Cl$, $m-Cl$, $p-Cl$.

These investigations are neither numerous nor very rigorous in the bibliography, however they give rise to some outstanding results (sometimes contradictories) in the knowledge of the kinetics and thermodynamics of the chemical reaction in solution.

EXPERIMENTAL

Instrumentation, materials and preparation. Kinetic measurements were carried out spectrophotometrically with the aid of a Bausch & Lomb model Sp—20 photocolorimeter at λ_{max} around 350 nm. The appropriate wavelengthwas determined from the UV/VIS spectra of the synthesized phenlhydrazones using a Perkin-Elmer 137-UV spectrophotometer. In the reaction with *p*-dimethylaminobenzaldehyde a superposition of the aldehyde and phenylhydrazone absorptions was observed, so that these reactions were carried out at an acid concentration greater than 0.5 $mol \cdot dm^{-3}$, where a negligible aldehyde absorption is verified.

Phenylhydrazine, benzaldehydes, HCl and NaCl were commercial products "for analysis" quality.

Solutions of benzaldehydes were prepared by dilution, in the solvent-mixture, of a stock solution of aldehyde to an initial concentration in the reactor 5.10^{-5} $mol \cdot dm^{-3}$ in all kinetic experiments.

Solutions of phenylhydrazine were prepared just prior to use from an exact amount of commercial product in the solvent-mixture so that its concentration was in a great excess (between 20—400 times) on the aldehyde concentration.

The solvent-mixture was an hydroalcoholic solution (20% ethanol) of HCl and NaCl to give an ionic strength of 1.5 $mol \cdot dm^{-3}$ and an acid concentration between 0.1—1.5 $mol \cdot dm^{-3}$.

The temperature was controlled by a conventional thermostate (±0.1°C). In all cases its values oscillated between 25—49°C.

Kinetics. In all cases, correlation of experimental measures was consistent with a pseudo-first order kinetic behavior. Since the reaction is bidirectional and the amine and water concentrations are constant in practice along the reaction, experimental rate constants were evaluated from slopes of plots lg $(A_\infty - A_t)$ against time in the usual manner :

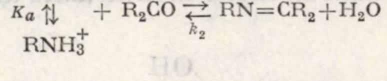

$$\begin{matrix} RNH_2 \\ K_a \upharpoonleft\downharpoonright \\ RNH_3^+ \end{matrix} + R_2CO \underset{k_2}{\overset{k_2}{\rightleftarrows}} RN{=}CR_2 + H_2O \qquad (2)$$

$$\ln \frac{A_\infty}{A_\infty - A_t} = k_{exp} \cdot t \qquad (3)$$

Second-order rate constants (and equilibrium constants) were obtained from slopes and plots intercepts of k_{exp} against the phenylhydrazine free-base concentration (a) :

$$k_{exp} = k_2 \cdot a + k_{-1} \qquad (4)$$

$$(k_{-1}/C_{H_2O} = k_{-2}) \qquad K = k_2/k_{-2} \qquad (5)$$

The free-amine concentration can be calculated from both acid and amine added concentrations and the pK_a of phenylhydrazinium ion.[3]

The kinetic measures are consistent with an over-all reaction order two (one for each reagent in the addition process, and one for the product in the hydrolysis process) so that the rate law is:

$$v = \frac{d[RN{=}CR_2]}{dt} = k_2[MNH_2]\,[R_2CO] - k_{-2}[RN{=}CR_2][H_2O] \qquad (6)$$

Catalytic constants for acid-catalyzed reaction and for uncatalyzed reaction were obtained from slopes and plots intercepts of second-order rate constants against the acid concentrations were modified:

$$k = k_0 + k_H C_H \qquad (7)$$

Finally, the rate constants were measured at five temperatures, and thermodynamic parameters were evaluated by the habitual correlations.

RESULTS

Kinetic parameters. The rate constants showed in table 1 are absolutes in that they do not depend on any external variable and therefore they represent the relative intrinsic reactivities of substrates; the reactivity differences only will be associated with the structural differences. This can be learnt by the free energy relationships (a good agreement can be shown between both rate or equilibrium constants and free energy changes). One of the well-known of these relationships is the Hammett equation[4,5] lg $k/k_0 = \sigma\rho$.

Good correlations can be observed between the logarithm of catalytic constants or equilibrium constants versus the substituents constants, but while the addition reaction (fig. 1.1) and over-all equilibrium (fig. 1.2) show a good correlation with σ-electrophilic substituent constants (with exception of p—NHMe$_2$ group), the hydrolysis reaction (fig. 1.2) shows a better correlation with σ-substituent constants.

A different behavior of the ρ-slope sign can also be observed, what points out that electronic substituent effects have a contrary influence in hydrolysis and in both equilibrium or addition processes. The ρ-amount is rather low for the addition process; the ρ-constants for hydrolysis and equilibrium are greater what points out that electronic efects are much more acute.

Substituent electronic effects are a sum of both inductive and resonance contributions. It can be supposed that in *meta* position no resonance exist with the side chain, so that $\sigma_I \cong \sigma_m$, and that in *meta* and *para* positions the inductive effect must be similar, so that $\sigma_R \cong \sigma_p - \sigma_I$. Notion of division of electronic effects in the inductive and resonance contributions has the corollary which these different ways of charge transfer may require for different ρ-values, in agreement with a double parameter equation lg $k/k_0 = \rho_I\sigma_I - \rho_R\sigma_R$.

We have evaluated these parameters from the σ_I, σ_R and the experimental rate constants (see table 1). The values show a large inductive effect in *meta* and *ortho* positions, when contribution of resonance is negligible, while in *para* position they contribute similarly.

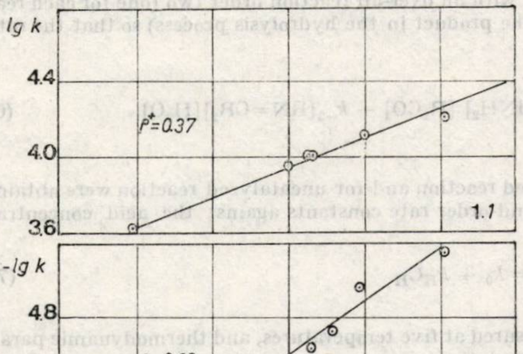

Fig. 1. — Hammett's correlations for phenylhydrazine addition to substituted benzaldehydes (1.1), hydrolysis of phenylhydrazones (1.2) and over-all equilibrium (1.3).

Table 1

ρ^+-constant for both inductive and resonance charge transfer in addition of phenylhydrazine to substituted benzaldehydes

constant	*ortho*	*meta*	*para*
ρ_I^+	0.33	0.40	0.39
ρ_R^+	0.07	0.01	0.37

Thermodynamic parameters. Table 2 shows that reactivity (k) or affinity (K) cannot be accounted for by ΔH or ΔS values in particular, since both parameters are changed in complex form. The ΔH variations are much simpler, what can be accounted for by the compensation effect between enthalpy and entropy due to solute-solvent interactions. The mathematical expression of this effect is the isokinetic law, and the isokinetic temperatures (approx. 260 −270 K) suggest that entropy is the

Table 2

k_H, $\Delta H^{\neq}$, $\Delta S^{\neq}$, $\Delta G^{\neq}$ and K values

Reagents : Phenylhydrazine and substitued benzaldehydes (XC_6H_3CHO)
Solvent mixture : ethanol-water 20 % v/v; HCl 0.1—1.5 mol · dm^{-3}; ionic strength 1.5 mol · dm^{-3} (compensating electrolyte : NaCl)
Temperature range : 25—37°C.

Addition reaction	X	o-Cl	p-NHMe$_2^+$	m-Cl	p-Cl	m-OH	H	p-OH
$k_H/10^4$ dm^{6}mol^{-1}s^{-1}		2.72	1.68	1.33	1.03	1.02	0.92	0.43
$\Delta H^{\neq}$/kJ · mol^{-1}		9	28	13	25	18	15	26
$\Delta S^{\neq}$/J · K^{-1} · mol^{-1}		−97	−37	−88	−50	−74	−120	−56
$\Delta G^{\neq}$/kJ · mol^{-1}		37.5	38.6	39.3	39.9	40.0	51.0	42.2
Hydrolysis reaction	X	p-NHMe$_2^+$	o-Cl	m-Cl	p-Cl	m-OH	H	p-OH
$k_H/10^{-5}$dm^{6}mol^{-1}s^{-1}		0.72	0.90	1.08	1.87	2.33	2.90	4.50
$\Delta H^{\neq}$/kJ · mol^{-1}		53	74	62	62	67	74	82
$\Delta S^{\neq}$/J · K^{-1} · mol^{-1}		−130	−58	−99	−92	−74	−82	−20
$\Delta G^{\neq}$/kJ · mol^{-1}		92.2	91.7	91.1	89.9	89.3	99	87.6
Over-all equilibrium	X	p-NHMe$_2^+$	o-Cl	m-Cl	p-Cl	m-OH	H	p-OH
K/10^8		25	19	12	6	4	3	0.6
ΔH/kJ · mol^{-1}		−54	−60	−40	−35	−43	−48	−43
ΔS/J · K^{-1} · mol^{-1}		1	−21	39	49	20	2	3
ΔG/kJ · mol^{-1}		−54.4	−53.8	−51.7	−50.1	−49.2	−48.6	−44.4

factor determining the magnitude of temperatures in which the experiments were carried out.

The $\Delta H^{\neq}$ values for the addition process are rather low with respect to typical values. The great negative values of heat of reaction ΔH are in agreement with the high values of equilibrium constants. The $\Delta S^{\neq}$ values are, in general, greatly negative, what appears to point out an active role of water in the solvation of activation complex.

These parameters can be analysed in more detail by division of $\delta\Delta H$ and $\delta\Delta S$ in both internal (imputed at electronic substituent effects) and external contributions (imputed at medium effects)$_6$. Figure 2 shows that $\delta\,\Delta H_{int}$ are parallel to the respective values of $\delta\Delta G$, what is a verification of the Hammett equation with the effect that the substituent influences can be accounted for by electronic factors (measured by ΔH_{int}), while over-all values of ΔH and ΔS show a much more complex variation caused by medium contributions. This fact is important since it is a test of the Hepler method [6] in these reactions, and moreover because it is a guarantee to quantify separately both electronic and solvent effects (see table 3).

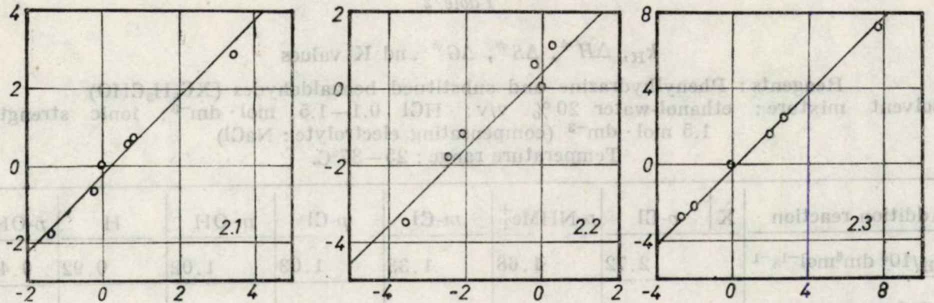

Fig. 2. — $\delta\Delta G$ vs. $\delta\Delta H_{\text{int}}$ for phenylhydrazine addition to substituted benzaldehydes (2.1), hydrolysis of phenylhydrazones (2.2) and over-all equilibrium (2.3).

Table 3

Internal and external contributions to ΔH and ΔS

$$\delta\Delta S \cong \delta\Delta S_{\text{ext}}$$
$$\delta\Delta H_{\text{ext}} \cong T\delta\Delta S_{\text{ext}} \cong T\delta\Delta S$$
$$\delta\Delta H = \delta\Delta H_{\text{int}} + \delta\Delta H_{\text{ext}} \cong \delta\Delta H_{\text{int}} + T\delta\Delta S$$
$$\delta\Delta H - T\delta\Delta S \cong \delta\Delta H_{\text{int}} \cong \delta\Delta G$$

Addition reaction substituent	$\delta\Delta H_{\text{ext}}$	$\delta\Delta H_{\text{int}}$	$\delta\Delta G$
p-OH	9.5	3.5	2.9
m-OH	4.2	0.8	0.7
p-Cl	11.3	0.7	0.6
m-Cl	0.0	0.0	0.0
p-NHMe$_2^+$	15.2	−0.2	−0.7
o-Cl	− 2.7	−1.3	−1.8

Equilibrium substituent	$\delta\Delta H_{\text{ext}}$	$\delta\Delta H_{\text{int}}$	$\delta\Delta G$
p-OH	−10.7	7.7	7.3
m-OH	− 5.7	2.7	2.5
p-Cl	3.0	2.0	1.6
m-Cl	0.0	0.0	0.0
o-Cl	−17.9	−2.1	−2.1
p-NHMe$_2^+$	−11.2	−2.7	−2.7

Hydrolysis reaction substituent	$\delta\Delta H_{\text{ext}}$	$\delta\Delta H_{\text{int}}$	$\delta\Delta G$
p-NHMe$_2^+$	26.5	2.5	2.0
o-Cl	15.2	0.8	0.3
m-Cl	0.0	0.0	0.0
p-Cl	8.3	−1.3	−1.0
m-OH	9.8	−1.8	−1.2
p-OH	20.3	−4.3	−4.4

Relative order of electron-extracting capacity:
o-Cl > p-NHMe$_2$ > m-Cl > m-OH ≅ p-Cl > H > p-OH

DISCUSSION

Structure-Reactivity Correlations

Correlation of rate constants for the addition process and constants for the over-all equilibrium, with electrophilic substituent constant σ^+ (better than σ) is consistent with the existence of a positive center (carbonyl) capable to resonate thoroughly with electron-donors substituents. In this way the extent of thorough conjugation present in the aldehyde is suppressed on the other side of the equilibrium. The justification of this requirement suggessts that the thorough conjugation in hydrazone must be limited by resonance itself with the adjacent nitrogen atom (eq. 8. b):

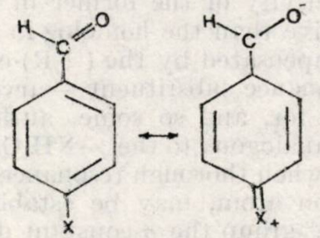

(8a)

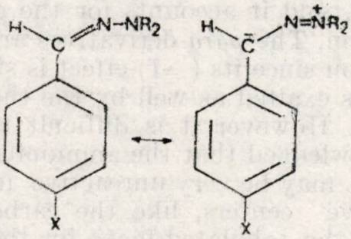

(8b)

After this, it can be expected that the rate constants for the hydrolysis process do not show any deviation in correlation with the unmodified constants σ, what means that they are in agreement with the observed behavior (fig. 1).

About the sign of the ρ-slopes, the observed positive value for the addition process and over-all equilibrium suggest that the mentioned processes are aided by electron-withdrawing substituents; on the other hand that it occurs in the hydrolysis process where ρ is negative. The interpretation of this behaviour is quite simple if we compare the species in equilibrium involved into the over-all mechanism:

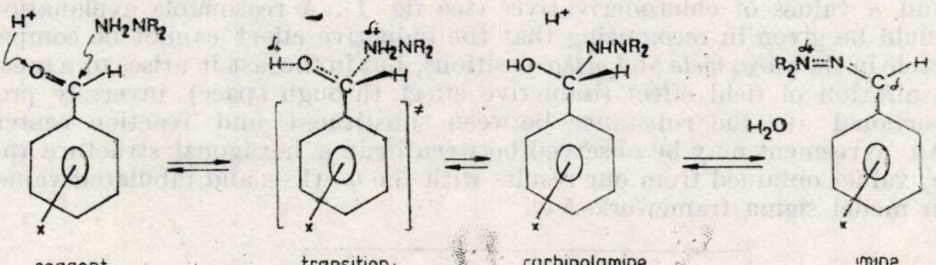

(9)

The amount of ρ is a measure of the reaction susceptibility for the electronic effects of the substituents. The greatest value for the over-all equilibrium is an evidence for the imine resonance stabilization (eq. 8. b) whose partially negative carbon atom behaves towards the electric influences in opposite form that the partially positive carbon atom of the aldehyde, and the influence of the substituents between both states arises notabily accentuated. However, the influence observed in the addition process is an evidence for the competence between the addition of nucleophile and proton, so that an effect which adds one of them will make difficult the other, logically.

In agreement with the criterion that the inductive effect of a substituent may be quantified by its σ_m-constant, and the resonance effect would be proportional to a $\sigma_p - \sigma_m$, it is evident that the —Cl and —OH groups are of the (—I + R)—type, while the $-NH(CH_3)_2^+$ group is practically of pure (—I)-type. The (—I)-effect of —Cl is greater than that of —OH, and it accounts for the greater reactivity of the former in *meta*-position. The *para*-derivatives are less reactive than the homolog in *meta*-position since its (—I)-effect is strongly compensated by the (+R)-effect, that is exalted as well by the thorough resonance substituent — aryl-carbonyl. However it is difficult to account for, and so some authors, [5] acknowledged that the ammonium groups, analogous to the $-NH(CH_3)_2^+$-group, may be very unreactive in reactions when thorough resonance with positive centers, like the carbonilic carbon atom, may be established (after the tabulated facts, for the $-N(CH_3)_3^+$-group the σ-constant decreases from $\sigma_p = 0.82$ [7] to $\sigma_p^+ = 0.41$). Our results show that this phenomenon is not relevant since the σ_p^+-value is near the tabulated σ_p-value for the $-N(CH_3)_3^+$-group.

Another contradictory point is the "*ortho* effect",[1,8] that consists in an exaltation of reactivity in many *ortho*-derivatives with respect to their homologs in *para*-position. The only explanation that the resonance donation in *ortho* is very hindered does not appear consistent with the observation that the *meta*-isomer, that cannot be conjugated with the carbonylic group, is also much less reactive than the *ortho*-isomer (see table 2). The loss of thorough conjugation, pointed by some authors, accounts for just a small part of the increase in reactivity of *ortho*-isomer, approx. three times greater than the *para*-isomer, if we compare both σ^* and σ values of chloroderivatives (see fig. 1). A reasonable explanation could be given in recognizing that the inductive effect cannot be comparable in the *para*, *meta* and *ortho* positions, but in the last it arises to a great exaltation of field effect (inductive effect through space) inversely proportional to the r-distance between substituent and reaction center. An agreement may be observed between 1/r in a hexagonal structure and σ_I values obtained from our results with the *o*—Cl— and tabulated values in model sigma frameworks.[5]

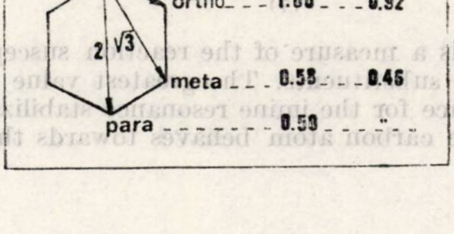

(10

Thermodynamic Parameters

The close relation between reactivity and internal contribution to ΔH (see table 3) accounts for the apparent anomalies that are observed if the over-all ΔH value, that includes the medium contribution, is compared. Only the *o*-chlorobenzaldehyde presents even some anomalies with respect to hydrolysis rates and over-all equilibrium constants : its ΔH_{int}-values are not consistent with the fact that the *o*-chloro is the most electron-extracting group. As an explanation it may be postulated an intramolecular hydrogen bond that may give rise to a cyclic hydrazone less stable due to the strain of framework (11).

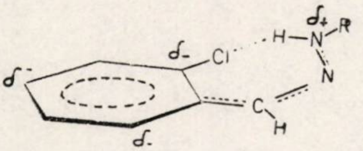

(11)

The ΔH_{ext}-values show a very great variation and difficult interpretation. In general, it may be observed that substituent electronic extraction reduces the ΔH_{ext}-values, what may be a reflex of the changes in polarity (and therefore in solvation) of the activated complex. The most remarkable anomalies correspond to groups that, as $o-\text{Cl}$ and $p-\text{NH(CH}_3)_2^+$ may show hardly quantifiable effects (sterics, intramolecular bonds, pure electric charge, . . .) whose influence in the external contributions is very difficult to anticipate.

REFERENCES

[1] W. P. Jencks, *Progr. Phys. Org. Chem.*, **2**, 63 (1964).

[2] P. Y. Sollenberg and R. B. Martin, "The Chemistry of Amino Group", John Wiley & Sons, New York, 1968.

[3] A. Rodriguez and F. Mata, *Afinidad*, **395**, 107 (1985).

[4] L. P. Hammett, "Physical Organic Chemistry", Mc Graw-Hill, New York, 1940.

[5] C. D. Jonhson, "The Hammett Equation", Cambridge University Press. 1973.

[6] L. G. Hepler and J. W. Larson, "In Solute-Solvent Interactions", Marcel Dekker, London, 1969.

[7] H. C. Brown and Y. Okamoto, *J. Amer. Chem. Soc.*, **80**, 4979 (1958).

[8] M. P. Bastos and L. do Amaral, *J. Ord. Chem.*, **43**, 4032 (1978) ; **44**, 980 (1979).

[9] F. Gutierrez, Doctoral Thesis, Universidad de Valladolid, Spain, 1983.

Revue Roumaine de Chimie, 32, *3*, 315–320 (1987)

PHOTOLYSIS OF MONO-, DI- AND TRIBENZYLAMINE AND THE NOVEL PHOTOCARBYLAMINE REACTION *

M. Z. A. BADR, M. M. ALY, S. A. MAHGOUB, A. M. FAHMY and F. F. ABDEL-LATIF
Chemistry Department, Faculty of Science, Assiut University, Assiut, Egypt, A.R.E.

Received January 25, 1986

The direct irradiation of (mono-, di) and tribenzylamine in isopropanol leads to the formation of benzaldehyde, toluene, dibenzyl and a mixture of mono, di- and tribenzylamine. In case of carbon tetrachloride or chloroform, in addition to the previous products, benzylisocyanide, benzyl chloride and the corresponding amine hydrochloride are formed through charge transfer complex between amine and solvent. A mechanism is postulated for isocyanide formation which is further separated from photolysis of arylamines, namely; aniline, *o*-, *m*- and *p*-toluidines, α— and β-naphthylamines. Descending the series from tri- to di- to monobenzylamine is assumed to go through initial C—N bond homolysis, whereas ascending the benzylamine series going through initial N—H bond homolysis is suggested.

Nitrogen-centered radicals were extensively studied[1] some years ago. Most of the present knowledge concerning their generation and properties is derived from dimethylamino free radicals formed on thermolysis or photolysis of tetramethyltetrazene, tetramethylurea or dimethylacetamide.[2–6] The results obtained by Ratcliff and Kochi[7] on irradiation of dibenzylamine in cyclohexane solution suggest a free radical mechanism through homolysis of the benzyl-nitrogen bond forming benzyl and N-benzylamino radicals. These subsequently undergo consecutive dark and secondary photolytic processes.

The present work deals with the partial photolysis of mono- di- and tribenzyl amine half time expose to avoid complications due to secondary photolysis of the initially formed products, in carbon tretrachloride, chloroform or isopropanol. Under these conditions the results obtained are quite different from those described by other workers.[7]

The non-sensitized irradiation of mono-benzylamine in carbon tetrachloride or chloroform give rise to benzyl chloride, benzaldehyde, toluene and dibenzyl as neutral products together with mono, di- and tribenzylamines, benzylamine hydrochloride and ammonium chloride as amino products in addition to evolution of benzylisocyanide. Similar results are also obtained on irradiation of di- or tri-benzylamine in carbon tetrachloride or chloroform solution. However, when the irradiation of di- or tribenzylamine is carried out in isopropanol solution we do not observe the formation of benzyl isocyanide, the amine hydrochloride, ammonium chloride or benzyl chloride. The variation of the products obtained under different conditions with different solvents suggests different routes for the reaction mechanism.

---

* Presented in part at the 10th International Conference on Photochemistry : University of Crete, Iraklion, Crete, Greece, Sep. 6–12 (1981), *J. Photochem.*, **17**, 83 (1981).

UV Irradiation of alkyl amines in tetrahalomethanes is reported[8] to form a charge transfer complex between both reactants and solvent. This complex subsequently dissociates into trihalomethyl radical and amino radical cation halonium salt. The trihalomethyl radicals may further initiate a chain reaction.[9] A similar mechanism is suggested to occur in the irradiation of mono- and dibenzylamines in carbon tetrachloride or chloroform and we consider it as the precursor of benzylchloride together with amines hydrochloride salts according to Scheme 1.

Scheme 1

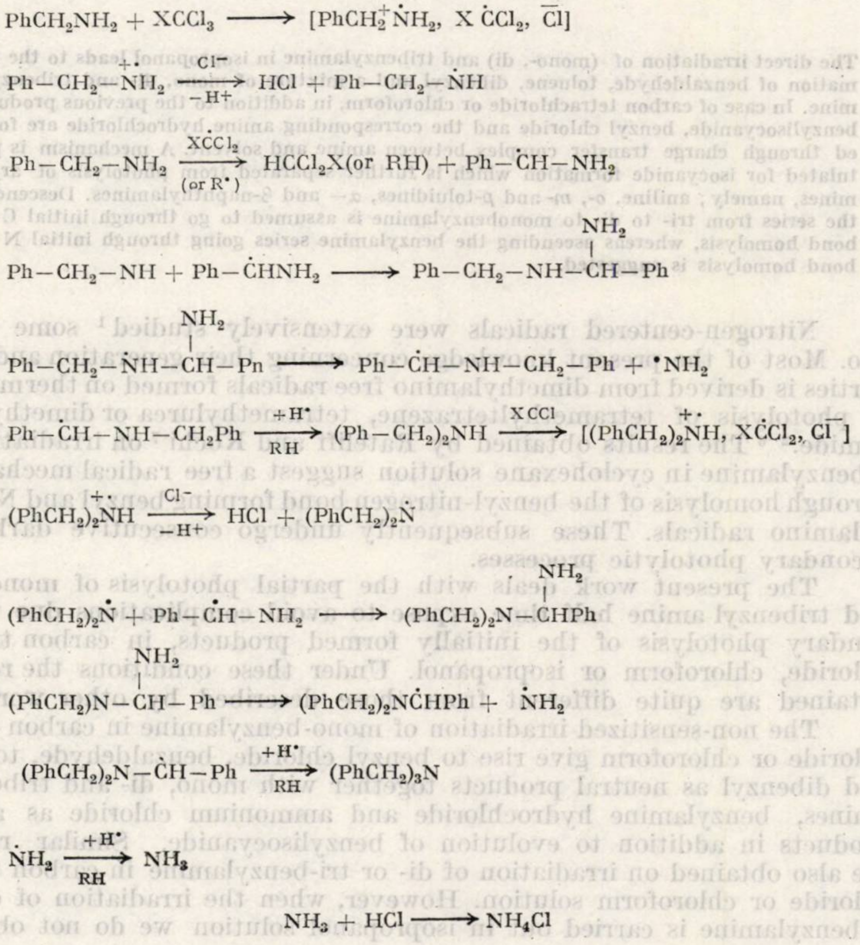

$$PhCH_2NH_2 + XCCl_3 \longrightarrow [PhCH_2^{+}\dot{N}H_2,\ X\dot{C}Cl_2,\ \bar{Cl}]$$

$$Ph-CH_2-\overset{+\cdot}{N}H_2 \xrightarrow[-H^+]{Cl^-} HCl + Ph-CH_2-\dot{N}H$$

$$Ph-CH_2-NH_2 \xrightarrow[(or\ R^{\cdot})]{X\dot{C}Cl_2} HCCl_2X(or\ RH) + Ph-\dot{C}H-NH_2$$

$$Ph-CH_2-NH + Ph-\dot{C}HNH_2 \longrightarrow Ph-CH_2-NH-\overset{\overset{NH_2}{|}}{C}H-Ph$$

$$Ph-CH_2-\dot{N}H-\overset{\overset{NH_2}{|}}{C}H-Pn \longrightarrow Ph-\dot{C}H-NH-CH_2-Ph + {}^{\bullet}NH_2$$

$$Ph-\dot{C}H-NH-CH_2Ph \xrightarrow[RH]{+H^{\cdot}} (Ph-CH_2)_2NH \xrightarrow{XCCl} [(PhCH_2)_2\overset{+\cdot}{N}H,\ X\dot{C}Cl_2,\ \bar{Cl}\ ]$$

$$(PhCH_2)_2\overset{+\cdot}{N}H \xrightarrow[-H^+]{Cl^-} HCl + (PhCH_2)_2\dot{N}$$

$$(PhCH_2)_2\dot{N} + Ph-\dot{C}H-NH_2 \longrightarrow (PhCH_2)_2N-\overset{\overset{NH_2}{|}}{C}HPh$$

$$(PhCH_2)N-\overset{\overset{NH_2}{|}}{C}H-Ph \longrightarrow (PhCH_2)_2N\dot{C}HPh + \dot{N}H_2$$

$$(PhCH_2)_2N-\dot{C}H-Ph \xrightarrow[RH]{+H^{\cdot}} (PhCH_2)_3N$$

$$\dot{N}H_2 \xrightarrow[RH]{+H^{\cdot}} NH_3$$

$$NH_3 + HCl \longrightarrow NH_4Cl$$

Moreover, the successive formation of monbenzylamine and dibenzylamine from their higher analogues as well as bibenzyl, toluene and bezaldehyde may be regarded to take place through another route involving the initial homolysis of the C—N bond into benzyl and the corresponding benzyl-amine radicals as depicted in Scheme 2.

Scheme 2

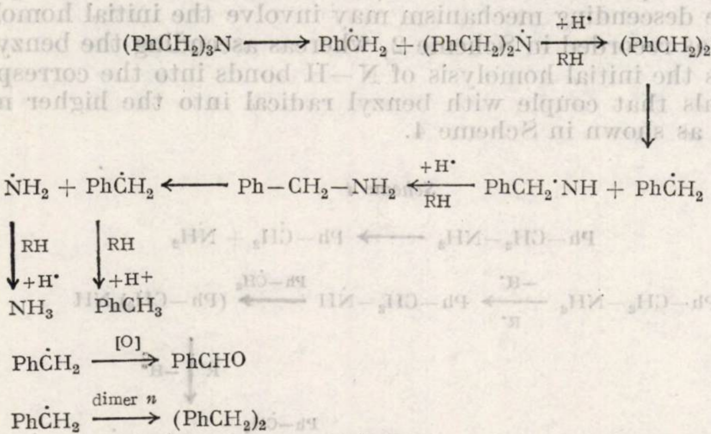

$$(PhCH_2)_3N \longrightarrow Ph\dot{C}H_2 + (PhCH_2)_2\dot{N} \xrightarrow[RH]{+H^{\cdot}} (PhCH_2)_2NH$$

$$\dot{N}H_2 + Ph\dot{C}H_2 \longleftarrow Ph-CH_2-NH_2 \xleftarrow[RH]{+H^{\cdot}} PhCH_2\dot{}NH + Ph\dot{C}H_2$$

$$\dot{N}H_2 \xrightarrow[+H^{\cdot}]{RH} NH_3 \qquad Ph\dot{C}H_2 \xrightarrow[+H^{+}]{RH} PhCH_3$$

$$Ph\dot{C}H_2 \xrightarrow{[O]} PhCHO$$

$$Ph\dot{C}H_2 \xrightarrow{\text{dimer } n} (PhCH_2)_2$$

An interesting feature on irradiation in CCl_4 or $HCCl_3$ as solvent but not in H_2CCl_2 is the formation of benzyl isocyanide. This is also show tobe the case of primary arylamines; namely, aniline, *o*-, *m*- and *p*-toluidines, α- and β-naphthylamines, where the corresponding isocyanides are detected.

The process appears to start with coupling of the alkyl or arylamino radicals (a) with halomethyl radicals followed by dehydrohalogenation through base catalysed β-elimination from (b) to form the isocyanide and the amine hydrochloride, as shown according to Scheme 3 :

Scheme 3

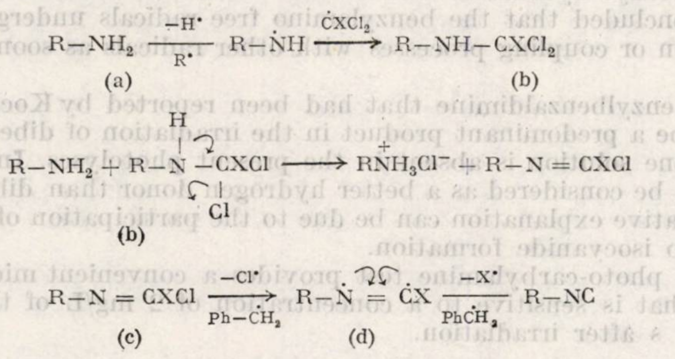

$$\underset{(a)}{R-NH_2} \xrightarrow[R^{\cdot}]{-H^{\cdot}} R-\dot{N}H \xrightarrow{\dot{C}XCl_2} \underset{(b)}{R-NH-CXCl_2}$$

$$R-NH_2 + \underset{(b)}{R-N(H)-CXCl(Cl)} \longrightarrow R\overset{+}{N}H_3Cl^- + R-N=CXCl$$

$$\underset{(c)}{R-N=CXCl} \xrightarrow[Ph-\dot{C}H_2]{-Cl^{\cdot}} \underset{(d)}{R-\dot{N}=\dot{C}X} \xrightarrow[Ph\dot{C}H_2]{-X^{\cdot}} R-NC$$

(R = $PhCH_2-$, Ph, (o) $CH_3C_6H_4-$, (*m*)$CH_3C_6H_4-$, (*p*) $CH_3C_6H_4-$,

α$-C_{10}H_7-$or β$-X_{10}H_7-$; X = H or Cl).

In such a scheme, benzyl free radicals abstract chlorine atoms from (c and d) in order to form benzyl chloride. No chlorine molecules are detected among the photolysates.

When irradiation of each of mono-, di- and tribenzyl amines is carried out in iso-propanol, the same products are obtained with the exception of benzyl chloride, isocyanide and hydrochloride salts of the amines or ammonia. These reactions proceed through a mechanism which is different from that reported for halomethanes as solvents. The most plausible route for the descending mechanism may involve the initial homolysis of C—N bonds as recorded in Scheme 2, whereas ascending the benzylamine series implies the initial homolysis of N—H bonds into the corresponding amino radicals that couple with benzyl radical into the higher member of the series as shown in Scheme 4.

Scheme 4

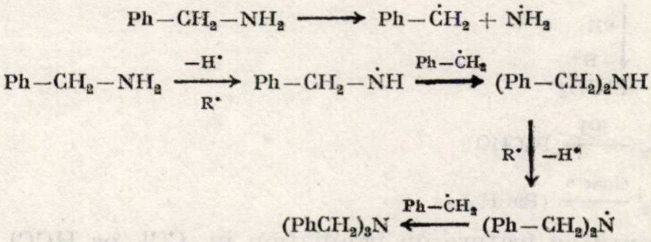

Although dibenzyl is formed through dimerization of benzyl radicals, the corresponding amino dimer, viz; symdibenzylhydrazine from benzylamino (or tetrabenzylhydrazine from dibenzylamino) free radicals is not detected among the products. Such a result can be explained by two different hypotheses:

i) The benzylamino dimers dissociate as soon as they are formed.

ii) The benzylamino radicals undergo preferentially other fast dark reactions and so they are unavailable for dimerization.

The first hypothesis is rejected on the basis of the great stability of such benzyl hydrazines under such irradiation conditions.[7] Hence it can be concluded that the benzylamino free radicals undergo hydrogen-abstraction or coupling processes with other radicals as soon as they are formed.

N-Benzylbenzaldimine that had been reported by Kochi and Ratcliff [7] to be a predominant product in the irradiation of dibenzylamine in cyclohexane solution is absent in the present photolyses. Indeed isopropanol can be considered as a better hydrogen donor than dibenzylamine. An alternative explanation can be due to the participation of the radicals leading to isocyanide formation.

The photo-carbylamine test provides a convenient microanalytical method that is sensitive to a concentration of 2 mg/L of the primary amine 30 s after irradiation.

EXPERIMENTAL

All m.ps. are uncorrected. Gas-liquid chromatographic analysis (g.l.c.) was carried out on a Pye-Unicam gas chromatograph, "Series 104", Dual flame ionization detector, Model 24 and the column used was 20% SE 30 on Chromsorb W (35—80 mesh) at 185°C using nitrogen as a carrier gas. Ultraviolet irradiation was carried out using a Mallinkrodt 150 W low pressure mercury discharge lamp and the solutions were contained in open-topped pyrex beakers.

The solvents used were of "AnalR" grade. Benzylamines were purified as recommended in the literature [7].

Photolysis of benzylamines or arylamines

The amine (1 g) in the solvent used (100 mL) was irradiated at room temp. (~25°) for 15 hours. The isocyanide evolved was absorbed on a filter paper strip moistened with dil. HCl whereby it was hydrolyzed to the corresponding primary amine hydrochloride. The benzylamine hydrochloride was identified by developing an intense violet-red colour on treating the filter paper strip with acetone and sod. nitroprusside (Rimini's test) while the arylamine hydrochloride was identified by diazotisation on treatment with sod. nitrite followed by coupling with alkaline β-naphthol developing a red azo-dye.

The photolysate was filtered off to separate the mixture of ammonium chloride and the amine HCl, from which ammonium chloride was separated by dissolution in water and detected by Nessler reagent. The filtrate was separated as indicated in previous work [11] into amine and neutral products and analysed by g.l.c. The results are summarized in Tables 1 and 2.

Table 1

Percentage composition of mono-, di- and tribenzylamine photolysates in different solvents

	Monobenzylamine			Dibenzylamine		Tribenzylamine	
Solvent	$CHCl_3$	CCl_4	iso-C_3H_7OH	CCl_4	iso-C_3H_7OH	CCl_4	iso-C_3H_7OH
Monobenzylamine	49.10	48.20	49.12	1.55	2.10	0.28	0.34
Dibenzylamine	8.58	8.75	3.20	47.87	48.00	2.25	1.30
Tribenzylamine	0.36	0.75	0.38	0.60	0.36	47.60	48.00
Toluene	6.77	6.70	7.80	18.90	11.40	11.69	10.86
Benzaldehyde	11.30	11.40	24.30	14.90	23.30	23.50	25.30
Dibenzyl	13.45	14.20	15.20	10.93	14.83	10.38	14.20
Benzyl chloride	11.20	10.0	—	5.25		4.30	
Other products	(a), (b)	(a), (b)	—	(a), (c)		(a), (b)	—

(a) Benzyl isocyanide evolved and gave positive Rimini's test.

(b) Benzylamine hydrochloride insoluble solid (0.052 g), m.p. and mixed m.p. 248–9° together with NH_4Cl.

(c) Dibenzylamine hydrochloride insoluble solid (0.056 g), m.p. and mixed m.p. 256° together with NH_4Cl.

(d) Tribenzylamine hydrochloride, insoluble solid (0.062 g), m.p. and mixed m.p. 227–8° together with NH_4Cl.

Table 2

Hydrochloride salts produced on photolysis of arylamines in chloroform

Arylamine	Amount in g(%)	m.p. °C
Aniline	0.070(7)	198
o-Toluidine	0.068(6.8)	215
m-Toluidine	0.072(7.2)	228
p-Toluidine	0.071(7.1)	243
α-Naphthylamine	0.056(5.6)	262
β-Napthylamine	0.063(6.3)	254

Micro photocarbylamine test

The primary amine (2 mg) mixed with chloroform (0.5 mL) contained in a small beaker or a watch glass was exposed to UV irradiation for 30 s whereby the odour of isocyanide can be distinguished and furthermore detected by chemical test as indicated previously.

Preparation of reference compounds

Dibenzyl : Cryst. from ethanol m.p. 52° ; 4,4′-dinitro deriv. m.p. 180°. (Lit (12) m.p. 52°).

Dibenzylamine : Colourless oil, b.p. b.p. 300°, n^{22} 1.5743 ; hydrochloride m.p. 256°. (Lit (13) b.p. 300°, n_D^{20} 1.5731.)

Tribenzylamine : Prisms from ether, m.p. 92° ; b.p. 228°/12 Torr. ; HCl salt m.p. 227—8°. (Lit (14) m.p. 91—94°).

N-Benzylbenzaldimine : b.p. 1670—5°/8 Torr ; HCl salt m.p. 148—150°. (Lit (15) b.p. 170—173°/8 Torr).

Sym-Dibenzylhydrazine : Colourless oil ; hydrochloride m.p. 213—4° dec. (Lit (16) m.p. 215—217°dec.).

Tetrabenzylhydrazine : Cryst. from ethanol ; m.p. 139—140°. (Lit (17) m.p. 139—140°).

REFERENCES

[1] S. G. Hadley and D. H. Volman, *J. Amer. Chem. Soc.*, **89**, 1053 (1967).
[2] W. C. Danen and T. T. Kensler, *J. Amer. Chem. Soc.*, **92**, 5235 (1970).
[3] P. W. Jones and H. D. Gesser, *J. Chem. Soc. B*, **1971**, 1873.
[4] B. R. Cowley and W. A. Waters. *J. Chem. Soc.*, **1961**, 1228.
[5] A. Good and J. C. J. Thynne, *J. Chem. Soc. B*, **1967**, 684.
[6] D. Mackay and W. A. Waters, *J. Chem. Soc. C*, **1966**, 813.
[7] M.A. Ratcliff and J. K. Kochi, *J. Org. Chem.*, **37**, 3268 (1972).
[8] D. P. Stevenson and G. M. Coppinger, *J. Amer. Chem. Soc.*, **84**, 149 (1962).
[9] J. L. Kurz, H. Hutton and F. H. Westheimer, *J. Amer. Chem. Soc.*, **84**, 584 (1961).
[10] A. I. Vogel, "Practical Org. Chem.", Longmans, London, 1971 p. 420.
[11] M. Z. A. Badr and M. M. Aly, *Canad. J. Chem.*, **52**, 293 (1974).
[12] L. Cannizaro and G. Rossi, *Ann.*, **251**, 121 (1962).
[13] W. M. Dehn, Kindle and Peschke, *Ann.*, **485**, 113 (1931).
[14] L. Cannizaro, *J. Chem. Soc.*, **1856** 581.
[15] G. Mignonac, *Ann. Chim.*, **2**, 225 (1934) ; *Chem. Abstr.*, **29**, 1074 (1935).
[16] A. F. Bickel and W. A. Waters, *Rec. Trav. Chim.*, **69**, 312 (1950).
[17] R. T. Marrow and R. Van Dolah, *J. Amer. Chem. Soc.*, **76**, 4522 (1954).

Revue Roumaine de Chimie, **32**, *3*, 321–324 (1987)

PROTON CATALYSED REARRANGEMENT OF N-ALKYL-NAPHTHALENE-SULPHONANILIDES TO *ORTHO*-ALKYL-AMINO-ARYL-NAPHTHALYL-SULPHONES.

PART IV*

B. C. JOSHI *, YOGESH JOSHI, D. KISHORE and S. S. SHRIMALI
Department of Chemistry, University of Rajasthan, Jaipur-302004,
India

Received October 26, 1985

N-Methylaniline and N-ethylaniline were condensed with 3-carboalkoxy-4-hydroxy napthalene-1-sulphonyl chloride and 3-carboalkoxy-2-hydroxy naphthalene-1-sulphonyl chlorides separately resulting in the formation of sulphonanilides (IA∼VIA. These sulphonanilides were rearranged in conc. sulphuric acid to the corresponding sulphones (IB∼VIB). The structures of (IA∼VIA) and (IB∼VIB) were established through elemental analysis, IR and ^{1}H-NMR spectral studies.

It has been observed that sulphuric acid causes rearrangement or hydrolysis of N-alkyl arene sulphonanilides.[1] Witt et al.[2] and later Halberkann [3] established that the rearrangement generally takes place at the *ortho* position. Gennaro and Zanger [4] synthesised a number of sulphones by rearranging 1,2,3,4-tetrahydroquinoline sulphonanilides with conc. sulphuric acid. In an earlier communication rearrangement of N-alkyl arene sulphonanilides with quinoline,[5] napththalene [6] and salicylic acid [7] moieties has been reported. The present communication describes the rearrangement of various sulphonanilides (having 1-hydroxy-2-naphthoic esters and 2-hydroxy-3-naphthoic esters as important moieties) to the corresponding sulphones.

Sulphonanilides (IA∼VIA) have been synthesised by the condensation of N-ethylaniline and N-methylaniline with 3-carboalkoxy-4-hydroxy naphthalene-1-sulphonyl chloride and 3-carboalkoxy-2-hydroxy naphthalene-1-sulphyl chlorides (methyl and ethyl esters only separately. Sulphonanilides (IA∼VIA) have been rearranged in conc. sulphuric acid to sulphones (IB∼VIB). The TLC pure sulphonanilides and sulphones have been characterised through elemental analysis, molecular weight determination (Rast's method) and spectral studies (IR and ^{1}H-NMR) (cf. Table 1).

---

* **Part III, Rev. Roumaine Chim, 32, 215 (1987).**

STRUCTURAL ELUCIDATION

On the basis of elemental analysis and molecular weight determination (Rast's method) the molecular formula to IA and IB was assigned as $C_{20}H_{19}O_5NS$. IR spectrum of (IA) showed characteristic absorption bands for various functional groups e.g. for carbomethoxy group at 1730–1720 cm^{-1}, for phenolic –OH at 3610 cm^{-1} and 1200 cm^{-1}, and for sulphonanilide group at 1175 cm^{-1} and 1330 cm^{-1}. ^1H–NMR spectrum of (IA) indicated signals for aromatic protons in the range of δ 6.6–8.1

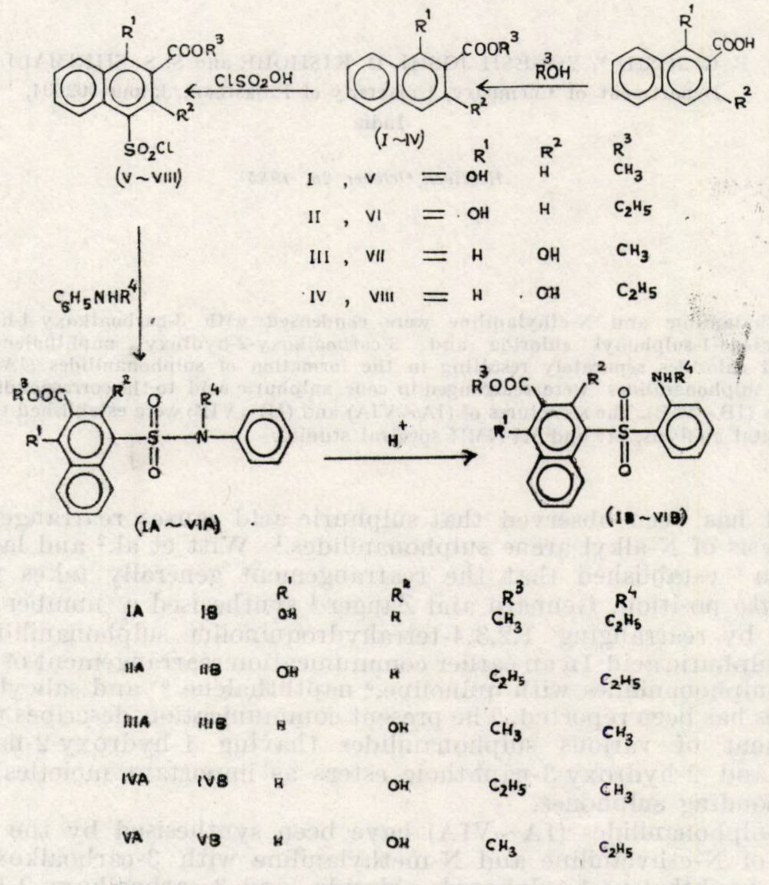
R¹
COOR³
ClSO₂OH
R²
SO₂Cl
(V~VIII)
R¹
COOR³
R³OH
R²
(I~IV)
R¹
COOH
R²
R¹ R² R³
I , V = OH H CH₃
II , VI = OH H C₂H₅
III , VII = H OH CH₃
IV , VIII = H OH C₂H₅
C₆H₅NHR⁴
R³OOC
R²
R¹
O
S
O
R⁴
N
H⁺
R³OOC
R²
NHR⁴
R¹
O
S
O
(IA~VIA)
(IB~VIB)
R¹ R² R³ R⁴
IA IB OH H CH₃ C₂H₅
IIA IIB OH H C₂H₅ C₂H₅
IIIA IIIB OH H CH₃ CH₃
IVA IVB H OH C₂H₅ CH₃
VA VB H OH CH₃ C₂H₅
VIA VIB H OH C₂H₅ C₂H₅

CHART-I

and the integration gave the value of ten to such proton. A quartet for two protons of $-CH_2-$ at δ 4.2, a triplet at δ 1.2–1.5 for three protons of $-C-CH_3$ group, a singlet for three protons at δ 4.05 for a carbomethoxy group were also observed. A broad peak at δ 5.40 (disappeared on D_2O

Table 1

^{1}H-NMR Spectra (δ ppm)

Compd. No.	Molecular formula	Aromatic Proton	N-CH$_2$ and C−CH$_2$ Protons	C−CH$_3$ Protons	COOCH$_3$ Protons	N−CH$_3$ Protons	OH Protons	−NH Protons
IA	$C_{20}H_{19}O_5NS$	6.6−8.1(m)−10H	4. 2−2H	1.2−1.5(t)−3H	4.06(s)−3H	—	5.40(b)−1H	
IIA	$C_{21}H_{21}O_5NS$	6.6−8.1(m)−10H	4.15−4.8(m) −4H	1.2−1.8(m)−6H	—	—	5.40(b)−1H	
IIIA	$C_{19}H_{17}O_5NS$	6.6−8.2(m)−10H	—	—	4.05(s)−3H	—	5.40(b)−1H	
IVA	$C_{20}H_{19}O_5NS$	6.6−8.2(m)−10H	4.25(q)−2H	1.2−1.5(t)−3H	—	3.1(s) −3H	5.40(b)−1H	
VA	$C_{20}H_{19}O_5NS$	6.6−8.2(m)−10H	4.25(q)−2H	1.2−1.5(t)−3H	4.05(s)−3H	3.1(s) −3H	5.45(b)−1H	
VIA	$C_{21}H_{21}O_5NS$	6.6−8. 2(m)−10H	4.15−4.80(m) −4H	1.2−1.8(m)−6H	—	—	5.45(b)−1H	
IB	$C_{20}H_{19}O_5NS$	6.8−8.15(m)−9H	4.25(q)−2H	1.2−1.5(t)−3H	4.05(a)−3H	—	5.45(b)−1H	
IIB	$C_{21}H_{21}O_5NS$	6.8−8.15(m)−9H	4.15−4.8(m) −4H	1.2−1.8(m)−6H	—	—	5.45(b)−1H	10.3(b)−1H
IIIB	$C_{19}H_{17}O_5NS$	6.8−8.15(m)−9H	—	—	4.05(s)−3H	2.95(s) −3H	5.45(b)−1H	10.3(b)−1H
IVB	$C_{20}H_{19}O_5NS$	6.8−8.20(m)−9H	4.25(q)−2H	1.2−1.5(t)−3H	—	2.95(s) −3H	5.45(b)−1H	10.3(b)−1H
VB	$C_{20}H_{19}O_5NS$	6.8−8.20(m)−9H	4.25(q)−2H	1.2−1.5(t)−3H	4.05(s)−3H	—	5.45(b)−1H	10.3(b)−1H
VIB	$C_{21}H_{21}O_5NS$	6.8−8.20(m)−9H	4.15−4.8(m) −4H	1.2−1.8(m)−6H	—	—	5.45(b)−1H	10.3(b)−1H

s = singlet, t = triplet, m = multiplet, b = broad, q = quartet.

addition) indicated the presence of a proton of a hydroxyl group. On the basis of these observations the structure to (IA) was assigned as 3-carbomethoxy-4-hydroxy-N-ethyl-naphthalene-1-sulphonanilide.

IR spectrum of IB showed absorptions at 1145 cm^{-1} and 1310 cm^{-1} for sulphonyl ($-SO_2-$) group and at 3350 cm^{-1} and 1600 cm^{-1} for secondary amino group; the rest of the spectrum was comparable to that of IA. ^1H-NMR spectrum of (IB) indicated the presence of nine aromatic protons in the range δ 6.8—8.15. A broad peak at δ 10.3 (disappeared on D_2O addition) for —NH proton confirmed the rearrangement of IA to IB. The rest of the spectrum was comparable to that of IA. On the basis of these observations the structure of IB was assigned as 3-carbomethoxy-4-hydroxy-1-naphthyl-2′-ethylaminophenyl sulphone. On similar arguments, structures to (IIA—VIA) and (IIB—VIB) were also assigned.

EXPERIMENTAL

All the melting points are uncorrected. The purity of the compounds was ascertained by TLC using 0.25 mm thick plates coated with silica gel-G as stationary phase and benzene : ethanol : ammonia (7 : 2 : 1 v/v upper layer) as mobile phase. The ^1H-NMR spectra were recorded on Perkin-Elmer spectrophotometer using TMS as internal reference standard and $CDCl_3$ as solvent.

3-Carbomethoxy-4-hydroxy-N-ethyl-naphthalene-1-sulphonanilide (IA)

3-Carbomethoxy-4-hydroxy-napthalene-1-sulphonyl chloride (I) (6.0 g; 0.02 m) dissolved in dioxane (30.0 mL) and anhydrous sodium acetate (2.0 g) was placed in a round bottomed flask (100 mL). N-ethyl aniline (2.90 g., 0.024 M) was added slowly. The reaction mixture was refluxed for 8 hr and then conc. HCl (50 mL) was added. The reaction mixture was left overnight. On dilution sulphonanilide (IA) precipitated out. It was filtered washed, dried and crystallised from alcohol water (Yield 6.9 g., 89.6 %, 0.018 M, Rf. 0.54, m.p. 123°C). On similar lines (IIA—VIA) were also synthesised.

3-Carbomethoxy-4-hydroxy-1-naphthyl-2-ethyl-aminophenyl sulphone (IB)

IA (3.85 g., 0.01M) was dissolved in A.R. sulphuric acid (10 mL). The mixture was heated at 100° for 5 min. when it acquired a dark green colour. The mixture was poured dropwise into crushed ice when a compound identified as sulphone (IB) precipitated out as a green solid. It was filtered, washed thoroughly with water, dried and crystallised from ethanol water (Yield, 1.90 g., 40 %, 0.005M, Rf 0.64 ; m.p. 185°C). On similar lines sulphones (IIB—VIB) were also synthesised by rearrangement of (IIA—VIA).

ACKNOWLEDGEMENT: The authors are thankful to the Head of Department of Chemistry, University of Rajasthan, Jaipur for providing the necessary research facilities.

REFERENCES

[1] O. N. Witt and D. Uermanyi, *Ber. dtsch. chem. Ges.*, **46**, 296 (1913); *Chem. Abstr.*, **7**, 1502 (1913).

[2] O. N. Witt and N. Truttwin, *Ber. dlsch. chem. Ges.*, **47**, 2786 (1914); *Chem Abstr.* **9**, 307 (1915).

[3] J. Halberkann, *J. Ber. dslsch. chem. Ges.*, **54**B, 1665 (1921); *Chem Abstr.*, **15**, 3994 (1921).

[4] A. R. Gennaro and M. Zanger, *J. Org. Chem.*, **36**, 1321 (1971).

[5] S. S. Shrimali, N. D. Sharma, S. Kumar and B. C. Joshi; *Rev. Roumaine Chim.*, **23**, 613 (1978).

[6] S. S. Shrimali, A. Iyer, R. K. Sinhva, D. Kishore and B. C. Joshi; *Rev. Roumaine Chim* **24**, 597 (1979).

[7] S. S. Shrimali, D. Kishore, Y. C. Joshi and B. C. Joshi, *Rev. Roumaine Chim.* (Communicated).

Revue Roumaine de Chimie, **32**, *3*, 325—328 (1987)

POLY-1,3,4-OXADIAZOLESTERIMIDES

MARIA BRUMĂ and ION SAVA
"P. Poni" Institute of Macromolecular Chemistry, Aleea Gr. Ghica Vodă 41 A — Iași
Romania

Received March 4, 1986

Poly-1,3,4-oxadiazolesterimides have been synthesized by solution polycondensation of certain diols containing preformed imide rings with a dichloride of a dicarboxylic acid which contains both oxadiazole and imide preformed rings. The thermal stability of these polymers is discussed.

Heterocyclic polymers containing 1,3,4-oxadiazolic ring into their macromolecular chain are of special interest due to their high thermal stability in oxidative atmosphere.[1] In a couple of previous papers we reported the synthesis of different poly-1,3,4-oxadiazoles containing amide, imide or both amide and imide groups and we studied the interrelations between the structure and properties of these polymers.[2-4]

In the present paper further investigation has been undertaken in order to prepare new polyoxadiazoles containing ester and imide groups and to evaluate their properties by comparing them with related polyoxadiazolamidimides.

RESULTS AND DISCUSSION

Poly-1,3,4,-oxadiazolesterimides have been synthesized by the polycondensations reaction of certain diols having preformed imide rings with a dichloride of a dicarboxylic acid containing both oxadiazole and imide preformed rings. The diols are N,N'-bis(hydroxyethyl) or (hydroxyaryl) pyromellitic or benzophenontetracarboxylic diimides. They have been prepared by the reaction between aminoethanol or *m*- or *p*-aminophenol with pyromellitic or benzophenontetracarboxylic dianhydride using dimethylformamide as a solvent, as can be seen in scheme 1.

The dichloride II was prepared by treating with thionyl chloride the dicarboxylic acid obtained from trimellitic anhydride and 2,5-bis (p-aminophenyl) 1, 3, 4,-oxadiazole, the latter being prepared by the reaction of p-aminobenzoic acid and hydrazine.[3] Scheme 2 shows the reaction sequences.

Polycondensation of equimolecular amounts of diols and dichloride using as solvent N-methylpyrolidone (NMP) containing 60 % lithium chloride, gave poly-1, 3, 4-oxadiazolesterimides III, according to scheme 3.

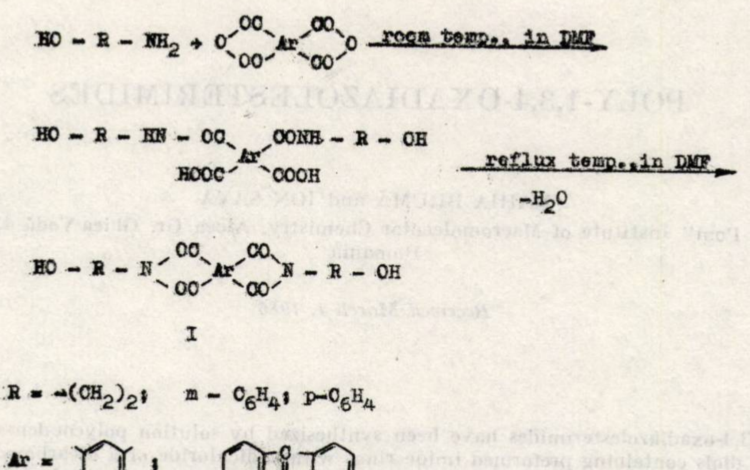
room temp., in DMF
reflux temp., in DMF
$-H_2O$
I
R = $-(CH_2)_2-$; m $-C_6H_4$; p$-C_6H_4$
Ar =

Scheme 1

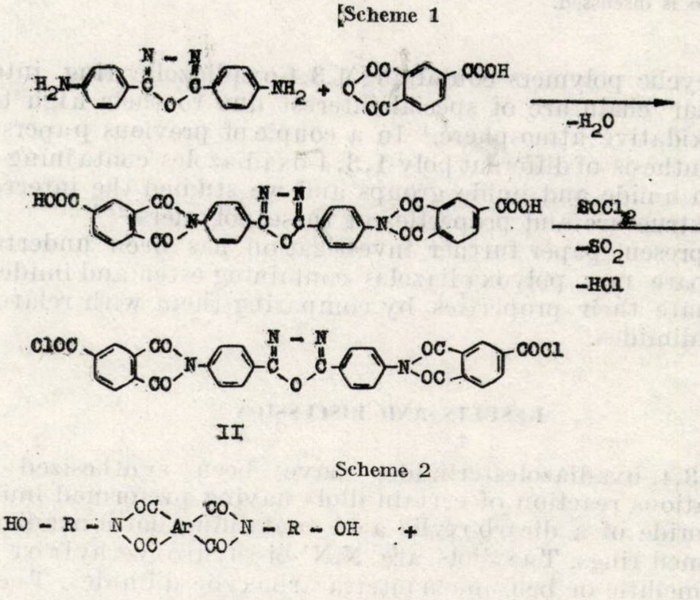
$-H_2O$
$SOCl_2$
$-SO_2$
$-HCl$
II

Scheme 2

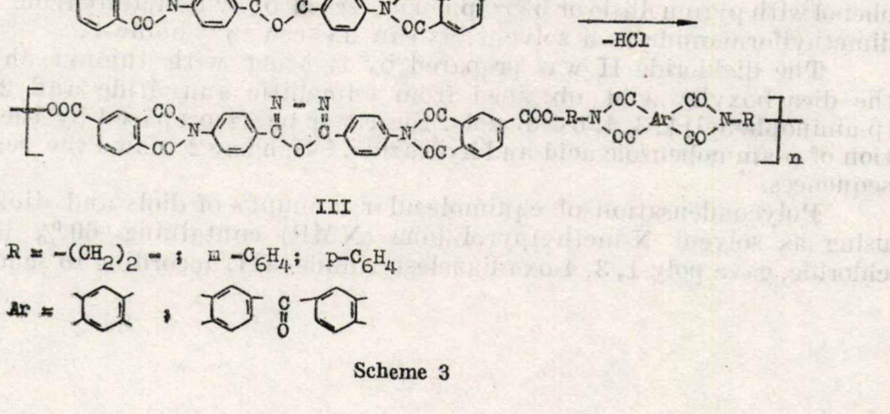
$-HCl$
III
R = $-(CH_2)_2-$; m $-C_6H_4$; p$-C_6H_4$
Ar =

Scheme 3

Inherent viscosity of these new polymers is in the range 0.15 – 0.21 (Table 1).

Experiments attempted in o-dichlorobenzene using quinoline as acid acceptor did not give higher viscosities.

All polymers reported in this paper are soluble in polar amidic solvents containing lithium chloride; those polymers which contain ethylene units are soluble even in (NMP) without LiCl. Because of their low viscosity, only brittle films could be obtained by casting a 15 % polymer solution on a glass plate.

Table 1

Properties of poly-1,3,4-oxadiazolesterimides :

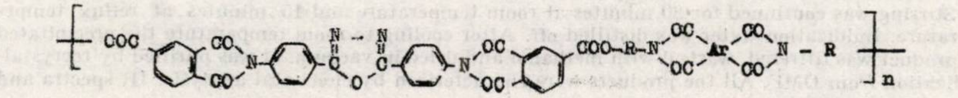

No.	Polymer	R	Ar	η inh[1] dL/g	Solubility		TGA, weight loss %[2]	
					in NMP	in NMP + 6 % LiCl	at 400°	at 500°
1	IIIa	$(CH_2)_2$	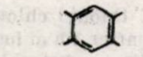	0.15	+	+	9.5	18.5
2	IIIb	$(CH_2)_2$	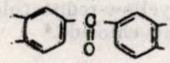	0.15	+	+	10.00	19.5
3	IIIc	p-C_6H_4	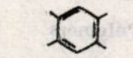	0.21	–	+	1.2	11.0
4	IIId	p-C_6H_4	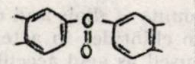	0.20	–	+	2.0	11.8
5	IIIe	m-C_6H_4	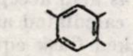	0.18	–	+	1.8	12.2
6	IIIf	m-C_6H_4	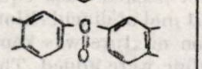	0.16	–	+	2.8	12.6

[1] Measured at a concentration of 0.5 g/100 mL NMP + 6 % LiCl, at 20°C.

[2] Determined in air on "Derivatograph" Paulik and Paulik, at a heating rate of 9.8°/minute.

Thermogravimetric analysis performed in air at a heating rate of 9.8°C/minute showed that polymers containing all aromatic and heterocyclic units do not decompose up to 430°, while the polymers having ethylene units lose weight rapidly at 370 – 390°C. If we compare these polyoxadiazolesterimides with polyoxadiazolamidimides reported earlier, we can see that polyoxadiazolesterimides have lower molecular weight, evaluated from inherent viscosity, due to the lower reactivity of hydroxy-groups compared to amino groups in monomer structure. However, these polyoxadiazolesterimides have a good thermal stability, similar to polyoxadiazolamidimides.

Thus, poly-1,3,4-oxadiazolesterimides reported in this paper are soluble in polar aprotic solvents and have a good thermal stability due to the oxadiazolic and imidic units which are present into the macromolecular chain.

EXPERIMENTAL

Preparation of Monomers

N,N′-bis(hydroxyethyl) or (hydroxyaryl) pyromellitic or benzophenontetracarboxylic diimides, I, have been prepared by the reaction of 2 mol of 2-aminoethanol or m- or p-aminophenol with 1 mol of pyromellitic or benzophenontetracarboxylic dianhydride, in dimethylformamide as solvent. The following example illustrates the general procedure : In a three-necked flask equipped with mechanical stirrer, reflux condenser and N_2-inlet and outlet, were placed 0.5 mol aminoethanol (or aminophenol) and 225 mL dimethylformamide. Then, 0.25 mol pyromellitic dianhydride or benzophenontetracarboxylic dianhydride were added gradually to the stirred solution while temperature of the reaction mixture increased rapidly up to 60°. Stirring was continued for 30 minutes at room temperature and 15 minutes at reflux temperature. Imidization water was distilled off. After cooling to room temperature the precipitated product was filtrered, washed with methanol and dried in vacuum. It was purified by recrystallization from DMF. All the products were characterized by elemental analysis, IR spectra and melting points.[5]

To prepare the diacid chloride, we synthesized 2,5-bis(p-aminophenyl)-1,3,4-oxadiazole from p-aminobenzoic acid and hydrazine, according to a known procedure.[6] 0.2 mol of 2.5-bis-(p-aminophenyl)-1,3,4-oxadiazole and 250 mL dimethylformamide were placed in a three-necked flask fitted with stirrer and reflux condenser and flushed with nitrogen. Then, 0.4 mol trimellitic anhydride were added to the stirred solution and stirring was continued for 1 h at room temperature and 30 minutes at reflux temperature. Imidization water was distilled off. The dicarboxylic acid precipitated from solution and it was filtered, washed with water and acetone, and then recrystallized from dimethylformamide.

25 grames of dicarboxylic acid and 100 mL thionyl chloride were heated under reflux for 2 h. then 1 mL of dimethylformamide was added after 1 h of heating. The formation of diacid chloride was indicated by changing colours : the yellow-redish colour of dicarboxylic acid changed into light-yellow corresponding to the diacid chloride.[4]

Preparation of Polymers

Polycondensation of equimolecular amounts of diols and diacid chloride was performed in N-methylpyrolidone containing 6% lithium chloride, in a temperature range of 70—90°, for 8—10 hr. Triethylamine or pyridine were used as acid acceptors. The general procedure is as follows : 0.1 mol diol and a quantity of solvent calculated as to obtain a concentration of 10—20% final polymer were placed in a three-necked flask equipped with stirrer and reflux condenser and flushed with nitrogen. Then, 0.1 mol of diacid chloride as a finely divided powder was added to the stirred solution. The reaction mixture was kept at room temperature for 40 minutes. Then, 0.1 mol triethylamine or pyridine were added. The flask content was heated at 70—90° for 8—10 hr. After cooling, the polymer solution was poured into water and the precipitated polymer was filtered and washed with water and methanol and dried in vacuum oven.

Inherent viscosity is in the range of 0.15—0.21 dL/g. IR spectra of polyoxadiazolesterimides shown characteristic absorption bands at 1770—1780 cm^{-1}, 1720—1730 cm^{-1} and 710—730 cm^{-1} assigned to imidic rings and at 960 cm^{-1} assigned to oxadiazolic rings.

REFERENCES

1. A. H. Frazer and T. A. Reed, *J. Polymer Sci.*, C, **19**, 8 (1967).
2. M. Brumă, L. Stoicescu-Crivetz and I. Zugrăvescu, *Rev. Roumaine Chim.*, **16**, 935 (1971).
3. M. Brumă, L. Stoicescu- Crivetz and I. Zugrăvescu, *Rev. Roumaine Chim.*, **16**, 1591 (1971).
4. M. Brumă and G. Neamțu, *Rev. Roumaine Chim.*, **26**, 87 (1981).
5. K. Y. Choi and S. K. Choi, *J. Polymer Sci.*, *Polymer Chem.*, *Ed.*, **20**, 1107 (1982).
6. A. Siegrist, Swiss Pat. 383.985 ; *Chem. Abstr.*, **62**, 14867 (1965).

Revue Roumaine de Chimie, 32, 3, 329–333 (1987)

as-TRIAZINE DERIVATIVES WITH POTENTIAL THERAPEUTIC ACTION. XXII *

A SIMPLIFIED METHOD FOR THE SYNTHESIS OF 1,2,4-TRIAZOLE NUCLEOSIDES AND 1,2,4-TRIAZINE-NUCLEOSIDES

CAROL CRISTESCU[a] and CLAUDIU SUPURAN[b]

[a] Chemical and Pharmaceutical Research Institute Sos. Vitan 112, 74351 Bucharest, Romania

Department of Chemistry, Polytechnic Institute of Bucharest, Romania

Received February 2, 1986

The syntheses of 1-β-D-ribofuranosyl-1,2,4-triazole-3-carboxamide (Ribavirin) and 2-β-D-ribofuranosyl-1,2,4-triazine-3,5(2H, 4H) dione (6-Azauridine) by silylation-glycosylation procedure in the presence of iodotrimethylsilane (*in situ*) as catalyst are described.

The recent discoveries of potential antiviral and antitumor activity in several classes of nucleosides have given impetus to acceleration of research in this area. The nucleosides of certain five- and six-membred heterocycles such as pyrazomycine,[1] showdomycine,[2] bredinin,[3] ribavirin[4], 6-azauridine[5] and 5-azacytidine[6] have exhibited a broad spectrum of biological activities.

In our present work we have investigated a simpliefied method for the synthesis of 1-β-D-ribofuranosyl-1,2,4-triazole-3-carboxamide-(Ribavirin) and 2-β-D-ribofuranosyl-1,2,4-triazine-3,5(2H,4H) dione (6-Azauridine).

The syntheses of 1(2′,3′,5′-tri-O-acyl-β-D-ribofuranosyl)-3-substituted-1, 2, 4-triazole and 2(2′,3′,5′-tri-O-acyl-β-D-ribofuranosyl)-6-substituted-1, 2, 4-triazine-3, 5 (2H, 4H) dione were achived by using two well-known procedures : *a.* by reaction of between fully silylated 3-substituted-1, 2, 4-triazole[7,8] or 6-substituted-1, 2, 4-triazine-3, 5 (2H, 4H) dione[9–12] with acyl-bloked ribosyl bromide or tetra-O-acyl-blocked ribose in an aprotic solvent in the presence of a Lewis acid at room temperature providing, in the case of 1, 2, 4-trizole-derivatives, a 1 : 1 mixture of the two nucleosides (N 1-β and N 4-β isomers) ; *b.* by acid-catalysed fusion procedure[7, 8,18] using tetra-O-acyl-blocked ribose and 3-substitued-1,2,4-triazole, providing the same nucleosides in a 1 :10 N 1-β and N 4-β isomers ratio.

Recently, the synthesis of pyrimidine nucleosides in high yield using the condensation of 1-0-acetyl sugars with the trimethylsilylated base in the presence of iodotrimethylsilane as catalyst was reported.[14,15] However, iodotrimethylsilane is rather expensive and requires extreme care in handling because of its sensitivity to air and moisture.[16]

---

* Part XXI : C. Cristescu, Rev. Roumaine Chim., 31, 881 (1986).

We have investigated the syntheses of 1,2,4-triazolenucleosides and 1,2,4-triazine-nucleosides by applyng the silylation-glycosylation procedure in the presence of iodotrimethylsilvane, generated *in situ*, as catalyst.

Treatment of 1-0-acetyl-2, 3, 5-tri-O-benzoyl-D-ribose with the easily to handle and inexpensive chlorotrimethylsilane and anhydrous sodium iodide in dry acetonitrile in the presence of molecular sieves followed by reaction with the trimethylsilyl derivative of methyl 1, 2, 4-triazole-3-carboxylate (II-a) (obtained from methyl 1,2,4-triazole-3-carboxylate (I-a) and hexamethyldisilazane) gives crystalline 1(2′, 3′, 5′-tri-O-benzoyl-β-D-ribofuranosyl)-1,2,4-triazole-3-carboxylic acid methyl ester (III) in 82% yield. No N-4-β-isomer was detected by TLC in the reaction mixture and the optimum reaction time was 20 hours at room temperature. The same treatment applied to 1,2,3,5-tetra-O-acetyl-D-ribofuranose followed by reaction with the trimethylsilyl derivative of 3-cyano-1,2,4-triazole (II-b) (obtained from 3-cyano-1,2,4-triazole[17] (I-b) and hexamethyldisilazane) led to the formation of 3-cyano-1 (2′, 3′, 5′-tri-O-acetyl-β-D-ribofuranosyl)-1,2,4-triazole (IV) in 85% yield.

Treatment of the bloked nucleoside III with methanolic ammonia ar room temperature provided 1-β-D-ribofuranosyl-1,2,4-triazole-3-carboxamide (V). On the other side IV heated with aqueous ammonia at

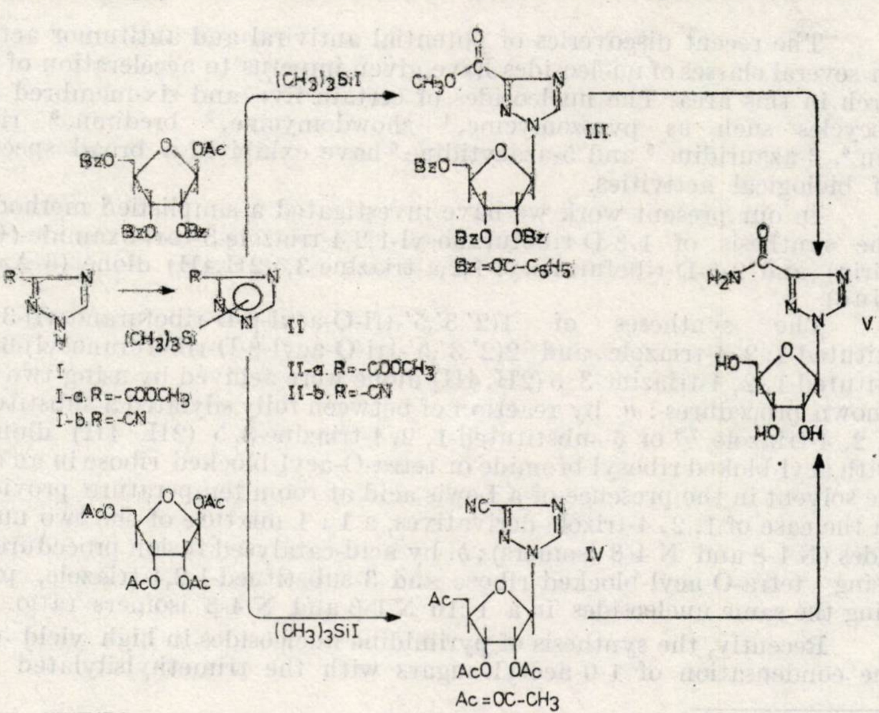

SCHEME 1

80°C, removes the acyl groups and the cyano moiety is converted to the carboxamide, affording V in 80 % yield.

The assignments of the glycosylation sites in the 3-and 5-substitued-1, 2 4-triazole were made by ^{1}H-NMR. The aromatic protons of 1,3-disubstituted 1,2,4-triazole occur downfield from the aromatic protons of 1,5-disubstituted-1, 2, 4-triazole.[18] In addition, a stricking difference in the ^{1}H-NMR spectra is the large downfield shift of the anomeric proton of the 5-substituted-1, 2, 4-triazole nucleosides as compared with the coresponding 3-substituted isomers.[18]

The position of signals for H-5 (δ 8. 91) and H-1′ (δ 5. 85) is in in close agreement with those reported [7] for the corresponsing 1-β-D-ribofuranosyl-1,2,4-triazole-3-carboxamide.

The preparations of the blocked nucleosides of 6-substituted 1,2, 4-triazine-3, 5 (2H, 4 H) dione (VIII) was performed as outlined in scheme 2.

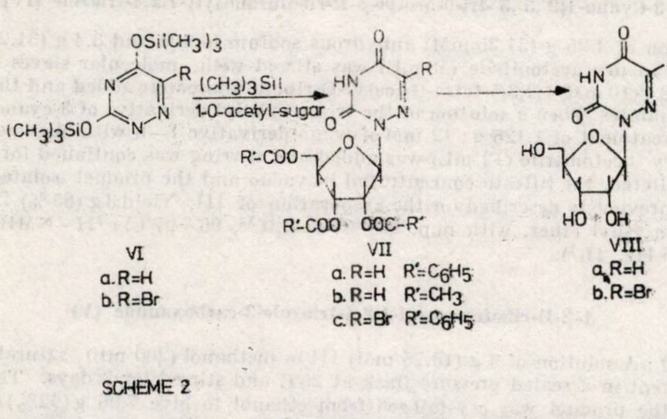

SCHEME 2

Treatment of 1-O-acetyl-sugar with chlorotrimethylsilane and anhydrous sodium iodide in dry acetonitrile followed by reaction with 3,5-bis(trimethylsilyloxy)-6-substituted-1, 2, 4-triazine (VI) afforded only N-2-glycosides (VII) in 90—92 % yield. No 0-glycoside was detected by TLC in the reaction mixture, and the optiumum reaction time was 8—10 hours at room temperature. Removal of the blocking groups of VII with sodium methoxide in anhydrous methanol gave ae 87 % yield of the nuclesides, 2-β-D-ribofuranosyl-6-substituted-1,2,4-triazine-3,5(2H,4H) dione (VIII). The anomeric configuration of the sugar was determined from the anomeric proton signals in the ^{1}H-NMR sectrum : δ 6.13 ppm ($J_{1',2'}$ = 3.6 Hz ; β — anomer) for VIII-a and δ 5.95 ppm ($J_{1',2'}$ = = 2.8 Hz ; β — anomer) for VIII-b.

EXPERIMENTAL

The melting points were determined on a heating-plate microscope and are not corrected. Optical rotation was measured on a Hilger and Watts automatic polarimeter. The ^{1}H—NMR spectra were recorded at 60 MHz on a Varian EM 360 spectrometer in the indicated solvents and the chemical shifts are reported parts per million (δ) with tetramethylsilane (TMS) as internal standard. The acetonitrile was twice distilled over P_2O_5 and 1-0-acetyl-sugars were dried carefully in high vacuum. Traces of alcohol or humidity in the solvent resulted in a dramatic lowering of the yield of the desired blocked nucleosides.

1(2′,3′,5′-tri-0-benzoyl-β-D-ribofuranosyl)-1,2,4-triazole-3-carboxylic acid methyl ester (III)

A solution of 9.5 g (62.5 mM) anhydrous sodium iodide and 6.8 g (62.5 mM) chlorotrimethylsilane in dry acetonitrile (100 mL) was stirred with molecular sieves 4Å (1g) for 10 minutes. 10 g (20 mM) 1-0-acetyl-2,3,5-tri-0-benzoyl-D-ribofuranoze were added and the mixture was stirred for 40 minutes. Then, a solution of the trimethylsilyl derivative of methyl-1,2,4-triazole-3-carboxylate (prepared by treatment of 3.06 g; 24 mM of the ester I-a with excess hexamethyldisilazane at reflux) in acetonitrile (25 mL) were added and stirring was continued for 20 hours at room temperature. The mixture was filtered, the filtrate concentrated in vacuo, and the residue was dissolved in 1,2-dichloroethane (150 mL). The dichloroethane solution was washed with saturated sodium hydrogen carbonate solution (2 × 75 mL), 10 % sodium thiosulphate solution (2 × 75 mL), water (2 × 75 mL) and dried on sodium sulphate. The solvent was removed and the residue was recrystallized from ethanol. Yield 9.38 g (82 %) III with m.p. 138—139.5°C (Lit.[7], 137—139°C); ^{1}H—NMR ($CDCl_3$): 6.26 (d, $J_{1',2'}$ = 3.2 Hz, $H_{1'}$).

3-Cyano-1(2′,3′,5′-tri-0-acetyl-β-D-ribofuranosyl)-1,2,4-triazole (IV)

A solution of 4.25 g (31.25 mM) anhydrous sodium iodide and 3.4 g (31.25 mM) chlorotrimethylsilane in dry acetonitrile (50 mL) was stirred with molecular sieves 4Å (0.5 g) for 10 minutes. 3.18 g (10 mM) 1,2,3,5-tetra-0-acetyl-D-ribofuranose were added and the mixture was stirred for 40 minutes. Then a solution of the trimethylsilyl derivative of 3-cyano-1,2,4-triazole (prepared by treatment of 1.125 g; 12 mM of cyano-derivative I—b with hexamethyldisilazane at reflux) in dry acetonitrile (12 mL) was added and stirring was continued for 20 hours. The mixture was filtered, the filtrate concentrated in vacuo and the product isolated according to the procedure previously described for the preparation of III. Yield 3 g (85 %) IV after recrystallization from ethyl ether, with m.p. 95—97°C (Lit.[13], 96—97°C); ^{1}H—NMR ($CDCl_3$): 6.03 (d, $J_{1',2'}$ = 2.5 Hz, $H_{1'}$).

1-β-D-ribofuranosyl-1,2,4-triazole-3-carboxamide (V)

Method 1: A solution of 9 g (15.75 mM) III in methanol (200 mL) saturated at 0°C with ammonia was kept in a sealed pressure flask at 25°C and stirred for 3 days. The solvent was removed, and the product was crystallized from ethanol to give 7.06 g (92%) of V with m.p. 174—176°C (Lit.[7]. 174—176°C); $(\alpha)_D^{25}$: −36.0° (c 1, H_2O); ^{1}H—NMR (DMSO-d_6/DSS): 5.5 (d, $J_{1',2'}$ = 3.6 Hz, H 1′).

Method 2: A mixture of 6 g (17 mM) IV and concentrated ammonium hydroxide (50 mL) was heated on the steam bath for 1 hours. The solvent removed and the product were crystalized from ethanol. Yield 3.32 g (80 %) of V with m.p. 174—176°C identical in all respect with a sample prepared by method 1.

2(2′,3′,5′-tri-0-benzoyl-β-D-ribofuranosyl)-1,2,4-triazine-3,5(2H,4H)dione (VII-a)

A solution of 9.5 g (62.5 mM) of anhydrous sodium iodide and 6.8 g (62.5 mM) chlorotrimethylsilane in dry acetonitrile (100 mL) was stirred with molecular sieves 4 Å (1 g) for 10 minutes. 10 g (20 mM) 1-0-acetyl-2,3,5-tri-0-benzoyl-D-ribofuranose were added and the mixture was stirred for 40 minutes. Then, a solution of 7.86 g (23.5 mM) 3,5-bis(trimethylsilyloxy)-1,2,4-triazine in acetonitrile (50 mL) was added and the stirring was continued for 8 hours at room temperature. The mixture was filtered, the filtrate concentrated in vacuo and the residue was dissolved in 1,2-dichloroethane (200 mL). The dichloroethane solution was washed with saturated sodium hydrogen carbonate solution (2 × 100 mL), 10 % sodium thiosulphate solution (2 × 100mL), water (2 × 100 mL) and dried on sodium sulphate. The solvent was removed and the residue was recrystallized from 2-propanol. Yield 10.25 g (92 %) VII-a with m.p. 192—194°C (Lit.[20] = 192—194°C); ^{1}H—NMR ($CDCl_3$): 6.4 (d, $J_{1',2'}$ = 3.5 Hz, $H_{1'}$).

2(2′,3′,5′-tri-0-acetyl-β-D-ribofuranosyl)-1,2,4-triazine-3,5(2H,4H)dione (VII-b)

The compound was obtained from 1,2,3,5-tetra-0-acetyl-D-ribofuranose (20 mM) and 3,5-bis(trimethylsilyloxy)-1,2,4-triazine (24 mM) following exactly the procedure reported for the synthesis of compound VII-a. The product was crystallized from ethanol to give a pure crystalline compound in 90% yield with m.p. 99–101°C (Lit.[19] 100–102°C); ^1H-NMR ($CDCl_3$): 6.22 (d, $J_{1',2'} = 3.5$ Hz, $H_{1'}$).

2(2′,3′,5′-tri-0-benzoyl-β-D-ribofuranosyl)-6-bromo-1,2,4-triazine-3,5 (2H, 4H) dione (VII-c)

The compound was obtained from 1-0-acetyl-2,3,5-tri-0-benzoyl-D-ribofuranose (10 mM) and 3,5-bis(trimethylsilyloxy)-6-bromo-1,2,4-triazine (12 mM) following exactly the procedure reported for the synthesis of compound VII-a. The product was crystallized from ethanol to afford VII-c in 90% yield with m.p.168–169°C (Lit.[10] = 168–169°C); ^1H-NMR: 6.38 (d, $J_{1',2'} = 3.1$ Hz, $H_{1'}$).

General procedure for the preparation of 2-β-D-ribofuranosyl-6-substituted-1,2,4-triazine-3,5(2H, 4H) dione (VIII a, b)

2 mM of VII a–c were dissolved in dry methanol and 1 N sodium methoxide (2 mM) was added. The mixture was stirred for two hours at room temperature. The solvent was evaporated under reduced pressure and the resulting oil was dissolved in water (20 mL) and extracted with ethyl acetate-ether (2 : 1 v/v; 2×10 mL). The aqueous layer was treated with DOWEX 50×8 (H^+) at pH 3, filtered and evaporated under reduced pressure. The residue crystallized from ethanol to afford VIII a, b was identical in all respects (melting point, UV, IR, ^1H-NMR) with the authentic samples.

ACKNOWLEDGEMENTS. The authors thank Mrs. Veronica Vişan and Mrs. Ileana Costea of the Analytical Department of our Institute for recording the IR and UV spectra and Mr. D. Ionescu for NMR spectra. The authors express their gratitude to Mrs. Anca Sava for her invaluable help.

REFERENCES

[1] K. Gerzon, D. C. Delong and J. C. Kline, *Pure Appl. Chem.*, **28**, 489 (1971).

[2] N. Nishimura M. Mayama, Y. Komatsu, H. Kato, N. Shimaoka and Y. Tanaka, *J. Antibiot., Ser. A*, **17**, 148 (1964).

[3] K. Mizuno, T. Tsugune, M. Takada, M. Hayashi, K. Atsumi, K. Asano and T. Matsuda, *J. Antibiot.*, **27**, 775 (1974).

[4] R. W. Sidwell, J. H. Huffman, G. P. Khare, L. B. Allen, J. T. Witkowski and R. K. Robins, *Science*, **177**, 705 (1972).

[5] F. Šorm, H. Heilová, *Experientia*, **14**, 215 (1958).

[6] F. Šorm, A. Piskala, A. Čihák and J. Veselý, *Experientia*, **20**, 202 (1964).

[7] J. T. Witkowski, R. K. Robins, R. W. Sidwell and L. N. Simon, *J. Med. Chem.*, **15**, 1150 (1972).

[8] S. R. Naik, J. T. Witkowski and R. K. Robins, *J. Heterocycle Chem.*, **11**, 57 (1974).

[9] U. Niedballa and H. Vorbrüggen, *Angew. Chem. (Internat. Ed)*, **9**, 461 (1970).

[10] C. Cristescu, *Rev. Roumaine Chim.*, **20**, 1287 (1975).

[11] C. Cristescu and S. Sitaru, *Rev. Roumaine Chim.*, **27**, 943 (1982).

[12] C. Cristescu, *Rev. Roumaine Chim.*, **30**, 117 (1985).

[13] J. T. Witkowski, R. K. Robins, G. P. Khare and R. W. Sidwell, *J. Med. Chem.*, **16**, 935 (1973).

[14] Z. Točik, R. A. Earl and J. Beranek, *Nucleic Acid Res.*, **8**, 4755 (1980).

[15] A. Matsuda, Y. Kurasawa and K. A. Watanabe, *Synthesis*, **1981**, 748.

[16] G. A. Olah, S. C. Narang, B. G. B. Gupta and R. Malhotra, *J. Org. Chem.*, **44**, 1247 (1979).

[17] G. I. Chipen and V. Ya. Grinshtein, *Chem. Heterocycl. Compounds* (USSR), **1**, 420 (1965).

[18] G. P. Kreishman, J. T. Witkowski, R. K. Robins and M. P. Schweizer, *J. Amer. Chem. Soc.*, **94**, 5894 (1972).

[19] J. Beránek and J. Pitha, *Coll. Czech. Chem. Comm.*, **29**, 625 (1964).

[20] V. Černeckij, S. Chládek, F. Šorm and J. Smrt, *Coll. Czech. Chem. Comm.*, **27**, **87** (1962).

Revue Roumaine de Chimie, 32, 3, 335–340 (1987)

COMPTES RENDUS

"Design and Synthesis of Organic Molecules Based on Molecular Recognition", edited by G. Van Binst, Springer Verlag, Berlin, 1986, 315 pages, hard cover, DM 166.

The proceedings of the 18th Solvay Conference on Chemistry with the above title, which took place in Brussels on Nov. 28 — Dec. 1, 1983 under the chairmanship of E. Katzir-Katchalski and V. Prelog, have been published. A comprehensive introduction by E. Katzir-Katchalski (23 pp.) delineates the general area of specific molecular interaction describing the "hot" research fields which are discussed in detail by the invited speakers. Four main topics are treated by reports and communications, followed by discussions reproduced *in toto*.

Topic 1: Molecular recognition in biochemical processes. R. Schwyzer's report describes specific reversible interactions in life processes: antenna function of membranes and their regioselective, conformation selective, and stereoselective interactions with regulatory peptides (ACTH, dynorphin and enkephalin peptides). This report is followed by three communications: R. A. Lerner on "Antibodies of predetermined specificity in biology and medicine"; R. J. P. Williams on "Calcium trigger proteins", and K. Wüthrich on "Glucagon conformation in different environments: implications for molecular recognition". The last author describes the use of ^{1}H–NMR for studying the interaction of glucagon (a linear polypeptide with 29 amino acid residues) and perdeuterated dodecylphosphocholine micelles. By means of the NOESY pulse sequence one can determine the secondary structure in solution, which is different from that determined by X-ray methods for single crystals.

Topic 2: Thermodynamic, kinetics and stereochemistry in molecular recognition. In his report entitled "On the economics of binding energies", W. P. Jencks describes the balance between entropy loss in exactly-bound-substrates and binding energy, cautioning that such binding may be therefore weak, unlike the energetically strong binding of substrates by enyzmes which have imprecise receptors. M. Karplus discusses "Dynamics of ligand binding to proteins" using hemoglobin as example in computer simulations of molecular motions. T. J. Franklin's report is entitled "Binding energy and the stimulation of hormone receptors". H. A. Scheraga's report on "Theoretical studies of molecular recognition and catalysis by enzymes" mentions the rationalization (using conformational energy calculations) of the right-handed twist of α-helices and β-sheets of proteins; then the interaction between chymotrypsin and oligopeptides explaining their hydrolysis is described: the acyl-enzyme intermediate involving Ser^{195} is depicted by calculations in its lowest-energy conformation in the cleft binding region. Finally, the lysozyme complex with oligosaccharides explaining their hydrolysis via a stabilized carbonium ion was calculated in good agreement with experimental data. Stereo views are provided, showing evidence for "the docking process". In the first short communication pertaining to this topic, A. R. Ubbelohde asks "Why water?" and replies that enzymes benefit from the multiple functions of water molecules (quasi crystalline liquid, formation of anticrystalline clusters); he suggests more extensive studies of the effect of temperature, elevated pressures, and additives influencing the anticrystalline properties of water. Finally H. Frauenfelder discusses "Experimental studies of protein dynamics through ligand binding".

Topic 3: Synthetic models of hosts. The four reporters are outstanding scientists and they present extensive well-illustrated reports of their recent results: D. J. Cram on "Designed host-guest relationships"; J. M. Lehn on "Molecular recognition: design of abiotic receptor molecules"; R. Breslow on "Biomimetic control of chemical selectivity"; and P. L. Luisi on "Biopolymers in reverse micelles as guest-host molecular systems". In the present reviewer's opinion, the 70 pages occupied by these reports present the best part of this book and amply justify its aquisition in terms of good value for money. The first two chemists have created a new area in chemistry (macrocyclic ligands, cryptands, spherands) interfacing organic, inorganic and biological chemistry. Breslow's modeled substrates react at centres predetermined by the length of flexible molecular moieties, and qualify as "honorary" catalysts because they do not yet possess turnover abilities. A host of interesting results were obtained by Luisi with enzymes in reverse micelles in a non-polar medium, e.g. n-heptane which is transparent to UV enabling spectrophotometric measurements to be made.

Topic 4: Design of new "guests". The report by M. Lahav and coworkers on "Molecular discrimination in crystal growth in the presence of tailor-made initiators" presents very interesting data, well illustrated with photographs, on the inhibition of crystal growth for one enantiomer of a racemic mixture leading to spectacular resolutions via single crystals which float and grow at the surface of the solution. Thus racemic glutamic acid hydrochloride or threonine afforded 100% enantiomeric excess of the (R) stereoisomer in the presence of (S) lysine or (S) glutamic acid, respectively, which act as inhibitors; the inhibited (S) stereoisomer of the racemic mixture appears as fine powder incorporating about 1% of the initiator; this powder coates the well-formed crystals of the (R) enantiomer which does not incorporate inhibitors, and therefore grow normally. It was surmised that such phenomena might explain the generation and amplification of the optical activity in an initially symmetric prebiotic soup.

V. J. Hruby and M. E. Hadley's report "Binding and information transfer in conformationally restricted peptides" describes the development of superpotent hormones and neurotransmitters: α-melanotropin agonist analogs, oxytocin and glucagon antagonist analogs, and selective enkephalins based on a simple idea: replacement of one (S) amino acid in a peptide by its (R) enantiomer, causing conformational changes.

Two communications (E. Gil-Av: "Chiral recognition in partitioning systems"; and H. Kessler: "Designing activitiy and receptor selectivity in cyclic peptide hormone analogs") conclude this topic.

In summary the broad range of first-class reports and communications constitute an important selection of current scientifically advanced areas in a rapidly progressing field.

Alexandru T. Balaban

"Characterization of Polymers in the Solid State II: Synchrotron Radiation, X-Ray Scattering and Electron Microscopy" (Advances in Polymer Science, vol. 67), Springer, Berlin, 1984, 233 pages, 128 DM (hard-co ver).

This volume contains six articles concerning different investigation techniques used in solid state polymers.

The first article "Synchrotron Radiation in Polymer Science", written by G. Elsner, Ch. Rieker and H. G. Zachmann, presents in its first part the historical development of this technique and the advantages of synchrotron radiation. Properties, production and instrumentation of synchrotron radiation are described in detail. This article is the first one which reviews (108 references) the applications of synchrotron radiation in solid state polymer investigation. Small angle scattering during crystallization, during annealing above the crystallization temperature, phase separation and crazing and wide angle scattering during crystallization and solid phase transitions are discussed for several polymers and rubber.

J. Hendrix presents in "Position Sensitive X-Ray Detectors" both single photon counting and integrating systems with their principles of operating and their properties. The author emphasizes that time resolved measurements are the most important applications of X-ray synchrotron radiation and they are meaningful only with electron area detectors. Combining synchrotron radiations (as a high intensity X-ray source) with electronic position sensitive detectors, it is possible to use X-ray diffraction as an investigation technique of structural changes in molecular systems during chemical reactions and phase transitions.

"Fluorescence Anisotropy Technique Using Synchrotron Radiation as a Powerful Means for Studying the Orientation Correlation Functions of Polymer Chains" is written by J. -L. Viovy and L. Monneric. The theoretical models of local dynamics are briefly reviewed. The fluorescence anisotropy decay techniques permitted by synchrotron radiation are used to study ocal dynamics in solutions and in molten polymers. New information about the mechanism lof backbone rearrangement are obtained using this technique.

H. B. Stuhrmann guides the reader in his article "Resonance Scattering in Macromolecular Structure Research" from well-established facts of resonance scattering to its application in new areas, where successful use of this technique became possible with the advent of synchrotron radiation. The analysis of the basic scattering functions in terms of a multipole expansion provides a promissing strategy, once the possibilities of synchrotron radiation are fully exploited so as to allow for the required high precision of the scattering measurements.

The last article, "X-Ray Line Shape Analysis. A Means for the Characterization of Crystalline Polymers" is written by G. Bodor from the Polymer Research Institute, Budapest, Hungary. The theoretical background for line shape analysis is given. Line broadening of the experimental spectra consists of an instrumental line broadening and a structural line broadening. The former can be measured using standard samples which have infinite large crystallites and have no strains. The second line broadening is connected with the average crystalline particle size of the polymer. The distorsion and crystalline particle size distributions are import-tant for better characterization of polymer structures. The strain and distorsions are directly connected with the mechanical properties.

All the reports included in this volume contain valuable up-dated information and are recommended to chemists studying modern methods of investigation of polymers in the solid state.

Ursula Bologa

"Modern Synthetic Methods 1986", edited by R. Scheffold, Springer Verlag, Berlin, 1986, 356 pp., soft cover, DM 68.

The fourth volume in this series is centered on two topics : 1) Sound and light in synthesis, and 2) Synthesis of enantiomerically pure compounds with C—C bond formation.

The preceding three volumes were published by Verlag Sauerländer, Aarau in 1976, 1980, and 1983. The last of the triennial Seminars sponsored by the Association of Swiss Chemists took place in Interlaken on April, 17—18, 1986 and the camera-ready manuscripts were rapidly processed into a "ready for use, practice-oriented" survey of rapidly developing areas of synthetic organic chemistry. The present volume is dedicated to V. Prelog.

On the first topic, K. E. Suslick presents "Ultrasound in synthesis" (60 pages), reviewing the nature of acoustic cavitation, reactor design and configuration, experimental factors influencing the reaction course and giving a survey of synthetic applications in homogeneous and heterogeneous systems, followed by a few representative experimental procedures. Sonolysis, pyrolysis and radiolysis of chemical bonds afford similar results but the reaction conditions are quite different. So far, most applications of sonochemistry involve organometallic derivatives but quite a few other applications are known. The bibliography includes 278 references.

"Photochemically generated building blocks" are reviewed in two parts. In the first part, by K. Schaffner and M. Demuth, the tricyclooctanone approach to polyquinane synthesis is presented with special emphasis on the underlying photochemistry streassing 1,3-acyl shifts and oxa di-π-methane processes of β, γ-unsaturated ketones. The second part by M. Demuth is dedicated to photochemical methods in cyclopentanoid natural product synthesis. Both parts together have 165 references and occupy 60 pages.

The second topic starts with an excellently illustrated review of "Enantiomerically pure compound (EPC) synthesis with C—C bond formation via acetals and enamines" by D. Seebach, R. Imwinkelried and T. Weber (135 pp., 326 references). Morrison's books on stereoselective syntheses (1971, 1985) indicated the explosive growth of this area with enormous application potential in pesticides, vitamines, pharmaceutical drugs, cosmetics, etc. Starting from basic definitions and criticizing sloppy use of stereochemical terms, the authors intersperse the description of case studies (tetrahydrocarbolines and tetrahydroisoquinolines), and of the three main pathways of enantioselective C—C bond formation (the use of enolates of cyclic α-aminoacid and α-hydroxyacid derived acetals ; substitution at acetal centers ; syntheses with enamines) with practical recipes from their own experience or from the literature.

G. Helmchen, R. Karge and J. Weetman continue the review of EPC syntheses with C—C bond formation by describing (in 45 pages with a complete bibliography of over 100 references) asymmetric Diels-Alder reactions with chiral enolates as dienophiles. The last seven years witnessed a sudden growth in this area, specially after the first author defined "concave" and "convex" alkoxy groups in esters of optically active alcohols acting as auxiliaries in such reactions.

The last chapter of the book, (50 pages and 57 references) by H. C. Brown, P. K. Jadhav and B. Singram, presents EPC via chiral boranes ; the auxiliary group is derived from α-pinene.

The high quality of the reviews and the short duration of the publishing process are high assets for all research chemists wishing to benefit from authoritative reviews of outstanding chemists in rapidly expanding areas.

Alexandru T. Balaban

"Initiators — Poly-Reactions — Optical Activity" (Advances in Polymer Science, vol. 62), Springer, Berlin, 1984, 184 pages, 98 DM (hard-cover).

"Cationic Polymerization — Iodonium and Sulfonium Salt Photoinitiators" is the first article written by J. V. Crivello. A characteristic aspect of cationic polymerization is that the counteranion attached in the vicinity of the cationic propagating species determines the pro-

pagation reactions, in contrast to radicalic polymerization. Both these polymerization reactions are extensively reviewed. Initiation of polymerization with irradiated cations is at its beginning. The review discusses the nature of the propagating species in polymerization of vinyl monomers when photoirradiated nonmetal halides are used as initiators. This is important in order to be able to control their life-time. When short-lived intermediates are involved as initiators, chain transfer reactions follow the propagation (e.g. selective dimerization); when the intermediate has an infinite life-time, living polymerization is possible. Diaryliodonium, triarylsulfonium, dialkylphenacylsulfonium and 4-hydroxyphenylsulfonium salts are described as initiators. Syntheses, mechanisms of photoinitiation and photosensitization (electron transfer and decomposition by free radicals) are presented in detail. These initiators have the following advantages with regard to strong acid initiators : they are stable, can be easily prepared, handled and dissolved in monomers to form homogeneous solutions, and are sources for the slow release of cations and radicals. They are also of interest because through the cations or radicals generated by photoirradiation, functional groups can be introduced into the polymer at the ends of the chain.

The second article "Living Polymerization and Selective Dimerization : Two Extremes of the Polymer Synthesis by Cationic Polymerization" written by T. Higashimura and M. Sawamoto, is closely related to the first one. The two reactions, selective dimerization and living polymerization, are discussed on the basis of the current understanding of the nature of the propagating species. Metal halides and nonmetal halides are used as initiators.

T. Corner is the author of the review "Free Radical Polymerization. The Synthesis of Graft Copolymers". Until now little attention has been paid to the synthesis of macromers as intermediates for an easy preparation of graft copolymers. Macromolecules were obtained by cationic and anionic polymerization, but the number of monomers which can be converted by ionic polymerization methods is small. The preparation of macromers by free radical polymerization is potentially much more important because a greater number of monomers can be utilized. The review emphasizes how to design the functionalization of macromers prepared by free radical polymerization methods.

E. Chiellini, R. Solaro, G. Galli and A. Ledwith are the authors of the article "Optically Active Synthetic Polymers Containing Pendant Carbazolyl Groups". The carbazole moiety has a pronounced molecular polarizability with a low ionization potential, a lower electron affinity compared to that of anthracene and participates in the formation of donor-acceptor complexes which can participate in charge transport and electron transfer processes. It seems to be advantageous to combine the unique electronic properties of carbazole with its incorporation into a polymer matrix. The most convenient method to prepare optically active polymers containing carbazole groups, attached via the nitrogen atom to the polymeric chain, is by copolymerization of a variety of optically active co-monomers with non-chiral carbazole-containing monomers. The review reports UV absorption, fluorescence emission, ^1H-NMR, and circular dichroism spectra in order to establish a correlation between photophysical behavior with secondary and primary structural features of the polymers.

This volume contains four articles which report different aspects of polymerization processes which are complementary to one another. The reader can easily get an image of modern aspects of polymer science. Future trends in this field are also stressed.

Ursula Bologa

W. P. Weber, "Silicon Reagents for Organic Synthesis" (Reactivity and Structure Concepts in Organic Chemistry, vol. 14), Springer, Berlin, 1983, 430 pages, 224 DM (hard-cover).

The author stresses out at the beginning of the book (chapter 1) some physical properties of silicon and carbon atoms in order to facilitate the understanding of organosilicon chemistry. These two elements have the same distribution of the valence electrons ($2s^22p^2$ for carbon and $3s^23p^2$ for silicon). Both elements are able to form four covalent bonds. As a consequence, organosilicon chemistry has much in common with carbon organic chemistry, but there are three main differences between silicon and carbon which are responsible for the differences of their chemical behavior.

i) The atomic radius of silicon (1.17 Å) is larger than that of carbon (0.77 Å); The C—C and C—H bonds are shorter than the Si—C and Si—H bonds. The Si—H bond length does not depend on the nature of the substituents as in the case of C—H bonds (e.g.in alkanes). The silicon compounds having Si=Si double bonds are very unstable.

ii) The electronegativity of silicon on Pauling's scale is lower ($\chi = 1.8$) compared to those of carbon and hydrogen ($\chi = 2.5$ and $\chi = 2.1$ respectively). Thus bond energies of Si—C and Si—H bonds are lower than those of C—C and C—H bonds, and Si—H bonds are slightly more polar than C—H bonds. Sylyl bases e.g. lithium 1,1-bis (trimethylsilyl) alkoxides, have a basicity intermediate between that of tertiary alkoxides and lithium amide bases. This behavior is attributed to the more pronounced releasing effect of the trimethylsilyl group. In triethylsilane, the hydrogen atom is the "electron reservoir" of the molecule. Thus hydride transfer from triethylsilane to carbocations occurs easily in reduction reactions of alkenes and polar multiple bonds.

Silicon forms stronger bonds with more electronegative elements (e.g. O, N, Cl, F) than carbon, their formation being favoured energetically. Separate chapters are devoted to silicon-sulfur, silicon-phosphorus and silicon-fluorine reagents. It is pointed out that in the case of ionic hydrogenation of alkenes with triethylsilane, the thermodynamic driving force of the transfer of a hydride ion from the silane to the carbocation results not only from the greater strength of the C—H bond formed compared to the Si—H bond broken, but also from the formation of a strong Si—O bond.

Another consequence of the enhanced polarity of the Si—H bond is that the trialkylsilyl group has a chemical behavior similar to that of a proton e.g. in trimethylsilyl cyanide and in reduction reactions. Nucleophilic additions of trimethylsilyl cyanide to polar cumulenes or carbonyl groups are similar to those of hydrogen cyanide.

iii) Being an element of the third row of the Periodic Table, silicon has unoccupied 3*d* orbitals of low energy. As a result, silicon can be penta- and hexacoordinated (e.g. in alkylpentafluorosilicates). These orbitals stabilize the carbocation to the silicon when 3*d* orbitals overlap with the adjacent filled 2*p* orbitals. The increased bond order and bond angles in $H_3Si-O-SiH_3$ are due to the interaction of 3*d* orbitals of silicon with the nonbonding oxygen 2*p* electrons. The stabilization of carbocations by β-trimethylsilylgroups is possible when nonclassical carbocations are formed. This is demonstrated by many examples (e.g. in the stereospecificity of *trans*-elimination reactions).

The book has 25 chapters, an author index and a subject index. References are given at the end of each chapter. A short introduction stresses out the goal of each chapter. Many examples of organic synthetic routes involving silicon reagents are presented in detail. For each class of reagents the most important preparation methods are mentioned.

One question arises when the reader has a first contact with the book : "Why are silicon reagents of such an interest for organic synthesis?" Reading attentively, the answer comes to mind. It seems that silicon reagents are used preferentially in fine organic syntheses where usual organic reagents fail to be efficient, when high regioselectivities and stereospecificities and mild reaction conditions are required. Since many of these reagents are commercially available, a more rapid development of organosilicon chemistry is expected.

The book is highly readable, excellently printed, formulas and tables are drawn with care. It is recommended to chemists concerned with organic synthesis and to all those who want to be well informed in fundamental silicon organic chemistry.

Ursula Bologa

"Analysis, Networks, Peptides" (Advances in Polymer Science, vol. 65), Springer, Berlin, 1984, 230 pages, 118 DM (hard-cover).

The book contains four articles which are concerned with new techniques used for structural determinations of polymers and biopolymers.

1. "Rheo-Optical Fourier-Transform Infrared Spectroscopy: Vibrational Spectra and Mechanical Properties" by H. W. Sie Siesler. Transient phenomena in polymer determination and relaxation are studied by rheo-optics which describes the relation between stress or strain and an optical parameter (birefrigence, infrared absorption, light scattering, X-ray diffraction) measured simultaneously with stress and strain as a function of time. The mechanical test is combined with one of these types of optical measurements. The advent of rapid-scanning Fourier Transform Infrared Spectroscopy (FTIR) has expanded the applications of vibrational spectroscopy. A similar development has occurred for X-ray diffraction since the availability of synchrotron radiation. The aim of the article is to review (270 references) the instrumental and theoretical background of polymer deformation and relaxation studies by simultaneous FTIR spectroscopy and mechanical measurements and to give some experimental results obtained by this technique.

2. "Analysis of the Fine Structure of Poly(oxymethylene) Prepared by Radiation-Induced Polymerization in the Solid State", by Y. Nakase, I. Kuriyama and A. Odajima is the second paper of the book. The fine structure of polymers is characterized by X-ray scattering, melting behavior, and radiolysis. The annealing effects on these behaviors gave valuable information to clarify the structure of the original material. Electron microscopic studies were also performed to confirm the suggested structure in the case of irradiated samples.

3. J. P. Queslel and J. E. Mark are the authors of the next paper, "Molecular Interpretation of the Moduli of Elastomeric Polymer Network of Known Structure". The understanding of the elastic properties exhibited by elastomer networks has been investigated for a long time. Nevertheless some controversies remain in the interpretation of experimental data. The paper presents a review of the molecular theories and analyses in term of the structure factor which relates the network modulus to the degree of crosslinking. The relevance and importance of branching theory is covered in detail.

4. "Conformational Studies on Model Peptides. Their Contribution to Synthetic, Structural and Funtional Innovations on Proteins" by F. Maser, K. Bode, V. N. Rajasekharen Pillai and M. Mütter is the fourth article. The authors present recent theoretical and experimental investigations of the interactions between sequences, structure and functions in peptides. The most popular methods for secondary structure predictions are discussed. A new designed host--guest approach represents a promising tool for the elucidation of the sequence dependence in secondary structure formation. In the final section the usefulness of conformational predictions is pointed out. Conformational studies are of interest in order to elucidate the biological activity, to allow the design of conformationally constrained analogs of biologically active molecules for rational drug design. The understanding of secondary structure formation opens new areas, not only in the field of the peptide chemistry but also in the field of genetic engineering.

The articles are readable and systematically presented. Attention is drawn on the understanding of the basic phenomena. Like all the other volumes in this series, this book is a main source of fundamental knowledge of structural determination of polymers and biopolymers.

Ursula Boioga

NOTE POUR LES AUTEURS

La Revue Roumaine de Chimie publie des articles en anglais, français, russe, allemand ou espagnol. Les auteurs sont priés d'envoyer des articles et des comptes rendus inédits.

Les manuscrits seront dactylographiés à double interligne. La bibliographie, les tableaux et la légende des figures seront placés après le texte.

Si l'article fait partie d'une série numérotée, la partie précédente sera donnée comme première référence.

Chaque article sera précédé d'un résumé comprenant quinze lignes au maximum.

Les références bibliographiques dans le texte seront faites par des exposants sans parenthèses et paraîtront à la fin de l'ouvrage.

Les publications périodiques mentionnées dans la bibliographie seront présentées suivant les prescriptions internationales : le nom de l'auteur précédé de l'initiale du prénom, le titre du périodique abrégé conformément à « Chemical Abstracts » et souligné par une ligne, le numéro du tome indiqué par des chiffres arabes et souligné par deux lignes, suivi de la première page de l'article ; à la fin, l'année de la parution sera placée entre parenthèses. Le numéro de la revue ne sera pas indiqué si les pages du volume sont numérotées consécutivement.

Les textes des livres ou traités incluront : le nom des auteurs, l'initiale du prénom, le titre du livre entre guillemets et sans être souligné, le numéro du tome précédé par l'abréviation « vol. » (ou « Bd »), le numéro de l'édition, les éditions (the publisher), la localité de la parution du livre, l'année de la parution et la page de la référence précédée(s) par l'abreviation « p » (ou « S. »).

Les brevets seront indiqués comme suit : l'auteur ou la firme, le pays et le numéro du brevet, la date et la revue (*Chem. Abstr.*). Par. ex : M. Jones (to Union Carbide Co.), Brit. Pat. 601 238, 2 Sept. 1959 ; cf. *Chem. Abstr.*, ***44***, 12808 (1960).

Si la référence n'a pas été lue en original, on indiquera aussi la revue de référence consultée.

Les diagrammes seront tracés à l'encre de Chine sur papier calque. Les tableaux et les figures (en nombre strictement nécessaire) ainsi que les courbes dans les figures seront numérotés par des chiffres arabes. Leur explication sera donnée dans la légende des figures. Prière de ne pas inscrire les mêmes données dans les tableaux et les figures. Chaque tableau aura un titre. On indiquera dans le texte la place approximative des tableaux et des figures. Les formules chimiques. seront incluses dans le texte ; en outre, elles seront transcrites sur papier calque à l'encre de Chine.

Les auteurs sont priés d'indiquer les caractères italiques (en soulignant les letttres au crayon), ainsi que tout autre caractère spécial ; les préfixes *ortho*, *meta*, *para*, *cis*, *trans*, etc. seront soulignés pour indiquer leurs caractères italiques et ne seront jamais écrits avec des majuscules.

Aucune correction à la main ne sera admise sur le manuscrit. Les corrections seront tapées à la machine. Les lettres grecques ou d'autres symboles spéciaux seront insérés à la main à l'encre clairement.

Le manuscrit sera signé par l'auteur.

Le titre-courant aura 50 lettres au maximum.

L'entière responsabilité du contenu des articles appartient aux auteurs.

Sur demande on peut obtenir une note plus complète.

PRINTED IN ROMANIA

M. I. Ch. — I. C. Ch.

IAMN

BUCUREȘTI

Ministry of Chemical Industry-
Chemical Research Institute
IAMN-Bucharest

PRODUCES:

ADS electrodes

Chromic anhydride

Benzoic aldehyde

Magnesium sulphate

Pickling salts

Naposil

Magnesium oxide

Ammonium bichromate

"Kollene" salts

Aluminium chloride

Sol. zinc chloride

Benzyl chloride

Benzoyl chloride

Calcium acetate

Stanex

Sodium aluminate

Anhydride ferric chloride

Potassium dichromate

Barrium carbonate

Potassium alumen

Magnesium chloride

Potassium silicate

Sol. chromic acid

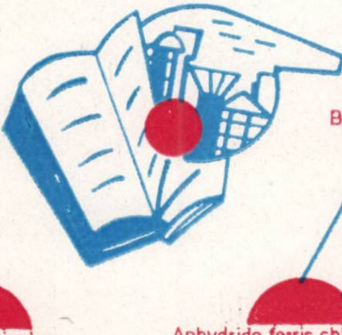

'TRANSILVANIA' RESEARCH DEPARTMENT
12 C Armata Roșie street
TURDA, ROMANIA

TRAVAUX PARUS AUX ÉDITIONS DE L'ACADÉMIE DE LA RÉPUBLIQUE SOCIALISTE DE ROUMANIE

ELENA CEAUŞESCU **Progrese în chimia şi tehnologia polimerilor**, 1986, 446 p.

ELENA CEAUŞESCU, **Forschungen im Bereich der Chemie und Technologie der Polymere**, 1986, 444 p.

RAUL MIHAIL, ION GROZEANU, **Estimarea secvenţială aplicată sistemelor chimice**, 1986, 406 p.

M. BREZEANU, L. PATRON, M. ANDRUH, **Combinaţii complexe polinucleare şi aplicaţiile lor**, 1986, 244 p.

A. T. BALABAN, I. GĂLĂŢEANU, G. GEORGESCU, L. SIMIONESCU, **Labelled compounds applied in nuclear medicine**, coédition avec John Wiley and Sons, 1986, 742 p.

D. PURDELA, **Nomenclatura chimiei organice** — IUPAC, 1986, 454 p.

PETRU BUDRUGEAC, **Probleme de chimie**, 1986, 280 p.

V. DRĂGUŢAN, A. T. BALABAN, M. DIMONIE, **Olefin Metathesis and Ring-Opening Polymerization of Cyclo-olefins**, Coédition avec John Wiley and Sons, 1985, 544 p.

C. LITEANU, I. RÎCĂ, **Optimizarea proceselor analitice**, 1985, 360 p.

N. PERESCU, **Chimia extracţiei cu solvenţi şi aplicaţii**, 1985, 212 p.

V. E. SAHINI, M. HILLEBRAND, **Chimie cuantică în exemple şi aplicaţii**, 1984, 378 p.

GH. MARCU, **Chimia compuşilor coordinativi**, 1984, 415 p.

E. CORDOŞ, C. MANOLIU, **Spectrometria de absorbţie şi fluorescenţa atomică**, 1984, 178 p.

C. BODEA, **Tratat de biochimie vegetală**, p. II, vol. 5, 1984, 438 p.

ELENA CEAUŞESCU, **Cercetări în chimia şi tehnologia polimerilor**, 1983, 519 p.

N. ASANDEI, A. GRIGORIU, **Chimia şi structura fibrelor**, 1983, 395 p.

N. IONESCU, M. CĂLDĂRARU, **Oxidarea catalitică a olefinelor inferioare**, 1983, 178 p.

C. CAŞCAVAL, **Studiul polimerilor prin piroliză şi cromatografie de gaze**, 1983, 220 p.

C. I. SIMIONESCU, F. DANEŞ, **Originea vieţii**, 1983, 110 p.

C. BODEA (sous la direction), **Tratat de biochimie vegetală**, 2 partie, t. IV, 1982, 408 p.

I. G. MURGULESCU, RODICA VÎLCU, **Introducere în chimia fizică. Vol. III. Termodinamica chimică**, 1982, 624 p.

I. G. MURGULESCU, J. PĂUN, **Introducere în chimia fizică. Vol. I. 3. Nucleul atomic, reacţii nucleare, particule elementare**, 1982, 606 p.

ELENA CEAUŞESCU, **Noi cercetări în domeniul compuşilor macromoleculari**, 1981, 536 p.

I. G. MURGULESCU, TATIANA ONCESCU, E. SEGAL, **Introducere în chimia fizică. Vol. II, 2, Cinematică chimică şi cataliză**, 1981, 1024 p.

I. GĂLĂŢEANU, **Procese şi metode radiochimice în energetica nucleară**, 1981, 234 p.

CR. SIMIONESCU, VALERIA GORDUZA, **Polimeri biocompatibili şi biologic activi**, 1980, 479 p.

ELENA CEAUŞESCU, **Polimerizarea stereospecifică a izoprenului**, 1979, 307 p.

C. GH. MACAROVICI, **Analiza chimică cantitativă anorganică**, 1979, 457 p.

M. FLORESCU, **Metode ştiinţifice în dezvoltarea industriei chimice moderne**, 1979, 256 p.

I. G. MURGULESCU, E. SEGAL, **Introducere în chinia fizică, Vol. II. 1. Teoria molecular-cinetică a materiei**, 1979, 1036 p.

I. G. MURGULESCU, V. EM. SAHINI, **Introducere în chimia fizică, Vol. I 2. Structura şi proprietăţile moleculelor**, 1978, 604 p.

I. ZUGRĂVESCU, MAGDA PETROVANU, **N-ylid chemistry**, coédition avec McGraw-Hill International Book Company U.S.A., 1977, 396 p.

I. G. MURGULESCU, **Introducere în chimia fizică, Vol. I. 1. Atomi, molecule, legătură chimică**, 1976, 560 p.

ELENA CEAUŞESCU, **Research work on synthesis and characterization of macromolecular compounds. Contributions**, 1974, 251 p.

ISSN 0035–3930

c. 2759—I. P. INFORMAŢIA

43 426

Lei 40

$ 80 (pour un abonnement annuel)

F 1103 04

ACADÉMIE DE LA RÉPUBLIQUE SOCIALISTE DE ROUMANIE

REVUE ROUMAINE DE CHIMIE

TOME 32
Nº 4
Avril 1987

Rev. Roumaine Chim. RRCHAX, 32, 4, p. 341–454 (1987), Bucarest

EDITURA ACADEMIEI REPUBLICII SOCIALISTE ROMANIA

ACADÉMIE DE LA RÉPUBLIQUE SOCIALISTE DE ROUMANIE

COMITÉ DE RÉDACTION

Rédacteur en chef :

I. G. MURGULESCU, membre de l'Académie de la République Socialiste de Roumanie

Rédacteurs en chef adjoints :

A. T. BALABAN et V. EM. SAHINI, membres correspondants de l'Académie de la République Socialiste de Roumanie

Collège de rédaction :

EM. BRATU, ELENA CEAUŞESCU, ECATERINA CIORĂNESCU-NENITZESCU, CR. SIMIONESCU, membres de l'Académie de la République Socialiste de Roumanie; P. SPACU, membre correspondant de l'Académie de la République Socialiste de Roumanie; M. BANCIU, M. D. GHEORGHIU, I. HAIDUC, D. I MARCHIDAN, G. NIAC et D. SĂNDULESCU.

La Revue Roumaine de Chimie paraît 10 fois par an. Toute commande de l'étranger sera adressée à ROMPRESFILATELIA — sectorul Export-Import Presă, P.O. Box 12—201, télex 10376, prsfi r 78 104, 64—66, Calea Griviței, Bucarest, Roumanie

Les manuscrits, les livres et les revues proposés en échange, ainsi que toute correspondance seront envoyés à la rédaction

REVUE ROUMAINE DE CHIMIE

125, Calea Victoriei, 79717 Bucarest, Roumanie, téléphone 50 76 80

EDITURA ACADEMIEI REPUBLICII SOCIALISTE ROMÂNIA
125, Calea Victoriei 79717 Bucarest, Roumanie, téléphone 50 76 80

REVUE ROUMAINE DE CHIMIE

Tome 32, Nº 4 Avril, 1987

TATIANA ONCESCU, MIHAELA ȘTEFAN and O. HÖRER, On the acid-base equilibria of proflavine in ground and excited electronic states 343–352
A. COUTURE, A. LABLACHE COMBIER, G. SURPĂȚEANU and M. CONSTANTINESCU, Theoretical study on the photocyclization of enamides and thioenamides 353–357
D. POPESCU, B. ALBU, D. OANCEA, N. I. IONESCU, V. GOȘA and D. GEANĂ, The explosive combustion of propylene. IV. The maximum explosion pressure in adiabatic and non-adiabatic constant volume combustion 359–367
DAN CARTIANU, Rate-constrained chemical equilibrium method for solving complex mass action kinetic systems 369–386
P. L. LÓPEZ DE ALBA and L. LÓPEZ M., Potentiometric study of reactions of thorium nitrate and various sodium orthoarsenates in solutions (in Spanish) 387–392
V. V. KORSHAK, E. S. KRONGAUZ, N. M. BELOMOINA, M. BRUMĂ, I. SAVA and C. I. SIMIONESCU, Polyphenylquinoxaline-oxadiazole-imide-amides 393–399
M. BEZDADEA, GH. MIHĂILĂ, N. BÎLBĂ and N. NAUM, Polymerisation of some vinylic monomers in the presence of synthetic zeolites. 401–406
CLEOPATRA VASILIU-OPREA and ALEXANDRU C. CONSTANTINESCU, Mechanochemical reactions of some polyurethane elastomers. 5. Study of modifications of some physico-chemical properties induced by uniaxial tensile creep and UV irradiation 407–415
IRINA V. SHCHERBAKOVA, EVGENII V. KUZNETSOV, LEV YU. UKHIN, MIRCEA D. GHEORGHIU, AURELÍA MEGHEA, JEAN HERDAN and ALEXANDRU T. BALABAN, 2-Benzopyrylium salts. XXXII. Synthesis and some chemical and spectral properties of 1- and/or 3-(3,5-di-t-butyl-4-hydroxyphenyl)-substituted 2-benzopyrylium salts . 417–426
M. M. KAMEL, M. T. EL-WASSIMI, F. H. OSMAN and G. EL-SARRAF, Some reactions on 3-[(2-Hydroxy-4-quinolyl)methyl]-2,4-pentanediones 427–429
O. ANAÇ, The synthesis of an azo-dye 431–433
A. F. EL-FARARGY, A. Y. SOLIMAN, M. EL-MOBAYED and S. EL-ESSER, Synthesis and studies of 3-N-arylcarbamidocoumarins 435–441
METODIU RĂILEANU, Solvent effects. VI. The mechanism of increase, differentiation and leveling of R_f values in the chromatographic separation of substances 443–448
BOOK REVIEWS 449–451
ANNOUNCEMENT 453

Rev. Roumaine Chim. **32**, *4*, 341–454 (1987), Bucarest

Revue Roumaine de Chimie, **32**, *4*, 343–352 (1987)

ON THE ACID-BASE EQUILIBRIA OF PROFLAVINE IN GROUND AND EXCITED ELECTRONIC STATES

TATIANA ONCESCU*, MIHAELA ŞTEFAN** and O. HÖRER***

* Polytechnic Institute, Department of Physical Chemistry, Blvd. Republicii 13, Bucharest, R-70346

** Institute of Chemical Pharmaceutical Research, Şos. Vitan 112, Bucharest, R-74379

*** Institute of Virology "St. Nicolau", Şos. Mihai Bravu 285, Bucharest, R-74339

Received April 14, 1986

Values of the acid-base equilibria involving the four protonated forms of proflavine in their ground and excited electronic states were determined by using various experimental methods and Förster's cycle. These values are important because they correlate with the electron donating capacity of the dye used as photosensitizer in the systems converting photochemically the solar energy.

I. INTRODUCTION

Photochemical conversion of visible quanta is one of the most interesting objects of researches devoted to obtain fuels. The literature mentions a series of systems which produce photohydrogen from water[1-5] using various dyes as photosensitizers. Among them 3,6-diaminoacridine (proflavine) was often used, its photochemistry being better known.[6]

The electron donating ability of the photosensitizer being correlated with its basicity, pK_a values are important in characterizing both the ground and excited state. Since the literature indicates for one of the protonated forms of proflavine only one datum and for another, two different pK_a values, we considered necessary the determination with more accuracy of their pK_a, particularly because we investigate a photochemical system containing proflavine.

II. EXPERIMENTAL

Materials. Proflavine, $C_{13}H_{12}N_3 \cdot HSO_4$ (Serva, Feinbiochemica Heidelberg) r.g., was used as such. Buffer solutions (pH 1 — 14) were prepared from "spectroscopy purity" reagents. In the range of Hammett acidities sulphuric aqueous solutions prepared from H_2SO_4 99% UCB. Belgium were used.

Apparatus and methods. pH-Measurements and potentiometric titration were performed with a pH/mV-meter automatic titration device (Radiometer). For the spectrophotometric investigation of the acid-base equilibria in the ground state of proflavine, the electronic absorption spectra at the desired pH (or H_0) were recorded by a SP 8000 Spectrophotometer Pye-Unicam at 25°C using silica cells with the path length $d = 1$ cm. The spectrophotometric titration of proflavine, 2×10^{-5}M, with concentrated H_2SO_4 was also carried out directly into the cell using microliter pipettes (Pedersen, Denmark). The corrected emission fluorescence spectra were recorded by an Aminco SPF 500 spectrofluorimeter equipped with a Felix M18 microcomputer. The relative fluorescence intensity and the corresponding wavelengths were automatically tabulated on the basis of an adequate program. Proflavine solutions, 1×10^{-6} M, at various pH's (H_0) were used.

III. RESULTS AND DISCUSSION

Proflavine can be involved in the following prototropic equilibria, dependent on the medium acidity:

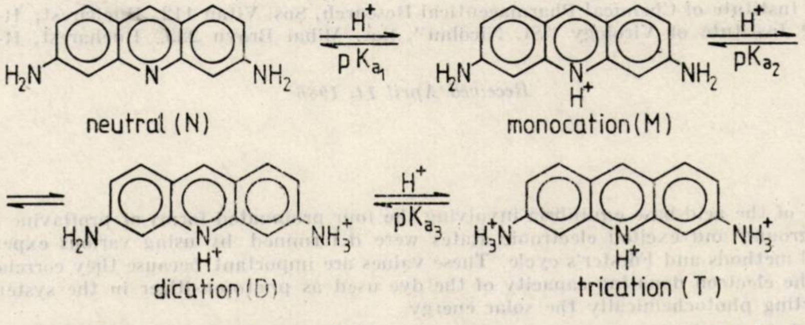

(1)

The spectral characteristics of these species are presented in Table 1 and are in good agreement with those of Shulman[7]. We determined in addition their molar absorptivities ε.

Table 1

Spectral characteristics of absorption ($\lambda_{^1L_a}$ and $\lambda_{^1L_b}$)* and fluorescence emission (λ_f) of protonated proflavine forms in aqueous and sulphuric acid media

Species	$\lambda_{^1L_a}$, nm	$\lambda_{^1L_b}$, nm	$\varepsilon \times 10^{-4}$, M^{-1} cm^{-1}	λ_f, nm
neutral	395	–	1.97	518
monocation	444	–	4.07	512
dication	458	363	1.50 (^1L_a); 1.21 (^1L_b)	540
trication	403	351	0.42 (^1L_a); 2.30 (^1L_b)	477

* ^1L_a ; ^1L_b are bands in the Klevens and Platt nomenclature.[8]

a) Acid-base equilibria in the ground state

The strong dependence of the absorption band position on pH allowed to estimate the acid-base dissociation constants, eq. (1). Figure 1 presents the absorption spectra associated to the equilibrium $M \rightleftharpoons N$ (pH 5.95 – 13.00). One observes that in the pH range 11.83 – 13.00 there exists only the neutral species of amine (λ_{max}=395 nm) whereas between pH 1.95 – 5.95, only the monocationic form (λ_{max} = 444 nm).

Craig et al.[9] showed that the first stage of the protonation corresponds to the attachment of a proton to the ring nitrogen. We calculated from the following equation [10] the pK_{a_1} value:

$$pK_{a_1} = pH - \log \frac{A - A_{BH^+}}{A_B - A} \qquad (2)$$

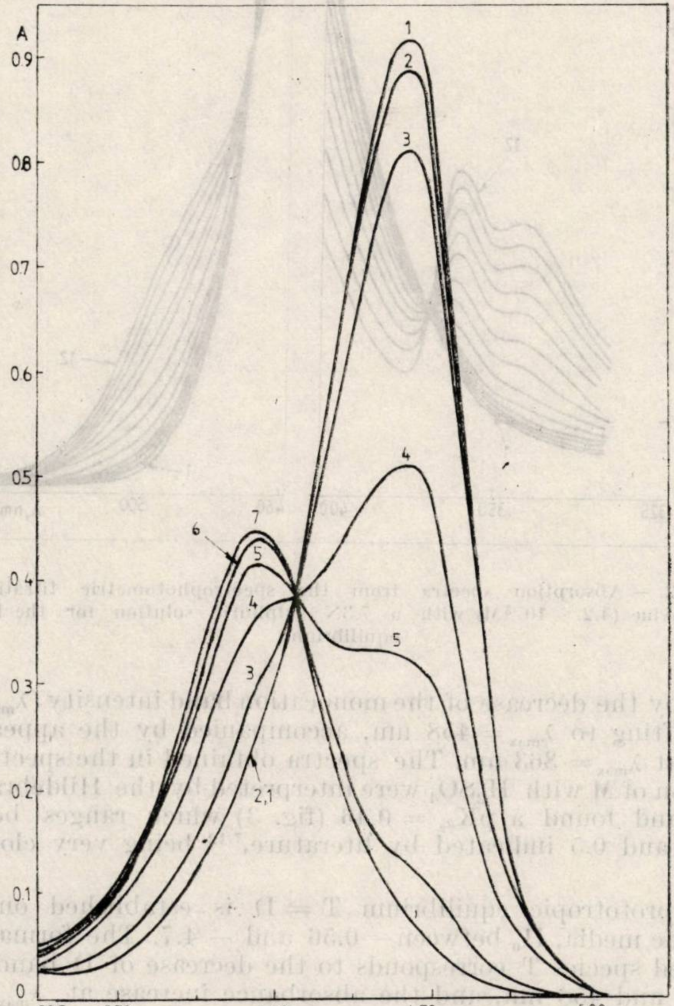

Fig. 1. — Absorption spectra of proflavine (3.15×10^{-5}M) corresponding to M ⇌ N equilibrium at 25°C : 1) pH 1.9 — 5.95 ; 2) pH 7 ; 3) pH 8.85 ; 4) pH 9.62 ; 5) pH 10.6 ; 6) pH 10.8 ; 7) pH 11.85 — 13.

where A, A_{BH^+}, A_B are the absorbances of the sample, protonated species and neutral one, for $\lambda = 444$ nm and a certain pH. We determined a pK_{a_1} of 9.49 in good agreement with the values indicated by literature[7,11,12] using other methods.

The acidity increase of the medium favors the attachment of the second proton to the molecule characteristic to the equilibrium $D \rightleftharpoons M$ evidenced by the decrease of the monocation band intensity ($\lambda_{max} = 444$ nm) and its shifting to $\lambda_{max} = 458$ nm, accompanied by the appearence of a new band at $\lambda_{max} = 363$ nm. The spectra obtained in the spectrophotometric titration of M with H_2SO_4 were interpreted by the Hildebrand-Benessi method[13] and found a $pK_{a_2} = 0.46$ (fig. 3) which ranges between the values 0.3 and 0.5 indicated by literature,[7,12] being very closely to the last one.

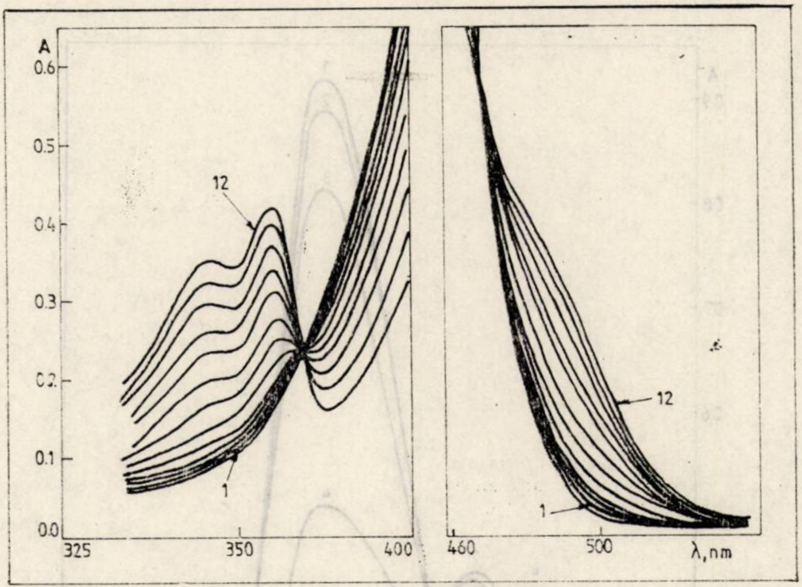

Fig. 2. — Absorption spectra from the spectrophotometric titration of proflavine (4.2×10^{-5}M) with a 7.3N sulphuric solution for the $D \rightleftharpoons M$ equilibrium.

The prototropic equilibrium $T \rightleftharpoons D$ is established only in very strong acidic media, H_0 between -0.56 and -4.7. The formation of the tripotonated species T corresponds to the decrease of D band intensities at 363 nm and 458 nm, and the absorbance increase at $\lambda_{max} = 351$ nm (fig.4). This new absorption band is positioned similarly to that of an unsubstituted acridinium ion $\lambda_{max} = 350$ nm, because of the lone pairs absence on both exocyclic nitrogens. We applied to this equilibrium the method described by David and Geissman[14] (fig. 5) and obtained a value of -2.87 for pK_{a_3}, the only one reported by literature[7] being -2.70.

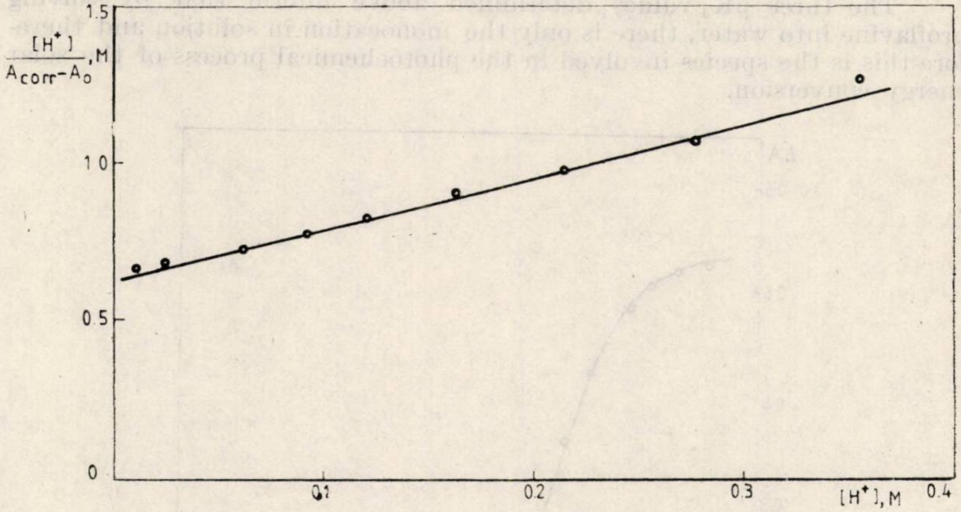

Fig. 3. — The determination of pK_{a_2} value from spectral data of Fig. 2 ($\lambda = 363$ nm); A_{corr}, A_0 are the corrected values for the dilution during the titration, of the proflavine absorbance and the initial one, respectively.

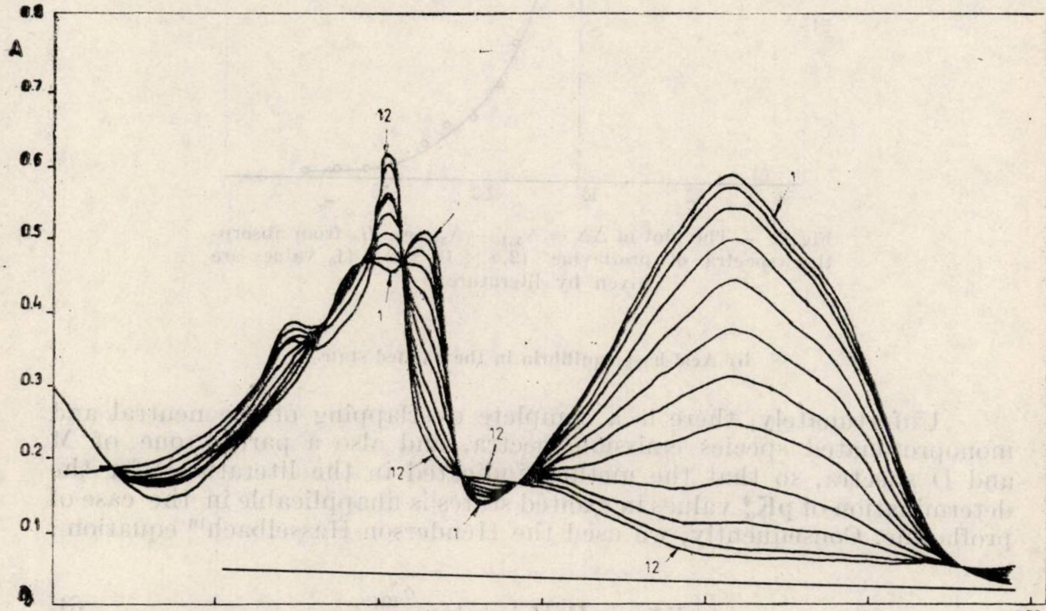

Fig. 4. — Absorption spectra of proflavine (2.5×10^{-5}) in the acidity range 0.24 — 9.3 M H_2SO_4, corresponding to the T ⇌ D equilibrium.

The three pK_a values determined above inform that by solving proflavine into water, there is only the monocation in solution and therefore this is the species involved in the photochemical process of the solar energy conversion.

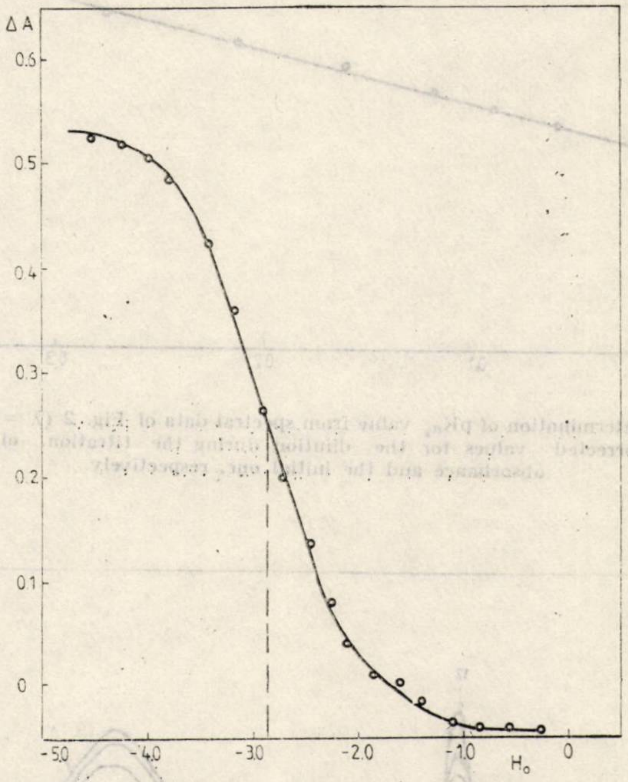

Fig. 5. — The plot of $\Delta A = A_{351} - A_{480}$ *vs.* H_0 from absorption spectra of proflavine $(2.5 \times 10^{-5} M)$; H_0 values are given by literature.[16]

b) Acid-base equilibria in the excited state

Unfortunately, there is a complete overlapping of the neutral and monoprotonated species emission spectra, and also a partial one of M and D spectra, so that the method indicated in the literature[15] for the determination of pK_a^* values in excited states is unapplicable in the case of proflavine. Consequently, we used the Henderson-Hasselbach[16] equation :

$$pK_a^* = pH(H_0) + \log \frac{c^*_{BH^+}}{c^*_B} \qquad (3)$$

and adapted it for the fluorescence measurements on the basis of the fluorescence intensity additivity as well as of the proportionality of these with the emissive excited species concentrations :

$$\frac{c_{\mathrm{B}}^*}{c_{\mathrm{BH}^+}^*} = \frac{I_{0\mathrm{BH}^+} - I_f}{I_f - I_{0\mathrm{B}}} \tag{4}$$

where $\overset{*}{c}_{\mathrm{BH}^+}$, c_{B}^* are the excited state concentrations of the protonated and basic form respectively, $I_{0\mathrm{BH}^+}+I_{0\mathrm{B}}$, the relative intensity fluorescence at a given wavelength under certain conditions of pH(H_0), at which only the protonated, respectively the basic species exist and I_f the relative fluorescence intensity of the sample at various pH's (H_0), measured at the wavelength at which both species involved in the prototropic equilibrium emit. By plotting eq. (3) we calculated the pK_a^* value at the pH(H_0) for which $c_{\mathrm{B}}^* = \overset{*}{c}_{\mathrm{BH}^+}$. Applying this equation to the equilibrium $M^* \rightleftharpoons N^*$ (fig. 6) we determined a $pK_{a_1}^*$ value of 12.5 which corresponds to that indicated by Mataga.[12] The difference between this value and that corresponding to the ground state confirms the basicity increase of N-heterocycle aromatic molecules in their excited states. The fluorescence spectrum change occurs at a far greater pH value than that of the absorption one. Thus the shift to form M* is associated with a slight shift of the maximum emission from $\lambda_f = 518$ nm (pH 14) to $\lambda_f = 512$ nm (pH 4.10). The constant value of the fluorescence intensity (fig. 7) in the range of pH 4—9 evidenced only the presence of the excited monocation in solution. It can be also noticed that in basic media stronger than H^-(NaOH) > 14,

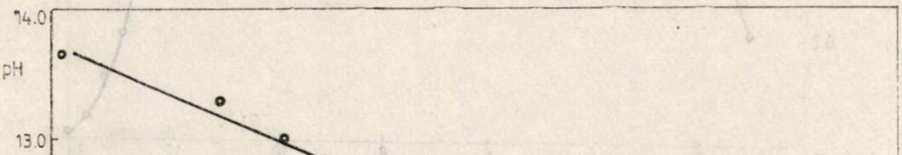

Fig. 6. — The plot of pH vs. log $\frac{c_{\mathrm{B}}^*}{c_{\mathrm{BH}+}^*}$ in which $c_{\mathrm{B}}^* = [\mathrm{Pf}^*]$ and $\overset{*}{c}_{\mathrm{BH}+} = [\mathrm{PfH}^{+*}]$, for $\lambda_f = 512$ nm.

the proflavine fluorescence is quenched. The inflection point of the curve in the range of pH 8.5—11 corresponds to the value 9.7 and that situated between pH 11—14, to the value 12.4. These can be assigned to pK_{a_1} and pK^* respectively, according to the theoretical interpretation of Parker.[17]

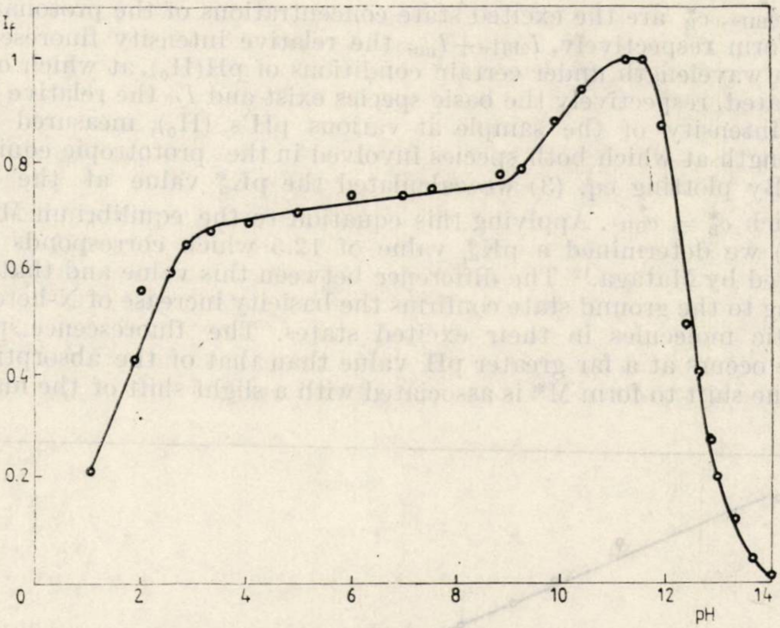

Fig. 7. — The plot of the relative fluorescence intensity vs. pH, for $\lambda_f = 512$ nm.

The increase of the medium acidity to $H_0 = -4.8$ (9.5 M H_2SO_4) induces significant changes in the proflavine fluorescence spectrum ($\lambda_{excit} = 360$ nm). Thus, the fluorescence band intensity at 512 nm diminishes and a new emission appears at $\lambda_f = 540$ nm, assigned to the dication D*. One can assert that in the range of Hammett acidities -3.0 and -4.8 the fluorescence intensity remains practically constant indicating the presence only of D* species. The value of 2.03 obtained for $pK^*_{a_2}$ (applying equation (3)) characterising the equilibrium $D^* \rightleftharpoons M^*$ is greater than the corresponding one in the ground state, what suggests the basicity increase of the proflavine exocyclic aminogroup in the excited state. This value differs somehow from those mentioned in the literature 1.5 [12,18] and 1.6[7] but is very closely to the value which we calculated from Förster's cycle[19] (Table 2).

The investigation of the prototropic equilibrium $T^* \rightleftharpoons D^*$ was carried out in strong sulphuric acid media ($H_0 = -4.8$ and $-y$ 10.5.[20] Under such conditions we observed the flourescence maximum shifting from 540 nm to shorter wavelengths where appears a new intense fluorescence band with vibrational structure ($\lambda = 477$ nm) characteristic

Table 2

The determined pK_a^* and pK_a values of the acid-base equilibria involving proflavine protonated forms

Equilibrium	pK_a^*		pK_a
	Fluorim. titr.	Förster cycle	
$M \rightleftharpoons N$	12.50	12.35	9.49
$D \rightleftharpoons M$	2.03	2.06	0.46
$T \rightleftharpoons D$	−8.60	−8.49	−2.87

of the trication. The value of − 8.6 for $pK_{a_3}^*$ resulted from our experimental data by plotting eq. (3) is in good agreement with that indicated in literature,[7] namely − 9.0.

The three pK_a^* values were also calculated by Förster's cycle[19]:

$$pK_a^* = pK_a - 2.1 \times 10^{-3}(\tilde{\nu}_{BH^+} - \tilde{\nu}_B). \tag{5}$$

where $\tilde{\nu}_{BH+}$ and $\tilde{\nu}_B$ is the arithmetical mean of the wave numbers corresponding to the absorption and fluorescence maxima for the acidic and basic form, respectively. These values listed in Table 2 agree very well with our experimental data.

CONCLUSION

The results obtained in this paper give information upon the prototropic equilibria involving proflavine, both in the ground and its excited state. The increase of the proflavine basicity under excitation and its redox potential value in excited state[6] recommends this dye as photosensitizer in redox photosystems for the generation of photohydrogen.

REFERENCES

[1] B. V. Koriakin, T. S. Dzhabiev and E. Shilov, *Doklandy Akad. Nauk SSSR*, **253,** 620 (1977).

[2] M. Kirch, J. M. Lehn and J. P. Sauvage, *Helv. Chim. Acta*, **62**, 1345 (1979).

[3] A. I. Krasna, *Photochem. Photobiol.*, **29**, 267 (1979).

[4] K. Kalyanasundaran and M. Grätzel, *J. Chem. Soc. Chem. Commun.*, **1979,** 1137.

[5] K. Kalyanasundaran and D. Dung, *J. Phys. Chem.*, **84**, 2551 (1980).

[6] M. P. Pileni and M. Grätzel, *J. Phys. Chem.*, **84**, 2402 (1980).

[7] S. Schulman, D. Naik, A. Capomacchia and T. Roy, *J. Pharm. Sci.*, **64**, 982 (1975)

[8] W. B. Klevens and J. R. Platt, *J. Chem. Phys.*, **1949**, 470.

[9] D. P. Craig and L. N. Short, *J. Chem. Soc.*, **1945**, 419.

[10] A. Albert and E. P. Serjeant, "The Determination of Ionization Constants", 2nd ed., Chapman and Wall, London, 1971.

[11] A. Albert, *J. Chem. Soc.*, **1965**, 4653.

[12] a) N. Mataga, Y. Kaifu and M. Koizumi, *Bull. Chem. Soc. Japan*, **83**, 373 (1965); b) R. C. Kaye and H. I. Stonehill, *J. Chem. Soc.*, **1951**, 2638.

[13] H. A. Benesi and J. W. Hildebrand, *J. Amer. Chem. Soc.*, **71**, 2703 (1949).

[14] C. T. Davis and T. A. Geissman, *J. Amer. Chem. Soc.*, **76**, 3504 (1954).

[15] E. Vander Donckt, in "Éléments de photochimie avancée", Pierre Courtot, Ed. Hermann, Paris 1972, p. 79.

[16] M. A. Paul and F. A. Long, *Chem. Rev.*, **1957**, 1.

[17] C. A. Parker, "Photoluminescence of Solutions", Elsevier Publishing Co., Amsterdam 1968, p. 328.

[18] G. R. Haugen and W. H. Melhuish, *Trans. Faraday Soc.*, **60**, 386 (1964).

[19] T. Förster, *Z. Elektrochem.*, **54**, 42 (1950).

[20] M. J. Jorgensen and D. Hatter, *J. Amer.Chem.Soc.*, **85**, 878 (1963).

Revue Roumaine de Chimie, **32**, *4*, 353–357 (1987)

THEORETICAL STUDY ON THE PHOTOCYCLIZATION OF ENAMIDES AND THIOENAMIDES

A. COUTURE [a], A. LABLACHE COMBIER[a], G. SURPĂŢEANU [b]
and M. CONSTANTINESCU [b]

[a] Physical Organic Chemistry Department, University of Lille, 59655 Villeneuve d'Ascq Cedex, France

[b] Organic Chemistry Department, Polytechnic Institute Iaşi, Splai Bahlui Stg. 71., Iaşi, 6600, Romania

Received February 3, 1986

Using the MO-CNDO/2 method, the total energies of some isomers of N-(1-isobutenyl) benzamide **3a**, and N-(1-isobutenyl) thiobenzamide **1a** have been calculated. The obtained results explain the absence of photoreactivity of enamide **3a** supposing a rotation around N_1-C_2 bond (**7a** ⇒ **6a**), by irradiation. The photoreactivity of thioenamide **1a** as a mechanism shown in Scheme 5, is proved.

INTRODUCTION

In a previous paper[1] we reported a fast efficient and novel method for preparing a wide variety of thiazolines from thioenamides as easily available starting materials

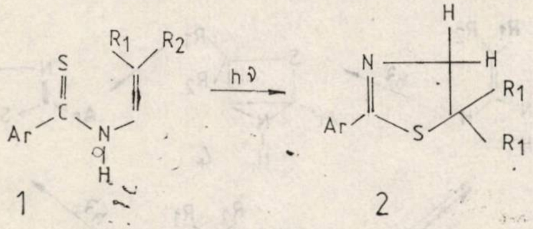

a, Ar = Ph ; $R_1 = CH_3$
b, Ar = α-naphthyl ; $R_1 = CH_3$
c, Ar = o-biphenylyl ; $R_1 = CH_3$
d, Ar = Ph ; R_1, $R_1 = (CH_2)_5$
e, Ar = α-naphthyl ; R_1, $R_1 = (CH_2)_5$
f, Ar = β-nyphthyl ; R_1, $R_1 = (CH_2)_5$
g, Ar = o-biphenylyl ; R_1, $R_1 = (CH_2)_5$
h, Ar = CH_2Ph ; R_1, $R_1 = (CH_2)_5$
Ph = phenyl

Irradiation of thioenamides **1a–c** in hexane (10^3 M, Rayonet PRP 208, 3000 Å lamps) led to the formation of 5,5-dimethyl-thiazolines **2a-c** with fairly good yields (75 – 80 %). In this way it was possible to obtain from thioenamides **1d-g**, spiro heterocyclic framework, one of the most restricted processes in organic synthesis.[2] Irradiation of thioenamides **1d-g** under the conditions described previously, furnished the expected spirocyclohexanethiazolines **2d-g** with yields of 78 — 82%.

RESULTS AND DISCUSSION

The irradiation of secondary enamides **3a-c**, in neutral medium as well as under various conditions left the starting compounds unchanged.

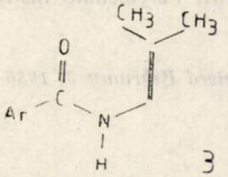

a, Ar = phenyl
b, Ar = — naphtyl
c, Ar = — biphenylyl

The degradation products and polymeric material resulted mainly by long time irradiation. The absence of photoreactivity was also observed for rather similar systems.[3,4] It was then thought that it might be of interest to investigate the photochemical behaviour of enamides and thioenamides from the theoretical viewpoint.

The next qualitative Scheme for the explanation of the photocyclization of thioenamides to the thiazoline derivate **2** is proposed.[1]

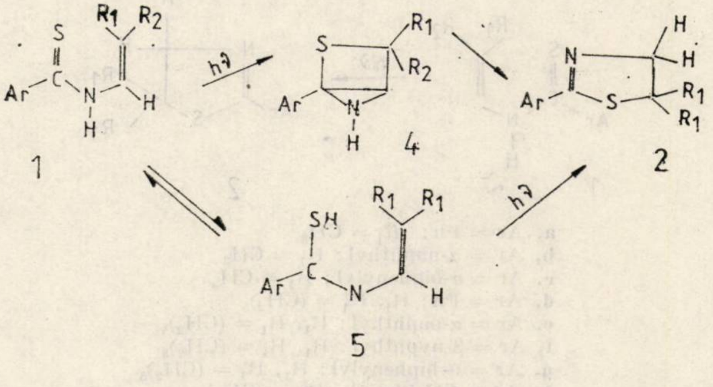

Although not identified, the presence of enols and thioenols as isomer forms of amides and thioamides was reported.[5-7]

Taking into account all the above data we have tried to explain the difference in the photochemical behaviour of enamides and thioenamides.

As method of investigation we have used the calculation of total energies of some isomer forms of enamides and thioenamides. Thus, we have chosen for our study N-(1-isobutenyl) benzamide **3a**, and N-(1-isobutenyl) thiobenzamide **1a**.

Literature data on the X-ray crystal structure of enamides[8-11] and thioenamides[12,13], recall the spatial arrangement of these molecular structures of the type **7**.

C=O 1.22 Å
C=S 1.62 Å

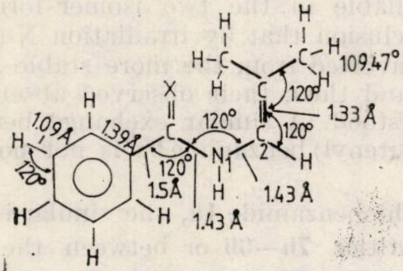
H
H–C
C–H
H
109.47°
X
H
120°
1.33 Å
1.09Å
1.39Å
120°
120°
120°
N1
2
1.5Å
1.43 Å
1.43 Å
H
H
H
H

6a, X=O E_t=-73890.3 Kcal/mol
6b, X=S divergence

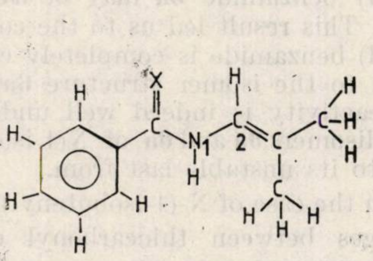
X
H
H
C–H
H
C
N1
2
C
H
H
H
H
H
H

7a, X=O E_t =-74045.2 Kcal/mol
7b, X=S E_t =-69404.2 Kcal/mol

H–O 1.02 Å ∢HSC 92°
H–S 1.30 Å ∢HOC 105°
C–O 1.43 Å
C–S 1.82 Å

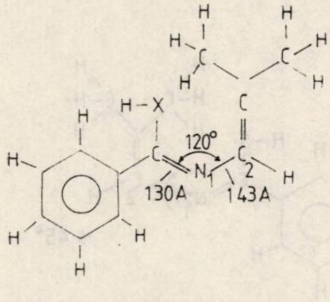
H
H
H
H
H
H–X
H
120°
N1
2
130A
143A
H
H
H
H
H

8a, X=O divergence
8b X=S divergence

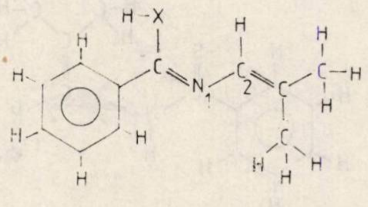
H–X
H
H
H
C
N1
2
C–H
H
H
H
H
H
H

9a, X=O E_t = -74055.3 Kcal/mol
9b X=S E_t = -69359.9 Kcal/mol

Thus, we may write the N-(1-isobutenyl) benzamide **3a** and N-(1-isobutenyl) thiobenzamide **1a** as in Scheme 3. The passing from the structures **7** and **9**, to the structures **6** and **3** respectively, could be explained by a rotation around the N_1—C_2 single bond. On the other hand the passing between structures **6** and **7** to **8** and **9**, respectively, involves a proton isomerization.

In Scheme 3 the geometries of all isomers of enamide **3a** and thioenamide **1a**, taken into account in calculations, are given.

These geometries have been approximated by analogy to previous ones by determined structures.[8-13]

The numerical values of the total energies of all isomers **6**—**9** by the MO-CNDO/2 method have been calculated.[14] Their values are given in Scheme 3.

Due to the steric hindrance in isomers **6b**, **8a,b** by their H(CH$_3$) and X atoms, the iterative calculations of their energies failed and therefore we may appreciate the unstability of these molecules. Only the N-(1-isobutenyl) benzamide **3a** may be available in the two isomer forms **6a** and **7a**. This result led us to the conclusion that by irradiation N-(1-isobutenyl) benzamide is completely converted from the more stable structure **7a** to the isomer structure **6a** and thus, their observed absence of photoreactivity is indeed well understood. A similar exchange between the enolisomers **9a** and **8a** of N(1-isobutenyl) benzamide **9a** is not possible owing to its unstable last from.

In the case of N-(1-isobutenyl) thiobenzamide **1a**, the similar isomer exchanges between thiocarbonyl entities **7b**—**6b** or between the form bearing thioenol group **9b** are not possible. The structures **6b** and **8b** are forbidden from sterical viewpoint. The mechanisms given in Scheme 2, which take into account the addition of thioenol entity or cycloaddition of thiocarbonyl entity to the double bond failed.

The formation of the five-membered heterocyclic compound **2a** may be explained by a photochemical excitation of molecule **1a**; by irradiation that is increased from its ground state **7b** to an intermediate high energy state **10** (Scheme 4).

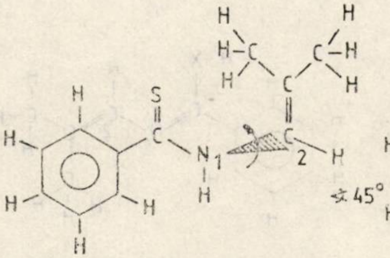

10 E_t = -69428.9 Kcal/mol

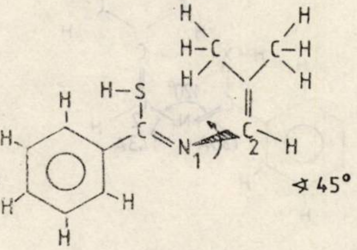

11 E_t = -69394·9 Kcal/mol

The high difference of 44.3 kcal/mol between the energies of isomers **9b** and **7b** allows the appointment, the form **7b** as ground state.

Taking into account all previous data presented in this paper, we propose the mechanism shown in Scheme 5 for the explanation of this type of photocyclization reactions.

In this way, a solution to a problem often encountered in the photochemistry of enamides and thioenamides is provided. Such compounds can indeed rise to new heterocycles with thiazole or spirocyclohexanethiazoline structures with fairly good yields. The obtained results permit us to try to avoid the absence of photocyclization enolenamides by their submission to irradiation.

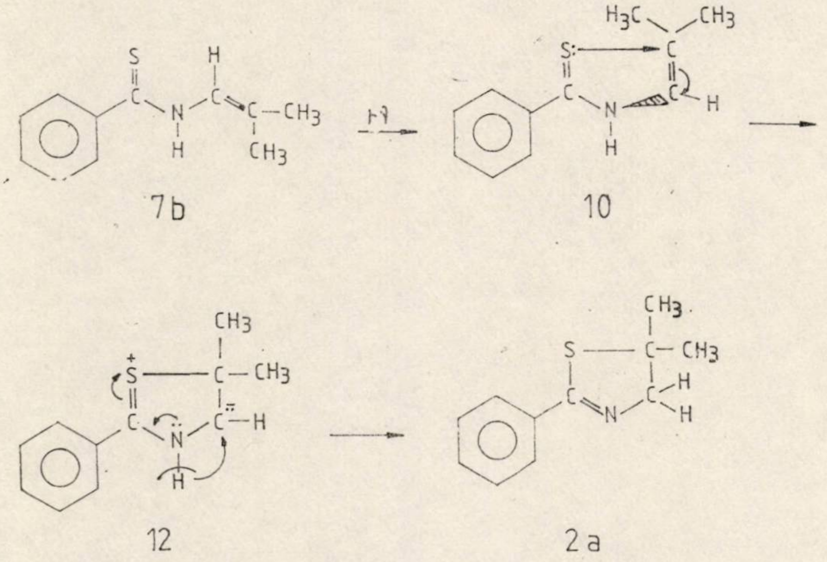

7b 10 12 2a

REFERENCES

[1] A. Couture, R. Dubiez and A. Lablache-Combier, *J. Org. Chem.*, **49**, 714 (1984).
[2] A. P. Krapcho, *Synthesis*, **1978**, 77.
[3] J. C. Gramain, Y. Troin and D. Vallee, *J. Chem. Soc., Chem. Commun.*, **1981**, 832.
[4] I. Ninomiya, T. Kiguchi and T. Naito, *J. Chem. Soc.*, Perkin-Trans., **1**, 2257 (1973).
[5] C. D. Nenițescu, "Chimie organică", vol. I, p. 828, Ed. Didactică și Pedagogică, București, 1973.
[6] P. Beak, *Acc. Chem. Ress*, **10**, 186 (1976).
[7] S. Tobias and H. Gunter, *Tetrahedron Letters*, **23**, 4785 (1982).
[8] M. Kimura and M. Aoki, *Bull. Chem. Soc. Japan*, **26**, 429 (1953).
[9] R. A. Pasternak, *Acta Cryst.*, **6**, 808 (1953).
[10] C. J. Brown and D.E.C. Corbridge, *Acta Cryst.*, **7**,711 (1954).
[11] J. D. Turner and E. C. Lingafelter, *Acta Cryst.*, **8**, 551 (1955).
[12] B. Long, P. Markey and P. J. Wheatley, *Acta Cryst.*, **7**, 140 (1954).
[13] B. R. Penfold, *Acta Cryst.*, **6**, 707 (1953).
[14] J. A. Pople and D. L. Beveridge, "Aproximate Molecular Orbital Theory", McGraw-Hill London, 1970.

Revue Roumaine de Chimie, 32, 4, 359–367 (1987)

THE EXPLOSIVE COMBUSTION OF PROPYLENE. IV.

THE MAXIMUM EXPLOSION PRESSURE IN ADIABATIC AND NON-ADIABATIC CONSTANT VOLUME COMBUSTION

D. POPESCU*, B. ALBU*, D. OANCEA**, N. I. IONESCU*, V. GOȘA* and D. GEANĂ*

* Center of Physical Chemistry, Spl. Independenței 202, Bucharest 77208, Romania
** The Polytechnic Institute, Department of Physical Chemistry and Electrochemical Technology, Blvd. Republicii 13, Bucharest, Romania

Received April 14, 1986

The maximum explosion pressure attained in the adiabatic constant volume combustion of propylene in air, as well as the flame temperature and the equilibrium composition of the reaction mixture have been calculated by means of a computer programme. The adiabatic coefficient of the pressure rise during the constant volume combustion is compared with the coefficients of the pressure rise for non-adiabatic cases, measured in three cylindrical bombs with different sizes and ratios diameter/height.

The maximum pressure attained durring the explosion of a gaseous mixture in a closed vessel ("maximum explosion pressure" or MEP) is a useful parameter, required to design the equipment containing explosive mixtures or its safety devices. At the same time, the maximum explosion pressures can be used in the calculation of normal burning velocities, according to the models of flame propagation in a constant volume bomb with central ignition. [1–3]

The measured values of MEP are always inferior to the theoretical values, obtained on the basis of chemical equilibrium calculations for an adiabatic combustion. The experimental values of MEP are obtained in non-adiabatic conditions, when the heat losses are controlled by the shape and size of the explosion vessel, by the degree of turbulence of the explosive mixture and by the symmetry of flame propagation, corresponding to a central or lateral ignition.[4]

This paper presents the values of MEP measure din several cylindrical bombs having different volumes and different ratios diameter to height, as compared to the adiabatic MEP computed for the constant volume combustion of propylene in air, at different propylene concentrations within its flammability range.

EXPERIMENTAL

The explosions of propylene-air mixtures were performed in three cylindrical stainless steel bombs, as follows:

Vess l no. I: $\varnothing_i = 4.7\cdot10^{-2}$ m; $h = 9.2\cdot10^{-2}$ m.
Vessel no. II: $\varnothing_i = 6.0\cdot10^{-2}$ m; $h = 6.0\cdot10^{-2}$ m.
Vessel no. III: $\varnothing_i = 10.0\cdot10^{-2}$ m; $h = 15.0\cdot10^{-2}$ m.

Each vessel was provided with a lower and an upper demountable lid, made of stainless steel and of a plexiglas plate respectively; a screwed cap on both sides and silicone rubber gaskets ensured a good tightness of the vessels. In some experiments, vessel no. II was supplied with a mixing device, formed by a fan with two blades. This fan, mounted in the upper plexiglas plate, was driven from outside by a magnetic stirrer.

The explosion was initiated of by an inductive-capacitive spark produced between two stainless steel electrodes having plane surfaces. Usually, the spark gap was centrally mounted; however, in vessel no. III, the ignition was realised also asymmetrically, in the median part of the cylindrical wall or in the upper part of the vessel, at the joint between the cylinder and the top plate.

The pressure evolution during the explosion was recorded with a piezoelectric transducer Kistler type 601 A, mounted in the center of the bottom plate: the transducer surface was coated with silicone grease to avoid the direct contact with the flame.

A ball tap mounted in the cylindrical wall of each vessel provided a minimum dead space in the vessel and ensured a tight connection with the vacuum pump and with the gas storage vessel, respectively. Other details concerning the installation, the preparation and storage of the explosive gaseous mixtures can be found in a previous paper.[1]

Several mixtures of propylene and air, with a propylene content of 3 — 9% vol., were studied. For each explosive mixture, 5 — 7 experiments were performed in each vessel, at different initial pressures varying between 40 and 150 kPa. Likewise, for each explosive mixture, the adiabatic maximum explosion pressures, the adiabatic flame temperatures and the equilibrium composition in flame were calculated, for the constant volume combustion, using the computer programme previously described.[5] The following 15 species were considered as combustion products: C(graphite), H_2O, CO, CO_2, O_2, N_2, H_2, CH_4, C_2H_6, C_3H_8, C_2H_4, C_3H_6, H, OH and O. Their theromodynamic functions were taken from.[6–8] The programme was run on the computer "Independent-100" from the Center of Physical Chemistry-ICECHIM.

RESULTS AND DISCUSSION

The MEP's attained in the adiabatic constant volume combustion of several propylene-air mixtures with various concentrations of propylene, computed at different initial pressures, are given in table 1. It can be seen that for this initial pressure range, the adiabatic MEP's are proportional to the initial pressures (figure 1); the slope of the function $p_{\max}^{\mathrm{ad}} = f(p_0)$ is the adiabatic coefficient of pressure rise in the constant volume combustion, k_V^{ad}.[9] In a similar manner, the maximum explosion pressures attained in different closed vessel explosions follow a linear correlation with the initial pressures, according to the equation:

Table 1

The adiabatic maximum explosion pressures (kPa) of several propylene-air mixtures, at different compositions and initial pressures

$[C_3H_6]$ (vol %) \ p_0(kPa)	50.7	76.0	101.3	152.0	202.7	405.3
3.03	399	598	798	1199	1599	3206
4.52	476	719	964	1454	1947	3931
5.65	496	757	998	1510	2016	4030
6.12	495	744	996	1496	1996	4002

$$p_{\max} = a\,p_0 - b \qquad (1)$$

For a given mixture, the parameters a and b of equation (1) depend on the vessel volume and its asymmetry ratio ($\varnothing/h$), as follows from the results in table 2.

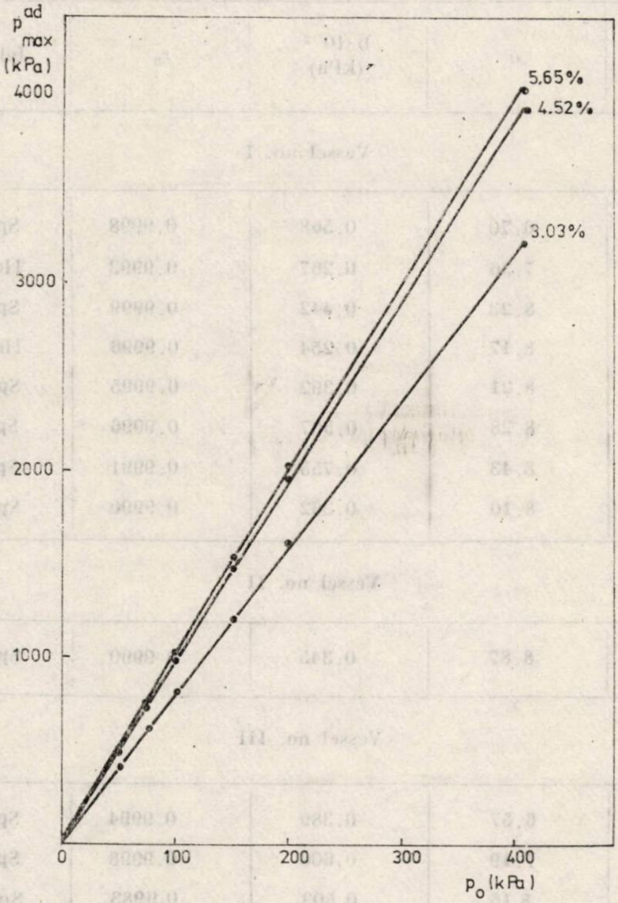

Fig. 1. — The adiabatic maximum explosion pressures of several propylene-air mixtures, at different initial pressures (calculated values).

The analysis of heat balance for the constant volume combustion in cylindrical vessels has shown[9] that the slopes and intercepts of equations (1) depend on the heat transferred to the vessel. The experiments performed with a stoichiometric propylene-air mixture in cell no. III, when the initiation spark was produced in different points of the cell, showed indeed a significant change of both parameters a and b. For instance:

$$p_{\max} = 8.97\, p_0 - 0.325, \text{ for central ignition} \tag{2}$$

and respectively

$$p_{\max} = 8.15\, p_0 - 0.646, \text{ for lateral ignition} \tag{3}$$

Table 2

The parameters of the linear correlation $p_{\max} = ap_0 - b$, for the explosion of several propylene-air mixtures in closed vessels (r_n is the correlation coefficient)

$[C_3H_6]$ (vol %)	a	$b \cdot 10^{-2}$ (kPa)	r_n	Ignition source
Vessel no. I				
3.22	6.70	0.568	0.9998	Spark
3.67	7.36	0.267	0.9993	Hot wire
4.08	8.23	0.442	0.9999	Spark
4.49	8.17	0.254	0.9996	Hot wire
4.52	8.21	0.392	0.9995	Spark
4.55	8.28	0.507	0.9996	Spark
5.05	8.43	0.755	0.9991	Spark
6.12	8.10	0.362	0.9990	Spark
Vessel no. II				
4.53	8.87	0.345	0.9990	Spark
Vessel no. III				
3.03	6.57	0.389	0.9994	Spark
3.22	7.19	0.600	0.9998	Spark
3.67	8.16	0.503	0.9983	Spark
4.08	8.54	0.595	0.9994	Spark
4.55	8.97	0.325	0.9990	Spark
5.05	8.72	0.531	0.9996	Spark
5.65	9.28	0.225	0.9992	Spark
6.12	8.72	0.531	0.9994	Spark
7.07	8.30	0.830	0.9997	Spark
7.60	7.24	0.250	0.9998	Spark
7.65	7.16	0.263	0.9993	Spark
8.11	7.15	1.367	0.9923	Spark
8.48	6.34	0.785	0.9990	Spark

The overall result of lateral ignition is the decrease of effective maximum pressure attained during the explosion.

Using the linear correlations found between the experimental MEP and the initial pressure, the effective coefficients of pressure rise in constant volume explosions taking place at initial atmospheric pressure, $(k_V^{\text{eff}})_0$, have been calculated:

$$(k_V^{\text{eff}})_0 = \frac{a p_{\text{atm}} - b}{p_{\text{atm}}} \tag{4}$$

Their values, for propylene-air mixtures with various propylene concentrations, are given in figure 2, as well as the values of the adiabatic coefficients, k_V^{ad}.

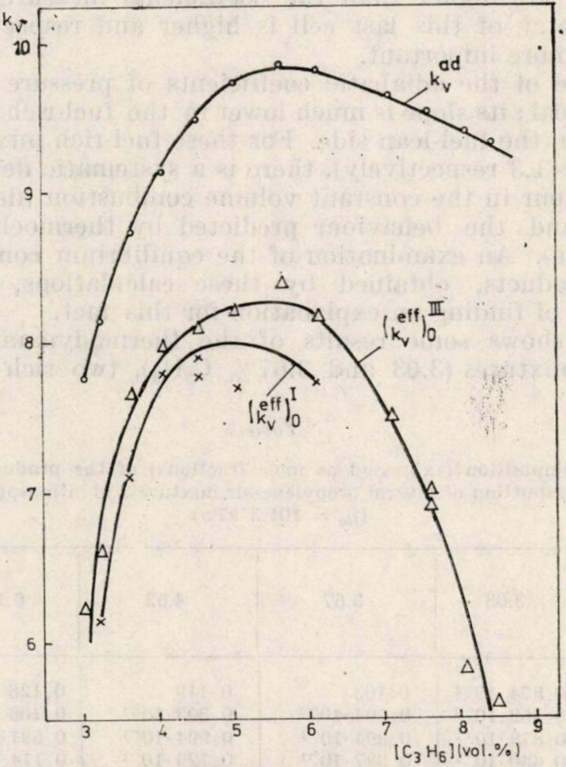

Fig. 2. — The coefficients of pressure rise in explosions taking place at atmospheric initial pressure: (o) — the adiabatic coefficients, k_V^{ad}; (x) — the effective coefficient of pressure rise, measured in bomb no. I, $(k_V^{\text{eff}})_0^{\text{I}}$; (Δ) — the same in bomb no. III, $(k_V^{\text{eff}})_0^{\text{III}}$.

The curves in figure 2 are different from the point of view of their shape and position. The $(k_V^{\text{eff}})_0$—curves are symmetrical and have a parabolic shape, with a maximum in the concentration range 5.0 — 5.5% propylene (equivalence ratio, $\varphi \simeq 1.1$). For bomb no. III, this curve could be described by the equation :

$$(k_V^{\text{eff}})_0 = -0.273\,[C_3H_6]^2 + 2.909\,[C_3H_6] + 0.582 \tag{5}$$

from which it can be seen that the effective coefficients of the pressure rise do not approach zero, as the propylene concentration is closer to the lower or the upper flammability limit (2.0 – 9.9% [10]); in fact, the behaviour of the propylene-air system near the flammability limits was not studied, as the ignition becomes more and more difficult in the near-limit mixtures.

For each propylene-air mixture, the coefficients $(k_V^{\text{eff}})_0$ measured in cell no. III are higher than the coefficients measured in cell no. I, as the asymmetry of this last cell is higher and respectively, the heat losses become more important.

The curve of the adiabatic coefficients of pressure rise, k_V^{ad}, is no more symmetrical; its slope is much lower in the fuel-rich side part of the diagram than in the fuel-lean side. For these fuel-rich mixtures ($[C_3H_6] > 6\%$ and $\varphi > 1.3$ respectively), there is a systematic deviation between the real behaviour in the constant volume combustion (described by the $(k_V^{\text{eff}})_0$-curves) and the behaviour predicted by thermochemical calculations (k_V^{ad}-curve). An examination of the equilibrium composition of the combustion products, obtained by these calculations, could be useful in the attempt of finding an explanation for this fact.

Table 3 shows some results of the thermodynamic calculations, for two lean mixtures (3.03 and 3.67% C_3H_6), two rich mixtures (6.12 and 8.48% C_3H_6) and respectively, for the stoichiometric mixture propylene-air (4.52%). It can be seen that even for the lean mixtures, the burned gas contains two main products (CO_2 and H_2O) and significant amounts of CO and H_2. The increase of propylene content in the initial

Table 3

The equilibrium composition (expressed as mole fractions) of the products obtained in the constant volume combustion of several propylene-air mixtures, at atmospheric initial pressure (p_0 = 101.3 kPa)

Species \ $[C_3H_2]_0$ (vol. %)	3.03	3.67	4.52	6.12	8.48
H_2O	$0.874 \cdot 10^{-1}$	0.103	0.119	0.128	$0.834 \cdot 10^{-1}$
CO	$0.152 \cdot 10^{-2}$	$0.794 \cdot 10^{-2}$	$0.303 \cdot 10^{-1}$	0.106	0.184
CO_2	$0.878 \cdot 10^{-1}$	$0.994 \cdot 10^{-1}$	$0.994 \cdot 10^{-1}$	$0.591 \cdot 10^{-1}$	$0.220 \cdot 10^{-1}$
O_2	$0.660 \cdot 10^{-1}$	$0.387 \cdot 10^{-1}$	$0.126 \cdot 10^{-1}$	$0.114 \cdot 10^{-3}$	$0.109 \cdot 10^{-6}$
N_2	0.753	0.742	0.722	0.667	0.587
CH_4	—	—	$0.252 \cdot 10^{-14}$	$0.661 \cdot 10^{-11}$	$0.377 \cdot 10^{-8}$
H_2	$0.257 \cdot 10^{-3}$	$0.125 \cdot 10^{-2}$	$0.520 \cdot 10^{-2}$	$0.347 \cdot 10^{-1}$	0.123
H	$0.574 \cdot 10^{-2}$	$0.357 \cdot 10^{-4}$	$0.139 \cdot 10^{-2}$	$0.265 \cdot 10^{-2}$	$0.834 \cdot 10^{-3}$
OH	$0.330 \cdot 10^{-2}$	$0.663 \cdot 10^{-4}$	$0.861 \cdot 10^{-2}$	$0.236 \cdot 10^{-2}$	$0.877 \cdot 10^{-4}$
O	$0.479 \cdot 10^{-3}$	$0.118 \cdot 10^{-2}$	$0.139 \cdot 10^{-2}$	$0.109 . 10^{-3}$	$0.823 \cdot 10^{-7}$

mixture is followed by a continuous increase of CO and H_2 concentrations, as CO_2 and H_2O are formed in smaller amounts; beside these compounds, methane is present in very small concentrations, only in the fuel-rich flames. The radicals H, HO and O also apear in rather high concentrations, for all mixtures; however, the thermochemical calculations do not reveal the soot formation, for none of the initial compositions taken into account. Experimental studies have shown that the lower limit for carbon formation ("the soot threshold") for the combustion of propylene in air is 7.15 – 7.25 % C_3H_6[10,11] and the amount of soot increases dramatically as the propylene concentration is closer to the upper flammability limit. A similar behaviour was observed in the combustion of rich methane-air mixtures; the threshold concentration for soot formation corresponds to a considerably weaker equivalence ratio than that which is suggested by equilibrium calculations.[12] This could be one of the reasons which explains the difference in the slopes of the k_V^{ad} and $(k_V^{eff})_0$-curves, in the fuel-rich domain. At the same time, one cannot eliminate the possibility that, in these mixtures, the thermodynamic equilibrium in the burned gas is not reached, so that the thermochemical calculations do not reveal the real composition of the burned gas.

The maximum values of the k-coefficients, in both adiabatic and non-adiabatic combustion, correspond to propylene-air mixtures with the maximum reactivity, having also a maximum flame temperature, maximum mole fractions of the free radicals (figure 3) and maximum values of normal burning velocities.[13] At the same time, these maximum reactivity mixtures can be characterized by minimum values of the time lag between ignition and the development of the MEP ("time to maximum pressure", θ_{max}). Within the studied range of initial pressures, the θ_{max} values depend to a small extent on the initial pressure, but are strongly influenced by the propylene concentration and by the total volume of the explosive mixture (figure 4).

It is obvious that, at high values of θ_{max}, which appear in the combustion of near-limit mixtures, the contact time of the flame with the side walls of the cylindrical bombs is longer, leading to an increase of the thermal losses and of the difference between the adiabatic and non-adiabatic coefficents of pressure rise.

A turbulence created in the gaseous explosive mixture just before ignition or during the combustion leads to a decrease of θ_{max} values; this effect is stronger when the turbulence degree of the explosive mixture is greater (table 4). A slight increase of the MEP could be observed when the turbulence degree of the gas increased, in good agreement with literature data for other hydrocarbon-air mixtures.[14]

CONCLUSIONS

The coefficients of the pressure rise during the explosion of gaseous propylene-air mixtures in a closed vessel are strongly dependent on the hydrocarbon concentration; this correlation has a parabolic shape, with a maximum in the fuel-rich side of the diagram. For a given propylene

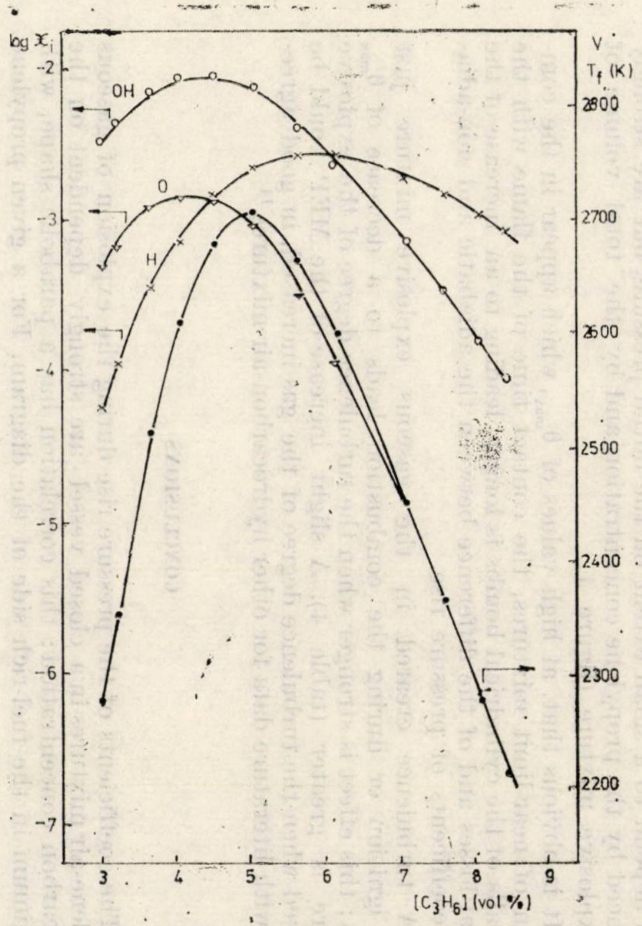

Fig. 3. — The dependence of free radical mole fractions in the flame and respectively, of adiabatic flame temperature (T_f^V) on the initial propylene concentration of the explosive mixtures (explosions at atmospheric initial pressure).

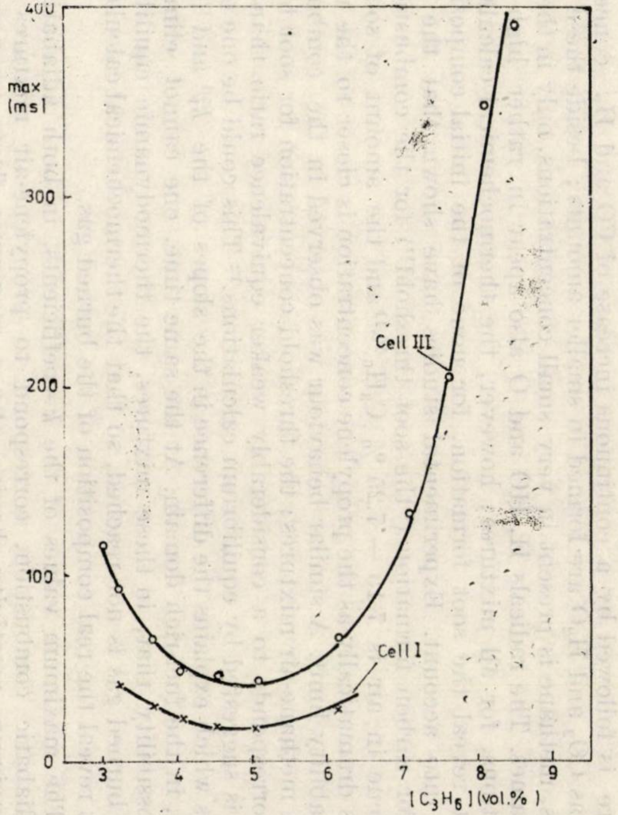

Fig. 4. — The influence of initial propylene concentration, in the explosive mixture on the values of explosion time, θ_{max} in experiments taking place at atmospheric initial pressure.

Table 4

The characteristic parameters of the explosion, for a propylene-air mixture (4.52% C_3H_6) at $p_0 = 58$ kPa, in a closed vessel having $Ø = h = 6.10^{-2}$ m

p_{max} (kPa)	Time to maximum explosion pressure (ms)	Observations
443	26	Quiescent mixture
453	21	Turbulent mixture, minimum fan speed
458	18	Turbulent mixture, fan operation stopped before ignition
463	15	Turbulent mixture, maximum fan speed

concentration, the effective value of the coefficient of pressure rise depends on the explosion vessel size and shape, on the position of the initiation source and on the turbulence of the gas. These experimental values are always lower than the computed values, obtained for the adiabatic combustion.

REFERENCES

[1] Part III: D. Popescu, D. Oancea, V. Goşa, N. I. Ionescu and B. Albu, *Rev. Roumaine Chim.*, **29**, 253 (1984).

[2] B. Lewis and G. von Elbe, "Combustion, Flames and Explosion of Gases", 2nd Edition, Academic Press, New York and London, 1961, chapter V.

[3] C. Rallis, A. Garforth and J. Steinz, *Combustion and Flame*, **9**, 345 (1965).

[4] H. Phillips, *J. Hazardous Materials*, **8**, 251 (1984).

[5] D. Geană, D. Popescu, M. Mihai and L. Adomnică, *Rev. Chim. (Bucureşti)*, **36**, 708 (1985).

[6] D. Stull, E. Westrum and G. Sinke, "The Chemical Thermodynamics of Organic Compounds", J. Wiley, New York, 1969: Russian Translation, Izd. Mir, Moskva, 1971.

[7] I. Barin and O. Knacke, "Thermochemical Properties of Inorganic Substances", Springer Verlag, Berlin, 1973.

[8] I. Barin, O. Knacke and O. Kubascheswki, "Thermochemical Properties of Inorganic Substances", Suppl., Springer Verlag, Berlin, 1977.

[9] D. Oancea, V. Goşa, N. I. Ionescu and D. Popescu, *Rev. Roumaine Chim.*, **30**, 767 (1985).

[10] D. Popescu, V. Goşa, R. H. Schuster, N. I. Ionescu and D. Oancea, *Rev. Roumaine Chim.*, **26**, 927 (1981).

[11] F. Takahashi and I. Glassman, *Combust. Sci. Technol.*, **37**, 1 (1984).

[12] J. Macfarlane, *Combustion and Flame*, **14**, 67 (1970).

[13] A. Sen and G. Ludford, Proc. of the XIX-th Symp. (International) on Combustion, The Combustion Institute, 1982, p. 267.

[14] G. Harris, *Combustion and Flame*, **11**, 17 (1967).

Revue Roumaine de Chimie, **32**, *4*, 369–386 (1987)

RATE-CONSTRAINED CHEMICAL EQUILIBRIUM METHOD FOR SOLVING COMPLEX MASS ACTION KINETIC SYSTEMS

DAN CARTIANU

Center of Physical Chemistry, Splaiul Independenţei 202, Bucureşti, Romania

Received October 7, 1985

The paper clarifies the relationship between the methods of calculation of the chemical equilibria and the solution of certain complex kinetic systems whose rate-determining steps are assumed to be known. A characterization of quasithermodynamic systems in terms of quantities describing the associated chemical graph is first presented. There follows an extension of the definition of the entropy to systems maintained far from thermodynamic equilibrium and the method of determination of the rate-determining step of kinetic models. The constrained equilibrium method introduces into the usual chemical equilibrium calculation additional constraints whose slow time evolution is just the relaxation of the far from equilibrium condition towards a quasithermodynamic evolution.

1. INTRODUCTION

The importance of a study of the computational methods for the quasithermodynamic kinetic systems originates in the fact that these systems delimit the category of dynamical systems exhibiting dissipative structures.

In the publications$^{1-6}$ methods for calculation of the dissipative structures are devised, based on the most recent advances of nonlinear mathematics. A theory of the synchronization of chemical oscillations is proposed as a new basis for the calculation and prediction of dissipative structures.

In this paper a useful method of solving the quasithermodynamic kinetic systems is devised by taking advantage of the computational methods proposed in the papers.$^{7-9}$ This method drastically reduces the number of ordinary differential equations to be integrated, since otherwise such kinetic systems are a challenge even to the biggest computers.

Quasithermodynamic systems are those reaction systems which have only one stoechiometrically accessible steady state for each set of realistic initial conditions, and which always approach this steady state.$^{10-17}$

2. THE ANALYSIS OF THE CONDITIONS FOR QUASITHERMODYNAMIC EVOLUTION

Detailed balance kinetic systems, whose forward and reverse rates for each reaction are equal at steady state, are quasithermodynamic.

A broader class of quasithermodynamic systems is formed by the complex balanced reaction systems, in which all complexes, i.e. the vectors formed by the stoechiometric coefficients of each side of the elementary reactions, and which have a dimension equal to the total numbers of species, are at steady state. Each complex $C(j)$, $j = 1,\ldots,n$ is defined by

$$C(j) = \sum_{i=1}^{m} y^i(j)B(i) \tag{2.1}$$

$B(i)$ being the chemical species and $y(j) = (y^1(j), \ldots, y^n(j))^T$, being the m-tuple or list of molecularities of the total number of species or stoechiometric coefficients of the respective elementary reaction of the kinemechanism. The m by n matrix Y formed by the complex vectors is called the complex matrix.

The rate matrix $R(\mathbf{c})$ at species concentration vector $\mathbf{c}$ is $r_{ij}(\mathbf{c})$, $j = 1,\ldots,n$, and the rate of creation of a complex is the sum of the rates of all reactions leading to the complex considered : $\sum_{j=1}^{n} r_{ij}(\mathbf{c})$. Similarly is defined the rate of annihilation of a complex $\sum_{j=1}^{n} r_{ij}(\mathbf{c})$. Their difference is the rate of formation of a complex. The vector of the rates of formation of complexes or the complex formation vector is

$$\mathrm{g}(\mathbf{c}) = (\mathrm{R}(\mathbf{c}) - R^T(\mathbf{c}))\mathbf{e}_w \tag{2.2}$$

where $\mathbf{e}_w$ is a unit vector in the n-dimensional complex space, R^T being the transpose. The species formation rate vector at concentration $\mathbf{c}$ is defined by

$$f(c) = \sum_{i=1}^{n} \sum_{j=1}^{m} r_{ij}(\mathbf{c})(y(i) - y(j)) \tag{2.3}$$

and satisfies

$$\mathrm{f}(\mathbf{c}) = Yg(\mathbf{c}) \tag{2.4}$$

Complex balance systems are those for which $g(\mathbf{c}) = 0$, and obviously they satisfy also $f(\mathbf{c}) = 0$, for the species formation rate. A kinetic system is called detailed balanced at $\mathbf{c}$ if the rate matrix R is symmetric

$$R(\mathbf{c}) = R^T(\mathbf{c}) \tag{2.5}$$

Every detailed balanced kinetic system is complex balanced. Complex balancing holds for all steady states of many reaction systems which are not detailed balanced. A system has mass action kinetics if $r_{ij} = k(i,j) \prod_{\nu=1}^{m} (c^{\nu})y^{\nu}(j)$, k being the rate constant. This rates law is a consequence of reactive collisions between molecules.

A mass action system is quasithermostatic if there is a vector $\mathbf{a}$ in the positive orthant of species space such that $\mathbf{c}$ satisfies $f(\mathbf{c}) = 0$ if and only if $\ln \mathbf{c} - \ln \mathbf{a}$ is in the orthogonal complement of the stoechiometric space S, the space spanned by the elementary reaction vectors $\mathbf{x}(i,j) = \mathbf{y}(i) - \mathbf{y}(j)$. The kinetics is of the M-molar mass action type if all complexes have the same molarity $M_i = \sum_{j=1}^{m} y^i(j)$. A mass action kinetic system which is not M-molar is called mixed molar. In[17] it is demonstrated that every mixed molar mass action kinetic system can be transformed into a M-molar one.

A mass action system is quasithermodynamic if there is a vector $\mathbf{a}$ in the positive orthant of species space such that: (a) the system is quasithermostatic with respect to $\mathbf{a}$ and: (b) for all $\mathbf{c}$ for which $f(\mathbf{c}) \neq 0$, the stability property holds

$$(\ln \mathbf{c} - \ln \mathbf{a}) f(\mathbf{c}) < 0 \tag{2.6}$$

A quasithermodynamic system exhibits certain regular statics and dynamics similar to that which can be found in closed systems.

If a mass action system is quasithermostatic, then for any $f(\mathbf{c}) \neq 0$ and any $\mathbf{x} \in S$,

$$(\ln \mathbf{c} - \ln \mathbf{a})\mathbf{x} = 0 \tag{2.7}$$

Then $f(\mathbf{c}) = 0$ if and only if

$$\mathbf{c}^{x(i,j)} = \mathbf{a}^{x(i,j)} \tag{2.8}$$

The right side is just the equilibrium constant of the reaction $C(j) \rightarrow C(i)$.

A complex balanced mass action kinetic system is quasithermodynamic.[10-16] The demonstration of this theorem proceeds by a decomposition into cyclic systems, for which the result is shown to hold.

Complex balancing is however not a necessary condition for quasithermodynamic behavior. For mass action kinetics it ensures the stability usually associated with the narrower class of detailed balanced mass action kinetics.

If a mass action kinetic system is complex balanced at one concentration $\mathbf{c}$ for which $f(\mathbf{c}) = 0$, then it is complex balanced at all concentrations satisfying $f(\mathbf{c}) = 0$. It is thus possible to infer from the properties of a mass action kinetic system at only one point that the chemical dynamics must exhibit a certain global regularity and may not exhibit cartain exotic phenomena such as sustained chemical oscillations or bistability.[1-6]

To preclude the possibility that the set of reaction exhibits such interesting phenomena that form the subject of[1-6], the number of independent relations δ that must be satisfied by the rate constants for complex balancing to hold should be zero.

All steady states of mechanisms with $\delta = 0$ are complex balanced and hence quasithermodynamic.

In the set of complexes of arbitrary kinetic systems several equivalence relations take place. The relation $\rightarrow$ (reacts to) is defined if $i = j$ or $r_{ji} > 0$. The kinetic system is reversible if the relation $\rightarrow$ is symmetric, i.e. if $i \rightarrow j$ implies $j \rightarrow i$. Detailed balanced systems are reversible. The relation $i \Rightarrow j$ (forms) holds if there are complexes $i_1, i_2, \ldots, i_\alpha$ such that there exists a pathway leading from i to j : $i = i_1 \rightarrow i_2 \rightarrow \ldots \rightarrow i_\alpha = j$.

A kinetic system is weakly reversible if the relation $\Rightarrow$ is symmetric i.e. if $i \Rightarrow j$ imples $j \Rightarrow i$. The relation $i \leftrightarrow j$ is defined if $i \rightarrow j$ or $j \rightarrow i$. It differs hereby from the relation $i \rightleftarrows j$ often used in reaction diagrams. The relation $i \equiv j$ is defined if there are complexes such that : $i = i_1 \leftrightarrow i_2 \leftrightarrow \ldots \leftrightarrow i_\alpha = j$.

The equivalence classes determined by the relation $\equiv$ are called linkage classes, and their number is denoted by l. If s is the dimension of the stoechiometric space and n is the number of complexes then if the quantity $\delta = n - l - s$ is zero, the kinetic system is complex balanced at every concentration $\mathbf{c}$ such that $f(\mathbf{c}) = 0$ [0–15]. — δ is just the cyclomatic number or first Betti number of the graph whose vertices and edges are the complexes and the reaction paths respectively.

If $\delta = n - l - s = 0$, then

(a). For arbitrary kinetics there can exist an equilibrium composition only if the kinetic mechanism is weakly reversible. If not then there are like in ecology extinct species, or even explosions.

(b). If the kinetic mechanism is weakly reversible, then for mass action kinetics with any choice of positive rate constants, there exists in each stoechiometric compatibility class of the positive orthant of the species space, exactly one composition $\mathbf{c}$ with $f(\mathbf{c}) = 0$. Every such composition is asymptotically stable relative to its stoechiometric compatibility class, and the dynamic equations cannot give rise to periodic solutions.

$\delta = 0$ is thus a criterion for delimiting or screening the kinetic mechanisms which do produce oscillations, or bistability, i.e. memory or switching phenomena[1–6].

In[16] a reaction diagram is devised in which a line is drawn between two complexes if they are connected by an elementary reaction.

It is proved that all weakly reversible mass action kinetics with three short complexes (containing only molecularities 0,1 or 2) are quasithermodynamic. Further, all these systems are complex balanced provided they are not of some exceptional kinds in which case further conditions on the rate constants must be satisfied.

3. THE DESCRIPTION OF KINETIC SYSTEMS IN TERMS OF THERMODYNAMIC CONCEPTS

A mass action system is conservative if there is a positive vector in the orthogonal complement of the stoechiometric space. A nonconservative mass action kinetics can only be the model of an open physical system while conservative systems may model both, open and closed physical systems.

In nonideal systems described by certain nonideal chemical potentials [18] multiple thermodynamic equilibria can take place, just as for certain kinetic systems.

If the kinetics are modelled by mass action rate laws, the kinetic and thermodynamic equilibrium points coincide, the thermodynamic equilibrium point being defined just as in[7-9], by the vanishing of the affinity of each reaction.

One could thus take advantage of the methods described in[7-9] in order to solve the chemical kinetics equations, a problem with great computational complexity.

These methods are based on or are equivalent to the extremum condition of certain thermodynamic potentials, in closed systems. A recent development consists in the demonstration[19-21], that a σ function analogous to the entropy can be defined on the nonequilibrium steady state by extending the Einstein definition of the entropy in terms of the fluctuations. The stability property of the dissipative steady state exhibits many analogies to that of the thermodynamic equilibrium, but is more strongly influenced by noise.[22] A maximum entropy formalism is thus available by which equilibrium themodynamics is extended to nonequilibrium steady states just was mentioned in[3], relative to the extension of the fluctuation-dissipation theorem to steady states.

The σ function on the steady state, which extends the definition of the equilibrium entropy is related to the nonequilibrium fluctuations $W^s(\mathrm{n})$ by the local equilibrium extension of the Einstein formula

$$W^s(\mathrm{n}) \sim \exp(\delta^2\Sigma/2k_B) \tag{3.1}$$

where

$$\delta^2\Sigma = \sum_i (n_i - n_i^s)(\partial^2\Sigma/\partial n_i^s \partial n_j^s)(n_j - n_j^s) \tag{3.2}$$

and to the covariance matrix σ_{ij} at steady state, by

$$k_B \sigma_{ij}^{-1}(\mathbf{n}^s, \mathbf{n}) = \partial^2\Sigma\,(\mathbf{n}^s, \mathbf{n})/\partial n_i^s \partial n_j^s \tag{3.3}$$

An extension of the definition of the temperature, for steady states is provided by the relation derived by evaluating the covariance matrix for steady states involving heat conduction

$$\delta\Sigma/\delta\,\varepsilon\,(\mathbf{r}) = (T^s(\mathbf{r}))^{-1} \tag{3.4}$$

ε ($\mathbf{r}$) being the energy density. T^s for steady states resulting thus from Fourier's law is just the familiar absolute temperature.

Close to a stable noncritical state, the second differential of the σ function is a Ljapunov function:

$$\delta^2\Sigma < 0, \text{ and } \partial\delta^2\Sigma/\partial t \geqslant 0 \tag{3.5}$$

Thus the σ function depends on all the variables characterizing the steady state, including fluxes of the extrinsic variables and reservoir parameters.

In[19] calculations of the σ function have been outlined for several multicomponent systems of experimental interest.

A related development is the derivation of the kinetic microscopic, Boltzmann-like, besides the kinetic macroscopic and hydrodynamic equations for the reactive systems, as well as their solutions, the distribution functions, assuming local chemical equilibrium.[23]

This is the mathematical framework for the phenomena encountered in continuous flow reactors.[8]

The advantage of a purely thermodynamic description of phenomena at steady states is its inherent simplicity.

The properties of the σ function are all based on the steady state fluctuation-dissipation theorem.[19] This result relates the covariance matrix σ_{ij} at steady state to the linearized relaxation matrix H_{ij} of the extensive variables and to the strength of the molecular noise in the system γ_{ij}:

$$\mathbf{H}\boldsymbol{\sigma} + \boldsymbol{\sigma}\mathbf{H}^T = -\boldsymbol{\gamma} \tag{3.6}$$

where

$$\gamma_{ij} = \sum_k (n_{ki}^- - n_{ki}^+)(r_k^+ + r_k^-)(n_{kj}^- - n_{kj}^+) \tag{3.7}$$

$r_k^\pm$ being the rates of the forward and reverse reactions and H_{ij} results by linearizing the average nonlinear evolution equations with respect to $\mathbf{n}$, around the steady state. The rigorous mathematical basis of the definition of the σ function is the Hahn-Banach theorem on the extension of functionals[24].

The demonstration of the effectiveness of stoechiometric techniques in the chemical equilibrium problem, done in [7–9], justifies their wider use, e.g. for the stiff differential equations with stoechiometry, like the mass action kinetic systems.

The crossover of quasithermodynamic mass action kinetic systems from the nonequilibrium steady state towards the eventual thermodynamic equilibrium state, as the conditions on the reservoirs are relaxed, is governed by the slowest reactions, or evolution equations of the relaxed constraints, the other, faster reactions being assumed at chemical equilibrium.

The mass action model has played a dominant role for chemical processes proceeding far from thermodynamic equilibrium. This model has been successful in predicting rates of dilute gas reactions. Its intuitive appeal in terms of molecular collision picture has determined its use even for solution reactions, by introducing various artifices, such as fractional reaction orders, fugacity coefficients and concentration-dependent rate constants.

When dealing with a reaction system wherein certain species relax to their equilibrium concentrations much more rapidly than others it may be convenient or necessary to use perturbation approximations whereby one assumes that the fast reactions relax instantly to their equilibrium values and the motion of the slow reactions is subsequently confined to the nonlinear submanifold defined by the set of equilibrium équations. This is the quasiequilibrium or pseudo-steady state approximation, valid for closed systems.

Concentration-clamp experiments can be done by maintaining a chemical system at a nonequilibrium distribution of chemical concentrations, by means of electronic circuitry analogous to the voltage-clamp apparatus.

Not all the extensive variables of reaction systems are independent. These dependences can be removed in several ways. One way to remove conservation constraints is to provide contact with species reservoirs. The reservoirs fix the equilibrium values of the extensive variables and by exchanging energy (in heat transfer), molecules or charge with the system, remove the conservation constraints. The conservation constraints are holonomic constraints. They have a geometric structure analogous to that of the holonomic constraints of mechanics (finite or integrable constraint expressed by exact total differentials).

In[13] the possibility of a description of chemical dynamics within a framework similar to the classical mechanics is analyzed. The constraint of symplectic flows, with their restriction to even-dimensional systems is however too narrow to encompass dissipative chemical processes.

A capacitive constitutive relation for the ideal dilute solution is defined by

$$n_i \to \mu_i^c + RT \ln \frac{n_i}{V} \tag{3.8}$$

In the thermodynamic case, by using again the analogy to electrical circuit theory, a resistive or dissipative constitutive relation expresses the rate completely by the chemical affinity $\alpha_\xi \to j_\xi$. The resistive constitutive relation is analogous to a nonholonomic constraint on the reaction advancements ξ.

For reactions proceeding far from thermodynamic equilibrium, in general the affinity $\alpha = -A^T\mu$, does not uniquely determine the reaction rate. To maintain the law of definite proportions (i.e. one parameter the advancement ξ characterizing each reaction), one extends the definition of the reaction manifold to allow for a broadened concept of chemical affinity while maintaining the usual notion of reaction advancement and reaction rate. This is a quasithermodynamic construction. Forward and reverse affinities $\hat{\alpha}$ and reaction advancements $\hat{\xi}$ are defined so that a quasithermodynamic constitutive relation results $\hat{\alpha}_{\hat{\xi}} \to \hat{j}_{\xi}$.

Thus closed, and a large class of open mass action type systems are drawn into a common framework. The description of the influx and efflux of several chemical species is accounted for. The physico-chemical structure of many open systems can be described by a set of pseudo-reactions, just like the chemistry of closed systems. These result from reactions in open systems by stripping off the constant concentration species. For entrance or exit reactions including reservoirs, a zero complex is used in pseudoreactions. The pseudoreactions need not reflect compatibility with principles associated with chemical mechanism like conservation of mass or detailed balance.

The $\delta = 0$ criterion for quasithermodynamic behavior provides a relationship between the algebraic structure of the set of pseudoreactions which described an open system and the qualitative dynamics of the system. For closed systems this description is simply the set of elementary reactions themselves.

Certain principles like detailed balance, appropriate for closed systems might restrict the class of rate constant sets. The δ of a kinetic mechanism obtained by stripping (or taking pseudoreactions) does not exceed that of the initial mechanism. These facts help to calculate the set of rate constants which lead to exotic dynamics.

4. THE DETERMINATION OF THE RATE-DETERMINING STEP OF KINETIC MODELS

A simple calculation will show the consistency of certain kinetic and thermodynamic equilibrium expressions.

A frequent expression for the rate, the mass action type kinetics can be written as

$$f(n, Z) = \vec{k}(Z)\prod_{s=1}^{s}(n^s)^{\vec{\beta}^s} - \overleftarrow{k}(Z)\prod_{s=1}^{s}(n^s)^{\overleftarrow{\beta}^s} \tag{4.1}$$

in which the reaction orders are $\vec{\beta}^s$ and $\overleftarrow{\beta}^s$ and Z denotes a pair of thermodynamic variables. The reaction rate vanishes when

$$\prod_{s=1}^{s}(n^s)^{\overleftarrow{\beta}^s - \vec{\beta}^s} = \vec{k}(Z)/\overleftarrow{k}(Z) \tag{4.2}$$

This condition should define the same surface in $(\mathbf{n}, Z)$ space as the equilibrium condition

$$\prod_{s=1}^{s}(n^s)^{A^s} = K(Z) \tag{4.3}$$

A^s being the stoechiometric coefficients. This takes place when for some suitable function F,

$$\vec{k}/\overleftarrow{k} = F(K) \text{ and } \prod_{s=1}^{s}(n^s)^{\overleftarrow{\beta}^s - \vec{\beta}^s} = f\left[\prod_{s=1}^{s}(n^s)^{A_s}\right] \tag{4.4}$$

It is obvious that $f(x) = x^{1/\chi}$, $\chi > 0$ is a satisfactory function and implies that $\overleftarrow{\beta}^s - \vec{\beta}^s = A^s/\chi$, and

$$\vec{k}/\overleftarrow{k} = K^{1/\chi} \tag{4.5}$$

In[25] its unicity is demonstrated.

Let us comment on the significance of the quantity χ. For a sequence of s elementary reactions, open or closed, the sum of which is a stoechiometric equation for a reaction with the net rate r, the identity is valid, r_i, r_{-i} being the forward and reverse rates of step i

$$(r_1 - r_{-1}) r_2 r_3 \ldots r_s + r_{-1}(r_2 - r_{-2}) r_3 \ldots r_s + \ldots + r_{-1} r_{-2} r_{-3} \ldots (r_s - r_{-s}) =$$

$$= r_1 r_2 r_3 \ldots r_s - r_{-1} r_{-2} \ldots r_{-s} \tag{4.6}$$

At the steady state,

$$r_i - r_{-i} = \chi_i r, \qquad (i = 1, \ldots, s) \tag{4.7}$$

where χ_i is called the stoechiometric number of step i, and denotes the number of times the elementary reaction appears in the overall reaction, i.e. in that reaction which contains no intermediates but only initial reactants and products. The rate of this overall reaction is

$$r = \frac{r_1 r_2 \ldots r_s - r_{-1} r_{-2} \ldots r_{-s}}{\chi_1 r_2 \ldots r_s + r_{-1} \chi_2 r_3 \ldots r_s + \ldots + r_{-1} r_{-2} \ldots \chi_s} \tag{4.8}$$

If any step from left to right is irreversible $(r_{-i} = 0)$ the reaction is proceding irreversibly at a rate $r = \vec{r}$. Similarly if any step is irreversible from right to left, $(r_i = 0)$, then $r = \overleftarrow{r}$. Then

$$\vec{r}/\overleftarrow{r} = \prod_{i=1}^{s} (r_i/r_i) \tag{4.9}$$

For every elementary reaction which has rates r_i and r_{-i} described by the equilibrium formulation of the transition state theory, $r_i/r_{-i} = \exp(\alpha_i/RT)$ where α_i is the affinity of step i in the forward direction, equal to $-\Delta G_i$, the Gibbs free energy in the reaction. Then

$$\vec{r}/\overleftarrow{r} = \exp\left(\sum_{i=1}^{s} \alpha_i/RT\right) \tag{4.10}$$

The average stoechiometric number $\bar{\chi}$ is defined by

$$\bar{\chi} = \sum_{i=1}^{s} \chi_i \alpha_i \Big/ \sum_{i=1}^{s} \alpha_i = \alpha \Big/ \sum_{i=1}^{s} \alpha_i \tag{4.11}$$

α being the total affinity of the overall reaction, $\alpha = \sum_{i=1}^{s} \chi_i \alpha_i$.

The ratio of the rates of the overall reaction becomes

$$\overrightarrow{r}/\overleftarrow{r} = \exp(\alpha/\bar{\chi}RT) \tag{4.12}$$

$\bar{\chi}$ depends on the composition and may vary with the extent of reaction. If there exists a rate-determining step σ so that $\alpha_i \simeq 0$ except for $i = \sigma$, then $\chi = \chi_\sigma$ and

$$\overrightarrow{r}/\overleftarrow{r} = \exp(\alpha/\chi_\sigma RT) = r_\sigma/r_{-\sigma} \tag{4.13}$$

since $r_i \simeq r_{-i}$ except for $i = \sigma$.

Both expressions express the consistency between thermodynamic requirements that apply to equilibrium and define how far a reaction will proceed, and the kinetic parameters which define how fast the reaction will take place.

From [7] the affinity α is written in terms of the standard affinity α° of the reaction:

$$\alpha = \alpha^\circ - RT \ln \prod_{j=1}^{c} n_j^{A_j}, \quad 0 = \prod_{j=1}^{c} A_j n_j \tag{4.14}$$

A_j are the stoechiometric coefficients and c the number of components

$$\alpha^\circ = RT \ln K \tag{4.15}$$

Hence $\overrightarrow{r}/\overleftarrow{r} = \left[K \prod_{j=1}^{c} (n_j)^{-A_j}\right]^{1/\bar{\chi}}$. For mass action kinetics with orders of kinetics $\overrightarrow{\beta}_j$ and $\overleftarrow{\beta}_j$, and kinetic coefficients $\overrightarrow{k}$ and $\overleftarrow{k}$,

$$\overrightarrow{r}/\overleftarrow{r} = (\overrightarrow{k}/\overleftarrow{k}) \prod_{j=1}^{c} (n_j)^{\overrightarrow{\beta}_j - \overleftarrow{\beta}_j} = K^{1/\bar{\chi}} \left[\prod_{j=1}^{c} (n_j)^{-A_j}\right]^{1/\bar{\chi}} \tag{4.16}$$

The ratio of the kinetic coefficients and the equilibrium constant depends only on the temperature, the other factors being independent of T, hence the ratio

$$(\overrightarrow{k}/\overleftarrow{k})(K^{-1/\bar{\chi}}) = \prod_{j=1}^{c} (n_j)^{[-A_j/\bar{\chi} - \overrightarrow{\beta}_j + \overleftarrow{\beta}_j]} = \text{const.} \tag{4.17}$$

The constant must be unity, for all the exponents of concentrations must be zero for the relation to be true for arbitrary concentrations. This is the interpretation of the exponent $\bar{\chi}$ in (4.5).

In the transition state picture of the rate constants k, the rate-determining step corresponds to a steep decrease in the free enthalpy as results from (4.5) and from the expression of the equilibrium constant[7].

$$\chi_\sigma = \frac{-\Delta G^\circ}{RT \ln (\overrightarrow{r}/\overleftarrow{r})} \tag{4.18}$$

This expression serves to determine the stoechiometric number of the rate-determining step and is useful in the determination of the location of the rate-determining step of a reaction mechanism from the rates of the overall reaction and the total free enthalpy balance.

The steady state conditions are expressed in terms of stoechiometric numbers :

$$\begin{aligned} r &= r_\sigma / \chi_\sigma \\ r &= r_i / \chi_i \end{aligned} \tag{4.19}$$

A consequence of relation (4.5) is that a catalyst changes $\vec{k}$ and $\overleftarrow{k}$ individually, but not the ratio $\vec{k}/\overleftarrow{k}$, as long as χ is unchanged, and that a catalyst can change the ratio $\vec{k}/\overleftarrow{k}$ if it shifts the rate-determining step.

There may be several sets of stoechiometric numbers associated to a kinetic mechanism. They satisfy the relation [26,27], S being the number of stages,

$$\sum_{k=1}^{S} \chi_{lk} A_{ki} = 0 \tag{4.20}$$

Each vector of stoechiometric numbers defines a possible reaction route. It should be stressed that the above derivation of the consistency relation (4.5) between kinetics and thermodynamics is valid only for single route reactions. For such reactions the notion of a rate-determining step can be defined. For reactions with several basic routes the concept of forward and reverse rates is not always applicable.

The number of basic routes P, that are linearly independent satisfies the relation

$$P = S - I \tag{4.21}$$

where S is the number of reaction stages and I the number of independent intermediates.

For several routes overall reactions the steady state condition on intermediates leads to the relation

$$\sum_{p=1}^{P} \chi_s^{(p)} r^{(p)} = r_s - r_{-s} \tag{4.22}$$

where $\chi_s^{(p)}$ is the stoechiometric number of stage s for the basic route $N^{(p)}$, $r^{(p)}$ is the rate along the basic route, and r_s, r_{-s} are the rates for stage s.

Denoting by A and $\bar{A}$ the stoechiometric coefficients for stages and routes, they are related by

$$\bar{A}_{li} = \sum_{k=1}^{s} \chi_{li} A_{ki}, \; (i = 1, \ldots, n) \tag{4.23}$$

the indices l, k, i denote respectively the route, the stage and the species.

For each route a formal kinetic equation can be witrten:

$$r_i = \sum_{l=1}^{P} \bar{A}_{li}\bar{R}_l, \ (i = 1, \ldots, m) \tag{4.24}$$

where $\bar{R}_l$ is the overall rate on the route l.

The initial stoechiometric equations are:

$$r_i = \sum_{k=1}^{S} A_{ki}R_k \ (i = 1, \ldots, m) \tag{4.25}$$

From the equality of (4.24) and (4.25) and using (4.23) results

$$R_k = \sum_{l=1}^{P} \chi_{lk}\bar{R}_l \ (k = 1, \ldots, S) \tag{4.26}$$

This equation correlates the unknown overall rates $\bar{R}_i$ on the routes with known rates on the stages R_k.

The steady state condition of the intermediate species is $r_i = 0$, for $i = m' + 1, \ldots, m$, where m' is the number of initial reactants and reaction products.

By using (4.24) and (4.23) in (4.26) results (4.20) where $l = 1, \ldots, P$, $i = m' + 1, \ldots, m$.

Among the solutions of equations (4.20) a number of $P = S - I$ are independent. These are the basic routes of the kinetic mechanism.

From the equation (4.26) for mass action kinetics, solved in terms of the rates on the basic routes and the concentrations of intermediates in terms of the concentrations of reactants and products the rates of the reaction stages and the rates of accumulation of each species can be derived, thus permitting to prove the validity of the kinetic mechanisms devised for a certain overall reaction.[28,29]

The independence of the routes does not mean that the corresponding stoechiometric equations are independent.

If the ranks of the matrices A and χ(Q and P) differ, the number of independent empty routes or routes of the from $O = O$ on which no chemical transformations take place is $P - Q$, if $P > Q$. Q is the number of basic overall reactions and it can thus differ from the number of basic routes. $Q = m - c$, where m is the number of reaction participants and c the number of independent components. The basis of routes with Q nonempty and $P - Q$ empty routes is the stoechiometric basis of routes, since it also determines the basis of the stoechiometric overall reactions.

If a stoechiometric basis of routes is chosen then the observable chemical transformation is fully described by Q reaction rates along nonempty routes. A knowledge of $P - Q$ reaction rates on empty routes is not necessary. This however does not mean that the rates along the empty routes are zero.

The relation (4.22) is analogous to the relation [30]

$$\mathbf{v}^{\circ} = \mathbf{E}\mathbf{j} \tag{4.27}$$

for the steady state rates of "currents", expressing the steady state rates on stages in terms of a matrix of extremal currents E, or extremal steady state rates, defined by

$$\mathbf{A}\cdot\mathbf{E} = 0 \tag{4.28}$$

and whose columns are just the stoechiometric numbers of (4.19).

The rate $\mathbf{j}$ along the basic routes is transformed contravariantly when a new basis of routes is introduced.

The empty routes show that for a reaction with a given overall stoechiometric equation, several kinetic mechanisms can be devised.

The summation of the molecular equations corresponding to two kinetic schemes each with one route gives a scheme with two routes, each having the same overall stoechiometric equation. The reverse problem in spite of its nonunicity is important in the planification of kinetic experiments and for organic syntheses as an addition to the tree exploration method starting with the target species.

Practically these systems of equations are overdetermined due to the availability of a great number of measured quantities. The reaction rates are thus determined by a least-squares method supplemented with the requirement that the rates be nonnegative, or with the Tschebyscheff method which includes the nonnegativity of the rate constants.

5. THE CONSTRAINED EQUILIBRIUM METHOD

From (4.20) together with (2.9) of[7] which expresses the rule of definite proportions, the equation of the constraints on composition or invariants results:

$$\sum_j \chi_{ij}^T n_j = b_l = \text{const.} \tag{5.1}$$

The net production of subunit l due to the production of n_i in reaction j is $\chi_{lt}A_{ij}$. For a conserved unit, relation (4.20) is again obtained.

In the quasisteady state of closed reaction systems, some concentrations of species may vary slowly according to differential equations. They govern the rate-determining step. The other concentrations are at their equilibrium values.

The equation (5.1) derived for the constraints in a kinetic system is an extension of the equation of the stoechiometric constraints used in the calculations of chemical equilibria [7-9].

Such constraints describe e.g. the fixed concentration inputs of species in a steady-state reactor.

By relaxing the constraints (5.1) one obtains a set of differential equations that govern the slow rate-determining step of quasi-steady state reaction systems. The other reactions are assumed at equilibrium.

This is the constrained equilibrium method, and provides also for constraints of thermal of hydrodynamic, i.e. other than chemical nature.

Practically for ideal gas mixtures one has to minimize the free enthalpy

$$G(T,\, p) = \sum_{j=1}^{m} n_j \left[E_j(T) + RT - TS_j(p,\, T,\, n_j)\right] \tag{5.2}$$

with the constraints

$$\sum_{i=1}^{m} a_{ij}\, n_i = b_j,\ (j = 1,\ldots,s + r) \tag{5.3}$$

the first s of which are the conservation equations for chemical equilibrium[7–9] and the other r constraints of the form (5.1).

By introducing the Lagrange multipliers γ_k conjugate to these constraints, one obtains

$$\ln\ n_j^c = \ln\ Q_j(T) + \ln V - \sum_{k=1}^{s+r} \gamma_k\, a_{jk} \tag{5.4}$$

where $Q(T) = Q_j(T,\, V)/V$ is the canonical partition function of statistical mechanics per unit volume for molecules of species j and whose logarithm gives standard thermodynamical functions tabulated e.g. in[31].

Equation (5.4) has to be solved for n_j^c in terms of T and p, by using the equation of state

$$pV = RT \sum_{j=1}^{m} n_j^c \tag{5.5}$$

An artifice is to introduce an additional unknown

$$n_0 = \sum_{j=1}^{m} n_j^c \tag{5.6}$$

By introducing (5.4) into (5.3) the equations result :

$$b_l = n_0 \sum_{j=1}^{m} a_{jl} \exp\left[-\sum_{1=1}^{s+r} \gamma_k\, a_{jk} - G_j(p,\, T)\right],\ l = 1,\ldots,s + r \tag{5.7}$$

and

$$1 = \sum_{j=1}^{m} \exp\left[\sum_{k=1}^{s+r} \gamma_k\, a_{jk} - G_j(p,\, T)\right] \text{ where}$$

where $G_j(T, p) = -\ln\ Q_j(T) - \ln(p/RT)$ (5.8)

which may be solved for the $n + r + 1$ unknowns

$$\gamma_k = \gamma_k(T, p,\, b_1,\ldots,b_{n+r}),\ k = 1,\ldots,s + r$$

and

$$n_0 = n_0(T,\, p,\, b_1,\ldots,b_{n+r}) \tag{5.9}$$

Introducing back (5.9) into (5.4) one obtains the constrained equilibrium composition

$$n_j = n_j^c(T,\, p,\, b_1,\ldots,b_{n+r}) \tag{5.10}$$

Once the composition of the gas mixture has been determined, all its other thermodynamic properties can be easily calculated. In particular, the chemical potential and the free enthalpy are :

$$\mu_j = RT \ln \, n_j/Q_j = \sum_{k=1}^{s+r} \lambda_k \, a_{jk} \tag{5.11}$$

$$G = \sum_{j=1}^{m} \mu_j \, n_j = \sum_{k=1}^{s+r} \gamma_k \, b_k \tag{5.12}$$

in which the parameter $\lambda_k = - RT\gamma_k$ (5.13)
It follows that

$$\mu_j = (\partial \, G/\partial \, n_j)_{T,p,n} \tag{5.14}$$

and

$$\lambda_k = (\partial \, G/\partial b_k)_{T,p,b} \tag{5.15}$$

also

$$\sum_{j=1}^{m} n_j \, \mathrm{d}\mu_j = \sum_{k=1}^{s+r} b_k \, d\lambda_k \tag{5.16}$$

$$\sum_{j=1}^{m} \mu_j \, \mathrm{d}n_j = \sum_{k=1}^{s+r} \lambda_k \, \mathrm{d}b_k \tag{5.17}$$

Introducing (5.17) into the Gibbs equation

$$T\mathrm{d}s = \mathrm{d}E + p\mathrm{d}V - \sum_{j=1}^{m} \mu_j \, \mathrm{d}n_j \tag{5.18}$$

the equation results

$$T\mathrm{d}s = \mathrm{d}E + p\mathrm{d}V - \sum_{k=1}^{s+r} \lambda_k \, \mathrm{d}b_k \tag{5.19}$$

The parameters λ_k play precisely the same role with respect to the constraints b_k as the chemical potentials μ_j play with respect to the numbers of mols n_j.

It should be stressed that the number of constraints $s + r$ is much smaller than the number of species m, so it is far more efficient to determine the composition in terms of λ_k than in terms of μ_j.

A condition for chemical equilibrium is

$$\lambda_k^0 = 0 \text{ if } \mathrm{d}b_k \neq 0 \tag{5.20}$$

If the constraints b_k on the composition of the gas mixture are slowly varying functions of time, the temperature $T(t)$, may also be slowly varying with time. The variation of the composition of the gas is assumed to be the result of chemical reactions of the type

$$\sum_j A^{+}_{i} \, B_j \underset{R_i^{+}}{\overset{R_i^{-}}{\rightleftarrows}} \sum_j A^{-}_{ji} \, B_j \tag{5.21}$$

with rate equations for the individual species of the mass action type :

$$\dot{n}_j = \sum_i A_{ji}(R_i^+ - R_i^-) \tag{5.22}$$

where

$$\begin{aligned} A_{ji} &= (A_{ji}^- - A_{ji}^+) \\ R_i^\pm(T, V, n) &= k_i^\pm(T) V \prod_j [n_j]^{A_{ji}^\pm} \end{aligned} \tag{5.23}$$

where $[n_j] = n_j/V$ is the concentration of species B_j.

The detailed balance condition which is sufficient for equilibrium is

$$R_i^+ = R_i^- = R_i^0 \tag{5.25}$$

The following rate quotient rule is obtained from (5.24) and (5.25)

$$k_i^+/k_i^- = \prod_{j=1}^{m} [Q_j]^{A_{ij}} = K_i(T) \tag{5.26}$$

where K (T) is the equilibrium constant of reaction i. This relation assumes the individual molecules are in equilibrium at a temperature T and is a particular case of relation (4.5).

The relaxation times τ_{B_j} and τ_{R_i} for the relaxation of species B_j or reaction R_i to equilibrium can be defined by

$$\tau_{B_j}^{-1} = |\partial \ln n_j/\partial t|_{TV} \tag{5.27}$$

and

$$\tau_{R_i}^{-1} = |\partial \ln (R_i^+ - R_i^-)/\partial t| \tag{5.28}$$

By using (5.22) — (5.25) the formulas results :

$$\tau_{B_j}^{-1} = (n_j^0)^{-1} \sum_i A_{ij} R_i \tag{5.29}$$

$$\tau_{R_i}^{-1} = R_i^0 \sum_j A_{ij}(n_j^0)^{-1}. \tag{5.30}$$

These expressions are useful in determining the rate-determining step and the species that are close to equilibrium.

The rate equations for the constraints are written :

$$\dot{b}_k = \sum_{j=1}^{m} a_{jk}\, n_j, \; k = 1, \ldots, s + r \tag{5.31}$$

or

$$\dot{b}_k = \sum_{i=1}^{s} c_{ik}(R_i^+ - R_i^-),\ k = 1,\ldots,s + r \tag{5.32}$$

where

$$c_{ik} = \sum_{j=1}^{m} a_{ji} A_{jk} = \sum_{j=1}^{m} a_{ji}(A_{jk}^- - A_{jk}^+) \tag{5.33}$$

is the variation of the constraint b_k due to the reaction i. Assuming the elements are conserved in all reactions that are detailed balanced,

$$c_{ki} = 0,\ k = 1,\ldots,s,\ \text{or}\ b_k(t) = b_k,\ k = 1,\ldots,s \tag{5.34}$$

A set of differential equations,

$$\dot{b}_k(t) = \dot{b}_k(T(t),\ V(t),\ b_1,\ldots,b_s,\ b_{s+1}(t),\ldots,b_{s+r}(t)),\ k = s + 1,\ldots,s + r, \tag{5.35}$$

remains to be solved in conjunction with the equations of state and the conservation equations of thermodynamics and fluid mechanics.

When $\dot{b}_k = 0$, the system is maintained at steady state, far from equilibrium. The method thus applies to closed quasithermodynamic systems. This results also by evaluating the entropy production due to chemical reactions, σ_R. From (5.18) one has

$$T\dot{S} = \dot{E} + p\dot{V} + T\sigma_R \tag{5.36}$$

where

$$\sigma_R = -\frac{1}{T}\sum_{k=1}^{s+r} \lambda_k \dot{b}_k = -\frac{1}{T}\sum_i \left(\sum_{k=1}^{s+r} \lambda_k b_{jk}\right)(R_j^+ - R_j^-) \tag{5.37}$$

By using the relation

$$R_j^-/R_j^+ = (k_j^-/k_j^+)\prod_{j=1}^{m} [Q_j]^{A_{ji}} \exp\left(\sum_{k=1}^{s+r} \gamma_k b_{jk}\right) = \exp\left(-\sum_{k=1}^{s+r} \gamma_k b_{jk}\right) \tag{5.38}$$

or

$$\ln\ (R_j^-/R_j^+) = -\sum_{k=1}^{s+r} \lambda_k b_{jk} = (RT)^{-1} \lambda_k b_{jk} = (RT)^{-1}\sum_{i=1}^{m} \mu_i A_{ji} \tag{5.39}$$

one has

$$\sigma_R = R\sum_i (R_i^+ - R_i^-)\ \ln (R_i^+/R_i^-) \tag{5.40}$$

which is a positive definite form.

The expression (5.39) is a measure of the distance from equilibrium, and vanishes for detailed balance conditions. For a set of reactions which vary only a single constraint b_l, results

$$b_{il}^{-1} \ln\ (R_i^-/R_i^+) = (RT)^{-1}\lambda_l \tag{5.41}$$

This relation is useful for establishing the validity of the constrained equilibrium assumption and for determining the rate-determining reaction.

In combustion reactions which exhibit both oscillatory and quasithermodynamic behaviors, 50 or more interesting species should be taken into account, which react in thousands of significant reactions so the above method is the only way of determining the composition of these systems. Moreover most of the rate constants will depend strongly on the estimated rate constants. The practical way is to limit the number of equations to those for which the reaction rates are known and to use the constrained equilibrium assumption to determine the other unknowns.

If a steady-state approximation is used, by letting some species to be constant in time instead of some constraints, the above proof of the positive definite form of the entropy production does not apply. The system may not evolve towards a unique stable equilibrium.

It should be mentioned that computationally, since the conservation laws enter explicitly as constraints, they are satisfied at all times and do not give rise to round-off errors.

The precision of the calculation can be improved by taking account of the constraints one at a time.

REFERENCES

[1] D. Cartianu, *Rev. Roumaine Chim.*, **31**, 175 (1986).
[2] D. Cartianu, *Rev. Roumaine Phys.*, **30**, 327 (1985).
[3] D. Cartianu, *Rev. Chim. (București)*, **30**, 126 (1985).
[4] D. Cartianu, *Stud. Cercet. Fiz.*, **36**, 762 (1984).
[5] D. Cartianu, *Stud. Cercet. Fiz.*, **35**, 360 (1983).
[6] D. Cartianu, "National Conference of Energy", **24**, 152 (1983).
[7] D. Cartianu, *Stud. Cercet. Fiz.*, **31**, 503 (1979).
[8] D. Cartianu, *Rev. Chim., (București)*, **30**, 241 (1979).
[9] D. Cartianu, *Rev. Chim., (București)*, **30**, 754 (1979).
[10] M. Feineberg, *Arch. Rat. Mech. Analys.*, **49**. 187 (1972).
[11] M. Feinberg, *Arch. Rat. Mech. Analys.*, **46**, 1 (1972).
[12] M. Feinberg, and F. J.M. Horn, *Chem. Eng. Sci.*, **29**, 775 (1984).
[13] G. F. Oster and A. Perelson, *Arch. Rat. Mech. Analys.*, **55**, 230 (1974).
[14] F. Horn and R. Jackson, *Arch. Rat. Mech. Analys.*, **47**, 82 (1972).
[15] F. Horn, *Arch. Rat. Mech. Analys.*, **49**, 172 (1972).
[16] F. Horn, *Proc. Roy. Soc. Lond.*, A**334**, 299, 313, 331 (1973).
[17] K. D. Williamowski, *Z. Naturforsch.*, **33**a, 983 (1978).
[18] H. G. Othmer, *Chem. Eng. Sci.*, **31**, 393 (1976).
[19] J. Keizer, *J. Chem. Phys.*, **69**, 2609 (1978), **64**, 1679 (1976), **65**, 4431 (1976), **64**, 4466 (1976), **67**, 1473 (1977), **63**, 5037 (1975), **63**, 398 (1975).
[20] J. Keizer, *J. Stat. Phys.*, **6**, 67 (1972).
[21] G. Lindblad, "Nonequilibrium Entropy and Irreversibility", *Mathemathical Physics Studies* Vol. **5**, D. Reidel, Dordrecht, 1983.
[22] R. Landauer, *Physics Today*, **31**, 24 (1978).
[23] Byung Chan Eu, *J. Chem. Phys.*, **74**, 2998 (1974).
[24] M. Feinberg, *Arch. Rat. Mch. Analys.*, **82**, 203 (1983).
[25] R. Aris, *Arch. Rat. Mech. Analys.*, **27**, 356 (1968).
[26] J. Horiuti and T. Nakamiya, *Adv. Catalysis*, **17**, 1 (1967).
[27] K. D. Williamowski, *Z. Naturforsch.*, **33**a, 983 (1978).
[28] V. N. Pisarenko and A. G. Pogorelov, "Planirovanie kinsiceskinh issledovanii", Nauka Moscow, 1969.
[29] O. Sinanoglu and L. S. Lee, *Theor. Chim. Acta*, **51**, 1 (1979).
[30] B. L. Clarke, *Adv. Chem. Phys.*, **43**, 1 (1980).
[31] "JANAF Thermochemical Tables", Dow. Chem. Comp., Thermal Res. Lab., NSRDS-NBS −37,2ndEd.,1971.

Revue Roumaine de Chimie, 32, *4*, 387–392 (1987)

ESTUDIO POTENCIOMÉTRICO DE LAS REACCIONES EN SOLUCIÓN DEL NITRATO DE TORIO Y DIFERENTES ORTOARSENATOS DE SODIO

P. L. LÓPEZ DE ALBA* y L. LÓPEZ M.

Universidad de Guanajuato, Instituto de Investigaciones Científicas, L. de Retana # 5,
Guanajuato, Gto., 36000 México

Recibido el 24 de marzo de 1986

Se presenta un estudio potenciométrico de las reacciones en solución del nitrato de torio y tres diferentes ortoarsenatos de sodio, comprobándose por esta técnica electroanalítica la estequiometría del $Th_3(AsO_4)_4$, $Th(HAsO_4)_2$ y $Th(H_2AsO_4)_4$ preparados a partir de soluciones milimolares de nitrato de torio y su ortoarsenato de sodio correspondiente. Los valores de pH de precipitación de estos ortoarsenatos resultó para el ortoarsenato neutro entre 5.5 y 5.7, el monobásico entre 3.9 y 4.1, y para el dibásico entre 4.7 y 4.9.

A potentiometric study of reactions of thorium nitrates and three sodium orthoarsenates is presented. The electro-analytical technique used permitted the establishment of the stoichiometry of $Th_3(AsO_4)_4$, $Th(HAsO_4)_2$ and $Th(H_2AsO_4)_4$ prepared starting from millimolar solutions of thorium nitrate and sodium orthoarsenates. The precipitation pH's were : 5.5 — 5.7 for neutral orthoarsenate : 3.9 — 4.1 for monobasic orthoarsenate and 4.7 — 4.9 for dibasic orthoarsenate.

INTRODUCCION

Una búsqueda exhaustiva de la bibliografía reveló que existen varias referencias sobre el estudio de la formación de arsenatos de torio. Barberi 1 trató soluciones acuosas de ácido arsénico al 40 % en caliente con nitrato de torio al 2%, obteniendo un precipitado cristalino de arsenato monoácido de torio, $Th(H\,As\,O)_2 \cdot 6H_2O$; mientras que el arsenato diácido de torio, $Th(H_2AsO_4) \cdot 4H_2O$ fue obtenido usando 50% de ácido arsénico acuoso y solución de nitrato de torio conteniendo 3% de torio. Pierre Castel[2] obtuvo cristales de $Th(H_2AsO_4) \cdot 6H_2O$ y $Th(HAsO_4)_2 \cdot 5H_2O$ mezclando ThO_2 y As_2O_5 en relaciones molares de 0.05 :0.14 y 1.63 : 2.80 respectivamente y fundiéndolos. Le Flem, Lamic y Hagenmuller[3] observaron que calentando fuertemente el gel de $As_2O_5 \cdot ThO_2$ se obtiene un producto de dos formas el hexaarsenato $Th_3As_6O_{23}$ y el ortoarsenato $Th_3(AsO_4)_4$. Prasad y Saxena[4] estudiaron la preparación del ortoarsenato neutro de sodio, a partir de soluciones de pentóxido de arsénico e hidróxido de sodio en relación molar 1 a 6 y llevado a ebullición.

No existen referencias en la literatura sobre un estudio electroanalítico de la formación de diferentes ortoarsenatos de torio a partir de soluciones de nitrato de torio y los ortoarsenatos de sodio correspondients.

En la presente investigación se involucra un estudio potenciométrico de estas reacciones, así como la conformación de las relaciones estequiométricas de los differentes ortoarsenatos de torio.

EXPERIMENTAL

Los reactivos son Merck grado analítico, nitrato de torio, pentoxido de sodio, hidróxido de sodio, p-benzoquinona e hidroquinona fueron usados y sus soluciones preparadas con agua tridestilada libre de oxígeno. Los ortoarsenatos de sodio fueron preparados de acuerdo a sus relaciones molares a partir de soluciones de pentóxido de arsénico e hidróxido de sodio como se muestra en la Tabla 1; dichas soluciones se llevaron a ebullición durante 15 minutos. Las soluciones de los ortoarsenatos de sodio preparadas fueron valoradas como piroarsenatos de magnesio[5] y el torio en solución de nitrato de torio como ThO_2 vía su oxalato[5] y por el método complejométrico con EDTA[6].

Tabla 1

Preparación de los Diferentes Ortoarsenatos de Sodio

Ortoarsenato Neutro

$$6\ NaOH + As_2O_5 \xrightarrow{100°C} 2Na_3AsO_4$$

Ortoarsenato Monoácido

$$4NaOH + As_2O_5 \xrightarrow{100°C} 2Na_2HAsO_4$$

Ortoarsenato Diácido

$$As_2O_5 + 3H_2O \rightarrow 2H_3AsO_4$$

$$2H_3AsO_4 + 2NaOH \xrightarrow{100°C} 2NaH_2AsO_4$$

Diferentes cantidades tanto de nitrato de torio aproximadamente 0.001M como del ortoarsenato de sodio aproximadamente 0.001 M fueron tomados y una serie de titulaciones potenciométricas fueron corridas en una celda para definir la estequiometría de los ortoarsenatos de torio formados.

La fem se midió con un potenciómetro construído por A. García T., de esta misma Institución. Se usaron diferentes tipos de electrodos metálicos (Pt, Au, W, Cu/Al) en (la determinación potenciométrica, combinados con el de quinhidrona (solución de p-benzoquinona e hidroquinona en relación molar (1 :1) en referencia al electrodo de plata/cloruro de plata[7]. Los pares de electrodos utilizados fueron: platino-quinhidrona, oro-quinhidrona, tungsteno-quinhidrona y cobre, aluminio-quinhidrona. Las curvas de titulación para la formación del ortoarsenato neutro de torio con diferentes electrodes se muestra en la figura 1; en la figura 2, se muestra la curva de titulación para el orotarsenato monoácido de torio; y la formación del ortoarsenato diácido de torio se presenta en la figura 3.

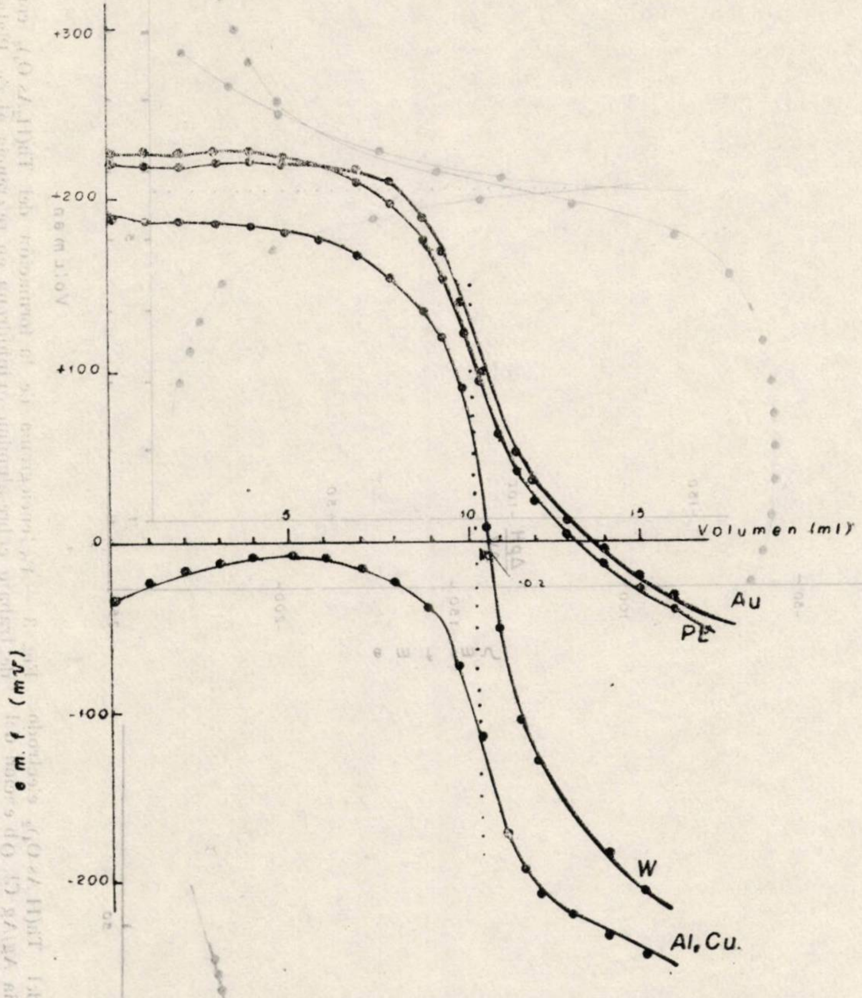

Fig. 1. — Formación del $Th_3(AsO_4)_4$. Curvas potenciométricas con diferentes electrodos metálicos.

RESULTADOS Y DISCUSIÓN

El examen de los resultados revela que las reacciones en solución de los diferentes ortoarsenatos de sodio con el nitrato de torio son factibles de determinar potenciométricamente utilizándolos como reactivos titulantes. El punto final obtenido del máximo de dE/dV y la deflección en la curva de titulación ocurre cuando la reacción está en unarelación molar de torio : AsO_4, 3 :4 para el ortoarsenato neutro; torio : $HAsO_4$, 1 :2 para el orotarsenato monoácido; y de torio : H_2AsO_4, 1 :4 para el ortoarsenato diácido de torio en los valores de pH, 5.6, 4.8 y 4.0 respec-

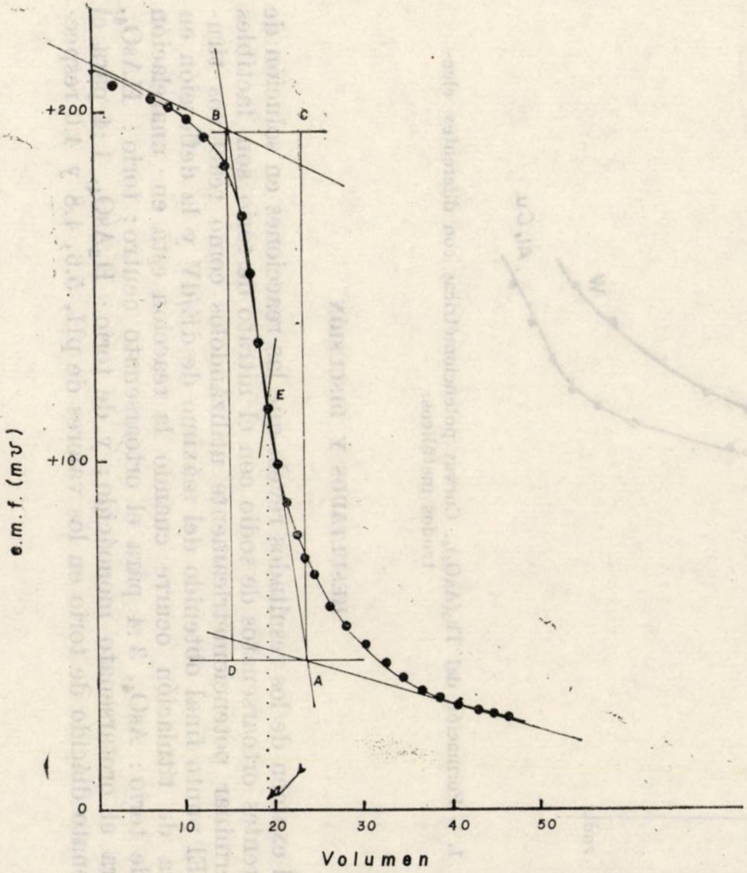

Fig. 2. — Potenciograma de la formación del $Th(H\,As\,O_4)_2$ electrodo indicator de tungsteno-quinhidrona en referencia Ag/Ag Cl. Obtencion del punto de inflexión (E) por el método geométrico.

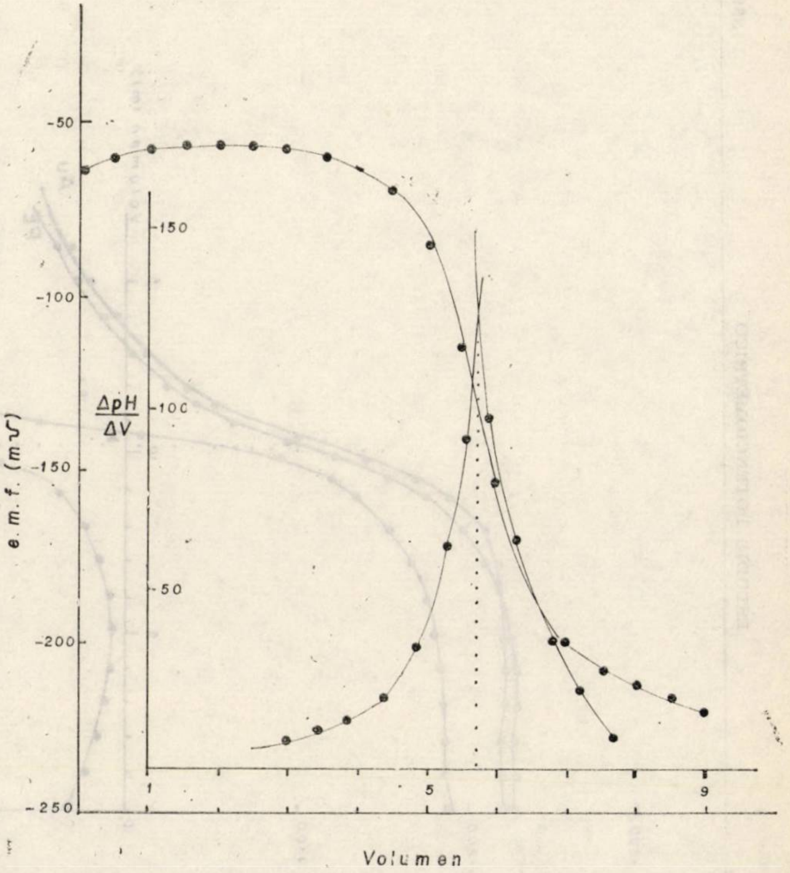

Fig. 3. — Potenciograma de la formación del $Th(H_2As\,O_4)_4$ con electrodo de trabajo cobre-aluminio-quinhidrona en referencia al de Plata-Cloruro de plata.

tivamente. Las reacciones de obtención de los diferentes ortoarsenatos de torio son mostradas en la Tabla 2, mientras que los cálculos para la confirmación de los ortoarsenatos de torio formados son tabulados en la Tabla 3.

Tabla 2

Reacciones de Obtención de los Ortoarsenatos de Torio

Ortoarsenato Neutro

$$4Na_3AsO_4 + 3Th(NO_4)_4 \rightarrow Th_3(AsO_4)_4 + 12\ NaNO_3$$

pH de precipitación : 5.5 a 5.7

Ortoarsenato Monoácido

$$2Na_2HAsO_4 + Th(NO_3)_4 \rightarrow Th(HAsO_4)_2 + 4\ NaNO_3$$

pH de precipitación : 4.7 a 4.9

Ortoarsenato Diácido

$$4NaH_2AsO_4 + Th(NO_3)_4 \rightarrow Th(H_2AsO_4)_4 + 4NaNO_3$$

pH de precipitación : 3.9 a 4.1

Tabla 3

Cálculos Confirmativos de la Obtención de los Diferentes Ortoarsenatos de Torio

	Ortoarsenato Neutro	Ortoarsenato Monoácido	Ortoarsenato Diácido
Alícuota de Torio en ml.	10.0	5.0	10
Volumen gastado en la sol. de ortoarsenato en la titulación, en ml.	10.4	19.0	5.8
mg. de torio en la alícuota	3.38	1.69	3.38
mg. del anión correspondiente en el volumen gastado en la titulación	2.89	2.14	8.1
Moles de Torio	1.46×10^{-2}	7.28×10^{-3}	1.46×10^{-2}
Moles del anión correspondiente	2.8×10^{-2}	1.53×10^{-4}	5.80×10^{-2}
Relación de Torio : Anión	3 :4.2	1 :2.09	1 :3.98
Fórmula	$Th_3(AsO_4)_4$	$Th(HAsO_4)_2$	$Th(H_2AsO_4)_4$

CONCLUSIONES

La presente investigación confirmó la formación de los diferentes ortoarsenatos de torio a partir de soluciones milimolares de nitrato de torio y los diferentes ortoarsenatos de sodio.

Además, se observó que cualquiera de estas reacciones puede ser utilizada en la determinación potenciométrica cuantitative del torio, como ortoarsenato.

AGRADECIMIENTO. Se agradece al Ing. Alvaro García T., Director de este Instituto, por las facilidades prestadas para el desarrollo de este trabajo.

BIBLIOGRAFIÁ

[1] Atli Barberi, *Reale Accad. Naz. Lincei,* **19**, 11, 462 (1910).
[2] Pierre Castell, *C. R. Hebd. Seances Acad. Sci.*, **208**, 37 (1939).
[3] G. Leflem, J. Lamic and P. Hagenmuller, *Bull. Soc. chim. France,* **6**, 188 (1966).
[4] R. S. Saxena and S. Prasad, *J. Inorg. Nucl. Chem.*, **31**, 3338 (1969); Z. *Naturforsch.*, **24 b** 795 (1969).
[5] A. I. Vogel, "A Text Book of Quantitative Inorganic Analysis", Longmans, Green and Co.,
[6] London 1962 pp. 500 y 541.
[7] J. Apple and S. White, *Chemist-Analyst.*, **49**, 42 (1961).
[8] P. L. López de Alba, "Determinación Potenciométrica de la relación Estequiométrica del $Th_3(AsO_4O)_4$con Diferentes Electrodos Metálicos", en Memorias del VI Congreso Mexicano de Quimicos Inorgánicos, San Luis Potosi, S.L.P., México, Junio (1984).

Revue Roumaine de Chimie, **32**, *4*, 393—399 (1987)

POLYPHENYLQUINOXALINE-OXADIAZOLE-IMIDE-AMIDES

V. V. KORSHAK[a], E. S. KRONGAUZ[a], N. M. BELOMOINA[a], M. BRUMĂ[b],
I. SAVA[b] and C. I. SIMIONESCU[b]

[a] Institute of Element-Organic Compounds, Moscow, USSR
[b] Institute of Macromolecular Chemistry, Iaşi, Romania

Received April 14, 1986

New polyphenylquinoxaline-oxadiazole-imide-amides have been synthesized by low temperature solution polycondensation of two aromatic diamines containing preformed phenylquinoxaline and oxadiazole units respectively with diacid chlorides containing preformed imide rings. The thermal stability as well as electrical properties of these copolymers are discussed.

INTRODUCTION

Considerable work has been concentrated in the last two decades on the synthesis of new heterocyclic thermostable polymers with improved processing properties in order to facilitate their utilization into practice. Thus polyphenylquinoxalines have shown remarkable improvement in solubility over their nonphenylated analogs and many other heterocyclic polymers.[1] Likewise, it has been established that among heterocyclic structures, poly-1,3,4-oxadiazoles had the best thermal stability in oxidative atmosphere, owing to some factors concerning the nature of oxadiazole ring. The following order has been written regarding the stability of different polyheterocyclic structures:[2]

1,3,4-oxadiazole > imide > 4-phenyl-1,2,4-triazole > benzimidazole > thiazole.

Since polyimide type polymers show high resistance at elevated temperatures together with good electrical insulating properties,[3] it appeared interesting to us to synthesize new structures which should contain all these heterocyclic units alternating with flexible amide groups and to compare the properties of these polymers with related structures previously reported.

It is the purpose of this paper to describe the preparation of a series of co-polyphenylquinoxaline-1,3,4-oxadiazole-imideamides using two heterocyclic diamines, one of which contains the phenylquinoxaline system and the other the oxadiazole ring, and a diacid chloride which incorporates a preformed imide unit.

RESULTS AND DISCUSSION

Diaminophenylquinoxalines I used in the copolycondensation process have been synthesized by the reaction of 3,4,4′-triaminodiphenylether with bis(α-diketones),[4] according to scheme 1 :

Scheme 1

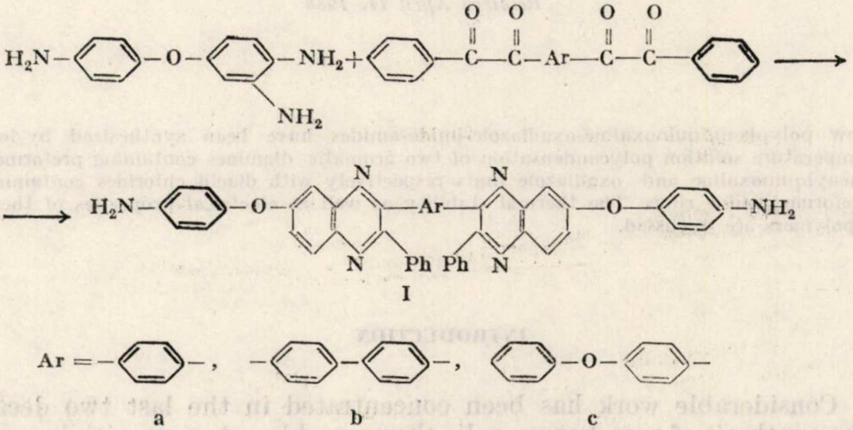

The other diamine, 2,5-bis(*p*-aminophenyl)-1,3,4-oxadiazole, used in the copolycondensation reaction has been obtained from *p*-aminobenzoic acid and hydrazine in polyphosphoric acid (PPA),[5] according to scheme 2.

Scheme 2

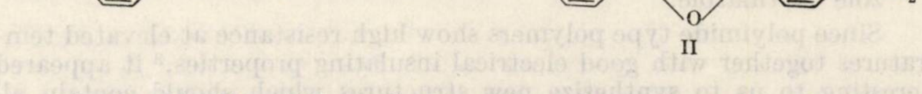

II

Diacid chlorides III used for polycondensation with the above-mentioned heterocyclic diamines have been prepared by treating with thionyl chloride the corresponding dicarboxylic acids which had been synthesized from trimellitic anhydride and certain aromatic diamines, such as 4,4′-diaminodiphenylmethane, 4,4′-diaminodiphenylether and 4,4′-

diaminodiphenylsulphone,[6] as shown in scheme 3 :

Scheme 3

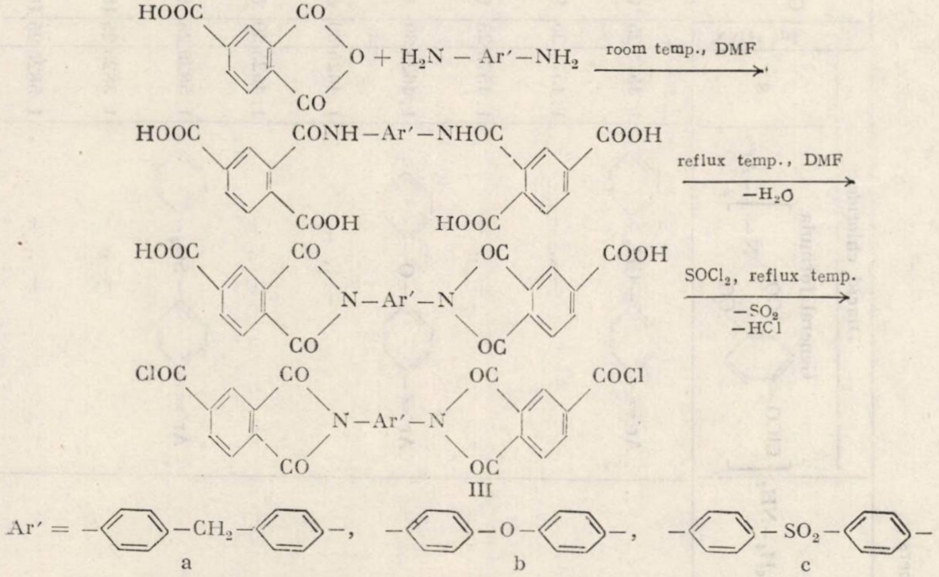
room temp., DMF
reflux temp., DMF
$-H_2O$
$SOCl_2$, reflux temp.
$-SO_2$
$-HCl$
III
Ar' =
a
b
c

Low temperature solution polycondensation of 1 mol of diamines (0.5 mol of diamine I and 0.5 mol of diamine II) and 1 mol of diacid chloride in N-methylpyrrolidone (NMP) at a concentration of 8–10% using Pyridine as acid acceptor, gave polyphenyl-quinoxaline-oxadiazole-imide-amides IV, according to scheme 4 :

Scheme 4

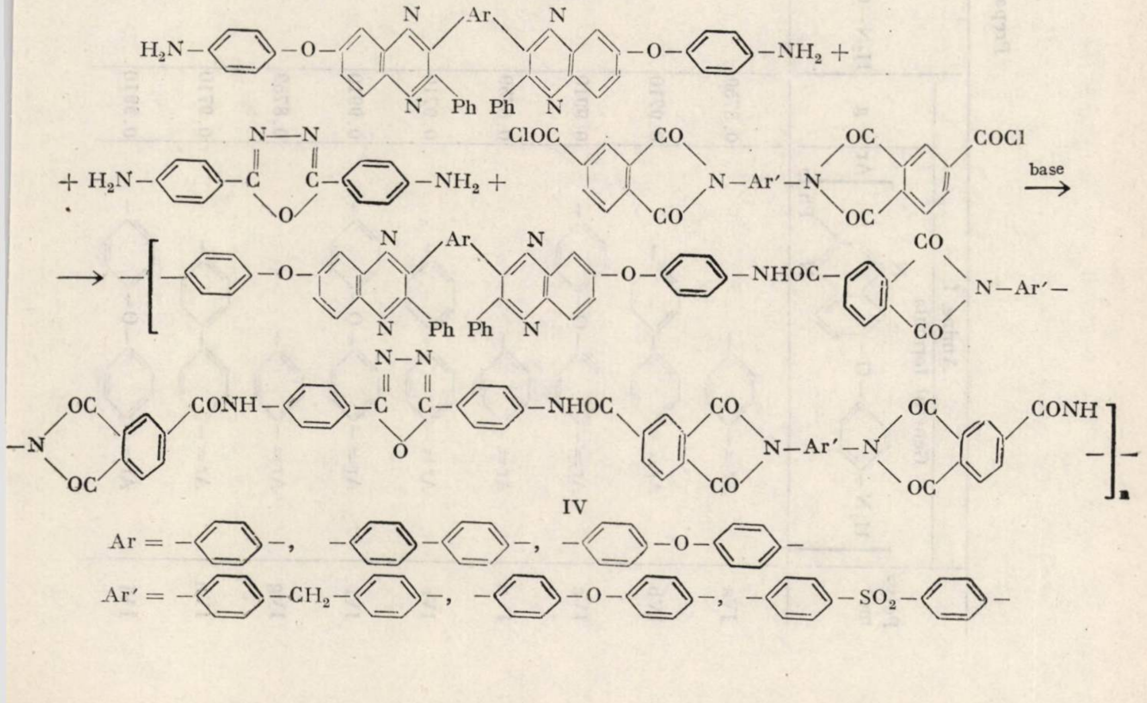
base
IV
Ar =
Ar' =

Table 1

Preparation of copolymers

Polymer	Amine I		Amine II	Diacid chloride		NMP mL	Conc. %
	General formula 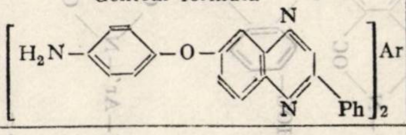	g	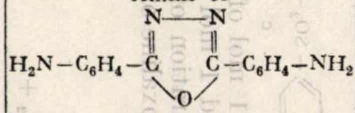	General formula 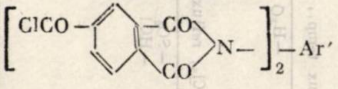	g		
IVa	Ar = 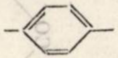	0.8759	0.3153	Ar′ = 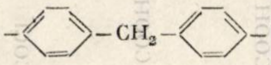	1.4575	25	9.25
IVb	Ar = 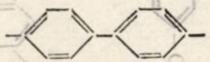	0.9710	0.3153	— ,, —	1.4575	25	9.89
IVc	Ar = 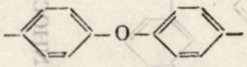	0.9910	0.3153	— ,, —	1.4575	25	9.95
IVd	Ar = 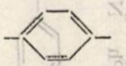	0.8759	0.3153	Ar′ = 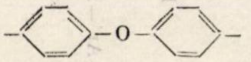	1.4625	30	8.07
IVe	Ar = 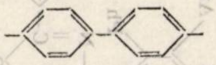	0.9710	0.3153	— ,, —	1.4625	30	8.39
IVf	Ar = 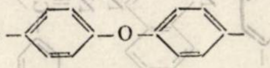	0.9910	0.3153	— ,, —	1.4625	30	8.45
IVg	Ar = 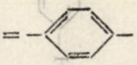	0.8759	0.3153	Ar′ = 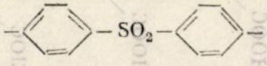	1.5825	25	9.99
IVh	Ar = 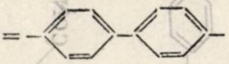	0.9710	0.3153	— ,, —	1.5825	25	10.29
IVi	Ar = 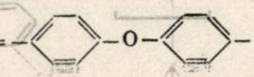	0.9910	0.3153	— ,, —	1.5825	25	10.36

The clear viscous solution which resulted after reaction has been diluted with NMP and then precipitated by pouring into water. The fibrous polymer was filtered, washed with water and acetone and dried. In the case of polycondensation run with diacid chloride IIIb, dilution was requested even during the reaction as the solution became so viscous that the stirring was impossible. The preparation of copolymers is shown in table 1.

The structure of polyphenylquinoxaline-oxadiazole-imide-amides was identified by IR spectra and elemental analyses. Strong bands appeared at 1770 — 1780 cm^{-1}, 1710 — 1720 cm^{-1} and 715 — 720 cm^{-1} assigned to the imide ring. Also all spectra showed wide absorption bands at 3350 cm^{-1} characteristic for NH and 1660 — 1670 cm^{-1} due to CO in amide group. Absorption situated at 960 — 990 cm^{-1} was assigned to oxadiazole ring. Elemental analysis data for C, H, N and S are in good agreement with the calculated values.

All these copolymers are soluble in polar aprotic solvents such as dimethylacetamide and N-methylpyrrolidone up to 40% concentration. Inherent viscosities are 0.30 — 1.5 dl/g, measured in NMP at a concentration of 0.5 g polymer/100 mL solvent, at 20°C (Table 2). Polymers containing SO_2 groups gave lower viscosities than those containing — — CH_2 — and — O — bonds. This fact could be explained by the lower reactivity of the monomer — diacid chloride IIIc — which contains SO_2 linkage.

The thermal stability of these copolymers was evaluated by thermogravimetric analysis (TGA) performed in air at a heating rate of 12°/minute. All polymers begin to decompose after 410° and at 500° the total weight loss is 10 — 12%. Comparison of these polymers with polyphenylquinoxaline-amide-imides previously reported [7] which had related structures but did not contain oxadiazole units, shows that their thermal stabilities are very similar. That means that the introduction of oxadiazole units into the chain of phenylquinoxaline-amide-imide polymers did not lead to higher thermostability. At the same time, if we compare the present polyphenylquinoxaline-oxadiazole-imide-amides with polyoxadiazole-imide-amides reported earlier,[8] it can be noticed that the latest decompose at about 30° higher than the former which can be explained by strong packing between the macromolecular chains containing oxadiazole rings of small volume, which also permit strong hydrogen bonds through amide linkages. In the case of related phenylquinoxaline polymers, due to the big volume of phenylquinoxaline unit, the packing of those macromolecular chains is somewhat disturbed and decomposition can begin with the destruction of amide linkages, no matter of what kind of other highly thermostable heterocycles are introduced into the chain. But, on the other hand, the disturbed packing of macromolecular chains leads to a better solubility. As can be seen, polyoxadiazole-imide-amides are little soluble only in NMP + lithium chloride, while related polyphenylquinoxaline polymers are easily soluble, at high concentration in NMP.

Electrical insulating properties of the polymers synthesized in the present paper have been studied using polymer films of 30 microns thickness. These films have been prepared by pouring onto glass plates

Table 2

Properties of copolymers

Polymer	$\eta_{inh.}$*	Elemental Analysis								TGA***	
		C%		H%		N% **		S%		Initial decomp. temp.°C.	Weight loss at 500°%
		Calcd.	Found	Calcd.	Found	Calcd.	Found	Calcd.	Found		
IVa	0.9	74.41	72.83	3.71	3.45	9.49	8.22	—	—	415	12
IVb	0.43	74.99	75.52	3.74	3.67	9,57	7.75	—	—	410	11
IVc	0.76	74.23	71.52	3.68	3.47	9.94	9.67	—	—	415	10
IVd	1.5	72.87	70.23	3.46	3.60	9.92	7.87	—	—	415	12
IVe	1.03	73.67	71.63	3.53	3.83	9.55	7.65	—	—	415	10
IVf	1.12	73.11	73.45	3.51	4.02	9.47	7.20	—	—	420	10
IVg	0.36	71.15	67.51	3.38	3.46	9.68	8.43	1.58	2.00	410	12
IVh	0.35	71.99	68.52	3.45	3.18	9.33	8.11	1.55	2.47	410	12
IVi	0.30	71.45	70.22	3.43	3.40	9.26	8.77	1.51	2.13	415	11

* Measured at a concentration of 0.5 g/100 mL in NMP, at 20°C ; ** Determined by the Kjeldahl method : *** Determined in air on "Paulik-Paulik — Erderly Derivatograph", at a heating rate of 12°/minute.

the polymer solutions which resulted at the end of polycondensation reactions. The films obtained from polymers IV a-f were flexible, but those prepared from polymers IV g-i were brittle. The values of dielectric loss tangent, dielectric constant and volume resistivity (Table 3) evidenced good electrical insultating properties comparable with those of polyimide film obtained from pyrromellitic dianhydride and 4,4′-diaminodiphenylether (film H).

Table 3

Insulating properties of polyphenylquinoxaline-oxadiazole-imide-amides*

Polymer	Dielectric loss tangent	Dielectric constant	Volume resistivity Ω·cm.
IVa	4.8×10^{-3}	3.1	7.9×10^{15}
IVb	6.1×10^{-3}	2.9	4.5×10^{15}
IVc	2.5×10^{-3}	3.2	$6{\cdot}3\times10^{15}$
IVd	4.1×10^{-3}	3.0	8.3×10^{15}
IVe	3.2×10^{-3}	2.8	2.1×10^{16}
IVf	2.4×10^{-3}	2.9	3.1×10^{16}
Film H	$3{\cdot}0\times10^{-3}$	3.5	9×10^{16}

* All data were obtained on polymer films of 30 microns, at room temperature, frequency 800 Hz, using a differential bridge for dielectric constants and dielectric loss tangent, of the type TR — 9701 (Hungary).

EXPERIMENTAL

Synthesis of the monomers

Diaminophenylquinoxalines I were synthesized by condensation of 3,4,4′-triaminodiphenylether (2 mol) with bis (α-diketones) such as 1,4-bis (phenylglyoxalyl)benzene, 4,4′-bis(phenylglyoxalyl)diphenyl and 4,4′-bis (phenylglyoxalyl)diphenylether (1 mol) in ethanol at reflux temperature, according to a method indicated in the literature.[4]

2,5-Bis(p-aminophenyl)-1,3,4,-oxadiazole II was prepared from *p*-aminobenzoic acid (2 mol) and hyzdrazine hydrate (1 mol) in polyphosphoric acid, at 120 — 130°, following a method described in the literature.[5]

Diacid chlorides III were obtained by treating with excess thionyl chloride at reflux temperature the corresponding dicarboxylic acids resulted from the reaction of trimellitic anhydride with 4,4′-diaminodiphenylmethane, 4,4′-diaminodiphenylether and 4,4′-diaminodiphenylsulphone respectively.[6]

N-methylpyrrolidone (NMP) was dried over sodium hydroxide pellets and distilled over phosphorous pentoxide under reduced pressure.

Synthesis of the polymers

Polycondensation was run with equimolecular amounts of total diamines and of diacid chloride, using N-methylpyrrolidone as solvent. A three-necked flask fitted with stirrer and N_2-inlet and outlet was charged with 0.00125 mol diaminophenylquinoxaline and 0.00125 mol 2,5-bis-(*p*-aminophenyl)-1,3,4-oxadiazole. 25 — 30 mL N-methylpyrrolidone were added and the mixture was stirred until complete dissolution. Then the flask was cooled below —5°C and 0.0025 mol finely powdered diacid chloride was added in a heterogeneous system with rapid stirring under inert atmosphere. The flask content was kept below — 5°C for 30 minutes then slowly raised to room temperature within other 30 minutes and kept at room temperature for 2 — 3 h. The clear yellow viscous solution was then neutralized with a few drops of pyridine. Half quantity of this solution was used to prepare a film by casting on a glass plate and evaporating the solvent at 100° for 30 minutes at 150° for 1 h and at 200° for 30 minutes. Films were used to measure electrical properties. The other half of the polymer solution was diluted with 10 — 15 mL NMP and then it was poured into water under rapid stirring. The precipitated polymer was washed for three times with water and then with acetone and dried. Inherent viscosity is 0.3 — 1.5 dL/g.

CONCLUSIONS

New polyphenylquinoxaline-oxadiazole-imide-amides have been synthesized by low temperature solution polycondensation of two heterocyclic diamines, one containing the phenylquinoxaline unit and the other the 1,3,4-oxadiazole ring with diacid chlorides incorporating preformed imide rings. These polymers show high thermal stability, their decomposition beginning over 410°, which is very similar to related polyphenylquinoxaline-imide-amides. They have also a remarkable solubility in polar aprotic solvents and can be cast into transparent films with good electrical insulating properties comparable to those of film H.

REFERENCES

[1] E. S. Krongauz, *Vysokomol. Soedineniya Ser. A*, **26**, 227 (1984).

[2] J. Preston and W. B. Black, *J. Polymer Sci.*, A-1, **9**, 2429 (1967).

[3] C. E. Sroog, *J. Polymer Sci., Macromol. Reviews*, **11**, 161 (1976).

[4] V. V. Korshak, E. S. Krongauz, N. M. Belomoina, H. Raubach and D. Hein, *Acta Polymerica*, **34**, 213 (1983).

[5] M. Brumă, Thesis, Institute "P. Poni" Iași (1971).

[6] G. Neamțu and M. Brumă, *Angew. Makromol. Chem.*, **103**, 19 (1982).

[7] V. V. Korshak, E. S. Krongauz, N. M. Belomoina, M. Brumă, I. Diaconu and C. I. Simionescu, *Angew. Makromol. Chem.*, **144**, 129 (1986).

[8] M. Brumă, G. Neamțu, *Rev. Roumaine Chim.*, **26**, 87 (1981).

Revue Roumaine de Chimie, 32, 4, 401—406 (1987)

POLYMERISATION OF SOME VINYLIC MONOMERS IN THE PRESENCE OF SYNTHETIC ZEOLITES

M. BEZDADEA, GH. MIHĂILĂ, N. BÎLBĂ and N. NAUM
Department of Chemical Technology, Polytechnic Institute, Splai Bahlui 71, Iași, Romania

Received March 24, 1986
Revised October 6, 1986

The present paper deals with a study on the matrix polymerisation of some vinylic monomers in the presence of synthetic zeolites by a radicalic mechanism. The experimental data obtained on polymerisation of vinyl acetate (VAc) in the presence of CaX zeolite and UV or γ irradiations allowed us to evidence the "host" role of zeolite in matrix polymerisation, finding a reaction mechanism similar to that promoted by enzymes in the bifunctional catalysis. Evidence for stereoregular polymerisation in zeolite as a matrix was provided by NMR spectra.

INTRODUCTION

In classical polymerisation, i.e. block, emulsion or suspension polymerisation, the monomer molecules are disorderly arranged during the process. In order to obtain stereoregular polymers, new ways of catalytic and matrix polymerisation are investigated. This important aim can be reached by the following procedures:

a. Crystallisation, which has as result the regular disposing of molecules in tridimensional space;

b. Adsorption at phase interface in mono- or polymolecular film, when the molecules are arranged bidimensionally;

c. Insertion of the monomers in cavities of different crystalline structures with mono, bi- or tridimensional arrangement of the molecules.

The matrix polymerisation is a relatively new method that allows to obtain macromolecules with extra properties depending on the matrix nature.

The synthetic zeolites, having organized structure, can be used successfully as "host" in order to control some polymerisation reactions of vinylic monomer "guests", forming stereoregular synthetic polymers. The zeolite matrix facilitates selective reactions similar to the biochemical ones. Thus, the inorganic matrix of zeolite type, having many channels, pores and cavities, reminds us, on the one hand, of the adductional polymerisation of urea due to the crystalline network and, on the other hand, of the effect of high selectivity of reactions controlled also by other matrices such as cyclodextrines and modified dextrines, Sephadex.[1-3]

The results reported in this paper show the role of zeolite matrix in polymer development and the most probable mechanism controlled by the host.

EXPERIMENTAL

Zeolites. Taking into account how important is the amount of monomer adsorbed on zeolite before polymerisation, the adsorption of VAc and acrylonitrile (AN) on 12 synthetic zeolites was investigated, using both statical and dynamical methods.[4] The results allowed as to select the best "host", i.e. CaX zeolite for polymeristion of VAc under UV and γ irradiation. Both adsorption capacity and catalytical activity of the tested zeolites are higher against VAc than against AN.

The adsorption capacity of zeolites against VAc, determined under dynamic conditions, is presented in table 1.

Table 1

Adsorption da'a of zeolites against VAc

Run	Zeolite	Molar ratio SiO_2/Al_2O_3	Exchange degree, %	Adsorption capacity, %
1	NaX	2.50	—	23.4
2	CaX	2.50	80.00	22.4
3	NaY	4.25	—	19.0
4	HM	10.00	100.00	13.4
5	HZe	10.00	—	12.2
6	NaM	10.00	—	8.5
7	CaHX	3.10	—	14.0
8	CeX	3.10	87.00	4.5
9	CeY	4.25	79.75	1.7
10	NiY	4.25	80.00	7.2
11	LaM	10.00	—	3.8
12	LaY	4.25	81.75	3.0

The statical adsorption of VAc and AN was investigated on NaX, CaX and NaY zeolites only, at 20°C, and the adsorption isotherms obtained are set out in figure 1.

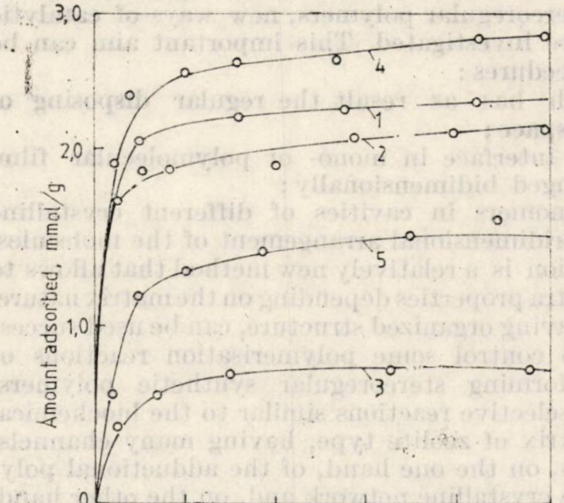

Fig. 1. — Adsorption isotherms of NaX, CaX and NaY (1, 2, 3) against VAc and of NaY and CaX (4, 5) against AN.

Monomers. The commercial VAc (Schuchardt — Munich) having b.p. = 72.5 °C, d_4^{20} = = 0.9342 and n_D^{20} = 1.3956 and AN (Merck) with b.p. = 77.5 — 77.8 °C, purified by vacuum distillation, were employed. Their polar characteristics and specific reactivities as well as standard distances between atoms are summarized in table 2. In table 2:

$$Q = \exp^{-q/RT}$$

Table 2

Specific reactivity Q, polar characteristics e and μ standard distances L, l and g between atoms, corresponding to valencestates for investigated monomers

Monomer	Q	e	μ, eV	L, Å	l, Å	g, Å
VAc	0.03	−0.22	1.7	7.39	3.9	2.8
AN	2.7	1.91	3.88	7.1	4.7	3.5

where q is the resonance energy, kj·mol^{-1}, R is the perfect gas constant, kj·mol^{-1}·K^{-1} and T is the absolute temperature, K.

$$e = \varepsilon/(HDRT)^{1/2}$$

where ε is electric charge, D is dielectric constant of the reaction medium and H is the distance between electric charges.

The specific reactivity Q is dependent on the UV maximum absorption of monomers, providing information on the π electrons in the molecule.[5]

Under identical reaction conditions, using the same zeolite CaX, AN does not polymerize although its Q, e and μ are larger than those of VAc.

Synthesis of the matrix polymers. The photopolymerisation of VAc was performed by irradiation with UV light using a Hg lamp (125 W) with $I_0 = 7.32 \cdot 10^{15}$ s^{-1}. The ratio "host" to "guest" ranged from 0.1 to 5.0 and the temperature from + 50°C down to −25°C. The same experiments were carried out with γ radiations from a ^{60}Co source with dose rate of 60 mrad.h^{-1}.

The separation of PVAc from the zeolite was done by its dissolution in acetone, centrifugation, filtration, slow evaporation and vacuum drying at 30 °C.

The obtained product has either a paraffinous form or is a white powder with melting point between 290 and 350 °C.

RESULTS AND DISCUSSION

The polymerisation rate of VAc on NaX is slower than on CaX. Under the same experimental conditions, on the same matrix, AN does not polymerise. The polar characteristics, the different specific reactivities as well as the standard distances between atoms, corresponding to valence state (table 2) show the different behaviour of the two monomers.

Photopolymerisation of VAc at 50°C in the presence of a little amount of CaX zeolite, with the ratio zeolite to VAc of about 0.1, gives a conversion of 80 – 100%, and the obtained PVAc has $\bar{M}_n = 146300$. For this ratio, at temperatures below 0 °C, no polymer results. If the ratio host to guest was larger than unity, the polymerisation reaction took place at temperatures below 0 °C and $\bar{M}_n = 800$. This behaviour is a proof of reaction inside the channels, due to a high density of active sites.

The synthesis of PVAc in the presence of CaX zeolite by γ irradiation gave a higher yield in comparison with those obtained by UV irradiation under similar experimental conditions. Thus, the samples irradiated with γ radiation with dose rates of 129 or 242 mrad.h^{-1} gave ^{1}H-NMR spectra that show larger amounts of PVAc than those obtained by UV irradiation. The ^{1}H-NMR spectra of the samples are represented in figure 2.

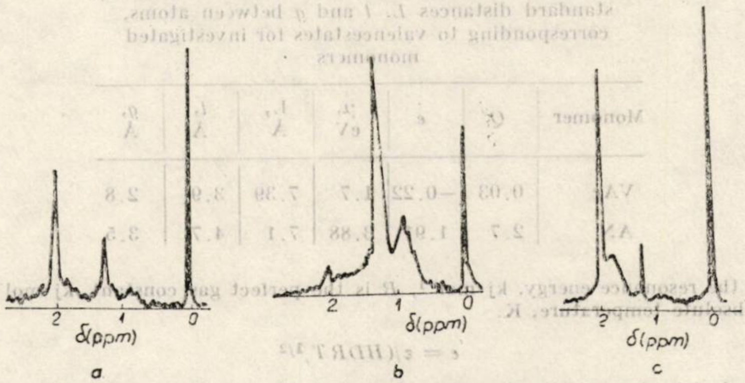

Fig. 2. — The NMR spectra of PVAc samples obtained at 20°C ; *a* — in the presence of zeolite CaX by γ irradiation ; *b* — in the presence of zeolite CaX by UV irradiation ; *c* — as "inclusion" in Sephadex G 50 by UV irradiation.

The ^{1}H-NMR spectrum of a polymer sample obtained by γ irradiation at room temperature on zeolite is similar to that of the Sephadex sample.[1] The larger amount of PVAc in the case of γ irradiation may be explained by increasing of the number of paramagnetic sites in zeolite.

An interaction between monomer and zeolite is possible, that proves the role of hydroxylic groups in polymerisation and consequently, a possible similarity between reaction mechanism of the two matrices Sephadex and zeolite.[5-7]

According with certain investigators, dextrines are complexing agents, their hydroxylic groups being both electron donors by base effect "electron pressure" and electron acceptors by hydrogen bond "electron depression", therefore an "attraction-repulsion" mechanism is possible. The stereochemistry of interaction host-guest allows to apply the "lock and key" theory for this mechanism of matrix polymerisation similar to that exercised by cyclodextrines,[8,9] mechanism I.

The formation of the active sites on zeolite in the presence of water is mentioned in literature.[5] For the polymerisation of VAc in the presence of CaX zeolite the mechanism II is suggested.

CONCLUSIONS

We summarize our results in the following statements :

1. The CaX synthetic zeolite has an effect on polymerisation of VAc similar to enzymes or bifunctional catalysis.

2. Zeolites are selective catalysts for the polymerisation of vinylic monomers. Vinyl acetate does polymerize in the presence of CaX zeolite, while acrylonitrile does not.

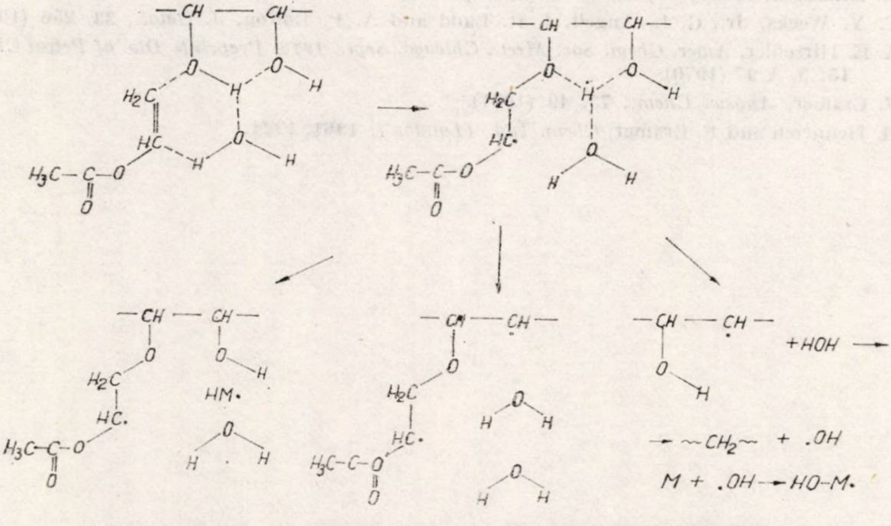

I. Polymerisation mechanism of VAc in the presence of Sephadex.

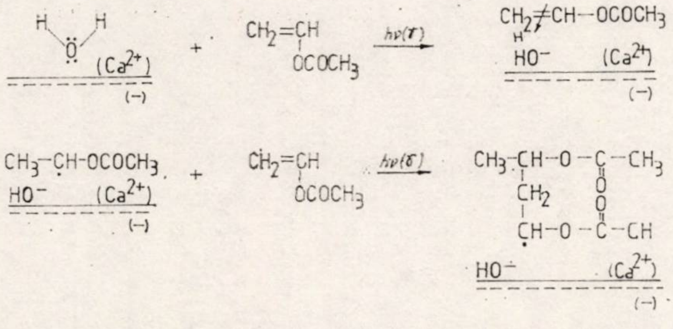

II. Polymerisation mechanism of VAc in the presence of the zeolite CaX.

3. The reaction mechanism due to the CaX zeolite justifies a similarity of its action with biological systems; it exhibits sites of certain polarity and the lattice water is in a structural state between ice and liquid.

REFERENCES

[1] M. Bezdadea, Matrix Polymerisation, Doctoral Thesis, "Gh. Asachi" Polytechnic Institute, Iași, September, 1982.

[2] M. Bezdadea and C. N. Cașcaval, Proc. of the First Symp.on Zeolites in Modern Technology, October 28 – 29, 1983, Iași, p. 325.

[3] M. Bezdadea and C. N. Caşcaval, *Brit. Polym. J.*, **16**, 151 (1984).

[4] Gh. Mihăilă, N. Bilbă, M. Bezdadea and N. Naum, Proc. of the First Symp. on Zeolites in Modern Technology, October 28 – 29, 1983, Iaşi, p. 167.

[5] M. Bezdadea, *Materiale plastice*, 1985, in print.

[6] T. Y. Weeks, Jr., C. L. Angell, I. R. Ladd and A. P. Bolton, *J. Catal.*, **33**, 256 (1974).

[7] A. E. Hirschler, *Amer. Chem. Soc. Meet., Chicago. Sept., 1970, Preprints Div. of Petrol Chem.* **15**, 3, A 97 (1970).

[8] F. Cramer, *Angew. Chem.*, **73**, 49 (1961).

[9] H. Hennrich and F. Cramer, *Chem. Ind. (London)*, **1961**, 1224.

Revue Roumaine de Chimie, **32**, *4*, 407–415 (1987)

MECHANOCHEMICAL REACTIONS OF SOME POLYURETHANE ELASTOMERS. 5

STUDY OF MODIFICATIONS OF SOME PHYSICO-CHEMICAL PROPERTIES INDUCED BY UNIAXIAL TENSILE CREEP AND UV IRRADIATION

CLEOPATRA VASILIU-OPREA* and ALEXANDRU C. CONSTANTINESCU

Macromolecular Chemistry Department, Polytechnic Institute of Jassy, Calea 23 August 11 A, 6600 — Jassy Romania

Received March 24, 1986

The accelerated UV ageing of polyurethane thermoplastic elastomers correlated with the uniaxial tensile creep straining induce important modifications of the molecular and supermolecular structure of the polymer. The structural transformations were proved by following the modification of some physico-chemical properties (swelling at equilibrium, thermal and chemical stabilities) as well as by means of the transmission electronic microscopy (TEM).

I. INTRODUCTION

The photochemical destruction of polymers is one of the major consequences of the environment action.[1-2] Generally, polyurethanes show a good stability to light due to their saturated character. However, in the case of those synthesized from aromatic diisocyanates their photodegradation by UV irradiation and the formation of quinoide structures was noticed.[3] Tarakanov[4-5] showed that the oxidative photodegradation of the polyurethanes proceeds by a radicalic mechanism leading to polyconjugated sytems inhibiting the further photooxidative degradation.

In the present paper the modifications induced at the molecular and supermolecular levels of some polyurethane thermoplastic elastomers by the accelerated UV irradiation and uniaxial tensile creep are studied, these conditions existing frequently in operating these polymers.

II. EXPERIMENTAL

The polyurethane under study is a thermoplastic elastomer obtained from 4,4′-dibenzyl-diisocyanate with a 98.63% NCO group content, poly(ethyleneglycoladipates) with $\bar{M} = 2000$ and ethyleneglycol of 99.8% purity.

The uniaxial tensile creep conditions were carried out as described previously.[6] The UV irradiation was performed by a high-pressure mercury-vapour lamp (PEK BH-61 B). The accelerated ageing of the samples before the uniaxial tensile creep straining was achieved at 80 °C by UV irradiation for 200 hours.

The equilibrium swelling degree was estimated by the Dogatkin method,[7] using the phenol-water (9 :1 vol) mixtures, at (30 ± 1) °C. The maximum swelling duration was of 200 hours. The following calculating relation was applied :

$$\alpha = \frac{m - m_0}{m_0} \cdot 100 \qquad (1)$$

where : α — swelling degree (%) ;
m_0 — initial weight of the polymer (g) ;
m — polymer weight after swelling (g).

The swelling rate constant was estimated graphically by using the relation :

$$k = \frac{\operatorname{tg} \varphi}{0.434} \qquad (2)$$

where : k — swelling rate constant at equilibrium (hrs^{-1}) ;
φ — angle between the lines in $\log(\alpha_{max} - \alpha)$-time coordinates and Ox axis.

The termal degradation was studied by means of a MOM Budapest derivatograph (heating rate = 10 °C/min, nitrogen as working medium). The energy of activation and reaction order for the thermal decomposition were estimated by the Freeman — Carroll method,[8] by means of a programme implemented on a Felix C-256 computer.

The chemical stability was determined in several media (water, mineral oil and 10% H_2SO_4 solution, by weight), at 65 °C and for 200 hours. These agents were chosen by taking into account the operating conditions of the polymers. The variation of sample stabilities was followed gravimetrically and expressed as percentage.

The modifications in the supermolecular structure of the stressed and UV irradiated samples were investigated in comparison with a broken sample, after an immersion of 30 min. into liquid nitrogen (—197 °C), by using the transmission electronic microscopy (TEM). The fracture surfaces was examined by the two stages replica method, on a Tesla BS 513 A microscope.

III. RESULTS AND DISCUSSION

After the uniaxial tensile creep by a 9.0 MPa unit load the stressed and unaged sample and that fast aged for 200 hours before stressing did not fail after 1000 hours, while that simultaneously stressed and UV irradiated broke after 55 hours (Fig. 1). The calculation of the characteristic deformations (Table 1) reveals that the sample simultaneously uniaxially stressed and UV irradiated is the most strained and breaks macroscopically after a stressing of 55 hours. With the other two samples the appearance of plastic deformations is noticed after removing the load, the deformation being larger for the UV preirradiated sample (Table 1).

The concomitantly stressed and UV irradiated sample cracks before the macroscopic breaking, an effect which can be seen by eye. The microphotographs of the unstressed and unirradiated sample, fractured after immersion into liquid nitrogen, show the presence of globular supermolecular formations which are typical for amorphous polymers of the same type as the elastomers under study (Fig. 2).

The study of transmission electronic microscopy was performed in two zones characteristic of the broken samples : the fracture zone and the

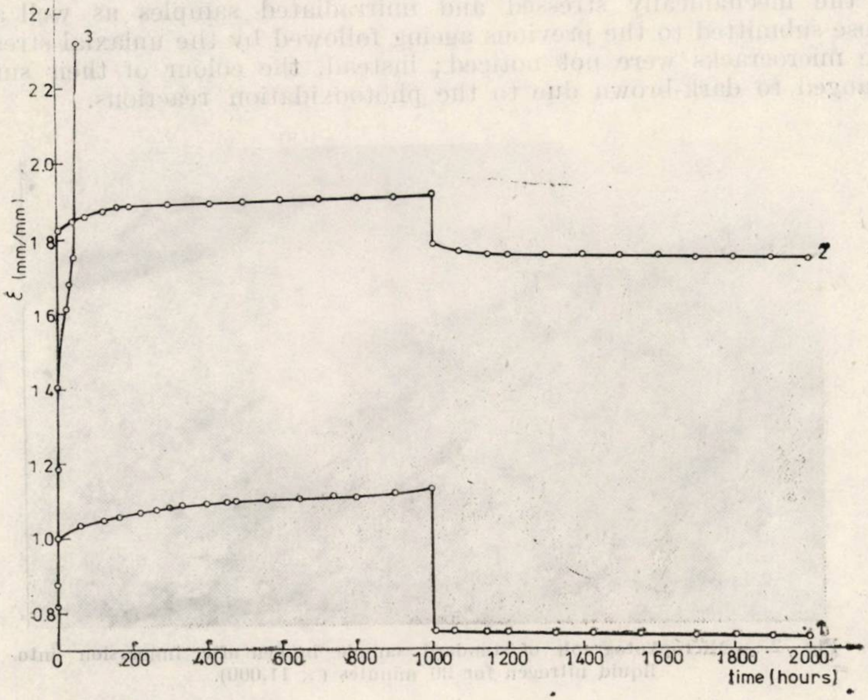

Fig. 1. — Strain-time creep curves: *1* — 9.0 MPa tensile creep tested sample; *2* — 200 hrs UV accelerated ageing and then 9.0 MPa tensile creep tested sample; *3* — simultaneously 9.0 MPa tensile creep tested and UV irradiated sample.

Table 1

The strain values in the case of Moldotan D uniaxial tensile creep and UV irradiation tests

Test conditions / Strain, mm/mm	9.0 MPa	9.0 MPa after accelerated ageing (200 hrs)	9.0 MPa simultaneously with UV irradiation *
Instantaneous elastic strain	0.880	1.790	0.885
Total strain	1.135	1.920	2.320
Instantaneous elastic recovery	0.375	0.350	—
Delayed elastic recovery	0.020	0.040	—
Permanent deformation	0.740	1.745	—

* Failure took place after 55 hrs of tensile creep simultaneously with UV irradiation.

deformation one preceding the first. In the fracture zone (Fig. 3) the disappearance of the globular formations and the appearance of a rough surface are noticed, due to the formations of many microcracks. The microphotographs of the adjacent straining zone (Fig. 4) show the presence of the fibrilar formations consisting of packed macromolecules. This fact indicates the splitting of the globules due to the uniaxial stress which resulted in a longitudinal ordering but without crystallization. In the case of the mechanically stressed and unirradiated samples as well as of those submitted to the previous ageing followed by the uniaxial stressing the microcracks were not noticed; instead, the colour of their surface changed to dark-brown due to the photooxidation reactions.

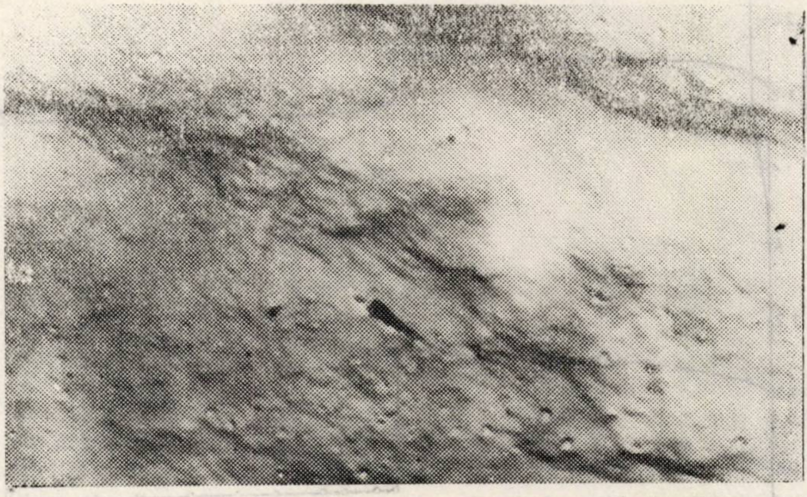

Fig. 2. — Microphotograph of standard sample broken after immersion into liquid nitrogen for 30 minutes (× 11,000).

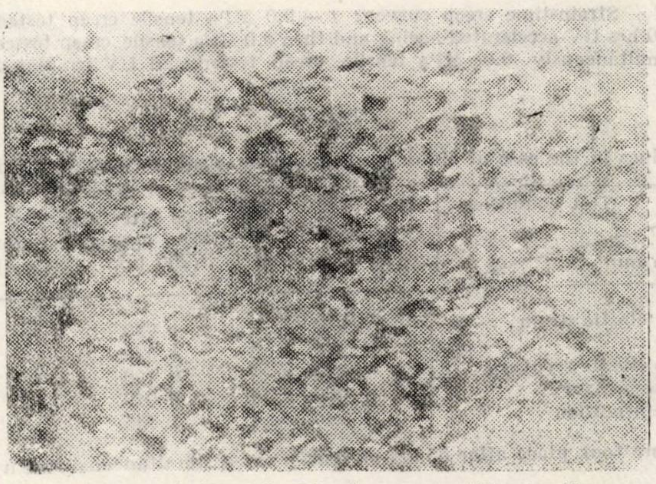

Fig. 3. — Microphotograph of fracture zone of the simultaneously creep stressed and UV irradiated sample (× 11,000).

The UV irradiation and the uniaxial tensile creep induced the modification of some physico-chemical properties (equilibrium swelling, thermostability and chemical stability in different media), as a consequence of the transformations at the molecular level.

The swelling study (Fig. 5) reveals the samples concomitantly strained and UV irradiated (curve 4) to suffer a stronger swelling than those stressed and unirradiated (curve 2) and those fast aged and subsequently stressed (curve 3) due to a more pronounced loosening of molecular and supermolecular structure. Generally, all samples show a limited swelling in the phenol-water (9 :1 vol) mixture, the unstressed sample having the least maximum swelling degree. The swelling rate constant calculated graphically (Fig. 6) varies in the same manner being maximum with the samples simultaneously stressed and UV irradiated.

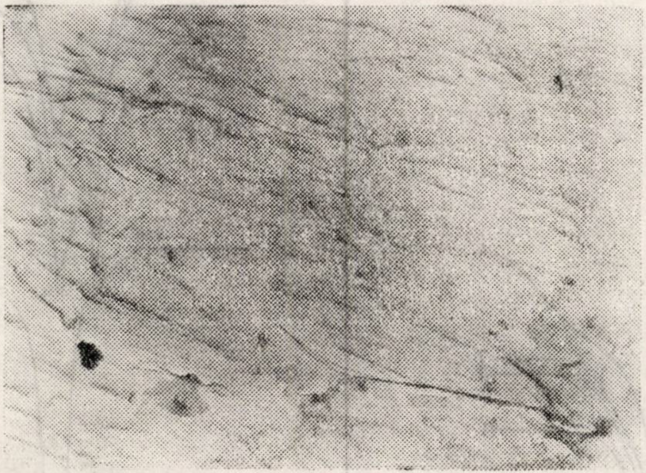

Fig. 4. — Microphotograph of adjacent straining zone of the simultaneously creep stressed and UV irradiated sample (× 11,000).

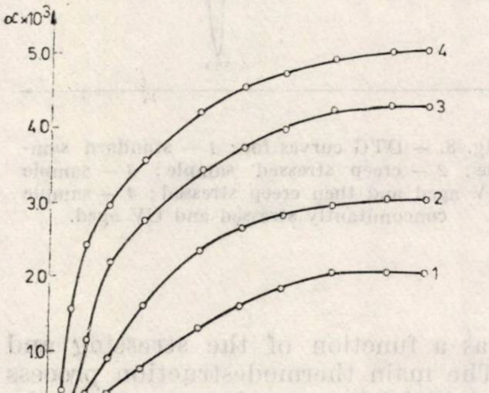

Fig. 5. — Swelling kinetical curves in phenol-water (9 :1) mixture for : *1* — standard sample ; *2* — 9.0 MPa tensile creep tested sample ; *3* — 200 hrs UV accelerated ageing and then 9.0 MPa tensile creep tested sample ; *4* — simultaneously 9.0 MPa tensile creep tested and UV irradiated sample.

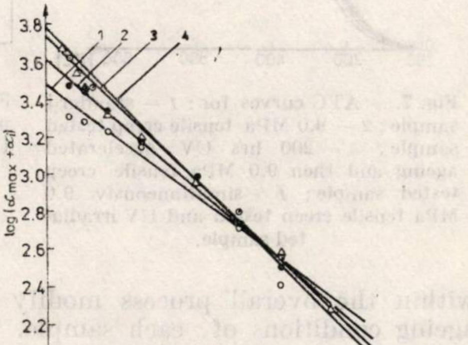

Fig. 6. — Swelling rate constants estimated graphically for : *1* — standard sample ; *2* — 9.0 MPa tensile creep tested sample ; *3* — 200 hrs UV accelerated ageing and then 9.0M Pa tensile creep tested sample ; *4* — simultaneously 9.0 MPa tensile creep tested and UV irradiated sample.

The thermogravimetrical analysis (ATG) (Fig. 7) shows the creep stressed and UV irradiated sample to be the least stable (maximum weight loss of 98%, at 550 °C) and the standard one the most stable (weight loss 52% at the same temperature). The differential curves (DTG) (Fig. 8) reveal three processes of thermal destruction whose intensity and weight within the overall process modify as a function of the stressing and ageing conditions of each sample. The main thermodestruction process corresponding to the temperature of 360°C is more intense with the simultaneously stressed and UV irradiated sample while the process proceeding at 320 – 330°C shows lower intensity (Fig.8). If the process at 280°C were supposed to proceed by the scission of the Van der Waals bonds, that at 320 – 330°C by the hydrogen bond splittings and that at 360°C by the homolytical scission of the valence bonds the intensity increase of the last for the simultaneously stressed and UV irradiated sample would be in agreement with the appearance of microcracks preceding the macroscopic failure.

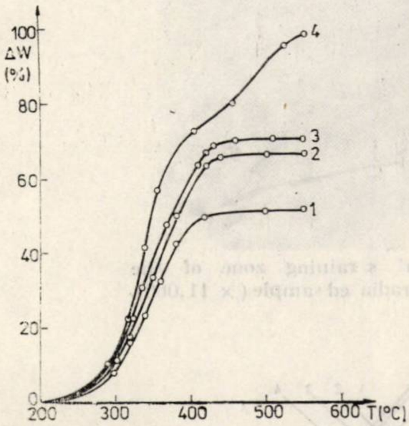

Fig. 7. — ATG curves for: *1* — standard sample; *2* — 9.0 MPa tensile creep tested sample; *3* — 200 hrs UV accelerated ageing and then 9.0 MPa tensile creep tested sample; *4* — simultaneously 9.0 MPa tensile creep tested and UV irradiated sample.

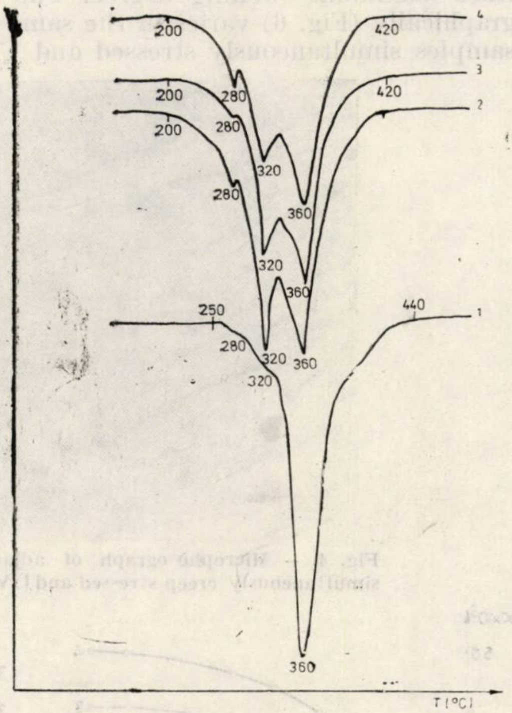

Fig. 8. — DTG curves for: *1* — standard sample; *2* — creep stressed sample; *3* — sample UV aged and then creep stressed; *4* — sample concomitantly stressed and UV aged.

The great number of hydorgen bonds in the elastomer under study would explain the intensity of the process at 320 – 330 °C.[8] In case of the tensioned sample submitted to the concomitant creep straining and UV ageing this process is practically superposed on that corresponding to the valence bond scissions whose intensity prevails. With the other samples these two processes are of equivalent intensities and clearly differentiated (Fig. 8). The same might be said about the process corresponding to the scission of the Van der Waals bonds (280 °C).

Table 2

Energies of activation and thermal decomposition reaction order for the mechanically stressed and UV irradiated samples

Test conditions	0	9.0 MPa	9.0 MPa after accelerated ageing (200 hrs)	9.0 MPa simultaneouysly with UV irradiation*
Energy of activation $\times 10^5$ kcal/mol	−0.16428	−0.16856	−0.17011	−0.26033
Reaction order	1.0	1.0	1.1	2.5

* **Failure** tooke place after 55 hrs of tensile creep simultaneously with UV irradiation.

The activation energy of the thermal decomposition (Table 2) has negative values corresponding to endothermal processes being minimum for the the concomitantly strained and UV irradiated sample and maximum for the standard sample. The reaction order increases from 1.0 (standard sample) to 2.5 (concomitantly strained and UV irradiated sample) (Table 2).

The elastomer stability in different inert liquid (mineral oil, water) as well as active (10% H_2SO_4 solution) media, at 65 °C, was studied in comparison with an unstrained sample. In mineral oil (Fig. 9) and water (Fig. 10) the samples swell to a rather limited extent the process being more intense with simultaneously strained and UV irradiated sample. The highest stability is shown by the standard sample (1.6% in oil and 1.3% in water, after 200 hours). The least stable sample shows however a weight increase less than 2%, hence it is stable enough in oil and water. In acid solution all samples show a low stability, the process of chemical destruction being very intense (Fig. 11). The sample stressed by a load of 9.0 MPa and concomitantly UV irradiated decomposes completely after about 150 hours while the standard one after 220 hours.

The presented data reveal that UV irradiation has an accelerating effect on the mechanochemical destruction of 4,4′-dibenzyldiisocyanate polyurethane elastomers. The simultaneous UV irradiation and uniaxial tensile creep stress accelerate the scission of valence bonds and finally the polymer macroscopic failure. The scission of macromolecular chains caused by the mechanical and UV irradiation energies accumulates in destroyed microvolumes and results in a pronounced loosening of the sample structure and would explain their resistance decrease on the action of solvents, heat and some chemical agents.

During the accelerated UV ageing at 80°C a great number of valence bonds suffer a thermally activated photooxidative scission without recovering under the subsequent mechanical stress which results in the increase in the plastic deformation of the samples and the decrease in the thermal and chemical stabilities in comparison with a uniaxial tensile creep strained sample only.

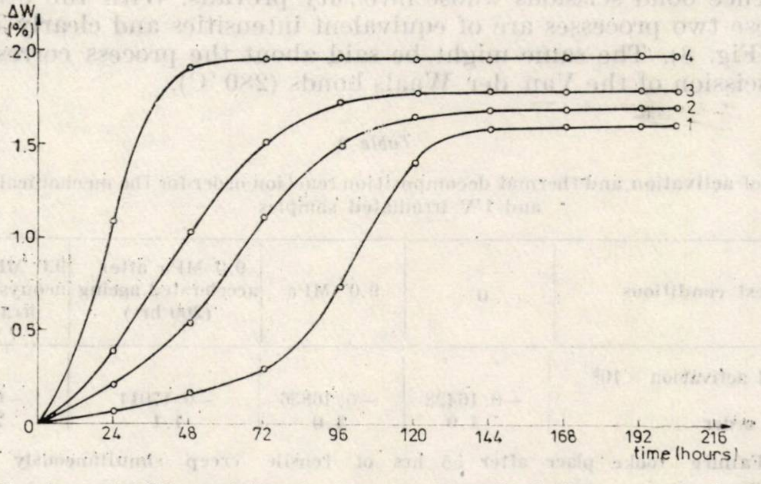

Fig. 9. — Stability variation in time in mineral oil for: *1* — standard sample; *2* — 9.0 MPa tensile creep tested sample; *3* — 200 hrs UV accelerated ageing and then 9.0 MPa tensile creep tested sample; *4* — simultaneously 9.0 MPa tensile creep tested and UV irradiated sample.

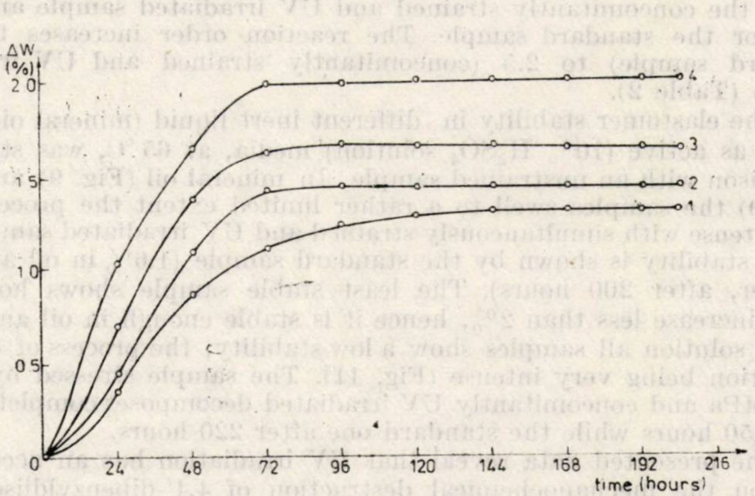

Fig. 10. — Stability variation in time in water for: *1* — standard sample; *2* — creep stressed sample; *3* — sample UV aged and then creep stressed; *4* — concomitantly stressed and UV aged sample.

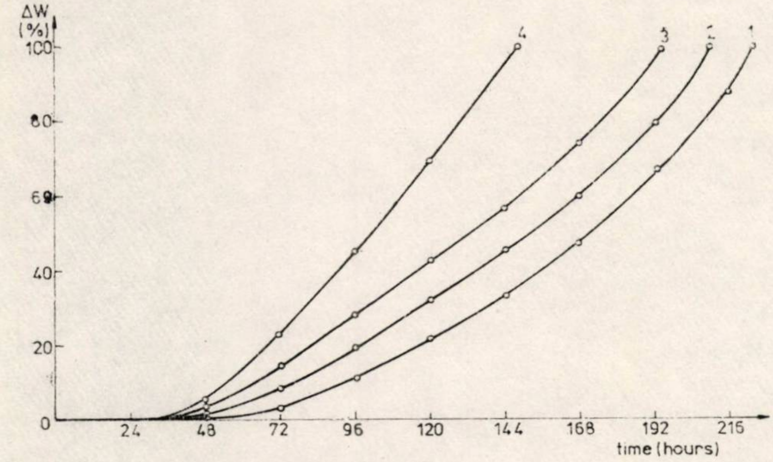

Fig. 11. — Stability variation in time in 10% H_2SO_4 solution for : *1* — standard sample ; *2* — creep stressed sample ; *3* — UV aged and then creep stressed sample ; *4* — concomitantly stressed and UV aged sample.

IV. CONCLUSIONS

1. The UV irradiation accelerates the scission of the valence bonds due to the uniaxial tensile creep straining.

2. At the supermolecular level the disappearance of globular formations characteristic of the unstressed and unirradiated polymer is noticed as well as the formation of microcracks preceding the macroscopic failure.

3. Under the concomitant mechanical stress and UV irradiation the thermal and chemical stabilities decrease and the equilibrium swelling degree increases.

4. The previous UV ageing determines the photochemical scission of the valence bonds, this process increasing under the creep straining.

REFERENCES

[1] B. Ranby and F. J. Rabek, "Photodegradation, Photo-oxidation and Photostabilization of Polymers. Principles and Applications", J. Wiley, New York, 1975, p. 423.

[2] W. Schnabel and J. Kiwi in "Aspects of Degradation and Stabilization of Polymers" (H. H. G. Jellinek, Editor), Elsevier, Amsterdam, 1978, p. 149.

[3] Z. Osawa, E. L. Chen and K. Nagashima, *J. Polym. Sci., Polymer Chem. Ed.*, **15**, 445 (1977).

[4] A. A. Berlin, K. A. Belyakov, V. L. Newski and G. O. Tarakanov, *Vysokomol. Soed.*, **A9**, 1677 (1967).

[5] G. O. Tarakanov, V. L. Newski and K. A. Belyakov, *J. Polym. Sci., Part C*, **23**, 193 (1968).

[6] C. Vasiliu-Oprea and A. C. Constantinescu, Proceedings of the IUPAC 29th Macromolecular Symposium, Bucharest, 1983, Section IV, p. 697.

[7] S. S. Voinitskii and R. M. Panici, "Praktikum po koloidnoi himii i electronnoi mikroscopii", Himia, Moscka, 1974, p. 151.

[8] E. S. Freeman and B. Carroll, *J. Phys. Chem.*, **73**, 751 (1969).

[9] J.H.Saunders in "Polymer Chemistry of Synthetic Elastomers", (J. P. Kennedy and E.G.M. Törnqvist, Editors), Part II, Wiley-Interscience New York, 1969, p. 745.

Revue Roumaine de Chimie, **32**, *4*, 417–426 (1987)

2-BENZOPYRYLIUM SALTS. XXXII [1]

SYNTHESIS AND SOME CHEMICAL AND SPECTRAL PROPERTIES OF 1- AND/OR 3-(3,5-DI-t-BUTYL-4-HYDROXYPHENYL)-SUBSTITUTED 2-BENZOPYRYLIUM SALTS

IRINA V. SHCHERBAKOVA, [a] EVGENII V. KUZNETSOV, [a]
LEV YU. UKHIN, [a] MIRCEA D. GHEORGHIU, [b] AURELIA MEGHEA, [b]
JEAN HERDAN, [c] and ALEXANDRU T. BALABAN [b,*]

[a] Institute for Physical Organic Chemistry, Rostov-on-Don University, U.S.S.R.

[b] Polytechnic Institute, Organic Chemistry Department, Splaiul Independenței 313, 76206 Bucharest, Romania

[c] Institute of Technological Engineering, Research and Refinery Design (I.C.I.T.P.R.), Ploiești, Romania

Received November 16, 1986

Four new 2-benzopyrylium salts IIIa–d bearing one or two 3,5-di-t-butyl-4-hydroxyphenyl groups in positions 1 and/or 3 were prepared. Treatment with bases in aqueous or anhydrous media causes deprotonation of the phenolic group attached to position 1 when such a group is present, leading to a fairly stable betaine IVa–c; otherwise the phenolic group attached to position 3 is deprotonated affording a less stable *ortho*-quinonoid betaine VIId. Oxidation of compounds IIIa–d affords stable aroxyl radical-cations whose ESR spectra were recorded.

A recent communication[2] described 3-(3,5-di-t-butyl-4-hydroxyphenyl)-substituted 2-benzopyrylium salts; either as such or as their derivatives, these salts may be interesting for their antioxidant activity and for the aroxyl radicals they form on oxidation. The variation of the number and positions of such 2,6-di-t-butyl-4-hydroxyphenyl substituents in 2-benzopyrylium cations may influence the persistency of free radicals and at the same time may lead to the appearance of other centres (hydroxyl groups) for nucleophilic attack of the molecule, but no comparison of such possibilities for this class of compounds has yet been reported.

The present paper describes the synthesis of newly prepared 1-mono-, 3-mono-, and 1,3-bis-(3,5-di-t-butyl-4-hydroxyphenyl)-substituted 2-benzopyrylium salts and a few derivatives, as well as their reactions with alkali hydroxides and triethylamine, including the electronic and ESR spectral investigations.

Salts IIIa—c were obtained by acylation of ketones Ia—c with acids IIa, d in the presence of polyphosphoric ester (PPE) (preparative yields 30—50 %) (see Scheme 1).

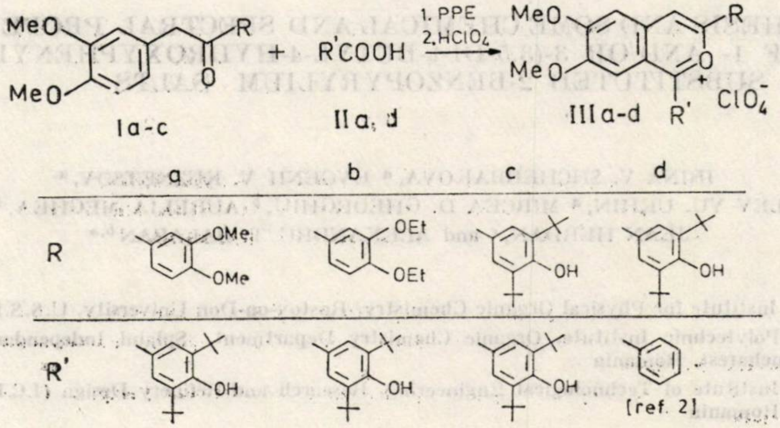
MeO
MeO
R
O
+ R'COOH
1. PPE
2. HClO4
MeO
MeO
R
O
+
ClO4-
R'
Ia-c
IIa, d
IIIa-d
a
b
c
d
R
OMe
OMe
OEt
OEt
OH
OH
R'
OH
OH
OH
[ref. 2]

Scheme 1

The identification of these deep orange-coloured salts posed no difficulties. Some of their characteristics are given in the experimental part.

It was observed that the addition of 30% aqueous alkali hydroxide solutions to the solutions of salts IIIa—c in acetone led to the appearance of dark violet precipitates, which were extracted with ethyl ether; after evaporation of the solvent, compounds IVa—c were obtained (Scheme 2).

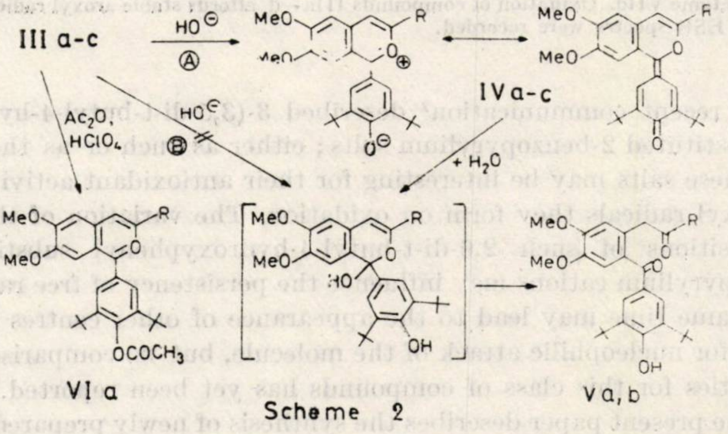
III a-c
HO⊖
A
MeO
MeO
R
O⊕
O⊖
MeO
MeO
R
O
O
IVa-c
Ac2O,
HClO4
HO⊖
B
+ H2O
MeO
MeO
R
O
OCOCH3
VI a
MeO
MeO
R
O
HO
OH
MeO
MeO
R
O
O
OH
Va, b

Scheme 2

Two resonant structures for such compounds may be written, a quinonoid and a zwitterionic one; for convenience we shall use for compounds IV the term "betaines" (the same term will be applied to compound VIId in Scheme 4).

The sharp stretching vibration of the hydroxyl group in $CHCl_3$ at 3610 cm^{-1} for salts IIIa—c is absent in the IR spectra of betaines IVa, b, and it changes its position to 3480 cm^{-1} for betaine IVc. The disappearance of the hydroxyl group of salt IIIa on conversion into the betaine IVa is also manifest in the ^1H-NMR spectrum (the singlet at 6.53 ppm vanishes). It is necessary to point out that the crystalline betaines IVa—c are stable towards air, and the solutions in neutral and dry organic solvents can be conserved. In the presence of perchloric acid in any organic solvents and even as suspensions in acidic water the betaines are reconverted very easily into the initial salts IIIa—c. Unlike methyleneisobenzopyrones (anhydrobases of 2-benzopyrylium salts), which are formal analogs of quinonoid structures IV and which are stable towards aqueous or alcoholic solutions of alkali hydroxides,[3] compounds IV present a different behaviour. Betaines IVa,b are stable in concentrated aqueous solutions of alkali hydroxides, but in organic solvents in the presence of water even traces of bases cause their conversion into the corresponding colourless diketones Va,b. The diketones were purified by means of column chromatography for betaines IVa,b (or salts IIIa, b) on neutral alumina with moist chloroform as eluent. It was impossible to use this method for the synthesis of pure diketones from the salts IIIc, d; in these cases complicated mixtures of colourless compounds were obtained.

It is known from quantum-chemical calculations that the largest positive charge density is in position 1 of the 2-benzopyrylium cation,[4] therefore the expected pathway for hydroxyl ion attack ought to be pathway B in Scheme 2, as it was described earlier.[5] However in our case this attack leads to deprotonation of the phenolic group (pathway A). It is interesting that products of direct interaction between 2-benzopyrylium salts and hydroxyl ion (diketones Va, b) were obtained only through betaines IVa, b. This was indicated by the very characteristic violet colour of betaines which appeared instantaneously and then disappeared during the synthesis of the diketones from the salts IIIa,b. Literature data on analogous quinonoid forms derived from *p*-hydroxyphenyl-substituted pyrylium salts are known.[6-8]

The acetylation of the phenolic hydroxyl group in IIIa proceeds easily under conditions described earlier, yielding the acetate VIa.

In order to investigate optical properties of the newly prepared compounds, electronic absorption spectra were recorded for salts IIIa—c and betaines IVa—c in different solvents. Interestingly, it was impossible to obtain good UV spectra of the salts III in 96% ethanol: the intial orange colour became violet and then colourless. Probably processes which are similar to syntheses of diketones Va, b take place in this solvent. However, acidic ethanol leads to good results for all salts, and UV spectral data are given in Table 1. There are two main bands for salts IIIa—c with λ_{max} around 390 and 480 nm in the visible region. The positions of these bands give a good correlation with the polarity of solvents. The spectra of betaines IVa—c have also two bands: the first one with λ_{max} 360 — 390 nm, which sometimes appears as a shoulder, and the second one with λ_{max} 510 nm. The bathochromic shift of the longest-wavelength band for betaines relative to the salts is due to increased

Table 1

UV Spectral data[a] a for salts IIIa—d and for betaines IVa—c

Compound	Solvent	λ_{max}; nm(ε)		
IIIa	CH_2Cl_2	400 (15800),	498(17500)	
	$(CH_3)_2CO$	390 (14800),	492(16000)	
	CH_3CN	390 (17300),	479(15500)	
IIIb	$(CH_3)_2CO$	388 (12000),	480(10600)	
	CH_3CN	388 (15400),	480(12100)	
IIIc	CH_2Cl_2	395 (18300),	485(15200)	
	$(CH_3)_2CO$	382 (15000),	484(14000)	
	CH_3CN	382 (14300),	473(12500)	
	1 %Et_3N/CH_2Cl_2[b]	300 (12100),	534[b](19000)	
IVa	CH_2Cl_2	—	485(12800)	
	$(CH_3)_2CO$	—	472(12800)	
	CH_3CN	—	470(14500)	
IVa	CH_2Cl_2	400 (8300),	512(13200)	
	$(CH_3)_2CO$	359 (10700),	535(15200)	
	CH_3CN	360(sh),	530(10400)	
	Et_2O	355(sh),	515(16300)	
IVb	$(CH_3)_2CO$	360(13600),	533(18800)	
	CH_3CN	360(sh),	510(15000)	
IVc	$(CH_3)_2CO$	360(10400),	535(16300)	
	CH_3CN	360(9600),	537(14400)	
	Et_2O	355(sh),	515(15600)	
IIId	CH_2Cl_2	358(sh),	478(12900)	
	CH_3CN	350(sh),	467(11000)	
	1 %$HClO_4$/EtOH	353(sh),	472(10200)	
	1 %Et_3N/CH_3CN[b]	340(15300),	460(31600),	770[b] (4900)
	1 %Et_3N/CH_2Cl_2[b,c]	341(17600),	467(44800),	820[c] (9300)

[a] Concentrations were in the range 20 to 50 μmol/liter.

[b] In the presence of Et_3N the spectrum is due to betaine.

[c] On longer standing the spectrum undergoes the following changes: after 30 min., band at 340 nm moves towards 320 nm; after one hour the band at 820 nm vanishes, and after two hours only the band at 320 nm remains.

electronic delocalization. The spectrum of the salt IIIc in the presence of triethylamine coincided with the spectrum of betaine IVc. No removal of the acetyl group in salt VIa in the presence of Et_3N was observed; the visible region of the spectrum was transparent and did not change in time. As it was described earlier,[2] the acetylated phenolic hydroxyl is stable under similar conditions also in 3-(3,5-di-t-butyl-4-hydroxyphenyl)-substituted 2-benzopyrylium salts.

It is easy to notice that salt IIIc possesses two alternative possibilities for deprotonation from the two phenolic substituents under alkaline conditions, along with the nucleophilic addition; UV-visible spectral data indicate that betaine IVc (deprotonation of the substituent in position 1) is the only product of this reaction. The nucleophilic attack is always directed regiospecifically towards the stepwise formation of products involving the 1-aryl group (steps 1 and 2 in Scheme 3 in analogy to Scheme 2).

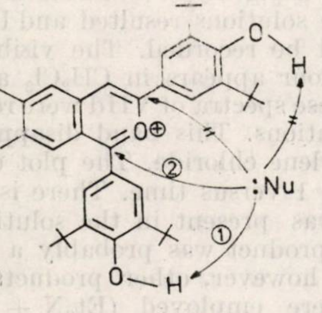

III c

Scheme 3

The structure of betaine IVc is supported also by data on the behaviour of salt IIId under conditions for betaine synthesis. In the last case a deep green colour appeared at first, then it was changed to light yellow and disappeared within 30 minutes in the ethereal extract. We suppose that the unstable betaine VIId was the compound with the deep green colour; this colour may be due to the "*ortho*-quinonoid" limiting structure VIId with quite different charge distribution in comparison with "benzenoid" betaines IVa—c. At the same time betaine VIId, derived from a 3-(*p*-hydroxyphenyl) group, is not as stable as betaines IVa—c, which are derived from 1-(*p*-hydroxyphenyl) group, probably because of reduced aromaticity in the 2-benzopyrylium system, as seen by comparing the neutral resonance structures IV with VIId (Scheme 4).

Scheme 4

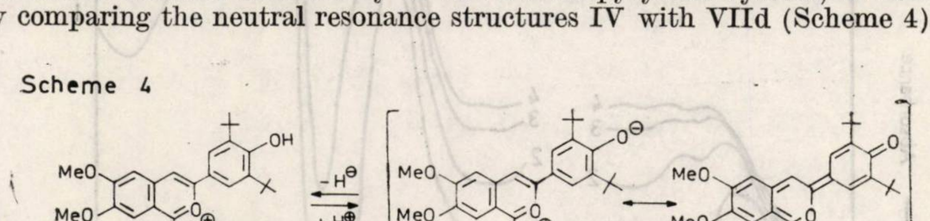

Thus betaine VIId reacts under nucleophilic attack more easily than betaines IVa—c leading to a complicated mixture of products. It remains to be seen if these products are derived from nucleophilic attack of OH anions in position 3 followed by ring opening, or if alternative reactions take place (nucleophilic attack in position 1, polymer formation, etc.). The only example so far reported of a similar perturbation of aromaticity for isobenzopyrylium salts involved the attack of secondary amines to position 3 of 1,3-dialkyl-substituted 2-benzopyrylium cations resulting in the formation of naphthylamines;[5] however no intermediate products of nucleophilic addition could be evidenced. Therefore it was interesting to try and obtain conditions under which betaine VIId could be stable, so that one may prove its existence. It seems obvious to exclude water and to use tertiary amines as bases for its formation. However, the first attempts failed to yield positive results, for example in 1% solutions of Et_3N in non-polar solvents such as dry ether or benzene; the disappearance of the green colour was too fast even for recording electronic absorption spectra. On using Et_3N + dichloromethane or acetonitrile as solvents, more stable solutions resulted and UV spectra at different intervals of time could be recorded. The visible absorption band responsible for the green colour appears in CH_2Cl_2 at λ_{max} 820 nm and in CH_3CN at λ_{max} 770 nm. These spectra of VIId were recorded immediately after preparation of the solutions. This band disappeared more quickly in acetonitrile than in methylene chloride. The plot of its disappearance in CH_3CN is given in Figure 1 versus time. There is no isosbestic point in the spectra. When water was present in the solution of betaine VIId, TLC showed that the major product was probably a diketone analogous to compounds Va and Vb; however, other products were also present. When anhydrous media were employed ($Et_3N + CH_2Cl$ or $Et_3N + CH_3CN$) the disappearance of VIId was due to the formation of mixtures containing addition and/or ring-opened products.

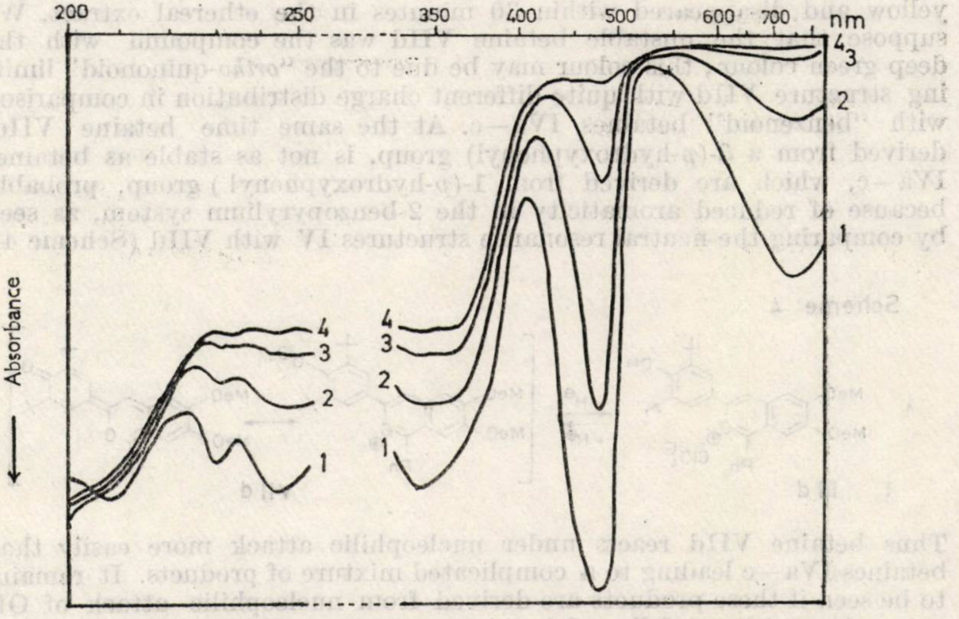

Fig. 1. — Ultraviolet and visible absorption spectrum of the salt IIId in acetonitrile containing 1% triethylamine: *1*, immediately after preparation; *2*, after 10 min.; *3*, after 20 min.; *4*, after 35 minutes.

According to these data it is possible to conclude that the aromaticity in the benzenoid ring of 2-benzopyrylium salts can be perturbed enabling nucleophilic attack in position 3 of isobenzopropyrylium cations to occur under definite conditions.

ESR SPECTRA

Oxidation with lead tetraacetate converts compounds III into the corresponding aroxyl radical cations whose ESR spectra were recorded. Compounds IIIa and IIId were oxidized in benzene containing 1% polyisoprenic rubber for increasing the viscosity of the medium and for obtaining thus line narrowing; these compounds (and IIIa which was not studied in detail) afford well-resolved 1 :2 :1 triplets with total width 0.4 mT, and with a coupling constant of the two *meta*-hydrogens equal to about 0.2 mT in both cases, as indicated in Table 2. Both the coupling constants and the *g*-values presented in Table 2 agree with data for other aroxyls.[9]

Table 2

ESR spectral data for radicals from salts IIIa, c, d

Compound	g	a_H, mT	$a_{^{13}C}(1)$	$a_{^{13}C}(2)$
IIIa	2.0050	0.205	1.301	0.628
IIId	2.0042	0.208	—	—
	Monoradical		Diradical	
	g	a_H	g	a_H
IIIc	2.0050	0.204	2.0044	0.098

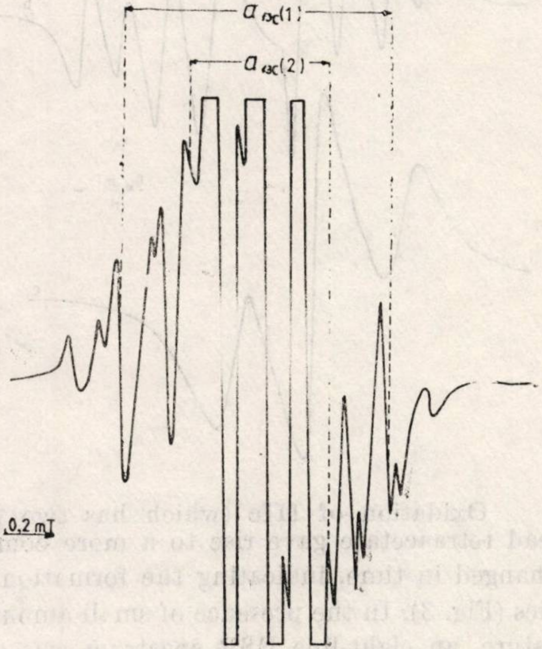

Fig. 2. — First-derivative ESR spectrum of the free radical obtained by oxidizing IIIa, amplified so much as to show the ^{13}C-hyperfine couplings as side-bands on the 1 :2 :1 triplet caused by the ^{1}H-hyperfine coupling.

The aroxyl prepared from IIIa was obtained in high concentration and its solution proved to be quite stable, unlike its congener obtained from IVd. The ESR spectra of the former radical (Fig. 2) reveal low-intensity peaks due to coupling with ^{13}C nuclei in natural abundance. Two larger such coupling constants are easily seen (as 1 :2 :1 triplet patterns, repeating the central intense triplet), namely 1.301 and 0.628 mT; they may be assigned to the *o*- and *p*-standing carbons of the phenoxyl ring.

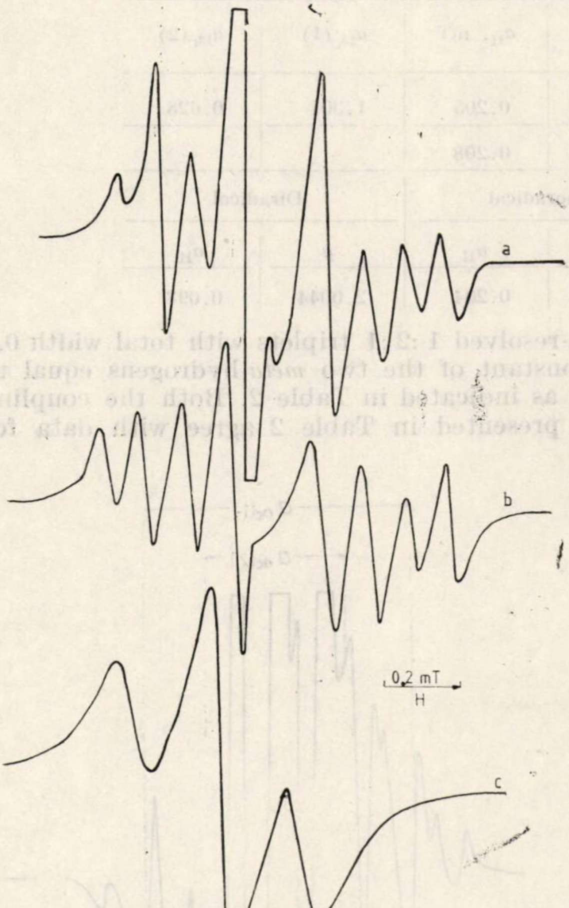

Fig. 3. — First-derivative ESR spectrum of the radical obtained by oxidizing IIIc: *a*, immediately after oxidation without any precaution; *b*, idem but with small amounts of $Pb(OAc)_4$; *c*, 25 minutes after adding oxidant.

Oxidation of IIIc (which has two *p*-hydroxyphenyl groups) with lead tetraacetate gave rise to a more complicated ESR spectrum which changed in time, indicating the formation of mono- and diradicalic species (Fig. 3). In the presence of small amounts of oxidant, at room temperature, an eight-line ESR spectrum was obtained; it attained maximal intensity after about 10 minutes after which in another ten minutes it decreased leaving a 1 :2 :1 triplet. We suppose that this signal is due to the diradical because its width (about 0.8 mT) is twice as large as for the monoradicals, and the distance between neighbouring lines (0.098 mT) is practically half as large as for the monoradicals.

ACKNOWLEDGEMENT. The experimental assistance of Florin Omota is acknowledged.

EXPERIMENTAL PART

IR spectra were determined with a Specord 71-IR Jena instrument in chloroform solutions. ^{1}H-NMR spectra were recorded with a Varian EM-360L instrument in $CDCl_3$; UV spectra were measured with a Specord UV-VIS instrument. ESR spectra were recorded on a Romanian-made ART-5 spectrometer, in the X-band frequency (9060 MHz), using peroxylamine-disulphonate as internal standard ($a_N = 1.3$ mT ; $g = 2.0055$).

3,4-Diethoxy-3,4-dimethoxydeoxybenzoin (*Ib*) was obtained from homoveratric acid and *o*-diethoxybenzene as in ref.[10]; yield 70%, m.p.89° (from n-propanol). IR bands are at 1670, 1590, 1210 cm^{-1}. ^{1}H-NMR Spectrum : $\delta = 1.47$ (6H, t, $2CH_3CH_2$), 3.83 (3H, s, CH_3O), 3.90 (3H, s, CH_3O),4.13 (4H, q, 2 CH_3CH_2), 6.76 — 7.73 ppm (6H, m, aromatic protons).

Preparation of the 2-benzopyrylium salts IIIa—c

The mixture of ketone I (10 mmoles) and acid II (15 mmoles) in 20 mL polyphosphoric ester was heated for 1.5 hrs at 80 — 85° with stirring, then the mixture was poured into 60 mL of cold water containing 6 mL of 70% $HClO_4$. After one hour, 20 mL of ether were added, the mixture was left overnight and then the crystalline perchlorate was filtered off. Yields 30—40% after recrystallisation from glacial acetic and or ethanol.

The salts IIIa—c afforded satisfactory elemental analyses. The IR spectra present the free OH stretching band at 3610 cm^{-1} and characteristic bands of the cation at 1620 and 1220 cm^{-1} (the bands at 1100 and 625 cm^{-1} are due to the anion).

1-(4-Hydroxy-3,5-di-t-butylphenyl)-3-(3,4-dimethoxyphenyl)-6,7-dimethoxy-2-benzopyrylium perchlorate (*III a*), m.p. 295°. Its ^{1}H-NMR spectrum has peaks at δ 1.60 (18H, s, 6 CH_3), 3.98 (3H, s, CH_3O), 4.01 (3H, s, CH_3O), 4.08 (3H, s, CH_3O), 4.14 (3H,s, CH_3O), 6.53 (1H, s, OH), 8.73 (1H, s, aromatic H) in addition to seven other aromatic protons as multiplet at 6.93 — 8.07 ppm.

1-(4-Hydroxy-3,5-di-t-butylphenyl)-3-(3,4-diethoxyphenyl)-6,7-dimethoxy-2-benzopyrylium perchlorate (*III b*), m.p. 250°.

1,3-Di-(4-hydroxy-3,5-di-t-butylphenyl)-6,7-dimethoxy-2-benzopyrylium perchlorate (*III c*), m.p. 298°.

1-(4-Acetoxy-3,5-di-t-butylphenyl)-6,7-dimethoxy-2-benzopyrylium perchlorate (VIa) was obtained with yield 80% under conditions described earlier.[2] Compound IIIa was suspended in excess acetic anhydride, and 70% perchloric acid was added dropwise with cooling under stirring. Then ether was added, the precipitated VIa was filtered off and recrystallized from acetic acid, m.p. 262°. IR spectrum : 1760, 1620, 1100, 625 cm^{-1}.

Preparation of betaines IVa—c

The solution of the salt III (one mmole) in 5 mL of acetone was added to 20 mL of 30% aqueous sodium hydroxide solution. The dark violet precipitate which appeared immediately was extracted with ether. After evaporation in vacuum of the dried solution, pure betaines IVa—c were obtained with yields 70—75%. The IR spectra present bands at 1645, 1230 and 1040 cm^{-1} for betaines IVa,b and the additional OH streching band at 3480 cm^{-1} for betaine IVc.

1-(3,5-Di-t-butylphenyl-4-oxide)-3-(3,4-dimethoxyphenyl)-6,7-dimethoxy-2-benzopyrylium (*IVa*), m.p. 215° (from ether). The ^{1}H-NMR spectrum has peaks at $\delta = 1.44$ (18H, s, 6 CH_3), 3.96

(3H, s, CH_3O), 4.00 (6H, s, 2 CH_3O), 7.89 (1H, s, aromatic H) in addition to seven other aromatic protons as multiplet at 6.87–7.73 ppm.

1-(3,5-Di-t-butylphenyl-4-oxide)-3-(3,4-diethoxylphenyl)-6,7-dimethoxy-2-benzopyrylium (*IVb*), m.p. 193°. The ^{1}H-NMR spectrum : $\delta = 1.43$ (24H, m, 6 CH_3 and $2CH_3CH_2$), 4.00 (10H, m, $2CH_3O$ and 2 CH_3CH_2), 6.67 – 7.43 (7H, m, aromatic 7H), 7.80 ppm (1H, s, aromatic 1H).

1-(3,5-Di-t-butylphenyl 4-oxide)-3-(4-hydroxy-3,5- di-t-butylphenyl)-6,7- di-methoxy-2-benzopyrylium (*IVc*), m.p. 260°.

3,5-Di-t-butyl-4-hydroxy-3,4′-dimethoxy-2′-(3,4-dimethoxyphenacyl)-benzophenone (*Va*). The solution of one mmole of salt IIIa or betaine IVa in 5 mL of moist chloroform was poured into a chromatographic column (4 cm diameter, height 30 cm), containing neutral Al_2O_3 without solvent. Using wet chloroform the colourless diketone Va (R_f 0.9) was eluted with yield 80%, m.p. 152° (from ethanol). IR bands at 3600 (νOH), 1680 ($\nu COCH_2$), 1640 (νCO), 1580, 1270 cm^{-1}. The ^{1}H-NMR spectrum has peaks at $\delta = 1.43$ (18H, s, 6 CH_3), 3.83 (3H, s, 2 CH_3O), 3.93 (3H, s, CH_3O), 4.37 (2H, s, CH_2), 5.73 (1H, s, OH) in addition to aromatic protons appearing at 6.70 – 6.96 as multiplet (3H) and at 7.26 (1H), 7.50 (1H) and 7.67 ppm (2H) as singlets.

3,5-Di-t-butyl-4-hydroxy-3,4′-dimethoxy-2′-(3,4-diethoxyphenacyl)-benzophenone (*Vb*) was obtained by the same method with yield 70%, m.p. 128°, and its IR spectrum is similar to the IR spectrum of ketone Va.

REFERENCES

[1] Previous part, A. T. Balaban, M-D. Gheorghiu, I. V. Shcherbakova, E. V. Kuznetzov and I. A. Yudilevich, *Tetrahedron*, **43**, 409 (1987).

[2] I. V. Shcherbakova, L. Yu. Ukhin, V. N. Komissarov, E. V. Kuznetsov, A. V. Poliakov, A. I. Yanovskii and Yu. T. Struchkov, *Khim. Geterotsikl. Soedin.*, in press (1986).

[3] I. V. Korobka, I. V. Shcherbakova and E. V. Kuznetzov, *Khim. Geterotisikl. Soedin.*, **1982**, 1184.

[4] G. N. Dorofeenko, E. I. Sadekova and V. M. Gancharova, *Khim. Geterotsikl. Soedin.*, **1970**, 1308.

[5] G. P. Safaryan, I. V. Shcherbakova, G. N. Dorofeenko and E. V. Kuznetsov, *Khim. Geterotsikl Soedin.*, **1981**, 1608.

[6] A. T. Balaban, A. Dinculescu, G. N. Dorofeenko, G. W. Fischer, A. V. Koblik, V. V. Mezheritskii and W. Schroth, "Pyrylium Salts. Synthesis, Reactions and Physical Properties", *Adv. Heterocyclic Chem.*, Suppl. vol. 2 (ed. A. R. Katritzky), Academic Press, New York, 1982, p. 61, 225, 237.

[7] W. Dilthey, *Ber. dtsch. chem. Ges.*, **59**, 1195 (1919); W. Dilthey et al., *ibid.*, **53**, 252 (1920); **54**, 825 (1921); *J. prakt. Chem.*, **774**, 113 (1926).

[8] A. T. Balaban, M. Gavăt, P. T. Frangopol, M. Mocanu and C. D. Nenitzescu, *Rev. Roum. Chim.*, **9**, 79 (1964).

[9] See e.g. J. Herdan, A. T. Balaban, N. Negoiță and N. Grecu, *Rev. Roum. Chim.*, **28**, 129 (1983); J. Herdan, G. Iordache, N. Negoiță, N. Grecu and T. Balaban, *ibid.*, **27**, 69 (1982).

[10] G. N. Dorofeenko and E. V. Kuznetsov, *Khim. Geterotsikl. Soedin.*, Sbornik **2**, 207 (1970).

Revue Roumaine de Chimie, 32, *4*, 427–429 (1987)

SOME REACTIONS ON 3-[(2-HYDROXY-4-QUINOLYL) METHYL]-2,4-PENTANEDIONES

M. M. KAMEL*, M. T. EL-WASSIMI**, F. H. OSMAN* and G. EL-SARRAF**
* National Research Centre, Dokki, Cairo, Egypt
** Faculty of Science, Sohag-Assiut University, Egypt

Received March 24, 1986

The reaction of 3-[(2-hydroxy-4-quinolyl) methyl]2,4-pentanediones (**2a,b**) with hydrazine hydrate, phenyl hydrazine, hydroxylamine, urea and thiourea gave the corresponding pyrazoles (**3**), isoxazoles (**4**), 2-pyrimidones (**5a,b**) and pyrimidine-2-thiones (**5c,d**).

The interesting pharmacological properties of pyrazoles,[1] isoxazoles[2] and pyrimidines[3] prompted us to introduce these types of heterocycles as substituents in the carbostyril molecule to obtain new compounds of expected biological activity[4] especially against bacteria and fungi.[1,2]

For this purpose, the key intermediates 3-(2-hydroxy-4-quinolyl)methyl]-2,4-pentanediones (**2a, b**) were prepared by the reaction of 4-bromomethylcarbostyril (**1a, b**)[5] with acetyl acetone in the presence of sodium ethoxide.

Condensation of **2a, b** with 98% hydrazine hydrate in ethanol afforded the corresponding 4-[(2-hydroxy-4-quinolyl)methyl]-3,5-dimethylpyrazoles (**3a, b**). In this way both **2a** and **2b** were condensed with phenyl hydrazine giving the corresponding N-phenyl-3,5-dimethyl pyrazoles (**3c**) and (**3d**). The IR spectrum of **3a** showed bands attributable to OH (3450 cm^{-1}) and amidic C=O and C=N, respectively (1660 cm^{-1} and 1550 cm^{-1}).

The isoxazoles **4a** and **4b** were obtained by condensation of **2a** and **2b** with hydroxylamine hydrochloride in the presence of pyridine. The IR spectrum of **4b** showed the absorption bands at 3420 cm^{-1} (OH), 1650 cm^{-1} (C=O) and 1550 cm^{-1} (—C=N).

Furthermore, treatment of diketone **2a,b** with urea and/or thiourea in acidified ethanol, followed by neutralization with sodium hydroxide solution, gave the corresponding 4,6-dimethylpyrimidine-2-ones (**5a,b**) and/or 4,6-dimethylpyrimidine-2-thiones (**5c, d**), respectively. The IR spectrum of **5d** showed absorption bands at 3420 cm^{-1} (OH), 1665 cm^{-1} (C=O), 1605 cm^{-1} (—C=N), 1265 cm^{-1} (C=S) and 1470 cm^{-1} (—N—C=S).

Preliminary anti-bacterial evaluation of these compounds is under progress and the results will be published elsewhere.

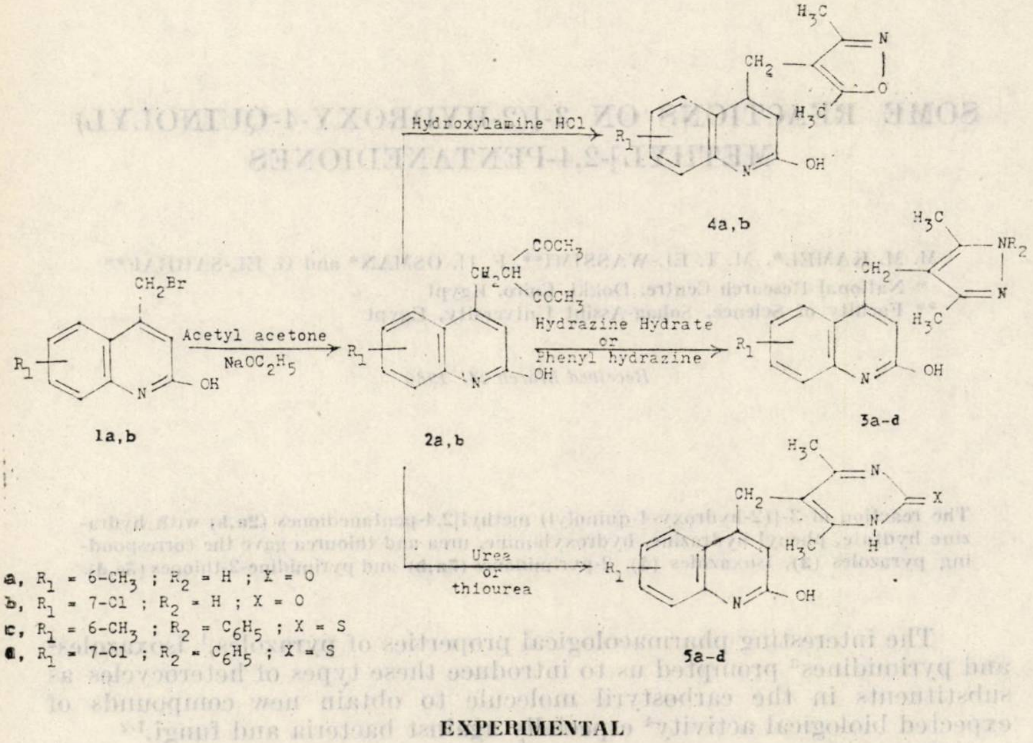

a, R_1 = 6-CH_3 ; R_2 = H ; X = O
b, R_1 = 7-Cl ; R_2 = H ; X = O
c, R_1 = 6-CH_3 ; R_2 = C_6H_5 ; X = S
d, R_1 = 7-Cl ; R_2 = C_6H_5 ; X = S

EXPERIMENTAL

All melting points are uncorrected and were determined on a Gallenkamp apparatus. The IR spectra were taken in KBr, with a Unicam Sp 1000 Infracord spectrophotometer. 4-Bromomethyl-6-methylcarbostyril (**1a**) and 7-chloro-derivative (**1b**) were prepared by established procedure.[5]

3-[(2-Hydroxy-6-methyl-4-quinolyl) methyl]-2,4-pentanedione (**2a**). Acetyl acetone (1 g, 0.01 mole) was added to an alcoholic sodium ethoxide solution (0.1 g sodium metal in 30 mL absolute ethanol) with stirring. After 1 h, 4-bromomethyl-6-methylcarbostyril (**1a**) (2.5 g, 0.01 mole) was added and the reaction mixture was refluxed for 4 h. The precipitate was filtered off, washed with water and crystallized from dilute acetic acid to give colourless crystals of **2a**, m.p. 220 — 222°C in 55% yield.

Analysis for $C_{16}H_{17}NO_3$; Calcd C 70.80 H 6.27 N 5.16 ; Found C 70.90 H 6.10 N 5.02.

Similarly, compound **2b** was produced as colourless crystals by the action of acetyl acetone on 4-bromomethyl-7-chlorocarbostyril (**1b**).

3-[(7-Chloro-2-hydroxy-4-quinolyl)methyl]-2,4-pentanedione (**2b**) was crystallized from dilute acetic acid with m.p. 210 — 212°C in 50% yield.

Analysis for $C_{15}H_{14}ClNO_3$; Calcd C 61.70 H 4.80 N 4.80 ; Found C 61.34 H 4.66 N 4.60.

4-[(2-Hydroxy-6-methyl-4-quinolyl)methyl]-3,5-dimethyl pyrazole (**3a**). A mixture of diketone **2a** (0.5 g, 0.002 mole) in ethanol was treated with 98% hydrazine hydrate (0.1 g, 0.002 mole) in ethanol and heated under refux for 3 h. The precipitate was filtered off, washed with water and crystallized from dilute acetic acid to give **3a** as colourless crystals, m.p. 274 — — 276°C in 55% yield.

Analysis for $C_{12}H_{17}N_3O$; Calcd C 71.90 H 6.30 N 15.73 ; Found C 72.40 H 6.34 N 15.61.

In the same manner as described for compound **3a**, **3b** was prepared by the action of **2b** on hydrazine hydrate and also, compounds **3c** and **3d** were obtained by the action of **2a** and **2b** on phenyl hydrazine.

4-[(7-chloro-2-hydroxy-4-quinolyl)methyl]-3,5-dimethylpyrazole (**3b**) was crystallized from dilute acetic acid, m.p. 262 — 264°C in 52% yield.

Analysis for $C_{15}H_{14}ClN_3O$; Calcd C 62.60 H 4.86 N 14.60; Found C 62.20 H 4.70 N 14.30.

N-Phenyl-4-[(2-hydroxy-6-methyl-4-quinolyl) methyl]-3,5-dimethylpyrazole (**3c**) was crystallized from dilute acetic acid, m.p. > 320°C in 57% yield.

Analysis for $C_{22}H_{21}N_3O$; Calcd C 76.96 H 6.12 N 12.24; Found C 76.80 H 6.19 N 12.15.

N-Phenyl-4-[(7-chloro-2-hydroxy-4-quinoly)methyl]-3,5-dimethylpyrazole (**3d**), was crystallized from dilute acetic acid, m.p. > 320°C in 60% yield.

Analysis for $C_{21}H_{18}ClN_3O$; Calcd C 69.30 H 4.95 N 11.55; Found C 69.49 H 5.05 N 11.46;

4-[(2-Hydroxy-6-methyl-4-quinolyl)methyl]-3,5-dimethylisoxazole **4a**. A mixture of diketone **2a** (0.5 g, 0.002 mole), hydroxylamine hydrochloride (0.14 g, 0.002 mole) and a few drops of pyridine in ethanol was heated under reflux for 4 h. After cooling and neutralisation with dilute hydrochloric acid solution, the precipitate was filtered off, washed with water and crystallized from dilute acetic acid to give **4a** as colourless crystals, m.p. 258 — —260°C in 50% yield.

Analysis for $C_{16}H_{16}N_2O_2$; Calcd C 71.64 H 5.97 N 10.41; Found C 71.50 H 5.81 N. 10.33.

Similarly, compound **4b** was obtained from the reaction of **2b** with hydroxylamine hydrochloride.

4-[(7-Chloro-2-hydroxy-4-quinolyl)methyl]-3,5-dimethylisoxazole (**4b**) was crystallized from dilute acetic acid, m.p. 244 — 245°C in 53% yield.

Analysis for $C_{15}H_{13}ClN_2O_2$; Calcd C 62.39 H 4.50 N 9.70; Found C 62.30 H 4.42 N 9.62.

5-[(2-Hydroxy-6-methyl-4-quinolyl)methyl]-4,6-dimethyl-2-pyrimidone (**5a**). To a mixture of diketone 2a (0.5 g, 0.002 mole) and urea (2.0 g, 0.0032 mole) in absolute ethanol (25 mL), a few drops of concentrated hydrochloric acid solution was added. The reaction mixture was heated under reflux with continuous stirring for 3 h. After cooling and neutralization with cold solution of sodium hydroxide, the precipitate was filtered off, washed with water and crystallized from diluted acetic acid to give **5a** with m.p. 273 — 275°C in 60% yield.

Analysis for $C_{17}H_{17}N_3O_2$; Calcd C 69.15 H 5.76 N 14.23; Found C 69.30 H 5.71 N 14.16.

Under similar experimental conditions, compound **5b** was obtained by the reaction of diketone **2b** with urea.

5-[(7-Chloro-2-hydroxy-4-quinolyl) methyl]-4,6-dimethyl-2-pyrimidone (**5b**) was crystallized from dilute acetic acid, m.p. 252 — 254°C in 58% yield.

Analysis for $C_{16}H_{14}ClN_3O_2$; Calcd C 60.86 H 4.43 N 13.31; Found C 60.72 H 4.51 N 13.22.

5-[(2-Hydroxy-6-methyl-4-quinolyl)methyl]-4,6-dimethylpyridimine-2-thione (**5c**). A mixture of diketone **2a** (0.5 g, 0.002 mole) and thiourea (0.2 g, 0.0025 mole) in absolute ethanol (15 mL) was treated with concentrated solution of sulfuric acid (1 mL). The reaction mixture was kept with continuous stirring at ambient temperature for 24 h. After heating under reflux (bath temperature 40°C) for 15 minutes and neutralization with cold solution of sodium carbonate, the precipitate was filtered off, washed with water and crystallized from dilute acetic acid to give **5c** with m.p. > 320 °C in 65% yield.

Analysis for $C_{17}H_{17}N_3OS$; Calcd C 65.60 H 5.46 N 13.50; Found C 65.43 H 5.32 N 13.39

Compound **5d** was prepared in the same manner as described for **5c** by the action of **2b** on thiourea.

5-[(7-Chloro-2-hydroxy-4-quinolyl)methyl]-4,6-dimethylpyrimidine-2-thione (**5d**) was crystallized from dilute acetic acid, m.p. > 320 °C in 65% yield.

Analysis for $C_{16}H_{14}ClN_3OS$; Calcd C 57.90 H 4.22 N 12.66; Found C 57.82 H 4.18 N 12.57

REFERENCES

[1] E. Herrman and J. Gabliks, *Cancer Chemotherapy Rept.*, **14**, 85 (1961).

[2] A. R. Katritzky, "Advances in Heterocyclic Chemistry", Academic Press, New York, Vol. 6, 1966, p. 345.

[3] J. Skoda, A. Cihal, J. Gut, M. Prystas, A. Piskala, C. Parkanyi and F. Sorm, *Coll. Czech. Chem. Comm.*, **27**, 1736 (1962).

[4] M. T. El-Wassimi, M. M. Kamel and G. El-Sarraf, *Die Pharmazie*, **38**, 201 (1983).

[5] R. J. Chudgar and K. N. Trivedi, *J. Indian Chem. Soc.*, **46**, 537 (1969).

Revue Roumaine de Chimie, **32**, *4*, 431–433 (1987)

THE SYNTHESIS OF AN AZO-DYE

O. ANAÇ
Department of Chemistry, Istanbul Technical University, Maslak-Istanbul-Turkey

Received April 14, 1986

This study describes the synthesis of an azo-dye, Reddish Navy (C. I. Acid Blue 113). The specifications and qualifications of the obtained dye are determined and compared with a commercial sample. Satisfactory results are obtained.

INTRODUCTION

Azo-dyes constitute numerically the most important class of synthetic coloring materials and in money value they are second only to the anthraquinonoid vat dyes. [1] Azo dyes are a distinct and clearly defined class, characterized by the presence of one or more azo ($-\bar{N}=\bar{N}-$) groups. They are all prepared by a common process involving two reactions: (1) diazotizing an aromatic primary amine; and (2) coupling the diazonium salt with a phenol or aromatic amine with a free *o*- and/or *p*-position (Scheme 1).

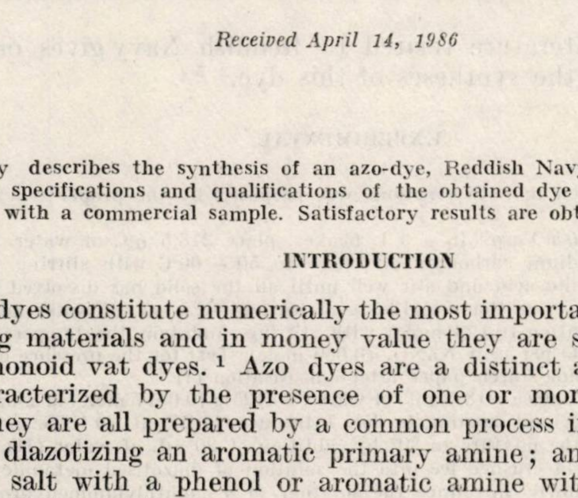

Scheme 1—C.I. Acid Blue 113.

Metanilic Acid → 1-Naphythylamine → N-Phenyl Peri Acid → Reddish Navy

Aromatic amines couple with diazonium salts under neutral or weakly acid conditions (pH 4 to 7). Because, under these conditions, the positively polarized diazonium ion ArN_2^+ which is strongly electrophilic attacks the nucleophilic *p*-center when this is unsubstituted, and otherwise to the *o*-center as may be expected from the resonance structure of an aromatic amine (Scheme 2).

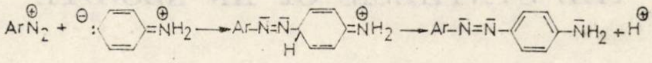

Scheme 2

Except for some special dyes, the diazotization reactions occur in aqueous solution.

The actual literature related to Reddish Navy gives only limited information about the syntheses of this dye.[2-5]

EXPERIMENTAL

Metanilic acid used in both reactions was prepared by the proper reactions, starting from nitrobenzene.[6]

Synthesis of Reddish Navy : In a 3 L beaker, place 218.5 mL of water, 5.6 g (0.0528 mole) of anhydrous sodium carbonate and heat to 50 — 60°C with stirring. Add 15.32 g (0.0885 mole) of metanilic acid and stir well until all the solid has dissolved.Then cool the mixture to about 20° by addition of 112.5 g of ice and 62.5 mL of water and add 13 mL of 30 per cent HCl solution (0.123 mole) with stirring. Maintain the temperature to about 20° and pour 17 mL of 30 per cent $NaNO_2$ (0.089 mole). Test for the presence of free nitrous acid with potassium iodide-starch paper after diazotisation (I).

In a 1 L beaker place 218.5 mL of water, 13.125 g (0.0917 mole) of α-naphthylamine. Dissolve it with stirring and heating to 85°. Introduce 11.25 mL (0.1078 mole) of 30 per cent HCl solution. Cool the mixture to 30° by addition of 20 mL of water (II).

Add about 125 g of crushed ice into the solution of diazotised metanilic acid (I) and cool it to 10°. Then slowly introduce the solution of α-naphthlylaminehydrochloride (II) and stir continuously. As the amount of α-naphthylamine (0.0917 mole) is a little higher than the metanilic acid (0.0885 mole) test for the absence of free diazotised metanilic acid with alkali H-acid solution to ensure the end of coupling. When coupling takes place, add 58.75 mL of 10 per cent NaOH solution until the pH : 6.5 — 7.

In order to dissolve the brown-coloured dye III, add 11.25 mL of 30 per cent NaOH solution (0.1096 mole) until pH : 8 — 9. The mixture will assume a uniform orange colour due to the solution of sodium salt of III. Pour 21.55 mL of 30 per cent $NaNO_2$ (0.1114 mole) solution and 131.25 g of NaCl with stirring. Then add quickly a solution of 12.5 mL of 96 per cent H_2SO_4 (0.223 mole) in 75 mL of crushed ice. The temperature must be kept at about 10° during diazotisation. After addition of 88 g of NaCl test for the presence of free nitrous acid with potassium iodide-starch paper. Filter off the new diazocompound at the pump (IV).

Dissolve 27.5 g (0.087 mole) of ammonia salt of phenyl-Peri acid in 219 mL of water at 60° with stirring (V).

Cool the solution V and add 350 g of crushed ice to maintain the temperature below 5°. Pour 44 mL of 25 per cent sodium acetate solution having 0.5 mL of acetic acid. Then add the suspension of filtered diazocompound IV in 250 mL of water with stirring. When coupling takes place (VI) add 17 mL of 30 per cent NaOH solution for the separation of the sodium salt of the blue dye (VI). The pH must equal 8.

Cool the dye to about 0° by addition of 350 g of crushed ice, add 219 g of NaCl and stir. Filter-press the dye, dry at the air-drier first at 50° and then at 80°. The yield is 65.90 g. This value also includes the contribution of some present NaCl. The theoretical yield is expected to be equal to 59.26 g, in the absence of NaCl.

Test for Reddish Navy[3] :

a) Soluble in water (violet), ethanol (Violet blue) and Cellosolve
b) Slightly soluble in acetone
c) Insoluble in other organic solvents
d) Aqueous solution + HCl conc. → corinth
e) Aqueous solution + NaOH conc. → bordeaux

f) Aqueous solution + H_2SO_4 conc. → dullish greenish blue ; on dilution → dark greenish blue to greyish violet.

g) Aqueous solution + HNO_3 conc. → orange brown solution.

IR (not neat to the presence of NaCl) : 3400, 1620 (s, N—H), 1220, 1180 (SO_3^-) cm^{-1}.

Comparison of the dye with the commercial sample using Visible Spectrophotometer showed that this dye was stronger than the available commercial sample (Cyanin 5R-South Korean) by a factor of 1.5.

In order to convert the sodium salt of the dye having residual NaCl to the acid form of the dye having no NaCl, a sample of the dye was dissolved by addition of cold aqueous solution of HCl. The greenish-blue solution was boiled for 1—2 min. and a red solution with a purple precipitate was obtained. No decomposition occurred under these conditions.[2]

This precipitate was filtered off then washed with a small quantity of water and dried in vacuum oven at 70°C.

Elemental analysis : calculated for $C_{32}H_{23}N_5S_2O_2$: C 60.28 ; H 3.61 ; N 10.99 ; found C 60.26 ; H 3.63 ; N 10.98 IR (neat) : 3400, 1620 (s, N—H), 1220, 1180 (SO_3^-) cm^{-1}.

In conclusion high quality Reddish Navy can be easily produced by the method proposed in this study.

ACKNOWLEDGEMENTS. I thank Imdat ANAÇ, the manager of Gökçe Tekstil A.Ş. for assistance in obtaining visible spectra, technical information and supplying the chemicals and commercial dye sample. I also thank Prof. Dr. Bahattin BAYSAL for helpful comments on the manuscripts.

REFERENCES

[1] K. Venkataraman, "The Chemistry of Synthetic Dyes", Ed.L F Fieser and M Fieser, Academic Press, New York, 1972.

[2] Rowe and Dangerfield, *J. Soc. Dyers and Colourists*, **52**, 55 (1954).

[3] Rowe, "Coloured Index" Ed. The Society of Dyers and Colourists, Bradford, 1971 Vol. IX, 4230.

[4] Bayer Co., G. P. 118655.

[5] FIAT 764.

[6] A. I. Vogel, "A Text-Book of Practical Organic Chemistry" Longman, London, 1970, p. 589.

Revue Roumaine de Chimie, 32, 4, 435–441 (1987)

SYNTHESIS AND STUDIES OF 3-N-ARYLCARBAMIDOCOUMARINS

A. F. EL-FARARGY, A. Y. SOLIMAN*, M. EL-MOBAYED and S. EL-ESSER
Chemistry Department, Faculty of Science, Zagazig University, Zagazig, Egypt

Received April 26, 1986

3 N-aryl carbamido coumarins **1** were prepared by the action of aromatic amines on 3-carbethoxy coumarin. 4-Substituted 3,4-dihydrocoumarins **2** and **3** were prepared by the Michael condensation of **1** with ethylacetoacetate and/or acetylacetone in the presence of sodium ethoxide. But the Michael condensation of **1** with acetophenone in the presence of ammonium acetate gave benzopyrano(3,4-c)-pyridine diones **4**, with aliphatic ketones gave 2-alkyl-4-oxo-3,4,5,6-tetrahydro-2,6-methano [2H]-1,3- benzoxazocines-5-carboxamides **5**, and/or with excess cyclic ketones gave 12-oxo-hexahydro (o-pentahydro) 4a,9-imino-[4a-H]-xanthone-11-carboxamides **6**.

Coumarins which are a class of 5,6-benzopyran-2-one, were found to have wide medical applications.[1,2] 3-Carbethoxy coumarin was reacted with benzylamine and/or *p*-anisidine in boiling ethanol to give the corresponding 3-N-benzyl- and 3-N-(p-methoxy)-phenyl carbamido coumarin (**1a**–**b**) respectively.[3] The structures of (**1a**–**b**) were established by independent synthesis, by heating coumarin-3-carbonyl chloride with the corresponding amines in dry ether.

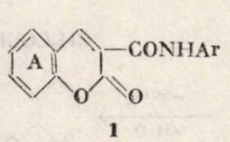

1

a, Ar $= C_6H_5CH_2-$
b, Ar $= p-CH_3OC_6H_4-$

The structures of (**1a**–**b**) were confirmed by correct analytical data. The IR spectra of (**1a**–**b**) exhibited bands at 1650 cm^{-1} (νCO of amide), 1690 cm^{-1} (νCO of unsaturated lactone) and at 3310 cm^{-1} (νNH). The ^{1}H-NMR ($CDCl_3$) spectrum of (**1b**) showed signals at δ 3.8 (s, 3H of OCH_3) at δ 6.84–7.68 (m, 9H of Ar–H, the olefinic proton and the ring A) and at δ 8.9 (s, 1H of NH).

---

* **Faculty of Teachers at El-Fayoum, University of Cairo.**

The Michael condensation of (**1a**—**b**) with ethylacetoacetate or acetyl acetone in the presence of sodium ethoxide [4,5] at the boiling point of the reaction mixture yielded 4-acetonyl-3,4-dihydro-coumarin (**2**) and 4(3-pentan-2,4-dionyl)-3,4-dihydro-coumarin (**3**). The infrared spctrum of (**2**) and (**3**) exhibited bands at 1740 cm^{-1}, 1670 cm^{-1} and 1640 cm^{-1} attributable to (νCO) of lactone and ketone. An explanation for the formation of compounds (**2**) and (**3**) involves the Michael addition of ethylacetoacetate or acetylacetone to the coumarin derivatives (**1a**—**b**) with subsequent fission and cyclization of heterocyclic ring *via* the following mechanism (cf. Scheme 1).

Scheme 1

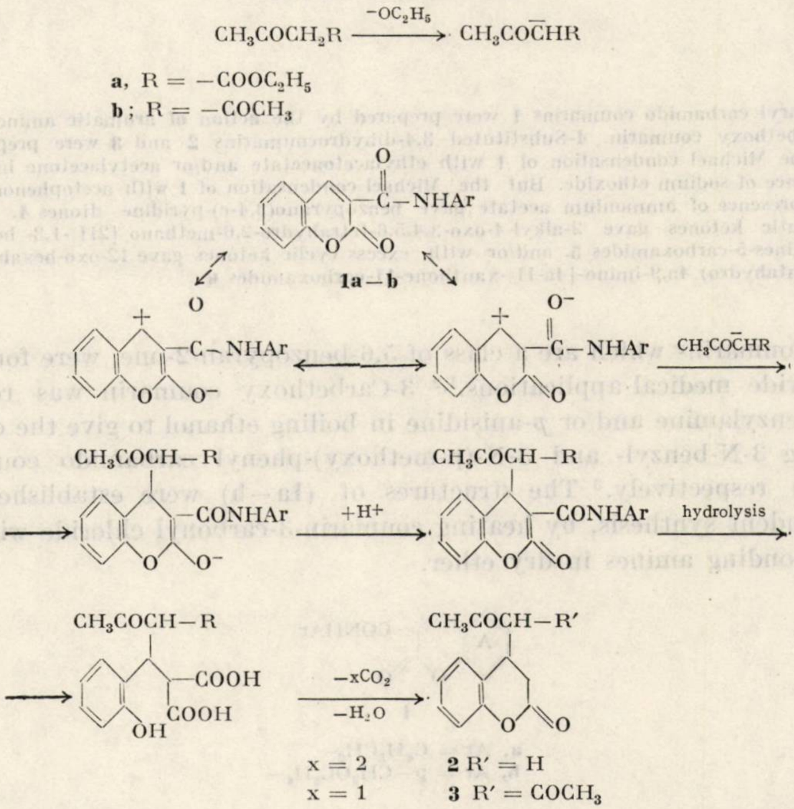

$CH_3COCH_2R \xrightarrow{-OC_2H_5} CH_3CO\overline{C}HR$
a, R = $-COOC_2H_5$
b; R = $-COCH_3$
C—NHAr
1a—b
C—NHAr
C—NHAr
$CH_3CO\overline{C}HR$
$CH_3COCH—R$
—CONHAr
+H+
—CONHAr
hydrolysis
$CH_3COCH—R$
—COOH
COOH
OH
$-xCO_2$
$-H_2O$
$CH_3COCH—R'$
x = 2
x = 1
2 R′ = H
3 R′ = $COCH_3$

Recently, [6-8] it was found that 3-(N-phenyl carbonyl) coumarins reacted with ketones in the presence of ammonium acetate or amines at room temperature or at the boiling point of the reaction mixture to give 3,4,5,6-tetrahydrobenzoxazocines. 3-N-Aryl carbamido coumarines (**1a**—**b**) reacted with acetophenone in the presence of ammonium acetate at the boiling point of the reaction mixture and gave 3,4,4a,10b tetrahydro (1)benzopyrano(3,4-c)pyridine-4,5(H)diones (**4**). The structure of (**4**) was confirmed by its correct analytical data and by infrared spectrum which showed bands at 1750 cm^{-1} (νCO of saturated δ-lactone), 1640 cm^{-1} (νCO of cyclic amide) and 3420 cm^{-1} (νNH). The reaction possibly takes place by the following mechanism (cf. Scheme 2);

Scheme 2

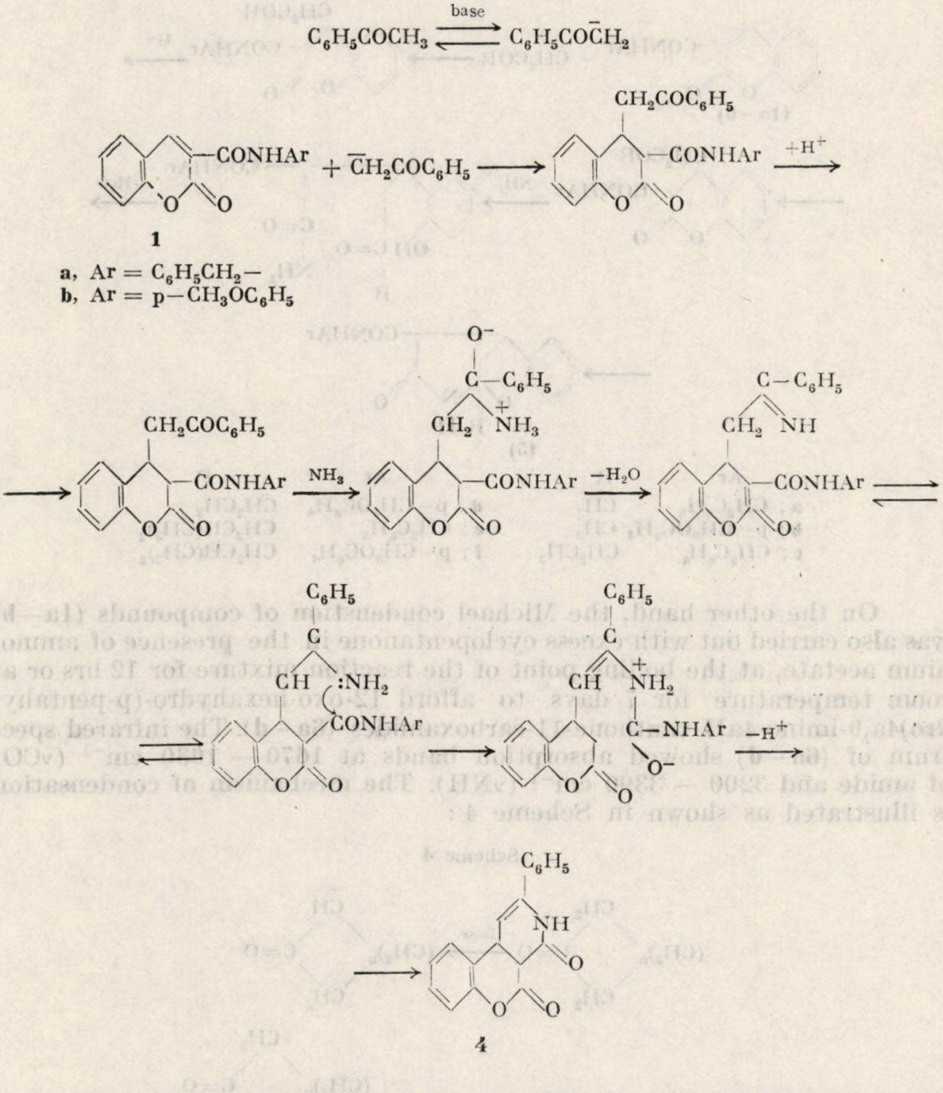
base
C6H5COCH3
C6H5COCH2
CH2COC6H5
CONHAr
+ CH2COC6H5
+H+
O
1
a, Ar = C6H5CH2—
b, Ar = p—CH3OC6H5
O−
C—C6H5
CH2
NH3
NH3
−H2O
C—C6H5
NH
C6H5
C
CH
:NH2
CONHAr
C—NHAr
−H+
4

Also 3-N-arylcarbamido coumarins (**1a**—**b**) reacted with excess acetone, ethyl methyl ketone and/or isobutyl methyl ketone in the presence of ammonium acetate to give 2-alkyl-4-oxo-3,4,5,6-tetrahydro-2,6-methano [2H]-1,3-benzoxazocine-5-carboxamides (**5a**—**f**). The infrared spectrum of (**5a**—**f**) exhibited bands at **1670**—**1630** cm^{-1} (νCO of amide) and 3390 — 3200 cm^{-1} (νNH). The reaction possibly takes place by the following mechanism (cf. Scheme 3):

Scheme 3

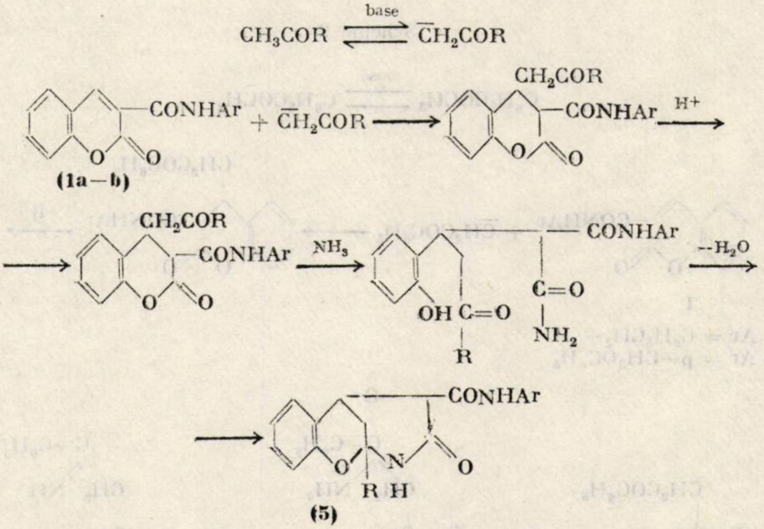
base
$CH_3COR \rightleftharpoons \bar{C}H_2COR$
CONHAr
$\bar{C}H_2COR$
CH_2COR
H^+
(1a—b)
NH_3
OH
C=O
R
NH_2
$-H_2O$
R H

(**5**)

Ar	R	Ar	R
a; $CH_2C_6H_5$	CH_3	**d**; $p-CH_3OC_6H_4$	CH_2CH_3
b; $p-CH_3OC_6H_4$	CH_3	**e**; $CH_2C_6H_5$	$CH_2CH(CH_3)_2$
c; $CH_3C_6H_4$	CH_2CH_3	**f**; $p-CH_3OC_6H_4$	$CH_2CH(CH_3)_2$

On the other hand, the Michael condenstion of compounds (**1a—b**) was also carried out with excess cyclopentanone in the presence of ammonium acetate, at the boiling point of the reaction mixture for 12 hrs or at room temperature for 7 days to afford 12-oxo-hexahydro-(p-pentahydro)4a,9-imino-4aH-xanthone-11-carboxamides (**6a—d**). The infrared spectrum of (**6a—d**) showed absorption bands at 1670 — 1630 cm^{-1} (νCO) of amide and 3200 — 3390 cm^{-1} (νNH). The mechanism of condensation is illustrated as shown in Scheme 4:

Scheme 4

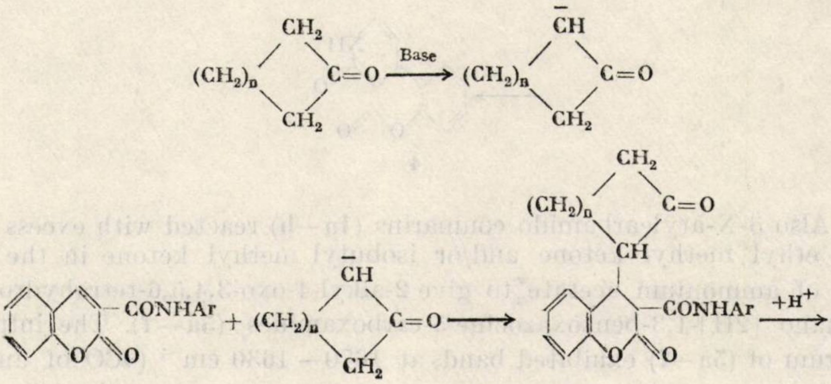
CH_2
$(CH_2)_n$
C=O
CH_2
Base
$\bar{C}H$
CONHAr
$+H^+$

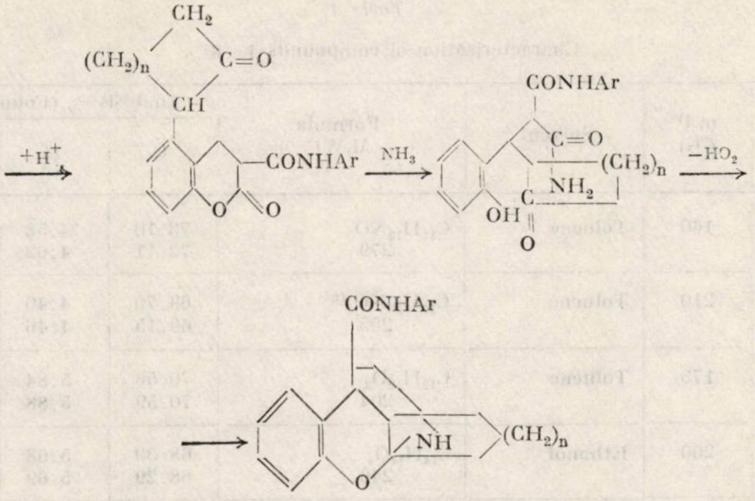

(6)

a ; $Ar = CH_2C_6H_5$; $n = 4$ **c** ; $Ar = p-CH_3OC_6H_4$; $n = 4$

b : $Ar = CH_2C_6H_5$; $n = 3$ **d** ; $Ar = p-CH_3OC_6H_5$; $n = 3$

EXPERIMENTAL

Melting points are not corrected. Infrared spectra (KBr) were measured on a Perkin Elmer infracord 137 spectrophotometer, the ^{1}H-NMR spectra on a Varian A 60 equipment using TMS as internal standard; mass spectra at a Varian Mat 711 mass-spectrometer. The analytical and physical data of all the products are described in Table 1.

Reaction of 3-carbethoxy coumarin with benzylamine and/or p-*anisidine ; formation of* **(1a — b)** :

To a solution of 3-carbethoxy coumarin (0.01 mol) in 50 mL ethanol was added benzylamine and/or *p*-anisidine (0.01 mol). The mixture was refluxed for 5 hrs. The solid product was filtered off and crystallised from the suitable solvent to give **(1a—b)**.

Condensation of **(1a—b)** *with active methylene compounds or ketones in the presence of sodium ethoxide ; formation of* **2** *and* **3** :

A mixture of **(1a—b)** and ethylacetoacetate or acetylacetone (0.01 mol) and sodium ethoxide (0.025 mol) was heated at the boiling point of the reaction mixture for 12 hrs. The products were stirred with conc. HCl (20 mL), washed with water and crystallised from suitable solvent to give (**2**) and (**3**).

Condensation of (**1a—b**) *with ketones and cyclic ketones ; Formation of* (**4**), (**5a—f**) *and* (**6a—d**) :

A mixture of (**1a—b**) (0.01 mol), 30 mL ketones (acetophenone, acetone, ethylmethyl ketone, cyclopentanone or cyclohexanone) and ammonium acetate (0.025 mol) was heated at the boiling point of the reaction mixture for 12 hrs or stirred at room temperature for 7 days. The solid products were filtered off and crystallised from the proper solvent.

Table 1

Characterisation of compounds **1**–**6**.

Compound	m.P (°C)	Solvent	Formula M.Wt	Analysis % (Found/Calc.)		
				C	H	N
1a	160	Toluene	$C_{17}H_{13}NO_3$ 279	73.10 73.11	4.58 4.62	4.88 5.00
1b	210	Toluene	$C_{17}H_{13}NO_4$(a) 295	69.70 69.15	4.40 4.46	5.02 4.74
2	173	Toluene	$C_{12}H_{12}O_3$ 204	70.56 70.59	5.84 5.88	
3	200	Ethanol	$C_{14}H_{14}O_4$ 246	68.30 68.29	5.68 5.69	
4	250	Acetic acid	$C_{18}H_{13}NO_3$ 291	74.20 74.22	4.43 4.46	4.79 4.81
5a	205	Xylene	$C_{20}H_{20}N_2O_3$(b) 336	71.30 71.43	6.00 5.95	8.31 8.33
5b	193	Benzene	$C_{20}H_{20}N_2O_4$(c) 352	68.70 68.18	4.90 5.68	7.63 7.95
5c	184	Benzene	$C_{21}H_{22}N_2O_3$ 350	72.00 72.00	6.00 6.28	7.80 8.00
5d	164	Benzene	$C_{21}H_{22}N_2O_4$(d) 366	68.20 68.85	6.04 6.01	6.50 7.65
5e	174	Toluene	$C_{23}H_{26}N_2O_3$ 378	73.06 73.02	6.85 6.87	7.40 7.41
5f	190	Toluene	$C_{23}H_{26}N_2O_4$ 394	70.10	6.58	7.10
6a	130	Benzene	$C_{25}H_{30}N_2O_2$ 390	76.89 76.92	7.71 7.69	7.14 7.17
6b	183	Methanol	$C_{24}H_{28}N_2O_2$ 376	76.58 76.59	7.46 7.44	7.40 7.44
6c	210	Benzene	$C_{25}H_{30}N_2O_3$ 406	73.88 73.89	7.36 7.39	6.87 6.90
6d	250	Acetic acid	$C_{24}H_{28}N_2O_3$ 392	73.44 73.47	7.11 7.14	7.10 7.14

(a) *m/e* 295 (M^+), 218, 173 (100%), 146, 145.
(b) *m/e* 336 (M^+), 243, 228, 202 (100%), 184, 106, 91.
(c) *m/e* 352(M^+), 259, 202(100%),184, 145.
(d) *m/e* 366 (M^+), 273, 244, 218, 216 (100%), 200, 183.

REFERENCES

[1] Olson, *Canad. J. Biochem.*, **43**, 1565 (1965).

[2] C. N. Matur *et al.*, *Ach. Int. Pharmacodyn*, **153**, 218 (1965); *Chem. Abstr.*, **63**, 12154 (1965).

[3] M. El-Kady, G. H. Sayed, A. Mansour and M. El-sherif, *Polish. J. Chem.* **56**, 1393 (1982).

[4] A. Sammour, M. Abdalla, and M. El-Kady, *Acta. Chem.* (Budapest), **82**, 369 (1974).

[5] A. I. Essawy, M. El-Kady and A. Y. Mohamed, *Indian J. Chem.* **19**, 567 (1980).

[6] M. El-Kady, *Pakistan. J. Sci. Res.* **31**, 163 (1979).

[7] M. El-Kady, M. A. El-Hashash, M. A. Sayed and M. El-Sherif, *Indian J. Chem.* **20**, 491 (1981).

[8] M. El-Kady, G. H. Sayed, R. M. Saleh and H. M. Mosa, *J. Chem. Soc.* (in Press).

Revue Roumaine de Chimie, 32, 4, 443—448 (1987)

SOLVENT EFFECTS. VI[1]

THE MECHANISM OF INCREASE, DIFFERENTIATION AND LEVELING OF R_f VALUES IN THE CHROMATOGRAPHIC SEPARATION OF SUBSTANCES

METODIU RĂILEANU
Craiova University, Department of Chemistry, Str. A. I. Cuza 13, Craiova, Romania

Received March 4, 1986

The paper gives an explanation of the mechanism of increasing, differentiation and leveling of R_f values under the influence of activating solvent from a binary mobile phase. Two notions, namely, the active and saturation concentrations were introduced in order to understand the variation manner of R_f values, when the concentration of the activating solvent increases. An optimum interval for the concentration of activating solvent in the mobile phase allowing a good chromatographic separation of the substances is proposed.

1. INTRODUCTION

In our previous papers[1,2] the notions of activating and deactivating solvents were introduced in order to suggest slightly the manner of the influence of the solvent from a binary mobile phase on the R_f values.

An activating solvent is defined as a solvent which in a pure state determines the increase and a leveling of R_f values of the substances which are separated from the mixture. Unlike the activating solvent, a deactivating solvent in similar conditions decreases and levels the R_f values of the polar substances. The mixture in different proportions of the activating and deactivating solvents generates binary mobile phases which determine medium R_f values with a certain degree of differentiation.

An activating solvent is always polar and attracts predominantly polar substances (by dipole-dipole forces or by hydrogen bonds) from the mixture to be separated. The deactivating solvent is unpolar or slightly polar; that's why it attracts (by dispersion forces) unpolar molecules of the mixture.

It is important to specify that in the chromatographical practice the symmetrical molecules, without permanent dipole, are considered polar, if they have polar groups which can be adsorbed on the polar surface of the two phases, the stationary and mobile one.[3]

In this paper the influence of the activating und deactivating solvents on the variation, differentiation and leveling of R_f values was studied. To this purpose, using the thin layer chromatography on silicagel, the following phenothiazinic and phenothiazonic compounds were separated : phenothiazine(I), 1,3,7,9-tetranitrophenothiazine-5-oxide (II), 4-nitrophenothiazone-(3)(III), phenothiazone-(3)(IV), 3,7-dinitrophenothiazine-5-oxide(V) and phenothiazine-5-oxide (VI).

For separation of the mentioned compounds, which possess different polarities, binary mobile phases in different concentrations of the activating solvent were utilized.

As deactivating solvents the benzene and toluene were chosen. The activating solvents used were : acetone, methyl acetate, propanol-1, propanol-2 and butanol-1. The first two solvents (acetone and methyl acetate) are aprotic ; they attract the polar substances especially by dipole-dipole forces. The last three alcohols are protic solvents ; they attract the polar substances by dipole-dipole forces and by hydrogen bonds.

The silicagel from the stationary phase adsorbs predominantly the polar substances by dipole-dipole forces and by hydrogen bonds. It is important to mention that the adsorption power of a molecule on silicagel depends not only on the number of the polar groups, but also on its geometry, *i.e.* on the positions of these groups in the molecule.[4]

2. RESULTS AND DISCUSSION

Table 1 presents the R_f values of compounds I—VI in pure deactivating and activating solvents as well as in binary mobile phases with different concentrations of the activating solvent.

As was expected, phenothiazine (I), which is very little polar, has in benzene the R_f values equal to 0.80. This great value for the R_f points out that benzene, being unpolar, transports phenothiazine(I) in the mobile phase by dispersion forces. The addition of an activating solvent (acetone, alcohol) determines an increase of R_f value for phenothiazine (I) up to 0.95 ; this fact suggests that, under the influence of the activating solvent, an induced dipole in phenothiazine molecule (which is slightly polarisable) occurs. So, in the presence of the activating solvent, phenothiazine(I) is transported from the mobile phase by dispersion forces to which weak dipole-dipole forces are added.

With an increase of the substances polarity beyond a certain limit the dispersion forces become negligible in comparison which dipole-dipole forces or hydrogen bonds. Indeed, phenothiazine-5-oxide (VI) differs from phenothiazine(I) only by a sulphoxidic polar group $>S\rightarrow O$, but it is strongly adsorbed on the stationary phase of the silicagel and cannot be displaced from the benzene in the mobile phase ($R_f = 0$). In this manner the deactivating solvent separates easily the unpolar from polar substances.

Table 1 shows how the gradual concentration increase of the activating solvent determines an increase of R_f values of substances I—IV. The maximum R_f values in the pure activating solvents are recorded.

Table 1

The R_f values variation for compounds I — VI in pure solvents and in binary solvent mixtures *)

Substance	B	B/MA(37.38/1, V/V)	B/MA(18.69/1, V/V)	B/MA(9.34/1, V/V)	MA
I	0.80	0.85	0.88	0.91	0.98
II	0.17	0.43	0.59	0.74	0.97
III	0.03	0.21	0.31	0.53	0.97
IV	0.01	0.16	0.25	0.46	0.96
V	0	0	0	0	0.90
VI	0	0	0	0	0.78
		B/A(40/1, V/V)	B/A (20/1, V/V)	B/A (10/1, V/V)	A
I		0.86	0.88	0.90	0.99
II		0.31	0.61	0.72	0.99
III		0.26	0.42	0.65	0.96
IV		0.18	0.33	0.56	0.96
V		0	0	0.02	0.96
VI		0	0	0.02	0.90
		B/PA(40/1, V/V)	B/PA (20/1, V/V)	B/PA(10/1, V/V)	PA
I		0.90	0.93	0.95	0.98
II		0.51	0.61	0.74	0.98
III		0.22	0.35	0.61	0.87
IV		0.18	0.31	0.56	0.85
V		0.01	0.08	0.29	0.85
VI		0.01	0.07	0.29	0.85
		B/IA(40/1, V/V)	B/IA (20/1, V/V)	B/IA (10/1, V/V)	IA
I		0.94	0.95	0.95	0.95
II		0.64	0.76	0.88	0.88
III		0.41	0.68	0.84	0.83
IV		0.33	0.54	0.75	0.83
V		0.01	0.08	0.23	0.83
VI		0.01	0.07	0.22	0.80
	T	T/BA (18,58/1, V/V)	T/BA (9.29/1, V/V)	T/BA (4.64/1, V/V)	BA
I	0.70	0.79	0.80	0.88	0.97
II	0.14	0.30	0.51	0.78	0.97
III	0.02	0.28	0.49	0.73	0.84
IV	0.02	0.27	0.49	0.73	0.84
V	0	0.05	0.25	0.54	0.84
VI	0	0.04	0.20	0.46	0.84

*) B = benzene ; T = toluene ; MA = methyl acetate ; A = acetone ; PA = proypl alcohol ; IA = isopropyl alcohol ; BA = n-butyl alcohol

In order to explain the variation mechanism of R_f values, it is important to study the graphical representation of relation (1) in which C represents the concentration of the activating solvent from the mobile phase. In figure 1 the variation of R_f values for compounds I—VI and VI is graphically represented, using propanol-2 as activating solvent and benzene as deactivating solvent.

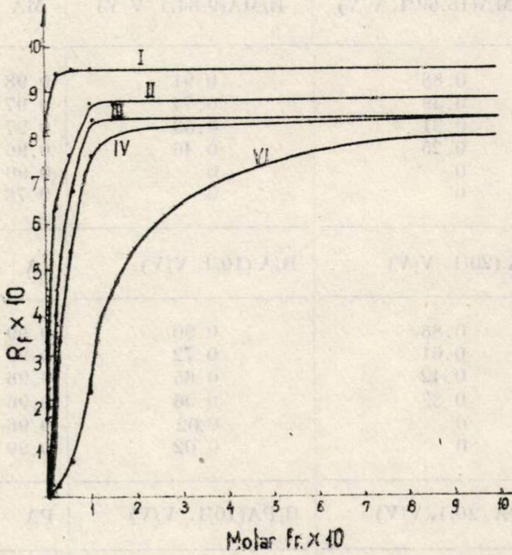

Fig. 1. — The graphical representation of the relation $R_f = f(C)$ for compounds I—IV and VI in benzene/propanol-2 mixture. The concentration C of the activating solvent (propanol-2) is expressed in molar fractions.

$$R_f = f(C) \tag{1}$$

Figure 1 shows that at identical concentrations of the activating solvent the studied compounds present different R_f values, because they have different polarities. The compound to be separated with the greatest polarity is evidently displaced more easily from the mobile phase from the silicagel surface and in this case the R_f values are greater than for a compound with a smaller polarity.

On the other hand, one can see that a concentration increase of the activating solvent determines an increase of R_f values for all separated compounds.

This phenomenon is normal, because a greater concentration of the activating solvent determines a more powerful adsorption of a polar substance to be separated on the mobile phase, where it remains a longer time.

In the case of the substances with a strong polarity, II, III and IV, one can see in figure 1 a straight portion, where the R_f values increase practically proportionally to the concentration of the activating solvent, and a curve portion, where R_f values increase more slowly. The proportionality of the R_f values with the concentration in a certain interval suggests that all molecules of the activating solvent present chromatographical activity. Therefore, for the linear portion *active concentrations* of the activating solvent correspond, but for the curve portion *saturation* *concentrations* of the activating solvent correspond (where R_f values increase more slowly).

In the case of the saturation concentrations only a part of the solvent molecules present chromatographic activity ; a fraction from the molecules of this solvent loses their mobility because at these great concentrations they disturb one another by dipole-dipole forces or by hydrogen bonds. A similar phenomenon is also found at the osmotic pressure, which is proportional to the concentration of the dissolved substances up to certain limit, then increases more slowly. The effect of the saturation concentration for the leveling of R_f values is evident. Indeed, compound II has the same R_f value equal to 0.96 in three pure different alcohols : in methanol which contains 53.12% —OH groups, in propanol-1 with 28.33% —OH groups and in n-butanol-1 with 22.97% —OH groups. The equalization of the R_f values for compound II in three alcohols with a very different content of —OH groups points out that one can imagine a minimum saturation in active —OH groups for which the R_f value becomes maximm.

Introduction of the notions of active and saturation concentration of the activating solvent presents a remarkable importance for the chromatographic separation of the substances. Indeed, in figure 1 one can see that in the field of the active concentrations, which is very narrow, the R_f values of the polar compounds increase rapidly. Also in this interval a more stressed differentiation of the R_f values takes place for the polar separated substances.

The saturation concentrations of the activating solvent are not favorable to the chromatographic separation, because they level the R_f values. The leveling phenomenon of the R_f values can be explained. When the concentration of the activating solvent increases, the R_f values of all substances increase and crowd in a more and more narrow interval which is displaced towards the maximum value $R_f = 1$.

The R_f values leveling in the activating concentrated or pure solvent can be also caused by the unequal polarization of the molecules of the substances to be separated. Thus, it can be considered that a less polar molecule polarizes more powerfully than one more polar at the great concentrations of the activating solvent. The polarization phenomenon adds to the permanent dipole an induced dipole, resulting thus an increase of the total polarity of the molecule to be separated and of the correspondent R_f values. This explains, for example, how two substances with different polarities and R_f values at a small concentration of the activating solvent, present equal R_f values in the pure activating solvent (see the curves $R_f = f(C)$ for compounds III and IV from fig. 1).

For all the other activating solvents (protic or aprotic) studied in benzene the shape of the curves $R_f = f(C)$ for compounds I—VI is the same as in figure 1; also for the butanol-1 in toluene.

The study of the shape of the curves $R_f = f(C)$ established that the saturation phenomenon in activating solvent manifests in the same manner at the polar protic and aprotic solvents. It results that at great concentrations of the activating solvent a part of the molecules can be in the same manner immobilized by dipole-dipole attraction forces or by hydrogen bonds formation.

3. EXPERIMENTAL

The substances used in this paper were obtained and purified according to the methods described in the literature.[5–8] Solvents of advanced purity were utilized. The HR silicagel plates were prepared at the Chemical Institute of Cluj-Napoca. No supplementary activation of the silicagel was made.

The identification of the substances on the chromatogram was done according to the following colours: phenothiazine (I) is coloured brown-green with bromine vapours and 3,7-dinitrophenothiazine-5-oxide(V) in red with ammonia vapours; phenothazine-5-oxide(VI) becomes brownish by treatment with 30% HNO_3. Phenothiazone-(3)(IV) is coloured in dark red, 4-nitrophenothiazone-(3) (III) in orange and 1,3,7,9-tetranitrophenothiazine-5-oxide (II) in yellow.

An ascendent development for 0.5 h at room temperature was performed.

4. CONCLUSIONS

The notions of activating and deactivating solvents proposed in the previous papers [1,2] are particularly useful, because they suggest the strong influence of the solvent on the R_f values.

The notions of active and saturation concentrations introduced in this paper are also important, because they show the variation, differentiation and leveling manner of the R_f values, when the concentration of the activating solvent in the mobile phase increases.

The leveling of R_f values is caused by their increasing and crowding in a smaller interval which is displaced towards the maximum value 1, when the concentration of the activating solvent increases.

The strong leveling of the R_f values can be also caused by the unequal polarization of the molecules of the substances to be separated, when the concentration of the activating solvent increases, because, generally, the less polar molecules polarize more strongly than those with a great permanent dipole.

The optimum concentration of the activating solvent in a binary mobile phase for the differentiation of R_f values can be placed in the molar fraction interval $0.05 \div 0.15$.

REFERENCES

[1] Part V: M. Răileanu, *Rev. Chim. (Bucureşti)*, **36**, 164 (1985).

[2] M. Răileanu, *Rev. Chim. (Bucureşti)*, **35**, 1119 (1984).

[3] J. P. Garel, *Bull. Soc. chim. France*, **1964**, 653.

[4] M. Răileanu, "Influenţa mediului asupra reactivităţii chimice", Ed. Scrisul Românesc, Craiova, 1981, pp. 374–378.

[5] M. Răileanu, *Rev. Chim. (Bucureşti)*, **33**, 1102 (1982).

[6] M. Răileanu, *Rev. Chim. (Bucureşti)*, **34**, 111 (1983).

[7] C. Bodea and M. Răileanu, *Studii şi Cercetări Chim. Fil. Cluj*, **11**, 325 (1960).

[8] C. Bodea, M. Terdic and E. Broser, *Liebigs Ann. Chem.*, **715**, 122 (1968).

Revue Roumaine de Chimie, 32, 4, 449–451 (1987)

COMPTES RENDUS

"Mathematical Modelling in Science and Technology", (eds. X. J. R. Avula, R. E. Kalman, A. I. Liapis and E. Y. Rodin), Proceedings of the Fourth International Conference, Zürich, Aug. 1983. Pergamon Press, New York, 1984. Hard-cover large format volume, 1006 pp, ISBN: 0-08-030156-8, $ 200.

International Conferences on Mathematical Modelling are held every two years. They provide an interdisciplinary forum on mathematical modelling in engineering, economics, biological, medical, environmental, social and other sciences. The 6th Conference will be held on August 10–13, 1987 at the Washington University in St. Louis, Missouri. The International Association for Mathematical Modelling and the international journal *Mathematical Modelling* (eds. X. J. R. Avula and E. Y. Rodin) are the sponsors of these conferences.

The excellently printed volume contains the seven invited general lectures (two of which are present only as summaries) and the 173 communications (some of which are only one-page abstracts). All are printed from camera-ready manuscripts following carefully-designed guidelines: abstract on one column, text on two columns, length not exceeding 12 pages for lectures and 8 pages for communications. Each communication stands on a separate page, and the layout is unified by the fact that all authors followed the guidelines.

It will be impossible to deal at length with all interdisciplinary papers. The lectures were: 1) Deterministic control of uncertain systems, by G. Leitman; 2) The use of interactive graphics in the analysis and design of complex feedback systems, by A. G. J. MacFarlane; 3) General software for computer-aided synthesis of control for manipulation robots, by M. K. Vukobratović, a Yugoslav author from the Robotic Department in the Institute "Mihailo Pupin", Beograd, 4) Multiplication decisions in systems with feedback, by T. L. Saaty; in this lecture, complex decision patterns are exemplified by means of graphs illustrating the objectives of an optimal word processing systems, or the cost/benefit hierarchies for power generation alternatives, or the Munich terrorist massacre of the Israel olympic team in 1972; 5) Mathematical modelling and long range planning, by S. E. Dreyfus and S. Sen (Babi), a discussion (with two divergent conclusions) whether expert modelling is really possible for long range planning in uncertain times; 6) Modelling and identification (Abstract), by R. E. Kalman; 7) Statistical methods for experimental planning in chemical engineering (Abstract), by D. W. T. Ripkin.

The communications (their number is given in brackets) are grouped in the following sections: Methodology (5); Systems Theory (12); Parameter estimation and system identification (9); Optimisation (15); Stochastic modelling (11); Simulation (6); Numerical modelling (15); Chemical engineering (9); Solid mechanics (17); Fluid mechanics (11); Water resources (3); Biomedical models (17); Modelling in economics (12); Transportation (7); Industrial applications (6); Populations (4); Mathematical modelling education (5); General topics (7); and Late abstracts (2).

The whole section on chemical engineering and many communications from the section on fluid mechanics, optimization, mathematical modelling education, biological models, and general topics will be interesting for chemists and chemical engineers. Of special interest to the reviewer was the communication "Neighborhood complexities and symmetry of chemical graphs, and their biological applications" by A. B. Roy, S. C. Basak, D. K. Harris and V. R. Magnuson.

In an interdisciplinary conference the main attractiveness is not so much to find something of immediate interest, but rather to become familiar with contingent areas, to be able to seize analogies in problems or methods. For all those wishing to browse for this purpose, this book will be an inexhaustible source of inspiration.

A. T. Balaban

V.E. Zubarev, "Metod spinovykh lovushek; primenenie v khimii, biologii i meditsine (Method of spin traps; application in chemistry, biology and medicine)", 185 pp, Izd. Moskovskogo Universiteta, Moscow, 1984, 1.70 rbl.

Spin traps are compounds such as nitrones or nitroso-derivatives which react with short-lived free radicals by adding them to C=N or N=O bonds, respectively, and which form thereby persistent nitroxidic free radicals. The latter may be studied by various methods, especially by ESR spectroscopy, providing information on the short-lived free radicals.

The review contains six chapters :

1) The ESR method in chemical research
2) Spin traps
3) Methodology of experiments
4) Chemistry of spin traps
5) Use of the spin trapping method for investigating the mechanism of chemical reactions
6) Use of the spin trapping method in medical-biological investigations.

The book contains 423 references up to 1983. The author's Ph. D. thesis (1976) concerned the investigation of free radicals formed in the radiolysis of alcohols in liquid or solid phases and he conserved an interest in this area.

The book is informative and well-writen, containing personal views of the author in a field he is thoroughly familiar with. He discusses methods for selecting the optimal spin trap and solvent for the required purpose, because there exist no universally optimal spin traps.

The book will be useful to all chemists who wish to be informed about a valuable method for investigating reaction mechanisms and structures of unstable or stable free radicals, as well as to biochemists and biologists.

A. T. Balaban

"Flavonoids and Bioflavonoids 1985". L. Farkas, M Gabor and F. Kallay (editors), Akadémiai Kiadó, Budapest, 1986, 466 pages,

The present book contains the 44 lectures held by the participants at the 7th Hungarian Bioflavonoid Symposium. This meeting, attended by participants from 15 countries, was organized in Szeged, the town in which Rusznyak and Szent-Györgyi discovered — 50 years ago — the therapeutical effects of flavonoids.

As in the previous volumes dedicated to Flavonoid Symposia, the papers, presented in camera-ready form and including rich reference lists, cover all the main topics of the domain : syntheses of flavonoids and related compounds, physical investigations of flavonoids, reactions, isolation of new flavonoids as well as biologic activities in animal and human organism.

From the interesting papers contained in the book we could only mention some examples such as :

1) Syntheses : "The synthesis and biological activity of the latinones" (D.M.X. Donnelly and P.G.M. Cannon) ; "Synthesis of americanin —D" (S. Antus, R. Bauer, A Gottsegen, O. Seligmann and H. Wagner) ; "Synthesis of natural pyranochromones" (C.S.R. Iyer and R. P. Iyer)

2) Reactions : "Kinetic investigations of the elimination reeaction of 3-bromoflavanones" (E. Peli, T. Patonay, M. Zsuga and Gy. Litkey) ; "Ethylene carbonate, a regioselective reactant for hydroxyethylation of flavonoids" (D. Rehn and G. Wurm) ; "Reactions of 3-mesyloxyflavonones with S-nucleophiles" (T. Patonay and Gy. Litkey).

3) Physical investigations : "Quantum chemical studies of the UV spectra of parent flavonoids" (Z. Dinya, S. Kiss, J. Balint and R. Bognar) "Characteristic constituents of the Cherry peduncle extract novicardin : HPLC fingerprint" (M. Gellert, K. Szendrei, Z.Dinya and J. Répasi) ; "Investigation of the chemical constituents, particularly the flavonoid components, of propolis and *Populi gemma* by the GC/MS method" (E. Nagy, V. Pappay, Gy. Litkey and Z. Dinya).

4) Isolation of new flavonoids (8 papers) : "New flavonol glycosides from *Mespilus germanica* L." (N. Nikolov, O. Seligmann and H. Wagner) : "Identification of the anthocyanin of *Consolida orientalis* Schröd " (Gy. Sulyak and J. Balint) : "Isolation of anthocyanidins from natural sources" (E. Gabor and O. Herczegh).

5) Biologic activities (18 papers) : "New results in the pharmacology of benzopyrone derivatives and related compounds" (M. Gabor) ; "Isoflavones and arteriosclerosis" (A. L. Kazakov, V. P. Khilya and V. A. Kompantsev) ; 'Flavonoids inhibit enzymic thyroid hormone deiodination" (J. Köhrle, M. Auf'mkolk, M. Spanka, G. Sonyi, V. Cody and R. D. Hesch), "The effect of flavonoids on the natural killer activity of human lymphocytes" (I. Beladi, Y. Mandi, Gy. Seprényi, R. Pusztai and A. Veckenstedt).

A detailed subject index ends this interesting and useful book containing the newest results in flavonoid research.

M. Banciu

Şerban Dan Cartianu, "Synchronization Phenomena in Reaction-Diffusion Systems", B. G Teubner Verlagsgesellschaft, Leipzig, 1986, 283 pp.

The present book (the 8th volume in the recent and methodologically very interesting series "Teubner Texte zur Physik", Leipzig, D.D.R.) is concerned with the interdisciplinary aspects of self-organizational chemistry (chemical synergetics), considering such phenomena as the oscillatory phenomena in dissipative, nonhamiltonian systems (especially the Belousov — Zhabotinskii systems) and the interactions of such systems when coupled by diffusion. After a general introduction (chapter I), the book reviews the following aspects (Section Headings):

— Phase and Frequency Synchronization in Reaction-Diffusion Equations;

— Dissipative Structures in Reaction-Diffusion Systems as Synchronization Phenomena;

— The Improvement of the Energetic Efficiency of Chemical Processes in the Oscillatory Mode;

— Cooperative Phenomena in Dissipative Systems Far from Thermodynamic Equilibrium. Bifurcation of Reaction-Diffusion Systems

— Synchronization Phenomena of Periodically Stimulated Dissipative Systems in Bifurcation Theory and in the Alternative Theory of Averaging;

— Rate-Constrained Chemical Equilibrium Method for Solving Complex Mass Action Kinetic Systems.

Several chapters give special attention to the conceptual and mathematical premises towards a theory of synchronization, based mainly on the author's own works, printed in Romanian scientific journals. As is well known, the concept of time is much more complex than we thought (I. Prigogine), but the author's research sheds new light on the complexities of this theory.

For the readers interested in the improvement of the energetic efficiency of free energy conversion for open chemical systems (by varying the stimulus frequency up to the resonance with the intrinsic oscillations) the results of chapter 4 are of particular relevance. There is, too, a brief but consistent discussion of the close relationship between resonance and synchronization — two crucial self-organizational categories (states) that are nontrivially correlated.

The 20 suggestive figures are uneqully distributed in the 7 chapters (chapter 5 contains 14 bifurcation diagrams); 319 references including "classics" P. Glansdorf, I. Prigogine, H. Haken, A. Pacault, D. Ruelle and W. Ebeling (first editor of Teubner series) — are given for each chapter.

Finally, needless to say, the entire book of Dan Cartianu has important conceptual and methodological implications for the development of the space-time framework of contemporary nonlinear physical chemistry.

Florin Pelecan

ANNOUNCEMENT

The seventh international symposium on olefin metathesis and polymerization, ISOM 7, will be held at Humberside College of Higher Education, Hull, 24—28 August, 1987. Information from Dr. A. Ellison, School of Science, Humberside College of Higher Education, Cottingham Road, Hull HU6 7RT, N. Humberside, England.

NOTE POUR LES AUTEURS

La Revue Roumaine de Chimie publie des articles en anglais, français, russe, allemand ou espagnol. Les auteurs sont priés d'envoyer des articles et des comptes rendus inédits.

Les manuscrits seront dactylographiés à double interligne. La bibliographie, les tableaux et la légende des figures seront placés après le texte.

Si l'article fait partie d'une série numérotée la partie précédente sera donnée comme première référence.

Chaque article sera précédé d'un résumé comprenant quinze lignes au maximum.

Les références bibliographiques dans le texte seront faites par des exposants sans parenthèses et paraîtront à la fin de l'ouvrage.

Les publications périodiques mentionnées dans la bibliographie seront présentés suivant les prescriptions internationales : le nom de l'auteur précédé de l'initiale du prénom, le titre du périodique abrégé conformément à « Chemical Abstract » et souligné par une ligne, le numéro du tome indiqué par des chiffres arabes et souligné par deux lignes, suivi de la première page de l'article : à la fin, l'année de la parution sera placée entre parenthèses. Le numéro de la revue ne sera pas indiqué si les pages du volume sont numérotées consécutivement.

Les textes des livres ou traités inclueront : le nom des auteurs, précédés de l'initiale du prénom, le titre du livre entre guillemets et sans être souligné, le numéro du tome précédé par l'abréviation « vol. » (ou « Bd. »), le numéro de l'édition, les éditions (the publisher), la localité de la parution du livre, l'année de la parution et la page de la référence précédée(s) par l'abréviation « p » (ou « S »).

Les brevets seront indiqués comme suit : l'auteur ou la firme, le pays et le numéro du brevet, la date de la revue (*Chem. Abstr.*). Par ex. : M. Jones (to Union Carbide Co.). Brit. Pat. 610 238, 2 Sept. 1959 : cf. *Chem. Abstr.*, **54**, 12808 (1960).

Si la référence n'a pas été lue en original, on indiquera aussi la revue de références consultée.

Les diagrammes seront tracés à l'encre de Chine sur papier calque. Les tableaux et les figures (en nombre strictement nécessaire), ainsi que les courbes dans les figures seront numérotés par des chiffres arabes. Leur explication sera donnée dans la légende des figures. Prière de ne pas inscrire les mêmes données dans les tableaux et les figures. Chaque tableau aura un titre. On indiquera dans le texte la place approximative des tableaux et des figures. Les formules chimiques seront incluses dans le texte ; en outre, elles seront transcrites sur papier calque à l'encre de Chine.

Les auteurs sont priés d'indiquer les caractéres italiques (en soulignant les lettres au crayon), ainsi que tout autre caractère spécial : les préfixes, *ortho*, *meta*, *para*, *cis*, *trans*, etc. seront soulignés pour indiquer leurs caractères italiques, et ne seront jamais écrits avec des majuscules.

Aucune correction à la main ne sera admise sur le manuscrit. Les corrections seront frappées à la machine. Les lettres grecques ou d'autres symboles spéciaux seront insérés à la main à l'encre clairement.

Le manuscrit sera signé par l'auteur.

Le titre courant aura 50 lettres au maximum.

L'entière responsabilité du contenu des articles appartient aux auteurs.

Sur demande on peut obtenir une note plus complète.

PRINTED IN ROMANIA

ORSZÁGOS MŰSZAKI INFORMÁCIÓS KÖZPONT ÉS KÖNYVTÁR

M. I. Ch. — I. C. Ch.

IAMN

BUCUREȘTI

Ministry of Chemical Industry-
Chemical Research Institute
IAMN-Bucharest

PRODUCES:

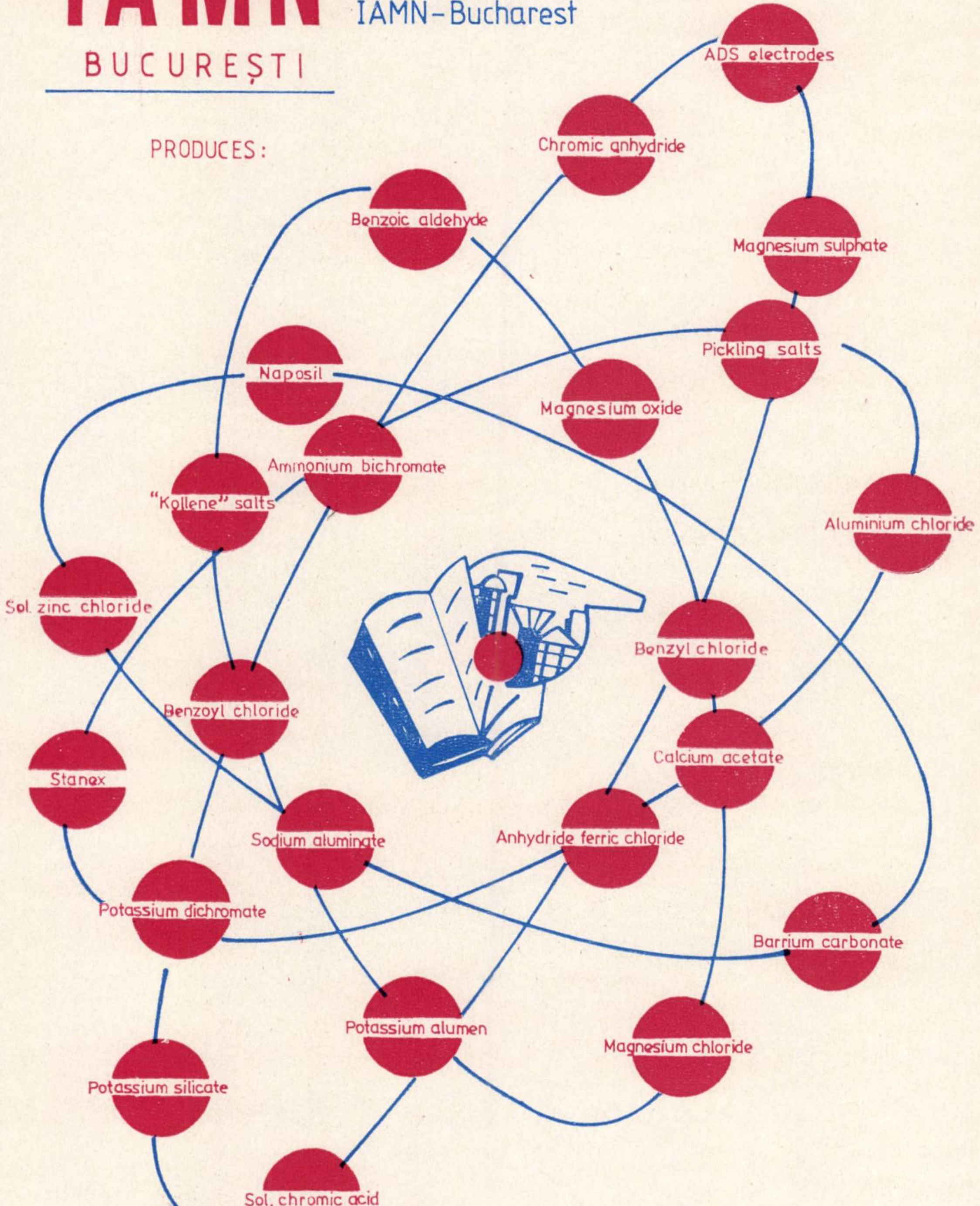

- ADS electrodes
- Chromic anhydride
- Benzoic aldehyde
- Magnesium sulphate
- Pickling salts
- Naposil
- Magnesium oxide
- Ammonium bichromate
- "Kollene" salts
- Aluminium chloride
- Sol. zinc chloride
- Benzyl chloride
- Benzoyl chloride
- Calcium acetate
- Stanex
- Sodium aluminate
- Anhydride ferric chloride
- Potassium dichromate
- Barrium carbonate
- Potassium alumen
- Magnesium chloride
- Potassium silicate
- Sol. chromic acid

'TRANSILVANIA' RESEARCH DEPARTMENT
12 C Armata Roșie street
TURDA, ROMANIA

ORSZÁGOS MŰSZAKI INFORMÁCIÓS KÖZPONT ÉS KÖNYVTÁR * 1983 *

TRAVAUX PARUS AUX ÉDITIONS DE L'ACADÉMIE DE LA RÉPUBLIQUE SOCIALISTE DE ROUMANIE

ELENA CEAUŞESCU, **Progrese în chimia şi tehnologia polimerilor**, 1986, 446 p.
ELENA CEAUŞESCU, **Forschungen im Bereich der Chemie und Technologie der Polymere**, 1986, 444 p.
A. T. BALABAN et al., **Labelled Compounds and Radiopharmaceuticals Applied in Nuclear Medicine**, coédition avec John Wiley and Sons, 1986, 742 p.
M. BUDRUGEAC, **Probleme de chimie**, 1986, 280 p.
M. BREZEANU, L. PATRON, M. ANDRUH, **Combinaţii complexe polinucleare şi aplicaţiile lor**, 1986, 224 p.
R. MIHAIL, I. GROZEANU, **Estimarea secvenţială aplicată sistemelor chimice**, 1986, 406 p.
I. G. MURGULESCU, O. M. RADOVICI, **Introducere în chimia fizică, vol. IV, Electrochimia**, 1986, 416 p.
D. PURDELA, **Nomenclatura chimiei anorganice**, 1986, 454 p.
T. ONCESCU, S. G. IONESCU, **Conversie fotochimică şi stocare de energie solară**, 1985, 272 p.
V. DRĂGUŢAN, A. T. BALABAN, M. DIMONIE, **Olefin Metathesis and Ring-Opening Polymerization of Cyclo-Olefins**, coédition avec John Wiley and Sons, 1985, 544 p.
C. LITEANU, I. RÎCĂ, **Optimizarea proceselor analitice**, 1985, 360 p.
N. PERESCU, **Chimia extracţiei cu solvenţi şi aplicaţii**, 1985, 212 p.
V. EM. SAHINI, M. HILLEBRAND, **Chimie cuantică în exemple şi aplicaţii**, 1985, 378 p.
GH. MARCU, **Chimia compuşilor coordinativi**, 1984, 415 p.
E. CORDOŞ, C. MANOLIU, **Spectrometria de absorbţie şi fluorescenţa atomică**, 1984, 178 p.
C. BODEA, **Tratat de biochimie vegetală**, p. II, t 5, 1984, 438 p.
N. ASANDEI, A. GRIGORIU, **Chimia şi structura fibrelor**, 1983, 395 p.
N. IONESCU, M. CĂLDĂRARU, **Oxidarea catalitică a olefinelor inferioare**, 1983, 178 p.
C. CAŞCAVAL, **Studiul polimerilor prin piroliză şi cromatografie de gaze**, 1983, 220 p.
C. I. SIMIONESCU, F. DANEŞ, **Originea vieţii**, 1983, 110 p.
C. BODEA, **Tratat de biochmie vegetală**, p. II, t. 4, 1982, 408 p.
I. G. MURGULESCU, RODICA VÎLCU, **Introducere în chimia fizică. Vol. III. Termodinamica chimică**, 1982, 624 p.
I. G. MURGULESCU, J. PĂUN, **Introducerea în chimia fizică. Vol. I. 3, Nucleul atomic, reacţii nucleare, particule elementare**, 1982, 606 p.
ELENA CEAUŞESCU, **Noi cercetări în domeniul compuşilor macromoleculari**, 1981, 536 p.
I. G. MURGULESCU, TATIANA ONCESCU, E. SEGAL, **Introducere în chimia fizică Vol. II. 2. Cinematică chimică şi cataliză**, 1981, 1024 p.
I. GĂLĂŢEANU, **Procese şi metode radiochimice în energetica nucleară**, 1981, 234 p.
CR. SIMIONESCU, VALERIA GORDUZA, **Polimeri biocompatibili şi biologic activi**, 1980, 479 p.
ELENA CEAUŞESCU, **Polimerizarea stereospecifică a izoprenului**, 1979, 307 p.
C. GH. MACAROVICI, **Analiza chimică cantitativă anorganică**, 1979, 457 p.
M. FLORESCU, **Metode ştiinţifice în dezvoltarea industriei chimice moderne**, 1979, 256 p.
I. G. MURGULESCU, E. SEGAL, **Introducere în chimia fizică. Vol. II. 1. Teoria molecular-cinetică a materiei**, 1979, 1036 p.
I. G. MURGULESCU, V. EM. SAHINI, **Introducere în chimia fizică. Vol. I. 2. Structura şi proprietăţile moleculelor**, 1978, 604 p.
I. G. MURGULESCU, **Introducere în chimia fizică. Vol.I. 1. Atomi, molecule, legătură chimică**, 1976, 560 p.
ELENA CEAUŞESCU, **Research work on synthesis and characterization of macromolecular compounds. Contributions**, 1974, 251 p.

ISSN 0035–4090

1987 MAJ 15

I.P. INFORMAŢIA c. 1003

43 426

Lei 40

$ 80 (pour un abonnement annuel)

1103

04

ACADÉMIE DE LA RÉPUBLIQUE SOCIALISTE DE ROUMANIE

96

REVUE ROUMAINE DE CHIMIE

TOME 32

Nº 5

Mai 1987

Rev. Roumaine Chim.

RRCHAX, 32, 5, p. 455–548 (1987), Bucarest

EDITURA ACADEMIEI REPUBLICII SOCIALISTE ROMÂNIA

ACADÉMIE DE LA RÉPUBLIQUE SOCIALISTE DE ROUMANIE

COMITÉ DE RÉDACTION

Rédacteur en chef:

I. G. MURGULESCU, membre de l'Académie de la République Socialiste de Roumanie

Rédacteurs en chef adjoints:

A. T. BALABAN et V. EM. SAHINI, membres correspondants de l'Académie de la République Socialiste de Roumanie

Collège de rédaction:

EM. BRATU, ELENA CEAUŞESCU, ECATERINA CIORĂNESCU-NENITZESCU, CR. SIMIONESCU, membres de l'Académie de la République Socialiste de Roumanie ; P. SPACU, membre correspondant de l'Académie de la République Socialiste de Roumanie ; M. BANCIU, M. D. GHEORGHIU, I. HAIDUC, D. I. MARCHIDAN, G. NIAC et D. SĂNDULESCU

La Revue Roumaine de Chimie paraît 10 fois par an. Toute commande de l'étranger sera adressée à ROMPRESFILATELIA — sectorul Export-Import Presă, P. O. Box 12—201, télex 10376 prsfi r 78 104 Bucarest, Calea Griviţei nr. 64—66, Bucureşti, Roumanie

Les manuscrits, les livres et les revues proposés en échange, ainsi que toute correspondance seront envoyés à la rédaction :

REVUE ROUMAINE DE CHIMIE

125, Calea Victoriei, 79717 Bucarest, Roumanie, téléphone 50 76 80

EDITURA ACADEMIEI REPUBLICII SOCIALISTE ROMÂNIA
125, Calea Victoriei, 79717 Bucarest, Roumanie, téléphone 50 76 80

REVUE ROUMAINE DE CHIMIE

Tome 32, N° 5 **Mai, 1987**

S. STERNBERG, A. MATEESCU, V. BRÂNZOI and LILIANA APĂTEANU, The coulometric study of the Pb, PbO_2, $O_2/PbSO_4$ system 457–465
MARIANA CIUREANU, MIHAELA HILLEBRAND, ELENA VOLANSCHI and DANIELA GHEȚU, Optical spectra and electronic structure of some nitrothioamide anion radicals 467–475
RAM KUMAR AGARWAL and SUNIL KUMAR GUPTA, Magneto, spectral and thermal investigations of coordination compounds of lanthanides(III) with 2-ethoxycarbonylaminopyridine 477–487
V. V. KORSHAK, E. S. KRONGAUZ, N. M. BELOMOINA, M. BRUMĂ, G. MANDRIC and C. I. SIMIONESCU, New copolymers containing phenylquinoxaline units 489–494
A. RASHEED KHAN, TEHZEEB AKHTER and A. H. K. YOUSUFZAI, Chain transfer constants for some aromatic solvents in the cationic polymerization of α-methyl styrene 495–499
ALEXANDRU T. BALABAN, NICOLAE NEGOIȚĂ, S. M. SHEIN and A.D. KHMELINSKAYA, Factors affecting stability and equilibria of free radicals. XVIII. Capto-dative (Push-pull) diarylaminyls with 2,4,6-tri-(methanesulphonyl)-phenyl or 2,4,6-tri-(N,N-dimethyl-sulphonamido)-phenyl groups 501–508
MIRCEA IOVU and STELIAN RADU, 4-benzyloxyazobenzenes synthesized by condensation of benzyl chloride with sodium salts of 4-hydroxy-azobenzenes 509–513
M. F. ABDEL MEGGED, M. EL BORAI, M. FAHMY and EL-SAIED A. ALY, Studies on the pyridyl-pyrazolone system. I. Some reactions with 3-(3′-pyridyl)-1-phenyl-2-pyrazolin-5-one 515–518
N. NAUM, GH. MIHĂILĂ, F. VITAN, P. ONU and D. GÂNJU, Alkylation of benzene with isopropanol 519–524
EMIL DUMITRIU, SPIRIDON OPREA and VASILE HULEA, Activity and selectivity of zeolite catalysts in *m*-xylene isomerization 525–532
GR. POP, M. BOZEȘANU, N. I. IONESCU, I. IOSIF and G. MUSCĂ, Distribution of products in methanol conversion over H–ZSM-5 type zeolites . 533–538
VICTOR DAVID, Informational entropy of the probability field events of a chemical control analysis 539–545

BOOK REVIEW 547–548

Rev. Roumaine chim. 32, 5, 455–548 (1987), Bucarest

Revue Roumaine de Chimie, 32, 5, 457–465 (1987)

THE COULOMETRIC STUDY OF THE Pb, PbO_2, $O_2/PbSO_4$ SYSTEM

S. STERNBERG*, A. MATEESCU**, V. BRÂNZOI* and LILIANA APĂTEANU***
* Polytechnic Institute of Bucharest, Dept. of Physical Chemistry, Bucharest, Romania
** Acumulatorul Entreprise of Bucharest, Romania
*** Biochemical and Chemical Energetics Institute of Bucharest, Romania

Received February 3, 1986

The polarization behaviour of the lead microelectrode, within the (+800 to +1650) mV potential range was studied using the potentiodynamic technique. Experimental results show that at the anodic potential sweep, $PbSO_4$ oxidation to PbO_2 takes place simultaneously with the O_2 evolution ; at the reverse potential scan a reduction peak is obtained, corresponding to the $PbO_2 \rightarrow PbSO_4 + 2e^-$ process. The coulometric ratios, calculated as a function of the higher limit of the potential scan range pointed out the following : the oxygen evolution is considerably reduced at potential up to +1600 mV ; within the potential ranges, with the superior limit of +1400 and +1500 mV, the main anodic reaction is that of the PbO_2 formation, while within the (+ 800 ÷ +1300) mV potential range, $Pb^{2+} \rightarrow Pb^{4+}$ oxidation process is in the incipient period. The values of the medium anodic and cathodic currents, calculated by us, by means of the coulometric measurements and of the polarization curves, confirm the behaviour of the PbO_2, $O_2/PbSO_4$ electrode, explained on the basis of the coulometric ratios.

INTRODUCTION

The lead and sulphate lead oxidation to lead dioxide, in sulphuric acid solutions, was studied because of the lead dioxide importance as positive electrode in the lead acid batteries. The literature[1-9] points out that in sulphuric acid solutions, by means of the successive recyclings, the $PbO_2/PbSO_4$ electrode capacity progressively increases, and after about 10 cycles a porous microelectrode is obtained, with both sufficiently high capacity and reproductible properties.

A similar behaviour displays sulphuric acid solutions with cobalt sulphate additions.[10]

The present paper shows the experimental results concerning the electrochemical behaviour of the PbO_2 positive electrode, obtained on pure lead by repeated cyclings, in sulphuric acid solutions. The potential was scanned in the anodic range ; the start potential was, for all determinations, +800 mV vs.$Hg/Hg_2SO_4/SO_4^{2-}$ reference electrode and the end potential was changed between +1300 and +1650 mV.

Unlike the paper [11] which showed the influence of the H_2SO_4 concentration within a constant range of the potential scan, the present paper shows the influence of the potential scan range (+800 mV — changeable end potential) on the complex electrode process, Pb, PbO_2 $O_2/PbSO_4$.

The anodic (Q_a) and cathodic (Q_c) electricity amounts were coulometrically measured.

EXPERIMENTAL PART

The determinations were carried out by means of the linear voltammetry method of low potential scan rate. The duration of the determinations was maintained constant but since the potetial range was changed, the potential scan rates were modified, within very small limits (see Table 1). The working electrodes were from pure lead, the surface exposed to the electrolyte being of 50 mm^2.

Table 1

Th e coulcmeter parameters of the polarization curves obtained on pure lead (for the 10th cycle) in 4.15 M H_2SO_4 solution

Potential range (mV)	Potential scan rate (mV/sec)	Q_a (C)	Q_c (C)	a	b	c	d
800 – 1650	6.85	2.303	0.1993	100	100	9.47	8.65
800 – 1600	6.45	2.100	0.1516	94.47	76.06	7.64	7.22
800 – 1500	5.64	0.1942	0.1249	3.30	62.66	180.14	63.32
800 – 1400	4.83	0 0877	0.05192	1.70	26.05	145.00	59.20
800 – 1300	4.03	0.02052	0.0055	0.71	2.75	36.66	26.82

Note : The coulometric parameters a, b, c and d were calculated by means of equations (3)–(6).

Before each deteimiation the electrodes were submitted to a mechanical and chemical cleaning treatment[8] and then they were electroetched (for 3 minutes) at a tension of 45 V/cel in a solution of $CH_3COOH + HClO_4$. Further the working electrodes were immersed in the cell for the electrochemical polarization. After the stabilization of the steady state potential the working electrode potential was scanned in the anodic range, starting from +800 mV, (vs. $Hg/Hg_2SO_4/SO_4^{2-}$ electrode, which will be denoted by MSE). The superior limit of the potential range was modified by steps of 50 mV starting from +1300 mV up to +1650 mV.

The potential scan was carried out by means of a Model 173 potentiostat-galvanostat (Princeton Applied Research) with coulometer (Model 179 Digital Coulometer).

The potential-current curves (the cyclovoltammograms) were registered by means of an X recorder.

The total anodic (Q_a) and cathodic (Q_c) electricity amounts were registered on the digital coulometer, simultaneously with the cyclovoltammograms recording. The electrolytes were 4.15 M sulphuric acid soutions and the temperature was 25 ± 0.1°C.

RESULTS AND DISCUSSION

Figure 1 shows the first ten successive cyclovoltammograms obtained on pure lead in 4.14 M sulphuric acid solutions, at the potential scan between +800 and +1300 mV (vs. MSE).

The polarization curves, from fig. 1, show that after 6–7 successiv cycles the shape of the voltammograms behaves reproductibly, with, an anodic (A_1) peak, corresponding to the oxidation reaction of

$3pPbO \cdot PbSO_4 \cdot H_2O$ to Pb_3O_4[12-14] and a cathodic (B_1) peak which represents the formed compounds reduction to lead sulphate.

Other authors[15-17] suppose that within this anodic potential range the α-PbO_2 formulation occurs, too, the peak corresponding to this crystallographic form of the PbO_2, being masked by the oxygen evolution wave. Comparison of fig. 1 with figures 2, 3 and 4 shows that the anodic electricity amounts (Q_a) as well as the cathodic one (Q_c) are much smaller within the (+800 ÷ +1300 mV) potential range. Hence, the main

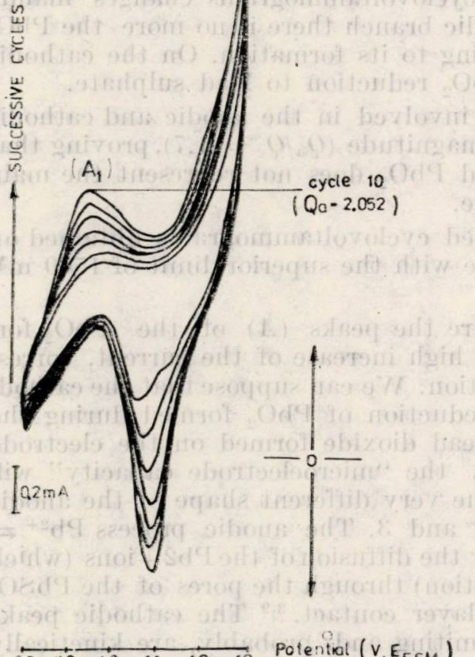

Fig. 1. — Polarization curves obtained on pure lead in 4.15 M H_2SO_4 solution. The (+800 ÷ +1300 mV) potential range.

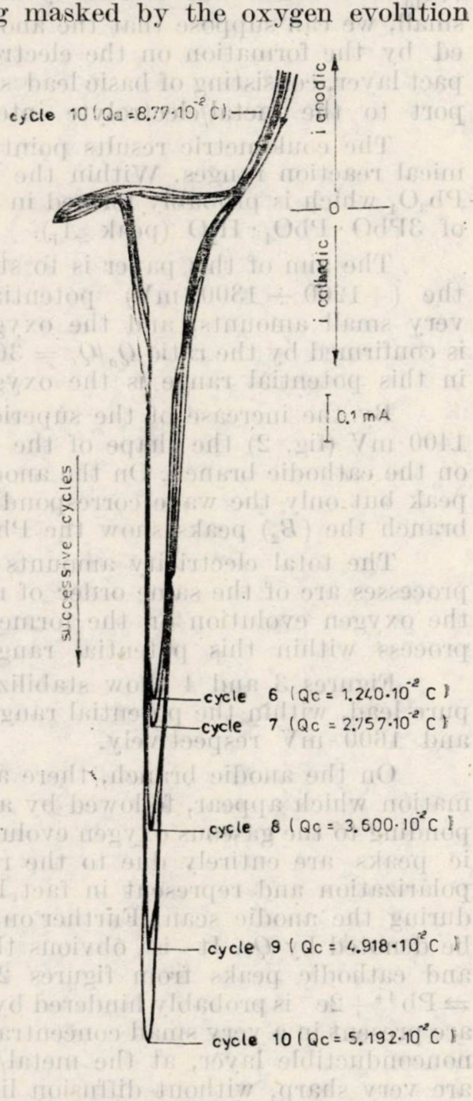

Fig. 2. — Polarization curves on pure lead, in 4.15 M H_2SO_4 solution. The (+800 — +1400 mV) potential range.

process of oxido-reduction, $PbO_2/PbSO_4$, occurs with very small currents within this range.

In our experiments, both anodic ($Q_{a_{10}} = 2.052 \cdot 10^{-2}C$) and cathodic ($Q_{a_{10}} = 0.055 \cdot 10^{-2}C$) electricity amounts, for the 10th cycle, being very small, we can suppose that the anodic and cathodic reactions are inhibited by the formation on the electrode surface of an adherent and compact layer, consisting of basic lead sulphates, which hinder the ions transport to the metal/electrolyte interface.

The coulometric results point out the existence of two electrochemical reaction ranges. Within the ($+800 \div +1100$ mV) range it is the Pb_3O_4 which is probably formed in very small amounts, by the oxidation of $3PbO \cdot PbO_4 \cdot H_2O$ (peak A_1).

The aim of this paper is to study the $PbO_2/PbSO_4$ process. Within the ($+1200 \div 1300$ mV) potential range the formation of PbO_2, in very small amounts, and the oxygen evolution start. This supposition is confirmed by the ratio $Q_a/Q_c = 36$, which shows that the main reaction in this potential range is the oxygen evolution.

By the increase of the superior limit of the potential range up to 1400 mV (fig. 2) the shape of the cyclovoltammograms changes mainly on the cathodic branch. On the anodic branch there is no more the PbO_2 peak but only the wave corresponding to its formation. On the cathodic branch the (B_2) peaks show the PbO_2 reduction to lead sulphate.

The total electricity amounts involved in the anodic and cathodic processes are of the same order of magnitude ($Q_a/Q_c = 1.7$), proving that the oxygen evolution on the formed PbO_2 does not represent the main process within this potential range.

Figures 3 and 4 show stabilized cyclovoltammograms obtained on pure lead, within the potential range with the superior limit of 1500 mV and 1600 mV respectively.

On the anodic branch, there are the peaks (A) of the PbO_2 formation which appear, followed by a high increase of the current, corresponding to the gaseous oxygen evolution. We can suppose that the cathodic peaks are entirely due to the reduction of PbO_2 formed during the polarization and represent in fact lead dioxide formed on the electrode during the anodic scan. Further on, the "microelectrode capacity" will be denoted by Q_c. It is obvious the very different shape of the anodic and cathodic peaks from figures 2 and 3. The anodic process $Pb^{2+} \rightleftarrows Pb^{4+} + 2e^-$ is probably hindered by the diffusion of the Pb2+ions (which are present in a very small concentration) through the pores of the $PbSO_4$ nonconductible layer, at the metal/layer contact.[3,9] The cathodic peaks are very sharp, without diffusion limiting and, probably, are kinetically controlled by the reduction of PbO_2, which is semiconductor and allows a cathodic process $Pb^{4+} + 2e^- \rightleftarrows Pb^{2+}$ occurring directly on the electrode surface. Hence the cathodic peaks represent a stripping processes (the reduction of PbO_2 without diffusion limiting).

It must be mentioned that in the conditions of the potential scan up to values higher than +1600 mV, the anodic oxidation occurs with a high excess of oxygen ($Q_a/Q_c = 11$).

Table 1 shows the coulometric parameters of cyclovoltammograms obtained on pure lead (for the 10th cycle) in 4.15 M H_2SO_4 solutions.

The Q_c amount practically equals the PbO_2 amount which forms during the anodic oxidation. Considering that the main electrode processes involved in Q_a and Q_c are the $Pb^{2+} \rightleftarrows Pb^{4+}$ oxidoreduction and the evolution of the gaseous oxygen, we can write the following relations:

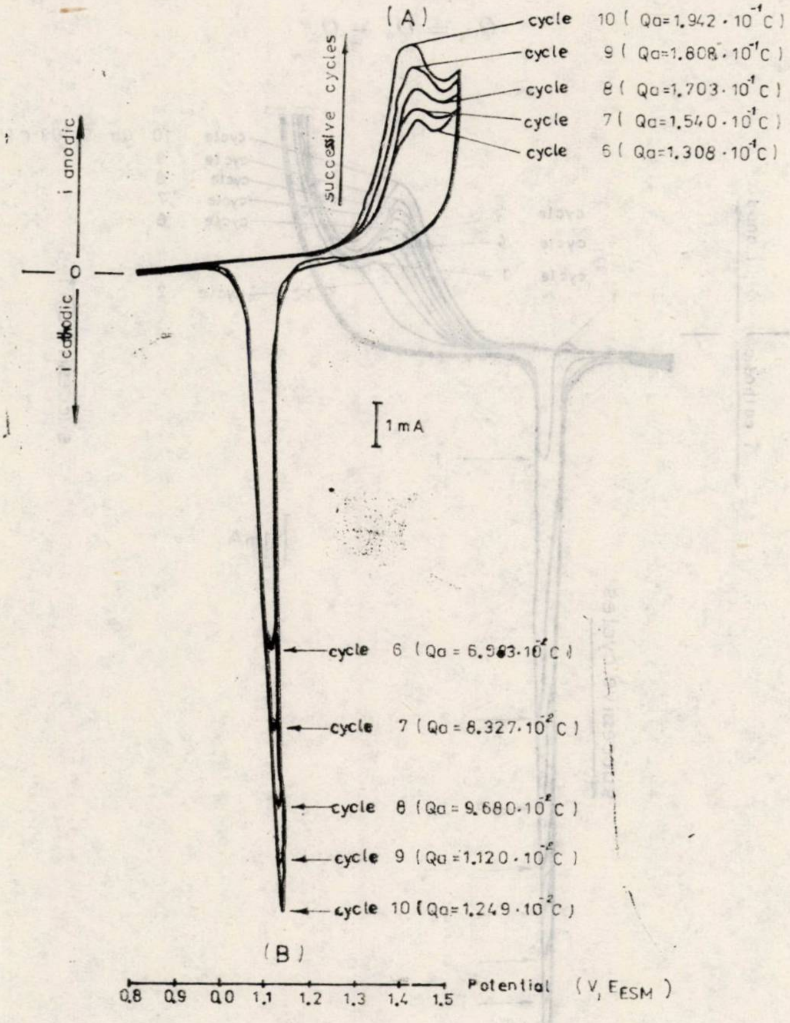

Fig. 3. — Polarization curves obtained on pure lead, in 4.15 M H_2SO_4 solution. The (+800 ÷ +1500 mV) potential range.

$$Q_a = Q_{PbO_2} + Q_{O_2} = Q_c + Q_{O_2} \tag{1}$$

where :

$$Q_{PbO_2}\ (\text{anodic}) = Q_{PbO_2}\ (\text{cathodically reduced}) = Q_c$$

Hence :

$$Q_{O_2} = Q_a - Q_c \qquad (2)$$

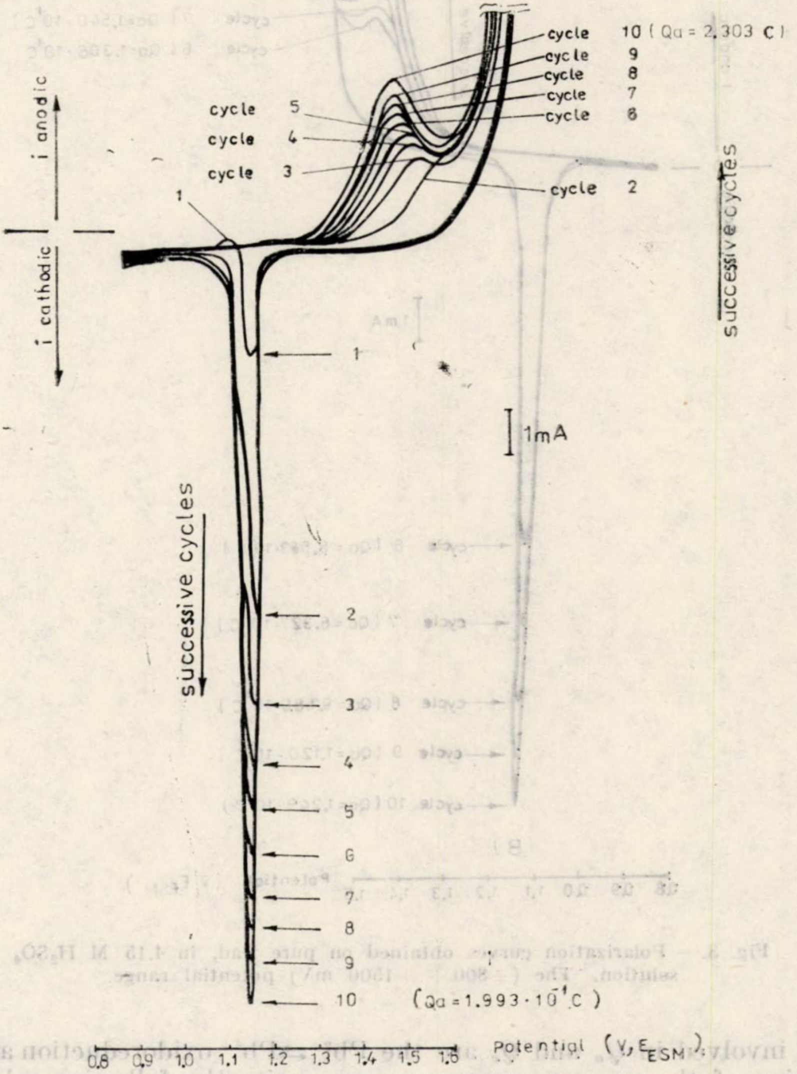

Fig. 4. — Polarization curves obtained on pure lead, in 4.15 M H_2SO_4 solution. The (+800 ÷ +1600 mV) potential range.

We can write also the following equations :

$$a = \frac{Q_{O_2}}{Q^0_{O_2}} \cdot 100 = \frac{Q_a - Q_c}{Q^0_a - Q^0_c} \cdot 100 \tag{3}$$

$$b = \frac{Q_{PbO_2}}{Q^0_{PbO_2}} \cdot 100 = \frac{Q_c}{Q^0_c} \cdot 100 \tag{4}$$

$$c = \frac{Q_{PbO_2}}{Q_{O_2}} \cdot 100 = \frac{Q_c}{Q_a - Q_c} \cdot 100 \tag{5}$$

$$d = \frac{Q_{PbO_2}}{Q_{total}} \cdot 100 = \frac{Q_c}{Q_a} \cdot 100 \tag{6}$$

where the superscript refers to the results obtained in the (+800 ÷ + +1650 mV) potential range.

The coulometric ratios a, b, c and d, defined by equations (3)—(6), give some interesting information concerning the influence of different factors on the electrode processes.

It is remarkable the fact that the "a" ratio decreases very much with the decrease of the potential range, proving that the O_2 evolution is disfavoured by the potential decrease, being well reduced at potentials below +1600 mV. Within the potential ranges with the maximum limits of +1400 mV and +1500 mV, the Q_a and Q_c amounts are of the same order of magnitude, showing that anodic reaction is mainly that of PbO_2 formation, accompained by the a reduction of oxygen evolution.

The "b" ratio shows also a decrease but of a smaller degree. The $Pb^{2+} \rightarrow Pb^{4+}$ oxidation process is disfavoured, especially within the potential range with the maximum limit of +1300 and +1400 mV ; the process of the formation of the Pb^{4+} ions is in the incipient period, if we take into account that the characteristic potential of the (A)—PbO_2-peak is of about +1467 mV (vs. MSE). [18]

Analysis of the "c" coulometric ratios shows that thery are of about 10% within the potential range with the maximum limit of +1650 mV, but become of about 180% when the potential changes till +1500 mV only. The coulometric ratio "d" shows a similar behaviour.

The "c" and "d" ratios give, in fact, the relative efficiency of the PbO_2 production vs. the oxygen ("c") or vs. the total anodic current ("d") respectively. The efficiency is most favourable at about +1500 mV, which is in fact the functioning way at the battery charging. At higher potentials, of +1600 and +1650 mV respectively, the "c" and "d" relative efficiencies decrease very much ; the coulometric ratio "b" increases at these potentials, showing that in the conditions of the high oxygen evolution, there is a supplementary amount of PbO_2 which forms, too. For example, the absolute amount of PbO_2 is higher at +1650 mV($Q_{c_{10}} = 1.993 \cdot 10^{-1}$C) than at +1600 mV ($Q_{c_{10}} = 1.516 \cdot 10^{-1}$C). The present coulometric analysis proves that the optimum conditions for the development of the $PbSO_4 \rightarrow PbO_2$ process are within the potential range with the maximum limit of +1500 mV. At potentials below 1500 mV (hence below A peak) the overvoltage of the PbO_2 formation is insufficient although within this range the oxygen concurrent evolution is negligible (the "*a*" parameter); however the absolute amount of PbO_2 is under that obtained in optimum conditions and "*b*" is respectivelly small.

Figure 5 shows the dependence of the medium anodic ($\bar{I}_a$) and cathodic ($\bar{I}_c$) currents on the maximum limit of each potential range under study.

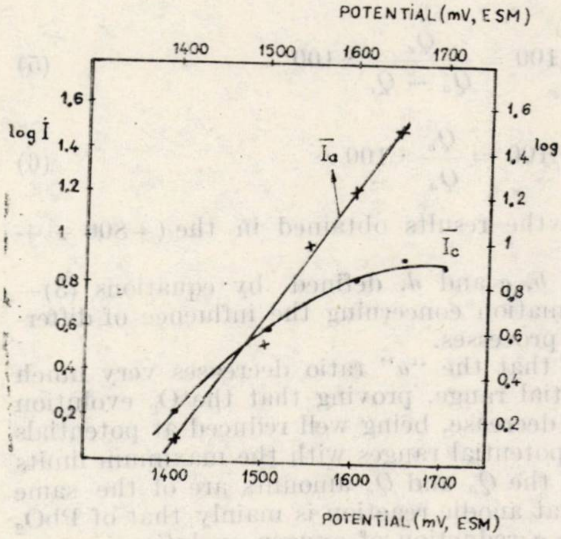

Fig. 5.— The dependence of the the medium anodic (I_c) and cathodic (I_c) currents on the maximum limit of the potential ranges under study.

The total electricity amount "Q" is given by the relation

$$Q = \int_{t_1}^{t_2} I \cdot \mathrm{d}t = \bar{I} \cdot t \qquad (7)$$

hence:

$$\bar{I}_a = \frac{Q_a}{t_{anodic}}$$

$$\bar{I}_c = \frac{Q_c}{t_{cathodic}}$$

The medium currents were obtained by dividing the total electricity amounts, for the anodic and cathodic processes, by a corrected time (anodic or cathodic). The anodic or cathodic corrected time was obtained by substracting from the total anodic or cathodic time the periods of quasi-null current, in which the intensity of processes is very small. For Q_a and Q_c this correction is negligible, while for the time it has significant values. By this way it is possible to obtain the medium currents for the main processes, $Pb^{2+} \rightleftarrows Pb^{4+}$ and the oxygen evolution, respectively. Hence, the coulometric measurements can be used for the calculation of the medium anodic and cathodic currents.

Figure 5 shows the existence of the ranges of the current variation as a function of the limit potential. Within the first range, till +1500 +1500 mV, the $\bar{I}_a$ anodic current is smaller than the cathodic one. Within this range, the main process is $PbSO_4 \rightleftarrows PbO_2$. The anodic current is smaller, proving a more increased irreversibility of the oxidation process, controlled by diffusion, comparatively with the reduction process, controlled by charge transfer. Within the +1500 ÷ 1550 mV there is a sudden increase of the anodic current, which, at +1650 mV becomes much higher than the cathodic one, because of the oxygen evolution. Hence, the method of the medium currents confirms, too, the electrochemical behaviour of the $PbO_2/PbSO_4$ electrode, found by discussion of the coulometric parameters and of the polarization curves.

REFERENCES

[1] G. W. Vinal, "Storage Batteries", Wiley, New York, 1965.

[2] P. Delahay and C. W. Tobias, "Advances in Electrochemistry and Electrochemical Engineering" vol. 8, Wiley, New York, 1971.

[3] P. Casson, N. A. Hampson and K. Peters, *J. Electrochem. Soc.*, **11**, (1977), p. 1655.

[4] J. E. Puzey and R. Taylor, in "Batteries 2", Edited by D. H. Collins, 1965, p. 29.

[5] L. Antropov, "Theoretical Electrochemistry", Mir, Moscow, 1975, p. 470.

[6] S. Sternberg, V. Brânzoi and L. Apăteanu, *Rev. Roumaine Chim.*, (in press).

[7] B. K. Mahato, *J. Electrochem. Soc.*, **126**, (1979) **365**.

[8] S. Sternberg, V. Brânzoi, L. Apăteanu and A. Mateescu, *Rev. Roumaine Chim.*, **28**, 583, (1983).

[9] S. Sternberg, A. Mateescu, V. Brânzoi and L. Apăteanu, *Rev. Roumaine Chim.*, **29**, 727, (1984).

[10] S. Sternberg, A. Mateescu, V. Brânzoi and L. Apăteanu, *Rev. Roumaine Chim.*, **30**, 955 (1985).

[11] S. Sternberg, A. Mateescu, V. Brânzoi and D. Mateescu, *Rev. Chim.* (*Bucureşti*), **33**, 1108, (1984).

[12] S. Sternberg and A. Mateescu, *Rev. Chim.* (*Bucureşti*), **35**, 510 (1984).

[13] S. Sternberg, A. Mateescu, V. Brânzoi and L. Apăteanu, *Rev. Roumaine Chim.*, **29**, 727 (1984).

[14] P. Ruetschi and R. T. Angstadt, *J. Electrochem. Soc.*, **111**, 1323 (1964).

[15] D. Pavlov and Z. Dinev, *J. Electrochem. Soc.*, **127**, 855, (1980).

[16] T. F. Sharpe, *J. Electrochem. Soc.*, **124**, 168, (1977).

[17] D. Pavlov and N. Iordanov, *J. Electrochem. Soc.*, **117**., 1103, (1970).

[18] T. Sharpe, *J. Electrochem. Soc.*, **122**, 845, (1975).

Revue Roumaine de Chimie, 32, 5, 467–475 (1987)

OPTICAL SPECTRA AND ELECTRONIC STRUCTURE OF SOME NITROTHIOAMIDE ANION RADICALS

MARIANA CIUREANU, MIHAELA HILLEBRAND, ELENA VOLANSCHI
and DANIELA GHEȚU
Department of Physical Chemistry, Polytechnic Institute Bdul. Republicii 13, Bucharest,
Romania

Received April 14, 1986

The electronic spectra of some nitrothioamide anion radicals are presented and discussed in terms of the influence of the relative position of the nitro and thioamide moieties and of the nature of the thioamide. MO calculations in the frame of the restricted method of Longuet-Higgins and Pople account well for the experimental transitions and for the main features of the electronic structure of these anion radicals.

Previous papers dealt with the electronic structure of the anion radicals provided by some nitrothiobenzamides and nitrocynammoylthioamides as reflected by the ESR spectra and spin density calculations. [1-3]

Further insight on the electronic structure of the anion radicals is provided by the study of the optical spectra.

It is the aim of this paper to report the visible spectra of the anion radicals presented in fig. 1 and to establish to which extent the results of the MO calculations account for the experimentally observed trends and, in general, for the main features of the electronic structure of these anion radicals.

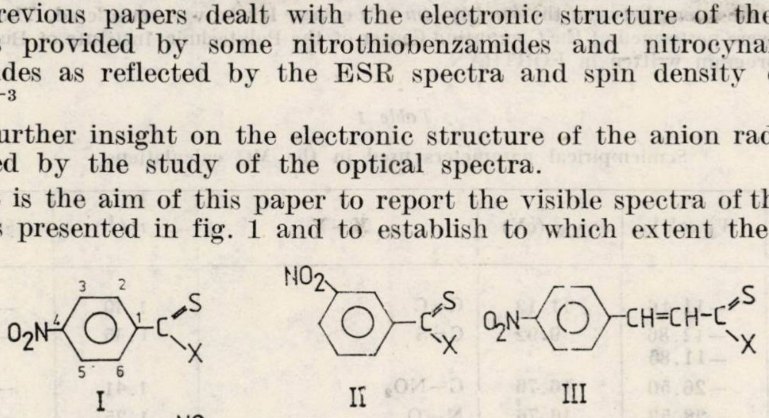

Fig. 1. — Investigated nitrothioamides. *a* — X = pyrrolidine ; *b* — X = = piperidine ; *c* — X = morpholine ; *d* — X = 3,5-dimethyl-morpholine ; *e* — X = homopiperidine.

As the UHF method used in the spin density calculations is not suitable for the electronic spectra, we used the restricted semiempirical PPP selfconsistent method in the version of Longuet-Higgins and Pople,[4] with the configurational interaction in the formalism of Ishitani and Nagakura,[5] and Carsky-Zahradnik.[6]

EXPERIMENTAL PART

The electronic spectra were recorded during the electrochemical reduction in a 1 cm-cell equipped with three electrodes. The two compartments were separated by a fritted glass and only the cathodic compartment was in the light-path. As solvent and supporting electrolyte dimethylsulphoxide (DMSO) and tetra-*n*-butylammonium perchlorate (TBAP) 0.1 M were used. The concentration of the substrate was in the range of $10^{-2}-10^{-3}$M. The chemical reduction in dimethylformamide (DMF) was performed in inert atmosphere using alkali metals (Li, Na, K) as reducing agents.

The optical spectra were registered on a SPECORD-UV-VIS spectrophotometer in the visible range.

MO calculations. The MO calculations were carried out by the method of Longuet-Higgins and Pople, using the parameters in Table 1. For the sulphur atom two values of the W_S parameter were tried, in order to evidence its influence on the energy levels.

From the thioamide saturated ring only the nitrogen atom was considered, with a different W_N parameter. For the nitrocynnamoyl thioamides two geometries were taken into account, corresponding to the *cis* and *trans* isomers.

The bielectronic mono- and bi-centric repulsion integrals were evaluated by the method of Pariser-Parr and, respectively Nishimoto-Mataga.

The configurational interaction (*CI*) of the ground (*G*) with 31 doublet excited states implying transitions between the $(m-4)\rightarrow(m+3)$ energy levels was considered. The MO calculations were performed at the Computing Center of the Polytechnic Institute of Bucharest, using a program written in FORTRAN.

Table 1

Semiempirical parameters used in the MO calculations

X	W_X (eV)	γ_{XX} (eV)	X−Y	r (Å)	β (eV)
$\dot{C}$	−11.16	11.13	C=C	1.40	−2.39
$\dot{S}$	−12.86 −11.86	9.92	C=S	1.65	−1.83
$\ddot{N}$	−26.50	16.76	$C-NO_2$	1.41	−2.60
$\ddot{N}(NO_2)$	−28.53	16.76	N−O	1.25	−2.60
$\dot{O}$	−17.28	15.23	$C-N_{(thioamide)}$	1.32	−2.32
			$C=C_{(vinyl)}$	1.34	−2.78
			$C_{(thioamide)}-C_{(ring)}$		−1.65
			$C_{(thioamide)}-C_{(vinyl)}$		−2.39
			$C_{(vinyl)}-C_{(ring)}$		−2.39

RESULTS AND DISCUSSION

a) Electronic spectra

Previous ESR studies pointed out that the main products of the electrochemical reduction of the investigated compounds are the anion radicals. The electronic spectra obtained in similar experimental conditions revealed two or several absorption bands in the visible range of the spectra, which could all be assigned either to the anion radicals, or to some secondary diamagnetic compounds, not identifiable by the ESR spectroscopy.

As the longest wavelength absorption band is the first to decay when the electrolysis is interrupted and the solution exposed to air (figure 2), it was assigned to the anion radicalic species.

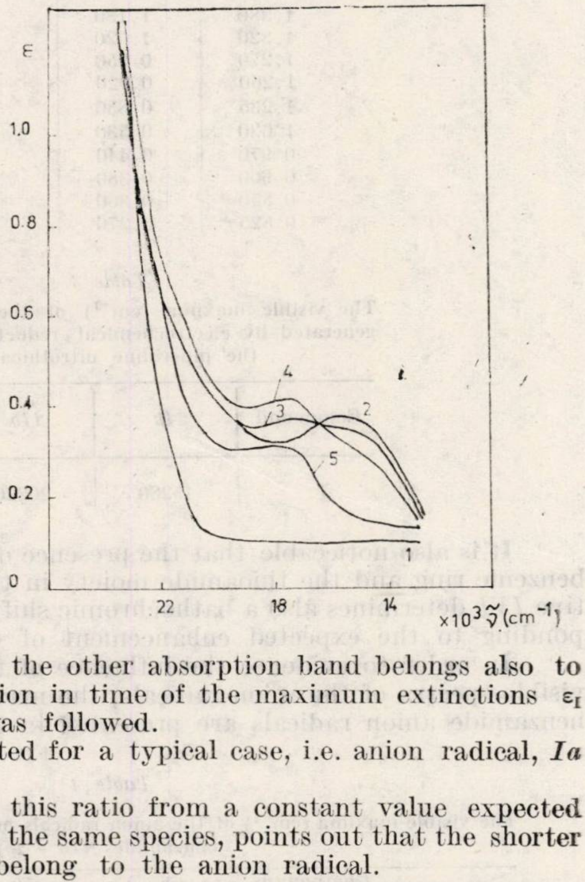

Fig. 2. — Time evolution of the electronic spectrum of anion radical *Ia* : *1* — initial ; *2* — on electrolysis ; *3*—*5* — on decay.

In order to establish if the other absorption band belongs also to the anion radical, the variation in time of the maximum extinctions ε_I and ε_{II} of the two bands was followed.

The ratio $\varepsilon_I/\varepsilon_{II}$, calculated for a typical case, i.e. anion radical, *Ia* is given in Table 2.

The large departure of this ratio from a constant value expected if both bands would belong to the same species, points out that the shorter wavelength band does not belong to the anion radical.

The position of the absorption band of the anion radicals is determined by two factors : firstly, by the relative positions of the nitro and thioamide groups, and secondly, by the structure of the thioamidic moiety.

The effect of the position of the nitro group is evidenced by the data in Table 3, which contains the absorption bands of the anion radicals provided by the piperidine nitrothiobenzamide and cynnamoyl derivatives.

Examination of the data in Table 3 reveals a significant bathochromic shift of the absorption of the *para*-(*Ib*) as compared to the *meta*-nitrothiobenzamide (*IIb*) anion radical, consistent with the increased conjugation between the two groups in the *para* position.

Table 2

The extinction values measured during the decay of the reduction products of *4*-nitropyrrolidine thiobenzamide (*Ia*)
($\tilde{\nu}_I = 18.000$ cm^{-1} ; $\tilde{\nu}_{II} = 16.000$ cm^{-1})

ε_I	ε_{II}	$\varepsilon_I/\varepsilon_{II}$
1.380	1.180	1.17
1.320	1.020	1.29
1.270	0.950	1.34
1.260	0.920	1.37
1.235	0.850	1.45
1.030	0.530	1.94
0.970	0.440	2.20
0.900	0.380	2.37
0.850	0.300	2.83
0.825	0.270	3.05

Table 3

The visible maxima (cm^{-1}) of the anion radicals generated by electrochemical reduction (DMSO) of the piperidine nitrothicamides

Compound	*Ib*	*IIb*	*IVb*
$\tilde{\nu}$	15280	20320	17920

It is also noticeable that the presence of a double bond between the benzenic ring and the thioamide moiety in the *3*-nitrocynnamoyl derivative *IVb* determines also a bathochromic shift as compared to *IIb*, corresponding to the expected enhancement of the aromatic conjugation.

In order to evidence the influence of the thioamide moiety on the visible spectra of the anion radicals, the maxima of different *4*-nitrothiobenzamide anion radicals are presented in Table 4. Inspection of these data points out a smaller influence of the nature of the thioamide, as compared to the relative positions of the nitro and thioamide groups. It may be also noted that the pyrrolidine and homopiperidine-thioamide

Table 4

The visible maxima (cm^{-1}) of the anion radicals provided by several *4*-nitrothiobenzamides (*Ia* — *Ie*).

Compounds / Reduction conditions	*Ia*	*Ib*	*Ic*	*Id*	*Ie*
Electrochemical (DMSO)	16080	15280	14560	15000	16000
Chemical (Na, DMF)	16000	—	15160	15040	16560

anion radicals exhibit absorption in the same range, while the absorption of the piperidine-, morpholine- and dimethylomorpholine-thioamide derivatives is shifted towards longer wavelengths.

In order to get more information about the reduction products, the chemical reduction using alkali metals was performed too ; the electronic spectra obtained are more complex than those registered during the electrochemical reduction, but the bands of the anion radicals are easily identified, as they are not significantly shifted (see i.e. the data in Table 4).

In conditions of prolonged chemical reduction and especially when potassium is used as reducible agent, a new band appeared at shorter wavelengths, which was assigned to a diamagnetic dianion (fig. 3).

A previous ESR study concerning the *4*-nitro-cynnamoylthioamide anion radical (*IIIc*) attested that during the reduction process a secondary reaction occurs leading to the anion radical of *4*-nitrobenzaldehyde. It was therefore expected that the study of the optical spectra of the reduction products will provide further information about this process. The electronic spectra obtained in different experimental conditions starting from *4*-nitrocynnamoyl thioamide (*IIIc*) were registered and are presented in Table 5.

The data in Table 5 point out that at the electrochemical reduction of *IIIc* one maximum is observed, while at chemical reduction an asymmetric band is obtained, the peak of which is shifted in time from about 14000 cm^{-1} towards 16700–17500 cm^{-1}. We assigned the peak at 14000 cm^{-1}, which appears from the very beginning of the reduction, to the anion radical of *IIIc*, and the maximum which appears in time

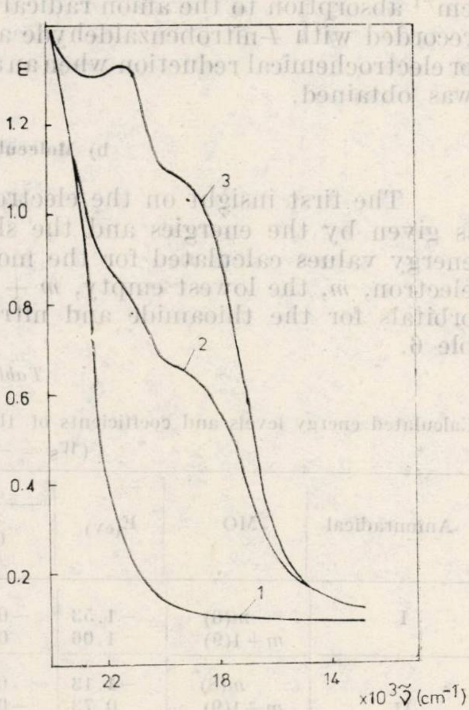

Fig. 3. — Electronic spectrum of anion radical *IVb* in conditions of prolonged reduction (K, DMF): 1 — initial; 2,3 — in time.

Table 5

Visible absorption bands (cm^{-1}) obtained at the reduction of *IIIc* in different experimental conditions

Conditions	electro (MDSO)	Li (DMF)	Na (DMF)	K (DMF)
$\tilde{\nu}$		14240	14000(sh)	14000(sh)
		14880	15200	15040
	17200	17500(sh)	16720	17000

(16700—17500 cm^{-1}) to the anion radical of a secondary product, that is the anion radical of 4-nitrobenzaldehyde (*V*). As the registration of the electronic spectrum at the *in situ* electrolysis requires an accumulation of the species, it is explainable that using this kind of reduction only the second radicalic species was obtained. The assigment of the 17500 cm^{-1} absorption to the anion radical *V* is further supported by the spectra recorded with *4*-nitrobenzaldehyde as starting material for both chemical or electrochemical reduction when an absorption band centered at 18000 cm^{-1} was obtained.

b) Molecular orbitals

The first insight on the electronic structure of the anion radicals is given by the energies and the shapes of the molecular orbitals. The energy values calculated for the molecular orbitals occupied by the odd electron, *m*, the lowest empty, $m + 1$, and the coefficients of the atomic orbitals for the thioamide and nitro group atoms are collected in Table 6.

Table 6

Calculated energy levels and coefficients of the A.O's in the *m*, *m + 1* molecular orbitals ($W_S = -12.86$)

Anionradical	MO	$E_{(eV)}$	Thioamide		Nitro-group		
			C_C	C_S	C_N	C_O	C_O
I	$m(8)$	−1.53	−0.27	0.26	−0.34	0.41	0.41
	$m+1(9)$	1.06	0.60	−0.39	−0.33	0.28	0.28
II	$m(8)$	−1.13	0.20	−0.17	−0.37	0.43	0.43
	$m+1(9)$	0.73	−0.61	0.43	−0.21	0.21	0.20
IV_{trans}	$m(9)$	−1.58	−0.25	0.25	−0.32	0.36	0.39
	$m+1(10)$	−0.11	0.37	−0.32	−0.32	0.33	0.34
IV_{cis}	$m(9)$	−1.73	−0.20	0.21	−0.34	0.39	0.36
	$m+1(10)$	−0.19	−0.37	0.32	0.28	0.29	−0.29

Examination of these data points out that in all the investigated compounds the molecular orbital of the odd electron is mainly delocalized on the nitro group, while the $m = 1$ orbital presents a larger contribution from the thioamide moiety, in agreement with previous UHF spin density calculations and ESR hyperfine patterns. The difference between the features of the *m*, and *m + 1* molecular orbitals is dependent on the extent of conjugation between the two fragments as determined by their relative positions and/or the presence of the vinylic bond. The greatest difference is thus observed for the anion radical *II*, for which the nitro and thioamide groups are in *meta* to each other and no vinylic bond is present.

The geometry chosen for the cynnamoyl anion radicals does not influence the preferential delocalization of the *m* orbital on the nitro group, which remains, like in anion radicals *I* and *II* very similar to the molecular orbital of the odd electron in a nitrobenzene derivative.

The energies of the *m* molecular orbitals are in agreement with the trend of the reducibility of the compounds, as evidenced by the previous experimental data, i.e. in the order *IV* > *I* > *II*. A higher reducibility of the *m*-nitrocynnamoylthiobenzamide when supposed in a *cis* as compared to a *trans* configuration is also to be noted.

The influence of the sulphur parameter W_S was also investigated and is reflected by the results for anion radical *I* (Table 7). It may be inferred that the change of W_S from −11.86 to −12.86 lowers the energy of both *m*, *m + 1* molecular orbitals, but does practically not affect their shape.

Table 7

The influence of the sulphur parameter (W_S) on the energy and shape of the *m*, and $m + 1$ molecular orbitals of a.r. *I*

W_S	MO	E(eV)	C_C	C_S	C_N	C_O	C_O
−11.86	*m*	−1.36	−0.22	0.27	−0.35	0.42	0.42
	m+1	1.28	0.59	−0.44	−0.31	0.26	0.26
−12.86	*m*	−1.53	−0.27	0.26	−0.34	0.41	0.41
	m+1	1.06	0.60	−0.39	−0.33	0.28	0.28

The charge distributions calculated for the ground state indicate in all the investigated compounds a high degree of polarisation of the nitro group, that is net charges of about −0.6 on the oxygen and +0.6 on the nitro group nitrogen atoms.

c) Electronic transitions

The experimental and calculated energies for the visible bands of the anion radicals are listed in Table 8, together with the contributions (percent) of the A, B, C_α, α and C_β– type configurations to the CI-excited states.

As the visible maxima are somewhat sensitive to the nature of the thioamide group or/and the reduction method, the spectral range within which the experimental values are found is given in Table 8.

For anion radical *IV*, the results for the two geometries used are listed and it may be observed that the differences noted are minor for both transition energies and CI-doublet state componence.

For all the investigated anion radicals the first two calculated transitions, mainly due to *m* → *m + 1* excited configurations, are situated in the near IR-range and were therefore not considered. The next calculated values listed in Table 8 are in good agreement with the experimental ones. They reflect the bathochromic shift in the sequence *II* → *I* → *IV* already discussed and dependent on the extension of the π-electronic system.

The data in Table 8 point out that, excepting anion radical *II*, the higher energy values belong to a transition from the ground to an excited CI-state with a major contribution of the B ($m \rightarrow m + 2$) excited configuration. As in our case the $m + 2$ orbital has in all the anion radicals a predominant benzenic character, the excited B($m \rightarrow m + 2$) state is to a great extent connected with an intramolecular charge transfer from the nitro group to the benzenic ring. This is evidenced by the calculated charge diagrams for the ground and excited $m \rightarrow m + 2$ states of i.e. anion radical *I* (Fig. 4).

Table 8

Experimentel and calculated transition energies and C.I. excited doublet states*
($W_S = -12.86$)

Anion radical	$h\nu_{exp}$ (eV)	$h\nu_{calc}$ (eV)	C.I., doublet states** (%)
I	1.82–2.33	2.25	22.00 A($m-1$, m) ; 33.64 B(m, $m+2$)
		2.37	10.89 A($m-1$, m) ; 62.41 B(m, $m+2$) ; 13.69 C($m-1$, $m+1$)
II	2.50–2.59	2.27	64.00 B(m, $m+2$) ; 21.16 B(m, $m+3$)
		2.54	16.81 A($m-2$, m) ; 59.29 C($m-2$, $m+1$)
IV	2.18–2.24	*cis*	
		1.87	27.04 A($m-1$, m) ; 42.25 C($m-1$, $m+1$)
		2.30	67.24 B(m, $m+2$) ; 26.01 B(m, $m+3$)
		trans	
		2.10	36.00 A($m-1$, m) ; 36.06 C($m-1$, $m+1$)
		2.32	70.56 B(m, $m+2$) ; 20.25 B(m, $m+3$)

* Only the doublet configurations with a contribution greater than 10% were considered.
** ($m-i$, m) stands for an excited configuration involving transitions between the ($m-i$) and m orbitals.

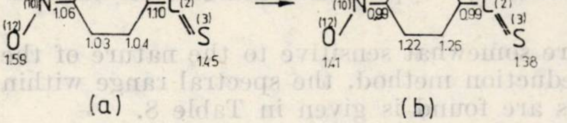

Fig. 4. — Calculated charge diagrams of the ground (a) and excited $m \rightarrow m + 2$ states (b), of anion radical *I*.

This behaviour is in agreement with the results found for the nitrobenzene anion radical, for which the visible band is generally interpreted in terms of a transition characterised by a significant charge transfer from the nitro to the benzenic ring.[7]

Taking into account this analogy with the nitrobenzene anion radical, we can ascertain that the MO calculations reflect the main features of the electronic structure of these anion radicals and outline the conclusion drawn from the experimental work on the dominant role of the nitro group as against the thioamide moiety.

REFERENCES

[1] C. Cercasov, F. Cornea, M. Ciureanu, M. Hillebrand, V. E. Sahini and E. Volanschi, *Org. Magn. Reson.*, **20**, 217 (1982).

[2] C. Cercasov, F. Cornea, M. Ciureanu, M. Hillebrand, V. E. Sahini and E. Volanschi, *Rev. Roumaine Chim.*, **20**, 25 (1984).

[3] M. Ciureanu, M. Hillebrand, V. E. Sahini and E. Volanschi, *Rev. Roumaine Chim.*, **30**, 97 (1985).

[4] H. C. Longuet-Higgins and J. A. Pople, *Proc. Phys. Soc.* (London), **A 68**, 591 (1955).

[5] A. Ishitani and S. Nagakura, *Theor. Chim. Acta.*, **4**, 236 (1966).

[6] P. Carsky and R. Zahradnik, *J. Phys. Chem.*, **74**, 1235 (1970).

[7] T. Shida and S. Iwata, *J. Phys. Chem.*, **75**, 2591 (1971).

Revue Roumaine de Chimie, **32**, 5, 477–487 (1987)

MAGNETO, SPECTRAL AND THERMAL INVESTIGATIONS OF COORDINATION COMPOUNDS OF LANTHANIDES(III) WITH 2-ETHOXYCARBONYLAMINOPYRIDINE

RAM KUMAR AGARWAL* and SUNIL KUMAR GUPTA

Department of Chemistry, Lajpat Rai Post-Graduate College, Sahibabad-201 005, Ghaziabad, India

Received April 26, 1986

Lanthanide(III) coordinated compounds of 2-ethoxycarbonylaminopyridine (Ecap) of the general composition $LnX_3.nEcap$ ($X = Cl$ or NCS ; $n = 3$; $X = NO_3$; $n = 2$; $X = ClO_4$; $n = 4$ and Ln = La, Pr, Nd, Sm, Gd, Tb, Dy, Ho or Yb) have been prepared in nonaqueous medium and characterized by chemical analyses, molar conductance, molecular weight, magnetism, IR and electronic spectral data. Ecap behaves as bidentate ligand and forms a six-membered chelate ring with metal ion. Conductance data of the compounds indicate 1 : 3 electrolytic nature of perchlorato complexes while the chloro, nitrato and thiocyanato complexes are nonelectrolytes. The coordination numbers of lanthanide(III) in these complexes have tentatively been assigned to be 8, 9 or 10 depending upon the nature of anions. Thermal properties of some of the representative complexes have also been investigated through t.g.a.

INTRODUCTION

Lanthanide(III) ions generally present very high coordination number and the type of polyhedron obtainable is influenced by the nature of the ligands.[1-7] Many good reviews and monographs on the coordination chemistry of lanthanides have appeared. The high coordination number in lanthanide complexes (six to twelve) may be attributed to steric factors and electrostatic forces of attraction and repulsion, rather than bond orientation by the well shielded 4f orbitals of the metal ion. Thus the relatively large size of the lanthanide ions and high positive charge (+3) generally allow accommodation of more than six donor atoms in the coordination sphere.[8] In this view, in the present work, we have synthesised a series of coordination compounds of 2-ethoxycarbonylaminopyridine (Ecap) with lanthanide(III) ions and studied the influence of anions in these coordination compounds.

EXPERIMENTAL

Analytical grade reagents were used in the present investigations. The ligand 2-ethoxycarbonylaminopyridine was prepared from 2-aminopyridine as follows. Ethyl chloroformate (66 mL) was added dropwise at 0°C to 2-aminopyridine (50 g) in pyridine (150 mL) with constant stirring. After *ca.* 2 hrs, the mixture was poured into ice cold water, which gives 2-ethoxycarbonylaminopyridine (Ecap). On crystallization, fine crystals of the Ecap were obtained.

---

* Author for correspondence.

Lanthanide chlorides, nitrates and oxide were obtained from Indian Rare Earths Ltd., Kerala State (India). The hydrated lanthanide perchlorates were prepared by dissolving the corresponding oxides in perchloric acid and evaporating the solution on a steam bath. Lanthanide(III) thiocyanates were prepared from nitrates as follows. A warm ethanolic solution (20 mL) of lanthanide nitrate (1.0 m mole) was added to a warm ethanolic solution (40 mL) of potassium thiocyanate (3.0 mmole). The solution evaporated to half volume was left overnight for complete precipitation of potassium nitrate, which was removed by filtration. The filtrate was used for complexation.

Isolation of the complexes

(a) *Preparation of the lanthanide chloride compounds*

1 mmole of the lanthanide chloride dissolved in 15 mL of methanol was mixed with 3.5 mmole of the ligand (in 30 mL of methanol) and heated on the steam bath, with stirring. On continuous heating ands stirring, a solid compound formed which was stirred with about 10 mL of benzene, filtered, washed with benzene and anhydrous diethyl ether, dried and preserved over phosphorus (V) oxide in a vacuum desiccator.

(b) *Preparation of the lanthanide nitrate compounds*

Lanthanide nitrate (1 mmole) dissolved in 15 mL of acetone was mixed with ligand (2.5 mmole in 20 mL of methanol) and heated on a steam bath with stirring for 1/2h. On cooling a solid mass was obtained, which was filtered, washed with acetone and anhydrous diethyl ether and dried over phosphosus (V) oxide in a vacuum desicator.

(c) *Preparation of the lanthanide(III) isothiocyanate compounds*

Lanthanide(III) thiocyanate (1mmole) in ethanol was mixed with the solution of Ecap (3.3 mmole) in methanol. The reaction contents were refluxed for about 1/2h. The mixtur was concentrated to one forth of its volume and on cooling a solid mass was obtained. The compound was filtered and dried as above.

(d) *Preparation of the lanthanide(III) perchlorate compounds*

Lanthanide(III) perchlorate (1 mmole) dissolved in ethyl acetate (10 mL) was added drop by drop to a solution of Ecap (4.5 mmole) in methanol (30 mL) with constant stirring and left the required reaction mixture overnight. The compound was obtained gradually, filtered, washed with ether and dried as above.

All the analyses and physical measurements were performed as reported earlier.[9,10]

RESULTS AND DISCUSSION

The analytical data presented in tables 1—4 indicate the general composition of the compounds as $LnX_3 \cdot nEcap$ ($X = Cl$, or NCS ; $n = 3$; $X = NO_3$; $n = 2$; $X = ClO_4$; $n = 4$ and $Ln =$ La, Pr, Nd, Sm, Gd, Tb, Dy, Ho or Yb). All the compounds are generally soluble in common organic solvents and the electrical conductances measured in nitrobenzene are consistent with the nonelectrolytic nature of chloro, nitrato and thiocyanato compounds, while the perchlorate compounds are 1 : 3 electrolytes. The molecular weights, determined cryoscopically in freezing nitrobenzene, support the same electrolytic behaviour of the compounds.

Table 1

Analytical, conductance and magnetic data of lanthanide(III) chlorides complexes of Ecap

Complex	Colour	Analysis % Found (Calcd.)			ΩM ohm^{-1}cm^2 mole^{-1}	Mol. wt. Found (Calcd.)	μ_{eff} B.M.
		Metal	N	Anion			
[La(Ecap)$_3$Cl$_3$]	White	18.56 (18.69)	11.19 (11.29)	14.20 (14.32)	3.9	736 (743.5)	Diamag.
[Pr(Ecap)$_3$Cl$_3$]	Light green	18.78 (18.91)	11.18 (11.26)	14.16 (14.28)	4.3	738 (745.5)	3.69
[Nd(Ecap)$_3$Cl$_3$]	Dull white	19.11 (19.23)	11.11 (11.22)	14.10 (14.22)	4.6	740 (748.5)	3.58
[Sm(Ecap)$_3$Cl$_3$]	White	19.73 (19.88)	11.02 (11.13)	13.91 (14.11)	3.8	745 (754.5)	1.82
[Gd(Ecap)$_3$Cl$_3$]	Dull white	20.43 (20.61)	10.92 (11.03)	13.81 (13.98)	4.9	751 (761.5)	7.77
[Tb(Ecap)$_3$Cl$_3$]	Yellowish white	20.68 (20.82)	10.89 (11.00)	13.78 (13.94)	4.1	753 (763.5)	9.39
[Dy(Ecap)$_3$Cl$_3$]	Dirty white	21.06 (21.20)	10.87 (10.95)	13.76 (13.89)	3.7	755 (766.5)	10.50
[Ho(Ecap)$_3$Cl$_3$]	White	21.31 (21.44)	10.80 (10.91)	13.72 (13.84)	4.8	759 (769.5)	10.45
[Yb(Ecap)$_3$Cl$_3$]	Yellowish white	22.13 (22.25)	10.69 (10.80)	13.57 (13.69)	3.8	768 (777.5)	4.63

Table 2

Analytical, conductance and magnetic data of lanthanide(III) nitrates complexes of Ecap

Complex	Colour	Analysis% Found (Calcd.)		ΩM ohm^{-1} cm^2 mole^{-1}	Mol. wt Found (Calcd.)	μ_{eff} B.M.
		Metal	N			
[La(Ecap)$_2$(NO$_3$)$_3$]	Dull white	20.92(21.15)	14.73(14.91)	3.9	649(657)	Diamag.
[Pr(Ecap)$_2$(NO$_3$)$_3$]	Pale yellow	21.26(21.39)	14.69(14.87)	3.6	651(659)	3.73
[Nd(Ecap)$_2$(NO$_3$)$_3$]	Dull white	21.63(21.75)	14.62(14.80)	4.3	655(662)	3.52
[Sm(Ecap)$_2$(NO$_3$)$_3$]	Pinkish white	22.32(22.45)	14.52(14.67)	4.2	658(668)	1.63
[Gd((Ecap)$_2$(NO$_3$)$_3$]	Dirty white	23.12(23.25)	14.36(14.51)	3.3	667(675)	7.68
[Tb(Ecap)$_2$(NO$_3$)$_3$]	White	23.37(23.48)	14.32(14.47)	3.9	669(677)	9.27
[Dy(Ecap)$_2$(NO$_3$)$_3$]	Dull white	23.69(23.87)	14.26(14.40)	4.6	671(680.5)	10.43
[Ho(Ecap)$_2$(NO$_3$)$_3$]	White	24.02(24.15)	14.26(14.34)	4.7	676(683)	10.52
[Yb(Ecap)$_2$(NO$_3$)$_3$]	Pinkish white	24.87(25.03)	14.06(14.18)	4.5	685(691)	4.53

Magnetic studies

Ion La^{3+} is diamagnetic as may be expected from its closed shell electronic configuration and absence of unpaired electrons. All other tripositive lanthanide ions are paramagnetic due to the presence of 4f electrons which are effectively shielded by 5s^{2}p^2 electrons. Since these electrons are well shielded from external influences, both their spin and orbital motions are significant in determining the overall observed magnetic moment for the coordination compound. Generally speaking the magnetic moment of a coordination compound should indicate whether or not

Table 3

Analytical, conductance and magnetic data of lanthanide(III) thiocyanate complexes of Ecap

Complex	Colour	Analysis % Found (Calcd.)			ΩM ohm^{-1} cm^2 mole^{-1}	Mol. wt. Found (Calcd.)	μ_{eff} B.M.
		Metal	N	Anion			
$[La(Ecap)_3(NSC)_3]$	Dull white	17.03 (17.13)	15.42 (15.53)	21.31 (21.45)	4.3	806 (811)	Diamag.
$[Pr(Ecap)_3(NCS)_3]$	Dirty white	17.26 (17.34)	15.38 (15.49)	21.25 (21.40)	4.9	808 (813)	3.69
$[Nd(Ecap)_3(NCS)_3]$	Dull white	17.55 (17.64)	15.35 (15.44)	21.18 (21.32)	3.9	809 (816)	3.62
$[Sm(Ecap)_3NCS)_3]$	Dull white	18.15 (18.24)	15.21 (15.32)	21.02 (21.16)	3.8	815 (822)	1.69
$[Gd(Ecap)_3(NCS)_3]$	Pale yellow	18.84 (18.93)	15.08 (15.19)	20.74 (20.98)	4.6	819 (829)	7.71
$[Tb(Ecap)_3(NCS)_3]$	Light brown	19.04 (19.13)	15.06 (15.16)	20.77 (20.93)	4.2	820 (831)	9.61
$[Dy(Ecap)_3(NCS)_3]$	Light brown	19.38 (19.48)	15.01 (15.10)	20.69 (20.86)	3.8	823 (834)	10.39
$[Ho(Ecap)_3(NCS)_3]$	White	19.60 (19.71)	14.94 (15.05)	20.62 (20.78)	4.6	832 (837)	10.61
$[Yb(Ecap)_3(NCS)_3]$	Reddish brown	20.35 (20.47)	14.81 (14.91)	20.43 (20.59)	4.8	839 (845)	4.63

Table 4

Analytical conductance and magnetic data of lanthanide (III) perchlorates complexes of Ecap

Complex	Colour	Analysis % Found (Calcd.)			ΩM ohm^{-1} cm^2 mole^{-1}	Mol. wt. Found (Calcd.)	μ_{eff} B.M.
		Metal	N	Anion			
$[La(Ecap)_4](ClO_4)_3$	Light yellow	12.51 (12.61)	10.06 (10.16)	26.82 (27.09)	78.9	279 (1101.5)	Diamag.
$[Pr(Ecap)_4](ClO_4)_3$	With	12.69 (12.77)	10.03 (10.14)	26.79 (27.05)	79.9	283 (1103.5)	3.71
$[Nd(Ecap)_4](ClO_4)_3$	Dull white	12.89 (13.01)	10.06 (10.12)	26.68 (26.97)	83.2	285 (1106.5)	3.60
$[Sm(Ecap)_4](ClO_4)_3$	Greenish yellow	13.31 (13.48)	9.95 (10.06)	26.63 (26.83)	81.9	286 (1112.5)	1.58
$[Gd(Ecap)_4](ClO_4)_3$	Light yellow	13.89 (14.92	9.91 (10.00)	26.58 (26.66)	80.6	288 (1119.5)	7.96
$[Tb(Ecap)_4](ClO_4)_3$	Dirty white	14.06 (14.17)	9.86 (9.98)	26.53 (26.61)	78.8	290 (1121.5)	9.51
$[Dy(Ecap)_4](ClO_4)_3$	Very light brown	14.32 (14.44)	9.83 (9.95)	26.42 (26.53)	82.9	292 (1125)	10.63
$[Ho(Ecap)_4](ClO_4)_3$	White	14.51 (14.63)	9.81 (9.93)	26.35 (26.47)	83.1	293 (1127.5)	10.57
$[Yb(Ecap)_4](ClO_4)_3$	Dull white	15.11 (15.23)	9.78 (9.86)	26.12 (26.28)	80.9	295 (1135.5)	4.62

these 4f electrons are involved in bond formation. The magnetic moments of the lanthanides coordination compounds show deviation from reported values.[11-15] The magnetic moments of the coordination compounds remain unchanged upon coordination with Ecap, indicating thereby that 4f electrons do not participate in bond formation. Furthermore, the magnetic moments of isolated coordination compounds are within the range of paramagnetic lathanide ions.[16,17] Similar behaviour of some lanthanide coordination compounds was recently reported.[18-20]

Infrared spectral studies

Assignments of the substituted pyridine bands are based on Katritzky's data for uncomplexed Ecap [21] and other works on monosubstituted pyridines. [22,23] There is as usual in such coordination compounds, a slight shift of most ring bands to higher wavenumbers on coordination. Of the amide bands, the CO stretching (amide I) and out-of-plane bending (amide VI) modes can be used to diagnose O or N coordination (Table 5). The decrease in frequency of band I and the increase in frequency of band VI on coordination confirm that the amide group is O-bonded in all complexes. Thus, Ecap acts as a bindentate ligand, coordinating through hetero N-atom and O of the amide group forming a stable six-membered ring. [24]

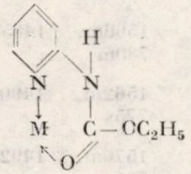

In far IR region ν (Ln—O) and ν (Ln—N) have been assigned at 435—410 cm^{-1} and 390—360 cm^{-1} region respectively. [4,25]

In nitrato compounds, the nonelectrolytic behaviour of these compounds in nitrobenzene suggests that all the nitrate groups are covalently bound, this being confirmed by the absence of a band at *ca.* 1360 cm^{-1} attributed to ionic nitrate. [7,26] Five bands attributed to the nitrate ions were observed for the corresponding compounds, indicating these ions are coordinated to the tripositive lanthanides. The nature of binding of the nitrate groups to the metal can be predicted by examining the combination bands in the 1700—1800 cm^{-1} region of the IR spectrum. [27-31] The spectrum of the coordination compounds of lanthanide nitrates containing only two combination bands with a separation of 30—45 cm^{-1} which lies in the range (30—55 cm^{-1}) reported for bidentate nitrate groups[29,31] reveals bidentate bonding of the nitrate groups in these coordination compounds.

The thiocyanato compounds show three bands in the region 2030—2020 cm^{-1}, 795—780 cm^{-1} and 475—465 cm^{-1}.[32] The perchlorate compounds show three bands at 1110—1105 cm^{-1} (ν_3), 930—925 cm^{-1} (ν_1)- and 625—620 cm^{-1} (ν_4) unsplit ν_3 and ν_4 a bands are consistent with the tetrahedral symmetry of the ionic perchlorate group in the coordination compounds.[33] The ν_1 band is normally not observed for it is a forbidden one for T_d perchlorate ion, however, it sometimes appears due to solid state effects.[34] In all the chloro compounds Ln—Cl stretching mode was assigned to the regions 250—230 cm^{-1}.[35]

Table 5

Partial infrared frequencies (cm^{-1}) of lanthanide(III) salts of Ecap

Complex	Pyridine vibrations ν(C=C), ν(C=N) ν(ring, vibration)	Amide I	Amide VI	ν(MO)	ν(M–N)
Ecap	1580s, 1545m, 1470m, 1000s, 770s	1720s	550m	—	—
$[La(Ecap)_3Cl_3]$	1605s, 1568m, 1480m, 1008m, 790s	1690s	582m	418m	362m
$[Pr(Ecap)_3Cl_3]$	1595s, 1562m, 1488m, 1015m, 782s	1702s	580m	410m	357m
$[Nd(Ecap)_3Cl_3]$	1592s, 1572m, 1486m, 1005m, 776s	1695s	590m	415m	350w
$[Sm(Ecap)_3Cl_3]$	1600s, 1560m 1485m, 1003m, 775m	1695s	588m	415m	362m
$[Gd(Ecap)_3Cl_3]$	1602s, 1566m, 1485m, 1018m, 780m	1698s	572m	412m	355m
$[Tb(Ecap)_3Cl_3]$	1592s, 1562m, 1490m, 1010m, 775s	1695s	580m	420m	360m
$[Dy(Ecap)_3Cl_3]$	1602s, 1570m, 1492m, 1010m, 785s	1703s	575m	416m	363w
$[Ho(Ecap)_3Cl_3]$	1602s, 1558w, 1482m, 1012m, 782s	1700s	575m	415w	362w
$[Yb(Ecap)_3Cl_3]$	1595s, 1562m, 1486m, 1015m, 780s	1698s	580m	412w	376w
$[La(Ecap)_2(NO_3)_3]$	1598s, 1572w, 1490m, 1012m, 778m	1699s	578m	418m	362m
$[Pr(Ecap)_2(NO_3)_3]$	1603s, 1560w, 1486m, 1015m, 782s	1695s	568m	422w	368m
$[Nd(Ecap)_2(NO_3)_3]$	1590s, 1562w, 1480m, 1005m, 780s	1700s	572m	415m	365m
$[Sm(Ecap)_2(NO_3)_3]$	1599s, 1557m, 1482m, 1008m, 785m	1706s	576m	418m	365m
$[Gd(Ecap)_2(NO_3)_3]$	1600s, 1555m, 1482m, 1006m, 786m	1702s	582m	410m	362m
$[Tb(Ecap)_2(NO_3)_3]$	1600s, 1568w, 1485m, 1010m, 785m	1705s	586m	415m	364m
$[Dy(Ecap)_2(NO_3)_3]$	1598s, 1565m, 1490m, 1010m, 785s	1702s	578m	412m	370m
$[Ho(Ecap)_2(NO_3)_3]$	1605s, 1565m, 1490m, 1012m, 788s	1698s	575m	416m	364m
$[Yb(Ecap)_2(NO_3)_3]$	1602s, 1566m, 1488m 1010m, 782m	1700s	576m	415m	360m

Table 5 (continued)

Complex	Pyridine vibrations $\nu(C=C)$, $\nu(C=N)$, ν(ring vibration)	Amide I	Amide VI	$\nu_{(MO)}$	$\nu_{(M-N)}$
$[La(Ecap)_3(NCS)_3]$	1600s, 1562m, 1482m, 1015m, 786m	1700s	582m	412m	365m
$[Pr(Ecap)_3(NCS)_3]$	1598s, 1568m, 1488m, 1002m, 780s	1695s	586m	410m	362m
$[Nd(Ecap)_3(NCS)_3]$	1595s, 1568w, 1485m, 1003m, 780s	1698s	578m	416m	368m
$[Sm(Ecap)_3(NCS)_3]$	1601s, 1565m, 1485m, 1012m, 780m	1705s	680m	415m	365m
$[Gd(Ecap)_3(NCS)_3]$	1596s, 1566m, 1490m, 1018m, 788m	1696s	582m	420m	365m
$[Tb(Ecap)_3(NCS)_3]$	1594s, 1560m, 1485m, 1018m, 788s	1708s	582m	415m	370m
$[Dy(Ecap)_3(NCS)_3]$	1601s, 1568w, 1486m, 1005m, 785m	1700s	586m	418m	364m
$[Ho(Ecap)_3(NSC)_3]$	1595s, 1570m, 1485m, 1010m, 780s	1698s	575m	418m	362m
$[Yb(Ecap)_3(NCS)_3]$	1598s, 1570w, 1490m, 1008m, 780s	1702s	570m	412m	362m
$[La(Ecap)]_4(ClO_4)_3$	1592s, 1560m, 1476m, 1018m, 782m	1693s	588m	410m	360m
$[Pr(Ecap)_4](ClO_4)_3$	1603s, 1568m, 1488m 1015m, 785m	1701s	590m	418w	362m
$[Nd(Ecap)_4](ClO_4)_3$	1596s, 1565m, 1480m, 1015m, 790s	1695s	576m	418m	362m
$[Sm(Ecap)_4](ClO_4)_3$	1605s, 1566m, 1480m, 1010m, 775s	1695s	576m	424m	365m
$[Gd(Ecap)_4](ClO_4)_3$	1600s, 1565w, 1482m, 1020m, 780m	1698s	575m	415m	366m
$[Tb(Ecap)_4](ClO_4)_3$	1598s, 1568w, 1480m, 1008m, 785s	1698s	580m	412m	365m
$[Dy(Ecap)_4](ClO_4)_3$	1592s, 1565m, 1485m, 1010m, 786m	1700s	576m	412w	362m
$[Ho(Ecap)_4](ClO_4)_3$	1660s, 1565m, 1482m, 1015m, 782m	1695s	584m	412w	370m
$[Yb(Ecap)_4](ClO_4)_3$	1702s, 1562w, 1488m, 1016m, 785s	1595s	576m	415m	368m

Electronic spectral studies

The utility of absorption spectra in ascertaining the nature of the band between the lanthanide ion and the surrounding donor group is limited. The observed bands are due to the transitions within the 4f levels which are least affected by changes in the environment and, therefore, there is substantial identity on the absorption spectra of the ion whether it is solvated or associated with any chelating group. However, small splittings of the characteristic bands are due to crystal field effects on J levels of the central ion.[36,37] Lanthanide(III) has no significant absorption in the visible region. The absorption bands of praseodymium(III), neodymium(III), samarium(III), gadolinium(III) and dysprosium(III) in the visible and near IR region appear due to transitions from the ground levels $^3H_4$, $^4I_{9/2}$, $^6H_{5/2}$, $^8S_{7/2}$ and $^6H_{15/2}$ to the excited J levels of 4f configuration, respectively. Some red shift or nephelauxetic effect is observed in DMF solution of these coordination compounds. This red shift is usually accepted as evidence of a higher degree of covalency than existing in the aquo compounds.[37,38] In all the coordination compounds marked enhancement in the intensity of the bands has been observed.

Thermal studies

Thermogravimetric results of the present coordination compounds are given in tables 6–9. There is no apparent weight loss up to 100°, and this clearly indicates the absence of water molecules in these coordination compounds. In chloro compounds 1.5 mole of ligand has been lost in 240–320°C temperature region and at ca. 500°C, all the ligand molecules have been lost. Finally at 710°C, stable lanthanide oxides are formed (Table 6).[18,39] Similar to chloro compounds, thiocyanato compounds lost 1.5 mole of ligand in 265–315°C and at 720°C, stable lanthanide oxides are formed (Table 7).

Table 6

Thermoanalytical results obtained for the complexes of formula $LnCl_3 \cdot 3Ecap$

Ln	Sample weight (mg)	Residual mass (mg)	Ligand mass loss (%)				Residue % ca. 710°C	
			240–320°C		340–500°C			
			Theor.[a]	Exp.	Theor.[b]	Exp.	Theor.[c]	Exp
La	26.56	6.14	33.49	34.94	66.98	68.82	21.92	23.12
Pr	27.32	6.57	33.40	34.86	66.80	68.62	22.84	24.06
Nd	21.39	5.05	33.26	34.52	66.53	68.29	22.44	23.64
Dy	23.20	5.91	32.48	33.98	64.97	66.92	24.33	25.50
Yb	25.10	6.70	32.02	33.32	64.05	65.54	25.33	26.72

[a] Calculated for 1.5 mole of ligand.
[b] Calculated for 3 mole of ligand
[c] Calculated as lanthanide oxide Ln_2O_3 and Pr_6O_{11}

Table 7

Thermoanalytical results obtained for the complexes of formula $Ln(NCS)_3 \cdot 3Ecap$

Ln	Sample weight (mg)	Residual mass (mg)	Ligand mass loss (%)				Residue %	
			265−315°C		350−510°C		ca. 720°C	
			Theor.[a]	Exp.	Theor.[b]	Exp.	Theor.[c]	Exp.
La	21.92	4.62	30.70	31.21	61.40	63.20	20.09	21.12
Pr	25.22	5.58	30.62	31.98	61.25	63.06	20.95	22.15
Tb	24.01	5.74	29.96	31.26	59.92	61.54	22.50	23.92
Ho	26.92	6.42	29.74	31.06	59.49	61.32	22.58	23.85
Yb	23.06	5.68	29.46	30.92	58.93	60.26	23.61	24.63

[a] Calculated for 1.5 mole of ligand.

[b] Calculated for 3 mole of ligand.

[c] Calculated as lanthanide oxide, Ln_2O_3. Pr_6O_{11} and Tb_4O_7.

Table 8

Thermoanalytical results obtained for the complexes of formula $Ln(NO_3)_4 \cdot 2Ecap$

Ln	Sample weight (mg)	Residual mass (mg)	Ligand mass loss (%)				Residue (%)	
			265−300°C		330−490°C		ca. 715°C	
			Theor.[a]	Exp.	Theor.[b]	Exp.	Theor.[c]	Exp.
La	26.62	6.97	25.26	26.62	50.53	52.16	24.80	26.20
Nd	28.92	7.69	25.07	26.49	50.15	51.52	25.37	26.62
Sm	25.10	6.85	24.85	26.08	49.70	51.30	26.04	27.32
Gd	23.69	6.66	24.59	25.96	49.18	50.62	26.81	28.12
Tb	24.39	7.31	24.51	25.92	49.03	50.42	27.62	29.98

[a] Calculated for 1 mole of ligand.

[b] Calculated for 2 mole of ligand.

[c] Calculated as lanthanide oxide, Ln_2O_3 and Tb_4O_7

Table 9

Thermoanalytical results obtained for the complexes of formula $Ln(ClO_4)_3 \cdot 4Ecap$

Ln	Sample weight (mg)	Residual mass (m)	Ligand mass loss (%)				Residue (%)	
			260−330°C		360−510°C		ca. 730°C	
			Theor.[a]	Exp.	Theor.[b]	Exp.	Theor.[c]	Exp.
Pr	25.49	4.17	37.60	39.56	60.17	62.56	15.43	16.39
Sm	23.79	3.92	37.30	39.20	59.68	62.41	15.64	16.49
Gd	21.72	3.76	37.07	39.12	59.31	62.06	16.16	17.32
Tb	27.31	4.89	37.00	39.96	59.20	62.01	16.67	17.92
Ho	26.05	4.67	36.80	38.82	58.89	61.98	16.76	17.96

[a] Calculated for 2.5 mole of ligand.

[b] Calculated for 4 mole of ligand.

[c] Calculated as lanthanide oxide Ln_2O_3, Pr_6O_{11} and Tb_4O_7.

The thermogravimetric curves of $Ln(NO_3)_4 \cdot 2$ Ecap indicate that above 265° the compounds start to lose mass with partial evaporation of the ligand. Up to the temperature of 300°C the loss of mass corresponds to one ligand. At temperatures close to 490°C the second mole of ligand is lost. The residues obtained after heating at 715°C to constant weight, are very close to that expected for the lanthanide oxides (Table 8). In perchlorato compounds within the temperature region 260—330°C, the loss of mass corresponds to 2.5 mole of ligands and at temperatures close to 510°C all the ligand is lost. Finally at ca. 730°C, stable lanthanide oxides are formed (Table 9). The decomposition temperature of these coordination compounds indicates that in general the thermal stability of the compounds falls in the order :

Nitrate $\sim$ Thiocyanate $>$ Perchlorate $>$ Chloride

ACKNOWLEDGEMENTS. The authors are thankful to the Council of Scientific and Industrial Research, New Delhi for financial support and Dr. G.D. Sharma, Principal, Lajpat Rai Post-Graduate College (Meerut University), Sahibabad (Ghaziabad) for taking keen interest throughout the work.

REFERENCES

[1] D. G. Karraker, *J. Chem. Educ.*, **47**, 424 (1970).

[2] T. Moeller, D. F. Martin, L. C. Thompson, R. Ferrus, G. R. Feistel and W. J. Randall *Chem. Rev.*, **65**, 1 (1975).

[3] T. Moeller, M.T.P. "International Review of Sciences. Lanthanides and Actinides" (Ed Bagnall, K.W.), Series 1, **7**, 275 (1972) Butterworths, London.

[4] J. H. Forsberg, *Coordination Chem. Rev.*, **10**, 195 (1973).

[5] T. Moeller, E. R. Birnbanu, J. H. Forshberg and R. B. Gayhart, "Progress in the Science and Technology of the Rare Earths" **3**, 61 (1968), Pergamon Press, Oxford.

[6] S. P. Sinha, "Complexes of the Rare Earths", Pergamon Press, Oxford (1966).

[7] S. Soundararajan, *Proc. Chem. Symp.*, Ist Sept. 1969, **1**, 203 (1970).

[8] D. Brown, "Inorganic Chemistry, Series 1 Lanthanides and Actinides" **7**, 87 (1972), Butterworths, London.

[9] M. C. Jain, R. K. Sharma, A. K. Srivastava and P. C., Jain, *J. Inorg. Nuclear Chem.*, **41**, 1305 (1979).

[10] R. K. Agarwal, Q. K. Srivastava and T. N. Srivastava, *Transition Met. Chem.*, **5**, 95 (1980).

[1] J. H. Van Vleck and A. Frank, *Phys. Rev.*, **34**, 1496, 1625 (1929).

[12] J. Zer Nicke and C. James, *J. Amer. Chem. Soc.*, **48**, 2827 (1926).

[13] B. Cabrera and A. Duperier, *Compt. rend.*, **188**, 1640 (1929).

[14] B. N. Figgis and J. Lewis, *Tech. Inorg. Chem.*, **4**, 137 (1965).

[15] T. Moeller, "Comprehensive Inorganic Chemistry", Pergamon Press, Oxford, 1973.

[16] A. Iandelli, "Rare Earth Research" Ed. Kleber, E.V. Macmillan.

[17] R. Didchenkov and F. P. Gortsema, *J. Phys. Chem. Solids*, **24**, 683 (1963).

[18] R. K. Agarwal and S. K. Gupta, *Thermochim. Acta*, **195**, 99 (1985).

[19] R. K. Agarwal, M.B.L. Sharma, and A. K. Srivastava, *Acta Chim.* (in press).

[20] R. K. Agarwal and S. K. Gupta, *Rev. Roumaine Chim.* (in press).

[21] A. R. Katritzky, *J. Chem. Soc.*, **1958**, 2202.

[22] J. H. S. Green, W. Kynaston and H. M. Paisley, *Spectrochim. Acta*, **19**, 549 (1963).

[23] R. E. Yingst and B. E. Douglas, *Inorg. Chem.*, **3**, 1177 (1964).

[24] J. Bould and B. J. Brisdon, *Inorg. Chim. Acta.*, **19**, 169 (1976).

[25] D. Y. West and C. L. Bielinski, *J. Inorg. Nucl. Chem.*, **42**, 229 (1980).

[26] N. S. Navaneetham and S. Soundararajan, *Current Sci.* (India), **47**, 655 (1978).

[27] N. F. Curtis, and Y. M. Curtis, *Inorg. Chem.*, **4**, 804 (1965).

[28] C. C. Addison, N. Logan, S. C. Wallwork and C. D. Garner, *Quart. Rev. Chem. Soc.*, **25**, 289 (1971).

[29] A. B. P. Lever, E. Montovani and B. S. Ramaswamy, *Canad. J. Chem.*, **49**, 1957 (1971).
[30] R. J. Foster and D. G. Hendriker, *Inorg. Chim. Acta*, **6**, 371 (1972).
[31] J. R. Ferraro, C. Cristallini and K. Fox, *J. Inorg. Nuclear Chem.*, **29**, 139 (1967).
[32] J. L. Burmeister, *Coord. Chem. Rev.*, **1**, 205 (1966); **3**, 225 (1968).
[33] D. M. Mehs and S. K. Mdan, *J. Inorg. Nuclear Chem.*, **30**, 3017 (1968).
[34] K. Nakamoto, "Infrared Spectra of Inorganic and Coordination Compounds", Wiley Interscience, New York, 1963.
[35] L. J. Basile, D. L. Gronert and J. R. Ferraro, *Spectrochim. Acta Part A.*, **24**, 707 (1968).
[36] C. K. Jorgen, *Progr. Inorg. Chem.*, **4**, 73 (1962).
[37] C. K. Jorgensen, *Z. Naturforsch.*, **19w**, 424 (1964).
[38] S. P. Sinha, *Spectrochim. Acta.*, **22**, 57 (1966).
[39] R. K. Agarwal and S. K. Gupta, *Thermochim. Acta* (in press).

Revue Roumaine de Chimie, **32**, 5, 489–494 (1987)

NEW COPOLYMERS CONTAINING PHENYLQUINOXALINE UNITS

V.V. KORSHAK*, E.S. KRONGAUZ*, N.M. BELOMOINA*, M. BRUMĂ**,
G. MANDRIC**,+ and C.I. SIMIONESCU**

* Institute of Element-Organic Compounds, Moscow, USSR
** P. Poni Institute of Macromolecular Chemistry, Iași, Romania

Received May 23, 1986

New polyphenylquinoxaline-benzimidazole-imide-amides have been synthesized by low temperature solution polycondensation of a diacid chloride containing preformed imide rings with two aromatic diamines one of which contains a preformed phenylquinoxaline while the other contains preformed benzimidazole units. The thermal stability as well as electrical properties of these copolymers are discussed and compared with related polymers previously synthesized.

INTRODUCTION

Previously reported papers on polyphenylquinoxalines showed that these polymers are of special interest owing to a convenient balance of properties such as high thermal stability and remarkable solubility and processability.[1] On the other hand polyimide[2] and polybenzimidazole[3] type polymers are also known for their excellent stability at high temperature along with good mechanical and electrical properties. A combination between all these structures into one macromolecular chain was a tentation to us, particularly when starting from monomers which contain already formed such heterocyclic rings.

The present paper describes the synthesis of new polyphenylquinoxaline-benzimidazole-imide-amides from monomers which incorporate each of these preformed heterocycles, introducing amide groups between aromatic and heteroaromatic rings.

RESULTS AND DISCUSSION

Polyphenylquinoxaline-benzimidazole-imide-amides have been synthesized by low temperature solution polycondensation of diaminophenylquinoxaline I and diaminobenzimidazole II taken into the molar ratio 1 : 1 with diacid chloride III, so that the amounts of diacid chloride and

---

+ Deceased

total diamine monomer are equimolecular. This reaction is shown in scheme 1 :

Scheme 1

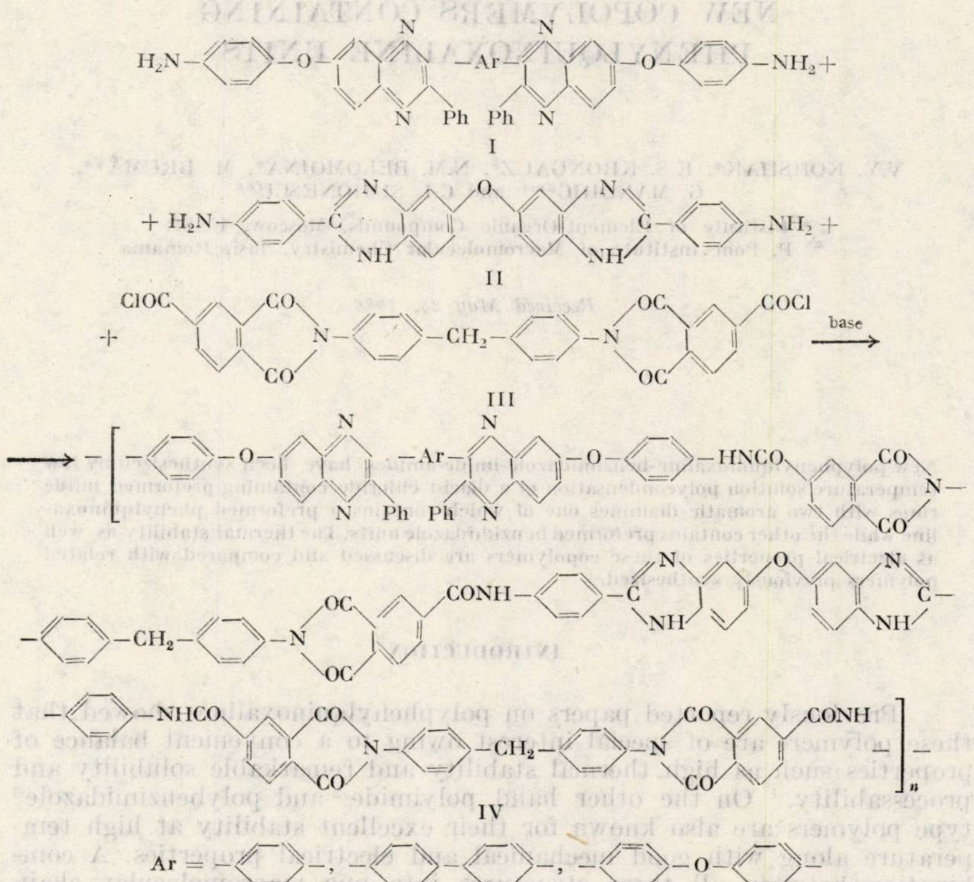

Table

Preparation of polyphenylquinoxaline-

Polymer	Diaminophenylquinoxaline 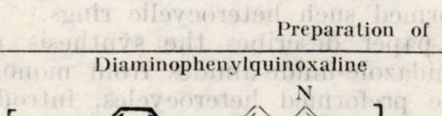	g
IVa	Ar = 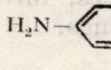	0.8759
IVb	Ar = 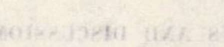	0.9710
IVc	Ar = 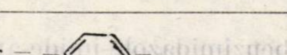	0.9911

The reaction was performed by adding the powdered diacid chloride to the mixture of the two diamines dissolved in N-methylpyrrolidone, the final polymer concentration being around 10%. In the end the viscous polymer solution was neutralized with pyridine, then diluted with N-methylpyrrolidone and precipitated by pouring into water. The fibrous polymer was filtered, washed with water and acetone and dried. The preparation of these copolymers is shown in table 1.

The structure of polyphenylquinoxaline-benzimidazole-imide-amides was identified by IR spectra and elemental analysis. Strong bands appeared at 1770—1780 cm^{-1}, 1710—1720 cm^{-1} and 710—720 cm^{-1} assigned to the imide ring. Likewise all spectra showed wide absorption bands at 3350 cm^{-1} characteristic for NH and 1660—1670 cm^{-1} due to CO in amide group. Absorptions situated at 1620, 1400 and 965 cm^{-1} were assigned to benzimidazole unit. Elemental analysis data for C, H, N are in good agreement with the calculated values.

All these polymers are soluble in polar aprotic solvents such as dimethylacetamide and N-methylpyrrolidone up to 35% concentration. Inherent viscosity is 0.6—0.7 dL/g measured in NMP at a concentration of 0.5 g polymer/100 mL at 20°C (Table 2).

The thermal stability of these copolymers was evaluated by thermogravimetric analysis (TGA) performed in air at a heating rate of 12°/minute. All polymers begin to decompose after 410° and at 500° the total weight loss is 13—16%. By comparing the thermal stability of the present polyphenylquinoxaline-benzimidazole-imide-amides with the other related polybenzimidazole copolymers such as polybenzimidazole-imide-amides[4] and polybenzimidazole-imides[5] the following order was found: polybenzimidazole — imides > polyphenylquinoxaline-benzimidazole-imide-amides ≈ polybenzimidazole-imide-amides. That means that the introduction of phenylquinoxaline unit into the macromolecular chain of polybenzimidazole polymers gave similar thermostabilities, but the solubility of these copolymers was much improved.

Comparison of polyphenylquinoxaline-benzimidazole-imide-amides with polyphenylquinoxaline-amide-imides previously reported[6] which had related structures but did not contain benzimidazole units, shows that their thermal stabilities are very similar. At the same time if

1

benzimidazole-imide-amides

Diaminobenzimidazole 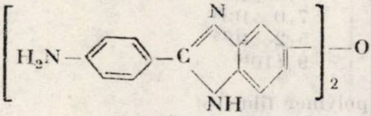 g	Diacid chloride 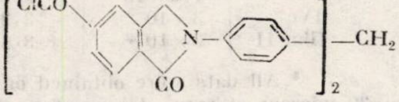 g	NMP mL	Conc. %
0.5406	1.4575	25	10.3
0.5406	1.4575	25	10.6
0.5406	1.4575	25	10.7

we compare the present polyphenylquinoxaline-benzimidazole-imide-amides with polyphenylquinoxaline-oxadiazole-imide-amides synthesized earlier,[7] we can see that the thermal stability of these two types of copolymers is almost the same. That means that the introduction of another heterocyclic unit into the chain of polyphenylquinoxaline-imide-amide polymers, even if this heterocycle is more thermostable, does not help to get higher thermostability of the final copolymers. The conclusion is that in all these quinoxaline-amide-imide polymers and copolymers the decomposition begins with the destruction of amide linkages. The important advantage of the introduction of phenylquinoxaline unit into these polymers is their remarkable solubility.

Table 2

Properties of polyphenylquinoxaline-benzimidazole-imide-amides

Polymer	$\eta_{inh.}$ *)	Elemental analysis						TGA***)	
		C %		H %		N %**)		Initial decomposition temperature, °C	Weight loss at 500°C, %
		Calcd.	Found	Calcd.	Found	Calcd.	Found		
IVa	0.7	74.58	72.51	3.74	4.51	10.47	9.82	415	13
IVb	0.6	75.27	73.55	3.97	4.32	10.11	9.60	410	15
IVc	0.6	74.73	72.96	3.76	4.19	10.04	9.41	410	16

*) Measured at a concentration of 0.5 g/100 mL NMP, at 20°C.

**) Determined by the Kjeldahl method.

***) Determined in air on "Paulik-Paulik — Erderly Derivatograph", at a heating rate of 12°/minute.

Electrical insulating properties of the polymers synthesized in this paper have been studied using polymer films of 30 microns thickness. These films have been obtained by pouring onto glass plates polymer solutions which resulted at the end of polycondensation reaction. All films were transparent and flexible. The values of dielectric loss tangent,

Table 3

Electrical insulating properties of polyphenylquinoxaline-benzimidazole-imide-amides*

Polymer	Dielectric loss tangent	Dielectric constant	Volume resistivity $\Omega \cdot$cm
IVa	6.4×10^{-3}	2.72	9.4×10^{14}
IVb	7.2×10^{-3}	3.6	7.0×10^{16}
IVc	3×10^{-3}	3.3	5.2×10^{15}
film H	3×10^{-3}	3·5	9×10^{16}

* All data were obtained on polymer films of 30 microns at room temperature, frequency 800 Hz, using a Differential bridge for dielectric constants and dielectric loss tangent, cf the type TR—9701 (Hungary).

dielectric constant and volume resistivity (Table 3) evidenced good electrical insulating properties comparable to those of polyimide film obtained from pyrromellitic dianhydride and 4,4′-diaminodiphenylether (filmH).

EXPERIMENTAL

Synthesis of monomers

Diaminophenylquinoxalines I were synthesized by condensation reaction of 3,4,4′-triaminodiphenylether (2 mol) with bis(α-diketones) such as 1,4-bis(phenylglioxalyl)benzene, 4,4′-bis(phenylglioxalyl)diphenyl and 4,4′-bis(phenylglioxalyl)diphenylether (1 mol) in ethanol at reflux temperature, according to a method indicated in the literature.[8]

2,2′-Bis(p-aminophenyl)-5,5′-bis(benzimidazolyl)ether II was obtained from 3,3′,4,4′-tetraaminodiphenylether and p-nitrobenzoic acid chloride using polyphosphoric acid as dehydrating reagent, following a method described previously.[5]

Methylene-bis-(N-(phenylene)-4′-(chloroformyl)phthalimide III was prepared by treating with excess thionyl chloride at reflux temperature the corresponding dicarboxylic acid which resulted from the reaction of 4,4′-diaminodiphenylmethane with trimellitic anhydride, as earlier reported.[9]

N-methylpyrrolidone (NMP) was dried over sodium hydroxide pellets and distilled over phosphorous pentoxide under reduced pressure.

Synthesis of polymers

Polycondensation was run under anhydrous conditions, in a nitrogen atmosphere, equimolecular amounts of diacid chloride and total diamine monomer being used in N-methylpyrrolidone as solvent. The following example illustrates the general procedure.

A three-necked flask equipped with mechanical stirrer and N_2-inlet and outlet was charged with 0.00125 mol diaminophenylquinoxaline and 0.00125 mol 2,2′-bis(p-aminophenyl)-5,5′-bis(benzimidazolyl)ether. 25 mL NMP were added and the mixture was stirred under nitrogen until complete dissolution. Then the solution was cooled to −5°C and 0.0025 mol diacid chloride was added under rapid stirring. The flask content was kept below −5° for 30 minutes then slowly raised to room temperature within other 30 minutes and kept at room temperature for 2 h. The clear yellow viscous solution was then neutralized with a few drops of pyridine. Half part of this solution was poured onto a glass plate (size 200 × 200 mm) and after evaporating the solvent at 100°C for 30 minutes, 150° for 1 h and 200° for other 30 minutes a flexible transparent film was obtained; it was used to measure electrical properties. The other part of polymer solution was dilluted with 10 mL NMP and was poured into 250 mL water under rapid stirring. The precipitated yellow polymer was filtered, washed there times each with 200 mL water, then with 100 mL acetone and dried in an oven at 150°C. Inherent viscosity is 0.6−0.7 dL/g. Electrical properties were measured on polymer films at room temperature using a Differential bridge for dielectric constants and dielectric loss tangent of type TR-9701 (Hungary).

CONCLUSIONS

Polyphenylquinoxaline-benzimidazole-imide-amides have been synthesized by low temperature solution polycondensation of two aromatic diamines containing preformed phenylquinoxaline and respectively benzimidazole units with a diacid chloride containing preformed imide rings. These polymers show high thermal stability, their decomposition temperature being over 410° which is very similar to related polyphenylquinoxaline-imide-amides and polyphenylquinoxaline-oxadiazole-imide-amides. Insulating properties measured on polymer films are comparable to those of polyimide film H.

REFERENCES

[1] E. S. Krongauz, *Vysokomol. Soedineniya*, A, **26**, 227 (1984).

[2] C. E. Sroog, *J. Polymer Sci., Macromol. Reviews.*, **11**, 161 (1976).

[3] G. Mandric, *Stud. Cercet. Chim.*, **20**, 1001 (1972).

[4] G. Mandric, G. Neamţu, S. Pecincu and G. Răcaru, *Rev. Roumaine Chim.*, **31**, 25 (1986).

[5] V. V. Korshak, A. I. Pavlov, G. Mandric and I. Zugrăvescu, *Rev. Roumaine Chim.*, **22** 1521 (1977).

[6] V. V. Korshak, E. S. Krongauz, N. M. Belomoina, M. Brumă, I. Diaconu and C. I. Simionescu, *Angew. Makromol. Chem.*, **144**, 129 (1986).

[7] V. V. Korshak, E. S. Krongauz, N. M. Belomoina, M. Brumă, I. Sava and C. I. Simionescu, *Rev. Roumaine Chim.*, **32**, 393 (1987).

[8] V. V. Korshak, E. S. Krongauz, N. M. Belomoina, H. Raubach and D. Hein, *Acta Polymerica*, **34**, 213 (1983).

[9] G. Neamţu and M. V Brumă, *Angew. Makromol. Chem.*, **103**, 19 (1982).

Revue Roumaine de Chimie, **32**, 5, 495–499 (1987)

CHAIN TRANSFER CONSTANTS FOR SOME AROMATIC SOLVENTS IN THE CATIONIC POLYMERIZATION OF α-METHYL STYRENE

A. RASHEED KHAN, TEHZEEB AKHTER and A.H.K. YOUSUFZAI
Pakistan Council of Scientific and Industrial Research
Laboratories, Karachi — 39, Pakistan

Received April 26, 1986

Cationic polymerization of α-methyl styrene in benzene, toluene and xylene has been carried out at 10°C using anhydrous aluminium chloride as initiator. The results indicate that rate of polymerization in different solvents is in the following order benzene ⊳ toluene ⊳ xylene. Molecular weight of the polymer depends upon solvent to solvent. Not only the solvents facilitate the initiation of cationic polymerization of α-methyl styrene but also partially serve as a chain transfer agent. The values of chain transfer constants measured for benzene, toluene and xylene are 19×10^{-3}, 15×10^{-3} and 9×10^{-3} respectively.

INTRODUCTION

The substitution of the α-hydrogen of styrene by a methyl group alters its tendency towards polymerization. Radical polymerization of the pure monomer proceeds very slowly[1–3] apparently because the double bond is made more negative. Homopolymers of α-methyl styrene may be easily prepared by cationic polymerization of the monomer in aromatic hydrocarbons (benzene, toluene etc.) using anhydrous aluminium chloride as catalyst. It is observed that the yield, viscosity, molecular weight even colour change with the solvents used as diluents. The lowering of molecular weight and viscosity of product might be due to the reaction between the reactive species and solvent. It needs the determination of chain transfer constants of such solvents. This paper deals with the cationic polymerization of α-methyl styrene in benzene, toluene and xylene using 5% anhydrous aluminium chloride as catalyst.

EXPERIMENTAL

Materials

1. α-Methyl styrene (BDH) was first washed with a sodium hydroxide to remove the inhibitor and then dried over anhydrous calcium chloride. It was then distilled at 165°C. The middle fraction was collected.
2. Anhydrous aluminium chloride (BDH) was used without further purification.
3. Laboratory reagent grade benzene, toluene, xylene were distilled before use.

Procedure of polymerization

The polymerization of α-methyl styrene was carried out in a three-neck round bottom flask fitted with a thermometer, stirrer and funnel and kept in an ice cold bath. Known quantities of solvent (Tables 1, 2, 3) and monomer in different proportions were added in the reaction flask. The mixture was stirred for 15 minutes and then 2.6 g anhydrous $AlCl_3$ were gradually added. During the addition of $AlCl_3$, the temperature was maintained at 10°C. The reactants were stirred for 4 hours. After the required reaction time, an aqueous solution of methanol (20 %) was added to the reactants. This was then transferred to a separating funnel and shaken well to remove castalyst residue. Methanol was added and shaken. The lower layer was collected. The solvents and unreacted monomer were distilled off. A semi-solid amber color substance was obtained. It became solid at freezing temperature. The substance was found soluble in most of the organic solvents. The softening range of the product is 38—45°C. The viscosity of dilute solutions of products prepared in toluene was measured at 30 ± 0.5°C using an ostwald type viscometer.

RESULTS AND DISCUSSION

Tables 1, 2 and 3 describe the results on cationic polymerization of α-methyl styrene in aromatic solvents e.g., benzene, toluene and xylene. In fig. 1 the rate of polymerization of α-methyl styrene ($R_p \times 10^{-5}$ moles/L) increases with increase of the monomer concentration. The rate of polymerization of α-methyl styrene in benzene, toluene and xylene was found in the following order: benzene>toluene>xylene.

Table 1

Cationic polymerization of α-methyl styrene in benzene using 5% anhydrous aluminium chloride as catalyst at 10°C for 4 hours

α-methyl styrene [M] moles/L	Benzene [S] moles/L	Conversion (g)	Number average molecular weight $\overline{Mn}$	Degree of polymerization $\overline{DP} \times 10^{-1}$
3.0158	6.8437	10.624	1735	147
3.7883	5.7234	14.530	2230	189
4.5513	4.5902	18.398	2903	246
6.1056	2.3092	20.654	3044	258

Table 2

Cationic polymerization of α-methyl styrene in toluene using 5% anhydrous aluminium chloride as catalyst at 10°C for 4 hours

α-methyl styrene [*M*] moles/L	Toluene [*S*] moles/L	Conversion (g)	Number average molecular weight $\overline{Mn}$	Degree of polymerization $\overline{DP} \times 10^{-1}$
2.9886	5.7498	9.418	2100	178
3.7528	4.8137	12.823	2490	211
4.5246	3.8689	13.465	3186	270
6.0880	1.9521	17.773	3328	282

Table 3

Cationic polymerization of α-methyl styrene in xylene using 5% anhydrous aluminium chloride as catalyst at 10° for 4 hours

α-methyl styrene $[M]$ moles/L	Xylene $[S]$ moles/L	Conversion (g)	Number average weight $\overline{Mn}$	Degree of polymerization $\overline{DP} \times 10^{-1}$
1.4726	6.5570	3.453	1876	159
2.9760	4.9696	7.546	3222	273
4.5109	3.3477	13.084	3363	285
6.0780	1.6916	15.392	4130	350

This might be due to the propagating species (solvent — separated ion pair and free ions) produced by the polymerization of α-methyl styrene in benzene which are more efficient than those produced in toluene and xylene. Beside this α-methyl styrene was also polymerized in the absence of any diluent (solvent). The resulting less viscous polymer with low conversion shows that the solvents are advantageous for obtaining uniform high polymers instead of dimers, trimers etc.

The viscosity of the dilute solutions of poly(α-methyl styrene) was measured at 30 ± 0.5°C. The average molecular weight $(\overline{Mn})$ of the polymer samples was calculated by using the following relationship[4]:

$$[\eta] = 0.923 \times 10^{-4}\, \overline{Mn}^{0.72} \qquad (1)$$

where $[\eta]$ is the intrinsic viscosity in dL/g of the polymer solution prepared in toluene. It is obtained by the intercept of the plot η_{sp}/C VSC. Here η_{sp} is the specific viscosity and C is the concentration of solution. The number average molecular weight of poly(α-methyl styrene) prepared in benzene was in the range 1735—3044 (Table 1) whereas in toluene and xylene, the range was 2100—3328 and 1876—4130 respectively (Tables 2 and 3). These results indicate that the average molecular weight of poly(α-methyl styrene) depends upon the solvent used.

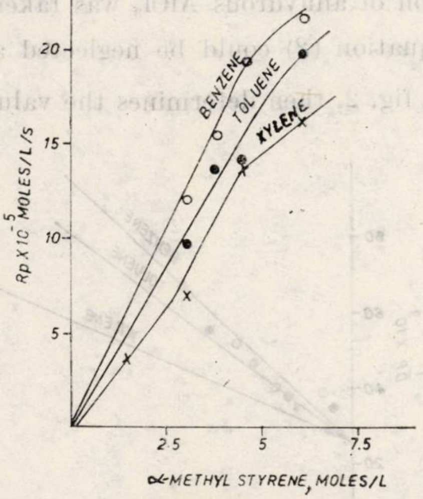

Fig. 1. — Plot showing the rate of polymerization of α-methyl styrene in the presence of benzene (○) toluene (●) and xylene (x).

The results summarized in tables 1, 2 and 3 indicate that the degree of polymerization $(\overline{DP})$ of α-methyl styrene decreases with increase of the solvent concentration. It varies from solvent to solvent. The value of $\overline{DP}$ is higher in the solvent possessing the higher dielectric constant (benzene 2.2628, toluene, 2.3661 and xylene 2.374).[5] The conversion of the monomer into polymer, its molecular weight and degree of polymerization of α-methyl styrene show that not only benzene, toluene and xylene serve as reaction medium but also help in transferring and terminating the grown polymer chain of α-methyl styrene. Furthermore at an early stage, α-methyl styrene in the form of dimers or trimers[6] also acts as an active hydrocarbon chain transfer agent. The chain transfer constant due to aromatic solvents may be determined by the following equation of Mayo [7]:

$$\frac{1}{\overline{DP}} = \frac{(K_1K_3)^{1/2}B^{1/2}}{K_2[M]^{1/2}} + \frac{K_4}{K_2} + Cs\frac{[S]}{[M]} \qquad (2)$$

where $[M]$, $[S]$ and B are respectively the concentration of monomer, solvent and catalyst, $\overline{DP}$ is the degree of polymerization, and K_1, K_2, K_3 and K_4 represent the rate constants for initiation, propagation, termination and monomer transfer respectively. Since the fixed concentration of anhydrous $AlCl_3$ was taken in each experiment, the first term of equation (2) could be neglected and the slope of the plot $\frac{1}{\overline{DP}}$ *vs* $\frac{S}{M}$ in fig. 2, then determines the value of chain transfer constant. The chain transfer constant thus obtained from this plot for benzene is 19×10^{-3} while for toluene and xylene these are 15×10^{-3} and 9×10^{-3} respectively. It can be concluded from these findings that the molecular weight of the polymer depends upon the nature of the reaction medium or diluents. It increases with increase in dielectric constant of the solvent. Not only the solvents serve as reaction medium (solvation effect) but also partially act as chain transfer agents. The higher the value of chain transfer constant, the lower the molecular weight of the polymer formed in the presence of a given amount of a chain transfer agent.

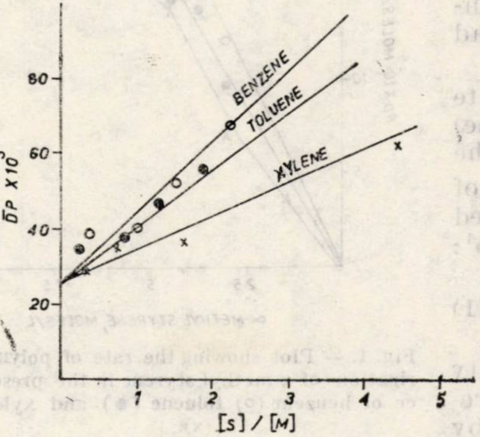

Fig. 2.—Effect of benzene (○), toluene(●) and xylene(x) on the degree of polymerization of α-methyl styrene.

All the polymer samples are semisolid amber colour substances which softens at 38—45°C. The low molecular weight poly(α-methyl styrene) is commercially very important and is widely usedas plasticiz)er in paints, waxes, polishes, adhesives and plastics. It may be used in the preparation of pressure sensitive tapes by blending with elastomers.

REFERENCES

[1] A. Rasheed Khan and A. H. K. Yousufzai, *J. Macromole Sci-Chem.* (in press).
[2] A. Rasheed Khan, A. H. K. Yousufzai and Tehzeeb Akhtar, *Pakistan J. Sci. Ind. Res.* (in press).
[3] Cf. G. Smets and L. D. Haes, *Bull. Soc. chim. belges*, **59**, 13 (1950).
[4] "Encyclopedia of Polymer Science and Technology", Vol. 13, Wiley-Interscience, New York 1970, p. 187.
[5] D. C. Pepper, *Nature London*, **158**, 789 (1941).
[6] "Encyclopedia of Chemical Technology", Vol. 19, Wiley New York, 1969, p. 115.
F. R. Mayo, *J. Amer. Chem. Soc.*, **65** 2324 (1943).

Revue Roumaine de Chimie, 32, 5, 501–508 (1987)

FACTORS AFFECTING STABILITY AND EQUILIBRIA OF FREE RADICALS. XVIII.[1]

CAPTO-DATIVE (PUSH-PULL) DIARYLAMINYLS WITH 2,4,6-TRI-(METHANESULPHONYL)-PHENYL OR 2,4,6-TRI-(N,N-DIMETHYL-SULPHONAMIDO)-PHENYL GROUPS

ALEXANDRU T. BALABAN,[a] NICOLAE NEGOIŢĂ,[b] S. M. SHEIN[c] and
A. D. KHMELINSKAYA[c]

[a] Polytechnic Institute, Department of Organic Chemistry, Splaiul Independenţei 313, 76206 Bucharest, Romania

[b] Institute of Nuclear and Engineering Physics, Bucharest

[c] Institute of Organic Chemistry of the Siberian Branch of the U.S.S.R. Academy of Sciences, Novosibirsk 90, U.S.S.R.

Received November 22, 1986

2,4,6-Tri-(methanesulphonyl)-phenyl-4′-tolylaminyl (Ia), and -4′-anisylaminyl (Ib), 2,4,6-tri-(dimethylamino-sulphonyl)-4′-tolylaminyl (IIa) and -4′-anisylaminyl (IIb) were prepared by oxidizing the corresponding diarylamines. These persistent capto-dative (psuh-pull) free radicals can be conserved in benzene solution at room temperature. Their ESR spectra were recorded and their hyperfine coupling constants were determined. Most of the spin density is located on the donor group, and no splitting is observed for protons or nitrogens attached to sulphonyl groups.

INTRODUCTION

A previous paper in this series [2] described push-pull (capto-dative, using the denomination introduced by Viehe [3]) diarylaminyls which were persistent in solution at room temperature; they had one acceptor aryl group (2,4,6-trinitrophenyl or 2,6-dinitrophenyl) and one donor aryl group (4-methoxyphenyl, 4-dimethylaminophenyl, or 4-diarylaminophenyl). A 2-, 3-, or 4-tolyl group as donor gave no detectable aminyls in these conditions, apparently because it was too weak a donor. On using a 2,4-dinitrophenyl group as an acceptor, no persistent aminyls were detected under the same conditions, probably because in this case the aminyl nitrogen was no longer sterically hindered.

More recently, Katritzky and coworkers [4] called such push-pull electronic stabilization "merostabilization" and gave other instances where it operated. Viehe and coworkers[3,5] introduced the term "capto-dative" for push-pull stabilization, and prepared new capto-dative carbon free radicals which were persistent. Other references on capto-dative free radicals are quoted in recent papers.[6]

Not only did 2,4-dinitrophenyl groups as acceptor yield undetectable diarylaminyls, [2] such groups also led to less persistent hydrazyls[7,8] than 2,6-dinitrophenyl or picryl groups. Again, this may be due to a steric effect (in 2,4-dinitro-substituted compounds only one *ortho*-position relative to the aminyl nitrogen is sterically shielded, while in the other cases this aminyl nitrogen is completely screened by the two bulky *ortho*-nitro groups), or to the effect of blocking a reactive position (in 2,4-dinitro-substituted compounds, the remaining *ortho*-hydrogen may undergo inter- or intramolecular substitutions).

Earlier, we reported the preparation of polynitrophenyl-alkoxyamines, having 2,4-di-, 2,6-di-, or 2,4,6-trinitrophenyl acceptor groups, and methoxy, ethoxy, or isopropoxy donor groups. [9] In all these cases, persistent aminyls were obtained on oxidation at 0—30° with lead tetraacetate in oxygen-free benzene, having fairly complicated ESR spectra; the initially formed radicals with 2,4- or 2,6-dinitrophenyl groups underwent a conversion into different radicals with simpler ESR spectra presenting a triplet of multiplets due to one larger nitrogen hyperfine coupling constant (hfc), probably owing to disproportionation into picryl-derivatives; again, the 2,4-dinitrophenyl-derivatives underwent this conversion faster than the other derivative. [10]

Since polynitrophenyl groups have so many atoms with non-zero nuclear spins (two or three protons, three or two nitrogens), the ESR spectra of all the above aminyls are so complicated that only the major splitting due to the aminyl nitrogen can be obtained in most cases. On the other hand, previous results indicated that sulphonyl groups are bulky, strongly acceptor substituents like nitro groups, but they relay little[11-14] spin density so that the ESR spectra are much simpler in arylsulphonyl-hydrazyls than in polynitrophenyl-hydrazyls having the same donor groups.

Having developed in USSR on the hand convenient syntheses for halobenzenes with methanesulphonyl or dimethylamino-sulphonyl (dimethylsulphonamido) substituents, which facilitate nucleophilic substitution of the halogen by arylamino groups, and on the other hand possessing in Romania experience in preparing aminyls and in interpreting their ESR spectra, we now report the synthesis of four capto-dative (push-pull) diarylamines (IHa, IHb, IIHa, IIHb) and of the corresponding diarylaminyls (Ia, Ib, IIa, IIb) with 4-methyl (a) or 4-methoxy substintuets (b). Compounds I have as acceptor group 2,4,6-tri-(methanesulphonyl)-phenyl, while compounds II have 2,4,6-tri-(N,N-dimethylsulphonamido)-phenyl or -(dimethylamino-sulphonyl)-phenyl substituents.

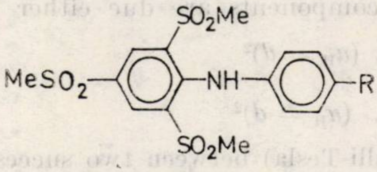
SO2Me
MeSO2
NH
R
SO2Me

I-H

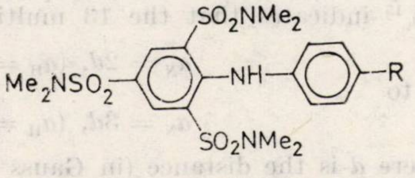
SO2NMe2
Me2NSO2
NH
R
SO2NMe2

II-H

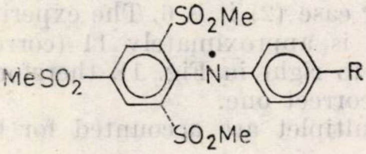
SO2Me
MeSO2
N
R
SO2Me

I

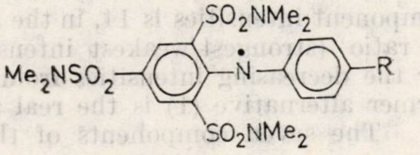
SO2NMe2
Me2NSO2
N
R
SO2NMe2

II

a, R=Me; b, R=OMe

ELECTRON SPIN RESONANCE (ESR) SPECTRA OF AMINYLS

All aminyls were prepared by oxidizing the diarylamines in benzene solution at room temperature in a static degassed vial with lead tetraacetate or lead dioxide, and their ESR spectra were recorded in the same closed vial. [2]

p-Tolyl-2,4,6-tri-(methanesulphonyl)-phenyl-aminyl (Ia) affords an ESR spectrum (Fig. 1) consisting of 79 lines grouped in 13 multiplets. Assuming free rotation of the aryl groups, this ESR spectrum must be

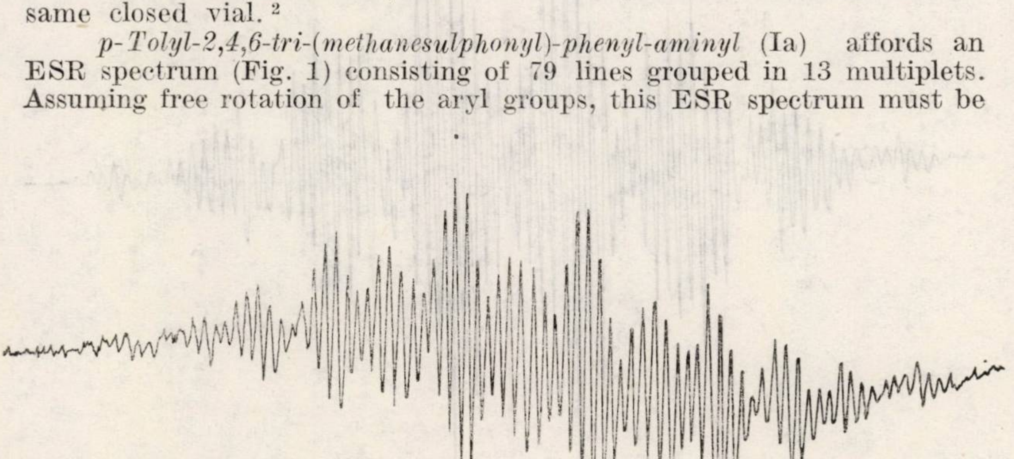

Fig. 1. — First-derivative ESR spectrum of radical Ia in benzene.

due to $1a_N$ (aminyl nitrogen hfc), $2a_{m-\mathrm{H}}$ (acceptor aryl group), $2a_{o-\mathrm{H}}$, $2a_{m-\mathrm{H}}$, and $3a_{\mathrm{CH_3}}$ (all these seven hfc's due to the donor *para*-tolyl group). A computer-obtained list of all possible ESR spectra with equidistant lines [15] indicates that the 13 multiplet components are due either to :*

$$a_{\mathrm{N}} = 2d,\ (a_{\mathrm{H}} = 2d)^3,\ (a_{\mathrm{H}} = d)^2 \tag{1}$$

or to

$$a_{\mathrm{N}} = 3d,\ (a_{\mathrm{H}} = 2d)^2,\ (a_{\mathrm{H}} = d)^2 \tag{2}$$

where d is the distance (in Gauss or milli-Tesla) between two successive multiplet centres, and exponents indicate the number of hfc's (nuclei equally coupled to the odd electron).

In the former case (1), the ratio of strongest to smallest (weakest) component intensities is 14, in the latter case (2) it is 6. The experimental ratio (strongest/weakest intensities) is approximately 11 (correcting for the decreasing intensities from left to right in Fig. 1), therefore the former alternative (1) is the real and correct one.

The seven components of the multiplet are accounted for by :

$$(a_{\mathrm{H}} = 2d')^2,\ (a_{\mathrm{H}} = d')^2 \tag{3}$$

where d' is the distance between two adjacent (successive) lines in each multiplet. For this radical, $d = 6d'$.

p-Tolyl-2,4,6-tri-(N,N-dimethylsulphonamido)-phenyl-aminyl (*II*a) has an ESR spectrum (Fig. 2) with 76 lines grouped in 8 multiplets.

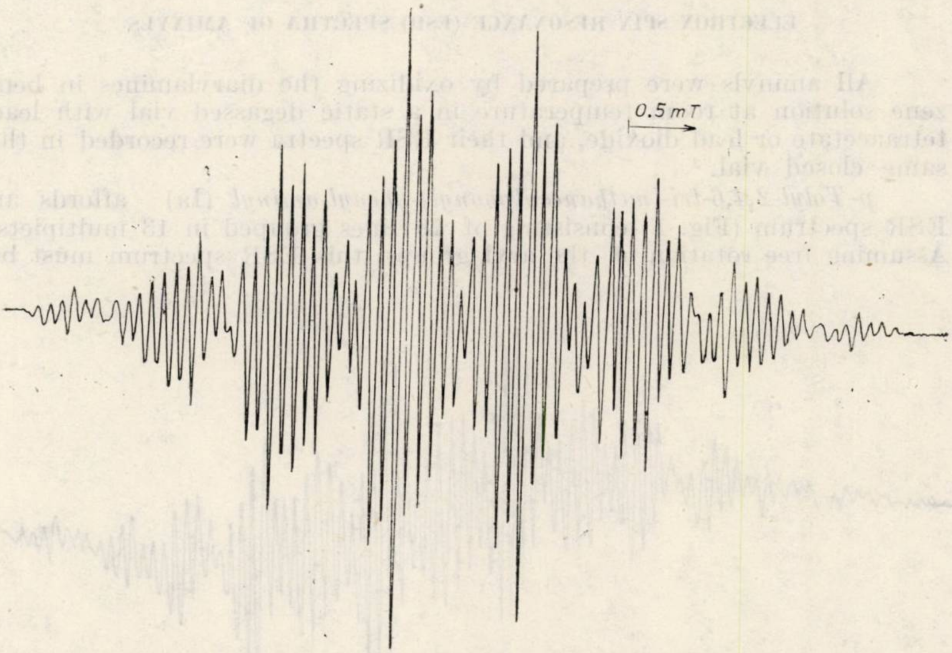

Fig. 2. — First-derivative ESR spectrum of radical IIa in benzen

---

* We use the notation $(a_{\mathrm{H}} = d)^k$ when k hfc's are equal to d.

The multiplet pattern may be accounted for by:

$$a_N = d,\ (a_H = d)^3,\ (a_H = d)^2 \tag{4}$$

leading to an intensity ratio (central to outer components of the multiplet) of 25. The experimental ratio is about 17. The remaining coupling constants are approximately

$$(a_H = 2d')^2,\ (a_H = d')^2 \tag{5}$$

as in the preceding radical. Here, however, $d' = 10d$.

Thus the difference between these two free radicals consists in the fact that in IIa a set of two proton coupling constants (which we assign to the *ortho*-tolyl protons) is approximately as large as the a_N and a_{CH_3} (namely, $10d'$), whereas in Ia the same *ortho*-tolyl protons have a smaller coupling constant ($6d'$) than the aminyl nitrogen and methyl protons (which are equal to $12d'$). In both radicals Ia and IIa the *meta* pairs of protons have the smallest hfc's of $2d'$ and d'.

p-Anisyl-2,4,6-tri-(methanesulphonyl)-phenyl-aminyl (Ib) presents an ESR spectrum with 47 lines grouped in 5 multiplets (Fig. 3). This five-component multiplet corresponds to:

$$a_N = d,\ (a_H = d)^2. \tag{6}$$

Further splittings within each component of the multiplet are accounted for by:

$$(a_H = 2d')^3,\ (a_H = d')^4 \tag{7}$$

with $d = 9d'$ (approximately).

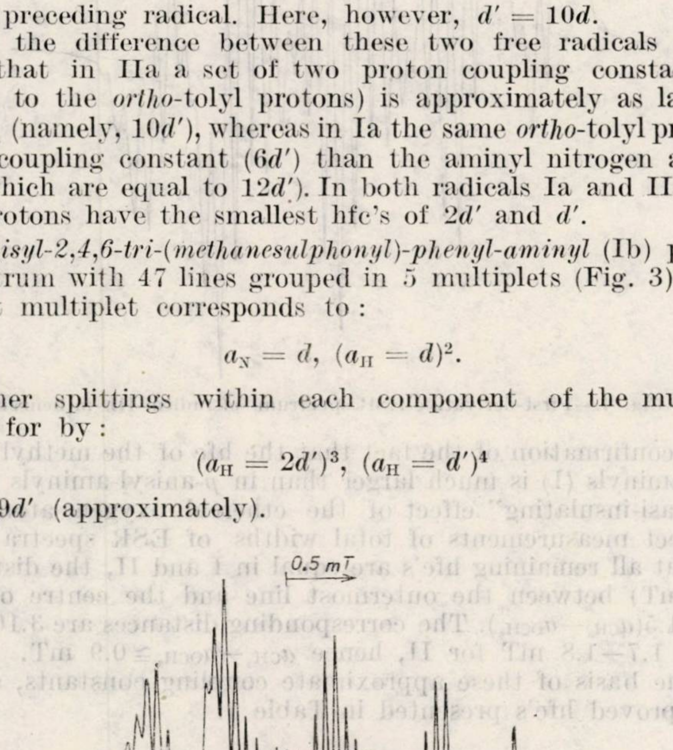

Fig. 3. — First-derivative ESR spectrum of radical Ib in benzene.

p-Anisyl-2,4,6-tri-(N,N-dimethylsulphonamido)-phenyl-aminyl (IIb) yielded an ESR spectrum consisting of 34 lines grouped again in 5 multiples (Fig. 4), with the same relative ratios between multiplet and submultiplet components as (6) and (7), but with $d = 7d'$ (approximately).

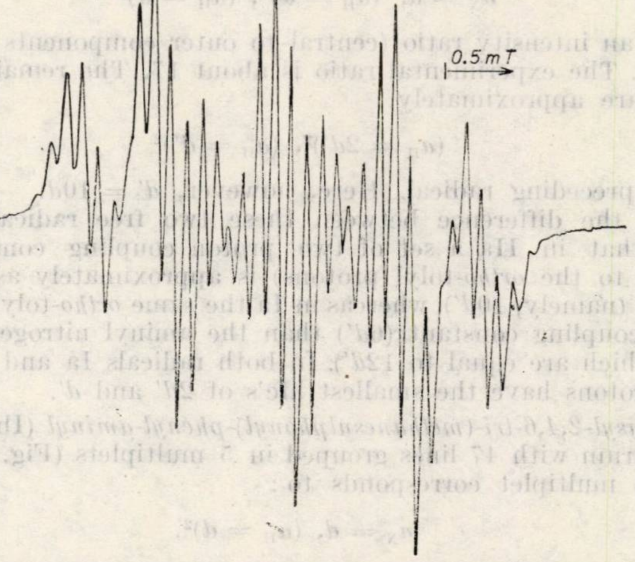

Fig. 4. – First-derivative ESR spectrum of radical IIb in benzene

As a confirmation of the fact that the hfc of the methyl hydrogens in *p*-tolyl-aminyls (I) is much larger than in *p*-anisyl-aminyls (II), owing to the "quasi-insulating" effect of the ethereal oxygen atom, we employed direct measurements of total widths of ESR spectra. Assuming roughly that all remaining hfc's are equal in I and II, the distance difference (in mT) between the outermost line and the centre of the ESR spectra is $1.5(a_{CH_3} - a_{OCH_3})$. The corresponding distances are 3.16 – 3.20 mT for I, and 1.7 – 1.8 mT for II, hence $a_{CH_3} - a_{OCH_3} \cong 0.9$ mT.

On the basis of these approximate coupling constants, simulations lead to improved hfc's presented in Table 1.

Table 1

ESR Hyperfine coupling constants (mT) of diarylaminyls in benzene solution (line half-widths about 0.03 mT)

Radical	Donor	Acceptor	a_N	Acceptor	Donor			Centre*
				a_{m-H}	a_{CH_3}	a_{o-H}	a_{m-H}	mT
Ia	C_6H_4-Me	$C_6H_2(SO_2Me)_3$	1.00	0.083	1.00	0.50	0.166	335.50
IIa	C_6H_4-Me	$C_6H_2(SO_2NMe_2)_3$	0.95	0.085	0.95	0.60	0.170	335.45
Ib	C_6H_4-OMe	$C_6H_2(SO_2Me)_3$	0.77	0.077	0.154	0.62	0.077	335.30
IIb	C_6H_4-OMe	$C_6H_2(SO_2NMe_2)_3$	0.88	0.110	0.110	0.55	0.110	335.30

* Position of the centre (in mT) of the ESR spectrum; the instrument has $f_0 = 9411$ MHz.

The results indicate that:

a) No couplings appear with sulphonyl group atoms;

b) *p*-tolyl groups are satisfactory donor groups, unlike capto-dative aminyls with polynitrophenyl as acceptor groups;

c) a_{H} for the methyl hydrogens is about as high as a_{N} when the donor is *p*-tolyl, with the methyl directly bonded to the phenyl ring, but 6—9 times smaller when the donor is *p*-anisyl (in the latter case, the spin density is relayed through the methoxy oxygen atom). For the *p*-tolyl radicals, a_{H} is in the range 0.8—1.0 mT, normal for *pi*-radicals of this type.

d) the nitrogen spin density, reflected in the a_{N} hfc, is somewhat smaller in *p*-anisyl- than in *p*-tolyl-substituted radicals, indicating a higher delocalization of the unpaired spin in the former radicals with the stronger donor group, in agreement with the expectations.

e) as it was found earlier in 3,5-di-t-butylphenyl-polynitrophenylaminyls, [1b] and in N-alkoxy-N-polynitrophenylaminyls, [8] most of the spin density is located on the donor group and very little on the acceptor group. This is in agreement with observation (a) above because ESR lines have half-widths of about 0.02 mT, making it impossible to see smaller splittings relayed through sulphonyl groups. Moreover, this is in agreement with the intuitive image of capto-dative stabilization in aminyls where the donor group delocalizes preferentially the odd electron, whereas the acceptor group interacts mainly with the unshared electron pair of the aminyl nitrogen, even when the two aryl rings are not mutually orthogonal, but only tilted out of coplanarity.

EXPERIMENTAL PART

ESR Spectra were recorded with a Jeol JES-ME-3X instrument at room temperature in benzene, in deaerated solutions.

Diarylamines were recrystallized from ethanol and gave correct elemental analyses. Aminyls were not isolated; their ESR spectra were determined in solution.

2,4,6-Tris (methylsulphonyl)-4′-methyl-diphenylamine (IHa), $C_{16}H_{19}NO_6S_3$, was obtained from *p*-toluidine and 1-chloro-2,4,6-tris(methylsulphonayl)benzene which had m.p. 327°. The purified diarylamine has m.p. 255°.

2,4,6-Tris(methylsulphonyl)-4′-methoxy-diphenylamine (IHb), $C_{16}H_{19}NO_7S_3$, was prepared similarly from *p*-anisidine. The purified product has m.p. 214° and presents in ethanol an electronic absorption band with λ_{max} 317 nm (log ε 2.88).

2,4,6-Tris(N,N-dimethylsulphonamido)-4′-methyl-diphenylamine (IIHa), $C_{19}H_{28}N_4O_6S_3$ was obtained similarly from *p*-toluidine and 1-chloro-2,4,6-tris(N,N-dimethylsulphonamido)-benzene. The product has m.p, 196° and presents in ethanol a band with λ_{max} 339 nm (log ε 2.86).

2,4,5-Tris(N,N-dimethylsulphonamido)-4′-methoxy-diphenylamine (IIHb), $C_{19}H_{28}N_4O_7S_3$, was prepared analogously from *p*-anisidine. The product has m.p. 194° and in ethanol presents an electronic absorption band with λ_{max} 338 nm (log ε 2.91).

Diarylaminyls (I and II) were prepared in benzene solution by oxidizing the corresponding diarylaminyls with PbO_2 or $Pb(OAc)_4$ in benzene. At room temperature, the radicals were persistent: their ESR spectra showed no change during one hour.

ACKNOWLEDGEMENT. Thanks are addressed to Dr. R. Baican for ESR spectral determinations.

REFERENCES

[1a] Preceding part., A. T. Balaban, U. Bologa, M. T. Căproiu, N. Grecu, N. Negoiţă and R. I. Walter, *J. Chem. Soc. Perkin I*, submitted; [b]. M. T. Căproiu, N. Negoiţă and A. T. Balaban, *Tetrahedron*, **23**, 3943 (1983), part XII.

[2] A. T. Balaban, P. T. Frangopol, M. Frangopol and N. Negoiță, *Tetrahedron*, **23**, 4661 (1967).

[3] H. G. Viehe, R. Merenyi, L. Stella and Z. Janousek, *Angew. Chem. Internat. Ed. Engl.*, **18**, 917 (1979); L. Stella, Z. Janousek, R. Merenyi and H. G. Viehe, *ibid.*, **17**, 691 (1978); H. G. Viehe, Z. Janousek, R. Merenyi and L. Stella, *Acc. Chem. Res.*, **18**, 148 (1985).

[4] A. R. Katritzky and F. Soti, *J. Chem. Soc. Perkin I*, 1427 (1974); R. W. Baldock, P. Hudson, A. R. Katritzky and F. Soti, *Heterocycles*, **1**, 67 (1972).

[5] H. G. Viehe, Z. Janousek and R. Merenyi (eds.), "Substituent Effects in Radical Chemistry", D. Reidel Publ., Dordrecht, 1986.

[6] A. T. Balaban, *Bul. Inst. Politehnic București, Ser. Chim. Metalurg.*, **43**, No. 4, 65 (1981); M. Hillebrand and A. T. Balaban, *Rev. Roum. Chim.*, **25**, 995 (1980); M. J. S. Dewar, *J. Am. Chem. Soc.*, **74**, 3353 (1952); D. Crans, T. Clark and P. von R. Schleyer, *Tetrahedron Lett.*, **21**, 3681 (1980); G. Leroy, D. Peeters, M. Sana and C. Wilante, in ref. 5, p. 1; G. Leroy and D. Peeters, *J. Mol. Struct. Theochem*, **2**, 133 (1981).

[7] A. T. Balaban, P. T. Frangopol, M. Mărculescu and I. Bally, *Tetrahedron*, **13**, 258 (1961).

[8] A. T. Balaban, M. Mărculescu, I. Pascaru, M. Rotaru, A. Valeriu and M. Weiner, *Z. physik. Chem. (Leipzig)*, **219**, 285 (1962).

[9] A. T. Balaban, M. Frangopol, N. Negoiță, P. T. Frangopol and M. Paraschiv, *Rev. Roumaine Chim.*, **14**, 941 (1969).

[10] G. Stănciuc, M. T. Căproiu, A. Caragheorgheopol, H. Căldăraru, A. T. Balaban and R. I. Walter, in press.

[11] J. B. Hine, *Organic Reactivity*, **5**, 886 (1968); R. M. Wisghert and I. E. Kachanko, *ibid.*, **5**, 9 (1968); L. M. Litvinenko and N. F. Levchenko, *Zhurn. Obshchei Khim.*, **30**, 1673 (1960).

[12] A. T. Balaban and N. Negoiță, *Rev. Roumaine Chim.*, **17**, 1227 (1972); A. T. Balaban, M. T. Căproiu, N. Negoiță and R. Baican, *Tetrahedron*, **33**, 2249 (1977).

[13] M. Teeninga, W. C. Nieuwpoort and J. B. F. N. Engberts, *Z. Naturforsch.*, **36b**, 279 (1981).

[14] Y. Miura, K. Kakamura and M. Minoshita, *Bull. Chem. Soc. Japan*, **51**, 947 (1978).

[15] A. T. Balaban and C. Pomponiu, *Rev. Roum. Chim.*, **19**, 581 (1974); A. T. Balaban, *ibid.*, **17**, 9, (1972).

Revue Roumaine de Chimie, 32, 5, 509–513 (1987)

4-BENZYLOXYAZOBENZENES SYNTHESIZED BY CONDENSATION OF BENZYL CHLORIDE WITH SODIUM SALTS OF 4-HYDROXY-AZOBENZENES

MIRCEA IOVU* and STELIAN RADU**

* Faculty of Pharmacy, str. Traian Vuia 6, Bucharest, Romania

** Faculty of Sciences, Department of Chemistry, Calea Bucureşti, 165, Craiova, Romania

Received February 15, 1985

This paper studies the synthesis of 4-benzyloxyazobenzenes (azomonoethers) by condensation of benzyl chloride with sodium salts of 4-hydroxy-azobenzenes. The following 4-hydroxyazobenzenes were used: 4-hydroxyazobenzene, 3-chloro-4-hydroxyazobenzene, 3-bromo-4-hydroxyazobenzene, 2′-methyl-4-hydroxyazobenzene, 4′-methyl-4-hydroxyazobenzene, 3-methyl-4-hydroxyazobenzene, 2,3-dimethyl-4-hydroxyazobenzene, 2,6-dimethyl-4-hydroxyazobenzene and 2′,3-dimethyl-1-4-hydroxyazobenzene. The new azoethers were characterized by spectral analysis in UV and IR and by thermogravimetric analysis.

INTRODUCTION

In our previous papers, [1,2] some azobisethers were synthesized by the condensation of sodium salt of dihydroxy azobenzenes and monochloromethylated derivatives of substituted and unsubstituted benzene and by condensation of sodium salt of hydroxy azobenzenes with bis(chloromethylated) derivatives of substituted and unsubstituted benzene. We synthesized also polyazoethers [3] by polycondensation of sodium salt of hydroxy azobenzenes with bis(chloromethylated) derivatives of substituted and unsubstituted benzene: 1,4-bis(chloromethyl)benzene, 1,4-bis(chloromethyl)-2,5-dimethylbenzene and 1,3-bis(chloromethyl)-4,6-dimethylbenzene.

In the present study, the above condensation was extended for the preparation of azomonoethers by the reaction of benzyl chloride with sodium salt of 4-hydroxy azobenzenes.

As the first step of azoethers synthesis, sodium salts of 4-hydroxyazobenzenes were prepared by the condensation of 4-hydroxyazobenzenes with sodium hydroxide. Because the reaction occurs better in an anhydrous medium, the resulted water was removed through distillation as a benzene-ethanol-water ternary azeotropic mixture.

The anhydrous mixture of solvents (ethanol-benzene) also permits the condensation of the sodium salts with the monochloromethylated derivative, with good results.

The reaction takes place due to the nucleophilic attack of the phenolate ion on the benzyl chloride :

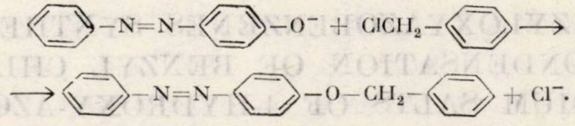

The sodium chloride which is formed in the reaction medium together with the azoether (solid) is removed by washing with water.

The reaction takes place with a good yield.

The azoethers presented in this paper possess a mixed aliphatic-aromatic character. The azoetheric structure was investigated by means of spectrometric and thermogravimetric methods.

RESULTS AND DISCUSSION

Table 1 gives the structural formulae, the molecular formulae the quantitative results of carbon, hydrogen, nitrogen and halogen elemental analysis, λ_{max} and ε_{max} from electronic spectra, the melting points and yields.

The azoethers presented in this table are solid, yellow compounds, excepting the compound synthesized from 2,6-dimethyl-4-hydroxyazobenzene which has a red colour.

The azoethers melting points were determined after repeated recrystallizations from ethanol or ethanol-benzene mixtures. The influence of the substituent nature and position on the melting temperatures is obvious. For instance, 4′-methyl-1-benzyloxyazobenzene has the highest melting point while 2′,3-dimethyl-4-benzyloxyazobenzene has the lowest melting point. One observes also that the azomonoether which contains bromine in its molecule (in *ortho* to the etheric function) has a lower melting temperature than the similar derivative substituted with chloride.

The melting points were determined in capillaries and by thermogravmietric analysis.

The infrared spectra of the synthesized azoethers showed characteristic azo absorptions at 1600–1566 and 1430–1400 cm^{-1}, a strong absorption at 1315–1245 cm^{-1} due to the asymmetric valency vibration of the C–O–C bond and a weaker absorption at 1055–1010 cm^{-1} due to the symmetric valency vibration of the C–O–C bond.

It must be shown that the second band due to the symmetric vibration of the C–O–C bond can be superposed with the bands due to the in-plane deformation of the C–H bands of the aromatic nuclei and those due to the ring vibrations.

For example the azoethers have their absorption maxima due to the asymmetric and symmetric vibration of the C–O–C– bond, as follows : at 1250 and 1040 cm^{-1} for 4-benzyloxyazobenzene, 1255 and 1043 cm^{-1} for 3-methyl-4-benzyloxyazobenzene, and 1252 and 1041 cm^{-1} for 4′-methyl-4-benzyloxyazobenzene.

Strong absorption bands appear in the region 1200–1100 cm^{-1} due to the Ph–N bond e.g. 4-benzyloxyazobenzene at 1145 cm^{-1}

Table 1

4-Benzyloxyazobenzenes

Azomonoether	Molecular formula	C % calc. found	H % calc. found	N % calc. found	Halogen % calc. found	nm λ_{max}	ε_{max}	M.p.°C	Yield %
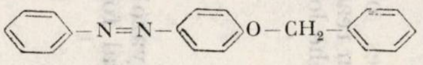	$C_{19}H_{16}ON_2$	79.14 79.20	5.59 5.55	9.71 9.80	—	205.3 235.4 345.9 439.1	7261 2594 6281 1005	116	70.4
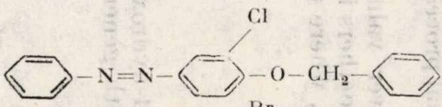	$C_{19}H_{15}ON_2Cl$	70.70 70.65	4.68 4.69	8.68 8.75	10.99 11.05	207 237.3 346.6 440	12590 2851 6383 1019	91.5	70.5
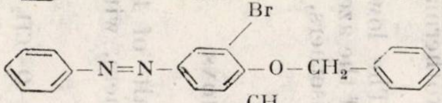	$C_{19}H_{15}ON_2Br$	62.14 62.23	4.12 4.15	7.63 7.52	21.76 21.80	207 224.6 346.8 438.3	13966 3097 6324 1040	94—84.5	55.8
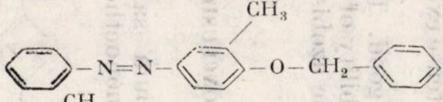	$C_{20}H_{18}ON_2$	79.44 79.23	6.00 6.05	9.26 9.45	—	206.5 234.9 350 439.1	15383 2987 4989 1076	86.5—87	51.7
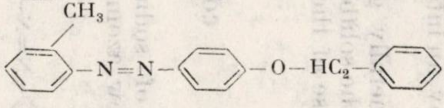	$C_{20}H_{18}ON_2$	79.44 79.45	6.00 6.00	9.26 9.35	—	207 237.9 349.1 442.6	24211 3590 5624 1040	91.5	81.2
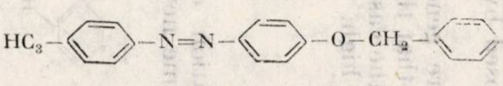	$C_{20}H_{18}ON_2$	79.44 79.31	6.00 5.95	9.26 9.41	—	206.1 238.7 348.6 443.8	10965 3319 6638 1076	128.5—129	87.8
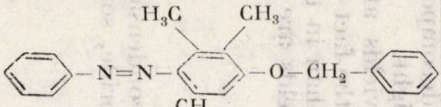	$C_{21}H_{18}ON_2$	79.72 79.80	6.37 6.31	8.85 8.97	—	206.7 253.7 355.8 447	17865 2489 3918 1067	110.5	64
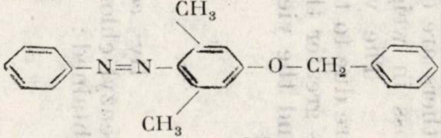	$C_{21}H_{20}ON_2$	79.72 79.41	6.37 6.34	8.85 9.02	—	207.8 348 458.6	18198 3573 1045	98—98.5	80.6
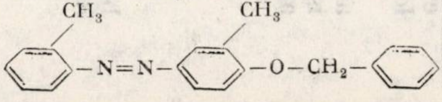	$C_{12}H_{20}ON_2$	79.72 79.63	6.37 6.44	8.85 9.14	—	207.3 214.4 353.5 442.6	13805 2630 3819 1043	61	73.8

3-methyl-4-benzyloxyazobenzene at 1156 cm^{-1} and 4′-methyl-4-benzyloxyazobenzene at 1155 cm^{-1}.

The absorption bands due to the azo group appear in two regions : 1600—1566 cm^{-1} and 1430—1400 cm^{-1} e.g. at 1600, 1578 and 1412 cm^{-1} for 4-benzyloxyazobenzene, at 1598 and 1415 cm^{-1} for 3-methyl-4-benzyloxyazobenzene and at 1600, 1582 and 1414 cm^{-1} for 4′-methyl-4-benzyloxyazobenzene.

The absorption bands which appear in the region 1600—1566 cm^{-1} are more intense than that in the region 1430—1400 cm^{-1}.

The values found for the azo group agree with the results reported in the literature.[4,5]

Comparison of the results obtained for azoethers with those previously presented[1,2] shows that they are very close.

The ultraviolet and visible spectra exhibited three absorption bands : a characteristic low-intensity R-band due to the azo group, a high-intensity K-band due to the conjugated system Ar—N=N—Ar and a low-intensity B-band due to the conjugated aromatic system.

Our results agree with the values presented in the literature by other authors.[6-9]

The description of the UV spectra is given in table 1.

Examining table 1 it may be observed that the R-band appears at 438.3—458.6 nm, the K-band appears at 345.9—355.8 nm and the B-band at 234.6—253.7 nm.

We observed also a band at 205.3—207.3 nm which can be due to the solvent (the ultraviolet and visible spectra were recorded in ethanol).

The molar extinction coefficients have smaller values for R-bands in comparison with B-bands and K-bands. The highest molar extinction coefficients have been found at the K-bands. The R-bands and the K-bands are rather broad.

The spectral properties of the azomonoethers are comparable with those observed for the azobisethers.

By thermal analysis, in the air, we established that the azoethers are decomposed by an intense exothermal process at 267—335° with loss in weight.

The yields are generally good. The lower values of some yields are due to the fact that the solubility of the azoethers in reaction medium is greater than in the case of the azobisethers, where the losses are small and the yields are high.

CONCLUSIONS

By condensation of sodium salt of 4-hydroxyazobenzene with benzyl chloride, some new azomonoethers, with general formula **1** were obtained :

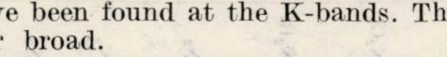

1

These compounds are yellow or red solids which were investigated by UV, IR and thermogravimetric analysis.

EXPERIMENTAL

4-Hydroxyazobenzene and the substituted 4-hydroxyazobenzene used in this paper were synthesized as shown in a previous paper.[2]

Benzyl chloride was a commercial Riedel de Häen product.

The infrared absorption spectra were obtained on a Perkin-Elmer 157 infrared spectrophotometer, in KBr pellets, within the range 4000–650 cm^{-1}.

The electronic spectra were recorded on a Specord-Carl Zeiss apparatus. All the spectra were recorded in ethanol, after storing the samples for 24 hours in a dark place before the measurements. The spectra were recorded within the range 200–700 nm.

DTA, DTG, TG and T curves were obtained by a Setaram thermal balance.

Synthesis of 4-benzyloxyazobenzenes

4-Hydroxyazobenzene (1.98 g, 0.1 mole) and sodium hydroxide (0.4 g, 0.1 mole) together with an ethanol-benzene mixture, 40 mL (1 : 1 in volumes) as solvent, were introduced in a 100 mL flask, equipped with a condenser (to which a tube with anhydrous calcium chloride is connected) and a thermometer. The reaction mixture was heated up to the boiling point till the sodium hydroxide reacts with 4-hydroxyazobenzene, forming the sodium salt.

After the formation of sodium salt, the reflux condenser is replaced by a distillation one to remove the reaction water.

Benzyl chloride (1.265 g, 0.1 mole) was added, the distillation condenser was replaced by a reflux one and the mixture was maintained at 55–60° for 5 j hours, in which time the reaction of sodium salt with benzyl chloride respectively the formation of 4-benzyloxyazobenzene and sodium chloride were accomplished.

After cooling the reaction flask at room temperature 4-benzyloxyazobenzene and sodium chloride are separated by filtering ; the precipitate is washed on the filter with a large amount of water to remove the sodium chloride. The resulting precipitate with yellow colour was dried in a heating chamber at 105°. The yield was 2.03 g (70.4%). After two recrystallizations from ethanol, the melting point was 116°.

The other azoethers mentioned in this paper were obtained in a similar way.

REFERENCES

[1] M. Iovu and S. Radu, *Rev. Roumaine Chim.*, **18**, 473 (1973).
[2] M. Iovu and S. Radu, *Rev. Roumaine Chim.*, in press.
[3] M. Iovu and S. Radu, *Makromol. Chem.*, **176**, 883 (1975).
[4] P. Bassignana and C. Cogrossi, *Tetrahedron*, **20**, 2361 (1964).
[5] A. J. Fatiadi, *J. Res. Nat. Bur. Stand.*, **71A**, 277 (1967).
[6] A. Burawoy, *J. Chem. Soc.*, **1973**, 1865.
[7] A. Burawoy and J. T. Chamberlain, *J. Chem. Soc.*, **1952**, 3734.
[8] W. R. Brode, J. H. Gould and G. H. Wyman, *J. Amer. Chem. Soc.*, **75**, 1856 (1953)
[9] P. Tomasik, *Roczniki Chem.*, **44**, 1369 (1970).

Revue Roumaine de Chimie, **32**, *5*, 515–518 (1987)

STUDIES ON THE PYRIDYL-PYRAZOLONE SYSTEM. I. SOME REACTIONS WITH 3-(3′-PYRIDYL)-1-PHENYL-2-PYRAZOLIN-5-ONE

M.F. ABDEL MEGGED, M.EL BORAI, M. FAHMY* and EL-SAIED A. ALY
Chemistry Department, Faculty of Science, Tanta University, Tanta, Egypt

Received April 20, 1986

The methylene group in the 4-position of 3-(-3′-pyridyl)-1-phenyl-2-pyrazolin-4-one(**1**) has been shown to undergo condensation reaction with aldehydes, ketones, chalcones, acetoacetic ester and acetone dicarboxylate to give compounds **2**, **3** and **4**. It also undergoes the Mannich reaction to give compounds **5** and **6**. The structures of the synthesised compounds were determined from analytical data, IR and ^{1}H-NMR spectral analysis.

INTRODUCTION

In view of the potential biological activity of pyrazolone and pyridine systems,[1–4] it seemed worthwhile to prepare some molecules containing these two moieties in the hope that such condensed systems could possess potential biological activity.

RESULTS AND DISCUSSION

It is known that the 4-position of 2-pyrazolin-5-ones is very reactive and undergoes the characteristic condensation reactions of active methylene groups.[5–7] Thus, 3-(3′-pyridyl)-1-phenyl-2-pyrazolin-5-one (**1**) was condensed with various aldehydes and ketones to give the coloured 4-arylidine-pyrazolin-5-one derivatives **2a—e**.

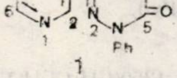

1

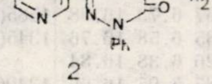

2

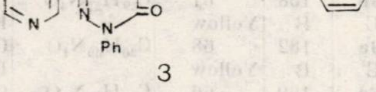

3

2	R_1	R_2
a	H	$C_6H_3-(OCH_3)_2$-2,4
b	H	C_6H_4-CH-p
c	H	$C_6H_4-N-(C_2H_5)_2$-*p*
d	$C_6H_5-CH_2$	$C_6H_5-CH_2$
e	$CH_2CO_2C_6H_5$	$CH_2CO_2H_6H_5$

a Ar = C_6H_5
b Ar = $C_6H_5-CH_3$-*p*

The structures of the prepared compounds were determined by their analytical data, IR and ^1H-NMR spectral analysis (see Tables 1 and 2). The mass spectrum of compound **2a** shows its molecular ion peak (M^+) at $m/e = 385$ (95.2%) and the base peak at $m/e = 354$ ($M^+ - 31$).

The pyrazolone **1** was also condensed with chalcones to give the deep coloured compounds **3a** and **3b**.

Table 1

Experimental results for compounds **2,3,4,5** and **6**

Comp. Method	M.p°C Solvent	Yield % Colour	Formula	Analysis %	C	H	N	IR data ν cm^{-1}
2a	168	85	$C_{23}H_{19}N_3O_3$	Calcd	71.68	4.39	10.90	1685 (C=O) ;1610(C)Pz. ;
A	E	Orange		Found	71.42	4.73	10.98	1585(C=N)Pyd ; 1540(C=C). ;
2b	247	91	$C_{21}H_{15}N_3O_2$	Calcd	73.90	4.39	12.31	1535(C=C) ;3350(OH).
A	E	Orange		Found	73.71	4.32	12.43	
2c	128	78	$C_{25}H_{24}N_4O$	Calcd	75.35	5.96	14.14	1535(C=C).
A	B	Red		Found	75.75	6.06	14.02	
2d	04	65	$C_{29}H_{23}N_3O$	Calcd	81.11	5.36	9.79	1665(C=O) ;1540(C=C).
A	B	Red		Found	81.45	5.49	9.29	
2e	219	63	$C_{23}H_{23}N_3O_5$	Calcd	65.55	5.46	9.98	1665(C=O) ;1540(C=C) ;
A	T	Brown		Found	65.76	5.26	9.68	1715(C=O) ester.
3a	222	72	$C_{29}H_{21}N_3O$	Calcd	81.49	4.91	9.83	1685−1665(C=C−C=O).
A	X	Deep red	Found	Found	81.26	4.75	9.59	
3b	237	70	$C_{30}H_{23}N_3O$	Calcd	81.63	5.21	9.52	1685−1665(C=C−C=O)
A	X	Deep red		Found	81.39	5.36	9.49	
4a	212	68	$C_{18}H_{13}N_3O_2$	Calcd	71.28	4.29	13.86	1775(C=O) αpyrone.
A	X	Beige		Found	71.05	4.58	13.49	
4b	223	55	$C_{21}H_{17}N_3O_4$	Calcd	67.20	4.29	11.20	1775(C=O) αpyrone
A	X	Beige		Found	67.57	4.64	11.65	
5a	158	6	$C_{21}H_{18}NO_4$	Calcd	73.68	5.26	16.37	3380(NH) ;1670(C=O) ;
B	M	Yellow		Found	73.41	5.45	16.71	1615(C=N) ;1600(C=N) Pyd
5d	136	70	$C_{22}H_{18}N_4O$	Calcd	74.57	5.08	15.81	3390(NH) ;1675(C=O).
B	M	Yellow		Found	74.39	5.19	15.63	
5c	149	72	$C_{22}H_{18}N_4O_3$	Calcd	69.39	4.66	14.50	3370(NH) ;2840(OH) ;
B	M	Yellow		Found	68.81	4.37	14.29	1705(C=O) acid.
5d	140	68	$C_{22}H_{18}N_4O_3$	Calcd	68.39	4.66	14.50	3370(NH) ;2845(OH) ;
B	M	Yellow		Found	68.72	4.31	14.87	1710(C=O) acid.
5e	156	68	$C_{25}H_{20}N_4O$	Calcd	76.53	5.10	14.28	3390(NH) ;1670(C=O).
B	M	Orange		Found	76.31	5.29	14.61	
6a	158	62	$C_{17}H_{18}N_4O$	Calcd	69.38	6.12	19.04	1680(C=O) ;1600(C=N)Pz
C	B	Yellow		Found	69.19	6.25	17.76	1590(C=N)Pyd.
6b	168	61	$C_{19}H_{22}N_4O$	Calcd	70.80	6.83	16.66	1665(C=O) ;1610(C=N)Pz
C	B	Yellow		Found	70.67	6.73	16.98	1585(C=N)Pyd.
6c	182	68	$C_{20}H_{22}N_4O$	Calcd	71.85	6.58	16.76	1345(C−N).
C	B	Yellow		Found	72.26	6.38	16.84	
6d	169	66	$C_{19}H_{20}N_4O_2$	Calcd	67.85	5.95	16.66	1340(C−N) ;1260(CH_2OCH_2)
C	B	Yellow		Found	67.96	5.89	16.90	asym ;1040(CH_2OCH_2)sym

The mass spectrum of compound **3a** shows its molecular peak at $m/e = 427$ (28%), along with peaks at $m/e = 191$ (26%) for $C_6H_5-CH{=}{=}CH-C^+-C_6H_5$ and $m/e = 207$ for $M^+ - 191$, then $-CO$.

Table 2

^1H-NMR data for compounds **2,3,4,5** and **6**

Comp.	^1H-NMR δ(ppm)
2a	H_2 d/1 9.00 ; H_4 d/1 7.52 ; H_5 d/1 7.45 ; H_6 d/1 8.90 ; CH exocyclic s/1 8.25 ; Aromatic protons m/3 6.60 ; N−Ph m/5 8.35 ; OCH_3 s/3 3.85 and 3.90
2b	CH exo. s/1 8.29 ; Arom. protons m/4 6.55 ; OH (broad) s/1 1.95.
2c	CH exo. s/1 8.26 ; Arom. protons m/4 6.45 ; $N-CH_2$ q/4 3.65 ; CH_3 t/6 1.28,
2d	CH_2 s/4 4.44 ; Benzylic protons m/10 7.65.
2e	CH_2 S/4 3.96 ; CH_2 ester q/4 4.12 ; CH_3 t/6 1.4.
3a	H_2 d/1 8.94 ; H_4, H_5 m/2 7.65 ; H_6 d/1 8.90 ; Arom. protons m/10 6.85 ; N−Ph m/5 8.35 ; CH=CH d/2 5.9 ; J=6 Hz.
3b	Arom. protons m/9 6.85 ; CH_3 s/3 1.2 ; CH=CH d/2 5.92 ; J=5.9 Hz.
4a	H_2 d/1 9.04 ; H_4, H_5 m/2 7.55 ; H d/1 8.85 ; N−Ph m/5 8.35 ; CH s/1 7.85 ; CH_3 s/3 2.87.
4b	CH s/1 7.82 ; CH_2 q/2 4.30 ; CH_3 t/3 1.52.
5a	H_2 d/1 9.00 ; H_4, H_5 m/2 7.75 ; H_6 d/1 8.88 ; N−Ph m/5 8.35 ; CH s/1 9.38 ; CH_2 s/2 4.25 ; NH (broad) s/1 3.15 ; Arom. protons m/5 6.50.
5b	CH s/1 9.40 ; CH_2 s/2 4.30 ; NH (broad) s/1 3.18 ; Arom. protons m/4 6.65 ; CH_3 s/3 2.10.
5e	CH s/1 9.40 ; CH_2 s/2 4.25 ; NH(broad) s/1 3.20 ; Arom. protons m/4 6.70.
5c	CH s/1 9.40 ; CH_2 4.24 ; NH (broad) s/1 3.18 ; Arom. protons m/4 6.65.
5e	CH s/1 9.40 ; CH_2 s/2 4.25 ; NH (broad) s/1 3.18 ; Arom. protons m/7 6.85
6a	H_2 d/1 9.00 ; H_4, H_5 m/2 7.65 ; H_6 d/1 8.90 ; N−Ph m/5 8.35 ; CH s/1 9.39 ; CH_2 s/2 4.28 ; $N(CH_3)_2$ s/6 2.60.
6b	CH s/1 9.40 ; CH_2 s/2 4.30 ; $N(CH_2)_2$ q/4 3.70 ; $(CH_3)_2$ t/6 1.90.
6c	CH s/1 9.40 ; CH_2 s/2 4.32 ; $N(CH_2)_2$ m/4 3.74 ; $(CH_2)_3$ m/6 1.90.
6d	CH s/1 9.40 ; CH_2 4.30 ; $O(CH_2)_2$ m/4 3.22 ; $N(CH_2)_2$ m/4 3.86.

s : singlet ; d : doublet ; t : triplet ; q : quadruplet ; m : multiplet.

The condensation of pyrazolone **1** with acetoacetic ester and with acetone-1,3-diethyl-carboxylate at elevated temperature, gave the corresponding pyrazolo-pyrone derivatives **4a** and **4b** respectively.

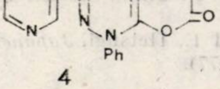

4

a $R=CH_3$
b $R=CH_2COQC_2H_5$

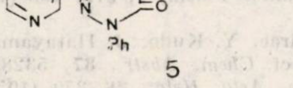

5

a $Ar = C_6H_5$
b $Ar = C_6H_4-CH_3$-*m*
c $Ar = C_6H_4-COOH$-*o*
d $Ar = C_6H_4-COOH$-*p*
e $Ar = C_{10}H_7$

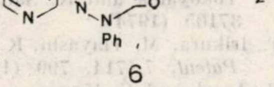

6

a $R_1 = R_2 = CH_3$
b $R_1 = R_2 = C_5H_5$

c
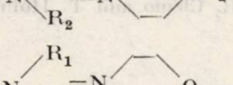

d
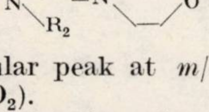

The mass spectrum of **4a** shows its molecular peak at *m/e* = 303 (30%) and its base peak at *m/e* = 259 ($M^+ - CO_2$).

Moreover, the active methylene group in pyrazolone **1** reacts in the Mannich reaction with primary aromatic amines in ethanol to give 4-N-arylamino-methyl-pyrazolones **5a−e.**

The Mannich reaction with secondary amines was carried out in acetic acid and affords 4-N-dialkyl-methyl-pyrazolones **6a—d.**

The mass spectrum of **6e** shows its molecular peak at $m/e =$ $= 334$ (15%) and its base peak at $m/e = 207$.

EXPERIMENTAL

The 3-(3′-pyridyl)1-phenyl-2-pyrazolin-5-one (**1**) was prepared according to Clemo *et al.*[10] The ^1H—NMR spectra were recorded in $CDCl_3$ on a Jeol C-90 MHo spectrometer with TMS as internal standard. The IR spectra were recorded on Finnigan 3000 spectrometer operating at 70 eV, with direct inlet and a source temperature of 90°C.

The usual preparative procedure consisted in diluting the reaction mixture with water extraction with $CHCl_3$,washing the extract with water, drying on magnesium sulphate, removing the solvent under reduced pressure and purification by column chromatography on silica G 60 (Merk).

The experimental results are grouped in Table 1.

Method A : *Condensation with aldehydes, ketones, chalcones, ethyl acetoacetate, and acetone-1-,3-diethylcarboxylate*

A mixture of **1** (0.01 mole) and the appropriate reagent (0.015 mole) was heated in an oil bath at 140—150°C for 3 hrs. The reaction mixture was left to cool and worked-up as described above.

Method B : *Mannich reaction with primary aromatic amines*

A mixture of **1** (0.01 mole), 300 mg of paraformaldehyde, the appropriate aromatic amine (0.015 mole) 10 mL of HCl 3N and 50 mL of ethyl alcohol was refluxed for 6 hrs. The products were separated after dilution with water, and addition of 10% NaOH solution until the pH become 10. The products were filtered oil and purified as usual.

Method C : *Mannich reaction with secondary amines*

A mixture of **1**(0.01 mole), 5 mL of formaldehyde, and the appropriate amine (0.015 mole) in 50 mL of acetic acid was heated at 80°C for 4 hrs. The reaction mixture was left to cool and worked-up as usual.

REFERENCES

[1] H. Hoehn, *U.S. Patent* 4, 048, 184 (1977); cf. Chem. Abstr. **88**, 6878 (1978).

[2] J. Krapcho and C. F. Turk, *Swiss Patent* 594, 667 (1978); cf. *Chem. Abstr.*, **88**, 13666 (1978).

[3] T. Okamoto, T. Irikura, S. Suzue, K. Ushiyama, Y. Matsui, Y. Nagatsu, S. Sato, M. Yokoyama and K. Saito, *Japanese Patent*, 7, 372, 193 (1973); cf. *Chem. Abstr.*, **80**, 37105 (1974).

[4] T. Irikura, M. Hayashi, K. Koshirae, Y. Kudo, J. Hatayama and E. Hetsugi, *Japanese Patent*, 7, 714, 799 (1977); cf. *Chem. Abstr.*, **87**, 53282 (1977).

[5] H. Amal and C. Kapuano, *Pharm. Acta. Helv.*, **26**, 379 (1951).

[6] R. M. Anker and A. H. Cook, *J. Chem. Soc.*, **1944**, 489.

[7] W. Cocker and G. Turnet, *J. Chem. Soc.*, **1940**, 57.

[8] E. Stollé, *Chem. Ber.*, **38**, 3027 (1905).

[9] B. Pathak and T. N. Ghosh, *J. Ind. Chem. Soc.*, **26**, 371 (1949).

[10] G. R. Clemo and T. Holmes, *J. Chem. Soc.*, **1934**, 1739.

Revue Roumaine de Chimie, **32**, 5, 519–524 (1987)

ALKYLATION OF BENZENE WITH ISOPROPANOL

N. NAUM, GH. MIHĂILĂ, F. VITAN, P. ONU and D. GÂNJU
Department of Chemical Technology, Polytechnic Institute, Splai Bahlui 71, Iași, Romania

Received January 10, 1986

The thermodynamic study of the alkylation reaction of benzene with isopropanol, carried out on the basis of standard thermal data, has pointed out that the equilibrium composition strongly depends on the benzene : isopropanol molar ratio and on the presence of inert gas, but is not greatly influenced by temperature changes in the range of 473–673 K. Alkylation of benzene with isopropanol at 533 K, on zeolite catalyst in the Ce, La or H form of faujazite Y, for 4 :1 benzene : isopropanol molar ratio, led to a conversion equal to the thermodynamical one. If the molar ratio is lower than 4 :1, di- and polyalkylates occur as secondary reaction products.

INTRODUCTION

Alkylation of benzene is one of the most important processes, applied now on industrial scale, for ethylbenzene and cumene manufacture. A selective alkylation with great reaction rate and high yield greatly depends on the catalyst employed. For this reaction, many types of catalysts, various alkylation agents as well as different reaction conditions, have been investigated.[1–3] During the last decade, much atention has been paid to utilization of synthetic zeolites with molecular sieve properties as alkylating catalysts.[4–7] Taking into account the great practical importance of alkylation product obtained by alkylation of benzene with isopropanol, this paper presents a thermodynamic study of the alkylation as well as the results concerning the alkylation performed on zeolite catalyst of faujazite Y, modified by ion-exchange in the Ce, La and H form, activated thermally at 773 K.

The mathematical model connecting the initial composition, temperature and equilibrium composition, established thermodynamically, allowed the determination of the conditions for maximum yield obtention as well as the programming of the experiments to be performed.

THERMODYNAMIC STUDY

For the thermodynamic study, we have taken into consideration only the reaction

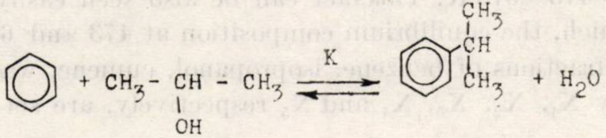

(1)

Besides reaction (1) also secondary reactions can take place such as cumene alkylation or, at higher temperatures, decomposition reactions. In order to avoid these secondary reactions alkylation will be performed with large amounts of benzene in a limited temperature range.

As a first step of the thermodynamic study, using the entropical method[8-9] and standard thermal data of the reaction components (Table 1) the dependence of equilibrium constant on temperature has been determined :

Table 1

Thermal data of the reaction components[6]

Components	H^0_{298} kcal·mol^{-1}	S^0_{298} cal·mol^{-1}·K^{-1}	$C_p = f(T)$ cal·mol^{-1}·K^{-1}
Benzene	19.82	64.34	$-5.04 + 0.09563T - 4.06 \cdot 10^{-5}T^2$
Isopropanol	−64.20	73.20	$7.41 + 0.06745T - 2.32 \cdot 10^{-5}T^2$
Cumene	0.94	92.87	$0.7 + 0.13\,T - 4.357 \cdot 10^{-5}T^2$
Water	−57.79	45.106	$6.89 + 3.283T - 6.1365 \cdot 10^{-5}T^2$

$$\ln K = -11.9923 + \frac{391.5074}{T} + 2.6284 \ln T - 7.5017 \,.\, 10^{-3} T - 3.4521 \,.\, 10^{-6} T^2 \qquad (2)$$

Some values of the equilibrium constant, calculated with equation (2) for the temperature range of 473–673 K, are listed in Table 2.

Table 2

Values of the equilibrium constant at different temperatures

T(K)	473	493	513	533	553	573	613	633	653	673
$K \cdot 10^{-3}$	456.88	237.99	129.74	72.897	42.054	24.836	14.975	9.1848	5.7281	2.3215

As it can be seen in Table 2, the equilibrium constant strongly depends on temperature, but its value being very high, it means that the equilibrium composition does not change significantly in the temperature range of 473–673 K. This fact can be also seen easily in Tables 3, 4 and 5 in which, the equilibrium composition at 473 and 673 K, expressed in molar fractions of benzene, isopropanol, cumene, water and nitrogen, noted by X_1, X_2, X_3, X_4 and X_5 respectively, are set out.

Table 3

Equilibrium composition of the system, for different molar ratios, benzene : isopropanol, in the presence of nitrogen

T(K)	Molar ratio	Composition, molar fractions				
		X_1	X_2	X_3	X_4	X_5
473	1 : 1	0.0092	0.0092	0.3628	0.3628	0.2560
	2 : 1	0.2456	0.0001	0.2463	0.2463	0.2608
	3 : 1	0.3685	0.0000	0.1841	0.1841	0.2631
	4 : 1	0.4413	0.0000	0.1471	0.1471	0.2644
673	1 : 1	0.0118	0.0011	0.3601	0.3601	0.2560
	2 : 1	0.2466	0.0002	0.2461	0.2461	0.2608
	3 : 1	0.3685	0.0001	0.1841	0.1841	0.2631
	4 : 1	0.4413	0.0000	0.1471	0.1471	0.2644

Table 4

Equilibrium composition of the system, for different benzene : isopropanol molar ratios, without nitrogen

T(K)	Molar ratio	Composition, molar fraction			
		X_1	X_2	X_3	X_4
473	1 : 1	0.0123	0.0123	0.4876	0.4876
	2 : 1	0.3334	0.0001	0.3331	0.3331
	3 : 1	0.5000	0.0000	0.2499	0.2499
	4 : 1	0.5999	0.0000	0.2000	0.2000
673	1 : 1	0.0159	0.0159	0.4841	0.4841
	2 : 1	0.3336	0.0003	0.3329	0.3329
	3 : 1	0.5001	0.0001	0.2498	0.2498
	4 : 1	0.6001	0.0000	0.1999	0.1999

Table 5

Equilibrium composition of the system for different benzene : isopropanol ratios, without nitrogen and water vapour

T(K)	Molar ratio	Composition, molar fractions		
		X_1	X_2	X_3
473	1 : 1	0.0241	0.0241	0.9518
	2 : 1	0.5000	0.0002	0.4998
	3 : 1	0.6667	0.0000	0.3333
	4 : 1	0.7499	0.0000	0.2501
673	1 : 1	0.0308	0.0308	0.9387
	2 : 1	0.5002	0.0005	0.4993
	3 : 1	0.6667	0.0002	0.3300
	4 : 1	0.7501	0.0000	0.2499

A careful examination of the data presented in Tables 3, 4 and 5 shows that the equilibrium composition strongly depends on the benzene : isopropanol molar ratio, only.

The equilibrium composition of the system was calculated on the basis of the following mathematical model:

$$K = \frac{X_3 \cdot X_4}{X_1 \cdot X_2} \tag{3}$$

$$X_1^0 = X_1 + X_2 \tag{4}$$

$$X_2^0 = X_2 + X_3 \tag{5}$$

$$X_2^0 = X_2 + X_4 \tag{6}$$

representing the mass-action law and the mass balance of phenyl, isopropyl and hydroxyl radicals, respectively, and X_1^0 and X_2^0, the molar fraction of benzene and isopropanol in the initial mixture.

Combining the mass-action law and mass balances equations, a new equations system that allows to calculate X_1, X_2, X_3 and X_4 from the equilibrium constant and initial composition, can be obtained:

$$X_3^2 + \frac{K}{1-K}(X_1^0 - X_2^0)X_3 - \frac{K}{1-K}X_1^0X_2^0 = 0 \tag{7}$$

$$X_1 = X_1^0 - X_3 \tag{8}$$

$$X_2 = X_2^0 - X_3 \tag{9}$$

$$X_4 = X_3 \tag{10}$$

For the benzene : isopropanol molar ratios of 1 : 1, 2 : 1, 3 : 1 and 4: 1, and nitrogen flow-rate of 20 cm^3/min., at reactants feed of 0.2 cm^3/min., the values of X_1^0, X_2^0 and X_5^0 are those summarized in Table 6.

Table 6

Composition of the initial mixture for different benzene : isopropanol ratios

Molar ratic	Composition, molar fractions		
	X_1^0	X_2^0	X_3^0
1 : 1	0.3720	0.3720	0.2560
2 : 1	0.4928	0.2464	0.2608
3 : 1	0.5527	0.1842	0.2631
4 : 1	0.5884	0.1471	0.2644

EXPERIMENTAL

Heating the two reactants up to a temperature ranging between 473 and 673 K without a corresponding catalytic system, no alkylation occurs. In order to find out how the performances pointed out thermodynamically can be obtained, the alkylation reaction was carried out in the presence of zeolite catalysts prepared from synthetic faujazite Y, modified by ion-exchange in the La, Ce and H form. Manufacture and structural-adsorptive and physico-textural characterization of the catalyst employed in this work was reported in two previous papers.[10,11]

The alkylation of benzene with isopropanol, in gaseous phase was carried out in a flow plant fully described in the literature. Alkylation was investigated for the initial benzene : isopropanol molar ratio of 1 : 1, 2 : 1, 3 : 1 and 4 : 1 at 0.2 cm^3/min. feed, on 10 cm^3 catalyst, at temperatures from 473 to 573 K and nitrogen flow-rate of 20 cm^3/min. The data concerning the catalytic activity, expressed by cumene yield (% mol), reported to initial isopropanol are represented in figures 1, 2 and 3.

Quantitative determination of the composition was carried out chromatographically.

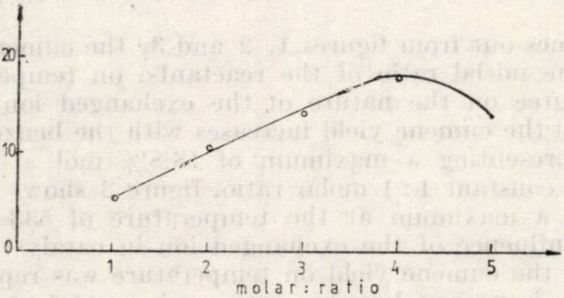

Fig. 1. — Dependence of the cumene yield on the benzene : isopropanol molar ratio, at 533 K on CeY catalyst.

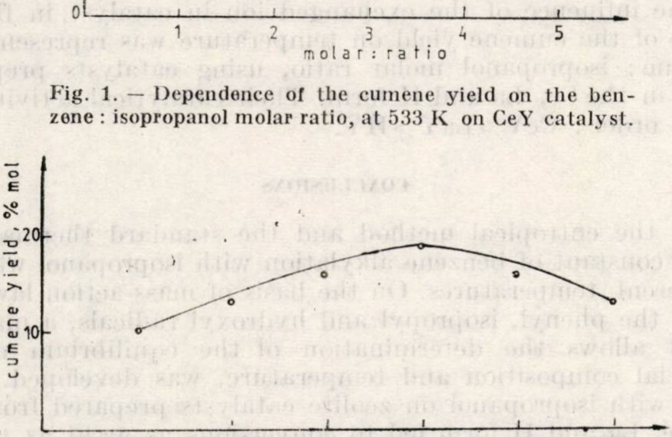

Fig. 2. — Effect of the temperature on the cumene yield for the 4 : 1 benzene : isopropanol molar ratio, on CeY catalyst.

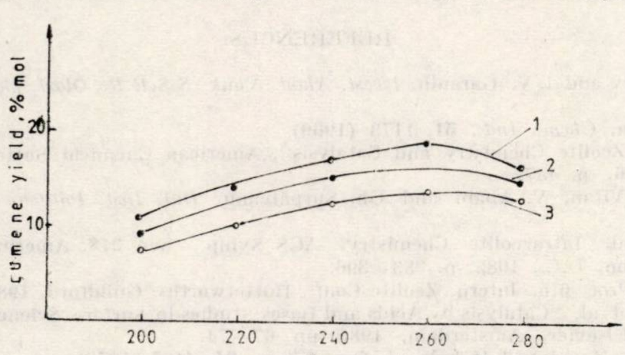

Fig. 3. — Effect of the exchanged ion on the cumene yield for the 4 : 1 benzene : isopropanol molar ratio, *1* — Ce, *2* — La, *3* — H.

DISCUSSION

Under the conditions considered above from all experiments the principal product was cumene, amounts of di- and polyalkylate products being negligible. This fact shows the high selectivity of the catalysts prepared on the basis of synthetic zeolites against the classical ones (at which formation of many di- and polyalkylates troubles the cumene separation).

As it comes out from figures 1, 2 and 3, the cumene yield strongly depends on the initial ratio of the reactants, on temperature and only to a little degree on the nature of the exchanged ion. Thus, figure 1 points out that the cumene yield increases with the benzene : isopropanol molar ratio, presenting a maximum of 18.8% mol at the molar ratio of 4 : 1. For a constant 4 : 1 molar ratio, figure 2 shows that the cumene yield exhibits a maximum at the temperature of 533 K. In order to find out the influence of the exchanged ion in catalyst, in figure 3 the dependence of the cumene yield on temperature was represented for the 4 : 1 benzene : isopropanol molar ratio, using catalysts prepared from faujazite Y in the Ce, La and H form. Their catalytical activity is situated in the order : CeY>LaY>HY.

CONCLUSIONS

Using the entropical method and the standard thermal data, the equilibrium constant of benzene alkylation with isopropanol was calculated for different temperatures. On the basis of mass-action law and mass balances of the phenyl, isopropyl and hydroxyl radicals, a mathematical model that allows the determination of the equilibrium composition against initial composition and temperature, was developed. Alkylation of benzene with isopropanol on zeolite catalysts prepared from faujazite Y in the Ce, La and H form led to conversions as great as those determined thermodynamically for the temperature of 533 K and 4 : 1 benzene : isopropanol molar ratio. The secondary reactions can be avoid using a large excess of benzene.

REFERENCES

[1] M. H. Minachev and I. V. Garanin, *Izvest. Akad. Nauk. S.S.R.R., Otdel. khim. Nauk*, **1963**, 999.

[2] F. G. Giappeta, *Chem. Ind.*, **51**, 1173 (1969).

[3] J. A. Rabo, "Zeolite Chemistry and Catalysis", American Chemical Society Washington, D.C., 1976, p. 437.

[4] N. Naum, F. Vitan, V. Ababi and Gh. Surpățeanu, *Bul. Inst. Politeh. Iași*, **24**, (3–4), 58(1978).

[5] W. E. Garwood, Intrazeolite Chemistry, ACS Symp., Ser. 218, American Chem. Soc., Washington, D.C., 1983, p. 383–396.

[6] W. O. Haag, Proc. 6th. Intern. Zeolite Conf., Butterworths, Guildford, 1984, pp. 466–479.

[7] S. M. Garces et al, "Catalysis by Acids and Bases Studies in Surface Science and Catalysis" vol. 20, Elsevier, Amsterdam, 1985, pp. 67–74.

[8] G. A. Olah, J. Kaspi and Bukala, *J. Org. Chem.*, **24**, 4187 (1977).

[9] ** * "Manualul inginerului chimist", vol. II, Ed. tehnică, Bucharest, 1952, p. 1454, 1560.

[10] N. Naum, P. Onu, N. Bîlbă and Gh. Mihăilă, *Rev. Chim (Bucureşti)*, **33**, 715 (1982).

[11] N. Naum, V. Ababi, Gh. Mihăilă and Ev. Popovici, *Bul. Inst. Politech. Iași*, **26**, fasc. 3–4, 62 (1980).

Revue Roumaine de Chimie, **32**, *5*, 525–532 (1987)

ACTIVITY AND SELECTIVITY OF ZEOLITE CATALYSTS IN *m*-XYLENE ISOMERIZATION

EMIL DUMITRIU, SPIRIDON OPREA and VASILE HULEA

Department of Organic Chemical Technology, Faculty of Chemical Technology, Jassy 6600, Romania

Received April 12, 1986

The catalytic properties of three zeolites, namely SK-500, HNdY and HZSM-5, in the reaction of *m*-xylene isomerization were investigated. Two kinetic models, the first taking into account only *m*-xylene isomerization to *p*- and *o*-xylene and the second connsidering the isomerization and disproportionation reactions of xylene, were adopted. The catalytic properties of zeolites were analysed on the basis of the rate constants determined by these kinetic models. It was found that HNdY showed a high activity, especially in the disproportionation reaction, but HZSM-5 had the best selectivity both for the isomerization reaction and for *p*-xylene formation.

As is known, the kinetic measurements offer the best method both for the catalyst characterization, in relation to its activity and selectivity, and for the comparison of various catalysts; in the last case the kinetic measurements must be carried out in the same conditions for all catalysts. Moreover, this method supplies a series of data which are useful in the improvement of the actual catalysts as well as to elucidate the mechanism of catalytic processes. Some of these aspects are found in the field of the catalytic reactions of xylenes.

Thus, the reaction of *m*-xylene isomerization is of great interest for the organic chemical industry where the demand for the *para* and *ortho* isomers exceeds the offer. That is why many studies on the reaction mechanism of isomerization and the activity of various catalysts were undertaken. The good activity of zeolite catalysts was proved in the gaseous phase isomerization of *m*-xylene [1-3] but, in respect of kinetics, relatively few catalysts were investigated (e.g. mordenite, [4] dealuminated Y zeolites [5] etc.). It can be also cited here the kinetic studies on the Friedel-Crafts catalysts, [6] silica-alumina, [7-10] silica-alumina supported platinum [11] etc., but these kinetic studies were approached in a very different manner so that an eventual comparison of the catalysts is difficult to be made.

The aim of this study is to investigate, on the one hand, the behaviour of some catalysts whose activity and selectivity data have not been yet reported, and on the other hand, the manner in which the experimental data verify the kinetic models.

EXPERIMENTAL

Catalysts. Three types of zeolite catalyts were used in the isomerization reaction, namely SK-500, HNdY and HZSM-5. The first catalyst was delivered by VENTRON and the composition of the anhydrous SK-500 extrudate zeolite was: 65.0% SiO_2, 22.7% Al_2O_3, 1.6% Na_2O and 10.7% RE_2O_3 (by weight). The specific area was about 550 m^2/g.

HNdY catalyst was prepared as follows: NaY (LZ-Y52 extrudate, VENTRON) was subjected to exchange with ammonium chloride solution under reflux conditions, followed by washing with distilled water and drying for 3 hr at 120°C to get NH_4NaY which on calcination at 500°C in a dry air stream resulted in the H^+ form. The residual Na^+ ions of HNaY sample were also exchanged for Nd^{3+} with 0.1 N $Nd(NO_3)_3$ solution. Finally, the percentage of natrium ions exchanged by ammonium was 53.0% and that by neodymium of 34.0% in equivalents. It was proved by X-ray diffraction that the zeolites did not lose their crystallinity during the process of ionic exchange. The specific area was about 600 m^2/g.

HZSM-5 was prepared according to U.S.Pat. 4, 199, 556. The *X*-ray analysis proved that the product had about 90% crystallinity. Inorganic oxides were used as binder.

Isomerization procedure. The isomerization reaction of *m*-xylene was carried out on an integral fixed-bed flow reactor operated under isothermal and plug-flow conditions at atmospheric pressure. The feed rate of *m*-xylene was accurately maintained by a calibrated syringe pump. Nitrogen was used as diluent and carrier gas.

Kinetic measurements. The kinetic experiments were performed by modifying the contact time as a result of different flow rates of *m*-xylene. All runs were carried out at constant molar ratio N_2/F and on the same amount of catalyst.

Analysis. The reaction products were analysed by GC using a column of benton 34 — dinonyl phthalate on Chromosorb W.

RESULTS AND DISCUSSION

It must be emphasised from the beginning that the catalysts used in the isomerization reaction of *m*-xylene have been chosen on the basis of their different catalytic properties. This assertion is supported by the results obtained in a series of preliminary experiments which pointed out the influence of the catalyst nature, contact time etc., on the catalytic activity and especially on the selectivity.

As is observed from Figure 1, the activities of the three catalysts, expressed as conversion of *m*-xylene vs. contact time, are approximately close but the small differences observed allow the following disposal of the catalysts according to their catalytic activity:

$$\text{HNdY} > \text{SK}-500 \geqslant \text{HZSM}-5$$

This order is also valuable for the catalytic activity in relation to the secondary reactions.

The data on the selectivity of zeolite catalysts (in respect of the isomerization reaction the selectivity is expressed as mole ratio between the resulted *p*- and *o*-xylene) are shown in Figure 2. As can be observed HZSM-5 shows the best selectivity. This behaviour is generally explained on the basis of the geometrical constrictions exerted on certain hydrocarbons by the internal structure of ZSM zeolite.

SK-500 zeolite does not show a distinct selectivity; the ratio between the xylene isomers formed in the presence of this catalyst and that obtained from the thermodynamic data (the composition at the thermodynamic equilibrium) are very close to one another. Therefore, the zeolites used as catalysts for the isomerization of *m*-xylene are disposed about their selectivity as follows :

$$\text{HZSM-5} > \text{HNdY} > \text{SK-500}$$

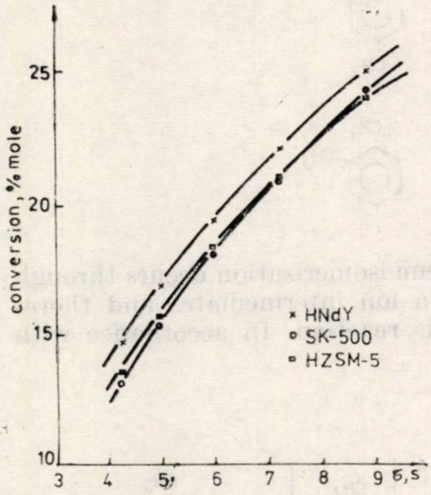

Fig. 1. — The *m*-xylene conversion *vs.* contact time ; T = 673 K, $N_2/F = 5/1$, $V_{cat} = 8.83\ cm^3$.

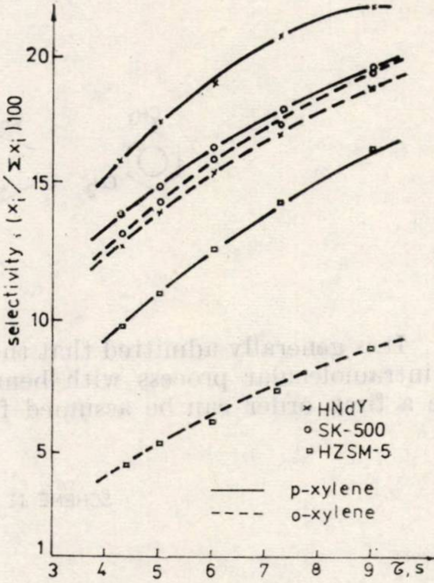

Fig. 2. — The selectivity for xylene isomers vs. contact time.

The above presented data allow only a qualitative estimation of the catalytic properties of the three zeolites. Consequently, we shall try to describe the catalytic properties of these zeolites by means of the kinetic parameters.

The experimental conditions were chosen in such a way that the bulk-mass transfer and intraparticle diffusional effects can be neglected. The influence of the external diffusion on the reaction rate was studied modifying the amount of catalyst while the temperature, pressure and the feed rate were kept constant. With reference to the intraparticle diffusional effects we must underline that the molecular sieve catalysts consist of small crystals of zeolites pelleted with binder and two distinct diffusional processes are therefore involved : (i) — diffusion through the macropores of the pellet and (ii) — diffusion within the micropores of the zeolite crystals. If the diffusional effect through the macropores can be avoided by the choice of proper pellet dimensions, the second effect involves the crystal size of zeolite. This effect could be studied modifying the conditions of zeolite synthesis affecting diffusivity characteristics. The kinetic rates presented here include the last micropore diffusional effect, if any.

On the basis of the above mentioned data it may be admitted that the process of catalytic isomerization of *m*-xylene was carried out in the kinetic range.

The first kinetic model which was adopted takes into account only the isomerization reaction (Scheme I):

SCHEME I

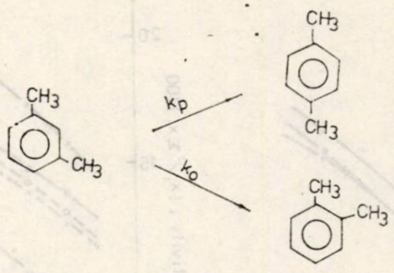

It is generally admitted that the xylene isomerization occurs through an intramolecular process with benzenium ion intermediates and therefore a first order can be assumed for this reaction. In accordance with the equation developed by Hiroshige and Yoshiro[12] for the first order reactions, the rate constant could be obtained by the following expression:

SCHEME II

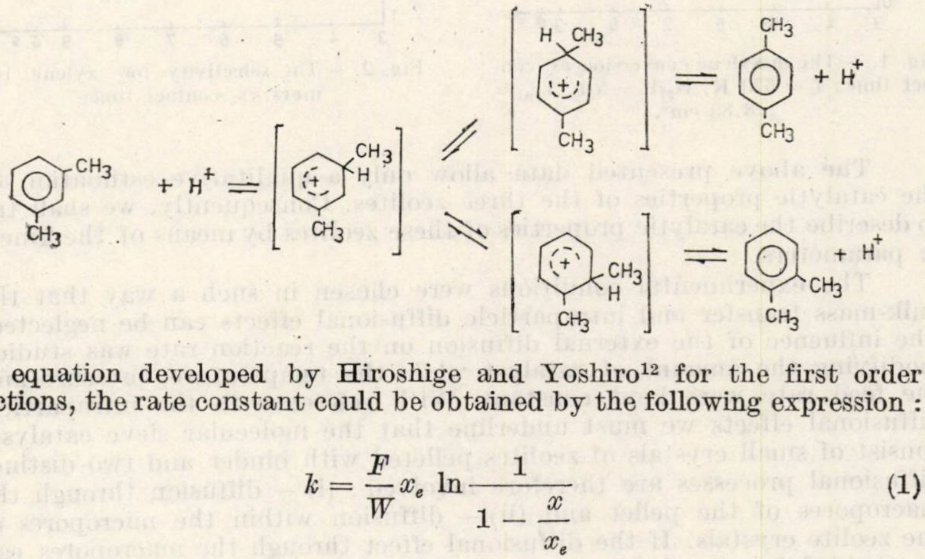

$$k = \frac{F}{W} x_e \ln \frac{1}{1 - \frac{x}{x_e}} \tag{1}$$

where W — the amount of catalyst,

F — the feed rate,

x_e — the mole fraction of xylene isomer at the equilibrium composition.

The equilibium composition of xylene isomers was calculated from the thermodynamic data and it is shown in Table 1.

Acid zeolites catalyze the isomerization of xylenes and also their disproportionation into trimethylbenzenes and toluene. It was admitted for the xylene disproportionation that the reaction mechanism involves the same benzenium ion intermediates as for the isomerization :

Table 1

The equilibrium composition of xylene isomers

Temperature (K)	Composition, mole fraction		
	$x_{m,e}$	$x_{p,e}$	$x_{o,e}$
623	0.5144	0.2444	0.2410
673	0.5086	0.2432	0.2486
698	0.5061	0.2417	0.2521
723	0.5035	0.2408	0.2556

SCHEME III

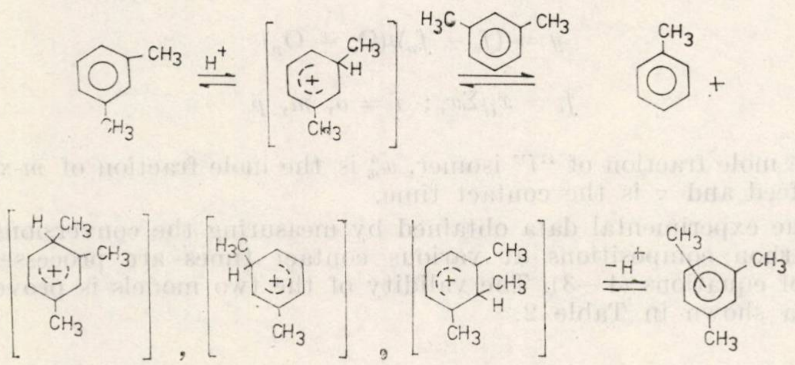
CH3
H+
CH3
H
CH3
H3C
CH3
CH3
+
CH3
H
CH3
CH3
CH3
H3C
H
CH3
CH3
CH3
H
CH3
CH3
−H+
CH3
CH3
CH3

Mathematical model for the simultaneous isomerization and disproportionation is based on a kinetic model involving a "triangular" scheme :

SCHEME IV

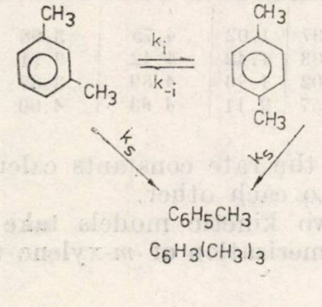
CH3
CH3
k_1
k_{-1}
CH3
CH3
CH3
CH3
ks
ks
$C_6H_5CH_3$
$C_6H_3(CH_3)_3$

Taking into account the following suppositions : (i) — the surface reactions are rate controlling and first order with respect to the hydrocarbon components, (ii) — the rate constants for the various disproportionation reactions of xylenes (i.e., *ortho* + *metha*, *ortho* + *para* etc.) have the same value, and (iii) — the toluene disproportionation and the catalyst deactivation by coking during the process are negligible, we could adapt here the kinetic model developed by Beltrame.[13] The rate constants k_i and k_s can be obtained by the following equations :

$$k_i = \frac{(1 - \O)\ \ln(1 - y)}{\tau} \tag{2}$$

$$k_s = -\frac{\ln \sigma}{\tau} \tag{3}$$

where

$$\O_m = x_{m,e}/(x_{o,e} + x_{p,e} + x_{m,e})$$

$$\sigma = (x_o + x_m + x_p)/x_m^o$$

$$y = (f_o + f_p)/(\O_o + \O_p)$$

$$f_i = x_i/\Sigma x_i\ ;\ \ i = o,\ m,\ p$$

x_i is the mole fraction of "i" isomer, x_m^o is the mole fraction of *m*-xylene in the feed and τ is the contact time.

The experimental data obtained by measuring the conversions and hydrocarbon compositions at various contact times are processed by means of equations (1—3). The validity of the two models is proved by the data shown in Table 2.

Table 2

The test of validity of the kinetic models ; HZSM-5 catalyst, T = 673 K

Contact time (s)	Composition of reaction products % mole					$k_s \times 10^3$ (s^{-1})	$k_i \times 10^2$ (s^{-1})	$k_p \times 10^5$ (s^{-1})	$k_0 \times 10$ (s^{-1})
	T	p−X	*m*−X	*o*−X	TMB				
4.61	1.00	9.51	84.10	4.37	1.02	4.75	3.98	9.58	3.83
6.48	1.21	12.27	79.07	6.03	1.42	4.42	3.91	9.64	3.91
7.81	1.68	13.95	75.54	7.02	1.70	4.89	3.87	9.71	3.88
9.73	1.98	15.74	71.60	8.57	2.11	4.63	4.00	9.54	3.97

It can be observed that the rate constants calculated at different contact times are very close to each other.

As stated above, the two kinetic models take into account, on the one hand, the catalytic isomerization of *m*-xylene to *o*- and *p*-xylene

(Scheme I) and on the other hand, the isomerization and disproportionation of xylenes (Scheme IV). Therefore, the rate constants obtained by means of eqs. (1—3) allow a quantitative estimation of the catalytic activity and selectivity (both for the *para* isomer, which is of great interest among the xylene isomers, and for the isomerization reaction in relation to the disproportionation). In respect of the catalytic activity, the data from Table 3 allow a more accurate comparison of the zeolite catalysts than that presented at the beginning. One can observe the good performances of HZSM-5.

Table 3

The rates constants of iomerization process for various catalysts; $T = 673$K

Catalyst	$k_i \times 10^2$ (s^{-1})	$k_s \times 10^2$ (s^{-1})	$k_p \times 10^5$ (s^{-1})	$k_0 \times 10^5$ (s^{-1})
HNdY	10.12	15.20	7.68	5.94
SK-500	8.61	10.20	6.28	8.53
HZSM-5	3.94	0.47	9.62	3.90

If we define the relative activity as ratio of rate constants corresponding to the various catalysts, e.g. $A = (k_i)_{\mathrm{HNdY}}/(k_i)_{\mathrm{HZSM\text{-}5}}$, and the selectivity as ratio $S = k_p/k_0$ or $S = k_i/k_s$, we can obtain the following results (see Table 4).

Table 4

The catalytic properties of zeolites in the isomerization process at 673 K

Catalytic properties	Catalyst		
	HZSM-5	SK-500	HNdY
Relative activity for			
— isomerization (model II)	1.0	2.18	2.56
— disproportionation	1.0	21.70	32.34
— isomerization to *p*-xylene (model I)	1.0	0.65	0.80
Selectivity for:			
— isomerization	8.38	0.84	0.66
— *p*-xylene	2.46	0.74	1.29

As shown in Table 4 the relative activity for the isomerization reaction increases in the order:

HZSM-5> SK-500 <HNdY

but the relative activity for the disproportionation increases in the same order, too. In addition, we can remark that the zeolites exchanged with rare earth are more active in the disproportionation than in the isomerization reaction. This aspect is clearly pointed out by the selectivity which drastically decreases from HZSM-5 to HNdY. An approximately similar remark can be made only on the isomerization reaction. The selectivity for *p*-xylene decreases as follows:

HZSM-5>HNdY>SK-500

The same disposal is kept for the relative activity in the isomerization reaction of *m*-xylene to *p*-xylene. Another interesting aspect consists in the relative high activity of SK-500 zeolite for the isomerization reaction of *m*-xylene to *p*-xylene.

The influence of temperature on the rate constants is shown in Figures 3 and 4. As the temperature is raised the rate constants are also increased, but the rate constant for *m*-xylene isomerization to *p*-xylene (k_p) and the rate constant for isomerization (k_i) are much stronger influenced by the temperature rising when the reaction is carried out in the presence of HZSM-5.

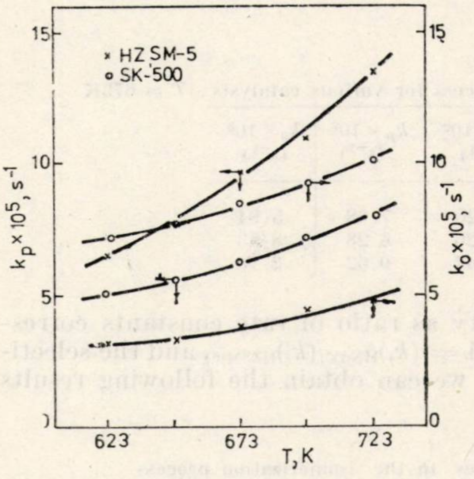

Fig. 3. — The influence of temperature on the rate constants k_0 and k_p.

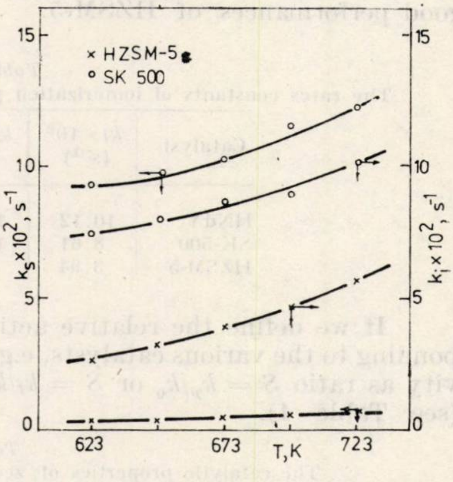

Fig. 4. — The influence of temperature on the rate constants k_i and k_s.

To conclude we can affirm that the calculations in terms of the rate constants indicate HZSM-5 as a proper catalyst for *m*-xylene isomerization ; though its activity is smaller than that of zeolites exchanged with rare earth, the selectivity of HZSM-5 is undoubtedly higher.

REFERENCES

[1] H. Matsumoto, J. Take and Y. Yoneda, *J. Catal.*, **11**, 211 (1968).

[2] M. F. Savits, Yu. G. Egiazarov and B. V. Romanovskii, *Kinetka i Kataliz*, **17**, 527 (1979).

[3] P. B. Weiszi, *Pure Appl. Chem.*, **52**, 2175 (1980).

[4] H. G. Norman, S. D. Shigemura and R. J. Hopper, *Ind. Eng. Chem.*, *Prod. Res Dev.*, **15**, 41 (1976).

[5] F. Gajewski and B. Sulikowski, *React. Kinet. Catal. Lett.*, **9**, 395 (1978).

[6] H. C. Brown and H. J. Jung. *J. Amer. Chem. Soc.*, **77**, 5579 (1955).

[7] A. J. Silvestri and C. D. Prater, *J. Phys. Chem.*, **68**, 3268 (1964).

[8] K. L. Hanson and A. J. Engel, *A.I. Ch. Eng. J.*, **13**, 260 (1967).

[9] A. Cortés and A. Corma, *J. Catal.*, **51**, 338 (1978).

[10] A. Corma, A. Cortés, I. Nebot and F. Tomás, *J. Catal.*, **57**, 444 (1979).

[11] S. Rașeev and B. Olteanu, *Rev. Chim. (București)*, **28**, 521 (1977).

[12] M. Hiroshige and M. Yoshiro, *J. Chem. Soc. Japan, Ind. Chem. Sect.*, **71**, 1496 (1968).

[13] P. Beltrame, P. L. Beltrame, P. Carniti and M. Magnoni, *Gazz. chim. Ital.*, **108**, 651 (1979).

Revue Roumaine de Chimie, **32**, 5, 533–538 (1987)

DISTRIBUTION OF PRODUCTS IN METHANOL CONVERSION OVER H–ZSM-5 TYPE ZEOLITES

GR. POP [1], M. BOZEŞANU [2], N.I. IONESCU, [2] I. IOSIF[2] and G. MUSCĂ [1]

[1] Institute of Chemical and Biochemical Energetics, Splaiul Independenţei 202, Bucharest, Romania

[2] ICECHIM – Center of Physical Chemistry, Splaiul Independenţei 202, Bucharest, Romania

Received June 16, 1986

The conversion reaction of methanol over H–ZSM-5 Zeolite catalyst diluted in a SiO_2 framework leads manly to the formation of methane and dimethylether. It is probable that methane formation is different from the formation of the other olefins.

In order to elucidate the mechanism of the methane formation over zeolite catalysts, a study of the reaction in its initial stage is necessary, that is at low conversions. These conditions are fulfilled by several methods :[1,2]

- less active catalysts
- high spatial velocities
- adequate temperature range
- inert diluent.

In our previous papers[3,4] where the autocatalytic character of the reaction has been evidenced and a global kinetic model has been worked out, the catalyst was diluted with inert material, the spatial velocities were high and the temperatures low.

In the present paper, we try to determine the distribution of the reaction products over a H–ZSM-5 catalyst.

EXPERIMENTAL

The experiments were carried out in a flow system at atmospheric pressure using a previously described [3] apparatus over a H–ZSM-5 catalyst whose catalytic activity was lowered by diluting it in a SiO_2 framework so as to obtain low methanol conversions. The catalyst/inert material (glass) ratios were 1 : 2, 1.25 : 1 and without dilution, corresponding to space velocities of 16.8, 10.2 and 5.5 h^{-1} within the 440–590°C temperature range.

The analysis of the reaction products was made by means of gas-chromatographic method. [3]

The main reaction products were : dimethylether, methane, ethene, propene and water. Hydrogen was not determined because in order to enhance the sensibility of the analytical method the analysis was carried out using hydrogen as eluent.

RESULTS AND DISCUSSION

The values for methanol conversion and distribution of the main reaction products are given in figures 1—4.

Figure 1 shows that the conversion for the catalyst diluted 1 : 2 with inert material lies on a curve having a maximum whose value decreases when the temperature rises.

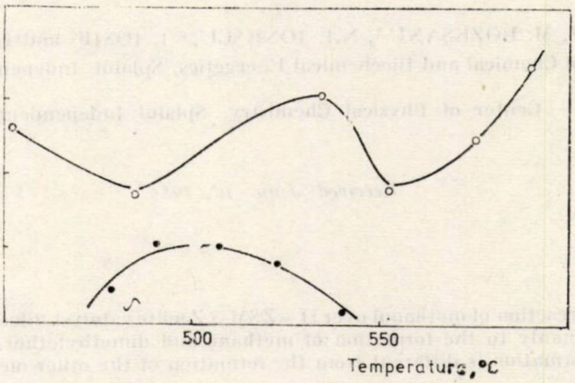

Fig. 1. — The variation of methanol conversion with temperature : ● — catalyst/inert material = 1 : 2 ; ○ — without dilution.

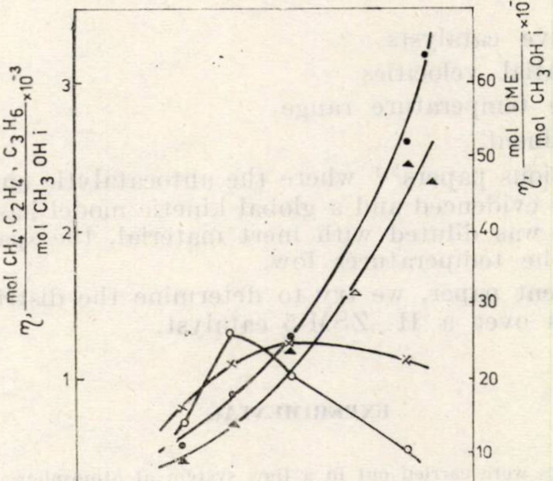

Fig. 2. — The variation of reaction products yields with temperature on diluted catalyst with ratio catalyst/inert material = 1 : 2 ● — CH_4, x — C_2H_4, ○ — C_3H_6, ▲ — DME.

The results obtained with the nondiluted catalyst present the shape characteristic of reactions with an autocatalytic character.

The yields of the main reaction products are presented in figures 2–4 as a function of temperature.

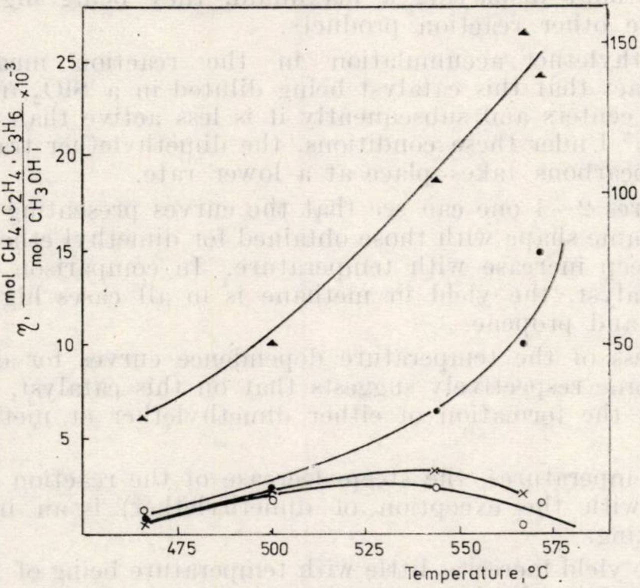

Fig. 3. — The variation of reaction products yields with temperature on diluted catalyst with ratio catalyst/inert material =1.25 : 1
● — CH_4, x — C_2H_4, o — C_3H_6, ▲ — DME.

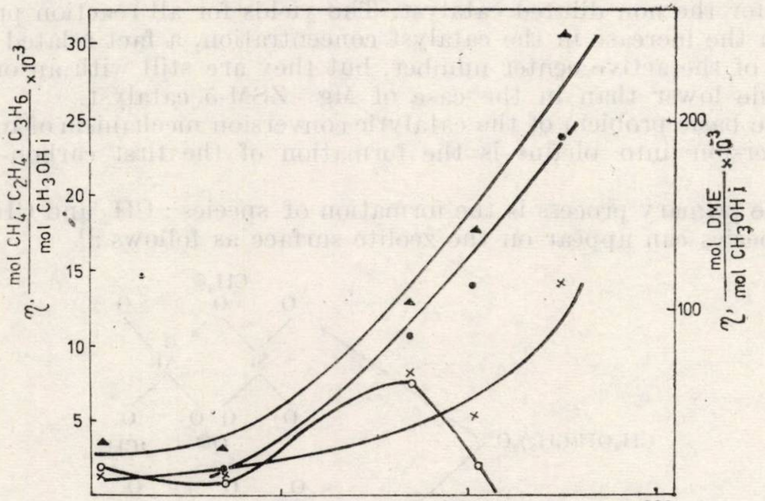

Fig. 4. — The variation of reaction products yields with temperature on catalyst without inert material.
● — CH_4, x — C_2H_4, o — C_3H_6, ▲ — DME

In all the three sets of experiments carried out on this catalyst, the conversion values are much lower than those obtained with the Mg—ZSM-5 catalyst. [3]

The yields in dimethylether in all the experiments increase with temperature without displaying a maximum, they being higher than those of all the other reaction products.

The dimethylether accumulation in the reaction medium can be due to the fact that this catalyst being diluted in a SiO_2 framework has less active centers and subsequently it is less active than the Mg-ZSM-5 catalyst. [5] Under these conditions, the dimethylether transformation into hydrocarbons takes place at a lower rate.

From figures 2—4 one can see that the curves presenting methane yield have the same shape with those obtained for dimethyl ether, that is they show a steep increase with temperature. In comparison with the Mg—ZSM-5 catalyst, the yield in methane is in all cases higher than that in ethene and propene.

The likeness of the temperature dependence curves for dimethylether and methane respectively suggests that on this catalyst, the conditions favoring the formation of either dimethylether or methane are the same.

At high temperatures, the steep decrease of the reaction products concentration (with the exception of dimethylether) is an indication of catalyst coking.

The ethene yield increases little with temperature being of the same order of magnitude with that for propene.

In all the three sets of experiments, the curves presenting the propene yield as a function of temperature show a maximum which is better marked for the non diluted catalyst. The yields for all reaction products rise with the increase in the catalyst concentration, a fact related to the increase of the active center number, but they are still with an order of magnitude lower than in the case of Mg—ZSM-5 catalyst.

The basic problem of the catalytic conversion mechanism of methanol conversion into olefins is the formation of the first carbon-carbon bond.

The primary process is the formation of species : CH_2 and CH_3^+.[5-11] These species can appear on the zeolite surface as follows :[11]

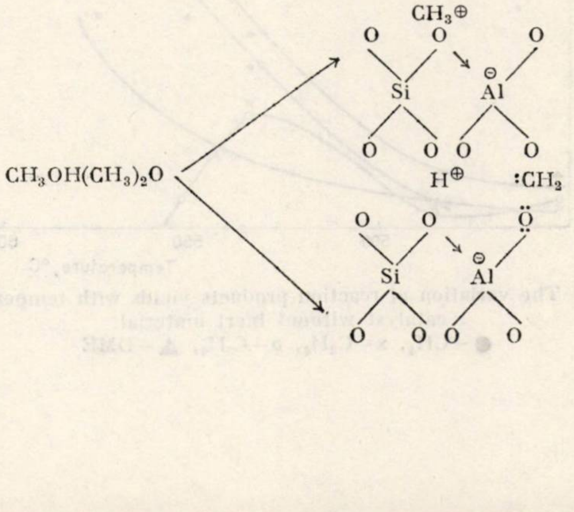

(I)

(II)

The species I and II can react subsequently as below.

$$(I) + CH_3OH \longrightarrow CH_4 + CH_3O^+ \ Zeol^-$$

or

$$2(II) \longrightarrow C_2H_4$$

Another way of methane transformation is based on the ability of either methanol or dimethylether to act as agents for hydrogen transfer :

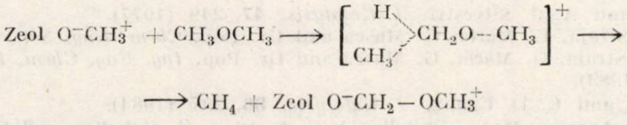

$$Zeol\ O^-CH_3^+ + CH_3OCH_3 \longrightarrow \left[\begin{array}{l} H \\ CH_3 \end{array} \!\!> CH_2O{-}CH_3\right]^+ \longrightarrow$$

$$\longrightarrow CH_4 + Zeol\ O^-CH_2-OCH_3^+$$

$CH_2-O-CH_3^+$ species can react on, leading to e other products.[12]

Methane could be also formed by intermediary radicalic reactions of the type :[13]

$$CH_3OH \longrightarrow CH_3^{\bullet} + OH.$$

which take place with the participation of the catalyst active centers. The methyl radicals are the precursors of some consecutive reaction sequences of the type :

$$CH_3^{\bullet} + CH_3^{\bullet} \longrightarrow CH_3-CH_3$$

$$CH_3^{\bullet} + CH_3-CH_2 \longrightarrow CH_4 + CH_3-CH_2.$$

$$CH_3-CH_2^{\bullet} \longrightarrow CH_2 = CH_2 + H.$$

$$CH_3^{\bullet} + H. \longrightarrow CH_4$$

The methyl radicals can be formed too following a radicalic mechanism, by dimethylether pyrolysis.[14,15]

$$CH_3-O-CH_3 \longrightarrow CH_3^{\bullet} + {\cdot}O-CH_3$$

The fact that the methane concentration on this diluted catalyst, which has few active centers, is generally higher than that of the other hydrocarbons, suggests that its formation is not related to these centers but it follows an independent reaction path. It is known that dimethylether formation needs the presence of some weakly acid centers, while the olefin formation needs some strongly acid ones.

No matter its nature, the reaction path for methane formation is independent of the other reaction products.

Besides the indicated probable mechanisms, ethene can appear either by dimethylether dehydration[16] or by an attack of the methylcarbenium ion on the carbon-hydrogen bond in methanol or dimethylether.[17]

Propene could appear from ethene reaction with methanol by insertion in a carbon-hydrogen bond.[18]

In conclusion, our experiments have shown that diluting H—ZSM-5 catalyst with a SiO_2 framework favors mainly the formation of dimethylether and methane. It is possible that this is the difference between methane and olefine formation respectively.

REFERENCES

[1] C. D. Chang, *Catal. Rev.-Sci. Eng.*, **26**, 323 (1984).

[2] M. M. Wu and W. W. Kaeding, *J. Catalysis*, **88**, 478 (1984).

[3] Gr. Pop, I. Iosif, M. Bozeșanu and N. I. Ionescu, *Rev. Chim. București*, **95**, 1078 (1984).

[4] N. I. Ionescu, B. Albu, I. Iosif, M. Bozeșanu, G. Musca and Gr. Pop, *React. Kinet. Catal. Lett*, **28**, 437 (1985).

[5] M. B. Sayed and R. P. Cooney, *Austral. J. Chem.*, **35**, 2483 (1982).

[6] G. Peret, F. X. Cormerais and M. Guisnet, *J. Mol. Catalysis*, **17**, 255 (1982).

[7] D. Kagi, *J. Catalysis*, **69**, 242 (1981).

[8] C. D. Chang and A. J. Silvestri, *J. Catalysis*, **47**, 249 (1977).

[9] R. Mihail, S. Straja, G. Maria, G. Musca and Gr. Pop, *Chem. Eng. Sci.*, **38**, 1581 (1983).

[10] R. Mihail, S. Straja, G. Maria, G. Musca and Gr. Pop, *Ing. Eng. Chem. Prod. Des. Dev.*, **22**, 532 (1983).

[11] C. T. W. Chu and C. D. Chang, *J. Catalysis*, **86**, 297 (1984).

[12] P. Dejaife, A. Auroux, P. C. Gravelle, J. C. Vedrine, Z. Gabelica and E. G. Derouane, *J. Catalysis*, **70**, 123 (1981).

[13] W. Zatorski and S. Krzyznowski, *Acta Physica et chimica*, **24**, 347 (1978).

[14] S. W. Benson and D. V. Jains, *J. Chem. Phys.*, **31**, 1008 (1959).

[15] K. H. Anderson and S. W. Benson, *J. Chem. Phys.*, **39**, 1681 (1963).

[16] E. G. Derouane, J. B. Nagy, P. Dejaifve, I. H. van Hoof, B. P. Spekman, J. C. Vedrine and C. Naccache, *J. Catalysis*, **53**, 40 (1978).

[17] Y. Ono, E. Imai and T. Mori, *Z. phys. Chem.* (*Frankfurt*), **115**, 99 (1979).

[18] M. S. Spencer and T. V. Witam, *J. Mol. Catalysis*, **17**, 271 (1982).

Revue Roumaine de Chimie, **32**, 5, 539–545 (1987)

INFORMATIONAL ENTROPY OF THE PROBABILITY FIELD EVENTS OF A CHEMICAL CONTROL ANALYSIS

VICTOR DAVID
Institute of Hygiene and Occupational Health, Str. Pop de Băsești 59, 72244–Bucharest, Romania

Received April 21, 1986

A new way of estimating the informational entropy of the results of an analytical experiment is proposed. This method can be applied to qualitative, semiquantitative and quantitative analyses and depends on several factors, such as the number of constituents of the analyzed sample, the number of concentration intervals (in the case of semiquantitative and quantitative analyses), the standard deviation, and the confidence interval of the analytical results.

INTRODUCTION

Analytical measuring systems behave as communication systems; they transmit chemico-analytical information about a sample or about a set of samples. The source of the analytical measuring system, modelled as a communication system, is the analyzed sample, to which a probability field may be assigned by means of information theory. Depending on the intended purpose of the chemical analysis – qualitative, semiquantitative or quantitative – the events related to a certain sample determine the *a priori* probability field of the analytical experiment. In the case of a qualitative chemical analysis, the events of the probability field, before the experiment, are the possible constituents X_i of the sample (elements, isotopes, radicals, compounds, phases, etc.), having the corresponding probabilities $p_i(i = 1, n$, where n is the maximum number of constituents of the sample). The probability field so defined will be noted by $\{X_i, p_i\}_{i=1,n}$. In the case of a semiquantitative analysis, the events of the probability field are the concentration intervals within whose limits the concentration of one or several analyzed components may lie. For a quantitative analysis, the events of the probability field may be defined if the concentration intervals set up by semiquantitative analysis, in which the concentrations of the analyzed components may lie, are divided by that value of the concentration (called sensitivity and noted by S) which depends on the performance of the analytical system. All three types of probability fields are characterized by their informational entropies, given by Shannon's relation:[1]

$$H = -\sum_i p_i \log_2 p_i \qquad (1)$$

This topic has been given much attention in the literature and different points of view on the application of the information theory to analytical chemistry have been published.[2-11]

The purpose of this paper is to present a novel method of estimating the total informational entropy related to the probability fields corresponding to the events of the qualitative, semiquantitative or quantitative chemical control analyses.

THEORETICAL CONSIDERATIONS

The qualitative composition of a sample is determined by analyzing it *qualitatively*; the sample constituents may be elements, isotopes, radicals, inorganic and/or organic compounds, phases, and so on. If the sample contains n components, the events of the probability field before the experiment are all the combinations of the n constituents taken $l = 0, n$ at a time; assuming that these events are independent of one another, their number is $\sum_{l=0}^{n} C_n^l = 2^n$ and their probabilities 2^n. The informational entropy of the events of a qualitative analysis, estimated before the analytical experiment by means of Shannon's relation, is given by

$$H(\text{qual}) = n(\text{bits}) \qquad (2)$$

The *semiquantitative* analysis of a sample consists in setting up some intervals $[c_{inf}, c_{sup}]$ within which the concentrations of the analyzed constituents of the analytical sample are situated. The concentration intervals within which the value of the concentration of a certain component i may lie could be practically represented as follows:

$$\begin{array}{lll} \text{Interval } 1: & 100-10\,\%; & c^1_{\text{sup}} = 10\, c^1_{\text{inf}} \\ \text{Interval } 2: & 10-1\,\%; & c^2_{\text{sup}} = 10\, c^2_{\text{inf}} \\ \text{Interval } 3: & 1-0.1\,\%; & c^3_{\text{sup}} = 10\, c^3_{\text{inf}} \qquad (3) \\ \ldots\ldots & \ldots\ldots & \ldots\ldots \\ \text{Interval } \nu: & 10^{3-\nu} - 10^{2-\nu}\,\%; & c^{\nu}_{\text{sup}} = 10\, c^{\nu}_{\text{inf}} \end{array}$$

The probability q_{ij} that the value of the concentration of the component i lie in one of these ν intervals is

$$q_{ij} = \frac{1}{\nu}\,; \quad \sum_{j=1}^{\nu} q_{ij} = 1, \; i = 1,n \qquad (4)$$

Therefore, the informational entropy corresponding to the probability field of a semiquantitative analysis for a component i is

$$H_i(\text{semiquant}) = \log_2 \nu \qquad (5)$$

For instance, if a semiquantitative analysis for a certain component is carried out down to the ppm level, the informational entropy of the events of this analysis has the value of 2.57 bits, whereas if the analysis is carried out down to the ppb level, the value is 3.14 bits.

The informational entropy corresponding to the events of a semiquantitative analysis of all the components of the sample has the expression

$$H(\text{semiquant}) = \sum_{i=1}^{n} H_i(\text{semiquant}) = n \log_2 \nu \tag{6}$$

By carrying out a *quantitative* chemical analysis for a certain component, a confidence interval $\overline{c} \pm \mu\sigma$ is set up, within which the value $\overline{c}$ of the true concentration of the analyzed component can be situated; here σ is the standard deviation of the analytical result c and μ is a number, set after analysis, which indicates the magnitude of the confidence interval in σ units (usually the value $\mu = 3$ is considered). To carry out a quantitative analysis, one or several analytical methods are used, either physical or physico-chemical, which are affected by a series of physico-chemical factors; the value of the standard deviation σ and the response function (the calibration curve) can be usually known before the analytical experiment for each method used for analyzing the sample. The value of the concentration of a certain component i, after the analytical experiment had been carried out, is $\overline{c}_{ij} \pm \mu_{ij}\sigma_{ij}$, $\overline{c}_{i,} \in [c^j_{\text{sup}}, c^j_{\text{inf}}]$, $j = 1, \nu$. Hence, the events of the probability field, before a quantitative, analysis has been carried out, are certain concentration microintervals, with a magnitude of $2\mu_{ij}\sigma_{ij}$, $j = 1, \nu$, $i = 1, n$. Besides, the events of the probability field corresponding to a quantitative analysis depend on the events of a semiquantitative analysis.

If $2_{ij}\mu\sigma_{ij}$ is the magnitude of the confidence interval for the quantitative analytical results, relative to the chemical component i and to the concentration interval j, the interval j can be subdivided into s_{ij} microintervals of magnitude $2\mu_{ij}\sigma_{ij}$, their number is given by the relation

$$s_{ij} = \frac{c^j_{\text{sup}} - c^j_{\text{inf}}}{2\mu_{ij}\sigma_{ij}} = \frac{9\times 10^{2-\nu}}{2\mu_{ij}\sigma_{ij}} \tag{7}$$

Since the obtained microintervals are independent of one another, the probability of a microinterval of the interval j, for a component i is the reverse of s_{ij},

$$p'_{ij} = \frac{2\mu_{ij}\sigma_{ij}}{9\times 10^{2-\nu}} \tag{8}$$

The described procedure of dividing before the experiment an interval j into microintervals of magnitude $2\mu_{ij}\sigma_{ij}$ implies another probability, after the experiment had taken place, namely the probability that the corresponding microinterval represents the true concentration $\overline{c}_{ij}$. The probability that a result $\overline{c}_{ij}$ deviates from the true value $\overline{c}_{ij}$ is a Gauss function. Therefore, the probability that a certain obtained result $c_{ij} \in [c^j_{\text{sup}}, c^j_{\text{inl}}]$ belongs to an interval $\overline{c}_{ij} \pm \mu_{ij}\sigma_{ji}$ can be estimated : it is equal to the probability that the corresponding interval represents the true value :

$$p''_{ij} = \frac{1}{\sigma_{ij}\sqrt{2\pi}} \int\limits_A^B \exp\left[\frac{(c_{ij} - \overline{c}_{ij})^2}{2\sigma^2_{ij}}\right] \mathrm{d}c_{ij} \tag{9}$$

$$(A = \overline{c}_{ij} - \mu_{ij}\sigma_{ij}\,; \quad B = \overline{c}_{ij} + \mu_{ij}\sigma_{ij})$$

After performing the variable change $z = (c_{ij} - \overline{c}_{ij})/\sigma_{ij}$, the integral (9) becomes

$$p''_{ij} = 2\left[\frac{1}{\sqrt{2\pi}} \int\limits_0^{\mu_{ij}} \exp\left(-\frac{z^2}{2}\right) \mathrm{d}z\right] = 2\Phi(\mu_{ij}) \tag{10}$$

where $\Phi(\mu_{ij})$ is the Laplace function, which is usually tabulated or can be easily estimated by computer for various values of μ_{ij}.

If multiplied by p''_{ij}, the probability p_{ij} gives the probability p_{ij} of obtaining a microinterval of magnitude $2\mu_{ij}\sigma_{ij}$ which would represent the true value $\overline{c}_{ij}$. Hence, p_{ij} is given by

$$p_{ij} = \frac{4\mu_{ij}\sigma_{ij}\Phi(\mu_{ij})}{9 \times 10^{2-j}} \tag{11}$$

The probability of obtaining by quantitative analysis a microinterval of the interval j, of magnitude $2\mu_{ij}\sigma_{ij}$, when the interval k had been determined previously by semiquantitative analysis, represents the probability $\pi(2\mu_{ij}\sigma_{ij}|k)$ of an event of the quantitative analysis conditioned by an event of a semiquantitative analysis : with a very good approximation this is given by the following equation :

$$\pi(2\mu_{ij}\sigma_{ij}|k) = p_{ij}\delta_{jk} \tag{12}$$

where δ_{jk} is the Kronecker symbol ($\delta_{jj} = 1$, $\delta_{jk} = 0$ if $j \neq k$). The entropy of the probability field which has as events the microintervals of magnitude $2\mu_{ij}\sigma_{ij}$ and the probabilities p_{ij}, conditioned by the event k of a semiquantitative analysis, is

$$H(2\mu_{ij}\sigma_{ij}|k) = -s_{ij}\pi(2\mu_{ij}\sigma_{ij}|k)\ \log_2 \pi(2\mu_{ij}\sigma_{ij}|k) \tag{13}$$

The entropy of the probability field corresponding to a quantitative analysis of a component i, conditioned by the probability field corresponding to a semiquantitative analysis, noted by H_i (quant|semiquant), has the expression

$$H_i(\text{quant}\,|\text{semiquant}) = \sum_{k=1}^{\nu}\sum_{j=1}^{\nu} q_{ij} H(2\mu_{ij}\sigma_{ij}\,|k) =$$

$$= -\sum_{k=1}^{\nu}\sum_{j=1}^{\nu} s_{ij} q_{ij} p_{ij} \delta_{jk} \log_2 p_{ij} \qquad (14)$$

Replacing expressions (4) and (11) by q_{ij} and p_{ij}, respectively, the following expression is obtained for the informational entropy of the probability field corresponding to the events of a quantitative analysis of a component i, depending on the probability field of the events of a semiquantitative analysis :

$$H_i(\text{quant}\,|\text{semiquant}) = \frac{2}{\nu}\sum_{j=1}^{\nu} \Phi(\mu_{ij}) \log_2 \frac{9\times 10^{2-j}}{4\mu_{ij}\sigma_{ij}\Phi(\mu_{ij})} \qquad (15)$$

Taking into account all the components of the sample, expression (15) becomes

$$H(\text{quant}\,|\text{semiquant}) = \frac{2}{\nu}\sum_{i=1}^{n-1}\sum_{j=1}^{\nu} \Phi(\mu_{ij}) \log_2 \frac{9\times 10^{2-j}}{4\mu_{ij}\sigma_{ij}\Phi(\mu_{ij})} \qquad (16)$$

The informational entropy H corresponding to the events of the complete control analysis of an analytical sample is

$$H = H\,(\text{qual}) + H(\text{semiquant}) + H(\text{quant}\,|\text{semiquant}) \qquad (17)$$

or, more explicitly,

$$H = n\log_2 2\nu + \frac{2}{\nu}\sum_{i=1}^{n-1}\sum_{j=1}^{\nu} \Phi(\mu_{ij}) \log_2 \frac{9\times 10^{2-j}}{4\mu_{ij}\sigma_{ij}\Phi(\mu_{ij})} \qquad (18)$$

Expression (18) depends on 4 variables : n, ν, σ_{ij} and $\mu_{ij}(i = 1, n,\ j = 1, \nu)$. The informational entropy H is a linear function of n and a logarithmic function of ν and σ_{ij} ; it is a convex function of μ, so that a value of μ can be found for which the function $H(\mu)$ has a maximum.

APPLICATIONS AND CONCLUSIONS

The standard deviation σ_{ij} for a component $i = 1, n$ and a concentration interval $j = 1, \nu$ may be expressed as a function of proportionality of the lower limit of the corresponding concentration interval, $c^j_{\text{inf}} = 10^{2-j}$,

$$\sigma_{ij} = \beta_{ij} 10^{2-j} \qquad (19)$$

In this case, the function H can be written in a simpler form :

$$H = n \log_2 2\nu + \frac{2}{\nu} \sum_{i=1}^{n-1} \sum_{j=1}^{\nu} \Phi(\mu_{ij}) \log_2 \frac{9}{4\beta_{ij}\mu_{ij}\Phi(\mu_{ij})} \tag{20}$$

In what follows, we will give some examples of estimating H, considering the ideal case in which β_{ij} and μ_{ij} are constant, having the values β and μ for any $i = 1, n$ and $j = 1, \nu$. The following expression of H is thus obtained :

$$H = n \log_2 2\nu + 2(n-1)\Phi(\mu) \log_2 \frac{9}{2\beta\mu\Phi(\mu)} \tag{21}$$

The values of the informational entropy obtained for a set of $n = 10$ analyzed constituents as a function of β and μ parameters, for an analysis carried out down to the ppm ($\nu = 6$) and the ppb ($\nu = 9$) levels, are given in Table 1. It can be a seen that the informational entropy of the results of the control analysis increases with the increase of the precision of the analytical measuring process, represented by the parameter β.

Table 1

The values of the informational entropy (in bits) for a set of $n=10$ components, as a function of β and μ ; the quantitative analysis is carried out down to the ppm ($\nu = 6$) and the ppb ($\nu = 9$) levels

μ	$\Phi(\mu)$	$\beta = 0.1$		$\beta = 0.01$		$\beta = 0.001$	
		$\nu = 6$	$\nu = 9$	$\nu = 6$	$\nu = 9$	$\nu = 6$	$\nu = 9$
		H	H	H	H	H	H
0.25	0.0987	53.32	59.17	59.22	65.07	65.12	70.97
0.50	0.1915	63.00	68.85	74.45	80.30	85.90	91.75
0.75	0.2734	69.20	75.05	85.55	91.40	101.90	107.75
1.00	0.3413	72.98	78.83	83.38	99.23	113.79	119.64
1.25	0.3944	74.98	80.83	98.56	104.42	122.15	128.00
1.50	0.4332	75.72*	81.57*	101.62	107.48	127.53	133.38
1.75	0.4599	76.62	81.47	103.13	108.98	130.63	136.48
2.00	0.4772	75.01	80.86	103.55*	109.40*	132.08	137.93
2.25	0.4878	74.11	79.96	103.28	109.13	132.45*	138.30*
2.50	0.4938	73.07	78.92	102.60	108.45	132.12	137.97
2.75	0.4970	72.00	77.85	101.72	107.57	131.44	137.29
3.00	0.4987	70.95	76.80	100.77	106.62	130.59	136.44

* Indicates the maximum of H for constant ν and β.

An important application of the proposed model consists in setting up an optimum value of the sensitivity of the measurement of that physical property which is being used in the analytical process as a function of the standard deviation of the whole analytical process used in the chemical analysis (from sampling and sample processing to the displayed result). It results from the described model that the optimum value of the measurement sensitivity, noted by S_{opt}, is that value which corresponds to a maximum of the informational entropy of the analytical results as a function of μ_{ij} and σ_{ij}, that is $S_{opt} = \mu_{ij}\sigma_{ij}$ so that $H(\mu_{ij}\sigma_{ij}) = \max$; for $S < \mu_{ij}\sigma_{ij}$ one would obtain a large number s_{ij} of concentration micro-intervals, but with a low probability of representing the true value, whereas for $S > \mu_{ij}\sigma_{ij}$ one would obtain a small number s_{ij} and a high probability of representing the true value of the concentration of the component i. In this way, one can select the measuring process or the outcome of the results as a function of the standard deviation for the corresponding analytical process, so that the obtained analytical results carry the maximum possible amount of information.

To exemplify, we will consider here the quantitative determination of a component in the range of parts per million, that is [1, 1000]ppm, with a standard deviation of the analytical results $\sigma = 0.1$ ppm, assumed to be constant over the entire given concentration range. According to Table 1, the value $\mu = 1.5$ corresponds to a maximum informational entropy of the analytical results, so that the analytical results of maximum informational entropy are those from the series

$$[1\,;\ 1.15\,;\ 1.30\,;\ 1.45\,;\ 1.60\,;\ldots\,;1000]\text{ppm}$$

The above series of results has therefore an informational entropy larger than the series of results given below, obtained with a similar standard deviation :

$$[1\,;\ 1.01\,;\ 1.02\,;\ 1.03\,;\ 1.04\,;\ 1.05\,;\ldots\,;1000]\text{ppm}$$

To conclude, by means of this procedure one can estimate and optimize the value of the informational entropy of the analytical results as a function of the number of analyzed components, the number of concentration domains, the standard deviation and the sensitivity of the measuring process.

REFERENCES

[1] C. E. Shannon, *Bell Syst. Tech. J.*, **27**, 379, 623 (1948).

[2] K. Eckschlager and V. Stepanek, "Information Theory as Applied to Chemical Analysis", John Wiley & Sons, New York, 1979.

[3] C. Liteanu and I. Rîcă, "Statistical Theory and Methodology of Trace Analysis", Ellis Horwood, Chichester, 1980.

[4] C. Liteanu and I. Rîcă, "Optimizarea proceselor analitice", Ed. Academiei, Bucharest, 1985.

[5] H. Kaiser, *Anal. Chem.*, **42**, 24A(2), 26A(4), (1970).

[6] K. Eckschlager, *Anal. Chem.*, **49**, 1265 (1977).

[7] K. Eckschlager and V. Stepanek, *Anal. Chem.*, **54**, 1115A (1982).

[8] C. Liteanu and I. Rîcă, *Anal. Chem.*, **51**, 1986 (1979).

[9] I. Frank, G. Veress and E. Pungor, *Hung. Sci. Instr.*, **54**, 1 (1982).

[10] V. David and D. Ciomîrtan, *Rev. Roumaine Chim.*, **30**, 777 (1985).

[11] V. David and D. Ciomîrtan, *Rev. Roumaine Chim.*, to be published.

the measurement sensitivity, noted by S_{opt}, is that value which corresponds to a maximum of the informational entropy of the analytical results as a function of μ_i and σ_i, that is $S_{opt} = \mu_i\sigma_i$, so that $H(\mu_i\sigma_i) = \max$; for $S < \mu_i\sigma_i$ one would obtain a large number s_1 of concentration intervals, but with a low probability of representing the true value, whereas for $S > \mu_i\sigma_i$ one would obtain a small number s_2 and a high probability of representing the true value of the concentration of the component i. In this way, one can select the measuring process, or the outcome of the results as a function of the standard deviation for the corresponding analytical process, so that the obtained analytical results carry the maximum possible amount of information.

To exemplify, we will consider here the quantitative determination of a component in the range of parts per million, that is (1, 1000) ppm, with a standard deviation of the analytical results $\sigma = 0.1$ ppm, assumed to be constant over the entire given concentration range. According to Table 1, the value $\mu = 1.5$ corresponds to a maximum informational entropy of the analytical results, so that the analytical results of maximum informational entropy are those from the series

$$[1;\ 1.15;\ 1.30;\ 1.45;\ 1.60;\ \ldots;\ 1000]\ \text{ppm}$$

The above series of results has therefore an informational entropy larger than the series of results given below, obtained with a similar standard deviation:

$$[1;\ 1.01;\ 1.02;\ 1.03;\ 1.04;\ 1.05;\ \ldots;\ 1000]\ \text{ppm}$$

To conclude, by means of this procedure one can estimate and optimize the value of the informational entropy of the analytical results as a function of the number of analyzed components, the number of concentration domains, the standard deviation and the sensitivity of the measuring process.

REFERENCES

[1] C. E. Shannon, Bell Syst. Tech. J., 27, 379, 623 (1948).
[2] K. Eckschlager and V. Štěpánek, "Information Theory as Applied to Chemical Analysis", John Wiley & Sons, New York, 1979.
[3] C. Liteanu and I. Rîcă, "Statistical Theory and Methodology of Trace Analysis", Ellis Horwood, Chichester, 1980.
[4] C. Liteanu and I. Rîcă, "Optimizarea proceselor analitice", Ed. Academiei, Bucureşti, 1985.
[5] H. Kaiser, Anal. Chem., 42, 24A(2), 26A(4), (1970).
[6] K. Eckschlager, Anal. Chem., 49, 1265 (1977).
[7] K. Eckschlager and V. Štěpánek, Anal. Chem., 54, 1115A (1982).
[8] C. Liteanu and I. Rîcă, Anal. Chem., 51, 1986 (1979).
[9] I. Frankó, G. Veress and E. Pungor, Hung. Sci. Instr., 54, 5 (1982).
[10] V. David and G. Gheorghiu, Rev. Roumaine Chim., 30, 277 (1985).
[11] V. David and G. Gheorghiu, Rev. Roumaine Chim., to be published.

Revue Roumaine de Chimie, **32**, 5, 547–548 (1987)

BOOK REVIEW

John G. Verkade, "A Pictorial Approach to Molecular Bonding", Springer-Verlag, New York, 1986, 282 pp, ISBN 3–540–96271–9, Hard cover, DM 125

We welcome the appearance of an undergraduate-level textbook on elementary quantum chemistry using visual, intuitive and conceptual aids, and allowing (on the basis of only high school level chemistry, geometry, physics and trigonometry) to find localized and delocalized molecular orbitals (MOs) as well as normal vibrational modes in organic, inorganic and organometallic molecules.

Although initially developed and taught together with Klaus Ruedenberg and David K. Hoffman, the new concept of the generator orbital **(GO)**" method is authored here by J.G. Verkade with due acknowledgement of the others' earlier contributions. The present volume is the outcome of almost 20 years of evolution of undergraduate courses at Iowa State University on the basic elements of chemical bonding.

The gradual and fully logical introduction of basic principles and laws governing atomic orbitals (the first two chapters, i.e. 50 pages) is eminently pedagogical. No fact is considered too trivial to be left undefined, and if certain mathematical deductions or physical laws are introduced without justification (in order to keep the Appendixes to a minimum) this is explicitly stated.

The remaining nine chapters, i.e. 200 pages, are devoted to the systematic survey of molecules : diatomic (chapter 3), linear triatomic (ch. 4), triangular and related ones (ch. 5), bent triatomic (ch. 6), polygonal (ch. 7), octahedral (ch. 8), tetrahedral and related ones (ch. 9), bipyramidal (ch. 10) and prismatic molecules (ch. 11). The book has five Appendixes dealing with symmetry, with the description of a simple kit for constructing and visualizing three-dimensional styrofoam models of MOs, patented by J.G. Verkade and K. Ruedenberg, and with mathematical developments which would have lengthened the text. A subject index is included, but it does not include the names of the molecules discussed in various chapters.

Of course, the main theme of the book is the use of **GOs** (fictitious orbitals, placed in the center of a molecule, with appropriate symmetries and having quantum numbers n and l beyond those used in any atomic ground states). The excellent illustrations and printing conditions make the book highly readable and enjoyable. Actually, it is as exciting to read as Coulson's classical "Valence" or his lecture notes edited by O'Leary and Mallion, because despite the elemental presentation, one senses that this is purposeful, and is derived from a deep understanding of the subject. Only a good specialist can write an enjoyable textbook at an elementary level.

Highly commendable are the contour plots of mixtures of s and p atomic orbitals in various ratios from $\infty : 1$ to $1 : \infty$ (p. 37) as well as the continuous progression from one hybrid orbital set to another (p. 49).

Some of the questions that would be raised by the text in the mind of the potential reader are treated as problems at the end of each chapter. Some of the problems are connected with equations developed in the respective chapters, but most of them ask the student to develop pictorial representations of the bonding in molecular species. Some of the problems are actually linked with published papers (in some cases, authors' names are presented). Understandably (but regrettably) for a textbook, no bibliography is appended, nor are solutions to problems included.

An interesting and pedagogical idea is the developement of a set of rules for using **GOs** which is updated in a stepwise manner in consecutive chapters. Unfortunately, no open-shell molecule except O_2 is discussed. Curiously, Hund's rule, although used is not named, and the mnemonic device (p. 33) for the filling sequence of AOs is not called by its usual name (the $n + l$ rule). Although electron dash structures are used, double-headed arrows are not.

It would have been interseting to discuss isolobal groups and to mention on one hand NO_2^+ as a linear molecule isoelectronic with CO_2, and on the other hand the closed-shell SO_2 and the open-shell molecule NO_2 as further examples of bent triatomic molecules in addition to NO_2^-. These are, however, very minor improvements which may be suggested.

Although most abbreviations are of wide usage and all of them are explicitly defined on first encounter, a future edition would profit from the inclusion of a page dedicated to notation.

It should be stressed that this book encompasses both organic and inorganic molecules. This book induces the student to think in unified terms of chemical bonding for covalent of coordinative bonds, to understand hydrogen bonding and the two-electron three-center bonds or electron-deficient compounds, to realize how it is that N_3^+, $(CH)_3^+$, Te_4^{2+}, $CH)_5^-$, $(CH)_6$, $(CH)_7^+$, and $(CH)_8^{2-}$ are, and that ferrocene possesses planar rings with aromatic character. The geometry of molecules is based on Gillespie and Nyholm's VSEPR theory, but its limitations are frankly mentioned for 50-electron molecules such as XeF_6 and for transition metal complexes.

Brief expositions of the Jahn-Teller effect in cyclobutadiene, of hypervalency in molecules such as xenon fluorides, and of the ligand field and crystal field theories in metal complexes find their place naturally in the book.

Having already likened this book to the "Coulsin spirit", the reviewer hopes that it will find the success it deserves. He recommends it warmly to all teaching staff of chemistry departments at any level, and to all students who wish to become acquainted with a simple and useful method for visualizing MOs and (without the aid of group theory), who desire to determine the appearance of normal vibrational modes of moolecules.

A.T. Balaban

Polytechnic Institute, Bucharest

CORRIGENDUM

The author wishes to correct the following errors in his article published in *Revue Roumaine de Chimie*, **31**, 309 (1986), p. 318:

Line 2: "geminal anisochroneous protons" should be written correctly "geminal chemical shift nonequivalent protons" (see also A.O. Fulea, in "Abstracts", "Magnetic Resonance in Physics, Chemistry, Biology, Medicine", 9th Meeting of ISMAR held between June 29/July 5, 1986; A24, p. 38, Rio de Janeiro, Brasil).

Line 6: "for the observation of the geminal chemical shift nonequivalence" sthould be replaced by "for the geminal chemical shift nonequivalence".

Line 19: "(more precisely a symmetry plane)" should be corrected to "(more precisely a C_2 symmetry operation)".

ORSZÁGOS MŰSZAKI INFORMÁCIÓS KÖZPONT ÉS KÖNYVTÁR
1983

AZOMUREŞ
TÎRGU MUREŞ

L'USINE DE

matériaux PHOTOSENSIBLES azo

produit et offre:

- **FILM MICROSCOPIE ÉLECTRONIQUE AZO-AME**
- FILM RADIOGRAPHIQUE MÉDICAL **AZOIX RX$_{R-2}$**
- FILM CINÉANGIOGRAPHIQUE **AZOIX AX-1**
- FILM SÉRIOGRAPHIQUE **AZOIX SX-1**
- FILM SÉRIOANGIOGRAPHIQUE **AZOIX ASX-1**
- FILM MICRO-RADIO-PHOTO **AZOIX MX-1**
- FILM NÉGATIF POUR RÉPRODUCTIONS PHOTOGRAPHIQUES DES DOCUMENTS **AZOCOPY DN-3**
- FILM POSITIF POUR RÉPRODUCTIONS PHOTOGRAPHIQUES DES DOCUMENTS **AZOCOPY DP-1**
- PAPIER DÉRIVATOGRAPHE **AZOGRAF ID-2**
- FILMS PHOTOTECHNIQUES, PAPIERS PHOTOGRAPHIQUES NOIR ET BLANC ET EN COULEURS, PELLICULES CINÉMATOGRAPHIQUES NÉGATIVES, POSITIVES RÉVERSIBLES, ETC. . . .

TELEX: 065—246 AZOMUREŞ

ORSZÁGOS MŰSZAKI

NOTE POUR LES AUTEURS

La Revue Roumaine de Chimie publie des articles en anglais, français, russe, allemand ou espagnol. Les auteurs sont priés d'envoyer des articles et des comptes rendus inédits.

Les manuscrits seront dactylographiés à double interligne. La bibliographie, les tableaux et la légende des figures seront placés après le texte.

Si l'article fait partie d'une série numérotée, la partie précédente sera donnée comme première référence.

Chaque article sera précédé d'un résumé comprenant quinze lignes au maximum.

Les références bibliographiques dans le texte seront faites par des exposants sans parenthèses et paraîtront à la fin de l'ouvrage.

Les publications périodiques mentionées dans la bibliographie seront présentées suivant les prescriptions internationales : le nom de l'auteur précédé de l'initiale du prénom, le titre périodique abrégé conformément à « Chemical Abstracts » et souligné par une ligne, le numéro du tome indiqué par des chiffres arabes et souligné par deux lignes, suivi de la première page de l'article ; à la fin, l'année de la parution sera placée entre parenthèses. Le numéro de la revue ne sera pas indiqué si les pages du volume sont numérotées consécutivement.

Les textes des livres ou traités inclueront : le nom des auteurs, l'initiale du prénom, le titre du livre entre guillemets et sans être souligné, le numéro du tome précédé par l'abréviation « vol. » (ou « Bd »), le numéro de l'édition, les éditions (the publisher), la localité de la parution du livre, l'année de la parution et la page de la référence précédée(s) par l'abreviation « p » (ou « S. »).

Les brevets seront indiqués comme suit : l'auteur ou la firme, le pays et le numéro du brevet, la date et la revue (*Chem. Abstr.*) Par ex : M. Jones (to Union Carbide Co.), Brit. Pat. 601 238, 2 Sept. 1959 ; cf. *Chem. Abstr.*, **54**, 12808 (1960).

Si la référence n'a pas été lue en original, on indiquera aussi la revue de référence consultée.

Les diagrammes seront tracés à l'encre de Chine sur papier calque. Les tableaux et les figures (en nombre strictement nécessaire) ainsi que les courbes dans les figures seront numérotés par des chiffres arabes. Leur explication sera donnée dans la légende des figures. Prière de ne pas inscrire les mêmes données dans les tableaux et les figures. Chaque tableau aura un titre. On indiquera dans le texte la place approximative des tableaux et des figures. Les formules chimiques seront incluses dans le texte ; en outre elles seront transcrites sur papier calque à l'encre de Chine.

Les auteurs sont priés d'indiquer les caractères italiques (en soulignant les lettres au crayon), ainsi que tout autre caractère spécial ; les prefixes *ortho*, *meta*, *para*, *cis*, *trans*, etc. seront soulignées pour indiquer leurs caractères italiques et ne seront jamais écrits avec des majuscules.

Aucune correction à la main ne sera admise sur le manuscrit. Les corrections seront tapées à la machine. Les lettres grecques ou d'autres symboles spéciaux seront insérés à la main à l'encre clairement.

Le manuscrit sera signé par l'auteur.

Le titre-courant aura 50 lettres au maximum.

L'entiére responsabilité du contenu des articles appartient aux auteurs.

Sur demande on peut obtenir une note plus complete.

PRINTED IN ROMANIA

1987 JUN 16

TRAVAUX PARUS AUX ÉDITIONS DE L'ACADÉMIE DE LA RÉPUBLIQUE SOCIALISTE DE ROUMANIE

ELENA CEAUŞESCU, **Progrese în chimia şi tehnologia polimerilor**, 1986, p. 446.

ELENA CEAUŞESCU, **Forschungen im Bereich der Chemie und Technologie der Polymere**, 1986, 444 p.

M. BUDRUGEAC, **Probleme de chimie**, 1986, 280 p.

I. G. MURGULESCU, O. M. RADOVICI, **Introducere în chimia fizică, vol. IV. Electrochimia**, 1986, 416 p.

D. PURDELA, **Nomenclatura chimiei anorganice**, 1986, 454 p.

T. ONCESCU, S. G. IONESCU, **Conversie fotochimică şi stocare de energie solară**, 1985, 272 p.

A. T. BALABAN, I. GĂLĂŢEANU, G. GEORGESCU, L. SIMIONESCU, **Labelled compounds and radiopharmaceuticals applied in nuclear medicine**, coédition avec J. Wiley & Sons, 1986, 742 p.

RAUL MIHAIL, ION GROZEANU, **Estimarea secvenţială aplicată sistemelor chimice**, 406 p.

B. BREZEANU, L. PATRON, M. ANDRUH, **Combinaţii complexe polinucleare şi aplicaţiile lor**, 224 p.

V. Em. SAHINI, M. HILLEBRAND, **Chimia cuantică în exemple şi aplicaţii**, 1985, 380 p.

N. PERESCU, **Chimia extracţiei cu solvenţi şi aplicaţii**, 1985, 212 p.

V. DRĂGUŢAN, A. T. BALABAN, M. DIMONIE, **Olefin metathesis and ring-opening polymerization of cyclo-olefins**, coédition avec John Wiley & Sons, 1985, 544 p.

GH. MARCU, **Chimia compuşilor coordinativi**, 1984, 415 p.

E. CORDOŞ, C. MANOLIU, **Spectrometria de absorbţie şi fluorescenţă atomică**, 1984, 178 p.

C. BODEA **Tratat de biochimie vegetală**, p. II, vol. 5, 1984, 438 p.

N. ASANDEI, A. GRIGORIU, **Chimia şi structura fibrelor**, 1983, 395 p.

N. IONESCU, M. CĂLDĂRARU, **Oxidarea catalitică a olefinelor inferioare**, 1983.

C. I. SIMIONESCU, F. DANEŞ, **Originea vieţii**, 1983, 110 p.

C. BODEA, (editeur), **Tratat de biochimie vegetală**, II, Vol. IV, 1982, 408 p.

I. G. MURGULESCU, RODICA VÎLCU, **Introducere în chimia fizică, Vol. III. Termodinamica chimică**, 1982, 624 p.

I. G. MURGULESCU, J. PĂUN, **Introducere în chimia fizică, Vol. I.3. Nucleul atomic, reacţii nucleare, particule elementare**, 1982, 606 p.

ELENA JERCAN, **Analiza cromatografică**, 1982, 286 p.

ELENA CEAUŞESCU, **Noi cercetări în domeniul compuşilor macromoleculari**, 1981, 536 p.

I. G. MURGULESCU, TATIANA ONCESCU, E. SEGAL, **Introducere în chimia fizică. Vol. II, 2. Cinematică chimică şi cataliză**, 1981, 1024 p.

I. GĂLĂŢEANU, **Procese şi metode radiochimice în energia nucleară**, 1981, 234 p.

CR. SIMIONESCU, VALERIA GORDUZA, **Polimeri biocompatibili şi biologic activi**, 1980, 479 p.

ELENA CEAUŞESCU, **Polimerizarea stereospecifică a izoprenului**, 1979, 307 p.

CONST. GH. MACAROVICI, **Analiza chimică cantitativă anorganică**, 1979, 457 p.

M. FLORESCU, **Metode ştiinţifice în dezvoltarea industriei chimice moderne**, 1979, 256 p.

I. G. MURGULESCU, E. SEGAL, **Introducere în chimia fizică. Vol. II.1. Teoria molecular cinetică a materiei**, 1979, 1036 p.

S. STERNBERG, FL. DANEŞ, **Termodinamica chimică aplicată**, 1978, 400 p.

I. G. MURGULESCU, V. EM. SAHINI, **Introducere în chimia fizică, Vol. I.2. Structura şi proprietăţile moleculelor**, 1978, 604 p.

I. ZUGRĂVESCU, MAGDA PETROVANU, **N-ylid chemistry**, coédition avec McGraw-Hill, International Book Company, U.S.A., 1977, 396 p.

I. G. MURGULESCU, **Introducere în chimia fizică. Vol. I.1. Atomi, molecule, legătură chimică**, 1976, 560 p.

ELENA CEAUŞESCU, **Research work on synthesis and characterization of macromolecular compounds. Contributions**, 1974, 251 p.

ISSN 0035–4090

I- P. Informaţia c. 1049

43 426

Lei 40

$ 80 (pour un abonnement annuel)

F1103 ~~04~~ ~~66~~

ACADÉMIE DE LA RÉPUBLIQUE SOCIALISTE DE ROUMANIE

REVUE ROUMAINE DE CHIMIE

TOME 32

N° 6

Juin 1987

Rev. Roumaine Chim.

RRCHAX, **32**, *6*, p. 549 - 616 (1987), Bucarest

EDITURA ACADEMIEI REPUBLICII SOCIALISTE ROMÂNIA

ACADÉMIE DE LA RÉPUBLIQUE SOCIALISTE DE ROUMANIE

COMITÉ DE RÉDACTION

Rédacteur en chef:

I. G. MURGULESCU, membre de l'Académie de la République Socialiste de Roumanie

Rédacteurs en chef adjoints:

A. T. BALABAN et V. EM. SAHINI, membres correspondants de l'Académie de la République Socialiste de Roumanie

Collège de rédaction:

EM. BRATU, ELENA CEAUŞESCU, ECATERINA CIORĂNESCU-NENITZESCU, CR. SIMIONESCU, membres de l'Académie de la République Socialiste de Roumanie ; P. SPACU, membre correspondant de l'Académie de la République Socialiste de Roumanie ; M. BANCIU, M. D. GHEORGHIU, I. HAIDUC, D. I. MARCHIDAN, G. NIAC et D. SĂNDULESCU

La Revue Roumaine de Chimie paraît 10 fois par an. Toute commande de l'étranger sera adressée à « ROMPRESFILATELIA » — sectorul Export-Import, Presă, P.O. Box 12—201, télex 10376 prsfi r 78104, Calea Griviţei nr. 64—66, Bucureşti, Roumanie

Les manuscrits, les livres et les revues proposés en échange, ainsi que toute correspondance seront envoyés à la rédaction :

REVUE ROUMAINE DE CHIMIE

125, Calea Victoriei, 79717 Bucarest, Roumanie, téléphone 50 76 80

EDITURA ACADEMIEI REPUBLICII SOCIALISTE ROMÂNIA
125, Calea Victoriei, 79717 Bucarest, Roumanie, téléphone 50 76 80

REVUE ROUMAINE DE CHIMIE

ORSZÁGOS MŰSZAKI INFORMÁCIÓS KÖZPONT ÉS KÖNYVTÁR

Tome 32, N° 6 **Juin, 1987**

IULIANA VARTIRES, VERONICA POPESCU, ANGELA MIHELIS and N. SPĂTARU, Electrochemical behavior of the electroactive spinel type Co_3O_4 coatings 551–562
N. BÎLBĂ, D. BÎLBĂ, GH. MIHĂILĂ and N. NAUM, Exchange of Zn^{2+} and Mn^{2+} in synthetic zeolites NaA, NaX and mordenite 563–569
ASHOK KUMAR, MOHAN KATYAL and B. K. PURI, Polarographic study of lead with δ-valerolactam and its analytical applications 571–575
MIRCEA IOVU and STELIAN RADU, Aromatic azoxybisethers 577–582
M. APETROAE, CL. SINGER, RALUCA BOZGA, ST. CILIANU, RODICA CECLAN, TAMARA BÂNZARU and Z. SIMON, Structure activity relations by the free-Wilson and MTD methods for substances with a potential psychotropic activity. I. Diphenylether derivatives with neuroleptic activity 583–590
MOHAMED F. ABDEL-MEGEED, Studies on pyridylpyrazolone system. V. Cyclocondensation of 1-phenyl-3-(3′-pyridyl)-2-pyrazolin-5-one with ethyl acetoacetate and related compounds 591–597
GH. JUNCU, O. MUNTEAN and R. MIHAIL, Gas absorption with a complex chemical reaction in a perfectly mixed chemical reactor 599–610
ROMULUS POMOJE-MARCU and LIVIA MAGYAR, The ionic-molecular flotation of Cu(II) using Ponilit CP_1 as collector. pH Influence on the flotation efficiency (in French) 611–616

Rev. Roumaine Chim. **32**, *6*, 549–616 (1987), Bucarest

Revue Roumaine de Chimie, 32, 6, 551–562 (1987)

ELECTROCHEMICAL BEHAVIOR OF THE ELECTROACTIVE SPINEL TYPE Co_3O_4 COATINGS

IULIANA VARTIRES, VERONICA POPESCU, ANGELA MIHELIS and N. SPĂTARU
Center of Physical Chemistry — ICECHIM,
Spl. Independenţei 202 — Bucharest, Romania

Received July 12, 1986

The present investigation aims at establishing the electrochemical performances of Co_3O_4 coatings through evaluation of the kinetic parameters of the chlorine evolution reaction, and of the reversible voltammetric charge. An attempt has been made to establish correlations between the measured parameters, in order to understand how the structure of the surface affects the electrode electrocatalytic activity. A mechanism for the anodic discharge of chloride ions is proposed and the dependence of electrode active area on oxide loading is established.

INTRODUCTION

Extensive application of the electrocatalytic processes requires unexpensive and easily available materials of high catalytic activity. This is why the main trend in the selection of catalytic materials rests now upon the investigation of the electrode properties of the oxidic semiconductors.

In recent years attempts have been made to obtain electrocatalytic coatings without utilization of noble metal oxides.[1-5]

In spite of some shortcomings, like not very high specific surface and rather high resistivity,[6] complex oxides with spinelic structure are very promising as they are active, thermodynamically stable and are recommended for alkaline media.

Investigations on spinel-type coatings aim at establishing the link of the mechanism and kinetics of various reactions with the electric and structural properties of the catalyst. This would help at least in part, in understanding the way the molecules are activated on the oxidic electrocatalyst and how this activity can be controlled.

The paper deals with titanium electrodes covered with an active layer of Co_3O_4 and an intermediary semiconductor layer of $SnO_2 + Sb_2O_3$. An attempt is made to work out a mechanism for the anodic discharge of chloride ions on such electrodes, based on kinetic parameters of the reaction (Tafel slope *b*, stoichiometric number ν, and reaction order *r*).

The reversible voltammetric charge *Q*, employed by various authors for RuO_2 electrodes,[7-11] has also been determined in order to characterize the electrode active surface area.

THE MECHANISM FOR ANODIC DISCHARGE OF CHLORIDE IONS

The chlorine evolution reaction is in many respects similar to the hydrogen one.[12,13] Thus, assume an active center S on the electrocatalytic layer surface and a unique rate-controlling step, three mechanisms can be envisaged, which, in the first approximation, control the global process kinetics :

— The first mechanism assumes a slow discharge reaction, followed by a fast recombination and desorption of the products;

$$S + Cl^- \rightarrow S \cdots\cdots Cl + e^- \tag{Ia}$$

$$S \cdots\cdots Cl + S \cdots\cdots Cl \rightleftharpoons 2S + Cl_2 \tag{Ib}$$

Taking into account that the charge transfer reaction is the rate-controlling step, the kinetics of the global process can be described by the Butler—Volmer equation,

$$i = i_0 \left[\exp\left[\frac{\alpha F}{RT}\eta\right] - \exp\left[\frac{-(1-\alpha)F}{RT}\eta\right]\right] \tag{1}$$

where i is the total current density, i_0 the exchange current, α is the transfer coefficient for the anodic process, η the overvoltage, F Faraday's constant, R the universal gas constant and T is the absolute temperature.

At overvoltages higher than 5—10 mV, eqn. (1) can be rewritten in the Tafel form,

$$\eta = a + b \log i \tag{2}$$

where b $(= 2.303\ RT/\alpha F)$ is the Tafel slope.

For the above-discussed first mechanism the kinetic reaction order $r = 1$ and the stoichiometric number $\nu = 2$.

— The second mechanism consists of a fast charge transfer reaction followed by a slow recombination and desorption,

$$S + Cl^- \underset{v_{-a}}{\overset{v_a}{\rightleftharpoons}} S \cdots\cdots Cl + e^- \tag{IIa}$$

$$S \cdots\cdots Cl + S \cdots\cdots Cl \xrightarrow[v_b]{} Cl_2 + 2S. \tag{IIb}$$

Thus the recombination being the rate-determining step, one should take account of the surface coverage due to adsorption θ. At steady state, for a certain current density,

$$\frac{d\theta}{dt} = 0 = v_a - v_{-a} - v_b. \tag{3}$$

The rate equations for the reactions (II) can be written as :

$$v_a = k_a c_{Cl^-} (1 - \theta) \exp\left[\frac{\alpha F}{RT}\eta\right] \tag{4}$$

$$v_{-a} = k_{-a}\theta \exp\left[\frac{-(1-\alpha)F}{RT}\eta\right] \tag{5}$$

$$v_b = k_b \theta^2 \tag{6}$$

and eqn. (3) becomes,

$$k_b\theta^2 + \theta\left\{k_a c_{\mathrm{Cl}^-}\exp\left[\frac{\alpha F}{RT}\eta\right] + k_{-a}\exp\left[\frac{-(1-\alpha)F}{RT}\eta\right]\right\} - $$

$$- k_a c_{\mathrm{Cl}^-}\exp\left[\frac{\alpha F}{RT}\eta\right] = 0 \tag{7}$$

Considering that reaction (IIb) is rate-determining, the global process rate is given by eqn. (6) with the θ value resulting from eqn. (7).

As reaction (IIb) is a slow one (i.e. k_b is small) explicit equations for the reaction rate can be obtained only for the limiting cases :

(a) when $\theta \to 0$,

$$k_a c_{\mathrm{Cl}^-}\exp\left[\frac{\alpha F}{RT}\eta\right] \ll k_{-a}\exp\left[\frac{-(1-\alpha)F}{RT}\eta\right]$$

for which,

$$\theta \approx K_a c_{\mathrm{Cl}^-}\exp\left[\frac{F}{RT}\eta\right] \tag{8}$$

where K_a is the equilibrium constant of reaction (IIa) and,

$$v_b = k_b K_a^2 c_{\mathrm{Cl}^-}^2\exp\left[\frac{2F}{RT}\eta\right]. \tag{9}$$

Because the current density for the rate-controlling step is proportional to v_b, the Tafel slope assumes the value $b = 2.303\ RT/2F$, the kinetic reaction order and the stoichiometric number are $r = 2$ and $\nu = 1$, respectively;

(b) when $\theta \to 1$

$$k_{-a}\exp\left[\frac{-(1-\alpha)F}{RT}\eta\right] \ll k_a c_{\mathrm{Cl}^-}\exp\left[\frac{\alpha F}{RT}\eta\right]$$

and

$$v_b = k_b. \tag{10}$$

It results that $b = \infty$ $r = 0$, $\nu = 1$.

— The third mechanism, which can be considered for the chloride ions discharge reaction, assumes a fast charge transfer followed by a slow electrochemical desorption,

$$S + \mathrm{Cl}^- \underset{v_{-a}}{\overset{v_a}{\rightleftharpoons}} S \cdots\cdots \mathrm{Cl} + e^- \tag{IIIa}$$

$$S \cdots\cdots \mathrm{Cl} + \mathrm{Cl}^- \xrightarrow[v_c]{} S + \mathrm{Cl}_2 + e^-. \tag{IIIb}$$

The rate equations for reaction (IIIb) being of the type,

$$v_c = k_c\theta c_{\mathrm{Cl}^-}\exp\left[\frac{\alpha F}{RT}\eta\right] \tag{11}$$

the steady state condition,

$$\frac{d\theta}{dt} = v_a - v_{-a} - v_c = 0 \tag{12}$$

together with eqns. (4),(5) and (11) yield

$$\theta = \frac{k_a c_{\mathrm{Cl^-}} \exp\left[\frac{\alpha F}{RT}\eta\right]}{k_a c_{\mathrm{Cl^-}} \exp\left[\frac{\alpha F}{RT}\eta\right] + k_{-a} \exp\left[\frac{-(1-\alpha)F}{RT}\eta\right] + k_c c_{\mathrm{Cl^-}} \exp\left[\frac{\alpha F}{RT}\eta\right]} \tag{13}$$

Assuming that reaction (IIIb) is a slow one (i.e. k_c very small) explicit equations for the reaction rate can be obtained for the same limit cases as above:

(a) when $\theta \to 0$,

$$v_c = k_c K_a c^2_{\mathrm{Cl^-}} \exp\left[\frac{(1+\alpha)F}{RT}\eta\right] \tag{14}$$

with kinetical parameters $b = 2.303\ RT/((1+\alpha)F)$, $r = 2$, $\nu = 1$;

(b) when $\theta \to 1$,

$$v_c = k_c c_{\mathrm{Cl^-}} \exp\left[\frac{\alpha F}{RT}\eta\right] \tag{15}$$

with $b = 2.303\ RT/(\alpha F)$, $r = 1$, $\nu = 1$.

The kinetic parameters discussed above are summarized in Table 1 for comparison with experimental data.

Table 1

Theoretical values of the kinetic parameters for various reaction mechanisms

Mechanism	$\theta \to 0$			$\theta \to 1$		
	ν	r	b(mV)	ν	r	b(mV)
I $S + \mathrm{Cl^-} \rightarrow S\cdots\mathrm{Cl} + e^-$ $\mathrm{S}\cdots\mathrm{Cl} + \mathrm{S}\cdots\mathrm{Cl} \leftrightarrows 2S + \mathrm{Cl_2}$	2	1	$\frac{2.303\ RT}{\alpha F} = 140$	2	1	$\frac{2.303\ RT}{\alpha F} = 140$
II $S + \mathrm{Cl^-} \rightleftarrows S\cdots\mathrm{Cl} + e^-$ $S\cdots\mathrm{Cl} + S\cdots\mathrm{Cl} \rightarrow 2S + \mathrm{Cl_2}$	1	2	$\frac{2.303\ RT}{2F} = 35$	1	0	∞
III $S + \mathrm{Cl^-} \rightleftarrows S\cdots\mathrm{Cl} + e^-$ $S\cdots\mathrm{Cl} + \mathrm{Cl^-} \rightarrow S + \mathrm{Cl_2} + e^-$	1	2	$\frac{2.303\ RT}{(1+\alpha)F} = 46.6$	1	1	$\frac{2.303\ RT}{\alpha F} = 140$

EXPERIMENTAL

The electroactive Co_3O_4 coatings have been prepared by thermal decomposition of an aqueous solution of $Co(NO_3)_2$ at 300°C in air stream.

In order to avoid anodic oxidation of titanium substrate, an intermediary layer of complex oxide $SnO_2-Sb_2O_3$ has been deposited from alcohol solution of chlorides, by thermal decomposition at 500°C. The titanium substrate has been etched in oxalic acid solution in order to obtain the rough surface which ensures a good adherence of the oxidic layer.

The measurements have been performed in a Pyrex glass cell at constant temperature, with a working electrode of 1.24 cm^2 area and a platinum counter electrode of about 20 cm^2, in a cylindrical symmetry configuration.

Anodic polarization measurements have been carried out with a Tacussel PRT 20-2X potentiostat. A NaCl 5M solution, saturated with Cl_2 through electrolysis at 300 mA with platinum electrodes for 30 minutes, has been used as electrolyte. The pH has been 2.5 and the temperature 80°C.

The results were corrected for the ohmic drop, deduced through the interrupter technique, the signal was recorded with a Tektronix 7613 memoryscope.

The cyclic voltammgrams were recorded by a GSTP Tacussel generator, a PRT 20-2X Tacussel potentiostat and an EMG-EN 230 Orion chart plotter; the Q charge values being determined by integration (Radelkis integrator) of the voltammogram positive sweep. The charge measurements were carried out with 0.5 M H_2SO_4 solution, deaerated with purified argon for one hour prior to each run.

RESULTS AND DISCUSSIONS

Kinetics of chlorine evolution

The stoichiometric number has been determined by the equation

$$\nu = \frac{\partial \eta}{\partial i} \cdot i_0 \frac{nF}{RT} \tag{16}$$

where n stands for the number of electrons involved in the overall reaction.

In this case utilization of Tafel equation to calculate i_0 is not recommended because of the possible differences between the values of kinetic parameters at high overvoltage and about equilibrium. We preferred to use the following, more complete equation which is valid for any overvoltage value [14]

$$\ln\left[i/\left(1 - \exp\left(-\frac{nF}{RT}\eta\right)\right)\right] = \ln i_0 + \frac{\alpha nF}{RT} \tag{17}$$

Figs 1 and 2 show the data obtained on electrodes with different oxide loadings. Fig. 1 presents polarization curves around the equilibrium potential of the Cl^-/Cl_2 reaction (micropolarization curves). Fig. 2 presents a plot of η versus $\lg(i/(1 - \exp(-2F\eta/RT)))$ i.e. the polarization curves corrected for the reverse reaction, and it allows one to determine the exchange current i_0 (the intercept for $\eta = 0$) and Tafel slope. It is worth mentioning that each curve in Figs 1 and 2 represents average data for several similar electrodes.

Table 2 lists the kinetic parameters data for three types of electrodes.

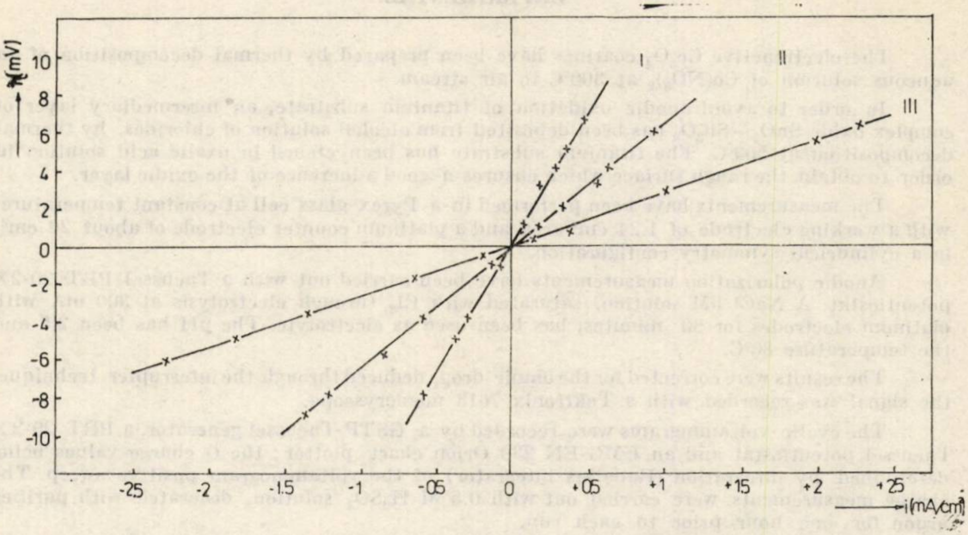

Fig. 1. — Micropolarization curves for electrodes with different oxide loadings in Cl_2 saturated 5M NaCl solution (pH ~ 2.5, at 80°C).

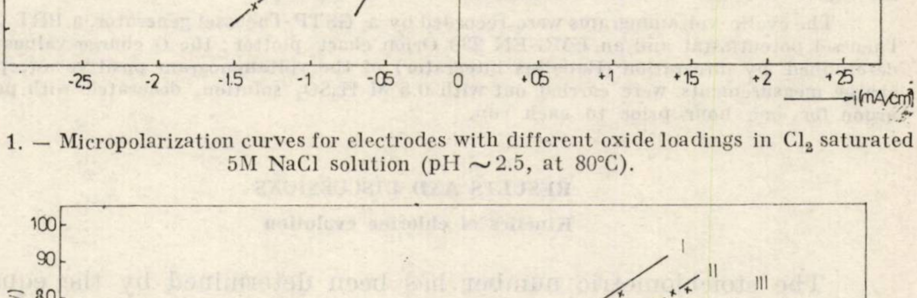

Fig. 2. — Anodic polarization behavior of electrodes with different oxide loadings, in Cl_2 saturated 5M NaCl solution (pH ~ 2.5, at 80°C).

Table 2

Kinetic parameters of the chlorine evolution reaction for electrodes with various Co_3O_4 loadings, at 80°C in 5M NaCl solution (pH = 2.5)

Electrode	Co_3O_4 (mg/cm²)	i_0 (mA/cm²)	$d\eta/di(\Omega)$	ν	b (mV)
I	3.31	1.3	13.0	1.11	41.0
II	6.61	2.5	6.5	1.07	42.5
III	13.2	5.5	2.7	0.98	42.0

The specific values have been obtained by taking into consideration the geometric surface area of the electrodes.

The kinetic reaction order (r) given by

$$r = \left(\frac{\partial \ln i}{\partial \ln a_{\text{Cl}^-}} \right)_{\varphi} \tag{18}$$

has been determined from i values, at a potential of 1.1 V (SCE) for NaCl solutions whose concentrations ranged within 0.5 – 5 M, at pH = 2.5 and 80°C.

Fig. 3 shows that for type I electrodes the kinetic reaction order $r = 1$. Similar values are also obtained for the other two types of electrodes.

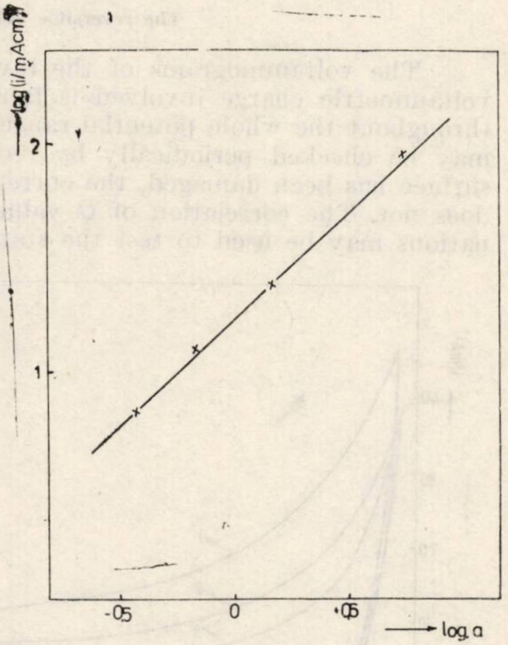

Fig. 3. — Log-log plot of current density at E = 1.1 V (SCE) in NaCl solutions (pH ∼ 2.5) as a function of mean ionic activity; the NaCl concentration ranges from 0.5M to 5M; electrode type I.

The comparison between the theoretical kinetic parameters in Table 1 and the experimental values ($\nu \approx 1$, $b \approx 42$ mV) supports the conclusion that the most probable mechanism for the chlorine evolution reaction is that of type III, in which a fast charge transfer is followed by a slow electrochemical desorption.

The surface coverage appears to be low ($\theta \approx 0$), i.e. the adsorption of the chloride species should be low. This is also supported by the good linearity of the curves in Fig. 3. If the surface coverage were high, an increase in NaCl concentration would not result in a proportional increase of the current density (under constant potential), as the surface would be inhibited by coverage.

The small difference between the experimental value of the Tafel slope (≈ 42 mV) and the calculated one (46.6 mV), may be assigned either to repulsive interactions between adsorbed species (which we did not consider), or to an $\alpha = 0.66$ instead of $\alpha = 0.5$.

The discrepancy between the experimental kinetic reaction order, and that yielded by the mechanism III, may be explained if one assumes that the chlorine evolution reaction follows a complex mechanism, in which the rate-controlling step is the oxidation of an unspecified $(S\text{--}Cl)^z$ surface complex.[15]

Another conclusion, which can be drawn from Table 2, is that there are no essential differences between the kinetic parameters for electrodes with different oxide loadings, which proves that the chloride ion discharge reaction is similar on all these electrodes. The increase in the exchange current values, with the Co_3O_4 loading, is only due to the associated increase in the active surface.

The reversible voltammetric charge

The voltammograms of the investigated electrodes show that the voltammetric charge involved is fairly large and uniformly distributed throughout the whole potential range. The state of the electrode surface may be checked periodically by recording the voltammograms. If the surface has been damaged, the current changes but the shape of curves does not. The correlation of Q value with the electrochemical determinations may be used to test the state of the surface.[16]

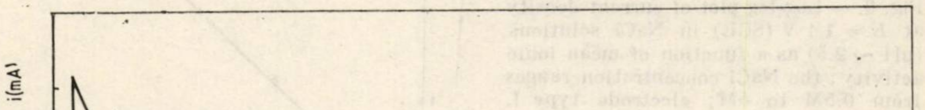

Fig. 4. — Voltammograms of type III electrode at various sweep rates in 0.5M H_2SO_4 : *1*) 100, *2*) 50, *3*) 25 mV/s.

In Fig. 4 are presented the voltammograms obtained by sweeping the potential within 0.4–1.4 V (SCE) range, at various sweeping rates.

In order to characterize the various electrodes the current has been integrated at potentials ranging within 0.4–1.2 V (SCE), so that reproducible, peak-free curves were obtained.

The value of reversible voltammetric charge Q decreases as the sweep rate increases up to a plateau, where Q is independent of the sweep rate (dE/dt), (Fig. 5) which shows that the electrode processes associated to a sweeping potential are fast redox surface reactions, which involve Co atoms.

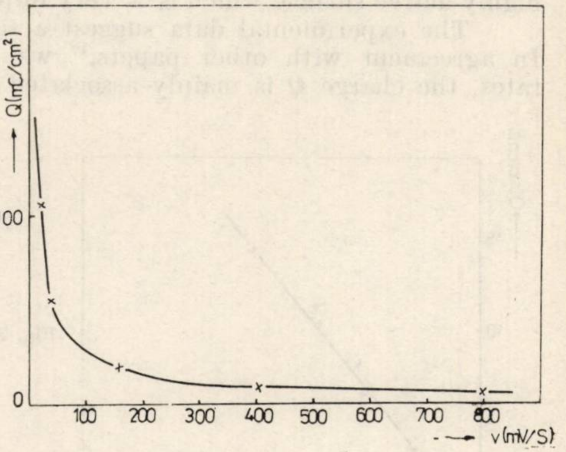

Fig. 5. — Dependence of reversible voltammetric charge Q on potential sweep rate; type II electrode.

The high Q values for low sweeping rates are interpreted in terms of bulk changes of the electroactive layer.

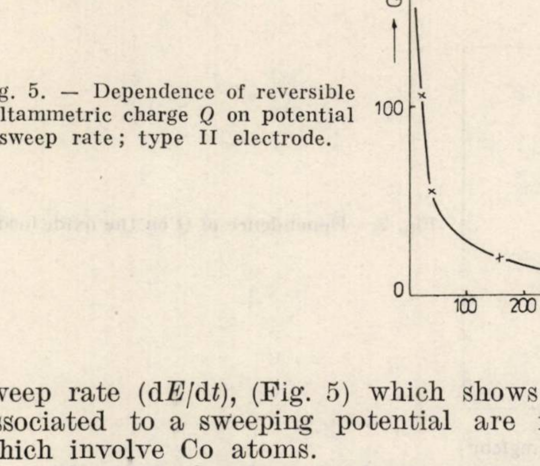

Fig. 6. — Log–log plot of the current density at $E = 1.1$ V (SCE), as a function of voltammetric charge Q.

Fig. 6 shows $\log i$ vs. $\log Q$ dependence at a constant potential of 1.1 V (SCE), for various electrodes. The resulting slope (1.2) is in fact the reaction order with respect to the number of active sites on the surface (assuming that the number of active sites is proportional to the surface area). The slope is close to unit, which proves once more that the chlorine evolution reaction on Co_3O_4 electrodes obeys a mechanism of the type III.

The real surface area (S) of the oxide layers is several orders of magnitude higher than the geometrical surface area, due to the porous structure of the deposited oxides, and this is why these layers have a highly active surface which is a very important electrode quality.

The experimental data suggest a simple evaluation of active area. In agreement with other papers,[17] we assume that, at high sweeping rates, the charge Q is mainly associated to the double layer. The linear increase of Q with the oxide loading — which is in turn proportional to the active surface area — (Fig. 7) clearly shows that the reversible voltammetric charge Q is directly related to the magnitude of the active surface.

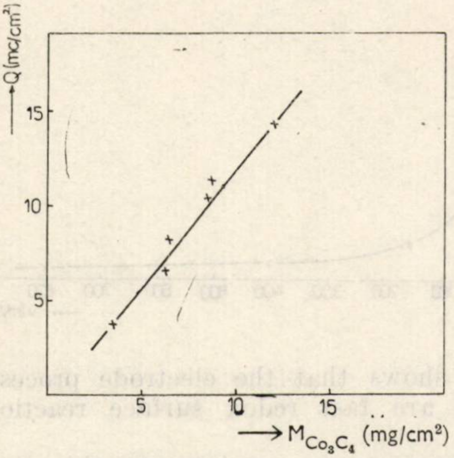

Fig. 7. — Dependence of Q on the oxide loading.

Measurements of Q and i_0 on the three investigated types of electrodes evidence the following linear dependences,

$$Q_{II,III} = f_{Q_{II,III}} Q_I \tag{19}$$

$$i_{0\,II,III} = f_{i0_{II,III}} i_{0I}$$

where f_Q and f_{i_0} are constants.

Fig. 8 illustrates the correlation between f_Q and f_{i_0} for the three types of electrodes. The resulting slope is very close to 1, and this allows one to draw the conclusion that the proportionality coefficients do not depend on the measured parameter, but only on the active area of the electrodes.

Then,

$$f_{Q_{II,III}} = f_{i_0\,II,III} = f_{S_{II,III}} \tag{20}$$

and eqn (19) becomes,

$$Q_{II,III} = f_{S\,II,III} Q_I \tag{21}$$

$$i_{0\,II,III} = f_{S_{II,III}} i_{0I}$$

Fig. 9 shows the linear increase of the coefficient f_S with the amount of deposited active substance ($\Delta M_{\mathrm{ox}_{\mathrm{II,III}}} = M_{\mathrm{ox}_{\mathrm{II,III}}} - M_{\mathrm{ox}_{\mathrm{I}}}$).

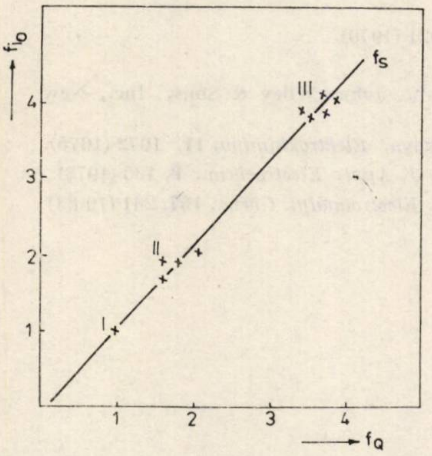

Fig. 8. — The correlation between f_Q and f_{i_0} coefficients for the three types of electrodes.

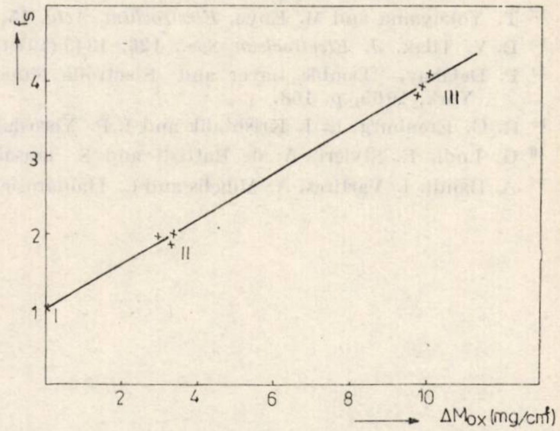

Fig. 9. — The dependence of f_S coefficient on the quantity of oxide, deposited on the electrode.

In a first approximation one assumes that the same dependence holds for the first oxide layers deposited on metal surface and that the specific surfaces of the two types of oxides (Co_3O_4 and $SnO_2 + Sb_2O_3$) are similar, so that one may write,

$$S_{\mathrm{I}} = f_S(M_{\mathrm{ox}_{\mathrm{I}}}) S_{\mathrm{geom}} \tag{22}$$

or, to turn it more general,

$$S_i = f_S(\Delta M_{\mathrm{ox}_{\mathrm{i}}}) S_{\mathrm{I}} \tag{23}$$

This supplies a confortable method for active surface evaluation representing a useful tool in caracterization of titanium electrodes, activated with oxide layers.

REFERENCES

[1] Pat. France — 2,094,051.

[2] Pat. France — 2,112,388.

[3] Pat. France — 2,128,667.

[4] Pat. Rom. — 71,200.

[5] Pat. U.S.A. — 4,208,450.

[6] S. Trasatti, "Electrodes of Conductive Metallic Oxides", Part A", Elsevier Scientific Publishing Company, Amsterdam — Oxford — New York, 1980, p. 221.

[7] L. D. Burke, O. J. Murphy and J. F. O'Neill, *J. Chem. Soc. Faraday I*, **73**, 1659 (1977).

[8] L. D. Burke and O. J. Murphy, *J. Electroanalyt. Chem.*, **109**, 99 (1980).

[9] L. D. Burke and O. J. Murphy, *J. Electroanalyt. Chem.*, **96**, 19 (1979).

[10] L. D. Burke and O. J. Murphy, *J. Electroanalyt. Chem.*, **112**, 39 (1980).

[11] D. V. Kokoulina, T. V. Ivanova, V. I. Krasovitskaya, Z. I. Kudryavtseva and L. Z. Krishtalik, *Elektrokhimiya*, **13**, 1511 (1977).

[12] T. Yokoyama and M. Enyo, *Electrochim. Acta*, **15**, 1921 (1970).

[13] B. V. Tilak, *J. Electrochem. Soc.*, **126**, 1343 (1979).

[14] P. Delahay, "Double Layer and Electrode Kinetics", John Wiley & Sons, Inc., New York, 1965, p. 163.

[15] R. G. Erenburg, L. I. Krishtalik and I. P. Yaroshevskaya, *Elektrokhimiya*, **11**, 1072 (1975).

[16] G. Lodi, E. Sivieri, A. de Battisti and S. Trasatti, *J. Appl. Electrochem.*, **8**, 135 (1978).

[17] A. Bandi, I. Vartires, A. Mihelis and C. Hainăroșie, *J. Electroanalyt. Chem.*, **157**, 241 (1983)

Revue Ro ımaine de Chimie, 32, 6, 563–569 (1987)

EXCHANGE OF Zn^{2+} and Mn^{2+} IN SYNTHETIC ZEOLITES NaA, NaX AND MORDENITE

N. BÎLBĂ, D. BÎLBĂ, GH. MIHĂILĂ and N. NAUM
Department of Chemical Technology, Polytechnic Institute of Iași,
Splai Bahlui 71, Romania

Received June 1, 1985
Revised November 25, 1986

The exchange of Zn^{2+} and Mn^{2+} with Na^+ ions in sodalite zeolites NaA and NaX as well as in natrium mordenite (NaM) was carried out to determine the selectivity coefficients, K_{Na}^{Me}, apparent thermodynamic equilibrium constant, K_a, free energy, ΔG, enthalpy, ΔH and entropy, ΔS. The exchange isotherms were measured at 2, 22 and 60°C. All isotherms showed that these metal ions cannot replace all sodium ions present in the network of zeolites, except Zn^{2+} ions in NaA.

INTRODUCTION

The zeolitic network contains excess negative charge, due to the $[AlO_4]$ tetrahedra, which is compensated by exchangeable cations.[1-6] From this stand point, zeolites belong to inorganic ion exchangers. The number, size, valence and site of the interchangeable cations in crystal network provide important effects on size and shape of the access pores of zeolites cavities, responsible for modification of their catalytical, adsorptive and "molecular sieves" properties. Moreover, zeolites exhibit a significant selectivity against certain cations, working as "ionic sieves", making possible the separation and concentration of some cations.[7]

Ion exchange in zeolites of any type is intersting, for the elucidation of the cation site positions in the zeolite as well as in production of the selective catalysts and adsorbents, widely employed in the catalytic and sorptive processes.

Detailed studies on thermochemistry and thermodynamics of ion exchange both in natural and synthetic zeolites belong to Barrer et al.[8-9] and to Sherry.[10-11]

As different cations occupy preferentially certain sites in zeolitic network, controlling their specific properties, the behaviour of the zeolites as ion-exchangers must be known against each cation separately.

The present paper deals with the results of the exchange of Zn^{2+} and Mn^{2+} with the Na^+ ions in synthetic zeolites NaA, NaX and NaM, zeolites with different Si/Al ratios and structure types.

Certain zeolites with either Zn^{2+} or metallic finely dispersed zinc are selective catalysts for dehydrogenation of olefines to dienes,[12] hydration of acetylene to acetaldehyde,[13] isomerisation of *n*-butenes,[14] cyclohexane and *n*-pentene[15] whereas Mn^{2+} containing zeolites are catalysts for oxidation of *n*-C_6 hydrocarbons[16] and *para*-xylene to carboxylic acids.[17]

EXPERIMENTAL

All zeolites investigated in this work were synthesized hydrothermally in our laboratory. Their structure, chemical composition and adsorptive properties were determined by usual methods before the ion-exchange test. In order to prevent the Na^+ ions hydrolysis during the washing process, zeolites were initially treated with 0.1 N NaCl solution, washed with bidistilled water up to the absence of Cl^- ion, dried and equilibrated with water vapour, in desiccator, over a saturated NH_4Cl solution at room temperature. The results of their chemical analysis are summarized in table 1 in terms of unit cell composition, Si/Al ratio and ion exhange capacity.

Table 1

Properties of studied zeolites

Type	Composition of elemental cell	Si/Al	Ion exchange capacity, mequiv./g hydrate zeolite
NaA	$Na_{12}(AlO_2)_{12}(SiO_2)_{12}\cdot 26{,}7\ H_2O$	1.0	5.5
NaX	$Na_{85}(AlO_2)_{85}(SiO_2)_{107}\cdot 241\ H_2O$	1.25	4.7
NaM	$Na_{85}(AlO_2)_{8}(SiO_2)_{40}\cdot 24\ H_2O$	5.0	2.3

In order to obtain the data for the exchange isoterms, the ion exchange was accomplished by weighing out suitable quantities (0.1 — 1.0 g) of dried sodium form of the zeolite and pipetting 25 mL isonormal solution of NaCl — $MeCl_2$, 0.1 N, in a three-necked flask fitted with a stirrer, at 60, 22 and 2°C, controlled in a water bath, for 24 hours. The concentrations of Zn^{2+}, Mn^{2+} and Na^+ in zeolite phase and in solution were determined complexometrically and flamphotometrically, respectively. It was found that 24 hours were enough for reaching equilibrium because after this time, the concentration of cations in solution showed no change.

RESULTS AND DISCUSSION

The ion-exchange isotherms measured for all systems under study, are represented in figures 1—6 where the abscissa is the equivalent fraction of the entering ion in the solution and the ordinate is the equivalent fraction of the same ion in the zeolite.

The isotherms of $Na^+ \rightleftharpoons 1/2\, Zn^{2+}$ ion exchange in zeolites NaA and NaX belong to *a*-type, the exchange degree has the maximum value, $X_{max.} \simeq 1$ (Figs 1 and 3); in the case of NaM, the exchange isotherms belong to *b*-type, sigmoidal ones. The affinity of NaM against Zn^{2+} appears up to an exchange degree as high as 40%, that corresponds favourably to the Na^+ ions located within uninterrupted channels of mordenite (Fig. 5). Both the exchange degree and shape of isotherms for NaA and NaX are similar to those obtained by Gal et al.[18] and Nikashina et al.[19]

The $Na^+ \rightleftharpoons 1/2\, Mn^{2+}$ ion exchange in the three zeolites exhibits *d*-type isotherms, i.e. the exchange is not entirely performed (Figs 2, 4

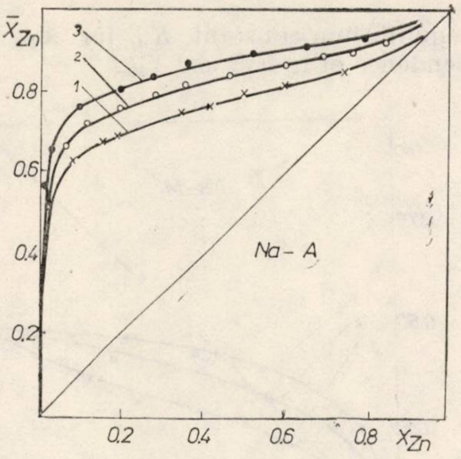

Fig. 1. — Isotherms of the Na⁺ ⇌ 1/2 Zn²⁺ ion exchange in NaA zeolite: *1* — 2°C; *2* — 22°C; *3* — 60°C.

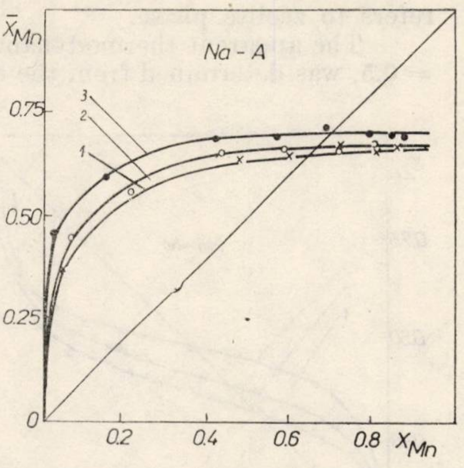

Fig. 2. — Isotherms of the Na⁺ ⇌ 1/2 Mn²⁺ ion exchange in NaA zeolite: *1* — 2°C; *2* — 22°C; *3* — 60°C

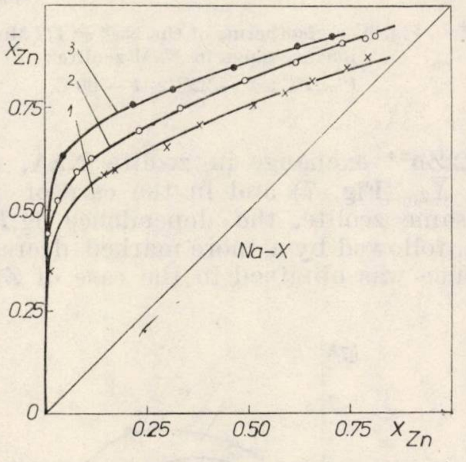

Fig. 3. — Isotherms of the Na⁺ ⇌ 1/2 Zn²⁺ ion exchange in NaX zeolite: *1* — 2°C; *2* — 22°C; *3* — 60°C

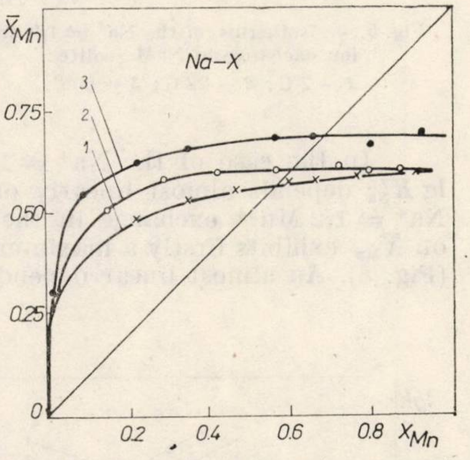

Fig. 4. — Isotherms of the Na⁺ ⇌ 1/2 Mn²⁺ ion exchange in NaX zeolite: *1* — 2°C; *2* — 22°C; *3* — 60°C.

and 6), its order being as follows: NaA > NaX > NaM. At 60°C, the maximum extent of exchange is 66, 65 and 50% in NaA, NaX and NaM, respectively. These values correspond to 8, 55 and 4 sodium ions replaced by Mn^{2+} per unit cell in NaA, NaX and NaM, respectively.

Based on the concentrations determined from the exchange isotherms, the selectivity coefficients, K_{Na}^{Me}, were calculated using the relation

$$K_{Na}^{Me} = \frac{\bar{X}_{Me}^{1/2} \cdot X_{Na}}{X_{Me}^{1/2} \cdot \bar{X}_{Na}}$$

where X is the equivalent fraction of ions and the above lined symbol refers to zeolite phase.

The apparent thermodynamic equilibrium constant, K_a, for $\overline{X}_{\mathrm{Me}} = 0.5$, was determined from the dependence of lg $K_{\mathrm{Na}}^{\mathrm{Me}}$ on $\overline{X}_{\mathrm{Me}}$.

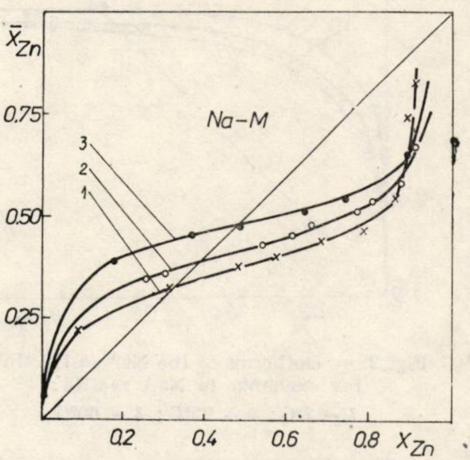

Fig. 5. — Isotherms of the $\mathrm{Na^+} \rightleftharpoons 1/2\ \mathrm{Zn^{2+}}$ ion exchange in NaM zeolite:
1 — 2°C; *2* — 22°C; *3* — 60°C.

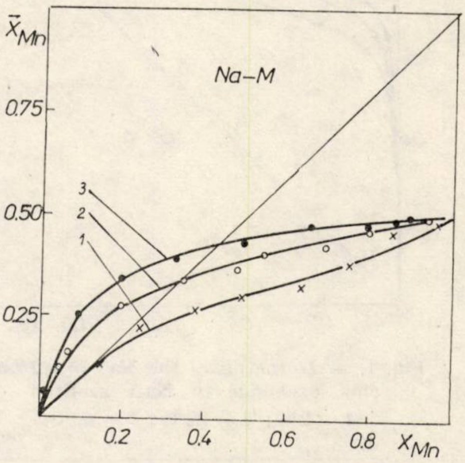

Fig. 6. — Isotherms of the $\mathrm{Na^+} \rightleftharpoons 1/2\ \mathrm{Mn^{2+}}$ ion exchange in NaM zeolite:
1 — 2°C; *2* — 22°C; *3* — 60°C.

In the case of the $\mathrm{Na^+} \rightleftharpoons 1/2\ \mathrm{Zn^{2+}}$ exchange in zeolite NaA, the lg $K_{\mathrm{Na}}^{\mathrm{Zn}}$ depends almost linearly on $\overline{X}_{\mathrm{Zn}}$ (Fig. 7) and in the case of the $\mathrm{Na^+} \rightleftharpoons 1/2\ \mathrm{Mn^{2+}}$ exchange in the same zeolite, the dependence lg $K_{\mathrm{Na}}^{\mathrm{Mn}}$ on $\overline{X}_{\mathrm{Mn}}$ exhibits firstly a maximum, followed by a more marked decrease (Fig. 8). An almost linear dependence was obtained in the case of $\mathrm{Zn^{2+}}$

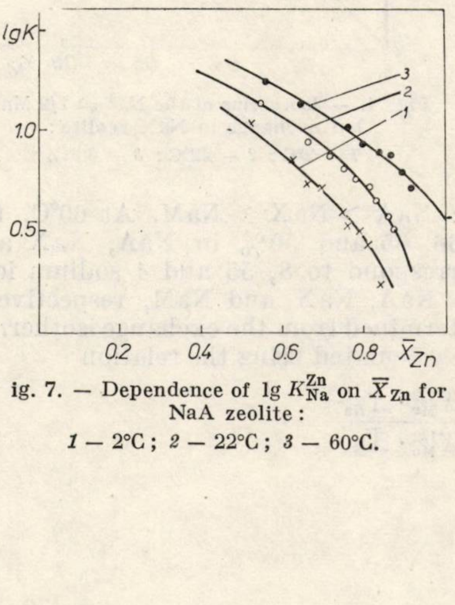

Fig. 7. — Dependence of lg $K_{\mathrm{Na}}^{\mathrm{Zn}}$ on $\overline{X}_{\mathrm{Zn}}$ for NaA zeolite:
1 — 2°C; *2* — 22°C; *3* — 60°C.

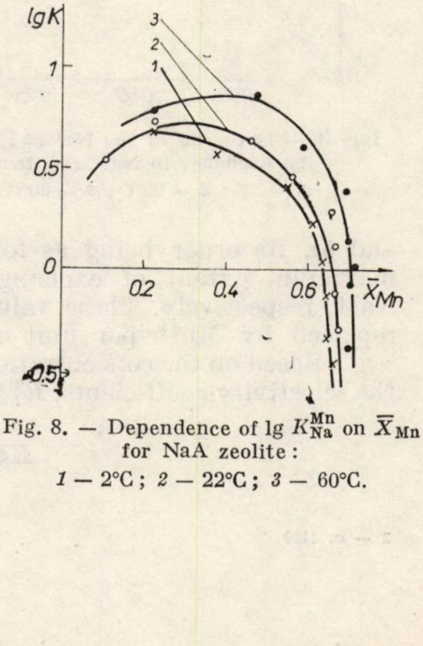

Fig. 8. — Dependence of lg $K_{\mathrm{Na}}^{\mathrm{Mn}}$ on $\overline{X}_{\mathrm{Mn}}$ for NaA zeolite:
1 — 2°C; *2* — 22°C; *3* — 60°C.

ions in zeolites NaX and NaM and a not linear one in the case of Mn^{2+} ions in the same zeolites. The plots of $\lg K_{Na}^{Me}$ versus $\bar{X}_{Me}$ are almost parallel to each other at 2 and 22°C and more uniform at 60°C, when the ion exchange is activated.

The free energies, ΔG, enthalpies, ΔH and entropies, ΔS were calculated using the relations : $\Delta G = -RT\ln K_a$, $d\lg K_a = -\frac{\Delta H}{R}d\left(\frac{1}{T}\right)$ and $T\Delta S = \Delta H - \Delta G$, respectively.

The thermodynamic data as regards the $Na^+ \rightleftharpoons 1/2\ Zn^{2+}$ and $Na^+ \rightleftharpoons 1/2\ Mn^{2+}$ ion exchanges in sodalite zeolites NaA and NaX as well as in natrium mordenite NaM are listed in table 2.

Table 2

Thermodynamic data of Zn^{2+} and Mn^{2+} exchange in zeolites NaA, NaX and NaM

Exchange reaction	Temp., °C	Isoterm type	X_{max}	lg K_a for $X_{Me} = 0.5$	ΔG, cal/mol.K	ΔH, cal/mol.K	ΔS, e.u.
			Zeolite NaA				
$Na^+ \rightleftharpoons \frac{1}{2} Zn^{2+}$	2	(a)	1	1.04	−1038.75	+2463.88	13.33
	22	(a)	1	1.18	−1595.20		
	60	(a)	1	1.32	−2012.40		
$Na^+ \rightleftharpoons \frac{1}{2} Mn^{2+}$	2	(d)	0.66	0.48	− 606.86	+2384.40	11.00
	22	(d)	0.68	0.60	− 809.32		
	60	(d)	0.70	0.82	−1251.15		
			Zeolite NaX				
$Na^+ \rightleftharpoons \frac{1}{2} Zn^{2+}$	2	(a)	1	0.72	− 907.56	+3311.67	16.28
	22	(a)	1	0.91	−1231.57		
	60	(a)	1	1.11	−1643.77		
$Na^+ \rightleftharpoons \frac{1}{2} Mn^{2+}$	2	(d)	0.60	0.30	− 337.24	+2781.80	11.80
	22	(d)	0.62	0.48	− 648.18		
	60	(d)	0.70	0.70	−1065.77		
			Zeolite NaM				
$Na^+ \rightleftharpoons \frac{1}{2} Zn^{2+}$	2	(b)	0.80	−0.60	+ 757.18	+3746.90	10.40
	22	(b)	0.80	−0.36	+ 479.27		
	60	(b)	0.80	−0.10	+ 145.63		
$Na^+ \rightleftharpoons \frac{1}{2} Mn^{2+}$	2	(d)	0.50	−1.15	+1454.28	+3808.40	9.75
	22	(d)	0.50	−0.87	+1196.38		
	60	(d)	0.50	−0.60	+ 920.14		

The values of ΔG are negative for the exchange of Zn^{2+} and Mn^{2+} in zeolites NaA and NaX and positive in mordenite, when the thermodynamic equilibrium constant $K_a < 1$. As the temperature increases, the exchange equilibrium becomes favourable to divalent cation.

Although Zn^{2+} and Mn^{2+} ions have almost the same radii, 0.74 Å, according to Pauling (0.83 Å, according to Ahrens) and 0.80 Å, respectively, their behaviour under exchange is not the same due to their different tendency to hydration. The Mn^{2+} ion proceeds from a transition metal in which the 5 orbitals (d) in level 3 are half occupied by electrons, fact that explains its great capacity of complexation with water dipols; thus, the radius of hydrated ion increases and its exchange degree decreases. The Zn^{2+} ion derives from a transition metal in which the 5 orbitals (d) in level 3 are completely occupied by electrons, whence their less hydration capacity and less radius of hydrated ion. The Zn^{2+} ions are more mobile than the Mn^{2+} ions in zeolites NaX, NaA and mordenite, because the latter has CN = 5, forming a trigonal bipyramidal arrangement [20] and the former has CN = 4, being a tetrahedric one.[21]

Also, it must be taken into account that in the case of more aluminous zeolites the electrostatic field of network is very strong, and contribution of the electrostatic attraction to energetics of the exchange is much greater than that corresponding to hydration, so that the ion with a smaller radius is preferred. In the case of zeolites with weak electrostatic field, siliceous zeolites, e.g. NaM, the contribution of the electrostatic field is not significant, involving much more the hydration energy of ions in solution; zeolite will prefer the ion with greater radius and less hydrated. Mordenite prefers neither Zn^{2+} nor Mn^{2+}, for both ions $\Delta G > 0$.

Mobility of the ions in zeolite is also controlled by its structure; while sodalite zeolites have a tridimensional structure of pores and cavities, mordenite has a bidimensional one of tubular pores with adjacent cavities.

CONCLUSIONS

From the experimental results presented above the following conclusions may be drawn:

1. The $Na^+ \rightleftharpoons 1/2\, Zn^{2+}$ ion exchange, in the sodalite zeolites NaA and NaX, takes place according to an *a* — type isotherm with maximum exchange degree, i.e. $X \simeq 1$ and, in NaM, it takes place according to a sigmoidal isotherm of the *b*-type, affinity of mordenite against Zn^{2+} being important only up to an exchange degree of about 40%.

2. The $Na^+ \rightleftharpoons 1/2\, Mn^{2+}$ ion exchange, in all cases, takes place according to isotherms of the *d*-type and maximum exchange degree is not reached; this is situated in the order: NaA > NaX > NaM.

3. Free energy of exchange is negative for the exchange of Zn^{2+} and Mn^{2+} in NaA and NaX zeolite and positive in mordenite. In both cases the temperature increase influence favourably the ion-exchange.

REFERENCES

[1] D. W. Breck, W. G. Eversole, R. M. Milton, T. B. Reed and T. L. Thomas, *J. Amer. Chem. Soc.*, **78**, 5963 (1956).

[2] R. M. Barrer and W. M. Meier, *Trans. Faraday Soc.*, **54**, 1074 (1958).

[3] L. Broussard and D. F. Schoemaker, *J. Amer. Chem. Soc.*, **82**, 1041 (1960).
[4] M. M. Dubinin, *Izvest. Akad. Nauk SSSR, Otdel. khim. Nauk*, **1961**, p. 1183.
[5] D. W. Breck and E. M. Flanigen, "Molecular Sieves", Soc. Chem. Ind., London, 1968, p. 47.
[6] W. M. Meier, "Molecular Sieves", Soc. Chem. Ind., London, 1969, p. 10.
[7] J. D. Sherman, *AIChE, Symp. Series*, **74**, 98 (1978).
[8] R. M. Berrer, L. V. C. Ress and M. Shamsuzzoha, *J. Inorg. Nuclear Chem.*, **28**, 629 (1966).
[9] R. M. Barrer, J. A. Davies and L. V. C. Rees, *J. Inorg. Nuclear Chem.*, **30**, 3333 (1968).
[10] H. S. Sherry, "Ion Exchange", vol. 2, Ed. J. A. Marinsky, New York, 1969, p. 89—133.
[11] H. S. Sherry, *Adv. Chem. Ser.*, **101**, 350 (1971).
[12] P. V. Venuto and P. S. Landis, *Adv. Catalysis*, **18**, 259 (1968).
[13] G. Gutt and K. Aufderlgen, *Helv. Chim. Acta*, **57**, 441 (1974).
[14] N. E. Cross, C. Kemball and H. F. Leach, *Adv. Chem. Ser.*, **102**, 389 (1971).
[15] Kh. Minachev, V. Garanin, T. Isakova, V. Kharlamov and V. Bogomolov, "Molecular Sieves Zeolite II", ACS 102, **76**, 444 (1970).
[16] J. Rouchard, L. Sendegam and J. J. Firipiat, *Bull. Soc. chim. belges*, **77**, 537 (1968).
[17] J. Rouchaud, P. Mulkay and J. J. Fripiat, *Bull. Soc. chim. belges*, **77**, 537 (1968).
[18] I.J. Gal, O. Iankovic, S. Malcic, P. Radovarov and M. Todorovic, *Trans. Faraday Soc.*, **67**, 999 (1971).
[19] V. A. Nikashina, L. I. Zvereva, K. M. Olshanova and M. A. Potapova, *J. Chromatog.*, **120**, 155 (1976).
[20] R. Y. Yanagida. T. B. Jr. Vance and K. Seff, *Inorg. Chem.*, **13**, 723 (1974).
[21] A. A. Amaro, C. L. Kovacing, K. B. Kunz, P. E. Roley, T. B. Jr. Vance, R. Y. Yanagida and K. Seff, "Molecular Sieves", Leuven Univ. Press., Belgium, 1973, p. 113.

Revue Roumaine de Chimie, **32**, *6*, 571–575 (1987)

POLAROGRAPHIC STUDY OF LEAD WITH δ-VALEROLACTAM AND ITS ANALYTICAL APPLICATIONS

ASHOK KUMAR *, MOHAN KATYAL ** and B. K. PURI ***

* Department of Chemistry, D. A. University of Indore, Indore-452 003, India
** St. Stephen's College, Delhi-110007, India
*** Department of Chemistry, Indian Institute of Technology, Hauz Khas, New Delhi-110 016 India

Received August 30, 1986

The polarographic behaviour of lead has been studied using δ-valerolactam as complexing agent at a constant ionic strength (0.1 M postassium nitrate) and pH 6.5. A well defined diffusion-controlled reversible wave is obtained. The overall stability constants were evaluated by Deford and Hume's method. Lead is found to form 1 : 1 and 1 : 2 complexes having $\log \beta_1 = 0.74$, 0.79, 0.85 and $\log \beta_2 = 1.81$, 1.99, 2.16 at 303, 313, and 323 K respectively. The percentage distribution of various complex species has been presented. The values of thermodynamic parameters, ΔG, ΔH and ΔS have also been obtained. The value of diffusion current constant (I) was calculated and found to be 3.47 which is constant over concentration range 1.0–3.5 mM. The method has been employed for the determination of lead in certain alloys.

INTRODUCTION

Polarographic reduction of lead has been studied in various supporting electrolytes such as hydroxylamine,[1] pyridine,[1] imidozol,[2] ethanolamine,[3] EDTA,[4] N-N′-dihydroxyethylglycine,[5] hexamine,[6] glutamic acid,[7] pyrrolidinone-2,[8] caproloctam.[9] It is found that in most of these cases mixed electrolytes have been used and in certain cases a maximum supressor is also required. Thus, the sensitivity and accuracy in the measurement of the diffusion-current tend to decrease. Less attention is paid to the thermodynamics of complex formation which has the potentiality to provide good insight into complex phenomenon. The present work deals with the determination of the thermodynamic parameters and the stability constants of the complexes formed by lead with δ-valerolactam at different temperatures. The interference of various ions has been studied in detail and conditions have been developed for the quantitative determination of lead in pure solution as well as in complex materials such as alloys. There is no need of a maximum supresser or of an auxiliary electrolyte.

EXPERIMENTAL

Solutions

The stock solution of δ-valerolactam (Fluka, GR grade) was prepared in doubly distilled water. Solution of lead was prepared by dissolving $Pb(NO_3)_2$ in distilled water in the presence of a few drops of HNO_3 and standardized.[10] Ionic strength was maintained constant with potassium nitrate.

Apparatus and Procedure

A balancing type [11] manual polarograph was set up to obtain current-potential curves. A saturated calomel electrode was used as reference electrode. All polarographic measurements were carried out in a water thermostat (accuracy ± 0.1°C). pH of the test solutions was measured with an Elico pH meter. Oxygen was expelled by passing a slow stream of purified nitrogen through the test solution for 5 min. The dropping-mercury electrode had the following characteristics : $m = 2.90$ mg s^{-1} ; $t = 2.9$ s ; $m^{2/3} t^{1/6} = 2.93$ mg$^{2/3}$ s$^{-1/2}$; and $h_{\text{corr}} = 58.7$ cm in 0.1 M potassium nitrate solution. The number of electrons (n) involved in the reduction process was determined by the millicoulometric method of Devries and Kroon.[12]

RESULTS AND DISCUSSION

A number of polarograms recorded in 0.1 M δ-valerolactam showed that a well-defined wave was obtained in a pH range 3.0—7.5. As the pH was lowered below 3.0 the lower plateau was distorted while above pH 7.5 a slight turbidity appeared. It was observed that the negative shift in $E_{1/2}$ was maximum at pH 6.5 and hence this pH was chosen for studying the complex formation between Pb(II) and δ-valerolactam.

The plots of i_d vs $h^{1/2}$ were found to be linear and passing through the origin, thereby indicating that the reduction is diffusion controlled. This is also supported [13] by the fact that the temperature coefficient of the diffusion current is 1.15 percent per degree. The plots of log $i(i_d - i)$ vs $E_{d.e}$ were found to be linear with a slope of the order (32 ± 2 mV) showing the reversibility of the reduction. The value of n was found to be 2 at pH 6.5. A negative shift in $E_{1/2}$ values with increasing concentration of δ-valerolactam indicates the formation of complexes.

A plot of $E_{1/2}$ vs log C_x (where C_x is the total ligand concentration) was found to be smooth curve, showing the formation of more than one complex species. Lead is found to form 1 : 1 and 1 : 2 complexes with the values of the constants $\beta_1 = 5.5 \pm 1$ and $\beta_2 = 65.0 \pm 2$ at 303 K. The stability constants (Table 1) obtained at 303, 313 and 323 K were used to calculate [14,15] various thermodynamic functions. The percetnt age distribution of various species present at different ligand concentrations has been presented(Fig. 1).

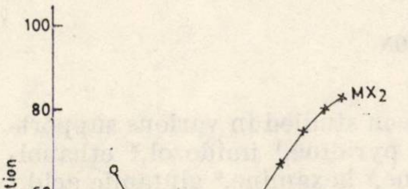

Fig. 1.—Distribution diagram for Pb(II)—valerolactam system.

The stability of complex changes with the change in temperature, depending upon the thermodynamics of complexation. The stability of complexes was found to enhance by an increase in temperature (Table 1) showing the endothermic nature of reaction.

Table 1

Stability constant and thermodynamic functions
$Pb(II) = 1.0 \times 10^{-3}$ M, pH 6.5, $\mu = 0.1$ M KNO_3

Complex	log			$-\Delta F^\circ$ kcal mol^{-1}			ΔH° kcal mol^{-1}	ΔS° caldeg^{-1} mol^{-1}
	303 K	313 K	323 K	303 K	313 K	323 K		
Pb(δ-val.)	0.74	0.79	0.85	1.03	1.14	1.27	2.52	3.39
$Pb(\delta\text{-val.})_2$	1.81	1.99	2.16	2.53	2.87	3.21	5.49	9.16

Effect of Metal Ion Concentration

Polarograms over the concentration range of $Pb(II) = 1.00-3.50$ mM were drawn under the above-mentioned conditions. The diffusion current was measured by the extrapolation method. The value of diffusion current constant (I) was calculated using Ilkovic equation, $I = i_d/c\ m^{2/3}t^{1/6}$, and found to be 3.47 which is constant over the Pb(II) concentration range of 1.00 – 3.50 mM. Therefore the polarographic results are used for the quantitative determination of lead. Ten replicate determinations for the sample solution containing 1 mM of Pb(II) gave a mean diffusion current of 8.44 with a standard deviations of 0.092 and a relative standard deviation of 1.10%.

General Procedure for the Determination of Pb(II)

A calibration curve for Pb(II) was prepared by recording the polarograms of the lead at various concentrations in 0.1 M δ-valerolactam at pH 6.5. The i_d values of polarograms were plotted against concentration of Pb(II) and then, polarogram of the solution containing the metal in unknown concentration was recorded under identical conditions. The *id* values of this wave were referred to calibration curve (which was linear) and the concentration of the lead in the solution was determined (Table 2).

Table 2

Polarographic determination of Pb(II) with δ-valerolactam. δ-valarolactam = = 0.1 M, pH 6.5 sensitivity = 1/50

Amount taken (mg)	Amount found * (mg)	Error (%)
0.865	0.874	+1.04
1.220	1.206	−1.15
1.850	1.868	+0.97
2.115	2.136	+0.99
2.860	2.800	−0.21
3.250	3.280	+0.92

* Average of ten replicate determinations.

Determination of Lead in Alloys

A 0.1 g of the alloy was dissolved in 10 mL of concentrated hydrochloric acid and 5 10 mL of concentrated nitric acid. The solution was heated till reduced to about 5 mL. After cooling, 5 mL of concentrated nitric acid were added and the solution diluted to 100 mL in a standard flask with distilled water. An alliquot of this solution was taken and lead was determined as described above. The results are given in Table 3.

Table 3

Determination of lead in alloys
δ-valerolactam = 0.1 M, pH 6.5, sensitivity = 1/50

Alloy	Certified composition (%)	Amount taken (mg)	Amount found * (mg)	Error (%)
Gun metal	Zn : 4.4 Pb : 6.3 Sn : 5.3 Cu : 84.0	2.532	2.550	+0.71
Standard sample No. 54 D	Sn : 88.54, Cu : 3.61 Sb : 7.06, Pb : 0.62 As : 0.09, Bi : 0.048 Fe : 0.028, Ag : 0.003 Ni : 0.002	3.050	3.024	−0.85

* Average of ten replicate determinations.

Effect of Various Ions

The effect of the various anions and metal ions at a certain concentration (1 mM) has been ascertained. The effect of sulphate, nitrate, acetate, oxalate, salicylate, citrate and formate on the polarograms of the metal was studied. In all instances the $E_{1/2}$ value remained almost constant. Ti(IV), W(VI), Sc(VI), Cr(III), Fe(III), Ba(II), Ca(II), Sr(II), Ag(I), Pt(IV) were not reduced under these conditions and could be tolerated up to 10-fold excess. U(VI), Cu(II) were reduced at low potentials while Zn(II), Sn(II), As(III), Sb(III), Ni(II), Pd(II), Mn(II) at higher potentials and they could be tolerated up to 5-fold excess in the determination of lead.

REFERENCES

[1] J. W. Grenier and L. Meites, *Analyt. Chim. Acta*, **14**, 482 (1956).
[2] Madhu Shivhare and M. Singh, *J. Inorg. Chem.*, **43**, 1599 (1981).
[3] R. S. Subrahmanya, *Proc. Indian Acad. Sci.*, **46A**, 433 (1957).
[4] W. Christmann, Z. Luka Szewski and R. Neeb, *Z. analyt. Chem.*, **302**, 132 (1980).

[5] R. C. Kapoor and J. Krishan, *Indian J. Chem.*, **13A**, 1078 (1980).

[6] K. Saraswati and D. R. Prasad, *Indian J. Chem.*, **15A** 251 (1977).

[7] J. N. Gaur and M. M. Palreeha, *Talanta*, **15**, 583 (1968).

[8] B. K. Puri and Ashok Kumar, *Chemical Acta Turcica*, **12**, 11 (1984).

[9] B. K. Puri and Ashok Kumar, *Microchem. J.* (in press).

[10] A. I. Vogel, "Text Book of Quantitative Inorganic Analysis", Longmans, London 1969.

[11] I. M. Kolthoff and J. J. Lingane, "Polarography", Interscience Pub., New York, 1946.

[12] T. De Vries and J. L. Kroon, *J. Amer. Chem. Soc.*, **75**, 2484 (1953 .

[13] L. Meites, "Polarographic Techniques", Interscience, New York 1965.

[14] J .K. Gupta and C. M. Gupta, *Ind. J. Chem.*, **6**, 50 (1968).

[15] S. S. Kelkar and B. I. Gemede , *J. Electrochem. Soc.*, **30**, 228 (1981).

Revue Roumaine de Chimie, 32, 6, 577–582 (1987)

AROMATIC AZOXYBISETHERS

MIRCEA IOVU * and STELIAN RADU **
* Faculty of Pharmacy, Str. Traian Vuia 6, Bucharest, Romania
** Faculty of Sciences, Department of Chemistry, Calea Bucureşti, 165, Craiova, Romania

Received February 15, 1986

The paper describes the possibility of obtaining aromatic azoxybisethers : a) by oxidising the corresponding azobisethers with hydrogen peroxide in the presence of acetic acid and b) by condensation of sodium salt of 4,4′-dihydroxy azobenzene with monochloromethylated derivatives of substituted and unsubstituted benzene. The new azoxybisethers were characterized by spectral (IR and UV) and thermal analysis.

INTRODUCTION

The oxidation of aromatic azo-compounds by hydrogen peroxide in acetic acid was used in this paper to obtain a new class of derivatives of azoxybisethers.

Using this oxidant, Bigiavi and Carrara,[2] obtained 4,4′-azoxydiphenol and its derivatives.

We present here the synthesis of azoxybisethers by oxidation of azobisethers, synthesized from sodium salt of 4,4′-dihydroxy azobenzene and monochloromethyiated derivatives of substituted and unsubstituted benzene,[2] using the same oxidant.

This reagent yielded 4,4′-bis(benzyloxy)azoxybenzene from 4,4′-bis(benzyloxy)azobenzene ; 4,4′-bis(4-methylbenzyloxy) azoxybenzene from 4,4′-bis(4-methylbenzyloxy)azobenzene ; 4,4′bis-(2,4-dimethylbenzyloxy)azoxybenzene from 4,4′-bis-(2,4-dimethylbenzyloxy) azobenzene ; 4,4′-bis(2,5-dimethylbenzyloxy) azoxybenzene from 4,4′-bis(2,5-dimethylbenzyloxy) azobenzene and 4,4′-bis(4-phenylbenzyloxy)azobenzene.

The azoxy group results due to the attack of the atomic oxygen from the oxidation reagent on the azo group of azobisethers :

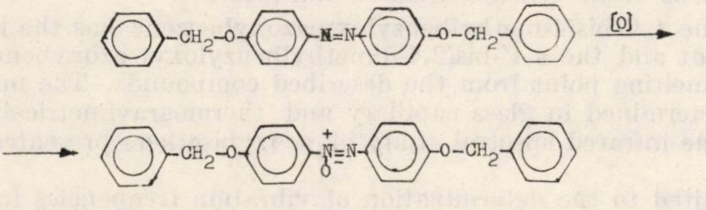

The acetic acid is used as reaction medium.

The disappearance of the oxidant in the reaction medium is verified with iodine-starched paper.

The above-mentioned azoxybisethers were synthesized by condensation of sodium salts of 4,4′-dihydroxy azoxybenzene with monochloromethylated derivatives of substituted and unsubtituted benzene : chloromethylbenzene, chloromethyl-4-methylbenzene, chloromethyl-2,4-dimethylbenzene, chloromethyl-2,5-dimethylbenzene and chloromethyl-4-phenylbenzene. To obtain sodium salts we used the method previously presented,[3,2] which consists in the reaction of 4,4′-dihydroxyazoxybenzene with sodium hydroxide in a mixture (1 : 1 by volumes) of ethanol and benzene, as solvent. The sodium salts can be obtained anhydrous if the resulting water is removed by azeotropic distillation (as an azeotropic mixture of ethanol-benzene-water).

The condensation of anhydrous phenoxide with halogeno-derivative takes place at 60 – 65°, through nucleophilic attack of phenoxide anion on the monochloromethylated derivatives, as follows :

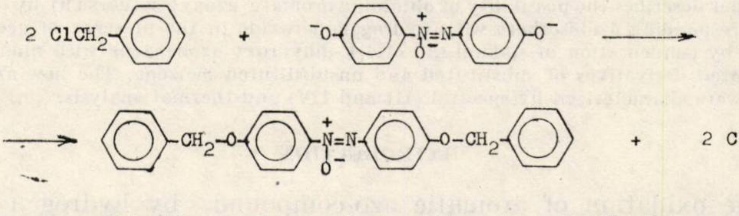

The azoxybisethers obtained by the two methods are identical, having the same melting points and spectral properties. The yields have higher values in the case of oxidation. The azoxybisethers were investigated spectrometrically and thermogravimetrically.

RESULTS AND DISCUSSION

Table 1 lists the synthesized compounds, the structural formulae, the molecular formulae, the quantitative results of carbon, hydrogen and nitrogen elemental analysis, λ_{max} and ε_{max} from UV spectra, their melting points and yields.

The azoxybisethers synthesized by the two methods described above are solid products, weakly coloured in green.

They are more soluble in ethanol and benzene than the corresponding azobisethers. Their melting points were determined after repeated recrystallizations from ethanol-benzene mixtures.

The 4,4′-bis(4-methylbenzyloxy)azoxybenzene has the highest melting point and the 4,4′-bis(2,4-dimethylbenzyloxy) azoxybenzene has the lowest melting point from the described compounds. The melting points were determined in glass capillary and thermogravimetrically.

The infrared spectral study of azoxybisethers presented in Table 1 was limited to the determination of vibration frequencies for 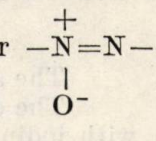 $-\underset{\underset{O^-}{|}}{\overset{+}{N}}=N-$ and C – O – C characteristic bonds.

Table 1

Aromatic azoxybisethers

Azoxybisethers	Molecular formula	C % calc. found	H % calc. found	N % calc. found	λ_{max} nm	ε_{max}	M.p. °C	Yield %
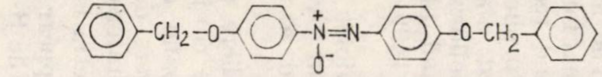	$C_{26}H_{22}N_2O_3$	76.08 75.32	5.40 5.41	6.82 6.88	257.3 356.3	1260 2986	153	91.1
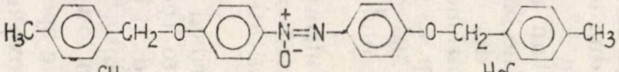	$C_{28}H_{26}O_3N_2$	76.69 76.21	5.98 5.90	6.39 6.25	256.7 357.7	1261 2918	183	96.4
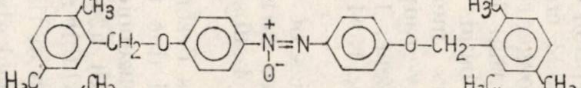	$C_{30}H_{30}O_3N_2$	77.23 76.98	6.48 6.30	6.00 6.17	258.1 356.7	1318 3373	178.5— 179	91.8
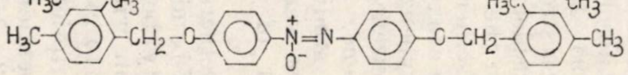	$C_{30}H_{30}O_3N_2$	77.23 76.71	6.48 6.20	6.00 6.29	257.3 357.0	1355 3484	145.5— 146.5	77.3
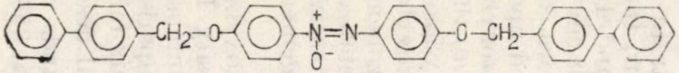	$C_{38}H_{30}O_3N_2$	81.117 80.74	5.37 5.29	4.98 4.73	260.0 356.5	5129 4667	147.5— 149	91.5

The infrared spectra of azoxybisethers mentioned in Table 1 present a characteristic strong band at 1253–1213 cm^{-1} due to the antisymmetric valency vibration of the C–O–C bond and a weaker band at 1029–997 cm^{-1} due to the symmetric valency vibration of the C–O–C bond. The second band due to the symmetric vibration of the C–O–C bond can be superposed upon the bands due to the in-plane deformation of the C–H bonds of the aromatic nucleus and of the ring vibrations.

For the azoxybisethers presented in table 1, we assigned the following values of the absorption maxima due to the antisymmetric and symmetric vibration of the νC–O–C bond : 1253 and 1029 cm^{-1} for 4,4′-bis(benzyloxy) azoxybenzene, 1213, 1246 and 1008 cm^{-1} for 4,4′-bis(4-methylbenzyloxy) azoxybenzene, 1232, 1253 and 998 cm^{-1} for 4,4′-bis(2,5-dimethylbenzyloxy) azoxybenzene.

It could be observed that the band due to the antisymmetric valency vibration is split into two peaks, for the last two compounds mentioned above.

As is known, the azo-group vibration frequencies of aromatic and aliphatic azocompounds are difficult to recognize and therefore they have been the least studied.[5]

The literature also reports a few data on 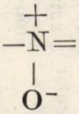 $-\underset{O^-}{\underset{|}{\overset{+}{N}}}=N-$ vibration frequencies. Langley and coworkers[6] gave two characteristic frequencies of azoxy-group for some aliphatic azoxyderivatives : a symmetric stretching at 1344–1285 cm^{-1} and an antisymmetric stretching at 1531–1495 cm^{-1}.

The azoxybisethers synthesized here present azoxy-group absorption bands similar to those assigned for the corresponding aromatic azobisethers.[2,4] Thus, the absorption due to the azoxygroup appears at 1410–1408 cm^{-1} and 1595–1593 cm^{-1}. The absorption band which appears at 1410–1408 cm^{-1} is stronger than that for the corresponding azobisethers, In addition, we consider that the band recorded at 1595–1593 cm^{-1} can be superposed upon the bands due to phenyl-ring absorption.

The azoxybisethers mentioned above possess their absorption maxima due to the azoxy-group, as follows : 1594 and 1410 cm^{-1} for 4,4′-bis(benzyloxy)azoxybenzene, 1593 and 1410 cm^{-1} for 4,4′-bis(4-methylbenzyloxy)azoxybenzene, 1594 and 1409 cm^{-1} for 4,4′-bis(2,5-dimethylbenzyloxy)azobenzene.

The detailed studies of ultraviolet and visible spectra for azoxybenzene derivatives were carried out by Hahn and Jaffé[7] performing the rearrangement of 4-substituted azoxybenzenes into hydroxyazobenzenes.

The azoxybisethers described here present two absorption bands : a high-intensity K-band due to the conjugated system Ar–N=N–Ar and a low-intensity benzenoid B-band due to the aromatic systems.

In comparison with azobisethers described in a previous paper,[8] azoxybisethers fail to exhibit a low-intensity R-band.

The full description of the spectra is given in table 1.

The bands mentioned above appear for azoxybisethers, as follows : the K-band at 356.3–357.7 nm and the B-band at 256.7–260 nm.

The K- and B-bands are shifted (hypsochromically) in comparison with those corresponding to the azobisethers.

The molar extinction coefficients have smaller values for B-bands than for K-bands.

The yields depend on the preparation method; they are larger for synthesis by oxidation and smaller for synthesis by condensation.

CONCLUSIONS

In this paper we have presented a new class of compounds, aromatic azoxybisethers, with the general formula :

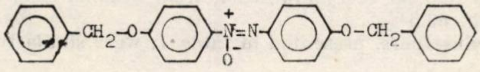

These compounds were obtained either starting from azobisethers by oxidation or from sodium salt of 4,4′-dihydroxy azoxybenzene and monochloromethylated derivatives of benzene, by condensation.

The azoxybisethers were characterized by spectral (infrared, ultraviolet, visible) and thermogravimetric analysis.

EXPERIMENTAL

The aromatic azobisethers used in the synthesis were obtained as shown in a previous paper.[2] Hydrogen peroxide was a Carlo Erba product. Acetic acid was a "Reactivul" commercial product. 4,4′-Dihydroxyazoxybenzene was obtained by oxidation of 4,4′-dihydroxyazobenzene with hydrogen peroxide and acetic acid.[1] Chloromethylbenzene was a Riedel de Häen commercial product. 1-Chloromethyl-1-4-mehylbenzene was synthesised by photochemical chlorination of *p*-xylene with sulphuryl chloride, using benzoyl peroxide as initiator. 1-Cloromethyl-2,4-dimethylbenzene and 1-chloromethyl-2,5-dimethylbenzene were synthesized by chloromethylation of *m*-xylene and *p*-xylene, using paraformaldehyde, hydrochloric acid and phosphoric acid.[9] 4-Chloromethylbiphenyl was obtained by chloromethylation of biphenyl, using paraformaldehyde, hydrochloric acid, $ZnCl_2$ in acetic acid and petroleum ether.

Infrared spectra were recorded with a Perkin-Elmer spectrophotometer model 157, in KBr pellets, within the range 4000—650 cm^{-1}. The electronic spectra were obtained with a Specord, Carl-Zeiss spectrophotometer, within the range 200—700 nm, using dioxane as solvent.

The DTA, DTG, TG and T curves were obtained by a Setaram thermal balance.

Synthesis of 4,4′-bis(benzyloxy)azoxybenzene by oxidation of 4,4′-bis(benzyloxy)azobenzene with hydrogen peroxide and acetic acid

In a 500 mL flask equipped with ascending condenser and a thermometer, 2 g(0.005 moles) of 4,4′-bis(benzyloxy)-azobenzene and 100 mL acetic acid were placed. The mixture was heated up to the boiling point to obtain a homogeneous solution. The solution obtained was cooled to keep the temperature at 75—80°. Under these conditions, 3.5 mL H_2O_2 30% (excess) were added in the flask.

The reaction mixture was heated at 75—80° for 25 hours, after which the flask was cooled. The total oxidation can be tested by identification of peracetic acid in excess with iodine starched paper. 4,4,-Bis(benzyloxy)azobenzene was precipitated with water ; after filtering, the precipitate was washed with a great amount of water on the filter, in order to remove acetic acid, then dried. After recrystallization from ethanol-benzene mixture, 4,4′-bis(benzyloxy)azoxybenzene had m.p. 153°. The yield : 91.1 %.

Synthesis of 4,4′-bis(benzyloxy)azoxybenzene by condensation of sodium salt of 4,4′-dihydroxyazoxybenzene with benzyl chloride

In a 100 mL two-necked flask equipped with a reflux condenser with a drying tube and a thermometer, 1.15 g (1/200 mol) 4.4′-dihydroxyazoxybenzene, 0.4 g (1/100 mol) NaOH and 40 mL of ethanol-benzene mixture (1 : 1 by volume) were introduced.

The mixture was heated under reflux for one hour, when the sodium salt was formed. After removing the resulting water as an ethanol-benzene-water ternary azeotropic mixture 1.265 g (1/100 mol) benzyl chloride were added over the sodium salt and brought to the boiling point for 10 hours.

The resulting precipitate was recovered by filtration, washed successively with a great amount of water and a little ethanol on the filter, then dried at a 105° in a heating chamber. Azoxybisether was purified by recrystallization from ethanol-benzene-mixture. The melting point : 153°. The yield : 83.6 %.

The other azoxybisethers, presented in table 1, were similarly synthesized by the two procedures.

REFERENCES

[1] D. Bigiavi and G. Carrara, *Gazz. chim. Ital.*, **53**, 285 (1923).

[2] M. Iovu and S. Radu, *Rev. Roumaine Chim.*, **18**, 473 (1973).

[3] M. Iovu, *Rev. Roumaine Chim.*, **16**, 1223 (1971).

[4] M. Iovu, *Rev. Roumaine Chim.*, **17**, 1261 (1972).

[5] C. N. Rao, "Chemical Applications of Infrared Spectroscopy", Academic Press Inc., New York, 1963, p. 267.

[6] B. W. Langley, E. Lythgoe and L. S. Rayner, *J. Chem. Soc.*, **1952**, 4191.

[7] C. S. Hahn and H. H. Jaffé, *J. Amer. Chem. Soc.*, **84**, 946 (1962).

[8] M. Iovu and S. Radu *Rev. Roumaine Chim.*, in press.

[9] A. A. Vansedt, E. P. Mlelnikova and L. V. Kuhareva, *Zhur. priklad Khim.*, **23**, 2151 (1960).

Revue Roumaine de Chimie, 32, 6, 583–590 (1987)

STRUCTURE ACTIVITY RELATIONS BY THE FREE-WILSON AND MTD METHODS FOR SUBSTANCES WITH A POTENTIAL PSYCHOTROPIC ACTIVITY. I

DIPHENYLETHER DERIVATIVES WITH NEUROLEPTIC ACTIVITY

M. APETROAE, CL. SINGER, RALUCA BOZGA, ST. CILIANU, RODICA CECLAN,
TAMARA BÂNZARU * and Z. SIMON *

Chemical Pharmaceutical Research Institute, Sos. Vitan 112, 73 619, Bucharest
* Medicinal Institute of Timişoara, Department of Biophysics, Pţa 23 August 2, 1900,
Timişoara, Romania

Received July 7, 1986

The simultaneous use of both Free-Wilson and MTD methods in QSAR analysis gives supplementary information about structural features which are essential for a certain type of biological activity. These two methods are used in a QSAR analysis of a series of 20 diphenylether derivatives which intensify the barbituric sleep in mice. A correlation coefficient of r = 0.771 is obtained by the Free-Wilson method with 17 structural fragments in four positions, while r = 0.811 is obtained by the MTD method with two supplementary indicator variables and r = 0.870 if two compounds are eliminated out of the series. There is a general agreement between the orders of the contributions to biological activity of the different substituents in each of the four positions, as indicated by the two methods.

INTRODUCTION

The quantitative structure activity analysis, the so-called QSAR, is recognised as a useful tool for drug design.[1] The QSAR method which is to be considered in searching substances with a certain biological activity depends both upon the nature of the pertinent receptor effector interactions, drug transport characteristics etc., and upon the synthesis availabilities of the respective laboratory. These items are considered here, in connection with the use of Free-Wilson and MTD methods in the QSAR analysis of a series of diphenylether derivatives with neuroleptic activity.

Three types of structural factors are considered to determine biological activity [2]: i) sterical factors connected with the fit of the drug molecule in the receptor site; ii) electronic factors connected with reactivity and intermolecular force characteristics and iii) partition effects connected especially with transport characteristics. Our experimental data refer to *in vivo* physiological effects and may depend not only upon drug-receptor interactions but also upon transport and other phenomena. The QSAR analysis may, eventually, yield information also on some of these phenomena.

METHOD

Experimental activities. The chemical formulae of the 20 substances tested for neuroleptic activity are given in Table 1. Most of them are new compounds; their synthesis and physico-chemical characteristics will be described elsewhere.

The neuroleptic activity, A_{exp}, is defined as the prolongation of barbituric (amital) sleep in mice, expressed as percentage with respect to the test batch. Details upon these tests will be given elsewhere. The logarithm of this activity, $\log A_{exp}$, is used for the correlations.

Free-Wilson method.[3] This method calculates the contributions to the biological activity of substituents (structural fragments) introduced in certain positions of a molecular core. The correlational equation is of the general form:

$$\log A^{i}_{FW} = a_0 + a_1 x_{1i} + \ldots + a_n x_{ni} \qquad (1)$$

with a_0 the mean activity value for the tested series, $x_{1i} \ldots x_{ni}$ — the indicator variables for the presence of certain structural fragments and $a_1 \ldots, a_n$ their contributions to biological activity. Steric, electronic and partition effects of each structural fragment are implicitly included in the a_j contributions.

MTD method.[4] This method accounts specifically for the stereochemical aspects of biological activity. The correlational equation is of the type:

$$\log A^{i}_{MTD} = \alpha - \beta \, MTD_i \qquad (2)$$

with MTD_i as a measure for the steric misfit of the i molecule in the receptor site. Indicator variables for specific structural features or other structural variables may be also added to equation (2).

In this method the hypermolecule, a topological network, is constructed by an approximate atom per atom superposition of the molecules, with M vertices "j". The receptor space, S, investigated by the molecules of the series is characterized by a set of ternary parameters:

$$S : \varepsilon_1, \varepsilon_2, \ldots, \varepsilon_M$$

with $\varepsilon_j = -1$ for beneficial (cavity) vertices, $\varepsilon_j = +1$ for detrimental (wall) vertices and $\varepsilon_j = 0$ for irrelevant (external) vertices.

Comparison of the Free-Wilson and MTD methods. The Free-Wilson method includes, implicitly, both steric, electronic and partition effects without distinguishing between them, while the MTD method accounts specifically for stereochemical features, but is not able to discern the nature of the atom (group) occupying a certain vertex. A comparison of the results of these methods may give indications concerning electronic and hydrophobicity effects of groups occupying certain positions. If the effect of hydrophobicity (partition) characteristics of the molecules is also considered, some general indications about drug transport phenomena may be also obtained.

A special problem is the reliability of the results, as both methods use a large number of parameters in characterizing the structures of the molecules. If both methods yield the same results concerning the contributions of structural fragments, the reliability is certainly increased, but a comparison of experimental and calculated activities for some new molecules is highly desirable.

RESULTS

Free-Wilson method. The computation of the a_j contributions is performed according to a multiple regression program, developed at the Chemical Pharmaceutical Research Institute, which performs the computation of the a_j coefficients and their statistical analysis (confidence

TABLE 1. COMPOUNDS WITH NEUROLEPTICAL ACTIVITY STRUCTURE AND ACTIVITIES

	STRUCTURE	$\log A_{exp}$	$\log A_{FW}$
1.	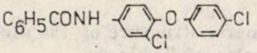	2.55	2.45
2.	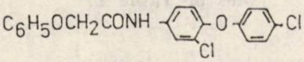	2.45	2 39
3.	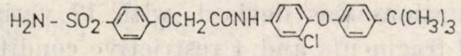	2.33	2.17
4.	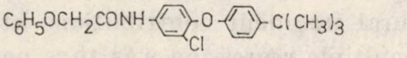	2.30	2.20
5.	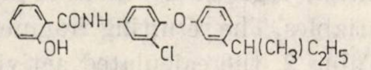	2.285	2.20
6.	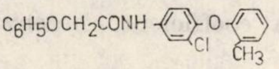	2.28	2·10
7.	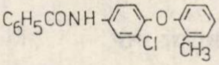	2.24	2.24
8.	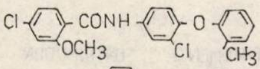	2.24	1.96
9.	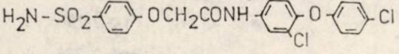		
10.	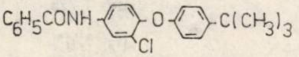	2.17	2.27
11.	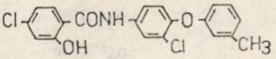	2.15	2.13
12.	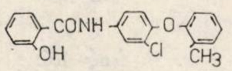	2.09	2.17
13.	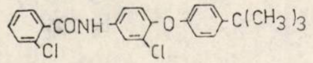	2.08	2.24
14.	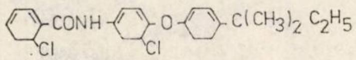	2.06	1.90
15	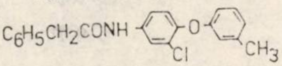	2.06	2.06
16.	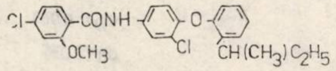	1.91	1.99
17.	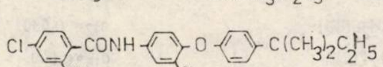	1.86	2.07
18	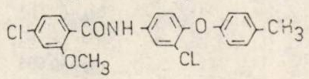	1.87	1.88
19.	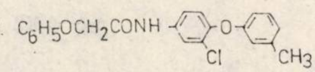	1.79	1.99
20.	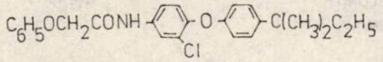	1.72	1.86

For the definition of $\log A_{exp}$-values see Method (Experimental activities) section; $\log A_{FW}$ is calculated according to eq (1) with the structural fragment contributions of Table 2.

interval, dispersional analysis, multiple correlation coefficient etc.). The basic structure (molecular core) selected for the series of Table 1 is depicted in Fig. 1.

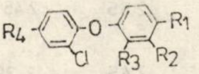

Fig. 1. – General structure of the molecules of Table 1.

A system of 20 equations was devised, with 17 variables corresponding to the structural fragments and 4 restrictive conditions selected such that the sum of structural fragment contributions at each of the four positions is zero.[3] The multiple regression was thus performed for a system of 20 equations and 13 variables. The resulting fragmental structure contributions, a_j, are listed in Table 2, the calculated activities, log A_{FW} in Table 1. The multiple correlation coefficient, hereby obtained is $r = 0.771$, the free term $a_0 = 2.131$.

TABLE 2. STRUCTURAL FRAGMENT CONTRIBUTIONS FOR FREE WILSON CALCULATIONS

POSITION	SUBSTITUENT (STRUCTURAL FRAGMENT)	CONTRIBUTION
		$a_0 = 2.131$
R_1	A: tC_4H_9-	$a_1 = 0.226$
	B: Cl-	$a_2 = 0.411$
	C: H-	$a_3 = -0.186$
	D: iC_5H_{11}-	$a_4 = -0.116$
R_2	E: H-	$a_5 = -0.063$
	F: CH_3-	$a_6 = 0.152$
R_3	G: H-	$a_7 = -0.064$
	H: CH_3-	$a_8 = 0.138$
	I: i C_4H_9-	$a_9 = 0.171$
R_4	J: 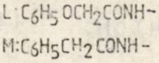	$a_{10} = -0.064$
	K: C_6H_5CONH-	$a_{11} = 0.030$
	L: $C_6H_5OCH_2CONH$-	$a_{12} = -0.030$
	M: $C_6H_5CH_2CONH$-	$a_{13} = 0.040$
	N: 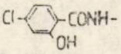	$a_{14} = 0.103$
	O: 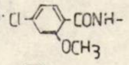	$a_{15} = -0.006$
	P: 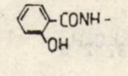	$a_{16} = -0.062$
	R 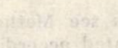	$a_{17} = 0.151$

MTD method. The hypermolecule for the 20 molecules of Table 1 is depicted in Fig. 2 and was obtained by maximal superposition of the molecules, such that the common core occupies always the same vertices. Only the vertices occupied in not all molecules are numerated, while the groups of vertices j : 2, 2′, 2″; 6, 6′, 6″; 7, 7′; 14, 14′; 15, 15′, 15″, 15‴ which are either all occupied or all empty for these molecules are indicated by the first, unprimed, number. A total number of $M = 24$ vertices results hereby. The vertices occupied in the 20 molecules are listed in the $(x_{ij} = 1)$ column of Table 3.

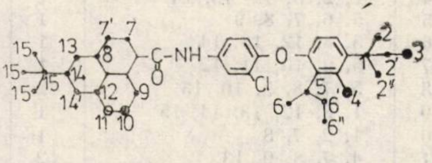

Fig. 2. — Hypermolecule and vertex numbering. Beneficial vertices ($\varepsilon_j = -1$) are marked by white circle (o), detrimental vertices ($\varepsilon_j = +1$), by black circles (—), irrelevant vertices ($\varepsilon_j = 0$) by dots.

The optimised receptor map was obtained by trial and error and verified as optimal by the Y_j criterion[4] and consists of the following vertex attributions :

$$S^* \begin{cases} j(\varepsilon = -1) : 11 \\ j\ (\varepsilon = +1) : 3,\ 4,\ 10 \\ j\ (\varepsilon = 0) : 1,\ 2,\ 5,\ 6-9,\ 12 \text{ (including all primed vertices)} \end{cases} \tag{3}$$

The MTD values corresponding to S* are also listed in Table 3. As the log A_{exp} vs. MTD correlation coefficient is low ($r = -0.716$) 2 indicator variables σ_1 and σ_2 were introduced such as to correct, as much as possible, the deviations from the log A_{exp} vs. MTD antiparallelism. These variables are defined as :

$\sigma_1 = 1$ if vertex $j = 1$ is occupied by a Cl-atom ; otherwise $\sigma_1 = 0$

$\sigma_2 = 1$ if vertex $j = 1$ is occupied by Cl and $j = 15-15'''$ by SO_2NH_2 ; otherwise $\sigma_2 = 0$

The corresponding correlational equation is :

$$\log A_{MTD} = 2.480 - 0.259\,MTD + 0.278\,\sigma_1 - 0.310\,\sigma_2 \tag{4}$$

$$r = 0.811;\ s = 0.128;\ F = 7.19;\ EV = 0.593;\ N = 20$$

The computations were performed upon the M-18 computer of the Medicinal Institute of Timişoara.

If molecules $i = 8$ and 20, for which the differences between experimental and calculated activities are larger than 0.2 log units are eliminated, the correlation is significantly improved :

$$\log A_{MTD} = 2.485 - 0.264\,MTD + 0.279\,\sigma_1 - 0.310\,\sigma_2 \tag{5}$$

$$r = 0.870;\ s = 0.102;\ F = 10.13;\ EV = 0.705;\ N = 18$$

The variations of the regressional coefficients from eq (4) to eq (5) are remarkably small. Partial correlation and intercorrelation coefficients for both equations are presented in Table 4.

Table 3

Vertex occupancy and MTD results

i	$j(x_{ij} = 1)$	MTD	σ_1	σ_2	log A_{exp}	log A_{MTD}	
						(e 4)	(e 5)
1	1, 7, 8	1	1	0	2.55	2.50	2.50
2	1, 8, 12, 13, 14	1	1	0	2.45	2.50	2.50
3	1, 2, 8, 12, 13, 14, 15	1	0	0	2.33	2.22	2.22
4	1, 2, 8, 12, 13, 14	1	0	0	2.30	2.22	2.22
5	5, 6, 7, 8, 9	1	0	0	2.28	2.22	2.22
6	5, 8, 12, 13, 14	1	0	0	2.28	2.22	2.22
7	5, 9, 10, 11, 12	1	0	0	2.24	2.22	2.22
8	5, 7, 8, 9, 10, 13	2	0	0	2.24	1.96	—
9	1, 8, 12, 13, 14, 15	1	1	1	2.19	2.19	2.19
10	1, 2, 7, 8	1	0	0	2.17	2.22	2.22
11	4, 7, 8, 9, 13	2	0	0	2.15	1.96	1.96
12	5, 7, 8, 9	1	0	0	2.09	2.22	2.22
13	1, 2, 7, 8, 9	1	0	0	2.08	2.22	2.22
14	1, 2, 3, 7, 8, 9	2	0	0	2.06	1.96	1.96
15	4, 9, 10, 11, 12	2	0	0	2.06	1.96	1.96
16	5, 6, 7, 8, 9, 10, 13	2	0	0	1.91	1.96	1.96
17	1, 2, 3, 7, 8, 9, 13	2	0	0	1.86	1.96	1.96
18	1, 7, 8, 9, 10, 13	2	0	0	1.87	1.96	1.96
19	4, 8, 12, 13, 14	2	0	0	1.79	1.96	1.96
20	1, 2, 3, 8, 12, 13	2	0	0	1.72	1.96	—

The i-molecules are depicted in Table 1. The $j(x_{ij} = 1)$ indicates the j-vertices (Fig. 2), occupied by the i-molecule ; if there are also primed vertices they are all occupied or non-occupied as the corresponding j-vertex (e.g : if $j = 15$ is occupied, all vertices $j : 15, 15', 15'', 15''$. are also occupied). MTD values are calculated according to the receptor map S* : $\sigma_1 = 1$ if a Cl atom occupies $j : 1$; $\sigma_2 = 1$ if there are both Cl in $j : 1$ and H_2N-SO_2 in $j : 15-15'''$

Table 4

Partial correlation and intercorrelation coefficients
(MTD method)

	A	MTD	σ_1	σ_2
MTD	−0.716 (−0.759)	1		
$\sigma1$	0.523 (0.555)	−0.380 (−0.357)	1	
σ_2	0.063 (0.193)	−0.207 (−0.193)	0.546) (0.542)	1

The indicated figures correspond to the whole series of 20 molecules and eq (4) ; figures in parenthesis correspond to the reduced series ($i = 8$ and 20, eliminated) and eq (5).

Hydrophobicities were also calculated, based upon additivity rules, using log P_{oct} values and increments listed by Leo, Hansch and Elkins [5] (log P_{oct} values for benzamide, diphenyloxide, phenoxyacetic acid and benzenesulphonamide). For the most active molecule $i = 1$ of Table 1, a hydrophobicity, $\pi \cong 5.4$ results ; the most hydrophobic is molecule i = 14 which has $\pi_{14} \cong 6.9$, the less one, i = 9 which has $\pi_9 \cong 3.0$. There is no correlation between the π values and the log $A_{\exp}$ values or the differences between experimental and calculated values, but all molecules in Table 1 have a rather strong hydrophobic character.

DISCUSSIONS AND CONCLUSIONS

The multiple regressional coefficients, r, are rather poor for both methods, due probably to the fact that the log $A_{\exp}$ values, related to the prolongation of barbituric sleep are parallel to the affinity of the molecules to some pertinent receptor, but the relation between them may be far from linear.

The predictions of the two methods, concerning the contribution of substituents in various positions, compare rather favourable. For position R_1, the Free-Wilson method predicts the order $Cl > t-C_4H_9 > i-C_5H_{11} > H$. According to the MTD method these substituents occupy irrelevant vertices, except for $i-C_5H_{11}$ which occupies also the detrimental vertex j : 3 (while Cl as R_1 corresponds to $\sigma_1 = 1$ with positive regressional coefficients), the predicted order would be $Cl > tC_4H_9 = H > i-C_5H_{11}$. The inversion of H and iC_5H_{11} suggests a hydrophobic interaction at R_1 in the molecule-receptor complex.

For position R_2 the methods disagree : according to the Free-Wilson method $CH_3 > H$ while according to the MTD method CH_3 occupies the detrimental vertex j : 4.

A disagreement exists also for the predictions for position R_3. According to the Free-Wilson method $i-C_4H_9 > CH_3 > H$, while only irrelevant vertices are occupied. The substituents should have the same contributions according to the MTD method. A hydrophobic interaction at R_3 could explain the difference.

For R_4, according to the Free-Wilson method $R > N > M \cong K > O > L > P \cong J$, while according to the MTD method, all substituents should be equipotent occupying only irrelevant vertices, or a beneficial and a detrimental one. Exceptions are P which occupies the detrimental vertex j : 10 and J found in molecules i = 3 and 9, in the last, corresponding to $\sigma_2 = 1$ for this detrimental indicator variable (see eqs. 4 and 5). Thus, the order indicated by the MTD method R, N, M, K,O, L > P, J is in partial agreement with the one of the Free-Wilson method.

Some new molecules predicted more active than those of Table 1, are depicted in Fig. 3. Molecules (a) and (b) are predicted by the Free-Wilson method to have log A values of 3.16 and 2.98, while the MTD method predicts log A_{MTD} (ed 4) values of 2.50 and 2.22. These molecules have been synthesized and their log $A_{\exp}$ values found to be 2.51 and 2.40 near to the top of the experimental activity values of the Table 1 molecules. Molecules c, d, e are predicted by the MTD method to have log A_{MTD} (eq 4) values of 2.76 (MTD = 1 vertex j : 11 occupied j : 10 nonoccupied, $\sigma_1 = 1$) ; no Free-Wilson predictions can be done as they contain structural fragments absent in the molecules of Table 1.

The receptor or sites implied in the neuroleptic activity should have a rather hydrophobic character. Eventually the hydrophobic diphenoxidic moiety dissolves into some nervous membrane and prevents transmission of excitation pulses. The more polar moiety (at position R_4) may allow an interaction with the surrounding water, possibly important for a sufficient rapid transport of the drug. There seem to be few steric constraints for the drug-receptor interaction, most vertices in the receptor map S'' being irrelevant ($\varepsilon = 0$). The site seems restricted towards the R_1 and R_2 substituents ($\varepsilon_3 = \varepsilon_1 = +1$). Hydrophobic interactions seem to take place at positions R_1 and R_3, as indicated by comparison of the Free-Wilson and MTD predictions, while the beneficial effect of Cl in j : 1 indicates also some polar interactions with groups in the R_1 position (the beneficial σ_1 indicator variable). The detrimental effect of the presence of both Cl in j : 1 and SO_2NH_2 in j : 15 – 15''' ($\sigma_2 = 1$) suggests a folding of the molecule in the complex with the receptor such as to bring near the two ends of the molecule (repulsion between the two electronegative groups).

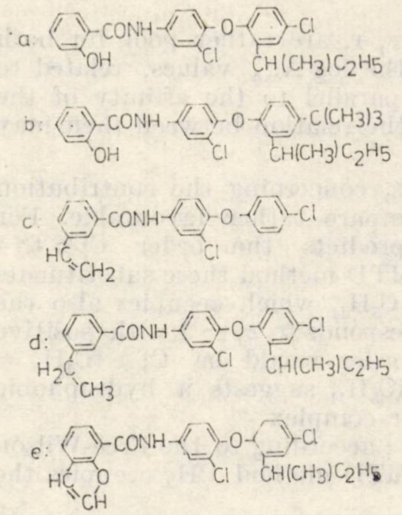

Fig. 3. — Molecules with predicted high neuroleptic activity ; *a* and *b* — by the Free-Wilson method, *c*, *d* and *e* — by the MTD-method.

As a whole, most predictions of the Free-Wilson and MTD methods either agree or the disagreements can be explained by some local, hydrophobic effects. The most active molecules predicted by the Free-Wilson method (*a* and *b* in Fig. 3) are predicted to have a high activity also by the MTD method, in agreement with the experimental activity measurements. A comparison of the results given by several different QSAR methods may thus be recommended for drug design.

REFERENCES

[1] C. Hansch and J. M. Blaney, The New Look in QSAR, in "Drug Design, Fact or Fantasy" Academic Press, London 1984, 185.

[2] A. Camarata, in "Molecular Orbital Studies Chem. Pharmacol. Symp.", L. B. Kier and B. Lemont editors, Springer, New York 1970, 156.

[3] W. E. Purcell, G. E. Bass and J. M. Clayton, "Strategy of Drug Design. A Guide to Biological Activity", John Wiley, New York, 1973, chap. III.

[4] Z. Simon, A. Chiriac, S. Holban, D. Ciubotariu and G. I. Mihalaş, "Minimum Steric Difference. The MTD Method for QSAR Studies", Res. Stud. Press, Letchworth Herts., 1984.

[5] A. Leo, C. Hansch and D. Elkins, *Chem. Revs.*, **71**, 525 (1971).

Revue Roumaine de Chimie, **32**, *6*, 591–597 (1987)

STUDIES ON PYRIDYLPYRAZOLONE SYSTEM. V

CYCLOCONDENSATION OF 1-PHENYL-3-(3′-PYRIDYL)-2-PYRAZOLIN-5-ONE WITH ETHYL ACETOACETATE AND RELATED COMPOUNDS

MOHAMED F. ABDEL-MEGEED
Chemistry Department, Faculty of Science, Tanta University, Tanta, Egypt

Received September 3, 1986

The reaction of 1-phenyl-3-(3′-pyridyl)-2-pyrazolin-5-one (IV) with ethyl acetoacetate, diethylacetone dicarboxylate and diethylterphthaloyl bisacetate yielded the corresponding pyrazolo-α-pyrone which was readily converted to pyrazolo-α-pyridone. Compound (IV) was formulated by Vilsmeier reagent to the corresponding 4-formyl derivative which reacts readily with ethyl acetoacetate to give pyrazolo-pyrane and pyrazolo-α-pyrone depending on the reaction condition. The products were identified by their IR-, ^{1}H-NMR-, ^{13}C-NMR- and mass spectral data.

INTRODUCTION

Although the cyclocondensation of ethyl acetoacetate with 1,3 disubstituted-5-aminopyrazoles has been studied by several investigators[1-8] and the analogy reaction with 1,3-disubstituted-2-pyrazolin-6-one has not been studied much [9,10] there still exists a disparity in the assignements of structure of the products (scheme 1).

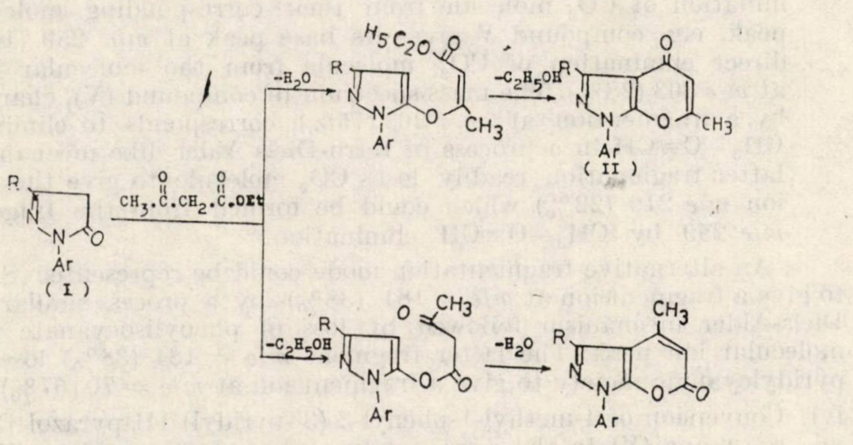

Scheme (1)

RESULTS AND DISCUSSION

In order to establish fully the assignments of the structure of products of this condensation, the reactions between 1-phenyl-3-(3′-pyridyl)-2-pyrazolin-5-one (IV) with ethyl acetoacetate, diethylacetone dicarboxylate and diethylterphthaloyl biacetate were investigated at elevated temperatures (150–160°C). The isolated products were fully identified as V, VI and VII, respectively. Structural elucidation of compounds V, VI and VII was carried out by the following means :

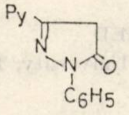

(IV)

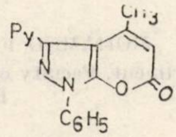

(V)

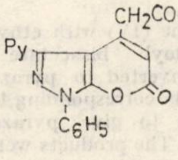

(VI)

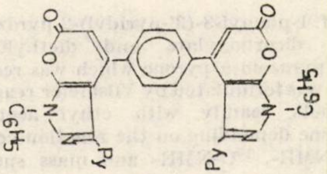

(VII)

- i) Compound V failed to give the styryl condensation product with the aromatic aldehyde as the analogous reactions.
- ii) The IR-spectra of compounds V, VI and VII are characterised by a very strong band at 1775–1780 cm^{-1} region which could be interpreted as the stretching vibration mode of the α-pyrone carbonyl group.
- iii) The mass spectra of these compounds show their base peak by elimination of CO_2 molecule from their corresponding molecular ion peak, e.g. compound V gives its base peak at *m/e* 259 (100%) by direct elimination of CO_2 molecule from the molecular ion peak at *m/e* 303 (28%). The mass spectrum of compound (V), characterised by a fragmention at *m/e* 263 (75%), corresponds to elimination of $CH_3-C\equiv CH$ in a process of retro-Diels-Alder like mechanism. The latter fragmention readily loses CO_2 molecule to give the fragment ion *m/e* 219 (22%) which could be formed from the fragment ion *m/e* 259 by $CH_3-C\equiv CH$ elimination.

An alternative fragmentation mode could be represented (Scheme 3) to give a fragment ion at *m/e* = 184 (38%) by a process similar to retro-Diels-Alder mechanism followed by loss of phenylisocyanate from the molecular ion peak. The latter fragment *m/e* = 184 (38%) loses readily pyridylcyanide moiety to give a fragment ion at *m/e* = 70 (67%).

- iv) Conversion of 4-methyl-1-phenyl-3-(3′-pyridyl)-1H-pyrazol [3,4-b]pyran-6-one (V) to the corresponding pyrazolo-α- pyridone (XII) was

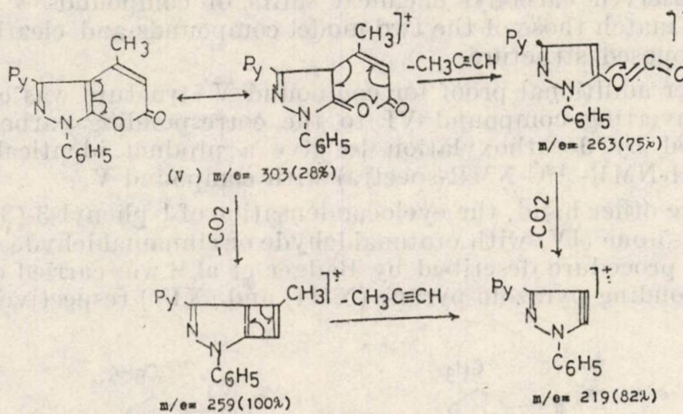
(V) m/e= 303(28%)
-CH3C≡CH
m/e= 263(75%)
-CO2
-CO2
m/e= 259(100%)
-CH3C≡CH
m/e= 219(82%)

Scheme (2)

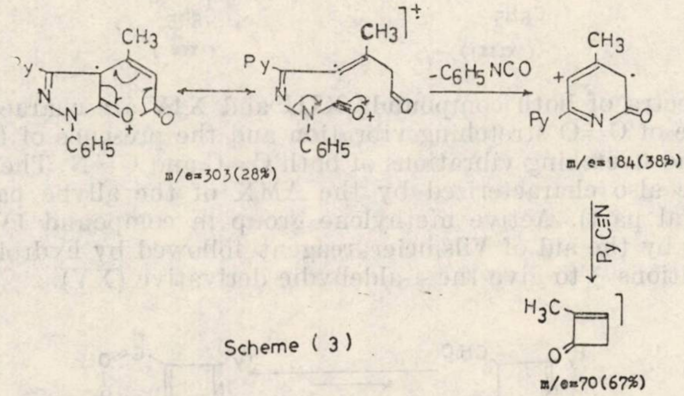
m/e=303(28%)
-C6H5NCO
m/e=184(38%)
-PyC≡N
m/e=70(67%)

Scheme (3)

carried out using either alcoholic ammonia or ammonium carbonate. The structures of both compounds V and XII were obtained from ^{13}C-NMR-spectral data by comparing the significant difference between the carbonyl chemical shifts of the isomeric models.

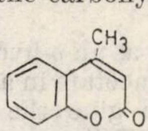

(VIII)

δCO= 167.8 ppm

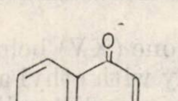

(IX)

δCO= 182.3 ppm

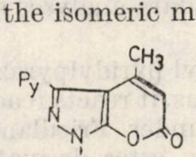

(V)

δCO= 168.2 ppm

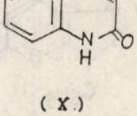

(X)

CO= 162.9 ppm

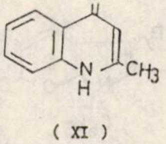

(XI)

CO= 177.9 ppm

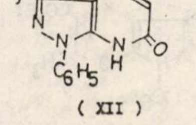

(XII)

CO= 163.5 ppm

The observed carbonyl chemical shifts of compounds V and XII closely match those of the two model compounds and clearly support the proposed structure.

v) Another additional proof for compound V structure was carried out by converting compound VI to the corresponding carboxylic acid followed by decarboxylation to give a product identical (m.mp., IR-, ^{1}H-NMR- ^{13}C-NMR-spectra) with compound V.

On the other hand, the cyclocondensation of 1-phenyl-3-(3′-pyridyl)-2-pyrazolin-5-one (IV) with crotonaldehyde or cinnamaldehyde employing a modified procedure described by Badger et al.[11] was carried out to give the corresponding pyrazolo-pyrane (XIII) and (XIV) respectively.

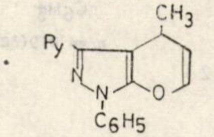

(XIII))

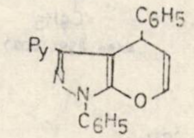

(XIV)

The IR-spectra of both compounds XIII and XIV are characterized by the absence of C=O stretching vibration and the presence of two strong bands of the stretching vibrations of both C=C and C=N. The ^{1}H-NMR-spectra are also characterized by the AMX of the allylic pattern (see experimental part). Active methylene group in compound IV was also fromylated by the aid of Vilsmeier reagent followed by hydrolysis under basic conditions [12] to give the 4-aldehydic derivative (XV).

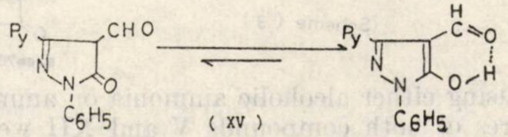

(XV)

The spectral data analyses show the predominance of the hydroxy tautomeric form.

4-Formyl pyridylpyrazolone (XV) behaves as an *o*-hydroxy aromatic aldehyde. Thus, it reacts readily with ethyl acetoacetate in a basic catalysis (piperidine under Friedlander condition [13]) to give the corresponding pyrazolopyran ester derivative (XVI). Ester (XVI) was hydrolysed by alkali to give the corresponding carboxylic acid (XVII). Consequently, acid (XVII) was decarboxylated to give 6-methyl-1-phenyl-3-(3′-pyridyl)-1H-pyrazolo[3,4-b]pyran (XVIII).

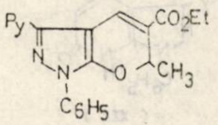

(XVI)

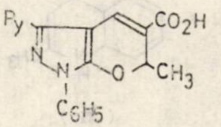

(XVII)

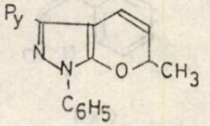

(XVIII)

Another cyclocondensation pathway of compound XV with ethyl acetoacetate was carried out by direct fussion at elevated temperatures following the method described by Fehnel [14] to yield the acetylpyrazolo-α-pyrone derivative (XIX).

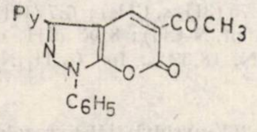

(XIX)

The spectral data of compound XIX were in agreement with the proposed structure (see experimental part).

EXPERIMENTAL

Unless otherwise stated, IR-spectra were determined using Bechmann Spectrometer Model 4240. Potassium bromide technique was used, and ^{1}H-NMR and ^{13}C-NMR-spectra were recorded using VARIAN Model CFT-20 and 20.0 MHz for ^{13}C-NMR spectra. Mass spectra were measured using PERKIN ELMER Model PMU-6E using a direct inlet source temperature 90°C and beam energy of 70 eV. When compounds are stated to be identical their identity has been established by comparing m.p. and by mixed m.p. and where appropriated by comparison of IR-, NMR- and t.l.c. behaviours.

4-Methyl-1-phenyl-3-(3'-pyridyl)-1H-pyrazolo-(3,4-b)-pyran-6-one (V)

A mixture of 1-phenyl-3-(3′-pyridyl)-2-pyrazolin-5-one (IV) (2.49; 0.01 mole) and equimolecular amount of ethylacetoacetate and 50 mL of glacial acetic acid was heated on a steam bath for 3—4 hours and later heated at reflux temperature for 15 minutes. The reaction mixture was cooled, filtered off, the harvested crystals were washed with ethanol and finally dried in vacuo at 100°. The yield was 1.9 g (63%) m.p. 212°C; ν_{max}: 1775 cm^{-1} (C=O) δ(CDCl$_3$) 2.87(3H, s, CH$_3$); 7.35(1H, six., H^5-py); 7.46(1H, six., H^4-py); 7.8 (1H, s, =CH); 7.88(5H, m, N—C$_6$H$_5$); 8.52(1H, q, H^6-py); 9.22 (1H, q, H^2-py) ($J_{5,4}$ = 8.03 Hz; $J_{4,6}$ = 1.76 Hz; $J_{2,6}$ = 1.13 Hz; $J_{2,5}$ = 0.88 Hz; $J_{5,6}$ = 4.87 Hz) found: C, 71.05%; H, 4.58%; N, 13.49% for $C_{18}H_{13}N_3O_2$; Cal: C, 71, 28%; H, 4.29%; N, 13.86%; *m/e* 303 ($M^{\overset{+}{\cdot}}$).

4-Methylcarboethoxy-1-phenyl-3-(3'-pyridyl)-1H-pyrazolo-(3,4-b)pyran 6-one (VI)

Cyclocondensation of pyridylpyrazolone (V) with diethyl acetonedicarboxylate was carried out as previously described to give compound (VI) m.p. 223°. The yield was 1.8 g (58%) ν_{max} 1778 cm^{-1} and 1755 cm^{-1} (C=O, α-pyrone) and (C=O, ester) respectively; δ(CDCl$_3$): 1.5 (3H, s, CH$_3$); 4.3 (2H, q, CH$_2$); 5.1(2H, s, CH$_2$); 7.4(1H, six., H^5-py.); 7.52(1H, six, H^4-py.); 8.82(1H, s, =CH); 7.90(5H, m, N—C$_6$H$_5$); 8.60(1H, q, H^6-py.); 9.22(1H, q, H^2-py.); found: C, 67.47%; H, 4.61%; N, 11.37%, for $C_{21}H_{17}N_3O_4$, calc.: C, 67.20%; H, 4.53%, N, 11.20%; *m/e* 375 ($M^{\overset{+}{\cdot}}$).

p-Bis(1-phenyl-3-(3'-pyridyl)-1H-pyrazolo(3,4-b)pyran-6-one)benzene (VII)

Cyclocondensation of pyridylpyrazolone (V) with diethyl terphthaloyl-bis-acetate was carried out as previously described to yield compound (VII) m.p. 328°. The yield was 2.3 g (65%); ν_{max}: 1775 cm^{-1} (C=O); δ(DMSO-d$_6$): 7.19(4H, d, p-C$_6$H$_4$, J = 8 Hz); 7.35(1H, six, H^5-py); 7.55 (1H, six., H^4-py); 7.88(1H, S, =CH); 7.90(5H, m, N—C$_6$H$_5$); 8.62 (1H, q,- H^6-py.) 9.22(1H, q, H^2-py.) found: C, 73.52%; H, 3.50%; N, 13.12% for $C_4OH_{24}N_6O_4$, calc.: C, 73.61% H, 3.71%; N, 12.88%.

4-Methyl-1-phenyl-3-(3'-pyridyl)-1H-pyrazolo(3,4-b)-pyridin-6-one (XII)

Method A

4-Methyl-1-phenyl-3-(3′-pyridyl)-1H-pyrazolo[3,4-b] Pyran 6-one (V) 3.0 g was dissolved in 50 mL ethanol. A stream of ammonia was dried and bubbled for three hours. The yellow solid was filtered off, washed with ethanol for several times and recrystallised as pale yellow needles m.p. 278° 2.39 (78%).

Method B

Pyrazolo-α-pyrone (V) 3.0 g was fused with 10 g ammonium carbonate in an oil bath. The reaction mixture was heated for 1.5 hours until no longer ammonia gas was evolved. The caky material was washed with water and ethanol for several times. The pale yellow product was crystallised from ethanol 2.1 g (67 %) m.p. 278° ; ν_{max} : 1680^{-1} (C=O) ; 3310 cm^{-1} (NH and/or OH) δ(DMSO-d_6) : 2.75 (3H, s, CH_3) ; 6.7 (1H, s, =CH) ; 7.38 (1H, six., H^5-py.) ; 7.45 (1H, six, H-py.) ; 7.88 (5H, m, N-CH) ; 8.53 (1H, q, H-py.) ; 9.15 (1H, q, H-py.), Found : C, 71.60 % ; H, 4.50 % ; N, 18.32 %, for $C_{18}H_{14}N_4O$, calc. : C, 71.51 % ; H, 4.67 % ; N, 18.53 % ; *m/e* = 302 (M^+).

4-(Methyl or phenyl) 1-phenyl-3(3′-pyridyl)-1H-pyrazolo(3,4-b)pyrane (XIII) or (XIV)

Employing a modification of a procedure described by Badger and coworkers [11] a solution of 1-phenyl-3-(3′-pyridyl)-2-pyrazolin-5-one (IV) (4.89, 0.02 mole) in glacial acetic acid (100 mL), was cooled, while concentrated sulfuric acid (2 mL) was introduced with stirring. To this, a solution of anhydrous crotonaldehyde or cinnamaldehyde (0.021 mole) in glacial acetic acid (30 mL) was added. The resulting reaction mixture was stirred for one hour at room temperature and heated at reflux temperature for another hour. The coloured reaction solution was concentrated in vacuo, the residue dissolved in 300 mL of water, rendered basic with sodium hydroxide 15 % and extracted with chloroform. The combined extracts were dried over anhydrous magnesium sulfate and finally the solvent removed in vacuo. The solid product was crystallised from benzene compound XIII : m.p. 132°, 2.5 g (53 %) ; ν_{max} : 1600 cm^{-1} (C=O) ; δ($CDCl_3$) : 2.8 (3H, d, CH_3) ; 3.8 (1H, m, C_4−CH) ; 4.8 (1H, q, C_5−CH) ; 6.70 (1H, d, C_6−CH) ; 7.35(1H, six., H^5-py.) ; 7.52(1H, six., H^4-py.) ; 7.92 (5H, m, N−C_6H_5) ; 8.55 (1H, q, H^6-py), 9.20 (1H, q, H^2-py.) ; found ; C, 74.64 % ; H, 5.18 % ; N, 14.50 % for $C_{18}H_{15}N_3O$; calc. : C, 74.72 % ; H, 5.23 % ; N, 14.52 % ; *m/e* 289 ($M^{\overset{+}{\cdot}}$).

Compound XIV : m.p. 158° 3.1 g (48 %) ; ν_{max} : 1600 cm^{-1} (C=C) ; δ($CDCl_3$) : 3.9(1H, m, C_4−CH), 5.1(1H, q, C_5−CH) ; 6.95 (1H, d, C_6−CH) ; 7.1 (5H, m−C_6H_5) ; 7.30 (1H, six, H^5, py.), 7.65 (1H, six., H^4-py.) ; 7.90(5H, m, N−C_6H_5) ; 8.43(1H, q, H^6-py.) ; 9.15 (1H, q, H^6-py.) ; found ; C, 78.81 % ; H, 4.80 % ; N, 11.90 % for $C_{23}H_{17}N_3O$; calc. : C, 78.84 % ; H, 4.88 % ; N, 11.96 % : *m/e* 351 ($M^{\overset{+}{\cdot}}$).

4-Formyl-1-phenyl-3-(3-pyridyl)-2-pyrazolin-5-one (XV)

A solution of pyridyl-2-pyrazolin-5-one (IV) (11.8 g ; 0.5 mole) in dimethylformamide (146 g ; 2.0 mole) was treated with phosphorous oxychloride (32.1 g, 2.1 mole) in a dropwise fashion over a period of 2 hours with stirring. The reaction mixture was stirred at 80−90° for additional 2.5 hours and then allowed to remain at room temperature overnight. The mixture was poured in ice and neutralised with sodium hydroxide (50 %) solution. The coloured oily layer which separated was extracted with several portions of chloroform. The combined extract was washed with water, dried over anhydrous magnesium sulfate and filtered. The creamy coloured solid was collected after evaporation of solvent *in vacuo* and crystallised from pet. ether 50−70° to give 5.6 g (43 %), m.p. 88−90° ; ν_{max} : 1710 and 1700 cm^{-1} (2C=O) ; δ($CDCl_3$) : 6.2 (1H, d, C_4=CH) ; 4.8 (1H, bs, OH) ; 7.43 (1H, six., H^5-py.) ; 7.55 (1H, six., H^4-py.) ; 7.93 (5H, m, N−C_6H_5), 8.62 (1H q, H^6-py.) ; 9, 20 (1H, q, H^2-py.) ; 9.95 (1H, s, CHO) found : C, 67.80 % ; H, 4.15 % ; N, 15.62 % for $C_{15}H_{11}N_3O_2$; calc. : C, 67.92 % ; H, 4.18 % ; N, 15.84 % ; *m/e* = 265 ($M^{\overset{+}{\cdot}}$).

5-Carbethoxy-6-methyl-1-phenyl-3-(3'-pyridyl)-1H-pyrazolo-(3,4-b)pyrane (XVI)

A stirred mixture of 4-formyl-2-pyrazolin-5-one (XV) (6.6 g ; 0.025 mole), ethyl acetoacetate (6.8 g ; 0.05 mole) and piperidine 150 mL was heated at reflux temperature for 3 hours, filtered while hot and allowed to cool. Upon concentration a pale yellow substance was separated ; crystallised from benzene afforded 4.2 g (53 %) of the ester (XVI) as colourless needles m.p. 123−4°) ; ν_{max} : 1775 cm^{-1} (C=O) ; δ(DMSO-d_6) : 1.5 (3H, t, CH_3) ; 1.9 (3H, d−C_6−CH_3) ; 4.2 (2H, q, CH_2) ; 4.8 (1H, q, OCH) ; 7.95 (5H, m, N−C_6H_5) ; 7.45 (1H, six., H^5-py.) ; 7.63 (1H, six., H^4-py.) ; 8.55 (1H, S, =CH), 8.65 (1H, 1q, H^6-py.) ; 9.15 (1H, q, H^2-py.) ; found : C, 69.62 % ; H, 5.15 % ; N, 11.72 % ; for $C_{21}H_{19}N_3O_3$; calc. : C, 69.79 % ; H, 5.30 %, N, 11.63 % ; *m/e* = 361 ($M^{\overset{+}{\cdot}}$).

6-Methyl-1-phenyl-3-(3'-pyridyl)-1H-pyrazolo(3,4-b)-pyran-5-carboxylic acid (XVII)

A mixture of pyrazolo-pyrane ester (XVI) (3.6 g; 0.01 mole), potassium hydroxide solution (100 mL) 6N and ethanol (300 mL) was stirred at reflux temperature of 3 hours, cooled and then acidified with hydrochloric acid 6N. The crude acid was filtered and washed with water and crystallised from ethanol-water (2 : 1 by volume). After drying in vacuo at 90°, the yield was 3.1 g (92 %) m.p. 302° ; ν_{max} : 1690 cm^{-1} C=O ; 3500 cm^{-1} (OH) ; $\delta(CF_3COOH)$: 2.05 (3H, d, CH_3) ; 4.35 (1H, q, OCH) ; 7.90 (5H, m, $N-C_6H_5$) ; 7.45 (1H, six., H^5-py.) ; 7.62 (1H, six., H^4-py.) ; 8.55 (1H, S, =CH) ; 8.65 (1H, q, H_6-py.) ; 9.15 (1H, q, H^2-py.) ; 11.5 (1H, bs, OH) ; found : C, 68.22 % ; H, 4.38 % ; N, 12.48 % for $C_{19}H_{15}N_3O_3$; calc. : C, 68.46 % ; H, 4.54 % ; N, 12.61 % ; *m/e* = 333 ($M^{\overset{+}{\cdot}}$).

6-Methyl-1-phenyl-3-(3'-pyridyl)-1H-pyrazolo(3,4-b)pyran (XVIII)

The finely pulverized potassium salt of acid (XVIII) (5.5 g ; 0.051 mole) was thoroughly mixed with calcium oxide 10.5 g and the mixture was heated in a Pyrex flask, fitted for distillation over full flame of Meker burner. The decarboxylation product was collected as a yellow coloured distilate in a yield 3.6 g ; (60 %). This sample was dissolved in ether, dried over anhydrous sulfate, filtered and evaporated in vacuo to afford a pale yellow crude product recrystallised from benzene, m.p. 112.3° ; ν_{max} ; 1620 (C=C) ; $\delta(CDCl_3)$: 1.90 (3H, d, CH_3) ; 4.35 (1H, m, O—CH) ; 5.62 and 6.68 (2,H q, CH=CH) ; 7.45 (1H, six., H^5-py.) ; 7.55 (1H, six., H^4-py.) ; 7.90 (5H, m, $N-C_6H_5$), 8.65 (1H, 1, H^6-py.) ; 9.10 (1H, q, H^2-py.) ; found : C, 74.52 % ; H, 5.12 % ; N, 14.30 % for $C_{18}H_{15}N_3O$; calc. : C, 74.72 % ; H, 5.23 % ; N, 14.52 % ; *m/e* 289 ($M^{\overset{+}{\cdot}}$).

5-Acetyl-1-phenyl-3-(3'-pyridyl)-1H-pyrazolo(3,4-b)pyran-5-one (XIX)

A mixture of 4-formylpyridylpyrazolone (XV), (2.7 g ; 0.01 mole) and 50 mL ethylacetoacetate was heated for one hour in an oil bath maintained at 160—170°.[14] The white solid obtained upon cooling was collected and washed with ethanol, crystallised from ethanol and dried at 90° in *vacuo* to give 1.5 g (65 %) ; m.p. 169.8° ; ν_{max} : 1775 cm^{-1}, 1715 (2 × C=O) ; $\delta(DMSO\text{-}d_6)$: 2.49 (3H, s, $COCH_3$) ; 7.44 (1H, six., H^5-py.) ; 7.58 (1H, six., H^4-py.) ; 7.95 (5H, m, $N-C_6H_5$) ; 8.45 (1H, s, =CH) ; 8.65 (1H, q, H^6-py.) ; 9.22 (1H, q, H^2-py.) ; found : C, 68.62 % ; H. 3.58 % ; N, 12.60 % for $C_{19}H_{13}N_3O_3$; calc. : C, 68.88 % ; H, 3.95 % ; N, 12.6 %8 ; *m/e* 331 ($M^{\overset{+}{\cdot}}$).

REFERENCES

[1] C. Bülow, *Ber. dtsch. chem. Ges.*, **43**, 3401 (1910).

[2] Y. Makisumi, *Chem. Pharm. Bull.* (Tokyo), **10**, 612 (1962).

[3] H. Dorn and A. Zubek, *Angew. Chem. Intern. Ed. Engl.*, **6**, 858 (1967).

[4] H. Dorn and A. Zubek, *Chem. Ber.*, **101**, 3265 (1968).

[5] S. V. Tabak, I. I. Grandberg, and A. N. Kost., *J. Gen. Chem.*, U.S.S.R., **34**, 2778 (1964).

[6] S. Checchi, M. Ridi and P. Papini, *Gazz. chim. Ital.*, **85**, 1160 (1955).

[7] M. Ridi, P. Papini and S. Checchi, *Gazz. chim. Ital.*, **91**, 973 (1961).

[8] S. V. Tabak, I. I. Grandberg and A. N. Kost, *Chem. Heterocyclic compounds*, **1**, 79 (1965).

[9] R. Stolle, *Ber. dtsch. chem. Ges.*, **38**, 3027 (1905).

[10] M. F. Abdel-Megeed, M. El-Borai and E. A. Aly, part. II of this series submitted for publication.

[11] G. M. Baiger, H. P. Crockers, B. C. Ennis, J. A. Gayler, W. E. Mathews, W. G. G. Raper, E. L. Samuel and T. M. Spotswood, *Austral. J. Chem.*, **16**, 814 (1963).

[12] I. Y. Kvitoko and T. M. Loginova, *Zhur. Org. Khim.*, **10**, 1088 (1974).

[13] P. Friedländer and C. T. Gohring, *Ber. dtsch. chem. Ges.*, **16**, 1833 (1883).

[14] E. A. Fehnel, *J. Heterocyclic chem.*, **4**, 505 (1967).

Revue Roumaine de Chimie, **32**, *6*, 599 – 610 (1987)

GAS ABSORPTION WITH A COMPLEX CHEMICAL REACTION IN A PERFECTLY MIXED CHEMICAL REACTOR

GH. JUNCU, O. MUNTEAN and R. MIHAIL *
Polytechnic Institute of Bucharest, Department of Chemical Engineering, Polizu 1, 78126, Bucharest, Romania

Received May 26, 1986

The effect of the reactor operating conditions upon the values of the absorption-reaction parameters for the complex gas-liquid reaction $A_1 + A_2 \rightleftarrows A_3$, $A_1 + A_3 \rightleftarrows A_4$ taking place in a perfectly mixed reactor is investigated on the basis of the film theory. A multigrid algorithm was used to solve the diffusion-reaction equations. The key operating parameters are : the ratio of the bulk to film volume, α, and the Damköhler number β. The results are presented in terms of the enhancement factor E_1, film selectivity Y_f and profiles of dimensionless concentration of intermediate A_3 across the film. It was found that both α and β can strongly affect the performances of the gas-liquid reactor.

INTRODUCTION

In chemical reaction engineering much work has been done with respect to modelling and computing the rate of gas absorption followed by complex chemical reactions. The diversity of the reaction mechanisms and stoichiometric relations is a characteristic of the gas-liquid reactions encountered in practice. The quantitative analysis of such a process requires the formulation of a mathematical model, as completely as possible, describing the interaction between the chemical reactions and the mass transfer steps. Many evaluations, some rather recent,[1] regarding the influence of the physical model chosen to represent the mass transfer in the liquid phase upon the values of the main parameters of the gas-liquid reactions, show that the presently used mass transfer theories (film, penetration, surface-renewal) are quasi-equivalent and for the sake of simplicity the film theory is almost unanimously accepted. In the latter case the mathematical model is described by the steady-state diffusion-reaction equations for the stagnant liquid film. Excepting the case of the first order reaction, which can be analytically solved, the model equations are nonlinear and numerical methods have to be developed. The numerical techniques employed so far belong to two main classes : finite differences and orthogonal collocation.

---

* Deceased in 1985.

The results of the computation are usually given synthetically by the enhancement (reaction) factor, which is a measure of the augmentation of the mass transfer due to the chemical reaction and it is directly used in design.

Recently,[1] it has been shown that if the knowledge of the enhancement, factor is sufficient for the estimation of the performance of a gas-liquid reactor for singular reactions, for a multiple reaction scheme the enhancement factor gives only a partial answer. This becomes quite obvious if one takes into account that for the enhancement factor only the concentration distribution of the gas reactant near the G—L interface is needed ; for other parameters (selectivity, yield) the concentration profiles for other chemical species across the whole liquid film are required.

The boundary condition to be used in the bulk of the liquid deserves some comment. If the reaction is fast enough and if the volume of the liquid in the bulk is much greater than that of the film or the penetration depth then the concentration of the unreacted gas component in the bulk must be negligibly small in the case of irreversible reaction or negligibly different from the equilibrium value in the case of reversible reaction.[2] For more complicated reaction mechanisms these assumptions do not apply. Most of the developments so far have neglected the fact that in continuous reactors at the film-bulk boundary an elemental volume of bulk fluid is subject to specific environmental conditions. Froment and Bischoff [3] drew attention on the importance of the proper formulation of the film-bulk boundary conditions. From some recent papers [4,5] it can be seen that the performances of the perfectly mixed gas-liquid reactor in which a complex chemical reaction occurs are strongly limited by mass transfer and reactor operating conditions.

The aim of the present paper is to extend the results presented in [4] by considering a new reaction scheme and to evidence the results in a more systematic way.

THE MATHEMATICAL MODEL

Many complex gas-liquid reactions, for example the hydrogeneration of diolefins, the sulfonation of aromatics and olefins, the chlorination and the oxidation of hydrocarbons, etc. may be viewed as combinations of parallel and/or consecutive reaction steps. In order to simulate a general reaction scheme the following parallel-consecutive reversible reactions were chosen :

$$\nu_{11}A_1(G) + \nu_{12}A_2(L) \underset{k-1}{\overset{k_1}{\rightleftarrows}} \nu_{13}A_3(L) \tag{1}$$

$$\nu_{21}A_1(G) + \nu_{23}A_3(L) \underset{k-2}{\overset{k_2}{\rightleftarrows}} \nu_{24}A_4(L) \tag{2}$$

The rate expressions for the two reactions may have in the general case the form :

$$r_1 = k_1 c_1^m c_2^n - k_{-1} c_3^0 \tag{3}$$

$$r_2 = k_2 c_1^s c_3^t - k_{-2} c_4^w \tag{4}$$

In the present paper all partial reaction orders were considered equal to unity and therefore:

$$r_1 = k_1c_1c_2 - k_{-1}c_3 \tag{5}$$

$$r_2 = k_2c_1c_3 - k_{-2}c_4 \tag{6}$$

The mathematical model is based upon the following assumptions:

i) the liquid phase is perfectly mixed;
ii) the two-film theory is valid;
iii) the mass transfer resistance in the gas phase is negligibly small;
iiii) the temperature of the liquid phase is constant;
iiiii) the chemical species A_2, A_3 and A_4 are nonvolatile;
iiiiii) the solubility of the gaseous species A_1 in the liquid phase follows Henry's law.

Under these suppositions the differential molar balance equations describing diffusion and reaction, for the reaction components, in the stagnant liquid film, are:

$$D_j \frac{d^2c_j}{dx^2} + \sum_{i=1}^{2} \nu_{ij}r_i = 0 \quad j = 1, 2, 3, 4 \tag{7}$$

where D_j represents the diffusion coefficient of the chemical species j in the reaction mixture. The system equations (7) are solved for the boundary conditions given in Table 1. The fourth condition at x = 0 results

Table 1

Boundary conditions for the film theory

x = 0		x = δ_L
$c_1 = c_{1,I}$		$-a_vD_1\frac{dc_1}{dx} = \left(-\sum_{i=1}^{2}\nu_{i1}r_i\right)[(1-\varepsilon_G) - a_v\delta_L] + \frac{F_Lc_{1,L}}{V}$
$\frac{dc_2}{dx} = 0$		$c_2 = c_{2,L}$
$\frac{dc_3}{dx} = 0$	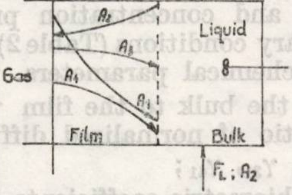 A1L, A2L A3L, A4L A2 Liquid A3 δ Gas A4 A1 Film Bulk FL ; A2	$-a_vD_3\frac{dc_3}{dx} = \left(-\sum_{i=1}^{2}\nu_{i3}r_i\right)[(1-\varepsilon_G) - a_v\delta_L] + \frac{F_Lc_{3,L}}{V}$
$\frac{dc_4}{dx} = 0$		$-a_vD_4\frac{dc_4}{dx} = \left(-\sum_{i=1}^{2}\nu_{i4}r_i\right)[(1-\varepsilon_G) - a_v\delta_L] + \frac{F_Lc_{4,L}}{V}$

from the assumptions iiiii) and iiiiii). For an R_L reactor, which is characterized by the concentrations at $x = \delta_L$, the boundary conditions at the stagnant film-bulk liquid hypothetical interface are represented by the continuity of the molar fluxes. For the liquid reactant A_2 we assume a constant concentration at $x = \delta_L$.

The enhancement factor and the selectivity are defined as:

$$E_1 = \frac{N_1|_{x=0}}{k_L c_1|_{x=0}} \tag{8}$$

$$Y_f = \left.\frac{N_3}{N_2}\right|_{x=0} \tag{9}$$

where N_j represents the molar flux of the j species.

In dimensionless variables equations (7) and the boundary conditions are listed in Table 2.

The dimensionless enhancement factor and selectivity are:

$$E_1 = -\left.\frac{dA}{dX}\right|_{x=0} \tag{10}$$

$$Y_f = \left|\left.\frac{1}{q}\frac{dC}{dB}\right|_{x=1}\right| \tag{11}$$

where the modulus has been taken in eq. (11) in order to alleviate the possible negative values of the selectivity.

The model equations were discretized by finite difference of second-order accuracy. The nonlinear system obtained was solved by a FAS-FULL ADAPTIVE multigrid technique.[6] The prolongation and restriction operators are those defined in[7]. For high order interpolation the finite difference operator was used.[8] The iteration was stopped when dynamical residuals achieve the truncation error.[6,9]

NUMERICAL RESULTS AND DISCUSSIONS

Numerical simulations of the mathematical model have been performed to investigate the effect of the mass transfer and kinetic parameters upon enhancement factor, selectivity and concentration profiles. The dimensionless equations and the boundary conditions (Table 2) are governed by several dimensionless physico-chemical parameters. These are:

i) physical parameters: ratio of the bulk to the film volume (α), Damköhler number β and ratio of normalized diffusive fluxes between chemical species γ_{21}, γ_{31}, γ_{41};

ii) reaction parameters: the stoichiometric coefficients ν_{ij}, reaction orders, dimensionless equilibrium constants K_1, K_2 and intrinsic selectivity p;

iii) physico-chemical interrelated parameters: the ratio between the reaction rate and the liquid film mass transfer rate, the Hatta number, Ha.

Table 2

Dimensionless model equations and boundary conditions

Chemical species	Film equations	Boundary conditions	
		$X = \frac{x}{\delta_L} = 0$	$X = \frac{x}{\delta_L} = 1$
A_1	$\frac{d^2A}{dX^2} = Ha\left[AB - \frac{C}{qK_1} + \frac{p}{q}\left(AC - \frac{P}{K_2}\right)\right]$	$A = 1$	$-\frac{dA}{dX} = \alpha Ha\left[AB - \frac{C}{K_1 q} + \frac{p}{q}\left(AC - \frac{P}{K_2}\right)\right] + \frac{A}{\beta}$
A_2	$\gamma_{21} q \frac{d^2B}{dX^2} = Ha\left(AB - \frac{C}{qK_1}\right)$	$\frac{dB}{dX} = 0$	$B = 1.0$
A_3	$\gamma_{31} \frac{d^2C}{dX^2} = Ha\left[-AB + \frac{C}{qK_1} + \frac{p}{q}\left(AC - \frac{P}{K_2}\right)\right]$	$\frac{dC}{dX} = 0$	$\gamma_{31} \frac{dC}{dX} = \alpha Ha\left[AB - \frac{C}{K_1 q} - \frac{p}{q}\left(AC - \frac{P}{K_2}\right)\right] - \frac{C}{\beta}$
A_4	$\gamma_{41} \frac{d^2P}{dX^2} = -Ha\,\frac{p}{q}\left(AC - \frac{P}{K_2}\right)$	$\frac{dP}{dX} = 0$	$\gamma_{41} \frac{dP}{dX} = \alpha Ha\,\frac{p}{q}\left(AC - \frac{P}{K_2}\right) - \frac{P}{\beta}$

Except for the reaction parameters the others are dependent on each other. An exhaustive search for the effects of all these parameters is a difficult task and is not made here.

Several restrictions were considered. All stoichiometric coefficients were taken equal to unity. According to van de Vusse [10] we may also consider the diffusivity ratios equal to unity without losing in generality. For the numerical calculations the ratio between the bulk concentration of A_2 to interface concentration of A_1, q, was taken in all situations equal to two. The Hatta modulus is considered the independent variable and it takes, in this work, values from 1 to 10.

A delicate problem is represented by the choice of the values for K_1, K_2 and p. What we are interested in are the effects of dimensionless parameters α and β. Therefore we select from the general reaction scheme the following situations:

$$A_1 + A_2 \rightleftarrows A_3 \tag{12a}$$

$$A_1 + A_3 \underset{\leftarrow}{\longrightarrow} A_4 \tag{12b}$$

$$A_1 + A_2 \rightleftarrows A_3 \tag{13a}$$

$$A_1 + A_3 \rightleftarrows A_4 \tag{13b}$$

$$A_1 + A_2 \underset{\leftarrow}{\longrightarrow} A_3 \tag{14a}$$

$$A_1 + A_3 \rightleftarrows A_4 \tag{14b}$$

The relative length of the arrows shows the relative magnitude of kinetic constants. The numerical values of K_1, K_2 and p for each reaction are depicted in Table 3 and are chosen as to present some interesting situations which have correspondence in practice. In the first mechanism, eq. (12), the absorption takes place by a former reversible reaction, in which the inverse reaction is comparable in rate with the direct reactions, followed by a quasi-irreversible reaction. The second scheme, eq. (13), includes reactions which have approximately the same rate. In the third mechanism, eq. (14), the former quasi-irreversible reaction is followed by a reversible one. For the sake of simplicity of language we shall name the first scheme R_1 reaction, the second scheme R_2 reaction and the third scheme the R_3 reaction.

Table 3

Values of kinetic parameters

K_1	K_2	p	Reaction
2.5	100.0	0.8	R_1
1	1.125	1.2	R_2
50.0	1.125	0.8	R_3

In all situations α was varied from 0.1 to 100 and β from 0.01 to 10. Usually the film volume is a small fraction of the total volume of liquid; this means a large value of α as commonly met in gas-liquid reactors. But small values of α may also be encountered, if the liquid is in the form of a froth, in slug flow and in some biological reactors. Huang et al.[1] employ values of α as low as 1. Using the data of Ho and Lee[4] ($k_L = 3.4 \cdot 10^{-4}$ cm/s, $a_v = 5$ cm^{-1}, $\varepsilon_G = 0.1$), with $D = 5 \cdot 10^{-5}$ cm^2/s it results that even in a CSTR a value $\alpha \sim 0.2$ may arise. For a perfectly mixed reactor the product $k_L a_v$ has usually values in the range of 10° — 10^{-4} s. The residence time of the liquid phase in the reactor depends on the rate of the chemical reaction.

In our situation, $1 \leqslant \mathrm{Ha} \leqslant 10$, a rapid chemical reaction takes place in reactor and, for such a reaction, a maximum residence time of approximately 10^2 s is a good choice. From these assumptions we conclude that β values between 0.01 and 10 cover the situations of practical interest.

For the sake of thoroughness, results in E_1 and Y_f are presented in a three-dimensional form. Only two response surfaces corresponding to extreme values of α, 0.1 and 100, are depicted. For a given β the variation of E_1 and Y_f with α being monotonuous, any other value of α between 0.1 and 100 will lead to a response surface comprised between those depicted.

The dependence of the enhancement factor E_1 on Ha, α and β is shown in Fig. 1 for the R_1 reaction, in Fig. 2 for the R_2 reaction and in Fig. 3 for the R_3 reaction. It can be seen that irrespective of the reaction type, at low values of β all response surfaces converge and the model becomes intensitive to α and β variations. Otherwise, for β values greater than 0.1 each reaction has a particular behaviour depending on α and β values. For the R_1 reaction at $\beta = 10$ the effect of α and β on E_1 is rather small and at large values of Ha the two α surfaces converge. For the R_2 reaction at $\beta \to 10$ the increase in Ha increases the difference between the $\alpha = 0.1$ surface and the $\alpha = 100$ surface. In the case of R_3 reaction, at $\beta > 1$, E_1 grows rapidly with the increase in Ha. At $\beta \approx 10$ the increase in Ha increases the difference between the two extreme α surfaces.

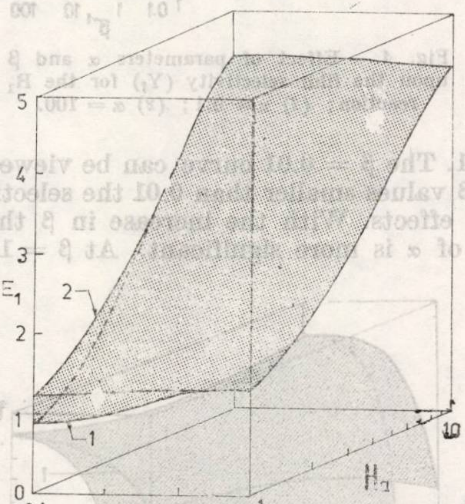

Fig. 1. — Reponse surfaces in the space (E_1, β, Ha) for the R_1 reaction ; (1) $\alpha = 0.1$; (2) $\alpha = 100$.

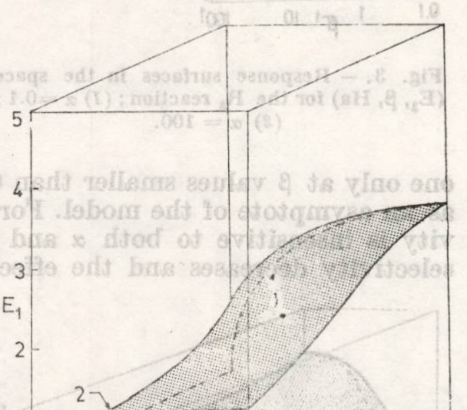

Fig. 2. — Response surfaces in the space (E_1, β, Ha) for the R_2 reaction ; (1) $\alpha = 0.1$; (2) $\alpha = 100$.

The effects of α and β parameters on the film selectivity are shown in Figs 4, 5 and 6 for R_1, R_2, and R_3 reactions respectively. As can be seen β has a more marked influence upon the selectivity than upon the enhancement factor. Small values of β improve the selectivity. The response surfaces generated by various values of α converge to a unique one only at β values smaller than 0.1. The β = 0.01 curve can be viewed as an asymptote of the model. For β values smaller than 0.01 the selectivity is insensitive to both α and β effects. With the increase in β the selectivity decreases and the effect of α is more significant. At β = 10

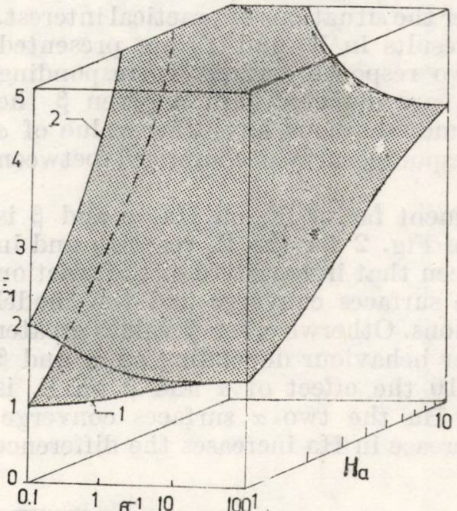

Fig. 3. — Response surfaces in the space (E_1, β, Ha) for the R_3 reaction; (*1*) α = 0.1; (*2*) α = 100.

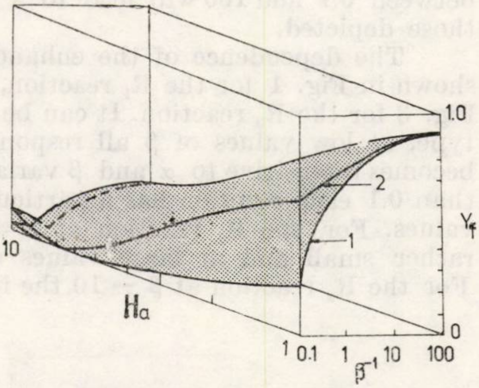

Fig. 4. — Effect of parameters α and β upon the film selectivity (Y_f) for the R_1 reaction; (*1*) α = 0.1; (*2*) α = 100.

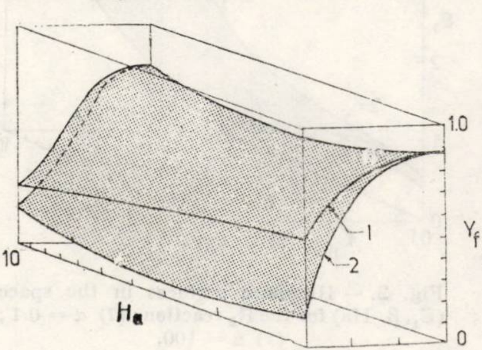

Fig. 5. — Effect of parameters α and β upon the film selectivity (Y_f) for the R_2 reaction; (*1*) α = 0.1; (*2*) α = 100.

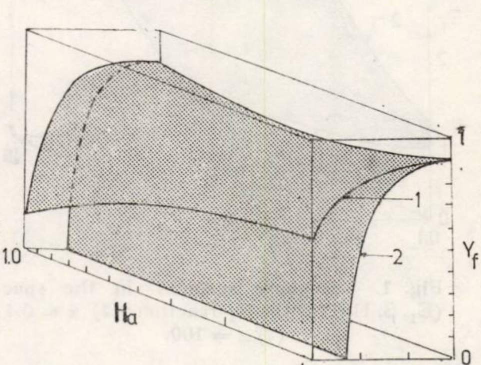

Fig. 6. — Effect of parameters α and β upon the film selectivity (Y_f) for the R_3 reaction; (*1*) α = 0.1; (*2*) β = 100.

the two α surfaces remain distinct over the whole variation domain of Ha. In the limit $\beta \to 10$ the R_3 reaction has a specific variation in regard to Ha, α and β.

The concentration profiles of the A_3 species, across the film which can be viewed as the key product, are depicted in Figs 7 to 12. Some

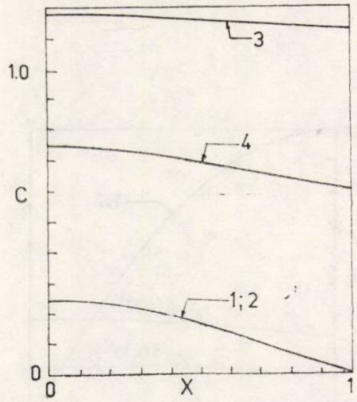

Fig. 7. — Dimensionless concentration profiles for intermediate A_3 across the liquid film; Ha = 1; R_1 reaction; (*1*) α = = 0.1; β = 0.01; (*2*) α = 100, β = 0.01; (*3*) α = 0.1, β = 10; (*4*) α = 100, β = 10.

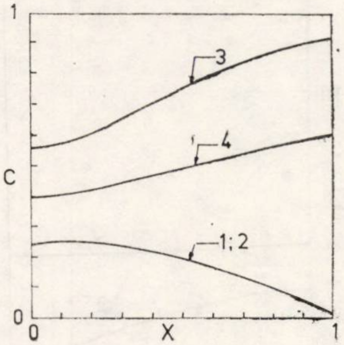

Fig. 8. — Dimensionless concentrations profiles for intermediate A_3 across the liquid film; Ha=10; R_1 reaction; (*1*) α = 0.1, β=0.01; (*2*) α = 100, β = 0.01; (*3*) α=0.1, β = 10; (*4*) α = 100, β = 10.

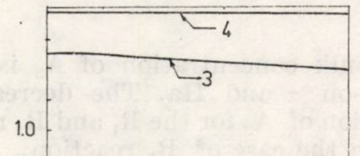

Fig. 9. — Dimensionless concentration profiles for intermediate A_3 across the liquid film; Ha = 1; R_2 reaction; (*1*) α = 0.1, β = 0.01; (*2*) α = 100, β = 0.01; (*3*) α =0.1, β = 10; (*4*) α = 100, β = 10.

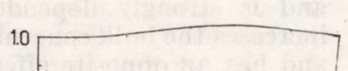

Fig. 10. — Dimensionless concentration profiles for intermediate A_3 across the liquid film; Ha=10; R_2 reaction; (*1*) α = 0.1, β=0.01; (*2*) α = 100, β = 0.01; (*3*) α=0.1, β = 10; (*4*) α = 100, β = 10.

conclusions can be drawn concerning the bulk value of A_3 and its profile across the film:

- for low values of β, for instance $\beta = 0.01$, the bulk concentration of A_3 tends to zero; the profile is independent of α for all reaction types and quasiindependent of Ha only for R_1 reaction;

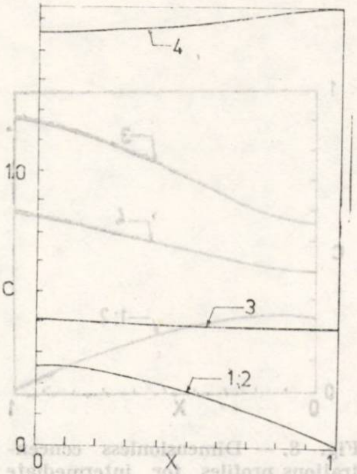

Fig. 11. — Dimensionless concentration profiles for intermediate A_3 across the liquid film; Ha = 1; R_3 reaction; (*1*) $\alpha=0.1$, $\beta=0.01$; (*2*) $\alpha=100$, $\beta=0.01$; (*3*) $\alpha=0.1$, $\beta=10$; (*4*) $\alpha=100$, $\beta=10$.

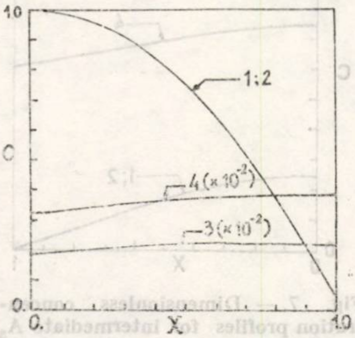

Fig. 12. — Dimensionless concentration profiles for intermediate A_3 across the liquid film; Ha=5; R_3 reaction; (*1*) $\alpha=0.1$, $\beta=0.01$; (*2*) $\alpha=100$, $\beta=0.01$; (*3*) $\alpha=0.1$, $\beta=10$; (*4*) $\alpha=100$, $\beta=10$.

- at larger values of β the bulk concentration of A_3 is greater and is strongly dependent on α and Ha. The decrease in α increases the bulk concentration of A_3 for the R_1 and R_2 reactions and has an opposite effect in the case of R_3 reaction.

Notice that in the limit $\beta = 0.01$, the A_1 and A_4 dimensionless concentrations tend to zero too. For other values of β, i.e. $\beta \geqslant 0.1$, the bulk concentrations of A_1 are significantly greater than zero even at large values of Ha.

CONCLUSIONS

The effects of the mass transfer and reactor operating conditions upon the absorption of a gas followed by a complex chemical reaction in a perfectly mixed reactor are investigated. Three possible chemical reactions observed from a general one were taken into consideration. The multigrid method has been used to solve the system equations from which the species concentration in both the bulk and film have been computed. The numerical parametric study revealed that the preformances of the gas-liquid reactors, expressed as enhancement factor and film selectivity are strongly affected by mass transfer and reactor operating conditions for a given value of the kinetic parameters.

As a result, depending on the operating conditions, more care must be given to the design of gas-liquid reactors in which complex chemical reactions occur in order to avoid the formation of undesirable reaction products.

Symbols used

A — dimensionless concentration of A_1, c_1/c_{1I}
A_1, A_2, A_3, A_4 — the chemical species presented in system
a_V— interfacial area per unit dispersion volume
B — dimensionless concentration of A_2, c_2/c_{2L}
C — dimensionless concentration of A_3, c_3/c_{1I}
c_1, c_2, c_3, c_4 — molar concentration of A_1, A_2, A_3, A_4
D_1, D_2, D_3, D_4 — diffusion coefficient of A_1, A_2, A_3, A_4
E_1 — enhancement factor defined in eq. 8.
F_L — liquid flow rate
Ha — Hatta number, $\sqrt{k_1 D_1 c_{2L}/k_L}$.
k_1, k_{-1}, k_2, k_{-2} — reaction rates constants
k_L — liquid film mass transfer coefficient
K_1, K_2 — dimensionless equilibrium constants
m — partial order of reaction
N_1, N_2, N_3, N_4 — molar flux of A_1, A_2, A_3, A_4
n — partial order of reaction
o — partial order of reaction
p — intrinsic selectivity, k_1/k_2
P — dimensionless concentration of A_4, c_4/c_{1I}
q — the ratio c_{2L}/c_{1I}
r_1, r_2 — reaction rates
s — partial order of reaction
t — partial order of reaction
V — volume of gas-liquid dispersion
x — film coordinate normal to interface
X — dimensionless coordinate across the film
Y_f — film selectivity defined in eq. (9)
w — partial order of reaction

Greek letters

α — ratio of the bulk to film volume
β — Damköhler number, $k_L a_V \tau$
δ_L — film thickness
ε — volumetric fraction
γ_{ij} — ratio of the diffusion coefficient, D_i/D_j
ν_{ij} — stoichiometric coefficient of the j component in the i reaction
τ — residence time of the liquid phase, V/F_L

Indices

G — gas phase
i — chemical reaction
I — gas-liquid interface
j — chemical species
L — liquid phase or liquid bulk

REFERENCES

[1] D. T.-J. Huang, J. J. Carberry and A. Varma, *A.I.Ch.E.J.*, **26**, 832 (1980).
[2] P. W. Danckwerts, "Gas-Liquid Reaction", McGraw Hill, New York, 1970.
[3] G. F. Froment and K. B. Bischoff, "Chemical Reactor Analysis and Design", Wiley, New York, 1979.
[4] Shi-Phing Ho. and Sheng-Tai Lee, *Chem. Eng. Sci.*, **35**, 1139 (1980).
[5] T. Darde, N. Midoux and J.-S. Charpentier, *Int. Chem. Eng.*, **25**, 67 (1985).
[6] A. Brandt, *Math. Comp.*, **31**, 330 (1977).
[7] C. C. Douglass, *S.I.A.M.J. Num. Anal.*, **21**, 236 (1984).
[8] J. M. Hyman, *J. Comput. Phys.*, **23**, 124 (1977).
[9] J. E. Dendy Jr., *J. Comput. Phys.*, **48**, 366 (1982).
[10] J. G. van de Vusse, *Chem. Eng. Sci.*, **21**, 631 (1966).

Revue Roumaine de Chimie, 32, 6, 611–616 (1987)

LA FLOTTATION IONO-MOLÉCULAIRE DU Cu(II) AVEC COLLECTEUR PONILIT CP. 1

L'INFLUENCE DU pH SUR LE RENDEMENT DE LA FLOTTATION

ROMULUS POMOJE-MARCU et LIVIA MAGYAR

La Faculté de Technologie Chimique de l'Institut Polytechnique «Traian Vuia», Timişoara, Bd. 30 Decembrie 2, La chaire de Chimie minérale et Technologie chimique minérale

Reçu le 19 juillet, 1986

This paper deals with the ionic-molecular flotation of Cu(II) aqueous dilute solutions as a method of extraction and concentration using the collector Ponilit CP 1. The optimum values of the parameters which influence the flotation have been established. The optimum pH range for various concentrations of the coligand Cu(II) has also been determined.

On présente la flottation iono-moléculaire dans le cas de certaines solutions aqueuses diluées de Cu(II) comme méthode d'extraction et de concentration, en employant le collecteur Ponilit CP 1. On a établi les valeurs optimales des paramètres qui influencent le processus de flottation. On a suivi la détermination de l'intervalle de pH optimal pour différentes concentrations du coligand Cu(II).

En considérant le fait que les cations aqueux de forme générale simple $[Me(OH_2)_x]^{n+}$ sont pour la plupart stables aux petits pH, la forme aqueuse du ion concourt par stabilité le produit qu'il formerait avec le collecteur. En échange, les hydroxo-aqua espèces de la forme de certains polymères minéraux $[Me_p(OH)_y(OH_2)_x]^{np-y}$, par les ponts de OH et les liaisons collatérales avec OH_2 représentent des espèces polynucléaires qui déterminent la floconnation de la solution de Cu(II). La flottation de telles espèces s'encadre dans la catégorie de flottation des précipités. Ce type de flottation nécessite des consommations réduites de collecteur, a lieu à une grande vitesse de flottation en obtenant des rendements de grandes extractions, or, les autres électrolytes libres de la solution n'exercent aucune influence sur l'interaction collecteur-coligand. Avec ces avantages, la variante de la flottation des précipités est devenue prioritaire par rapport à la flottation des ions simples.[1-6]

La littérature spécialisée accorde une importance à l'application de la méthode de la flottation dans le cas du Cu(II), en montrant que dans le cas des espèces polynucléaires, elle est plus avantageuse que celle des systèmes solubles.[1,2] Les hydroxo-aqua espèces du coligand Cu(II), sont plus fortement liées aux collecteurs qui contiennent de l'azote, existant une affinité du Cu(II) pour les ligands comme la pyridine,[7] la lauryl-amine [8] et stéaryl-amine.[8] D'autres collecteurs efficients existent aussi pour la flottation du Cu(II), comme par exemple le triphénylarsénoxyde.[9] Un autre avantage au niveau des macroespèces complexes qui se forment entre l'espèce polynucléaire du coligand et du collecteur est une meilleure portance dans l'écume par le flux gazeux.

Il existe un certain intervalle de pH optimal dans lequel la flottation se réalise avec un rendement maximal qui doit être établi concrètement pour chaque système analytique, compte tenu de la nature du coligand, du collecteur et leur concentration.[10]

En ce qui concerne les rendements et les sources volumineuses de solutions diluées du Cu(II) des eaux résiduaires industrielles, des eaux de mine, on considère comme rentable la récupération du Cu(II) de ces sources permanentes.

RÉSULTATS EXPÉRIMENTAUX

On a poursuivi la modalité d'extraire et de concentrer le Cu(II) des solutions diluées par flottation iono-moléculaire des précipités, ayant comme gaz portant l'air, à différents pH, en maintenant les valeurs optimales constantes préétablies pour les autres paramètres qui influencent le processus : le temps de contact collecteur-coligand avant la flottation, le temps nécessaire à la flottation et le nécessaire de collecteur, le débit de gaz. On a établi par voie expérimentale les suivantes valeurs optimales avec des rendements $R\%$ jusqu'à 99%.

$$R\% = \frac{C_{flottée}}{C_{initiale}} \cdot 100$$

— le temps de contact collecteur-coligand sous agitation, $\tau_c = 300$ s ;
— le temps minimal nécessaire à la flottation, $\tau_{fl.} = 180$ s ;
— le volume de la solution d'étanol : de l'eau = 1 : 1 de collecteur Ponilit CP.1 — 0,9% égal avec 0,5 mL/50 mL échantillon de Cu(II) ;
— le débit volumique d'air : $q_v = 6{,}62$ mL/s. On a constaté que les débits plus grands redispersent le sublat de l'écume ;[11]
— la température de travail est la température de la chambre.

Pour chaque expériment initial de 50 ml solution de Cu(II), on a effectué la correction du pH, en employant une solution de NaOH 2M sous agitation, puis on a ajouté le collecteur et on l'a maintenu pendant 300 s sous agitation. L'addition de collecteur ne modifie pas sensiblement le pH de la solution.

On a poursuivi, aux différentes concentrations en coligand, d'établir les limites du pH entre lesquelles découle la flottation à des rendements élevés. Dans les tableaux 1, 2, 3 on donne les rendements de la flottation aux différents pH et pour différentes concentrations initiales (C_i) en Cu(II).

Les notations *, **, *** de l'ouvrage ont les significations suivantes :
* le moyen de deux déterminations ;
** la portance ultérieure de sublat dans l'écume ;
*** ne flotte pas

On a collecté les expériments pour la détermination de la concentration résiduaire en Cu(II), de la hauteur de 1 cm au-dessus de la fritte de la colonne, la hauteur totale de la colonne de solution étant de 7 cm.

Tableau 1

Rendements de la flottation du Cu(II) pour des solutions à $C_i = 9{,}72 \cdot 10^{-3}$M aux différents pH

n	1	2	3	4	5	6	7	8	9	10	11	12
pH	6,20	6,40	6,60	6,70	6,80	7,00	7,20	7,30	7,40	7,60	7,80	8,0
* R %	51,90	80,51	84,74	91,75	92,59	97,52	98,64	98,84	99,25	99,48	**	***

On a déterminé par spectrométrie d'absorption atomique les concentrations résiduaires en Cu(II) non-flottées, respectivement les concentrations initiales en Cu(II).

Tableau 2

Rendements de la flottation du Cu(II) pour des solutions à $C_i = 4{,}62 \cdot 10^{-3}$M aux différents pH

n°	1	2	3	4	5	6	7	8	9	10	11	12
pH	6,30	6,60	6,90	7,20	7,25	7,30	7,35	7,40	7,50	7,60	8,15	8,75
* R %	48,49	78,46	90,23	95,54	95,60	96,03	96,52	98,12	98,22	99,47	**	***

Tableau 3

Rendements de la flottation du Cu(II) pour des solutions à $C_i = 2{,}64 \cdot 10^{-3}$M aux différents pH

n	1	2	3	4	5	6	7	8	8	10
pH	7,40	7,50	8,10	8,25	8,30	8,35	8,40	8,50	8,75	9,4
* R %	1,80	3,00	94,06	94,44	97,50	97,60	97,75	97,87	98,18	***

En examinant les résultats des tableaux 1, 2, 3 il résulte le fait qu'aux concentrations plus grandes en coligand Cu(II) le pH optimal devient plus petit. Un motif pour passer vers des valeurs plus grandes de pH optimal avec la diminution de la concentration en coligand peut être l'atteinte de la valeur du produit de sublation, ce qui nécessite une plus grande concentration en ions hydroxyle. On observe même le fait, qu'aux concentrations plus grandes en coligand, l'intervalle du pH est plus large pour de bons rendements malgré qu'il soit, en général, relativement restreint. Le motif probable est le domaine d'existence acido-basique restreint des macroespèces qui se forment par condensation qui, ayant l'avantage du grand volume, sont liées plus puissamment au collecteur et portées par les flux gazeux dans l'écume. Les valeurs plus élevées du pH provoquent la rupture de ces macrostructures et leur passage en hydroxyde de Cu(II), qui reste dispersé dans la solution, puis se dépose sur la fritte de la cellule de flottation.

On observe aussi une baisse des valeurs des rendements maximaux atteints avec la baisse de la concentration en coligand. On a testé des solutions de différentes concentrations en coligand tout en gardant invariables les autres conditions de travail. Les résultats sont présentés dans la tableau 4.

Tableau 4

La baisse du rendement maximal de la flottation avec la baisse de la concentration en Cu(II)

C_i – Cu(II)	pH	R %*	pH	R %*	pH	R %*
$4,22\cdot10^{-4}$ M	9,00	69,83	9,25	74,67	9,80	* * *
$2,88\cdot10^{-5}$ M	9,00	11,00	9,60	18,00	10,20	* * *

On a suivi la reproductibilité de la méthode de flottation iono-moléculaire pour l'extraction et la concentration du ion de Cu(II) des solutions aqueuses diluées en employant comme collecteur Ponilit CP.1. En ce but on a appliqué le calcul statistique d'une série de neuf déterminations qui ont été effectuées dans des conditions identiques de travail.[12,13]

$$\mathrm{pH} = 7{,}25\ ;\ C_i = 4{,}62\cdot10^{-3}\mathrm{M\ en\ Cu(II)}\ ;\ q_{v(\mathrm{air})} = 6{,}62\ \mathrm{mL/s}$$

$$\tau_{fl.} = 180\ \mathrm{s}\ ;\ \tau_c = 300\ \mathrm{s}$$

$$V_{\mathrm{collecteur}}/V_{\mathrm{expériment\ \ coligand\ Cu(II)}} = 0{,}5\ \mathrm{mL}/50\ \mathrm{mL}$$

Les résultats de ces déterminations sont donnés, dans des conditions de flottation identiques, dans le tableau 5.

Le calcul statistique, comme il résulte du tableau 5, montre qu'avec une probabilité $P = 99{,}9\%$ la méthode est précise et exacte et n'est pas affectée par des erreurs systématiques.

LES RÉACTIFS

- On a préparé les solutions de Cu(II) de cuivre métallique et acide azotique, réactifs p.a.
- Le collecteur Ponilit CP 1 – poly [chlorure de N,N-dimetyl-N,N-diallyle ammonium], élaboré dans l'Institut de Chimie Macromoléculaire « Petru Poni » de Jassy, le collectif de recherche dirigé par Dr. ing. Adrian Karpov.

Appareillage

- cellule de flottation en verre, avec prise pour collecter des expériments, ayant montée à la base une fritte du type G4.[14]
- régulateur de débit étalonné ayant une résistance de 164 MP1.
- pH-mètre « Radelkis » type O.P. 205, ayant monté un agitateur magnétique.
- spectrophotomètre d'absorbtion atomique « Pye Unicam » type S.P. 1900.

Tableau 5

Les rendements pour des déterminations exécutés dans des conditions de flottation identique

n	R		Δ	Δ²
	$R\%$ les valeurs déterminées	$R'\%$ exprimés en pourcentage enraport avec $\bar{R}\%$		
1	97,10	100,50	+0,5	0,25
2	97,90	101,30	+1,3	1,69
3	95,50	98,90	−1,1	1,21
4	97,50	100,90	+0,9	0,81
5	98,10	101,50	+1,5	2,25
6	95,60	99,00	−1,0	1,00
7	94,50	97,90	−2,1	4,41
8	96,60	100,00	0	0
9	96,50	99,90	−0,1	0,01
	$\bar{R}\%=96,60$	$\bar{R}'\%=99,90$		$\sum\Delta^2=11,63$

$n = 9$; $k = 8$; $P = 99,9\%$; $t_{(P)} = 5,04$

$S^2 = 1,46$; $S_R = 1,21$; $S_{\bar{R}} = 0,403$; $t_{(P)} \cdot S_{\bar{R}} = 2,03$

$R_i = \bar{R} \pm t_{(P)} \cdot S_{\bar{R}} = 96,60 \pm 2,03$ l'intervalle de confiance ;

$$t_c = \frac{|\bar{R}' - A|}{S_{\bar{R}}} = \frac{99,90 - 100,00}{0,403} = 0,25,$$

on vérifie la condition ; $t_c < t_{(P)}$;

la vraie valeur $A = 100,00\,\%$[13] ;

on vérifie la condition : $t_{(P)} \cdot S_{\bar{R}} \geqslant |\bar{R}' - A|$.

CONCLUSIONS

En considérant les résultats expérimentaux présentés il résulte les suivantes conditions de travail pour obtenir les rendements élevés dans l'extraction et la concentration du Cu(II) des solutions aqueuses par flottation avec Ponilit CP.1.

— la concentration en coligand $C_l \geqslant 10^{-4}$M en Cu(II) ;
— le pH optimal s'établit en fonction de la concentration en coligand ;
— le temps maximal de flottation, $\tau_{\text{fl.}} = 180$ s ;
— le temps de contact collecteur-coligand sous agitation $\tau_c = 300$ s.
— le débit volumique d'air $q_v = 6,62$ mL/s
— la température de travail est la température ambiante.

On constate que cette méthode est efficiente, elle prétend une consommation minimale de réactifs de production indigènes, suppose une exécution simple, conduit à de grands rendements, elle est reproductible, sollicite un temps de développement très court par rapport à d'autres méthodes et elle ne nécessite pas des consommations énergétiques différenciées.

BIBLIOGRAPHIE

[1] R. Lemlich, "Adsorptive bubble separation techniques", Academic Press, New York, 1972, p. 78.

[2] I. Scheiham et T. A. Pinfold, *J. Appl. Chem.*, **18**, 217 (1968).

[3] E. J. Mahne et T. A. Pinfold, *J. Appl. Chem.*, **18**, 52 (1968).

[4] E. J. Mahne et T. A. Pinfold, *J. Appl. Chem.*, **18**, 140 (1968).

[5] E. J. Mahne et T. A. Pinfold, *J. Appl. Chem.*, **19**, 57 (1969).

[6] T. A. Pinfold et E. J. Mahne, *J. Appl. Chem.*, **19**, 188 (1969).

[7] J. V. Quagliano et J. Fujita, G. Franz, D. I. Phillips, I. A. Walmsley, S. Y. Tyree, *J. Amer. Chem. Soc.*, **83**, 3770 (1961).

[8] L. Stoica, I. Jitaru, M. Dinculescu, M. Georgescu, A. German, A. Lupu, *Rev. Chim. (București)*, **31**, 54 (1980).

[9] D. J. Phillips et S. Y. Tyree, *J. Amer. Chem. Soc.*, **83**, 1806, 1961.

[10] C. Liteanu, S. Gocan et A. Bold, Separatologie analitică, Ed. Dacia, Cluj-Napoca, 1981, p. 338.

[11] I. H. Newson, *J. Appl. Chem.*, **16**, 47 (1966).

[12] C. Liteanu et I. Rîcă, Teoria și metodologia statistică a analizei urmelor, Ed. Scrisul Românesc, Craiova, 1979, p. 30.

[13] D. Oprescu et M. Oprescu, *Rev. Chim. (București)*, **35**, 634 (1984).

[14] Al. Duca et L. Stoica, *Bul. Inst. Politeh. București*, **1**, 53 (1978).

NOTE POUR LES AUTEURS

La **Revue Roumaine de Chimie** publie des articles en anglais, français, russe, allemand ou espagnol. Les auteurs sont priés d'envoyer des articles et des comptes rendus inédits.

Les manuscrits seront dactylographiés à double interligne. La bibliographie, les tableaux et la légende des figures seront placés après le texte.

Si l'article fait partie d'une série numérotée, la partie précédente sera donnée comme première référence.

Chaque article sera précédé d'un résumé comprenant quinze lignes au maximum.

Les références bibliographiques dans le texte seront faites par des exposants sans parenthèses et paraîtront à la fin de l'ouvrage.

Les publications périodiques mentionnées dans la bibliographie seront présentées suivant les prescriptions internationales : le nom de l'auteur précédé de l'initiale du prénom, le titre du périodique abrégé conformément à « Chemical Abstracts » et souligné par une ligne, le numéro du tome indiqué par des chiffres arabes et souligné par deux lignes, suivi de la première page de l'article : à la fin, l'année de la parution sera placée entre parenthèses. Le numéro de la revue ne sera pas indiqué si les pages du volume sont numérotées consécutivement.

Les textes des livres ou traités incluront : le nom des auteurs, précédés de l'initiale du prénom, le titre du livre entre guillemets et sans être souligné, le numéro du tome précédé par l'abréviation « vol. » (ou « Bd. »), le numéro de l'édition, les éditions (the publisher), la localité de la parution du livre, l'année de la parution et la page de la référence précédée(s) par l'abréviation « p » (ou « S »).

Les brevets seront indiqués comme suit : l'auteur ou la firme, le pays et le numéro du brevet, la date de la revue (*Chem. Abstr.*). Par ex. : M. Jones (to Union Carbide Co.). Brit. Pat. 610 238,2 Sept. 1959 : cf. *Chem. Abstr.*, **54**, 12808 (1960).

Si la référence n'a pas été lue en original, on indiquera aussi la revue de références consultée.

Les diagrammes seront tracés à l'encre de Chine sur papier calque. Les tableaux et les figures (en nombre strictement nécessaire), ainsi que les courbes dans les figures seront numérotés par des chiffres arabes. Leur explication sera donnée dans la légende des figures. Prière de ne pas inscrire les mêmes données dans les tableaux et les figures. Chaque tableau aura un titre. On indiquera dans le texte la place approximative des tableaux et des figures. Les formules chimiques seront incluses dans le texte ; en outre, elles seront transcrites sur papier calque, à l'encre de Chine.

Les auteurs sont priés d'indiquer les caractères italiques (en soulignant les lettres au crayon), ainsi que tout autre caractère spécial : les préfixes *ortho*, *meta*, *para*, *cis*, *trans*, etc. seront soulignés pour indiquer leurs caractères italiques, et ne seront jamais écrits avec des majuscules.

Aucune correction à la main ne sera admise sur le manuscrit. Les corrections seront frappées à la machine. Les lettres grecques ou d'autres symboles spéciaux seront insérés à la main à l'encre clairement.

Le manuscrit sera signé par l'auteur.

Le titre courant aura 50 lettres au maximum.

L'entière responsabilité du contenu des articles appartient aux auteurs.

Sur demande on peut obtenir une note plus complète.

PRINTED IN ROMANIA

1987 JUL 6

TRAVAUX PARUS AUX ÉDITIONS DE L'ACADÉMIE DE LA RÉPUBLIQUE SOCIALISTE DE ROUMANIE

ELENA CEAUŞESCU, **Progrese în chimia şi tehnologia polimerilor**, 1986, 446 p.
ELENA CEAUŞESCU, **Forschungen im Bereich der Chemie und Technologie der Polymere**, 1986, 444 p.
I. G. MURGULESCU, O. M. RADOVICI, **Introducere în chimia fizică, vol. IV, Electrochimia**, 1986, 416 p.
RAUL MIHAIL, ION GROZEANU, **Estimarea secvenţială aplicată sistemelor chimice**, 1986, 406 p.
M. BREZEANU, L. PATRON, M. ANDRUH, **Combinaţii complexe polinucleare şi aplicaţiile lor**, 1986, 244 p.
A. T. BALABAN et al., **Labelled Compounds Applied in Nuclear Medicine**, coédition avec John Wiley and Sons, 1986, 742 p.
D. PURDELA, **Nomenclatura chimiei organice — IUPAC**, 1986, 454 p.
PETRU BUDRUGEAC, **Probleme de chimie**, 1986, 280 p.
T. ONCESCU, S. G. IONESCU, **Conversie fotochimică şi stocare de energie**, 1985, 272 p.
V. DRĂGUŢAN, A. T. BALABAN, M. DIMONIE, **Olefin Metathesis and Ring-Opening Polymerization of Cyclo-olefins**, coédition avec John Wiley and Sons, 1985, 544 p.
C. LITEANU, I. RÎCĂ, **Optimizarea proceselor analitice**, 1985, 360 p.
N. PERESCU, **Chimia extracţiei cu solvenţi şi aplicaţii**, 1985, 212 p.
V. E. SAHINI, M. HILLEBRAND, **Chimie cuantică în exemple şi aplicaţii**, 1984, 378 p.
GH. MARCU, **Chimia compuşilor coordinativi**, 1984, 415 p.
E. CORDOŞ, C. MANOLIU, **Spectrometria de absorbţie şi fluorescenţă atomică**, 1984, 178 p.
C. BODEA, **Tratat de biochimie vegetală, p. II, t. V**, 1984, 438 p.
N. ASANDEI, A. GRIGORIU, **Chimia şi structura fibrelor**, 1983, 395 p.
N. IONESCU, M. CĂLDĂRARU, **Oxidarea catalitică a olefinelor inferioare**, 1983, 178 p.
C. CAŞCAVAL, **Studiul polimerilor prin piroliză şi cromatografie de gaze**, 1983, 220 p.
C. I. SIMIONESCU, F. DANEŞ, **Originea vieţii**, 1983, 110 p.
C. BODEA, **Tratat de biochimie vegetală, p. II, t. IV**, 1982, 408 p.
I. G. MURGULESCU, RODICA VÎLCU, **Introducere în chimia fizică. Vol. III. Termodinamica chimică**, 1982, 624 p.
I. G. MURGULESCU, J. PĂUN, **Introducere în chimia fizică, Vol. I. 3. Nucleul atomic, reacţii nucleare, particule elementare**, 1982, 606 p.
ELENA CEAUŞESCU, **Noi cercetări în domeniul compuşilor macromoleculari**, 1981, 536 p.
I. G. MURGULESCU, TATIANA ONCESCU, E. SEGAL, **Introducere în chimia fizică. Vol.II.2. Cinematică chimică şi cataliză**, 1981, 1024 p.
I. GĂLĂŢEANU, **Procese şi metode radiochimice în energetica nucleară**, 1981, 234 p.
CR. SIMIONESCU, VALERIA GORDUZA, **Polimeri biocompatibili şi biologic activi**, 1980, 479 p.
ELENA CEAUŞESCU, **Polimerizarea stereospecifică a izoprenului**, 1979, 307 p.
C. GH. MACAROVICI, **Analiza chimică cantitativă anorganică**, 1979, 457 p.
M. FLORESCU, **Metode ştiinţifice în dezvoltarea industriei chimice moderne**, 1979, 256 p.
I. G. MURGULESCU, E. SEGAL, **Introducere în chimia fizică. Vol. II. 1. Teoria molecular-cinetică a materiei**, 1979, 1036 p.
I. G. MURGULESCU, V. EM. SAHINI, **Introducere în chimia fizică, Vol. I, 2. Structura şi proprietăţile moleculelor**, 1979, 604 p.
I. ZUGRĂVESCU, MAGDA PETROVANU, **N-ylid chemistry**, coédition avec McGraw-Hill International Book Company U.S.A., 1977, 396 p.
I.G. MURGULESCU, **Introducere în chimia fizică, Vol. I. 1. Atomi, molecule, legătură chimică**, 1976, 560 p.
ELENA CEAUŞESCU, **Research work on synthesis and characterization of macromolecular compounds. Contributions**, 1974, 251 p.

ISSN 0035—3930

c. 1120—I. P. INFORMAŢIA

43 426

Lei 40
$ 80 (pour un abonnement annuel)

F 1103

ACADÉMIE DE LA RÉPUBLIQUE SOCIALISTE DE ROUMANIE

REVUE ROUMAINE DE CHIMIE

TOME 32
N° 7
Juillet 1987

Rev. Roumaine Chim.

RRCHAX, 32, 7, p. 617–736 (1987), Bucarest

EDITURA ACADEMIEI REPUBLICII SOCIALISTE ROMÂNIA

ACADÉMIE DE LA RÉPUBLIQUE SOCIALISTE DE ROUMANIE

COMITÉ DE RÉDACTION

Rédacteur en chef :

I. G. MURGULESCU, membre de l'Académie de la République Socialiste de Roumanie

Rédacteurs en chef adjoints :

A. T. BALABAN et V. EM. SAHINI, membres correspondants de l'Académie de la République Socialiste de Roumanie

Collège de rédaction :

EM. BRATU, ELENA CEAUŞESCU, ECATERINA CIORĂNESCU, NENITZESCU, CR. SIMIONESCU, membres de l'Académie de la République Socialiste de Roumanie ; P. SPACU, membre correspondant de l'Académie de la République Socialiste de Roumanie ; M. BANCIU, M. D. GHEORGHIU-I. HAIDUC, D. I. MARCHIDAN, G. NIAC et D. SĂNDULESCU

La Revue Roumaine de Chimie paraît 10 fois par an. Toute commande de létranger sera adressée à ROMPRESFILATELIA — sectorul Export-Import Presă, P. O. Box 12—201, télex 10376 prsfi r 78104 Bucarest, Calea Griviţei nr. 64—66, Bucureşti, Roumanie

Les manuscrits, les livres et les revues proposés en échange, ainsi que toute correspondance seront envoyés à la rédaction :

REVUE ROUMAINE DE CHIMIE

125, Calea Victoriei, 79717 Bucarest, Roumanie, téléphone 50 76 80

EDITURA ACADEMIEI REPUBLICII SOCIALISTE ROMÂNIA
125, Calea Victoriei 79717 Bucarest, Roumanie, téléphone 50 76 80

ORSZÁGOS MŰSZAKI INFORMÁCIÓS KÖZPONT ÉS KÖNYVTÁR

REVUE ROUMAINE DE CHIMIE

Tome 32, N° 7 **Juillet, 1987**

THE 2nd SYMPOSIUM ON THE CHEMISTRY OF COLLOIDS AND SURFACES 619

MIHAIL FLORESCU, The chemistry of colloids and surfaces 621–626

EMIL CHIFU, ALEXANDRA CHIFU, MARIA TOMOAIA-COTIŞEL and JÁNOS ZSAKÓ, Specific interactions in monomolecular membranes of biological interest 627–636

TATIANA ONCESCU, M. CONTINEANU, S. G. IONESCU, MIHAELA OLTEANU, MINODORA LECA and LUCIA MEAHCOV, Photoinduced H_2 generation from water in micellar systems 637–646

MIHAELA OLTEANU, Mixed solutions of cationic and nonionic surfactants 647–652

M. MARINESCU, V. BUTUCEA, GEORGETA POPESCU, ADRIANA SÎRBU, ADRIANA IONESCU, CECILIA GEORGESCU and B. ALBU, Physicochemical characterization of the two-phase system employed in emulsion polymerization of vinyl chloride. 653–661

MARIA TOMOAIA-COTIŞEL, JÁNOS ZSAKÓ and EMIL CHIFU, Ejection curves and miscibility of egg lecithin with some carotenoid derivatives 663–670

VIORICA TRANDAFIR, MINODORA LECA, DAN DEMBINSCHI, ELENA PUICĂ and GABRIEL ZĂINESCU, Interactions between polyacrylic dispersions and biopolymers hydrolysates 671–675

HORIA VAIS and DORU G. MĂRGINEANU, Bacterial immobilization in membraneous supports for amperometric probing of organic compounds 677–682

EMIL CHIFU, MARIUS SĂLĂJAN, IOAN DEMETER-VODNÁR and MARIA TOMOAIA-COTIŞEL, Fatty acid films at the benzene / water interface 683–691

STELA FLORESCU, AURELIA ŞTEFĂNESCU, MARIA ROB and ION FĂTU, The influence of sodium toluene sulfonate on surface and colloidal properties of sodium alkylbenzene sulfonates 693–699

LIVIU ONICIU, DAN A. LÖWY, MARIA JITARU, IOAN A. SILBERG and BOGDAN C. TOMA, Electrosynthesis of propionitrile. II. Phase equilibria in the acrylonitrile–propionitrile–water system in the presence of cationic surfactants and electrolytes 701–706

EVELINE POPOVICI, MIHAELA GRECU, ANGELA POPA, MARIA ALEXANDROAIE, AURELIA VASILE, MIHAI CRUCEANU and NICOLETA DUMITRU, Detergent suspension for hard washings. Study of fluidity and stability 707–712

M. M. MARINESCU, MARIETA BALCAN, B. G. ALBU, GEORGETA POPESCU and N. N. WEISSMAN, Polymer-surfactant interaction. Surface-active properties 713–721

ION CREŢU, MIHAI IONESCU and MARIA STOICESCU, Some aspects of polymer flooding in oil reservoirs 723–728

BOOK REVIEWS 729–735

Rev. Roumaine Chim. 32, 7, p. 617–736 (1987), Bucarest

Revue Roumaine de Chimie, 32, 7, 619 (1987)

THE 2nd SYMPOSIUM ON THE CHEMISTRY OF COLLOIDS AND SURFACES

The 2nd Symposium on the Chemistry of Colloids and Surfaces was held between 8 –10 September, 1986 at the University of Cluj-Napoca, Department of Chemical Engineering. It was organized jointly by the Ministry of Chemical Industry, ICECHIM, CNST and the Ministry of Education; the symposium was dedicated to the 65th Anniversary since the founding of the Romanian Communist Party.

The proceedings developed within four sections: interfacial phenomena; disperse systems; biological membranes and synthesis, and colloidal systems in technological processes. They were intended to evidence the contribution of Romanian research to technological progress, to higher grade utilization of raw materials, development of new products and materials, reduction of specific consumption of materials and energy, etc., according to the requirements formulated by Acad. Elena Ceaușescu, D. Sc. Chem. at the recently held Congress of Science and Technology.

The opening address was given by Prof. Dr. Aurel Negucioiu, the rector of the host institution, the University of Cluj-Napoca. The message of the National Council for Science and Technology, delivered by Mihail Florescu, minister secretary of State, emphasized the importance of Colloidal and Surface Chemistry in the most diverse areas of modern science and technology.

The proceedings included 155 contributions by 332 authors that covered such diverse areas of colloidal and surface chemistry as: stability of colloidal systems used in complex industrial processes, obtainment of high quality products, physico-chemical and mathematical modelling of some biological processes, characterization and utilization of synthesis membranes correlated with data for natural membranes, etc.

In plenary sessions a number of major topics were broached: Supermolecular chemistry and supermolecular catalysis (Prof. Constantin Luca), Modern problems in the chemistry of liquid interfaces (Prof. Emil Chifu), Synthesis membranes in separation processes (Dr. Gheorghe Rădulescu), Interaction of polymers with surfactants (Dr. Georgeta Popescu and Mircea Marinescu).

The discussions had an interdisciplinary character, bearing upon the ways of implementing new technologies and procedures and emphasizing the topical problems of colloidal and surface chemistry.

This volume of the proceedings papers gathers all contributions; it is intended to evidence the research programs underway in research and higher education institutes, programs that are basically oriented towards elucidating either fundamental problems or practical questions of industrial relevance.

THE ADVISORY BOARD

THE 2nd SYMPOSIUM ON THE CHEMISTRY OF COLLOIDS AND SURFACES

The 2nd Symposium on the Chemistry of Colloids and Surfaces was held between 8—10 September 1986 at the University of Cluj-Napoca, Department of Chemical Engineering. It was organized jointly by the Ministry of Chemical Industry, ICECHIM, CSEC and the Ministry of Education; the symposium was dedicated to the 65th anniversary since the founding of the Romanian Communist Party.

The proceedings developed within four sections: interfacial phenomena; disperse systems; biological membranes and synthesis; and colloidal systems in technological processes. They were intended to evidence the contribution of Romanian research to technological progress, to higher grade utilization of raw materials, development of new products and materials, reduction of specific consumption of materials and energy, etc., according to the requirements formulated by Acad. Dr. Eng. Elena Ceaușescu at the recently held Congress of Science and Technology.

The opening address was given by Prof. Dr. Aurel Negruciu, rector of the host institution, the University of Cluj-Napoca. The message of the National Council for Science and Technology, delivered by Mihail Florescu, minister-secretary of State, emphasized the importance of Colloidal and Surface Chemistry in the most diverse areas of modern science and technology.

The proceedings included 135 contributions of 333 authors that covered such diverse areas of colloidal and surface chemistry as: stability of colloidal systems used in complex industrial processes, obtainment of high quality products, physico-chemical and mathematical modelling of some biological processes, characterization and utilization of synthetic membranes correlated with data for natural membranes, etc.

In plenary sessions a number of major topics were presented: Supramolecular chemistry and supramolecular catalysis (Prof. Constantin Luca), Modern problems in the chemistry of liquid interfaces (Prof. Emil Chifu), Synthetic membranes in separation processes (Dr. Gheorghe Răducanu), Interaction of polymers with surfactants (Dr. Georgeta Popescu and Mircea Marinescu).

The discussions had an interdisciplinary character, bearing upon the ways of implementing new technologies and procedures and emphasizing the topical problems of colloidal and surface chemistry.

This volume of the proceedings papers gathers all contributions; it is intended to evidence the research programs underway in research and higher education institutes, programs that are basically oriented towards elucidating either fundamental problems or practical questions of industrial relevance.

[illegible]

Revue Roumaine de Chimie, 32, 7, 621–626 (1987)

THE 2nd SYMPOSIUM ON THE CHEMISTRY OF COLLOIDS AND SURFACES

Cluj-Napoca, 8 –10 September, 1986

THE CHEMISTRY OF COLLOIDS AND SURFACES

MIHAIL FLORESCU

Received November 24, 1986

The 2nd Symposium on the Chemistry of Colloids and Surfaces took place at a time when new and efficient measures for the implementation of the Programme of Romania's economic and social development during the 1986 –1990 five-year plan and the prospective economic development up to the year 2000 and subsequently are being discussed.

The President of Romania, Nicolae Ceaușescu, has often emphasized the importance of science and technology for the economic and social development of the country, pointing out that "The fulfillment of our strategic goals and an intensive objective development impose full commitment to promoting the technical and scientific revolution, to achieving a new and revolutionary transformation of the management and organization of our activity based on the latest developments in the world of science and technology, on the social laws, on human knowledge, in general."

Since its beginnings, chemistry has always played a revolutionary role in the history of civilization by its theories on the Universe, Life and Society, on one side, and by the development of a material basis for human existence, on the other.

Being a fundamental science of nature, chemistry has always played an important part in the scientific and technological progress of modern times, due to its essentially applied character, which reasonably extends to its role in the future. As a fundamental science, it has provided a wider scope to human knowledge in related fields such as physics, biology, medicine, agriculture, as well as in interdisciplinary areas like physical chemistry, and more recently, astrochemistry, biochemistry and molecular biology.

Chemistry will further play an important part in the design of new materials such as composites and polymeric alloys, pure and ultrapure metals and substances without which one could not speak of a revolution in microelectronics and informatics. In the framework of the new scientific and technical revolution and its technological and industrial aftermath at the end of this millennium, the role of chemistry in the revolutionary development of biotechnology and bioengineering constitutes the basis of a new field of great scope and breadth, namely industrial microbiology.

The chemistry of polymers, of fine organic syntheses, of electrochemical organic syntheses, of colloids and surfaces, and such fields as plasmochemistry, laser photochemistry and astrochemistry are nowadays domains of intensive research.

Within this broad framework of scientific and technological activity, the 2nd Symposium on the Chemistry of Colloids and Surfaces is one of the manifestations through which the contributions of Romanian research teams to the economic and social development of our country become known to a wide range of specialists.

The papers presented meet Acad. Elena Ceaușescu's request made at the Congress of Science and Education for "The existing chemical technologies to be improved and new technologies elaborated, with a view to better putting to use crude oil and natural gas, to chemicalizing coal and cokeoven tar, and extracting hydrocarbons from the biomass and from other non-petroleum sources. It is necessary to continue searching for new sorts of plastics, rubbers, synthetic fibers, drugs, dyes and catalysts, as well as other products of fine organic synthesis having low energy requirements."

The Symposium was attended by researchers, engineers, professors and other specialists from various fields, concerned with the study of systems and phenomena specific to the chemistry of colloids, a science of supermolecular entities and interactions through physical forces. The colloid state exists everywhere and requires the presence of an interface; this led to the development of surface chemistry. The colloid state (according to Oparin's hypothesis) lies at the basis of life inception on earth.

The beginnings of colloid chemistry can be traced to mid 19th century, when Graham divided the substances into two classes: crystalloids and colloids. Well-known scientists such as Langmuir, Einstein, Smoluchowski, Jean Perrin, Staudinger, Svedberg, McBain, Rehbinder and the Romanian professor Eugen Angelescu, contributed to the progress of this science.

I would recall here the important role played by the chemistry of colloids in the successful assertion of the atomic theory. After a century of scientific disputes, at the end of the 19th century, there were still many scientists who did not accept the atomist theory. Among the most important experiments carried out by Perrin on Brownian motion there were six types of emulsions used in calculating Avogardo's number. As Jean Perrin wrote in his book *Les atomes*, published in 1913: "The laws of perfect gases can be applied in all details to emulsions, which gives a solid experimental basis to molecular theories." The laws of Brownian motion established by Einstein and Smoluchowski, and their theory, which comes close to the kinetic theory, have been confirmed by many experiments.

The applications of the chemistry of colloids and surfaces to industrial processes are wide-ranging. The important achievements of this border discipline over the last decades and the wide diversity of the theoretical and practical aspects involved are unanimously recognized. The development of synthetic detergents has focused the interest on the investigation of such aspects as the formation of micelles and the role of tensides. There are few scientific or technological activities which could do without the tensides from the detergent industry, the polymerization processes in emulsion, flotation, oil drilling and extraction, the drug and cosmetics industry, machine building industry, to the study of phenomena or systems modelling their counterparts in cell biochemistry or space science. These fields, though extremely varied, share a common working methodology and scientific basis.

The study of the colloid structure has a lot in common with the investigation of tensides. Investigating the behaviour of substances which in aqueous or organic media give birth to colloid particles, one draws conclusions about their shape, structure and size. The presence of colloidal particles in solution confers the system specific colloidal properties, leading to their utilization as detergents, wetting agents, foaming agents, dispersion agents, etc.

The development of the polymer industry has stimulated the investigation of dispersions. Water-soluble polymers became efficient stabilizing agents, which transform the irreversible lyophobic dispersions into reversible ones, namely :

— polymer mixtures can be considered disperse systems whose properties are influenced by interface compatibility ;

— highly dispersed materials with large surface areas can be used for separations, purifications, catalyst supports, etc.

— the properties of composite materials are largely determined by the nature of interface reactions and the dispersed state of at least one component ;

— hydrophobic binding and monolayer techniques underlie the understanding of processes in biological membranes.

The first biotechnologies for the production of biopolymers have been discovered in the past few decades. The latter can be used in any new fields as for instance the increase of the recovery factor of crude oil. This is a promising field for scientific and technological research.

Acad. Cristofor Simionescu and Valeria Gorduza show in their book *Biocompatible and Biologically Active Polymers* (Ed. Academiei, Bucharest, 1980) that polymers are very widely employed in the pharmaceutical industry and in medicine. "Biopolymers are the basic units of regenerative systems of cells (nucleic acids), of oxygen and carbon dioxide carriers (hemoglobin) and of the control agents of biochemical catalysts (enzymes). The results of research carried out during the last two decades have led to the ever wider use of biopolymers, both as testing instruments and remedies in many serious diseases."

The beginnings of the tenside industry in Romania recorded the production of a narrow range of washing agents, mainly soaps, and of some auxiliaries used in the textile and leather processing industries, such as sulphated natural oils and sulphonic acids resulting from oil refining. In the second half of the fifties, in parallel with the world progress of this field, the tradition and experience of our specialists in the processing of oil derivatives and natural fats grew into a Romanian school in the area of the synthesis of tensides ; many original processes could be applied in industry. The development of this industry allowed, on one side, a high growth rate in the production of detergents, from 10,000 tons in 1958 –1959 to 130,000 tons/ year nowadays, and, on the other side, the increase in the tenside-based auxiliaries production, with applications in many industries.

Romanian research has played an important role in the multiplication of the sorts of tensides in current production. All the four main classes of tensides are now being produced in this country, the sorts and quantities meeting the demand. The anionic tensides, recording the highest outputs in Romania, comprise alkylbenzenesulphonates, alkyl sulphates, alkyl- and alkylamidophosphates (with or without ethoxy groups), sulphosuccinates and sulphated or sulphited triglycerides. The nonionic tensides include a wide range of polyethoxylated products derived from alkylphenols, fatty acids and alcohols, alkylamides, esters of fatty acids, natural or synthetic triglycerides and newer products like block copolymers of ethylene oxide and propylene oxide, and propoxylated products.

A new field, developed over the last years, includes cationic tensides like primary, secondary and tertiary fatty amines, alkylphenolamines, alkylamidopolyamines, and their quaternary derivatives : tetraalkylammonium and trialkylbenzylammonium halides. The amphoteric tensides are produced in small quantities : alkylbetaines, alkylamineoxides and alkylyaminoacids.

The wide range of products belonging to all known classes – a mark of a modern chemical industry – requires a diversified amount of new materials and intermediary products, both natural (oils and vegetal or animal fats) and synthetic (petrochemical). The use of different classes of tensides has continuously been extended ; 30 years ago they produced only 22 sorts, while nowadays more than 250 products are being manufactured. They meet almost all the demands of our industry, from traditional uses in the textile and leather processing industries, oil drilling and extraction, metallurgical industry, to the more recently developed fields such as rubber and plastics processing, flotation, corrosion, inhibition, cosmetics, food processing and public health. The existing technologies and those under study cover the present and future uses of tensides in Romania. The research and development programmes for the next years provide for the improvement of the technologies in the tensides, detergents and auxiliaries industries.

Another promising field is the use of membranes in medicine and industrial applications, after the model of natural cell membranes. Interest in this field is now focused on the practical applications in many modern processes. The unique properties of membranes facilitated the development of less conventional technologies which otherwise could not have existed.

The membrane is a boundary between two phases and constitutes the very place where important processes like the transport of substance, separation and electric potential processes occur, which are relevant for chemistry, physics, biology, medicine, agronomy, ecology, etc. The most important membrane processes which have found practical applications are : osmosis, reverse osmosis, dialysis, electrodialysis, ultrafiltration, thermo-osmosis and others. The essential role of membranes is to act as a selective barrier between the gaseous or liquid components of a mixture.

The oldest application of membranes in the Romanian chemical industry is the regeneration of lyes by dialysis in the manufacture of artificial fibers. The membrane evolved from a cloth impregnated with magnesium hydroxide to a film of synthetic polymers supported on a polyamidic tissue ; this product has until recently been imported, but due to the research conducted within the Central Institute for Chemical Research it could be replaced by Romanian-made materials. Great progress has been made in the industrial applications of membrane-based technologies and in the manufacture of membranes with different separation properties.

The National programme for membrane manufacturing and application has been sponsored by the National Council for Science and Technology and its responsibility lies with the Central Institute for Chemical Research. This programme provides for the study of the following major processes : dialysis, electrodialysis, osmosis, ultrfiltration and hemodialysis. Researchers are involved both in the manufacture and use of membranes. Some of the projects concern homogeneous and heterogeneous ion-exchange membranes, membranes for dialysis and osmosis and a very important product, namely the apparatus and membranes for hemodialysis.

The Central Institute for Chemical Research has recently obtained important results in the research of electrodialysis that will widen the range of its applications. A special programme has been developed for ion separation in organic syntheses, purification and the recycling of some substances or their recovery from waste waters. The advantages of this process are economy of energy, high yields and purity of final products. The work is focused on such priorities as the recovery of sulphuric acid, its salts and other organic and inorganic acids used in large quantities and which are still found in waste waters at concentrations too high to be disintegrated. The most important contributions to the solution of this problem have been made by the research teams that manufactured their own membranes (Research and Design Institute for Waste Water Management in Bucharest, Săvinești Research Center, "P. Poni" Polymer Research Institute in Iași, a.o.). Equally important are the membranes for filtration and ultrafiltration, for gas separation and reverse osmosis, which are extensively studied. The Committee for Membranes and Membrane Technologies will revise and update this programme based on the results obtained in 1986 so as to be applicable to several important technologies for which no satisfactory solutions could be found by using ordinary materials. The departments interested in the application of these technologies are the Ministeries of chemical industry, food industry, health, and education.

The investigation techniques used by colloid and surface chemistry have been continuously improved from the current physical and chemical methods such as viscosimetry, electrical conductivity measurements, dialysis, chromatography and the usual spectroscopic methods (IR, UV, NMR) to modern procedures, e.g. pulse radiolysis, dielectric relaxation spectroscopy, chemical relaxation techniques or ESR. These methods of investigation have provided information concerning the aggregation states of colloidal systems and new data on the interactions in complex systems (e.g. polymer-tenside, biliary salts-lipides, polyelectrolyte — or tenside-induced hydrophobic interactions of hydrocarbons) and, generally speaking, on the identification of the specific experimental factors which control hydrophobic binding.

The intensive research done in the field of colloids is reflected by four important journals: Journal of Colloids and Interface Science, Kolloid Zeitschrift, Tensides, Kolloidnyi zhurnal, and by the symposia where the latest advances in this area are presented, e.g. micellization in aqueous and non-aqueous media, thermodynamics and kinetics of micellization, micellar catalysis, microemulsion and reactions in emulsions.

Out of the many industrial applications of colloid chemistry we would mention the purification of waste waters, detergents, flotation, emulsioning, foaming, solubilization with tensides, hydrophobization and hydrophyllization (mainly in the textile and leather industries), polymer latexes, electrophoretic deposition, enrichment and purification of raw ceramic materials, separation and purification by membrane processes, modifications in the behaviour of building materials, recovery of substances from aerosuspensions by electric filtration, tertiary recovery of crude oil by the injection of micellar solutions.

At this Symposium, organized by the Central Institute for Chemical Research and the Cluj-Napoca University, more than 150 papers were presented, which shows that the science of colloids has gained a place of its own in Romania.

The proceedings developed within the four sections of the symposium:

— interface phenomena
— disperse systems
— synthetic and biological membranes
— colloidal systems in technological processes.

The subjects approached are quite relevant for the development of the Romanian economy. We hope that both the papers and the discussions enabled a better understanding of the investigated phenomena and will no doubt promote a faster application of research results in industry.

Revue Roumaine de Chimie, **32**, 7, 627–636 (1987)

SPECIFIC INTERACTIONS IN MONOMOLECULAR MEMBRANES OF BIOLOGICAL INTEREST

EMIL CHIFU, ALEXANDRA CHIFU *, MARIA TOMOAIA-COTIŞEL
and JÁNOS ZSAKÓ
University of Cluj-Napoca, Physical Chemistry Department, 3400 Cluj-Napoca, Romania
*Institute of Isotopic and Molecular Technology, 3400 Cluj-Napoca, Romania

Received November 24, 1986

Collapse surface pressure *vs.* composition curves are presented for some two-component monolayers consisting of lipids (A) and carotenoids (B) viz. : (1) egg lecithin : β-cryptoxanthin ; (2) egg lecithin : β-cryptoxanthin palmitate ; (3) egg lecithin : zeaxanthin monopalmitate ; (4) distearoyl lecithin : zeaxanthin ; (5) distearoyl lecithin : astaxanthin, and (6) distearoyl digalactosyl glycerol : astaxanthin. Experimental data, interpreted by using the surface phase rule, lead to total miscibility of the constituents in both monolayer (M) and collapsed bulk phase (C). System (1) bears a perfect solution behaviour, systems (2) and (3) can be described by means of the regular solutions theory. A new approximation is advanced for the systems (4)–(6), admitting formation of AB_n-type molecular associations. Stability constants of the carotenoid-lipid complexes are evaluated. Stability of the molecular associations is discussed in terms of molecular structure.

INTRODUCTION

The simplified models are often used in the study of phenomena occurring at the level of cell membranes. A widely used biomembrane model[1] is the surfactant monolayer – also called monomolecular membrane – spread at the air/water interface, which presents some advantages : it is stable and provides adequate frame for experimental investigations on conformation and packing of the molecules and on the specific interactions, which could occur between the film forming molecules, under close to *in vivo* conditions.

Six systems were investigated of two-component monomolecular membranes consisting of substances of biological interest – lipids (A) and carotenoids (B) – spread at the air/water interface namely :

(1) egg lecithin : β-cryptoxanthin (EL : C) ;
(2) egg lecithin : β-cryptoxanthin palmitate (EL : CP) ;
(3) egg lecithin : zeaxanthin monopalmitate (EL : ZP) ;
(4) distearoyl phosphatidyl choline : zeaxanthin (DSPC : Z) ;
(5) distearoyl phosphatidyl choline : astaxanthin (DSPC : AX) and
(6) distearoyl digalactosyl glycerol : astaxanthin (DGDG : AX).

RESULTS AND DISCUSSION

The monolayers of pure components and of the mixtures were investigated by means of compression isotherms: surface pressure as a function of mean molecular area, using the Wilhelmy method. Details on the experimental techniques were presented elsewhere.[2,3] Of the study on the compression isotherms for all the six systems of two-component membranes a similar effect was found namely the collapse pressure was dependent on the composition of the mixed film throughout the investigated composition range. Upon collapse the monolayer (M) was in equilibrium with a new tridimensional phase denoted as collapsed bulk phase (C).[4]

In establishing the miscibility degree of the components in the system under consideration the surface phase rule[4-9] was applied to the collapse pressure of the mixed films. In a capillary system with plane interfaces at constant temperature and external pressure, the two-dimension phase rule takes the form:

$$w = (c - \varphi) - (\psi - s) \tag{1}$$

where w stands for the variance of the system; s represents the surface types; φ is the number of bulk phases; ψ – the number of surface phases, and; c is the number of independent components in the system.

Let us take, as an example, the case of a surface phase in equilibrium with a collapsed phase. Under the given circumstances, $c = 4$ (water, the monolayer-forming components A and B, inert gas-air); $\varphi = 3$ (water, air, collapsed phase); $s = 3$ (collapsed phase/ water, collapsed phase/ air, air/ water) and all the surface types carry only one single surface phase, $\psi = 3$, for instance – the air/ water surface carries one single surface phase only – corresponding to the mixed monomolecular membrane. It goes without saying that in such type discussions air is considered as monocomponent.

Given the above, according to Eq. (1) the system variance is $w = 1$ and, consequently the collapse surface pressure (π, mN/m) varies with composition of the monolayer – e.g. expressed by the molar fraction of the lipid in the monolayer ($x_A^M = x^M$) : $\pi = \pi(x^M)$, obtaining thus equilibrium isotherms termed as monolayer curves or still collapse curves.

To illustrate, in Figs 1, 2*a* and 3*a* the monolayer curves are given for some of the investigated systems namely: EL : C, EL : ZP and DSPC : AX, respectively. As can be seen the collapse pressures continuously vary with composition of the systems throughout the possible composition range. Such situation is found with all the considered systems, being in agreement with the phase rule; the system variance is $w = 1$, what indicates that the two components are totally miscible in both M and C.

The experimentally obtained monolayer isotherms of the six systems were discussed to the end of getting information on the behaviour of surface solutions. Upon the collapse of a monolayer consisting of components A and B, insoluble in water subphase, an equilibrium of the phases M and C is usually assumed, what implies equality of the chemical potentials, $\mu_i^M = \mu_i^C$, of all the components i present in both phases. The

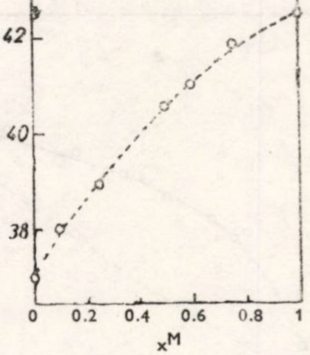

Fig. 1. — Monolayer curve of EL : C system, dashed line, calculated by means of Eq. (4) and the experimental collapse pressures. $T = 295$ K.

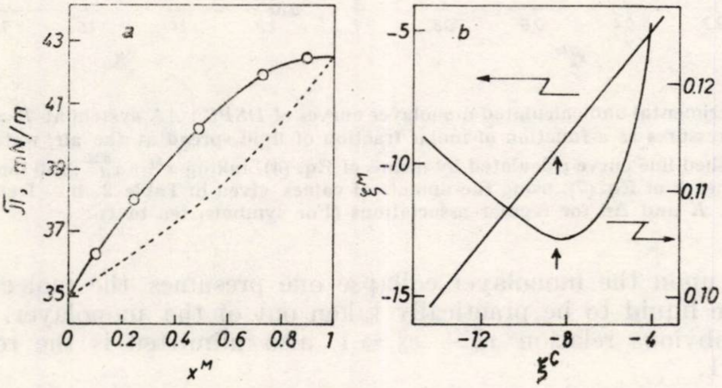

Fig. 2. — Deriving of interaction parameters for the EL : ZP system, at $T = 295$ K. a — Experimental collapse pressures and calculated monolayer curves : — dashed line, calculated for a perfect system by using Eq. (4) ; — solid line, calculated by means of Eqs (5) with $\xi_m^M = -9.48$ and $\xi_m^C = -8.67$; b — ξ^M and Δ as a function of ξ^M (For symbols, see text).

chemical potential of the components in the monolayer can be given under the form : [5,10]

$$\mu_i^M = \mu_i^{\Phi M} + kT \ln_i^M x_i^M + \pi A_i' \qquad (2)$$

and in the collapsed bulk phase as :

$$\mu_i^C = \mu_i^{oC} + kT \ln f_i^C x_i^C \qquad (3)$$

where $\mu_i^{\Phi M}$ and μ_i^{oC} stand for the standard chemical potential of the component i in M and the chemical potential of the pure component i in C, respectively; f_i^M and f_i^C are activity coefficients of i in M and C, respectively; x_i^M and x_i^C stand for the corresponding molar fractions; π is the monolayer surface pressure; and, A'_i is the partial molecular area of i.

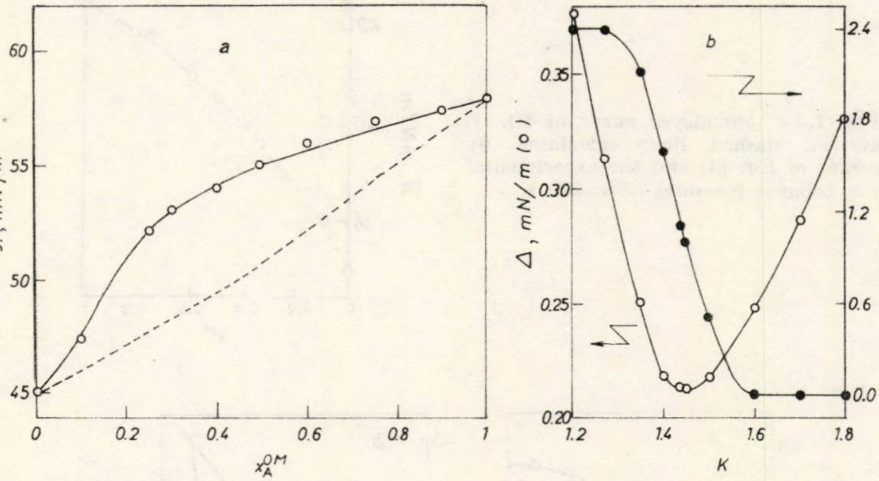

Fig. 3. — Experimental and calculated monolayer curves of *DSPC* : AX system at $T = 295$ K. a — Collapse pressures as a function of molar fraction of lipid spread at the air/ water interface (x_A^{oM}) : dashed line curve calculated by means of Eq. (4), taking $x^M = x_A^{oM}$; full line curve : calculated by means of Eq. (7), using the numerical values given in Table 2. b — Deriving of K and $\Delta\pi$ for regular associations (For symbols, see text).

Frequently, upon the monolayer collapse one presumes the molecules of the subphase liquid to be practically taken out of the monolayer. Thus, beside the obvious relation $x_A^C + x_B^C = 1$, also admitted is the relation $x_A^M + x_B^M = 1$.

The shape of the monolayer curve can be described by using varied simplifying approximations. By most simple approximation, both phases, M and C, are presumed as perfect solutions of A and B, $f_i^C = f_i^M = 1$, and upon collapse, the following relation is valid:

$$x^M \exp[(\pi - \pi_A)A_A/kT] + (1 - x^M)\exp[(\pi - \pi_B)A_B/kT] = 1 \qquad (4)$$

which results from Eqs (2) and (3) and from the above assumptions noting that $x_A^M = x^M$ and $x_B^M = 1 - x^M$. In Eq. (4), π, π_A and π_B stand for the collapse pressure of the mixed monolayer and of the pure monolayers A and B respectively; A_A and A_B are the mean molecular areas of A and B, respectively, upon collapse of the monocomponent monolayers. The values π_A, π_B, A_A and A_B have been obtained from the experimental compression isotherms of the pure monolayers and are given in Tables 1 and 2.

Table 1

Collapse pressure, π, area per molecule at collapse for pure monolayers, A, interaction parameters in monolayer (ξ_m^M) and collapsed phase (ξ_m^C) and minimum standard deviation Δ_m

System	Component		π, mN/m		A, nm²		ξ_m^M	ξ_m^C	Δ_m mN/m
	A	B	A	B	A	B			
(1)	EL	C	42.5	37	0.54	0.23	0	0	—
(2)	EL	CP	42.5	28	0.54	0.44	−2.65	−1.73	0.169
(3)	EL	ZP	42.5	35	0.54	0.52	−9.48	−8.67	0.105

Table 2

Surface characteristics, stability constants and surface pressure increments of the regular associations and their minimum standard deviation

System	Component		π, mN/m		A, nm²		K	$\Delta\pi$ mN/m	Δ_m mN/m
	A	B	A	B	A	B			
(4)	DSPC	Z	58	40	0.38	0.30	3.9	2.50	0.340
(5)	DSPC	AX	58	45	0.38	0.25	1.45	1.00	0.213
(6)	DGDG	AX	68	45	0.39	0.25	1.17	0.05	0.172

The dashed line curves in Figs 1, 2*a* and 3*a* give the plots of the theoretical monolayer curves computed by Eq. (4), employing the surface characteristics listed in Tables 1 and 2. As seen in Fig. 1, there is a good agreement of the experimental data with the calculated ones, what points to a perfect solution behaviour for the EL : C system throughout the composition range of the membrane. The positive deviations from perfect behaviour, noticeable in Figs 2*a* and 3*a*, point to the strong interactions between the molecules of xanthophylls and lipids.

Assuming the two surfactants to form regular solutions in both M and C, the following equations are valid : [5,8,10,11]

$$\begin{aligned} \ln(1 - x^C) + \xi^C(x^C)^2 &= \ln(1 - x^M) + \xi^M(x^M)^2 + (\pi - \pi_B)A_B/kT \\ \ln x^C + \xi^C(1 - x^C)^2 &= \ln x^M + \xi^M(1 - x^M)^2 + (\pi - \pi_A)A_A/kT \end{aligned} \tag{5}$$

where x^C and ξ^C stand for the molar fraction of the lipid and the interaction parameter, respectively, that characterizes the interaction between the lipid and carotenoid molecules A : B in the collapsed bulk phase, while x^M and ξ^M are the values of the monolayer parameters.

Eq. (5) allows the calculation of the values ξ^M and ξ^C which should provide for best description of the experimental monolayer curve.

Using the theory of regular solutions, one can show that for $\pi_B < \pi_A$ the maximum deviation from perfect behaviour appears at $x^M > 0.5$.

Returning to Fig. 2*a*, a maximum deviation of the experimental data from the perfect behaviour can be observed for the systems EL : ZP at x^M greater than 0.5. The same holds good for the EL : CP system. Thus, the shape of the monolayer curve for systems (**2**) and (3) can be described by the Eqs (5), ξ^M and ξ^C being obtained from the experimental data (see Fig. *2b*). The calculation procedure lies in the double minimization of the standard deviation (Δ) of the experimental values (π) from the calculated ones, using this time the approximation of the regular solutions. The values ξ_m^M and ξ_m^C are given in Table 1, and the system of Eqs (5) satisfactorily describes the experimental monolayer curve for both systems (2) and (3) (see full line in Fig. *2a*).

With the systems (4) — (6) the maximum deviation of the experimental data from the perfect behaviour was recorded for $x^M < 0.5$ and, in consequence, the approximation of the regular solutions cannot account for the deviations noticed. To the end of accounting for the molecular interactions encountered with the last three systems in discussion, the formation of the A_mB_n-type molecular associations was presumed. Obviously, the collapse pressure of the monolayers containing $\mathrm{A}_m\,\mathrm{B}_n$ molecular species only must be greater than both π_A and π_B, and the point of maximum deviation from the perfect behaviour is dependent on the stability of the $\mathrm{A}_m\mathrm{B}_n$ association as well as on the $m : n$ ratio.

As with the DSPC : AX system (Fig. *3a*) the maximum deviation from perfect behaviour is found at $x_A^{oM} < 0.5$, the molecular association must contain more molecules of carotenoids than of lipids. Therefore, let us presume the formation of the AB_n-type molecular association, which implies in M an equilibrium between the molecular species A, B, AB, $\mathrm{AB}_2, \ldots, \mathrm{AB}_n$. The reactions $\mathrm{AB}_{i-1} + B \rightleftharpoons \mathrm{AB}_i$ can be described by the equilibrium constants :

$$K_i = \frac{a^M_{AB_i}}{a^M_{AB_{i-1}} \cdot a^M_B}$$

where $a^M_{AB_i}$, $a^M_{AB_{i-1}}$ and a^M_B stand for the activity in M of the corresponding molecular species, which in the approximation of the perfect solutions turn :

$$K_i = \frac{x^M_{AB_i}}{x^M_{AB_{i-1}} \cdot x^M_B} \tag{6}$$

In what regards the magnitude n the reasonable maximum value appears to be 6, having in mind both the experimental results and our calculations using the molecular models.

Assuming that both M and C are perfect solutions consisting of A and B and of the six AB_i-type molecular species, the collapse pressure of the mixed monolayer will abide by the relation obtained by generalization of the Eq. (4), becoming :

$$\begin{aligned} &x_A^M \exp\left[(\pi - \pi_A)\frac{A_A}{kT}\right] + \sum_{i=1}^{6} x^M_{AB_i} \exp\left[(\pi - \pi_{AB_i})\frac{A_{AB_i}}{kT}\right] + \\ &+ x_B^M \exp\left[(\pi - \pi_B)\frac{A_B}{kT}\right] = 1 \end{aligned} \tag{7}$$

Eq. (7), beside the molar fraction of all the molecular species, also comprises the collapse pressures π_{AB_i} and the molecular areas A_{AB_i}. Calculation of the molar fractions implies the knowledge of the equilibrium constants given by Eq. (6). These magnitudes cannot be directly measured; it follows that eighteen parameters must be calculated from the experimental curves π as function of x_A^{oM}.

A new simplified method is advanced to the end of overcoming the above difficulties, which is called approximation of the perfect solution of regular molecular associations, the monolayer being considered as perfect solution of regular associations. The regular characteristic of the molecular associations is given by:

1. All the equilibrium constants K_i have the same value, i.e. $K_i = K$ for $1 \leqslant i \leqslant 6$;

2. If B is attached to A or AB_{i-1}, that will entail the same collapse pressure increment $\Delta\pi$ of the pure monolayer, i.e. $\pi_{AB_i} = \pi_A + i\Delta\pi$;

3. The molecular area of the complex AB_i is the sum of molecular areas of the components, i.e. $A_{AB_i} = A_A + iA_B$.

On the basis of these hypotheses, the molar fractions $x_{AB_i}^M$ in Eq. (7) can be calculated by the relation:

$$x_{AB_i}^M = \frac{(1 - x_B^M)\,(x_B^M K)^i}{\left[1 + \sum_{i=1}^{6} (x_B^M K)^i\right]} \tag{8}$$

As seen in Eq. (6), if the surfactants form up regular associations, the following relation will be between the molar fractions of the species AB_i:

$$x_{AB_i}^M = x_{AB_{i-1}}^M x_B^M K$$

It can also be shown that $x_A^M = (1 - x_B^M) \Big/ \left[1 + \sum_{i=1}^{6} (x_B^M K)^i\right]$ viz. $x_{AB_i}^M = x_A^M (x_B^M K)^i$, irrespective of the value of i. As in the event of great excess of B (if $K > 1$) one must have $x_{AB}^M < x_{AB_2}^M < \ldots < x_{AB_6}^M$, which means that $x_B^M K > 1$, while with A in great excess it is just the opposite, viz. $x_{AB}^M > x_{AB_2}^M > \ldots > x_{AB_6}^M$; according to the condition $x_B^M K < 1$, there must be one composition where with $x_B^M K = 1$ and accordingly all the molecular species, except B, will have the same molar fraction. This very composition is denoted as point iso-$x_{AB_i}^M$. It can easily be inferred that this point is characterized by the following properties:

$$x_B^M = 1/K\,;\; x_A^M = x_{AB}^M = x_{AB_2}^M = \ldots = x_{AB_6}^M = \frac{K-1}{7K} \text{ and}$$

$$x_A^{oM} = \frac{K-1}{4K-3} \tag{8'}$$

The equilibrium molar fraction of B, x_B^M, is obtained as solution of an equation of the order 7, equation resulting from the expression of K as well as from the balance equations of material and it takes the form of Eq. (9):

$$x_A^{oM}(1-x_B^M)\sum_{i=1}^{3} i(x_B^M\,K)^i = (1-x_A^{oM}-x_B^M)\left[1+\sum_{i=1}^{6}(x_B^M\,K)^i\right] \qquad (9)$$

Of the above equation x_B^M can be calculated as a function of K and of the apparent molar fraction x_A^{oM} of lipid initially spread in the monolayer.

Therefore, the system of Eqs (7)–(9) contains only two unknown parametres, K and $\Delta\pi$, which can be calculated from the experimental data by using, for instance, the following procedure of double minimization: — aK value for all x_A^{oM} is presumed for which the collapse pressure has been experimentally determined, x_B^M is calculated as solution of Eq. (9) and then all the molar fractions are calculated by Eq. (8). The collapse pressures are further calculated using Eq. (7) assuming different $\Delta\pi$ values. By systematically varying $\Delta\pi$, one of its values is found which ensures the minimum standard deviation Δ of the values of the experimental collapse pressure from the calculated ones. Likewise, by repeating these calculations for different K values the resulting graphs of Δ as a function of K present a minimum which indicates the best values of K and $\Delta\pi$.

Assuming the formation of regular associations of the type AB, AB_2, AB_3, AB_4, AB_5 and AB_6, the above procedure was used in processing our experimental data. The minimum standard deviations of the experimental points from the calculated ones, for varied K values presumed in the case of DSPC : AX system are illustrated in Fig. 3*b*. As can be seen the curve touches an evident minimum that corresponds to $K = 1.45$. This same figure also exhibits the $\Delta\pi$ value ensuring the minimum standard deviation as a function of K.

The set forth calculus procedures allowed for calculation of the values of K and $\Delta\pi$ from our experimental data. These data as well as the corresponding standard deviations are given in Table 2 for the systems DSPC : Z, DSPC : AX and DGDG : AX.

The full line curve in Fig. 3a has been calculated by Eq. (7), using the values given in Table 2. As can be seen in Table 2, our model of molecular associations can describe very well the experimental data of the three systems investigated, with a standard deviation which does not outpass the experimental errors of the collapse pressure determinations (± 0.5 mN/m). Hence the assumed formation of regular associations appears to be real.

The obtained values of K enable us to calculate the monolayer composition for the varied apparent molar fractions of the lipid initially spread in the film. The curves plotted on Fig. 4 give the molar fraction of the varied molecular species as a function of the apparent molar fraction of the lipid for the DSPC : AX system. Similar isotherms are obtained for the system (4) and (6). Fig. 4 shows an important alteration in the molar fraction of the AB$_i$-type species, especially at greater i values. That is easily understood since the stability constant of the AB$_i$ complex, $\beta_i = \prod_{k=1}^{i} K_k$, equals K^i. Thus, in the region $0 < x_A^{oM} < 0.5$, the number of the molecules of the complex, particularly of those with high i values, increases greatly, leading to the alteration of the maximum collapse

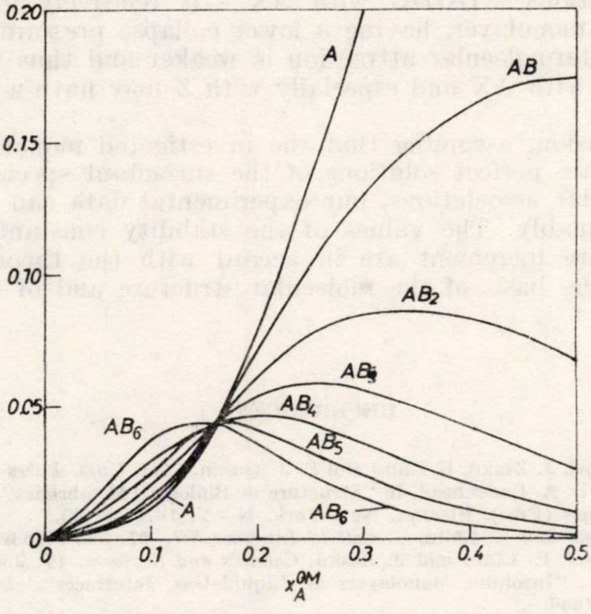

Fig. 4. — Composition of DSPC-AX films as a function of x_A^{oM}. Curves were calculated by means of Eq. (8), using $K = 1.45$. The type of the molecular species of i is given near each curve.

pressure deviation from the perfect behaviour towards the lower x_A^{oM} values.

In Fig. 4 there can be also noticed the existence of the iso-$x_{AB_i}^M$ point situated at $x_A^{oM} = 0.16$, in agreement with Eq. (8′).

According to our results, the AB$_n$-type associations appear to approximately have the same stability for the systems with astaxanthin, being a little higher with the DSPC : AX system as compared to the DGDG : AX one. This suggests that the intermolecular interaction could lie in the formation of the hydrogen bonds with participation of the OH group of AX and of the O-atoms of the stearic ester of glycerol. The higher stability of the DSPC : AX associations could be due to the inductive effect of the negative charge placed in the phosphate group.

The AB$_n$-type molecular associations seem to have a higher stability for the system (4) (i.e. DSPC : Z) than with the systems (5) and (6) (i.e. with AX). This suggests that in the formation of molecular associations the xanthophyll OH group plays an important role, while the carbonyl groups of AX apparently disfavour association.

As regards the stabilizing effect of the monolayer expressed by the collapse pressure increment $\Delta\pi$, the greater value found with the mixed films of xanthophylls and DSPC, as compared to those of DGDG, also seems reasonable. The high value of the collapse pressure of the "pure" monolayer of DGDG is due to the very important intermolecular forces acting between the galactosyl groups.[12] Therefore, the stabilizing effect of the associations – DGDG with AX – is relatively low. With the "pure" DSPC monolayer, having a lower collapse pressure than that of DGDG, the intermolecular attraction is weaker and thus the formation of associations with AX and especially with *Z* may have a greater stabilizing effect.

In conclusion, assuming that the investigated monolayers for systems (4) –(6) are perfect solutions of the surfactant species and of the regular molecular associations, our experimental data can be accounted for quite reasonably. The values of the stability constants and of the collapse pressure increment are in accord with the theoretical results envisaged on the basis of the molecular structure and of the electronic effects.

REFERENCES

[1] M. Tomoaia-Cotişel, J. Zsakó, E. Chifu and P. J. Quinn, *Stud. Univ. Babeş-Bolyai Chem.* **32,** (1), in press ; D. A. Cadenhead, in "Structure of Biological Membranes", S. Abrahamsson and I. Pascher (Eds.), Plenum, New York, N–Y, 1976, p. 63.

[2] M. Tomoaia-Cotişel and E. Chifu, *J. Colloid Interface Sci.*, **95**, 355 (1983).

[3] M. Tomoaia-Cotişel, E. Chifu and J. Zsakó, *Colloids and Surfaces*, **14**, 239 (1985).

[4] G. L. Gaines, Jr., "Insoluble Monolayers at Liquid-Gas Interfaces", Interscience, New York, NY, 1966.

[5] R.Defay, I. Prigogine, A. Bellemans and D. H. Everett, "Surface Tension and Adsorption", Longmans and Green, London, 1969.

[6] D. J. Crisp, "Surface Chemistry", Supplement to Research, London, 1949, pp. 17–23.

[7] M. C. Phillips and P. Joos, *Kolloid-Z. Z. Polym.*, **238**, 499 (1970).

[8] M. Nakagaki and N. Funasaki, *Bull. Chem. Soc. Japan*, **47**, 2482 (1974).

[9] E. Chifu and M. Tomoaia-Cotişel, *Rev. Roumaine Chim.*, **27**, 27 (1982).

[10] J. Zsakó, M. Tomoaia-Cotişel and E. Chifu, *J. Colloid Interface Sci.*, **102**, 186 (1984).

[11] P. Joos and R. A. Demel, *Biochim. Biophys. Acta*, **183**, 447 (1969).

[12] M. Tomoaia-Cotişel, A. Sen and P. J. Quinn, *J. Colloid Interface Sci.*, **94**, 390 (1983).

Revue Roumaine de Chimie, 32, 7, 637–646 (1987)

PHOTOINDUCED H_2 GENERATION FROM WATER IN MICELLAR SYSTEMS

TATIANA ONCESCU, M. CONTINEANU, S. G. IONESCU, MIHAELA OLTEANU, MINODORA LECA and LUCIA MEAHCOV
Polytechnical Institute of Bucharest, Department of Physical Chemistry,
Bd. Republicii 13, R-70346

Received October 30, 1986

Photoredox reactions in micellar systems have been more and more investigated lately in order to reduce the rate of back electron transfer from electron relay to the photosensitizer. This reaction competes strongly with the electron transfer from the relay to water molecule which generates H_2. Our experiments carried out in three types of detergents (cationic, anionic and nonionic) evidence some possibilities to increase the amount of evolved H_2.

INTRODUCTION

Photochemical conversion of solar energy via redox processesis one of the promising ways to obtain H_2 from water. It involves a system with a photosensitizer Ps, a relay species R, a sacrificial electron donor D (usually a tertiary amine) and a catalyst C_{red}. Such a system operates in many steps as follows:

– light absorption:

$$Ps + h\nu \rightarrow Ps^* \qquad (1)$$

forward electron transfer by oxidative quenching:

$$Ps^* + R \rightarrow Ps^{\cdot +} + R^{\cdot -} \qquad (2)$$

– fast back reduction of $Ps^{\cdot +}$ with $D^{\cdot -}$ and its subsequent decomposition:

$$Ps^{\cdot +} + D \rightarrow Ps + D^{\cdot +} \qquad (3)$$

$$D^{\cdot +} \rightarrow \text{decomposition}$$

– H_2 production by water reduction:

$$2R^{\cdot -} + 2H^+ \xrightarrow{C_{red}} 2R + H_2 \qquad (4)$$

In this oxidative quenching scheme the photosensitizer and the electron relay follow catalytic cycles while H^+ (from water, and D are consumed as figure 1 shows. Of course, reaction (2) can also be replaced by a reductive quenching process to yield the reduced species $Ps^{\cdot -}$ which undergoes further transformation leading to H_2 generation.

The choice of the respective components in such a system must fulfil a number of requirements with respect to excited-state properties, redox potentials and reaction kinetics.[1] In any case the $R/R^{\cdot -}$ redox potential of the relay must lie between those of H^+/H_2 and $Ps^{\cdot +}/Ps^*$.

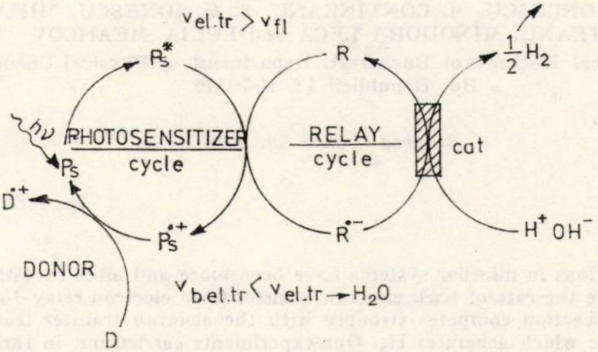

Fig. 1. — Scheme of hydrogen generation from water by an oxidative quenching.

Irradiation with visible light of an aqueos solution (pH 7) containing these components leads to H_2 generation and its efficiency is dictated by the competition between the opposite processes involved in the two homogeneous catalytic cycles of Ps and R, respectively. So, in the photochemical cycle of Ps there is a competition between the emission process and the forward electron transfer from Ps* to R; evidently, the rate of the last one must be greater than the rate of fluorescence emission : $v_{fl} <$ $< v_{el.tr.}$. In the thermal cycle of R the competition is between the electron transfer from $R^{\cdot -}$ to H_2O and the back electron transfer from $R^{\cdot -}$ to $Ps^{\cdot +}$. In this stage of experiments the presence of D (usually EDTA or TEOA) prevents the back electron transfer from the reduced relay to the oxidized photosensitizer by consuming rapidly the $Ps^{\cdot +}$ species. To increase the cycle efficiency it is necessary for the back transfer electron to be slower than the rate of electron transfer to H_2O. The presence of catalyst provides the increase of this last reaction. It is also necessary to minimize the rate of the back electron transfer process from $R^{\cdot -}$ to $Ps^{\cdot -}$: $v_{b.el.tr.} < v_{eltr} \rightarrow H_2O$.

On this purpose the micellar systems may be useful owing to their microheterogeneous character which offers a double advantage :

— the apolar interior of the aggregates is distinguished from the aqueous phase through its hydrocarbon-like character which facilitates the solubilization of hydrophobic species (the photosensitizer or the electron relay);

— the double-layer formed around ionic micelles which gives rise to surface potentials, frequently exceeding values of 150 mV.[2] This charged lipid-water interface provides a microscopic barrier for prevention of thermal back-transfer of the electron so that its role may be compared to that of the depletion or accumulation layer present at the semiconductor/ electrolyte interface.

The following examples offered by literature illustrate this point :

a) both sensitizer ($ZnTMPyP^{4+}$) and electron relay (CM_nV^{2+}), a viologen derivative, are dissolved in the aqueous phase. Under irradiation with visible light the electron transfer process takes place in this phase by an oxidative quenching :

$$\begin{tikzcd}
ZnTMPyP^{4+} \arrow[r, "h\nu"] & {}^3(ZnTMPyP^{4+})^* \arrow[r] \arrow[d, "C_nMV^{2+}"] & h\nu' \\
ZnTMPyP^{5+} + C_nMV^{\cdot +} \arrow[u, "\Delta"] \arrow[r, "H^+OH^-"] & C_nMV^{2+} + OH^- + \frac{1}{2}H_2 &
\end{tikzcd} \tag{5}$$

M. Grätzel et al. [3] studied the kinetics of this process by laser flash photolysis techniques. Decay of the porphyrin triplet at 980 nm (Fig. 2a) is accompanied by formation of redox products $C_{14}MV^{\cdot +}$ and $ZnTMPyP^{5+}$ (Fig. 2b) which undergo a rapid back reaction (Δ) carried out at 600 nm where absorb $C_{14}MV^{\cdot +}$ and $ZnTMPyP^{5+}$. In the presence of a cationic micelle, cetyl trimethyl ammonium chloride (CTAC), (Fig. 6c), the intervention of the back reaction is not noticed ; the kinetic analysis shows that CTAC micelles retard the reverse electron transfer by at least a factor of 10^3.

The explanation is that in the reduced state the viologen relay acquires hydrophobic properties [4,5] and it solves rapidly in the CTAC assemblies. On the other hand, the oxidized porphyrine is prevented from approaching the micelles by the positive surface charge (Fig. 3). Under these conditions, as the ζ-potential of CTAC is at least $+100$ mV[2], the probability of encounter with $ZnTMPyP^{5+}$ is less than 2×10^{-9}. This explains the effective micellar inhibition of the back reaction that in the scheme (fig. 1) is equivalent of $v_{b.el.tr.} < v_{el.tr \to H_2O}$. Under such conditions, the transfer electron from $C_{14}MV^{\cdot +}$ to H_2O molecule and therefore the amount of evolved H_2 are favorized.

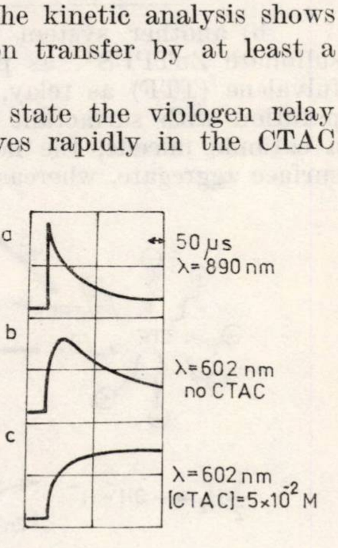

Fig. 2. — Laser flash experiments with the system[3] : $ZnTMPy^{4+}$ (5×10^{-5} M) and $C_{14}MV^{2+}$ (10^{-3} M) ; a — triplet decay ; b — growth and decay of redox products in the absence of CTAC ; c — in the presence of CTAC.

Grätzel mentioned also that in the case of $Ru(bipy)_3^{2+}$ as sensitizer and $C_{14}MV^{2+}$ as electron relay, it is not necessary to use a surfactant because $C_{14}MV^{\cdot +}$ forms small aggregates as positive microspheres which repulse Ru (II) complex that delayed substantially the back electron transfer. He

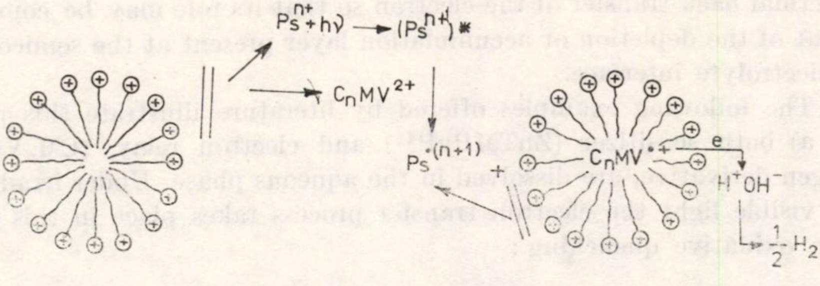
$Ps^{n+} + h\nu \rightarrow (Ps^{n+})^*$
C_nMV^{2+}
$Ps^{\cdot(n+1)}$
+
$C_nMV^{\cdot+}$
e
$H^+ OH^-$
$\frac{1}{2}H_2$

Fig. 3. — Charge-separation effect [3] induced by the cationic micelle in the system Zn porphirine-$C_{14}MV^{2+}$.

considers that such a system offers a model for a photochemical conversion cell to generate concomitantly H_2 and O_2 by water decomposition :

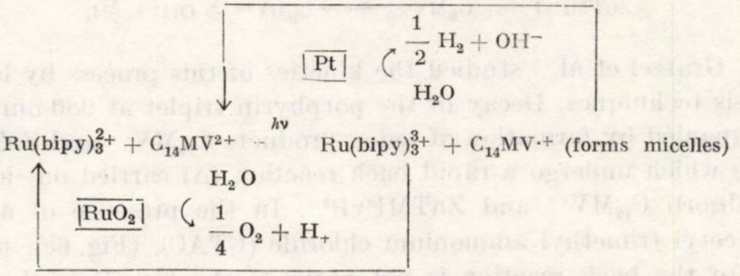

$$C_{14}MV^{\cdot+} + H_2O \xrightarrow{|Pt|} \frac{1}{2}H_2 + OH^-$$

$$Ru(bipy)_3^{2+} + C_{14}MV^{2+} \xrightarrow{h\nu} Ru(bipy)_3^{3+} + C_{14}MV^{\cdot+} \text{ (forms micelles)} \tag{6}$$

$$Ru(bipy)_3^{3+} + H_2O \xrightarrow{|RuO_2|} \frac{1}{4}O_2 + H_+$$

b) another system is the hydrophilic zinc-tetraphenylporphyrinsulfonate $ZnTPPS^{4-}$ as photosensitizer and the hydrophobic tetrathiofulvalene (TTF) as relay, which under visible light induced charge separation with surfactant assemblies by a reductive quenching. [6] Using a cationic micelle, the negative porphyrin associates with the positive surface aggregate, whereas TTF solves inside the micelle (Fig. 4). Visible

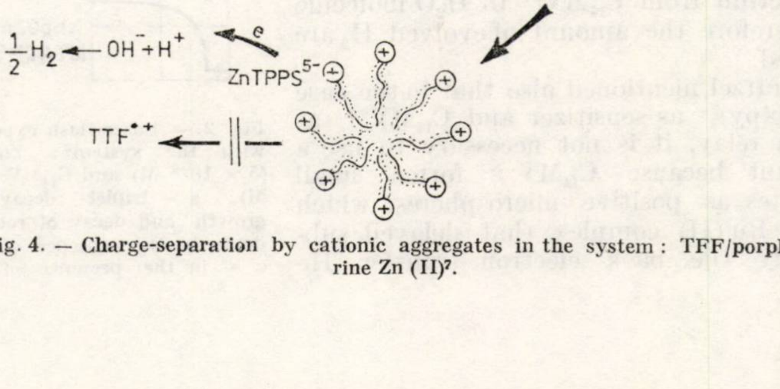
$h\nu$
$ZnTPPS^{4-}$
TTF
e
$(ZnTPPS^{4-})^*$
TTF
$ZnTPPS^{5-}$
$TTF^{\cdot+}$
$\frac{1}{2}H_2 \leftarrow OH^- + H^+$
e
$ZnTPPS^{5-}$
$TTF^{\cdot+}$

Fig. 4. — Charge-separation by cationic aggregates in the system : TFF/porphirine Zn (II)[7].

light absorption transforms excited porphyrin into a good electron acceptor from TTF by tunnelling micelle. The radical redox pair TTF$^{\cdot +}$ and ZnTPPS^{5-} is thereby produced within the aggregate. In this case, TTF$^{\cdot +}$ is destabilized with respect to the aqueous phase so that when it reaches the surface it will be ejected into the water. At the same time ZnTPPS^{5-} radical is electrostatically more stable in the micellar than in the aqueous phase and remains associated with the surfactant surface. Under these conditions the diffusional reencounter of the two radicals is obstructed by the ultrathin barrier of the micellar double layer and their life time is prolonged by several orders of magnitude.

We have also investigated in micellar solutions, another system: proflavine/Co(bipy)$_3^{2+}$/TEOA/Pt which we studied previously in water [8] to appreciate comparatively its behaviour in both cycles presented in figure 1.

We carried out our experiments in three types of micelle: anionic, cationic and nonionic.

EXPERIMENTAL

We studied the photosensitizer cycle by the fluorescence quenching method and the relay one measuring gaschromatographically the amount of hydrogen evolved under irradiation with visible light, as described elsewhere. [9] We used as photosensitizer proflavine monoclorhydrate Merck, as electron relay Co(bipy)$_3$Cl$_2$ which we synthetized from CoCl$_2$ · 6H$_2$O p.a. Merck and Bypiridil Merck, under reductive atmosphere, triethanolamine (TEOA) Merck, as electron donor and PtCl$_6$K$_4$ prepared by precipitating hexachloroplatinic acid with a KCl solution, as catalyst. We used as micellar medium three tensides: sodium dodecyl sulphate (NaDS), cetyl dibezylammonium chloride (CDBAC) and Tween 20.

RESULTS AND DISCUSSION

We carried out our experiments using a proflavine solution of 10^{-5}M concentration with various amounts of Co(bipy)$_3^{2+}$ in the three detergents, in order to verify the Stern-Volmer equation from fluorescence measurements. Figure 5 exemplifies one of our experiments carried out in a NaDS solution of 8.8×10^{-3}M. The value of the electron transfer rate constant was calculated from the plot of the Stern-Volmer equation (7):

$$\frac{I_e}{(I_e)_R} = 1 + k_{\mathrm{el.tr}}\tau_{\mathrm{Ps^*}}[R] \qquad (7)$$

We used also the same method for the other two micellar solutions approximating the same life time of excited proflavine $\tau_{\mathrm{Ps^*}}$, in the three detergents and in water. The results obtained are summarized in table 1.

One notices that the photochemical electron transfer from Ps_S^* to Co(II) complex is more efficient in micellar solutions than in water. At the same time one observes that in NaDS the rate constant $k_{\mathrm{el.tr.}}$ has the highest value, probably because both partners PfH$^+$ and Co(bipy)$_3^{+2}$ with positive charges are associated to the surfactant negative surface. [3]

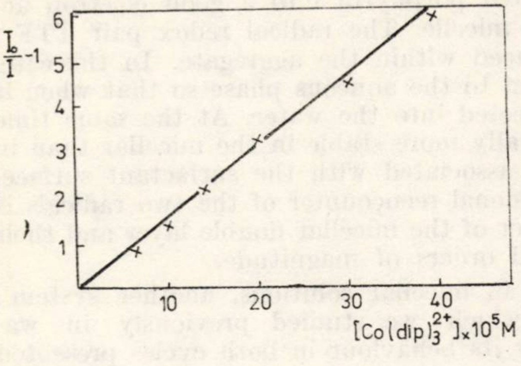

Fig. 5. — The plot of the Stern-Volmer equation for proflavine/$Co(bipy)_3^{2+}$ system in NaDS solution ($8.8 \times 10^{-3}M$).

Table 1

Rate constants of the electron transfer process and the corresponding amounts of H_2 evolved on irradiation with visible light

Medium	$k_{el.tr.}$, $M^{-1}s^{-1}$	H_2, μmoles
H_2O	8.2×10^9	72
NaDS $8.8\times10^{-3}M$	9.0×10^{11}	9
CDBAC $3.5\times10^{-3}M$	3.4×10^{10}	51
Tween 20 $8.4\times10^{-3}M$	6.8×10^{10}	85

In the cationic micelle the rate constant is only of about three times higher than in water due to the fact that the positive surface of tenside repels the photosensitizer as well as the electron relay to the aqueous phase where the electron transfer takes place similarly as in water (of course, with another distribution of the partners).

In the nonionic micelle the rate constant differs with an order of magnitude higher than in the cationic surfactant and lower than in the anionic one.

The results concerning the relay thermal cycle are also summarized in Table 1 by the amounts of H_2 evolved under three hours irradiation of 5 ml solution samples, with visible light of a Hg lamp (250 W). One notices that the smallest amount of hydrogen determined gas-chromatographically is obtained in NaDS where the electron transfer rate constant is the highest. This denotes that the back electron transfer is also favorized in this micelle on the same ground as for the forward one. At the same time the highest value for the H_2 evolved amount is, in Tween 20 solution, in a concentration much higher than its c.m.c. one. Therefore, we considered of interest to investigate our system: proflavine/Co $(bipy)_3^{2+}$/ TEOA/Pt cat., by analysing the behaviour of its components in this nonionic micelle.

Figure 6 presents the absorption spectrum of proflavine in Tween 20 of different concentration solutions.

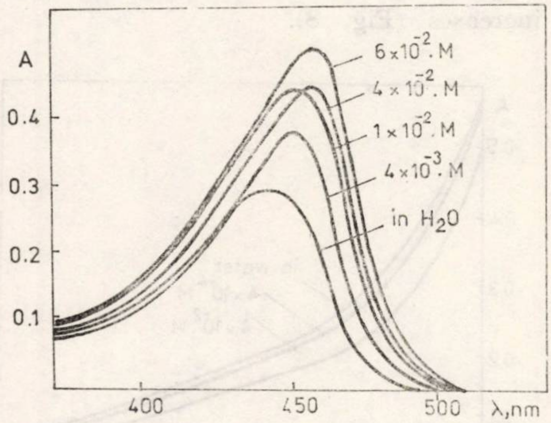

Fig. 6. — Absorption spectrum of 10^{-5}M proflavine in solutions of various Tween 20 concentrations.

With the increase of Tween 20 concentration one observes hyperchromic and bathochromic effect in comparison with the aqueous solution. Such behaviour suggests the formation of a proflavine-micelle complex by outside hydrogen bonding where the polyethoxylated chains are concentrated. For one of the investigated Tween 20 solutions, 10^{-2}M, we proceed to the optimization of the proflavine concentration in terms of the H_2 amounts, as figure 7 shows. The increase of photosensitizer concentration up to 1.5 10^{-3}M increases also the evolved amount of H_2 after which it remains constant in agreement with the limited capacity of detergent to bound proflavine, at the used micelle and PfH^+ concentrations.

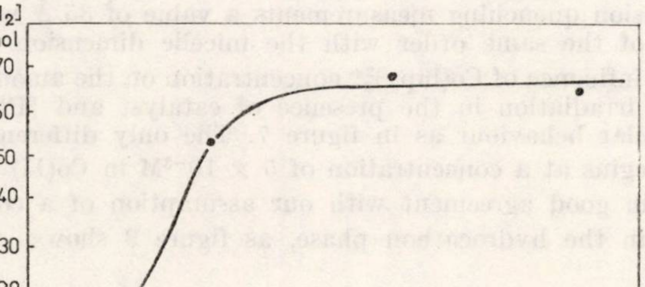

Fig. 7. — The plot $H_2\mu$ moles versus proflavine concentration in Tween 20 10^{-2}M.

Similar experiments were also carried out with the eletron relay. The absorption spectrum of $Co(bipy)_3^{2+}$ in aqueous solutions of Tween 20 points out the decrease of the absorbance when tenside concentration increases (Fig. 8).

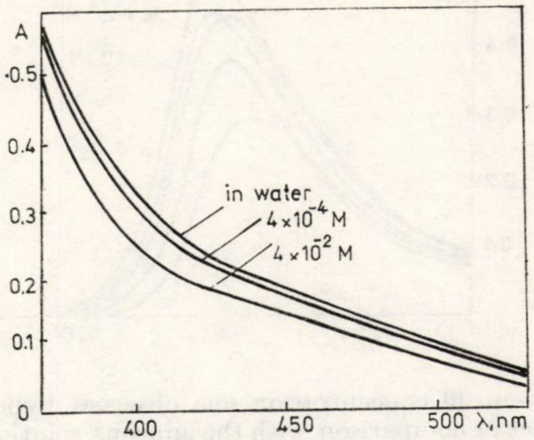

Fig. 8. — Absorption spectrum of $Co(bipy)_3^{2+}$ in solutions of different Tween 20 concentrations.

This behaviour suggests the Co(II) complex solvation in the micellar phase so that the electron transfer from the proflavine bounded at the micelle surface takes place by tunnelling to inside. This conclusion is supported also by the value of the critical distance R_c for which the electron transfer rate is equal to the fluorescence emission rate. We determined from emission quenching measurements a value of 35 Å which is approximately of the same order with the micelle dimension.

The influence of $Co(bipy)_3^{2+}$ concentration on the amount of evolved H_2 under irradiation in the presence of catalyst and $[PfH^+] = 10^{-3}M$, has a similar behaviour as in figure 7. The only difference is that the plateau begins at a concentration of $5 \times 10^{-3}M$ in Co(II) complex. This result is in good agreement with our assumption of a complex limited solvation in the hydrocarbon phase, as figure 9 shows.

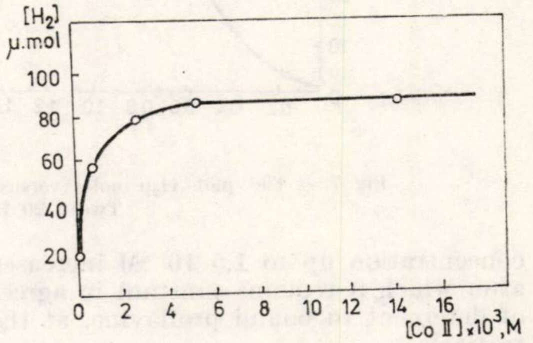

Fig. 9. — The variation of the H_2 amounts evolved under irradiation in the presence of various Co(II) complex concentrations.

Finally we carried out in the same manner experiments with the Pt catalyst and obtained the behaviour shown in figure 10. One notices that for a catalyst concentration of 2.5 10^{-4}M, is obtained the maximum amount of H_2. We interpret it by the fact that at this concentration the colloidal Pt in solution under irradiation, which acts as a filter for the proflavine light absorption, can be already observed. But it is surprising the absorption spectrum of the catalyst in a Tween 20 solution of 10^{-2}M, the same concentration we used at the photochemical electron transfer process investigation. Its absorption is smaller than that in water as figure 11 shows.

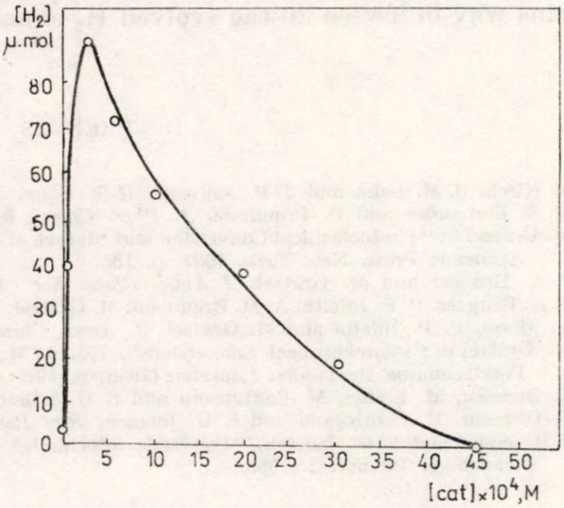

Fig. 10. — The plot H_2 μ moles versus catalyst concentration.

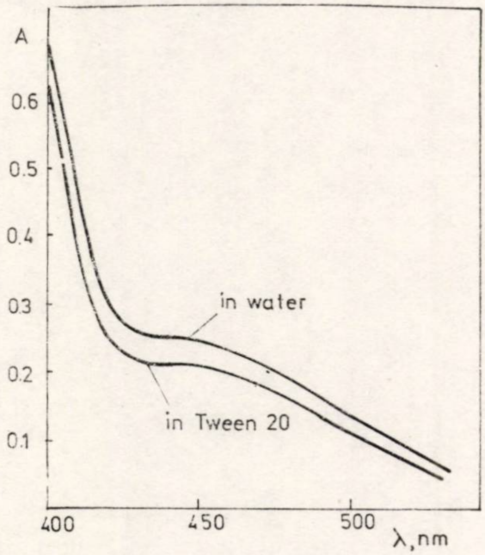

Fig. 11. — The absorption spectrum of $PtCl_6K_4$ in water and in a 10^{-2}M Tween 20 solution.

This behaviour shows also that the catalyst is solved in a small amount in the core of the aggregate. In this case Co(I) species appeared inside the aggregate reduce the water molecules existent at the micelle core periphery in the presence of the catalyst. Under such conditions the back electron transfer to the bounded proflavine is prevented and explains why in Tween 20 the evolved H_2 amount has the highest value.[10]

REFERENCES

[1] M. Kirch, J. M. Lehn and J. P. Sauvage, *Helv. Chim. Acta*, **62**, 1345 (1979).

[2] M. S. Fernandez and P. Fromherz, *J. Phys. Chem.*, **81**, 1755 (1977).

[3] M. Grätzel in "Photochemical Conversion and Storage of Solar Energy", Ed. J. S. Connolly, Academic Press, New York, 1981, p. 136.

[4] P. A. Brugger and M. Grätzel, *J. Amer. Chem. Soc.*, **102**, 2461 (1980).

[5] P. A. Brugger, P. P. Infelta, A. M. Braun and M. Grätzel, *J. Amer. Chem. Soc.*, **103**, 320 (1981).

[6] Y. Moroi, P. P. Infelta and M. Grätzel, *J. Amer. Chem. Soc.*, **101**, 573 (1979).

[7] M. Grätzel in "Photochemical Conversions", Ed. A. M. Braun, IOCD, UNESCO, Presses Polytechnique Romandes, Lausanne (1983) p. 191.

[8] T. Oncescu, M. Stefan, M. Contineanu and S. G. Ionescu, *Solar Energy* (in press).

[9] T. Oncescu, M. Contineanu and S. G. Ionescu, *Rev. Roumaine. Chim.*, **27**, 95, (1982).

[10] T. Oncescu and S. G. Ionescu, "Conversie fotochimică şi stocare de energie solară", Ed. Academiei, Bucharest, 1985.

Revue Roumaine de Chimie, 32, 7, 647–652 (1987)

MIXED SOLUTIONS OF CATIONIC AND NONIONIC SURFACTANTS

MIHAELA OLTEANU
Department of Physical Chemistry, Polytechnic Institute, Blvd. Republicii, 13,
Bucharest, Romania

Received November 25, 1986

Critical micelle concentration (CMC) of dodecylpyridinium iodide and dodecylpolyoxyethyleneglycol mixture was studied by the variation of surface tension, electrical conductivity and light absorption with molar ratio N_1 and concentration of the cationic surfactant. Up to $N_1 = 0 - 0.5$, the critical micelle concentration of the mixture takes values which are lower than CMC_1 of cationic surfactant, and higher than CMC_1, for N_1 ranging within 0.5 – 1. Increase of CMC may be explained by decreasing the dielectric constant, the polarity at micelle surface of the cationic surfactant in the mixture.

The mixtures of solutions of amphyphilic molecules with various chemical structures exhibit non-ideal behaviour compared to that of mixtures of compounds of similar chemical structure depending on the type of polar group and the length of hydrocarbon chain.[1,2] The theories advanced in the literature [3,4] for non-ideal mixtures apply to a restricted number of systems.

The mixtures of cationic and non-ionic amphyphilic molecules which were scarcely studied deviate strongly from ideality throughout the whole range of values of molar ratios with respect to their capacity of micellization [5] and micellar weight. [6]

The solutions of alkyltrimethylammonium halide cationic surfactants with polyoxyethyleneglycol non-ionic surfactants form mixed micelles whose critical micelle concentrations are lower than those calculated for single surfactants. [5-8]

In this contribution mixtures of dodecylpyridinium iodide cationic surfactants with polyethylenglycol non-ionic surfactants are studied. Amphyphilic molecules with the same hydrocarbon chain were selected because some specific interactions between I^- and pyridinium ions may occur with formation of charge transfer complexes. [9-10] In the case of surfactants with equivalent hydrocarbon chain the interactions between polar groups take the largest share in the determination of interaction parameter β.[4]

The behaviour of surfactant mixture was studied by surface tension, electrical conductivity and light absorption measurements.

EXPERIMENTAL

Dodecylpyridinium iodide (Do Py I) was synthesized and purified as described elsewhere. [11] The variation of surface tension and optical density have yielded a critical micelle concentration (CMC_1) of $5.3 \cdot 10^{-3}$ mole/L while the corresponding value contributed by the variation of electrical conductivity was $5.0 \cdot 10^{-3}$ mole/L. These values agree well with the data in literature.[10-12]

Dodecylpolyoxyethyleneglycol ($C_{12}E_{10}$) exhibited an average degree of ethoxylation of 10.3 and a CMC_2 of $1 \cdot 10^{-4}$ mole/L as coming out of the concentration variation of surface tension.

A Du Nouy tensiometer with platinum ring was employed in surface tension measurements; the accuracy was $\pm$ 0.1 dyne/cm. The electrical conductivity was determined with a Radelkis conductometer and the light absorption with a Unicam SP800 spectrophotometer.

Solutions were prepared with distilled water whose specific conductivity was $2 \cdot 10^{-6}$ ohm$^{-1} \cdot$ cm^{-1} and kept at 25 $\pm$ 0.1 °C during the runs.

RESULTS AND DISCUSSION

Figures 1 and 2 show the variation of surface tension and specific conductivity of Do PyI – $C_{12}E_{10}$ mixtures at various molar fractions of cationic surfactant.

Depending on component ratio, the breakpoints of the curves corresponding to the formation of some mixed micelles (or micelles whose properties are different from those of purely ionic ones) take values which are lower than CMC_1 up to cationic surfactant mole fraction $N_1 = 0.5 - 0.7$ and higher than CMC_1 for N_1 ranging within $0.5 - 1.0$ (Fig. 3).

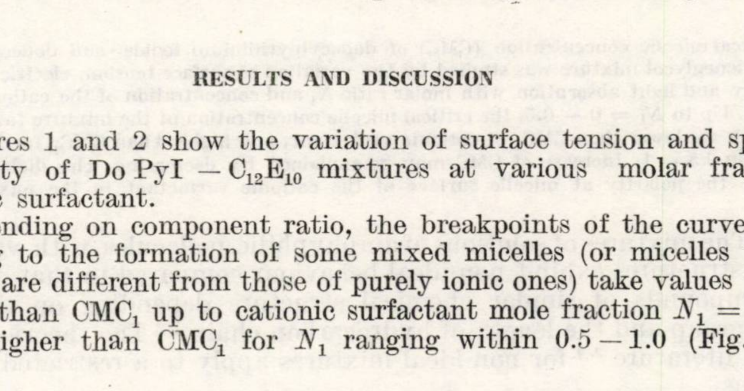

Fig. 1. — Surface tension for mixture of DoPyI – $C_{12}E_{10}$ for different molar ratios N_1.

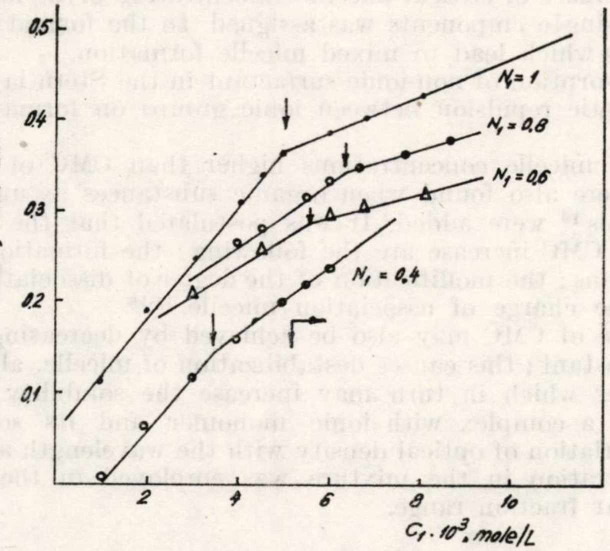

Fig. 2. — Dependence of specific conductivity on concentration for DoPyI — $C_{12}E_{10}$ mixture for different molar ratios.

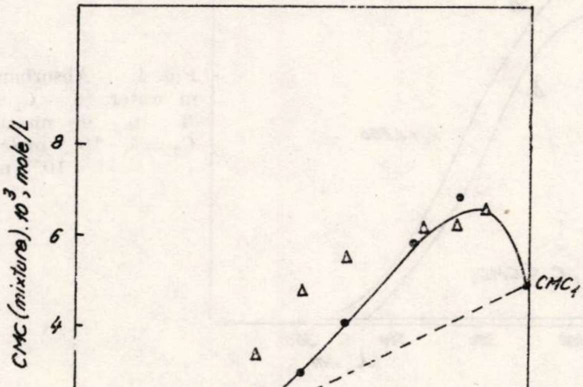

Fig. 3. — Critical micelle concentration for mixture DoPyI — $C_{12}E_{10}$ vs. molar ratio N_1 : surface tension data (●); specific conductivity data (Δ).

The decrease of critical micelle concentration of the mixture against the CMC of single cmponents was assigned to the formation of hydrophobic bonds which lead to mixed micelle formation.

The adsorption of non-ionic surfactant in the Stern layer diminishes the electrostatic repulsion between ionic groups on formation of mixed micelles. [4-7]

Critical micelle concentrations higher than CMC of pure cationic surfactant were also found when organic substances as urea[13] and aromatic alcohols[14] were added. It was postulated that the factors which play part in CMC increase are the following: the formation of ion pairs of complex ions; the modification of the degree of dissociation of surfactant ions; the charge of association micelle. [15,16]

Increase of CMC may also be achieved by decreasing the medium dielectric constant; this causes destabilization of micelle, alters the structure of water which in turn may increase the solubility of monomer, formation of a complex with ionic monomer and its solubilization. [14]

The variation of optical density with the wavelength and the surfactant concentration in the mixture was employed in the investigation of high molar fraction range.

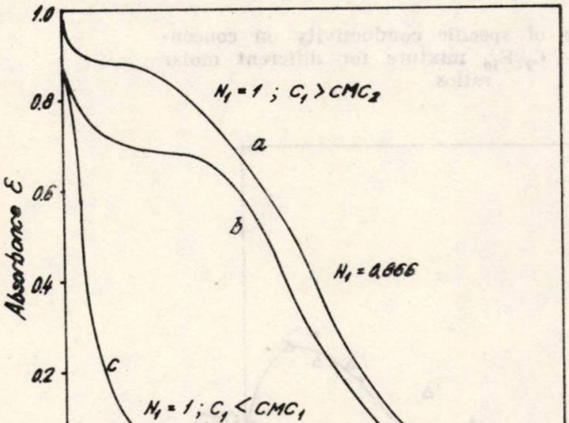

Fig. 4. — Absorbance data of DoPyI in water: a — $C_1 = 6.5 \cdot 10^{-3}$ mole/ /L; b — in mixture with, $C_{12}E_{10}$ $C_2 = 1 \cdot 10^{-3}$ mole/L; c — $C_1 = 2 \cdot 10^{-3}$ mole/L.

Fig. 4 shows that the micelles absorb stronger than non-micellar solution, the addition of non-ionic surfactant to a micellar solution of Do Py I lowers the absorbance and shifts the maximum from 285 nm towards 295 nm ($N_1 = 0.866$). This behaviour points to a demicellization of ionic solution accompanied by a decrease of polarity at micellar surface indicated by the shift towards higher wavelength. [10]

Figs 5 and 6 support the results of surface tension and electrical conductivity measurements. At mole fractions, about $N_1 = 0.8 - 0.9$, the non-ionic surfactant destabilizes cationic micelles. The breakpoint on the curve for the mixture with $N_1 = 0.864$ is located at $C_1 = 6.38 \cdot 10^{-3}$ mole/L (Fig. 5) a value which is close to $C_i = 6.3 \cdot 10^{-3}$ mole/L resulted from k vs. c (Fig. 2) and $C_1 = 6.4 \cdot 10^{-3}$ mole/L from γ vs. c (Fig. 1). In Fig. 6 one can note that at constant concentration of cationic surfactant higher than CMC_1 and mole fractions $N_1 = 0.8 - 0.9$ there are absorption minima due to destabilization of cationic micelles.

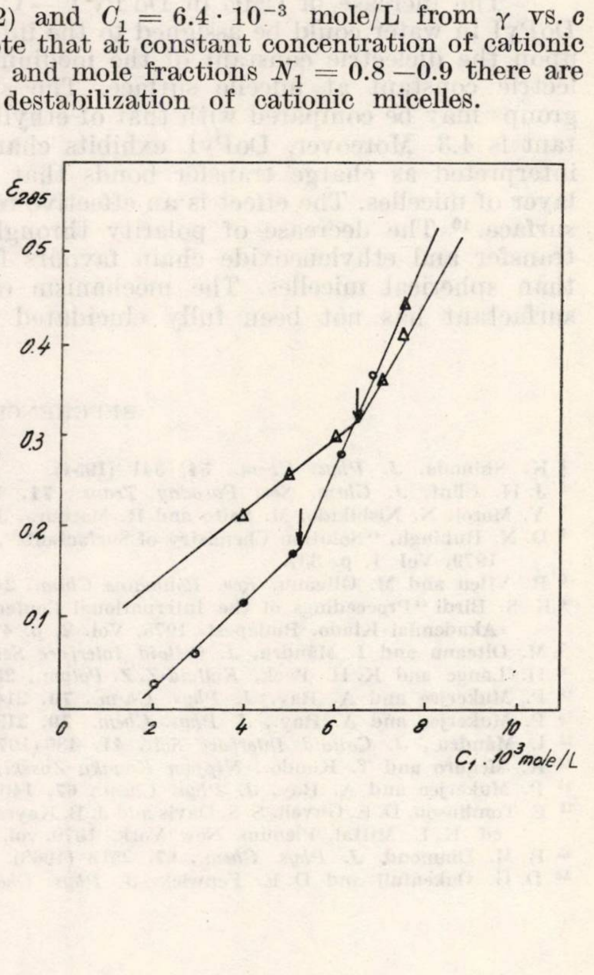

Fig. 5. — Absorbance data at $\lambda = 285$ nm for DoPyI in water (●) and in mixture with $C_{12}E_{10}$, $C_2 = 1 \cdot 10^{-3}$ mole/L (Δ).

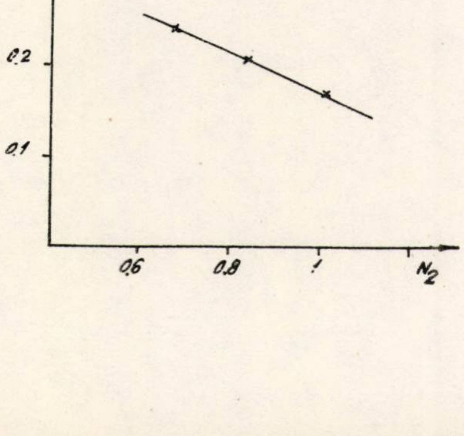

Fig. 6. — Absorbance data at $\lambda = 285$ nm for mixture of DoPyI$-C_{12}E_{10}$ vs. molar ratio N_1 : × — $C_1 = 4.5 \cdot 10^{-3}$ mole/L ; ○ — $C_1 = 6.5 \cdot 10^{-3}$ mole/L ; ● — $C_1 = 7.5 \cdot 10^{-3}$ mole/L.

The increase of CMC in Do Py I $-$ $C_{12}E_{10}$ mixture above CMC_1 of DoPyI in water could be assigned to the influence of non-ionic surfactant upon the dielectric constant of the medium and to the decrease of dielectric constant at micelle surface. The structure of polyoxyethylenic groups may be compared with that of ethylic ether whose dielectric constant is 4.3. Moreover, DoPyI exhibits characterstic spectra which were interpreted as charge transfer bonds that modify the electrical double layer of micelles. The effect is an effective reduction of polarity at micelle surface.[10] The decrease of polarity through the two effects i.e. charge transfer and ethyleneoxide chain favours formation of ion pairs rather than spherical micelles. The mechanism of CMC increase for cationic surfactant has not been fully elucidated so far.

REFERENCES

[1] K. Shinoda, *J. Phys. Chem.*, **54**, 541 (1954).

[2] J. H. Clint, *J. Chem. Soc. Faraday Trans.*, **71**, 1327 (1975).

[3] Y. Moroi, N. Nishikido, M. Saito and R. Matuura, *J. Colloid Interface Sci.*, **52**, 356 (1975).

[4] D. N. Rubingh, "Solution Chemistry of Surfactants", ed. K. L. Mittal, Plenum, New York, 1979, Vol. 1, p. 337.

[5] R. Vîlcu and M. Olteanu, *Rev. Roumaine Chim.*, **24**, 509 (1979).

[6] K. S. Birdi "Proceedings of the International Conference on Colloid and Surface Science", Akademiai Kiado, Budapest, 1975, Vol. 2, p. 473.

[7] M. Olteanu and I. Mândru, *J. Colloid Interface Sci.*, **106**, 247 (1985).

[8] H. Lange and K. H. Beck, *Kolloid-Z. Z. Polym.*, **251**, 424 (1973).

[9] P. Mukerjee and A. Ray, *J. Phys. Chem.*, **70**, 2144 (1966).

[10] P. Mukerjee and A. Ray., *J. Phys. Chem.*, **70**, 2150 (1966).

[11] I. Mândru , *J. Colloid Interface Sci.*, **41**, 430 (1972).

[12] K. Meguro and T. Kondo., *Nippon Kagaku Zasski*, **80**, 818 (1959).

[13] P. Mukerjee and A. Ray, *J. Phys. Chem.*, **67**, 140 (1963).

[14] E. Tomlinson, D. E. Guveli, S. S. Davis and J. B. Kayes, "Solution Chemistry of Surfactants", ed. K. L. Mittal, Plenum, New York, 1979, vol. 1, p. 355.

[15] R. M. Diamond, *J. Phys. Chem.*, **67**, 2513 (1963).

[16] D. G. Oakenfull and D. E. Fenwick, *J. Phys. Chem.*, **78**, 1759 (1974).

Revue Roumaine de Chimie, 32, 7, 653–661 (1987)

PHYSICO-CHEMICAL CHARACTERIZATION OF THE TWO-PHASE SYSTEM EMPLOYED IN EMULSION POLYMERIZATION OF VINYL CHLORIDE

M. MARINESCU, V. BUTUCEA *, GEORGETA POPESCU, ADRIANA SÎRBU*, ADRIANA IONESCU*, CECILIA GEORGESCU* and B. ALBU
ICECHIM – Center of Physical Chemistry, Bucharest, Romania
*ICECHIM – Research Center for Plastic Materials, Bucharest, Romania

Received October 30, 1986

A physicochemical study was carried out on a two-phase system similar to that employed in emulsion polymerization of vinyl chloride. The influence of the ternary system of emulsifiers and the modifications it may exert upon the physico-chemical characteristic of the obtained polyvinylchloride was studied. The methods employed were : conductometric titration, interface tension measurements, differential scanning calorimetry (DSC) and wide band nuclear magnetic resonance (NMR), applied either to the biphasic system water-trichlorethylene (TCE)-emulsifier system, or to the preemulsion reaction mixture that represents one third of the aqueous phase with the entire ternary system of emulsifiers. On the basis of these data, the biphasic system was characterised and information was acquired about its structure. The part played by each of the three emulsifiers utilized i.e. unsulphated C_{16-18} alcohol, 30% sulphated C_{16-18} alcohol and nonylphenol ethoxylated with 30 moles ethylene oxide was evidenced and described.

INTRODUCTION

The emulsion polymerization of vinyl chloride (VC) is a process which has not been only studied but technologically applied, throughout the past three decades.

This contribution achieves a physico-chemical characterization of some two-phase systems similar to those employed for emulsion polymerization of VC according to the technology currently applied at Turda Chemical Factory.

A ternary emulsifier system consisting of :

- ionic surfactant – sulphated cetanic alcohol C_{16-18} (SCA) ;
- cosurfactant – nonsulphated cetanic alcohol C_{16-18} (NCA) ;
- nonionic surfactant – nonylphenol ethoxylated with 30 moles ethylene oxide (NF_{30})

was employed to obtain special qualities of polyvinylchloride (PVC) by emulsion polymerization of VC. This choice was determined by the need of controlling the properties of PVC resulted, i.e. of its particle size ; this requires the control of the monomer in water emulsion drop size which in turn controls the polymerization process.

Polyvinylchloride latex of higher quality is conditioned by the obtention of a primar polymer particle of 1 –2 μ which may be achieved only through the adjustment of concentration ratios of the three components of the emulsifier system.

Likewise, it is necessary that the monomer emulsions in water possess higher stability against diffusive degradation to avoid initiation of the reaction outside monomer drops, taking into account that the initial emulsion drop size distribution ranges within 0.2 – 1.0 μ. Besides exerting some effects upon this stability, the surfactant-cosurfactant concentration ratio influences the kinetics of polymerization and the geometry of resulted PVC particle.

Previous studies $^{1-4}$ came to the following conclusions :

– the surfactant-cosurfactant ratio is determined for the degree of dispersion of the monomer in water, being directly related to the interface tension in the system ;

– the stabilizing effect of the cosurfactant and its efficiency against the diffusive degradation of the monomer water emulsion are higher, the more insoluble in water the monomer is ;

– when interface tension drops below a certain value i.e. the monomer dispersion in aqueous phase decreases below 0.7 μ, one may speak of a predetermined initiation in monomer drops, the initiation in micelles remaining a secondary aspect of the process.

As we were aware of all these facts we have tried to acquire information about the physico-chemistry of the system and the way it is influenced by changes of emulsifier system to enable us to improve the control of the process – the polymerization reaction of VC in emulsion.

We have utilized conductometric titration, which consists of monitoring the variation of the conductivity of the system as one phase mixes with the other, determinations of interface tension, differential scanning calorimetry (DSC) and wide band nuclear magnetic resonance (NMR).

The results obtained have allowed not only the confirmation of optimum solution applied in industry for a better control of the process but, at the same time, the advancement of a hypothesis regarding the structure of the system before initiation i.e. before polymerization reaction starts.

EXPERIMENTAL PART

Polymerization was conducted in a system consisting of :

– aqueous phase : water (H_2O/monomer ratio 2 : 1) ;

– organic phase : VC monomer supplied by Brazi Chemical Works ;

– emulsifier system : surfactant–sulphated cetanic alcohol (SCA), cosurfactant–nonsulphated cetanic alcohol (NCA), nonionic surfactant (NF_{30}), all supplied by "Detergentul" Timişoara Factory ;

– initiator : p.a. grade potassium persulphate "Reactivul" Bucharest.

This system was polymerized two hours at 6.6 atm. and 50°C. Then the polymer latex was separated from the aqueous phase and characterized from the standpoint of conversion and particle size.

The conductometric titration was achieved pouring aqueous phase over the organic phase – that was trichlorethylene (TCE) instead of VC which is volatile in normal solutions and may not be utilzed – in the presence of the already mentioned emulsifier system ; a Radiometer conductometer was employed with a calibrated cell of known constant. The interface tension measurements were made with the volume drop method [5] utilizing metallic capillaries of known radius.

Differential scanning calorimetries were carried out with a Du Pont DSC 1090 Thermal Analyzer while those of broad line NMR with a Romanian spectrometer (IFTAR-Bucharest).

RESULTS AND DISCUSSION

Table 1 shows the influence of emulsifier system, its concentration and of surfactant-cosurfactant concentration ratio, upon the kinetics of polymerization or particle size of latex obtained; there are listed the results of several experiments of polymerization carried out in conditions mentioned above. In case nonionic surfactant NF_{30} is added to the anionic one (SCA) the rate of polymerization drops first, then it increases, as cosurfactant C_{16-18} is added, close to the initial value which is obtained with ionic surfactant as single emulsifier added to the system. One can notice in table 1 that the size of PVC particles is improved: they rise from 0.3 to 0.8 μ.

Tabel 1

The dependence of VC polymerization on the emulsifier concentration and emulsifiers concentration ratio

System*	Conc. g/L	NCA/SCA ratio	Polym. rate g PVC/hour	Average particle diameter μ	Obs.
NCA	0				
SCA	1.8	—	50	0.3	
NF_{30}	0				
NCA	0				
SCA	1.8	—	7	—	too little conversion
NF_{30}	4.7				
NCA	1.8				
SCA	1.8	1 :1	28	0.5	
NF_{30}	4.7				
NCA	3.6				
SCA	1.8	2 :1	45	0.8	
NF_{30}	4.7				
NCA	7.2				
SCA	1.8	4 : 1	48	0.8	
NF_{30}	4.7				

* Polymerizations were conducted under the conditions mentioned in the text (6 atm., 50°C); concentrations (gram/Liter) given in the table refer to the entire reaction mixture volume; the volume phase ratio VC : water was 1 : 2.

Polymerization data have shown that the optimum surfactant-cosurfactant is 1 : 4 whenever the concentration of nonionic emulsifier is about twice that of the ionic one; this is shown in Table 1 entry no. 5.

The data in Table 1 show that the three components of surfactant system employed influence the polymerization process, determining the monomer drop size distribution in aqueous phase, as well as the initiation and kinetics of the whole process.

To interpret these results several physico-chemical measurements were carried out on the two-phase system aqueous phase-organic phase (TCE) in the presence of emulsifier.

Conductometric titration is a technique developed in order to characterize other two phase systems studied in relation with polymerization in heterogeneous system of another acrylic monomer, the acrylamide.[6] It is achieved through titration of organic phase (TCE) with aqueous phase at 50°C in the presence of the presented emulsifier system as such, or modified as the study requires. Each phase contains that part of the emulsifier which is compatible with it; the cosurfactant, cetanic alcohol (NCA), solves in TCE whereas the ionic SCA and nonionic NF_{30} surfactants solve in about 1/3 of aqueous phase, calculated for the ratio water : TCE 2 : 1 system; this 1/3 part of aqueous phases is called "preemulsion flota". The TCE titration is first effected with this aqueous preemulsion and then continued with pure water. Thus the whole emulsifiers complex (whatever their concentration in the system) is present in the system at nominal concentrations when the titration volume ratio $V_{H_2O}/V_{TCE} = 0.7$ is reached.

The method supplies basically the following information[6]:

— volume jump ratio, $(V_{H_2O}/V_{TCE})_{jump}$, as ratio of phase volumes for which the system reverses from an *A*/*U* emulsion to a *U*/*A* one; this transition is accompanied by a sudden increase of conductivity;

— the magnitude conductivity jump, λ_{jump}, which we regard as the maximum λ value; the conductivity reaches a plateau during titration wich occurs after the inversion of the system took place.

Both quantities are sensitively dependent on the nature and concentration of emulsifiers employed, on the concentration or nature of the salt if its presence in the system was considered useful.

Figure 1 shows several conductometric titrations effected on some emulsifier systems in which the cosurfactant : surfactant ratio was modified through the increase of the amount of cetanic alcohol (NCA) in the system. Examination of Fig. 1 shows that on the abscissa one can easily locate the point where jump occurs i.e. the jump volume ratio $(V_{H_2O/TCE})_{jump}$ while on ordinate the jump conductivity λ_{jump}. In Fig. 1 the jump appears as the maximum of titration curves.

One can notice on the figure that both these quantities vary with the cosurfactant/surfactant ratio; the system whose cosurfactant/surfactant ratio is 4 : 1 exhibits a $(V_{H_2O}/V_{TCE})_{jump}$ ratio of 0.25, while λ_{jump} is maximum for a volume ratio approximately equal to that for which all emulsifiers are already introduced in the system (0.7). Figure 1 also shows that $(V_{H_2O}/V_{TCE})_{jump}$ and λ_{jump} increase and respectively decrease gradually either with the increase of cosurfactant/surfactant ratio from 5 : 1 to 6 : 1 or with its decrease from 3 : 1 to 2 : 1. All these data point to a maximum stabilty of the system reached for NCA : SCA ratio of 4 : 1 which was indicated as optimal by polymerization experiments (Table 1 entry 5).

These data are better emphasized if the two quantities $(V_{H_2O}/V_{TCE})_{jump}$ and λ_{jump} are plotted versus the concentration of cetanic alcohol in the sample (Fig. 2). For easier comparison the concentration of cetanic alcohol is expressed as the ratio of NCA concentration in titrated sample over that in the sample with NCA : SCA = 4 : 1.

Figures 1 and 2 suggest that the stability of the system is higher for phase ratios (aqueous over organic phase) lower than 2 : 1. This has suggested the decrease of aqueous volume in *VC* emulsion polymerization which entails a slight increase of latex particle size without marked modification of conversion kinetics. Similar data were obtained from conductometric titration and variation of nonionic emulsifier NF_{30} concentration in the system. These results are displayed in Fig. 3; the emulsifier concentration is like in Fig. 2 expressed as the ratio of NF_{30} in the sample

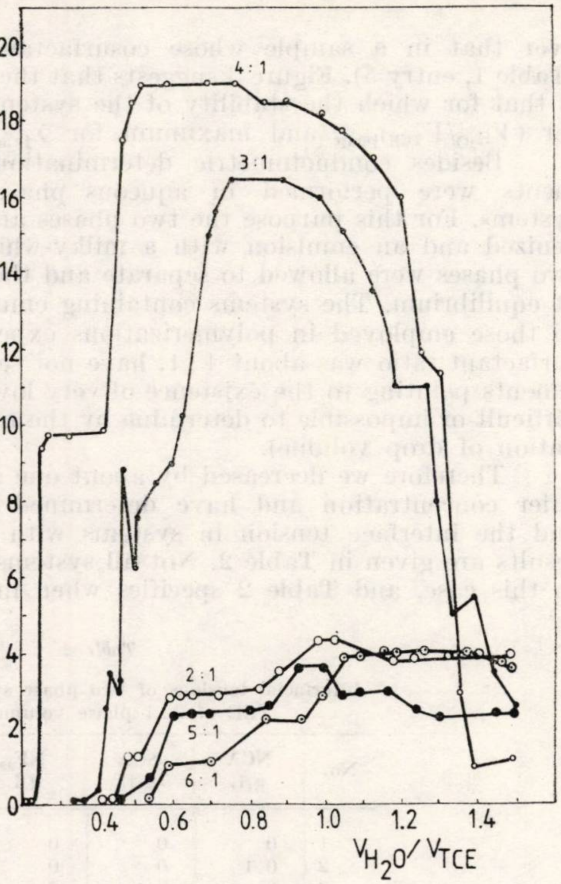

Fig. 1. — **Conductometric titration of TCE phase (with cosurfactant NCA added) with the aqueous phase (containing the sulphated cetanic alcohol SCA and NF_{30}), at different cosurfactant-surfactant volume phase ratios: 2 : 1, 3 : 1, 4 : 1, 5 : 1 and 6 : 1**

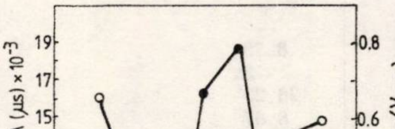

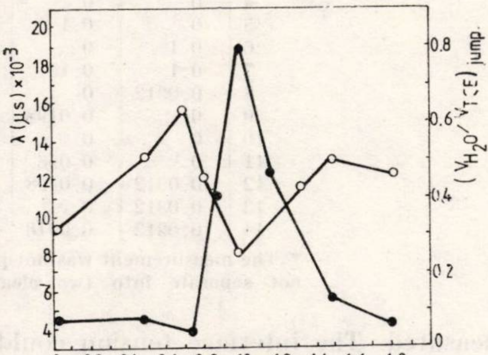

Fig. 2. — **The dependency of $(V_{H_2O}/V_{TCE})_{jump}$ and λ_{jump} obtained from conductometric titration curves on the cosurfactant NCA concentration in the titrated probe; the NCA concentration over NCA concentration in 4 : 1, NCA : SCA probe, ratio, was used instead the simple NCA concentration.**

Fig. 3. — **The dependency of $(V_{H_2O}/V_{TCA})_{jump}$ and λ_{jump}, obtained from conductometric titrations curveson the nonionic emulsifie¹ concentration NF_{30}; the NF_{30} concentration was expressed as (NF_{30} concentration in titrated probe)/(NF_{30} concentration in 4 : 1 NCA SCA probe) ratio.**

over that in a sample whose cosurfactant/ surfactant ratio was 4 : 1 (Table 1, entry 5). Figure 3 suggests that the concentration of NF_{30} chosen is that for which the stability of the system is optimum ; it is minimum for $(V_{H_2O}/V_{TCE})_{jump}$ and maximum for λ_{jump}.

Besides conductometric determinations, interface tension measurements were performed in aqueous phase : organic phase : emulsifier systems. For this purpose the two phases and the emulsifiers were homogenized and an emulsion with a milky-white aspect was obtained ; the two phases were allowed to separate and then the system was considered at equilibrium. The systems containing emulsifier in concentrations close to those employed in polymerizations experiments, whose cosurfactant/ surfactant ratio was about 4 : 1, have not separated even in lasting experiments pointing to the existence of very low interface tensions which are difficult or impossible to determine by the method we employed (determination of drop volume).

Therefore we decreased by about one order of magnitude the emulsifier concentration and have determined the emulsifier concentration and the interface tension in systems with one or two emulsifiers. The results are given in Table 2. Not all systems have been equilibrated even in this case, and Table 2 specifies when interface tension could not be measured. The interface tension could not be measured in the systems whose emulsifier concentrations was two-three times lower, except for the systems containing only either cosurfactant NCA, or surfactant SCA, either nonionic surfactant NF_{30}.

Table 2

Interfacial tensions of two phase systems water : TCE of 2 : 1 phase volume ratio

No.	NCA g/L	SCA g/L	NF_{39} g/L	γ dyn/cm
1	0	0	0	23.58
2	0.1	0	0	27.33
3	0	0.1	0	—*
4	0	0	0.1	—
5	0	0.1	0.1	—
6	0.1	0	0.1	8.79
7	0.1	0.1	0.1	−3
8	0.0312	0	00	26.23
9	0	0.0198		8.67
10	0	0	0.0219	10.72
11	0	0.098	0.0219	—
12	0.0312	0.0198	0	11.5
13	0.0312	0	0.0219	—
14	0.0312	0.0918	0.0219	5.78

* The measurement was not possible ; the system does not separate into two clear phases.

In these systems, whose emulsifier concentration was one order of magnitude lower, the interface tension was measurable in almost all cases (Table 2 entries 3, 10, 11, 13, 14). Table 2 suggests the following conclusions :

— NCA is the only emulsifier which raises the interface tension between the two phases i.e. H_2O and TCE (entries 2, 9);

— SCA appears as the component which strongly lowers the interface tension (Table 2, entry 10); thus it is the component which determines the curvature of interface;

— NF_{30} participates in formation of the interface, by contributing to a better mixing of phases and lowering interface tension wherever it is present;

— the synergetic effects are noticeable for NCA and NF_{30} (entry 7), for NCA and SCA (entry 13) and for all three emulsifiers in concentrations ten times lower than in polymerization mixture (entry 14);

— the interface tension for the two phases without emulsifier is reduced to one fifth by the presence of all the three components of the system of emulsifiers.

Figure 4 shows some of the results obtained by differential scanning calorimetry (DSC) for three preemulsion reaction mixtures at cosurfactant/ surfactant ratios of 4 : 1, 2 : 1, 1 : 1. Examination of Fig. 4 shows that the major thermal effect due to transformation of water in the system increases in the same sequence; the more water in the system, the higher the enthalpy effect of rising temperature. Also in Fig. 4 the DSC curve drawn for 4 : 1 system shows another effect observed at about –20°C (curve 1).

Figure 5 shows a detail of this thermal effect; the figure also shows the value of thermal exchange, about 0.61 J/g, close to the resolution

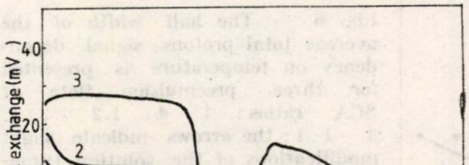

Fig. 4. — Differential scanning calorimetry (DSC) of some preemulsion flota characterized by different NCA : SCA ratios : 1 — 4 : 1 2 — 2 : 1; 3 — 1 : 1.

Fig. 5. — The enlarged enthalpic effect presented in fig. 4 on curve 1 for 4 : 1 NCA : SCA, preemulsion flota; the magnitude of the thermal effect, in J/g, as well as its thermal points, are also represented.

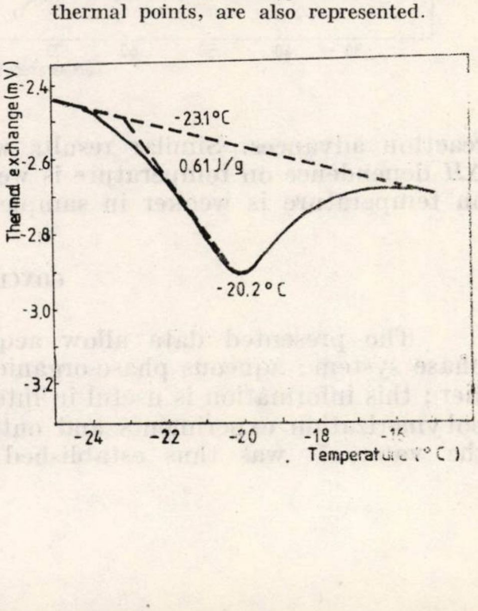

limit of the apparatus. This effect points to a mesophasic transition occurring at this temperature below 0°C.

Such mesophasic transitions are usually specific to liquid crystal systems with a high degree of ordering. These determinations were thought to evidence changes occurring in preemulsion reaction mixtures i.e. only in aqueous phase, by variations of cosurfactant/ surfactant ratio. For a cosurfactant/ surfactant ratio of 4 : 1 it is likely that the system structure shows a certain degree of mesophasic ordering, originating in lamellar micelles present in aqueous phase at higher concentration of surfactant. [7] In fact, such systems look like a milky paste of high viscosity. The preemulsion reaction mixture is brought to this state by previous heating to 70°C, followed by cooling to room temperature.

The same samples were subjected to wide band NMR measurements. In each of the three samples the dependence of the half width of averaged signal for all protons in the sample on the sample temperature, was recorded and represented. The results are shown in Fig. 6. It is also simple with 4 : 1 cosurfactant/ surfactant ratio, which exhibits obvious phase transition ; a minimum of line halfwidth is correlated with a maximum proton mobility. Such a minimum of ΔH is seen for that sample (Fig. 6, curve 1) at about 50°C which is the temperature where polymerization reaction advances. Similar results were obtained for 1 : 1 sample ; the ΔH dependence on temperature is weaker in sample ; the ΔH dependence on temperature is weaker in sample 2 : 1.

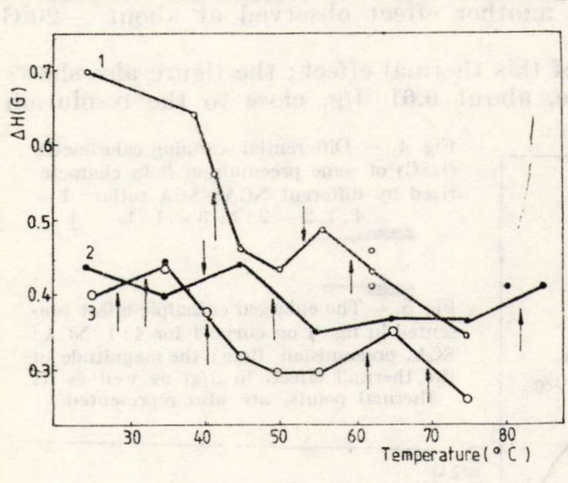

Fig. 6. — The half width of the average total protons signal dependency on temperature is presented for three preemulsion flota of SCA ratios : 1 — 4 : 1, 2 — 2 : 1, 3 — 1 : 1 ; the arrows indicate slight modifications of the solution turgescence.

CONCLUSIONS

The presented data allow acquiring information upon the three phase system : aqueous phase-organic phase (TCE instead of CV)-emulsifier ; this information is useful in interpretation of the results supplied by polymerization experiments and outlines new trends of the research on the vater. It was thus established that :

— SCA plays the main role in the emulsifier system; it is the surfactant that determines the interface curvature and is determining in emulsifying of TCE (CV) in water as well as in microemulsifying water in TCE (CV); it also determines the interface charge and together with NF_{30} ensures its curvature;

— the system structure is probably that of a double emulsion; this statement is based on the existence in the system, at those emulsifier concentrations favourable to polymerization reaction, of very low interface tension;

— NCA, cosurfactant plays the main part in hardening the interface towards its nonpolar side; together with the other two components of the system it ensures the stability of shape and dimensions of emulsion drops which is very important during polymerization;

— NF_{30}, together with SCA, ensure a better dispersion of two phases and stabilize the interface on its polar side. All these data may serve to further optimization of technologies VC emulsion polymerization in order to improve the quality of PVC obtained.

REFERENCES

[1] A.R.M. Azad, J. Ugelstadt, R. M. Fitch and F. K. Hansen, *ACS Series 24, Emulsion Polymerization*, **24**, 1 (1976).

[2] J. Ugelstad, *Makromol. Chem.*, **179**, 815 (1978).

[3] J. Ugelstad, K. Herder Kaggerund, F. K. Hansen and A. Berge, *Makromol. Chem.*, **180** 737 (1979).

[4] J. Ugelstad, P. C. Mørk, K. Herder Kaggerund, T. Ellingsen and A. Berge, *Advances in Colloid and Interface Science*, **13**, 101 (1980).

[5] I. Mîndru and D. M. Ceacăreanu, "Chimia Coloizilor și Suprafețelor", Editura Tehnică, Bucharest, 1976.

[6] M. V. Dimonie, C. M. Boghină, N. N. Marinescu, M. N. Marinescu, C. I. Cincu and C. G. Oprescu, *Eur. Polym. J.*, **18**, 639 (1982).

[7] L. D. Prince, "Microemulsions. Theory and Practice", Academic Press, New York, San Francisco, London, 1977.

Revue Roumaine de Chimie, **32**, 7, 663–670 (1987)

EJECTION CURVES AND MISCIBILITY OF EGG LECITHIN WITH SOME CAROTENOID DERIVATIVES

MARIA TOMOAIA-COTIŞEL, JÁNOS ZSAKÓ and EMIL CHIFU
University of Cluj-Napoca, Faculty of Chemical Technology, Physical Chemistry Department, 3400 Cluj-Napoca, Romania

Received December 2, 1986

Ejection curves, i.e. surface pressure (π) *vs.* A/x_1^{OM} curves are given for ethyl ester of β-apo-8'carotenoic acid (EEC) : egg lecithin (EL) and zeaxanthin monopalmitate (ZP) : EL mixed monolayers, spread at the air/ water interface (A-mean molecular area, x_1^{OM} — molar fraction of EL in the monolayer before collapse). Immiscibility of EEC with EL, both in the monolayer (M) and in the collapsed bulk phase (C) is observed. On the contrary, ZP and EL are completely miscible both in M and in C. Theoretical ejection curves are constructed for the ZP : EL system, by using the regular solution approximation and phase diagrams were calculated from interaction parameters. The results are compared with the other ones obtained in EL with β-cryptoxanthin palmitate system. Conclusions are drawn concerning the nature of collapse equilibria and the area necessity of the C phase.

INTRODUCTION

At the compression of monolayers of surfactants, insoluble in subphase liquid, spread at the gas/ liquid interface at a certain surface pressure (π), which will be referred to as collapse pressure (π_c), the collapse of the monolayer occurs, viz. a new bulk phase is formed from the monolayer. Upon collapse, a thermodynamic equilibrium may be presumed between the monolayer phase/phases (M) and the freshly collapsed bulk phase/phases (C).

According to the two-dimensional phase rule of Defay-Crisp,[1,2] applied to a binary mixture of surfactants, at constant external pressure and temperature, the following situations may arise : [3]

(*a*) One mixed surface phase in equilibrium with one collapsed bulk phase. The variance of the system is $w = 1$, i.e. the surface collapse equilibrium pressure is a function of the composition of the monolayer, e.g. of the molar fraction of one of the surfactants.

(*b*) One mixed surface phase in equilibrium with two collapsed bulk phases. The phase rule gives $w = 0$, i.e. the three phases may coexist only at a single equilibrium collapse pressure which is independent of system composition.

(*c*) Two surface phases in equilibrium with one collapsed bulk phase. The variance of the system is also $w = 0$ and the surface collapse pressure does not depend on composition.

The coexistence of four phases in equilibrium is thermodynamically impossible.

The possible types of phase diagrams reflecting these heterogeneous equilibria have been discussed in our previous paper, [4] considering that in M and/ or C the surfactants may be completely miscible (*m*), partially miscible (*p*) or immiscible (*i*).

Experimentally, phase diagrams can be obtained by recording compression isotherms, i.e. π *vs.* mean molecular area (A) curves, for monolayers of different compositions. The collapse of the monolayer is indicated by a sudden slope change of these isotherms at high π values. Instead of π *vs.* A curves also π *vs.* A/x_1^{oM} curves, i.e. ejection curves, may be used, [1] where x_1^{oM} stands for the molar fraction of surfactant 1 in the initially spread M, by taking for component 2 the more easily collapsible surfactant, i.e. one has $\pi_{2c} < \pi_{1c}$, by denoting the collapse pressure of the pure monolayer, containing only the component i, by π_{ic}.

The ejection curves are presented in this paper for two binary systems, namely: ethyl ester of β-apo-8′-carotenoic acid (EEC) with egg lecithin (EL) and zeaxanthin monopalmitate (ZP) with EL. The results are discussed in comparison with the others obtained on β-cryptoxanthin palmitate (CP) : EL system reported earlier. [5] It is mentioned that all three carotenoid derivatives were of all-*trans*-configuration.

Details concerning the provenience of the surfactants studied, spreading conditions and obtention of the compression isotherms, have been reported elsewhere. [6]

RESULTS AND DISCUSSION

Since the collapse pressure of EL is higher than π_c of both EEC and ZP (Table 1), egg-lecithin is taken for component 1. The ejection curves of several EEC : EL mixed monolayers are given in Fig. 1. a.

As seen from Fig. 1, the collapse pressure of the mixtures is the same, irrespective of their composition and it is equal to the collapse pressure of pure EEC (π_{EEC}) (see dashed horizontal line in Fig. 1.a and full lower line in Fig. 1.b). This means, that at the collapse of the mixed monolayer situation (*c*) appears, i.e. the surfactants are immiscible in M. At high surface pressures all the ejection curves are superposed over the compression isotherm of EL, indicating a second collapse pressure equal to collapse pressure of pure EL (π_{EL}) (see arrow in Fig. 1.a. and full upper line in Fig. 1.b). Consequently, the surfactants are also immiscible in C and at the collapse of mixed monolayers the pure EEC is ejected. The phase diagram of this *i*M-*i*C system is visualized in Fig. 1.b.

From Fig. 1.a it is obvious that after π_{EEC} is attained some over compression phenomena occur, i.e. the equilibrium π value slightly surpasses π_{EEC} (see horizontal dashed line), but practically the ejection curve has a horizontal portion as expected for *i*M-*i*C systems.

The experimental ejection curves of several ZP : EL mixtures are presented in Fig. 2 (full line curves).

As seen, in all the composition range investigated, π_c is a function of x_1^{OM}, i.e. at collapse only situation (*a*) appears. Consequently, the surfactants are completely miscible in M. Fig. 2 shows for high π values a

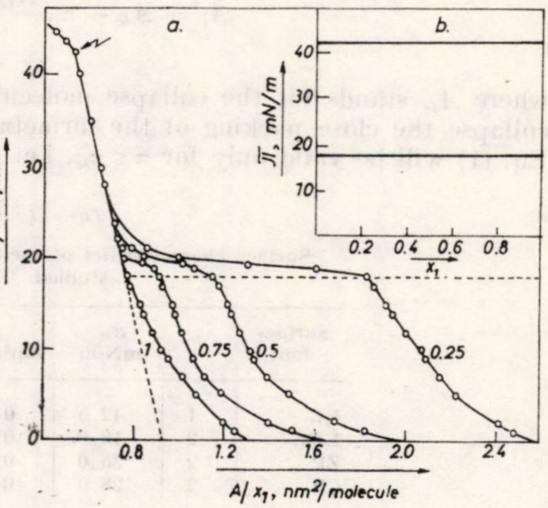

Fig. 1. — Ejection curves (a), and phase diagram (*i*M-*i*C) (b) for EL : EEC system. a — figures near the curves indicate x_1^{OM}, denoted on the abscissa simply by x_1.

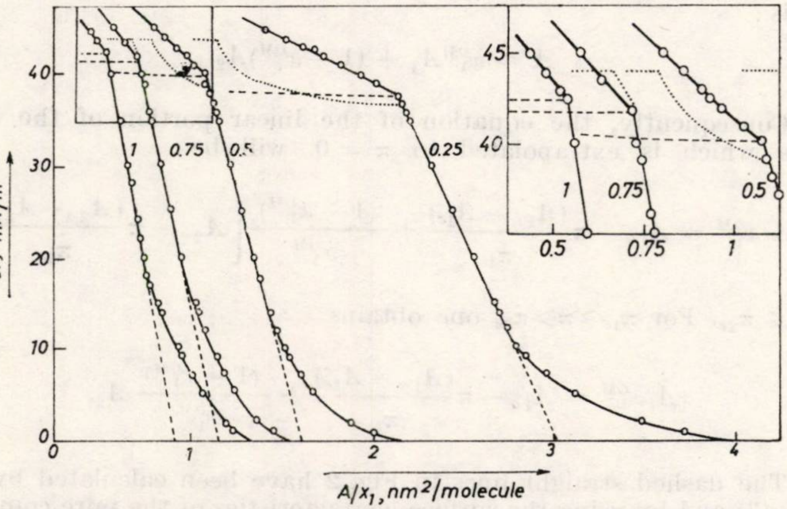

Fig. 2. — Ejection curves for EL : ZP monolayers; Figures near the curves indicate x_1^{OM}, denoted by x_1 on abscissa, as in Fig. 1a. Full lines — experimental curves; Dashed lines — for $\pi \leqslant 35$ mN/m, calculated by means of Eq. (3); for $35 < \pi \leqslant 42.5$, calculated by Eq. (3') (see Table 1); for the after-collapse region with Eq. (6), for each x_1^{OM} chosen; Dotted lines — calculated for *m*M-*i*C systems by using *approach 2*.

linear portion of the ejection curves, up to π_c, corresponding to the liquid condensed state of the monolayer (see dashed lines-extrapolated to $\pi \to 0$). In the case of the pure component i, by extrapolating this linear portion to $\pi = 0$, one obtains the limiting molecular area A_{io}. Obviously, the equation of the straight line will be

$$A_i = A_{io} - \pi \frac{A_{io} - A_{ic}}{\pi_{ic}} \tag{1}$$

where A_{ic} stands for the collapse molecular area of i (Table 1). Since at collapse the close packing of the surfactant molecules may be assumed, Eq. (1) will be valid only for $\pi \leqslant \pi_{ic}$, i.e. A_i cannot be less than A_{ic}.

Table 1

Surface characteristics of the pure components studied

Surfactant	i	π_{ic} mN/m	A_{ic} nm²/molec.	A_{io} nm²/molec.
EL	1	42.5	0.54	0.92
EEC	2	18.0	0.35	0.46
ZP	2	35.0	0.52	0.70
CP	2	28.0	0.44	0.83

By presuming as a first approximation, for the mixed films, the additivity of the molecular areas, before collapse the mean molecular area is :

$$A = x_1^{OM} A_1 + (1 - x_1^{OM}) A_2 \tag{2}$$

Consequently, the equation of the linear portion of the ejection curves which is extrapolated to $\pi = 0$, will be :

$$A/x_1^{OM} = A_{1o} - \pi \frac{(A_{1o} - A_{1c})}{\pi_{1c}} + \frac{(1 - x_1^{OM})}{x_1^{OM}} \left[A_{2o} - \pi \frac{(A_{2o} - A_{2c})}{\pi_{2c}} \right] \tag{3}$$

if $\pi \leqslant \pi_{2c}$. For $\pi_{1c} \geqslant \pi > \pi_{2c}$ one obtains

$$A/x_1^{OM} = A_{1o} - \pi \frac{(A_{1o} - A_{1c})}{\pi_{1c}} + \frac{(1 - x_1^{OM})}{x_1^{OM}} A_{2c} \tag{3'}$$

The dashed straight lines in Fig. 2 have been calculated by means of Eq. (3) and by using the surface characteristics of the pure components given in Table 1. As seen, at high π values the experimental points are situated on the straight lines calculated, indicating the validity of Eqs (2) and (3) in the liquid state of the monolayers, as a first approximation.

At the collapse of the mixed monolayer, the bulk phase ejected may consist of the pure component 2 (if the system is of mM $-i$C type), or of a mixed phase C, richer in component 2, as compared to the M (if the system is of mM$-m$C type). Consequently, the composition of the remaining M is modified and, unlike with the iM$-i$C system, the equilibrium π will gradually increase during the ejection of the mixed bulk phase C, as observed experimentally. If ZP and EL were immiscible in C, a simple calculation performed by means of the relation derived for perfect mM$-$ iC systems [4] shows that there would be a concollapse point at which a monolayer with $x_1^M = 0.803$ would be in equilibrium with two pure C phases, each consisting of pure components 1 or 2, corresponding to a maximum value of collapse pressure $\pi_c = 43.93$ mN/m, i.e. to a surface pressure higher than π_{1c}.

Since in the case of all mixed monolayers investigated one has $\pi_{1c} > \pi_c > \pi_{2c}$, the system may be presumed to be of mM$-m$C type, as also the CP$-$EL one, studied earlier. [5]

The hypothesis that ZP and EL form regular solutions both in M and C, allowed us to derive interaction parameters (ξ^M and ξ^C in both phases) from the experimental monolayer curve (collapse pressure *vs.* composition in monolayer). The values obtained, viz. $\xi^C = -8.67$ and $\xi^M = -9.48$, respectively, [6] can be used for the construction of the phase diagram, containing the monolayer curve (π_c *vs.* x_1^M) and the bulk curve (π_c *vs.* x_1^C). Both curves are given in Fig. 3.b. For the sake of comparison, in the same figure also the equilibrium curves corresponding to a perfect system ($\xi^C = \xi^M = 0$) are given with dashed lines.

The phase diagram enables us to construct the portion of theoretical ejection curve, corresponding to $\pi > \pi_c$ for each system of a given composition x_1^{0M}.

For this purpose the following model was used.

At the compression of the monolayer with $x_1^M = x_1^{0M} = x_1$ the C phase appears at $\pi_c(x_1^{0M})$ and at $\pi_c + \Delta\pi$ a thermodynamic equilibrium is established between the M and C phases of the composition x_1^{1M} and x_1^{1C}, respectively, corresponding to the molar fraction values given by the phase diagram for $\pi_c + \Delta\pi$. The collapse of the remaining M leads to a new equilibrium at $\pi_c + 2\Delta\pi$ corresponding to x_1^{2M} and x_1^{2C}, respectively. At $\pi_c + {}_j\Delta\pi$ the equilibrium phases correspond to x_1^{jM} and x_1^{jC}, respectively. Consequently, the thermodynamic equilibrium is presumed to be established between the M and only the newly collapsed portion of the C phase. By using the phase diagram, the lever rule concerning the amount of the equilibrium phases, and by taking a certain surface pressure step $\Delta\pi$, a theoretic ejection curve can be constructed for each x_1^{0M} value used.

Concerning the area necessity of the C phase (A^C), two approximations were used. In *approach* 1 this area necessity is pressumed to be neglectingly small ($A^C \approx 0$).

In this case the equation of the ejection curve for a certain initial composition x_1^{0M} in monolayer can be given as:

$$A^{(n)}/x_1^{0M} = \prod_{j=1}^{n} \frac{x_1^{(j-1)M} - x_1^{jC}}{x_1^{jM} - x_1^{jC}} \left[\frac{x_1^{nM}}{x_1^{0M}} A_1 + \frac{1 - x_1^{nM}}{x_1^{0M}} A_{2c} \right] \qquad (4)$$

where A_1 means:

$$A_1 = A_{1\,0} - \pi \frac{A_{1\,0} - A_{1c}}{\pi_{1c}} \tag{5}$$

obtained from Eq. (1) for $i = 1$, and with $\pi = \pi_c + n\Delta\pi$ by presuming the phase equilibrium to be established at each step (j) for the same inrement of surface pressure equal to $\Delta\pi$, π_c being $\pi_c = \pi_c(x_1^{OM}$ and $A^{(n)}$ is the mean molecular area after n such steps. In *approach 2*, at the collapse of the monolayer the formation of a trilayer is assumed according to a collapse mechanism proposed in the literature,[7] which seems to be in agreement with our results concerning the kinetics of relaxation phenomena in apocarotenoid monolayers.[8] $A^{(n)\prime}$ being the apparent mean molecular area, by also taking into account the area necessity of the C phase as trilayers $(A - A^{(n)})/3$, in *approach 2* one obtains:

$$A^{(n)}/x_1^{OM} = A^{(n)}/x_1^{OM} + (A - A^{(n)})/3x_1^{OM} \tag{6}$$

where $A^{(n)}$ and A were obtained from Eq. (4) and (3′), repectively.

The ejection curves constructed for $x_1^{OM} = 0.25$; 0.50; 0.75 and 1.00, by performing the calculations stepwise of $\Delta\pi = 0.1$ mN/m, are presented in Fig. 3.a in *approach 1*, and in Fig.3.c in *approach 2*.

In Fig. 3c the vertical portions of the ejection curves for $\pi > \pi_{1c}$ correspond to:

$$\frac{A}{x_1^{OM}} = \frac{A^{(n)\prime}}{x_1^{OM}} = \frac{1}{3}\left[A_{1c} + \frac{(1 - x_1^{OM})}{x_1^{OM}} A_{2c}\right], \text{ obtained from}$$

Eq. (6) for $A^{(n)} = 0$, and $A = x_1^{OM} A_{1c} + (1 - x_1^{OM}) A_{2c}$ by taking into account that for $\pi \geqslant \pi_{1c}$ one has $A_1 = A_{1c}$. The after collapse portions of the ejection curves are also partially given in Fig. 2, in which the dashed line curves were calculated in *approach 2*, by means of Eq. (6), since these are nearer to the experimental curves, than the ejection curves calculated by means of Eq. (4) and given in Fig.3.a. In Fig.3.a and 3.*c* the dotted lines indicate the collapse pressure $\pi_c(x_1^{OM})$ *vs.* A/x_1^{OM} curve for all initial molar fractions comprised between about 0.25 and 1.00. This curve can be easily calculated by means of Eq. (3′), by taking for π the π_c a value corresponding to x_1^{OM} and actually it represents the monolayer curve of the phase diagram (Fig. 3.*b*), now in a plot $\pi_c(x_1^{OM})$ *vs.* $\dfrac{A}{x_1^{OM}}$.

Results obtained for the ZP – EL system can be compared with those reported earlier[5] for the CP – EL one, which is also of mM – mC type. The phase diagram of the latter system can be seen in Fig.4.b ejection curves in *approach 1* and *2* in Fig.4.a and 4.c, respectively. As seen, the higher negative values of the interaction parameters in ZP – EL monolayers, as compared to the CP – EL ones, modify essentially the shape of both phase diagrams and ejection curves. The presence of the OH group in the air phase ionone ring of ZP leads to enhanced intermolecular interactions, entailing, presumably, even a dimerization of ZP in the

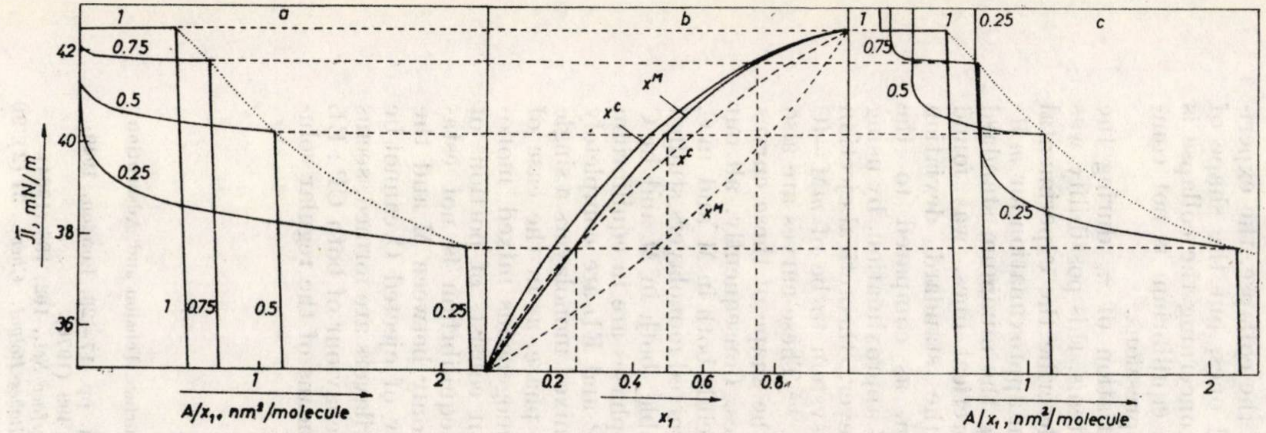

Fig. 3. — Theoretical ejection curves and phase diagrams for EL :ZP system; a — Ejection curves calculated in *approach 1*. Full lines — calculated by means of Eq. (4), for regular solution. Figures as in Fig. 1. Dotted line — collapse pressure curve calculated by means of Eq. (3'), for regular solution.[6] b — Phase diagram (*m*M-*m*C). Full lines — regular solution approximation, calculated by using $\xi^C = -8.67$ and $\xi^M = -9.48$. Dashed lines — perfect solution approximation, calculated for $\xi^C = \xi^M = 0$. c — Ejection curves in *approach 2*. Full lines — calculated by means of Eq. (6) for regular solution. Figures and dotted line curve as in Fig. 3. a.

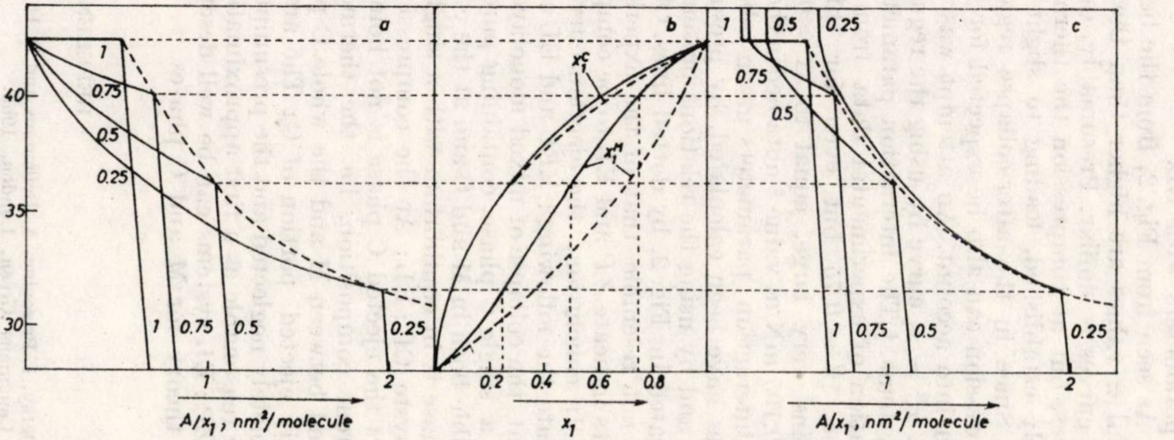

Fig. 4. — Theoretical ejection curves and phase diagram for EL : CP monolayers. a — Ejection curves in *approach 1*. Full lines — calculated by means of Eq. (4). Figures as in Fig. 1. Dashed line — collapse pressure curve calculated by means of Eq. (3') for regular solution; b — Phase diagram (*m*M-*m*C). Full lines — regular solution approximation calculated with $\xi^C = -1.73$ and $\xi^M = -2.65$. Dashed lines — perfect solution approximation calculated for $\xi^C = \xi^M = 0$; c — Ejection curves in *approach 2*. Full lines — calculated by means of Eq. (6) for regular soolution. Figures and dashed line curve as in Fig. 4. a.

monolayer, which could be responsible both for the higher π_c value of ZP, as compared to CP in pure monolayers, and for the increased interaction parameters with EL.

As seen from Fig. 2, from the beginning of the collapse, the experimental π values are higher than the calculated ones, but the shape of both curves is similar. Presumably, our model concerning the collapse is correct, but at compression the thermodynamic equilibrium is not completely established, leading to slight over compressions.

Since in the after-collapse region the variation of π_c during the compression can also be expected for *m*M-*i*C systems, this possibility was taken into account. An attempt was made to describe the experimental π_c *vs.* $x_1^M = x_1$ curve by using the regular solution approximation for *mM-iC* systems.[4] The interaction parameter ensuring the minimum standard deviation of experimental data from the theoretical ones, was found to be $\xi^M = 0.75$ but even for this value the standard deviation remains very large, equal to $\Delta = 0.819$ mN/m, as compared to the $\Delta = 0.105$ mN/m value[6] obtained in the *m*M —*m*C approximation, by using the interaction parameters given above. However, theoretical ejection curves have been calculated, by presuming the system to be of *m*M —*i*C type and by using the relations presented earlier.[4,5] These curves are also indicated in Fig. 2, by dotted lines. Obviously, the shape of these curves does not resemble that of the experimental ones. Consequently, all our results indicate *ZP* and EL to be completely miscible both in M and in C.

In conclusion, the ejection curves of the mixed monolayers studied indicate the following : EEC and EL are immiscible both in M and in C and at the collapse of mixed monolayers two M phases are in equilibrium with a single C phase, containing pure EEC ; ZP and EL are completely miscible both in M and C and at the collapse of mixed monolayers a single M phase is in equilibrium with a single mixed C phase, as in the case of the syste CP : EL ; At the compression of homogeneous mixed monolayers the ejected C phase is not homogeneous, it consists of portions of different composition, i.e. the thermodynamic equilibrium is not established between M and the whole C phase, but only between M and the freshly ejected portion of C ; The area necessity of ejected C cannot be completely neglected and the presumption that trilayers are formed, seems to be reasonable as a first approximation ; The behaviour of both CP : EL and ZP : EL systems can be well described by means of the regular solution theory for M and C phases.

REFERENCES

[1] R. Defay, I. Prigogine, A. Bellemans and D. H. Everett, "Surface Tension and Adsorption" Longmans Green, London, 1966.

[2] D. J. Crisp, "Surface chemistry", Supplement to Research, pp. 17—23, London, 1949.

[3] M. C. Phillips and P. Joos, *Kolloid. -Z.Z — Polym.*, **238**, 499 (1970).

[4] J. Zsakó, M. Tomoaia-Cotişel and E. Chifu, *J. Colloid Interface Sci.*, **102**, 186 (1984).

[5] E. Chifu, J. Zsakó and M. Tomoaia-Cotișel, *Studia Univ. Babeș-Bolyai, Chem.*, **31** (2), 90 (1986).

[6] M. Tomoaia-Cotişel, E. Chifu and J. Zsakó, *Colloids and Surfaces*, **14**, 239 (1985).

[7] H. E. Ries, Jr., *Nature*, **281**, 287 (1979).

[8] J. Zsakó, M. Tomoaia-Cotişel, I. Stan, V. Coman, V. Tămaş and E. Chifu, "Proc. 3rd National Conference on Biophysics", Jassy (Romania), 1985, p. 63.

Revue Roumaine de Chimie, **32**, *7*, 671–675 (1987)

INTERACTIONS BETWEEN POLYACRYLIC DISPERSIONS AND BIOPOLYMERS HYDROLYSATES

VIORICA TRANDAFIR*, MINODORA LECA, ** DAN DEMBINSCHI*,
ELENA PUICĂ* and GABRIEL ZĂINESCU*

*** Leather and Footwear Research Institute, Bucharest, Romania**
**** Polytechnic Institute of Bucharest, Physical Chemistry Department, Bucharest, Romania**

Received November 25, 1986

The microheterogeneous dispersed systems composed of polyacrylic latexes and collagen hydrolysates having low molecular weights of the order of 6000 to 10000 (PA/HF) were studied, the hydrolysate being obtained by the alkaline hydrolysis of the tanned finished leather waste products. These microheterogeneous systems are stable on wide pH (4.5–8.5), mixing ratio (10–70% acrylic polymer), and temperature (20–60°C) ranges. The above systems have a pseudoplastic non-Newtonian fluid behaviour, their viscosities being much larger than those of the individual components, which indicate a strong interaction between acrylic dispersion and collagen hydrolysate molecules. The dispersed systems PA/HF are compatible with aqueous caseine solutions, producing an increase of its viscosity up to a weight ratio of 30–40%. The above mentioned dispersed systems are used to prepare some auxiliary for leather finishing, as lustre agents, and pigment pastes.

INTRODUCTION

The compatibility of polyacrylic dispersions (latexes) with hydrolysates obtained from the collagen biopolymer (the basic protein from the connective tissue) was the subject of a previous paper, which pointed out their rheologic behaviour.[1] These hydrolysates of the type HO used were characterised by a high degree of purity (about 98–99% protein) and average molecular weights of 20 000 –250 000 ; they are obtained from un-tanned skin waste products. The rheologic behaviour of polyacrylic latexes—collagen hydrolysates mixtures is of the pseudo-plastic non-Newtonian type.

The perfectly reproductible rheological curves indicate that the microheterogeneous systems have a kinetic stability within some limits of pH, temperature, concentration, and the nature of the acrylic dispersion. The considerable increase of the mixture viscosity compared to that of each of the components shows that the aggregation of the polyacrylic latex particles with the hydrolysate macroions is due to electrostatic attraction forces, the mixture maintaining its stability.

The films formed of these microheterogeneous systems were also studied and it was established that certain amounts of collagen hydrolysates improved the rheological properties of polyacrylic films, the latter passing from the "rigid and resistant" type to the "soft and resistant" one.

The present work is oriented to the stability of the microheterogeneous systems obtained from polyacrylic latexes (PA) and collagen hydrolysates of another type (HF), extracted by alkaline hydrolysis of waste products from tanned and finished leather, where the collagen is chemically cross-linked. HF contain polypeptides with low molecular weights (6 000 to 10 000) and have a lower degre of purity : about 5 –10% are mineral salts and about 10% organic nitrogen free components.

The above microheterogeneous systems are used to prepare auxiliary products for the lather industry (pigment pastes and lustre agents).

EXPERIMENTAL

The acrylic polymers used are aqueous dispersions showing the following characteristics : PA_1-acrylic acid co-ethylacrylate, 35.8% dry substance, pH = 3.5 ; PA_2-acrylic acid co-ethyl acrylate – acrylonitrile, 22% dry substance, pH = 3.5. The collagen hydrolysate HF used have the following physical-chemical characteristics : 18.5% dry substance, 79.7%* proteic substance, 10.0%* ash, 0.5%* fat matters, 9.5%* nitrogen organic matters – free, pH = 9.3 (*-recalculated values under moisture-free conditions).

The average molecular weight $\overline{M}$ of the hydrolysate is 8500. Mixing the two components, a kinetically stable microheterogeneous system in the range of 10 to 70% polyacrylic latex concentration at a pH between 4.5 and 8.5 and for a temperature of 20 to 60°C is almost instantaneously formed.

The order of component addition is important for the stability of the system. Therefore, the PA latexes were added under stirring on HF.

The system PA_2/HF is used to replace partially caseine (30–40%) that is used to prepare pigment pastes. The study also concentrated on the compatibility of the compound (PA/HF/ caseine solution).

The viscosities of the studied microheterogeneous systems were determined with a Rheoviscometer. The molecular weight distributions were determined by gel permeation chromatography on Sephadex G-200, detection being made by UV absorption at 230 nm.

RESULTS AND DISCUSSION

The studied microheterogeneous systems, due to their stability in certain conditions, are similar to soluble inter-polymeric complexes or to the polyelectrolyte complexes that are studied nowadays as a new class of synthetic polyelectrolites.[2]

The specific rheologic behaviour of the studied systems shows the existence of some strong interactions between components due to physical and chemical cross-linking (ex. electrostatic, hydrogen, and hydrophobe bonds) determined by their different reactivity and leading to an increase in the particle mass.

The dispersions PA_1 and PA_2 contain two major fractions with different molecular weights (Figs 1a, 2a) and HF has a major fraction with $\overline{M}$ = 8500 (Figs 1b, 2b). The distribution of the molecular weight in the PA_1/HF and PA_2/HF systems (Figs 1c, 1d, 1d, 2d) shows the pre-

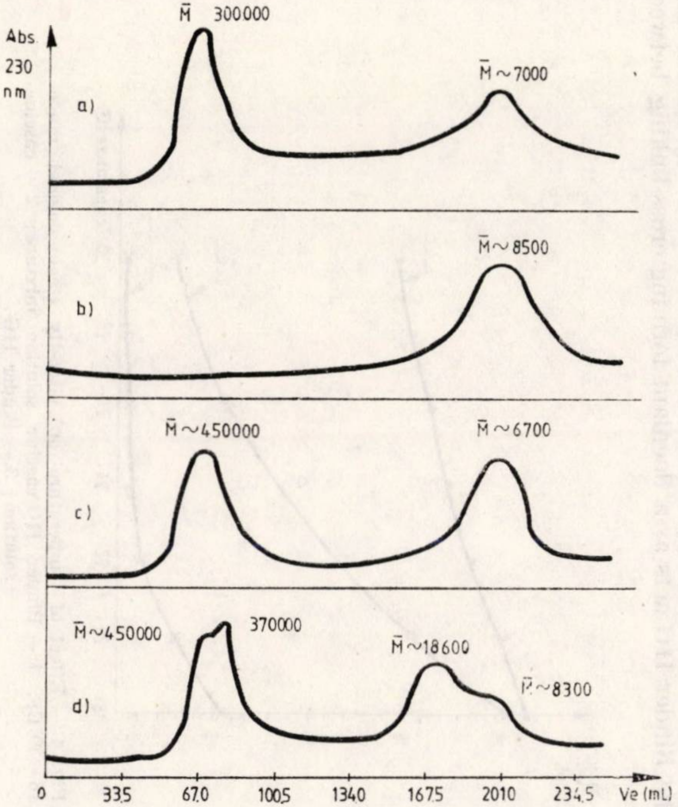

Fig. 1. — Molecular weight distribution obtained by gel permeation chromatography on Sephadex G-200 : a) acrylic polymer PA_1 ; b) hydrolysate HF ; c) PA_1/HF mixture at 20°C ; d) PA_1/HF mixture at 45°C.

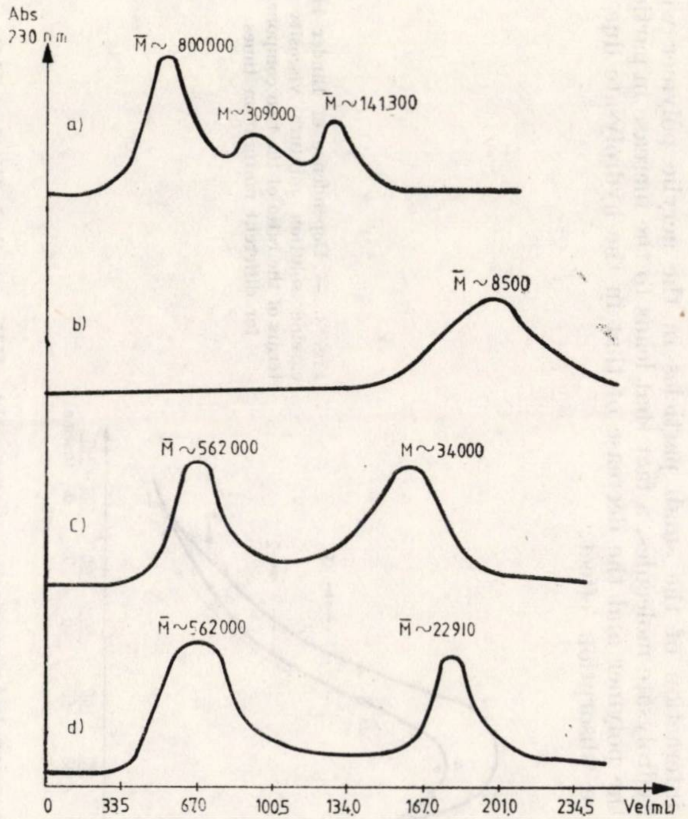

Fig. 2. — Molecular weight distribution obtained by gel permeation chromatography on Sephadex G-200 : a) acrylic polymer PA_2 ; b) hydrolysate HF ; c) PA_2/HF mixture at 20°C ; d) PA_2/HF mixture at 45°C.

ferential interaction of the small particles in the acrylic polymer with collagen hydrolysate molecules, a fact that leads to the increase in particle mass of the polymer and the decrease of that in the hydrolysate due to a selective absorption effect.

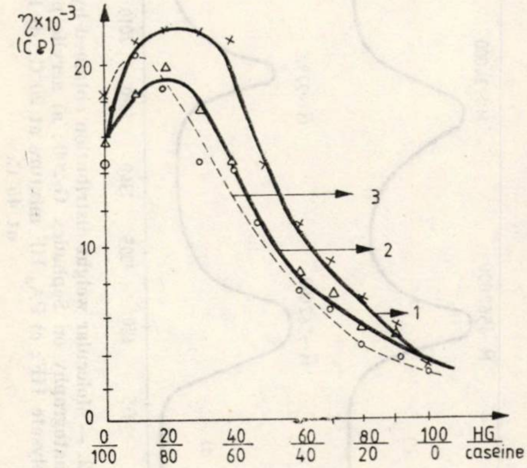

Fig. 3. — Dependence of Binder HG/caseine solution mixture viscosity in terms of the ratio of the two components for different maturation times.

The microheterogeneous system PA_2/HF — called Binder HG — is compatible with the caseine solution, resulting in the increase of the viscosity of caseine solution up to an amount of 30—40% Binder HG (Fig. 3). The Binder HG acts as a floculant forming cross-linking between

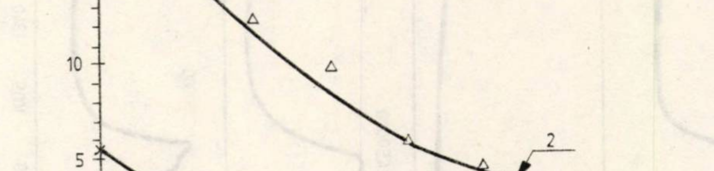

Fig. 4. — Effect of temperature on viscosity (technological range 18—30°C) : 1 — Binder HG/caseine solution mixture ; 2 — caseine solution ; 3 — Binder HG.

the caseine particles (micelles), increasing the volume fraction of the dispersed phase and the viscosity of the system. Exceeding 30 – 40% leads to a decrease of the viscosity due to the prevalence of the Binder HG with smaller molecules.

The lower value in the decrease of the viscosity with temperature in the Binder HG/ caseine solution system can be explained by the increase in the particle mass due to physical and chemical cross-linking. A similar behavior is observed for melt and concentrated polymer solutions (Fig. 4).

The dependence of viscosity on temperature in Binder HG/ caseine solution mixture is substantially turned off from Arrhenius type behaviour, a fact that is also present in the case of concentrated polymer solutions.

CONCLUSIONS

Under certain conditions, collagen hydrolysates and polyacrylic latexes form stable microheterogeneous systems as a result of the intermolecular interactions between components having a different reactivity.

In their turn, these systems are compatible, under certain conditions, with caseine solutions resulting in a stable microheterogeneous system with a specific rheologic behaviour similar to that of the concentrated polymer solutions.

The above studied systems, due to their stability and specific physical properties, are used to prepare some auxiliary products needed in the leather industry.

REFERENCES

[1] M. Olteanu, V. Trandafir, I. Mîndru, M. Leca, I. Ionescu-Bujor and I. Brădescu, *Industria Uşoară*, **12**, 522 (1980).

[2] V. A. Kabanov and A. B. Zezin, *IUPAC – Macro' 83*, Bucharest, Romania, Sept. 5–9, 1983.

the caseine particles (micelles), increasing the volume fraction of the dispersed phase and the viscosity of the system. Exceeding 30 – 40% leads to a decrease of the viscosity due to the prevalence of the Binder (H) with smaller molecules.

The lower value in the decrease of the viscosity with temperature in the Binder H/caseine solution system can be explained by the increase in the particle mass due to physical and chemical cross linking. A similar behaviour is observed on melt and concentrated polymer solutions (Fig. 4).

The dependence of viscosity on temperature in Binder H/caseine solution mixture is substantially turned off from Arrhenius type behaviour, a fact that is also present in the case of concentrated polymer solutions.

CONCLUSIONS

Under certain conditions, collagen hydrolysates and poly-acrylic latexes form stable macroheterogeneous systems as a result of the intermolecular interactions between components having a different reactivity.

In their turn, these systems are compatible, under certain conditions, with caseine solutions resulting in a stable microheterogeneous system with a specific rheologic behaviour similar to that of the concentrated polymer solutions.

The above studied systems, due to their stability and specific physical properties, are used to prepare some auxiliary products needed in the leather industry.

REFERENCES

[illegible] Olteanu, V. [illegible], [illegible] Mihalcea, M. [illegible] and [illegible], *Industria Textila*, [illegible] (1969).

[illegible] and [illegible], *[illegible]*, [illegible], Sept. [illegible] 1985.

Revue Roumaine de Chimie, **32**, 7, 677–682 (1987)

BACTERIAL IMMOBILIZATION IN MEMBRANEOUS SUPPORTS FOR AMPEROMETRIC PROBING OF ORGANIC COMPOUNDS

HORIA VAIS* and DORU G. MĂRGINEANU**
* Membrane Biophysics Group, Institute of Biological Sciences, Spl. Independenţei 296, Bucharest, R-77748
** Laboratory of Biophysics, Faculty of Biology, Bucharest University, Spl. Independenţei 91–95, Bucharest R-76201, Romania

Received November 28, 1986

The electrodes with immobilized whole cells in membrane-like supports are promising for quantitative analysis of several classes of organic compounds. Their interest lies in the longer lifetime and the much lower cost, as compared with the enzyme electrodes, but by now they are beset by severe limitations as concerns the specificity and the speed of response.

A kinetic model of the amperometric response of such a type of electrodes, as developed here, is a prerequisite for expressing the functional parameters of the electrodes in terms of their designing features : bacterial density, permeability constants, and geometrical constraints.

INTRODUCTION

The electrodes with immobilized bacteria are considered[1,2] as a possible alternative of the enzyme electrodes, [3] for the electrical probing of several classes of dissolved organic compounds.

The construction of a bacterial electrode does not significantly differ from an enzyme-membrane probe. No matter if the overall result is a potentiometric or an amperometric measurement, the problem is to place, close to the surface of the product-sensing electrode, or to that of the oxygen cathode, a catalyst which, in this case, is represented by the living bacterial cells. The bacteria must be attached in such a manner as to form a membraneous barrier, compatible with the geometry of the main electrode and with good permeability characteristics for both the organic molecules whose concentration has to be detected, and for the final product (or the oxygen) whose concentration is actually measured. At this stage, the problems of cell immobilization appear, at least compared with enzyme immobilization, much less difficult.

Generally, most of the attempts reported as bacterial immobilization procedures revolve around the entrapment of cells either in gels,[4,5] or in porous materials, [6,7] or even simply to keep a certain amount of cells onto the surface of the main electrode with a dyalisis membrane. [8–10] The immobilized bacteria perform the chemical transformation of the analyte into a chemically simpler compound for which the electrochemical detection is already achieved, the whole electrochemical transduction thus being complete. Besides this, if the bacterial metabolism is specific towards a given organic compound, the chemoelectrical transduction can then be achieved simply by monitoring the oxygen consumption, due to the specific metabolic activity.

KINETIC MODEL

A biosensor based on an entrapped catalyst, can be modelled by a series arrangement of three phases, as in Fig. 1.[11]

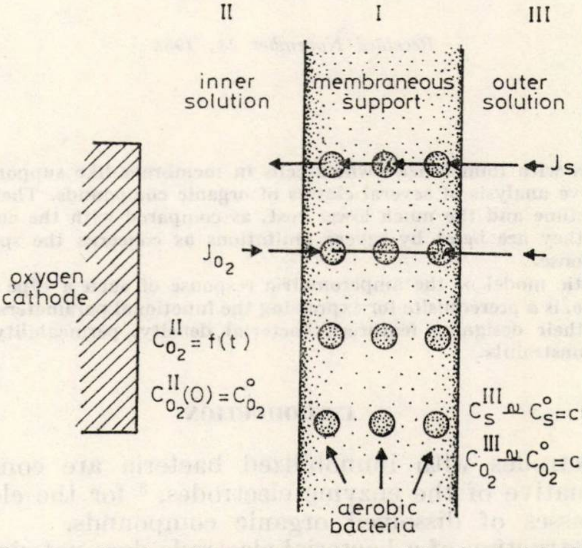
II
I
III
inner solution
membraneous support
outer solution
J_s
J_{O_2}
oxygen cathode
$C^{II}_{O_2} = f(t)$
$C^{II}_{O_2}(0) = C^{\circ}_{O_2}$
$C^{III}_{S} \simeq C^{\circ}_{S} = ct$
$C^{III}_{O_2} \simeq C^{\circ}_{O_2} = ct$
aerobic bacteria

Fig. 1. — A schematic representation of the bacterial electrode, consisting in a conventional oxygen cathode, covered by a membraneous support with immobilized aerobic bacteria, which probes an organic compound dissolved in the outer solution. The notations are : J_s and JO_2 — the flows of substrate and oxygen respectively ; c's stand for concetrations of the substances indicated by lower scripts, while the upper script (°) indicates the initial values.

Phase I represents the membraneous support, having a surface A, in which N microorganisms, randomly distributed, are enclosed. This phase imposes a permeability barrier between the external solution, that one in which the analytical detection of the dissolved organic compound is performed (phase III), and the internal compartment (phase II), close to the oxygen cathode, whose volume V^{II} is by some orders of magnitude smaller than the external one.

In the internal compartment, c_{O_2} is time dependent, due to the aerobic metabolism of the organic substrate, the rate of oxygen consumption being related to that of substrate metabolization by the stoechiometric coefficient γ :

$$r_{O_2} = \gamma \cdot r_s \tag{1}$$

The electrical output of the oxygen cathode is simply $I = k \cdot c^{II}_{O_2}$ where $k = 0.326 \times 10^5$ nA/cm³ O_2, per cm³ of solution, in our case, [5] so that the objective is to express the concentration of the dissolved oxygen in the inner compartment as a function of time, as well as of the designing features : bacterial density in the support, permeability constants of both the substrate and the oxygen, and geometrical constraints. For this, we have to solve a system of differential equations which are constructed by superposing the consumption by bacterial metabolism and the simple diffusion through the membrane :

$$\frac{dc_i^{II}}{dt} = \frac{P_i \cdot A}{V^{II}} (c_i^{III} - c_i^{II}) - N \cdot r_i \quad (i = s, O_2) \tag{2}$$

The bacterial metabolism of the substrate has an enzymatic kinetics, so r_s is given by a Michaelis-Menten type of equation :

$$r_s = R \cdot c_s/(K_m + c_s), \tag{3}$$

where R and K_m have the usual meanings. With the help of relation (1), the rate of oxygen consumption can be thus related to the substrate concentration. As the compartment III was presumed to be a reservoir for s, the concentration c which appears in equation (3) is c_s^{II}. Thus,

$$r_{O_2} = \gamma \cdot R \cdot c_s^{II} / (K_m + c_s^{II}) \tag{4}$$

With these preliminary remarks, the equation (2), corresponding to $i = O_2$, can be analytically resolved in two particular cases :

1. High substrate concentrations ($c_s \gg K_m$)

In this case, the exact solution of equation (2) is the following :

$$c^{II}_{O_2} = c^{III}_{O_2} - \frac{\gamma N R}{P_{O_2} \cdot A} \left[1 - \exp\left(\frac{-P_{O_2} \cdot A}{V^{II}} \cdot t \right) \right] \tag{5}$$

As one can easily observe, this case has no meaning for the analytical probing of the organic substrate. Nevertheless, this equation provides a possibility to measure P_{O_2}, as in the steady conditions ($t \to \infty$) $c^{II}_{O_2}$ depends solely on it, the other parameters being independently known.

2. Low substrate concentrations ($c_s \ll k_m$)

The exact solution of equation (2) is now:

$$c_{O_2}^{II} = c_{O_2}^{III} - c_s^{III} \frac{\gamma NR\,(P_s/P_{O_2})}{P_s A K_m + NR}\left[1 - \exp\left(-\frac{P_{O_2}\cdot A}{V^{II}}\cdot t\right)\right]\left\{1 - \right.$$

$$\left. - \exp\left[-\frac{P_s\cdot A}{V^{II}}\left(1 + \frac{NR}{P_s\cdot A\cdot K_m}\right)t\right]\right\} \tag{6}$$

Thus, this is the case of analytical interest, the stationary value of oxygen concentration being proportional to the substrate concentration in the tested medium.

Once the time dependence of the oxygen concentration in the inner electrode compartment is established, the response of the electrode ($I = k\cdot c_{O_2}^{I}$) to different substrate concentrations present in the tested medium will be as in Fig. 2. As noted on this figure, the final response

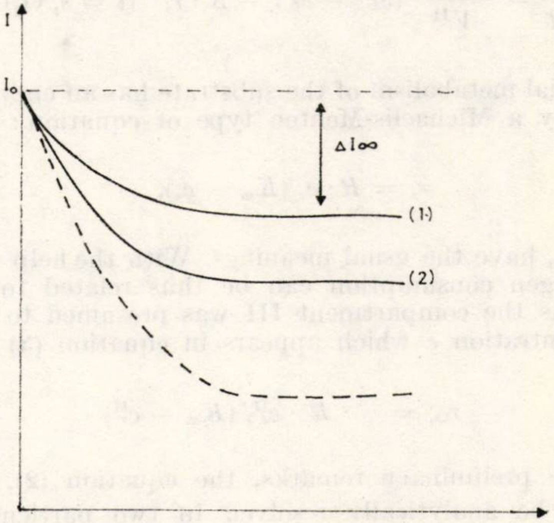

Fig. 2 — The general shape of the time course of the amperometric response, for two increasing substrate concentrations (curves 1 and 2)and for the limiting case $c \gg K_m$ (interrupted line). The curves 1 and 2 correspond to equation (6), and the interrupted curve to equation (5), both arbitrarily scaled.

ΔI_∞ for such amperometric electrodes is defined with the aid of the stationary value: $\Delta I_\infty = I_0 - I(\infty)$. With the notations: $\frac{N\cdot R}{A\cdot K_m} = P_b$ and $p_i = P_i/P_{O_2}$ $(i = s, b)$; the electrical response has the following analytical form:

$$\Delta I_\infty = \gamma\cdot k\cdot c_s^{III}/(p_s^{-1} + p_b^{-1}) \tag{7}$$

P_b has the dimensions of a permeability coefficient, while p_i are dimensionless.

On the basis of equation (7) it appears possible to derive functional characteristics of such type of biosensors in terms of their designing features.[11]

The practical response time is taken as the time τ which elapses between the instant at which the organic compound is added to the solution (or its concentration is changed) and the moment at which the electrical response becomes a fraction a of the stationary value (a ranging from 90% to 99%, depending on the desired accuracy). According to this definition, the derived analytical expression for τ is:

$$\tau = \frac{V^{II}}{A} \frac{2 + \ln a}{P_s + P_b + P_{O_2}} \tag{8}$$

The limit of detection is defined as the minimal substrate concentration which induces an electrical response not greater than the residual current of the oxygen cathode ($\simeq 1$ nA,[12]). Following this definition, the limit of detection c_s is given by the formula:

$$c_s^{\min} = \frac{1}{\gamma \cdot k} (p_s^{-1} + p_b^{-1}) \tag{9}$$

By comparing the electrical response depicted by equation (7) with the corresponding one obtained from equation (5), the maximal substrate concentration which could be electrically detected can be evaluated:

$$c_s^{\max} = K_m p_b (p_s^{-1} + p_b^{-1}) \tag{10}$$

From this, the linearity domain, defined as $\Delta c_s = c_s^{\max} - c_s^{\min}$, is analytically depicted by the formula:

$$\Delta c_s = (1 + p_b/p_s)(K_m - 1/\gamma k p_b) \tag{11}$$

DISCUSSION AND CONCLUSIONS

A general evaluation of the advantages and drawbacks of the bacterial electrodes as compared with the enzyme electrodes is beyond our scope here, because it was done elsewhere.[13] However, we recall that their advantage lies in the fact that the time consuming and costly extraction and purification procedures are avoided, and a sensible longer lifetime is ensured, due to the fact that the enzymes are kept in their natural environment within the cell. On the other hand, the selectivity and the speed of response are poorer.

This model is not conceived to account for either selectivity or the lifetime. However, it can be extended to incude the selectivity problem, too, if the simultaneous oxidative metabolization of several substrates is considered.

From equation (8) it appears that the speed of response will be higher for smaller depth (i.e. V^{II}/A) of the inner compartment and for immobilization supports with high permeabilities P_s and P_{O_2} and with high bacterial density N/A. P_{O_2} can be estimated from the response of the bacterial electrode itself, in the limiting case of high substrate concentration, as mentioned above, while P_s can be independently measured by various analytical procedures as for instance, by an immersion weighing method.[14,15]

The equations (10, 11) modulate the second requirement mentioned above for improving τ, in the sense that the efforts must be focused on rising P_b, that is to obtain a bacterial density in the support as high as possible.

REFERENCES

[1] G. A. Rechnitz, *Science*, **214**, 287 (1981).

[2] H. Vais and D. -G. Mărgineanu, *Amer. Biotechnol. Lab.*, **2**, 8 (1984).

[3] G. G. Guilbault, *Appl. Biochem. Biotechnol.*, **7**, 85 (1982).

[4] I. Karube, S. Mitsuda and S. Suzuki, *Eur. J. Appl. Microbiol. Biotechnol.*, **7**, 343 (1979).

[5] H. Vais, F. Oancea, A. M. Faghi, C. Delcea and D. G. Mărgineanu, *Rev. Roum. Biochim.*, **21**, 57 (1985).

[6] I. Karube, T. Nakahara, T. Matsunaga and S. Suzuki, *Analyt. Chem.*, **54**, 1725 (1982).

[7] B. J. Vincke, M. J. Devleeschouwer and G. J. Patriarche, *J. Pharm. Belg.*, **38**, 225 (1983).

[8] G. A. Rechnitz, S. J. Riechel, R. K. Kobos and M. E. Meyerhoff, *Science*, **199**, 440 (1978).

[9] R. R. Walters, B. E. Moriaty and R. P. Buck, *Analyt. Chem.*, **52**, 1680 (1980).

[10] H. Y. Neujahr, *Appl. Biochem. Biotechnol.*, **7**, 107 (1982).

[11] H. Vais and D. G. Mărgineanu, *Bioelectrochem. Bioenerg.*, **16**, (1986), in press.

[12] P. W. Davies, in Physical Techniques in Biological Research" (W. L. Nastuk, ed.), 157, Academic Press, 1962.

[13] D. G. Mărgineanu, H. Vais and I. Ardelean, *J. Biotechnol.*, **3**, 1 (1985).

[14] D. G. Mărgineanu and M. L. Flonta, *J. Biophys. Biochem. Methods*, **3**, 129 (1980).

[15] H. Vais and D. G. Mărgineanu, *J. Biomed. Eng.*, **5**, 340 (1983).

Revue Roumaine de Chimie, 32, 7, 683–691 (1987)

FATTY ACID FILMS AT THE BENZENE/WATER INTERFACE

EMIL CHIFU, MARIUS SĂLĂJAN, IOAN DEMETER-VODNÁR and
MARIA TOMOAIA-COTIȘEL

University of Cluj-Napoca, Physical Chemistry Department, 3400 Cluj-Napoca, Romania

Received November 27, 1986

The adsorbed film of stearic acid at the benzene/ water (pH = 2) interface was investigated by means of interfacial tension measurements as a function of time by pendant drop method. The characteristics of the uncharged adsorbed stearic acid film, estimated by using the equilibrium values of the interfacial tension, are discussed in comparison with those of stearic acid film spread at the air/ water (pH = 2) interface, the adsorbed film being more expanded than the spread one. The behaviour of the stearic acid in the twophase systems of oil and water in presence of NaOH was also investigated at various mole ratios R = [NaOH]/ [fatty acid], (pH ranging between 6 and 11), and the extreme (minimum) value of the interfacial tension at the mole ratio $R = 1$ was recorded. This points to the formation of the sodium salt of the fatty acid at the benzene/ water interface, which was also confirmed by the study of adsorption of sodium stearate, leading to the same equilibrium value of the interfacial tension for a given concentration in surfactant and obviously for a mole ratio $R = 1$ in systems with stearic acid. Similar results were also obtained for the systems with caprinic acid at the benzene/ water (pH = 10) interface.

INTRODUCTION

The physico-chemical behaviour of surfactant films is of great interest because of their wide use in many different fields such as: detergent industry, synthetic materials, pharmaceuticals, cosmetics, tertiary oil recovery, froth flotation, etc. Due to their reproducible behaviour both at liquid/ gas and at liquid/ liquid interfaces, saturated fatty acids are largely utilized as reference substances.

The interfacial properties of the adsorbed films of two fatty acids, stearic acid ($C_{17}H_{35}COOH$) and caprinic acid ($C_9H_{19}COOH$) at benzene/ water interface were studied by interfacial tension measurements at constant temperature. In order to determine the interfacial tension of the films with time, the pendant drop method was utilized because of the following advantages [1,2]: it is an absolute method appropriate for the determination of interfacial tensions in a wide range of values (0.3 –hundreds of mN/m), also suitable for pure liquids and polycomponent systems, adequate to investigate the kinetics of interfacial processes; it allows for automatic data processing.[3,4]

EXPERIMENTAL

The substances utilized were of high purity: benzene and HCl p.a. Reactivul", NaOH ,,Chemapol", stearic acid p.a. "Schuchardt", caprinic acid puriss. "Fluka AG" and sodium stearate Riedel-de Haen AG". Solutions of NaOH and HCl were prepared with doubly distilled water. Interfacial tension measurements were performed in benzene/ water systems in presence of fatty acid at various pH values of aqueous phase: pH = 2; and ranging between 6 and 11. The experimental arrangement is presented in Fig. 1. Throughout the experiments temperature was maintained at 20 ± 0.1°C. Drop images were recorded on an AZOPAN PS-21 film in order to determine the characteristic dimensions of the drops (equatorial and selected diameters) necessary to obtain interfacial tension values. To this end a computer program in *BASIC* language was worked out. The accuracy of interfacial tension measurements was ± 0.1 mN/m, in agreement with literature data. [5]

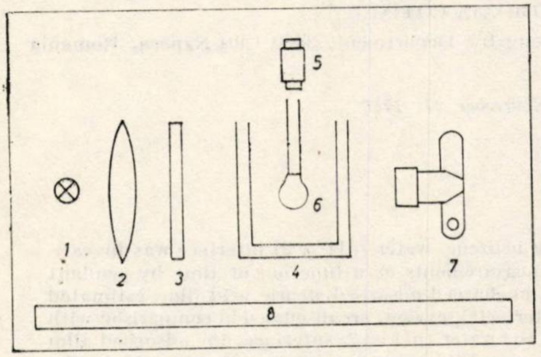

Fig. 1. — Experimental equipment: 1 — light-source, 2 — condensor lens, 3 — mat filter, 4 — thermostated cell, 5 — drop forming device, 6 — drop, 7 — camera, 8 — optical bench.

RESULTS AND DISCUSSION

The interfacial film of stearic acid at the benzene/ water (pH = 2) interface was obtained by adsorption of the fatty acid from benzene phase. We mention that at pH = 2 the stearic acid molecules are practically un-ionized. [6,7]

Interfacial tension (σ, mN/m) at the benzene solution of fatty acid/ water (pH = 2) interface was measured as a function of time for systems with various concentrations (*C*, moles/litre, M) of fatty acid (Fig. 2). It is found that σ varies strongly with time, the adsorption equilibrium being reached in approximately 100 min, which is indicated by the constancy of the interfacial tension values and the appearance of a horizontal slope on the isotherm.

By employing the equilibrium values of the interfacial tension, σ vs. *C* isotherm was constructed (Fig. 3). It is to be noticed that the stearic acid is surface-active at the benzene/ water interface within the concentration range of 10^{-5} and 10^{-1} M, the decrease in the interfacial tension is about 24 mN/m.

The processing of the isotherm (Fig. 3) by a computer, according to the Gibbs equation:

$$\left(\frac{\partial \sigma}{\partial \ln C}\right) = -RT\Gamma \tag{1}$$

allows to obtain the adsorption (Γ) for a certain interfacial tension, and the corresponding molecular area ($A = 1/\Gamma \cdot N_A$; N_A being Avogadro's constant); R and T having their usual meanings. Taking into account that, it is possible to estimate the interfacial pressure (π) from the following relation:

$$\pi = \sigma_0 - \sigma \tag{2}$$

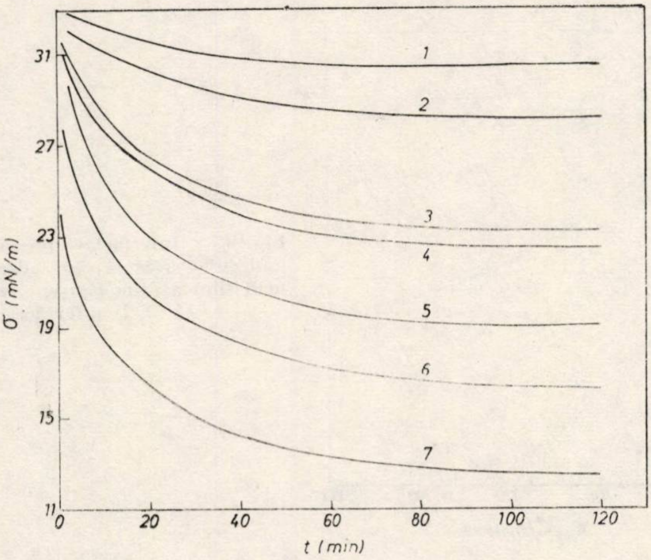

Fig. 2. — Interfacial tension, σ, as a function of time, t, isotherms for benzene solutions of stearic acid/ water (pH = 2). The concentrations of stearic acid (M) are: curve 1 — 1×10^{-3}; 2 — 1.78×10^{-3}; 3 — 2.75×10^{-3}; 4 — 5.7×10^{-3}; 5 — 1.2×10^{-2}; 6 — 1.8×10^{-2}; 7— 5.1×10^{-2}.

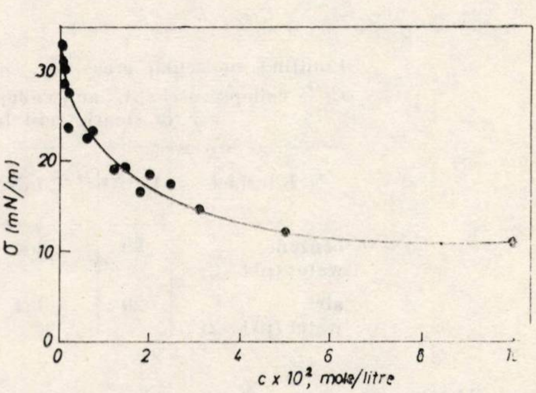

Fig. 3. — Concentration dependence of equilibrium interfacial tension in the system: benzene solutions of stearic acid/ water (pH = 2).

σ_0 being the interfacial tension of "pure" benzene/ water interface and σ for the benzene solution of stearic acid/ water interface, corresponding to the chosen mole concentration of fatty acid, finally π versus A isotherm was calculated for the adsorbed stearic acid film (Fig.4.). By extrapolating to $\pi = 0$, the high pressure linear portion of the π vs. A isotherm, the limiting molecular area A_0 was obtained (Fig. 4, dashed line ; and Table 1.).

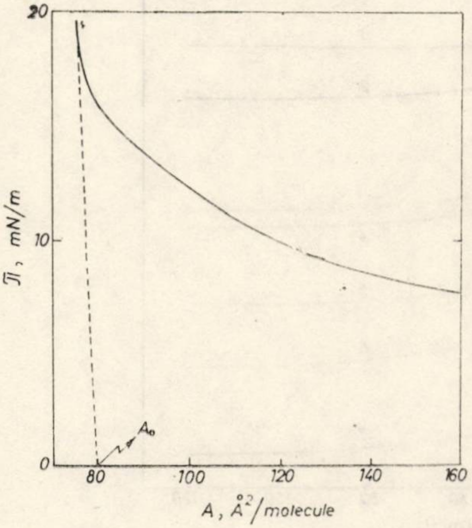

Fig. 4. — Interfacial pressure, π, vs. molecular area A, for adsorbed stearic acid film at the benzene/ water (pH = = 2) interface.

Table 1

Limiting molecular areas, A_0, compressional moduli, C_s^{-1}, collapse area, A_c, and collapse surface pressure, π_c, for stearic acid films.

Interface	A_0, Å²	C_s^{-1}, mN/m	A_c, Å²	π_c, mN/m
benzene/ water (pH=2)	80	304	—	—
air/ water (pH=2)	20	454	18	40.8

For comparison, the surface pressure, π, vs. A compression isotherm[7] for spread stearic acid monolayer, at the air/ water (pH = 2) interface was plotted in Fig. 5. With the help of the compression isotherm, the monolayer properties of stearic acid at the air/ water interface were obtained : A_0 value for solid state of the monolayer (dashed line, for $\pi = 0$, Fig. 5) as well as the collapse characteristics : collapse molecular area, A_c, and collapse surface pressure, π_c, as coordinates of the point where a sudden slope change appears at high surface pressure. Using the $\pi_{vs.} A$ isotherms (Fig. 4 and 5), the compressional moduli [8,9]

$$C_s^{-1} = -A\left(\frac{\partial \pi}{\partial A}\right)_T \tag{3}$$

were estimated by using the linear-region slope of the isotherm for high pressures, with $A = A_0$ (Table 1).

By comparing the limiting molecular areas for stearic acid, oriented at the two interfaces air/ water and benzene/water leads us to the conclusion that the film at the benzene and/ water is more expanded than that at the air/ water interface. The area increase in adsorbed film as compared to spread film for each value of the two-dimensional pressure (Fig. 4 and Fig. 5 is due to those benzene molecules which penetrate betweenand the hydrocarbon chains of the interfacial film, tending to reduce the attraction among the chains. Moreover, the limiting areas obtained for stearic acid in both adsorbed film at the benzene/water interface and in the film spread at the air/ water interface are greater than those found for the cross molecular section (A_c) at the collapse point (Fig. 5 and Table 1). It is worth mentioning that the collapse pressure is the highest surface pressure to which a monolayer can be compressed without detectable expulsion of molecules to form a new bulk phase called collapsed phase. At the collapse of the monolayer the orientation of the molecular chain axis is perpendicular to interface, being favoured by the cohesion forces between the chains of the molecules in spread film, leading to high π_c values.

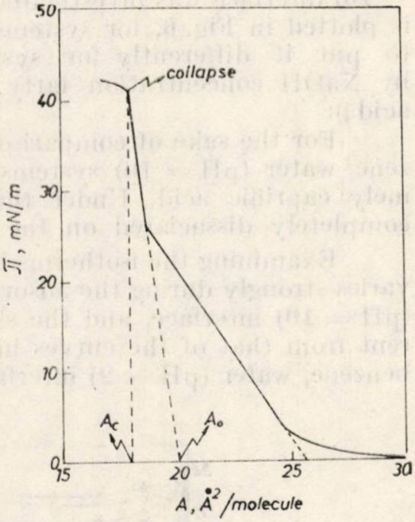

Fig. 5. — Surface pressure, π, vs. molecular area, A, compression isotherm for stearic acid film spread at the air/ water (pH = 2) interface.

Therefore, the chains of the stearic acid molecules in adsorbed film appear to remain in an essentially hydrocarbon environment at the benzene/ water (pH = 2) interface. This fact is supported by the constancy of the free standard energy values for adsorption from the oil phase for alkanols of different chain lengths [10,11] and probably the state of the hydrocarbon chain at the oil/ water interface is similar to that in bulk oil.

The values of the compressional modulus for the adsorbed film at the benzene/ water interface, as well as the monomolecular film at the air/ water characterize the film in a hypothetic state corresponding to close packing of the stearic acid molecules in monolayers at the two types of interfaces, but having $\pi = 0$. However, C_s^{-1} can characterize generally into somewhat the behaviour of the surfactant films, namely the value of the compressional modulus is lower at the benzene/ water interface as compared to the air/ water interface (Table 1), the film being relatively more expanded in the first case as primarily illustrated by the values of the limiting molecular areas as well.

Next, the adsorption of stearic acid from the benzene phase at the benzene/aqueous solution of NaOH constant concentration (pH = = 10) interface was investigated. The interfacial tension vs. time isotherm is plotted in Fig. 6, for systems of various concentrations in stearic acid to put it differently for systems of certain mole ratio (*R*) defined by NaOH concentration/ fatty acid concentration (R = [NaOH]/ [fatty acid]).

For the sake of comparison, Fig. 6 also gives the isotherms for benzene/ water (pH = 10) systems which contain another organic acid, namely caprinic acid. Under these circumstances both acids are almost completely dissociated on the liquid/ liquid interface.

Examining the isotherms in Fig. 6, it is found that interfacial tension varies strongly during the adsorption of stearic acid at the benzene/ water (pH = 10) interface, and the shape of the isotherms is completely different from that of the curves in Fig. 2 recorded for its adsorption at the benzene/ water (pH = 2) interface. Moreover, it is to be noticed in Fig. 6

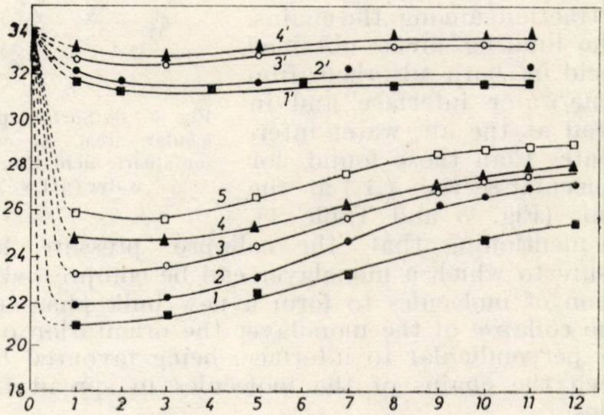

Fig. 6. — Interfacial tension vs. time isotherms for fatty acid benzene solutions/ water (pH = 10) realized with NaOH. The concentrations (M) of stearic acid and respectively mole ratio ($R = C_{NaOH}/C_{fatty\ acid}$) were :

curve 1 – 5.48×10^{-4} ($R = 1$) ;
2 – 6.09×10^{-4} (0.9) ;
3 – 3.78×10^{-4} (1.45) ;
4 – 2.88×10^{-4} (1.9) ;
5 – 1.57×10^{-4} (3.5)

and for systems with caprinic acid were :

1' – 4.93×10^{-4} (R = 1) ;
2' – 4.29×10^{-4} (1.15) ;
3' – 9.86×10^{-4} (0.5) ;
4' – 2.00×10^{-4} (2.47)

that during the first instances from adsorption onset, the interfacial tension takes much lower values than those of the "pure" interface without surfactant ($\sigma_0 = 34$ mN/m) (Fig. 6, dashed line), following then a slow increase of σ with time, having a trend to reach equilibrium values; in Fig. 7 (dashed line), is replotted the curve (1) of Fig. 6 yet this time to values of $t \approx 120$ min from the onset of the adsorption of stearic acid at the benzene/ water (pH = 10) interface.

The shape of the isotherms in Fig. 6 could be accounted for by instant formation of reaction products at the interface — in this case natrium salts of the fatty acids — following then their desorption and transfer in the aqueous bulk phase. In both the system with stearic acid and that with caprinic acid minima of the interfacial tension vs. time occur, which are much more marked in the presence of the fatty acid having the longer hydrocarbon chain. That could be ascribed to the quite different surface activity of the reaction products in the two systems. Due to the high rate of reaction at interface, a real minimum of the interfacial tension vs. time could not be observed because the experimental method did not permit to obtain accurate interfacial tension values during the first minute.

It is necessary to investigate further the adsorption of the natrium stearate from the aqueous phase to the benzene/ water interface (Fig. 7, full line) with a stearate concentration equal to that of stearic acid in the benzene phase for the system with $R = 1$ (Fig. 7, dashed line).

Comparing the isotherms σ vs. time of Fig. 7 for the two systems it is found that the interfacial tension has a trend towards one and the same common equilibrium value. This finding supports the idea of formation of natrium salts of the fatty acids at benzene / alkaline aqueous solution interface as well as the transfer of the reaction products from the interface onto the aqueous bulk phase until the distribution equilibria are reached.

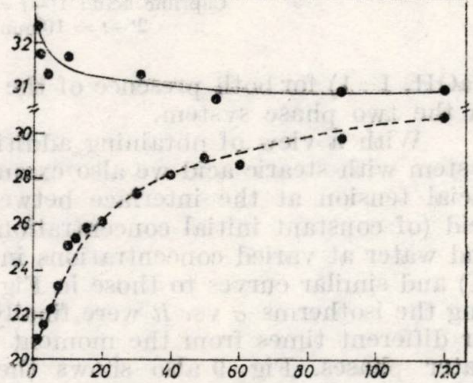

Fig. 7. — Interfacial tension versus time isotherms for benzene/ Na-stearate aqueous solution of 5.42×10^{-4} M concentration (full line), and for stearic acid benzene solution of 5.48×10^{-4}M concentration/ water (pH = 10) (dashed line).

Figure 8 gives the isotherms: interfacial tension as a function of R, for the systems with stearic acid and those of caprinic acid, respectively, recorded at a certain t from the instant the oil and water phases were put in contact; the isotherms were obtained by processing the curves of the type of those drawn in Fig. 6. It is found in Fig. 8 that there is an extreme value of the interfacial tension, a minimum that maintains with time and corresponds to the same mole ratio ($R = 1$, fatty acid: NaOH, 1 : 1) for both presence of the stearic acid and of the caprinic acid in the two phase system.

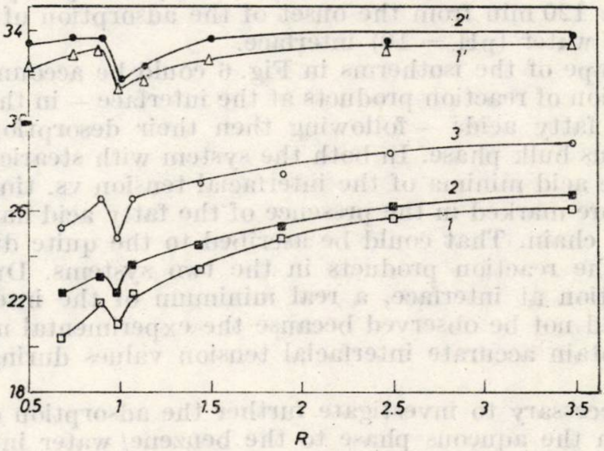

Fig. 8. — Interfacial tension, σ, vs. mole ratio, R, curve for the system with fatty acids at benzene/ water (pH =10) interface at various time periods from onset of adsorption.
Stearic acid: 1 — $t = 1$ min;
2 — $t = 5$ min;
3 — $t = 10$ min;
Caprinic acid: 1'— $t = 3$ min;
2'— $t = 10$ min.

With a view of obtaining additional information on the twophase system with stearic acid we also examined the time variance of the interfacial tension at the interface between the benzene solution of stearic acid (of constant initial concentration in stearic acid, i.e. 5.57×10^{-4} M) and water at varied concentrations in NaOH (pH ranging between 6 and 11) and similar curves to those in Fig. 6 were obtained, by which processing the isotherms σ vs. R were finally obtained; they are given in Fig. 9 for different times from the moment of putting into contact the oil and water phases. Fig. 9 also shows the occurrence of the minimum values of the interfacial tensions which maintain along time for one and the same mole ratio ($R = 1$), as with the systems given in Fig. 8.

Comparing the experimental results of Fig. 9 with those of Fig. 8 it is to be noticed that the extreme values of the interfacial tensions for $R = 1$ are practically the same for similar times from the moment of putting into contact the twophases, although in one case the initial concentration in fatty acid was maintained constant, while in the other that of NaOH (Fig. 8).

The extreme value of the interfacial tension for a certain bulk mole ratio of the reactants in the twophase system can be related to the formation of reaction products in the interface.[12–16] It is noteworthy that at the extreme value of the interfacial tension, even the ratio of the stoichiometric coefficients of reactants in interface is equal to the ratio of their bulk concentration.[12] Therefore, it follows that the extreme value of the interfacial tension obtained in the investigated systems with fatty acids can be correlated to the formation of interfacial reaction compounds, namely, sodium stearate and sodium caprinate.

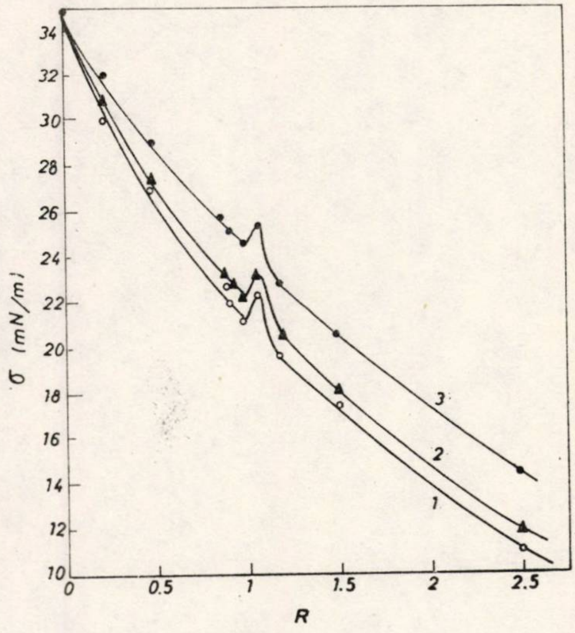

Fig. 9. — Interfacial tension vs. mole ratio (R) curves for systems benzene solution of a constant concentration of stearic acid $5.57 \times \times 10^{-4}$M-aqueous solution at various concentrations of NaOH (pH 6 to 11). Time values at which interfacial tension was considered: 1 — 1 min; 2 — 5 min; 3 — 10 min;

REFERENCES

[1] J. M. Andreas, E. A. Hauser and W. B. Tucker, *J. Phys. Chem.*, **42**, 1001 (1938).

[2] S. Fordham, *Proc. Roy. Soc. (London)*, **A. 194**, 1 (1948).

[3] H. H. Girault, D. J. Schiffrin and B. D. V. Smith, *J. Electroanalyt. Chem.*, **137**, 207 (1982).

[4] J. F. Boyce, S. Schrürch, Y. Rotenberg and A. W. Neumann, *Colloids Surf.*, **9**, 307 (1984).

[5] W. Drost-Hansen, *Ind. Eng. Chem.*, **57** (3), 38 (1965).

[6] G. L. Gaines, Jr., "Insoluble Monolayers at Liquid-Gas Interface", Interscience, New York, 1966.

[7] M. Tomoaia-Cotișel, J. Zsakó, A. Mocanu, M. Lupea and E. Chifu, *J. Colloid Interface Sci.*, **117**, 464 (1987).

[8] M. Tomoaia-Cotișel, "Ph. D. Thesis", University of Cluj-Napoca, 1979.

[9] J. T. Davies and E. K. Rideal, "Interfacial Phenomena", Academic Press, New York, London, 1963.

[10] R. Aveyard, in "Surfactants", Edited by Th. F. Tadros, Academic Press, London, 1984, p. 153.

[11] R. Aveyard and B. Vincent, *Progress in Surface Sci.*, **8**, 59 (1977).

[12] R. Defay, I. Prigogine, A. Bellemans and D. H. Everett, "Surface Tension and Adsorption", Longmans, Green, London, 1966.

[13] E. Chifu and G. Gabrielli, *Gazz. chim. Ital.*, **98**, 1213 (1968).

[14] E. Chifu and I. Albu, *Studia Univ. Babeș-Bolyai, Chem.*, **18** (1), 81 (1973).

[15] M. Tomoaia, Z. Andrei and E. Chifu, *Rev. Roumaine Chim.*, **18**, 1547 (1973).

[16] E. Chifu, *Studia Univ. Babeș-Bolyai, Chem.*, **17** (2), 143 (1972).

Revue Roumaine de Chimie, 32, 7, 693–699 (1987)

THE INFLUENCE OF SODIUM TOLUENE SULFONATE ON SURFACE AND COLLOIDAL PROPERTIES OF SODIUM ALKYLBENZENE SULFONATES

STELA FLORESCU, AURELIA ŞTEFĂNESCU, MARIA ROB
and ION FĂTU
Chemical Research Institute — Detergent Section, 202 Splaiul Independenţei,
Bucharest, Romania

Received November 15, 1986

The research work has been done in order to establish the influence of sodium toluenesulfonate on surface and colloidal properties of sodium l-alkylbenzene sulfonates. The final aim of this work is to improve the building technology and properties of the detergents based on sodium l-alkylbenzene sulfonates, by the addition of sodium toluene sulfonate in their formulations.

INTRODUCTION

Linear-alkylbenzene sulfonates (LAS) represent the predominant class of surfactants in the detergent industry, on account of their high detergence, wetting- and foam properties as well as on their relatively low cost.

It is a well known fact that the aqueous solubility of LAS is increased by the presence of a hydrotropic additive, [1] so that we decided to study the influence of sodium toluenesulfonate (TS) on surface and colloidal properties of LAS. The research work has been done in order to improve some properties of the LAS-based detergents.

In the first part of the present work we studied some surface and colloidal properties of mixtures comprising 2.5 ; 5.0 ; 10.0 and 15.0 g TS in 100 g LAS. In the second part we studied the effect of TS on most important properties of a detergent.

EXPERIMENTAL

Surfactant, TS and builders used

— LAS with 11.9 carbon atoms in the hydrocarbon chain, produced by Dero Ploieşti Factory;

— *p*-Toluenesulfonic acid from Hoechst Co., neutralized by Dero Ploieşti Factory;

— Builders: sodium tripolyphosphate, sodium sulphate, sodium ethylenediaminetetraacetate, carboxymethylcellulose, fluorescent whiteners and perfume of technical grade (Romanian products).

Test Methods

— Critical micelle concentration (cmc) estimated from the surface tension (γ) versus log. concentration curves, at 25°C; surface tension was measured by the ring method;

— The wetting was found by the time necessary for the sample of fabric to be immersed into an aqueous solution of surfactant, at 25°C;

— Viscosity (η) was measured with Rheotest 2 at 80°C;

— The foaming power (P_{sp}) was estimated from the foam volume made in certain circumstances by an aqueous solution of surfactant, at 25°C; foam stability (S_{sp}) represents the ratio between foam volume after a certain time of rest and the initial foam volume;

— The washing power (S_{abs}) was estimated by measuring the reflectance of an artificially soiled fabric after its wash in the aqueous solution of surfactant; the test was done on a polyesteric-cotton fabric, at 60°C;

— The solubilization rate of a detergent in water was found by the time necessary to obtain 100 mL solution of 10 g detergent/L, at 25°C.

RESULTS AND DISCUSSION

Part. I. The influence of sodium toluenesulfonate on the surface and colloidal properties of sodium alkylbenzene sulfonates

The properties studied on the mixtures of LAS and TS were: critical micelle concentration, wetting- and washing power. The results of these tests are shown in figures 1—3.

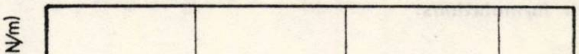

Fig. 1. — Surface tension versus log. concentration for the mixtures of LAS + TS (● % TS; ■ 2.5% TS; ○ 5.0% TS; × 15% TS).

(The symbols are the same for all the figures: ● LAS + 0% TS; ■ LAS + 2.5% TS; ○ LAS + 5.0% TS; □ LAS + 10.0% TS; × LAS + 15.0% TS).

As can be seen there are no important differences in cmc value of the mixtures of LAS and TS and the cmc value of LAS. So we can say that TS has no effect on the cmc value of LAS.

The washing power of the mixtures of LAS and TS is a little higher than the washing power of LAS. However these differences

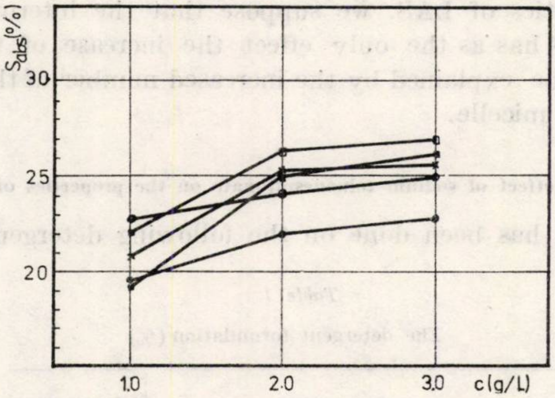

Fig. 2. — Washing power versus concentration for the mixtures of LAS + TS (● % TS; ■2.5% TS; ● 5.0% TS; ○ 10%TS; × 15% TS).

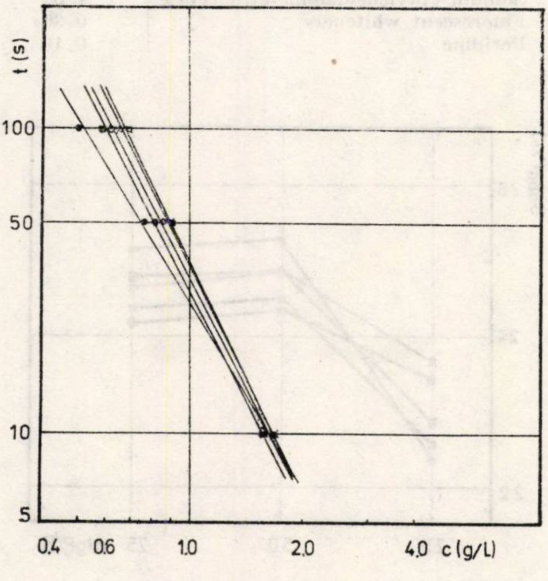

Fig. 3. — Wettability-immersion time versus concentration for the mixtures of LAS + TS (●% TS; ■2.5% TS; ○ 5.0% TS; □ 10% TS; × 15% TS).

are not essential, so we can say that TS has practically no effect on the washing power.

The wettability of mixtures of LAS and TS is almost equal to that of the LAS alone. Therefore the wettability is not influenced by the addition of TS.

According to the fact that TS does not influence the surface- and colloidal properties of LAS, we suppose that the intermolecular action of LAS with TS has as the only effect the increase of the solubility of LAS. This can be explained by the increased number of the solubilization groups in LAS micelle.

Part II. **The effect of sodium toluenesulfonate on the properties of a detergent**

Our study has been done on the following detergent formulation:

Table 1

The detergent formulation (%)

Component	Detergent
Sodium l-alkylbenzene sulfonate	16.00
Sodium tripolyphosphate	30.00
Sodium sulphate	51.00
Carboxymethylcellulose	1.60
Sodium ethylenediaminetetraacetate	1.00
Fluorescent whiteners	0.30
Perfume	0.10

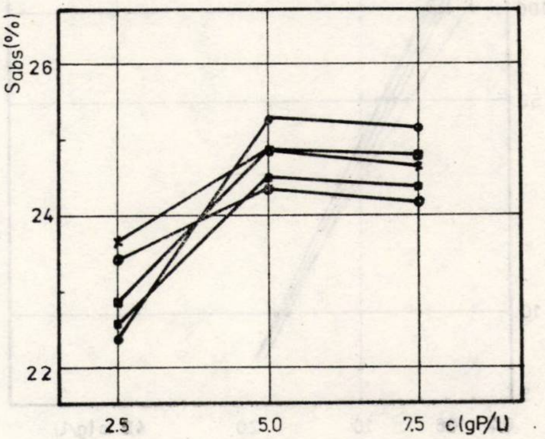

Fig. 4. — **Washing power versus concentration for one detergent comprising TS (● % TS ; ■ 2.5 % TS ; O 5.0 % TS : □ 10 % TS ; × 15 % TS)**

The named detergent was built with 2.5 ; 5.0 ; 10.0 and 15.0 g TS/100 g LAS and the following properties were investigated : the washing power, the foaming power and foam stability, the solubilization rate and viscosity of the detergent slurry (65% concentration). The results of all these tests are shown in figures 4–8.

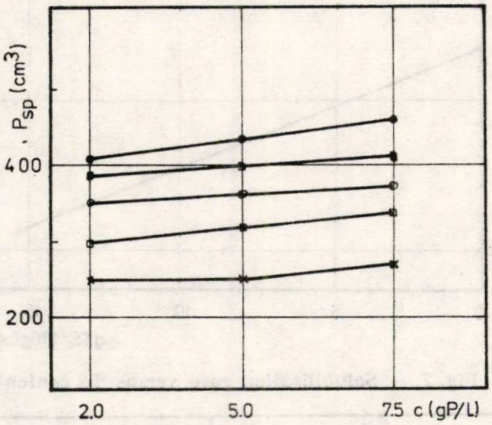

Fig. 5. — Foaming power versus concentration for a detergent comprising TS (● % TS; ■ 2.5% TS; ○ 5.0%; TS; □ 10% TS; × 15% TS).

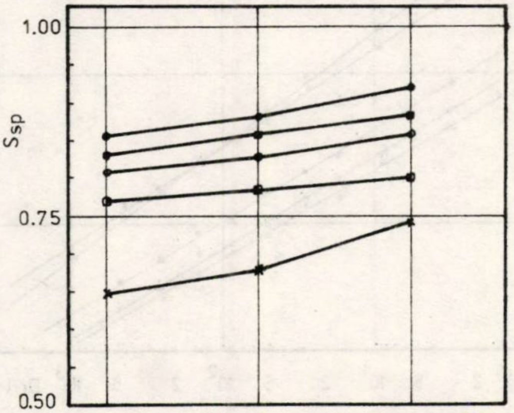

Fig. 6. — Foam stability versus concentration for one detergent comprising TS (● % TS; ■ 2.5% TS; ○ 5% TS; □ 10% TS; × 15% TS).

The washing power of the detergent with TS is practically equal to that of the detergent without TS.

The foaming power and foam stability progressively decrease with the content of TS.

The solubilization time also decreases with the content of TS.

Viscosity of the slurries of detergent comprising TS progressively decreases with the content of TS.

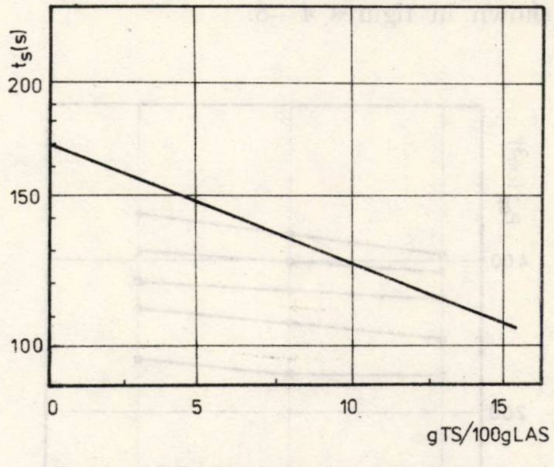

Fig. 7. — Solubilization rate versus TS content.

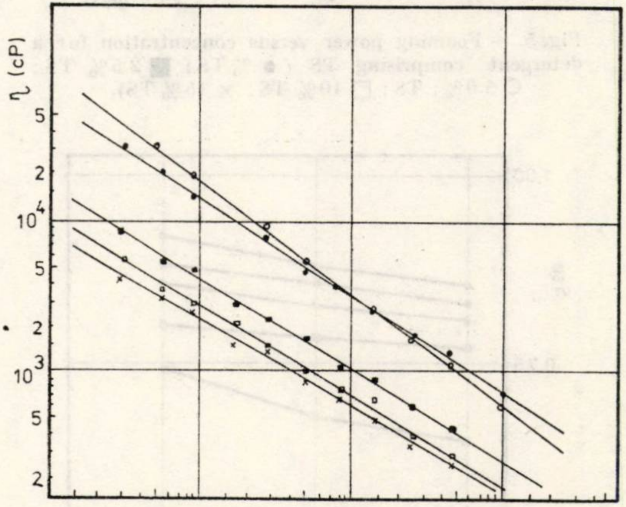

Fig. 8. — Viscosity versus the shear rate for the slurries of detergent comprising TS (● % TS ; ■ 2.5 % TS ; ○ 5.0 % TS ; □ 10 % TS ; × 15 % TS).

CONCLUSIONS

The present work proved that the addition of TS to the LAS-based detergents has the following advantages :

— decreases the viscosity of slurries ;

– decreases the foaming power and foam stability of the detergent;

– increases the solubilization rate of the detergent.

The results of this study will be applied at the detergent factories in order to improve the building technology and the detergents quality.

ACKNOWLEDGEMENTS. The authors wish to thank Mr. P. Ionescu for his support to this investigation.

REFERENCES

[1] M. J. Rosen, "Surfactants and Interfacial Phenomena", N4, Toronto, 1978, p. 8.

Revue Roumaine de Chimie, 32, 7, 701–706 (1987)

ELECTROSYNTHESIS OF PROPIONITRILE. II*

PHASE EQUILIBRIA IN THE ACRYLONITRILE–PROPIONITRILE–WATER SYSTEM IN THE PRESENCE OF CATIONIC SURFACTANTS AND ELECTROLYTES

LIVIU ONICIU[a], DAN A. LÖWY[b], MARIA JITARU[b], IOAN A. SILBERG[b] and BOGDAN C. TOMA[b],

[a] University of Cluj-Napoca, Department of Physical Chemistry, Cluj-Napoca, Romania

[b] ICECHIM – Institute of Chemical and Biochemical Energetics Cluj-Napoca Research Group, Cluj-Napoca, Romania

Received December 23, 1986

The experiments herewith reported were carried out as a consequence of the practical necessity of effectuating a rigorous material balance of propionitrile manufacturing by the non-dimerizant acrylonitrile electroreduction.

In this order, the individual solubilities in aqueous phosphate buffer of pure acrylonitrile, propionitrile, and of their mixtures in different proportions were studied. Determinations were carried out in the presence and the absence of a cationic surfactant in approximately micellar concentrations. An empirical additivity rule obeyed by global solubility is put forward.

INTRODUCTION

The electrochemistry of acrylonitrile, having as the most significant result the synthesis of adiponitrile, applied at industrial scale, offers the possibility of obtaining several other products – like propionitrile, allylamine, propylamine, etc. – in advantageous conditions from the economic, energetical and ecological point of view.[1–4]

The selectivity of the acrylonitrile (ACN) electroreduction to propionitrile (PN), avoiding the electrohydrodimerization to adiponitrile, is controlled mainly by the nature and concentration of the cationic surfactant, as well as by its behaviour in the synthesis medium, consisting of an electrolyte based on an approximately neutral phosphate buffer, in contact with an organic phase: a mixture of ACN and PN.[5,6]

The experiments reported in the present paper were carried out as a consequence of the practical necessity of effectuating a rigorous material balance of the PN manufacturing by the non-dimerizant ACN electroreduction.

Since in the literature there are data concerning only the reciprocal solubilities in the binary and ternary systems formed by ACN, PN and

---

* Part. I. *Stud. Univ. Babeș–Bolyai, Chem.*, 31, 80 (1986).

H_2O [7,8] we set ourselves as a goal to investigate these systems in the presence of electrolytes and a quaternary ammonium salt in submicellar concentrations, compositions similar to the working medium of the propionitrile electrosynthesis, and which modify the solubility values.

EXPERIMENTAL

The materials used in the equilibrium experiments were :

— acrylonitrile (99 %) — *Combinatul Petrochimic* Pitești

— propionitrile (98—99 %) — *I.C.P.A.O.* Mediaș

— alkyltrimethylammonium chloride (ATA^+Cl^-) — *Intreprinderea de Detergenți* Timișoara. The surfactant is of technical grade. It has thea verage molecular weight of 275.5 and contains approximately 60 % C_{12} and 40 % C_{14} alkyl chains.

The individual solubilities in an aqueous phosphate buffer of pure ACN, PN, and of their mixtures in different proportions were studied. The system was magnetically stirred for 2 hours at constant temperature, until equilibrium was reached. The densities of the organic and of the aqueous phase were measured before and after partition. The composition of the organic phase at equilibrium was determined by a previously described gas-chromatographic method, [9] while the concentration of the cationic surfactant in the aqueous phase was monitored by potentiometric titration, using an original liquid-membrane surfactant-selective electrode, [10] respectively a coated-wire electrode. [11] Both electrodes are based on the same active principle : the tetraphenylborate of the alkyltrimethylammonium ion used in electrosynthesis. [10]

RESULTS AND DISCUSSION

For evaluating the optimal duration of the experiments, a kinetic study of the partition process, at a given ratio of the organic and of the aqueous phase and in the presence of approximately micellar concentrations of the cationic surfactant, was carried out. As seen in Figure 1, the partition equilibrium is complete in 2 hours, attaining a proportion of 89.1% in 30 minutes.

Under the conditions of PN electrosynthesis, the concentration of the quaternary ammonium salt in the aqueous phase decreases in time as seen in Figure 2 by the simultaneous action of two phenomena :

1. its extraction by organic phase and
2. a slight consumption in the electrochemical process.

Taking into account the recommendation of the literature to run the electrosynthesis by using cationic surfactants in concentrations less than equal to the critical micellar concentration (CMC),[12] it was necessary to determine the CMC of the quaternary ammonium salt involved in the electroreduction of ACN to PN. Since this surfactant is not a unitary product there is no well-defined value for the CMC, but a concentration range, which can be estimated by adequate methods.

In this paper the CMC determinations were carried out by 4 different methods : by means of the selective liquid-membrane electrode, [10] respectively a coated wire electrode, [11] the conductivity method and the Wilhelmy method. Table 1 contains the CMC values of the cationic surfactant in aqueous and phosphate buffer media. A rather good reproducibility of the results obtained in aqueous solution by different methods can be observed. The best agreement with the CMC values found in the literature (*e.g.* $4.47 \cdot 10^{-3}$ M $\cdot$ L^{-1} for the tetradecyltrimethylammonium chloride, [13] respectively $3.51 - 3.6 \cdot 10^{-3}$ for the corresponding

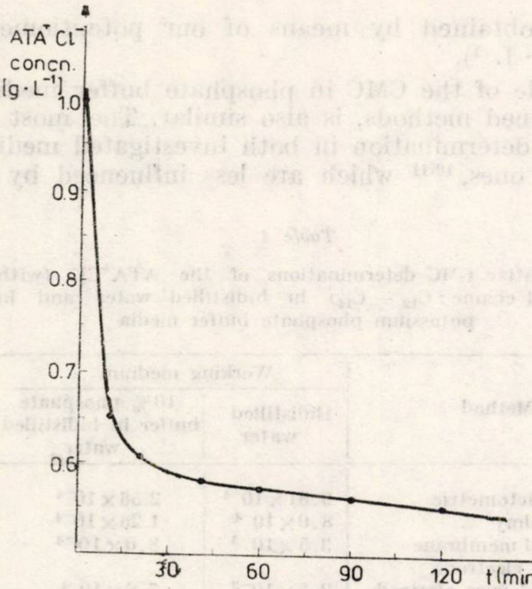

Fig. 1. — Kinetics of the ATA$^+$Cl$^-$ partition between a 10% potassium-phosphate aqueous buffer and an organic phase consisting of ACN and PN (3.22 : 1, W/W), at a volume ratio of the organic phase *vs.* the aqueous phase equal to 0.325.

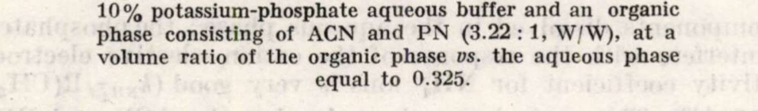

Fig. 2. — The decrease in time of the ATA$^+$Cl$^-$ concentration by multiple extraction with organic phase (curve a, k — number of extractions), respectively under the conditions of PN electrosynthesis (curve b), by the initial partition of ATA$^+$Cl$^-$ and its consumption in the electrochemical process.

bromide,[14,15] was obtained by means of our potentiometric methods ($2.5 - 3.5 \cdot 10^{-3}$ M $\cdot$ L^{-1}).

The magnitude of the CMC in phosphate buffer medium, obtained by the four mentioned methods, is also similar. The most suitable methods for the CMC determination in both investigated media seem to be the potentiometric ones,[10,11] which are less influenced by the presence of the components dissolved in the aqueous phase; the phosphate anions do not interfere with the response of the cation-selective electrode, and its selectivity coefficient for NH_4^+ ions is very good ($k_{NH_4^+}/R(CH_3)_3N^+ = 3.9 \cdot 10^{-4}$ [10]). The neutral organic molecules, the ACN and PN in our case, have no influence upon the electrode potential.

Table 1

Comparative CMC determinations of the ATA^+Cl^- (with an alkyl chaine : $C_{12} - C_{14}$) in bidistilled water and in potassium phosphate buffer media

Method	Working medium	
	Bidistilled water	10% phosphate buffer in bidistilled water
Conductometric	9.61×10^{-4}	2.56×10^{-4}
Wilhelmy	8.0×10^{-4}	1.26×10^{-4}
Liquid membrane electrode	3.5×10^{-3}	8.0×10^{-4}
Coated wire electrode	2.5×10^{-3}	7.6×10^{-4}

In the reciprocal solubility determinations carried out at an organic/ aqueous phase ratio of 0.325 the values given in Table 2 were obtained. These results point out to the salting out effect of electrolytes

Table 2

The individual solubilities of pure ACN and PN and of their mixtures in water and in phosphate buffer solution, respectively in the presence and absence of approximately micellar concentrations of the ATA^+Cl^- (* values from the literature [7,8])

Working medium	ionic strength	ATA^+Cl^- concen. /$g \times L^{-1}$/	Solubility/ g/ 100 mL/					
			ACN	PN	ACN/PN = 3.222		ACN/PN=1.000	
					calcd.	found	calcd.	found
Distilled water	0	—	7.92	9.94	8.41	8.40	8.95	9.50
	~0	1.0	9.48	11.68	9.99	9.82	10.58	10.81
KH_2PO_4 + K_2HPO_4	1.14	—	6.12	7.18	6.37	6.45	6.65	6.58
		1.0	6.23	7.21	6.46	6.42	6.72	6.63
$NH_4H_2PO_4$	4.04	—	4.01	4.64	4.16	4.15	4.33	4.33
$(NH_4^+)_2HPO_4$		1.0	5.04	6.90	5.49	5.48	5.99	5.96

$$S_{g1} = X_{ACN} \times S_{ACN} + X_{PN} \times S_{PN} \quad (1)$$

present in the aqueous phase upon the solubility of ACN and PN, the cationic surfactant exerts, as expected, a salting in effect, which is rather marked in distilled water and in ammonium buffer. A higher ionic strength medium consisting of a 30% K^+ and NH_4^+ phosphate buffer ($j = 5.19$) produces a more advanced insolubilization of the organic molecules, the global solubility decreasing to approximately 3.5 g ACN + PN (1 : 1, W/W) per 100 mL solvent.

Data in Table 2 are relevant for the fact that the global solubility obeys an additivity rule given by the equation 1 in Table 2, where: Sgl — global solubility; S_{ACN} and S_{PN} — individual solubilities of ACN and PN; X_{ACN} and X_{PN} — molar fractions of ACN and PN in the initial organic phase. This empirical relationship, which can be deduced theoretically on the assumption that the chemical potentials of the compounds in pure state and in mixtures have a constant value,[16] is a proof of the ideal behaviour of the ACN-PN-H_2O system at equilibrium. The explanation of the phenomenon is to be found in the chemical similitude of the two organic molecules present in the system.

By means of the determined solubility data, a complete material balance of the propionitrile electrosynthesis can be accomplished.

The entire quantity of the PN obtained in a non-dimerizant electroreduction experiment, is to be calculated by the summation of the PN, determined by a gas-chromatographic method[19], from the spontaneously separated organic phase and from the organic phase resulting when distilling the ACN-PN-H_2O azeotrope, with the PN extracted by ethyl ether from the remaining aqueous phase.

The PN amounts obtained by the described summation method (see column 4 in Table 3) are in agreement with the results calculated from the independently determined solubility data.

CONCLUSIONS

The reciprocal solubility determinations, herewith reported, enabled us to abandon the laborious methodology of gas-chromatographic analysis of the aqueous phase and multiple extractions with ethyl ether. In the ulterior experiments both the current efficiency and the conversion could

Table 3

The complete material balance of 3 representative experiments of PN electrosynthesis (Organic phase 1 — the organic phase spontaneously separated at the end of the experiment; Organic phase II — the organic phase resulting from the distilled ACN-PN-H_2O azeotropic mixture; Aqueous phase — the phase remaining after the distillation of the azeotrope)

Experiment no.	Found				Calculated
	Organic phase I	Organic phase II	Aqueous phase	Total	
1	23.35	16.14	24.50	63.99	64.75
2	25.73	16.53	24.80	67.04	67.27
3	24.75	16.42	24.75	65.92	66.34

be determined by correlating the gas-chromatographic analysis of the separated organic phase with the corresponding solubility data, the latter giving the exact amounts of PN and ACN retained by the aqueous phase.

Further investigations of the thermodynamics and other fundamental aspects of these systems will form the object of a future paper.

REFERENCES

[1] N. Tsutomu and S. Kiichiro, *J. Electrochem. Soc.*, **114**, 1255 (1967).

[2] Yu. D. Smirnov, L. I. Saltikova and A. P. Tomilov, *Zhur. priklad. Khim.*, **43**, 1620 (1970).

[3] N. Watanabe, T. Hirai and I. Tasato, *Pat. Japan*, 77 31 313, 13 Aug. 1977 ; *Chem. Abstr.*, **88**, 13637 (1978).

[4] I. L. Knunyants, S. L. Varshavskii, A. P. Tomilov and L. V. Kabak, *Pat. Fr.* 1401175, June 4, 1965 (*Chem. Abstr*, **64**, 1660 (1966)) and *Pat. Brit.* 1014428, Dec. 1965 (*Chem. Abstr.*, **64**, 7683 (1966)).

[5] L. Oniciu, I. A. Silberg, D. A. Löwy, M. Jitaru and F. Ciomoş, *Stud. Univ. Babeş-Bolyai Chem.*, **31**, 80 (1986).

[6] L. Oniciu, I A. Silberg, I. Bâldea, F. Ciomoş, M. Jitaru, D. A. Löwy, O. H. Oprea and L. Radu, *Kinetics of competing reactions of acrylonitrile electroreduction to adiponitrile and propionitrile*, in "Proceedings of the 36th Meeting of the International Society of Electrochemistry", Salamanca, Spain, September 23–28, 1985, pp. 13010–12.

[7] V. V. Prokhorova, L. A. Serafimov, R. I. Novoselova and L. S. Takhtamysheva, *Zhur. fiz. Khim.*, **38**, 1488 (1964).

[8] L. A. Serafimov, V. V. Prokhorova and R. I Novoselova, *Zhur. fiz. Khim.*, **38**, 1662 (1964).

[9] D. A. Löwy, I. A. Silberg and L. Oniciu, *Rev. Chim.* (*Bucureşti*, **36**, 354 (1985).

[10] L. Oniciu, D. A. Löwy, I. A. Silberg and D. F. Anghel, *Analysis* **14**, 456 (1986).

[11] L. Oniciu, D. A. Löwy, I. A. Silberg, D. F. Anghel, F. Ciomoş, and M. Jitaru, *Electroanalytical methods for determination of cationic surfactants involved in adiponitrile electrosynthesis*, in "Proceedings of the Second Symposium of Applied Electrochemistry", Timişoara, 4–5 October 1985, Tome I, p. 207.

[12] L. Oniciu, I. A. Silberg and F. Ciomoş, *Rev. Chim. (Bucureşti)*, **36**, 406 (1985).

[13] H. W. Hoyer and A. Marmo, *J. Phys. Chem.*, **65**, 1807 (1961).

[14] R. L. Vanable and R. V. Nauman, *J. Phys. Chem.*, **68**, 3498 (1964).

[15] H. J. L. Trap and J. J. Hermans, *Proc. Koninkl. Ned. Akad. Wetenschap*, **58 B**, 97 (1955) ; Chem. Abstr., **49** : 12918 (1956).

[16] I. Zsakó, personal communication.

Revue Roumaine de Chimie, **32**, 7, 707–712 (1987)

DETERGENT SUSPENSION FOR HARD WASHINGS

STUDY OF FLUIDITY AND STABILITY

EVELINE POPOVICI, MIHAELA GRECU*, ANGELA POPA, MARIA ALEXANDROAIE, AURELIA VASILE, MIHAI CRUCEANU and NICOLETA DUMITRU*

Faculty of Chemical Technology, Polytechnic Institute Iași, R-6600 Iași, Romania
* ICECHIM-Bucharest, Romania

Received November 12, 1986

In the manufacturing process of detergent suspension for hard washings the necessity to ensure a fluid and stable character is an important problem. With the view of optimizing the stages in obtaining and storing detergent suspension the paper approaches the study of rheological tests of H type detergent suspensions comparatively with some witness products. The rheological properties correlated with the washing performances have revealed the efficiency of the H type detergent suspensions.

INTRODUCTION

Present necessities which impose certain detergent formulas demonstrated the advantage of obtaining and utilizing detergent suspensions. Unlike the liquid detergents, which contain 25–30 active substances, the detergent suspensions allow the reduction of active substance content simultaneously with the increase of the washing process efficiency.[1] The utilization of detergent suspension is favourable due to the fact that in their manufacturing process the specific consumption of energy is lower than for granulated detergents.[2,7]

With the view of optimizing the stages in obtaining and storage of detergent suspensions, out of the necessity to ensure their fluid and stable character, the present paper studies rheological tests for some detergent suspensions for hard washings comparatively with some control products (Romy and Azur from Czechoslovakia).

EXPERIMENTAL

The detergent suspensions for hard washings were prepared in standard conditions with reference to the order of addition, temperature and stirring speed.[8]

A mixture of 16% tensioactive agents, 17% sequestration agents against Ca and Mg ions, 1–3% carboxymethylcellulose (preventing the redepositing and thickening of suspension), 5% silica gel (as a conditioning agent) and 56–60% water were included in the composition of suspensions (Table 1).

Table 1

Chemical composition of the detergent suspensions for hard washings

Code	Tensioactive agents, %			Sequestration agents, %		Anti-redeposit agents, % CMC	Conditioning agents, %		Water, %
	Anionic	Nonionic	Soap	TPPNa	EDTA 40%		Silica gel	NaCl	
H_1	6	6	4	15	2	1	5	—	61
H_2	10	6	—	15	2	3	5	—	59
H_3	8	8	—	15	2	1	5	—	61
H_4	12	—	4	15	2	1	5	—	61
H_5	8	8	—	15	2	2	5	—	60
H_6	8	8	—	15	2	3	5	—	59
H_7	8	8	—	15	2	—	5	3	59

The preparation of samples lasted 120 minutes. This was considered the zero point in the experiments. Fluidity and flow properties of detergent suspensions were tested through viscosity determinations, using a Rheotests 2 apparatus with the ratio of coaxial rollers $r/R = 0.9$.

The experiments were made at temperatures varying between 20 and 60 C. The detergent suspensions were analysed for a four-months storage without stirring.

The anti-redeposit power was determined with a Zeiss, leuchometer while the washing capacity was analysed by titrating the dilute detergent suspension with oil. [9]

RESULTS AND DISCUSSION

The study of viscosity variation of detergent suspensions versus the shear rate shows that the viscosity decreases with the increase of the shear rate. This is a result of a destructuration process which brings about a decrease of internal friction. This behaviour — specific also to standard suspensions — is evident throughout the analysed interval of temperature.

It could be mentioned that the analysed detergent suspensions, except for H_4 suspension, are less viscous than the standard products. During storage the viscosity of the standard suspensions prepared long before remains constant. The determinations carried out at temperatures of 20 and 60°C show that during the storage the viscosity of the H type suspensions changes within the first week then becomes stabilized.

This behaviour is noted in a four-months storage period.

The non-linear dependence of the shear stress versus the shear rate proves a nonnewtonian behaviour caused by the modification of the structure of the suspensions under the action of the frictional forces. A curve with hysteresis is obtained by continuously modifying the shear rate, either increasing or decreasing it. This proves the interactions between the flow elements and the dispersion medium determining a tixotropical behaviour.

The quantitative estimation of these phenomena was performed by determination of the consistence index (k) and the flow index (n) using the rheological Oswald de Waale model for different values of the shear rate. [10] At the zero point, the analysed detergent suspensions, except for H_4 suspension, show values of consistence indexes lower than of standard products, though they possess a higher flow index.

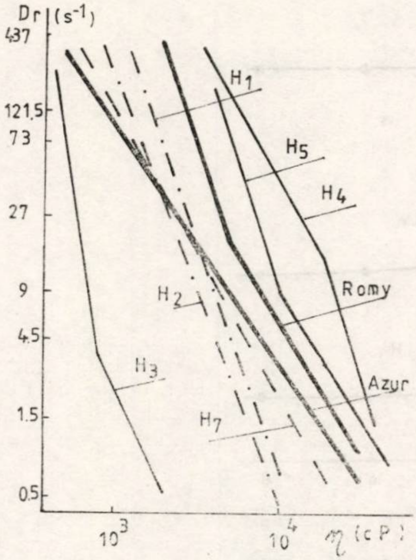

Fig. 1. — Variation of viscosity versus shear rate, at 20°C.

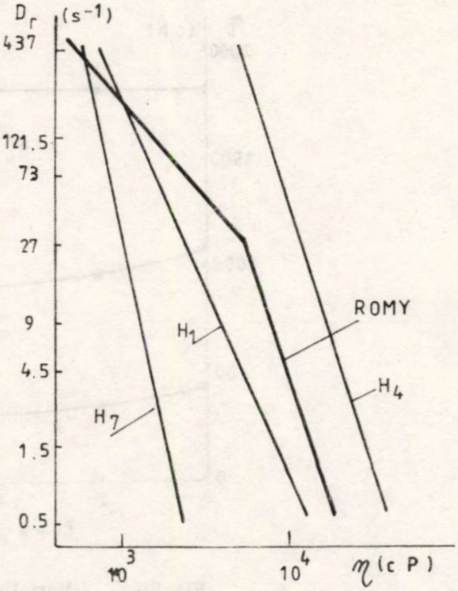

Fig. 2. — Variation of viscosity versus shear rate, at 60°C.

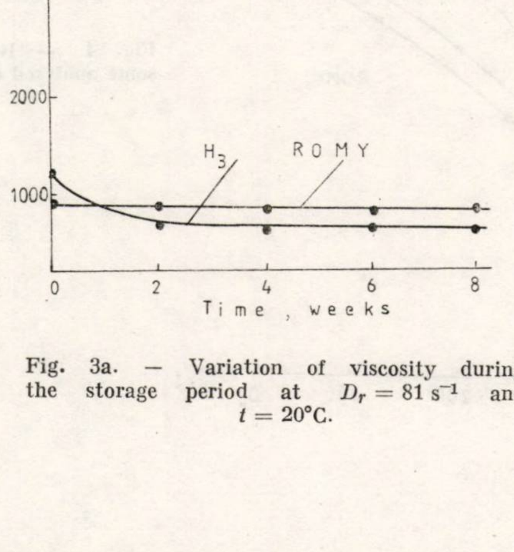

Fig. 3a. — Variation of viscosity during the storage period at $D_r = 81\ s^{-1}$ and $t = 20°C$.

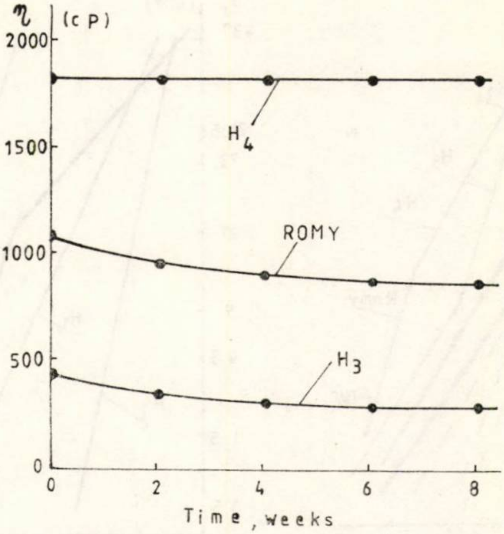

Fig. 3b. — Variation of viscosity during the storage period at $D_r = 81\ s^{-1}$ and $t = 60°C$.

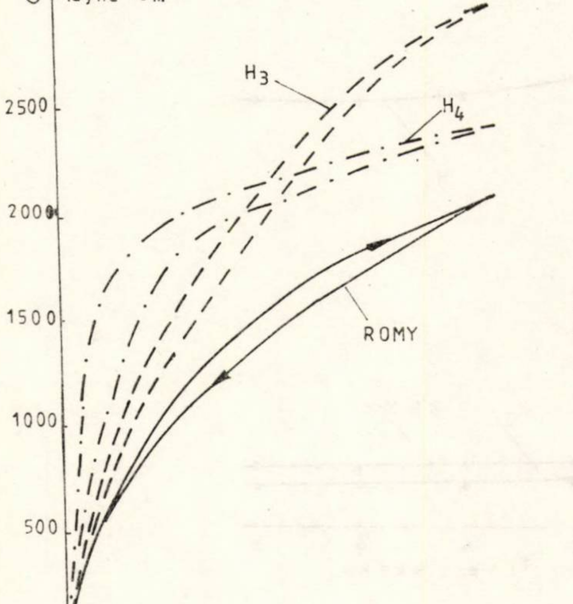

Fig. 4. — Rheological curves of some analysed detergent suspensions.

The rheological behaviour of H_4 suspension shows the influence of an increased content of anionic tensioactive substance and soap in the composition of the sample.

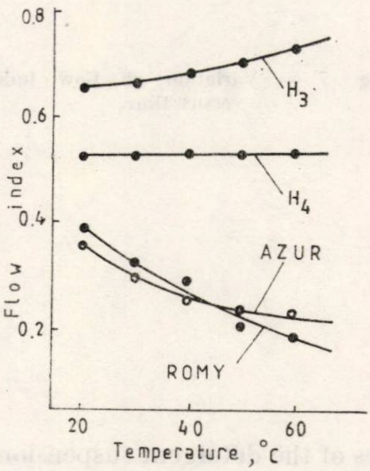

Fig. 5. — Variation of flow index versus temperature.

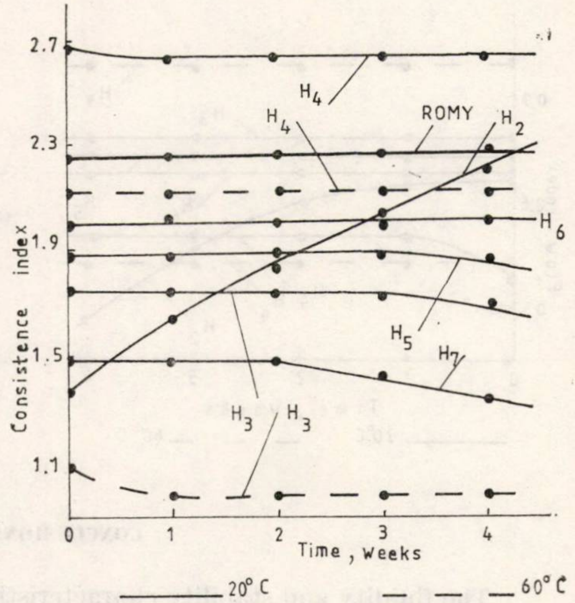

Fig. 6. — Variation of consistence index versus time.

The flow index increases with the increase of temperature whereas a decreasing variation was observed for the standard products (Fig. 5). This observation reveals the facility in operating with H type suspensions at increased temperatures. At standard products a decreasing variation of the consistence index with the increase of temperature was observed.

Generally, during storage at 20 and 60°C, the values of the consistency index show a slight tendency of decrease in the first part of storing followed by a further stabilization of this parameter (Fig. 6)

The flow index remains constant during storing. H_1 and H_2 suspensions have a particular behaviour with respect to both the variation of the consistence index (Fig. 6) and to the flow index. The constant maintenance of the k and n values during storing is a criterion for the stability in time of these suspensions and from this point of view we notice that all the analysed detergent suspensions are stabilized in storing, except for H_1 and H_2 suspensions.

The increase of viscosity (with an order of magnitude — Fig. 1) and of the consistence index (Fig. 6) simultaneously with the decrease of the flow index (Fig. 7) are due to the addition of 1—3% carboxymethyl-cellulose.

The determination of the anti-redeposit power and of the washing capacity have shown similar values of the utilization index for all the analysed detergent suspensions as well as for the standard products.

The washing performances correlated with the estimations referring to the stability in storage reveal the efficiency of the analysed detergent formulas, except for H_1 and H_2 samples.

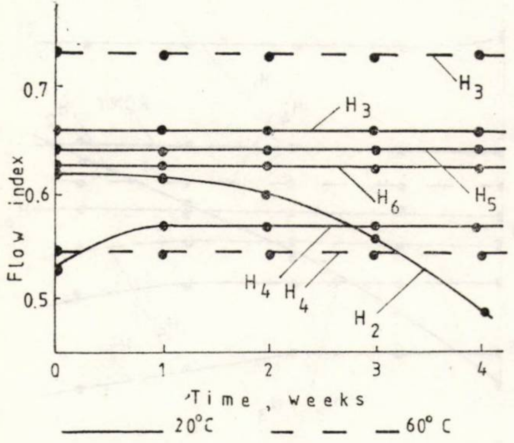

Fig. 7. — Variation of flow index versus time.

CONCLUSIONS

The fluidity and stability characteristics of the detergent suspensions for hard washings were appreciated by analysing the viscosity, the flow index and the consistence index during a storage period. It resulted that the constant maintenance of the k and n indices in storage is a criterion of the stability in time of these suspensions. From this point of view the remarkable behaviour of H_3-H_7 suspensions should be stressed.

The effect of the carboxymethylcellulose addition bringing about an increase of the viscosity and consistence index was revealed.

The anionic tensioactive agent and the soap ensure a good stability of the detergent suspensions during storage.

REFERENCES

[1] A. M. Schwartz and J. W. Perry, "Surface Active Agents and Their Chemistry and Technology", New York, 1978, pp. 459–464.

[2] Jpn. Kokai Tokkyo Koho J. Pat. 8 234 017 (1982) ; *Chem. Abstr.*, **97**, 8153 (1982).

[3] E. Popovici, *Rev. Chem.*, **36**, 310 (1985).

[4] Sorbe Guenter, Bollwerk Juergen (Hoechst A. G.) Ger. Pat. Appl. Ep. 46.171 (1982) ; *Chem. Abstr.*, **96**, 219684 (1982).

[5] Jpn. Kokai Tokkyo Koho J. Pat. 8234016 1982 ; *Chem. Abstr.*, **97**, 81546 (1982).

[6] Jpn. Kokai Tokkyo Koho J. Pat. 5 938 299 (8438299) 1984 ; *Chem. Abstr.*, **101**, 25418 (1984).

[7] Jpn. Kokai Tokkyo Koho J. Pat. 5 949 298, 1984 ; *Chem. Abstr.*, **101**, 40244 (1984).

[8] E. Popovici, Proceedings, Slovzeo, Conference, 1984, 2nd vol., p. 88.

[9] H. E. Tschakert, *Seifen Ölle Fette Wachse*, **93**, 421 (1967).

[10] R. Tudose, "Reologia compușilor macromoleculari", Ed. Tehnică, Bucharest, 1982.

Revue Roumaine de Chimie, **32**, 7, 713–721 (1987)

POLYMER-SURFACTANT INTERACTION SURFACEACTIVE PROPERTIES

M. M. MARINESCU, MARIETA BALCAN, B. G. ALBU,
GEORGETA POPESCU and N. N. WEISSMAN
ICECHIM Center of Physical Chemistry, Splaiul Independenței 202,
79611 Bucharest, Romania

Received December 8, 1986

The interaction of sodium dodecylsulphate (SDS) with non-ionic (polyvinylpyrrolidone – PVP) or ionic (bovine serum albumin – BSA) polymers has been studied by surface tension measurements of their aqueous solutions; use has been made of drop volume method. The surface tension and adsorption isotherms in systems with and without polymers have allowed us to calculate the molar adsorption coefficients, the surface area per molecule at interface and the thickness of adsorbed molecular layer at solution–air interface. The results obtained were employed in a comparative study of the adsorption of the surfactant in systems containing different polymers and in an analysis of the way the adsorption of the surfactant at the solution – air interface is influenced by the presence of the polymer. A comparison of this method with other methods (e.g. liquid membrane ion specific electrodes) suggests that although it is outstandingly simple it provides only qualitative information. However this information is useful when combined with results from other experimental methods.

INTRODUCTION

This contribution is an attempt to study the interaction of some soluble nonionic (polyvinylpyrrolidone – PVP) or ionic (bovine serum albumin – BSA) polymers with surfaceactive substances (sodium dodecylsulphate – SDS) in aqueous solutions by simple measurements of surface tension.

Our previous data [1,2] as well as data in the literature, [3–5] have suggested the conclusion that surface tension of a surfactant solution (SDS) is modified by the presence of the polymer, in at least two distinct ways (Fig. 1).

Figure 1 shows the variation of surface tension of a surfactant solution with its concentration i.e. the so-called surface tension isotherm (Fig. 1a) and how these isotherms of surface tension behave when a polymer is added to the system (Fig. 1b and c). It is well known from the literature [6,7] that a surface tension plateau corresponds to the critical micellar concentration (c.m.c.); at this concentration, activity of surface active ions becomes approximately constant, because when one exceeds the c.m.c. all the excess ions associate in the form of micelles.[8]

The addition of polymer alters the aspect of surface tension isotherm of the surfactant solution, according to one of curves b or c (Fig. 1) : — curve b is a two-level isotherm and is so referred to in the literature ; [3,4]

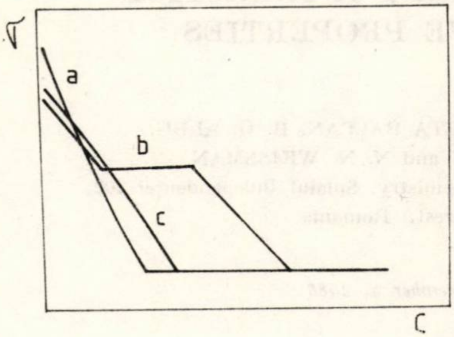

Fig. 1. — Surface tension isotherms of some aqueous solutions : a — pure surfactant solution ; b — two level isotherm of a polymer-surfactant solution ; c — simple isotherm of a polymer-surfactant solution.

it is accounted for by a two step saturation of the interface. This behaviour is due to the adsorption on the polymer ; within a certain concentration range the macromolecules present in the system adsorb on their surface the excess of free ions produced at concentration increase. Above the c.m.c. the second plateau is reached, coinciding with that of the surface tension isotherm of the pure surfactant solution. Type c isotherm does not exhibit an intermediate plateau ; however the slope corresponding to the adsorption at the solution air interface is modified and so is the coordinate where the curve flattening begins (c.m.c.).

These sections of the surface tension isotherms along which the surface tension varies with concentration (plateaus excepted) have allowed us to calculate the following parameters :

Γ_m — the coefficient of adsorption at the air-solution interface (number of moles of surfactant adsorbed at interface), according to equation :

$$\Gamma_m = -\frac{d\sigma}{dc}\frac{c}{RT} \qquad (1)$$

where σ stands for surface tension, c for concentration, R for the gas constant and T for temperature ;

S_0 — the effective surface occupied by a molecule at the air solution interface :

$$S_0 = \frac{1}{N_A \Gamma_m} \qquad (2)$$

where N_A is Avogadro number ;

δ — the thickness of surface active layer adsorbed on interface :

$$\delta = \frac{M\Gamma_m}{d} \qquad (3)$$

where M and d are the surfactant molecular weight and density respectively.

The values of these parameters were calculated by regression of experimental points of surface tension isotherms with straight lines, second and third order equations. The second order has proved to be satisfactory for the most experimental data and therefore was employed in all cases. The coefficients of the polynomials obtained by regression analysis allowed the calculation of derivate values $d\sigma/dc$ at each point and hence Γ_m (adsorption isotherm), S_0 and δ.

MATERIAL AND METHODS

The following chemicals were used: Merck reagent grade sodium dodecylsulphate — SDS; Riedel polyvinylpyrrolidone — PVP, K 25, of approximate molecular weight 28000; Fluka A. G. bovine serum albumin — BSA.

Surface tension measurements were made by the drop volume method[9] using a calibrated Traube capillary tube which was thermostated at a temperature of 25° ± 0.1°C.

RESULTS AND DISCUSSION

We present next some of our results obtained for the polymers studied. Figure 2 presents the surface tension isotherms for the SDS-PVP system. These data as well as other reported in literature [3] on a similar system (SDS-PVP) were analyzed in accordance with equation (1). The curves in Fig. 2 as well as those from reference [3] indicate the b type curve (surface tension two-level isotherm).

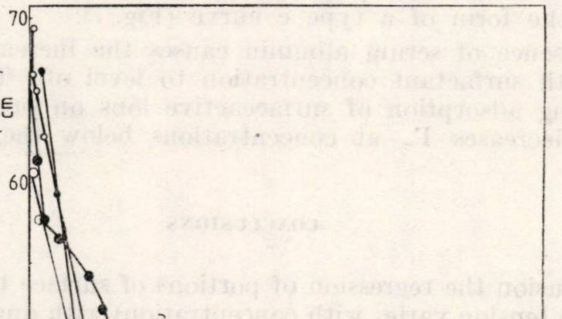

Fig. 2. — Surface tension isotherms of SDS + PVP system: 1 — SDS pure solution; 2 — SDS + PVP 0.1 %; 3 — SDS + PVP 0.33 %; 4 — SDS + PVP 0.66 %.

The adsorption isotherms obtained are presented in Figures 3, 4 (our data) and in Figures 5, 6 (H. Lange's data [3]). Curves in Fig. 3 – 6 are the adsorption isotherms for the first (Figs 3 and 5) and second (Figs 4 and 6) level variation of the surface tension. A comparison of Fig. 3 with Fig. 5 and of Fig. 4 with Fig. 6 shows that the values of the adsorption coefficients and their dependence on surfactant concentration are not identical for the two experimental sets calculated – Fig. 2 and ref. 3 – but the range of Γ_m values is similar for the first plateau – Figs 3 and 5 – and for the second one – Figs 4 and 6. This may be partially due to the different batches of polymers employed i.e. K 25 and K 30 respectively. [3]

Table 1 lists the S and δ parameters calculated from the same sets of data – Fig. 2 and ref. 3. These parameters are proportional to $1/\Gamma_m$ and Γ_m respectively. This gives little additional information regarding the dependence of surface properties on the surfactant concentration. As Table 1 shows the parameter S (effective interfacial area per surfactant molecule) increases and δ (thickness of surfactant molecular layer at solution air interface) diminishes with increasing surfactant concentration; the presence of the first plateau on isotherms breaks this variation for both parameters.

Figures 7 and 8 show the experimental results for the SDS – BSA system : the surface tension isotherms (Fig. 7) and the adsorption isotherms (Fig. 8). In this case the influence of the polymer on the adsorption coefficient is more obvious (Fig. 8). The surface tension isotherms have in this case the form of a type c curve (Fig. 7).

The presence of serum albumin causes the increase of adsorption coefficient with surfactant concentration to level off. This may be the effect of strong adsorption of surfaceactive ions on protein macromolecules which decreases Γ_m at concentrations below the c.m.c. [10]

CONCLUSIONS

In conclusion the regression of portions of surface tension isotherms (where surface tension varies with concentration) with quadratic equations allows calculation of the derivative $\frac{d\sigma}{dc}$ and hence the values of Γ_m (adsorption isotherm), S and δ, according to equations 1, 2 and 3 respectively.

The influence of some soluble polymers upon surfaceactive properties of SDS solutions has been described. The results show that there are various types of interactions for various polymers introduced into the system. The parameters obtained can be employed for a comparative study of the adsorption of surfaceactive substances on various water-soluble polymers. However the information obtained regarding this interaction is rather qualitative unlike that provided by other methods, e.g. those based on ion-sensitive electrodes. [11] Further studies using other methods will provide additional information and should allow a better understanding of this interaction.

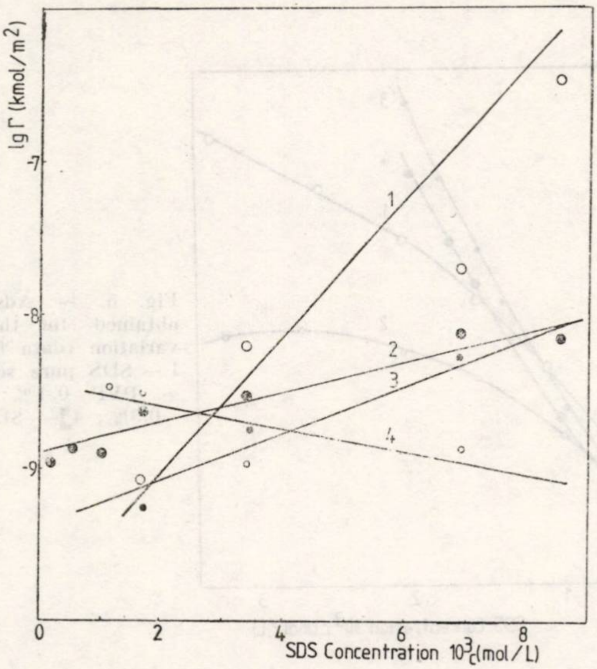

Fig. 3. — Adsorption isotherms obtained for the first plateau σ variation (results presented in Fig. 2) : 1 — SDS pure solution ; 2 — SDS + PVP 0.1% ; 3 — SDS + PVP 0.33% ; 4 — SDS + PVP 0.66%.

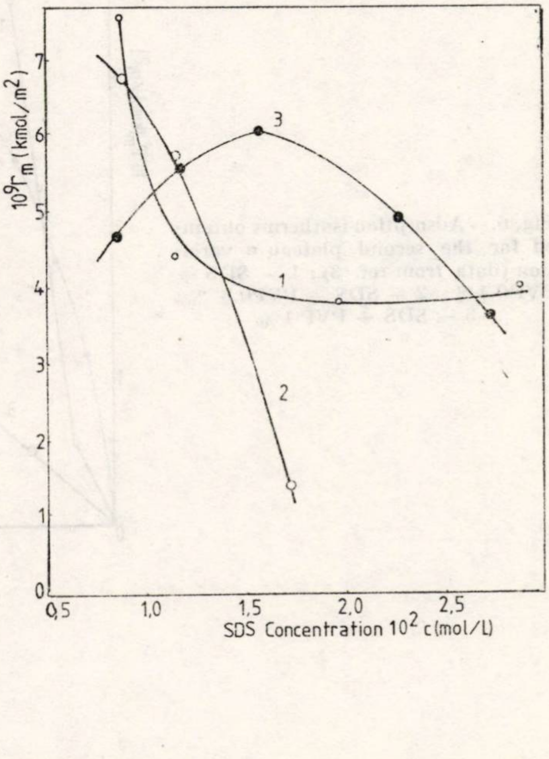

Fig. 4. — Adsorption isotherms obtained for the second plateau σ variation (Fig. 2) : 1 — SDS pure solution : 2 — SDS + PVP 0.1% ; 3 — SDS + PVP 0.33% ; 4 — SDS+ PVP 0.66%.

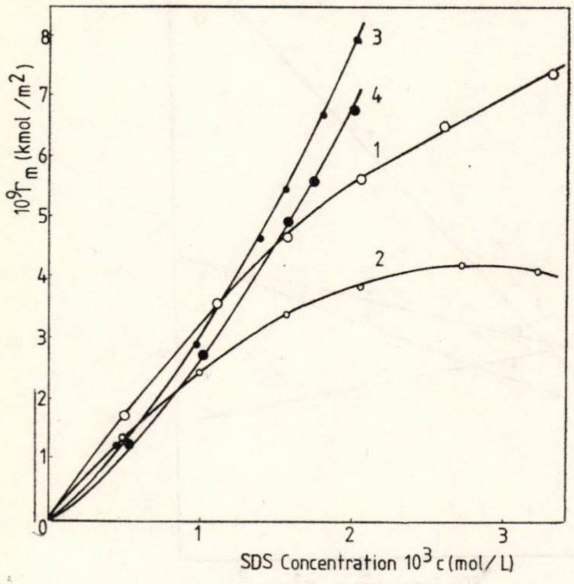

Fig. 5. — Adsorption isotherms obtained for the first plateau σ variation (data from reference 3): 1 — SDS pure solution; 2 — SDS + PVP 0.1%; 3 — SDS + PVP 0.3%; 4 — SDS + PVP 1%.

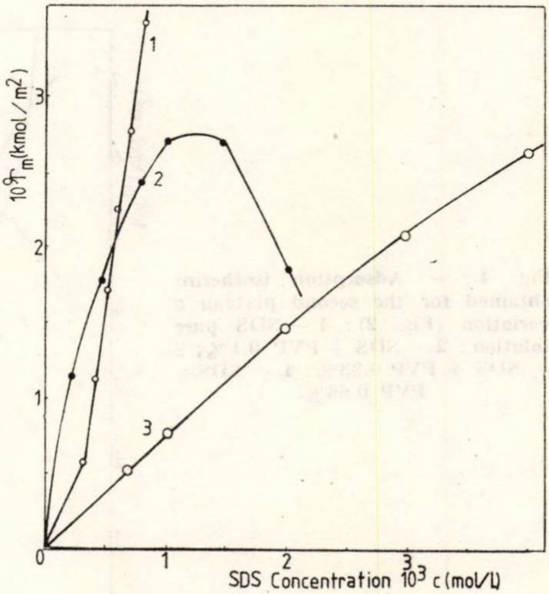

Fig. 6. — Adsorption isotherms obtained for the second plateau σ variation (data from ref. 3): 1 — SDS + PVP0.1%; 2 — SDS + PVP0.3 %; 3 — SDS + PVP 1%.

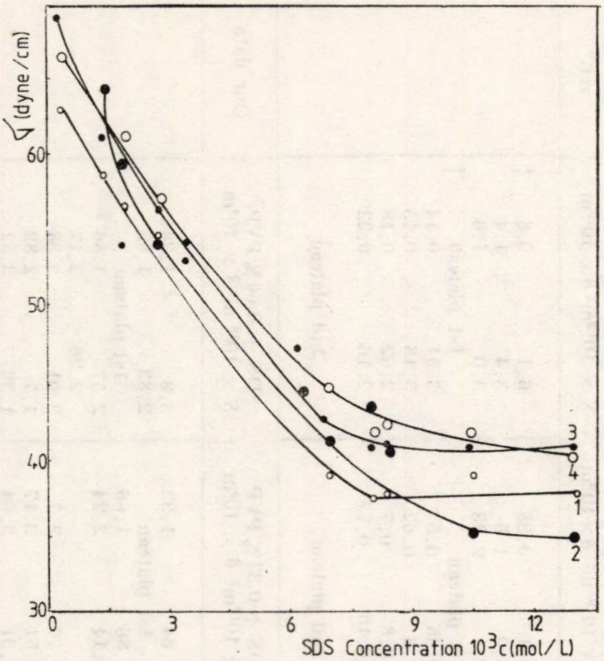

Fig. 7. — Surface tension isotherms for SDS + BSA system: 1 — SDS pure solution; 2 — ADS + BSA 0.01%; 3 — SDS + BSA 0.05%; 4 — SDS + BSA 0.1%.

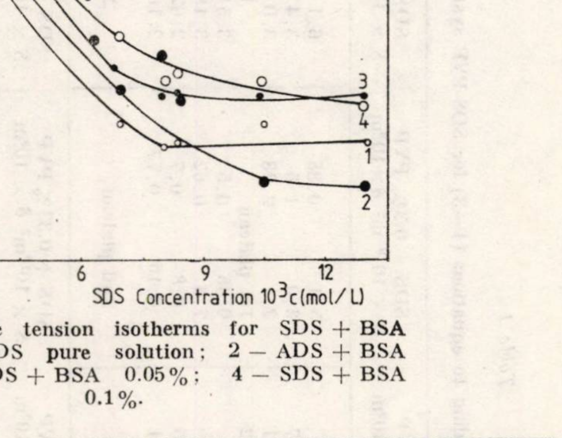

Fig. 8. — Adsorption isotherms for SDS + BSA system (Fig. 7): 1 — SDS pure solution; 2 — SDS + BSA 0.01%; 3 — SDS + BSA 0.05%; 4 — SDS + BSA 0.1%.

Table 1

S and δ values obtained according to equations (1—3) for SDS-PVP systems

Surfactant conc. × 10^3	SDS		SDS + 0.1% PVP		SDS + 0.3% PVP		SDS + 1% PVP		Data from ref.[3]
	$S \times 10^{19} m^2$	$\delta \times 10^9 m$	$S \times 10^{19} m^2$	$\delta \times 10^9 m$	$S \times 10^{19} m^2$	$\delta \times 10^9 m$	$S \times 10^{19} m^2$	$\delta \times 10^{19} m$	
1	4.7	1	6.8	0.7	5.1	0.85	6.1	0.8	
1.6	3.6	1.3	4.9	0.97	3.0	1.6	3.4	1.4	
2	3.0	1.6	4.3	1.1	2.1	2.28	3.0	1.6	
2.6	2.6	1.85	3.90	1.22	1st plateau		1st plateau		
5	2.5	1.92	1st plateau		9.45	0.5	3.51	0.14	
6	3.34	1.43	9.78	0.5	7.6	0.62	3.18	0.15	
6.7			7.37	0.65	6.8	0.7	2.62	0.18	
8	plateau		4.78	1.11	6.15	0.77	2.16	0.22	
10									
			2nd plateau		2nd plateau		2nd plateau		

Surfactant conc. × 10^3	SDS		SDS + 0.1% PVP		SDS + 0.33% PVP		SDS + 0.66% PVP		Our data
	$S \times 10^{19} m^2$	$\delta \times 10^9 m$	$S \times 10^{19} m^2$	$\delta \times 10^9 m$	$S \times 10^{19} m^2$	$\delta \times 10^9 m$	$S \times 10^{19} m^2$	$\delta \times 10^9 m$	
1.4	3.02	1.58	6.43	0.74	3.64	1.32	3.8	1.28	
2	2.6	1.84	4.4	1.09	1st plateau		2.83	1.69	
3.5	2.2	2.17	3.35	1.43	2.88	1.66	1st plateau		
7	1.21	3.28	1.81	2.64	2.14	2.24	2.57	1.86	
8	1.18	4.06					2.26	2.12	
8.6	plateau		1.51	3.17	1.77	2.7	2.01	2.38	
11.5			1.33	3.61	1.51	3.17	1.7	2.82	
17.3			1.3	3.68	1.31	3.64	1.36	3.52	
23			1st plateau		1.36	3.52	1.13	4.23	
29			1.26	3.79					
			2nd plateau		2nd plateau		2nd plateau		

REFERENCES

[1] G. Popescu, M. Radu and D. Anghel, *Kolloid Z und Z. Polymere*, **250**, 303, 875 (1972) ; **251**, 1039 (1973).

[2] G. Popescu, M. Radu and D. Anghel, "Proc. 6th. Int. Congress on Surface Active Substances", **II**, 953, Zürich, Sept. 1972.

[3] H. Lange, *Kolloid Z. und Z. Polymere*, **243**, 101 (1971).

[4] H. Lange, *Chem.-Ztg*, **96**, 192 (1972).

[5] T. Ildiko, F. Zsolt and W. Ervin, *Magyar Kém. Folyóirat*, **79**, 532 (1979).

[6] K. Shinoda, T. Nakagawa, B. Tamamushi and T. Isemura, "Colloidal Surfactants", Academic Press, New York, 1963, p 26.

[7] P. Mukerjee and K. J. Mysels, "Critical Micelle Concentrations of Aqueous Surfactant Systems", Nat. Stand. Ref. Data, Ser. Nat. Bur. Stand. (U.S.), 1971, p 8.

[8] P. Ekwall, I. Danielsson and P. Stenius, in "Surface Chemistry and Colloids", M. Kerker Editor, Butterworths, London, University Park Press, Baltimore, 1972, p. 97.

[9] I. Mîndru and D. M. Ceacăreanu, "Chimia Coloizilor și Suprafețelor", Editura Tehnică, Bucharest, 1976.

[10] J. Steinhardt and J. A. Reynolds, "Multiple Equilibria in Proteins", Academic Press, New York, 1969.

[11] M. M. Marinescu, D. F. Anghel, B. G. Albu, G. Popescu and P. N. Pavel, Paper presented at the 1st Symposium on Colloid and Surface Chemistry, Bucharest, May, 1983.

REFERENCES

1 G. Popescu, M. Haus and G. Anghel, Kolloid Z. und Z. Polymere 250, 703, 575 (1972); 251, 1029 (1973).

2 G. Popescu, M. Haus and G. Anghel, "Proc. 6th Int. Congress on Surface Active Substances", II, 965, Zürich, Sept. 1972.

3 H. Lange, Kolloid Z. und Z. Polymere, 243, 101 (1971).

4 H. Lange, Chem.-Ztg. 96, 182 (1972).

5 [illegible], Trans. Faraday Soc., 73, [illegible]

6 K. Shinoda, T. Nakagawa, B. Tamamushi and T. Isemura, "Colloidal Surfactants", Academic Press, New York, 1963, p. 26.

7 P. Mukerjee and K. J. Mysels, "Critical Micelle Concentrations of Aqueous Surfactant Systems", Nat. Stand. Ref. Data Ser. Nat. Bur. Stand. (U.S.), 1971, p. 36.

8 P. Ekwall, I. Danielsson and P. Stenius, in "Surface Chemistry and Colloids", M. Kerker Editor, Butterworths, London, University Park Press, Baltimore, 1972, p. 97.

9 I. Mihaila and D. M. Georgescu, "Chimia Coloizilor şi Suprafeţelor", Editura Tehnică, Bucharest, 1974.

10 J. Steinhardt and J. A. Reynolds, "Multiple Equilibria in Proteins", Academic Press, New York, 1969.

11 M. M. Marinescu, D. F. Anghel, B. G. Albu, G. Popescu and R. N. Pavel, Paper presented at the 1st Symposium on Colloid and Surface Chemistry, Bucharest, May, 1983.

Revue Roumaine de Chimie, **32**, 7, 723–728 (1987)

SOME ASPECTS OF POLYMER FLOODING IN OIL RESERVOIRS

ION CREŢU, MIHAI IONESCU and MARIA STOICESCU
Institute of Petroleum and Gas, Blvd. Bucureşti no. 39, 2000 Ploieşti, Romania

Received January 15, 1987

Polymer flooding is an oil recovery method with a better recovery factor than the conventional water flooding. Its versatility was proved both by laboratory researches and field tests. This paper presents some data on scientific researches in polymer flooding, the types of polymers used for oil displacement, the rheological behavior of polymer solutions and its implications on injection parameters. The polymer systems stability, and the polymer adsorption and retention phenomena in porous media are also described. In the end some problems on polymer solutions injection are treated.

INTRODUCTION

Polymer flooding was designed to improve sweep efficiency by improving the mobility ratio. Since the early 1900's the oil industry recognized the inefficiency of oil recovery by conventional methods. Since then, extensive research has been conducted on improvement of displacement and sweep efficiency in petroleum recovery. Muskat[3] first pointed out that fluid mobilities would affect waterflood performance. The use of increased viscosity water to improve sweep efficiency in oil reservoirs was proposed in 1944, when Detling[4] patented some additives designed to increase water viscosity. The high cost of the additives proposed (glycerine, sugar, glycols) made inapplicable this method up to 1964 when Pye[5] established that water mobility can be reduced efficiently by dissolving in it little amounts of polymer. The first Romanian studies on using increased mobility water for the displacement of oil in reservoirs were accomplished in 1956, when polysaccharides were used. Since 1965 the Romanian research has been orientated to the use of polymer solutions.

POLYMER TYPES FOR OIL DISPLACEMENT

Polymer solutions used for oil displacement in reservoirs are obtained by dissolving a little amount of polymer in the injection water, corresponding to concentrations between 250 and 1,500 ppm. Polymer solution mobility depends upon a series of factors as : polymer type, petrophysical characteristics of the porous medium, ionic composition of the solvent (water) and injection rate. In reservoir processes two kinds of polymer were usually used[6] : a synthetic polymer classified as a polyacrylamide (partially hydrolyzed) and a biologically produced polymer known as xanthan gum.[7] Two other types of polymer were studied in the laboratory : hydroxyethyl cellulose and polyethylene oxide. They were not used in field applications because of the high concentration needed to realize the same viscosity increase as the previously presented polymers.

The molecular structure of the partially hydrolyzed polyacrylamide (PAA) consists of long chains of carbon atoms alternatively coupled with both sodium carboxyl groups and amidic groups. The average size of these molecules is less than 1 μ and their molecular weight is about 10^6.

The partially hydrolyzed PAA is a white dry powder, nontoxic and uncorrosive. It can be rapidly dissolved in water in an appropriate plant in which the surrounding of every polymer particle by water is ensured. Polymer solution can be stored for a short time only in a tank containing nitrogen to avoid contact with the atmosphere. By dissolving in fresh water, the partially hydrolyzed PAA has the carboxyl groups situated among the molecular chains in an ionic form. That makes the negative charges to push back, leading to an expansion of the molecules which has a result a viscosity increase. Consequently, any action which amplifies or diminishes the expansion of the molecules determines the increase, respectively the decrease of polymer viscosity. Thus, by decreasing the pH value or by adding a little amount of NaCl, a part of the carboxyl ions become nonionized groups, determining a viscosity decrease.

PAA reduces injection water mobility both by increasing its viscosity as previously shown, and by reducing porous medium permeability as a result of polymer adsorption and retention in the rock pores. This permeability decrease is irreversible and cannot be diminished by waterflooding. Therefore, fresh water (total dissolved solids less than 10,000 ppm) is desirable to prepare these polymer solutions. PAA can be mechanically degraded by shear stress; special care in surface handling is required to avoid this shear degradation.

The xanthan gum solutions are relatively insensitive to salinity and can tolerate shearing effects. The main disadvantages of this polymer are formation plugging characteristics and susceptibility to bacterial attack.

RHEOLOGICAL BEHAVIOR OF POLYMER SOLUTIONS

Both partially hydrolyzed PAA and xanthan gum solutions have a pseudoplastic behavior. In addition, the PAA solutions can also show a viscoelastic behavior. [6] The rheological behavior of polymer solutions in porous media can be divided in four zones [2,10] as shown in fig. 1. These

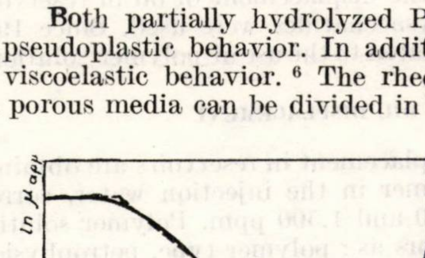

Fig. 1. — Typical rheological behavior of polymer solutions in porous media.

zones are characterized by: a maximum value for the apparent viscosity which is approximately constant for low velocities; a decreasing apparent viscosity with increasing velocity corresponding to a pseudoplastic behavior; a minimum apparent viscosity which is approximately constant at higher velocities; an increasing viscosity with increasing velocity at very high velocities, corresponding to a dilatant behavior. Admitting that the dilatant domain is absent, polymer solution behavior can be approximated by the straight lines traced in fig. 1, corresponding to the Newtonian behaviors defined by $\mu_{\max}$ and $\mu_{\min}$, respectively to the pseudoplastic one described by the power law modified by Blake and Kozeny as

$$\mu_{\text{app}} = Hv^{n-1}, \tag{1}$$

where the parameters H and n can be either calculated directly from data on flow through core material or estimated from viscosimetric measurements. If the power-law coefficient and exponent, K and n, are calculated from viscosimetric data, then H can be estimated as

$$H = \frac{K}{12}\left(\frac{9n+3}{n}\right)^{n}(150\,k_a\,m_a)^{\frac{1-n}{2}}, \tag{2}$$

where k_a is introduced in mD and $m_a = ms_a$.

Laboratory experiments accomplished at the Hydraulics Laboratory of I.P.G. Ploiești, with a Fann viscosimeter using polymer solutions of the PAA type originated in Romania and in the USA, for various concentrations between 250 and 1,500 ppm, confirmed the previously presented rheological behavior. For example, the curves corresponding to a concentration of 1,500 ppm are presented in fig. 2.

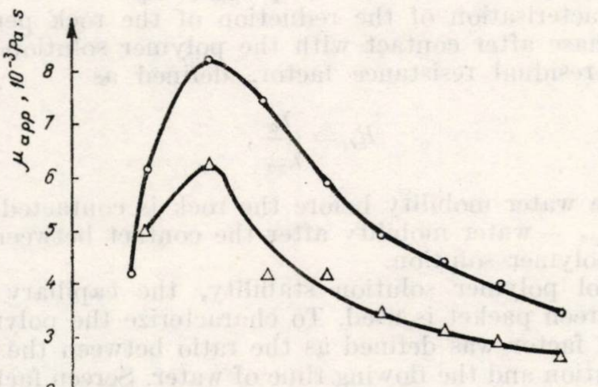

Fig. 2. — Rheological behavior of Romanian and American originated polymers of the partially hydrolyzed polyacrylamide type (concentration of the solution — 1,500 ppm).

DYNAMICS OF POLYMER FLOODING

In order to express the decrease of polymer solution mobility versus that of the fresh water used to prepare the solution, Pye[5] defined the resistance factor R_r as

$$R_r = \frac{I_a}{I_{p0}} = \frac{Q_a \Delta p_{p0}}{Q_{p0} \Delta p_a}, \tag{3}$$

which becomes

$$R_r = \frac{Q_a}{Q_{p0}} \tag{4}$$

when waterflooding and polymer flooding carry on at the same differential pressure ($\Delta p_a = \Delta p_{p0}$), respectively

$$R_r = \frac{\Delta p_{p0}}{\Delta p_a} \tag{5}$$

when $Q_a = Q_{p0}$. On the other hand, on the basis of Darcy's law, equation (3) can be written as

$$R_r = \frac{\lambda_a}{\lambda_{p0}}, \tag{6}$$

where λ_a is the water mobility at residual oil saturation and λ_{p0} – polymer solution mobility.

The resistance factor increases with increasing total volume of injected solution in the core, tending to a constant value which shows that the porous medium will be not plugged up.

The characterisation of the reduction of the rock permeability to the aqueous phase after contact with the polymer solution can be done by using the residual resistance factor, defined as

$$R_{rr} = \frac{\lambda_a}{\lambda_{pa}}, \tag{7}$$

where λ_a is the water mobility before the rock is contacted by polymer solution and λ_{pa} – water mobility after the contact between the porous medium and polymer solution.

To control polymer solution stability, the capillary viscosimeter which has a screen packet is used. To characterize the polymer degradation the screen factor was defined as the ratio between the flowing time of polymer solution and the flowing time of water. Screen factor is usually correlated with polymer molecular weight and permeability reduction, reflected by resistance factor.

In accordance with relationship (6), high values of the resistance factor correspond to low polymer solution mobilities. Laboratory tests accomplished with various polymer solutions showed that high values of R_r are indeed obtained as a result of both permeability decrease by retention of polymer molecules in pores, and water viscosity increase in the presence of the polymer.

POLYMER STABILITY

The achievement of a polymer flooding process requires the polymer solution to remain stable for a long time at reservoir conditions. However, polymers are sensitive to mechanical, chemical, thermal and microbial degradations. Degradation can be prevented or minimized using special equipment and techniques.

Mechanical degradation of polymer solutions is the effect of shear tensions and high velocities which can appear both in valves and orifices, in the equipment for polymer dissolving and for filtering and pumping the solution, and in porous media having a low permeability.[11] The degradation appears if local pressure drops are greater than 0.15 –0.2 MPa. Higher values can be accepted if using special devices as the coil nozzle.[1] Shear degradation has a moderate effect on viscosity (less than 5% loss in most cases) and a severe effect on screen factors (up to 90% loss).

Chemical degradation occurs when a polymer solution is exposed to oxygen or oxidizing agents in the presence of certain transition metal ions, as a result of hydrolysis under acidic or basic conditions, or as a result of the presence of corrosion inhibitors, biocides and even suspended solids. Chemical degradation may be aggravated by temperature, aging and even exposure to certain ranges of light spectrum.

Thermal degradation is manifested by a continuous viscosity decrease in the temperature domain 120 –150°C. Few data about the thermal stability of different polymer solutions for extended periods of time (greater than 6 months) have been published. However, the criteria for long-term stability in various media have not been established for any type of polymer. Thermal degradation is aggravated under aerobic conditions, and also by increased pH values and in the presence of metal ions.

Bactericides are required to prevent microbial attack. Low concentrations of formaldehyde have been successfully used both in laboratory and in field tests. Xanthan gums are more susceptible than PAA to microbial attack. This is because many microbes can excrete enzymes that hydrolyze the polysaccharides into monosaccharides, which then can be transported through cell membranes and used in metabolism.

POLYMER ADSORPTION

The amount of polymer adsorbed depends on the nature of the polymer and the rock surface. Both physical adsorption of polymer on solid surfaces and polymer retention in the pores play a role in total polymer retention in the reservoir. Typical field adsorption values range from 80 to 2,000 kg/(ha.m). Laboratory results often cannot be extrapolated to predict polymer adsorption in the reservoir. The low flow rates in the reservoir can decrease the amount of polymer retented in mechanical entrapment in field conditions versus laboratory conditions.

POLYMER INJECTION

In the sixties, polymer slugs were injected at constant concentration during field operations. As a polymer bank propagates through porous media, the front edge is gradually stripped of polymer, which is adsorbed on the rock. Also, when the low-mobility polymer slug is followed by a higher-mobility brine, viscous fingering tends to occur at the interface as a result of the unfavorable mobility ratio. To provide favorable mobility ratios both ahead and behind the slug, polymer slug programming was proposed. The slug starts at a relatively high concentration which fairly decreases, touching in the end a relatively low value. At present, the programmed slug is used in almost all polymer or micellar-polymer flooding field operations.

A modified variant of the programmed slug method is the gradual increase of the concentration up to a value which is constant for an injection period and then the continuous decrease of the concentration up to a minimum value. For improving sweep efficiency when using polymer solutions, the use of polymer preserver agents, of cations designed either to reduce the rate of water produced or to plug up high permeability zones, and of various polymer combinations was proposed.

REFERENCES

[1] A. Cârcoană and Gh. Aldea, "Mărirea factorului final de recuperare la zăcămintele de hidrocarburi", Ed. tehnică, Bucharest, 1976.

[2] I. Crețu, "Modelarea numerică a mișcării fluidelor în medii poroase", Ed. tehnică, Bucharest, 1980.

[3] M. Muskat, "The Flow of Homogeneous Fluids Through Porous Media", McGraw-Hill, New York, 1937.

[4] K. D. Detling, U.S. Patent 2341500, Febr. 1, 1944.

[5] D. J. Pye, *J. Petroleum Techn.*, Aug. (1964).

[6] H. L. Chang, *J Petroleum Techn.*, Aug. (1970).

[7] F. W. Smith, *J. Petroleum Techn.*, Aug. (1970).

[8] A. Jeanes, J. E. Pittsley and F. R. Senti, *J. Appl. Polymer Sci.*, 5 (1961).

[9] N. Mungan, *World Oil*, Febr., March, May, June, July, Aug., Sept. (1981), Febr., March May (1982).

[10] P. L. Bondor, G. J. Hirasaki and M. J. Tham, *Soc. Petroleum Eng. J.*, Oct. (1972).

[11] J. M. Maerker, *Soc. Petroleum Eng. J.*, Aug., (1975).

Revue Roumaine de Chimie, **32**, 7, 729–735 (1987)

COMPTES RENDUS

B. Giese, "Radicals in Organic Synthesis : Formation of Carbon-Carbon Bonds", Pergamon Books, Oxford, 1986. 294 pp., flexicover, US $ 25.00, ISBN 0–08–032194–0 (there exists also a hardcover version, with ISBN 0–08–32493–2, US $ 50.000)

This is a timely book summarizing recent advances in the use of homolytic reactions for organic synthesis involving C–C bond formation. The author developed himself some of these reactions ; he presents systematically and pedagogically what can be done with the help of reactive free radicals.

After a two-page introductory chapter, general aspects of syntheses with radicals are examined in the chapter entitled "Basic Principles" ; based upon the example of the reaction between alkyl halides, alkenes, and tributyltin hydride leading to tributyltin halides and to reductive C–C addition products, the author indicates the thermodynamic and especially kinetic requirements that have to be met for a chain reaction to occur. The five types of reactions between radicals and non-radicals are discussed briefly on the basis of SOMO–LUMO and SOMO-HOMO interactions ; it is stressed that such reactions are more convenient for synthetic purposes than reactions between radicals. A comparison between ions and radicals in syntheses indicates that chemoselectivity, regioselectivity and (more seldom) stereoselectivity can be in favour of homolytic reactions. Thus, α, β-unsaturated carbonyl compounds add radicals only at the olefinic and never at the carbonylic carbon atom, owing to the difference in energy between the π/σ electrons in C=C and C=O bonds. Also, carbocations cyclize intramolecularly yielding six-membered rings whereas radicals afford predominantly five-membered rings (Baldwin's rules) owing to the unsymmetrical transition state in the latter case.

The bulk of the book (230 pages) is devoted to a well-structured survey of C-C bond formation processes, organized in three chapters : inter-, then intra-molecular formation of aliphatic C–C bonds, and C–C bond formation of aromatic systems (including heteroaromatic tones). It is shown how polar and stearic factors can be put to work for designing useful synthetic reactions. Within the chapters on aliphatic C–C bond formation, the material is ordered according to the types of reactions which can trap radicals with hydrogen donors (RHgH, R_3SnH, R_3GeH, and various organic hydrogen donors such as R_2CHOH, RCHO, $CHCl_3$, etc.), heteroatom donors (Hal, SR, BR_2), electron transfer reactions, fragmentations. Also, radical–radical reactions are considered both for inter- and intramolecular processes (Kolbe electrolysis of carboxylates, pinacol dimerization, acyloin formation, Viehe's dehydrodimerization involving radicals formed by addition to capto-dative 1, 1-disubstituted olefins, etc.). It is shown that the electrophilic/ nucleophilic nature of the radicals, and the electron-rich/ electron-poor character of the non-radicalic reaction partners is decisive for the outcome of the reaction.

The chapter on aromatic C–C bond formation highlights Minisci's alkylation and acylation of electron-deficient heterocyclics (these reactions supplement the Friedel-Crafts substitutions of electron-rich systems), and presents also the use of carbocyclic aromatic radicals. Meerwein's reaction, the use of N-nitrosoace tanilide going back to Bamberger and explained by Hey forty years later, Bunnett's, Kornblum's and Russel's $S_{RN}1$ reactions, the use of aromatic radical-ions and other homolytic processes find their place in the systematic discussion of synthetically useful reactions.

A final retrospective survey presents schematically on 15 pages all methods for the rupture of C–X bonds leading to carbon-centered radicals which are used for C–C bond formation : X = Hal, OH, SR, NH_2, NO_2, N_2^+, N_2R, COOH, BR_2, HgR, cyclopropanes, alkenes, carbanions, carbonyl or cobalt derivatives ; the reader is referred to pages of the book where the corresponding reaction is mentioned. An author index for the 450 references and a short subject index conclude the book. Literature references up to 1986 are included.

The book is reproduced photographically from the typewritten manuscript, including excellently stencil-produced formulas ; thus the text is completely free of typesetting errors. The non-standard colloquial Anglo-American style does not impede the flow of ideas from author to readers.

The fact that nowadays homolytic C–C bond formations have become accepted as synthetically important reactions emerges from the numerous syntheses of natural products described in the book. The fact that both H. C. Brown and D. H. R. Barton developed and applied homolytic reactions based upon boron and sulfur compounds, respectively, also illustrates the synthetic importance of such reactions.

A substantial advantage of syntheses involving radicals is that important functional groups such as OH or NH_2 are compatible with homolytic reactions and do not need therefore to be protected and then deprotected as in ionic reactions. Professor Giese's interests lie in the use of such radicalic reactions for obtaining non-conventional saccharides, and many such examples are given; some of these have already been published, while some are under press.

The book is highly recommended for its direct and concise exposition, for the formulas depicting clearly steric relationships, for the modern and economical way of presenting chain reactions *via* circularly-arranged formulas (as in biochemical pathways), and for the exemplary way of compressing an impressive amount of up-to-date information in a small number of pages, words, and formulas.

Alexandru T. Balaban

Atta-Ur-Rahman, "Nuclear Magnetic Resonance: Basic Principles", Springer-Verlag, New York, 1986, 358 pp, ISBN 3–540–96243–3, hard-cover, DM 128.

Professor Atta-ur-Rahman's book on Nuclear Magnetic Resonance (NMR) is a useful and practical introduction to the field of ^1H- and ^{13}C-NMR as well as a guide to the newer techniques which make use of pulsed Fourier Transformed (FT) NMR.

Very pedagogically written, the text refinement, probably as the result of teaching for many years the basic concepts of NMR spectroscopy, is visible. The book has five chapters and two Appendices.

The first two chapters are concerned with continuous-wave ^1H-NMR spectroscopy and present in detail gradually, after an introduction, the factors affecting the chemical shifts (in Chapter 1) and coupling constants (in Chapter 2). A Table of Chemical Shifts convenient for use is given for CH_3, CH_2 and CH protons attached to different functional groups. Aromatic protons are listed separately. Coupling constants of protons in the more frequently encountered systems, are listed after the exemplification of the different spin systems ranging from two coupled nuclei (AX, AB and A_2 systems) to five interacting nuclei (in A_2X_3, A_2B_3 and AA′BB′C spin systems).

Chapter 3, "Experimental procedures in NMR spectroscopy" starts by giving some hints concerning sample preparation and a list of useful NMR solvents, after which the reader is introduced to pulsed FT-NMR spectroscopy. The rotating frame reference, free induction decay, pulse angles are amply described and exemplified. Examples are also given for correct phase setting and signal weighing as well as for the sampling of data points. Double resonance techniques, the nuclear Overhauser effect (NOE), T_1 (spin lattice relaxation time) and T_2 (spin-spin relaxation time) are exemplified and their use for structural elucidation is described. A short section of this chapter deals with dynamic effects observable by NMR. As before, the mathematical treatment is kept to a minimum, only the final equations, to be used directly by the practitioner, are given.

Chapter 4 considers ^{13}C-NMR spectroscopy together with some newer applications of NMR, namely solid state spectra (obtained by Magic Angle Spinning (MAS), Cross-Polarization (CP) enhancement, or a combined technique (CP-MAS)) and NMR imaging. A large number of ^{13}C-chemical shifts are given either in Tables or as additivity relationships. Coupling constants are also listed. A mild criticism concerns citations of literature references. These are given at the end of Tables, as footnotes, in block form so that the actual reference for a given compound is hard to identify among the very numerous other references. The fact that references are given is a bonus which this book offers, but if numbers had been used for each individual reference, this bonus could have been actually given instead of only displayed. A more general "recommended reading" list of books and reviews is, however, given at the end of each chapter and is useful.

The last chapter is entitled "Special Pulse Sequences and Two-Dimensional NMR Spectroscopy" and is the largest chapter having 110 pages. A list of 146 references is given as recommended reading while a few other references are given as footnotes throughout the chapter. It is one of the first texts to deal comprehensively and unbiased with these modern techniques. Drawbacks as well as advantages are put before the reader who is regarded as a potential user of these techniques, which are exemplified and discussed, again, without the mathematical complexity which hinders the readability, but nevertheless, without oversimplification. Among the spectra exemplified and the structural elucidation gained through them are the following: 1) Gated Spin Echo (GASPE, APT or SEFT) spectra for differentiating between CH_3, CH_2, CH and quaternary carbons (the first and third may give negative" ^{13}C-NMR signals; 2) Cross Polarization (CP) spectra for enhancing signal intensities of nuclei of low abundance when these are coupled to protons ; 3) Insensitive Nuclei Enhanced by Polarization Transfer (INEPT) spectra for enhancement and observation of only the ^{13}C doublets (CH groups), only triplets (CH_2), only quartets (CH_3), or all carbons irrespective of the multiplicity, or, as in APT spectra, the triplets out of phase with respect to doublets and quartets (positive and negative peaks) ; 4) Distorsionless Enhancement by Polarization Transfer (DEPT) spectra which are superior to INEPT spectra as they can give also only quaternary carbons, in addition to the desired CH, CH_2 or CH_3 signals ; 5) Incredible Double Quantum Transfer Experiment (INADEQUATE) spectra for giving the carbon-carbon connectivities ; 6) Two-Dimensional (2D) NMR spectra (homo-and heteronuclear) *J*-resolved and *J*-correlated spectra with their multiple applications. Pulse sequences are given for gated decoupling, spin-flip, selective spin-flip, semi-selective spin-flip, 2D-*J*-resolved spectra with INEPT, semiselective refocused heteronuclear correlated spectra, 2D-DEPT spectra heteronuclearly correlated, XCOR spectra, heteronuclear shift correlation spectra *via* long range coupling (COLOC) which are useful for the assignment of carbonyl groups, homonuclear shift correlated 2D-NMR spectra (COSY, SECSY, FOCSY, DISCO), chemical shift correlated spectra through cross-relaxation and exchange (NOESY, HOESY-2D-NOE which gives spatial proximity between carbons and protons), relayed NOESY, simultaneous 2D-correlated (COSY) and 2D-NOE (NOESY) spectra (also known as combined correlated NOE spectra with simultaneous COSY and NOESY i.e. COCONOSY which are spectra without long aquisition times), relayed coherence transfer (RCT) for determining carbon-carbon connectivities, 2D-INADEQUATE also for determining the carbon-carbon connectivity plot (CCP), 2D-double quantum coherence echo correlated spectra (DECSY), relayed double quantum 2D-NMR spectra and others.

The book has as Appendices 26 problems in ^1H-and 16 problems in ^{13}C-NMR consisting in giving the molecular formula and the NMR spectrum (only the broad band decoupled spectrum for the ^{13}C problems), with the answers listed separately. The fairly large subject index is useful, particularly as it facilitates the entry to the various pulse sequences.

With relatively few mistakes and with a graphical presentation which although clear, could have been professionally drawn, the text is recommeded both for students as an advanced guide in NMR and for practising spectroscopists for a view on the newer techniques (those published until 1985 have been included in the text).

Teodor-Silviu Balaban

R. Schoenfeld, "The Chemist's English", Second, revised edition, VCH Verlagsgesellschaft, Weinheim, 1986. Hard cover, 173 pages, DM 48, ISBN 3–527–26309–8 (for USA and Canada, VCH Publishers, New York, ISBN 0–89573–599–7)

The author of the book under discussion is the editor of the *Australian Journal of Chemistry*. He is multilingual, having been born in Austria, and he used also to be a playwright. During his career as editor, he has encountered many examples of poorly written papers. Although he declares that the skill of good writing cannot be taught, just as the skill of doing research cannot be taught, he provides a series of essays for chemists who wish to write better in the language he calls CE, i.e. Chemist's English (as different from Standard Written English, SWE, which again differs from Standard Spoken English. SSE). This volume gathers essays that were published over several years in *Proc. Roy. Austral. Chem. Inst.*, *Chemistry in Australia*, and *CHEMTECH*. All essays are written in an amusing, highly readable, humorous style, even when they discuss serious grammar problems. Some of the titles of these sketches are intended to be provocative : Tetravalency of Carbon Disproved ! To Reflux or not to Reflux. Amazing Revelations : English Scientists Secretly Practise German Vice ! Now, from the Pen that Gave You Monglish, Comes Gerglish.

The essay "How Good is Your English ? How Good is English ?" analyses the predominance of English as the language of science in the world nowadays. To quote from that chapter : "Did this marriage between chemistry and English take place because the bride was so beautiful, or because her parents were so rich ? It must be admitted that the wealth of the parents had something to do with it. Consider some of the bridegroom's past flirtations, and how they were discreetly abandoned when family fortunes declined. The present bride certainly brings with her a resplendent dowry : the huge American research budget, the substantial contributions from Great Britain, Ireland, Canada, and Australia.. But it would be most ungallant to deny her personal charms and virtues". Then the author goes on to demonstrate the simplicity of English with only 26 characters, unlike French, German, Italian or Spanish which have accents or umlaut (diaeresis) multiplying thereby the number of characters, or Slav languages which have more than 30 letters ; the simplicity of the English grammar is well-known. There are, however, some problems to be faced : the lack of an ablative or instrumental case, the formal equivalence between gerund and present participle, or between past tense and past participle, or between noun and verb forms.

A few hints on style are given in the essay ''Instant Stylistics'' by borrowing the theater phrase : ''In the first ten minutes, somebody must kick the cat, or else the play will fall flat''. In trying to convey to the reader knowledge which should be acquired at a rate around one bit per second, authors must provide stimulants for the attention of readers with a low boredom threshold, therefore authors should from time to time kick the cat. Both terseness and verbosity are to be avoided, because they slow down the rate at which knowledge is acquired by the reader.

A host of interesting data are provided on how to edit a manuscript, to differentiate hyphens from en dashes (nuts), em rules (muttons) and minus signs. How does one divide at the end of a line an English word? The answer is provided in the essay ''On the Divisibility of Earth/ Worms'', and the conclusion is that there exist two systems, namely the SWE and the CE rules (the latter is according to morphemes).

Although this is not a book on rules for writing ''good English'' but rather a collection of essays about some of these rules, all chemists and scientists, irrespective if they are proficient in SSE/ SWE or if they use English only for communicating with fellow scientists, will benefit from this book ; it is fun to read and it provides matter for thought ; moreover, it will certainly improve the quality of CE.

A. T. Balaban

''Biotechnology'', edited by H.-J. Rehm and G. Reed, VCH Verlagsgesellschaft, Weinheim. Vol 4 (volume editors H. Pape and H.-J. Rehm), 1986. Hard cover, 673 pp., DM 495, ISBN 3–527–25764–0

The comprehensive treatise ''Biotechnology'' in eight volumes (ten, actually, because volumes 6 and 7 will each have two parts) is published over a period of several years : 1981–1987.

The (192) contributors are from 20 countries : Austria (6), Australia (1), Belgium (5), Canada (8), Chile (1), Czechoslovakia (5), Finland (1), Federal Republic of Germany (66), France (3), German Democratic Republic (1), Hungary (1), Israel (1), Italy (2), Japan (20), Netherlands (5), Spain (3), Sweden (1), Switzerland (13), United Kingdom (18) and USA (31) ; they have written alone or collaborating among them the 175 chapters of the book.

Volume 4 (Microbial Products II) continues the description that began in volume 3. That volume dealt with biomass, ethanol, organic acids, energy from renewable resources and microorganisms for special applications. The present volume has twenty chapters covering products of secondary metabolism : nucleotides and related compounds, vitamins, coenzymes, lipids, siderophores, antibiotics (7 chapters), antitumor agents, ergot alkaloids, and further secondary products of biotechnological interest.

We shall highlight only a few of the aspects discussed in vol. 4. The first chapter, by R. Hütter (ETH, Zürich), discusses the overproduction of microbial metabolites ; secondary metabolites are viewed as products of overproduction due to selected strains (monoclonal in the ideal case) ; this overproduction is a reflection of differential flux rates. Chapter 2, by L. C. Vinnig (Dalhousie Univ., Halifax, Canada) presents a brief but comprehensive overview of secondary metabolism, and chapter 3, by V. S. Malik (Philip Morris Research Center, Richmond, VA, USA) discusses the genetics of secondary metabolism, including technical details on recombinant DNA technology. Chapter 5, by J. Florent (Rhône-Poulenc Santé, Vitry-sur-Seine, France) presents the 13 vitamins for humans, from which vitamin B 12 is exclusively produced by fermentation ; with vitamin B 12 (riboflavin), in terms of sales, these vitamins are at the middle of the scale. The largest sales, of course, are of vitamin C, followed by vitamin A and B-carotene on the second place and by vitamin E (the tocopherols, which are not discussed in this chapter) in the third place. At the end of the scale, in terms of sales, are biotin (vitamin B 8 or H) and provitamin D 2 (ergosterol). Closely related to this chapter is the following one by Japanesse authors (S. Shimizu and H. Yamada) on coenzymes, which presents ATP, NAD, NADP, coenzyme A, pyridoxal, biotin (again), etc. Chapter 7, on lipids (by C. Ratledge, Univ. of Hull, UK) indicates that microbial oils may penetrate the market for the case of higher value oils such as cocoa butter and olive oil; the source of such microbial oils is constituted by products from waste recycling.

Antibiotics (A) are surveyed separately in the following chapters : B-Lactam **A**, peptide **A**, aminoglycoside **A**, macrolide **A**, tetracyclines (by Z. Hostalek and Z. Vanek from the Institute of Microbiology of the Czechoslovak Academy of Sciences, Prague), ansamycins (e.g. rifamycins), and further **A** with practical applications (this chapter, by J. Berdy from the Institute of Drug Research, Budapest, includes chloramphenicol).

The last chapters in this volume include surveys on antitumor substances (e.g. actinomycin D; the anthracyclines such as daunorubicin, adriamycin; bleomycin; etc.), glycosidase inhibitors (applied in medicine for reducing the digestion of di- or polysaccharides, and for treating metabolic discorders), ergot alkaloids, and other secondary products.

Each chapter is a source of rich and recent bibliographical information. All formulas are carefully drawn in order to ensure legibility and clarity. A subject index is appended.

Since biotechnology is nowadays an important component part of advanced technology, despite its high price, the treatise under discussion will be an invaluable help for all those nvolved in teaching, research, and development of biotechnological products, including producers of antibiotics.

A. T. Balaban

E. Breitmaier and W. Voelter, "Carbon-13 NMR Spectroscopy", 3rd Ed., VCH Verlagsgesellschaft, Weinheim, 1987. Hard cover, 515 pp., DM 240, ISBN 3-527-26466-3 (VCH Verlagsgesellschaft), ISBN 0-89573-493-1 (VCH Publishers, New York).

The book with the subtitle "High-Resolution Methods and Applications in Organic Chemistry and Biochemistry" is now at its third completely revised edition, after the previous two editions in 1974 and 1978. In the preface the authors indicate that new sections about coupling constants, organophosphorus and organometallic compounds, as well as synthetic polymers have been added; above all, the new computer-controllable pulse sequences for one- and two-dimensional NMR experiments, in particular those used for multiplicity analysis and homo- or heteronuclear shift correlations, have imposed drastic changes in the first half (i.e. the first three chapters) of the book.

The five chapters of the book are:

1) Introduction to NMR spectroscopy; here, after the basic laws have been stated, the rotating coordinate system is introduced, the Bloch equations are given, and the discussion is centered on chemical shift and spin-spin coupling.

2) Instrumental methods of ^{13}C NMR spectroscopy. Following a brief discussion of continuous wave NMR spectroscopy, the pulse Fourier transform NMR spectroscopy is presented in detail, with an illuminating comparison between CW and PFT; PFT has made ^{13}C NMR into a routine method of structure analysis for all organic molecules having the natural abundance of 1.1% ^{13}C. Double resonance techniques used as assignment aids (NOE enhancement, selective proton decoupling, and the new pulse sequences) are reviewed. The J-modulated spin-echo experiments permit more accurate CH_n multiplicity analyses than off-resonance techniques; the INADEQUATE sequence allows the measurement of carbon-carbon coupling constants without ^{13}C isotopic enrichment. Two-dimensional carbon-proton and proton-proton shift correlations enable spectacular determinations of connectivities via couplings. Two-dimensional COSY, RELAY, and INADEQUATE experiments enable "effortlessly" structure elucidations which would have been unimaginable two decennia ago. An algorithmic ^{13}C NMR strategy for structure elucidation involves (i) counting the nonequivalent carbon atoms from proton broadband decoupled ^{13}C NMR spectra; (ii) determining CH_n multiplicities from J-modulated spin-echo (APT) or non-selective polarization transfer (DEPT) spectra; (iii) alternatively, J-resolved two-dimensional ^{13}C NMR spectra may be used; (iv) 2D carbon-proton shift correlation identifies carbon-proton bonds and quaternary carbon atoms via long-range couplings, COLOC sequence; (v) alternatively, 2D proton-proton shift correlation (COSY experiment) identifies $CH_A - CH_X$ substructures; (vi) finally, two-dimensional carbon-carbon shift correlation (2D-INADEQUATE) enables the chemist to trace the entire carbon-carbon bonding network, in combination with DEPT experiments. *This is the most straightforward and convenient method for structure elucidation invented till now.*

3) ^{13}C NMR spectral parameters and structural properties. Chemical shifts, coupling constants, and relaxation times are surveyed, and various factors influencing these parameters are reviewed. The authors have included comprehensive tables with up-to-date information for these parameters.

4) ^{13}C NMR spectroscopy of organic compounds. The various classes are reviewed selectively: hydrocarbons (non-aromatic), halides, alcohols, ethers, carbonyl compounds, carboxylic acids, sulfur and nitrogen compounds, organophosphorus compounds, aromatics, heterocyclics, organometallic compounds, ions, synthetic polymers. In the final section, substituent increments are cited. No such SCS data are quoted for oxygen-containing aromatic heterocycles, however.

5) ^{13}C NMR spectra of natural products. Again, several classes are systematically discused: terpenes, steroids, alkaloids, carbohydrates, nucleosides and nucleotides, amino acids, peptides, porphyrins, coumarins, and flavonoids. The final section is on the elucidation of biosynthetic pathways with eleven examples, using ^{13}C-enriched precursors to culture media and then recording the ^{13}C NMR spectrum of the specifically labelled biosynthetic materials.

The book is an excellent presentation of the state-of-the-art in ^{13}C NMR spectroscopy. It equilibrates well the general and specific part (about half and half). Of course, omissions are inevitable in such a book. The printing is practically free of errors, but one error found its way both in a chapter heading and in the summary (not in the index, however): bicyclo[2.2.2] heptane, instead of bicyclo[2.2.1] heptane on p. 316. On pages 42 and 122 the assignment of quinoline carbons is contradictory for positions 7 and 8, although the experimental conditions (solvent) are the same.

The bibliography contains more than 1000 references, mostly post-1970, of course. A detailed subject index is included.

The book is a "must" in every laboratory of organic chemistry, even if it does not yet have a ^{13}C NMR instrument.

A. T. Balaban

J. K. Seydel(editor), "Qsar and Strategies in the Design of Bioactive Compounds", VCH Verlagsgesellschaft, Weinheim, 1985. 442 pp. softcover, DM 148, ISBN 3–527–26306–3.

The Proceedings of the Fifth European Symposium on Quantitative structure-activity relationships which was held on September 17–21, 1984 in Bad Segeberg, Federal Republic pf Germany, have been published in a volume edited by J. K. Seydel. The previous symposia were held in Prague (1973), Suhl (1976), Budapest (1979) and Bath (1982). Although the meeting involved mainly 17 European countries, non- European ones such as USA, India and Japan also were represented.

Six plenary lectures were presented, followed by several orally presented papers; the main emphasis was placed on poster sessions which were grouped in three sessions. All communications and posters are included in the present volume, prepared from camera-ready manuscripts, except for C. Hansch's plenary lecture "QSAR and Graphics, Ligand Receptors Interaction" which is presented only as an one-page summary because the color stereo picture could not be included in the volume for economic reasons; this lecture in modified form was published by C. Hansch and T. E. Klein in *Acc. Chem. Res.*, **12**, 392 (1986) in full with the pictures.

It will not be possible to deal with each of the 26 lectures and the 43 posters, but a few of them will be highlighted. The opening lecture (16 pages) by H. Lüllmann and A. Ziegler, "To which extent can receptor events be extrapolated from drug-induced responses?" cautions against such extrapolations on the basis of own data.

The six sessions and the corresponding plenary lectures are:

1) Methods in QSAR: M. Wise, "Evaluation of QSAR methodology and the role of newer computational techniques" (21 pages).

2) QSAR Parameters: R. Franke (same title) discusses on 20 pages interaction parameters (among which the MTD, MSD and MCD methods of Z. Simon and the SIBIS method of I. Moţoc are discussed comprehensively), quantum chemical indices, LFER parameters, hydrophobicity parameters, electronic and stearic parameters.

3) Molecular Modelling: G. R. Marshall, I. Motoc et al., "Applications of systematic search to structure-activity studies" (9 pages).

4) Application of QSAR Analysis in Medicinal Chemistry: C. Hansch (title mentioned above).

5) Application of QSAR Analysis in Pharmacokinetics : K.-J. Schaper and J. K. Seydel, "Multivariate methods in QSAR" (17 pages).

6) Applications of QSAR in Agrochemistry : T. Fujita, "Applications of QSAR analyses to pesticides and growth regulators" (12 pages).

Among the other papers in these sessions, we shall mention : "A new approach in computer-aided derivation of QSAR" by B. Jerman-Blazié, M. Randié and J. Zerovnik, based on the enumeration of self-avoiding paths in the molecular graph; "Structure-activity analysis using hierarchically organized structural molecular descriptors" by W. Schubert, based on pruning one atom at a time from the molecule leading to new molecular descriptors, which can be used for QSAR; "Rapid calculation of electronic effects in organic molecules" by J. Gasteiger et al.; "The STERIMOL approach" by A. Verloop, with a vie towards receptor mapping.

The three poster sessions had the titles :

1) Methods and parameters in QSAR;

2) Application of QSAR in medicinal chemistry and pharmacokinetics;

3) QSAR in agrochemistry and in environmental safety.

We mention several posters of M. Charton (USA), R. Franke (GDR), and A. Lopata (Compudrug Ltd., Budapest). From our country, one poster by Z. Simon, D. Ciubotariu and A. T. Balaban, "Reactivity and stereochemical parameters in QSAR for carcinogenic polycyclic aromatic hydrocarbon derivatives", but no participant was present.

The high cost of drug synthesis and testing on animals and people is a strong incentive for developing new methods of drug design. The volume succeeds in indicating which are these novel directions. The whole QSAR community is aware that this field has changed from academic to more practical, as seen from the fact that quite a number of delegates from industry attended the symposium.

The volume is well-produced and, of course, free of printing errors — there are at most authors' errors — ; in spite of the varied origin of all manuscripts, the whole text is readily legible.

An author and a subject index are appended.

The book is highly recommended to research workers in chemistry, drug industry, and medicinal or environmental chemistry

A. T. Balaban

ORSZÁGOS MŰSZAKI INFORMÁCIÓS KÖZPONT ÉS KÖNYVTÁR 1988

NOTE POUR LES AUTEURS

La Revue Roumaine de Chimie public des articles en anglais, français, russe, allemand ou espagnol. Les auteurs sont priés d'envoyer des articles et des comptes rendus inédits.

Les manuscrits seront dactylographiés à double interligne. La bibliographie, les tableaux et la légende des figures seront placés après le texte.

Si l'article fait partie d'une série numérotée, la partie précédente sera donnée comme première référence.

Chaque article sera précédé d'un résumé comprenant quinze lignes au maximum.

Les références bibliographiques dans le texte seront faites par des exposants sans parenthèses et paraitront à la fin de l'ouvrage.

Les publications périodiques mentionnées dans la bibliographie seront présentées suivant les prescriptions internationales : le nom de l'auteur précédé de l'initiale du prénom, le titre du périodique abrégé conformément à « Chemical Abstracts » et souligné par une ligne, le numéro du tome indiqué par des chiffres arabes et souligné par deux lignes, suivi de la première page de l'article ; à la fin, l'année de la parution sera placée entre parenthèses. Le numéro de la revue ne sera pas indiqué si les pages du volume sont numérotées consécutivement.

Les textes des livres ou traités inclueront : le nom des auteurs, l'initiale du prénom, le titre du livre entre guillemets et sans être souligné, le numéro du tome précédé par l'abréviation « vol. » (ou « Bd. »), le numéro de l'édition, les éditions (the publisher), la localité de la parution du livre, l'année de la parution et la page de la référence précédée(s) par l'abréviation «p. » (ou « S. »).

Les brevets seront indiqués comme suit : l'auteur ou la firme, le pays et le numéro du brevet, la date et la revue *(Chem. Abstr.)*. Par ex. : M. Jones (to Union Carbide Co), Brit. Pat. 601 238, 2 Sept. 1959 ; cf. *Chem. Abstr.*, **54**, 12808 (1960).

Si la référence n'a pas été lue en original, on indiquera aussi la revue de référence consultée.

Les diagrammes seront tracés à l'encre de Chine sur papier calque. Les tableaux et les figures (en nombre strictement nécessaire) ainsi que les courbes dans les figures seront numérotés par des chiffres arabes. Leur explication sera donnée dans la légende des figures. Prière de ne pas inscrire les mêmes données dans les tableaux et les figures. Chaque tableau aura un titre. On indiquera dans le texte la place approximative des tableaux et des figures. Les formules chimiques seront incluses dans le texte ; en outre, elles seront transcrites sur papier calque, à l'encre de Chine.

Les auteurs sont priés d'indiquer les caractères italiques (en soulignant les lettres au crayon), ainsi que tout autre caractère spécial ; les préfixes *ortho*, *meta*, *para*, *cis*, *trans*, etc. seront soulignés pour indiquer leurs caractères italiques et ne seront jamais écrits avec des majuscules.

Aucune correction à la main ne sera admise sur le manuscrit. Les corrections seront tapées à la machine. Les lettres grecques ou d'autres symboles spéciaux seront insérés à la main à l'encre clairement.

Le manuscrit sera signé par l'auteur.

Le titre-courant aura 50 lettres au maximum.

L'entière responsabilité du contenu des articles appartient aux auteurs.

Sur demande on peut obtenir une note plus complète.

PRINTED IN ROMANIA

1987 SEP 04

TRAVAUX PARUS AUX ÉDITIONS DE L'ACADÉMIE DE LA RÉPUBLIQUE SOCIALISTE DE ROUMANIE

ELENA CEAUŞESCU, **Progrese în chimia şi tehnologia polimerilor**, 1986, 446 p.
ELENA CEAUŞESCU, **Forschungen im Bereich der Chemie und Technologie der Polymere**, 1986, 444 p.
I. G. MURGULESCU, O. M. RADOVICI, **Introducere în chimia fizică, vol. IV, Electrochimia**, 1986, 410 p.
RAUL MIHAIL, ION GROZEANU, **Estimarea secvenţială aplicată sistemelor chimice**, 1986, 406 p.
M. BREZEANU, L. PATRON, M. ANDRUH, **Combinaţii complexe polinucleare şi aplicaţiile lor**, 1986, 244 p.
A. T. BALABAN et al., **Labelled Compounds and Radiopharmaceuticals Applied in Nuclear Medicine**, coédition avec John Wiley and Sons, 1986, 742 p.
D. PURDELA, **Nomenclatura chimiei organice — IUPAC**, 1986, 454 p.
PETRU BUDRUGEAC, **Probleme de chimie**, 1986, 280 p.
T. ONCESCU, S. G. IONESCU, **Conversie fotochimică şi stocare de energie**, 1985, 272 p.
V. DRĂGUŢAN, A. T. BALABAN, M. DIMONIE, **Olefin Metathesis and Ring-Opening Polymerization of Cyclo-Olefins**, coédition avec John Wiley and Sons, 1985, 544 p.
C. LITEANU, I. RICĂ, **Optimizarea proceselor analitice**, 1985, 360 p.
N. PERESCU, **Chimia extracţiei cu solvenţi şi aplicaţii**, 1985, 212 p.
V. E. SAHINI, N. HILLEBRAND, **Chimie cuantică în exemple şi aplicaţii**, 1984, 378 p.
GH. MARCU, **Chimia compuşilor coordinativi**, 1984, 415 p.
E. CORDOŞ, C. MANOLIU, **Spectrometria de absorbţie şi fluorescenţa atomică**, 1984, 178 p.
C. BODEA, **Tratat de biochimie vegetală, p. II, t. V**, 1984, 438 p.
N. ASANDEI, A. GRIGORIU, **Chimia şi structura fibrelor**, 1983, 395 p.
N. IONESCU, M. CĂLDĂRARU, **Oxidarea catalitică a olefinelor inferioare**, 1983, 178 p.
C. CAŞCAVAL, **Studiul polimerilor prin piroliză şi cromatografie de gaze**, 1983, 220 p.
C. I. SIMIONESCU, F. DANEŞ, **Originea vieţii**, 1983, 110 p.
C. BODEA, **Tratat de biochimie vegetală, p. II, t. IV**, 1982, 408 p.
I. G. MURGULESCU, RODICA VILCU, **Introducerea în chimia fizică. Vol. III. Termodinamica chimică**, 1982, 624 p.
I. G. MURGULESCU, J. PAUN, **Introducere în chimia fizică, Vol. I. 3. Nucleul atomic, reacţii nucleare, particule elementare**, 1982, 606 p.
ELENA CEAUŞESCU, **Noi cercetări în domeniul compuşilor macromoleculari**, 1981, 536 p.
I. G. MURGULESCU, TATIANA ONCESCU, E. SEGAL, **Introducere în chimia fizică. Vol. II. 2. Cinematică chimică şi cataliză**, 1981, 1024 p.
I. GĂLĂŢEANU, **Procese şi metode radiochimice în energetica nucleară**, 1981, 234 p.
CR. SIMIONESCU, VALERIU GORDUZA, **Polimeri biocompatibili şi biologic activi**, 1980, 479 p.
ELENA CEAUŞESCU, **Polimerizarea stereospecifică a izoprenului**, 1979, 307 p.
C. GH. MACAROVICI, **Analiza chimică cantitativă anorganică**, 1979, 457 p.
M. FLORESCU, **Metode ştiinţifice în dezvoltarea industriei chimice moderne**, 1979, 256 p.
I. G. MURGULESCU, E. SEGAL, **Introducere în chimia fizică. Vol. II. 1. Teoria molecular-cinetică a materiei**, 1979, 1036 p.
:I. G. MURGULESCU, E. EM. SAHINI, **Introducere în chimia fizică, Vol. I, 2. Structura şi proprietăţile moleculelor**, 1979, 604 p.
I. ZUGRAVESCU, MAGDA PETROVANU, **N-ylid chemistry**, coédition avec McGraw-Hill International Book Company U.S.A., 1977, 396 p.
I. G. MURGULESCU, **Introducere în chimia fizică, Vol. I. 1. Atomi, molecule, legătură chimică** 1976, 560 p.
ELENA CEAUŞESCU, **Research work on synthesis and characterization of macromolecular compounds, Contributions**, 1974, 251 p.

ISSN 0035 — 3930

I.P. Informaţia c.1229

43 426

Lei 40

$ 80 (pour un abonnement annuel)

F 1103

~~04~~

ACADÉMIE DE LA RÉPUBLIQUE SOCIALISTE DE ROUMANIE

66

REVUE ROUMAINE DE CHIMIE

TOME 32

N° 8

Août 1987

Rev. Roumaine Chim.

RRCHAX, 32, 8, p. 737–836 (1987), Bucarest

EDITURA ACADEMIEI REPUBLICII SOCIALISTE ROMÂNIA

ACADÉMIE DE LA RÉPUBLIQUE SOCIALISTE DE ROUMANIE

COMITÉ DE RÉDACTION

Rédacteur en chef :

I. G. MURGULESCU, membre de l'Académie de la République Socialiste de Roumanie

Rédacteurs en chef adjoints :

A. T. BALABAN et V. EM. SAHINI, membres correspondants de l'Académie de la République Socialiste de Roumanie

Collège de rédaction :

EM. BRATU, ELENA CEAUȘESCU, ECATERINA CIORĂNESCU-NENITZESCU, CR. SIMIONESCU, membres de l'Académie de la République Socialiste de Roumanie ; P. SPACU, membre correspondant de l'Académie de la République Socialiste de Roumanie ; M. BANCIU, M. D. GHEORGHIU, I. HAIDUC, D. I MARCHIDAN, G. NIAC et D. SĂNDULESCU.

La Revue Roumaine de Chimie paraît 10 fois par an. Toute commande de l'étranger sera adressée à ROMPRESFILATELIA — sectorul Export-Import Presă, P.O. Box 12—201, télex 10376, prsfi r 78 104, 64—66, Calea Griviței, Bucarest, Roumanie

Les manuscrits, les livres et les revues proposés en échange, ainsi que toute correspondance seront envoyés à la rédaction

REVUE ROUMAINE DE CHIMIE

125, Calea Victoriei, 79717 Bucarest, Roumanie, téléphone 50 76 80

EDITURA ACADEMIEI REPUBLICII SOCIALISTE ROMÂNIA
125, Calea Victoriei 79717 Bucarest, Roumanie, téléphone 50 76 80

REVUE ROUMAINE DE CHIMIE

ORSZÁGOS MŰSZAKI INFORMÁCIÓS KÖZPONT ÉS KÖNYVTÁR 1883

Tome 32, N° 8 **Août 1987**

J. ZSAKÓ, V. NEAGU, MARIA TOMOAIA-COTIȘEL and E. CHIFU, Molecular structure and monolayer properties 739–748

ION NEACȘU and MARIANA BEZDADEA, Electric potential of some autochthonous synthetic membranes 749–757

GEORGE DRĂGAN, High resolution mixing calorimetry in studies of composite systems 759–765

G. DRĂGAN, S. IFRIM and GEORGETA POPESCU, Study by high resolution mixing calorimetry of adsorption of aqueous solutions of superplasticizer additive on cement 767–773

A. S. FOUDA, H. A. MOSTAFA and M. N. MOUSSA, Heterocyclic quaternary ammonium compounds as corrosion inhibitors for mild steel in H_3PO_4 . . 775–782

Z. SIMON, G. I. MIHALAS, M. APETROAIE, CL. SINGER, RALUCA BOZGA, RODICA CECLAN and ST. CILIANU, Structure activity relations by the free-Wilson and MTD methods for substances with a potential psychotropic activity. 2. Benzensulphonamide derivatives with anticonvulsive activity 783–791

C. I. CHIRIAC, N-aroylphthalimides by a new direct condensation reaction . . 793–796

M. F. ABDEL MEGEED, M. EL BORAI, M. FAHMY and EL-SAIED A. ALY, Studies on pyridyl-pyrazolone system. II. Some reactions with 4-arylidene-3-(3′-pyridyl)-1-phenyl-2-pyrazolin-5-one 797–801

OLCAY ANAÇ and KERIMAN GÜNAYDIN, Organochlorine (OCl) pesticide residues in human fats. Part I 803–806

R. Z. TUDOSE and H. KADI, Drying of a porous spherical grain (in French) . . 807–819

GHEORGHE MARIA, CRISTIAN TSAKIRIS, GRIGORE BOZGA and ALEXANDRU ISOPESCU, An adapted zone method for propane thermal cracking process simulation in a radiant furnace 821–832

BOOK REVIEWS 833–836

Rev. Roumaine Chim. **32**, *8*, 737–836 (1987), Bucarest

Revue Roumaine de Chimie, 32, 8, 739–748 (1987)

MOLECULAR STRUCTURE AND MONOLAYER PROPERTIES*

J. ZSAKÓ, V. NEAGU, MARIA TOMOAIA-COTIŞEL and E. CHIFU
Faculty of Chemical Technology, University of Cluj-Napoca, Romania

Received December 15, 1986

Surface pressure (π) *vs.* mean molecular area (A) curves of insoluble monolayers can be used to derive monolayer properties as limiting molecular area (A_o), collapse area (A_c), collapse pressure (π_c), surface compressional modulus (C_{so}^{-1}). By using a semi-empirical van der Waals type two-dimensional state equation› an interaction parameter (α) can be derived. Geometric molecular models allows the interpretation of the experimental A_o and A_c values in terms of orientation, conformation and packing of surfactant molecules. π_c, C_{so}^{-1} and α are correlated with the intermolecular dipole-dipole interactions and dispersion forces. For some carotenoid derivatives π-electron distribution and dipole moments computed by using semiempirical MO calculations, are in good agreement with the experimentally found parameters.

INTRODUCTION

The surfactants, insoluble in water, being spread at the air/water interface, form a unimolecular film. The molecules, having a polar headgroup and one or more, saturated or unsaturated hydrocarbon chains, are anchored in the aqueous subphase by their polar headgroup. By compressing this monolayer, the surface pressure (π) increases gradually and the plot of π *vs.* the mean molecular area (A) gives a characteristic curve, called compression isotherm. A typical compression isotherm is visualized in Figure 1. At low π values the monolayer occurs in an expanded state and this portion of the isotherm (*ab* in Fig. 1) can be described by means of state equations of different forms. [1-7] Rather good results are obtained by using two-dimensional van der Waals type state equations, thus, frequently, experimental curves are very well described

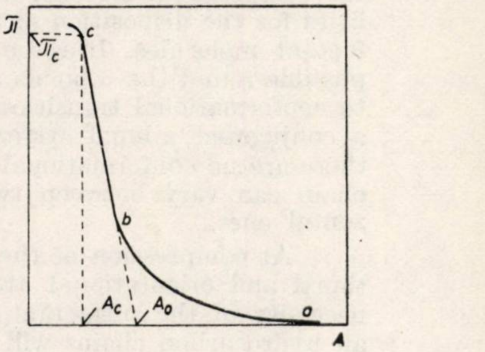

Fig. 1. — Typical compression isotherm of insoluble monolayer.

---

* Paper presented at the Symposium on Chemistry of Colloids and Surfaces, Cluj-Napoca, September, 8–10, 1986

by the following semiempirical variant:[8,9]

$$(\pi + \alpha/A^{2/3})(A - A_0') = kT \qquad (1$$

where α and A_0' are empirical parameters to be derived from the experimental curves. The parameter α characterizes the intermolecular forces, acting between the surfactant molecules and A_0 is correlated with the area necessity of the latter.

At higher π values, the compression isotherm becomes linear (*bc* in Fig. 1) and the high slope straight line indicates a condensed state of the monolayer, its slope being a measure of its compressibility. By extrapolating this linear portion to $\pi = 0$, one obtains the limiting molecular area A_0 (see Fig. 1), and from the slope of the straight line the surface compressional modulus[10] can be derived as:

$$C_{so}^{-1} = -A_0\left(\frac{\partial \pi}{\partial A}\right)_T = -A_0\frac{\pi_c}{A_c - A_o} \qquad (2)$$

At the compression of the monolayer, after this linear portion, a sudden slope change is observed, indicating the collapse of the film, i.e. the appearance of a new phase, of the collapsed bulk phase. This means that a part of the surfactant molecules is ejected from the monolayer, from the two-dimensional surface phase, into a three-dimensional bulk phase. Generally, the co-ordinates of this collapse point, called collapse pressure (π_c) and collapse area (A_c) (see Fig. 1), are quite well reproducible in a rather large region of compression speeds, i.e. a thermodynamic equilibrium may be presumed between the monolayer and the freshly collapsed bulk phase.[11]

On the basis of the shape of the π *vs.* A curves a hypothesis can be forwarded concerning the behaviour of the surfactant molecules during the compression. At high molecular areas there are great many possibilities for the disposition of the air phase hydrocarbon chains of the surfactant molecules. If these chains are saturated ones, free rotation is possible round the σ-bonds and the collisions between the molecules lead to conformational transitions. If the hydrocarbon chain is rigid, due to a conjugated π-bond system, as it occurs with carotenoid derivatives, there are no conformational transitions, only the orientation of the rigid chain can vary between two extreme positions, the vertical and horizontal ones.

At compression of the monolayer, due to the collisions, conformational and orientational transitions occur, leading to decreasing area necessity of the surfactant molecules in the monolayer, and eventually all hydrocarbon chains will adopt the most extended conformation and a vertical orientation, i.e. a two-dimensional lattice of oriented molecules is formed. Presumably, this condensed state gives the high slope linear portion of the isotherm at high surface pressures. At very high π values, this two-dimensional lattice is destroyed and the collapse of the monolayer occurs.

MOLECULAR MODELS

This image of what happens at the molecular level if monolayers are compressed, has been verified by molecular model calculations. In our previous papers a rotating rigid plate model was proposed for carotenoid derivatives [12] and a quasi-rigid prism model for surfactants having saturated hydrocarbon chains. [13] By taking into account internuclear distances, bond angles and van der Waals radii of the atoms, the linear dimensions of the molecules have been obtained for their more extended conformation. Area necessities of the vertically oriented surfactant molecules have been calculated in different approximations, viz. by presuming a tetragonal (A_4) or a hexagonal (A_6) close packing of some cylinders, obtained by the rotation of the vertically oriented surfactant molecules, as well as by presuming the close packing of non-rotating molecules (A_p).

Comparison of the calculated A_4, A_6 and A_p values with the experimental A_o and A_c ones, showed that A_0 corresponds approximately to the tetragonal close packing of rotating, vertically oriented, most extended molecules, i.e. $A_o \approx A_4$. At further compression, the rotation of the molecules gradually becomes hindered and before collapse an almost regular two-dimensional lattice of non-rotating molecules seems to be achieved, since $A_c \approx A_p$. Some examples [9,14] are given in Table 1.

Table 1

Calculated and experimental molecular areas in nm²/molecule

Surfactant	A_0	A_4	A_c	A_p
β-cryptoxanthin	0.42	0.40	0.23	0.24
β-cryptoxanthin acetate	0.48	0.50	0.27	0.27
β-cryptoxanthin palmitate	0.83	0.83	0.44	0.45
zeaxanthin	0.49	0.42	0.30	0.29
zeaxanthin diacetate	0.67	0.66	0.40	0.41
zeaxanthin monopalmitate	0.70	0.67	0.52	0.52
stearic acid	0.20			
	0.25	0.25	0.18	0.18
oleic acid	0.41	0.39	0.27	0.26
linoleic acid	0.48	0.47	0.31	0.30

Obviously, one has indeed $A_0 \approx A_4$ and $A_c \approx A_p$. A single exception is observed, viz. in the case of zeaxanthin A_0 is significantly higher than A_4. This anomaly can be easily understood, by taking into account that zeaxanthin has also an air phase OH group, allowing the dimerization of the surfactant molecules. This dimerization does not affect the area necessity if the molecular rotation is hindered (consequently, $A_c \approx \approx A_p$), but it increases very much if the dimer rotates.

In the case of stearic acid, for A_0 two values are given, since on the compression isotherm two successive linear portions appear, the first one corresponding to a liquid condensed state, giving $A_0 = 0.25$ nm^2/molecule and equal to A_4, as with the other surfactants studied. The second linear portion corresponds to the solid state of the film, giving $A_0 = 0.20$ nm^2/molecule, this value being very close to A_p, indicating a close packing of non-rotating molecules, as can be expected for a two-dimensional "solid" lattice.

Our results obtained in the case of carotenoid derivatives, [9,12] fatty acids, [14] phospholipids [13] and galactolipids [15] are in good agreement with

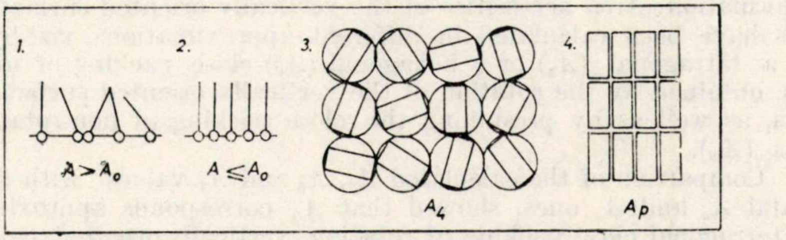

Fig. 2. — Structure of the monolayer. Model for rigid molecules. *1* — expanded monolayer; *2* — condensed monolayer; *3* — close packing of rotating molecules; *4* — close packing of non-rotating molecules.

the above given hypothesis concerning the transitions of the molecules during the compression of the monolayer. This mechanism is illustrated in Fig. 2 for rigid molecules. The first two situations are given in side-view (into the direction of the interface) for the expanded ($A > A_0$) and condensed ($A \leqslant A_0$) states, respectively. In the last two situations the molecules are thought to be looked at into a direction perpendicular to the interface and the structure of the surface lattice is given for the close packing of the rotating (A_4) and of the non-rotating (A_p) molecules.

We mention that these model calculations may reveal the conformation of the polar headgroup in the condensed state, or may explain the nature of phase transitions observed on the compression isotherms, if these are due to conformational transitions. [12,16]

INTERMOLECULAR INTERACTIONS

The intermolecular interactions in monolayers are rather complicated and are completely different in the expanded and in the condensed states. In expanded monolayers, where the vertical orientation of the surfactant molecules is not achieved yet, the main role is played by the dipole-dipole interactions. This is reflected by the interaction parameter α derived from the compression isotherms by means of Eq. (1). [9] As seen from Table 2, this parameter has higher values in the case of zeaxanthin derivatives, as compared to β-cryptoxanthin ones, since the former have one more OH group linked to the air phase ionone ring, as compared to the latter. The higher α values obtained for the acetates, as compared to the non-esterified xanthophylls, might be due to the polarity of the carboxyl group, but it might be also influenced by the interactions of the polar headgroup, which must be quite different in the case of esters, as compared to the free alcohols.

Table 2

Van der Waals type interaction parameters from Eq. (1), $\alpha \times 10^{30}$, Nm^2

xanthophyll		monoacetate
β-cryptoxanthin	3.08	4.98
zeaxanthin	5.46	6.35

In the condensed state, besides the dipole-dipole interactions, also the dispersion forces have an important part and near to the collapse, the polar headgroup — subphase liquid interactions become of major importance. The collapse pressure is a result of all these co-operative effects. Collapse pressures of a series of surfactants of different natures are given in Table 3. [9,12–15,17]

Table 3

Collapse pressure (π_c, mN/m) of monolayers at air/water interface

No	Surfactant	π_c
1	Retinylidene oxazolone	7
2	β-Apo-8′-carotenylidene oxazolone	13
3	Equinenone	32
4	Canthaxanthin	36
5	β-Cryptoxanthin	37
6	Zeaxanthin	40
7	Astaxanthin	45
8	β-Cryptoxanthin acetate	31.5
9	β-Cryptoxanthin palmitate	28
10	Egg lecithin	42.5
11	Dipalmitoyl lecithin	55
12	Distearoyl lecithin	58
13	Monogalactosyl dipalmitoyl glycerol	49
14	Digalactosyl dipalmitoyl glycerol	68
15	Stearic acid	40.8
16	Oleic acid	30
17	Linoleic acid	26

Inspection of Table 3 allows us to illustrate the effect of the interactions of different types. Surfactants 1 and 2 have the same polar headgroup, but 1 has a short air phase hydrocarbon chain, 2 has a long one, which entails enhanced London type hydrophobic interactions, leading to higher π_c value. Substances 3—9 have the same carotene skeleton and it is easy to understand the increase of π_c from 3 to 7, by taking into account that 3 has a single CO group anchored into the water phase, 4 has one more CO group in the air phase, 5 has a single OH group, which is more strongly anchored into the water phase than the CO group does, 6 has one more OH group in the air phase and 7 has both CO and OH groups, both in the water phase headgroup and in the air phase. This order of increasing π_c illustrates the effect of polar groups and of polar headgroup — subphase water interactions. The lower π_c values of 8 and 9, as compared to 5, are a consequence of the space necessity of the acetate, and especially of the palmitate moiety, hindering the close packing of the carotenoid molecular "plates" and consequently, leading to weaker dispersion forces. Also, the substitution of the hydroxylic H atom for an acyl group makes the polar headgroup to be less strongly anchored into the water phase.

π_c values of the lecithins reveal the importance of the short range dispersion forces. The unsaturated chains of 10 hinder the close packing of the molecules and consequently, lessens the intermolecular attraction. The hydrocarbon chains being saturated with 11 and 12, π_c becomes much higher due to the close packing of the molecules and the longer chains of 12, as compared to 11, entail higher π_c. Surfactants 13 and 14 differ between them with respect to their sugar moiety and the extremely high π_c of 14 is due to the great number of OH groups, leading to strong hydration and near to the collapse, presumably, also to hydrogen bridge formation between the adjacent surfactant molecules.

The fatty acids 15–17 illustrate newly the importance of close packing for the manifestation of the dispersion forces. These acids have the same number of C atoms, but whilst 15 is saturated, 16 and 17 have one and two double bonds, respectively. As shown by the molecular models, [14] the close packing of the molecules in their most extended conformation occurs easily with 15, but it is hindered in the case of 16 and especially of 17, which is reflected in their π_c values.

MO CALCULATIONS

The large conjugated π-bond system of the carotenoids allows us to perform MO calculations concerning the π-electron densities on the different atoms of the conjugated system and to compute the dipole moments of the individual bonds. For this purpose three carotenoids were chosen, containing carbonylic oxygen atoms, participating in the conjugated π-bond system.

The substances studied were 4-oxo-β-carotene (equinenone, OC), 4,4′-dioxo-β-carotene (canthaxanthin, DOC) and diapo-4,4′-carotenedial (CDA). Their molecular structure is presented in Figure 3. By recording compression isotherms, monolayer properties were derived. These are shown in Table 4. [18]

MO calculations were performed in two approximations, viz. :

Approach 1 is the simple Hückel method, applied earlier, [18] by using the following parameters : $\alpha_C = 0$; $\alpha_O = 1$; $\beta_{CC} = 1$ and $\beta_{OC} = 1$.

Approach 2, used in the present paper, applies inductive parameters in the case of the Coulomb integrals of C-atoms, to which instead of an H atom, a single-bonded C atom is linked. According to literature

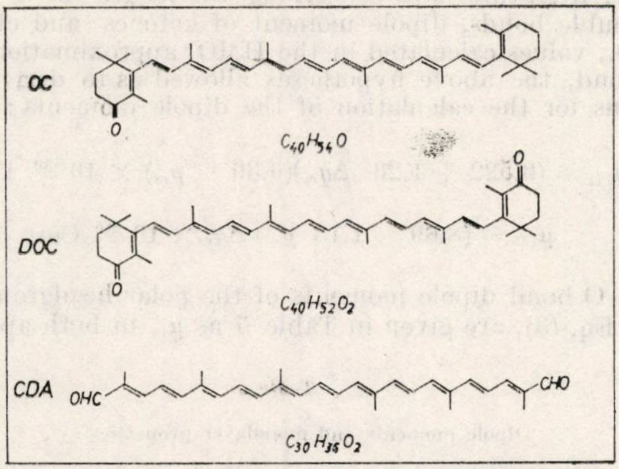

Fig. 3. — Molecular structure of the carotenoids studied: OC — 4-oxo-β-carotene; DOC — 4,4′-dioxo-β-carotene; CDA — diapo-4,4′-carotene-dial.

Table 4

Surface properties of certain carotenoids

Surfactant	π_c mN/m	C_{s0}^{-1} mN/m	$\alpha \times 10^{30}$ Nm^2
OC	32	151	9.02
DOC	36	145	8.74
CDA	32	95	6.71

data,[19] the following values were taken: $\alpha_C = -0.3$ for all C-atoms carrying a CH_3 group and $\alpha_C = -0.5$ for the C-atoms linked to the saturated part of the ionone ring.

In both approximations energy levels, LCAO MO coefficients, π-electron densities, q_r, and bond orders, p_{rs}, have been calculated.

The q_r and p_{rs} values have been used for the calculation of dipole moments of the individual C—O and C—C bonds. For this purpose a semiempirical method has been proposed,[18] based upon the following hypotheses:

1. The dipole moment of CO is the sum of the dipole moment of the C—O σ-bond and of that of the C—O π-bond, both are directly proportional to the internuclear distance, the latter one being a linear function of the π-bond order, p_{rs}.

2. The dipole moment of the C—C σ-bond is equal to zero.

3. The dipole moment of the π-bonds, both of C—O and of C—C ones, is directly proportional to the difference between the π-electron densities of the atoms linked to each other, $\Delta q_{rs} = q_r - q_s$.

By using literature data concerning the length of C—O and C—C single and double bonds, dipole moment of ketones and ethers, as well as Δq_{rs} and p_{rs} values calculated in the HMO approximation for a C—O localized π-bond, the above hypotheses allowed us to derive the following expressions for the calculation of the dipole moments : [18]

$$\mu_{CO} = (0.522 + 1.26\ \Delta q_{rs})(6.39 - p_{rs}) \times 10^{-30}\ \mathrm{Cm} \qquad (3)$$

$$\mu_{CC} = (8.69 - 1.13\ p_{rs})\,\Delta q_{rs} \times 10^{-30}\ \mathrm{Cm} \qquad (4)$$

The C—O bond dipole moments of the polar headgroup, calculated by means of Eq. (3), are given in Table 5 as μ_1, in both approaches.

Table 5

Dipole moments and monolayer properties

Magnitude	Approach 1			Approach 2		
	OC	DOC	CDA	OC	DOC	CDA
$\mu_1 \times 10^{30}$, Cm	9.14	9.09	9.09	9.94	9.92	8.65
$\mu_{3h} \times 10^{30}$, Cm	9.52	9.41	6.71	9.63	9.43	3.96
$\mu_{3v} \times 10^{30}$, Cm	2.35	2.31	−6.99	1.73	1.68	−6.23
$\mu_{3t} \times 10^{30}$, Cm	9.81	9.69	9.59	9.78	9.58	7.39
β, °	13.9	13.8	−46.2	10.2	10.1	−57.5
$\mu_{12h} \times 10^{30}$, Cm	6.15	7.14	8.98	13.0	14.3	1.65
α/μ_{3h}, Nm/C	0.947	0.929	1.00	0.937	0.926	1.69
α/μ_{3t}, Nm/C	0.919	0.902	0.692	0.922	0.912	0.908
$C_{so}^{-1}/\mu_{3h} \times 10^{-28}$, N/Cm^2	1.58	1.54	1.42	1.57	1.54	2.40
$C_{so}^{-1}/\mu_{3t} \times 10^{-28}$, N/Cm^2	1.54	1.50	0.98	1.54	1.51	1.29
$\Sigma\lvert\mu_h\rvert \times 10^{30}$, Cm	17.8	28.7	18.0	27.9	34.9	21.3

The dipole moments of the individual bonds are composed in the molecule and frequently, in the intermolecular interactions these individual dipole moments do not act separately, but their vector sum does,

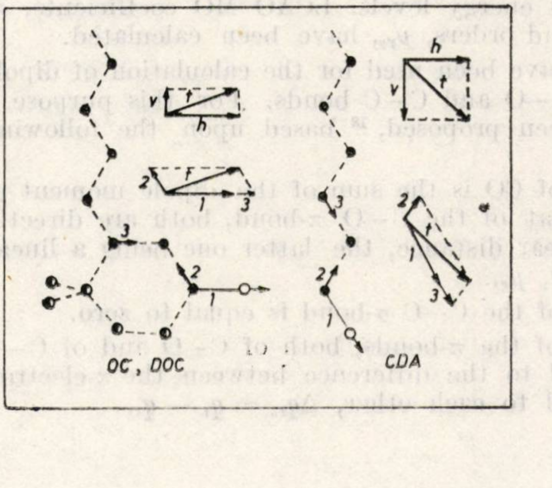

Fig. 4. — Composition of the dipole moments of the first 3 bonds. $h - \mu_{3h}$; $v - \mu_{3v}$; $t - \mu_{3t}$. ● — C-atom with sp^2 hybridization ; ◐ — C-atom with sp^3 hybridization ; ○ — C-atom with sp^2 hybridization.

viz. the overall dipole moment of the interacting moiety. Therefore, the dipole moments of the bonds have been summed up, by obtaining overall dipole moments, μ_{nt}, representing the vector sum of the first n bonds of the conjugated system, beginning from the headgroup C—O bond. These dipole moments have been decomposed into a horizontal, μ_{nh}, and a vertical, μ_{nv}, component for the vertical position of the whole surfactant molecule. Some examples are given in Table 5. Construction of μ_{3t}, μ_{3h} and μ_{3v} is visualized in Figure 4.

It is interesting to observe that μ_{3v} is oriented upwards in the case of OC and DOC, but downwards with CDA. The angle β, formed by μ_{3t} with the air/water interface is also indicated in Table 5. It seems to be reasonable to take μ_{3t} for the dipole moment of the polar headgroup and it may be presumed to play an important part in the expanded state of the monolayer. It is interesting therefore, to compare interaction parameters α with the calculated μ_{3h} and μ_{3t} values. The ratios α/μ_{3h} and α/μ_{3t} are given in Table 5. Since C_{so}^{-1} values vary in parallel with α, also C_{so}^{-1}/μ_{3h} and C_{so}^{-1}/μ_{3t} ratios were calculated and given in the same table. As seen, for OC and DOC, all four ratios in both approaches are rather close to each other, but the values obtained for CDA are sometimes quite different. In this respect approach 2 seems to give more reasonable results. In this approach α/μ_{3t} is practically the same for CDA as with OC and DOC; C_{so}^{-1}/μ_{3h} is higher, but C_{so}^{-1}/μ_{3t} is lower than with OC and DOC. By taking into account that α characterizes the expanded monolayer, C_{so}^{-1} the condensed one, with vertical orientation of the molecules, it seems reasonable α to be correlated with μ_{3t}, but in determining C_{so}^{-1} the horizontal component μ_{3h} to play a more important part, as reflected by the above mentioned ratios, obtained in approach 2.

Table 5 contains also μ_{12h} values, which are very different in the two approximations used, since the induction parameters introduced may change the polarity in the case of bonds with low dipole moments. Anyhow, there is no reason summing up dipole moments for a large portion of the molecule. Thus, due to the symmetry of the molecule, both for DOC and CDA, the overall dipole moment μ_{25t} is equal to zero. Nevertheless, between adjacent, vertically oriented molecules, important dipole-dipole interactions must occur, which might be characterized rather by means of the sum $\Sigma|\mu_h|$, representing the sum of the modulus of the horizontal components of all individual bond dipole moments, than with μ_{12h}, or with the overall dipole moment. These sums $\Sigma|\mu_h|$ are also given in Table 5 and they might be presumed to play an important role near to the collapse, when the close packing of oriented, non-rotating molecules occurs. This hypothesis is in good agreement with experimental data. As seen, the sum $\Sigma|\mu_h|$ is much higher for DOC, as compared to OC and CDA, and the same is observed with the corresponding collapse pressures (see Tables 4 and 5).

In conclusion, the dipole moments of the polar headgroup can be well correlated with the monolayer properties α and $C_{s_0}^{-1}$, derived from the experimental compression isotherms. The sum $\Sigma|\mu_h|$ is a measure of the dipole-dipole interactions between neighbouring molecules, near to the collapse of the monolayer and therefore, the higher this sum, the higher will be the collapse pressure of the monolayer.

REFERENCES

1. W. D. Harkins, "The Physical Chemistry of Surface Films", Reinhold Publ. Corp., 1952.
2. P. C. Hiemenz, "Principles of Colloids and Surface Chemistry", Marcel Dekker, Inc., New York—Basel, 1977, p. 268.
3. E. D. Glandt and A. L. Myers, *J. Chem. Phys.*, **70**, 4243 (1979).
4. W. Rettig, P. Hennersdorf and H. D. Dörfler, *Z. phys. Chem. Leipzig*, **262**, 820 (1981).
5. Y. Izumitani, H. Fukuoka and T. Nakamuro, *J. Colloid Interface Sci.*, **108**, 356 (1985).
6. F. J. Garfias, *J. Phys. Chem.*, **83**, 3126 (1979).
7. T. Smith, *J. Colloid Interface Sci.*, **23**, 27 (1967).
8. J. T. Davies, *J. Colloid Sci.*, **11**, 377 (1956).
9. E. Chifu, J. Zsakó and M. Tomoaia-Cotişel, *J. Colloid Interface Sci.*, **95**, 346 (1983).
10. J. T. Davies and E. K. Rideal, "Interfacial Phenomena", Academic Press, New York, 1963, p. 265.
11. G. L. Gaines, Jr., "Insoluble Monolayers at Liquid-Gas Interfaces," Wiley Interscience, New York, 1966.
12. J. Zsakó. E. Chifu and M. Tomoaia-Cotişel, *Gazz. chim. Ital.*, **109**, 663 (1979).
13. M. Tomoaia-Cotişel, J. Zsakó and E. Chifu, *Ann. Chimica (Rome)* **71**, 189 (1981).
14. M. Tomoaia-Cotişel, J. Zsakó, A. Mocanu, M. Lupea and E. Chifu, *J. Colloid Interface Sci.*, **117**, 464 (1987).
15. M. Tomoaia-Cotişel, J. Zsakó, E. Chifu and P. J. Quinn, *Chem. Phys. Lipids*, **34**, 55 (1983).
16. J. Zsakó, M. Tomoaia-Cotişel, V. Tămaş, V. Coman and E. Chifu, *Rev. Roumaine Chim.*, in press.
17. J. Zsakó, M. Tomoaia-Cotişel and E. Chifu, *J. Colloid Interface Sci.*, **102**, 186 (1984).
18. J. Zsakó, M. Tomoaia-Cotişel and E. Chifu in "Surfactants in Solution", — "Proceedings of the 6th international symposium on surfactants in solution", August 18—22, 1986, New Delhi, India, in press.
19. A. Streitwieser, "Molecular Orbital Theory for Organic Chemists". J. Wiley, New York, 1961.

Revue Roumaine de Chimie, 32, 8, 749–757 (1987)

ELECTRIC POTENTIAL OF SOME AUTOCHTHONOUS SYNTHETIC MEMBRANES*

ION NEACŞU and MARIANA BEZDADEA[a]

Center of Biological Research, 23 August 20 A, 6600 Iaşi
[a]Polytechnic Institute of Iaşi, Faculty of Chemical Technology,
Department of Physical, General and Technological Chemistry,
Splai Bahlui 71 A, 6600 Iaşi

Received December 28, 1986

The membrane potential has been determined from a series of synthetic membranes prepared by original methods, on the basis of polyvinylacetate (KA–7, KA–10, KA–11, KA–14) or cellulose acetate (CA) in comparison with an imported Sartorius membrane, in the presence of NaCl or KCl solutions (100 mmol/L) and of bidistilled water. The measurements have been taken at 10 minutes intervals, for two hours, at the room temperature (17–18°C), by means of an equipment used for determining the electric potential of biological membranes, using nonpolarizable electrodes (Ag/AgCl): a microelectrode with glass micropipette (the electric resistance 6–10 Mohm) and a reference macroelectrode. Potential values specific to each membrane type have been recorded. The obtained data evidence a likeness between the autochthonous membrane and the imported Sartorius one which suggests the possibility of the latter replacing in some uses.

Key words: synthetic membranes, membrane potential, selectivity

INTRODUCTION

One of the parameters characterizing the various membrane types is the membrane potential which is the potential difference occurring between two electrolyte solutions separated by a membrane. The value and the sign of the membrane potential depend on the physico-chemical properties of the membrane, the nature and concentration of the ions present in the adjacent phases and also on the interaction mode between the membranes and the solutions they are in contact with. This interaction implies the presence of fixed electric charges, the ion adsorption on the walls of membrane pores etc., which influences the diffusion degree and the mobility of ions.[1,2] It was found that in water the mobility ratio of K^+ to Na^+ ions is of 1.49 while in the case of solution separation by a collodium membrane this ratio is of 7.19.[1] The complex processes staying at the basis of membrane potential and of other phenomena taking place at the level of synthetic and biological membranes are much investigated at present, many theories on the membrane potential being known.[2,5] At the same time their application to the various technological processes is considered.[6]

---

* Paper presented at the Symposium on Chemistry of Colloids and Surfaces, Cluj-Napoca, September 8–10, 1986.

As a complex determined parameter, the membrane potential specific to various types of synthetic membranes has to be known for a better characterization of the membranes with the purpose of finding the most suitable uses.

In the present paper the membrane potential of some synthetic membranes based on polyvinylacetate or cellulose acetate, prepared by our own methods [7,8] has been studied, using for comparison an imported membrane of Sartorius type.

EXPERIMENTAL

The investigations were carried out on a series of synthetic membranes prepared by original methods [7,8] on the basis of polyvinylacetate (PVAc) (KA—6, KA—10, KA—11, KN—14) or cellulose acetate (CA), in comparison with an imported membrane, based on cellulose acetate, of Startorius type (S). Since the Sartorius membrane is a membrane of combined type, having the filtering material based on cellulose acetate arranged on a porous support, under a protective nylon cover, the filtering material was taken out the support to enssure experimental conditions identical to those used with the autochthonous membranes.

A plexiglass cell with two equal compartments separated by the investigated membranes of an areas of 1.24 cm^2 was used for measuring the membrane potential. One compartment was filled with 10 mL NaCl or KCl aqueous solution (100 mmol/L) and the other with an equal volume of bidistilled water or, in other cases, with isotonic glucose solution, to investigate the influence of osmotic pressure on the membrane potential.

Prior to the measurements the membrane was hept in bidistilled water for 12 hours for imbibing with water and for elasticity recovery to avoid the breakage during mounting in the measuring cell.

The membrane potential was measured by means of an electronic equipment (cathodic follover, preamplifier, cathodic oscilloscope), used for determining the electric potential of the biological membranes, adapted to our experimental conditions. To remove some undesired perturbing influences on the recorded values, the achievement of a good electric stability of the electrodes, as well as the reduction of the electrode and the liquid-liquid junction potentials [1,9,10] by using nonpolarizable Ag/AgCl electrodes with an agar-agar bridge in 3 M KCl solution were taken into account. A microelectrode with a glass micropipette attached to the agar-agar bridge and filled with 3 M KCl solution (having electrical resistance of 5—10 Mohm and tip potential below 5 mV) and a reference electrode were placed in the diluted and the concentrated solutions, respectively. Before measurements the required amplification was settled (10 mV/cm), the corresponding electrodes were selected, the measuring equipment regulated, a good shielding of the latter being assured, thus reducing the electrode noise and the electric signal deviation on the oscilloscope screen to minimum.[9,10] The measurements were taken without mixing the solutions, by keeping continuously the electrodes in fixed positions, at the same depth in the solution and the same distance to the membrane. The transmembrane electric potential was recorded at room temperature (17—18°C) for two hours, either continuously by setting the zero level on the oscilloscope screen only at the initial moment and reading the values at 10 minutes' intervals, or periodically, by setting the zero level at every 10 minutes and taking the values corresponding to each moment.

RESULTS AND DISCUSSION

In recording the membrane potential of the various types of membranes under investigation, characteristic values have been found, depending on the membrane type, the chemical composition of the solutions used, their osmotic equilibrium and the recording manner.

Thus, with the imported Sartorius membrane (S) by the continuous recording of the potential difference between the compartment with

NaCl (100 mmol/L) solution and that with bidistilled water (Fig. 1—A : W, NaCl), during the first ten minutes negative values of the membrane potential are found in the compartment with bidistilled water (—5 mV)

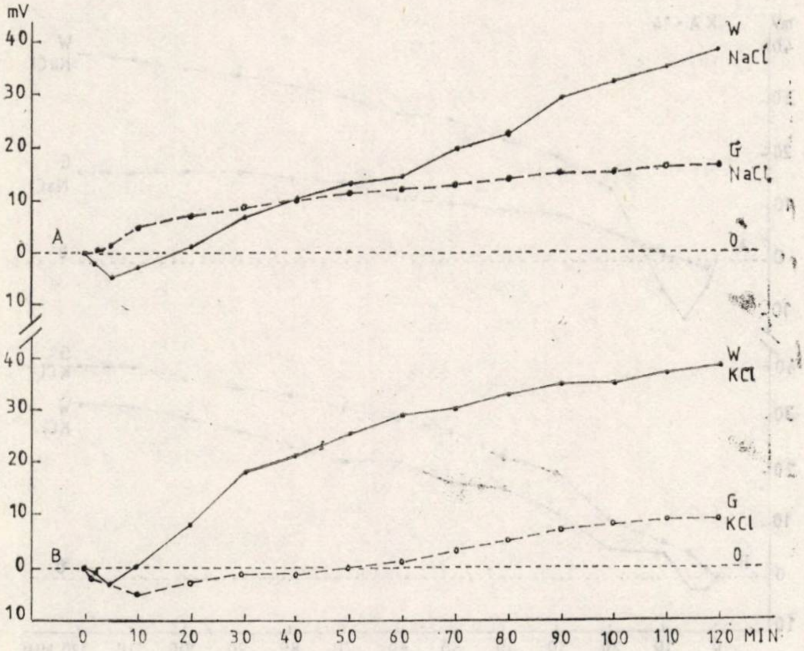

Fig. 1. — Membrane potential of the Sartorius type membrane, in a continuous recording. A — in the presence of NaCl and water (W) or glucose (G), B — in the presence of KCl and water (W) or of glucose (G).

ollowed by slowly increasing positive values (+14 mV after 60 minutes and +38 mV after 120 mintues). In the presence of NaCl solution on one side of the membrane and of an isotonic glucose solution on the other side (Fig. 1—A : G, NaCl) only positive potential values are recorded in the compartment with glucose solution which maintains, however, at low values (+16 mV at 120 minutes). The recording of the membrane potential in the presence of a KCl solution (100 mmol/L) and of bidistilled water (Fig. 1—B) evidences phenomena similar to those recorded with NaCl solution, but the initial negative values are smaller (—3 mV) while the positive ones occur earlier (+29 mV after 30 minutes and +3 mV after 120 minutes). If the recording is accomplished in the presence of KCl and isotonic glucose solutions the negative values prevail for a longer duration (40 minutes) and the positive ones are much lower (+ 9 mV after 120 minutes).

With the continuous recording of the potential in the presence of NaCl and bidistilled water, the membrane KA—14 (Fig. 2—A) exhibits a value dynamics of the membrane potential similar to that characteristic of the S membrane. Thus, negative values are recorded during the first

10 minutes (−11 mV after 5 minutes) followed by positive values which occur earlier (+28 mV after 60 minutes and +39 mV after 120 minutes). In the presence of NaCl and isotonic glucose solutions only low positive values are noticed (+17 mV after 120 min.) as in the case of S membrane. With KCl solution and bidistilled water (Fig. 2—B) values similar to those characteristic of the S membrane are found, which are slightly negative during the first 5 minutes (−2 mV) and then positive, increasing up to +33 mV after 120 minutes. The replacement of bidistilled water by isotonic glucose solution determines only positive values increasing slowly up to +40 mV after 120 minutes.

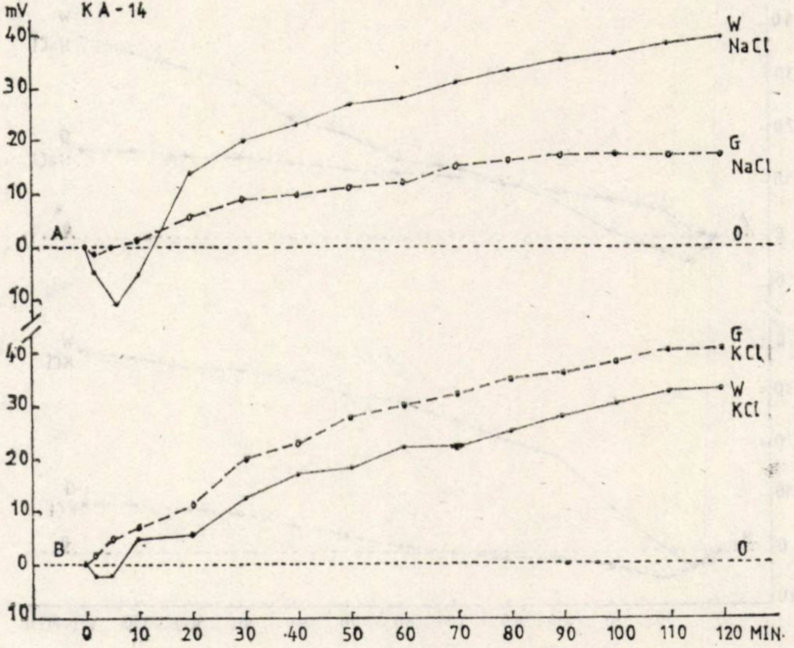

Fig. 2. — Membrane potential of the KA—14 membrane in a continuous recording. A and B the same as in Fig. 1.

With the continuous recording the membrane KA—7 exhibits a dynamics of potential values generally similar to that characteristic of the S and KA—14 membranes (Fig. 3). In the presence of NaCl and bidistilled water the values increase from −2 mV after two minutes up to +26 mV after 120 minutes. By replacing the bidistilled water by isotonic glucose solution the values slowly increase from +2 mV after 5 minutes up to +29 mV after 120 minutes. With the KCl solution and bidistilled water the values increase from −4 mV after 5 minutes up to +24 mV after 120 minutes and from +1 mV after 10 minutes up to +30 mV after 120 minutes, after the replacement of bidistilled water by isotonic glucose solution.

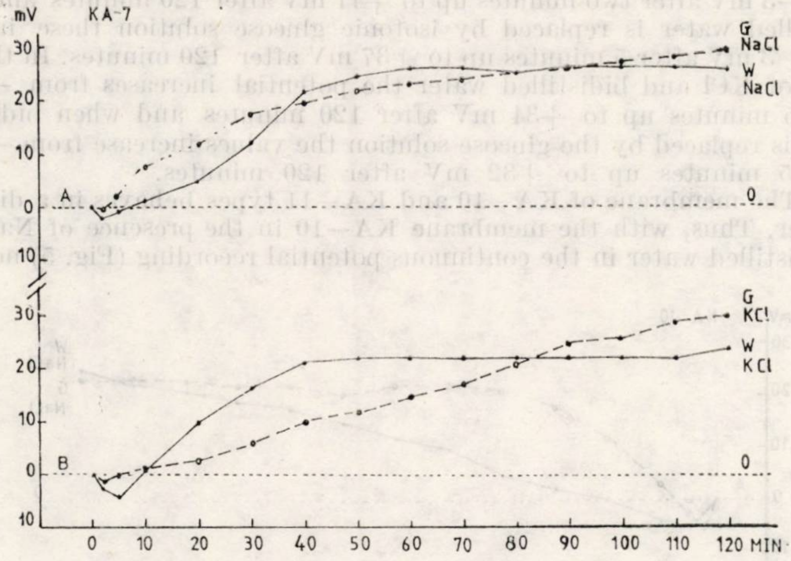

Fig. 3. — Membrane potential of KA—7 membrane in a continuous recording. A and B the same as in Fig. 1.

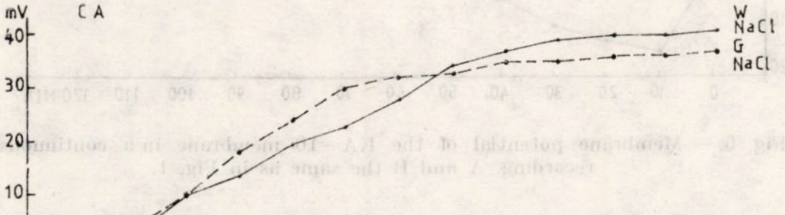

Fig. 4. — Membrane potential of the CA membrane in a continuous recording. A and B the same as in Fig. 1.

A similar situation is also noticed in the case of cellulose acetate membrane (CA) with the continuous recording of the membrane potential (Fig. 4). In the presence of NaCl and bidistilled water the values increase from −3 mV after two minutes up to +41 mV after 120 minutes and when bidistilled water is replaced by isotonic glucose solution these increase from −3 mV after 5 minutes up to +37 mV after 120 minutes. In the presence of KCl and bidistilled water the potential increases from −2 mV after 5 minutes up to +34 mV after 120 minutes and when bidistilled water is replaced by the glucose solution the values increase from −3 mV after 5 minutes up to +32 mV after 120 minutes.

The membrane of KA−10 and KA−11 types behaves in a different manner. Thus, with the membrane KA−10 in the presence of NaCl and of bidistilled water in the continuous potential recording (Fig. 5) negative values are noticed during the first 20 minutes (−5 mV after 5 minutes) followed by positive values which slowly increase up to +25 mV after 120 minutes. With the water replacement by an isotonic glucose solution the potential values increase rapidly from −5 mV after two minutes up to +22 mV after 60 minutes, remaining then almost constant. In the presence of KCl solution and of bidistilled water the values are much different, negative during the first 60 minutes (−15 mV after 10 minutes), then positive, but small (+8 mV after 120 minutes). By the replacement of bidistilled water by isotonic glucose solution small values of membrane potential are recorded (−3 mV after two minutes and +2 mV after 120 minutes).

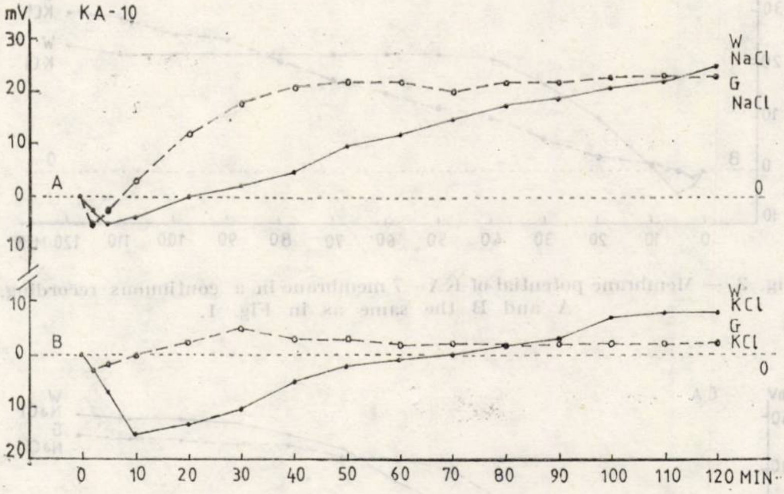

Fig. 5. — Membrane potential of the KA−10 membrane in a continuous recording. A and B the same as in Fig. 1.

With the membrane KA−11 small values of the membrane potential are generally noticed for continuous recording in the presence of both NaCl and KCl solutions (Fig. 6).

With the periodical recording of the membrane potential the value dynamics is different from that characteristic of continuous procedure, but specific to each membrane type, emphasizing a similar behaviour of KA−14, KA−10, CA and S membranes.

The obtained results indicated the membrane potential to have specific values for each membrane type, this parameter being otherwise one of the parameters characterizing a membrane.[2] The membrane potential was found to depend on membrane properties and on nature of the solutions separated by membranes.[1,2] The properties of a synthetic membrane depend on its microscopical and macroscopical structure.[2,11] The microscopical structure of the membrane studied in the present work was investigated by means of electronic scanning microscopy both for membranes based on cellulose acetate which have pores between 0.45 and 1 μm and for those based on polyvinylacetate. For the latter pores with variable sizes between 2 and 30 μm and a morphological "tubular" structure and of "schweitzer" type, with a certain regularity[7,11] have been found.

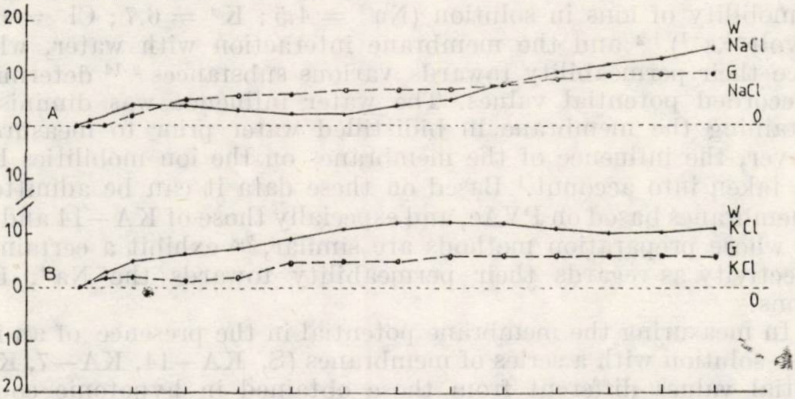

Fig. 6. — Membrane potential of KA—11 membrane in a continuous recording. A and B the same as in Fig. 1.

The dynamics of membrane potential values measured between a compartment with NaCl or KCl solutions and one with bidistilled water (hypotonic conditions), separated by the investigated membranes, evidences a different behaviour of the latter towards Na^+, K^+ and Cl^- ions in solution, which implies certain properties determining a different permeability towards these ions. Thus, during the first minutes negative potential values are recorded, which indicate that the passage of Cl^- ions (with negative charge) through the membrane from the compartment with NaCl or KCl solutions into that with bidistilled water prevails. Simultaneously a passage of Na^+ or K^+ ions (with positive charge) takes place, which after some time reach an equilibrium with Cl^- ions becoming predominant; in the compartment with more diluted solution only positive values are recorded. This phenomenon is more accentuated in the case of NaCl solution, especially with the membranes of S, KA—14, KA—7 and CA types. It derives from the properties of these membranes which determine a different behaviour towards the Cl^- ions, in comparison with Na^+ or K^+ ions. It is known that the mass transfer through the membrane depends both on their structure and the nature of the solutions they are in contact with as well as on the interaction forces between the membrane surfaces and the solute.[13] Thus, these properties together with the different mobility of ions in solution ($Na^+ = 4.5$; $K^+ = 6.7$; $Cl^- = 6.8\ 10^{-4}$ $cm^2 \cdot volt^{-1}.s^{-1}$)[1,2] and the membrane interaction with water, which influence their permeability towards various substances[2,14] determine also the recorded potential values. The water influence was diminished by maintaining the membrane in bidistilled water prior to measurements. However, the influence of the membranes on the ion mobilities has also to be taken into account.[1] Based on these data it can be admitted that the membranes based on PVAc, and especially those of KA–14 and KA–7 type, whose preparation methods are similar,[7,8] exhibit a certain degree of selectivity as regards their permeability towards the Na^+, K^+ and Cl^- ions.

In measuring the membrane potential in the presence of an isotonic glucose solution with a series of membranes (S, KA–14, KA–7, KA–10) potential values different from those obtained in hypotonic conditions are found, though the glucose used for the equilibration of the osmotic pressure in the two compartments separated by membranes has no electric charge. It may be deduced that the osmotic pressure influences the value of membrane potential, fact also noticed by other authors,[1,2] but the possibility also exists of an influence of glucose motion through the membrane.

The likeness of behaviour of synthetic membranes based on PVAc (KA–14 and KA–7) with that of imported Sartorius membrane suggests a possible replacement of the latter in some uses, which exhibits a series of advantages. Generally the fact is known that the membranes based on cellulose acetate are sensitive to hydrolysis at a pH of 4.5–6, slightly degraded by bacteria at temperatures above 30°C and have durations of about two years.[11] The synthetic membranes based on PVAc are insoluble in most of the common solvents, with thickness of about 0.30 mm, resistant, have duration of more than three years and are reproductible.

CONCLUSIONS

1. The dynamics of membrane potential values depends on the membrane type, the chemical nature of the solutions the membrane are in contact with, the osmotic conditions and the mode of potential recording.

2. The membrane based on PVAc exhibits a certain degree of selectivity as regards the permeability towards the Na^+, K^+ and Cl^- ions.

3. The behaviour of our synthetic membrane based on PVAc (KA–14 and KA–7) and of that based on cellulose acetate (CA) in the presence of Na^+, K^+ and Cl^- ions is similar to that of imported Sartorius membrane, which suggests a likeness of their properties and the possibility of replacing the imported membrane in certain uses.

REFERENCES

1. J. Bures, M. Petran and J. Zachar, "Electrophysiological Methods in Biological Research", Nakladatelstvi Cekoslovenské Akademie věd, Praha, 1960.
2. C. Liteanu and G. Rădulescu, "Bazele membranologiei", Ed. ştiinţifică şi enciclopedică, Bucharest, 1984.
3. I. Neacşu, "Acţiunea unor ioni şi a unor agenţi organici asupra proprietăţilor electrice ale membranei celulare", Thesis, Univ. "Al. I. Cuza", Iaşi, 1984.
4. P. Mazliak, "Les membranes protoplasmiques", Doin, Paris, 1971.
5. G. Benga, "Biologia moleculară a membranelor cu aplicaţii medicale" Ed. Dacia, Cluj-Napoca, 1979.
6. D.-G. Mărgineanu, "Biofizica membranelor : implicaţii şi aplicaţii tehnice", în "Revoluţia biologică", co-ordinators : M. Drăgănescu and G. Zarnea, Ed. Academiei, Bucharest, 1985, p. 99.
7. C. Simionescu and M. Bezdadea, Patent R.S.R. 84569, 1984.
8. M. Bezdadea and G. Grigoriu, Proposal of patent OSIM, 1985.
9. F. Topoliceanu and S. Lozneanu, "Bioelectrometrie", Ed. Tehnică, Bucharest, 1985.
10. R. Negoescu, "Instrumentaţia electronică biomedicală. Iniţiere", Ed. Tehnică, Bucharest, 1985.
1. M. Bezdadea, "Polimerizare matricială", Doctoral Thesis, Polytehnic Inst., Iaşi, 1982.
2. Berghof GMBH, "Membranfilter Laborakatalog 80, Abt. Labortechnik", 1980.
3. C. Kam, M. Takeshi and S. Sourirajan, *Ind. Eng. Chem. Prod. Res. Dev.*, **21**, 605, (1982).
4. N. I. Nicolaev, "Diffuziya v membranah", Izd. Himia, Moscow, 1980.

Revue Roumaine de Chimie, **32**, *8*, 759–765 (1987)

HIGH RESOLUTION MIXING CALORIMETRY IN STUDIES OF COMPOSITE SYSTEMS*

GEORGE DRĂGAN
Institute of Chemical Research, ICECHIM-CCF,
Spl. Independenţei 202, Bucharest 77208 Romania

Received November 24, 1986

High resolution mixing calorimetry (HRCM) recently introduced, represents an efficient, sensitive and low cost measuring system for studies of composite systems. Solubility behaviour of aqueous electrolyte solutions (NaOH, KOH, Na_2SO_4) with several alcohols (EtOH, MeOH, phenol) is studied as a function of electrolyte concentration and temperature. The composite and polymeric structure of water, aqueous electrolyte solutions and alcohols based on H-bonds is evidenced by these experiments. It results that the aqueous electrolyte solutions have stronger structure than liquid EtOH and MeOH which especially capture the free water, while phenol has a stronger structure in glassy state (below $T_g = 38°C$) than liquid KOH aqueous solutions. A value of approximately 80 J/g ($\simeq$ 7.6 kJ/mol) was found for the conformational energy associated to the glass transition of phenol both from water-phenol and KOH/H_2O solution-phenol solubility experiments.

INTRODUCTION

Calorimetry represents a universal tool in the studies of transforming systems due to the fact that any process of transformation is accompanied by a caloric flow. On the other hand, the transforming systems can be considered as composite systems, because at least two components interact during transformation. From this basic idea a new formalism in defining the behaviour of composite systems has been developed in the last decade [1–3] starting from some introductory notions of topological thermodynamics formally introduced by Oster and Auslander.[4] The problem solved by the topoenergetic theory of behaviour of composite systems mainly consists in the determination in relative units in respect to standard systems, the nature and the amplitude of the overall process and the coupling strength between the two components.

These notions were thoroughly defined in many of the recent works so that the aim of the present work is to apply them for suggestive and representative cases. The solubility behaviour of two component systems is a universal problem in topoenergetic terms and at which any problem of material science can be reduced.[5]

---

* Paper presented at the Symposium on Chemistry of Colloids and Surfaces, Cluj-Napoca, September, 8–10, 1986.

High resolution mixing calorimetry (HRMC) has been recently introduced as an efficient, sensitive and low cost device which can be adapted in studies of solubility behaviour for a large variety of systems. [5,6] Some of the disadvantages of the classical point of view on solubility problem calorimetrically evidenced mainly originate from the large deviations from the standard experimental conditions and these were previously reviewed. [6] These conditions are neglected in the majority of the actual calorimetric measurements so that the results are seriously incorrect and cannot be compared between them, even for the series of systems tested by the same operator on the same device. This basic aspect imposed by the topoenergetic principles is revealed in the present work and the results are qualitatively discussed as a first stage. The interaction of electrolyte-water is considered as a continuation of the previous extensive studies, [5-7] taking into account that the structure of the aqueous solutions plays an important role in the actual physical-chemistry of the liquid state.

EXPERIMENTAL

The standard experimental conditions for the present calorimetric measurements are suggestively given in Figure 1. Components 1 and 2 have always the same volumes of 0.7 mL and 0.2 mL, respectively. Component 1 contains the electrolyte (E) solution of concentration c_E in mol E/liter (E : NaOH, KOH, Na_2SO_4) ; component 2 represents an alcohol (EtOH, MeOH, phenol). The experiments can be grouped into two distinct series : A : experiments isothermally carried out for EtOH and MeOH ; and B : experiments with solutions of KOH and phenol at different temperatures : 26.2, 34.5, 45.2 and 51.0 (± 0.06)°C which include the glass transition of phenol (T_g). The standard experimental conditions have taken into account also the annealing time of the electrolyte solutions. The used HRMC device was recently described in every detail.[6]

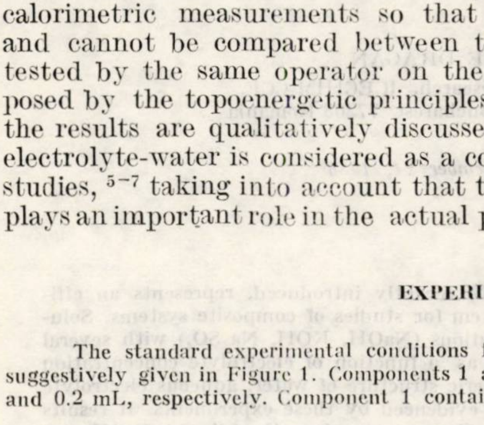

Fig. 1. — Schematic representation of standard mixing experiments by HRMC technique (see the text).

RESULTS AND DISCUSSION

The mixing experiments on aqueous solution-alcohol mainly reveal the H-bond structure of both components. In general liquid alcohol has smaller amount of H-bonds than liquid pure water, but ionic compounds catalyze formation of polymeric chains in water. [6,7] By mixing the alcohol especially captures the free water and also affects the polymeric chains, so that an exothermal flow results with specific overall energy, E in J, peak height, h in mm and their ratio h/E defining the intrinsic process rate. [6] Thus, two concurrent processes occur : the breaking effect of the alcohol on the structure of aqueous solution and the formation of molecular association of water-alcohol characterized by endothermal and exothermal flows, respectively. In glassy state (below T_g) alcohols have a high H-bond density, so that their mixing with liquid aqueous solutions is characterized by a predominant endothermal flow associated to breaking effect of water on glass structure of alcohols.

A. The results of the kinetic parameters defined by HRMC experiments of this series are given in Figures 2 and 3. The overall energy measured by E and h decreases wtih c_E as a general feature, showing a decrease

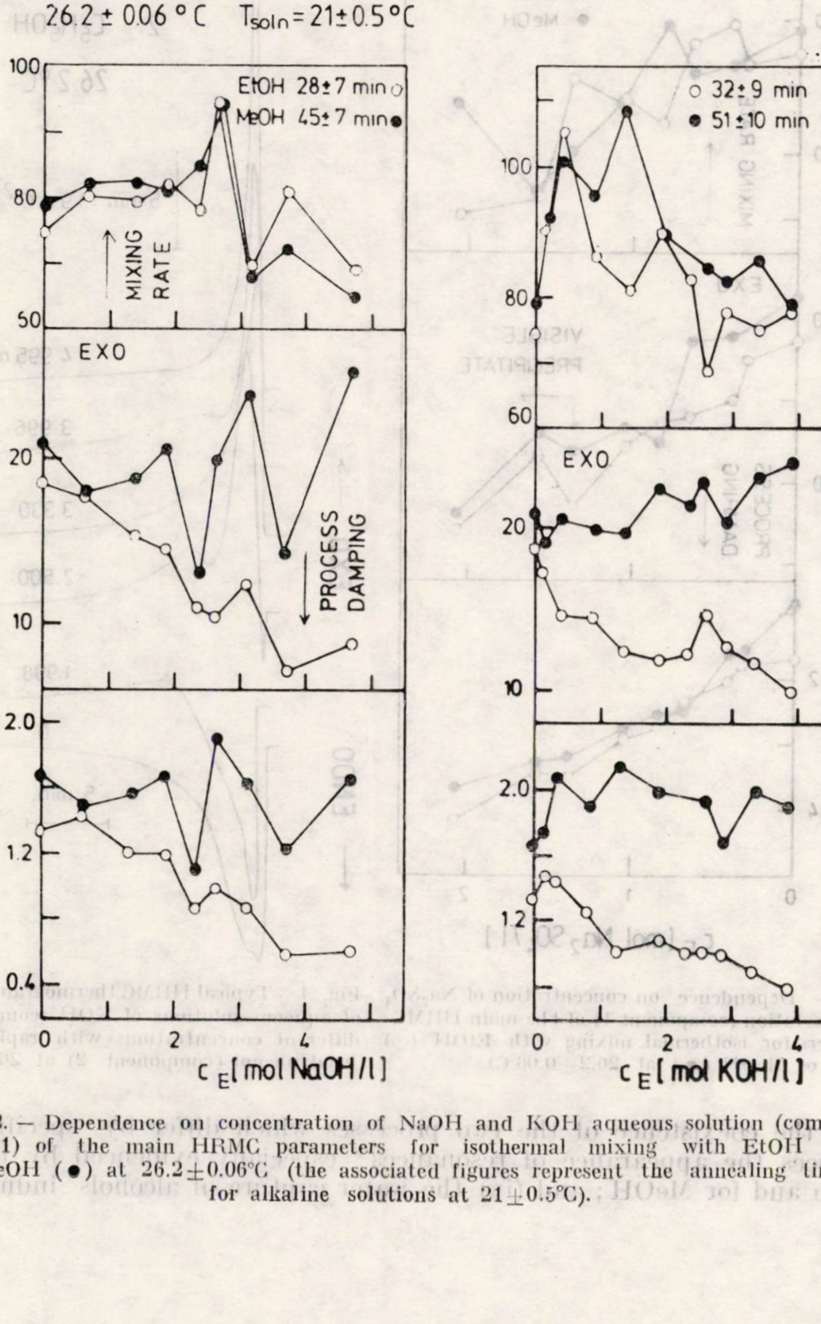

Fig. 2. — Dependence on concentration of NaOH and KOH aqueous solution (component 1) of the main HRMC parameters for isothermal mixing with EtOH (O) or MeOH (●) at 26.2±0.06°C (the associated figures represent the annealing times for alkaline solutions at 21±0.5°C).

of the free water content in the electrolyte solution, but several particularities should be mentioned, namely : (i) the process amplitude for MeOH is larger than for EtOH due to the specific molecular volume ; (ii) this fact makes the breaking efficiency of MeOH be larger than for EtOH ;

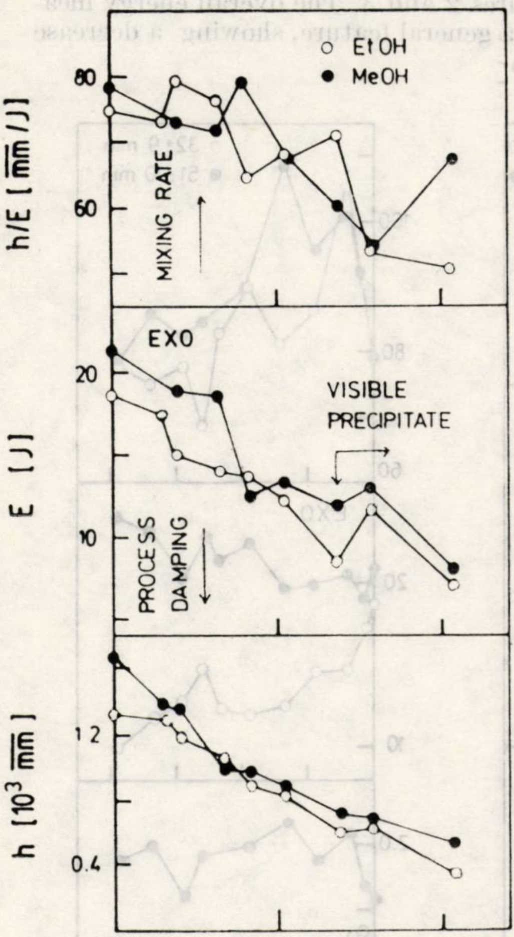

Fig. 3. — Dependence on concentration of Na_2SO_4 aqueous solution (component 1) of the main HRMC-parameters for isothermal mixing with EtOH (○) or MeOH (●) at 26.2±0.06°C).

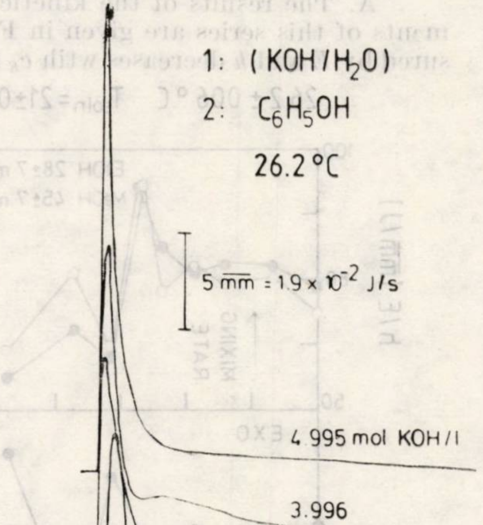

Fig. 4. — Typical HRMC thermograms for mixing of aqueous solutions of KOH (component 1) of different concentrations with rapidly crystallized phenol (component 2) at 26.2 ± 0.06°C.

(iii) the coexistence of the two processes which differ by specific rate, induces the appearance of resonances [6] especially evidenced by the h/E ratio and for MeOH ; and (iv) the water capture of alcohols induces the spontaneous crystallization of Na_2SO_4 in hydrated crystalline species above a value of c_E.

B. This series of experiments can be divided into three distinct stages as a function of temperature in respect to T_g of phenol : below (B1) and above (B2) T_g with different c_E values, and at different temperatures with pure water and c_E^0 (9.36 mol KOH) above the threshold values c_E^0 at which the predominance of the two processes is reversed.

B1. A series of thermograms for different c_E values are given in Figure 4. The following facts should be revealed : (i) the breaking effect (as endothermal flow) of the electrolyte solution on the phenol in glassy state is faster than the exothermal flow observed at higher c_E values ; (ii) for intermediary c_E values above c_E^0 an oscillatory behaviour occurs as superposition of the two processes ; and (iii) the exothermal flow predominantly observed at high c_E values shows the new stronger structure induced by KOH in alcohol.

B2. The HRMC kinetic parameters as a function of c_E for mixing experiments at 45.2 and 51.0°C are given in Figure 5. The value of c_E^0 of approximately 0.8 mol KOH can be evidenced in the three parameters and corresponds to a maximum intrinsic rate of mixing for both temperatures. This rate has a larger value for the higher temperature but E values are the same at each c_E.

B3. The solubility behaviour as a function of temperature for two extreme c_E values in respect to c_E^0 is given in Figure 6. In both cases T_g is evidenced as a steplike transition in the process amplitude expressed by E and h. For $c_E = 0$ the breaking effect of water against phenol drastically decreases at T_g due to thermally breaking of the glassy state based on H-bonds. For $c_E = 9.36$ mol KOH ($\gg c_E^0$), this transition favours the formation of the new structure of KOH-phenol polymeric chains strong-

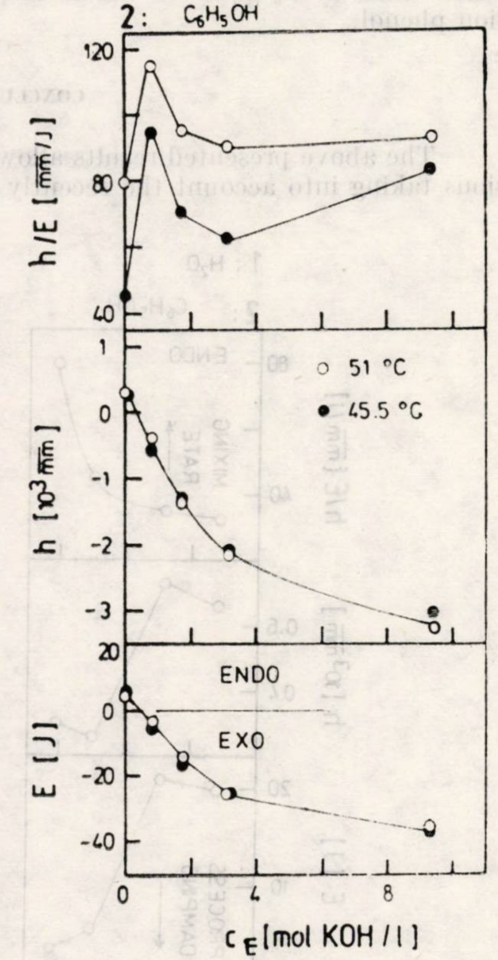

Fig. 5. — Dependence on concentration of KOH aqueous slolutions (component 1) of the main HRMC-parameters for isothermal mixing with phenol at 51 (○) and 45.5°C (●).

er than in KOH-water ones. From both behaviours a value of $\Delta E \simeq = 17$ J (81 $J/g \simeq 7.6$ kJ/mol) results, representing the conformational transition energy of phenol polymeric chains and fairly agrees with direct calorimetric measurements.[8] We can observe that interaction liquid water—liquid phenol ($T > T_g$) tends to zero and its amplitude has a transition value at T_g equal to the corresponding value for KOH/H_2O solution-phenol.

CONCLUSIONS

The above presented results allow to point out the following conclusions taking into account the recently reported results:[5–7]

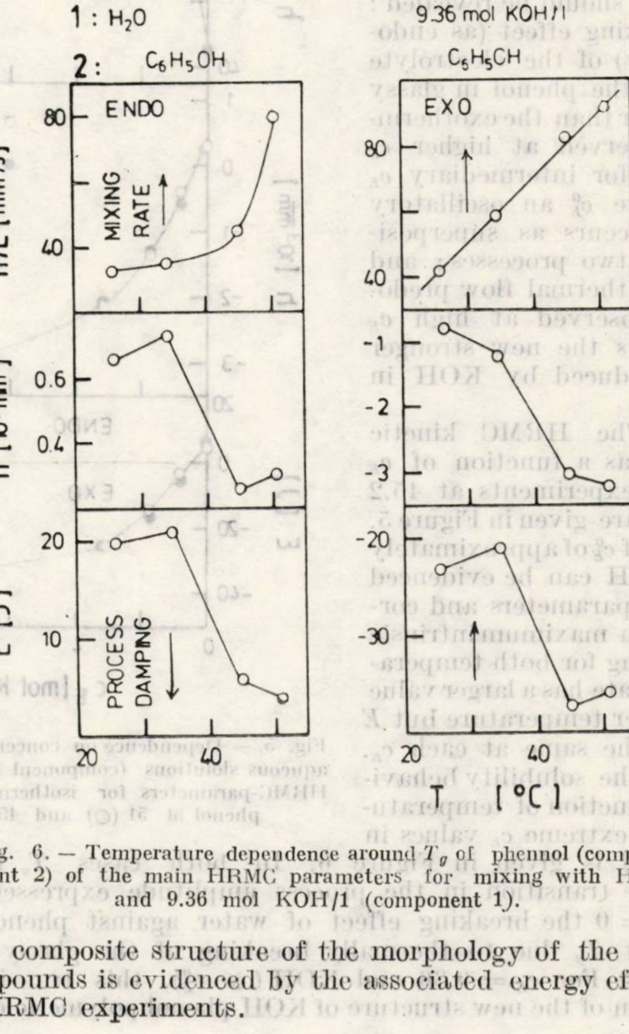

Fig. 6. — Temperature dependence around T_g of phennol (component 2) of the main HRMC parameters for mixing with H_2O and 9.36 mol KOH/1 (component 1).

(i) The composite structure of the morphology of the two types of X—OH compounds is evidenced by the associated energy effects of their mixing in HRMC experiments.

(ii) These processes show the difference in catalytic potential in H-bond forming or the hydrophillic power of the X-groups in the two compounds. The majority of experiments shows exothermal energies due to the structuring effect of the cations in electrolyte compounds upon the alcohols.[6,7]

(iii) It is important to notice that we call EtOH, MeOH and PhOH as alcohols from morphological point of view in which X-groups have low catalytic potentials (hydrophobic behaviour) in liquid state. Their glass transition can be assigned as a transition in this catalytic potential.

(iv) This composite structure is similar to the well-known shish-kebab morphology firstly evidenced in crystalline polymers[9,10] and recently detected in hydrated crystals[11] and in frozen aqueous electrolyte solutions.[7] This structural model agrees with the iceberg structure of water and aqueous solutions independently established also by solubility experiments.[12]

(v) HRMC technique is an efficient, sensitive and low cost technique for solubility studies on composite systems and can be extensively used in obtaining solubility data.

REFERENCES

1. G. Drăgan, *J. Thermal Anal.*, **9**, 405(1976); **15**, 297(1979); **23**, 173(1982).
2. G. Drăgan, *Acta Polymerica*, **31**, 293(1980); **34**, 1(1983); **35**, 499(1985).
3. G. Drăgan, "A Universal Representation of System Behaviour Based on Topoenergetic Principles", The 9th International CODATA Conference, Jerusalem, Israel, June 24—28, 1984.
4. G. F. Oster, and D. M. Auslander, *J. Franklin Inst.*, **292**, 77 (1971).
5. G. Drăgan, "Solubility Data Banks Based on Topoenergetic Principles", The 10th International CODATA Conference, Ottawa, Canada, July 14—17, 1986.
6. G. Drăgan, *J. Thermal Anal.*, **31**, 677, 941 (1986); **32**, 253(1987).
7. G. Drăgan, *Acta Polymerica*, **38**, 211, 270, 467 (1987).
8. S. M. Wolpert, A. Weitz and B. Wunderlich, *J. Polymer Sci.*, **A—2,9**, 1887 (1971).
9. W. Pechhold, S. Blasenbrey, and S. Woerner, *Kolloid Z.-Z. Polymere*, **189**, 14 (1963).
10. G. Drăgan, *Rev. Roumaine Chim.*, **20**, 687(1975); **21**, 1381, 1537 (1976); **23**, 261, 435, 629, 1313 (1978); **26**, 1315 (1981); *J. Polymer Sci., Polymer Symposium*, **64**, 141 (1978).
11. G. Drăgan, *Rev. Roumaine Phys.*, **27**, 297 (1982).
12. H. S. Frank and M. W. Evans, *J. Chem. Phys.*, **13**, 507 (1945).

Revue Roumaine de Chimie, **32**, *8*, 767–773 (1987)

STUDY BY HIGH RESOLUTION MIXING CALORIMETRY OF ADSORPTION OF AQUEOUS SOLUTIONS OF SUPERPLASTICIZER ADDITIVE ON CEMENT

G. DRĂGAN, S. IFRIM and GEORGETA POPESCU
Institute of Chemical Research, ICECHIM-CCF,
Spl. Independenţei 202, Bucharest, 77208, Romania

Received November 24, 1986

The calorimetric study of superficial interaction at short times by isothermal (30°C) mixing of aqueous solutions of Flubet® (Ca-salt) as superplasticizer with cement is presented by using the recently introduced technique of the high resolution mixing calorimetry. Three distinct samples of cement originating from the same grade but differing by the hydration coverage of grains in normal conditions are considered. The fresh sample of cement extracted from the current production line is the most representative for practical purposes with reproductible behaviour. Its results show that the mixing thermograms consist of two distinct exotherms corresponding to the adsorption of additive and/or water on the particle surface and the hydration of ionic salts, both processes specifically influenced by the superplasticizer.

INTRODUCTION

Tensioactive additives in polydisperse systems like water-cement (w/c) aggregate, improve the workability of the resulting mortars and concretes by increasing the fluidity at constant w/c ratio. An equivalent workability is obtained at a reduced w/c ratio and consequently the physical and mechanical properties of the hardened system are favourably affected. When small amounts (1–3%) of plasticizer are present in the mixture, both cement consumption and the pump energy required for placing are lowered.[1–4]

In the last decade, various superplasticizer additives mainly based on sulphonated naphthaline-formaldehyde condensates were proposed.[5–8] Superplasticizers are characterized by a highly polar macromolecular structure which ensures a high degree of dispersion most favorable to cement hydration. The surfactants are adsorbed together with less polar groups on the surface of cement grains so that the polar groups are located towards water. Adsorption on the surface of cement grains increases their hydrophily and favours their hydration. The electrically charged cement grains repulse each other, are dispersed and consequently the surface of phase separation increases. Thus, the action of additives upon the hydration-hydrolysis of the cement is complex and depends on the nature of the cement and additives and, obviously, on the concentration of the latter.

---

* Paper presented at the Symposium on Chemistry of Colloids and Surfaces, Cluj-Napoca, September, 8–10 1986.

The rheologic properties of concretes and mortars [9–11] are also strongly influenced because the adsorbed layers and the electric charges at grain surface raise the stability of c/w system. Therefore, the tendency of separation is lowered and so is the rate of sedimentation which ensures a higher homogeneity.

The interactions in w/c systems mainly consist in hydration-hydrolysis of a series of ionic salts associated with exothermal effects of H-bonding of water molecules in a new ordered structure. [12–14] These processes can be reproducibly revealed in calorimetric measuring systems with a view to studying their kinetics. The aim of the present work is to study by high resolution mixing calorimetry (HRMC) recently introduced just for such processes [15] the interactions between aqueous solutions of different concentrations of Flubet® as a superplasticizer and cement. The results of this introductory study could establish a new routine technique in the rapid, sensitive and low cost analysis both of cement and additives.

EXPERIMENTAL

The cement used in the study is of high early strength, P—42 type and free of organic additives. Three distinct samples of this kind of cement differing by the nature of the surface of the grains were studied, namely: (A) a sample with the free surface maintained in normal conditions (20±3°C and 65±5% RH) for approximately 1 month: (B) a fresh sample ex'tracted from a virgin container and immediately analyzed in a period of about 2 hours; and (C) a fresh sample as the previous one, but maintained in air at 500°C for 12 hours, preserved in a dry desiccator and analyzed also in about 5 hours.

Aqueous solutions in bidistilled water of Flubet® (calcium salt) were considered at the following concentrations: 0, 0.001, 0.005, 0.01, 0.02, 0.04, 0.05, 0.06, 0.08, 0.1, 0.2, and 0.4% w/w.

The HRMC experiments were carried out at 30°C by using the previously described device.[15]

RESULTS AND DISCUSSION

HRMC technique imposes as a basic requirement of reproducibility the preservation of strict standard experimental conditions [12–15] which correspond for the present experiments to the mixing of 0.7 mL solution at concentration c with an amount of (0.200±0.5%) g of cement placed in a glass bubble. Two typical thermograms of such experiments for the three samples of cement are reproduced in Figure 1. It can be noticed that sample A contains already hydrated species which reveal by mixing a starting endotherm of their solution, [12] on which a pronounced hydration exotherm is superimposed. Due to the fact that the prior hydration in the normal conditions is an uncontrolled process and occurs superficially, the thermograms of sample A are not reproducible and do not allow a quantitative study.

Samples B and C show only the hydration exotherm, but with a ratio of approximately 1 : 1.5 of their amplitude, respectively, which is in good agreement with the hydration potential. Both the samples for all concentrations *c* show a specific splitting shoulder of the exotherms corresponding to the early stage of hydration. On the other hand, sample C presents the first exotherm practically unchanged while the second one is considerably increased. These facts lead to the conclusion that the first part of the exotherms corresponds to the pure adsorption process of additives and/or water in the micropores of the cement grains, and the second one corresponds to the hydration-hydrolysis of the ionic salts. Sample B allows in these conditions to better separate contributions of the two processes because their amplitudes are closer than for sample C.

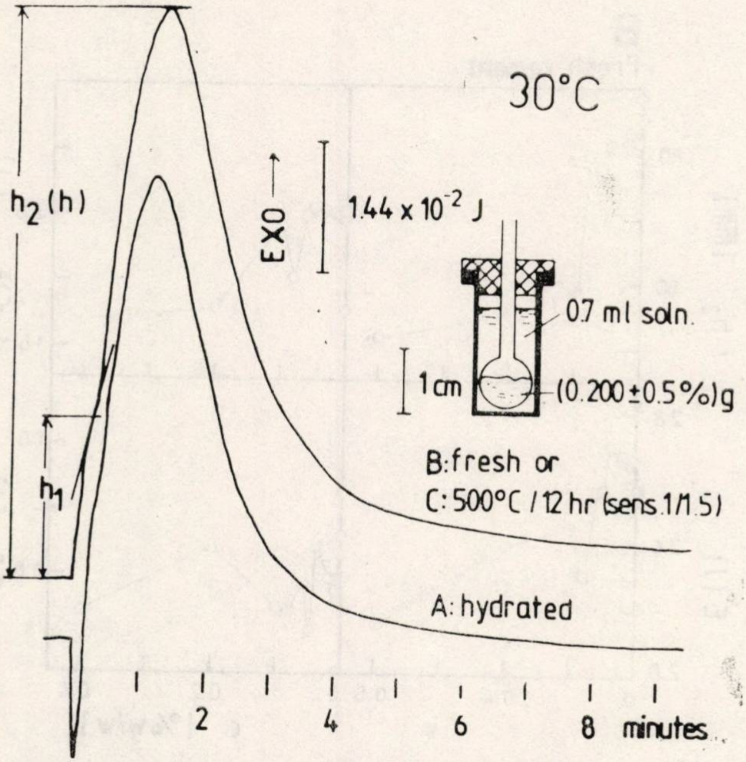

Fig. 1. — Schematic representation of HRMC standard experimental conditions of isothermal mixing of aqueous solutions of Flubet® (Ca-salt)-cement and two typical thermograms for the three series of cement samples.

The peak heights h_1 and h_2 (or h) of these two processes (in standard units, $\overline{\text{mm}}$ [15]), graphically determined (see Fig. 1) allow to evaluate the splitting coefficient of the overall process, $\alpha = h_1/(h_1 + h_2)$, in addition to the other kinetic parameters : E (in J) — the overall energy determined by integrating the exothermal peak, [15] αE (in J) — the energy fraction of the adsorption process, $(1 - \alpha)E$ (in J) — the energy fraction for the hydration process, and the intrinsic rate of the overall process, h/E (in mm/J). These parameters can be compared for all the samples as such, due to the same standard experimental conditions no matter the sample of cement and/or solution concentration.

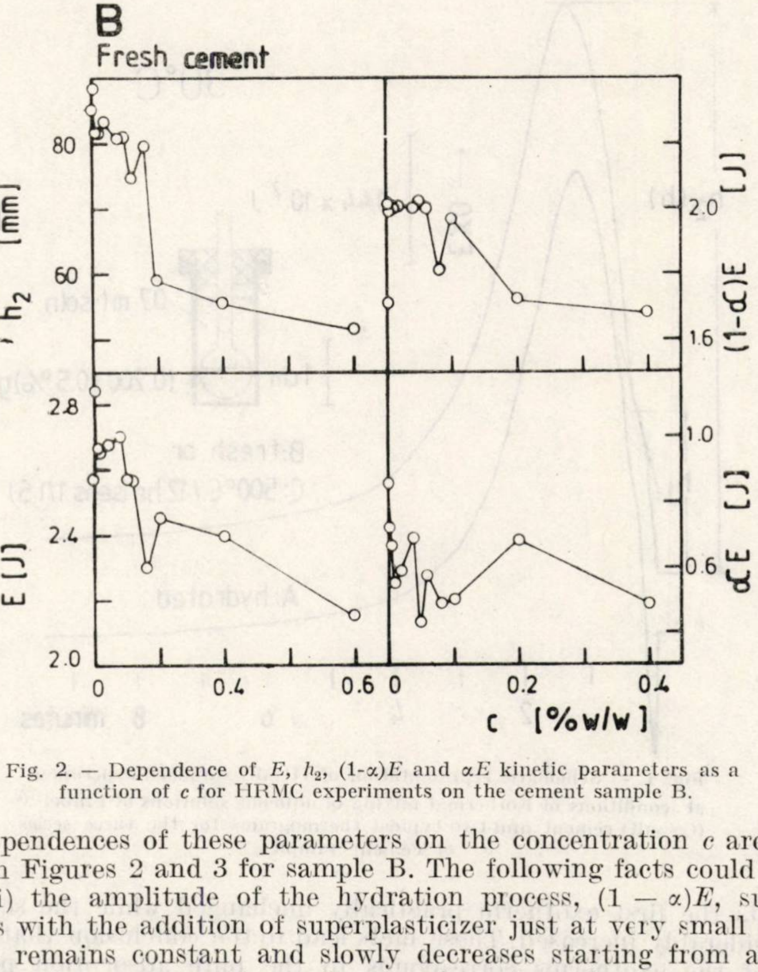

Fig. 2. — Dependence of E, h_2, (1-α)E and αE kinetic parameters as a function of c for HRMC experiments on the cement sample B.

Dependences of these parameters on the concentration c are represented in Figures 2 and 3 for sample B. The following facts could be noticed: (i) the amplitude of the hydration process, $(1 - \alpha)E$, suddenly increases with the addition of superplasticizer just at very small concentrations, remains constant and slowly decreases starting from approximately 0.1% to a saturation value equal to the value for pure water; (ii) the adsorption energy fraction, αE, abruptly decreases with c at small values of c and shows several maxima towards a saturation value for greater values of c; (iii) the overall energy measured by E and h and the intrinsic rate of the process h/E have a slow decrease with c up to approximately 0.1% from which an abrupt decrease occurs; and (iv) E and h show a decrease of approximately 20% in 24 hours, maintaining the samples in glass bubbles in normal conditions. The local jumps in these dependences can be explained by resonance phenomena excited by the hydrodynamic regime to mixing.[12,15]

The values of overall HRMC kinetic parameters for sample C are represented as a function of *c* in Figure 4, and the following observations should be made : (v) the overall process amplitude measured by *E* and *h* has a pronounced main maxima at approximately 0.1% with local resonance jumps : (vi) the *h*/*E* ratio increases with *c* towards a saturation value, and (vii) the local jumps in these dependences are more pronounced for this sample than for sample B.

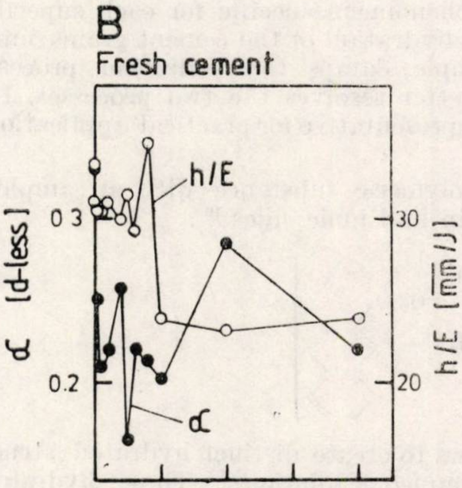

Fig. 3. — Dependence of α and h/E kinetic parameters as a function of *c* for HRMC experiments on cement sample B.

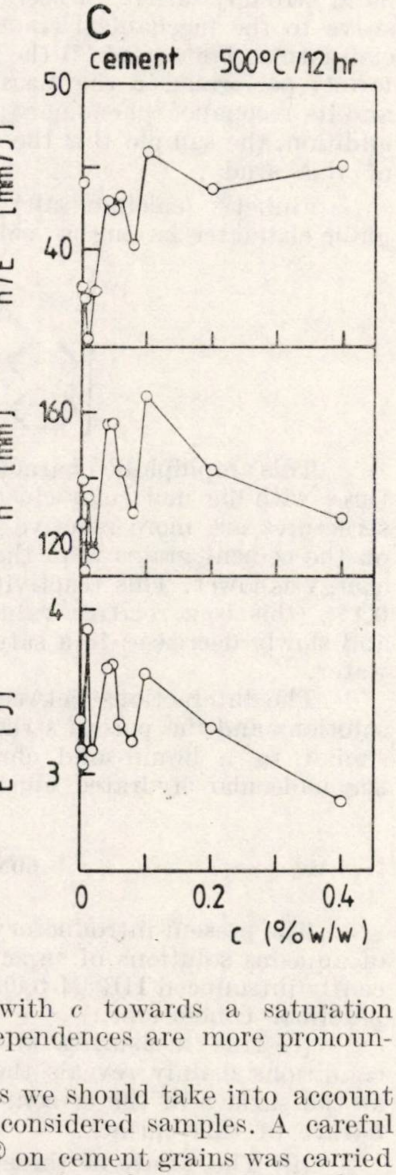

Fig. 4. — Dependence of *E*, *h* and *h*/*E* overall kinetic parameters as a function of *c* for HRMC experiments on the cement sample C.

For a better discussion of these results we should take into account the structure of cement grains in the two considered samples. A careful study on isothermal adsorption of Flubet® on cement grains was carried out spectroscopically for equilibrium concentration of suspension at long time.[16] We cannot compare these results with the present ones because the experimental conditions strongly differ both from the point of view of solution-cement ratio and the temporal scale of the involved processes.

We can mention that the isothermal adsorption at long time strongly differs for different solution-cement ratios showing a higher amplitude for smaller amounts of cement.[16]

The processes revealed by HRMC experiments mainly refer to the surface adsorption and hydration of the cement grains which, on the one hand strongly differ for the two samples, and on the other hand, are sensitive to the mechanical resonance phenomena specific for each superficial nature. For sample B the partial hydration of the cement grains uniformly performed in the mass of sample, damps the hydration process and its resonance phenomena, but better resolves the two processes. In addition, the sample B is the most representative for practical application of this study.

Flubet® (calcium salt) is a polymeric substance with an amphiphilic character having a polar chain and ionic sides[16]:

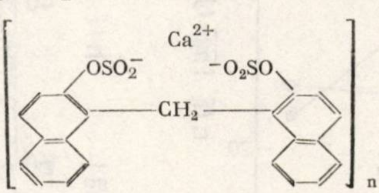

This amphiphilic character allows to create distinct hydrated structures with big molecular clusters in aqueous solution.[17] These hydrated structures are more reactive in the hydration process of the ionic salts on the cement grains than the free water molecules, but their adsorption energy is lower. This reactivity maintains constant up to approximately 0.1% (this is a relative value depending on the solution/cement ratio) and slowly decreases to a saturation value equal to the value of the free water.

The interactions between the composite structure of the aqueous solutions and the porous structure of the surface of the cement grains is similar to a liquid-solid chromatographic measuring system in which the molecular hydrated clusters are specifically adsorbed.

CONCLUDING REMARKS

The present introductory calorimetric study of the isothermal mixing of aqueous solutions of superplasticizer additive and cement by the recently introduced HRCM technique, allows to point out several important practical conclusions :

(i) This measuring system including the standard experimental conditions mainly reveals the interactions between the two components at the surface of the cement grains, so that it is highly sensitive to the nature of this surface.

(ii) The study of these interactions for fresh sample of cement reveals reproducible results and is important for practical purposes.

(iii) The amphiphilic character of the aqueous solutions of superplasticizer Flubet® (calcium salt) improves the hydration of cement grains even at very small concentrations both with the overall amplitude and the intrinsic rate of the process.

(iv) This experimental technique should be extended to a large number and variety of cements and additives with a view to establishing it as a standard, sensitive, rapid and low cost analysis of the two main components in the concrete and mortar industry.

REFERENCES

1. V. S. Gladkov and B. J. Polchkov, *Beton Zhelezobeton*, Moscow, **13—14**, 10 (1976).
2. I. Odler, J. Skalny and T. S. Brunauer, The VIth International Symposium on Chemistry of Cement, Moscow 1974, part II—6.
3. I. Teoreanu, *Materiale de Construcții*, **10**, 31—34 (1980).
4. V. M. Malhotra, *Concrete Constructions*, March, 142 (1978).
5. L. Hodkinson, and M. R. Rixom, Ger. Offen., 2.531.595, (1976).
6. L. Hodkinson, and M. R. Rixom, Can. Patent 1.066.584 (1979).
7. Y. V. Sinka, U. S. Patent, 4.164,426 (1979).
8. T. Murata, Japan Kokay Tokkyo Koho, 79.17.918 (1979).
9. G. Popescu, M. Muntean, H. Bălășoiu, S. Ifrim, D. F. Anghel and B. Albu, *Il Cemento*, **2**, 107 (1982).
10. G. Popescu, M. Muntean, H. Bălășoiu, S. Ifrim, D. F. Anghel, and B. Albu, *Materiale de construcții*, **2**, 28 (1980).
11. H. Bălășoiu, G. Popescu, M. Muntean, S. Ifrim, D. Anghel, and V. Popa, *Il Cemento*, **81**, 77 (1984).
12. G. Drăgan, *J. Thermal Anal.*, **31**, 941 (1986).
13. G. Drăgan, *J. Thermal Anal.*, **32**, 253 (1987).
14. G. Drăgan, *Acta Polymerica*, **38**, 211, 270, 467 (1986).
15. G. Drăgan, *J. Thermal Anal.*, **31**, 677 (1986).
16. S. Ifrim, G. Popescu, and I. Mândru, The IVth Conference on Chemistry and Engineering Chemistry, Polytechnic Institute of Bucharest, 1985.
17. G. Drăgan, I. Mândru, G. Popescu and S. Ifrim, "Thermal effects of micellization of surfactants", The IInd National Symposium on Chemistry of Colloids and Surfa ces, Cluj-Napoca, September 8—10, 1986.

groups [illegible] very small concentrations [illegible] with the system [illegible] and the irradiation rate of the process.

(b) This experimental technique should be extended to a large number and variety of reagents and [illegible] with a view to establishing it as a standard, sensitive, rapid and low cost analysis of the [illegible] components in the [illegible]

[illegible]

1. S. Glasstone and [illegible]
2. [illegible]
[illegible]
3. [illegible]
4. [illegible]
5. [illegible]
6. [illegible] Patent [illegible]
7. [illegible] Patent [illegible]
8. [illegible]
9. [illegible]
[illegible]
10. [illegible]
[illegible]
11. [illegible]
[illegible]
12. [illegible]
13. [illegible]
14. [illegible]
15. [illegible]
16. [illegible] Polytechnic Institute of Brooklyn [illegible]
17. [illegible] International Symposium on Chemistry of Cellulose [illegible] September [illegible]

Revue Roumaine de Chimie, **32**, *8*, 775–782 (1987)

HETEROCYCLIC QUATERNARY AMMONIUM COMPOUNDS AS CORROSION INHIBITORS FOR MILD STEEL IN H_3PO_4

A. S. FOUDA *, H. A. MOSTAFA and M. N. MOUSSA
Chemistry Department, Faculty of Science, Mansoura
University, Mansoura, Egypt

Received May 19, 1986

Quaternary ammonium compounds were prepared from some cycloaliphatic amines and were tested as corrosion inhibitors for mild steel in 50% H_3PO_4 by weight loss and polarization techniques. The two techniques gave the same order of inhibition. It is suggested that these heterocyclic quaternary ammonium compounds act mainly as cathodic inhibitors of the acid corrosion of mild steel. The degree of coverage of electrode surface was calculated from the corrosion rates with and without inhibitors. Likewise, thermodynamic parameters for adsorption are calculated using the Frumkin adsoprtion isotherm.

INTRODUCTION

N-Alkyl quaternary ammonium compounds, particularly when added as their halides, are good inhibitors of the acid corrosion of both pure iron [1] and mild steel. [2] This is attributed to the formation of an adsorbed layer of positively charged quaternary amonium ions at the negatively charged metal surface.

In has been shown previously that *n*-alkyltriethyl ammonium compounds are better inhibitors of acid corrosion of steel [3] and pure iron [1] than the corresponding n-alkyl-trimethylammonium compounds, presumably because there is less electrostatic repulsion between the ions with the bigger head groups, allowing them to pack more closely. Other workers [4,5] have reported that quaternary ammonium sulphates give very little inhibition, and that the presence of halide ion is necessary to obtain good inhibition.

In the previous electrochemical studies [1] of the corrosion inhibition of mild steel in 0.5M H_2SO_4, it was noted that the n-alkylquaternary ammonium compounds often caused a significant stimulation of the cathodic reaction at the lower levels of inhibition, the decrease in corrosion rate being due solely to inhibition of the anodic reaction. The results obtained in the present work suggest that stimulation of the cathodic reaction of steel in 50% H_3PO_4 is a general feature of corrosion inhibition by the heterocyclic ammonium ions and the possible significance of this is now discussed.

---

* To whom all correspondence should be addressed.

EXPERIMENTAL

Apparatus and working procedure

The inhibition efficiency of the substances studied was determined by weight loss measurements of mild steel samples of 20×20×0.2 mm cut from commercial purity sheets. They contain 0.44% Mn, 0.08% C, 0.05% Si and 0.02% S and Fe the rest. The surfaces were degreased and abraded successively down to 00 grade. The inhibition efficiency, τ, was calculated by the standard formula :

$$\tau = \frac{m_0 - m_i}{m_0} \times 100$$

where m_0 = weight loss in 50% H_3PO_4, m = weight loss in 50% H_3PO_4 containing the inhibitor. The results obtained over 3 experiments in the inhibited and uninhibited acid, gave corrosion rates which were reproducible to within ± 6.1%.

The current-polarization curves were measured using simple galvanostatic technique in the absence (blank) and presence of various concentrations of substances used. Current densities were calculated on the basis of apparent surface area. The working mild steel cathode was immerdsed in the electrolyte before the polarization measurements were started and the free corrosion potential was measured against saturated calomel electrode. The electrolyte used was 50% H_3OP_4, measurements were taken in a water thermostat adjusted to $\neq$ 1°C. The potential at any given current under similar experimental conditions was reproducible within $\neq$ 8%.

Materials

Preparation of N,N-dialkyl ammonium salts

To 0.015 mole of the N-alkylimine dissolved in 25 mL petroleum ether (B.p. 100–120°C) is added 0.015 mole of the corresponding alkyl halide. The reaction mixture is refluxed for 30 minutes, allowed to stand over night. The product is filtered, washed with petrol ether (B.p. 100–120°C) twice, dried and kept in a vacuum desiccator.

The structures of these compounds were identified by methods of elementary, IR and NMR analysis.

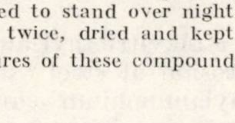

I

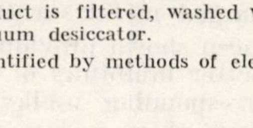

III

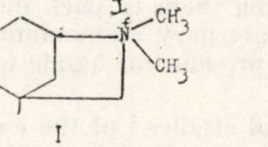

II

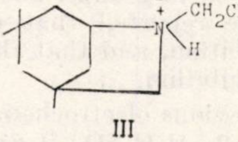

IV

RESULTS AND DISCUSSION

Weight loss measurements

The penetration P (depth of corrosion) was calculated from the weight loss by the relation:

$$P = \frac{\text{Weight loss due to corrosion}}{\text{area of corrosion} \times \text{density of metal}}$$

The penetration for different concentrations of H_3PO_4 at 300°K (Fig. 1) is described by the expression:

$$\log P = x + y \log t \qquad (1)$$

and

$$\frac{\mathrm{d}P}{\mathrm{d}t} = kP^n \qquad (2)$$

where x, y, k and n are constants and t the time. Smith and Hatfield[6] have shown that equations (1) and (2) describe the results of the corrosion of pure iron in H_3PO_4.

Although information on the corrosion mechanism is contained in the parameters x, y, k and n, this can rarely be extracted to give an unambiguous interpretation of the data without the establishment of a model which incorporates the chemistry of the corrosion reactions and the structure of the protective adsorbed layer on the surface.

Integrating equation (2) yields:

$$\log P = [\log(1-n) + \log k + \log t]/(1-n) \qquad (3)$$

and comparison of equations (3) and (1) enables n to be expressed as:

$$n = (y-1)/y \qquad (4)$$

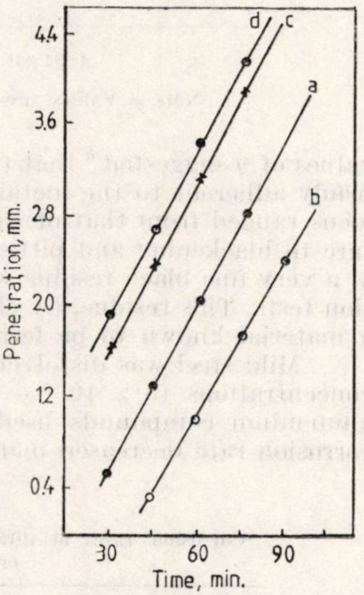

Fig. 1. — The penetration of mild steel by H_3PO_4 at 300K. a — 100 % H_3PO_4; b — 75 % H_3PO_4; c — 50 % H_3PO_4; d — 25 % H_3PO_4.

Values of y have been computed from Fig. 1 and from these the values of n obtained. Table 1 summarizes the results for mild steel in acid solutions of different concentrations.

It can be seen from the table that despite an apparent trend towards lower values of y at higher acid concentrations, the spread of data does not allow an unequivocal deduction that the corrosion mechanism is changing with acid concentration. Moreover, because all four y values are close to unity, equation (4) shows that the values of n are essentially zero. The linearity of the plots in Fig. 1 implies that the mechanism of corrosion does not change at least up to corrosion times of the order 2 h.

The values of y (Table 1) for the tests in 50.75 and 100% H_3PO_4 were slightly but significantly less than unity, the rate of corrosion decreased as the amount of corrosion increased, indicating that a reaction product had kinetic significance. The small differences from unity of the values of y suggested[6] that the reaction product is either very thin or not firmly adherent to the metal. The visible effect of the acid on the specimens ranged from that of slightly polishing the specimen on short exposure to blackening and pitting its surface on prolonged exposure. A trace of a very fine black residue was found in the acid after each of the corrosion tests. This residue, by chemical analysis, suggested that it was Fe_2P, a material known to be ferromagnetic.[7]

Table 1

Kinetic parameters for corrosion of mild steel in orthophosphoric acid

Acid conc. %	25	50	75	100
y	$1.04 \neq 0.25$	$0.94 \neq 0.22$	$0.86 \neq 0.17$	$0.82 \neq 0.16$

Note ≠ Values are the standard errors.

Mild steel was dissolved for 1 h in 50% H_3PO_4 containing different concentrations ($5 \times 10^{-3} - 10^{-5}$M) of the four heterocyclic quaternary ammonium compounds used under unstirred conditions at 300K. The corrosion rate decreased markedly even by the traces of these inhibitors.

Table 2

Corrosion rates at different concentrations of inhibitors in 50% orthophosphoric at 300°K

Inhibitor concentration (M)	Corrosion rate mg cm^{-2} min^{-1})			
	I	II	III	IV
1×10^{-5}	2.39	2.18	2.07	1.97
5×10^{-5}	1.87	1.79	1.76	1.66
1×10^{-4}	1.45	1.35	1.24	1.14
5×10^{-4}	1.24	1.04	0.99	0.93
1×10^{-3}	1.14	0.93	0.83	0.73
5×10^{-3}	1.09	0.83	0.62	0.52

Table 2 shows the variation of corrosion rate with inhibitor concentration. The extent of inhibition of corrosion was found to depend on the nature and concentration of the inhibitor. The type of dependence of corrosion rate with inhibitor concentration was the same for all the inhibitors. Even at a low concentration of inhibitor (1×10^{-5}M), the degree of corrosion inhibition was higher with I or II or III than with IV. The corrosion rate decreased considerably with an increase in concentration of each inhibitor. The steric hindrance of these compounds increases in the order : I > II > III > IV. This confirms the inhibition order of the heterocyclic quaternary ammonium compounds used which is the reverse to the increasing steric hindrance.

Polarization measurements

Cathodic polarization of mild steel was carried out under galvanostatic conditions in 50% H_3PO_4 containing different concentrations of inhibitors at 300K. At all current densities during polarization, the potentials were recorded at regular intervals of time. Fig. 2 shows a plot of the current density (logarithmic scale) as a function of potential in the presence and in the absence of different concentrations of inhibitor I. The figure reveals that the inhibitor concentration has a strong effect on the corrosion behaviour of the steel. As the inhibitor concentration increases, it is seen that the free corrosion potential and the Tafel line are shifted to more cathodic potentials relative to the blank curve. Furthermore, the Tafel slope slightly increases. These results suggest that inhibitor I is a cathodic inhibitor. Similar results were obtained for all inhibitors used.

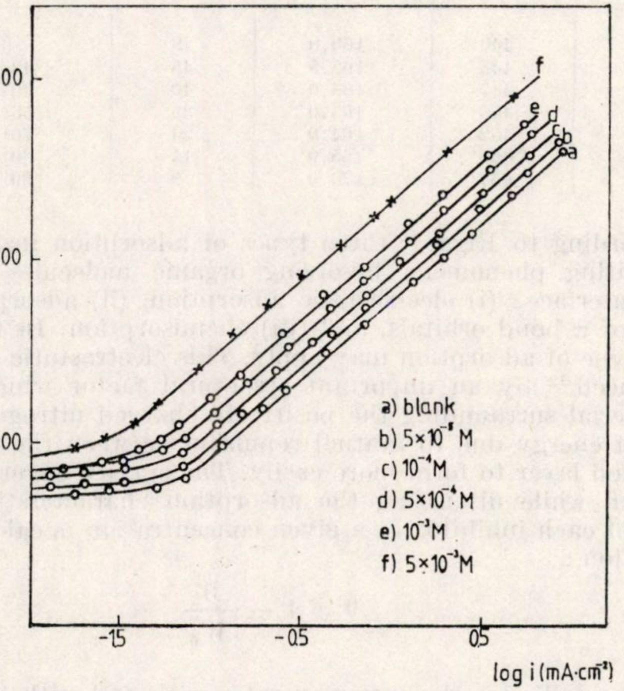

Fig. 2. — Tafel relationships for mild steel in 50% H_3PO_4 at 300K with inhibitor I.

Table 3 shows the effect of inhibitor I concentration on : free corrosion potential E_{corr}, Tafel slope, corrosion c.d. and percentage inhibition. The decrease in i_{corr}. with increasing concentration demonstrates the efficiency of the heterocyclic quaternary ammonium compounds as inhibitors.

Recently, the nature of inhibitor interaction on the corroding surface during corrosion inhibition of metals and alloys has been deduced in terms of adsorption characteristics [8-10] of the inhibitor.

Table 3

Cathodic behaviour of mild steel in the presence and absence of various concentrations of inhibitor I

Concentration, M	$-E_{\text{corr.}}$, mV	$-b_c$ (mV/decade)	$i_{\text{corr.}}$, μA cm^{-2}	% Inhibition from: Polarization	Weight loss
0	440	160.0	79	—	—
5×10^{-5}	445	162.8	45	43	80.1
1×10^{-5}	447	165.0	40	49	82.4
5×10^{-4}	450	165.0	35	55	91.6
1×10^{-4}	452	164.0	24	70	93.9
1×10^{-3}	455	165.9	11	86	97.8
5×19^{-3}	457	170.0	9	89	98.5

According to Riggs,[11] three types of adsorption may take place in the inhibiting phenomena involving organic molecules at the metal/solution interface: (i) electrostatic adsorption, (ii) adsorption due to the influence of π bond orbitals, and (iii) chemisorption. In the present case the first type of adsorption may apply. This electrostatic adsorption may be influenced[12] by an important structural factor which is: the non-polar material surrounding the positively charged nitrogen atom reduces the loss of energy due to mutual repulsion between the ions, allowing a close packed layer to form more easily. The surface coverage (θ) data are very useful while discussing the adsorption characterstics. The surface coverage of each inhibitor at a given concentration is calculated by using the equation:

$$\theta = 1 - \frac{W}{W_0}$$

where W and W_0 are the corrosion rates with and without inhibitor, respectively. For each inhibitor, the plot of θ vs. log of inhibitor concentration (Fig. 3) followed an *S*-type curve, characteristic of the Frumkin adsorption isotherm.[13]

$$\frac{\theta}{(1-\theta)} \exp(-f\theta) = KC_1,$$

where K (equilibrium constant) and f are constants. C_1 is the concentration of the inhibitor in the bulk of the solution. The value of f is characteristic of the range of values of θ (0.25 — 0.87). It depends on the molecular interactions in the adsorption layer and the degree of the heterogeneity of the surface. K is related to the free energy of adsorption ($\Delta G^\circ_{\text{ads}}$) by the relation:

$$K = \exp\left(-\frac{\Delta G^\circ_{\text{ads.}}}{RT}\right)$$

The values of f and K were calculated (Table 4) by choosing values of θ in the range (0.25 — 0.87) and the corresponding values of C_1 and then solving the two simultaneous equations. The values of f indicate [14] that molecular interactions are not predominant in the adsorption layer, being less under the influence of heterogeneity of the surface.

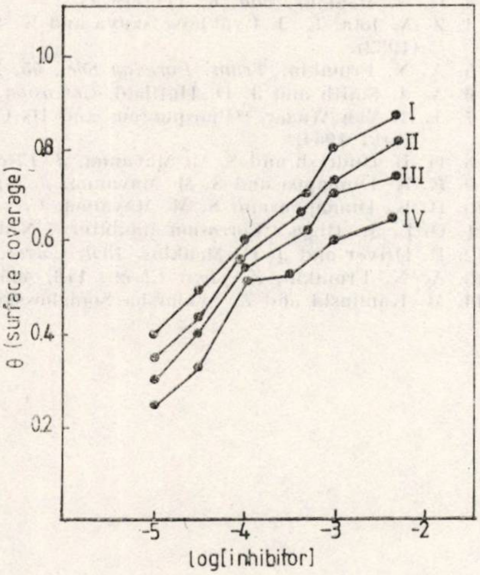

Fig. 3. — The relationships between degree of coverge θ, and the concentration of inhibitor at 300K.

The values of free energy of adsorption for each concentration of inhibitors are calculated. The negative values of ΔG°_{ads} indicate the spontaneous adsorption of the inhibitors on mild steel. One could expect the degree of adsorption by these inhibitors on mild steel to be in the order : IV > III > II > I. This is also in agreement with the observed order of corrosion inhibition (Table 4).

Table 4

Values of thermodynamical parameters, f and K, during adsorption of inhibitors (10^{-4}M) on mild steel in 50 % H_3PO_4 at 300 °K

Inhibitors	$-f$	K	$-\Delta G^0_{ads.}$ kJ mol^{-1}	% Inhibition from :	
				Polarization	Weight loss
IV	11.7	1.7×10^7	41.598	70	93.4
III	11.9	1.2×10^7	40.595	60	92.8
II	12.0	9.2×10^6	40.001	57	92.2
I	12.4	6.7×10^6	39.204	55	91.6

ACKNOWLEDGEMENTS : The authors are grateful to Dr. Y. M. Darwish for providing facilities during this work.

REFERENCES

1. R. Driver and R. J. Meakins, *Brit. Corros. J.*, **9**, 233 (1974).
2. R. J. Meakins, *J. Appl. Chem. Lond.*, **13**, 339 (1963).
3. R. J. Meakins, *ibid*, **6**, 111 (1971).
4. Z. A. Iofa, E. J. Lyakhovetskaya and K. Sharifov, *Doklady Akad. Nauk. SSSR*, **84**, 543 (1952).
5. A. N. Frumkin, *Trans. Faraday Soc.*, **55**, 156 (1959).
6. A. J. Smith and J. D. Hatfield, *Corrosion*, **26**, 246 (1970).
7. J. R. Van Wager, "Phosphorous and Its Compounds", Interscience Publishers Inc. New York, 1964.
8. H. B. Rudresh and S. M. Mayanna, *J. Electrochem. Soc.*, **124**, 340 (1977).
9. R. K. Dinnappa and S. M. Mayanna, *J. Appl. Electrochem.*, **11**, 111 (1981).
10. R. K. Dinnappa and S. M. Mayanna, *Corrosion*, **38**, 525 (1982).
11. O. L. Jr. Riggs "Corrosion Inhibitors" NACE, Houston, Texas, **7** (1973).
12. R. Driver and J. R. Meakins, *Brit. Corros. J.*, **15**, 18 (1980).
13. A. N. Frumkin, *Z. phys. Chem.*, **116**, 466 (1925).
14. M. Kaminski and Z. Syklarsha Sonialowska, *Corrosion Sci.*, **13**, 557 (1973).

Revue Roumaine de Chimie, 32, 8, 783–791 (1987)

STRUCTURE ACTIVITY RELATIONS BY THE FREE-WILSON AND MTD METHODS FOR SUBSTANCES WITH A POTENTIAL PSYCHOTROPIC ACTIVITY. 2

BENZENSULPHONAMIDE DERIVATIVES WITH ANTICONVULSIVE ACTIVITY

Z. SIMON, G. I. MIHALAS, M. APETROAIE *, CL. SINGER *,
RALUCA BOZGA *, RODICA CECLAN * and ST. CILIANU *
Medicinal Institute of Timişoara, Department of Biophysics,
Pţa 23 August 2, 1900 Timişoara, Romania
*Chemical Pharmaceutical Research Institute, Sos. Vitan 112, 73619,
Bucharest, Romania

Received July 7, 1986

The Free-Wilson and QSAR methods are used in a QSAR analysis of a series of 22 benzensulphonamides with a protecting action against convulsions induced by cardiazol in mice. A correlation coefficient $r = 0.874$ is obtained by the Free-Wilson method with 23 structural fragments in 6 positions, while $r = 0.807$ is obtained by the MTD method with two supplementary indicator variables and $r = 0.905$ if three compounds are eliminated out of the series. There is a general agreement in the results of the two methods. The fact that the MTD method gives a better result for the series analysed in the first part of this work, while the Free-Wilson method gives better results in the series analysed here indicates different weights of steric or other effects in determining the biological activities of the two series of compounds.

INTRODUCTION

In Part 1 of this work[1] the comparative use of Free-Wilson and MTD methods in QSAR analyses was discussed and applied upon a series of diphenylether derivatives with neuroleptic activity. This comparison allowed some tentative conclusions about sterical and conformational aspects, about local hydrophobicity effects important for neuroleptic activity. Here we shall use the same procedure for the QSAR analysis of a series of 22 benzensulphonamide derivatives with anticonvulsive activity.

The protection index against cardiazol induced convulsions, expressed in percentages with respect to the control group are used as experimental biological activity. The logarithm of this index is used, as log A^{exp}, for the correlations.

Most of the tested substances are new compounds. Details upon their synthesis and physicochemical characterisation and upon the biological tests will be given elsewhere.

The 22 compounds and the log A_{exp} values are listed in Table 1.

Table 1

Compounds with anticovulsive activity. Structure and activity data

1	Structure 2	log A exp 3	log AFW 4
1.	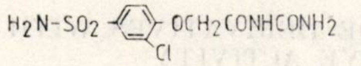	0.91	0.88
2.	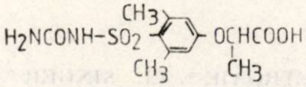	0.83	0.78
3.	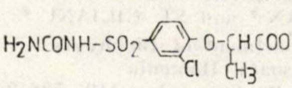	0.81	0.70
4.	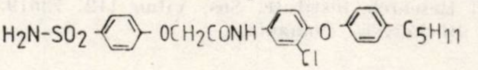	0.81	0.81
5.	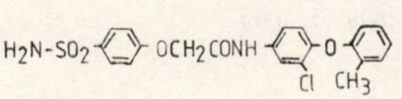	0.81	0.81
6.	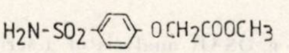	0.79	0.79
7.	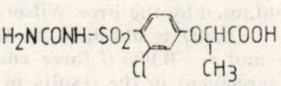	0.76	0.76
8.	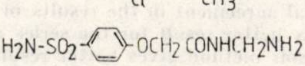	0.75	0.75
9.	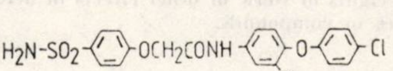	0.75	0.75
10.	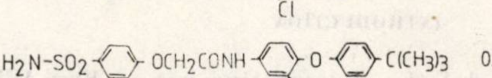	0.74	0.74
11	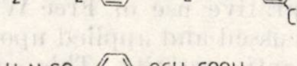	0.74	0.74
12.	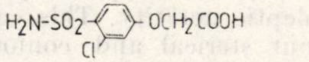	0.74	0.77
13.	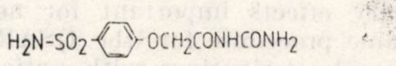	0.67	0.52
14	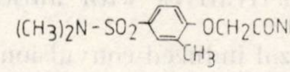	0.65	0.70
15.	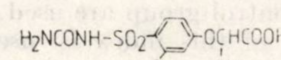	0.63	0.59
16.	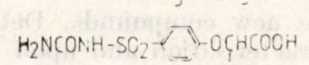	0.62	0.57

1	2	3	4
17	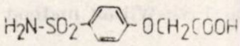	0.60	0.60
18	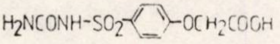	0.60	0.65
19	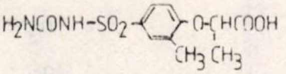	0.50	0.64
20	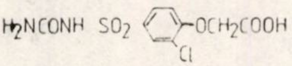	0.48	0.48
21	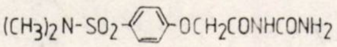	0.46	0.47
22	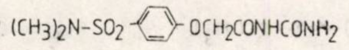	0.45	0.58

RESULTS

Some basic features of the Free Wilson and MTD[3] methods are given in Part 1 of this work.[1]

Free Wilson method. The molecular core and substituent positions for the Free Wilson method are depicted in Figure 1. There are 23 variables corresponding to the structural fragments existing in the compounds of Table 1, out of which 6 are subtracted corresponding to the restrictional equations for the 6 positions (see Fig. 1). The programme used for the computations is the same as for Part 1. The calculated activities, log A_{FW}, are listed in Table 1, the substituent contributions (a_1, a_2, . . ., a_{17}) in Table 2. The multiple correlation coefficient is $r = 0.874$, $a_0 = 0.686$.

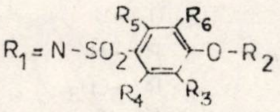

Fig. 1. — General structure of the molecules of Table 1.

MTD method. The hypermolecule resulted by the superposition of the 22 molecules of Table 1 is depicted in Fig. 2. A total number of 16 vertices and groups of vertices (all occupied or all empty) result, the occupation of which is given by the $j(x_{ij} = 1)$ column of Tab. 3.

The optimised receptor map was obtained with an optimisation method based upon the increase of the r — correlation coefficient (the MTDR-procedure, see[3]-Appendix II) on a M—18 computer. The start map, S° was characterised by the following vertex attributions :

$$S^\circ(\varepsilon_1 = +1, \ \varepsilon_2 = \varepsilon_3 = \ldots = \varepsilon_{16} = 0) \ r^\circ = 0.497$$

Table 2

Structural fragment contributious for the Free-Wilson method

Position	Substituent (structural fragment)	$a_0 = 0.686$
R_1	A H H	$a_1 = 0.608$
	B H HCONH$_2$	$a_2 = -0.080$
	C CH$_3$ CH$_3$	$a_3 = -0.157$
R_2	D-CH$_2$CONH$_2$NHCOOC$_2$H$_5$	$a_4 = 0.012$
	E - CH$_2$COOH	$a_5 = 0.012$
	F - CH$_2$CONH 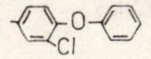	$a_6 = -0.178$
	G - CH$_2$CONH 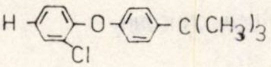	$a_7 = -0.038$
	H - CH$_2$CONH 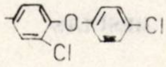	$a_8 = -0.028$
	I - CH(CH$_3$)COOH	$a_9 = 0.033$
	J - CH$_2$CONHCONH$_2$	$a_{10} = -0.010$
	K - CH$_2$CONH 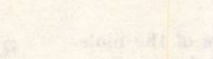	$a_{11} = 0.032$
	L - CH$_2$CONH 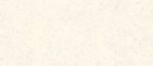	$a_{12} = 0.032$
R_3	M -H	$a_{13} = -0.020$
	N -CH$_3$	$a_{14} = 0.034$
	O -Cl	$a_{15} = 0.093$
R_4	P -H	$a_{16} = 0.017$
	R -CH$_3$	$a_{17} = 0.092$
	S -Cl	$a_{18} = 0.152$
R_5	T -H	$a_{19} = -0.015$
	U -CH$_3$	$a_{20} = 0.065$
	V -Cl	$a_{21} = 0.155$
R_6	W H	$a_{22} = 0.004$
	X Cl	$a_{23} = 0.085$

while the optimised receptor map S* is characterised by

$$S^* \begin{cases} j(\varepsilon = -1) : 4, 6 \\ j(\varepsilon = +1) : 1, 2 \\ j(\varepsilon = 0) \ : 3,\ 5,\ 7-16 \text{ (including the ``primed'' vertices)}; \end{cases}$$

$$r = 0.681$$

The MTD values calculated with S* are also given in Table 2. One may observe that the molecules i : 7, 14, 18 may exist in two approximately equienergetic conformations, with Cl or CH_3 either in j : 4 or in j : 6. For both conformations in all these molecules, the same MTD values are obtained with the S* receptor map.

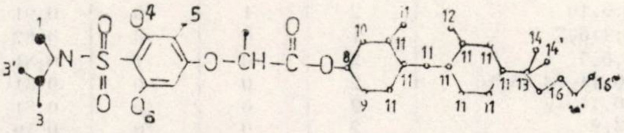

Fig. 2. – Hypermolecule and vertex numbering. Beneficial vertices ($\varepsilon_j = -1$) are marked by white circles (○), detrimental vertices ($\varepsilon_j = +1$), by black circles (●).

The following indicator variables were used in an attempt to improve the correlation :

$\sigma_1 = 1$ if vertices j : 8–10 are occupied by a CONH group
$\sigma_2 = 1$ if a CH_3-group is in j : 7 simultaneously with Cl in j : 5
$\sigma_3 = 1$ if j : 5 is occupied by a CH_3-group
$\sigma_4 = 1$ if j : 4 is occupied by a CH_3-group
$\sigma_5 = 1$ if j : 2 is occupied by a CH_3-group

With these 5 indicator variables the following correlational equation results :

$$\log A_{MTD} = 1.180 - 0.216\ MTD + 0.0758\ \sigma_1 + 0.276\ \sigma_2 + 0.102\ \sigma_3 - \\ - 0.128\ \sigma_4 + 0.128\ \sigma_5 \qquad (1)$$

$$r = 0.830\ ;\ s = 0.073\ ;\ F = 4.42\ ;\ EV = 0.564\ ;\ N = 22$$

If one renounces to the σ_3, σ_4, σ_5 – variables, the correlation coefficient decreases only slightly, but F and EV increase

$$\log A'_{MTD} = 1.020 - 0.150\ MTD + 0.150\ \sigma_1 + 0.241\ \sigma_2 \qquad (2)$$

$$r' = 0.807\ ;\ s = 0.77\ ;\ F = 7.92\ ;\ EV = 0.592\ ;\ N = 22$$

If molecules i : 13,17,18 (for which the $\log A_{exp} - \log A'_{MTD}$ difference is larger than ± 0.10 log units) are eliminated the correlation is sensibly improved :

$$\log A''_{MTD} = 1.089 - 0.174\ MTD = 0.072\ \sigma_1 = 0.242\ \sigma_2 \qquad (3)$$

$$r'' = 0.905\ ;\ s = 0.058\ ;\ F = 15.81\ ;\ EV = 0.782\ ;\ N = 19$$

Partial correlation coefficients and intercorrrelation coefficients are listed in Table 4.

The hydrophobicities, π, of Table 1 – molecules were calculated on an additive basis using $\log P_{oct}$ values of Leo, Hansch and Elkins [4] (for phenoxyacetic acid benzensulphonamide, urea, diphenylether) and hydrophobicity increments of Rekker [7] and of Hansch et al [6]. Most molecules result as markedly hydrophilic, for example for i : 16, $\pi_{16} \cong -9$ (considering the carboxilic group ionised at pH = 7), but the molecules

Table 3

Vertex occupancy and MTD results

i	$j(x_{ij}=1)$	MTD	σ_1	σ_2	log A_{exp}	log A_{MTD}	
						(eq 2)	(eq 3)
1	5,8,9,10	2	1	0	0.91	0.83	0.81
2	2,3,4,6,7	1	0	0	0.83	0.87	0.91
3	2,3,5,7	3	0	1	0.81	0.81	0.81
4	8,9,10,11,13,15,16	2	0	0	0.81	0.72	0.74
5	8,9,10,11,12	2	0	0	0.81	0.72	0.74
6	8,9	2	0	0	0.79	0.72	0.74
7	{2,3,4,7, {2,3,6,7	2	0	0	0.76	0.72	0.74
8	8,9	2	0	0	0.75	0.72	0.74
9	8,9,10,11,13	2	0	0	0.75	0.72	0.74
10	8,9,10,11,13,14,15	2	0	0	0.74	0.72	0.74
11	{2,3,4, {2,3,6	2	0	0	0.74	0.72	0.74
12	8,9,10	2	1	0	0.74	0.83	0.81
13	1,2,5,8,9,10	4	1	0	0.67	0.53	—
14	{2,3,4,7, {2,3,6,7	2	0	0	0.65	0.72	0.74
15	2,3,7	3	0	0	0.63	0.57	0.57
16	2,3	3	0	0	0.62	0.57	0.57
17	—	2	0	0	0.60	0.72	—
18	{2,3,4 {2,3,6	2	0	0	0.60	0.72	—
19	2,3,5,7	3	0	0	0.50	0.57	0.57
20	2,3,5	3	0	0	0.48	0.57	0.57
21	1,2,8,9,10	4	1	0	0.46	0.53	0.47
22	1,2,5,8,9,10	4	1	0	0.45	0.53	0.47

Legend. As for Table 3 of Part 1. For σ_1, σ_2 see Method (MTD)-section. Molecules i : 7,11,14 and 18 can exist in two approximately isoenergetic conformations with Cl or CH_3 in either j : 4 or j : 6, differing by a 180° rotation of the phenylic moiety.

Table 4

Partial correlation and intercorrelation coefficients

	A	MTD	σ_1	σ_2	σ_3	σ_4	σ_5
MTD	−0.681 (−0.809)	1	0.517 (0.400)	0.152 (0.182)	−0.427	−0.400	0.785
σ_1	−0.112 (−0.217)		1	−0.183 (−0.122)	0.206	−0.215	0.733
σ_2	0.203 (0.209)			−1	−0.069	−0.087	−0.087
σ_3	−0.149				1	−0.126	0.335
σ_4	0.009					1	−0.158
σ_5	−0.414						1

The values refer to the whole series of 22 molecules of Table 1 (eqs 1 and 2); values in parentheses to the reduced series of 19 molecules (molecules i : 13, 17, 18 eliminated, eq. 3). For definitions of the indicator variables $\sigma_1, \sigma_2, \ldots, \sigma_5$ see RESULTS section, MTD method.

with a diphenyloxidic moiety in R_2 are markedly hydrophobic, up to $\pi_{10} \cong +4.6$ for i : 10. There is no correlation between the π and the log A_{exp} – values, or the log A_{exp} – log A_{calc} differences.

DISCUSSION AND CONCLUSIONS

The largest differences between fragment contributions, as predicted by the Free Wilson method are for position R_1, the order being

$$\mathrm{H,H} > \mathrm{H,HCONH_2} > \mathrm{CH_3,CH_3}$$

in agreement with the MTD predictions, as these fregments occupy 0, 1 and respectively 2 detrimental vertices (j : 1, 2) in the hypermolecule (Fig. 2).

For position R_2 the fragment contributions, as predicted by the Free-Wilson method, are rather small also in agreement with the MTD predictions, as all the substituents occupy only irrelevant ($\varepsilon_j = 0$) vertices.

The CH_3 or Cl – substituents in R_3 and R_6 occupy an irrelevant vertex ($\varepsilon_5 = 0$); the Free-Wilson order for R_3 is $H < CH_3 < Cl$, while for R_6 : $Cl > H$, but these fragment contributions are generally small.

Positions R_4 and R_5 correspond to the beneficial vertices j : 6 and respectively 4. The order of Free-Wilson contributions is $H < CH_3 < Cl$; the one predicted by the MTD method (**H** atoms are neglected); $H < < CH_3 = Cl$. The higher polarisation of the Cl-atom, as compared to CH_3, may allow a stronger van der Waals substituent receptor attraction for these positions.

The most active structures, as predicted by the MTD method (a and b) and by the Free-Wilson method (c–h) are depicted in Fig. 3. The activities predicted for these molecules, according to the structural fragment contributions (Free-Wilson method) and according to eq. (2) (MTD metohd) are listed in Table 5. The activities predicted by the Free-Wilson method are somewhat larger than those predicted by MTD method, but all predicted activities are higher than those listed in Table 1.

The fact that large variations, especially in the hydrophobicity contributions of substituents in R_2 produce only minor changes in the activities (cca. 0.2 log units) suggests that the R_2 substituents are rapidly hydrolysed within the organism, to $-CH_2COO^-$ or $-CH(CH_3)COO^-$ (at pH = 7). The active species should all be strongly hydroyphlic, anionic and thus the passive transport across cell membranes should be rather difficult.

According to the MTD receptor map S*, the "left hand" side of the molecules (Fig. 2) should interact with a relatively rigid receptor region : substituents at the SO_2NH_2 group interfere with the receptor wall ($\varepsilon_1 = \varepsilon_2 = +1$), while CH_3 and Cl atoms at R_4 and R_5 interfere favourably with the receptor ($\varepsilon_4 = \varepsilon_6 = -1$). Alternatively, the two **H** atoms of the sulphonamide group may be necessary for hydrogen bonding within the receptor. The beneficial effect of the –CONH– group

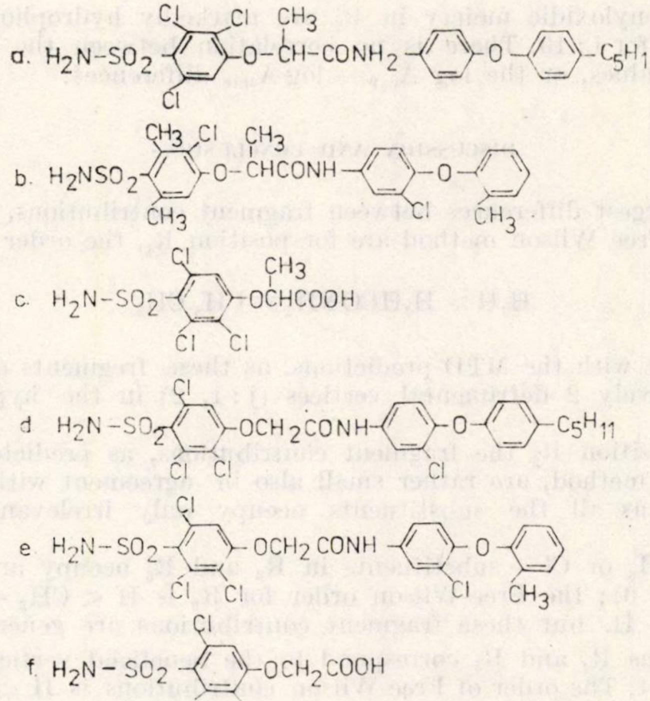
a. H_2N-SO_2 O-CH-CONH$_2$ O C_5H_{11} Cl Cl CH$_3$ Cl
b. H_2NSO_2 O-CHCONH O CH$_3$ Cl CH$_3$ CH$_3$ Cl CH$_3$
c. H_2N-SO_2 OCHCOOH CH$_3$ Cl Cl Cl
d H_2N-SO_2 OCH$_2$CONH O C_5H_{11} Cl Cl Cl Cl
e H_2N-SO_2 OCH$_2$ CONH O Cl CH$_3$ Cl Cl Cl
f. H_2N-SO_2 OCH$_2$COOH Cl Cl
g. H_2N-SO_2 O-CH-COOH CH$_3$ Cl Cl Cl
h. H_2N-SO_2 OCHCOOH CH$_3$ CH$_3$ CH$_3$ CH$_3$

Fig. 3. — Molecules with predicted high activity (see also Table 5).

Table 5

Predicted activities for the molecules of Fig. 3

Molecule	a	b	c	d	e	f	g	h
log A_{FW}	1.73	1.54	1.73	1.73	1.73	1.71	1.67	1.62
log A_{MDT}	1.41	1.41	1.02	1.17	1.17	1.02	1.02	1.02

log A_{FW} calculated with substituent contributions of Table 2
log A_{MDT} according to eq (2); for all molecules MTD $=0$, $\sigma_1 = 1$ for a, b, d and e ($\sigma_1 = 0$ for the rest), $\sigma_2 = 1$ for a and b.

in j : 8—10 ($\sigma_1 = 1$) may be connected with the early, rapid, hydrolysis process. The beneficial effect of the simultaneous presence of the electronegative Cl-atom in j : 5 and the electropositive CH_3-group in j : 7 ($\sigma_2 = 1$) suggests a conformation within the drug-receptor complex, in which these groups interact.

As a whole, there is an acceptable agreement between the Free-Wilson and the MTD results, for both the neuroleptic diphenyl-ether derivatives of Part 1[1] and the anticonvulsant benzen-sulphonamide derivatives of this second part. For the first series, the MTD method gives a better result ($r = 0.81$) than the Free-Wilson method ($r = 0.77$), for the second series the Free-Wilson results are better ($r = 0.87$ and $r = 0.81$). For the first type of activity, steric requirements are probably more stringent, for the second —other types of effects. The agreement of predicted log A_{FW} and log A_{MTD} activities and in two cases also with experimental activities (log A_{exp}) for new molecules — see Part 1, is also satisfactory, which increases the reliability of the comparativ eprocedure used here.

REFERENCES

1. Part 1, *Rev. Roumaine Chim.*, **32**, in print (1987).
2. W. E. Purcell, G. E. Bass and J. M. Clayton, "Strategy of Drug Design. A Guide to Biological Activity", John Wiley, New York, 1973, chap. III.
3. Z. Simon, A. Chiriac, S. Holban, D. Ciubotariu and G. I. Mihalaş, "Minimum Steric Difference. The MTD Method for QSAR Studies", Res. Stud. Press, Letchworth, Herts, 1984.
4. A. Leo, C. Hanasch and D. Elkins, *Chem. Rev.*, **71**, 525 (1971).
5. R. F. Rekker, "The Hydrophobic Fragmental Constant", Elsevier, Amsterdam.
6. C. Hansch, A. Leo, B. H. Unger, K. H. Kim, D. Nikaitani and E. J. Lien, *J. Medic. Chim.*, **16**, 1207 (1973).

in 1 : 8 -16 ($c_\gamma = 1$) may be connected with the early, rapid, hydrolysis process. The beneficial effect of the simultaneous presence of the electronegative Cl atom in 1 : 5 and the electropositive CH$_3$ group in 1 : 7 ($c_\gamma = 1$) suggests a conformation, within the drug-receptor complex, in which these groups interact.

As a whole, there is an acceptable agreement between the Free-Wilson and the MTD results, for both the neuroleptic diphenyl-ether derivatives of Part 1 and the anticonvulsant benzenesulphonamide derivatives of this second part. For the first series, the MTD method gives a better result ($r = 0.81$) than the Free-Wilson method ($r = 0.77$); for the second series the Free-Wilson results are better ($r = 0.87$ and $r = 0.81$). For the first type of activity, steric requirements are probably more stringent, for the second – other types of effects. The agreement of predicted log A_W and log A_{MTD} activities and in two cases also with experimental activities (log A_{exp}) for new molecules – see Part 1, is also satisfactory, which increases the reliability of the comparative procedure used here.

REFERENCES

1. Part 1. Rev. Roumaine Chim., 32, in print (198[illegible]).
2. W. P. Purcell, G. E. Bass and J. M. Clayton, "Strategy of Drug Design. A Guide to Biological Activity", John Wiley, New York, 1973, chap. 11.
3. Z. Simon, A. Chiriac, S. Holban, D. Ciubotariu and G. I. Mihalas, "Minimum Steric Difference. The MTD Method for QSAR Studies", Res. Stud. Press, Letchworth, Herts, 1984.
4. A. Leo, C. Hansch and D. Elkins, Chem. Rev., 71, 525 (1971).
5. R. F. Rekker, "The Hydrophobic Fragmental Constant", Elsevier, Amsterdam.
6. C. Hansch, A. Leo, S. H. Unger, K. H. Kim, D. Nikaitani and E. J. Lien, J. Med. Chem., 16, 1207 (1973).

Revue Roumaine de Chimie, 32, *8*, 793–796 (1987)

N-AROYLPHTHALIMIDES BY A NEW DIRECT CONDENSATION REACTION

C. I. CHIRIAC
"P. Poni" Institute of Macromolecular Chemistry,
Aleea Gr. Ghica-Vodă 41 A, Jassy, Romania

Received February 15, 1986

By a direct condensation reaction between aromatic carboxylic acids and phthalimide in the presence of benzensulfonyl chloride in pyridine as reagent at reflux for 4–5 hours, N-aroylphthalimides resulted.

N-Acylphthalimides are commonly obtained by the acylation of K-phthalimide with acyl halides [1–3] or ketenes.[4] Other general methods of preparing N-acylphthalimides involve the acylation of amides with phthaloyl dichloride,[5,6] or by the reaction of diphenylphosphorophthalimide (prepared from phthalimide and diphenyl phosphorochloridate) with carboxylic acids in the presence of triethylamine.[7]

RESULTS AND DISCUSSION

Aromatic sulfonyl halides in pyridine have been used as reagents for the Beckmann [8] and Lossen [9] rearrangements, the dehydration of aldoximes [10] and primary amides [11] to nitriles, etc.

It is now reported that N-aroylphthalimides are easily obtained by a direct condensation reaction from phthalimide and aromatic carboxylic acids with benzensulfonyl chloride in pyridine as a new reagent, which has not been used until now in this field. Thus a solution of an aromatic carboxylic acid in pyridine is treated with benzenesulfonyl chloride and then with phthalimide. After heating at reflux for 4–5 hours, the corresponding aroylphthalimides resulted (with aliphatic acids impure products resulted). By the addition of benzenesulfonyl chloride to a solution of an aromatic carboxylic acid (I) in pyridine, mixed anhydrides (II) [11] result, which can further react with phthalimide (weak nucleophilic reagent). The high reactivity of the mixed anhydrides ($Ar-COOSO_2Ar'$) was proved also in other cases.[12,13] The pyridine is a suitable solvent and serves as acceptor for hydrochloric acid.

We propose the following mechanism of reaction :

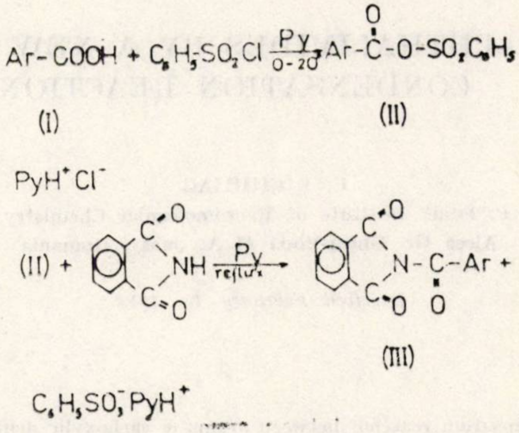

We supposed, similar as in other cases, [14-16] that this reaction involves a four-centered transition state (IV) :

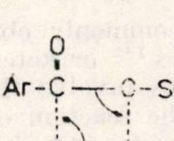

In a general procedure, to a solution of one mole + 10% excess (I) in dried pyridine cooled to 0—5°, one mole + 10% excess benzenesulfonyl chloride was added under stirring (a small excess improves the yield). After the formation of the anhydride (II), for about 1 hour at room temperature, 1 mole phthalimide was added and the obtained solution was refluxed for 4—5 hours at 120—130° (at lower temperatures, the yield was smaller). Table 1 shows the N-aroylphthalimides (III) obtained in this way.

The IR spectra of the compounds (III) present absorption bands between 1600—1800 cm^{-1} for carbonyl group.[7] The absorption band for N—H group at 3400 cm^{-1} of phthalimide is absent in the spectra of the aroylphthalimides (III). The yields ranged from 57 to 72% (Table 1). The lower yield in the case of o-chlorobenzoid acid may be determined by an effect of steric hindrance.

In conclusion, by this direct synthesis, we obtained N-aroylphthalimide, directly from carboxylic acids, although the phthalimide is a weak nucleophilic reagent.

Table 1

N-Aroylphthalimides obtained from aromatic carboxylic acids and phthalimide in the presence of benzenosulfonyl chloride/Py as reagent

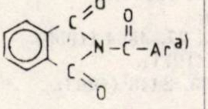 Ar:	Yield[b] %	M.p.[c] °C	Reported m.p. °C
C_6H_5	68	167—169	166—168 [7]
p—CH_3—C_6H_4	70	107—209	new comp.[d]
p—CH_3—O—C_6H_4	72	203—205	new comp.[e]
p—Cl—C_6H_4	65	200—202	199—200[7]
m—Br—C_6H_2	63	191—193	new comp.[f]
o—Cl—C_6H_4	57	175—177	new comp.[g]

[a] The products were identified by comparison of the m.p. and IR spectra with those of authentic samples.

[b] Yields calculated on phthalimide employed.

[c] After recrystallisation from ethyl acetate.

[d] Anal. Found : C, 67.91 ; H, 4.06 ; N, 5.14%.
Calculated for : $C_{16}H_{11}NO_3$; C, 67.36 ; H, 3.85 ; N, 4.91%.

[e] Anal. Found : C, 68.80 ; H, 3.94 ; N, 5.33%
Calculated for : $C_{16}H_{11}NO_4$; C, 68.32 ; H, 3.91 ; N, 4.98%.

[f] Anal. Found : C, 55.02 ; H, 2.38 ; N, 4.63%.
Calculated for : $C_{15}H_8BrNO_3$; C, 54.54 ; H, 2.42 ; N, 4.24%.

[g] Anal. Found : C, 63.61 ; H, 3.18 ; N, 5.27%.
Calculated for : $C_{15}H_8ClNO_3$; C, 63.04 ; H, 2.80 ; N, 4.90%.

EXPERIMENTAL

N-Benzoylphthalimide

To a stirred cooled (0°) solution of 2.68 g (0.02 mole + 10% excess) of benzoic acid in 15 mL dried pyridine, 2.75 mL benzenesulfonyl chloride were added in 2—3 minutes. After stirring for 1 hour at room temperature, 2.94 g (0.02 mole) phthalimide were added and the obtained solution was refluxed for 4—5 hours (120—130°). At the end of reaction, the still hot solution was poured into a large volume of water with ice (40—60 mL), when the N-benzoyl-phthalimide precipited. Then this mixture was treated with 2% NaOH solution till pH = 9—10 and the product was collected by filtration. The N-benzoylphthalimide was washed three times with 15—20 mL water and dried under vacuum at 80—100°. After recrystallisation from ethyl acetate, 3.27 g N-benzoylphthalimide with m.p. 167—169° were obtained (mixed m.p. with pure N-benzoylphthalimide undepressed). Yield 68% (calculated on phthalimide employed).

Anal. calculated for : $C_{15}H_9NO_3$; C, 71.71 ; H, 3.58 ; N, 5.57%. Found : C, 72.06 ; H, 5.63 ; N, 5.89%.

In similar conditions, the other N-aroylphthalimides (presented in table 1) were prepared.

REFERENCES

1. A. M. Titherley, *J. Chem. Soc.*, **1906**, 708.
2. C. H. Hurd and M. F. Dull, *J. Amer. Chem. Soc.*, **54**, 2432 (1932).
3. A. J. Mc. Alees and R. Crindle, *J. Chem. Soc.*, (*C*), **1969**, 2425.

4. R. E. Dubar and W. M. Swenson, *J. Org. Chem.*, **23**, 1973 (1958).
5. T. W. Evans and W. M. Dehn, *J. Amer. Chem. Soc.*, **51**, 3651 (1929).
6. H. T. Laronde and C. B. Davis, *J. Org. Chem.*, **35**, 77 (1970).
7. C. Palomo, *Synthesis*, **1981**, 993.
8. P. Oxley and W. F. Short, *J. Chem. Soc.*, **1947**, 382 ; **1948**, 1519.
9. C. D. Hurd and L. Bauer, *J. Amer. Chem. Soc.*, **76**, 2791 (1954).
10. A. Werner and A. Piquet, *Chem Ber.*, **37**, 4295 (1904).
11. J. H. Brewster and C. H. Kucera, *J. Amer. Chem. Soc.*, **77**, 4564 (1955).
12. M. H. Karger and Y. Mazur, *J. Org. Chem.*, **36**, 540 (1971).
13. C. G. Overberger and E. Sarlo, *J. Amer. Chem. Soc.*, **85**, 2448 (1963).
14. C. I. Chiriac, *Rev. Roumaine Chim.*, **26**, 1001 (1981).
15. W. Gerrard and J. A. Cade, *J. Chem. Soc.*, **1954**, 2034.
16. H. O. Becker and K. F. Funk, *J. prakt. Chem*, **14**, 55 (1961).

Revue Roumaine de Chimie, 32, 8, 797–801 (1987)

STUDIES ON PYRIDYL-PYRAZOLONE SYSTEM. II.

SOME REACTIONS WITH 4-ARALIDENE-3-(3′-PYRIDYL)-1-PHENYL-2-PYRAZOLIN-5-ONE

M. F. ABDEL MEGEED, M. EL. BORAI, M. FAHMY * and EL-SAIED A. ALY
Chemistry Department, Faculty of Science, Tanta University, Tanta, Egypt

Received April 20, 1986

4-Arylidene-3(3′-pyridyl)-1-phenyl-2-pyrazolin-5-one (1) reacts with hydrazine to give the benzalazine 2. Also, it undergoes addition reactions with piperidine, morpholine, thiophenol, *p*-thiocresol, nitromethane and nitroethane to give the addition products 3a–d and 4a–b. The Michael reaction of ethyl cyanoacetate and ethyl acetoacetate with 1 gives compounds 5–8 depending on the experimental conditions.

INTRODUCTION

In extension to our studies on the 3,3′-pyridyl-pyrazolone system [1] and keeping in mind their vital importance in biological systems,[2–5] we report here on some reactions of 4-arylidene-3(3′-pyridyl)-1-phenyl-2-pyrazolin-5-one (1).

RESULTS AND DISCUSSION

The reactivity of the exocyclic C=C in the four position of the pirazolone ring is due to conjugation with the adjacent carbonyl group. The reaction of hydrazine with the arylidene derivatives 1 gives the benzalazines 2. This result is in contrast to the results previously reported in the case of 4-arylidene-3-methyl or phenyl-1-phenyl-2-pyrazolin-5-one.[6,7]

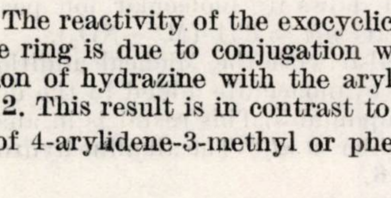

1

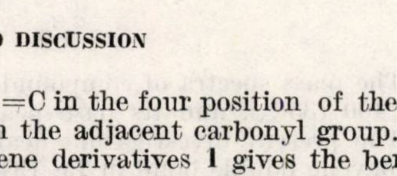

2

	R^1	R^2
a,	OCH_3	OCH_3
b,	H	$-N(C_2H_5)_2$

The structures of compounds **2** were inferred from the analytical data as well as from IR, M.S. and ^1H-NMR spectral analysis. The mass spectral fragmentation pattern of compound **2a** shows its molecular ion peak at $m/e = 328$ (38%); this fragment readily eliminates 31 mass units (corresponding to OCH_3 radical) producing a fragment ion at $m/e = 297$ (45%).

The addition of piperdine, morpholine, thiophenol, and *p*-thiocresol to the olefinic double bond in the four position of compound **1a** gives the corresponding addition products **3a-d**.

3	R
a	$N(CH_2)_5$
b	$N(CH_2CH_2)_2O$
c	SC_6H_5
d	SC_6H_4-CH_3p.

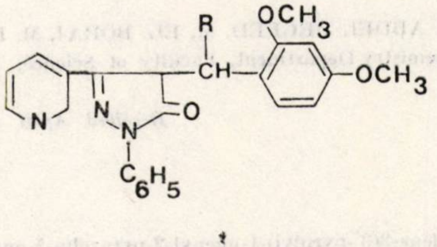

3

The mass spectrum of compound **3c** shows its molecular ion peak at $m/e = 449$ (27%), and its base peak at $m/e = 329$ ($M^+ - C_6H_5SH$).

Also, the nitroalkanes are known to add to the C=C bond in the $\alpha - \beta$ unsaturated compounds in the presence of a basic catalyst;[8-9] in the present case the addition of nitromethane and nitroethane leads to the formation of compounds **4a** and **4b**.

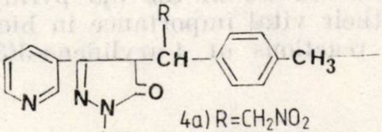

4a) $R=CH_2NO_2$
b) $R=CH_3$-CH-NO_2

The mass spectra of compound **4a** shows its molecular ion peak at $m/e = 400$ (35%), and its base peak at $m/e = 354$ ($M^+ - NO_2$).

The present investigation deals also with the Micheal addition on the exocyclic double bond in **1a**. Ethyl cyanoacetate added to the double bond of compound **1a** affording the compound **5**. This result is in analogy with the previous work reported by Kohler *et al.*[10] The alkaline hydrolysis of **5** gave the corresponding diacid **6**.

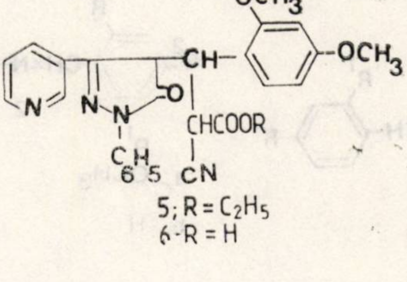

5; $R = C_2H_5$
6-R = H

The mass spectra of compound **6** shows its molecular ion peak at $m/e =$ $= 489$ (14%), and its base peak at $m/e = 445$ ($M^+ - CO_2$).

Also, ethyl acetoacetate reacts with **1a** to give compounds **7** and **8** depending on the basic catalyst as shown in the scheme.

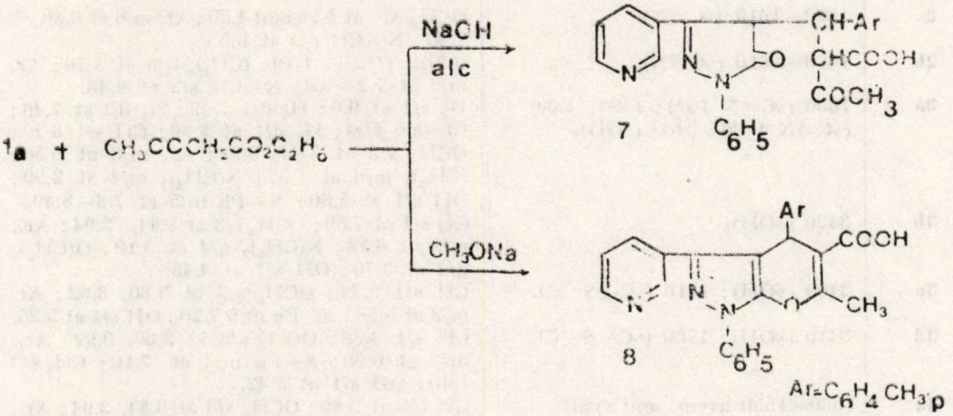

Table 1

Experimental results for compounds **2**, **3**, **4**, **5**, **6**, **7**, and **8**

Comp.	M.P °C Solvent*	Yield % Colour	Mol. Formula	Analysis %				
					C	H	N	S
2a	194	62	$C_{18}H_{29}N_2O_4$	Calcd	65.85	6.09	8.53	
	E	Yellow		Found	65.97	6.22	8.67	
2b	183	68	$C_{22}H_{30}N_4$	Calcd	75.42	8.57	16.00	
	E	Yellow		Found	75.87	8.72	16.23	
3a	208	79	$C_{28}H_{30}N_4O_3$	Calcd	71.48	6.38	11.91	
	B-H(2 : 1)	Colourless		Found	71.01	6.31	11.62	
3b	220	82	$C_{27}H_{28}N_4O_4$	Calcd	68.64	5.93	11.86	
	B-H(2 : 1)	Colourless		Found	68.42	5.63	11.57	
3c	214	58	$C_{29}H_{25}N_3O_3S$	Calcd	70.30	5.05	8.48	6.43
	B-H(2 : 1)	Yellow		Found	70.61	6.19	8.63	6.27
3d	229	63	$C_{30}H_{27}N_3O_3S$	Calcd	70.72	5.30	8.25	6.28
	B-H(2 : 1)	Yellow		Found	70.91	5.47	8.42	6.08
4a	186	62	$C_{24}H_{22}N_4O_5$	Calcd	64.57	4.93	12.56	
	E	Yellow		Found	64.82	5.11	12.67	
4b	198	58	$C_{25}H_{24}N_4O_5$	Calcd	65.22	5.21	12·17	
	E	Yellow		Found	65.44	5.32	12.39	
5	138	71	$C_{28}H_{26}N_4O_5$	Calcd	67.47	5.22	11.24	
	E	Yellow		Found	67.98	5.11	11.74	
6	102	78	$C_{26}H_{23}N_3O_7$	Calcd	63.80	4.70	8.58	
	B-H(1 : 1)	Colourless		Found	63.41	4.92	8.87	
7	229	70	$C_{27}H_{25}N_3O_6$	Calcd	66.53	5.13	8.62	
	M	Yellow		Found	66.92	5.32	8.87	
8	252	64	$C_{27}H_{23}N_3O_5$	Calcd	69.08	4.90	8.96	
	M	Yellow		Found	69.37	5.08	9.07	

* B. Benzene ; E : Ethanol ; H : Hexane ; M : Methanol.

Table 2

Spectroscopic data for compounds **2**, **3**, **4**, **5**, **6**, **7**, and **8**

Comp.	IR data in cm^{-1}	^1H-NMR data in δ ppm
2a	1620–1610 ($\nu C{=}N$).	OCH_3 s/6 at 4.18 and 4.20 ; Ar. m/6 at 6.80 – 7.20 ; N–CH s/2 at 9.55.
2b	1620–1610 ($\nu C{=}N$).	$(CH_3)_4$ t/12 at 1.19 ; $(CH_2)_4$ q/8 at 3.70 ; Ar. m/8 at 7.2–7.8 ; N–CH s/2 at 9.48.
3a	1600 ($\nu C{=}N$ Pz[a]) ; 1590–1580 ($\nu C{=}N$ Py[b]) ; 3400 (νOH).	H_2 s/1 at 9.0 ; H_4 d/1 7.52 ; H_5 d/l at 7.46 ; (J=5.6 Hz) ; H_2 d/1 at 8.90 ; CH s/1 8.20 ; OCH_3 s/3 at 3.84, 3.92 ; Ar. m/3 at 6.50 ; $(CH_2)_3$ m/6 at 1.57 ; $N(CH_2)_2$ m/4 at 2.99 ; OH s/1 at 5.30 ; N–Ph m/5 at 7.8–8.40.
3b	3420 (νOH)	CH s/1 at 7.80 ; OCH_3 s/3 at 3.84, 3.94 ; Ar., m/3 at 6.58 ; $N(CH_2)_2$ q/4 at 3.10 ; $O(CH_2)_2$ q/4 at 3.70 ; OH s/1 at 4.45.
3c	3400 (νOH) ; 1710 ($\nu C{-}S{-}C$).	CH s/1 3.44 ; OCH_3 s/3 at 3.80, 3.92 ; Ar. m/3 at 6.58 ; S–Ph m/5 7.20 ; OH s/1 at 5.25.
3d	3410 (νOH) ; 1700 ($\nu C{-}S{-}C$).	CH s/1 3.58 ; OCH_3 s/3 at 3.80, 3.92 ; Ar., m/3 at 6.60 ; S–Ph m/4 at 7.10 ; CH_3 s/3 1.40 ; OH s/1 at 5.42.
4a	1530–1550 asym. and sym (νNO_2).	CH t/1 at 5.80 ; OCH_3 s/3 at 3.84, 3.94 ; Ar., m/3 at 6.54 ; CH_2 d/2 at 4.24 ; OH s/1 at 5.26.
4b	1530–1550 asym. and sym (νNO_2).	CH t/1 at 5.78 ; OCH_3 s/3 at 3.84, 3.94 ; Ar., m/3 at 6.54 ; CH_2q/2 at 3.82 ; CH_2 t/2 at 4.26 ; OH s/1 at 5.28.
5	1725 ($\nu C{=}O$ ester) ; 3550 (OH)	CH s/1 3.90 ; OCH_3 s/3 at 3.84, 3.94 ; Ar. m/3 at 6.50 ; CH_2 q/2 at 4.35 ; CH_3 t/3 at 1.52 ; OH s/1 5.68.
6	1720–1710 ($\nu C{=}O$ acid) ; 3540 (νOH).	CH s/1 3.92 ; OCH_3 s/3 at 3.84 ; 3.94 ; Ar. m/3 at 6.52 ; OH s/1 5.58.
7	1720–1710 ($\nu C{=}O$ acid) ; 2650 (νOH acid) ; 1690 ($\nu C{=}O$).	CH s/1 at 3.90 ; OCH_3 s/3 at 3.84, 3.94 ; Ar., m/3 6.50 ; CH_3 s/3 2.30 ; OH s/1 5.68.
8	1740 ($\nu C{=}O$ acid) ; 2630 (νOH acid).	OCH_3 s/3 at 3.80, 3.92 ; Ar. m/3 at 6.54 ; CH_3 s/3 at 1.84 ; CH s/1 at 4.82.

a : Pyrazolone ring ; b : Pyridine ring ; s : singlet ; d : doublet ; t : triplet ; q : quadruplet ; m : multiplet.

The mass spectrum of compound **7** shows its molecular ion peak at $m/e = 487$ (27%), and the base peak at $m/e = 443$ ($M^+{-}CO_2$) while compound **8** shows its molecular ion peak at $m/e = 469$ (14%), and its base peak at $m/e = 425$ ($M^+{-}CO_2$).

EXPERIMENTAL

The IR spectra were recorded on a Unicam SP 200G, using KBr Wafer technique, the ^1H-NMR spectra were recorded in $CDCl_3$ with TMS as internal reference with a Jeol C–90 MHz spectrometer. The mass spectra were recorded on a Finnigan 3000 spectrometer operating at 70 eV, with direct inlet and a source of temperature of 90°C. Melting points were taken on a Thomas-Hoover apparatus, and are uncorrected. The usual preparative procedure consisted of diluting the reaction mixture with water, extraction with CH_2Cl_2, drying on $MgSO_4$, removing the solvents under reduced pressure and purification by column chromatography on silica G 60 (Merk). The starting compound **1** was prepared according to the method previously reported by El Borai *et al.*[1] The experimental results are grouped in Table 1.

Reaction of **1** *with hydrazine. Formation of* **2**.

A mixture of 1.9 g (0.005 mole) of **1**, and 0.5 g hydrazine hydrate in 50 mL ethanol was refluxed for 4 hr. The reaction mixture was concentrated to half volume and diluted with water. The separated solid was filtered, and dried.

Reaction of **1a** *with piperdine morpholine, thiophenol and p-thiocresol.*

A solution of 1.9 g (0.005 mole) of **1a** and (0.005 mole) of the appropriate reagent dissolved in 30 mL dry benzene was stirred for one hour and allowed to stand overnight at room temperature. The coloured solution faded gradually, light petroleum ether was added, the formed solid was filtered off, and purified by column chromatography using CH_2Cl_2 — hexane (2 : 1) as eluent.

Reaction of **1a** *with nitroalkanes. Formation of* **4a** *and* **4b**.

A mixture of 1.9 g (0.005 mole) of **1a** and (0.01 mole) of the appropriate nitroalkane in 30 mL ethanol was treated at 0°C with a solution of (0.005 mole) sodium ethoxide in ethanol. The reaction mixture was stirred for 30 minutes, then poured on ice/water, acidified with dilute acetic acid and worked-up as usual. The product was purified by column chromatography using CH_2Cl_2-hexane (2 : 1) as eluent.

Reaction of **1a** *with ethyl cyanoacetate. Formation of* **5**.

A mixture of 1.9 g (0.005 mole) of **1a**, ethyl cyanoacetate (0.01 mole) and few drops of piperdine in 50 mL dry chloroform was refluxed for 4 hr. The solvent was evaporated under reduced pressure and worked-up as usual. The product was purified by column chromatography using CH_2Cl_2-hexane (3 : 1) as eluent.

Alkaline hydrolysis of **5**. *Formation of* **6**.

Compound **5** was hydrolysed by shaking 1.9 g (0.005 mole) with 20 mL 10% methanolic potassium hydroxide solution for one hour. The reaction mixture was left overnight at room temperature. The alkaline solution was diluted with water and acidified with dilute H_2SO_4. The formed solid was filtered off, washed with water and dried.

Reaction of **1a** *with ethyl acetoacetate. Formation of* **7**.

A mixture of 1.9 g (0.005 mole) of **1a** and 2 mL ethyl acetoacetate in 20 mL ethanol was added dropwise to 5 mL of a 10% sodium hydroxide solution, the mixture was stirred at room temperature for 24 hr. The reaction mixture was poured into 5 mL 5% HCl. The formed solid was filtered, washed with water and dried.

Reaction of **1a** *with ethylacetoacetate. Formation of* **8**.

A mixture of 1.9 g (0.005 mole) of **1a** and 2 mL ethyl acetoacetate and (0.01 mole) of sodium methoxide in methanol was refluxed for 3 hr. The solvent was evaporated under reduced pressure, acidified at 0°C with 2N HCl and worked-up as usual. The product was purified by column chromatography using CH_2Cl_2 as eluent.

REFERENCES

1. A. Sammour, T. Zimaity, and M. El. Borai, *J. prakt. Chem.*, **314**, 612 (1972).
2. S. G. Farid Soliman and R. M. Shafik, *Pharmazie*, **30**, 436 (1975).
3. S. P. Suman and S. C. Bahel, *J. Indian. Chem. Soc.*, **56**, 374 (1979).
4. H. Hoffman and I. Hamman, *Ger. Offen*; 2, 420, 360 (1973); cf. Chem. Abstr., **84**, 44043 (1976).
5. M. Wolf and J. F. Donald, *U. S. pat.*, 3, 190, 888 (1965); cf. *Chem. Abstr.*, **63**, 9951 (1965).
6. El-Sayed Afsah, F. A. Amer, M. Soafan, *Z. Naturforsch*, **35b**, 1313 (1980).
7. A. Sammour, A. Abd-El Raouf, M. El-Kasaby and M. A. Hasses, *Egypt. J. Chem.*, **15**, 429 (1972).
8. E. P. Kohler, *J. Amer. Chem. Soc.*, **46**, 503 (1924).
9. H. J. Bacher, W. Meijer, and W. Derivs, *Rec. Trav. Chem.*, **54**, 82 (1926).
10. E. P. Kohler, *J. Amer. Chem. Soc.*, **38**, 869 (1916).

Revue Roumaine de Chimie, **32**, *8*, 803–806 (1987)

ORGANOCHLORINE (OCl) PESTICIDE RESIDUES IN HUMAN FATS. PART I

OLCAY ANAÇ and KERIMAN GÜNAYDIN
Faculty of Science, Department of Chemistry
Technical University of Istanbul, Turkey

Received June 16, 1986

In this study, six samples of human fat tissue from Turkey were analyzed by glass capillary gas chromatography for chlorinated pesticides. Only two groups of pesticides, DDT and its derivatives, and chlordan were regularly found. Lindane, heptachlor, aldrin and endrin could not be found in any samples.

INTRODUCTION

As known, organochlorine pesticides are relatively inert to chemical attack and, being sparingly soluble in aqueous media, are not, in any case, readily available to microbial degradation. On the other hand, their solubility in fats results in their frequent absorption by plants and animal and their storage, chemically unchanged, for long periods of time.[1]

With the assistance of the examinations of pesticide residues in foodstuffs, some tolerances and restrictions on import, sale and application were accepted.[2,3]

Some of the important persistent organochlorine pesticides are DDT, DDE (normal metabolite of DDT in body tissues), Lindane, Chlordan, Heptachlor, Aldrin, Dieldrin, and Endrin.

The use of most of the chlorinated pesticides has been prohibited in some countries like West Germany, Sweden, Great Britain etc.[4,5]

The amounts of OCl pesticides used in Turkey between 1981–1983 are listed in Table 1.[6]

Table 1

Chlorinated pesticides used in Turkey

Year	OCl pesticides (ton)	Total pesticides (ton)	% Percentage of OCl pesticides
1981	9.966,0	33.695,4	29.5767
1982	8.641,9	26.586.2	23.6206
1983	5.865,1	43.245,5	13.5623

More than 30 studies have been made on the pesticide residues in foodstuffs of Turkey by Güvener.[7] But there is no study about OCl insecticides in the body fat of Turkish people.

As known, Gas Chromatography continues to be the most satisfactory procedure for the separation, identification, and quantitation of pesticide residues. The previous problems such as decomposition by metallic construction and stationary phase supports of columns have been solved by using glass capillary GC in case of chlorinated pesticides.[8] The capillary columns with suitable stationary phases and F.I.D. give good separations at nanogram levels.[9,10]

Table 2

The samples of human fats

Sample No	Sex	Age
1	F	39
2	M	25
3	F	60
4	F	45
5	F	45
6	F	30

EXPERIMENTAL

The six samples of human fat reported here have been obtained from Medical Faculty of Istanbul University (Table 2).

About 2 g of samples were extracted according to the procedure of Hoffman and co-workers.[11] Extracts were cleaned-up on Florisil topped with a layer of anhydrous sodium sulfate eluted by hexane containing 12 per cent ethyl ether. The effluent was concentrated to 5 mL then transferred to a centrifuge tube with small hexane washings, and evaporated to 0.5 mL. Then 0.1 mL of xylene was added, and the mixture concentrated to exactly 0.1 mL.

Recoveries were calculated by adding known amounts of pesticides to a sample of fat (No : 2) proved by previous analysis not to contain the pesticide and carrying the fat sample through the whole clean-up. The recoveries were changed from 0.75 to 0.88.

Gas Chromatographic Studies :
Apparatus : Shimadzu 5A (F.I.D.)
Capillary Column : Type WCOT, 20 m.L., 0.25 mm. I.D. (SUS Glass)
Liquid Phase : PEG-20 M
Temperature Programme : 5′ isothermal at 190°C,
190°→230° at 5°/min heating rate, isothermal at 230°.
Detector Temperature : Injector Temperature : 250°C
Carrier Gas : 1 mL/min
Scavenger Rate : 50 mL/min
H_2 : 55 mL/min
Air : 0.9 kg/cm^2
Range : 0.16 V
Sensitivity : 10^3 MΩ
Chart Speed : 5 mm/min
Integrator : ITG—4A

The standard pesticide chemicals from Fluka, Supelco and Pestanal were used as purchased.

Relative detector response factors were determined by analyzing the standard solutions having known amounts of pure standards at ppm levels. *o,p′*-DDT and *o,p′*-DDE were also added to standard solutions as *o,p′*-DDT which was present in commercial *p,p′*-DDT could be metabolized to *o,p′*-DDE. An example of chromatograms is illustrated in Figure 1.

The analyses of these six samples are presented in Table 3.

Table 3

Concentrations of chlorinated hydrocarbon pesticides in the body fat of people in Turkey (mg/kg)

Sample No	Age	Chlordan	*o,p′*-DDE	*p,p′*-DDE	*o,p′*-DDE	*p,p′*-DDT	Total DDT
1	39	—	2.66	—	9.28	18.25	30.19
2	25	—	—	—	—	—	—
3	60	—	51.84	70.81	241.84	—	364.49
4	45	34.3	11.64	—	90.13	—	101.77
5	45	41.29	15.11	—	67.57	—	83.68
6	30	38.26	0.597	—	11.09	3.62	15.30

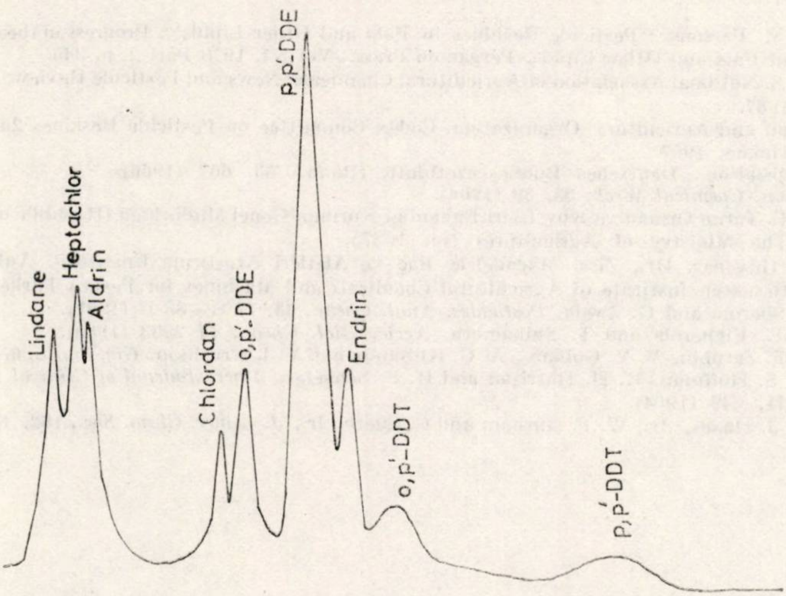

Fig. 1 GC of Some of the OCl Pesticides

RESULTS AND DISCUSSION

Under the presented condition of GC a satisfactory resolution could be achieved for the analysis of OCl pesticide.

Residues could not be found in the sample having number two, which is the youngest among the investigated samples. An increase in amount of total DDT, according to the ages, could be seen. In the samples 3, 4, 5 the values of total DDT were significantly higher than the moderate limits of 30.2—1.75 mg/kg although there are some exceptional values such as 1131 mg/kg.[11,12]

As can be seen from Table 3, lindane, heptachlor, aldrin, and endrin could not be found in any samples, but chlordan was detected in three of them.

To identify the storage of OCl pesticides in body fat of people in Turkey with environmental, occupational, or other special exposure to insecticides we are planning to continue our study and publish the findings in a future paper.

ACKNOWLEDGEMENT. The authors are grateful to Prof. A. Uras, from Medical Faculty of Istanbul University and N. Mumcuoğlu, from Unilever-Iş for their kind interest and providing fat samples and some standard chemicals.

REFERENCES

1. A. M. Parsons, "Pesticide Residues in Fats and Other Lipids", Progress in the Chemistry of Fats and Other Lipids, Pergamon Press. Vol XI, 1970 Part 2, p. 245.
2. U. S. National Association of Agricultural Chemicals, News and Pesticide Review, February, 1967.
3. Food and Agriculture Organization, Codex Committee on Pesticide Residues 2nd Session, Hague, 1967.
4. Legislation : Deutsches Bundesgezetblatt, (Bonn,) **53**, 667 (1966).
5. Anon. *Chemical Week*, **95**, 59 (1964).
6. T. C. Tarim Orman ve Köy Işleri Bakanliği Koruma Genel Müdürlüğü (Republic of Turkey, The Ministry of Agriculture) No. 16275.
7. A. Güvener, Dr., Zirai Mücadelele Ilaç ve Aletleri Araştırma Enstitüsü, Ankara (The Research Institute of Agricultural Chemicals and Machines for Pests.) Turkey.
8. J. Sherma and G. Zweig, *Pesticides, Anal. Chem.*, **53**, 77 R—88 R (1981).
9. F. E. Figuerola and T. Shibamotu, *Agric. Biol. Chem.*, **47** 2933 (1983).
10. G. P. Zarubin, V. Y. Golikov, A. G. Khromov and V. I. Krushkin, *Gig. Sanit.*, **6**, 78 (1983).
11. W. S. Hoffman, R. H. Harrison and R. F. Schaefer, *Amer. Journal of Clinical Pathology*, **41**, 649 (1964).
12. W. J. Haxes, Jr., W. P. Durham and C. Cueto, Jr., *J. Amer. Chem. Soc.*, **162**, 890 (1956).

Revue Roumaine de Chimie, **32**, *8*, 807–819 (1987)

SÉCHAGE D'UN GRAIN POREUX SPHÉRIQUE

R. Z. TUDOSE et H. KADI
Institut polytechnique, Faculté de technologie chimique, 228, rue 23 August,
Iași, Roumanie

Reçu le 14 avril 1986

Une théorie permettant le calcul de la distribution de l'humidité, du temps et de la vitesse de séchage d'un grain sphérique a été mise au point. Dans cette théorie, on considère que le mécanisme essentiel du processus de séchage est basé sur la migration de l'humidité à l'état liquide dans le matériau.
On a étudié l'évolution de la vitesse de séchage d'un grain poreux et l'influence que peuvent avoir sur cette vitesse de séchage : la porosité du matériau, la température et la vitesse de l'air. Les résultats théoriques sont vérifiés par l'expérience.

A model for the calculation of the humidity distribution, time and drying rate of a spherical grain is proposed. In this theory the essential mechanism of the drying process is based on the humidity migration in liquid state in material. The influence of the material porosity, temperature and air flow-rate are also considered. The theoretical results are checked up experimentally.

1. INTRODUCTION

Le processus de séchage d'un matériau présente une période à vitesse constante et une ou deux périodes à vitesse décroissante. La détermination de l'allure de séchage dans la période à vitesse constante ne présente pas de difficulté grâce à des simplifications du phénomène. Par contre, la période du ralentissement de la vitesse est beaucoup plus complexe. Plusieurs chercheurs [1,2] ont essayé d'expliquer la mécanisme et d'établir les relations permettant le calcul de la vitesse de séchage et de la distribution de l'humidité dans le matériau. Certains auteurs ont tenté de faire un modèle en considérant que le mécanisme essentiel du séchage est basé sur la migration de l'humidité à l'état liquide dans le matériau.

L'épaisseur de la zone de migration de l'humidité dépend de la vitesse de migration de l'humidité et de la vitesse de séchage, c'est-à-dire du rapport D_l/UR. À l'épaisseur r_m de cette zone, on fait correspondre trois modèles de séchage :

- modèle avec une zone limite de migration d'humidité quand $0 < (r_m/R) < 1$;
- modèle avec une zone complète de migration d'humidité quand $(r_m/R) = 1$;
- modèle sans zone de migration d'humidité quand $(r_m/R) = 0$.

2. MODÈLE AVEC UNE ZONE COMPLÈTE DE MIGRATION DE L'HUMIDITÉ

Dans ce cas, la courbe de la vitesse de séchage ne présente que deux périodes. L'évaporation se fait d'abord à vitesse constante à partir de la surface extérieure du matériau, la migration de l'humidité se faisant sur toute l'épaisseur du matériau vers la surface où a lieu l'évaporation, c'est-à-dire que dans le matériau, il existe une seule zone, la zone de migration de l'humidité. La vitesse de séchage demeure constante tant que l'humidité à la surface du matériau est supérieure à l'humidité d'équilibre.

Dans la seconde étape de séchage, la surface d'évaporation se déplace vers l'intérieur du matériau. La vitesse de séchage diminue de façon continue puisqu'à la résistance de la couche limite vient s'ajouter la résistance à la diffusion des vapeurs d'eau à travers la zone séchée. Dans le matériau, il existe deux zones : la zone séchée à l'extérieur et la zone humide à l'intérieur (fig. 1). L'épaisseur de la zone séchée augmente avec le temps de séchage.

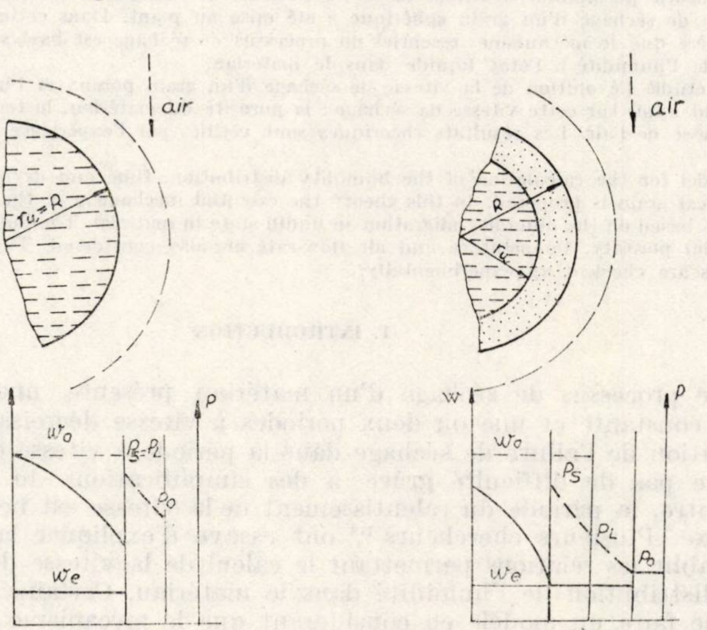

Fig. 1. — Modèle avec une zone complète de migration de l'humidité.

3. MODÈLE AVEC UNE ZONE LIMITE DE MIGRATION DE L'HUMIDITÉ

Ce modèle présente toutes les étapes de séchage. Le procédé commence à partir de la surface qui est directement en contact avec l'agent thermique. L'évaporation de l'humidité conduit à un gradient de concentration qui fait migrer l'humidité à l'état liquide. La vitesse de séchage dépend des phénomènes d'humectation et de capillarité.

Tant que l'humidité à la surface extérieure du matériau est supérieure à l'humidité d'équilibre, la vitesse de séchage demeure constante. Dans cette première étape, il existe deux zones dans le matériau : une zone à humidité initiale et une zone de migration de l'humidité. Quand l'humidité à la surface devient égale à l'humidité d'équilibre, la pression de vapeur à la surface diminue : c'est la fin de la première étape (fig. 2).

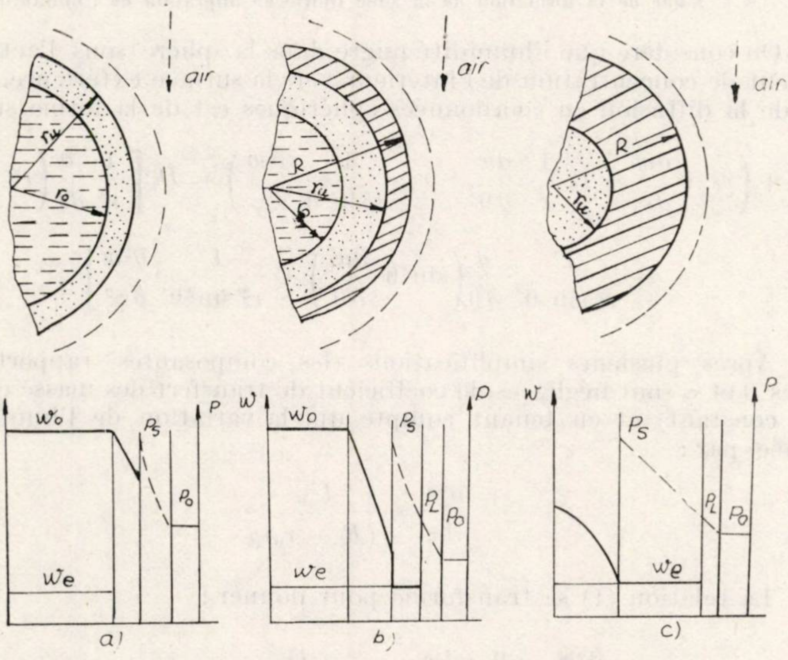

Fig. 2. — Modèle avec une zone limite de la migration de l'humidité.

Dans la seconde étape, la surface d'évaporation se déplace vers l'intérieur du matériau. La vitesse de séchage diminue puisqu'à la résistance de la couche limite vient s'ajouter la résistance à la diffusion qui devient de plus en plus grande : c'est la première période du ralentissement de la vitesse de séchage. Dans le matériau, il y a alors trois zones : une zone séchée à l'extérieur, une zone de migration de l'humidité et une zone à humidité initiale tout à fait à l'intérieur (fig. 2). La fin de cette étape de séchage se manifeste par la disparition de la dernière zone.

Dans la dernière étape, il n'existe dans le matériau que la zone séchée à l'extérieur et la zone de migration à l'intérieur. La vitesse de séchage décroît plus rapidement que dans le second stade puisque l'humidité liquide migre moins rapidement. La surface d'évaporation se déplace à une vitese plus grande vers l'intérieur, ce qui augmente l'épaisseur de la zone séchée, voire la résistance à la diffusion des vapeurs formés à la surface d'évaporation. Le procédé de séchage prend fin quand l'humidité est partout égale à l'humidité d'équilibre.

4. ÉQUATIONS DE LA VITESSE ET DU TEMPS DE SÉCHAGE

Conformément au modèle avec une zone limite de migration de l'humidité, le séchage d'un matériau se fait en trois étapes. Nous présentons dans ce travail les équations permettant le calcul de la vitesse et du temps de séchage quand le matériau à sécher est de forme sphérique.

4.1. Stade de la formation de la zone limite de migration de l'humidité

On considère que l'humidité migre dans la sphère sous l'action d'un gradient de concentration de l'intérieur vers la surface extérieure. L'équation de la diffusion en coordonnées sphériques est de la forme suivante :

$$\frac{\partial w}{\partial \tau} + \left(v_r + \frac{\partial w}{\partial r} + v_\theta \frac{1}{r} \cdot \frac{\partial w}{\partial \theta} + v_\varphi \frac{1}{r \sin \theta} \frac{\partial w}{\partial \varphi} \right) = D_l \left[\frac{1}{r^2} \frac{\partial}{\partial r} \left(r^2 \frac{\partial w}{\partial r} \right) + \right.$$

$$\left. + \frac{1}{r^2 \sin \theta} \cdot \frac{\partial}{\partial \theta} \left(\sin \theta \frac{\partial w}{\partial \theta} \right) + \frac{1}{r^2 \sin^2 \theta} \cdot \frac{\partial^2 w}{\partial \varphi^2} \right] \tag{1}$$

Après plusieurs simplifications (les composantes rapportées aux angles θ et φ sont négligées, le coefficient de transfert des masse est considéré constant) et en tenant compte que la variation de l'humidité est donnée par :

$$- \frac{\partial w}{\partial \tau} = \frac{U_M}{(R - r_0) \rho} \tag{2}$$

La relation (1) se transforme pour donner :

$$\frac{\mathrm{d}^2 w}{\mathrm{d} r^2} + \frac{2}{r} \cdot \frac{\mathrm{d} w}{\mathrm{d} r} + \frac{U_M}{D_l (R - r_0) \rho} = 0 \tag{3}$$

qui aura pour solution :

$$w = \frac{C_1}{r} + \frac{U_M}{6 D_l (R - r_0) \rho} r^2 + C_2 \tag{4}$$

Dans cette première étape, la vitesse de séchage est constante et les conditions aux limites sont :

$$\left. \begin{aligned} \frac{\mathrm{d} w}{\mathrm{d} r} &= 0 \text{ pour } r = r_0 \\ w &= w \text{ pour } r = R \end{aligned} \right. \tag{5}$$

La solution de l'équation sera donc :

$$w = w_1 + \frac{U_M}{3 D_l (R - r_0) \rho} \left[r_0^3 \left(\frac{1}{R} - \frac{1}{r} \right) + \frac{1}{2} (R^2 - r^2) \right] \tag{6}$$

L'humidité moyenne du matériau durant la première étape sera déterminée à partir de l'équation suivante :

$$w_1 = \frac{w_0 r_0 + \int_{r_0}^{R} w \,\mathrm{d}r}{R} \tag{7}$$

On trouve :

$$w_1 = w_0 + \frac{U_M}{3D_l(R - r_0)\rho} \frac{r_0^3}{R} \ln \frac{r_0}{R} - \frac{U_M}{18D_l(R - r_0)\rho} \cdot \frac{R^3 - r^3}{R} + \frac{U_M}{2D_1 \rho} \cdot \frac{r_0^2}{R} \tag{8}$$

La première humidité critique peut être calculée à partir de l'équation (7) où on utilise, pour la distribution de l'humidité l'équation (8) ou $w_i = w_e$:

$$w_{\mathrm{cr}1} = w_e + (w_0 - w_e) \frac{r_0}{R} + \frac{U_M}{3D_l \rho} \frac{r_0^3}{R(R - r_0)} \mathrm{lu} \frac{r_0}{R} - \frac{U_M}{18D_1 \rho} \cdot \frac{R^3 - r^3}{R(R - r_0)} + \frac{U_M}{6D_l \rho} \cdot \frac{R^3 + 2r^3}{R^2} \tag{9}$$

On détermine le temps de séchage dans la première étape en considérant l'équation suivante :

$$\mathrm{d}\tau = - \frac{\rho}{U_M} (R - r_0) \,\mathrm{d}w \tag{10}$$

En utilisant l'équation de la distribution de l'humidité, on trouve le temps total de séchage :

$$\tau_{1t} = \frac{r_0^3}{3D_l} \left(\frac{1}{R_1} - \frac{1}{r_0} \right) + \frac{1}{6D_l} (R^2 - r_0^2) \tag{11}$$

4.2. Stade du déplacement de la zone de migration de l'humidité

L'équation de la vitesse de séchage dans la période du ralentissement se détermine en utilisant la loi de Fick et la distribution de la pression de vapeur de l'eau à travers la zone séchée du matériau qui est donnée par la relation suivante :

$$\frac{\partial p}{\partial \tau} = D_v \frac{\partial^2 p}{\partial r^2} \tag{12}$$

A l'aide des conditions limites :

$$\begin{aligned} - D_v \frac{\mathrm{d}p}{\mathrm{d}r} &= k_g(p - p_g) \quad \text{pour} \quad r = R \\ p &= p_v \qquad\qquad\quad \text{pour} \quad r = r_u \end{aligned} \tag{13}$$

on obtiendrait :

$$p = p_v - \frac{k_g(p_v - p_g)}{D_v + k_g(R - r_u)}(r - r_u) \tag{14}$$

L'expression de la vitesse de séchage dans la période de ralentissement est obtenue en combinant les équations (14) et $U = -(D_v/RT)(\mathrm{d}p/\mathrm{d}\tau)$:

$$U = \frac{U_M}{1 + \frac{k_g}{D_v}(R - r_u)} \tag{15}$$

La variation de l'humidité avec la temps est donnée par la relation suivante :

$$-\frac{\partial w}{\partial \tau} = \frac{U}{(r_u - r_0)\rho} \tag{16}$$

L'équation permettant le calcul de la distribution de l'humidité est déterminée en combinant les équations (1), après simplifications, et (16) :

$$\frac{\mathrm{d}^2 w}{\mathrm{d}r^2} + \frac{2}{r}\frac{\mathrm{d}w}{\mathrm{d}r} + \frac{U_M}{1 + \frac{k_g}{D_v}(R - r_u)} \cdot \frac{r^2}{D_1 \rho (r_u - r_0)} = 0 \tag{17}$$

Avec les conditions aux limites suivantes :

$$\begin{aligned} w &= w_e \qquad \text{pour } r = r_u \\ w &= w_0 \qquad \text{pour } r = r_0 \end{aligned} \tag{18}$$

on obtient la distribution de l'humidité dans la zone de migration :

$$\begin{aligned} w = w_0 &+ \frac{U_M}{6\left[1 + \frac{k_g}{D_v}(R - r_u)\right]} \cdot \frac{r_0 r_u}{D_l\, \rho(r_0 - r_u)} \left[\frac{r_0 + r_u}{r} - \frac{r_0 + r_u}{r_0}\right] - \\ &- \frac{U_M}{6\left[1 + \frac{k_g}{D_v}(R - r_u)\right]} \cdot \frac{r^2 - r_0^2}{r_u - r_0} + (w_0 - w_e)\frac{r_u r_0}{r_0 - r_u}\left[\frac{1}{r_0} - \frac{1}{r}\right] \end{aligned} \tag{19}$$

L'humidité moyenne w_2 sera évoluée grâce à l'équation suivante :

$$w_2 = \frac{w_0 r_0 + \int_{r_0}^{r_u} w \,\mathrm{d}r + w_e(R - r_u)}{R} \tag{20}$$

Avec l'équation (19), on obtient :

$$w_2 = w_0 - (w_0 - w_c)\frac{1}{R}\frac{r_0 r_u}{r_0 - r_u}\ln\frac{r_u}{r_0} +$$

$$\frac{U_M}{6D_l\rho\left[1 + \frac{k_g R}{D_v}\left(1 - \frac{r_u}{R}\right)\right]R}\left[\frac{r_0 r_u}{r_0 - r_u}(r_0 - r_u)\ln\frac{r_u}{r_0} + r_u(r_0 + r_u) + r_0^2\right] -$$

$$-\frac{U_M}{18D_l\rho\left[1 - \frac{k_g R}{D_v}\left(1 - \frac{r_v}{R}\right)\right]R}\frac{r_u^3 - r_0^3}{r_u - r_0} \tag{21}$$

La seconde humidité critique est déterminée en considérant $r_0 = 0$:

$$w_{cr2} = w_0 + \frac{U_M}{9\left[1 + \frac{k_g}{D_v}(R - r_u)\right]}\frac{r_u^2}{D_l\rho R} \tag{22}$$

Le temps total de séchage sera :

$$\tau_{2t} = \frac{1}{6D_l}R^2 + \frac{(w_0 - w_c)}{U_M}\left[1 + \frac{k_g}{D_v}(R - r_0)\right]r_u \tag{23}$$

4.3. Stade de la disparition de la zone de migration de l'humidité

La distribution de la pression partielle de vapeur de l'eau à travers la zone séchée est donnée par la relation (14) et la vitesse de séchage, dans la troisième étape, par la relation (15). En combinant l'équation de la distribution de l'humidité (1) par le relation suivante :

$$-\frac{\partial w}{\partial \tau} = \frac{U_M}{1 + \frac{k_g}{D_v}(R - r_u)}\frac{1}{\rho r_u} \tag{24}$$

nous aboutissons à l'équation différentielle suivante :

$$\frac{\mathrm{d}^2 w}{\mathrm{d}r^2} + \frac{2}{r}\frac{\mathrm{d}w}{\mathrm{d}r} + \frac{U_M}{1 + \frac{k_g}{D_v}(R - r_u)}\cdot\frac{1}{D_l\rho r_u} = 0 \tag{25}$$

Avec les conditions limites suivantes :

$$\begin{aligned} w &= w_c \qquad \text{pour } r = r_u \\ \frac{\mathrm{d}w}{\mathrm{d}r} &= 0 \qquad \text{pour } r = 0 \end{aligned} \tag{26}$$

on trouve :

$$w = w_e + \frac{U_M}{6\left[1 + \frac{k_g}{D_v}(R - r_u)\right]} \frac{r_u^2 - r^2}{D_l \rho\, r_u} \tag{27}$$

L'humidité moyenne dans cette troisième étape se calcule à l'aide de la relation :

$$w_3 = \frac{\int_0^{r_u} w \,\mathrm{d}r + w_e(R - r_u)}{R} \tag{28}$$

On trouve :

$$w_3 = w_e + \frac{U_M}{9\left[1 + \frac{k_g}{D_v}(R - r_u)\right]} \cdot \frac{r_u^2}{D_l \rho R} \tag{29}$$

Le temps de séchage dans la dernière étape se détermine à partir de l'équation (23) :

$$\tau_3 = \frac{1}{6\,D_l}(R^2 - r^2) + \frac{(w_0 - w_e)\rho}{U_M}\left[1 + \frac{k_g}{D_v}(R - r_u)\right] r_u \tag{30}$$

5. RÉSULTATS EXPÉRIMENTAUX

Une sphère en matériau poreux est soumise à un écoulement d'air chaud (fig. 3) dont on fait varier la température et la vitesse. Les figures (3) et (4) représentent l'effet de ces paramètres sur la vitesse de séchage. La figure (5) donne l'influence de la porosité sur l'allure du séchage.

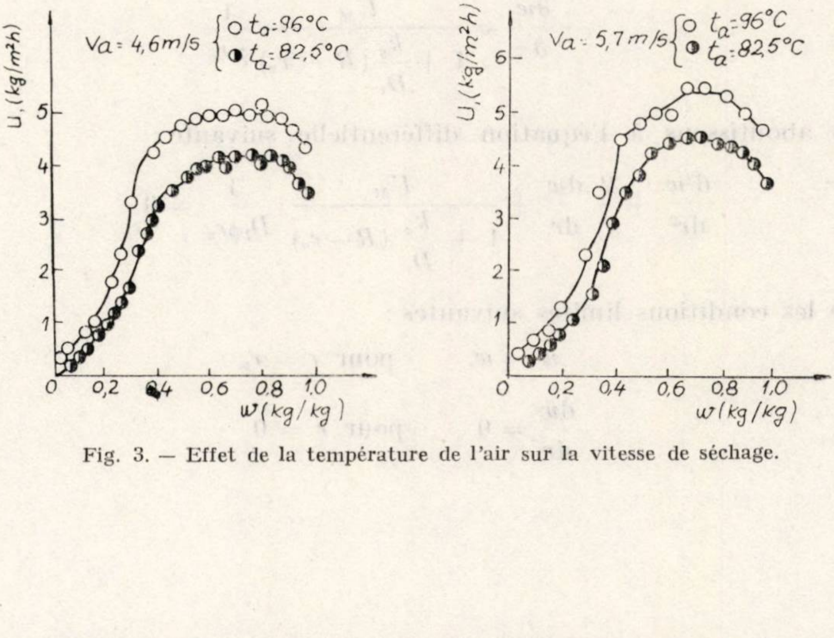

Fig. 3. — Effet de la température de l'air sur la vitesse de séchage.

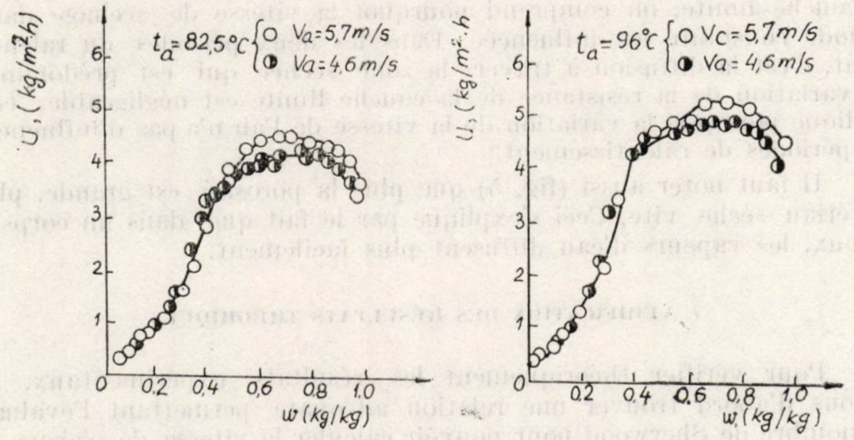

Fig. 4. — Effet de la vitesse de l'air sur la vitesse de séchage.

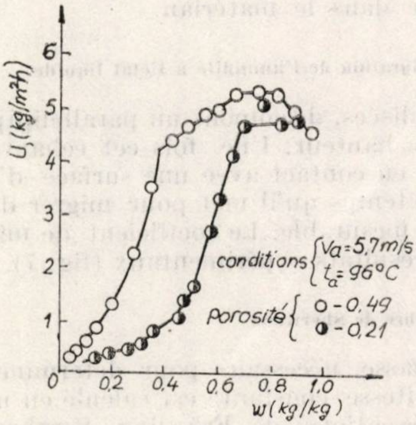

Fig. 5. — Effet de la porosité sur la vitesse de séchage.

6. INTERPRÉTATION DES RÉSULTATS EXPÉRIMENTAUX

On constate que la vitesse de séchage croît avec la température de l'air (fig. 3). L'effet de cette dernière est sensible même sur les deux périodes à vitesse de séchage décroissante. Cela est dû au fait que la variation de la température de l'air modifie les coefficients de transfert de masse (k_g) et de migration de l'humidité à l'état liquide (D_l) et a une influence sur la température de la sphère.

On note d'après la figure (4) que la vitesse de séchage augmente aussi avec la vitesse de l'air. L'effet de cette dernière se fait ressentir sur la période à vitesse constante et à un degré moindre sur la première période du ralentissement de la vitesse. La vitesse de l'air n'a pratiquement pas d'influence sur la dernière période. L'explication pourrait être la suivante : dans la période à vitesse constante, la diffusion à travers la couche limite est déterminante. Comme la variation de la vitesse modifie la couche limite, on comprend pourquoi la vitesse de séchage dans la période constante est influencée. Dans les deux périodes du ralentissement, c'est la diffusion à travers la zone séchée qui est prédominante. La variation de la résistance de la couche limite est négligeable, ce qui explique pourquoi la variation de la vitesse de l'air n'a pas d'influence sur les périodes de ralentissement.

Il faut noter aussi (fig. 5) que plus la porosité est grande, plus le matériau sèche vite. Ceci s'explique par le fait que dans un corps plus poreux, les vapeurs d'eau diffusent plus facilement.

7. VÉRIFICATION DES RÉSULTATS THÉORIQUES

Pour vérifier théoriquement les résultats expérimentaux, nous devons d'abord trouver une relation adéquate permettant l'évaluation du nombre de Sherwood pour pouvoir calculer la vitesse de séchage dans la période constante. Dans les périodes de ralentissement, nous pouvons utiliser soit le coefficient de diffusion des vapeurs (4), soit celui de la migration de l'humidité à l'état liquide dans le matériau.

7.1. Détermination du coefficient de migration de l'humidité à l'état liquide

De l'une des sphères poreuses utilisées, découpons un parallélipipède que nous graduons dans le sens de la hauteur. Une fois cet échantillon complètement séché, mettons sa base en contact avec une surface d'eau. Le liquide humidifie le matériau et le temps qu'il met pour migrer d'une graduation à une autre est facilement mesurable. Le coefficient de migration de l'humidité est calculé par les résultats expérimentaux (fig. 7).

7.2. Calcul du nombre de Sherwood

Le coefficient de transfert de masse, nécessaire pour déterminer la vitesse de séchage dans la période à vitesse constante est calculé en utilisant le nombre de Sherwood. Les équations de Frössling, Serghev et Nesterenko (5) ne donnent pas un nombre de Sherwood correspondant à la valeur expérimentale. Nos expériences nous ont permis de proposer l'équation suivante :

$$\mathrm{Sh} = -0{,}217 + 0{,}504\, Re^{0.244} Sc^{0.701}$$

dans le domaine expérimental $10.000 \leqslant \mathrm{Re} \leqslant 14.000$

7.3. Calcul de la vitesse dans la période de ralentissement

La vitesse de séchage dans la période de ralentissement peut être évaluée en utilisant :

a) le coefficient de diffusion déterminé en utilisant les résultats expérimentaux (fig. 6) ;

b) le coefficient de migration de l'humidité à l'état liquide dans le matériau (fig. 7).

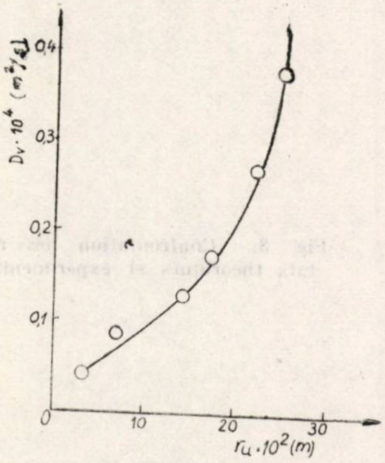

Fig. 6. — Coefficient de diffusion en fonction du rayon r_u.

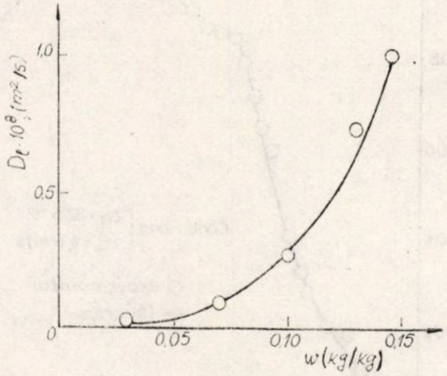

Fig. 7. — Coefficient de migration de l'humidité à l'état liquide en fonction de l'humidité w.

Notons que le rayon de la surface d'évaporation est donné par la relation suivante :

$$\frac{r_u}{R} = \left(\frac{w}{w_{cr}}\right)^{1/n}$$

ou $n = 3$, $w_{er} = w_{cr1}$ pour la première du ralentissement et

$n = 1$, $w_{cr} = w_{cr2}$ pour la seconde.

7.4. Comparaison des résultats théoriques et expérimentaux

La courbe théorique de la vitesse de séchage a été vérifiée expérimentalement (fig. 8) pour :

— toutes les périodes de séchage en utilisant le coefficient de diffusion des vapeurs ;

— seulement la dernière période en utilisant le coefficient de migration de l'humidité liquide dans le matériau. Les calculs sont faits à l'aide de l'équation (27).

CONCLUSIONS

Nous avons constaté que l'allure de séchage augmente avec la vitesse et la température de l'agent thermique ainsi qu'avec la porosité du matériau.

Dans la période à vitesse de séchage constante, la diffusion à travers la couche limite est déterminante. La vitesse de l'air, ne faisant varier que la structure de la couche limite n'influence que cette période.

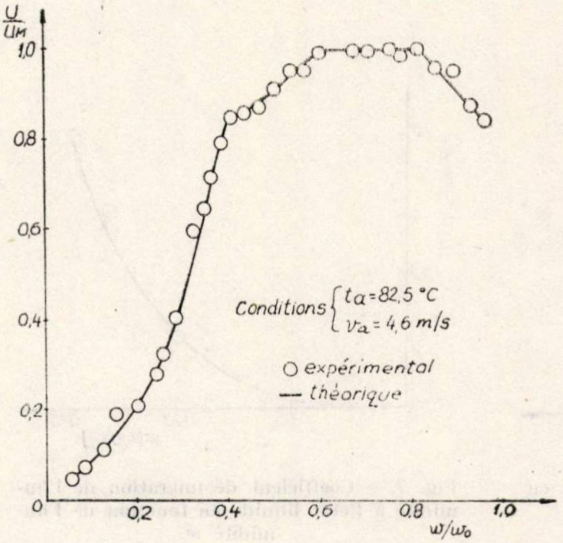

Fig. 8. — Confrontation des résultats théoriques et expérimentaux

La température de l'air modifie les coefficients de transfert de masse, de migration de l'humidité à l'état liquide et la température de la sphère. Elle a donc une influence sur presque tous les paramètres qui régissent le phénomène de séchage, d'ou son influence sur toutes les périodes de la vitesse de séchage.

Les équations de Frössling, de Serghev et de Nesterenko n'offrent pas un nombre de Sherwood correspondant à celui de nos expériences. Conformément à ces dernières, nous proposons une nouvelle relation.

La courbe de la vitesse de séchage expérimentale a été retrouvée par la théorie sur toutes les périodes en utilisant le coefficient de diffusion mais seulement sur la dernière période avec le coefficient de migration de l'humidité à l'état liquide. Le dernier coefficient offre plus d'avantages puisqu'il permet la prévision de la cinétique du séchage sans soumettre le matériau à l'évaporation. Cependant, cette méthode présentera toujours des lacunes tant que l'on ne sait pas évaluer de façon assez précise l'épaisseur de la zone de migration de l'humidité.

NOTATIONS

D_l : Coefficient de migration de l'humidité liquide, m²/s
D_v : Coefficient effectif de diffusion des vapeurs, m²/s
k_g : Coefficient de transfert de masse, m/s
R : Rayon du grain, m
Re : Nombre de Reynolds
r : Coordonnée radiale, m
r_m : Epaisseur de la zone de migration de l'humidité, m
r_0 : Rayon de la zone à humidité initiale, m

r_u : Rayon de la zone humide, m
t_a : Température de l'air, °C
U : Vitesse de séchage, $Kg/m^2 \cdot s$
U_M : Vitesse maximale de séchage $kg/m^2 \cdot s$
v_a : Vitesse de l'air, m/s
w : **H**umidité, %
w_{cr} : **H**umidité critique, %
w_e : umidité d'équilibre, %
ρ : Densité, Kg/m^3
ψ : Porosité.

RÉFÉRENCES

1. Gh. Christian et R. Z. Tudose, *Rev. Chim. (București)*, **22**, 9 (1971).
2. R. Z. Tudose et Gh. Christian, *Bul. Inst. Polytek. Iași*, **22**, 1 (1976).
3. Kadi, H. Thèse de dctorat, Institut Polytechnique Iași, 1984.
4. R. B. Bird, W. E. Stewart et E. N. Lightfoot, « Transport Phenomena », Wiley, New York , (1960).
5. C. Mihăilă, V. Caluianu- M. Marinescu et A. Dănescu, « Procese și instalații industriale de uscare », Ed. tehnică, București, (1983).

Revue Roumaine de Chimie, **32**, *8*, 821–832 (1987)

AN ADAPTED ZONE METHOD FOR PROPANE THERMAL CRACKING PROCESS SIMULATION IN A RADIANT FURNACE

GHEORGHE MARIA[a]*, CRISTIAN TSAKIRIS[b], GRIGORE BOZGA[c]
and ALEXANDRU ISOPESCU[d]
[a] ICECHIM, Chemical and Biochemical Energetics Institute, Splaiul Independenței 202A, Bucharest 77208, Romania
[b] Brazi Petrochemical Works, Romania
[c] Department of Chemical Engineering, Polytechnic Institute of Bucharest, Romania
[d] Computer Center of Chemical Industry, Bucharest, Romania

In order to decrease the computational time for the cracking process simulation in a radiant furnace, an adapted Hottel zone method was used. A flexible rectangular division of the combustion chamber and an elaborated strategy to solve the coupled fire box-tubular reactor model, give a good agreement with the industrial experimental data.

1. INTRODUCTION

In order to obtain an accurate simulation of the hydrocarbon cracking process, a detailed model for the radiative and convective transfer in the fire box is necessary. The simulation procedures of the radiant enclosures, containing tubular reactors, solve the radiant box and thermal cracking coil uncoupled model, or adversely, the coupled model in an iterative schema.

The uncoupled reactor models impose either a tube wall temperature profile, or a heat flux profile. The approximate evaluation of these profiles may be separately accomplished by using several fire box models : i) semiempirical models, ii) ideal stirred gas models, and iii) zone models. Some reviews of these models are available from references.[1–3] The flux profiles depend on the radiative properties of the combustion products, the characteristics of the burners, and geometry of the furnace. The accurate computation of these profiles is usually performed using two radiant enclosure simulation methods : the flux method, based on the differential form of the radiative transport equation, and the zone method of Hottel [4,5] based on the integrated transport equation between each pair of zones. A comparison of these two methods for a typical radiant furnace simulation is given by Filla and Chiappetta[6] ; the flux method seems to be faster and requires less storage than the zone method.

The coupled fire box and tubular reactor simulation allows to obtain simultaneously the tridimensional temperature box field, and the reactor performances for several operating conditions.[7–10] The main difficulties of the coupled simulation, as revealed by Filla and Chiappetta,[6] are the great size of the computer memory storage, and the computer time necessary to solve iteratively the radiant and reaction program sections. For this reason, the best compromise between refinement and computational time is necessary.

---

* Author to whom correspondence should be addressed.

The aim of this paper is to present a coupled method, based on Hottel's zone method, to simulate an industrial furnace for propane cracking using a flexible division of the box, adequate compromise concerning the calculus refinements, and a good strategy to solve the enclosure model. These adaptations can save computer time for several different operating condition simulations.

2. RADIANT ENCLOSURE MODEL

Hottel's zone method [1,4,5] requires the division of the combustion chamber (see Fig. 1) into a number of isothermal zones : volume zones and surface wall zones. An increasingly refined zoning of the enclosure leads, after simulation, to a more accurate tridimensional temperature box field, necessary for the reactor simulation. At the same time the required storage and the necessary computer time increase with respect to the number of zones, with a power law. A realistic compromise is possible using the particularities of each simulated enclosure. In our case the

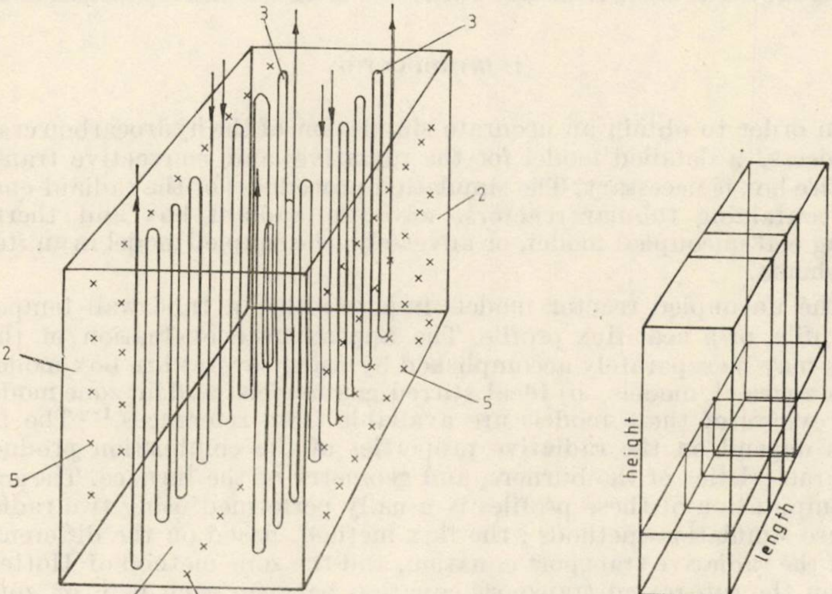

Fig. 1. — Fire box division (1 — central section ; 2 — lateral section ; 3 — coils ; 4 — central inferior burners ; 5 — lateral burners).

central combustion section and the lateral sections are separately simulated. The spatial arrangement of coils and burners suggests a temperature field symmetry with respect to the vertical symmetry planes of the parallelepipedic enclosure. A square-cubic division simulation for a similar combustion chamber [11,12] confirms such a conclusion. In order to obtain a minimum necessary number of zones with the advantages as underlined, a rectangular-parallelepipedic division is performed.

In our example (Fig. 1), the industrial furnace was divided into 28 rectangular surface zones and 8 parallelepipedic volume zones for each of three sections. This division into unequal zones is more flexible for various operating condition simulations, because zone dimensions can be varied according to the experimental information concerning the temperature gradients and the burner working, without introducing new zones for a finer division.

Using the radiative and convective heat transfer equation, the zone temperature computation involves, according to Hottel's rule, more steps as indicated below.

Estimation of the direct interchange areas $(\overline{ss}, \overline{gs}, \overline{gg})$. Using the view factors, i.e. the fraction of the radiation leaving a radiant zone that is emitted in the direction of a receptor, multiplied by A for an emitting surface, and by $4kV$ for an emitting gas volume, the direct interchange areas are thus obtained. The resulted expressions :

$$\overline{s_i s_j} = \int_{A_i}\int_{A_j} \tau(r)\cos\hat{\theta}_i \cos\hat{\theta}_j/(\pi r^2)\mathrm{d}A_i\mathrm{d}A_j, \qquad \text{for } i \neq j, \tag{1}$$

$$\overline{g_i s_j} = \int_{V_i}\int_{A_j} \tau(r)k_i\cos\hat{\theta}_j/(\pi r^2)\mathrm{d}V_i\mathrm{d}A_j, \qquad \text{for } i \neq j, \tag{2}$$

$$\overline{g_i g_j} = \int_{V_i}\int_{V_j} \tau(r)k_i k_j/(\pi r^2)\mathrm{d}V_i\,\mathrm{d}V_j, \qquad \text{for } i \neq j, \tag{3}$$

$$\overline{g_i g_i} = 4k_i V_i(1 - \Phi_i), \tag{4}$$

are difficult to evaluate by direct analytical integration. The multiple integrals may be computed for several zone geometry using the Monte-Carlo method,[13,14] the "shape-factor algebra",[1,5,15] or by using combinated numerical method and "shape-factor algebra".[16] In the above direct interchange area formulas, the medium transmittance may be approximated with the relationship :

$$\tau(r) = \exp(-\bar{k}\,r), \tag{5}$$

and the escape factor Φ is evaluated numerically using multiple integration Hottel's rule.[5] Explicit solutions are givens by Hottel et al.[1,5] for square-cubic zones, by Gross et al.[15] for rectangular surface zones, and by Hottel et al.[1,17] and Mihail and Maria [16] for cylindrical and elliptical zones. The influence of the geometrical coil arrangement on the radiative transfer around tubes is given by Hottel.[17]

In our example the multiple integrals were evaluated numerically using Simpson's rule,[12] adapted for rectangular and parallelepipedic zone cases. The direct interchange areas for the coil plane zones, considered by projecting the reactor tubes, were corrected owing to the void space between the tube rows, and to the cylindricity of tubes.[16]

Estimation of the total interchange areas ($\overline{SS}$, $\overline{GS}$, $\overline{GG}$), takes into account the direct radiation, the absorbed radiation and, in addition, multiple reflections on the surface zones. Using Hottel's rule, the energy balance for radiant surface zones (index k) :

$$\sum_i \overline{s_i s_j}({}_{s_k}R_{s_j}) - A_{s_i}({}_{s_i}R_{s_i})/\rho_{si} = -\varepsilon_{s_k}\,\overline{s_i s_k}, \tag{6}$$

gives the solutions :

$$\overline{S_i S_j} = \overline{S_j S_i} = ({}_{s_i}R_{s_j})A_{s_j}\,\varepsilon_{s_j}/\rho_{s_j}, \tag{7}$$

The energy balance for radiant gas zones (index k) :

$$\sum_j \overline{s_i s_j}\,({}_{g_k}R_{s_j}) - A_{s_i}({}_{g_k}R_{s_i})/\rho_{s_i} = -\overline{g_k s_i}, \tag{8}$$

gives the solutions :

$$\overline{G_k S_j} = \overline{S_j G_k} = ({}_{g_k}R_{s_j})A_{s_j}\,\varepsilon_{s_j}/\rho_{s_j}. \tag{9}$$

The total gas-gas exchange areas are obtained using the formula :

$$\overline{G_i G_j} = \overline{g_i g_j} + \sum_k ({}_{g_i}R_{s_k})\overline{s_k g_j}. \tag{10}$$

Taking satisfactory the one-gray-gas model for the radiative properties of the combustion products,[6] and using the gas emissivity correlated with the formula :

$$\varepsilon = a(T)(1 - \exp(-kpr)), \tag{11}$$

the total exchange areas must be ponderated by means of the relationships :

$$\overline{S_i S_j} = a(T_{s_i})[\overline{S_i S_j}]_k + (1 - a(T_{s_i}))[\overline{S_i S_j}]_{k=0} \tag{12}$$

$$\overline{G_i S_j} = a(T_{g_i})[\overline{G_i S_j}]_k \tag{13}$$

$$\overline{G_i G_j} = a\,(T_{g_i})[\overline{G_i G_j}]_k \tag{14}$$

The wall and coil emissivities were locally correlated using a temperature power law[1,12] (see Table 1).

Formulation of energy balances for each zone. The total energy balance includes radiative and nonradiative terms as enthalpy flux, convective flux, and energy storage terms, when conditions are not steady in time. For a surface zone (i), the balance equation is :

Table 1

Reaction scheme for propane cracking[19]

No.	Reaction	A	E_a
1	$C_3H_8 \rightarrow C_2H_4 + CH_4$	4.692×10^{10}	50.60
2	$C_3H_8 \rightleftharpoons C_3H_6 + H_2$	5.888×10^{10}	51.29
3	$C_3H_8 + C_2H_4 \rightarrow C_2H_6 + C_3H_6$	2.536×10^{13} *	59.06
4	$2C_3H_6 \rightarrow 3C_2H_4$	1.514×10^{11}	55.80
5	$2C_3H_6 \rightarrow 0.5C_6 + 3CH_4$	1.423×10^{9}	45.50
6	$C_3H_6 \rightleftharpoons C_2H_2 + CH_4$	3.794×10^{11}	59.39
7	$C_3H_6 + C_2H_6 \rightarrow C_4H_8 + CH_4$	5.553×10^{14} *	60.01
8	$C_2H_6 \rightleftharpoons C_2H_4 + H_2$	4.652×10^{13}	65.26
9	$C_2H_4 + C_2H_2 \rightarrow C_4H_6$	1.026×10^{12} *	41.20
10	$C_4H_8 \rightarrow C_6$	6.960×10^{7}	34.32
	Coke model :		
	$C_3H_6 \rightarrow$ coke	5.82×10^{14}	73.58

* second order reaction

$$E_{s_i}(\overline{S_iS_i} - \varepsilon_{s_i} A_{s_i}) + \sum_{j\neq i} E_{s_j}\overline{S_jS_i} + \sum_j E_{g_j}\overline{G_jS_i} - \sum_j h_{s_j} A_{s_ig_j}\cdot$$

$$\cdot(T_{s_i} - T_{g_j}) - h_{s_i} A_{s_i}(T_{s_i} - T_{\mathrm{ext},i}) = \bar{C}_{s_i}\mathrm{d}T_{s_i}/\mathrm{d}t, \qquad (15)$$

and for a gas zone (index k) :

$$E_{g_k}(\overline{G_kG_k} - 4kaV_{gk}) + \sum_{j\neq k} E_{g_j}\overline{G_jG_k} + \sum_j E_{s_j}\overline{G_kS_j} + \sum_j G_j(H_s + H_c)_j -$$

$$\sum_j h_{s_j}A_{s_jg_k}(T_{sj} - T_{gk}) = \bar{C}_{g_k}\mathrm{d}T_{g_k}/\mathrm{d}t. \qquad (16)$$

The chemical enthalpy terms, H_{cj}, were computed using experimental fuel gas composition before and after combustion. The convective coefficients gas-wall, h, were evaluated using the relationship :[18]

$$\mathrm{Nu} = 0.644\ \mathrm{Re}^{0.5}\mathrm{Pr}^{0.33} \qquad (17)$$

If the surface zone contains burners with surface diffused flame, the gas-wall heat transfer coefficient was computed using the experimental wall temperature data. In our example, this coefficient has been found

300–360 W.m^{-2}grd^{-1}. The heat transfer coefficient inner wall surface-ambient medium was computed with the common formula :

$$1/h = 1/h_{\mathrm{ext}} + \sum_i \delta_i/\lambda_i, \tag{18}$$

where h_{ext} corresponds to natural convection.[18] The heat transfer coefficients coil–reaction medium are computed using the relationships presented in Section 3.

The obtained balance equations are nonlinear with respect to the zone temperatures. Solving the total energy balance nonlinear set, by means of a successive approximation method,[11] the unknown zone temperatures are thus obtained.

3. TUBULAR REACTOR MODEL

To obtain the product distribution, reaction temperature, and pressure profiles along the cracking coil, a set of mass and enthalpy balance and pressure drop equations is required. These are written using the wide accepted assumptions of plug-flow, one-dimensional, ideal model :

$$\frac{\mathrm{d}\xi_i}{\mathrm{d}z} = \frac{v_{R_i}}{\dot{G}},\ i = 1,2,\ \ldots\ \text{(index of reaction)};\ \xi_i\,(z = 0) = 0, \tag{19}$$

$$\frac{\mathrm{d}T}{\mathrm{d}z} = \left(\sum_i v_{R_i}(-\Delta H_i) + \frac{4}{\mathrm{d}_t}\,h_s(T_{\mathrm{ext}} - T)\right)/(\dot{G}c_g);\ T(z = 0) = T_0, \tag{20}$$

$$\frac{\mathrm{d}p}{\mathrm{d}z} = -f\frac{1}{d_t}\frac{w^2}{2}\,\rho_g;\ p(z = 0) = p_0. \tag{21}$$

The kinetic of propane cracking is described by molecular reaction scheme derived and published by Sundaram and Froment,[19] given in Table 1. The kinetic parameters are assumed to obey the Arrhenius law, with the specified frequency factors and activation energies.

The inside heat transfer coefficient, h_s, is computed with the Dittus-Boelter equation corrected by Sundaram and Froment :[20]

$$\mathrm{Nu} = h_s\mathrm{d}_t/\lambda_g = \mathrm{Nu}_{\mathrm{DB}} + 429.2\,z_1^{-0.0706} - 544.3(x/100)^{-0.0437}, \tag{22}$$

where :

$$z_1 = 4z/(\mathrm{Re}\ \mathrm{Pr}\ \mathrm{d}_t);\ \mathrm{Nu}_{\mathrm{DB}} = 0.023\ \mathrm{Re}^{0.8}\mathrm{Pr}^{0.4}$$

4. COUPLED SIMULATION OF THE REACTOR AND RADIANT ENCLOSURE. RESULTS AND CONCLUSIONS

The simulation of the radiant box starts from a uniform proposed temperature field, and uses the gas temperature and heat transfer coefficient profiles inside the reaction tubes. After the evaluation of the direct

Scheme 1. Flow diagram for cracking furnace simulation

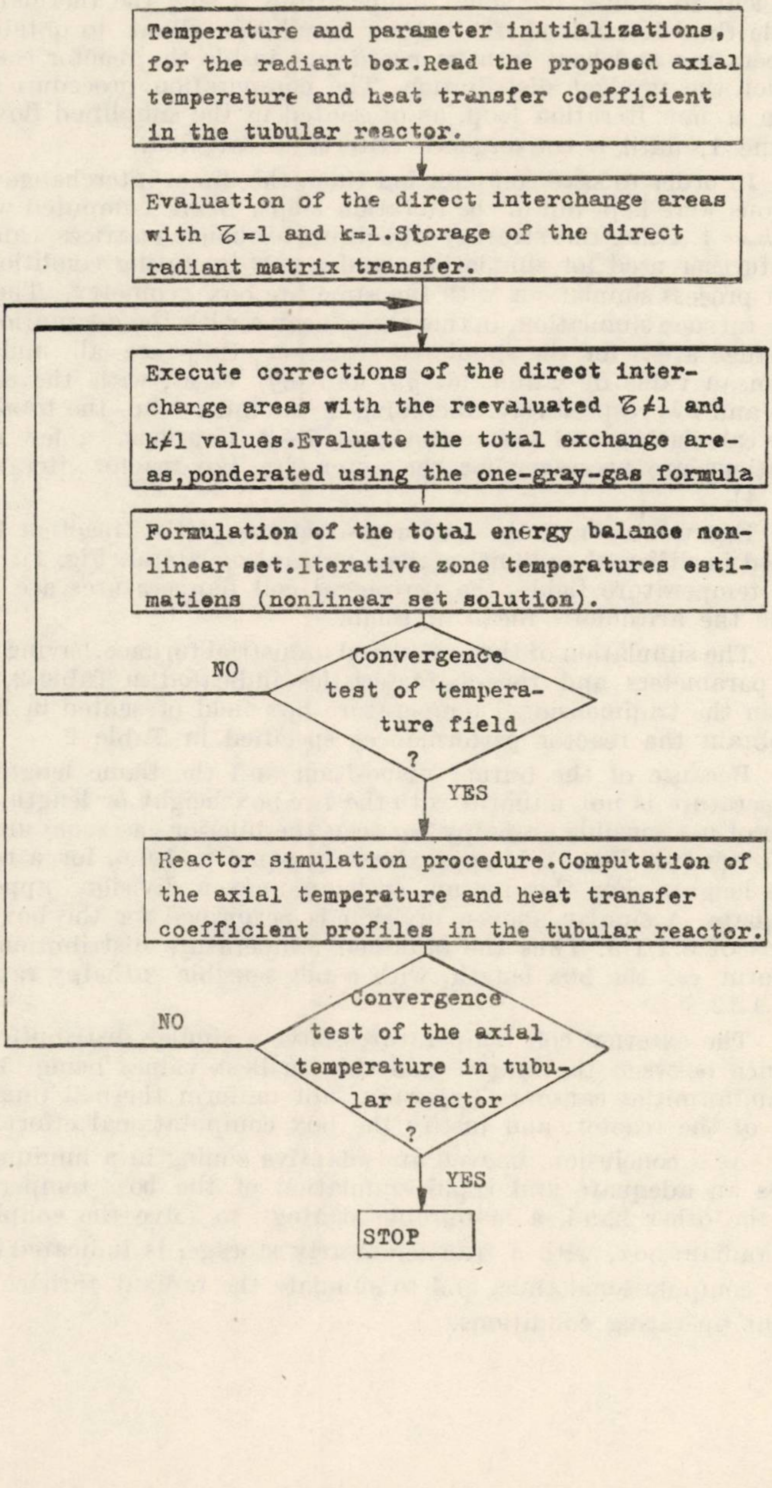
Temperature and parameter initializations, for the radiant box. Read the proposed axial temperature and heat transfer coefficient in the tubular reactor.
Evaluation of the direct interchange areas with τ=1 and k=1. Storage of the direct radiant matrix transfer.
Execute corrections of the direct interchange areas with the reevaluated τ≠1 and k≠1 values. Evaluate the total exchange areas, ponderated using the one-gray-gas formula
Formulation of the total energy balance nonlinear set. Iterative zone temperatures estimations (nonlinear set solution).
Convergence test of temperature field ?
NO
YES
Reactor simulation procedure. Computation of the axial temperature and heat transfer coefficient profiles in the tubular reactor.
Convergence test of the axial temperature in tubular reactor ?
NO
YES
STOP

interchange areas for $k = 0$ and $k \neq 0$ (one-gray-gas model), and the total exchange areas (dependent on the temperature), the nonlinear total energy balance set is solved. A few numbers of iterations (20. . .40) are sufficient to obtain the zones temperatures. Using the thermal flux coil profile thus determined, the reactor simulation allows to obtain the new temperature and heat transfer coefficient inside the reactor coils, and to predict the product distribution. The computation procedure is restarted in a new iteration loop, as presented in the simplified flow diagram scheme 1, until a convergence criteria is satisfied.

In order to save computation time, the direct interchange area evaluations were kept out of the iteration loops, being computed with $\tau = 1$ and $k = 1$. Using this strategy the direct exchange matrices can be stored and further used for simulations under new operating conditions, or for other process simulations with the same fire box geometry. The approximate furnace simulation, in this cases, begins with the adaptation of direct exchange areas for the simulated situation; they are all multiplied by the mean value of τ and, for $\overline{g_i s_j}$ and $\overline{g_i g_j}$ cases, with the mean value of k_i and $k_i k_j$ respectively. Including in the inner loop the total exchange area calculation and performing gest 2—3 iterations, a few number of iterations are necessary for the outer fire box-reactor iteration cycle (2. . .4).

Because each of the half cross-sections of the reaction tube is included in different radiant sections (central or lateral, Fig. 1), with different temperature fields, the peripheral coil temperatures are considered to be the arithmetic mean of them.

The simulation of the considered industrial furnace, having the operating parameters and the characteristics indicated in Table 2, allows to obtain the tridimensional temperature box field presented in Fig. 2, and to obtain the reactor performances specified in Table 2.

Because of the burner disposition and the flame length, the gas temperature is not uniform with the fire box height or length. Thus the ratio of net sensible enthalpy between the inferior gas zones and superior gas zones (see Fig. 1), is approximately equal to 1/0.6, for a ratio 1/4 of zone heights. For this reason, such an uneven division appears to be adequate. A similar uneven division is performed for the box length in ratios of 3/1/1/3. Thus the obtained temperature distributions are more uniform *vs.* the box length, with a net sensible enthalpy ratio of 1.12/ /1/1/1.12.

The external coil temperatures have a similar distribution, the difference between the largest and the smallest values being 53°C. These nonuniformities cause an important not uniform thermal flux along the axis of the reactor, and justify the box computational effort.

As a conclusion, uneven and adaptive zoning in a minimum number gives an adequate and rapid simulation of the box temperature field. On the other hand, a favourable strategy to solve the coupled reactor and radiant box, with a transfer matrix storage, is indicated in order to save computational time, and to simulate the radiant furnace under different operating conditions.

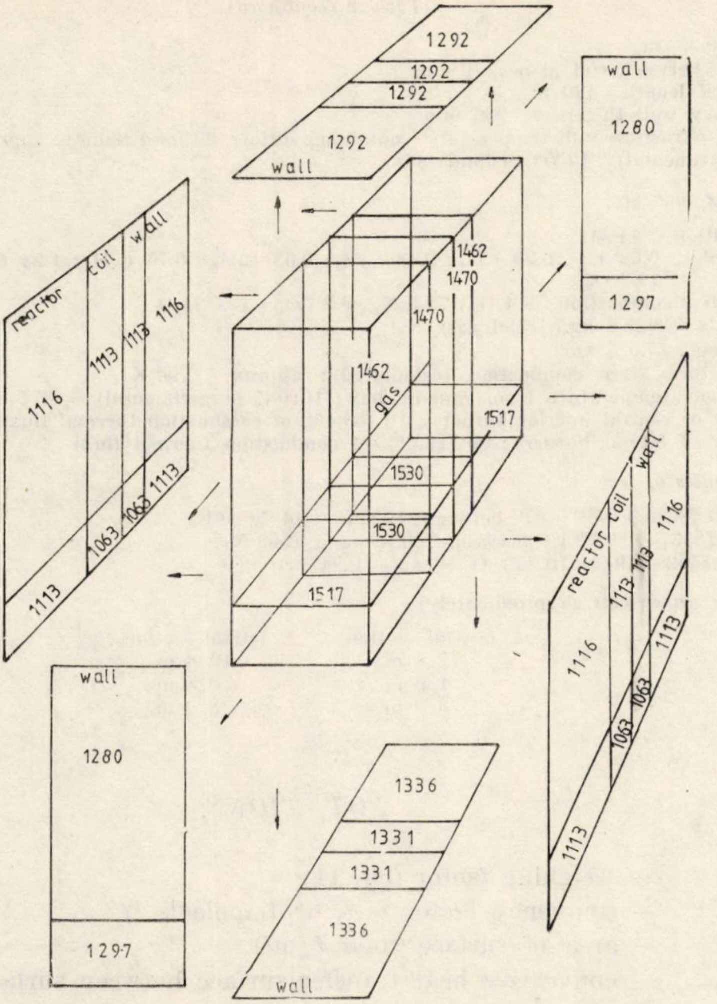
1292
1292
1292
1292
wall
wall
1280
1297
1462
1470
1470
1462
gas
1517
1530
1530
1517
reactor
coil
wall
1116
1113
1113
1116
1116
1113
1063
1063
1113
1113
wall
1280
1297
1336
1331
1331
1336
wall
reactor
coil
wall
1116
1113
1113
1113
1116
1063
1063
1113

Fig. 2. — Fire box (central section) temperature field (°K).

Table 2

Furnace configuration, operating condition and simulated results

Feed gas properties for the cracking reactor:

Feed flow rate: 55 kmoles C_3H_8/hr.
Dilution: 0.4 kg steam/kg C_3H_8
Inlet temperature in radiant section: 600°C
Inlet pressure: 3 atm. abs.
Resulted propane conversion: 92.0% (experimental); 94.1% (simulated)
Outlet product temperature: 840°C (experimental); 851°C (simulated)

Reactor coil and refractory walls:

External coil diameter: 0.123 m
Internal coil diameter: 0.105 m

Table 2 (continued)

Pitch : 0.37 m
Distance between coil planes : 1.6 m
Total coil length : 120 m
Refractory wall thickness : 285 mm
Internal refractory wall temperature (containing surface diffused flame) : approx. 1300°C (experimental) ; 1270°C (simulated)

Fuel gas and air:

Composition (% mol)
inlet : 0.08 H_2 ; 0.29 CH_4 ; 0.48 C_2H_4 ; 0.53 C_2H_6 ; 0.76 C_3H_8 ; 1.24 C_4H_{10} ; 77.2 N_2 ; 19.3 O_2
after combustion : 3.4 O_2 ; 75.2 N_2 ; 9.2 CO_2 ; 12.0 H_2O
Feed rate : 3651.8 kg/h (fuel gas)
Air excess : 17.5% vol.
Temperature after combustion (calculated) : approx. 1700°K
Outlet gas temperature from radiant box : 1010°C (experimental) ;
Number of central inferior burners : 10 (83.4% of combustion thermal flux)
Number of lateral burners : 96 (16.6% of combustion thermal flux)

Emissivities of

walls : 0.48036 $T^{0.08207}$ (T between 1000°K and 2000°K)
coil : 0.15337 $T^{0.16209}$ (T between 700°K : and 1500°K)
gas : $(0.8352-1.942\times10^{-4}T)$ $(1-\exp(-0.642\ r))$

Furnace dimensions (approximately) :

	central section	lateral section
Length :	12.8 m	12.8 m
Width :	1.6 m	0.8 m
Height :	8.0 m	8.0 m

NOTATIONS

a — weighing factor (eq. 11)
A — frequency factor (s^{-1}, or $L.mole^{-1}s^{-1}$)
A_i — area of surface zone i (m^2)
$A_{s_j g_k}$ — convective heat transfer surface between surface j and gas volume k (m^2)
c — molal specific heat ($J.mole^{-1}K^{-1}$)
C — heat capacity ($J.K^{-1}$)
d_t — reactor tube diameter (m)
$E(=\sigma T^4)$ — radiation-emission rate ($W.m^{-2}$)
E_a — activation energy ($kcal.mole^{-1}$)
f — friction factor in the drop pressure eq. (21)
$\overline{g_i g_j}$ — direct interchange area between two gas zones indexed i and j (m^2)
$\overline{g_i s_j}$ — direct interchange area between a gas zone i and a surface zone j (m^2)
$\overline{G_i G_j}$ — total interchange area between two gas zones indexed i and j, including reflections at all surfaces (m^2)

$\overline{G_iS_j}$ — total interchange area between a gas zone i and a surface zone j, including reflections at all surfaces (m^2)
G — molal gas flow rate entering or leaving a gas zone (moles.s^{-1})
$\dot{G}$ — molal flow rate per unit area of reactor cross-section (moles.m^{-2}.s^{-1})
h, h_s — heat transfer convective coefficient between a surface zone and a neighbouring gas volume, ambient or reaction medium (W.m$^{-2}\cdot$K^{-1})
$H_{c,s}$ — molal chemical or sensible enthalpy (J.mole^{-1})
ΔH — heat of reaction (J.mole^{-1})
k — gas absorption coefficient (m^{-1}, or atm^{-1}m^{-1})
Nu — Nusselt number
p — partial or total gas pressure (atm)
Pr — Prandtl number
r — linear distance between two elements (m)
$g_iR_{s_j}$ — flux density away from the j-th surface zone, due solely to radiation originating within the i-th gas zone (W.m^{-2})
Re — Reynolds number
$\overline{s_is_j}$ — direct interchange area between two surface zones, indexed i and j (m^2)
$\overline{S_iS_j}$ — total interchange area between two surface zones, indexed i and j, including reflections at all surfaces (m^2)
t — time (s)
T — temperature (K)
v_R — reaction rate (moles.m^{-3}s^{-1})
V_i — volume of gas zone i (m^3)
x — propane conversion (%)
w — gas velocity (m.s^{-1})
z — reactor length (m)

Greek letters:

δ — material thickness (m)
ε — emissivity
$\hat{\theta}$ — angle with the normal (rad.)
λ — thermal conductivity of the material (W.m^{-1}.K^{-1})
ξ — molal transformation in the i-th reaction
$\rho(=1-\varepsilon)$ — reflectivity
ρ_g — gas density (kg.m^{-3})
σ — Stefan-Boltzmann constant (W.m^{-2}.K^{-4})
τ — gas transmissivity
Φ — escape factor for radiation from a gas zone (ratio of energy leaving boundaries to energy originating within volume)

Subscripts

g — gas zone
ext — external medium
s — surface zone

REFERENCES

1. H. C. Hottel and A. F. Sarofim, "Radiative transfer", McGraw-Hill, New York, 1967.
2. R. Nogay and A. Prasad, *Hydroc. Process.*, **64** (11), 91(1985).
3. A. Nicoară and G. C. Suciu, *Rev. Chim.* (*Bucureşti*), **35**, 519(1984).
4. H. C. Hottel, "Radiant heat transmission" (in : W. H. McAdams, "Transmission", McGraw-Hill, New York, 1954).
5. H. C. Hottel and E. S. Cohen, *Amer. Inst. Chem. Engineers J.*, **4**, 3(1958).
6. M. Filla and M. Chiappetta, *Comp. Chem. Eng.*, **9**, 527(1979).
7. W. F. Petryschuk and A. I. Johnson, *Canad. J. Chem. Eng.*, **46**, 172(1968).
8. E. Eckert, V. Hlavacek, M. Marek and J. Mikulas, Scientific papers of the Institute of Chemical Technology, Prague, **K3**, 71(1969).
9. M. Filla and G. Maresca, *Ing. Chim. Ital.*, **12**, 143(1976).
10. H. A. J. Vercammen and G. F. Froment, paper presented at ISCRE 1978, Houston (Texas), published in *A.C.S. Symp. Series*, **65**, 271(1978).
11. R. Mihail, G. Maria and A. Isopescu, *Rev. Chim. (Bucureşti)*, **32**, 988(1981).
12. R. Mihail, G. Maria and A. Isopescu, *Rev. Chim. (Bucureşti)*, **33**, 157(1982).
13. H. A. J. Vercammen and G. F. Froment, *Int. J. Heat Mass Transfer*, **23**, 329(1980).
14. S. Osuwan and F. Steward, *Canad. J. Chem. Eng.*, **50**, 450 (1972).
15. U. Gross, K. Spindler and E. Hahne, *Lett. Heat Mass Transfer*, **8**, 219 (1981).
16. R. Mihail and G. Maria, *Int. J. Heat Mass Transfer*, **26**, 1783 (1983).
17. H. C. Hottel, *Ind. Eng. Chem. Fundls.*, **22**, 153 (1983).
18. V. P. Isachenko, V. A. Osipova and A. S. Sukomel, "Heat transfer", MIR, Moscow, 1980.
19. K. M. Sundaram and G. F. Froment, *Chem. Eng. Sci.*, **34**, 635(1979).
20. Ibidem, *Chem. Eng. Sci.*, **35**, 364(1980).

Revue Roumaine de Chimie, 32, 8, 833–836 (1987)

COMPTES RENDUS

I. Hargittai and M. Hargittai, "Symmetry through the Eyes of a Chemist", VCH Verlagsgesellschaft, Weinheim, 1986. 458 pp., hard cover, ISBN 3–527–26409–4 (0–89573–520–2 for VCH Publishers), 156 DM

The husband and wife team succeeded in authoring a book which is at the same time serious and enjoyable to read. This is no easy task when wishing to make readers with a scant knowledge of mathematics familiar with group theory and its applications in quantum chemistry, vibrational spectroscopy, and crystallography. The main topic of the book is symmetry; however, unlike other well-known books on the same topic, such as those by Mislow, by Cotton, or by Jaffé and Orchin, here the stress is laid upon the intuitive approach, and numerous illustrations from everyday life (many photographs are made by the authors themselves) serve to achieve the authors' purpose, namely to make the reader "feel" what symmetry is, and how it can be put to use in simple mathematical terms. Thus, this book is also related to more general treatments such as those dedicated by Weyl and by Shubnikov to symmetry.

The first author has edited recently a first volume of an unusual book, "Symmetry Unifying Human Understanding" and has published in 1957–1977 books on the structure of volatile sulfur compounds, and of coordination compounds in the vapour phase. Thus the present book represents the outcome of a lifelong acquaintance with symmetry. from the standpoint of a chemist. A shorter version of this book appeared in Hungarian in 1983, by the same author, "Szimmetria — egy kémikus szemével".

After a brief introduction, the second chapter presents examples for simple symmetries, introducing rotation axes, inversion, mirror rotation, chirality, assymetry and dissymmetry. Not only chemical, but all types of examples are beautifully illustrated, from galaxies through painting, sculpture and music, to flowers and snowflakes.

The third chapter is more chemical in nature and discusses the shape and geometry of molecules, guiding gradually the reader so that he or she should be able to establish molecular point gruops. Then many examples illustrate the point groups, both chemical and non-chemical (trademark logos, coins, stamps, etc.). It is probably due to the authors' reluctance to burden the reader with mathematics at this stage that, in the discussion of isomers due to substitution in aromatics or in tetrahedral or octahedral complexes, Pólya's important and useful theorem is not mentioned. A discussion of the VSEPR model, including contributions by I. Hargittai, concludes this chapter.

Chapter 4 introduces groups, matrices, character tables and operations with these tools. The reader is gradually made to understand what lies beyond mathematical symbols, and by means of examples, is persuaded in highly pedagogical manner that character tables compress in a very efficient fashion all the relevant information for point groups. In order to make the text more palatable, antisymmetry is illustrated by a text from a short story of Frigyes Karinthy (another such text was used earlier to exemplify inversion).

The fifth chapter uses the point-group symmetry of molecules for deducing the number, symmetry, and type of normal vibrations. Again, all the discussion is conducted by means of examples. A similar approach is followed in the next chapter for the electronic structure of atoms and molecules. From one-electron wave functions through many-electron atoms, the reader is presented with electronic configurations of the elements. Then molecular orbitals are presented and discussed for homodiatomic molecules and polyatomic molecules. The Jahn-Teller effect is illustrated by several examples.

Chapter 7 discusses chemical reactions in terms of potential energy hypersurfaces, transition state theory with symmetry rules for the reaction coordinate, and the Woodward-Hoffmann rules for pericyclic reactions. Hückel-Möbius aromaticity, and the isolobal analogy are also mentioned.

Whereas till now only point groups have been discussed and used, the last two chapters deal with space groups. Chapter 8 presents the mathematical aspects, and chapter 9 discusses the chemical counterparts, starting from the 32 crystal groups and the 230 space groups. Beautiful drawings by Escher from McGillavry's book illustrate chapter 8, alongside with Hungarian needlework patterns and with authors' photographs of tilings or decorations of the Capitol building in Washington, D.C. Similarly, the molecular packings are exemplified by assemblies of cannon balls in the USA and Hungary.

A subject and an author index conclude this well-produced and highly readable volume.

In conclusion, the authors have skilfully produced an interesting, stimulating book, addressed especially to those organic and inorganic chemists who have not received specialized training in group theory. They will discover how easy it is to master this theory by means of an intuitive approach and of a thoroughly delectable monograph.

A. T. Balaban
Polytechnic Institute, Bucharest

G. Beckmann and P. V. Gilli, "Thermal Energy Storage" (Basics—Design—Applications to Power Generation and Heat Supply) in "Topics in Energy" Eds. M. Grenon, S. Srinivasan and G. Woite, Springer-Verlag, Wien, New York, 1984, 230 pp., XI, 176 figs., hard cover, DM 86, ISBN 3—211—81764—6

The book presents aspects associated with storage of energy for power generation and heat supply. It has the following eight chapters :

1. Introduction ; 2. Basics ; 3. Storage systems ; 4. Storage vessels ; 5. Thermal energy storage in industry ; 6. Thermal energy storage in space heating and cooling ; 7. Power plants with thermal energy storage ; 8. Thermal energy storage in vehicles.

Each chapter has a separate bibliography, but all are placed at the end of the book so there is not much difference between this approach and the usual one. Another aspect is that almost half of the 199 references are in German.

The importance of energy storge can hardly be overestimated. The increase of nuclear power, the utilization of solar energy and the need for oil substitution in industry as well as at home, induced a substantial increase of thermal storage systems and their applications.

According to these new trends, the authors give a comprehensive survey of the worlds' recent achievements in thermal energy storage, but the book is far to be narrative. It is a professional one, well illustrated by mathematical formulae, tables and diagrams, which are very useful for those who are facing the difficult problem of thermal energy storage.

The stress is put both on technological and design aspects : storage systems and storage vessels, storage media and heat transfer media, charge and discharge equipments, specific mass and specific heat storage capacity, types of accumulators, thermochemical data, and so on. Special stress is laid on economic parameters : cost of installation and fuel, investment cost, storage efficiency, etc. A short history of thermal energy storage is also presented.

Despite its professional character, the book is accessible to a broad group of specialists from other fields of activity. It is written in a fluent language and has a very helpful basics chapter. The quality of the printing is excellent, and the book is highly recommended.

A. Dinculescu

Z. Slanina, "Contemporary Theory of Chemical Isomerism", D. Reidel Publ. Comp., Dordrecht, and Academia, Praha, 1986. 254 pp., 105 Kcs.

The author, who is a research worker at the "J. Heyrovský" Institute of Physical Chemistry and Electrochemistry of the Czechoslovak Academy of Sciences in Prague, is a theoretical chemist ; he started to work on physical-chemical problems about 20 years ago and defended his Ph. D. Thesis in 1971. He published in Czech an earlier, smaller, version of this book in 1981, which was translated into Russian in 1984 (Mir, Moscow). The present book was completed in 1982, and then translated into English ; for updating the references, the book contains an 4-page postscript with 158 references published in 1983—1985.

The first chapter is a brief introduction indicating how mathematical methods have helped theoretical chemists, both numerically for obtaining better and better procedures for solving Schrödinger's equation applied to larger and larger assemblies of atoms, and non-numerically for obtaining direct insight into the intrinsic logical structure behind chemical problems without numerical computations leading to algebraic or mathematical chemistry which became a new field. Thus isomerism is elucidated by combining the methods of quantum and algebraic chemistry.

The second chapter discusses basic concepts of chemical isomerism. Since the experiments of Gay-Lussac, Liebig and Wöhler on silver cyanate and fulminate, or on ammonium cyanate and urea, followed by work done by Berzelius on tartaric acid isomers, the phenomenon of isomerism has intrigued chemists. Berzelius introduced the term "isomerism" in 1830. A brief and non-exhaustive description of a few types of isomers from the thirty odd ones so far known concludes this chapter. The author emphasizes the importance of time scale and temperature in any definition and classification of isomers.

The following four chapters constitute the main part of the book. Chapters 3 and 4 are devoted to quantum-chemical and quantum-mechanical descriptions of isomerism. The adiabatic and the Born-Oppenheimer approximations permit assignment of a potential energy hypersurface to each electronic state of any N-atomic molecule, representing the energy of the system in a hypothetical state of fixed nuclei as a function of $3N-6$ ($3N-5$ for a linear molecule) independent coordinates of the nuclear positions. Minima on this hypersurface correspond to isomers, but the problem is complicated by the uncertainty principle. Only by abandoning the Born-Oppenheimer approximation and by using more advanced approximations is it possible to retain the concept of molecular structure. Thus the theory of quantum topology and other methods within quantum-mechanical approaches are able to account for rate processes in simple systems, including tunnelling in bonded ensembles of atoms.

Algebraic aspects of isomerism are reviewed in chapter 5 briefly but comprehensively. Starting with Cayley, Körner and van't Hoff, algebraic methods for isomer counting were introduced in 1874 and even earlier. With the help of set theory, graph theory, group theory and information theory, chemists can nowadays rationalize isomerism. The author presents with examples Polya's theorem and other graph-theoretical methods for isomer enumeration, and emphasizes the need for such enumerations in estimating the number of stationary points on the energy hypersurface. Mention is also made of computer-assisted organic syntheses. A particular emphasis is placed on Mezey's topologization of nuclear configuration space which allows the classification of stationary points on energy hypersurfaces.

Chapter 6 discusses interactions between isomerism and the theory of chemical reactivity, with many contributions by the author of the book, based on the concept of isomerism of reaction components.

Each chapter is followed by references, totalling more than 1000 quotations and by a summary. The book mentions that isomerism is not limited to chemical systems, but exists at the atomic and biological levels. The book is highy recommended to organic and theoretical chemists.

A.T.Balaban
Polytechnic Institute, Bucharest

"Recent Developments in the Chemistry of Natural Carbon Compounds" (edited by R. Bognár and Cs. Szántai), vol. 10 : "Syntheses of the Benzo[c]phenanthridine Alkaloids" by I. Ninomiya and T. Naito, and "The Chemistry of the Vancomycin Group of Antibiotics" by F. Sztaricskai and R. Bognár, Akadémiai Kiadó, Budapest, 1984, 209 pp., ISBN 963-05-3255-7

The tenth volume of the series "Recent Developments in the Chemistry of Natural Carbon Compounds" is formed from two approximately equally long reviews, written by first-class scientists, directly involved in research in their respective fields.

The first part, written by two Japanese chemists from Kobe, describes the chemistry and syntheses of two groups of benzo[c]phenanthridine alkaloids : nitidine and related compounds, which are quaternary N-methyl fully aromatic systems (azonia-chrysene compounds), and chelidonine, corynoline, and related systems which are tertiary amines with the same skeleton as the former compounds, but have hydrogenated B/C rings mainly with *cis*-fusion of these rings; however, isocorynoline has *trans*-fusion. These skeletons possess various substituents, mostly methoxy or *ortho*-methylenedioxy. The finding that some of these alkaloids are active against leukemia has triggered a marked interest in their synthesis. The authors present a systematic overview of all reported syntheses, grouped according to the final ring formed during these syntheses ; this is either ring B (the pyridine/pyridinium ring), or ring C (the non-terminal ring adjacent to the heterocyclic one). After the exhaustive and well-illustrated enumeration of these syntheses, a brief table presents pharmacological data. The bibliography contains 83 references, 14 of which originate from the authors' laboratory. These isoquinoline type alkaloids have biosynthetic pathways starting from tyrosine, via substituted 1-benzyl-1,2,3,4-tetrahydroisoquinolines, and a rearrangement step converting an azonia-benz[a]anthracene into an azonia-chrysene system. The introduction of a new chromatographic separation technique, the droplet countercurrent chromatography (DCCC), considerably assisted the direct isolation and separation of the quaternary salts, which had presented difficult problems.

The second part is a review written by two Hungarian chemists; Professor Bognár, from the Kossuth Lajos University in Debrecen is one of the two editors of the series of which this book is the tenth volume; Dr. Sztaricskai works in the Research Group for antibiotics of the Hungarian Academy of Sciences. The vancomycin-type antibiotics are cyclic glycopeptides: heptapeptides with neutral sugar residues such as D-glucose, D-mannose, D-arabinose, L-rhamnose, L-fucose, and with a variety of deoxy-amino-hexoses: vancosamine, ristosamine, acosamine, actinosamine, etc., all belonging to the L series.

Several research groups study the structure and synthesis of this group of antibiotics, in USSR, USA, UK, and Hungary. Some of these products have been introduced as antibacterial antibiotics or as laboratory diagnostic agents in haematology for diagnosing Willebrand's disease; also, veterinary application and feed additivation has been approved in some countries, even before the elucidation of the chemical structure.

The review is structured in a general characterization, followed by five chapters describing the main groups of antibiotics from this class: vancomycin, actinoidin, avoparcin, ristocetin—ristomycin, and the antibiotic complex A—35512. For each of these, the isolation, biological activity, detailed structural studies, and the mechanism of antibiotic action (when known) are described.

Each chapter has its own references listed at the end, and its numbering of formulas. The difficulties encountered in elucidating the chemical structures are demonstrated by the fact that till now ristocetin is the only glycopeptide antibiotic with a molecular weight higher than 2000 (actually, 2063 dalton) with completely known structure: its elucidation after the initial discovery of these antibiotics and the elaboration of satisfactory methods for purification and selective chemical degradation needed more than 20 years.

The excellent printing conditions and the clearly drawn formules together with the fluent and easily readable English make the perusal of this book an enjoyable enterprise. The book is highly recommended to all those interested in biologically active natural products, and to all organic chemists interested in the complicated task of structure elucidation and total synthesis of interesting naturally occurring compounds.

Alexandru T. Balaban
Polytechnic Institute, Bucharest

ORSZÁGOS MŰSZAKI INFORMÁCIÓS KÖZPONT ÉS KÖNYVTÁR 1983

NOTE POUR LES AUTEURS

La Revue Roumaine de Chimie publie des articles en anglais, français, russe, allemand ou espagnol. Les auteurs sont priés d'envoyer des articles et des comptes rendus inédits.

Les manuscrits seront dactylographiés à double interligne. La bibliographie, les tableaux et la légende des figures seront placés après le texte.

Si l'article fait partie d'une série numérotée, la partie précédente sera donnée comme première référence.

Chaque article sera précédé d'un résumé comprenant quinze lignes au maximum.

Les références bibliographiques dans le texte seront faites par des exposants sans parenthèses et paraîtront à la fin de l'ouvrage.

Les publications périodiques mentionnées dans la bibliographie seront présentée suivant les prescriptions internationales : le nom de l'auteur précédé de l'initiale du prénom, le titre du périodique abrégé conformément à « Chemical Abstracts » et souligné par une ligne, le numéro du tome indiqué par des chiffres arabes et souligné par deux lignes, suivi de la première page de l'article ; à la fin, l'année de la parution sera placée entre parenthèses. Le numéro de la revue ne sera pas indiqué si les pages du volume sont numérotées consécutivement.

Les textes des livres ou traités incluront : le nom des auteurs, l'initiale du prénom, le titre du livre entre guillemets et sans être souligné, le numéro du tome précédé par l'abréviation « vol. » (ou « Bd. », le numéro de l'édition, les éditions (the publisher), la localité de la parution du livre, l'année de la parution et la page de la référence précédée(s) par l'abréviation « p. » (ou « S. »).

Les brevets seront indiqués comme suit : l'auteur ou la firme, le pays et le numéro du brevet, la date et la revue (*Chem. Abstr.)*. Par. ex. : M. Jones (to Union Carbide Co), Brit. Pat. 601 238, 2 Sept. 1959 ; cf. *Chem. Abstr.*, **54**, 12808 (1960).

Si la référence n'a pas été lue en original, on indiquera aussi la revue de référence consultée.

Les diagrammes seront tracés à l'encre de Chine sur papier calque. Les tableaux et les figures (en nombre strictement nécessaire) ainsi que les courbes dans les figures seront numérotés par des chiffres arabes. Leur explication sera donnée dans la légende des figures. Prière de ne pas inscrire les mêmes données dans les tableaux et les figures. Chaque tableau aura un titre. On indiquera dans le texte la place approximative des tableaux et des figures. Les formules chimiques seront incluses dans le texte ; en outre, elles seront transcrites sur papier calque, à l'encre de Chine.

Les auteurs sont priés d'indiquer les caractères italiques (en soulignant les lettres au crayon), ainsi que tout autre caractère spécial; les préfixes *ortho*, *meta*, *para*, *cis*, *trans*, etc. seront soulignés pour indiquer leurs caractères italiques et ne seront jamais écrits avec des majuscules.

Aucune correction à la main ne sera admise sur le manuscrit. Les corrections seront tapées à la machine. Les lettres grecques ou d'autres symboles spéciaux seront insérés à la main à l'encre clairement.

Le manuscrit sera signé par l'auteur.

Le titre-courant aura 50 lettres au maximum.

L'entière responsabilité du contenu des articles apartient aux auteurs.

Sur demande on peut obtenir une note plus complète.

PRINTED IN ROMANIA

TRAVAUX PARUS AUX ÉDITIONS DE L'ACADÉMIE DE LA RÉPUBLIQUE SOCIALISTE DE ROUMANIE

ELENA CEAUȘESCU, **Progrese în chimia și tehnologia polimerilor**, 1986, 446 p.
ELENA CEAUȘESCU, **Forschungen im Bereich der Chemie und Technologie der Polymere**, 1986, 444 p.
I. G. MURGULESCU, O. M. RADOVICI, **Introducere în chimia fizică, vol. IV, Electrochimia**, 1986, 410 p.
RAUL MIHAIL, ION GROZEANU, **Estimarea secvențială aplicată sistemelor chimice**, 1986, 406 p.
M. BREZEANU, L. PATRON, M. ANDRUH, **Combinații complexe polinucleare și aplicațiile lor**, 1986, 244 p.
A. T. BALABAN et al., **Labelled compounds applied in nuclear medicine**, coédition avec John Wiley and Sons, 1986, 742 p.
D. PURDELA, **Nomenclatura chimiei organice — IUPAC**, 1986, 454 p.
PETRU BUDRUGEAC, **Probleme de chimie**, 1986, 280 p.
T. ONCESCU, S. G. IONESCU, **Conversie fotochimică și stocare de energie**, 1985, 272 p.
V. DRĂGUȚAN, A. T. BALABAN, M. DIMONIE, **Olefin Metathesis and Ring-Opening Polymerization of Cyclo-olefins**, coédition avec John Wiley and Sons, 1985, 544 p.
C. LITEANU, I. RÎCĂ, **Optimizarea proceselor analitice**, 1985, 360 p.
N. PERESCU, **Chimia extracției cu solvenți și aplicații**, 1985, 212 p.
V. E. SAHINI, M. HILLEBRAND, **Chimie cuantică în exemple și aplicații**, 1984, 378 p.
GH. MARCU, **Chimia compușilor coordinativi**, 1984, 415 p.
E. CORDOS, C. MANOLIU, **Spectrometria de absorbție și fluorescența atomică**, 1984, 178 p.
C. BODEA, **Tratat de biochimie vegetală, p. II, t. 4**, 1984, 438 p.
N. ASANDEI, A. GRIGORIU, **Chimia și structura fibrelor**, 1983, 395 p.
N. IONESCU, M. CĂLDĂRARU, **Oxidarea catalitică a olefinelor inferioare**, 1983, 178 p.
C. CAȘCAVAL, **Studiul polimerilor prin piroliză și cromatografie de gaze**, 1983, 220 p.
C. I. SIMIONESCU, F. DANEȘ, **Originea vieții**, 1983, 110 p.
C. BODEA, **Tratat de biochimie vegetală, p. II, t. IV**, 1982, 408 p.
I. G. MURGULESCU, RODICA VÎLCU, **Introducerea în chimia fizică. Vol. III. Termodinamica chimică**, 1982, 624 p.
I. G. MURGULESCU, J. PĂUN, **Introducere în chimia fizică, Vol. I. 3. Nucleul atomic, reacții nucleare, particule elementare**, 1982, 606 p.
ELENA CEAUȘESCU, **Noi cercetări în domeniul compușilor macromoleculari**, 1981, 536 p.
I. G. MURGULESCU, TATIANA ONCESCU, E. SEGAL, **Introducere în chimia fizică. Vol. II. 2. Cinematică chimică și cataliză**, 1981, 1024 p
I. GĂLĂȚEANU, **Procese și metode radiochimice în energia nucleară**, 1981, 234 p.
CR. SIMIONESCU, VALERIA GORDUZA, **Polimeri biocompatibili și biologic activi**, 1980, 479 p.
ELENA CEAUȘESCU, **Polimerizarea stereospecifică a izoprenului**, 1979, 307 p.
C. GH. MACAROVICI, **Analiza chimică cantitativă anorganică**, 1979, 457 p.
M. FLORESCU, **Metode științifice în dezvoltarea industriei chimice moderne**, 1979, 256 p.
I. G. MURGULESCU, E. SEGAL, **Introducere în chimia fizică. Vol. II. 1. Teoria molecular-cinetică a materiei**, 1979, 1036 p.
I. G. MURGULESCU, V. EM. SAHINI, **Introducere în chimia fizică, Vol. I, 2. Structura și proprietățile moleculelor**, 1979, 604 p.
I. ZIGRĂVESCU, MAGDA PETROVANU, **N-ylid chemistry**, coédition avec McGraw-Hill International Book Company U.S.A., 1977, 386 p.
I. G. MURGULESCU, **Introducere în chimia fizică, Vol. I. 1. Atomi, molecule, legătură chimică**, 1976, 560 p.
ELENA CEAUȘESCU, **Research work on synthesis and characterization of macromolecular compounds, Contributions**, 1974, 251 p.

ISSN 0035–3930

I. P. Informația c. 1263

43 426

Lei 40

$ 80 pour un abonnement annuel

F1103

~~66~~ 04

ACADÉMIE DE LA RÉPUBLIQUE SOCIALISTE DE ROUMANIE

REVUE ROUMAINE DE CHIMIE

TOME 32

N°s 9 – 10

Septembre – Octobre 1987

Rev. Roumaine Chim.

RRCHAX, 32, *9–10*, p. 837 – 1010 (1987), Bucarest

EDITURA ACADEMIEI REPUBLICII SOCIALISTE ROMÂNIA

ACADÉMIE DE LA RÉPUBLIQUE SOCIALISTE DE ROUMANIE

COMITÉ DE RÉDACTION

Rédacteur en chef:

I. G. MURGULESCU, membre de l'Académie de la République Socialiste de Roumanie

Rédacteurs en chef adjoints:

A. T. BALABAN et V. EM. SAHINI, membres correspondants de l'Académie de la République Socialiste de Roumanie

Collège de rédaction:

EM. BRATU, ELENA CEAUŞESCU, ECATERINA CIORĂNESCU-NENITZESCU, CR. SIMIONESCU, membres de l'Académie dd la République Socialiste de Roumanie ; P. SPACU, membre correspondant de l'Académie de la République Socialiste de Roumanie ; M. BANCIU, M. D. GHEORGHIU, I. HAIDUC, D. I. MARCHIDAN, G. NIAC et D. SĂNDULESCU

La Revue Roumaine de Chimie parait 10 fois par an. Toute commande de l'étranger sera adressée à ROMPRESFILATELIA — sectorul Export-Import Presă, P. O. Box 12—201, télex 10376 prsfi r 78 104 Bucarest, Calea Griviţei nr. 64—66, Bucureşti, Roumanie

Les manuscrits, les livres et les revues proposés en échange, ainsi que toute correspondance seront envoyés à la rédaction :

REVUE ROUMAINE DE CHIMIE

125, Calea Victoriei, 79717 Bucarest, Roumanie, téléphone 50 76 80

EDITURA ACADEMIEI REPUBLICII SOCIALISTE ROMÂNIA
125, Calea Victoriei, 79717 Bucarest, Roumanie, téléphone 50 76 80

REVUE ROUMAINE DE CHIMIE

Tome 32, N°s 9–10 **Septembre–Octobre, 1987**

EDITORIAL 839–842

V. EM. SAHINI and C. PODINĂ, Partition coefficients on the basis of atomic charge density 843–845

RODICA VÎLCU and EUGENIA SĂLĂGEAN, Micelle formation in aqueous-sodium dodecyl sulfate solutions 847–853

H.-H. EMONS, D. KIEßLING, W. HORLBECK and K. WITTENBECHER, Vapour pressures of molten salt mixtures alkali halide – alkaline earth halide 855–862

DAN GEANĂ, VIOREL FEROIU and ORTANSA LANDAUER, Computation of saturation pressure and orthobaric densities by a general cubic equation of state 863–875

P. SPACU, SILVIA PLOȘTINARU, LUMINIȚA PATRON, ADRIANA CONȚESCU, D. CRIȘAN and N. STĂNICĂ, Rare earth mixed oxides with transition metals. I. Mixed oxides with Co(III) and Ni(III) having a Perovskite structure 877–881

S. STERNBERG, T. VIȘAN, N. BONCIOCAT and ADINA COTÂRȚĂ, Electrode processes in the system : lead(liquid)/lithium chloride-potassium chloride-lead chloride 883–893

VALENTINA LĂZĂRESCU, O. RADOVICI, M. VASS, Sintering effects on anodic oxidation of vacuum deposited silver films 895–899

CECILIA VASS, Lead electrodeposits on graphite support 901–905

IULIANA VARTIRES, ANGELA MIHELIS, VERONICA POPESCU and N. SPĂTARU, On the semiconducting character of Spinel-type electrocatalytic oxide layers 907–912

G. HORÁNYI and E. M. RIZMAYER, Radiotracer study of the adsorption of DL-asparaginic acid at a platinized platinum electrode 913–923

MARIA ZAHARESCU, CONSTANȚA PÎRLOG, D. CRIȘAN, N. DRĂGAN, ANA BRĂILEANU, M. ILISIE and T. SURDEANU, Protonic conductors with beta-alumina type structure 925–933

M. O. VLAD, V. T. POPA and E. SEGAL, A nonlinear transformation for the reaction extents within the framework of the Horiuti-Temkin theory . . 935–938

N. I. IONESCU and MONICA CĂLDĂRARU, Mobility of lattice oxygen and activity of multicomponent oxide catalysts for oxidation of propylene . . 939–943

EMIL CHIFU and CĂLIN-IOAN GHEORGHIU, Surface mobility of surfactant solutions. XII. Remarks concerning the Marangoni flow through an inclined surface canal 945–951

Rev. Roumaine Chim. | **32**, *9–10*, 837–1010 (1987), Bucarest

TATIANA ONCESCU, MIHAELA STEFAN, M. CONTINEANU and S.G. IONESCU, Optimisation of hydrogen production from water using proflavine as photosensitizer 953–960

M. BANCIU, ANCA BANCIU, M. ELIAN, C. DRĂGHICI and ECATERINA CIORĂNESCU, Synthesis and pyrolysis of 10,21-dithia-9, 10, 11, 20, 21, 22-hexahydrodiphenanthro [a, f] cyclodecene-S, S, S′, S′-tetraoxide. . . . 961–967

MICHAELA STĂNESCU, MIHAI ELIAN and ECATERINA CIORĂNESCU, Carbonium ion reactions. XVIII^1. Substituent effect in solvolytic reactions. Solvolysis of the tosylate of 10-methyl-5H-dibenzo [a, d] cyclohepten-5-carbinol 969–973

MICHAELA-CARMEN BALABAN, IOSIF SCHIKETANZ, ALEXANDRU T. BALABAN, ANA SCHIKETANTZ and MIRCEA D. GHEORGHIU, Aminoketone and oxazole synthesis. X. Acylation and alkylation of arenes with the azlactone of cinnamoylglycine 975–978

MIRCEA D. GHEORGHIU, MARINA MIHAI, LUMINIȚA PÂRVULESCU, ANGHELUSIS VAIOS and FLORIN NICULESCU, Nuclear magnetic resonance investigations of small rings. 4. ^{13}C-NMR spectra of 2-t-butyl-2-cyanocyclobutanones as probes for configurational assignments 979–984

G. BLIZNAKOV, D. KLISSURSKI and Y. PESHEVA, Selective oxidation of methanol to formaldehyde on modified vanadia catalysts 985–994

DUMITRU DOBRESCU, MIRCEA IOVU, CORNEL GEORGESCU, VASILE STOICESCU and AURELIA CRISTEA, Relations between chemical structure and analgesic action of some diamines and aminoethers . . . 995–1000

NICULAE OLARU and ZENO SIMON, Quantitative structure-activity relations for the inhibition of guanine phosphoribosyltransferase from *Escherichia coli* 1001–1009

Revue Roumaine de Chimie, **32**, *9–10*, 839–842 (1987)

EDITORIAL

PROFESSOR I. G. MURGULESCU
Member of the Academy of the Socialist Republic of Romania

Professor I. G. Murgulescu, Member of the Academy of the Socialist Republic of Romania, Professor Emeritus of Physical Chemistry at the Bucharest University and formerly Director of the Centre of Physical Chemistry celebrates the 85th anniversary of his birthday. We take this opportunity to express our high esteem for his great contribution to the creation of a modern school of physical chemistry in Romania, for his multiple activities in scientific research and teaching.

His prominent scientific personality has deeply marked the development of physical chemistry in Romania. The present volume is meant as a tribute from his students, colleagues and friends who have benefited from his remarkable work and kind friendship. It is also a proof of the stimulating influence of his discoveries and achievements on current researches as well as on future ones.

Professor I. G. Murgulescu was born at Cornu, Oltenia in 1902. He studied at the elementary school of his native village and attended the high school in Craiova. As a student at the Science Faculty of the Cluj University he proved his ingenuity on many occasions.

He began his didactic activity at the Science Faculty of the Cluj University where he was appointed assistant in 1928 after having graduated from the same Faculty with the highest honours. In 1930 he obtained his Ph.D. degree with a thesis on Copper Thiosulphate Complexes which was approved "Magna Cum Laude" by the Cluj University.

During the period 1932—1933, he worked with Professor F. Weigert at the Institute of Physical Chemistry, of the Leipzig University and after his returning home in 1934 he became a reader in Analytical and Physical Chemistry at the Timişoara Polytechnic Institute. He held this position until 1945, when he was nominated professor at the same Institute.

In 1949 he was appointed professor of physical chemistry at the Bucharest University, where he gave lectures until he retired in 1972.

Professor Murgulescu's research work covers a wide field : kinetics, thermodynamics, electrochemistry, spectroscopy, inorganic and analytical chemistry, molten salts chemistry.

Starting from the studies of complex compounds, he discovered new types of silver and copper thiosulphate complexes. These investigations were extended by spectrophotometric, cryoscopic and conductimetric measurements which led him to determining the composition of Durand's salt. He also studied spectrophotometrically the copper and cobalt salts in solution and the nature of the chemical bond of complex chromium, iron and cobalt oxalates.

On the basis of the refractometric properties of acqueous solutions of electrolytes, Professor Murgulescu elaborated new methods for calculating the refractive index of electrolytes and the individual ionic refractions. One of these methods was applied to obtain the refractive indices of ferricyanide and ferrocyanide ions.

His studies in photochemistry have been directed towards the quantum efficiency and the mechanism of the photochemical decomposition of potassium cobaltic oxalates and of diphenyldiazomethane in solution, as well as towards the kinetics of the decomposition of diphenyldiazomethane.

Professor I. G. Murgulescu studied the kinetics of the alcoholysis of several benzyl halides and decomposition of the cobaltic oxalate in acqueous solution.

Another matter in which Professor I. G. Murgulescu became interested was the anodic passivation of metals and alloys. He particularly studied the electrochemical behaviour of thin films and the measurement of electrode potentials.

His contribution to chemical thermodynamics was mainly felt in the field of thermal decomposition of calcium carbonate, thermodynamic activity of solutions and alloys, and free energy of chemical substances. By ebullioscopy he obtained the dissociation constant of alpha-nitroso--beta-naphthol in solution, and by calorimetry, heat of dissolution of sodium iodate, both anhydrous and hydrated.

Likewise, Professor I. G. Murgulescu elaborated new analytical methods for mercury and other elements. He was the first who used the *o*-chlorobenzoic acid in alkalimetry and acidimetry. He developed a new conductimetric method for titrating molybdates and tungstates using silver nitrate, thus enriching the theory of precipitation processes in the physico-chemical analysis. He has also paid attention to the equivalence point in titrimetry and to the determination of normal electrode potential.

He was particularly interested in the physical chemistry of molten salts and concentrated his theoretical and experimental studies on the thermodynamic properties of binary mixture of molten salts by the methods of electromotive forces, cryometry and vapour pressure measurements, transport properties of molten salts, refractive indices, heat of mixing, heat of melting, heat capacity of molten salts, a.s.o.

Chemisorption focused the interest of Professor Murgulescu on strong and weak interaction of gases with solid surfaces, aiming at clarifying the importance of the elementary act of adsorption in simple catalytic reactions.

The main results of his scientific research have been published in Romanian and foreign journals.

Professor I. G. Murgulescu has been not only a remarkable scientist, but also an excellent, stimulating teacher whose textbooks have been widely used in universities all over Romania. In 1976, he started the publication of "Introduction to Physical Chemistry". The work has been issued in four volumes, subdivided into seven parts : I, 1 *Atoms. Molecules. Chemical Bond*; I, 2 *Structure and properties of molecules*; I, 3 *Atomic nucleus. Nuclear reactions. Elementary particles;* II, 1 *Molecular theory of the states of matter*; *gas*, *solid*, *liquid and solutions*; II, 2 *Chemical kinetics. Catalysis*; III. *Chemical thermodynamics*; IV. *Electrochemistry*.

These volumes represent an extension of the lectures given by the author for almost a quarter of a century of teaching and scientific activity. They are also an illustration of Professor Murgulescu's interest in permanently updating them with the newest achievemets in the field.

The year 1948 was marked by the election of Professor Murgulescu as a Member of the Romanian Academy. Due to his merits he was elected Vicepresident of the Academy between 1959–1963 and President between 1963–1966.

In 1960, when the Commission of Spectroscopy came into being as part of the Chemical Sciences Section of the Academy, Professor Murgulescu became its Chairman. Some years later, in 1971, he became editor-in-chief of Revue Roumaine de Chimie.

On his initiative, the Centre of Physical Chemistry (founded in 1963 under his leadership) assisted by central Government institutions

(National Council for Science and Technology, the Academy of the Socialist Republic of Romania, Ministry of Education, Ministry of Chemical Industry) organized the five "National Conferences on Pure and Applied Physical Chemistry", between 1968 and 1976.

By the stimulating atmosphere created both at the Centre of Physical Chemistry and at the Bucharest University, Professor Murgulescu provided an excellent starting point for many Romanian young scientists. This was also beneficial for a few young scientists from abroad, while studying at the Centre of Physical Chemistry.

Professor Murgulescu is an excellent example of a scientific personality in whom devotion to teaching and research have made a successful combination.

Due to his organizing aptitudes, Professor Murgulescu was nominated Rector of the Timişoara Polytechnic Institute (1947–1949), Rector of the Bucharest University (1949–1950), Deputy Minister and Minister of Education (1950–1956) and again Minister of Education (1960–1963).

As an international recognition of his scientific merits, he was elected Member of the USSR Academy of Sciences, of the Czechoslovak Academy of Sciences, of the Hungarian Academy of Sciences, of the Bulgarian Academy of Sciences, of the New York Academy of Sciences.

He is also a Member of the American Chemical Society, of the International Society of Electrochemistry and of the American Association for the Advancement of Science.

He was editor-in-chief of *Studii şi cercetări de chimie – Academia R. S. România* and presently is editor-in-chief of the chemical scientific journal *Revue Roumaine de Chimie.*

For his scientific and public activity, Professor Murgulescu has been awarded distinctions, medals, and prizes such as : Romanian State Prize (1963), Professor Emeritus (1964), Emeritus Scientist (1969), Gold Medal of the 39th International Congress of Industrial Chemistry (1970), Hero of Socialist Labour (1971).

Professor Murgulescu's personality is held in high esteem by all Romanian scientists.

Now, as before, his many friends, students and colleagues warmly wish Professor Murgulescu many happy years to come.

THE EDITORIAL BOARD OF
REVUE ROUMAINE DE CHIMIE

Revue Roumaine de Chimie, **32**, *9–10*, 843–845 (1987)

Dedicated to Professor I. G. MURGULESCU
on his 85th anniversary

PARTITION COEFFICIENTS ON THE BASIS OF ATOMIC CHARGE DENSITY

V. EM. SAHINI and C. PODINĂ
Laboratory of Physical Chemistry,
Polytechnic Institute, Bd. Republicii 13, Bucharest, Romania

Received April 2, 1987

A method for the calculation of the octanol/water partition coefficient is established based on the resultant charge density of atomic group.

INTRODUCTION

The biological activity of substances can be correlated with some of their physical characteristics ;[1] from this point of view, the partition coefficient (P) between a lipidic phase (usually n–1-octanol) and water[2] is of a particular importance, describing, to a great extent, the transport properties of the biologically active substances in living organisms[3] and also their interactions with the receptive molecules.[4] Many attempts were made previously to find out computation methods of partition coefficients, among which well known is Hansch's method of fragments. Though empirical, it leads to good results in most of the cases, but there are some difficulties for more complex molecules, when inside them there take place interactions between various fragments such as bond dipole-dipole interactions, hydrogen bonds and other electronic and/or steric effects. In 1981 Klopman and Iroff [5] proposed a polynomial relation for the calculation of log P based on the charge densities (obtained by Hückel and MINDO/3 SCF molecular orbital methods) of the "heavy" atoms and neglecting the charge of the hydrogen atoms. The aim of the present paper is to find out a method for the calculation of log P taking into account the charge density of all the molecule atoms.

METHOD OF CALCULATION

We have obtained the charge density using the Del Re[6] method, which allows for getting such values for every atom in the molecule, including the hydrogen ones. We have considered that it is important especially for the hydroxyl and other groups able to achieve hydrogen bonds, to particularly know the charge existing at the hydrogen atoms which may be involved in such interactions. In large organic molecules and in the models of their interaction with the biological substrates, it is expected that an important role should be played not only by the resultant dipole moment of the molecule, but also by the interaction with the substrate of the local (bond) dipole existing in the so-called reactive points of the molecule. Therefore, in our calculations we used the values of "group charge" (q^*) obtained by algebraic addition of the charge of the atoms forming a group (CH_3, CH_2, OH, NH_2 etc.). We have also, used a polynomial relation (the terms p represent empirical coefficients referring to atom (i) or group (g) and give the contribution of three factors : the nature of the atoms, their number and charges)

$$\log P = \sum_i p_i + \sum_i n_i p_i^* + \sum_g p_g^* \; q_g^{*2}$$

in which by the first term (p_i) we take into account the presence of the i-class atoms in the molecule ; the second term (p_i^*) includes the number of atoms from each class ; the third term denotes the potential electrostatic interactions of various local dipoles and the dipoles of the molecules from the solvent cage.

The set of parameters used for calculating the atom charge densities is given in Table 1.[7]

Table 1

Parameters used in atom charge density calculation

Bond / Parameter	C—H	C—C	C—N	C—O	N—H	O—H
ε_{ij}	1.00	1.00	1.00	0.95	0.45	0.45
$\gamma_{i(j)}$	0.30	0.10	0.10	0.10	0.30	0.30
$\gamma_{j(i)}$	0.40	0.10	0.10	0.10	0.40	0.40
δ_i^0	0.07	0.07	0.07	0.07	0.24	0.40
δ_j^0	0.00	0.07	0.24	0.40	0.00	0.00

The following is the calculation relation we have used :

$$\log P = 0.344 + 0.2078\ n_H + 0.093\ n_C - 2.119\ n_N - 1.937\ n_O - 1.389\ \Sigma q_C^{*2} - 17.28\ \Sigma\ q_N^{*2} + 0.7316\ \Sigma\ q_O^{*2}$$

where n_H, n_C, n_N and n_O stand for the number of hydrogen, carbon, nitrogen and oxygen — atoms in the molecule while q_C^* is the group charge density for the carbon group in the molecule (CH_3, CH_2, CH), q_N^* is the group charge density for the nitrogen group (NH_2) and q_O^* represents the same value for oxygen group (OH).

RESULTS

The results are given in table 2.

Table 2

Experimental and computed values of partition coefficient

log P / Molecule	Experimental	Present paper	Computed MINDO/3 SCF	HÜCKEL	HANSCH
CH_3OH	−0.66	−0.68	−0.69	−0.66	−0.66
CH_3CH_2OH	−0.15	−0.17	−0.22	−0.20	−0.16
$CH_3CH_2CH_2OH$	0.30	0.32	0.30	0.31	0.34
$CH_3(CH_2)_2CH_2OH$	0.88	0.85	0.81	0.82	0.84
$CH_3(CH_2)_3CH_2OH$	1.40	1.36	0.31	1.34	1.34
$CH_3(CH_2)_4CH_2OH$	2.03	1.87	1.83	1.85	1.84
$(CH_3)_3COH$	0.37	0.85	0.74	0.54	0.37
CH_3OCH_3	0.10	−0.16	−0.15	−0.05	0.03
$C_2H_5OC_2H_5$	0.77	0.87	0.86	0.86	1.03
CH_3NH_2	−0.57	−0.78	−0.69	−0.77	−0.69
$CH_3CH_2NH_2$	−0.13	−0.29	—	—	—

For comparison we have also recorded the experimental values of log *P*, as well as those computed on the basis of the charge densities obtained by other calculation methods and by the method of fragments. The figures listed in table 2 show that the method proposed leads, in many cases, to results in satisfactory accordance with the experimental values, particularly in the case of larger molecules and of those having an increasing lipidic character. This result stresses the particular significance to be ascribed to the charge of hydrogen atoms in the bio-molecules and offers a new argument for a mechanism of the local anaesthetic action we dealt with in our previous papers.[8,9] We assume that binding of these substances at the level of the receptor is controlled by charge and that hydrogen bonds might be formed between a hydrogen acceptor on the receptor and hydrogen atoms from the anaesthetic molecule.

REFERENCES

[1] R. B. Barlow, "Quantitative Aspects of Chemical Pharmacology", Croom Helm, London, 1980, pp 20–35.

[2] A. Leo, C. Hansch and D. Elkins, *Chem. Rev.*, **71**, 525 (1971).

[3] W. H. Oldendorf, *Proc. Soc. Exp. Biol. Med.*, **147**, 813 (1984).

[4] R. F. Rekker, in "Biological Activity and Chemical Structure" (J. A. Keverling Buisman Editor), Elsevier, Amesterdam, 1977, p. 107–130.

[5] G. Klopman and Linda D. Iroff, *J. Comput. Chem.*, **2** (2), 157 (1981).

[6] G. del Re, *J. Chem. Soc.*, **1958**, 4031.

[7] V. Em. Sahini and Mihaela Hillebrand, "Chimie cuantică", Ed. Academiei, Bucharest, 1985, p. 201.

[8] Mioara Tripşa, V. Em. Sahini and V. Vasilescu, in "Water and Ions in Biological Systems" (A. Pulman, V. Vasilescu and L. Packer, Editors), Union of Societies for Medical Sciences, Bucharest, 1985, p. 131.

[9] M. Tripşa, V. E. Sahini, C. Nae and V. Vasilescu, *Gen. Physiol. Biophys.*, **5**, 371 (1986).

Revue Roumaine de Chimie, 32, *9–10*, 847–853 (1987)

Dedicated to Professor I. G. MURGULESCU
on his 85th anniversary

MICELLE FORMATION IN AQUEOUS SODIUM DODECYL SULFATE SOLUTIONS

RODICA VÎLCU and EUGENIA SĂLĂGEAN
Department of Physical Chemistry, Polytechnic Institute Bucharest,
Bd. Republicii 13, Bucharest

Received April 6, 1987

Micellization in aqueous sodium dodecyl sulfate (SDS) was investigated at two temperatures, by calorimetry and by an equilibrium method. From calorimetric and van't Hoff heats of micelle formation, the fraction of counterions bound into the micelle was estimated.

Thermodynamic functions of micelle formation, ΔG^{mic}, ΔH^{mic} and ΔS^{mic}, result through the approach of the equilibrium between monomers and micelles, an equilibrium rather questionable both in the its existence and in its nature. The only thermodynamic function accessible without any equilibrium assumption is the heat of micelle formation, so it could be used as validity test for equilibrium approaches.

For nonionic surfactants, heats of micellization from calorimetry and from van't Hoff equation agree quite well. For ionic surfactants, a direct comparison is not possible due to the fraction of counterions bound into micelle, which cannot be directly determined. The values quoted in literature for the fraction of counterions bound into micelle are widespread, making irrelevant any comparison between calorimetric and equilibrium heats of micelle formation. Other cumbersome aspects come from the sensible *cmc* dependence upon the method used for its determination, as well as from the fact that calorimetric and equilibrium data come out from various sources,[2] in many cases obtained on substances of different purity grades.

This paper aims to obtain the fraction of counterions bound into micelle. We have performed calorimetric measurements of the micellization heats, on a CALVET MS 70 differential calorimeter, and conductometric measurements on a conductometer of RADIOMETER type.

In order to check the method, we have used the most investigated ionic surfactant – sodium dodecyl sulfate (SDS), SERVA, of 99 % purity, without further purification.

CALORIMETRIC HEATS OF MICELLES FORMATION

The enthalpy of micelle formation, per mole of monomer bound into micelle, is defined as the difference bwetween partial molal heats of the micellar and monomeric SDS :

$$\Delta H^{\mathrm{mic}} = H_2^M - \overline{H}_2 \tag{1}$$

The integral heat of solution of solid SDS into water,

$$\Delta^i H^{\mathrm{dis}} = \frac{cmc}{c}(\overline{H}_2 - H_2^s) + \frac{c - cmc}{c}(H_2^M - H_2^s) + \frac{n_1}{n_2}(\overline{H}_1 - H_1) \tag{2}$$

where subscript 1 refers to the solvent and 2 to the solute, may be simplified in the *cmc* range, trough the assumption that the partial molal enthalpy of water, $\overline{H}_1$, is equal to its molal enthalpy :

$$\overline{H}_1 = H_1 \tag{3}$$

Then,

$$\Delta^i H^{\mathrm{dis}} = \overline{H}_2 - H_2^s + \Delta H^{\mathrm{mic}} - \frac{cmc}{c}\,\Delta H^{\mathrm{mic}} \tag{4}$$

At concentrations inferior to *cmc*, equation (4) reduces to :

$$\lim_{c < cmc} \Delta^i H^{\mathrm{dis}} = \overline{H}_2 - H_2^s \tag{5}$$

At concentrations higher than *cmc*, the heat balance equation predicts a linear dependence of the integral heat of solution on the reciprocal of concentration. If we admit that the partial molal enthalpies of the solute in the monomeric and micellar form are also concentration independent, from the equations (4) and (5) we get both the heat of micelles formation and the *cmc* value.

If equation (4) is valid over a larger range of concentrations, then at very high concentrations :

$$\lim_{c \gg cmc} \Delta^i H^{\mathrm{dis}} = \overline{H}_2 - H_2^s + \Delta H^{\mathrm{mic}} \tag{6}$$

The above equation offers another possibility to obtain the heat of micellization.

The heat balance equations were obtained under some approximations, so they need a very careful handling in order to give reliable results.

Besides the approximations concerning the partial molal entahlpies $\overline{H}_1$ and $\overline{H}_2$, we have also neglected other association phenomena, like pre *cmc* dimerization and micellar growth above *cmc*.

Another apparent drawback of equation (4) is the explicit presence of *cmc*, whose value is rather dependent on the method of determination.

The heat flow curves were recorded both without and with external Peltier compensation, and Joule calibration of each thermal effect.

The curves recorded without Peltier compensation show only a peak in the range of low concentrations, and two peaks in the range of high concentrations.

Two typical curves are presented in figure 1.

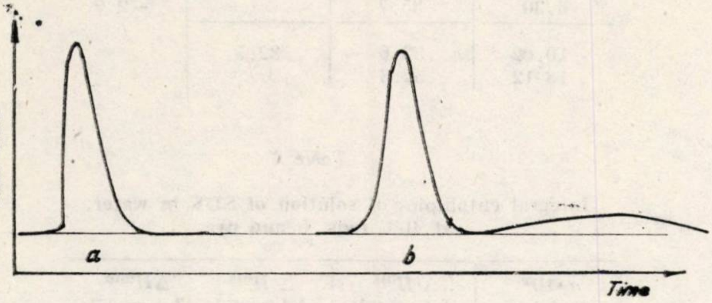

Fig. 1. — Heat flow curves: a.) at $c < cmc$; b) at $c > cmc$.

On both curves, the first peaks are delivered at about the same time ($\approx 30'$), representing the major part of the heat effect. The second peak, of a very low amplitude, extends over a much longer time (few hours).

On the curves recorded at the lower temperature, the second peak appeared only at very high concentrations.

The heats corresponding to the first peaks are rather constant relative to the concentrations, giving rise to two different values, namely a higher one at much lower concentrations than *cmc* and a smaller one at concentrations near and above *cmc*.

In the range of higher concentrations the whole heats obtained from the two peaks show the expected concentration dependence.

We consider as responsible for this behaviour the lack of agitation within our calorimeter, so that at the beginning of the heat flow, all the solute is in a kind of micellar form, and then, through a slow demicellization (the second broad peak) it comes to the equilibrium corresponding to the given concentration.

Thus, if our representation of the phenomena is right, we can get the heat of micelle formation, from the first peaks only, with equations (5) and (6), as well as from the entire curve, with equations (4) and (5). From the entire curves, the *cmc* is also accesible.

The fact that on the lower temperature curves the second peak appears only at very high concentrations, suggests, through equation (4), a low heat of micelle formation at this temperature. The micellization heats at this temperature were obtained only from equations (5) and (6).

The results are presented in tables 1, 2 and 3 each entry being a mean of three measurements with standard deviation of $0.2-0.3\ \mathrm{kJ.mol^{-1}}$

Table 1

Integral enthalpies of solution of SDS in water, at 31.5°C (eqs. 5 and 6)

$c\cdot10^3$ $\mathrm{mol\cdot L^{-1}}$	$\Delta^i H^{\mathrm{dis}}$ kJ, $\mathrm{mol^{-1}}$	$\Delta^i H^{\mathrm{dis}}$ $\mathrm{kJ\cdot mol^{-1}}$	ΔH^{mic} $\mathrm{kJ\cdot mol^{-1}}$
0.76	35.0	35.4	−2.9
2.51	35.6		
6.30	35.7		
10.02	32.6	32.5	
13.12	32.3		

Table 2

Integral entahlpies of solution of SDS in water, at 40°C (eqs. 5 and 6)

$c\cdot10^3$ $\mathrm{mol\cdot L^{-1}}$	$\Delta^i H^{\mathrm{dis}}$ $\mathrm{kJ\cdot mol^{-1}}$	$\Delta^i H^{\mathrm{dis}}$ $\mathrm{kJ\cdot mol^{-1}}$	ΔH^{mic} $\mathrm{kJ\cdot mol^{-1}}$
1.53	40.1	40.1	−7.1
3.97	40.1		
7.96	33.1	33.0	
10.86	33.0		
13.29	32.8		
20.97	33.1		

Table 3

Integral enthalpies of solution of SDS in water, at 40°C (eqs. 4 and 5)

$c\cdot10^3$ $\mathrm{mol\cdot L^{-1}}$	$\Delta^i H^{\mathrm{dis}}$ $\mathrm{kJ\cdot mol^{-1}}$	$\Delta^i H^{\mathrm{dis}} = f(c)$ $\mathrm{kJ\cdot mol^{-1}}$	ΔH^{mic} $\mathrm{kJ\cdot mol^{-1}}$	$cmc\cdot10^3$ $\mathrm{mol\cdot L^{-1}}$
1.53	40.1	40.1	−7.1	9.02
3.97	40.1			
7.96	40.0			
10.86	38.9	$32.9+0.06497\cdot\frac{1}{c}$		
13.29	37.7			
20.97	36.0			

EQUILIBRIUM APPROACH OF THE MICELLE FORMATION

For an ionic surfactant the micelles result through the equilibrium;

$$nL^- + mX^+ \rightleftarrows M^{-(n-m)} \qquad (7)$$

for which ΔG^{mic} per mole of monomer bound into micelle may be written :

$$\frac{\Delta G^{\mathrm{mic}}}{nRT} = \frac{\ln\,[\mathrm{M}]}{n} + \ln\,[L^-] + \frac{m}{n}\ln\,[\mathrm{X}^+] \tag{8}$$

where all the terms have the usual meaning, and $\frac{m}{n}$ stands for the fraction of counterions bound into micelle.

Approximating in the *cmc* range :

$$\frac{\ln\,[\mathrm{M}]}{n} - \text{negligible}$$

$$[\mathrm{L}^{-1}] \cong cmc \tag{9}$$

$$[\mathrm{X}^+] = c - \frac{m}{n}(c - cmc) \approx cmc$$

we get simplified expressions for ΔG^{mic} and ΔH^{mic} per mole of monomer bound into micelle :

$$\frac{\Delta G^{\mathrm{mic}}}{nRT} = \ln\, cmc + \frac{m}{n}\ln\, cmc \tag{10}$$

$$\frac{\Delta H^{\mathrm{mic}}}{n} = -RT^2\frac{\mathrm{d}\ln cmc}{dT}\left(1 + \frac{m}{n}\right) - RT^2\,\frac{\mathrm{d}\left(\frac{m}{n}\right)}{\mathrm{d}T}\ln cmc \tag{11}$$

In order to estimate the fraction of counterions bound into micelle, m/n, we suppose that in a narrow temperature range, the ratio m/n depends linearly on temperature, so

$$\frac{\mathrm{d}\left(\frac{m}{n}\right)}{\mathrm{d}T} = A \tag{12}$$

This assumption, and eqution (11) with the calorimetric values of micellization heats at two temperatures, give the system :

$$\Delta H^{\mathrm{mic}}_{T_1} = -RT_1^2\left(\frac{\mathrm{d}\ln cmc}{dT}\right)_{T_1}\left[1 + \left(\frac{m}{n}\right)_{T_1}\right] - RT_1^2\cdot A\cdot\ln\,(cmc)_{T_1}$$

$$\Delta H^{\mathrm{mic}}_{T_2} = -RT_2^2\left(\frac{\mathrm{d}\ln cmc}{\mathrm{d}T}\right)_{T_2}\left[1 + \left.\frac{m}{n}\right)_{T_1} + A(T_2 - T_1)\right] - RT_2^2\cdot A\cdot\ln(cmc)_{T_2}$$

which may be solved for m/n.

The critical micellar concentrations needed were obtained from specific conductance, following the usual procedure. The values of *cmc*'s at different temperatures are given in table 4.

Experimental values of *cmc* were correlated with temperature through a polynomial function:

$$\ln cmc = aT^2 + bT + c$$

to which an extreme condition was imposed at 295.65 K; the resulting correlation equation is:

$$\ln cmc = 2.0045 . 10^{-4} T(T - 2 \times 295.65) + 8.68837 \tag{14}$$

Solving the system (13) we obtain the value of the fraction of counterions bound into micelle (0.48) and its temperature coefficient $A = 1.78 . .10^{-4}\ \mathrm{K}^{-1}$.

With the fraction of counterions bound into micelle we estimated the thermodynamic micellization functions, presented in table 5, per mole of monomer bound into micelle. The ΔH^{mic} values are those obtained by calorimetry.

Table 4

Cmc of SDS in water

t, °C	$cmc \cdot 10^3$ mol·L^{-1}
30.2	8.20
35.0	8.35
40.4	8.64

Table 5

Thermodynamic micellization function of SDS in water

t, °C	$-\dfrac{\Delta G^{\mathrm{mic}}}{nRT}$	$-\dfrac{\Delta H^{\mathrm{mic}}}{nRT}$	$\dfrac{\Delta S^{\mathrm{mic}}}{nR}$
31.5	13.05	1.14	11.9
40.0	12.98	2.74	10.2

DISCUSSION OF THE RESULTS

We have investigated a very classical system is order to check the capabilities of our calorimetric method which is a modification of that used by Mazer and Olofsson[3]; their method has the great advantage of a direct heat of micellization determination, but with our calorimeter it does not work, due to a slight but ungovernable foaming which compromises the reprouctibility of the measurements. The determination of micellization enthalpy, entirely from the integral heats of solution which we adopted, implied a lot of simplifying assumptions. In spite of these assumptions, our results agree surprinsingly well with the most recent results on calorimetric determinations.[2,3]

The *cmc* values obtained from calorimetric measurements differ with 4% from that obtained from conductibility measurements, but still remain in the normal range of *cmc* at this temperature, taking into account the numerous values quoted for this property. [4–6]

The estimated fraction of bound counterions, as such, and through the micellization thermodynamic functions, ranges well with the various literature values.[1,7,8] Our value, although a bit smaller than the most values in literature, falls within a 0.1 deviation from these ones.

REFERENCES

[1] P. Mukerjee, *Adv. Colloid Interface Sci.*, **1**, (1967).
[2] G. Pilcher, M. N. Jones, L. Espada and H. A. Skinner, *J. Chem. Thermodyn.*, **1**, 381 (1969).
[3] N. A. Mazer and G. Olofsson, *J. Phys. Chem.*, **86**, 4584 (1982).
[4] A. Packter and M. Donbrow, *J. Pharm. Chem.*, **67**, 1713 (1963).
[5] F. Huisman, *Proc. Koninkl. Ned. Akad. Wentenchap.*, **B**, 67 (1964).
[6] M. F. Emerson and A. Holtzer, *J. Phys. Chem.*, **71**, 1898 (1967).
[7] D. Stigter and K. J. Mysels, *J. Phys. Chem.*, **59**, 45 (1955).
[8] D. Stigter, *J. Phys. Chem.*, **68**, 3603 (1964).

The estimated fraction of bound counterions, as such, and through the micellization thermodynamic functions, ranges well with the various literature values.[illegible] Our value, although a bit smaller than the most values in literature, falls within a 0.1 deviation from these ones.

REFERENCES

[1] [illegible] Mukerjee, Adv. Colloid Interface Sci. 1, 1 (1967).
[2] G. Pilcher, M. N. Jones, L. Espada and H. A. Skinner, J. Chem. Thermodynamics 1, 381 (1969).
[3] [illegible] and [illegible], J. Phys. Chem. 66, [illegible]84 (1962).
[4] A. Packter and M. Donbrow, J. Pharm. [illegible] 65, 1119 (1963).
[5] [illegible], [illegible] Acad. [illegible] 6[illegible] (1964).
[6] M. F. Emerson and A. Holtzer, J. Phys. Chem. 71, 1898 (1967).
[7] [illegible] and [illegible], J. Phys. Chem. 59, 45 (195[illegible]).
[8] [illegible], J. Phys. Chem. 68, [illegible] (1964).

Revue Roumaine de Chimie, **32**, *9–10*, 855–862 (1987)

Herrn Professor Dr. ILIE G. MURGULESCU,
dem Nestor der Physikalischen Chemie der
Sozialistischen Republik Rumänien, in Verehrung und langjähriger Verbundenheit
gewidmet

VAPOUR PRESSURES OF MOLTEN SALT MIXTURES ALKALI HALIDE–ALKALINE EARTH HALIDE

H.-H. EMONS, D. KIEẞLING, W. HORLBECK and K. WITTENBECHER
Bergakademie Freiberg, Sektion Chemie, Freiberg, DDR-9200

Received March 25, 1987

Vapour pressures of binary molten mixtures alkali halide — alkaline earth halide were determined by the Knudsen effusion method using the exact molar weight of vapours from mass-spectrometrical measurements. In all cases negative deviations of vapour pressure on ideality were found. A correlation between these maximum deviations and ionic parameters (radius and ion charge) of cations is discussed.

INTRODUCTION

In the previous papers [1–4] we reported on vapour pressure measurements of pure alkali and alkaline earth halides and their binary molten chloride mixtures. The Knudsen effusion method[5] was used, which needs the knowledge of molar weight of vapours to calculate vapour pressures. Because of the lack of data of vapour composition over the chloride mixtures the molar weight of monomeric alkali chloride molecules was used as approximate molar weight of the vapour.[2] The results of mass spectrometric investigations of gaseous phases over pure halides[3,4,6] and their binary mixtures [7] show that the relatively high contents of alkali halide dimers in the vapours cannot be neglected. Especially in the case of iodide mixtures the main species in the vapour except the alkali iodide are molecules of alkaline earth iodides and gaseous heterocomplexes.

In the present paper the vapour pressures of binary molten mixtures

$(Na, K, Rb, Cs)Br - CaBr_2$
$(Na, K, Rb, Cs)Br - SrBr_2$
$(Na, K, Rb, Cs)Br - BaBr_2$
$NaI - (Ca, Sr, Ba)I_2$

were measured. In literature vapour pressure data of these systems do not exist.

Considering the more exact vapour compositions of chloride mixtures the vapour pressure values published[1] were corrected.

EXPERIMENTAL METHOD

A principal scheme of the vapour pressure apparatus is shown in Fig. 1. The quartz glass tube (1), which contains the Knudsen cell (2), a condensing tube (3), and a platinum/platinum-10%-rhodium thermocouple (4) for temperature measurements are placed in a furnace (5). After reaching the temperature the filled Knudsen cell was brought in the zone of constant temperature by a magnetic sliding rod (6). The pressure in the quartz glass tube was maintained at an apparent vacuum of 10^{-4} Pa or lower.

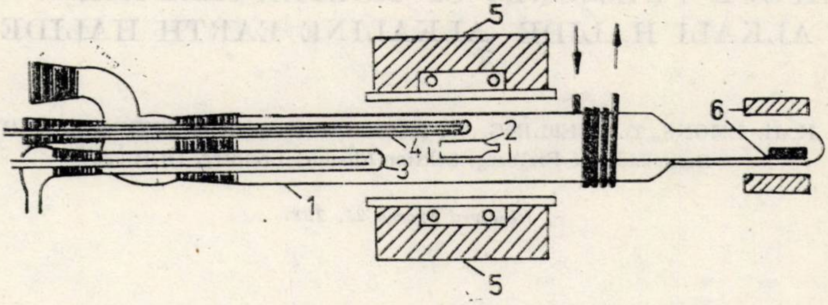

Fig. 1. — Apparatus of vapour pressure measurements by means of the Knudsen method.

From the weight loss W accompanying the effusion process in the time t the vapour pressure p can be calculated by the Knudsen equation [5]

$$p = \frac{W}{A_{\mathrm{eff}} \cdot t} (2\pi RT/M)^{1/2}, \tag{1}$$

were T is the absolute temperature, R the ideal gas constant, M the molar weight of the vapour, and A_{eff} the effective orifice area.

The effective orifice areas were determined microscopically considering the tabulated Clausing factors for geometry correction.[8,9] Molar weights of vapour were calculated from vapour compositions and consist of the parts of alkali halide monomers and dimers in a good approximation.[7] The validity of the molecular effusion formula (1) and its applicability to the measurements of small vapour pressures was first established by Knudsen's detailed studies on gaseous flow.[5] Carlson[10] stated by effusion experiments with Hg that molecular flows exist to a pressure $\leqslant$ 10 Pa. In this region the molecules of the gas passing through the small effusion orifice move nearly independently of one another. At higher pressures the mean free path of molecules is small enough in relation to the orifice dimensions that dependent motion prevails. The effusion can be described by a hydrodynamical flow for which equation (2)

$$p = \frac{W}{A_{\mathrm{eff}} \cdot t} (eRT/M)^{1/2} \tag{2}$$

is valid.

Different limits of transition from "molecular flow" to "hydrodynamical flow" expressed by the ratio Λ/d (Λ — mean free path; d — diameter of effusion orifice) are given in the literature.[5,11,12] These limits are in the region $> 4 - 10$ (mol. fl.) and $< 0.1 - 0.01$ (hydr. fl.), respectively. In this paper equation (2) was used to calculate vapour pressures in the region $\Lambda/d < 0.05$.

Considering all sources of errors a relative error of vapour pressure measurements of mixtures was found $< 10\%$. The highest contribution results from mass spectrometric determination of molar weight of vapour ($\leqslant 5\%$).

The preparation and purification of substances is given in[4,6]. The composition of premelted mixtures of alkali and alkaline earth halides was determined by analytical methods before and after vapour pressure measurements.

RESULTS AND DISCUSSION

Experimental vapour pressures could be described by a polynome equation of the type

$$p = a + bx + cx^2 + dx^3 + ex^4 + fx^5, \tag{3}$$

where x is the molar fraction of alkaline earth halide in molten mixtures. The vapour pressure isotherms of bromide and iodide mixtures fitted in this way are presented in Tables 1—4.

Table 1

Vapour pressures of mixtures calcium bromide — alkali bromide (p, Pa ; T, K)

$x^1_{CaBr_2}+$	NaBr	KBr	RbBr			CsBr		
T / p	1073	1073	1073	1120	1173	1033	1073	1173
0.0	103.0	141.4	190.8	428.7	983.9	193.0	364.5	1715.6
0.1	80.9	63.4	153.3	333.2	792.3	141.2	318.0	1378.8
0.2	61.7	48.6	111.9	249.3	636.0	95.5	245.2	1047.0
0.3	46.5	48.7	76.0	182.2	513.9	59.0	168.6	750.0
0.4	35.2	42.9	50.0	132.0	419.2	32.8	102.7	504.8
0.5	26.8	29.6	33.7	95.6	342.3	16.5	54.8	318.0
0.6	20.0	16.5	24.8	68.1	273.1	8.3	26.6	187.8
0.7	13.6	11.7	19.4	45.2	203.8	5.6	14.9	105.7
0.8	7.4	14.3	14.3	24.7	131.4	5.4	12.7	58.8
0.9	2.2	5.3	7.5	8.4	60.5	4.5	10.6	31.6
1.0	0.6	0.6	0.6	1.9	5.9	0.2	0.6	5.9

Table 2

Vapour pressures of mixtures strontium bromide — alkali bromide (p, Pa ; T, K)

$x^1_{SrBr_2}+$	NaBr	KBr	RbBr			CsBr		
T / p	1073	1073	1033	1073	1173	1033	1073	1173
0.0	103.8	137.6	87.3	183.4	1036.4	188.1	375.0	1698.7
0.1	83.2	98.6	65.2	153.7	690.9	156.1	323.0	1468.9
0.2	71.4	77.6	45.5	121.6	544.1	114.3	251.4	1202.9
0.3	61.3	63.0	29.7	91.6	485.0	78.6	179.8	938.8
0.4	50.1	49.6	18.3	66.2	445.7	54.7	119.5	701.2
0.5	38.4	36.4	11.0	46.4	392.7	41.4	75.2	503.0
0.6	28.3	25.0	7.1	32.0	317.7	33.6	46.7	347.4
0.7	21.5	17.2	5.4	21.9	228.5	25.5	30.3	230.6
0.8	17.9	13.4	4.6	14.7	140.5	14.1	20.8	143.1
0.9	13.7	10.3	3.2	8.8	66.6	2.0	12.7	72.5
1.0	0.3	0.3	0.1	0.3	3.4	0.1	0.3	3.4

Table 3

Vapour pressures of mixtures barium bromide — alkali bromide (p, Pa ; T, K)

$x^1_{BaBr_2}$ +	NaBr	KBr		RbBr			CsBr		
T / p	1153	1073	1153	1073	1136	1173	1073	1136	1173
0.0	458.8	141.2	538.0	187.9	550.6	959.4	373.5	998.7	1698.0
0.1	406.9	105.2	315.7	173.8	414.4	774.0	333.8	870.3	1510.9
0.2	357.7	85.8	221.3	145.5	339.4	663.6	267.6	723.2	1291.5
0.3	312.1	71.9	181.6	112.3	293.5	579.6	201.1	581.9	1061.0
0.4	269.5	58.5	156.0	80.6	256.8	497.6	146.5	457.9	837.6
0.5	228.0	44.7	128.3	53.9	218.6	410.6	106.2	353.2	635.3
0.6	185.5	31.8	97.5	33.5	175.5	321.7	76.4	264.1	463.2
0.7	140.7	22.0	70.2	19.3	128.8	237.9	51.3	185.1	323.7
0.8	93.2	15.8	51.0	10.0	82.2	162.5	27.1	112.8	211.6
0.9	45.0	—	34.8	—	39.1	89.1	—	49.2	112.6
1.0	1.3	—	1.3	—	0.9	2.1	—	0.9	2.1

Considering the content of dimeric alkali halide molecules in calculation of molar weight of vapour leads to a pressure, which is lower up to 20 % in the alkali halide rich region than the values obtained by using molar weight of monomers only. If both vapour pressure isotherms are compared, the differences in the concentration range $x^1_{M'X_2} > 0.6$ can be neglected (Fig. 2).

Table 4

Vapour pressures of mixtures sodium iodide — alkaline earth iodide (p, Pa ; T = 1073 K)

$x^1_{M'I_2}$ +	CaI$_2$	SrI$_2$	BaI$_2$
0.0	352.4	356.0	356.0
0.1	284.5	222.5	291.9
0.2	192.4	168.4	252.6
0.3	129.6	136.4	217.0
0.4	106.6	104.1	179.1
0.5	107.1	71.9	139.4
0.6	104.2	51.3	102.1
0.7	76.7	52.4	71.4
1.0	6.1	24.8	0.5

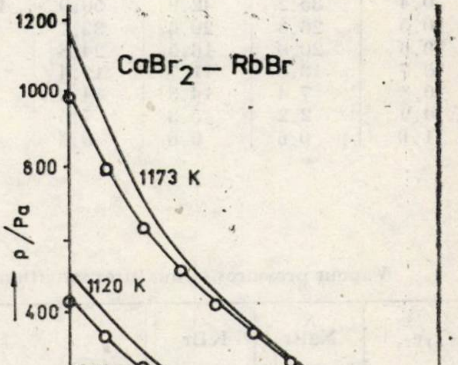

Fig. 2. — Vapour pressure of molten mixtures RbBr—CaBr$_2$; — calculated using molar weight of monomeric rubidium bromide ; ○ calculated with the exact molar weight

In all cases negative deviations from ideality were found, decreasing with increasing temperature. The dependence of these deviations on the alkali or alkaline earth cations in the mixtures is illustrated in Fig. 3

and Fig. 4 using the systems $MBr-SrBr_2$ and $CsBr-M'Br_2$ as examples. Negative deviations from ideality like the ionic interactions in mixtures increase in the order $Na^+ < K^+ < Rb^+ < Cs^+$ and $Ba^{2+} < Sr^{2+} < Ca^{2+}$. Analogous behaviour of the other chloride and bromide mixtures was also observed.

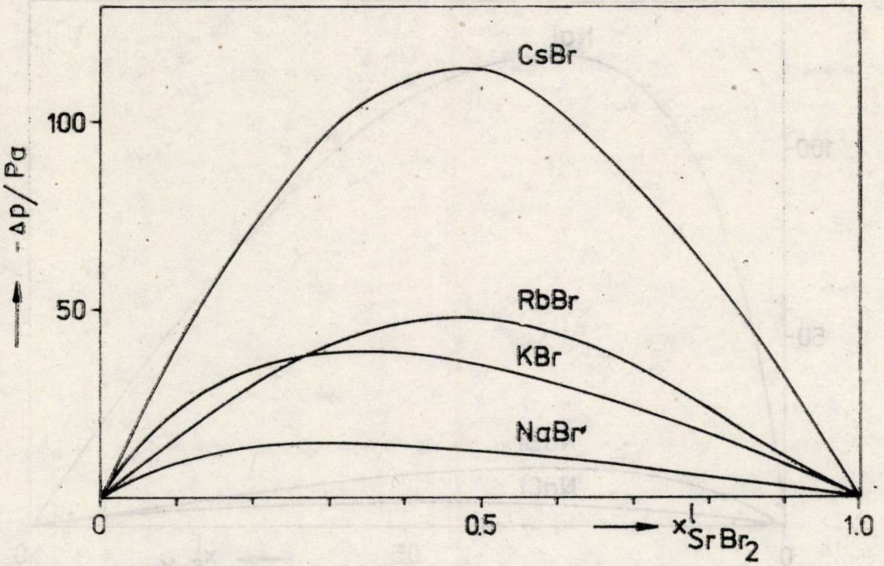

Fig. 3. — Deviations of vapour pressures on ideality; mixtures alkali bromide — strontium bromide; $T = 1073$ K.

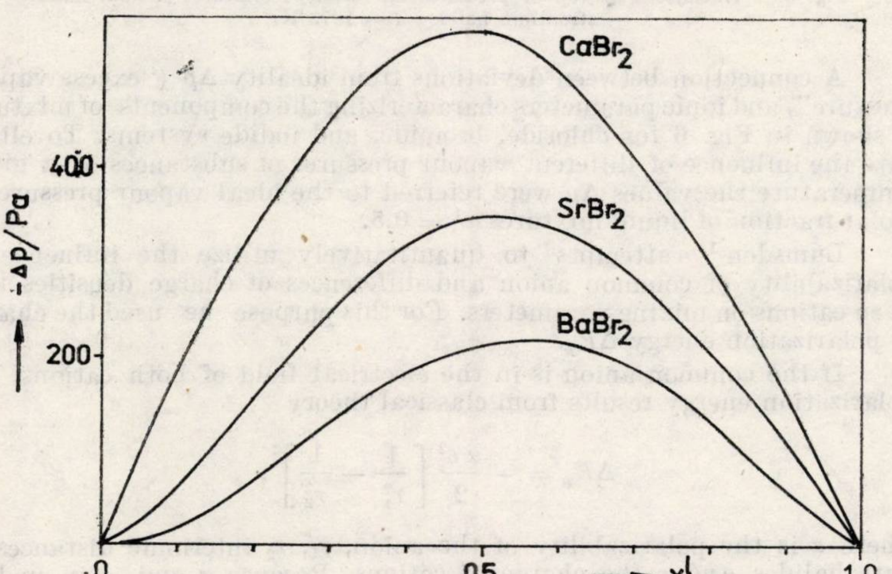

Fig. 4. — Deviations of vapour pressures on ideality: mixtures caesium bromide — alkaline earth bromide; $T = 1173$ K.

The influence of anions on the interactions depends above all on their polarizability increasing in the order $Cl^- < Br^- < I^-$ (Fig. 5). This is conformable to the increasing tendency of formation of gaseous heterocomplexes over mixtures alkali halide — alkaline earth halide.[7]

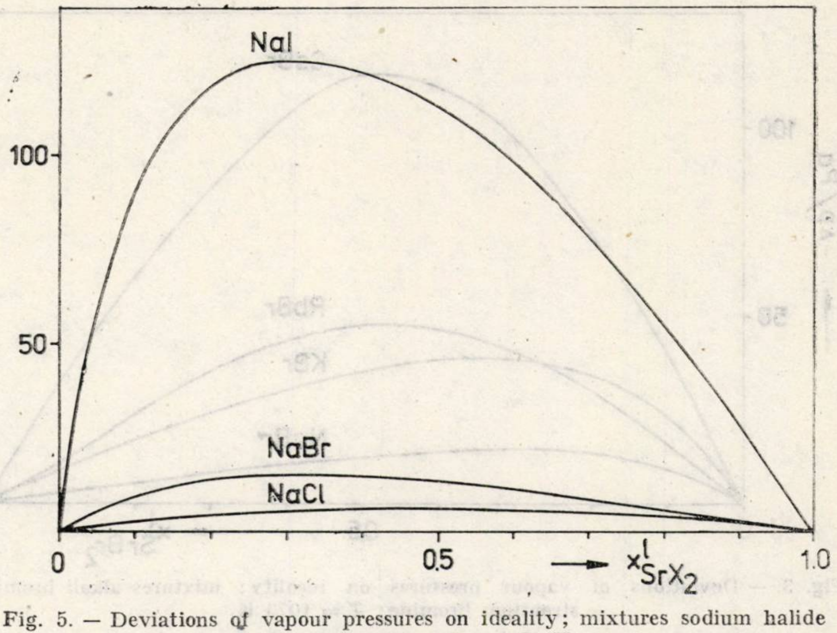

Fig. 5. — Deviations of vapour pressures on ideality; mixtures sodium halide — strontium halide; $T = 1073$ K.

A connection between deviations from ideality Δp ("excess vapour pressure") and ionic parameters characterizing the components of mixtures is shown in Fig. 6 for chloride, bromide, and iodide systems. To eliminate the influence of different vapour pressures of substances at a given temperature the values Δp were referred to the ideal vapour pressure at molar fraction of liquid mixtures $x^1 = 0.5$.

Lumsden[13] attempts to quantitatively utilize the influence of polarizability of common anion and differences of charge densities between cations on mixing parameters. For this purpose he used the change of polarization energy ΔE_p.

If the common anion is in the electrical field of both cations, the polarization energy results from classical theory

$$\Delta E_p = -\frac{\alpha e^2}{2}\left[\frac{1}{r_1^2} - \frac{1}{r_2^2}\right]^2, \tag{4}$$

where α is the polarizability of the anion, r_1, r_2 interionic distances of pure halides and e the charge of cations. Because r and α in molten salts are not exactly known, interionic distances data of crystals published by Pauling[14] and Wyckoff[15] and polarizabilities from Kordes[16] were used.

Generally the Δp-values are calculated at about 1073 K. In some cases vapour pressure data at higher temperatures were used. A systematic correlation between ionic parameters and the ionic interactions expressed by the "excess vapour pressure" is to be seen. Only in such molten mixtures, in which partially covalent interactions exist, like the systems (Na, K) Cl$-$MgCl$_2$ and LiCl$-$BaCl$_2$ (× in Fig. 6), results differ from this correlation.

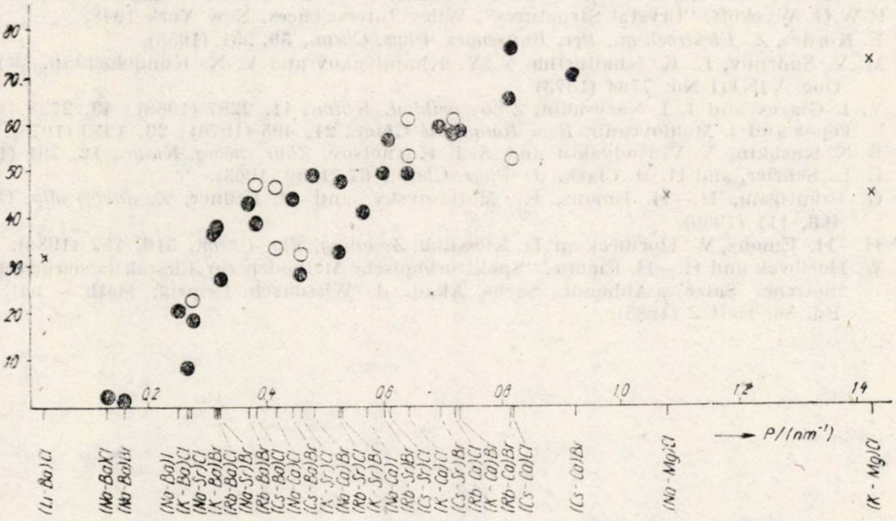

Fig. 6. — "Excess vapour pressures" of halide mixtures against polarization energy ΔE_p. ● — own values ; ○ — literature data : (Li, Cs) Cl$-$BaCl$_2$,[17] (Na, K) Cl$-$SrCl$_2$,[18] (Na, K, Rb, Cs)Cl$-$CaCl$_2$,[19] NaCl$-$MgCl$_2$,[20] KCl$-$MgCl$_2$.[20,21]

An analogous dependence was stated by Bräutigam et al.[22] in the case of electrical excess conductivities for the same type of mixtures. Thus different thermodynamic and transport properties of binary molten salt mixtures with Coulombic interactions can be described by ionic parameters of their components.

A comprehensive thermodynamic analysis of vapour pressure measurements is published in[23,24].

REFERENCES

[1] H.—H. Emons, G. Bräutigam and R. Thomas, *Chem. Zvesti*, **30**, 773 (1976).
[2] H.—H. Emons, G. Bräutigam and D. Kögler, *Z. Chem.*, **12**, 223 (1972).
[3] H.—H. Emons, W. Horlbeck and D. Kiessling, *Z. Chem.*, **21**, 416 (1981).
[4] H.—H. Emons, D. Kiessling and W. Horlbeck, *Z. anorg. allg. Chem.*, **488**, 219 (1982).
[5] M. Knudsen, *Ann. Physique*, **28**, 999 (1909).
[6] H.—H. Emons, W. Horlbeck and D. Kiessling, *Z. anorg. allg. Chem.*, **488**, 212 (1982).
[7] H.—H. Emons, W. Horlbeck and D. Kiessling, *Z. anorg. allg. Chem.*, **507**, 142 (1983).
[8] R. D. Freeman and J. G. Edwards, in "The Characterization of High Temperature Vapors", Wiley, New York 1967.
[9] T. E. Dunham and J. P. Hirth, *J. Chem. Phys.*, **49**, 4650 (1968).

[10] K. D. Carlson, P. W. Gilles and R. J. Thorn, *J. Chem. Phys.*, **38**, 2725 (1963).
[11] P. G. Wahlbeck, *J. Chem. Phys.*, **55**, 1709 (1971).
[12] W. Hirschwald, F. Stolze and I. N. Stranski, *Z. Phys. Chem. (Neue Folge)*, **42**, 96 (1964).
[13] J. Lumsden, "Thermodynamics of Molten Salt Mixtures", Academic Press, New York, London 1966.
[14] L. Pauling, "Die Natur der chemischen Bindung", Verlag Chemie, Weinheim 1962.
[15] R.W.G. Wyckoff, "Crystal Structures", Wiley Interscienccs, New York 1948.
[16] E. Kordes, *Z. Elektrochem., Ber. Bunsenges. Phys. Chem.*, **59**, 551 (1955).
[17] M. V. Smirnov, L. K. Khalturina, V. Y. Khundyakov and V. N. Khudolozhkin, Deposit. Doc. VINIII No. 7764 (1973).
[18] V. I. Glazov and I. I. Naryshkin, *Zhur. priklad. Khim.*, **41**, 2297 (1968); **43**, 2728 (1970).
[19] L. Topor and I. Moldoveanu, *Rev. Roumaine Chim.*, **21**, 495 (1976); **23**, 1353 (1978).
[20] B. N. Kushkin, V. V. Rodyakin and S. I. Kuznetsov, *Zhur. neorg. Khim.*, **12**, 791 (1967).
[21] E. E. Schrier, and H. M. Clark, *J. Phys. Chem.*, **67**, 1259 (1963).
[22] G. Bräutigam, H.—H. Emons, K. Matiasovsky and P. Fellner, *Z. anorg. allg. Chem.*, **468**, 111 (1980).
[23] H.—H. Emons, W. Horlbeck an D. Kiessling, *Z. anorg. allg. Chem.*, **510**, 152 (1984).
[24] W. Horlbeck and H.—H. Emons, "Spektroskopische Methoden zur Charakterisierung geschmolzener Salze"; Abhandl. Sächs. Akad. d. Wissensch. Leipzig, Math. — nat. Kl., Bd. 56, Heft 2 (1985).

Revue Roumaine de Chimie, **32**, *9–10*, 863–875 (1987)

Dedicated to Professor I. G. MURGULESCU
on his 85th anniversary

COMPUTATION OF SATURATION PRESSURE AND ORTHOBARIC DENSITIES BY A GENERAL CUBIC EQUATION OF STATE

DAN GEANĂ, VIOREL FEROIU and ORTANSA LANDAUER
Dept. Physical Chemistry/TSCO, Polytechnic Institute, Bucharest, Spl. Independenţei
313, Romania

Received April 25, 1987

The results of liquid-vapour equilibria calculations (saturation pressure and orthobaric densities) based on a general cubic equation of state[1] for water, sulphur dioxide and argon are presented. The computations were done over the range of temperature and pressure between the triple and critical points of the above substances. The results are compared with experimental data and with those predicted by the widely used Peng-Robinson equation. It is shown that our general cubic equation of state predicts more reliable results.

The equations of state are commonly used to calculate thermodynamic properties for the design of chemical processes. For engineering purposes, the most used equations of state are either empirical or semitheoretical, containing adjustable parameters that are fitted to experimental data. In two previous papers [1,2] we presented a new cubic general equation of state which was applied to PVT calculations of pure fluids as well as to phase equilibria computations of pure fluids and mixtures. The results obtained using this equation of state compared favorably with experimental data and with those predicted by other commonly used equations in the literature.

The properties of pure fluids, e.g. the vapor pressure and the orthobaric densities must be well done by an equation of state and this is a condition for further extension to mixtures. The computations reported with different cubic equations of state represent in a different way the phase behaviour of fluids over wide ranges of temperature and pressure. Many comparisons were presented in the literature[3–10] between experimental values and those predicted by cubic equations of state for orthobaric curve of pure substances. For example, in Soave's paper[3] the comparison is limited to vapor pressure in the range of temperature between the triple point and critical point. Peng and Robinson[5] motivated their equation by a better agreement with experimental data for the saturated liquid density, as compared with other equations. In other papers[8] the comparison is done for ranges of pressure $P \leqslant 1$ bar and respectively $P > 1$ bar.

In a previous work[11] we presented the results obtained with our general cubic equation of state for prediction of vapor pressure and orthobaric densities of three hydrocarbons : methane, ethane and *n*-butane. The results compared favorably with experimental data and are better than those obtained with the Peng-Robinson equation.

In this paper we report on vapor pressure and orthobaric densities predicted by our equation[1,2] and by the Peng-Robinson equation for three substances : argon, water and sulphur dioxide. The computations were done over the ranges of temperature and pressure, between triple and critical points of the above substances.

The results are compared with experimental data and with those predicted by the widely used Peng-Robinson equation. It is shown that generally, our equation of state predicts more reliable results.

CUBIC EQUATIONS OF STATE

For the computations of saturation pressure and orthobaric densities (or molar volumes) we have used two equations of state. First, we applied our general cubic equation of state.[1,2] Second, the common used Peng-Robinson (PR) equation is considered.

The general cubic equation developed by us, based on Himpan's equation[12] is :

$$P = \frac{RT}{V - b} - \frac{a/T^m}{(V - d)^2 + c} \tag{1}$$

or in reduced form :

$$P = \frac{T_r}{U + B} - \frac{A/T_r^m}{(U + D)^2 + C} \tag{2}$$

This reduced form was obtained by a procedure described in another paper.[1,2] Imposing the critical conditions (3 equations) and the critical point slope of the vapor pressure as suggested by Riedel[13]

$$\alpha_c = (\partial P_r/\partial T_r)V_r ; \quad V_r = 1 ; \quad T_r = 1$$

one obtains expressions for the four parameters :

$$A = \frac{(\alpha_c - 1)^3}{(\alpha_c + m)^3} ; \quad B = \frac{1 + m}{\alpha_c + m} \tag{2a}$$

$$C = \frac{(\alpha_c - 1)^2(3m + 4 - \alpha_c)}{4(\alpha + m)^3 ;} ; \quad D = \frac{\alpha_c - 1}{\alpha_c + m} \tag{2b}$$

where P_r, T_r, V_r are reduced pressure, temperature and volume respectively, and

$$U = Z_c(V_r - 1) \tag{2c}$$

with

$$Z_c = P_c V_c/(RT_c) \tag{2d}$$

The new parameter, m, has the role to modify the form of the isotherms thus increasing the flexibility of the equation. Written in the above form, the equation of state contains three parameters : Z_c (critical compressibility factor), α_c (Riedel's criterion) and m (called isotherm contraction parameter). In all calculations Z_c was obtained from experimental critical values (P_c, T_c, V_c) of the substances. The two parameters α_c and m were chosed as will be reported further.

The PR equation, in the original form[5] is :

$$P = \frac{RT}{V - b} - \frac{(T)}{V(V + b) + b(V - b)} \tag{4}$$

or

$$P = \frac{RT}{V - b} - \frac{a(T)}{(V + \delta_1 b)(V + \delta_2 b)} \tag{5}$$

We must remark that equation (5) is a particular form of equation (1) for the restrictions :

$$\gamma = \delta_1 b \quad \text{and} \quad \delta = \delta_2 b$$

with γ and δ as in the previous works[1,2].

The function $a(T)$ is :

$$a(T) = a \cdot \alpha(T_r)$$

with

$$\alpha(T_r) = [1 + K(1 - \sqrt{T_r})]^2$$

where K is a function of acentric factor (ω) :

$$K = 0.37464 + 1.54226\ \omega - 0.26992\ \omega^2$$

A recent modification[9] of the original equation has introduced

$$K = K_0 + K_1(1 + \sqrt{T_r})\ (0.7 - T_r)$$

with

$$K_0 = 0.378893 + 1.489153\ \omega - 0.17131848\ \omega^2 + 0.0196554\ \omega^3$$

and K_1 an adjustable parameter.

In this paper, the original expression of PR equation has been used, which in the reduced form becomes :

$$P_r = \frac{T_r}{Z_c V_r - 0.0778} - \frac{a(T_r)}{Z_c V_r (Z V_r + 0.0778) + 0.0778\ (Z_c V_r - 0.0778)} \tag{6}$$

with $a(T_r) = 0.457236 \cdot \alpha(T_r)$.

Equation (6) may be rearranged in the form :

$$P_r = \frac{T_r}{Z_c(V_r - b')} - \frac{a'(T_r)}{(V_r + b')^2 - 2(b')^2} \tag{7}$$

with

$$b' = 0.0778/Z_c \quad \text{and} \quad a'(T_r) = a(T_r)/Z_c^2$$

Comparing with our modification of Himpan's equation[1]

$$P_r = \frac{T_r}{Z_c(V_r - B')} - \frac{A'/T_r^m}{(V_r - D')^2 + C'} \tag{8}$$

the following results :

$$A' = 0.457236/Z_c^2 \,; \qquad B' = b'$$

$$C' = -2(b')^2 \,; \qquad D' = -b'$$

and $\alpha(T_r)$ taking the place of T_r^{-m}.

By the substitution of $U = Z_c(V_r - 1)$, one obtains for the constants A, B, C, D in equation (1) the following expressions :

$$A = A' \cdot Z_c^2 = 0.457236 \tag{9}$$

$$B = (1 - B')Z_c = (1 - b')Z_c \tag{10}$$

$$C = C'Z_c^2 = -2(b')^2 Z_c^2 \tag{11}$$

$$D = (1 - D')Z_c = (1 + b')Z_c \tag{12}$$

All the expressions deduced for our equation of state (8) in the previous papers[1,2] can be applied also to the PR equation with the constants (9–12). Of course, imposing the restrictions given by expressions (9–12), the PR equation did not verify the experimental value Z_c predicting for all the substances the value $Z_c^{PR} = 0.307$.

COMPUTATION OF SATURATION PRESSURE AND ORTHOBARIC DENSITIES

For liquid-vapour phase equilibrium calculations of pure substances (saturation pressure and orthobaric densities), a method based on the equality of chemical potential in both phases has been used. For a pure component it is obtained :

$$G^L = G^V \quad \text{or} \quad F^L + PV^L = F^V + PV^V$$

where G is the free enthalpy and F, the free energy.

The equilibrium equation can be written in the form :

$$P = \frac{F^L - F^V}{V^V - V^L} = \frac{\int\limits_{V^L}^{V^V} P dV}{V^V - V^L} \tag{13}$$

or for reduced parameters :

$$P = \frac{\int\limits_{V_r^V}^{V_r^V} P_r dV_r}{V_r^V - V_r^L} \tag{14}$$

The integral is calculated from the equation of state and for equation (1), it has the expression :

$$\int\limits_{V_r^L}^{V_r^V} P_r \mathrm{d} V_r = \frac{T_r}{Z_c} \ln \frac{U^V + B}{U^L + B} + \frac{A}{Z_c T_c^m} (E^V - E^L) \tag{15}$$

where :

$$E = \frac{1}{2\sqrt{-C}} \ln \frac{U + D + \sqrt{-C}}{U + D - \sqrt{-C}} \qquad \text{for } C < 0$$

$$E = \frac{1}{\sqrt{C}} \operatorname{arc\,tg} \frac{\sqrt{C}}{U + D} \qquad \text{for } C > 0 \tag{16}$$

$$E = \frac{1}{U + D} \qquad \text{for } C = 0$$

with U^V and E^V for the vapour phase, respectively U^L and E^L for the liquid phase.

For PR equation we used expressions (14—16) with the constants A, B, C, D given by equations (9—12). In this way, the calculation method is general, being independent of the used cubic equation of state.

The algorithm of the calculation procedure is :

a) For a given temperature, a saturation pressure value is estimated.

b) Using the equation of state the molar volumes of phases (by U^V and U^L values) are calculated.

c) A new estimation of pressure is done from equation (14) using the volumes obtained at (b). The calculation is repeated from (b) until the change in pressure from one iteration to the next is less than a given error ($|\Delta P/P| < 10^{-4}$).

It must be remarked that this procedure works only in the case when the equation of state has for the pressure for which the computation is done, three real roots, distinctive in volume, i.a. the isobar intersects the isotherm in three points. The situation can be met when the equation of state has a single real root in volume.

For using the algorithm in all the cases, the solving of the equation of state is done together with solving of the equation of the first derivative of pressure with respect to volume:

$$P' = \left(\frac{\partial P}{\partial V} \right)_T = 0 \tag{17}$$

From equation (17), the maximum respectively the minimum molar volumes (densities) are calculated, corresponding to vapour and liquid phases. One of this values is attached to the single real root of the equation of state, which was attributed to one phase molar volume (density). This procedure is in detail described in literature.[10] Numerical methods for solving equations (1) and (14) can be used: the secant method, the hyperbolic method, the Newton-Raphson's method, the Muller' method etc.[14,15] In this paper the secant and hyperbolic methods were used. Based on the above algorithm a computer code in BASIC was written.

DISCUSSION OF RESULTS

Computations of the saturation pressure and orthobaric densities for three pure substances: argon, water and sulphur dioxide were done using the equation of state (1) and PR equation (7). The computation results expressed as relative errors in pressure, $\varepsilon_P(\%)$, liquid density (volume) $\varepsilon_L(\%)$ and vapour density (volume) $\varepsilon_V(\%)$ are presented in figures 1–9, as a function of temperature.

The errors were calculated by the formula:

$$\varepsilon_M = \frac{M^{\text{exp}} - M^{\text{calc}}}{M^{\text{exp}}} \cdot 100 \tag{18}$$

where M = pressure, liquid density (volume) at equilibrium, vapour density (volume) at equilibrium.

The computations have been done in the whole range of temperature between triple and critical point. For comparison, experimental data in the literature[16,17] have been used.

The critical data and acentric factors which have been used in computation are presented in table 1.

The m and α_c parameters of our equation of state (1) were estimated for each substance from the values of saturation pressure and experimental liquid density at normal boiling temperature. The estimation was done by minimisation of the following expression:

$$S(\alpha_c, m) = \left[\left(\frac{P^{\text{exp}} - P^{\text{calc}}}{\sigma_P} \right)^2 + \left(\frac{\rho_L^{\text{exp}} - \rho_L^{\text{calc}}}{\sigma_{\rho_L}} \right)^2 \right]_{T=T_f} \tag{19}$$

Table 1

Critical data and acentric factors

Substance	T_c[K]	P_c[atm]	V_c[m^3/kg]	ω	Literature
Water	647.2	217.6	$3.108 \cdot 10^{-3}$	0.344	/16,17/
Sulphur dioxide	425.1	77.23	$1.906 \cdot 10^{-3}$	0.251	/16/
Argon	150.9	48.34	$1.867 \cdot 10^{-3}$	0	/16,17/

using Hooke-Jeeves or Rosenbrok's method.[18] The standard deviations were chosen as $\sigma_P = 10^{-3} \cdot P^{\text{exp}}$ and $\sigma_{\rho_L} = 10^{-3} \cdot \rho_L^{\text{exp}}$. The obtained parameter values for the three pure substances are presented in table 2. In the same table we give also the α_c values calculated by Riedel's relation:[13]

$$\alpha_c = 0.9076 \, [1 + T_f (T_c - T_f)^{-1} + \ln P_c] \tag{20}$$

Table 2

α_c and m Parameters for Equation (1)

Subst.	m(estimate)	α_c (estimate)	α_c (Riedel)	Observation
Water	0.35	8.15	7.559	From $P = 1$ atm $T_B = 373.15$ K $\rho_L = 957.492$ kg/m^3
Sulphur dioxide	0.4407	7.4008	7.308	From $P = 1.363$ bar $T = 270$ K $\rho_L = 1441.33$ kg/m^3
Argon	0.15	5.9125	5.739	From $P = 1$ atm $T_B = 87.3$ K $\rho_L = 1393.92$ kg/m^3
Sulphur dioxide	0.4213	7.3471	7.308	From data of: 90.4; 120; 150; 200; 250; 290 [K]

We have to remark that α_c values estimated with expression (19) do not differ too much from those predicted with equation (20).

The results obtained for the saturation pressure for the three substances are shown in figures 1–3.

PR equation used for water (Fig. 1) gives, for vapour pressure in the range of temperature between triple and critical point, greater errors, till 20%, while equation (1) gives only 10%. Both equations reproduce satisfactorily the experimental vapour pressure of water, giving errors less than 5% in the range of temperatures between the boiling and critical points.

PR equation used for sulphur dioxide (Fig. 2) gives strong deviations of vapour pressure in the range of temperature between the triple and critical points (40% at triple point) and they remain greater than

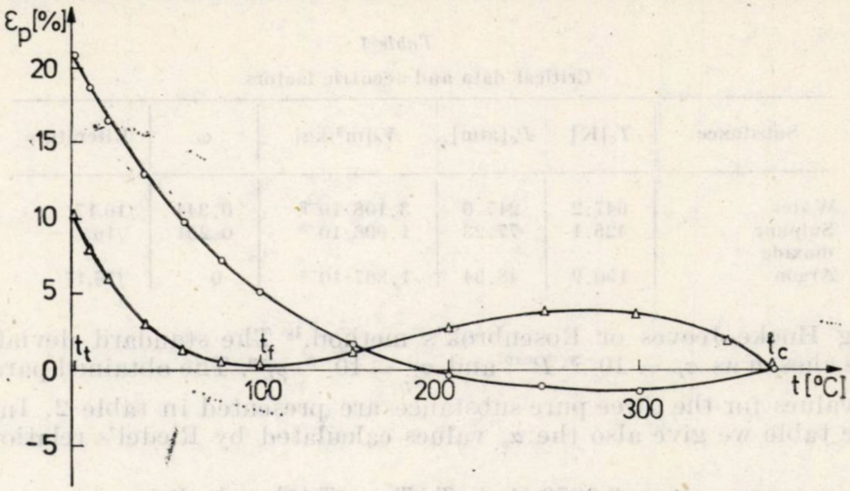

Fig. 1. — Deviation in saturation pressure for water: Δ — equation (1) with m and α_c, estimated parameters at boiling temperature; o — PR equation.

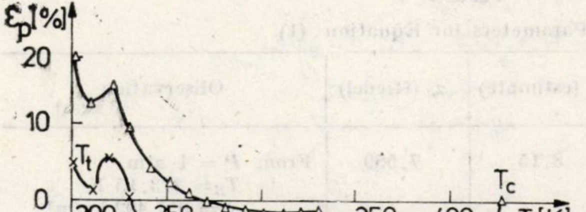

Fig. 2. — Deviation in saturation pressure for sulphur dioxide: Δ — equation (1) with m and α_c, estimated parameters at boiling temperature; o — PE equation; x — equation (1) with m and α_c, estimate parameters from data at: 90.4; 120; 150; 200; 250; 290 K.

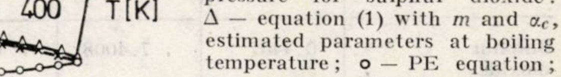

Fig. 3. — Deviation in saturation pressure for argon: Δ — equation (1) with m and α_c, estimated parameters at boiling temperature; o — PR equation.

10 % even in the range of temperature between the boiling and critical points. Equation (1) estimates better the vapour pressure of sulphur dioxide with a maximum error of 17 % at the triple point, remaining less than 10 % in another range.

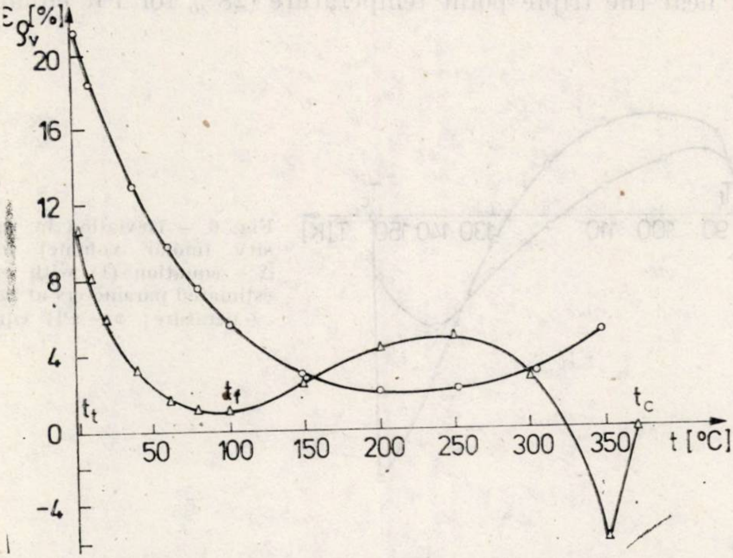

Fig. 4. — Deviation in vapour density (molar volume) for water: Δ — equation (1) with m and α_c, estimated parameters at boiling temperature; ○ — PR equation.

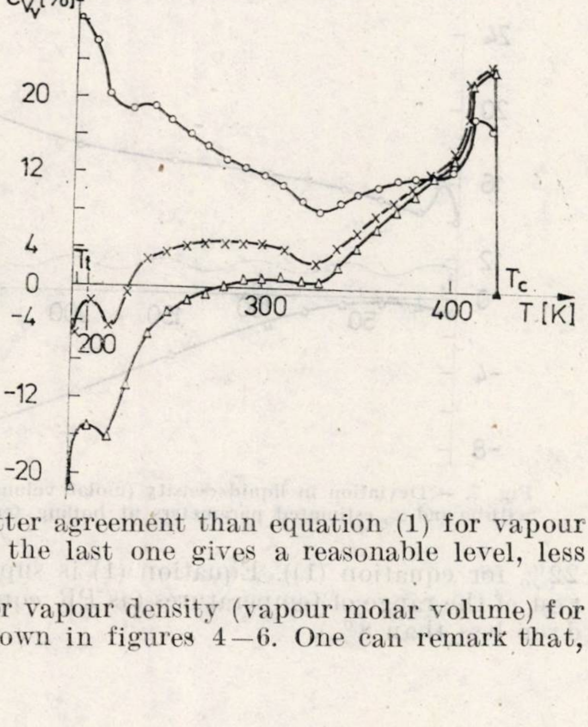

Fig. 5. — Deviation in vapour density (molar volume) for sulphur dioxide: Δ — equation (1) with m and α_c, estimated parameters at boiling temperature; ○ — PR equation; x — equation (1) with m and α_c, estimated parameters from data at: 90.4; 120; 150; 200; 250; 290 K.

PR equation yields better agreement than equation (1) for vapour pressure of argon, however the last one gives a reasonable level, less than 2.5 %.

The results obtained for vapour density (vapour molar volume) for the three substances are shown in figures 4—6. One can remark that, for water, as for the saturation pressure, PR equation yields the maximum error of 21% at the triple point, while equation (1) has a better accuracy, giving errors of 10.5%.

Both equations give maximum errors for sulphur dioxide (Fig. 5), especially near the triple point temperature (28% for PR equation and 22% for equation (1)). Equation (1) is superior to PR equation in the rest of the range of temperatures (as PR equation gives errors that never drop less than 8%).

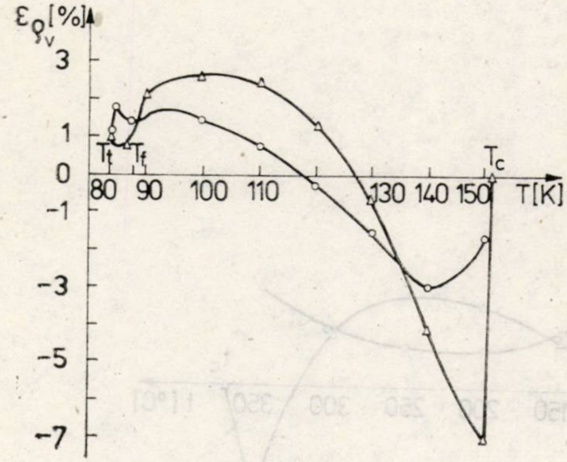

Fig. 6. — Deviation in vapour density (molar volume) for argon: Δ — equation (1) with m and α_c, estimated parameters at boiling temperature; o — PR equation:

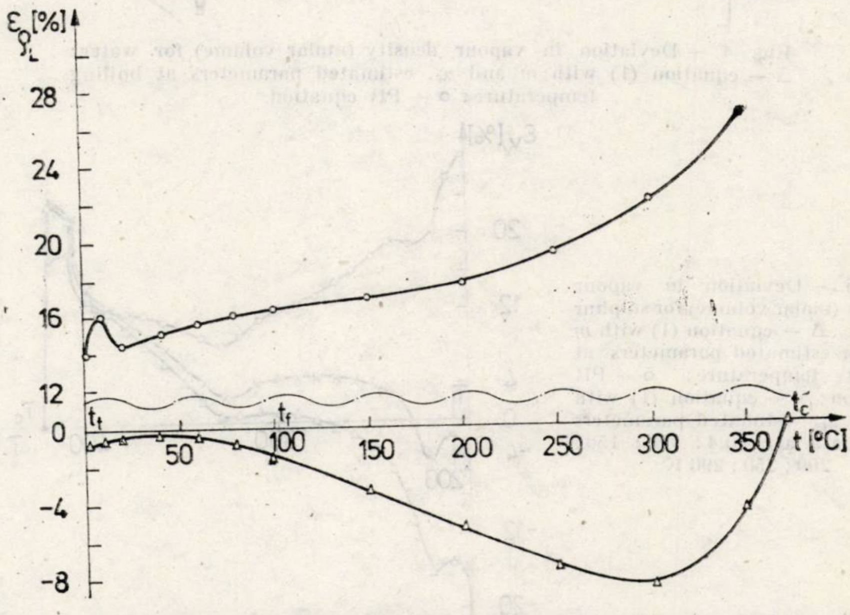

Fig. 7. — Deviation in liquid density (molar volume) for water: Δ — equation (1) with m and α_c, estimated parameters at boiling temperature; o — PR equation.

Both equations estimate acceptably the vapour density for argon, giving errors less than 3% in the most part of the range of temperatures, equation (1) giving greater errors near the critical point (7%).

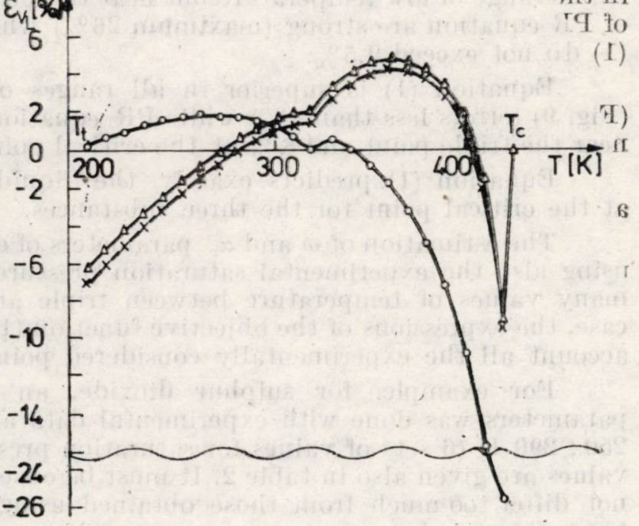

Fig. 8. — Deviation in liquid density (molar volume) for sulphur dioxide : Δ — equation (1) with m and α_c, estimated parameters at boiling temperature ; o — PR equation ; x — equation (1) with m and α_c, estimated parameters from data at : 90.4 ; 120 ; 150 ; 200 ; 250 ; 290 K.

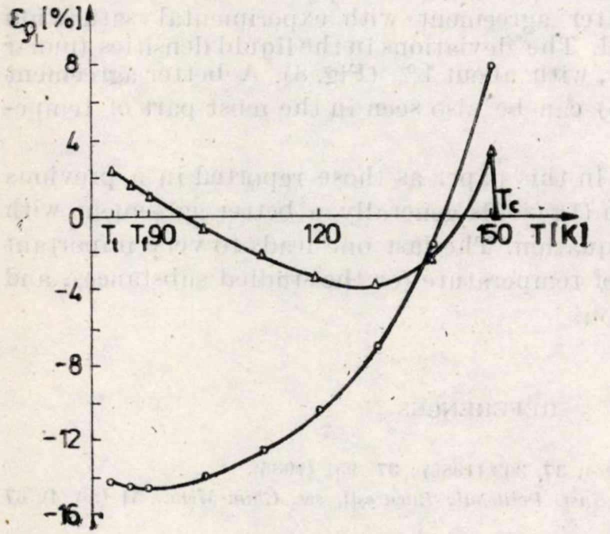

Fig. 9. — Deviation in liquid density (molare volume) for argon : Δ— Δ — equation (1) with m and α_c, estimated parameters at boiling temperature ; o — PR equation.

It must be remarked that equation (1) predicts exactly the values of vapour density (molar volume) at the critical point for all the three substances.

The deviations in liquid densities (molar volume) are shown in figures 7—9. Equation (1) is superior to PR equation in the whole range of temperature, for water, as shown in figure 7. PR equation yields errors between minimum 14% and maximum 26%, while equation (1) does not exceed 9%.

PR equation is slightly better than equation (1) for sulphur dioxide, in the range of low temperature but near the critical point the deviations of PR equation are strong (maximum 26%) while the errors of equation (1) do not exceed 9.5%.

Equation (1) is superior in all ranges of temperature for argon (Fig. 9) (errors less than 4%) while PR equation has derivations of 15% near the triple point and 8% at the critical point.

Equation (1) predicts exactly the liquid density (molar volume) at the critical point for the three substances.

The estimation of m and α_c parameters of equation (1) may be done using also the experimental saturation pressure and liquid densities for many values of temperature between triple and critical point. In this case, the expressions of the objective function (19) is modified taking into account all the experimentally considered points.[1]

For example, for sulphur dioxide, an estimation of m and α_c parameters was done with experimental data at : 90.4 ; 120 ; 150 ; 200 ; 250 ; 290 K (6 sets of values for saturation pressure-liquid density). The values are given also in table 2. It must be observed that these values do not differ too much from those obtained using the data at the boiling temperature only.

The errors which appear using this set of parameters are shown in figures 2, 5 and 8. A better agreement with experimental saturation pressure (Fig. 12) is observed. The deviations in the liquid densities (molar volume) are slightly smaller, with about 1% (Fig. 8). A better agreement for vapour densities (Fig. 5) can be also seen in the most part of temperature range.

The results presented in this paper as those reported in a previous work, [11] show that equation (1) yields generally a better agreement with the experiment than PR equation. The last one leads to very important deviations in some ranges of temperature for the studied substances, and it must be used with caution.

REFERENCES

[1] D. Geană, *Rev. Chim. (București)*, **37**, 303 (1986) ; **37**, 951 (1986).

[2] F. Daneș, and D. Geană, *Bul. Inst. Politehnic București, ser. Chim-Metal.*, **51** (no. 4), 67 (1979).

[3] G. Soave, *Chem. Eng. Sci.*, **27**, 1197 (1972).

[4] G. Soave, *I. Chem. E. Symposium* Series No. 56.

[5] D. Y. Peng and D. B. Robinson, *Ind. Eng. Chem. Fundam.*, **15**, 59 (1976).

[6] E. Usdin, J. C. Mc Auliffe, *Chem. Eng. Sci.*, **31**, 1077 (1976).

[7] G. Schmidt and H. Wenzel, *Chem. Eng. Sci.*, **35**, 1503 (1980).

[8] J. Vidal, *Fluid Phase Equil.*, **13**, 15 (1983).

[9] R. Stryjek and J. H. Vera, *Fluid Phase Equil.*, **25**, 279 (1986).

[10] T. F. Anderson and J. P. Prausnitz, *Ind. Eng. Chem. Proc. Des. Dev.*, **19**, 1 (1980).

[11] D. Geană, V. Feroiu and O. Landauer, *Rev. Chim. (București)*, in print.

[12] J. Himpan, *Monatsh. Chem.*, **84**, 787 (1953) ; **86**, 289 (1955).

[13] L. Riedel, *Chem. Ing. Techn.*, **26**, 83 (1954).

[14] J. Ortega and W. Rheinboldt, "Iterative Solution of Nonlinear Equation in Several Variables", Academic Press, New York, 1970.

[15] St. Maruşter, "Metode numerice de rezolvare a ecuaţiilor neliniare", Ed. Tehnică, Bucharest, 1981.

[16] Perry's Chemical Engineers'Handbook, 6th Edition, Edited by H. H. Perry and D. Green McGraw-Hill, New York, (1985).

[17] J. S. Rowlinson, "Liquids and Liduid Mixtures", 2nd Edition, Butterworths, London, (1969).

[18] V. Dumitru, "Programare neliniară", Ed. Academiei, Bucharest, 1975.

Revue Roumaine de Chimie, 32, *9–10*, 877–881 (1987)

Dedicated to Professor I. G. MURGULESCU
on his 85th anniversary

RARE EARTH MIXED OXIDES WITH TRANSITION METALS. I.

MIXED OXIDES WITH Co(III) AND Ni(III) HAVING A PEROVSKITE STRUCTURE

P. SPACU, SILVIA PLOȘTINARU, LUMINIȚA PATRON, ADRIANA CONȚESCU,
D. CRIȘAN and N. STĂNICĂ
Center of Physical Chemistry, Bucharest, Romania

Received December 13, 1986

The present paper deals with the study of the mixed oxides $LnCoO_3$, (Ln = La...Tb) and $LaNiO_3$ obtained using polynuclear coordination compounds as precursors. All oxides were analysed by X-ray diffraction and were characterized by physico-chemical methods (electronic and IR spectra, and magnetic measurements).

Mixed oxides of perovskite structure having the general formula ABO_3 (where A = Ln(III) and B = transition metal) represent a typical system which allows the correlation between physico-chemical properties and its possible application. Several data concerning the synthesis, structure and properties of such compounds can be found in the literature.

Perovskites containing Co^{III}, of the $LnCoO_3$ and $Ln_{0.8}Sr_{0.2}CoO_3$ type and those containing Ni^{III} were tested as catalysts in oxidation-reduction and hydrogenation reactions, respectively. It was also shown that these perovskites may be employed as catalysts in depolution reactions, as their activity is comparable with that of Pt catalysts currently used in this kind of reactions. It is known that the properties of oxide system (specific surface,[1,2] oxygen stoechiometry[3,4] and even catalytical activity [5,6]) depend on the way of synthesis.

Mixed oxides of perovskite type are generally obtained with methods involving high temperatures (ceramic method). Lately, in order to eliminate the disadvantage of the classical methods, unconventional methods have been used, such as decomposition of coprecipitates,[7,8] or complex compounds.[9,10]

The present paper deals with the study of the mixed oxides $LnCoO_3$ and $LaNiO_3$ obtained by the decomposition method of polynuclear complexes.

RESULTS AND DISCUSSION

Oxide compounds of type $LnMO_3$ ($M = (Co(III), Ni(III))$ were obtained using as precursors polynuclear complexes[9,10]:

$$[LnCo(Sal)_4(OH)]\cdot 4H_2O \quad \text{where:}$$

$$Ln(III) = La, Pr, Nd, Sm, Gd$$

$$Sal = C_6H_4\,(OH){-}COO^-$$

and $[LnM(RCOO)_5]\cdot nH_2O$ where:

$$M(II) = Co;\ Ln(III) = La\ldots Tb;\ n = 2$$

$$M(II) = Ni;\ Ln(III) = La\ldots Er;\ n = 3$$

$$R = C_6H_5 - CH - OH -$$

$$Cl - C_6H_4 - CH - OH -$$

$$C_{12}H_{10}\quad CH\quad OH$$

The product obtained from thermogravimetric decomposition has been analysed by X-ray diffraction. The spectra indicated the coexistence of perovskite phase and traces of oxide components. For this reason, the product was thermally treated until the diffraction data indicated the pure perovskite phase only. This phase was obtained by 6 – 7 hrs calcination at 800°C for the Ln – Co – O system. Table 1 presents the X-ray data for $LaCoO_3$ and for $NdCoO_3$. The data obtained are in agreement with those reported in the literature.[11] The ideal perovskite structure has the

Table 1

X-ray data for $LaCoO_3$ and $NdCoO_3$

hkl	$LaCoO_3$				*hkl*	$NdCoO_3$			
	Obs.		Calc.			Obs.		Calc.	
	dÅ	I/I_0	dÅ	I/I_0		dÅ	I/I_0	dÅ	I/I_0
012	3.84	28	3.82	60	200	3.76	19	3.77	12
110	2.725	100	2.711	100	210	3.36	6	3.37	2
104	2.693	99	2.679	100	220	2.666	100	2.668	100
202	2.221	27	2.213	60	222	2.178	16	2.179	18
006	2.183	11	2.178	30	400	1.886	30	1.886	35
024	1.912	58	1.909	80	410	1.829	8	1.830	6
122	1.718	8	1.719	10	420	1.688	6	1.688	8
116	1.697	8	1.701	10	412	1.643	4	1.646	5
214	1.566	38	1.563	80	422	1.5396	29	1.541	45
018	1.546	15	1.542	10					

cubic cell unit. These oxides present some distortions from the ideal perovskite structure. Excepting $LaCoO_3$ which belongs to rhombohedric structure (space group R_{3c}, D^6_{3d}), other oxides crystallize in the orthorhombic structure of the $GdFeO_3$ type (space group P_{bnm}). The higher the distortion the lower the rare earth ionic radius is.

The obtention of perovskite phase for Ln—Ni—O system is more difficult than for the Ln—Co—O system due to the reduced stability of Ni(III) ion. The classical methods indicate the preparation of Ni(III) perovskite either by calcination of a mixture of components under oxygen flow or by the presence of some oxidants.[12-14]

By application of a similar treatment to the Ln—Co—O system the products resulted by decomposition of polynuclear complex compounds lead to a mixture of phases of La_2NiO_4 and traces of oxides. The samples röntgenographically analysed after a calcination at 900°C for 40 hrs, indicated an obvious modification of phases, the main product being $LaNiO_3$.This oxide has a rhombohedric symmetry belonging to the R_{3c}, D^6_{3d} space group (Table 2).

Table 2

X-ray data for $LaNiO_3$

hkl	$LaNiO_3$			
	Obs.		Calc.	
	dÅ	I/I_0	dÅ	I/I_0
101	3.804	14	3.84	80
110	2.727	100	2.728	100
012	2.705	61	2.697	100
021	2.223	310	2.222	60
003	2.195	9	2.187	30
202	1.920	47	1.919	80

It is worth mentioning that the cobalt perovskites are more stable than the nickel ones within a large range of temperature, even higher than 1000°C. The nickel perovskites decompose over this temperature into La_2NiO_4 and NiO.

The obtained oxide compounds are black powders, easily soluble at warm in mineral acids and have specific surfaces betwen 6—8 m²/g.

The reflectance electronic spectra recorded in UV and visible range for $LnCoO_3$ and $LaNiO_3$ are very similar to those reported in the literature for Co(III) and Ni(III) octahedral compounds. Figure 1 shows the electronic spectrum of $LaCoO_3$ compared with that of Co_3O_4. The two absorption bands occurring in the visible range at 500 nm and 330 nm respectively can be assigned to the transitions $A^1_{1g} \rightarrow T^1_{1g}$ and $A^1_{1g} \rightarrow T^1_{2g}$.

IR spectra recorded for $LaCoO_3$ and $LaNiO_3$ have a strong absorption band at 630 and 650 cm^{-1} respectively, assigned to the stretching vibration ν_{M-O} (Fig. 2).

The mixed oxides present interesting electric and magnetic properties, due to the transitions from the low spin to high spin states of the transition metal ions. Such transitions were known for rare earth cobaltites only.[15] A detailed study of magnetic properties of $LnCoO_3$ shows that the Co(III) ions which are in the low spin state ($Co^{III}\ t^6_{2g}e_g$) at low temperatures partially pass over a critical temperature to the high state ($Co^{3+}\ t^4_{2g}\ e^2_g$). The magnetic moment (2.49 BM) for $LaCoO_3$ at 300 K cannot be compared with that reported in the literature for the high spin (3.9BM) or for low spin Co(III) ion which is diamagnetic. The found intermediate value could be explained by a mixture of electronic states for Co(III) ion. The explanation is supported by the fact that for similar compounds the contribution of transition metal ions to the magnetic moment occurs at temperature higher than 300 K. As an example, the magnetic moment of $GdCoO_3$ (7.669 BM) presents an increase at $T >$ > 500 K (8.31 BM), most likely due to the contribution of Co(III) ion.

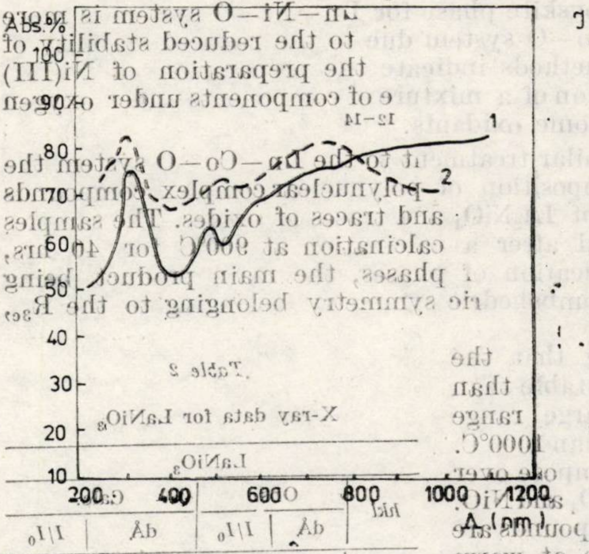

Fig. 1.—Electronic spectra of $LaCoO_3$ (1) and Co_3O_4 (2).

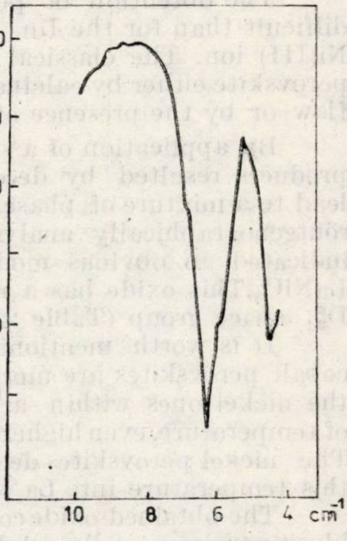

Fig. 2. — IR spectra of $LaCoO_3$.

EXPERIMENTAL

Mixed complex compounds used as precursors for mixed oxides were carried out as reported earlier.[9]

The techniques employed were the following:

- the differential thermal analyses were recorded with a MOM Budapest Paulik-Paulik Erdey derivatograph;
- the UV and visible spectra were recorded with a VSU-1 Zeiss-Jena spectrometer, in the 240—980 nm range with MgO as standard;
- the IR spectra were recorded with a UR-10 Zeiss Jena spectrometer; KBr pellets were employed;
- the magnetic measurements, on solid samples were effected by Farday method with Mohr salt as standard;
- the X-ray spectra were recorded with a TUR-M 62 diffractometer (Co K_α radiation)

REFERENCES

[1] D. W. Nohnson, P. K. Gallagher, F. Shrey and W. W. Rhodes, *Amer. Ceram. Soc. Bull.*, **55**, 520 (1976).

[2] L. Wachowski, S. Zielinski and A. Burewicz, *Acta Chim. Acad. Sci. Hung.*, **104**, 141 (1980).

[3] B. C. Tofield and W. R. Scott, *J. Solid State Chem.*, **10**, 183 (1974).

[4] E. M. Vogel, D. W. Johson and P. K. Gallagher, *J. Amer. Ceram. Soc.*, **60**, 31 (1977).

[5] Y. F. Yu-Yao, *J. Catalysis*, **36**, 266 (1975).

[6] O. Parkash, P. Ganguly, G. R. Rao and C.N.R. Rao, *Mat. Res. Bull.*, **9**, 1173 (1974).

[7] A. S. Nedil'ko and T. Vasiaghina, *Ukrain. khim. Zhur.*, **46**, 251 (198 0).

[8] A. S. Nedil'ko, *Zhur. neorg. Khim.*, **24**, 1395 (1979).

[9] P. Spacu, S. Ploștinaru, L. Patron, A. Conțescu and E. Segal, *Rev. Roumaine Chim.*, **30**, 658 (1985).

[10] P. Spacu, S. Ploștinaru, L. Patron, A. Conțescu and N. Stanică, *Rev. Roumaine Chim.*, **30**, 837 (1985).

[11] G. Demazeau, M. Pouchard and P. Hagenmuller, *J. Solid State Chem.*, **9**, 202 (1974).

[12] M. Crepin, P. Levitz and L. Gatineau, *J. Chem. Soc., Faraday Trans.*, **79**, 1181 (1983)

[13] P. Ganguly and C.N.R. Rao *Mat. Res. Bull.*, **8**, 405 (1973

[14] G. Demazeau and M. Puchard, *High temp.-High press.*, **8**, 624 (1976).

[15] W. H. Madhusudan, P. Ganguly and N.C.R. Rao, *J. Chem, Soc., Dalton Trans.*, **8**, 1397 (1980).

Revue Roumaine de Chimie, **32**, *9–10*, 883–893 (1987)

Dedicated to Professor I. G. MURGULESCU
on his 85th anniversary

ELECTRODE PROCESSES IN THE SYSTEM: LEAD(LIQUID)/LITHIUM CHLORIDE–POTASSIUM CHLORIDE–LEAD CHLORIDE

S. STERNBERG, T. VIȘAN, N. BONCIOCAT* and ADINA COTÂRȚĂ*
Polytechnic Institute, Laboratory for Applied Physical Chemistry, Faculty of Chemical Technology, Bucharest, Romania
* Institute of Chemical and Biochemical Energetics, Bucharest, Romania

Received April 16, 1987

A comparative study was made of the electrode processes on the liquid lead and graphite electrodes using cyclic voltammetry and chronoamperometry. Furthermore, the polarization curves were outlined in quasistationary conditions. Both methods attested the occurrence of cathodic currents which were far higher on liquid lead than on graphite electrode. This different behaviour of the liquid lead electrode in $LiCl-KCl+PbCl_2$ melts ($t = 500°C$) was explained by the existence of a number of reactions between metallic lead and lead ions as well as the formation of a surface reaction layer in which Pb_n^{2+} ions are generated in high concentration.

INTRODUCTION

The electrochemical technologies employing liquid electrodes in molten salts have developed the stock of data on the interactions between molten metal and salt melt, as well as on the peculiar features of electrode kinetics on molten metal electrodes.

Various physico-chemical methods, such as cryoscopy, for instance, are known to have proved the existence of true metal-molten salt solutions resulting from metal dissolution. Though the formation of similar solutions was noted as early as the 19th century, their systematic study was started rather late, that is in the 1955–1965 decade by Bredig *et al.* A new surge of interest in metal-molten salt solutions developed in recent years.[1] Owing to their physico-chemical properties these solutions may be divided into two large classes[2]: ionic-electronic solutions (melts, such as the alkali metal-alkali metal halide systems, having both ionic and electronic conductivity) and solutions that form subcompounds ($Bi-BiCl_3$ and $Cd-CdCl_2$ melts, as well as other systems that contain heavy metal salts).

According to Volkov,[2] Me^+-type monovalent subcompounds are less likely to form in the case of divalent non-transitional metals, being rather favoured the solvated ions. So, for instance, in the case of cadmium dissolved in a melt with a $CdCl_2$ content, the following reaction is assumed

$$(n - 1)\ Cd + Cd^2 \rightarrow Cd_n^{2+} \tag{1}$$

where n equals two in many cases.

As for solutions of metallic lead in lead chloride melt, we came across no relevant research work in the specialty literature; however, we do assume that a behaviour of the kind mentioned above is quite plausible. There is no clear distinction between the aforesaid two classes of metal-molten salt solutions. Nevertheless, the fact is noteworthy that, experimentally, the dissolution of the metal was noted to be favoured by the presence of its ion in the melt. So, for instance, metal dissolution in the case of Pb/alkali metal chloride + $PbCl_2$ melt system may be visualized in the form of a violet-coloured metallic haze.

Electrochemical kinetic measurements on liquid lead in molten LiCl—KCl electrolyte (450°C) containing Pb^{2+} ions were conducted by Laitinen et al.[3] and by Bek and Lifshits[4] who used double pulse galvanostatic technique and faradaic impedance method, respectively.

All these authors assessed that the exchange currents are higher than those recorded on solid inert electrodes by one order of magnitude.

One of our previous works[5] outlined the polarization curves in steady-state potentiostatic conditions for the Pb/$PbCl_2$(615°C) and Pb/LiCl—KCl + $PbCl_2$ 1 M (500°C) systems. In both cases the resulting curves are almost linear, with the cathodic and anodic branches in prolongation and symmetrically as to the steady-state potential. We attributed this result to the fact that lead deposition and, respectively, dissolution processes occur in conditions of a very low charge transfer overpotential. The largest weight in total polarization was held by the ohmic drop potential between the working and reference electrodes; which, at the high exchange currents, acquires substantial values. The attempt to obtain cyclic voltammograms in the two discussed systems proved futile; a perfectly linear shape resulted, the curve being identical with the steady-state potentiostatic curve and no additional information is yielded.

In the present paper the electrochemical investigations into more diluted LiCl—KCl+$PbCl_2$ melts are reported. The methods of cyclic voltammetry and chronoamperometry are applied comparatively on liquid lead and graphite electrodes.

EXPERIMENTAL TECHNIQUE

All measurements were performed at a constant temperature of 500°C. LiCl—KCl+ + $PbCl_2$ melts of various concentrations (0.02 M, 0.03 M, 0.04 M, 0.05 M, 0.06 M, 0.07 M and 0.08 M $PbCl_2$ in LiCl—KCl eutectic) were studied.

The cell in which the electrochemical measurements were conducted is shown in Fig. 1. The working electrode was made either of liquid lead or of graphite. The liquid lead electrode was a metallic lead ring with an area of about 0.25 — 0.30 cm². It is worth noting that to obtain significant results the surface area of metallic lead ring should be relatively small, of less than 0.5 cm². Otherwise, linear cyclovoltammograms are recorded owing to the very high cathodic currents. The same phenomenon occurs when very concentrated $PbCl_2$ solutions are employed.

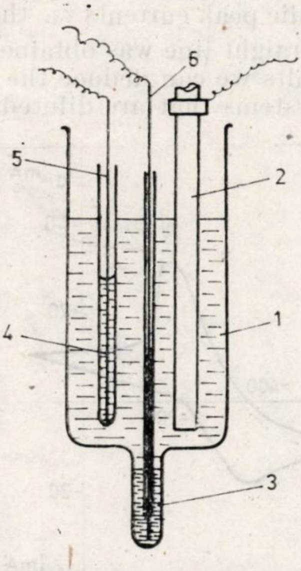

Fig. 1. — The experimental cell for the study of electrode processes on liquid lead: 1 — $LiCl-KCl + PbCl_2$ molten electrolyte; 2 — counterelectrode (graphite rod); 3 — liquid lead; 4 — $LiCl-KCl + AgCl$ electrolyte; 5 — Ag wire; 6 — tungsten wire sealed in Pyrex glass.

The working graphite electrode was made of a spectral graphite rod, welded to Pyrex glass, having a surface area on contact with the melt of 1 cm². The counterlectrode was a carbon rod with a large area and the reference electrode was an Ag wire immersed in a solution 0.1 mole/kg AgCl in LiCl—KCl eutectic.

All reactants employed had pro analysis purity and were dried at a temperature of 120°C for several days. Furthermore, inert gas (Ar) gas bubbled in the melts in order to completely remove water.

The usual technique was employed in the experiments of cyclic voltammetry and chronoamperimetry, using a P.A.R. Model 173 potentiostat, a low frequency pulse generator and an XY recorder with time base.

RESULTS AND DISCUSSION

Cyclic voltammetry measurements on graphite electrode (the systems with 0.02 M, 0.03 M and 0.05 M $PbCl_2$) show a marked cathodic peak when lead deposition occurs at the values of potential between $-0.3V - -0.5V$ (vs. Ag/Ag^+ electrode); an anodic peak also occurs on sweep return, which is assigned to the dissolution of lead that recently deposited. (Fig. 2.) A cyclovoltammogram yielded in the base electrolyte (LiCl—KCl eutectic) shows only a background current of ~ 1 mA in the potential range -2 V to $+1$ V at 0.5 V/s sweep rate.

Therefore, the elctrode reactions that take place on graphite electrode in the cyclovoltammogram from Fig. 2 correspond to the simple reactions with two electrons of lead deposition and dissolutions:

$$Pb^{2+} + 2\ e \rightarrow Pb \tag{2}$$

$$Pb - 2\ e \rightarrow Pb^{2+} \tag{3}$$

Our measurements made at various sweep rates show both cathodic and anodic peaks on the $i - E$ curves to have been more marked and in symmetrical shape. The experimental data were processed by plotting the cathodic peak currents *vs.* the square root of sweep rates ($I_{p_c} - v^{1/2}$), when a straight line was obtained which passes through the origin. From these results we can deduce the diffusive character of lead deposition in molten systems that are diluted in Pb^{2+} ions.

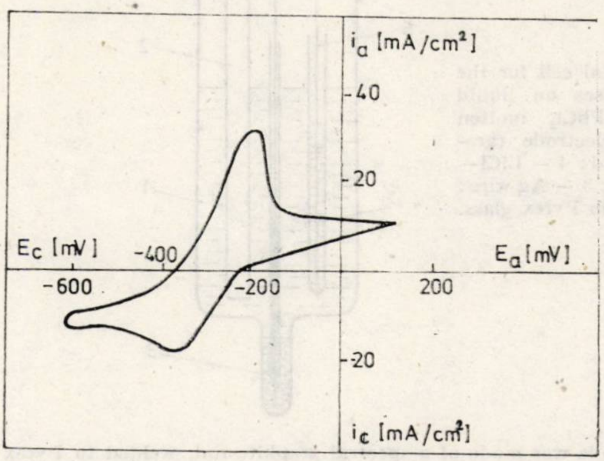

Fig. 2. — A cyclovoltammogram recorded on gaphite electrode in LiCl—KCl + 0.05 M $PbCl_2$ system; scan rate $v = 0.58$ V/s; $t = 500$°C.

On the basis of the $I_p - v^{1/2}$ dependence and according to the known relation

$$I_p = \frac{0.447\,(n\,F)^{3/2}\cdot c\cdot D^{1/2}\cdot v^{1/2}\cdot A}{(RT)^{1/2}} \tag{4}$$

the diffusion coefficient $D_{Pb^{2+}}$ could be evaluated; a quite plausible value of 4.10^{-5} cm²/s results. In the above expression very much used in cyclic voltammetry, F, R and T have their usual meanings, n is the number of electrons in electrochemical reaction ($n = 2$), c — concentration and A — the surface area. Early, by chronopotentiometric measurements, a value $D_{Pb^{2+}} = 3.1.10^{-5}$ cm²/s was reported, which was confirmed by other methods as well.[6]

The aforesaid results lead to the conclusion that the inert graphite electrode is only a support for the formation of a liquid lead film; afterwards, the cathodic process develops on this "mirror-like" surface of liquid metal.

The cyclovoltammograms obtained in concentrated solutions (for example 1 M $PbCl_2$ in LiCl—KCl eutectic) on graphite and, respectively, liquid lead electrode, are practically identical on the cathodic branch and in both cases a straight line is outlined (Fig. 3). A voltammetric peak develops on the graphite electrode on the anodic branch, as the amount of lead deposited on graphite is limited, while in the case of the lead electrode a free anodic dissolution of liquid metal occurs.

Figure 4 shows a cyclovoltammogram obtained on liquid electrode which is representative; a difference may be noted which is significant

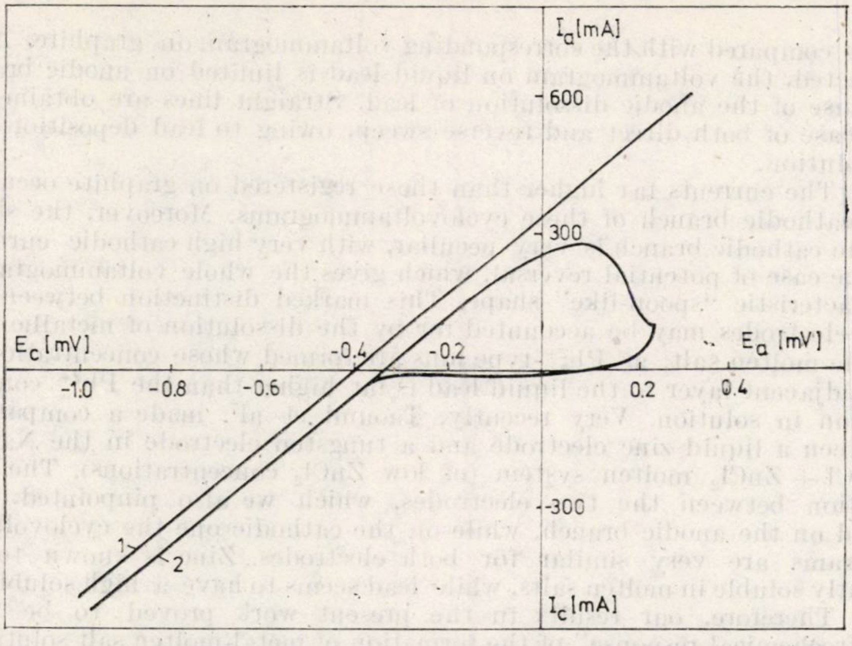

Fig. 3. — Representative cyclovoltammograms in concentrated LiCl—KCl+$PbCl_2$ electrolyte (1 M $PbCl_2$) : 1 — graphite electrode ($s = 1$ cm²) ; 2 — liquid lead electrode ($s = 0.5$ cm²).

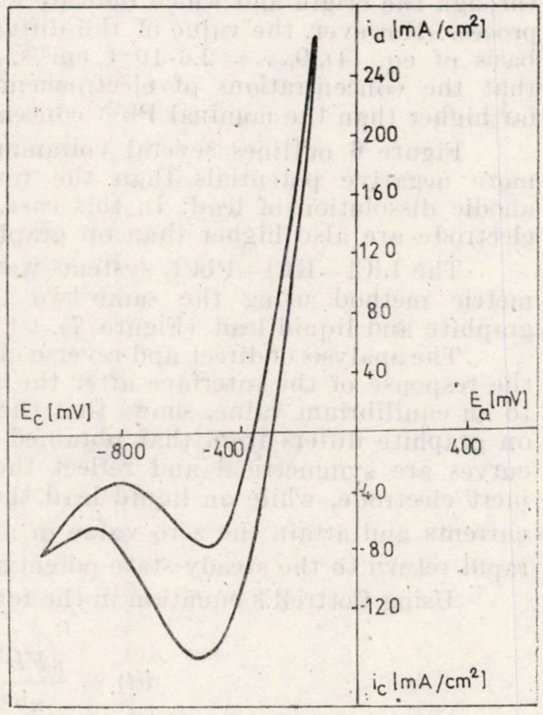

Fig. 4 — A cyclovoltammogram in the LiCl—KCl+0.05 M $PbCl_2$ system on liquid lead electrode ; $v = 0.72$ V/s.

when compared with the corresponding voltammogram on graphite. As is expected, the voltammogram on liquid lead is limited on anodic branch because of the anodic dissolution of lead. Straight lines are obtained in the case of both direct and reverse sweep, owing to lead deposition and dissolution.

The currents far higher than those registered on graphite occur on the cathodic branch of these cyclovoltammograms. Moreover, the shape of the cathodic branch is very peculiar, with very high cathodic currents in the case of potential reversal, which gives the whole voltammogram a characteristic "spoon-like" shape. This marked distinction between the two electrodes may be accounted for by the dissolution of metallic lead in the molten salt, as Pb_n^{2+}-type ions are formed whose concentration in the adjacent layer to the liquid lead is far higher than the Pb^{2+} concentration in solution. Very recently, Taoumi .et al[7]. made a comparison between a liquid zinc electrode and a tungsten electrode in the NaCl—KCl + $ZnCl_2$ molten system (of low $ZnCl_2$ concentrations). The distinction between the two electrodes, which we also pinpointed, was noted on the anodic branch, while on the cathodic one the cyclovoltammograms are very similar for both electrodes. Zinc is known to be slightly soluble in molten salts, while lead seems to have a high solubility.

Therefore, our results in the present work proved to be "the electrochemical response" of the formation of metal-molten salt solutions.

Figure 5 represents the $I_{p_c} - v^{1/2}$ dependence from voltammograms using liquid lead electrodes. Straight lines are also obtained which pass through the origin and which indicate a diffusive control of the electrode process. However, the value of the diffusion coefficient computed on the basis of eq. (4), $D_{Pb^{2+}} = 2.6 \cdot 10^{-3}$ cm^2/s, is unbelievably high, indicating that the concentrations of electrochemically active cations (Pb_n^{2+}) are far higher than the nominal Pb^{2+} concentrations.

Figure 6 outlines several voltammograms obtained in the case of more negative potentials than the reversible potential, to avoid the anodic dissolution of lead. In this case, the currents recorded on liquid electrode are also higher than on graphite.

The LiCl—KCl+$PbCl_2$ systems were also studied by chronoamperometric method using the same two types of electrodes, *viz*. spectral graphite and liquid lead (Figure 7).

The analysis of direct and reverse chronoamperograms, which express the response of the interface after the potential has been brought back to an equilibrium value, shows that the shape of the "reversed" curves on graphite differs from that obtained on liquid lead; on graphite the curves are symmetrical and reflect the dissolution of lead film on the inert electrode, while on liquid lead the reversal curves boast far lower currents and attain the zero value in a very short time, which proves a rapid return to the steady-state potential.

Using Cottrell's equation in the form

$$i(t) = \frac{nFD^{1/2} cA}{\pi^{1/2} . t^{1/2}} \qquad (5)$$

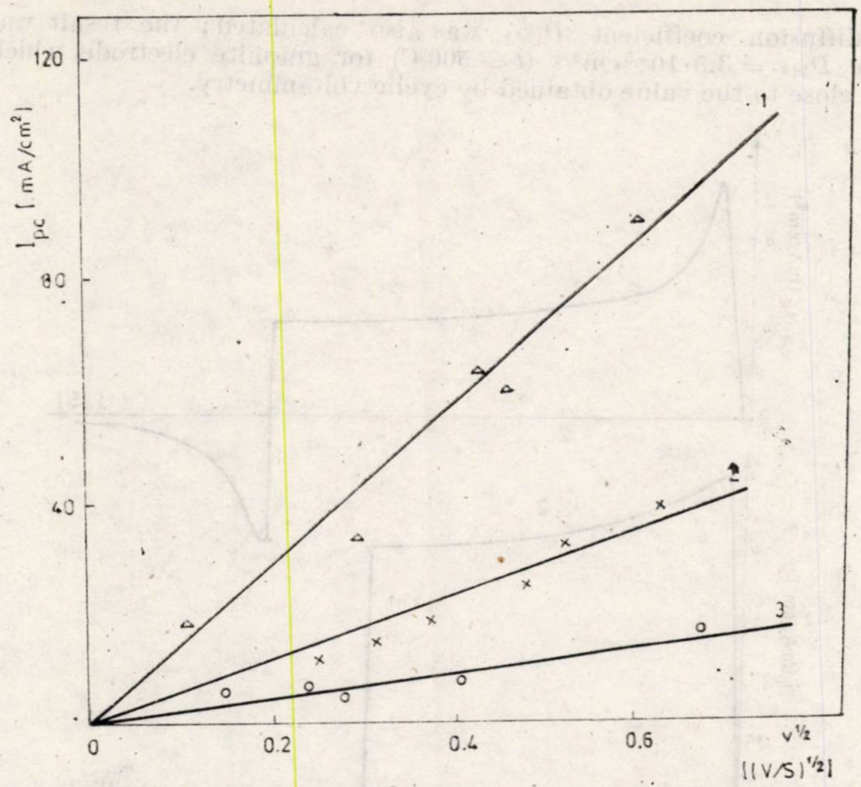

Fig. 5. — The $I_{pc} - v^{1/2}$ dependence on liquid electrode with various $PbCl_2$ concentrations : 1 — 0.05 M ; 2 — 0.03 M ; 3 — 0.02 M $PbCl_2$.

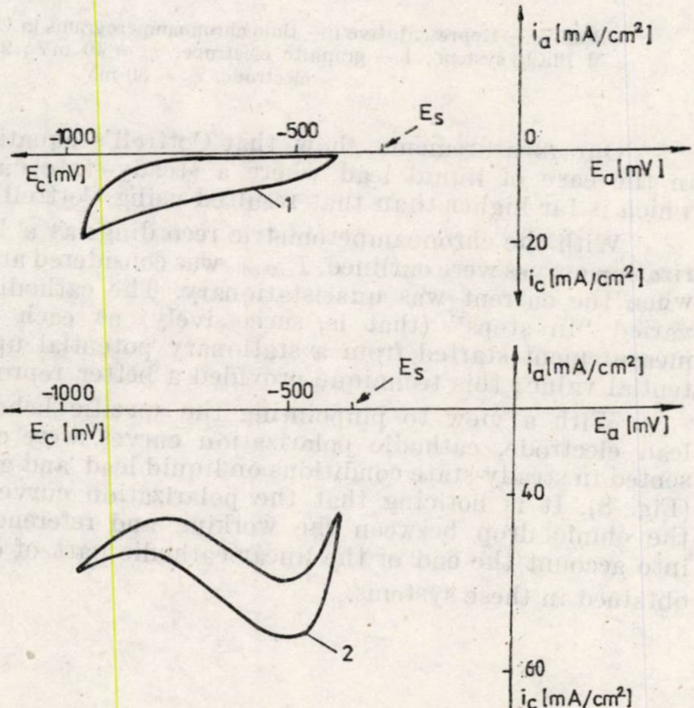

Fig. 6. — Cyclovoltammograms on graphite (1) and liquid lead (2) in the LiCl—KCl+0.05 M $PbCl_2$ system ; v=0.6 V/s.

the diffusion coefficient $D_{Pb^{2+}}$ was also calculated; the result was a value $D_{Pb^{2+}} = 3.5 \cdot 10^{-5}\,cm^2/s$ ($t = 500°C$) for graphite electrode, which is very close to the value obtained by cyclic voltammetry.

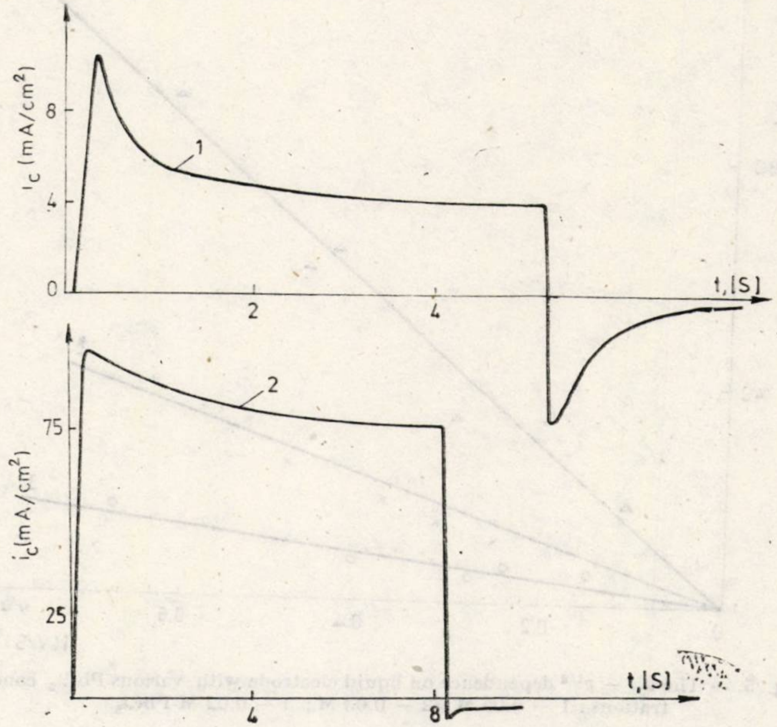

Fig. 7. — Representative i — time chronoamperograms in LiCl—KCl+0.05 M $PbCl_2$ system; 1 — graphite electrode, $\eta_c = 40$ mV; 2 — liquid lead electrode, $\eta_c = 30$ mV.

Our measurements show that Cottrell's equation does not apply in the case of liquid lead where a steady-state current is established which is far higher than that resulted using Cottrell's equation:

With the chronoamperometric recordings as a basis, $I = f(E)$ polarization curves were outlined. $I_{cathodic}$ was considered at a time of 10 seconds, when the current was quasistationary. The cathodic potential was not varied "in steps" (that is, successively) as each chronoamperometric measurement started from a stationary potential up to the desired potential value; this technique provided a better reproducibility of results.

With a view to pinpointing the specific behaviour of the liquid lead electrode, cathodic polarization curves were comparatively represented in steady-state conditions on liquid lead and graphite respectively, (Fig. 8). It is noticing that the polarization curve was corrected with the ohmic drop between the working and reference electrodes, taking into account the end of the linear cathodic part of cyclovoltammograms obtained in these systems.

The polarization curve obtained on liquid lead is altogether different, being characterized by a maximum (220 mA), after which a limiting current of roughly 100 mA occurs. The last value is four times higher than the limiting current recorded in the case of the graphite electrode.

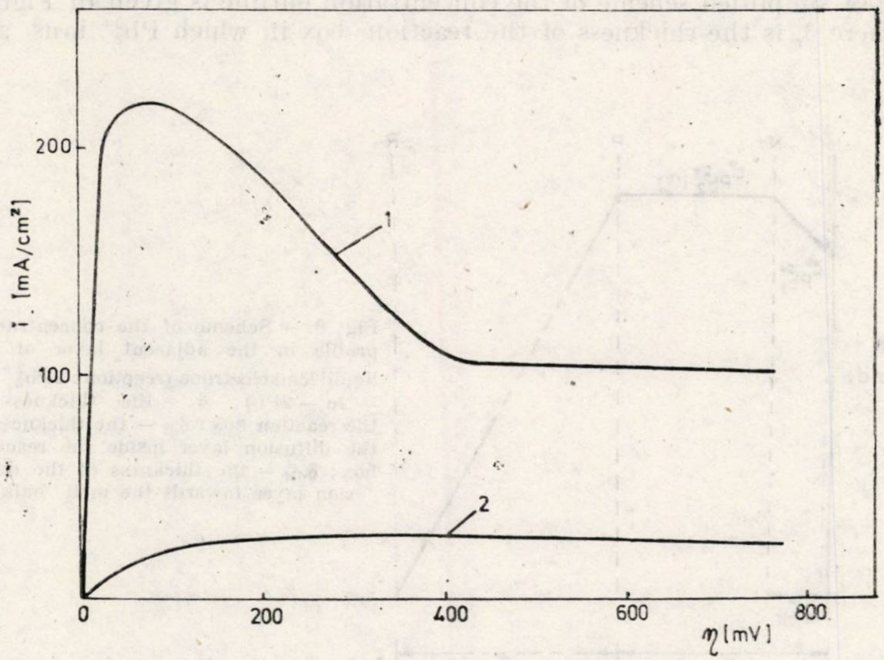

Fig. 8. — Cathodic polarization curve in $LiCl-KCl+0.05$ M $PbCl_2$ electrolyte ($t = 500°C$) : 1 — liquid lead electrode ; 2 — graphite electrode.

The maximum current increases with the $PbCl_2$ concentration in the melt and a $I_{max} \sim c^n_{PbCl_2}$ dependence (where n average 1.2) results.

The marked rise in cathodic currents in the case of polarization on liquid lead — which the present work highlights by several techniques — may be correlated with the existence of metal — molten salt solutions, respectively, with the existence of such reactions as

$$Pb + Pb^{2+} \rightarrow 2\,Pb^{+} \qquad (6)$$

or of the type

$$Pb + Pb^{2+} \rightarrow Pb_2^{2+} \qquad (7)$$

according to the conception metal — ionic melt with solvatation sphere.[2]

In what follows our discussion relies on reaction (7). Assuming reaction (7) to be very rapidly, one may agree with the fact that when the potential steps are relatively short, a "surface reaction box" is created, which is adjacent to the liquid lead electrode and in which the

Pb_2^{2+} concentration is far higher than the Pb^{2+} concentration in the solution bulk. If we pressume that the cathodic current is $i = i_{Pb_2^{2+}} + i_{Pb^{2+}}$, and $i_{Pb_2^{2+}} \gg i_{Pb^{2+}}$, it follows that $i_{Pb^{2+}}$ may be neglected and the cathodic current is therefore assessed by the Pb_2^{2+} concentration in a reaction box.

A simplified scheme of the concentration outline is given in Figure 9 where δ_r is the thickness of the reaction box in which Pb_2^{2+} ions are generated, δ_{dr} is the thickness of the diffusion layer inside the reaction box, and δ_{dif} is the thickness of the diffusion layer towards the melt bulk. According to this model, $\delta_{dif} \gg \delta_r$. We tried, in a first approximation, to use the general equation of cathodic current density for the reaction $0 + ne \rightleftharpoons R$, for the combined charge transfer and diffusion overpotential, that is

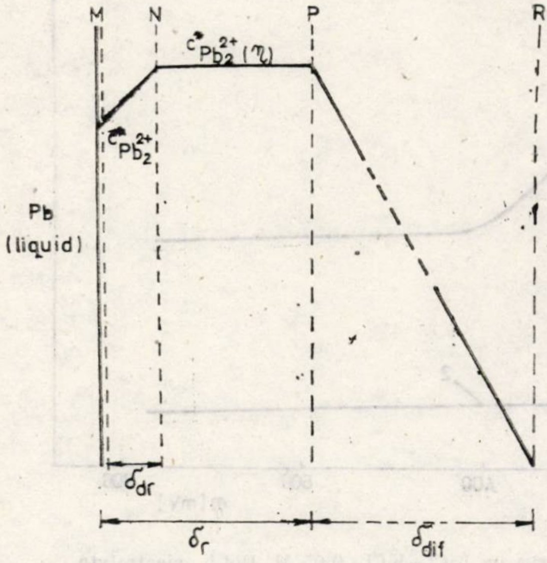

Fig. 9. — Scheme of the concentration profile in the adjacent layer of the liquid lead electrode (reaction : $2Pb_2^{2+} + 2e \rightarrow 2Pb$); δ_r — the thickness of the reaction box; δ_{dr} — the thickness of the diffusion layer inside the reaction box; δ_{dif} — the thickness of the diffusion layer towards the melt bulk.

$$i = i^0 \left[\frac{\bar{c}_0}{c_0} \cdot e^{-\frac{\alpha n F}{RT}\eta} - \frac{\bar{c}_R}{c_R} \cdot e^{\frac{(1-\alpha) n F}{RT}\eta} \right] \tag{8}$$

where $\bar{c}_0$, $\bar{c}_R$ are the concentrations of the species 0 and R on the surface of the electrode corresponding to the overpotential η and c_0, c_R are the concentrations of the same species in the bulk of electrolyte.

In our case, the species 0 and R are Pb_2^{2+} and Pb, and the volume of electrolyte means the volume of the reaction box. The $\bar{c}_R/c_R$ ratio is obviously equal to unity. Consequently (see Fig. 9), the $\bar{c}_0/c_0$ ratio becomes in this case $\bar{c}^*_{Pb_2^{2+}}/c^*_{Pb_2^{2+}}$, where $c^*_{Pb_2^{2+}}$ and $\bar{c}^*_{Pb_2^{2+}}$ are the concentrations o the electrochemically active species Pb_2^{2+} in the reaction box. In the lasf analysis, the cathodic current will depend only on the $c^{*}_{\mathrm{Pb}_2^{2+}}(\eta)/c^{*}_{\mathrm{Pb}_2^{2+}}$ $(\eta = 0)$ ratio.

In the works to follow[8,9] this ratio was computed as a function of the reaction rate and overpotential and a more general equation was obtained for the $i - \eta$ curves in the case of combined charge transfer, chemical reaction and diffusion mechanism.

It was pointed out that when reaction rate decreases with the overpotential, the polarization curves boasting a maximum and a limiting current might yield, in agreement with our results on liquid lead electrode.

REFERENCES

[1] W. W. Warren Jr., *Molten Salts Bulletin*, **28**, 3 (1985).

[2] S. V. Volkov, V. S. Naumov and A. A. Omelchuk, *Ukr. khim. Zhur.*, **50**, 154 (1984).

[3] M. A. Laitinen, R. P. Tischer and D. K. Roe, *J. Electrochem. Soc,*, **107**, 546 (1960).

[4] R. Iu. Bek and A. S. Lifshits, *Izvest. Sibirsk. Otdel. Akad. Nauk SSSR, Khim. Nauk*, No. 7, vyp. 3, 53 (1970).

[5] S. Sternberg, T. Vişan, A. Cotârţă and I. Lingvay, in vol. "Lucrările celui dintîi seminar naţional de electrochimie aplicată", Cluj-Napoca, 14–15 May 1982, vol. I, p. 141.

[6] C. E. Thalmayer, S. Bruckenstein and D. M. Gruen, *J. Inorg. Nuclear Chem.*, **26**, 347 (1964); C. Herdlicka, Thesis, Bucharest, 1972.

[7] M. Taoumi, J. Bouteillon and M. J. Barbier, *Electrochim. Acta*, **31**, 837 (1986).

[8] S. Sternberg, N. Bonciocat, T. Vişan and A. Cotârţă, *Rev. Roumaine Chim.*, to be published.

[9] N. Bonciocat, S. Sternberg, T. Vişan and A. Cotârţă, *Rev. Roumaine Chim.*, to be published.

Revue Roumaine de Chimie, 32, *9–10*, 895–899 (1987)

Dedicated to Professor I. G. MURGULESCU,
on his 85th anniversary

SINTERING EFFECTS ON ANODIC OXIDATION OF VACUUM DEPOSITED SILVER FILMS

VALENTINA LĂZĂRESCU*, O. RADOVICI**, and M. VASS*

* ICECHIM — Center of Physical Chemistry, Spl. Independenței 202, Bucharest 79611, Romania

** Polytechnic Institute, Faculty of Chemical Technology, Bucharest, Romania

Received April 27, 1987

Cyclic voltammetry investigations have been performed in 1M KOH solution on fresh and differently annealed silver evaporated films. A pronounced influence of the sintering process has been observed to be exerted on the penetration of O^{2-} ions into the subsurface layers of the metal, giving a further support to our previous assumptions.

INTRODUCTION

There exists good evidence about the close relations between phenomena occurring at solid/gas and solid/electrolyte interfaces.[1,2] We have recently shown that both atomic and molecular hydrogen adsorption and absorption take place on Raney — Cu in solid/gas as well as in solid//electrolyte system.[3,4]

The ability of silver to incorporate oxygen atoms in its bulk is well-known.[5-8] Certain peculiarities of the thin dense layer of Ag_2O, initially formed on anodic potential scans performed in alkaline solutions seem to indicate that this is the result of the oxygen penetration into the silver lattice, as we have previously reported.[9-11] The cyclic voltammetry investigations on silver evaporated films differently annealed give further support to the previous assumption.

EXPERIMENTAL

The film electrodes were prepared from 99.99% pure silver (Goodfellow Metals) by vacuum evaporation ($p < 10^{-6}$ Torr) on optically polished glass substrates (approx. 1 cm^2) heated at 570 K. The thickness was chosen to be greater than 3000Å to avoid the substrate influence.[12,13] After deposition, the films were further annealed at 570 K ($T_{\text{Tammann}} \cong \cong 0.3\ T_{\text{melting}}$) at a base pressure of 10^{-5} Torr, for various times. They were then transferred through air in a Pyrex three — compartment cell of conventional design. Two platinum wires embedded in the glass surface ensured the electrical connection to the measuring circuit.

The measurements were performed at room temperature, in 1M KOH solution prepared by analytical reagent dissolution in twice distilled water.

The control of the electrode potential (measured versus a saturated calomel reference, SCE) was carried out by means of a PAR-EG & G potentiostat (model 173) driven by a PAR-EG & G Universal Programmer (model 179). Cyclic voltammograms taken with a constant scan rate of 10 mVs^{-1} were recorded with a Hewlett — Packard X—Y recorder.

RESULTS AND DISCUSSION

Typical cyclic voltammograms of the silver film electrodes annealed for various times are shown in figures 1–3. As seen, under the heat treatment, the silver films undergo irreversible changes disturbing the anodic oxidation steps. The voltammogram of the freshly deposited silver film (Fig. 1) as well as the first stage of the metal anodic oxidation for the film annealed for a shorter period (Fig. 2) are dominated by the sharp peak B. Only the prolonged annealed film (Fig. 3) exhibits a behaviour similar to that observed for the compact electrode (Fig. 4).

The anodic oxidation of silver in alkaline solution takes place in several steps. The first process, A, was shown to be the metal dissolution[9–11] as $Ag(OH)_2^-$. The next one, B, is generally accepted to be the first step of the Ag_2O phase formation,[14–16] but its mechanism is still the object of a large dispute.[15–20] We have recently suggested[9–11] that the features of the process B may be correlated with the well-known ability of silver to retain oxygen in its bulk. The O^{2-} ions resulted in HO^- discharge reaction may penetrate the silver lattice forming the thin oxide layer indicated by X-ray diffraction and electron microscopy studies.[21]

The present results support well these assumptions. Silver films evaporated on glass at relatively high temperatures (470 – 570 K) are almost polycrystalline.[22] Annealing causes only small changes[22] in this respect but brings about metal agglomeration, associated with work function increase,[23] which is more pronounced[24] if oxygen is present (since the oxygen presence on the surface induces an increase in the self-diffusion coefficient of silver atom by a factor of 100)[25]. Therefore, a negative influence of the sintering process is expected to be exerted on the O^{2-} ions diffusion into the subsurface layers of silver. This phenomenon was really observed, giving a further support to the previous assumptions.[9–11]

The last two steps of the anodic oxidation of silver, C and D, are generally assigned[14–16,18] to the formation of a thick layer of Ag_2O (controlled by Ag^+ diffusion/migration through the initially formed dense oxide layer[26]) and the formation of a mixed oxide layer $Ag^IAg^{III}O_2$, respectively. The marked inhibition of process C on freshly or partially annealed silver films may be also a cosequence of the thicker subsurface O^{2-} layer, acting as a barrier for Ag^+ ions in their way to surface as in other similar cases.[9–11]

CONCLUSIONS

The cyclic voltammetry investigations performed on fresh and annealed silver films give a further support to the previous assumptions concerning the mechanism of the first stage in the anodic oxidation of Ag to Ag(I) in alkaline solutions, confirming the hypothesis of oxygen penetration in the metal lattice.

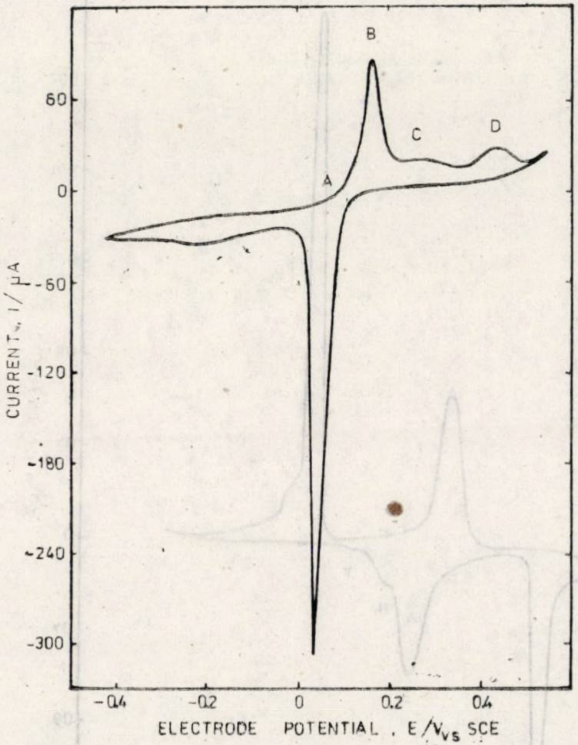

Fig. 1. — Typical cyclic voltammogram for freshly deposited silver films, recorded in 1M KOH at a scan rate of 10 mVs^{-1}.

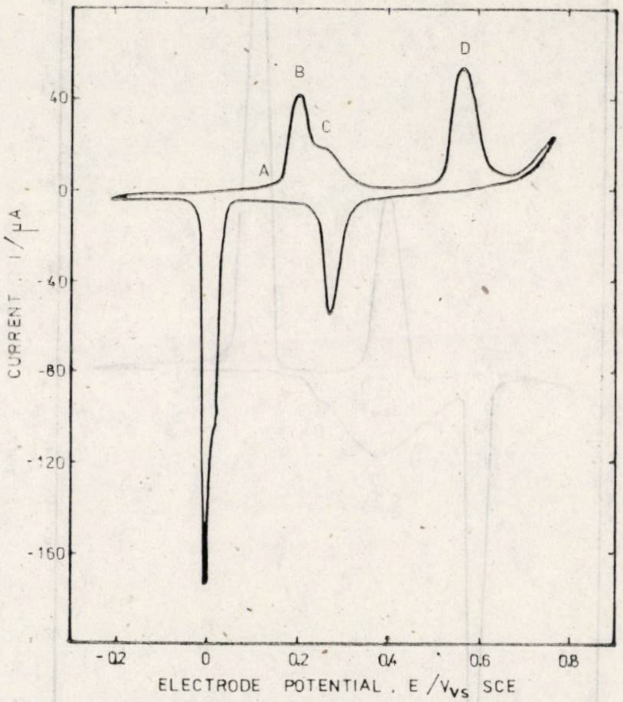

Fig. 2. — Typical cyclic voltammogram for silver films annealed for 30 min. in a residual pressure of 10^{-5} Torr, recorded in 1M KOH at a scan rate of 10 mVs^{-1}.

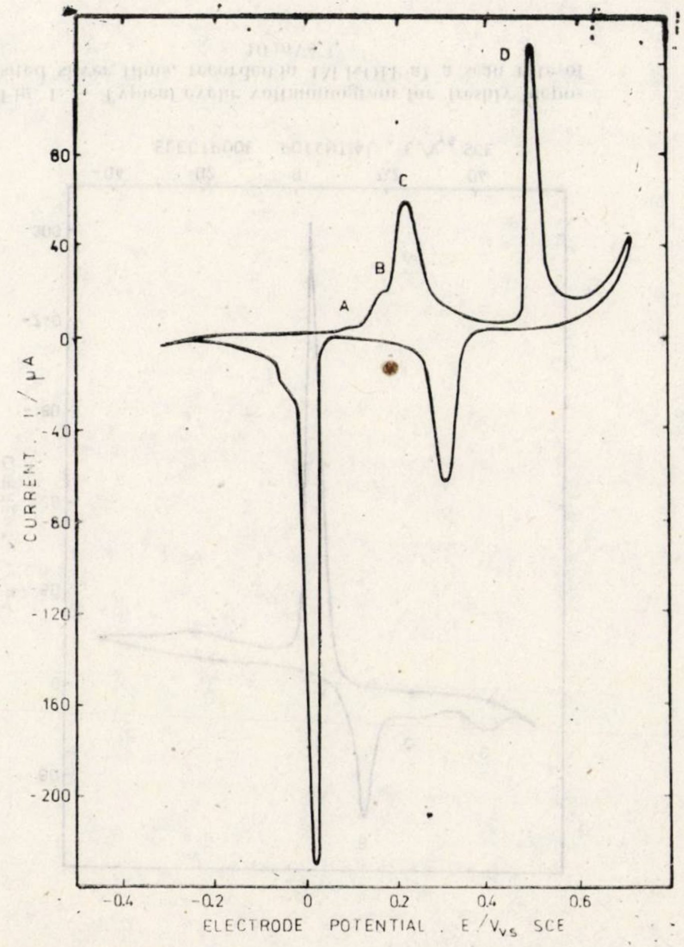

Fig. 3. — Typical cyclic voltammogram for silver films annealed for 70 min. in a residual pressure of 10^{-5} Torr, recorded in 1M KOH at a scan rate of 10 mVs^{-1}.

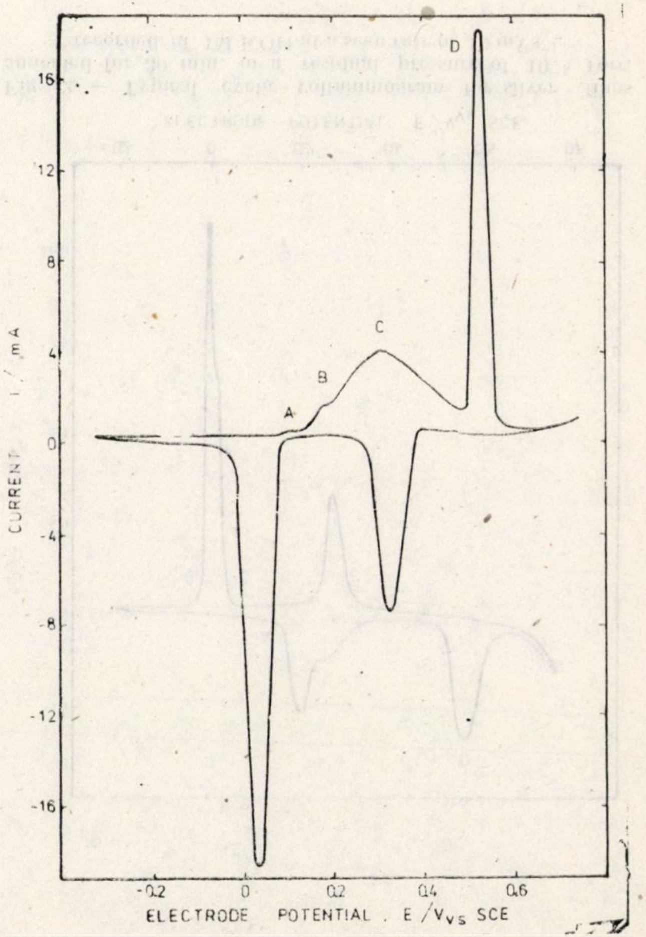

Fig. 4. — Typical cyclic voltammogram for the compact silver electrode, in 1M KOH at a scan rate of 10 mVs^{-1}.

REFERENCES

[1] J. K. Sass, *Vacuum*, **33**, 741 (1983).

[2] R. Parsons, *Surface Sci.*, **101**, 316 (1980).

[3] V. Lăzărescu, M. Vass, O. Radovici, E. Jugănaru, E. Gorlăteanu and T. Bota, "Proc. 2nd Symp. Appl. Electrochem.", Timişoara 4–5 oct. 1985" vol. 1, p. 260.

[4] V. Lăzărescu, M. Vass, O. Radovici, E. Jugănaru, E. Corlăteanu, T. Bota and A. Popa, "Proc. 2nd Symp. Appl. Electrochem.," Timişoara 4–5 Oct. 1985" vol. 1, p. 267.

[5] R. W. Joyner and M. W. Roberts, *Chem. Phys. Lett.*, **60**, 459 (1979).

[6] C. Backx, C.P.M. De Groot and P. Biloen, *Surface Sci.*, **104**, 300 (1981).

[7] G. Rovida, F. Pratesi and E. Ferroni, *Appl. Surface Sci.*, **5**, 121 (1980).

[8] W.M.H. Sachtler, C. Backx and R.A. Van Santen, *Catal. Rev.*, **23** 127 (1981).

[9] V. Lăzărescu, M. Vass, O. Radovici, C. Daşoveanu M. Stanciu and M. Tolan, *Rev. Roumaine Chim.*, **30**, 933 (1985).

[10] V. Lăzărescu, O. Radovici and M. Vass, *Electrochim. Acta*, **30**, 1407 (1985).

[11] V. Lăzărescu, O. Radovici and M. Vass, *Rev. Roumaine Chim.*, **31**, 461 (1986).

[12] M. E. Macovschi, *St. Cerc. Chim.*, **20**, 849 (1972).

[13] D. Henning and K. G. Weil, *Z. Phys. Chem. N.F.*, **98**, 143 (1975).

[14] Z. Takehara, Y. Namba and S. Yoshizawa, *Electrochim. Acta*, **13**, 1395 (1968).

[15] R. D. Giles and J. A. Harrison, *J. Electroanalyt. Chem.*, **27**, 161 (1970).

[16] B. V. Tilak, R. S. Perkins, H. A. Kozlowska and B. E. Conway, *Electrochim. Acta*, **17**, 1447 (1972).

[17] T. G. Clarke, N. A. Hampson, J. B. Lee, R. R. Morley and B. Scanlon, *Canad. J. Chem.*, **46**, 3437 (1968).

[18] P. Stonehart, *Electrochim. Acta*, **13**, 1789 (1968).

[19] B. Miller, *J. Electrochem. Soc.*, **117**, 49 (1970).

[20] B. G. Pound, D. B. Macdonald and J. W. Tomlinson, *Electrochim. Acta*, **25**, 563 (1980).

[21] G.W.D. Briggs, M. Fleishman, D. J. Lax and H. R. Thirsk, *Trans. Faraday Soc.*, **64**, 3120 (1968).

[22] M.S. Zei, Y. Nakai, G. Lehmpfuhl and D. M. Kolb, *J. Electroanalyt. Chem.*, **150**, 201 (1983).

[23] R. Bouwman, "Electron Emission, Surface Composition and Adsorption Phenomena of Metals and Alloys", Drukkerij Bronder – Offset N.V., Rotterdam, 1970.

[24] S. K. Sharma and J. Spitz, *Thin Solid Films*, **56**, L 17 (1979).

[25] G. E. Rhead, *Acta Metall.*, **13**, 223 (1965).

[26] M. Fleischmann, D. J. Lax, and H.R. Thirsk, *Trans. Faraday Soc.*, **64**, 3128 (1968).

Revue Roumaine de Chimie, **32**, *9–10*, 901–905 (1987)

Dedicated to Professor I. G. MURGULESCU
on his 85th anniversary

LEAD ELECTRODEPOSITS ON GRAPHITE SUPPORT

CECILIA VASS

Center of Physical Chemistry, 202 Spl. Independenţei, 77208 Bucharest, Romania

Received April 27, 1987

The obtention of lead electrodeposits with an intermediate copper layer on graphite support has been investigated. The obtained deposits were tested by polarization measurements and evaluation of surface profile and structure, specific surface area and porosity. The obtained results suggest that the lead plated graphite surfaces may be employed to replace solid lead electrodes utilized in electrosynthesis.

INTRODUCTION

Utilization, with good results, in electrosynthesis of some organic compounds of PbO_2[1] or Pd[2,3] – covered graphite electrodes is mentioned in literature, besides the metallic ones.[4–7]

An important condition imposed to electrolytically covered components is the low value of specific area. Concerning porosity, another work[8] mentions that the graphite samples employed had a porosity of about 20% while the surface was the visible one.

This contribution deals with formation and characterization of some lead electrodeposited layers on graphite support, aiming at replacing lead bipolar electrodes[9] employed in electrochemical synthesis.

In order to improve the adherence of lead electrodeposited layer to the covered surface the deposition of an intermediate copper or nickel layer was recommended.[10] It is known that electrodeposition of copper occurs at relatively lower overvoltages, the adherence and compactness of the resulted layer being of good quality regardless of the support (steel, brass, iron, zamak[11]). Classical procedures of copper plating recommend utilization of cyanide baths; however these baths present some disadvantages such as: low deposition rate, loss of surface quality with increasing thickness of deposited layer, the decrease of cathodic efficiency with the increase of free cyanide concentration as well as the toxicity.[12] To avoid the mentioned drawbacks the complexing pyrophosphate baths were employed.[13–15]

EXPERIMENTAL

Two types of graphite were employed, G1 (porosity 27–28%) and G2 (10–12%); the manufacturer controls porosity through additional treatment of embedding and baking. The graphite surface was prepared for plating according to indications in literature.[16] The anodes were made of Pb (99,9%) without impurities (e.g. Sb or Cu which turn the deposits rough). The brightening and levelling of the intermediate copper and lead layers was ensured by addition of 2,5-dimercapto-1,3,4-thiadiazole[17] and gelatine, respectively to the electrolyte. Lead depositions on surface areas of 1 cm^2 were carried out in plumbite electrolyte while those on larger surface areas in fluoborate electrolyte.

A PRT 20—20 X Tacussel potentiostat was employed in polarization measurements; galvanostatic measurements were carried out with Bipad type Tacussel bipotentiostat; the electrode potential was measured with a S 6 N Tacussel millivoltmeter against a saturated calomel electrode. Surface profiles were determined with a Taylor Hobson Talysurf — 4 Profilometer while surface structure was inspected with a Tesla BS-300 scanning electron microscope. A Carlo Erba A.G. 60 mercury porosimeter was utilized in porosity determinations while specific surfaces were measured by means of BET method with nitrogen at liquid nitrogen temperature using an adsorption volumetric device.

RESULTS AND DISCUSSION

Two graphite samples were selected for copper and lead plating of 73.2 m^2/g (G1) and 45.3 m^2/g (G2) specific surface as supports for copper and lead plating.

The electrochemical behaviour of electrodes obtained through electrodeposition of lead with intermediate copper layer on graphite, similar to solid lead electrodes, was estimated from polarization curves recorded with these electrodes. Fig. 1 shows the cathodic polarization curves of lead-plated graphite electrode (1) and solid Pb electrode (2) in an electrolyte containing 1% nitroguanidine in 30% $(NH_4)_2SO_4$.[18]

The obtained deposits were tested, besides usual methods as adherence, thickness and corrosion resistance, by evaluation of surface profile and structure, specific surface area and porosity.

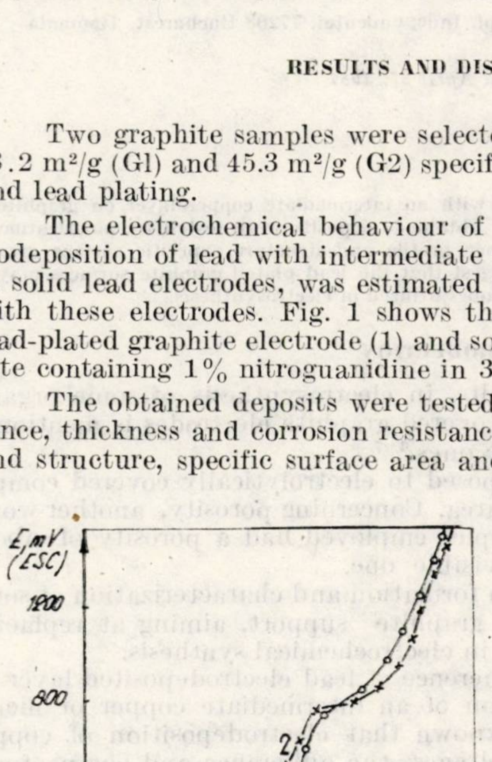

Fig. 1 — Cathodic polarization curve in 1% nitroguanidine in 30% $(NH_4)_2SO_4$; 1 — Pb plated graphite; 2 — Pb.

Table 1 lists the values of specific surface areas and maximum heights of surface profiles for G1 and G2 graphite electrodes unplated or plated with copper and lead.

Specific surface area determinations show the decreasing values as deposition of copper advances. Although the two types of graphite are initially different, they finally come to similar surface area values which points to a good covering of superficial pores. Maximum heights of 1μ are satisfactory[19] for achieving a uniform plating which may be further employed as electrosynthesis electrode.

The porosity measurements data for the two types of graphite, G1 and G2, were then processed by a computer program in order to obtain the pore volume distribution according to their radii (75—75 000Å).

Table 2 shows the distribution of pore volumes PV for various ranges of pore radii in G1 electrodes unplated and plated with lead and intermediate copper layer.

Table 1

Specific surface area ($S_{sp} \cdot m^2/g$) and maximum height of surface profile for graphite electrodes unplated (G1 and G2) and plated with copper (G1—Cu, G2 — Cu) and lead (G1 — Cu — Pb, G2 — Cu — Pb).

Electrode	$S_{sp} \cdot m^2/g$	h max., μ
G1	73.2	4.5
G2	45.3	2.5
G1—Cu	31.2	2.6
G2—Cu	31.5	1.6
G1—Cu—Pb	9.3	1.5
G2—Cu—Pb	4.7	1.0

Table 2

Distribution of pore volumes (PV, cm³/g and PV, %) versus pore radii for G1 electrodes unplated and plated with copper (G1—Cu) and lead (G1—Cu—Pb).

R, Å	G1		G1—Cu—Pb	
	PV, cm³/g	PV, %	PV, cm³/g	PV, %
75—100	0.0047	10.53	0.0025	5.71
100—300	0.0235	52.63	0.0134	31.43
300—600	0.0024	5.26	0.0086	20.00
600—1000	0.0000	0.00	0.0037	8.57
1000—5000	0.0141	31.58	0.0049	11.43
5000—10000	0.0000	0.00	0.0024	5.71
10000—75000	0.000	0.00	0.0073	17.14

Similar measurements led to the data shown in the histograms in Fig. 2a and 2b which present the percent distribution of pore volume versus their radius for G2 graphite unplated (Fig. 2a) and plated with lead and intermediate copper layer (Fig. 2b).

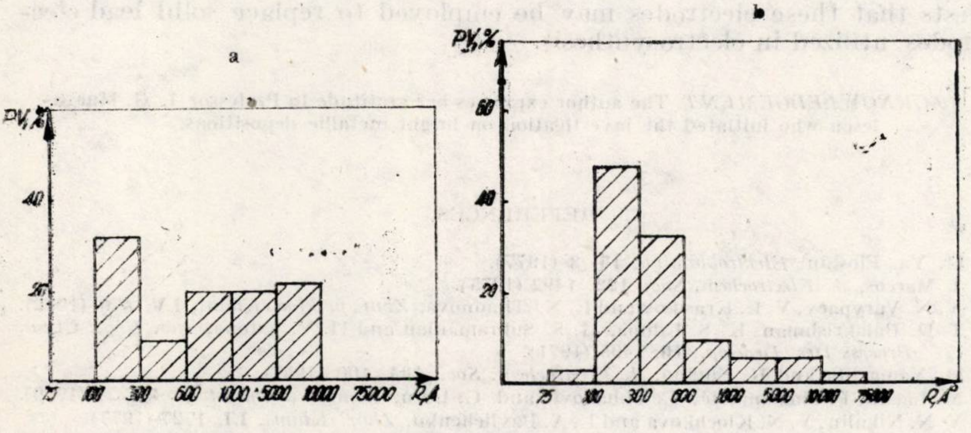

Fig. 2 — The percent distribution of pore volumes versus pore radii for G2 electrodes unplated (a) and plated with copper and lead (b).

Examination of the data presented in Table 2 and Fig. 2a shows that the overall pore volumes of the two types of graphite are similar: 0.04 cm^3/g in G1 and 0.06 cm^3/g in G2. However the pore distribution in the two samples points to G1 as more adequate for the obtaining of a compact deposit; the most pores in G1 (63%) are within 75 –'300 Å range of radii unlike G2 whose majority of pores (63%) range within 600–10 000 Å. Data in Table 2 and Fig. 2b suggest that the overall volume of pores in components plated with copper and lead (0.048 and 0.06 cm^3/g) are fairly similar to those unplated, G1 and G2, respectively. However the pore distribution for Pb layers electrodeposited on the two types of graphite show that in G2 the macropores are covered such that of the total of 63% only ~ 17% are not covered. The number of pores within 1000–5000 Å in lead-plated G1 is lower but a macropore structure appears which – due to its relatively low percent (17%) – surely cracks in the metallic layer.

Images of the surface of G1 graphite electrode unplated or plated with copper and then with lead as well as G2 graphite plated with copper are shown in Fig. 3 (a–d) respectively; they indicate a coverage of large cracks existing in the support and a uniformization of the structure of surface layers as deposition of metals advances.

CONCLUSIONS

Electrodeposition of lead on graphite with intermediate copper layer from baths of original composition was studied aiming to replace the solid lead electrodes employed in electrosynthesis.

The specific surface area of graphite suport (45.3–73.2 m^2/g) was reduced through lead plating (4.7–9.3 m^2/g).

About 83% of the total initial macropores (R = 5000–75 000 Å) was blocked through lead plating.

The plated lead surface unevenness was lowered from 4μ to 1μ through addition of brightener.

The electrochemical behaviour of Pb-plated graphite surfaces suggests that these electrodes may be employed to replace solid lead electrodes utilized in electrosynthesis.

ACKNOWLEDGEMENT. The author expresses her gratitude to Professor I. G. Murgulescu who initiated the investigation on bright metallic depositions.

REFERENCES

[1] M. Ya. Fioshin, *Elektrokhimiya*, **13**, 3 (1977).
[2] I. Marcos, *J. Electrochem. Soc.*, **122**, 1492 (1975).
[3] V. N. Varypaev, V. L. Krasikov and E. N. Timonova, *Zhur. priklad. Khim.*, **LV**, 470 (1982).
[4] T. D. Balakrishman, K. S. Udupa, G. S. Subramanian and H. V. Udupa, *Ind. Eng. Chem. Process Des. Develop.*, **10**, 495 (1971).
[5] M. Yamasjita and K. Sugino, *J. Electrochem. Soc.*, **104**, 100 (1957).
[6] M. Lacán, P. Maksimović, L. Thbakovic and G. Dźin, *Kemija u Industriji*, **5**, 227 (1970).
[7] V. N. Nikulin, V. N. Klochkova and L. A. Pavlichenko, *Zhur. Khim.*, **LI**, 1727 (1977).
[8] N.D. Viet, D. V. Kokoulina and L. I. Krishtalik, *Elektrokhimiya*, **8**, 221 (1972).
[9] D. J. Pickett, "Electrochemical Reactor Design", Elsevier, Amsterdam, 1977, p. 380.

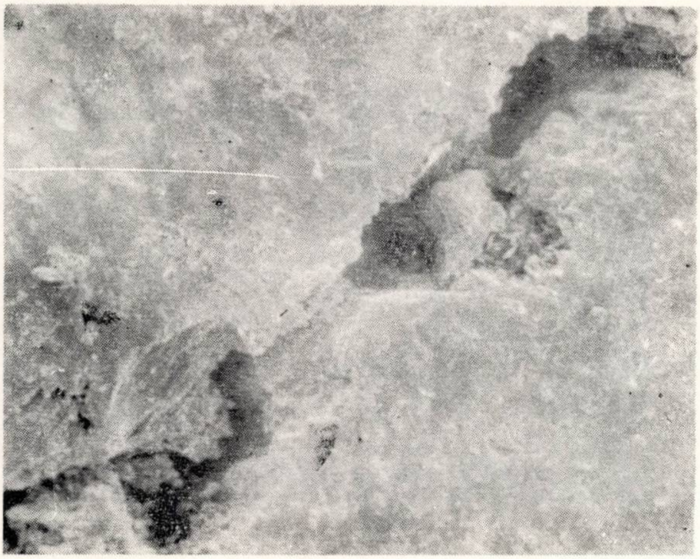

a

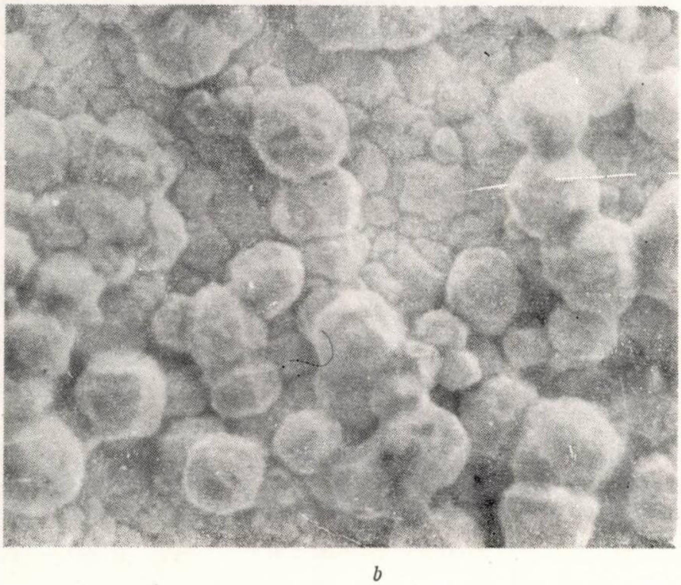

b

Fig. 3 — The surface structure of G1 graphite electrode unplated (a, 100 X); plated with copper (b, 2500 X); plated with copper and lead (c, 2500 X) and G2 graphite electrode plated with copper (d, 2500 X).

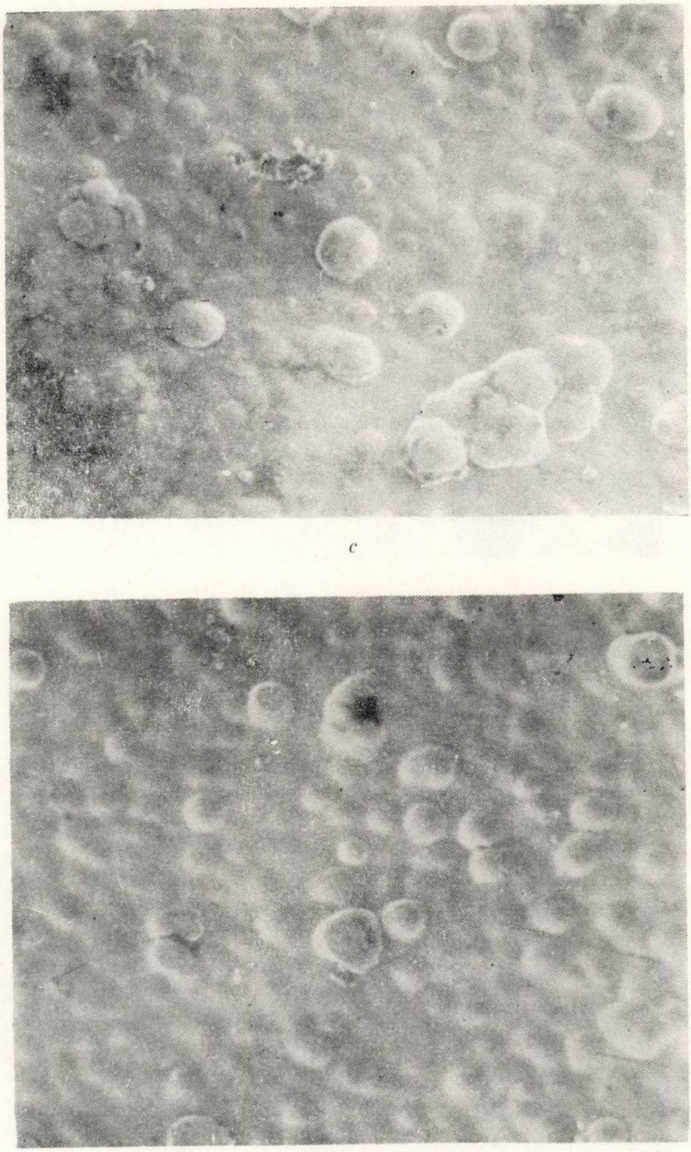

c

d

Fig. 3. – c, d.

[10] Yu. Yu. Matulis, "Blestyashchie Elektrolytycheskie Pokrytiya", Mintis, Vilnius, 1969, p. 350.
[11] C. Vass and I. Radovici, The Symposium "Chimia in Sprijinul Electronicii", Bucharest, 19–20 May, 1980.
[12] J. B. Mohler, "Electroplating and Related Processes", Chemical Publishing Co., New York, 1969, p. 134.
[13] O. Radovici, C. Vass, I. Solacolu and M. Marinescu, *Rom. Pat.*, 54.967/1972.
[14] C. Vass, Buletin de Informare tehnico-documentară "Coroziune", 1/1982, p. 21.
[15] H. Kouno and M. Nagayama, *Electrochim. Acta*, **22**, 353 (1977).
[16] V. N. Varypaev and V. L. Krasikov, *Zhur. priklad. Khim.*, **LIII**, 586 (1980).
[17] O. Radovici, C. Vass and I. Solacolu, *Electrodep. Surf. Treat.*, **2**, 263 (1973/19734).
[18] I. Vartieres, C. Vass and V. Toc, The Symposium of Applied Electrochemistry, Timișoara, 4–5 Oct. 1985, p. 289.
[19] E. Beltowska-Lehman and A. Riesenkampf, *Surface Technology*, **11**, 349 (1980).

Revue Roumaine de Chimie, **32**, *9–10*, 907–912 (1987)

Dedicated to Professor I. G. MURGULESCU
on his 85th anniversary

ON THE SEMICONDUCTING CHARACTER OF SPINEL-TYPE ELECTROCATALYTIC OXIDE LAYERS

IULIANA VARTIRES, ANGELA MIHELIS, VERONICA POPESCU and N. SPĂTARU

Center of Physical Chemistry, 202 Spl. Independenței, 77208 Bucharest, Romania

Received May 5, 1987

The paper aims at establishing the semiconducting character of the spinel-type oxide coating consisting of an active Co_3O_4 layer and an intermediary $SnO_2 + Sb_2O_3$ layer. Electrophysical properties of the system have been investigated through resistivity, ohmic drop and differential capacity measurements.

INTRODUCTION

Spinel-type oxides represent electrode materials which arose great interest in the chlorine-alkali industry because of their good electrocatalytic properties, ready availability and low cost.

The investigations, concerning spinels use for the chloride ion discharge reaction, have the purpose to find new materials with high electrocatalytic properties. Electrodes of titanium coated with an active layer of Co_3O_4 with an intermediary layer of $SnO_2 + Sb_2O_3$, have been investigated in an attempt to establish the reaction mechanism through kinetic parameters determination.[1]

Taking into account that the electrocatalytic performances are strongly related to the electrophysical properties of the material,[2] in the present work the semiconducting character of the material as well as the real surface area of the electrode are investigated. To this aim, measurements of resistivity, ohmic drop and differential capacity have been performed so that the electrochemical characterization should be completed.

EXPERIMENTAL

Electroactive layers of Co_3O_4, with an intermediary mixed-oxide $SnO_2 + Sb_2O_3$ layer, have been obtained by thermal decomposition of an appropriate mixture of metal salts. The method was described previously.[1]

For resistivity determinations the material has been deposited on glass substrates, and the resistivity has been determined using a Keithley 616 electrometer.

The resistivity of NaCl solution, with pH = 2.5, has been measured in a thermostated glass cell with platinated Pt electrodes, using an impedance bridge Wayne-Kerr B 641.

The ohmic drop has been measured under previously described conditions.[1]

The differential capacity has been measured in a 0.5M sodium acetate solution using the experimental setting in Fig. 1, in which the working cell has cylindrical symmetry. For the differential capacity and ohmic drop measurements the investigated electroactive layer has been deposited on cylindrical titanium electrodes.

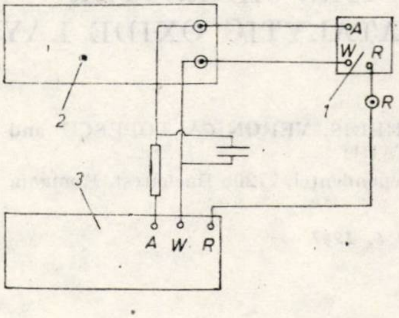

Fig. 1. — Measurement setting for differential capacity ; 1 — measurement cell ; 2 — impedance bridge ; 3—potentiostat ; W — working electrode ; A — counter-electrode ; R — reference electrode.

RESULTS AND DISCUSSION

The resistivity ρ is an important parameter as it reflects the free carrier concentration and is affecting the rate constants of the electrochemical reactions which take place at the electrode.

Table 1

The resistivity of the spinel-type oxide coatings, deposited on glass

Oxide	M_{ox}(mg/cm^2)	d(cm)	ρ(Ωcm)
$SnO_2 + Sb_2O_3$	1.7	0.00635	42.37
Co_3O_4	3.21	0.00875	92.84

Resistivity measurements (Table 1) give for the investigated oxide layers values of the order of ×10 Ω cm, which correspond to a semiconductor with a relatively high carrier concentration, with respect to other spinels described in the literature.[2] These values, correlated with the data concerning the geometry of the layers (Fig. 2), have allowed us to calculate the resistance of the oxide coating (Table 2).

Taking into account that these semiconducting layers can be used for dimensionally stable anodes (DSA), the effect of the titanium substrate and of the working solution (NaCl 5M, pH = 2.5) on layers resistance has been investigated. The resistivity of the NaCl solution has been first determined as a function of temperature and concentration at pH = 2.5 (Fig. 3). These values have been used to calculate the resistance R_s of the solution, between electrode surface and the tip of the Luggin capillary (Fig. 5).

One can determine electrochemically the total resistance of the oxide layer and of solution, $R_t = R_{ox} + R_s$ (Fig. 4), through the well known "interrupter" technique.

Fig. 5 shows measurement results for an electrode coated with 1.29 mg/cm² $SnO_2 + Sb_2O_3$ and 3.39 mg/cm² Co_3O_4. The resistance of the oxide layer ($R_{ox}(25°C) = 0.26\ \Omega$) is in agreement with the calculated values (Table 2), if one takes into account the contact between various layers.

Table 2

The resistance of the Co_3O_4 layer, with intermediary $SnO_2 + Sb_2O_3$ layer, on glass substrate

M_{ox}(mg/cm²)		d(cm)			$L(cm)$	$R(\Omega)$
$SnO_2 + Sb_2O_3$	Co_3O_4	Total	$SnO_2 + Sb_2O_3$	Co_3O_4		
1.69	3.95	0.007	0.0063	0.000635	1.67	0.127

The decrease of the R_{ox}, when the temperature increases, represents a characteristic behaviour for a semiconducting material.

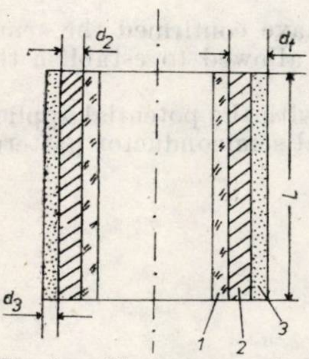

Fig. 2. — Electrode on glass substrate; 1 — glass; 2 — $SnO_2 + Sb_2O_3$; 3 — Co_3O_4.

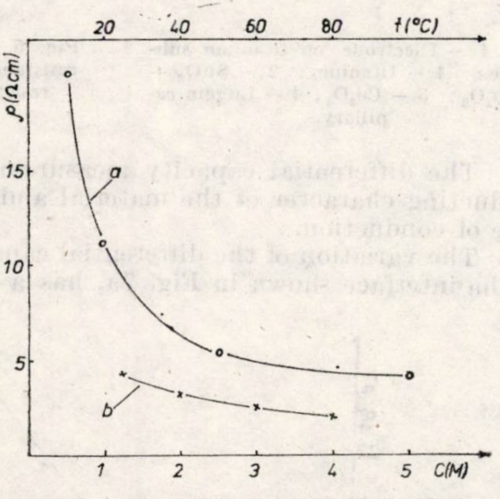

Fig. 3. — The resistivity of the NaCl solution, pH = 2.5; a — the dependence on concentration; b — the temperature dependence.

By investigating the variation of the resistance R_t with the quantity of Co_3O_4 deposited onto the electrode, the real surface area of the latter has been calculated.

The Fig. 6 shows the increase of the layer resistance with the quantity of deposited oxide. If the values of the geometrical surface area of the titanium and glass substrates are considered ($S_{Ti} = 1.24$ cm²; $S_g = 2.555$ cm²), it results that, depositing about 4.6 mg/cm² oxide, the electrode surface area increases by a factor of 15.38, that is the roughness factor is about 15. If, as a first approximation, one considers that the real surface area S of the electrodes increases linearly with the quantity of oxide M_{ox} deposited, it results, $S = 3.3 \times M_{ox} \times S_{geom}$.

However, it should be mentioned that the real surface area of the electrode is not the same with the active one, the latter being smaller.[1]

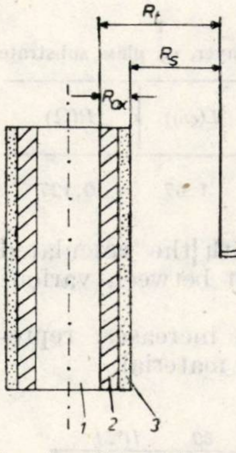

Fig. 4. — Electrode on titanium substrate: 1 — titanium; 2 — $SnO_2 + Sb_2O_3$; 3 — Co_3O_4; 4 — Luggin capillary.

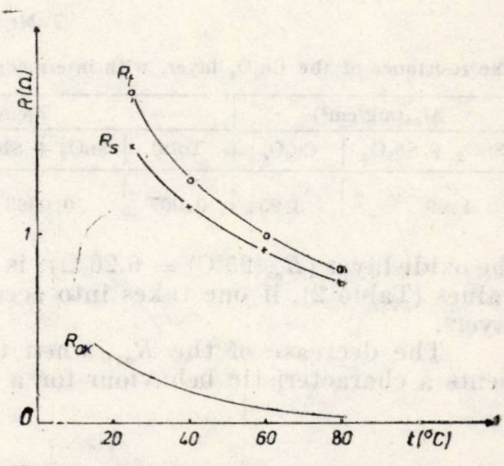

Fig. 5. — The temperature dependence of the resistance: R_t — total resistance; R_s — solution resistance; R_{ox} — oxide layer resistance.

The differential capacity measurements have confirmed the semiconducting character of the material and have allowed to establish the type of conduction.

The variation of the differential capacity with the potential applied to the interface shown in Fig. 7a, has a typical semiconductor pattern,

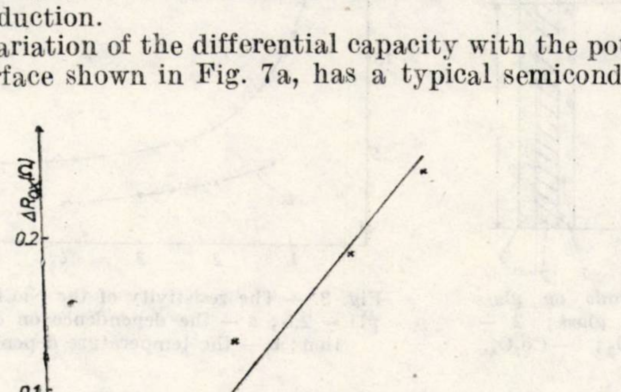

Fig. 6. — The dependence of R_{ox} resistance on the quantity of the deposited oxide.

with a specific capacity of 2–5 μF/cm², as usually found in the literature.[3]

In the Mott-Shottky representation one obtains for the anodic potentials range a characteristic straight line, with a negative slope which identifies a p-type semiconducting. The frequency variation (Fig. 8) shows the presence of surface states.

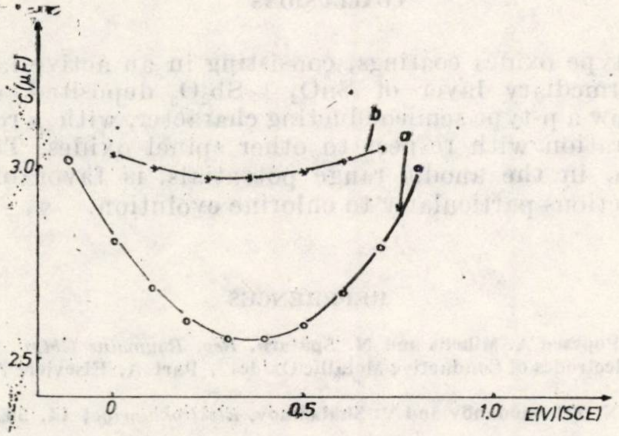

Fig. 7. — The dependence of the differential capacity on the applied potential: a — typical semiconductor pattern; b — high surface state density.

It has been found that some electrodes show a less pronounced dependence of the capacity on potential (Fig. 7b) but the values remain

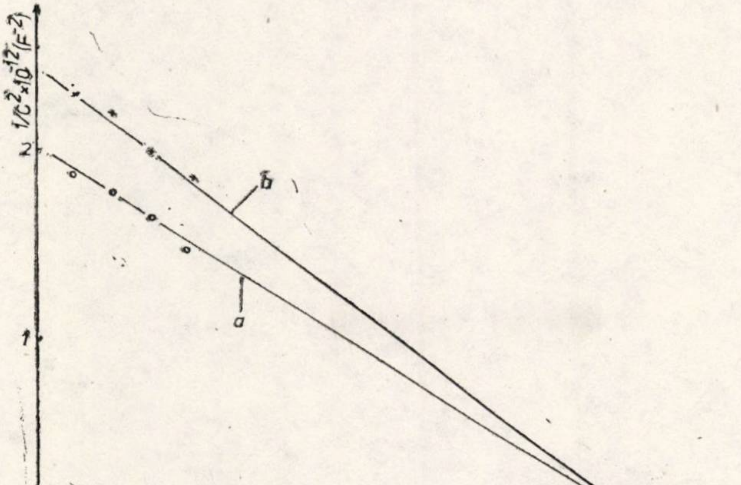

Fig. 8. — Potential and frequency dependence of $1/C^2$: a — $\omega =$ = 1.6 kHz; b — ω = 3 kHz.

within the 2–5 μF/cm² range. This behaviour is probably due to the high surface state density which quenches the polarization effect on differential capacity values.

CONCLUSIONS

Spinel-type oxides coatings, consisting in an active layer of Co_3O_4 and an intermediary layer of $SnO_2 + Sb_2O_3$ deposited on titanium substrate, show a p-type semiconducting character, with a relatively high hole concentration with respect to other spinel oxides. The high hole concentration, in the anodic range potentials, is favorable to anodic oxidation reactions particularly to chlorine evolution.

REFERENCES

[1] I. Vartires, V. Popescu A. Mihelis and N. Spătaru, *Rev. Roumaine Chim.*, **32**, 551 (1987).
[2] S. Trasatti, "Electrodes of Conductive Metallic Oxides", Part A, Elsevier, Amsterdam, 1980, p. 225.
[3] D. M. Sub, A. N. Tchemodanov and V. Shalaginov, *Elektrokhimiya*, **14**, 595 (1980).

Revue Roumaine de Chimie, 32, *9–10*, 913–923 (1987)

Dedicated to Professor ILIE G. MURGULESCU
on his 85th anniversary

RADIOTRACER STUDY OF THE ADSORPTION OF DL-ASPARAGINIC ACID AT A PLATINIZED PLATINUM ELECTRODE

G. HORÁNYI and E. M. RIZMAYER
Central Research Institute for Chemistry of the Hungarian Academy of Sciences, Budapest, H-1525, Hungary

Received March 30, 1987

Adsorption of ^{14}C labelled DL-asparaginic acid was studied in acid (1 mol dm^{-3} $HClO_4$) and in alkaline (0.1 mol dm^{-3} NaOH) media. The potential dependence of the adsorption and the mobility of adsorbed species were investigated. In acid medium loosely and strongly adsorbed species were found. In alkaline medium only the formation of strongly chemisorbed species was observed. The shapes of the amount adsorbed (Γ) vs. potential (E) curves obtained in acid and alkaline media significantly differ from each other owing to the difference in the behaviour of the adsorbed species. Results are compared with those obtained for other amino-acids and for succinic acid.

INTRODUCTION

In previous communications results obtained from the study of the adsorption of amino-acids at platinized platinum electrodes were reported.[1,2] Adsorption of glycine, alanine and γ-amino-butyric acid has been studied and the relevant literature data available for the adsorption of amino-acids at noble metal electrodes were overviewed (see, for instance, refs[3] and[4]). The aim of these studies was to investigate the role of amino group in the adsorption properties. In accordance with this aim, the adsorption behaviour of the amino-acids mentioned above was compared with that of the corresponding aliphatic acids as acetic, propionic and butyric acids. As the state of the functional groups involved in simple amino-acids strongly depends upon the pH ($-NH_3^+$ and COOH in strong acid, NH_2 and $-COO^-$ in strong alkaline media) a different adsorption behaviour was found in acid and alkaline media.

Our experimental study and considerations were hitherto restricted to monocarboxylic amino-acids.

In the present communication result obtained from the study of the adsorption of a dicarboxylic amino-acid, DL-asparaginic acid ($HOOCCH_2CH_2(NH_2)COOH$), will be reported. This amino-acid is a derivative of succinic acid the adsorption behaviour of which has been reported in ref.[5]

EXPERIMENTAL

The experimental procedure and methods described in the previous studies were used.[1,2] 1 mol dm^{-3} $HClO_4$ and 0.1 mol dm^{-3} NaOH were used as supporting electrolytes. The potential values quoted in this paper are given on the RHE scale. The roughness factors of the platinized platinum electrodes used were between 100 and 200. ^{14}C labelled DL-asparaginic acid (specific activity: 457 MBq mmol^{-1}) was used.

RESULTS

The potential dependence of the adsorption of DL-asparaginic acid in 1 mol. dm^{-3} $HClO_4$ and in 0.1 mol dm^{-3} NaOH supporting electrolytes is shown in Figs 1/a and 1/b respectively. In both cases the labelled species was added to the solution phase at low potential (0 mV) and the potential was shifted in 100 mV steps. At 700 mV the direction of the potential shisfts was reversed. A hysteresis may be observed between the ascending and descending branches. The attainment of the steady state following the potential shifts is a slow process at low potentials (0—300 mV) while a higher adsorption rate can be observed at higher potentials. This is shown in Fig. 2. It can be seen, that in acid medium there is a significant difference between the adsorption rates at 200 and 700 mV. On the other hand, in alkaline medium the slowness of the adsorption is very pronounced (curves 2′ and 3′ in Fig. 2).

The character of the potential dependence of the adsorption differs significantly in acid and alkaline media. In the former case two distinct steps can be distinguished on the Γ vs. E curve. In alkaline medium above 400 mV there is no significant change in the adsorption.

In order to gain some information about the nature of the adsorbed species their mobility was studied investigating the exchange of labelled adsorbed molecules with non-labelled species added to the solution phase in a great excess.

Fig. 3 shows the behaviour of labelled DL-asparaginic acid adsorbed at $E = 200$ mV in 1 mol. dm^{-3} $HClO_4$. It follows from Fig. 3 that practically no exchange of adsorbed species occurs at 200 mV, however, by shifting the potential to more negative values significant desorption takes place. In contrast to this, a remarkable exchange rate may be observed in the case of species formed at more positive potentials. Fig. 4 shows the behaviour observed at $E = 400$ mV. After the attainment of the equilibrium state (section 1) the addition of non-labelled species results in a significant decrease of the count-rate (section 2). However, the exchange process slows down rapidly and a significant part of the adsorbed species remains on the surface. This part can be removed by a potential shift to 0 mV (section 3).

Similar experiments were carried out at $E = 700$ mV. As Fig. 5 shows a potential shift to more positive values up to 1200 mV does not result in the complete removal of strongly adsorbed species, however, an almost complete elimination can be achieved by a subsequent potential switch to -25 mV. These experimental results attest that two types of adsorbed species, loosely adsorbed and strongly chemisorbed molecules, are formed in acid medium. The existence of mobile species is a characteristic feature in the case of saturated aliphatic acids. Only this type of species was found for succinic acid, the parent compound of asparaginic acid. [5]

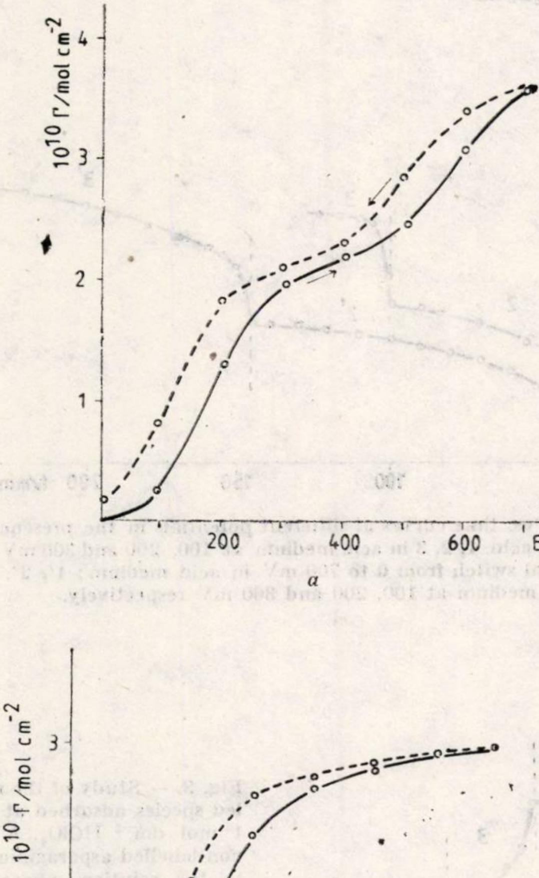

Fig. 1. — Potential dependence of the adsorption of asparaginic acid at $c = 5 \times 10^{-4}$ mol dm^{-3}. a) in 1 mol dm^{-3} $HClO_4$; b) in 0.1 mol dm^{-3} NaOH supporting electrolytes.

Results of a study of the simultaneous adsorption of asparaginic acid with acetic and succinic acids and chloride ions furnish further evidence proving the dynamic behaviour of a significant part of the adsorbed species formed at potentials above 300 mV. Fig. 6 shows the attainment of the equilibrium state with respect to the adsorption of asparaginic acid in the presence of acetic and succinic acids. Succinic acid exerts a significant influence on the adsorption of asparaginic acid when the concentration of the two acids is commensurable. This means that their adsorption strength (considering only the mobile part of asparaginic acid) is

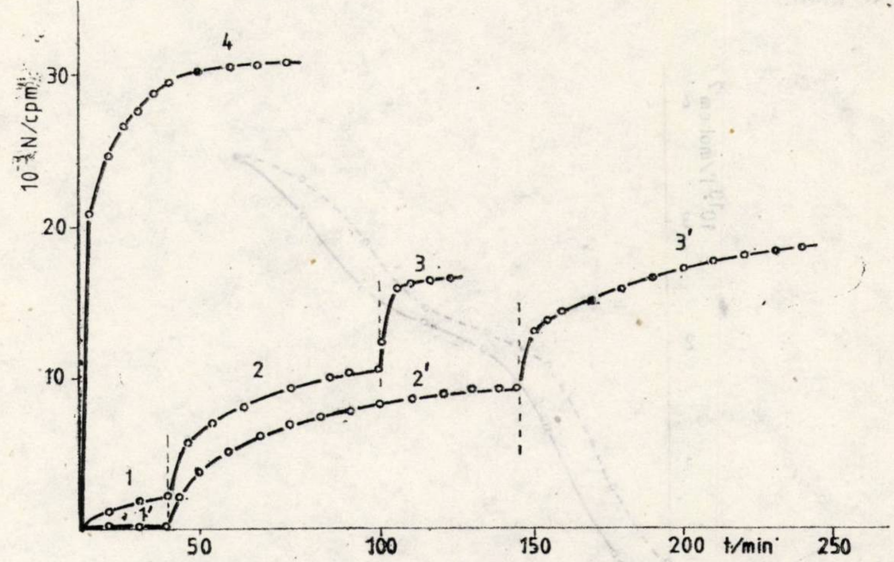

Fig. 2. — Count rate vs. time curves at different potentials in the presence of 5×10^{-4} mol dm^{-3} asparaginic acid. 1, 2, 3 in acid medium at 100, 200 and 300 mV respectively; 4 following a potential switch from 0 to 700 mV in acid medium; 1', 2', 3' in alkaline medium at 100, 200 and 300 mV respectively.

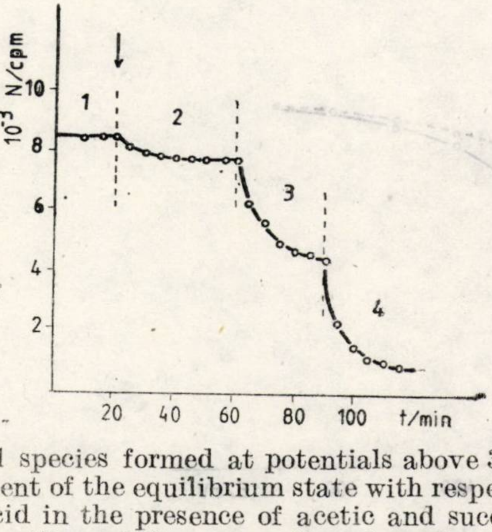

Fig. 3. — Study of the mobility of labelled species adsorbed at $E = 200$ mV in 1 mol dm^{-3} HClO$_4$. A great excess of non-labelled asparaginic acid was added to the solution phase at the moment indicated by the arrow. 1) and 2) 200 mV, 3) 100 mV, 4) 0 mV.

not far from each other. On the other hand, the concentration of acetic acid should be significantly higher in order to observe a remarkable decrease in the adsorption of the labelled asparaginic acid. i.e. there is a

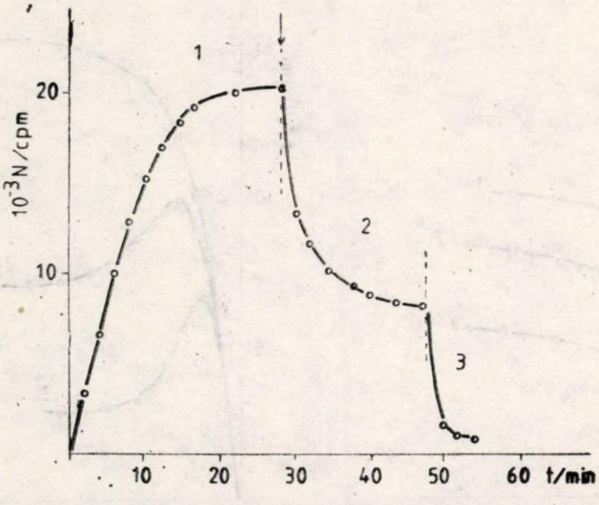

Fig. 4. — Study of the mobility of labelled species adsorbed at $E = 400$ mV in 1 mol dm^{-3} $HClO_4$. 1) and 2) 400 mV, 3) 0 mV. Non-labelled asparaginic acid was added at the moment indicated by the arrow.

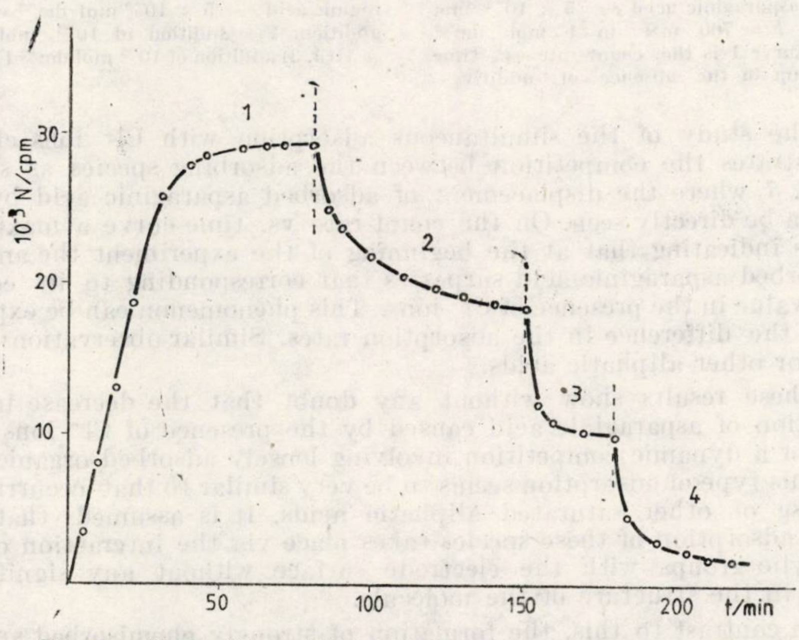

Fig. 5. — Study of the mobility of labelled species adsorbed at $E = 700$ mV. 1) and 2) 700 mV, 3) 1200 mV, 4) -25 mV.

great difference in the adsorption strengths of the these molecules, as it can be expected on the basis of results obtained from a similar study with acetic and succinic acids.[2]

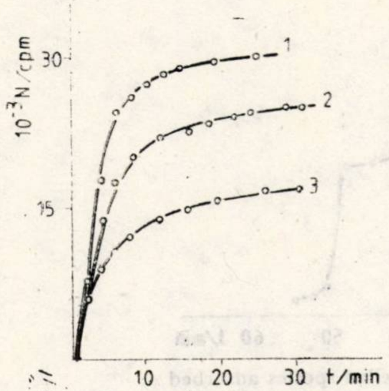

Fig. 6. — Effect of acetic acid (2) $c = 2 \times 10^{-3}$ mol dm^{-3} and succinic acid (3) $c = 5 \times 10^{-4}$ mol dm^{-3} on the adsorption of asparaginic acid $c = 5 \times 10^{-2}$ mol dm^{-3} at $E = 700$ mV in 1 mol dm^{-3} HClO$_4$. Curve 1 is the count rate vs. time relationship in the absence of additives.

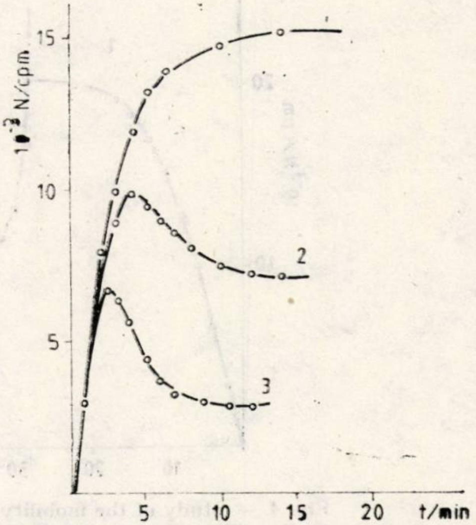

Fig. 7. — Adsorption competition of labelled asparaginic acid with Cl$^-$ ions at $E = 400$ mV in 1 mol dm^{-3} HClO$_4$. 1) Asparaginic acid $c = 5 \times 10^{-3}$ mol dm^{-3} without addition, 2) addition of 10^{-3} mol dm^{-3} HCl, 3) addition of 10^{-3} mol dm^{-3} HCl.

The study of the simultaneous adsorption with Cl$^-$ ions clearly demonstrates the competition between the adsorbing species as shown by Fig. 7 where the displacement of adsorbed asparaginic acid by Cl$^-$ ions can be directly seen. On the count-rate vs. time curve a maximum appears indicating that at the beginning of the experiment the amount of adsorbed asparaginic acid surpasses that corresponding to its equilibrium value in the presence of Cl$^-$ ions. This phenomenon can be explained by the difference in the adsorption rates. Similar observations were made for other aliphatic acids.

These results show without any doubt that the decrease in the adsorption of asparaginic acid caused by the presence of Cl$^-$ ions is a result of a dynamic competition involving loosely adsorbed organic species. This type of adsorption seems to be very similar to that occurring in the case of other saturated aliphatic acids. It is assumed that the mobile adsorption of these species takes place via the interaction of the carboxylic groups with the electrode surface without any significant change in the structure of the molecule.

In contrast to this, the formation of strongly chemisorbed species should involve a strong interaction with the electrode surface.

The potential dependence of the adsorption of strongly chemisorbed species can be studied separately in the presence of Cl^- ions. On the basis of the results presented in connection with the competitive adsorption studies it can be stated that at 1 :5 Cl^- ion and asparagic acid concentration ratio the adsorption of loosely adsorbing species is practically suppressed. Thus the Γ vs. E curve obtained in the presence of an excess of Cl^- ions corresponds to the strongly adsorbed species.

The result of this study is reflected by Fig. 8. The adsorption with respect to the strongly chemisorbed species practically does not change in the potential range between 300 and 700 mV. Above 700 mV a decrease in the adsorption can be observed, however, no significant change occurs up to 1000 mV. On the other hand, a predominant part of the chemisorbed molecules can be eliminated by shifting the potential to 0 mV.

Cyclic voltammetric and voltradiometric measurements furnish further information about the simultaneous charge transfer and adsorption processes. These studies were carried out at low sweep rates considering the slowness of the adsorption processes at the low concentrations used in tracer studies (1 mV s^{-1} and less). Fig. 9/a shows the cyclic voltammetric curves obtained in the absence and presence of labelled asparaginic acid in 5×10^{-4} mol dm^{-3} concentration. The periodical changes in the adsorption during consecutive cycles are shown in Fig. 9/b.

The most conspicuous changes in the voltammograms caused by the presence of asparaginic acid are as follows : Instead of the small second hydrogen peak on the anodic branch a relatively high peak appears with a small negative shift of the peak potential. Above 700 mV a continuous increase of the anodic current takes place. On the cathodic

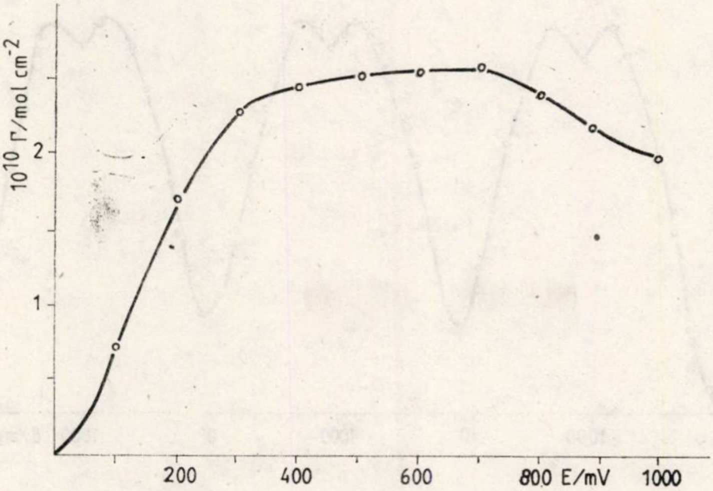

Fig. 8. — Potential dependence of the adsorption of asparaginic acid ($c = 5 \times 10^{-4}$ mol dm^{-3}) in the presence of 2.5×10^{-3} mol dm^{-3} HCl.

branch the oxygen reduction peak is suppressed and the hydrogen adsorption peaks are distorted. All this means that the adsorption of the organic species inhibits the oxygen adsorption and modifies the hydrogen adsorp-

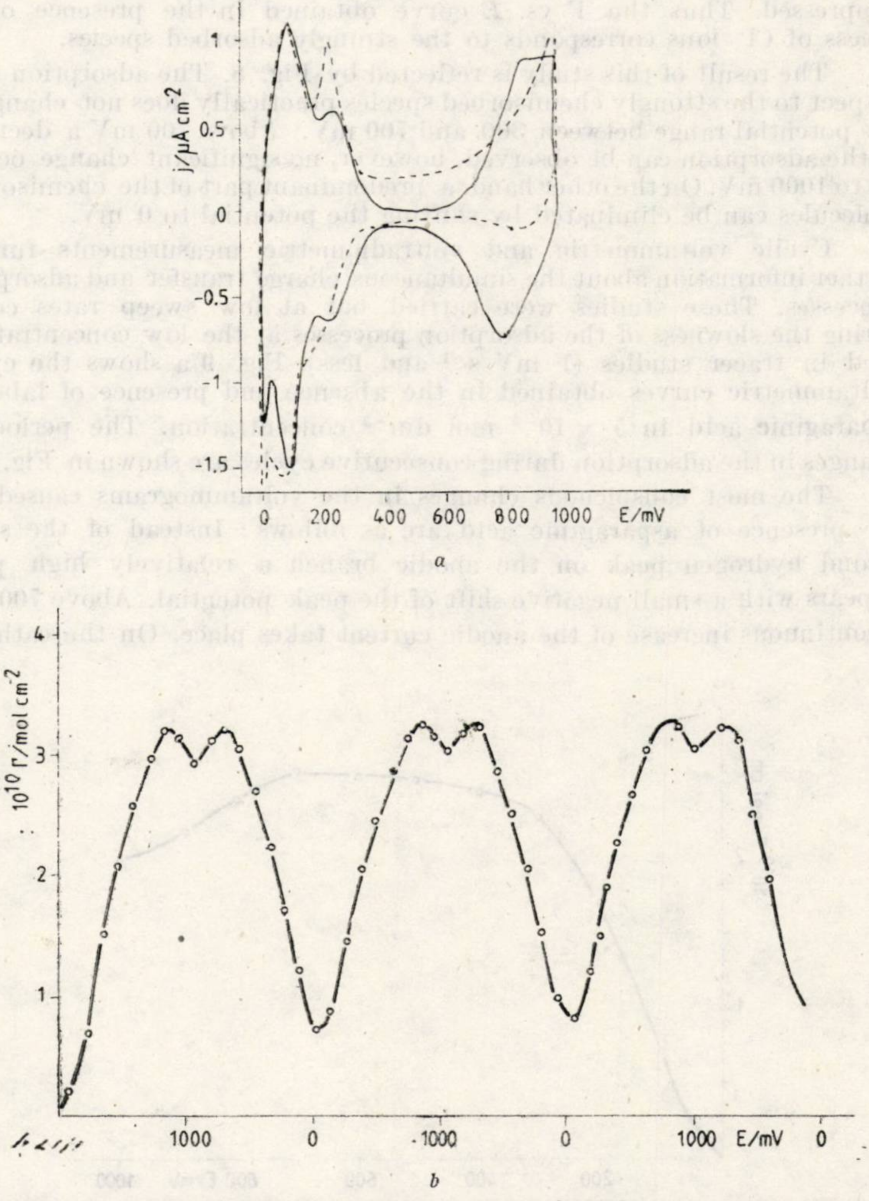

Fig.9. — a) cyclic voltammetric curves in 1 mol dm^{-3} HClO$_4$ in the absence (full line) and in the presence of labelled asparaginic acid (dotted line, $c = 5 \times 10^{-4}$ mol dm^{-3}), sweep rate 1 mV s^{-1}, potential range 0—1000 mV. b) Periodical changes in the count rate during consecutive cycles.

tion. At potentials above 700 mV the oxidation of the adsorbed organic species occurs. This observation is in accordance with the results of the tracer studies.

Cycling between 0 and 600 mV with a higher sweep rate (2.5 mV s^{-1}) the voltammograms become more symmetrical and the peaks on both branches can be distinctly seen as shown in Fig. 10.

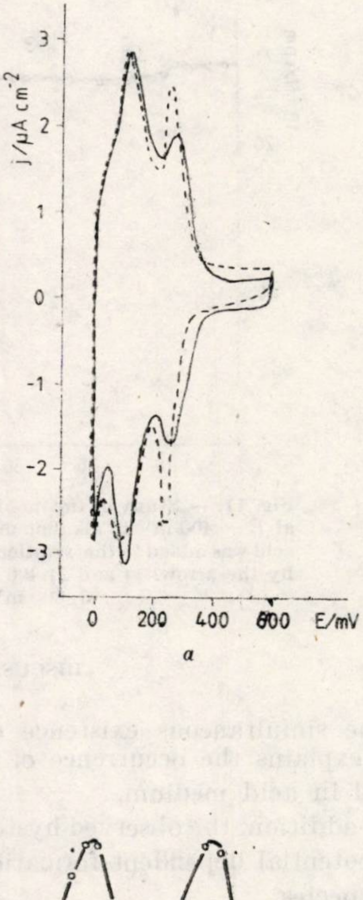

Fig. 10. — Cyclic voltammetric (a) and voltradiometric (b) studies with a sweep rate 2.5 mV s^{-1}. Potential range: 0—600 mV, the other data as in Fig. 9.

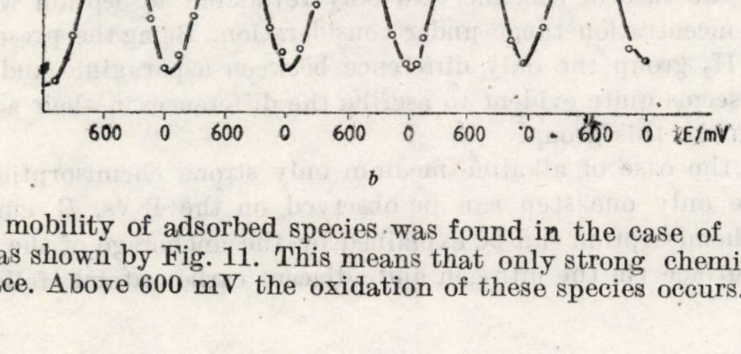

No mobility of adsorbed species was found in the case of alkaline medium as shown by Fig. 11. This means that only strong chemisorption takes place. Above 600 mV the oxidation of these species occurs. Below

200 mV a reductive elimination takes place. At 0 mV the chemisorbed species can be removed almost completely. This behaviour is very similar to that observed for other amino acids.[1,2]

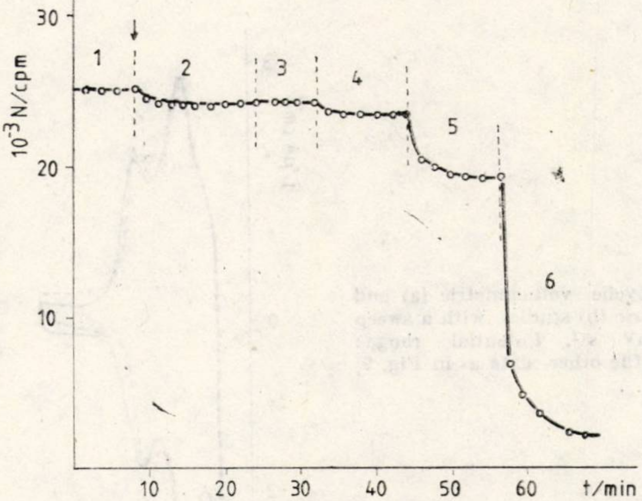

Fig. 11. — Study of the mobility of labelled species adsorbed at $E = 400$ mV in alkaline medium. Non-labelled asparaginic acid was added to the solution phase at the moment indicated by the arrow. 1) and 2) 400 mV ; 3) 500 mV ; 4) 600 mV ; 5) 800 mV ; 6) 0 mV.

DISCUSSION

The simultaneous existence of mobile and strongly chemisorbed species explains the occurrence of the two steps on the Γ vs. E curve obtained in acid medium.

In addition, the observed hysteresis phenomena can also be ascribed to the potential dependent formation and desorption of strongly chemisorbed species.

In the case of succinic acid only reversible adsorption was found in the concentration range under consideration. Being the presence of a single NH_2 group the only difference between asparaginic and succinic acids it seems quite evident to ascribe the differences in their adsorption behaviour to this group.

In the case of alkaline medium only strong chemisorption occurs therefore only one step can be observed on the Γ vs. E curve. The strong chemisorption can be explained by the anchorage of the molecule to the surface via the nitrogen and adjacent carbon atoms following an oxidative transformation (dehydrogenation). For instance:

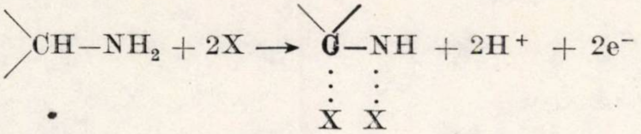

$$\rangle CH-NH_2 + 2X \longrightarrow \overset{\diagdown\,\diagup}{\underset{\underset{X}{\vdots}}{C}}-\underset{\underset{X}{\vdots}}{NH} + 2H^+ + 2e^-$$

It can be assumed that in the case of reductive desorption the opposite process takes place.

In acid medium the reversible adsorption leading the loosely adsorbed species (oriented by a COOH groups towards the surface) precedes the formation of strongly chemisorbed molecules. Presumably the slow oxidative transformation of the protonated $-CH-NH_2$ moiety occurs during strong chemisorption similarly to that assumed in the case of alkaline medium. There is no significant difference in the behaviour of chemisorbed species formed in alkaline and acid media, thus the above assumption seems acceptable. On the other hand, the occurence of some processes accompanied by the rupture of C—C bonds cannot be excluded.

REFERENCES

[1] G. Horányi and E. M. Rizmayer, *J. Electroanalyt. Chem.*, **64**, 15 (1975); **80**, 401 (1977); **198**, 393 (1986).

[2] G. Horányi and E. M. Rizmayer, *Electrochim. Acta*, in press.

[3] T. Ya. Safonova, Sh. Sh. Khidirov and O. A. Petrii, *Elektrokhimiya*, **20**, 1666 (1984).

[4] M. R. Tarasevich, A. Yu. Safronov, V. A. Bogdanovskaya and A. S. Chernyak, *Elektrokhimiya*, **19**, 167 (1983).

[5] G. Horányi and G. Inzelt, *Israel J. Chem.*, **18**, 136 (1979).

Revue Roumaine de Chimie, **32**, *9–10*, 925–933 (1987)

Dedicated to Professor I. G. MURGULESCU
on his 85th anniversary

PROTONIC CONDUCTORS WITH BETA-ALUMINA TYPE STRUCTURE

MARIA ZAHARESCU, CONSTANȚA PÎRLOG, D. CRIȘAN, N. DRĂGAN,
ANA BRĂILEANU, M. ILISIE and T. SURDEANU*
ICECHIM – Center of Physical Chemistry, Bucharest, 202 Splaiul Independenței, Romania
* SINTEROM Plant, Cluj-Napoca, 12 Podgoriei St., Romania

Received May 16, 1987

The conditions of synthesis of beta-aluminas with proton conduction are presènted; the influence of various steps of synthesis upon the structure, texture and transport properties of the materials resulted is discussed. The experimental methods employed were: X-ray diffraction, differential thermal analysis, textural properties measurements and impedance spectroscopy. The materials resulted possess adequate structure and texture; their electrical conductivity is in the range of solid electrolytes.

1. INTRODUCTION

Beta-aluminas are aluminates with variable amounts of mono- or divalent cations which due to their characteristic hexagonal structure[1] possess an unusually high ionic conduction for a ceramic material.[2] The conduction of beta″-alumina polymorph is higher than that of beta-alumina,[3] but this structure requires stabilization. Due to their high ionic conductivity and low electronic conductivity, beta-aluminas are an important class of solid electrolytes.

Hydronium beta-alumina is peculiar among these materials, as it cannot be prepared by the usual solid phase sintering method because its structure collapses at temperatures considerably lower than those required by the formation of beta-alumina structure.[4]

The only alternative left is to start up with sodium-beta-alumina and use an ionic exchange method.

In the series of isomorph beta-alumina (Table 1) the parameter "*a*" of the unit cell is almost unchanged, while the parameter "*c*" changes with the ionic radius of the monovalent cation in the structure. The expansion of "*c*" parameter occurred in the conduction plane containing the monovalent ions.

Due to the significant difference between the ionic radii of Na^+ and of hydronium, the exchange of these ions would induce stresses which affect the mechanical strength of sintered material, causing eventually its breakdown.

A possible way to avoid this difficulty is to achieve the exchange in several steps; it has recently been suggested to use a mixed Na/K beta-alumina as starting material.[6]

Table 1

Lattice constants of some beta and beta''-aluminas

Structure	Cation	Ionic radius Å	*a* Å	*c* Å	Δ*c* Å	References
beta	Na^+	0.95	5.594	22.530	—	5
	K^+	1.33	5.596	22.729	+0.199	5
	$Na^+/K^+(1/1)$	—	5.595	22.606	+0.076	5
	Li^+	0.60	5.596	22.570	+0.040	5
	Ag^+	1.26	5.596	22.498	−0.032	5
	H_3O^+	1.40	5.597	22.655	+0.155	5
beta''	Na^+	0.95	5.594	33.975	—	6
			5.623	33.59	—	7
	K^+	1.33	5.596	34.29	+0:315	6
	H_3O^+	1.40		34.16	+0.185	6
				34.51	+0.535	

Utilization of mixed Na/K beta-alumina in the obtention of hydronium beta-almina was suggested by the fact that the radius of K^+ ion is about the same with that of H_3O^+ whereas Na^+ ion favours formation of beta'' phase and lowers the sintering temperature.[6]

The present contribution reports the synthesis of a hydronium beta-alumina from a mixed beta-alumina resulted from utilization of two stabilizers, La_2O_3 and MgO, in a multistep ionic exchange. The influence of the different steps of the synthesis on the structure, texture and ionic transport properties of the sintered materials, was also investigated.

2. EXPERIMENTAL

2.1. Synthesis of Na/K beta-alumina

The preparation of ceramic materials of Na/K beta-alumina used in the ionic exchange resulting in hydronium beta-alumina started with the composition advanced by Nicholson[6] (with MgO as stabilizer). The composition mentioned elsewhere by the authors[8] was employed with La_2O_3 as stabilizer; the Na/K ratio was identical to that proposed by Nicholson.[6]

For the sake of comparison, a sodium beta-alumina was sintered with La_2O_3 as stabilizer.

The classical process for preparation of beta-alumina ceramics consists of two steps. The former is the synthesis of beta-alumina powders of adequate composition, and the latter consists of the shaping of green bodies and their sintering.

The raw materials employed were ceramic grade alpha-alumina (GDR) and analytical grade Na_2CO_3 (Reactivul), La_2O_3 (Loba Chemie) and MgO (Merck).

After a thorough homogenization, the mixture was heated for two hours at 1250°C. The reacted powders were ground in a planetary mill with alpha-alumina balls to the same particle size (90% below 32 μm).

From these powders 20 mm diameter disks were pressed at 2000 daN/cm². This pressure was determined from the compressibility curves of each powder.

In order to prevent Na losses upon heating the samples to be sintered were powdered with coarse beta-alumina of the same Na_2O/Al_2O_3 ratio as in the samples and were sintered in a gas furnance for one hour at 1600°C (MgO stabilized powder) and 1520 and 1600°C (La_2O_3 stabilized powder).

2.2. Synthesis of hydronium beta-alumina

Hydronium beta-alumina was prepared from sintered bodies of Na/K beta-alumina by ionic exchange in molten NaCl/KCl followed by chemical attack with concentrated H_2SO_4. The overall scheme of hydronium beta-alumina preparation is given below:

$$\text{Na/K-}\beta\text{-Al}_2\text{O}_3 \xrightarrow[800^\circ\text{C, 48 h}]{\text{NaCl/KCl}} \text{K-}\beta\text{-Al}_2\text{O}_3 \xrightarrow[350^\circ\text{C, 110 h}]{\text{H}_2\text{SO}_4} \text{H}_3\text{O}^+\text{-}\beta\text{-Al}_2\text{O}_3$$

2.3. Characterisation of beta-aluminas

The phase composition was determined by X-ray diffraction. A HZG-3 diffractometer was used, working with the $Co_{K\alpha}$ radiation. The beta/beta″ ratio was calculated with the equation developed by Johnson et al.[2], while for calculation of volume fraction $f(\beta)$ the X-ray line at 2.69 Å for beta phase was compared with that at 2.60 Å for beta″ phase.[12]

The conversion of mixed Na/K beta-aluminas into hydronium beta-alumina was determined by the evaluation of parameter "*c*" of unit cell and by simultaneous DTA and DTG using a MOM OD-102 Derivatograph with a heating rate of 10°/min.

The textural properties and their variation after ionic exchange was determined by density and porosity measurements.

Ionic transport properties were determined by impedance spectroscopy. The equipment and equations employed are discussed together with the present results.

3. RESULTS AND DISCUSSION

3.1. Na/K beta-alumina precursor powders

The phase compositions of the precursor powders prepared as shown above were determined by X-ray diffraction and are presented in Table 2.

In all cases these powders were mixtures of beta and beta″ phases, the latter being the major component. Small amounts of unconverted alpha-alumina were noted, too.

3.2. Ceramics of Na/K beta-alumina

The structure and texture of Na/K beta-alumina ceramics are compared in Table 3 with those of Na beta-alumina.

In the presence of La_2O_3 the temperatures required for sintering are lower and the density of the samples is closer to the theoretical value.

The presence of MgO favors the formation of beta″-alumina higher electrical conduction.

If the phase compositions of the precursor powder (Table 2) are compared with those of sintered bodies (Table 3), one will note that all alpha-alumina present in the fomer has been converted to beta-alumina.

Table 2

Phase composition and beta/beta″ ratio of the precursor powders

Sample of $\beta-Al_2O_3$	$\alpha-Al_2O_3$	$\beta-Al_2O_3$		$\beta''-Al_2O_3$		$f(\beta'')$**
	I(mm) (1.1.3) line $d = 2.085$ Å	I(mm) (0.2.5) line $d = 2.136$ Å	%*	I(mm) (2.0.10) line $d = 1.976$ Å	%*	
Na/K/Mg	14	26	34.67	112	65.33	1.88
Na/K/La	16	35	49.38	82	50.62	1.03
Na/La	59	31	39.40	109	60.60	1.54

* represents percentage of $\beta-Al_2O_3$, respectively $\beta''-Al_2O_3$ from all beta phases in samples. It was calculated with the equation :

$$\%\beta'' = \frac{35 I\beta''}{35\ I\beta'' + 80\ I\beta}\text{, according to}^9;$$

** according to[10].

Table 3

Structural and textural properties of Na/K beta-alumina ceramics

Sample of $\beta-Al_2O_3$	Sintering temperature (°C)	Density (g/cm^3)	Porosity (%)	Phase composition				$f(\beta'')$*
				$\beta-Al_2O_3$		$\beta''-Al_2O_3$		
				I(mm) (0.2.5.) line $d = 2.136$ Å	%*	I(mm). (2.0.10) line $d = 1.976$ Å	%*	
Na/K/Mg	1600	2.20	31.75	35	32.52	166	67.48	2.08
Na/K/La	1520	2.33	9.41	109	94.32	15	5.68	0.06
	1600	3.18	1.04	66	100	—	—	0
Na/La	1520	2.21	—	86	88.72	25	11.28	0.13
	1600	3.02	17.10	87	100	—	—	0

* according to Table 2

3.3. **Hydronium beta-alumina ceramics**

3.3.1. *Structure and texture*

The properties characterizing the structure and texture of the hydronium betá-alumina samples are given in Table 4, which also lists the properties of the starting materials and of the intermediate samples resulted after ionic exchange in molten salts.

In both cases the porosity of initial samples is rather high and decreases after the exchange, which yields dense ceramic whose porosity is practically zero. The density of La_2O_3 stabilized hydronium beta-alumina represents 96.36% of theoretical density.

According to Table 3 the major phase components of samples stabilized with MgO and La_2O_3 are beta″ and beta-alumina respectively.

The parameter "*c*" determined for the major component in the two ceramics obtained exhibits a successive increase in the two exchange steps (Table 1), in good agreement with the literature data. The ionic exchange of Na^+ with K^+ is accompanied by a sensitive increase of parameter "c" of crystalline lattice while in the exchange of K^+ with H_3O^+, due to the similar radii of the two ions, the variation of the same parameter is less obvious.

Table 4

Structural and ceramic properties of hydronium beta-alumina samples

Sample of $\beta-Al_2O_3$	Density g/cm³	Porosity %	Phase composition	"c" parameter variation	
				$\beta-Al_2O_3$	$\beta''-Al_2O_3$
Na/K/Mg sintered 1600°C	2.22	27.40	$\beta''-Al_2O_3$		33.835
Exchanged in molten NaCl/KCl	2.51	17.20	$\beta''-Al_2O_3$		33.950
Exchanged in conc. H_2SO_4	2.77	0.01	$\beta''-Al_2O_3$		34.112
Na/K/La sintered 1520°C	2.33	8.90	$\beta-Al_2O_3$	22.538	
Exchanged in molten NaCl/KCl	2.81	1.20	$\beta-Al_2O_3$	22.644	
Exchanged in conc. H_2SO_4	3.11	0.009	$\beta-Al_2O_3$	22.645	

For hydronium beta-alumina stabilized with La_2O_3 the value of parameter "c" is very close to the theoretical one (Table 1) pointing to a complete ionic exchange.

In MgO-stabilized sample the parameter "c" differs more significantly from the data in literature which may be assigned to an incomplete ionic exchange.

The synthesis of hydronium beta-alumina was confirmed by DTA and DTG, too. The DTA-DTG curves for the MgO-stabilized sample are shown in Figure 1.

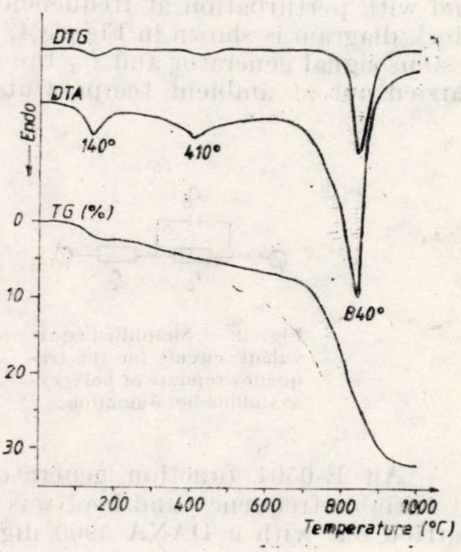

Fig. 1.—The DTA—DTG curves for the MgO stabilized hydronium beta—alumina sample.

The shapes of these curves are similar to those given elsewhere.[11] Besides the low temperature effect assigned to the loss of hydratation water of H_3O^+ ion there is a high temperature effect brought about by elimination of hydration water of the proton. The weak effect at 410°C is assigned to the existence in the sample of small amounts of incompletely converted intermediate species.

3.3.2. *Ionic transport properties*

The transport properties of hydronium beta/beta″-alumina were determined by impedance spectroscopy. A simple model suggested by Powers and Mitoff[12] was employed in the calculations; it makes use of the circuit shown in Figure 2. In this circuit r_c stands for the resistance of intragranular material (crystal), r_b for the resistance of intergranular material and c_b is the electrical capacity associated to intergranular regions. The component r_c may be regarded as the lower limit of the overall impedance. The separation of these components can be done by examining a plot of the specific impedance of the samples vs. frequency. A theoretical curve is given in Figure 3.

One may distinguish three regions on this plot:

— at low frequency there is a plateau at a value of the impedance about equal to the electrical resistance in d.c. of the sample i.e. $(r_b + r_c)$;

— within the second region, at higher frequencies, the impedance decreases monotonously; from electrical viewpoint the sample behaves as a capacitor in a.c.;

— finally, at even higher frequencies there is a second plateau at lower impedance than the previous one $(r_b \to 0)$, equal to the electrical resistance of the crystal, r_c.

The measurements were carried out by an open bridge, without and with perturbation at frequencies between 10 Hz and 250 kHz. The block diagram is shown in Figure 4, where U_1 is the voltage supplied by a sinus signal generator and U_2 the measured voltage. Measuremnts were carried out at ambient temperature.

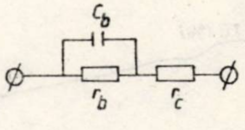

Fig. 2. — Simplified equivalent circuit for the frequency reponse of polycrystalline beta-alumina.

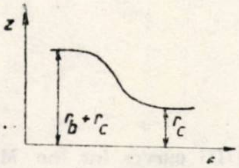

Fig. 3. — A plot of the specific impedance of beta-alumina vs. frequency.

An E-0504 function generator which supplied constant voltage at variable frequency and load was utilized; voltage measurements were carried out with a DANA 5900 digital multimeter.

The values of resistor R_0 (employed in measurements) and of the ceramic capacitor C_0 (perturbation) were determined by experiments such that the effects measured to be the highest. The following values were found : $R_0 = 4\ \mathrm{K\Omega}$ and $C_0 = 60\ \mathrm{nF}$.

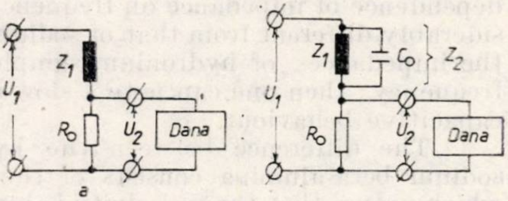

Fig. 4. — Block diagram for the impedance measurements. a) unperturbed circuit ; b) circuit perturbed with the condenser C_0 (Z_1 is the impedance of the sample).

To find out impedance Z_1, the complex impedances of the two circuits were written without any specification of the nature of reactance of the sample (X) :

$$(1)\quad \begin{cases} Z_1 = R_0 + jX \\ \dfrac{1}{Z_2} = \dfrac{1}{Z_1} + \dfrac{1}{j\omega C_0} \end{cases}$$

Processing of system (1) yields :

$$(2)\quad \begin{cases} x^2 + y^2 - Z_1^2 = 0 \\ x^2(1 - ax)^2 + y^2 + a^2y^4 - Z_2^2(1-ax)^2 + a^2y^2 - 2axy^2(1 - ax) = 0 \end{cases}$$

where : $a = C_0$; $x = X$ and $y = R_0$.

Solving the system by running an adequate computer program yielded the values of Z_1. Examination ot the imaginary part of Z_1 shows that the reactance is capacitive according to the model in Figure 2.

The results obtained after processing of data for hydronium beta/ /beta''-alumina stabilized with La_2O_3 (I= 1) and MgO ($I = 2$) are presented comparatively with the natrium beta-alumina ($I = 3$) in Figure 5.

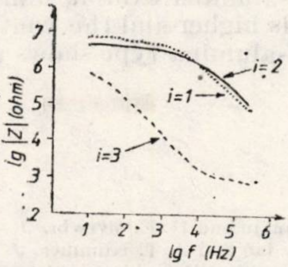

Fig. 5. — Impedance vs. frequency curves for the investigated beta-aluminas : $I = 1$ hydronium beta-alumina stabilized with La_2O_3 ; $I = 2$ hydronium beta''-alumina stabilized with MgO ; $I=3$ sodium beta-alumina

The curve for sodium beta-alumina is similar to the ideal one suggesting that the equivalent circuit of the sample may be represented by a resistor in parallel with a capacitor. The resistor is associated to the intergranular resistance, while the capacitor corresponds to the intergranular capacitive effect. The contribution of intragranular resistance is very low because the curve exhibits a tendency of slow decline towards zero with increasing frequency above 250 kHz.

The hydronium beta/beta″-alumina samples exhibit a similar dependence of impedance on frequency; however this dependence is considerably different from that of sodium beta-alumina. Thus below 5 kHz the impedances of hydronium samples do not vary significantly with frequency; then one can note a slow decrease which in fact points to a capacitive behaviour.

The difference between the hydronium beta/beta″-alumina and sodium beta-alumina consists of the higher value of the first plateau which proves that the resistivity is higher in the former case.

The curves representing the variation of impedance versus frequency approach zero slower in hydronium beta-aluminas than in sodium beta-alumina, which means that the intragranular contribution to the overall resistance is more important.

This finding is accounted for by the fact that in hydronium beta-alumina the conduction is protonic while in sodium beta-alumina it is due to sodium ions whose mobility is higher.

The measurements effected have come out with the following values of resistivities and conductivities, respectively:

$$\rho_{I=1} \simeq 8\cdot 10^{7}\ \Omega\mathrm{cm}; \quad \gamma_{I=1}\ \frac{1}{\rho_{I=1}} \simeq 10^{-8}\ (\Omega\mathrm{cm})^{-1}$$

$$\rho_{I=2} \simeq 5\cdot 10^{7}\ \Omega\mathrm{cm}; \quad \gamma_{I=2} = \frac{1}{\rho_{I=2}} \simeq 2\cdot 10^{-8}\ (\Omega\mathrm{cm})^{-1}$$

which are in the range accepted by literature for such materials.

The preliminary measurements of transport properties presented show that the conductivity of the materials obtained is similar although the major phase component differs i.e. it is beta or beta″ alumina.

We consider that the samples stabilized with La_2O_3 (beta-alumina as major component) and that stabilized with MgO whose major component is beta″-alumina exhibit similar conductivity because in the former the density is higher and the contribution of the secondary phases which are of beta″-alumina type shows up.

REFERENCES

[1] G. A. Rankin and H. E. Merwin, *J. Amer. Chem. Soc.*, **38**, 568 (1916); according to [23]
[2] Y. F. Y. Iao and J. T. Kummer, *J. Inorg. Nuclear Chem.*, **29**, 2453 (1967).
[3] J. T. Kummer, "Beta-Alumina Electrolytes", in "Progress in Solid State Chemistry", vol. 7, Edited H. Reiss and J. McCaldin, Pergamon Press, 1972, p. 141.
[4] Ph. Colomban, Y. P. Boilot, P. Chagnon and G. Guilloteau, *Bull. Soc. Ceram. France*, **1978**, 3.
[5] J. H. Kennedy, "The Beta-Aluminnas" in "Topics in Applical Physics", vol. 21, "Solid Electrolytes", Editor S. Geller, Springer Verlag, Berlin, Heidelberg, New York, 1977, p. 105.

[6] P. S. Nicholson, M. Nagai, K. Yamashita, M. Sayer and M. F. Bell, *Solid State Ionics*, **15**, 317 (1985).

[7] Ph. Colomban and A. Novak, *Solid State Communications*, **32**, 467 (1979).

[8] M. Zaharescu, VC. Pîrlog, V. Stancovschi, D. Crişan, A. Brăileanu, N. Drăgan and T. Surdeanu, "Proceedings of the Symposium on Applied Electrochemistry", Timişoara, 4–5 Oct. 1985, vol. I, p. 273.

[9] D. W. Johnson, S. M. Granstaff and W. W. Rhodes, *Amer. Ceram. Soc. Bull.*, **58**, 859 (1979).

[10] A. Teitsma, M. Sayer, S. L. Segel and P. S. Nicholson, *Mat. Res. Bull.*, **15**, 1611 (1980).

[11] M. W. Breiter, G. C. Farington, W. L. Roth and J. L. Duffy, *Mat. Res. Bull.*, **12**, 895 (1977).

[12] R. W. Powers and S. P. Mitoff, *J. Electrochem. Soc.*, **122**, 226 (1975).

[6] P. S. Nicholson, M. Nagai, K. Yamashita, M. Sayer and M. F. Bell, *Solid State Ionics*, **15**, 317 (1985).

[7] [illegible] and A. Nowick, *Solid State Communications*, **33**, 167 (1979).

[8] M. Zaharescu, V. C. Pârlog, V. Stanciovici, D. Crişan, A. Braileanu, N. Drăgan and E. Segal, "Proceedings of the Symposium on Applied Electrochemistry," Timişoara, 4–5 Oct. 1986, vol. 1, p. 278.

[9] D. W. Johnson, S. M. Granstaff and W. W. Rhodes, *Amer. Ceram. Soc. Bull.* **58**, 849 (1979).

[10] A. Tofield, M. Sayer, S. L. Segel and P. S. Nicholson, *Mat. Res. Bull.* **15**, 1611 (1980).

[11] W. Bruner, G. C. Farrington, W. L. Roth and J. L. Duffy, *Mat. Res. Bull.*, **12**, 395 (1977).

[12] W. Powers and S. P. Mitoff, *J. Electrochem. Soc.*, **122**, 226 (1975).

Revue Roumaine de Chimie, **32**, *9–10*, 935–938 (1987)

Dedicated to Professor I. G. MURGULESCU
on his 85th anniversary

A NONLINEAR TRANSFORMATION FOR THE REACTION EXTENTS WITHIN THE FRAMEWORK OF THE HORIUTI – TEMKIN THEORY

M. O. VLAD[a], V. T. POPA[b] and E. SEGAL[c]

[a]Industrial Central for Medicinal Drugs and Cosmetics, Blvd. Chimiştilor 50, CP 78014, Bucharest, Romania
[b]ICECHIM-CCF Bucharest, Splaiul Independenţei 202, 79611, Romania
[c]Polytechnic Institute, Department of Physical Chemistry and Electrochemical Technology, Blvd, Republicii 13, Bucharest 70346, Romania

Received December 29, 1986

This note deals with multi-route chemical systems for which a transformation law leading to a "one reaction representation" may exist. A critical analysis of the formalism used in literature is presented. Finally a general nonlinear transformation of the reaction extents is introduced.

The Horiuti-Temkin theory[1-3] allows to describe the dynamic behaviour of a complex chemical system by means of a simplified reaction scheme composed of overall reactions. Each overall reaction involves a succession of elementary steps and may be derived by eliminating the reactive intermediates from the full reactional scheme. For a given mechanism the number of linearly independent reaction routes is constant. Let us consider that the overall reactions corresponding to a basis of linearly independent reaction routes are:

$$\sum_{i=1}^{M} \psi_{il} A_i = 0, \quad l = 1, \ldots, P. \tag{1}$$

where ψ_{il} are the overall stoichiometric coefficients. To each of reactions (1) we may attach a stoichiometric vector:

$$\boldsymbol{\psi}_l = (\psi_{il}), \quad i = 1, \ldots, M, \tag{2}$$

an extent variable[4] ξ^l, a reaction rate:

$$r^l = \mathrm{d}\xi^l/\mathrm{d}t, \tag{3}$$

and a reaction affinity:

$$\mathscr{A}_l = -\partial G/\partial \xi^l, \tag{4}$$

where G is the free energy of the system.

Unlike the case of elementary reactions, the representation (1) is not unique. Performing a linear transformation of the route basis we get a new set of overall reactions :

$$\sum_{i=1}^{M} \psi'_{il'} A_i = 0, \quad l' = 1, \ldots, P, \tag{5}$$

with

$$\psi'_{il'} = (\mathbf{c})^{l}_{l'} \psi_{il}, \quad \boldsymbol{\psi}'_{l'} = (\mathbf{c})^{l}_{l'} \boldsymbol{\psi}_{l}, \tag{6}$$

$$\xi'^{l'} = (\mathbf{c}^{-1})^{l'}_{l} \xi^{l}, \quad r'^{l'} = (\mathbf{c}^{-1})^{l'}_{l} r^{l}, \tag{7),(8}$$

$$\mathscr{A}'_{l'} = (\mathbf{c})^{l}_{l'} \mathscr{A}_{l}, \tag{9}$$

and the transformation matrix $\mathbf{c}$ is nonsingular

$$\det \ \mathbf{c} \neq 0. \tag{10}$$

We note that $\boldsymbol{\psi}_l$ and $\mathscr{A}_l$ are transformed covariantly when a new basis of routes is introduced. On the contrary, ξ^l and r^l have a contravariant behaviour.

Generally speaking the transformation need to be independent of reaction parameters. However, the following transformation is commonly used[5] :

$$c^{1}_{l} = r^{1} \Big/ \sum_{q=1}^{P} r^{q}; \quad c^{l'}_{l} = \delta^{l'}_{l}, \quad l' \neq 1, \tag{11}$$

where $\delta^{l'}_{l}$ is the Kronecker delta. The transformation (11) leads to the so-called "one reaction representation". Indeed, from (8) and (11) we obtain :

$$r'^{1} = \sum_{q=1}^{P} r^{q}, \quad r'^{l'} = 0, \quad l' = 2, \ldots, P. \tag{12}$$

Only the reaction :

$$\sum_{i=1}^{M} \psi'_{i1} A_i = 0, \quad \psi'_{i1} = \sum_{l} \psi_{il} r^{l} \Big/ \sum_{l} r^{l}, \tag{13}$$

corresponding to $l' = 1$ has a nonvanishing reaction rate. Therefore, the entropy source of the system :

$$\sigma = \frac{1}{T} r^{l} \mathscr{A}_{l}, \tag{14}$$

can be written as :

$$\sigma = \frac{1}{T} r'^{1} \mathscr{A}'_{1}, \tag{15}$$

where $\mathscr{A}_1$ is the reaction affinity coresponding to Eq. (13). The dynamical behaviour of the system seems to be entirely described by the overall reaction (13). In our opinion this is not true, since the use of the transformation (11) is purely formal, unless the kinetic equations have a particular form. The main difficulty is to find a suitable definition for the reaction extent attached to reaction (13). Trying to use the de Donder definition[4] we get :

$$\mathrm{d}\xi'^1 = \mathrm{d}_1 N_i/\psi'_{i1}, \tag{16}$$

where $d_1 N_i$ are the variations of the numbers of molecular species A_i, $i=1,\ldots,M$ due to reaction (13). ψ'_{i1} depend on the reaction rates and then (16) are in fact a set of differential equations which can be integrated only in particular cases.

Another possible definition is based on Eqs. (3) :

$$\mathrm{d}\xi'^{l'}/\mathrm{d}t = \mathrm{r}'^{l'}. \tag{17}$$

Supposing that the kinetic equations corresponding to the overall equations (1) are given in the form :

$$\dot{\xi}^l = r^l = \beta^l(\xi), \tag{18}$$

and combining (3), (8) and (16) we see that (11) defines in fact an infinitesimal transformation of the reaction extents :

$$\mathrm{d}\xi'^1 = \left\{\beta^1(\xi)\Big/\sum_{q=1}^{\mathrm{P}} \beta^q(\xi)\right\}\mathrm{d}\xi^1, \tag{19}$$

$$\mathrm{d}\xi'^q = -\{\beta^q(\xi)/\beta^1(\xi)\}\mathrm{d}\xi^1 + \mathrm{d}\xi^q, \quad q = 2,\ldots,P. \tag{19'}$$

These equations provide us a transformation law for the reaction extents only if the expressions are total differentials, that is

$$-\partial\{\beta^q/\beta^1\}/\partial\xi^q = 0, \quad q = 2,\ldots,P,$$

i.e. if

$$\beta^q/\beta^1 = \text{independent of } \xi^q.$$

Equations (19) suggest us to consider a general infinitesimal transformation of the reaction extents :

$$\mathrm{d}\chi^j = a^j_i(\xi)\mathrm{d}\xi^i. \tag{20}$$

Provided that a^j_i fulfils the condition :

$$\partial a^j_i/\partial\xi^k = \partial a^j_k/\partial\xi^i, \tag{21}$$

$$\det|a^j_i(\xi)| = \text{finite} \neq 0, \tag{22}$$

(20) defines a finite transformation law :

$$\chi^j = \Phi^j(\xi) \tag{23}$$

with:

$$\partial a_i^j / \partial \xi^k = \partial a_k^j / \partial \xi^i = \partial^2 \Phi^j / \partial \xi^i \partial \xi^k. \tag{24}$$

Due to (22) we can express explicitly ξ^l from (23)

$$\xi^l = g^l(\chi), \qquad \chi = (\chi^j). \tag{25}$$

The dependences (25) are generally nonlinear. In order that the transformed reaction rates $r'^{l'}$ preserve the contravariance it is necessary to use the notion of absolute derivative.[6] We get the following transformation laws :

$$\xi'^{l'} = M_l^{l'} \xi^l, \tag{26}$$

and

$$r'^{l'} = \frac{\mathrm{d}\xi'^{l'}}{\mathrm{d}t} + \xi'^{l} \frac{\mathrm{d}\chi^i}{\mathrm{d}t} M_h^{l'} E_{li}^h, \tag{27}$$

where

$$M_i^l \partial g^i / \partial \chi^k = \mathrm{M}_k^i \partial g^l / \partial \chi^i = \delta_k^l, \tag{28}$$

and

$$E_{ij}^h = \frac{\partial^2 g^h}{\partial \chi^i \partial \chi^j}. \tag{29}$$

Expressed in terms of the curvilinear coordinates the transformed reaction rates $r'^{l'}$ can be written as

$$r'^{l'} = \frac{\mathrm{d}\chi^{l'}}{\mathrm{d}t}. \tag{30}$$

CONCLUSION

Although useful,[5] the transformation (11) must be handled with care. Eqs. (11) can be used to integrate the kinetic equations only in few particular cases. The transformation (11) could be viewed as a particular case of an infinitesimal transformation of the reaction extents.

ACKNOWLEDGEMENT. This work has been supported by CIMC Bucharest.

REFERENCES

[1] J. Horiuti, *Ann. New York Acad. Sci.*, **213**, 5 (1973).

[2] M. I. Temkin, *Int. Chem. Eng.*, **11**, 709 (1971).

[3] M. I. Temkin, *Adv. Catalysis*, **28**, 171 (1973).

[4] Th. de Donder, "L'Affinite", Gauthier-Villars, Paris, 1936., ch.1.

[5] N. Émanuel and D. Knorre, "Cinétique chimique", Mir, Moscow, 1975, pp. 257–260; 280–284.

[6] G. A. Korn and T. M. Korn, "Mathematical Handbook for Scientists and Engineers", McGraw-Hill, New York, 1961, p. 488–496.

Revue Roumaine de Chimie, 32, *9–10*, 939–943 (1987)

Dedicated to Professor I. G. MURGULESCU
on his 85th anniversary

MOBILITY OF LATTICE OXYGEN AND ACTIVITY OF MULTICOMPONENT OXIDE CATALYSTS FOR OXIDATION OF PROPYLENE

N. I. IONESCU and MONICA CĂLDĂRARU
ICECHIM–Center of Physical Chemistry, Spl. Independenţei 202, Bucharest, Romania

Received April 13, 1987

In order to find out the role of active phases in multicomponent catalysts used in the oxidation of propylene, two catalyst samples obtained from a Bi–Mo "reference" catalyst containing also Ni, Fe, Zn, P and K by complete substitution of iron (or nickel) by nickel (iron, respectively) have been studied by electrical conductivity, microgravimetric and catalytic activity measurements. The lower catalytic activity of both catalysts was explained by lower lattice oxygen mobility due to the absence of defective iron molybdate phase in these samples.

Olefin oxidation and ammoxidation over oxide catalysts (particularly over bismuth molybdate catalysts) occurs mainly by a Mars van Krevelen (redox) type mechanism.[1] To preserve the constant concentration of oxidized surface sites, the hydrocarbon catalyst reduction and its reoxidation with gaseous oxygen must occur with comparable rates. However for some oxide catalysts the reoxidation rate is lower than the reduction one, i.e. reduction-reoxidation cycle is not entirely reversible (the catalyst operates in partially reduced state).[2–6] This means that the catalyst surface gradually loses oxygen and the subsequent evolution of the reaction is conditioned by the rate of restoration of the oxidized sites (through oxygen diffusion from bulk and/or through reoxidation with gaseous oxygen).

The easiness of oxygen losing is controlled mainly by the strength of metal – oxygen bond in the solid catalyst; however, there are some other factors as the deviations from stoichiometry (anionic and cationic vacancies, interstitial ions) which also control the lattice oxygen mobility.

In multicomponent, multiphasic catalysts, containing metal – oxygen bonds whose strengths are different it is difficult to establish the origin of lattice oxygen involved in hydrocarbon oxidation, due to the already mentioned deviations from the stoichiometry of each component phase and to the reciprocal interactions between phases.

A possible way for elucidating the role of a component phase in the multicomponent systems is to change its concentration into the remaining host matrix, not necessarily catalytically inert. Starting from this point of view, in the present work we have studied a Bi-Mo multicomponent catalyst containing iron and nickel, whose composition was changed by complete substitution of iron (or nickel) by nickel (or iron, respectively).

EXPERIMENTAL

Three multicomponent catalysts of the general formula $Ni_aFe_bBi_{3.1}Zn_{0.7}P_{0.9}K_{0.02}Mo_{15.7}O_x/$ 25% SiO_2 where $a = 4.8$, $b = 7.5$ (catalyst I), $a = 0$, $b = 11.3$ (catalyst II), $a = 11.3$, $b = 0$ (catalyst III) were studied in the reaction of selective propylene oxidation. All the catalysts were prepared in similar conditions by coprecipitation from aqueous solutions of the corresponding nitrates and ammonium paramolybdate. The catalysts were supported on SiO_2 (25% weight) by using an ammonium stabilized silica sol. After drying the samples were calcinated in air flow for 6 h at 673 K and 6 h at 773 K.

The catalytic activity measurements were carried out in flow system using a special integral reactor which allows also the determination of electrical conductance simultaneously.[7] The catalytic activity for propylene oxidation was measured at 673 K by using a propylene : air feed as 1 :10 and contact time of 2 s.

A.c. electrical conductance was measured with a semiautomatic precision RLC bridge Tesla BM 484, with a fixed frequency of 1592 Hz.

In order to establish the initial temperature at which catalyst starts to be reduced by propylene, microgravimetric measurements were performed by using a vacuum microbalance Sartorius 4102. Reduction occurred in static system at 150 torr propylene pressure, by rising the temperature with 5°C/min rate.

RESULTS AND DISCUSSION

Fresh catalysts samples are a mixture of phases including a complex bismuth molybdate phase BM in poorly crystallized form described by Lo Jacono[8–10] (in all three catalysts), β-$NiMoO_4$ (in catalysts I and III) (β-phase) and $Fe_2(MoO_4)_3$ (in catalysts I and II) (FM-phase); traces of MoO_3 were also found in catalysts I and III.

The amounts of β and FM phases follow the concentration of Ni and Fe in the samples, as it was already mentioned for a number of multicomponent catalysts with the same structure[9,10]; this suggests a relative constant composition of the BM phase. It can be emphasized that iron preferentially enters the FM phase, rather than the BM phase.

The activity data for propylene oxidation are presented in Table 1. In spite of their composition including active iron (nickel) bismuth and molybdenum oxides, the activity of the catalysts II and III appears unusually low.

After performing the catalytic activity measurements samples II and III were reduced for 0.5 h in dynamic system at 673 K with propylene : argon flow 1 : 3 ($\tau = 2$ s) and the electrical conductance was measured after this operation. Finally, propylene : air feed 1 : 10 was again passed at 673 K over the reduced sample and the catalytic activity test was repeated (Table 1); the propylene conversion over the catalyst II has significantly increased (from — 2 to 54%) and the product distribution has completely changed after this procedure.

The direction of the changes of the conductance G in reductive or oxidative atmosphere was in agreement with the well-known behaviour of the n-type oxide semiconductors. If we assume that a given conductance corresponds to a definite oxidation state of the surface and underlying layers, we can emphasize that the changes of *G* values are unambiguously connected with the changes of the oxidation level of the catalyst surface in comparison with the fresh sample.

Table 1

Conversion of propylene and the selectivities for carbon dioxide and acrolein, in oxidation of propylene over catalysts I, II and III (C_3H_6 : air 1 :10, 673 K, $\tau = 2s$).

Catalyst	C (%)	S_{CO_2} (%)	S_{acrol} (%)
I	92.1	8.5	76.4
II	2.0	100.0	0.0
II*	54.6	10.5	89.5
III	11.0	8.0	92.0
III*	13.3	6.7	93.3

* after reduction for 0.5 h at 673 K in propylene : argon flow (1 : 3), $\tau = 2$ s.

Figure 1 presents these changes of conductivity for the catalyst II. The fact that the final *G* value in propylene : air mixture is higher than the initial one indicated that the "activated" catalyst sample was in a partially reduced state. No detectable Fe^{3+} reduction of the "activated" sample in comparison with the fresh sample could be evidenced by ESR spectroscopy, indicating a very low level of Fe^{3+} reduction.

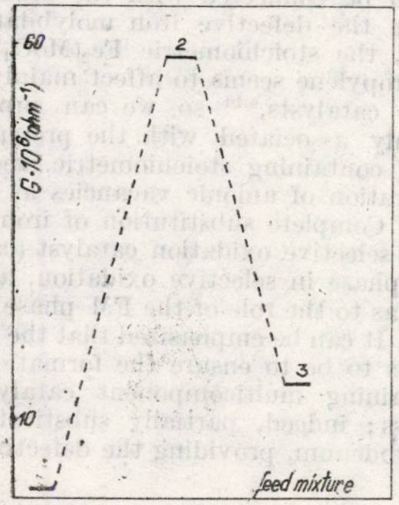

Fig. 1. — The variation of electrical conductance *G* for the catalyst II at 673 K. 1 — in C_3H_6 : air flow (1 : 10), $\tau = 2s$; 2 — in C_3H_6 : argon flow (1 : 3), $\tau = 2$ s, after 0.5 h reduction; 3 — in C_3H_6 : air flow (1 : 10), $\tau = 2$ s, after stabilization.

Microgravimetric measurements in static system indicated that the catalyst reduction by propylene starts at 593 K for catalyst I, 673 K for catalyst II and 703 K for catalyst III. Taking these temperatures as an indication for the relative reducibility (or lattice oxygen mobility), we can conclude that in catalysts II and III the reducibility is lower in comparison to that of the reference sample (catalyst I).

The experimental results presented above together with the structural information obtained on the studied catalysts[9,10] could be rationalized in the following way.

It was already mentioned[9,10] that the FM phase of some multicomponent catalysts, including catalyst I, has expanded lattice due to the presence of molybdenum excess, which substitutes Fe^{3+} in the lattice in the way proposed by Fagherazzi and Pernicone.[11] The partial substitution of Mo^{6+} for Fe^{3+} involves the appearance of the interstitial oxygen ions as well as cationic vacancies.

The importance of cationic vacances in oxidation catalysis has been mentioned for scheelitic catalysts.[12-14] It has been proposed that cationic vacancies (representing electron rich centers) make the neighbour oxygen ions more basic, favouring the proton abstraction from the hydrocarbon molecule. On the other hand, the mobility of oxygen species connected with cationic vacancy is higher, thus explaining the facile loss of oxygen in many oxide catalysts, and consequently the facile appearance of anionic vacancies.[4] The anionic vacancies act as olefin adsorption sites favouring the olefin-cation interaction and electron transfer to cation.[15,16]

The lower reducibility of the catalyst II in comparison with the catalyst I (reference sample) could be due to the large Fe/Mo ratio in the former, i.e. to the lack of molybdenum excess; thus, the concentration of cationic vacancies in the FM phase appears to be very small and could be connected with the lower activity of the catalyst II. Indeed, while the defective iron molybdate oxidizes C_3H_6 mainly to CO_2 and H_2O, the stoichiometric $Fe_2(MoO_4)_3$ is practically inactive.[17] Reduction of propylene seems to affect mainly the FM phase of these multicomponent catalysts,[9,10] so we can suppose that oxidation of propylene is mainly associated with the presence of defective FM phase; in catalysts containing stoichiometric, reduction resistent FM phase, the concentration of anionic vacancies as olefin adsorption sites is much lower.

Complete substitution of iron by nickel produces a low active but high selective oxidation catalyst (catalyst III) pointing to the role of the BM phase in selective oxidation, as it has already been mentioned,[10] as well as to the role of the FM phase in propylene conversion.

It can be emphasized that the role of Ni^{2+} (as well as of other Me^{2+}) seems to be to ensure the formation of the defective FM phase in iron-containing multicomponent catalysts, by controlling the molybdenum excess; indeed, partially substitution of Fe^{3+} by Ni^{2+} induces excess molybdenum, providing the defective FM phase, as in catalyst I.

REFERENCES

[1] P. Mars and D. W. van Krevelen, *Chem. Engn. Sci. Suppl.*, **3**, 41 (1954).
[2] F. Brazdil, D. D. Suresh and R. K. Grasselli, *J. Catalysis*, **66**, 347 (1980).
[3] M. Căldăraru, B. Albu and N. I. Ionescu, in "Proc. 5th Intern. Symp. Heterogeneous Catalysis, Varna 1983", D. Shopov, A. Andreev, A. Palazov, L. Petrov (Eds), Publishing House of the Bulgarian Acad. of Sci., Sofia 1983, vol. I, p. 51.

[4] M. Căldăraru, Ph. D. Thesis, Center of Physical Chemistry, Bucharest, 1983.

[5] J. M. Peacock, A. J. Parker, P. G. Ashmore and J. A. Hockey, *J. Catalysis*, **15**, 387 (1969).

[6] M. Căldăraru and N. I. Ionescu, in "Proc. 6-th Intern. Symp. Heterogeneous Catalysis, Varna 1987", vol. I, 382. Publishing House of the Bulgarian Academy of Sciences, 1987.

[7] N. I. Ionescu and M. Căldăraru, *React. Kinet. Catal. Lett.*, **8**, 477 (1978).

[8] M. Lo Jacono, Th. M. Notermann and G. W. Keulks, *J. Catalysis*, **40**, 19 (1975).

[9] H. Căldăraru, R. Mănăilă, G. Filoti, M. Căldăraru, P. Banyai and N. I. Ionescu, in "Proc. 5th Intern. Symp. Heterogeneous Catalysis, Varna 1983", D. Shopov, A. Andreev, A. Palazov, L. Petrov (Eds.), Publishing House of the Bulgarian Acad. of Sci., Sofia 1983, vol. I, pag. 69.

[10] R. Mănăilă, N. I. Ionescu and M. Căldăraru, *Z. anorg. allgem. Chem.*, **466**, 221 (1980).

[11] G. Fagherazzi and N. Pernicone, *J. Catalysis*, **16**, 321 (1970).

[12] A. W. Sleight and W. J. Linn, *Ann. New York Acad. Sci.*, **272**, 22 (1976).

[13] A. W. Sleight, in "Advanced Materials in Catalysis", J. J. Burton, R. L. Garten (Eds.), Acad. Press, New York, 1976, p. 181.

[14] K. Aykan, D. Halvorson, A. W. Sleight and D. B. Rogers, *J. Catalysis*, **35**, 401 (1974).

[15] G.C.A. Schuit, *Chim. Ind.*, **51**, 1307 (1969).

[16] Ph. A. Batist, B. C. Lippens and G.C.A. Schuit, *J. Catalysis*, **5**, 55 (1966).

[17] G. Filoti, R. Mănăilă, H. Căldăraru, M. Căldăraru, N. I. Ionescu, M. Selenina and K. H.Schnabel, to be published.

Revue Roumaine de Chimie, **32**, *9–10*, 945–951 (1987)

Dedicated to Professor I. G. MURGULESCU
on his 85th anniversary

SURFACE MOBILITY OF SURFACTANT SOLUTIONS. XII*

REMARKS CONCERNING THE MARANGONI FLOW THROUGH AN INCLINED SURFACE CANAL

EMIL CHIFU* and CĂLIN-IOAN GHEORGHIU**
* University of Cluj-Napoca, Faculty of Chemical Technology, Romania
** Polytechnic Institute of Cluj-Napoca, Romania

Received April 3, 1987

The Marangoni flow of an incompressible viscous fluid through an inclined canal having triangular section and a free liquid/gas surface is discussed. In comparison with the previously proposed models,[1,2,4,5] in the present one the existence of a surface viscosity of the liquid and the fact that the process is non-steady are taken into account. A numerical analysis of the mathematical model is done, by using a Galerkin-Crank-Nicolson algorithm. By taking notice of the non-stationarity of the process the occurrence of the Marangoni-type flow in competition with the gravity flow is elucidated.

INTRODUCTION

In previous works[1-2] some processes of surface flow have been analysed by using the model of flow in a thin liquid layer of thickness δ and infinitely wide, situated on an inclined solid plane. The axis Ox_1 is oriented along the maximum slope, Ox_3 is perpendicular to the plane, and Ox_2 joins the points found at the same level (Fig. 1).

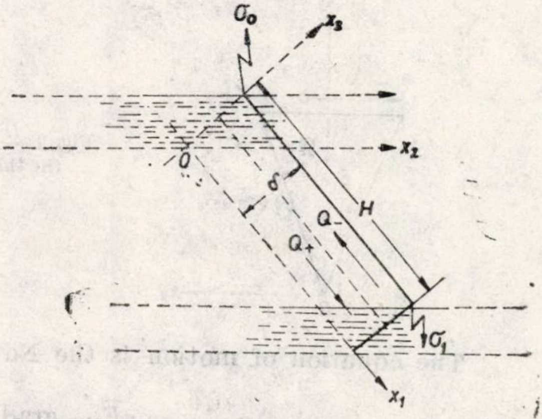

Fig. 1. — Transverse section of the semi-infinite thin liquid layer: along the Ox_2 axis the layer is indefinitely expanded.

---

* Part XI; see reference 5.

The surface tension σ at the liquid/gas interface varies along the Ox_1 axis. This variation may originate in several causes.

Thus for instance, Van den Bogaert and Joos[3] have studied the forced flow in a horizontal canal of rectangular section, under the action of a hydrostatic pressure gradient. Here the surface tension gradient is produced by the mechanical compression of a surfactant film.

In our above-cited works the surface tension gradient occurs between two reservoirs : one, holding the surfactant solution and situated at the distance $x_1 = H$; another, containing the pure solvent (or a diluted surfactant solution) and situated at the distance $x_1 = 0$.

In a recent paper[4] we have studied the case when the surface tension gradient arises as a result of temperature changes.

From the theoretical point of view, electrical charge variations could also lead to the occurrence of surface tension gradients at interfaces.

By re-examining the model of the above-described semi-infinite liquid layer, we found it too approximate in fitting the experimental results and attempted to refine it. Thus, in a subsequent paper,[5] the flow of an incompressible viscous fluid under the simultaneous action of a surface tension gradient and of gravity has been considered, when developing along a "surface canal -slit-" of triangular transverse section (Fig. 2).

GOVERNING EQUATIONS

By referring now to this second physical model,[5] much more realistic, we shall try to give it a mathematical formulation.

As the fluid flowing along the canal is incompressible, the continuity equation is :

$$\operatorname{div} \vec{v} = 0. \tag{1}$$

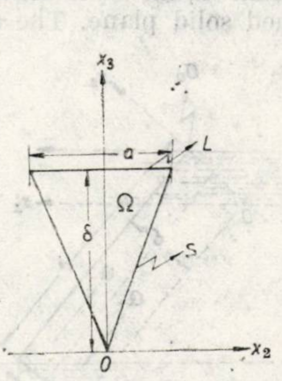

Fig. 2. — Transverse section assumed for the thin liquid layer in the calculus.

The equation of motion is the Navier-Stokes equation :

$$\rho \frac{\mathrm{d}\vec{v}}{\mathrm{d}t} = \rho \vec{F} - \operatorname{grad} p + \mu \Delta \vec{v}. \tag{2}$$

In equations (1) and (2) $\vec{v}$ represents the velocity vector, p is the pressure, ρ the density, μ the viscosity and $\vec{F}$ the external forces.

If thermal phenomena are taken into account, the set of equations (1) and (2) should be completed with the energy equation (see for example, L. Howarth[6]).

When the flow is considered as symmetrical with respect to the x_1Ox_3 plane, what is very plausible, then we have :

$$v_2 = v_3 = 0 \tag{3}$$

and, from (1),

$$v_1 = v_1(x_2, x_3). \tag{4}$$

Another possible simplification consists of considering the pressure as constant along the canal, then grad $p = 0$; or of giving a certain variation law to the pressure. In this second case the term grad p in Eq.(2) will be known.

The boundary condition on the solid walls, denoted by S in Fig. 2, will be that of adherence of the viscous fluid, namely :

$$v_1 = 0. \tag{5}$$

The boundary condition on the liquid/gas interface, denoted by L in Fig. 2, will be given by the equation of flow of the interface[7-9] :

$$\frac{d\vec{w}}{dt} = \vec{F}_S + \text{grad}\,\sigma + (\varepsilon + k)\Delta\vec{w}, \tag{6}$$

with the supplementary condition :

$$\vec{w} = \vec{v}\,|_{x_3=\delta}.$$

In Eq. (6), $\Gamma(ML^{-2})$ represents the surface density ($\Gamma \approx 10^{-7}$ g.cm^{-2}), ε is the shear surface viscosity, and k the dilatational surface viscosity of the interface. The notation $\mu_S = \varepsilon + k$, (MT^{-1}) is also used occasionally.

The external forces $\vec{F}_S$ applied on the surface unit of the liquid/gas interface are the resultant of two components : the first originates in the field of external forces $\vec{F}_{\text{ext}}$ (which may be the gravity field, or an electrical field); the second is the traction exerted by the two phases (in our case $\vec{T}_l$, by the liquid, and $\vec{T}_g$, by the gas). Thus, $\vec{F}_S = \vec{F}_{\text{ext}} + \vec{T}_l - \vec{T}_g$. If the field of external forces is reduced to gravity, $\vec{F}_{\text{ext}} = \Gamma g$ and, as a rule, this component is neglected because Γ has a very small value as compared with μ_S. For the same reason the left-hand side in Eq. (6) will be cancelled. The traction upon the gaseous phase is also negligible in the expression of $\vec{F}_S$, while the traction upon the liquid phase has the following expression :

$$\vec{T}_l = -\mu\left(\frac{\partial \vec{v}}{\partial x_3}\right)\Bigg|_{x_3=\delta}.$$

Relationship (4), showing that the flow velocity of the liquid inside the canal depends only on the x_2 and x_3 coordinates, implies the fact the flow velocity of the liquid/gas interface — denoted by w — will depend only on the variable x_2 (as the interface is contained in the plane $x_3 = \delta$).

Taking these into account, equation (6) is written :

$$\mu_S \frac{d^2 w_1}{d x_2^2} - \mu \frac{\partial v_1}{\partial x_3} + \frac{\partial \sigma}{\partial x_1} = 0 \tag{7}$$

with the supplementary condition $w_1 = v_1 |_{x_3=\delta}$.

Here it was taken account of the fact that the movement of the interface occurs only with the Ox_1 direction, so that the component w_2 of the $\vec{w}$ vector is identically null.

The following boundary condition will be attached to the differential equation (7) in the unknown w_1 :

$$w_1(\pm a/2) = 0 \tag{8}$$

meaning that also the liquid in the layer is viscous and therefore it adheres to the canal walls.

By integrating Eq. (7) with the conditions (8), and taking into account that $\partial(\ \ )/\partial x_3 = \partial(\ \ )/\partial n$ on L, the equation of motion of the interface is :

$$\frac{\partial v_1}{\partial n} + \left[1\Big/\left(\frac{a^2}{4} - x_2^2\right)\right] \frac{2\mu_S}{\mu}\, v_1 = \frac{1}{\mu} \frac{\partial \sigma}{\partial x_1}. \tag{9}$$

Like this, the equation of flow, with the boundary conditions, leads to the system :

$$\left\{ \begin{array}{ll} \rho \dfrac{\partial v_1}{\partial t} - \mu \left(\dfrac{\partial^2 v_1}{\partial x_2^2} + \dfrac{\partial^2 v_1}{\partial x_3^2} \right) = \rho g \sin \alpha \text{ in } \Omega,\ t \in (0, T) & \\ \qquad\qquad v_1 = 0 & \text{on } S \\ \dfrac{\partial v_1}{\partial n} + v_1 \left[1\Big/\left(\dfrac{a^2}{4} - x_2^2 \right) \right] \dfrac{2\mu_S}{\mu} = \dfrac{1}{\mu} \dfrac{\partial \sigma}{\partial x_1} & \text{on } L. \end{array} \right. \tag{10}$$

The signification of the angle α is given in Fig. 3.

With regard to the initial conditions for the system (10) an entire series of speculations can be done.

Taking into account the experimental conditions, we have thought that at the initial moment, the field of velocities could be the solution of the following problem :

$$\begin{cases} -\left(\dfrac{\partial^2 v_1}{\partial x_2^2}+\dfrac{\partial^2 v_1}{\partial x_3^2}\right)=\dfrac{h}{H}\,\dfrac{\rho g}{\mu} & \text{in } \Omega \\ v_1 = 0 & \text{on } S \\ \dfrac{\partial v_1}{\partial n} = 0 & \text{on } L. \end{cases} \tag{11}$$

This problem corresponds to the flow of an incompressible viscous fluid along the canal having a free surface — the condition on L.

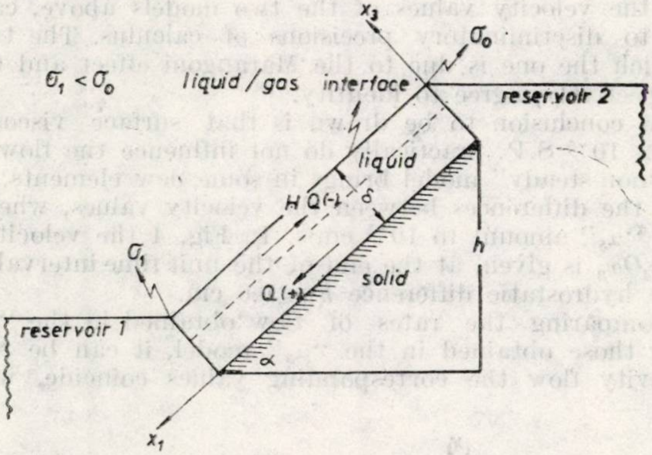

Fig. 3. — Longitudinal section of the thin liquid layer in which the Marangoni flow is in competition with the gravity flow.

NUMERICAL RESULTS AND DISCUSSION

The problem (11) is a mixed boundary value problem, attached to Laplace equation. It is a particular case of a problem treated in the work[5]. We have integrated it numerically, as in Ref[5], and used the finite element method in simplex form. We underline once again that the solution of this equation gives the initial condition for the problem (10). From the mathematical point of view it is a Cauchy-Dirichlet problem, attached to a linear parabolic equation. We have solved this problem by a finite element — finite differences method, of the Galerkin-Crank-Nicolson type.

Details on the numerical integration of problems (10) and (11), including implementation of the used algorithms, are found in ref. [10]

In the numerical tests performed we have also tried to do the numerical integration of the steady model, by making allowance for the surface viscosity μ_S. This model corresponds to the system (10) without the term $\rho \partial v_1/\partial t$ and we shall refer to it as the model "μ_S". That one treated in the work[5] will be referred to as the model "μ" and it corresponds in fact to the system (10) in which the derivative with respect to time is neglected and μ_S is taken as equal to zero on L. Finally, the most complete model is the one which corresponds to (10) and we shall refer to it as the "nonsteady" model.

In the following we try to compare, from the qualitative point of view, the numerical results obtained by using these three models, and to possibly refer to the experimental results discussed in Ref [5].

Thus, for values of the surface viscosity μ_S about 1×10^{-5} S.P. (μ being considered of the order of 5.49×10^{-3} P.), the models "μ" and "μ_S" lead practically to the same results.

The small differences, of 2×10^{-2} cm/s at the most, obtained by comparing the velocity values of the two models above, can be easily attributed to discriminatory precisions of calculus. The two rates of flow, of which the one is due to the Marangoni effect and the other to gravity respectively, agree to identity.

A first conclusion to be drawn is that surface viscosities of the order of 1×10^{-5} S.P. practically do not influence the flow.

The "non-steady" model brings in some new elements.

Thus, the differences between the velocity values, when compared with model "μ_S" amount to 10^{-1} cm/s. In Fig. 4 the velocity profile in the plane x_1Ox_3 is given, at the end of the unit time interval corresponding to the hydrostatic difference $h = 0.6$ cm.

By comparing the rates of flow obtained in the "non-steady" model with those obtained in the "μ_S" model, it can be realized that or the gravity flow the corresponding values coincide, while for the Marangoni flow the "non-steady" values are significantly larger. This time also, the comparison is done at the end of the unit time interval $T = 1$.

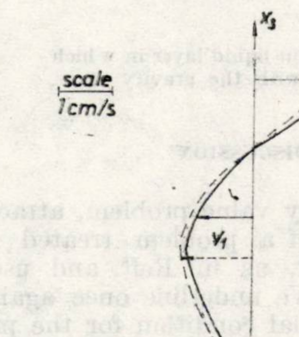

Fig. 4. — Velocity profiles in the x_1Ox_3 plane, corresponding to the "non-steady" and "μ_S" models, for $\Delta\sigma = 5.29$ mN/m.

Referring now only to the "non-steady" model, we can notice that it leads to certain observations not detected experimentally. Namely, the moment of occurrence for the "antiparallel" flow (the gravity flow in competition with the motion due to the surface tension gradient) has been established as being $\frac{1}{3}T$ with regard to the above-mentioned initial condition.

Further on, it has been evidenced that the "antiparallel" flow appears in close vicinity of the solid wall and then develops towards the middle of the surface L. This fact is plausible, because near to the canal walls the thickness of the layer is small as compared to its maximum thickness δ.

It can also be noticed that an important rate of flow, comparable with the positive one, arises at the time $\frac{2}{3}T$.

Finally, some observations are to be done on the simplifications used.

From the phenomenological point of view, the molecular diffusion effect, appearing together with the antiparallel flow, has not been taken into account.

From the point of view of the algorithm of calculus it can be said that the simplest form has been chosen. Simplex finite elements have been considered (linear variation), and the interface liquid/gas L has been approximated with a plane.

Nevertheless, it can be concluded that, in a first approximation, the "non-stationary" model elucidates the transition state from the flow on an inclined plane with a free surface to the flow under the action of the surface tension gradient.

REFERENCES

[1] E. Chifu, *Stud. Univ. Babeş-Bolyai, Chem.*, **10** (2), 85(1965); E. Chifu, R. Dentsch, *Rev. Roumaine Chim.*, **11**, 873 (1966).

[2] E. Chifu and I. Stan, *Rev. Roumaine Chim.*, **27**, 703 (1982).

[3] R. Van den Bogaert and P. Joos, *S. Colloid Interface Sci.*, **69**, 301 (1979).

[4] E. Chifu, I. Albu, C. I. Gheorghiu, E. Gavrilă, M. Sălăjan and M. Tomoaia-Cotişel, *Rev. Roumaine Chim.*, **31**, 105 (1986).

[5] E. Chifu, C. I. Gheorghiu and I. Stan, *Rev. Roumaine Chim.*, **29**, 31 (1984).

[6] L. Howarth, "Modern Developments in Fluid Dynamics. High Speed Flow", vol. I, Oxford 1953.

[7] L. E. Scriven, *Chem. Eng. Sci.*, **12**, 98 (1960).

[8] R. Aris, "Vectors Tensors and the Basic Equations of the Fluid Mechanics", Chap. X, Prentice Hall, New Jersey, 1962.

[9] E. Chifu, I. Stan, Z. Finta and E. Gavrilă, *J. Colloid Interface Sci.*, **93**, 140 (1983).

[10] C. I. Gheorghiu, Ph. D. thesis, University of Bucharest, Faculty of Mathematics (1984).

Revue Roumaine de Chimie, **32**, *9–10*, 953–960 (1987)

Dedicated to Professor I. G. MURGULESCU
on his 85th anniversary

OPTIMISATION OF HYDROGEN PRODUCTION FROM WATER USING PROFLAVINE AS PHOTOSENSITIZER

TATIANA ONCESCU, MIHAELA ŞTEFAN[a], M. CONTINEANU and S. G. IONESCU
Department of Physical Chemistry, Polytechnic Institute of Bucharest, Bd. Republicii 13, R-70346, Romania
[a] Chemical and Pharmaceutical Research Institute, Sos. Vitan 112, Bucharest, Romania

Received May 7, 1987

Proflavine photosensitized electron transfer to $Co(bipy)_3^{2+}$ in aqueous solutions was used to reduce water to hydrogen gas. The formation of H_2 was dependent upon the concentrations of the system components, the irradiation time and the light intensity. These factors were optimised for H_2 production. The efficiency of the couple photosensitizer – electron relay we used was expressed by the turnover numbers (TO).

INTRODUCTION

Recently, there has been considerable interest in the research of H_2 photoproduction from water via visible light redox reactions, as means of solar energy conversion and storage.[1–6] For this purpose, different systems were used, where the essential ingredients are a photosensitizer (PS), an electron relay (R) and a catalyst (C). The photosensitizer excitation induces the electron transfer :

$$PS + R \xrightarrow{h\nu} PS^+ + R^- \qquad (1)$$

followed by the catalytic step leading to H_2 generation :

$$R^- + H_2O \xrightarrow{C} 1/2H_2 + R + OH^- \qquad (2)$$

Reaction (1) represents the so-called "oxidative quenching cycle" of the photosensitizer. PS may be regenerated by adding a sacrificing electron donor, through irreversible oxidation :

$$PS^+ + D \longrightarrow PS + D^+ \qquad (3)$$

Alternatively, the photosensitizer regeneration may be achieved by coupling this "half reaction" to the photosensitized water oxidation.

It is known that these systems must fulfil certain thermodynamic requirements, i.e., the reduction potential of the relay $E_{(R/R^-)}$ must be more negative than that of water $E_{(H_2O/H_2)} = -0.41$ V and also the reduction potential of the photosensitizer excited state $E_{(PS/PS^*)}$ must be more negative than that of the relay.

In this paper we investigated the model system for generating photohydrogen : proflavine (PS) – $Cobipy_3Cl_2$(R) – K_2PtCl_6(C), under visible light irradiation in aqueous solution using triethanolamine (TEOA) as donor (D). We used the same relay, $Cobipy_3Cl_2$, as in our previous paper,[7] but with another photosensitizer.

EXPERIMENTAL

Materials. Proflavine sulphate, $C_{13}H_{12}N_3 \cdot HSO_4$ (Serva, Feinbiochemica, Heidelberg) reagent grade and triethanolamine (BDH) reagent grade, were used as received. The $Cobipy_3Cl_2$ complex was prepared modifying the literature procedure,[8] and the catalyst by precipitat, ing K_2PtCl_6 from H_2PtCl_6 with KCl.

Apparatus and method. Absorption spectra were recorded by a SP 8000 Pye Unicam spectrophotometer, using thermostatted silica cells with the path length $d = 1$ cm. The quenching determinations were carried out with an atomic absorption SP 90 Pye Unicam spectrophotometer adapted for fluorescence measurements. The evolved H_2 was analysed with a Carlo Erba Gas-Chromatograph, using argon as carrier gas. Irradiation with visible light was carried out using a mercury lamp of 250 W. The 5 mL solution samples were purged beforehand with argon. The temperature reached by samples under irradiation was 55°C.

RESULTS AND DISCUSSION

We utilized TEOA as sacrificial electron donor in aqueous solutions of 4×10^{-2}M. This amine has a suitable redox potential $E_0(+0.82\ V)$ for irreversible oxidation, and its pK_a (7.9) renders a weak alkaline medium for optimum hydrogen generation.

In order to optimise the H_2 producing reaction, we studied the dependence of the evolved hydrogen amount on the concentration of each component using the same procedure described by J. M. Lehn et al.[9]

In 4×10^{-2} M TEOA solutions (pH ~ 9.5), the acid – base equilibrium of the excited proflavine is practically shifted towards the monocation[10] $(PfH^+)^*$, $pK_a^* = 12.5$. In the investigated concentration range $5 \times 10^{-5} - 10^{-3}$ M proflavine, we found a maximum value of hydrogen yield for 2.4×10^{-4} M (Fig. 1). At higher concentrations in proflavine the H_2 quantity decreases probably due to the presence of the dimer. In the absence of the photosensitizer no hydrogen evolution was observed.

The relay $Cobipy_3Cl_2$ is photochemically stable and has a redox potential $E_{0(Co^{2+}/Co^+)} = -0.95$V, more negative than the water reduction potential $E_{0(H_2O/H_2)} = -0.41$ V vs. NHE. Thus, it acts efficiently in the electron transfer process to water, generating H_2. In our investigated system, the variation of the relay concentration evidenced a concentration range ($10^{-3} - 4 \times 10^{-3}$ M) where the maximum value of evolved H_2 is constant (Fig. 2).

The produced hydrogen amount depends also on the catalyst concentration. Our experimental data show this behaviour in figure 3. The hydrogen obtained increases with the amount of Pt catalyst up to a maximum value of 10^{-4} M. After this value, the H_2 quantity decreases

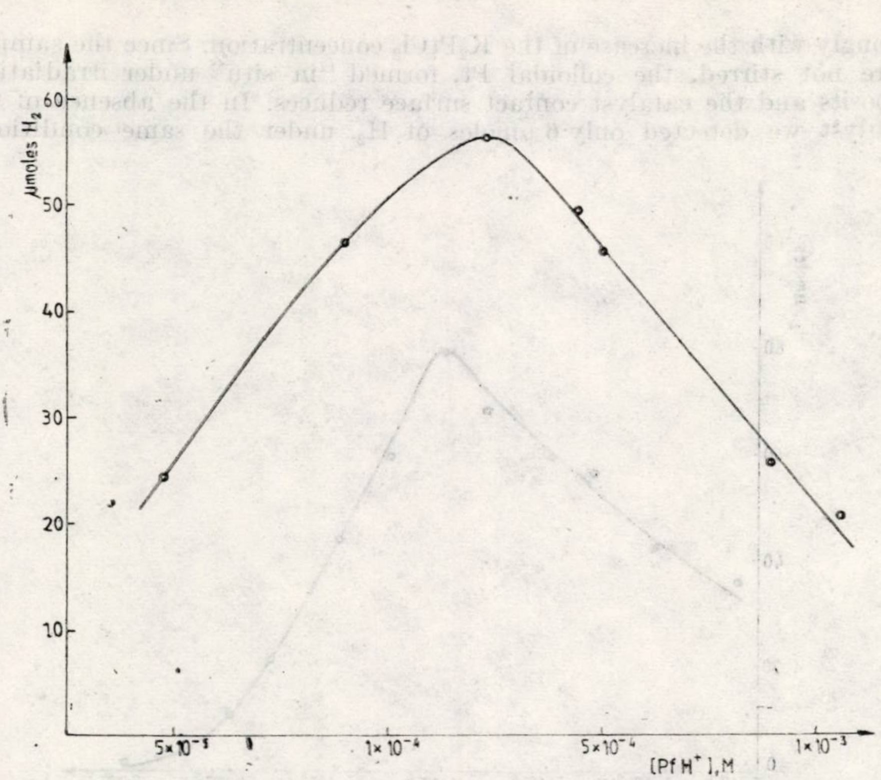

Fig. 1. — Dependence of the H_2 amount upon the proflavine concentration after 3 hours' irradiation. $[\mathrm{Cobipy}_3^{2+}] = 4.25 \times 10^{-3}$ M, $[\mathrm{PtCl_6K_2}] = 2.5 \times 10^{-4}$M.

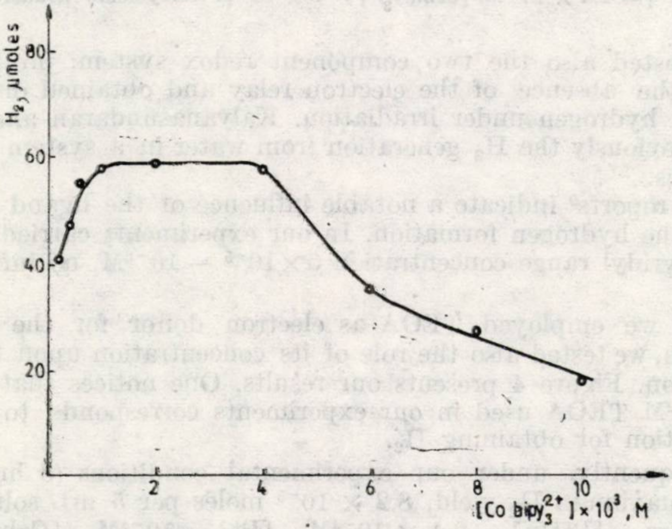

Fig. 2. — The plot of the H_2 amount evolved, against the Co(II) complex concentration. $[\mathrm{PfH^+}] = 2.4 \times 10^{-4}$M, $[\mathrm{K_2PtCl_6}] = 2.5 \times 10^{-4}$M (three hours' irradiation).

strongly with the increase of the K_2PtCl_2 concentration. Since the samples were not stirred, the colloidal Pt, formed "in situ" under irradiation, deposits and the catalyst contact surface reduces. In the absence of the catalyst we detected only 6 μmoles of H_2, under the same conditions.

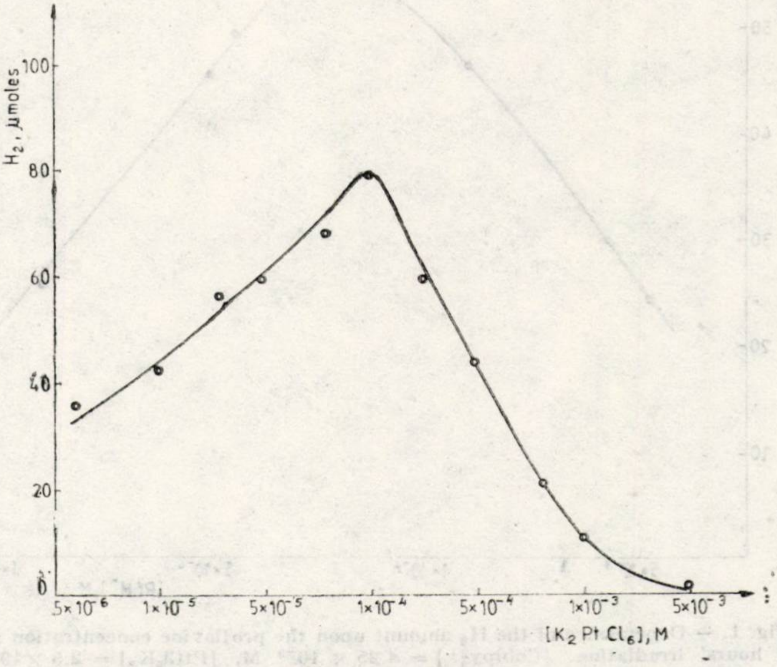

Fig. 3. — Dependence of the H_2 quantity upon the catalyst concentration. $[PfH^+] = 2.4 \times 10^{-4}M$, $[Cobipy_3^{2+}] = 1 \times 10^{-3}M$ (three hours' irradiation)

We tested also the two component redox system, proflavine and TEOA, in the absence of the electron relay and obtained only a small quantity of hydrogen under irradiation. Kalyanasundaran and Grätzel[11] reported previously the H_2 generation from water in a system free of the relay species.

Some reports[9] indicate a notable influence of the ligand concentration upon the hydrogen formation. In our experiments carried out under a large bipyridyl range concentration $5 \times 10^{-5} - 10^{-2}M$, no influence was observed.

Since we employed TEOA as electron donor for the proflavine regeneration, we tested also the role of its concentration upon the hydrogen evolution. Figure 4 presents our results. One notices that the value of $4 \times 10^{-2}M$ TEOA used in our experiments corresponds to the optimum condition for obtaining H_2.

Consequently, under our experimental conditions (3 hrs' irradiation), the maximum H_2 yield, 8.2×10^{-5} moles per 5 mL solution, was obtained for: $[PfH^+] = 2.4 \times 10^{-4}M$, $[Pt] = 10^{-4}M$, $[Cobipy_3Cl_2] = 10^{-3}M$ and $[TEOA] = 4 \times 10^{-2}M$.

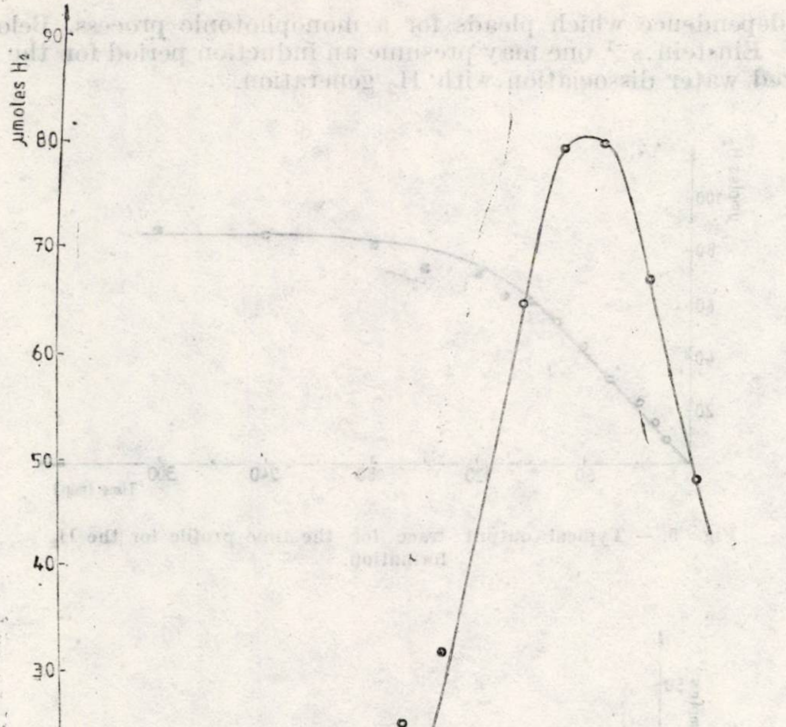

Fig. 4. — The influence of TEOA concentration of H_2 evolution for 3 hours' irradiation. $[PfH^+] = 2.4 \times 10^{-4}M$, $[Cobipy_3^{2+}] = 1 \times 10^{-3}M$, $[K_2PtCl_6] = 1 \times 10^{-4}M$.

The samples were irradiated for three hours because after this period, a limiting value of hydrogen production is reached (Fig. 5). One notices a linear dependence during 90 minutes' irradiation, for which one calculated a zero-order rate constant $k_0 = 1.2 \times 10^{-8}M^{-1}s^{-1}$, for an irradiation flux $\Phi = 9 \times 10^{-6}$ Einstein.s^{-1}. This reaction order is typical for a strongly absorbing system.

For a 30 minutes' irradiation time (linear dependence in Fig. 5), we investigated the influence of the light intensity on the optimised system and obtained the behaviour shown in Fig. 6. One notices a linear dependence which pleads for a monophotonic process. Below 4×10^{-6} Einstein.s^{-1} one may presume an induction period for the photosensitized water dissociation with H_2 generation.

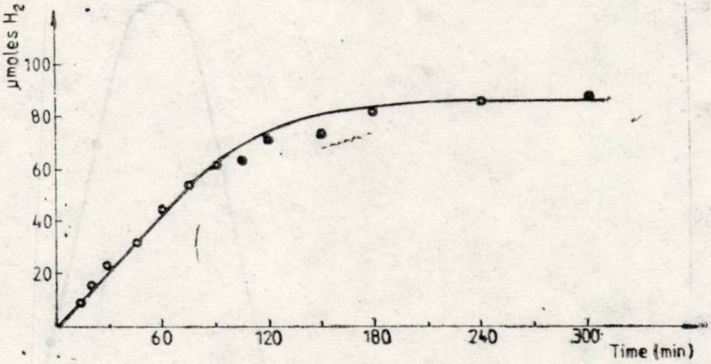

Fig. 5. — Typical output trace for the time profile for the H_2 formation.

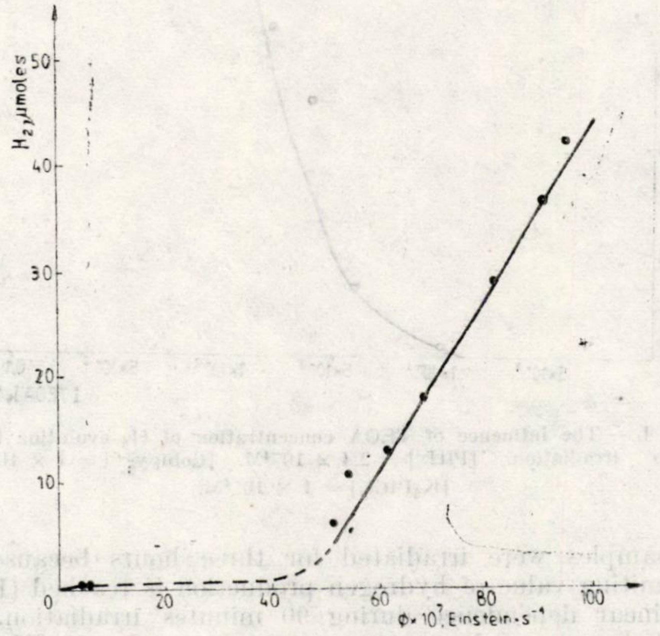

Fig. 6. — Dependence of the H_2 formation upon the incident light intensity.

As pointed above, the photochemical hydrogen generation reaction described here comprises two catalytic cycles with respect to the photosensitizer (proflavine) and to the electron relay ($Cobipy_3Cl_2$). The overall reaction is given in figure 7. In this system the eletron donor TEOA, the water protons and the visible light quanta are consumed.

In order to study the oxidative quenching of proflavine cycle, we used fluorescence measurements. Whereas the emission of the excited proflavine is unaffected by high concentrations of TEOA in aqueous solutions, marked quenching of the fluorescence is observed when $Cobipy_3^{2+}$ is added instead. From a Stern-Volmer plot (Fig. 8), the rate constant of the quenching process, $k_q = (8.2 \pm 0.8) \times 10^9 \ M^{-1}s^{-1}$ at 25°C was calculated. This value is typical for a diffusion-controlled process.

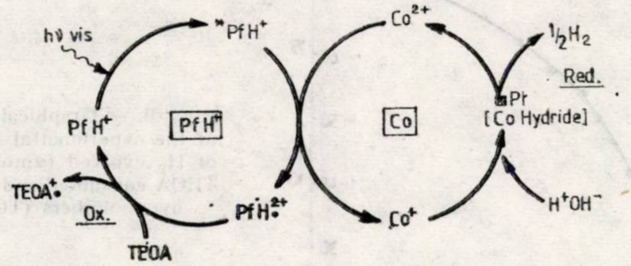

Fig. 7. — Schematic representation of the hydrogen generation by the oxidative quenching of proflavine cycle.

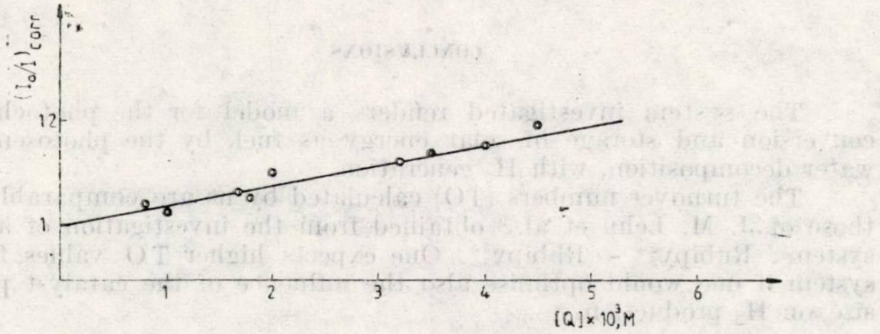

Fig. 8. — Stern-Volmer plot for quenching of proflavine fluorescence by $Cobipy_3^{2+}$.

A very important parameter describing the efficiency of the system is the observed turnover number (TO) of the various components. Also, we calculated the turnover number (TO) of the photosensitizer (proflavine) and of the electron relay ($Cobipy_3^{2+}$) and presented our results in figure 9. Both partners are involved in monoelectronic cyclic processes. Thus, the effective numbers of catalytic cycles are 2(TO) namely: 125 for proflavine and 30 for Co(II) complex, under three hours' irradiation.

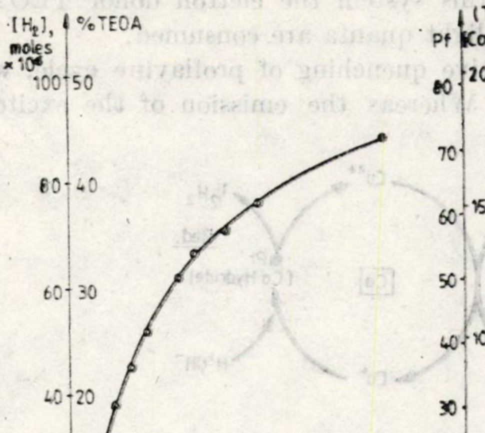

Fig. 9. — Graphical representation of the experimental results: amount of H_2 evolved (μmoles), fraction of TEOA consumed and observed turnover numbers (TO).

CONCLUSIONS

The system investigated renders a model for the photochemical conversion and storage of solar energy as fuel, by the photosensitized water decomposition, with H_2 generation.

The turnover numbers (TO) calculated by us are comparable with those of J. M. Lehn et al.,[9] obtained from the investigation of another system: $Rubipy_3^{2+}$ — $Rhbipy_3^{3+}$. One expects higher TO values for our system if one would optimise also the influence of the catalyst particle size on H_2 production.

REFERENCES

[1] J. M. Lehn and J. P. Sauvage, *Nouv. J. Chim.*, **1**, 449 (1977).
[2] B. V. Koryakin, T. S. Dzhabiev and A. E. Shilov, *Dokl. Acad. Nauk SSSR*, **233**, 620 (1977).
[3] K. Kalyanasundaran, J. Kiwi and M. Grätzel, *Helv. Chim. Acta*, **61**, 2720 (1978).
[4] N. Sutin, *J. Photochem.*, **10**, 19 (1979).
[5] P. Keller and A. Moradpour, *J. Amer. Chem. Soc.*, **102**, 7193 (1980).
[6] A. Harriman and A. Mills, *J. Chem. Soc. Faraday Trans.*, **77**, 2111 (1981).
[7] Tatiana Oncescu, M. Contineanu and S. G. Ionescu, *Rev. Roum. Chim.*, **27**, 95 (1982).
[8] F. H. Burstall and R. S. Nyholm, *J. Chem. Soc. London*, 3570 (1952).
[9] M. Kirch, J. M. Lehn and J. P. Sauvage, *Helv. Chim. Acta*, **62**, 1345 (1979).
[10] Tatiana Oncescu, Mihaela Ştefan and O. Hörer, *Rev. Roum. Chim.*, **4**, 343 (1987).
[11] K. Kalyanasundaran and M. Grätzel, *J. Chem. Soc. Chem. Comm.*, 1137 (1979).

Revue Roumaine de Chimie, **32**, *9—10*, 961—967 (1987)

Dedicated to Professor I. G. MURGULESCU
on his 85th anniversary

SYNTHESIS AND PYROLYSIS OF 10,21-DITHIA-9,10,11,20,21,22-HEXAHYDRODIPHENANTHRO*[a,f]*CYCLODECENE-S,S,S′,S′-TETRAOXIDE

M. BANCIU [a], ANCA BANCIU [b], M. ELIAN [b], C. DRĂGHICI [b]
and ECATERINA CIORĂNESCU [a,b]

[a] Organic Chemistry Department, The Polytechnic, TCH, Spl. Independenţei 313,
76206 Bucharest, Romania
[b] Centre of Organic Chemistry — ICECHIM, Spl. Independenţei 202 B, 78100 Bucharest

Received April 1, 1987

Reaction of 9,10-bis(bromomethyl)phenanthrene (**19**) with thiourea afforded 9,10-bis(mercaptomethyl)phenanthrene (**20**) or 2,3-dithia-1,2,3,4-tetrahydrotriphenylene (**21**) depending on the presence or absence of inert atmosphere. Coupling of **19** with **20** produced the symmetric cyclic disulphide **22** which was oxidized to the title disulphone **16**. Flow-vacuum pyrolysis of **16** afforded 9, 10-dimethylphenanthrene (**23**) and phenanthro[9,10-c]thiophene (**24**) instead of the expected 1:2,5:6-bis(9,10-phenanthro)cycloocta-1,5-diene (**6**). The reaction mechanism is discussed.

INTRODUCTION

Pyrolysis of cyclic sulphones — reaction first developed by Vögtle[1] — has become in our days a versatile general method in the construction of cyclic and polycyclic compounds.[2] Utilizing this approach Staab and Haenel[3] synthesized the *para*-cyclophanes **1**, **2** and **3** whereas we[4] obtained **4** and **5**. The missing member in the latter series should be **6**, isomeric with **3** from the former series.

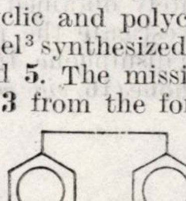

1

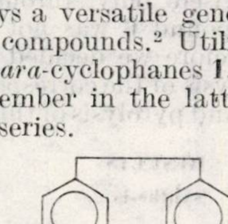

2

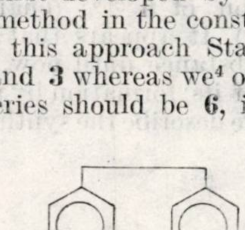

3

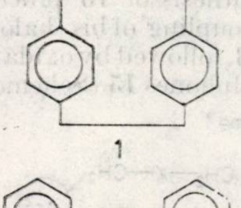

4

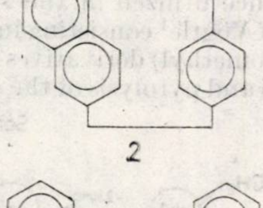

5

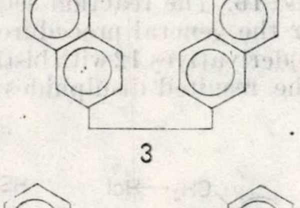

6

The 1 :2,5 :6-bis(9, 10-phenanthro)cycloocta-1,5-diene (**6**) was claimed to be obtained by Stille and Foster[5] in 1963 in pyrolyses of **7**, **8** or **9** but this structure (**6**) was later corrected[6] to tetrabenzo[*a*, *c*, *h*, *j*] anthracene (**10**), a compound known since 1952.[7,8]

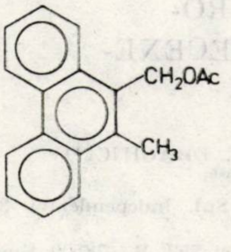

7

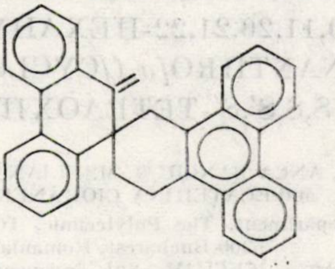

8

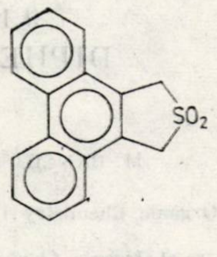

9

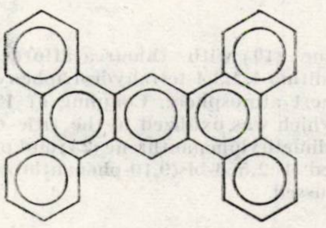

10

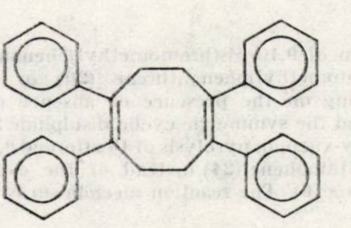

11

On the other hand, UV-irradiation of **11** led "to the *apparent* formation of **6**"[9,6] (characterised only through UV-spectrum of the solution). It appears that compound **6** was not definitely obtained as a pure substance until now, therefore we decided to investigate the possibility of its formation by pyrolysis of the corresponding disulphone. In this paper we describe the synthesis and pyrolysis of this sulphone (**16**, *vide infra*).

RESULTS

Synthesis

The key-intermediate in the attempted synthesis of **6** is the disulphone **16**. The reaction sequence utilized in the synthesis of **16** proceeds after the general procedure of Vögtle[1] consisting in coupling of bis (halomethyl)derivatives **12** with bis(thiomethyl) derivatives **13**, followed by oxidation of the resulted disulphides **14** and pyrolysis of the sulphones **15** (Scheme 1).

Scheme 1

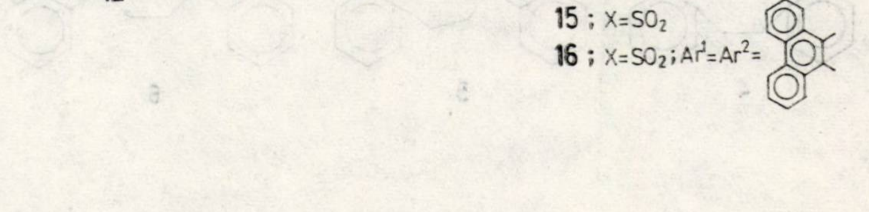

The starting intermediate 9,10-bis(bromomethyl)phenanthrene (**19**), was obtained by the improved synthesis of Staab *et al.*,[10] beginning with 9,10-phenanthrenequinone, *via* the diol **17** which underwent successive brominations with phosphorus tribromide to **18** then with N-bromosuccinimide to **19**.

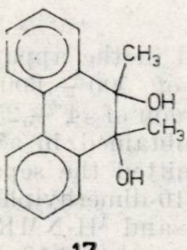
CH3
OH
CH3
OH

17

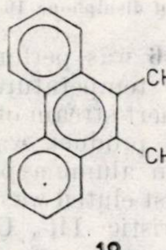

18

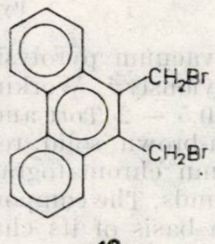
CH2Br
CH2Br

19

The conversion of **19** into 9,10-bis(mercaptomethyl)phenanthrene (**20**) was performed after Hauptmann,[11] by treatment with thiourea followed by alkaline hydrolysis of the intermediate bis-(isothiuronium) salt under inert atmosphere.

When the above reaction was carried out without inert atmosphere a cyclic disulphide **21**, m.p. 180 – 3°, was obtained by air-oxidation of **20**. The structure of **21** results from its ^{1}H-NMR spectrum, presenting along with phenanthrenic proton signals, only an unresolved singlet at $\delta = 4.17$ ppm due to CH_2 protons.

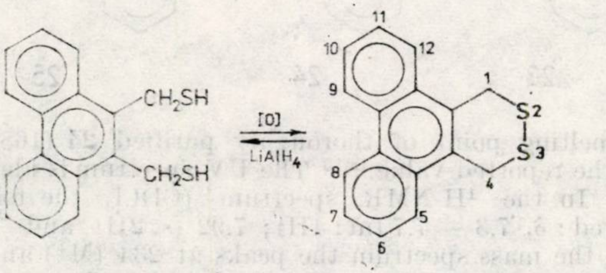
CH2SH
CH2SH
[O]
LiAlH4
11
10
12
9
1
S2
S3
8
4
7
5
6

20 **21**

A further confirmation of the structure **21** was brought by its $LiAlH_4$ reduction, affording quantitatively **20**.

Coupling of **19** with **20**, performed with KOH in boiling ethanol under inert atmosphere, afforded the very little soluble cyclic disulphide **22** m.p. 360–5°.

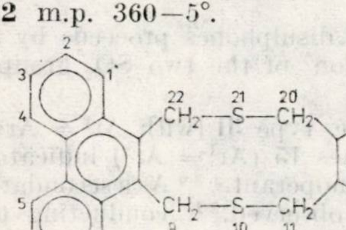
2
3
1
4
22
21
20
CH2—S—CH2
5
CH2—S—CH2
9
10
11
6
8
7

22

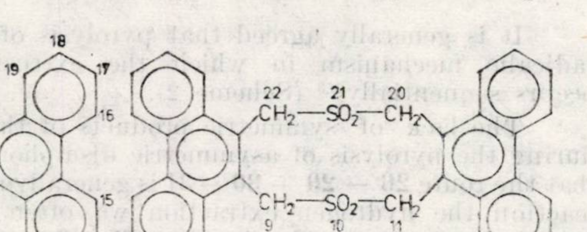
18
19
17
16
22
21
20
CH2—SO2—CH2
15
CH2—SO2—CH2
9
10
11
12
14
13

16

Oxidation of **22** with 30% hydrogen peroxide in acetic acid furnished the desired disulphide **16** as a slight yellowish solid, mp. 370–372°, presenting in IR spectrum the characteristic absorptions of SO_2 groups at 1120 cm^{-1} ($\nu_{SO_2}^{symm}$) and 1305 cm^{-1} ($\nu_{SO_2}^{asymm}$).

Pyrolysis of disulphone 16

Flow-vacuum pyrolysis of **16** was perfomed in the apparatus described previously.[4] Working at temperatures of 500 – 600°C with a vacuum of 0.5 – 2 Torr and an inert stream of argon of 4 – 25 mL/min, a yellowish-brown solid reaction product was obtained in about 52% yield. Column chromatography on alumina permitted the separation of two compounds. The compound first eluted was 9,10-dimethylphenanthene (**23**), on the basis of its characteristic IR-, UV- and ^{1}H-NMR spectra). For the second product the structure of phenanthro[9,10c]thiophene (**24**) was proved on the basis of physico-chemical evidence presented below.

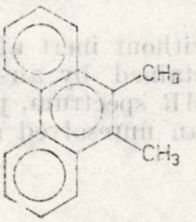

23

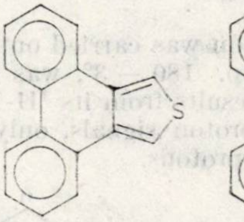

24

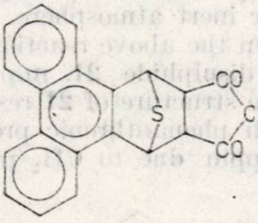

25

The melting point of thoroughly purified **24** (168°C) is in agreement with the reported value.[12,13] The UV spectrum is identical with that described.[13] In the ^{1}H-NMR spectrum ($CDCl_3$) the following signals were observed : δ, 7.3 – 7.7 (m ; 4H) ; 7.92 (s, 2H) and 7.95 – 8.5 ppm (m, 4H). In the mass spectrum the peaks at 234 (M^+) and 117 (M^{2+}) are relevant. On the other hand, reaction of **24** with maleic anhydride afforded a Diels-Alder adduct **25**, identical to that described in literature.[14]

DISCUSSION

It is generally agreed that pyrolysis of disulphones proceeds by a radicalic mechanism in which the extrusion of the two SO_2 groups occurs sequentially[2,3] (Scheme 2).

The lack of symmetric products of the type **31** (with $Ar^1 = Ar^2$) during the pyrolysis of asymmetric disulphones **15** ($Ar^1 \neq Ar^2$) indicates that the route **26** → **29** + **30** → **31** is generally inoperant.[2,3,4] As a secondary reaction the hydrogen extraction was often observed,[3,15] conducting to dimethylderivatives **23** *via* **26** → **28** → **32**. This reaction occurs to a low extent (1 – 5%) in gas-phase pyrolyses[3] but could become important in pyrolysis conducted in condensed phase.[15]

Scheme 2

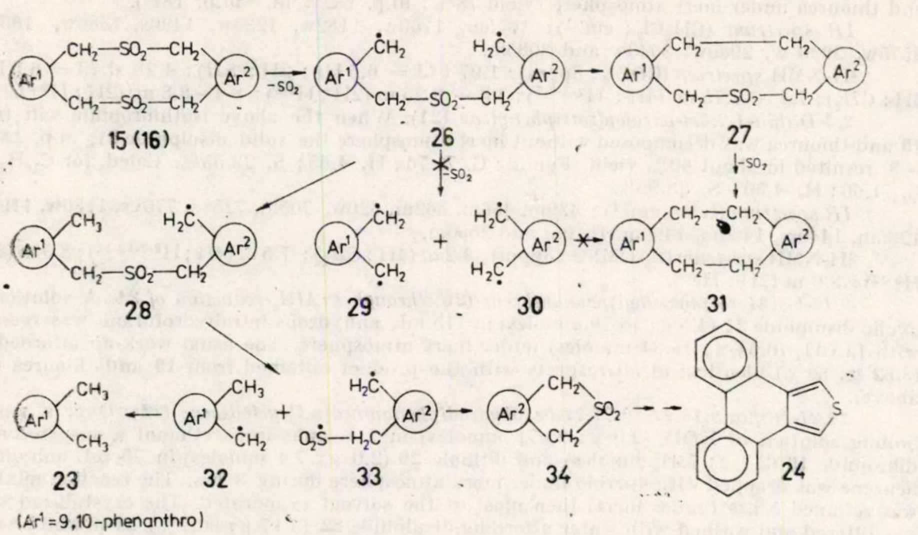

(Ar¹ = 9,10-phenanthro)

In the case of pyrolysis of **16** the exclusive formation of **23** and **24** indicates without doubt that the reactions of the type **26** → **28** are predominant. Very probably the 9,10-dimethylphenanthrene (**23**) appears from radical **28** *via* **32** whereas phenanthrothiophene (**24**) occurs from the same intermediate **28** *via* **33**. The collapse of **33** affords probably the cyclic sulphone **34** which could be a direct precursor of **24**.

In the reaction conditions utilized in the present work the formation of **6** (i.e. **31** with Ar^1 = Ar^2 = 9,10-phenanthro) is replaced by the far more efficient competing reaction of hydrogen abstraction. Thus the present results become quite similar to those of pyrolyses in condensed phase. In order to prove this assumption some control experiments were conducted by eliminating the electrical oven, all the heating being achieved by a free flame (see Experimental). The reaction products as well as their distribution were the same as in the pyrolyses described above. Thus the hypothesis mentioned before was proved : the disulphone **16**, due to its high melting point, was not converted into vapours in the conditions used, and reacted instead practically in condensed phase. The possibility of synthesis of **6** through pyrolysis of **16** using a higher vacuum apparatus is presently investigated in our laboratory.

EXPERIMENTAL

Melting points are uncorrected. IR spectra were registered with an UR-20 C. Zeiss Jena double beam spectrophotometer, UV spectra with a SPECORD-UV/VIS spectrophotometer and the ^{1}H-NMR spectra with a VARIAN A-60A spectrometer using TMS as internal standard. The mass-spectrum was performed on a VARIAN MAT-SM1 apparatus with direct inlet.

9,10-bis(Bromomethyl)phenanthrene (**19**) was obtained starting with **17**[16] after Staab *et al.*,[10] m.p. 232–3° (from CHCl$_3$) ; lit.[10] m.p. 229–231°.

IR spectrum (KBr ; cm^{-1}) : 490m, 525s, 728vs, 768vs, 1214s, 1459m, 1497m, 2860 (broad) and 2930 (broad).

9,10-bis(Mercaptomethyl)phenanthrene (**20**) was obtained after Hauptmann[11] from **19** and thiourea under inert atmosphere (yield 78%; m.p. 182°; lit.[11] m.p. 181°).

IR spectrum (CH_2Cl_2; cm^{-1}): 1055m, 1160w, 1182w, 1235w, 1490s, 1580w, 1600w, 2575w, 2930 w, 2980w, 3040w and 3085m.

^{1}H-NMR *spectrum* ($CDCl_3$; δppm): 1.97 t (J = 6.5 Hz; 2H; S*H*); 4.28 d (J = 6.5 Hz; 4H; CH_2); 7.4 – 7.75 m (4H; H^{2,3,6,7}); 7.8 – 8.25 m (2H; H^{1,8}); 8.4–8.8 m (2H; H^{4,5}).

2,3-Dithia-1,2,3,4-tetrahydrotriphenylene (**21**). When the above isothiuronium salt from **19** and thiourea was decomposed without inert atmosphere the solid disulphide **21**, m.p. 180—3° resulted in about 60% yield. Found: C. 71.76; H, 4.65; S, 23.55%. Calcd. for $C_{16}H_{12}S$: C, 71.60; H, 4.50; S. 23.90%.

IR spectrum (KBr, cm^{-1}): 439m, 486m, 562m, 620w, 705m, 725vs, 770vs, 1180w, 1195w, 1235m, 1440m, 1460m, 1490m, 1510m and 2550m.

^{1}H-NMR *spectrum* (d_6-DMSO; δppm): 4.2 m (4H; CH_2); 7.5 m (4H; H^{6,7,10,11}); 8.0 m (2H; H^{5,12}); 8.6 m (2H; H^{8,9}).

9,10-bis(Mercaptomethyl)phenanthrene (**20**) *through* $LiAlH_4$*-reduction of* **21**. A solution of cyclic disulphide **21** (4.5 g; 16.79 mmoles) in 115 mL anhydrous tetrahydrofurane was reduced with $LiAlH_4$ (0.64 g; 16.84 mmoles) under inert atmosphere. The usual work-up afforded **20** (3.62 g; 80%) identical in all respects with the product obtained from **19** and thiourea (see above).

10,21-Dithia-9,10,11,20,21,22-hexahydrodiphenanthro[a,f]*cyclodecene* (**22**). Over a stirred boiling solution of KOH (2.0 g; 35.71 mmoles) in 1 L anhydrous ethanol a suspension of dibromide **19** (2.7 g; 7.41 mmoles) and dithiole **20** (2.0 g; 7.4 mmoles) in 75 mL anhydrous benzene was dropped with stirring under inert atmosphere during 3 hrs. The reaction mixture was refluxed 5 hrs (under inert) then most of the solvent evaporated. The crystallized solid was filtered and washed with water affording disulphide **22** (3.17 g; 90.7%) as a white solid, m.p. 360–365°, practically unsoluble in all usual solvents.

IR spectrum (KBr; cm^{-1}) 442w, 485w, 560w, 720vs, 732m, 764vs, 780m, 952w, 1155w, 1182w, 1248m, 1422s, 1440m, 1490w, 2925w, 3005w, and 3070w.

10,21-Dithia-9,10,11,20,21,22-hexahydrodiphenanthro[a,f]*cyclodecene-S,S,S',S'-tetraoxide* (**16**). Over a stirred suspension of disulphide **22** (2 g; 4.23 mmoles) in 50 mL anhydrous acetic acid heated at 100° a solution of 30% hydrogen peroxide (5g; 44 mmoles) was dropped during 1 hr. After 6 hrs of heating at 100° a new portion of 5 g (44 mmoles) hydrogen peroxide was added and the mixture heated for another 1.5 hrs. The solid disulphone was filtered and washed with 20 mL $CHCl_3$. The disulphone **16** (2g; 88%), m.p. 370–372° is a pale yellow solid unsoluble in all usual solvents. Found: C, 72.02; H, 4.75; S, 11.70%. Calcd. for $C_{32}H_{24}O_4S_2$: C, 71.64; H, 4.48; S, 11.94%.

IR spectrum (KBr, cm^{-1}): 434w, 492w, 520w, 580w, 728s, 750s, 765s, 850w, 1040m, 1120s (νSO_2), 1160m, 1250m 1305s, (νSO_2), 1440 m, 3020w and 3075w.

Pyrolysis of disulphone **16**. The pyrolysis was performed in the apparatus described previously.[4] The sample of disulphone **16** (1g; 1.86 mmoles) was introduced in a small quartz tube with both ends fitted with glass wool. The tube was introduced in the pyrolysis quartz tube in front of the electrically heated zone. The sample was sublimated with an exterior flame in a constant flow of argon (5 mL/min) maintaining a vacuum of 0.5 Torr and the vapours enter directly in the empty pyrolysis zone of the tube (30 cm length; 20 mm diameter) heated at 500° with an electrical oven. The reaction product crystallizes in the final unheated zone of the pyrolysis tube whereas some black untratable material remains in the sample tube. The yellowish-brown reaction mixture (0.40 g; 52.6%) was chromatographed on neutral Al_2O_3 (Merck; activity II) with petroleum ether (b.p. 30–50°) as eluent.

The first separated product was *9,10-dimethylphenanthrene* (**23**) (0.22 g; 29%) m.p. 139–142° (from ethanol) lit.[16] m.p. 139°.

^{1}*H-NMR spectrum* ($CDCl_3$; δppm): 2.6 s (6H; CH_3); 7.35–7.70 m (4H; H^{2,3,6,7}); 7.8 – 8.2 m(2H; H^{1,8}) and 8.40–8.75 m (2H; H^{4,5}) was in agreement with the reported one.[17]

The second separated product of pyrolysis was phenanthro-[9,10c]thiophene (**24**) (0.18 g; 20.6%) m.p. 168° (from ethanol); lit.[13] m.p. 168–9°.

IR spectrum (CS_2; CCl_4; cm^{-1}): 752vs, 778w, 875w, 1173m, 1235w, 1405w, 1440m, 1465m, 3025m, 3060m, 3085m and 3100w.

UV spectrum (MeOH; λ max nm, lg ε max): 254(4.77); 263(4.76); 278(3.90); 289 (3.96); 303(3.90); 320(3.80) and 336(3.58).

^{1}*H-NMR spectrum* (see text).

Adduct **25** was obtained after the procedure of Dann *et al*[14]; m.p. 220–2°; lit[14] m.p. 219–220°. The UV spectrum of **25** was identical with that reported.[14]

ACKNOWLEDGEMENTS : We express our thanks to Dr. N. Palibroda and Dr. Monica Culea for mass spectrum and to Eng. Maria Dezsö for help in synthesis of some starting materials.

REFERENCES

[1] a) F. Vögtle, *Chem Ber.*, **102**, 3077 (1969) ; b) F. Vögtle, *Angew. Chem.*, **81**, 258 (1969) ; c) F. Vögtle, *Liebigs Annal. Chem.*, **728**, 17 (1969).

[2] a) F. Vögtle and L. Rossa, *Angew. Chem.*, **91**, 534 (1979) ; b) A. Ruland and H.A. Staab, *Chem. Ber.*, **111**, 2997 (1978) ; R.F.C. Brown, "Pyrolytic Methods in Organic Chemistry", Academic Press, New York, 1980, p. 196.

[3] a) M. Haenel and H. A. Staab, *Tetrahedron Letters*, **1970**, 3585 ; b) H. A. Staab and M. Haenel, *Chem. Ber.*, **106**, 2190 (1973).

[4] M. Banciu, I. Pogany, D. Mosora, P. Rusu, R. Stănciulescu and M. Dezsö, *Rev. Roumaine Chim.*, **30**, 703 (1985).

[5] J. K. Stille and R. T. Foster, *J. Org. Chem.*, **28**, 2708 (1963).

[6] J. P. Anhalt and E. H. White, *Tetrahedron*, **28**, 2921 (1972).

[7] P. Lambert and R. H. Martin, *Bull. Soc. Chim. Belges*, **61**, 124 (1952).

[8] J. van Thuijl and C. Romers, *Req. Trav. Chim. Pays-Bas*, **87**, 5 (1968).

[9] E. H. White and J. P. Anhalt, *Tetrahedron Letters*, **1965**, 3937.

[10] H. A. Staab, U. E. Meissner, W. Weinacht and A. Gensler, *Chem. Ber.*, **112**, 3895 (1979).

[11] S. Hauptmann, *Chem. Ber.*, **93**, 2604 (1960).

[12] O. Hinsberg, *Ber. dtsch. chem. Ges.*, **4**, 901 (1910).

[13] J. E. Shields, D. E. Remy, and J. Bornstein, *J. Org. Chem.*, **40**, 477 (1975).

[14] O. Dann, M. Kokorudz and R. Gropper, *Chem. Ber.*, **87**, 140 (1954).

[15] a) F. Vögtle, *Angew. Chem.*, **81**, 258 (1969) ; b) E. J. Moriconi, R. E. Misner and T.E. Brady, *J. Org. Chem.*, **34**, 1651 (1969) ; c) M.P. Cava and A. A. Deana, *J. Amer. Chem. Soc.*, **81**, 4266, (1959).

[16] T. Zincke and W. Tropp, *Liebigs Annal. Chem.*, **362**, 242 (1908).

[17] P.M.G. Bavin, K.D. Bartle and J.A.S. Smith, *Tetrahedron*, **21**, 1087 (1965).

Revue Roumaine de Chimie, **32**, *9–10*, 969–973 (1987)

Dedicated to Professor I. G. MURGULESCU
on his 85th anniversary

CARBONIUM ION REACTIONS. XVIII[1]

SUBSTITUENT EFFECT IN SOLVOLYTIC REACTIONS. SOLVOLYSIS OF THE TOSYLATE OF 10-METHYL-5H-DIBENZO[*a*, *d*]CYCLOHEPTEN-5-CARBINOL

MICHAELA STĂNESCU, MIHAI ELIAN and ECATERINA CIORĂNESCU
Centre of Organic Chemistry, Spl. Independenţei 202 B, 78100 Bucharest, Romania

Received April 29, 1987

The synthesis and acetolysis of tosylate of 10-methyl-5H-dibenzo[*a*,*d*]cyclohepten-5-carbinol (**4**-OTs) were performed. The solvolysis product consisted of bridged compounds (**7**, **8** and **9**) generated by the remote double bond assistance (π-route). The results were compared with those obtained in the solvolysis of the unsubstituted analogue **1a** which yielded by ring expansion compounds with dibenzocyclooctatriene skeleton (phenonium route).

The acetolyses of tosylates **1** with a side-chain of one, two or three carbon atoms were described in previous papers.[2–4] Depending on the chain length, one of the three possible routes shown in Scheme 1 prevails.

Scheme 1

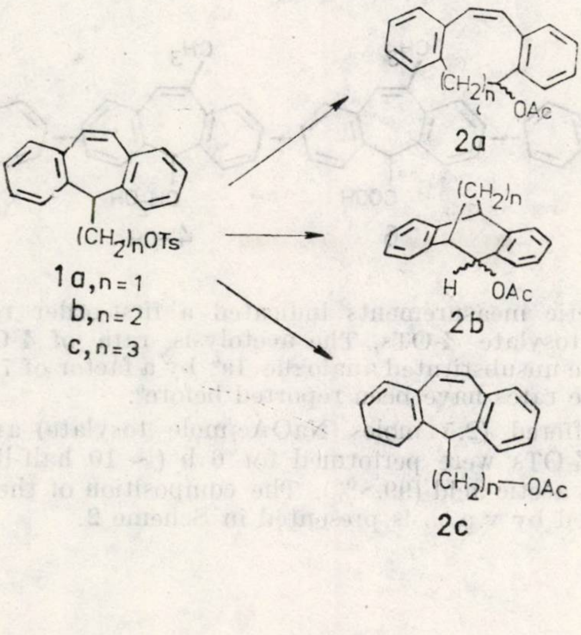

The phenonium route, leading to a reaction product with enlarged median ring (**2a**, $n = 1$), is the main route in the buffered (sodium acetate) acetolysis of the tosylate **1a**. Only small quantities (6–8%) of bridged compounds (**2b**, $n = 1$) generated by remote double bond participation (π-route) were identified. The phenonium route is ruled out for $n > 1$. The buffered acetolysis of tosylate **1b** proceeds almost entirely through π-route (90% **2b**, $n = 2$), while that of tosylate **1c** leads to the acetate corresponding to the starting material (**2c**, $n = 3$).

The substituted analogues of **1b**, namely the tosylates **3**, parallel the solvolytic behaviour of the unsubstituted congener.[5]

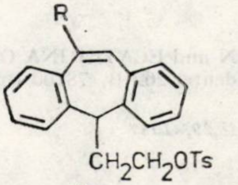

3 (R=CH$_3$,C$_6$H$_5$)

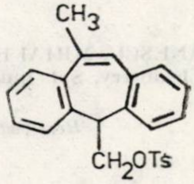

4–OTs

The present paper reports the solvolysis of the tosylate of 10-methyl-5H-dibenzo[a,d]cyclohepten-5-carbinol (**4**-OTs) possessing a methyl group on the double bond of the median ring. In this case, a higher yield in the π-route products is expected due to the enhanced nucleophilicity of the methyl-substituted double bond.[6]

RESULTS AND DISCUSSION

The synthesis of the tosylate **4**-OTs was performed by starting from the ketone **5**,[7] through the acid **6** prepared by a known method:[8]

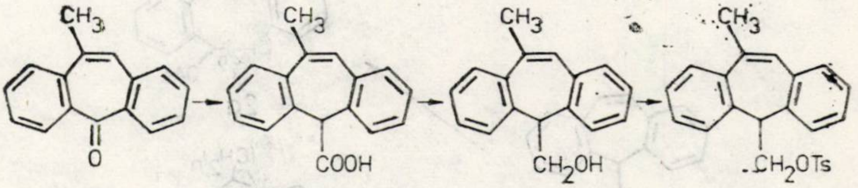

5 6 4–OH 4–OTs

The kinetic measurements indicated a first-order reaction in the solvolysis of tosylate **4**-OTs. The acetolysis rate of **4**-OTs is higher than that of the unsubstituted analogue **1a**[9] by a factor of 7.5 ($t = 110°C$). Similar relative rates have been reported before[6].

Both buffered (2.5 moles NaOAc/mole tosylate) and unbuffered acetolyses of **4**-OTs were performed for 6 h (~ 10 half-lives) at reflux temperature in acetic acid (99.8%). The composition of the reaction mixture, determined by v.p.c., is presented in Scheme 2.

Scheme 2

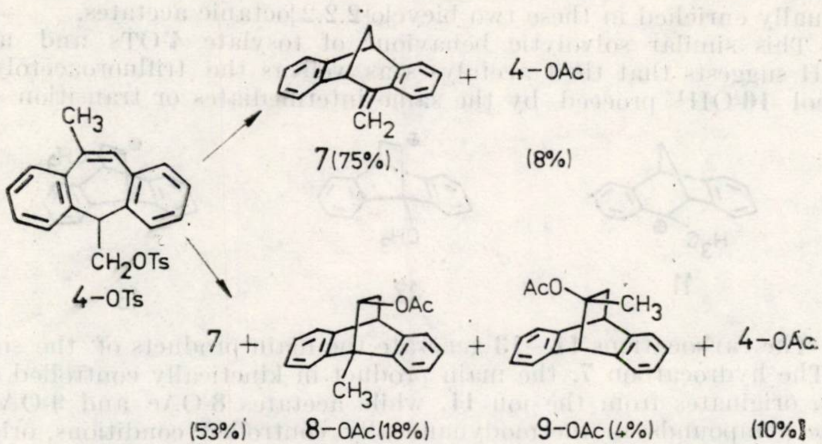

The main product of the buffered acetolysis was the exomethylene hydrocarbon **7**, with a dibenzobicyclo[3.2.1]octane skeleton. The unbuffered acetolysis yielded, besides the hydrocarbon **7**, acetates **8**-OAc and **9**-OAc with a dibenzobicyclo[2.2.2]octane skeleton. Small quantities of the acetate with unchanged skeleton **4**-OAc were identified. In both solvolyses, unidentified compounds were also obtained, each one in less than 5% of the reaction mixture. The hydrocarbon **7**[10] and the alcohols **8**-OH[11] and **9**-OH[12] are known.

New evidence concerning the relative stability and interconversion of reaction products was provided by the acetolyses of the alcohol **10**-OH.[13] The corresponding acetate **10**-OAc was expected among the solvolytic products in the buffered acetolysis of **4**-OTs.

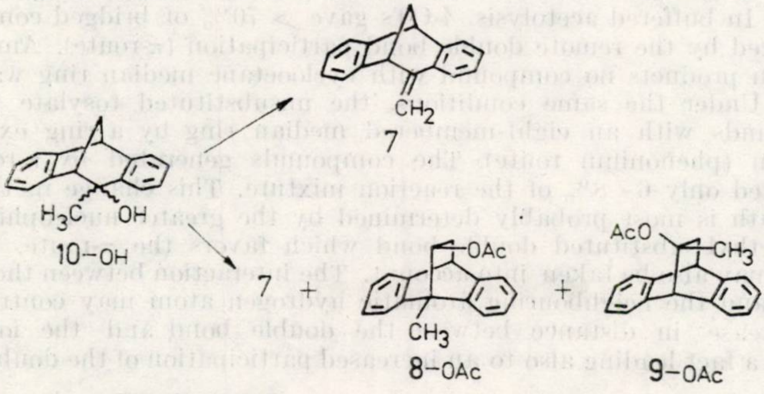

time 2h	84%	5%	.2%
6h	21%	61%	11%

On reflux in acetic acid (99.8%), the alcohol **10**-OH gave only the hydrocarbon **7**, indicating the lack of stability of the acetate **10**-OAc (whose structure is both benzylic and tertiary). In acetic acid containing three added equivalents of *p*-toluenesulphonic acid, besides the hydrocarbon

7, acetates **8**-OAc and **9**-OAc were formed. The reaction mixture became gradually enriched in these two bicyclo[2.2.2]octanic acetates.

This similar solvolytic behaviour of tosylate **4**-OTs and alcohol **10**-OH suggests that their acetolyses as well as the trifluoroacetolysis of alcohol **10**-OH[1] proceed by the same intermediates or transition states.

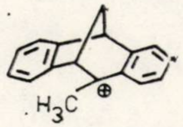

11

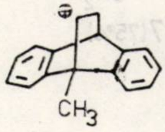

12

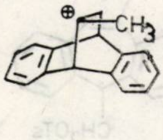

13

The carbocations **11**—**13** generate the main products of the solvolyses. The hydrocarbon **7**, the main product in kinetically controlled conditions, originates from the ion **11**, while acetates **8**-OAc and **9**-OAc, the stable compounds in thermodynamically controlled conditions, originate from the ions **12** and **13**, respectively. The existence of ions **14**—**17** as intermediates or transition states was taken into account to explain the reaction course.

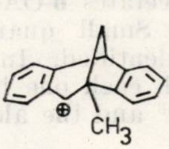

14

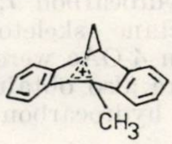

15

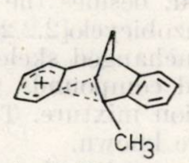

16

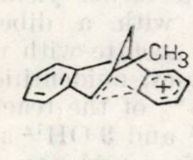

17

The difference between the tosylates **4**-OTs and **1a** consists in the presence of a methyl group attached to the double bond of the median ring in **4**-OTs. This difference leads to a dramatic change in the reaction course. In buffered acetolysis, **4**-OTs gave > 70% of bridged compounds generated by the remote double bond participation (π-route). Among the reaction products no compound with cyclooctane median ring was identified. Under the same conditions, the unsubstituted tosylate **1a** gave compounds with an eight-membered median ring by a ring expansion reaction (phenonium route). The compounds generated by π-route represented only 6—8% of the reaction mixture. This change in the reaction path is most probably determined by the greater nucleophilicity of the methyl-substituted double bond which favors the π-route. A steric factor may also be taken into account. The interaction between the methyl group and the neighbouring aromatic hydrogen atom may contribute to a decrease in distance between the double bond and the ionization center, a fact leading also to an increased participation of the double bond.

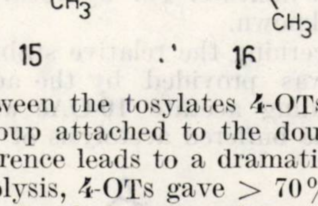

EXPERIMENTAL

Melting points are uncorrected, IR spectra were recorded with a double-beam C. Zeiss Jena UR-20 spectrophotometer and ^1H-NMR spectra on a Varian EM-360 spectrometer using TMS as internal standard. The v.p.c. analyses were performed on a Carlo Erba model D, with flame ionization detector, 2 m column (10% silicone oil QF1 on Chromosorb Q, 80—100 mesh), carrier gas nitrogen at 180°C. For kinetic determinations the ampoule technique was used. The *p*-toluenesulphonic acid, formed during the reaction, was determined by titration with 0.05 M NaOAc/HOAc solution. For recordings, a potentiograph A Metrohm E-336 with platinum and graphite capillary electrodes was used.

*10-Methyl-5*H*-dibenzo*[a,d]*cyclohepten-5-carboxilic acid* (**6**) was obtained with 60% yield from 10, 11-dihydro-10-methyl-5H-dibenzo[*a,d*]cyclohepten-5-one in an analogous manner as previously described.[8] The acid **6** is a white solid, m.p. 190°C.

Found: C, 81.58; H, 5.64%. $C_{17}H_{14}O_2$ requires: C, 81.40; H, 5.55%.

IR spectrum (CCl_4; cm^{-1}): 1240 m, 1280 m, 1722 vs, 2300—3400 m.

NMR spectrum ($CDCl_3$; δppm): 2.3 (d, 3H, CH_3, J = 1 Hz), 4.8 (s, 1H, H_5), 6.9 (d, 1H, H_{11}), 7.1—7.6 (m, 8H, H_{arom}), 9.7 (s. large, 1H, COOH).

*The tosylate of 10-methyl-5*H*-dibenzo*[a,d]*cyclohepten-5-carbinol* (**4**—OTs). From the acid **6**, by usual procedures, alcohol **4**-OH was prepared. The corresponding tosylate **4**-OTs is a crystalline solid, m.p. 85—6°C (methanol).

Found: C, 74.01; H, 6.00%. $C_{24}H_{22}O_3S$ requires: C, 73.82; H, 5.68%.

IR spectrum (CCl_4; cm^{-1}): 1182 vs, 1374 s.

NMR *spectrum* ($CDCl_3$; δppm): 2.2 (d, 3H, CH_3, J = 1 Hz), 2.4 (s, 3H, CH_{3-Ts}), 4.1—4.5 (m, 3H, H_5 + CH_2), 6.6 (d, 1H, H_{11}, J = 1 Hz), 7.0—7.5 (m, 12H, H_{arom}).

The acetolyses of the tosylate **4**-OTs. The tosylate **4**-OTs was treated with acetic acid (99.8%), with (2.5 moles/mole **4**-OTs), or without sodium acetate at reflux for 6 h (~ 10 half-lives). The residue obtained after the usual work up (88—90% yield) was v.p.c. analysed. After $LiAlH_4$ reduction of the reaction product, the alcohols **4**-OH, **8**-OH and **9**-OH were identified by comparison with authentic samples.

*The acetolyses of 10,11-dihydro-11-methyl-5,10-methano-5*H*-dibenzo*[a,d]*cyclohepten-11-ol* (**11**). The alcohol **11** was treated with acetic acid, at reflux, with (3 moles/mole **11**) or without p-toluenesulphonic acid. The residue was worked up as previously described.

ACKNOWLEDGEMENTS: We wish to thank Mrs. Ligia Stănescu and dr. M. D. Gheorghiu for their help with physical measurments.

REFERENCES

[1] Note XVII. M. Stănescu, M. Elian and E. Ciorănescu, *Rev. Roumaine Chim.*, **31**, 1001 (1986).

[2] E. Ciorănescu, A. Bucur, M. Elian, M. Banciu, M. Voicu and C. D. Nenitzescu, *Tetrahedron Letters*, **1964**, 3855; E. Ciorănescu, A. Bucur, M. Elian and C. D. Nenitzescu, *Rev. Roumaine Chim.*, **10**, 149 (1965); E. Ciorănescu, A. Bucur, F. Badea, M. Rentzea and C. D. Nenitzescu, *Tetrahedron Letters*, **1969**, 1867.

[3] E. Ciorănescu, M. Banciu, R. Jelescu, M. Rentzea, M. Elian and C. D. Nenitzescu, *Tetrahedron Letters*, **1969**, 1971; *Rev. Roumaine Chim.*, **14**, 911 (1969).

[4] M. Banciu, R. Vlad and C. Drăghici, *Rev. Roumaine Chim.*, **25**, 1221 (1980).

[5] M. Stănescu, G. Mihai, L. Stănescu and E. Ciorănescu, *Rev. Roumaine Chim.*, **24**, 197 (1979).

[6] P. D. Bartlett and G. D. Sargent, J. *Amer. Chem. Soc.*, **87**, 1297 (1965); H. Felkin and C. Lion, *Tetrahedron*, **27**, 1375 (1971).

[7] J. R. Geigy, *Fr. Pat.*, 1.522.973 26 Apr. 1968.

[8] M. A. Davis, F. A. Sunahara, F. Herr and R. Gaudry, *J. Med. Chem.*, **6**, 513 (1963).

[9] M. Voicu and F. Badea, *Rev. Roumaine Chim.*, **17**, 1551 (1972).

[10] D. A. Cullison and R. K. Hill, *Tetrahedron Letters*, **1972**, 3747.

[11] H. Hart, D. L. Dean and D. N. Buchanan, *J. Amer. Chem. Soc.*, **95**, 6294 (1973).

[12] V. J. Shiner and J. S. Humphrey, *J. Amer. Chem. Soc.*, **85**, 2416 (1963).

[13] M. Avram, I. G. Dinulescu and C. D. Nenitzescu, R. A. Y. Jones, A. R. Katritzky and R. J. Wyatt, *Rev. Roumaine Chim.*, **18**, 441 (1973).

EXPERIMENTAL

Melting points are uncorrected. IR spectra were recorded with a double-beam C. Zeiss Jena UR-20 spectrophotometer and ¹H-NMR spectra on a Varian EM-360 spectrometer using TMS as internal standard. The v.p.c. analyses were performed on a Carlo Erba model D, with flame ionization detector, 2 m column (10% silicone oil OV-1 on Chromosorb Q, 80–100 mesh), carrier gas nitrogen (at 180°C). For kinetic determinations the ampoule technique was used. The p-toluenesulphonic acid, formed during the reaction, was determined by titration with 0.05 N NaOAc/HOAc solution. For recordings, a potentiograph, a Metrohm E-336 with platinum and graphite capillary electrodes was used.

[illegible] acid (6) was obtained with 60% yield from [illegible] in an analogous manner as previously described.[8] The acid 6 is a white solid, m.p. 180°C.

Found: C, 81.36; H, 5.64%. [illegible] requires: C, 81.40; H, 5.53%.

IR spectrum (CCl_4; cm^{-1}): 1240 m, 1290 m, 1732 vs, 2500–3400 m.

NMR spectrum ($CDCl_3$; δppm): 1.3 (d, 3H, CH_3, J = 1 Hz), 1.8 (s, 2H), [illegible] 7.1–7.6 (m, 8H, H_{arom}), 9.5 (s, large, 1H, COOH).

The tosylate of [illegible] (4-OTs). From the acid 6 by usual procedure, alcohol 4-OH was prepared. The corresponding tosylate 4-OTs is a crystalline solid, m.p. [illegible] °C (decomposed).

Found: C, 74.01; H, 5.60%. [illegible]O_3S requires: C, 73.82; H, 5.35%.

IR spectrum (CCl_4; cm^{-1}): 1192 vs, 1374 s.

NMR spectrum (CCl_4; δppm): 2.2 (d, 3H, CH_3, J = 1 Hz), 2.4 (s, 3H, CH_3-tyl), 3.1 [illegible] (m, 1H), 4.5 (d, 1H, [illegible] J = 1 Hz), 7.0–7.5 (m, 12H, H_{arom}).

The acetolysis of the tosylate 4-OTs. The tosylate 4-OTs was treated with acetic acid (0.05 M), with 2.5 moles/mole 4-OTs, or without sodium acetate, at reflux for 4 h (> 10 half-lives). The residue obtained after the usual work up (85–90% yield) was v.p.c. analysed. After $LiAlH_4$ reduction of the reaction product, the alcohols 5-OH, 8-OH and 9-OH were identified by comparison with authentic samples.

The acetolysis of [illegible] (11). The alcohol 11 was treated with acetic acid, at reflux, with 10 moles/mole 11, or without p-toluenesulphonic acid. The residue was worked up as previously described.

ACKNOWLEDGEMENTS. We wish to thank Mrs. Elena Stănescu and dr. M. D. Gheorghiu for their help with physical measurements.

REFERENCES

[1] Note XVII: M. Stănescu, M. Elian and E. Ciorănescu, *Rev. Roumaine Chim.*, **31**, 1001 (1986).
[2] E. Ciorănescu, A. Bucur, M. Elian, M. Banciu, M. Voicu and C. D. Nenitzescu, *Tetrahedron Letters*, **1964**, 3835; E. Ciorănescu, A. Bucur, M. Elian and C. D. Nenitzescu, *Rev. Roumaine Chim.*, **10**, 141 (1965); E. Ciorănescu, A. Bucur, F. Badea, M. Rentea and C. D. Nenitzescu, *Tetrahedron Letters*, **1965**, 1867.
[3] E. Ciorănescu, M. Banciu, R. Jelescu, M. Rentea, M. Elian and C. D. Nenitzescu, *Tetrahedron Letters*, **1969**, 1871; *Rev. Roumaine Chim.*, **14**, 911 (1969).
[4] M. Banciu, D. Vlad and C. Drăghici, *Rev. Roumaine Chim.*, **25**, 1221 (1980).
[5] M. Stănescu, A. Bucur, L. Stănescu and E. Ciorănescu, *Rev. Roumaine Chim.*, **24**, 127 (1979).
[6] P. D. Bartlett and G. D. Sargent, *J. Amer. Chem. Soc.*, **87**, 129 (1965); H. Tanida and C. Lowe, *Tetrahedron*, **27**, 1275 (1971).
[7] J. R. Geigy, Fr. Pat. 1,523,673 26 Apr. 1968.
[8] M. A. Davis, S. O. Winthrop, R. Herr and D. Gaudry, *J. Med. Chem.*, **8**, 318 (1965).
[9] M. Voicu and F. Badea, *Rev. Roumaine Chim.*, **17**, 1551 (1972).
[10] D. A. Cullison and E. K. Hill, *Tetrahedron Letters*, **1972**, 374.
[11] H. Hart, D. E. Dean and D. N. Buchanan, *J. Amer. Chem. Soc.*, **95**, 6294 (1973).
[12] J. Sicher and S. Humphrey, *J. Amer. Chem. Soc.*, **85**, 2419 (1963).
[13] M. Avram, I. G. Dinulescu and C. D. Nenitzescu, R. A. V. Jones, A. R. Katritzky and R. J. Wyatt, *Rev. Roumaine Chim.*, **16**, 141 (1971).

Revue Roumaine de Chimie, 32, *9–10*, 975–978 (1987)

Dedicated to Professor I. G. MURGULESCU
on his 85th anniversary

AMINOKETONE AND OXAZOLE SYNTHESIS. X.[1]

ACYLATION AND ALKYLATION OF ARENES WITH THE AZLACTONE OF CINNAMOYLGLYCINE

MICHAELA-CARMEN BALABAN, IOSIF SCHIKETANZ, ALEXANDRU T. BALABAN*,
ANA SCHIKETANZ and MIRCEA D. GHEORGHIU
Polytechnic Institute, Department of Organic Chemistry, Splaiul Independenţei 313,
76206 Bucharest, Roumania

Received January 20, 1987

The azlactone **2** obtained from cinnamoylglycine simultaneously acylates and alkylates benzene in the presence of $AlCl_3$ leading to the saturated α-acylaminoketone N-(β,β-diphenylpropionyl)-phenacylamine **3** which was obtained also by an unambiguous synthesis from phenacylamine and β,β-diphenylpropionyl chloride. With toluene, in addition to the analogous reaction, an exchange of the phenyl group from the cinnamoyl residue with a tolyl group occurs. The acylaminoketones are easily dehydrated to 2,5-disubstituted oxazoles which may be dehydrogenated *via* bromination with NBS and dehydrobromination with pyridine affording 2-(β,β-diphenylvinyl)-5-phenyloxazole, whose conjugated double bond is manifested in a bathochromic shift of the electronic absorption spectrum.

So far we have explored systematically the Friedel-Crafts acylaminoacylation of aromatic hydrocarbons with azlactones or bis-azlactones prepared from aroylglycine derivatives.[2,3] In the present paper we report that the azlactone derived from an unsaturated acid (cinnamoylglycine) affords both electrophilic addition and substitution, namely an acylation (substitution of aromatics, as with other azlactones) and an alkylation reaction involving the C=C double bond (addition of an arene across a C=C double bond, or substitution of an arene with an alkyl cation obtained by protonation of a C=C double bond).

Cinnamoylglycine **1** was prepared as described earlier,[4] and it was converted into its azlactone **2**. Among the reagents for effecting this conversion, acetic anhydride proved to be unsuitable; ethyl chloroformate with triethylamine[5] gave less satisfactory results than dicyclohexylcarbodiimide in methylene chloride. The yellow crystalline azlactone **2** was dissolved in excess of benzene and treated at 0° with powdered aluminium chloride. A crystalline product **3** was obtained which was shown by IR, elemental analysis, ^{1}H-NMR and mass spectrometry to originate in the reaction of one mole azlactone with two moles of benzene.

The structure of **3** as N-(β,β-diphenylpropionyl)-phenacylamine was proved by independent synthesis from phenacylamine and β,β-diphenylpropionyl chloride[6] in the presence of pyridine.

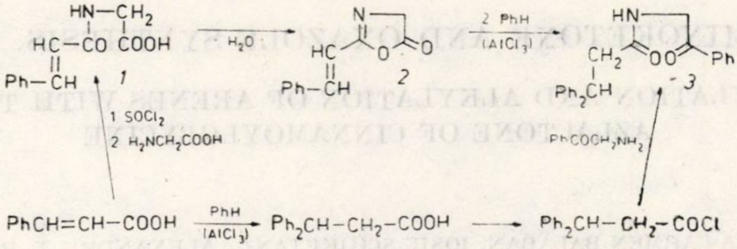
HN—CH₂
HC—CO COOH
Ph—CH
1
H₂O
2
2 PhH
(AlCl₃)
3
Ph
1 SOCl₂
2 H₂NCH₂COOH
PhCOCH₂NH₂
PhCH=CH—COOH
PhH
(AlCl₃)
Ph₂CH—CH₂—COOH
Ph₂CH—CH₂—COCl

When the same reaction was performed with azlactone **2** in toluene, the final reaction product **6** presented ^{1}H-NMR and mass spectral evidence that three and not two moles of toluene were involved in the reaction (in the formulas below we denote the *p*-tolyl residue by Tol):

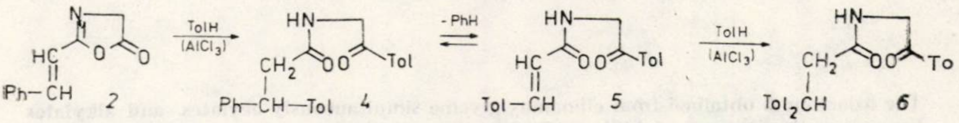
2
TolH
(AlCl₃)
4
- PhH
5
TolH
(AlCl₃)
6
Ph—CH—Tol
Tol—CH
Tol₂CH

Taking into account the reversibility of aromatic alkylation, it can be assumed that the first reaction product **4**, involving only two moles of toluene, may equilibrate *via* alkylation-dealkylation with the hydrocarbon medium leading *via* **5** to **6** because toluene is in marked excess.

According to literature data, such equilibrations were already observed in the reaction of cinnamic acid with chlorobenzene which afforded β,β-di-*p*-chlorophenylpropionic acid.[7] Also, the reaction of 4-arylidene-5-oxazolones (unsaturated azlactones, which like **1** also possess an α,β-unsaturated carbonyl moiety) with arenes in the presence of $AlCl_3$ involves addition of the arene to the C=C double bond, as shown by Filler and coworkers;[8,9] the reaction product under anhydrous conditions in the arene as solvent is a saturated azlactone. In the presence of water,[10] or in other solvents;[8–10] the reaction takes other courses.

The α-acylaminoketone **3** was converted into the corresponding oxazole **7** by refluxation with phosphorus oxychloride.

For obtaining an oxazole absorbing at longer wavelengths than **7**, the saturated side-chain was dehydrogenated *via* bromination with N-bromosuccinimide and dehydrobromination in refluxing pyridine.[11] The bromoderivative **8** was not purified but was converted directly into the unsaturated oxazole **9**.

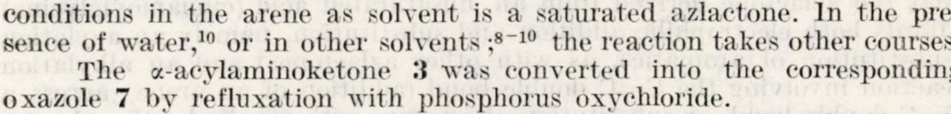
3
- H₂O
7
NBS
8
- HBr
9
Ph₂CH
Ph₂CBr
Ph₂C
Ph

While the saturated oxazole **7** presented UV maxima at 270 and 280 nm (in ethanol), the unsaturated oxazole **9** had a pronounced bathochromic shift (in the same solvent) with absorption maxima at 260 and 352 nm.

We have presented a method for obtaining saturated and unsaturated oxazoles from cinnamoylglycine and aromatic hydrocarbons; the oxazoles have a 2-alkyl or vinylene group, and a 5-aryl group. The conversion of the α-acylaminoketone **3** into the corresponding saturated and unsaturated thiazoles is described in the following part of this series.

EXPERIMENTAL PART

N-Cinnamoylglycine, **1**, m.p. 192°, was prepared from cinnamoyl chloride and glycine in excess aqueous sodium hydroxide followed by acidification.[4] Its ^{1}H-NMR spectrum in $(D_3C)_2SO$ (δ, ppm): 3.97 (2H, d, CH_2, $J = 6$ Hz); 6.79 (1H, d, $J = 16$ Hz, $-CH=$); 7.55 (1H, d, $J = 16$ Hz, $-CH=$), 7.3–7.5 (5H, m); 8.50 (1H, broad triplet, $J = 6$ Hz, NH); 10.80 (1H, broad, COOH). Decoupling experiments of $CH=CH$ and $NH-CH_2$ groups as well as deuterations of COOH and NH groups confirmed the assignments.

2-Styryl-5-oxazolone, **2**, was prepared from the preceding compound either with ethyl chloroformate and triethylamine according to the method described in the literature[5], or with more satisfactory results using dicyclohexylcarbodiimide in methylene chloride with stirring at room temperature for six hours, followed by filtering off dicyclohexylurea, evaporating the solvent and recrystallization from benzene-ligroin (3 :7 vol :vol). Found : N, 7.69. $C_{11}H_9NO_2$ requires : N, 7.48%. Yellow crystals, m.p. 123°. ^{1}H-NMR spectrum in $(CD_3)_2CO$ (δ, ppm) : 3.1 (2H, s, CH_2); 6.73 (1H, d, $J = 16$ Hz, $-CH=$); 7.43 (1H, d, $J = 16$ Hz, $-CH=$); 7.3–7.7 (5H, m).

Acylation of benzene with 2-styryl-5-oxazolone. To the benzenic solution of the preceding azlactone (4 g in 100 mL benzene), 8 g $AlCl_3$ were added with external cooling at 0°, then the mixture was stirred for one hour at room temperature and finally hydrolyzed with ice and dilute hydrocloric acid. The separated benzene layer was washed acid-free with sodium hydrogen carbonate, dried, evaporated, and the residue was recrystallized from ethanol, yielding (70% yield) N-(β,β-diphenylpropionyl)-phenacylamine, m.p. 152°.

An independent synthesis of the same compound was carried out by preparing β,β-diphenylpropionic acid from cinnamic acid, benzene and anhydrous aluminium chloride,[6] m.p. 152–3° (from methanol), conversion with $SOCl_2$ into the acid chloride, and reaction with phenacylamine (obtained from phenacyl bromide[12] and hexamethylenetetramine, as hydrochloride[13]) by refluxation in pyridine for 30 minutes, using conditions similar to those described by Hayes et al.[14]

^{1}H-NMR spectrum in $CDCl_3$ (δ,ppm) : 3.10 (2H, d, $J = 8$ Hz, CH_2-CH); 4.67 (2H, d, $J = 5$ Hz, CH_2-NH); 4.70 (1H, t, $J = 8$ Hz, $CH_2-\mathbf{CH}$), 6.60 (1H, NH, broad); 7.33–8.10 (15H, m).

Decoupling experiments and deuteration of the NH group confirmed the assignment.

Mass spectrum : parent and base peak $m/z = 343$; isotopic peaks at 344 (34.5%) and 345 (6.6%); 180 (75%, $Ph_2CH=CH$), 167 (83%, Ph_2CH), 165 (30%, fluorenyl), 152 (14%, biphenylene), 136 (17%), 105 (35%, PhCO) and 77 (15%, Ph).

Acylation of toluene with 2-styryl-5-oxazolone. The mass spectrum and the ^{1}H-NMR spectrum of the product obtained analogously to the preceding compound revealed that it contained mostly the tritolyl-derivative $Tol_2CH-CH_2CO-NH-CH_2-CO-Tol$ with the parent peak at $m/z = 385$ (73%) and with the peak at 371 (37%) due to $M - CH_2$ and/or $Tol-CHPh-CH_2-CO-NH-CH_2-CO-Tol$. The base peak is at $m/z = 208$ ($Tol_2C=CH_2$) with the peak at 195 (57%, Tol_2CH) and 181 (26%, due either to PhCHTol or to Tol_2CH which had lost a CH_2 group); TolCO has m/z 119 (71%), and tropylium 91 (22%).

In the ^{1}H-NMR spectrum there are two methyl peaks as singlets at $\delta = 2.25$ (4.5H) and 2.37 (3H); the latter peak is the TolCO peak, and the former one is due to the Tol_2CH and TolCHPh groups. The remaining peaks are at 2.93 (CH_2, d, $J = 7$ Hz) coupled to 4.50 ($CHAr_2$, t) and at 4.52 (d, CH_2, $J = 5$ Hz) coupled to 6.47 (NH, broad). The *p*-tolyl aromatic AA′BB′ multiplet appears at 7.13 and 7.73 ppm in addition to a phenyl singlet at 7.02 ppm.

2-(2,2-Diphenylethyl)-5-phenyloxazole **7** was prepared on dehydrocyclizing the compound obtained in the acylation of benzene by refluxing it for 3 hrs in excess of phosphorus oxychloride, removing the unreacted reagent under vacuum, and treating the residue with ice-water overnight. The product was filtered off and recrystallized from 80% aqueous ethanol, m.p. 123°, 82% yield. Found: N, 4.10. $C_{23}H_{19}NO$ requires N, 4.30 %.

^{1}H-NMR spectrum in $CDCl_3$ (δ, ppm) : 3.60 (2H, d, $J = 8$ Hz, CH$-$**CH$_2$**) ; 4.71 (1H, t, $J = 8$ Hz, **CH**$-$CH$_2$) ; 7.14 (1H, s, 4-H) and 7.2 $-$ 7.3 (15H, m, aromatic H).

UV spectrum in ethanol : λ_{max} 270 and 280 nm.

2-(2,2-Diphenylvinyl)-5-phenyloxazole **9** was prepared by brominating the aforementioned oxazole (0.5 g, 1.5 mmol) in dry CCl_4 (30 mL) with 0.275 g (1.5 mmol) N-bromosuccinimide and a few milligrams of benzoyl peroxide at reflux temperature for 8 hrs. After filtering off succinimide, the solvent was evaporated under reduced pressure, the residue was dissolved in 20 mL pyridine and refluxed for two hours. After dilution with water, extraction with ether, washing with dilute hydrochloric acid, evaporation of the solvent and recrystallization from ethanol, off-white crystals were obtained in 53% yield, m.p. 135 $-$ 136°. Found: N, 4.08. $C_{23}H_{17}NO$ requires N, 4.33%.

^{1}H-NMR Spectrum in DCl_3 (δ, ppm) : 7.00 (1H, s, 4-H) ; 7.2 $-$ 7.4 (16H, aromatic H).

UV spectrum in ethanol : 260 and 352 nm.

p-Methylcinnamoylglycine was prepared from glycine and *p*-methyl-cinnamoyl chloride with aqueous sodium hydroxide, followed by acidification ; m.p. 162° from ethanol.

2-p-Methylstyryl-5-oxazolone. The preceding compound (2.2 g, 10 mmol) was stirred for 6 hrs in methylene chloride (80 mL) with 2.1 g dicyclohexylcarbodiimide (10 mmol). The orange-coloured solution was filtered, the solvent was removed under reduced pressure, and the azlactone was recrystallized from benzene$-$ligroin (3 :7 vol : vol) m.p. 141°, 97% yield. ^{1}H-NMR /Spectrum in $(CD_3)_2CO$(δ, ppm) : 2.33 (3H, s, *p*-CH$_3$) ; 2.95 (2H, s, CH$_2$) ; 6.60 (1H, d, $J = 16$ Hz, $-$CH$=$) ; 7.17 (2H, d, $J = 8$ Hz, *m*-H) ;7.43 (1H, d, $J = 16$ Hz, $-$CH$=$) ; 7.57 (2H, d, $J = 8$ Hz, *o*-H).

Acylation of benzene and toluene. With the usual procedure, 10 mmol (2 g of the foregoing azlactone) in 50 mL aromatic hydrocarbon was treated gradually with $AlCl_3$ (30 mmol, 4 g) with cooling. After 5 hrs' stirring, the mixture was left overnight, then decomposed with ice and HCl, and extracted with ether. After evaporating the solvent the oily residue was analyzed by ^{1}H-NMR and mass spectroscopy.

REFERENCES

[1] Peceding part, A. T. Balaban, I. Schiketanz, M. D. Gheorghiu and A. Schiketanz, *Rev. Roum. Chim.*, **30**, 977 (1985).

[2] See parts III$-$IX of this series.

[3] I. Schiketanz, A. Schiketanz, M. D. Gheorghiu and A. T. Balaban, *Rev. Roum. Chim.*, **30**, 969 (1985).

[4] H. Staudinger, *Ber. dtsch. chem. Ges.*, **56**, 654 (1923).

[5] Method described by P. Kumar, H. D. Mishra and A. K. Mukerjee, *Synthesis*, 836 (1980).

[6] W. Wilsicenus and K. Ebbe, *Ber. dtsch. chem. Ges.*, **50**, 253 (1917).

[7] J.F.J. Dippy and J. T. Young, *J. Chem. Soc.*, 1817 (1952).

[8] R. Filler and L. M. Hebron, *J. Org. Chem.*, **23**, 1815 (1958) ; R. Filler and Y. S. Rao, *J. Org. Chem.*, **26**, 2055 (1961) ; *J. Heterocyclic Chem.*, **1**, 292 (1965).

[9] R. Filler, *Adv. Heterocyclic Chem.*, **4**, 75 (1965).

[10] E. Ciorănescu, L. Bîrlădeanu, A. T. Balaban and C. D. Nenitzescu, *Tetrahedron Lett.*, **349**, 887 (1962) ; W. I. Awad and M. S. Hafez, *J. Org. Chem.*, **26**, 2055 (1961).

[11] S. Israelashvili and F. Bergman, *J. Chem. Soc.*, 1070 (1953).

[12] R. M. Cowper and L. H. Davidson, *Org. Synth.*, Coll. Vol. 2, p. 480 (1943).

[13] S. Gabriel, *Ber. dtsch. chem. Ges.*, **40**, 2649 (1907) ; C. Mannich, *ibid.*, **44**, 1542 (1911).

[14] F. N. Hayes, B. S. Rogers and D. G. Ott, *J. Am. Chem. Soc.*, **77**, 1850 (1955).

Revue Roumaine de Chimie, **32**, *9–10*, 979–984 (1987)

Dedicated to Professor I. G. MURGULESCU
on his 85th anniversary

NUCLEAR MAGNETIC RESONANCE INVESTIGATIONS OF SMALL RINGS. 4.

^{13}C-NMR SPECTRA OF 2-t-BUTYL-2-CYANOCYCLOBUTANONES AS PROBES FOR CONFIGURATIONAL ASSIGNMENTS[1]

MIRCEA D. GHEORGHIU,* MARINA MIHAI, LUMINIŢA PÂRVULESCU,
ANGHELUSIS VAIOS and FLORIN NICULESCU

Department of Organic Chemistry, Polytechnic Institute – TCH,
Bucharest 16, Romania 76 206

Received May 11, 1987

The configuration of fourteen cyclobutanones obtained from the cycloaddition of t-butylcyanoketene with vinylarenes, fulvenes, cyclopentadiene or bicyclo[2.2.1]heptene derivatives, is either α or β depending if the bulky group of the ketenophile and the t-Bu group are *cis* or *trans*, respectively. Two vinylarenes (p-methoxyphenyl- and 9-vinylanthracene) and dimethyl- and diphenylfulvenes gave *trans*-substituted cyclobutanones; all the remaining examples led to kinetically-controlled *cis*-cyclobutanones. A good diagnosis for configurational assignment is the ^{13}C-NMR chemical shift of cyano group carbon atom; for *trans*- substituted cyclobutanones $\delta_{C(C\equiv N)}$ is very close to 115 ppm, while in the *cis*-substituted cyclobutanones $\delta_{C(C\equiv N)}$ is centered around 119 ppm. The cyclobutanone and t-Bu carbon atoms have less significant chemical shifts for the configurational assignments of the title compounds.

INTRODUCTION

The Woodward-Hoffmann $_2\pi_s + {}_2\pi_a$ reaction mode for concerted cycloaddition of ketenes to carbon-carbon double bonds predicts the formation of the kinetically-favored (contra-thermodynamic) cyclobutanone.[2] Conventionally the isomer regarded as favored thermodynamically, is the isomer having the two bulky groups (originating from the ketene and the ketenophile, respectively) in *trans* configuration. The latter compound is resulting if the cycloaddition of ketene is stepwise.

In our previous contributions, we have presented evidence that t-butylcyanoketene (TBCK) is reacting with norbornene derivatives[3] and vinylarenes[4] giving contra-thermodynamic cyclobutanones. There was, however, an exception, in the case of cyclobutanone isolated from the reaction of p-methoxystyrene and TBCK[4c] whose aryl and t-butyl groups had *trans* configuration.

Since the contrathermodynamic cyclobutanones outnumber the corresponding thermodynamically stable isomers, we believe that TBCK chemistry with respect to nonactivated double bonds, is a good experimental support for the Woodward-Hoffmann $_2\pi_s + _2\pi_a$ reaction mode.

In this contribution we present results regarding the ^{13}C-NMR spectra of fourteen 2-t-butyl-2-cyanocyclobutanes, obtained from the reaction of TBCK with vinylarenes, cyclopentadiene, norbornenes and fulvenes. Additionally, to the thermodynamically favored cyclobutanone obtained from p-methoxystyrene and TBCK, we shall present here evidence that 9-vinylanthracene, dimethyl- and diphenylfulvene react similarly with TBCK. Also we point out that according to our best knowledge there is no literature precedent dedicated to the discussion of ^{13}C-NMR spectra of 2-t-butyl-2-cyanocyclobutanones.

RESULTS AND DISCUSSION

The configuration of α-naphthyl-substituted cyclobutanone **1d** was established by X-ray measurements;[5] the α-naphthyl and t-butyl groups are vicinal and *cis*. Prior to the availability of this result, we have predicted the same configuration for the related cyclobutanones obtained from styrene, indene, acenaphthalene,[4a,b] p-nitrostyrene, p-phenylstyrene and β-vinylnaphthalene,[4c] based on an extensive analysis of their ^{1}H-NMR spectra. Thus, the relatively shielded signal for the t-butyl group protons, due to the aromatic ring proximity, and the relatively deshielded signal of the benzylic proton (bounded to C_3) as result of the anisotropic effects of the vicinal cyano group were instrumental for the proposed configuration.

A similar conclusion, *e.g.*, the formation of contrathermodynamic cyclobutanone, was reached from the analysis of ^{1}H-NMR spectra of compounds obtained from norbornene derivatives and TBCK. The best agreement between calculated and experimental ^{1}H-NMR spectra with $Eu(fod)_3$ for compounds **4** have resulted if the model cyclobutanone had an *exo*-configuration of the four-membered ring and the *t*-Bu the α-configuration (e.g. pointing toward the methylene bridge). The adduct **3a** obtained from cyclopentadiene and TBCK is also displaying in the ^{1}H-NMR spectra similar patterns. In compound **2a**, the configuration of p-methoxyphenyl group is *trans* with respect to the vicinal t-Bu group. This conclusion has resulted from the X-ray measurements[5] carried out for the cyclobutanone resulted from TBCK and p-methoxystyrene. The ^{1}H-NMR spectrum of **2b** has a different pattern compared with the similar spectra of **1a** – **1d**. Thus the signal of t-Bu group protons is relatively deshielded, while the protons belonging to the cyclobutanone ring are spread over a narrower range (0.6 ppm) than in the case of cyclobutanones **1a** – **1d**, and is centered at higher field (3.5 pm). Therefore, there is no deshielding effect of the cyano group. In many respects, the cyclobutanone obtained from TBCK and 9-vinylanthracene is displaying a similar pattern in the ^{1}H-NMR spectrum.

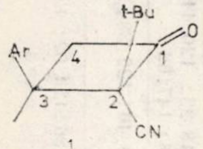

1

a C_5H_5 -
b $C_6H_5-C_5H_4$ -
c p-$NO_2-C_5H_4$-
d α-naphthyl-

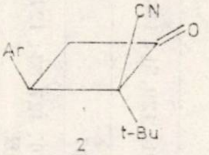

2

a p-$CH_3O-C_6H_4$-
b 9-anthryl-

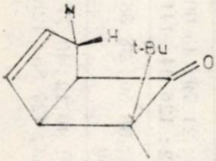

3a

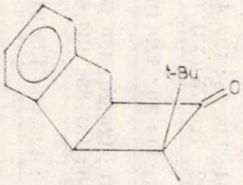

3b

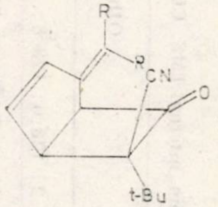

3c R=Me–
3d R=C_6H_5–

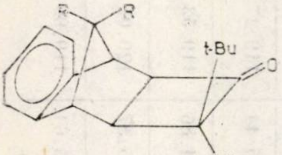

4a R=H
4b R=dimethylmethylidene-

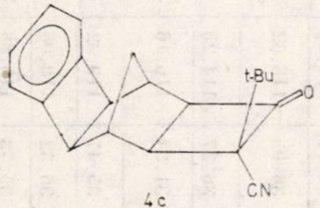

4c

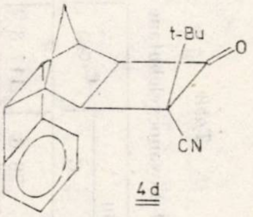

4d

Thus we have at hand the two configurational isomers at C_2 and C_3 in 1-t-butyl-cyanocyclobutanones.

Now let us point out the relevant characteristic of the two groups of compounds according to their ^{13}C-NMR spectrum, and discuss accordingly also the configuration of the adducts between TBCK and cyclopentadiene, dimethyl- and diphenylfulvenes.

In the Table are presented the assignments of the ^{13}C-chemical shifts for the four-membered ring, for the t-butyl and cyano carbon atoms, as well as the non-assigned chemical shifts for the remaining carbon atoms. We consider as relevant for the configuration assignment, the chemical shift of the cyano group carbon atom. For all cyclobutanones, **1a** – **1d**, **3b** and **4**, previously considered as contrathermodynamic reaction products,[3,4] including the product from cyclopentadiene and TBCK,[6] the average $\delta_{C(CN)}$ is 119.04 ppm. For the remaining four thermodynamically stable cyclobutanones, **2a**, **2b**, **3c** and **3d**, the average chemical shift for the cyano group carbon atom $\delta_{C(CN)}$ is 115.47 ppm. We suggest as a good diagnosis for the configurational assignments of 1-butyl-1-cyanocyclobutanones the actual value for the chemical shift of cyano group carbon atoms, according to the above mentioned pattern.

Table

^{13}C-NMR chemical shifts of 2-t-butyl-2-cyanocyclobutane (δ ppm, internal TMS, $CDCl_3$)

Compound	C_1 (C=O)	C_2	C_3	C_4	t-Bu		$C_{(CN)}$	Other signals
					$C_{(CH_3)}$	C		
1a	195.8	69.8	41.5	48.8	26.6	36.6	117.8	127.2 ; 128.0 ; 128.8 ; 133.6
1b	196.53	71.22	41.39	49.11	26.82	36.88	118.95	126.98 ; 127.07 ; 127.71 ; 128.91 ; 129.81 ; 133.03 ; 140.01 ; 140.89
1c	195.09	71.90	41.39	49.31	26.89	38.17	118.06	123.73 ; 130.39 ; 141.98 ; 147.67
1d	196.50	71.39	41.91	49.16	26.88	36.95	118.62	126.64 ; 126.78 ; 127.41 ; 127.76 ; 127.83 ; 127.89 ; 128.22 ; 128.75 ; 131.65 ; 133.02
2a	198.14	76.13	36.27	51.69	25.90	36.27	114.25	55.23 ; 114.10 ; 129.16 ; 129.71 ; 159.32
2b	200.00	75.43	38.01	54.08	26.21	31.34	116.16	124.81 ; 126.20 ; 126.68 ; 127.17 ; 129.68 ; 130.28 ; 130.60 ; 131.88 ; 134.07
3a	200.85	72.98	49.85	60.71	27.05	35.47	119.32	33.11 ; 128.36 ; 135.91
3b	201.74	73.09	49.81	61.13	26.32	36.32	119.08	125.54 ; 127.23 ; 128.21 ; 128.73 ; 137.98 ; 144.46
3c	198.46	73.90	42.85	66.05	25.87	35.73	115.88	21.11 ; 22.36 ; 129.11 ; 131.22 ; 134.21 ; 135.89
3d	198.88	73.557	43.98	68.19	26.02	37.78	115.59	127.44 ; 127.64 ; 128.07 ; 129.14 ; 129.30 ; 130.04 ; 133.96 ; 138.28 ; 140.92 ; 141.31
4a	199.55	75.58	46.0	66.32	27.49	35.44	119.27	45.38 ; 45.54 ; 121.25 ; 121.85 ; 126.81 ; 145.32 ; 147.54
4b	197.90	67.37	47.15	66.14	27.44	34.86	119.53	20.35 ; 21.79 ; 45.00 ; 46.37 ; 118.23 ; 120.44 ; 121.22 ; 126.64 ; 141.64 ; 145.28 ; 147.62
4c	199.85	72.05	44.42	65.88	27.51	35.57	120.05	28.74 ; 38.56 ; 38.88 ; 47.86 ; 50.46 ; 122.33 ; 128.31 ; 144.50
4d	200.95	73.16	42.79	64.38	27.54	35.64	119.99	39.99 ; 40.12 ; 40.77 ; 48.97 ; 50.86 ; 124.02 ; 124.53 ; 127.53 ; 127.85 ; 128.05 146.06

Note at this point that dimethylfulvene and the diphenylfulvene give with TBCK the cyclobutanones with β-oriented t-butylgroup, as a result of a stepwise reaction. Presumably, the remaining conjugated system, after the electrophilic attack of the ketene, is a good positive charge stabilizer.[4c] In the case of 9-vinylanthracene reaction with TBCK, the stepwise reaction is envisaged both on steric and electronic grounds.

As it results from the data collected in the Table, the cyclobutanone ring and the t-butyl carbon atoms are so far less relevant for configurational assignments. Thus the carbonyl group carbon chemical shift is virtually insensitive to the configuration of the four-membered ring, the average value of the chemical shift being $\delta = 198.59$ ppm. Apparently, the two possible configurations at C_2, as in fact our X ray measurements have revealed,[5] induces important geometrical distorsions in the cyclobutanone ring. A crowded configuration (*e.g. cis*) results in folding the four-membered ring up to 22°, while the less strained configuration (e.g. *trans*) leaves the cyclobutanone planar.[5] These geometric modifications, however, are not reflected in the actual magnitude of the chemical shift at C_1.

The ^{13}C chemical shifts of both the methyl group (with one exception) and the quaternary carbon atoms (for all compounds) are not dependent upon configuration. Thus the average chemical shift for the methyl group carbon atom is at $\delta = 36.18$ ppm. The signal of the methyl group carbon atom at $\delta = 31.34$ ppm for the compound **2b**, obtained from 9-vinylanthracene and TBCK is remarkable. At present, only speculative rationalization is at hand based mainly on the assumption that the bulky 9-anthryl group causes severe geometric distorsions. The quaternary carbon atom of the t-butyl group has an average $\delta = 26.75$ ppm.

We believe that so far the chemical shifts of C_2, C_3 and C_4 are reluctant to generalization.

In conclusion we believe that one can define the stereochemistry of cyclobutanones obtained from TBCK and non-activated alkenes, *via* the actual shift of the carbon atom belonging to the cyano group. A δ value close to 119.8 ppm is indicative of an α-configuration for the t-butyl group, while a δ value close to 115.5 ppm indicates the β-configuration for the t-butyl group. Our examples, presented here, are supporting a concerted cycloaddition of TBCK to all non-activated alkanes, with the exception of the systems which can be good positive charge stabilizer, and/or possessing, as result of intrinsic polarization, π-excessive double bonds, as in the case of fulvenes.

EXPERIMENTAL

The ^{13}C spectra were recorded on a Varian FT80-A instrument, in $CDCl_3$, with TMS as internal standard. The spectral width was 5000 H6z, pulse width 18μs, pulse delay 4 s, acquisition time 1.6 s. The signal assignment was established by off-resosnance spectra.

The cyclobutanones were obtained from the corresponding alkenes and TBCK,[7] in benzene at reflux during 4 — 10 hours. Analytically pure samples were obtained by column chromatography on silicagel, using benzene as eluent. The newly obtained cyclobutanones **2b**, **3a**, **3b**, and **3c** have elemental analyses, IR, ^1H-NMR and/or mass spectra consonant with the proposed structure.

ACKNOWLEDGEMENTS. We express our thanks to M. Mironescu, I. V. Gheorghiu, I. Mihutz and P. Rutz (Varian-Zug, Switzerland) for support in implementation of the present project.

REFERENCES

[1] Taken in part from the Ph. D. Thesis of M.M. and BSc. Thesis of A.V. (Polytechnic Bucharest, 1983) and F.N. (Polytechnic Bucharest, 1987). For part 3, see: M. D. Gheorghiu and E. Olteanu, J. *Org. Chem.*, in press.

[2] R. Woodward and R. Hoffmann, "The Conservation of Orbital Symmetry", Academic Press, New York, 1970, p. 163.

[3] L. Ghosez and M. J. O'Donnell in "Pericyclic Reactions", A. P. Marchand and R. E. Lehr. Eds, vol. 2, Academic Press, New York 1977 ; M. D. Gheorghiu, P. Filip, C. Drăghici and L. Pârvulescu, J. *Chem. Soc. Chem. Commun*, **1975**, 635 ; M. D. Gheorghiu, C, Drăghici and L. Pârvulescu, *Tetrahedron*, **33**, 3295 (1977) ; M. D. Gheorghiu, L. Pârvulescu and C. Drăghici, *Rev. Roumaine Chim.*, **24**, 1005 (1979).

[4] (a) M. D. Gheorghiu, F. Kerek and M. Avram, *Rev. Roumaine Chim.*, **20**, 75 (1975) ; (b) M. D. Gheorghiu, L. Pârvulescu, C. Drăghici and M. Elian, *Tetrahedron*, **37**, Suppl. 1, 143 (1981) ; (c) M. D. Gheorghiu, M. Mihai, L. Pârvulescu, S. V. Sereda and Yu. T. Struchkov, to be submitted.

[5] M. D. Gheorghiu, M. Mihai, L. Pârvulescu, S. V. Sereda and Yu. T. Struchkov, manuscript in preparation.

[6] M. D. Gheorghiu, L. Pârvulescu and C. Florea, manuscript in preparation.

[7] W. Weyler, Jr., W. G. Duncan, M. S. Liewen and H. W. Moore, *Org. Synth.*, **55**, 32 (1976) ; M. D. Gheorghiu and M. Avram, *Org. Prep. Proc. Int.*, **6**, 231 (1973) ; M. D. Gheorghiu, L. Pârvulescu, R. Ceclan, I. Manolescu, D. Constantinescu, C. Florea and M. Stănescu, *Rev. Roumaine Chim.*, **33**, 000 (1988).

Revue Roumaine de Chimie, **32**, *9–10*, 985–994 (1987)

Dedicated to Professor I. G. MURGULESCU
on his 85th anniversary

SELECTIVE OXIDATION OF METHANOL TO FORMALDEHYDE ON MODIFIED VANADIA CATALYSTS

G. BLIZNAKOV, D. KLISSURSKI and Y. PESHEVA
Institute of General and Inorganic Chemistry, Bulgarian Academy of Sciences, Sofia 1040

Received April 10, 1987

The selectivity of V_2O_5 catalyst for conversion of methanol to formaldehyde was increased by adding TeO_2 and MoO_3. The binary system $V_2O_5-TeO_2$ gave an unsatisfactory degree of conversion, while the three-component $V_2O_5-MoO_3-TeO_2$ catalyst had a stable activity and oxidized methanol with a specific rate comparable with industrial iron-molybdenum catalyst.

INTRODUCTION

The production of formaldehyde by direct selective oxidation of methanol on oxide catalysts has an increasing application in industry. After the classical works of Adkins and Peterson,[1] the catalyst used in this process is iron molybdate with a high excess of molybdenum trioxide. However, this catalyst loses its activity due to the evolution of part of the molybdenum trioxide, besides the pressure drop of the catalyst layer which quickly increases whereas its thermal stability is relatively low.

Boreskov *et al.*[2] and Bliznakov *et al.*[3] proposed a catalyst based on chromium (III) molybdate which proved to be thermally stable.

Up to now studies on the catalytic activity and selectivity of simple metal oxides towards the reaction under consideration have shown V_2O_5 to have an activity commensurable with that of iron molybdate but an unsatisfactory selectivity.[4-6]

Our investigations aimed at increasing the selectivity of V_2O_5 by introducing promoting additives without changing the specific catalytic activity. The phase diagrams of the systems $V_2O_5-TeO_2$ and $V_2O_5-TeO_2-MoO_3$ were studied. The results obtained were reported in previous papers. The present work contains results from a study of the catalytic properties of some definite compositions.

EXPERIMENTAL

The TeO_2-modified V_2O_5 and $V_2O_5-MoO_3$ catalysts were prepared by melting the oxide mixtures. After quick cooling, the melts obtained were grounded and tabletted. A 0.3–0.6 mm fraction was used for the kinetic measurements.

Preliminary studies showed TeO_2-rich samples to have a low specific activity and a low thermal stability. For this reason, catalysts with a low TeO_2 concentration were preferred.

The specific catalytic activity and selectivity of the samples with respect to methanol oxidation to formaldehyde were investigated by a flow-circulation method in the apparatus described elsewhere. [7-9]

The content of formaldehyde in the reaction mixture was determined by a bisulphite method whereas the gas phase was analyzed chromatographically for CO and CO_2.

The specific surface areas of the samples were determined by the BET method using low-temperature adsorption of krypton.

To determine the $V^{4+}$and V^{5+} contents, the catalysts were analysed by two methods;

— spectrophotometric analysis for V^{4+} based on the blue colouring of the vanadyl ion V^{++}.[10]

— the method of Niwa and Murakami[11].

V-Te-O CATALYSTS

Table 1 contains data on the compositions and specific surface areas of the catalysts.

Table 1

Data on the composition and specific surface areas of the samples

TeO_2 (g)	V_2O_5 (g)	V_{exp} (g)	V^{4+} (g)	V^{5+} (g)	V^{4+}/V_{exp} (%)	S (m²/g)
—	100	55.80	2.30	53.50	4.1	1.90
1	99	56.05	2.25	53.80	4.2	0.61
5	95	53.75	2.00	51.75	3.7	0.44
10	90	50.70	1.92	48.78	3.8	0.34

The V^{4+}/V_{exp} ratio does not change with the composition, *i.e.* the introduction of TeO_2 into the samples causes no change in the ionic state of vanadium in the catalysts volume.

IR studies of mixed $V_2O_5-TeO_2$ catalysts showed in the 400–1100 cm^{-1} range the three absorption bands characteristic of the main component V_2O_5. The shift in the low-frequency region and the broadening of the bands can be ascribed to deformations in the V_2O_5 lattice followed by a change in character of the bonds in the main component under the effect of TeO_2.

The effect of temperature on the specific rate of methanol oxidation over catalysts with different TeO_2 concentrations is illustrated in Fig. 1.

For samples with 5 and 10% TeO_2, the curves show a monotonic increase. No carbon monoxide is observed over the whole temperature range investigated. This can be attributed to the relatively low conversion degree of methanol to formaldehyde. However, if the catalytic activity is estimated on the basis of the specific rate of methanol oxidation and a comparison with the catalytic activity of V_2O_5 is made (Table 2), it can be seen that methanol is oxidized with commensurable rates on V_2O_5 and $V_2O_5-TeO_2$ catalysts.

A difference is observed in the temperature ranges where the maximum conversion degree and the highest selectivity are attained.

However, to make a definite estimation of selectivity, one has to achieve a relatively high conversion degree of methanol. Table 3 presents the results from a study of the temperature dependence of the conversion degrees $Y_{CH_2O}(\%)$ and $Z_{CO}(\%)$ as well as of the selectivity with increasing amount of catalyst.

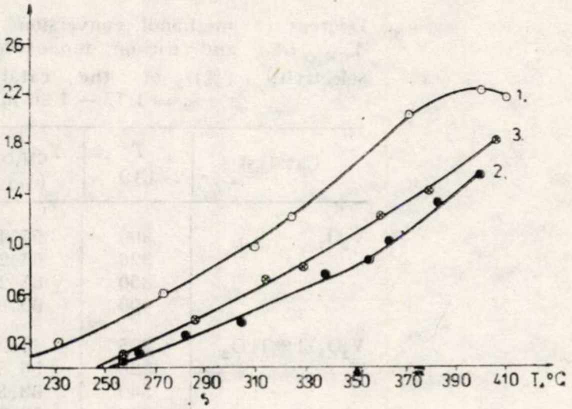

Fig. 1. — Temperature dependence of W_1; (1), $V_2O_5 \cdot 1\,\mathrm{wt}\,\%\,TeO_2$; (2), $V_2O_5 \cdot 5\,\mathrm{wt}\,\%\,TeO_2$; (3), $V_2O_5 \cdot 10\,\mathrm{wt}\,\%\,TeO_2$.

Table 2

Specific rates, W_1 (mkmol/m²s) and selectivity $S(\%)$ of $V_2O_5-TeO_2$ catalysts ($V_0/gS = 3.13$ mL/m²s)

Catalyst	350°C		400°C	
	W_1	S	W_1	S
V_2O_5	1.8751	79	1.6954	71
$V_2O_5 \cdot 1\%TeO_2$	1.6379	100	2.1854	98
$V_2O_5 \cdot 5\%TeO_2$	0.8224	100	1.5226	100
$V_2O_5 \cdot 10\%TeO_2$	1.0865	100	1.7048	100

The degrees of methanol conversion to formaldehyde on the catalysts under consideration are commensurable with those on V_2O_5. The introduction of 1 wt.% TeO_2 essentially increases the catalyst selectivity.

In addition, a high selectivity is observed over a significantly broader temperature range than with V_2O_5. However, the catalysts investigated exhibit a low thermal stability compared to V_2O_5, which determines their lower catalytic activity for the same period of time.

Investigations on the effect of methanol concentration upon the reaction rate have shown a first order rate for all samples. The activation energy of methanol oxidation is determined from the temperature dependence of the rate (Fig. 2). A trend to rising activation energy, E_1, with increasing TeO_2 concentration is observed:

$V_2O_5 \cdot 1\,\mathrm{wt}\%\ TeO_2$	$E_1 = 11$ kcal/mol
$V_2O_5 \cdot 5\,\mathrm{wt}\%\ TeO_2$	$E_1 = 16$ kcal/mol
$V_2O_5 \cdot 10\,\mathrm{wt}\%\ TeO_2$	$E_1 = 17$ kcal/mol

The calculated rate constants K_1 for catalysts with 1 and 10 wt% TeO_2 at 326°C are 2.41 and 2.70 mL/m²s, respectively. They are of the same order of magnitude as the calculated rate constant of V_2O_5.

Table 3

Degrees of methanol conversion to formaldehyde Y_{CH_2O} (%) and carbon monoxide Z_{CO} (%) and selectivity (%) of the catalysts (V_0/gS = = 1.77 — 1.96 mL/m²s)

Catalyst	T (°C)	Y_{CH_2O} (%)	Z_{CO} (%)	S (%)
V_2O_5	300	57.4	7.2	89
	326	66.2	11.0	86
	350	65.2	17.3	79
	400	60.9	24.9	71
$V_2O_5 \cdot 1\,\%TeO_2$	295	43.2	—	100
	320	56.8	1.2	98
	340	63.8	1.9	97
	369	58.2	2.3	96
$V_2O_5 \cdot 10\,\%TeO_2$	295	36.8	—	100
	318	54.2	—	100
	326	58.0	—	100
	342	60.5	—	100
	372	61.2	0.2	99.7

The sharp increase in selectivity of vanadium-tellurium catalysts compared with the selectivity of V_2O_5 is of a definite theoretical and practical interest. A possibility is found to regulate this important catalyst property by varying the $V_2O_5:TeO_2$ ratio. On the basis of previous studies with a view to selecting catalysts[12,13] as well as on the basis of the above results it may be assumed that the introduction of TeO_2

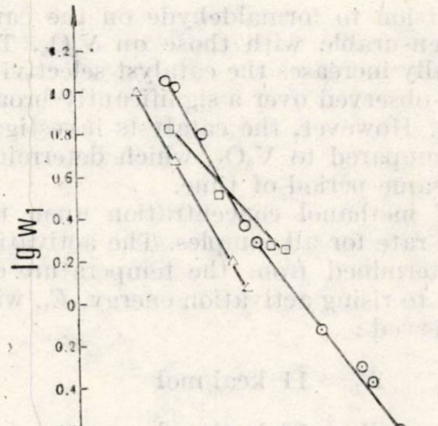

Fig. 2. — Temperature dependence of W_1 for (⊙) V_2O_5; (□) $V_2O_5 \cdot 1wt\,\%TeO_2$; (○) $V_2O_5 \cdot 10wt\,\%TeO_2$ and (Δ) $V_2O_5 \cdot 5$ wt % TeO_2.

leads to the formation of stable surface structures in which the energy of the oxygen bond is higher than in the initial V_2O_5. Besides, it is known that in most cases the effect of various additives is attributed to changes in the catalyst surface structure.

Qualitative information on the change in strength of the oxygen bound under standard experimental conditions can be obtained from the behaviour of the catalysts during the reduction with hydrogen. For that purpose, V_2O_5 and $V_2O_5 \cdot 10$ wt% TeO_2 were investigated at a temperature of 450°C and a hydrogen pressure $P_{H_2} = 80$ mm Hg. The investigations were carried out by the static-circulation method. The reduction degree versus time dependence is presented in Fig. 3. Obviously, the reduction degree attained over V_2O_5 is several times higher than that reached over a TeO_2-containing sample.

The reduction degree was also controlled spectrophotometrically. Part of the reduced samples was preheated in an alkali medium and formed no white precipitate of $V(OH)_3$. The results of spectrophotometric analysis are given in Table 4. The results obtained show that under standard conditions oxygen removal from the mixed catalysts surface is

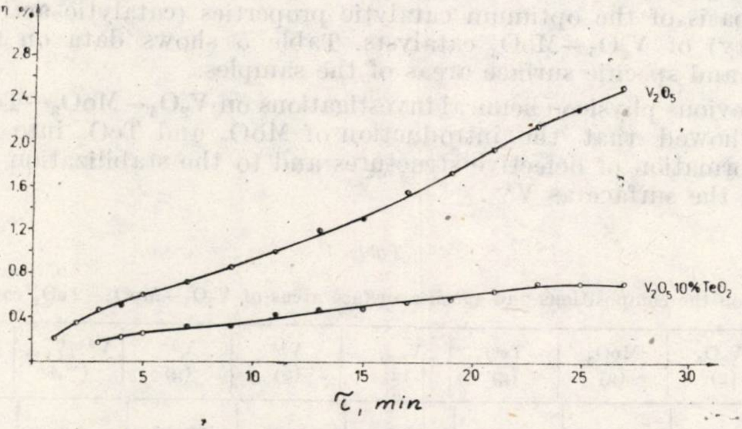

Fig. 3. — Dependence of the reduction degree on time; (1), V_2O_5; (2) $V_2O_5 \cdot 10$ wt%TeO_2.

Tble 4

Spectrophotometric analysis of V^{4+} and V^{5+} in fresh and reduced samples (The calculations are made for 100 g V_2O_5)

Sample	V^{5+} (g)	V^{4+} (g)	Reduction degree (%)
fresh			
V_2O_5	53.00	2.4	
$V_2O_5 \cdot 10$ wt% TeO_2	52.00	2.5	
reduced			
V_2O_5	47.00	5.0	4,9
$V_2O_5 \cdot 10$ wt% TeO_2	48.00	3.6	2.1

twice as much as from a V_2O_5 catalysts surface. This experimentally established fact confirms the assumption about the participation of tellurium in the formation of surface structures in which the oxygen bond is stronger than in V_2O_5. Simultaneously, the higher standard acidity of TeO_2 would favour the adsorption of the methanol molecule on the catalyst surface.

Irrespective of the high selectivity of mixed $V_2O_5-TeO_2$ catalysts, the conversion degree of methanol to formaldehyde in the temperature range, where the catalysts show a high selectivity, is not satisfactory. With rising temperature the conversion degree also increases but the catalysts have an instable activity in this case due to their low thermal stability.

It was attempted to preserve the high selectivity along with a stable activity by modifying the mixed $V_2O_5-MoO_3$ catalysts with TeO_2.

V-Mo-Te-O CATALYSTS

The catalysts under investigation ($V_2O_5-MoO_3-TeO_2$) were chosen on the basis of the optimum catalytic properties (catalytic activity and selectivity) of $V_2O_5-MoO_3$ catalysts. Table 5 shows data on the composition and specific surface areas of the samples.

Previous physico-chemical investigations on $V_2O_5-MoO_3-TeO_2$ catalysts[5] showed that the introduction of MoO_3 and TeO_2 into V_2O_5 led to the formation of defective structures and to the stabilization of vanadium on the surface as V^{4+}.

Table 5

Data on the compositions and specific surface areas of $V_2O_5-MoO_3-TeO_2$ catalysts

No	V_2O_5 (g)	MoO_3 (g)	TeO_2 (g)	V_{exp} (g)	V^{4+} (g)	V^{5+} (g)	V^{4+}/V_{exp} (%)	S (m^2/g)
	100	—	—	55.80	2.30	53.50	4.1	1.9
1	75	25	—	47.51	6.55	40.96	13.8	0.55
2	74.25	24.75	1	44.10	5.50	38.50	12.5	0.57
3	71.25	23.75	5	40.55	6.35	34.20	15.8	0.62
4	67.50	22.50	10	39.05	6.00	33.05	15.0	0.57
5	63.75	21.25	15	37.60	5.50	32.19	14.8	0.66

Formaldehyde is the main product of methanol oxidation over $V_2O_5-MoO_3-TeO_2$ catalysts. Small amounts of carbon monoxide are also formed whereas carbon dioxide and hydrogen are not found. The temperature dependences of the specific oxidation rate of methanol, W_1, and formaldehyde, W_2, are given in Figs. 4 and 5, respectively. All curves of the dependence $W_1 = f(T)$ pass through a maximum within the range 380—410°C, after which the rate of methanol oxidation decreases at the expense of the proceeding of the secondary reaction of formaldehyde oxidation. The oxidation rate of formaldehyde, W_2, for all TeO_2-containing catalysts is much lower (0.006—0.28 mkmol/m^2) than in cases where

TeO_2 is absent, which determines the high selectivity of the catalysts over a very large temperature range. Part of the results are shown in Table 6. Obviously, already with 1 wt% TeO_2 the selectivity of mixed catalysts increases.

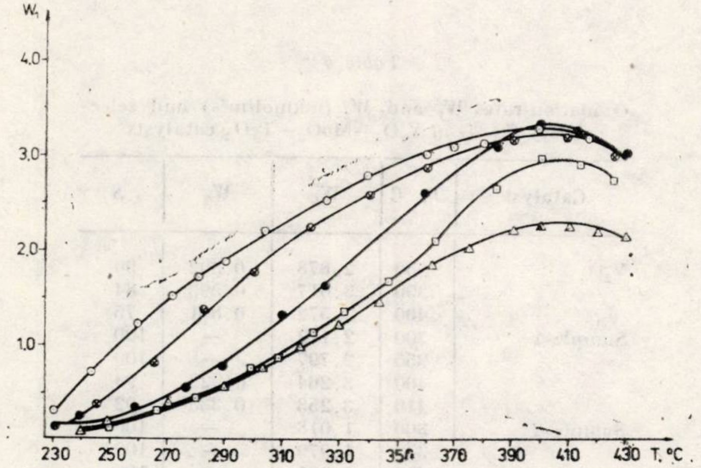

Fig. 4. — Temperature dependence of W_1 for : (○), sample 1 ; (●) sample 2 ; (△), sample 3 ; (□), sample 4 and (⊗), sample 5.

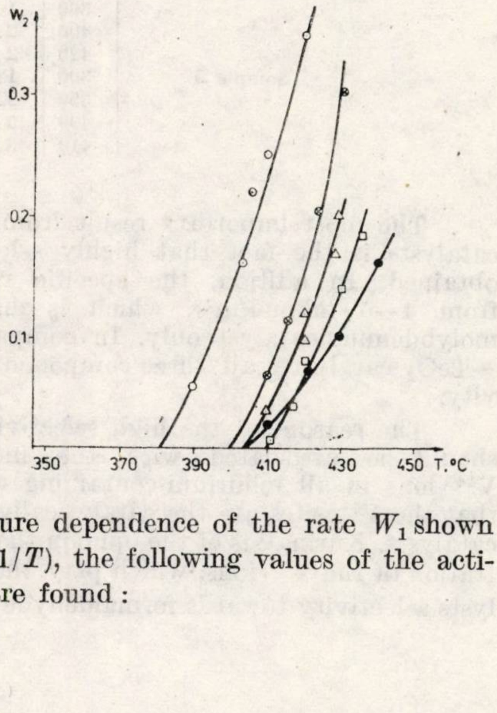

Fig. 5. — Temperature dependence of W_2 (symbols as in Fig. 6).

On the basis of the temperature dependence of the rate W_1 shown in Fig. 6 in coordinates lg $W_1 = f(1/T)$, the following values of the activation energy E_1 of the reaction are found :

Catalyst	E_1, kcal/mol
sample 1	14
sample 2	13
sample 3	15
sample 4	13
sample 5	15
V_2O_5	12
MoO_3	18

Table 6

Oxidation rates W_1 and W_2 (mkmol/m^{2}s) and selectivity S (%) of $V_2O_5-MoO_3-TeO_2$ catalysts

Catalyst	T, °C	W_1	W_2	S
V_2O_5	300	2.878	0.302	90
	350	3.017	0.593	84
	400	2.572	0.801	75
Sample 1	300	2.172	—	100
	350	2.797	—	100
	400	3.264	0.222	94
	410	3.253	0.338	92
Sample 2	300	1.018	—	100
	340	1.979	—	100
	400	3.331	—	100
	420	3.216	0.053	98
Sample 3	310	0.862	—	100
	360	1.822	—	100
	400	2.258	—	100
	420	2.199	0.103	96
Sample 4	320	1.032	—	100
	360	1.926	—	100
	400	2.958	—	100
	420	2.886	0.073	98
Sample 5	300	1.786	—	100
	350	2.769	—	100
	400	3.208	—	100
	410	3.154	0.069	98

The most important result from the study of the three-component catalysts is the fact that highly selective catalysts based on V_2O_5 are obtained. In adition, the specific rates of methanol oxidation range from 4—5 mkmol/m^{2}s, which is characteristic of the industrial iron-molybdenum catalyst only. In comparison with two-component $V_2O_5-TeO_2$ catalysts, all three-component compositions have a stable activity.

The reason for the high selectivity of $V_2O_5-MoO_3-TeO_2$ catalysts should be associated with the increased surface concentration of V^{4+} ions in all tellurium-containing catalysts. It is generally accepted that the V^{4+} sites are the catalytically active centers of V_2O_5-containing catalysts. Kurina[14] is of the opinion that with the increase in total concentration of the V^{4+} ions, which play the role of lattice defects, the catalysts selectivity towards formaldehyde increases. Evidently, the modifying effect of TeO_2 consists in stabilization of the surface concentration of vanadium in the V^{4+} valence state which is probably maintained during the process.

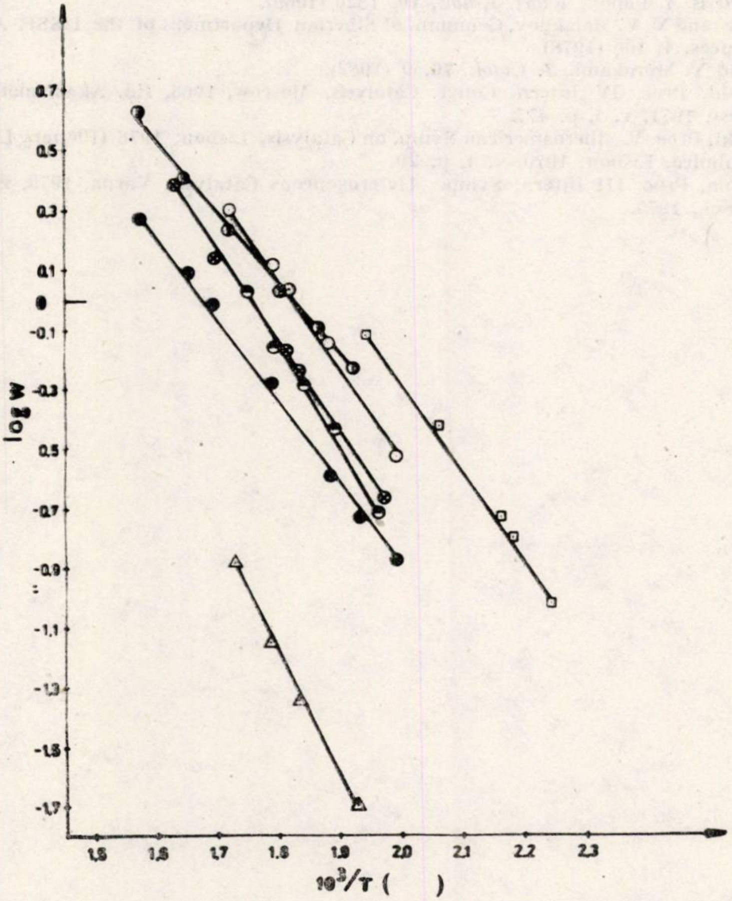

Fig. 6. — Temperature dependence of the rate, W_1, of : (○), sample 1 ; (●), sample 2 ; (⊗), sample 3 ; (◑), sample 4 ; (◓), sample 5 ; (□), V_2O_5 ; (Δ), MoO_3.

REFERENCES

[1] H. Adkins and W. R. Peterson, *J. Amer. Chem. Soc.*, **53**, 1512 (1931).

[2] T. Popov, B. I. Popov, V. N. Bibin, G. K. Boreskov and G. M. Bliznakov, Pat. USSR, N 408504, 1973.

[3] T. S. Popov, V. N. Bibin, G. M. Bliznakov and G. K. Boreskov, *React. Kinet. Catal. Lett.*, **3** (2), 169 (1975).

[4] G. K. Boreskov, B. I. Popov, V. N. Bibin and E. S. Kozishnikova, *Kinet. Katal.*, **9, 796,** (1968).

[5] G. Bliznakov, Y. Pesheva, D. Klissurski, M. Marinov and V. Kozhukharov, *Appl. Catal.*, **29**, 211 (1987).

[6] D. Klissurski and Y. Pesheva, *React. Kinet. Catal. Lett.*, **32**, (1), 77 (1986).

[7] G. Bliznakov, M. Marinov, D. Klissurski, V. Kozhukharov and Y. Pesheva, Commun. of the Depart. Chem. Bulg. Acad. Sci., **15**, 261 (1982).

[8] V. Bibin and B. I. Popov, *Kinet. Katal.*, **9**, 618 (1968).

[9] V. Bibin and B. I. Popov, *Kinet. Katal.*, **10**, 1326 (1969).

[10] T. Bocharov and V. V. Malakhov, Commun. of Siberian Department of the USSR Academy of Sciences, **4**, 106 (1978).

[11] M. Niwa and Y. Murakami, *J. Catal.*, **76**, 9 (1982).

[12] D. Klissurski, Proc. IV Intern. Congr. Catalysis, Moscow, 1968, Ed. Akademiai Kiado, Budapest, 1971, v. I, p. 477.

[13] D. Klissurski, Proc. V. Iberoamerican Symp. on Catalysis, Lisbon, 1976 (Plenary Lectures), Ed. Quimica, Lisbon, 1979, v. I, p. 29.

[14] L. N. Kurina, Proc. III Intern. Symp. Heterogeneous Catalysis, Varna, 1975, Ed. Bulg. Acad. Sci., 1975.

Revue Roumaine de Chimie, **32**, *910*, 995–1000 (1987)

Dedicated to Professor I. G. MURGULESCU
on his 85th anniversary

RELATIONS BETWEEN CHEMICAL STRUCTURE AND ANALGESIC ACTION OF SOME DIAMINES AND AMINOETHERS

DUMITRU DOBRESCU, MIRCEA IOVU, CORNEL GEORGESCU, VASILE STOICESCU
and AURELIA CRISTEA
Faculty of Pharmacy, Str. Traian Vuia 6, Bucharest, Romania

Received November 15, 1986

The analgesic activity of numerous α,α′-diaminoxylenes, terephthaldiamides and monoaminomethylenealkylethers was investigated. Using the calculation model of Free-Wilson, the contribution of the different parts of the molecules to the analgesic activity was established. The results permitted the estimation of the analgesic action values for some yet unknown substances belonging to the same chemical classes.

INTRODUCTION

Starting with the finding that *tremorine* (1,4-dipyrrolidino-2-butyne), *oxotremorine* [1-(2′-oxo-1′-pyrrolidino)-4-(1′-pyrrolidino)-2-butyne] and *dioxotremorine* [1,4-di-(2′-oxo-pyrrolidino)-2-butyne] possess analgesic action,[1,2] we have synthesized analogous compounds in which the acetylenic triple bond with 4π electrons was replaced by benzenic nuclei with 6π electrons.[3]

It has been expected on the one hand that the benzenic nuclei can exert a similar action with the triple bond towards the amino groups and, on the other hand, that the action of the benzenic nuclei may influence the analgesic properties through the reciprocal position of the substituted aminomethylene groups as well as through the existence of some methyl groups on the benzenic nucleus. We synthesized new analgesic compounds with the general formula **1**, where $n = 0 - 4$, and the nitrogen belongs to acyclic tertiary amines[3].

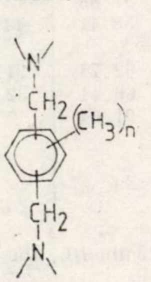

1

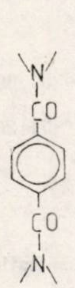

2

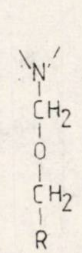

3

Taking into account that the α,α'-diaminoxylenes could be oxidized metabolically into terephthaldiamides, we have also synthesized the terephthaldiamides with the general formula **2** corresponding to the α, α'-diamino-*p*-xylene.

Taking into account the interaction between the unshared electrons of the nitrogen atom and the π electrons of the benzenic nucleus as responsible for the analgesic action, we have also synthesized compounds in which the aromatic radical was replaced by an oxygen atom which could exert a similar action. As diaminomethylenethers are not stable splitting off formaldehyde and yielding diaminomethane derivatives, we have synthesized monoaminomethylenethers[4] with the general formula **3**, where R is a phenyl, furfuryl or cycloalkyl.

All synthesized compounds exhibit a superior or comparable analgesic action with that of noraminophenazone.

As the analgesic action depends on the molecular structure of the new compounds, we tried to establish some correlations between the analgesic action and the molecular structure (taking into account data for a great number of compounds).

PHARMACODYNAMICAL TESTS

The pharmacodynamical tests have been effected on mice, using the test of the contortions induced by chemical stimulus (acetic acid), the most frequently utilized for non-narcotics.[5] The results have been referred to noraminophenazone. In table 1 there the analgesic actions (in %) for 25 moles per liter are noted.

Table 1

The percentage values of the analgesic action for 25 μM solutions *
(experimental data)

μ a	$\mu_{1,1}$	$\mu_{1,2}$	$\mu_{1,3}$	$\mu_{1,4}$	μ_2	$\mu_3 + a_{30}$	$\mu_4 + a_{23}$	$\mu_4 + a_{24}$	$\mu_4 + a_{25}$
a_2					51.66	50.04	61.23	40.38	61.27
a_7					44.15		60.27	44.34	54.45
a_8	52.48	34.61	85.02						
a_{11}	29.30	10.45	38.00	51.03	52.36	16.63			
a_{12}	48.67	36.31	47.81		68.31	55.21	62.16	31.64	
a_{13}	5.05	12.59	30.80	38.23	39.98	14.51			
a_{14}	51.98				51.55				
a_{15}	20.54				58.41	44.74			
a_{16}	44.9	54.74	85.72						
a_{19}	6.43	8.24	19.91	50.60	62.74	31.19	67.97		51.68
a_{21}					66.41	32.98			
a_{22}	52.96	51.47	68.27	71.30	91.64				
a_{23}									
a_{24}									
a_{25}									
a_{30}									

*) For noraminophenazine at concentration 25 μmol/L, the analgesic action is 17.8 %

CALCULATION METHOD

We used the Free-Wilson[6-9] method which relies on the hypothesis that the biological activity is an additive property of the substituents of a molecule. The analgesic activity, S, of the n-th new compounds ($n = 1$ to 54) was considered as the sum of contributions of the two parts of the molecule: the "central" one with the actions μ_j and the "peripheral" ones with the actions a_i, so that the basic equation becomes:

$$\mu_j + \sum_i a_i = S_n \qquad n = 1, 2 \ldots N$$

N corresponds to the 54 substances tested pharmacodynamically; S_n represents the activity.

According to the model, the activity of the central part of the molecule results as the average activity of the series of compounds which contain this central part (the sum corresponding to the substructures on each position is annulled); therefore it has been possible to calculate the values for the central part action.

Therefore, the following equations follow:

$$\overline{\mu}_j \frac{1}{M} \sum_{k=1}^{M} S_k \qquad k = 1.$$

$$\sum_i a_i = S_n - \mu_j = S'_n$$

Introducing the predictor variables X_{ij} with known values (0 or 1) which indicate the frequency of the substructure i within the structure j, the equations could be rewritten:

$$\sum_j \sum_i X_{ij} a_i = S'_j \qquad \begin{matrix} j = 1, 2 \ldots N = 54 \\ i = 1, 2 \ldots L = 19 \end{matrix}$$

The activities a_i are computed using the least squares method.

The total correlation coefficient of the 54 equations with 19 unknowns was $R = 0.776$.

RESULTS AND DISCUSSION

Table 2 gives the a_i values for different substructures radicals o tertiary amino(cycloalkyl or phenyl) and in table 3 the μ_j values for the central parts of α,α'-xylene, terephthalyl and ether are noted.

Table 4 presents the values of the action resulting from the calculation for the synthesized compounds as well as for the compounds of the same series yet unsynthesized.

Following the data of the tables it was found that from the central parts of the molecules of α,α'-diaminoxylenes, those compounds which have the benzenic nucleus substitute by four methyl groups ($\mu_{1,4}$) have a greater contribution to the analgesic action than those with unsubstituted benzenic nuclei ($\mu_{1,1}$) or those substituted by only two methyl radicals ($\mu_{1,2}$ and $\mu_{1,3}$).

Comparing the action of the unsubstituted α, α'-diamino-p-xylenes ($\mu_{1,1}$) with the action of the corresponding terephthaldiamides (μ_2) which can be considered as oxidation products of the α,α'-diminoxylenes, it was found that the terephthaldimides are much more active.

Table 2

The contributions (*a*) of the peripherical parts

Compound	Group	Contribution a
2	C_2H_5-	$a_2 = -2.03$
7	$i-C_3H_7-$	$a_2 = -6.48$
8	$sec-C_4H_9$	$a_2 = +14.16$
11	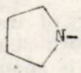	$a_{11} = 5.76$
12	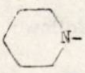	$a_{12} = +2.21$
13	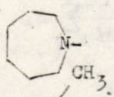	$a_{13} = -12.13$
14	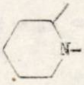	$a_{14} = +1.04$
15	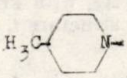	$a_{15} = -3.87$
16	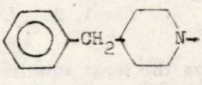	$a_{16} = +15.11$
19	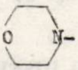	$a_{19} = -7.22$
21	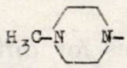	$a_{21} = +1.51$
22	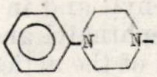	$a_{22} = +11.51$
23	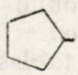	$a_{23} = +5.23$
24	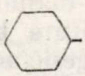	$a_{24} = -0.41$
25	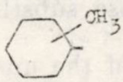	$a_{25} = +8.18$
30	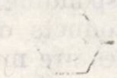	$a_{30} = +4.18$

From the aminoethers, those which have two methylene groups (μ_3 and a_{30}) attached to the oxygen atom are less active than those which have one methylene – and one cycloalkyl group ($\mu_4 + a_{23}$, $\mu_4 + a_{24}$, $\mu_4 + a_{25}$).

Table 3

The contributions (μ) of the central parts

Compound	Group	Contribution
1,1	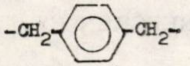	$\mu_{1,1} = 39.65$
1,2	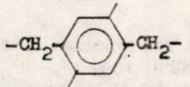	$\mu_{1,2} = 38.80$
1,3	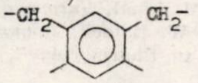	$\mu_{1,3} = 41.21$
1,4	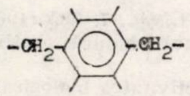	$\mu_{1,4} = 51.19$
2	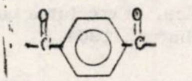	$\mu_2 = 59.72$
3	$-CH_2-O-CH_2-$	$\mu_3 = 34.60$
4	$-CH_2-O-$	$\mu_4 = 53.44$

Table 4

The percent values of the calculated analgesic activity

a \ μ		$\mu_{1,1}$ 39.65	$\mu_{1,2}$ 38.80	$\mu_{1,3}$ 41.21	$\mu_{1,4}$ 51.19	μ_2 59.72	μ_3+a_{30} 38.78	μ_4+a_{23} 58.67	$\mu_4 + a_{24}$ 53.03	$\mu_4 + a_{25}$ 61.62
a_2	−2.03	35.59	34.74	37.15	47.13	55.56	36.75	56.64	51.00	59.59
a_7	−6.48	26.69	25.84	28.25	38.23	46.76	32.3	52.19	46.55	55.14
a_8	14.16	67.98	67.12	69.53	79.51	88.04	52.94	72.83	67.19	75.78
a_{11}	−5.76	28.13	27.28	29.69	39.67	48.20	33.02	52.91	47.27	55.86
a_{12}	2.21	44.07	43.22	45.63	55.61	64.14	40.99	60.88	55.24	63.83
a_{13}	−12.13	15.39	14.53	16.95	26.93	35.46	26.65	46.54	40.90	49.49
a_{14}	1.04	41.73	40.88	43.29	53.27	61.80	39.82	59.71	54.07	62.66
a_{15}	−3.87	31.91	31.06	33.47	43.45	51.98	34.91	54.80	49.16	57.75
a_{16}	15.11	69.87	69.02	71.43	81.41	89.94	53.89	73.78	68.14	76.73
a_{19}	−7.22	25.21	24.36	26.77	36.75	45.28	31.45	51.45	45.81	54.40
a_{21}	1.51	42.67	41.82	44.23	54.21	62.74	40.29	60.18	54.54	63.13
a_{22}	11.51	62.67	61.82	64.23	74.21	82.74	50.29	50.29	60.18	73.13
a_{23}	5.23	50.11	49.26	51.67	61.65	70.18	44.01	63.90	58.26	66.85
a_{24}	−0.41	38.83	37.98	40.30	50.37	58.90	38.37	58.26	52.62	61.21
a_{25}	8.18	56.01	55.16	57.57	67.55	76.08	46.96	66.85	61.21	69.80
a_{30}	4.18	48.01	47.16	49.57	59.55	68.08	42.96	62.85	57.21	65.8
		$\mu + 2a$					$\mu + a_n + a_m$			

From the peripheral amino groups ($a_1 - a_{30}$) the most important contributions were : di-*sec*-butylamino (a_3), benzylpiperidine (a_{16}) and N-phenylpiperazine (a_{22}).

From the most active compounds, some were synthesized before the mathematical prospection : $\mu_{1.3} + a_{16}$; $\mu_2 + a_{22}$, $\mu_4 + a_{23} + a_8$; $\mu_4 + a_{25} + a_8$; $\mu_{1.4} + a_{16}$; $\mu_2 + a_{16}$; $\mu_4 + a_{23} + a_{16}$; $\mu_4 + a_{25} + a_{16}$; $\mu_{1.4} + a_{22}$; $\mu_4 + a_{23} + a_{22}$; $\mu_4 + a_{25} + a_{22}$.

All calculations were performed with a computer program on a PRAE-M microcalculator.

REFERENCES

[1] G. Chen, J. *Pharmacol.*, **224**, 73 (1958).

[2] G. M. Keranen, V. L. Zorotzian and R. Colman, *Toxicol. and Appl. Pharmacol.*, **3**, 481 (1961) ; cf. Chem. Abstr. **55**, 23.829i, 1961.

[3] D. Dobrescu, M. Iovu, A. Cristea and M. Iqbal, *Farmacia*, **31**, 65 (1983).

[4] D. Dobrescu, M. Iovu, E. Cristea and W. Balock, *Romanian Patent*, 66758 (1977).

[5] R. A. Turner", "Screening Methods in Pharmacolgy", Academic Press, New York, 1965, vol. I, p. 14.

[6] S. M. Free and J. W. Wilson, *J. Med. Chem.*, **7**, 395 (1964).

[7] I. Simiti and I. Schwartz, "Structură chimică. Activitate biologică,", Editura Dacia, Cluj-Napoca, 1980.

[8] I. Moțoc, "Structura moleculelor și activitatea biologică", Editura Facla, Timișoara, 1980.

[9] M. Simionovici, A. Cristea and C. Vlădescu, "Cercetarea farmacologică și prospectarea medicamentelor", Editura Medicală, Bucharest, 1964.

Revue Roumaine de Chimie, 32, *9–10*, 1001–1009 (1987)

Dedicated to Professor I. G. MURGULESCU
on his 85th anniversary

QUANTITATIVE STRUCTURE-ACTIVITY RELATIONS FOR THE INHIBITION OF GUANINE PHOSPHORIBOSYLTRANSFERASE FROM *ESCHERICHIA COLI*

NICULAE OLARU and ZENO SIMON*
Institute of Macromolecular Chemistry "P. Poni" Aleea Gr. Ghica-Vodă 41 A Iași-6600, Romania
* Institute of Medicine, Timișoara–1900, Romania

Received May 4, 1987

Elecronic parameters calculated by HMO and Del Re methods and steric parameters calculated by MTD method are correlated with biological activities for a series of 39 purinic derivatives tested as inhibitors of guanine phosphoribosyltransferase (GPRT) from *Escherichia Coli*. The best correlational equations thus obtained were tested on a series of 23 purinic derivatives for which inhibition constants are quoted as lower than 3 by Miller et al. The correlational equations show that interactions between inhibitors and the active site of GPRT are controlled by both electronic and steric factors.

Inhibition constants for the inhibition of guanine phosphoribosyltransferase (GPRT) from *Escherichia Coli* by a large series of nitrogen heterocycle derivatives were determined by Miller et al.[1] This series containing 62 purine derivatives and 38 derivatives of other nitrogen heterocycles, is well suited for a QSAR study, allowing to select a series upon which correlational equations are established and also a test series. Only the purine derivatives are discussed here as other inhibition mechanisms may occur for derivatives of different heterocycles.

Biological activity is generally determined by electronic, steric and hydrophobicity effects. The number of structural parameters required to characterize these effects will be rather large : each atomic centre should be characterized by indices for all the three types of effects. In order to obtain a meaningful correlational equation, one has to select a limited set of those structural parameters. The predictive power of the "best" correlational equation can be evaluated only by using a test series, which will be done in this paper.

Here we use the superposition procedure and the hypermolecule of the MTD-method,[3] but the vertices of the hypermolecule will be characterized not only by their occupation or nonoccupation in the respective molecule, but also by electronic indices characterizing the atom which occupies the corresponding vertex.

METHOD

The experimental activities, A_i, of the 62 purine derivatives are listed in Table 1. They are calculated as $A_i = -\log K_i$, where K_i represents the inhibition constants determined by Miller et al.[1]

The generalized perturbational theory of Klopman[4] in the variant used by Cammarata[2] to describe receptor-effector interactions is used here as a general framework for electronic effects. The electronic indices used by Cammarata, net atomic charges q, electrophilic and nucleophilic superdelocalizabilities S^E and S^N, respectively, of different atomic centres are also used here. These electronic indices for the 62 purine derivatives were calculated in a previous paper[5] by the simple Hückel + Del Re methods. One may argue that more advanced molecular orbital methods should have been used, but a comparison of electronic indices calculated by these simple methods and more advanced methods indicates a satisfactory correlation of relative atomic chages.[6] Details of the HMO + Del Re calculations and of some results can be found in the above mentioned papers. [5,6] Only the indices actually used in our correlations are given here (Table 2).

The comparison of different atomic centres is based upon the vertex j, occupied in the hypermolecule constructed by the atom per atom (hydrogen atoms are neglected) superposition of the 39 molecules, according to the procedure described in other previous papers. [3,7,8] The hypermolecule is depicted in Figure 1 together with numbering of vertices. The numbering of vertices is as close as possible to the usual numbering of atoms in the purine ring. For example, vertices $j = 1-9$ correspond to the numbering of the purine ring atoms, vertex 10 to the guanine 0 (oxo)-atom, vertex 11 to the guanine NH_2 (amino)-group. The substituents of the ring positions, 1, 3, 7, 8, having only one atom different from hydrogen (i.e. CH_3, NH_2, etc.), occupy vertices 15, 16, 14, 12, respectively.

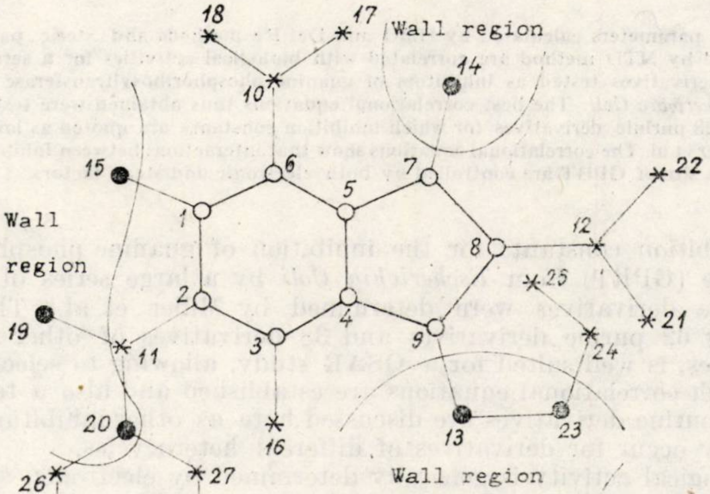

Fig. 1. — Hypermolecule and vertex-attributions. Figures indicate numbering of the vertices j. Cavity vertices ($\varepsilon_j = -1$) are marked by open circles (○), wall vertices ($\varepsilon_j = +1$) by black circles (●), irrelevant, exterior vertices ($\varepsilon_j = 0$) by asterisks (✳); wall regions, presenting steric repulsion are specially marked.

Of the 62 purine derivatives, a number of 23 quoted as inactive ($K_i > 10^{-3}$M) are considered as test series. The other 39 for which inhibition constants are listed (i.e. $K_i < 10^{-3}$M) constitute the series for optimization, for which correlational equations are established. The best

Table 1

Experimental, A_i, and calculated with Eq. (10), (11), (12), activities and MTD parameter for the 62 purine derivatives

i	Inhibitor name	6 Substituent	2 Substituent	Other	A_i	$\hat{A}_i^{10}$	$\hat{A}_i^{11}$	$\hat{A}_i^{12}$	MTD_i
0	1	2	3	4	5	6	7	8	9
1	2-Hydroxypurine	H	OH	—	3.469	3.550	3.386	3.449	0
2	2-Mercaptopurine	H	SH	—	3.081	2.836	2.873	2.871	0
3	Adenine	NH_2	H	—	3.000	2.787	3.179	2.901	0
4	Hypoxanthine	OH	H	—	3.745	3.893	3.891	3.912	0
5	Guanine	OH	NH_2	—	5.569	5.446	5.030	5.219	0
6	Xanthine	OH	OH	—	4.319	4.067	4.076	4.095	0
7	2-Mercapto-6-hydroxypurine	OH	SH	—	3.538	3.777	3.855	3.854	0
8	6-Mercaptopurine	SH	H	—	4.420	4.320	4.193	4.289	0
9	2-Amino-6-mercaptopurine	SH	NH_2	—	6.041	5.877	5.334	5.600	0
10	2-Hydroxy-6-mercaptopurine	SH	OH	—	4.337	4.646	4.479	4.585	0
11	2,6-Dimercaptopurine	SH	SH	—	3.638	4.064	4.048	4.105	0
12	2-Methyl-6-mercaptopurine	SH	CH_3	—	4.959	4.633	4.430	4.555	0
13	2-Amino-6-chloropurine	Cl	NH_2	—	3.155	3.223	3.311	3.221	0
14	8-Methylguanine	OH	NH_2	8-CH_3	5.000	5.066	4.677	4.825	0
15	8-Aminoguanine	OH	NH_2	8-NH_2	5.337	5.402	5.154	5.408	0
16	8-Hydroxyguanine	OH	NH_2	8-OH	4.509	4.719	4.651	4.566	0
17	8-Mercaptoguanine	OH	NH_2	8-SH	5.131	4.946	5.095	5.011	0
18	8-Bromoguanine	OH	NH_2	8-Br	3.523	3.540	3.848	3.769	0
19	8-Methylxanthine	OH	OH	8-CH_3	4.004	3.984	3.937	3.944	0
20	7-Methylxanthine	OH	OH	7-CH_3	3.387	6.099	3.006	3.466	1
21	6-Mercapto-7-methylpurine	SH	H	7-CH_3	3.108	6.143	3.032	3.025	1
22	2-Amino-6-mercapto-7-methylpurine	SH	NH_2	7-CH_3	3.886	8.023	4.242	4.447	1
23	1-Methylguanine	O	NH_2	1-CH_2	3.284	5.563	4.037	4.200	1
24	3-Methylguanine	O	NH_2	3-CH_3	4.523	4.256	4.359	4.260	0
25	9-Methylguanine	OH	NH_2	9-CH_3	3.328	4.048	3.459	3.541	1
26	8-Methylthioguanine	OH	NH_2	8-SCH_3	4.444	4.265	4.370	4.438	0
27	2-Methylamino-6-hydroxypurine	OH	$NHCH_3$	—	4.208	5.367	3.934	4.180	1
28	2-Anilino-6-hydroxypurine	OH	NHC_6H_5	—	3.699	5.289	3.877	4.115	1
29	2-Dimethylamino-6-hydroxypurine	OH	$N(CH_3)_2$	—	3.420	5.312	2.855	3.161	2
30	1-Methylxanthine	O	OH	1—CH_3	3.357	4.489	3.302	3.466	1
31	1,3-Dimethylxanthine	O	O	1,3-DiCH_3	3.137	4.398	3.228	3.832	1
32	2-Methylthio-6-hydroxypurine	OH	SCH_3	—	3.357	5.378	3.928	4.182	1

Table 1 (continued)

0	1	2	3	4	5	6	7	8	9
33	6-Mercapto-9-methylpurine	SH	H	9-CH_3	3.076	2.920	2.624	2.614	1
34	1-Methyl-2-amino-6-thiopurine	S	NH_2	1-CH_3	3.108	6.004	4.438	4.728	1
35	2-Amino-6-mercapto-9-methylpurine	SH	NH_2	9-CH_3	3.337	4.479	3.764	3.921	1
36	2-Amino-6-mercapto-9-n-butylpurine	SH	NH_2	9-n-C_4H_9	3.222	4.541	2.769	3.004	2
37	2-Acetylamino-6-mercaptopurine	SH	$NHCOCH_3$	—	4.678	5.753	4.204	4.522	1
38	2-Amino-6-methylthiopurine	SCH_3	NH_2	—	3.319	3.541	3.617	3.538	0
39	2-Hydroxy-6-methylthiopurine	SCH_3	OH	—	3.237	3.154	3.484	3.314	0
40	Purine	H	H	—	<3	1.019	1.600	1.240	0
41	2-Aminopurine	H	NH_2	—	<3	2.283	2.536	2.343	0
42	2,6-Diaminopurine	NH_2	NH_2	—	<3	3.246	3.369	3.213	0
43	1-Methylhypoxanthine	O	H	1-CH_3	<3	4.017	2.904	3.039	1
44	3-Methylhypoxanthine	O	H	3-CH_3	<3	3.373	3.683	3.523	0
45	7-Methylhypoxanthine	OH	H	7-CH_3	<3	5.732	2.742	2.661	1
46	9-Methylhypoxanthine	OH	H	9-CH_3	<3	2.478	2.314	2.224	1
47	7-Methylguanine	OH	NH_2	7-CH_3	<3	7.075	3.711	3.776	1
48	8-Phenylguanine	OH	NH_2	8-C_6H_5	<3	5.472	3.186	2.572	3
49	3-Methylxanthine	OH	O	3-CH_3	<3	4.274	4.216	3.353	0
50	9-Methylxanthine	OH	OH	9-CH_3	<3	2.959	2.714	2.653	1
51	Uric acid	OH	OH	8-OGH	<3	3.440	3.684	3.432	0
52	8-Chloroxanthine	OH	OH	8-Cl	<3	2.837	3.387	3.256	0
53	2-Amino-6-methoxypurine	OCH_3	NH_2	—	<3	3.360	3.471	3.370	0
54	1-Methyl-6-thiopurine	S	H	1-CH_3	<3	4.442	2.958	3.383	1
55	2-Amino-6-mercapto-9-ethylpurine	SH	NH_2	9-C_6H_5	<3	4.557	2.762	2.994	2
56	2-Amino-6-mercapto-9-n-propylpurine	SH	NH_2	9-n-C_3H_7	<3	4.560	2.769	3.003	2
57	2-Chloro-6-mercaptopurine	SH	Cl	—	<3	3.094	3.133	3.051	0
58	2-Amino-6-methylpurine	CH_3	NH_2	—	<3	2.269	2.537	2.331	0
59	2-Amino-6-cyanopurine	CN	NH_2	—	<3	1.703	1.944	1.747	0
60	6-Carbethoxypurine	$COOC_2H_5$	H	—	<3	0.339	0.291	0.605	0
61	6-Carboxypurine	COOH	H	—	<3	0.211	0.810	0.476	0
62	6-Thiocarboxamidopurine	$CSNH_2$	H	—	<3	0.724	1.284	0.977	0

Table 2

Electronic indices for GPRT inhibitors

i	q_{i1}	q_{i2}	S^E_{i7}	q_{i7}	q_{i8}	q_{i9}	S^E_{i10}	q_{i10}
0	1	2	3	4	5	6	7	8
1	−0.229	0.452	1.224	−0.563	0.315	−0.208		
2	−0.197	0.358	1.223	−0.562	0.318	−0.205		
3	−0.518	0.313	1.108	−0.558	0.317	−0.192	1.132	−0.439
4	−0.245	0.392	1.049	−0.539	0.259	−0.178	0.978	−0.369
5	−0.253	0.548	1.075	−0.539	0.129	−0.183	1.021	−0.371
6	−0.322	0.463	1.049	−0.541	0.229	−0.173	0.822	−0.349
7	−0.293	0.376	1.049	−0.541	0.230	−0.173	0.823	−0.348
8	−0.214	0.397	1.053	−0.541	0.266	−0.178	1.670	−0.352
9	−0.223	0.551	1.079	−0.542	0.246	−0.183	1.757	−0.355
10	−0.296	0.464	1.054	−0.543	0.234	−0.173	1.352	−0.317
11	−0.266	0.377	1.054	−0.543	0.235	−0.173	1.353	−0.317
12	−0.221	0.446	1.053	−0.541	0.266	−0.176	1.670	−0.352
13	−0.502	0.467	1.119	−0.555	0.310	−0.194	0.971	−0.100
14	−0.253	0.548	1.075	−0.547	0.289	−0.190	1.021	−0.371
15	−0.255	0.532	1.479	−0.610	0.426	−0.197	1.117	−0.374
16	−0.252	0.539	1.633	−0.315	0.456	−0.291	1.315	−0.392
17	−0.252	0.540	1.653	−0.280	0.367	−0.258	1.316	−0.391
18	−0.253	0.545	1.131	−0.506	0.344	−0.147	1.035	−0.371
10	−0.322	0.463	1.049	−0.549	0.279	−0.180	0.822	−0.349
20	−0.323	0.463	0.978	−0.083	0.282	−0.555	0.852	−0.349
21	−0.218	0.390	0.991	−0.083	0.297	−0.552	1.712	−0.352
22	−0.227	0.542	1.019	−0.087	0.297	−0.558	1.795	−0.357
23	−0.157	0.531	1.075	−0.539	0.239	−0.183	1.021	−0.373
24	−0.684	0.553	1.047	−0.543	0.241	−0.175	1.047	−0.386
25	−0.253	0.548	1.075	−0.541	0.223	−0.087	1.021	−0.371
26	−0.254	0.536	1.338	−0.565	0.408	−0.170	1.085	−0.373
27	−0.255	0.538	1.075	−0.539	0.239	−0.183	1.021	−0.371
28	−0.255	0.529	1.075	−0.539	0.240	−0.183	1.021	−0.371
29	−0.256	0.531	1.075	−0.539	0.239	−0.123	1.021	−0.371
30	−0.226	0.447	1.049	−0.541	0.229	−0.173	0.822	−0.351
31	−0.228	0.431	1.490	−0.541	0.229	−0.175	0.822	−0.351
32	−0.228	0.547	1.067	−0.539	0.244	−0.181	1.008	−0.370
33	−0.211	0.397	1.053	−0.544	0.250	−0.081	1.670	−0.352
34	−0.126	0.535	1.079	−0.542	0.247	−0.183	1.757	−0.357
35	−0.223	0.551	1.078	−0.544	0.231	−0.087	1.757	−0.355
36	−0.223	0.551	1.078	−0.544	0.230	−0.092	1.757	−0.355
37	−0.224	0.537	1.077	−0.542	0.248	−0.183	1.752	−0.355
38	−0.514	0.466	1.119	−0.556	0.309	−0.194	1.019	−0.235
39	−0.623	0.458	1.072	−0.545	0.258	−0.172	0.985	−0.228
40	−0.474	0.308	1.101	−0.563	0.335	−0.192		
41	−0.507	0.461	1.114	−0.562	0.322	−0.194		
42	−0.552	0.465	1.120	−0.573	0.408	−0.209	1.131	−0.438
43	−0.149	0.376	1.049	−0.539	0.259	−0.178	0.978	−0.371
44	−0.602	0.417	1.046	−0.543	0.244	−0.175	1.020	−0.375
45	−0.249	0.385	0.992	−0.081	0.291	−0.553	1.004	−0.371
46	−0.245	0.392	1.049	−0.541	0.243	−0.081	0.978	−0.369
47	−0.256	0.538	1.019	−0.085	0.291	−0.558	1.045	−0.373
48	−0.252	0.553	1.217	−0.539	0.281	−0.202	1.031	−0.367
49	−0.324	0.447	1.049	−0.541	0.229	−0.175	0.822	−0.349
50	−0.322	0.462	1.049	−0.543	0.213	−0.077	0.822	−0.349
51	−0.323	0.462	1.554	−0.321	0.455	−0.284	1.002	−0.365
52	−0.322	0.463	1.268	−0.555	0.401	−0.151	0.847	−0.350
53	−0.553	0.466	1.121	−0.555	0.301	−0.194	1.025	−0.158
54	−0.131	0.379	1.053	−0.542	0.266	−0.178	1.670	−0.354

Table 2 (continued)

0	1	2	3	4	5	6	7	8
55	−0.223	0.551	1.078	−0.544	0.230	−0.091	1.757	−0.355
56	−0.223	0.551	1.078	−0.544	0.230	−0.092	1.757	−0.355
57	−0.188	0.557	1.070	−0.542	0.499	−0.181	1.728	−0.354
58	−0.513	0.460	1.114	−0.563	0.322	−0.194		
59	−0.499	0.460	1.102	−0.562	0.332	−0.194	0.462	0.312
60	−0.465	0.307	1.095	−0.563	0.341	−0.101	0.319	0.341
61	−0.460	0.307	1.094	−0.564	0.344	−0.191	0.283	0.381
62	−0.467	0.308	1.092	−0.562	0.342	−0.191	0.482	0.202

equations are thereafter used to calculate the activities of the test series compounds and the prediction is considered successful if a sufficiently low calculated activity, $\hat{A} < 3$, results.

The selection of electronic parameters is done as follows. The most active compounds are those with an amino-group in position 2 and an oxo-group in position 6. Therefore a first series of $n = 13$ compounds with small substituents in positions 2 and/or 6 is considered. We first attempted to correlate the activities, A_i, with net electronic charges[5], q_{ij}. The best monoparametric correlation is obtained for the charge of the atomic position 2, q_{i2} (in parenthesis is given the Student t-test value):

$$\hat{A}_i = -5.437 + 10.844\, q_{i2} \qquad (1)$$
$$(4.297)$$

$$r = 0.792; \quad F = 18.462$$

To this monoparametric equation a second parameter was added and a significant increase of the correlation coefficient, r, and Fischer test, F, was obtained for the following biparametric equations:

$$\hat{A}_i = -6.533 + 0.382 q_{i2} + 0.706 S^{E}_{i10} \qquad (2)$$
$$(4.515) \qquad (2.719)$$

$$r = 0.886; \quad F = 18.295$$

$$\hat{A}_i = 25.654 + 8.933\, q_{i2} + 46.419\, q_{i7} \qquad (3)$$
$$(4.379) \qquad (2.953)$$

$$r = 0.895; \quad F = 20.069$$

$$\hat{A}_i = -1.400 + 10.887\, q_{i2} - 2.967\, q_{i10} \qquad (4)$$
$$(6.141) \qquad (-3.506)$$

$$r = 0.912; \quad F = 24.859$$

Biparametric equations having statistical significance were also obtained by using S^{E}_{i7}, q_{i8}, and q_i^9 as a second parameter:

$$\hat{A}_i = 5.750 + 10.330\, q_{i2} - 5.533\, S^{E}_{i7} \qquad (5)$$
$$(4.809) \qquad (-2.313)$$

$$r = 0.870; \quad F = 15.553$$

$$\hat{A}_i = 2.691 + 9.279 q_{i2} - 9.652\, q_{i8} \qquad (6)$$
$$(4.026) \qquad (-2.138)$$

$$r = 0.862; \quad F = 14.513$$

$$\hat{A}_i = 4.901 + 10.54\, q_{i2} + 28.924\, q_{i9} \qquad (7)$$
$$(4.984) \qquad (2.391)$$

$$r = 0.873; \quad F = 15.046$$

We next added a third electronic parameter to the equations (1) — (3). The best correlation for three electronic parameters obtained by us is given by Eq. (8).

$$\hat{A}_i = 0.682 + \underset{(2.740)}{2.997\, q_{i_1}} + \underset{(4.870)}{8.167\, q_{i_2}} + \underset{(3.739)}{0.759 S^{\mathrm{E}}_{i10}} \tag{8}$$

$$r = 0.940\,; \quad F = 22.636$$

As small substituents at position 8 exhibit only moderate decreases of activity (i.e. steric repulsion is improbable), this series is completed with other 6 compounds ($i = 14-19$). For the series of $n = 19$ molecules the regression coefficients are calculated by using the parameters of Eq. (2). Eq. (9) is thus obtained, which is significant from the statistical point of view.

$$\hat{A}_i = 1.513 + \underset{(2.089)}{3.051 q_{i_1}} + \underset{(3.464)}{5.963\, q_{i_2}} + \underset{(3.042)}{0.810\, S^{\mathrm{E}}_{i10}} \tag{9}$$

$$r = 0.855\,; \quad F = 13.354$$

This equation was completed with the parameters q_{i_7}, $q_{i_{10}}$, S^{E}_{i10}, q_{i_8}, and q_{i_9} (used in Eq. (3) — (7)), to obtain Eq. (10) which shows a significant increase of r and F.

$$\hat{A}_i = -\,7.436 + \underset{(2.900)}{2.487 q_{i_1}} + \underset{(6.984)}{7.428 q_{i_2}} + \underset{(2.625)}{2.936 S^{\mathrm{E}}_{i10}} - \underset{(-5.186)}{8.344 q_{i_7}} -$$

$$-\,\underset{(-4.672)}{11.266 q_{i_8}} - \underset{(-3.273)}{16.615\, q_{i_9}} + \underset{(2.769)}{0.580\, S^{\mathrm{E}}_{i7}} - \underset{(-2.870)}{2.283\, q_{i_{10}}} \tag{10}$$

$$r = 0.973\,; \quad F = 22.027$$

Equation (10) is used to calculate the activities for the rest of the molecules of the series for optimization ($i = 20-39$). Most of the calculated activities are much larger than the experimental ones, due to the neglect of steric repulsion effects produced by some substituents. The minimal steric difference, MTD , is introduced as an additional parameter to consider these effects. The vertices $j = 1-9$ occupied by the purine ring are considered as cavity vertices ($\varepsilon_j = -1$), while some vertices occupied by detrimental substitutents ($j = 13-15$, 19, 20, 23) are considered as wall vertices ($\varepsilon_j = +1$). Each occupied wall vertex contributes one unit to MTD_i ; the MTD_i values are listed also in Table 1. These vertex attributons are illustrated in Figure 1. The corresponding correlational equation is :

$$\hat{A}_i = \underset{(2.011)}{-\,4.070} + \underset{(4.216)}{1.388\; q_{i_1}} + \underset{(2.821)}{5.334 q_{i_2}} + 3.155\, S^{\mathrm{E}}_{i7} - \underset{(-2.688)}{4.990\, q_{i_7}} - \tag{11}$$

$$-\,\underset{(-2.971)}{8.843 q_{i_8}} - \underset{(-3.118)}{7.107\, q_{i_9}} + \underset{(1.979)}{0.446 S^{\mathrm{E}}_{i10}} - \underset{(2.-211)}{2.170\, q_{i_{10}}} - \underset{(-6.158)}{1.040\, \mathrm{MTD}_i}$$

$$r = 0.866\,; \quad F = 9.679\,; \quad n = 39$$

As seen in Table 1, the calculated activities for three compounds ($i = 23$, 32, 34) are much higher than the experimental ones. If these three compounds are eliminated from the series the correlational equation becomes :

$$\hat{A}_i = -\,5.753 + \underset{(3.994)}{2.022\, q_{i_1}} + \underset{(6.650)}{6.102\, q_{i_2}} + \underset{(4.430)}{3.550\, S^{\mathrm{E}}_{i7}} - \underset{(-5.046)}{6.903\, q_{i_7}} - \tag{12}$$

$$-\,\underset{(-4.805)}{10.291\, q_{i_7}} - \underset{(-5.511)}{9.196\, q_{i_3}} + \underset{(3.129)}{0.528\, S^{\mathrm{E}}_{i10}} - \underset{(-3.177)}{2.257\, q_{1i0}} - \underset{(-8.039)}{0.974\, \mathrm{MTD}_i}$$

$$r = 0.938\,; \; F = 21.042\,; \; n = 36$$

The corresponding receptor map (13) illustrated by the vertex attributions of Figure 1 is optimal according to the *Y*-criterion [3,7].

$$S^{\circ}\begin{cases} j(\varepsilon = -1)\,;\ 1-9 \\ j(\varepsilon = 0)\,;\ 10,\ 11\ 12,\ 17,\ 18,\ 21,\ 22,\ 24-30 \\ j(\varepsilon = +1)\,;\ 13-15,\ 19{,}20,\ 23 \end{cases} \qquad (13)$$

RESULTS AND DISCUSSION

An inspection of the test series ($i = 40-62$) shows that 15 of the 23 molecules have the activities $\hat{A}_i^{12}$ (see Table 1) calculated by Eq. (12), not higher than the limit of 3.000. For 8 molecules the calculated activities, $\hat{A}_i^{12}$, are somewhat higher than this limit, but nevertheless low if the whole activity scale (3.000–6.041) of the first 39 compounds of Table 1 is considered. The approximate character of our method, the neglect of hydrophobic effects, may explain these differences. The introduction of the MTD_i-parameter (Eq. (12)) corrects significantly the calculated activities, $\hat{A}_{12}^i$, as compared to activities, $\hat{A}_{10}^i$, calculated only with electronic parameters.

According to the receptor map S° (13) (see also Figure 1) the receptor cavity should correspond, largely, to the purine ring with opening in the "left up" ($j = 10,\ 17,\ 18$), "left down" ($j = 16,\ 26-30$) and the "right hand"-region designated by vertices $j = 12,\ 21,\ 22,\ 24,\ 25$. The $\varepsilon_{11} = 0$ – attribution may correspond to a position within the receptor cavity, but rather near to the wall, with a compensation of attractive and steric repulsive effects. The rather high values of the Student t-test for the regressional coefficients of electronic indices in Eq. (12), suggest that electronic factors play an important part in the interaction of the inhibitor and the enzyme site.

The effect of q_{i7}, q_{10}, S_{i10}, S_{i10}^{E}, in $\hat{A}_i^{12}$ may correspond to an interaction of the atoms which occupy the vertices $j = 7,\ 10$ with an electrophilic zone of the receptor cavity of GPRT or with Mg^{2+}-ion (the inhibition constants were determined in a solution containing $MgSO_4$); the shape of electrostatic potential in the plane of guanine shows a well-evidenced negative hole next to the atoms 7 and 10 corresponding to the basicity of these positions.[9]

The signs of the regressional coefficients for q_{i1} and q_{i2} in Eq. (12) suggest that the vertices $j = 1,\ 2$ are situated in a nucleophilic zone of the enzyme. It is possible to occur a hydrogen bond between a proton acceptor from this zone and the hydrogen atom of purinic N_1 atom.

Eq. (12) also suggests that the vertices $j = 8,\ 9$ are situated in an electrophilic zone of the active site of GPRT.

Therefore, we may conclude that the binding of purinic derivatives to GPRT is controlled by both electronic and steric factors. The hypermolecule of MTD procedure, which delimits the investigated enzyme-space, may be used as a framework for approximate localization of these interactions.

REFERENCES

[1] R. L. Miller, G. A. Ramsey, J. A. Krenitsky and G. B. Elion, *Biochemistry*, **11**, **4723** (1972).

[2] A. Cammarata, in "Molecular Orbitals Studies in Chemical Pharmacology", Ed. L. B. Kier, Springer-Verlag, N. York, p. 156, 1970.

[3] Z. Simon, A. Chiriac, S. Holban, D. Ciubotariu and G. I. Mihalas, "Minimum Steric Difference", Research Studies Press Ltd., Letchworth (1984).

[4] G. Klopman and R. F. Hudson, *Theor. Chim. Acta*, **8**, 165 (1967); G. Klopman, *J. Amer. Chem. Soc.*, **90**, 223 (1968).

[5] N. Olaru and Z. Simon, *Rev. Roum. Chim.*, **32**, 63 (1987).

[6] N. Olaru and Z. Simon, *Rev. Roum. Chim.*, **32**, 83 (1987).

[7] Z. Simon, N. Dragomir, M. G. Plauchithiu, S. Holban, F. Glatt and F. Kerek, *Eur. J. Med. Chem.*, **15**, 521 (1980).

[8] A. Chiriac, V. Chiriac, D. Ciubotariu, S. Holban and Z. Simon, *Eur. J. Med. Chem.*, **18**, 507 (1983).

[9] R. Bonaccorsi, E. Scrocco, J. Tomasi and A. Pullman, *Theor. Chim. Acta*, **36**, 3917 (1975).

NOTE POUR LES AUTEURS

La **Revue Roumaine de Chimie** publie des articles en anglais, français, russe, allemand ou espagnol. Les auteurs sont priés d'envoyer des articles et des comptes rendus inédits.

Les manuscrits seront dactylographiés à double interligne. La bibliographie, les tableaux et la légende des figures seront placés après le texte.

Si l'article fait partie d'une série numérotée, la partie précédente sera donnée comme première référence.

Chaque article sera précédé d'un résumé comprenant quinze lignes au maximum.

Les références bibliographiques dans le texte seront faites par des exposants sans parenthèses et paraitront à la fin de l'ouvrage.

Les publications périodiques mentionnées dans la bibliographie seront présentées suivant les prescriptions internationales : le nom de l'auteur précédé de l'initiale du prénom, le titre du périodique abrégé conformément à « Chemical Abstracts » et souligné par une ligne, le numéro du tome indiqué par des chiffres arabes et souligné par deux lignes, suivi de la première page de l'article : à la fin, l'année de la parution sera placée entre parenthèses. Le numéro de la revue ne sera pas indiqué si les pages du volume sont numérotées consécutivement.

Les textes des livres ou traités inclueront : le nom des auteurs, précédés de l'initiale du prénom, le titre du livre entre guillemets et sans être souligné, le numéro du tome précédé par l'abréviation « vol. » (ou « Bd. »), le numéro de l'édition, les éditions (the publisher), la localité de la parution du livre, l'année de la parution et la page de la référence précédée(s) par l'abréviation « p » (ou « S »).

Les brevets seront indiqués comme suit : l'auteur ou la firme, le pays et le numéro du brevet, la date de la revue (*Chem. Abstr.*).Par ex.: M. Jones (to Union Carbide Co.). Brit. Pat. 610 238,2 Sept. 1959 : cf. *Chem. Abstr.*, 54, 12808 (1960).

Si la référence n'a pas été lue en original, on indiquera aussi la revue de références consultée.

Les diagrammes seront tracés à l'encre de Chine sur papier calque. Les tableaux et les figures (en nombre strictement nécessaire), ainsi que les courbes dans les figures seront numérotés par des chiffres arabes. Leur explication sera donnée dans la légende des figures. Prière de ne pas inscrire les mêmes données dans les tableaux et les figures. Chaque tableau aura un titre. On indiquera dans le texte la place approximative des tableaux et des figures. Les formules chimiques seront incluses dans le texte ; en outre, elle seront transcrites sur papier calque, à l'encre de Chine.

Les auteurs sont priés d'indiquer les caractères italiques (en soulignant les lettres au crayon), ainsi que tout autre caractère spécial : les préfixes *ortho*, *méta*, *para*, *cis*, *trans*, etc. seront soulignés pour indiquer leurs caractères italiques, et ne seront jamais écrits avec des majuscules.

Aucune correction à la main ne sera admise sur le manuscrit. Les corrections seront frappés à la machine. Les lettres grecques ou d'autres symboles spéciaux seront insérés à la main à l'encre clairement.

Le manuscrit sera signé par l'auteur.

Le titre courant aura 50 lettres au maximum.

L'entière responsabilité du contenu des articles appartient aux auteurs.

Sur demande on peut obtenir une note plus complète.

PRINTED IN ROMANIA

[illegible]

TRAVAUX PARUS AUX ÉDITIONS DE L'ACADÉMIE DE LA RÉPUBLIQUE SOCIALISTE DE ROUMANIE

ELENA CEAUŞESCU, **Progrese în chimia şi tehnologia polimerilor**, 1986, 446 p.
ELENA CEAUŞESCU, **Forschungen im Bereich der Chemie und Technologie der Polymere**, 1986, 444 p.
I. G. MURGULESCU, O. M. RADOVICI, **Introducere în chimia fizică, vol. IV, Electrochimia**, 1986, 416 p.
RAUL MIHAIL, ION GROZEANU, **Estimarea secvenţială aplicată sistemelor chimice**, 1986, 406 p.
M. BREZEANU, L. PATRON, M. ANDRUH, **Combinaţii complexe polinucleare şi aplicaţiile lor**, 1986, 244 p.
A. T. BALABAN et al., **Labelled Compounds and Radiopharmaceuticals Applied in Nuclear Medicine**, coédition avec John Wiley and Sons, 1986, 742 p.
D. PURDELA, **Nomenclatura chimiei organice — IUPAC**, 1986, 454 p.
PETRU BUDRUGEAC, **Probleme de chimie**, 1986, 280 p.
T. ONCESCU, S. G. IONESCU, **Conversie fotochimică şi stocare de energie**, 1985, 272 p.
V. DRĂGUŢAN, A. T. BALABAN, M. DIMONIE, **Olefin Metathesis and Ring-Opening Polymerization of Cyclo-olefins**, coédition avec John Wiley and Sons, 1985, 544 p.
C. LITEANU, I. RÎCĂ, **Optimizarea proceselor analitice**, 1985, 360 p.
N. PERESCU, **Chimia extracţiei cu solvenţi şi aplicaţii**, 1985, 212 p.
V. E. SAHINI, M. HILLEBRAND, **Chimie cuantică în exemple şi aplicaţii**, 1984, 378 p.
GH. MARCU, **Chimia compuşilor coordinativi**, 1984, 415 p.
E. CORDOŞ, C. MANOLIU, **Spectrometria de absorbţie şi fluorescenţă atomică**, 1984, 178 p.
C. BODEA, **Tratat de biochimie vegetală**, p. II, t. 4, 1984, 438 p.
N. ASANDEI, A. GRIGORIU, **Chimia şi structura fibrelor**, 1983, 395 p.
N. IONESCU, M. CĂLDĂRARU, **Oxidarea catalitică a olefinelor inferioare**, 1983, 178 p.
C. CAŞCAVAL, **Studiul polimerilor prin piroliză şi cromatografie de gaze**, 1983, 220 p.
C. I. SIMIONESCU, F. DANEŞ, **Originea vieţii**, 1983, 110 p.
C. BODEA, **Tratat de biochimie vegetală, p. II, t. 4**, 1982, 408 p.
I. G. MURGULESCU, RODICA VÎLCU, **Introducere în chimia fizică. Vol. III. Termodinamica chimică**, 1982, 624 p.
I. G. MURGULESCU, J. PĂUN, **Introducere în chimia fizică, Vol. I. 3. Nucleul atomic, reacţii nucleare, particule elementare**, 1982, 606 p.
ELENA CEAUŞESCU, **Noi cercetări în domeniul compuşilor macromoleculari**, 1981, 536 p.
I. G. MURGULESCU, TATIANA ONCESCU, E. SEGAL, **Introducere în chimia fizică. Vol.II.2. Cinematică chimică şi cataliză**, 1981, 1024 p.
I. GĂLĂŢEANU, **Procese şi metode radiochimice în energetica nucleară**, 1981, 234 p.
CR. SIMIONESCU, VALERIA GORDUZA, **Polimeri biocompatibili şi biologic activi**, 1980, 479 p.
ELENA CEAUŞESCU, **Polimerizarea stereospecifică a izoprenului**, 1979, 307 p.
C. GH. MACAROVICI, **Analiza chimică cantitativă anorganică**, 1979, 457 p.
M. FLORESCU, **Metode ştiinţifice în dezvoltarea industriei chimice moderne**, 1979, 256 p.
I. G. MURGULESCU, E. SEGAL, **Introducere în chimia fizică. Vol. II. 1. Teoria molecular-cinetică a materiei**, 1979, 1036 p.
I. G. MURGULESCU, V. EM. SAHINI, **Introducere în chimia fizică, Vol. I. 2. Structura şi proprietăţile moleculelor**, 1979, 604 p.
I. ZUGRĂVESCU, MAGDA PETROVANU, **N-ylid chemistry**, coédition avec McGraw-Hill International Book Company U.S.A., 1977, 396 p.
I.G. MURGULESCU, **Introducere în chimia fizică, Vol. I. 1. Atomi, molecule, legătură chimică**, 1976, 560 p.
ELENA CEAUŞESCU, **Research work on synthesis and characterization of macromolecular compounds. Contributions**, 1974, 251 p.

1987 NOV

ISSN 0035—3930

c. 1373—I. P. INFORMAŢIA

43 426

Lei 40
$ 90 (pour un abonnement annuel)

F 1103

~~04-66~~

ACADÉMIE DE LA RÉPUBLIQUE SOCIALISTE DE ROUMANIE

REVUE ROUMAINE DE CHIMIE

TOME 32

N°s 11 – 12

Novembre – Décembre 1987

Rev. Roumaine Chim.

RRCHAX, 32, *11–12*, p. 1011–1242 (1987), Bucarest

EDITURA ACADEMIEI REPUBLICII SOCIALISTE ROMÂNIA

ACADÉMIE DE LA RÉPUBLIQUE SOCIALISTE DE ROUMANIE

COMITÉ DE RÉDACTION

Rédacteur en chef:

I. G. MURGULESCU, membre de l'Académie de la République Socialiste de Roumanie

Rédacteurs en chef adjoints:

A. T. BALABAN et V. EM. SAHINI, membres correspondants de l'Académie de la République Socialiste de Roumanie

Collège de rédaction:

EM. BRATU, ELENA CEAUŞESCU, ECATERINA CIORĂNESCU-NENITZESCU, CR. SIMIONESCU, membres de l'Académie de la République Socialiste de Roumanie; P. SPACU, membre correspondant de l'Académie de la République Socialiste de Roumanie; M. BANCIU, M. D. GHEORGHIU, I. HAIDUC, D. I. MARCHIDAN, G. NIAC et D. SĂNDULESCU

La Revue Roumaine de Chimie paraît 10 fois par an. Toute commande de l'étranger sera adressée à ROMPRESFILATELIA — sectorul Export-Import Presă, P. O. Box 12—201, télex 10376 prsfi r 78104 Bucarest, Calea Griviței nr. 64—66, București, Roumanie

Les manuscrits, les livres et les revues proposés en échange, ainsi que toute correspondance seront envoyés à la rédaction :

REVUE ROUMAINE DE CHIMIE

125, Calea Victoriei, 79717 Bucarest, Roumanie, téléphone 50 76 80

EDITURA ACADEMIEI REPUBLICII SOCIALISTE ROMÂNIA
125, Calea Victoriei 79717 Bucarest, Roumanie, téléphone 50 76 80

REVUE ROUMAINE DE CHIMIE

Tome 32, Nos 11–12 **Novembre–Décembre, 1987**

ANNIVERSARY 1013–1023

RODICA VÎLCU, VIELKA LANGSHAW and ZOICA CENUȘE, Isothermal liquid-vapour equilibrium in the acetonitrile-propionitrile system 1025–1031
MARIUS ANDRUH, C. I. LEPADATU and MARIA BREZEANU, Angular overlap model (AOM) calculations for the coordination compounds with macrocyclic ligands. I. AOM parameters for nickel(II) coordination compounds with tetrakis-anhydro-aminobenzaldehyde macrocyclic ligand 1033–1037
ECATERINA JURCONI, TATIANA ONCESCU and GEORGETA RĂCĂȘANU, Kinetics of the substitution reaction between CoC_2O_4 $Bipy_2I$ and bipyridyl in aqueous solution 1039–1044
CRISTINA MANDRAVEL and LIGIA ANASTASESCU, The influence of various factors on the optical activity of some essential aminoacids. I. Applications 1045–1050
MIHAELA HILLEBRAND, MIRCEA MORARU and ELENA VOLANSCHI, ESR spectral study of some substituted 2,4-dinitroanilines 1051–1057
VOICU CONSTANTIN, Calculation of mass spectra of some oxygen- and sulphur-containing heterocycles 1059–1068
A. SAVIN, H. PREUSS and H. STOLL, Why are caesium clusters more difficult to ionize than their monoxides ? 1069–1070
A. M. SAPSE, Theoretical studies of the decomposition of lithiated nitrosoureas 1071–1074
I. B. BERSUKER, S. A. BORSHCH and I. N. KOTOV, The vibronic theory of magnetic properties of trinuclear mixed-valence clusters 1075–1084
GERHARD RASCH and SVEN TOBISCH, The insertion reaction of Ni and Ni_2 into O–H, S–H, O–O and S–S bonds. A CNDO treatment 1085–1095
AL. IVANOV, Counting observables of chemical species 1097–1101
Z. SIMON, Stereochemical and informational aspects in QSAR and MTD . . 1103–1107
IOANA ILIE, MARIA BREZEANU, LUMINIȚA PATRON, E. SEGAL and G. FILOTI, Synthesis of nickel ferrite from polynuclear coordination compounds. Part I. Study of the dry ferritization process 1109–1115
JOSETTE WEINBERG and ALEXANDRINA DONESCU, β-Lactam antibiotics. I. Structure-neurotoxic activity of benzylpenicillin 1117–1121
S. STERNBERG and MIHAELA UNGUREANU, Heterogeneous electrocatalysis for nitrobenzene and phenol reduction 1123–1128
ORTANSA LANDAUER, CORNELIA MATEESCU, OLGA IULIAN and D. GEANĂ, Models for the viscosity of liquid mixtures. Application to the binary system water-dioxan 1129–1139
AGNETA CARAGHEORGHEOPOL and ILEANA DRĂGUȚAN, An electron spin resonance study of conformational inversion in iminoxy radicals derived from benzocycloheptene and heterocyclic analogs 1141–1149
H. CĂLDĂRARU, Molecular motion in solid bicyclo[3.3.1]nonan-9-one and adamantanone oximes studied by the electron spin resonance spectra of the corresponding iminoxy radicals 1151–1154
C. BENDIC and C. PODINĂ, Dipole moments of ground and excited states of 7-chloro-2,3-dihydro-4-quinolone (in French) 1155–1159

Rev. Roumaine Chim. **32**, *11–12*, 1011–1242 (1987) Bucarest

M. BANCIU, MICHAELA STĂNESCU, CRISTINA FLOREA, A. T. BALABAN and ECATERINA CIORĂNESCU, Ring contraction and additional annelation in the dibenzobullvalone system . . . . 1161—1170
NICOLETA ŞTEFAN, ILIE G. DINULESCU and MARGARETA AVRAM, 1,3-Di-t-butylcyclobutane derivatives . . . . 1171—1174
IOSIF SCHIKETANZ, ANDREI ŞTEFĂNESCU, MICHAELA-CARMEN BALABAN, ANA SCHIKETANZ, MIRCEA D. GHEORGHIU and ALEXANDRU T. BALABAN, Aminoketone and oxazole synthesis. XI. Extension to the synthesis of thiazoles from 2-aza-1,4-diketones or *via* electrophilic substitution of arenes with 2-thiazolin-5-ones (thioazlactones) . . . 1175—1180
MIRCEA D. GHEORGHIU, MARINA MIHAI, LUMINIŢA PÂRVULESCU, ANGHELUSSIS VAIOS and MIHAI ELIAN, Nuclear magnetic resonance investigations of small rings. Part. 5. The exact analysis for the four-membered ring three-proton system of 3-aryl-2-t-butyl-2-cyclobutanones as evidence for configurational assignments . . . . 1181—1186
M. IOVU and ELENA TUDORACHE, Homopolycondensation of dichloromethylderivatives in the presence of tetrachloroethene or trichloroethene (in French) 1187—1192
J. ZSAKÓ, MARIA TOMOAIA-COTIŞEL, V. TĂMAŞ, VIRGINIA COMAN and E. CHIFU, Monomolecular films of some apocarotenoid derivatives . 1193—1202
CONSTANTIN MARIAN SPOITU, SORIN SPOITU and OVIDIU MUNTEAN, Approximate solution for isothermal effectiveness factor . . . . . . 1203—1210
D. OANCEA, DOMNINA POPESCU and N. I. IONESCU, On the significance of the minimum ignition energy of an explosive gaseous mixture . . . . 1211—1218
A. HAAS, M. LIEB and B. SCHWEDERSKI, Perhalogenomethyl-thioheterocycles. XXV. Electrophilic substitution of 2,4-diaminopyrimidines with perhalogenomethyl—chalcogenohalides (in German) . . . . 1219—1224

AUTHOR INDEX . . . . 1225—1236

SUBJECT INDEX . . . . 1237—1242

Revue Roumaine de Chimie, 32, *11–12*, 1013–1023 (1987)

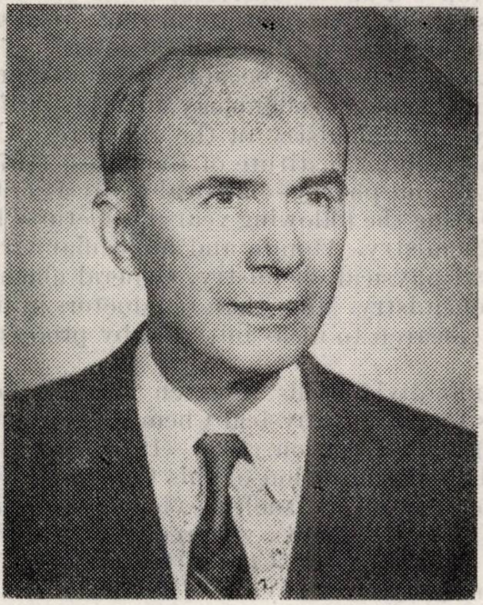

PROFESSOR V. E. SAHINI'S 60th ANNIVERSARY

For professor Victor E. Sahini's 60th anniversary, the Editorial Board of Revue Roumaine de Chimie expresses the best wishes for a long and productive life, for good health and new successes in his multiple activities.

Victor Emanuel M. Sahini was born in Galatzi on the 30th August 1927. After starting elementary school in Galatzi, he moved to Bucharest where he studied at the Gheorghe Lazăr Lyceum in 1938–1946. He enrolled as a student at the Faculty of Chemistry of the Bucharest University where he became a graduate in 1950. As a bright student, in the final year he was retained as a member of the teaching staff at the Chair of Physical Chemistry and he embarked on a Ph. D. thesis under the supervision of Acad. Prof. I. G. Murgulescu. His thesis (1962) had the title "Contributions to the Theory of the Coordinative Bond". In 1970 he became docent (dr. habil.).

After graduation, dr. Sahini had two post-doctoral assignments in quantum chemistry and molecular structure : in 1960 at the Moscow Institute of Inorganic Chemistry (professors I. K. Syrkin and M. E. Dyatkina) and the Leningrad Institute of Macromolecular Chemistry, and in 1962 at the Department of Theoretical Chemistry, Cambridge University (professor H. C. Longuet-Higgins).

Professor Sahini's didactic career started in 1949 as preparator; he became an assistant in 1950, lecturer in 1955, reader in 1962 and full professor in 1968 at the Chair of Physical Chemistry. The Chemistry Faculty of the Bucharest University became integrated in the Polytechnic Institute, Faculty of Chemical Technology, in 1974. Professor Sahini headed a Chair of Physical Chemistry in the Bucharest University (1966—1974) and in the Polytechnic Institute of Bucharest (1977—1985). He lectured for the first time on physico-chemical analysis (1951) and quantum chemistry (1954). During the following years his lectures had various topics such as Physical Chemistry, Atomic and molecular structure, Quantum Chemistry, Biological physical chemistry, General chemistry, Electrochemistry and Colloid chemistry. More than ten doctors in physical chemistry owe their début in research to ideas initiated by professor Sahini's school in Bucharest.

Professor Sahini divided his research activity between the Chair and the Academy's Centre of Physical Chemistry, where he was head of sector (1960—1963) and of section (1963—1973), becoming scientific deputy director till the reorganization of this Centre (1973—1975).

He held various functions, such as vice-dean of the Chemistry Faculty, Bucharest University (1953), vice-rector of the University (1970—1972), Rapporteur of the Expert Committee for the Foundation of the United Nations University in Tokyo (1971—1973).

Currently, professor Sahini combines his teaching duties with the functions of Director of the Library of the Romanian Academy (since 1980), president of the Spectroscopy Commission of the Romanian Academy (since 1986), president of the Bucharest Branch of the Society for Teaching Physics and Chemistry (since 1971) and National Representative of the Romanian Academy for the International Council of Scientific Unions (since 1963). He is also a vice-president of Romanian Association of Scientists.

Since the foundation of *Revue Roumaine de Chimie*, professor Sahini has been a member of the Editorial Board and he is currently a Deputy Head Editor.

He was elected as a corresponding member of the Academy of Romania in 1963. He is an annual active member of the New York Academy of Sciences.

For his scientific activity, professor Sahini was decorated with the Order of Labour (1973).

Professor Sahini was Secretary of the Organizing Committee for the National Conferences on Physical Chemistry held in Bucharest in 1968, 1970, 1972, 1974, 1976. Since 1962, he has taken part with communications in numerous scientific congresses in Romania and abroad.

Professor Sahini authored till now three books and over 100 papers. His scientific research is centered on molecular structure and quantum theory of chemical bonding. He studied a variety of problems in the area of covalent and coordinative bond, using numerous experimental techniques such as IR, Raman, UV, ESR, NMR spectroscopy, refractometry, interferometry etc. Using the methods of Quantum Chemistry, professor Sahini initiated in Romania their application to various problems of chemistry.

Polycyclic aromatic hydrocarbons. A criterion for the classification of the Kekule formula of condensed aromatic hydrocarbons has been proposed, a perfect aromatic limiting structure being defined, which is invariant to all molecular symmetry operations. MOs that minimize the bond resonance energy were defined and used as a foundation for the perfect aromatic limiting structure and for some liniar relationships of the delocalisation energy. Atom-localised MOs were defined and applied to alternant hydrocarbons in the HMO approximation.

Heterocyclic and aromatic compounds. The barrier to internal rotation about the C—N bond in several thiopiperidides was determined, by 'H—DNMR, finding that it increases in the series : cynnamoylthiopiperidide < thiobenzoylpiperidide < phenylthioacetylpiperidide ; these results are well explained in the framework of a HMO-treatment of data. In the case of m- and p-substituted compounds, the barriers increase with the electron-withdrawing character of the substituent in the aromatic ring. The activation parameters for the hindered internal rotation of both N-(p-chlorothiocinnamoyl) and its CT-complex with iodine revealed a considerable increase of the rotational barrier on molecular complexing. Computer programs for SCF—CI—Mo calculation of closed-shell and open-shell π-electron systems have been established.

The ESR — spectra of mono- and di-nitrophenoxatellurin anion-radicals in different solvents have been interpreted in terms of solvent-induced line-width alternation and the effect of the substituents on the nitro-stilbene anion-radicals was observed from ESR-spectra and interpreted by means of MO-calculations. Also, from ESR-spectra and MO calculations there was established that in the anion-radicals of m- and p-nitrosubstituted derivatives of several classes of N-(thioacyl)-piperidines and morpholines, the radicals are centered on the nitro group and the conjugation between the thiocarbonyl group and the aromatic moiety influences the distribution of the unpaired electron. ESR and optical spectra of radical anions have been studied in different solvents and the hfs and optical results have been analysed in terms of MO computation. UHF spin-density-calculations of substituted nitroaromatic anion-radicals have been correlated with some experimental results and new values for the nitrogen spin polarisation parameters were obtained. UHF computations have been performed in order to calculate the spin distribution in heteroaromatic ions. Computed electronic structure of cation radicals provided by isatin and N-methyl isatin, carbozole cation-radical and carbozolium ion heteroanalogs of anthracene and also for diphenyl-amine anion radicals account for their optical spectra.

Some papers have been devoted to the ESR spectra and MO computations of σ-radicals ; in the case of iminoxy radicals, hfs have been correlated with the long-range interaction and with the *cis*-interaction. EHT calculations described correctly the experimental splittings observed in ESR spectra of iminoxy radicals of pyrimidine derivatives. The isomerism effect in ESR spectra of iminoxy radicals of 1-benzoxepin-5-one derivatives has been studied as well as the hfs due to hydrogen atoms lying *anti* to the iminoxy group oxygen in (z)-α-keto-iminoxy radicals.

The correlation of UV spectra with HMO and SCF—CI—PPP—MO computations of dibenzo-thiepines, thioacylpiperidides and morpholides revealed the role of different structural entities of the molecules. UV spectra and basicity constants of xylidine isomers have been correlated with the results of HMO-technique and SCF—PPP—MO computation. UV spectra and electronic energy levels, resulting from PPP—MO computations of benzenesulphonic acids, disubstituted benzenes, and monosubstituted naphthalenes have been correlated. Assignment of electronic transitions from the correlation of molecular structure with the spectral data has been obtained for alkyl- and phenyl-substituted pyrylium salts and for nitrophenol isomers. SCF—CI—MO method has been used in order to interpret the substituent influence on electronic spectra of aminodiphenylstilbenes. Energy levels and electronic transitions calculated by the same method for phenoxaselenine have been discussed with respect to the similar values of phenoxathin. A new NMR method to study the self-association equilibria of aromatic amines in solution was established.

The study of reactivity of *m*-nitrophenyl acetate in excited state leads to a mechanism explaining some particularities of the photochemical reaction, the specific *meta* activation by nitro group being correlated with the change in the electronic structure induced by excitation.

EHT and point charge computations of *o*- and *p*-chlorobenzamide account for the non-planarity of the *o*-isomer. The dipole moment values of 2,4- and 2,6-xylidine were computed by CNDO/2 methods and the dipole moments of all xylidine isomers were analysed in the frame of an SCF—PPP—MO calculation; HMO calculation of chemical reactivity have been applied to the polymerisation of acetylene derivatives and FG-matrix method for the calculation of CO stretching frequency of symmetrically halogen-substituted benzophenones.

An experimental and theoretical study of the modification of the dipole moments of aminodiphenyl ethers and nitrodiphenyl ethers in their electronic ground and first excited states was attributed as being due to the change of nitrogen charge density. The dipole moments in the first excited single state of xylidine isomers were obtained experimentally and by an SCF—MO computation.

Charge-transfer complexes and coordination compounds. A perturbation treatment has been established and applied to the CT complexes formed by iodine with several five-membered heteroaromatic molecules.

Spectrophotometric studies were carried out on iodine complexes with some xylidine isomers, their dipole moment, pKa and HNH angle values in ground state being obtained. For a series of molecular complexes of phenyl-substituted pyrylium salts with tetracyano *para*-quinodimethane anions, spectrophotometric, conductometric and dipole data were obtained, solvocromy and stability-constants being established. By different experimental physical-chemical methods and MO computation, he studied the complexation of di-p-tolyl selenide with iodine and the CT complexes of iodine with several heterocycles in the azoles series; these complexes are of an n-σ type, values of Δ^0_f and ΔS^0_f being obtained both experimentally and theoretically. CT spectra and equilibrium constants of iodine-aromatic amines have been studied and the two-center overlap integral for the selenium-iodine bond of donor-acceptor type has been computed. He developed an isolated binary collision model of light scattering in liquids, in order to obtain an analytical expression for the spectral intensity of IR simultaneous transition spectrum in liquid mixtures.

The partial ionic character of the coordination bond in complex oxalates has been calculated from IR spectra and a new method for the individual ionic refraction has been established. The variation of atomic refraction *versus* the element electronegativity was obtained. Roothaan's SCF—MO method has been applied in order to calculate the electronic energy levels of $[Co(NH_3)_6]^{3+}$ and $[Co(NH_3)_5Cl]^{2+}$ ions. The stereochemistry of tetrahedral complexes and the relative stability of hexacoordinated Co^{3+} and Co^{2+} complexes have been analysed in terms of the second order perturbation. A corrected Gauss function applied to the visible absorption band of Co(III) halogenopentaamines gave the precise value of the two maxima. IR spectra have been used in the study of molecular structure of some complex thiosulphates, chlorates and coordination isomers of chromium diaquo-oxalate complexes.

Molecular interactions. A group of other papers has been devoted to the study of the solvent effects on carbonyl group; solvent effects on some IR bands of benzophenone have been correlated with solvent effect on the shape of singlet $n-\pi^*$ electronic band. The effect of weak hydrogen bond formation on the mechanical and electrical anharmonicity of the $C=O$ vibration has also been studied. The influence of alcohols on the frequency and intensity of carbonyl group vibration and the formation of hydrogen bond have been studied in the Raman spectrum of acetophenone. Furthermore, a progression of totally-symmetrical stretching vibration of $C=O$ group was evidenced in the $n-\pi^*$ electronic transition of acetophenone. The consequence of the dissolution on the depolarisation ratios of the Raman lines corresponding to some vibrations of acetophenone was observed and the Raman spectra of some beryllium oxalate complexes have been investigated in solid state. The solvent effect on the carbonyl stretching frequency of benzophenone and anthrone enables the study of the complexes arising at their solvation in mixtures of *m*-cresol and cyclohexane. From the IR spectra of carbonyl group in aromatic anion radicals and also by MO calculation, it was found that the CO stretching frequency and force constant change gradually in respect to the neutral molecules in benzophenone, fluorenone, phenanthrenequinone and anthrone. Electronic and ESR spectra of some aromatic metal ketyls, correlated with HMO computation results, revealed the influences of both the solvent and metal cation.

The solvent effect on the optical spectra of phenoxatellurine and some of its tellurium- and ring-substituted derivatives has been observed and the results were correlated with HMO calculations.

The solvent and temperature effects on the vibrational structure of the visible absorption band of $UO_2(NO_3)_2 \cdot 6H_2O$ have been studied, some molecular parameters of the excited state being obtained.

Force constant computations. In a study of IR spectra of hexahaloethanes and hexahalodisilanes, a modified Urey-Bradley force field was proposed, which enabled the assignment of all their vibrational bands. The $C-C$ stretching frequency in C_2H_6, C_2D_6 and C_2T_6 was studied in correlation with the mass effects in molecular vibration. From the isotopic effect in the vibrational spectra of PH_4^+ and PD_4^+, the anharmonicity factors, the harmonic wave numbers, the symmetry force constants and the constants of the most general square potential have been obtained. The force constants of $^{12}CF_4$ and $^{13}CF_4$ as well as of $^{10}BF_4^-$ and $^{11}BF_4^-$ have been calculated using the FG-matrix method.

Gaseous-phase radicals. Using an original improvement of the MI–1305 mass-spectrometer, Professor Sahini and his coworkers obtained the mass spectra of several heterocycles and established the main fragmentation pathways as well as the ionisation and appearence potentials for the more relevant fragments. The effect of isomerism in the mass spectra of toluidine, nitrianiline and picoline was studied in connection with mechanisms of main fragmentation processes and in correlation with MO results.

HMO and SCF–CI–PPP computation of the electronic structure of thioacylpiperidides, dibenzo-[b, e]-thiepine and morpholide derivatives as well as the correlation of these results with mass and UV spectra revealed the role of different structural entities of the molecules.

In *bio-physical chemistry*, the electronic structure data and physical chemical properties of xylidines and chloro-benzene isomers were correlated with their biological activity. HMO calculation of π-electron structure of β-lactam antibiotics enables the correlation of their electronic structure with the bio-activity spectrum and explains an adverse reaction of benzyl-penicillin. From the correlation of electronic structure and partition coefficients of certain local anaesthetics with their capacity of the reversible block of the nerve action potential, an active part in these molecules has been shown to be primarily involved in the action of local anaesthetics. A new method for partition coefficient calculation was established. Some molecular modifications of irradiated plant tissues after dehydration have been proved by ESR spectra.

A significant part of Professor Sahini's scientific activity has been devoted to some *applicative aspects of psysical chemistry*, the main topics being the relations of physico-chemical properties, particularly molecular and electronic structure, with the biological activity; he also studied physico-chemical aspects of the environment.

A new procedure for the preparation of the sodium salt of benzenesulphonic acid has been patented.

A spectrographic method has been established for the determination of traces of Cu, Pb, Cr, Ni, Mo and Co in natural waters as well as a new and precise procedure for the determination of magnetic susceptibility using the Gouy method.

With this anniversary volume, Professor Sahini's many students, friends, and colleagues enclose the warmest wishes for many happy years to come.

SCIENTIFIC PUBLICATIONS

BOOKS

D. Bârcă-Gălăţeanu, M. Giurgea, I. Iova, V. Sahini, A. Truţia and R. Ţiţeica, "Introducere în spectroscopia experimentală", Ed. Tehnică, Bucharest, 1966.

I. G. Murgulescu and V. Em. Sahini, "Introducere în chimia fizică", vol. I, 2 "Structura şi proprietăţile moleculelor", Ed. Academiei, Bucharest, 1975.

V. Em. Sahini and M. Hillebrand, "Chimie cuantică", Ed. Academiei, Bucharest, 1985.

PAPERS

1. V. Sahini, "Asupra unor relații între electronegativitatea și refracția atomică a elementelor", *Anal. Univ. C. I. Parhon — Bucharest, Series. St. Nat.*, **13**, 85 (1957).
2. I. G. Murgulescu and V. Sahini, "Despre refracțiile ionilor. III", *Stud. Cercet. Chim.*, **1**, 15 (1959).
3. I. G. Murgulescu and V. E. Sahini, „Spectre d'absorption dans l'infrarouge de quelques exalates complexes", *Revue Universelle des Mines*, 9e series (XV), **5**, 1 (1959).
4. V. E. Sahini, M. Leonte and E. Keplinger, "Contributions à l'étude des hydrazones de l'aldéhyde", *Anal. Univ. "Al. I. Cuza" — Iași*, **5**, 167 (1959).
5. A. T. Balaban, V. E. Sahini and E. Keplinger, "Electronic absorption spectra of alkyl- and phenyl-substituted pyrylium salts", *Tetrahedron*, **9**, 163 (1960).
6. V. Sahini and Z. Simon, "Studiul spectral în infraroșu al izomeriei *cis-trans* la combinațiile coordinative. II", *Stud. cercet. chim.*, **3**, 573 (1961).
7. V. E. Sahini, M. Feldman and I. Pîrcălăbescu, "Spectrele de absorbție în infraroșu ale cloraților unor metale", *Anal. Univ. C.I. Parhon, Series St. Nat.*, **30**, 43 (1961).
8. V. E. Sahini, "Asupra legăturii de coordinație în complecșii oxalici de crom, mangan, fier și cobalt din date spectrale în infraroșu", *Anal. Univ. C. I. Parhon, Series St. Nat., Chimie*, **30**, 49 (1961).
9. I. G. Murgulescu, V. E. Sahini and L. Bolfa, "Studiul spectral în infraroșu al izomeriei *cis-trans.* I", *Stud. cercet. Chim.*, **4**, 585 (1961).
10. T. ONCESCU and V. E. SAHINI, "Studiul spectral în infraroșu al izomeriei *cis-trans.* III", *Stud. cercet. Chim.*, **4**, 663 (1961).
1. V. Em. Sahini, "Sur la stabilité des hydrocarbures aromatiques condensés. I", *J. Chim. phys.*, **21**, 177 (1962).
2. V. E. Sahini, "Sur le caractère ionique de la liaison coordinative", *Revue de Chimie, Acad. R.P.R..*, **1**, 495 (1962).
3. V. E. Sahini, "Sur la stabilité de hydrocarbures aromatiques condensés. II", *Revue de Chimie, Acad. R.P.R..*, **2**, 1265 (1962).
4. V. E. Sahini and M. Damaschin, "On the vibration frequencies of the coordinated carbonic anion", *Revue de chimie, Acad. R.P.R.*, **2**, 193 (1963).
5. I. G. Murgulescu, V. Em. Sahini, M. Segal and M. Damaschin, "Spectre de vibrație și structura complecșilor tiosulfatului de cupru și argint", *Stud. cercet. Chim.*, **12**, (1), 27 (1964).
6. V. E. Sahini, "Asupra stabilității hidrocarburilor aromatice condensate. III", *Revista Chim. (București)*, 551 (1964).
7. L. Ciurea, V. E. Sahini, and C. Volanschi, "Absorption spectra of some metal-ketyls", *Rev. Roumaine Chim.*, **9**, 819 (1964).
8. I. G. Murgulescu, V. E. Sahini and A. Greff, "The influence of solvents on the electronic absorption spectra of substituted aromatics" in "Molecular Structure and Spectroscopy", Science Council of Japan, Tokyo, 1962, p. 108.
- V. E. Sahini and A. O. Fulea, "About the evaluation of the force constants of some tetrahedral molecules", *Rev. Roumaine Chim.*, **11**, 1045 (1966).
- V. E. Sahini, R. Beldie and M. Damaschin, "Ramanspektrum der freien und koordinierten Oxalate", *Rev. Roumaine Chim.*, **11**, 1361 (1966).
- V. Em. Sahini, V. Bender, S. Verzea and H. Bednar, "O nouă metodă de prezentare a orbitalelor", *Rev. fiz. chim., series A*, **III**, 9 (1966).
- V. Em. Sahini, C. I. Ghirvu and V. C. Macovei, "On the elctronic structure and spectrum of the benzensulphonated anion", *Rev. Roumaine Chim.*, **12**, 237 (1967).
- V. Em. Sahini and V. Brezuleanu, "SCF-MO calculation of the electronic energy levels of $[Co(NH_3)_6]^{3+}$", *Rev. Roumaine Chim.*, **12**, 367 (1967).
- V. E. Sahini, E. Keplinger and M. Hillebrand, "On electronic absorption spectra of nitrophenols", *Rev. Roumaine Chim.*, **12**, 361 (1967).
- V. E. Sahini, L. Ciurea and E. Volanshi, "Spectral study of some metal ketyls", *Rev. Roumaine Chim.*, **12**, 355 (1967).
- A. Caragheorgheopol, M. Hartmann, R. Kühmstedt and V. E. Sahini, "Electron spin resonance spectra of some iminoxy-radicals", *Tetrahedron Letters*, **42**, 4161 (1967).
- V. E. Sahini, V. Constantin and C. Podină, "L'étude des toluidines par spectrométrie de masse", *Rev. Roumaine Chim.*, **12**, 1405 (1967).
- V. E. Sahini and C. I. Ghirvu, "A Pariser-Parr treatment of substituted benzenes in the approximation of inductive model. I", *Rev. Roumaine Chim.*, **13**, 851 (1968).
- V. E. Sahini and M. Feldman, "Solvent effects of benzophenone infrared spectrum", *Rev. Roumaine Chim.*, **13**, 527 (1968).

30. V.E. Sahini, Th. Pirtea and Al. Butucelea, "Visible absorption spectrum of uranyl nitrate hexahydrate", *Rev. Roumaine Chim.*, **13**, 985 (1968).
31. V. E. Sahini and V. Brezuleanu, "On tetracoordinated complexes", *Rev. Roumaine Chim.*, **13**, 1119 (1968).
32. V. E. Sahini and V. Mincu, "Sur l'aplicabilité de la méthode Gouy aux poudres", *Univ. C. I. Parhon, Series St. Nat.*, **2**, 33 (1968).
33. S. Dumitrescu, G. I. Ghirvu, C. Simionescu and V. E. Sahini, "Etude de la polymerisation des derivés acétyléniques. II", *Bul. Inst. Politeh. Iași*, **XIV**, (XVIII) 1–2 (1968).
34. V. E. Sahini and A. O. Fulea, "The force constants of $PH_4^+ (T_d)$", *Rev. Roumaine Chim.* **14**, 17 (1969).
35. V. E. Sahini and L. Telea, "On the electronic spectra of Co(III)halogeno-pentaamines", *Rev. Roumaine Chim.*, **14**, 157 (1969).
36. V. E. Sahini and C. I. Ghirvu, "On the electronic structure and spectra of the monosubstituted naphthalenes", *Rev. Roumaine Chim.*, **14**, 275 (1969).
37. R. Beldie and V. E. Sahini, "Raman spectra of beryllium oxalate complexes", *Rev. Roumaine Chim.*, **14**, 419 (1969).
38. V. E. Sahini and L. Ciurea, "Electron spin resonance spectra of some aromatic metal ketyls", *Rev. Roumaine Chim.*, **14**, 689 (1969).
39. V. E. Sahini and M. Olteanu, "Solvent effect on the infrared spectra of benzophenone and anthrone", *Rev. Roumaine Chim.*, **14**, 831 (1969).
40. V. E. Sahini and Al. Butucelea, "On the n–π* electronic transition in aromatic ketones", *Rev. Roumaine Chim.*, **14**, 981 (1969).
41. M. Hilebrand, O. Maior, V. E. Sahini and E. Volanschi, "Spectral study of some phenoxathin derivatives and their positive ions", *J. Chem. Soc.*, (B), 775 (1969).
42. V. E. Sahini and L. Ciurea, "Electronic spectra of some aromatic metal ketyls", *Rev. Roumaine Chim.*, **14**, 1093 (1969).
43. V. E. Sahini and C. I. Ghirvu, "Pariser-Parr Treatment of substituted benzenes. II", *Rev. Roumaine Chim.*, **15**, 11 (1970).
44. M. Hillebrand, O. Maior and V. E. Sahini, "Charge transfer heterocomplexes of the aromatic heterocycles. I", *Rev. Roumaine Chim.*, **15**, 149 (1970).
45. V. E. Sahini, C. Podină and V. Constantin, "L'étude des picolines par spectrométrie de masse", *Rev. Roumaine Chim.*, **15**, 495 (1970).
46. A. Gioabă, V. E. Sahini and E. Volanschi, "Charge transfer complexes of the aromatic heterocycles. II", *Rev. Roumaine-Chim.*, **15**, 309 (1970).
47. A. Gioabă, V. E. Sahini and E. Volanschi, "Spectral study of phenoxatellurine and some of its derivatives", *Rev. Roumaine Chim.*, **15**, 501 (1970).
48. V. E. Sahini and M. Craiu, "Depolarisation ratio of the Raman lines of molecules containing carbonyl group", *Rev. Roumaine Chim.*, **15**, 675 (1970).
49. V. E. Sahini and M. Dobrescu, "On the carbonyl stretching frequency of halogen-substituted benzophenones", *Rev. Roumaine Chim.*, **15**, 679 (1970).
50. V. E. Sahini and M. Craiu, "Raman spectrum of acetophenone. II", *Bull. Inst. Politeh Iași*, **XVI**, 183 (1970).
51. V. E. Sahini and C. I. Ghirvu, "Pariser-Parr treatment of substituted benzenes. III", *Rev Roumaine Chim.*, **16**, 149 (1971).
52. V. E. Sahini and C. I. Ghirvu, "Charge transfer study on the electronic structure an spectra of the monosubstituted naphthalenes", *Rev. Roumaine Chim.*, **16**, 321 (1971)
53. V. E. Sahini and V. Tufoi, "SCF-MO calculation of the electronic energy levels c $Co[(NH_3)_5Cl]^{2+}$", *Rev. Roumaine Chim.*, **16** 789 (1971).
54. V. E. Sahini, M. Dobrescu and C. Bendic, "Electronic structure and electronic spectra carbazole positive ions", *Rev. Roumaine Chim.*, **16**, 1131 (1971).
55. M. Hillebrand, O. Maior and V. E. Sahini, "Radical cation-dimer equilibrium in strongl acidic solutions of phenoxaselenine", *Rev. Roumaine Chim.*, **16**, 1489 (1971).
56. V. E. Sahini and J. Weinberg, "Electronic structure of xylidine isomers", *Anal. Uni Bucharest* (XX), **2**, 19 (1971).
57. V. E. Sahini and L. Ciurea, "Infrared spectra of carbonyl aromatic ion radicals. I" *Re Roumaine Chim.*, **17**, 273 (1972).
58. V. E. Sahini, V. Tufoi and A. Ivanov, "Considerations about the stability of complex con binations of cobalt", *Rev. Roumaine Chim.*, **17**, 617 (1972).
59. H. Căldăraru, A. Caragheorgheopol and V. E. Sahini, "Electron spin resonance study the iminoxy-radicals of some pyrimidine derivatives", *J. Magnetic Resonance*, **11**, 3 (1973).

60. Al. Gioabă, V. E. Sahini and E. Volanschi, NMR spectra of some phenoxatellurine derivatives", *Rev. Roumaine Chim.*, **18**, 531 (1973).

61. V. E. Sahini and M. Olteanu, "Solvent effect on the anharmonicity of the C=O vibration of acetophenone and benzophenone", *Rev. Roumaine Chim.*, **18**, 361 (1973).

62. M. Dobrescu-Ciureanu and V. E. Sahini, "A perturbation treatment of molecular complexes. III", *Rev. Roumaine Chim.*, **18**, 921 (1973).

63. V. E. Sahini, C. Podină and M. Strul, "Etude des isomers de la nitroaniline par spectrométrie de masse", *Rev. Roumaine Chim.*, **18**, 1283 (1973).

64. V. E. Sahini and J. Weinberg, "Xilidine isomers. II", *Rev. Roumaine Chim.*, **18**, 1493 (1973).

65. A. Caragheorgheopol, H. Căldăraru and V. E. Sahini, "Assignement of proton hyperfine splitting constants in cyclic α-keto-iminoxy radicals", *Rev. Roumaine Chim.*, **18**, 1497 (1973).

66. V. Em. Sahini, M. Craiu and E. Ivana, "Spectrographic determination of traces of copper, lead, chromium, nickel, molybdenum and cobalt in natural waters", *Rev. Roumaine Chim.*, **19**, 165 (1974).

67. C. Simionescu, S. Dumitrescu, T. Lixandru, M. Dăringă, B. Simionescu, M. Viţă, V. E. Sahini and J. Weinberg, "Polimeri *orto* i *para*-fenil-atsetilena", *Vysokomol. Soedineniya*, tom (A) **16**, 7 (1974).

68. R. Beldie, A. Butucelea and V. E. Sahini, "The carbon-carbon stretching frequency in ethane, ethane-d_6 and ethane-t_6", *Rev. Roumaine Chim.*, **21**, 327 (1976).

69. R. Grigorovici, A. Butucelea, V. E. Sahini and M. K. Dehrmond, "Normal coordinate analysis of hexahaloethanes", *Rev. Roumaine Chim.*, **21**, 965 (1976).

70. V. E. Sahini, J. Weinberg and M. Vasilescu, "Xylidine isomers. IV. Dipole moments in the first excited singlet state", *Rev. Roumaine Chim.*, **21**, 112 (1976).

71. L. Ciurea, V. Em. Sahini and A. Mateescu, "Spectral study of 4,7-phenanthroline-5,6-dione radical anion" *Rev. Roumaine Chim.*, **21**, 1445 (1976).

72. M. Hillebrand, V. Em. Sahini and E. Volanschi, "Electronic structure of the chloro-benzenes in connection with their biological activity", *Bul. Inst. Politeh. Bucharest, Series Chimie-Metalurgie*, **39**, 27 (1977).

73. Al. Gioabă, V. Em. Sahini and E. Volanshi, "Electron spin resonance spectra and electronic structure of nitrophenoxatellurin anion-radicals", *J. Chem. Soc.* (*Perkin II*). **1977**, 529.

74. V. E. Sahini and A. Savin, "On the stability of aromatic hydrocarbons. IV. On the linearity of the delocalization energy relationships', *Rev. Roumaine Chim.*, **22**, 39 (1977).

75. L. Ciohodaru, V. Em. Sahini and E. Volanschi, ,,The electronic structure of some stilbene derivatives. IV. ESR spectra of some nitro-containing stilbene anion-radicals", *Rev. Roumaine Chim.*, **22**, 171 (1977).

76. V. Em. Sahini and S. Bădilescu, "Collision-induced light absorption in liquid mixtures" *Rev. Roumaine Chim.*, **22**, 811 (1977).

77. M. Ciureanu and V. E. Sahini, "A spectroscopic study of iodine complexes with some heterocycles in the azoles series", *Rev. Roumaine Chim.*, **22**, 1441 (1977).

78. C. Bendic, M. Hillebrand and V. E. Sahini, "Computer program for S.C.F.-C.F. Calculations. I. Closed shell systems", *Rev Roumaine Chim.*, **23**, 3 (1978).

79. V. E. Sahini, V. Constantin, I. Şerban and C. Vlădescu, "Electron-impact-induced fragmentation of dibenzo [b, e] oxepin-11-one and dibenzo-[b,e]thiepin-11-one, *Rev. Roumaine Chim.*, **23**, 163 (1978).

80. V. E. Sahini, V. Constantin, I. Şerban and C. Vlădescu, "Electron-impact-induced fragmentation of some dibenzo[b,e]thiepines", *Rev. Roumaine Chim.*, **23**, 315 (1978).

81. V. E. Sahini, V. Constantin and I. Şerban, "Determination of ionization potential using a MI-1305 mass spectrometer", *Rev. Roumaine Chim.*, **23**, 479 (1978).

82. V. E. Sahini, R. Grigorovici and A. Butucelea, "A modified Urey-Bradley force field for hexahalodisilanes", *Rev. Roumaine Chim.*, **23**, 643 (1978).

83. A. Căilean, C. Mandravel and V. E. Sahini, "Studiul fizico-chimic al complexării de tip donor-acceptor în sistemul : Di-P-Tolilseleniura-Iod I", *Rev. chim. (Bucureşti)*, **29**, 939 (1978).

84. V. E. Sahini and A. Savin, "On the stability of aromatic hydrocarbons. V. Use of localised molecular orbitals in delocalization energy relationships", *Rev. Roumaine Chim.*, **24**, 165 (1979).

85. A. Căilean, C. Mandravel and V. E. Sahini, "The evaluation of the two-center overlap integral for selenium-iodine bond of the donor-acceptor type", *Rev. Roumaine Chim.*, **24**, 391 (1979).

86. M. Ciureanu and V. E. Sahini, "A spectroscopic study of iodine complex, with aromatic amines", *Rev. Roumaine Chim.*, **24**, 655 (1979).

87. M. Contineanu, M. Ciureanu and V. E. Sahini, "Nuclear magnetic resonance study of self-association equilibria of aromatic amines in carbon tetrachloride", *Rev. Roumaine Chim.*, **24**, 663 (1979).

88. J. Weinberg and V. Em. Sahini, "Xylidine isomers. VI. Cndo calculations on 2,4- and 2,6-xylidine", *Rev. Roumaine Chim.*, **25**, 9 (1980).

89. V. E. Sahini and A. Savin, "On a possible improvement of localized molecular orbitals", *Chem. Phys. Letters*, **69**, 514 (1980).

90. A Caragheorgheopol, H. Căldăraru, I. I. Bădilescu and V. E. Sahini "An electron spin resonance study of the iminoxy radicals of 1-Benzoxepin-5-one derivatives", *Rev. Roumaine Chim.*, **25**, 307 (1980).

91. M. Hillebrand and V. Em. Sahini, "The electronic structure of phenoxaselenine' " *Rev. Roumaine Chim.*, **25**, 625 (1980).

92. M. Hillebrand and V. Em. Sahini, "Unrestricted Hartree-Fock spin densities of some heteroaromatic cation-radicals", *Rev. Roumaine Chim.*, **25**, 631 (1980).

93. V. E. Sahini, S. Moldoveanu and C. Mihailciuc, "On chlorobenzamide molecular structure", *Rev. Roumaine Chim.*, **25**, 1055 (1980).

94. V. Em. Sahini, E. Volanschi and A. Meghea, "ESR spectra and electronic structure of some diphenylamine anion-radicals", *Rev. Roumaine Chim.*, **25**, 449 (1980).

95. C. Bendic, I. Ciurea and V. Em. Sahini, "Structura electronică a unor aminodifenileteri", *Bul. Inst. Politeh. Bucharest, Series Chimie-Metalurgie*, **XLII**, 61 (1981).

96. J. Weinberg and V. Em. Sahini, "Xylidine isomers. VII. Structure-hepatotoxic activity relationships of some xylidines", *J. Theor Biol.*, **88**, 153 (1981).

97. M. Ciureanu, V. Sahini, F. Cornea, C. Cercasov and M. Contineanu, "Dynamic NMR study of hindered rotation around the C.N. bond in thiopiperidides", *Org. Magn. Reson*, **15**, 148 (1981).

98. V. E. Sahini and A. Savin, "On the use of atom-localized molecular orbitals", *Z. Naturforsch.*, **36a**, 415 (1981).

99. J. Weinberg and V. Em. Sahini, "Xylidine isomers. V. Molecular complex spectra of iodine with xylidines", *Rev. Roum. Chim.*, **26**, 521 (1981).

100. L. Ciurea, C. Bendic and V. Em. Sahini, "II. Dipol moments of some Aminodiphenylethers", *Bul. Inst. Politeh. Bucharest, Series Chimie-Metalurgie*, **XLIII**, 39 (1981).

101. V. Em. Sahini, C. Bendic and L. Virag, "Reactivity of *m*-nitrophenyl acetate in excited state", *Rev. Roumaine Chim.*, **27**, 129 (1982).

102. C. Bendic, L. Ciurea and V. Em. Sahini, "III. Electronic structure of some nitrodiphenylethers", *Bul. Inst. Politeh. Bucharest, Series Chimie-Metalurgie*, **XLIV**, 53 (1982).

103. C. Cercasov, F. Cornea, M. Ciureanu, M. Hillebrand, V. Em. Sahini and E. Volanschi, "Electron spin resonance studies of several anion radicals of nitro-substituted thyoacylpiperidines and morpholines, *Org. Magn. Reson.*, **20**, 221 (1982).

104. J. Weinberg, A. Dănescu and V. Em. Sahini, "MO-LCAO Hüchel calculations of some β-lactam antibiotics", *Studia biophysica*, **93**, (3), 161 (1983).

105. M. Ciureanu, F. Cornea, V. Sahini and C. Cercasov, "Studies on the electronic spectra of thioacylpiperidides and morpholides", *Rev. Roumaine Chim*, **28**, 555 (1983).

106. V. Em. Sahini and El. Volanschi, "Electronic structure and UV-spectral of some dibenzo-b, e-thiepine derivatives", *Rev. Roumaine Chim.*, **28**, 785 (1983).

107. M. Ciureanu, V. Em. Sahini, M. Contineanu, F. Cornea and C. Cercasov, "Internal rotation in change transfer complexes", *Rev. Roumaine Chim.*, **28**, 875 (1983.)

108. C. Cercasov, F. Cornea, M. Ciureanu, M. Hillebrand, V. Em. Sahini and El. Volanschi, "ESR and ^{1}H-NMR spectra of some nitrosubstituted thiobenzamides", *Rev. Roumaine Chim.*, **29**, 25 (1984).

109. V. Em. Sahini, "A method for partition coefficient calculation", in Vol. "New trends in the study of water and ions in biological systems" (V. Vasilescu, C. F. Hazlewood, Eds., Biophysical Laboratory, Medical Faculty, Bucharest, 1984).

110. V. Em. Sahini, "On the significance of the chemical bond concept", *Noesis*, **10**, 111 (1984).

111. M. Ciureanu, M. Hillebrand, V. Em. Sahini and El. Volanschi, "U.M.F. spin density calculations on substituted nitroaromatic anions radicals", *Rev. Roumaine Chim.*, **30**, 97 (1985).

112. V. Em. Sahini, "Molecular modifications of irradiated plant tissues after dehydration as revealed by ESR spectra", "Water and Ions in Biological Systems" (B. Pullman, V. Vasilescu L. Packer Eds., U.S.M.S. Bucharest, 1985, p. 131).

113. M. F. Tripșa, V. Em. Sahini and V. Vasilescu, "Anaesthetics and excitability", "Water and Ions in Biological Systems" (B. Pullman, V. Vasilescu L. Packer Eds., U.S.M.S., Bucharest, 1985, p. 417).

114. M. Tripșa, V. Em. Sahini, C. Nae and V. Vasilescu, "Structure-nerve membrane effect relationships of some local anaesthetics", *Gen. Physiol. Biophys.*, **5**, 371 (1986).

115. M. Hillebrand and V. Em. Sahini, "Electronic spectra of some heteroaromatic cation-radicals", *Rev. Roumaine Chim.*, **31**, 649 (1986).

116. M. Bugeanu, V. Em. Sahini, V. T. Ciorba and A. T. Balaban, "Molecular complexes with aromatic cations as electron acceptors, VII", *Rev. Roumaine Chim.*, **31**, 1013(1986).

Revue Roumaine de Chimie, **32**, *11—12*, 1025—1031 (1987)

Dedicated to Professor V. E. SAHINI
on his 60th anniversary

ISOTHERMAL LIQUID-VAPOUR EQUILIBRIUM IN THE ACETONITRILE-PROPIONITRILE SYSTEM

RODICA VÎLCU, VIELKA LANGSHAW and ZOICA CENUȘE
Chair of Chemical Thermodynamics and Electrochemical Technology, Department of Chemical Technology, Polytechnic Institute, Blvd Republicii 13, Bucharest
Romania

Received June 27, 1987

The present paper reports data on the liquid-vapour equilibrium in the acetonitrile-propionitrile binary system, under isothermal conditions at 25, 30, 35, 40, 45 and 50°C. The molar fractions of the vapour phase in equilibrium were calculated on the basis of the experimental data obtained, $P = f(x)$, by integrating the coexistence equation under isothermal conditions. The final data were correlated with the Wilson equation and compared with those predicted by the UNIFAC equation.

It is well known that nitriles are important components of several mixtures that appear in the synthesis of plastics or as a result of the extractive distillation in certain industrial processes. They are also highly interesting in that the specialty literature offers — on liquid-vapour equilibrium — many experimental data not corroborating the various models existing for their generalization.

For a complete understanding of the acetonitrile behaviour in other solvents than hydrocarbons or alcohols we have studied the acetonitrile (1)-propionitrile(2) system.

The experimental calculations started with the measurement of the vapour pressures of pure propionitrile, with the view of determining the Antoine equation. These results were generalized within the temperature range in which the isothermal equilibrium data were obtained for the acetonitrile(1)—propionitrile(2) binary.

For these measurements the installation described in a previous paper was used. [1]

The data of the saturated pressures obtained experimentally, the saturation pressures recalculated according to the Antoine equation — whose parameters are suggested by us — as well as the relative deviation for predicting the saturation pressure are given in table 1.

Table 1

Experimentally determined and calculated saturation pressures of propionitrile

t (°C)	P_{exp} (mmHg)	$P_{calcd.}$ with the Antoine eq. suggested (mmHg) $A = 6.782116$ $B = 1202.837$ $C = 211.000$ $t_{f_{760}} = 97.317$	$\frac{\Delta p}{P}$	$P_{calcd.}$ with the Antoine eq. in the lit. (mmHg)	$\frac{\Delta p}{P}$
20.1	37.69	37.64	0.0013	36.44	0.03
30.75	64.18	64.05	0.002	61.65	0.039
40.2	98.83	98.5	0.003	94.95	0.034
51.05	155.62	155.47	0.001	150.40	0.033
55.8	187.58	187.68	0.0005	181.94	0.031
60.0	220.39	220.48	0.0004	214.19	0.029
relative average deviation			0.00136		0.033

Our own experimental data on the saturation pressure of propionitrile, correlated with the relative average deviation, 0.00136, are slightly higher than the values obtained by Hala; [2] but as they were often measured, either by incresing the temperature or by decreasing it to reproducibility we consider them correct and use them in the correlation of the binary systems.

Acetonitrile has the same physical properties as that used in the study of the methanol—acetonitrile binary system.[3]

Table 3 shows the experimental values of acetonitrile(1)—propionitrile(2) binary system, obtained in the same installation, [1] at different concentrations and temperatures, and also the data correlated with the Antoine-type equation.

Table 3 presents the total saturation pressures of the acetonitrile (1)—propionitrile(2) system, at 25, 30, 35, 40, 45 and 50°C, recalculated by the Antoine equation. These saturation pressures are given at different temperatures and concentrations as a function of the molar fraction of acetonitrile (x_1) in Fig. 1.

Examination of figure 1 shows that the acetonitrile-propionitrile system has an ideal behaviour within the whole concentration range. As a matter of fact we envisaged this behaviour due to the likeness of the molecules making up the system.

The data of vapour pressures (Table 3) were correlated with the first degree equation whose constants a_0 and a_1 are likewise indicated in the table.

The molar fraction of the vapour phase in equilibrium with the liquid phase was calculated by integrating the coexistence equation transposed under isothermal conditions. It has the following working form:

$$\frac{\mathrm{d}y}{\mathrm{d}x} = \frac{Uy_1\,(1 - y_1)}{(y_1 - x_1)} \cdot \frac{\mathrm{d}P}{\mathrm{d}x} \tag{1}$$

Table 2

Total saturation pressure in the acetonitrile(1)-propionitrile(2) system

x_1	t(°C)	P_{exp} (mmHg)	P_{calcd} (mmHg)	A	B	C	$\Delta P/P \cdot 100$	Relative average deviation
0.0410	20.5	37.16	37.01	6.901027	1263.7484	217.00	0.32	0.25
	25.5	49.19	48.94				0.51	
	30.1	61.00	61.19				−0.31	
	34.75	76.00	76.06				−0.08	
	45.50	112.45	112.15				0.27	
	50.55	150.49	150.53				−0.03	
0.1376	20.0	42.98	42.22	6.994316	1309.9782	224.00	0.14	0.22
	25.3	54.95	54.91				0.07	
	30.7	71.37	70.97				0.56	
	40.1	108.58	108.18				0.37	
	45.0	133.22	133.20				0.02	
	50.9	169.74	169.44				0.18	
0.2052	20.0	44.52	44.47	7.017874	1320.9725	226.0	0.11	0.25
	25.1	57.77	57.17				1.04	
	30.5	73.97	73.77				0.27	
	35.7	93.30	93.37				0.08	
	40.1	113.17	113.16				0.01	
	50.9	176.70	176.72				−0.01	
0.3707	20.0	50.00	49.98	7.143635	1382.9790	234.0	0.04	0.178
	25.5	65.35	65.20				0.02	
	30.1	80.36	80.73				−0.5	
	34.75	99.57	99.46				0.1	
	43.5	144.26	144.56				−0.2	
	50.55	191.98	192.04				−0.03	
0.4619	20.0	52.98	53.03	7.206909	1414.4595	238.0	0.09	0.0625
	25.9	68.78	68.69				0.13	
	30.5	86.82	86.88				0.07	
	35.5	108.43	108.45				0.02	
	50.55	201.80	201.81				0.00	
0.6939	20.1	61.81	61.04	7.29695	1455.5516	244.0	1.25	0.45
	24.7	75.08	75.85				1.03	
	30.1	97.10	96.97				0.13	
	35.5	123.00	122.82				0.50	
	40.3	150.58	150.38				0.3	
	50.3	224.40	224.46				0.03	

Table 3

Total saturation pressures at 25, 30, 35, 40, 45 and 50°C in the acetonitrile(1)-propionitrile (2) system

x_1	P(mmHg) (25°C)	P (30°C)	P (35°C)	P (40°C)	P (45°C)	P (50°C)
0.0	48.49	61.81	78.04	97.64	121.10	148.99
0.041	50.17	63.86	80.53	100.65	124.71	153.30
0.1376	54.12	68.69	86.40	107.72	133.20	168.44
0.1852	56.08	71.08	89.29	111.22	137.40	169.44
0.2025	56.89	72.08	90.51	112.67	139.13	170.51
0.3268	61.87	78.17	97.89	121.59	149.85	183.32
0.3707	63.67	80.37	100.57	124.81	153.72	187.93
0.4619	67.41	84.93	106.11	131.50	161.74	197.51
Correlation constants a_0	48.49	61.81	78.04	97.64	121.10	148.99
a_1	40.96	56.05	60.77	73.33	87.99	105.02

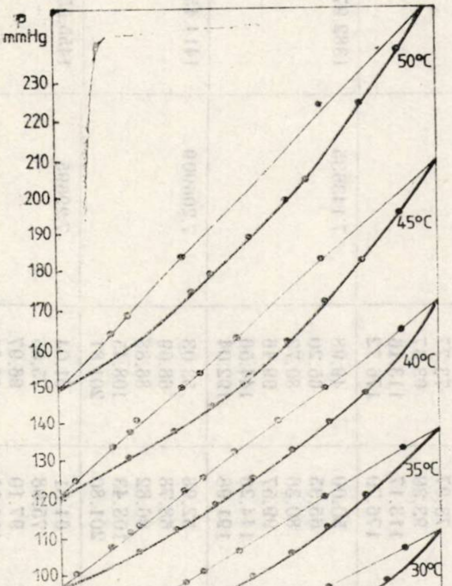

Fig. 1. — Total saturation pressures in the acetonitrile-propionitrile system.

where the U function is calculated either by the P—V—T data or by a state equation. Using the virial state equation for the vapour phase, U will become :

$$U = \frac{x_1B_{11} + x_2B_{22} - V^2}{R_T} + \frac{1}{P} \tag{2}$$

where the virial coefficients of the pure substances were appreciated by a Tsonopoulos type equation.[4]

The volume of the liquid mixture was considered a linear function of the molar fraction in respect of the molar volumes of the pure elements :

$$V^L = x_1V_1 + x_2V_2 \tag{3}$$

as the neglection of the volume variation after mixing does not influence the calculation owing to the magnitude values that appear in the expression of U.

The numerical integration was achieved by applying the Runge—Kutta method;[2] for starting the integration — due to the form of the working equation that has singular points at the extreme values of the concentration $x_1 = 0$ and $x_1 = 1$ — the development in the Taylor series was used in the vicinity of these extreme points.

As the system has an ideal behaviour in liquid state, the coexistence equation was continously integrated between the two limit values of the concentration.

The calculated values of the vapour phase composition were given in table 4.

In this system the ideal behaviour was immediately recorded by the Λ_{ij} parameters of the Wilson equation for which $\lambda_{ij} - \lambda_{ii} = 0$. In this case Λ_{ij} depends only on the ratio of the molar volumes of the two liquids in V_j/V_i.

This situation was also reconfirmed by the constant value of the relative volatility $\alpha = 1.857$.

Table 5 gives the values of the saturation pressures recalculated with the parameters used for the generalization of the saturation pressure variation as a function of molar fraction of the liquid phase versus the pressures predicted by the UNIFAC model.

Examination of the table shows a good agreement of the experimentally obtained data with those calculated with the UNIFAC model,[5] an agreement also explained by the ideal character of the studied binary.

Table 4

Molar fraction of the vapour phase at equilibrium, calculated by integration of the coexistence equation

P (mmHg)	x_1	y_1	
$t=25°$			
50.537994	0.0500	0.0881	$B_{11}=-6121.49$ cm^3/mol
52.585999	0.1000	0.1693	$B_{22}=-4295.78$ cm^3/mol
56.682007	0.2000	0.3141	$V_1=52.53$ cm^3
60.778000	0.3000	0.4396	$V_2=70.93$ cm^3
64.873993	0.4000	0.5493	
68.970001	0.5000	0.6461	
73.059998	0.6000	0.7322	
77.162003	0.7000	0.8094	
81.257996	0.8000	0.8789	
85.354004	0.9000	0.9421	
87.462006	0.9500	0.9717	
$t=30°$C			
64.311996	0.5000	0.0863	$B_{11}=-5605.15$
66.815002	0.1000	0.1665	$B_{22}=-3966.67$
71.820007	0.2000	0.3098	$V_1=52.83$
76.824997	0.3000	0.4348	$V_2=71.3$
81.830002	0.4000	0.5443	
96.839996	0.5000	0.6415	
91.839996	0.6000	0.7282	
96.845001	0.7000	0.8062	
101.250000	0.8000	0.8761	
106.854996	0.9000	0.9420	
109.356995	0.9500	0.9711	
$t=35°$C			
81.078003	0.0500	0.0851	$B_{11}=-5143.69$
84.117004	0.1000	0.1640	$B_{22}=-3672.35$
90.194000	0.2000	0.3060	$V_1=53.24$
96.270004	0.3000	0.4302	$V_2=71.78$
102.350006	0.4000	0.5397	
108.425003	0.5000	0.6372	
114.501999	0.6000	0.7245	
120.578995	0.7000	0.8032	
126.656006	0.8000	0.8741	
132.733002	0.9000	0.9399	
135.770004	0.9500	0.9705	
$t=40°$C			
101.306000	0.0500	0.0838	$B_{11}=-4730.34$
104.973007	0.1000	0.1617	$B_{22}=-3197.22$
112.306000	0.2000	0.3024	$V_1=53.61$
119.639008	0.3000	0.4260	$V_2=72.22$
126.972000	0.4000	0.5355	
134.304993	0.5000	0.6330	
141.638000	0.6000	0.7211	
148.970993	0.7000	0.8001	
156.304001	0.8000	0.8726	
163.636993	0.9000	0.8382	
168.770004	0.9500	0.9700	

Table 4 (continued)

$t=45°C$

P	x_1	y_1	
125.500000	0.0500	0.0828	$B_{11}=-4359.27$
129.899002	0.1000	0.1597	$B_{22}=-3170.11$
138.697998	0.2000	0.2993	$V_1=72.67$
147.469994	0.3000	0.4223	$V_2=53.98$
156.296005	0.4000	0.5317	
165.095001	0.5000	0.6291	
182.692993	0.7000	0.7979	
173.893997	0.6000	0.7979	
191.490005	0.8000	0.8710	
200.289993	0.9000	0.9380	
204.690002	0.9500	0.9690	

$t=50°C$

154.240005	0.0500	0.0817	$B_{11}=-4025.43$
159.492004	0.1000	0.1580	$B_{22}=-2955.31$
169.994003	0.2000	0.2968	$V_1=54.37$
180.496002	0.3000	0.4193	$V_2=73.13$
191.000000	0.4000	0.5288	
201.500000	0.5000	0.6267	
212.001999	0.6000	0.7153	
222.503998	0.7000	0.7959	
233.005997	0.8000	0.8695	
243.507996	0.9000	0.9372	
248.769003	0.9500	0.9692	

Table 5

Values of the saturation pressures calculated by the UNIFAC model for the acetonitrile (1)-propionitrile(2) system

x_1	P_{exp} (mmHg) (25°C)	$P_{calcd.}$ UNIFAC	P_{exp} (mmHg) (30°C)	$P_{calcd.}$ UNIFAC	P_{exp} (mmHg) (35°C)	$P_{calcd.}$ UNIFAC	P_{exp} (mmHg) (40°C)	$P_{calcd.}$ UNIFAC
0.1	52.59	52.66	66.91	66.815	84.117	84.24	104.97	105.12
0.2	56.58	56.81	71.98	71.82	90.191	90.39	112.31	112.55
0.3	60.78	60.93	77.02	76.825	96.271	96.52	119.64	119.94
0.4	64.87	65.04	82.04	81.83	102.35	102.61	126.97	127.29
0.5	68.97	69.13	87.03	86.835	108.42	108.67	134.31	134.61
0.6	73.07	73.21	92.02	91.84	114.50	114.72	141.64	141.91
0.7	77.16	77.28	96.99	96.845	120.57	120.76	148.97	149.12
0.8	81.26	81.34	101.95	101.85	126.65	126.78	156.30	156.46
0.9	85.39	85.35	106.91	106.855	132.73	132.8	163.64	163.72

REFERENCES

[1] R. Vîlcu, Z. Cenuşe, F. Gothard and V. Langshaw, *Rev. Roumaine Chim.*, **28**, 891 (1983).

[2] E. Hala, I. Wichterle and J. F. Boublik, "Vapour Liquid Equilibria Data at Normal Pressures", Pergamon Press, Oxford, 1968.

[3] R. Vîlcu, V. Langshaw and Z. Cenuşe, *Bull. Inst. Politeh. Bucureşti*, **XLVI–XLVII**, 32 (1985).

[4] C. Tsonopoulos, *Amer. Inst. Chem. Engineers J.*, **20**, 263 (1974).

[5] A. Fredeslund, J. Ghehling and P. Rasmussen, "Vapour Liquid Equilibria Using UNIFAC", Amsterdam, 1977.

Revue Roumaine de Chimie, **32**, *11–12*, 1033–1037 (1987)

Dedicated to Professor V. E. SAHINI
on his 60th anniversary

ANGULAR OVERLAP MODEL (AOM) CALCULATIONS FOR THE COORDINATION COMPOUNDS WITH MACROCYCLIC LIGANDS. I

AOM PARAMETERS FOR NICKEL(II) COORDINATION COMPOUNDS WITH TETRAKIS-ANHYDRO-AMINOBENZALDEHYDE MACROCYCLIC LIGAND

MARIUS ANDRUH [*], C. I. LEPADATU [**] and MARIA BREZEANU [*]

[*] Laboratory of Inorganic Chemistry, Faculty of Chemical Technology, Polytechnic Institute, str. Dumbrava Roșie no. 23, Bucharest, Romania

[**] Center of Physical Chemistry, ICECHIM, Splaiul Independenței no. 202, Bucharest, Romania

Received May 20, 1987

The Angular Overlap Model parameters, taking into account the complete configuration interaction, for nickel(II) coordination compounds with tetrakis-anhydro-aminobenzaldehyde (TAAB) macrocyclic ligand are calculated. The input data were derived from the electronic spectra reported for two complexes : $[Ni(TAAB)(NCS)_2]$ and $[Ni(TAAB)(N_3)_2]$ (Busch, 1977). The corresponding parameters give information on the relative σ and π magnitude interactions of the metal ion with the ligands involved and emphasize the π-acceptor ability of the macrocyclic ligand.

1. INTRODUCTION

The appearance of the coordination chemistry with macrocyclic ligands, twenty years ago, has stimulated, during the last ten years, theoretical approaches and more sophisticated experimental studies. [1]

Complexes of the type **1** are ideally suited to the study of the effects of tetragonal fields on the electronic states of the metal ions ; on the other hand, the experimental data, as well as, the semiempirical calculations emphasize the occurrence of the so-called "macrocyclic effect" [2], whose explanation is still contradictory. [3-7]

The ligand tetrakis-anhydro-aminobenzaldehyde, TAAB, **2**, is among the most extensively studied macrocyclic ligands, especially in the nickel

(II) coordination chemistry.[8-11] The semiempirical calculations carried out by Busch *et al.*[4] using both weak and strong field approaches emphasized some electronic particularities of this ligand. The aim of this paper is to calculate the Angular Overlap Model (AOM) and Racah parameters

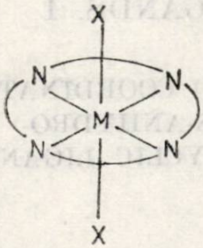

1.

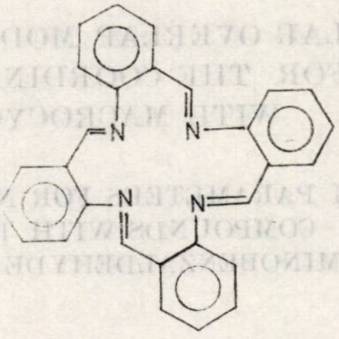

2.

by fitting the excited state energies, in order to get information on the relative σ and π magnitude interactions of the metal ion with the nitrogen atoms of the macrocyclic ligand.

2. RESULTS AND DISCUSSION

The complexes studied in this paper are [Ni(TAAB)(NCS)$_2$] and [Ni(TAAB)(N$_3$)$_2$], characterized by a high spin electronic configuration, *i.e.* a $^3B_{1g}$ ground state in D_{4h} symmetry.[4,8,9] Our calculation procedure is that usually employed for *trans*- Nia$_4$b$_2$ chromophores,[12], including the complete configuration interaction between the three E_g levels and between the two A_{2g} levels. The calculations assumed the following equations:

$$\begin{array}{c|ccc|l} & {}^3E_g^a & {}^3E_g^b & {}^3E_g^c & \\ {}^3E_g^a & A_{11}-E & A_{12} & A_{13} & \\ {}^3E_g^b & A_{21} & A_{22}-E & A_{23} & =0 \\ {}^3E_g^c & A_{31} & A_{32} & A_{33}-E & \end{array}$$

$$\begin{array}{c|cc|l} & {}^3A_{2g}^a & {}^3A_{2g}^b & \\ {}^3A_{2g}^a & B_{11}-E & B_{12} & =0 \\ {}^3A_{2g}^b & B_{21} & B_{22}-E & \end{array}$$

Thus, with all configuration interactions included, the energies of the six transitions are given by a linear equation, a two by two secular determinant and a three by three secular determinant. The A_{ij} and B_{ij} matrix elements are respectively[13]:

$$A_{11} = \langle {}^3E_g^a | {}^3E_g^a \rangle = 3/2e_\sigma^a + 3/2e_\sigma^b - 2e_\pi^a - 2e_\pi^b$$

$$A_{12} = A_{21} = \langle {}^3E_g^a | {}^3E_g^b \rangle = \sqrt{3}/2(e_\sigma^a - e_\sigma^b)$$

$$A_{22} = \langle {}^3E_g^b | {}^3E_g^b \rangle = 5/2e_\sigma^a + 1/2e_\sigma^b - 2e_\pi^a - 2e_\pi^b + 12B$$

$$A_{23} = A_{32} = \langle {}^3E_g^b | {}^3E_g^c \rangle = 6B$$

$$A_{13} = A_{31} = \langle {}^3E_g^b | {}^3E_g^a \rangle = 0$$

$$A_{33} = \langle {}^3E_g^c | {}^3E_g^c \rangle = 4e_\sigma^a + 2e_\sigma^b - 6e_\pi^a - 2e_\pi^b + 3B$$

$$B_{11} = \langle {}^3A_{2g}^a | {}^3A_{2g}^a \rangle = e_\sigma^a + 2e_\sigma^b - 4e_\pi^a + 12B$$

$$B_{22} = \langle {}^3A_{2g}^b | {}^3A_{2g}^b \rangle = 4e_\sigma^a + 2e_\sigma^b - 4e_\pi^a - 4e_\pi^b + 3B$$

$$B_{12} = B_{21} = \langle {}^3A_{2g}^a | {}^3A_{2g}^b \rangle = 6B$$

The sets of AOM and Racah parameters were estimated by fitting the spectral data[4] using a computer program based on the Davidon–Fletcher–Powell optimization method.[14] The input data are collected from ref. [4]. Table 1 shows the AOM parameters calculated by us.

Table 1

Angular Overlap Model Parameters (kK)*

Parameters	[Ni(TAAB)(NCS)$_2$]	[Ni(TAAB)(N$_3$)$_2$]
e_σ^N(MAC)	4.670	4.513
e_σ^N(X)	2.060	1.880
e_π^NMAC)	−0.162	−0,290
e_π^N(X)	−0.450	−0.135
B	0,850	0.880

* MAC stands for the macrocyclic ligand and X the NCS$^-$ or N$_3^-$ anions; 1 kK = 1000 cm^{-1}.

In order to check up our results and taking into account that the two approaches are not strictly homomorphous, we calculated the parameters Dq^{xy}, Ds, Dt, $d\sigma$ and $d\pi$ which are inter-related with those calculated in the strong field approach.[12] The data collected in Table 2 show a very good agreement between the two semiempirical methods.

According to the results obtained herewith, the ligands involved in the two coordination compounds seem to be π-acceptors, in agreement with earlier observations[4,15]: the relative significance of the π- *vs.* the σ-bonding effect can be judged by the importance of conjugative effects which lowers the energy of the ligands π^* orbitals, favouring metal-ligand back-bonding.

Table 2

Correlation between Semiempirical Parameters (kK)

Parameters	$[Ni(TAAB)(NCS)_2]$		$[Ni(TAAB)(N_3)_2]$	
	AOM	strong field	AOM	strong field
D_q^{xy}	1.465	1.465	1.473	1.473
Dt	0.382	0.379	0.487	0.485
Ds	0.828	0.823	0.708	0.705
$d\sigma$	−1.958	−1.947	−1.975	−1.967
$d\pi$	0.288	0.286	0.155	0.156
B	0.850	0.882	0.880	0.867

It is interesting to note that the $e_\sigma^N(MAC)$ value is fairly close to that calculated for pyridine[13,16]; however, the $NiPy_4X_2$—type complexes are all paramagnetic ($X = Cl, Br, NCS, N_3$) whereas only $[Ni(TAAB)(NCS)_2]$ and $[Ni(TAAB)(N_3)_2]$ have a normal paramagnetic behaviour.

The explanation of this behaviour may be found in the π-donor property of pyridine which lowers the Dq^{xy} parameter, whereas the π-acceptor ability of TAAB macrocyclic ligand increases it. The greatest Dq^{xy} values favour a diamagnetic behaviour or a high spin $\rightleftharpoons$ low spin equilibrium[17]:

$$10\,Dq^{xy}(\mathrm{Py}) = 3e_\sigma^N - 4e_\pi^N = 11.73 \text{ kK}$$

$$10\,Dq^{xy}(\mathrm{TAAB}) = 3e_\sigma^N - 4e_\pi^N = 14.65 \text{ kK, where :}$$

$$e_\sigma^N(\mathrm{Py}) = 4.67 \text{ kK} ;\ e_\pi^N(\mathrm{Py}) = 0.57 \text{ kK}^{13}$$

$$e_\sigma^N(\mathrm{TAAB}) = 4.67 \text{ kK} ;\ e_\pi^N(\mathrm{TAAB}) = -0.162 \text{ kK}.$$

The $e_\sigma^N(X)$ values are in agreement with the position of the NCS^- and N_3^- ions in the spectrochemical series.

In the following papers we shall present similar calculations carried out for nickel(II) coordination compounds with saturated macrocyclic ligands.

REFERENCES

[1] K. B. Yatsimirskii and Ia. D. Lampeka, "Fiziko-himiia komplexov metalov s makrotsiklicheskimi ligandami", Kiev Naukova Dumka, 1985.

[2] D. K. Cabbiness and D. W. Margerum, *J. Amer. Chem. Soc.*, **91**, 6540 (1969).

[3] Y. Hung, L. Y. Martin, S. C. Jackels, A. M. Tait and D. H. Busch, *J. Amer. Chem. Soc.*, **99**, 4029 (1977).

[4] L. Y. Martin, C. R. Sperati, and D. H. Busch, *J. Amer. Chem. Soc.*, **99**, 2968 (1977).

[5] D. H. Busch, *Acc. Chem. Res.*, **11**, 392 (1978).

[6] R. D. Hancock and G. J. McDougall, *J. Amer. Chem. Soc.*, **102**, 6551 (1980).

[7] V. J. Thom, J. C. A. Baeyens, G. J. McDougall and R. D. Hancock, *J. Amer. Chem. Soc.*, **106**, 3198 (1984).

[8] G. A. Melson and D. H. Busch, *J. Amer. Chem. Soc.*, **86**, 4830 (1966).

[9] G. A. Melson and D. H. Busch, *J. Amer. Chem. Soc.*, **86**, 4834 (1966).

[10] K. B. Yatsimirskii and Ia. D. Lampeka, *Zhur. neorg. Khim.*, **27**, 2541 (1982).

[11] M. Andruh, C. I. Lepădatu and M. Brezeanu, *Rev. Roumaine Chim.*, **31**, 943 (1986).

[12] A. B. P. Lever, *Coord. Chm. Rev.*, **3**, 119 (1968).

[13] M. A. Hitchman, *Inorg. Chem.*, **11**, 2387 (1972).

[14] I. Dancea, "Optimization Methods" (in Romanian), Dacia, Cluj-Napoca, 1979.

[15] P. Krumholtz, *Structure and Bonding*, **9**, 139 (1970).

[16] M. Andruh, C. I. Lepădatu, and M. Brezeanu, *Inorg. Chim. Acta*, **131**, 159 (1987).

[17] J. K. Burdett, *Inorg. Chem.*, **14**, 931 (1975).

Revue Roumaine de Chimie, 32, *11—12*, 1039—1044 (1987)

Dedicated to Professor V. E. SAHINI
on his 60th anniversary

KINETICS OF THE SUBSTITUTION REACTION BETWEEN CoC_2O_4 $Bipy_2I$ AND BIPYRIDYL IN AQUEOUS SOLUTION

ECATERINA JURCONI, TATIANA ONCESCU and GEORGETA RĂCĂŞANU
Department of Physical Chemistry, Polytechnic Institute of Bucharest, Bd. Republicii 13, R—70346, Romania

Received April 26, 1987

The kinetics of the substitution reaction between $CoC_2O_4Bipy_2^+$ and 2,2-bipyridyl in aqueous solution have been studied and the corresponding activation parameters are reported. The obtained data show a slow rate process, a significant shift of the equilibrium to the right and the photosensitivity of the reaction product.

INTRODUCTION

The characterization, from the kinetic point of view, of the transition metal complexes with bidentate ligands such as 2,2′-bipyridyl is important also for the investigations concerning the photochemical conversion and storage of solar energy. It is known that these coordination compounds play the role either of the photosensitizer or of the relay, depending on the electron donor-acceptor couple used in such investigations. $CoBipy_3Cl_3$ and $CoBipy_3Cl_2$ are among such complexes.

The literature refers[1] to the synthesis of some Co(III) complexes in crystalline state, starting from solutions of $Co(C_2O_4)_3K_3$ and bipyridyl. Broomhead et al. did not isolate $CoBipy_3Cl_3$ from these solutions. This suggested a study [2] of the kinetics and mechanism of the substitution reaction between the trisoxalato Co(III) complex and bipyridyl, and the following mechanism was proposed :

$$CoOx_3^{-3} + Bipy \rightleftharpoons CoOx_2Bipy^- + Ox^{-2} \quad (1)$$

$$CoOx_2Bipy^- + Bipy \rightleftharpoons CoOxBipy_2^+ + Ox^{-2} \quad (2)$$

$$CoOxBipy_2^+ + Bipy \rightleftharpoons CoBipy_3^{+3} + Ox^{-2} \quad (3)$$

which involves two steps with the formation of the mixed complexes up to the total substitution of the oxalate ligand.

EXPERIMENTAL

$CoC_2O_4Bipy_2I$ was prepared using Broomhead's[1] method by mixing 2,2′-bipyridyl (LOBA p.a.) with $Co(C_2O_4)_3K_3 \cdot 3H_2O$ synthesized in our laboratory according to the Bailar [3] procedure. We also synthesized the reaction final products $CoBipy_3(ClO_4)_3$ and $CoBipy_3(ClO_4)_2$ by modifying for the latter, the procedure described in the literature[4].

The kinetic measurements were carried out at a SP-800 Pye-Unicam spectrophotometer in two ways : the absorption spectrum recorded at different reaction times, or the absorption change during the reaction recorded at a fix wavelength.

RESULTS AND DISCUSSION

We considered necessary to previously test the thermal and photochemical stability of the reaction participants. Their absorption spectra served this purpose. After 5—6 hours at 50°C under continuous irradiation in the spectrophotometer cell, with $\lambda = 500$ nm, the $CoC_2O_4Bipy_2^+$ solution did not change significantly its absorption : from 1.04 to 1.00. Therefore we concluded that this complex is stable thermally as well as photochemically. The reaction product $CoBipy_3^{+3}$ is also practically stable at this temperature, but photochemically not : a small change appears in the

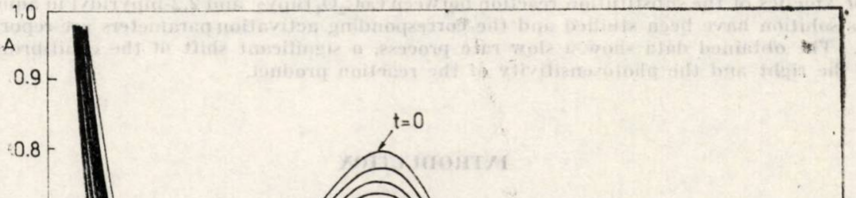

Fig. 1. — Kinetic evolution of the substitution reaction between $CoC_2O_4Bipy_2^+$ and bipyridyl (1 :1) at 50°C ($c = 2.24 \times 10^{-3}$M, $d = 5$ cm).

visible spectrum but the change is much more evident in UV region, manifested by the spectral shifting towards the short wavelengths. Consequently, in order to avoid the photochemical effect, we obturated the spectrophotometer light beam during the reaction and measured only from time to time at fix wavelength, the absorption of the solution in the thermostated cell of the spectrophotometer.

Fig. 1 presents the kinetic evolution of the substitution reaction between $CoC_2O_4Bipy_2^+$ and bipyridyl (1 : 1) at 50°C. The presence of an isosbestic point *at*$\lambda = 468$ nm is a first indication for an equilibrium reaction, therefore we investigated the forward as well as the back process. Kinetic runs carried out at $\lambda = 500$ nm verified a first order kinetics with respect to the $CoC_2O_4Bipy_2^+$ complex, illustrated in Fig. 2.

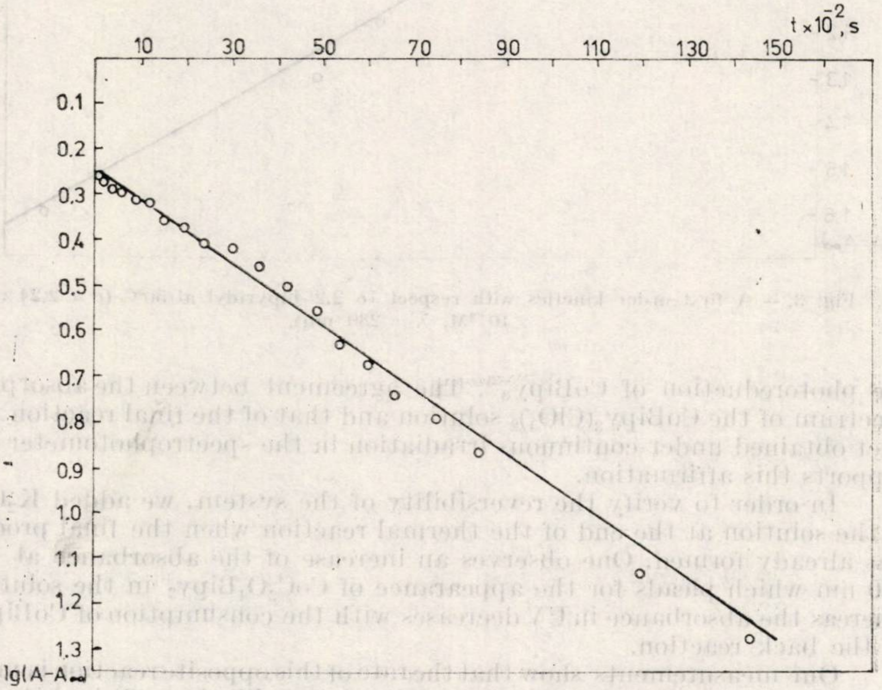

Fig. 2. — A first order kinetics with respect to the $CoC_2O_4Bipy_2^+$ complex at 50°C ($c = 2.24 \times 10^{-3}$ M, $\lambda = 500$ nm).

By following the reaction at $\lambda = 280$ nm, where the bipyridyl presents its absorption maximum, a first order kinetics has also been found (Fig. 3).

The rate constants calculated from the kinetics of both reactants $k_1 = 2.6 \times 10^{-5}s^{-1}$ are in good agreement. Therefore, the overall kinetics of this substitution reaction is of the second order. The formation of $CoBipy_3^{+3}$ during the reaction in the solution kept in the dark at 50°C is confirmed by the similitude between the absorption spectra of the reaction product and of $CoBipy_3(ClO_4)_3$ solution.

In the presence of the light, at the same temperature, another product was obtained namely the $CoBipy_3^{+2}$ complex resulted from

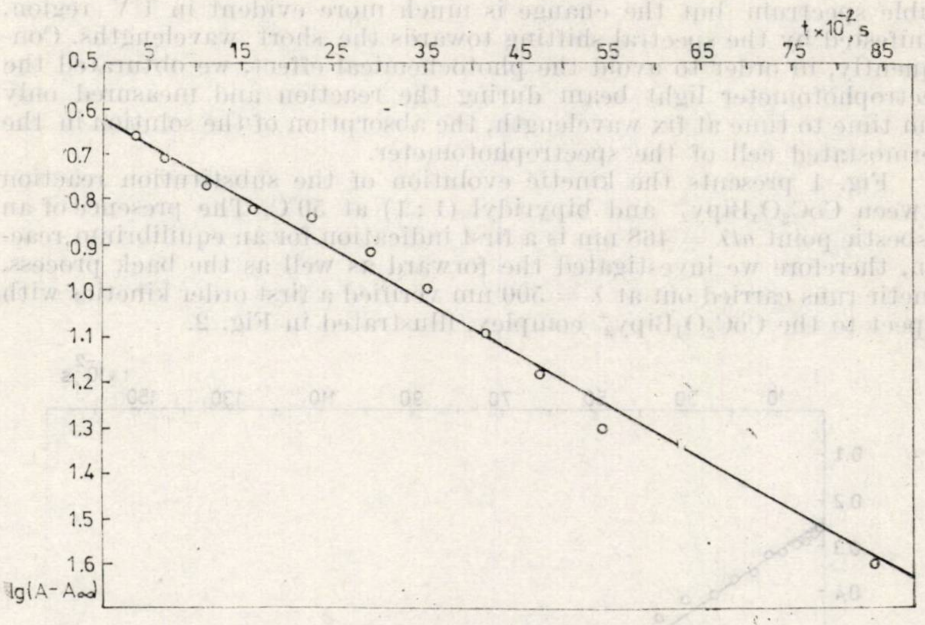

Fig. 3. — A first order kinetics with respect to 2,2′-bipyridyl at 50°C ($c = 2.24 \times \times 10^{-3}$M, λ = 280 nm).

the photoreduction of $CoBipy_3^{+3}$. The agreement between the absorption spectrum of the $CoBipy_3(ClO_4)_2$ solution and that of the final reaction product obtained under continuous irradiation in the spectrophotometer cell, supports this affirmation.

In order to verify the reversibility of the system, we added $K_2C_2O_4$ in the solution at the end of the thermal reaction when the final product was already formed. One observes an increase of the absorbance at λ = 500 nm which pleads for the appearance of $CoC_2O_4Bipy_2^+$ in the solution, whereas the absorbance in UV decreases with the consumption of $CoBipy_3^{+3}$ in the back reaction.

Our measurements show that the rate of this opposite reaction is much slower than the direct one. Consequently, the equilibrium (3) is shifted to the right. In order to annihilate the contribution of the back reaction, we followed the kinetics of the substitution reaction between $CoC_2O_4Bipy_2^+$ and bipyridyl in the dark in excess of bipyridyl (1 : 10). The reaction has been studied at three temperatures : 40°, 50° and 60°C. The determined pseudofirst order rate constant for one of the above temperatures is presented in table 1.

Table 2 presents the obtained $\bar{k}_1$ values at these three temperatures as well as the corresponding calculated k_2 rate constants, $k_2 = \frac{k_1}{c_{Bipy}}$ in which c_{Bipy} is the excess concentration.

From the Arrhenius equation we obtained an activation energy $E^{\neq}$ of 10.5 kcal/mol and a preexponential coefficient $A = 3.16\ 10^{11} s^{-1}$. With these values one calculated the activation parameters of the substitution reaction as follows : $\Delta H^{\neq} = 9.9$ kcal/mol, $\Delta S^{\neq} = -6.12$ cal/mol. degree and $\Delta G^{\neq} = 12.0$ kcal/mol. The negative value of $\Delta S^{\neq}$ attests a reduced freedom of motion in the transition state and therefore a slow reaction.

Table 1

Kinetic data of the thermal substitution reaction at 40°C

t, s	Δt, s	A	$\Delta \lg A$	$k_1/2.303$, s^{-1}
0		0.540		—
840	840	0,530	0.0081	1.0×10^{-5}
1800	960	0.515	0.0210	2.2×10^{-5}
3720	1920	0.490	0.0131	1.4×10^{-5}
7620	3960	0.447	0.0399	1.0×10^{-5}
10860	3180	0.420	0.0271	0.9×10^{-5}
13920	3060	0.380	0.0321	1.0×10^{-5}
16320	2400	0.360	0.0348	1.5×10^{-5}
19200	2880	0.340	0.0248	0.9×10^{-5}

$\bar{k}_1 = 2.8\times10^{-5} s^{-1}$

Table 2

Kinetic parameters of the substitution reaction for three different temperatures

t, °C	T, K	$1/T$, K^{-1}	k_1, s^{-1}	k_2, M^{-1} s^{-1}
40	313	0.00319	2.8×10^{-5}	2.5×10^{-3}
50	323	0.00310	4.1×10^{-5}	4.0×10^{-3}
60	333	0.00300	7.8×10^{-5}	7.0×10^{-3}

We conclude that the substitution of the only one oxalate ligand does not take place easily because bpyridyl is more voluminous than this group, so that there is a steric impediment for the entrance of the third bipyridyl molecule. These results show that concerning the suggested reaction mechanism (1)—(3), the process (3) has not to be taken into account during the short time in which steps (1) and (2) occur. In this system is more probably to take place the association between the anionic and cationic complexes with the formation of the double salt reported in literature : [1]

$$CoOx_2Bipy^- + CoOxBipy_2^+ \rightleftharpoons CoOxBipy_2CoOx_2Bipy \qquad (4)$$

In conclusion, the kinetic data of the present study emphasize the slow rate process of the substitution, the significant shift of the equilibrium to the right and the photosensitivity of its reaction product.

REFERENCES

[1] J. A. Broomhead, M. Dwyer and N. Kane-Maguire, *Inorg. Chem.*, **7**, 1388 (1968)

[2] Ecaterina Jurconi and Tatiana Oncescu, the 4th Conference on Chemistry and Chemical Engineering, Bucharest, 1985.

[3] J. C. Bailar and E. M. Jones, *Inorg. Synt*, **1**, 37 (1939).

[4] F. H. Burstall and R. S. Nyholm, *J. Chem. Soc.* (London), 3570 (1952).

Revue Roumaine de Chimie, **32**, *11–12*, 1045–1050 (1987)

Dedicated to Professor V. E. SAHINI
on his 60th anniversary

THE INFLUENCE OF VARIOUS FACTORS ON THE OPTICAL ACTIVITY OF SOME ESSENTIAL AMINOACIDS. I

APPLICATIONS

CRISTINA MANDRAVEL and LIGIA ANA STASESCU
Department of Physical Chemistry and Electrochemical Technology, Electrofar Factory, Blvd. Republicii 13, Bucharest, Romania

Received June 15, 1987

The purpose of this paper is the study of the dependence of the optical activity on the wavelength, temperature and on the character of the medium, for three aminoacids : L-cysteine, L-histidine and L-tyrosine. As the methods of theoretical computations estimate only the order of magnitude of optical rotation for symmetrical-top and spherical-top molecules, information regarding the influence of different factors on the optical activity are of interest for organic fine synthesis and pharmaceutical industry.

INTRODUCTION

The index, based on the magnitude of optical activity of optically active component in a pharmaceutical product, as enantiomeric purity (or optical purity), presents theoretical and practical interest. Theoretically diminution of the optical purity during a reaction may often give valuable information about its mechanism, if we know this index for reactants and products. In practice of polypeptide synthesis a small quantity of optical impurity in the initial monomer may conduct to polymeric products with substracted homogenity.

Using polarimetry, isotope dilution and, in the last years, NMR spectroscopy and differential calorimetry, simultaneous analysis of stereo isomers components in a mixture may be realised without separation.[1]

In polarimetry, enantiomeric purity of enantiomer L is the ratio of the rotatory power for the mixture, at definite λ and T, to the optical rotatory power of the pure enantiomer L at the same λ and T $[\alpha_{\mathrm{abs}}]_{\lambda}^{T}$ (where the usual reference parameters : $T = 293$ K, $\lambda = 589$ nm).

By spectropolarimetry in some mixtures of the aminoacids and their aminoesters [2] enantiomeric purity may be obtained using reactives for complexation which allow to distinguish interesting species by spectral and polarimetric studies at different wavelengths.

RESULTS AND DISCUSSION

The three aminoacids studied may be considered under the general formula $CR_1R_2R_3R_4$ where $R_1 = H$, $R_2 = COOH$, $R_3 = NH_2$ and $R_4 = CH_2-SH$ for L-cysteine. $HCl \cdot H_2O$; $CH_2-C_3H_3N_2$ for L-histidine. $HCl \cdot H_2O$ and $CH_2-C_6H_5OH$ for L-tyrosine. The molecular weight of the R_4-radicals increases in this series.

From structural point of view the nature of radical R_4 is very interesting in these aminoacids where $R_1R_2R_3$ — radicals are the same. The literature data concerning $[\alpha_{abs}]_D^{20}$ of these aminoacids [3] are given in the experimental part.

Analysis of our experimental data concerning the dependence of the optical activity on λ (in the range 366 to 578 nm) at different temperatures (between 20 and 85°C) reveals for L-cysteine and L-histidine chlorhydrates a positive ORD and for L-tyrosine the fact that the optical power tends to a minimum. For temperatures of 20, 25 and 30°C this minimum is at $\lambda = 446$ nm and at temperatures higher than 60°C this minimum disappears (see Tables 1, 2 and Fig. 1). For many biopolymers [4] a dependence of the optical activity on λ is observed symbatically with the variation of molecular extinction coefficient on the wavelength. Considering the UV-spectrum of L-tyrosine ($\lambda_{max} = 274.5$ nm in 0.01 HCl 1 N solution and $\lambda_{max} = 293.5$ nm in 0.01% NaOH 1 N solution) the observed variation of the optical activity may be explained as a specifical anomalous variation near the absorption band. In the case of L-cysteine and L-histidine-chlorhydrates their absorption bands ($\lambda_{max} = 212$ nm and, respectively, $\lambda_{max} = 215$ nm, both in 0.01% HCl 1 N solution) are disposed to the far-side of the UV-spectrum (in accordance with their smaller molecular weight and smaller number of chromophore groups in their R_4 radical). The variation of the molecular extinction coefficient does not change the dependency of the optical activity on λ. Therefore, if we test the experimental variation of optical activity of L-tyrosine with the relation [5]

$$[\alpha] = \frac{K}{\lambda^2 - \lambda_i^2} \tag{1}$$

(where K — constant, λ_i — current wavelength, λ — the UV-absorption wavelength) convergent values for constant *K* were obtained only for $\lambda_i > 546$ nm. From the shape of the function $[\alpha] = f(\lambda)$, presented in figure 1 it may be considered that this phenomenon is dependent on the disorder grade in solutions, this being further determined by temperature. Until now,[6-13] theoretical computational models predict only the order magnitude of the optical activity for symmetrical-top and spherical-top molecules and sometimes [8-12] the sign of the optical activity in homolog series.

From tables 1 and 2 and from figure 1, the variation of the optical activity on temperature (at different λ) may be extracted for the three aminoacids. In our study the temperature range is extended to 85°C i.e. in the interesting range of temperatures for industrial processes.

For different concentrations of L-cysteine chlorhydrate the value of the slope of the decreasing curves $[\alpha]_\lambda = f(T)$ is the highest at smaller λ.

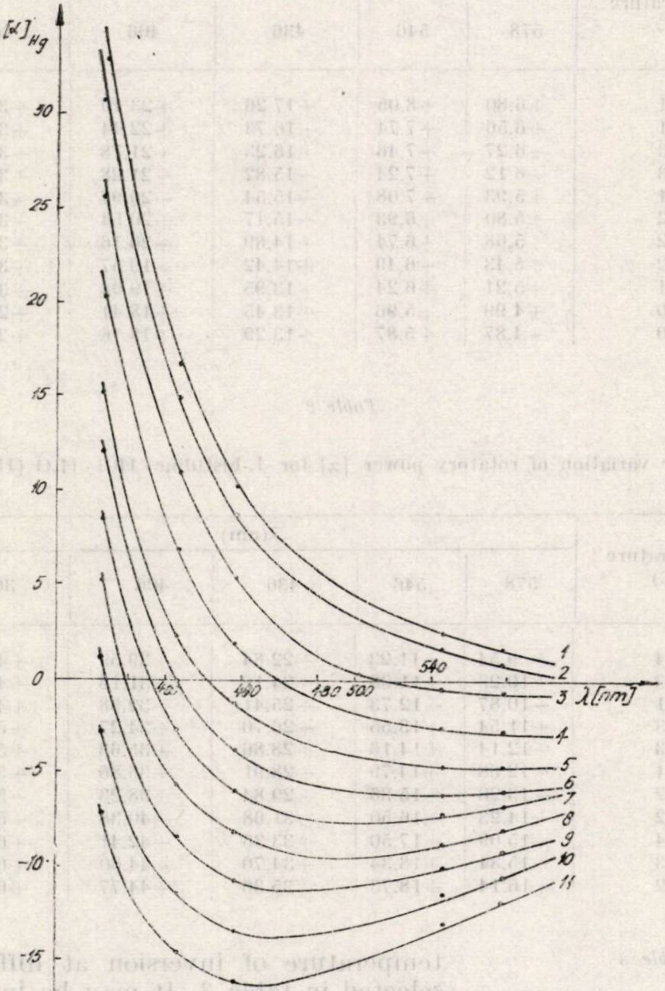

Fig. 1 — The variation of optical rotatory power for L-Tyrosine (c = 5 % in HCl 1 N) with λ (nm) 1— 85.4°C ; 2— 80.2°C ; 3 — 70.°C ; 4— 60.2°C ; 5 — 45.1°C ; 6 — 40.1°C ; 7— 35.1°C ; 8 — 35.2°C ; 9— 30.1°C ; 10 — 25.2°C ; 11— 20.2°C.

For L-histidine chlorhydrate raising curves $[\alpha]_\lambda = f(T)$ are observed, but their slope changes in the same manner. Only for L-tyrosine an inversion of the rotatory power for the studied temperature range is observed. The

Table 1

The variation of rotatory power [α] for L-cysteine · HCl · H_2O(I)

Temperature °C	λ(nm)				
	578	546	436	406	366
20.1	+6.80	+8.05	+17.26	+23.10	+36.21
25.1	+6.56	+7.74	+16.73	+22.44	+35.27
30.3	+6.27	+7.46	+16.23	+21.78	+34.27
35.3	+6.12	+7.24	+15.82	+21.28	+33.58
40.1	+5.93	+7.08	+15.54	+20.97	+33.08
45.2	+5.80	+6.93	+15.17	+20.54	+32.52
50.2	+5.68	+6.74	+14.89	+20.16	+32.08
60.2	+5.43	+6.49	+14.42	+19.57	+31.15
70.1	+5.21	+6.24	+13.95	+19.04	+30.27
80.0	+4.99	+5.96	+13.45	+18.41	+29.34
85.0	+4.87	+5.87	+13.29	+18.16	+28.96

Table 2

The variation of rotatory power [α] for L-histidine · HCl · H_2O (II)

Temperature (°C)	λ(nm)				
	578	546	436	406	366
20.4	+ 9.54	+11.23	+22.84	+29.59	+44.70
25.3	+10.23	+11.98	+24.16	+31.16	+46.82
30.1	+10.87	+12.73	+25.41	+32.68	+48.79
35.3	+11.54	+13.55	+26.70	+34.27	+50.86
40.3	+12.14	+14.16	+28.86	+35.63	+52.63
45.4	+12.68	+14.79	+28.91	+36.86	+54.32
50.2	+13.20	+15.36	+29.84	+38.23	+56.09
60.2	+14.23	+16.50	+31.68	+40.38	+58.91
70.4	+15.09	+17.50	+33.36	+42.41	+61.50
80.3	+15.84	+18.34	+34.70	+44.00	+63.50
85.2	+16.14	+18.73	+35.36	+44.77	+64.68

Table 3

The temperature of inversion for L-tyrosine

λ(nm)	T(°C)
366	30.1
406	50.3
436	60.2
546	80.2
578	80.2

temperature of inversion at different λ is selected in table 3. It may be inferred that the smaller temperature of inversion corresponds to $\lambda = 366$ nm which is nearest to λ_{max} characteristic of the absorption band in the UV spectrum of L-tyrosine in acid medium. It may be also observed that working with concentrations of 1 and 4 %L-tyrosine in the same range of temperatures, but in basic solvent (KOH 11.6 %), the inversion of optical activity does not occur.

In conclusion, the values now reported for the variation of the optical activity on the temperature, wavelength and character of the medium can be used to obtain the optical purity in the range of temperatures of interest for synthesis and extraction processes.

EXPERIMENTAL PART

APPARATUS AND CALIBRATION

Optical activity measurements were performed with a polarimeter Polamat A — Carl Zeiss Jena which allows an objective reading with a precision smaller than 0.005° and a stabilisation rate of marker of 12°/s, in the working range from −75° to +75°. The set of interferential filters for 366, 406, 436, 546 and 578 nm was used. For the explored temperature range two thermostates were used : one for thermostation of the polarimetric appropiate cell, the second one for room of the cell. Precision of thermostation correspondents to 0.05°C but reading precision of the two thermometers was 0.1°C. The calibration was realised with normal slides of silica and lead to the following data.

Table 4

The calibration data

Temperature (°C)	Obtained values	Theoretical values
20	10.29	10.29
25	10.30	10.32
30	10.31	10.34

UV-Spectra were recorded on a Unicam-SP 8000 spectrophotometer for absorbance range 0—1 with a path length of 10.02 mm.

SUBSTANCES, SOLUTIONS AND MEASUREMENT TECHNIQUE

L-cysteine. HCl$\cdot H_2O$(I), L-histidine · HCl · H_2O (II) and L-tyrosine (III) used in this work were Merck products p.a.

The literature concerning optical activity gives the following data.

Table 5

The reference data

Substance	$[\alpha_{\text{abs}}]_D^{20}$	$\Delta\alpha/1^0$ (between 15—35°C)	Conditions
I	+6.3	−0.03	$c=$ 8 % in HCl 1 N
II	+9.3	+0.14	$c=$11 % in HCl 6 N
III	−11.8	+0.23	$c=$ 5 % in HCl 1 N

Reactives for the preparation of solution. KOH, HCl — products Chemapol p.a. and doublly distilled water were utilised. Conventional formulas [2,5] to translate our measurements at $[\alpha]_D$ and to verify our set of values with references data[3] were used. The range of temperatures is considerably extended in this work.

REFERENCES

[1] Raban and K. Nislow, "Topics in stereochemistry" edited by N. L. Alinger, J. Wiley & Sons New York, London 1967, p. 199.
[2] M. Spaski, M. Reix, M. O. Sepulcre and J. P. Guette, *Analysis*, **8**, 130 (1980).
[3] * * * Ajinomoto Co "Tables and Charts of Amino Acids", Tokyo, Part 4, 3—7 (1972).
[4] O. Hörer "The Structure of Biopolymers", Abacus Press, Tunbridge Walls, Kent, 1972, p. 180.
[5] F. Badea and I. Kerek "Stereochimie" Ed. Ştiinţifică, Bucharest, 1974, p. 149.
[6] F. Boys, *Proc. Roy. Soc.*, A **144**, 655(1934).
[7] Y. Tinoco and R. W. Woody, *J. Chem. Phys.* **40**, 160 (1964).
[8] S. Yamana, *Bull. Kyoto Univ. Educ.*, ser. B, **46**, 9 (1975).
[9] S. Yamana, *Bull. Kyoto Univ. Educ.*, ser. B, **50**, 16 (1977)
[10] S. Yamana, *Bull. Kyoto Univ. Educ.* ser. B, **54**, 1 (1979).
[11] S. Yamana, *Bull. Kyoto Univ. Educ.*, ser. B, **56**, 40 (1979).
[12] S. Yamana, *Bull. Kyoto Univ. Educ.*, ser. B, **56**, 1 (1980).
[13] Ying Nan Chiu, *J. Chem. Phys.* **52**, 3 (1970).

Revue Roumaine de Chimie, 32, *11–12*, 1051–1057 (1987)

Dedicated to Professor V. E. SAHINI
on his 60th anniversary

ESR SPECTRAL STUDY OF SOME SUBSTITUTED 2,4-DINITROANILINES

MIHAELA HILLEBRAND*, MIRCEA MORARU** and ELENA VOLANSCHI *
*Department of Physical Chemistry
** Department of Organic Chemistry
Polytechnic Institute, Blvd. Republicii 13, Bucharest, Romania

Received June 18, 1987

ESR and electronic spectra of the anion-radicals provided by the electrochemical reduction of N-methyl- and N, N-dimethyl-2,4-dinitroaniline are presented and discussed in terms of the steric and hydrogen bond interaction between the amine and vicinal nitro groups The different behaviours in reduction processes of the secondary and tertiary amines, respectively, characteristic for a large number of previously investigated *m*-dinitroanilines, is outlined. LCAO-HMO calculations account well for the experimental trends.

Previous studies on *meta*-dinitrosubstituted tertiary anilines[1] have pointed out specific features of the ESR spectra that can be accounted for by sterical and electronic effects, due to the proximity of the bulky amine and nitro groups. In spite of the presence of two nitro groups, the ESR spectra present a typical aspect for a mono nitroanion radical and were rationalised in terms of a large nitrogen splitting in the range of 0.8–1.1 mT and two quasiequivalent protons (0.30–0.36 mT), assigned to the protons in *ortho vs.* the 4-nitro group. The presence of a single nitrogen splitting was explained by the out of plane position of the nitro group, vicinal to the tertiary amine. [2,3]

Another striking statement of our previous study concerns the instability of this radicalic species. In time, the nitro-centered anion-radical (A) decays, and a second, more stable radicalic species (B) is accumulated. On the basis of its hyperfine splitting constants and *g*-factor, this species was assigned to a nitroso anion radical, formed during the further reduction of anion radical A.

In contrast with the behaviour of the tertiary nitrosubstituted anilines, the reduction of one secondary amine, namely N-isobutyl-2,4-dinitroaniline evidenced a single stable radicalic species, with the ESR features of the above discussed species A.

It is the aim of this paper to provide further information on the different behaviours at reduction of the tertiary and secondary 2,4-dinitroanilines choosing for this purpose two model compounds.

The compounds in fig. 1 were selected to have a small alkyl substituent, in order to verify if the statements already discussed are also valid in conditions of reduced steric hindrance.

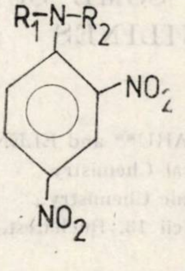

Fig. 1. — Investigated compounds.
I : $R_1 = R_2 = CH_3$
II : $R_1 = CH_3$; $R_2 = H$.

EXPERIMENTAL PART

The compounds were synthesised by literature methods (I, $R_1 = R_2 = CH_3-$, m.p. = 86–87° (C_6H_6) ; II, $R_1 = H$, $R_2 = CH_3$,— m.p. = 178–179° (EtOH). The electrochemical reduction was performed by *in situ* techniques previously described, [2] using dimethylsulphoxide (DMSO) as solvent and 0.1 M tetra-*n*-butyl-ammonium perchlorate as supporting electrolyte. The ESR spectra were registered on a JES-3B spectrometer in the X-band frequency, using peroxylamine disulphonate as internal standard. ($a_{N^-} = 1.300$ mT, $g = 2.0055$).

The visible spectra of the anion radicals were registered during the electrolysis on a Specord-UV-VIS spectrophotometer, K. Zeiss Jena. The LCAO-HMO calculations were performed using standard parameters on a TIM-S micro computer.

RESULTS AND DISCUSSION

a) *ESR Spectra.* The ESR spectrum registered at the very beginning of the electrochemical reduction of I is consistent with a mixture of two radicalic species with different g-values (Fig. 2 a). In time, only the radicalic species at higher g-value is accumulated (Fig. 2b), and was interpreted in terms of the ESR parameters listed in Table 1.

The results in Table 1 point out that this radicalic species presents all the features mentioned above for the type B anion-radical, obtained when starting with other tertiary amines, and can therefore be assigned to a nitroso anion radical. The strong unequivalence of the *ortho* protons is explained by the locked in plane position of the nitroso group.[5–7]

Differing from the other cases, when the time variation of the ESR spectrum was low enough to allow the analysis of both radicalic species A and B, in this case only the second radical, (B), could be described. The experimental data point out that N, N-dimethyl-2,4-dinitroaniline behaves in the same manner as the other tertiary amines, in spite of the smaller size of the methyl substituent.

Starting from compound **II** (Fig. 3) only one radicalic species of type A was detected. The low resolution ESR spectrum of the anion-radical **II** (Fig. 3 a) was analysed in terms of one nitrogen splitting of 1.100 mT and two nonequivalent protons of 0.261 and 0.507 mT, respectively. At

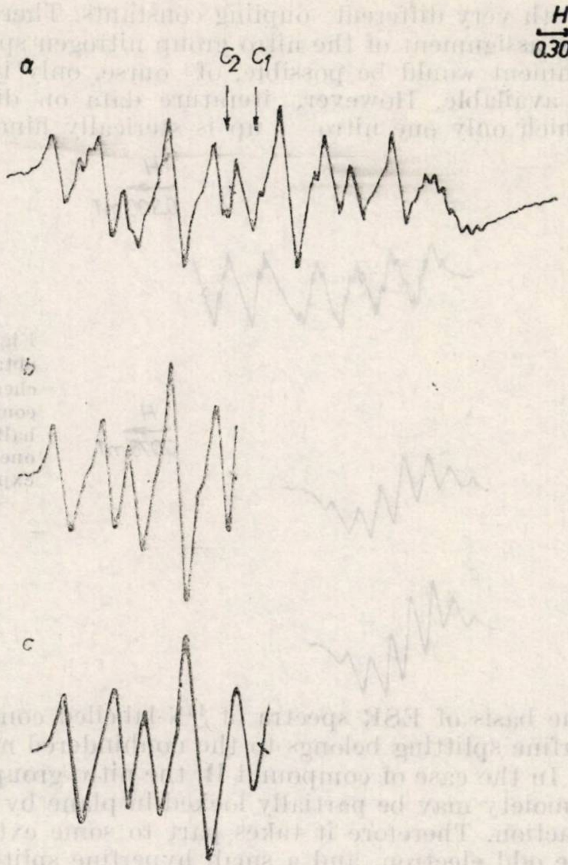

Fig. 2. — ESR spectrum obtained at the electrochemical reduction of compound I. a) mixture of anion-radicals A and B. b) ESR spectrum of radicalic species B (experimental). c) Simulated with hfs. in Table 1.

Table 1

ESR parameters (mT) for the investigated anion-radicals

Anion-radical	$a_1^{N(H)}$	$a_2^{NO_2}$	a_3	$a_4^{NO_2}$	a_5	a_6	δ	g
I(spB)	—	—	0.338	0.853	0.531	—	0.048	2.0064
II	0.039 (N ~ H)	0.031	0.261	1.100	0.507	0.043	0.023	2.0045

this degree of resolution, the spectrum is quite similar to that obtained from N-isobutyl-2,4-dinitroaniline, in both splitting constants and *g*-factor. However, at higher resolution further splittings from the remaining molecule were apparent (Fig. 3 b), reflecting the hyperfine interaction with the amino nitrogen and proton, the nitro group nitrogen and the proton in site 6.

Therefore, the possibility of formation of a nitroso-type anion-radical starting from II was ruled out.

An interesting feature in the ESR pattern of compound II consists in the detection of hyperfine splittings from both nitrogroup nitrogen atoms, but with very different coupling constants. Therefore, a problem arises as to the assignment of the nitro group nitrogen splittings. An unambiguous assignment would be possible, of course, only if ^{15}N-labelled compounds were available. However, literature data on dinitrobenzene derivatives in which only one nitro group is sterically hindered [8] have pointed out,

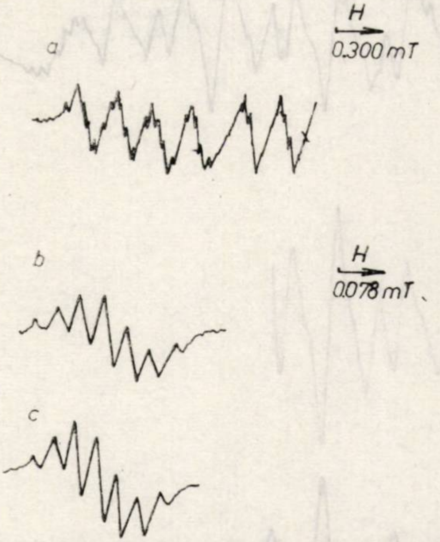

Fig. 3. — ESR spectrum obtained at the electrochemical reduction of compound **II**. a) low-field half of the spectrum. b) one line of spectrum (a), expanded, (experimental) and c) simulated.

on the basis of ESR spectra of ^{15}N-labelled compounds, that the largest hyperfine splitting belongs to the nonhindered nitrogroup nitrogen.

In the case of compound **II**, the nitro group in *ortho* to the NH-methyl moiety may be partially locked in plane by a hydrogen-bonding type interaction. Therefore it takes part to some extent to the delocalization of the odd electron, and a small hyperfine splitting is observed.

In order to verify these assumptions, MO-calculations in the frame of the simple LCAO–HMO method were performed. The parameters were those usually employed for nitroaromatic anion-radicals. [9]

The hindered nitro-group was taken into account by a reduced resonance integral, $\beta_{C_2-N} < \beta_{C_4-N}$, in agreement with the usually employed angular dependence : $\beta_{CN} = \beta^{\circ}_{CN} \cdot \cos\theta$, where θ is the twisting angle of the nitro group *vs.* the aromatic ring.[8]

The results of the calculations are presented in Table 2. It may be observed that when two equivalent nitro groups are considered (model 1), two quasidegenerated MO's ($\Delta\varepsilon_{m+1,m+2} = 0.0158$) are obtained, explaining the enhanced probability of further reduction to a diamagnetic dianion. In this model the odd electron is delocalized on both nitro groups, preferentially on the nitro group in site 2, as pointed out by the values of the nitro group AO's in the $(m + 1)$ molecular orbital and by the calculated a_N values. So this model would account satisfactorily for the instability of radicalic species A, in the case of the tertiary amines (i.e. compound **I**) but not for the general ESR pattern of this species.

On the contrary, if the bulky amino group forces the nitro group in site 2 to be out of plane (model 2), the energy difference between ε_{m+1} and ε_{m+2} is enhanced and the odd electron is almost exclusively delocalized

Table 2

Splitting constants (mT) and coefficients of the nitro group AO's in the MO's of anion-radical **II**

(a) Model	M.O.	ε M.O.	Site 2 N	Site 2 O	Site 2 O	Site 4 N	Site 4 O	Site 4 O
1	$m+1^{(b)}$	−0.4640	0.4303	−0.3855	−0.3855	−0.2307	0.2067	0.2067
	$m+2$	−0.4798	0.2689	−0.2389	−0.2389	0.4654	−0.4134	−0.4134
			$a_N^{(c)} = 0.768$			$a_N = 0.221$		
2	$m+1^{(b)}$	−0.4750	0.0228	−0.0203	−0.0203	−0.5150	0.4588	0.4588
	$m+2$	−0.5650	0.6057	−0.5148	−0.5148	0.0469	−0.0399	−0.0399
			$a_N = 0.002$			$a_N = 1.183$		
3	$m+1^{(b)}$	−0.4751	0.0539	−0.0434	−0.0480	−0.5123	0.4563	0.4563
	$m+2$	−0.5149	−0.6156	0.4861	0.5368	−0.0716	0.0625	0.0625
			$a_N = 0.014$			$a_N = 1.107$		

(a) Model 1 : symmetrical nitro groups with $h_N = 2.2$; $h_O = 1.4$ and $k_{C(ring)\text{-}NO_2} = 1.0$; model 2 : for the nitro group in site 2, $k_{C(ring)\text{-}NO_2} = 0.4$; model 3 : hydrogen-bond in site 2 (see text).

(b) M.O. of the odd electron in the anion-radical.

(c) $a_N = 9.9\ \rho_N^{\pi} - 3.58 \times \Sigma\rho_O^{\pi}$, [9] ρ_N^{π} and ρ_O^{π} being the Hückel spin densities.

on the unhindered nitro group in site 4. This is in agreement with the ESR pattern specific to the radicalic species A, which involves either one large nitro nitrogen hyperfine splitting or two very different ones.

If a hydrogen bond is assumed for the nitro group in site 2 (introduced in terms of an enhanced coulombian parameter for one oxygen atom, $k_0 = 1.6$ (model 3)), it may be noted that, although the severe nonequivalence between the two nitro groups is maintained, a slightly higher hf splitting is obtained for the site 2 nitro group nitrogen, in agreement with the hf coupling measured for it.

Therefore, it may be stated that this model accounts reasonably for both the stability and specific features of the spin distribution in radicalic species A, formed by the electrochemical reduction of the secondary amines.

b) *Electronic spectra.* In order to get more information about the behaviour of the investigated compounds in reduction processes, the electronic spectra were registered during the electrolysis. The spectra are presented in Figures 4 and 5 and the relevant data are collected in Table 3.

Table 3

Electronic spectra of the anion-radicals

	Parent compound	Anion radicals	
I	386 nm	422 nm;	555 nm
II	362 nm	431 nm;	500 nm; 545 nm

For both compounds new absorption bands appear in the visible range of the spectra, simultaneously with the decrease in intensity of the peak of the parent compound. As the longest wavelength maxima are the first ones to disappear when the electrolysis is interrupted, they were assigned to the anion-radicals.

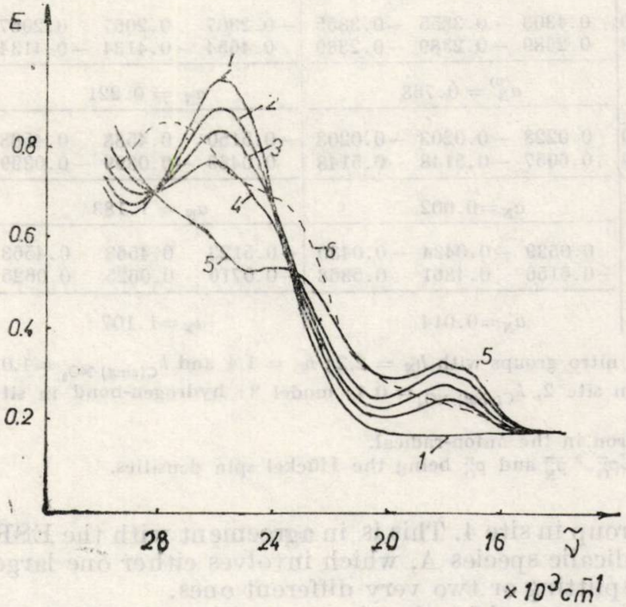

Fig. 4. — Visible spectra obtained at the electrochemical reduction of I. 1—5, in time, during electrolysis; 6 — registered several hours after the electrolysis was interrupted.

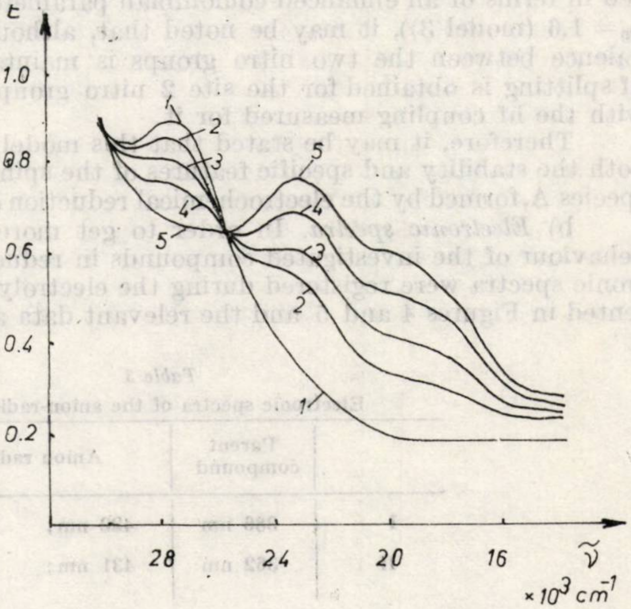

Fig. 5. Visible spectra obtained at electrochemical reduction of II. 1—5 in time.

In the case of compound **I** (Fig. 4) it may be observed that, when the parent compound is totally reduced, another maximum is evidenced at 422 nm. This absorption peak was assigned to the nitroso anion-radical, on the basis of the ESR spectra and literature data [10] on the electronic spectra of the nitroso anion-radical. Ishitani and Nagakura reported for the anion-radical of nitroso benzene three bands located at 416, 530 and 610 nm, respectively, the peak at 610 nm being of very low intensity. In our spectra only the most intense peak at 422 nm could be located, the band at about 530 nm being probably overlapped by the absorption of the type A radicalic species, and leading to a broad and slightly asymmetric absorption band. When the reduction is stopped and the solution is exposed to air, the parent compound is not recovered; instead of it, a compound absorbing at 363 nm is formed, presumably a reduction product.

Differing from this behaviour, the reduction of compound **II** is reversible and the parent compound is recovered quantitatively (Fig. 5). However two absorption bands are apparent in the visible range of the spectrum, and the variation of their absorbance in time proves that they do not belong to the same species. The longer wavelength band was assigned to the anion-radical; the other is presumably due to some diamagnetic species (i.e. dianion) arising during the reversible reduction of the nitro group.

The reversibility of the reduction process of compound **II**, noted in the study of the optical spectra is in agreement with the ESR statements about the formation in this case of a single radicalic species of type A.

In conclusion it may be stated that the behaviour at the electrochemical reduction of compounds **I** and **II**, as outlined by the study of their ESR and optical spectra, as well as by the MO calculations performed, matches the general pattern evidenced by a large number of previously investigated derivatives and characteristic for the tertiary and, respectively, secondary *meta*-dinitrosubstituted anilines.

REFERENCES

[1] M. Hillebrand, Em. Ionescu and E. Volanschi, *Rev. Roumaine Chim.*, to be published.

[2] V. M. Kazakova, V. B. Piscov, *Zhur. strukt. Khim.*, **14**, 734 (1973).

[3] V. M. Kazakova, V. I. Kopper, I. G. Makarov, V. B. Piscov, *Zhur. strukt. Khim.*, **15**, 1071 (1974).

[4] I. Baciu, M. Hillebrand, V. Em. Sahini and E. Volanschi, *Rev. Roumaine Chim.*, **21**, 485 (1976).

[5] G. Cauquis, M. Genies, H. Lemaire, A. Rassat and J. Ravet, *J. Chem. Phys.*, **47**, 4642 (1967).

[6] V. F. Staricenko, V. A. Riabinin, S. M. Shein, *Izvest. Akad. Nauk. S.S.S.R.*, **3**, 520 (1976).

[7] V. Kaminski and K. Möbius, *Z. Naturforsch.*, **25 a**, 635 (1970).

[8] D. H. Geske, J. L. Ragle, M. A. Bambenek, A. L. Balch, *J. Amer. Chem. Soc.*, **86**, 987 (1964).

[9] P. H. Rieger, G. K. Fraenkel, *J. Chem. Phys.*, **39**, 609 (1963).

[10] A. Ishitani and S. Nagakura, *Theor. Chim. Acta.*, **4**, 236 (1965).

Revue Roumaine de Chimie, **32**, *11–12*, 1059–1068 (1987)

Dedicated to Professor V. E. SAHINI
on his 60th anniversary

CALCULATION OF MASS SPECTRA OF SOME OXYGEN- AND SULPHUR-CONTAINING HETEROCYCLES

VOICU CONSTANTIN
Polytechnic Institute, Department of Physical Chemistry,
Bd. Republicii 13, Bucharest, Romania

Received June 1, 1987

The relative abundances of the main peaks in the 50 eV mass spectra of dibenzo[b,e]oxepine-11-one and dibenzo[b,e]thiepine-11-one-5,5 dioxide have been calculated using the classical approximation of the quasi-equilibrium theory. A good agreement was found between calculated and experimental data.

In the quasi-equilibrium theory (QET) of mass spectra, [1] the molecular ion formed in the electron-impact process is treated as an isolated system in a state of internal equilibrum. The excited molecular ions were assumed to decompose adiabatically from the stable electronic states, leading, by a series of competing, consecutive unimolecular reactions, to the mass spectrum.

To carry out QET-calculations for the mass spectrum of a compound the following factors must be considered : (1) the excitation energy distribution of the molecular ion, (2) the partition of internal energy between products, (3) the form of the QET rate equation, (4) the kinetic equations for the unimolecular decompositions, (5) the reaction pathways of the compound under consideration, (6) the frequency factors and (7) the activation energies for the reactions taken into account.

This paper reports the calculation of the mass spectra of dibenzo [b, e]oxepine-11-one (DBO) and dibenzo[b, e]thiepine-11-one-5,5-dioxide (DBTDIOX), using the classical approximation of the QET.

DISCUSSION

(1) *The internal energy distribution.* For the present calculations we have used a simplified energy distribution in agreement with the general shape of 70 eV-energy distributions obtained by McLafferty et al. [2] for several substituted 1,2-diphenylethanes. This distribution is defined by

the following equations :

$$\left.\begin{array}{c} F(E)=2E \text{ for } 0\leqslant E\leqslant 0.5,\ F(E)=1 \text{ for } 0.5\leqslant E\leqslant 5.5, \\ F(E)=6.5-E \text{ for } 5.5\leqslant E\leqslant 6, \\ F(E)=(11-E)/10 \text{ for } 6\leqslant E\leqslant 10 \text{ and } F(E)=(40-E)/300 \\ \text{for } 10\leqslant E\leqslant 40 \end{array}\right\} \quad (1)$$

Since the ionization potentials of DBO and DBTDIOX are nearly equal, the maximum internal energy ($E_{\max}=E_{\mathrm{el}}-IP$) has been taken as $E_{\max}=40$ eV for both compounds. To normalize the energy distribution, the above equations for $F(E)$ must be divided by a factor of 8.325.

(2) *The partition of the internal energy between fragments*. If the molecular ion M^+ is formed with the internal energy E, and ε_{0i}, ε_{ij} and ε_{jr} are the activation energies in the respective stages of the following reaction sequence

$$\mathrm{M}^+ \xrightarrow[-\mathrm{N}_i]{\varepsilon_{0i}} \mathrm{A}^+(i) \xrightarrow[-\mathrm{N}_{ij}]{\varepsilon_{ij}} \mathrm{B}^+(j) \xrightarrow[-\mathrm{N}_{jr}]{\varepsilon_{jr}} \mathrm{C}^+(r), \qquad (2)$$

the internal energy of the molecular ion in excess of that required to attain the transition state for $\mathrm{A}^+(i)$, namely $E^{\mathrm{ex}}_{0i}=E-\varepsilon_{0i}$, will be partitioned between the fragment ion $\mathrm{A}^+(i)$ and the neutral species N_i. If g_i is the function which describes this partition, the internal energy of $\mathrm{A}^+(i)$ is

$$E_i = g_i(E-\varepsilon_{0i}) \qquad (3)$$

and from this, the excess energy available for further reaction of $\mathrm{A}^+(i)$ to give $\mathrm{B}^+(j)+\mathrm{N}_{ij}$, will be $E^{\mathrm{ex}}_{ij}=g_i(E-\varepsilon_{0i})-\varepsilon_{ij}$.

Similarly, for the subsequent stage, the internal energy of $\mathrm{B}^+(j)$ is

$$E_j = g_j(g_i(E-\varepsilon_{0i})-\varepsilon_{ij}) \qquad (4)$$

and the excess energy of $\mathrm{B}^+(j)$ to give $\mathrm{C}^+(r)+\mathrm{N}_{jr}$ will be $E^{\mathrm{ex}}_{jr}=E_j-\varepsilon_{jr}$ where g_j is the function which describes the partition of the excess energy E^{ex}_{ij} of $\mathrm{A}^+(i)$ between $\mathrm{B}^+(j)$ and N_{ij}.

Neglecting the statistical fluctuations, the g_i and g_j functions can be readily calculated assuming that the excess energy of the reactant is equipartitioned only between the internal degrees of freedom of the ionic and neutral products : [3]

$$g_i = S_{\mathrm{A}^+(i)}/(S_{\mathrm{A}^+(i)}+S_{\mathrm{N}_i}),\ g_j = S_{\mathrm{B}^+(j)}/(S_{\mathrm{B}^+(j)}+S_{\mathrm{N}_{ij}}) \qquad (5)$$

where S_k ($k=\mathrm{A}^+(i)$, N_i, $\mathrm{B}^+(j)$ or N_{ij}) is the number of internal degrees of freedom for the species under consideration.

(3) *The rate constant equation*. For any stage parent (p) — fragment (f) in the reaction sequence (2), the expression of the rate constant used in the present calculations is

$$k_{p,f}(E) = Z_{p,f}(1-\varepsilon_{p,f}/E_p)^{P_p} \qquad (6)$$

in which

$$Z_{p,f} = \sigma \nu_{rc} \prod_{i=1}^{S_p-1} \nu_i / \nu_i^{\neq}$$

where σ is the number of the equivalent ways of choosing the reaction coordinate (rc), ν_{rc} is the stretching vibration of the reactant ion which becomes rc in the transition state, $\varepsilon_{p,f}$ is the activation energy for the reaction, E_p is the internal energy of the parent ion (i.e., E, E_i or E_j defined above), P_p is the effective number of oscillators in the decomposing ion and the ν's are the vibrational frequencies of the reactant ion (ν_i) and of the activated complex ($\nu_i^{\neq}$). For the index P_p the expression $P_p = (S_p - 1)\cdot x$ was used, x being either 1/3 or a linear function on the excess energy (see Results).

(4) *The kinetic equation of unimolecular decompositions.* Consider the unimolecular reactions which lead to the mass spectrum of a molecule ion

$$M^+ \xrightarrow[-N_i]{k_{0i}} A^+(i) \xrightarrow[-N_{ij}]{k_{ij}} B^+(j) \xrightarrow[-N_{jr}]{k_{jr}} C^+(r)$$

in which $i = 1 \div l$, $j = 1 \div m$, $r = 1 \div n$, and k_{0i}, k_{ij} and k_{jr} are the rate constants in the respective stages of the reaction sequence. The differential equations governing this system are the following *

$$\left.\begin{aligned}
\frac{dM}{dt} &= -\sum_{i=1}^{l} k_{0i}M \\
\frac{dA(i)}{dt} &= \sum_{i=1}^{l} k_{0i}M - \sum_{J=1}^{m} k_{ij}A(i) \\
\frac{dB(j)}{dt} &= \sum_{j=1}^{m} k_{ij}\,A(i) - \sum_{r=1}^{n} k_{jr}B(j) \\
\frac{dC(r)}{dt} &= \sum_{r=1}^{n} k_{jr}B(j)
\end{aligned}\right\} \qquad (7)$$

For a single-focusing mass spectrometer, operated at the usual accelerating voltages, the residence time T of a ion in the ionization chamber is in the range 1—5 μs and the time τ at which it is collected is in the range 10—15 μs. [4] The collected molecular ions are those which are not decomposed until time τ, and the collected fragment ions are those which are formed before time T.

Let M_0 be the number of molecular ions formed with the internal energy E at zero time. The solution of the differential equations (7) for the appropriate times on the mass spectrometer time scale, weighted according to the energy distribution $F(E)$ and integrated over appropriate energies, leads to the relative amounts of the corresponding ionic species ;

---

* For sake of simplicity, in all the following equations the sign (+) of the ions was omitted.

$$\left.\begin{aligned}
[\mathrm{M}] &= \int_{0}^{E_{\max}} \exp(-\tau S_1)\cdot F(E)\mathrm{d}E \\
[A(i)] &= \int_{E_{0i}^{\mathrm{ex}}=0}^{E_{\max}} (k_{0i}/(S_2 - S_1))(\exp(-TS_1) - \exp(-TS_2))\cdot F(E)\mathrm{d}E \\
[B(j)] &= \int_{E_{ij}^{\mathrm{ex}}=0}^{E_{\max}} \sum_{i=1}^{l} k_{ij}k_{0i}(B_1(j) + B_2(j) + B_3(j))\cdot F(E)\,\mathrm{d}E \\
[C(r)] &= \int_{E_{jr}^{\mathrm{ex}}=0}^{E_{\max}} \sum_{j=1}^{m} k_{jr} \sum_{i=1}^{l} k_{ij}k_{0i}(C_1(r) + C_2(r) + C_3(r))\cdot F(E)\,\mathrm{d}E
\end{aligned}\right\} \quad (8)$$

where : $[\mathrm{M}] = \mathrm{M}/\mathrm{M}_0$, $[\mathrm{A}(i)] = \mathrm{A}(i)/\mathrm{M}_0$, $[\mathrm{B}(j)] = \mathrm{B}(j)/\mathrm{M}_0$, $[\mathrm{C}(r)] = \mathrm{C}(r)/\mathrm{M}_0$

$$S_1 = \sum_{i=1}^{l} k_{0i}, \quad S_2 = \sum_{j=1}^{m} k_{ij}, \quad S_3 = \sum_{r=1}^{n} k_{jr},$$

$$\mathrm{B}_1(j) = \frac{\exp(-TS_1)}{(S_1 - S_2)(S_1 - S_3)}, \quad \mathrm{B}_2(j) = \frac{\exp(-TS_2)}{(S_2 - S_1)(S_2 - S_3)},$$

$$\mathrm{B}_3(j) = \frac{\exp(-TS_3)}{(S_3 - S_1)(S_3 - S_2)},$$

$$\mathrm{C}_1(r) = \frac{1 - \exp(-TS_1)}{S_1(S_1 - S_2)(S_1 - S_3)}, \quad \mathrm{C}_2(r) = \frac{1 - \exp(-TS_2)}{S_2(S_2 - S_1)(S_2 - S_3)},$$

$$C_3(r) = \frac{1 - \exp(-TS_3)}{S_3(S_3 - S_1)(S_3 - S_2)}$$

In the present calculations we have taken $T = 1$ µs and $\tau = 10$ µs.

(5) *Unimolecular reaction in the DBO and DBTDIOX mass spectra.* The 50 eV mass spectra of DBO and DBTDIOX have been reported in the previous works. [5] The major fragmentation pathways of the molecular ions have been reasonably ascertained by using the observed metastable transitions and the low voltage patterns.

The reaction sequences assumed to account for the DBO and DBT-DIOX mass spectra are given in Fig. 1. In order to obtain a suitable comparison between calculated and experimental data, many of the minor peaks have been included in the peaks listed theoretically. In DBO reaction scheme, the subsequent reactions of the secondary ions have been sorted out by comparison with the mass spectra of some related compounds (fluorene, biphenyl, biphenylene). The mass spectrum of DBTDIOX at mass numbers lower than m/e 165 is similar to those of anthrone and fluorene compounds. From this lower region, the m/e 90 and m/e 83 ions are included in the most probable precursor m/e 166 ion, and the major part

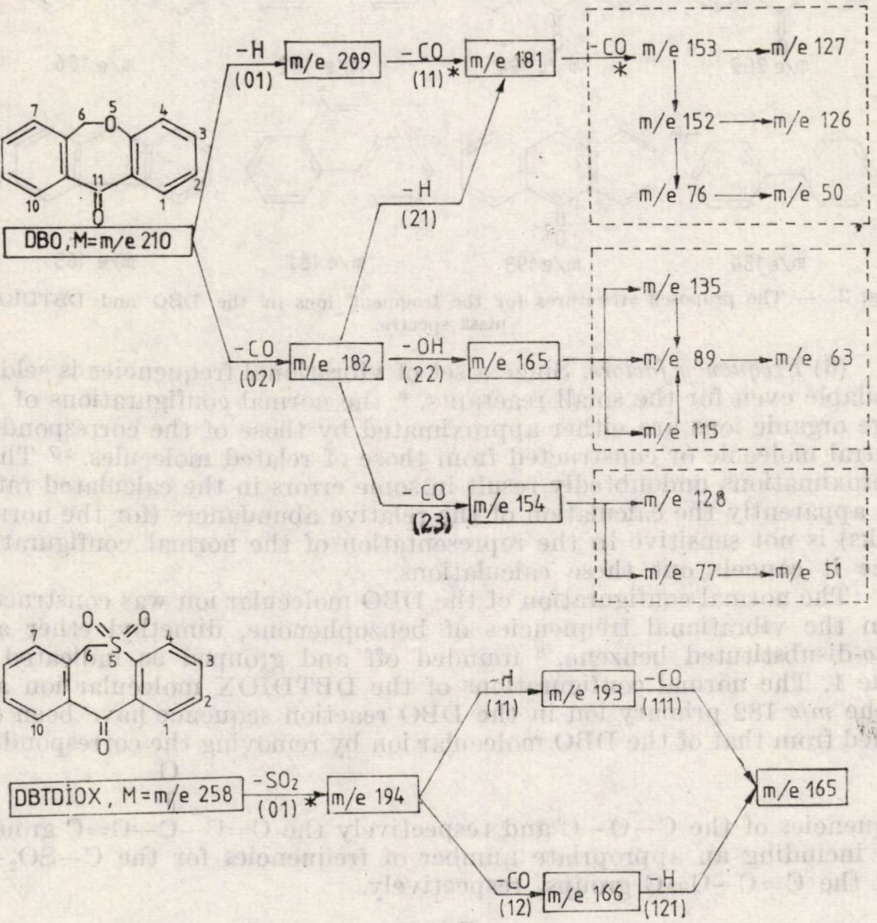
DBO, M=m/e 210
-H
(01)
m/e 209
-CO
(11)
*
m/e 181
-CO
*
m/e 153
m/e 127
m/e 152
m/e 126
m/e 76
m/e 50
-H
(21)
-CO
(02)
m/e 182
-OH
(22)
m/e 165
m/e 135
m/e 89
m/e 63
m/e 115
-CO
(23)
m/e 154
m/e 128
m/e 77
m/e 51
DBTDIOX, M=m/e 258
-SO₂
(01)
*
m/e 194
-H
(11)
m/e 193
-CO
(111)
m/e 165
-CO
(12)
m/e 166
-H
(121)

Fig. 1. — Reaction sequences assumed to account for the DBO and DBTDIOX mass spectra. The numbers under the arrows are used to identify the reactions and the ionic products. The asterisk denotes a metastable transition.

of the minor products are added to the relative abundance of the m/e 165 ion. The remaining peaks, those which cannot be certainly framed in the reaction scheme due to the difficulty of assigning the precursors, have been neglected. The amount of the omitted peaks is about 15% and respectively 5% from the total ionization of DBO and DBTDIOX.

The most significant ionic products in both mass spectra result by successive elimination of atom groups from the central seven membered ring. The fragment ions in the two reaction sequences have been assumed in closed ring structure as usually suggested in organic mass spectrometry. These structures are shown in Fig. 2.

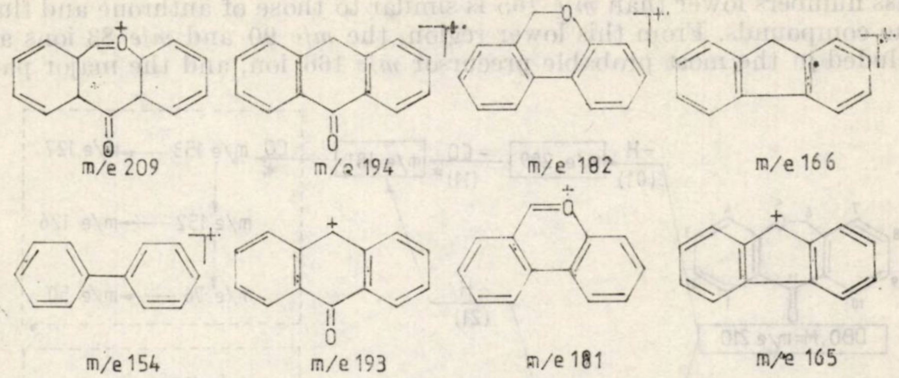

Fig. 2. — The proposed structures for the fragment ions in the DBO and DBTDIOX mass spectra.

(6) *Frequency factors.* Since a set of vibrational frequencies is seldom available even for the small reactants, * the normal configurations of the large organic ions are either approximated by those of the corresponding neutral molecule or constructed from those of related molecules. [2,7] These approximations undoubtedly result in some errors in the calculated rates, but apparently the calculation of the relative abundances (for the normal peaks) is not sensitive to the representation of the normal configuration since it cancels out these calculations.

The normal configuration of the DBO molecular ion was constructed from the vibrational frequencies of benzophenone, dimethyl ether and *ortho*-disubstituted benzene, [8] rounded off and grouped as indicated in table 1. The normal configurations of the DBTDIOX molecular ion and of the *m/e* 182 primary ion in the DBO reaction sequence have been obtained from that of the DBO molecular ion by removing the corresponding frequencies of the C—O—C and respectively the $C{=}C{-}\overset{\overset{O}{\|}}{C}{-}C{=}C$ groups, and including an appropriate number of frequencies for the $C{-}SO_2{-}C$ and the C=C—C=C groups, respectively.

Table 1

Construction of the activated-complex configurations

DBO : C—H stretching : 3000(1—8) ; 2900(9—10) ; C—C stretching : 1550(11—12), 1150 (23—24), 1200 (25) ;C—O stretching : 1200(26), 1000(27), 1700(28) ; C—H bending ; 1100(29 — 36), 1000(37—40), 800(41—44) ; CH_2 bending : 1400(45—46) ; CH_2 deformation : 1000(47—48) ; Bending of skeleton : 800(49—50), 700(51—52), 600(53—54), 500(55—59), 400(60—64), 300 (65—68), 200(69—72)

DBTDIOX :** C—S stretching : 800(26), 700(27) ; S—O stretching : 1250(73—74) ; SO_2 bending 600(75—76) ; SO_2 deformation : 500(77—78)

** The other frequencies (1—25 and 28—72) of DBTDIOX are assumed to be equal to those of DBO, respectively.

---

* E.g., such a set was occasionally obtained for the molecular ion of phenol[6].

Table 1 (continued)

m/e 182 : C—H stretching : 3000(1—8), 2900(9—10) ; C—C stretching : 1550 (11—22), 1300(23), 1200(24) ; C—O stretching : 1200(25), 1000(26) ; C—H bending : 1100 (27—34), 1000(35—38), 800(39—42) ; CH_2 bending : 1400 (43—44) ; CH_2 deformation : 1000(45—46) ; Bending of skeleton : 800(47—48), 700(49—50), 600 (51—52), 500(53—55), 400(56—59), 300(60—62), 200(63—66)

Frequency changes for assumed activation complexes :

Complex **A** : $\nu_9 = rc$, $\nu_{45} = 1000$, $\nu_{57} = 700$, $\nu_{62} = 800$; $\nu_{64} = 600$, $\nu_{65} = 500$, $\nu_{71} = 400$
Complex **B** : $\nu_{23} = rc$, $\nu_{24} = 288$, $\nu_{58-59} = 300$, $\nu_{63,65-66} = 200$, $\nu_{72} = 100$
Complex **C** : $\nu_{27} = rc$, $\nu_{26} = 200$, $\nu_{57} = 800$, $\nu_{62,64} = 600$, $\nu_{65} = 500$, $\nu_{71} = 300$, $\nu_{77-78} = 400$
Complex **D** : $\nu_{26} = rc$, $\nu_{25} = 300$, $\nu_{43} = 900$, $\nu_{60} = 600$, $\nu_{65} = 300$
Complex **E** : $\nu_{25} = rc$, $\nu_{24} = 300$, $\nu_{43-44} = 900$, $\nu_{55} = 800$, $\nu_{58} = 600$, $\nu_{59} = 200$

The activated complex configuration was considered in detail only for the following reactions :

A — the elimination of a hydrogen atom from the methylene bridge (*01* primary reaction of the DBO molecular ion)
B — the elimination of the carbonyl group as CO neutral molecule (*02* primary reaction of the DBO molecular ion)
C —the elimination of the SO_2 molecule (*01* primary reaction of the DBTDIOX molecular ion)
D — the elimination of an OH radical from the *m/e* 182 ion (*22* secondary reaction of DBO) and
E — the elimination of a CO molecule from the *m/e* 182 ion (*23* secondary reaction of DBO)

The other reactions taken into account occur either by elimination of the carbonyl group (the reactios *11* for DBO, *12* and *111* for DBTDIOX) or by elimination of a H atom from the methylene bridge (the reactions *21* for DBO, *11* and *121* for DBTDIOX). These reactions have been assumed to proceed through the same activated complex (and therefore to have the same frequency factor) as in the corresponding reactions of type **B** and **A**, respectively.

The activated complex configurations for the reactions of type **A**—**E** were selected consistent with the usual procedure employed in the QET calculations. [9] These configurations are given in table 1.

Based on the assumption that both the reactant ions and the resulted ionic products present closed ring structures, all the reactions taken into account may be described as rearrangement processes, in which the transition state results, in the absence of possible internal rotations, only from combined bond breaking and bond formation into the intermediate cycle.

The reactions of type **A** lead to the stable (even-electron) ionic species assumed with a completely conjugated structure. This suggests that the H atom is lost from an intermediate, in which partial bond formation has occurred. The activated complex for this process has been represented as tight ring structure. This is the "tightest" activated complex used in the present calculations.

The reactions of type **B**—**E** are rearrangement processes and it would be expected for these reactions to be also represented by tight transition state. However, because the activation energies for the reactions of type **B** are in all cases higher than the concurrent reactions of type **A**, a substantial reduction in the "tightness" of the B-activated complex is required for a reasonable fit with experimental data. For the reactions of type **B**—**E**, which involve the rupture of the two bonds from the intermediate cycle of the reactants, one bond stretching has been taken as reaction coordinate and the other bond stretching has been reduced by a factor of 4 in the activated complex configuration.

(7) *Activation energies*. The activation energy is usually estimated from the difference between the appearance potential (AP) of the relevant fragment ion and the AP of the precursor parent ion. However, the appearance potential difference (ΔAP) is only an approximate measure of the activation energy because it is also dependent on the thermal energy, the kinetic and competitive shifts and the activation energy for the reverse reaction.

The appearance potentials for the DBO and DBTDIOX compounds have been obtained by the direct evaporation of the sample in the approach of the ionization chamber, so that the initial molecules had acquired a certain amount of thermal energy prior to ionization. In accordance with the QET, this thermal energy produces a "thermal shift" in onset potential measurement which acts in opposite direction to the kinetic shift. [10]

The final values for the activation energies as given in table 3 have been arrived at by starting with differences in measured AP's and adjusting until the calculated relative abundances were in reasonable agreement, with the experimental data.

The activation energies for the reactions of type **A** are represented whithin the limits of experimental error, by the respective differences in measured AP's. For the other reactions, an appreciable kinetic shift and/or reverse activation energy may be expected, especially for the secondary or tertiary reactions. However, the deviation of the activation energy from the corresponding ΔAP is in reasonable limits for five such reactions. A larger deviation appears only for *12* secondary reaction and *111* tertiary reactions in the reaction sequence of DBTDIOX.

RESULTS

The rate constants for the reactions figured in the reaction sequences of DBO and DBTDIOX (Fig. 1) have been calculated by means of Eq. (6). The parameters used in the rate calculations are summarized in Table 2.

The relative amounts $[I(E)]$, ($I = M, A(i), B(j)$ or $C(r)$), of the several ions produced in given instrumental conditions were calculated as a function of the internal energy E at intervals of 0.1 eV, by using Eqs. (8). The required numerical integrations to obtain the relative abundances (RA) of each ion are performed by the summation of the products $[I(E)] \cdot F(E)$ over the appropriate energy range. The final values of the RA's are given in Table 3 where they are compared with the corresponding RA's from the experimental mass spectra (normalized into monoisotopic form).

An alternative approach in the classical approximation of the QET has been proposed by Yeo and Williams. [3] In this approach the effective number of oscillators in the rate equation (6) is taken as $P_p = (S_p - 1) \cdot x$, where x varies linearly with the excess energy rom 0.2 at threshold to

Table 2

Parameters used in the calculation of the rate constants

Compound	Reaction number[a]	σ	rc[b]	S_p	g_i or g_j	ε(eV)	Z
DBO	01	2	2900	72		1.27	1.74×10^{13}
	02	1	1150	72		1.62	3.45×10^{15}
	11	1	1150	69	1.0	1.30	3.45×10^{15}
	21	2	2900	66	0.985	0.85	1.74×10^{13}
	22	2	1000	66	0.985	1.50	1.50×10^{14}
	23	1	1200	66	0.985	2.15	3.00×10^{14}
DBTDIOX	01	1	700	78		0.35	1.46×10^{13}
	11	2	2900	69	0.958	1.15	1.74×10^{13}
	12	1	1150	69	0.985	1.50	3.45×10^{15}
	111	1	1150	66	1.0	0.85	3.45×10^{15}
	121	2	2900	63	0.984	1.15	1.74×10^{13}

[a] As given in the respective reaction sequences (Fig. 1)

[b] Reaction coordinate.

0.5 at the maximum internal energy assumed in the energy distribution function. Following this suggestion, we have repeated the calculations for DBO and DBTDIOX mass spectra using the same values for the other parameters (i.e., Z, ε, $F(E)$, g_i or g_j). The resulted RA's of the new calculations are also given in Table 3. At lower internal energies, this approach produces a sharper rise of $k(E)$ with E. Therefore, the calculated RA for the molecular ion will be decreased and, in effect, the RA's for some fragment ions will be increased in comparison with the respective RA's obtained in the previous calculations, where $x = 1/3$. However, the overall agreement of these calculations with experimental data is satisfactory, since it was obtained without the readjustment of the other parameters.

Table 3

Appearance potentials, calculated and experimental mass spectra

	m/e	210	209	182	181	165	154
DBO	AP(eV)	9.63	10.8	11.5	12.4	13.4	14.0
	RA(calc)[a]	24.8	6.7	3.0	45.5	13.1	6.9
	RA(calc)[b]	17.9	7.5	4.7	45.1	17.1	7.7
	RA(exp)	24.0	8.8	3.2	44.7	12.6	6.7
	m/e	258	194	193	166	165	
DBTDIOX	AP(eV)	9.7	10.0	11.1	12.2	13.25	
	RA(calc)[a]	4.9	22.8	3.6	8.5	60.2	
	RA(calc)[b]	2.8	18.6	6.4	9.4	62.8	
	RA(exp)	5.0	23.0	2.8	8.2	61.0	

[a] calculated with $P_p = (S_p-1)/3$ and [b] calculated with $P_p = (S_p-1)x$, where x varies linearly with the excess energy from 0.2 to 0.5.

A computer program was written to perform the calculation of the relative abundances from a mass spectrum using the classical approximation of the QET rate equation. For calculations the FELIX C-256 computer by the IPB Computation Center has been used.

REFERENCES

[1] H. M. Rosenstock, M. B. Wallenstein, A. L. Wahrhafting and H. Eyring, *Proc. Nat. Acad. Sci. U.S.A.*, **38**, 667 (1952).

[2] F. W. MaLafferty, T. Wachs, C. Lifshitz, G. Innorta and P. Irving, *J. Amer. Chem. Soc.*, **92**, 6867 (1970).

[3] A. N. H. Yeo and D. H. Williams, *Org. Mass Spectrom.*, **5**, 135 (1971).

[4] W. A. Chupka, *J. Cem. Phys.*, **30**, 191 (1959); I. Hove and D. H. Williams, *Chem. Commun.*, **1968**, 220.

[5] V. E. Sahini, V. Constantin, I. Serban and C. Vlădescu, *Rev. Roumaine Chim.*, **23**, 163 (1978); *ibid* , **23**, 315 (1978).

[6] M. L. Fraser-Monteiro, L. Frasser-Monteiro, J. de Wit and T. Baer, *J. Phys. Chem.*, **88**, 3622 (1984).

[7] J. M. Pechine, *Org. Mass Spectrom.*, **6**, 805 (1972); J. H. Chen, J. D. Hays and R. C. Dunbar, *J. Phys. Chem.*, **88**, 4759 (1984).

[8] L. M. Sverdlov, M. A. Kovner and E. P. Krainov, "Kolebatelnie spectri mnogoatomnih molecul", Izd. Nauka, 1970, p. 310–313, 427.

[9] A. Kropf, E. M. Eyring, A. L. Wahrhaftig and H. Eyring, *J. Chem. Phys.*, **32**, 149 (1960); E. M. Eyring and A. L. Wahrhafting, *J. Chem. Phys.*, **34**, 23 (1961); M. L. Vestal, *J. Chem. Phys.*, **43**, 1356 (1965); M. L. Vestal, in P. Ausloos Ed., "Fundamental Processes in Radiation Chemistry", Wiley-Interscience, New York, 1968.

[10] W. A. Chupka, *J. Chem. Phys.*, **54**, 1936 (1971).

Revue Roumaine de Chimie, 32, *11–12*, 1069–1070 (1987)

Dedicated to Prof. V. E. SAHINI
on his 60th birthday

WHY ARE CAESIUM CLUSTERS MORE DIFFICULT TO IONIZE THAN THEIR MONOXIDES?

A. SAVIN, H. PREUSS and H. STOLL
Institut für Theoretische Chemie, Universität Stuttgart, Pfaffenwaldring 55,
D-7000 Stuttgart 80

Received May 3, 1987

A curious trend has been observed experimentally by T. P. Martin and H. Limberger (Physica, to be published); Cs_nO clusters have lower ionization energies than the Cs_n ones. We explain it qualitatively by using an exclusion effect. In order to support this statement, SCF pseudopotential calculations were made for a typical case : Cs_4O.

Recently, T. P. Martin has observed that for several Cs_nO clusters the ionization potential is lower than for Cs_n ones. [1] The difference is largest for $n = 4$.

In order to support a qualitative explanation of this effect, we performed pseudopotential SCF calculations for Cs_4 and Cs_4O. The pseudopotential used for Cs is from reference [2]. The Gaussian basis sets were contracted : from (6s, 1p) to (3s, 1p) for Cs[3], and from (9s, 4p) to (3s, 2p) for oxygen.[4]

We assumed T_d symmetry for Cs_4O, as M_4O clusters are expected to have T_d symmetry (cf. the calculations for Li_4O[5]). We obtained a Cs–Cs distance of 8.3 bohr in Cs_4O and of 10.1 bohr in Cs_4 with T_d symmetry. The bond shortening may be explained by Cs–O interaction. The rhombic D_{2d} structure is more stable for Cs_4. The highest occupied orbital energy of Cs_4O is of -0.1 hartree, the Cs_4 clusters show values which are lower by a few mhartree. For the totally symmetric orbitals of the latter, the values obtained are about -0.15 hartree.

As the SCF calculations show the same trends as the experimental values, let us now try to find the effect responsible for the change in the ionization energy. Some simple qualitative explanations fail :

1) Charge consideration. More positive ions have larger ionization potentials. O is more electronegative than Cs_n and will thus take away electronic charge from Cs_n.

2) The structure of molecular orbital levels. M_4 clusters have two electrons in a totally symmetric orbital and two in higher ones. As O will

tend to fill its shell up to an octet, only the lower, totally symmetric, orbital will remain occupied. Thus one must ionize from a deeper level in Cs_4O than in Cs_4.

The effect, opposite to the preceding ones, leading to the trend observed relies on a detail overseen at point 2. There we did not take into account the existence of a_1 (=s) orbitals on the oxygen atom. The Cs_4-orbital builds up density within the tetrahedron. As this space is now excluded by the Pauli principle, the a_1 orbital is destabilized and this makes it easier to remove electrons from it.

Finally, we would like to thank Dr. T. P. Martin for drawing our attention to the problem treated in this paper. We are also grateful to Dr. J. Flad for stimulating discussions.

REFERENCES

[1] T. P. Martin and H. Limberger, *Physica*, to be published.

[2] P. Fuentealba, H. Stoll, L. von Szentpaly, P. Schwerdtfeger and H. Preuss, *J. Phys.*, **B16**, L323 (1983).

[3] G. H. Jeung, J. P. Malrieu and J. P. Daudey, *J. Chem. Phys.*, **77**, 3571 (1982).

[4] T. H. Dunning and P. J. Hay, in : H. F. Schaeffer III, ed., "Methods of electronic structure theory", Plenum, New York, 1977, p. 1.

[5] P.v. R. Schleyer, E.-U. Würthwein and J. A. Pople, *J. Amer. Chem. Soc.*, **104**, 5839 (1982).

Revue Roumaine de Chimie, 32, *11–12*, 1071–1074 (1987)

I would like to dedicate this paper to Professor Doctor V. E. SAHINI, a great scholar, teacher and human being. I wish him happiness in the future, with the occasion of his 60th birthday.

A. M. SAPSE

THEORETICAL STUDIES OF THE DECOMPOSITION OF LITHIATED NITROSOUREAS

A. M. SAPSE

Department of Chemistry, City University of N.Y., John Jay College and Graduate Center, New York City, N. Y., 10019 and Rockefeller University, N. Y., 10021

Received May 10, 1987

An explanation is sought for the fact that E isomers of diazohydroxides are obtained from the decomposition of *anti* haloethyl nitrosureas. It is found that in the presence of cations the most stable structure of nitrosurea is conducive to decomposition which leads to the formation of E isomers.

The place of 2-haloethylnitrosoureas (HENU's) has been established in the clinical treatment of human cancer, for example Burkitt's lymphoma, Hodgin's disease and cerebral neoplasm. [1-3] It has been shown that HENU's decompose spontaneously under physiological conditions, producing electrophiles, which attack cellular macromolecules, mainly DNA. Specific lesions have been identified, such as base alkylation, including cyclic nucleotide adduct formation, and interstrand cross-linking, a lethal event to the cell. [3-6]

Nitrosoureas, such as methyl nitrosourea, are highly mutagenic and carcinogenic but more complex analogs, for example HENU's, have much higher anti-tumor activity in relation to mutagenicity. [7] It was shown that the extent of the cross-linking correlates with activity against L-1210 murine leukemia and with the G+C content of DNA. [8,9] The sequence of reactions leading to cross-link formation by HENU's begins with the generation of reactive intermediates responsible for the transfer of the haloethyl group to nucleophilic sites on the DNA bases. The mono adduct so formed can then react with a nucleophilic site on another base, eliminate the halogen and generate a cross-link consisting of an ethylene bridge. It has been shown that nucleophilic sites alkylated by haloethyl groups comprise the O_6 site on guanine as well as the N_7 site, while the cross-linking seems to occur with a cytosine amine group.[6,10,11] The O_6 alkylation leads to interstrand cross-linking, while the alkylation at N_7 seems to be harmless.

The ability to repair the alkylation at O_6 before crosslinking can occur has been related to the selective toxic action of HENU's. The tumor-cell strains were found to be deficient in the removal of O_6-methylguanine from their DNA and thus were found to belong to the phenotype termed Mer^-, while normal cells belong to the phenotype Mer^+, that is, show proficiency in removing O_6-methylguanine from DNA.

Nitrosoureas decompose to diazohydroxides and isocyanate, according to the scheme shown below. [13]

Scheme

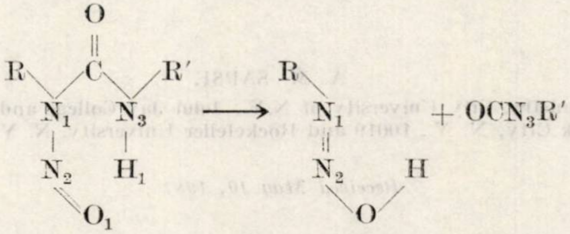

One of the facts related to nitrosoureas' carcinostatic activity is that H_1 cannot be replaced by another group, leading to the conclusion that its presence plays an essential role in the decomposition.[14] It might be presumed that H_1 is released in solution, while a proton or another cation from the solution is attached to O_1, to form diazohydroxides or some of their salts.

The diazohydroxides such obtained will then exhibit an E or Z structure, according to the *syn* or *anti* positioning of the N–O group to N_3, respectively.

E :

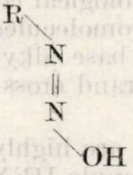

Z :

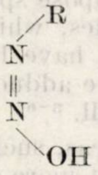

Indeed, an *anti* NO group will lead to the formation of a Z isomer. The conversion barrier between isomers is quite high, for both inversion and rotation of the NOH group around the N_1-N_2 bond. Indeed, N_1-N_2 is a double bond which leads to a high rotational barrier and the inversion energy has been calculated to be around 48 kcal/mole. [15] In methylnitrosourea, the rotational barrier around the N_1-N_2 bond has a value of 13 kcal/mole (theoretically calculated), value consistent with the fact that the π electrons of the N–O bond are delocalized on the N_1-N_2 bond, giving it partial double bond character.[16] Therefore, the distribution between *syn* and *anti* nitrosourea should reflect in the E *vs* Z diazohydro xide isomers distribution. NMR experiments and theoretical calculations show methylnitrosourea to exhibit a *syn* structure, while chloroethyl nitrosourea and fluoroethyl nitrosurea exhibit an *anti* structure presumably in the first case due to the hydrogen bond formation between O_1 and H_1 and, in the second case, due to the stabilization provided by the proximity of the negatively charged O_1 and the increased positive charge on the CH_2 group which is attached to C.[16,17] Indeed, in methyl diazohydroxide, the methyl group has a 0.246 e.u. charge, while in chloroethyl diazohydroxide, the group adjacent to N has a 0.335 e.u. charge (as calculated by Mulliken Population Analysis). However, the distribution of E and Z isomer shows a much larger population of the E isomer. The explanation of this fact might involve the experimental procedure which deals with salts of the diazohydroxides. Indeed, when a cation such as Li^+ approaches nitrosourea, it can bind in several ways as shown in Figure 1.

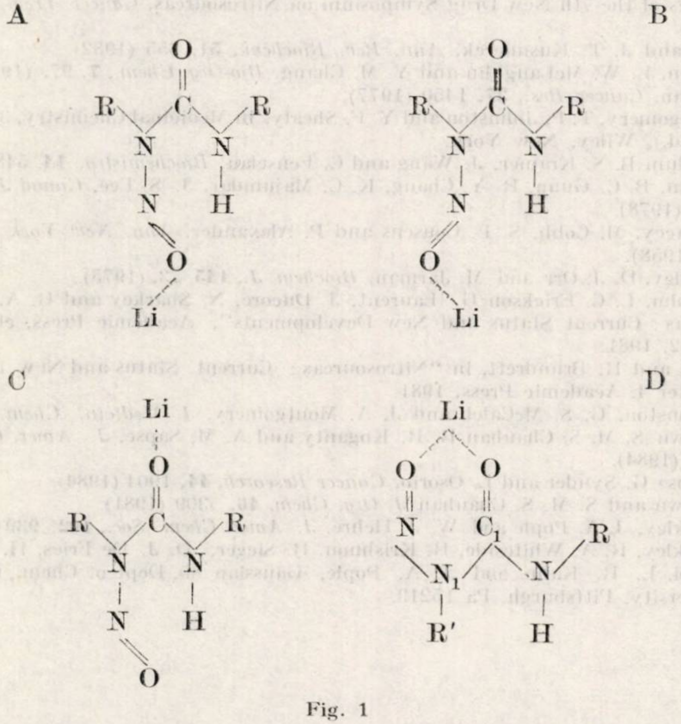

Fig. 1

The total energies of these structures, calculated with quantum chemical calculations using the 3-21G gaussian basis set (as implemented by the Gaussian-80 computer program), for $R=R'=H$, are shown in Table 1.[18,19]

It can be seen that structure D is the most stable, by 2 kcal/mole. It has also been calculated that the barrier to rotation around the C_1-N_1 bond is very high for structure D (27 kcal/mole). It can thus be presumed that the structure D will be quite stable.

Table 1

	Energy (a.u.)
A	−357.8853
B	−357.8913
C	−357.9102
D	−357.9133

Structure D, upon breakage of the C_1-N_1 bond will lead to the formation of E isomers of the Li^+ diazotate and this could be the reason why E isomers are found experimentally to result from the decomposition of *syn* and *anti* nitrosourea, when the experiment is performed in the presence of cations.

ACKNOWLEDGEMENT. I thank City University of N. Y. for computer time and for the Grant 666275.

REFERENCES

[1] D. B. Ludlum, "Mechanism of Action of 2-halooethylnitrosoureas". In : F. F. Becker, ed. "Cancer, a Comprehensive Treatise", vol. 5. Plenum Press, New York, p. 285ff, 1975.

[2] G. P. Wheeler, "A Review of Studies on the Mechanism of Action of Nitrosureas", ACS Symp, Ser., No. 30, Washington, D.C., p. 87, 1975.

[3] Proceedings of the 7th New Drug Symposium on Nitrosoureas, *Cancer Treat. Rep.*, **60**, 651, (1976).

[4] B. Singer and J. T. Kusmierek, *Ann. Rev. Biochem.*, **51**, 655 (1982).

[5] J. W. Lown, L. W. McLaughlin and Y. M. Chang, *Bio-Org. Chem.*, **7**, 97, (1978).

[6] K. M. Kohn, *Cancer Res.*, **37**, 1450 (1977).

[7] J. A. Montgomery, T. P. Johnston and Y. F. Shealy, in Medicinal Chemistry, 3rd ed., (Burger, A., Ed.), Wiley, New York.

[8] D. B. Ludlum B. S. Kramer, J. Wang and C. Fenselau, *Biochemistry*, **14**, 5480, 1975.

[9] J. W. Lown, B. C. Gunn, R. Y. Chang, K. C. Majumdar, J. S. Lee, *Canad J. Biochem.*, **56**, 1006 (1978).

[10] K. A. Stacey, M. Cobb, S. F. Cousens and P. Alexander, *Ann. New York Acad. Sci.*, **68**, 682 (1958).

[11] P. D. Lawley, D. J. Orr and M. Jarman, *Biochem. J.*, **145**, 73, (1975).

[12] K. W. Kohn, L. C. Erickson G. Laurent, J. Ducore, N. Sharkey and R. A. Ewig, "Nitrosoureas : Current Status and New Developments", Academic Press, chapter 6, pages 69—82, 1981.

[13] M. Colvin and R. Brundrett, in "Nitrosoureas : Current Status and New Developments", Chapter 4, Academic Press, 1981.

[14] T. P. Johnston, G. S. McCaleb and J. A. Montgomery, *J. Medicin. Chem.*, **9**, 892 (1963).

[15] J. W. Lown S. M. S. Chauhan R. R. Koganty and A. M. Sapse, *J. Amer. Chem Soc.*, **106**, 6401 (1984).

[16] A. M. Sapse G. Synder and L. Osorio, *Cancer Research*, **44**, 1904 (1984).

[17] J. W. Lown and S. M. S. Chauhan *J. Org. Chem.* **46**, 5309 (1981).

[18] J. S. Binkley, J. A. Pople and W. J. Hehre, *J. Amer. Chem. Soc.*, **102**, 939 (1980).

[19] J. S. Binkley, R. A. Whiteside, R. Krishnon, R. Sieger, D. J. De Fries, H. B. Schlegel, S. Topiol, L. R. Kahn and J. A. Pople, Gaussian 80, Dept of Chem., Carnegie-Mellon University, Pittsburgh, Pa 15213.

Revue Roumaine de Chimie, **32**, *11–12*, 1075 – 1084 (1987)

Dedicated to Professor V. E. SAHINI
on his 60th anniversary

THE VIBRONIC THEORY OF MAGNETIC PROPERTIES OF TRINUCLEAR MIXED-VALENCE CLUSTERS

I. B. BERSUKER, S. A. BORSHCH and I. N. KOTOV
Institute of Chemistry, Academy of Sciences, Moldavian SSR, 277028 Kishinev, USSR

Received June 15, 1987

The effect of vibronic interactions on magnetic properties of trinuclear mixed-valence clusters with intramolecular electron transfer is considered. A method of calculation of spin-vibronic states of these clusters is suggested. For a simple trimeric system with the $d^1-d^1-d^2$ electronic configuration of the centers the calculation of the temperature dependence of the effective magnetic moment is carried out. It is shown that for intermediate values of vibronic constants the magnetic properties of mixed-valence trimers cannot be described correctly either in the HDVV model, or by the double-exchange theory (i.e. in electronic models explicit consideration of vibronic interaction). The analysis of magnetochemistry experiments requires independent determination of the parameters of vibronic interactions.

1. INTRODUCTION

The magnetochemistry is a powerful method of investigation of coordination compounds containing two or more transition metal ions. Traditionally, the temperature and field dependence of the magnetic characteristics obtained from the experimental data are described by means of the energy spectrum of the molecule and allow to evaluate the parameters of intercenter interactions. Most often the electronic energy levels in these cases are obtained within the Heisenberg–Dirac–Van Vleck (HDVV) model. Sometimes also weaker non-Heisenberg interactions (in addition to the Heisenberg exchange interaction) are taken into account.

A special place among the exchange clusters is occupied by the mixed-valence ones containing ions of the same element in different valent states.[1] In these systems the migration of the "extra" electron between the equivalent metal ions may take place. Naturally, the question arises whether the HDVV model based on the assumption of fixed atomic spins is applicable to systems with intramolecular electron transport. The calculation of the electronic energy levels of dimeric [2,3] and trimeric [4,5] mixed-valence clusters shows that the peculiarities of the magnetic properties of such systems are determined by the effects of double exchange. The latter is demonstrated in the resonance splitting of the spin multiplets (of the HDVV model) which is complicated by the interactions of the multiplets with the same spin.

However, the electronic interaction only does not describe the tendency of the migrating electron toward localization. The latter is due mostly to the interaction with the totally symmetric displacements of the near-neighbour surrounding of the metal ion. These displacements are not totally symmetric with respect to the cluster as a whole ; the interaction with them results in a mixing of the electronic states, being thus an example of vibronic interactions.

For exchange-coupled mixed-valence dimers it was shown[7] that the taking account of the vibronic interactions results in a temperature dependent magnetic moment which is intermediate between that predicted by the theory of double exchange and the HDVV model. Among the trinuclear mixed-valence clusters the carboxylates of transition metals (in particular, iron) are most studied by magnetochemistry methods.[8-11] Although it was shown by Mössbauer spectroscopy that in these compounds there is an intramolecular electron transport, the temperature dependence of the magnetic moment is considered in these works by the HDVV model. Therefore a question arises : how correct the experimental exchange parameters obtained in this way reflect the true magnitudes of intercenter electron interactions in the cluster. The fact that the transition of the "extra" electron from the localized state to the delocalized one is checked by the gamma-resonance methods having a characteristic time of 10^{-7} s. shows that the electron transfer is strongly reduced by vibronic interactions. However, as it was shown for exchange-coupled mixed-valence dimers,[12] even if the spectral methods testify to the delocalized state, the contribution of the double exchange to the magnetic properties may be not completely reduced.

In the present paper a method is suggested for taking account of the vibronic interactions in exchange-coupled mixed-valence trimeric clusters, and the results of calculations of the magnetic properties of a model system with the electronic configuration $d^1 - d^1 - d^2$ are given. The consideration allows to reveal the essential changes in the magnetic properties introduced by the vibronic interactions.

2. ELECTRONIC ENERGY SPECTRUM

In order to calculate the spin-vibronic states of the mixed-valence cluster, the electronic energy spectrum has to be determined first. This can be done by constructing the multielectron wave functions with a definite total spin and localized electron followed by the diagonalization of the matrix of Coloumb intercenter interactions in this basis.[4] However, the bulky procedure of constructing wave functions can be avoided by using the generalized Hamiltonian of Anderson-Hasegawa, which in case of trimeric clusters has the following form[5]:

$$\mathcal{H}_{\mathrm{AH}}=\begin{pmatrix} \begin{matrix}-2J_0\vec{S}_1\vec{s}-2J_2\vec{S}_2\vec{S}_3-\\ -2J_1(S_1+\vec{s})(S_2+S_3)\end{matrix} & B\cdot\hat{1} & B\cdot\hat{1} \\ B\cdot\hat{1} & \begin{matrix}-2J_0\vec{S}_2\vec{s}-2J_2\vec{S}_1\vec{S}_3-\\ -2J_1(\vec{S}_2+\vec{s})(\vec{S}_1+\vec{S}_3)\end{matrix} & B\cdot\hat{1} \\ B\cdot\hat{1} & B\cdot\hat{1} & \begin{matrix}-2J_0\vec{S}_3\vec{s}-2J_2\vec{S}_1\vec{S}_2-\\ -2J_1(S_3+\vec{s})(S_1+S_2)\end{matrix} \end{pmatrix} \quad (1)$$

where J_0 is the intra-atomic exchange integral, J_1 is the exchange integral between the heterovalent ions d^n and d^{n+1}, J_2 is the same between the d^n ions. $\vec{S}_1$, $\vec{S}_2$ and $\vec{S}_3$ are the spin operators for the ionic cores, $\vec{s}$ is the spin operator of the migrating electron. B is the parameter of the resonance intercenter interaction, $\hat{1}$ is a unit matrix. The method of treatment of the Hamiltonian (1) is given in ref.[5] If one neglects the high-in-energy non-Hund states, i.e if one assumes that $B/J_0 \to 0$ then the energy levels obtained from Eq. (1) coincide with the energies given in ref.[4] For a four-electron system $d^1 - d^1 - d^2$ with fixed electron localization there are four spin multiplets: with $S = 0$, $S = 2$ and two ones with $S = 1$. Each of these multiplets, beyond the spin degeneracy, possesses also three-fold degeneracy due to the three possibilities of localization of the "extra" electron at three centers. The electron transfer splits the orbital triplet into a doublet E and singlet A (with some exceptions), not changing the spin multiplicity. Besides, the electron transfer mixes the states having the same spin multiplicity. Here we neglect the mixing of different states with $S = 1$; it will be taken into account later at the stage of spin-vibronic state calculations.

In these approximations the Hamiltonian (1) results in the following energy levels of exchange-isotropin ($J_1 = J_2 = J$) mixed-valence trinuclear clusters of the type $d^1 - d^1 - d^2$:

$$\begin{gathered} \varepsilon(^1A) = 2J - B;\quad \varepsilon(^1E) = 2J + B/2, \\ \varepsilon(^5A) = -4J + 2B;\quad \varepsilon(^5E) = -4J - B; \\ \varepsilon(^3A') = -B;\quad \varepsilon(^3E') = B/2; \\ \varepsilon(^3A'') = 0;\quad \varepsilon(^3E'') = 0. \end{gathered} \quad (2)$$

The eigenfunctions of these states are:

$$\begin{gathered} \varphi(^{2S+1}A) = (^{2S+1}\varphi_1 + {}^{2S+1}\varphi_2 + {}^{2S+1}\varphi_3)/\sqrt{3}, \\ \varphi_\theta(^{2S+1}E) = (2\,{}^{2S+1}\varphi_1 - {}^{2S+1}\varphi_2 - {}^{2S+1}\varphi_3)/\sqrt{6}, \\ \varphi_\varepsilon(^{2S+1}E) = (^{2S+1}\varphi_2 - {}^{2S+1}\varphi_3)/\sqrt{2}. \end{gathered} \quad (3)$$

where ${}^{2S+1}\varphi_i$ are the multielectron wave functions with the spin and the "extra" electron localized at the i-th center.

3. THE METHOD OF CALCULATION OF SPIN-VIBRONIC STATES

All the known vibronic theories of mixed-valence clusters so far are based on the following main assumptions :

1) At each center of the cluster the "extra" electron occupies a non-degenerate orbital and interacts with the totally symmetric displacements of the near-neighbour environment ; 2) The frequency of the totally symmetric vibration of the near-neighbour environment of the metal center is the same for both valent states. Taking into account that the vibronic interaction does not mix different spin states, one can write for each triad of the states (3) the following Hamiltonian, obtained in ref. [13].

$$\hat{\mathcal{H}} = \hat{\mathcal{H}}_{el} + \hat{\mathcal{H}}_{vib} + \hat{\mathcal{H}}_{ev} = E_S + \Delta_S \begin{pmatrix} 2 & 0 & 0 \\ 0 & -1 & 0 \\ 0 & 0 & -1 \end{pmatrix} + \hat{\mathcal{H}}_{vib} + \frac{A}{\sqrt{3}} \begin{pmatrix} Q_A & Q_\theta & Q_\varepsilon \\ Q_\theta & Q_A + Q_\theta/\sqrt{2} & -Q_\varepsilon/\sqrt{2} \\ Q_\varepsilon & -Q_\varepsilon/\sqrt{2} & Q_A - Q_\theta/\sqrt{2} \end{pmatrix} \qquad (4)$$

In Eq. (4) $\hat{\mathcal{H}}_{el}$ and $\hat{\mathcal{H}}_{vib}$ are the Hamiltonians of the electronic and nuclear subsystems, respectively $\hat{\mathcal{H}}_{ev}$ describes their interaction, A is the constant of interaction of the localized electron with the totally symmetric vibrations Q_i ($i = 1, 2, 3$), which are taken in symmetrized combinations :

$$\begin{aligned} Q_A &= (Q_1 + Q_2 + Q_3)/\sqrt{3}, \\ Q_\theta &= (2Q_1 - Q_2 - Q_3)/\sqrt{6}, \qquad (5) \\ Q_\varepsilon &= (Q_2 - Q_3)/\sqrt{2}. \end{aligned}$$

For different spin states the Hamiltonian (4) differs by different energy read off

$$E_0 = 2J \,;\; E_2 = -4J \,;\; E_1' = 0 \,;\; E_1'' = 0, \qquad (6)$$

and by the parameter of the energy gap

$$\Delta_0 = -B/2 \,;\; \Delta_2 = B \,;\; \Delta_1' = -B/2 \,;\; \Delta_1'' = 0 \qquad (7)$$

The operator of interaction with the Q_A vibrations is commutative with the full Hamiltonian and therefore it can be separated. Let us pass also to the more convenient complex basis of states ψ_μ ($\mu = 0 \pm 1$)

$${}^{2S+1}\psi_0 = {}^{2S+1}\varphi_0 \,;\; {}^{2S+1}\psi_{\pm 1} = ({}^{2S+1}\varphi_\theta \pm {}^{2S+1}i\varphi_\varepsilon)/\sqrt{2} \qquad (8)$$

Then the part of the Hamiltonian describing the vibronic interactions is as follows

$$\hat{\mathcal{H}}_{\mathrm{ev}} = \frac{A}{\sqrt{3}} \begin{pmatrix} 0 & Q_- & Q_+ \\ Q_+ & 0 & Q_- \\ Q_- & Q_+ & 0 \end{pmatrix} \tag{9}$$

where

$$Q_\pm = (Q_\theta \pm \mathrm{i} Q_\varepsilon)/\sqrt{2} \tag{10}$$

The eigenfunction of the Hamiltonian (4) can be sought for in the form:

$${}^{2S+1}\Phi^{(n)} = \sum_{\mu v l} {}^{S}C^{(n)}_{\mu v l} | S, \mu, v, l\rangle, \tag{11}$$

i.e. as an expansion with respect to the eigenfunctions of $\hat{\mathcal{H}} - \hat{\mathcal{H}}_{\mathrm{ev}}$ having the following form:

$$| S, \mu, v, l\rangle \equiv {}^{2S+1}\psi_\mu \chi_{v,l} \tag{12}$$

where $\chi_{v,l}$ are the wave functions of the dimeric isotropic harmonic oscillator. Thus we come to the system of linear equations:

$$\sum_{\substack{\lambda \neq \mu \\ v', l'}} \langle v, l | \hat{\mathcal{H}}^e_{\mu\lambda} | v', l'\rangle \, {}^{S}C^{(n)}_{\lambda v' l'} + [\hat{\mathcal{H}}^e_{\mu\mu} + v + 1 - E_S^{(n)}] \, {}^{S}C^{(n)}_{\mu v l} = 0,$$

$$\mu = 0, \pm 1; \; v = 0, 1, 2, \ldots; \; l = -v, -v + 2, \ldots, v, \tag{13}$$

where $E^{(n)}_S$ are the energies of the vibronic states and $\hat{\mathcal{H}}^e = \hat{\mathcal{H}}_{\mathrm{el}} + \hat{\mathcal{H}}_{\mathrm{ev}}$. The dimensionality of the secular equation which has to be solved for evaluation of $E^{(n)}_S$ can be reduced by means of a group-theoretical classification of the vibronic states. For this purpose we introduce the quantum number of the electron-vibrational moment

$$j = l - \mu \tag{14}$$

Taking j in the following form

$$j = 3m - \Lambda \tag{15}$$

where m is an integer, one can easily show that the states with $\Lambda = 0$ transform after the representation $\bar{A}$ (A_1 and A_2), and the states with $\Lambda = +1$ and -1 transform respectively as the E_+ and E_- components of the representation of the C_{3v} group.[14,15] In practice we have to limit the vibrational basis by some maximum value $v_{\max}$. The partition of the basis wave functions after the irreducible representations reduces the problem to the diagonalization of two matrices of $(v_{\max} + 1)(v_{\max} + 2)/2$ dimensions (the matrices for E_+ and E_- representations coincide) instead of diagonalization of one matrix of three times larger dimension. Schematically, these matrices can be presented as follows

$$\hat{\mathcal{H}}_{\Lambda} = \left[\begin{array}{c|c|c|c|c} \ddots & & 0 & & \cdot^{\cdot^{\cdot}} \\ \hline & h(j-3,\, j-3) & h(j-3,\, j) & 0 & \\ \hline 0 & h(j,\, j-3) & h(j,\, j) & h(j,\, j+3) & 0 \\ \hline & 0 & h(j+3,\, j) & h(j+3,\, j+3) & \\ \hline \cdot^{\cdot^{\cdot}} & & 0 & & \ddots \end{array}\right] \tag{16}$$

The matrix elements $h(j, j')$ are given in ref [16]. The eigenfunctions of Eq. (16) have the form :

$$ {}^{2\mathbf{S}+1}\boldsymbol{\Phi}_{\boldsymbol{\Lambda}}^{(n)} = \sum_{\substack{\boldsymbol{\mu}=0,\pm 1\\ k=0,1,2\ldots}} \; \sum_{m=0,\pm 1,\pm 2,} {}^{\mathbf{S}}C_{\boldsymbol{\mu} mk}^{\boldsymbol{\Lambda}(n)} \,|\, \mathbf{S}, \boldsymbol{\mu}, |3m - \boldsymbol{\Lambda} + \boldsymbol{\mu}| + 2k, 3m - \boldsymbol{\Lambda} + \boldsymbol{\mu} \rangle , \tag{17}$$

where the summation is performed under the condition

$$|3m - \boldsymbol{\Lambda} + \boldsymbol{\mu}| + 2k \leqslant v_{\max} \tag{18}$$

After the calculation of the vibronic states the interaction between the states with the same spin $S = 1$ has to be taken into account. The group-theoretical analysis shows that only those components of the spin triplet mix that transform after the "orbital" E representation. Using Eqs. (1) and (17) one can show that only the following matrix elements are nonzero

$$\langle {}^{3}\boldsymbol{\Phi}_{+1}^{(n)} \,|\, \hat{\mathcal{H}}_{\mathrm{AH}} \,|\, {}^{3}\boldsymbol{\Phi}_{-1}^{(n')} \rangle =$$

$$= \mathrm{i}\sqrt{\frac{3}{2}}\, B \sum_{mk} \left({}^{1}C_{+1mk}^{+1(n)}\, {}^{1}C_{-1mk}^{-1(n')} - {}^{1}C_{-1\,mk}^{+1(n)}\, {}^{1}C_{+1mk}^{-1(n')} \right). \tag{19}$$

Thus, after the diagonalization of the matrix (16), the diagonalization of the matrix constructed by the basis ${}^{3}\boldsymbol{\Phi}_{\boldsymbol{\Lambda}}^{(n)}$ has to be carried out, the diagonal elements of this matrix being the appropriate vibronic energies, while its nondiagonal elements are given by Eq. (19). The eigenvalues obtained in this way represent the "correct" energies of the spin-vibronic states with $S = 1$.

4. TEMPERATURE DEPENDENCE OF THE EFFECTIVE MAGNETIC MOMENT

For the local totally symmetric vibration frequencies about several hundreds cm^{-1} and temperatures ~ 300 K only 1—2 vibronic levels (of given symmetry) of the vibronic spectrum of the Hamiltonian (4) are populated. This means that, considering the behaviour of the magnetic moment within room temperatures for any J and B values, one has to take the $v_{\max}$ magnitude great enough in order to get reliable energy values for the ground and first excited states only (for reasonable A values). The calculations show that for $A/\sqrt{\hbar\omega^3} < 3$ one can limit the $v_{\max}$ value by $v_{\max} = 9$. For this latter the problem reduces to the diagonalization of two matricies of the dimension 55×55 for each spin multiplet. Then the basis including 10 vibronic states from each electronic multiplet with $S = 1$ transforming after the E representation is used to get the corrected energies.

The magnetic moment is calculated by the usual formula

$$\mu^2 = g^2\,\beta^2\,\frac{\sum\limits_{S,n} \nu_n S(S+1)\,(2S+1)\exp(-E_S^{(n)}/kT)}{\sum\limits_{S,n} \nu_n(2S+1)\exp(-E_S^{(n)}/kT)} \tag{20}$$

For trimeric mixed-valence complexes the sign of the matrix element of intercenter interaction can be either positive or negative dependent on the type of orbital occupied by the "extra" electron and on the kind of bridge through which the electron transfers.[17] Similarly, the parameter of exchange interaction J can be either positive or negative describing ferro and antiferromagnetic exchange, respectively. Accordingly, four cases of vibronic interaction effects in the magnetic properties can be considered :

1) $B > 0$, $J > 0$ (Fig. 1). In this case the vibronic interaction does not cause qualitative changes in the $\mu(T)$ dependence, the increase of the vibronic interaction approching it to that expected in the HDVV model in the absence of electron transfer. The ground state is always $S = 2$. When the A value increases the energy gap to the next spin multiplets somewhat decreases reducing more sharply the magnetic moment.

2) $B > 0$, $J < 0$ (Fig. 2). In this case of antiferromagnetic exchange the taking account of only the electronic effects of double exchange results in spin-singlet ground state for any positive B values[4] (similar to the HDVV model). However, since for the low-lying triplet states the energy gap (caused by the electron transfer) is smaller and hence the vibronic interaction is stronger than in the singlet state, for some of the A values the state with $S = 1$ becomes the ground one, and the $\mu(T)$ dependence becomes nonmonotonous. In mixed-valence dimers the vibronic interaction acts toward strengthening the antiferromagnetic behaviour.[7] But here we face a situation when it results in an increase of the spin of the ground state, i.e. in a strengthening of the ferromagnetic behaviour. Note that the tunneling splitting, the energy gap between the lowest A and E vibronic levels, for appropriate values of the vibronic constants is almost completely quenched. This means that the spectral data should demonstrate a localized, or almost localized (e.g. in the Mössbauer effect

time scale) picture. For $A \gg 1$ the energies of the spin-vibronic levels become independent of B, and the ground state becomes again singlet, as required by the HDVV model. However, the essential extention of the basis set needed in order to reach this region of A values, goes beyond the possibilities of this calculation.

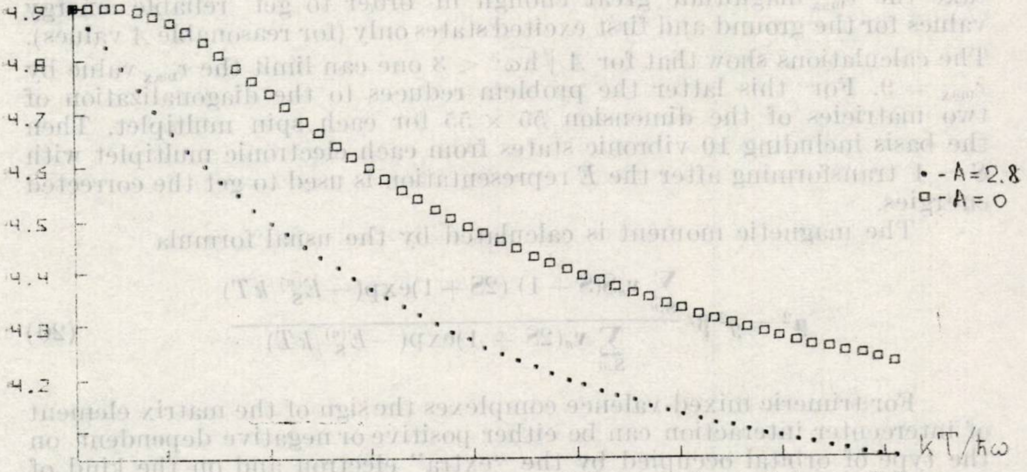

Fig. 1. — Temperature dependence on the effective magnetic moment for the case of ferromagnetic exchange coupling ($J/\hbar\omega = 0.1$). The parameter $A/\sqrt{\hbar\omega^3}$ labels the curves, $B/\hbar\omega = 1$.

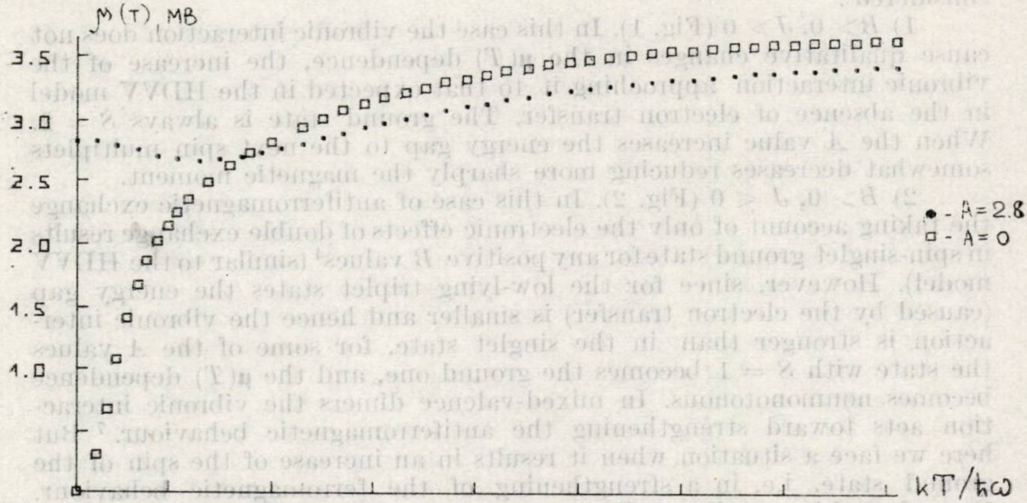

Fig. 2. — Temperature dependence of the effective magnetic moment for the antiferromagnetic case ($J/\hbar\omega = -0.1$). Notation as in Fig. 1.

Revue Roumaine de Chimie, 32, *11–12*, 1085–1095 (1987)

Dedicated to Professor V. E. SAHINI
on the occasion of his 60th anniversary

THE INSERTION REACTION OF Ni AND Ni_2 INTO O–H, S–H, O–O AND S–S BONDS. A CNDO TREATMENT

GERHARD RASCH and SVEN TOBISCH
Technische Hochschule Leuna-Merseburg "Carl Schorlemmer", Sektion Chemie, Merseburg 4200, German Democratic Republic

Received May 22, 1987

Energetical and structural behaviour during insertion reactions has been investigated using the modified Fischer-Kollmar CNDO method. In general the reactions with S compounds are favoured. Otherwise the insertion of Ni_2 is favoured against Ni. The reactions are of the oxidational addition type. The structure of the transition states is discussed.

In the field of heterogenous catalysis the hydrogenation of hydrocarbons on an Ni surface is an important reaction. Several mechanisms have been proposed.[1,6] One of these is the adsorption with subsequent break-up of the H–H and C–C bonds on a surface and the recombination of Ni–H and Ni–C to Ni–Ni and C–H. Here Ni stands for a distinct Ni atom on an excellent position of the surface, and Ni_2 for a greater part of the surface with the properties determined mainly by a pair of neighbouring Ni atoms.

The good results of this model[1] induced us to expand the consideration to other bonds. Because oxygen and sulphur compounds influence the catalytic activity, we explored the insertion of Ni or Ni_2 into the O–H bond, the S–H bond, the O–O bond and the S–S bond.

MODEL

The Ni surface was reduced to one or two Ni atoms. Therefore we distinguish between the Ni mechanism and the Ni_2 mechanism. Because in an insertion reaction the distance of the bonded atoms will be lengthened to form the product with one or two Ni atoms inside, this distance could be handled as a reaction coordinate (RC), or in some cases as the reaction path. This corresponds to a cross-section through the potential hyperface of all degrees of freedom. For different fixed points on RC all other distances can be optimized and so we received energies between the ground of the reaction valley and the transition state. We do not need the full curves because we are only interested in four points :

- *F* — Free molecules with infinite distance of the metal atoms from the bond considered as references for the energy
- *E* — It is known that the reacting molecules form a precomplex, the educt
- *T* — The transition state
- *P* — The endpoint of the reaction with the inserted atoms, the product.

—With a single Ni atom, for the insertion reaction in a bond X—Y the following structures for *E*, *T* and *P* must be discussed.

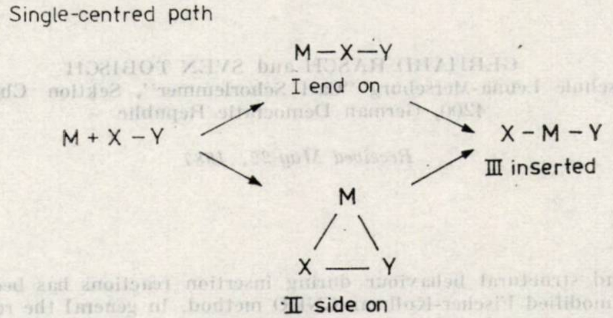
Single-centred path
M—X—Y
I end on
M + X − Y
X − M − Y
III inserted
M
X
Y
II side on

Scheme 1

From the three possible products the π-complexes have been considered earlier.[7,8] We will therefore look at the insertion product III and the σ-complex II.

With two Ni atoms for the insertion we obtain several possibilities :

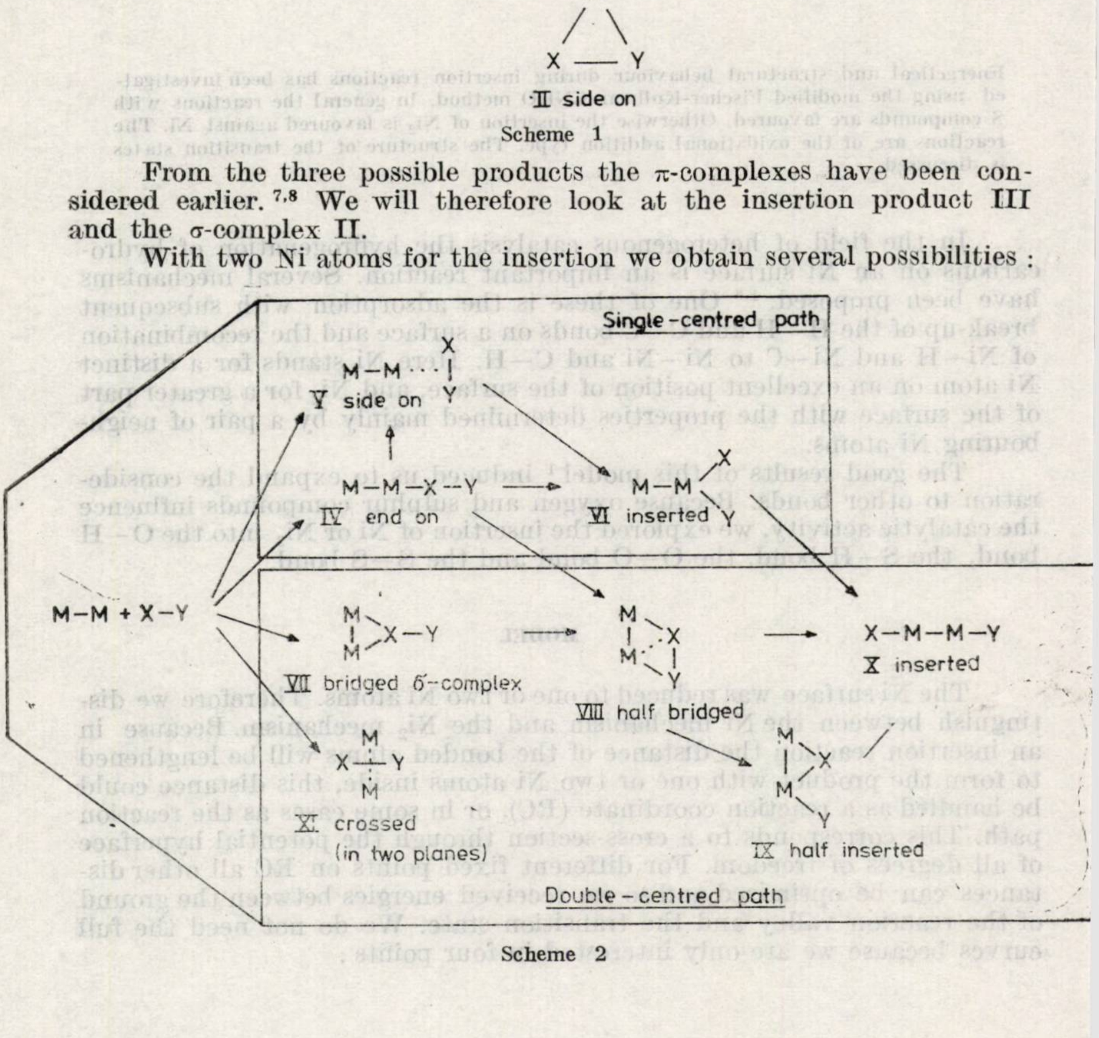
Single-centred path
M—M···X—Y
V side on
M—M—X—Y
IV end on
M—M X Y
VI inserted
M—M + X—Y
M M X—Y
VII bridged σ-complex
M M X Y
VIII half bridged
X—M—M—Y
X inserted
M X Y M
XI crossed (in two planes)
M X M Y
IX half inserted
Double-centred path

Scheme 2

Therefore we must distinguish between two general routes, viz. the single-centred path and the double-centred path. It seems that starting with Ni_2 we have a branch identical with the single-centred path. But here we have additionally the rearrangement from VI to X and also we can take into account the influence of a second Ni atom.

As model for a O—H bond we take the molecule of water, for the S—H bond one of dihydrogensulphide, for the O—O bond one of hydrogenperoxide, and for S—S one of hydrogendisulphide. We use the abbreviation X = OH, SH and Y = H, X. The real symmetries of the different molecules are therefore other than in schemes 1 and 2.

METHOD

We used the CNDO Version of Fischer—Kollmar [5] with some modification, [6,9] called CNDO—FK/M, a semiempirical quantum-chemical method. This approximation gives good results for hydrocarbons and related oxygen and sulphur compounds [5,11] and is able to include transition metals e.g. nickel or copper. The parameters are tabulated in [6] and [10].

The method is a single determinant method and therefore the question of correlation effects must be regarded. This influence has been proven as configuration interaction in [12]. But there the parameters are fitted to experimental results only for the single determinant version of the method. Therefore we cannot use the numerical results. But we notice that the energy will be lowered more for the transition state and we can only state that our calculated values for the transition states are too high.

The method permits geometrical optimization [13] and a vibrational analysis. [14] This gives the possibility to characterize excellent points of the potential hyperface. Otherwise we are able to complete the energies with the zero-point parts. With this we obtain for the reaction the ergicities and instead of the activation barriers the threshold energies.

For the bond strength we use the well known Wiberg Index WB. The energies are declared in kJ/mol, distances in pm and electron density by Mulliken population analysis in electrons.

But we could not determine the transition states in every case. In these cases we give estimated values of the activation energies.

RESULTS

1. INSERTION INTO O—H

1.1. Insertion of Ni

As precomplex *E* we always find, independent of the starting geometry, a structure corresponding to I, an end on σ-complex with C_h symmetry. The systematically lengthened O—H bond leads to the transition state at $R_{OH} = 150$ pm in C_h. The structure of *T* is II nearly an equilateral triangle. Its character is proven by vibrational analysis. The imaginary decay vibration is $i\nu = 2012\ \mathrm{cm}^{-1}$. The product *P* is an angled molecule in C_h ($\sphericalangle$ HNiO $= 147°$) and corresponds to III. Descending calculations starting near T yield either E or P, both in C_h. This demonstrates the undistorted way from E about T to P in C_h. The results for the ergicity and the threshold energies as an upper limit are listed in table 1 and other data in table 2.

Table 1

Threshold energies, activation energies and ergicities for insertion reactions

Reaction	Centres	Threshold energies (upper limit)		Activation energies		Ergicities
		$\longrightarrow$	$\longleftarrow$	$\longrightarrow$	$\longleftarrow$	
$Ni+H-OH$	1	252	274	273	280	−22
$Ni+H-CH_3$[6]	1	117	303	135	307	−186
$Ni+H-SH$	1	54	354	63	328	−300
Ni_2+H-OH	1	229	223	250	230	6
Ni_2+H-OH	2	279	478	298	480	−199
Ni_2+H-CH_3[6]	2	180	502	198	509	−322
Ni_2+H-SH	2	(70)	(415)	(85)	(428)	(−346)
$Ni+HO-OH$	1			760	580	(182)
$Ni+H_3C-CH_3$[6]	1			380	515	(−134)
$Ni+H-H$[6]	1			176	337	(−190)
$Ni+HS-SH$	1			−64	342	(−406)
Ni_2+H-H[6]	2	68	409	78	425	−341
$Ni_2+H_3C-CH_3$[6]	2	180	617	200	625	−437

Table 2

Bond energies E_B. zero point energies E_{ZP}, and atomic net charges Q for insertion

Reaction	Character	Structure	E_B	E_{ZP}	Q		
					Ni	X	H(1)
$Ni+H_2O$	E	I	−102.7	78.6	−.280	−.237	.259
	T	II	170.0	58.2	−.017	−.332	.180
	P	III	−109.2	63.7	.212	−.335	−.039
$Ni+H_2S$	E	I	−128.9	50.7	−.277	.012	.132
	T	II	−66.1	41.8	−.055	−.235	−.177
	P	III	−421.1	45.9	.273	−.306	−.087

Figure 1 shows on the top the chemical formulae during the reaction, below this the energetic behaviour and at the foot the changing of the bonds as Wiberg indices. We notice that:

1. The energy curve is continual and therefore the reaction is allowed in C_h symmetry.
2. During the reaction the charges of the Ni atom and the separated H(1) atom change in an opposite way. In the transition state the Ni atom is nearly neutral.

The reaction has the character of an oxidational addition.

3. The WBs indicate the bond changes well. At the start the bond, which is later destroyed, has a high value and at the end this falls to zero. Vice versa, the new bond was built up.
   For the bond relations in *T* compare figure 2.

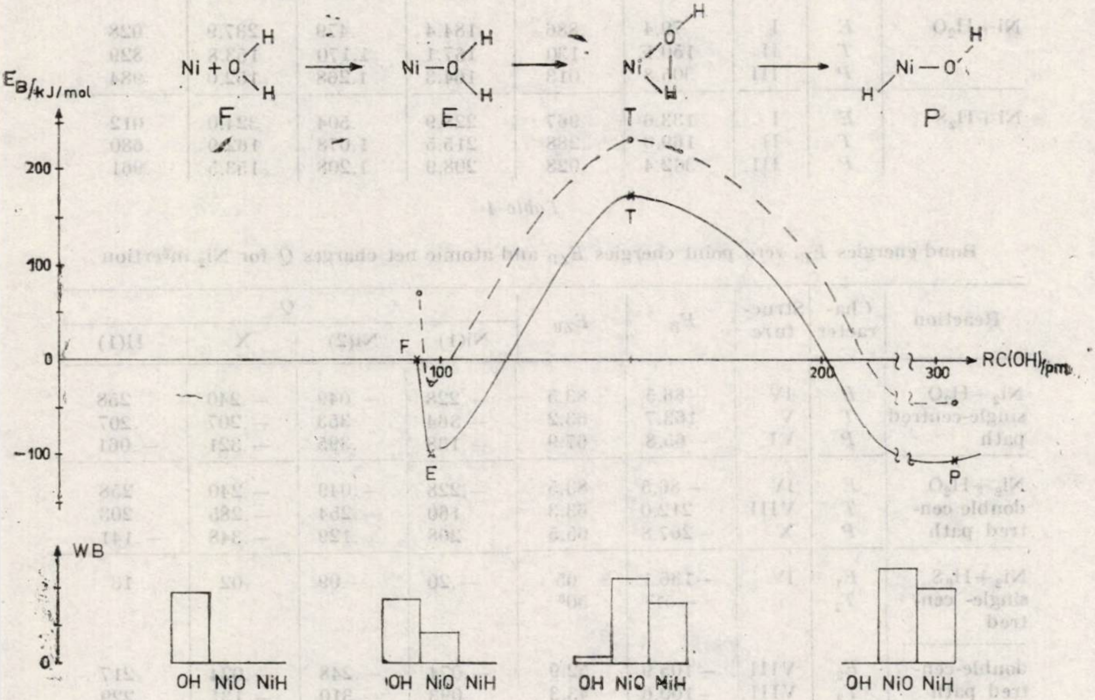

Fig. 1. — Course of the insertion of Ni in an O—H bond.

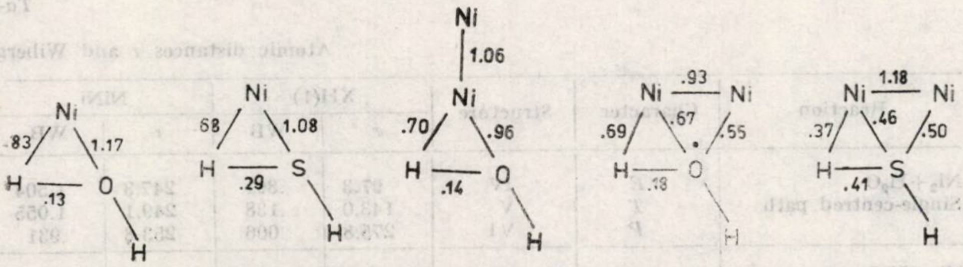
Ni
.83
1.17
H
.13
O
H
Ni
.68
1.08
H
.29
S
H
Ni
1.06
Ni
.70
.96
H
.14
O
H
Ni
.93
Ni
.69
.67
.55
H
.18
O
H
Ni
1.18
Ni
.37
.46
.50
H
.41
S
H

Fig. 2.— Some Wiberg indices for transition states of insertion reactions.

1.2. Insertion of Ni_2

For the precomplex *E* we have a stable non-linear structure (C_h) end on IV. In following RC we receive different transition states. We can divide into the single- and the double-centred paths.

Table 3

Atomic distances r and Wiberg indices WB fir Ni insertion

Reaction	Character	Structure	XH(1)		NiX		NiH(1)	
			r	WB	r	WB	r	WB
$Ni+H_2O$	E	I	79.4	.886	184.4	.479	237.9	.028
	T	II	150.E	.130	167.1	1.170	153.8	.829
	P	III	305.8	.013	164.3	1.268	152.0	.984
$Ni+H_2S$	E	I	133.6	.967	228.9	.504	324.0	.012
	T	II	169.0	.288	215.5	1.078	162.9	.680
	P	III	362.4	.028	208.9	1.208	153.5	.961

Table 4

Bond energies E_B, zero point energies E_{ZP} and atomic net charges Q for Ni_2 insertion

Reaction	Character	Structure	E_B	E_{ZP}	Q			
					Ni(1)	Ni(2)	X	H(1)
Ni_2+H_2O single-centred path	E	IV	−86.5	83.5	−.228	−.049	−.240	.258
	T	V	163.7	63.2	−.364	.353	−.207	.207
	P	VI	−65.8	67.9	−.138	.395	−.321	−.061
Ni_2+H_2O double centred path	E	IV	−86.5	83.5	−.228	−.049	−.240	.258
	T	VIII	212.0	63.3	.160	−.254	−.285	.203
	P	X	−267.8	65.5	.208	.129	−.348	−.141
Ni_2+H_2S single-centred	E_1	IV	−136.1	65	−.20	−.09	.02	.13
	T_1		−51[a]	50[a]				
double-centred path	E_2	VIII	−105.9	52.9	−.074	−.248	−.024	.217
	T_2	VIII	−100.6	43.3	.093	−.310	−.131	.229
	P	IX	−479.0	62.4	.144	.068	−.226	−0.97

[a] estimated.

Ta-

Atomic distances r and Wiberg

Reaction	Character	Structure	XH(1)		NiNi	
			r	WB	r	WB
Ni_2+H_2O Single-centred path	E	IV	97.3	.891	247.3	1.504
	T	V	143.0	.138	249.1	1.055
	P	VI	275.8	.006	253.8	.931
Ni_2+H_2O Double-centred path	E	IV	97.3	.891	247.3	1.504
	T	VIII	136.0	.184	246.4	.932
	P	X	572.6[a]	.003	254.7	1.012
Ni_2+H_2S Double-centred path	E_1	IV	133.8	.96[a])	245.8	
	E_2	VIII	138.7	.866	247.1	1.335
	T_2	VIII	151,0	.412	246.4	1.170
	P	IX	345.1	.014	250.0	.943.

[a] estimated.

At first T_1 corresponds to the side on complex V (C_h). This is a saddle point ($i\nu = 2167\ cm^{-1}$). P_1 has the inserted structure VI (C_h). The course of the reaction is nearly the same as in the case of the insertion of Ni alone. But now we notice an influence of the second Ni atom as a buffer for the electrons. The positive charge is no longer on Ni(1) but on Ni(2). The double-centred path started likewise in IV. It has a T_2 with the surprising half bridged structure VIII (C_h) as a saddle point ($i\nu = 2337\ cm^{-1}$). In P_2, Ni_2 is fully inserted to X (C_1). For data see tables 1, 4 and 5.

Both reaction branches are allowed. The single-centred path has a lower threshold energy, but the double-centred path is clearly favoured by its ergicity.

2. INSERTION INTO S—H

2.1. Insertion of Ni

The structure of E corresponds to I (C_{2v}). Besides E we find a less stable structure in the form of a four ring system with two Ni—H bonds. T is not fully even. Ni atom lies about the HSH plane. The structure is near to II and belongs to C_1. It was characterized as a saddle point ($i\nu = 1887\ cm^{-1}$). Starting in C_h a similar structure was found with only 1.9 kJ/mol energy lower. As with P we find in C_1 a point with 0.5 kJ/mol more stable than a point in C_h. In both $\measuredangle HNiS = 175°$. A third point in $C_{\infty v}$ is localized not far from the others. We think this method can distinct these three points numerically, but the differences are too small for conclusions. The data for the most stable structures are listed in tables 1, 2 and 3. All three points E, T and P have negative energies compared with the non bonded state F. Therefore the reaction will hardly be hindered. It is allowed in C_1, perhaps also in C_h.

ble 5

indices WB for Ni_2 insertion

Ni(1X)		Ni(1)H(1)		Ni(2)X		Ni(2)H(1)	
r	WB	r	WB	r	WB	r	WB
187.2	.445	241.4	.024	363.4	.016	405.2	.001
169.9	.958	155.6	.699	359.4	.104	402.6	.111
165.2	1.174	153.7	.912	364.0	.058	358.5	.078
187.2	.445	241.4	.024	363.4	.016	405.2	.001
193.1	.553	307.6	.084	184.7	.673	157.4	.690
165.9	1.237	407.9	.021	419.1	.013	153.4	.956
229.3		334.5					
244.9	.384	318.2	.021	257.6	.256	199.4	.122
240.6	.498	315.6	.085	246.4	.458	174.2	.368
223.8	.820	404.2	.036	233.1	.588	154.3	.940

2.2. Insertion of Ni_2

The most stable precomplex E_1 has a single-centred structure end on IV (C_h). It is more stable than the comparable precomplex $NiSH_2$ in 1.2. Searching for T results in only a half bridged structure T_2 VIII (C_1) with $i\nu = 1335$ cm^{-1}. Descending calculations lead to the product IX (C_1) which is half inserted. But the starting point E_1 could not have been reached. Instead of this we get a structure similar to the half bridged VIII (C_1). We term this point E_2. It was characterized as a minimum. Therefore between E_1 and E_2 there must be a transition state of a rearrangement. We estimated the values for this state T_1 and for the zero-point energies of E_1 and T_1. For this reaction we assumed a way from E_1 about T_1 to the intermediate E_2 end then to T_2 and P. The data are listed in tables 1, 4 and 5. The reaction is allowed in C_1. Three peculiarities must be noticed :

1. The threshold energy determined by the estimated T_1 is very small.
2. For the second threshold a negative energy value results. The activation energy is positive but because of the differences in the zero-point energy the threshold energy is negative and has no influence on the reaction.
3. The product structure suggests the influence of other Ni atoms. It is already clear that a second Ni atom favours the reaction, although it is not clear to what extent. Moreover, the product has a bridged structure and shows the position of sulphur atoms on a nickel surface in agreement with the experimental results. [15]

To generalize the results we complete tables 1 and 6 with the values for the insertion into C−H, H−H and C−C. [5,6]

Table 6

Relative change of the Wiberg indices during an insertion reaction of Ni into an X−H bond

	X=O			C			S		
	OH	NiO	NiH	CH	NiC	NiH	SH	NiS	NiH
$\frac{WB(E)-WB(T)}{WB(E)-WB(P)}$	.87	.87	.84	.75	.87	.73	.72	.81	.71
$\frac{WB(T-WB(P)}{WB(E)-WB(P)}$	.13	.13	.16	.25	.13	.27	.28	.19	.29

In the range O−H, C−H and S−H the ergicities show that the S−H bond is favoured. The same holds for the threshold energies. In table 6 we compare the change in the Wiberg indices during the reaction. In all three cases the behaviour is similar. The greatest part of change happens between E and T. Only a small percentage remains for T to P. Obviously the electron structure and the behaviour of the wave function for the way from T to P in all three cases are similar. On the other hand, by geometrical considerations, T are more similar to E.

3. INSERTION INTO O–O

3.1. Insertion of Ni

For this single-centred reaction (related to Ni) we distinguish between a symmetrical way (to O–O) and an asymmetrical one. For the symmetrical way for E a saddle point ($i\nu = 231$ cm^{-1}) results. In the direction O–O–Ni there is another saddle point ($i\nu = 323$ cm^{-1}). The most stable structure for E corresponds to the asymmetrical II, a bent precomplex ($\sphericalangle$OONi $= 131°$). It belongs to an energy minimum. The dihedral angle HOOH is 19°. This value is not very reliable, because the method approximates the interaction between free electron pairs in a spherical way. The symmetry of E is therefore C_1. For P it results in a structure III. Its symmetry is C_1. A transition state T could not have been fixed. Starting from E it results in another configuration than for the starting point P. The data in table 7 show equal energies but otherwise different NiO distances, different charges and different WB's for RC = 170 pm. We assume a pseudocrossing of two hyperfaces of different configurations. The crossing point is only a bad value for the transition energy because configuration interactions are not taken into account, because the hamiltonian of both configurations is different and because the zero-point energy was neglected. In table 1 we therefore only give the estimated values of activation energies. The reaction is forbidden.

Table 7

Bond energies E_B, zero point energies E_{ZP}, atomic net charges Q, atomic distances r and Wiberg indices WB for insertion into an X–X bond

Reaction	Character	Structure	E_B	E_{ZP}	Q		NiX(1)		XX	
					Ni	X(1)	r	WB	r	WB
Ni + H$_2$O$_2$	E	II	−53.2	98.5	−.253	−.050	189.	.428	115.8	.985
		II	706.0	—	−.369	−.062	170.9	.793	170.0	.555
asymmetrical	T_1/T_2	II	706.0	—	.253	−.278	164.0	1.176	170.0	.029
	P	III	114.3	113.0	.21	−.289	161.5	1.325	323.0	.019
Ni + H$_2$S$_2$	E	II	166.1	53.1	−.344	−.034	234.4	.461	202.8	.935
		II	−64.1	—	−.385	−.024	229.3	.541	235.0	.875
symmetrical	T_1/T_2	II	64.1	—	.341	−.219	211.8	1.162	235.0	.047
	P	III	−588.8	70.4	.332	−.285	209.6	1.184	418.3	.034

3.2. Intertion of Ni$_2$

For the precomplex E we received a typical first centre structure IV end on (C_1). But its energy was only −28.6 kJ/mol. T and P could not be determined.

4. INSERTION INTO S—S

4.1. Insertion of Ni

In contrast to O—O we find a symmetrical way. *E* has a side on structure II (C_{2v}). But in this case it results in a five ring system with two Ni—H bonds. With the hydrogen atoms directly bonded to S—S yields that the energy is 15 kJ/mol less stable and belongs to a saddle point ($i\nu = 113$ cm^{-1}). *P* in C_{2v} has a different configuration to *E*. Once more we have a forbidden reaction. *T* will correspond to II. The S—S distance alone is a bad *RC*. The data in table 7 show two values for $r_{SS} = 235$ pm. In table 1 the estimated activation energy is given. The reaction is forbidden.

4.2. Insertion of Ni_2

E, *T* and *P* could not be determined. But calculation modelling an S—S bond break point leads to a reaction without kinetic inhibition.

CONCLUSION

We can take most information from table 1. We always find a range $S < H < C < O$ either for the ergicities or for the threshold energiese Exceptions for the ergicities are only the inverse range of Ni_2 insertion. nto CC or HH. But the threshold energies for H are lower than for C. In all cases the sulphur compounds will react with Ni or Ni_2 better than the others.

In all cases the insertion of Ni_2 over the double-centred path is favoured. For the Ni insertion into a symmetrical bond the chosen model is not successful. With this the reactions are forbidden. It yields different configurations for the educts and products.

The insertion reaction can be characterized in every case as an oxidational addition onto Ni. This is clearer for the single-centred reactions.

During the reaction the greatest change in the wave function for the electrons results between the educt and the transition state.

From figure 2 we can see that the structure of the transition state for Ni or Ni_2 insertion is similar. In the case of Ni_2 insertion the bridged structure is important. In most cases this ring will be opened in the product structure, but for sulphur this ring remains. This points to the strong poisonous effects of sulphur compounds for Ni catalysts.

At last in the products we find enlarged Ni—Ni distances referring to the well known balloon effect.[16] This gives order to investigate the influence of surface places and defects.

REFERENCES

[1] J. H. Sinfelt, *J. Phys. Chem.* **68**, 334 (1964).
[2] J.H. Sinfelt, W.F. Taylor and D.J.C. Yates, *J. Phys. Chem.* **69**, 95 (1965).
[3] G.A. Martin, *J. Catalysis*, **60**, 345 (1979).
[4] J. R. Anderson and B. G. Baker, *Proc. Roy. Soc.*, **A271**, 402 (1963).
[5] E. Bauwe and G. Rasch, *Z. physik. Chem. (Leipzig)*, **265**, 1009 (1984).
[6] E. Bauwe, Dissertation Merseburg 1985 and therein.
[7] H. Bögel and G. Rasch, *Z. Chem.* **22**, 191 (1982).
[8] H. Bögel, *Theor. Chim. Acta (Berl.)* **63**, 395, (1983).
[9] H. Fischer and H. Kollmar, *Theor. Chim. Acta (Berl.)*, **13**, 213 (1969).
[10] G. Rasch and E. Bauwe, *Z. physik. Chem. (Leipzig)*, im Druck.
[11] E. Bauwe, A. M. Richter, G. Rasch and E. Fanghänel, *Z. Chem.*, **24**, 418 (1984).
[12] E. Bauwe and G. Rasch, *Z. Chem.*, **24**, 304 (1984).
[13] J. Reinhold, H. Zwanziger and Ch. Nieke, Universität Leizig Programmsystem CNDOCX.
[14] H.-J. Köhler, Universität Leipzig, contained in Program system MINDO/3.
[15] D. W. Goodman, *Acc. Chem. Res.*, **17**, 194, (1984).
[16] H. Müller and Ch. Opitz, *Z. phys. Chem. (Leipzig)*, **257**, 482 (1976).

Revue Roumaine de Chimie, **32**, *11–12*, 1097–1101 (1987)

Dedicated to Professor V. E. SAHINI
on his 60th anniversary

COUNTING OBSERVABLES OF CHEMICAL SPECIES

AL. IVANOV
Center of Physical Chemistry, ICECHIM,
Spl. Independenței 202, Bucharest, Romania

Received May 27, 1987

The notion of counting observable associated with a chemical species is introduced. By using the methods of the theory of orthomodular lattices, certain conditions ensuring a "classical description" of the systems of many chemical species in the framework of standard quantum mechanics are established.

1. THE PROBLEM

The notion of chemical species is inferred from empirical chemical facts. Roughly speaking, a chemical species is a material entity which may be distinguished from other material entities in terms of an empirically defined set of chemical properties.

In what follows it will be supposed that *any chemical species is characterized by a specific type of particles.* Therefore, we may assume that there exists — at least in principle — an experimental procedure of "counting" the particles of an arbitrarily given chemical species. In other words, any chemical species S may be characterized by a measurable physical quantity which might be called *the number of particles of the species S.* If a given physical theory is able to describe the chemical species S, then it must contain a mathematical object corresponding to this physical quantity.

This work deals with the description of chemical species in the framework of standard quantum mechanics, i.e. in a theory which uses as basic mathematical object a separable Hilbert space. Since in the standard quantum mechanics any physical quantity is described by a self-adjoint operator, the number of particles of the species S will be represented by an operator N_S, called *the counting observable of the species S.*

We want to discuss here a problem arising when two different chemical species — S_1 and S_2 — are described in the same separable Hilbert space $\mathscr{H}$. The physical meaning of our problem will be more transparent if we will use the formulation of standard quantum mechanics in terms of projection operators (projectors).

Let us denote by $\Pi_{\mathscr{H}}$ the set of all orthogonal projectors of the Hilbert space $\mathscr{H}$. It is well known that the basic objects of the standard quantum mechanics – the states and the observables – may be defined in terms of projection operators.[1] Indeed, any state – density operator – is completely described by a function $p : \Pi_{\mathscr{H}} \to [0,1]$ whose restriction to any Boolean algebra of projectors is a probability, and any observable – self-adjoint operator – is completely described by a function $\omega : \mathcal{B}(\mathbb{R}) \to \Pi_{\mathscr{H}}$, which is a σ-homomorphism of orthomodular lattices[2] (here $\mathcal{B}(\mathbb{R})$ denotes the σ-algebra of Borel subsets of the real line). It results that $\Pi_{\mathscr{H}}$ may be used as a basic mathematical object of the standard quantum mechanics. This fact is important since $\Pi_{\mathscr{H}}$ has a more clear physical meaning than the Hilbert space $\mathscr{H}$. Indeed, according to von Neumann's interpretation, any projector corresponds to a "yes-no experiment" (YNE).[3] This interpretation offers a clear physical meaning to the order relation on $\Pi_{\mathscr{H}}$($E_1 \leqslant E_2$, E_1, $E_2 \in \Pi_{\mathscr{H}}$, iff $E_2 - E_1$ is a positive operator) and to the orthocomplementation $\Pi_{\mathscr{H}} \ni E \mapsto 1 - E \equiv E^{\perp}$, where 1 is the identity of $\mathscr{H}$. The order "$\leqslant$" and the orthocomplementation "$\perp$" define on $\Pi_{\mathscr{H}}$ a structure of orthomodular lattice. These facts and certain similar observations concerning classical theories led to the conclusion that the structure of orthomodular lattice is fundamental for physical theories.[4,5]

Let us return now to the description of the chemical species S_1, S_2, in the theory $\Pi_{\mathscr{H}}$. The counting observables N_{S_1}, N_{S_2}, may be written in the form:

$$N_{s_i} = \sum_{k \geqslant 0} k\, E_k^{(i)}, \quad 1 \leqslant i \leqslant 2 \tag{1}$$

where $E_k^{(i)}$ is the spectral projector corresponding to the eigenvalue k of the operator N_{S_i}. By using relation (1) we may say that – in terms of the orthomodular lattice $\Pi_{\mathscr{H}}$ – the counting observable N_{S_i} is represented by the complete sublattice of $\Pi_{\mathscr{H}}$ generated by the family $\{E_k^{(i)}\ ;\ k \in \mathbb{N}\}$ of spectral projectors of N_{S_i} ($\mathbb{N} = \{0, 1, 2, \ldots\}$ is the set of all positives integers). Let us denote this sublattice by $\mathcal{N}_{S_i}$. It is obvious that $\mathcal{N}_{S_i}$ is a Boolean algebra of projectors. The object we want to study is the complete sublattice of $\Pi_{\mathscr{H}}$ generated by the union $\mathcal{N}_{S_1} \cup \mathcal{N}_{S_2}$. This sublattice will be denoted by $\mathcal{C}_{\mathscr{H}}$. Since the elements of the sublattice $\mathcal{C}_{\mathscr{H}}$ represent YNE referring to the determination of the number of particles of the species S_1 and S_2, it will be called the sublattice of counting YNE of the family $\{S_1, S_2\}$. Our study refers to the properties of the sublattice $\mathcal{C}_{\mathscr{H}}$.

Let us remark now that, if the "classical concept" of particle is applied to the particles of species S_1, S_2, then we may accept the existence of YNE determining simultaneously the number of particles of these species in any arbitrarily given state. In other words, to any pair (k_1, k_2) of positive integers we may associate a YNE whose answer is "yes" when the determined number of particles of the species S_1, S_2 is k_1 and k_2 respectively. It results that, from classical point of view, the lattice of counting YNE is isomorphic to the Boolean algebra of all subsets of the Cartesian product $\mathbb{N} \times \mathbb{N}$; it will be denoted by $\mathcal{C}$. Obviously, the Boolean character of the orthomodular lattice $\mathcal{C}$ has as physical support the compatibility of all counting YNE.

The problem of this paper is to find those physically interpretable conditions which ensure the existence of an isomorphism between $\mathcal{C}_{\mathcal{H}}$ and $\mathcal{C}$. Since we consider that the compatibility of counting observables of any two chemical species is hard to be considered as an empirically obvious fact, the conditions we look for must have physical interpretations which do not use the compatibility of counting YNE.

2. A SOLUTION OF THE PROBLEM

Some of the results of this section will refer to a general orthomodular lattice, which will be denoted by $(L, \leqslant, \perp)$ (here L is a nonempty set, "$\leqslant$", "$\perp$", the order and the orthocomplementation which define on L a structure of orthomodular lattice). If $A \subseteq L$ is an arbitrarily given subset of L, then we will denote by $\vee A$, $\wedge A$ the *least upper bound* and the *greatest lower bound* of A respectively.

The central result of this section is the following theorem.

Theorem 2. *Let us denote by* Ω_{12} *the set of all elements* $E^{(1)}_{k_1} \wedge E^{(2)}_{k_2}$ (see (1)), $(k_1, k_2) \in \mathbb{N} \times \mathbb{N}$. *Suppose that the following two conditions are satisfied:*

(C_1) *it does not exist a state* $p : \Pi_{\mathcal{H}} \to [0, 1]$ *such that* $p(E) = 0$ *for all* $E \in \Omega_{12}$;

(C_2) *for any pair* $(k_1, k_2) \in \mathbb{N} \times \mathbb{N}$ *there exists a state* p *such that* $p(E^{(1)}_{k_1}) = p(E^{(2)}_{k_2}) = 1$.

Then $\mathcal{C}_{\mathcal{H}}$ *is isomorphic to* $\mathcal{C}$.

The physical interpretation of the conditions (C_1) and (C_2) is obvious. We may say that, if (C_1) and (C_2) are true, then the description of the chemical species S_1, S_2 in the framework of the standard quantum mechanics is a classical one.

The proof of Theorem 2 is a straightforward consequence of the following two lemmas.

Lemma 3. *Let* $(L, \leqslant, \perp)$ *be an orthomodular lattice and* $\mathcal{A}$, $\mathcal{B} \subseteq L$ *atomic Boolean sublattices of* L. *Let us denote by* Ω *the set of all elements of the form* $\alpha \wedge \beta$, *where* α, β *are respectively atoms of* $\mathcal{A}$, $\mathcal{B}$, and *by* $[\mathcal{N}]$ *the smallest sublattice of* L *having the property*: $A \subseteq \mathcal{N}$ *and* $\vee A$ *exists in* $L \Rightarrow \vee A \in [\mathcal{N}]$. *Then the following assertions are equivalent*:

(i) $\mathcal{A}, \mathcal{B} \subseteq [\Omega]$;

(ii) $\vee \Omega = 1$ *(1 is the greatest element of* L*)*;

(iii) $[\mathcal{A} \cup \mathcal{B}]$ *is a Boolean sublattice of* L.

Proof. For any two elements $a, b \in L$ we write $(a, b)\,K$ if $a = (a \wedge b) \vee (a \wedge b^{\perp})$. We say that a, b are compatible elements of L. If $L = \Pi_{\mathcal{H}}$, then a, b are projectors in $\mathcal{H}$ and $(a, b)\,K$ iff $ab = ba$. It may be proved easily that L is a Boolean algebra iff $(a, b)\,K$ for all pairs $(a, b) \in L \times L$.

We will prove first the implication (ii) $\Rightarrow$ (i). For any atom $\alpha \in \mathcal{A}$, we may write $(\alpha, \gamma)K$ if $\gamma \in \Omega$, so that $\alpha = \bigvee_{\gamma \in \Omega} (\alpha \wedge \gamma)$ and we get $\mathcal{A} \subseteq [\Omega]$. In order to prove the implication (i) $\Rightarrow$ (iii), it is sufficient to use the fact that the elements of Ω are mutually orthogonal (if $\alpha, \alpha' \in \mathcal{A}$, $\beta, \beta' \in \mathcal{B}$ are atom and $\beta \neq \beta'$, we may write $\alpha \wedge \beta \leqslant \beta \leqslant \beta'^{\perp} \leqslant \alpha'^{\perp} \vee \beta'^{\perp} = (\alpha' \wedge \beta')^{\perp}$). Since the orthogonal elements of L are also compatible, it results that

$[\Omega]$ is a Boolean sublattice of L. Therefore $[\mathcal{A} \cup \mathcal{B}]$ is a Boolean sublattice since $[\mathcal{A} \cup \mathcal{B}] \subseteq [\Omega]$. It remains to prove the implication (iii) $\Rightarrow$ (ii), which is trivial since the least upper bound of the set of atoms of $\mathcal{A}$ (or $\mathcal{B}$) is 1.

The following lemma has been proved by J. M. Jauch. [6] The proof we give below is interesting since it uses mainly geometric properties of the Hilbert space (or, equivalently, algebraic properties of the set $\Pi_{\mathcal{H}}$).
Lemma 4. *Let* $\mathcal{H}$ *be a Hilbert space of dimension greater than 3 and* $p : \Pi_{\mathcal{H}} \to [0, 1]$ *a state. Then* $p(E) = p(E') = 1 \Rightarrow p(E \wedge E') = 1$.
Proof. Let $e \in \Pi_{\mathcal{H}}$ be an atom and $\delta_e : \Pi_{\mathcal{H}} \to [0, 1]$ the unique state having the property $\delta\,(e) = 1$. According to Gleason's theorem [7], we may write for any arbitrarily given state p :

$$p = \sum_{n \geqslant 1} c_n \delta_{e_n}. \tag{5}$$

where $\{e_n\}_{n \geqslant 1}$ is a set of mutually orthogonal atoms of $\Pi_{\mathcal{H}}$ and $\{c_n\}_{n \geqslant 1}$ is a set of positive real numbers having the property $\sum\limits_{n \geqslant 1} c_n = 1$. We will prove first that, given $E, e \in \Pi_{\mathcal{H}}$, where e is an atom, there exists $e' \in \Pi_{\mathcal{H}}$, $e' \leqslant E$ an atom such that $\delta_e(E) = \delta_e(e')$. This statement is obvious when E is an atom, $e \leqslant E$ or $(e, E) \perp$ (here $(a, b) \perp$ denotes that $a, b \in \Pi_{\mathcal{H}}$ are orthogonal). Therefore, let us suppose that $e \nleqslant E$ and e, E are not orthogonal. Then there exists an atom e'' such that $E \vee e = E \vee e''$, $(e'', E) \perp$. Then $\delta_e(E \vee e) = \delta_e(E) + \delta_e(e'') = 1$. On the other hand there exists an atom e' such that $(e', e'') \perp$ and $e \vee e'' = e' \vee e''$. It results $\delta_e(e \vee e'') = \delta_e(e') + \delta_e(e') = 1$. By combining these equalities, we get $\delta_e(E) = \delta_e(e')$. It remains to show that $e' \leqslant E$. But $e' \leqslant e \vee e'' \leqslant E \vee e = E \vee e''$ and $(e', e'') \perp$ imply $e' \leqslant E$ since $e' \leqslant e \vee e''$, $e' \leqslant e''^{\perp} \Rightarrow e' \leqslant (E \vee e'') \vee e''^{\top} = E \wedge e''^{\perp}$.

Let p be an arbitrarily fixed state with the property $p(E) = p(E') = 1$. Taking account of the relation (5), we may write $p(E) = \sum\limits_{n \geqslant 1} c_n \delta_{e_n}(E)$. It results $\delta_{e_n}(E) = 1$ for all $n \geqslant 1$ (it is supposed that $c_n > 0$ for all $n \geqslant 1$). Therefore, there exists e', an atom of $\Pi_{\mathcal{H}}$, such that $e'_n \leqslant E$ and $\delta_{e_n}(E) = \delta_{e_n}(e'_n) = 1$. But we know that $\delta_{e_n}(e'_n) = 1$ implies $e_n = e'_n$, so that we get $\bigvee\limits_{n \geqslant 1} e_n \leqslant E$. Similarly, we may prove that $\bigvee\limits_{n \geqslant 1} e_n \leqslant E'$. Consequently $p(E \wedge E') \geqslant \sum\limits_{n} c_n \delta_{e_n}(\bigvee\limits_{k \geqslant 1} e_k) = \sum\limits_{n \geqslant 1} c_n = 1$, and it results $p(E \wedge E') = 1$.

Proof of Theorem 2

Suppose that $\vee \Omega_{12} < 1$. Then there exists a projector E, $0 < E < 1 - \vee \Omega_{12}$ and we may find a state p such that $p(E) = 1$. It results that $p(E') = 0$ for all $E' \in \Omega_{12}$, which contradicts the condition (C_1). Consequently, $\vee \Omega_{12} = 1$ and – according to Lemma 3 – $\mathcal{C}_{\mathcal{H}} = [\Omega_{12}]$ is an atomic Boolean sublattice. By using Lemma 4 we find that $E^{(1)}_{k_1} \wedge E^{(2)}_{k_2} > 0$ for all $(k_1, k_2) \in \mathbb{N} \times \mathbb{N}$. Since $0 \notin \Omega_{12}$, it results that Ω_{12} is the set of atoms of $\mathcal{C}_{\mathcal{H}}$, which proves that $\mathcal{C}_{\mathcal{H}}$ and $\mathcal{C}$ are isomorphic Boolean algebras.

3. COMMENTS

The results of this paper may be generalized to any finite family of chemical species. If we have in view a system of n chemical species, then by $\mathcal{C}$ we understand the orthomodular lattice of all subsets of the Cartesian product of n copies of the set $\mathbb{N}$.

When we want to construct a theory of the systems of n chemical species in a Hilbert space $\mathcal{H}$, we have to accept as fundamental certain empirical facts. The final result of such a construction is the sublattice $\mathcal{C}_{\mathcal{H}}$.

If (C_1) and (C_2) are considered as empirical facts, we get a classical description of particles of the systems of many chemical species, in the sense that $\mathcal{C}_{\mathcal{H}}$ is isomorphic to $\mathcal{C}$. But it is also possible to get a sublattice $\mathcal{C}_{\mathcal{H}}$ which is not isomorphic to $\mathcal{C}$. This is generally the case when the particles of chemical species are considered as molecules constituted from electrons and nuclei. An example is offered by the formalism of quantum theory of scattering, where counting YNE of chemical species may be identified with projection operators on subspaces of asymptotic states.[8] It may be verified that, if such a description of counting YNE is adopted, then at least one of the conditions (C_1), (C_2) is not satisfied. We may say that, in such a theory, the particles of the systems of more then one chemical species have not a "classical behaviour".

REFERENCES

[1] E. Prugovecki, "Quantum Mechanics in Hilbert Space", Academic Press, New Work, 1971, pp. 226, 390.

[2] J. M. Jauch, "Foundations of Quantum Mechanics", Addison-Wesley Publishing Company, 1968, p. 98.

[3] G. W. Mackey, "Mathematical Foundations of Quantum Mecanics", W. A. Benjamin, Inc., 1963, p. 74.

[4] C. Piron, "Foundations of Quantum Physics", W. A. Benjamin, Inc., 1976, p. 19.

[5] V. S. Varadarajan, "Geometry of Quantum Theory", D. von Nostrand Company, Inc., 1968, Vol. I, p. 105.

[6] J. M. Jauch, "The Quantum Probability Calculus", in "Logic and Probability in Quantum Mechanics", Ed. Patrick Suppes, D. Reidel Publishing Company, 1976, p. 123.

[7] A M. Gleason, *J. Math. Mech.*, **6**, 885,(19 75).

[8] M. Reed and Barry Simon, "Methods of Modern Mathematical Physics", III "Scattering Theory", Academic Press, 1979, p. 90.

Revue Roumaine de Chimie, **32**, *11–12*, 1103–1107 (1987)

Dedicated to Professor V. E. SAHINI
on his 60th anniversary

STEREOCHEMICAL AND INFORMATIONAL ASPECTS IN QSAR AND MTD

Z. SIMON
Institute of Medicine Timișoara — 1900, Pța. 23 August 2, Romania

Received May 28, 1987

The relation between the quantity of information required to specify the receptor-effector interaction and the one contained in the series of experimental biological activities studied for quantitative structure-activity relations is discussed, with special reference to the MTD method. The reliability of QSAR results can be assessed by test-series of molecules for which calculated and experimental activities are compared. For the MTD-method, $r \cong 0.85-0.95$ are usually obtained for the corresponding QSAR's and $r \cong 0.70-0.85$ for the test series, if certain connectivity restrictions are respected.

INTRODUCTION

The usefulness of the quantitative structure activity methods (QSAR) in the design of drugs was stressed, recently, by Hansch.[1,2] Nevertheless the large number of explicitely or implicitely adjustable parameters used in such methods may introduce a large degree of chance correlation in the results.[3-6] The result of QSAR, the regressional equation, or the result of methods like pattern recognition is actually an approximative relation between parameters for molecular structure and the affinity of molecules towards a biological receptor, or eventually a combination of such receptors. To describe the molecule-receptor interaction a certain quantity of information is required. This is given by the structures and biological activities of the studied series of molecules. The lack of sufficient available information cannot be substituted by methodological sophistications.

It is not easy to express quantitatively these quantities of information, but they are produced mostly by the stereochemical aspects of the interaction problem. Such quantities of information are calculated out of the number W of possible situations among which there is also the required situation. Such a calculation was performed by Crippen[7] for a somewhat particularised case. Here we shall use also a particularised case, the one corresponding to the MTD method,[8] the first method to use, for QSAR, the comparison of molecular shapes by approximative atom per atom superposition. Recent results of the MTD-method will be also analysed here from an informational point of view.

INFORMATION QUANTITY CALCULATIONS IN THE MTD METHOD

Consider a series of N molecules with known experimental activities, A_i, $(i = 1, 2, \ldots, N)$ included in the $A_{\min} \div A_{\max}$ interval and determined with a precision (mean standard deviation), ΔA. We have, thus:

$$n = (A_{\max} - A_{\min})/\Delta A \tag{1}$$

activity intervals, within which the activities must be predicted. For QSAR, the regressional equation is of the general form:

$$A_i = a_0 + a_1\sigma_{1i} + \ldots + a_k\sigma_{ki} \tag{2}$$

We consider that each term $a_1\sigma_{1i}$ has comparable values on a scale of n intervals. The number W_1 of combinations of "discrete" values for the k regressional coefficients a_i and the quantity of information I_1 required to establish eq. (2) are:

$$W_1 = n^k\,;\; I_1 = \ln_2 W_1 = k \ln_2 n \tag{3}$$

If the k structural parameters describe with a sufficient approximation the molecule-receptor interactions, I_1 will be at least equal to the quantity of information I_2 required to describe these interactions.

In the MTD method [9,10] one compares molecular shapes by approximative atom per atom superpositions (neglecting H-atoms). The hypermolecule results hereby, which divides the investigated receptor space (IRS [11,12]) into M cells of q types characterising the interactions between the corresponding receptor zone and an atom of the molecules. Three such types are considered in the MTD-method: (i) surrounding aqueous solution, (ii) repulsive zone in the interior of the receptor walls, and (iii) interior of the receptor cavity, corresponding to the values 0, +1, −1 of the ε_j-parameter or to the i, w and o-zones of the SIBIS variant. The atom of the molecule "i" which occupies the vertex j can be present $(x_{ij} = 1)$ or absent $(x_{ij} = 0)$ in the MTD method. If this characterisation does not yield a satisfactory approximation for the receptor-effector interaction, the number q of types can be enlarged by introduction of supplementary structural variables (σ_{1i}, σ_{2i} etc.) for receptor zones of hydrophobic, of proton donor/acceptor nature etc.

The regressional equation of the MTD-method is:

$$A_i = a_0 + a_1\,\sigma_{1i} \ldots - \beta\,\mathrm{MTD}_i \tag{4}$$

with MTD_i the number of cavity (c) vertices unoccupied by molecule "i" plus the number of wall (w) vertices occupied by the same molecule in the low energy conformation which allows the best fit of the molecule in the receptor cavity, i.e. the lowest MTD_i-value.

Let us suppose that by q types of atoms occupying the M vertices of the hypermolecule one obtains a satisfactory approximation for the molecule receptor interactions. The number W_2 of molecules, distinguishable within this approximation and the quantity of information I_2 required to describe these interactions are :

$$W_2 = q^M ; \; I_2 = \ln_2 W_2 = M \ln_2 q \qquad (5)$$

We shall not try to calculate the quantity of information contained in the experimental biological activities, A_i and in the structure of the N molecules of the series considered for QSAR. Instead, we shall use the result of Topliss [5, 6] concerning simulations of chance correlations in QSAR. Accordingly, in order to obtain a reliable regressional equation with k structural parameters, one requires at least 3—4 times more A_i values :

$$N \gtrsim 3\,k \qquad (6)$$

By comparing eqs (3) and (5) for $I_1 = I_2$, the following requirement results for the MTD-method :

$$N \gtrsim 3M(\ln_2 q/\ln_2 n) \cong 3\mathrm{M} \qquad (7)$$

In the series studied for QSAR by the MTD-method, [10] condition (7) is usually not satisfied; large hypermolecules result and one has rather $N \cong M$ in most cases. Nevertheless, the topological character of the hypermolecule allows to introduce some supplementary information for setting up the QSAR, [11] information which corresponds to what may be termed as chemical intuition. Namely, a receptor map with several interdispersed i, w and c-type vertices is unlikely to correspond to a real, very intricate structure of the receptor cavity. To avoid such situations one can use restrictions, based upon the connectivity of vertices of a certain type, in the process of attributing the M-vertices to i, w or c-zones.

One may especially recommend to consider only those receptor maps in which all cavity (c) vertices are connected into a single network, together with the vertices occupied by all molecules which are also considered as c-vertices. [10] This corresponds to a single receptor cavity. If there are supplementary data concerning the receptor cavity (for example X-ray crystallography) the single connected network restriction can be extended also to wall (w) and external (i) vertices.

CONCLUSIONS CONCERNING THE RELIABILITY OF MTD RESULTS

A real evaluation of reliability, of any QSAR result, can be performed only by comparing predicted and experimental activities for a test series of molecules not used in establishing the QSAR. Test series were used for several QSAR's established with the MTD-method. [10] Correlation coefficients $r \cong 0.85—0.95$ are usually obtained for the series for optimisation and $r \cong 0.70—0.85$ for test series. Some relevant and more recent results are listed in Table 1. Satisfactory results for test series are obtained when the connectivity restriction is used for the cavity (c) vertices. One exception is the QSAR for auxinic activity of substituted acetic acid derivatives (No. 1, Table 1) in which attractive interactions are accounted for mostly by hydrophobic interactions.[13] For cardiotoxic steroids (No. 2, Table 1) the SIBIS method[11] with connectivity restrictions for both the *c*- and *i*-vertices yields unsatisfactory results, refuting the hypothesis of a cavity with the shape of a sack opened at one end.[14]

Table 1

Correlational results by the MTD method with test series

No.	Biol. activity	Series for optimisation Test series	Parameters (connectivity)	r (r_{Test})
1.	Auxinic activity[10,13]	Aryl and alkyl derivs of acetic acid, $N = 55$	δ, π, π^2 MTD*	0.872 (0.826)
		The same, different authors, $N = 22$		
2.	Cardiotoxicity in cats[14,15,16]	Cardenolides, bufadienolides, $N = 30$	MTD (−) MTD (c) SIBIS ($c+i$)	0.916(0.635) 0.884(0.792) 0.820(0.100)
		The same, $N = 16$		
3.	Alpha-adrenergic agonists[10,17]	β-phenylethylamines derivs, clonidine, $N = 18$	MTD (c)	0.841 (0.750)
		Clonidine derivs, $N = 9$		
4.	Alpha chymotrypsine hydrolysis rates[18,19,20]	Me-esthers of N−Ac−-L-aminoacids ($N = 14$); nitrophenyl esters of carboxylic acids ($N = 11$)	MTD (−) MTD(c)	0.948 ;0.809 0.947 ;0.720
		Nitrophenyl ester of L- and D-aminoacids and carb. ac., $N = 42$	π,σ,MTD(−) π,σ,MTD(c) π,σ,ES	(0.814) (0.852) 0.676
5.	Dedifferentiation reversal[21]	Retinoids, $N = 53$	δ, π, MTD(c)	0.853 (0.916)
		The same, $N = 15$		
6.	Acetylcholinesterase inhibition[22]	Methylphenylcarbamates, $N = 97$	π,R,EC,HB, MTD (−)	0.876
		Phenylthiophosphates, $N = 8$; Methylarylcarbamates, N= 8		(0.787) (0.518)
7.	Sarcoma and papilloma induction[23]	Benz[a]anthracene derivs. $N = 29$	DE,MTD(c)	0.860
		Methylbenzo[a]pyrene derivs, $N = 10$		(0.941)

Legends : r — correlation coefficient, series for optimisation, values in parentheses — for test series ; π — relative hydrophobicities, σ — Hammett parameter ; ES — Taft parameter ; δ— indicator variables ; DE — delocalisation energy (HMO) ; R, EC, HB — molar refraction, charge, hydrogen bonding parameters. Connectivity restrictions : (—) — without restriction, (*) without + hydrophobic attractive interactions ; (c)—restriction for cavity vertices ; ($c+i$) — restriction for cavity and irrelevant vertices.

As a conclusion, for QSAR studies concerning receptors for which detailed X-ray crystallography data are not available, the first step should be the use of a MTD-type method, to suggest a receptor model for a second step in which receptor-effector molecule interactions are to be calculated by quantum chemical methods, semiempiric potential functions etc.

REFERENCES

[1] C. Hansch and J. M. Blaney, in "Drug Design. Fact or Fantasy", Academic Press, London, 1984, p. 185.
[2] C. Hansch, *Drug Metabolism Revs.*, **15**, 1279 (1984/85).
[3] S. Wold and W. J. Dunn III, *J. Chem. Inf. Comput. Sci.*, **23**, 6 (1983).
[4] D. Bawden, *J. Chem. Inf. Comput. Sci.*, **23**, 14 (1983).
[5] J. G. Topliss and R. J. Costello, *J. Medic Chem.*, **15**, 1066 (1972).
[6] J. G. Topliss and P. P. Edwards, *J. Medic. Chem.*, **22**, 1238 (1979).
[7] G. M. Crippen, *J. Medic. Chem.*, **23**, 599 (1980).
[8] Z. Simon and Z. Szabai, *Studia Biophys. (Berlin)*, **39**, 123 (1973).
[9] Z. Simon, A. Chiriac, I. Motoc, S. Holban, D. Ciubotariu and Z. Szabadai, *Studia Biophys. (Berlin)*, **55**, 217 (1976).
[10] Z. Simon, A. Chiriac, S. Holban, D. Ciubotariu and G. I. Mihalaş : "Minimum Steric Difference", Res. Studies Press, Letchworth (England) 1984 ;
[10a] A. T. Balaban, A. Chiriac, I. Motoc and Z. Simon, "Steric Fit in QSAR", Springer Lecture Notes in Chemistry, **15**, (1980), Springer, Heidelberg, 1980.
[11] I. Motoc and O. Dragomir-Filimonescu, *Mat. Chem.*, **12**, 117 (1981).
[12] I. Motoc and G. Marschall, *Z. Naturforsch.*, **40** (a), 85 (1985).
[13] A. Chiriac, Veronica Chiriac, D. Ciubotariu, S. Holban and Z. Simon, *Eur. J. Med. Chem.*, **18**, 507 (1983).
[14] Z. Simon, *Math. Chem.*, **13**, 357 (1982).
[15] Z. Simon, N. Dragomir, M. G. Plauchithiu, H. Glatt and F. Kerek, *Eur. J. Med. Chem.*, **15**, 521 (1980).
[16] I. Motoc, *Topics in Current Chem.*, **114**, 94 (1984).
[17] V. Abelj and H. Hazdi, in "QSAR and Strategies in the Design of Bioactive Compounds", editor J. K. Seydel, Weinheim 1985, p. 83.
[18] Z. Simon, S. Holban, I. Motoc, M. Mracec, A. Chiriac, F. Kerek, D. Ciubotariu, Z. Szabadai, R. D. Pop and I. Schwartz, *Studia Biophys. (Berlin)*, **59**, 181 (1976).
[19] S. Holban, D. Ciubotariu, I. Motoc and Z. Simon, *Rev. Roumaine Biochimie*, **16**, 99 (1979).
[20] Z. Simon and A. Chiriac. Preprint, Univ. Timişoara, Ser. Chim., **5** (1985).
[21] I. Niculescu-Duvăz, Z. Simon and N. Voiculeţ, *Carcinogenesis*, **6**, 479 (1985).
[22] I. I. Bădilescu, A. Stepan, A. Chiriac and Z. Simon, *Analele Univ. Timişoara. Ser. St. Chimice*, **XIV** (2), 29 (1976).
[23] Z. Simon , A. T. Balaban, D. Ciubotariu and T. S. Balaban, *Rev. Roumaine Chim.*, **30**, 985 (1985).

Revue Roumaine de Chimie, 32, *11–12*, 1109–1115 (1987)

Dedicated to Professor V. E. SAHINI
on his 60th anniversary

SYNTHESIS OF NICKEL FERRITE FROM POLYNUCLEAR COORDINATION COMPOUNDS. I

STUDY OF THE DRY FERRITIZATION PROCESS

IOANA ILIE[a], MARIA BREZEANU[b], LUMINIȚA PATRON[c], E. SEGAL[d] and G. FILOTI[e]

[a] Institute of Chemical and Biomedical Energetics, ICECHIM, Splaiul Independenței no. 202 Bucharest, Romania

[b] Chair of Inorganic Chemistry and Technology, Faculty of Chemical Technology, IPB, Dumbrava Roșie no. 23, Bucharest, Romania

[c] Center of Physical Chemistry, ICECHIM, Splaiul Independenței no. 202, 77208 Bucharest, Romania

[d] Chair of Physical Chemistry and Electrochemical Technology, Faculty of Chemical Technology, IPB, Bdul. Republicii no. 13, Bucharest, Romania

[e] Institute of Physics and Materials Technology, I. C. Fiz., Postal Box 07, Măgurele, Romania

Received October 20, 1986

Thermal decomposition at 400°C of some PCC's with ligands such as acetate, formate and oxalate yields $NiFe_2O_4$ or solid solutions of Fe_3O_4 ($\gamma-Fe_2O_3$)$-NiFe_2O_3$ and NiO. X-Ray diffraction and Mössbauer spectroscopy show that the properties of $NiFe_2O_4$ depend on the nature of polynuclear precursor and the thermal treatment. The crystallinity and degree of inversion of $NiFe_2O_4$ increase with temperature and time of calcination. Thermal decomposition at temperatures higher than 400°C is not recommended because the ferritic phase is impurified with hematite.

The needs of oxidic materials with reproducible structure and properties, have determined the development of some new "nonconventional" methods of which the thermal decomposition of polynuclear coordination compounds (PCC) is even more frequently mentioned in literature.[1–10]

Utilization of this method in the preparation of $NiFe_2O_4$ has required extensive studies on the formation conditions of some PCC's containing Fe and Ni and on the possibilities of their thermal decomposition to yield the ferrite phase.

EXPERIMENTAL

X-Ray diffraction patterns were recorded with a Philips PW 140/10 diffractometer using the chromium K_α radiation.

The Mössbauer spectroscopy measurements were carried out with an IFTM Mössbauer spectrometer, with variable speed and symmetrical wave shape; a Co^{57} radioactive source in Cr matrix, whose activity was 2.5 GBk was employed.

RESULTS AND DISCUSSION

We have obtained and characterized several PCC's from which we selected for the purpose mentioned the following[11]:

$[Fe_2NiO(CH_3COO)_6(H_2O)_3]\cdot 3H_2O$

$[Fe_2NiO(HCOO)_8(H_2O)](NH_4)_2\cdot 2H_2O$

$[Fe_2Ni(C_2O_4)_3(H_2O)_2](NH_4)_8\cdot 6H_2O$

The selection of these PCC's as precursors in the preparation of $NiFe_2O_4$ was justified by several factors : firstly, the compounds selected contain the two metals in a 2 : 1 ratio, required by formation of spinel ferrite, and ligands which decompose at low temperature according to a simple mechanism and generating volatile products. Secondly, these PCC's are obtained in a good yield, in spite of variation of parameters controlling the coordination process within broad limits (these parameters are the Fe : Ni and metal : ligand ratios, the pH of reaction medium, the nature of solvents, bases and salts employed as raw materials).

The kinetic study of thermal decomposition of these PCC's by thermal analysis showed that within 300—400°C range all thermal conversion stages are complete and the ferrite phase is formed. [12]

The minimum temperature required by formation of $NiFe_2O_4$ was considered 400°C ; studies were conducted at higher temperatures to evidence the modifications of structural properties of $NiFe_2O_4$ due to the nature of generating PCC and the thermal treatment. Use has been made of elemental chemical analysis, X-ray diffraction and Mössbauer spectroscopy.

The following indices were used for tracing the samples (Table 1).

Table 2 shows the results of elemental chemical analysis ; the stoichiometry of the oxide phase corresponds to $NiFe_2O_4$ regardless of the polynuclear precursor employed.

The results of X-ray diffraction were interpreted according to ASTM assignments, taking into account that the structure of $NiFe_2O_4$ is of inverse spinel type. [13]

Table 1

Indices of $NiFe_2O_4$ samples obtained by dry ferritization

Complex precursors	Temperatures of thermal decomposition (°C)			
	400	600	800	1000
$[Fe_2NiO(CH_3COO)_6(H_2O)_3] \cdot 3H_2O$	Ac—400	Ac—600	Ac—800	Ac—1000
$[Fe_2NiO(HCOO)_8(H_2O)](NH_4)_2 \cdot 2H_2O$	F—400	F—600	F—800	F—1000
$[Fe_2Ni(C_2O_4)_8(H_2O)_2](NH_4)_8 \cdot 6H_2O$	OX—400	OX—600	OX—800	OX—1000

The data listed in table 3 show that :

(a) The samples obtained by thermal decomposition at 400°C of all complex precursors studied exhibit the diffraction lines specific to a spinel structure ;

(b) The crystallinity of samples is improved if heating up to 400°C lasts 1 to 5 or 10 hours ;

(c) Samples obtained from $[Fe_2NiO(CH_3COO)_6 (H_2O)_3] \cdot 3H_2O$ by thermal decomposition at 600, 800 and 1000°C (one hour) and to a lesser extent those obtained by thermal decomposition at 600°C and 800°C of $[Fe_2NiO(HCOO)_8 (H_2O)](NH_4)_2 \cdot 2H_2O$ yield $\alpha-Fe_2O_3$ together with spinel structure phase ; however $\alpha-Fe_2O_3$ is absent in oxide phases obtained from trinuclear oxalates, regardless of the temperature range.

Table 2

The results of elemental chemical analysis of oxide phases

Index of sample	Composition (wt, %)			Fe(III): Ni(II) ratio
	Fe(e/c)	Ni(e/c)	O(e/c)	
Ac—400	48.24/47.66	25.10/25.11	27.30/27.23	2 : 1
Ac—600	48.00	25.45	27.33	2 : 1
Ac—800	47.90	25.20	27.11	2 : 1
Ac—1000	47.50	25.00	27.40	2 : 1
F—400	48.25	25.11	27.00	2 : 1
F—600	48.03	25.00	27.23	2 : 1
F—800	47.53	26.00	26.16	2 : 1
F—1000	47.66	24.83	26.00	2 : 1
OX—400	47.25	25.55	27.80	2 : 1
OX—600	47.14	25.67	26.82	2 : 1
OX—800	48.50	25.35	26.15	2 : 1
OX—1000	48.24	25.70	26.03	2 : 1

The Mössbauer spectroscopy study served to determine the oxide phase structure, to establish the source of hematite in some samples and to issue a mechanism of dry ferritization. This study allows the correlation of Mössbauer parameters i.e. the hyperfine field (H), quadrupolar splitting ΔQ, isomeric shift Γ, line width δ and relative surface area (A) with local assignments, the modification of iron valence, concentration of lattice defects and the number of iron ions lying in the O (B) or T (A) position.

The data thus obtained, listed in Table 4, suggest the following conclusions :

(a) Sample Ac—400 (1 h) shows the existence of a solid solution of Fe_3O_4—$NiFe_2O_4$ type. Because Fe_3O_4 and $NiFe_2O_4$ are not present as separate sublattices, we consider that $NiFe_2O_4$ forms on a spinelic structure of Fe_3O_4 type, whose growth is a priority of the early stages of thermal treatment. The increase of duration from 1 to 5 hours causes the spinel solid solution Fe_3O_4—$NiFe_2O_4$ to pass gradually into a nickel ferrite whose degree of inversion increases with heating time.

(b) The Mössbauer spectrum of OX—400 (1 h) shows formation of a nickel ferrite without impurities ; because only 1/2 of tetrahedral sites are occupied by Fe^{3+}, the degree of inversion is 50%.

(c) In sample F—400 (1 h) there are two separate spinelic phases : 93% $NiFe_2O_4$ and 7% Fe_3O_4 — γ-Fe_2O_3.

Table 3

The results of X-ray diffraction of oxide phases :

Index of sample	d(Å)	d(ASTM)	Index of samples	d(Å)	d(ASTM)
Ac—400 (1 h)	2.949 2.508 2.410 2.081	2.948 2.513 2.408 2.085	F—1000	2.949 2.508 2.402	2.948 2.513 2.408
Ac—400 (5 h)	2.949 2.508 2.410		OX-400(1h)	2.949 2.508 2.402	
Ac—400 (10 h)	2.949 2.508 2.402		OX-400(10h)	2.941 2.517 2.418	
Ac—600 (1 h)	2.949 2.724 2.525 2.418 2.098	 α-Fe$_2$O$_3$	OX-600(1h)	2.949 2.508 2.402 2.087 1.691	
Ac—800 (1 h)	4.824 3.678 2.944 2.694 2.516 2.410 2.206 2.081 1.84 1.691 1.60	 α-Fe$_2$O$_3$ α-Fe$_2$O$_3$ α-Fe$_2$O$_3$	OX-1000(1h)	2.949 2.508 2.402	
Ac—1000 (1 h)	2.936 2.693 2.508 2.402	 α-Fe$_2$O$_3$	F-400(1h)	2.949 2.534 2.426 2.098	
F—400 (10 h)	2.949 2.508 2.402		F-600(1h)	2.941 2.704 2.517 2.410 2.212	α-Fe$_2$O$_3$
F—800 (1 h)	2.941 2.517 2.410 2.087				

Table 4

The results of Mössbauer spectroscopy for the oxide phases

Index of sample	Subsp.	H(KOe)	ΔQ(mm/s)	δ(mm/s)	Γ(mm/s)	Relative area (%)	Oxide phases
Ac−400 (1h)	1	510.9	−0.06	0.54	0.31	0.1450	Fe_3O_4+ $NiFe_2O_4$
	2	485.6	−0.02	0.50	0.58	0.3571	
	3	463.0	−0.04	0.36	1.14	0.4495	
	4	440.5	0.20	0.77	0.44	0.0475	
Ac−600 (1h)	1	513.4	−0.30	0.50	0.53	0.5440	$NiFe_2O_4$+ $\alpha-Fe_2O_3$
	2	482.1	−0.06	0.43	0.59	0.4560	
Ac−800 (1h)	1	516.0	−0.14	0.54	0.46	0.5517	$NiFe_2O_4$+ $\alpha-Fe_2O_3$
	2	488.7	0.02	0.40	0.61	0.4483	
Ac−1000 (1h)	1	517.8	−0.14	0.52	0.44	0.5331	$NiFe_2O_4$+ $\alpha-Fe_2O_3$
	2	492.5	−0.02	0.40	0.66	0.4699	
OX−400	1	497.6	−0.04	0.47	0.73	1.0000	$NiFe_2O_4$

The value of hyperfine field for Fe^{3+} in T_a position and the line of Fe^{3+} in $NiFe_2O_4$ decrease in the sequence :

$$\mathrm{OX}-400\ (1\ \mathrm{h}) > \mathrm{F}-400\ (1\ \mathrm{h}) > \mathrm{Ac}-400\ (1\ \mathrm{h})$$

so that the best formed nickel ferrite is OX−400 (1 h) and the worst is Ac−400 (1 h).

Heating at 600, 800 and 1000°C increases the size of $NiFe_2O_4$ crystallites but the amount of Fe^{3+}(B) remains practically the same (45−56 %), also it appears as impurity $\alpha-Fe_2O_3$ with $NiFe_2O_4$ phase.

Formation of $NiFe_2O_4$ from magnetite which appears first and stands in the early stages of the thermal treatment suggests that Fe_3O_4 acts as a nucleus for the spinel lattice, which was also assumed in sintering of α-Fe_2O_3 and NiO mixture. [14] Thus, one may consider that the complex precursors decompose in the first stage to generate magnetic intermediate phases which involve the modification of iron valence, of the type Fe_3O_4, or partially oxidised to $\gamma-Fe_2O_3$ and NiO. These oxides interact quickly to form structurally ordered solid solutions of $Fe_3O_4-NiFe_2O_4$ type which gradually turn into $NiFe_2O_4$. Thus the degree of inversion and the dimensions or crystallites of $NiFe_2O_4$ thus formed increase with temperature and duration of thermal treatment.

The hematite found in samples obtained at temperatures higher than 400°C is accounted for strong oxidation of incipient Fe_3O_4 which hinders the gradual substitution of Fe^{2+} with Ni^{2+} to form $NiFe_2O_4$

The mechanism of $NiFe_2O_4$ formation through thermal decomposition of PCC which we refer to as dry ferritization, may be represented as follows:

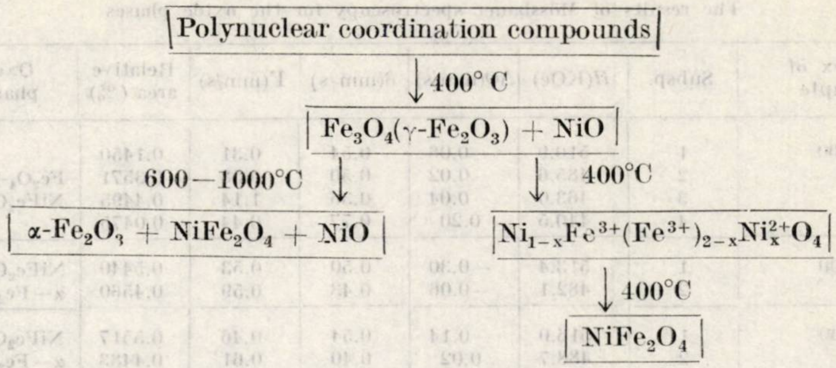
Polynuclear coordination compounds
400° C
$Fe_3O_4(\gamma\text{-}Fe_2O_3) + NiO$
600—1000°C
400°C
$\alpha\text{-}Fe_2O_3 + NiFe_2O_4 + NiO$
$Ni_{1-x}Fe^{3+}(Fe^{3+})_{2-x}Ni_x^{2+}O_4$
400°C
$NiFe_2O_4$

To achieve a well formed ferritic material phase a thermal treatment at 400°C suffices, provided that it lasts 5—10 hours (the crystallinity and the degree of inversion increase with duration of calcination). Higher temperatures cause formation of hematite as impurities together with $NiFe_2O_4$.

This mechanism explains the influence of thermal treatment and nature of complex precursors upon oxide phase composition; during thermal conversion PCC's with oxalate and formate ligands yield a reducing gas mixture (because the presence of CO favours partial reduction of Fe^{3+} to Fe^{2} and implicitely maintains Fe_3O_4 in the system). As formation of $NiFe_2O_4$ includes Fe_3O_4 as intermediate it becomes obvious why the reaction yields and the structural features of $NiFe_2O_4$ improve in the sequence:

acetate < formate < oxalate

The temperature and duration of calcination which are considerably lower in the procedure proposed here (400°C, 10 hours), compared to classical methods, are possible due to the unusual reactivity of oxidic species obtained through decomposition of PCC and to the homogeneous distribution (at molecular level) of nickel and iron ions.

Replacement of Fe^{III} and Ni^{II} oxides with salts containing these metals eliminate some energy and difficult-technologic steps; ferritization at lower temperature and shorter duration of heating as well as the reproducibility of properties of $NiFe_2O_4$ thus obtained are only some of the advantages which dry ferritization ensures.[9]

REFERENCES

[1] G. C. Macarovici and Gh. Morar, *Rev. Roumaine Chim.*, **17**, 1051 1972.
[2] M. Zaharescu and G. C. Macarovici. *Rev. Roumaine Chim.*, **16**, 1323 (1971).
[3] G. C. Macarovici and G. Schmidt, *Rev. Roumaine Chim.*, **16**, 1759 (1971).

[4] J. Paris and R. Paris, *Bull. Soc. chim. France*, **4**, 1138 (1965).

[5] M. Brezeanu L. Patron, I. Nesfîntu, O. Brezeanu, E. Segal and V. Mincu, Roumanian Patent no. 69300, (1978), CA.

[6] M. Brezeanu, L. Patron, I. Nesfîntu, O. Brezeanu, V. Mincu and E. Segal, Roumanian Patent no. 71644, (1979), CA

[7] M. Brezeanu, E. Segal, V. Mincu, L. Patron and S. Ciobanu, Roumanian Patent no. 77972 (1981) CA

[8] M. Brezeanu, E. Segal, V. Mincu, L. Patron and S. Ciobanu, Roumanian Patent no. 77973 (1981) CA

[9] I. Anastasiu, I. Nesfîntu, M. Brezeanu, E. Segal, L. Patron and V. Mincu, Romanian Patent no. 79364 (1977).

[10] L. Patron, A. Conţescu, G. Munteanu and M. Brezeanu, *Rev. Roumaine Chim.*, in press.

[11] I. Ilie, Doctoral Dissertation, Polytechnic Institute of Bucharest, Inorganic Chemistry Dep., Bucahrest, 1985.

[12] I. Ilie, M. Brezeanu and E. Segal, *Thermochim. Acta*, **94**, 393 (1985)

[13] S. Cedighean, "Ferite", Ed. Tehnică, Bucharest, 1966.

[14] J. Beretka, M. J. Ridge, *Nature*, London, **216**, 473 (1967).

Revue Roumaine de Chimie, 32, *11–12*, 1117–1121 (1987)

Dedicated to Professor V. E. SAHINI
on his 60th anniversary

β-LACTAM ANTIBIOTICS. I

STRUCTURE-NEUROTOXIC ACTIVITY OF BENZYLPENICILLIN

JOSETTE WEINBERG and ALEXANDRINA DONESCU
ICECHIM – Centre of Physical Chemistry, Splaiul Independenţei 202, Bucharest, Romania

Received May 18, 1987

Electronic structure data are correlated with neurotoxic activity of benzylpenicillin. One possible biochemical mechanism based on reactivity parameters is advanced.

This contribution employs the Hückel and Pariser–Parr–Pople methods in a theoretical study on whole molecules and molecular fragments of benzylpenicillin, aiming at correlating its electronic structure with the antibacterial activity spectrum and, especially, at explaining its neurotoxicity (as an adverse reaction) in terms of these theoretical parameters.

RESULTS AND DISCUSSION

1. QUANTUM MECHANICAL CALCULATIONS OF BENZYLPENICILLIN

We have first considered only the 6-position side chain of benzylpenicillin (Fig. 1) in the Hückel calculation (variant 1) and the Pariser–Parr–Pople calculation.

The Hückel method was then extended to β-lactam ring and to 6-position side chain (variant 2) and finally, the same formalism was applied to the whole molecule of antibiotic (variant 3).

The Pariser–Parr–Pople and the first Hückel variant were applied by considering the coplanarity of the side chain. The atomic coordinates are taken from X-ray crystallographic study. [1] This side chain was selected because it is the molecular fragment responsible for the activity spectrum specificity.

The second Hückel variant was applied by considering the coplanarity of the β-lactam ring; this approximation is not so drastic because the X-ray studies have confirmed the coplanarity. [2]

In the third variant, the correction factor for β-lactam and thiazolidine rings nonplanarity were applied.[4] In the second and the third variants a certain degree of unsaturation of the two rings was considered.

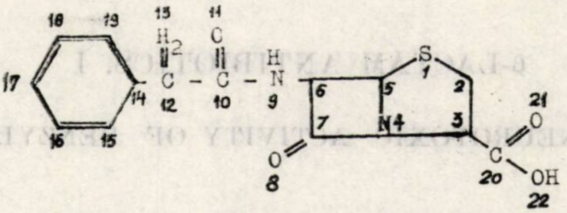

Fig. 1.—The notation of molecular centres in benzylpenicillin.

Tables 1—3 show the theoretical reactivity indices. The variants 2 and 3 of the Hückel method show that the net charge on carbonylic carbon C_7 confirms its high reactivity in the initial acylation stage of a nucleophilic reaction; the net charge in table 1 agrees with Boyd's data.[3] In accordance with the Fukui theory,[5] the frontiers are the most susceptible to electron transfer. Thus, due to the reaction capacity of C_7 and N_4 with a nucleophilic agent, the frontier electron density in a nucleophilic substitution (f_4^N — table 2) proves their reactivity in acylation reaction. The mobile bond order $P_{N_4-C_7}$ (Table 1) which is the lowest in β-lactam ring confirms its easy break during acylation reaction; this way it is possible to evaluate indirectly the antibacterial activity.

On the other hand, the large value of $P_{C_5-C_6}$, points to the stability of the antibiotic during the antimicrobian reaction, preserving its initial structure.

The large Coulomb density (Table 1) as well as the relatively high electrophile substitution density (Table 2) on nitrogen atom N_9 demonstrate a certain stability to hydrolysis.

Table 3 lists the literature data[6] concerning the antibacterial activity of benzylpenicillin and oxacillin towards three grampositive and gramnegative strains, as well as the lowest unoccupied molecular orbital (LUMO) parameters. These data are obtained by the Hückel application only on the side chain. In the same table are also presented our LUMO data obtained through the three Hückel variants. Our data are in good agreement with those in the literature, as long as the method is applied only to the side chain. However, it results that benzylpenicillin has a sensibly high activity against oxacillin.

Therefore this higher activity specificity may be correlated to the better electron acceptor properties of benzylpenicillin.

2. THE BENZYLPENICILLIN NEUROTOXIC ACTIVITY

The literature data[7,8] mention the frequent neurotoxic activity of benzylpenicillin. Tests carried out on rabbits have shown that after i.v. administration of benzylpenicillin and oxacillin, the former, unlike the

Table 1

The Coulson density, the mobile bond order and the net charge in the ground state of benzylpenicillin

Atom (p)	q_p				Bond pq	P_{pq}				Q_p	
	Hückel (1)	Hückel (2)	PPP	Hückel (3)		Hückel (1)	Hückel (2)	PPP	Hückel (3)	H(2)	H(3)
N_4	—	1.7952	—	1.7279	N_4-C_7	—	0.3496	—	0.4434	0.2048	0.2721
C_7	—	0.5952	—	0.5999	C_7-C_6	—	—	—	0.4744	0.4048	0.4001
C_6	—	1.2143	—	1.2502	C_5-C_6	—	0.8011	—	0.7509	-0.2143	-0.2502
C_5	—	1.4622	—	0.8477	C_6-N_9	—	0.3012	—	0.3069	-0.4622	$+0.1523$
N_9	1.7699	1.6742	1.7699	1.6407	N_9-C_{10}	0.5593	0.5598	0.5086	0.5858	0.3258	0.3593
C_{10}	0.6188	0.6631	0.8756	0.7532	$C_{10}-C_{12}$	0.2092	0.2068	0.0169	0.2147	0.3369	0.2468
C_{12}	1.0949	1.0896	1.3912	1.0919	$C_{12}-H_{(2)(13)}$	0.9547	0.9384	0.8972	0.9533	-0.0896	-0.0919
C_{14}	1.0338	1.0282	1.1226	1.0339	$C_{12}-C_{14}$	0.1789	0.2517	0.1939	0.1789	-0.0282	-0.0339
$H_{2(13)}$	0.8663	0.8667	0.6057	0.8712							

Table 2

Fukui density in the second and the third Hückel variants on benzylpenicillin

Atom (p)	f_p^E		f_p^R		f_p^N	
	(2)	(3)	(2)	(3)	(2)	(3)
N_4	0.4764	0.3134	0.2395	0.1615	2.73×10^{-3}	0.97×10^{-2}
C_7	4.68×10^{-3}	0.85×10^{-2}	0.3249	0.3062	0.6453	0.6038
C_6	0.6620	0.5093	0.4112	0.2493	0.1619	0.1221
C_5	0.3882	0.1266	0.5925	—	0.7968	0.8309
N_9	0.2812	0.1631	0.1473	—	0.0134	4.3×10^{-3}
C_{10}	0.0797	7.97×10^{-2}	0.0608	—	0.0419	5.65×10^{-2}
C_{12}	0.7×10^{-3}	5.41×10^{-4}	0.3×10^{-3}	1.65×10^{-6}	—	5×10^{-9}

Table 3

The antibacterial activity and the parameter LUMO on benzylpenicillin and oxacillin

Antibiotic	Antimicrobial activity (mkg/mL)				LUMO		
	hemolytic streptococcus	pneumo-coccus	entero-coccus	Lit.[6]	our calculations		
					variant 1	variant 2	variant 3
Benzylpenicillin	0.004	0.020	0.100	−1.00	−0.9527	−0.5094	−0.5026
Oxacillin	0.030	0.100	6.000	−0.57	−0.5741	—	−0.4789

latter, induces a pronounced epileptogenic activity. After benzylpenicillin administration to cats, the cortex of a whole brain hemisphere has proved the direct action of this penicillin upon the neurons.

A very important hormone in maintaning an equilibrium of processes occurring in brain is serotonine.[9] This hormone exists in animal and humain brain and its presence in a certain amount seems to be necessary to maintain this equilibrium.[10] The substances that modify the serotonine function in the central nervous system may cause important mental troubles.

The BAS antimetabolite (1-benzyl-2.5-dimethyl-serotonine) is a benzylic analog of serotonine (Fig. 2).

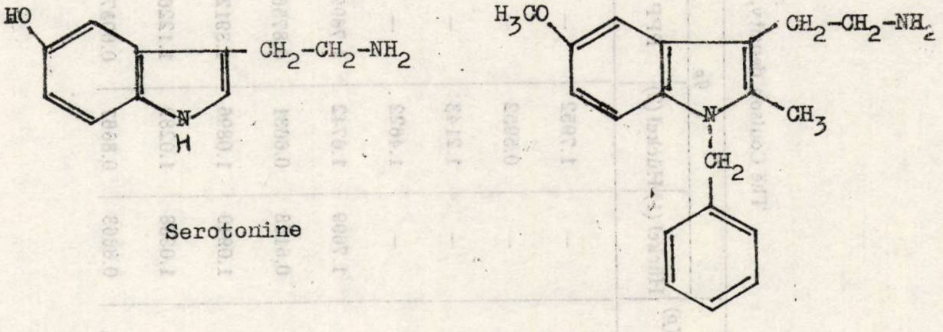

Serotonine

BAS

Fig. 2.—Serotonine and its antimetabolite.

As its chemical structure is similar to that of serotonine, it may be accepted into the serotonine receiver and thus hampers the normal inlet which causes a specific deficiency of the hormone. At the same time the brain enzyme (aminoxidase) is inhibited. This enzyme destroys the serotonine excess.

The finding that benzylpenicillin is a strong neurotoxic has determined us to advance the following hypothesis : in subjects that have been administered the drug, the benzyl radical detaches from penicillin molecule (perhaps by an enzymatical mechanism) and generates its antimetabolite with serotonine.

Table 1 lists the bond orders on benzyl chain in the molecule ; the very low value for $P_{C_{10}-C_{12}}$ is remarked, which points to a weak bond from the energy viewpoint ($\sim$ 0.20 in the three Hückel variants and 0.017 in the PPP method).

Likewise the bonding of methylene carbon to nitrogen atom in serotonine is justified by the strong electron acceptor character of this atom (f_{12}^{N} in table 2).

REFERENCES

[1] "Tables of interatomic distances and configuration in molecules and ions", London, The Chemical Society, 1958, M 247.

[2] D. B. Boyd, *Int. J. Quant. Chem.* ; *Quantum Biology Symp.*, **4**, 161, (1977).

[3] D. B. Boyd and W. H. W Lunn, *J. Antibiotics*, **32**, 855 (1979).

[4] A. Streitwieser Jr., "Molecular Orbital Theory for Organic Chemistry", John Wiley and Sons., Inc., New York, London 1962, p. 105.

[5] K. Fukui, T. Yonezawa and co., *J. Chem. Phys.*, **22**, 1433 (1954) ; **26**, 831 (1957).

[6] E. A. Rudzit, A. C. Kobankin and M. A. Landau, *Antibiotiki*, **21**, 127 (1976).

[7] R. Kolb and co., *Arch. Int. Pharmacodyn. Ther.*, **222**, 149 (1976).

[8] J. J. Hablitz and co., *Exp. Neurol.*, **62**, 463 (1978).

[9] "Progress in Neurobiology. III Psychopharmacology", Chap. VII. Ed. H. H. Pennes, Copyright 1958, USA.

[10] B. Pullman and A. Pullman, "Quantum Biochemistry", Interscience Publishers 1963.

Revue Roumaine de Chimie, 32, *11–12*, 1123–1128 (1987)

Dedicated to Professor V. E. SAHINI
on his 60th anniversary

HETEROGENEOUS ELECTROCATALYSIS FOR NITROBENZENE AND PHENOL REDUCTION

S. STERNBERG and MIHAELA UNGUREANU
Laboratory for Applied Physical Chemistry, Faculty of Chemical Technology, Polytechnic Institute, Bucharest, Romania

Received April 30, 1987

The electrochemical reduction of nitrobenzene and phenol on platinum, copper and mercury electrodes was studied by potentiostatic method. The polarization curves were discussed on the basis of the half-wave potential and the limiting current related to the cathode nature. Electrocatalytical factors were calculated for nitrobenzene reduction. In comparison with mercury they are 576 and 6112 on copper and platinum, respectively.

INTRODUCTION

It is known that the aromatic ring and the double bounds can be reduced on some metals, like platinum, while the functional groups can be reduced especially on metals with high hydrogen overpotential, like copper and mercury.[1] The cathodic reduction of nitrobenzene ($PhNO_2$) and phenol (PhOH) in aqueous sulphuric acid solutions on platinum, copper and mercury was studied in order to obtain information on the influence of he cathodical nature on the reduction process of the organic substance

EXPERIMENTAL PART

Measurements were carried out by potentiostatic technique using a Model 173 Princeton Applied Research potentiostat.

The working cell had two separate compartments. The working electrodes were successively a bright platinum plate (geometrical area 0.85 cm^2), a platinized-platinum plate Pt—Pt (geometrical area 0.85 cm^2, roughness factor 160) and mercury (geometrical area 1.2 cm^2) A platinum net was used as a counterelectrode. All the potentials were measured vs. the $Hg/Hg_2SO_4/2\ M\ H_2SO_4$ reference electrode (MSE), having a standard potential of +0.58 V (s HNE). The working electrode was polarized by steps of 40 mV. For each step the value of the steady state current was registered after 2 minutes of polarization.

RESULTS AND DISCUSSION

The electrochemical reduction of $PhNO_2$ on platinum, copper and mercury electrodes was studied by the potentiostatic method. Figure 1 shows polarization curves obtained in 1 M aqueous sulphuric acid solution containing $5 \cdot 10^{-3}$ M $PhNO_2$ and in 1 N aqueous sulphuric acid solution respectively (curves B and A respectively). On platinum the $PhNO_2$ cathodic reduction process starts at about $= -0.4$ V and the hydrogen discharge begins at about -0.7 V. Because the electrode surface is blocked by the $PhNO_2$ adsorption the current for the simultaneous processes of hydrogen discharges and the $PhNO_2$ reduction is smaller than the current for the background.

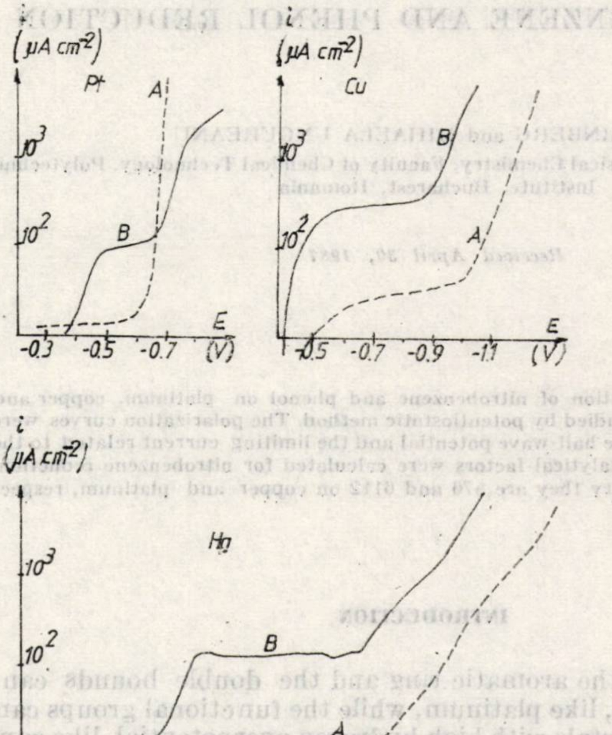

Fig. 1. — Polarization curves obtained on platinum, copper and mercury electrodes in 1 N sulphuric acid solution (curve A) and 1 N sulphuric acid solution containing 5.10^{-3} M nitrobenzene (curve B).

On copper the $PhNO_2$ reduction process occurs at about -0.5 V and the hydrogen discharge (occurring at more electropositive potentials than in the background) superposes it. The current for both processes (at potentials more negative than −0.9 V) is much higher than that obtained by simply summing the currents obtained for both processes taken independently.

On mercury the $PhNO_2$ reduction process begins at about − 0.4 V and the hydrogen discharge superposes it at about −1.1 V. There is a high value of the current in the potential range in which both processes occur simultaneously, much higher than the current obtained by simply summing the currents of both processes taken independently.

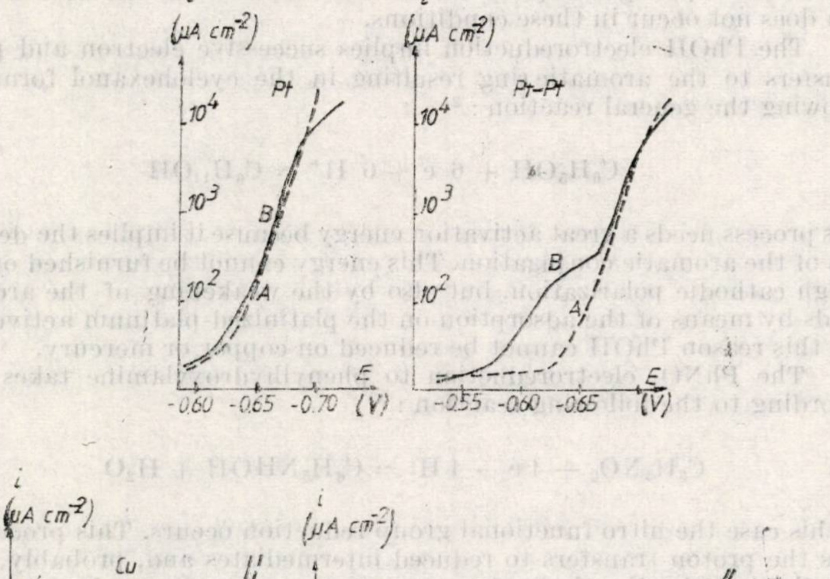

Fig. 2. — Polarization curves obtained on platinum, copper and mercury electrodes in 1 N sulphuric acid solution (curve A) and 1 N sulphuric acid solution containing 10^{-2}M phenol (curve B).

Figure 2 shows the polarization curves obtained in 1 N aqueous sulphuric acid solution containing 10^{-2} M phenol and in 1 N aqueous sulphuric solution respectively, on platinum, copper and mercury (curves B and A respectively).

On bright platinum the PhOH reduction process occurs very slowly, being masked by hydrogen discharge. The PhOH reduction is more evident on platinized-platinum starting at about −0.55 V. At potentials higher than −0.7 V at which the PhOH reduction and the hydrogen evolution simultaneously occur, there is an inversion of the curves, because the surface is blocked by the PhOH adsorption.

On copper and mercury the PhOH presence in the electrolyte does not change the shape of the background polarization curves and there is only a small hydrogen depolarization. That means that the PhOH reduction does not occur in these conditions.

The PhOH electroreduction implies successive electron and proton transfers to the aromatic ring resulting in the cyclohexanol formation, following the general reaction : [2]

$$C_6H_5OH + 6\ e + 6\ H^+ = C_6H_{11}OH \tag{a}$$

This process needs a great activation energy because it implies the destruction of the aromatic conjugation. This energy cannot be furnished only by a high cathodic polarization, but also by the weakening of the aromatic bonds by means of the adsorption on the platinized-platinum active sites. For this reason PhOH cannot be reduced on copper or mercury.

The $PhNO_2$ electroreduction to phenylhydroxylamine takes place according to the following reaction : [3]

$$C_6H_5NO_2 + 4\ e + 4\ H^+ = C_6H_5NHOH + H_2O \tag{b}$$

In this case the nitro functional group reduction occurs. This process implies the proton transfers to reduced intermediates and, probably, could be influenced by the electrode nature in the same way as hydrogen discharge. It is known that the hydrogen discharge overpotential decreases in the sequence — mercury, copper, platinum.

The $PhNO_2$ reduction occurs on platinum and also on copper and mercury, but with different rates. This reduction rate increases in the sequence-mercury, copper, platinum. Our research tries to find some quantitative equations in order to show the influence of the "indifferent" electrode nature on the $PhNO_2$ electroreduction rate.

For an irreversible electrode process, at small concentrations of the active substance the charge transfer and also the concentration overpotential must be taken into account, according to the eqution (1). [4]

$$\frac{i}{i_o} = \left(1 - \frac{i}{i_L}\right) \exp\left\{-\frac{\alpha n F \eta}{RT}\right\} \tag{1}$$

In equation (1) i, i_0, i_L, α, n, F, R and T are respectively, the current obtained at η overpotential, the exchange current, the limiting current, the charge transfer coefficient, the number of exchanged electrons, Faraday's constant, Regnault's constant and temperature.

If one considers a reduction process taking place on different metals M, M′, at the same concentration of active substance and at value of

$i = i_L/2$, then the ratio $i_{o,\mathrm{M}}/i_{o,\mathrm{M}'}$ can be obtained between the exchange current on the metals M and M′, by assuming that the reduction standard potential is the same on both metals $E_{o,\mathrm{M}} = E_{o,\mathrm{M}'}$;

$$\frac{i_{o,\mathrm{M}}}{i_{o,\mathrm{M}'}} = \frac{i_{L,\mathrm{M}}}{i_{L,\mathrm{M}'}} \exp\left\{-\frac{\alpha n F}{RT}\,[E_{1/2,\mathrm{M}} - E_{1/2,\mathrm{M}'}]\right\} \tag{2}$$

where $E_{1/2,M}$ and $E_{1/2,M'}$, are the half-wave potentials of the reduction process on the metal M_0 and M′, respectively. This ratio represents the intensification of the reduction process on metal M compared with the process taking place on "reference" metal, M′. We call it heterogeneous catalysis factor and denote it by γ :

$$\gamma = \frac{i_{o,\mathrm{M}}}{i_{o,\mathrm{M}'}} \tag{3}$$

The ratio $i_{L,M}/i_{L,M'}$ represents the process activation by surface increase and it is denoted by γ_s :

$$\gamma_s = \frac{i_{L,\mathrm{M}}}{i_{L,\mathrm{M}'}} \tag{4}$$

The exponential term from equation (2), denoted γ_E, represents the process activation by shifting the half-wave potential on M compared with M′ :

$$\gamma_E = \exp\left\{-\frac{\alpha n F}{RT}\,[E_{1/2,\mathrm{M}'} - E_{1/2,\mathrm{M}}]\right\} \tag{5}$$

Mercury was considered as a "reference" metal M′ (liquid electrode with definite surface). The γ factors were calculated for the $\mathrm{PhNO_2}$ reduction on platinum and copper in comparison with mercury, by means of the $E_{1/2}$ and i_L values, obtained from the polarization curves. For this reduction process we consider $n = 4$; $\alpha = 0.5$; $T = 293$ K ; $F = 96\,485$ C.

The calculation was done starting from the assumptions that the reduction reaction (b) is the same on each of the electrodes studied and that phenylhydroxylamine is the main reduction product.

Table 1

γ-Factors for the $\mathrm{PhNO_2}$ reduction on the mercury electrode scale

Electrode	Hg	Cu	Pt
$E_{1/2}$, V	−0.55	−0.48	−0.44
i_L, μA/cm^2	170	380	170
γ_s	1	2,24	1
γ_E	1	257	6112
$\gamma=\gamma_s\gamma_E$	1	576	6112

The analysis of the γ values shows that the electrocatalytic effect acts by means of the γ_E factor on platinum and by the γ_s and also γ_E factors on copper. It is also remarkable the great effect of hydrogen discharge depolarization produced by $\mathrm{PhNO_2}$. However, the electrocatalytical factor γ is not the only important factor in choosing the electrode material for electrolysis. In the $\mathrm{PhNO_2}$ reduction on platinum (that has the highest value for γ) the hydrogen discharge occurs simultaneously, leading thus to the decrease of the current yield. That is why the cathodes with a great hydrogen overpotential, such as mercury and copper, are preferred.

REFERENCES

[1] L. Antropov, "Theoretical electrochemistry" Mir Publishers, Moscow, 1977, p. 487.
[2] K. Sasaki, A. Kunai, J. Harada and S. Nakabori, *Electrochim. Acta*, **28**, 671 (1983).
[3] H. Lund, in "Organic Electrochemistry", ed. by M. Baizer, New York, Dekker (1970).
[4] A. Bard and L. Faulkner, "Electrochemical Methods", Wiley, New York, p. 109 (1980).
[5] A. P. Tomilov, M. Ia. Fiosin and V. A. Smirnov, "Elektrohimicheskii sintez organicheskikh veshcestv", Khimia, Leningrad, 1976, p. 155.

Revue Roumaine de Chimie, 32, *11–12*, 1129–1139 (1987)

Dedicated to Professor V. E. SAHINI
on his 60th anniversary

MODELS FOR THE VISCOSITY OF LIQUID MIXTURES. APPLICATION TO THE BINARY SYSTEM WATER-DIOXAN

ORTANSA LANDAUER, CORNELIA MATEESCU, OLGA IULIAN and D. GEANĂ

Dept. Physical Chemistry/TSCO, Polytechnic Institute, Bucharest, Spl. Independenței 313, Romania

Received May 15, 1987

A review of some of the models presented in the literature for representing the viscosity of the binary systems of liquids is presented. A new model recently developed based on Eyring's equation from the activated complex theory and NRTL (non-random two-liquids) expression from the thermodynamics of mixtures is discussed. The new suggested model and some of the models in the literature are applied to the system water-dioxan.

INTRODUCTION

The viscosity of liquid mixtures mainly the binary ones has been the subject of many studies.[1,2] Theoretical studies have been focussed both on the possibilities of predicting the viscosity of liquid mixtures from the properties of their components and on certain statistic molecular models that are able to represent the variety of practical mixtures. Experimental studies related to a lot of binary mixtures are presented in the literature.

The aim of this work is to review some of the models suggested in the literature for representing the viscosity of the binary systems of liquids. A new model recently developed [3] for the viscosity of liquid mixtures based on Eyring's equation from the theory of the activated complex for kinematic viscosity (ν) and NRTL (non-random two-liquids) expression[2] for thermodynamics of mixtures is presented. The new suggested model[3] and some of the models in the literature [4,5] are applied to the system water-dioxan.

MODELS FOR THE VISCOSITY OF LIQUID MIXTURES

The experimental data on the viscosity of the binary mixtures have been correlated to different empiric models. Relations of additivity [2] have been tested in the form :

$$Y = X_1Y_1 + X_2Y_2 \tag{1}$$

where X_1, X_2 are the mole fractions of the components and Y, Y_1, Y_2 are respectively

a) η, η_1, η_2
b) $\ln\ \eta$, $\ln\ \eta_1$, $\ln\ \eta_2$
c) $\eta^{1/3}$, $\eta_1^{1/3}$, $\eta_2^{1/3}$
d) ν, ν_1, ν_2
e) $\ln\ \nu$, $\ln\ \nu_1$, $\ln\ \nu_2$

where η is the dynamic viscosity and $\nu = \eta/\rho$ is the kinematic viscosity.

It has been noticed that no expression of this type can represent the real behaviour of the mixtures. Consequently, following the idea of excess functions of chemical thermodynamics, expressions of the type

$$Y^E = Y - (X_1Y_1 + X_2Y_2) \tag{2}$$

have been proposed, where Y, Y_1, Y_2 can be considered respectively $\ln \eta$, $\ln \eta_1$ and $\ln \eta_2$. The excess function which is thus defined was empirically expressed either by a model taken from the theory of regular solutions (of the type $A(T)X_1X_2$) or by a model of the type Redlich-Kister [6]

$$Y^E = \ln\ \eta^E = \sum_{i=0}^{n} A_i(T)(X_1 - X_2)^i X_1X_2 \tag{3}$$

where n is chosen in general 3 or 4. The A_i parameters as temperature functions are obtained by regression. It is obvious that the parameters that are introduced in this manner cannot be associated with a physical significance. They are used only to represent the data in an analytical form. The choice of the function $\ln\ \eta^E$ may be motivated by the empirical relation

$$\eta = A\ e^{B/T} \tag{4}$$

where for B, which is adopted as an "energy of activation" a relation of the type

$$B_{\rm mix} = X_1B_1 + X_2B_2 + B^E \tag{5}$$

is accepted and for A one supposes that $A_{\rm mix} = A_1 = A_2$.

Other correlations have been also tried for ν, among which we can mention those which have been proposed by Mc Allister [4] and respectively by Lobe. [5]

The Mc Allister model [4] can be considered as having more advanced physical motivation if compared with the models above. The cubic expression, which is considered to represent interactions of trimolecular type is :

$$\begin{aligned}\ln \nu = X_1^3 \ln \nu_1 + 3\ X_1^2X_2 \ln \nu_{12} + 3X_1X_2^2 \ln \nu_{21} + X_2^3 \ln \nu_2 - \\ - \ln(X_1 + X_2M_2/M_1) + 3X_1^2X_2 \ln[(2 + M_2/M_1)/3] + \\ + 3X_1X_2^2 \ln[(1 + 2M_2/M_1)/3] + X_2^3 \ln(M_2/M_1)\end{aligned} \tag{6}$$

Equation (6) contains two parameters ν_{12} and ν_{21} which can be calculated by regression from experimental data.

The model proposed by Lobe [5] has the form

$$\nu = \Phi_1 \nu_1 \exp(\Phi_2 \alpha_2^*) + \Phi_2 \nu_2 \exp(\Phi_1 \alpha_1^*) \tag{7}$$

the parameters of the model being $\alpha_1^* = \alpha_1/RT$ and $\alpha_2^* = \alpha_2/RT$, and Φ_1, Φ_2 are volume fractions.

A new model recently developed [3] is also discussed. The starting point as in Mc Allister's model [4] is the expression

$$\eta = \frac{\lambda_1 h}{\lambda_2 \lambda_3 \lambda^2} \exp(\Delta G^*/RT) \tag{8}$$

which is obtained on the basis of the theory of activated complex. [1] λ and λ_1, λ_2, λ_3 represent the distances between the molecules of the liquid.

Adopting the hypothesis $\lambda = \lambda_1$ and $\lambda_1 \lambda_2 \lambda_3 = \mathbf{V}/N$ (molecular volume) with $\mathbf{V}$ as molar volume and N as Avogadro's number, we get

$$\nu = \eta/\rho = \frac{hN}{M} \exp(\Delta G^*/RT) \tag{9}$$

where M is the molar mass and h is Planck's constant.

Applying equation (9) to a mixture we may introduce the hypothesis that

$$\Delta G^*_{\text{mix}} = X_1 G_1^* + X_2 \Delta G_2^* + G_E^* \tag{10}$$

where G_E^* is an excess term as compared to the simple additivity, determined by molecular interactions in the mixture. Considering the following relation for the pure components

$$\nu_1 = \frac{hN}{M_1} \exp(\Delta G_1^*/ERT) \tag{11}$$

$$\nu_2 = \frac{hN}{M_2} \exp(\Delta G_2^*/RT)$$

and combining expressions (9—11) we get

$$\ln \nu = X_1 \ln \nu_1 + X_2 \ln \nu_2 + X_1 \ln M_1 + X_2 \text{ in } M_2 - \ln M + G_E^*/RT \tag{12}$$

This expression was proposed in the literature, e.g. [7] At this point the central problem is the modelling of an expression for G_E^*. As a theoretical model does not seem possible, empirical expressions can be taken into account (may be with certain molecular motivations).

A possible choice is based on the equation NRTL (non random two-liquids) used for the excess free enthalpy (G^E) in the thermodynamics of mixtures[8]

$$\frac{G_E^*}{RT} = X_1X_2\left(\frac{\tau_{21}\theta_{21}}{X_1 + \theta_{21}X_2} + \frac{\tau_{12}\theta_{12}}{X_2 + \theta_{12}X_1}\right) \tag{13}$$

where

$$\tau_{12} = \frac{g_{12} - g_{22}}{RT}; \quad \tau_{21} = \frac{g_{21} - g_{11}}{RT}$$
$$\theta_{12} = \exp(-\alpha\tau_{12}); \quad \tau_{21} = \exp(-\alpha\tau_{21}) \tag{14}$$

The preliminary tests have shown that the most useful expression corresponds to the choice

$$\alpha = -1 \tag{15}$$

called LEMF variant.[9] Thus the expression of the viscosity of the mixtures remains dependent on two parameters $g_{21}-g_{11}$ and $g_{12}-g_{22}$ which can be motivated molecularly (within the two-fluid model[10]), as representing the energy differences between the interactions of the type 1—2 and respectively 1—1 or 2—2.

Another hypothesis must be introduced regarding the molar mass of mixture, M. The simplest of them is the expression

$$M = X_1M_1 + X_2M_2 \tag{16}$$

The expression obtained by combining equations (12—16) was called the model NRTL/ν2 :[3]

$$\ln \nu = X_1 \ln(\nu_1 M_1) + X_2 \ln(\nu_2 M_2) - \ln(X_1M_1 + X_2M_2) + \\ + X_1X_2\left(\frac{\tau_{21}\theta_{21}}{X_1 + \theta_{21}X_2} + \frac{\tau_{12}\theta_{12}}{X_2 + \theta_{12}X_1}\right) \tag{17}$$

Taking also into account the possibility that $\lambda \neq \lambda_1$ for the mixture, we may write

$$\nu = \frac{hN}{\beta M}\exp(\Delta G^*/RT) \tag{18}$$

where $\beta = (\lambda/\lambda_1)^2$. Expression (17) becomes

$$\ln \nu = X_1 \ln(\nu_1 M_1) + X_2 \ln(\nu_2 M_2) - \ln(\beta M) + \\ + X_1X_2\left(\frac{\tau_{21}\theta_{21}}{X_1 + \theta_{21}X_2} + \frac{\tau_{12}\theta_{12}}{X_2 + \theta_{12}X_1}\right) \tag{19}$$

having three parameters $g_{12}-g_{22}$, $g_{21}-g_{11}$ and β. We called this expression[3] model NRTL/ν3. One of the advantages of the models of the type NRTL is the possibility of their extension to multicomponent systems, in the form :

$$\ln \nu = \sum_{i=1}^{C} X_i \ln(\nu_i M_i) - \ln(\beta M) + \sum_{i=1}^{C} X_i \left[\left(\sum_{j=1}^{C} \tau_{ji} \theta_{ji} X_j \right) \Big/ \left(\sum_{k=1}^{C} \theta_{ki} X_k \right) \right] \tag{20}$$

where β may be calculated from the binary β_{ij} parameters or considered a mixture parameter independent of the binary values.

In order to appreciate the quality of the experimental data and of the models that have been proposed, we may also use, for G_E^* in equation (12), an expression of the Redlich-Kister type :

$$\frac{G_E^*}{RT} = \sum_{i=0}^{n} B(T)(X_1 - X_2)^i X_1 X_2 \tag{21}$$

or an expression based on Legendre polynomials having the advantage of the latter's orthogonality.

APPLICATION TO THE SYSTEM WATER-DIOXAN

The mixed solvent water-dioxan is frequently used as a reaction medium, so that its physical properties for the whole range of compositions as well as their dependence on the temperature should be known.

The viscosity and density of the system water-dioxan have been determined experimentally for the temperature of 20, 30 and 40°C.

Pure liquids, bidistilled water and dioxan purified according to the methods indicated in the literature have been used for the measurements.[11] The viscosity of pure liquids and of the mixtures was determined by using an Ubbelohde viscometer, and the density picnometrically.[12,13]

The experimental results that have been obtained for the three temperatures are given in tables 1—3.

As we can observe the mixtures present extreme maximum values both for the density and for the viscosity for mole fractions of about $X_{H_2O} = 0.65$ at all the temperatures. The excess, values are negative and present maximum values for the same compositions.

Taking into account the peculiar behaviour of the mixture water-dioxan, we consider it proper for the testing of the viscosity models that have been proposed.

In tables 4—5 we present the values of the coefficients of the polynomials correlating the density

$$\rho = \sum_{i=0}^{n} a_i X_{H_2O}^{i} \tag{22}$$

Table 1

Density, viscosity and excess volume for water-dioxan mixtures at $t=20°C$

X_{H_2O}	ρ, /cm³	η, cP	ν, cST	V^E, cm³/mole
0	1.0339	1.3125	1.2694	0
0.3420	1.0378	1.6399	1.5801	−0.44006
0.5378	1.0405	1.9730	1.8962	−0.63471
0.6642	1.0417	2.2928	2.2010	−0.70284
0.7531	1.0411	2.2369	2.1486	−0.69197
0.8195	1.0384	2.2028	2.1213	−0.62442
0.8712	1.0334	2.0253	1.9598	−0.51451
0.9127	1.0270	1.7655	1.7191	−0.39545
0.9470	1.0185	1.5038	1.4766	−0.25525
0.9756	1.0092	1.2068	1.1958	−0.12340
1	0.9992	1.0050	1.0050	0

Table 2

Density, viscosity and excess volume for water-dioxan mixtures at $t=30°C$

X_{H_2O}	ρ, g/cm²	η, cP	ν, cSt	V^E, cm³/mole
0	1.0225	1.1127	1.0882	0
0.3420	1.0272	1.2967	1.2623	−0.44980
0.5378	1.0304	1.6816	1.6320	−0.63401
0.6642	1.0225	1.8514	1.7931	−0.70977
0.7531	1.0321	1.7539	1.6993	−0.67980
0.8195	1.0301	1.7238	1.6734	−0.61139
0.8712	1.0260	1.5705	1.5307	−0.50494
0.9127	1.0200	1.7775	1.3505	−0.37663
0.9470	1.0125	1.1960	1.1812	−0.24091
0.9756	1.0045	0.9888	0.9844	−0.11873
1	0.9956	0.8007	0.8042	0

Table 3

Density, viscosity and excess volume for water-dioxan mixtures at $t=40°C$

X_{H_2O}	ρ, g/cm³	η, cP	ν, cSt	V^E, cm³/mole
0	1.0121	0.9603	0.9488	0
0.3420	1.0150	1.0923	1.0761	−0.30315
0.5378	1.0211	1.2961	1.2693	−0.63101
0.6642	1.0226	1.4729	1.4403	−0.65867
0.7531	1.0222	1.4797	1.4476	−0.61367
0.8195	1.0212	1.4195	1.3900	−0.56256
0.8712	1.0177	1.2395	1.2179	−0.45804
0.9227	1.0133	1.0920	1.0776	−0.35407
0.9470	1.0063	0.9541	0.9481	−0.21433
0.9756	1.0004	0.8003	0.8000	−0.12035
1	0.9922	0.6560	0.6611	0

Table 4

Coefficients of the polynomials for correlating the density with X_{H_2O} for the system water-dioxan

a_i \ t °C	20	30	40
a^1	1.0339007	1.022500	1.012055
$\overset{*}{a_1}$	—	—	—
a_2	−0.1057575	−0.0713496	—
a_3	0.8710158	0.6429766	0.0590163
a_4	−2.359328	−1.778626	−0.325116
a_5	2.805608	2.177961	0.682377
a_6	−1.246184	−0.9969027	−0.434946
σ^2	$2.74 \cdot 10^{-8}$	$3.66 \cdot 10^{-8}$	$1.45 \cdot 10^{-6}$
r_{cor}	0.9993	0.99987	0.99251

* Not given coefficients were eliminated by a significance test.

Table 5

Redlich-Kister parameters for correlating $V^E - X_{H_2O}$ in the system water-dioxan

t°C \ a_i	20	30	40
a_0	−2.389083	−2.42865	−2.32966
a_1	−2.115979	−1.60020	−2.35922
a_2	−0.651199	−1.50294	1.65234
a_3	2.020647	−1.68128	−2.097
a_4	−8.594968	2.19247	—
a_5	6.557173	—	—
σ^2	$1.28 \cdot 10^{-3}$	$2.25 \cdot 10^{-3}$	$3.66 \cdot 10^{-2}$
r_{cor}	0.9995	0.999	0.9856

Table 6

Redlich-Kister parameters for correlating $\ln \eta^E - X_{H_2O}$ in the system water-dioxan

a_i \ t, °C	20	30	40
a_0	1.5699	2.1509	1.8689
a_1	9.0543	3.2186	1.7377
a_2	−4.7715	−0.44307	5.0987
a_3	−53.301	−1.0343	9.2134
a_4	126.03	5.6655	−31.583
a_5	−71.451	—	22.846
σ^2	0.04473	0.0123	0.01397
r_{cor}	0.9957	0.9989	0.9986

Table 7

Parameters for the models of viscosity in the system water-dioxan

Model	Paramteers	t, °C 20	 30	 40
Lobe (eq. 7)	α_1^*	0.4074 ± 0.238	0.1999 ± 0.286	1.1466 ± 0.328
	α_2^*	1.8463 ± 0.129	1.8726 ± 0.147	1.7823 ± 0.184
NRTL/ν2 (eq.(17))	$g_{12} - g_{22}$, cal/mole	-123.2 ± 111	-87.08 ± 130	-186.6 ± 184
	$g_{21} - g_{11}$ cal/mole	1131.0 ± 22	1150.2 ± 28	1186.1 ± 35
NRTL/ν 3 (eq.(19))	$g_{12} - g_{22}$ cal/mol	9.884 ± 64	30.51 ± 111	-11.97 ± 113
	$g_{21} - g_{11}$ cal/mole	1207.9 ± 25	1221.6 ± 46	1281.3 ± 42
	β	1.146 ± 0.05	1.128 ± 0.08	1.170 ± 0.08
Redlich-Kister (eq. (12), (16), (21))	B_0	2.9064 ± 0.063	3.3039 ± 0.083	3.1416 ± 0.095
	B_1	3.2356 ± 0.164	2.9747 ± 0.231	2.8818 ± 0.250
	B_2	2.4531 ± 0.663	-0.9081 ± 0.901	1.7298 ± 1.004
	B_3	0.8190 ± 0.910	5.3265 ± 1.235	2.8986 ± 1.361

and respectively of the Redlich-Kister equation for the excess molar volume

$$V^E = \sum_{i=0}^{n} a_i(T)(X_{H_2O} - X_{DO})^i \, X_{H_2O} \, X_{DO} \tag{23}$$

These correlations are presented both for evaluating the quality of experimental data (by means of the standard deviation, σ^2 and correlation coefficient, r_{cor}) and for introducing the data in computer data bases.

The results of the testing of the viscosity models are presented in tables 6–8. Table 6 presents the values of the Redlich-Kister parameters according to equation (3). These values are also useful for evaluating the quality of the data (by σ^2 and r_{cor}) and for introducing the results in data bases.

The parameters presented in tables 4–6 have been obtained by a multilinear regression procedure.[14] For the density the following criterion was used

$$\min S_\rho = \sum_{i=1}^{N_{ex}} (\rho_i^{ex} - \rho_i^{c})^2 \tag{24}$$

and for the excess functions (V^E, $\ln \eta^E$)

$$\min S_Y = \sum_{i=1}^{N_{ex}} \left(\frac{Y_i^{ex}}{X_1 X_2} - \frac{Y_i^{c}}{X_1 X_2} \right)^2 \tag{25}$$

where N_{ex} is the number of experimental points. The indices "ex" and "c" respectively refer to experimental and calculated values.

Table 8

Relative errors, 100 $(\nu^c - \nu^{ex})/\nu^{ex}$, of different viscosity models applied to the system water-dioxan

X_{H_2O}	20°C				30°C				40°C			
	Lobe	NRTL/ν2	NRTL/ν3	RK (eq. (12), (21))	Lobe	NRTL/ν2	NRTLν3	RK (eq. (12), 21))	Lobe	NRTL/ν2	NRTL/ν3	RK (eq. (12), (21))
0												
0.3420	8.6	5.4	0.9	−0.35	13.2	10.5	6.5	−0.34	10.7	7.8	2.5	−0.15
0.5378	4.3	2.6	1.9	1.6	−0.7	−2.1	−2.4	1.3	4.6	2.9	2.2	0.62
0.6642	−4.6	−4.6	−3.6	−3.1	−5.1	−5.1	−4.2	−2.7	−3.9	−4.1	−2.9	−0.93
0.7531	−1.5	−0.3	1.3	2.5	0.05	0.9	2.4	2.5	−4.8	−3.8	−1.9	0.58
0.8195	−3.2	−1.6	−0.1	0.37	−2.1	−0.9	0.4	−0.3	−4.5	−3.2	−1.4	−0.78
0.8712	−1.6	−0.3	0.3	−0.62	−0.1	0.8	1.4	0.05	1.7	3	3.8	1.9
0.9127	2.0	2.3	1.3	−0.58	2.4	2.7	1.7	0.25	4.2	4.8	3.7	0.34
0.9470	4.0	3.1	−0.5	−1.4	0.02	1.7	−1.6	−1.7	3.9	3.5	−0.8	−2.6
0.9756	7.6	5.8	−1.9	1.7	3.1	1.9	−4.8	−1.1	3.8	2.7	−6.0	−2.1
1.0												
S(eq.(28))	0.0552	0.0297	0.0099	0.0097	0.0403	0.0299	0.0197	0.0053	0.0336	0.0227	0.0105	0.0018
σ^2	$7.9.10^{-3}$	$4.2.10^{-3}$	$1.6.10^{-3}$	$1.9.10^{-3}$	$5.7.10^{-3}$	$4.2.10^{-3}$	$3.2.10^{-3}$	$1.1.10^{-3}$	$4.8.10^{-3}$	$3.2.10^{-3}$	$1.7.10^{-3}$	$3.7.10^{-4}$

The standard deviation was calculated on the basis of the relation

$$\sigma^2 = \frac{\min S}{N_{\mathrm{ex}} - \mathfrak{M}} \tag{26}$$

where $\mathfrak{M}$ is the number of the parameters in the model, and the correlation coefficient is

$$r_{\mathrm{cor}} = \left(1 - \frac{\sigma^2}{\sigma_y^2}\right)^{1/2} \tag{27}$$

The number of the terms, n, in the expressions (22—23) was established after successive tests with $n = 1-6$, observing the optimum of the correlation by means of the statistic values σ^2 and r_{cor}.

The respective capacities of correlation of the Mc Allister, Lobe, NRTL/ν2 and NRTL/ν3 models were tested. The correlation with the Mc Allister model led to altogether unsatisfactory results for the system water-dioxan. For this reason the results related to this model are not presented in the tables.

Table 7 shows the values of the parameters of the Lobe (7), NRTL/ν2 (17) and NRTL/ν3 (19) models with the corresponding standard deviations. The parameter values of a Redlich-Kister model (12,21) are presented for comparison.

The parameters of table 7 have been calculated by a non-linear parameter estimation method [14] using the criterion function

$$\min S_\nu = \sum_{i=1}^{N_{\mathrm{ex}}} (\ln \nu_i^{\mathrm{ex}} - \ln \nu_i^{\mathrm{c}})^2 \tag{28}$$

Table 8 shows the capacities of correlation of the tested models, expressed by the relative error

$$\varepsilon_\nu = 100\, (\nu^{\mathrm{ex}} - \nu^{\mathrm{c}})/\nu_{\mathrm{ex}} \tag{29}$$

We can notice that the NRTL/ν2 model represents the viscosity of the mixture water-dioxan better than the Lobe model. Better results can be obtained using the NRTL/ν3 model. The fact that parameter β has values greater than 1 should be remarked.

The three models are all still inferior to the Redlich-Kister expression (21) with 4 or 5 parameters. It should be noticed also that the standard deviations of some parameters in table 7 are very great, indicating a low statistical significance of the model.

It is obvious that a great number of systems should be studied to draw ultimate conclusions. However we consider that the new NRTL/ν2 and NRTL/ν3 models[3] represent a starting point for the developing of new expressions taking also into account the advantages determined by the possibility of extending them to multicomponent systems (20).

REFERENCES

[1] S. Glasstone, K. J. Leidler and H. Eyring, "The Theory of Rate Processes", Mc Graw-Hill, New York, 1941.

[2] R. C. Reid, J. M. Prausnitz and T. K. Sherwood, "The Properties of Gases and Liquids", 3rd ed., Mc Graw-Hill, New York, 1977.

[3] D. Geană, *Rev Chim. (București)*, in press.

[4] R. A. McAllister, *Amer Inst. Chem. Engineers J.*, **6**, 427 (1960).

[5] V. M. Lobe, MS thesis, University of Rochester, Rochester N. Y., 1973 (cited in lit. [2]).

[6] O. Redlich and A. T. Kister, *Ind. Eng. Chem.*, **40**, 345 (1945).

[7] M. S. Dhillon and J. Kaur, *Z. Phys. Chem. (Leipzig)*, **264**, 525 (1983).

[8] H. Renon and J. M. Prausnitz, *Amer. Inst. Chem. Engineers J.*, **15**, 785 (1969).

[9] J. M. Marina and D. P. Tassios, *Ind. Eng. Chem. Proc. Des. Dev.*, **12**, 67 (1973).

[10] R. L. Scott, *J. Chem Phys.*, **25**, 193 (1956).

[11] C. J. Clement, E. Forest and P. Smith, *J. Chem. Phys.*, **40**, 2129 (1964).

[12] O. Landauer, G. Costeanu and C. Mateescu, *Rev. Roumaine Chim.*, **19**, 1429 (1974).

[13] O. Landauer, G. Costeanu and C. Mateescu, *Rev. Roumaine Chim.*, **24**, 1021 (1979).

[14] Y. Bard, "Non-linear Parameter Estimation", Academic Press, New York, 1974.

Revue Roumaine de Chimie, 32, *11—12*, 1141—1149 (1987)

Dedicated to Professor V. E. SAHINI
on his 60th anniversary

AN ELECTRON SPIN RESONANCE STUDY OF CONFORMATIONAL INVERSION IN IMINOXY RADICALS DERIVED FROM BENZOCYCLOHEPTENE AND HETEROCYCLIC ANALOGS

AGNETA CARAGHEORGHEOPOL* and ILEANA DRĂGUŢAN**

* Institute of Physical Chemistry, Spaiul Independenţei 202, Bucharest, Romania
** Institute of Organic Chemistry, Splaiul Independenţei 202, Bucharest, Romania

Received May 27, 1987

The effect of temperature on the ESR spectra of α-ketoiminoxy radicals derived from benzocycloheptenone and heterocyclic analogs has been investigated. The radical derived from 2,3-dihydro-1-benzoxepin-5(4*H*)-one (I) was conformationally mobile down to −80°C, whereas the radicals derived from 6,7,8,9-tetrahydro-5*H*-benzocyclohepten-5-one (II), 2,3-dihydro-1-benzothiepin-5-(4*H*)-one (III) and 2,3-dihydro-1-benzothiepin-1,1-dioxid-5(4*H*)-one (IV) yielded coalescence temperatures (T_c) and demonstrated line broadening effects above and below T_c. Treatment of theline-broadening data yielded (for the *Z*-isomers of these α-keto-iminoxy radicals) rate constants and thermodynamic activation parameters for the ring inversion ($\Delta G_c^{\neq} = 5.9$ kcal/mol, $T_c = -53$°C for II, $\Delta G_c^{\neq} = 6.2$ kcal/mol, $T_c = -44$°C fr III and $\Delta G_c^{\neq} = 9.5$ kcal/mol, $T_c = 69$°C for IV).

INTRODUCTION

In a previous paper[1] we reported on α-keto-iminoxy radicals derived from 1-benzoxepin-5-one and 1-benzothiepin-5-one. The radicals were prepared from the corresponding ketones by reaction with nitrogen dioxide, a general method for obtaining α-keto-iminoxy radicals : [2]

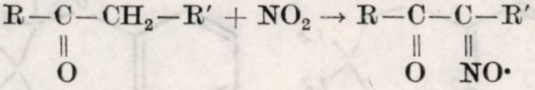

$$R-\underset{\displaystyle O}{\underset{\|}{C}}-CH_2-R' + NO_2 \rightarrow R-\underset{\displaystyle O}{\underset{\|}{C}}-\underset{\displaystyle NO\cdot}{\underset{\|}{C}}-R'$$

The equivalence of all pairs of geminal hydrogen hyperfine splitting (hfs) constants at room temperature was an indication for rapid conformational inversion of the seven rings in the above mentioned radicals.

We have now studied the spectra of these radicals and other two analogs at various temperatures in order to obtain thermodynamic data for the conformational inversion process in the seven membered carbocyclic and heterocyclic rings.

RESULTS

The investigated parent ketones were (I—IV).

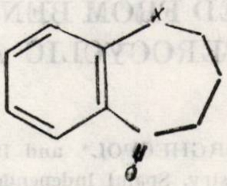

I X = O
II X = CH_2
III X = S
IV X = SO_2

By reaction with nitrogen dioxide, in all cases the spectra of both isomers, *E* and *Z*, of the iminoxy group have been obtained. The nitrogen hfs (a_N) values of the two isomers differ by several gauss, the relation being $a_N(Z) < a_N(E)$, [2] so the assignment of the spectra to the corresponding isomers was straightforward. As the outer lines of the two nitrogen triplets do not overlap clear proton hfs patterns were obtained. An unequivocal assignment of the proton hfs constants resulted by analogy with previously studied alicyclic and bicyclic α-keto-iminoxy radicals. [3]

The spectra of both isomers, *E* and *Z*, were temperature dependent; however, only the spectra of the *Z*-isomer — with higher intensity and a very simple 1 : 2 : 1 hfs pattern — could be used for a full line-shape analysis. The concentration of the *E*-isomers was always, lower, and — due to the adverse effect of low temperature on radical concentration, probably connected with the dimerization of the radicals — the spectra of these isomers could not be measured over a large temperature range. On the other hand, a second hfs causes line overlapping in these spectra, a fact having negative consequences on the accuracy of the line-shape analysis.

1-Benzoxepin-5-one (I)

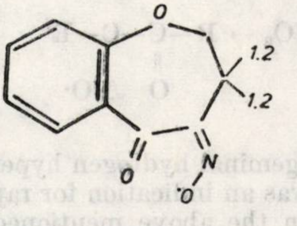

$a_N = 28.2$ G

Z–I

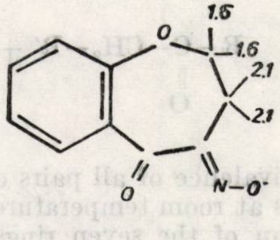

$a_N = 33.7$ G

E–I

The equivalence of all geminal hfs constants at room temperature is an indication for rapid interconversion between limiting conformations. Upon cooling no alternating line-width effect has been observed down to −80°C.

As found before,[3] the angular dependence of *α-anti* hfs constants is described by a Heller-McConnell type equation :

$$a_{\mathrm{H}}(\alpha\text{-}anti) = 0.6 + 1.6 \cos^2 \varphi \tag{1}$$

where φ is the angle defined in Figure 1a.

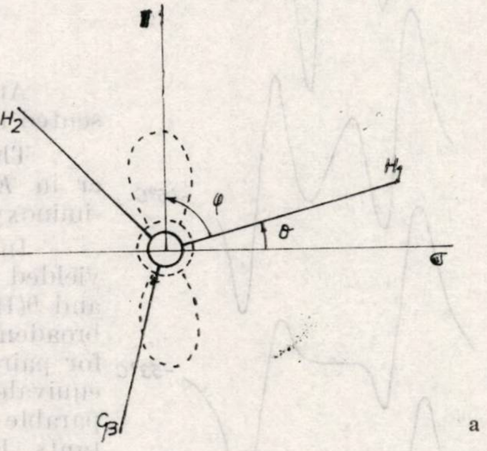

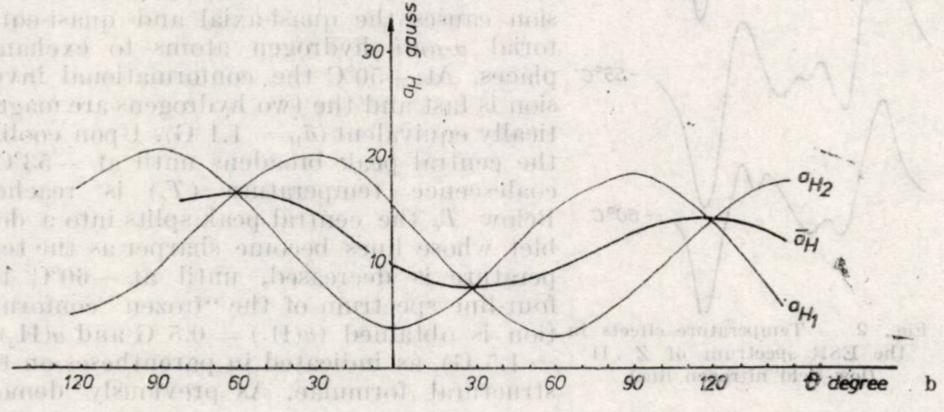

Fig. 1. — a) View along the $C_{im} - C_\alpha$ bond of the p_π orbital on C_{im} and of the α-methylene group. σ represents the plane containing the C=NO group.
b) *α-anti* proton hfs dependence on the dihedral angle θ (Eq. 1).

By using the $\bar{a}_{\mathrm{H}}(\alpha\text{-}anti)$ curve in Figure 1b, the dihedral angles $\theta(H_1) = 0°$ and $\theta(\mathrm{H}_2) = 120°$, corresponding to $\bar{a}_{\mathrm{H}}(\alpha\text{-}anti) = 1.2$ G have been obtained. These angles are characteristic of pure axial and equatorial positions as in cyclohexane.

The hfs constants in the *E*-isomer are slightly lower than the corresponding ones in the α-keto-iminoxy radical of cyclohexanone.[4]

Benzocyclohepten-5-one (II)

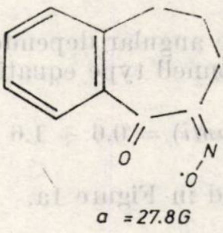

Z-II

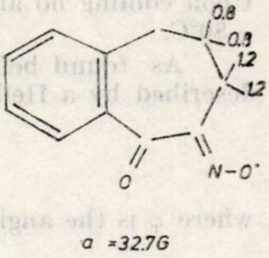

E-II

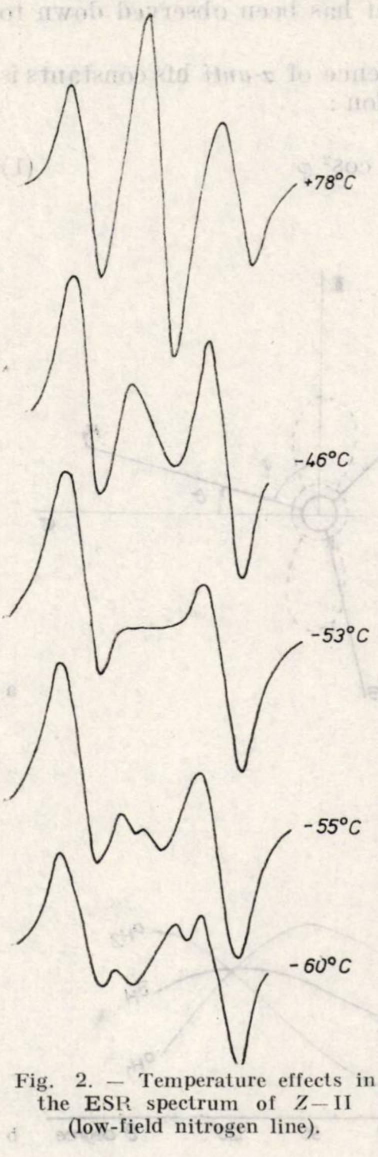

Fig. 2. — Temperature effects in the ESR spectrum of Z–II (low-field nitrogen line).

At room temperature both isomers presented time-averaged spectra.

The average $\bar{a}_{\mathrm{H}}(\alpha\text{-}syn)$ value is much lower in E-II than in E-I and in other α-keto-iminoxy radicals in six-membered rings. [3,4]

In the Z-II isomer the $\bar{a}_{\mathrm{H}}(\alpha\text{-}anti)$ value yielded the dihedral angles $\theta(\mathrm{H}_1) > 0°(\sim 10°)$ and $\theta(\mathrm{H}_2) > 120°$ $(\sim 130°)$. Upon cooling line broadening was observed in a way typical for pairs of hydrogen atoms exchanging nonequivalent environments at a frequency comparable to the difference in their hfs constants. Figure 2 illustrates the phenomenon for radical Z-II, where conformational inversion causes the quasi-axial and quasi-equatorial α-*anti* hydrogen atoms to exchange places. At +50°C the conformational inversion is fast and the two hydrogens are magnetically equivalent ($\bar{a}_{\mathrm{H}} = 1.1$ G). Upon cooling the central peak broadens until at −53°C a coalescence temperature (T_c) is reached. Below T_c the central peak splits into a doublet whose lines become sharper as the temperature is decreased, until at −60°C the four-line spectrum of the "frozen" conformation is obtained ($a(\mathrm{H}_1) = 0.5$ G and $a(\mathrm{H}_2) = 1.5$ G), as indicated in parentheses on the structural formulae. As previously demonstrated,[3] the higher hfs value has to be assigned to the axial hydrogen, the lower one to the equatorial.

The time-averaged a_{H} value equals the arithmetical mean of the two hfs constants in the fixed conformation, which implies that : (i) both hfs constants are of the same sign, and (ii) the conformations involved in the exchange are equivalent.

1-Benzothiepin-5-one (III)

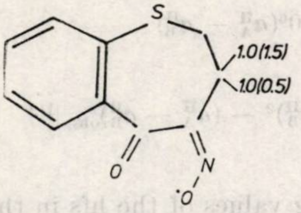

=28.2 G
Z-III

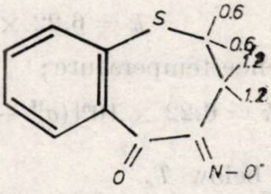

a = 33.0
E-III

The radicals obtained from this compound were in all regards, including the temperature dependence of the spectra, similar to the corresponding Z-II and E-II radicals. In this case the coalescence temperature was $T_c = -44$°C.

1-Benzothiepin-1,1-dioxide-5-one (IV)

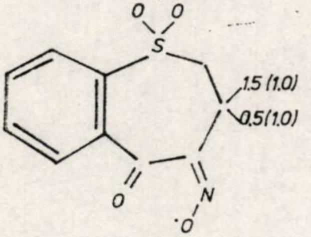

$a_N = 28.8$ G
Z-IV

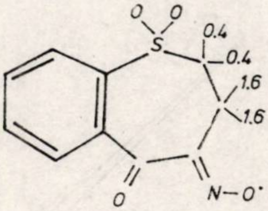

$a_N = 32.7$ G
E-IV

The sulphone IV proved to be more rigid than III. Indeed, the α-*anti* geminal hydrogen atoms in the Z-isomer were not equivalent at room temperature, this spectrum corresponding to a frozen conformation with $a(H_1) = 0.6$ G, $a(H_2) = 1.5$ G. Upon heating the sample, the inner lines coalesce at $T_c = +69$°C and above this temperature a three line pattern appears, the central line becoming more intense as the temperature is raised. At 100°C the intensity ratio was 1 : 1 : 1 ; above this temperature the radicals decompose.

The a_H(α-*anti*) values in the radical Z-IV correspond to the same dihedral angles as in Z-II and Z-III.

The radical E-IV had a time averaged spectrum at room temperature. Regarding the α-*syn* hfs in this radical, the same remarks as for E-II and E-III hold true.

The rate constants k for ring inversion were calculated with the following approximate equations, derived from the Bloch equations modified for exchange (the "two-site jump" model) : [5]

$$k = 4.4 \times 10^6 (a_A^H - a_B^H)^2/\Delta \qquad (2)$$

which is valid above T_c, for gaussian lines;

$$k = 6.22 \times 10^6 (a_A^H - a_B^H) \tag{3}$$

at the coalescence temperature;

$$k = 6.22 \times 10^6 [(a_A^H - a_B^H)^2 - (a_A^H - a_B^H)^2_{obs.}]^{1/2} \tag{4}$$

which is valid below T_c.
Here a_A^H and a_B^H represent the limiting values of the hfs in the frozen conformation and Δ is the increase, due to exchange, in full line-width of the central peak, relative to the wing peaks. When a_H and Δ are measured in gauss, k results in sec^{-1}.

Treatment of the line-broadening experimental data above the coalescence temperature (eq. (2)), at the coalescence temperature (eq. (3)), and peak separation below the coalescence temperature (eq. (4)) yielded the rate constants for ring inversion plotted in Figure 3. Thermodynamic data obtained from Figure 3 are summarized in Table 1.

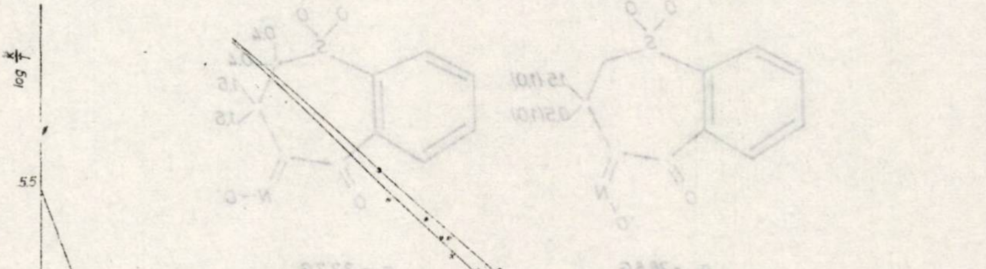

Fig. 3. — Computer least-squares plot of log k/T vs $1/T$ for the conformational interconversion of $Z-$II (1), $Z-$III (2) and $Z-$IV (3) α-keto-iminoxy radicals.

Table 1

Activation parameters for ring inversion of the *Z*-I — *Z*-IV α-keto-iminoxy radicals

Radical	T_c, °C	$\Delta G_c^{\neq}$, kcal/mol	$\Delta H^{\neq}$, kcal/mol	$\Delta S^{\neq}$, cal/°, mol
$Z-I$	<-100	<4		
$Z-II$	-53	5.9	4.3	-7.3
$Z-III$	-44	6.2	4.5	-6.7
$Z-IV$	$+69$	9.5	13.0	10.0

DISCUSSION

Comparison of $\Delta G_c^{\neq}$ data in Table 1 with literature data on related compounds suggests the following observations :

(a) The $\Delta G_c^{\neq}$ values of *Z*-I—*Z*-IV radicals are all lower with ~5 kcal/mol than the corresponding values of diheterosubstituted benzocycloheptenes having the same heteroatoms. [6-14] The observed decrease of the free enthalpy of activation seems to be related to the presence of the two $C_{sp}{}^2$ atoms in the seven ring.

This interpretation is supported by the results of dynamic NMR which yields for benzocycloptenones [15] much lower $\Delta G_c^{\neq}$ values (~5 kcal/mol) than for benzocycloheptene (10.7 kcal/mol).

The effect of one $C_{sp}{}^2$ on the $\Delta G_c^{\neq}$ value in benzocycloheptene derivatives is best emphasized by a comparison between iminoxy radicals *Z*-V and *Z*-VI[1] — conformationally frozen up to +60°C — and the α-keto-iminoxy radicals *Z*-I and *Z*-III, having fast inversion rates under the same conditions.

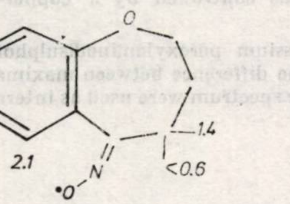

Z–V

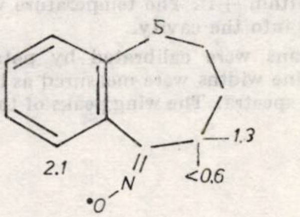

Z–VI

(b) The $\Delta G_c^{\neq}$ values of radicals *Z*-I—*Z*-III increased in the same sequence, i.e. $O < CH_2 \leqslant S$ as the values resulted from dynamic NMR[6-14] in three series of compounds of the general formulae :

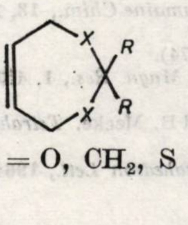

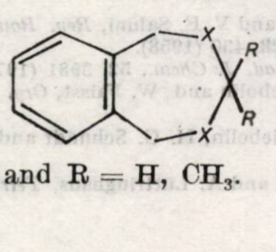

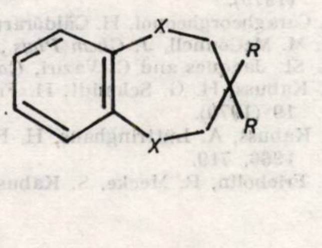

where $X = O$, CH_2, S and $R = H$, CH_3.

Literature data indicate high $\Delta G_c^{\neq}$ values for other heterocyclic sulphur compounds as well. [8] For sulphones the $\Delta G_c^{\neq}$ values are still higher than for the corresponding sulphur-derivatives.[16]

The sequence of $\Delta G_c^{\neq}$ values is not correlated either with the position of the heteroatoms or with the conformation of the cycle (some of these compounds have a chair conformation, others a twist-boat one). Instead it seems to follow the degree of "puckering" of the seven ring, which is favoured by the long C—S bond (1.82 Å) and small C—S—C angle (103°). In the other limit the oxygen compound, with the shortest C—O bond and largest C—O—C angle is the flattest one.

NMR data, yielding the value of the R parameter $(R = (J_{aa} + J_{ee})/(J_{ae} + J_{ea}))$ confirm the fact that seven rings are always more puckered than cyclohexane, the degree of puckering increasing in the $O < C < S$ sequence; [17] on the other hand sp^2 C atoms or O atoms in the seven-membered rings always exert a flattening effect. [18]

EXPERIMENTAL

Materials. 2,3-dihydro-1-benzoxepin-5(4*H*)-one, [19]2,3-dihydro-1-benzothiepin-5(4*H*)-one, [19] 2,3-dihydro-1-benzothiepin-1,1-dioxide--5(4*H*)-one and 6,7,8,9-tetrahydro-5*H*-benzocyclohepten-5-one [20] were prepared as previously described. Benzene was dried on sodium wire and distilled. Nitrogen dioxide was prepared as described in the literature. [21]

Radicals. The α-keto-iminoxy radicals were prepared by adding a saturated solution of nitrogen dioxide in benzene over the ketone in the sample tube.

ESR spectra. The ESR spectra were measured using a JES-3B (JEOL) spectrometer with 100 kHz field modulation. Variable temperature measurements were performed using the variable temperature cavity and the temperature control unit which reproducibly yielded temperatures within ±1°. The temperature was controlled by a copper-constantan thermocouple inserted into the cavity.

Field scans were calibrated by potassium peroxylaminedisulphonate ($a_N = 13.0$ G, $g = 2.0055$). Line widths were measured as the difference between maxima and minima of the first derivative spectra. The wing peaks of the spectrum were used as internal standars for line width.

REFERENCES

[1] A. Caragheorgheopol, H. Căldăraru, I. I. Bădilescu and V. E. Sahini, *Rev. Roumaine Chim.*, **24**, 307 (1980).

[2] W. M. Fox, J. A. McRae and M. C. R. Symons, *J. Chem Soc* (A), **1967**, 1773.

[3] H. Căldăraru, A. Caragheorgheopol, M. Moraru and V. E. Sahini, *J. Phys. Chem.*, **79**, 646 (1975).

[4] A. Caragheorgheopol, H. Căldăraru and V. E. Sahini, *Rev. Roumaine Chim.*, **18**, 1497 (1973).

[5] H. M. McConnell, *J. Chem Phys.*, **28**, 430 (1958).

[6] M. St. Jacques and C. Vaziri, *Canad. J. Chem.*, **52**, 3581 (1974).

[7] A. Kabuss, H. G. Schmidt, H. Friebolin and W. Faisst, *Org. Magn. Res.*, **1**, 451 (1969); **2**, 19 (1970).

[8] S. Kabuss, A. Lüttringhaus, H. Friebolin, H. G. Schmidt and R. Mecke, *Tetrahedron Lett.* **1966**, 719.

[9] H. Friebolin, R. Mecke, S. Kabuss and A. Lüttringhaus, *Tetrahedron Lett.*, **1964**, 1929.

[10] A. Blanchette, F. Sauriol-Lord and M. St. Jacques, *J. Amer. Chem. Soc.*, **100**, 4055 (1978).

[11] F. Sauriol-Lord and M. St. Jacques, *Canad. J. Chem.*, **57**, 3221 (1979).

[12] D. Menard and M. St. Jacques, *Canad. J. Chem.*, **59**, 1160 (1981).

[13] M. S. Jacques and C. Vaziri, *Canad. J. Chem.*,**49**, 1256 (1971).

[14] M. St. Jacques and C. Vaziri, *Org. Magn. Res.*, **4**, 77 (1972).

[15] G. Bodennec and M. St. Jacques, *Canad. J. Chem.*, **55**, 1199 (1977).

[16] I. O. Sutherland, M. V. J. Ramsay, *Tetrahedron*, **21**, 3401 (1965).

[17] J. B. Lambert, *Acc. Chem. Res.*, **4**, 87 (1971).

[18] L. Canuel and M. St. Jacques, *Canad. J. Chem.*, **52**, 3581 (1974).

[19] I. I. Bădilescu, *Rev. Roumaine Chim.*, **20**, 761 (1975).

[20] R. C. Gilmore and W. J. Horton, *J. Amer. Chem. Soc.*, **73**, 1413 (1951).

[21] Brauer, "Handbook of Preparative Inorganic Chemistry", Academic Press, New York, London, 1963, pp. 488, 767.

Revue Roumaine de Chimie, **32**, *11–12*, 1151–1154 (1987)

Dedicated to Professor V. E. SAHINI
on his 60th anniversary

MOLECULAR MOTION IN SOLID BICYCLO[3.3.1]NONAN-9-ONE AND ADAMANTANONE OXIMES STUDIED BY THE ELECTRON SPIN RESONANCE SPECTRA OF THE CORRESPONDING IMINOXY RADICALS

H. CĂLDĂRARU

ICECHIM-Institute of Physical Chemistry, Spl. Independenţei 202, 77208 Bucharest, Romania

Received May 28, 1987

The iminoxy radicals II and III obtained "in situ" by γ-irradiation of powder bicyclo [331]nonan-9-one and adamantanone oximes respectively were studied by ESR spectroscopy. Substantial deviation of experimental values of their nitrogen hyperfine coupling tensor from the corresponding values obtained for a series of iminoxy radicals Ia-e pointed to molecular motion of radicals II and III and indicated that their parent lattice is of mesomorphic plastic nature. The variation of ESR parameters over a wide range of temperatures (77—340 K) was measured. Motionally narrowed spectra of radical III were analyzed allowing calculation of an activation energy for reorientation of ~1.7 kcal/mole.

INTRODUCTION

Plastic crystals (orientationally disordered crystals) form the class of molecular crystals whose constituent molecules residing in a well-defined lattice undergo rapid reorientation. The experimental evidence concerning molecular motion in these crystals has been based on thermal, dielectric, X-ray diffraction, neutron scattering, infrared, Raman and nuclear magnetic resonance measurements.[1,2] Few electron spin resonance (ESR) studies of plastic cyrstals have been carried out, all supplying information about molecular motion by means of solubilized spin probes (nitroxides) in the corresponding matrices.[3-5]

This contribution investigates the possibility of using ESR spectra of radicals obtained "in situ" from the crystal matrix constituent in order to obtain information about molecular motion of the matrix itself. Thus, we have studied the temperature variation of the ESR parameters of the iminoxy radicals Ia—e, II and III obtained by γ-irradiation of the corresponding substituted bicyclo[331]nonan-9-one and adamantanone oximes (in powders).

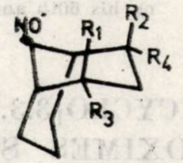

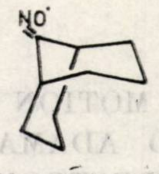

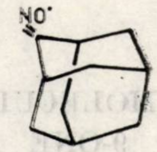

Ia, $R_1 = R_2 = H$; $R_3 = R_4 = Ph$
b, $R_1 = R_4 = H$; $R_2 = R_3 = Ph$
c, $R_1 = R_2 = H$; $R_3 = Ph$; R_4 = N-morpholinyl
d, $R_1 = R_4 = H$; $R_2 = Ph$; R_3 = N-morpholinyl
e, $R_3 = R_4 = H$; $R_1 = Ph$; R_2 = N-morpholinyl

II

III

RESULTS AND DISCUSSION

The principal values of the ^{14}N hyperfine coupling tensor of the iminoxy radicals Ia-e measured from their spectra as indicated in Fig. 1a, [6] as well as molecular parameters (orbital spin populations, spin density on the nitrogen atom, aparent bond angle) derived from these values [6] are listed in Table 1. The same data were obtained both at room (298 K) and liquid nitrogen (77 K) temperatures. They confirm the general features of iminoxy radicals in solid state [6] and are characteristic for strongly immobilized radicals in the parent lattice.

Table 1

ESR and molecular parameters of the iminoxy radicals Ia—e

Radicals	A_{zz}	A_{yy}	A_{xx}	$\%s$	$\%p$	p/s	ρ_N	∢ CNO
Ia	42.9	23.7	23.7	5.5	37.6	6.8	43.1	140.5°
b	44.6	24.5	23.6	5.6	39.4	7.0	45.0	141.0°
c	43.7	24.5	25.4	5.7	37.6	6.6	43.3	140.0°
d	44.6	23.6	23.6	5.6	41.2	7.4	46.8	142.0°
e	43.9	24.5	24.9	5.7	38.2	6.9	43.9	140.5°

Compared to a typical spectrum of strongly immobilized iminoxy radicals (Fig. 1a), the 298 K spectra of radicals II (Fig. 1b) and III (Fig. 1c) evidence the molecular motion of the radicals in the parent lattice; this motion partially averages the ^{14}N hyperfine coupling tensor. ESR spectra measured at 77 K are relevant for this interpretation. Indeed, on passing from 298 K (Fig. 1b) to 77 K (Fig. 1d) the spectrum of II changes essentially, the measured A_{zz} value at 77 K (43.3 G) being much higher than that at 298 K (35.8 G). The A_{zz} value at 77 K for this radical is close to the values of substituted radicals Ia—e (Table 1) indicating that at 77 K the radical II is immobilized to a great extent. For radical III the change is more evident, the motionally narrowed three line spectrum at 298 K (Fig. 1c) yields at 77 K a motionally slowed spectrum (Fig.

1e) with an A_{zz} of 41.4 G; this value compared to those of strongly immobilized radicals Ia—e indicates that there still exists some residual motion of radical III at 77 K.

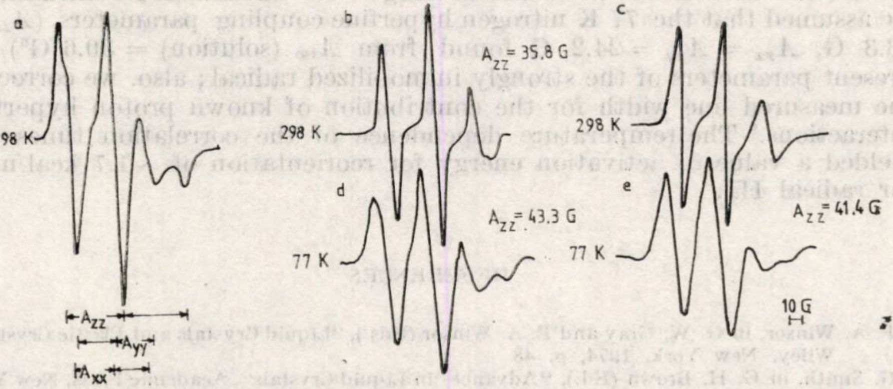

Fig. 1. — The ESR spectra of the iminoxy radicals a) Ib ; b, d) II ; c, e) III at the specified temperatures.

It is well known that adamantane and bicyclo[331]nonane [2] and their corresponding ketones [7] possessing globular shape, are plastic crystals in a certain temperature range. Our results regarding molecular motion of the "in situ" generated iminoxy radicals II and III indicate that the parent lattice (oxime) is also of mesomorphic plastic nature. The lack of mobility of radicals Ia—e may be accounted for by their deviation from globular shape brought about by the substituent groups.

The temperature dependence of the ESR spectra has been studied in the 77—340 K range. In this temperature range the molecular motion for radical II has been found to be only in the slow region (Fig. 2), while

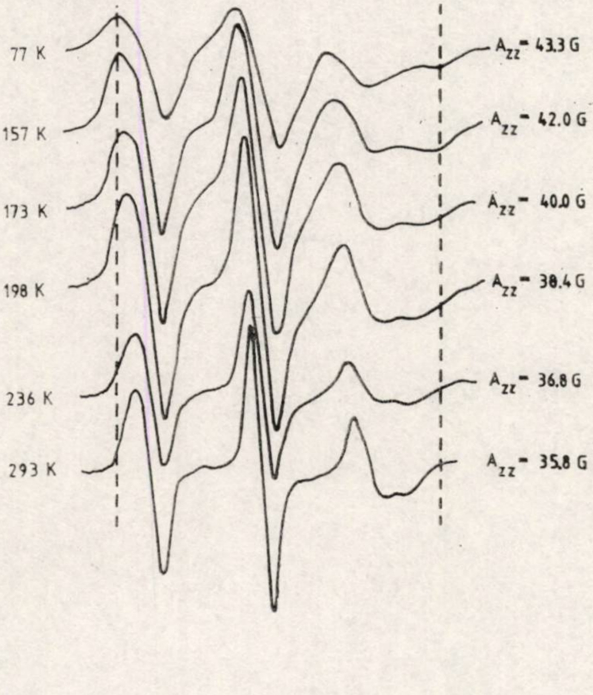

Fig. 2. The ESR spectra of the iminoxy radical II at different temperatures.

for radical III both in the slow and in the narrow region. For the latter region, using the Kivelson theory for isotropic motion[8] the rotational correlation times in the 293—340 K range were calculated. In calculations we assumed that the 77 K nitrogen hyperfine coupling parameters ($A_{zz} =$ 43.3 G, $A_{xx} = A_{yy} = 24.2$ G found from A_{iso} (solution) $= 30.6$ G[9]) represent parameters of the strongly immobilized radical; also, we corrected the measured line width for the contribution of known proton hyperfine interactions.[9] The temperature dependence of the correlation times has yielded a value of activation energy for reorientation of ~1.7 kcal/mole for radical III.

REFERENCES

[1] P. A. Winsor, in G. W. Gray and P. A. Winsor (Eds.), "Liquid Crystals and Plastic Crystals", Wiley, New York, 1974, p. 48

[2] G. Smith, in G. H. Brown (Ed.), "Advances in Liquid Crystals", Academic Press, New York, 1975, p. 189.

[3] F. Volino and A. Rousseau, *Mol. Cryst. Liq. Cryst.*, **16**, 247, (1972).

[4] H. Verdun, B. Meerovici and F. Volino, *J. Chem. Phys.*, **57**, 2414 (1972).

[5] S. H. Glarum and J. H. Marshall, *J. Chem. Phys.*, **62**, 956 (1975).

[6] W. M. Fox and M. C. R. Symons, *J. Chem. Soc. (A)*, **1966**, 1503.

[7] R. E. Wasylishen and K. J. Friesen, *Org. Magn. Reson.*, **13**, 343 (1980).

[8] D. Kivelson, *J. Chem. Phys.*, **33**, 1094 (1960).

[9] H. Căldăraru and M. Moraru, *J. Amer. Chem. Soc.*, **96**, 149 (1974).

Revue Roumaine de Chimie, **32**, *11—12*, 1155—1159 (1987)

Dédié au Professeur V. E. SAHINI
à l'occasion de son 60e anniversaire

LES MOMENTS DIPOLAIRES DE LA 7-CHLORO-2,3-DIHYDRO-4-QUINOLONE DANS LES ÉTATS FONDAMENTAL ET EXCITÉ

C. BENDIC et C. PODINĂ
Institut Polytechnique de Bucarest, Département de Chimie Physique, Bd. Republicii, 13, Bucarest, Roumanie

Reçu le 28 mai 1987

The dipole moments of 7-chloro-2,3-dihydro-quinolone in the ground and first excited states were determined. The methods based on the solvent shifts of the absorption and fluorescence spectra were used for the S_1 state. The experimental values were compared with the theoretical ones obtained by vectorial addition of σ and π moments (μ_σ and μ_π). The μ_π values were calculated from the ground and excited state charge densities obtained by CSF—CI method. The μ_σ value was evaluated from σ charge densities, obtained by Del Re method and by vectorial addition of the bond moments. A modification of Lippert's equation by the introduction of the Onsager cavity radius associated with the excited state was proposed.

On a déterminé les moments dipolaires de la 7-chloro-2,3,dihydro-4-quinolone dans les états fondamental et excité S_1. Pour le premier état excité on a utilisé des méthodes basées sur les spectres d'absorption et de fluorescence. Les valeurs expérimentales ont été comparées avec celles obtenues par l'addition vectorielle de moments σ et π (μ_σ, μ_π). Les valeurs μ_π ont été calculées à partir des densités de charge dans les états fondamental et excité obtenues par la méthode SCF-CI. La valeur de μ_σ a été évaluée tant à partir des densités de charge σ obtenues par la méthode de Del Re, que par l'addition vectorielle de moments de liaison.

La transition d'une molécule de son état fondamental dans un état excité, singulet ou triplet, conduit d'habitude à un changement substantiel dans la distribution de la densité électronique. On peut obtenir des renseignements sur la densité de charge dans les états fondamental et excité par des mesures indépendantes, tant des équilibres protolitiques [1,2] que des effets du solvant sur les spectres d'absorption et de fluorescence.[3-8]

Dans ce travail on a déterminé les moments dipolaires de la 7-chloro-2,3-dihydro-4-quinolone (CDHQ), un important intermédiaire dans la synthèse de la chloroquine, dans l'état foundamental et le premier état excité, S_1.

PARTIE EXPÉRIMENTALE

Le moment dipolaire dans l'état fondamental a été déterminé par la méthode de Guggenheim[9] en utilisant des solutions benzéniques obtenues par des dilutions successives d'une solution 0,1 mole/L. Les constantes diélectriques et les indices de réfraction ont été mesurés à l'aide d'un dielcomètre DK-METER 700 RL et d'un réfractomètre ABBE. Pour obtenir le moment dipolaire dans le premier état excité on a appliqué les méthodes qui utilisent l'effet du solvant sur les spectres d'absorption et de fluorescence.[3-8] Les spectres ont été enregistrés a l'aide d'un spectrophotomètre SPECORD UV-VIS et d'un spectrofluorimètre PERKIN-ELMER. Les moments dipolaires mesurés ont été comparés avec les valeurs théoriques calculées à partir des densités de charge.

CALCULS

Les valeurs théoriques des moments dipolaires ont été obtenues par l'addition vectorielle de moments σ et π (μ_σ et μ_π). Les valeurs μ_π ont été calculées à partir de densités de charge π-électronique, dans les états fondamental et excité obtenues par la méthode SCF—CI en utilisant les paramètres recommandés par Hinze et Jaffe.[10] Puisqu'on n'a pas disposé de données cristallographiques concernant la géometrie de la molécule de CDHQ, on a utilisé pour modèle théorique la molécule de la 2-amino-4-chloroacétophénone avec le groupe acétyl tourné autour de la liaison carbone-cycle par $\varphi = 30°$. Cette conformation de la molécule diminue l'intégrale d'échange ($\beta = \beta_{c-c} \cdot \cos \varphi$). Les intégrales de répulsion biélectroniques bicentriques ont été evaluées en utilisant l'approximation de Nishimoto—Mataga.[11] Les valeurs μ_σ ont été évaluées à partir des densités de charge σ-électroniques obtenues par la méthode de Del Re[12] ou par l'addition vectorielle des moments de liaison. Les paramètres utilisés dans la méthode de Del Re sont ceux recommandés par Del Re[15] et Berthold.[13,14]

Les moments de liaison σ sont ceux habituels[15] à l'exception de ceux pour les liaisons N—H et C—Cl pour lesquels on a considéré les valeurs 0,38 D et respectivement 2,26 D. Ces valeurs donnent la meilleure concordance entre les moments dipolaires expérimentaux et théoriques pour l'aniline et le chlorobenzène dont les électrons p non partagés participent à la conjugaison. Par conséquent, il ne faut pas les considérer dans le calcul du moment dipolaire de la liaison σ. En même temps on a pris la valeur 1,52 D pour les orbitales hibrides sp^2 de l'atome d'oxygène.[16] Pour l'état excité on a supposé que μ_σ ne sont pas affectés par l'excitation.

RÉSULTATS ET DISCUSSIONS

Dans le tableau 1 sont présentés les nombres d'onde pour les maximums d'absorption ($\tilde{\nu}_A$) et de fluorescence ($\tilde{\nu}_F$) dans des solvants différents.

A partir de ces données on a déterminé les moments dipolaires dans le premier état excité (μ^*_{exp}) par les méthodes de Varma et Groenen[3] (I), Legder et Suppan[4] (II), qui utilisent seulement les spectres d'absorption et aussi, par les méthodes de Lippert[5,6] (III) et Kawski[7,8] (IV) qui utilisent tant les spectres d'absorption que les spectres de fluorescence. Dans toutes ces méthodes on a utilisé pour le rayon de la cavité d'Onsager la valeur $a_0 = 3{,}6$ Å.

Tableau 1

Les nombres d'ondes correspondant aux maximums d'absorption et de fluorescence

Solvant	$\tilde{\nu}_A$(cm^{-1})	$\tilde{\nu}_F$(cm^{-1})
Benzène	27808	23697
Toluène	27744	23585
Éther éthylique	27632	23474
Tétrachlorure de carbone	28112	24096
Térahdyrofurane	27328	23041
Diméthylformamide	26592	22026

Les résultats obtenus sont présentés dans le tableau 2 à côté de la valeur expérimentale du moment dipolaire dans l'état fondamental et les valeurs théoriques calculées pour les deux états (μ_{calc} et μ^*_{calc}).

Tableau 2

Les moments dipolaires dans les états fondamental et excité S_1

μ_{exp} (D)	μ_{calc} (D)	μ^*_{exp} (D)				μ^*_{calc} (D)	θ (rad)
		I	II	III	IV		
4,45	4,43[a] 5.31[b]	11,73	10,67	6,89	6,82	10.69[a] 11,14[b]	0,12[a] 0,28[b]

[a] μ_σ calculé par la méthode de Del Re.
[b] μ_σ calculé par l'addition vectorielle des moments de liaison.

Dans toutes les méthodes mentionnées on considère que les moments dipolaires dans les états fondamental et excité sont parallèles. Cette approximation est plausible en tenant compte des valeurs des angles entre les moments dipolaires théoriques (θ), valeurs qui sont aussi données dans le tableau 2.

On peut observer que pour l'état fondamental il existe une bonne concordance entre les valeurs expérimentales et celles calculées. Pour le premier état excité les méthodes (III) et (IV) prévoient que la transition de la molécule dans l'état excité doit être accompagnée d'une variation similaire du moment dipolaire d'approximativement 2,4 D qui est bien différente de la variation prévue par les méthodes (I) et (II) (environ 6—7 D). Les méthodes de Lippert et Kawski conduisent, dans le cas de la CDHQ à des valeurs assez basses pour le moment dipolaire dans l'état excité, valeurs qui ne sont pas en accord avec le transfert puissant de charge de l'atome d'azote ($\Delta q_N = -0{,}312$) et non plus avec les valeurs calculées pour cet état.

Les différences élevées entre les valeurs du moment dipolaire obtenues en utilisant les deux groupes de méthodes pourraient être dues au fait que tant la méthode de Lippert que celle de Kawski ne font pas la distinction entre le rayon de la cavité d'Onsager dans l'état fondamental et celui dans l'état excité. L'application de la méthode de Varma et Groenen aux spectres de fluorescence conduit a une équation contenant un terme de dispersion et un rayon de la cavité d'Onsager spécifiques pour l'état excité. [3] La représentation graphique de cette équation en utilisant les données du tableau 1 concernant les spectres de fluorescence donne la possibilité de déterminer le rayon de la cavité dans l'état excité si on prend pour $(\vec{\mu}^* - \vec{\mu})$ et $\vec{\mu}^*$ les valeurs respectives obtenues à partir des spectres d'absorption. On a obtenu ainsi la valeur de ce rayon de la cavité dans l'état excité, $a = 4{,}54$ Å, bien différente de la valeur correspondant à l'état fondamental ($a_0 = 3.6$Å). Ce résultat montre que l'approximation $a \cong a_0$ utilisée dans les méthodes de Lippert et Kawski n'est pas valable dans le cas de la CDHQ.

Dans l'équation obtenue par Lippert [5] pour l'énergie de stabilisation de l'état excité nous avons introduit le rayon a de la cavité d'Onsager pour l'état excité et après on a développée en série de Taylor autour de la valeur a_0 et on a obtenu ainsi l'équation :

$$\Delta\tilde{\nu}_{00} = \frac{2(\vec{\mu}^* - \vec{\mu})}{hca_0^3}\,\Delta F - \frac{2\vec{\mu}^*(\vec{\mu}^* - \vec{\mu})}{hca_0^3}\left[\frac{3\,\Delta a}{a_0} - \frac{6\,\Delta a^2}{a_0^2} + \frac{10\,\Delta a^3}{a_0^3}\dots\right]\Delta F \qquad (1)$$

avec :

$$\Delta F = \frac{\varepsilon - 1}{2\varepsilon + 2} - \frac{n^2 - 1}{2n^2 + 1}\;;\quad \Delta a = a - a_0$$

où : $\Delta\nu_{00}$ représente la différence entre les nombres d'onde correspondant à la transition $0-0$ dans le spectre d'absorption et celui de fluorescence; ε et n sont la constante diélectrique et respectivement l'indice de réfraction du solvant; h — la constante de Planck et c — la vitesse de la lumière dans le vide.

En utilisant les valeurs $a_0 = 3{,}6$ Å et $a = 4{,}54$ Å l'équation (1) devient :

$$\Delta\tilde{\nu}_{00} = \frac{1}{hca_0^3}(\vec{\mu}^* - \vec{\mu})(\vec{\mu}^* - 2\vec{\mu}) \qquad (2)$$

La valeur du moment dipolaire de la CDHQ dans son état excité S_1, déterminée à l'aide de cette équation donne $\mu^* = 10{,}76$ D ce qui est une valeur beaucoup plus proche de celle obtenue par les méthodes qui utilisent seulement les spectres d'absorption. Ce résultat confirme notre supposition en ce qui concerne les différences entre les valeurs du moment dipolaire dans l'état excité obtenues par les deux groupes de méthodes.

Les résultats expérimentaux présentés et les valeurs calculées pour le moment dipolaire de la CDHQ dans son premier état excité, singulet montrent que par l'excitation, le moment dipolaire augmente d'environ 6—7 D et par conséquent le caractère donneur ou accepteur de substituants de la molécule, augmente lui aussi.

BIBLIOGRAPHIE

[1] T. Förster, *Z. Electrochem.*, **54**, 42 (1950) ; *ibid.*, **54**, 531 (1950).

[2] A. Weller dans « Progress in Reaction Kinetics » (G. Porter, Editeur), vol. 1, Pergamon Press London, 1961, p. 187.

[3] C. A. G. O. Varma et E. J. J. Groenen, *Rec. Trav. chim.*, **91**, 296 (1972).

[4] M. B. Ledger et Suppan, *Spectrochim. Acta*, **23A**, 641 (1967).

[5] E. Lippert, *Z. Naturforsch.*, **10A**, 541 (1955).

[6] E. Lippert, *Z. Electrochem.*, **61**, 962 (1957).

[7] A. Kawski, *Acta Phys. Polon.*, **29**, 506 (1966).

[8] L. Janic et A. Kawski, *Bull. Acad. polon. Sci., Ser. Sci. math., astronom., phys.*, **20**, 519 (1972).

[9] E. A. Guggenheim, *Trans. Faraday Soc.*, **45**, 714 (1949).

[10] J. Hintz et H. H. Jaffé, *J. Amer. Chem. Soc.*, **84**, 540 (1962) ; *ibid., J. Phys. Chem.*, **67**, 1501 (1963).

[11] K. Nishimoto et N. Mataga, *Z. phys. Chem. (Frankfurt)*, **13**, 140 (1957).

[12] G. Del Re, *J. Chem. Soc.*, **1958**, 4031.

[13] H. Berthod et A. Pullman, *J. Chim. phys.*, **62**, 942 (1965).

[14] H. Berthod, G. G. Prettre et A. Pullman, *Theor. Chim. Acta*, **8**, 212 (1967).

[15] C. P. Smyth, « Dielectric Behavior and Structure », McGraw-Hill Book Co., Inc. New York Toronto, London, 1965, p. 239.

[16] R. D. Brown et B. A. W. Coller, *Theor. Chim. Acta*, **7** , 259 (1967).

Revue Roumaine de Chimie, 32, *11–12*, 1161–1170 (1987)

Dedicated to Professor V. E. SAHINI
on his 60th anniversary

RING CONTRACTION AND ADDITIONAL ANNELATION IN THE DIBENZOBULLVALONE SYSTEM

M. BANCIU,[a] MICHAELA STĂNESCU,[b] CRISTINA FLOREA[b], A. T. BALABAN[a] and ECATERINA CIORĂNESCU[a,b]

[a] Laboratory of Organic Chemistry, Polytechnic Institute, TCH, Spl. Independenţei 313, 76206 Bucharest, Romania

[b] Centre of Organic Chemistry — ICECHIM, Spl. Independenţei 202B, 78100 Bucharest, Romania

Received May 30, 1987

The dibenzobullvalone 1 was converted successively into its formyl derivative 5 (which is completely tautomerized to the hydroxymethylene ketone 5b) then into the corresponding diazoketone 4. UV-irradiation of 4 afforded dibenzobarbarallane-9-carboxylic acid (6) or its methyl ester 7 as products of ring contraction. On the other hand reaction of the same hydroxymethylene derivative 5b with acetophenone in the presence of perchloric acid leads to the pyrylium salt 11, further converted into the pyridine 13 by reaction with ammonia. Compounds 11 and 13 are the first bullvalenes annelated with three aromatic rings.

INTRODUCTION

In connection with our interest in the syntheses and interconversions of dibenzo$(CH)_{10}$-hydrocarbons[1] we have obtained[1a,c] dibenzobullvalone **1** through intramolecular ring closure of diazoketone **2**. The ketone **1** was the

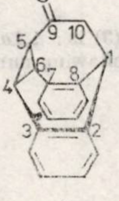

1

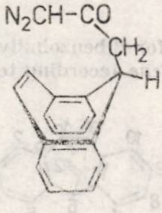

2

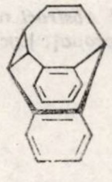

3

key-intermediate in the synthesis of dibenzobullvalene **3***, either through the corresponding alcohol [1a,c] or *via* Bamford-Stevens reaction.

In this paper we describe two other conversions of dibenzobullvalone system namely : a) photochemical ring contraction of diazoketone **4** (related to **1**) to dibenzobarbarallane derivatives and b) additional annelation of **1** by a new aromatic ring of pyrylium- or pyridinium-type.

RESULTS AND DISCUSSION

PHOTOCHEMICAL RING CONTRACTION OF DIAZOKETONE 4

The diazoketone **4** was prepared from ketone **1** *via* its formyl derivative **5**.

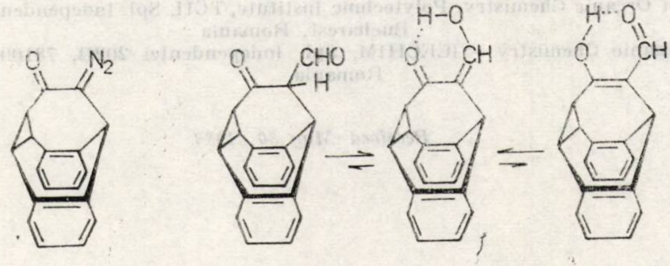

4 5a 5b 5c

Treatment of ketone **1** with ethyl formate and sodium methoxide afforded the formyl derivative **5** as a solid with m.p. 218–220° ; elemental analysis corresponds to formula $C_{19}H_{14}O_2$. Analysis of its ^1H–NMR and IR spectra proved that the equilibrium **5a** $\rightleftarrows$ **5b** $\rightleftarrows$ **5c** is totally shifted towards **5b**, in agreement with literature data [2] showing the complete enolization of other α-formylketones. Thus the ^1H–NMR signal of the O–H proton appears at $\delta = 15$ ppm (in $CDCl_3$) indicating a strong chelatization by hydrogen bonds (as in tautomer **5b**) ; the signal of the vinylic = CH–O proton appears at 8–8.25 ppm. No aldehydic proton signal is visible in the spectrum of **5**. In the IR spectrum of **5** a strong absorption at 1622 cm^{-1} and a medium one at 1601 cm^{-1} could be attributed to $\nu_{C=O}$ and $\nu_{C=C}$ vibrations respectively in a C=C–C=O conjugated system whereas a broad absorption between 2750 and 3600 cm^{-1} suggests a ν_{OH}^{assoc} frequency. No aldehydic absorption between 2700–2750 cm^{-1} is visible in the spectrum of **5**. Thus, all the above data are in agreement with the structure **5b**.

---

* The *Chemical Abstract* name for dibenzobullvalene (3) is : 1,1*a*,6,10*b*-*Tetrahydro*-1,6-*ethenodibenzo*[a,e]*cyclopropa*[c]*cycloheptene* according to the following numbering of the fundamental system :

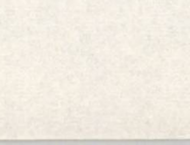

Conversion of hydroxymethyleneketone **5b** into the diazoketone **4** was performed — using the procedure of Rosenberger *et al.* [3] — by treatment with *p*-toluenesulfonylazide and triethylamine. The diazoketone **4**, a yellow solid with m.p. 202—205°, presents in its IR spectrum strong absorptions at 1605 cm^{-1} ($\nu_{C=O}$) and 2094 cm^{-1} (ν_{N_2}). The ^1H-NMR spectrum (see Experimental) is also in agreement with the proposed structure **4**.

Irradiation of the diazoketone **4** using a medium-pressure Hg—UV lamp, in dioxane — water solution, afforded as reaction product the acid **6** whereas irradiation in methanol solution gave rise to the corresponding ester **7**. The "dibenzobarbarallanic" structures **6** and **7** for the above reaction products were inferred from spectral data as well as by comparison of their ^1H-NMR spectra with those of the known related compounds **8**,[4] **9**,[5] and **10**. (Table 1).

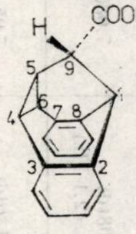

6

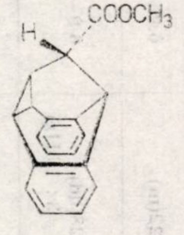

7

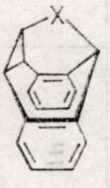

8 $X = CH_2$

9 $X = CO$

10 $X = CHBr$

The δ-values of **6** and **7** are in agreement with the proposed structures. The strong deshielding of the H^9 proton and the smaller one for H^1 in **6** and **7** in comparison with **8** is due to the electron-withdrawing effect of the COOR group ($R=H$, CH_3). The signals for cyclopropanic protons appear in the same domain as in ketone **9** or in bromide **10**. Moreover, the triplet pattern of the signal for H^9 in **7** (less visible for **6**) is the same as in **8**. The signal of H^1 in **7** is a double doublet due to its couplings with H^9 and H^5 and its coupling constants are similar to those observed for **10** (see Table 1).

It should be added that treatment of the acid **6** with ethereal diazomethane afforded the ester **7**, identical with that obtained by irradiation of **4** in methanol.

The formation of ring-contracted compounds in the photochemical Wolff rearrangement [6] of diazoketones was the subject of interesting recent mechanistic studies.[7] Conformational studies[7a–c] postulated a *concerted* rearrangement for *s*—Z conformation of diazoketones and a non-concerted one for *s*-E conformations. However, a convincing proof for *stepwise* Wolff rearrangement of cyclic diazoketones (*s*-Z) was brought by Chapman *et al.* [7d] in 1985 by spectrochemical characterization of intermediate α-ketocarbenes formed on photochemical extrusion of nitrogen from matrix-isolated *s*-Z diazoketones (e.g. 2-diazo-1(2H)-acenaphthylenone). Subsequent irradiation of α-ketocarbenes results in ring contraction to strained cyclic ketenes.[7d]

Table 1

^{1}H-NMR data for dibenzobarbarallane derivatives **6**–**10**$^{(a)}$

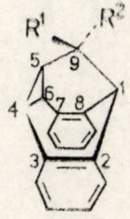

6 – 10

Compound \ Proton	$H^{4,5,6}$	H^9	H^1	Harom	Other signals	Ref.
6 ($R^1 = H$; $R^2 = COOH$)$^{(b)}$	2.5–2.75(m)	2.82(m)	4.22(m)	6.9–7.3(m)	8.18(COOH)	This work
7 ($R^1 = H$; $R^2 = COOCH_3$)$^{(b)}$	2.5–2.75(m)	2.85(t)	4.28(dd) (J=3 ; 1.5Hz)	6.9–7.5(m)	3.48s(CH_3)	This work
8 ($R^1 = R^2 = H$)$^{(b)}$	1.9–2.7(m)	1.70(t ;2H)	3.77(sextet)	7.02(s)	–	4
9 (R^1, $R^2 = 0<\ )$)$^{(c)}$	2.50(m ; 1H) 3.02(d ;2H)	–	4.08(d) (J=2.1 Hz)	7.08(m)	–	5
10 ($R^1 = H$; $R^2 = Br$)$^{(b)}$	2.56–2.9(m)	4.64(dd) (J=3.5 ; 3 Hz)	4.13(dd) J=3.5 ;1.5Hz	7.05–7.35(m)	–	9b

(a) The *Chemical Abstracts* name for dibenzobarbarallane (**8**) is ; 1, 1a,6,10b-Tetrahydro-1,6-methano[a,*e*] cyclopropa[*c*]cycloheptene, in accord with the principle of numbering noted above for dibenzobullyalene (**3**) ;

(b) in $CDCl_3$; (c) in CCl_4.

In agreement with these results, the formation of **6** and **7** from the cyclic *s*-Z diazoketone **4** could be explained by scheme 1.

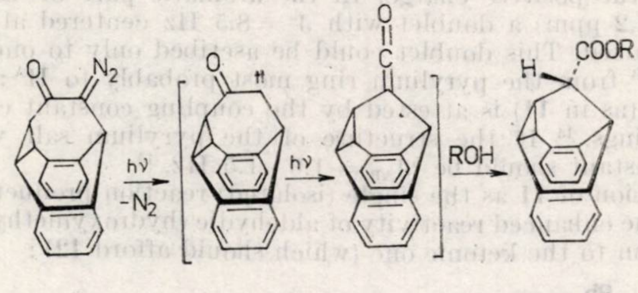

4(*s*-*Z*)

Scheme 1

6(R=H)

7(R=CH_3)

The symmetrical intermediate ketene could be attacked by solvent molecules from either side affording a unique product (**6** in dioxane : water or **7** in methanol).

A similar reactivity of other related dibenzoannelated diazoketones was recently observed in our laboratory. [2,8]

Preparation of functionalized dibenzobarbarallanes (**6** and **7** could present some interest in connection with the sparingly investigated chemistry of this system. [4,5,9]

ADDITIONAL ANNELATION OF THE DIBENZOBULLVALONE SYSTEM: SYNTHESIS OF PYRYLIUM SALT 11 AND PYRIDINE 13

The hydroxymethylene ketone **5b** may be used as an intermediate for the synthesis of pyrylium salts e.g. **11**, **12**, keeping in mind the general reaction [10,11] between methyl(ene)ketones and 1,3-diketones respectively β-ketoaldehydes, affording pyrylium salts. [12] This reaction was recently applied in our laboratory [13] in the preparation of pyrylium salts with oxonia-homotriptycene skeleton.

Reaction of hydroxymethylene ketone **5b** with purified acetophenone in the presence of perchloric acid (1.5 hrs at 105–110°) afforded — after usual work-up — a brownish-grey precipitate in 14% yield. The IR spectrum proves the formation of a perchlorate by characteristic absorptions of ClO_4^- ion at 625 cm^{-1} and 1100 cm^{-1}. The ^1H–NMR spectrum (in F_3C–COOH) is in agreement with structure **11**.

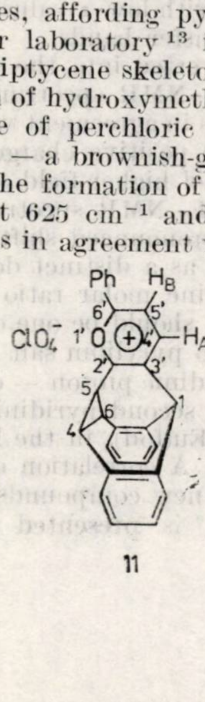

11

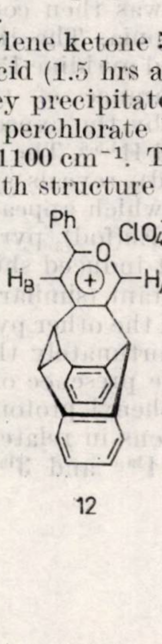

12

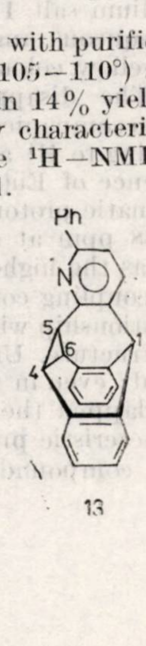

13

The low-field position of H^1 signal ($\delta = 4.96$ ppm) as well as of cyclopropanic protons $H^{4,5,6}$($\delta = 3.76$ ppm) could be ascribed to the deshielding induced by the positive charge. In the aromatic part of the spectrum ($\delta = 6.85-8.2$ ppm) a doublet with J = 8.5 Hz centered at 8.1 ppm is easily recognized. This doublet could be ascribed only to one of the two protons $H^{A,B}$ from the pyrylium ring most probably to H^A; their *ortho*-relationship (as in **11**) is attested by the coupling constant characteristic for ^3J couplings.[14] If the structure of the pyrylium salt were **12** the coupling constant should be $^5J_{AB} = 1.0-1.5$ Hz.[14]

Formation of **11** as the single (isolated) reaction product is in agreement with the enhanced reactivity of aldehydic (hydroxymethylenic) group in comparison to the ketonic one (which should afford **12**):

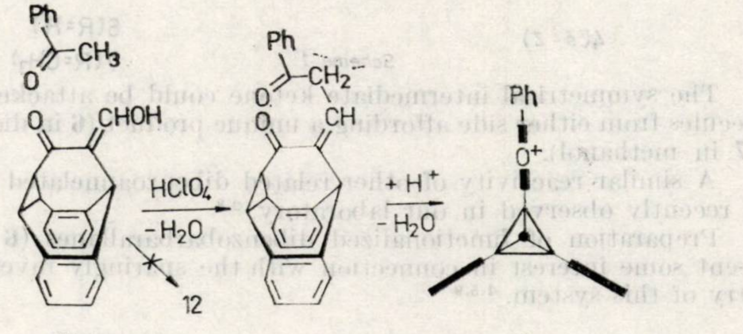

5b **12** **11**

The propeller shape of the molecule **11** suggests the possibility of occurrence of some interactions between π-electrons of the benzenic ring(s) with the positive pyrylium charge (of the type described by Murata et al.[15] and by us[13] for triptycene and homotriptycene derivatives). Indeed, in the electronic spectrum of **11** absorptions with low ε values from 492 and 526 nm may be considered as charge transfer bands.

The pyrylium salt **11** was then converted into the pyridine **13** by reaction with aqueous ammonia. The ^1H-NMR spectrum (see Experimental) of the yellow coloured pyridine **13** is in agreement with the proposed structure. The disappearance of the positive charge in conversion of **11** to **13** is accompanied by the expected higher field shift of the signals corresponding to H^1 and $H^{4,5,6}$. The ^1H-NMR spectrum of pyridine **13** in the presence of $Eu(fod)_3$ reveals a pronounced shift towards lower field of an aromatic proton which appears as a distinct doublet (J = 8.5 Hz) at $\delta = 8.38$ ppm at a $Eu(fod)_3$/pyridine molar ratio of 0.226. This proton which has the highest induced shift should be one of the pyridinic protons whose coupling constant (similar to pyrylium salt **11**) is evidence for an *ortho*-relationship with the other pyridinic proton — confirming thus the proposed structure. Unfortunately the second pyridinic proton could not be observed; even in the presence of $Eu(fod)_3$ in the highest concentration, it overlapped the phenyl protons. A correlation of the chemical shifts for characteristic protons in related new compounds **5b**, **4**, **11**, and **13** and known compounds **1**[1a,c] and **3**[1a,c,e] is presented graphically in fig. 1.

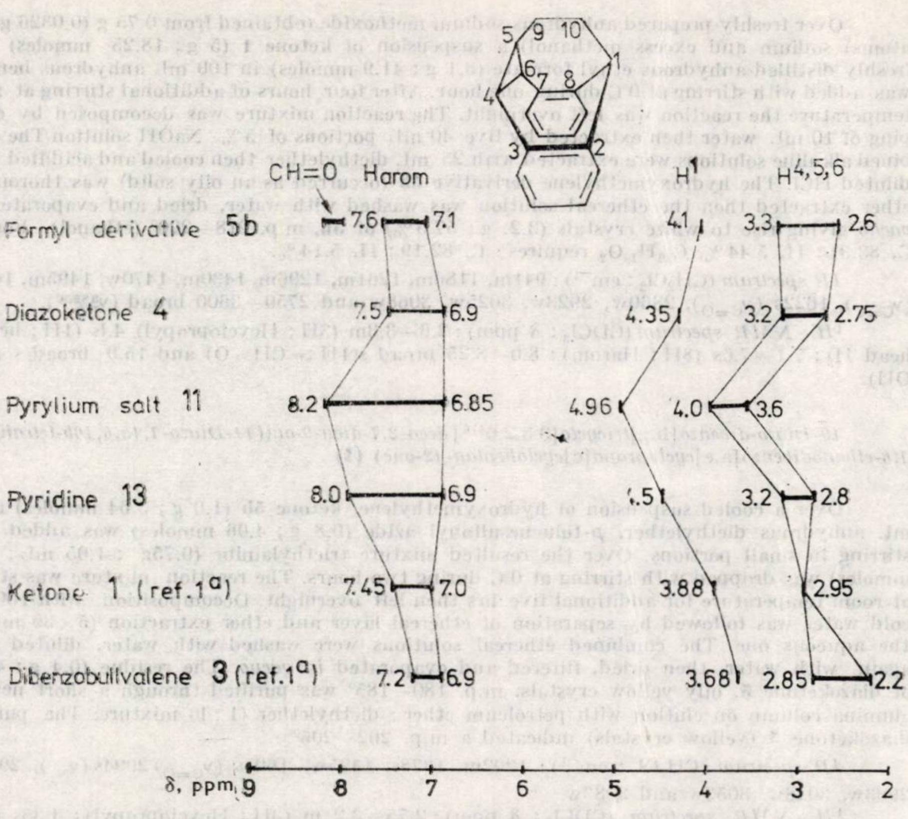

Fig. 1. — Correlation of ^{1}H-NMR spectra of compounds **1**, **3**, **4**, **5**, **11** and **13**

The pyrylium salt **11** and the pyridine **13** are the first bullvalenes annelated with three aromatic rings.

In conclusion this work has proved: a) the possibility of photochemical ring contraction of derivatives with dibenzobullvalone skeleton to functional derivatives of the sparingly investigated dibenzobarbarallane system and b) the facile additional annelation of dibenzobullvalone derivative **5** affording the first bullvalenes annelated with three aromatic rings (two benzenoid and one heterocyclic).

EXPERIMENTAL

Melting points are uncorrected. IR spectra were recorded with a double beam UR-20 Carl Zeiss Jena spectrophotometer, UV spectra with a SPECORD UV-VIS Carl Zeiss Jena double beam spectrometer and ^{1}H-NMR spectra with a VARIAN A-60A apparatus with TMS as internal standard.

Dibenzo[b,g]*tricyclo*[3.3.2.0^{4,6}]*deca-2,7-dien-9-one* (*1,1a,6,10b-Tetrahydro-1,6-ethanodibenzo*[a,c]*cyclopropa*[c]*cyclohepten-12-one*) (*"dibenzobullvalone"*) (**1**)

The ketone **1** was obtained as previously described from the 5H-dibenzo[*a,d*]cycloheptene-5-acetic acid *via* its acid chloride and diazoketone **2**.

10-Hydroxymethylene-dibenzo[b,g]*tricyclo*[3.3.2.0^{4,6}]*deca-2,7-dien-9-one* (*11-Hydroxymethylene-1,1a,6,10b-tetrahydro-1,6-ethanodibenzo*[a,c]*cyclopropa*[c]*cyclohepten-12-one*) (**5b**)

Over freshly-prepared anhydrous sodium methoxide (obtained from 0.75 g (0.0326 gram-atoms) sodium and excess methanol) a suspension of ketone **1** (5 g ; 18.25 mmoles) and freshly distilled anhydrous ethyl formate (3.1 g ; 41.9 mmoles) in 100 mL anhydrous benzene was added with stirring at 0°C during one hour. After four hours of additional stirring at room temperature the reaction was left overnight. The reaction mixture was decomposed by dropping of 10 mL water then extracted by five 40 mL portions of 5 % NaOH solution.The combined alkaline solutions were extracted with 25 mL diethylether then cooled and acidified with diluted HCl. The hydroxymethylene derivative **5b** (occurred as an oily solid) was thoroughly ether extracted then the ethereal solution was washed with water, dried and evaporated *in vacuo* giving rise to white crystals (3.2. g ; 57.5 %) of **5b**, m.p. 218—220° (ethanol). Found : C, 83.31 ; H, 5.44 %. $C_{19}H_{14}O_2$ requires : C, 82.19 ; H, 5.14 %.

IR spectrum (CH_2Cl_2 ; cm^{-1}) : 941m, 1186m, 1261m, 1296m, 1430m, 1470w, 1495m, 1601s-($\nu_{C=C}$), 1622s ($\nu_{C=O}$). 2860w, 2923w, 3025w, 3068w and 2750—3600 broad (ν_{HO}^{assoc}).

^{1}*H—NMR spectrum* ($CDCl_3$; δ ppm) : 2.6—3.3m (3H ; Hcyclopropyl) 4.ls (1H ; bridgehead H) ; 7.1—7.6s (8H ; Harom) ; 8.0—8.25 broad s(1H ;=CH—O) and 15.0 broad s (1H ; OH).

10-Diazo-dibenzo[b,g]*tricyclo*[3.3.2.$0^{4,6}$] *deca-2,7-dien-9-on*((*11-Diazo-1,1a,6,10b-tetrahydro-1,6-ethanodibenzo*[a,e]*cyclopropa*[c]*cycloheptan-12-one*) **(4)**

Over a cooled suspension of hydroxymethylene ketone **5b** (1.0 g ; 3.64 mmoles) in 35 mL anhydrous diethylether, *p*-toluenesulfonyl azide (0.8 g ; 4.06 mmoles) was added with stirring in small portions. Over the resulted mixture triethylamine (0.75g ; 1.05 mL ; 5.56 mmoles) was dropped with stirring at 0°C during two hours. The reaction mixture was stirred at room temperature for additional five hrs then left overnight. Decomposition with 100 mL cold water was followed by separation of ethereal layer and ether extraction (5 × 30 mL) of the aqueous one. The combined ethereal solutions were washed with water, diluted HCl, again with water, then dried, filtered and evaporated *in vacuo*. The residue (0.4 g ; 40 %) of diazoketone **5**, oily yellow crystals, m.p. 180—185° was purified through a short neutral alumina column on elution with petroleum ether : diethylether (1 : 1) mixture. The purified diazoketone **5** (yellow crystals) indicated a m.p. 202—205°.

IR spectrum (CH_2Cl_2 ; cm^{-1}) : 1202m, 1378s, 1495w, 1605s ($\nu_{C=O}$) 2094s (ν_{N_2}), 2925w, 2963w, 3028w, 3053w and 3083w.

^{1}*H—NMR spectrum* ($CDCl_3$; δ ppm) : 2.75—3.2 m (3H ; Hcyclopropyl) ; 4.35s (1H ; bridgehead) ; 6.9—7.5m (8H ; Harom).

Dibenzo[b, g]*tricyclo*[3.3.1.$0^{4,6}$]*nona-2,7-dien-9-carboxylic acid* (*1,1a,6,10b-Tetrahydro-1,6-methano-dibenzo*[a, e]*cyclopropa*[c]*cyclohepten-11-carboxylic acid*) (*dibenzobarbarallane-9-carboxylic acid*) (**6**) *and its methyl ester* **7**

A solution of diazoketone **4** (0.3 g, 1.1 mmoles) in 100 mL dioxane : water (5 : 1) mixture was irradiated in a quartz vessel with a medium pressure Hg UV-lamp (150 watt) through-a Pyrex filter for 18 hrs. After this time the evolution of nitrogen failed. The solution was filtered from small quantities of unsoluble material, then evaporated *in vacuo*. The oily residue dissolved in 30 mL diethylether was treated with 10 % NaOH solution (30mL) and stirred for 0.5 hr. The aqueous layer was separated and evaporated *in vacuo* affording a pale yellow solid (0.15 g ; 52 %) with m.p. 205—208°. After recrystallization from ethanol the acid **6** indicated a m.p. of 211—213°.

IR spectrum (KBr, cm^{-1}) : 712m, 738m, 755s, 798m, 943m, 1245m, 1318m, 1420m, 1460m, 1488m, 1698s ($\nu_{C=O}$), 2850w,2920w, 3020w, 3060w, and 2400—3300 large (ν_{OH}^{assoc}).

^{1}*H—NMR spectrum* (see Table 1).

When the UV irradiation of the diazoketone **4** was performed in methanol solution for 36 hrs the reaction product was the methyl ester **7** obtained in crude form as a yellow oil (62 % yield). Purification through a short neutral alumina column afforded (on elution with chloroform) the ester **7** as a white solid with m.p. 104—105°.

IR spectrum (CS_2 ; CCl_4 ; cm^{-1}) : 713m, 732m, 750s, 785w, 793w, 1020m, 1085m, 1190m, 1210s (ν_{C-O}) ; 1230m, 1435m, 1470m,1495m, 1735s ($\nu_{C=O}$), 2950m, 3020m and 3070w.

UV spectrum (methanol ; λ_{max}^{nm} ; ε_{max}) ; 217.5 (25500) ; 271 (1100) and 278.5 (925).

^{1}*H-NMR spectrum* (see Table 1).

The same methyl ester **7**, m.p. 102—104°, was obtained on treatment of the acid **6** with an excess of ethereal diazomethane solution at room temperature. The IR and ^{1}H-NMR spectra of ester **7** obtained by both methods were identical.

6′-Phenyl-oxoniabenzo[j]*dibenzo*[b,g]*tricyclo*[3.3.2.$0^{4,6}$]*deca-2,7,9-triene perchlorate* (*13-Phenyl. 1,1a,6,10b-tetrahydro-oxoniabenzo*[h]*dibenzo*[a,e]*cyclopropa*[c]*cycloheptene perchlorate* **(11)**

A mixture of hydroxymethylene ketone **5b** (0.5 g ; 1.82 mmoles), freshly distilled acetophenone (0.45 g ; 3.75 mmoles), 70 % perchloric acid (0.5 mL ; 0.835 g ; 5.63 mmoles) and 5 mL anhydrous acetic acid was heated on an oil bath at 105—110° for 1.5 hrs. The dark solution was cooled and poured over 100 mL anhydrous diethylether. The brownish-gray precipitate formed was filtered and washed with diethylether affording the pyrylium salt **11**, m.p. 232° (dec.) (0.120g ; 14.5 %).

IR spectrum (KBr ; cm^{-1}) ; 625m(ClO_4^-), 750m ; 1100s (ClO_4^-) ; 1450m, 1478s, 1495m.

UV spectrum (CH_2Cl_2 ; λ_{max}^{nm} ; ε_{max}) ; 239 (18500) ; 259 (17500) 400 (8900) ; 492.5 (3100), and 526.5 (1500).

^{1}*H-NMR spectrum* (see text)

6-Phenyl-pyridino[j]*dibenzo*[b,g]*tricyclo*[3.3.2.$0^{4,6}$]*deca-2,7,9-triene* (*13-Phenyl-1, 1a, 6, 10b-tetrahydro-pyridino*[h]*dibenzo*[a,e]*cyclopropa*[c]*cycloheptene*) **(13)**

The pyrylium salt **11** (0.1 g ; 0.218 mmoles) was treated with 10 mL methanol, then with 5 mL conc. solution of ammonia and heated at 50° for 2—3 minutes. The reaction mixture becomes orange coloured and was filtered from small quantities of unsoluble material. The filtrate was diluted with 5 mL water then ether-extracted, the ethereal layer was washed, dried and evaporated affording a thick orange oil 0.050 g ; 64 %. This oil was dissolved in 2 mL $CHCl_3$ and chromatographed through a short neutral alumina column. On elution with $CHCl_3$ yellow crystals of pyridine **13** with m.p. 155° were obtained.

IR spectrum ($CHCl_3$; cm^{-1}) ; 905w, 1465s, 1495w, 2865w, 2930m, 3020m and 3070m.

^{1}*H-NMR spectrum* ($CDCl_3$; δ ppm) ; 2.8—3.2 (3H ; Hcyclopropyl) ; 4.5 s (1H ; 6.9—8.0 (8H ; Harom).

ACKNOWLEDGEMENTS. The authors express their thanks to Eng. Ana Schiketanz, Drs. F. Chiraleu and C. Drăghici for performing the ^{1}H-NMR spectra and to Dr. Mihai Elian for helpful discussions.

REFERENCES

[1] a) M. Banciu, M. Elian, E. Ciorănescu and C. D. Nenitzescu, *Tetrahedron Letters*, **1972**, 2573 ; b) M. Banciu, M. Elian, C. Drăghici and E. Ciorănescu, *Rev. Roumaine Chim.*, **19**, 1179 (1974) ; c) M. Elian, M. Banciu, L. Stănescu and E. Ciorănescu, *Rev. Roumaine Chim.*, **21**, 89 (1976) ; d) M. Banciu, M. Elian, Phan Le Thuy, C. Drăghici and E. Ciorănescu *Rev. Roumaine Chim.*, **27**, 19 (1982) ; e) R. Vlad and M. Banciu, *Rev. Roumaine Chim.*, **30**, 1001 (1985) ; f) M. Banciu, D. Elian, M. Elian, L. Stănescu and E. Ciorănescu, *Rev., Roumaine Chim.*, **31**, 503 (1986) ; g) A. T. Balaban, M. Banciu and V. Ciorba, "Annulenes, Benzo-, Hetero-, Homo-Derivatives and Their Valence Isomers", CRC Press, Boca Raton Fl., 1987.

[2] a) K. v. Auvers and H. Jacobsen, *Liebigs Annal. Chem.*, **426**, 161, 182, 224 (1922) ; b) M. Banciu, M. Elian, A. Banciu, C. Drăghici and E. Ciorănescu, *Rev. Roumaine Chim.*, **31**, 1019 (1986).

[3] M. Rosenberger, P. Yates, J. B. Hendrickson and W. Wolf, *Tetrahedron Letters*, **1964**, 2285.

[4] E. Ciorănescu, M. Banciu, R. Jelescu, M. Rentzea, M. Elian and C. D. Nenitzescu, *Rev. Roumaine Chim.*, **14**, 911 (1969).

[5] V. Ioan, M. Popovici and C. D. Nenitzescu, *Tetrahedron Letters*, **1965**, 3383.

[6] a) W. Kirmse, „Carbene Chemistry", Academic Press, New York, 1964, p. 120 ; b) H. Maier and K. P. Zeller, *Angew. Chem.*, **87**, 52 (1975).

[7] a) H. Tomiola, H. Okuno and Y. Izawa, *J. Org. Chem.*, **45**, 5278 (1980) ; b) F. Kaplan and M. L. Mitchell, *Tetrahedron Letters*, **1979**, 759 ; c) H. Tomioka, M. Kondo and Y. Izawa, *J. Org. Chem.*, **46**, 1090 (1981) ; d) R. J. McMahon, O. L. Chapman, R. A. Hayes, T.C. Hess and H.- P. Krimmer, *J. Amer. Chem. Soc.*, **107**, 7597 (1985).

[8] M. Banciu, *Rev. Roumaine Chim.*, **27**, 769 (1982).

[9] a) S. J. Cristol, R. M. Sequeira and G. O. Mayo, *J. Amer. Chem. Soc.*, **90**, 5564 (1968) ; b) S. J. Cristol, D. P., Stull, and R. D. Daussin, *J. Amer. Chem. Soc.*, **100**, 6674 (1978) ; c) S. J. Cristol, M. W. Klein, M. H. Henderoerk and R. D. Daussin, *J. Org. Chem.*, **46**, 4992 (1981).

[10] W. Dilthey and J. Fischer, *Ber. dtsch. chem. Ges.*, **57**, 1653 (1924).

[11] G. N. Dorofeenko and G. I. Junghietu, *Zhur. obschei Khim.*, **35**, 589 (1965).

[12] A. T. Balaban, A. Dinculescu, G. N. Dorofeenko, G. W. Fischer, A. V. Koblik, V. V. Mezheritskii and W. Schroth, "Pyrylium Salts, Syntheses, Reactions and Physical Properties", *Adv. Heterocyclic Chem.*, Suppl. 2, 1982, Academic Press, New York, 1982.

[13] M. Banciu, A. T. Balaban, C. Drăghici and R. Vlad, *Rev. Roumaine Chim.*, **27**, 1037 (1982).

[14] P. Sándor and L. Radics, *Org. Magn. Reson.*, **14**, 98 (1980).

[15] a) A. Tajiri, M. Hatano, T. Nazakawa and I. Murata, *Chem. Phys. Lett.*, **76**, 490 (1980) ; b) T. Nakazawa, N. Abe, K. Kubo and I. Murata, *Tetrahedron Letters*, **1979**, 4995 ; c) T. Nakazawa and I. Murata, *J. Amer. Chem. Soc.*, **99**, 1996 (1977).

Revue Roumaine de Chimie, 32, *11–12*, 1171–1174 (1987)

Dedicated to Professor V. E. SAHINI
on his 60th anniversary

1,3-Di-t-BUTYLCYCLOBUTANE DERIVATIVES[1]

NICOLETA ŞTEFAN, ILIE G. DINULESCU and MARGARETA AVRAM *
Center of Organic Chemistry, Spl. Independenţei 202 B, 78100 Bucharest 12, Romania

Received May 6, 1987

The synthesis of 2,4-di-t-butylcyclobutane-1,3-dione (**1**) and of 1,3-dihydroxy-2,4,di-t-butylcylobutane (**2**), starting from 2,4-diisopropylidenecyclobutanone (**3**), is described.

In the course of our investigations in the cyclobutane field, it seemed interesting to study the synthesis and the properties of the diketone **1** and of the dihydroxy-derivative **2**. The results of this investigation are given in the present paper.

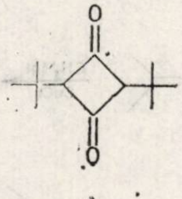
1

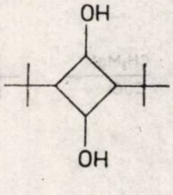
2

For the synthesis of these compounds, 2,4-diisopropylidene-cyclobutanone (**3**)[2] was used as starting material.

The diisopropylidene-derivative 3, by reaction with N-bromosuccinimide, undergoes bromination in the bis-allylic position, affording 3-bromo-2,4-diisopropylidenecyclobutanone (4), m.p. 52°. The assigned structure was supported by IR and ^{1}H-NMR spectra. The IR spectrum shows the characteristic absorption bands for an α,β-unsaturated ketone ($\nu_{C=O}$ 1745 and $\nu_{C=C}$ 1675 cm^{-1}). In the ^{1}H-NMR spectrum, the signal of H-3 appears at a low field (δ 5.30 ppm) due to the deshielding induced by the bromine atom. In the bromide 4, the bis-allylic bromine atom has a high reactivity. Thus, heated in methanolic solution, 4 undergoes solvolysis, yielding the methoxy-derivative 5. Similarly, 4 is hydrolysed in acetone-water solution affording the hydroxy-derivative 6, m.p. 143°. The IR

---

* Deceased October 28, 1983.

spectrum of **6** shows strong absorption bands for $\nu_{C=O}$ at 1748 cm^{-1}, $\nu_{C=C}$ at 1680 cm^{-1} and ν_{O-H} at 3615 cm^{-1}. In the ^{1}H-NMR spectrum, the signal of H-3 appears at δ 5.13 ppm and the signals of the methyls from the isopropylidene groups appear at δ 2.15 and 1.95 ppm.

The oxidation of the hydroxy-ketone **6** to the diketone **9** failed; the various experiments carried out using different oxidation reagents, led only to undefined products.

By treating the α,β-unsaturated ketone **6**, in the presence of catalytic amounts of cuprous chloride, with an excess of methyl magnesium iodide, in THF solution, **7** was formed. The assigned structure of **7** is supported by spectral data. The IR spectrum presents absorption bands of an α,β-unsaturated ketone ($\nu_{C=O}$ 1748 and $\nu_{C=C}$ 1680 cm^{-1}) and of a hydroxyl group (ν_{O-H} 3610 cm^{-1}). The ^{1}H–NMR spectrum shows characteristic chemical shifts for the isopropylidene group (δ 2.06 and 1.88 ppm) and for t-butyl group (δ 0.98 ppm).

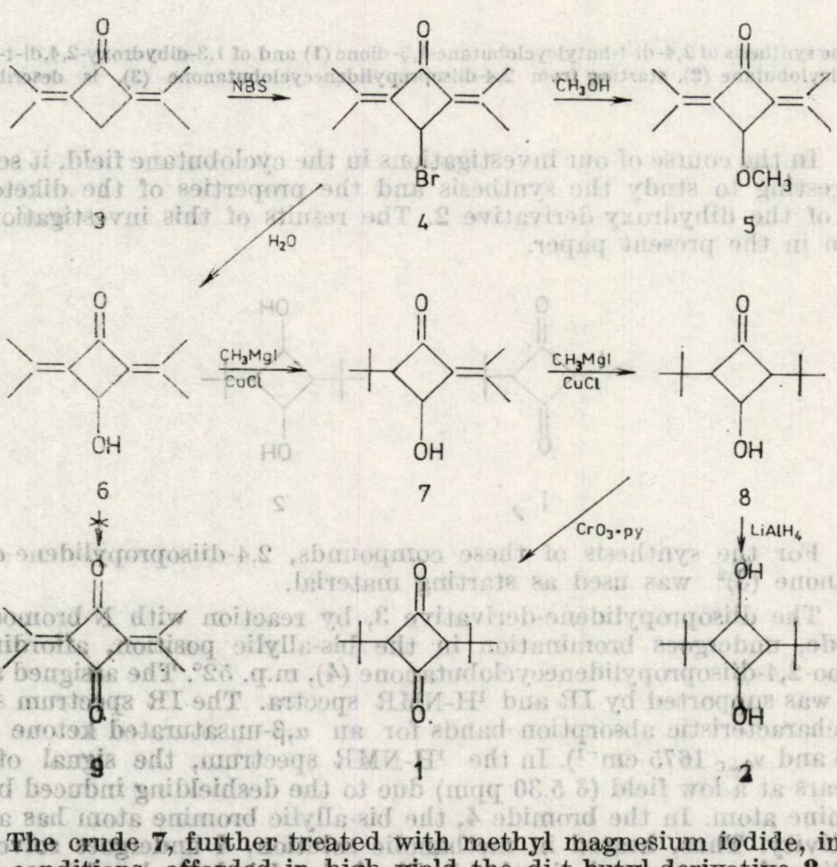

The crude **7**, further treated with methyl magnesium iodide, in the same conditions, afforded in high yield the di-t-butyl-derivative **8**, m.p. 121°. The spectra of this compound are in good accordance with the assigned structure. Thus, the IR spectrum indicates an unconjugated cyclobutanone ($\nu_{C=O}$ 1780 cm^{-1}). The ^{1}H-NMR spectrum exhibits the signal due of the two equivalent t-butyl groups (δ 0.98 ppm), while the signals of the isopropylidene groups are absent.

Oxidation of **8** with Sarrett reagent, in pyridine solution, led to the diketone **1**, m.p. 131°.

Reducing **8** with lithium aluminium hydride, in ethereal solution, the dihydroxy-derivative **2**, m.p. 165°, was obtained. In accordance with the spectral data (no intramolecular hydrogen bonds) and with Dreiding models, a conformation with pseudo-equatorial t-butyl and hydroxyl groups appears as very probable.

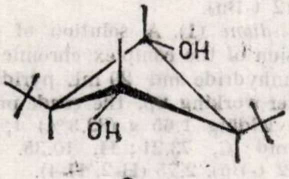

2

The attempts to synthesize the di-t-butylcyclobutadiene or its dichloro-derivative, starting from **2**, respectively **1** (by replacement of oxygenated groups with chlorine, followed by dehydrohalogenation) were unsuccessful.

Other aspects of this problem are under investigation .

EXPERIMENTAL

IR spectra were recorded with a double beam Jena UR-20 spectrophotometer. ^{1}H-NMR spectra were performed with a Varian A 60-A spectrometer.

3-Bromo-2,4-diisopropylidenecyclobutanone (**4**). A mixture of 3.0 g (20 mmoles) **3**, 3.56 g (20 mmoles) N- bromosuccinimide, 20 mg benzoyl peroxide and 50 mL anhydrous carbon tetrachloride, was heated until a strongly exothermal reaction started up and then refluxed for an additional 1/2 hr. After cooling, the succinimide was filtered off, the solvent evaporated *in vacuo* and the residue recrystallized from petroleum ether, yielding 3.0 g (65.0%) **4**, m.p. 52°. — $C_{10}H_{13}BrO$ (229.1) Calcd.: C, 52.42 ; H, 5.72 ; Br, 34.88. Found: C, 52.64 ; H, 5.98 ; Br, 34. 56. — IR (CCl_4, cm^{-1}): $\nu_{C=O}$ 1745, $\nu_{C=C}$ 1675. — ^{1}H-NMR (CCl_4, δ, ppm): 1.88 (2 CH_3), 2.18 (2 CH_3), 5.30 (H-3).

3-Methoxy-2,4-diisopropylidenecyclobutanone (**5**). A solution of 2.3 g (10 mmoles) **4** in 60 mL anhydrous methanol and 2.5 g (30 mmoles) sodium hydrogen carbonate was heated at 50°, under stirring, for 12 hrs. After evaporation of acetone, diethyl ether was added, the ethereal layer washed with water and evaporated, yielding 1.3 g (82.0%) **5**, m.p. 71°. — $C_{11}H_{16}O$ (164.2) Calcd.: C, 80.43 ; H, 9.81. Found: C, 80.36 : H, 10.05. — IR (CCl_4, cm^{-1}): $\nu_{C=O}$ 1750, $\nu_{C=C}$ 1680. — ^{1}H-NMR ($CDCl_3$, δ, ppm): 1.91 (2 CH_3), 2.18 (2 CH_3), 3.21 (OCH_3), 5.16 (H-3).

3-Hydroxy-2,4-diisopropylidenecyclobutanone (**6**). Working as above, but using 100 mL 80 % acetone instead of methanol, 1.4 g (86.0 %) **6**, m.p. 143°, were obtained. — $C_{10}H_{14}O$ (166.2) Calcd.: C, 72.26 ; H, 8.49. Found: C, 72.08 ; H, 8.62. — IR (CCl_4, cm^{-1}): $\nu_{C=O}$1748, $\nu_{C=C}$ 1680, ν_{O-H} 3615. — ^{1}H-NMR ($CDCl_3$, δ, ppm): 1.95 (2CH_3), 2.15 (2 CH_3), 5.13 (H-3).

Reaction of the ketoalcohol **6** *with oxidation reagents*. **6** treated with various oxidation reagents as $CrO_3 \cdot py_2$ in pyridine or in methylene chloride, chromic anhydride in acetic acid, sodium dichromate in water, undergoes advanced destruction, and no definite compound could be isolated.

3-Hydroxy-2,4-di-t-butylcyclobutanone (**8**). Into a solution of methyl magnesium iodide in THF (prepared from 2.4 g (100 mmoles) magnesium and 14.2 g (100 mmoles) methyl iodide in 100 mL THF), containing 30—40 mg anhydrous cuprous chloride, a solution of 4.2 g (25 mmoles) **6** in 25 mL THF was dropped, the temperature being maintained at 0°.

The mixture was further stirred fs 2 for at 0° and for 8 hrs at room temperature. After usual work up, 4.1 g (90.0 %) crude *3-hydroxy-2-t-butyl-4-isopropylidenecyclobutanone* (**7**), were obtained. — IR (CCl_4, cm^{-1}) : $\nu_{C=O}$ 1748, $\nu_{C=C}$ 1680, $\nu_{O=H}$ 3610. — ^1H-NMR (CCl_4, δ, ppm) : 0.98 (t-Bu), 1.88 (CH_3), 2.06 (CH_3), 2.55 (H-2) 4.62 (H-3).

The crude **7**, treated again with methyl magnesium iodide, in the same quantities and in the same conditions as above, afforded 4.0 g **8** (yield 90 % based on **7**, 81 %, based on **6**), m.p. 121° — $C_{12}H_{22}O_2$(198.3)Calcd. : C, 72.68 : H, 11.18. Found : 72.75 ; H, 11.48. — IR(CCl_4, cm^{-1}) ; : $\nu_{C=O}$1780, ν_{O-H}3625. — ^1H-NMR (CCl_4, δ, ppm) : 0,98 (2 t-Bu), 2.73 (H-2, H-4), 4.23 (H-3).

1,3-Dihydroxy-2,4-di-t-butylcyclobutane (**2**). Reduction of **8** with lithium aluminium hydride afforded with 85.0 % yield the dihydroxy-derivative **2**, m.p. 165°. — $C_{12}H_{24}O_2$ (200.3) Calcd. ; C, 71.95 ; H, 1.08. Found : C, 71.70 ; H, 11.97. — IR (CCl_4, cm^{-1}) ; ν_{O-H} 3640. — ^1H-NMR ($CDCl_3$, δ, ppm) ; 0.98 (2 t-Bu).

2,4-Di-t-butylcyclobutane-1,3-dione (**1**). A solution of 2.0 g (10 mmoles) **8** in 20 mL pyridine was added to a suspension of the complex chromic anhydride — pyridine, prepared from 2.0 g (20 mmoles) chromic anhydride and 20 mL pyridine, and the mixture was left at room temperature for 24 hrs. After working up, the crude product was chromatographed on alumina with petroleum ether, yielding 1.65 g (83.3 %) 1, m.p. 131°. — $C_{12}H_{20}O_2$ (196.3) Calcd. : C, 73.42 ; H, 10.27. Found : C, 73.21 ; H, 10.35. — IR (CCl_4, cm^{-1}) : $\nu_{C=O}$1770. — ^1H-NMR ($CDCl_3$, δ, ppm) : 0.98 (2 t-Bu), 2.75 (H-2, H-4).

REFERENCES

[1] Part LXI of the *Investigations in the Cyclobutane Series*. For part LX see : N. Ştefan, P. Filip, F. Chiraleu, I. G. Dinulescu and M. Avram, *Rev. Roumaine Chim.*, **30**, 791 (1985).

[2] J.-H. Conia and J.-P. Sandre, *Bull. Soc. Chim. France*, **1963**, **744**.

Revue Roumaine de Chimie. **32**, *11–12*, 1175–1180 (1987)

Dedicated to Professor V. E. SAHINI
on his 60th anniversary

AMINOKETONE AND OXAZOLE SYNTHESIS. XI[1]

EXTENSION TO THE SYNTHESIS OF THIAZOLES FROM 2-AZA-1,4-DIKETONES OR *via* ELECTROPHILIC SUBSTITUTION OF ARENES WITH 2-THIAZOLIN-5-ONES (THIOAZLACTONES)

IOSIF SCHIKETANZ, ANDREI ȘTEFĂNESCU, MICHAELA-CARMEN BALABAN, ANA SCHIKETANZ, MIRCEA D. GHEORGHIU and ALEXANDRU T. BALABAN
Polytechnic Institute, Organic Chemistry Department, Splaiul Independenței 313,
76206 Bucharest, Romania

Received January 20, 1987

2-Phenyl-5-thiazolone **5** reacts with arenes in the presence of anhydrous $AlCl_3$ affording directly thiazoles **8** without isolation of the intermediate substituted thiobenzoyl-phenacylamines **7**. An independent synthesis of thiobenzoylamine **7a** and its conversion with $AlCl_3$ into 2,5-diphenylthiazole **8a** were carried out for confirming the dehydration under the reaction conditions. ^{1}H-NMR and ^{13}C-NMR data of thiazoles are presented. For converting into thiazoles the 2-aza-1,4-diketones obtained in the previous parts of this series, in addition to the known method using P_4S_{10}, a new method was employed, namely using Lawesson's reagent **14**. Thus were prepared 2,5-diarylthiazoles with *p*-fluorophenyl substituents **20**, as well as a saturated and an unsaturated thiazole, **17** and **18**, respectively; the latter presents a bathochromic shift relatively to the former in its UV spectrum.

SYNTHESIS OF THIAZOLES FROM ARENES AND 2-PHENYLTHIAZOLIN-5-ONES

The importance of thiazoles for biologically active compunds (thiamine, penicillins, antiinflamatory and bactericidal compounds, pesticides, herbicides, fungicides, nematocides), natural flavors (in cereals, meat, tomatoes, tea, roasted coffee, etc.), dyes and thermostable polymers, needs hardly to be stressed. Many reviews are available.[2–7]

By analogy with the acylaminoacylation of arenes with azlactones and $AlCl_3$ leading to acylated α-aminoketones,[8] we investigated the analogous reaction of arenes with 2-thiazolin-5-ones in the presence of anhydrous aluminium chloride. The thio-analogue **5** of an azlactone (2-phenylthiazolin-5-one) is obtained by dehydrating thiobenzoyl-glycine **4** which is prepared[9] (i) by treating benzimido methyl ether hydrochloride **2**[10] with hydrogen sulfide to afford methyl thiobenzoate (O-methyl ester) **3**, which is then reacted with glycine and sodium hydroxide, or (ii) by benzoylating glycine ethyl ester hydrochloride and by converting the resulted ethyl hippurate into the thiono ester with phosphorus pentasulfide followed by alkaline hydrolysis and acidification. [11-12] Alternatively, the ester resulted from ethyl hippurate and P_4S_{10} may be converted directly into **5** by elimination of ethanol. The dehydration of **4** to **5** may be effected either with dicyclohexylcarbodiimide [13] or with ethyl chloroformate and triethylamine; the former alternative gave better results.

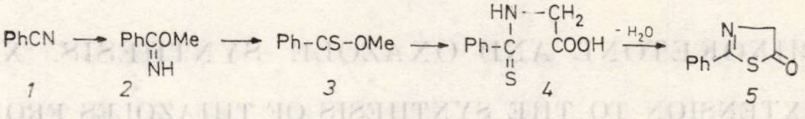
PhCN
PhCOMe
NH
Ph–CS–OMe
HN––CH2
Ph–C
COOH
S
- H2O
N
Ph
S
O
1
2
3
4
5

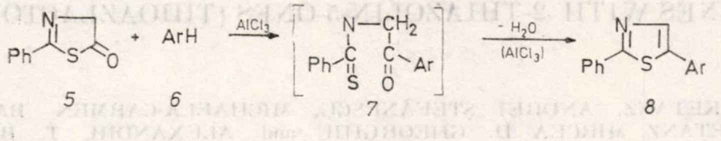
N
Ph
S
O
+ ArH
AlCl3
N–CH2
Ph–C
C–Ar
S
O
- H2O
(AlCl3)
N
Ph
S
Ar
5
6
7
8

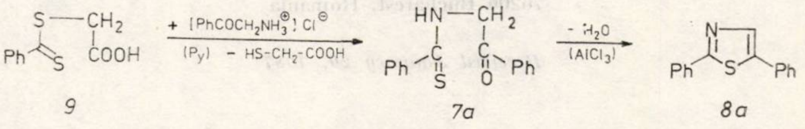
S——CH2
Ph
S
COOH
+ [PhCOCH2NH3⊕] Cl⊖
(Py) - HS-CH2-COOH
HN—CH2
Ph
C
S
C
O
Ph
- H2O
(AlCl3)
N
Ph
S
Ph
9
7a
8a

The reaction of 2-phenylthiazolin-5-one **5** with arenes **6** (benzene, toluene and *ortho*-xylene) in the presence of anhydrous aluminium chloride afforded aryl thiobenzoylaminomethyl ketones **7** which were not isolated because they underwent dehydration, under the reaction conditions, to the corresponding thiazoles **8**.

By an independent synthesis, we prepared N-thiobenzoyl-phenacylamine **7a** from phenacylamine hydrochloride and S-(thiobenzoyl)-thioglycollic acid **9**. [14] Treatment of **7a** with anhydrous aluminium chloride afforded smoothly and in quantitative yield the corresponding 2,5-diphenylthiazole **8a**. The same dehydration was described as being produced by sulfuric acid. [3]

Table 1 presents the structures and melting points of the resulted thiazoles **8** and of their hydrochlorides. Table 2 describes ^1H-NMR data of the same thiazoles. The latter table presents only the singlet peaks;

Table 1

Melting points (°C) of 2-phenyl-5-arylthiazoles **8** and corresponding hydrochlorides

Comp	Ar	M.p. Thiazole		M.p. Hydrochloride	
		Found	Lit.	Found.	Lit.
8a	Ph	105	$103-104^{15}$	148−153	—
8b	p-MeC_6H_4	120	$120-121^{16}$	168−173	$167-173^{16}$
8c	3,4-$Me_2C_6H_3$	95	—	160−165	—

the aryl protons give rise to multiplet splittings in the range δ = 7.0—7.7 ppm (and for the two *ortho*-standing protons of the 2-phenyl group, in the range 7.8—8.2 ppm). The attempt to resolve the accidental degeneracy of the two methyl peaks in **8c** by aromatic solvent induced shift failed: in C_6D_6 all methyl protons appeared together, too.

Table 2

^{1}H-NMR Singlets (δ, ppm) of 2-phenyl-5-arylthiazoles **8** in $CDCl_3$

Compound	Ar	CH_3	4-Thiazole-H
8a	Ph	—	8.00
8b	p-MeC_6H_4	2.33 (3H)	8.00
8c	3,4-$Me_2C_6H_3$	2.23 (6H)	7.90

For the 2-phenyl-5-*p*-tolylthiazole **8b**, the ^{13}C—NMR spectrum with its assignment is presented in the experimental part.

SYNTHESIS OF THIAZOLES FROM ARYL α-ACYLAMINOMETHYL KETONES AND P_4S_{10} OR LAWESSON'S REAGENT

Taking into account that acylaminoacylation of aromatic hydrocarbons ArH with azlactones **11** in the presence of Friedel—Crafts catalysts such as aluminium cloride affords α-acylaminoketones **12** in good yields we also present here the synthesis of thiazoles **4** using some of our α-acylaminoketones.[8]

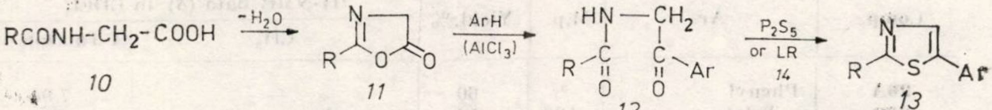

From the reported methods for the conversion of acylaminoketones into thiazoles [3,15] we applied the reaction with phosphorus pentasulfide, obtaining satisfactory yields. We also present a new method for performing the same conversion, namely using Lawesson's reagent (LR) **14** formed by heating in anisole phosphorus pentasulfide or phosphorus and sulfur.[16—18]

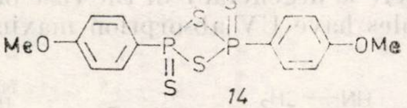

14

The first acylaminoketones for which we applied the above reactions were N-benzoyl-phenacylamine (**12**, R=Ar=Ph) and β,β-diphenylpropionyl-phenacylamine (**16**, or **12** with R = $Ph_2CH—CH_2$, Ar = Ph).

The former was prepared from benzene and hippuric acid azlactone while the latter was obtained via an acylation and alkylation of benzene with the azlactone (**15**) obtained by dehydrating cinnamoylglycine. [1]

When **16** was heated with P_4S_{10} at 180° for 30 minutes followed by decomposition with aqueous potassium hydroxide, 2-(2,2-diphenyl-ethyl)-5-phenylthiazole **17** was obtained in 63% yield.

In order to perform the same reaction we treated **16** with Lawesson's reagent **14** and the saturated thiazole **17** was obtained in comparable yield. Its UV absorption maximum in ethanol is at 284 nm.

Dehydrogenation to the unsaturated thiazole **18** was effected by bromination with N-bromosuccinimide followed by dehydrobromination in refluxing pyridine in analogy with established procedures. The resulted 2-(2,2-diphenylvinyl)-5-phenylthiazole **18** has λ_{max} bathochromically shifted at 362 nm (with another UV absorption band at 276 nm) in ethanol.

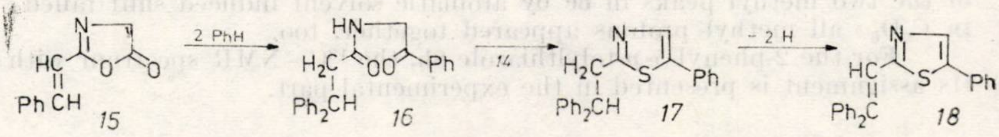

This reaction was applied to a series of N-(*p*-fluorobenzoyl)-phenacylamines **19** substituted in the phenacylamino ring and reported in an earlier part of the present series. [20] The conversion into thiazoles **20** was effected by refluxing in xylene the azadiketone with Lawesson's reagent **14**. Results are presented in table 3.

Table 3

2-*p*-Fluorophenyl-5-arylthiazoles

Comp.	Ar	M.p.	Yield, %	^{1}H-NMR data (δ) in $CDCl_3$	
				CH_3	4-Thiazole-H
20A	Phenyl	[a]	60	—	7.94
20B	p-Tolyl	130	54	2.35 (3H)	7.92
20C	3,4-Xylyl	97	70	2.28 (6H)	7.88
20D	2,4-Xylyl	53	72	2.33(3H), 2.38(3H)	7.70
20E	Mesityl	115	63	2.25(6H), 2.35(3H)	7.00

[a] Lit. m.p. [21] 137°.

As in the case of table 2, data for ^{1}H−NMR singlets are included in table 3; again there is degeneracy in the case of the 3,4-xylyl methyls. All 2,5-diaryl thiazoles have UV absorption maxima at 310−313 nm.

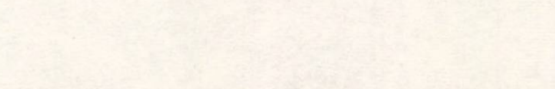

EXPERIMENTAL PART

Thionohippuric acid, Ph—CS—NH—CH$_2$—COOH, was prepared from glycine and methyl thiobenzoate with aqueous sodium hydroxide and ethyl ether at room temperature.[11,12] ^{1}H,NMR spectrum in $(CD_3)_2SO$, δ (ppm); 4.70 (d, 2H, $J = 5$ Hz, CH$_2$); 7.5—7.8 (m, 3H, *m*-,*p*-H); 7.9—8.2 (m, 2H, *o*-H); 10.67 (t, 1H, broad, $J = 5$ Hz, NH); 11.93 (1H, broad, COOH). M.p. 152° (from water, yield 70%).

This preparation started from benzonitrile which on treatment at 0° with methanol and hydrogen chloride afforded in 87% yield benzimido methyl ether hydrochloride, b.p. 106/24 Torr; IR data: 3360 cm^{-1} (NH), 1655 cm^{-1} (C=N) in CCl$_4$; ^{1}H-NMR data (CCl$_4$, δ; ppm): 3.67 (s, 3H, OCH$_3$); 7.67 (s, 1H, NH, vanishes with D$_2$O); 6.9—7.1 (m, 3H, *m*-, *p*-H; 7.2—7.4 (m, 2H, *o*-H). This compound was treated with hydrogen sulfide in ether at 0° to yield methyl thionobenzoate, b.p. 110—113/15 Torr, in 80% yield; ^{1}H-NMR data (CCl$_4$, δ, ppm); 4.13 (s, 3H, OCH$_3$); 7.1—7.4 (m, 3H, *m*-, *p*-H); 7.8—8.2 (m, 2H, *o*-H).

2-Phenylthiazolin-5-one was prepared analogously to other thioazlactones[13] by dehydrating 1.00 g (5 mmol) thionohippuric acid in 30 mL methylene chloride with 1.03 g (5 mmol) dicyclohexylcarbodiimide by stirring for 15 min. at room temperature. After filtering off dicyclohexylurea, the filtrate was evaporated and the residue was purified from petroleum ether yielding quantitatively the phenylthiazolinone, m.p. (dec.) 81°. Lit. m. p. 79—81° ([9]), 84° ([11,16]).

IR (CHCl$_3$) 1736 cm^{-1} (C=O stretch); ^{1}H-NMR, (CDCl$_3$, δ, ppm); 4.83 (s, 2H, CH$_2$); 7.3—7.6 (m, 3H, *m*-, *p*-H); 7.7—7.95 (m, 2H, *o*-H).

Reaction with arenes. To a stirrred solution of 2-phenylthiazolin-5-one (5 mmol) in 40 mL arene, 2 g (15 mmol) freshly sublimed AlCl$_3$ was added portionwise at 0°. The mixture was allowed to reach room temperature with strring for 4 hrs, and then it was left overnight. After decomposition with dilute hydrochloric acid, the organic layer was separated, washed and evaporated under vacuum. The residue was recrystallized from ethanol or 80% ethanol. Results are presented in Tables 1 and 2.

Alternative synthesis of N-thiobenzoyl-phenacylamine. Phenacylamine hydrochloride (1.7 g, 10 mmol) was dissolved in 30 mL dry pyridine, then 2.1 g (10 mmol) of S-(thibenzoyl)-thioglycollic acid[14] were added, and the mixture was heated at 50—60° for 2 hrs. Then the mixture was poured in water, the solid product was filtered off and recrystallized from ethanol. The yield was 32% (0.8 g, m.p. 110°). ^{1}H-NMR (δ, CDCl$_3$, ppm); 5.2 (d, 2H, CH$_2$, $J = 5$ Hz); 7.3—7.5 (m, 6H); 7.7—8.1 (m, 4H), 8.76 (t, 1H, broad, NH). Found; N, 5.50. $C_{15}H_{13}NOS$ requires N, 5.49%.

2,5-Diphenylthiazole. The above product (0.5 g, 2 mmol) was introduced in 20 mL dry benzene, then 0.8 g (6 mmol) anhydrous aluminium chloride was introduced portionwise at 0° with stirring, which was continued for 4 hrs. The next day the mixture was hydrolyzed with dilute hydrochloric acid, the organic layer was separated, washed acid-free, and evaporated leaving quantitatively 2,5-diphenylthiazole, whose properties agreed with those mentioned in the literature.[15]

^{13}C-NMR Spectrum of 2-phenyl-5-p-tolylthiazole in CDCl$_3$ (δ, ppm); 21.19 (CH$_3$); 126.31, 126.53, 128.92 and 129.75 (each for 2C, *o*-*m*-aromatic carbons); 128.55 (1C *ipso*-tolyl); 129.85 (1C, *p*-phenyl); 133.76 (1C, C—CH$_3$); 138.27 (1C, 5-thiazolyl); 138.80 (1C, 4-thiazolyl); 139.44 (1C, *ipso*-phenyl) and 166.52 (1C, 2-thiazolyl).

Preparation of thiazoles using Lawesson's reagent. Five mmol each of 2-aza-1,4-diketone and Lawessons' reagent (prepared according to ref. [19] were refluxed with stirring in 35 mL xylene. The reaction involves simultaneous thionation and dehydrative cyclization to a thiazole. The endpoint of the reaction was determined by TLC using ethyl acetate as eluent. The hot xylene solution was poured on a short alumina-filled column using n-hexane as eluent, then the solvents were evaporated under reduced pressure and the thiazoles were recrystallized from ethanol. Properties are indicated in table 3.

2-(2,2-Diphenylethyl)-5-phenylthiazole, **17**. Phosphorus pentasulfide (1.47 g, 6.6 mmol) was mixed thoroughly, in a mortar with 1.4 g N-(β, β-diphenylpropionyl)-phenacylamine, **16**,[1] then the mixture was heated at 180° till the foaming subsided (about half and hour). The hardened cool material was digested with 5% aqueous potassium hydroxide. The product was filtered off and recrystallized from 50% aqueous ethanol, yield 60%, m.p. 122°. Found N, 3.94; $C_{23}H_{19}NS$ requires N, 4.404%.

^{1}H-NMR Spectrum in CDCl$_3$ (δ, ppm); 3.75 (2H, d, $J = 8$ Hz, **CH$_2$** — CH); 4.60 (1H, t, $J = 8$ Hz, C**H**—CH$_2$); 7.2—7.3 (15 H, m); 7.78 (1H, s, thiazole-H).

Alternative synthesis using Lawesson's reagent. The azadiketone **6** (1.9g, 4 mmol) and 1.6 g Lawesson's reagent (4 mmol) were heated in 100 mL *p*-xylene at reflux temperature, then the mixture was worked as decribed above with chromatography on Al$_2$O$_3$.

2-(2,2-Diphenylvinyl)-5-phenylthiazole, **18**. The above thiazole (0.7 g) was brominated at reflux temperature in 50 mL CCl_4 with the equimolar amount (0.37 g) of N-bromosuccinimide with Bz_2O_2 and then without purifying the intermediate bromoderivative, this was dehydrobrominated as described in the previous part of this series,[1] by refluxation in pyridine. Yield 44 %, m.p. 115° (from ethanol). Found ; N, 4.10 ; $C_{23}H_{17}NS$ requires 4.12 %. ^{1}H-NMR Spectrum in $CDCl_3$ (δ, ppm) ; 7.88 (1H, s, 4-H) and overlapped multiplet patterns for the remaining protons.

REFERENCES

[1] M. C. Balaban, I. Schiketanz, A. T. Balaban, A. Schiketanz and M. D. Gheorghiu, *Rev. Roum. Chim.*, **32**, 975 (1987). Part X.

[2] J. V Metzger, in "Comprehensive Heterocyclic Chemistry" (eds. A. R. Katritzky and J. W. Rees) vol. 6, p. 235, Pergamon Press, Oxford, 1984.

[3] J. V. Metzger (ed.), "Thiazole and Its Derivatives", Part. I, Wiley-Interscience, New York, 1979, p. 395.

[4] J. Metzger, *Z. Chem.*, **9**, 99 (1969).

[5] H. Beyer, *Acta Chim. Acad. Sci. Hung.*, **12**, 225 (1957).

[5] J. M. Sprague and A. H. Land, in "Heterocyclic Compounds" (ed. R. C. Elderfield), vol. 5, pp. 484–772, Wiley, New York, 1957.

[7] R. H. Wiley, D. C. England and L. C. Behr, *Org. React.*, **6**, 367 (1951).

[8] See previous parts of this series (III–X).

[9] H. Muxfeldt, J. Behling, G. Grethe and W. Rogalski, *J. Am. Chem. Soc.*, **89**, 4991 (1967).

[10] A. W. Dox, *Org. Synth.* Coll. Vol. 1, 5 (1941).

[11] J. P. Jepson, A. Lawson and V. D. Lawton, *J. Chem. Soc.*, **1955**, 1791.

[12] M.D. Bachi, *J. Chem. Soc. Perkin I*, **1972**, 310.

[13] G. C. Barrett, *J. Chem. Soc.*, (C) **1971**, 1380.

[14] F. Kurzer and A. Lawson, *Org. Synth.* Coll. Vol. 5, **1973**, 1046.

[15] S. Gabriel, *Ber. dtsch. chem. Ges.*, **43**, 134 (1910).

[16] K. Rüdenburg, *Ber. dtsch. chem. Ges.*, **46**, 3555 (1913).

[17] P. B. Tasmusson, U. Pedersen, I. Thomsen, B. Yde, and S. O. Lawesson, *Bull. Soc. Chim. Fr.*, (1), 62 (1985).

[18] R. A. Cherkasov, G. A. Kutyrev and A. M. Pudovik, *Tetrahedron*, **41**, 2567 (1985).

[19] M. P. Cava and M. I. Levinson, *ibid.*, **41**, 5061 (1985).

[20] Part VIII of this series : I. Schiketanz, A. Schiketanz, M. D. Gheorghiu and A. T. Balaban, *Rev. Roum. Chim.*, **30**, 969 (1985).

[21] V. N. Kerr, F. N. Hayes, D. G. Ott and E. Hansbury, *J. Org. Chem.*, **24**, 1861 (1959).

[22] E. S. Gatewood and T. B. Johnson, *J. Am. Chem. Soc.*, **48**, 2904 (1926).

Revue Roumaine de Chimie, 32, *11–12*, 1181–1186 (1987)

Dedicated to Professor V. E. SAHINI
on his 60th anniversary

NUCLEAR MAGNETIC RESONANCE INVESTIGATIONS OF SMALL RINGS. PART 5[1]

THE EXACT ANALYSIS FOR THE FOUR-MEMBERED RING THREE-PROTON SYSTEM OF 3-ARYL-2-t-BUTYL-2-CYCLOBUTANONES AS EVIDENCE FOR CONFIGURATIONAL ASSIGNMENTS

MIRCEA D. GHEORGHIU, *[,a] MARINA MIHAI,[b] LUMINIȚA PÂRVULESCU,[a]
ANGHELUSIS VAIOS[a] and MIHAI ELIAN*[,b]

[a] Department of Organic Chemistry, Polytechnic Institute – TCH, 76206, Bucharest 16, Romania
[b] Centre of Organic Chemistry, ICECHIM, Bucharest, Romania

Received June 4, 1987

The exact analysis of the experimental spectra of 3-aryl-2-t-butyl-2-cyclobutanone (Ar : p-$NO_2-C_6H_4$, p-$C_6H_5-C_6H_4$, 1-naphthyl, and 2-naphthyl) has provided the spectral parameters (chemical shifts and coupling constants). The other five or seven theoretical solutions, correct as frequencies, but unacceptable as intensities, were rejected. Our option for the true solution was substantiated by the exact analysis for some cyclobutanones in a different solvent and by comparison with our previous result (see ref. 4b). The signal of the benzylic proton appears at $\delta > 4.3$ ppm (deshielded by comparison with appropiate models), indicating that H^1 and the cyano group are *cis*, while in cases when the same signal occurs at $\delta < 4$ ppm, the configuration is reversed.

INTRODUCTION

The archetypal evidence for the concerted on non concerted cycloaddition of ketenes to carbon-carbon double bond is the stereochemistry of the cyclobutanone resulted from the reaction with cyclopentadiene.[2] Should a cycloaddition proceed through a $_2\pi_s + {}_2\pi_a$ reaction mode,[3] then in the resulting cyclobutanone the largest substituents originating from the ketene and the cyclopentene fragment are in *cis* configuration. The alternative nonconcerted reaction mode has as result a cyclobutanone with the small substituent facing the five-membered ring.

We believe that vinylarenes[4] and bicyclo[2.2.1]heptene derivatives,[5] two less explored substrates, are also appropriate to gauge the stereochemistry of the cycloaddition reaction, and hence to learn more about the reaction mode.

In the present paper, extending our previous contributions,[4] we would like to bring new evidences that besides styrene, indene and acenaphthene, vinylarenes (Ar : $p-NO_2-C_6H_4$, $p-C_6H_5-C_6H_4$, 1-naphthyl and 2-naphthyl) are suitable ketenophiles in order to illustrate the Woodward – Hoffmann reaction mode.[3] Such an attempt has been virtually unexplored, to our best knowledge, since 1920 when Staudinger discovered the first example of cycloaddition of diphenylketene with styrene.

In our hand, vinylarenes have reacted with t-butylcyanoketene (TBCK)[7] to give overwhelmingly cyclobutanones with Ar and t–Bu groups vicinal and *cis*, and only in one case the isolated cyclobutanone had the stereochemistry *trans* (Ar : $p-CH_3O-C_6H_4$).[4c]

The configuration assignments, proposed here, are originating from the exact analysis of the ^1H-NMR spectrum of the ring protons. As in our previous contribution,[4b] we would like to present new evidence that the cyano group has an effective deshielding effect upon the proton facing this group, as it was stated by Moore.[8] In order to obtain a confident value for the chemical shift of the benzylic proton facing the cyano group, we carried out an exact analysis of the ^1H-NMR spectra for the 3-aryl-2-t-butyl-2-cyano-cyclobutanones **2**–**5**. In comparison with the cyclobutanone **6** (Ar = $p-MeO-C_6H_4$), whose structure is definitely known from X-ray measurements,[4c] the signals of H^1 in the case of cyclobutanones **2**–**5** are deshielded, as result of magnetic effects exerted by the vicinal cyano group. This outcome is fully in agreement with our previous discussion in the case of cyclobutanone **1**,[4] the $^{13}C-NMR$ results for a diversified substituted 2-t-butyl-2-cyano-cyclobutanones,[1a] and X-ray measurements for cyclobutanones **4** and **6**.[9]

RESULTS AND DISCUSSION

In order to ascertain the configuration of cyclobutanones **2**–**5**, our main goal is to establish unambiguously the chemical shift of benzylic protons, H^1. Our methodology was based on the exact analysis of the frequencies experimental spectra of the three-spin systems $H^1H^2H^3$, according to the procedure developed by Castellano and Waugh,[10] and Cavanaugh.[11] The actual solution was retained only after comparison of the intensities of the calculated and the experimental spectrum. Asin the case of 2-t-butyl-2-cyano-3-phenylcyclobutanone,[4b] among the six (or in some cases eight)

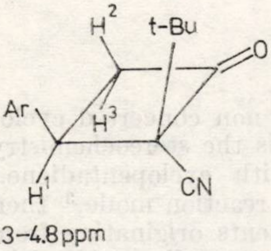

$1 = C_6H_5-$
$2 = p-NO_2-C_6H_4-$
$3 = C_6H_5-C_6H_4-$
4 = 1-naphthyl–
5 = 2-naphthyl–

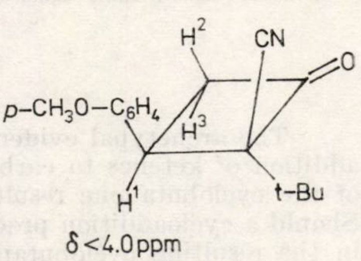

6

real frequencies, only two solutions had slight differences in some line intensities, the other four or six are easily rejected as we had shown in our previous paper.[4b] The true solution, *e.g.* with both frequencies and intensities fitted, had $J^{gem} < 0$, while the closely resembling one, hereafter called concurrent solution (CS), had $J^{gem} > 0$.

The spectral parameters of cyclobutanones **1**—**5** are collected in Table 1, and the stick representation of the cyclobutanone ring protons spectra, simulated with the corresponding spectral parameters are presented in the accompanying figure 1.

Table 1

Spectral parameters (true solution) obtained by exact analysis of the proton spectra of cyclobutanones **1**—**5**, (a) in $CDCl_3$ and (b) in C_6D_6

Compound		H^1	H^2	H^3	J^{trans}	J^{cis}	J^{gem}	No solutions
1	a	4.41	3.81	3.44	11.14	10.07	−18.24	6
	b	4.00	3.25	2.77	11.27	10.32	−18.31	6
2		4.49	3.88	3.53	11.02	9.67	−18.05	6
3	a	4.39	3.81	3.43	11.26	9.99	−18.38	6
	b	3.99	3.26	2.82	11.10	10.11	−18.04	6
4	a	4.81	4.04	4.44	11.73	9.88	−18.17	8
	b	4.35	3.34	2.64	11.12	10.20	−18.11	8
5		4.47	3.90	3.44	10.48	9.72	−18.12	6

In order to check the correct choice of solution for the spectra run in $CDCl_3$, we have analyzed in the case of cyclobutanone **3** ($\mathrm{Ar} = \mathrm{p}-C_6H_5-$ $-C_6H_4$) and **4** (Ar = 1-naphthyl) the experimental spectrum in C_6D_6. For the 3-(p-nitrophenyl)cyclobutanone **2**, the CS had the same chemical shifts as those quoted as true solution in Table 1, while the vicinal coupling constants had reversed magnitude, $J^{cis} = 11.3$ Hz and $J^{trans} = 9.2$ Hz, while the geminal coupling constant was positive, $J^{gem} = 17.43$ Hz. These spectral parameters gave a theoretical spectrum with a slightly decreased relative intensity for line 6 and an increased relative intensity for line 8 (see Fig. 1), when compared with the experimental spectrum. All the remaining signals of the CS spectrum had relative intensities identical with the experimental spectrum.

The same comment is valid in the case of CS simulated spectra for compounds **3**, **4** and **5**, when compared with the experimental spectrum of the corresponding cyclobutanones. However, in the case of cyclobutanone 5, in Fig. 1, instead of line 8, read line 7. The line 7 had an intensity of 2% from that corresponding to the most intense peak 9, and therefore was not represented.

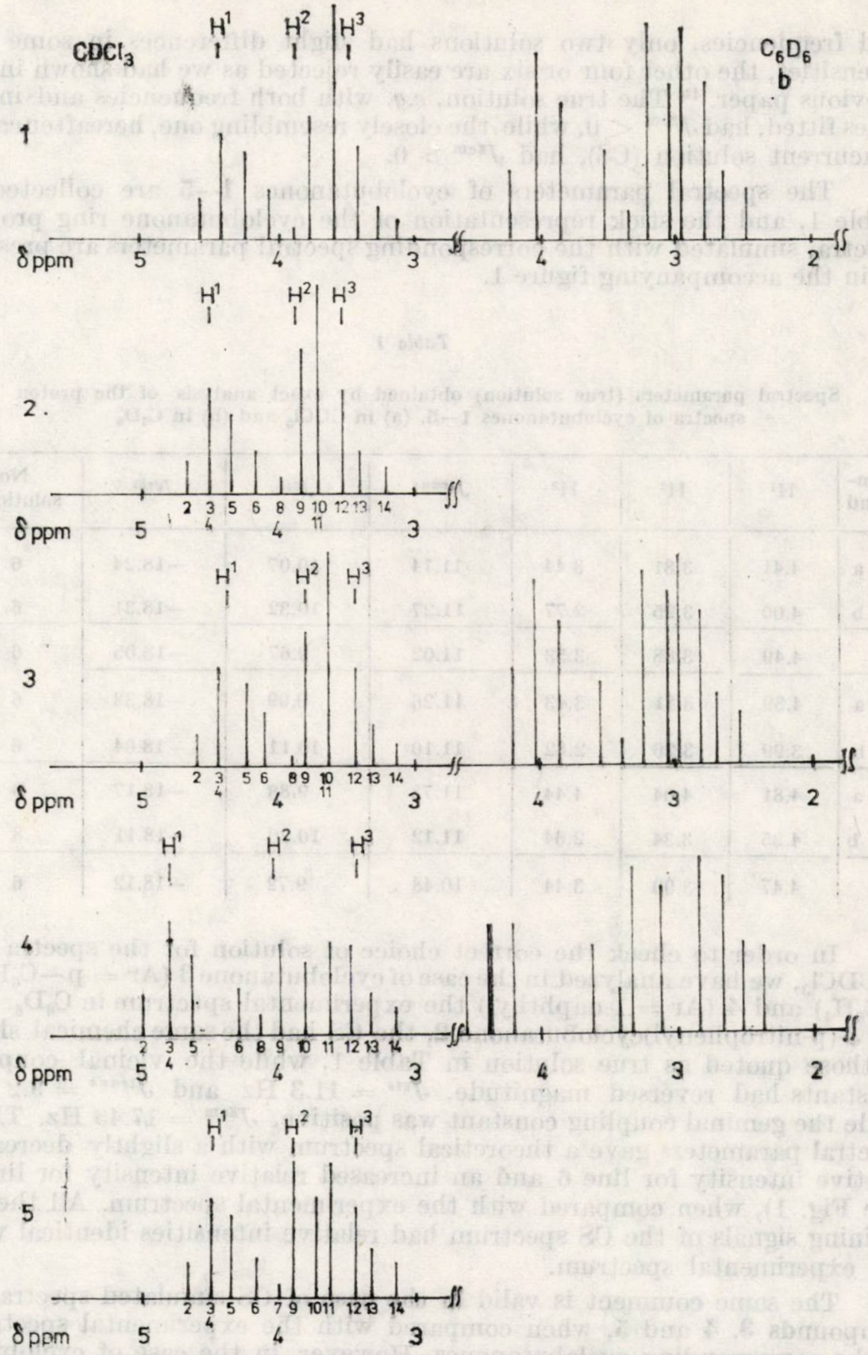

Fig. 1. — Stick representation of the experimental spectra of cyclobutanones 1—5 (a) in $CDCl_3$, (b) in C_6D_6. The missing lines (1, 7 and 15, in the case of cyclobutanones 1—4, and 1, 8 and 15 for the cyclobutanone 5) had intensities less than 2% from the most intense line 9.

Note the strongly resemblance of the spectral parameters obtained for the cyclobutanone **2**—**5**, with those proposed for the cyclobutanone **1**.[4b] Therefore, we believe *that the structures of cyclobutanone* **1**—**5** *are virtually identical.* There is however, obvious that the chemical shift of the benzylic proton, H^1, is dependent upon the anisotropic shift induced by the geminal aryl group. The chemical shift of the protons H^2 are spread over a narrower region around 3.90 ppm, while H^3 is located for all compounds at 3.4 ppm.

The choice of the true solution was supported also by the exact analysis of the experimental spectra of cyclobutanones **4** and **5** in C_6D_6. The aromatic solvent induces a displacement of all signals with about 0.5 ppm toward higher fields, leaving the coupling constants relatively unchanged as magnitude.

Having at hand the true spectral parameters, the configurational assignment is opportune.

The benzylic proton, H^1, is located for cyclobutanones **1**—**5** in the range of 4.3—4.8 ppm. The indene adduct with TBCK has the same proton signal at 4.65 ppm, while the acenaphthylene adduct with TBCK has $\delta_{H^1} = 5.5$ ppm. Therefore the cyclobutanones obtained from seven styrene-like ketenophiles display the location of the benzylic proton at $\delta > 4.3$ ppm. The location of the same proton signal in the cyclobutanone obtained from p-methoxystyrene and TBCK is less than 4 ppm. Our experiments in the latter case with shift reagents were unsuccessful in assigning the signal to a certain chemical shift, therefore we have quoted above the lower end of the multiplet belonging to the three-spin system. We believe that in the former examples the deshielding of H^1 signal is the result of the anisotropic effect of the vicinal *cis* cyano group, while the latter example is displaying a higher field signal as a result of a vicinal *trans* configuration of benzylic proton and the cyano group. The X-ray measurements obtained from 1-vinylnaphthalene, definitely established the configuration of the cyclobutanone as is presented in the structure **4**. [4c] Also the structure **6** was proposed as a result of **X**-ray measurements. [4c] By analogy, as the result of ^1H—NMR pattern resemblance with cyclobutanone **4**, the structures of the remaining compounds **1**—**3** and **5** have the configuration with the bulky aryl and t—Bu groups vicinal and *cis*. In our view, this conclusion suggests for the respective reaction mode a concerted $_2\pi_s + _2\pi_a$ mechanism.

EXPERIMENTAL PART

The ^1H-NMR spectra were recorded at 60 MHz with a Varian EM 360 L spectrometer. The cyclobutanones were obtained from TBCK[7] and the corresponding alkenes. Analytical samples of cyclobutanones **2**—**5** were obtained by chromatography on silica gel. All the newly obtained compounds have good elemental analysis, and spectroscopic properties (IR, ^1H-NMR, ^{13}C-NMR) according to the proposed structure.

The protocol for the exact analysis was described in our previous paper.

REFERENCES

[1] (a) Part 4 : M. D. Gheorghiu, M. Mihai, L. Pârvulescu, A. Vaios and F. Niculescu, *Rev. Roumaine Chim.*, **32**, 979 (1987) : (b) Taken in part from the Ph. D. Thesis of M. M. and B. Sc. Thesis of A. V. (Polytechnic Institute, Bucharest, 1983).

[2] R. W Holder, *J. Chem. Educ.*, **53**, 81 (1976); L. Ghosez and M. J. O'Donnell, "Pericyclic Reactions", vol. 2, A. P. Marchand and R. E. Lehr, Eds., Academic Press, New York, 1977; M. Rey, S. M. Roberts, A. Dieffenbacher and A. S. Dreiding, *Helv. Chim. Acta*, **53**, 417 (1970); M. Rey, S. M. Roberts, A. S. Dreiding, A. Roussel, H. Vanlierde, S. Toppet and L. Ghosez, *Helv. Chim. Acta*, **65**, 703 (1982).

[3] R. B. Woodward and R. Hoffmann, "The Conservation of Orbital Symmetry", Academic Press, 1970, p. 163.

[4] (a) M. D. Gheorghiu, F. Kerek and M. Avram, *Rev. Roumaine Chim.*, **20**, 75 (1975); M. D. Gheorghiu, L. Pârvulescu, C. Drăghici and M. Elian, *Tetrahedron*, **37**, Suppl. 1. 143 (1981); (b) M. D. Gheorghiu, O Ciobanu and M. Elian, *J. Mag. Resonance*, **44**, 330 (1981); (c) M. D. Gheorghiu, M. Mihai, L. Pârvulescu, S. V. Sereda and Yu. T. Struchkov, manuscript to be submitted.

[5] M. D. Gheorghiu, P. Filip, C. Drăghici and L. Pârvulescu, *J. Chem. Soc., Chem. Commun.*, **1975**, 635; M. D. Gheorghiu, C. Drăghici and I. Pârvulescu, *Tetrahedron*, **33**, 3295 (1979); M. D. Gheorghiu, L. Pârvulescu and C. Drăghici, *Rev. Roumaine Chim.*, **24**, 1005 (1979); C. Drăghici, M. D. Gheorghiu, L. Pârvulescu and M. Elian, manuscript to be submitted.

[6] H. Staudinger and E. Suter, *Ber. dtsch. chem. Ges.*, **53**, 1092 (1920).

[7] W. Weyler, Jr., W. G. Duncan, M. S. Liewen and H. W. Moore, *Org. Synth.*, **55**, 32 (1976); see also: M. D. Gheorghiu and M. Avram, *Org. Prep. Proc. Int.*, **6**, 631 (1979); M. D. Gheorghiu, L. Pârvulescu, R. Ceclan, I. Manolescu, D. Constantinescu, C. Florea and M. Stănescu, *Rev. Roumaine Chim.*, **33**, 000 (1988).

[8] W. Weyler, Jr., L. Byrd, M. B. Caserio and H. W. Moore, *J. Amer.Chem. Soc.*, **94**, 1027 (1971).

[9] S. V. Sereda, Yu. T. Struchkov, M. D. Gheorghiu, M. Mihai and L. Pârvulescu, manuscript to be submitted.

[10] S. Castellano and J. S. Waugh, *J. Chem. Phys.*, **34**, 295 (1961).

[11] J. R. Cavanaugh, *J. Chem. Phys.*, **39**, 2378 (1963).

Revue Roumaine de Chimie, **32**, *11–12*, 1187–1192 (1987)

Dédié au Professeur V. E. SAHINI à
l'occasion de son 60e anniversaire

HOMOPOLYCONDENSATION DE DÉRIVÉS DICHLOROMÉTHYLES EN PRÉSENCE DU TÉTRACHLOROÉTHYLÈNE OU DU TRICHLOROÉTHYLÈNE

M. IOVU[a] et ELENA TUDORACHE[b]
[a] Faculté de Pharmacie, Traian Vuia 6, Bucarest, Roumanie
[b] Institut Polytechnique, Bucarest, Faculté de Technologie Chimique

Reçu le 15 février 1986

It is shown, for the first time, that the homopolycondensation reaction of trichloromethylene and tetrachloromethylene (used as solvents) with dichloromethylated derivatives as 1,4-dichloromethylbenzene, 1,4-dichloromethyl-2,5-dimethylbenzene, 1,3-dichloromethyl-4,6-dimethylbenzene, 1,2-dichloro-1,2-diphenylethane, and 1,3-di(α-chloroethyl) benzene in the presence of $AlCl_3$ takes place. Macromolecular products of the reaction are different in comparison with the macromolecular products obtained by homopolycondensation from the same dichloroderivatives in inert solvents as CS_2.

On a mis en évidence, pour la première fois la participation du trichloroéthylène et du tétrachloroéthylène, (utilisés comme solvants), à la réaction d'homopolycondensation des composés dichlorométhylés comme les 1,4-dichlorométhylbenzène, 1,4-dichlorométhyle-2,5-diméthylbenzène, 1,3-dichlorométhyl-4,6-diméthyl-benzène, 1,2-dichloro-1,2-diphényléthane et du 1,3-di(α-chloroéthyl)benzène en présence de $AlCl_3$. Les produits macromoléculaires de réaction sont différents de ceux obtenus par l'homopolycondensation des mêmes composés dihalogénés dans des solvants inertes comme le sulfure de carbone.

INTRODUCTION

Dans cet article on étudie l'homopolycondensation des dérivés dichlorés tels que ceux du tableau 1.

Le 1,2-dichloro-1,2-diphényléthane à la différence d'autres dérivés dichlorométhylés, ne donne pas de réaction d'homopolycondensation en présence de $AlCl_3$, si on utilise des solvants inertes comme le sulfure de carbone.

Dans un travail antérieur[1] nous avons montré que le 1,4-dichlorométhylbenzène, le 1,3-dichlorométhyle-4,6-diméthyl-benzène, le 1,4-dichlorométhyle-2,5-diméthylbenzène et le 1,3-bis(α-chlorométhyl)benzène donnent lieu à des réactions d'homopolycondensation en présence de catalyseurs Friedel-Crafts en milieu de sulfure de carbone. Le 1,4-bis(α-chloroéthyl)benzène ne réagit pas dans ces conditions.

Tableau 1

Polycondensation des dérivés dihalogénés dans le milieu de tri- et tétrachloroéthylène

Derivé dihalogéné	Solvant et réactant	Quantité de produits % *)	Chlore %	Solubilité dans le benzène (g/dm^3)
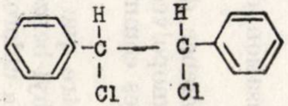	$Cl_2C{=}CCl_2$	49,3	18,44	58,1
	$Cl_2C{=}CHCl$	104,2	10,78	54,21
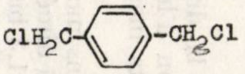	$Cl_2C{=}CCl_2$	43,70 (48,7)**	19,00 (10,86)	61,11
	$Cl_2C{=}CHCl_2$	236,0	8,23	51,44
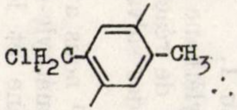	$Cl_2C{=}CCl_2$	98,0 (104,3)	14,65) (3,59	55,48
	$Cl_2C{=}CHCl$	212,9	7,248	53,25
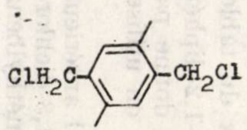	$Cl_2C{=}CCl_2$	94,6 (95,6	16,8 (7,63	53,24
	$Cl_2C{=}CHCl$	198,9	12,18	50,25
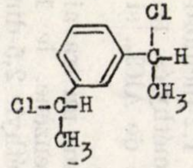	$Cl_2C{=}CCl_2$	88,5 (99,7)	17,23 (3,70)	53,10
	$Cl_2C{=}CHCl$	104,3	13,27	55,41

*) Les quantités des produits sont rapportées a la quantité de dérivé dichloré aromatique en considérant comme quantité optimale (théorique) celle qui correspond à un produit résultant de l'élimination complète du chlore sous forme d'acide chlorhydrique.

**) – Les données (entre parenthèses) obtenues dans du sulfure de carbone, qui ne participe pas à la réaction d'homopolycondensation, antérieurement publiée [1,2].

En essayant de réaliser l'homopolycondensation du 1,2-dichloro-1,2-diphényléthane, sous l'influence catalytique de AlCl$_3$, et dans le sulfure de carbone, on constate que cette réaction a eu lieu avec des rendements très faibles (15 %)[2]; c'est pour cette raison que nous avons utilisé le tétrachloroéthylène comme solvant (sa température d'ébullition est plus élevée que celle du sulfure de carbone) et la réaction a atteint un rendement de 49 %. En utilisant le trichloroéthylène comme solvant la quantité de produit croît jusqu'à 104 %. Ces faits nous ont déterminés d'effectuer des homopolycondensation avec d'autres dérivés halogénés dans ces solvants.

RÉSULTATS ET DISCUSSIONS

On remarque, en étudiant les données du tableau 1, que les quan-
s de produits * observées pour tous les composés dichlorés sont plus
ıdes (presque deux fois plus élevées) quand on utilise comme solvant
ichloroéthylène que dans le cas du tetrachloroéthylène.

La teneur en chlore est faible quand on utilise le trichloroéthylène
quantités des produits sont grandes. Dans le cas du tetrachloroéthy-
'est l'inverse.

a fait que les quantités de produits dépassent 100 % dans le cas du
oéthylène montre que le solvant participe à la réaction de conden-
u dérivé dichloré, en présence de AlCl$_3$. Le rapport molaire dichlo-
ant était dans tous les cas de 1/10.

plus, même quand on utilise le tétrachloroéthylène et que les
des produits sont inférieures à 100 %, la teneur en chlore du pro-
olycondensation prouve la participation du tétrachloroéthylène
on.

nnaît les travaux de Prins[3–5] d'où il ressort que le tétrachlor-
ut fixer du chloroforme et du hexachloropropène[3] en présence
que le 1,2,3,3-tétrachloropropène-1[5] se polycondense sur lui

igne de signaler que le 1,2-dichloroéthane, dans lequel les ato-
sont plus réactifs que dans les tri- et tétrachloroéthylènes, a
nme solvant dans les réactions d'homopolycondensation des
rométhyliques sans que les auteurs aient pu déceler la par-
solvant à la réaction.[6–8]

dérivés chlorés comme le 1,2-dichloro-1,2-diphényléthane,
de chlore se trouve en position α par rapport au noyau
conséquence la liaison C—Cl est affaiblie. En même temps
hlore sont en position β par rapport à l'autre noyau benzé-
est à l'origine de la désactivation de la liaison C—Cl. Cette
ctéristique du 1,2-dichloro-1,2-diphényléthane fait qu'il ne
icilement lieu à des réactions d'homopolycondensation.

ıtités des produits sont rapportées à la quantité de dérivé dichloré aromati-
ıt comme quantité optimale (théorique) celle qui correspond à un produit
nination complète du chlore sous forme d'acide chlorhydrique.

En présence de $AlCl_3$ les dérivés dihalogénés donnent naissance à des ions complexes après une réaction d'équilibre qui, dans le milieu solvant nonpolaire, sont déplacés vers la gauche en raison de l'impossibilité de solvation des ions.

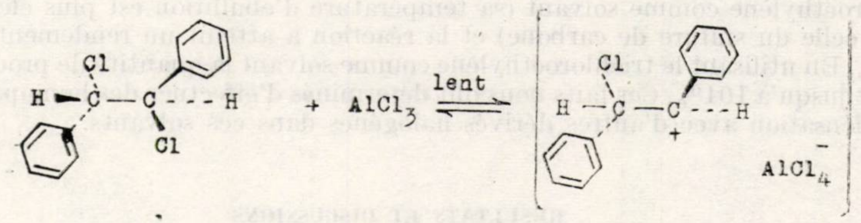

1 2

De plus, les ions formés restent sous forme de paires d'ions pour même raison. L'ion carbenium formé peut ainsi donner lieu à une atta électrophile d'un noyau benzénique d'une autre molécule.

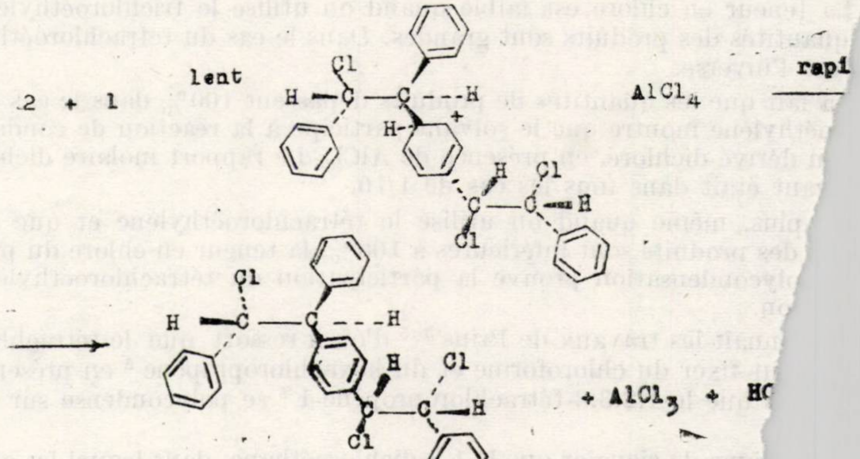

La réaction peut continuer par la formation d'une aut carbenium qui attaque un noyau benzénique d'une nouvell de la même molecule en donnant des produits tridimension

L'attaque électrophile de l'ion carbenium sur le tétra est difficile en raison de la symétrie de cette molécule qui ne p délocalisation électrophile.

Ce fait explique pourquoi les quantités des produits pas 100%.

Lorsque l'on utilise le trichloroéthylène, en raison de l cette molécule, les ions peuvent être solvatés. De plus, l'at phile des ions carbenium peut se produir non seulement su benzénique, mais sur la double liaison du trichloroéthylène qui est fortement polarisée :

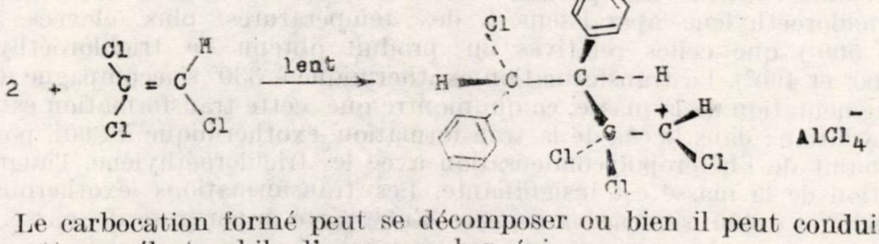

Le carbocation formé peut se décomposer ou bien il peut conduire à une attaque électrophile d'un noyau benzénique.

Les atomes de chlore qui proviennent du trichloroéthylene se trouvent, après la réaction, dans des positions benzyliques, réactives dans le produit intermédiaire de réaction, et ils peuvent donc réagir avec les autres noyaux benzéniques de façon intramoléclaire ou intermoléculaire augmentant la masse moléculaire.

La participation à la réaction d'homopolycondensation des composés chlorométhylés (en présence de $AlCl_3$) et des deux solvants (tétrachloroéthylène et trichloroéthylène) est mise en évidence aussi par les spectres IR. On peut comparer les spectres IR en pastille KBr du produit de l'homopolycondensation du 1,3-dichlorométhyle — 4,6-diméthylbenzène réalisée dans la sulfure de carbone (qui ne participe pas à la réaction) et les spectres IR des polycondensés du même dérivé dichloruré, obtenues dans le tétrachloroéthylène et le trichloroéthylène. Le produit d'homopolycondensation présente une bande d'absorption due à la vibration de valence C—Cl, située à 733 cm^{-1}, alors que le produit d'hétéropolycondensation dans le trichloroéthylène révèle en outre une bande intense à 800 cm^{-1}, due à ν_{C-Cl} relative à un atome de chlore lié à un atome de carbone engagé dans une double liaison $\rangle C=\overset{|}{C}-Cl$.

De même, dans la zone des vibrations de valence C—C des noyaux benzéniques qui correspondent aux fréquences comprises entre 1445 et 1620 cm^{-1} on remarque des différences. Le produit d'homopolycondensation présente une bande d'absorption étroite, mais intense, à 1510 cm^{-1}; cette bande ne se retrouve pas dans les produits d'hétéropolycondensation.

L'analyse thermogravimétrique des nouveaux produits de polycondensation révèle qu'il n'existe pas de transformations d'état d'agrégation (endothermiques).

Les produits de polycondensation au cours de l'échauffement selon la nature des matières premières ont un comportement différent.

Par exemple dans la figure 1 on peut voir que les produits de polycondensation du 1,3-di-

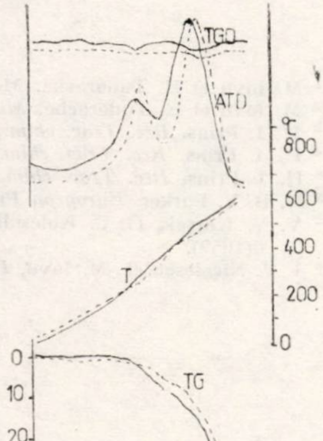

Fig. 1

chlorométhyle-4,6-diméthylbenzène avec le tétra chloroéthylène et avec le trichloroéthylène présentent deux transformations exothermiques importantes. Celles du produit macromoléculaire obtenu avec du tétrachloroéthylène aparaissent à des températures plus élevées (330° et 500°) que celles relatives au produit obtenu de trichloroéthylène (300° et 490°). La transformation exothermique à 330° s'accompagne d'une augmentation de la masse, ce qui montre que cette transformation est une oxydation; dans le cas de la transformation exothermique à 300°, pour le produit de l'hétéropolycondensation avec le trichloroéthylène, l'augmentation de la masse est insignifiante. Les transformations exothermiques à 525° et à 490° sont accompagnées d'une perte importante de masse.

PARTIE EXPÉRIMENTALE

POLYCONDENSATION DU 1,3-BIS(CHLOROMÉTHYLE)-6,6-DIMÉTHLBENZENE AVEC LE TÉTRACHLOROÉTHYLÈNE

Dans un ballon de 100 cm³ muni d'un agitateur, d'un réfrigérant scellé à tube de garde de $CaCl_2$, d'un piège pour HCl et d'un thermomètre, on introduit sous atmosphère de gaz inerte 2.030 g (0.01 mol) de 1,3-bis(chlorméthyle)-4,6-diméthylbenzène et 16,583 g (0,1 mol) tétrachloroéthylène en agitant pour accélérer la dissolution ; on ajoute 0,333 g de $AlCl_3$ (0.04 mol) et on chauffe a l'ébullition sous agitation pendant 9—010 h. Il se dégage du HCl qui est retenu par une solution aqueuse de NaOH. Le produit solide de la réaction se présente sous la forme d'une suspension dans la tétrachloroéthylène qui n'a pas réagi. Puis il est filtré et le précipité est lavé à l'éthanol, afin d'éliminer les traces des réactifs.

Le polymère est lavé a l'acide chlorhydrique à 10% pour séparer le catalyseur, puis à l'eau froide jusqu'à l'élimination totale des ions Cl^-. Le produit est séché a 110°. Rdt. 1,275 g (98%).

Les autres réactions de polycondensation ont été effectuées dans des conditions similares.

BIBLIOGRAPHIE

[1] M. Iovu et E. Tudorache, *Makromol. Chem.*, **147**, 101 (1971).
[2] M. Iovu et E. Tudorache, *Makromol. Chem.*, **176**, 1579 (1975).
[3] H. I. Prins, *Rec. Trav. chim.*, **54**, 249 (1935).
[4] H. I. Prins, *Rec. Trav. chim.*, **57**, 659 (1938).
[5] H. I. Prins, *Rec. Trav. chim.*,**68**, 217 (1949).
[5] D. B. V. Parker, *European Polym. J.*, **5**, 93 (1969).
[7] V. V. Korşak, G. C. Kolesnikov et A. V. Harghevnicova, *Doklady Akad. Nauk.*, **56**, **169** (1957).
[8] I. V. Nicolescu et M. Iovu, *Industrie des plastiques modernes*, **10**, 46 (1958).

Revue Roumaine de Chimie, 32, 11–12, 1193–1202 (1987)

Dedicated to Professor V. E. SAHINI
on his 60th anniversary

MONOMOLECULAR FILMS OF SOME APOCAROTENOID DERIVATIVES

J. ZSAKÓ, MARIA TOMOAIA-COTIȘEL, V. TĂMAȘ *, VIRGINIA COMAN and E. CHIFU
Faculty of Chemical Technology, University of Cluj-Napoca, 3400 Cluj-Napoca, Romania
* Institute of Agromomy, 3400 Cluj-Napoca, Romania

Received May 8, 1987

Compression isotherms, i.e. surface pressure (π) *vs.* mean molecular area (A) curves are reported for 5 apocarotenoid derivatives spread at the air/water interface, indicating a first order phase transition in the case of two derivatives studied. Surface properties are derived from the π *vs.* A curves and compared with those obtained earlier for other 4 similar derivatives. Molecular models are constructed for different conformations of the substances studied and area necessities of the molecules are calculated. The surface characteristics and the phase transition are discussed in terms of area necessities, polar headgroup interactions, hydrocarbon chain hydrophobic interactions. Surface compressibility modulus (C_s^{-1}) *vs.* π curves are derived indicating the liquid expanded character of the monolayers.

INTRODUCTION

Compression isotherms, i.e. surface pressure (π) *vs.* mean molecular area (A) curves have been reported in our previous paper [1] for β-*apo*-8′-carotenylidene-oxazolone (I), retinylidene-oxazolone (II), diethylamide of β-*apo*-7′-benzoylamino-6′-carotenoic acid (III) and diethylamide of β-*apo*-15′-benzoylamino-14′-carotenoic acid (IV). Surface characteristics derived from the π *vs.* A curves, viz. collapse pressure (π_c), collapse molecular area (A_c), limiting molecular area (A_0) and surface compressional modulus ($C_{s,0}^{-1}$), have been discussed in terms of molecular structure. For this purpose the rotating rigid plate model [2] was used. By assuming hydrocarbon chain to be like a rigid plate, due to the delocalized π-bond system, and at the compression of the monolayer spread at the air/water interface to adopt a vertical orientation, this molecular model allowed us to determine the area necessity of a molecule as the cross section of both the rotating molecule and the non-rotating one. The size of the cross section is characterized by its "length" a (the maximum distance) and by its "width" b (in the direction perpendicular to a). Thus, for a non-rotating molecule the area necessity will be $A_p = ab$, for a rotating one it will be $A_4 = a^2$ in the case of tetragonal close packing and $A_6 = (\sqrt{3}/2)a^2$, if a hexagonal close packing of the molecules occurs. Our experiments and calculations, performed on the basis of literature data concerning the internuclear distances, van der Waals radii and bond angles corresponding to the hybridization type, showed $A_c \approx A_p$ and $A_0 \approx A_4$. This suggests the idea that at the compression of the monolayer the apocarotenoid molecules gradually adopt a vertical orientation; for A_0 one has a tetragonal close packing of the rotating molecules, at collapse the rotation of the molecules becomes hindered and the close packing of the non-rotating molecules is achieved.

In the present paper other 5 apocarotenoid derivatives are studied, viz. aminoethyl amide of β-*apo*-7′-benzoylamino-6′-carotenoic acid (V), aminoethyl amide of β-*apo*-15′-benzoylamino-14′-carotenoic acid (VI), di-ethanolamide of β-*apo*-7′-benzoylamino-6′-carotenoic acid (VII), di-ethanolamide of β-*apo*-15′-benzoylamino-14′-carotenoic acid (VIII) and methylethanolamide of β-*apo*-7′-benzoylamino-6′-carotenoic acid (IX). Structure of substances I—IX is given in Figure 1.

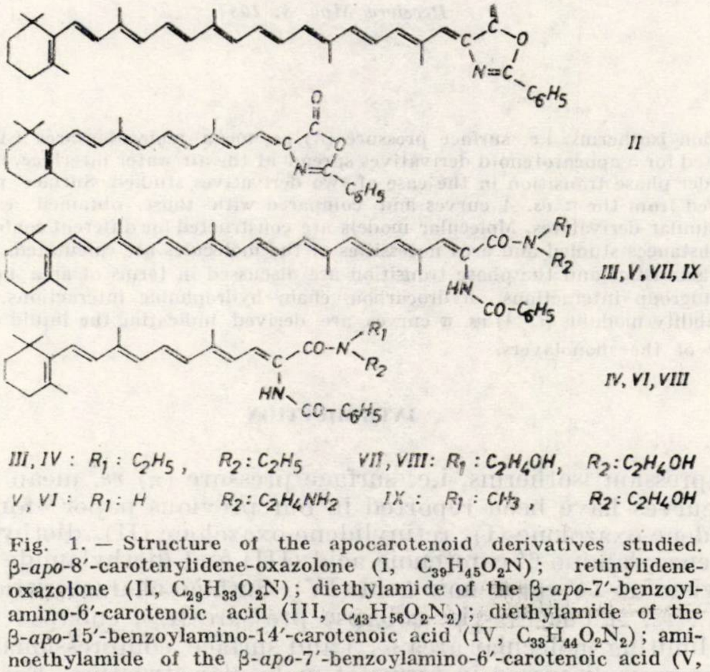

III, IV : R_1 : C_2H_5 , R_2 : C_2H_5 VII, VIII: R_1 : C_2H_4OH, R_2 : C_2H_4OH

V, VI : R_1 : H R_2 : $C_2H_4NH_2$ IX : R_1 : CH_3 , R_2 : C_2H_4OH

Fig. 1. — Structure of the apocarotenoid derivatives studied. β-*apo*-8′-carotenylidene-oxazolone (I, $C_{39}H_{45}O_2N$); retinylidene-oxazolone (II, $C_{29}H_{33}O_2N$); diethylamide of the β-*apo*-7′-benzoylamino-6′-carotenoic acid (III, $C_{43}H_{56}O_2N_2$); diethylamide of the β-*apo*-15′-benzoylamino-14′-carotenoic acid (IV, $C_{33}H_{44}O_2N_2$); aminoethylamide of the β-*apo*-7′-benzoylamino-6′-carotenoic acid (V, $C_{41}H_{53}O_2N_3$); aminoethylamide of the β-*apo*-15′-benzoylamino-14′-carotenoic acid (VI, $C_{31}H_{41}O_2N_3$); diethanolamide of the β-*apo*-7′-benzoylamino-6′-carotenoic acid (VII, $C_{43}H_{56}O_4N_2$); diethanolamide of the β-*apo*-15′-benzoylamino-14′-carotenoic acid (VIII, $C_{33}H_{44}O_4N_2$); methyl, ethanolamide of the β-*apo*-7′-benzoylamino-6-′-carotenoic acid (IX, $C_{42}H_{54}O_3N_2$).

EXPERIMENTAL

The apocarotenoid derivatives studied were synthetic products [3,4] of chromatographic purity and were utilized without further purification. Since carotenoid pigments are sensitive, especially to light, their purity was checked during the experiments by thin layer chromatography and no degradation was observed.

Compression isotherms were recorded at room temperature (22 ± 2°C). Details concerning the experimental procedure have been described elsewhere[1,5].

The surface pressure was measured by the Wilhelmy method, ensuring data reproducible within ± 0.5 mN/m in the case of π and within ± 0.01 to 0.04 nm^2/molecule with A. The compression of the films started 1 to 10 min after spreading, this time being sufficient for the evaporation of the solvent.

As subphase, doubly distilled water was used. The spreading solvent was benzene or benzene-ethanol mixtures with a content of 1 to 16% ethanol. Both benzene and ethanol were of p.a. purity, produced by "Reactivul", Bucharest.

Spreading area was varied between about 1 and 5 nm^2/molecule. Compression rate was maintained constant (approximately in the range between 0.02 to 0.08 nm^2/molecule · min, in which the isotherms were not dependent of the compression rate). Compression was discontinuous, allowing the internal equilibrium in the film to be established for each experimental point of the isotherm. The π *vs.* A curves given represent the mean of at least 10 isotherms recorded under identical conditions.

RESULTS AND DISCUSSION

The experimental compression isotherms of V–IX are given in Figures 2 and 3.

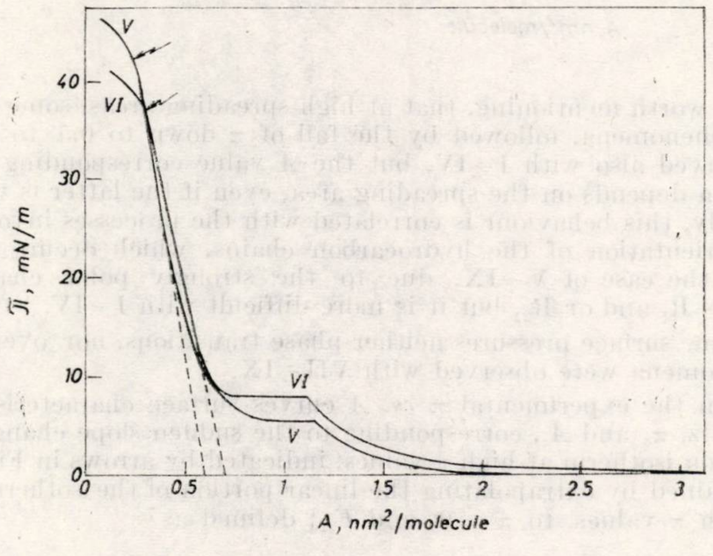

Fig. 2. — Compression isotherms of V and VI.

As seen, the π *vs.* A curves of V and VI present a horizontal portion, indicating a phase transition. In the case of high spreading areas (2 to 5 nm^2/molecule) this transition begins at about 1.1 nm^2/molecule, corresponding to $\pi \approx 6$ mN/m for V and $\pi \approx 8$ mN/m with VI. At decreasing spreading areas (from about 1.5 nm^2/molecule), the beginning of the transition is shifted towards lower A values. The horizontal portion becomes shorter and eventually is transformed into an inflexion point, to disappear completely at very low spreading areas. At higher surface pressures the isotherm is not affected by the spreading area. This behaviour might be assigned to the flexibility of the polar headgroup of the molecule. Similar phenomena were observed also with dipalmitoyl lecithin monolayers.[6]

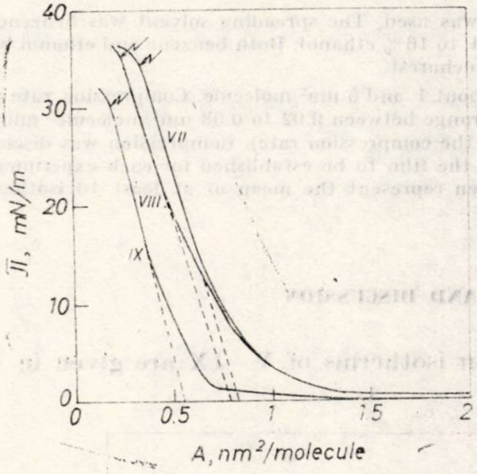

Fig. 3. — Compression isotherms of VII, VIII and IX.

It is worth mentioning, that at high spreading areas, some overcompression phenomena, followed by the fall of π down to 0.5 to 2 mN/m, were observed also with I—IV, but the A value corresponding to these phenomena depends on the spreading area, even if the latter is very high. Presumably, this behaviour is correlated with the processes involving the vertical orientation of the hydrocarbon chains, which occurs relatively easily in the case of V—IX, due to the strongly polar character of substitutes R_1 and/or R_2, but it is more difficult with I—IV.

At low surface pressures neither phase transitions, nor overcompression phenomena were observed with VII—IX.

From the experimental π *vs.* A curves surface characteristics were derived, viz. π_c and A_c, corresponding to the sudden slope change of the compression isotherm at high π values, indicated by arrows in Figs. 2 and 3, A_0 obtained by extrapolating the linear portion of the isotherm observed at high π values, to $\pi = 0$, and $F_{s,0}^{-1}$ defined as[7]

$$C_{s,0}^{-1} = -A_0\left(\frac{\partial \pi}{\partial A}\right)_T = -A_0\,\frac{\pi_c}{A_c - A_0}$$

These data are presented in Table 1. For the sake of comparison, this table contains also the characteristics of I—IV reported earlier.[1]

In order to correlate the surface characteristics with the molecular structure, molecular models were constructed. The polar headgroup anchored in the water phase is the following:

$$C_6H_5{-}CO{-}NH{-}\overset{\|}{C}{-}CO{-}NR_1R_2$$

where R_1, R_2 : C_2H_5 with III and IV; R_1 : H, R_2 : $CH_2-CH_2-NH_2$ with V and VI; R_1, R_2 : CH_2-CH_2-OH with VII and VIII; R_1 : CH_3, R_2 : CH_2-CH_2-OH with IX.

Table 1

Surface characteristics and theoretical molecular area calculated for the *C* conformation of the NR_1R_2 group

Substance	π_c mM/m	A_c nm²/molec.	A_p nm²/molec.	A_o nm²/molec	A_4 nm²/molec.	C_{so}^{-1} mM/m
I	12	0.36	0.30	0.47	0.56	35
II	7	0.48	0.30	0.63	0.56	30
III	12	0.54	0.53	0.68	0.69	59
IV	7	0.73	0.53	0.88	0.69	41
V	42	0.25	0.25	0.60	0.61	72
VI	37	0.30	0.25	0.70	0.61	65
VII	35	0.25	0.25	0.79	0.76	51
VIII	33	0.35	0.26	0.84	0.76	56
IX	30	0.20	0.23	0.56	0.61	46

For this moiety several conformations are possible. Since NH forms a bridge between two delocalized π-bond systems and the N atom has a non-participating electron pair, there would be possible to appear a single united conjugated system, leading to the configuration given in Fig. 4.A. In this case the *a* value would be at least 1.31 nm, corresponding to $A_4 = 1.72$ nm². Since A_0 values are far below this limit, we can conclude that practically, at least at higher surface pressures, this conjugation does not occur, i.e. rotation round the NH—CO bond remains free. Thus, at compression, the moiety C_6H_5-CO will be forced to adopt a conformation leading to a minimum area necessity. Two alternative possibilities for this minimum area conformation are visualized in Fig. 4B and C. We mention that the plane of the moiety C_6H_5-CO is slightly rotated as compared to the plane of the hydrocarbon chain, but this does not affect essentially the *b* value, i.e. the "thickenes" of the molecular plate.

As seen from Fig. 4 B and C, the *a* values will depend on the conformation of the NR_1R_2 group and obviously, also on the nature of the substituents R_1 and R_2. Therefore, calculations have been performed for two extreme conformations, which will be referred to as extended (*E*) and closed (*C*) ones. Calculated *a*, *b*, A_p, A_4 and A_6 values are given in table 2 for both *E* and *C* conformations.

The air phase hydrocarbon chain of the surfactants studied is the same "long" chain (*L*) in the case of I, III, V, VII and IX, and the same "short" one (*S*) with II, IV, VI and VIII. In the monolayers of *L* systems an enhanced van der Waals type hydrophobic interaction may be expected as compared to the corresponding *S* systems. The higher attraction between the hydrocarbon chains of *L* systems entails on the one hand higher π_c values, as observed with all *L*—*S* pairs having the same polar group (Table 1), and on the other hand, the vertical orientation of the molecule to occur more easily in the case of *L* systems, than of *S* ones. The latter effect leads to higher A_c and A_0 values for *S* systems, as compared to the *L* ones, as seen from Table 1.

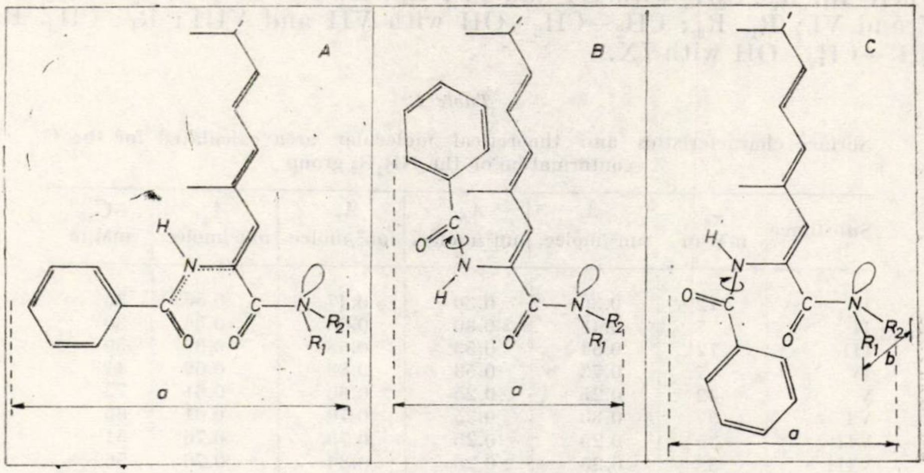

Fig. 4. — The polar headgroup of III—IX.

A — configuration for united conjugated π-bond system; *B*, *C* — conformations for two isolated delocalized π-bond systems, corresponding to minimum area necessity.

Table 2

Geometric characteristics of the vertically oriented surfactant molecules for the *E* and *C* conformations of the NR_1R_2 group

Substance	Conformation	*a* nm	*b* nm	A_p nm²/molec.	A_6 nm²/molec.	A_4 nm²/molec.
I, II	—	0.75	0.40	0.30	0.49	0.56
III, IV	*E*	1.00	0.64	0.64	0.87	1.00
	C	0.83	0.64	0.53	0.60	0.69
V, VI	*E*	1.07	0.34	0.36	0.99	1.14
	C	0.78	0.32	0.25	0.53	0.61
VII, VIII	*E*	1.07	0.45	0.48	0.99	1.14
	C	0.87	0.30	0.26	0.66	0.76
IX	*E*	1.07	0.34	0.36	0.99	1.14
	C	0.78	0.30	0.23	0.53	0.61

The dipole-dipole type interactions and/or hydrogen bond formation also influence the π_c values. The experimentally found order of π_c in the case of *L* systems, *viz.* I ≈ III < IX < VII < V is in perfect agreement with theoretical expectations. The polar headgroup interactions are the weakest for I and III, their headgroups being the least polar. Substance IX has one more OH group as compared to III, and VII has two more OH groups, as compared to the same III, which leads to the increase of π_c in the above-mentioned order. The highest collapse pressure observed with V might be due to the protonation possibility of its NH_2 group, leading to the appearance of charged species, and consequently to an electric double layer, which might hinder the collapse.

Concerning the molecular areas, the agreement between the experimental data and the calculated ones may be expected especially for the *L* type systems, since the close packing of vertically oriented molecules can be achieved more easily in this case, due to the enhanced hydrophobic interactions. Data presented in Table 1, where also the A_p and A_4 values are given, calculated for the *C* conformation of the NR_1R_2 group, show A_p and A_c, as well as A_4 and A_0 values to be very close to each other. If the polar headgroup interactions are weak (I and III) A_c is a little higher than A_p, but the opposite is observed with highly polar headgroups (V, VII and IX).

In the case of III and IV the *b* value is higher than with V–IX due to the non-polar character of R_1 and R_2, the latters being squeezed out from the aqueous phase. If R_1 and/or R_2 are polar groups, they can be readily accommodated beneath the air phase hydrocarbon chain.

Comparison of our experimental A_0 values with the calculated A_4 ones shows a quite good agreement for the conformation *C*, but not for the conformation *E*, suggesting the idea that at compression of the film conformation *E* is not preferrable, at least at high surface pressures. It is interesting to remark, that the molecular area at which the phase transition begins in the case of V and VI (1.1 nm²) is in very good agreement with the A_4 value calculated for the *E* conformation, visualized in Fig. 5, together with the *C* one of the $NH-CH_2-CH_2-NH_2$ moiety. This means, that presumably, the phase transition observed is a conformational transition *E* → *C*. A similar phase transition has not been observed if R_1 and/or R_2 are CH_2-CH_2-OH. This means that the OH group, being strongly hydrated, penetrates into the aqueous subphase even at high molecular areas. The possibility of the *E* conformation in the case of V and VI at high molecular areas might be correlated with the lower solubility of amines as compared to the corresponding alcohols (e.g. the solubility of 1-hexanol in water is of 0.59 g/100 ml, whereas 1-aminohexane is only sparingly soluble in water), [8] the NH_2 group forming less easy hydrogen bonds with the subphase water molecules, than the OH group.

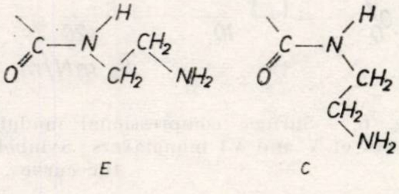

Fig. 5. — *E* and *C* conformations for the NR_1R_2 group of V and VI.

Concerning the compressional moduli of the films, generally $C_{s,0}^{-1}$ values given in Tab. 1 are higher with *L* systems as compared to the corresponding *S* ones, i.e. *S* systems are more easily compressible than the *L* ones. An inversion appears in the case of the pair VII–VIII, but one must take into account that the differences between the π_c, A_0 and $C_{s,0}^{-1}$ values in the case of this pair are much less, as compared to the pairs III–IV and

V—VI. Presumably, the OH group being strongly anchored in the aqueous subphase, the vertical orientation of the molecular plates occurs more easily than with the other derivatives studied and consequently, the above-mentioned inversion of order is only an apparent effect.

The surface compressional modulus, or elasticity[9] defined as $C_s^{-1} = -A(\partial\pi/\partial A)_T$ is a function of π, i.e. it varies during the compression of the film. C_s^{-1} *vs.* π curves were obtained by us by graphical derivation of the experimental π *vs.* A curves (Figs. 2 and 3). The C_s^{-1} *vs.* π curves obtained are given in Figs. 6 and 7.

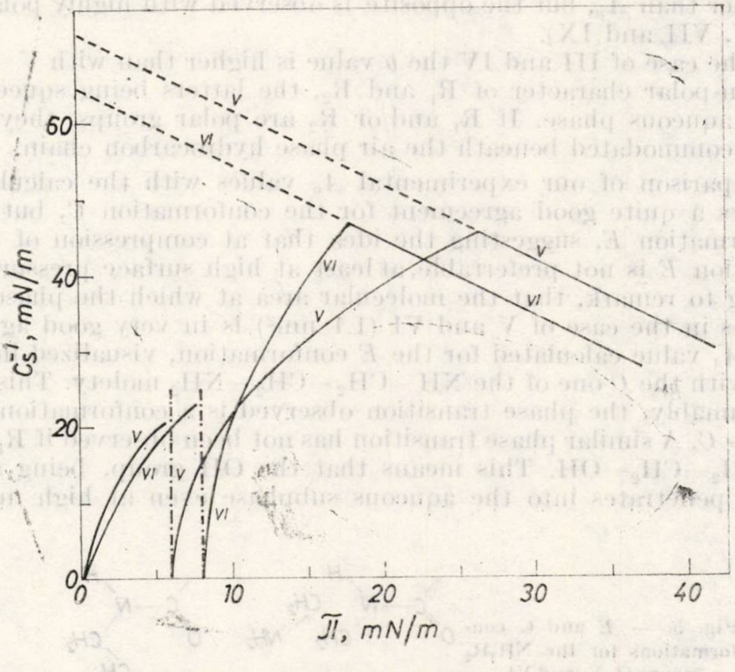

Fig. 6. — Surface compressional modulus vs. surface pressure curves of V and VI monolayers. Symbols of substances are near the curves.

As seen in Fig. 2, in the case of V and VI the curves show a plateau, indicating a first order phase transition, i.e. a discontinuity in the real molecular areas at a certain surface pressure. This discontinuity appears also in the case of the corresponding C_s^{-1} *vs.* π curves (Fig. 6). The curves of VII—IX are continuous (Figs. 3 and 7). All the compressional modulus curves (Figs. 6 and 7) pass through a maximum at π values comprised between 16.5 and 26.25 mN/m. The shape of the curves is similar to the elasticity curves of natural albumin monolayers.[9]

At all π values C_s^{-1} remains (Figs. 6 and 7) below the upper limit indicated for liquid expanded monoalyers,[10] although $C_{s,0}^{-1}$ slightly surpasses this limit with III, V—VIII. It is worth mentioning that by extrapolation of the linear portion of the C_s^{-1} *vs.* π curves to $\pi = 0$, one obtains

$C_{s,0}^{-1}$ (see Figs. 6 and 7). Therefore, $C_{s,0}^{-1}$ characterizes the monolayer in a hypothetical state, corresponding to the close packing of the rotating molecules, but having $\pi = 0$. Nevertheless, $C_{s,0}^{-1}$ characterizes to a certain extent the behaviour of the monolayer at high π values, since the order of $C_{s,0}^{-1}$ values for a series of surfactants is the same as the order of their C_s^{-1} values at a given π, providing that this π is higher than the surface pressure corresponding to the beginning of the high pressure linear portion of the compression isotherms.

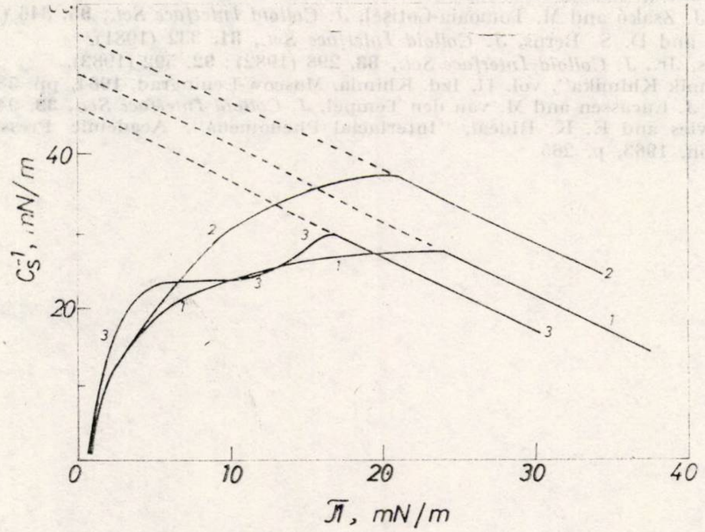

Fig. 7. — Surface compressional modulus *vs.* surface pressure curves of VII, VIII and IX monolayers.
1 — VII ; 2 — VIII ; 3 — IX.

We can conclude that our molecular model allows us to obtain pieces of information concerning the behaviour of surfactant molecules at the compression of insoluble monolayers, to have an idea of the formation of surface lattices of oriented molecules in the liquid expanded state and before the collapse of the film. The experimental surface characteristics may be correlated with the conformation of the flexible part of the molecule, with the intermolecular interactions occurring between both polar headgroups and hydrocarbon chains of neighbouring surfactant molecules, as well as between the polar headgroups and the subphase water molecules. These results might contribute to the understanding of phenomena occurring in natural membranes, by taking into account the importance of carotenoids in the living organisms.

REFERENCES

[1] M. Tomoaia-Cotişel, E. Chifu, V. Tămaş and V. Mărculeţiu, *Rev. Roumaine Chim.*, **25,** 175 (1980).

[2] J. Zsakó, E. Chifu and M. Tomoaia-Cotişel, *Gazz. chim. Ital.*, **109,** 663 (1979).

[3] V. Tămaş, V. Ciurdaru and C. Bodea, *Rev. Roumaine Chim.*, **18,** 1409 (1973).

[4] V. Tămaş and C. Bodea, *Rev. Roumaine Chim.*, **19,** 701 (1974).

[5] E. Chifu, J. Zsakó and M. Tomoaia-Cotişel, *J. Colloid Interface Sci.*, **95,** 346 (1983).

[6] R. Almog and D. S. Berns, *J. Colloid Interface Sci.*, **81,** 332 (1981).

[7] H. E. Ries, Jr., *J. Colloid Interface Sci.*, **88,** 298 (1982); **92,** 592 (1983).

[8] "Spravochnik Khimika", vol. II, Izd. Khimia, Moscow-Leningrad, 1964, pp. 584, 590.

[9] M. Blank, J. Lucassen and M. van den Tempel, *J. Colloid Interface Sci.*, **33,** 94 (1977).

[10] J. T. Davies and E. K. Rideal, "Interfacial Phenomena", Academic Press, New York-London, 1963, p. 265.

Revue Roumaine de Chimie, **32**, *11–12*, 1203–1210 (1987)

Dedicated to Professor V. E. SAHINI
on his 60th anniversary

APPROXIMATE SOLUTION FOR ISOTHERMAL EFFECTIVENESS FACTOR

CONSTANTIN MARIAN SPOITU,[a] SORIN SPOITU[b] and OVIDIU MUNTEAN[c]
[a] Romanian Chemical Factories, Panduri 71, Bucharest, Romania
[b] Territorial Electronic Calculus Centre, Ana Ipătescu 20, Slatina, jud. Olt, Romania
[c] Department of Chemical Engineering, Polytechnic Institute, Polizu 1, Bucharest, Romania

Received May 25, 1987

The paper peresents an approximate analytical method for solving the problem of diffusion with chemical reaction for catalytic gas-solid systems. This method improves the results of Bischoff.[1] The method uses a new function which provides an analytical solution for the problem. The error of the result tends to zero when the generalized Thiele modulus goes to infinity. The bounds of the error for finite values of the same modulus are indicated in the work. An application is also presented for a specific rate equation taken from the literature[1] and extensions of the method for general cases are suggested.

INTRODUCTION

The interest for approximate solutions for diffusion with catalytic chemical reaction is justified by the possibility to use such solutions for solving complex mathematical models of industrial catalytic reactors. In this way the computation time may be substantially reduced without losing too much in accuracy.

This paper presents an approximate analytical method for solving the problem of isothermal effectiveness factor improving the results obtained by Bischoff.[1] The method is an extension to catalytic gas-solid systems of an earlier technique.[2]

MATHEMATICAL MODEL

Consider a porous catalytic slab in which the following irreversible chemical reaction takes place:

$$A \rightarrow \text{products} \tag{1}$$

which is described by a general rate equation of the homogeneous type:

$$r = r(T_0,\ c) \tag{2}$$

If one admits that the effective diffusion coefficient is concentration independent the reactant concentration distribution within the pellet results by solving the mass balance on the reactant in the pore space of the pellet :

$$D\ddot{c} - r(T_0, c) = 0 \tag{3}$$

for the boundary conditions :

$$c(0) = c_0 \tag{4a}$$

$$\dot{c}(L) = 0 \tag{4b}$$

where L is the catalyst half width. The second boundary condition arises from the symmetry condition of the concentration profile.

In dimensionless form, Eq. (3) becomes :

$$\ddot{c}_1 - \varphi^2 v_R = 0 \tag{5}$$

and the boundary conditions (4) :

$$c_1(0) = 1 \tag{6a}$$

$$\dot{c}_1(1) = 0 \tag{6b}$$

where :

$$c_1 = c/c_0\,;\ \varphi^2 = L^2(c_0)/(Dc_0)\,;\ v_R = r(c)/r(c_0) \qquad \text{(7a), (7b), (7c)}$$

The quantity of interest is the catalyst effectiveness factor which is given by :

$$\eta = -D\,\frac{\dot{c}(0)}{L\,r(c_0)} \tag{8}$$

or in dimensionless form :

$$\eta = \frac{L}{\varphi^2}\,\dot{c}_1(0) \tag{9}$$

As can be seen from Eq. (9) the effectiveness factor may be obtained if one knows the dimensionless concentration gradient at the catalyst surface, $\dot{c}_1(0)$.

APPROXIMATE ANALYTICAL METHOD

By integrating once Eq. (5) with condition (4b) one obtains :

$$\dot{c}_1^2(0) = -2\varphi^2 \int_1^{c_1(1)} v_R\,\mathrm{d}\alpha \tag{10}$$

The right side integral may be analytically solved if one knows the primitive function of the integral and the upper limit $c_1(1)$. But to obtain $c_1(1)$ one has to integrate twice Eq. (5) which is a difficult or impossible task in a general case.

One may by-pass this difficulty by introducing a new function $\Phi(c_1)$ to replace $v_R(c_1)$ in Eq. (5) in such a way as to be able to analytically solve the approximate equation :

$$\ddot{\tilde{c}}_1 - \varphi^2 \Phi(\tilde{c}_1) = 0 \tag{11}$$

with the corresponding boundary conditions :

$$\tilde{c}_1(0) = 1 \tag{12a}$$

$$\dot{\tilde{c}}_1(1) = 0 \tag{12b}$$

The absolute error on the value of $\dot{c}_1^2(0)$ when one uses Eq. (11) instead of Eq. (5) is :

$$|\dot{c}_1^2(0) - \dot{\tilde{c}}_1^2(0)| = 2\varphi^2 \left| \int_1^{\tilde{c}_1(1)} \Phi \, \mathrm{d}\alpha - \int_1^{c_1(1)} v_R \, \mathrm{d}\alpha \right| \tag{14}$$

and on the effectiveness factor :

$$|\eta^2 - \tilde{\eta}^2| = \frac{2L^2}{\varphi^2} \left| \int_1^{\tilde{c}_1(1)} \Phi \, \mathrm{d}\alpha - \int_1^{c_1(1)} v_R \, \mathrm{d}\alpha \right| \tag{15}$$

Taking into account that :

$$\int_1^{c_1(1)} v_R \, \mathrm{d}\alpha = \int_1^{\tilde{c}_1(1)} v_R \, \mathrm{d}\alpha + \int_{\tilde{c}_1(1)}^{c_1(1)} v_R \, \mathrm{d}\alpha \tag{16}$$

one obtains from (15) :

$$|\eta^2 - \tilde{\eta}^2| = \frac{2L^2}{\varphi^2} \left| \int_1^{\tilde{c}_1(1)} \Phi \, \mathrm{d}\alpha - \int_1^{\tilde{c}_1(1)} v_R \mathrm{d}\alpha - \int_{\tilde{c}_1(1)}^{c_1(1)} v_R \, \mathrm{d}\alpha \right| \tag{17}$$

If the function Φ satisfies the condition :

$$I_\Phi = \int_1^{\tilde{c}_1(1)} \Phi \, \mathrm{d}\alpha = \int_1^{\tilde{c}_1(1)} v_R \, \mathrm{d}\alpha = I_v \tag{18}$$

Eq. (17) becomes :

$$|\eta^2 - \tilde{\eta}^2| = \frac{2L^2}{\varphi^2}\left|\int_{\tilde{c}_1(1)}^{c_1(1)} v_R \,\mathrm{d}\alpha\right| \tag{19}$$

The variables from Eq. (19) must have finite values (if v_R is a continuous function) so that the absolute error on the square of the effectiveness factor tends to zero when φ goes to infinity. The error in Eq. (19) is limited by :

$$\eta^2 - \tilde{\eta}^2 \leqslant \frac{2Dc_0}{r(c_0)} \max\left[\left|\int_{\tilde{c}_1(1)}^{1} v_R \,\mathrm{d}\alpha\right|, \left|\int_{\tilde{c}_1(1)}^{0} v_R \,\mathrm{d}\alpha\right|\right] \leqslant \frac{2Dc_0}{r(c_0)}\int_0^1 v_R \,\mathrm{d}\alpha\,\Big| \tag{19}$$

APPLICATION

Consider, similar to Bischoff, [1] that the rate equation has the form :

$$r(c) = k(T_0)\, c^n \tag{20}$$

and therefore the dimensionless reaction rate :

$$v_R = c_1^n \tag{21}$$

We exemplify here the case when the Φ function may be chosen to be of linear form :

$$\Phi = f^2 c_1 \tag{22}$$

From the Eq. (18) one obtains the values for the linearization factor f :

$$f^2 = \frac{2}{n+1}\,\frac{1 - \tilde{c}_1^{(n+1)}(1)}{1 - \tilde{c}_1^2(1)} \tag{23}$$

Solving Eq. (11) it results :

$$\tilde{c}_1(1) = \frac{1}{ch(\varphi f)} \tag{24}$$

and for the approximate effectiveness factor one obtains :

$$\tilde{\eta} = \frac{f}{\varphi}\, th(\varphi f) \tag{25}$$

In the references [1,3] the same approximate effectiveness factor is calculated from :

$$\eta_B = \frac{1}{m} th(m) \tag{26}$$

where :

$$m = \varphi f_B \tag{27}$$

and :

$$f_B^2 = \left[2 \int_0^1 v_R \, \mathrm{d}\alpha \right]^{-1} \tag{28}$$

Using Eq. (27) to correlate φ with the generalized Thiele modulus m, as Bischoff, [1] one obtains from Eq. (25) :

$$\tilde{\eta} = \frac{f f_B}{m} th \left(\frac{f m}{f_B} \right) \tag{29}$$

Another way or linearization, as indicated by DeLancey [4,5] is the least square method. The linearization factor, for this application, is obtained from the least square condition :

$$\min_f \int_1^{\tilde{c}_1(1)} (\Phi - v_R)^2 \, \mathrm{d}\alpha \tag{30}$$

and the result is :

$$f_D^2 = \frac{3}{n+1} \, \frac{1 - \tilde{c}_1^{(n+2)}(1)}{1 - \tilde{c}_1^3(1)} \tag{31}$$

Together with the relation :

$$\tilde{c}_1(1) = \frac{1}{ch(\varphi f_D)} \tag{32}$$

the approximate effectiveness factor may be calculated by :

$$\eta_D = \frac{f_D f_B}{m} th \left(\frac{f_D m}{f_B} \right) \tag{33}$$

One may compare now the values of three effectiveness factors, $\tilde{\eta}$ (29), η_B (26), η_D (33). Figure 1 presents these values as a function of the generalized modulus m. For the present example the precision decreases in the order $\tilde{\eta}$, η_D, η_B. The relative error is smaller than 5% for $\tilde{\eta}$, smaller than 7% for η_D and smaller than 8% for η_B when the reaction order lies between 0.5 and 3 in comparison with the analytical solution [6] of Eq. (3) with the rate expression (20).

CONCLUSIONS

The present suggested method gives an analytical approximate solution for the isothermal effectiveness factor which improves the results of Bischoff [1,3] but this must be balanced by the need of solving an algebraic nonlinear equation.

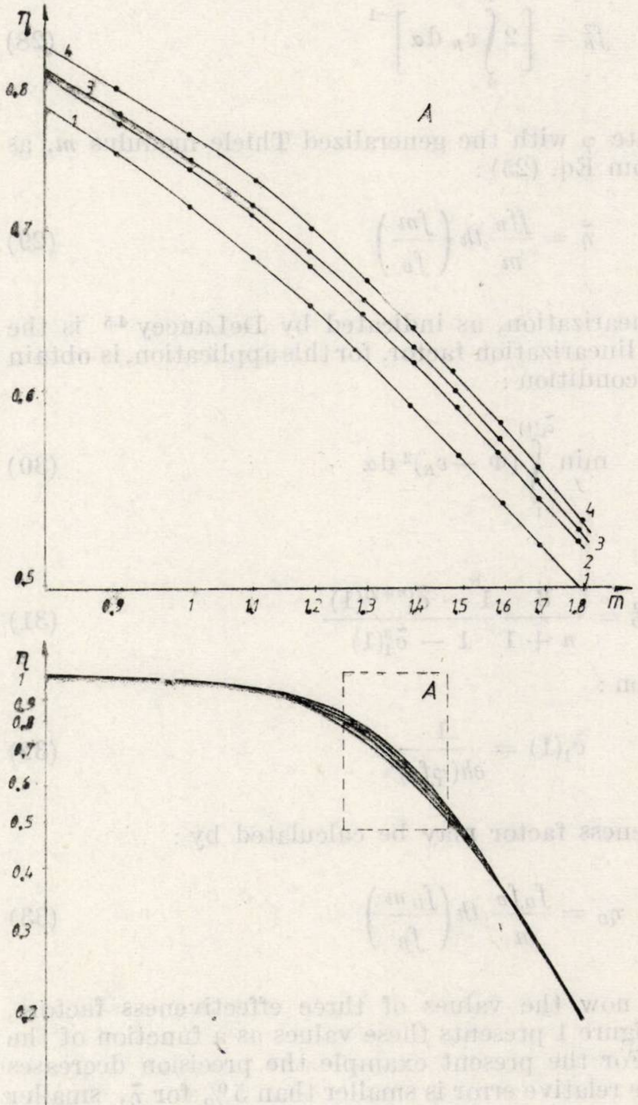

Fig. 1. — Plot of effectiveness factor versus m ($n=3$)
1 — numerical; 2 — η_B; 3 — η_D; 4 — $\bar{\eta}_B$

It has been also shown that the linearization of the reaction rate expression according to the least square method does not give always the best results.

The linearization is the most simple solution but for some v_R functions the use of a nonlinear "power-law" function as Φ and the results of Mehta-Aris [6] may be useful alternative.

The present method may be also extended to a reaction of the general form : [7,8]

$$\sum_{j=1}^{s} \nu_j A_j = 0 \tag{34}$$

if one uses for the limiting species the effective diffusion coefficient in a multicomponent mixture.

NOTATIONS

A — reactive component of reaction (1)
A_j — components of reaction (34)
c — concentration of A
c_1 — dimensionless concentration of A
c_0 — surface concentration of A
D — diffusion coefficient of A
f — linearization factor
k — reaction rate coefficient
L — catalyst half width
m — general modulus
n — reaction rate order
r — reaction rate
s — number of components in reaction (34)
v_R — dimensionless reaction rate

Greek symbols

η — effectiveness factor
φ — Thiele modulus
Φ — proposed function to replace v_R
ν_j — stoichiometric coefficient of A in reaction (34)

Subscripts

B — values obtained by the Bischoff technique [1]
D — values obtained by the DeLancey technique [4,5]

Superscripts

$\sim$ — approximate values obtained in this paper
$\dot{}$ — first derivative with respect to the distance from the surface
$\ddot{}$ — second derivative with respect to the distance from the surface

REFERENCES

[1] K. B. Bischoff, *AICHEJ.*, **11**, 351 (1965).
[2] C. M. Spoitu and O. Muntean *Rev. Chim.*, *(București)*, **37**, 780 (1986).
[3] G. F. Froment and K. B. Bishoff "Chemical Reactor Analysis and Design", John Wiley & Sons, New York, 1979.
[4] G. B. DeLancey, *Chem. Eng. Sci.*, **29**, 2315 (1974).
[5] S. T. Lee and G. B. DeLancey, *Chem. Eng. Sci.*, **29**, 2325 (1974).
[6] B. N. Mehta, R. Aris *Chem. Eng. Sci.*, **26**, p. 1699 (1971).
[7] D. J. Gunn *Chem. Eng. Sci.* **22**, p. 1435 (1967).
[8] J. B. Gros, R. Bugarel *Chem. Eng. Sci* **29**, p. 1465 (1974).

Revue Roumaine de Chimie, 32, *11–12*, 1211–1218 (1987)

Dedicated to Professor V. E. SAHINI,
on his 60th anniversary

ON THE SIGNIFICANCE OF THE MINIMUM IGNITION ENERGY OF AN EXPLOSIVE GASEOUS MIXTURE

D. OANCEA*, DOMNINA POPESCU** and N. I. IONESCU**
* The Polytechnic Institute, Department of Physical Chemistry and Electrochemical Technology, Bdul. Republicii 13, Bucharest, Romania
** Center of Physical Chemistry, Spl. Independenţei 202, Bucharest 77208, Romania

Received June 30, 1987

A model is proposed, based on the assumption that the minimum ignition energy (MIE) is identical with the expansion work of the burned gases during the initiation stage. On the basis of this model, the MIE can be calculated if the quenching distance and the initial pressure of the gaseous explosive mixture are known. The calculated values of MIE using the literature data on the quenching distances are in good agreement with the corresponding measured values for fuel-air mixtures, also available in literature.

1. INTRODUCTION

The concept of MIE is connected with the use of capacitive electric sparks to ignite the gaseous explosive mixtures.[1] MIE has specific values for mixtures of different compositions and is dependent on the pressure and temperature.[1–6] At a specified pressure and temperature, MIE seems to be an intrinsic property of a given explosive mixture. Some studies indicated that MIE can however be significantly modified by both electrode and discharge characteristics.[7] These instrumental factors can partly explain the differences between MIE values obtained in different laboratories for the same mixture. When measured under similar instrumental conditions, MIE is an important property of an explosive mixture having numerous theoretical and practical implications.[1] Besides some practical problems connected with the ignition of fuel-oxidant mixtures and with the assignment of safety standards in relation to possible explosion hazards,[3] MIE is a subject of a wide theoretical interest, especially for the understanding of the initiation stage of an explosion. The large number of experimental data available in literature, due to the continuous improvement of experimental techniques initiated by Lewis and von Elbe,[1] offers the opportunity to get a new insight into the physical significance of MIE. It was initially conceived[1] as the minimum energy of a spark necessary to be supplied to a small volume of a gaseous mixture in order to obtain a flame of minimum size (radius), just capable of self-propagation. As the calculations carried out on the basis of simplified models provide theoretical values which seldom agree with the measured ones,[1] and the endeavour to correlate the measured values of MIE with the molecular structure of the fuel did not exceed the qualitative level,[2] the question of the theoretical significance of MIE remains still open.

2. THE MODEL

When a gaseous explosive mixture is subjected to a capacitive electric spark (having a short discharge time), it can be ignited only if the energy delivered by the spark is sufficient to bring the initial nucleus of burned gases to a size equal to or larger than the minimal flame volume, when the burning process becomes self-propagating.[1] Let us consider an explosive gaseous mixture filling a sphere of volume V_0, and having the initial pressure and temperature p_i and T_i, respectively. If v_f^* is the minimal flame volume (considered also of spherical form), then generally $v_f^* \ll V_0$ and the ignition stage occurs at constant pressure, p_i. The burned gases within the critical volume v_f^* have the pressure p_i and temperature T_i, equal to the flame temperature at pressure p_i, and result from the combustion of a volume v_i of unburned gases at pressure p_i and temperature T_i. During the ignition process, the expansion of the unburned gases from the volume v_i to the minimal flame volume v_f^* is accompanied by an expansion work lost by the burned gas. As a first approximation, this quantity can be calculated as the reversible expansion work from v_i to v_f^* :

$$W_{e,\mathrm{rev}} = p_i(v_f^* - v_i) = p_i v_f^* \cdot \frac{E_0 - 1}{E_0} \tag{1}$$

where $E_0 = v_f^*/v_i$ is the expansion factor at constant pressure p_i. The minimal flame volume can easily be calculated if the quenching distance (or quenching diameter) d_q is known.

$$v_f^* = \frac{4\pi(d_q/2)^3}{3} \tag{2}$$

The expansion factor E_0 can be calculated from the state equations of gases before and after burning, assuming an ideal behaviour :

$$p_i v_i = n_i\ RT_i \tag{3}$$

$$p_i v_f^* = n_f\ RT_f \tag{4}$$

where R is the molar constant of an ideal gas and n_f is the mole number in the flame volume resulted from n_i mole number in initial volume v_i. In this case E_0 becomes

$$E_0 = \frac{n_f}{n_i} \cdot \frac{T_f}{T_i} \tag{5}$$

For air-fuel explosive mixtures, when nitrogen is usually in excess, the burning molar ratio n_f/n_i approaches unity and hence

$$\frac{E_0 - 1}{E_0} \simeq \frac{T_f - T_i}{T_f} \tag{6}$$

For common flame temperatures (1700 to 2500 K) the ratio given by eqn. (6) ranges from 0.82 to 0.88. A mean value of 0.85 simplifies the calculations without introducing a significant error. Equation (1) becomes now:

$$W_{e,\mathrm{rev}} = \frac{\pi}{6} \cdot p_i \cdot d_q^3 \cdot \frac{T_f - T_i(n_f/n_i)}{T_f} \simeq \frac{0.85\,\pi}{6} \cdot p_i d_q^3 \tag{7}$$

One can assume that the ignition occurs if the energy lost as the expansion work by the burned gases of the minimal flame is compensated through the spark energy: $W_{e,\mathrm{rev}} = H'_m$. *If* p_i is expressed in (N/m^2) and d_q in (m), then H'_m can be calculated using the equation:

$$H'_m = 0.445 \cdot p_i \cdot d_q^3 = k \cdot p_i \cdot d_q^3 \ (\mathrm{J}) \tag{8}$$

and compared with the measured value H_m.

On the other hand, if H_m is known, the corresponding quenching distance can be calculated:

$$d'_q = \left(\frac{H}{0.445 \cdot p_i}\right)^{1/3} = \left(\frac{H_m}{k \cdot p_i}\right)^{1/3} \tag{8'}$$

3. APPLICATION OF THE MODEL TO THE LITERATURE DATA

The quenching distances d_q and the minimum ignition energies H_m reported in literature for gaseous explosive mixtures of air with different fuels are given in table 1. The quenching distances measurements were based upon the method initiated by Lewis and von Elbe, using flanged electrodes. For a few systems the quenching distances measured by other methods are also given. The minimum ignition energy measurements were based upon the method of capacitance discharge, also initiated by Lewis and von Elbe. The measurements based upon the expanding capacitor plate technique,[8,9] leading to larger values of MIE as compared to standard technique were not taken into account, although sometimes they were in the favour of the model, because of the small number of available data. The mixture composition was given as the stoichiometric ratio, φ_s. The most numerous data were reported for the stoichiometric composition ($\varphi_s = 1$) and for the composition which has the lowest value of MIE. This "minimum" composition was designated by "*m*", without any other specification. In table 1 are also given the calculated values H'_m and d'_q

Table 1

Quenching distances and minimum ignition energies of air-fuel gaseous mixtures ($p_i = 1$ atm; $T_i = 298$ K)

No.	Fuel	φ_s	d_q (mm)	Ref	H_m (mJ)	H'_m (mJ)	d'_q (mm)	H_m/H'_m	d_q/d'_q	$(H_m/d_q^3)\cdot 10^4 (N/m^2)$
a	b	c	d	e	f	g	h	i	j	k
1	**Methane**	0.7	2.9	1	0.75	1.100	2.55	0.682	1.44	3.075
2	,,	0.8	2.2	1	0.42	0.480	2.10	0.875	1.05	3.944
3	,,	0.9	2.0	1	0.30	0.361	1.88	0.831	1.06	3.750
4	,,	1.0	2.1	1	0.30	0.418	1.88	0.718	1.12	3.239
5	,,	1.0	2.54	3	0.33	0.739	1.94	0.447	1.31	2.014
6	,,	1.0*	—	2	0.47	—	2.18	—	—	—
7	,,	1.0*	2.08	3	—	0.406	—	—	—	—
8	,,	1.1	2.5	1	0.46	0.705	2.17	0.653	1.15	2.944
9	,,	1.25	4.5	1	1.67	4.110	3.33	0.407	1.35	1.833
10	,,	m	2.03	3	0.29	0.377	1.86	0.769	1.09	3.467
11	**Ethane**	1.0	2.29	3	0.42	0.542	2.10	0.776	1.09	3.497
12	,,	1.0*	—	2	0.285	—	1.85	—	—	—
13	,,	m	1.78	3	0.24	0.254	1.75	0.944	1.02	4.256
14	,,	m*	—	3	0.25	—	1.77	—	—	—
15	,,	m	1.80	1	0.25	0.263	1.77	0.951	1.02	4.287
16	**Propane**	0.7	4.2	1	2.22	3.34	3.66	0.664	1.15	2.996
17	,,	0.7*	3.43	5	—	1.82	—	—	—	—
18	,,	0.9	2.4	1	0.59	0.624	2.36	0.946	1.02	4.268
19	,,	1.0	1.9	1	0.39	2.05	2.05	1.26	0.925	5.686
20	,,	1.0	1.75	2	0.305	0.242	1.89	1.26	0.925	5.691
21	,,	1.0	2.03	3	0.305	0.377	1.89	0.808	1.07	3.646
22	,,	1.0*	1.73	4	—	0.234	—	—	—	—
23	,,	1.28	1.70	1	0.25	0.222	1.77	1.13	0.961	5.088
24	,,	1.40	2.0	1	0.26	0.361	1.79	0.721	1.12	3.250
25	,,	1.50	2.5	1	0.29	0.705	1.86	0.412	1.34	1.856
26	,,	m	1.78	3	0.26	0.254	1.79	1.02	0.993	4.610
27	**n-Butane**	1.0	3.05	3	0.76	1.28	2.56	0.594	1.19	2.679
28	,,	1.0*	2.16	4	—	0.455	—	—	—	—
29	,,	m	1.78	3	0.26	0.254	1.79	1.02	0.993	4.610
30	**n-Pentane**	1.0	2.07	2	0.51	0.400	2.24	1.28	0.922	5.750
31	,,	1.0	3.30	3	0.82	1.62	2.63	0.506	1.26	2.282
32	,,	1.0*	2.00	4	—	0.361	—	—	—	—
33	,,	m	1.78	3	0.22	0.254	1.70	0.865	1.05	3.901
34	**n-Hexane**	1.0*	1.82	5	—	0.272	—	—	—	—
35	,,	1.0	3.56	3	0.95	2.03	2.76	0.467	1.29	2.106
36	,,	m	1.78	3	0.23	0.254	1.72	0.904	1.03	4.078
37	**n-Heptane**	1.0	2.2	2	0.70	0.480	2.49	1.46	0.882	6.574
38	**isobutane**	1.0	2.2	2	0.52	0.480	2.26	1.08	0.974	4.884
39	**isooctane**	1.0	3.47	2	1.35	1.88	3.11	0.716	1.12	3.231
40	**2,2-dimethyl-butane**	1.0	4.57	3	1.64	4.31	3.31	0.381	1.38	1.718
41	,,	m	1.78	3	0.25	0.254	1.77	0.983	1.01	4.433
42	**cyclopropane**	1.0	1.78	3	0.24	0.254	1.75	0.944	1.02	4.255
43	,,	1.0*	—	2	0.24	—	1.75	—	—	—
44	,,	m	1.78	3	0.23	0.254	1.72	0.906	1.03	4.078
45	**cyclopentane**	1.0	3.30	3	0.83	1.62	2.64	0.512	1.25	2.310
46	,,	1.0*	—	2	0.54	—	—	—	—	—
47	**cyclohexane**	1.0	3.0	2	1.38	1.22	3.13	1.13	0.959	5.111
48	,,	1.0	3.06	3	1.38	1.29	3.13	1.07	0.978	4.816
49	,,	1.0*	2.95	4	—	1.16	—	—	—	—

Table 1 (continued)

a	b	c	d	e	f	g	h	i	j	k
50	,,	m	1.78	3	0.223	0.254	1.70	0.877	1.05	3.954
51	ethylene	1.0	1.27	3	0.096	0.0924	1.29	1.04	0.987	4.687
52	,,	1.0	1.20	3	0.095	0.0779	1.28	0.82	0.936	5.498
53	,,	1.0*	—	2	0.096	—	1.29	—	—	—
54	1,3-butadiene	1.0	1.25	2	0.175	0.0881	1.57	1.99	0.796	8.960
55	,,	1.0	1.78	3	0.235	0.254	1.73	0.924	1.03	4.167
56	,,	m	1.27	3	0.125	0.0924	1.41	1.35	0.904	6.102
57	cyclohexene	1.0	2.10	2	0.525	0.418	2.27	1.26	0.927	5.669
58	,,	1.0	3.30	3	0.86	1.62	2.67	0.531	1.24	2.393
59	acetylene	1.0	0.65	2	0.020	0.0124	0.763	1.61	0.852	7.283
60	,,	1.0	0.76	3	0.011	0.0198	0.625	0.556	1.22	2.506
61	,,	m*	0.60	3	—	0.00974	—	—	—	—
62	1-heptyne	1.0	1.85	2	0.56	0.286	2.32	1.96	0.799	8.845
63	diisobutylene	1.0	3.2	2	0.96	1.478	2.77	0.650	1.15	2.930
64	benzene	1.0	1.95	2	0.55	0.334	2.30	1.64	0.847	7.418
65	,,	1.0	2.79	3	0.55	0.979	2.30	0.562	1.21	2.533
66	,,	1.0*	1.9	4	—	0.309	—	—	—	—
67	,,	1.0*	1.71	5	—	0.226	—	—	—	—
68	,,	m	1.78	3	0.225	0.254	1.71	0.885	1.04	3.990
69	methanol	1.0	1.78	3	0.215	0.254	1.68	0.845	1.06	3.812
70	,,	1.0*	—	2	0.215	—	1.68	—	—	—
71	,,	m	1.52	3	0.14	0.158	1.46	0.884	1.04	3.987
72	ethanol	m	1.75	3	0.14	0.242	1.46	0.579	1.20	2.612
73	diethylether	1.0	1.85	2	0.49	0.286	2.22	1.72	0.835	7.739
74	,,	1.0	2.54	3	0.49	0.739	2.22	0.663	1.15	2.990
75	,,	m	1.78	3	0.19	0.254	1.62	0.747	1.10	3.369
76	diisopropylether	1.0	3.00	2	1.14	1.22	2.94	0.936	1.02	4.222
77	acetone	1.0	3.81	3	1.15	2.49	2.94	0.461	1.29	2.079
78	,,	1.0*	—	2	1.15	—	2.94	—	—	—
79	ethylene oxide	1.0	1.18	2	0.087	0.0741	1.25	1.17	1.06	5.295
80	,,	1.0	1.27	3	0.105	0.0924	1.33	1.14	0.959	5.126
81	,,	m	1.00	3	0.06	0.0451	1.10	1.33	0.909	6.000
82	,,	m	1.02	3	0.062	0.0479	1.11	1.29	0.917	5.842

Table 1 (continued)

a	b	c	d	e	f	g	h	i	j	k
83	,,	1.0*	1.17	4	—	0.0722	—	—	—	—
84	propylene oxide	1.0	1.3	2	0.19	0.0991	1.62	1.92	0.805	8.648
85	,,	1.0	1.78	3	0.19	0.254	1.62	0.747	1.10	3.369
86	,,	m	1.52	3	0.14	0.158	1.46	0.884	1.04	3.987
87	methyl formate	1.0	1.65	2	0.40	0.203	2.07	1.97	0.797	8.905
88	ethyl acetate	1.0	4.32	3	1.42	3.64	3.16	0.391	1.37	1.761
89	,,	1.0*	—	2	1.42	—	—	—	—	—
90	,,	m	2.54	3	0.48	0.739	2.20	0.650	1.16	2.929
91	propionaldehyde	1.0	1.75	2	0.325	0.242	1.93	1.34	0.906	6.064
92	vinyl acetate	1.0	2.35	2	0.70	0.585	2.49	0.836	0.942	5.394
93	tetrahydropyrane	1.0	3.81	3	1.21	2.49	2.99	0.485	1.27	2.188
94	,,	m	1.78	3	0.22	0.254	1.70	0.865	1.05	3.901
95	ethylamine	1.0	5.33	3	2.4	6.83	3.76	2.85	1.42	1.585
96	acrylonytrile	1.0	2.32	3	0.36	0.563	2.00	0.639	1.16	2.883
97	,,	m	1.52	3	0.16	0.158	1.53	1.01	1.00	4.556
98	50 %C_2H_4+ +50 %CH_4	1.0	1.40	3	0.21	0.124	1.67	1.70	0.838	7.653
99	50 %C_2H_4+50 %H_2	1.0	1.05	3	0.05	0.0522	1.04	0.958	1.02	4.319
100	50 %CH_4+50 %H_2	1.0	1.38	3	0.11	0.119	1.35	0.928	1.03	4.186
101	SH_2	1.0	1.02	3	0.077	0.0479	1.19	1.61	0.853	7.256
102	,,	1.0*	—	2	0.068	—	1.15	—	—	—
103	CS_2	1.0	0.55	2	0.015	0.00750	0.693	2.00	0.794	9.016
104	,,	1.0	0.51	3	0.015	0.00598	0.693	2.51	0.736	11.308
105	,,	1.0*	—	4	0.053	—	1.06	—	—	—
106	H_2	1.0	0.6	2	0.020	0.00974	0.763	2.05	0.787	9.259
107	,,	1.0	0.52	3	0.016	0.00634	0.708	2.52	0.735	11.379
108	,,	1.0	0.64	3	0.02	0.0118	0.763	1.69	0.839	7.630
109	,,	1.0*	—	4	0.0585	—	1.09	—	—	—
110	,,	1.0*	—	5	0.0495	—	1.03	—	—	—
111	,,	m	0.61	3	0.013	0.0102	0.661	1.27	0.923	5.727
112	,,	0.6	0.71	1	0.026	0.0161	0.832	1.61	0.853	7.264
113	,,	1.01	0.64	1	0.019	0.0118	0.750	1.61	0.854	7.248
114	,,	1.58	0.76	1	0.028	0.0198	0.853	1.41	0.891	6.378
115	,,	3.15	1.65	1	0.21	0.203	1.67	1.04	0.988	4.675

(cf. eqn. 8 and 8′) and the ratios H_m/H'_m, d_q/d'_q and H_m/d_q^3 used as criteria to test the validity of the model. All the data refer to $p_i = 1$ atm and $T_i = 298$ K. It can be observed that for many systems the reported values of H_m and d_q, measured by different authors, are significantly different, which can explain the relatively large dispersion of the sought correlations. Frequently, the scatter of the experimental data originates in the choice of the ignition probability level, as well as in the difficulties of achieving the identical discharge conditions when experimental techniques are different. The data in table 1 marked with an asterisk were not included in the calculation and consequently the total number of pairs used for correlations was 91. When all the pairs were used for correlation the following results were obtained: $H_m/H'_m = 1.07 \pm 0.51$, $d_q/d'_q = 1.03 \pm 0.16$ and $H_m/(p_i d_q^3) = k' = 0.466 \pm 0.21$. If only 22 pairs were used, referring to the mixtures with the lowest MIE, having also a lower dispersion for the reported data, the correlations were better: $H/H' = 0.91 \pm 0.20$; $d_q/d'_q = 1.03 \pm 0.07$ and $H_m/(p_i d_q^3) = k' = 0.424 \pm 0.089$.

The ratios H_m/H'_m and d_q/d'_q have mean values very closed to unity and the deviations seem to be due to the dispersion of the experimental data. The correlations seem to be better for the ratios d_q/d'_q as compared to H_m/H'_m, but in the first case the deviations are attenuated and in the second one magnified as a result of raising the scattered experimental data to the powers 1/3 and 3, respectively (eqns. 8′ and 8). The mean values of the correlation parameter $k' = H_m/(d_q^3 \cdot p_i)$ are very close to the expected theoretical value in equations 8 and 8′ (namely 0.445), the deviations being at most 5%, which is well within the range of the experimental data dispersion.

Table 2

Quenching distances and minimum ignition energies of oxygen-fuel mixtures ($p_i = 1$ atm; $T_i = 298$ K)

No.	Fuel	φ_s	d_q (mm)	Ref	H_m (mJ)	H'_m (mJ)	d'_q (mm)	H_m/H'_m	d_q/d'_q	(H_m/d_q^3), 10^{-4} (N/m²)
1	methane	0.22	0.78	1	0.025	0.0214	0.822	1.168	0.949	5.268
2	methane	0.35	0.50	1	0.0079	0.00564	0.600	1.401	0.833	6.320
3	methane	0.67	0.35	1	0.0042	0.00193	0.453	2.176	0.773	9.796
4	methane	1.47	0.50	1	0.018	0.00564	0.736	3.192	0.679	14.40
5	methane	2.00	1.60	1	0.397	0.185	2.07	2.146	0.773	9.692
6	propane	0.4	0.36	1	0.0059	0.00210	0.508	2.810	0.709	12.65
7	propane	0.8	0.26	1	0.0020	0.000793	0.354	2.522	0.735	11.38
8	propane	1.2	0.29	1	0.0027	0.00110	0.391	2.455	0.742	11.07
9	propane	1.4	0.34	1	0.0031	0.00177	0.410	1.751	0.829	7.887
10	propane	1.47	0.37	1	0.0039	0.00228	0.442	1.711	0.837	7.699

The trend is quite different for the oxygen-fuel mixtures, given in table 2.

In this case $H_m/H'_m = 2.13 \pm 0.60$, $d_q/d'_q = 0.786 \pm 0.075$ and $H_m/(p_i d_q^3) = k' = 0.949 \pm 0.266$, indicating that the experimentally measured MIE is about twice larger than the value expected from the model. The deviations can be explained qualitatively within the frame work of the same model. On the one hand, the MIE of oxygen-fuel mixtures are at least two orders of magnitude smaller than those of air-fuel mixtures. In this case the fraction of the spark energy transfered to electrodes can become of the same order of magnitude as MIE, leading to an apparent increase of the measured value of MIE. On the other hand, at smaller quenching distances, the symmetry of the volume occupied by burned gases during the initiation stage can be far from spherical, as supposed in the model.

Table 3

Quenching distances and minimum ignition energies of stoichiometric methane—air mixture at different initial pressures ($T_i = 298$ K)

No.	p_i (atm)	d_q (mm)	H_m (mJ)	H'_m (mJ)	d'_q (mm)	H_m/H'_m	d_q/d'_q	$(H_m/p_0 \cdot d_q^3)$
1	0.20	8.6	6.5	5.74	0.897	1.132	0.959	0.504
2	0.25	6.9	3.4	3.70	0.671	0.9189	1.028	0.409
3	0.33	4.8	2.1	1.65	0.521	1.273	0.9213	0.568
4	0.50	3.6	1.2	1.05	0.376	1.143	0.9574	0.508
5	0.67	3.0	0.84	0.816	0.303	1.029	0.9901	0.458
6	1.00	2.1	0.47	0.418	0.218	1.124	0.9633	0.501

The form of equation (8) indicates the pressure dependence of MIE in agreement with some empirical correlations found in literature.[5,6,10]

It is obvious that MIE is also pressure dependent through the quenching distance, but this is not shown explicitely in eqn. (8).

Several data[1] which can be used to check the validity of the model are given in table 3.

On the basis of these data the following results were obtained: $H_m/H'_m = 1.10 \pm 0.11$, $d_q/d'_q = 0.970 \pm 0.033$ and $H_m/(p_i d_q^3) = k' = 0.049 \pm \pm 0.049$, which again support the suggested model.

The proposed model leads to a good correlation between the MIE and the quenching distance for fuel-air mixtures and represents an alternative explanation concerning the significance of the minimum ignition energy.

REFERENCES

[1] B. Lewis and G. von Elbe, "Combustion, Flames and Explosions of Gases" 2nd edition, Academic Press, New York, 1961, p. 323.

[2] H. F. Calcote, C. A. Gregory Jr., C. M. Barnett and R. B. Gilmer, *Ind.Eng. Chem.*, **44**, 2656 (1952).

[3] V. A. Bondar, V. I. Verevkin and B. G. Popov, *J. Vses. Himicesk. Obscestv.*, **12**, 291 (1967).

[4] H. Phillips, *Combust. and Flame*, **7**, 129 (1963).

[5] A. E. Potter and A. L. Berlad, Sixth Internat. Symp. on Combustion, Reinhold, New York, 1957, p. 30.

[6] J. B. Fenn, *Ind. Eng. Chem.*, **43**, 2865 (1951).

[7] H. E. Rose and T. Priede, Seventh Internat. Symp. on Combustion, London, Butterworth Sci. Publ., 1959, p. 436, 454.

[8] D. Y. Cheng, *Combust. and Flame*, **11**, 517 (1967).

[9] J. Moorhouse, A. Williams and T. E. Maddison, *Combust. and Flame*, **23**, 203 (1974).

[10] H. Morris, Third Internat. Symp. on Combustion, Williams and Wilkins, Baltimore, 1949 p. 361.

Revue Roumaine de Chimie, **32**, *11–12*, 1219–1224 (1987)

Herrn Prof. Dr. V. E. SAHINI
zu seinem 60. Geburtstag gewidmet

PERHALOGENMETHYLTHIOHETEROCYCLEN, XXV[1]

ELEKTROPHILE SUBSTITUTION VON 2,4-DIAMINOPYRIMIDINEN MIT PERHALOGENMETHYLCHALCOGENOHALOGENIDEN

A. HAAS, M. LIEB und B. SCHWEDERSKI
Ruhr – Universität Bochum, Lehrstuhl für Anorganische Chemie II, Postfach 102148,
4630 Bochum 1, West Germany

Received August 15, 1987

Reactions of the biologically active 2,4-diamino-pyrimidines Trimethoprim and Pyrimethamin with perhalogenomethylchalcogen halides have been studied. It was found that reactions selectively took place at the exocyclic amino-functions. Ring substitution was observed with selenyl halides only in the presence of perfluoromethylsulfonic acid.

2,4-Diamino-pyridimine zeichnen sich durch eine Vielzahl biologischer Aktivitäten aus. Hierbei hervorzuheben sind die Folsäure-Antagonisten,[2] deren bakterizide Wirkung zu einer Vielzahl chemotherapeutisch wichtiger Substanzen geführt hat. Grund dafür ist die Tatsache, daß Bakterien- und Säugetierenzyme unterschiedliche Affinitäten zu den Chemotherapeutika zeigen und daraus eine selektive Toxizität resultiert.[3,4] Hervorzuheben sind in diesem Zusammenhang Substanzen des Pyrimethamin-Types (Typ A) und des Trimethoprim-Typs (Typ B).

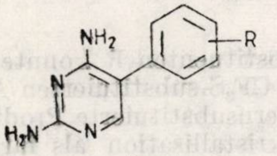

Typ A

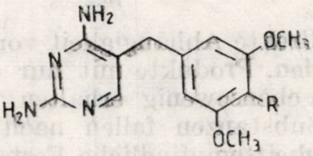

Typ B

Während sich Typ A als ausgesprochen wirksam gegen Malariaerreger erweist, wobei ein elektronenziehender Rest in *para*-Stellung am Benzolring zu einer Wirkungssteigerung führt, zeichnen sich die Vertreter des Typs B durch hohe Aktivitäten gegen gram-positive und gram-negative Bakterien und Mikro-organismen aus.

Da aus eigenen früheren Arbeiten[5,6] wie auch aus Literaturdaten[7] erhebliche Wirkungssteigerungen von Aktivstoffen durch Einführung von Perhalogenmethylthio-Resten bekannt waren, lag es nahe, auch im falle der 2,4-Diamino-pyrimidine des Typs A und B Substitutionen mit Perhalogenmethylcahlcogenhalogeniden zu versuchen. Interessant erschien in diesem Zusammenhang die Frage, ob bei der Reaktion solch komplexer Moleküle mit Sulfenylchloriden eine selektive Reaktion am exocyklischen Aminostickstoff durchführbar ist.

Betrachtet man das Trimethoprimgerüst des Typs B, so ergeben sich mehrere potentielle Substitutionspunkte, jedoch sind die 2-, 4- und 6-Positionen im Pyrimidinring, bedingt durch die elektronenziehende Wirkung der benachbarten Stickstoffatome, elektrophil nicht substituierbar, ebenso sollten die Alkoxygruppen bzw. die Methinbrücke gegenüber elektrophilen Angriffen inert sein. Substitutionen am Benzolring sollten unter Friedel-Crafts-Bedingungen möglich sein, so daß auf den Einsatz von Lewis-Säure-Katalysatoren verzichtet werden sollte. Demnach erschien es sinnvoll, Vertreter des Typs A und B unter milden elektrophilen Reaktionsbedingungen mit Perhalogenmethylchalcogenhalogeniden umzusetzen. So wurden, um Nebenreaktionen weitestgehend zu unterdrücken, Tetrahydrofuran als Lösungsmittel und Pyridin als HCl-Fänger gewählt. Unter Beibehaltung dieser Reaktionsbedingungen gelingt die Umsetzung von Vertretern des Typs B mit Trifluoromethylsulfenylchlorid CF_3SCl in guten Ausbeuten nach Gleichung I.

Gleichung I:

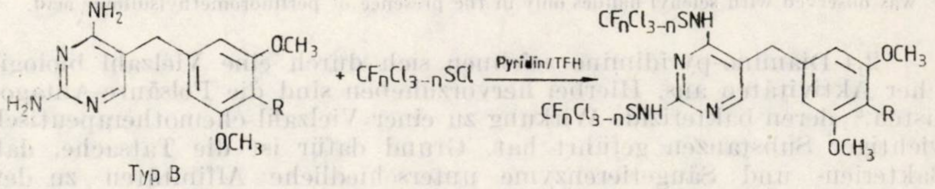

R	Ausbeute I : n = 3	II : n = 2
a OCH_3	59 %	12 %
b Br	81,7 %	8 %
c $OCH_2CH_2OCH_3$	35 %	9 %
d SCH_3	76,2 %	

+ Pyridin/HCl

n = 2 : I
n = 3 : II

Eine direkte Abhängigkeit vom Substituenten R konnte nicht festgestellt werden. Produkte mit nur einer CF_3S-substituierten Aminofunktion wurden ebensowenig erhalten wie kernsubstituierte Produkte.

Alle Substanzen fallen nach Umkristallisation als farblose, luft- und feuchtigkeitsempfindliche Feststoffe an.

Ganz analog verlaufen die Reaktionen mit dem Sulfensäurechlorid Chlordifluorsulfenylchlorid $CClF_2SCl$, jedoch liegen hier die Ausbeuten erheblich unter denen der Trifluoroanalogen, während im Falle von Id sogar kein Umsatz mehr erzielt werden konnte. Dieser Trend setzt sich im Falle des Dichlorfluormethyl-sulfenylchlorids und des Perchlormethylmercaptans fort, mit dem in allen Fällen kein Umsatz bei gleichzeitiger Verteerung und Zersetzung des Edukts erzielt werden konnte.

Diese Beobachtung abnehmender Produktausbeuten bei steigendem Chlorierungsgrad des Sulfensäurechlorids steht in Einklang mit früheren Beobachtungen[8,9]. Begründet wird dieses Phänomen durch die höhere Reaktivität der hochfluorierten Spezies und die damit verbundene erhöhte Elektrophilie des Anions.

Versuche, die Derivate des Trimethoprims trotz der eingangs erwähnten Vorbehalte unter Friedel-Crafts-Bedingungen umzusetzen, schlugen fehl. Hierbei kam es lediglich zur Adduktbildung zwischen dem basischen Substrat und der als Katalysator eingesetzten Trifluormethansulfonsäure, die bei vergleichbaren Problemstellungen beste Ergebnisse erbracht hat.[10]

In Analogie zu den Sulfenylhalogeniden sind in den letzten Jahren Selenylhalogenide vorgestellt worden.[11] Daher erschien es interessant, mit diesen Edukten Analogreaktionen mit Trimethoprimen durchzuführen. Bei Umsetzungen der Verbindungen des Typs B mit CF_3SeBr und CF_3SeCl konnten jedoch keine Umsätze erzielt werden. Erst bei Zusatz von Trifluormethansulfonsäure als Katalysator konnte in diesen Fällen eine Substitution im Benzolring bei gleichzeitiger Adduktbildung mit dem Katalysator konstatiert werden (Gleichung II).

Gleichung II:

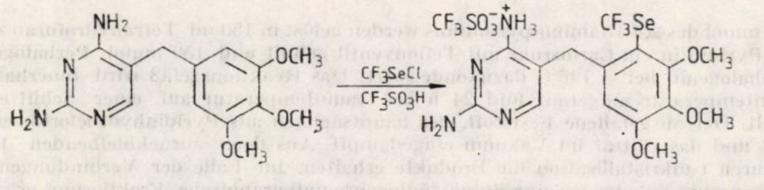

III 65 % Ausbeute

Reaktionen am exozyklischen Aminostickstoff wurden nicht beobachtet

Alle diese Reaktionen konnten auch auf einen Vertreter der Pyrimethamin-Stoffgruppe (Typ A) übertragen werden. Hierbei stand das 2,4-Diamino-5-(p-chlorphenyl)-6-ethyl-pyrimidin zur Verfügung, das nach Gleichung III mit CF_3SCl und CF_2ClSCl zu den Verbindungen IVa und b umgesetzt werden konnte (Gleichung III).

Gleichung III:

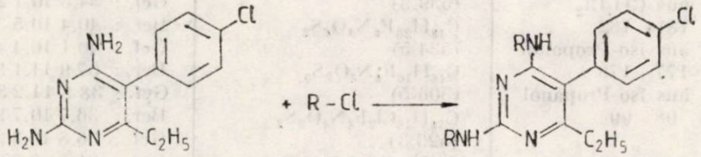

IV

R	Ausbeute
a) SCF_3	27,5%
b) $SCClF_2$	13,7%

Die Art der Umsetzung sowie die Entwicklung der Ausbeuten entspricht denen des Typs B, ebenso konnten mit $CFCl_2SCl$, CCl_3SCl und Selenylhalogeniden unter den beschriebenen Reaktionsbedingungen keine Umsetzungen erzielt werden.

Mit allen neu synthetisierten Substanzen sind Folgereaktionen versucht worden. Hierbei stand die Substitution der restlichen Aminoprotonen im Vordergrund des Interesses, jedoch scheiterten alle Versuche zur elektrophilen Direktsubstitution ebenso wie Metallierungsreaktionen die bei ähnlichen Problemstellungen zu Erfolgen geführt haben.[12]

Versuche, die eingeführten Perhalogenmethylthiosubstituenten oxidativ mittels konz. Salpetersäure, *meta*-Chlorperbenzoesäure, Wasserstoffperoxyd/Eisessig oder Chromsäure in die korrespondierenden Sulfone zu überführen, führten zur Totalzersetzung der Moleküle.

EXPERIMENTELLER TEIL

IR-Spektren: Feststoffe als KBr-Preßlinge.

Gitterspektrophotometer Perkin-Elmer 325; schwache Banden und Schultern werden nicht aufgeführt. NMR-Spektren; Bruker WM 250 FT und Bruker HX 60/5-Spektrometer (^{19}F), interne Locksubstanz C_6D_6; ^{1}H-NMR: Interner Standard: $Si(CH_3)_4$; ^{19}F-NMR: Interner Standard C_6F_6, Werte auf $CFCl_3$ umgerechnet. Alle Messungen in gesättigter DMSO-d_6 (20°) Lösung. Massenspektren: Varian MAT CH-5 und CH-7, Emission 100 μA. Es werden nur M^+ und M (100%) aufgeführt.

VERSUCHSVORSCHRIFT A

50 mmol des 2,4-Diamino-pyrimidins werden gelöst in 150 ml Tetrahydrofuran zusammen mit 15 g Pyridin in ein Cariusrohr mit Teflonventil gefüllt und 150 mmol Perhalogenmethylchalcogenhalogenid bei − 196°C dazukondensiert. Das Reaktionsgefäß wird innerhalb von 2h auf Raumtemperatur aufgetaut und 24 h bei Raumtemperatur auf einer Schüttelmaschine geschüttelt. Der ausgefallene Feststoff, der hauptsächlich aus Pyridinhydroclorid besteht, wird abfiltriert und das Filtrat im Vakuum eingedampft. Aus dem zurückbleibenden Rückstand werden durch Umkristallisation die Produkte erhalten. Im Falle der Verbindungen II konnten analysenreine Substanzen nur durch säulenchromatographische Fraktierung erhalten werden; Laufmittel; Methanol/Wasser (70/30); Säulenmaterial: Silica gel S 70−230 mesh.

Verbindung	Smp. [°C]	Bruttoformel (Molgewicht)	Elem. Analyse				
				C	N	H	S
Ia	178−180	$C_{16}H_{16}F_6N_4O_3S_2$	Ber.:	39.2	14.4	3.3	13.1
	aus $CHCl_3$	(490.4)	Gef.:	39.0	14.6	3.1	12.8
Ib	152−154	$C_{15}H_{13}BrF_6N_4O_2S_2$	Ber.:	35.5	10.4	2.4	12.0
	aus CH_2Cl_2	(539.3)	Gef.:	34.5	10.1	2.8	12.4
Ic	181−182	$C_{18}H_{20}F_6N_4O_4S_2$	Ber.:	40.4	10.5	3.7	—
	aus iso-Propanol	(534.5)	Gef.:	40.1	10.4	4.0	—
Id	177−179	$C_{16}H_{16}F_6N_4O_2S_3$	Ber.:	37.9	11.1	3.2	—
	aus iso-Propanol	(506.5)	Gef.:	38.8	11.2	3.1	—
IIa	98−99	$C_{16}H_{16}Cl_2F_4N_4O_3S_2$	Ber.:	36.7	10.7	3.1	—
		(523.3)	Gef.:	36.8	10.3	3.2	—
IIb	177−178	$C_{15}H_{13}BrCl_2F_4N_4O_2S_2$	Ber.:	31.5	9.8	2.3	—
		(572.2)	Gef.:	30.5	9.2	3.3	—
IIc	122−124	$C_{18}H_{20}Cl_2F_4N_4O_4S_2$	Ber.:	38.1	9.9	2.5	—
		(567.4)	Gef.:	39.0	9.6	3.6	—
IVa	129−131	$C_{14}H_{11}ClF_6N_4S_2$	Ber.:	37.5	12.5	2.4	14.3
	aus $CHCl_3$	(448.8)	Gef.:	37.6	12.5	2.5	14.1
IVb	132−134	$C_{14}H_{11}Cl_3F_4N_4S_2$	Ber.:	34.8	11.6	2.3	—
	aus iso-Propanol	(481.7)	Gef.:	35.5	11.4	2.5	—

VERSUCHSVORSCHRIFT B

Zu einer Suspension von 10 mmol 2,4-Diamino-pyrimidin in ca. 30 ml THF werden bei — 40°C einige Tropfen CF_3SO_3H und 25 mmol CF_3SeCl gegeben. Es wird auf Raumtemperatur erwärmt, wobei die Suspension in eine orangerote Lösung übergeht, und noch 24 h gerührt. Das Lösungsmittel wird abdestilliert, der Rückstand mit Eiswasser neutral gewaschen und aus Ethanol/H_2O (80 :20) umkristallisiert.

Verbindung	Smp. [°C]	Bruttoformel (Molgewicht)	Elementaranalyse
III	121—124	$C_{15}H_{17}F_3N_4O_3Se$ (438.2)	C N H Ber. : 35.5 10.4 3.5 Gef. : 34.6 9.7 3.5

Spektroskopische Daten der neu dargestellten Verbindungen

	^{19}F [ppm]	^{1}H [ppm]	IRν [cm^{-1}]	Ms [M^+, M^{100}]
Ia	51.4 (s) 52.7 (s)	3.67 (s); 3.74 (s); 3.87 (s); 6.53 (s); 7.97 (s)	1599 (s) 1431 (s) 1123 (vs)	490 (100)
Ib	50.9 (s) 52.1 (s)	3.82 (s); 4.0 (s); 6.83 (s); 8.03 (s)	1603 (s) 1419 (s) 1125 (vs)	538 (100) 540 (100)
Ic	51.0 (s) 52.3 (s)	3.33 (s); 3.61 (s); 3.68 (t); 3.79 (s); 3.94 (t); 6.56 (s); 8.0 (s)	3235 (s) 1600 (vs) 1180 (vs)	59 (100) 534 (45)
Id	51.1 (s) 52.1 (s)	2.18 (s); 3.78 (s); 3.88 (s); 6.58 (s); 8.05 (s); 9.02 (s); 9.12 (s)	1482 (s) 1130 (vs) 1120 (vs)	506 (100)
IIa	37.1 (s) 37.8 (s)	3.60 (s); 3.72 (s); 3.83 (s); 6.56 (s); 8.03 (s); 9.18 (s); 9.36 (s)	1600 (s) 1431 (vs) 1132 (vs)	523 (100) 524 (74)
IIb	37.1 (s) 37.9 (s)	3.79 (s); 3.91 (s); 6.68 (s); 7.55 (s); 7.72 (s); 8.08 (s)	1415 (vs) 1090 (vs)	572 (100) 574 (52)
IIc	37.1 (s) 37.8 (s)	3.28 (s); 3.55 (t); 3.72 (s); 3.83 (t); 3.85 (s); 6.55 (s); 8.03 (s); 89.89(s); 9.95 (s)	1600 (vs) 1475 (vs) 1138 (vs)	59 (100) 566 (23)
III	35.4 (s) 78.0 (s)	3.35 (s); 3.80 (s); 3.85 (s); 3.88 (s); 6.90 (s); 7.00 (s); 7.55 (as); 7.88 (s); 8.3 (s)	3415 (s) 1665 (vs) 1110 (vs)	289 (100) 438 (12)
IVa	51.5 (s) 52.4 (s)	1.1 (t); 2.35 (q); 7.4 (m)	3380 (s) 1590 (s) 1110 (vs)	448 (100) 449 (30) 450 (44)
IVb	36.85 (s) 37.60 (s)	1.03 (t); 2.28 (q); 7.35 (m); 8.35 (s); 9.43 (s)	3380 (vs) 1458 (vs) 1090 (vs)	482 (100) 483 (27) 484 (39)

LITERATUR

[1] A. Haas und M. Lieb, *J. Heterocyclic Chem.*, **23**, 1079 (1986).
[2] G. H. Hitchings und J. J. Burchall, *Adv. Enzymol.*, **27**, 416 (1965).
[3] B. R. Baker und B. T. Ho, *J. Pharm. Sci.*, **53**, 1137 (1964).
[4] G. H. Hitchings und J. J. Burchall, *Fed. Proc.*, **23**, 429 (1964).
[5] S. Dorn, P. Eggenberg, M. Gerstenberger, A. Haas, U. Niemann und P. Zobrist, *Helv. Chim. Acta*, **62**, 1442 (1979).
[6] A. Haas, *L'Actualite*, im Druck.
[7] R. Braden und E. Klauke, *Pestic. Sci.*, **17**, 418 (1986).
[8] A. Haas und V. Hellwig, *Chem. Ber.*, **108**, 334 (1975).
[9] A. Haas und U. Niemann, *Chem. Ber.*, **110**, 67 (1977).
[10] A. Haas und V. Hellwig, *Chem. Ber.*, **109**, 2475 (1976).
[11] A. Darmadi, A. Haas und B. Kock, *Z. Naturforschung*, **35B**, 526 (1980).
[12] A. Haas und V. Plass, *Chem. Ber.*, **105**, 2047 (1972).

Revue Roumaine de Chimie, 32, *11–12*, 1225–1236 (1987)

INDEX DES AUTEURS

ABDEL BADEI M. M. and E. A. EL SAWI, Microdetermination of reducing sugars and ascorbic acid by indirect method using ferricyanide — thymolphthalin reagent . . . 141

ABD-ELFATTAH A. M., voir ALI M. I. . . . 297

ABDEL-LATIF F.F., voir BADR M.Z.A. . . . 315

ABDEL-MEGEED F.M., Studies on pyridylpyrazolone system. V. Cyclocondensation of 1-phenyl-3-(3'-pyridyl)-2-pyrazolin-5-one with ethyl acetoacetate and related compounds . . . 591

ABDEL MEGEED M. F. and M. EL BORAI, M. FAHMY, EL-SAIED A. ALY, Studies on the pyridyl-pyrazolone system. I. Some reactions with -3-(3'-pyridyl)-1-phenyl-2-pyrazolin-5-one . . . 515

ABDEL MEGEED M. F. and M. EL BORAI, M. FAHMY, EL-SAIED A. ALY, Studies on pyridyl-pyrazolone system. II. Some reactions with 4-arylidene-3-(3'-pyridyl)-1-phenyl-2-pyrazolin-5-one . . . 797

AGARWAL RAM KUMAR and SUNIL KUMAR GUPTA, Magneto, spectral and thermal investigations of coordinations of coordination compounds of lanthanides(III) with 2-ethoxycarbonylaminopyridine . . . 477

AGARWAL R.K. and M.B.L. SHARMA, A. K. SRIVASTAVA, Magneto, spectral and thermal studies of rare earth nitrate chelates of N,N', N'-tetramethyl thiuram disulphide . . . 263

AGARWAL R. and G. K. OBEROI, D.C. JAIN, R. L. MITAL, Studies in the synthesis of 10H-8-trifluoromethyl-1-azaphenothiazine *via* the Smiles rearrangement . . . 37

AGHERGHINEI I., voir LUCA C. . . . 41

AKHTER T., voir KHAN A. R. . . . 495

ALBU B., voir POPESCU D. . . . 350

ALBU B., voir MARINESCU M. . . . 653

ALBU B., voir MARINESCU M. . . . 713

ALEXANDROAIE M., voir POPOVICI EV. . . . 707

ALBU B., voir MARINESCU M. . . . 713

ALEXANDROAIE M., voir POPOVICI EV. . . . 707

ALI M. I. an. A. M. ABD-ELFATTAH, H. A. HAMMOUDA, S. M. HUSSAIN, Reactions of homophthalic anhydride with some compounds containing owo amino groups . . . 297

ALY M.M., voir BADR M.Z.A. . . . 315

ANAÇ O., The synthesis of an azo-dye . . . 431

ANAÇ O. and GÜNAYDIN K., Organochlorine (OCl) pesticide residues in human fats. Part I . . . 803

ANAND MADHU, voir TAMBI S.B. . . . 33

ANASTASESCU L., voir MANDRAVEL C. . . . 1045

ANDRUH M. and C. I. LEPĂDATU, M. BREZEANU, Angular overlap model (AOM) calculations for the coordination compounds with macrocyclic ligands. I. AOM parameters for nickel(II) coordination compounds with tetrakis-anhydro-aminobenzaldehyde macrocyclic ligand . . . 1033

APĂTEANU L., voir S. STERNBERG . . . 121

APĂTEANU L., voir S. STERNBERG . . . 457

APETROAE M. and CL. SINGER, R. BOZGA, ST. CILIANU, R. CECLAN, T. BÂNZARU, Z. SIMON, Structure activity relations by the free-Wilson and MTD methods for substances with a potential psychotropic activity. I. Diphenylether derivatives with neuroleptic activity . . . 583

APETROAIE M., voir SIMON Z. . . . 783

ARIAS-CARBAJAL A. and R. CAO, Interaction product of N,N'-bis (Furfurylidene) ethylenediamine with cobalt(II) chloride . . . 47

AVRAM MARGARETA, voir ŞTEFAN N. 1171
BADAU EL., voir NEGOIU D. 91
BADEA F., voir VLAD R. 179
BADR M.Z.A. and M. M. ALY, S. A. MANGOUB, A. M. FAHMY, F. F. ABDEL-LATIF, Photolysis of mono-, di-, and tribenzylamine and novel photocarbylamine reaction 315
BALABAN A. T. and C. DELEANU, Chemical graphs. Part 47. Valence isomers of (14)annulene 271
BALABAN A.T. and E. STEPAN, Reactions of pyrylium salts with nucleophiles. XIX. Novel bispyridinium salts with potential biological activity 155
BALABAN A.T., voir SHCHERBAKOVA I.V. 417
BALABAN A.T. and N. NEGOIŢĂ, S.M. SHEIN, A. D. KHMELINSKAIA, Factors affecting stability and equilibria of free radicals. XVIII. Capto-dative (Push-pull) diarylaminyls with 2,4,6-tri-(methanesulphonyl)-phenyl or 2,4,6-tri-(N,N-dimethyl-sulphonamido)-phenyl groups 501
BALABAN A.T., voir BALABAN MICHAELA CARMEN 975
BALABAN A.T., voir BANCIU M. 1161
BALABAN A.T., voir SCHIKETANZ I. 1175
BALABAN MICHAELA-CARMEN and I. SCHIKETANZ, A. T. BALABAN, ANA SCHIKETANZ, M. D. GHEORGHIU, Aminoketone and oxazole synthesis. X. Acylation and alkylation of arenes with the azlactone of cinnamoyl-glycine 975
BALABAN MICHAELA-CARMEN, voir SCHIKETANZ I. . . . . . .
BALCAN M., voir MARINESCU M. 713
BANCIU M., voir VLAD R. 179
BANCIU M., voir VLAD R. 179
BANCIU M. and ANCA BANCIU, M. ELIAN, C. DRĂGHICI, ECATERINA CIORĂNESCU, Synthesis and pyrolysis of 10,21-dithia-9, 10, 11, 20, 21, 22-hexahydrodephenanthro [*a*, *f*] cyclodecene-S,S,S', S'-tetraoxide 961
BANCIU M. and M. STĂNESCU, C. FLOREA, A. T. BALABAN, E. CIORĂNESCU, Ring contraction and additional annelation in dibenzobulvalone system 1161
BANCIU ANCA, voir BANCIU M. 961
BÂNZARU T., voir APETROAE M. 583
BELOMOINA N.M., voir KORSHAK V.V. 393
BENDIC C. and C. PODINĂ, Dipole moments of ground and excited states of 7-chloro-2,3-dihydro-4-quinolone 1155
BERSUKER I.B. and S.A. BORSHCH, I. N. KOTOV, The vitronic theory of magnetic properties of trinuclear mixed-valence clusters 1075
BEZDADEA M. and GH. MIHĂILA, N. BÎLBA, N. NAUM, Polymerisation of some vinylic monomers in the presence of synthetic zeolites . . . .
BEZDADEA M., voir NEACSU I. 749
BHARGAVA N., voir TAMBI S.B. 33
BÎLBA D., voir BÎLBA N. 563
BÎLBA N., voir BEZDADEA M. 563
BÎLBA N., voir LUCA C. 41
BÎLBA N. and D. BÎLBA, GH. MIHĂILĂ, N. NAUM, Exchange of Zn^{2+} and Mn^{2+} in synthetic zeolites NaA, NaX and mordenite 563
BLIZNAKOV G. and D. KLISSURSKI, Y. PESHEVA, Selective oxidation of methanol to formaldehyde on modified vanadia catalysts 985
BONCIOCAT N., voir STERNBERG S. 883
BORDEIANU R., voir CEAUŞESCU ELENA 3
BIRSCH S.A., voir BERSUKER I.B. 1075
BOZEŞANU M., voir POP GR. 533
BOZGA GR., voir MARIA GH. 821
BOZGA R., voir APETROAIE M. 583
BOZGA R., voir SIMON Z. 783
BRĂILEANU ANA, voir ZAHARESCU M. 925
BREZEANU M., voir ANDRUH M. 1025
BREZEANU M., voir ILIE I. 1109

BRÂNZOI V., STERNBERG S. 121

BRÂNZOI V., voir STERNBERG S. 457

BRUMA M. and I. SAVA, Poly-1,3,4-oxadiazolesterimides 325

BRUMA M., voir V. V. KORSHAK 393

BUTUCEA V., voir MARINESCU M. 653

BUZDUGAN V., voir MARINESCU M. 653

BUZDUGAN E., voir CEAUȘESCU ELENA 3

CĂLDĂRARU H., Molecular motion in solid bicyclo[3.3.3] nonen-9-one and adamentanone eximes studies by the electron spin resonances spectra of the correspondig iminoxy radicals 1151

CĂLDĂRARU M., voir IONESCU N.I. 939

CĂLUȘARU A. and E. SAVIUC, Rate constants and activation energies of Fe(II) to Fe(III) oxidation reaction by hydroxylamine in normal and heavy water 101

CAO R., voir A. ARIAS-CARBAJAL 47

CAPITÁN F. and P. ESPINOSA, F. MOLINA, L. F. CAPITÁN-VALLVEY, Study of the metallic complexes of Schiff bases derived from 2-thiophenecarboxyaldehyde, 2-2-pyridiecarboxyaldehyde and *ortho*-aminobenzenethiole (in Spanish) 151

CAPITÁN-VALLVEY L. F., voir CAPITÁN F. 151

CARAGHEORGHEOPOL A. and I. DRĂGUȚAN, An electron spin resonance study of conformational inversion in iminoxy radicals derived from benzocycloheptene and heterocyclic analogs 1141

CARTIANU D., Rate-constrained chemical equilibrium method for solving complex mass action kinetic systems 369

CEAUȘESCU ELENA and R. BORDEIANU, P. GHIOCA, I. CERCHEZ, E. BUZDUGAN, R. STANCU, Dilute block copolymer systems. VI. Effect of polymeric diluents 3

CECAL A., voir MATEI F. 133

CECLAN R., voir APETROAE M. 583

CENUȘE Z., voir VÎLCU R. 1025

CERCHEZ I., voir CEAUȘESCU ELENA 3

CHIFU A., voir CHIFU E. 627

CHIFU E. and A. CHIFU, M. TOMOAIA-COTIȘEL, J. ZSAKÓ, Specific interactions in monomolecular membranes of biological interest 627

CHIFU E., voir TOMOAIA-COTIȘEL M. 663

CHIFU E. and M. SĂLĂJAN, I. DEMETER-VODNÁR, M. TOMOAIA-COTIȘEL, Fatty acid film at the benzene/water interface 683

CHIFU E., voir ZSAKÓ J. 739

CHIFU E. and CĂLIN-IOAN GHEORGHIU, Surface mobility of surfactant solutions. XII. Remarks concerning the Marangoni flow through an inclined surface canal 945

CHIFU E., voir ZSAKÓ J. 739

CHIFU E., voir ZSAKÓ J. 1193

CHIRIAC C.I., A new synthesis of aromatic ureas from carbon dioxide and diamines using ethylene chlorophosphite in pyridine as reagent 29

CHIRIAC C.I., Dimethyldichlorosilane as reagent for the synthesis of 1,3,4-oxadiazoles from diaroylhydrazines 223

CHIRIAC C.I, N-aroylphthalimides by a new direct condensation reaction 793

CID N.P. and O. GARCIA VIOR, Oxidation of mordant blue 9 with bromate catalyzed by vanadium (V). Part I. Influence of variables (in Spanish) 51

CID N.P. and O. GARCIA VIOR, Oxidation of mordant blue 9 with bromate catalyzed by vanadium (V). Part II. Kinetics and mechanism 203

CILIANU ST., voir APETROAE M. 583

CIORĂNESCU ECATERINA, voir BANCIU M. 961

CIORĂNESCU ECATERINA, voir STĂNESCU M. 969

CIORĂNESCU ECATERINA, voir BANCIU M. 1161

CIUREANU M. and M. HILLEBRAND, E. VOLANSCHI, D. GHEȚU, Optical spectra and electronic structure of some nitrothioamide anion radicals 467

COMAN V., voir ZSAKÓ J. 1193

CONSTANTIN VOICU, Calculation of mass spectra of some oxygen- and sulphur-containing heterocycles 1159

CONSTANTINESCU A., voir VASILIU OPREA CL. 407

CONSTANTINESCU M., voir COUTURE A. 353
CONȚESCU A., voir SPACU P. 249
CONȚESCU A., voir SPACU P. 877
CONTINEANU M., voir ONCESCU T. 637
CONTINEANU M., voir ONCESCU T. 953
COTÂRȚĂ A., voir STERNBERG S. 883
COUTURE A. and LABLANCHE COMBIER, C. SURPĂȚEANU, M. CONSTANTANTINESCU, Theoretical study on the photocyclization of enamides and thioenamides 353
CREȚU I. and M. IONESCU, M. STOICESCU, Some aspects of polymerflooding in oil reservoirs 723
CRIȘAN D., voir SPACU P. 249
CRIȘAN D., voir SPACU P. 877
CRIȘAN D., voir ZAHARESCU M. 925
CRISTESCU C. and C. SUPURAN, *as*-Triazine derivatives with potential therapeutic action. XXII. A simplified method for the synthesis of 1,2,4-triazole nucleosides and 1,2,4-triazine nucleosides 229
CRUCEANU M., voir POPOVICI EV. 707
DAVID V., Informational entropy of the probability field events of a chemical control analysis 539
DELEANU C., voir A. T. BALABAN 271
DEMBINSCHI D., voir V. TRANDAFIR 671
DEMETER-VODNÁR I., voir CHIFU E. 683
DINULESCU I. G., voir ȘTEFAN N. 1171
DOBRESCU D. and M. IOVU, C. GEORGESCU, V. STOICESCU, A. CRISTEA, Relations between chemical structure and analgesis activion of some diamines and aminoethers 995
DOCA N. and E. SEGAL, Dehydrogenation kinetics of low aliphatic alcohols on copper catalysts. III. Metallic copper with Fe and Ni as addition elements 199
DONESCU A., voir WEINBERG J. 1117
DRĂGAN G., High resolution mixing calorimetry in studies of composite systems 759
DRĂGAN G. and S. IFRIM, GEORGETA POPESCU, Study by high resolution mixing calorimetry of adsorption of aqueous solutions of superplasticizer additive on cement 767
DRĂGAN N., voir ZAHARESCU M. 925
DRĂGHICI C., voir BANCIU M. 961
DRĂGUȚAN I., voir CARAGHEORGHEOPOL A. 1141
DUCA A., voir MATEI F. 133
DUCA A. voir MATEI F. 235
DUMITRIU E. and S. OPREA, V. HULEA, Kinetic studies on the catalytic alkylation of toluene with methanol 191
DUMITRIU E. and S. OPREA, V. HULEA, Activity and selectivity of zeolite catalyts in *m*-xylene isomerization 525
DUMITRU N., voir POPOVICI EV. 707
EL-ASKLANY A. H., voir GOMAA E. A. 243
EL-BORAI M., voir ABDEL MEGEED M.F. 515
EL-BORAI M., voi ABDEL MEGEED M.F. 797
EL-ESSER S., voir El-FARARGY A. F. 435
EL-FARARGY A.F. and A. Y. SOLIMAN, M. EL-MOBAYED, S. EL-ESSER, Synthesis and studies of 3-N-arylcarbamidocoumarins 435
ELIAN M., voir BANCIU M. 961
ELIAN M., voir STĂNESCU M. 969
ELIAN M., voir GHEORGHIU M. 1181
EL-MOBAYED M., voir EL-FARARGY A. F. 435
EL-SAIED A. ALY, voir ABDEL MEGEED 515
EL-SAIED A. ALY voir ABDEL MEGEED 797
EL-SARRAF G., voir KAMEL M.M. 427
EL SAWI E.A., voir ABDEL BADEI M. M. 141
EL-WASSIMI M.T., voir KAMEL M.M. 427

EMONS H.-H. and D. KIEßLING, W. HORLBECK, K. WITTENBECHER, Vapour pressures of molten salt mixtures alkali halide-alkaline earth halide 855

ESPINOSA P., voir CAPITÁN F. 155

FAHMY A. M., voir BADR Z.A. 315

FAHMY M., voir ABDEL MEGEED M.F. 515

FAHMY M., voir ABDEL MEGEED M.F. 797

FĂTU I., voir FLORESCU S. 693

FEROIU V., voir GEANA D. 863

FLOREA CRISTINA, voir BANCIU M. 1161

FLORESCU M., The chemistry of colloids and surfaces 621

FLORESCU S. and A. ȘTEFĂNESCU, M. ROB, I. FĂTU, The influence of sodium toluene sulfonate on surface and colloidal properties of sodium alkylbenzene sulfonates 693

FILOTI G., voir ILIE I. 1109

FOUDA A. S. and H. A. MOSTAFA, M. N. MOUSSA, Heterocyclic quaternary ammonium compounds as corrosion inhibitors for mild steel in H_3PO_4 775

GĂNESCU I. and CS. VÁRHELYI, Metal- and metal(III)-amine salts of the $H_2[Pt(SCN)_4]$ and $H_2[Pt(SCN)_6]$ acids 255

GÂNJU D., voir NAUM N. 519

GARCIA VIOR O., voir CID N.P. 51

GARCIA VIOR O., voir CID N.P. 203

GEANA D., voir POPESCU D. 359

GEANĂ D. and V. FEROIU, O. LANDAUER, Computation of saturation pressure and orthobaric densities by a general cubic equation of state 863

GEANĂ D., voir LANDAUER O. 1129

GEORGESCU C., voir MARINESCU M. 653

GEORGESCU C., voir DOBRESCU D. 995

GHAFOOR RUBINA, voir KHAN M.A. 295

GHEORGHIU C.I., voir CHIFU E. 945

GHEORGHIU M.D., voir SHCHERBAKOVA I.V. 417

GHEORGHIU M.D., voir BALABAN A.T. 975

GHEORGHIU M.D. and M. MIHAI, L. PÂRVULESCU, A. VAIOS, F. NICULESCU, Nuclear magnetic resonance investigations of small rings. 4. ^{13}C-NMR spectra of 2-t-butyl-2-cyanocyclobutanones as probes for configurational assignments 979

GHEORGHIU M.D. and M. MIHAI, L. PÂRVULESCU, A. VAIOS, M. ELIAN, Nuclear magnetic resonance investigations of small rings. Part 5. The exact analysis for the four-membered ring three-proton system of 3-aryl-2-t-butyl-2-cyclobutamines as evidence for configurational assignments 1181

GHEORGHIU M.D., voir SCHIKETANZ I. 1175

GHERMAN E., voir NEGOIU D. 91

GHEȚU D., voir CIUREANU M. 467

GHIOCA P., voir CEAUȘESCU ELENA 3

GOMMA E. A. and A. H. EL-ASKLANY, M.N.H. MOUSSA, Dissociation of KCl in mixed hexamethylphosphortriamide-water solvents 243

GOȘA V., voir POPESCU D. 359

GRECU M., voir POPOVICI EV. 707

GUNAYDIN K., voir ANAÇ O. 803

GUPTA S.K., voir AGARWAL R.K. 477

GUTIERREZ-MARTIN F. and A. RODRIGUEZ-PASTOR, F. MATA-PÉREZ, Phenylhydrazone formation from substituted benzaldehydes : substituent effect and structure-reactivity correlations 305

HAAS, A. and M. LIEB, B. SCHWEDERSKI, Perhalogenomethyl-thioheterocycles. XXV. Electrophilic substitution of 2,4-diaminopyrimidine with perhalogenomethyl-chalcogenohalides (in German) 1219

HAMMOUDA H.A., voir ALI M. I. 297

HERDAN J., voir SHCHERBAKOVA I. V. 417

HILLEBRAND M., voir CIUREANU M. 467

HILLEBRAND M. and M. MORARU, E. VOLANSCHI, ESR-spectral study of some substituted 2,4-dinitroanilines 1051

HORÁNYI G. and E. M. RIZMAYER, Radiotracer study of the adsorption of DL-asparaginic acid at a platinized platinum electrode 913

HÖREB O., voir T. ONCESCU 343
HORLBECK W., voir H.-H. EMONS 855
HULEA V., voir DUMITRIU E. 191
HULEA V., voir DUMITRU E. 525
HUSSAIN S.M., voir ALI M. I. 297
ILIE I. and M. BREZEANU, L. PATRON, E. SEGAL, G. FILOTI, Synthesis of nickel ferrite from polynuclear coordination compounds. Part I. Study of the dry ferritization process 1109
ILISIE M., voir ZAHARESCU M. 925
IONESCU A., voir MARINESCU M. 653
IONESCU GH., voir F. MATEI 133
IONESCU GH. voir MATEI F. 235
IONESCU GH., voir ONCESCU T. 637
IONESCU M., voir CREȚU I. 723
IONESCU N.I., voir POPESCU D. 359
IONESCU N.I., voir POP GR 533
IONESCU N.I.and M. CĂLDĂRARU, Mobility of lattice oxygen and activity of multicomponent oxide catalysts for oxidation of propylene 939
IONESCU N.I., voir OANCEA D. 1211
IONESCU S.G., voir ONCESCU T. 953
IOSIF I., voir POP GR. 533
IOVU M. and RADU S., 4-Benzyloxyazobenzenes synthesized by condensation 359
of benzyl chloride with sodium salts of 4-hydroxy-azobenzenes 509
IOVU M., voir DOBRESCU D. 995
IOVU M. and E. TUDORACHE, Homopolycondensation of dichloromethylderivatives in the presence of tetrachloroethene or trichloroethene (in French) 1185
ISOPESCU A., voir MARIA GH. 821
IULIAN OLGA, voir LANDAUER O. 1129
IVANOV AL., Counting observables of chemical species 1097
JAIN D.C., voir AGARWAL R. 37
JITARU M., voir ONICIU L. 701
JOSHI B.C. and Y.C. JOSHI, D. KISHORE, S.S. SHRIMALI, Proton catalysed rearrangement of N-alkyl arene sulphonanilides to *ortho*-alkylamino sulphones. Part III 215
JOSHI B.C. and YOGESH JOSHI, D. SKIHORE, S. S. SHRIMALI, Proton catalysed rearrangement of N-alkyl-naphthalene-sulphonanilides to *ortho*-alkylamino-aryl-naphthalyl-sulphones. Part IV 321
JOSHI Y.C., voir JOSHI B.C. 215
JOSHI Y.C., voir JOSHI B.C. 321
JURCONI E. and T. ONCESCU, G. RĂCĂȘANU, Kinetics of the substitution rection between CoC_2O_3 Bipy I and bipyridyl in aqueous solution 1039
JUNCU GH. and O. MUNTEAN, R. MIHAIL, Gas absorption with a complex chemical reaction in a perfectly mixed chemical reactor 599
KADI H., voir TUDOSE R. Z. 807
KAMEL M.M. and M.T.EL-WASSIMI, F.H. OSMAN, G. EL-SARRAF, Some reactions on 3-[(2-Hydroxy-4-quinolyl)methyl]-2,4-pentanediones 427
KATYAL M., voir KUMAR A. 571
KUMAR ASHOK and M. KATYAL, B. K. PURI, Polarographic study of lead with δ-valerolactam and its analytical applications 571
KHAN MISBAHUL AIN and RUBINA GHAFOOR, *IPSO*-Substitution of heterocyclic compounds. I. Nitration of 5-bromo-3-4-dimethyl-1-phenyl-1*H*, 6*H*-pyrano [2,3,*c*] pyrazol-6-one 295
KHAN A. RASHEED and T. AKHTER, A. H. K. YOUSUFZAL, Chain transfer constants for some aromatic solvents in the cationic polymerization of α-methyl styrene 495
KHMELINSKAYA A. D., voir A. T. BALABAN 501
KIEßLING D., voir EMONS H.-H. 855
KISHORE D., voir JOSHI B.C. 215
KISHORE D., voir JOSHI B.C. 321
KLISSURSKI D., voir BLIZNAKOV G. 985
KORSHAK V.V. and E. S. KRONGAUZ, N.M. BELOMOINA, M. BRUMĂ, I. SAVA, C. I. SIMIONESCU, Polyphenylquinoxaline-oxadiazole-amides 393

KORSHAK V.V. and E. S. KRONGAUZ, N M. BELOMOINA, M. BRUMĂ, G. MANDRIC C. I. SIMIONESCU, New copolymers containing phenylquinoxaline units 489

KOTOV I.N., voir BERSUKER I.B. 1075

KRONGAUZ E.S., voir KORSHAK V.V. 393

KRONGAUZ E.S., voir KORSHAK V.V. 489

KUZNETSOV E.V., voir SHCHERBAKOVA V.I. 417

LABLACHE COMBIER, A., voir A. COUTURE 353

LANDAUER O., voir GEANĂ D. 83

LANDAUER O. and C. MATEESCU, O. IULIAN, D. GEANĂ, Models for the viscosity of liquid mixtures. Application to the binary system water-dioxan 1129

LANGSHAW V., voir VÎLCU R. 1025

LĂZĂRESCU V. and O. RADOVICI, M. VASS, Sintering effects on anodic oxidation of vacuum deposited silver films 895

LECA M., voir ONCESCU T. 637

LECA M. voir TRANDAFIR V. 671

LEPĂDATU C.I., voir ANDRUH M. 1033

LIEB M., voir HAAS A. 1219

LOPEZ DE ALBA P.L. and L. LOPEZ M., Potentiometric study of reactions of thorium nitrate and various sodium orthoarsenates in solutions (in Spanish) 387

LOPEZ L.M., voir LOPEZ DE ALBA 387

LÖWY D.A., voir ONICIU L. 701

LUCA C. and N. BÎLBĂ, GH. MIHĂILĂ, I. AGHERGHINEI, Inclusion compounds of perhydrotriphenylene with aliphatic monocarboxylic acids . . 41

MAGYAR L., voir POMOJE-MARCU R. 611

MAHGOUB S.A., voir BARD M.Z.A. 315

MANDRAVEL C. and L. ANASTASESCU, The influence of various factors on the optical activity of some essential aminoacids. I. Applications. . . . 1045

MARIA GH. and C. TSAKIRIS, GR. BOGZA, AL. ISOPESCU An adapted zone method for propane thermal cracking process simulation in a radiant furnace 821

MĂRGINEANU G.D., voir VAIS H. 677

MARINESCU M. and V. BUTUCEA, G. POPESCU, A. SÎRBU, A. IONESCU, G. GEORGESCU, B. ALBU, Physico-chemical characterization of the two-phase system employed in emulsion polymerization of vinyl chloride 653

MĂRGINEANU G.D., voir VAIS H. 677

MARINESCU M. M. and M. BALCAN, B. G. ALBU, G. POPESCU, N. N WEISSMAN, Polymer -surfactant interaction. Surface-active properties 713

MATA-PÉREZ F., voir GUTIERREZ-MARTIN F. 305

MATEESCU A., voir STERNBERG S. 457

MATEESCU C., voir LANDAUER O. 1129

MATEI F. and GH. IONESCU, A. CECAL, A. DUCA, Study on Co^{2+} and Zn^{2+} behaviour in dialysis process 133

MATEI F. and GH. IONESCU, AL. DUCA, Theoretical and experimental features of electrodialysis of $Cr_2O_7^{2-}$ ion on ion-exchange membranes 235

MEGHEA A., voir SHCHERBAKOVA I.V. 417

MEAHCOV L., voir ONCESCU T. 637

MIHAI MARINA, voir GHEORGHIU M.D. 1181

MIHAIL R., voir JUNCU GH. 599

MIHĂILĂ GH., voir BEZDADEA M. 401

MIHĂILĂ GH, voir N. BÎLBĂ 563

MIHĂILĂ GH., voir NAUM N. 519

MIHALAS G. I., voir SIMON Z. 783

MIHAI MARINA, voir GHEORGHIU M.D. 979

MIHAI MARINA, voir GHEORGHIU M.D. 1181

MIHELIS A., voir VARTIRES I. 551

MIHELIS A., voir VARTIRES I 907

MITAL R.L., voir TAMBI S.B. 33

MITAL R.L., voir AGRAWAL R. 37

MOLINA F., voir CAPITAN F. 151

MORARU M., voir HILLEBRAND M. 1051
MOUSSA M.N.H., voir GOMAA E.A. 243
MOUSSA M.N.H., voir FOUDA A. S. 775
MUNTEAN O., voir JUNCU GH. 599
MUNTEAN O., voir SPOITU C.M. 1203
MUSCA G., voir POP GR. 533
NAUM N. and GH. MIHĂILĂ, F. VITAN, P. ONU, D. GÂNJU, Alkylation of benzene with isopropanol 519
NAUM N., voir BEZDADEA M. 401
NAUM M., voir BILBA N. 653
NEACŞU I. and M. BEZDADEA, Electric potential of some autochthonous synthetic membranas 749
NEAGOE S., voir NEGOIU D. 91
NEAGU V., voir ZSAKO J. 739
NEGOIŢĂ N., voir BALABAN A.T. 501
NEGOIU D. and S. NEAGOE, MARIA NEGOIU, EL. BADAU, EL. GHERMAN, Complex compounds of Pd(II) with thioethers. I. Investigation of some compounds of Pd(II) with thioethers of the bis (phenylthiomethyl) ether series 91
NEGOIU M., voir NEGOIU D. 91
NICULESCU F., voir GHEORGHIU M.D. 979
OANCEA D., voir POPESCU D. 359
OANCEA D. and DOMNINA POPESCU, N.I. IONESCU, On the significane of the minimum ignition energy of an explosive gaseous mixture 1211
OBEROI G.K., voir AGRAWAL R. 37
OLARU N. and Z. SIMON, Electronic structure and reactivity indices for a series of purine derivatives, inhibitors of guanine phosphoribosyl-transferase from *Escherichia Coli* 63
OLARU N. and Z. SIMON, Comparison between empirical and advanced molecular orbital calculations for some derivatives of nitrogen heterocycles 83
OLARU N. and Z. SIMON, Quantitative struture-activity relations for the inhibition of guanine phosphoribosyl-transferase from *Escherichia Coli* 1001
OLTEANU M., voir ONCESCU T. 637
OLTEANU M., Mixed solution of cationic and nonionic surfactants 647
ONCESCU T. and M. STEFAN, O. HÖRER, On the acid-base equilibria of proflavine in ground and excited electronic states 343
ONCESCU T. and M. CONTINEANU, S.G. IONESCU, M. OLTEANU, M. LECA, L. MEAHCOV, Photoinduced H_2 generation from water in micellar systems 637
ONCESCU T. and M. ŞTEFAN, M. CONTINEANU, S. G. IONESCU, Optimisation of hydrogen production from water using proflavine as photosensitizer 953
ONCESCU T., voir E. JURCONI 1039
ONICIU D. and D. A. LÖWY, M. JITARU, I. A. SILBERG, B. C. TOMA, Electrosynthesis of propionitrile. II. Phase equilibria in the acrylonitrile-proprionitrile-water system in the presence of cationic surfactants and electrolytes 701
ONU P., voir NAUM N. 519
OPREA S., voir DUMITRIU E. 191
OPREA S., voir DUMITRIU E. 525
OSMAN F.H., voir KAMEL M.M., 427
PANDEY O.P. and S. K. SENGUPTA, S.C. TRIPATHI, Synthesis characterization, antifungal and antiviral activity of some transition metal complexes of cycloalkyl dithiocarbamate 145
PARVULESCU L., voir GHEORGHIU M.D. 979
PARVULESCU L., voir GHEORGHIU M.D. 1181
PATRON L., voir SPACU P. 249
PATRON L., voir SPACU P. 877
PATRON L., voir ILIE I. 1109
PESHEVA Y., voir BLIZNAKOV G. 985
PÎRLOG C., voir ZAHARESCU M. 925
PLOŞTINARU S., voir SPACU P. 249
PLOŞTINARU S., voir SPACU P. 877
PODINĂ C., voir SAHINI V. EM. 843

PODINA C., voir BENDIC C. 1155

POMOJE-MARCU R. and L. MAGYAR, The ionic-molecular flotation of Cu(II) using Ponilit CP_1 as collector. pH influence on the flotation efficiency (in French) 611

POPA A., voir POPOVICI EV. 707

POPA V.T., voir VLAD M.O. 935

POP GR. and BOZEȘANU M., N. I. IONESCU, I. IOSIF, G. MUSCĂ, Distribution of products in methanol conversion over H-ZSM-5 type zeolites 533

POPESCU D. and H. ALBU, D. OANCEA, N. I. IONESCU, V. GOȘA, D. GEANĂ, The explosive combustion of propylene. IV. The maximum explosion pressure in adibatic and non-adiabatic constant volume combustion . . . .

POPESCU D., voir OANCEA D. 359

POPESCU G., voir MARINESCU M. 653

POPESCU G., voir MARINESCU M. 713

POPESCU V., voir VARTIRES I. 551

POPESCU V., voir VARTIRES I. 907

POPOVICI EV. and M. GRECU, A. POPA, M. ALEXANDROAIE, A. VASILE, M. CRUCEANU and N. DUMITRU, Detergent suspension for hard washings. Study of fluidity and stability 707

PREUSS H., voir A. SAVIN 1069

PUICA E., voir TRANDAFIR V. 671

PURI K., voir KUMAR A. 571

RĂCĂȘANU G., voir JURCONI E. 1039

RADOVICI O., voir LĂZĂRESCU V. 895

RADU S., voir IOVU M., ... 509

RADU S., voir IOVU M. 577

RĂILEANU M,, Solvent effects. VI. The mechanism of increase, differentiation and leveling of R_f values in the chromatographic separation of substances 443

RASCH G. and S. TOBISCH, The insertion reaction of Ni and Ni_2 into O—H, S—H, O—O and S—S bonds. A CNDO treatment 1085

RIZMAYER E.M., voir HORANYI G. 913

ROB M., voir FLORESCU S. 693

RODRIGUEZ-PASTOR A., voir GUTIERREZ-MARTIN F., ... 305

SAHINI V. EM. and C. PODINĂ, Partition coefficients on the basis of atomic charge density 843

SĂLĂGEAN EUGENIA, voir VÎLCU R. 847

SĂLĂJAN M., voir CHIFU E. 683

SĂNDESCU M., voir CHIFU E. 683

SĂNDESCU F. and CR. I. SIMIONESCU, Interfacial phenomena on concentrated polymer solutions in the spinning process 21

SAPSE A. M. Theoretical studies of the decomposition of lithiated nitrosoureas 1071

SAVA I., voir BRUMĂ M. 325

SAVA L., voir KORSHAK V. V. 393

SAVIN A. and H. PREUSS, H. STOLL, Why are caesium clusters more dificult to ionize than their monoxides? 1069

SCHIKETANZ ANA, voir BALABAN M.-C. 975

SCHIKETANZ ANA, voir SCHIKETANZ I. 1075

SCHIKETANZ I., voir BALABAN M.-C. 975

SCHIKETANZ I. and A. STEFĂNESCU, M.-C. BALABAN, A. SCHIKETANZ, M. D. GHEORGHIU, A. T. BALABAN, Aminoketone and oxazole synthesis. XI. Extension to the synthesis of thiazoles from 2-aza-1,4-diketones or *via* electrophilic substitution of arenes with 2-thiazolin-5-ones (thioazolactones) 1075

SCHWEDERSKI B., voir HAAS A. 1219

SEGAL E., voir DOCA N. 199

SEGAL E., voir VLAD M.O. 229

SEGAL E., voir VLAD M. O. 935

SEGAL E., voir ILIE I. 1109

SENGUPTA S.K., voir PANDEY O.P. 145

SHARMA M.B.L., voir AGARWAL R.K., ... 263

SHCHERBAKOVA I.V. and E. V. KUZNETSOV, LEV YU. UKHIN, M. D. GHEORGHIU, A. MEGHEA, J. HERDAN, A. T. BALABAN, 2-Benzopyrylium salts. XXXII. Synthesis and some chemical and spectral properties of 1- and/or 3-(3,5-di-t-butyl-4-hydroxyphenyl)-substituted 2-benzopyrylium salts 417
SHEIN S.M., voir A. T. BALABAN 501
SHRIMALI S.S., voir B.C. JOSHI 215
SHRIMALI S.S., voir B.C. JOSHI 321
SILBERG I.A., voir ONICIU L. 701
SIMIONESCU I.CR., voir SĂNDESCU F. 21
SIMIONESCU I. CR. voir KORSHAK V.V. 393
SIMON ZENO voir N. OLARU 63
SIMON ZENO, voir N. OLARU 83
SIMON ZENO, voir N. OLARU 83
SIMON ZENO, voir APETROAE M. 583
SIMON ZENO and G. I. MIHALAS, M. APETROAIE, CL. SINGER, R. BOZGA, R. CECLAN, ST. CILIANU, Structure activity relations by the free-Wilson and MTD methods for substances with a potential psychotropic activity. 2. Benzensulphonamide derivatives with anticonvulsive activity 783
SIMON ZENO, voir N. OLARU 1001
SIMON ZENO, Stereochemical and informational aspects in QSAR and MTD . 1103
SINGER CL., voir APETROAE M. 583
SINGER CL.,, voir SIMON ZENO 783
GH. SINGUREL, Study of the influence of the hydrogen bond on the electronic absorption bands of mandelic and 4-chloromandelic acids 113
SÎRBU A., voir MARINESCU M. 653
SOLIMAN A.Y., voir EL-FARARGY A.F. 435
SPACU P. and L. PATRON, S. PLOŞTINARU, A. CONŢESCU, D. CRIŞAN, N. STĂNICĂ, Coordination compounds as raw materials for mixed oxides. IV. Mixed coordination compounds of lanthanides and Ni(II) with hydroxydiphenylacetic acid, as precursors of mixed Ln_2NiO_4 type oxides . . . 249
SPACU P. and S. PLOŞTINARU, L. PATRON, A. CONŢESCU, D. CRIŞAN, N. STĂNICĂ, Rare earth mixed oxides with transition metals. I. Mixed oxides with Co(III) and Ni(III) having a Perovskite structure 877
SPĂTARU N., voir VARTIRES I. 551
SPĂTARU N., voir VARTIRES I. 907
SPOITU C. MARIAN and SORIN SPOITU, O. MUNTEAN, Approximate solution for isothermal effectiveness factor 1203
SPOITU S., voir SPOITU C.M. 1203
SRIVASTAVA A.K., voir AGARWAL R.K. 263
STANCU R., voir CEAUŞESCU ELENA 3
STĂNESCU M. and M. ELIAN, ECATERINA CIORĂNESCU, Carbonium ion reactions. XVIII. Substituent effect in solvolytic reactions. Solvolysis of the tosylate of 10-methyl-5H-dibenzo [*a*,*d*] cyclohepten-5-carbinol 969
STĂNESCU M., voir BANCIU M. 1161
STĂNICA N., voir SPACU p. 249
STĂNICĂ N., voir SPACU P. 877
STEPAN E., voir BALABAN A.T. 155
ŞTEFAN MIHAELA, voir ONCESCU T. 343
ŞTEFAN MIHAELA, voir ONCESCU T. 953
ŞTEFAN NICOLETA and I. G. DINULESCU, M. AVRAM, 1,3-Di-t-butylcyclobutane derivatives 1171
ŞTEFĂNESCU AURELIA, voir FLORESCU S. 693
ŞTEFĂNESCU AURELIA, voir SCHIKETANZ I. 1175
STERNBERG S. and V. BRANZOI, L. APATEANU, Effect of $CoSO_4$ additions with $Pb/PbSO_4$ electrode 121
STERNBERG S. and A. MATEESCU, V. BRÂNZOI, L. APĂTEANU, The coulometric study of the Pb, PbO_2, $O_2/PbSO_4$ system 457
STERNBERG S. and T. VIŞAN, N. BONCIOCAT, A. COTÂRŢĂ, Electrode processes in the system : lead (liquid)/lithium chloride-potassium chloride-lead chloride 883

STERNBERG S. and M. UNGUREANU, Heterogeneous electrocatalysis for nitrobenzen and phenol reduction 1123
STOICESCU M., voir CREȚU I. 723
STOICESCU V., voir DOBRESCU D. 995
STOLL H., voir SAVIN A. 1069
SUPURAN CL., voir CRISTESCU C. 329
SURDEANU T., voir ZAHARESCU M. 925
SURpĂȚEANU G.. voir COUTURE A. 353
TAMBI S.B. and M. ANAND, N. BHARGAVA, R.L. MITAL, Synthesis of some new fluorosubstituted tricyclic heterocycles. II. 3-Alkoxy-7-fluoro-10--{3-[4-(2-hydroxyethyl)-1-piperazinyl]-propyl}-2-methoxy phenothiazine derivatives 33
TOMA C.B., voir ONICIU L. 701
TOMOAIA-COTIȘEL M. and J. ZSAKÓ, E. CHIFU, Ejection curves and miscibility of egg lecithin with some carotenoid derivatives 663
TOMOAIA-COTIȘEL M. voir CHIFU E. 627
TOMOAIA-COTIȘEL M., voir ZSAKÓ J. 739
TOMOAIA-COTIȘEL M., voir ZSAKÓ J. 1193
TOBISCH S., voir G. RASCH 1085
TRANDAFIR V. and M. LECA, D. DEMBINSCHI, E. PUICA, G. ZĂINESCU, Interaction between polyacrylic dispersions and biopolymers hydrolysates 671
TRIPATHI S.C., voir PANDEY O.P. 145
TSAKIRIS C., voir MARIA GH. 821
TUDORACHE E., voir IOVU M. 1087
TUDOSE R.Z. and H. KADI, Drying of a porous spherical grain (in French) 807
UKHIN LEV YU., voir SHCHERBAKOVA I. V. 417
UNGUREANU M., voir STERNBERG S. 1123
VAIOS A., voir GHEORGHIU M.D. 979
VAIOS A., voir GHEORGHIU D.M. 1181
VAIS H. and D. G. MĂRGINEANU, Bacterial immobilization in membraneous supports for amperometric probing of organic compounds 677
VARHELYI CS., voir I. GĂNESCU 255
VARTIRES I. and V. POPESCU, A. MIHELIS, N. SPĂTARU, Electrochemical behaviour of the electroactive spinel type Co_3O_4 coatings 551
VARTIRES and A. MIHELIS, V. POPESCU, N. SPĂTARU, On the semiconducting character of spinel type electrocatalytic oxide layers 907
VASILE A., voir POPOVICI EV., 707
VASILIU-OPREA CLEOPATRA and ALEX. C. CONSTANTINESCU, Mechanochemical reactions of some polyurethane elastomers. 5. Study of modifications of some physico-chemical properties induced by uniaxial tensile creep and UV irradiation 407
VASS C., Lead electrodeposits on graphite support 901
VASS M., voir LĂZĂRESCU V. 895
VÎLCU R. and E. SĂLĂGEAN, Micelle formation in aqueous sodium dodecyl sulfate solutions 847
VÎLCU R. and V. LANGSHAW, Z. CENUȘE, Isothermal liquid vapour equilibrium in the acetonitrile-proprionitrile system 1025
VIȘAN T., voir STERNBERG S. 883
VITAN F., voir NAUM N. 519
VLAD M.O. and E. SEGAL, The probability of reaction events in nonequilibrium chemical systems 229
VLAD M.O. and V.T. POPA, E. SEGAL, A nonlinear transformation for the reaction events within the framework of the Horiuti-Temkin theory 935
VLAD RODICA and F. BADEA, M. BANCIU, Kinetics of the acetolysis of 10,12-dihydro-10, 5-propeno-5H-dibenzo [*a,d*] cyclohepten-11-yl bromide. Another example of double bond participation in ionisation 179
VOLANSCHI E., voir CIUREANU M. 467
VOLANSCHI E., voir HILLEBRAND M. 1051
WEINBERG J. and A. DONESCU, β-lactam antibiotics. I. Structure-neurotoxic activity of benzylpenicillin 1171
WEISSMAN N.N., voir MARINESCU M.M. 713

WITTENBECHER K., voir EMONS H.-H. 855
ZAHARESCU M. and C. PÎRLOG, D. CRIŞAN, N. DRĂGAN, A. BRĂILEANU, M. ILISIE, T. SURDEANU, Protonic conductors with beta-alumina type structure 925
ZĂINESCU G., voir TRANDAFIR V. 671
ZSAKÓ J. and V. NEAGU, M. TOMOAIA-COTIŞEL, E. CHIFU, Molecular structure and monolayer properties 739
ZSAKÓ J., voir CHIFU E. 627
ZSAKÓ J., voir TOMOAIA-COTIŞEL M. 663
ZSAKÓ J. and M. TOMOAIA-COTIŞEL, V. TĂMAŞ, V. COMAN, E. CHIFU, Monomolecular film of some apocarotenoid derivatives 1193
YOUSUFZAL A.H.K., voir KHAN A.R. 495

Revue Roumaine de Chimie, 32, *11–12*, 1237–1242 (1987)

INDEX DES SUJETS

Acetolysis of 10,11-dihydro-10,5-propeno-5H-dibenzo[*a,d*] cyclohepten-11-yl bromide. Another example of double bond participation in ionisation. Kinetics of the — R. VLAD, F. BADEA and M. BANCIU 179

Acid-base equilibria of proflavine in ground and excited electronic states. On the — T. ONCESCU, M. ŞTEFAN, O. HÖRER. 343

Aliphatic alcohols on copper catalysts. Dehydrogenation kinetics of low-III. Metallic copper with Fe and Ni as addition elements. N. DOCA and E. SEGAL 199

Alkylation of benzene with isopropanol, N. NAUM, GH. MIHĂILĂ, F. VITAN, P. ONU,D. GÂNJU 519

Amine salts of the $H_2[Pt(SCN_4)]$ and $H_2[(Pt(SCN)_6]$ acids. Metal- and metal (III) — I. GĂNESCU and G. VÁRHELYI 255

Aminoacids I. The influence of various factors on the optical activity of some essential —. Aplications, C. MANDRAVEL and L. ANASTASESCU 1045

Aminoketone and oxazole synthesis. X. Acylation and alkylation of arenes with the azlactone of cinnamoylglycine, M.-C. BALABAN, I. SCHIKETANZ, A. T. BALABAN, ANA SCHIKETANZ and M. D. GHEORGHIU 975

Aminoketone and oxazole synthesis. XI. Extension to the synthesis of thiazoles from 2-aza-1,4-diketones or *via* electrophilic substitution or arenes with 2-thiazolin-5-ones (thioazolactones), I. SCHIKETANZ, A. STEFANESCU, M.-C. BALABAN, A. SCHIKETANZ, M.D. GHEORGHIU and A. T. BALABAN 1075

Anodic oxidation of vacuum deposited silver film. Sintering effects on — V. LĂZĂRESCU, O. RADOVICI and M. VASS 895

Angular overlap model (AOM) calculations for the coordination compounds with the macrocyclic ligands. I. AOM parameters for nickel (II) coordination compounds with tetrakis-anhydro-aminobenzaldehyde macrocyclic ligand — M. ANDRUH, C. I. LEPĂDATU and M. BREZEANU 1033

Antifungal and antiviral activity of some transition metal complexes of cycloalkyl dithiocarbamates. Synthesis, characterization — O. I. PANDEY, S. K. SENGUPTA and S.C. TRIPATHI 145

Apocarotenoid derivatives. Monomocular film of some. — J. ZSAKÓ, M. TOMOAIA-COTIŞEL, V. TAMAS, V. COMAN and E. CHIFU 1193

Aromatic azoxybisethers. M. IOVU and S. RADU 577

Aromatic ureas from carbon dioxide and diamines using ethylene chlorophosphite in pyridine as reagent. A new synthesis of — C. I. CHIRIAC 29

N-Aroylphthalimides by a new direct condensation reaction, C. I. CHIRIAC . . 793

3-N-Arylcarbamidocoumarins. Synthesis and studies of—A. F. EL-FARARGY, A. Y. SOLIMAN, M. EL-MOBAYED and S. EL-ESSER 435

Azo-dye. The synthesis of an—O. ANAÇ 431

Bacterial immobilization in membraneous supports for amperometric probing of organic compounds, H. VAIS and D. G. MĂRGINEANU 677

2-Benzopyrylium salts. XXXII. Synthesis and some chemical and spectral properties of 1- and/or 3-(3,5-di-t-butyl-4-hydroxyphenyl)-substituted 2-benzopyrylium salts, I. V. SHCHERBAKOVA, E. V, KUZNETSOV, L. YU. UKHIN, M. D. GHEORGHIU, A. MEGHEA, J. HERDAN and A. T. BALABAN . 417

4-Benzyloxyazobenzenes synthesized by condensation of benzyl chloride with sodium salts of 4-hydroxy-azobenzenes, M. IOVU, S. RADU 509

BOOK REVIEWS. 109—110, 325—340, 449—451, 547—548, 729—735, 833—836

Caesium clusters more difficult to ionize than their monoxides? Why are—A. SAVIN, H. PREUSS and H. STOLL 1069

Carbonium ion reactions. XVIII. Substituent effect in solvolytic reactions. Solvolysis of the tosylate of 10-methyl-5H-dibenzo[*a,d*] cyclohepten-5-carbinol, MICHAELA STĂNESCU, M. ELIAN and ECATERINA CIORĂNESCU 969

Catalytic alkylation of toluene with methanol. Kinetic studies on the — E. DUMITRU, S. OPREA and V. HULEA 191

Cationic polymerization of α-methyl styrene. Chain transfer constants for some aromatic solvents in the — A. R. KHAN, T. AKHTER and A. H. K. YOUSUFZAL 495

Chelates of N,N,N′, N′-tetramethyl thiuram disulphide. Magneto, spectral and thermal studies of rare earth nitrate — R. K. AGARWAL, M.B.L. SHARMA and A. K. SRIVASTAVA 263

Chemical equilibrium method for solving complex mass action kinetic system. Rate-constrained — D. CARTIANU 369

Chemical graphs. Part 47. Valence isomers of [14] annulene, A. T. BALABAN and C. DELEANU 271

Chemical species. Counting observables of — AL. IVANOV 1097

Colloids and surfaces. The chemistry of — M. FLORESCU 621

Composite systems. High resolution mixing calorimetry in studies of — G. DRĂGAN 759

Computation of saturation pressure and orthobaric densities by a general cubic equation of state, D. GEANĂ, V. FEROIU and O. LANDAUER 863

Coordination compounds of lanthanides(III) with 2-ethoxycarboxylamino-pyridine. Magneto, spectral and thermal investigations of — R. K. AGARWAL and S. K. GUPTA 477

Coordination compounds as raw materials for mixed oxides. IV. Mixed coordination compounds of lanthanides and Ni(II) with hydroxydiphenylacetic acid, as precursors of mixed Ln_2NiO_4 type oxides, P. SPACU, L. PATRON, S. PLOȘTINARU, A. CONȚESCU, D. CRIȘAN and N. STĂNICĂ 249

Copolymers containing phenylquinoxaline units, V. V. KORSHAK, E. S. KRONGAUZ, N. M. BELOMOINA, M. BRUMĂ, G. MANDRIC and C. I. SIMIONESCU 489

Corrosion inhibitors for steel in H_3PO_4. Heterocyclic quaternary ammonium compounds as — A. S. FOUDA, H. A. MOSTAFA and M. N. MOUSSA . . . 775

Coulometric study of the Pb, PbO_2, $O_2/PbSO_4$ system, S. STERNBERG, A. MATEESCU, V. BRÂNZOI and L. APĂTEANU 457

Detergent suspension for hard washings. Study of fluidity and stability, EV. POPOVICI, M. GRECU, A. POPA, M. ALEXANDROAIE, A. VASILE, M. CRUCEANU and N. DUMITRU 707

Dialysis process. Study on Co^{2+} and Zn^{2+} behaviour in — F. MATEI, GH. IONESCU, A. CECAL and A. DUCA 133

Diamines and aminoethers. Relations between chemical structure and analgesic action of some — D. DOBRESCU, M. IOVU, C. GEORGESCU, V. STOICESCU and A. CRISTEA 995

Dichloromethylderivatives in the presence of tetrachloroethene or trichloroethene. Homopolycondensation of — M. IOVU and G. TUDORACHE 1185

Dilute block copolymer systems. VI. Effect of polymeric diluents, E. CEAUȘESCU, R. BORDEIANU, P. GHIOCA, I. CERCHEZ, E. BUZDUGAN and R. STANCU 3

Dimethylchlorosilane as reagent for the synthesis of 1,3,4-oxadiazoles from diaroylhydrazines, C. I. CHIRIAC 223

Dipole moments of ground and excited states of 7-chloro-2,3-dihydro-4-quinolone (in French), C. BENDIC and C. PODINA 1155

Dissociation of KCl in mixed hexamethylphosphortriamide-water solvents, E. A. GOMAA, A. H. EL-ASKLANY and M.N.H. MOUSSA 243

1,3, Di-t-butylcyclobutane derivatives. N. STEFAN, I. G. DINULESCU and M. AVRAM 1171

10,21-Dithia-9,10, 11, 20, 21, 22-hexahydrodephenanthro[*a, f*] cyclodecene-S,S,S′-S′,-tetraoxide. Synthesis and pyrolysis of—, M. BANCIU, ANCA BANCIU, M. ELIAN, C. DRĂGHICI and ECATERINA CIORĂNESCU 961

Drying of a porous spherical grain (in French), R. Z. TUDOSE and H. KADI . 807

Effect of $CoSO_4$ additions on the Pb/$PbSO_4$ electrode, S. STERNBERG, V. BRÂNZOI and L. APĂTEANU 121

Egg lecithin with some carotenoid derivatives. Ejection curves and miscibility of — M. TOMOAIA-COTIȘEL, J. ZSAKÓ and E. CHIFU 663

Electrode processes in the system : lead (liquid)/lithium chloride-potassium chloride-lead chloride, S. STERNBERG, T. VIȘAN, N. BONCIOCAT and A. COTÂRȚĂ 883

Electrodialysis of $Cr_2O_7^{2-}$ ion on ion-exchange membranes. Theoretical and experimental features of — F. MATEI, GH. IONESCU and AL. DUCA 235

Electronic absorption bands of mandelic and 4-chloromandelic acids. Study of the influence of the hydrogen bond on the — GH. SINGUREL 113

Electron spin resonance study of conformational inversion in iminoxy radicals derived from benzocycloheptene and heterocyclic analogs, A. CARAGHEORGHEOPOL and I. DRĂGUȚAN 1141

Electrosynthesis of propionitrile. II. Phase equilibria in the acrylonitrile-propionitrile-water system in the presence of cationic surfactants and electrolytes.. L. ONICIU, D. A. LÖWY, M. JITARU, I.A. SILBERG and B. C. TOMA 701

ESR spectral study of some substituted *meta*-dinitroanilines, M. HILLEBRAND, M. MORARU and E. VOLANSCHI 1051

Exchange of Zn^{2+} and Mn^{2+} in synthetic zeolites NaA, NaX and mordenite, N. BÎLBĂ, D. BÎLBĂ, GH. MIHĂILĂ and N. NAUM 563

Explosive combustion of propylene. IV.The maximum explosion pressure in adiabatic and non-adiabatic constant volume combustion, D. POPESCU, B. ALBU, D. OANCEA, N. I. IONESCU, V. GOȘA and D. GEANĂ . . 359

Fatty acid films at the benzene water interface, E. CHIFU, M. SĂLĂJAN, I. DEMETER-VODNAR and M. TOMOAIA-COTIȘEL 683

Fluorosubstituted tricyclic heterocycles. II. 3-Alkoxy-7-fluor-10-{3[4-(2-hydroxyethyl)-1-piperazinyl]-propyl}-2-methoxy phenothiazine derivatives. Synthesis of some new—S. B. TAMBI, M. ANAND, N. BHARGAVA and R.L. MITAL 33

Free radicals. XVIII. Capto-dative (Push-pull) diarylaminyls with 2,4,6-tri- (methane-sulphonyl)-phenyl or 2,4,6-tri-(N,N-dimethyl-sulphonamido)-phenyl groups. Factors affecting stability and equilibria of — A. T. BALABAN, N. NEGOIȚĂ, S. M. SHEIN and A. D. KHMELINSKAYA 501

Free-Wilson and MTD methods for substances with a potential psychotropic activity. Structure activity relations by the —. 1. Diphenylether derivatives with neuroleptic activity, M. APETROAE, Cl. SINGER, R. BOZGA, ST. CILIANU, R. CECLAN, T. BÂNZARU and Z. ȘIMON 583

Free-Wilson and MTD methods for substances with a potential psychotropic activity. Structure activity relations by the — 2. Benzensulphonamide derivatives with anticonvulsive activity, Z. SIMON, G. I. MIHALAS, M. APETROAIE, CL. SINGER, R. BOZGA, R. CECLAN, and ST. CILIANU . 783

Gas absorption with a complex chemical reaction in a perfectly mixed chemical reactor, GH. JUNCU, O. MUNTEAN and R. MIHAIL 599

Guanine phosphorilosyltransferase from *Escherichia coli*. Quantitative structure-activity relations for the inhibition of — N. OLARU and Z. SIMON . . . 1001

Heterogeneous electrocatalysis for nitrobenzene and phenol reduction, S. STERNBERG and M. UNGUREANU 1123

High resolution mixing calorimetry of adsorption of aqueous solutions of superplasticizer additive on cement. Study by — G. DRĂGAN, S. IFRIM and G. POPESCU 767

Homophthalic anhydride with some compounds containing two amino groups. Reactions of—M. I. ALI, A. M. ABD-ELFATTAH, H. A. HAMMPUDA and and S. M. HUSSAIN 297

Horiuti-Temkin theory. A nonlinear transformation for the reaction extents within the framework of the — M. O. VLAD, V. T. POPA and E. SEGAL . . . 935

Hydrogen production from water using proflavine as photosensitizer. Optimistion of — T. ONCESCU, M. ȘTEFAN, M. CONTINEANU and S. G. IONESCU 953

3-[(2-Hydroxy-4-quinolyl)methyl]-2,4-pentanediones. Some reactions on — M. KAMEL, M. T. ELWASSIMI, F. H. OSMAN and G. EL. SARRAF . . 427

Inclusion compounds of perhydrotriphenylene with aliphatic monocarboxylic acids, C. LUCA, N. BÎLBĂ, GH. MIHĂILĂ and I. AGHERGHINEI . 41

Informational entropy of the probability field events of a chemical control analysis, V. DAVID 539

Insertion reaction of Ni and Ni_2 into O—H, S—H, O—O and S—S bonds. A CNDO treatment, G. RASCH. and S. TOBISCH 1085

Interaction product of N, N′-bis (Furfurylidene) ethylenediamine with cobalt (II) chloride, AIMEE ARIAS-CARBAJAL and ROBERTO CAO 47

Interfacial phenomena on concentrated polymer solutions in the spinning process, F. SĂNDESCU and CR. I SIMIONESCU . . . 21

Ionic-molecular flotation of Cu(II) using Ponilit CP_1 as collector. pH Influence on the flotation efficiency (in French), R. POMOJE-MARCU and L. MAGYAR . . . 611

IPSO-Substitution of heterocyclic compounds. I. Nitration of 5-bromo-3,4-dimethyl-1-phenyl-1*H*, 6*H*-pyrano [2,3-*c*]pyrazol-6-one, M. AIN KHAN and R. GHAFOOR . . . 295

Isothermal effectiveness factor. Approximate solution for —, C. M. SPOITU, S. SPOITU and O. MUNTEAN . . . 1203

Isothermal liquid-vapour equilibrium in the acetonitrile-propionitrile system, R. VÎLCU, V. LANGSHAW and Z. CENUȘE. . . . 1025

Kinetics of the substitution reaction between Co C_2O_4Bi Py_2 I and bipyridyl in aqueous solution, E. JURCONI, T. ONCESCU and S. RACĂȘANU . . . 1039

Lead electrodeposits on graphite support, C. VASS . . . 901

Lactam antibiotics. I. Structure-neurotoxic activity of benzylpenicillin. J. WEINBERG and A. DONESCU . . . 1171

Lithiated nitrosources's decomposition. Theoretical studies of — A. M. SAPSE . 1071

Mass spectra of some oxygen and sulphurcontaining heterocycles. V. CONSTANTIN 1059

Membranes. Electric potential of some autochtonous synthetic, I. NEACȘU and M. BEZDADEA . . . 749

Metallic complexes of Schiff bases derived from 2-thiophene-carboxyaldehyde, 2-pyridinecarboxyaldehyde and *ortho*-aminobenzene-thiole. Study of the — (in Spanish), F. CAPITAN, P. ESPINOSA, F. MOLINA and L. F. CAPITAN-VALLVEY . . . 151

Methanol conversion over H-ZSM-5 type zeolites. Distribution of products in — GR. POP, M. BOZEȘANU, N. I. IONESCU, I. IOSIF and G. MUSCĂ 533

Methanol to formaldehyde on modified vanadia catalysts. Selective oxidation of G. BLIZNAKOV, D. KLISSURSKI and Y. PESHEVA . . . 985

Micelle formation in aqueous sodium dodecyl sulfate solutions, R. VÎLCU and E. SĂLĂGEAN . . . 847

Minimum ignition energy of an explosive gaseous mixture. On the significance of — D. OANCEA, DOMNINA POPESCU and N. I. IONESCU . . . 1211

Mixed solutions of cationic and nonionic surfactants, M. OLTEANU . . . 647

Model for the viscosity of liquid mixtures. Application to the binary system water-dioxan. O. LANDAUER, C. MATEESCU, O. IULIAN and D. GEANA 1129

Molecular motion in solid bicyclo[3,3]nonan 9 one and adamantanone oximes studies by the electron spin resonance spectra of the corresponding iminoxy radicals, H. CĂLDĂRARU . . . 1151

Molecular structure and monolayer properties, J. ZSAKO, V. NEAGU, M. TOMOAIA-COTIȘEL and E. CHIFU . . . 739

Molten salt mixtures alkali halide—alkaline earth halide. Vapour pressures of — H.-H. EMONS, D. KIEẞLING, W. HORLBECK and K. WITTENBECHER . . . 855

Monomolecular membranes of biological interest. Specific interaction in —, CHIFU, A. CHIFU, M. TOMOAIA-COTIȘEL and J. ZSAKO . . . 627

Mordant blue 9 with bromate catalyzed by vanadium (V). Part I. Influence of variables. Oxidation of — (in Spanish), N.P. CID and L. O. GARCIA VIOR . . . 51

Mordant blue 9 with bromate catalyzed by vanadium (V). Part II. Kinetics and mechanism. Oxidation of — (in Spanish), N.P.CID and L. O. GARCIA VIOR . . . 203

Nickel ferrite from polynuclear coordination compounds. Part I. Study of the dry ferritization process. Synthesis of — I. ILIE, M. BREZEANU, L. PATRON, E. SEGAL and G. FILOTI . . . 1104

Nitrothioamide anion radicals. Optical spectra and electronic structure of some—, M. CIUREANU, M. HILLEBRAND, E. VOLANSCHI and D. GHEȚU 467

Nitrogen heterocycles. Comparison between empirical and advanced molecular orbital calculations for some —, N. OLARU and Z. SIMON . . . 83

Nuclear magnetic resonance investigations of small rings. 4.^{13}C-NMR spectra of 2-t-butyl-2-cyanocyclobutanones as probes for configurational assignments, M.D. GHEORGHIU, M. MIHAI, L. PARVULESCU, A. VAIOS and F. NICULESCU . . . 979

Nuclear magnetic resonance investigations of small rings. Part 5. The exact analysis for the four-membered ring three proton system of 3-aryl-2-t-butyl-2-cyclobutanones as evidence for configurational assignments. M. D. GHEORGHIU, M. MIHAI, L. PARVULESCU, A. VAIOS and M. ELIAN 1181

Organochlorine (OCl) pesticide residues in human fats. Part I, O. ANAÇ and K. GÜNAYDIN 803

Oxidation reaction by hydroxylamine in normal and heavy water. Rate constants and activation energies of Fe(II) to Fe(III) — A. CĂLUŞARU and E. SAVIUC. 101

Partition coefficients on the basis of atomic charge density, V. EM. SAHINI and C. PODINĂ 843

Perhalogenomethyl-thioheterocycles. XXV. Electrophilic substitution of 2,4-diaminopyrimidines with perhalogenomethyl-chalcogenohalides (in German). A. HAAS, M. LIEB and B. SCHWEDERSKI 1219

Phenylhydrazone formation from substitutionted benzaldehydes: substituent effect and structure-reactivity correlations, F. GUTIERREZ-MARTIN, A. RODRIGUEZ-PASTOR and F. MATA-PEREZ 305

Photocyclization on enamides and thioenamides. Theoretical study on the — A. COUTURE, A. LABLACHE COMBIER, G. SURPĂŢEANU and M. CONSTANTINESCU 353

Photoinduced H_2 generation from water in micellar systems. T. ONCESCU, M. CONTINEANU, S. G. IONESCU, M. OLTEANU, M. LECA and L. MEAHCOV 637

Photolysis of mono-, di- and tribenzylamine and the novel photocarbylamine reaction, M.Z.A. BADR, M.M. ALY, S. A. MAHGOUB, A. M. FAHMY and F. F. ABDEL-LATIF 315

Polarographic study of lead with δ-valerolactam and its analytical applications, A. KUMAR, M. KATYAL and B. K. PURI 571

Polyacrylic dispersion and biopolymers hydrolysates. Interactions between — V. TRANDAFIR, M. LECA, D. DEMBINSCHI, E. PUICĂ and G. ZĂINESCU 671

Polymer flooding in oil reservoirs. Some aspects of — I. CREŢU, M. IONESCU and M. STOICESCU 723

Polymerisation of some vinylic monomers in the presence of synthetic zeolites, M. BEZDADEA, GH. MIHĂILĂ, N. BÎLBĂ and N. NAUM 401

Polymer surfactant interaction. Surface-active properties, M. M. MARINESCU, M. BALCAN, B. G. ALBU, G. POPESCU and N. N. WEISSMAN 713

Poly-1,3,4-oxadiazolesterimides, M. BRUMĂ and I. SAVA 325

Poly-phenylquinoxaline-oxadiazole-imide-amides, V. V. KORSHAK, E. S. KRONGAUZ, N. M. BELOMOINA, M. BRUMA, I. SAVA and C. I. SIMIONESCU 393

Polyurethene elastomers. Mechanochemical reactions of some — 5. Study of modifications of some physico-chemical properties induced by uniaxial tensile creep and UV irradiation, Cl. VASILIU-OPREA and ALEX. C. CONSTANTINESCU 407

Propane thermal cracking process simulation in a radiant furnace. An adapted zone method for —, GH. MARIA, CR. TSAKIRIS, GR. BOZGA and AL. ISOPESCU 821

Propylene. Mobility of lattic oxygen and activity of multicomponent oxide catalysts for oxidation of — N. I. IONESCU and M. CĂLDĂRARU 939

Proton catalysed rearragement of N-alkyl arene sulphonanilides to *ortho*-alkylamino sulphones. Part III, B.C. JOSHI, Y. C. JOSHI, D. KISHORE and S. S. SHRIMALI 215

Proton catalysed rearrangement of N-alkyl-naphthalene-sulphoanilides to *ortho*-alkylamino-aryl-naphthalyl-sulphones. Part IV, B. C. JOSHI, Y. JOSHI, D. KISHORE and S. S. SHRIMALI 321

Protonic conductors with beta-alumina type structure, M. ZAHARESCU, C. PÎRLOG, D. CRIŞAN, N. DRĂGAN, ANA BRĂILEANU, M. ILISIE and T. SURDEANU 925

Purine derivatives, inhibitors of guanine phosphoribosyl-transferase from *Escherichia Coli*. Electronic structure and reactivity indices for a series of — N. OLARU and Z. SIMON 63

Pyridyl-pyrazolone system. I. Some reactions with 3-(3′-pyridyl)-1-phenyl-2-pyrazolin-5-one. Studies on the — M. F. ABDEL MEGEED, M. EL BORAI, M. FAHMY and EL-SAIED A. ALY 515

Pyridyl-pyrazolone system. II. Some reactions with 4-arylidene-3-(3′-pyridyl)-1-phenyl-2-pyrazolin-5-one. Studies on — M. F. ABDEL MEGEED, M. EL BORAI, M. FAHMY and EL-SAIED A. ALY 797

Pyridyl-pyrazolone system. V. Cyclocondensation of 1-phenyl-3-(3′-pyridyl)-2-pyrazolin-5-one with ethyl acetoacetate and related compounds. Studies on — M. F. ABDEL-MEGEED 591

Pyrylium salts with nucleophiles. XIX. Novel bispyridinium salts with potential biological activity. Reactions of — A. T. BALABAN and E. STEPAN . . 155

QSAR and MTD. Stereochemical and informational aspects in — Z. SIMON

Rare earth mixed oxides with transition metals. I. Mixed oxides with Co(III) and Ni(III) having a Perovskite structure, P. SPACU, S. PLOȘTINARU, L. PATRON, A. CONȚESCU, D. CRIȘAN and N. STANICĂ 87

Radiotracer study of the adsorption of DL-asparaginic acid at a platinized platinum electrode, G. HORANYI and E. M. RIZMAYER 913

Reaction events in nonequilibrium chemical systems. The probability of — O. M. VLAD and E. SEGAL 229

Ring contraction and additional annelation in dibenzobullvalone system. M. BANCIU, M. STĂNESCU, C. FLOREA, A. T. BALABAN and ECATERINA CIORĂNESCU 1161

Spinel-type Co_3O_4 coatings. Electrochemical behavior of the electroactive, I. VARTIRES, V. POPESCU, A. MIHELIS and N. SPĂTARU 551

Spinel-type electrocatalytic oxide layers. On the semiconducting character of — I. VARTIRES, A. MIHELIS, V. POPESCU and N. SPĂTARU . . . 907

Solvent effects VI. The mechanism of increase, differentiation and leveling of R_f values in the chromatographic separation of substances, M. RĂILEANU 443

Sugars and ascorbic acid by indirect method using ferricyamide — thymolphthalin reagent. Microdetermination of reducing — M. M. ABDEL BADEI, and E. A. EL SAWI 141

Surface and colloidal properties of sodium alkylbenezene sulfonates. The influence of sodium toluene sulfonate on — S. FLORESCU, A. ȘTEFĂNESCU, M. ROB and I. FĂTU 693

Surface mobility of surfactant solutions. XII. Remarks concerning the Marangoni flow through an inclined surface canal, E. CHIFU and C.-I. GHEORGHIU 945

Thioethers. I. Complex compounds of Pd(II) with—. Investigation of some compounds of Pd(II) with thioethers of the bis(phenylthio-methyl) ether series, D. NEGOIU, S. NEAGOE, M. NEGOIU, E. BADAU and E. GHERMAN 91

as-Triazine derivatives with potential therapeutic action. XXII. A simplified method for the synthesis of 1,2,4-triazole nucleosides and 1,2,4-triazine-nucleosides, C. CRISTESCU and CL. SUPURAN 329

10H-8-Trifluoromethyl-1-azaphenothiazine *via* the Smiles rearrangements. Studies in the synthesis of — R. AGRAWAL, G. K. OBEROI, D. C. JAIN and R.L. MITAL 37

Vibronic theory of magnetic properties of trinuclear mixed-valence clusters, I. B. BERSUKER, S. A. BORSHCH and I. N. KOTOV 1075

Vinyl chloride. Physico-chemical characterization of the two-phase system employed in emulsion polymerization of — M. MARINESCU, V. BUTUCEA, G. POPESCU, A. SIRBU, A. IONESCU, C. GEORGESCU and B. ALBU 653

Zeolite catalysts in *m*-xylene isomerization. Activity and selectivity of — E. DUMITRIU, S. OPREA and V. HULEA 525

I.C.I.T.P.R. PLOIEŞTI

ur address : B-dul Republicii nr. 291 A, Cod 2000 Telefon 3 18 75 — 3 17 25
TELEX : 1.93.40

TECHNOLOGY FOR THE PREPARATION OF α-PYRROLIDONE

I.C.I.T.P.R. PLOIEŞTI (Research Institute in Engineering and Design for Refi- ries) developed a licensed technology for the preparation of high purity pyrroli- ne, required in the synthesis of N-vinyl-pyrrolidone and of PIRACETAM ug.

This technology consists in direct ammonolysis of γ-butyrolactone with hydrous liquid ammonia.

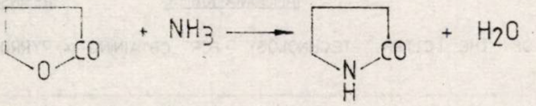

This technology differs from other known processes by splitting butyrolactone o γ-hydroxybutyramide and cyclization of amide into pyrrolidone, in a single action step, in absence of water.

Brief description of technology

The ammonolysis reaction of γ-buty- actone with anhydrous liquid ammo- occurs in a tubular reactor R, with al displacement.

The reactants in the molar ratio –1.2/1 (ammonia/γ-butyrolactone) er preheating at 170–180°C, under –90 at, are discharged to the bottom the ammonolysis reactor R, in series- w through the three reaction ele- nts.

The isothermicity of reaction tubes is hieved by a thermal agent (termo- ted oil) which circulates through the actor, keeping the temperature in the 0–300°C range.

The reaction water and excess of monia are separated from the effluent er quenching to 40–50°C, in a frac- nation column C_1 ; at the top the product withdrawn from the bottom of C_1 consists of 85–87% pyrrolidone, 5–7% butyrolactone and 6–7% resins. This product is discharged to the column C_2, which separates at the top the unreacted butyrolactone containing a small concentration of water and pyrrolidone, which are recycled into the feed.

The top temperature in C_2 is 105–107°C and the pressure 50 mm Hg.

From the bottom product of C_2, the high purity pyrrolidone is separated in a distillation column C_3.

Pyrrolidone of min. 99% purity is separated at the top of C_3 at 128–130°C under 20 mm col Hg and a reflux ratio of 1.5/1.

The heavy products are withdrawn from the bottom of C_3.

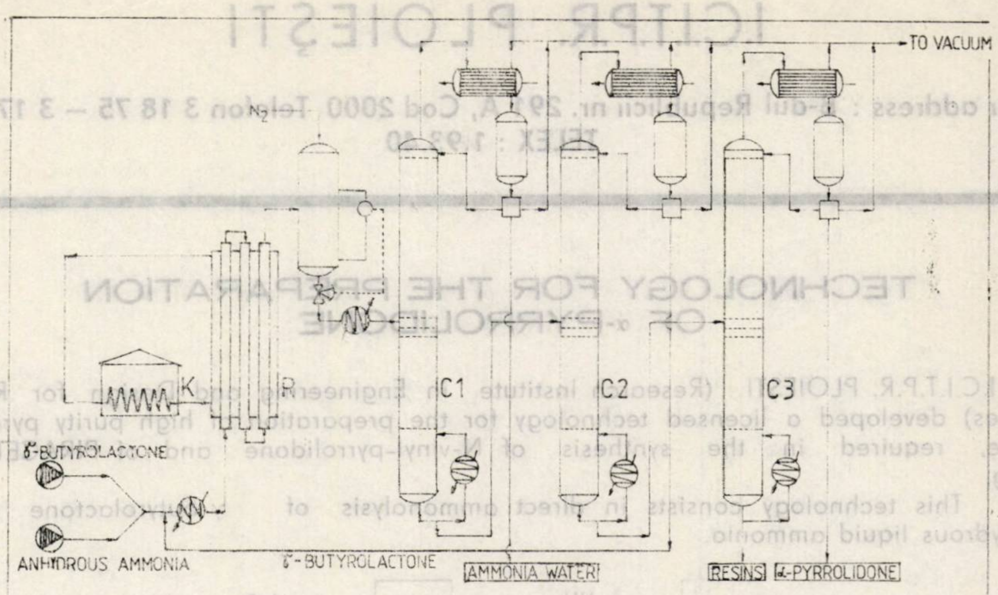
TO VACUUM
N_2
K
R
C1
C2
C3
γ-BUTYROLACTONE
ANHYDROUS AMMONIA
γ-BUTYROLACTONE
AMMONIA WATER
RESINS
α-PYRROLIDONE

FLOW-SHEET OF THE I.C.I.T.P.R TECHNOLOGY FOR OBTAINING α-PYRROLIDONE

Process performance

Yield in α-pyrrolidone = 90–92%; Conversion of butyrolactone = 93–94%.

Characteristics of the finished product

Content of α-pyrrolidone	99–99.5%
Content of γ-butyrolactone	max. 0.2%
Content of γ-butyramide	max. 0.2%
Content of propioamide	max. 0.1%
Content of water	max. 0.1%
Melting point	24.6°C

Feed requirements and utilities/tone pyrrolidone

γ-butyrolactone = 1.2 t; Anhydrous ammonia =0.35 t; Steam 14 ata 6 t; Cooling water ($\Delta t = 10^\circ$) =75 m³; Electricity = 100 kWh; Conventio fuel = 1 t.

Commercial application

One commercial plant in operation in Romania.

NOTE POUR LES AUTEURS

La Revue Roumaine de Chimie publie des articles en anglais, français, russe, allemand ou espagnol. Les auteurs sont priés d'envoyer des articles et des comptes rendus inédits.

Les manuscrits seront dactylographiés à double interligne. La bibliographie, les tableaux et la légende des figures seront placés après le texte.

Si l'article fait partie d'une série numérotée, la partie précédente sera donnée comme première référence.

Chaque article sera précédé d'un résumé comprenant quinze lignes au maximum.

Les références bibliographiques dans le texte seront faites par des exposants sans parenthèses et paraitront à la fin de l'ouvrage.

Les publications périodiques mentionnées dans la bibliographie seront présentées suivant les prescriptions internationales : le nom de l'auteur précédé de l'initiale du prénom, le titre du périodique abrégé conformément à « Chemical Abstracts » et souligné par une ligne, le numéro du tome indiqué par des chiffres arabes et souligné par deux lignes, suivi de la première page de l'article ; à la fin, l'année de la parution sera placée entre parenthèses. Le numéro de la revue ne sera pas indiqué si les pages du volume sont numérotées consécutivement.

Les textes des livres ou traités incluеront : le nom des auteurs, l'initiale du prénom, le titre du livre entre guillemets et sans être souligné, le numéro du tome précédé par l'abréviation « vol. » (ou « Bd. »), le numéro de l'édition, les éditions (the publisher), la localité de la parution du livre, l'année de la parution et la page de la référence précédée(s) par l'abréviation «p. » (ou « S. »).

Les brevets seront indiqués comme suit : l'auteur ou la firme, le pays et le numéro du brevet, la date et la revue *(Chem. Abstr.)*. Par ex. : M. Jones (to Union Carbide Co), Brit. Pat. 601 238, 2 Sept. 1959 ; cf. *Chem. Abstr.*, **54**, 12808 (1960).

Si la référence n'a pas été lue en original, on indiquera aussi la revue de référence consultée.

Les diagrammes seront tracés à l'encre de Chine sur papier calque. Les tableaux et les figures (en nombre strictement nécessaire) ainsi que les courbes dans les figures seront numérotés par des chiffres arabes. Leur explication sera donnée dans la légende des figures. Prière de ne pas inscrire les mêmes données dans les tableaux et les figures. Chaque tableau aura un titre. On indiquera dans le texte la place approximative des tableaux et des figures. Les formules chimiques seront incluses dans le texte ; en outre, elles seront transcrites sur papier calque, à l'encre de Chine.

Les auteurs sont priés d'indiquer les caractères italiques (en soulignant les lettres au crayon), ainsi que tout autre caractère spécial ; les préfixes *ortho*, *meta*, *para*, *cis*, *trans*, etc. seront soulignés pour indiquer leurs caractères italiques et ne seront jamais écrits avec des majuscules.

Aucune correction à la main ne sera admise sur le manuscrit. Les corrections seront tapées à la machine. Les lettres grecques ou d'autres symboles spéciaux seront insérés à la main à l'encre clairement.

Le manuscrit sera signé par l'auteur.

Le titre-courant aura 50 lettres au maximum.

L'entière responsabilité du contenu des articles appartient aux auteurs.

Sur demande on peut obtenir une note plus complète.

PRINTED IN ROMANIA

CHEMICAL FERTILIZERS UNIT

—Craiova—Romania—

Telephone : 86405 ; 86496 Telex : 41246 ; 41353 ciich-r

PRODUCES AND DELIVERS

- **Chemical fertilizers :**
  - with nitrogen (urea, ammonium nitrate, liquid fertilizers with nitrogen)
  - with phosphorus (simple superphosphate, simple superphosphate with boron, concentrated superphosphate)
  - complexes (NPK – various types, diammonium phosphate, foliar fertilizers)
- **Inorganic and organic chemical products**
- **Condensed and liquefied gases (NH_3, O_2, N_2, SO_2 Ar)**
- **Polymers**
- **Catalysts for chemical industry**
- **Salts for treatment of metallic surfaces (degreasing salts, pickling, phosphatization, passivation)**

EXPORTERS:

CHIMICA

Foreign trade enterprise
Bucharest – ROMANIA
Splaiul Independenței 202A
Telephone : 495060
Telex : 11489 DANAZ-R
P.O. Box : 3915

DANUBIANA

Foreign trade enterprise
Bucharest – ROMANIA
Blvd. Republicii 10
Telephone : 156051 ; 156052
Telex : 11184 DANEX
P.O. Box : 1–74

DUNĂREA

Foreign trade enterprise
Bucharest – ROMANIA
Str. Varșovia 4
Telephone : 331681
Telex : 10435 DUNEX-R
P.O. Box : 63124

SYNTHETIC FIBRES WORKS JASSY

a modern unit of advanced technology, much ahead in the Romanian chemical industry, produces and delivers a wide range of polyester fibres, yarns and films, as well as equipment and spare parts for chemical and textile industries as follows:

- **Polyester synthetic fibres :**
  polyester fibres of cotton type ; polyester fibres of wool type (staple, top and tow) ; polyester fibres of flax type ; polyester fibres high shrinkage.
- **Polyester synthetic textile yarns :**
  polyester continuous filament, textile twisted yarns for sewing thread ; polyester continuous filament textured yarn (semi-dull or bright, round or profiles, raw white or dyed) for knittings tissues or clothes.
- **Polyester industrial yarns for different technical end-uses**
- **Polyester films (transparent or light dull) for electrotechnical industry**
- **Complex equipments for fibre production and for chemical industry**
- **Yarn guides from sintered alumina for textile industry**

For any additional details regarding its products and services please write directly to :

COMBINATUL DE FIBRE
SINTETICE IAȘI
19 Țuțora Street,
6600 IAȘI,
Telex : 022251,
ROMANIA

THE SYNTHETIC FIBRES
WORKS JASSY
EXPORTS ITS PRODUCTS BY :

I.C.E. DANUBIANA BUCHAREST,
service E. 9, telex 11184
- **FOR FIBRE AND YARNS**

I.C.E. TEXTILE MACHINE
HEADQUARTER –
– "TISCEMA"
BUCHAREST telex 11185
- **FOR EQUIPMENTS AND SPARE PARTS.**

1988 JAN 2

TRAVAUX PARUS AUX ÉDITIONS DE L'ACADÉMIE DE LA RÉPUBLIQUE SOCIALISTE DE ROUMANIE

ELENA CEAUŞESCU, **Progrese în chimia şi tehnologia polimerilor**, 1986, 446 p.

ELENA CEAUŞESCU, **Forschungen im Bereich der Chemie und Technologie der Polymere**, 1986, 444 p.

ELENA CEAUŞESCU, **Noi cercetări în domeniul compuşilor macromoleculari**, 1981, 536 p.

ELENA CEAUŞESCU, **Polimerizarea stereospecifică a izoprenului**, 1979, 307 p.

ELENA CEAUŞESCU, **Research work on synthesis and characterization of macromolecular compounds, Contributions**, 1974, 251 p.

I. G. MURGULESCU, **Introducere în chimia fizică, Vol. I. 1. Atomi, molecule, legătură chimică** 1976, 560 p.

I. G. MURGULESCU, V. EM. SAHINI, **Introducere în chimia fizică, Vol. I, 2. Structura şi proprietăţile moleculelor**, 1979, 604 p.

I. G. MURGULESCU, E. SEGAL, **Introducere în chimia fizică. Vol. II. 1. Teoria molecular-cinetică a materiei**, 1979, 1036 p.

I. G. MURGULESCU, TATIANA ONCESCU, E. SEGAL, **Introducere în chimia fizică. Vol. II. 2. Cinematică chimică şi cataliză**, 1981, 1024 p.

I. G. MURGULESCU, J. PĂUN, **Introducere în chimia fizică, Vol. I. 3. Nucleul atomic, reacţii nucleare, particule elementare**, 1982, 606 p.

I. G. MURGULESCU, RODICA VÎLCU, **Introducerea în chimia fizică. Vol. III. Termodinamica chimică**, 1982, 624 p.

I. G. MURGULESCU, O. M. RADOVICI, **Introducere în chimia fizică, vol. IV, Electrochimia**, 1986, 410 p.

R. VÎLCU, M. LECA, **Termodinamica polimerilor prin cromatografie de gaze**, 1987, 238 p.

RAUL MIHAIL, ION GROZEANU, **Estimarea secvenţială aplicată sistemelor chimice**, 1986, 406 p.

M. BREZEANU, L. PATRON, M. ANDRUH, **Combinaţii complexe polinucleare şi aplicaţiile lor**, 1986, 244 p.

A. T. BALABAN et al., **Labelled Compounds and Radiopharmaceuticals Applied in Nuclear Medicine**, coédition avec John Wiley and Sons, 1986, 742 p.

D. PURDELA, **Nomenclatura chimiei organice — IUPAC**, 1986, 454 p.

PETRU BUDRUGEAC, **Probleme de chimie**, 1986, 280 p.

T. ONCESCU, S. G. IONESCU, **Conversie fotochimică şi stocare de energie**, 1985, 272 p.

V. DRĂGUŢAN, A. T. BALABAN, M. DIMONIE, **Olefin Metathesis and Ring-Opening Polymerization of Cyclo-Olefins**, coédition avec John Wiley and Sons, 1985, 544 p.

C. LITEANU, I. RICĂ, **Optimizarea proceselor analitice**, 1985, 360 p.

N. PERESCU, **Chimia extracţiei cu solvenţi şi aplicaţii**, 1985, 212 p.

V. E. SAHINI, M. HILLEBRAND, **Chimie cuantică în exemple şi aplicaţii**, 1984, 378 p.

GH. MARCU, **Chimia compuşilor coordinativi**, 1984, 415 p.

E. CORDOŞ, C. MANOLIU, **Spectrometria de absorbţie şi fluorescenţa atomică**, 1984, 178 p.

C. BODEA, **Tratat de biochimie vegetală, p. II, t. V**, 1984, 438 p.

N. ASANDEI, A. GRIGORIU, **Chimia şi structura fibrelor**, 1983, 395 p.

N. IONESCU, M. CĂLDĂRARU, **Oxidarea catalitică a olefinelor inferioare**, 1983, 178 p.

C. CAŞCAVAL, **Studiul polimerilor prin piroliză şi cromatografie de gaze**, 1983, 220 p.

C. I. SIMIONESCU, F. DANEŞ, **Originea vieţii**, 1983, 110 p.

C. BODEA, **Tratat de biochimie vegetală, p. II, t. IV**, 1982, 408 p.

I. GĂLĂŢEANU, **Procese şi metode radiochimice în energetica nucleară**, 1981, 234 p.

CR. SIMIONESCU, VALERIA GORDUZA, **Polimeri biocompatibili şi biologic activi**, 1980, 479 p.

C. GH. MACAROVICI, **Analiza chimică cantitativă anorganică**, 1979, 457 p.

M. FLORESCU, **Metode ştiinţifice în dezvoltarea industriei chimice moderne**, 1979, 256 p.

I. ZUGRĂVESCU, MAGDA PETROVANU, **N-ylid chemistry**, coédition avec McGraw-Hill International Book Company U.S.A., 1977, 396 p.

ISSN 0035 — 3930

I.P. Informaţia c. 1470

43 426

Lei 40

$ 90 (pour un abonnement annuel)